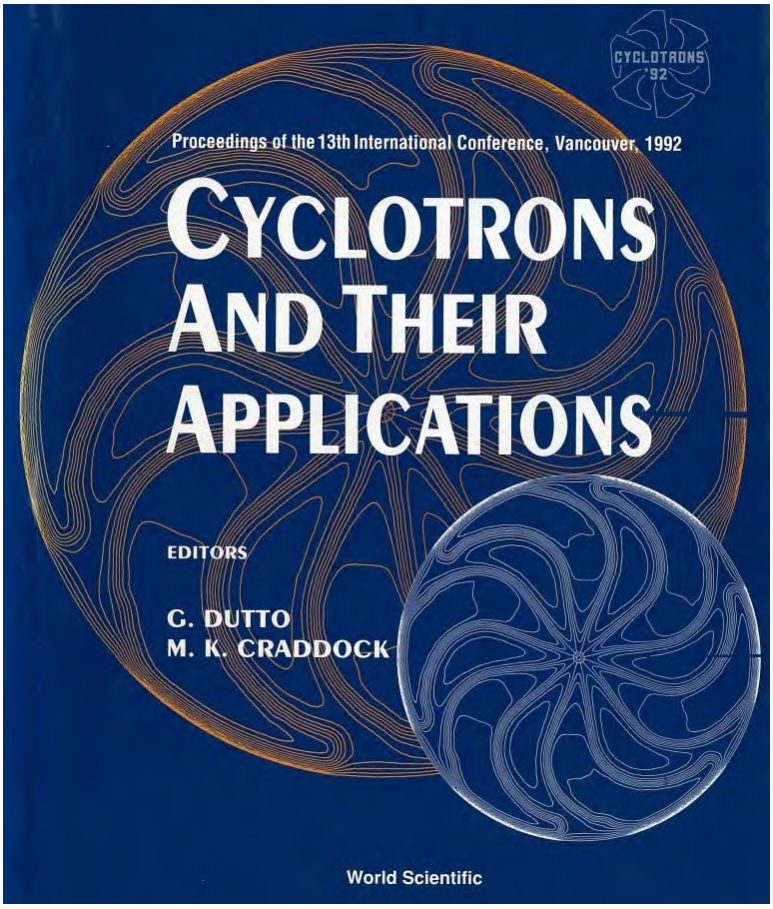
Cyclotrons 1992

Vancouver, BC, Canada
6-10 July, 1992

The links below lead to more detailed listings and eventually to Acrobat Format (PDF) files containing the papers.



Foreword
Conference Organization
Industrial Exhibitors and Sponsors
Opening Address

Index of Papers by:
Session
Authors
Keywords
Institutes

List of Participants
Conference Photographs
Cyclotron Data
International Cyclotron Conferences

First published by World Scientific, Singapore in 1993: ISBN 9810211309
Electronic edition produced with financial assistance from CERN and TRIUMF and with the permission of World Scientific, Singapore
Copyright © 1993 by World Scientific Publishing Co. Pte. Ltd.

Single photocopies of single articles may be made for private study or research. Illustrations and short extracts from the text of individual contributions may be copied provided that the source is acknowledged.

October 2013 JP Scientific (Nantwich) Ltd, UK

FOREWORD

The XIII International Conference on Cyclotrons and Their Applications was held at the Hotel Vancouver in Vancouver, British Columbia, from July 6-10, 1992. This was the 20th anniversary of the Sixth Conference, held in Vancouver in July 1972, and TRIUMF was honoured to have been chosen to host the conference a second time. The purpose of this conference series is to provide a forum for communication between all scientists and engineers involved with cyclotrons -- designers, builders and users. The organizers have therefore been delighted with the very supportive response from the community: both the attendance (241) and the number of papers submitted (181) have broken the records for previous conferences held in North America. We were especially pleased to see so many delegates from eastern European and Asian countries. The number of industrial exhibitors (26) was also a very gratifying record.

These statistics indicate the continuing vitality of the field. Although the construction of large cyclotrons for nuclear and particle physics seems to be reaching the point of saturation, the demand for smaller cyclotrons for other applications, particularly radioisotope production, seems to be unquenchable. Moreover, the intense beams from cyclotrons have made possible the conception and construction of much more exotic post-accelerator projects -- pion and kaon factories, cooling rings and, most recently, radioactive ion accelerators. For cyclotrons themselves, the application of superconducting magnets and rf systems continues to provide a fruitful source of novel designs. The last word on cyclotron design seems very far from being spoken!

The conference itself consisted of 15 oral sessions, with 24 invited and 36 contributed papers, and three poster sessions, with 130 papers. For the purposes of the proceedings we have arranged all the papers in sections according to the topics of the oral sessions, so that oral and poster papers on the same topic appear together. The remarks of welcome by Professor E.W. Vogt, Director of TRIUMF, and those of the Conference Chairman following the conference dinner are also included.

The organizers are happy to acknowledge the official sponsorship of the conference by the International Union of Pure and Applied Physics, the Canadian Association of Physicists, and the American Physical Society, through its Division of Physics of Beams. They are also very grateful for financial sponsorship by the Natural Sciences and Engineering Research Council of Canada (speakers' travel expenses), by AECL Research (a major contribution to the conference dinner), and by TRIUMF (additional travel funds). The Welcome Reception was generously sponsored by Nordion, Inc., summer support for a student assistant was provided by Ebco, Inc., and individual coffee breaks were sponsored by Alphatech International and Group 3, Inverpower Controls, and Varian Canada.

The initial planning for the conference was helped enormously by advice from members of the International Organizing Committee. Here there was a big turnover in membership from the previous conference and this is perhaps a suitable place to acknowledge the cyclotron community's debt to those who stepped down in 1989 for their many years of service; B.W. Allardyce (CERN), A.H. Botha (NAC), Y.N. Denisov (JINR), J. Fermé (GANIL), H.L. Hagedoorn (TUE), E.J. Jones (Harwell), Y. Jongen (UCL), J.M. Loiseaux (Grenoble), M.L. Mallory (MSU), J.A. Martin (ORNL), J.H. Ormrod (AECL), C. Yang (IMP) and K. Ziegler (VICKSI). John Martin, in particular, has served the committee and community faithfully since the very first conference held at Sea Island in 1959. The new members have been M. Fruneau (Grenoble), S. Gales (Orsay), H. Homeyer (VICKSI), A. Joubert (GANIL), R. Maier (Jülich), N.K. Mukhopadhyay (Calcutta), R. Ts. Oganessian (LNR, Dubna), D.K. Olsen (ORNL), D. Reitmann (NAC), G.H. Ryckewaert (UCL), H.

Schmeing (AECL), U. Trinks (Munchen), B-W. Wei (IMP) and, temporarily, J.A. Nolen (MSU). Another batch of members have announced their intention of retiring following this meeting, and again we salute them for their many years of service: H. Blosser (MSU), V.P. Dmitrievsky (LNP, Dubna), W. Joho (PSI), H. Kamitsubo (RIKEN) and D.H. Youngblood (Texas A&M).

The detailed organization of the scientific program was of course the responsibility of the Program Committee, and here we are indebted to our colleagues David Clark, Werner Joho, George Mackenzie, Reg Richardson and Harvey Schneider for their hard work over the last year, both inside and outside committee meetings. For the smooth running of the program we are grateful to the session chairmen, who ran what must have been one of the most punctual conferences ever. But our most profound thanks must go to the 663 authors, without whom there would have been no papers and no conference.

For the smooth operation of all other aspects of the conference, we are indebted to the dedicated efforts of the Local Committee members and their helpers. The secretariat, responsible for registration, was led initially by Maureen Iqbal and subsequently by Pat Stewart, with the help of Deanna Warner. The pressure in this job may be gauged from the fact that Maureen apparently decided that it would be less trouble to look after a new baby! Peter Grant created and nurtured the all-encompassing data base, while George Ludgate has had the dual responsibilities of budget and printing. Special credit must go to David Ross for design of the conference logo. Lorraine King has handled all the abstracts and papers and been responsible for the production of the proceedings. Bob Laxdal has looked after the Data Sheets, providing new ones for storage rings and trying to make the cyclotron list as up to date as possible. Harvey Schneider was responsible for all equipment and arrangements at the hotel, including the computer terminal room, and also for arranging the poster sessions and for coordinating the post-conference tour to Seattle. Milos Zach organized the very successful industrial exhibition, which ran from July 6-8.

The all-important social events -- the welcome reception on Sunday, the tour of TRIUMF and salmon barbecue at the UBC Museum of Anthropology on Monday, the excursions on Wednesday afternoon and the conference dinner on Thursday -- were coordinated very effectively by Elly Driessen. The TRIUMF tour was organized by Paul Schmor with the help of numerous staff members. Special mention should perhaps be made of the intrepid leaders of the Wednesday afternoon excursions -- Klaus Reiniger who led a 250 km tour of coast and mountain scenery, George Mackenzie whose group were obliged to break into a 19th century fort in order to see it after closing hours, and Jack Carey who monitored the smooth operation of the bar during the boat cruise. No less than 31 participants reached the top of Hollyburn mountain, with the women's gold medal going to Helena Lindquist and the men's to George Hendry. Finally, our particular thanks must go to our own secretaries, Maureen White and Lynn DeCaire, for their outstanding efforts in handling multifarious matters over many months.

The International Organizing Committee met in Vancouver during the conference to consider the traditional questions of whether the conference series should be continued, and if so, where the next conference should be held. The first question was answered with a rapid and resounding yes. The second took longer to decide, because of considerable competition, but a clear majority emerged in favour of accepting the long-standing invitation from the National Accelerator Centre at Faure in South Africa. We therefore look forward to the 1995 conference being held in Cape Town, probably in April, under the chairmanship of Dr. D. Reitmann.

M.K. Craddock, Conference Chairman
G. Dutto, Program Chairman

CONFERENCE COMMITTEES

International Organizing Committee

E. Acerbi (Univ. Milan)
H. Blosser (NSCL, East Lansing)
D. J. Clark (LBL, Berkeley)
M. K. Craddock (UBC/TRIUMF, Chairman)
V. P. Dmitrievsky (LNP, Dubna)
M. Fruneau (ISN, Grenoble)
S. Gales (IPN, Orsay)
Y. Hirao (NIRS, Chiba)
S. Holm (Univ. Uppsala)
H. Homeyer (VICKSI, Berlin)
W. Joho (PSI, Villigen)
A. Joubert (GANIL, Caen)
H. Kamitsubo (RIKEN, Saitama)
M. Kondo (RCNP, Osaka)
N. N. Krasnov (IPE, Obninsk)
E. Liukkonen (Univ. Jyväsklyä)
R. Maier (KFA, Jülich)
N. K. Mukhopadhyay (VEC, Calcutta)
R. Ts. Oganessian (LNR, Dubna)
D. K. Olsen (ORNL, Oak Ridge)
R. E. Pollock (IUCF, Bloomington)
D. Reitmann (NAC, Faure)
J. R. Richardson (UCLA/TRIUMF)
G. H. Ryckewaert (CRC, Louvain-la-Neuve)
H. Schmeing (AECL, Chalk River)
H. W. Schreuder (KVI, Groningen)
H. Schweickert (KFK, Karlsruhe)
U. Trinks (Tech. Univ. München)
B.-W. Wei (IMP, Lanzhou)
D. H. Youngblood (Texas A&M)

Program Committee

G. Dutto (Chairman)
D. J. Clark
M. K. Craddock
W. Joho
G. H. Mackenzie
J. R. Richardson
H. Schneider

Local Organizing Committee

M. K. Craddock (Chairman)
G. Dutto (Scientific Program)
E. Driessen (Social Events)
P. Grant (Database)
M. Iqbal (Secretariat)
L. King (Proceedings)
R. Laxdal (Data Sheets)
G. A. Ludgate (Budget & Printing)
H. Schneider (Equipment)
P. Stewart (Secretariat)
D. Warner (Secretariat)
M. White (Secretary)
M. Zach (Exhibits)

INDUSTRIAL EXHIBITORS

ALPHATECH INTERNATIONAL INC.
BALZERS
CERAMASEAL
CTS OF CANADA LTD
DYNAPOWER CORP.
DYNAPRO SYSTEMS INC
EBCO TECHNOLOGIES INC
EDWARDS HIGH VACUUM
EEV LTD
GMW/DANFYSIK
GROUP 3 TECHNOLOGY LTD
HEWLETT PACKARD (CANADA) LTD
ION BEAM APPLICATIONS SA
INVERPOWER CONTROLS LTD
LEYBOLD INC
MDC VACUUM PRODUCTS CORP
MKS INSTRUMENTS CANADA LTD
NORDION INTERNATIONAL INC
NTG NEUE TECHNOLOGIEN GMBH & CO KG
PERKIN ELMER
PRINCETON SCIENTIFIC CORP
RICHARDSON ELECTRONICS LTD
SWAGELOK CANADA LTD
TEKTRONIX CANADA INC
VARIAN CANADA INC
VAT INCORPORATED
VISTA CONTROL SYSTEMS INC

INDUSTRIAL SPONSORS

NORDION INTERNATIONAL INC
EBCO TECHNOLOGIES INC
ALPHATECH INTERNATIONAL INC
GROUP 3 TECHNOLOGY LTD
INVERPOWER CONTROLS INC
VARIAN CANADA INC

WELCOMING REMARKS

ERICH W. VOGT
Director of TRIUMF

It is my privilege and honour to welcome the return of this cyclotron conference to Vancouver. When you last convened here, twenty years ago, we were in the midst of building the world's largest and most complex cyclotron— the TRIUMF H^- spiral-ridge 520 MeV machine. As you will find on this visit, that cyclotron experienced a timely and healthy delivery, and its science program was nurtured by the stimulating climate of ideas associated with the standard model of quarks and leptons and unified forces. It has now led to the much-anticipated KAON factory.

You will also find a warm welcome to Vancouver, a city sprung magically in a drought-stricken rainforest. For conferences such as this one Vancouver has acted as an accretion-disk : some participants who come here never board their planes to return home. Anyone here wishing to explore such possibilities is urged to contact the genial Head of our Cyclotron Division, Gerardo Dutto.

We now have a sixty-two year history for cyclotrons, which were some of the first accelerators and continue to be among the most proliferative. It is fitting that you are meeting here in Reg Richardson's home town. Although he was not born in Vancouver he moved here at a very early age and his most magnificent work is connected with this city. Richardson's long scientific career has spanned the entire cyclotron era. He contributed greatly to Lawrence's early cyclotrons. He developed seminal ideas for accelerators which earned him the Wilson prize last year. Thirty years ago he conceived — at his summer estate on nearby Galiano Island — the ideas which led to the TRIUMF cyclotron. He headed TRIUMF during the crucial years in which our cyclotron was commissioned. Subsequently, and to this day, Richardson has contributed greatly to the accelerator ideas pertaining to our KAON factory and he has also proudly watched TRIUMF spawn a whole generation of small cyclotrons for isotope production. With this meeting we continue to honour Richardson's leadership in all matters pertaining to cyclotrons.

Vancouver has become a crossroads in the world of accelerators. This may seem unusual because, until rather recently, this was regarded as one of the remotest areas of the globe. Just over a century ago not a single European lived here. Exactly two centuries ago (June 6, 1792) Captains Galiano (for Spain) and Vancouver (for Britain), had first contact with our first peoples and they accidentally met, near the present site of TRIUMF. The state of European politics was such that British interests prevailed and this became British Columbia.

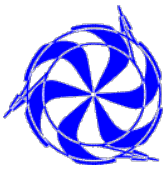
The first peoples whom Galiano and Vancouver encountered on Canada's west coast had a magnificent culture. According to the French anthropologist, Levi-Strauss, the art and mythology of our Haida and Kwakuitl Indians was the richest — next to the Greeks — that our world has produced. I urge you to experience some of this richness at the Anthropology Museum of the University of British Columbia when you visit it this evening.

With the large jets Vancouver is no longer remote. We regard this now as the hub of the world of accelerators, roughly equidistant (8-9 hours) from CERN, KEK and Waxahachie.

KAON will make Vancouver an exciting hub. We are ready to proceed toward construction and we know that the whole world of particle and nuclear physics is waiting for Canada to proceed. The final decision for KAON and the start to construction now only appear a few months away. The Governments of British Columbia and Canada have expressed their firm intent to provide two-thirds of KAON's construction costs (total $708M Cdn.). Everything now hinges on reconfirming that Canada's international partners will provide the remaining third of construction funds. Half of this international support is expected from the U.S., a quarter from Japan and the remaining quarter from a number of countries. Just ten days ago the federal government announced here that the Canadian delegation to secure this international funding will be headed by Stanley Hagen — a former British Columbia cabinet minister who is an exceptionally strong and visionary KAON supporter. KAON construction could be completed in six years. This project will make Vancouver the world centre for strong interaction physics and will maintain our great interest in cyclotrons. You will all want to return here, hopefully in less than 20 years time.

May your scientific sessions prosper.

August 31, 1992



Cyclotrons 1992

Vancouver, BC, Canada

Table of Sessions

I Opening Session - Cyclotrons New and Old

II Compact Cyclotrons

III TRIUMF and KAON (Tour Introduction)

IV Applications

V Medical Applications I - Radioisotopes

VI Medical Applications II - Radiotherapy

VII Storage Rings

VIII Ion Sources

IXa Theoretical Beam Dynamics

IXb Experimental Beam Dynamics

IXc Injection and Extraction Studies

IXd Beam Diagnostics

Xa Radiofrequency Systems

Xb Magnets

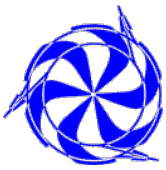
Xc Injection and Extraction Systems

Xd Beam Transport Systems

XI Control

Click on a session to display a list of papers.

	Systems
XII	Novel Cyclotrons
XIII	Radioactive Beam Facilities
XIV	Final Session
XV	Propriety of Accelerators (After-dinner talk)



Cyclotrons 1992

Vancouver, BC, Canada

List of Authors

A B C D E F G H I J K L M N O P Q R S T U V W X Y Z

Click on an author to display a list of papers.

A

Abe, J.
Abrosimov, N.K.
Adam, S.
Agematsu, T.
Albrand, S.
Alenitskiy, Ju.
Alessandria, F.
Alton, G.D.
Anderson, S.
Ando, A.
Antaya, T.A.
Aoki, K.
Arakaki, Y.
Arakawa, K.
Arnott, D.W.
Artamonov, S.A.
Arzumanov, A.A.
Audi, G.
Auger, G.

B

Bachman, D.A.
Bailey, J.
Bajard, M.
Baktash, C.
Ball, M.S.
Barnéoud, D.
Baron, E.
Batischev, V.
Bechtold, V.
Beeckman, W.
Bejsovec, V.
Bekhterev, V.
Bellomo, G.
Belmont, J.L.
Belov, V.P.
Berger, V.
Bergmark, T.
Bertsche, K.J.
Beuscher, H.
Bibet, D.

Biri, S.
Bizouard, G.
Blache, P.
Blaker, G.C.
Bloemhard, P.
Blosser, H.G.
Böge, H.G.
Bogdanov, P.V.
Bogomolov, S.L.
Bojovic, B.
Bony, J.
Borisov, O.
Bosotti, A.
Botha, A.H.
Botman, J.I.M.
Bouly, J.L.
Bourgarel, M.P.
Boux, R.
Bräutigam, W.
Brassart, N.
Briand, P.
Bricault, P.
Brigham, M.
Brings, R.
Brossard, S.
Brown, R.
Bru, B.
Bruandet, J.F.
Buchmann, L.
Buranov, V.
Burbeza, C.D.
Burger, S.J.
Busse, W.

C

Calabretta, L.
Campillo, G.
Capshew, T.
Carter, H.K.
Celliers, P.J.
Chabert, A.
Chang, H.
Chaudhri, M.A.
Chauvel, P.
Cherix, J.
Chervyakov, P.V.
Chesnov, A.
Chesnova, S.
Chida, K.
Ciavola, G.
Clark, D.J.
Clark, J.C.
Cole, D.
Collins, D.
Collins, J.C.

Commeaux, C.
Conard, E.
Conradie, J.L.
Cooper, M.
Cornell, J.C.
Corti, D.
Courdi, A.
Craddock, M.K.
Cronje, P.M.
Cui, X.
Cuttone, G.

D

Dale, D.J.
Dam, J.A.M.
Dambre, P.
D'Auria, J.M.
Davies, W.G.
de Conto, J.M.
De Martinis, C.
de Villiers, J.G.
Delhez, J.L.
Derenchuk, V.
Derrig, G.
Dewees, W.
Di Biasi, G.
Di Giacomo, M.
Diamond, W.T.
Didyk, A.Yu.
Dmitriev, S.N.
Dmitriev, S.P.
Dolinsky, A.V.
Dombsky, M.
Dowling, D.T.
du Toit, Z.B.
Dufour, J.P.
DuPlantis, D.
Dutto, G.

E

East, G.
Efremov, A.
Eiche, M.
Ekström, C.
Eliseev, V.A.
Ellison, T.J.P.
Enchevich, I.B.
Endo, K.
Erdman, K.L.
Ershov, B.D.

F

Farley, F.
Fehsenfeld, P.
Fenemore, R.E.F.
Fermé, J.
Fietier, N.
Fifield, K.
Fisch, R.K.
Fominenko, V.P.
Fong, K.
Fourie, D.T.
Frame, D.W.
Franklin, E.J.S.
Fraser, J.S.
Frei, H.
Fridén, C.-J.
Friesel, D.L.
Fruneau, M.
Fujita, M.
Fukuda, M.
Fukumoto, S.
Fukumoto, Y.

G

Gajewski, K.
Gammino, S.
Gangrski, Yu.P.
Garrett, J.D.
Gaudart, L.
Gelbart, W.Z.
Gerasimov, V.
Gikal, B.
Gillibert, A.
Gimond, G.
Giove, D.
Glazov, A.
Glushko, A.
Gmaj, P.
Golovanivsky, K.
Goodman, G.B.
Gorcovets, M.
Gordon, M.M.
Goto, A.
Gotovtsev, O.
Graham, J.
Grey-Morgan, T.
Grimmett, G.
Guisset, M.
Gulamov, I.
Gulbekyan, G.G.
Guo, M.
Gustafsson, S.

H

Hagedoorn, H.L.
Halbach, K.
Hamidov, N.K.
Hamilton, B.
Hardy, J.C.
Hatanaka, K.
Hayakawa, Y.
Hayashi, Y.
Haynes, D.L.
Heikkinen, P.
Hendry, G.O.
Herault, J.
Hermansson, L.
Herschbach, M.
Hicks, J.W.
Hirao, Y.
Hoffmann, C.R.
Hogan, M.E.
Holm, S.
Holmgren, B.
Hoshika, K.
Hosono, K.
Houtman, H.
Hubbard, R.E.
Humbel, M.

I

Ichac, J.P.
Ichida, S.
Ikegami, H.
Iljasov, O.
Inada, T.
Irie, Y.
Ishibori, I.
Ishigaki, T.
Ishii, K.
Iso, K.
Isoya, Y.
Itahashi, T.
Itano, A.
Ito, K.
Itoh, S.
Iudin, L.I.
Ivanenko, A.
Ivanov, E.M.

J

Jacky, J.
Jahnke, P.
Jayamanna, K.
Jenner, D.
Jeon, D.
Jiang, J.Z.

Jiang, W.M.
Joh, K.
Johansson, A.
Johansson, O.
Joho, W.
Jones, C.M.
Jones, F.W.
Jones, W.P.
Jongen, Y.
Josipovic, M.
Joubert, J.
Jungwirth, H.N.
Juras, R.C.

K

Kadantsev, S.
Kageyama, T.
Kalet, I.
Kamiya, T.
Kanazawa, M.
Kaplanski, J.M.
Karamian, S.A.
Karasawa, T.
Kase, M.
Kasugai, Y.
Katayama, T.
Kato, T.
Keitel, R.
Kennepohl, K.
Khalkin, V.A.
Kibayashi, M.
Kiewiet, H.H.
Kim, J.W.
Kimura, Y.
King, J.
Kitagawa, A.
Kleeven, W.J.G.M.
Kleinrahm, A.
Ko, J.
Kochkin, V.
Kodaira, K.
Kohler, I.H.
Kohno, T.
Kokorin, A.M.
Kolesov, I.
Komissarov, P.Yu.
Kondo, M.
Korenev, S.A.
Kormicki, J.
Korolev, L.E.
Kost, C.J.
Kozin, A.I.
Krasnikov, Yu.M.
Kritzinger, J.J.
Krivánek, M.

Kucera, J.
Kuchar, J.
Kuligin, V.S.
Kumada, M.
Kumata, Y.
Kunkel, W.B.
Kuo, T.Y.T.
Kutner, V.B.

L

Laborie, G.
LaForge, C.
Lafoux, A.
Laisné, A.
Lane, S.N.
Lanz, P.
Latushkin, S.T.
Launé, B.
Laxdal, R.E.
Lee, I.Y.
Leonov, V.V.
Leroy, R.
Leung, K.N.
Levy, C.D.P.
Lewitowicz, M.
Li, C.Y.
Liang, C.F.
Liatard, E.
Lindqvist, E.H.
Lipnicki, M.
Liu, C.
Liu, Z.
Liukkonen, E.
Lofnes, T.
Loiseaux, J.M.
Loiselet, M.
Ludgate, G.A.
Lundgren, S.A.
Lundström, B.
Lyneis, C.M.

M

Ma, Y.
Ma, Z.
Mackay, D.B.
Mackenzie, G.H.
Maeckelburg, D.
Märki, M.
Maier, R.
Makarov, A.A.
Mallory, M.L.
Malyshev, O.N.
Mandrillon, P.

Marie, H.
Markov, B.N.
Marti, F.
Martin, S.A.
Maruhashi, A.
Maruyama, M.
Maughan, R.
May, D.P.
McCammon, D.
McDonald, D.S.
McDonald, M.
McNeely, P.
Meads, Jr., P.F.
Meigs, M.J.
Meshkov, I.N.
Mezger, A.C.
Michelato, P.
Mikhailov, V.G.
Mikheev, G.F.
Miller, P.
Mills, G.D.
Milton, B.F.
Mironov, Yu.T.
Misawa, T.
Mitchel, G.R.
Mitra, A.K.
Mittig, W.
Miura, I.
Montsanglant, B.
Morduev, A.
Morelle, J.-L.
Mormiche, M.
Moryakov, V.P.
Moscatello, M-H.
Moshkin, V.N.
Mosko, S.W.
Mouat, M.
Mouchaty, G.
Mouris, J.F.
Mudrolyubov, V.G.
Müller, A.
Mueller, A.C.
Mukherjee, B.N.
Muminov, A.I.
Murakami, T.
Muto, K.

N

Nagayama, K.
Nakagawa, T.
Nakamura, Y.
Nara, T.
Naumov, I.V.
Nel, W.A.G.
Nifenecker, H.

Nishiguchi, M.
Nishino, M.
Nitschke, J.M.
Noda, K.
Nolen, J.A.
Norman, G.
Novikov, D.
Novikov, V.

O

Obert, J.
Oganessian, R.Ts.
Oganessian, Yu.Ts.
Ogata, H.
Ogawa, H.
Ohshiro, Y.
Okamura, T.
Okumura, S.
Olivetto, C.
Olsen, D.K.
Onishchenko, L.M.
Orzechowski, J.
Osakabe, M.
Osberg, E.A.
Ota, T.

P

Paans, A.M.J.
Pacquet, J.Y.
Pagani, C.
Panvier, R.
Papash, A.I.
Parhomchuk, V.V.
Paris, P.
Pattyn, E.
Pavlov, S.N.
Pearce, D.R.
Pearson, J.B.
Pedroni, E.
Pei, A.
Pei, X.
Pelzer, W.
Penco, C.
Petri, H.
Pfister, U.
Pieterman, K.
Pisman, A.Ya.
Pitatelev, G.
Plagnol, E.
Pálinkás, J.
Poe, D.
Poirier, R.L.
Pokrovskii, A.S.

Pollock, R.E.
Popeko, G.S.
Popov, S.
Postiau, N.
Pronin, N.V.
Pugatch, V.
Putaux, J.C.

Q

Qiao, Q.

R

Raadu, M.A.
Raia, G.
Rattray, T.
Reid, D.D.
Reistad, D.
Reitmann, D.
Rezvov, V.A.
Riabov, G.A.
Ricaud, Ch.
Rifuggiato, D.
Rinta-Nikkola, M.
Risler, R.
Rodin, A.M.
Roels, L.M.M.
Rogers, J.P.
Rogers, R.C.
Rogge, M.
Rohwer, P.F.
Root, L.
Roshchin, A.A.
Rossi, L.
Roy, G.
Rudchik, A.T.
Ruegg, R.
Ruth, T.J.
Ryckewaert, G.
Rykov, A.

S

Saito, T.
Sakuma, S.
Samsonov, E.
Sano, M.
Sarkisyan, A.L.
Sarkisyan, L.A.
Sato, K.
Sato, M.
Sato, Y.
Satoh, S.

Satoh, T.
Savalle, A.
Schippers, J.M.
Schmeing, H.
Schmor, P.W.
Schneider, H.R.
Schreuder, H.W.
Schukeilo, I.A.
Schutz, Y.
Schwandt, P.
Sedlacek, M.
Sekiguchi, M.
Semenov, M.
Sery, A.A.
Severgin, Yu.P.
Shen, Z.
Sherrill, B.
Shida, Y.
Shiltsev, V.D.
Shimizu, A.
Shukeylo, I.A.
Shychikov, G.I.
Sidorchuk, S.I.
Sigg, P.K.
Sivtsov, G.
Sklyarenko, V.I.
Sloan, T.
Smelser, P.
Smit, H.A.
Smolin, V.A.
Snyder, S.
Sokol, Ye.A.
Sokolov, G.L.
Sortais, P.
Soudée, M.
Sowinski, J.
Spinney, G.
Sprenger, H.
Stammbach, Th.
Starodub, G.Ya.
Steckmeyer, J.C.
Stepantsov, S.V.
Stetson, J.
Stevenson, N.R.
St-Laurent, M.G.
Stogov, Yu.I.
Strokach, A.P.
Stursa, J.
Sudou, M.
Suit, H.D.
Sura, J.
Susini, A.
Syresinm, Ye.M.

T

Tachibana, M.
Tachikawa, T.
Tada, J.
Tadokoro, M.
Takada, E.
Takada, Y.
Takahashi, N.
Takayama, T.
Tamura, K.
Tanaka, R.
Tang, J.Y.
Tarovik, M.N.
Tatum, B.A.
Tazawa, S.
ten Kate, H.J.H.
Ter-Akopian, G.M.
Theron, P.J.
Thornton, A.F.
Tihomirova, S.T.
Tilbury, R.
Timakov, V.A.
Timmermans, C.J.
Toda, Y.
Tomizawa, M.
Toporkov, D.
Toth, K.S.
Tran, D.
Trejbal, Z.
Trinks, U.
Tsuji, H.
Tsujii, H.

U

Unezhev, V.N.
Uraki, M.

V

Valek, A.
Val'Kov, A.E.
van Rooyen, D.M.
Varisco, G.
Vasilenko, A.
Vasiliev, A.A.
Venikov, N.I.
Verbruggen, R.
Vienet, R.
Vignon, B.
Vincent, D.
Vincent, J.
Vincent, J.S.
Vishnevsky, I.N.
Voitsechovsky, B.
Volchenkov, V.A.

Vorobiev, A.A.
Vorogushin, M.F.

W

Wagner, Jr., H.N.
Wang, F.
Wang, Q.
Wang, Y.
Watanabe, S.
Watanabe, T.
Webers, G.A.
Wedberg, R.
Wedekind, M.
Weehuizen, H.F.
Wei, B.W.
Wei, J.
Wells, R.P.
Westerberg, L.
Whittemore, W.L.
Wilkinson, N.A.
Winger, J.
Wootton, P.
Wu, D.
Wucherer, P.
Wüstefeld, G.

X

Xia, J.
Xie, K.
Xie, X.
Xie, Z.Q.

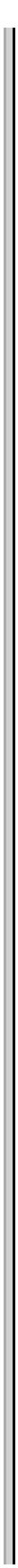
Y

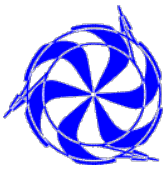
Yamada, S.
Yamada, T.
Yamamoto, H.
Yamamoto, Y.
Yamashita, Y.
Yamazaki, N.
Yamazaki, T.
Yang, D.
Yano, Y.
Yarosh, V.E.
Ye, F.
Yin, Q.
Yin, Y.
Yokota, W.
Yoshizawa, M.
Young, A.T.
Yuan, P.
Yudin, L.I.

Yurkon, J.

Z

Zach, M.
Zaika, N.I.
Zaitseva, N.G.
Zaplatin, E.
Zaplatin, N.
Zelenskii, A.N.
Zhang, J.
Zhang, W.
Zhang, X.
Zhao, H.
Zhmendak, A.V.
Zhou, X.H.
Zhu, X.
Ziai, F.
Zibra, F.
Ziegler, K.
Zlomanczuk, J.





Cyclotrons 1992

Vancouver, BC, Canada

Keyword Index

A

acceleration
accumulation
AGOR
ALICE

B

background
beam-losses
beam-transport
betatron
BNL
booster
bunching

C

cathode
cavity
CERN
closed-orbit
controls
COSY
coupling
cryogenics
cyclotron

D

diagnostics
dipole

E

ECR
ECRIS
electromagnetic-fields
electron
emittance
extraction

Click on a keyword to display a list of papers.

F

factory
feedback
focusing

H

heavy-ion
high-voltage

I

impedance
injection
insertion
instrumentation
interlocks
ion
ion-source
ISAC
ISOL
isotope-production

J

JAERI

K

kaon
kicker
klystron

L

laser
lattice
light-ion
linac
luminosity

M

MCP
micro-particles
microtron
monitoring
multipole

N

neutron

O

octupole
optical-matching
optics

P

permanent-magnet
photon
pick-up
plasma
polarization
positron
power-supply
proton

Q

quadrupole

R

radiation
radioactivity
resonance
rf-amplifier
rfq

S

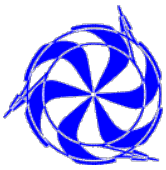
scattering
septum
sextupole
shielding
simulation
site
solenoid
space-charge
status
storage-ring
survey
synchro-cyclotron
synchrotron

T

tandem-accelerator
target
TRIUMF

V

vacuum



Cyclotrons 1992

Vancouver, BC, Canada

List of Institutes

ANL
Argonne, Illinois, USA

ANSTO
Menai, NSW, Australia

Ansaldo Componenti
Genoa, Italy

Associated Universities Oak Ridge
Oak Ridge, Tennessee, USA

Atomic Energy of Canada
Chalk River, Ontario, Canada

Austin Hospital & University of Melbourne
Melbourne, Australia

Australian National University
Canberra , Australia

BESSY
Berlin, Germany

CEN-Grenoble
Grenoble, France

CEN/Saclay
Gif-sur-Yvette, France

CERN
Geneva,

Click on an institute to display a list of authors.

Switzerland

CSNSM
Orsay, France

Center for Applied Physics and Technology
Lipetsk, Russia

Centre Antoine Lacassagne
Nice, France

Cryocon B.V.
Amersfoort, The Netherlands

Cyclotron Inc.
Napa, California, USA

Cyclotron Isotopes Manufacturing
Buckinghamshire, England

Czechoslovak Academy of Sciences
Rez, Czechoslovakia

D.V. Efremov Scientific Research Institute of Electrophysical Apparatus
St. Petersburg, Russia

Ebco Technologies Ltd
Richmond, BC, Canada

Eindhoven University of Technology
Eindhoven, The Netherlands

FZJ
Jülich, Germany

FZK
Karlsruhe,

Germany

GANIL
Caen, France

General Atomics
San Diego,
California, USA

Graduate School of
Nuclear Industry
Beijing, People's
Republic of China

HMI
Berlin, Germany

Hammersmith
Hospital
London, England

Harper Hospital
Detroit, Michigan,
USA

Harvard Medical
School
Boston,
Massachusetts,
USA

INFN/LASA
Segrate, Italy

INFN/LNS
Catania, Italy

IPN
Orsay, France

Indiana University
Bloomington,
Indiana, USA

Institute for
Nuclear Physics
Novosibirsk, Russia

Institute for
Nuclear Research
Kiev, Ukraine

Institute of Modern
Physics
Lanzhou, People's
Republic of China

Institute of Nuclear

Physics
Tashkent, Republic of Uzbekistan

Institute of Nuclear Research of the Hungarian Academy of Sciences
Debrecen, Hungary

Institute of Nuclear Research
Shanghai, People's Republic of China

Institute of Nuclear Research, Russian Academy of Sciences
Moscow, Russia

Ion Beam Applications
Louvain-la-Neuve, Belgium

JAERI
Gunma, Japan

JINR
Dubna, Russia

Japan Steel Works Ltd.
Tokyo, Japan

Japan Steel Works Ltd., Research Center for Advanced Technologies
Chiba, Japan

KEK
Ibaraki, Japan

Kazakhstan Academy of Sciences
Alma-Ata, Republic of Kazakhstan

Kernfysisch Versneller Instituut
Groningen, The Netherlands

Kurchatov Institute
Moscow, Russia

LBL
Berkeley,
California, USA

LPC
Caen, France

Medi + Physics
Inc.
Arlington Heights,
Illinois, USA

Moscow Institute-
Internate
Moscow, Russia

NIRS
Chiba, Japan

NSCL
East Lansing,
Michigan, USA

Nagoya University
Nagoya, Japan

National
Accelerator Centre
Faure, Republic of
South Africa

National Medical
Cyclotron
Camperdown,
NSW, Australia

ORNL
Oak Ridge,
Tennessee, USA

Osaka University
Osaka, Japan

PSI
Villigen,
Switzerland

Petersburg Nuclear
Physics Institute
Gatchina, Russia

RIKEN
Saitama, Japan

Royal Institute of

Technology
Stockholm, Sweden

Simon Fraser University
Burnaby, BC, Canada

Sumitomo Heavy Industries Systems Engineering Laboratory
Tokyo, Japan

Sumitomo Heavy Industries
Ehime, Japan

Sumitomo Heavy Industries, Toyo-shi
Toyo-shi, Japan

TRIUMF
Vancouver, Canada

TU München
Garching, Germany

TU Twente
Enschede, The Netherlands

Texas A&M University
College Station, Texas, USA

The Johns Hopkins University
Baltimore, Maryland, USA

The University of Texas
Houston, Texas, USA

Thomson Tubes Electroniques
Velizy-Villacoublay, France

Université Catholique de Louvain
Louvain-la-Neuve,

Belgium

Université Joseph Fourier
Grenoble, France

University Hospital Groningen, The Netherlands

University of Alberta
Edmonton, Alberta, Canada

University of British Columbia
Vancouver, Canada

University of Jyväskylä
Jyväskylä, Finland

University of Tokyo
Tanashi-shi, Tokyo, Japan

University of Toronto
Toronto, Ontario, Canada

University of Tsukuba
Ibaraki, Japan

University of Washington
Seattle, Washington, USA

Uppsala University
Uppsala, Sweden





LIST OF PARTICIPANTS

AUSTRALIA

Department of Medical Physics
Austin Hospital
Heidelberg Victoria 3084
CHAUDHRI, M.A.

Occupational Health and Safety Program
National Medical Cyclotron
ANSTO, PMB-1
Menai NSW 2234
MUKHERJEE, B.

AUSTRIA

Magnet Technology Department
Industrial Plants
Elin Energieanwendung GmbH
Elin-Sud-Str. 20
A-8160 Weiz
WENGER, S.

BELGIUM

Ion Beam Applications (IBA)
2 Chemin du Cyclotron
B-1348 Louvain-la-Neuve
CONARD, E.
JONGEN, Y.

Centre de Recherches du Cyclotron
Université Catholique de Louvain
2 Chemin Du Cyclotron
B-1348 Louvain-la-Neuve
LOISELET, M.
POSTIAU, N.
RYCKEWAERT, G.H.

CANADA

AECL Research
Chalk River, ON K0J 1J0
DAVIES, W.G.
DIAMOND, W.T.
HARDY, J.C.
HOFFMANN, C.R.
LINDQVIST, E.H.
SCHMEING, H.

British Columbia Cancer Agency
600 West 10th Ave.
Vancouver, B.C.
GOODMAN, G.B. (retired)

Dynapro Systems
800 Carleton Court
Annacis Island
New Westminster, B.C. V3M 6L3
CARLSON, N.L.

Ebco Technologies
4004 Wesbrook Mall
Vancouver, B.C. V6T 2A3
CLINE, R.W.
DAWSON, R.J.
EICHE, M.
EPPICH, R.
ERDMAN, K.L.
LUDWIG, D.

Department of Science and Technology
Medicine Hat College
Medicine Hat, Alberta T1A 3Y6
TSONG, F.

Nordion
4004 Wesbrook Mall
Vancouver, B.C. V6T 2A3
ABEYSEKERA, B.F.
DICKIE, W.J.
WEBSTER, B.A.

Department of Chemistry
Simon Fraser University
Burnaby Mountain
Burnaby, B.C. V5A 1S6
D'AURIA, J.M.

TRIUMF
4004 Wesbrook Mall
Vancouver, B.C. V6T 2A3
ADAM, M.
BAARTMAN, R.A.
BLACKMORE, E.W.
BLAKER, G.C.
BURGERJON, J.J.
CRADDOCK, M.K.
DUTTO, G.
ENCHEVICH, I.
FONG, K.
GELBART, W.Z.
HOUTMAN, H.
HURST, A.
JONES, F.

TRIUMF Continued...
KEITEL, R.
KOSCIELNIAK, S.
KOST, C.J.
LAVERTY, M.
LAXDAL, R.E.
LEE, R.
LEVY, C.D.P.
MACKENZIE, G.H.
MAMMERELLA, F.
MILTON, B.F.
MITRA, A.K.
MOUAT, M.
PEARCE, D.R.
POIRIER, R.L.
RAWNSLEY, W.
RICHARDSON, J.R.
ROOT, L.
SAMPLE, J.
SCHMOR, P.W.
SCHNEIDER, H.R.
STANFORD, G.
STEVENSON, N.R.
STINSON, G.M.
THORSON, I.M.
UZAT, B.
VAN DEN ELZEN, R.
WILKINSON, N.A.
YIN, Y.
ZACH, M.

University of British Columbia/TRIUMF PET Program
2211 Wesbrook Mall
Vancouver, B.C. V6T 2B5
RUTH, T.J.

Department of Physics
Université de Montréal
Montréal, PQ H3C 3J7
LESSARD, L.

CHINA, PEOPLE'S REPUBLIC OF
Institute of Electrical Appliances
No. 15 Wei Yuan Rd.
Lanzhou 73000
LI, Zhen

Institute of Modern Physics (IMP)
Academia Sinica
POB 57, 253 Nanchang Road
Lanzhou 730000
WEI, B.W.
YE, F.

CHINA, REPUBLIC OF
Institute of Nuclear Energy Research (INER)
1000 Wen-Hua Rd. POB 3-27
Lung-Tan 32500
SONG, P-S.
TING, G.
TONG, Y-C.

CZECHOSLOVAKIA
Nuclear Physics Institute (NPI)
Czechoslovak Academy of Sciences
250 68 Rez, near Prague
STURSA, J.

FINLAND
Accelerator Laboratory
University of Jyväskylä
P.O. Box 35
SF-40351 Jyväskylä
HEIKKINEN, P.
LIUKKONEN, E.
RINTA-NIKKOLA, M.

FRANCE
Laboratoire du Cyclotron
Centre Antoine Lacassagne
227 Ave. de la Lanterne
F-06200 Nice Cedexycercon
MANDRILLON, P.
TANG, J.Y.

CNRS-CERI
3A Rue de la Ferollerie
45071 Orleans Cedex 2
BRIAUD, J.
LE POLOTEC, L.

Cyceron
Bd. H. Becquerel, B.P. 5027
F-14021 Caen Cedex
LE POEC, C.L.

GANIL
BP 5027
F-14021 Caen Cedex
BARON, E.
BIBET, D.
BRICAULT, P.
RICAUD, Ch.

AGOR Project
Institut de Physique Nucléaire (IPN)
B.P. 1
F-91406 Orsay Cedex
LAUNÉ, B.

Institut des Sciences Nucléaire (ISN)
53 Avenue des Martyrs
F-38026 Grenoble Cedex
BELMONT, J.L.
FRUNEAU, M.

Thomson Tubes Electroniques
CP 121 405
Velizy-Villacoublay Cedex
ICHAC, J.P.

GERMANY

Bruker Analytische Meβtechnik GmbH
Wikinger Str. 13
D-7500 Karlsruhe 21
BEDAU, J.

Institut für Kernphysik
Forschungszentrum Jülich GmbH (KFA)
Postfach 1913
D-5170 Jülich 1
BRÄUTIGAM, W.
KENNEPOHL, K.
MAIER, R.
ZAPLATIN, E.

Gesellschaft für Schwerionforschung mbH (GSI)
Postfach 11 05 52
D-6100 Darmstadt
HARTWIG, D.

Bereich Schwerionphysik
Hahn-Meitner Institut (HMI)
Glienickerstr 100
D-1000 Berlin 39
BUSSE, W.
HOMEYER, H.
PELZER, W.
ZIEGLER, K.

Institut für Kernphysik III/Z
Kernforschungszentrum Karlsruhe GmbH (KFK)
Postfach 3640
D-7500 Karlsruhe
BECHTOLD, V.
FEHSENFELD, P.

Siemens AG
Friedrich-Ebert-Strasse
W-5060 Bergisch-Gladbach 1
ANTON, F.

Physics Dept. E12
Technische Universität München
James-Franck-Strasse
D-8046 Garching
TRINKS, U.

HUNGARY

Institute of Nuclear Research of the Hungarian Academy of Sciences (ATOMKI)
H-4001 Debrecen, Pf. 51
VALEK, A.

INDIA

Variable Energy Cyclotron Centre
Department of Atomic Energy
Government of India
Sector 1, Block AF
Bidhan Nagar,Calcutta 700 064
MUKHOPADHYAY, N.K.

ITALY

Laboratorio Acceleratori e Superconduttivita Applicata (LASA), INFN
Universita di Milano
Via F.lli Cervi 201
I-20090 Segrate (MI)
BOSOTTI, A.
PAGANI, C.

Laboratorio Nazionale del Sud (LNS-INFN)
Viale A. Doria Ang. S. Sofia
95125 Catania
CALABRETTA, L.
DI GIACOMO, M.
GMAJ, P.
MOSCATELLO, M.H.
SURA, J.

JAPAN

Takasaki Radiation Chemistry Research Estabmt.
Japan Atomic Energy Research Institute (JAERI)
1233 Watanuki-machi, Takasaki
Gunma-ken 370-12
ARAKAWA, K.
FUKUDA, M.

Division of Accelerator Research
National Institute for Radiological Sciences (NIRS)
9-1 Anagawa 4-chome
Chiba-shi 260
NODA, K.

Chiba Facility
Nihon Medi-Physics Co. Ltd.
3-1 Kitasoda
Sodegaura 299-02
SANO, T.
TAKAHASHI, M.

Quantum Equipment Division
Engineering Team
NKK Corporation
2-1 Suehiro-cho Tsurumi-ku
Yokohama 230
SHIMIZU, M.

Research Center for Nuclear Physics (RCNP)
Osaka University
10-1 Mihogaoka, Ibaraki-shi
Osaka 567
ITAHASHI, T.
KONDO, M.
MIURA, I.

Cyclotron Laboratory
Institute of Physical and Chemical Research (RIKEN)
2-1 Hirosawa, Wako-Shi
Saitama 351-01
GOTO, A.
YANO, Y.

Quantum Equipment Division
Sumitomo Heavy Industries
Sobiraki-cho 5-2
Niihama-city, Ehime 792
KUMATA, Y.
TAZAWA, S.

Systems Engineering Laboratory
Sumitomo Heavy Industries
2-4-15 Yato-cho, Tanashi-city
Tokyo 188
OKAMURA, T.

Institute for Nuclear Study (INS)
University of Tokyo
Midori-cho 3-2-1, Tanashi-shi
Tokyo 188
FUJITA, M.
SEKIGUCHI, M.
WATANABE, S.
YAMASHITA, Y.
YAMAZAKI, T.

Institute of Clinical Medicine
Proton Medical Research Center
University of Tsukuba
Tsukuba-shi, Ibaraki-ken 305
FUKUMOTO, S.

KAZAKHSTAN
Institute of Nuclear Physics (INP)
Kazakhstan Academy of Sciences
Alma-Ata 480082
ARZUMANOV, A.A.

NETHERLANDS
Cryocon B.V.
Algolweg 2
3821 BH Amersfoort
PIETERMAN, K.

Cyclotron Laboratory
Eindhoven University of Technology
Postbus 513
5600 MB Eindhoven
KLEEVEN, W.J.G.M.
QUEENS, M.P.A.

Kernfysisch Versneller Instituut (KVI)
Zernikelaan 25
9747 AA Groningen
SCHIPPERS, J.M.
SCHREUDER, H.W.

Cyclotron Group
Vrije Universiteit
De Boele Laan 1081
HV Amsterdam
HOEKSTRA, C.

POLAND
Heavy Ion Laboratory
Warsaw University
ul. Banacha 4
Warszawa 02-097
SLIWINSKI, A.

RUSSIA

D.V. Efremov Scientific Research Institute of Electrophysical Apparatus (NIIEFA)
St. Petersburg 189631
VOROGUSHIN, M.F.

Institute for Nuclear Research (INR) of the Russian Academy of Sciences
Profsojuznaja 7A
Moscow 117312
PARAMONOV, V.V.
ZELENSKII, A.N.

Joint Institute for Nuclear Research (JINR), Dubna
P.O. Box 79, Head Post Office
Moscow 101000
Flerov Laboratory of Nuclear Reactions
GULBEKYAN, G.
OGANESSIAN, Yu.
Laboratory for Computing & Automation
KADANTSEV, S.
Laboratory for Nuclear Problems
GLAZOV, A.

Kurchatov Institute of Atomic Energy (KIAE)
Moscow 123182
YAROSH, V.E.

Moscow Institute-Internate
Losinoostrovskaya st. 49
Moscow 107150
SARKISYAN, L.A.

Moscow Radiotechnical Institute (MRTI) of the Russian Academy of Sciences
Warshawskoe sh., 132
Moscow, 113519
KONOVALOV, V.A.

Accelerator Department
Petersburg Nuclear Physics Institute (PNPI)
St. Petersburg District
GATCHINA 188350
RIABOV, G.A.

SAUDI ARABIA

King Faisal Specialist Hospital
POB 3354
Riyadh 11211
MILIEBARI, S.

SOUTH AFRICA

National Accelerator Centre (NAC)
P.O. Box 72
Faure 7131
CELLIERS, P.J.
DU TOIT, Z.B.
JUNGWIRTH, H.N.
REITMANN, D.

SWEDEN

The Svedberg Laboratory
University of Uppsala
Box 533
Uppsala S-75121
HOLM, S.
LUNDSTRÖM, B.
REISTAD, D.V.

SWITZERLAND

Proton Synchrotron Division
CERN
CH-1211 Geneva 23
ALLARDYCE, B.W.
GASE, K.
SPINNEY, G.
SUSINI, A.

Paul Scherrer Institute (PSI)
CH-5232 Villigen
ADAM, S.
JOHO, W.
LANZ, P.
OLIVO, M.A.
PEDRONI, E.
REZZONICO, L.
SIGG, P.K.
STAMMBACH, Th.

UKRAINE

Institute of Nuclear Research (INR)
Academy of Science of the Ukraine
Prospekt Nauki, 47
Kiev 252028
PAPASH, A.I.
ZAIKA, N.I.

UNITED KINGDOM

Amersham International plc
White Lion Road
Amersham
Bucks HP7 9LL
BEASLEY, C.P.
GREY-MORGAN, T.
LEWIS, D.M.

MRS Cyclotron Unit
Hammersmith Hospital
Ducane Road
London W12 0HS
MACKAY, D.B.

Oxford Instruments Ltd.
Osney Mead
Oxford 0X2 0DX
FINLAN, M.F.
KRUIP, M.J.M.

UNITED STATES OF AMERICA

CTI Cyclotron Systems
950 Gilman St.
Berkeley, CA 94710
CARROLL, L.
PEKRUL, E.
RAMSEY, F.

Cyclotron Inc.
3104 Redwood Road
Napa CA 94558
HENDRY, G.O.
MILLER, J.

DuPont Merck Pharmaceuticals
331 Treble Cove Rd.
N. Billerica MA 01862
HOLTON, P.S.
SCHWARTZ, C.R.
SEIDEL, C.W.

EG&G Nuclear Instruments
100 Midland Rd.
Oak Ridge TN 37830
MCDONOUGH, J.

Indiana University Cyclotron Facility (IUCF)
2401 Milo B. Sampson Lane
Bloomington, IN 47405
DERENCHUK, V.P.
ELLISON, T.J.P.
FRAME, D.W.
JENNER, D.
PEI, X.
POLLOCK, R.E.
REID, D.D.

Nuclear Medicine and Radiation Division
Johns Hopkins Hospital
615 North Wolfe St.
Baltimore MA 21205-2179
WAGNER, H.N.

Lawrence Berkeley Laboratory
1 Cyclotron Road
Berkeley, CA 94720
ALONSO, J.R.
CLARK, D.J.
COLLINS, D.
LEUNG, K.N.
LUNDGREN, S.A.
LYNEIS, C.M.
NITSCHKE, J.M.
XIE, Z.Q.
YOUNG, A.T.

Mallinckrodt Medical Inc.
2703 Wagner Place
Maryland Heights, MO 63043
RUBIO, F.

Department of Radiology
Massachusetts General Hospital
32 Fruit Street
Boston, MASS 02114
THORNTON, A.F.

Brobeck Division
Maxwell Laboratories
4905 Central Ave.
Richmond, CA 94804
THOMAS, K.M.

MedCyc Corp.
609 Beech Street
East Lansing, MI 48823
BLOSSER, G.F.

Medi+Physics Inc.
3350 N. Ridge Ave.
Arlington Heights, IL 60004
HUBBARD, R.E.

National Superconducting Cyclotron Laboratory (NSCL)
Michigan State University
South Show Lane
East Lansing, MI 48824-1321
ANTAYA, T.
BAILEY, J.
BLOSSER, H.G.
JEON, D-O.
KIM, J.W.
KUO, T.
MILLER, P.
STETSON, J.

Oak Ridge National Laboratory
P.O. Box 2008
Oak Ridge, TN 37831-6368
MOSKO, S.W.
OLSEN, D.K.
TATUM, B.A.

Department of Nuclear Medicine
State University of New York
Rm 105 Parker Hall
3435 Main St.
Buffalo, NY 14214
ACKERHALT, R.E.
ORLOSKY, P.
VILANI, J.W.

Technical Edge Development Inc.
Suite A-200
2700 S. King St.
Honolulu, HI 96826
UYEMURA, D.K.

Cyclotron Institute
Texas A&M University
College Station, TX 77843-3366
ABEGGLEN, F.
MAY, D.P.
MOUCHATY, G.
ROGERS, R.C.

University of Pennsylvania
429 Johnson Pavilion
Philadelphia PA 19104-6063
GONZALEZ, C.

M.D. Anderson Cancer Center
University of Texas
1515 Holcombe Blvd, Box 94
Houston, TX 77030
MALLORY, M.L.

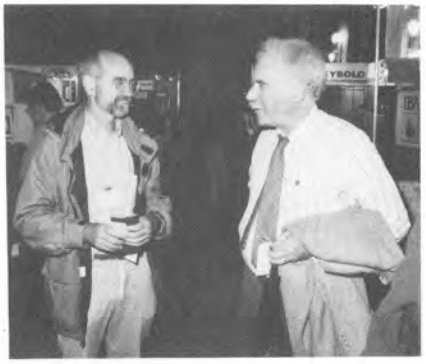
Department of Radiation Oncology
University of Washington
1959 NE Pacific Street
Seattle, WA 98195
JACKY, J.
RISLER, R.
ZIAI, F.

Varian
391 Industrial Way
San Carlos, CA 94070
LORING, Jr., C.M.

UZBEKISTAN
Institute of Nuclear Physics (INP)
Tashkent, Ulugbek 702132
MUMINOV, A.I.

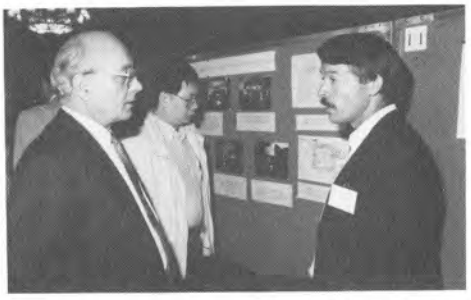

CONFERENCE ON CYCLOTRONS AND THEIR APPLICATIONS

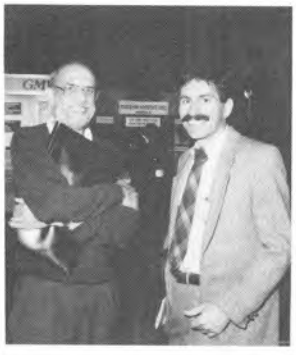





Connectors
New Products
Alumina Bushing



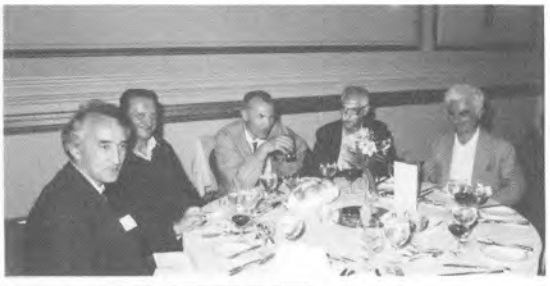




















































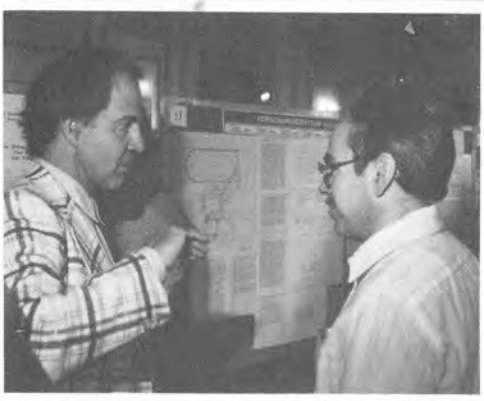






















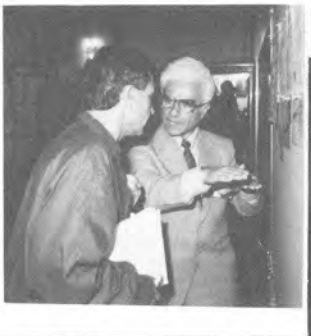








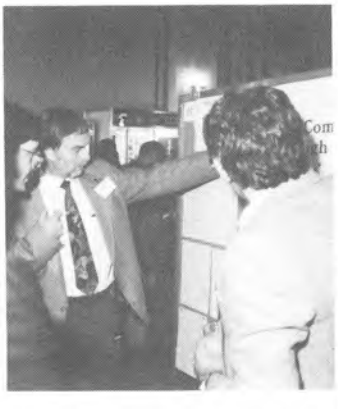
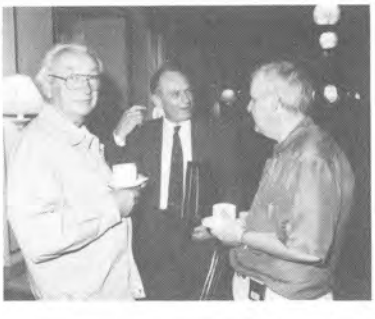


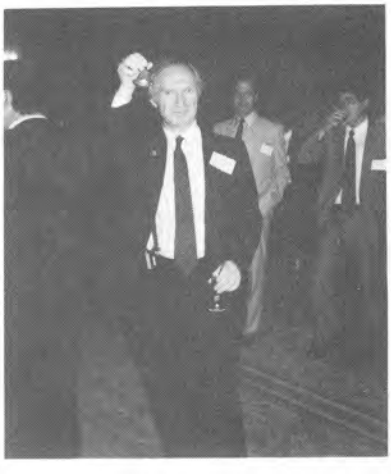









LISTS OF CYCLOTRONS AND COOLER-BOOSTER RINGS

For these proceedings, we have attempted to make the listings more comprehensive by including, with the assistance of their manufacturers and users, many small cyclotrons which had previously been overlooked. To avoid repetition and keep the listings to a manageable length, data sheets from commercial cyclotron users and manufacturers have been restricted to one column. For convenience, the listings have been divided into five sections, as follows:

- Cyclotrons - Individual Designs: - Entries C1-C74
- Commercial Cyclotrons - Manufacturers: - Entries CM1-CM29
- Commercial Cyclotrons - Users: - Entries CU1-CU124
- Synchrocyclotrons: - Entries FM1-FM7
- Cyclotron Cooler-Booster Rings: - Entries CB1-CB4

The last category is a new one which we hope will prove useful. If there are any errors or omissions in the listings, please send corrections to the undersigned.

R.E. Laxdal, TRIUMF

abbrev.: h.i. - heavy ion; s/c - superconducting

notations: * no data sheet received, Berlin 1989 data used; ** some new data added to Berlin 1989 entry; • cyclotron exists but no data available

Click on the Entry # below to view the particular data sheet

Cyclotrons - Individual Designs

Entry #	Location	Description		Name	First Beam
	BELGIUM				
C1	Louvain-la-Neuve	95 MeV p,...,h.i., K=115	4 sect	CYCLONE	1972
	CANADA				
C2	Chalk River (AECL)	h.i., K=520	4 sect, s/c	TASCC	1985
C3*	Winnipeg (U. of Man.)	50 MeV p,...	4 sect	Spiral Ridge	1965
C4	Vancouver (TRIUMF)	520 MeV H^-	6 sect	TRIUMF	1974
	CHILE				
C5*	Santiago (U. de Chile)	10 MeV p,...	3 sect	from U.C. Davis	1967
	CHINA, PEOPLE'S REPUBLIC OF				
C6*	Beijing (IAE)	15 MeV p,...	—		1958
C7	Lanzhou (IMP)	h.i., K=69	3 sect	HIRFL Inj.	-
C8	Lanzhou (IMP)	h.i., K=450	4 sect	HIRFL Cyc.	1988
C9	Shanghai (INR)	30 MeV p,...	3 sect	INRC	1983
	CZECHOSLOVAKIA				
C10	Rez (NPI)	37 MeV p,...	4 sect	U-120M	1977
	FINLAND				
C11	Jyväskylä (U. of)	70 MeV p,...,h.i., K=130	3 sect	K130	1992

	FRANCE				
C12	Caen (GANIL)	h.i., K=28	3 sect	C01 and C02	1982
C13	Caen (GANIL)	h.i., K=380	4 sect	SSC1 and SSC2	1982
C14	Grenoble (ISN)	h.i., K=90	4 sect	SARA inj.	1968
C15	Grenoble (ISN)	h.i., K=160	4 sect	SARA	1981
C16	Nice (CAL)	65 MeV p	4 sect	MEDICYC	1990
C17	Orleans (CNRS-CERI)	36 MeV p,...	4 sect	OIC	1974
C18*	Orsay (IPN)	h.i., K=75	3 sect	ALICE	1965
	GERMANY				
C19	Berlin (HMI)	50 MeV p,...,h.i., K=130	4 sect	VICKSI	1977
C20	Bonn (U. of Bonn)	h.i., K=60	3 sect	BIC	1968
C21	Jülich (KFA)	22 MeV p,...,h.i., K=180	3 sect	JULIC	1968/1969
C22	Karlsruhe (KFK)	26 MeV/u d,...	3 sect	KIZ	1962/1964
C23*	Munich (Tech. U.)	22 MeV p,...	4 sect	AEG Comp. Cyc.	1973
C24•	Munich (Tech. U.)	43.5 MeV p,...,h.i.	s/c	TRITRON	(—)
C25*	Rossendorf (ZIKFR)	14 MeV d,...	—	U-120	1958
	INDIA				
C26	Chandigarh (Panjab U.)	7 MeV p,...	—	CVEC	1971
C27	Calcutta (VECC)	30 MeV p,...	3 sect	VEC	1977/78
	ITALY				
C28	Catania (INFN)	h.i., K=800	3 sect, s/c	LNS-SCC	(1993)
	JAPAN				
C29	Osaka (RCNP)	85 MeV p,..., K=140	3 sect	AVF Cyc.	1974
C30	Osaka (RCNP)	400 MeV p,..., K=400	6 sect	Ring Cyc.	1991
C31	Saitama (RIKEN)	10 MeV p,...,h.i., K=70	4 sect	715 Cyc.	1989
C32	Saitama (RIKEN)	210 MeV p,...,h.i., K=540	4 sect	Ring Cyc.	1986
C33	Takasaki (JAERI)	90 MeV p,...,h.i., K=110	4 sect	AVF Cyc.	1991
C34	Tokyo (INS)	45 MeV p,...,h.i., K=68	3 sect	INS-SFC	1974
	KAZAKHSTAN				
C35*	Alma Ata (INP)	30 MeV p,...	3 sect	KVEIC	1971
	NETHERLANDS				
C36	Amsterdam (Vrije U.)	28 MeV p,...	3 sect	V.U.AVF (Philips)	1965
C37	Eindhoven (U. of Tech.)	3 MeV p	4 sect	ILEC	1989
C38	Eindhoven (U. of Tech.)	29.5 MeV p,...	3 sect	AVF Cyc. (Philips)	1963
C39*	Groningen (KVI)	200 MeV,...,h.i., K=600	3 sect, s/c	AGOR	(1993)
	POLAND				
C40*	Krakow (INP)	60 MeV p,...	4 sect	AIC-144	1987
C41*	Otwock-Swierk (Soltan I.)	30 MeV H^-	4 sect	C-30	1989
C42	Warsaw (Warsaw U., HIL)	h.i., K=180	4 sect	U-200P	(1992)
	RUSSIA				
C43**	Dubna (JINR,LNR)	h.i., K=145	4 sect	U-200	1968
C44**	Dubna (JINR,LNR)	h.i., K=540	4 sect	U-400M	1989
C45**	Dubna (JINR,LNR)	h.i., K=625	4 sect	U-400	1978
C46**	Dubna (JINR,LNR)	13 MeV $^{12}C^{2+}$	4 sect	CI-100	1985
C47	Gatchina (PNPI)	80 MeV H^-	4 sect		(—)
C48	Moscow (KIAE)	30 MeV p,...	3 sect	KIAEC	1976
	SOUTH AFRICA				
C49	Faure (NAC)	8 MeV p,...	4 sect	Inj. Cyc. I	1983
C50	Faure (NAC)	8 MeV p,...,h.i., K=11	4 sect	Inj. Cyc. II	(1993)
C51	Faure (NAC)	220 MeV p,...,h.i., K=220	4 sect	SSC	1985

	SWEDEN				
C52	Uppsala (Svedberg Lab)	h.i., K=200	3 sect	conv. s-cyc	1951/86/87
	SWITZERLAND				
C53	Villigen (PSI)	72 MeV p,...	4 sect	Inj. I (Phillips)	1974
C54	Villigen (PSI)	72 MeV p	4 sect	Inj. II	1984
C55	Villigen (PSI)	590 MeV p	8 sect	Ring Cyc.	1974
	UKRAINE				
C56	Kiev (INR-UAS)	78 MeV p,...	3 sect	U-240	1976
	UNITED KINGDOM				
C57**	Birmingham (U. of)	7 MeV p,...	3 sect	Radial Ridge	1963
C58**	Birmingham (U. of)	p,...	—	Nuffield 60-inch	1948
	UNITED STATES				
C59**	Argonne (ANL)	21 MeV d,...	—	60-inch	1952
C60	Berkeley (LBL)	h.i., K=160	3 sect	88-inch	1961/62
C61•	Bloomington (IUCF)	15 MeV p,...	4 sect	Inj. Cyc.	1972
C62	Bloomington (IUCF)	205 MeV p,...	4 sect	IUC	1975
C63*	Cleveland (LRC)	50 MeV p,...	3 sect		1972
C64	College Stat. (Texas A&M)	h.i., K=520	3 sect, s/c	K500	1988
C65	Davis (U. of Cal.)	68 MeV p,...	3 sect	Davis 76-inch	1966
C66	Detroit (Harper Hosp.)	50 MeV d	3 sect, s/c	K100	1988
C67	East Lansing (NSCL-MSU)	h.i., K=500	3 sect, s/c	K500	1982
C68	East Lansing (NSCL-MSU)	h.i., K=1200	3 sect, s/c	K1200	1988
C69	Oak Ridge (ORNL)	h.i., K=100	3 sect	ORIC	1963
C70*	Princeton (U.)	50 MeV p	3 sect	P. AVF Cyc.	1968
C71*	St. Louis (Wash. U.)	30 MeV α,...	3 sect	WUSFC	1965
C72	Upton (BNL)	34 MeV p,...	3 sect	60-inch	1968
C73*	Washington DC (NRL)	70 MeV p,...	3 sect	NRLC	1967/68
	UZBEKISTAN				
C74	Tashkent (INP)	20 MeV p,...	4 sect	JINR U-115T	(—)

Commercial Cyclotrons – Manufacturers

Entry #	Model	Description		# sold/oper.
ION BEAM APPLICATIONS (IBA) — Louvain-la-Neuve, Belgium				
CM1	CYCLONE 3	1.9 MeV/u d	4 sect	3/2
CM2	CYCLONE 10/5	10 MeV H^-, 2.5 MeV/u D^-	4 sect	2/2
CM3	CYCLONE 18/9	18 MeV H^-, 4.5 MeV/u D^-	4 sect	5/2
CM4	CYCLONE 30	30 MeV H^-	4 sect	14/10
EBCO TECHNOLOGIES — Vancouver, Canada				
CM5	TR-30	30 MeV H^-	4 sect	2/1
THE JAPAN STEEL WORKS, LTD. — Tokyo, Japan				
CM6	BC168	16 MeV p, 8 MeV d	4 sect	4/4
CM7	BC1710	17 MeV p, 10 MeV d	4 sect	8/8
CM8	BC2211	22 MeV p, 11 MeV d	4 sect	1/1
CM9	BC3015	30 MeV p, 15 MeV d	4 sect	1/1
SUMITOMO HEAVY INDUSTRIES, LTD. — Tokyo, Japan				
CM10	HM-18	18 MeV H^-, 10 MeV D^-	4 sect	2/1

CM11	480 AVF	30 MeV p	4 sect	1/1
CM12	750 AVF	70 MeV p	4 sect	2/2
CM13	930 AVF	90 MeV p, 35 MeV d	4 sect	5/5
D.V. EFREMOV INSTITUTE — St. Petersburg, Russia				
CM14	PIC-10	11 MeV H^-	4 sect	—/—
CM15	MGC-20	18 MeV p, 5 MeV/u d,…	3 sect	—/—
CM16	U-250	40 MeV/u $2H^+$,…,h.i., K=200	4 sect	—/—
SCANDITRONIX — Uppsala, Sweden				
CM17•	MC-17	17 MeV p,d	now sold to GE Medical Systems	
CM18	MC-30	30 MeV p	3 sect	1/1
CM19	MC-32 NI	32 MeV H^-, D^-	4 sect	2/2
CM20	MC-35,40	40 MeV p,…	3 sect	12/11
CM21	MC-50	50 MeV p,…	3 sect	2/2
CM22	MC-60 P	60 MeV p,…	3 sect	1/1
OXFORD INSTRUMENTS — Oxford, U.K.				
CM23	OSCAR	12 MeV H^-	3 sect, s/c	3/—
CTI – SIEMENS – TCC — Knoxville, USA				
CM24	TCC CS-15	15 MeV p, 8 MeV d,…	3 sect	3/3
CM25	TCC CS-22	22 MeV p, 12 MeV d,…	3 sect	4/3
CM26	TCC CV-28	24 MeV p, 14 MeV d,…	3 sect	5/5
CM27	TCC CS-30	26 MeV p, 15 MeV d,…	3 sect	15/16
CM28	TCC CP-42	42 MeV H^-	3 sect	5/4
CM29	RDS-112	11 MeV H^-	3 sect	—/—

Commercial Cyclotrons – Users

Entry #	Location	Description	Model	First Beam
	AUSTRALIA			
CU1•	Victoria (Austin Hosp.)	10 MeV H^-,D^-	CYCLONE 10/5	—
CU2	Camperdown (NMC)	30 MeV H^-	CYCLONE 30	1991
CU3•	Lucas Heights (Aus. Nuc. Sc. & T. Org.)	30 MeV H^-	CYCLONE 30	—
	BELGIUM			
CU4•	Bruxelles (ULB Erasmus Hosp.)	30 MeV H^-	CYCLONE 30	—
CU5	Fleurus (Nordion)	30 MeV H^-	CYCLONE 30	1992
CU6	Fleurus (Nordion)	80 MeV p	CGR-MeV 930S	1983
CU7	Gent (INS)	24 MeV p,…	CGR-MeV 520	1977
CU8*	Liege (U. de Liege, CRC)	20 MeV p,…	CGR-MeV 520	1975
CU9•	Louvain-la-Neuve (U. de Louvain)	10 MeV H^-, D^-	CYCLONE 10/5	—
CU10•	Louvain-la-Neuve (U. de Louvain)	30 MeV H^-	CYCLONE 30	—
	BRAZIL			
CU11*	Rio de Janeiro (IEN)	24 MeV p,…	TCC CV-28	1974
CU12*	San Paolo (IPEN)	24 MeV p,…	TCC CV-28	1981
	CANADA			
CU13	Hamilton (McMaster U.)	10.5 MeV H^-	RDS-112	1989
CU14•	Montreal (MNU, McGill U.)	18 MeV H^-, D^-	CYCLONE 18/9	—

CU15*	Montreal (MNU, McGill U.)	10 MeV p, d	JSW BC107	—
CU16	Toronto (Clarke Inst.)	17 MeV p, d	MC-17	1992
CU17	Vancouver (Nordion/TRIUMF)	30 MeV H^-	TR-30	1990
CU18	Vancouver (Nordion/TRIUMF)	42 MeV H^-	TCC CP-42	1979
	CHINA			
CU19•	Beijing (IAE)	30 MeV H^-	CYCLONE 30	—
	DENMARK			
CU20	Copenhagen (Rigshospitalet)	32 MeV H^-, D^-	MC-32	1992
	FINLAND			
CU21	Turku (Abo Akad. U.)	19 MeV p,...	MGC-20	1974
CU22	Turku (Turku U. Cent. Hosp.)	3.85 MeV d	CYCLONE 3	1992
	FRANCE			
CU23	Orsay (CEA-DRIPP/SHFJ)	20 MeV p, d	CGR-MeV 520	1975
CU24	Lyon (CERMEP)	16 MeV p, d	CYPRIS 325 (CGR-MeV)	1988
	GERMANY			
CU25	Braunschweig (Phys. Tech. Bund.)	24 MeV p, d	TCC CV-28	1973
CU26**	Essen (IMSS, U. Essen)	24 MeV p,...	TCC CV-28	1975
CU27	Heidelberg (DKFZ)	32 MeV H^-, D^-	MC-32 NI	1972
CU28	Hannover (MHH)	35 MeV p, d	MC-35	1977
CU29	Jülich (KFA-INC)	17 MeV p, d	JSW BC1710	1987
CU30*	Jülich (KFA-JCC)	24 MeV p	TCC CV-28	1975
CU31	Karlsruhe (KFZ)	42 MeV H^-	TCC CP-42	1983
CU32	Köln (Max Planck Inst.)	17 MeV p, d	MC-17	1987
	HUNGARY			
CU33	Debrecen (ATOMKI)	20 MeV p,...	MGC-20	1985
	ITALY			
CU34*	Ispra (JRC-AMI)	38 MeV p,...	MC-40	1982
CU35	Milano (INT)	17 MeV p,d	MC-17F	(1993)
CU36	Napoli (FSP)	17 MeV p, d	MC-17	1991
CU37	Pisa (CNR-ICP)	16 MeV p,d	CYPRIS 325 (CGR-MeV)	1986
CU38•	Rome (Ist. Tecn. Biomed. Av.)	40 MeV p,...	MC-40	—
	JAPAN			
CU39	Akita City (RIBBV-Akita)	16 MeV p, d	JSW BC168	1983
CU40*	Chiba City (CMSH)	18 MeV p,...	SHI/CGR-MeV 370	1985
CU41*	Chiba City (NIRS)	89 MeV p,...	CGR-MeV 930	1973
CU42•	Fukuoka (Kyushu U. Sch. of Med.)	17 MeV p, d	JSW BC1710	1983
CU43•	Kanazawa (Kanazawa Cardiov. Hosp.)	17 MeV p, d	JSW BC1710	1991
CU44•	Kyoto (Nishijin Hosp.)	17 MeV p,d	JSW BC1710	1985
CU45	Kyoto (U. Hosp.)	15 MeV p, d	SHI/CGR-MeV 325	1982
CU46•	Maebashi (Gunma U. Sch. of Med.)	17 MeV p, d	JSW BC1710	1983
CU47•	Nagoya (Nagoya U. Sch. of Med.)	17 MeV p, d	JSW BC1710	1989
CU48	Sanbugun (Diichi Rad. Labs/Chiba)	30 MeV H^-	CYCLONE 30	1991
CU49	Sanbugun (Diichi Rad. Labs/Chiba)	30 MeV p	MC-40	1984
CU50	Sanda City (Nihon Medi-Physics/Hyogo)	30 MeV H^-	CYCLONE 30	1990
CU51	Sanda City (Nihon Medi-Physics/Hyogo)	30 MeV H^-	CYCLONE 30	(1992)
CU52	Sendai (Tohoku U., CRC)	40 MeV p,...	CGR-MeV 680	1977
CU53	Sodegaura (Nihon Medi-Physics/Chiba)	28 MeV p	SHI/CGR-MeV 480 pF	1985
CU54	Sodegaura (Nihon Medi-Physics/Chiba)	70 MeV p	SHI/CGR-Mev 750 pV	1986

CU55*	Takarazuka (Nihon Medi-Physics)	26 MeV p	TCC CS-30	1974
CU56*	Takarazuka (Nihon Medi-Physics)	26 MeV p	TCC CS-30	1981
CU57•	Takarazuka (Nihon Medi-Physics)	30 MeV H^-	CYCLONE 30	—
CU58•	Takarazuka (Nihon Medi-Physics)	30 MeV H^-	CYCLONE 30	—
CU59*	Tokyo (IMS)	26 MeV p,…	TCC CS-30	1973
CU60•	Tokyo (Nat. Nakano Ch. Hosp.)	10 MeV p,d	JSW BC105	1979
CU61	Tokai (Nippon T&T)	16 MeV p, d,…	JSW BC168	1984
CU62	Tsukuba (NRIM)	17 MeV p, d,…	JSW BC1710	1986
CU63	Yokohama (NKK Corp.)	12 MeV H^-	OSCAR	1991
	NETHERLANDS			
CU64	Groningen (U. Hosp., PET)	17 MeV p, d	MC-17F	1991
CU65*	Petten (Mallinckrodt Diag.)	28 MeV p,…	Philips	1964
CU66•	Petten (Mallinckrodt Diag.)	30 MeV H^-	CYCLONE 30	—
	NORWAY			
CU67	Blindern (U. of Oslo)	35 MeV p,…	MC-35	1979
	RUSSIA			
CU68•	St. Petersburg (Inst. of Hum. Brain)	17 MeV p,d	MC-17	—
	SAUDI ARABIA			
CU69	Riyadh (King Faisal SHRC)	26 MeV p,…	TCC CS-30	1982
	SOUTH KOREA			
CU70*	Seoul (KAERI)	50 MeV p,…	MC-50	1986
	SWEDEN			
CU71	Stockholm (Karolinska Hosp.)	17 MeV p, d	MC-17	1981
CU72	Uppsala (U. PET Center)	17 MeV p, d	MC-17	1991
	TAIWAN			
CU73•	Taipei (Vet's Gen. Hosp.)	17 MeV p,d	MC-17	—
CU74	Taiwan (INER)	30 MeV H^-, D^-	TR30/15	(1993)
	UNITED KINGDOM			
CU75•	Aberdeen (U. of Aberdeen)	15 MeV d, a	TCC CS-30 (from WGH, Edinburgh)	
CU76	Amersham (Amersham Int.)	27 MeV p, d	Philips	1966
CU77	Amersham (Amersham Int.)	42 MeV H^-	TCC CP-42	1981
CU78	Amersham (Amersham Int.)	35 MeV p	MC-40	1986
CU79*	Bebington (Clatterbridge H.)	60 MeV p	MC-60	1984
CU80	London (Hammersmith Hosp.)	40 MeV p,…	MC-40	1986
CU81	London (Hammersmith Hosp.)	1.8 MeV/u d	CYCLONE 3	1991
	UNITED STATES			
CU82	Ann Arbor (U. of Mich. Med. Sch.)	26 MeV p, d	TCC CS-30	1982
CU83	Arlington Heights (Medi-Physics)	40 MeV p	MC-40	1979
CU84	Arlington Heights (Medi-Physics)	40 MeV p	MC-40	1982
CU85	Arlington Heights (Medi-Physics)	70 MeV p	PV-750	1986
CU86	Baltimore (Johns Hopkins U.)	16 MeV p, d	MC-16F	1982
CU87•	Baltimore (Johns Hopkins U.)	1.9 MeV/u d	CYCLONE 3	—
CU88	Bethesda (NIH Clinical Cent.)	17 MeV p, d	JSW BC1710	1985
CU89	Bethesda (NIH Clinical Cent.)	26.5 MeV p	TCC CS-30	1985
CU90	Billerica (DuPont Merck)	22 MeV p	TCC CS-22	1970
CU91	Billerica (DuPont Merck)	26 MeV p	TCC CS-30	1976
CU92	Billerica (DuPont Merck)	26 MeV p	TCC CS-30	1978
CU93	Billerica (DuPont Merck)	26 MeV p	TCC CS-30	1980
CU94	Billerica (DuPont Merck)	30 MeV p	MC-35	1989
CU95	Billerica (DuPont Merck)	30 MeV H^-	CYCLONE 30	1990

CU96•	Boston (Mass. Gen. Hosp.)	17 MeV p,d	MC-17	—
CU97	Buffalo (SUNY Nuc. Med.)	30 MeV H^-	CYCLONE 30	1992
CU98*	Chicago (FMMRI)	15 MeV p,...	TCC CS-15	1969
CU99*	Emeryville (Medi-Physics)	22 MeV p,...	TCC CS-22	1970
CU100	Cincinnati (Christ Hosp.)	11 MeV H^-	RDS-112	1991
CU101•	Cleveland (U. Hosp.)	17 MeV p,d	MC-17	1985
CU102	Houston (M.D. Anderson)	42 MeV H^-	TCC CP-42	1981
CU103•	Houston (U. of Texas, HSC)	35 MeV p,d	MC-35	1984
CU104•	Irvine (U. of Cal.)	17 MeV p,d	MC-17	1989
CU105•	Iowa City (U. of Iowa)	17 MeV p,d	MC-17	—
CU106*	Los Angeles (U. of Cal.)	22 MeV p,...	TCC CS-22	1971
CU107•	Los Angeles (UCLA Sch. of Med.)	18 MeV H^-, D^-	CYCLONE 18/9	—
CU108	Los Angeles (USC/SYNCOR)	11 MeV H^-	RDS-112	1992
CU109	Madison (U. of Wisconsin)	11 MeV H^-	RDS-112	1986
CU110•	Manhasset (NSUHRC)	17 MeV p,d	MC-17	1987
CU111	Miami Beach (Mt. Sinai M.C.)	27 MeV p	TCC CS-30	1972
CU112•	Minneapolis (Vet's Admin. Med. Cent.)	40 MeV p,...	MC-40	1989
CU113	Nashville (Vanderbilt U. Med. Cent.)	11 MeV H^-	RDS-112	1989
CU114	Peoria (Methodist Med. Cent.)	11 MeV H^-	RDS-112	1991
CU115•	Philadelphia (U. of Penn., Sch. of Med.)	30 MeV p,d	JSW BC3015	1987
CU116	Sacramento (N. Cal. PET Cent.)	11 MeV H^-	RDS-112	1992
CU117•	St. Louis (Wash. U., Mallinckrodt Med.)	40 MeV p,...	MC-40	1984
CU118•	St. Louis (Wash. U., Mallinckrodt Med.)	16 MeV p, d	JSW BC168	1990
CU119*	St. Louis (Wash. U.)	7 MeV d	Allis-Chalmers	1964
CU120*	St. Louis (Wash. U.)	15 MeV p,...	TCC CS-15	1978
CU121	Seattle (U. of Wash.)	50 MeV p,...	MC-50	1982
CU122	South Plainfield (Medi-Physics)	22 MeV p	TCC CS-22	1973
CU123	South Plainfield (Medi-Physics)	30 MeV H^-	CYCLONE 30	1989
CU124	Upton (BNL)	17 MeV p, d	JSW BC1710	1982

Synchrocyclotrons

Entry #	Location	Description		Name	First Beam
	CANADA				
FM1*	Montreal (McGill U.)	100 MeV p,...		McGill S-Cyc	1949
	FRANCE				
FM2*	Lyon (U. Claude Bernard)	28 MeV d,...		S-Cyc Lyon	1963
FM3*	Orsay (IPN)	201 MeV p,...		S-Cyc 200	1977
	GERMANY				
FM4	Gottingen (U. of)	13.5 MeV/u a,d			1962
	RUSSIA				
FM5	Dubna (JINR,LNP)	680 MeV p	4 sect	Phasotron	1984
FM6	St. Petersburg (PNPI)	1000 MeV p			1967
	UNITED STATES				
FM7	Cambridge (Harvard U.)	159 MeV p			1949

Cyclotron Cooler-Booster Rings

Entry #	Location	Description	Name	First Beam

	GERMANY			
CB1	Jülich (KFA)	2500 MeV p	COSY	(—)
	JAPAN			
CB2	Tokyo (INS)	220 MeV/u a	TARN-II	1989
	SWEDEN			
CB3	Uppsala (Svedberg Lab)	1300 MeV p,…	CELSIUS	1988
	UNITED STATES			
CB4	Bloomington (IUCF)	500 MeV p,…	Indiana Cooler	1987

REFERENCE DATA ON INTERNATIONAL CYCLOTRON CONFERENCES

Place	Year	Organizer	Registered Participants	Cyclotron Projects Listed	Operating
1) Sea Island	1959	ORNL	85	14	2
2) Los Angeles	1962	UCLA	139	41	11
3) Geneva	1963	CERN	146	42	15
4) Gatlinburg	1966	ORNL	224	61	27
5) Oxford	1969	AERE Harwell	202	72	45
6) Vancouver	1972	TRIUMF	195	70 + 17 FM	
7) Zürich	1975	SIN	231	74 + 14 FM	49 + 17 FM
8) Bloomington	1978	IUCF	205	95 + 14 FM	82 + 12 FM
9) Caen	1981	GANIL	225+GANIL Staff	106 + 11 FM	91 + 11 FM
10) East Lansing	1984	MSU	222	111 + 11 FM	99 + 11 FM
11) Tokyo	1986	INS, RIKEN, RCNP	206	131 + 12 FM	122 + 11 FM
12) Berlin	1989	HMI	213	131 + 9 FM	131 + 9 FM
13) Vancouver	1992	TRIUMF	241	199 + 7 FM + 4 CB	188 + 7 FM + 3 CB

The next conference is scheduled for 1995 in Cape Town, South Africa.

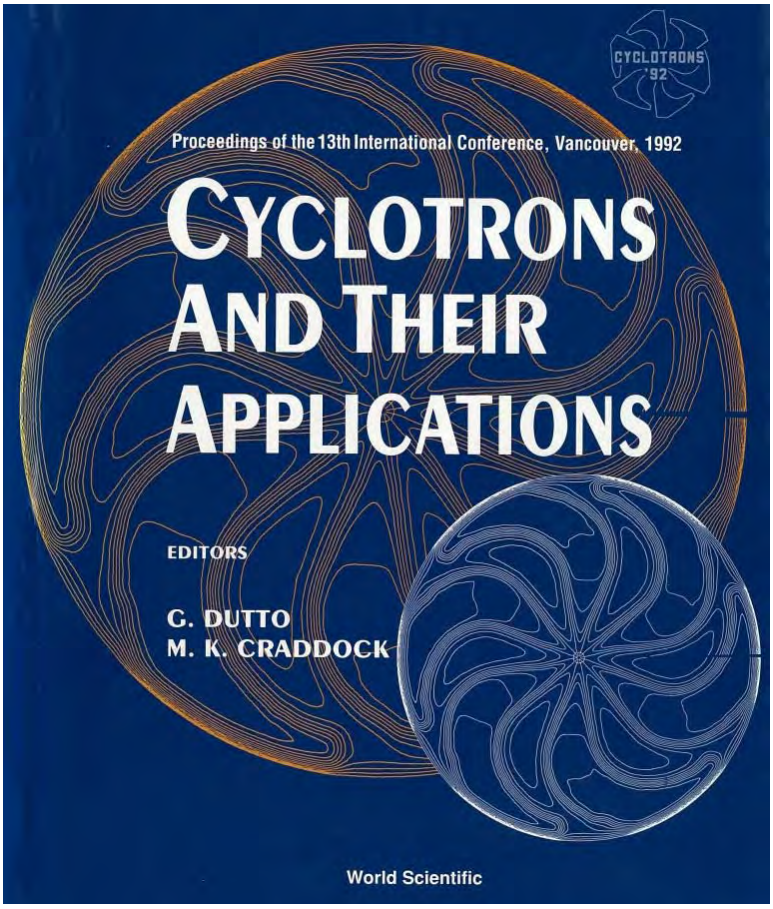
References

1. Informal conference on sector-focused cyclotrons: Sea Island, GA, USA 2-4 February 1959 (considered as the 1st international cyclotron conference). Proceedings: ed. F.T. Howard, National Academy of Sciences - National Research Council, Washington, DC; NAS-NRC Publ. 656 (1959), 303 pp.
2. International conference on sector-focused cyclotrons: Los Angeles, CA, USA, 17-20 April 1962 (considered as the 2nd international cyclotron conference). Proceedings: ed. K. Siegbahn and F.T. Howard, Nuclear Instruments and Methods **18, 19** (1962), 647 pp.
3. International conference on sector-focused cyclotrons and meson factories: Geneva, Switzerland, 23-26 April 1963 (considered as the 3rd international cyclotron conference). Proceedings: ed. F.T. Howard and N. Vogt-Nilsen, CERN 63-19 (1963), 430 pp.
4. International conference on sector-focused cyclotrons: Gatlinburg, TN, USA, 2-5 May 1966 (considered as the 4th international cyclotron conference). Proceedings: ed. F. Howard, IEEE Transactions on Nuclear Science **NS-13** (4), (1966), 531 pp.
5. 5th international cyclotron conference: Oxford, UK, 17-20 September 1969. Proceedings: ed. R.W. McIllroy, Butterworth, London (1971), 807 pp.
6. 6th international cyclotron conference: Vancouver, BC, Canada, 18-21 July 1972. Proceedings: "Cyclotrons - 1972", ed. J.J. Burgerjon and A. Strathdee, American Institute of Physics, New York; AIP Conf. Proc. no. 9 (1972), 846 pp.
7. 7th international conference on cyclotrons and their applications: Zürich, Switzerland, 19-22 August 1975. Proceedings: ed. W. Joho, Birkhäuser, Basel (1975), 656 pp.
8. 8th international conference on cyclotrons and their applications: Bloomington, IN, USA, 18-21 September 1978. Proceedings: ed. J.W. Hicks, IEEE Transactions on Nuclear Science, **NS-26** (2) (1979), 815 pp.
9. 9th international conference on cyclotrons and their applications: Caen, France, 7-10 September, 1981. Proceedings: ed. G. Gendreau, les Editions de Physique, Paris (1982), 884 pp.
10. 10th international conference on cyclotrons and their applications: East Lansing, MI, USA, 29 April-3 May, 1984. Proceedings: ed. F. Marti, IEEE, New York (1984), 755 pp.
11. 11th international conference on cyclotrons and their applications: Tokyo, Japan, 13-17 October 1986. Proceedings: ed. M. Sekiguchi, Y. Yano and K. Hatanaka, Ionics Publishing, Tokyo (1987), 921 pp.
12. 12th international conference on cyclotrons and their applications: Berlin, Germany, 8-12 May 1989. Proceedings: ed. B. Martin, K. Ziegler, World Scientific Publishing Co., Singapore (1991), 772 pp.
13. 13th international conference on cyclotrons and their applications: Vancouver, BC, Canada, 6-10 July 1992. Proceedings: ed. G. Dutto, M.K. Craddock, World Scientific Publishing Co., Singapore

Cyclotrons 1992

Vancouver, BC, Canada
6-10 July, 1992

The links below lead to more detailed listings and eventually to Acrobat Format (PDF) files containing the papers.



Foreword
Conference Organization
Industrial Exhibitors and Sponsors
Opening Address

Index of Papers by:

Session
Authors
Keywords
Institutes

List of Participants
Conference Photographs
Cyclotron Data
International Cyclotron Conferences

First published by World Scientific, Singapore in 1993: ISBN 9810211309
Electronic edition produced with financial assistance from CERN and TRIUMF and with the permission of World Scientific, Singapore
Copyright © 1993 by World Scientific Publishing Co. Pte. Ltd.

Single photocopies of single articles may be made for private study or research. Illustrations and short extracts from the text of individual contributions may be copied provided that the source is acknowledged.

October 2013 JP Scientific (Nantwich) Ltd, UK

I — Opening Session - Cyclotrons New and Old

Chairmen: G. Dutto / H. Schmeing

Paper	Title	Page
I-01	**Commissioning of the RCNP Ring Cyclotron (Invited Paper)**	3
	• **I. Miura**, A. Ando, K. Hatanaka, K. Hosono, H. Ikegami, T. Itahashi, M. Kibayashi, M. Kondo, H. Ogata, T. Saito, A. Shimizu, K. Tamura, M. Uraki, T. Yamazaki Osaka University, Osaka, Japan • J. Abe Sumitomo Heavy Industries, Ehime, Japan	
I-02	**New Development at the JINR Heavy Ion Cyclotron Facility (Invited Paper)**	11
	• **G.G. Gulbekyan**, V. Bekhterev, O. Borisov, B. Gikal, A. Ivanenko, I. Kolesov, V.B. Kutner, A. Morduev, Yu.Ts. Oganessian JINR, Dubna, Russia	
I-03	**New K130 Cyclotron at Jyväskylä (Invited Paper)**	22
	• **E. Liukkonen** University of Jyväskylä, Jyväskylä, Finland	
I-04	**Experience with the High Current Operation of the PSI Cyclotron Facility (Invited Paper)**	28
	• **Th. Stammbach** PSI, Villigen, Switzerland	
I-05	**The Commissioning of PSI Injector 2 for High Intensity, High Quality Beams**	36
	• **J. Stetson** NSCL, East Lansing, Michigan, USA • S. Adam, M. Humbel, W. Joho, Th. Stammbach PSI, Villigen, Switzerland	
I-06	**AGOR: Recent Achievements (Invited Paper)**	40
	• **H.W. Schreuder** IPN, Orsay, France	
I-07	**Thoughts on Decommissioning the CERN Synchro Cyclotron**	47
	• **G. Spinney** CERN, Geneva, Switzerland	
I-08	**Parameters, Present State and Application Perspectives of the U-250 Cyclotron**	50

- **A.I. Muminov**
  Institute of Nuclear Physics, Tashkent, Republic of Uzbekistan
- M.F. Vorogushin
  D.V. Efremov Scientific Research Institute of Electrophysical Apparatus, St. Petersburg, Russia

I-09 **GANIL Status Report** 54

- **M. Bajard**
  GANIL, Caen, France

I-10 **Gatchina Isochronous Cyclotron** 58

- **N.K. Abrosimov**, S.A. Artamonov, P.V. Chervyakov, S.P. Dmitriev, V.A. Eliseev, V.P. Fominenko, E.M. Ivanov, G.F. Mikheev, Yu.T. Mironov, A.S. Pokrovskii, G.A. Riabov, V.A. Smolin, G.L. Sokolov, V.A. Volchenkov, A.A. Vorobiev
  Petersburg Nuclear Physics Institute, Gatchina, Russia
- P.V. Bogdanov, B.D. Ershov, V.S. Kuligin, V.N. Moshkin, V.G. Mudrolyubov, Yu.I. Stogov, A.P. Strokach
  D.V. Efremov Scientific Research Institute of Electrophysical Apparatus, St. Petersburg, Russia

I-11 **Status Report of SARA** 62

- **M. Fruneau**, S. Albrand, D. Barnéoud, J.L. Belmont, G. Bizouard, J.L. Bouly, G. Campillo, M. Guisset, G. Laborie
  Université Joseph Fourier, Grenoble, France

I-12 **Commissioning of the Injector Complex of COSY-Jülich** 67

- **W. Bräutigam**, H. Beuscher, R. Brings, H.G. Böge, R. Maier, M. Rogge, P. Wucherer
  FZJ, Jülich, Germany

I-13 **Current Status and Future Project of Cyclotron Laboratory in Alma-Ata** 71

- **A.A. Arzumanov**, V. Batischev, V. Berger, V. Gerasimov, M. Gorcovets
  Kazakhstan Academy of Sciences, Alma-Ata, Republic of Kazakhstan

I-14 **Initial Operation of HIRFL** 74

- **B.W. Wei**, F. Ye
  Institute of Modern Physics, Lanzhou, People's Republic of China

I-15 **Upgrading the SFC** 78

- **F. Ye**, M. Guo, Z. Ma, Q. Qiao, Y. Wang, Q. Yin, X. Zhu
  Institute of Modern Physics, Lanzhou, People's Republic of China

I-16 **Status Report of Cyclone** 82

- **M. Loiselet**, N. Postiau, G. Ryckewaert
  Université Catholique de Louvain, Louvain-la-Neuve, Belgium

I-17 **Performance of the K1200 Cyclotron at MSU** 86

- **P. Miller**, T.A. Antaya, F. Marti, D. Poe, B. Sherrill, J. Stetson, J. Winger
  NSCL, East Lansing, Michigan, USA
- J.A. Nolen
  ANL, Argonne, Illinois, USA

I-18 **Status Report on the Heavy Ion Facility at LNS** 90

- **F. Alessandria**, G. Bellomo, A. Bosotti, C. De Martinis, D. Giove, P. Michelato, C. Pagani, L. Rossi
  INFN/LASA, Segrate, Italy
- L. Calabretta, G. Ciavola, G. Cuttone, M. Di Giacomo, S. Gammino, P. Gmaj, G. Raia, D. Rifuggiato, J. Sura
  INFN/LNS, Catania, Italy

I-19 **Development of the NAC Accelerator Facilities** 95

- **J.L. Conradie**, A.H. Botha, P.M. Cronje, R.E.F. Fenemore, H.N. Jungwirth, J.J. Kritzinger, W.A.G. Nel, D. Reitmann, L.M.M. Roels, P.F. Rohwer, H.A. Smit
  National Accelerator Centre, Faure, Republic of South Africa

I-20 **Heavy Ion Facility in ATOMKI** 99

- **S. Biri**, J. Pálinkás, A. Valek
  Institute of Nuclear Research of the Hungarian Academy of Sciences, Debrecen, Hungary

I-21 **Recent Achievements at the RIKEN Ring Cyclotron** 102

- **Y. Yano**
  RIKEN, Saitama, Japan

I-22 **Status Report on the Gustaf Werner Cyclotron in Uppsala** 106

- **S. Holm**
  Uppsala University, Uppsala, Sweden

II — Compact Cyclotrons

Chairman: A. Arzumanov

Paper	Title	Page
II-01	**Commercially Available Compact Cyclotrons for Isotope Production (Invited Paper)** • **V. Bechtold** FZK, Karlsruhe, Germany	110
II-02	**The Operation of Cyclotrons Used for Radiopharmaceutical Production** • **T. Grey-Morgan** Cyclotron Isotopes Manufacturing, Buckinghamshire, England • R.E. Hubbard Medi + Physics Inc., Arlington Heights, Illinois, USA	115
II-03	**Construction and First Year's Operation of the JAERI AVF Cyclotron** • **K. Arakawa**, T. Agematsu, M. Fukuda, I. Ishibori, T. Karasawa, T. Nara, Y. Nakamura, S. Okumura, R. Tanaka, W. Yokota JAERI, Gunma, Japan • A. Shimizu Osaka University, Osaka, Japan • Y. Hayashi, K. Ishii, T. Satoh, T. Tachikawa Sumitomo Heavy Industries, Ehime, Japan	119
II-04	**20 MeV Cyclotron for Isotope Production** • **A. Glazov**, Ju. Alenitskiy, A. Chesnov, S. Chesnova, V. Kochkin, D. Novikov, E. Samsonov, M. Semenov, A. Vasilenko, E. Zaplatin, N. Zaplatin JINR, Dubna, Russia • I. Gulamov, O. Iljasov, A. Rykov Institute of Nuclear Physics, Tashkent, Republic of Uzbekistan	123
II-05	**Status of a Compact H^- Cyclotron at the Kurchatov Institute of Atomic Energy** • **N.I. Venikov**, C.D. Burbeza, P.Yu. Komissarov, Yu.M. Krasnikov, S.T. Latushkin, V.V. Leonov, V.P. Moryakov, I.V. Naumov, A.Ya. Pisman, V.A. Rezvov, A.A. Vasiliev, V.E. Yarosh, L.I. Yudin Kurchatov Institute, Moscow, Russia	126
II-06	**A Newly Developed Compact Cyclotron for Neutron Therapy and Positron Nuclear Medicine** • **K. Ito**, T. Ishigaki, S. Itoh, Y. Kasugai, T. Kato, T. Misawa, M. Nishino, M. Osakabe, T. Ota, S. Sakuma, M. Tadokoro, H. Yamamoto Nagoya University, Nagoya, Japan • Y. Toda, Y. Yamamoto	129

Japan Steel Works Ltd., Tokyo, Japan

II-07 **Performance of the Harper Hospital Cyclotron; Effect of Pulsed Radio Frequency** 133

- **H.G. Blosser**, J. Vincent
  NSCL, East Lansing, Michigan, USA
- R. Maughan
  Harper Hospital, Detroit, Michigan, USA

III — TRIUMF and KAON (Tour Introduction)

Chairman: P.W. Schmor

Paper	Title	Page
III-01	**The TRIUMF 520 MeV Cyclotron: Recent and Future Developments**	138
	• **G. Dutto** TRIUMF, Vancouver, Canada	
III-02	**The KAON Factory at TRIUMF**	143
	• **M.K. Craddock** University of British Columbia, Vancouver, Canada	

IV — Applications

Chairman: M. Fruneau

Paper	Title	Page
IV-01	**Material Research with Beams at Cyclotron Energies (Invited Paper)**	149

- **K. Ziegler**
  HMI, Berlin, Germany

IV-02	**A Cyclotron as a Mass Spectrometer**	158

- **P. Bricault**, G. Auger, M. Bajard, E. Baron, D. Bibet, A. Chabert, J. Fermé, L. Gaudart, J. Joubert, M. Lewitowicz, W. Mittig, E. Plagnol, Ch. Ricaud, Y. Schutz
  GANIL, Caen, France
- G. Audi
  CSNSM, Orsay, France
- A. Gillibert
  CEN/Saclay, Gif-sur-Yvette, France
- K. Fifield
  Australian National University, Canberra , Australia

IV-03	**The Use of Heavy Ion Cyclotrons of the Flerov Laboratory of Nuclear Reactions in Condensed Matter Investigations**	162

- **R.Ts. Oganessian**, A.Yu. Didyk
  JINR, Dubna, Russia

IV-04	**^{178m2}Hf and ^{237}Pu Isotopes Production on the U-200 Cyclotron**	167

- **S.L. Bogomolov**, S.N. Dmitriev, Yu.P. Gangrski, G.G. Gulbekyan, S.A. Karamian, V.B. Kutner, B.N. Markov, Yu.Ts. Oganessian, N.V. Pronin, G.Ya. Starodub
  JINR, Dubna, Russia

IV-05	**Radionuclide Technique in Mechanical Engineering (RTM)**	171

- **P. Fehsenfeld**, A. Kleinrahm
  FZK, Karlsruhe, Germany
- V. Novikov
  Kurchatov Institute, Moscow, Russia

IV-06	**A P.E.T. Study of Proton Induced Radioactivity in Different Materials**	175

- **J.M. Schippers**
  Kernfysisch Versneller Instituut, Groningen, The Netherlands
- A.M.J. Paans
  University Hospital, Groningen, The Netherlands

IV-07	**Neutron Productions from Carbon by Charged Particle Bombardment at Different Energies**	178

- **M.A. Chaudhri**
  Austin Hospital & University of Melbourne, Melbourne, Australia

IV-08 **Analytical Applications of Cyclotrons in Biomedical Fields - Charged Particle Activation Analysis** 181

- **M.A. Chaudhri**
  Austin Hospital & University of Melbourne, Melbourne, Australia

IV-09 **A Simple Method for Estimating Activation Sensitivities of Different Elements / Isotopes with Cyclotron Produced Neutrons** 187

- **M.A. Chaudhri**
  Austin Hospital & University of Melbourne, Melbourne, Australia

IV-10 **A Proposal for an Intense Cyclotron-Based Thermal Neutron Source** 191

- **S. Tazawa**
  Sumitomo Heavy Industries, Toyo-shi, Toyo-shi, Japan
- W.L. Whittemore
  General Atomics, San Diego, California, USA

IV-11 **External High Current Targetry for Radioisotope Production** 196

- **N.R. Stevenson**, W.Z. Gelbart
  TRIUMF, Vancouver, Canada

IV-12 **A Remotely Controlled Robotic Vehicle for Work Within Radioactive Environments** 198

- **N.R. Stevenson**, P. Bloemhard, M. Brigham, J. Ko, C. LaForge, J. Orzechowski, E. Pattyn, T. Rattray
  TRIUMF, Vancouver, Canada

V — Medical Applications I - Radioisotopes

Chairman: M. Kondo

Paper	Title	Page
V-01	**The New Molecular Medicine** • **H.N. Wagner, Jr.** The Johns Hopkins University, Baltimore, Maryland, USA	202
V-02	**The Production of Radionuclides for the Biosciences (Invited Paper)** • **T.J. Ruth** TRIUMF, Vancouver, Canada	206
V-03	**A Facility for Radioisotope Production at TRIUMF with 70-110 MeV Protons** • **D.R. Pearce**, J.S. Vincent TRIUMF, Vancouver, Canada	209
V-04	**Possibility of Producing Some Radionuclides for Medicine Using JINR Accelerators** • **S.N. Dmitriev**, G.G. Gulbekyan, V.A. Khalkin, R.Ts. Oganessian, L.M. Onishchenko, G.Ya. Starodub, N.G. Zaitseva JINR, Dubna, Russia	213
V-05	**Radiopharmaceutical "Thallium-201-Chloride" Production using Thallium-203 Irradiation by Helium-3 Ions** • **A.A. Arzumanov**, N.K. Hamidov, A.I. Kozin, G.I. Shychikov, S.T. Tihomirova Kazakhstan Academy of Sciences, Alma-Ata, Republic of Kazakhstan	216
V-06	**Experiences with the Cyclone 3 Oxygen 15 Generator** • **E. Conard**, J.-L. Morelle Ion Beam Applications, Louvain-la-Neuve, Belgium • J.C. Clark, D.B. Mackay Hammersmith Hospital, London, England	218
V-07	**Dual Chemical Station for Cyclotron Produced ^{18}F** • **M.L. Mallory**, G. Grimmett, R. Tilbury, D. Yang The University of Texas, Houston, Texas, USA	222

VI — Medical Applications II - Radiotherapy

Chairman: J. Alonso

Paper	Title	Page
VI-01	**Accelerators for Charged Particle Therapy: Performance Criteria from the User Point of View (Invited Paper)** • **E. Pedroni** PSI, Villigen, Switzerland	226
VI-02	**Current and Potential Clinical Indications of Proton Irradiation (Invited Paper)** • **A.F. Thornton**, H.D. Suit Harvard Medical School, Boston, Massachusetts, USA	234
VI-03	**Pion Therapy for Cancer - What are the Prospects?** • **G.B. Goodman** University of British Columbia, Vancouver, Canada	242
VI-04	**Progress Report on the IBA-SHI Proton Therapy System** • **Y. Jongen**, W. Beeckman, J.P. Dufour, A. Laisné, H. Marie, R. Verbruggen Ion Beam Applications, Louvain-la-Neuve, Belgium • M. Sano, S. Satoh, N. Takahashi, T. Takayama Sumitomo Heavy Industries, Ehime, Japan	244
VI-05	**Recent Activities of the Cyclotron Laboratory in Nice** • **P. Mandrillon**, N. Brassart, P. Chauvel, A. Courdi, F. Farley, N. Fietier, J. Herault, J.Y. Tang Centre Antoine Lacassagne, Nice, France	248
VI-06	**Health Physics Data Acquisition System at the National Medical Cyclotron** • **B.N. Mukherjee** ANSTO, Menai, NSW, Australia • D.W. Arnott National Medical Cyclotron, Camperdown, NSW, Australia	252
VI-07	**Design Consideration of Neutron Therapy Facility Utilizing Existing Cyclotron** • **H. Chang**, X. Cui, J. Wei, J. Zhang, K. Xie Institute of Nuclear Research, Shanghai, People's Republic of China	255
VI-08	**A Proton Therapy Facility Plan** • **S. Fukumoto**, Y. Hayakawa, T. Inada, A. Maruhashi, M. Sato, J. Tada, Y. Takada,	258

H. Tsuji, H. Tsujii
University of Tsukuba, Ibaraki, Japan
- K. Endo, Y. Irie, K. Muto
KEK, Ibaraki, Japan

VI-09 **Continued Operation of the Seattle Clinical Cyclotron Facility** 262

- **R. Risler**, S. Brossard, J. Jacky, I. Kalet, P. Wootton, F. Ziai
University of Washington, Seattle, Washington, USA

VII — Storage Rings

Chairman: S. Holm

Paper	Title	Page
VII-01	**Recent Commissioning Results at Celsius (Invited Paper)**	266

- **D. Reistad**, T. Bergmark, C. Ekström, C.-J. Fridén, K. Gajewski, L. Hermansson, P. Jahnke, A. Johansson, O. Johansson, T. Lofnes, G. Norman, R. Wedberg, L. Westerberg, J. Zlomanczuk
  Uppsala University, Uppsala, Sweden
- M.A. Raadu, M. Sedlacek
  Royal Institute of Technology, Stockholm, Sweden

VII-02	**Beam Diagnosis for Unmeasurably Cold Beams (Invited Paper)**	274

- **T.J.P. Ellison**
  Indiana University, Bloomington, Indiana, USA

VII-03	**COSY-Jülich - A Synchrotron and Storage Ring for Medium Energy Physics**	282

- **R. Maier**, U. Pfister
  FZJ, Jülich, Germany

VII-04	**Study of Beam Dynamics at Cooler Synchrotron TARN-II**	286

- **S. Watanabe**, Y. Arakaki, K. Chida, T. Katayama, M. Tomizawa, T. Watanabe, M. Yoshizawa
  University of Tokyo, Tanashi-shi, Tokyo, Japan
- K. Noda, M. Kanazawa
  NIRS, Chiba, Japan

VII-05	**Dubna Project of the Heavy Ion Storage Ring Complex K4-K10**	290

- **Yu.Ts. Oganessian**, O.N. Malyshev, G.S. Popeko, A.M. Rodin, S.I. Sidorchuk, Ye.A. Sokol, S.V. Stepantsov, G.M. Ter-Akopian, V.A. Timakov
  JINR, Dubna, Russia
- V.V. Parhomchuk, A.A. Sery, V.D. Shiltsev
  Institute for Nuclear Physics, Novosibirsk, Russia
- I.N. Meshkov, Ye.M. Syresinm
  Center for Applied Physics and Technology, Lipetsk, Russia
- V.P. Belov, A.A. Makarov, Yu.P. Severgin, I.A. Shukeylo, M.N. Tarovik
  D.V. Efremov Scientific Research Institute of Electrophysical Apparatus, St. Petersburg, Russia

VII-06	**The New Project of INR (Kiev's) Storage-Accelerating Complex**	294

- **A.V. Dolinsky**, A.I. Papash, S.N. Pavlov, A.T. Rudchik, A.E. Val'Kov, I.N. Vishnevsky, A.V. Zhmendak
  Institute for Nuclear Research, Kiev, Ukraine

V.P. Belov, A.M. Kokorin, A.A. Makarov, I.A. Schukeilo, Yu.P. Severgin
D.V. Efremov Scientific Research Institute of Electrophysical Apparatus, St. Petersburg, Russia

VII-07 **Superthin Internal Target for Storage Rings** 297

- **V. Pugatch**, A. Glushko, G. Pitatelev, G. Sivtsov
  Institute for Nuclear Research, Kiev, Ukraine
- S. Popov, D. Toporkov, B. Voitsechovsky
  Institute for Nuclear Physics, Novosibirsk, Russia

VIII — Ion Sources

Chairman: D.P. May

Paper	Title	Page
VIII-01	**ECR Ion Sources for Accelerators (Invited Paper)** • **C.M. Lyneis** LBL, Berkeley, California, USA	301
VIII-02	**Performance of the LBL AECR Source at Various Frequencies** • **Z.Q. Xie**, D. Collins, S.A. Lundgren, C.M. Lyneis LBL, Berkeley, California, USA	308
VIII-03	**Ion Sources for Cyclotron Application** • **K.N. Leung**, D.A. Bachman, D.S. McDonald, A.T. Young LBL, Berkeley, California, USA	312
VIII-04	**A Review of Polarized Ion Sources for Cyclotrons (Invited Paper)** • **P.W. Schmor** TRIUMF, Vancouver, Canada	316
VIII-05	**Status of the TRIUMF Optically-Pumped Polarized H^- Ion Source** • **C.D.P. Levy**, K. Jayamanna, M. McDonald, R. Ruegg, P.W. Schmor TRIUMF, Vancouver, Canada • A.N. Zelenskii Institute of Nuclear Research, Russian Academy of Sciences, Moscow, Russia	322
VIII-06	**An ECR Ion Source for Multiply-Charged Heavy Ions at 14 GHz** • **M. Sekiguchi**, M. Fujita, Y. Ohshiro, T. Yamazaki University of Tokyo, Tanashi-shi, Tokyo, Japan • Y. Isoya, T. Yamada, Y. Yamashita Japan Steel Works Ltd., Research Center for Advanced Technologies, Chiba, Japan • A. Kitagawa NIRS, Chiba, Japan	326
VIII-07	**Performance and Status of the IUCF High Intensity Polarized Ion Source**	330

- **V. Derenchuk**, R. Brown, T.J.P. Ellison, D.L. Friesel, J.W. Hicks, D. Jenner, A. Pei, H. Petri, P. Schwandt, J. Sowinski, M. Wedekind
  Indiana University, Bloomington, Indiana, USA

VIII-08 **Ion Source of Discharge Type** 334

- **I.B. Enchevich**
  TRIUMF, Vancouver, Canada
- S.A. Korenev
  JINR, Dubna, Russia

VIII-09 **Operation of Ion Sources and Beam Transport to JAERI AVF Cyclotron** 336

- **W. Yokota**, T. Agematsu, K. Arakawa, M. Fukuda, I. Ishibori, Y. Nakamura, T. Nara, S. Okumura
  JAERI, Gunma, Japan
- Y. Hayashi, K. Ishii, T. Tachikawa
  Sumitomo Heavy Industries, Ehime, Japan

VIII-10 **Spin Dynamics and Polarized Ion Sources on Isochronous Cyclotron U-240** 340

- **N.I. Zaika**
  Institute for Nuclear Research, Kiev, Ukraine

VIII-11 **Study on the Magnetic Field of Caprice Type ECR Source** 344

- **B.W. Wei**, Z. Liu, Y. Ma, D. Wu, P. Yuan, W. Zhang, X. Zhang, H. Zhao
  Institute of Modern Physics, Lanzhou, People's Republic of China
- A. Efremov
  JINR, Dubna, Russia

VIII-12 **The Super Gas Mixing Technique for Highly Charged Uranium Ions** 348

- **T.A. Antaya**, D. Cole
  NSCL, East Lansing, Michigan, USA

VIII-13 **Recent Development of Internal H^-/D^- Source for Compact Cyclotrons** 352

- **T.Y.T. Kuo**
  TRIUMF, Vancouver, Canada
- G.O. Hendry
  Cyclotron Inc., Napa, California, USA

VIII-14 **Plan for the Ion Source Emittance Measurement Under the RF Extraction** 357

- **J.W. Kim**, H.G. Blosser

NSCL, East Lansing, Michigan, USA

VIII-15 **Progress with the NAC Injector Cyclotron for Heavy and Polarized Ions** 361

- **Z.B. du Toit**, S.J. Burger, P.J. Celliers, J.G. de Villiers, H.N. Jungwirth, A. Müller, P.F. Rohwer, D.M. van Rooyen
  National Accelerator Centre, Faure, Republic of South Africa

VIII-16 **Plasma Cathode Method for RIKEN ECRIS** 365

- **T. Nakagawa**, A. Goto, T. Kageyama, M. Kase, Y. Yano
  RIKEN, Saitama, Japan

VIII-17 **Performance of the Texas A&M ECRIS** 369

- **G. Mouchaty**, D.P. May, R.C. Rogers, P. Smelser
  Texas A&M University, College Station, Texas, USA

IXa — Theoretical Beam Dynamics

Chairman: S. Adam

Paper	Title	Page
IXA-01	**Advantage of Using Differential Algebra and Lie Algebra in the Orbit Dynamics of Cyclotrons (Invited Paper)**	372
	• **W.G. Davies** Atomic Energy of Canada, Chalk River, Ontario, USA	
IXA-02	**The Influence of Magnetic Field Imperfections on the Beam Quality in an H^- Cyclotron**	380
	• **W.J.G.M. Kleeven**, H.L. Hagedoorn Eindhoven University of Technology, Eindhoven, The Netherlands • B.F. Milton, G. Dutto TRIUMF, Vancouver, Canada	
IXA-03	**Emittance Growth in Nonlinear Beam Guiding and Focusing Elements**	384
	• **W.J.G.M. Kleeven**, J.I.M. Botman, J.L. Delhez, H.L. Hagedoorn, C.J. Timmermans, G.A. Webers Eindhoven University of Technology, Eindhoven, The Netherlands	
IXA-04	**Ion_Tracker, a Trace Tracking Program for Cyclotron Design**	388
	• **M. Rinta-Nikkola** University of Jyväskylä, Jyväskylä, Finland	
IXA-05	**Ion Optics in the Jyväskylä K130 Cyclotron**	392
	• **P. Heikkinen**, M. Rinta-Nikkola University of Jyväskylä, Jyväskylä, Finland	
IXA-06	**Nonlinear Transport of Accelerator Beam Phase Space**	396
	• **X. Xie** Graduate School of Nuclear Industry, Beijing, People's Republic of China • J. Xia Institute of Modern Physics, Lanzhou, People's Republic of China	
IXA-07	**Deriving the General Expressions of Nonlinear Transport Coefficients of Accelerator Beam Phase Space by Artificial Intelligence**	400
	• **J. Xia**	

Institute of Modern Physics, Lanzhou, People's Republic of China
- C. Liu, X. Xie
  Graduate School of Nuclear Industry, Beijing, People's Republic of China

IXA-08 **Evaluation of Third-Harmonic Voltage Flattopping for a Superconducting Cyclotron** 404

- **M.M. Gordon**, D. Jeon
  NSCL, East Lansing, Michigan, USA

IXA-09 **Crossing of Resonances** 408

- **L.A. Sarkisyan**, A.L. Sarkisyan
  Moscow Institute-Internate, Moscow, Russia

IXA-10 **Increase of Beam Intensity** 409

- **L.A. Sarkisyan**, A.L. Sarkisyan
  Moscow Institute-Internate, Moscow, Russia

IXA-11 **Developments in RELAX3D, a 2D/3D Laplace and Poisson Equation Solver** 411

- **H. Houtman**, F.W. Jones, C.J. Kost
  TRIUMF, Vancouver, Canada

IXA-12 **Beam Quality Investigations for H^- Extraction at TRIUMF** 415

- **R.E. Laxdal**, G.H. Mackenzie, J.B. Pearson, L. Root
  TRIUMF, Vancouver, Canada

IXb — Experimental Beam Dynamics

Chairman: S. Adam

Paper	Title	Page
IXB-01	**Cyclotron Tuning as a Rebuncher** • **D. Bibet**, M-H. Moscatello GANIL, Caen, France	419
IXB-02	**Beam Studies of Injection to Extraction System for JAERI AVF Cyclotron** • **M. Fukuda**, T. Agematsu, K. Arakawa, I. Ishibori, T. Karasawa, Y. Nakamura, T. Nara, S. Okumura, W. Yokota JAERI, Gunma, Japan	423
IXB-03	**K1200 Cyclotron Beam Development Techniques** • **T.A. Antaya**, D. Cole, P. Miller, D. Poe NSCL, East Lansing, Michigan, USA	427
IXB-04	**Selection and Measurement of RF Phase Width of the K1200 Cyclotron Beam** • **J. Bailey**, J. Kuchar, F. Marti, J. Yurkon NSCL, East Lansing, Michigan, USA • J.A. Nolen ANL, Argonne, Illinois, USA • D. Rifuggiato INFN/LNS, Catania, Italy	431
IXB-05	**Internal Beam Dynamics Studies with a TV Probe** • **F. Marti**, S. Snyder NSCL, East Lansing, Michigan, USA	435
IXB-06	**Effect of the Main-Coil Position on the Accelerated Beam of the K500 Cyclotron** • **D.P. May**, G. Mouchaty Texas A&M University, College Station, Texas, USA	439
IXB-07	**Beam Test Results Using the Auxiliary Accelerating Cavity** • **R.E. Laxdal**, G.H. Mackenzie, L. Root	442

TRIUMF, Vancouver, Canada

IXc — Injection and Extraction Studies

Chairman: S. Adam

Paper	Title	Page
IXC-01	**Commissioning of the New High Intensity Axial Injection System for GANIL** • **Ch. Ricaud**, E. Baron, J. Bony, M.P. Bourgarel, B. Bru GANIL, Caen, France • R. Vienet CEN/Saclay, Gif-sur-Yvette, France	446
IXC-02	**A Formulation of Spiral Inflector Design and Its Application to SF Cyclotron** • **M. Sekiguchi**, M. Fujita, M. Nishiguchi, Y. Ohshiro, Y. Shida, N. Yamazaki, T. Yamazaki University of Tokyo, Tanashi-shi, Tokyo, Japan	450
IXC-03	**Preliminary Design of a New Central Region for the LNS Superconducting Cyclotron** • **M-H. Moscatello** GANIL, Caen, France	454
IXC-04	**Non-Linear Beam Transport Effects in Highly Charged Positive Ion Beams Extracted From ECR Ion Sources** • **T.A. Antaya** NSCL, East Lansing, Michigan, USA • Z.Q. Xie LBL, Berkeley, California, USA	457
IXC-05	**Numerical Studies for Suppression of Vertical Oscillations in the K1200 Cyclotron** • **K. Joh**, F. Marti NSCL, East Lansing, Michigan, USA • J.A. Nolen ANL, Argonne, Illinois, USA	461
IXC-06	**Experiments on the Axial Injection System of the Cyclotron U-120M** • **Z. Trejbal**, M. Krivánek, J. Kucera, V. Bejsovec, J. Stursa Czechoslovak Academy of Sciences, Rez, Czechoslovakia	465

IXd — Beam Diagnostics

Chairman: S. Adam

Paper	Title	Page
IXD-01	**The New Phase Detection System of the Cosy-Injector** • **K. Kennepohl**, W. Bräutigam, M. Herschbach, D. Maeckelburg FZJ, Jülich, Germany	469
IXD-02	**High-Sensitive Ionization Detectors of Transverse Distribution of Accelerated Particles Beam** • **V.G. Mikhailov**, V.A. Rezvov, A.A. Roshchin, V.I. Sklyarenko, L.I. Iudin Kurchatov Institute, Moscow, Russia	473
IXD-03	**A Beam Profile Monitor Using the Ionization of Residual Gas** • **J.M. Schippers**, H.H. Kiewiet Kernfysisch Versneller Instituut, Groningen, The Netherlands	477
IXD-04	**Emittance Measurements in the HIRFL Beam Line** • **H. Zhao**, Z. Shen, B.W. Wei Institute of Modern Physics, Lanzhou, People's Republic of China	479
IXD-05	**High Sensitivity Electronic System for the Phase Probes of the LNS/MILANO Superconducting Cyclotron** • **A. Bosotti**, D. Corti, C. Pagani, G. Varisco, F. Zibra INFN/LASA, Segrate, Italy • M. Di Giacomo INFN/LNS, Catania, Italy	483
IXD-06	**The Diagnostics System for the AGOR Superconducting Cyclotron** • **B. Launé**, P. Dambre, J.M. Kaplanski, B. Montsanglant, C. Olivetto, D. Vincent IPN, Orsay, France	487
IXD-07	**Beam Diagnostics in the RCNP Ring Cyclotron** • **T. Itahashi**, T. Saito, I. Miura Osaka University, Osaka, Japan • S. Ichida Sumitomo Heavy Industries, Ehime, Japan	491

IXD-08 **Signal Processing for the Internal Phase Probe in the TRIUMF Cyclotron** 495

- **K. Fong**
  TRIUMF, Vancouver, Canada

IXD-09 **A DC Current Transformer for TRIUMF** 498

- **Y. Yin**
  TRIUMF, Vancouver, Canada

Xa — Radiofrequency Systems

Chairman: A. Glazov

Paper	Title	Page
XA-01	**Advances in RF Technology for Cyclotrons** • **C. Pagani** INFN/LASA, Segrate, Italy	501
XA-02	**The RF Coupling System of the VINCY Cyclotron** • **B. Bojovic**, M. Josipovic, A. Susini CERN, Geneva, Switzerland	511
XA-03	**Dual Frequency Resonator System for a Compact Cyclotron** • **M. Eiche**, K.L. Erdman Ebco Technologies Ltd, Richmond, BC, Canada • P. Lanz, M. Lipnicki, M. Zach TRIUMF, Vancouver, Canada	515
XA-04	**The RF-System for a VICKSI Injector Cyclotron** • **W. Pelzer** HMI, Berlin, Germany	519
XA-05	**Low Frequency RF System for the Indiana University Cooler Ring** • **X. Pei**, S. Anderson, V. Derenchuk, G. East, D.L. Friesel, D. Jenner, D. McCammon, T. Sloan Indiana University, Bloomington, Indiana, USA	523
XA-06	**A Modified RF System of JAERI AVF Cyclotron** • **Y. Kumata**, Y. Fukumoto Sumitomo Heavy Industries, Ehime, Japan • K. Arakawa, M. Fukuda, T. Karasawa JAERI, Gunma, Japan • A. Shimizu Osaka University, Osaka, Japan	526
XA-07	**Multi-Point Cavity Excitation** • **E. Zaplatin** FZJ, Jülich, Germany	530
XA-08	**Experience with the PSI-Cyclotron RF-System Under Heavy Beam Loading**	534

- **P.K. Sigg**, J. Cherix, H. Frei, M. Märki
  PSI, Villigen, Switzerland

XA-09 **Initial Operation of the RF System for the RCNP Ring Cyclotron** 538

- **T. Saito**, I. Miura, A. Shimizu, M. Uraki
  Osaka University, Osaka, Japan

XA-10 **RF Transmitter for ECR Ion Sources** 542

- **R. Boux**, J.P. Ichac, M. Soudée
  Thomson Tubes Electroniques, Velizy-Villacoublay, France

XA-11 **TRIUMF Cyclotron RF System Improvements** 545

- **G.C. Blaker**, A.K. Mitra, R.L. Poirier
  TRIUMF, Vancouver, Canada

XA-12 **Improvements to the RF Separator in the M9 Muon Channel at TRIUMF** 549

- **G.C. Blaker**, A.K. Mitra, R.L. Poirier
  TRIUMF, Vancouver, Canada

XA-13 **The RF System of the Gustaf Werner Cyclotron/Synchrocyclotron** 553

- **B. Lundström**, B. Holmgren
  Uppsala University, Uppsala, Sweden

Xb — Magnets

Chairman: A. Glazov

Paper	Title	Page
XB-01	**Low Temperature Tests of the AGOR Superconducting Coil System**	557

- **K. Pieterman**, J.A.M. Dam
  Cryocon B.V., Amersfoort, The Netherlands
- C. Commeaux
  IPN, Orsay, France
- C. Penco
  Ansaldo Componenti, Genoa, Italy

XB-02	**A Permanent Magnet System for a Cyclotron Used as a Mass Spectrometer**	561

- **C.Y. Li**, M. Cooper, K. Halbach, W.B. Kunkel, K.N. Leung, R.P. Wells, A.T. Young
  LBL, Berkeley, California, USA

XB-03	**Sector Magnet of the RCNP Ring Cyclotron and the Isochronization**	565

- **K. Hosono**, M. Kibayashi, I. Miura
  Osaka University, Osaka, Japan

Xc — Injection and Extraction Systems

Chairman: A. Glazov

Paper	Title	Page
XC-01	**The Electrostatic Deflector for the Chalk River Superconducting Cyclotron** • **W.T. Diamond**, C.R. Hoffmann, G.R. Mitchel, H. Schmeing Atomic Energy of Canada, Chalk River, Ontario, Canada	569
XC-02	**Potential Enhancement of Magnetic Deflection in the Chalk River Superconducting Cyclotron Extraction System** • **C.R. Hoffmann**, E.H. Lindqvist Atomic Energy of Canada, Chalk River, Ontario, Canada	573
XC-03	**Model Study of an Electrostatic Deflector Configuration with an Intermediate Electrode** • **C.R. Hoffmann**, J.F. Mouris Atomic Energy of Canada, Chalk River, Ontario, Canada	577
XC-04	**Performance of Beam Chopping System for JAERI AVF Cyclotron** • **W. Yokota**, T. Agematsu, K. Arakawa, M. Fukuda, I. Ishibori, Y. Nakamura, T. Nara, S. Okumura JAERI, Gunma, Japan • Y. Hayashi, Y. Kumata, T. Tachikawa Sumitomo Heavy Industries, Ehime, Japan	581
XC-05	**The AGOR Superconducting Extraction Channel EMC2** • **K. Pieterman**, J.A.M. Dam Cryocon B.V., Amersfoort, The Netherlands • H.J.H. ten Kate TU Twente, Enschede, The Netherlands • S. Gustafsson IPN, Orsay, France	585
XC-06	**Material Consideration for Magnetic Channels** • **J. Sura**, L. Calabretta, G. Di Biasi, P. Gmaj, D. Rifuggiato INFN/LNS, Catania, Italy	589
XC-07	**Design of Passive Magnetic Channels** • **G. Bellomo** INFN/LASA, Segrate, Italy	592

XC-08 **Deflector Development for the K1200 Cyclotron** 596

- **T.Y.T. Kuo**
  TRIUMF, Vancouver, Canada
- J.A. Nolen
  ANL, Argonne, Illinois, USA

XC-09 **Results from the Deflector Test Stand at Texas A&M University** 602

- **D.P. May**, G. Derrig, W. Dewees, P. Smelser, D. Tran, R.C. Rogers
  Texas A&M University, College Station, Texas, USA

Xd — Beam Transport Systems

Chairman: A. Glazov

Paper	Title	Page
XD-01	**Some Perspectives in the Beam Transport and Analyzing System Design for the U-250 Cyclotron** • **L.E. Korolev** D.V. Efremov Scientific Research Institute of Electrophysical Apparatus, St. Petersburg, Russia	606
XD-02	**Beam Transport System for the IUCF High Intensity Polarized Ion Source** • **W.P. Jones**, M.S. Ball, J.C. Collins, D. DuPlantis, T.J.P. Ellison, D.L. Friesel, B. Hamilton, J.W. Hicks, P. Schwandt Indiana University, Bloomington, Indiana, USA	609
XD-03	**Superconducting Focussing Channel for the AGOR Cyclotron** • **H.W. Schreuder**, P. Blache, C. Commeaux, S. Gustafsson, A. Lafoux, M. Mormiche, R. Panvier IPN, Orsay, France	612
XD-04	**The Beam-Guiding System of AGOR** • **J.M. Schippers** Kernfysisch Versneller Instituut, Groningen, The Netherlands	615
XD-05	**Buncher in the Beam Line from ECR to SFC** • **J.Z. Jiang**, X.H. Zhou, Q. Wang, F. Wang, W.M. Jiang Institute of Modern Physics, Lanzhou, People's Republic of China	618
XD-06	**Beamlines for a Second Injector Cyclotron at NAC** • **J.C. Cornell**, J.L. Conradie, D.T. Fourie National Accelerator Centre, Faure, Republic of South Africa	621
XD-07	**Beam Transport System for the HIMAC** • **K. Noda**, Y. Hirao, A. Itano, M. Kanazawa, A. Kitagawa, T. Kohno, M. Kumada, H. Ogawa, K. Sato, Y. Sato, M. Sudou, E. Takada, S. Yamada, T. Yamada NIRS, Chiba, Japan • K. Endo KEK, Ibaraki, Japan	625
XD-08	**Design of a Beam Buncher Using a Half-Cosine Driving Function**	629

- **R.C. Rogers**
  Texas A&M University, College Station, Texas, USA

XI — Control Systems

Chairman: W. Joho

Paper	Title	Page
XI-01	**Integrated Tools for Cyclotron Operation (Invited Paper)**	634
	• **W. Busse** HMI, Berlin, Germany	
XI-02	**The IUCF High Intensity Polarized Ion Source Control System**	641
	• **T. Capshew**, J.C. Collins, D. DuPlantis, D.W. Frame, J. Graham, D.D. Reid Indiana University, Bloomington, Indiana, USA	
XI-03	**An Operator Assistance System for the AVF Cyclotron**	644
	• **T. Okamura**, T. Murakami Sumitomo Heavy Industries Systems Engineering Laboratory, Tokyo, Japan • T. Tachikawa Sumitomo Heavy Industries, Ehime, Japan • T. Agematsu, S. Okumura, K. Arakawa JAERI, Gunma, Japan	
XI-04	**Control System for JAERI AVF Cyclotron**	648
	• **S. Okumura**, T. Agematsu, K. Arakawa, M. Fukuda, I. Ishibori, T. Kamiya, Y. Nakamura, T. Nara, W. Yokota JAERI, Gunma, Japan • K. Hoshika, K. Iso, M. Maruyama, M. Tachibana Sumitomo Heavy Industries, Ehime, Japan	
XI-05	**Automatic Control System of Magnetic Separator for Kurchatov IAE Cyclotron**	652
	• **N.I. Venikov**, V. Buranov, O. Gotovtsev, L.I. Iudin, P.Yu. Komissarov, V.N. Unezhev Kurchatov Institute, Moscow, Russia	
XI-06	**The New Distributed Control System of the NAC**	656
	• **H.F. Weehuizen**, R.K. Fisch, E.J.S. Franklin, M.E. Hogan, I.H. Kohler, J.P. Rogers, P.J. Theron National Accelerator Centre, Faure, Republic of South Africa	
XI-07	**Ion Spectra Identification Software for the ECR Ion Source at NAC**	660
	• **E.J.S. Franklin**, J.G. de Villiers National Accelerator Centre, Faure, Republic of South Africa	
XI-08	**Micro-Controlled Vacuum Systems at NAC**	664

- **P.J. Celliers**, E.J.S. Franklin
  National Accelerator Centre, Faure, Republic of South Africa

XI-09 **Two Dimensional Scans with Adaptive Domain Control** 668

- **S. Adam**, A.C. Mezger
  PSI, Villigen, Switzerland

XI-10 **Construction and System Tuning of Control System for the RCNP Ring Cyclotron and Beam Lines** 672

- **T. Yamazaki**, A. Ando, K. Hosono, T. Itahashi, M. Kibayashi, I. Miura, K. Nagayama, H. Ogata, T. Saito, A. Shimizu, K. Tamura, M. Uraki
  Osaka University, Osaka, Japan
- K. Aoki, Y. Kimura, M. Maruyama, M. Tachibana, S. Yamada
  Sumitomo Heavy Industries, Ehime, Japan
- K. Kodaira
  Sumitomo Heavy Industries Systems Engineering Laboratory, Tokyo, Japan

XI-11 **Early Experience with DECwindows/Motif in the TRIUMF Central Control System** 676

- **S. Kadantsev**
  JINR, Dubna, Russia
- M. Mouat
  TRIUMF, Vancouver, Canada

XI-12 **Application of Object Oriented Techniques in the TRIUMF Beam Line 2C Control System (Invited Paper)** 681

- **N.A. Wilkinson**, E.A. Osberg, G.A. Ludgate
  TRIUMF, Vancouver, Canada

XI-13 **The TR30 Control System - A Case for Off-the-Shelf Software** 685

- **R. Keitel**, D.J. Dale, B.F. Milton
  TRIUMF, Vancouver, Canada

XI-14 **Formal Specifications for a Cyclotron Control System** 689

- **J. Jacky**, R. Risler
  University of Washington, Seattle, Washington, USA

XII — Novel Cyclotrons

Chairman: N.K. Mukhopadhyay

Paper	Title	Page
XII-01	**The Superconducting Separated-Orbit Cyclotron Tritron (Invited Paper)**	693

- **U. Trinks**
  TU München, Garching, Germany

XII-02	**Study of an FFAG Synchrocyclotron for a Pulsed Neutron Source**	701

- **S.A. Martin**, E. Zaplatin
  FZJ, Jülich, Germany
- P.F. Meads, Jr.
  Private Address, Oakland, California, USA
- G. Wüstefeld
  BESSY, Berlin, Germany
- K. Ziegler
  HMI, Berlin, Germany

XII-03	**Design of a Compact Permanent Magnet Cyclotron Mass Spectrometer for the Detection and Measurement of Trace Isotopes**	705

- **A.T. Young**, K.J. Bertsche, D.J. Clark, K. Halbach, W.B. Kunkel, K.N. Leung, C.Y. Li
  LBL, Berkeley, California, USA

XII-04	**A New Design Proposal for a 200 MeV Superconducting Ring-Cyclotron Magnet**	709

- **H.N. Jungwirth**, J.G. de Villiers
  National Accelerator Centre, Faure, Republic of South Africa

XIII — Radioactive Beam Facilities

Chairman: B. Allardyce

Paper	Title	Page
XIII-01	**Accelerated Radioactive Nuclear Beams: Existing and Planned Facilities (Invited Paper)** • **J.M. Nitschke** LBL, Berkeley, California, USA	713
XIII-02	**A Conceptual Design for a Primary Cyclotron for the ISL Radioactive Beam Project** • **D.J. Clark** LBL, Berkeley, California, USA	721
XIII-03	**An On-Line Isotopic Separator Test Bench at GANIL** • **P. Bricault**, R. Leroy, M. Lewitowicz, J.Y. Pacquet, M.G. St-Laurent, P. Sortais GANIL, Caen, France • A.C. Mueller, J. Obert, J.C. Putaux IPN, Orsay, France • C.F. Liang, P. Paris CSNSM, Orsay, France • J.C. Steckmeyer LPC, Caen, France	725
XIII-04	**The PIAFE Project at Grenoble: Beam Transport and Acceleration** • **J.L. Belmont**, J.F. Bruandet, J.M. de Conto, M. Fruneau, G. Gimond, K. Golovanivsky, E. Liatard, J.M. Loiseaux, H. Nifenecker, A. Savalle, B. Vignon Université Joseph Fourier, Grenoble, France • P. Briand CEN-Grenoble, Grenoble, France	729
XIII-05	**High Intensity Superconducting Cyclotron Beams for a Radioactive Ion Beam Facility** • **L. Calabretta**, D. Rifuggiato INFN/LNS, Catania, Italy	733
XIII-06	**Radioactive Ion Beam Production Using the Louvain-La-Neuve Cyclotrons: Present Status and Future Developments** • **G. Ryckewaert**, M. Loiselet, N. Postiau Université Catholique de Louvain, Louvain-la-Neuve, Belgium	737

XIII-07 **The ORNL Radioactive Ion Beam Project with the ORIC Accelerator** 741

- **D.K. Olsen**, G.D. Alton, C. Baktash, D.T. Dowling, J.D. Garrett, D.L. Haynes, C.M. Jones, R.C. Juras, S.N. Lane, I.Y. Lee, M.J. Meigs, G.D. Mills, S.W. Mosko, B.A. Tatum, K.S. Toth
  ORNL, Oak Ridge, Tennessee, USA
- H.K. Carter, J. Kormicki
  Associated Universities Oak Ridge, Oak Ridge, Tennessee, USA

XIII-08 **Research and Development Studies with Radioactive Beams at TRIUMF** 745

- **J.M. D'Auria**, M. Dombsky
  Simon Fraser University, Burnaby, BC, Canada
- L. Buchmann, H. Sprenger, J.S. Vincent
  TRIUMF, Vancouver, Canada
- J. King
  University of Toronto, Toronto, Ontario, Canada
- P. McNeely, G. Roy
  University of Alberta, Edmonton, Alberta, Canada

XIII-09 **Post-Accelerator Studies for the ISOL Facility at TRIUMF** 749

- **L. Root**, H.R. Schneider, J.S. Fraser
  TRIUMF, Vancouver, Canada

XIV — Final Session

Chairman: J.R. Richardson

Paper	Title	Page
XIV-01	**Future Cyclotrons (Invited Paper)**	
	• **H.G. Blosser** NSCL, East Lansing, Michigan, USA	
XIV-02	**The Use of Cyclotrons for Physics Experiments, Past, Present and Future (Invited Paper)**	
	• **J.C. Hardy** Atomic Energy of Canada, Chalk River, Ontario, Canada	
XIV-03	**Physics with Storage Rings (Invited Paper)**	753
	• **R.E. Pollock** Indiana University, Bloomington, Indiana, USA	
XIV-04	**Conference Summary (Invited Paper)**	758
	• **D.J. Clark** LBL, Berkeley, California, USA	

XV — Propriety of Accelerators (After-dinner talk)

Paper	Title	Page
XV-01	**Proper and Improper Accelerators - In Praise of Cyclotrons and Their Builders**	765

- **M.K. Craddock**
  University of British Columbia, Vancouver, Canada

A B C D E F G H I J K L M N O P Q R S T U V W X Y Z

Abe, J.

Paper	Title	Page
I-01	**Commissioning of the RCNP Ring Cyclotron (Invited Paper)**	3

- **I. Miura**, A. Ando, K. Hatanaka, K. Hosono, H. Ikegami, T. Itahashi, M. Kibayashi, M. Kondo, H. Ogata, T. Saito, A. Shimizu, K. Tamura, M. Uraki, T. Yamazaki
  Osaka University, Osaka, Japan
- J. Abe
  Sumitomo Heavy Industries, Ehime, Japan

A B C D E F G H I J K L M N O P Q R S T U V W X Y Z

Abrosimov, N.K.

Paper	Title	Page
I-10	**Gatchina Isochronous Cyclotron**	58

- **N.K. Abrosimov**, S.A. Artamonov, P.V. Chervyakov, S.P. Dmitriev, V.A. Eliseev, V.P. Fominenko, E.M. Ivanov, G.F. Mikheev, Yu.T. Mironov, A.S. Pokrovskii, G.A. Riabov, V.A. Smolin, G.L. Sokolov, V.A. Volchenkov, A.A. Vorobiev
  Petersburg Nuclear Physics Institute, Gatchina, Russia
- P.V. Bogdanov, B.D. Ershov, V.S. Kuligin, V.N. Moshkin, V.G. Mudrolyubov, Yu.I. Stogov, A.P. Strokach
  D.V. Efremov Scientific Research Institute of Electrophysical Apparatus, St. Petersburg, Russia

A B C D E F G H I J K L M N O P Q R S T U V W X Y Z

Adam, S.

Paper	Title	Page
I-05	**The Commissioning of PSI Injector 2 for High Intensity, High Quality Beams**	36

- **J. Stetson**
  NSCL, East Lansing, Michigan, USA
- S. Adam, M. Humbel, W. Joho, Th. Stammbach
  PSI, Villigen, Switzerland

XI-09	**Two Dimensional Scans with Adaptive Domain Control**	668

- **S. Adam**, A.C. Mezger
  PSI, Villigen, Switzerland

A B C D E F G H I J K L M N O P Q R S T U V W X Y Z

Agematsu, T.

Paper	Title	Page
II-03	**Construction and First Year's Operation of the JAERI AVF Cyclotron**	119

- **K. Arakawa**, T. Agematsu, M. Fukuda, I. Ishibori, T. Karasawa, T. Nara, Y. Nakamura, S. Okumura, R. Tanaka, W. Yokota
  JAERI, Gunma, Japan
- A. Shimizu
  Osaka University, Osaka, Japan
- Y. Hayashi, K. Ishii, T. Satoh, T. Tachikawa
  Sumitomo Heavy Industries, Ehime, Japan

VIII-09	**Operation of Ion Sources and Beam Transport to JAERI AVF Cyclotron**	336

- **W. Yokota**, T. Agematsu, K. Arakawa, M. Fukuda, I. Ishibori, Y. Nakamura, T. Nara, S. Okumura
  JAERI, Gunma, Japan
- Y. Hayashi, K. Ishii, T. Tachikawa
  Sumitomo Heavy Industries, Ehime, Japan

IXB-02	**Beam Studies of Injection to Extraction System for JAERI AVF Cyclotron**	423

- **M. Fukuda**, T. Agematsu, K. Arakawa, I. Ishibori, T. Karasawa, Y. Nakamura, T. Nara, S. Okumura, W. Yokota
  JAERI, Gunma, Japan

XC-04	**Performance of Beam Chopping System for JAERI AVF Cyclotron**	581

- **W. Yokota**, T. Agematsu, K. Arakawa, M. Fukuda, I. Ishibori, Y. Nakamura, T. Nara, S. Okumura
  JAERI, Gunma, Japan
- Y. Hayashi, Y. Kumata, T. Tachikawa
  Sumitomo Heavy Industries, Ehime, Japan

XI-03	**An Operator Assistance System for the AVF Cyclotron**	644

- **T. Okamura**, T. Murakami
  Sumitomo Heavy Industries Systems Engineering Laboratory, Tokyo, Japan
- T. Tachikawa
  Sumitomo Heavy Industries, Ehime, Japan
- T. Agematsu, S. Okumura, K. Arakawa
  JAERI, Gunma, Japan

XI-04	**Control System for JAERI AVF Cyclotron**	648

- **S. Okumura**, T. Agematsu, K. Arakawa, M. Fukuda, I. Ishibori, T. Kamiya,

Y. Nakamura, T. Nara, W. Yokota
JAERI, Gunma, Japan
- K. Hoshika, K. Iso, M. Maruyama, M. Tachibana
Sumitomo Heavy Industries, Ehime, Japan

A B C D E F G H I J K L M N O P Q R S T U V W X Y Z

Albrand, S.

Paper	Title	Page
I-11	**Status Report of SARA**	62

- **M. Fruneau**, S. Albrand, D. Barnéoud, J.L. Belmont, G. Bizouard, J.L. Bouly, G. Campillo, M. Guisset, G. Laborie
  Université Joseph Fourier, Grenoble, France

A B C D E F G H I J K L M N O P Q R S T U V W X Y Z

Alenitskiy, Ju.

Paper	Title	Page
II-04	**20 MeV Cyclotron for Isotope Production**	123

- **A. Glazov**, Ju. Alenitskiy, A. Chesnov, S. Chesnova, V. Kochkin, D. Novikov, E. Samsonov, M. Semenov, A. Vasilenko, E. Zaplatin, N. Zaplatin
  JINR, Dubna, Russia
- I. Gulamov, O. Iljasov, A. Rykov
  Institute of Nuclear Physics, Tashkent, Republic of Uzbekistan

A B C D E F G H I J K L M N O P Q R S T U V W X Y Z

Alessandria, F.

Paper	Title	Page
I-18	**Status Report on the Heavy Ion Facility at LNS**	90

- **F. Alessandria**, G. Bellomo, A. Bosotti, C. De Martinis, D. Giove, P. Michelato, C. Pagani, L. Rossi
  INFN/LASA, Segrate, Italy
- L. Calabretta, G. Ciavola, G. Cuttone, M. Di Giacomo, S. Gammino, P. Gmaj, G. Raia, D. Rifuggiato, J. Sura
  INFN/LNS, Catania, Italy

A B C D E F G H I J K L M N O P Q R S T U V W X Y Z

Alton, G.D.

Paper	Title	Page
XIII-07	**The ORNL Radioactive Ion Beam Project with the ORIC Accelerator**	741

- **D.K. Olsen**, G.D. Alton, C. Baktash, D.T. Dowling, J.D. Garrett, D.L. Haynes, C.M. Jones, R.C. Juras, S.N. Lane, I.Y. Lee, M.J. Meigs, G.D. Mills, S.W. Mosko, B.A. Tatum, K.S. Toth
  ORNL, Oak Ridge, Tennessee, USA
- H.K. Carter, J. Kormicki
  Associated Universities Oak Ridge, Oak Ridge, Tennessee, USA

A B C D E F G H I J K L M N O P Q R S T U V W X Y Z

Anderson, S.

Paper	Title	Page
XA-05	**Low Frequency RF System for the Indiana University Cooler Ring**	523

- **X. Pei**, S. Anderson, V. Derenchuk, G. East, D.L. Friesel, D. Jenner, D. McCammon, T. Sloan
  Indiana University, Bloomington, Indiana, USA

A B C D E F G H I J K L M N O P Q R S T U V W X Y Z

Ando, A.

Paper	Title	Page
I-01	**Commissioning of the RCNP Ring Cyclotron (Invited Paper)**	3

- **I. Miura**, A. Ando, K. Hatanaka, K. Hosono, H. Ikegami, T. Itahashi, M. Kibayashi, M. Kondo, H. Ogata, T. Saito, A. Shimizu, K. Tamura, M. Uraki, T. Yamazaki
  Osaka University, Osaka, Japan
- J. Abe
  Sumitomo Heavy Industries, Ehime, Japan

XI-10	**Construction and System Tuning of Control System for the RCNP Ring Cyclotron and Beam Lines**	672

- **T. Yamazaki**, A. Ando, K. Hosono, T. Itahashi, M. Kibayashi, I. Miura, K. Nagayama, H. Ogata, T. Saito, A. Shimizu, K. Tamura, M. Uraki
  Osaka University, Osaka, Japan
- K. Aoki, Y. Kimura, M. Maruyama, M. Tachibana, S. Yamada
  Sumitomo Heavy Industries, Ehime, Japan
- K. Kodaira
  Sumitomo Heavy Industries Systems Engineering Laboratory, Tokyo, Japan

A B C D E F G H I J K L M N O P Q R S T U V W X Y Z

Antaya, T.A.

Paper	Title	Page
I-17	**Performance of the K1200 Cyclotron at MSU** • **P. Miller**, T.A. Antaya, F. Marti, D. Poe, B. Sherrill, J. Stetson, J. Winger NSCL, East Lansing, Michigan, USA • J.A. Nolen ANL, Argonne, Illinois, USA	86
VIII-12	**The Super Gas Mixing Technique for Highly Charged Uranium Ions** • **T.A. Antaya**, D. Cole NSCL, East Lansing, Michigan, USA	348
IXB-03	**K1200 Cyclotron Beam Development Techniques** • **T.A. Antaya**, D. Cole, P. Miller, D. Poe NSCL, East Lansing, Michigan, USA	427
IXC-04	**Non-Linear Beam Transport Effects in Highly Charged Positive Ion Beams Extracted From ECR Ion Sources** • **T.A. Antaya** NSCL, East Lansing, Michigan, USA • Z.Q. Xie LBL, Berkeley, California, USA	457

A B C D E F G H I J K L M N O P Q R S T U V W X Y Z

Aoki, K.

Paper	Title	Page
XI-10	**Construction and System Tuning of Control System for the RCNP Ring Cyclotron and Beam Lines**	672

- **T. Yamazaki**, A. Ando, K. Hosono, T. Itahashi, M. Kibayashi, I. Miura, K. Nagayama, H. Ogata, T. Saito, A. Shimizu, K. Tamura, M. Uraki
  Osaka University, Osaka, Japan
- K. Aoki, Y. Kimura, M. Maruyama, M. Tachibana, S. Yamada
  Sumitomo Heavy Industries, Ehime, Japan
- K. Kodaira
  Sumitomo Heavy Industries Systems Engineering Laboratory, Tokyo, Japan

A B C D E F G H I J K L M N O P Q R S T U V W X Y Z

Arakaki, Y.

Paper	Title	Page
VII-04	**Study of Beam Dynamics at Cooler Synchrotron TARN-II**	286

- **S. Watanabe**, Y. Arakaki, K. Chida, T. Katayama, M. Tomizawa, T. Watanabe, M. Yoshizawa
  University of Tokyo, Tanashi-shi, Tokyo, Japan
- K. Noda, M. Kanazawa
  NIRS, Chiba, Japan

A B C D E F G H I J K L M N O P Q R S T U V W X Y Z

Arakawa, K.

Paper	Title	Page
II-03	**Construction and First Year's Operation of the JAERI AVF Cyclotron**	119

- **K. Arakawa**, T. Agematsu, M. Fukuda, I. Ishibori, T. Karasawa, T. Nara, Y. Nakamura, S. Okumura, R. Tanaka, W. Yokota
  JAERI, Gunma, Japan
- A. Shimizu
  Osaka University, Osaka, Japan
- Y. Hayashi, K. Ishii, T. Satoh, T. Tachikawa
  Sumitomo Heavy Industries, Ehime, Japan

VIII-09	**Operation of Ion Sources and Beam Transport to JAERI AVF Cyclotron**	336

- **W. Yokota**, T. Agematsu, K. Arakawa, M. Fukuda, I. Ishibori, Y. Nakamura, T. Nara, S. Okumura
  JAERI, Gunma, Japan
- Y. Hayashi, K. Ishii, T. Tachikawa
  Sumitomo Heavy Industries, Ehime, Japan

IXB-02	**Beam Studies of Injection to Extraction System for JAERI AVF Cyclotron**	423

- **M. Fukuda**, T. Agematsu, K. Arakawa, I. Ishibori, T. Karasawa, Y. Nakamura, T. Nara, S. Okumura, W. Yokota
  JAERI, Gunma, Japan

XA-06	**A Modified RF System of JAERI AVF Cyclotron**	526

- **Y. Kumata**, Y. Fukumoto
  Sumitomo Heavy Industries, Ehime, Japan
- K. Arakawa, M. Fukuda, T. Karasawa
  JAERI, Gunma, Japan
- A. Shimizu
  Osaka University, Osaka, Japan

XC-04	**Performance of Beam Chopping System for JAERI AVF Cyclotron**	581

- **W. Yokota**, T. Agematsu, K. Arakawa, M. Fukuda, I. Ishibori, Y. Nakamura, T. Nara, S. Okumura
  JAERI, Gunma, Japan
- Y. Hayashi, Y. Kumata, T. Tachikawa
  Sumitomo Heavy Industries, Ehime, Japan

XI-03	**An Operator Assistance System for the AVF Cyclotron**	644

- **T. Okamura**, T. Murakami

Sumitomo Heavy Industries Systems Engineering Laboratory, Tokyo, Japan
- T. Tachikawa
  Sumitomo Heavy Industries, Ehime, Japan
- T. Agematsu, S. Okumura, K. Arakawa
  JAERI, Gunma, Japan

XI-04 **Control System for JAERI AVF Cyclotron** 648

- **S. Okumura**, T. Agematsu, K. Arakawa, M. Fukuda, I. Ishibori, T. Kamiya, Y. Nakamura, T. Nara, W. Yokota
  JAERI, Gunma, Japan
- K. Hoshika, K. Iso, M. Maruyama, M. Tachibana
  Sumitomo Heavy Industries, Ehime, Japan

A B C D E F G H I J K L M N O P Q R S T U V W X Y Z

Arnott, D.W.

Paper	Title	Page
VI-06	**Health Physics Data Acquisition System at the National Medical Cyclotron**	252

- **B.N. Mukherjee**
  ANSTO, Menai, NSW, Australia
- D.W. Arnott
  National Medical Cyclotron, Camperdown, NSW, Australia

A B C D E F G H I J K L M N O P Q R S T U V W X Y Z

Artamonov, S.A.

Paper	Title	Page
I-10	**Gatchina Isochronous Cyclotron**	58

- **N.K. Abrosimov**, S.A. Artamonov, P.V. Chervyakov, S.P. Dmitriev, V.A. Eliseev, V.P. Fominenko, E.M. Ivanov, G.F. Mikheev, Yu.T. Mironov, A.S. Pokrovskii, G.A. Riabov, V.A. Smolin, G.L. Sokolov, V.A. Volchenkov, A.A. Vorobiev
  Petersburg Nuclear Physics Institute, Gatchina, Russia
- P.V. Bogdanov, B.D. Ershov, V.S. Kuligin, V.N. Moshkin, V.G. Mudrolyubov, Yu.I. Stogov, A.P. Strokach
  D.V. Efremov Scientific Research Institute of Electrophysical Apparatus, St. Petersburg, Russia

A B C D E F G H I J K L M N O P Q R S T U V W X Y Z

Arzumanov, A.A.

Paper	Title	Page
I-13	**Current Status and Future Project of Cyclotron Laboratory in Alma-Ata**	71

- **A.A. Arzumanov**, V. Batischev, V. Berger, V. Gerasimov, M. Gorcovets
  Kazakhstan Academy of Sciences, Alma-Ata, Republic of Kazakhstan

Paper	Title	Page
V-05	**Radiopharmaceutical "Thallium-201-Chloride" Production using Thallium-203 Irradiation by Helium-3 Ions**	216

- **A.A. Arzumanov**, N.K. Hamidov, A.I. Kozin, G.I. Shychikov, S.T. Tihomirova
  Kazakhstan Academy of Sciences, Alma-Ata, Republic of Kazakhstan

A B C D E F G H I J K L M N O P Q R S T U V W X Y Z

Audi, G.

Paper	Title	Page
IV-02	**A Cyclotron as a Mass Spectrometer**	158

- **P. Bricault**, G. Auger, M. Bajard, E. Baron, D. Bibet, A. Chabert, J. Fermé, L. Gaudart, J. Joubert, M. Lewitowicz, W. Mittig, E. Plagnol, Ch. Ricaud, Y. Schutz
  GANIL, Caen, France
- G. Audi
  CSNSM, Orsay, France
- A. Gillibert
  CEN/Saclay, Gif-sur-Yvette, France
- K. Fifield
  Australian National University, Canberra , Australia

A B C D E F G H I J K L M N O P Q R S T U V W X Y Z

Auger, G.

Paper	Title	Page
IV-02	**A Cyclotron as a Mass Spectrometer**	158

- **P. Bricault**, G. Auger, M. Bajard, E. Baron, D. Bibet, A. Chabert, J. Fermé, L. Gaudart, J. Joubert, M. Lewitowicz, W. Mittig, E. Plagnol, Ch. Ricaud, Y. Schutz
  GANIL, Caen, France
- G. Audi
  CSNSM, Orsay, France
- A. Gillibert
  CEN/Saclay, Gif-sur-Yvette, France
- K. Fifield
  Australian National University, Canberra , Australia

A B C D E F G H I J K L M N O P Q R S T U V W X Y Z

Bachman, D.A.

Paper	Title	Page
VIII-03	**Ion Sources for Cyclotron Application**	312

- **K.N. Leung**, D.A. Bachman, D.S. McDonald, A.T. Young
  LBL, Berkeley, California, USA

A B C D E F G H I J K L M N O P Q R S T U V W X Y Z

Bailey, J.

Paper	Title	Page
IXB-04	**Selection and Measurement of RF Phase Width of the K1200 Cyclotron Beam**	431

- **J. Bailey**, J. Kuchar, F. Marti, J. Yurkon
  NSCL, East Lansing, Michigan, USA
- J.A. Nolen
  ANL, Argonne, Illinois, USA
- D. Rifuggiato
  INFN/LNS, Catania, Italy

A B C D E F G H I J K L M N O P Q R S T U V W X Y Z

Bajard, M.

Paper	Title	Page
I-09	**GANIL Status Report**	54

- **M. Bajard**
  GANIL, Caen, France

Paper	Title	Page
IV-02	**A Cyclotron as a Mass Spectrometer**	158

- **P. Bricault**, G. Auger, M. Bajard, E. Baron, D. Bibet, A. Chabert, J. Fermé, L. Gaudart, J. Joubert, M. Lewitowicz, W. Mittig, E. Plagnol, Ch. Ricaud, Y. Schutz
  GANIL, Caen, France
- G. Audi
  CSNSM, Orsay, France
- A. Gillibert
  CEN/Saclay, Gif-sur-Yvette, France
- K. Fifield
  Australian National University, Canberra , Australia

Baktash, C.

Paper	Title	Page
XIII-07	**The ORNL Radioactive Ion Beam Project with the ORIC Accelerator**	741

- **D.K. Olsen**, G.D. Alton, C. Baktash, D.T. Dowling, J.D. Garrett, D.L. Haynes, C.M. Jones, R.C. Juras, S.N. Lane, I.Y. Lee, M.J. Meigs, G.D. Mills, S.W. Mosko, B.A. Tatum, K.S. Toth
  ORNL, Oak Ridge, Tennessee, USA
- H.K. Carter, J. Kormicki
  Associated Universities Oak Ridge, Oak Ridge, Tennessee, USA

A B C D E F G H I J K L M N O P Q R S T U V W X Y Z

Ball, M.S.

Paper	Title	Page
XD-02	**Beam Transport System for the IUCF High Intensity Polarized Ion Source**	609

- **W.P. Jones**, M.S. Ball, J.C. Collins, D. DuPlantis, T.J.P. Ellison, D.L. Friesel, B. Hamilton, J.W. Hicks, P. Schwandt
  Indiana University, Bloomington, Indiana, USA

A B C D E F G H I J K L M N O P Q R S T U V W X Y Z

Barnéoud, D.

Paper	Title	Page
I-11	**Status Report of SARA**	62

- **M. Fruneau**, S. Albrand, D. Barnéoud, J.L. Belmont, G. Bizouard, J.L. Bouly, G. Campillo, M. Guisset, G. Laborie
  Université Joseph Fourier, Grenoble, France

A B C D E F G H I J K L M N O P Q R S T U V W X Y Z

Baron, E.

Paper	Title	Page
IV-02	**A Cyclotron as a Mass Spectrometer**	158

- **P. Bricault**, G. Auger, M. Bajard, E. Baron, D. Bibet, A. Chabert, J. Fermé, L. Gaudart, J. Joubert, M. Lewitowicz, W. Mittig, E. Plagnol, Ch. Ricaud, Y. Schutz
  GANIL, Caen, France
- G. Audi
  CSNSM, Orsay, France
- A. Gillibert
  CEN/Saclay, Gif-sur-Yvette, France
- K. Fifield
  Australian National University, Canberra , Australia

Paper	Title	Page
IXC-01	**Commissioning of the New High Intensity Axial Injection System for GANIL**	446

- **Ch. Ricaud**, E. Baron, J. Bony, M.P. Bourgarel, B. Bru
  GANIL, Caen, France
- R. Vienet
  CEN/Saclay, Gif-sur-Yvette, France

A B C D E F G H I J K L M N O P Q R S T U V W X Y Z

Batischev, V.

Paper	Title	Page
I-13	**Current Status and Future Project of Cyclotron Laboratory in Alma-Ata**	71

- **A.A. Arzumanov**, V. Batischev, V. Berger, V. Gerasimov, M. Gorcovets
  Kazakhstan Academy of Sciences, Alma-Ata, Republic of Kazakhstan

A B C D E F G H I J K L M N O P Q R S T U V W X Y Z

Bechtold, V.

Paper	Title	Page
II-01	**Commercially Available Compact Cyclotrons for Isotope Production (Invited Paper)**	110

- **V. Bechtold**
  FZK, Karlsruhe, Germany

A B C D E F G H I J K L M N O P Q R S T U V W X Y Z

Beeckman, W.

Paper	Title	Page
VI-04	**Progress Report on the IBA-SHI Proton Therapy System**	244

- **Y. Jongen**, W. Beeckman, J.P. Dufour, A. Laisné, H. Marie, R. Verbruggen
  Ion Beam Applications, Louvain-la-Neuve, Belgium
- M. Sano, S. Satoh, N. Takahashi, T. Takayama
  Sumitomo Heavy Industries, Ehime, Japan

A B C D E F G H I J K L M N O P Q R S T U V W X Y Z

Bejsovec, V.

Paper	Title	Page
IXC-06	**Experiments on the Axial Injection System of the Cyclotron U-120M**	465

- **Z. Trejbal**, M. Krivánek, J. Kucera, V. Bejsovec, J. Stursa
  Czechoslovak Academy of Sciences, Rez, Czechoslovakia

A B C D E F G H I J K L M N O P Q R S T U V W X Y Z

Bekhterev, V.

Paper	Title	Page
I-02	**New Development at the JINR Heavy Ion Cyclotron Facility (Invited Paper)**	11

- **G.G. Gulbekyan**, V. Bekhterev, O. Borisov, B. Gikal, A. Ivanenko, I. Kolesov, V.B. Kutner, A. Morduev, Yu.Ts. Oganessian
  JINR, Dubna, Russia

A B C D E F G H I J K L M N O P Q R S T U V W X Y Z

Bellomo, G.

Paper	Title	Page
I-18	**Status Report on the Heavy Ion Facility at LNS**	90

- **F. Alessandria**, G. Bellomo, A. Bosotti, C. De Martinis, D. Giove, P. Michelato, C. Pagani, L. Rossi
  INFN/LASA, Segrate, Italy
- L. Calabretta, G. Ciavola, G. Cuttone, M. Di Giacomo, S. Gammino, P. Gmaj, G. Raia, D. Rifuggiato, J. Sura
  INFN/LNS, Catania, Italy

XC-07	**Design of Passive Magnetic Channels**	592

- **G. Bellomo**
  INFN/LASA, Segrate, Italy

A B C D E F G H I J K L M N O P Q R S T U V W X Y Z

Belmont, J.L.

Paper	Title	Page
I-11	**Status Report of SARA**	62

- **M. Fruneau**, S. Albrand, D. Barnéoud, J.L. Belmont, G. Bizouard, J.L. Bouly, G. Campillo, M. Guisset, G. Laborie
  Université Joseph Fourier, Grenoble, France

Paper	Title	Page
XIII-04	**The PIAFE Project at Grenoble: Beam Transport and Acceleration**	729

- **J.L. Belmont**, J.F. Bruandet, J.M. de Conto, M. Fruneau, G. Gimond, K. Golovanivsky, E. Liatard, J.M. Loiseaux, H. Nifenecker, A. Savalle, B. Vignon
  Université Joseph Fourier, Grenoble, France
- P. Briand
  CEN-Grenoble, Grenoble, France

A B C D E F G H I J K L M N O P Q R S T U V W X Y Z

Belov, V.P.

Paper	Title	Page
VII-06	**The New Project of INR (Kiev's) Storage-Accelerating Complex**	294

- **A.V. Dolinsky**, A.I. Papash, S.N. Pavlov, A.T. Rudchik, A.E. Val'Kov, I.N. Vishnevsky, A.V. Zhmendak
  Institute for Nuclear Research, Kiev, Ukraine
- V.P. Belov, A.M. Kokorin, A.A. Makarov, I.A. Schukeilo, Yu.P. Severgin
  D.V. Efremov Scientific Research Institute of Electrophysical Apparatus, St. Petersburg, Russia

Paper	Title	Page
VII-05	**Dubna Project of the Heavy Ion Storage Ring Complex K4-K10**	290

- **Yu.Ts. Oganessian**, O.N. Malyshev, G.S. Popeko, A.M. Rodin, S.I. Sidorchuk, Ye.A. Sokol, S.V. Stepantsov, G.M. Ter-Akopian, V.A. Timakov
  JINR, Dubna, Russia
- V.V. Parhomchuk, A.A. Sery, V.D. Shiltsev
  Institute for Nuclear Physics, Novosibirsk, Russia
- I.N. Meshkov, Ye.M. Syresinm
  Center for Applied Physics and Technology, Lipetsk, Russia
- V.P. Belov, A.A. Makarov, Yu.P. Severgin, I.A. Shukeylo, M.N. Tarovik
  D.V. Efremov Scientific Research Institute of Electrophysical Apparatus, St. Petersburg, Russia

A B C D E F G H I J K L M N O P Q R S T U V W X Y Z

Berger, V.

Paper	Title	Page
I-13	**Current Status and Future Project of Cyclotron Laboratory in Alma-Ata**	71

- **A.A. Arzumanov**, V. Batischev, V. Berger, V. Gerasimov, M. Gorcovets
  Kazakhstan Academy of Sciences, Alma-Ata, Republic of Kazakhstan

A B C D E F G H I J K L M N O P Q R S T U V W X Y Z

Bergmark, T.

Paper	Title	Page
VII-01	**Recent Commissioning Results at Celsius (Invited Paper)**	266

- **D. Reistad**, T. Bergmark, C. Ekström, C.-J. Fridén, K. Gajewski, L. Hermansson, P. Jahnke, A. Johansson, O. Johansson, T. Lofnes, G. Norman, R. Wedberg, L. Westerberg, J. Zlomanczuk
  Uppsala University, Uppsala, Sweden
- M.A. Raadu, M. Sedlacek
  Royal Institute of Technology, Stockholm, Sweden

A B C D E F G H I J K L M N O P Q R S T U V W X Y Z

Bertsche, K.J.

Paper	Title	Page
XII-03	**Design of a Compact Permanent Magnet Cyclotron Mass Spectrometer for the Detection and Measurement of Trace Isotopes**	705

- **A.T. Young**, K.J. Bertsche, D.J. Clark, K. Halbach, W.B. Kunkel, K.N. Leung, C.Y. Li
  LBL, Berkeley, California, USA

A B C D E F G H I J K L M N O P Q R S T U V W X Y Z

Beuscher, H.

Paper	Title	Page
I-12	**Commissioning of the Injector Complex of COSY-Jülich**	67

- **W. Bräutigam**, H. Beuscher, R. Brings, H.G. Böge, R. Maier, M. Rogge, P. Wucherer
  FZJ, Jülich, Germany

A B C D E F G H I J K L M N O P Q R S T U V W X Y Z

Bibet, D.

Paper	Title	Page
IV-02	**A Cyclotron as a Mass Spectrometer**	158

- **P. Bricault**, G. Auger, M. Bajard, E. Baron, D. Bibet, A. Chabert, J. Fermé, L. Gaudart, J. Joubert, M. Lewitowicz, W. Mittig, E. Plagnol, Ch. Ricaud, Y. Schutz
  GANIL, Caen, France
- G. Audi
  CSNSM, Orsay, France
- A. Gillibert
  CEN/Saclay, Gif-sur-Yvette, France
- K. Fifield
  Australian National University, Canberra , Australia

IXB-01	**Cyclotron Tuning as a Rebuncher**	419

- **D. Bibet**, M-H. Moscatello
  GANIL, Caen, France

List of Authors

A

Abe, J.
Abrosimov, N.K.
Adam, S.
Agematsu, T.
Albrand, S.
Alenitskiy, Ju.
Alessandria, F.
Alton, G.D.
Anderson, S.
Ando, A.
Antaya, T.A.
Aoki, K.
Arakaki, Y.
Arakawa, K.
Arnott, D.W.
Artamonov, S.A.
Arzumanov, A.A.
Audi, G.
Auger, G.

B

Bachman, D.A.
Bailey, J.
Bajard, M.
Baktash, C.
Ball, M.S.
Barnéoud, D.
Baron, E.
Batischev, V.
Bechtold, V.
Beeckman, W.
Bejsovec, V.
Bekhterev, V.
Bellomo, G.
Belmont, J.L.
Belov, V.P.
Berger, V.
Bergmark, T.
Bertsche, K.J.
Beuscher, H.
Bibet, D.
Biri, S.
Bizouard, G.
Blache, P.
Blaker, G.C.
Bloemhard, P.
Blosser, H.G.
Böge, H.G.
Bogdanov, P.V.

Bogomolov, S.L.
Bojovic, B.
Bony, J.
Borisov, O.
Bosotti, A.
Botha, A.H.
Botman, J.I.M.
Bouly, J.L.
Bourgarel, M.P.
Boux, R.
Bräutigam, W.
Brassart, N.
Briand, P.
Bricault, P.
Brigham, M.
Brings, R.
Brossard, S.
Brown, R.
Bru, B.
Bruandet, J.F.
Buchmann, L.
Buranov, V.
Burbeza, C.D.
Burger, S.J.
Busse, W.

C

Calabretta, L.
Campillo, G.
Capshew, T.
Carter, H.K.
Celliers, P.J.
Chabert, A.
Chang, H.
Chaudhri, M.A.
Chauvel, P.
Cherix, J.
Chervyakov, P.V.
Chesnov, A.
Chesnova, S.
Chida, K.
Ciavola, G.
Clark, D.J.
Clark, J.C.
Cole, D.
Collins, D.
Collins, J.C.
Commeaux, C.
Conard, E.
Conradie, J.L.
Cooper, M.
Cornell, J.C.
Corti, D.
Courdi, A.
Craddock, M.K.

Cronje, P.M.
Cui, X.
Cuttone, G.

D

Dale, D.J.
Dam, J.A.M.
Dambre, P.
D'Auria, J.M.
Davies, W.G.
de Conto, J.M.
De Martinis, C.
de Villiers, J.G.
Delhez, J.L.
Derenchuk, V.
Derrig, G.
Dewees, W.
Di Biasi, G.
Di Giacomo, M.
Diamond, W.T.
Didyk, A.Yu.
Dmitriev, S.N.
Dmitriev, S.P.
Dolinsky, A.V.
Dombsky, M.
Dowling, D.T.
du Toit, Z.B.
Dufour, J.P.
DuPlantis, D.
Dutto, G.

E

East, G.
Efremov, A.
Eiche, M.
Ekström, C.
Eliseev, V.A.
Ellison, T.J.P.
Enchevich, I.B.
Endo, K.
Erdman, K.L.
Ershov, B.D.

F

Farley, F.
Fehsenfeld, P.
Fenemore, R.E.F.
Fermé, J.
Fietier, N.
Fifield, K.
Fisch, R.K.

Fominenko, V.P.
Fong, K.
Fourie, D.T.
Frame, D.W.
Franklin, E.J.S.
Fraser, J.S.
Frei, H.
Fridén, C.-J.
Friesel, D.L.
Fruneau, M.
Fujita, M.
Fukuda, M.
Fukumoto, S.
Fukumoto, Y.

G

Gajewski, K.
Gammino, S.
Gangrski, Yu.P.
Garrett, J.D.
Gaudart, L.
Gelbart, W.Z.
Gerasimov, V.
Gikal, B.
Gillibert, A.
Gimond, G.
Giove, D.
Glazov, A.
Glushko, A.
Gmaj, P.
Golovanivsky, K.
Goodman, G.B.
Gorcovets, M.
Gordon, M.M.
Goto, A.
Gotovtsev, O.
Graham, J.
Grey-Morgan, T.
Grimmett, G.
Guisset, M.
Gulamov, I.
Gulbekyan, G.G.
Guo, M.
Gustafsson, S.

H

Hagedoorn, H.L.
Halbach, K.
Hamidov, N.K.
Hamilton, B.
Hardy, J.C.
Hatanaka, K.
Hayakawa, Y.

Hayashi, Y.
Haynes, D.L.
Heikkinen, P.
Hendry, G.O.
Herault, J.
Hermansson, L.
Herschbach, M.
Hicks, J.W.
Hirao, Y.
Hoffmann, C.R.
Hogan, M.E.
Holm, S.
Holmgren, B.
Hoshika, K.
Hosono, K.
Houtman, H.
Hubbard, R.E.
Humbel, M.

I

Ichac, J.P.
Ichida, S.
Ikegami, H.
Iljasov, O.
Inada, T.
Irie, Y.
Ishibori, I.
Ishigaki, T.
Ishii, K.
Iso, K.
Isoya, Y.
Itahashi, T.
Itano, A.
Ito, K.
Itoh, S.
Iudin, L.I.
Ivanenko, A.
Ivanov, E.M.

J

Jacky, J.
Jahnke, P.
Jayamanna, K.
Jenner, D.
Jeon, D.
Jiang, J.Z.
Jiang, W.M.
Joh, K.
Johansson, A.
Johansson, O.
Joho, W.
Jones, C.M.
Jones, F.W.

Jones, W.P.
Jongen, Y.
Josipovic, M.
Joubert, J.
Jungwirth, H.N.
Juras, R.C.

K

Kadantsev, S.
Kageyama, T.
Kalet, I.
Kamiya, T.
Kanazawa, M.
Kaplanski, J.M.
Karamian, S.A.
Karasawa, T.
Kase, M.
Kasugai, Y.
Katayama, T.
Kato, T.
Keitel, R.
Kennepohl, K.
Khalkin, V.A.
Kibayashi, M.
Kiewiet, H.H.
Kim, J.W.
Kimura, Y.
King, J.
Kitagawa, A.
Kleeven, W.J.G.M.
Kleinrahm, A.
Ko, J.
Kochkin, V.
Kodaira, K.
Kohler, I.H.
Kohno, T.
Kokorin, A.M.
Kolesov, I.
Komissarov, P.Yu.
Kondo, M.
Korenev, S.A.
Kormicki, J.
Korolev, L.E.
Kost, C.J.
Kozin, A.I.
Krasnikov, Yu.M.
Kritzinger, J.J.
Krivánek, M.
Kucera, J.
Kuchar, J.
Kuligin, V.S.
Kumada, M.
Kumata, Y.
Kunkel, W.B.
Kuo, T.Y.T.

Kutner, V.B.

L

Laborie, G.
LaForge, C.
Lafoux, A.
Laisné, A.
Lane, S.N.
Lanz, P.
Latushkin, S.T.
Launé, B.
Laxdal, R.E.
Lee, I.Y.
Leonov, V.V.
Leroy, R.
Leung, K.N.
Levy, C.D.P.
Lewitowicz, M.
Li, C.Y.
Liang, C.F.
Liatard, E.
Lindqvist, E.H.
Lipnicki, M.
Liu, C.
Liu, Z.
Liukkonen, E.
Lofnes, T.
Loiseaux, J.M.
Loiselet, M.
Ludgate, G.A.
Lundgren, S.A.
Lundström, B.
Lyneis, C.M.

M

Ma, Y.
Ma, Z.
Mackay, D.B.
Mackenzie, G.H.
Maeckelburg, D.
Märki, M.
Maier, R.
Makarov, A.A.
Mallory, M.L.
Malyshev, O.N.
Mandrillon, P.
Marie, H.
Markov, B.N.
Marti, F.
Martin, S.A.
Maruhashi, A.
Maruyama, M.
Maughan, R.

May, D.P.
McCammon, D.
McDonald, D.S.
McDonald, M.
McNeely, P.
Meads, Jr., P.F.
Meigs, M.J.
Meshkov, I.N.
Mezger, A.C.
Michelato, P.
Mikhailov, V.G.
Mikheev, G.F.
Miller, P.
Mills, G.D.
Milton, B.F.
Mironov, Yu.T.
Misawa, T.
Mitchel, G.R.
Mitra, A.K.
Mittig, W.
Miura, I.
Montsanglant, B.
Morduev, A.
Morelle, J.-L.
Mormiche, M.
Moryakov, V.P.
Moscatello, M-H.
Moshkin, V.N.
Mosko, S.W.
Mouat, M.
Mouchaty, G.
Mouris, J.F.
Mudrolyubov, V.G.
Müller, A.
Mueller, A.C.
Mukherjee, B.N.
Muminov, A.I.
Murakami, T.
Muto, K.

N

Nagayama, K.
Nakagawa, T.
Nakamura, Y.
Nara, T.
Naumov, I.V.
Nel, W.A.G.
Nifenecker, H.
Nishiguchi, M.
Nishino, M.
Nitschke, J.M.
Noda, K.
Nolen, J.A.
Norman, G.
Novikov, D.

Novikov, V.

O

Obert, J.
Oganessian, R.Ts.
Oganessian, Yu.Ts.
Ogata, H.
Ogawa, H.
Ohshiro, Y.
Okamura, T.
Okumura, S.
Olivetto, C.
Olsen, D.K.
Onishchenko, L.M.
Orzechowski, J.
Osakabe, M.
Osberg, E.A.
Ota, T.

P

Paans, A.M.J.
Pacquet, J.Y.
Pagani, C.
Panvier, R.
Papash, A.I.
Parhomchuk, V.V.
Paris, P.
Pattyn, E.
Pavlov, S.N.
Pearce, D.R.
Pearson, J.B.
Pedroni, E.
Pei, A.
Pei, X.
Pelzer, W.
Penco, C.
Petri, H.
Pfister, U.
Pieterman, K.
Pisman, A.Ya.
Pitatelev, G.
Plagnol, E.
Pálinkás, J.
Poe, D.
Poirier, R.L.
Pokrovskii, A.S.
Pollock, R.E.
Popeko, G.S.
Popov, S.
Postiau, N.
Pronin, N.V.
Pugatch, V.
Putaux, J.C.

Q

Qiao, Q.

R

Raadu, M.A.
Raia, G.
Rattray, T.
Reid, D.D.
Reistad, D.
Reitmann, D.
Rezvov, V.A.
Riabov, G.A.
Ricaud, Ch.
Rifuggiato, D.
Rinta-Nikkola, M.
Risler, R.
Rodin, A.M.
Roels, L.M.M.
Rogers, J.P.
Rogers, R.C.
Rogge, M.
Rohwer, P.F.
Root, L.
Roshchin, A.A.
Rossi, L.
Roy, G.
Rudchik, A.T.
Ruegg, R.
Ruth, T.J.
Ryckewaert, G.
Rykov, A.

S

Saito, T.
Sakuma, S.
Samsonov, E.
Sano, M.
Sarkisyan, A.L.
Sarkisyan, L.A.
Sato, K.
Sato, M.
Sato, Y.
Satoh, S.
Satoh, T.
Savalle, A.
Schippers, J.M.
Schmeing, H.
Schmor, P.W.
Schneider, H.R.
Schreuder, H.W.
Schukeilo, I.A.

Schutz, Y.
Schwandt, P.
Sedlacek, M.
Sekiguchi, M.
Semenov, M.
Sery, A.A.
Severgin, Yu.P.
Shen, Z.
Sherrill, B.
Shida, Y.
Shiltsev, V.D.
Shimizu, A.
Shukeylo, I.A.
Shychikov, G.I.
Sidorchuk, S.I.
Sigg, P.K.
Sivtsov, G.
Sklyarenko, V.I.
Sloan, T.
Smelser, P.
Smit, H.A.
Smolin, V.A.
Snyder, S.
Sokol, Ye.A.
Sokolov, G.L.
Sortais, P.
Soudée, M.
Sowinski, J.
Spinney, G.
Sprenger, H.
Stammbach, Th.
Starodub, G.Ya.
Steckmeyer, J.C.
Stepantsov, S.V.
Stetson, J.
Stevenson, N.R.
St-Laurent, M.G.
Stogov, Yu.I.
Strokach, A.P.
Stursa, J.
Sudou, M.
Suit, H.D.
Sura, J.
Susini, A.
Syresinm, Ye.M.

T

Tachibana, M.
Tachikawa, T.
Tada, J.
Tadokoro, M.
Takada, E.
Takada, Y.
Takahashi, N.
Takayama, T.

Tamura, K.
Tanaka, R.
Tang, J.Y.
Tarovik, M.N.
Tatum, B.A.
Tazawa, S.
ten Kate, H.J.H.
Ter-Akopian, G.M.
Theron, P.J.
Thornton, A.F.
Tihomirova, S.T.
Tilbury, R.
Timakov, V.A.
Timmermans, C.J.
Toda, Y.
Tomizawa, M.
Toporkov, D.
Toth, K.S.
Tran, D.
Trejbal, Z.
Trinks, U.
Tsuji, H.
Tsujii, H.

U

Unezhev, V.N.
Uraki, M.

V

Valek, A.
Val'Kov, A.E.
van Rooyen, D.M.
Varisco, G.
Vasilenko, A.
Vasiliev, A.A.
Venikov, N.I.
Verbruggen, R.
Vienet, R.
Vignon, B.
Vincent, D.
Vincent, J.
Vincent, J.S.
Vishnevsky, I.N.
Voitsechovsky, B.
Volchenkov, V.A.
Vorobiev, A.A.
Vorogushin, M.F.

W

Wagner, Jr., H.N.
Wang, F.

Wang, Q.
Wang, Y.
Watanabe, S.
Watanabe, T.
Webers, G.A.
Wedberg, R.
Wedekind, M.
Weehuizen, H.F.
Wei, B.W.
Wei, J.
Wells, R.P.
Westerberg, L.
Whittemore, W.L.
Wilkinson, N.A.
Winger, J.
Wootton, P.
Wu, D.
Wucherer, P.
Wüstefeld, G.

X

Xia, J.
Xie, K.
Xie, X.
Xie, Z.Q.

Y

Yamada, S.
Yamada, T.
Yamamoto, H.
Yamamoto, Y.
Yamashita, Y.
Yamazaki, N.
Yamazaki, T.
Yang, D.
Yano, Y.
Yarosh, V.E.
Ye, F.
Yin, Q.
Yin, Y.
Yokota, W.
Yoshizawa, M.
Young, A.T.
Yuan, P.
Yudin, L.I.
Yurkon, J.

Z

Zach, M.
Zaika, N.I.
Zaitseva, N.G.

Zaplatin, E.
Zaplatin, N.
Zelenskii, A.N.
Zhang, J.
Zhang, W.
Zhang, X.
Zhao, H.
Zhmendak, A.V.
Zhou, X.H.
Zhu, X.
Ziai, F.
Zibra, F.
Ziegler, K.
Zlomanczuk, J.

A B C D E F G H I J K L M N O P Q R S T U V W X Y Z

Biri, S.

Paper	Title	Page
I-20	**Heavy Ion Facility in ATOMKI**	99

- **S. Biri**, J. Pálinkás, A. Valek
  Institute of Nuclear Research of the Hungarian Academy of Sciences, Debrecen, Hungary

A B C D E F G H I J K L M N O P Q R S T U V W X Y Z

Bizouard, G.

Paper	Title	Page
I-11	**Status Report of SARA**	62

- **M. Fruneau**, S. Albrand, D. Barnéoud, J.L. Belmont, G. Bizouard, J.L. Bouly, G. Campillo, M. Guisset, G. Laborie
  Université Joseph Fourier, Grenoble, France

A B C D E F G H I J K L M N O P Q R S T U V W X Y Z

Blache, P.

Paper	Title	Page
XD-03	**Superconducting Focussing Channel for the AGOR Cyclotron**	612

- **H.W. Schreuder**, P. Blache, C. Commeaux, S. Gustafsson, A. Lafoux, M. Mormiche, R. Panvier
  IPN, Orsay, France

A B C D E F G H I J K L M N O P Q R S T U V W X Y Z

Blaker, G.C.

Paper	Title	Page
XA-11	**TRIUMF Cyclotron RF System Improvements**	545

- **G.C. Blaker**, A.K. Mitra, R.L. Poirier
  TRIUMF, Vancouver, Canada

Paper	Title	Page
XA-12	**Improvements to the RF Separator in the M9 Muon Channel at TRIUMF**	549

- **G.C. Blaker**, A.K. Mitra, R.L. Poirier
  TRIUMF, Vancouver, Canada

A B C D E F G H I J K L M N O P Q R S T U V W X Y Z

Bloemhard, P.

Paper	Title	Page
IV-12	**A Remotely Controlled Robotic Vehicle for Work Within Radioactive Environments**	198

- **N.R. Stevenson**, P. Bloemhard, M. Brigham, J. Ko, C. LaForge, J. Orzechowski, E. Pattyn, T. Rattray
  TRIUMF, Vancouver, Canada

A B C D E F G H I J K L M N O P Q R S T U V W X Y Z

Blosser, H.G.

Paper	Title	Page
II-07	**Performance of the Harper Hospital Cyclotron; Effect of Pulsed Radio Frequency**	133

- **H.G. Blosser**, J. Vincent
  NSCL, East Lansing, Michigan, USA
- R. Maughan
  Harper Hospital, Detroit, Michigan, USA

VIII-14	**Plan for the Ion Source Emittance Measurement Under the RF Extraction**	357

- **J.W. Kim**, H.G. Blosser
  NSCL, East Lansing, Michigan, USA

XIV-01	**Future Cyclotrons (Invited Paper)**	

- **H.G. Blosser**
  NSCL, East Lansing, Michigan, USA

A B C D E F G H I J K L M N O P Q R S T U V W X Y Z

Böge, H.G.

Paper	Title	Page
I-12	**Commissioning of the Injector Complex of COSY-Jülich**	67

- **W. Bräutigam**, H. Beuscher, R. Brings, H.G. Böge, R. Maier, M. Rogge, P. Wucherer
  FZJ, Jülich, Germany

A B C D E F G H I J K L M N O P Q R S T U V W X Y Z

Bogdanov, P.V.

Paper	Title	Page
I-10	**Gatchina Isochronous Cyclotron**	58

- **N.K. Abrosimov**, S.A. Artamonov, P.V. Chervyakov, S.P. Dmitriev, V.A. Eliseev, V.P. Fominenko, E.M. Ivanov, G.F. Mikheev, Yu.T. Mironov, A.S. Pokrovskii, G.A. Riabov, V.A. Smolin, G.L. Sokolov, V.A. Volchenkov, A.A. Vorobiev
  Petersburg Nuclear Physics Institute, Gatchina, Russia
- P.V. Bogdanov, B.D. Ershov, V.S. Kuligin, V.N. Moshkin, V.G. Mudrolyubov, Yu.I. Stogov, A.P. Strokach
  D.V. Efremov Scientific Research Institute of Electrophysical Apparatus, St. Petersburg, Russia

A B C D E F G H I J K L M N O P Q R S T U V W X Y Z

Bogomolov, S.L.

Paper	Title	Page
IV-04	^{178m2}Hf and ^{237}Pu Isotopes Production on the U-200 Cyclotron	167

- **S.L. Bogomolov**, S.N. Dmitriev, Yu.P. Gangrski, G.G. Gulbekyan, S.A. Karamian, V.B. Kutner, B.N. Markov, Yu.Ts. Oganessian, N.V. Pronin, G.Ya. Starodub
  JINR, Dubna, Russia

A B C D E F G H I J K L M N O P Q R S T U V W X Y Z

Bojovic, B.

Paper	Title	Page
XA-02	**The RF Coupling System of the VINCY Cyclotron**	511

- **B. Bojovic**, M. Josipovic, A. Susini
  CERN, Geneva, Switzerland

A B C D E F G H I J K L M N O P Q R S T U V W X Y Z

Bony, J.

Paper	Title	Page
IXC-01	**Commissioning of the New High Intensity Axial Injection System for GANIL**	446

- **Ch. Ricaud**, E. Baron, J. Bony, M.P. Bourgarel, B. Bru
  GANIL, Caen, France
- R. Vienet
  CEN/Saclay, Gif-sur-Yvette, France

A B C D E F G H I J K L M N O P Q R S T U V W X Y Z

Borisov, O.

Paper	Title	Page
I-02	**New Development at the JINR Heavy Ion Cyclotron Facility (Invited Paper)**	11

- **G.G. Gulbekyan**, V. Bekhterev, O. Borisov, B. Gikal, A. Ivanenko, I. Kolesov, V.B. Kutner, A. Morduev, Yu.Ts. Oganessian
  JINR, Dubna, Russia

A B C D E F G H I J K L M N O P Q R S T U V W X Y Z

Bosotti, A.

Paper	Title	Page
I-18	**Status Report on the Heavy Ion Facility at LNS**	90

- **F. Alessandria**, G. Bellomo, A. Bosotti, C. De Martinis, D. Giove, P. Michelato, C. Pagani, L. Rossi
  INFN/LASA, Segrate, Italy
- L. Calabretta, G. Ciavola, G. Cuttone, M. Di Giacomo, S. Gammino, P. Gmaj, G. Raia, D. Rifuggiato, J. Sura
  INFN/LNS, Catania, Italy

IXD-05	**High Sensitivity Electronic System for the Phase Probes of the LNS/MILANO Superconducting Cyclotron**	483

- **A. Bosotti**, D. Corti, C. Pagani, G. Varisco, F. Zibra
  INFN/LASA, Segrate, Italy
- M. Di Giacomo
  INFN/LNS, Catania, Italy

A B C D E F G H I J K L M N O P Q R S T U V W X Y Z

Botha, A.H.

Paper	Title	Page
I-19	**Development of the NAC Accelerator Facilities**	95

- **J.L. Conradie**, A.H. Botha, P.M. Cronje, R.E.F. Fenemore, H.N. Jungwirth, J.J. Kritzinger, W.A.G. Nel, D. Reitmann, L.M.M. Roels, P.F. Rohwer, H.A. Smit
  National Accelerator Centre, Faure, Republic of South Africa

A B C D E F G H I J K L M N O P Q R S T U V W X Y Z

Botman, J.I.M.

Paper	Title	Page
IXA-03	**Emittance Growth in Nonlinear Beam Guiding and Focusing Elements**	384

- **W.J.G.M. Kleeven**, J.I.M. Botman, J.L. Delhez, H.L. Hagedoorn, C.J. Timmermans, G.A. Webers
  Eindhoven University of Technology, Eindhoven, The Netherlands

A B C D E F G H I J K L M N O P Q R S T U V W X Y Z

Bouly, J.L.

Paper	Title	Page
I-11	**Status Report of SARA**	62

- **M. Fruneau**, S. Albrand, D. Barnéoud, J.L. Belmont, G. Bizouard, J.L. Bouly, G. Campillo, M. Guisset, G. Laborie
  Université Joseph Fourier, Grenoble, France

A B C D E F G H I J K L M N O P Q R S T U V W X Y Z

Bourgarel, M.P.

Paper	Title	Page
IXC-01	**Commissioning of the New High Intensity Axial Injection System for GANIL**	446

- **Ch. Ricaud**, E. Baron, J. Bony, M.P. Bourgarel, B. Bru
  GANIL, Caen, France
- R. Vienet
  CEN/Saclay, Gif-sur-Yvette, France

A B C D E F G H I J K L M N O P Q R S T U V W X Y Z

Boux, R.

Paper	Title	Page
XA-10	**RF Transmitter for ECR Ion Sources**	542

- **R. Boux**, J.P. Ichac, M. Soudée
  Thomson Tubes Electroniques, Velizy-Villacoublay, France

A B C D E F G H I J K L M N O P Q R S T U V W X Y Z

Bräutigam, W.

Paper	Title	Page
I-12	**Commissioning of the Injector Complex of COSY-Jülich**	67
	• **W. Bräutigam**, H. Beuscher, R. Brings, H.G. Böge, R. Maier, M. Rogge, P. Wucherer FZJ, Jülich, Germany	
IXD-01	**The New Phase Detection System of the Cosy-Injector**	469
	• **K. Kennepohl**, W. Bräutigam, M. Herschbach, D. Maeckelburg FZJ, Jülich, Germany	

A B C D E F G H I J K L M N O P Q R S T U V W X Y Z

Brassart, N.

Paper	Title	Page
VI-05	**Recent Activities of the Cyclotron Laboratory in Nice**	248

- **P. Mandrillon**, N. Brassart, P. Chauvel, A. Courdi, F. Farley, N. Fietier, J. Herault, J.Y. Tang
  Centre Antoine Lacassagne, Nice, France

A B C D E F G H I J K L M N O P Q R S T U V W X Y Z

Briand, P.

Paper	Title	Page
XIII-04	**The PIAFE Project at Grenoble: Beam Transport and Acceleration**	729

- **J.L. Belmont**, J.F. Bruandet, J.M. de Conto, M. Fruneau, G. Gimond, K. Golovanivsky, E. Liatard, J.M. Loiseaux, H. Nifenecker, A. Savalle, B. Vignon
  Université Joseph Fourier, Grenoble, France
- P. Briand
  CEN-Grenoble, Grenoble, France

A B C D E F G H I J K L M N O P Q R S T U V W X Y Z

Bricault, P.

Paper	Title	Page
IV-02	**A Cyclotron as a Mass Spectrometer**	158

- **P. Bricault**, G. Auger, M. Bajard, E. Baron, D. Bibet, A. Chabert, J. Fermé, L. Gaudart, J. Joubert, M. Lewitowicz, W. Mittig, E. Plagnol, Ch. Ricaud, Y. Schutz
  GANIL, Caen, France
- G. Audi
  CSNSM, Orsay, France
- A. Gillibert
  CEN/Saclay, Gif-sur-Yvette, France
- K. Fifield
  Australian National University, Canberra , Australia

XIII-03	**An On-Line Isotopic Separator Test Bench at GANIL**	725

- **P. Bricault**, R. Leroy, M. Lewitowicz, J.Y. Pacquet, M.G. St-Laurent, P. Sortais
  GANIL, Caen, France
- A.C. Mueller, J. Obert, J.C. Putaux
  IPN, Orsay, France
- C.F. Liang, P. Paris
  CSNSM, Orsay, France
- J.C. Steckmeyer
  LPC, Caen, France

A B C D E F G H I J K L M N O P Q R S T U V W X Y Z

Brigham, M.

Paper	Title	Page
IV-12	**A Remotely Controlled Robotic Vehicle for Work Within Radioactive Environments**	198

- **N.R. Stevenson**, P. Bloemhard, M. Brigham, J. Ko, C. LaForge, J. Orzechowski, E. Pattyn, T. Rattray
  TRIUMF, Vancouver, Canada

A B C D E F G H I J K L M N O P Q R S T U V W X Y Z

Brings, R.

Paper	Title	Page
I-12	**Commissioning of the Injector Complex of COSY-Jülich**	67

- **W. Bräutigam**, H. Beuscher, R. Brings, H.G. Böge, R. Maier, M. Rogge, P. Wucherer
  FZJ, Jülich, Germany

A B C D E F G H I J K L M N O P Q R S T U V W X Y Z

Brossard, S.

Paper	Title	Page
VI-09	**Continued Operation of the Seattle Clinical Cyclotron Facility**	262

- **R. Risler**, S. Brossard, J. Jacky, I. Kalet, P. Wootton, F. Ziai
  University of Washington, Seattle, Washington, USA

A B C D E F G H I J K L M N O P Q R S T U V W X Y Z

Brown, R.

Paper	Title	Page
VIII-07	**Performance and Status of the IUCF High Intensity Polarized Ion Source**	330

- **V. Derenchuk**, R. Brown, T.J.P. Ellison, D.L. Friesel, J.W. Hicks, D. Jenner, A. Pei, H. Petri, P. Schwandt, J. Sowinski, M. Wedekind
  Indiana University, Bloomington, Indiana, USA

A B C D E F G H I J K L M N O P Q R S T U V W X Y Z

Bru, B.

Paper	Title	Page
IXC-01	**Commissioning of the New High Intensity Axial Injection System for GANIL**	446

- **Ch. Ricaud**, E. Baron, J. Bony, M.P. Bourgarel, B. Bru
  GANIL, Caen, France
- R. Vienet
  CEN/Saclay, Gif-sur-Yvette, France

A B C D E F G H I J K L M N O P Q R S T U V W X Y Z

Bruandet, J.F.

Paper	Title	Page
XIII-04	**The PIAFE Project at Grenoble: Beam Transport and Acceleration**	729

- **J.L. Belmont**, J.F. Bruandet, J.M. de Conto, M. Fruneau, G. Gimond, K. Golovanivsky, E. Liatard, J.M. Loiseaux, H. Nifenecker, A. Savalle, B. Vignon
  Université Joseph Fourier, Grenoble, France
- P. Briand
  CEN-Grenoble, Grenoble, France

A B C D E F G H I J K L M N O P Q R S T U V W X Y Z

Buchmann, L.

Paper	Title	Page
XIII-08	**Research and Development Studies with Radioactive Beams at TRIUMF**	745

- **J.M. D'Auria**, M. Dombsky
  Simon Fraser University, Burnaby, BC, Canada
- L. Buchmann, H. Sprenger, J.S. Vincent
  TRIUMF, Vancouver, Canada
- J. King
  University of Toronto, Toronto, Ontario, Canada
- P. McNeely, G. Roy
  University of Alberta, Edmonton, Alberta, Canada

A B C D E F G H I J K L M N O P Q R S T U V W X Y Z

Buranov, V.

Paper	Title	Page
XI-05	**Automatic Control System of Magnetic Separator for Kurchatov IAE Cyclotron**	652

- **N.I. Venikov**, V. Buranov, O. Gotovtsev, L.I. Iudin, P.Yu. Komissarov, V.N. Unezhev
  Kurchatov Institute, Moscow, Russia

A B C D E F G H I J K L M N O P Q R S T U V W X Y Z

Burbeza, C.D.

Paper	Title	Page
II-05	**Status of a Compact H^- Cyclotron at the Kurchatov Institute of Atomic Energy**	126

- **N.I. Venikov**, C.D. Burbeza, P.Yu. Komissarov, Yu.M. Krasnikov, S.T. Latushkin, V.V. Leonov, V.P. Moryakov, I.V. Naumov, A.Ya. Pisman, V.A. Rezvov, A.A. Vasiliev, V.E. Yarosh, L.I. Yudin
  Kurchatov Institute, Moscow, Russia

A B C D E F G H I J K L M N O P Q R S T U V W X Y Z

Burger, S.J.

Paper	Title	Page
VIII-15	**Progress with the NAC Injector Cyclotron for Heavy and Polarized Ions**	361

- **Z.B. du Toit**, S.J. Burger, P.J. Celliers, J.G. de Villiers, H.N. Jungwirth, A. Müller, P.F. Rohwer, D.M. van Rooyen
  National Accelerator Centre, Faure, Republic of South Africa

A B C D E F G H I J K L M N O P Q R S T U V W X Y Z

Busse, W.

Paper	Title	Page
XI-01	**Integrated Tools for Cyclotron Operation (Invited Paper)**	634

- **W. Busse**
  HMI, Berlin, Germany

A B C D E F G H I J K L M N O P Q R S T U V W X Y Z

Calabretta, L.

Paper	Title	Page
I-18	**Status Report on the Heavy Ion Facility at LNS** • **F. Alessandria**, G. Bellomo, A. Bosotti, C. De Martinis, D. Giove, P. Michelato, C. Pagani, L. Rossi INFN/LASA, Segrate, Italy • L. Calabretta, G. Ciavola, G. Cuttone, M. Di Giacomo, S. Gammino, P. Gmaj, G. Raia, D. Rifuggiato, J. Sura INFN/LNS, Catania, Italy	90
XC-06	**Material Consideration for Magnetic Channels** • **J. Sura**, L. Calabretta, G. Di Biasi, P. Gmaj, D. Rifuggiato INFN/LNS, Catania, Italy	589
XIII-05	**High Intensity Superconducting Cyclotron Beams for a Radioactive Ion Beam Facility** • **L. Calabretta**, D. Rifuggiato INFN/LNS, Catania, Italy	733

A B C D E F G H I J K L M N O P Q R S T U V W X Y Z

Campillo, G.

Paper	Title	Page
I-11	**Status Report of SARA**	62

- **M. Fruneau**, S. Albrand, D. Barnéoud, J.L. Belmont, G. Bizouard, J.L. Bouly, G. Campillo, M. Guisset, G. Laborie
  Université Joseph Fourier, Grenoble, France

A B C D E F G H I J K L M N O P Q R S T U V W X Y Z

Capshew, T.

Paper	Title	Page
XI-02	**The IUCF High Intensity Polarized Ion Source Control System**	641

- **T. Capshew**, J.C. Collins, D. DuPlantis, D.W. Frame, J. Graham, D.D. Reid
  Indiana University, Bloomington, Indiana, USA

A B C D E F G H I J K L M N O P Q R S T U V W X Y Z

Carter, H.K.

Paper	Title	Page
XIII-07	**The ORNL Radioactive Ion Beam Project with the ORIC Accelerator**	741

- **D.K. Olsen**, G.D. Alton, C. Baktash, D.T. Dowling, J.D. Garrett, D.L. Haynes, C.M. Jones, R.C. Juras, S.N. Lane, I.Y. Lee, M.J. Meigs, G.D. Mills, S.W. Mosko, B.A. Tatum, K.S. Toth
  ORNL, Oak Ridge, Tennessee, USA
- H.K. Carter, J. Kormicki
  Associated Universities Oak Ridge, Oak Ridge, Tennessee, USA

A B C D E F G H I J K L M N O P Q R S T U V W X Y Z

Celliers, P.J.

Paper	Title	Page
VIII-15	**Progress with the NAC Injector Cyclotron for Heavy and Polarized Ions**	361

- **Z.B. du Toit**, S.J. Burger, P.J. Celliers, J.G. de Villiers, H.N. Jungwirth, A. Müller, P.F. Rohwer, D.M. van Rooyen
  National Accelerator Centre, Faure, Republic of South Africa

XI-08	**Micro-Controlled Vacuum Systems at NAC**	664

- **P.J. Celliers**, E.J.S. Franklin
  National Accelerator Centre, Faure, Republic of South Africa

A B C D E F G H I J K L M N O P Q R S T U V W X Y Z

Chabert, A.

Paper	Title	Page
IV-02	**A Cyclotron as a Mass Spectrometer**	158

- **P. Bricault**, G. Auger, M. Bajard, E. Baron, D. Bibet, A. Chabert, J. Fermé, L. Gaudart, J. Joubert, M. Lewitowicz, W. Mittig, E. Plagnol, Ch. Ricaud, Y. Schutz
  GANIL, Caen, France
- G. Audi
  CSNSM, Orsay, France
- A. Gillibert
  CEN/Saclay, Gif-sur-Yvette, France
- K. Fifield
  Australian National University, Canberra , Australia

A B C D E F G H I J K L M N O P Q R S T U V W X Y Z

Chang, H.

Paper	Title	Page
VI-07	**Design Consideration of Neutron Therapy Facility Utilizing Existing Cyclotron**	255

- **H. Chang**, X. Cui, J. Wei, J. Zhang, K. Xie
  Institute of Nuclear Research, Shanghai, People's Republic of China

A B C D E F G H I J K L M N O P Q R S T U V W X Y Z

Chaudhri, M.A.

Paper	Title	Page
IV-07	**Neutron Productions from Carbon by Charged Particle Bombardment at Different Energies** • **M.A. Chaudhri** Austin Hospital & University of Melbourne, Melbourne, Australia	178
IV-08	**Analytical Applications of Cyclotrons in Biomedical Fields - Charged Particle Activation Analysis** • **M.A. Chaudhri** Austin Hospital & University of Melbourne, Melbourne, Australia	181
IV-09	**A Simple Method for Estimating Activation Sensitivities of Different Elements / Isotopes with Cyclotron Produced Neutrons** • **M.A. Chaudhri** Austin Hospital & University of Melbourne, Melbourne, Australia	187

A B C D E F G H I J K L M N O P Q R S T U V W X Y Z

Chauvel, P.

Paper	Title	Page
VI-05	**Recent Activities of the Cyclotron Laboratory in Nice**	248

- **P. Mandrillon**, N. Brassart, P. Chauvel, A. Courdi, F. Farley, N. Fietier, J. Herault, J.Y. Tang
  Centre Antoine Lacassagne, Nice, France

A B C D E F G H I J K L M N O P Q R S T U V W X Y Z

Cherix, J.

Paper	Title	Page
XA-08	**Experience with the PSI-Cyclotron RF-System Under Heavy Beam Loading**	534

- **P.K. Sigg**, J. Cherix, H. Frei, M. Märki
  PSI, Villigen, Switzerland

A B C D E F G H I J K L M N O P Q R S T U V W X Y Z

Chervyakov, P.V.

Paper	Title	Page
I-10	**Gatchina Isochronous Cyclotron**	58

- **N.K. Abrosimov**, S.A. Artamonov, P.V. Chervyakov, S.P. Dmitriev, V.A. Eliseev, V.P. Fominenko, E.M. Ivanov, G.F. Mikheev, Yu.T. Mironov, A.S. Pokrovskii, G.A. Riabov, V.A. Smolin, G.L. Sokolov, V.A. Volchenkov, A.A. Vorobiev
  Petersburg Nuclear Physics Institute, Gatchina, Russia
- P.V. Bogdanov, B.D. Ershov, V.S. Kuligin, V.N. Moshkin, V.G. Mudrolyubov, Yu.I. Stogov, A.P. Strokach
  D.V. Efremov Scientific Research Institute of Electrophysical Apparatus, St. Petersburg, Russia

A B C D E F G H I J K L M N O P Q R S T U V W X Y Z

Chesnov, A.

Paper	Title	Page
II-04	**20 MeV Cyclotron for Isotope Production**	123

- **A. Glazov**, Ju. Alenitskiy, A. Chesnov, S. Chesnova, V. Kochkin, D. Novikov, E. Samsonov, M. Semenov, A. Vasilenko, E. Zaplatin, N. Zaplatin
  JINR, Dubna, Russia
- I. Gulamov, O. Iljasov, A. Rykov
  Institute of Nuclear Physics, Tashkent, Republic of Uzbekistan

A B C D E F G H I J K L M N O P Q R S T U V W X Y Z

Chesnova, S.

Paper	Title	Page
II-04	**20 MeV Cyclotron for Isotope Production**	123

- **A. Glazov**, Ju. Alenitskiy, A. Chesnov, S. Chesnova, V. Kochkin, D. Novikov, E. Samsonov, M. Semenov, A. Vasilenko, E. Zaplatin, N. Zaplatin
  JINR, Dubna, Russia
- I. Gulamov, O. Iljasov, A. Rykov
  Institute of Nuclear Physics, Tashkent, Republic of Uzbekistan

A B C D E F G H I J K L M N O P Q R S T U V W X Y Z

Chida, K.

Paper	Title	Page
VII-04	**Study of Beam Dynamics at Cooler Synchrotron TARN-II**	286

- **S. Watanabe**, Y. Arakaki, K. Chida, T. Katayama, M. Tomizawa, T. Watanabe, M. Yoshizawa
  University of Tokyo, Tanashi-shi, Tokyo, Japan
- K. Noda, M. Kanazawa
  NIRS, Chiba, Japan

A B C D E F G H I J K L M N O P Q R S T U V W X Y Z

Ciavola, G.

Paper	Title	Page
I-18	**Status Report on the Heavy Ion Facility at LNS**	90

- **F. Alessandria**, G. Bellomo, A. Bosotti, C. De Martinis, D. Giove, P. Michelato, C. Pagani, L. Rossi
  INFN/LASA, Segrate, Italy
- L. Calabretta, G. Ciavola, G. Cuttone, M. Di Giacomo, S. Gammino, P. Gmaj, G. Raia, D. Rifuggiato, J. Sura
  INFN/LNS, Catania, Italy

A B C D E F G H I J K L M N O P Q R S T U V W X Y Z

Clark, D.J.

Paper	Title	Page
XII-03	**Design of a Compact Permanent Magnet Cyclotron Mass Spectrometer for the Detection and Measurement of Trace Isotopes** • **A.T. Young**, K.J. Bertsche, D.J. Clark, K. Halbach, W.B. Kunkel, K.N. Leung, C.Y. Li LBL, Berkeley, California, USA	705
XIII-02	**A Conceptual Design for a Primary Cyclotron for the ISL Radioactive Beam Project** • **D.J. Clark** LBL, Berkeley, California, USA	721
XIV-04	**Conference Summary (Invited Paper)** • **D.J. Clark** LBL, Berkeley, California, USA	758

A B C D E F G H I J K L M N O P Q R S T U V W X Y Z

Clark, J.C.

Paper	Title	Page
V-06	**Experiences with the Cyclone 3 Oxygen 15 Generator**	218

- **E. Conard**, J.-L. Morelle
  Ion Beam Applications, Louvain-la-Neuve, Belgium
- J.C. Clark, D.B. Mackay
  Hammersmith Hospital, London, England

A B C D E F G H I J K L M N O P Q R S T U V W X Y Z

Cole, D.

Paper	Title	Page
VIII-12	**The Super Gas Mixing Technique for Highly Charged Uranium Ions**	348

- **T.A. Antaya**, D. Cole
  NSCL, East Lansing, Michigan, USA

IXB-03	**K1200 Cyclotron Beam Development Techniques**	427

- **T.A. Antaya**, D. Cole, P. Miller, D. Poe
  NSCL, East Lansing, Michigan, USA

A B C D E F G H I J K L M N O P Q R S T U V W X Y Z

Collins, D.

Paper	Title	Page
VIII-02	**Performance of the LBL AECR Source at Various Frequencies**	308

- **Z.Q. Xie**, D. Collins, S.A. Lundgren, C.M. Lyneis
  LBL, Berkeley, California, USA

A B C D E F G H I J K L M N O P Q R S T U V W X Y Z

Collins, J.C.

Paper	Title	Page
XD-02	**Beam Transport System for the IUCF High Intensity Polarized Ion Source**	609

- **W.P. Jones**, M.S. Ball, J.C. Collins, D. DuPlantis, T.J.P. Ellison, D.L. Friesel, B. Hamilton, J.W. Hicks, P. Schwandt
  Indiana University, Bloomington, Indiana, USA

XI-02	**The IUCF High Intensity Polarized Ion Source Control System**	641

- **T. Capshew**, J.C. Collins, D. DuPlantis, D.W. Frame, J. Graham, D.D. Reid
  Indiana University, Bloomington, Indiana, USA

A B C D E F G H I J K L M N O P Q R S T U V W X Y Z

Commeaux, C.

Paper	Title	Page
XB-01	**Low Temperature Tests of the AGOR Superconducting Coil System**	557

- **K. Pieterman**, J.A.M. Dam
  Cryocon B.V., Amersfoort, The Netherlands
- C. Commeaux
  IPN, Orsay, France
- C. Penco
  Ansaldo Componenti, Genoa, Italy

XD-03	**Superconducting Focussing Channel for the AGOR Cyclotron**	612

- **H.W. Schreuder**, P. Blache, C. Commeaux, S. Gustafsson, A. Lafoux, M. Mormiche, R. Panvier
  IPN, Orsay, France

A B C D E F G H I J K L M N O P Q R S T U V W X Y Z

Conard, E.

Paper	Title	Page
V-06	**Experiences with the Cyclone 3 Oxygen 15 Generator**	218

- **E. Conard**, J.-L. Morelle
  Ion Beam Applications, Louvain-la-Neuve, Belgium
- J.C. Clark, D.B. Mackay
  Hammersmith Hospital, London, England

A B C D E F G H I J K L M N O P Q R S T U V W X Y Z

Conradie, J.L.

Paper	Title	Page
I-19	**Development of the NAC Accelerator Facilities**	95

- **J.L. Conradie**, A.H. Botha, P.M. Cronje, R.E.F. Fenemore, H.N. Jungwirth, J.J. Kritzinger, W.A.G. Nel, D. Reitmann, L.M.M. Roels, P.F. Rohwer, H.A. Smit
  National Accelerator Centre, Faure, Republic of South Africa

XD-06	**Beamlines for a Second Injector Cyclotron at NAC**	621

- **J.C. Cornell**, J.L. Conradie, D.T. Fourie
  National Accelerator Centre, Faure, Republic of South Africa

A B C D E F G H I J K L M N O P Q R S T U V W X Y Z

Cooper, M.

Paper	Title	Page
XB-02	**A Permanent Magnet System for a Cyclotron Used as a Mass Spectrometer**	561

- **C.Y. Li**, M. Cooper, K. Halbach, W.B. Kunkel, K.N. Leung, R.P. Wells, A.T. Young
  LBL, Berkeley, California, USA

A B C D E F G H I J K L M N O P Q R S T U V W X Y Z

Cornell, J.C.

Paper	Title	Page
XD-06	**Beamlines for a Second Injector Cyclotron at NAC**	621

- **J.C. Cornell**, J.L. Conradie, D.T. Fourie
  National Accelerator Centre, Faure, Republic of South Africa

A B C D E F G H I J K L M N O P Q R S T U V W X Y Z

Corti, D.

Paper	Title	Page
IXD-05	**High Sensitivity Electronic System for the Phase Probes of the LNS/MILANO Superconducting Cyclotron**	483

- **A. Bosotti**, D. Corti, C. Pagani, G. Varisco, F. Zibra
  INFN/LASA, Segrate, Italy
- M. Di Giacomo
  INFN/LNS, Catania, Italy

A B C D E F G H I J K L M N O P Q R S T U V W X Y Z

Courdi, A.

Paper	Title	Page
VI-05	**Recent Activities of the Cyclotron Laboratory in Nice**	248

- **P. Mandrillon**, N. Brassart, P. Chauvel, A. Courdi, F. Farley, N. Fietier, J. Herault, J.Y. Tang
  Centre Antoine Lacassagne, Nice, France

A B C D E F G H I J K L M N O P Q R S T U V W X Y Z

Craddock, M.K.

Paper	Title	Page
III-02	**The KAON Factory at TRIUMF**	143

- **M.K. Craddock**
  University of British Columbia, Vancouver, Canada

Paper	Title	Page
XV-01	**Proper and Improper Accelerators - In Praise of Cyclotrons and Their Builders**	765

- **M.K. Craddock**
  University of British Columbia, Vancouver, Canada

A B C D E F G H I J K L M N O P Q R S T U V W X Y Z

Cronje, P.M.

Paper	Title	Page
I-19	**Development of the NAC Accelerator Facilities**	95

- **J.L. Conradie**, A.H. Botha, P.M. Cronje, R.E.F. Fenemore, H.N. Jungwirth, J.J. Kritzinger, W.A.G. Nel, D. Reitmann, L.M.M. Roels, P.F. Rohwer, H.A. Smit
  National Accelerator Centre, Faure, Republic of South Africa

A B C D E F G H I J K L M N O P Q R S T U V W X Y Z

Cui, X.

Paper	Title	Page
VI-07	**Design Consideration of Neutron Therapy Facility Utilizing Existing Cyclotron**	255

- **H. Chang**, X. Cui, J. Wei, J. Zhang, K. Xie
  Institute of Nuclear Research, Shanghai, People's Republic of China

A B C D E F G H I J K L M N O P Q R S T U V W X Y Z

Cuttone, G.

Paper	Title	Page
I-18	**Status Report on the Heavy Ion Facility at LNS**	90

- **F. Alessandria**, G. Bellomo, A. Bosotti, C. De Martinis, D. Giove, P. Michelato, C. Pagani, L. Rossi
  INFN/LASA, Segrate, Italy
- L. Calabretta, G. Ciavola, G. Cuttone, M. Di Giacomo, S. Gammino, P. Gmaj, G. Raia, D. Rifuggiato, J. Sura
  INFN/LNS, Catania, Italy

A B C D E F G H I J K L M N O P Q R S T U V W X Y Z

Dale, D.J.

Paper	Title	Page
XI-13	**The TR30 Control System - A Case for Off-the-Shelf Software**	685

- **R. Keitel**, D.J. Dale, B.F. Milton
  TRIUMF, Vancouver, Canada

A B C D E F G H I J K L M N O P Q R S T U V W X Y Z

Dam, J.A.M.

Paper	Title	Page
XB-01	**Low Temperature Tests of the AGOR Superconducting Coil System**	557

- **K. Pieterman**, J.A.M. Dam
  Cryocon B.V., Amersfoort, The Netherlands
- C. Commeaux
  IPN, Orsay, France
- C. Penco
  Ansaldo Componenti, Genoa, Italy

XC-05	**The AGOR Superconducting Extraction Channel EMC2**	585

- **K. Pieterman**, J.A.M. Dam
  Cryocon B.V., Amersfoort, The Netherlands
- H.J.H. ten Kate
  TU Twente, Enschede, The Netherlands
- S. Gustafsson
  IPN, Orsay, France

A B C D E F G H I J K L M N O P Q R S T U V W X Y Z

Dambre, P.

Paper	Title	Page
IXD-06	**The Diagnostics System for the AGOR Superconducting Cyclotron**	487

- **B. Launé**, P. Dambre, J.M. Kaplanski, B. Montsanglant, C. Olivetto, D. Vincent
  IPN, Orsay, France

A B C D E F G H I J K L M N O P Q R S T U V W X Y Z

D'Auria, J.M.

Paper	Title	Page
XIII-08	**Research and Development Studies with Radioactive Beams at TRIUMF**	745

- **J.M. D'Auria**, M. Dombsky
  Simon Fraser University, Burnaby, BC, Canada
- L. Buchmann, H. Sprenger, J.S. Vincent
  TRIUMF, Vancouver, Canada
- J. King
  University of Toronto, Toronto, Ontario, Canada
- P. McNeely, G. Roy
  University of Alberta, Edmonton, Alberta, Canada

A B C D E F G H I J K L M N O P Q R S T U V W X Y Z

Davies, W.G.

Paper	Title	Page
IXA-01	**Advantage of Using Differential Algebra and Lie Algebra in the Orbit Dynamics of Cyclotrons (Invited Paper)**	372

- **W.G. Davies**
  Atomic Energy of Canada, Chalk River, Ontario, USA

A B C D E F G H I J K L M N O P Q R S T U V W X Y Z

de Conto, J.M.

Paper	Title	Page
XIII-04	**The PIAFE Project at Grenoble: Beam Transport and Acceleration**	729

- **J.L. Belmont**, J.F. Bruandet, J.M. de Conto, M. Fruneau, G. Gimond, K. Golovanivsky, E. Liatard, J.M. Loiseaux, H. Nifenecker, A. Savalle, B. Vignon
  Université Joseph Fourier, Grenoble, France
- P. Briand
  CEN-Grenoble, Grenoble, France

A B C D E F G H I J K L M N O P Q R S T U V W X Y Z

De Martinis, C.

Paper	Title	Page
I-18	**Status Report on the Heavy Ion Facility at LNS**	90

- **F. Alessandria**, G. Bellomo, A. Bosotti, C. De Martinis, D. Giove, P. Michelato, C. Pagani, L. Rossi
  INFN/LASA, Segrate, Italy
- L. Calabretta, G. Ciavola, G. Cuttone, M. Di Giacomo, S. Gammino, P. Gmaj, G. Raia, D. Rifuggiato, J. Sura
  INFN/LNS, Catania, Italy

A B C D E F G H I J K L M N O P Q R S T U V W X Y Z

de Villiers, J.G.

Paper	Title	Page
VIII-15	**Progress with the NAC Injector Cyclotron for Heavy and Polarized Ions**	361

- **Z.B. du Toit**, S.J. Burger, P.J. Celliers, J.G. de Villiers, H.N. Jungwirth, A. Müller, P.F. Rohwer, D.M. van Rooyen
  National Accelerator Centre, Faure, Republic of South Africa

XI-07	**Ion Spectra Identification Software for the ECR Ion Source at NAC**	660

- **E.J.S. Franklin**, J.G. de Villiers
  National Accelerator Centre, Faure, Republic of South Africa

XII-04	**A New Design Proposal for a 200 MeV Superconducting Ring-Cyclotron Magnet**	709

- **H.N. Jungwirth**, J.G. de Villiers
  National Accelerator Centre, Faure, Republic of South Africa

A B C D E F G H I J K L M N O P Q R S T U V W X Y Z

Delhez, J.L.

Paper	Title	Page
IXA-03	**Emittance Growth in Nonlinear Beam Guiding and Focusing Elements**	384

- **W.J.G.M. Kleeven**, J.I.M. Botman, J.L. Delhez, H.L. Hagedoorn, C.J. Timmermans, G.A. Webers
  Eindhoven University of Technology, Eindhoven, The Netherlands

A B C D E F G H I J K L M N O P Q R S T U V W X Y Z

Derenchuk, V.

Paper	Title	Page
VIII-07	**Performance and Status of the IUCF High Intensity Polarized Ion Source**	330

- **V. Derenchuk**, R. Brown, T.J.P. Ellison, D.L. Friesel, J.W. Hicks, D. Jenner, A. Pei, H. Petri, P. Schwandt, J. Sowinski, M. Wedekind
  Indiana University, Bloomington, Indiana, USA

XA-05	**Low Frequency RF System for the Indiana University Cooler Ring**	523

- **X. Pei**, S. Anderson, V. Derenchuk, G. East, D.L. Friesel, D. Jenner, D. McCammon, T. Sloan
  Indiana University, Bloomington, Indiana, USA

A B C D E F G H I J K L M N O P Q R S T U V W X Y Z

Derrig, G.

Paper	Title	Page
XC-09	**Results from the Deflector Test Stand at Texas A&M University**	602

- **D.P. May**, G. Derrig, W. Dewees, P. Smelser, D. Tran, R.C. Rogers
  Texas A&M University, College Station, Texas, USA

A B C D E F G H I J K L M N O P Q R S T U V W X Y Z

Dewees, W.

Paper	Title	Page
XC-09	**Results from the Deflector Test Stand at Texas A&M University**	602

- **D.P. May**, G. Derrig, W. Dewees, P. Smelser, D. Tran, R.C. Rogers
  Texas A&M University, College Station, Texas, USA

A B C D E F G H I J K L M N O P Q R S T U V W X Y Z

Di Biasi, G.

Paper	Title	Page
XC-06	**Material Consideration for Magnetic Channels**	589

- **J. Sura**, L. Calabretta, G. Di Biasi, P. Gmaj, D. Rifuggiato
  INFN/LNS, Catania, Italy

A B C D E F G H I J K L M N O P Q R S T U V W X Y Z

Di Giacomo, M.

Paper	Title	Page
I-18	**Status Report on the Heavy Ion Facility at LNS**	90

- **F. Alessandria**, G. Bellomo, A. Bosotti, C. De Martinis, D. Giove, P. Michelato, C. Pagani, L. Rossi
  INFN/LASA, Segrate, Italy
- L. Calabretta, G. Ciavola, G. Cuttone, M. Di Giacomo, S. Gammino, P. Gmaj, G. Raia, D. Rifuggiato, J. Sura
  INFN/LNS, Catania, Italy

Paper	Title	Page
IXD-05	**High Sensitivity Electronic System for the Phase Probes of the LNS/MILANO Superconducting Cyclotron**	483

- **A. Bosotti**, D. Corti, C. Pagani, G. Varisco, F. Zibra
  INFN/LASA, Segrate, Italy
- M. Di Giacomo
  INFN/LNS, Catania, Italy

A B C D E F G H I J K L M N O P Q R S T U V W X Y Z

Diamond, W.T.

Paper	Title	Page
XC-01	**The Electrostatic Deflector for the Chalk River Superconducting Cyclotron**	569

- **W.T. Diamond**, C.R. Hoffmann, G.R. Mitchel, H. Schmeing
  Atomic Energy of Canada, Chalk River, Ontario, Canada

A B C D E F G H I J K L M N O P Q R S T U V W X Y Z

Didyk, A.Yu.

Paper	Title	Page
IV-03	**The Use of Heavy Ion Cyclotrons of the Flerov Laboratory of Nuclear Reactions in Condensed Matter Investigations**	162

- **R.Ts. Oganessian**, A.Yu. Didyk
  JINR, Dubna, Russia

A B C D E F G H I J K L M N O P Q R S T U V W X Y Z

Dmitriev, S.N.

Paper	Title	Page
IV-04	**^{178m2}Hf and ^{237}Pu Isotopes Production on the U-200 Cyclotron**	167

- **S.L. Bogomolov**, S.N. Dmitriev, Yu.P. Gangrski, G.G. Gulbekyan, S.A. Karamian, V.B. Kutner, B.N. Markov, Yu.Ts. Oganessian, N.V. Pronin, G.Ya. Starodub
  JINR, Dubna, Russia

V-04	**Possibility of Producing Some Radionuclides for Medicine Using JINR Accelerators**	213

- **S.N. Dmitriev**, G.G. Gulbekyan, V.A. Khalkin, R.Ts. Oganessian, L.M. Onishchenko, G.Ya. Starodub, N.G. Zaitseva
  JINR, Dubna, Russia

A B C D E F G H I J K L M N O P Q R S T U V W X Y Z

Dmitriev, S.P.

Paper	Title	Page
I-10	**Gatchina Isochronous Cyclotron**	58

- **N.K. Abrosimov**, S.A. Artamonov, P.V. Chervyakov, S.P. Dmitriev, V.A. Eliseev, V.P. Fominenko, E.M. Ivanov, G.F. Mikheev, Yu.T. Mironov, A.S. Pokrovskii, G.A. Riabov, V.A. Smolin, G.L. Sokolov, V.A. Volchenkov, A.A. Vorobiev
  Petersburg Nuclear Physics Institute, Gatchina, Russia
- P.V. Bogdanov, B.D. Ershov, V.S. Kuligin, V.N. Moshkin, V.G. Mudrolyubov, Yu.I. Stogov, A.P. Strokach
  D.V. Efremov Scientific Research Institute of Electrophysical Apparatus, St. Petersburg, Russia

A B C D E F G H I J K L M N O P Q R S T U V W X Y Z

Dolinsky, A.V.

Paper	Title	Page
VII-06	**The New Project of INR (Kiev's) Storage-Accelerating Complex**	294

- **A.V. Dolinsky**, A.I. Papash, S.N. Pavlov, A.T. Rudchik, A.E. Val'Kov, I.N. Vishnevsky, A.V. Zhmendak
  Institute for Nuclear Research, Kiev, Ukraine
- V.P. Belov, A.M. Kokorin, A.A. Makarov, I.A. Schukeilo, Yu.P. Severgin
  D.V. Efremov Scientific Research Institute of Electrophysical Apparatus, St. Petersburg, Russia

A B C D E F G H I J K L M N O P Q R S T U V W X Y Z

Dombsky, M.

Paper	Title	Page
XIII-08	**Research and Development Studies with Radioactive Beams at TRIUMF**	745

- **J.M. D'Auria**, M. Dombsky
  Simon Fraser University, Burnaby, BC, Canada
- L. Buchmann, H. Sprenger, J.S. Vincent
  TRIUMF, Vancouver, Canada
- J. King
  University of Toronto, Toronto, Ontario, Canada
- P. McNeely, G. Roy
  University of Alberta, Edmonton, Alberta, Canada

A B C D E F G H I J K L M N O P Q R S T U V W X Y Z

Dowling, D.T.

Paper	Title	Page
XIII-07	**The ORNL Radioactive Ion Beam Project with the ORIC Accelerator**	741

- **D.K. Olsen**, G.D. Alton, C. Baktash, D.T. Dowling, J.D. Garrett, D.L. Haynes, C.M. Jones, R.C. Juras, S.N. Lane, I.Y. Lee, M.J. Meigs, G.D. Mills, S.W. Mosko, B.A. Tatum, K.S. Toth
  ORNL, Oak Ridge, Tennessee, USA
- H.K. Carter, J. Kormicki
  Associated Universities Oak Ridge, Oak Ridge, Tennessee, USA

A B C D E F G H I J K L M N O P Q R S T U V W X Y Z

du Toit, Z.B.

Paper	Title	Page
VIII-15	**Progress with the NAC Injector Cyclotron for Heavy and Polarized Ions**	361

- **Z.B. du Toit**, S.J. Burger, P.J. Celliers, J.G. de Villiers, H.N. Jungwirth, A. Müller, P.F. Rohwer, D.M. van Rooyen
  National Accelerator Centre, Faure, Republic of South Africa

A B C D E F G H I J K L M N O P Q R S T U V W X Y Z

Dufour, J.P.

Paper	Title	Page
VI-04	**Progress Report on the IBA-SHI Proton Therapy System**	244

- **Y. Jongen**, W. Beeckman, J.P. Dufour, A. Laisné, H. Marie, R. Verbruggen
  Ion Beam Applications, Louvain-la-Neuve, Belgium
- M. Sano, S. Satoh, N. Takahashi, T. Takayama
  Sumitomo Heavy Industries, Ehime, Japan

A B C D E F G H I J K L M N O P Q R S T U V W X Y Z

DuPlantis, D.

Paper	Title	Page
XD-02	**Beam Transport System for the IUCF High Intensity Polarized Ion Source**	609

- **W.P. Jones**, M.S. Ball, J.C. Collins, D. DuPlantis, T.J.P. Ellison, D.L. Friesel, B. Hamilton, J.W. Hicks, P. Schwandt
  Indiana University, Bloomington, Indiana, USA

Paper	Title	Page
XI-02	**The IUCF High Intensity Polarized Ion Source Control System**	641

- **T. Capshew**, J.C. Collins, D. DuPlantis, D.W. Frame, J. Graham, D.D. Reid
  Indiana University, Bloomington, Indiana, USA

A B C D E F G H I J K L M N O P Q R S T U V W X Y Z

Dutto, G.

Paper	Title	Page
III-01	**The TRIUMF 520 MeV Cyclotron: Recent and Future Developments**	138

- **G. Dutto**
  TRIUMF, Vancouver, Canada

Paper	Title	Page
IXA-02	**The Influence of Magnetic Field Imperfections on the Beam Quality in an H^- Cyclotron**	380

- **W.J.G.M. Kleeven**, H.L. Hagedoorn
  Eindhoven University of Technology, Eindhoven, The Netherlands
- B.F. Milton, G. Dutto
  TRIUMF, Vancouver, Canada

A B C D E F G H I J K L M N O P Q R S T U V W X Y Z

East, G.

Paper	Title	Page
XA-05	**Low Frequency RF System for the Indiana University Cooler Ring**	523

- **X. Pei**, S. Anderson, V. Derenchuk, G. East, D.L. Friesel, D. Jenner, D. McCammon, T. Sloan
  Indiana University, Bloomington, Indiana, USA

A B C D E F G H I J K L M N O P Q R S T U V W X Y Z

Efremov, A.

Paper	Title	Page
VIII-11	**Study on the Magnetic Field of Caprice Type ECR Source**	344

- **B.W. Wei**, Z. Liu, Y. Ma, D. Wu, P. Yuan, W. Zhang, X. Zhang, H. Zhao
  Institute of Modern Physics, Lanzhou, People's Republic of China
- A. Efremov
  JINR, Dubna, Russia

A B C D E F G H I J K L M N O P Q R S T U V W X Y Z

Eiche, M.

Paper	Title	Page
XA-03	**Dual Frequency Resonator System for a Compact Cyclotron**	515

- **M. Eiche**, K.L. Erdman
  Ebco Technologies Ltd, Richmond, BC, Canada
- P. Lanz, M. Lipnicki, M. Zach
  TRIUMF, Vancouver, Canada

A B C D E F G H I J K L M N O P Q R S T U V W X Y Z

Ekström, C.

Paper	Title	Page
VII-01	**Recent Commissioning Results at Celsius (Invited Paper)**	266

- **D. Reistad**, T. Bergmark, C. Ekström, C.-J. Fridén, K. Gajewski, L. Hermansson, P. Jahnke, A. Johansson, O. Johansson, T. Lofnes, G. Norman, R. Wedberg, L. Westerberg, J. Zlomanczuk
  Uppsala University, Uppsala, Sweden
- M.A. Raadu, M. Sedlacek
  Royal Institute of Technology, Stockholm, Sweden

A B C D E F G H I J K L M N O P Q R S T U V W X Y Z

Eliseev, V.A.

Paper	Title	Page
I-10	**Gatchina Isochronous Cyclotron**	58

- **N.K. Abrosimov**, S.A. Artamonov, P.V. Chervyakov, S.P. Dmitriev, V.A. Eliseev, V.P. Fominenko, E.M. Ivanov, G.F. Mikheev, Yu.T. Mironov, A.S. Pokrovskii, G.A. Riabov, V.A. Smolin, G.L. Sokolov, V.A. Volchenkov, A.A. Vorobiev
  Petersburg Nuclear Physics Institute, Gatchina, Russia
- P.V. Bogdanov, B.D. Ershov, V.S. Kuligin, V.N. Moshkin, V.G. Mudrolyubov, Yu.I. Stogov, A.P. Strokach
  D.V. Efremov Scientific Research Institute of Electrophysical Apparatus, St. Petersburg, Russia

A B C D E F G H I J K L M N O P Q R S T U V W X Y Z

Ellison, T.J.P.

Paper	Title	Page
VII-02	**Beam Diagnosis for Unmeasurably Cold Beams (Invited Paper)**	274

- **T.J.P. Ellison**
  Indiana University, Bloomington, Indiana, USA

Paper	Title	Page
VIII-07	**Performance and Status of the IUCF High Intensity Polarized Ion Source**	330

- **V. Derenchuk**, R. Brown, T.J.P. Ellison, D.L. Friesel, J.W. Hicks, D. Jenner, A. Pei, H. Petri, P. Schwandt, J. Sowinski, M. Wedekind
  Indiana University, Bloomington, Indiana, USA

Paper	Title	Page
XD-02	**Beam Transport System for the IUCF High Intensity Polarized Ion Source**	609

- **W.P. Jones**, M.S. Ball, J.C. Collins, D. DuPlantis, T.J.P. Ellison, D.L. Friesel, B. Hamilton, J.W. Hicks, P. Schwandt
  Indiana University, Bloomington, Indiana, USA

A B C D E F G H I J K L M N O P Q R S T U V W X Y Z

Enchevich, I.B.

Paper	Title	Page
VIII-08	**Ion Source of Discharge Type**	334

- **I.B. Enchevich**
  TRIUMF, Vancouver, Canada
- S.A. Korenev
  JINR, Dubna, Russia

A B C D E F G H I J K L M N O P Q R S T U V W X Y Z

Endo, K.

Paper	Title	Page
VI-08	**A Proton Therapy Facility Plan**	258

- **S. Fukumoto**, Y. Hayakawa, T. Inada, A. Maruhashi, M. Sato, J. Tada, Y. Takada, H. Tsuji, H. Tsujii
  University of Tsukuba, Ibaraki, Japan
- K. Endo, Y. Irie, K. Muto
  KEK, Ibaraki, Japan

Paper	Title	Page
XD-07	**Beam Transport System for the HIMAC**	625

- **K. Noda**, Y. Hirao, A. Itano, M. Kanazawa, A. Kitagawa, T. Kohno, M. Kumada, H. Ogawa, K. Sato, Y. Sato, M. Sudou, E. Takada, S. Yamada, T. Yamada
  NIRS, Chiba, Japan
- K. Endo
  KEK, Ibaraki, Japan

A B C D E F G H I J K L M N O P Q R S T U V W X Y Z

Erdman, K.L.

Paper	Title	Page
XA-03	**Dual Frequency Resonator System for a Compact Cyclotron**	515

- **M. Eiche**, K.L. Erdman
  Ebco Technologies Ltd, Richmond, BC, Canada
- P. Lanz, M. Lipnicki, M. Zach
  TRIUMF, Vancouver, Canada

A B C D E F G H I J K L M N O P Q R S T U V W X Y Z

Ershov, B.D.

Paper	Title	Page
I-10	**Gatchina Isochronous Cyclotron**	58

- **N.K. Abrosimov**, S.A. Artamonov, P.V. Chervyakov, S.P. Dmitriev, V.A. Eliseev, V.P. Fominenko, E.M. Ivanov, G.F. Mikheev, Yu.T. Mironov, A.S. Pokrovskii, G.A. Riabov, V.A. Smolin, G.L. Sokolov, V.A. Volchenkov, A.A. Vorobiev
  Petersburg Nuclear Physics Institute, Gatchina, Russia
- P.V. Bogdanov, B.D. Ershov, V.S. Kuligin, V.N. Moshkin, V.G. Mudrolyubov, Yu.I. Stogov, A.P. Strokach
  D.V. Efremov Scientific Research Institute of Electrophysical Apparatus, St. Petersburg, Russia

A B C D E F G H I J K L M N O P Q R S T U V W X Y Z

Farley, F.

Paper	Title	Page
VI-05	**Recent Activities of the Cyclotron Laboratory in Nice**	248

- **P. Mandrillon**, N. Brassart, P. Chauvel, A. Courdi, F. Farley, N. Fietier, J. Herault, J.Y. Tang
  Centre Antoine Lacassagne, Nice, France

A B C D E F G H I J K L M N O P Q R S T U V W X Y Z

Fehsenfeld, P.

Paper	Title	Page
IV-05	**Radionuclide Technique in Mechanical Engineering (RTM)**	171

- **P. Fehsenfeld**, A. Kleinrahm
  FZK, Karlsruhe, Germany
- V. Novikov
  Kurchatov Institute, Moscow, Russia

A B C D E F G H I J K L M N O P Q R S T U V W X Y Z

Fenemore, R.E.F.

Paper	Title	Page
I-19	**Development of the NAC Accelerator Facilities**	95

- **J.L. Conradie**, A.H. Botha, P.M. Cronje, R.E.F. Fenemore, H.N. Jungwirth, J.J. Kritzinger, W.A.G. Nel, D. Reitmann, L.M.M. Roels, P.F. Rohwer, H.A. Smit
  National Accelerator Centre, Faure, Republic of South Africa

A B C D E F G H I J K L M N O P Q R S T U V W X Y Z

Fermé, J.

Paper	Title	Page
IV-02	**A Cyclotron as a Mass Spectrometer**	158

- **P. Bricault**, G. Auger, M. Bajard, E. Baron, D. Bibet, A. Chabert, J. Fermé, L. Gaudart, J. Joubert, M. Lewitowicz, W. Mittig, E. Plagnol, Ch. Ricaud, Y. Schutz
  GANIL, Caen, France
- G. Audi
  CSNSM, Orsay, France
- A. Gillibert
  CEN/Saclay, Gif-sur-Yvette, France
- K. Fifield
  Australian National University, Canberra , Australia

A B C D E F G H I J K L M N O P Q R S T U V W X Y Z

Fietier, N.

Paper	Title	Page
VI-05	**Recent Activities of the Cyclotron Laboratory in Nice**	248

- **P. Mandrillon**, N. Brassart, P. Chauvel, A. Courdi, F. Farley, N. Fietier, J. Herault, J.Y. Tang
  Centre Antoine Lacassagne, Nice, France

A B C D E F G H I J K L M N O P Q R S T U V W X Y Z

Fifield, K.

Paper	Title	Page
IV-02	**A Cyclotron as a Mass Spectrometer**	158

- **P. Bricault**, G. Auger, M. Bajard, E. Baron, D. Bibet, A. Chabert, J. Fermé, L. Gaudart, J. Joubert, M. Lewitowicz, W. Mittig, E. Plagnol, Ch. Ricaud, Y. Schutz
  GANIL, Caen, France
- G. Audi
  CSNSM, Orsay, France
- A. Gillibert
  CEN/Saclay, Gif-sur-Yvette, France
- K. Fifield
  Australian National University, Canberra , Australia

A B C D E F G H I J K L M N O P Q R S T U V W X Y Z

Fisch, R.K.

Paper	Title	Page
XI-06	**The New Distributed Control System of the NAC**	656

- **H.F. Weehuizen**, R.K. Fisch, E.J.S. Franklin, M.E. Hogan, I.H. Kohler, J.P. Rogers, P.J. Theron
  National Accelerator Centre, Faure, Republic of South Africa

A B C D E F G H I J K L M N O P Q R S T U V W X Y Z

Fominenko, V.P.

Paper	Title	Page
I-10	**Gatchina Isochronous Cyclotron**	58

- **N.K. Abrosimov**, S.A. Artamonov, P.V. Chervyakov, S.P. Dmitriev, V.A. Eliseev, V.P. Fominenko, E.M. Ivanov, G.F. Mikheev, Yu.T. Mironov, A.S. Pokrovskii, G.A. Riabov, V.A. Smolin, G.L. Sokolov, V.A. Volchenkov, A.A. Vorobiev
  Petersburg Nuclear Physics Institute, Gatchina, Russia
- P.V. Bogdanov, B.D. Ershov, V.S. Kuligin, V.N. Moshkin, V.G. Mudrolyubov, Yu.I. Stogov, A.P. Strokach
  D.V. Efremov Scientific Research Institute of Electrophysical Apparatus, St. Petersburg, Russia

A B C D E F G H I J K L M N O P Q R S T U V W X Y Z

Fong, K.

Paper	Title	Page
IXD-08	**Signal Processing for the Internal Phase Probe in the TRIUMF Cyclotron**	495

- **K. Fong**
  TRIUMF, Vancouver, Canada

A B C D E F G H I J K L M N O P Q R S T U V W X Y Z

Fourie, D.T.

Paper	Title	Page
XD-06	**Beamlines for a Second Injector Cyclotron at NAC**	621

- **J.C. Cornell**, J.L. Conradie, D.T. Fourie
  National Accelerator Centre, Faure, Republic of South Africa

A B C D E F G H I J K L M N O P Q R S T U V W X Y Z

Frame, D.W.

Paper	Title	Page
XI-02	**The IUCF High Intensity Polarized Ion Source Control System**	641

- **T. Capshew**, J.C. Collins, D. DuPlantis, D.W. Frame, J. Graham, D.D. Reid
  Indiana University, Bloomington, Indiana, USA

A B C D E F G H I J K L M N O P Q R S T U V W X Y Z

Franklin, E.J.S.

Paper	Title	Page
XI-06	**The New Distributed Control System of the NAC**	656

- **H.F. Weehuizen**, R.K. Fisch, E.J.S. Franklin, M.E. Hogan, I.H. Kohler, J.P. Rogers, P.J. Theron
  National Accelerator Centre, Faure, Republic of South Africa

XI-07	**Ion Spectra Identification Software for the ECR Ion Source at NAC**	660

- **E.J.S. Franklin**, J.G. de Villiers
  National Accelerator Centre, Faure, Republic of South Africa

XI-08	**Micro-Controlled Vacuum Systems at NAC**	664

- **P.J. Celliers**, E.J.S. Franklin
  National Accelerator Centre, Faure, Republic of South Africa

A B C D E F G H I J K L M N O P Q R S T U V W X Y Z

Fraser, J.S.

Paper	Title	Page
XIII-09	**Post-Accelerator Studies for the ISOL Facility at TRIUMF**	749

- **L. Root**, H.R. Schneider, J.S. Fraser
  TRIUMF, Vancouver, Canada

A B C D E F G H I J K L M N O P Q R S T U V W X Y Z

Frei, H.

Paper	Title	Page
XA-08	**Experience with the PSI-Cyclotron RF-System Under Heavy Beam Loading**	534

- **P.K. Sigg**, J. Cherix, H. Frei, M. Märki
  PSI, Villigen, Switzerland

A B C D E F G H I J K L M N O P Q R S T U V W X Y Z

Fridén, C.-J.

Paper	Title	Page
VII-01	**Recent Commissioning Results at Celsius (Invited Paper)**	266

- **D. Reistad**, T. Bergmark, C. Ekström, C.-J. Fridén, K. Gajewski, L. Hermansson, P. Jahnke, A. Johansson, O. Johansson, T. Lofnes, G. Norman, R. Wedberg, L. Westerberg, J. Zlomanczuk
  Uppsala University, Uppsala, Sweden
- M.A. Raadu, M. Sedlacek
  Royal Institute of Technology, Stockholm, Sweden

A B C D E F G H I J K L M N O P Q R S T U V W X Y Z

Friesel, D.L.

Paper	Title	Page
VIII-07	**Performance and Status of the IUCF High Intensity Polarized Ion Source**	330

- **V. Derenchuk**, R. Brown, T.J.P. Ellison, D.L. Friesel, J.W. Hicks, D. Jenner, A. Pei, H. Petri, P. Schwandt, J. Sowinski, M. Wedekind
  Indiana University, Bloomington, Indiana, USA

XA-05	**Low Frequency RF System for the Indiana University Cooler Ring**	523

- **X. Pei**, S. Anderson, V. Derenchuk, G. East, D.L. Friesel, D. Jenner, D. McCammon, T. Sloan
  Indiana University, Bloomington, Indiana, USA

XD-02	**Beam Transport System for the IUCF High Intensity Polarized Ion Source**	609

- **W.P. Jones**, M.S. Ball, J.C. Collins, D. DuPlantis, T.J.P. Ellison, D.L. Friesel, B. Hamilton, J.W. Hicks, P. Schwandt
  Indiana University, Bloomington, Indiana, USA

A B C D E F G H I J K L M N O P Q R S T U V W X Y Z

Fruneau, M.

Paper	Title	Page
I-11	**Status Report of SARA**	62

- **M. Fruneau**, S. Albrand, D. Barnéoud, J.L. Belmont, G. Bizouard, J.L. Bouly, G. Campillo, M. Guisset, G. Laborie
  Université Joseph Fourier, Grenoble, France

XIII-04	**The PIAFE Project at Grenoble: Beam Transport and Acceleration**	729

- **J.L. Belmont**, J.F. Bruandet, J.M. de Conto, M. Fruneau, G. Gimond, K. Golovanivsky, E. Liatard, J.M. Loiseaux, H. Nifenecker, A. Savalle, B. Vignon
  Université Joseph Fourier, Grenoble, France
- P. Briand
  CEN-Grenoble, Grenoble, France

A B C D E F G H I J K L M N O P Q R S T U V W X Y Z

Fujita, M.

Paper	Title	Page
VIII-06	**An ECR Ion Source for Multiply-Charged Heavy Ions at 14 GHz**	326

- **M. Sekiguchi**, M. Fujita, Y. Ohshiro, T. Yamazaki
  University of Tokyo, Tanashi-shi, Tokyo, Japan
- Y. Isoya, T. Yamada, Y. Yamashita
  Japan Steel Works Ltd., Research Center for Advanced Technologies, Chiba, Japan
- A. Kitagawa
  NIRS, Chiba, Japan

IXC-02	**A Formulation of Spiral Inflector Design and Its Application to SF Cyclotron**	450

- **M. Sekiguchi**, M. Fujita, M. Nishiguchi, Y. Ohshiro, Y. Shida, N. Yamazaki, T. Yamazaki
  University of Tokyo, Tanashi-shi, Tokyo, Japan

A B C D E F G H I J K L M N O P Q R S T U V W X Y Z

Fukuda, M.

Paper	Title	Page
II-03	**Construction and First Year's Operation of the JAERI AVF Cyclotron**	119

- **K. Arakawa**, T. Agematsu, M. Fukuda, I. Ishibori, T. Karasawa, T. Nara, Y. Nakamura, S. Okumura, R. Tanaka, W. Yokota
  JAERI, Gunma, Japan
- A. Shimizu
  Osaka University, Osaka, Japan
- Y. Hayashi, K. Ishii, T. Satoh, T. Tachikawa
  Sumitomo Heavy Industries, Ehime, Japan

VIII-09	**Operation of Ion Sources and Beam Transport to JAERI AVF Cyclotron**	336

- **W. Yokota**, T. Agematsu, K. Arakawa, M. Fukuda, I. Ishibori, Y. Nakamura, T. Nara, S. Okumura
  JAERI, Gunma, Japan
- Y. Hayashi, K. Ishii, T. Tachikawa
  Sumitomo Heavy Industries, Ehime, Japan

IXB-02	**Beam Studies of Injection to Extraction System for JAERI AVF Cyclotron**	423

- **M. Fukuda**, T. Agematsu, K. Arakawa, I. Ishibori, T. Karasawa, Y. Nakamura, T. Nara, S. Okumura, W. Yokota
  JAERI, Gunma, Japan

XA-06	**A Modified RF System of JAERI AVF Cyclotron**	526

- **Y. Kumata**, Y. Fukumoto
  Sumitomo Heavy Industries, Ehime, Japan
- K. Arakawa, M. Fukuda, T. Karasawa
  JAERI, Gunma, Japan
- A. Shimizu
  Osaka University, Osaka, Japan

XC-04	**Performance of Beam Chopping System for JAERI AVF Cyclotron**	581

- **W. Yokota**, T. Agematsu, K. Arakawa, M. Fukuda, I. Ishibori, Y. Nakamura, T. Nara, S. Okumura
  JAERI, Gunma, Japan
- Y. Hayashi, Y. Kumata, T. Tachikawa
  Sumitomo Heavy Industries, Ehime, Japan

XI-04	**Control System for JAERI AVF Cyclotron**	648

- **S. Okumura**, T. Agematsu, K. Arakawa, M. Fukuda, I. Ishibori, T. Kamiya,

Y. Nakamura, T. Nara, W. Yokota
JAERI, Gunma, Japan
- K. Hoshika, K. Iso, M. Maruyama, M. Tachibana
Sumitomo Heavy Industries, Ehime, Japan

A B C D E F G H I J K L M N O P Q R S T U V W X Y Z

Fukumoto, S.

Paper	Title	Page
VI-08	**A Proton Therapy Facility Plan**	258

- **S. Fukumoto**, Y. Hayakawa, T. Inada, A. Maruhashi, M. Sato, J. Tada, Y. Takada, H. Tsuji, H. Tsujii
  University of Tsukuba, Ibaraki, Japan
- K. Endo, Y. Irie, K. Muto
  KEK, Ibaraki, Japan

A B C D E F G H I J K L M N O P Q R S T U V W X Y Z

Fukumoto, Y.

Paper	Title	Page
XA-06	**A Modified RF System of JAERI AVF Cyclotron**	526

- **Y. Kumata**, Y. Fukumoto
  Sumitomo Heavy Industries, Ehime, Japan
- K. Arakawa, M. Fukuda, T. Karasawa
  JAERI, Gunma, Japan
- A. Shimizu
  Osaka University, Osaka, Japan

A B C D E F G H I J K L M N O P Q R S T U V W X Y Z

Gajewski, K.

Paper	Title	Page
VII-01	**Recent Commissioning Results at Celsius (Invited Paper)**	266

- **D. Reistad**, T. Bergmark, C. Ekström, C.-J. Fridén, K. Gajewski, L. Hermansson, P. Jahnke, A. Johansson, O. Johansson, T. Lofnes, G. Norman, R. Wedberg, L. Westerberg, J. Zlomanczuk
  Uppsala University, Uppsala, Sweden
- M.A. Raadu, M. Sedlacek
  Royal Institute of Technology, Stockholm, Sweden

A B C D E F G H I J K L M N O P Q R S T U V W X Y Z

Gammino, S.

Paper	Title	Page
I-18	**Status Report on the Heavy Ion Facility at LNS**	90

- **F. Alessandria**, G. Bellomo, A. Bosotti, C. De Martinis, D. Giove, P. Michelato, C. Pagani, L. Rossi
  INFN/LASA, Segrate, Italy
- L. Calabretta, G. Ciavola, G. Cuttone, M. Di Giacomo, S. Gammino, P. Gmaj, G. Raia, D. Rifuggiato, J. Sura
  INFN/LNS, Catania, Italy

A B C D E F G H I J K L M N O P Q R S T U V W X Y Z

Gangrski, Yu.P.

Paper	Title	Page
IV-04	^{178m2}Hf and ^{237}Pu Isotopes Production on the U-200 Cyclotron	167

- **S.L. Bogomolov**, S.N. Dmitriev, Yu.P. Gangrski, G.G. Gulbekyan, S.A. Karamian, V.B. Kutner, B.N. Markov, Yu.Ts. Oganessian, N.V. Pronin, G.Ya. Starodub
  JINR, Dubna, Russia

A B C D E F G H I J K L M N O P Q R S T U V W X Y Z

Garrett, J.D.

Paper	Title	Page
XIII-07	**The ORNL Radioactive Ion Beam Project with the ORIC Accelerator**	741

- **D.K. Olsen**, G.D. Alton, C. Baktash, D.T. Dowling, J.D. Garrett, D.L. Haynes, C.M. Jones, R.C. Juras, S.N. Lane, I.Y. Lee, M.J. Meigs, G.D. Mills, S.W. Mosko, B.A. Tatum, K.S. Toth
  ORNL, Oak Ridge, Tennessee, USA
- H.K. Carter, J. Kormicki
  Associated Universities Oak Ridge, Oak Ridge, Tennessee, USA

A B C D E F G H I J K L M N O P Q R S T U V W X Y Z

Gaudart, L.

Paper	Title	Page
IV-02	**A Cyclotron as a Mass Spectrometer**	158

- **P. Bricault**, G. Auger, M. Bajard, E. Baron, D. Bibet, A. Chabert, J. Fermé, L. Gaudart, J. Joubert, M. Lewitowicz, W. Mittig, E. Plagnol, Ch. Ricaud, Y. Schutz
  GANIL, Caen, France
- G. Audi
  CSNSM, Orsay, France
- A. Gillibert
  CEN/Saclay, Gif-sur-Yvette, France
- K. Fifield
  Australian National University, Canberra , Australia

A B C D E F G H I J K L M N O P Q R S T U V W X Y Z

Gelbart, W.Z.

Paper	Title	Page
IV-11	**External High Current Targetry for Radioisotope Production**	196

- **N.R. Stevenson**, W.Z. Gelbart
  TRIUMF, Vancouver, Canada

A B C D E F G H I J K L M N O P Q R S T U V W X Y Z

Gerasimov, V.

Paper	Title	Page
I-13	**Current Status and Future Project of Cyclotron Laboratory in Alma-Ata**	71

- **A.A. Arzumanov**, V. Batischev, V. Berger, V. Gerasimov, M. Gorcovets
  Kazakhstan Academy of Sciences, Alma-Ata, Republic of Kazakhstan

A B C D E F G H I J K L M N O P Q R S T U V W X Y Z

Gikal, B.

Paper	Title	Page
I-02	**New Development at the JINR Heavy Ion Cyclotron Facility (Invited Paper)**	11

- **G.G. Gulbekyan**, V. Bekhterev, O. Borisov, B. Gikal, A. Ivanenko, I. Kolesov, V.B. Kutner, A. Morduev, Yu.Ts. Oganessian
  JINR, Dubna, Russia

A B C D E F G H I J K L M N O P Q R S T U V W X Y Z

Gillibert, A.

Paper	Title	Page
IV-02	**A Cyclotron as a Mass Spectrometer**	158

- **P. Bricault**, G. Auger, M. Bajard, E. Baron, D. Bibet, A. Chabert, J. Fermé, L. Gaudart, J. Joubert, M. Lewitowicz, W. Mittig, E. Plagnol, Ch. Ricaud, Y. Schutz
  GANIL, Caen, France
- G. Audi
  CSNSM, Orsay, France
- A. Gillibert
  CEN/Saclay, Gif-sur-Yvette, France
- K. Fifield
  Australian National University, Canberra , Australia

Gimond, G.

Paper	Title	Page
XIII-04	**The PIAFE Project at Grenoble: Beam Transport and Acceleration**	729

- **J.L. Belmont**, J.F. Bruandet, J.M. de Conto, M. Fruneau, G. Gimond, K. Golovanivsky, E. Liatard, J.M. Loiseaux, H. Nifenecker, A. Savalle, B. Vignon
  Université Joseph Fourier, Grenoble, France
- P. Briand
  CEN-Grenoble, Grenoble, France

A B C D E F G H I J K L M N O P Q R S T U V W X Y Z

Giove, D.

Paper	Title	Page
I-18	**Status Report on the Heavy Ion Facility at LNS**	90

- **F. Alessandria**, G. Bellomo, A. Bosotti, C. De Martinis, D. Giove, P. Michelato, C. Pagani, L. Rossi
  INFN/LASA, Segrate, Italy
- L. Calabretta, G. Ciavola, G. Cuttone, M. Di Giacomo, S. Gammino, P. Gmaj, G. Raia, D. Rifuggiato, J. Sura
  INFN/LNS, Catania, Italy

A B C D E F G H I J K L M N O P Q R S T U V W X Y Z

Glazov, A.

Paper	Title	Page
II-04	**20 MeV Cyclotron for Isotope Production**	123

- **A. Glazov**, Ju. Alenitskiy, A. Chesnov, S. Chesnova, V. Kochkin, D. Novikov, E. Samsonov, M. Semenov, A. Vasilenko, E. Zaplatin, N. Zaplatin
  JINR, Dubna, Russia
- I. Gulamov, O. Iljasov, A. Rykov
  Institute of Nuclear Physics, Tashkent, Republic of Uzbekistan

A B C D E F G H I J K L M N O P Q R S T U V W X Y Z

Glushko, A.

Paper	Title	Page
VII-07	**Superthin Internal Target for Storage Rings**	297

- **V. Pugatch**, A. Glushko, G. Pitatelev, G. Sivtsov
  Institute for Nuclear Research, Kiev, Ukraine
- S. Popov, D. Toporkov, B. Voitsechovsky
  Institute for Nuclear Physics, Novosibirsk, Russia

A B C D E F G H I J K L M N O P Q R S T U V W X Y Z

Gmaj, P.

Paper	Title	Page
I-18	**Status Report on the Heavy Ion Facility at LNS**	90

- **F. Alessandria**, G. Bellomo, A. Bosotti, C. De Martinis, D. Giove, P. Michelato, C. Pagani, L. Rossi
  INFN/LASA, Segrate, Italy
- L. Calabretta, G. Ciavola, G. Cuttone, M. Di Giacomo, S. Gammino, P. Gmaj, G. Raia, D. Rifuggiato, J. Sura
  INFN/LNS, Catania, Italy

XC-06	**Material Consideration for Magnetic Channels**	589

- **J. Sura**, L. Calabretta, G. Di Biasi, P. Gmaj, D. Rifuggiato
  INFN/LNS, Catania, Italy

Golovanivsky, K.

Paper	Title	Page
XIII-04	**The PIAFE Project at Grenoble: Beam Transport and Acceleration**	729

- **J.L. Belmont**, J.F. Bruandet, J.M. de Conto, M. Fruneau, G. Gimond, K. Golovanivsky, E. Liatard, J.M. Loiseaux, H. Nifenecker, A. Savalle, B. Vignon
  Université Joseph Fourier, Grenoble, France
- P. Briand
  CEN-Grenoble, Grenoble, France

A B C D E F G H I J K L M N O P Q R S T U V W X Y Z

Goodman, G.B.

Paper	Title	Page
VI-03	**Pion Therapy for Cancer - What are the Prospects?**	242

- **G.B. Goodman**
  University of British Columbia, Vancouver, Canada

A B C D E F G H I J K L M N O P Q R S T U V W X Y Z

Gorcovets, M.

Paper	Title	Page
I-13	**Current Status and Future Project of Cyclotron Laboratory in Alma-Ata**	71

- **A.A. Arzumanov**, V. Batischev, V. Berger, V. Gerasimov, M. Gorcovets
  Kazakhstan Academy of Sciences, Alma-Ata, Republic of Kazakhstan

A B C D E F G H I J K L M N O P Q R S T U V W X Y Z

Gordon, M.M.

Paper	Title	Page
IXA-08	**Evaluation of Third-Harmonic Voltage Flattopping for a Superconducting Cyclotron**	404

- **M.M. Gordon**, D. Jeon
  NSCL, East Lansing, Michigan, USA

A B C D E F G H I J K L M N O P Q R S T U V W X Y Z

Goto, A.

Paper	Title	Page
VIII-16	**Plasma Cathode Method for RIKEN ECRIS**	365

- **T. Nakagawa**, A. Goto, T. Kageyama, M. Kase, Y. Yano
  RIKEN, Saitama, Japan

A B C D E F G H I J K L M N O P Q R S T U V W X Y Z

Gotovtsev, O.

Paper	Title	Page
XI-05	**Automatic Control System of Magnetic Separator for Kurchatov IAE Cyclotron**	652

- **N.I. Venikov**, V. Buranov, O. Gotovtsev, L.I. Iudin, P.Yu. Komissarov, V.N. Unezhev
  Kurchatov Institute, Moscow, Russia

A B C D E F G H I J K L M N O P Q R S T U V W X Y Z

Graham, J.

Paper	Title	Page
XI-02	**The IUCF High Intensity Polarized Ion Source Control System**	641

- **T. Capshew**, J.C. Collins, D. DuPlantis, D.W. Frame, J. Graham, D.D. Reid
  Indiana University, Bloomington, Indiana, USA

A B C D E F G H I J K L M N O P Q R S T U V W X Y Z

Grey-Morgan, T.

Paper	Title	Page
II-02	**The Operation of Cyclotrons Used for Radiopharmaceutical Production**	115

- **T. Grey-Morgan**
  Cyclotron Isotopes Manufacturing, Buckinghamshire, England
- R.E. Hubbard
  Medi + Physics Inc., Arlington Heights, Illinois, USA

A B C D E F G H I J K L M N O P Q R S T U V W X Y Z

Grimmett, G.

Paper	Title	Page
V-07	**Dual Chemical Station for Cyclotron Produced ^{18}F**	222

- **M.L. Mallory**, G. Grimmett, R. Tilbury, D. Yang
  The University of Texas, Houston, Texas, USA

A B C D E F G H I J K L M N O P Q R S T U V W X Y Z

Guisset, M.

Paper	Title	Page
I-11	**Status Report of SARA**	62

- **M. Fruneau**, S. Albrand, D. Barnéoud, J.L. Belmont, G. Bizouard, J.L. Bouly, G. Campillo, M. Guisset, G. Laborie
  Université Joseph Fourier, Grenoble, France

A B C D E F G H I J K L M N O P Q R S T U V W X Y Z

Gulamov, I.

Paper	Title	Page
II-04	**20 MeV Cyclotron for Isotope Production**	123

- **A. Glazov**, Ju. Alenitskiy, A. Chesnov, S. Chesnova, V. Kochkin, D. Novikov, E. Samsonov, M. Semenov, A. Vasilenko, E. Zaplatin, N. Zaplatin
  JINR, Dubna, Russia
- I. Gulamov, O. Iljasov, A. Rykov
  Institute of Nuclear Physics, Tashkent, Republic of Uzbekistan

A B C D E F G H I J K L M N O P Q R S T U V W X Y Z

Gulbekyan, G.G.

Paper	Title	Page
I-02	**New Development at the JINR Heavy Ion Cyclotron Facility (Invited Paper)**	11

- **G.G. Gulbekyan**, V. Bekhterev, O. Borisov, B. Gikal, A. Ivanenko, I. Kolesov, V.B. Kutner, A. Morduev, Yu.Ts. Oganessian
  JINR, Dubna, Russia

IV-04	**^{178m2}Hf and ^{237}Pu Isotopes Production on the U-200 Cyclotron**	167

- **S.L. Bogomolov**, S.N. Dmitriev, Yu.P. Gangrski, G.G. Gulbekyan, S.A. Karamian, V.B. Kutner, B.N. Markov, Yu.Ts. Oganessian, N.V. Pronin, G.Ya. Starodub
  JINR, Dubna, Russia

V-04	**Possibility of Producing Some Radionuclides for Medicine Using JINR Accelerators**	213

- **S.N. Dmitriev**, G.G. Gulbekyan, V.A. Khalkin, R.Ts. Oganessian, L.M. Onishchenko, G.Ya. Starodub, N.G. Zaitseva
  JINR, Dubna, Russia

A B C D E F G H I J K L M N O P Q R S T U V W X Y Z

Guo, M.

Paper	Title	Page
I-15	**Upgrading the SFC**	78

- **F. Ye**, M. Guo, Z. Ma, Q. Qiao, Y. Wang, Q. Yin, X. Zhu
  Institute of Modern Physics, Lanzhou, People's Republic of China

A B C D E F G H I J K L M N O P Q R S T U V W X Y Z

Gustafsson, S.

Paper	Title	Page
XC-05	**The AGOR Superconducting Extraction Channel EMC2**	585

- **K. Pieterman**, J.A.M. Dam
  Cryocon B.V., Amersfoort, The Netherlands
- H.J.H. ten Kate
  TU Twente, Enschede, The Netherlands
- S. Gustafsson
  IPN, Orsay, France

XD-03	**Superconducting Focussing Channel for the AGOR Cyclotron**	612

- **H.W. Schreuder**, P. Blache, C. Commeaux, S. Gustafsson, A. Lafoux, M. Mormiche, R. Panvier
  IPN, Orsay, France

A B C D E F G H I J K L M N O P Q R S T U V W X Y Z

Hagedoorn, H.L.

Paper	Title	Page
IXA-02	**The Influence of Magnetic Field Imperfections on the Beam Quality in an H^- Cyclotron**	380

- **W.J.G.M. Kleeven**, H.L. Hagedoorn
  Eindhoven University of Technology, Eindhoven, The Netherlands
- B.F. Milton, G. Dutto
  TRIUMF, Vancouver, Canada

Paper	Title	Page
IXA-03	**Emittance Growth in Nonlinear Beam Guiding and Focusing Elements**	384

- **W.J.G.M. Kleeven**, J.I.M. Botman, J.L. Delhez, H.L. Hagedoorn, C.J. Timmermans, G.A. Webers
  Eindhoven University of Technology, Eindhoven, The Netherlands

A B C D E F G H I J K L M N O P Q R S T U V W X Y Z

Halbach, K.

Paper	Title	Page
XB-02	**A Permanent Magnet System for a Cyclotron Used as a Mass Spectrometer**	561

- **C.Y. Li**, M. Cooper, K. Halbach, W.B. Kunkel, K.N. Leung, R.P. Wells, A.T. Young
  LBL, Berkeley, California, USA

XII-03	**Design of a Compact Permanent Magnet Cyclotron Mass Spectrometer for the Detection and Measurement of Trace Isotopes**	705

- **A.T. Young**, K.J. Bertsche, D.J. Clark, K. Halbach, W.B. Kunkel, K.N. Leung, C.Y. Li
  LBL, Berkeley, California, USA

A B C D E F G H I J K L M N O P Q R S T U V W X Y Z

Hamidov, N.K.

Paper	Title	Page
V-05	**Radiopharmaceutical "Thallium-201-Chloride" Production using Thallium-203 Irradiation by Helium-3 Ions**	216

- **A.A. Arzumanov**, N.K. Hamidov, A.I. Kozin, G.I. Shychikov, S.T. Tihomirova
  Kazakhstan Academy of Sciences, Alma-Ata, Republic of Kazakhstan

A B C D E F G H I J K L M N O P Q R S T U V W X Y Z

Hamilton, B.

Paper	Title	Page
XD-02	**Beam Transport System for the IUCF High Intensity Polarized Ion Source**	609

- **W.P. Jones**, M.S. Ball, J.C. Collins, D. DuPlantis, T.J.P. Ellison, D.L. Friesel, B. Hamilton, J.W. Hicks, P. Schwandt
  Indiana University, Bloomington, Indiana, USA

A B C D E F G H I J K L M N O P Q R S T U V W X Y Z

Hardy, J.C.

Paper	Title	Page
XIV-02	**The Use of Cyclotrons for Physics Experiments, Past, Present and Future (Invited Paper)**	

- **J.C. Hardy**
  Atomic Energy of Canada, Chalk River, Ontario, Canada

A B C D E F G H I J K L M N O P Q R S T U V W X Y Z

Hatanaka, K.

Paper	Title	Page
I-01	**Commissioning of the RCNP Ring Cyclotron (Invited Paper)**	3

- **I. Miura**, A. Ando, K. Hatanaka, K. Hosono, H. Ikegami, T. Itahashi, M. Kibayashi, M. Kondo, H. Ogata, T. Saito, A. Shimizu, K. Tamura, M. Uraki, T. Yamazaki
  Osaka University, Osaka, Japan
- J. Abe
  Sumitomo Heavy Industries, Ehime, Japan

A B C D E F G H I J K L M N O P Q R S T U V W X Y Z

Hayakawa, Y.

Paper	Title	Page
VI-08	**A Proton Therapy Facility Plan**	258

- **S. Fukumoto**, Y. Hayakawa, T. Inada, A. Maruhashi, M. Sato, J. Tada, Y. Takada, H. Tsuji, H. Tsujii
  University of Tsukuba, Ibaraki, Japan
- K. Endo, Y. Irie, K. Muto
  KEK, Ibaraki, Japan

A B C D E F G H I J K L M N O P Q R S T U V W X Y Z

Hayashi, Y.

Paper	Title	Page
VIII-09	**Operation of Ion Sources and Beam Transport to JAERI AVF Cyclotron**	336

- **W. Yokota**, T. Agematsu, K. Arakawa, M. Fukuda, I. Ishibori, Y. Nakamura, T. Nara, S. Okumura
  JAERI, Gunma, Japan
- Y. Hayashi, K. Ishii, T. Tachikawa
  Sumitomo Heavy Industries, Ehime, Japan

II-03	**Construction and First Year's Operation of the JAERI AVF Cyclotron**	119

- **K. Arakawa**, T. Agematsu, M. Fukuda, I. Ishibori, T. Karasawa, T. Nara, Y. Nakamura, S. Okumura, R. Tanaka, W. Yokota
  JAERI, Gunma, Japan
- A. Shimizu
  Osaka University, Osaka, Japan
- Y. Hayashi, K. Ishii, T. Satoh, T. Tachikawa
  Sumitomo Heavy Industries, Ehime, Japan

XC-04	**Performance of Beam Chopping System for JAERI AVF Cyclotron**	581

- **W. Yokota**, T. Agematsu, K. Arakawa, M. Fukuda, I. Ishibori, Y. Nakamura, T. Nara, S. Okumura
  JAERI, Gunma, Japan
- Y. Hayashi, Y. Kumata, T. Tachikawa
  Sumitomo Heavy Industries, Ehime, Japan

A B C D E F G H I J K L M N O P Q R S T U V W X Y Z

Haynes, D.L.

Paper	Title	Page
XIII-07	**The ORNL Radioactive Ion Beam Project with the ORIC Accelerator**	741

- **D.K. Olsen**, G.D. Alton, C. Baktash, D.T. Dowling, J.D. Garrett, D.L. Haynes, C.M. Jones, R.C. Juras, S.N. Lane, I.Y. Lee, M.J. Meigs, G.D. Mills, S.W. Mosko, B.A. Tatum, K.S. Toth
  ORNL, Oak Ridge, Tennessee, USA
- H.K. Carter, J. Kormicki
  Associated Universities Oak Ridge, Oak Ridge, Tennessee, USA

A B C D E F G H I J K L M N O P Q R S T U V W X Y Z

Heikkinen, P.

Paper	Title	Page
IXA-05	**Ion Optics in the Jyväskylä K130 Cyclotron**	392

- **P. Heikkinen**, M. Rinta-Nikkola
  University of Jyväskylä, Jyväskylä, Finland

A B C D E F G H I J K L M N O P Q R S T U V W X Y Z

Hendry, G.O.

Paper	Title	Page
VIII-13	**Recent Development of Internal H^-/D^- Source for Compact Cyclotrons**	352

- **T.Y.T. Kuo**
  TRIUMF, Vancouver, Canada
- G.O. Hendry
  Cyclotron Inc., Napa, California, USA

A B C D E F G H I J K L M N O P Q R S T U V W X Y Z

Herault, J.

Paper	Title	Page
VI-05	**Recent Activities of the Cyclotron Laboratory in Nice**	248

- **P. Mandrillon**, N. Brassart, P. Chauvel, A. Courdi, F. Farley, N. Fietier, J. Herault, J.Y. Tang
  Centre Antoine Lacassagne, Nice, France

A B C D E F G H I J K L M N O P Q R S T U V W X Y Z

Hermansson, L.

Paper	Title	Page
VII-01	**Recent Commissioning Results at Celsius (Invited Paper)**	266

- **D. Reistad**, T. Bergmark, C. Ekström, C.-J. Fridén, K. Gajewski, L. Hermansson, P. Jahnke, A. Johansson, O. Johansson, T. Lofnes, G. Norman, R. Wedberg, L. Westerberg, J. Zlomanczuk
  Uppsala University, Uppsala, Sweden
- M.A. Raadu, M. Sedlacek
  Royal Institute of Technology, Stockholm, Sweden

A B C D E F G H I J K L M N O P Q R S T U V W X Y Z

Herschbach, M.

Paper	Title	Page
IXD-01	**The New Phase Detection System of the Cosy-Injector**	469

- **K. Kennepohl**, W. Bräutigam, M. Herschbach, D. Maeckelburg
  FZJ, Jülich, Germany

A B C D E F G H I J K L M N O P Q R S T U V W X Y Z

Hicks, J.W.

Paper	Title	Page
VIII-07	**Performance and Status of the IUCF High Intensity Polarized Ion Source**	330

- **V. Derenchuk**, R. Brown, T.J.P. Ellison, D.L. Friesel, J.W. Hicks, D. Jenner, A. Pei, H. Petri, P. Schwandt, J. Sowinski, M. Wedekind
  Indiana University, Bloomington, Indiana, USA

XD-02	**Beam Transport System for the IUCF High Intensity Polarized Ion Source**	609

- **W.P. Jones**, M.S. Ball, J.C. Collins, D. DuPlantis, T.J.P. Ellison, D.L. Friesel, B. Hamilton, J.W. Hicks, P. Schwandt
  Indiana University, Bloomington, Indiana, USA

A B C D E F G H I J K L M N O P Q R S T U V W X Y Z

Hirao, Y.

Paper	Title	Page
XD-07	**Beam Transport System for the HIMAC**	625

- **K. Noda**, Y. Hirao, A. Itano, M. Kanazawa, A. Kitagawa, T. Kohno, M. Kumada, H. Ogawa, K. Sato, Y. Sato, M. Sudou, E. Takada, S. Yamada, T. Yamada
  NIRS, Chiba, Japan
- K. Endo
  KEK, Ibaraki, Japan

A B C D E F G H I J K L M N O P Q R S T U V W X Y Z

Hoffmann, C.R.

Paper	Title	Page
XC-01	**The Electrostatic Deflector for the Chalk River Superconducting Cyclotron** • **W.T. Diamond**, C.R. Hoffmann, G.R. Mitchel, H. Schmeing Atomic Energy of Canada, Chalk River, Ontario, Canada	569
XC-02	**Potential Enhancement of Magnetic Deflection in the Chalk River Superconducting Cyclotron Extraction System** • **C.R. Hoffmann**, E.H. Lindqvist Atomic Energy of Canada, Chalk River, Ontario, Canada	573
XC-03	**Model Study of an Electrostatic Deflector Configuration with an Intermediate Electrode** • **C.R. Hoffmann**, J.F. Mouris Atomic Energy of Canada, Chalk River, Ontario, Canada	577

A B C D E F G H I J K L M N O P Q R S T U V W X Y Z

Hogan, M.E.

Paper	Title	Page
XI-06	**The New Distributed Control System of the NAC**	656

- **H.F. Weehuizen**, R.K. Fisch, E.J.S. Franklin, M.E. Hogan, I.H. Kohler, J.P. Rogers, P.J. Theron
  National Accelerator Centre, Faure, Republic of South Africa

A B C D E F G H I J K L M N O P Q R S T U V W X Y Z

Holm, S.

Paper	Title	Page
I-22	**Status Report on the Gustaf Werner Cyclotron in Uppsala**	106

- **S. Holm**
  Uppsala University, Uppsala, Sweden

A B C D E F G H I J K L M N O P Q R S T U V W X Y Z

Holmgren, B.

Paper	Title	Page
XA-13	**The RF System of the Gustaf Werner Cyclotron/Synchrocyclotron**	553

- **B. Lundström**, B. Holmgren
  Uppsala University, Uppsala, Sweden

A B C D E F G H I J K L M N O P Q R S T U V W X Y Z

Hoshika, K.

Paper	Title	Page
XI-04	**Control System for JAERI AVF Cyclotron**	648

- **S. Okumura**, T. Agematsu, K. Arakawa, M. Fukuda, I. Ishibori, T. Kamiya, Y. Nakamura, T. Nara, W. Yokota
  JAERI, Gunma, Japan
- K. Hoshika, K. Iso, M. Maruyama, M. Tachibana
  Sumitomo Heavy Industries, Ehime, Japan

A B C D E F G H I J K L M N O P Q R S T U V W X Y Z

Hosono, K.

Paper	Title	Page
I-01	**Commissioning of the RCNP Ring Cyclotron (Invited Paper)**	3

- **I. Miura**, A. Ando, K. Hatanaka, K. Hosono, H. Ikegami, T. Itahashi, M. Kibayashi, M. Kondo, H. Ogata, T. Saito, A. Shimizu, K. Tamura, M. Uraki, T. Yamazaki
  Osaka University, Osaka, Japan
- J. Abe
  Sumitomo Heavy Industries, Ehime, Japan

XB-03	**Sector Magnet of the RCNP Ring Cyclotron and the Isochronization**	565

- **K. Hosono**, M. Kibayashi, I. Miura
  Osaka University, Osaka, Japan

XI-10	**Construction and System Tuning of Control System for the RCNP Ring Cyclotron and Beam Lines**	672

- **T. Yamazaki**, A. Ando, K. Hosono, T. Itahashi, M. Kibayashi, I. Miura, K. Nagayama, H. Ogata, T. Saito, A. Shimizu, K. Tamura, M. Uraki
  Osaka University, Osaka, Japan
- K. Aoki, Y. Kimura, M. Maruyama, M. Tachibana, S. Yamada
  Sumitomo Heavy Industries, Ehime, Japan
- K. Kodaira
  Sumitomo Heavy Industries Systems Engineering Laboratory, Tokyo, Japan

A B C D E F G H I J K L M N O P Q R S T U V W X Y Z

Houtman, H.

Paper	Title	Page
IXA-11	**Developments in RELAX3D, a 2D/3D Laplace and Poisson Equation Solver**	411

- **H. Houtman**, F.W. Jones, C.J. Kost
  TRIUMF, Vancouver, Canada

A B C D E F G H I J K L M N O P Q R S T U V W X Y Z

Hubbard, R.E.

Paper	Title	Page
II-02	**The Operation of Cyclotrons Used for Radiopharmaceutical Production**	115

- **T. Grey-Morgan**
  Cyclotron Isotopes Manufacturing, Buckinghamshire, England
- R.E. Hubbard
  Medi + Physics Inc., Arlington Heights, Illinois, USA

A B C D E F G H I J K L M N O P Q R S T U V W X Y Z

Humbel, M.

Paper	Title	Page
I-05	**The Commissioning of PSI Injector 2 for High Intensity, High Quality Beams**	36

- **J. Stetson**
  NSCL, East Lansing, Michigan, USA
- S. Adam, M. Humbel, W. Joho, Th. Stammbach
  PSI, Villigen, Switzerland

A B C D E F G H I J K L M N O P Q R S T U V W X Y Z

Ichac, J.P.

Paper	Title	Page
XA-10	**RF Transmitter for ECR Ion Sources**	542

- **R. Boux**, J.P. Ichac, M. Soudée
  Thomson Tubes Electroniques, Velizy-Villacoublay, France

A B C D E F G H I J K L M N O P Q R S T U V W X Y Z

Ichida, S.

Paper	Title	Page
IXD-07	**Beam Diagnostics in the RCNP Ring Cyclotron**	491

- **T. Itahashi**, T. Saito, I. Miura
  Osaka University, Osaka, Japan
- S. Ichida
  Sumitomo Heavy Industries, Ehime, Japan

A B C D E F G H I J K L M N O P Q R S T U V W X Y Z

Ikegami, H.

Paper	Title	Page
I-01	**Commissioning of the RCNP Ring Cyclotron (Invited Paper)**	3

- **I. Miura**, A. Ando, K. Hatanaka, K. Hosono, H. Ikegami, T. Itahashi, M. Kibayashi, M. Kondo, H. Ogata, T. Saito, A. Shimizu, K. Tamura, M. Uraki, T. Yamazaki
  Osaka University, Osaka, Japan
- J. Abe
  Sumitomo Heavy Industries, Ehime, Japan

A B C D E F G H I J K L M N O P Q R S T U V W X Y Z

Iljasov, O.

Paper	Title	Page
II-04	**20 MeV Cyclotron for Isotope Production**	123

- **A. Glazov**, Ju. Alenitskiy, A. Chesnov, S. Chesnova, V. Kochkin, D. Novikov, E. Samsonov, M. Semenov, A. Vasilenko, E. Zaplatin, N. Zaplatin
  JINR, Dubna, Russia
- I. Gulamov, O. Iljasov, A. Rykov
  Institute of Nuclear Physics, Tashkent, Republic of Uzbekistan

A B C D E F G H I J K L M N O P Q R S T U V W X Y Z

Inada, T.

Paper	Title	Page
VI-08	**A Proton Therapy Facility Plan**	258

- **S. Fukumoto**, Y. Hayakawa, T. Inada, A. Maruhashi, M. Sato, J. Tada, Y. Takada, H. Tsuji, H. Tsujii
  University of Tsukuba, Ibaraki, Japan
- K. Endo, Y. Irie, K. Muto
  KEK, Ibaraki, Japan

A B C D E F G H I J K L M N O P Q R S T U V W X Y Z

Irie, Y.

Paper	Title	Page
VI-08	**A Proton Therapy Facility Plan**	258

- **S. Fukumoto**, Y. Hayakawa, T. Inada, A. Maruhashi, M. Sato, J. Tada, Y. Takada, H. Tsuji, H. Tsujii
  University of Tsukuba, Ibaraki, Japan
- K. Endo, Y. Irie, K. Muto
  KEK, Ibaraki, Japan

A B C D E F G H I J K L M N O P Q R S T U V W X Y Z

Ishibori, I.

Paper	Title	Page
II-03	**Construction and First Year's Operation of the JAERI AVF Cyclotron** • **K. Arakawa**, T. Agematsu, M. Fukuda, I. Ishibori, T. Karasawa, T. Nara, Y. Nakamura, S. Okumura, R. Tanaka, W. Yokota, JAERI, Gunma, Japan • A. Shimizu, Osaka University, Osaka, Japan • Y. Hayashi, K. Ishii, T. Satoh, T. Tachikawa, Sumitomo Heavy Industries, Ehime, Japan	119
VIII-09	**Operation of Ion Sources and Beam Transport to JAERI AVF Cyclotron** • **W. Yokota**, T. Agematsu, K. Arakawa, M. Fukuda, I. Ishibori, Y. Nakamura, T. Nara, S. Okumura, JAERI, Gunma, Japan • Y. Hayashi, K. Ishii, T. Tachikawa, Sumitomo Heavy Industries, Ehime, Japan	336
IXB-02	**Beam Studies of Injection to Extraction System for JAERI AVF Cyclotron** • **M. Fukuda**, T. Agematsu, K. Arakawa, I. Ishibori, T. Karasawa, Y. Nakamura, T. Nara, S. Okumura, W. Yokota, JAERI, Gunma, Japan	423
XC-04	**Performance of Beam Chopping System for JAERI AVF Cyclotron** • **W. Yokota**, T. Agematsu, K. Arakawa, M. Fukuda, I. Ishibori, Y. Nakamura, T. Nara, S. Okumura, JAERI, Gunma, Japan • Y. Hayashi, Y. Kumata, T. Tachikawa, Sumitomo Heavy Industries, Ehime, Japan	581
XI-04	**Control System for JAERI AVF Cyclotron** • **S. Okumura**, T. Agematsu, K. Arakawa, M. Fukuda, I. Ishibori, T. Kamiya, Y. Nakamura, T. Nara, W. Yokota, JAERI, Gunma, Japan • K. Hoshika, K. Iso, M. Maruyama, M. Tachibana, Sumitomo Heavy Industries, Ehime, Japan	648

A B C D E F G H I J K L M N O P Q R S T U V W X Y Z

Ishigaki, T.

Paper	Title	Page
II-06	**A Newly Developed Compact Cyclotron for Neutron Therapy and Positron Nuclear Medicine**	129

- **K. Ito**, T. Ishigaki, S. Itoh, Y. Kasugai, T. Kato, T. Misawa, M. Nishino, M. Osakabe, T. Ota, S. Sakuma, M. Tadokoro, H. Yamamoto
  Nagoya University, Nagoya, Japan
- Y. Toda, Y. Yamamoto
  Japan Steel Works Ltd., Tokyo, Japan

A B C D E F G H I J K L M N O P Q R S T U V W X Y Z

Ishii, K.

Paper	Title	Page
VIII-09	**Operation of Ion Sources and Beam Transport to JAERI AVF Cyclotron**	336

- **W. Yokota**, T. Agematsu, K. Arakawa, M. Fukuda, I. Ishibori, Y. Nakamura, T. Nara, S. Okumura
  JAERI, Gunma, Japan
- Y. Hayashi, K. Ishii, T. Tachikawa
  Sumitomo Heavy Industries, Ehime, Japan

II-03	**Construction and First Year's Operation of the JAERI AVF Cyclotron**	119

- **K. Arakawa**, T. Agematsu, M. Fukuda, I. Ishibori, T. Karasawa, T. Nara, Y. Nakamura, S. Okumura, R. Tanaka, W. Yokota
  JAERI, Gunma, Japan
- A. Shimizu
  Osaka University, Osaka, Japan
- Y. Hayashi, K. Ishii, T. Satoh, T. Tachikawa
  Sumitomo Heavy Industries, Ehime, Japan

A B C D E F G H I J K L M N O P Q R S T U V W X Y Z

Iso, K.

Paper	Title	Page
XI-04	**Control System for JAERI AVF Cyclotron**	648

- **S. Okumura**, T. Agematsu, K. Arakawa, M. Fukuda, I. Ishibori, T. Kamiya, Y. Nakamura, T. Nara, W. Yokota
  JAERI, Gunma, Japan
- K. Hoshika, K. Iso, M. Maruyama, M. Tachibana
  Sumitomo Heavy Industries, Ehime, Japan

A B C D E F G H I J K L M N O P Q R S T U V W X Y Z

Isoya, Y.

Paper	Title	Page
VIII-06	**An ECR Ion Source for Multiply-Charged Heavy Ions at 14 GHz**	326

- **M. Sekiguchi**, M. Fujita, Y. Ohshiro, T. Yamazaki
  University of Tokyo, Tanashi-shi, Tokyo, Japan
- Y. Isoya, T. Yamada, Y. Yamashita
  Japan Steel Works Ltd., Research Center for Advanced Technologies, Chiba, Japan
- A. Kitagawa
  NIRS, Chiba, Japan

A B C D E F G H I J K L M N O P Q R S T U V W X Y Z

Itahashi, T.

Paper	Title	Page
I-01	**Commissioning of the RCNP Ring Cyclotron (Invited Paper)**	3

- **I. Miura**, A. Ando, K. Hatanaka, K. Hosono, H. Ikegami, T. Itahashi, M. Kibayashi, M. Kondo, H. Ogata, T. Saito, A. Shimizu, K. Tamura, M. Uraki, T. Yamazaki
  Osaka University, Osaka, Japan
- J. Abe
  Sumitomo Heavy Industries, Ehime, Japan

IXD-07	**Beam Diagnostics in the RCNP Ring Cyclotron**	491

- **T. Itahashi**, T. Saito, I. Miura
  Osaka University, Osaka, Japan
- S. Ichida
  Sumitomo Heavy Industries, Ehime, Japan

XI-10	**Construction and System Tuning of Control System for the RCNP Ring Cyclotron and Beam Lines**	672

- **T. Yamazaki**, A. Ando, K. Hosono, T. Itahashi, M. Kibayashi, I. Miura, K. Nagayama, H. Ogata, T. Saito, A. Shimizu, K. Tamura, M. Uraki
  Osaka University, Osaka, Japan
- K. Aoki, Y. Kimura, M. Maruyama, M. Tachibana, S. Yamada
  Sumitomo Heavy Industries, Ehime, Japan
- K. Kodaira
  Sumitomo Heavy Industries Systems Engineering Laboratory, Tokyo, Japan

A B C D E F G H I J K L M N O P Q R S T U V W X Y Z

Itano, A.

Paper	Title	Page
XD-07	**Beam Transport System for the HIMAC**	625

- **K. Noda**, Y. Hirao, A. Itano, M. Kanazawa, A. Kitagawa, T. Kohno, M. Kumada, H. Ogawa, K. Sato, Y. Sato, M. Sudou, E. Takada, S. Yamada, T. Yamada
  NIRS, Chiba, Japan
- K. Endo
  KEK, Ibaraki, Japan

A B C D E F G H I J K L M N O P Q R S T U V W X Y Z

Ito, K.

Paper	Title	Page
II-06	**A Newly Developed Compact Cyclotron for Neutron Therapy and Positron Nuclear Medicine**	129

- **K. Ito**, T. Ishigaki, S. Itoh, Y. Kasugai, T. Kato, T. Misawa, M. Nishino, M. Osakabe, T. Ota, S. Sakuma, M. Tadokoro, H. Yamamoto
  Nagoya University, Nagoya, Japan
- Y. Toda, Y. Yamamoto
  Japan Steel Works Ltd., Tokyo, Japan

A B C D E F G H I J K L M N O P Q R S T U V W X Y Z

Itoh, S.

Paper	Title	Page
II-06	**A Newly Developed Compact Cyclotron for Neutron Therapy and Positron Nuclear Medicine**	129

- **K. Ito**, T. Ishigaki, S. Itoh, Y. Kasugai, T. Kato, T. Misawa, M. Nishino, M. Osakabe, T. Ota, S. Sakuma, M. Tadokoro, H. Yamamoto
  Nagoya University, Nagoya, Japan
- Y. Toda, Y. Yamamoto
  Japan Steel Works Ltd., Tokyo, Japan

A B C D E F G H I J K L M N O P Q R S T U V W X Y Z

Iudin, L.I.

Paper	Title	Page
IXD-02	**High-Sensitive Ionization Detectors of Transverse Distribution of Accelerated Particles Beam**	473

- **V.G. Mikhailov**, V.A. Rezvov, A.A. Roshchin, V.I. Sklyarenko, L.I. Iudin
  Kurchatov Institute, Moscow, Russia

XI-05	**Automatic Control System of Magnetic Separator for Kurchatov IAE Cyclotron**	652

- **N.I. Venikov**, V. Buranov, O. Gotovtsev, L.I. Iudin, P.Yu. Komissarov, V.N. Unezhev
  Kurchatov Institute, Moscow, Russia

A B C D E F G H I J K L M N O P Q R S T U V W X Y Z

Ivanenko, A.

Paper	Title	Page
I-02	**New Development at the JINR Heavy Ion Cyclotron Facility (Invited Paper)**	11

- **G.G. Gulbekyan**, V. Bekhterev, O. Borisov, B. Gikal, A. Ivanenko, I. Kolesov, V.B. Kutner, A. Morduev, Yu.Ts. Oganessian
  JINR, Dubna, Russia

A B C D E F G H I J K L M N O P Q R S T U V W X Y Z

Ivanov, E.M.

Paper	Title	Page
I-10	**Gatchina Isochronous Cyclotron**	58

- **N.K. Abrosimov**, S.A. Artamonov, P.V. Chervyakov, S.P. Dmitriev, V.A. Eliseev, V.P. Fominenko, E.M. Ivanov, G.F. Mikheev, Yu.T. Mironov, A.S. Pokrovskii, G.A. Riabov, V.A. Smolin, G.L. Sokolov, V.A. Volchenkov, A.A. Vorobiev
  Petersburg Nuclear Physics Institute, Gatchina, Russia
- P.V. Bogdanov, B.D. Ershov, V.S. Kuligin, V.N. Moshkin, V.G. Mudrolyubov, Yu.I. Stogov, A.P. Strokach
  D.V. Efremov Scientific Research Institute of Electrophysical Apparatus, St. Petersburg, Russia

A B C D E F G H I J K L M N O P Q R S T U V W X Y Z

Jacky, J.

Paper	Title	Page
VI-09	**Continued Operation of the Seattle Clinical Cyclotron Facility**	262

- **R. Risler**, S. Brossard, J. Jacky, I. Kalet, P. Wootton, F. Ziai
  University of Washington, Seattle, Washington, USA

XI-14	**Formal Specifications for a Cyclotron Control System**	689

- **J. Jacky**, R. Risler
  University of Washington, Seattle, Washington, USA

A B C D E F G H I J K L M N O P Q R S T U V W X Y Z

Jahnke, P.

Paper	Title	Page
VII-01	**Recent Commissioning Results at Celsius (Invited Paper)**	266

- **D. Reistad**, T. Bergmark, C. Ekström, C.-J. Fridén, K. Gajewski, L. Hermansson, P. Jahnke, A. Johansson, O. Johansson, T. Lofnes, G. Norman, R. Wedberg, L. Westerberg, J. Zlomanczuk
  Uppsala University, Uppsala, Sweden
- M.A. Raadu, M. Sedlacek
  Royal Institute of Technology, Stockholm, Sweden

A B C D E F G H I J K L M N O P Q R S T U V W X Y Z

Jayamanna, K.

Paper	Title	Page
VIII-05	**Status of the TRIUMF Optically-Pumped Polarized H^- Ion Source**	322

- **C.D.P. Levy**, K. Jayamanna, M. McDonald, R. Ruegg, P.W. Schmor
  TRIUMF, Vancouver, Canada
- A.N. Zelenskii
  Institute of Nuclear Research, Russian Academy of Sciences, Moscow, Russia

A B C D E F G H I J K L M N O P Q R S T U V W X Y Z

Jenner, D.

Paper	Title	Page
VIII-07	**Performance and Status of the IUCF High Intensity Polarized Ion Source**	330

- **V. Derenchuk**, R. Brown, T.J.P. Ellison, D.L. Friesel, J.W. Hicks, D. Jenner, A. Pei, H. Petri, P. Schwandt, J. Sowinski, M. Wedekind
  Indiana University, Bloomington, Indiana, USA

XA-05	**Low Frequency RF System for the Indiana University Cooler Ring**	523

- **X. Pei**, S. Anderson, V. Derenchuk, G. East, D.L. Friesel, D. Jenner, D. McCammon, T. Sloan
  Indiana University, Bloomington, Indiana, USA

A B C D E F G H I J K L M N O P Q R S T U V W X Y Z

Jeon, D.

Paper	Title	Page
IXA-08	**Evaluation of Third-Harmonic Voltage Flattopping for a Superconducting Cyclotron**	404

- **M.M. Gordon**, D. Jeon
  NSCL, East Lansing, Michigan, USA

A B C D E F G H I J K L M N O P Q R S T U V W X Y Z

Jiang, J.Z.

Paper	Title	Page
XD-05	**Buncher in the Beam Line from ECR to SFC**	618

- **J.Z. Jiang**, X.H. Zhou, Q. Wang, F. Wang, W.M. Jiang
  Institute of Modern Physics, Lanzhou, People's Republic of China

A B C D E F G H I J K L M N O P Q R S T U V W X Y Z

Jiang, W.M.

Paper	Title	Page
XD-05	**Buncher in the Beam Line from ECR to SFC**	618

- **J.Z. Jiang**, X.H. Zhou, Q. Wang, F. Wang, W.M. Jiang
  Institute of Modern Physics, Lanzhou, People's Republic of China

A B C D E F G H I J K L M N O P Q R S T U V W X Y Z

Joh, K.

Paper	Title	Page
IXC-05	**Numerical Studies for Suppression of Vertical Oscillations in the K1200 Cyclotron**	461

- **K. Joh**, F. Marti
  NSCL, East Lansing, Michigan, USA
- J.A. Nolen
  ANL, Argonne, Illinois, USA

A B C D E F G H I J K L M N O P Q R S T U V W X Y Z

Johansson, A.

Paper	Title	Page
VII-01	**Recent Commissioning Results at Celsius (Invited Paper)**	266

- **D. Reistad**, T. Bergmark, C. Ekström, C.-J. Fridén, K. Gajewski, L. Hermansson, P. Jahnke, A. Johansson, O. Johansson, T. Lofnes, G. Norman, R. Wedberg, L. Westerberg, J. Zlomanczuk
  Uppsala University, Uppsala, Sweden
- M.A. Raadu, M. Sedlacek
  Royal Institute of Technology, Stockholm, Sweden

A B C D E F G H I J K L M N O P Q R S T U V W X Y Z

Johansson, O.

Paper	Title	Page
VII-01	**Recent Commissioning Results at Celsius (Invited Paper)**	266

- **D. Reistad**, T. Bergmark, C. Ekström, C.-J. Fridén, K. Gajewski, L. Hermansson, P. Jahnke, A. Johansson, O. Johansson, T. Lofnes, G. Norman, R. Wedberg, L. Westerberg, J. Zlomanczuk
  Uppsala University, Uppsala, Sweden
- M.A. Raadu, M. Sedlacek
  Royal Institute of Technology, Stockholm, Sweden

A B C D E F G H I J K L M N O P Q R S T U V W X Y Z

Joho, W.

Paper	Title	Page
I-05	**The Commissioning of PSI Injector 2 for High Intensity, High Quality Beams**	36

- **J. Stetson**
  NSCL, East Lansing, Michigan, USA
- S. Adam, M. Humbel, W. Joho, Th. Stammbach
  PSI, Villigen, Switzerland

A B C D E F G H I J K L M N O P Q R S T U V W X Y Z

Jones, C.M.

Paper	Title	Page
XIII-07	**The ORNL Radioactive Ion Beam Project with the ORIC Accelerator**	741

- **D.K. Olsen**, G.D. Alton, C. Baktash, D.T. Dowling, J.D. Garrett, D.L. Haynes, C.M. Jones, R.C. Juras, S.N. Lane, I.Y. Lee, M.J. Meigs, G.D. Mills, S.W. Mosko, B.A. Tatum, K.S. Toth
  ORNL, Oak Ridge, Tennessee, USA
- H.K. Carter, J. Kormicki
  Associated Universities Oak Ridge, Oak Ridge, Tennessee, USA

A B C D E F G H I J K L M N O P Q R S T U V W X Y Z

Jones, F.W.

Paper	Title	Page
IXA-11	**Developments in RELAX3D, a 2D/3D Laplace and Poisson Equation Solver**	411

- **H. Houtman**, F.W. Jones, C.J. Kost
  TRIUMF, Vancouver, Canada

A B C D E F G H I J K L M N O P Q R S T U V W X Y Z

Jones, W.P.

Paper	Title	Page
XD-02	**Beam Transport System for the IUCF High Intensity Polarized Ion Source**	609

- **W.P. Jones**, M.S. Ball, J.C. Collins, D. DuPlantis, T.J.P. Ellison, D.L. Friesel, B. Hamilton, J.W. Hicks, P. Schwandt
  Indiana University, Bloomington, Indiana, USA

A B C D E F G H I J K L M N O P Q R S T U V W X Y Z

Jongen, Y.

Paper	Title	Page
VI-04	**Progress Report on the IBA-SHI Proton Therapy System**	244

- **Y. Jongen**, W. Beeckman, J.P. Dufour, A. Laisné, H. Marie, R. Verbruggen
  Ion Beam Applications, Louvain-la-Neuve, Belgium
- M. Sano, S. Satoh, N. Takahashi, T. Takayama
  Sumitomo Heavy Industries, Ehime, Japan

A B C D E F G H I J K L M N O P Q R S T U V W X Y Z

Josipovic, M.

Paper	Title	Page
XA-02	**The RF Coupling System of the VINCY Cyclotron**	511

- **B. Bojovic**, M. Josipovic, A. Susini
  CERN, Geneva, Switzerland

A B C D E F G H I J K L M N O P Q R S T U V W X Y Z

Joubert, J.

Paper	Title	Page
IV-02	**A Cyclotron as a Mass Spectrometer**	158

- **P. Bricault**, G. Auger, M. Bajard, E. Baron, D. Bibet, A. Chabert, J. Fermé, L. Gaudart, J. Joubert, M. Lewitowicz, W. Mittig, E. Plagnol, Ch. Ricaud, Y. Schutz
  GANIL, Caen, France
- G. Audi
  CSNSM, Orsay, France
- A. Gillibert
  CEN/Saclay, Gif-sur-Yvette, France
- K. Fifield
  Australian National University, Canberra , Australia

A B C D E F G H I J K L M N O P Q R S T U V W X Y Z

Jungwirth, H.N.

Paper	Title	Page
I-19	**Development of the NAC Accelerator Facilities**	95

- **J.L. Conradie**, A.H. Botha, P.M. Cronje, R.E.F. Fenemore, H.N. Jungwirth, J.J. Kritzinger, W.A.G. Nel, D. Reitmann, L.M.M. Roels, P.F. Rohwer, H.A. Smit
  National Accelerator Centre, Faure, Republic of South Africa

VIII-15	**Progress with the NAC Injector Cyclotron for Heavy and Polarized Ions**	361

- **Z.B. du Toit**, S.J. Burger, P.J. Celliers, J.G. de Villiers, H.N. Jungwirth, A. Müller, P.F. Rohwer, D.M. van Rooyen
  National Accelerator Centre, Faure, Republic of South Africa

XII-04	**A New Design Proposal for a 200 MeV Superconducting Ring-Cyclotron Magnet**	709

- **H.N. Jungwirth**, J.G. de Villiers
  National Accelerator Centre, Faure, Republic of South Africa

A B C D E F G H I J K L M N O P Q R S T U V W X Y Z

Juras, R.C.

Paper	Title	Page
XIII-07	**The ORNL Radioactive Ion Beam Project with the ORIC Accelerator**	741

- **D.K. Olsen**, G.D. Alton, C. Baktash, D.T. Dowling, J.D. Garrett, D.L. Haynes, C.M. Jones, R.C. Juras, S.N. Lane, I.Y. Lee, M.J. Meigs, G.D. Mills, S.W. Mosko, B.A. Tatum, K.S. Toth
  ORNL, Oak Ridge, Tennessee, USA
- H.K. Carter, J. Kormicki
  Associated Universities Oak Ridge, Oak Ridge, Tennessee, USA

A B C D E F G H I J K L M N O P Q R S T U V W X Y Z

Kadantsev, S.

Paper	Title	Page
XI-11	**Early Experience with DECwindows/Motif in the TRIUMF Central Control System**	676

- **S. Kadantsev**
  JINR, Dubna, Russia
- M. Mouat
  TRIUMF, Vancouver, Canada

A B C D E F G H I J K L M N O P Q R S T U V W X Y Z

Kageyama, T.

Paper	Title	Page
VIII-16	**Plasma Cathode Method for RIKEN ECRIS**	365

- **T. Nakagawa**, A. Goto, T. Kageyama, M. Kase, Y. Yano
  RIKEN, Saitama, Japan

A B C D E F G H I J K L M N O P Q R S T U V W X Y Z

Kalet, I.

Paper	Title	Page
VI-09	**Continued Operation of the Seattle Clinical Cyclotron Facility**	262

- **R. Risler**, S. Brossard, J. Jacky, I. Kalet, P. Wootton, F. Ziai
  University of Washington, Seattle, Washington, USA

A B C D E F G H I J K L M N O P Q R S T U V W X Y Z

Kamiya, T.

Paper	Title	Page
XI-04	**Control System for JAERI AVF Cyclotron**	648

- **S. Okumura**, T. Agematsu, K. Arakawa, M. Fukuda, I. Ishibori, T. Kamiya, Y. Nakamura, T. Nara, W. Yokota
  JAERI, Gunma, Japan
- K. Hoshika, K. Iso, M. Maruyama, M. Tachibana
  Sumitomo Heavy Industries, Ehime, Japan

A B C D E F G H I J K L M N O P Q R S T U V W X Y Z

Kanazawa, M.

Paper	Title	Page
VII-04	**Study of Beam Dynamics at Cooler Synchrotron TARN-II**	286

- **S. Watanabe**, Y. Arakaki, K. Chida, T. Katayama, M. Tomizawa, T. Watanabe, M. Yoshizawa
  University of Tokyo, Tanashi-shi, Tokyo, Japan
- K. Noda, M. Kanazawa
  NIRS, Chiba, Japan

XD-07	**Beam Transport System for the HIMAC**	625

- **K. Noda**, Y. Hirao, A. Itano, M. Kanazawa, A. Kitagawa, T. Kohno, M. Kumada, H. Ogawa, K. Sato, Y. Sato, M. Sudou, E. Takada, S. Yamada, T. Yamada
  NIRS, Chiba, Japan
- K. Endo
  KEK, Ibaraki, Japan

A B C D E F G H I J K L M N O P Q R S T U V W X Y Z

Kaplanski, J.M.

Paper	Title	Page
IXD-06	**The Diagnostics System for the AGOR Superconducting Cyclotron**	487

- **B. Launé**, P. Dambre, J.M. Kaplanski, B. Montsanglant, C. Olivetto, D. Vincent
  IPN, Orsay, France

A B C D E F G H I J K L M N O P Q R S T U V W X Y Z

Karamian, S.A.

Paper	Title	Page
IV-04	^{178m2}Hf and ^{237}Pu Isotopes Production on the U-200 Cyclotron	167

- **S.L. Bogomolov**, S.N. Dmitriev, Yu.P. Gangrski, G.G. Gulbekyan, S.A. Karamian, V.B. Kutner, B.N. Markov, Yu.Ts. Oganessian, N.V. Pronin, G.Ya. Starodub
  JINR, Dubna, Russia

A B C D E F G H I J K L M N O P Q R S T U V W X Y Z

Karasawa, T.

Paper	Title	Page
II-03	**Construction and First Year's Operation of the JAERI AVF Cyclotron**	119

- **K. Arakawa**, T. Agematsu, M. Fukuda, I. Ishibori, T. Karasawa, T. Nara, Y. Nakamura, S. Okumura, R. Tanaka, W. Yokota
  JAERI, Gunma, Japan
- A. Shimizu
  Osaka University, Osaka, Japan
- Y. Hayashi, K. Ishii, T. Satoh, T. Tachikawa
  Sumitomo Heavy Industries, Ehime, Japan

IXB-02	**Beam Studies of Injection to Extraction System for JAERI AVF Cyclotron**	423

- **M. Fukuda**, T. Agematsu, K. Arakawa, I. Ishibori, T. Karasawa, Y. Nakamura, T. Nara, S. Okumura, W. Yokota
  JAERI, Gunma, Japan

XA-06	**A Modified RF System of JAERI AVF Cyclotron**	526

- **Y. Kumata**, Y. Fukumoto
  Sumitomo Heavy Industries, Ehime, Japan
- K. Arakawa, M. Fukuda, T. Karasawa
  JAERI, Gunma, Japan
- A. Shimizu
  Osaka University, Osaka, Japan

A B C D E F G H I J K L M N O P Q R S T U V W X Y Z

Kase, M.

Paper	Title	Page
VIII-16	**Plasma Cathode Method for RIKEN ECRIS**	365

- **T. Nakagawa**, A. Goto, T. Kageyama, M. Kase, Y. Yano
  RIKEN, Saitama, Japan

A B C D E F G H I J K L M N O P Q R S T U V W X Y Z

Kasugai, Y.

Paper	Title	Page
II-06	**A Newly Developed Compact Cyclotron for Neutron Therapy and Positron Nuclear Medicine**	129

- **K. Ito**, T. Ishigaki, S. Itoh, Y. Kasugai, T. Kato, T. Misawa, M. Nishino, M. Osakabe, T. Ota, S. Sakuma, M. Tadokoro, H. Yamamoto
  Nagoya University, Nagoya, Japan
- Y. Toda, Y. Yamamoto
  Japan Steel Works Ltd., Tokyo, Japan

A B C D E F G H I J K L M N O P Q R S T U V W X Y Z

Katayama, T.

Paper	Title	Page
VII-04	**Study of Beam Dynamics at Cooler Synchrotron TARN-II**	286

- **S. Watanabe**, Y. Arakaki, K. Chida, T. Katayama, M. Tomizawa, T. Watanabe, M. Yoshizawa
  University of Tokyo, Tanashi-shi, Tokyo, Japan
- K. Noda, M. Kanazawa
  NIRS, Chiba, Japan

A B C D E F G H I J K L M N O P Q R S T U V W X Y Z

Kato, T.

Paper	Title	Page
II-06	**A Newly Developed Compact Cyclotron for Neutron Therapy and Positron Nuclear Medicine**	129

- **K. Ito**, T. Ishigaki, S. Itoh, Y. Kasugai, T. Kato, T. Misawa, M. Nishino, M. Osakabe, T. Ota, S. Sakuma, M. Tadokoro, H. Yamamoto
  Nagoya University, Nagoya, Japan
- Y. Toda, Y. Yamamoto
  Japan Steel Works Ltd., Tokyo, Japan

A B C D E F G H I J K L M N O P Q R S T U V W X Y Z

Keitel, R.

Paper	Title	Page
XI-13	**The TR30 Control System - A Case for Off-the-Shelf Software**	685

- **R. Keitel**, D.J. Dale, B.F. Milton
  TRIUMF, Vancouver, Canada

A B C D E F G H I J K L M N O P Q R S T U V W X Y Z

Kennepohl, K.

Paper	Title	Page
IXD-01	**The New Phase Detection System of the Cosy-Injector**	469

- **K. Kennepohl**, W. Bräutigam, M. Herschbach, D. Maeckelburg
  FZJ, Jülich, Germany

A B C D E F G H I J K L M N O P Q R S T U V W X Y Z

Khalkin, V.A.

Paper	Title	Page
V-04	**Possibility of Producing Some Radionuclides for Medicine Using JINR Accelerators**	213

- **S.N. Dmitriev**, G.G. Gulbekyan, V.A. Khalkin, R.Ts. Oganessian, L.M. Onishchenko, G.Ya. Starodub, N.G. Zaitseva
  JINR, Dubna, Russia

A B C D E F G H I J K L M N O P Q R S T U V W X Y Z

Kibayashi, M.

Paper	Title	Page
I-01	**Commissioning of the RCNP Ring Cyclotron (Invited Paper)**	3

- **I. Miura**, A. Ando, K. Hatanaka, K. Hosono, H. Ikegami, T. Itahashi, M. Kibayashi, M. Kondo, H. Ogata, T. Saito, A. Shimizu, K. Tamura, M. Uraki, T. Yamazaki
  Osaka University, Osaka, Japan
- J. Abe
  Sumitomo Heavy Industries, Ehime, Japan

XB-03	**Sector Magnet of the RCNP Ring Cyclotron and the Isochronization**	565

- **K. Hosono**, M. Kibayashi, I. Miura
  Osaka University, Osaka, Japan

XI-10	**Construction and System Tuning of Control System for the RCNP Ring Cyclotron and Beam Lines**	672

- **T. Yamazaki**, A. Ando, K. Hosono, T. Itahashi, M. Kibayashi, I. Miura, K. Nagayama, H. Ogata, T. Saito, A. Shimizu, K. Tamura, M. Uraki
  Osaka University, Osaka, Japan
- K. Aoki, Y. Kimura, M. Maruyama, M. Tachibana, S. Yamada
  Sumitomo Heavy Industries, Ehime, Japan
- K. Kodaira
  Sumitomo Heavy Industries Systems Engineering Laboratory, Tokyo, Japan

A B C D E F G H I J K L M N O P Q R S T U V W X Y Z

Kiewiet, H.H.

Paper	Title	Page
IXD-03	**A Beam Profile Monitor Using the Ionization of Residual Gas**	477

- **J.M. Schippers**, H.H. Kiewiet
  Kernfysisch Versneller Instituut, Groningen, The Netherlands

A B C D E F G H I J K L M N O P Q R S T U V W X Y Z

Kim, J.W.

Paper	Title	Page
VIII-14	**Plan for the Ion Source Emittance Measurement Under the RF Extraction**	357

- **J.W. Kim**, H.G. Blosser
  NSCL, East Lansing, Michigan, USA

A B C D E F G H I J K L M N O P Q R S T U V W X Y Z

Kimura, Y.

Paper	Title	Page
XI-10	**Construction and System Tuning of Control System for the RCNP Ring Cyclotron and Beam Lines**	672

- **T. Yamazaki**, A. Ando, K. Hosono, T. Itahashi, M. Kibayashi, I. Miura, K. Nagayama, H. Ogata, T. Saito, A. Shimizu, K. Tamura, M. Uraki
  Osaka University, Osaka, Japan
- K. Aoki, Y. Kimura, M. Maruyama, M. Tachibana, S. Yamada
  Sumitomo Heavy Industries, Ehime, Japan
- K. Kodaira
  Sumitomo Heavy Industries Systems Engineering Laboratory, Tokyo, Japan

A B C D E F G H I J K L M N O P Q R S T U V W X Y Z

King, J.

Paper	Title	Page
XIII-08	**Research and Development Studies with Radioactive Beams at TRIUMF**	745

- **J.M. D'Auria**, M. Dombsky
  Simon Fraser University, Burnaby, BC, Canada
- L. Buchmann, H. Sprenger, J.S. Vincent
  TRIUMF, Vancouver, Canada
- J. King
  University of Toronto, Toronto, Ontario, Canada
- P. McNeely, G. Roy
  University of Alberta, Edmonton, Alberta, Canada

A B C D E F G H I J K L M N O P Q R S T U V W X Y Z

Kitagawa, A.

Paper	Title	Page
VIII-06	**An ECR Ion Source for Multiply-Charged Heavy Ions at 14 GHz**	326

- **M. Sekiguchi**, M. Fujita, Y. Ohshiro, T. Yamazaki
  University of Tokyo, Tanashi-shi, Tokyo, Japan
- Y. Isoya, T. Yamada, Y. Yamashita
  Japan Steel Works Ltd., Research Center for Advanced Technologies, Chiba, Japan
- A. Kitagawa
  NIRS, Chiba, Japan

XD-07	**Beam Transport System for the HIMAC**	625

- **K. Noda**, Y. Hirao, A. Itano, M. Kanazawa, A. Kitagawa, T. Kohno, M. Kumada, H. Ogawa, K. Sato, Y. Sato, M. Sudou, E. Takada, S. Yamada, T. Yamada
  NIRS, Chiba, Japan
- K. Endo
  KEK, Ibaraki, Japan

A B C D E F G H I J K L M N O P Q R S T U V W X Y Z

Kleeven, W.J.G.M.

Paper	Title	Page
IXA-02	**The Influence of Magnetic Field Imperfections on the Beam Quality in an H^- Cyclotron**	380

- **W.J.G.M. Kleeven**, H.L. Hagedoorn
  Eindhoven University of Technology, Eindhoven, The Netherlands
- B.F. Milton, G. Dutto
  TRIUMF, Vancouver, Canada

Paper	Title	Page
IXA-03	**Emittance Growth in Nonlinear Beam Guiding and Focusing Elements**	384

- **W.J.G.M. Kleeven**, J.I.M. Botman, J.L. Delhez, H.L. Hagedoorn, C.J. Timmermans, G.A. Webers
  Eindhoven University of Technology, Eindhoven, The Netherlands

A B C D E F G H I J K L M N O P Q R S T U V W X Y Z

Kleinrahm, A.

Paper	Title	Page
IV-05	**Radionuclide Technique in Mechanical Engineering (RTM)**	171

- **P. Fehsenfeld**, A. Kleinrahm
  FZK, Karlsruhe, Germany
- V. Novikov
  Kurchatov Institute, Moscow, Russia

A B C D E F G H I J K L M N O P Q R S T U V W X Y Z

Ko, J.

Paper	Title	Page
IV-12	**A Remotely Controlled Robotic Vehicle for Work Within Radioactive Environments**	198

- **N.R. Stevenson**, P. Bloemhard, M. Brigham, J. Ko, C. LaForge, J. Orzechowski, E. Pattyn, T. Rattray
  TRIUMF, Vancouver, Canada

A B C D E F G H I J K L M N O P Q R S T U V W X Y Z

Kochkin, V.

Paper	Title	Page
II-04	**20 MeV Cyclotron for Isotope Production**	123

- **A. Glazov**, Ju. Alenitskiy, A. Chesnov, S. Chesnova, V. Kochkin, D. Novikov, E. Samsonov, M. Semenov, A. Vasilenko, E. Zaplatin, N. Zaplatin
  JINR, Dubna, Russia
- I. Gulamov, O. Iljasov, A. Rykov
  Institute of Nuclear Physics, Tashkent, Republic of Uzbekistan

A B C D E F G H I J K L M N O P Q R S T U V W X Y Z

Kodaira, K.

Paper	Title	Page
XI-10	**Construction and System Tuning of Control System for the RCNP Ring Cyclotron and Beam Lines**	672

- **T. Yamazaki**, A. Ando, K. Hosono, T. Itahashi, M. Kibayashi, I. Miura, K. Nagayama, H. Ogata, T. Saito, A. Shimizu, K. Tamura, M. Uraki
  Osaka University, Osaka, Japan
- K. Aoki, Y. Kimura, M. Maruyama, M. Tachibana, S. Yamada
  Sumitomo Heavy Industries, Ehime, Japan
- K. Kodaira
  Sumitomo Heavy Industries Systems Engineering Laboratory, Tokyo, Japan

A B C D E F G H I J K L M N O P Q R S T U V W X Y Z

Kohler, I.H.

Paper	Title	Page
XI-06	**The New Distributed Control System of the NAC**	656

- **H.F. Weehuizen**, R.K. Fisch, E.J.S. Franklin, M.E. Hogan, I.H. Kohler, J.P. Rogers, P.J. Theron
  National Accelerator Centre, Faure, Republic of South Africa

A B C D E F G H I J K L M N O P Q R S T U V W X Y Z

Kohno, T.

Paper	Title	Page
XD-07	**Beam Transport System for the HIMAC**	625

- **K. Noda**, Y. Hirao, A. Itano, M. Kanazawa, A. Kitagawa, T. Kohno, M. Kumada, H. Ogawa, K. Sato, Y. Sato, M. Sudou, E. Takada, S. Yamada, T. Yamada
  NIRS, Chiba, Japan
- K. Endo
  KEK, Ibaraki, Japan

Kokorin, A.M.

Paper	Title	Page
VII-06	**The New Project of INR (Kiev's) Storage-Accelerating Complex**	294

- **A.V. Dolinsky**, A.I. Papash, S.N. Pavlov, A.T. Rudchik, A.E. Val'Kov, I.N. Vishnevsky, A.V. Zhmendak
  Institute for Nuclear Research, Kiev, Ukraine
- V.P. Belov, A.M. Kokorin, A.A. Makarov, I.A. Schukeilo, Yu.P. Severgin
  D.V. Efremov Scientific Research Institute of Electrophysical Apparatus, St. Petersburg, Russia

A B C D E F G H I J K L M N O P Q R S T U V W X Y Z

Kolesov, I.

Paper	Title	Page
I-02	**New Development at the JINR Heavy Ion Cyclotron Facility (Invited Paper)**	11

- **G.G. Gulbekyan**, V. Bekhterev, O. Borisov, B. Gikal, A. Ivanenko, I. Kolesov, V.B. Kutner, A. Morduev, Yu.Ts. Oganessian
  JINR, Dubna, Russia

A B C D E F G H I J K L M N O P Q R S T U V W X Y Z

Komissarov, P.Yu.

Paper	Title	Page
II-05	**Status of a Compact H^- Cyclotron at the Kurchatov Institute of Atomic Energy**	126

- **N.I. Venikov**, C.D. Burbeza, P.Yu. Komissarov, Yu.M. Krasnikov, S.T. Latushkin, V.V. Leonov, V.P. Moryakov, I.V. Naumov, A.Ya. Pisman, V.A. Rezvov, A.A. Vasiliev, V.E. Yarosh, L.I. Yudin
  Kurchatov Institute, Moscow, Russia

Paper	Title	Page
XI-05	**Automatic Control System of Magnetic Separator for Kurchatov IAE Cyclotron**	652

- **N.I. Venikov**, V. Buranov, O. Gotovtsev, L.I. Iudin, P.Yu. Komissarov, V.N. Unezhev
  Kurchatov Institute, Moscow, Russia

A B C D E F G H I J K L M N O P Q R S T U V W X Y Z

Kondo, M.

Paper	Title	Page
I-01	**Commissioning of the RCNP Ring Cyclotron (Invited Paper)**	3

- **I. Miura**, A. Ando, K. Hatanaka, K. Hosono, H. Ikegami, T. Itahashi, M. Kibayashi, M. Kondo, H. Ogata, T. Saito, A. Shimizu, K. Tamura, M. Uraki, T. Yamazaki
  Osaka University, Osaka, Japan
- J. Abe
  Sumitomo Heavy Industries, Ehime, Japan

A B C D E F G H I J K L M N O P Q R S T U V W X Y Z

Korenev, S.A.

Paper	Title	Page
VIII-08	**Ion Source of Discharge Type**	334

- **I.B. Enchevich**
  TRIUMF, Vancouver, Canada
- S.A. Korenev
  JINR, Dubna, Russia

Kormicki, J.

Paper	Title	Page
XIII-07	**The ORNL Radioactive Ion Beam Project with the ORIC Accelerator**	741

- **D.K. Olsen**, G.D. Alton, C. Baktash, D.T. Dowling, J.D. Garrett, D.L. Haynes, C.M. Jones, R.C. Juras, S.N. Lane, I.Y. Lee, M.J. Meigs, G.D. Mills, S.W. Mosko, B.A. Tatum, K.S. Toth
  ORNL, Oak Ridge, Tennessee, USA
- H.K. Carter, J. Kormicki
  Associated Universities Oak Ridge, Oak Ridge, Tennessee, USA

A B C D E F G H I J K L M N O P Q R S T U V W X Y Z

Korolev, L.E.

Paper	Title	Page
XD-01	**Some Perspectives in the Beam Transport and Analyzing System Design for the U-250 Cyclotron**	606

- **L.E. Korolev**
  D.V. Efremov Scientific Research Institute of Electrophysical Apparatus, St. Petersburg, Russia

A B C D E F G H I J K L M N O P Q R S T U V W X Y Z

Kost, C.J.

Paper	Title	Page
IXA-11	**Developments in RELAX3D, a 2D/3D Laplace and Poisson Equation Solver**	411

- **H. Houtman**, F.W. Jones, C.J. Kost
  TRIUMF, Vancouver, Canada

A B C D E F G H I J K L M N O P Q R S T U V W X Y Z

Kozin, A.I.

Paper	Title	Page
V-05	**Radiopharmaceutical "Thallium-201-Chloride" Production using Thallium-203 Irradiation by Helium-3 Ions**	216

- **A.A. Arzumanov**, N.K. Hamidov, A.I. Kozin, G.I. Shychikov, S.T. Tihomirova
  Kazakhstan Academy of Sciences, Alma-Ata, Republic of Kazakhstan

A B C D E F G H I J K L M N O P Q R S T U V W X Y Z

Krasnikov, Yu.M.

Paper	Title	Page
II-05	**Status of a Compact H^- Cyclotron at the Kurchatov Institute of Atomic Energy**	126

- **N.I. Venikov**, C.D. Burbeza, P.Yu. Komissarov, Yu.M. Krasnikov, S.T. Latushkin, V.V. Leonov, V.P. Moryakov, I.V. Naumov, A.Ya. Pisman, V.A. Rezvov, A.A. Vasiliev, V.E. Yarosh, L.I. Yudin
  Kurchatov Institute, Moscow, Russia

A B C D E F G H I J K L M N O P Q R S T U V W X Y Z

Kritzinger, J.J.

Paper	Title	Page
I-19	**Development of the NAC Accelerator Facilities**	95

- **J.L. Conradie**, A.H. Botha, P.M. Cronje, R.E.F. Fenemore, H.N. Jungwirth, J.J. Kritzinger, W.A.G. Nel, D. Reitmann, L.M.M. Roels, P.F. Rohwer, H.A. Smit
  National Accelerator Centre, Faure, Republic of South Africa

A B C D E F G H I J K L M N O P Q R S T U V W X Y Z

Krivánek, M.

Paper	Title	Page
IXC-06	**Experiments on the Axial Injection System of the Cyclotron U-120M**	465

- **Z. Trejbal**, M. Krivánek, J. Kucera, V. Bejsovec, J. Stursa
  Czechoslovak Academy of Sciences, Rez, Czechoslovakia

A B C D E F G H I J K L M N O P Q R S T U V W X Y Z

Kucera, J.

Paper	Title	Page
IXC-06	**Experiments on the Axial Injection System of the Cyclotron U-120M**	465

- **Z. Trejbal**, M. Krivánek, J. Kucera, V. Bejsovec, J. Stursa
  Czechoslovak Academy of Sciences, Rez, Czechoslovakia

A B C D E F G H I J K L M N O P Q R S T U V W X Y Z

Kuchar, J.

Paper	Title	Page
IXB-04	**Selection and Measurement of RF Phase Width of the K1200 Cyclotron Beam**	431

- **J. Bailey**, J. Kuchar, F. Marti, J. Yurkon
  NSCL, East Lansing, Michigan, USA
- J.A. Nolen
  ANL, Argonne, Illinois, USA
- D. Rifuggiato
  INFN/LNS, Catania, Italy

A B C D E F G H I J K L M N O P Q R S T U V W X Y Z

Kuligin, V.S.

Paper	Title	Page
I-10	**Gatchina Isochronous Cyclotron**	58

- **N.K. Abrosimov**, S.A. Artamonov, P.V. Chervyakov, S.P. Dmitriev, V.A. Eliseev, V.P. Fominenko, E.M. Ivanov, G.F. Mikheev, Yu.T. Mironov, A.S. Pokrovskii, G.A. Riabov, V.A. Smolin, G.L. Sokolov, V.A. Volchenkov, A.A. Vorobiev
  Petersburg Nuclear Physics Institute, Gatchina, Russia
- P.V. Bogdanov, B.D. Ershov, V.S. Kuligin, V.N. Moshkin, V.G. Mudrolyubov, Yu.I. Stogov, A.P. Strokach
  D.V. Efremov Scientific Research Institute of Electrophysical Apparatus, St. Petersburg, Russia

A B C D E F G H I J K L M N O P Q R S T U V W X Y Z

Kumada, M.

Paper	Title	Page
XD-07	**Beam Transport System for the HIMAC**	625

- **K. Noda**, Y. Hirao, A. Itano, M. Kanazawa, A. Kitagawa, T. Kohno, M. Kumada, H. Ogawa, K. Sato, Y. Sato, M. Sudou, E. Takada, S. Yamada, T. Yamada
  NIRS, Chiba, Japan
- K. Endo
  KEK, Ibaraki, Japan

A B C D E F G H I J K L M N O P Q R S T U V W X Y Z

Kumata, Y.

Paper	Title	Page
XA-06	**A Modified RF System of JAERI AVF Cyclotron**	526

- **Y. Kumata**, Y. Fukumoto
  Sumitomo Heavy Industries, Ehime, Japan
- K. Arakawa, M. Fukuda, T. Karasawa
  JAERI, Gunma, Japan
- A. Shimizu
  Osaka University, Osaka, Japan

XC-04	**Performance of Beam Chopping System for JAERI AVF Cyclotron**	581

- **W. Yokota**, T. Agematsu, K. Arakawa, M. Fukuda, I. Ishibori, Y. Nakamura, T. Nara, S. Okumura
  JAERI, Gunma, Japan
- Y. Hayashi, Y. Kumata, T. Tachikawa
  Sumitomo Heavy Industries, Ehime, Japan

A B C D E F G H I J K L M N O P Q R S T U V W X Y Z

Kunkel, W.B.

Paper	Title	Page
XB-02	**A Permanent Magnet System for a Cyclotron Used as a Mass Spectrometer** • **C.Y. Li**, M. Cooper, K. Halbach, W.B. Kunkel, K.N. Leung, R.P. Wells, A.T. Young LBL, Berkeley, California, USA	561
XII-03	**Design of a Compact Permanent Magnet Cyclotron Mass Spectrometer for the Detection and Measurement of Trace Isotopes** • **A.T. Young**, K.J. Bertsche, D.J. Clark, K. Halbach, W.B. Kunkel, K.N. Leung, C.Y. Li LBL, Berkeley, California, USA	705

A B C D E F G H I J K L M N O P Q R S T U V W X Y Z

Kuo, T.Y.T.

Paper	Title	Page
VIII-13	**Recent Development of Internal H^-/D^- Source for Compact Cyclotrons**	352

- **T.Y.T. Kuo**
  TRIUMF, Vancouver, Canada
- G.O. Hendry
  Cyclotron Inc., Napa, California, USA

XC-08	**Deflector Development for the K1200 Cyclotron**	596

- **T.Y.T. Kuo**
  TRIUMF, Vancouver, Canada
- J.A. Nolen
  ANL, Argonne, Illinois, USA

A B C D E F G H I J K L M N O P Q R S T U V W X Y Z

Kutner, V.B.

Paper	Title	Page
I-02	**New Development at the JINR Heavy Ion Cyclotron Facility (Invited Paper)**	11

- **G.G. Gulbekyan**, V. Bekhterev, O. Borisov, B. Gikal, A. Ivanenko, I. Kolesov, V.B. Kutner, A. Morduev, Yu.Ts. Oganessian
  JINR, Dubna, Russia

Paper	Title	Page
IV-04	**^{178m2}Hf and ^{237}Pu Isotopes Production on the U-200 Cyclotron**	167

- **S.L. Bogomolov**, S.N. Dmitriev, Yu.P. Gangrski, G.G. Gulbekyan, S.A. Karamian, V.B. Kutner, B.N. Markov, Yu.Ts. Oganessian, N.V. Pronin, G.Ya. Starodub
  JINR, Dubna, Russia

A B C D E F G H I J K L M N O P Q R S T U V W X Y Z

Laborie, G.

Paper	Title	Page
I-11	**Status Report of SARA**	62

- **M. Fruneau**, S. Albrand, D. Barnéoud, J.L. Belmont, G. Bizouard, J.L. Bouly, G. Campillo, M. Guisset, G. Laborie
  Université Joseph Fourier, Grenoble, France

A B C D E F G H I J K L M N O P Q R S T U V W X Y Z

LaForge, C.

Paper	Title	Page
IV-12	**A Remotely Controlled Robotic Vehicle for Work Within Radioactive Environments**	198

- **N.R. Stevenson**, P. Bloemhard, M. Brigham, J. Ko, C. LaForge, J. Orzechowski, E. Pattyn, T. Rattray
  TRIUMF, Vancouver, Canada

A B C D E F G H I J K L M N O P Q R S T U V W X Y Z

Lafoux, A.

Paper	Title	Page
XD-03	**Superconducting Focussing Channel for the AGOR Cyclotron**	612

- **H.W. Schreuder**, P. Blache, C. Commeaux, S. Gustafsson, A. Lafoux, M. Mormiche, R. Panvier
  IPN, Orsay, France

A B C D E F G H I J K L M N O P Q R S T U V W X Y Z

Laisné, A.

Paper	Title	Page
VI-04	**Progress Report on the IBA-SHI Proton Therapy System**	244

- **Y. Jongen**, W. Beeckman, J.P. Dufour, A. Laisné, H. Marie, R. Verbruggen
  Ion Beam Applications, Louvain-la-Neuve, Belgium
- M. Sano, S. Satoh, N. Takahashi, T. Takayama
  Sumitomo Heavy Industries, Ehime, Japan

A B C D E F G H I J K L M N O P Q R S T U V W X Y Z

Lane, S.N.

Paper	Title	Page
XIII-07	**The ORNL Radioactive Ion Beam Project with the ORIC Accelerator**	741

- **D.K. Olsen**, G.D. Alton, C. Baktash, D.T. Dowling, J.D. Garrett, D.L. Haynes, C.M. Jones, R.C. Juras, S.N. Lane, I.Y. Lee, M.J. Meigs, G.D. Mills, S.W. Mosko, B.A. Tatum, K.S. Toth
  ORNL, Oak Ridge, Tennessee, USA
- H.K. Carter, J. Kormicki
  Associated Universities Oak Ridge, Oak Ridge, Tennessee, USA

A B C D E F G H I J K L M N O P Q R S T U V W X Y Z

Lanz, P.

Paper	Title	Page
XA-03	**Dual Frequency Resonator System for a Compact Cyclotron**	515

- **M. Eiche**, K.L. Erdman
  Ebco Technologies Ltd, Richmond, BC, Canada
- P. Lanz, M. Lipnicki, M. Zach
  TRIUMF, Vancouver, Canada

A B C D E F G H I J K L M N O P Q R S T U V W X Y Z

Latushkin, S.T.

Paper	Title	Page
II-05	**Status of a Compact H^- Cyclotron at the Kurchatov Institute of Atomic Energy**	126

- **N.I. Venikov**, C.D. Burbeza, P.Yu. Komissarov, Yu.M. Krasnikov, S.T. Latushkin, V.V. Leonov, V.P. Moryakov, I.V. Naumov, A.Ya. Pisman, V.A. Rezvov, A.A. Vasiliev, V.E. Yarosh, L.I. Yudin
  Kurchatov Institute, Moscow, Russia

A B C D E F G H I J K L M N O P Q R S T U V W X Y Z

Launé, B.

Paper	Title	Page
IXD-06	**The Diagnostics System for the AGOR Superconducting Cyclotron**	487

- **B. Launé**, P. Dambre, J.M. Kaplanski, B. Montsanglant, C. Olivetto, D. Vincent
  IPN, Orsay, France

A B C D E F G H I J K L M N O P Q R S T U V W X Y Z

Laxdal, R.E.

Paper	Title	Page
IXA-12	**Beam Quality Investigations for H^- Extraction at TRIUMF**	415
	• **R.E. Laxdal**, G.H. Mackenzie, J.B. Pearson, L. Root TRIUMF, Vancouver, Canada	
IXB-07	**Beam Test Results Using the Auxiliary Accelerating Cavity**	442
	• **R.E. Laxdal**, G.H. Mackenzie, L. Root TRIUMF, Vancouver, Canada	

A B C D E F G H I J K L M N O P Q R S T U V W X Y Z

Lee, I.Y.

Paper	Title	Page
XIII-07	**The ORNL Radioactive Ion Beam Project with the ORIC Accelerator**	741

- **D.K. Olsen**, G.D. Alton, C. Baktash, D.T. Dowling, J.D. Garrett, D.L. Haynes, C.M. Jones, R.C. Juras, S.N. Lane, I.Y. Lee, M.J. Meigs, G.D. Mills, S.W. Mosko, B.A. Tatum, K.S. Toth
  ORNL, Oak Ridge, Tennessee, USA
- H.K. Carter, J. Kormicki
  Associated Universities Oak Ridge, Oak Ridge, Tennessee, USA

A B C D E F G H I J K L M N O P Q R S T U V W X Y Z

Leonov, V.V.

Paper	Title	Page
II-05	**Status of a Compact H^- Cyclotron at the Kurchatov Institute of Atomic Energy**	126

- **N.I. Venikov**, C.D. Burbeza, P.Yu. Komissarov, Yu.M. Krasnikov, S.T. Latushkin, V.V. Leonov, V.P. Moryakov, I.V. Naumov, A.Ya. Pisman, V.A. Rezvov, A.A. Vasiliev, V.E. Yarosh, L.I. Yudin
  Kurchatov Institute, Moscow, Russia

A B C D E F G H I J K L M N O P Q R S T U V W X Y Z

Leroy, R.

Paper	Title	Page
XIII-03	**An On-Line Isotopic Separator Test Bench at GANIL**	725

- **P. Bricault**, R. Leroy, M. Lewitowicz, J.Y. Pacquet, M.G. St-Laurent, P. Sortais
  GANIL, Caen, France
- A.C. Mueller, J. Obert, J.C. Putaux
  IPN, Orsay, France
- C.F. Liang, P. Paris
  CSNSM, Orsay, France
- J.C. Steckmeyer
  LPC, Caen, France

A B C D E F G H I J K L M N O P Q R S T U V W X Y Z

Leung, K.N.

Paper	Title	Page
VIII-03	**Ion Sources for Cyclotron Application** • **K.N. Leung**, D.A. Bachman, D.S. McDonald, A.T. Young LBL, Berkeley, California, USA	312
XB-02	**A Permanent Magnet System for a Cyclotron Used as a Mass Spectrometer** • **C.Y. Li**, M. Cooper, K. Halbach, W.B. Kunkel, K.N. Leung, R.P. Wells, A.T. Young LBL, Berkeley, California, USA	561
XII-03	**Design of a Compact Permanent Magnet Cyclotron Mass Spectrometer for the Detection and Measurement of Trace Isotopes** • **A.T. Young**, K.J. Bertsche, D.J. Clark, K. Halbach, W.B. Kunkel, K.N. Leung, C.Y. Li LBL, Berkeley, California, USA	705

A B C D E F G H I J K L M N O P Q R S T U V W X Y Z

Levy, C.D.P.

Paper	Title	Page
VIII-05	**Status of the TRIUMF Optically-Pumped Polarized H^- Ion Source**	322

- **C.D.P. Levy**, K. Jayamanna, M. McDonald, R. Ruegg, P.W. Schmor
  TRIUMF, Vancouver, Canada
- A.N. Zelenskii
  Institute of Nuclear Research, Russian Academy of Sciences, Moscow, Russia

A B C D E F G H I J K L M N O P Q R S T U V W X Y Z

Lewitowicz, M.

Paper	Title	Page
IV-02	**A Cyclotron as a Mass Spectrometer**	158

- **P. Bricault**, G. Auger, M. Bajard, E. Baron, D. Bibet, A. Chabert, J. Fermé, L. Gaudart, J. Joubert, M. Lewitowicz, W. Mittig, E. Plagnol, Ch. Ricaud, Y. Schutz
  GANIL, Caen, France
- G. Audi
  CSNSM, Orsay, France
- A. Gillibert
  CEN/Saclay, Gif-sur-Yvette, France
- K. Fifield
  Australian National University, Canberra , Australia

XIII-03	**An On-Line Isotopic Separator Test Bench at GANIL**	725

- **P. Bricault**, R. Leroy, M. Lewitowicz, J.Y. Pacquet, M.G. St-Laurent, P. Sortais
  GANIL, Caen, France
- A.C. Mueller, J. Obert, J.C. Putaux
  IPN, Orsay, France
- C.F. Liang, P. Paris
  CSNSM, Orsay, France
- J.C. Steckmeyer
  LPC, Caen, France

A B C D E F G H I J K L M N O P Q R S T U V W X Y Z

Li, C.Y.

Paper	Title	Page
XB-02	**A Permanent Magnet System for a Cyclotron Used as a Mass Spectrometer**	561

- **C.Y. Li**, M. Cooper, K. Halbach, W.B. Kunkel, K.N. Leung, R.P. Wells, A.T. Young
  LBL, Berkeley, California, USA

XII-03	**Design of a Compact Permanent Magnet Cyclotron Mass Spectrometer for the Detection and Measurement of Trace Isotopes**	705

- **A.T. Young**, K.J. Bertsche, D.J. Clark, K. Halbach, W.B. Kunkel, K.N. Leung, C.Y. Li
  LBL, Berkeley, California, USA

A B C D E F G H I J K L M N O P Q R S T U V W X Y Z

Liang, C.F.

Paper	Title	Page
XIII-03	**An On-Line Isotopic Separator Test Bench at GANIL**	725

- **P. Bricault**, R. Leroy, M. Lewitowicz, J.Y. Pacquet, M.G. St-Laurent, P. Sortais
  GANIL, Caen, France
- A.C. Mueller, J. Obert, J.C. Putaux
  IPN, Orsay, France
- C.F. Liang, P. Paris
  CSNSM, Orsay, France
- J.C. Steckmeyer
  LPC, Caen, France

A B C D E F G H I J K L M N O P Q R S T U V W X Y Z

Liatard, E.

Paper	Title	Page
XIII-04	**The PIAFE Project at Grenoble: Beam Transport and Acceleration**	729

- **J.L. Belmont**, J.F. Bruandet, J.M. de Conto, M. Fruneau, G. Gimond, K. Golovanivsky, E. Liatard, J.M. Loiseaux, H. Nifenecker, A. Savalle, B. Vignon
  Université Joseph Fourier, Grenoble, France
- P. Briand
  CEN-Grenoble, Grenoble, France

A B C D E F G H I J K L M N O P Q R S T U V W X Y Z

Lindqvist, E.H.

Paper	Title	Page
XC-02	**Potential Enhancement of Magnetic Deflection in the Chalk River Superconducting Cyclotron Extraction System**	573

- **C.R. Hoffmann**, E.H. Lindqvist
  Atomic Energy of Canada, Chalk River, Ontario, Canada

A B C D E F G H I J K L M N O P Q R S T U V W X Y Z

Lipnicki, M.

Paper	Title	Page
XA-03	**Dual Frequency Resonator System for a Compact Cyclotron**	515

- **M. Eiche**, K.L. Erdman
  Ebco Technologies Ltd, Richmond, BC, Canada
- P. Lanz, M. Lipnicki, M. Zach
  TRIUMF, Vancouver, Canada

A B C D E F G H I J K L M N O P Q R S T U V W X Y Z

Liu, C.

Paper	Title	Page
IXA-07	**Deriving the General Expressions of Nonlinear Transport Coefficients of Accelerator Beam Phase Space by Artificial Intelligence**	400

- **J. Xia**
  Institute of Modern Physics, Lanzhou, People's Republic of China
- C. Liu, X. Xie
  Graduate School of Nuclear Industry, Beijing, People's Republic of China

A B C D E F G H I J K L M N O P Q R S T U V W X Y Z

Liu, Z.

Paper	Title	Page
VIII-11	**Study on the Magnetic Field of Caprice Type ECR Source**	344

- **B.W. Wei**, Z. Liu, Y. Ma, D. Wu, P. Yuan, W. Zhang, X. Zhang, H. Zhao
  Institute of Modern Physics, Lanzhou, People's Republic of China
- A. Efremov
  JINR, Dubna, Russia

A B C D E F G H I J K L M N O P Q R S T U V W X Y Z

Liukkonen, E.

Paper	Title	Page
I-03	**New K130 Cyclotron at Jyväskylä (Invited Paper)**	22

- **E. Liukkonen**
  University of Jyväskylä, Jyväskylä, Finland

A B C D E F G H I J K L M N O P Q R S T U V W X Y Z

Lofnes, T.

Paper	Title	Page
VII-01	**Recent Commissioning Results at Celsius (Invited Paper)**	266

- **D. Reistad**, T. Bergmark, C. Ekström, C.-J. Fridén, K. Gajewski, L. Hermansson, P. Jahnke, A. Johansson, O. Johansson, T. Lofnes, G. Norman, R. Wedberg, L. Westerberg, J. Zlomanczuk
  Uppsala University, Uppsala, Sweden
- M.A. Raadu, M. Sedlacek
  Royal Institute of Technology, Stockholm, Sweden

A B C D E F G H I J K L M N O P Q R S T U V W X Y Z

Loiseaux, J.M.

Paper	Title	Page
XIII-04	**The PIAFE Project at Grenoble: Beam Transport and Acceleration**	729

- **J.L. Belmont**, J.F. Bruandet, J.M. de Conto, M. Fruneau, G. Gimond, K. Golovanivsky, E. Liatard, J.M. Loiseaux, H. Nifenecker, A. Savalle, B. Vignon
  Université Joseph Fourier, Grenoble, France
- P. Briand
  CEN-Grenoble, Grenoble, France

A B C D E F G H I J K L M N O P Q R S T U V W X Y Z

Loiselet, M.

Paper	Title	Page
I-16	**Status Report of Cyclone**	82

- **M. Loiselet**, N. Postiau, G. Ryckewaert
  Université Catholique de Louvain, Louvain-la-Neuve, Belgium

Paper	Title	Page
XIII-06	**Radioactive Ion Beam Production Using the Louvain-La-Neuve Cyclotrons: Present Status and Future Developments**	737

- **G. Ryckewaert**, M. Loiselet, N. Postiau
  Université Catholique de Louvain, Louvain-la-Neuve, Belgium

A B C D E F G H I J K L M N O P Q R S T U V W X Y Z

Ludgate, G.A.

Paper	Title	Page
XI-12	**Application of Object Oriented Techniques in the TRIUMF Beam Line 2C Control System (Invited Paper)**	681

- **N.A. Wilkinson**, E.A. Osberg, G.A. Ludgate
  TRIUMF, Vancouver, Canada

A B C D E F G H I J K L M N O P Q R S T U V W X Y Z

Lundgren, S.A.

Paper	Title	Page
VIII-02	**Performance of the LBL AECR Source at Various Frequencies**	308

- **Z.Q. Xie**, D. Collins, S.A. Lundgren, C.M. Lyneis
  LBL, Berkeley, California, USA

A B C D E F G H I J K L M N O P Q R S T U V W X Y Z

Lundström, B.

Paper	Title	Page
XA-13	**The RF System of the Gustaf Werner Cyclotron/Synchrocyclotron**	553

- **B. Lundström**, B. Holmgren
  Uppsala University, Uppsala, Sweden

A B C D E F G H I J K L M N O P Q R S T U V W X Y Z

Lyneis, C.M.

Paper	Title	Page
VIII-01	**ECR Ion Sources for Accelerators (Invited Paper)**	301
	• **C.M. Lyneis** LBL, Berkeley, California, USA	
VIII-02	**Performance of the LBL AECR Source at Various Frequencies**	308
	• **Z.Q. Xie**, D. Collins, S.A. Lundgren, C.M. Lyneis LBL, Berkeley, California, USA	

A B C D E F G H I J K L M N O P Q R S T U V W X Y Z

Ma, Y.

Paper	Title	Page
VIII-11	**Study on the Magnetic Field of Caprice Type ECR Source**	344

- **B.W. Wei**, Z. Liu, Y. Ma, D. Wu, P. Yuan, W. Zhang, X. Zhang, H. Zhao
  Institute of Modern Physics, Lanzhou, People's Republic of China
- A. Efremov
  JINR, Dubna, Russia

A B C D E F G H I J K L M N O P Q R S T U V W X Y Z

Ma, Z.

Paper	Title	Page
I-15	**Upgrading the SFC**	78

- **F. Ye**, M. Guo, Z. Ma, Q. Qiao, Y. Wang, Q. Yin, X. Zhu
  Institute of Modern Physics, Lanzhou, People's Republic of China

A B C D E F G H I J K L M N O P Q R S T U V W X Y Z

Mackay, D.B.

Paper	Title	Page
V-06	**Experiences with the Cyclone 3 Oxygen 15 Generator**	218

- **E. Conard**, J.-L. Morelle
  Ion Beam Applications, Louvain-la-Neuve, Belgium
- J.C. Clark, D.B. Mackay
  Hammersmith Hospital, London, England

A B C D E F G H I J K L M N O P Q R S T U V W X Y Z

Mackenzie, G.H.

Paper	Title	Page
IXA-12	**Beam Quality Investigations for H^- Extraction at TRIUMF**	415
IXB-07	**Beam Test Results Using the Auxiliary Accelerating Cavity**	442

- **R.E. Laxdal**, G.H. Mackenzie, J.B. Pearson, L. Root
  TRIUMF, Vancouver, Canada

- **R.E. Laxdal**, G.H. Mackenzie, L. Root
  TRIUMF, Vancouver, Canada

A B C D E F G H I J K L M N O P Q R S T U V W X Y Z

Maeckelburg, D.

Paper	Title	Page
IXD-01	**The New Phase Detection System of the Cosy-Injector**	469

- **K. Kennepohl**, W. Bräutigam, M. Herschbach, D. Maeckelburg
  FZJ, Jülich, Germany

A B C D E F G H I J K L M N O P Q R S T U V W X Y Z

Märki, M.

Paper	Title	Page
XA-08	**Experience with the PSI-Cyclotron RF-System Under Heavy Beam Loading**	534

- **P.K. Sigg**, J. Cherix, H. Frei, M. Märki
  PSI, Villigen, Switzerland

A B C D E F G H I J K L M N O P Q R S T U V W X Y Z

Maier, R.

Paper	Title	Page
I-12	**Commissioning of the Injector Complex of COSY-Jülich**	67

- **W. Bräutigam**, H. Beuscher, R. Brings, H.G. Böge, R. Maier, M. Rogge, P. Wucherer
  FZJ, Jülich, Germany

VII-03	**COSY-Jülich - A Synchrotron and Storage Ring for Medium Energy Physics**	282

- **R. Maier**, U. Pfister
  FZJ, Jülich, Germany

A B C D E F G H I J K L M N O P Q R S T U V W X Y Z

Makarov, A.A.

Paper	Title	Page
VII-06	**The New Project of INR (Kiev's) Storage-Accelerating Complex**	294

- **A.V. Dolinsky**, A.I. Papash, S.N. Pavlov, A.T. Rudchik, A.E. Val'Kov, I.N. Vishnevsky, A.V. Zhmendak
  Institute for Nuclear Research, Kiev, Ukraine
- V.P. Belov, A.M. Kokorin, A.A. Makarov, I.A. Schukeilo, Yu.P. Severgin
  D.V. Efremov Scientific Research Institute of Electrophysical Apparatus, St. Petersburg, Russia

Paper	Title	Page
VII-05	**Dubna Project of the Heavy Ion Storage Ring Complex K4-K10**	290

- **Yu.Ts. Oganessian**, O.N. Malyshev, G.S. Popeko, A.M. Rodin, S.I. Sidorchuk, Ye.A. Sokol, S.V. Stepantsov, G.M. Ter-Akopian, V.A. Timakov
  JINR, Dubna, Russia
- V.V. Parhomchuk, A.A. Sery, V.D. Shiltsev
  Institute for Nuclear Physics, Novosibirsk, Russia
- I.N. Meshkov, Ye.M. Syresinm
  Center for Applied Physics and Technology, Lipetsk, Russia
- V.P. Belov, A.A. Makarov, Yu.P. Severgin, I.A. Shukeylo, M.N. Tarovik
  D.V. Efremov Scientific Research Institute of Electrophysical Apparatus, St. Petersburg, Russia

A B C D E F G H I J K L M N O P Q R S T U V W X Y Z

Mallory, M.L.

Paper	Title	Page
V-07	**Dual Chemical Station for Cyclotron Produced ^{18}F**	222

- **M.L. Mallory**, G. Grimmett, R. Tilbury, D. Yang
  The University of Texas, Houston, Texas, USA

A B C D E F G H I J K L M N O P Q R S T U V W X Y Z

Malyshev, O.N.

Paper	Title	Page
VII-05	**Dubna Project of the Heavy Ion Storage Ring Complex K4-K10**	290

- **Yu.Ts. Oganessian**, O.N. Malyshev, G.S. Popeko, A.M. Rodin, S.I. Sidorchuk, Ye.A. Sokol, S.V. Stepantsov, G.M. Ter-Akopian, V.A. Timakov
  JINR, Dubna, Russia
- V.V. Parhomchuk, A.A. Sery, V.D. Shiltsev
  Institute for Nuclear Physics, Novosibirsk, Russia
- I.N. Meshkov, Ye.M. Syresinm
  Center for Applied Physics and Technology, Lipetsk, Russia
- V.P. Belov, A.A. Makarov, Yu.P. Severgin, I.A. Shukeylo, M.N. Tarovik
  D.V. Efremov Scientific Research Institute of Electrophysical Apparatus, St. Petersburg, Russia

A B C D E F G H I J K L M N O P Q R S T U V W X Y Z

Mandrillon, P.

Paper	Title	Page
VI-05	**Recent Activities of the Cyclotron Laboratory in Nice**	248

- **P. Mandrillon**, N. Brassart, P. Chauvel, A. Courdi, F. Farley, N. Fietier, J. Herault, J.Y. Tang
  Centre Antoine Lacassagne, Nice, France

A B C D E F G H I J K L M N O P Q R S T U V W X Y Z

Marie, H.

Paper	Title	Page
VI-04	**Progress Report on the IBA-SHI Proton Therapy System**	244

- **Y. Jongen**, W. Beeckman, J.P. Dufour, A. Laisné, H. Marie, R. Verbruggen
  Ion Beam Applications, Louvain-la-Neuve, Belgium
- M. Sano, S. Satoh, N. Takahashi, T. Takayama
  Sumitomo Heavy Industries, Ehime, Japan

A B C D E F G H I J K L M N O P Q R S T U V W X Y Z

Markov, B.N.

Paper	Title	Page
IV-04	^{178m2}Hf and ^{237}Pu Isotopes Production on the U-200 Cyclotron	167

- **S.L. Bogomolov**, S.N. Dmitriev, Yu.P. Gangrski, G.G. Gulbekyan, S.A. Karamian, V.B. Kutner, B.N. Markov, Yu.Ts. Oganessian, N.V. Pronin, G.Ya. Starodub
  JINR, Dubna, Russia

A B C D E F G H I J K L M N O P Q R S T U V W X Y Z

Marti, F.

Paper	Title	Page
I-17	**Performance of the K1200 Cyclotron at MSU**	86

- **P. Miller**, T.A. Antaya, F. Marti, D. Poe, B. Sherrill, J. Stetson, J. Winger
  NSCL, East Lansing, Michigan, USA
- J.A. Nolen
  ANL, Argonne, Illinois, USA

IXB-04	**Selection and Measurement of RF Phase Width of the K1200 Cyclotron Beam**	431

- **J. Bailey**, J. Kuchar, F. Marti, J. Yurkon
  NSCL, East Lansing, Michigan, USA
- J.A. Nolen
  ANL, Argonne, Illinois, USA
- D. Rifuggiato
  INFN/LNS, Catania, Italy

IXB-05	**Internal Beam Dynamics Studies with a TV Probe**	435

- **F. Marti**, S. Snyder
  NSCL, East Lansing, Michigan, USA

IXC-05	**Numerical Studies for Suppression of Vertical Oscillations in the K1200 Cyclotron**	461

- **K. Joh**, F. Marti
  NSCL, East Lansing, Michigan, USA
- J.A. Nolen
  ANL, Argonne, Illinois, USA

A B C D E F G H I J K L M N O P Q R S T U V W X Y Z

Martin, S.A.

Paper	Title	Page
XII-02	**Study of an FFAG Synchrocyclotron for a Pulsed Neutron Source**	701

- **S.A. Martin**, E. Zaplatin
  FZJ, Jülich, Germany
- P.F. Meads, Jr.
  Private Address, Oakland, California, USA
- G. Wüstefeld
  BESSY, Berlin, Germany
- K. Ziegler
  HMI, Berlin, Germany

A B C D E F G H I J K L M N O P Q R S T U V W X Y Z

Maruhashi, A.

Paper	Title	Page
VI-08	**A Proton Therapy Facility Plan**	258

- **S. Fukumoto**, Y. Hayakawa, T. Inada, A. Maruhashi, M. Sato, J. Tada, Y. Takada, H. Tsuji, H. Tsujii
  University of Tsukuba, Ibaraki, Japan
- K. Endo, Y. Irie, K. Muto
  KEK, Ibaraki, Japan

A B C D E F G H I J K L M N O P Q R S T U V W X Y Z

Maruyama, M.

Paper	Title	Page
XI-04	**Control System for JAERI AVF Cyclotron**	648

- **S. Okumura**, T. Agematsu, K. Arakawa, M. Fukuda, I. Ishibori, T. Kamiya, Y. Nakamura, T. Nara, W. Yokota
  JAERI, Gunma, Japan
- K. Hoshika, K. Iso, M. Maruyama, M. Tachibana
  Sumitomo Heavy Industries, Ehime, Japan

XI-10	**Construction and System Tuning of Control System for the RCNP Ring Cyclotron and Beam Lines**	672

- **T. Yamazaki**, A. Ando, K. Hosono, T. Itahashi, M. Kibayashi, I. Miura, K. Nagayama, H. Ogata, T. Saito, A. Shimizu, K. Tamura, M. Uraki
  Osaka University, Osaka, Japan
- K. Aoki, Y. Kimura, M. Maruyama, M. Tachibana, S. Yamada
  Sumitomo Heavy Industries, Ehime, Japan
- K. Kodaira
  Sumitomo Heavy Industries Systems Engineering Laboratory, Tokyo, Japan

A B C D E F G H I J K L M N O P Q R S T U V W X Y Z

Maughan, R.

Paper	Title	Page
II-07	**Performance of the Harper Hospital Cyclotron; Effect of Pulsed Radio Frequency**	133

- **H.G. Blosser**, J. Vincent
  NSCL, East Lansing, Michigan, USA
- R. Maughan
  Harper Hospital, Detroit, Michigan, USA

A B C D E F G H I J K L M N O P Q R S T U V W X Y Z

May, D.P.

Paper	Title	Page
VIII-17	**Performance of the Texas A&M ECRIS**	369

- **G. Mouchaty**, D.P. May, R.C. Rogers, P. Smelser
  Texas A&M University, College Station, Texas, USA

IXB-06	**Effect of the Main-Coil Position on the Accelerated Beam of the K500 Cyclotron**	439

- **D.P. May**, G. Mouchaty
  Texas A&M University, College Station, Texas, USA

XC-09	**Results from the Deflector Test Stand at Texas A&M University**	602

- **D.P. May**, G. Derrig, W. Dewees, P. Smelser, D. Tran, R.C. Rogers
  Texas A&M University, College Station, Texas, USA

A B C D E F G H I J K L M N O P Q R S T U V W X Y Z

McCammon, D.

Paper	Title	Page
XA-05	**Low Frequency RF System for the Indiana University Cooler Ring**	523

- **X. Pei**, S. Anderson, V. Derenchuk, G. East, D.L. Friesel, D. Jenner, D. McCammon, T. Sloan
  Indiana University, Bloomington, Indiana, USA

A B C D E F G H I J K L M N O P Q R S T U V W X Y Z

McDonald, D.S.

Paper	Title	Page
VIII-03	**Ion Sources for Cyclotron Application**	312

- **K.N. Leung**, D.A. Bachman, D.S. McDonald, A.T. Young
  LBL, Berkeley, California, USA

A B C D E F G H I J K L M N O P Q R S T U V W X Y Z

McDonald, M.

Paper	Title	Page
VIII-05	**Status of the TRIUMF Optically-Pumped Polarized H^- Ion Source**	322

- **C.D.P. Levy**, K. Jayamanna, M. McDonald, R. Ruegg, P.W. Schmor
  TRIUMF, Vancouver, Canada
- A.N. Zelenskii
  Institute of Nuclear Research, Russian Academy of Sciences, Moscow, Russia

A B C D E F G H I J K L M N O P Q R S T U V W X Y Z

McNeely, P.

Paper	Title	Page
XIII-08	**Research and Development Studies with Radioactive Beams at TRIUMF**	745

- **J.M. D'Auria**, M. Dombsky
  Simon Fraser University, Burnaby, BC, Canada
- L. Buchmann, H. Sprenger, J.S. Vincent
  TRIUMF, Vancouver, Canada
- J. King
  University of Toronto, Toronto, Ontario, Canada
- P. McNeely, G. Roy
  University of Alberta, Edmonton, Alberta, Canada

A B C D E F G H I J K L M N O P Q R S T U V W X Y Z

Meads, Jr., P.F.

Paper	Title	Page
XII-02	**Study of an FFAG Synchrocyclotron for a Pulsed Neutron Source**	701

- **S.A. Martin**, E. Zaplatin
  FZJ, Jülich, Germany
- P.F. Meads, Jr.
  Private Address, Oakland, California, USA
- G. Wüstefeld
  BESSY, Berlin, Germany
- K. Ziegler
  HMI, Berlin, Germany

A B C D E F G H I J K L M N O P Q R S T U V W X Y Z

Meigs, M.J.

Paper	Title	Page
XIII-07	**The ORNL Radioactive Ion Beam Project with the ORIC Accelerator**	741

- **D.K. Olsen**, G.D. Alton, C. Baktash, D.T. Dowling, J.D. Garrett, D.L. Haynes, C.M. Jones, R.C. Juras, S.N. Lane, I.Y. Lee, M.J. Meigs, G.D. Mills, S.W. Mosko, B.A. Tatum, K.S. Toth
  ORNL, Oak Ridge, Tennessee, USA
- H.K. Carter, J. Kormicki
  Associated Universities Oak Ridge, Oak Ridge, Tennessee, USA

A B C D E F G H I J K L M N O P Q R S T U V W X Y Z

Meshkov, I.N.

Paper	Title	Page
VII-05	**Dubna Project of the Heavy Ion Storage Ring Complex K4-K10**	290

- **Yu.Ts. Oganessian**, O.N. Malyshev, G.S. Popeko, A.M. Rodin, S.I. Sidorchuk, Ye.A. Sokol, S.V. Stepantsov, G.M. Ter-Akopian, V.A. Timakov
  JINR, Dubna, Russia
- V.V. Parhomchuk, A.A. Sery, V.D. Shiltsev
  Institute for Nuclear Physics, Novosibirsk, Russia
- I.N. Meshkov, Ye.M. Syresinm
  Center for Applied Physics and Technology, Lipetsk, Russia
- V.P. Belov, A.A. Makarov, Yu.P. Severgin, I.A. Shukeylo, M.N. Tarovik
  D.V. Efremov Scientific Research Institute of Electrophysical Apparatus, St. Petersburg, Russia

A B C D E F G H I J K L M N O P Q R S T U V W X Y Z

Mezger, A.C.

Paper	Title	Page
XI-09	**Two Dimensional Scans with Adaptive Domain Control**	668

- **S. Adam**, A.C. Mezger
  PSI, Villigen, Switzerland

A B C D E F G H I J K L M N O P Q R S T U V W X Y Z

Michelato, P.

Paper	Title	Page
I-18	**Status Report on the Heavy Ion Facility at LNS**	90

- **F. Alessandria**, G. Bellomo, A. Bosotti, C. De Martinis, D. Giove, P. Michelato, C. Pagani, L. Rossi
  INFN/LASA, Segrate, Italy
- L. Calabretta, G. Ciavola, G. Cuttone, M. Di Giacomo, S. Gammino, P. Gmaj, G. Raia, D. Rifuggiato, J. Sura
  INFN/LNS, Catania, Italy

A B C D E F G H I J K L M N O P Q R S T U V W X Y Z

Mikhailov, V.G.

Paper	Title	Page
IXD-02	**High-Sensitive Ionization Detectors of Transverse Distribution of Accelerated Particles Beam**	473

- **V.G. Mikhailov**, V.A. Rezvov, A.A. Roshchin, V.I. Sklyarenko, L.I. Iudin
  Kurchatov Institute, Moscow, Russia

A B C D E F G H I J K L M N O P Q R S T U V W X Y Z

Mikheev, G.F.

Paper	Title	Page
I-10	**Gatchina Isochronous Cyclotron**	58

- **N.K. Abrosimov**, S.A. Artamonov, P.V. Chervyakov, S.P. Dmitriev, V.A. Eliseev, V.P. Fominenko, E.M. Ivanov, G.F. Mikheev, Yu.T. Mironov, A.S. Pokrovskii, G.A. Riabov, V.A. Smolin, G.L. Sokolov, V.A. Volchenkov, A.A. Vorobiev
  Petersburg Nuclear Physics Institute, Gatchina, Russia
- P.V. Bogdanov, B.D. Ershov, V.S. Kuligin, V.N. Moshkin, V.G. Mudrolyubov, Yu.I. Stogov, A.P. Strokach
  D.V. Efremov Scientific Research Institute of Electrophysical Apparatus, St. Petersburg, Russia

A B C D E F G H I J K L M N O P Q R S T U V W X Y Z

Miller, P.

Paper	Title	Page
I-17	**Performance of the K1200 Cyclotron at MSU**	86

- **P. Miller**, T.A. Antaya, F. Marti, D. Poe, B. Sherrill, J. Stetson, J. Winger
  NSCL, East Lansing, Michigan, USA
- J.A. Nolen
  ANL, Argonne, Illinois, USA

IXB-03	**K1200 Cyclotron Beam Development Techniques**	427

- **T.A. Antaya**, D. Cole, P. Miller, D. Poe
  NSCL, East Lansing, Michigan, USA

A B C D E F G H I J K L M N O P Q R S T U V W X Y Z

Mills, G.D.

Paper	Title	Page
XIII-07	**The ORNL Radioactive Ion Beam Project with the ORIC Accelerator**	741

- **D.K. Olsen**, G.D. Alton, C. Baktash, D.T. Dowling, J.D. Garrett, D.L. Haynes, C.M. Jones, R.C. Juras, S.N. Lane, I.Y. Lee, M.J. Meigs, G.D. Mills, S.W. Mosko, B.A. Tatum, K.S. Toth
  ORNL, Oak Ridge, Tennessee, USA
- H.K. Carter, J. Kormicki
  Associated Universities Oak Ridge, Oak Ridge, Tennessee, USA

A B C D E F G H I J K L M N O P Q R S T U V W X Y Z

Milton, B.F.

Paper	Title	Page
IXA-02	**The Influence of Magnetic Field Imperfections on the Beam Quality in an H^- Cyclotron**	380

- **W.J.G.M. Kleeven**, H.L. Hagedoorn
  Eindhoven University of Technology, Eindhoven, The Netherlands
- B.F. Milton, G. Dutto
  TRIUMF, Vancouver, Canada

XI-13	**The TR30 Control System - A Case for Off-the-Shelf Software**	685

- **R. Keitel**, D.J. Dale, B.F. Milton
  TRIUMF, Vancouver, Canada

A B C D E F G H I J K L M N O P Q R S T U V W X Y Z

Mironov, Yu.T.

Paper	Title	Page
I-10	**Gatchina Isochronous Cyclotron**	58

- **N.K. Abrosimov**, S.A. Artamonov, P.V. Chervyakov, S.P. Dmitriev, V.A. Eliseev, V.P. Fominenko, E.M. Ivanov, G.F. Mikheev, Yu.T. Mironov, A.S. Pokrovskii, G.A. Riabov, V.A. Smolin, G.L. Sokolov, V.A. Volchenkov, A.A. Vorobiev
  Petersburg Nuclear Physics Institute, Gatchina, Russia
- P.V. Bogdanov, B.D. Ershov, V.S. Kuligin, V.N. Moshkin, V.G. Mudrolyubov, Yu.I. Stogov, A.P. Strokach
  D.V. Efremov Scientific Research Institute of Electrophysical Apparatus, St. Petersburg, Russia

A B C D E F G H I J K L M N O P Q R S T U V W X Y Z

Misawa, T.

Paper	Title	Page
II-06	**A Newly Developed Compact Cyclotron for Neutron Therapy and Positron Nuclear Medicine**	129

- **K. Ito**, T. Ishigaki, S. Itoh, Y. Kasugai, T. Kato, T. Misawa, M. Nishino, M. Osakabe, T. Ota, S. Sakuma, M. Tadokoro, H. Yamamoto
  Nagoya University, Nagoya, Japan
- Y. Toda, Y. Yamamoto
  Japan Steel Works Ltd., Tokyo, Japan

A B C D E F G H I J K L M N O P Q R S T U V W X Y Z

Mitchel, G.R.

Paper	Title	Page
XC-01	**The Electrostatic Deflector for the Chalk River Superconducting Cyclotron**	569

- **W.T. Diamond**, C.R. Hoffmann, G.R. Mitchel, H. Schmeing
  Atomic Energy of Canada, Chalk River, Ontario, Canada

A B C D E F G H I J K L M N O P Q R S T U V W X Y Z

Mitra, A.K.

Paper	Title	Page
XA-11	**TRIUMF Cyclotron RF System Improvements**	545

- **G.C. Blaker**, A.K. Mitra, R.L. Poirier
  TRIUMF, Vancouver, Canada

Paper	Title	Page
XA-12	**Improvements to the RF Separator in the M9 Muon Channel at TRIUMF**	549

- **G.C. Blaker**, A.K. Mitra, R.L. Poirier
  TRIUMF, Vancouver, Canada

A B C D E F G H I J K L M N O P Q R S T U V W X Y Z

Mittig, W.

Paper	Title	Page
IV-02	**A Cyclotron as a Mass Spectrometer**	158

- **P. Bricault**, G. Auger, M. Bajard, E. Baron, D. Bibet, A. Chabert, J. Fermé, L. Gaudart, J. Joubert, M. Lewitowicz, W. Mittig, E. Plagnol, Ch. Ricaud, Y. Schutz
  GANIL, Caen, France
- G. Audi
  CSNSM, Orsay, France
- A. Gillibert
  CEN/Saclay, Gif-sur-Yvette, France
- K. Fifield
  Australian National University, Canberra , Australia

A B C D E F G H I J K L M N O P Q R S T U V W X Y Z

Miura, I.

Paper	Title	Page
I-01	**Commissioning of the RCNP Ring Cyclotron (Invited Paper)**	3

- **I. Miura**, A. Ando, K. Hatanaka, K. Hosono, H. Ikegami, T. Itahashi, M. Kibayashi, M. Kondo, H. Ogata, T. Saito, A. Shimizu, K. Tamura, M. Uraki, T. Yamazaki
  Osaka University, Osaka, Japan
- J. Abe
  Sumitomo Heavy Industries, Ehime, Japan

IXD-07	**Beam Diagnostics in the RCNP Ring Cyclotron**	491

- **T. Itahashi**, T. Saito, I. Miura
  Osaka University, Osaka, Japan
- S. Ichida
  Sumitomo Heavy Industries, Ehime, Japan

XA-09	**Initial Operation of the RF System for the RCNP Ring Cyclotron**	538

- **T. Saito**, I. Miura, A. Shimizu, M. Uraki
  Osaka University, Osaka, Japan

XB-03	**Sector Magnet of the RCNP Ring Cyclotron and the Isochronization**	565

- **K. Hosono**, M. Kibayashi, I. Miura
  Osaka University, Osaka, Japan

XI-10	**Construction and System Tuning of Control System for the RCNP Ring Cyclotron and Beam Lines**	672

- **T. Yamazaki**, A. Ando, K. Hosono, T. Itahashi, M. Kibayashi, I. Miura, K. Nagayama, H. Ogata, T. Saito, A. Shimizu, K. Tamura, M. Uraki
  Osaka University, Osaka, Japan
- K. Aoki, Y. Kimura, M. Maruyama, M. Tachibana, S. Yamada
  Sumitomo Heavy Industries, Ehime, Japan
- K. Kodaira
  Sumitomo Heavy Industries Systems Engineering Laboratory, Tokyo, Japan

A B C D E F G H I J K L M N O P Q R S T U V W X Y Z

Montsanglant, B.

Paper	Title	Page
IXD-06	**The Diagnostics System for the AGOR Superconducting Cyclotron**	487

- **B. Launé**, P. Dambre, J.M. Kaplanski, B. Montsanglant, C. Olivetto, D. Vincent
  IPN, Orsay, France

A B C D E F G H I J K L M N O P Q R S T U V W X Y Z

Morduev, A.

Paper	Title	Page
I-02	**New Development at the JINR Heavy Ion Cyclotron Facility (Invited Paper)**	11

- **G.G. Gulbekyan**, V. Bekhterev, O. Borisov, B. Gikal, A. Ivanenko, I. Kolesov, V.B. Kutner, A. Morduev, Yu.Ts. Oganessian
  JINR, Dubna, Russia

A B C D E F G H I J K L M N O P Q R S T U V W X Y Z

Morelle, J.-L.

Paper	Title	Page
V-06	**Experiences with the Cyclone 3 Oxygen 15 Generator**	218

- **E. Conard**, J.-L. Morelle
  Ion Beam Applications, Louvain-la-Neuve, Belgium
- J.C. Clark, D.B. Mackay
  Hammersmith Hospital, London, England

A B C D E F G H I J K L M N O P Q R S T U V W X Y Z

Mormiche, M.

Paper	Title	Page
XD-03	**Superconducting Focussing Channel for the AGOR Cyclotron**	612

- **H.W. Schreuder**, P. Blache, C. Commeaux, S. Gustafsson, A. Lafoux, M. Mormiche, R. Panvier
  IPN, Orsay, France

A B C D E F G H I J K L M N O P Q R S T U V W X Y Z

Moryakov, V.P.

Paper	Title	Page
II-05	**Status of a Compact H^- Cyclotron at the Kurchatov Institute of Atomic Energy**	126

- **N.I. Venikov**, C.D. Burbeza, P.Yu. Komissarov, Yu.M. Krasnikov, S.T. Latushkin, V.V. Leonov, V.P. Moryakov, I.V. Naumov, A.Ya. Pisman, V.A. Rezvov, A.A. Vasiliev, V.E. Yarosh, L.I. Yudin
  Kurchatov Institute, Moscow, Russia

A B C D E F G H I J K L M N O P Q R S T U V W X Y Z

Moscatello, M-H.

Paper	Title	Page
IXB-01	**Cyclotron Tuning as a Rebuncher** • **D. Bibet**, M-H. Moscatello GANIL, Caen, France	419
IXC-03	**Preliminary Design of a New Central Region for the LNS Superconducting Cyclotron** • **M-H. Moscatello** GANIL, Caen, France	454

A B C D E F G H I J K L M N O P Q R S T U V W X Y Z

Moshkin, V.N.

Paper	Title	Page
I-10	**Gatchina Isochronous Cyclotron**	58

- **N.K. Abrosimov**, S.A. Artamonov, P.V. Chervyakov, S.P. Dmitriev, V.A. Eliseev, V.P. Fominenko, E.M. Ivanov, G.F. Mikheev, Yu.T. Mironov, A.S. Pokrovskii, G.A. Riabov, V.A. Smolin, G.L. Sokolov, V.A. Volchenkov, A.A. Vorobiev
  Petersburg Nuclear Physics Institute, Gatchina, Russia
- P.V. Bogdanov, B.D. Ershov, V.S. Kuligin, V.N. Moshkin, V.G. Mudrolyubov, Yu.I. Stogov, A.P. Strokach
  D.V. Efremov Scientific Research Institute of Electrophysical Apparatus, St. Petersburg, Russia

A B C D E F G H I J K L M N O P Q R S T U V W X Y Z

Mosko, S.W.

Paper	Title	Page
XIII-07	**The ORNL Radioactive Ion Beam Project with the ORIC Accelerator**	741

- **D.K. Olsen**, G.D. Alton, C. Baktash, D.T. Dowling, J.D. Garrett, D.L. Haynes, C.M. Jones, R.C. Juras, S.N. Lane, I.Y. Lee, M.J. Meigs, G.D. Mills, S.W. Mosko, B.A. Tatum, K.S. Toth
  ORNL, Oak Ridge, Tennessee, USA
- H.K. Carter, J. Kormicki
  Associated Universities Oak Ridge, Oak Ridge, Tennessee, USA

A B C D E F G H I J K L M N O P Q R S T U V W X Y Z

Mouat, M.

Paper	Title	Page
XI-11	**Early Experience with DECwindows/Motif in the TRIUMF Central Control System**	676

- **S. Kadantsev**
  JINR, Dubna, Russia
- M. Mouat
  TRIUMF, Vancouver, Canada

A B C D E F G H I J K L M N O P Q R S T U V W X Y Z

Mouchaty, G.

Paper	Title	Page
VIII-17	**Performance of the Texas A&M ECRIS**	369

- **G. Mouchaty**, D.P. May, R.C. Rogers, P. Smelser
  Texas A&M University, College Station, Texas, USA

Paper	Title	Page
IXB-06	**Effect of the Main-Coil Position on the Accelerated Beam of the K500 Cyclotron**	439

- **D.P. May**, G. Mouchaty
  Texas A&M University, College Station, Texas, USA

A B C D E F G H I J K L M N O P Q R S T U V W X Y Z

Mouris, J.F.

Paper	Title	Page
XC-03	**Model Study of an Electrostatic Deflector Configuration with an Intermediate Electrode**	577

- **C.R. Hoffmann**, J.F. Mouris
  Atomic Energy of Canada, Chalk River, Ontario, Canada

A B C D E F G H I J K L M N O P Q R S T U V W X Y Z

Mudrolyubov, V.G.

Paper	Title	Page
I-10	**Gatchina Isochronous Cyclotron**	58

- **N.K. Abrosimov**, S.A. Artamonov, P.V. Chervyakov, S.P. Dmitriev, V.A. Eliseev, V.P. Fominenko, E.M. Ivanov, G.F. Mikheev, Yu.T. Mironov, A.S. Pokrovskii, G.A. Riabov, V.A. Smolin, G.L. Sokolov, V.A. Volchenkov, A.A. Vorobiev
  Petersburg Nuclear Physics Institute, Gatchina, Russia
- P.V. Bogdanov, B.D. Ershov, V.S. Kuligin, V.N. Moshkin, V.G. Mudrolyubov, Yu.I. Stogov, A.P. Strokach
  D.V. Efremov Scientific Research Institute of Electrophysical Apparatus, St. Petersburg, Russia

A B C D E F G H I J K L M N O P Q R S T U V W X Y Z

Müller, A.

Paper	Title	Page
VIII-15	**Progress with the NAC Injector Cyclotron for Heavy and Polarized Ions**	361

- **Z.B. du Toit**, S.J. Burger, P.J. Celliers, J.G. de Villiers, H.N. Jungwirth, A. Müller, P.F. Rohwer, D.M. van Rooyen
  National Accelerator Centre, Faure, Republic of South Africa

A B C D E F G H I J K L M N O P Q R S T U V W X Y Z

Mueller, A.C.

Paper	Title	Page
XIII-03	**An On-Line Isotopic Separator Test Bench at GANIL**	725

- **P. Bricault**, R. Leroy, M. Lewitowicz, J.Y. Pacquet, M.G. St-Laurent, P. Sortais
  GANIL, Caen, France
- A.C. Mueller, J. Obert, J.C. Putaux
  IPN, Orsay, France
- C.F. Liang, P. Paris
  CSNSM, Orsay, France
- J.C. Steckmeyer
  LPC, Caen, France

A B C D E F G H I J K L M N O P Q R S T U V W X Y Z

Mukherjee, B.N.

Paper	Title	Page
VI-06	**Health Physics Data Acquisition System at the National Medical Cyclotron**	252

- **B.N. Mukherjee**
  ANSTO, Menai, NSW, Australia
- D.W. Arnott
  National Medical Cyclotron, Camperdown, NSW, Australia

A B C D E F G H I J K L M N O P Q R S T U V W X Y Z

Muminov, A.I.

Paper	Title	Page
I-08	**Parameters, Present State and Application Perspectives of the U-250 Cyclotron**	50

- **A.I. Muminov**
  Institute of Nuclear Physics, Tashkent, Republic of Uzbekistan
- M.F. Vorogushin
  D.V. Efremov Scientific Research Institute of Electrophysical Apparatus, St. Petersburg, Russia

A B C D E F G H I J K L M N O P Q R S T U V W X Y Z

Murakami, T.

Paper	Title	Page
XI-03	**An Operator Assistance System for the AVF Cyclotron**	644

- **T. Okamura**, T. Murakami
  Sumitomo Heavy Industries Systems Engineering Laboratory, Tokyo, Japan
- T. Tachikawa
  Sumitomo Heavy Industries, Ehime, Japan
- T. Agematsu, S. Okumura, K. Arakawa
  JAERI, Gunma, Japan

A B C D E F G H I J K L M N O P Q R S T U V W X Y Z

Muto, K.

Paper	Title	Page
VI-08	**A Proton Therapy Facility Plan**	258

- **S. Fukumoto**, Y. Hayakawa, T. Inada, A. Maruhashi, M. Sato, J. Tada, Y. Takada, H. Tsuji, H. Tsujii
  University of Tsukuba, Ibaraki, Japan
- K. Endo, Y. Irie, K. Muto
  KEK, Ibaraki, Japan

A B C D E F G H I J K L M N O P Q R S T U V W X Y Z

Nagayama, K.

Paper	Title	Page
XI-10	**Construction and System Tuning of Control System for the RCNP Ring Cyclotron and Beam Lines**	672

- **T. Yamazaki**, A. Ando, K. Hosono, T. Itahashi, M. Kibayashi, I. Miura, K. Nagayama, H. Ogata, T. Saito, A. Shimizu, K. Tamura, M. Uraki
  Osaka University, Osaka, Japan
- K. Aoki, Y. Kimura, M. Maruyama, M. Tachibana, S. Yamada
  Sumitomo Heavy Industries, Ehime, Japan
- K. Kodaira
  Sumitomo Heavy Industries Systems Engineering Laboratory, Tokyo, Japan

A B C D E F G H I J K L M N O P Q R S T U V W X Y Z

Nakagawa, T.

Paper	Title	Page
VIII-16	**Plasma Cathode Method for RIKEN ECRIS**	365

- **T. Nakagawa**, A. Goto, T. Kageyama, M. Kase, Y. Yano
  RIKEN, Saitama, Japan

A B C D E F G H I J K L M N O P Q R S T U V W X Y Z

Nakamura, Y.

Paper	Title	Page
II-03	**Construction and First Year's Operation of the JAERI AVF Cyclotron** • **K. Arakawa**, T. Agematsu, M. Fukuda, I. Ishibori, T. Karasawa, T. Nara, Y. Nakamura, S. Okumura, R. Tanaka, W. Yokota JAERI, Gunma, Japan • A. Shimizu Osaka University, Osaka, Japan • Y. Hayashi, K. Ishii, T. Satoh, T. Tachikawa Sumitomo Heavy Industries, Ehime, Japan	119
VIII-09	**Operation of Ion Sources and Beam Transport to JAERI AVF Cyclotron** • **W. Yokota**, T. Agematsu, K. Arakawa, M. Fukuda, I. Ishibori, Y. Nakamura, T. Nara, S. Okumura JAERI, Gunma, Japan • Y. Hayashi, K. Ishii, T. Tachikawa Sumitomo Heavy Industries, Ehime, Japan	336
IXB-02	**Beam Studies of Injection to Extraction System for JAERI AVF Cyclotron** • **M. Fukuda**, T. Agematsu, K. Arakawa, I. Ishibori, T. Karasawa, Y. Nakamura, T. Nara, S. Okumura, W. Yokota JAERI, Gunma, Japan	423
XC-04	**Performance of Beam Chopping System for JAERI AVF Cyclotron** • **W. Yokota**, T. Agematsu, K. Arakawa, M. Fukuda, I. Ishibori, Y. Nakamura, T. Nara, S. Okumura JAERI, Gunma, Japan • Y. Hayashi, Y. Kumata, T. Tachikawa Sumitomo Heavy Industries, Ehime, Japan	581
XI-04	**Control System for JAERI AVF Cyclotron** • **S. Okumura**, T. Agematsu, K. Arakawa, M. Fukuda, I. Ishibori, T. Kamiya, Y. Nakamura, T. Nara, W. Yokota JAERI, Gunma, Japan • K. Hoshika, K. Iso, M. Maruyama, M. Tachibana Sumitomo Heavy Industries, Ehime, Japan	648

A B C D E F G H I J K L M N O P Q R S T U V W X Y Z

Nara, T.

Paper	Title	Page
II-03	**Construction and First Year's Operation of the JAERI AVF Cyclotron** • **K. Arakawa**, T. Agematsu, M. Fukuda, I. Ishibori, T. Karasawa, T. Nara, Y. Nakamura, S. Okumura, R. Tanaka, W. Yokota, JAERI, Gunma, Japan • A. Shimizu, Osaka University, Osaka, Japan • Y. Hayashi, K. Ishii, T. Satoh, T. Tachikawa, Sumitomo Heavy Industries, Ehime, Japan	119
VIII-09	**Operation of Ion Sources and Beam Transport to JAERI AVF Cyclotron** • **W. Yokota**, T. Agematsu, K. Arakawa, M. Fukuda, I. Ishibori, Y. Nakamura, T. Nara, S. Okumura, JAERI, Gunma, Japan • Y. Hayashi, K. Ishii, T. Tachikawa, Sumitomo Heavy Industries, Ehime, Japan	336
IXB-02	**Beam Studies of Injection to Extraction System for JAERI AVF Cyclotron** • **M. Fukuda**, T. Agematsu, K. Arakawa, I. Ishibori, T. Karasawa, Y. Nakamura, T. Nara, S. Okumura, W. Yokota, JAERI, Gunma, Japan	423
XC-04	**Performance of Beam Chopping System for JAERI AVF Cyclotron** • **W. Yokota**, T. Agematsu, K. Arakawa, M. Fukuda, I. Ishibori, Y. Nakamura, T. Nara, S. Okumura, JAERI, Gunma, Japan • Y. Hayashi, Y. Kumata, T. Tachikawa, Sumitomo Heavy Industries, Ehime, Japan	581
XI-04	**Control System for JAERI AVF Cyclotron** • **S. Okumura**, T. Agematsu, K. Arakawa, M. Fukuda, I. Ishibori, T. Kamiya, Y. Nakamura, T. Nara, W. Yokota, JAERI, Gunma, Japan • K. Hoshika, K. Iso, M. Maruyama, M. Tachibana, Sumitomo Heavy Industries, Ehime, Japan	648

A B C D E F G H I J K L M N O P Q R S T U V W X Y Z

Naumov, I.V.

Paper	Title	Page
II-05	**Status of a Compact H^- Cyclotron at the Kurchatov Institute of Atomic Energy**	126

- **N.I. Venikov**, C.D. Burbeza, P.Yu. Komissarov, Yu.M. Krasnikov, S.T. Latushkin, V.V. Leonov, V.P. Moryakov, I.V. Naumov, A.Ya. Pisman, V.A. Rezvov, A.A. Vasiliev, V.E. Yarosh, L.I. Yudin
  Kurchatov Institute, Moscow, Russia

A B C D E F G H I J K L M N O P Q R S T U V W X Y Z

Nel, W.A.G.

Paper	Title	Page
I-19	**Development of the NAC Accelerator Facilities**	95

- **J.L. Conradie**, A.H. Botha, P.M. Cronje, R.E.F. Fenemore, H.N. Jungwirth, J.J. Kritzinger, W.A.G. Nel, D. Reitmann, L.M.M. Roels, P.F. Rohwer, H.A. Smit
  National Accelerator Centre, Faure, Republic of South Africa

A B C D E F G H I J K L M N O P Q R S T U V W X Y Z

Nifenecker, H.

Paper	Title	Page
XIII-04	**The PIAFE Project at Grenoble: Beam Transport and Acceleration**	729

- **J.L. Belmont**, J.F. Bruandet, J.M. de Conto, M. Fruneau, G. Gimond, K. Golovanivsky, E. Liatard, J.M. Loiseaux, H. Nifenecker, A. Savalle, B. Vignon
  Université Joseph Fourier, Grenoble, France
- P. Briand
  CEN-Grenoble, Grenoble, France

A B C D E F G H I J K L M N O P Q R S T U V W X Y Z

Nishiguchi, M.

Paper	Title	Page
IXC-02	**A Formulation of Spiral Inflector Design and Its Application to SF Cyclotron**	450

- **M. Sekiguchi**, M. Fujita, M. Nishiguchi, Y. Ohshiro, Y. Shida, N. Yamazaki, T. Yamazaki
  University of Tokyo, Tanashi-shi, Tokyo, Japan

A B C D E F G H I J K L M N O P Q R S T U V W X Y Z

Nishino, M.

Paper	Title	Page
II-06	**A Newly Developed Compact Cyclotron for Neutron Therapy and Positron Nuclear Medicine**	129

- **K. Ito**, T. Ishigaki, S. Itoh, Y. Kasugai, T. Kato, T. Misawa, M. Nishino, M. Osakabe, T. Ota, S. Sakuma, M. Tadokoro, H. Yamamoto
  Nagoya University, Nagoya, Japan
- Y. Toda, Y. Yamamoto
  Japan Steel Works Ltd., Tokyo, Japan

Nitschke, J.M.

Paper	Title	Page
XIII-01	**Accelerated Radioactive Nuclear Beams: Existing and Planned Facilities (Invited Paper)**	713

- **J.M. Nitschke**
  LBL, Berkeley, California, USA

A B C D E F G H I J K L M N O P Q R S T U V W X Y Z

Noda, K.

Paper	Title	Page
VII-04	**Study of Beam Dynamics at Cooler Synchrotron TARN-II**	286

- **S. Watanabe**, Y. Arakaki, K. Chida, T. Katayama, M. Tomizawa, T. Watanabe, M. Yoshizawa
  University of Tokyo, Tanashi-shi, Tokyo, Japan
- K. Noda, M. Kanazawa
  NIRS, Chiba, Japan

XD-07	**Beam Transport System for the HIMAC**	625

- **K. Noda**, Y. Hirao, A. Itano, M. Kanazawa, A. Kitagawa, T. Kohno, M. Kumada, H. Ogawa, K. Sato, Y. Sato, M. Sudou, E. Takada, S. Yamada, T. Yamada
  NIRS, Chiba, Japan
- K. Endo
  KEK, Ibaraki, Japan

A B C D E F G H I J K L M N O P Q R S T U V W X Y Z

Nolen, J.A.

Paper	Title	Page
I-17	**Performance of the K1200 Cyclotron at MSU**	86

- **P. Miller**, T.A. Antaya, F. Marti, D. Poe, B. Sherrill, J. Stetson, J. Winger
  NSCL, East Lansing, Michigan, USA
- J.A. Nolen
  ANL, Argonne, Illinois, USA

IXB-04	**Selection and Measurement of RF Phase Width of the K1200 Cyclotron Beam**	431

- **J. Bailey**, J. Kuchar, F. Marti, J. Yurkon
  NSCL, East Lansing, Michigan, USA
- J.A. Nolen
  ANL, Argonne, Illinois, USA
- D. Rifuggiato
  INFN/LNS, Catania, Italy

IXC-05	**Numerical Studies for Suppression of Vertical Oscillations in the K1200 Cyclotron**	461

- **K. Joh**, F. Marti
  NSCL, East Lansing, Michigan, USA
- J.A. Nolen
  ANL, Argonne, Illinois, USA

XC-08	**Deflector Development for the K1200 Cyclotron**	596

- **T.Y.T. Kuo**
  TRIUMF, Vancouver, Canada
- J.A. Nolen
  ANL, Argonne, Illinois, USA

A B C D E F G H I J K L M N O P Q R S T U V W X Y Z

Norman, G.

Paper	Title	Page
VII-01	**Recent Commissioning Results at Celsius (Invited Paper)**	266

- **D. Reistad**, T. Bergmark, C. Ekström, C.-J. Fridén, K. Gajewski, L. Hermansson, P. Jahnke, A. Johansson, O. Johansson, T. Lofnes, G. Norman, R. Wedberg, L. Westerberg, J. Zlomanczuk
  Uppsala University, Uppsala, Sweden
- M.A. Raadu, M. Sedlacek
  Royal Institute of Technology, Stockholm, Sweden

A B C D E F G H I J K L M N O P Q R S T U V W X Y Z

Novikov, D.

Paper	Title	Page
II-04	**20 MeV Cyclotron for Isotope Production**	123

- **A. Glazov**, Ju. Alenitskiy, A. Chesnov, S. Chesnova, V. Kochkin, D. Novikov, E. Samsonov, M. Semenov, A. Vasilenko, E. Zaplatin, N. Zaplatin
  JINR, Dubna, Russia
- I. Gulamov, O. Iljasov, A. Rykov
  Institute of Nuclear Physics, Tashkent, Republic of Uzbekistan

A B C D E F G H I J K L M N O P Q R S T U V W X Y Z

Novikov, V.

Paper	Title	Page
IV-05	**Radionuclide Technique in Mechanical Engineering (RTM)**	171

- **P. Fehsenfeld**, A. Kleinrahm
  FZK, Karlsruhe, Germany
- V. Novikov
  Kurchatov Institute, Moscow, Russia

A B C D E F G H I J K L M N O P Q R S T U V W X Y Z

Obert, J.

Paper	Title	Page
XIII-03	**An On-Line Isotopic Separator Test Bench at GANIL**	725

- **P. Bricault**, R. Leroy, M. Lewitowicz, J.Y. Pacquet, M.G. St-Laurent, P. Sortais
  GANIL, Caen, France
- A.C. Mueller, J. Obert, J.C. Putaux
  IPN, Orsay, France
- C.F. Liang, P. Paris
  CSNSM, Orsay, France
- J.C. Steckmeyer
  LPC, Caen, France

A B C D E F G H I J K L M N O P Q R S T U V W X Y Z

Oganessian, R.Ts.

Paper	Title	Page
IV-03	**The Use of Heavy Ion Cyclotrons of the Flerov Laboratory of Nuclear Reactions in Condensed Matter Investigations**	162

- **R.Ts. Oganessian**, A.Yu. Didyk
  JINR, Dubna, Russia

Paper	Title	Page
V-04	**Possibility of Producing Some Radionuclides for Medicine Using JINR Accelerators**	213

- **S.N. Dmitriev**, G.G. Gulbekyan, V.A. Khalkin, R.Ts. Oganessian, L.M. Onishchenko, G.Ya. Starodub, N.G. Zaitseva
  JINR, Dubna, Russia

A B C D E F G H I J K L M N O P Q R S T U V W X Y Z

Oganessian, Yu.Ts.

Paper	Title	Page
I-02	**New Development at the JINR Heavy Ion Cyclotron Facility (Invited Paper)**	11

- **G.G. Gulbekyan**, V. Bekhterev, O. Borisov, B. Gikal, A. Ivanenko, I. Kolesov, V.B. Kutner, A. Morduev, Yu.Ts. Oganessian
  JINR, Dubna, Russia

IV-04	**^{178m2}Hf and ^{237}Pu Isotopes Production on the U-200 Cyclotron**	167

- **S.L. Bogomolov**, S.N. Dmitriev, Yu.P. Gangrski, G.G. Gulbekyan, S.A. Karamian, V.B. Kutner, B.N. Markov, Yu.Ts. Oganessian, N.V. Pronin, G.Ya. Starodub
  JINR, Dubna, Russia

VII-05	**Dubna Project of the Heavy Ion Storage Ring Complex K4-K10**	290

- **Yu.Ts. Oganessian**, O.N. Malyshev, G.S. Popeko, A.M. Rodin, S.I. Sidorchuk, Ye.A. Sokol, S.V. Stepantsov, G.M. Ter-Akopian, V.A. Timakov
  JINR, Dubna, Russia
- V.V. Parhomchuk, A.A. Sery, V.D. Shiltsev
  Institute for Nuclear Physics, Novosibirsk, Russia
- I.N. Meshkov, Ye.M. Syresinm
  Center for Applied Physics and Technology, Lipetsk, Russia
- V.P. Belov, A.A. Makarov, Yu.P. Severgin, I.A. Shukeylo, M.N. Tarovik
  D.V. Efremov Scientific Research Institute of Electrophysical Apparatus, St. Petersburg, Russia

A B C D E F G H I J K L M N O P Q R S T U V W X Y Z

Ogata, H.

Paper	Title	Page
I-01	**Commissioning of the RCNP Ring Cyclotron (Invited Paper)**	3

- **I. Miura**, A. Ando, K. Hatanaka, K. Hosono, H. Ikegami, T. Itahashi, M. Kibayashi, M. Kondo, H. Ogata, T. Saito, A. Shimizu, K. Tamura, M. Uraki, T. Yamazaki
  Osaka University, Osaka, Japan
- J. Abe
  Sumitomo Heavy Industries, Ehime, Japan

XI-10	**Construction and System Tuning of Control System for the RCNP Ring Cyclotron and Beam Lines**	672

- **T. Yamazaki**, A. Ando, K. Hosono, T. Itahashi, M. Kibayashi, I. Miura, K. Nagayama, H. Ogata, T. Saito, A. Shimizu, K. Tamura, M. Uraki
  Osaka University, Osaka, Japan
- K. Aoki, Y. Kimura, M. Maruyama, M. Tachibana, S. Yamada
  Sumitomo Heavy Industries, Ehime, Japan
- K. Kodaira
  Sumitomo Heavy Industries Systems Engineering Laboratory, Tokyo, Japan

A B C D E F G H I J K L M N O P Q R S T U V W X Y Z

Ogawa, H.

Paper	Title	Page
XD-07	**Beam Transport System for the HIMAC**	625

- **K. Noda**, Y. Hirao, A. Itano, M. Kanazawa, A. Kitagawa, T. Kohno, M. Kumada, H. Ogawa, K. Sato, Y. Sato, M. Sudou, E. Takada, S. Yamada, T. Yamada
  NIRS, Chiba, Japan
- K. Endo
  KEK, Ibaraki, Japan

A B C D E F G H I J K L M N O P Q R S T U V W X Y Z

Ohshiro, Y.

Paper	Title	Page
VIII-06	**An ECR Ion Source for Multiply-Charged Heavy Ions at 14 GHz**	326

- **M. Sekiguchi**, M. Fujita, Y. Ohshiro, T. Yamazaki
  University of Tokyo, Tanashi-shi, Tokyo, Japan
- Y. Isoya, T. Yamada, Y. Yamashita
  Japan Steel Works Ltd., Research Center for Advanced Technologies, Chiba, Japan
- A. Kitagawa
  NIRS, Chiba, Japan

IXC-02	**A Formulation of Spiral Inflector Design and Its Application to SF Cyclotron**	450

- **M. Sekiguchi**, M. Fujita, M. Nishiguchi, Y. Ohshiro, Y. Shida, N. Yamazaki, T. Yamazaki
  University of Tokyo, Tanashi-shi, Tokyo, Japan

A B C D E F G H I J K L M N O P Q R S T U V W X Y Z

Okamura, T.

Paper	Title	Page
XI-03	**An Operator Assistance System for the AVF Cyclotron**	644

- **T. Okamura**, T. Murakami
  Sumitomo Heavy Industries Systems Engineering Laboratory, Tokyo, Japan
- T. Tachikawa
  Sumitomo Heavy Industries, Ehime, Japan
- T. Agematsu, S. Okumura, K. Arakawa
  JAERI, Gunma, Japan

A B C D E F G H I J K L M N O P Q R S T U V W X Y Z

Okumura, S.

Paper	Title	Page
II-03	**Construction and First Year's Operation of the JAERI AVF Cyclotron** • **K. Arakawa**, T. Agematsu, M. Fukuda, I. Ishibori, T. Karasawa, T. Nara, Y. Nakamura, S. Okumura, R. Tanaka, W. Yokota, JAERI, Gunma, Japan • A. Shimizu, Osaka University, Osaka, Japan • Y. Hayashi, K. Ishii, T. Satoh, T. Tachikawa, Sumitomo Heavy Industries, Ehime, Japan	119
VIII-09	**Operation of Ion Sources and Beam Transport to JAERI AVF Cyclotron** • **W. Yokota**, T. Agematsu, K. Arakawa, M. Fukuda, I. Ishibori, Y. Nakamura, T. Nara, S. Okumura, JAERI, Gunma, Japan • Y. Hayashi, K. Ishii, T. Tachikawa, Sumitomo Heavy Industries, Ehime, Japan	336
IXB-02	**Beam Studies of Injection to Extraction System for JAERI AVF Cyclotron** • **M. Fukuda**, T. Agematsu, K. Arakawa, I. Ishibori, T. Karasawa, Y. Nakamura, T. Nara, S. Okumura, W. Yokota, JAERI, Gunma, Japan	423
XC-04	**Performance of Beam Chopping System for JAERI AVF Cyclotron** • **W. Yokota**, T. Agematsu, K. Arakawa, M. Fukuda, I. Ishibori, Y. Nakamura, T. Nara, S. Okumura, JAERI, Gunma, Japan • Y. Hayashi, Y. Kumata, T. Tachikawa, Sumitomo Heavy Industries, Ehime, Japan	581
XI-03	**An Operator Assistance System for the AVF Cyclotron** • **T. Okamura**, T. Murakami, Sumitomo Heavy Industries Systems Engineering Laboratory, Tokyo, Japan • T. Tachikawa, Sumitomo Heavy Industries, Ehime, Japan • T. Agematsu, S. Okumura, K. Arakawa, JAERI, Gunma, Japan	644
XI-04	**Control System for JAERI AVF Cyclotron** • **S. Okumura**, T. Agematsu, K. Arakawa, M. Fukuda, I. Ishibori, T. Kamiya,	648

Y. Nakamura, T. Nara, W. Yokota
JAERI, Gunma, Japan
- K. Hoshika, K. Iso, M. Maruyama, M. Tachibana
Sumitomo Heavy Industries, Ehime, Japan

A B C D E F G H I J K L M N O P Q R S T U V W X Y Z

Olivetto, C.

Paper	Title	Page
IXD-06	**The Diagnostics System for the AGOR Superconducting Cyclotron**	487

- **B. Launé**, P. Dambre, J.M. Kaplanski, B. Montsanglant, C. Olivetto, D. Vincent
  IPN, Orsay, France

A B C D E F G H I J K L M N O P Q R S T U V W X Y Z

Olsen, D.K.

Paper	Title	Page
XIII-07	**The ORNL Radioactive Ion Beam Project with the ORIC Accelerator**	741

- **D.K. Olsen**, G.D. Alton, C. Baktash, D.T. Dowling, J.D. Garrett, D.L. Haynes, C.M. Jones, R.C. Juras, S.N. Lane, I.Y. Lee, M.J. Meigs, G.D. Mills, S.W. Mosko, B.A. Tatum, K.S. Toth
  ORNL, Oak Ridge, Tennessee, USA
- H.K. Carter, J. Kormicki
  Associated Universities Oak Ridge, Oak Ridge, Tennessee, USA

A B C D E F G H I J K L M N O P Q R S T U V W X Y Z

Onishchenko, L.M.

Paper	Title	Page
V-04	**Possibility of Producing Some Radionuclides for Medicine Using JINR Accelerators**	213

- **S.N. Dmitriev**, G.G. Gulbekyan, V.A. Khalkin, R.Ts. Oganessian, L.M. Onishchenko, G.Ya. Starodub, N.G. Zaitseva
  JINR, Dubna, Russia

A B C D E F G H I J K L M N O P Q R S T U V W X Y Z

Orzechowski, J.

Paper	Title	Page
IV-12	**A Remotely Controlled Robotic Vehicle for Work Within Radioactive Environments**	198

- **N.R. Stevenson**, P. Bloemhard, M. Brigham, J. Ko, C. LaForge, J. Orzechowski, E. Pattyn, T. Rattray
  TRIUMF, Vancouver, Canada

A B C D E F G H I J K L M N O P Q R S T U V W X Y Z

Osakabe, M.

Paper	Title	Page
II-06	**A Newly Developed Compact Cyclotron for Neutron Therapy and Positron Nuclear Medicine**	129

- **K. Ito**, T. Ishigaki, S. Itoh, Y. Kasugai, T. Kato, T. Misawa, M. Nishino, M. Osakabe, T. Ota, S. Sakuma, M. Tadokoro, H. Yamamoto
  Nagoya University, Nagoya, Japan
- Y. Toda, Y. Yamamoto
  Japan Steel Works Ltd., Tokyo, Japan

A B C D E F G H I J K L M N O P Q R S T U V W X Y Z

Osberg, E.A.

Paper	Title	Page
XI-12	**Application of Object Oriented Techniques in the TRIUMF Beam Line 2C Control System (Invited Paper)**	681

- **N.A. Wilkinson**, E.A. Osberg, G.A. Ludgate
  TRIUMF, Vancouver, Canada

A B C D E F G H I J K L M N O P Q R S T U V W X Y Z

Ota, T.

Paper	Title	Page
II-06	**A Newly Developed Compact Cyclotron for Neutron Therapy and Positron Nuclear Medicine**	129

- **K. Ito**, T. Ishigaki, S. Itoh, Y. Kasugai, T. Kato, T. Misawa, M. Nishino, M. Osakabe, T. Ota, S. Sakuma, M. Tadokoro, H. Yamamoto
  Nagoya University, Nagoya, Japan
- Y. Toda, Y. Yamamoto
  Japan Steel Works Ltd., Tokyo, Japan

A B C D E F G H I J K L M N O P Q R S T U V W X Y Z

Paans, A.M.J.

Paper	Title	Page
IV-06	**A P.E.T. Study of Proton Induced Radioactivity in Different Materials**	175

- **J.M. Schippers**
  Kernfysisch Versneller Instituut, Groningen, The Netherlands
- A.M.J. Paans
  University Hospital, Groningen, The Netherlands

A B C D E F G H I J K L M N O P Q R S T U V W X Y Z

Pacquet, J.Y.

Paper	Title	Page
XIII-03	**An On-Line Isotopic Separator Test Bench at GANIL**	725

- **P. Bricault**, R. Leroy, M. Lewitowicz, J.Y. Pacquet, M.G. St-Laurent, P. Sortais
  GANIL, Caen, France
- A.C. Mueller, J. Obert, J.C. Putaux
  IPN, Orsay, France
- C.F. Liang, P. Paris
  CSNSM, Orsay, France
- J.C. Steckmeyer
  LPC, Caen, France

A B C D E F G H I J K L M N O P Q R S T U V W X Y Z

Pagani, C.

Paper	Title	Page
I-18	**Status Report on the Heavy Ion Facility at LNS**	90

- **F. Alessandria**, G. Bellomo, A. Bosotti, C. De Martinis, D. Giove, P. Michelato, C. Pagani, L. Rossi
  INFN/LASA, Segrate, Italy
- L. Calabretta, G. Ciavola, G. Cuttone, M. Di Giacomo, S. Gammino, P. Gmaj, G. Raia, D. Rifuggiato, J. Sura
  INFN/LNS, Catania, Italy

IXD-05	**High Sensitivity Electronic System for the Phase Probes of the LNS/MILANO Superconducting Cyclotron**	483

- **A. Bosotti**, D. Corti, C. Pagani, G. Varisco, F. Zibra
  INFN/LASA, Segrate, Italy
- M. Di Giacomo
  INFN/LNS, Catania, Italy

XA-01	**Advances in RF Technology for Cyclotrons**	501

- **C. Pagani**
  INFN/LASA, Segrate, Italy

A B C D E F G H I J K L M N O P Q R S T U V W X Y Z

Panvier, R.

Paper	Title	Page
XD-03	**Superconducting Focussing Channel for the AGOR Cyclotron**	612

- **H.W. Schreuder**, P. Blache, C. Commeaux, S. Gustafsson, A. Lafoux, M. Mormiche, R. Panvier
  IPN, Orsay, France

A B C D E F G H I J K L M N O P Q R S T U V W X Y Z

Papash, A.I.

Paper	Title	Page
VII-06	**The New Project of INR (Kiev's) Storage-Accelerating Complex**	294

- **A.V. Dolinsky**, A.I. Papash, S.N. Pavlov, A.T. Rudchik, A.E. Val'Kov, I.N. Vishnevsky, A.V. Zhmendak
  Institute for Nuclear Research, Kiev, Ukraine
- V.P. Belov, A.M. Kokorin, A.A. Makarov, I.A. Schukeilo, Yu.P. Severgin
  D.V. Efremov Scientific Research Institute of Electrophysical Apparatus, St. Petersburg, Russia

A B C D E F G H I J K L M N O P Q R S T U V W X Y Z

Parhomchuk, V.V.

Paper	Title	Page
VII-05	**Dubna Project of the Heavy Ion Storage Ring Complex K4-K10**	290

- **Yu.Ts. Oganessian**, O.N. Malyshev, G.S. Popeko, A.M. Rodin, S.I. Sidorchuk, Ye.A. Sokol, S.V. Stepantsov, G.M. Ter-Akopian, V.A. Timakov
  JINR, Dubna, Russia
- V.V. Parhomchuk, A.A. Sery, V.D. Shiltsev
  Institute for Nuclear Physics, Novosibirsk, Russia
- I.N. Meshkov, Ye.M. Syresinm
  Center for Applied Physics and Technology, Lipetsk, Russia
- V.P. Belov, A.A. Makarov, Yu.P. Severgin, I.A. Shukeylo, M.N. Tarovik
  D.V. Efremov Scientific Research Institute of Electrophysical Apparatus, St. Petersburg, Russia

A B C D E F G H I J K L M N O P Q R S T U V W X Y Z

Paris, P.

Paper	Title	Page
XIII-03	**An On-Line Isotopic Separator Test Bench at GANIL**	725

- **P. Bricault**, R. Leroy, M. Lewitowicz, J.Y. Pacquet, M.G. St-Laurent, P. Sortais
  GANIL, Caen, France
- A.C. Mueller, J. Obert, J.C. Putaux
  IPN, Orsay, France
- C.F. Liang, P. Paris
  CSNSM, Orsay, France
- J.C. Steckmeyer
  LPC, Caen, France

A B C D E F G H I J K L M N O P Q R S T U V W X Y Z

Pattyn, E.

Paper	Title	Page
IV-12	**A Remotely Controlled Robotic Vehicle for Work Within Radioactive Environments**	198

- **N.R. Stevenson**, P. Bloemhard, M. Brigham, J. Ko, C. LaForge, J. Orzechowski, E. Pattyn, T. Rattray
  TRIUMF, Vancouver, Canada

A B C D E F G H I J K L M N O P Q R S T U V W X Y Z

Pavlov, S.N.

Paper	Title	Page
VII-06	**The New Project of INR (Kiev's) Storage-Accelerating Complex**	294

- **A.V. Dolinsky**, A.I. Papash, S.N. Pavlov, A.T. Rudchik, A.E. Val'Kov, I.N. Vishnevsky, A.V. Zhmendak
  Institute for Nuclear Research, Kiev, Ukraine
- V.P. Belov, A.M. Kokorin, A.A. Makarov, I.A. Schukeilo, Yu.P. Severgin
  D.V. Efremov Scientific Research Institute of Electrophysical Apparatus, St. Petersburg, Russia

A B C D E F G H I J K L M N O P Q R S T U V W X Y Z

Pearce, D.R.

Paper	Title	Page
V-03	**A Facility for Radioisotope Production at TRIUMF with 70-110 MeV Protons**	209

- **D.R. Pearce**, J.S. Vincent
  TRIUMF, Vancouver, Canada

A B C D E F G H I J K L M N O P Q R S T U V W X Y Z

Pearson, J.B.

Paper	Title	Page
IXA-12	**Beam Quality Investigations for H⁻ Extraction at TRIUMF**	415

- **R.E. Laxdal**, G.H. Mackenzie, J.B. Pearson, L. Root
  TRIUMF, Vancouver, Canada

A B C D E F G H I J K L M N O P Q R S T U V W X Y Z

Pedroni, E.

Paper	Title	Page
VI-01	**Accelerators for Charged Particle Therapy: Performance Criteria from the User Point of View (Invited Paper)**	226

- **E. Pedroni**
  PSI, Villigen, Switzerland

A B C D E F G H I J K L M N O P Q R S T U V W X Y Z

Pei, A.

Paper	Title	Page
VIII-07	**Performance and Status of the IUCF High Intensity Polarized Ion Source**	330

- **V. Derenchuk**, R. Brown, T.J.P. Ellison, D.L. Friesel, J.W. Hicks, D. Jenner, A. Pei, H. Petri, P. Schwandt, J. Sowinski, M. Wedekind
  Indiana University, Bloomington, Indiana, USA

A B C D E F G H I J K L M N O P Q R S T U V W X Y Z

Pei, X.

Paper	Title	Page
XA-05	**Low Frequency RF System for the Indiana University Cooler Ring**	523

- **X. Pei**, S. Anderson, V. Derenchuk, G. East, D.L. Friesel, D. Jenner, D. McCammon, T. Sloan
  Indiana University, Bloomington, Indiana, USA

A B C D E F G H I J K L M N O P Q R S T U V W X Y Z

Pelzer, W.

Paper	Title	Page
XA-04	**The RF-System for a VICKSI Injector Cyclotron**	519

- **W. Pelzer**
  HMI, Berlin, Germany

A B C D E F G H I J K L M N O P Q R S T U V W X Y Z

Penco, C.

Paper	Title	Page
XB-01	**Low Temperature Tests of the AGOR Superconducting Coil System**	557

- **K. Pieterman**, J.A.M. Dam
  Cryocon B.V., Amersfoort, The Netherlands
- C. Commeaux
  IPN, Orsay, France
- C. Penco
  Ansaldo Componenti, Genoa, Italy

A B C D E F G H I J K L M N O P Q R S T U V W X Y Z

Petri, H.

Paper	Title	Page
VIII-07	**Performance and Status of the IUCF High Intensity Polarized Ion Source**	330

- **V. Derenchuk**, R. Brown, T.J.P. Ellison, D.L. Friesel, J.W. Hicks, D. Jenner, A. Pei, H. Petri, P. Schwandt, J. Sowinski, M. Wedekind
  Indiana University, Bloomington, Indiana, USA

A B C D E F G H I J K L M N O P Q R S T U V W X Y Z

Pfister, U.

Paper	Title	Page
VII-03	**COSY-Jülich - A Synchrotron and Storage Ring for Medium Energy Physics**	282

- **R. Maier**, U. Pfister
  FZJ, Jülich, Germany

A B C D E F G H I J K L M N O P Q R S T U V W X Y Z

Pieterman, K.

Paper	Title	Page
XB-01	**Low Temperature Tests of the AGOR Superconducting Coil System**	557

- **K. Pieterman**, J.A.M. Dam
  Cryocon B.V., Amersfoort, The Netherlands
- C. Commeaux
  IPN, Orsay, France
- C. Penco
  Ansaldo Componenti, Genoa, Italy

XC-05	**The AGOR Superconducting Extraction Channel EMC2**	585

- **K. Pieterman**, J.A.M. Dam
  Cryocon B.V., Amersfoort, The Netherlands
- H.J.H. ten Kate
  TU Twente, Enschede, The Netherlands
- S. Gustafsson
  IPN, Orsay, France

A B C D E F G H I J K L M N O P Q R S T U V W X Y Z

Pisman, A.Ya.

Paper	Title	Page
II-05	**Status of a Compact H^- Cyclotron at the Kurchatov Institute of Atomic Energy**	126

- **N.I. Venikov**, C.D. Burbeza, P.Yu. Komissarov, Yu.M. Krasnikov, S.T. Latushkin, V.V. Leonov, V.P. Moryakov, I.V. Naumov, A.Ya. Pisman, V.A. Rezvov, A.A. Vasiliev, V.E. Yarosh, L.I. Yudin
  Kurchatov Institute, Moscow, Russia

A B C D E F G H I J K L M N O P Q R S T U V W X Y Z

Pitatelev, G.

Paper	Title	Page
VII-07	**Superthin Internal Target for Storage Rings**	297

- **V. Pugatch**, A. Glushko, G. Pitatelev, G. Sivtsov
  Institute for Nuclear Research, Kiev, Ukraine
- S. Popov, D. Toporkov, B. Voitsechovsky
  Institute for Nuclear Physics, Novosibirsk, Russia

A B C D E F G H I J K L M N O P Q R S T U V W X Y Z

Plagnol, E.

Paper	Title	Page
IV-02	**A Cyclotron as a Mass Spectrometer**	158

- **P. Bricault**, G. Auger, M. Bajard, E. Baron, D. Bibet, A. Chabert, J. Fermé, L. Gaudart, J. Joubert, M. Lewitowicz, W. Mittig, E. Plagnol, Ch. Ricaud, Y. Schutz
  GANIL, Caen, France
- G. Audi
  CSNSM, Orsay, France
- A. Gillibert
  CEN/Saclay, Gif-sur-Yvette, France
- K. Fifield
  Australian National University, Canberra , Australia

A B C D E F G H I J K L M N O P Q R S T U V W X Y Z

Pálinkás, J.

Paper	Title	Page
I-20	**Heavy Ion Facility in ATOMKI**	99

- **S. Biri**, J. Pálinkás, A. Valek
  Institute of Nuclear Research of the Hungarian Academy of Sciences, Debrecen, Hungary

A B C D E F G H I J K L M N O P Q R S T U V W X Y Z

Poe, D.

Paper	Title	Page
I-17	**Performance of the K1200 Cyclotron at MSU**	86

- **P. Miller**, T.A. Antaya, F. Marti, D. Poe, B. Sherrill, J. Stetson, J. Winger
  NSCL, East Lansing, Michigan, USA
- J.A. Nolen
  ANL, Argonne, Illinois, USA

IXB-03	**K1200 Cyclotron Beam Development Techniques**	427

- **T.A. Antaya**, D. Cole, P. Miller, D. Poe
  NSCL, East Lansing, Michigan, USA

A B C D E F G H I J K L M N O P Q R S T U V W X Y Z

Poirier, R.L.

Paper	Title	Page
XA-11	**TRIUMF Cyclotron RF System Improvements**	545

- **G.C. Blaker**, A.K. Mitra, R.L. Poirier
  TRIUMF, Vancouver, Canada

Paper	Title	Page
XA-12	**Improvements to the RF Separator in the M9 Muon Channel at TRIUMF**	549

- **G.C. Blaker**, A.K. Mitra, R.L. Poirier
  TRIUMF, Vancouver, Canada

A B C D E F G H I J K L M N O P Q R S T U V W X Y Z

Pokrovskii, A.S.

Paper	Title	Page
I-10	**Gatchina Isochronous Cyclotron**	58

- **N.K. Abrosimov**, S.A. Artamonov, P.V. Chervyakov, S.P. Dmitriev, V.A. Eliseev, V.P. Fominenko, E.M. Ivanov, G.F. Mikheev, Yu.T. Mironov, A.S. Pokrovskii, G.A. Riabov, V.A. Smolin, G.L. Sokolov, V.A. Volchenkov, A.A. Vorobiev
  Petersburg Nuclear Physics Institute, Gatchina, Russia
- P.V. Bogdanov, B.D. Ershov, V.S. Kuligin, V.N. Moshkin, V.G. Mudrolyubov, Yu.I. Stogov, A.P. Strokach
  D.V. Efremov Scientific Research Institute of Electrophysical Apparatus, St. Petersburg, Russia

A B C D E F G H I J K L M N O P Q R S T U V W X Y Z

Pollock, R.E.

Paper	Title	Page
XIV-03	**Physics with Storage Rings (Invited Paper)**	753

- **R.E. Pollock**
  Indiana University, Bloomington, Indiana, USA

A B C D E F G H I J K L M N O P Q R S T U V W X Y Z

Popeko, G.S.

Paper	Title	Page
VII-05	**Dubna Project of the Heavy Ion Storage Ring Complex K4-K10**	290

- **Yu.Ts. Oganessian**, O.N. Malyshev, G.S. Popeko, A.M. Rodin, S.I. Sidorchuk, Ye.A. Sokol, S.V. Stepantsov, G.M. Ter-Akopian, V.A. Timakov
  JINR, Dubna, Russia
- V.V. Parhomchuk, A.A. Sery, V.D. Shiltsev
  Institute for Nuclear Physics, Novosibirsk, Russia
- I.N. Meshkov, Ye.M. Syresinm
  Center for Applied Physics and Technology, Lipetsk, Russia
- V.P. Belov, A.A. Makarov, Yu.P. Severgin, I.A. Shukeylo, M.N. Tarovik
  D.V. Efremov Scientific Research Institute of Electrophysical Apparatus, St. Petersburg, Russia

A B C D E F G H I J K L M N O P Q R S T U V W X Y Z

Popov, S.

Paper	Title	Page
VII-07	**Superthin Internal Target for Storage Rings**	297

- **V. Pugatch**, A. Glushko, G. Pitatelev, G. Sivtsov
  Institute for Nuclear Research, Kiev, Ukraine
- S. Popov, D. Toporkov, B. Voitsechovsky
  Institute for Nuclear Physics, Novosibirsk, Russia

A B C D E F G H I J K L M N O P Q R S T U V W X Y Z

Postiau, N.

Paper	Title	Page
I-16	**Status Report of Cyclone**	82

- **M. Loiselet**, N. Postiau, G. Ryckewaert
  Université Catholique de Louvain, Louvain-la-Neuve, Belgium

Paper	Title	Page
XIII-06	**Radioactive Ion Beam Production Using the Louvain-La-Neuve Cyclotrons: Present Status and Future Developments**	737

- **G. Ryckewaert**, M. Loiselet, N. Postiau
  Université Catholique de Louvain, Louvain-la-Neuve, Belgium

A B C D E F G H I J K L M N O P Q R S T U V W X Y Z

Pronin, N.V.

Paper	Title	Page
IV-04	^{178m2}Hf and ^{237}Pu Isotopes Production on the U-200 Cyclotron	167

- **S.L. Bogomolov**, S.N. Dmitriev, Yu.P. Gangrski, G.G. Gulbekyan, S.A. Karamian, V.B. Kutner, B.N. Markov, Yu.Ts. Oganessian, N.V. Pronin, G.Ya. Starodub
  JINR, Dubna, Russia

A B C D E F G H I J K L M N O P Q R S T U V W X Y Z

Pugatch, V.

Paper	Title	Page
VII-07	**Superthin Internal Target for Storage Rings**	297

- **V. Pugatch**, A. Glushko, G. Pitatelev, G. Sivtsov
  Institute for Nuclear Research, Kiev, Ukraine
- S. Popov, D. Toporkov, B. Voitsechovsky
  Institute for Nuclear Physics, Novosibirsk, Russia

A B C D E F G H I J K L M N O P Q R S T U V W X Y Z

Putaux, J.C.

Paper	Title	Page
XIII-03	**An On-Line Isotopic Separator Test Bench at GANIL**	725

- **P. Bricault**, R. Leroy, M. Lewitowicz, J.Y. Pacquet, M.G. St-Laurent, P. Sortais
  GANIL, Caen, France
- A.C. Mueller, J. Obert, J.C. Putaux
  IPN, Orsay, France
- C.F. Liang, P. Paris
  CSNSM, Orsay, France
- J.C. Steckmeyer
  LPC, Caen, France

A B C D E F G H I J K L M N O P Q R S T U V W X Y Z

Qiao, Q.

Paper	Title	Page
I-15	**Upgrading the SFC**	78

- **F. Ye**, M. Guo, Z. Ma, Q. Qiao, Y. Wang, Q. Yin, X. Zhu
  Institute of Modern Physics, Lanzhou, People's Republic of China

A B C D E F G H I J K L M N O P Q R S T U V W X Y Z

Raadu, M.A.

Paper	Title	Page
VII-01	**Recent Commissioning Results at Celsius (Invited Paper)**	266

- **D. Reistad**, T. Bergmark, C. Ekström, C.-J. Fridén, K. Gajewski, L. Hermansson, P. Jahnke, A. Johansson, O. Johansson, T. Lofnes, G. Norman, R. Wedberg, L. Westerberg, J. Zlomanczuk
  Uppsala University, Uppsala, Sweden
- M.A. Raadu, M. Sedlacek
  Royal Institute of Technology, Stockholm, Sweden

A B C D E F G H I J K L M N O P Q R S T U V W X Y Z

Raia, G.

Paper	Title	Page
I-18	**Status Report on the Heavy Ion Facility at LNS**	90

- **F. Alessandria**, G. Bellomo, A. Bosotti, C. De Martinis, D. Giove, P. Michelato, C. Pagani, L. Rossi
  INFN/LASA, Segrate, Italy
- L. Calabretta, G. Ciavola, G. Cuttone, M. Di Giacomo, S. Gammino, P. Gmaj, G. Raia, D. Rifuggiato, J. Sura
  INFN/LNS, Catania, Italy

A B C D E F G H I J K L M N O P Q R S T U V W X Y Z

Rattray, T.

Paper	Title	Page
IV-12	**A Remotely Controlled Robotic Vehicle for Work Within Radioactive Environments**	198

- **N.R. Stevenson**, P. Bloemhard, M. Brigham, J. Ko, C. LaForge, J. Orzechowski, E. Pattyn, T. Rattray
  TRIUMF, Vancouver, Canada

A B C D E F G H I J K L M N O P Q R S T U V W X Y Z

Reid, D.D.

Paper	Title	Page
XI-02	**The IUCF High Intensity Polarized Ion Source Control System**	641

- **T. Capshew**, J.C. Collins, D. DuPlantis, D.W. Frame, J. Graham, D.D. Reid
  Indiana University, Bloomington, Indiana, USA

A B C D E F G H I J K L M N O P Q R S T U V W X Y Z

Reistad, D.

Paper	Title	Page
VII-01	**Recent Commissioning Results at Celsius (Invited Paper)**	266

- **D. Reistad**, T. Bergmark, C. Ekström, C.-J. Fridén, K. Gajewski, L. Hermansson, P. Jahnke, A. Johansson, O. Johansson, T. Lofnes, G. Norman, R. Wedberg, L. Westerberg, J. Zlomanczuk
  Uppsala University, Uppsala, Sweden
- M.A. Raadu, M. Sedlacek
  Royal Institute of Technology, Stockholm, Sweden

A B C D E F G H I J K L M N O P Q R S T U V W X Y Z

Reitmann, D.

Paper	Title	Page
I-19	**Development of the NAC Accelerator Facilities**	95

- **J.L. Conradie**, A.H. Botha, P.M. Cronje, R.E.F. Fenemore, H.N. Jungwirth, J.J. Kritzinger, W.A.G. Nel, D. Reitmann, L.M.M. Roels, P.F. Rohwer, H.A. Smit
  National Accelerator Centre, Faure, Republic of South Africa

A B C D E F G H I J K L M N O P Q R S T U V W X Y Z

Rezvov, V.A.

Paper	Title	Page
II-05	**Status of a Compact H^- Cyclotron at the Kurchatov Institute of Atomic Energy**	126

- **N.I. Venikov**, C.D. Burbeza, P.Yu. Komissarov, Yu.M. Krasnikov, S.T. Latushkin, V.V. Leonov, V.P. Moryakov, I.V. Naumov, A.Ya. Pisman, V.A. Rezvov, A.A. Vasiliev, V.E. Yarosh, L.I. Yudin
  Kurchatov Institute, Moscow, Russia

IXD-02	**High-Sensitive Ionization Detectors of Transverse Distribution of Accelerated Particles Beam**	473

- **V.G. Mikhailov**, V.A. Rezvov, A.A. Roshchin, V.I. Sklyarenko, L.I. Iudin
  Kurchatov Institute, Moscow, Russia

A B C D E F G H I J K L M N O P Q R S T U V W X Y Z

Riabov, G.A.

Paper	Title	Page
I-10	**Gatchina Isochronous Cyclotron**	58

- **N.K. Abrosimov**, S.A. Artamonov, P.V. Chervyakov, S.P. Dmitriev, V.A. Eliseev, V.P. Fominenko, E.M. Ivanov, G.F. Mikheev, Yu.T. Mironov, A.S. Pokrovskii, G.A. Riabov, V.A. Smolin, G.L. Sokolov, V.A. Volchenkov, A.A. Vorobiev
  Petersburg Nuclear Physics Institute, Gatchina, Russia
- P.V. Bogdanov, B.D. Ershov, V.S. Kuligin, V.N. Moshkin, V.G. Mudrolyubov, Yu.I. Stogov, A.P. Strokach
  D.V. Efremov Scientific Research Institute of Electrophysical Apparatus, St. Petersburg, Russia

A B C D E F G H I J K L M N O P Q R S T U V W X Y Z

Ricaud, Ch.

Paper	Title	Page
IV-02	**A Cyclotron as a Mass Spectrometer**	158

- **P. Bricault**, G. Auger, M. Bajard, E. Baron, D. Bibet, A. Chabert, J. Fermé, L. Gaudart, J. Joubert, M. Lewitowicz, W. Mittig, E. Plagnol, Ch. Ricaud, Y. Schutz
  GANIL, Caen, France
- G. Audi
  CSNSM, Orsay, France
- A. Gillibert
  CEN/Saclay, Gif-sur-Yvette, France
- K. Fifield
  Australian National University, Canberra , Australia

Paper	Title	Page
IXC-01	**Commissioning of the New High Intensity Axial Injection System for GANIL**	446

- **Ch. Ricaud**, E. Baron, J. Bony, M.P. Bourgarel, B. Bru
  GANIL, Caen, France
- R. Vienet
  CEN/Saclay, Gif-sur-Yvette, France

Rifuggiato, D.

Paper	Title	Page
IXB-04	**Selection and Measurement of RF Phase Width of the K1200 Cyclotron Beam**	431

- **J. Bailey**, J. Kuchar, F. Marti, J. Yurkon
  NSCL, East Lansing, Michigan, USA
- J.A. Nolen
  ANL, Argonne, Illinois, USA
- D. Rifuggiato
  INFN/LNS, Catania, Italy

I-18	**Status Report on the Heavy Ion Facility at LNS**	90

- **F. Alessandria**, G. Bellomo, A. Bosotti, C. De Martinis, D. Giove, P. Michelato, C. Pagani, L. Rossi
  INFN/LASA, Segrate, Italy
- L. Calabretta, G. Ciavola, G. Cuttone, M. Di Giacomo, S. Gammino, P. Gmaj, G. Raia, D. Rifuggiato, J. Sura
  INFN/LNS, Catania, Italy

XC-06	**Material Consideration for Magnetic Channels**	589

- **J. Sura**, L. Calabretta, G. Di Biasi, P. Gmaj, D. Rifuggiato
  INFN/LNS, Catania, Italy

XIII-05	**High Intensity Superconducting Cyclotron Beams for a Radioactive Ion Beam Facility**	733

- **L. Calabretta**, D. Rifuggiato
  INFN/LNS, Catania, Italy

A B C D E F G H I J K L M N O P Q R S T U V W X Y Z

Rinta-Nikkola, M.

Paper	Title	Page
IXA-04	**Ion_Tracker, a Trace Tracking Program for Cyclotron Design**	388
	• **M. Rinta-Nikkola** University of Jyväskylä, Jyväskylä, Finland	
IXA-05	**Ion Optics in the Jyväskylä K130 Cyclotron**	392
	• **P. Heikkinen**, M. Rinta-Nikkola University of Jyväskylä, Jyväskylä, Finland	

A B C D E F G H I J K L M N O P Q R S T U V W X Y Z

Risler, R.

Paper	Title	Page
VI-09	**Continued Operation of the Seattle Clinical Cyclotron Facility**	262

- **R. Risler**, S. Brossard, J. Jacky, I. Kalet, P. Wootton, F. Ziai
  University of Washington, Seattle, Washington, USA

Paper	Title	Page
XI-14	**Formal Specifications for a Cyclotron Control System**	689

- **J. Jacky**, R. Risler
  University of Washington, Seattle, Washington, USA

A B C D E F G H I J K L M N O P Q R S T U V W X Y Z

Rodin, A.M.

Paper	Title	Page
VII-05	**Dubna Project of the Heavy Ion Storage Ring Complex K4-K10**	290

- **Yu.Ts. Oganessian**, O.N. Malyshev, G.S. Popeko, A.M. Rodin, S.I. Sidorchuk, Ye.A. Sokol, S.V. Stepantsov, G.M. Ter-Akopian, V.A. Timakov
  JINR, Dubna, Russia
- V.V. Parhomchuk, A.A. Sery, V.D. Shiltsev
  Institute for Nuclear Physics, Novosibirsk, Russia
- I.N. Meshkov, Ye.M. Syresinm
  Center for Applied Physics and Technology, Lipetsk, Russia
- V.P. Belov, A.A. Makarov, Yu.P. Severgin, I.A. Shukeylo, M.N. Tarovik
  D.V. Efremov Scientific Research Institute of Electrophysical Apparatus, St. Petersburg, Russia

A B C D E F G H I J K L M N O P Q R S T U V W X Y Z

Roels, L.M.M.

Paper	Title	Page
I-19	**Development of the NAC Accelerator Facilities**	95

- **J.L. Conradie**, A.H. Botha, P.M. Cronje, R.E.F. Fenemore, H.N. Jungwirth, J.J. Kritzinger, W.A.G. Nel, D. Reitmann, L.M.M. Roels, P.F. Rohwer, H.A. Smit
  National Accelerator Centre, Faure, Republic of South Africa

A B C D E F G H I J K L M N O P Q R S T U V W X Y Z

Rogers, J.P.

Paper	Title	Page
XI-06	**The New Distributed Control System of the NAC**	656

- **H.F. Weehuizen**, R.K. Fisch, E.J.S. Franklin, M.E. Hogan, I.H. Kohler, J.P. Rogers, P.J. Theron
  National Accelerator Centre, Faure, Republic of South Africa

A B C D E F G H I J K L M N O P Q R S T U V W X Y Z

Rogers, R.C.

Paper	Title	Page
VIII-17	**Performance of the Texas A&M ECRIS**	369

- **G. Mouchaty**, D.P. May, R.C. Rogers, P. Smelser
  Texas A&M University, College Station, Texas, USA

XC-09	**Results from the Deflector Test Stand at Texas A&M University**	602

- **D.P. May**, G. Derrig, W. Dewees, P. Smelser, D. Tran, R.C. Rogers
  Texas A&M University, College Station, Texas, USA

XD-08	**Design of a Beam Buncher Using a Half-Cosine Driving Function**	629

- **R.C. Rogers**
  Texas A&M University, College Station, Texas, USA

A B C D E F G H I J K L M N O P Q R S T U V W X Y Z

Rogge, M.

Paper	Title	Page
I-12	**Commissioning of the Injector Complex of COSY-Jülich**	67

- **W. Bräutigam**, H. Beuscher, R. Brings, H.G. Böge, R. Maier, M. Rogge, P. Wucherer
  FZJ, Jülich, Germany

A B C D E F G H I J K L M N O P Q R S T U V W X Y Z

Rohwer, P.F.

Paper	Title	Page
I-19	**Development of the NAC Accelerator Facilities**	95

- **J.L. Conradie**, A.H. Botha, P.M. Cronje, R.E.F. Fenemore, H.N. Jungwirth, J.J. Kritzinger, W.A.G. Nel, D. Reitmann, L.M.M. Roels, P.F. Rohwer, H.A. Smit
  National Accelerator Centre, Faure, Republic of South Africa

Paper	Title	Page
VIII-15	**Progress with the NAC Injector Cyclotron for Heavy and Polarized Ions**	361

- **Z.B. du Toit**, S.J. Burger, P.J. Celliers, J.G. de Villiers, H.N. Jungwirth, A. Müller, P.F. Rohwer, D.M. van Rooyen
  National Accelerator Centre, Faure, Republic of South Africa

A B C D E F G H I J K L M N O P Q R S T U V W X Y Z

Root, L.

Paper	Title	Page
IXA-12	**Beam Quality Investigations for H⁻ Extraction at TRIUMF**	415
	• **R.E. Laxdal**, G.H. Mackenzie, J.B. Pearson, L. Root TRIUMF, Vancouver, Canada	
IXB-07	**Beam Test Results Using the Auxiliary Accelerating Cavity**	442
	• **R.E. Laxdal**, G.H. Mackenzie, L. Root TRIUMF, Vancouver, Canada	
XIII-09	**Post-Accelerator Studies for the ISOL Facility at TRIUMF**	749
	• **L. Root**, H.R. Schneider, J.S. Fraser TRIUMF, Vancouver, Canada	

A B C D E F G H I J K L M N O P Q R S T U V W X Y Z

Roshchin, A.A.

Paper	Title	Page
IXD-02	**High-Sensitive Ionization Detectors of Transverse Distribution of Accelerated Particles Beam**	473

- **V.G. Mikhailov**, V.A. Rezvov, A.A. Roshchin, V.I. Sklyarenko, L.I. Iudin
  Kurchatov Institute, Moscow, Russia

A B C D E F G H I J K L M N O P Q R S T U V W X Y Z

Rossi, L.

Paper	Title	Page
I-18	**Status Report on the Heavy Ion Facility at LNS**	90

- **F. Alessandria**, G. Bellomo, A. Bosotti, C. De Martinis, D. Giove, P. Michelato, C. Pagani, L. Rossi
  INFN/LASA, Segrate, Italy
- L. Calabretta, G. Ciavola, G. Cuttone, M. Di Giacomo, S. Gammino, P. Gmaj, G. Raia, D. Rifuggiato, J. Sura
  INFN/LNS, Catania, Italy

A B C D E F G H I J K L M N O P Q R S T U V W X Y Z

Roy, G.

Paper	Title	Page
XIII-08	**Research and Development Studies with Radioactive Beams at TRIUMF**	745

- **J.M. D'Auria**, M. Dombsky
  Simon Fraser University, Burnaby, BC, Canada
- L. Buchmann, H. Sprenger, J.S. Vincent
  TRIUMF, Vancouver, Canada
- J. King
  University of Toronto, Toronto, Ontario, Canada
- P. McNeely, G. Roy
  University of Alberta, Edmonton, Alberta, Canada

A B C D E F G H I J K L M N O P Q R S T U V W X Y Z

Rudchik, A.T.

Paper	Title	Page
VII-06	**The New Project of INR (Kiev's) Storage-Accelerating Complex**	294

- **A.V. Dolinsky**, A.I. Papash, S.N. Pavlov, A.T. Rudchik, A.E. Val'Kov, I.N. Vishnevsky, A.V. Zhmendak
  Institute for Nuclear Research, Kiev, Ukraine
- V.P. Belov, A.M. Kokorin, A.A. Makarov, I.A. Schukeilo, Yu.P. Severgin
  D.V. Efremov Scientific Research Institute of Electrophysical Apparatus, St. Petersburg, Russia

A B C D E F G H I J K L M N O P Q R S T U V W X Y Z

Ruegg, R.

Paper	Title	Page
VIII-05	**Status of the TRIUMF Optically-Pumped Polarized H^- Ion Source**	322

- **C.D.P. Levy**, K. Jayamanna, M. McDonald, R. Ruegg, P.W. Schmor
  TRIUMF, Vancouver, Canada
- A.N. Zelenskii
  Institute of Nuclear Research, Russian Academy of Sciences, Moscow, Russia

A B C D E F G H I J K L M N O P Q R S T U V W X Y Z

Ruth, T.J.

Paper	Title	Page
V-02	**The Production of Radionuclides for the Biosciences (Invited Paper)**	206

- **T.J. Ruth**
  TRIUMF, Vancouver, Canada

A B C D E F G H I J K L M N O P Q R S T U V W X Y Z

Ryckewaert, G.

Paper	Title	Page
I-16	**Status Report of Cyclone** • **M. Loiselet**, N. Postiau, G. Ryckewaert Université Catholique de Louvain, Louvain-la-Neuve, Belgium	82
XIII-06	**Radioactive Ion Beam Production Using the Louvain-La-Neuve Cyclotrons: Present Status and Future Developments** • **G. Ryckewaert**, M. Loiselet, N. Postiau Université Catholique de Louvain, Louvain-la-Neuve, Belgium	737

A B C D E F G H I J K L M N O P Q R S T U V W X Y Z

Rykov, A.

Paper	Title	Page
II-04	**20 MeV Cyclotron for Isotope Production**	123

- **A. Glazov**, Ju. Alenitskiy, A. Chesnov, S. Chesnova, V. Kochkin, D. Novikov, E. Samsonov, M. Semenov, A. Vasilenko, E. Zaplatin, N. Zaplatin
  JINR, Dubna, Russia
- I. Gulamov, O. Iljasov, A. Rykov
  Institute of Nuclear Physics, Tashkent, Republic of Uzbekistan

A B C D E F G H I J K L M N O P Q R S T U V W X Y Z

Saito, T.

Paper	Title	Page
I-01	**Commissioning of the RCNP Ring Cyclotron (Invited Paper)**	3

- **I. Miura**, A. Ando, K. Hatanaka, K. Hosono, H. Ikegami, T. Itahashi, M. Kibayashi, M. Kondo, H. Ogata, T. Saito, A. Shimizu, K. Tamura, M. Uraki, T. Yamazaki
  Osaka University, Osaka, Japan
- J. Abe
  Sumitomo Heavy Industries, Ehime, Japan

IXD-07	**Beam Diagnostics in the RCNP Ring Cyclotron**	491

- **T. Itahashi**, T. Saito, I. Miura
  Osaka University, Osaka, Japan
- S. Ichida
  Sumitomo Heavy Industries, Ehime, Japan

XA-09	**Initial Operation of the RF System for the RCNP Ring Cyclotron**	538

- **T. Saito**, I. Miura, A. Shimizu, M. Uraki
  Osaka University, Osaka, Japan

XI-10	**Construction and System Tuning of Control System for the RCNP Ring Cyclotron and Beam Lines**	672

- **T. Yamazaki**, A. Ando, K. Hosono, T. Itahashi, M. Kibayashi, I. Miura, K. Nagayama, H. Ogata, T. Saito, A. Shimizu, K. Tamura, M. Uraki
  Osaka University, Osaka, Japan
- K. Aoki, Y. Kimura, M. Maruyama, M. Tachibana, S. Yamada
  Sumitomo Heavy Industries, Ehime, Japan
- K. Kodaira
  Sumitomo Heavy Industries Systems Engineering Laboratory, Tokyo, Japan

A B C D E F G H I J K L M N O P Q R S T U V W X Y Z

Sakuma, S.

Paper	Title	Page
II-06	**A Newly Developed Compact Cyclotron for Neutron Therapy and Positron Nuclear Medicine**	129

- **K. Ito**, T. Ishigaki, S. Itoh, Y. Kasugai, T. Kato, T. Misawa, M. Nishino, M. Osakabe, T. Ota, S. Sakuma, M. Tadokoro, H. Yamamoto
  Nagoya University, Nagoya, Japan
- Y. Toda, Y. Yamamoto
  Japan Steel Works Ltd., Tokyo, Japan

A B C D E F G H I J K L M N O P Q R S T U V W X Y Z

Samsonov, E.

Paper	Title	Page
II-04	**20 MeV Cyclotron for Isotope Production**	123

- **A. Glazov**, Ju. Alenitskiy, A. Chesnov, S. Chesnova, V. Kochkin, D. Novikov, E. Samsonov, M. Semenov, A. Vasilenko, E. Zaplatin, N. Zaplatin
  JINR, Dubna, Russia
- I. Gulamov, O. Iljasov, A. Rykov
  Institute of Nuclear Physics, Tashkent, Republic of Uzbekistan

A B C D E F G H I J K L M N O P Q R S T U V W X Y Z

Sano, M.

Paper	Title	Page
VI-04	**Progress Report on the IBA-SHI Proton Therapy System**	244

- **Y. Jongen**, W. Beeckman, J.P. Dufour, A. Laisné, H. Marie, R. Verbruggen
  Ion Beam Applications, Louvain-la-Neuve, Belgium
- M. Sano, S. Satoh, N. Takahashi, T. Takayama
  Sumitomo Heavy Industries, Ehime, Japan

A B C D E F G H I J K L M N O P Q R S T U V W X Y Z

Sarkisyan, A.L.

Paper	Title	Page
IXA-09	**Crossing of Resonances**	408

- **L.A. Sarkisyan**, A.L. Sarkisyan
  Moscow Institute-Internate, Moscow, Russia

Paper	Title	Page
IXA-10	**Increase of Beam Intensity**	409

- **L.A. Sarkisyan**, A.L. Sarkisyan
  Moscow Institute-Internate, Moscow, Russia

A B C D E F G H I J K L M N O P Q R S T U V W X Y Z

Sarkisyan, L.A.

Paper	Title	Page
IXA-09	**Crossing of Resonances**	408

- **L.A. Sarkisyan**, A.L. Sarkisyan
  Moscow Institute-Internate, Moscow, Russia

Paper	Title	Page
IXA-10	**Increase of Beam Intensity**	409

- **L.A. Sarkisyan**, A.L. Sarkisyan
  Moscow Institute-Internate, Moscow, Russia

A B C D E F G H I J K L M N O P Q R S T U V W X Y Z

Sato, K.

Paper	Title	Page
XD-07	**Beam Transport System for the HIMAC**	625

- **K. Noda**, Y. Hirao, A. Itano, M. Kanazawa, A. Kitagawa, T. Kohno, M. Kumada, H. Ogawa, K. Sato, Y. Sato, M. Sudou, E. Takada, S. Yamada, T. Yamada
  NIRS, Chiba, Japan
- K. Endo
  KEK, Ibaraki, Japan

A B C D E F G H I J K L M N O P Q R S T U V W X Y Z

Sato, M.

Paper	Title	Page
VI-08	**A Proton Therapy Facility Plan**	258

- **S. Fukumoto**, Y. Hayakawa, T. Inada, A. Maruhashi, M. Sato, J. Tada, Y. Takada, H. Tsuji, H. Tsujii
  University of Tsukuba, Ibaraki, Japan
- K. Endo, Y. Irie, K. Muto
  KEK, Ibaraki, Japan

A B C D E F G H I J K L M N O P Q R S T U V W X Y Z

Sato, Y.

Paper	Title	Page
XD-07	**Beam Transport System for the HIMAC**	625

- **K. Noda**, Y. Hirao, A. Itano, M. Kanazawa, A. Kitagawa, T. Kohno, M. Kumada, H. Ogawa, K. Sato, Y. Sato, M. Sudou, E. Takada, S. Yamada, T. Yamada
  NIRS, Chiba, Japan
- K. Endo
  KEK, Ibaraki, Japan

A B C D E F G H I J K L M N O P Q R S T U V W X Y Z

Satoh, S.

Paper	Title	Page
VI-04	**Progress Report on the IBA-SHI Proton Therapy System**	244

- **Y. Jongen**, W. Beeckman, J.P. Dufour, A. Laisné, H. Marie, R. Verbruggen
  Ion Beam Applications, Louvain-la-Neuve, Belgium
- M. Sano, S. Satoh, N. Takahashi, T. Takayama
  Sumitomo Heavy Industries, Ehime, Japan

A B C D E F G H I J K L M N O P Q R S T U V W X Y Z

Satoh, T.

Paper	Title	Page
II-03	**Construction and First Year's Operation of the JAERI AVF Cyclotron**	119

- **K. Arakawa**, T. Agematsu, M. Fukuda, I. Ishibori, T. Karasawa, T. Nara, Y. Nakamura, S. Okumura, R. Tanaka, W. Yokota
  JAERI, Gunma, Japan
- A. Shimizu
  Osaka University, Osaka, Japan
- Y. Hayashi, K. Ishii, T. Satoh, T. Tachikawa
  Sumitomo Heavy Industries, Ehime, Japan

A B C D E F G H I J K L M N O P Q R S T U V W X Y Z

Savalle, A.

Paper	Title	Page
XIII-04	**The PIAFE Project at Grenoble: Beam Transport and Acceleration**	729

- **J.L. Belmont**, J.F. Bruandet, J.M. de Conto, M. Fruneau, G. Gimond, K. Golovanivsky, E. Liatard, J.M. Loiseaux, H. Nifenecker, A. Savalle, B. Vignon
  Université Joseph Fourier, Grenoble, France
- P. Briand
  CEN-Grenoble, Grenoble, France

A B C D E F G H I J K L M N O P Q R S T U V W X Y Z

Schippers, J.M.

Paper	Title	Page
IV-06	**A P.E.T. Study of Proton Induced Radioactivity in Different Materials**	175

- **J.M. Schippers**
  Kernfysisch Versneller Instituut, Groningen, The Netherlands
- A.M.J. Paans
  University Hospital, Groningen, The Netherlands

IXD-03	**A Beam Profile Monitor Using the Ionization of Residual Gas**	477

- **J.M. Schippers**, H.H. Kiewiet
  Kernfysisch Versneller Instituut, Groningen, The Netherlands

XD-04	**The Beam-Guiding System of AGOR**	615

- **J.M. Schippers**
  Kernfysisch Versneller Instituut, Groningen, The Netherlands

A B C D E F G H I J K L M N O P Q R S T U V W X Y Z

Schmeing, H.

Paper	Title	Page
XC-01	**The Electrostatic Deflector for the Chalk River Superconducting Cyclotron**	569

- **W.T. Diamond**, C.R. Hoffmann, G.R. Mitchel, H. Schmeing
  Atomic Energy of Canada, Chalk River, Ontario, Canada

A B C D E F G H I J K L M N O P Q R S T U V W X Y Z

Schmor, P.W.

Paper	Title	Page
VIII-04	**A Review of Polarized Ion Sources for Cyclotrons (Invited Paper)**	316

- **P.W. Schmor**
  TRIUMF, Vancouver, Canada

VIII-05	**Status of the TRIUMF Optically-Pumped Polarized H^- Ion Source**	322

- **C.D.P. Levy**, K. Jayamanna, M. McDonald, R. Ruegg, P.W. Schmor
  TRIUMF, Vancouver, Canada
- A.N. Zelenskii
  Institute of Nuclear Research, Russian Academy of Sciences, Moscow, Russia

A B C D E F G H I J K L M N O P Q R S T U V W X Y Z

Schneider, H.R.

Paper	Title	Page
XIII-09	**Post-Accelerator Studies for the ISOL Facility at TRIUMF**	749

- **L. Root**, H.R. Schneider, J.S. Fraser
  TRIUMF, Vancouver, Canada

A B C D E F G H I J K L M N O P Q R S T U V W X Y Z

Schreuder, H.W.

Paper	Title	Page
I-06	**AGOR: Recent Achievements (Invited Paper)**	40

- **H.W. Schreuder**
  IPN, Orsay, France

XD-03	**Superconducting Focussing Channel for the AGOR Cyclotron**	612

- **H.W. Schreuder**, P. Blache, C. Commeaux, S. Gustafsson, A. Lafoux, M. Mormiche, R. Panvier
  IPN, Orsay, France

A B C D E F G H I J K L M N O P Q R S T U V W X Y Z

Schukeilo, I.A.

Paper	Title	Page
VII-06	**The New Project of INR (Kiev's) Storage-Accelerating Complex**	294

- **A.V. Dolinsky**, A.I. Papash, S.N. Pavlov, A.T. Rudchik, A.E. Val'Kov, I.N. Vishnevsky, A.V. Zhmendak
  Institute for Nuclear Research, Kiev, Ukraine
- V.P. Belov, A.M. Kokorin, A.A. Makarov, I.A. Schukeilo, Yu.P. Severgin
  D.V. Efremov Scientific Research Institute of Electrophysical Apparatus, St. Petersburg, Russia

A B C D E F G H I J K L M N O P Q R S T U V W X Y Z

Schutz, Y.

Paper	Title	Page
IV-02	**A Cyclotron as a Mass Spectrometer**	158

- **P. Bricault**, G. Auger, M. Bajard, E. Baron, D. Bibet, A. Chabert, J. Fermé, L. Gaudart, J. Joubert, M. Lewitowicz, W. Mittig, E. Plagnol, Ch. Ricaud, Y. Schutz
  GANIL, Caen, France
- G. Audi
  CSNSM, Orsay, France
- A. Gillibert
  CEN/Saclay, Gif-sur-Yvette, France
- K. Fifield
  Australian National University, Canberra , Australia

A B C D E F G H I J K L M N O P Q R S T U V W X Y Z

Schwandt, P.

Paper	Title	Page
VIII-07	**Performance and Status of the IUCF High Intensity Polarized Ion Source**	330

- **V. Derenchuk**, R. Brown, T.J.P. Ellison, D.L. Friesel, J.W. Hicks, D. Jenner, A. Pei, H. Petri, P. Schwandt, J. Sowinski, M. Wedekind
  Indiana University, Bloomington, Indiana, USA

XD-02	**Beam Transport System for the IUCF High Intensity Polarized Ion Source**	609

- **W.P. Jones**, M.S. Ball, J.C. Collins, D. DuPlantis, T.J.P. Ellison, D.L. Friesel, B. Hamilton, J.W. Hicks, P. Schwandt
  Indiana University, Bloomington, Indiana, USA

A B C D E F G H I J K L M N O P Q R S T U V W X Y Z

Sedlacek, M.

Paper	Title	Page
VII-01	**Recent Commissioning Results at Celsius (Invited Paper)**	266

- **D. Reistad**, T. Bergmark, C. Ekström, C.-J. Fridén, K. Gajewski, L. Hermansson, P. Jahnke, A. Johansson, O. Johansson, T. Lofnes, G. Norman, R. Wedberg, L. Westerberg, J. Zlomanczuk
  Uppsala University, Uppsala, Sweden
- M.A. Raadu, M. Sedlacek
  Royal Institute of Technology, Stockholm, Sweden

A B C D E F G H I J K L M N O P Q R S T U V W X Y Z

Sekiguchi, M.

Paper	Title	Page
VIII-06	**An ECR Ion Source for Multiply-Charged Heavy Ions at 14 GHz**	326

- **M. Sekiguchi**, M. Fujita, Y. Ohshiro, T. Yamazaki
  University of Tokyo, Tanashi-shi, Tokyo, Japan
- Y. Isoya, T. Yamada, Y. Yamashita
  Japan Steel Works Ltd., Research Center for Advanced Technologies, Chiba, Japan
- A. Kitagawa
  NIRS, Chiba, Japan

IXC-02	**A Formulation of Spiral Inflector Design and Its Application to SF Cyclotron**	450

- **M. Sekiguchi**, M. Fujita, M. Nishiguchi, Y. Ohshiro, Y. Shida, N. Yamazaki, T. Yamazaki
  University of Tokyo, Tanashi-shi, Tokyo, Japan

A B C D E F G H I J K L M N O P Q R S T U V W X Y Z

Semenov, M.

Paper	Title	Page
II-04	**20 MeV Cyclotron for Isotope Production**	123

- **A. Glazov**, Ju. Alenitskiy, A. Chesnov, S. Chesnova, V. Kochkin, D. Novikov, E. Samsonov, M. Semenov, A. Vasilenko, E. Zaplatin, N. Zaplatin
  JINR, Dubna, Russia
- I. Gulamov, O. Iljasov, A. Rykov
  Institute of Nuclear Physics, Tashkent, Republic of Uzbekistan

A B C D E F G H I J K L M N O P Q R S T U V W X Y Z

Sery, A.A.

Paper	Title	Page
VII-05	**Dubna Project of the Heavy Ion Storage Ring Complex K4-K10**	290

- **Yu.Ts. Oganessian**, O.N. Malyshev, G.S. Popeko, A.M. Rodin, S.I. Sidorchuk, Ye.A. Sokol, S.V. Stepantsov, G.M. Ter-Akopian, V.A. Timakov
  JINR, Dubna, Russia
- V.V. Parhomchuk, A.A. Sery, V.D. Shiltsev
  Institute for Nuclear Physics, Novosibirsk, Russia
- I.N. Meshkov, Ye.M. Syresinm
  Center for Applied Physics and Technology, Lipetsk, Russia
- V.P. Belov, A.A. Makarov, Yu.P. Severgin, I.A. Shukeylo, M.N. Tarovik
  D.V. Efremov Scientific Research Institute of Electrophysical Apparatus, St. Petersburg, Russia

A B C D E F G H I J K L M N O P Q R S T U V W X Y Z

Severgin, Yu.P.

Paper	Title	Page
VII-05	**Dubna Project of the Heavy Ion Storage Ring Complex K4-K10**	290

- **Yu.Ts. Oganessian**, O.N. Malyshev, G.S. Popeko, A.M. Rodin, S.I. Sidorchuk, Ye.A. Sokol, S.V. Stepantsov, G.M. Ter-Akopian, V.A. Timakov
  JINR, Dubna, Russia
- V.V. Parhomchuk, A.A. Sery, V.D. Shiltsev
  Institute for Nuclear Physics, Novosibirsk, Russia
- I.N. Meshkov, Ye.M. Syresinm
  Center for Applied Physics and Technology, Lipetsk, Russia
- V.P. Belov, A.A. Makarov, Yu.P. Severgin, I.A. Shukeylo, M.N. Tarovik
  D.V. Efremov Scientific Research Institute of Electrophysical Apparatus, St. Petersburg, Russia

VII-06	**The New Project of INR (Kiev's) Storage-Accelerating Complex**	294

- **A.V. Dolinsky**, A.I. Papash, S.N. Pavlov, A.T. Rudchik, A.E. Val'Kov, I.N. Vishnevsky, A.V. Zhmendak
  Institute for Nuclear Research, Kiev, Ukraine
- V.P. Belov, A.M. Kokorin, A.A. Makarov, I.A. Schukeilo, Yu.P. Severgin
  D.V. Efremov Scientific Research Institute of Electrophysical Apparatus, St. Petersburg, Russia

A B C D E F G H I J K L M N O P Q R S T U V W X Y Z

Shen, Z.

Paper	Title	Page
IXD-04	**Emittance Measurements in the HIRFL Beam Line**	479

- **H. Zhao**, Z. Shen, B.W. Wei
  Institute of Modern Physics, Lanzhou, People's Republic of China

A B C D E F G H I J K L M N O P Q R S T U V W X Y Z

Sherrill, B.

Paper	Title	Page
I-17	**Performance of the K1200 Cyclotron at MSU**	86

- **P. Miller**, T.A. Antaya, F. Marti, D. Poe, B. Sherrill, J. Stetson, J. Winger
  NSCL, East Lansing, Michigan, USA
- J.A. Nolen
  ANL, Argonne, Illinois, USA

A B C D E F G H I J K L M N O P Q R S T U V W X Y Z

Shida, Y.

Paper	Title	Page
IXC-02	**A Formulation of Spiral Inflector Design and Its Application to SF Cyclotron**	450

- **M. Sekiguchi**, M. Fujita, M. Nishiguchi, Y. Ohshiro, Y. Shida, N. Yamazaki, T. Yamazaki
  University of Tokyo, Tanashi-shi, Tokyo, Japan

A B C D E F G H I J K L M N O P Q R S T U V W X Y Z

Shiltsev, V.D.

Paper	Title	Page
VII-05	**Dubna Project of the Heavy Ion Storage Ring Complex K4-K10**	290

- **Yu.Ts. Oganessian**, O.N. Malyshev, G.S. Popeko, A.M. Rodin, S.I. Sidorchuk, Ye.A. Sokol, S.V. Stepantsov, G.M. Ter-Akopian, V.A. Timakov
  JINR, Dubna, Russia
- V.V. Parhomchuk, A.A. Sery, V.D. Shiltsev
  Institute for Nuclear Physics, Novosibirsk, Russia
- I.N. Meshkov, Ye.M. Syresinm
  Center for Applied Physics and Technology, Lipetsk, Russia
- V.P. Belov, A.A. Makarov, Yu.P. Severgin, I.A. Shukeylo, M.N. Tarovik
  D.V. Efremov Scientific Research Institute of Electrophysical Apparatus, St. Petersburg, Russia

A B C D E F G H I J K L M N O P Q R S T U V W X Y Z

Shimizu, A.

Paper	Title	Page
I-01	**Commissioning of the RCNP Ring Cyclotron (Invited Paper)**	3

- **I. Miura**, A. Ando, K. Hatanaka, K. Hosono, H. Ikegami, T. Itahashi, M. Kibayashi, M. Kondo, H. Ogata, T. Saito, A. Shimizu, K. Tamura, M. Uraki, T. Yamazaki
  Osaka University, Osaka, Japan
- J. Abe
  Sumitomo Heavy Industries, Ehime, Japan

II-03	**Construction and First Year's Operation of the JAERI AVF Cyclotron**	119

- **K. Arakawa**, T. Agematsu, M. Fukuda, I. Ishibori, T. Karasawa, T. Nara, Y. Nakamura, S. Okumura, R. Tanaka, W. Yokota
  JAERI, Gunma, Japan
- A. Shimizu
  Osaka University, Osaka, Japan
- Y. Hayashi, K. Ishii, T. Satoh, T. Tachikawa
  Sumitomo Heavy Industries, Ehime, Japan

XA-06	**A Modified RF System of JAERI AVF Cyclotron**	526

- **Y. Kumata**, Y. Fukumoto
  Sumitomo Heavy Industries, Ehime, Japan
- K. Arakawa, M. Fukuda, T. Karasawa
  JAERI, Gunma, Japan
- A. Shimizu
  Osaka University, Osaka, Japan

XA-09	**Initial Operation of the RF System for the RCNP Ring Cyclotron**	538

- **T. Saito**, I. Miura, A. Shimizu, M. Uraki
  Osaka University, Osaka, Japan

XI-10	**Construction and System Tuning of Control System for the RCNP Ring Cyclotron and Beam Lines**	672

- **T. Yamazaki**, A. Ando, K. Hosono, T. Itahashi, M. Kibayashi, I. Miura, K. Nagayama, H. Ogata, T. Saito, A. Shimizu, K. Tamura, M. Uraki
  Osaka University, Osaka, Japan
- K. Aoki, Y. Kimura, M. Maruyama, M. Tachibana, S. Yamada
  Sumitomo Heavy Industries, Ehime, Japan
- K. Kodaira
  Sumitomo Heavy Industries Systems Engineering Laboratory, Tokyo, Japan

A B C D E F G H I J K L M N O P Q R S T U V W X Y Z

Shukeylo, I.A.

Paper	Title	Page
VII-05	**Dubna Project of the Heavy Ion Storage Ring Complex K4-K10**	290

- **Yu.Ts. Oganessian**, O.N. Malyshev, G.S. Popeko, A.M. Rodin, S.I. Sidorchuk, Ye.A. Sokol, S.V. Stepantsov, G.M. Ter-Akopian, V.A. Timakov
  JINR, Dubna, Russia
- V.V. Parhomchuk, A.A. Sery, V.D. Shiltsev
  Institute for Nuclear Physics, Novosibirsk, Russia
- I.N. Meshkov, Ye.M. Syresinm
  Center for Applied Physics and Technology, Lipetsk, Russia
- V.P. Belov, A.A. Makarov, Yu.P. Severgin, I.A. Shukeylo, M.N. Tarovik
  D.V. Efremov Scientific Research Institute of Electrophysical Apparatus, St. Petersburg, Russia

A B C D E F G H I J K L M N O P Q R S T U V W X Y Z

Shychikov, G.I.

Paper	Title	Page
V-05	**Radiopharmaceutical "Thallium-201-Chloride" Production using Thallium-203 Irradiation by Helium-3 Ions**	216

- **A.A. Arzumanov**, N.K. Hamidov, A.I. Kozin, G.I. Shychikov, S.T. Tihomirova
  Kazakhstan Academy of Sciences, Alma-Ata, Republic of Kazakhstan

Sidorchuk, S.I.

Paper	Title	Page
VII-05	**Dubna Project of the Heavy Ion Storage Ring Complex K4-K10**	290

- **Yu.Ts. Oganessian**, O.N. Malyshev, G.S. Popeko, A.M. Rodin, S.I. Sidorchuk, Ye.A. Sokol, S.V. Stepantsov, G.M. Ter-Akopian, V.A. Timakov
  JINR, Dubna, Russia
- V.V. Parhomchuk, A.A. Sery, V.D. Shiltsev
  Institute for Nuclear Physics, Novosibirsk, Russia
- I.N. Meshkov, Ye.M. Syresinm
  Center for Applied Physics and Technology, Lipetsk, Russia
- V.P. Belov, A.A. Makarov, Yu.P. Severgin, I.A. Shukeylo, M.N. Tarovik
  D.V. Efremov Scientific Research Institute of Electrophysical Apparatus, St. Petersburg, Russia

A B C D E F G H I J K L M N O P Q R S T U V W X Y Z

Sigg, P.K.

Paper	Title	Page
XA-08	**Experience with the PSI-Cyclotron RF-System Under Heavy Beam Loading**	534

- **P.K. Sigg**, J. Cherix, H. Frei, M. Märki
  PSI, Villigen, Switzerland

A B C D E F G H I J K L M N O P Q R S T U V W X Y Z

Sivtsov, G.

Paper	Title	Page
VII-07	**Superthin Internal Target for Storage Rings**	297

- **V. Pugatch**, A. Glushko, G. Pitatelev, G. Sivtsov
  Institute for Nuclear Research, Kiev, Ukraine
- S. Popov, D. Toporkov, B. Voitsechovsky
  Institute for Nuclear Physics, Novosibirsk, Russia

A B C D E F G H I J K L M N O P Q R S T U V W X Y Z

Sklyarenko, V.I.

Paper	Title	Page
IXD-02	**High-Sensitive Ionization Detectors of Transverse Distribution of Accelerated Particles Beam**	473

- **V.G. Mikhailov**, V.A. Rezvov, A.A. Roshchin, V.I. Sklyarenko, L.I. Iudin
  Kurchatov Institute, Moscow, Russia

A B C D E F G H I J K L M N O P Q R S T U V W X Y Z

Sloan, T.

Paper	Title	Page
XA-05	**Low Frequency RF System for the Indiana University Cooler Ring**	523

- **X. Pei**, S. Anderson, V. Derenchuk, G. East, D.L. Friesel, D. Jenner, D. McCammon, T. Sloan
  Indiana University, Bloomington, Indiana, USA

A B C D E F G H I J K L M N O P Q R S T U V W X Y Z

Smelser, P.

Paper	Title	Page
VIII-17	**Performance of the Texas A&M ECRIS**	369

- **G. Mouchaty**, D.P. May, R.C. Rogers, P. Smelser
  Texas A&M University, College Station, Texas, USA

Paper	Title	Page
XC-09	**Results from the Deflector Test Stand at Texas A&M University**	602

- **D.P. May**, G. Derrig, W. Dewees, P. Smelser, D. Tran, R.C. Rogers
  Texas A&M University, College Station, Texas, USA

A B C D E F G H I J K L M N O P Q R S T U V W X Y Z

Smit, H.A.

Paper	Title	Page
I-19	**Development of the NAC Accelerator Facilities**	95

- **J.L. Conradie**, A.H. Botha, P.M. Cronje, R.E.F. Fenemore, H.N. Jungwirth, J.J. Kritzinger, W.A.G. Nel, D. Reitmann, L.M.M. Roels, P.F. Rohwer, H.A. Smit
  National Accelerator Centre, Faure, Republic of South Africa

A B C D E F G H I J K L M N O P Q R S T U V W X Y Z

Smolin, V.A.

Paper	Title	Page
I-10	**Gatchina Isochronous Cyclotron**	58

- **N.K. Abrosimov**, S.A. Artamonov, P.V. Chervyakov, S.P. Dmitriev, V.A. Eliseev, V.P. Fominenko, E.M. Ivanov, G.F. Mikheev, Yu.T. Mironov, A.S. Pokrovskii, G.A. Riabov, V.A. Smolin, G.L. Sokolov, V.A. Volchenkov, A.A. Vorobiev
  Petersburg Nuclear Physics Institute, Gatchina, Russia
- P.V. Bogdanov, B.D. Ershov, V.S. Kuligin, V.N. Moshkin, V.G. Mudrolyubov, Yu.I. Stogov, A.P. Strokach
  D.V. Efremov Scientific Research Institute of Electrophysical Apparatus, St. Petersburg, Russia

A B C D E F G H I J K L M N O P Q R S T U V W X Y Z

Snyder, S.

Paper	Title	Page
IXB-05	**Internal Beam Dynamics Studies with a TV Probe**	435

- **F. Marti**, S. Snyder
  NSCL, East Lansing, Michigan, USA

A B C D E F G H I J K L M N O P Q R S T U V W X Y Z

Sokol, Ye.A.

Paper	Title	Page
VII-05	**Dubna Project of the Heavy Ion Storage Ring Complex K4-K10**	290

- **Yu.Ts. Oganessian**, O.N. Malyshev, G.S. Popeko, A.M. Rodin, S.I. Sidorchuk, Ye.A. Sokol, S.V. Stepantsov, G.M. Ter-Akopian, V.A. Timakov
  JINR, Dubna, Russia
- V.V. Parhomchuk, A.A. Sery, V.D. Shiltsev
  Institute for Nuclear Physics, Novosibirsk, Russia
- I.N. Meshkov, Ye.M. Syresinm
  Center for Applied Physics and Technology, Lipetsk, Russia
- V.P. Belov, A.A. Makarov, Yu.P. Severgin, I.A. Shukeylo, M.N. Tarovik
  D.V. Efremov Scientific Research Institute of Electrophysical Apparatus, St. Petersburg, Russia

A B C D E F G H I J K L M N O P Q R S T U V W X Y Z

Sokolov, G.L.

Paper	Title	Page
I-10	**Gatchina Isochronous Cyclotron**	58

- **N.K. Abrosimov**, S.A. Artamonov, P.V. Chervyakov, S.P. Dmitriev, V.A. Eliseev, V.P. Fominenko, E.M. Ivanov, G.F. Mikheev, Yu.T. Mironov, A.S. Pokrovskii, G.A. Riabov, V.A. Smolin, G.L. Sokolov, V.A. Volchenkov, A.A. Vorobiev
  Petersburg Nuclear Physics Institute, Gatchina, Russia
- P.V. Bogdanov, B.D. Ershov, V.S. Kuligin, V.N. Moshkin, V.G. Mudrolyubov, Yu.I. Stogov, A.P. Strokach
  D.V. Efremov Scientific Research Institute of Electrophysical Apparatus, St. Petersburg, Russia

A B C D E F G H I J K L M N O P Q R S T U V W X Y Z

Sortais, P.

Paper	Title	Page
XIII-03	**An On-Line Isotopic Separator Test Bench at GANIL**	725

- **P. Bricault**, R. Leroy, M. Lewitowicz, J.Y. Pacquet, M.G. St-Laurent, P. Sortais
  GANIL, Caen, France
- A.C. Mueller, J. Obert, J.C. Putaux
  IPN, Orsay, France
- C.F. Liang, P. Paris
  CSNSM, Orsay, France
- J.C. Steckmeyer
  LPC, Caen, France

A B C D E F G H I J K L M N O P Q R S T U V W X Y Z

Soudée, M.

Paper	Title	Page
XA-10	**RF Transmitter for ECR Ion Sources**	542

- **R. Boux**, J.P. Ichac, M. Soudée
  Thomson Tubes Electroniques, Velizy-Villacoublay, France

A B C D E F G H I J K L M N O P Q R S T U V W X Y Z

Sowinski, J.

Paper	Title	Page
VIII-07	**Performance and Status of the IUCF High Intensity Polarized Ion Source**	330

- **V. Derenchuk**, R. Brown, T.J.P. Ellison, D.L. Friesel, J.W. Hicks, D. Jenner, A. Pei, H. Petri, P. Schwandt, J. Sowinski, M. Wedekind
  Indiana University, Bloomington, Indiana, USA

A B C D E F G H I J K L M N O P Q R S T U V W X Y Z

Spinney, G.

Paper	Title	Page
I-07	**Thoughts on Decommissioning the CERN Synchro Cyclotron**	47

- **G. Spinney**
  CERN, Geneva, Switzerland

A B C D E F G H I J K L M N O P Q R S T U V W X Y Z

Sprenger, H.

Paper	Title	Page
XIII-08	**Research and Development Studies with Radioactive Beams at TRIUMF**	745

- **J.M. D'Auria**, M. Dombsky
  Simon Fraser University, Burnaby, BC, Canada
- L. Buchmann, H. Sprenger, J.S. Vincent
  TRIUMF, Vancouver, Canada
- J. King
  University of Toronto, Toronto, Ontario, Canada
- P. McNeely, G. Roy
  University of Alberta, Edmonton, Alberta, Canada

A B C D E F G H I J K L M N O P Q R S T U V W X Y Z

Stammbach, Th.

Paper	Title	Page
I-04	**Experience with the High Current Operation of the PSI Cyclotron Facility (Invited Paper)**	28

- **Th. Stammbach**
  PSI, Villigen, Switzerland

Paper	Title	Page
I-05	**The Commissioning of PSI Injector 2 for High Intensity, High Quality Beams**	36

- **J. Stetson**
  NSCL, East Lansing, Michigan, USA
- S. Adam, M. Humbel, W. Joho, Th. Stammbach
  PSI, Villigen, Switzerland

A B C D E F G H I J K L M N O P Q R S T U V W X Y Z

Starodub, G.Ya.

Paper	Title	Page
IV-04	^{178m2}Hf and ^{237}Pu Isotopes Production on the U-200 Cyclotron	167
	• **S.L. Bogomolov**, S.N. Dmitriev, Yu.P. Gangrski, G.G. Gulbekyan, S.A. Karamian, V.B. Kutner, B.N. Markov, Yu.Ts. Oganessian, N.V. Pronin, G.Ya. Starodub JINR, Dubna, Russia	
V-04	Possibility of Producing Some Radionuclides for Medicine Using JINR Accelerators	213
	• **S.N. Dmitriev**, G.G. Gulbekyan, V.A. Khalkin, R.Ts. Oganessian, L.M. Onishchenko, G.Ya. Starodub, N.G. Zaitseva JINR, Dubna, Russia	

A B C D E F G H I J K L M N O P Q R S T U V W X Y Z

Steckmeyer, J.C.

Paper	Title	Page
XIII-03	**An On-Line Isotopic Separator Test Bench at GANIL**	725

- **P. Bricault**, R. Leroy, M. Lewitowicz, J.Y. Pacquet, M.G. St-Laurent, P. Sortais
  GANIL, Caen, France
- A.C. Mueller, J. Obert, J.C. Putaux
  IPN, Orsay, France
- C.F. Liang, P. Paris
  CSNSM, Orsay, France
- J.C. Steckmeyer
  LPC, Caen, France

A B C D E F G H I J K L M N O P Q R S T U V W X Y Z

Stepantsov, S.V.

Paper	Title	Page
VII-05	**Dubna Project of the Heavy Ion Storage Ring Complex K4-K10**	290

- **Yu.Ts. Oganessian**, O.N. Malyshev, G.S. Popeko, A.M. Rodin, S.I. Sidorchuk, Ye.A. Sokol, S.V. Stepantsov, G.M. Ter-Akopian, V.A. Timakov
  JINR, Dubna, Russia
- V.V. Parhomchuk, A.A. Sery, V.D. Shiltsev
  Institute for Nuclear Physics, Novosibirsk, Russia
- I.N. Meshkov, Ye.M. Syresinm
  Center for Applied Physics and Technology, Lipetsk, Russia
- V.P. Belov, A.A. Makarov, Yu.P. Severgin, I.A. Shukeylo, M.N. Tarovik
  D.V. Efremov Scientific Research Institute of Electrophysical Apparatus, St. Petersburg, Russia

A B C D E F G H I J K L M N O P Q R S T U V W X Y Z

Stetson, J.

Paper	Title	Page
I-05	**The Commissioning of PSI Injector 2 for High Intensity, High Quality Beams**	36

- **J. Stetson**
  NSCL, East Lansing, Michigan, USA
- S. Adam, M. Humbel, W. Joho, Th. Stammbach
  PSI, Villigen, Switzerland

I-17	**Performance of the K1200 Cyclotron at MSU**	86

- **P. Miller**, T.A. Antaya, F. Marti, D. Poe, B. Sherrill, J. Stetson, J. Winger
  NSCL, East Lansing, Michigan, USA
- J.A. Nolen
  ANL, Argonne, Illinois, USA

A B C D E F G H I J K L M N O P Q R S T U V W X Y Z

Stevenson, N.R.

Paper	Title	Page
IV-11	**External High Current Targetry for Radioisotope Production**	196

- **N.R. Stevenson**, W.Z. Gelbart
  TRIUMF, Vancouver, Canada

Paper	Title	Page
IV-12	**A Remotely Controlled Robotic Vehicle for Work Within Radioactive Environments**	198

- **N.R. Stevenson**, P. Bloemhard, M. Brigham, J. Ko, C. LaForge, J. Orzechowski, E. Pattyn, T. Rattray
  TRIUMF, Vancouver, Canada

A B C D E F G H I J K L M N O P Q R S T U V W X Y Z

St-Laurent, M.G.

Paper	Title	Page
XIII-03	**An On-Line Isotopic Separator Test Bench at GANIL**	725

- **P. Bricault**, R. Leroy, M. Lewitowicz, J.Y. Pacquet, M.G. St-Laurent, P. Sortais
  GANIL, Caen, France
- A.C. Mueller, J. Obert, J.C. Putaux
  IPN, Orsay, France
- C.F. Liang, P. Paris
  CSNSM, Orsay, France
- J.C. Steckmeyer
  LPC, Caen, France

A B C D E F G H I J K L M N O P Q R S T U V W X Y Z

Stogov, Yu.I.

Paper	Title	Page
I-10	**Gatchina Isochronous Cyclotron**	58

- **N.K. Abrosimov**, S.A. Artamonov, P.V. Chervyakov, S.P. Dmitriev, V.A. Eliseev, V.P. Fominenko, E.M. Ivanov, G.F. Mikheev, Yu.T. Mironov, A.S. Pokrovskii, G.A. Riabov, V.A. Smolin, G.L. Sokolov, V.A. Volchenkov, A.A. Vorobiev
  Petersburg Nuclear Physics Institute, Gatchina, Russia
- P.V. Bogdanov, B.D. Ershov, V.S. Kuligin, V.N. Moshkin, V.G. Mudrolyubov, Yu.I. Stogov, A.P. Strokach
  D.V. Efremov Scientific Research Institute of Electrophysical Apparatus, St. Petersburg, Russia

A B C D E F G H I J K L M N O P Q R S T U V W X Y Z

Strokach, A.P.

Paper	Title	Page
I-10	**Gatchina Isochronous Cyclotron**	58

- **N.K. Abrosimov**, S.A. Artamonov, P.V. Chervyakov, S.P. Dmitriev, V.A. Eliseev, V.P. Fominenko, E.M. Ivanov, G.F. Mikheev, Yu.T. Mironov, A.S. Pokrovskii, G.A. Riabov, V.A. Smolin, G.L. Sokolov, V.A. Volchenkov, A.A. Vorobiev
  Petersburg Nuclear Physics Institute, Gatchina, Russia
- P.V. Bogdanov, B.D. Ershov, V.S. Kuligin, V.N. Moshkin, V.G. Mudrolyubov, Yu.I. Stogov, A.P. Strokach
  D.V. Efremov Scientific Research Institute of Electrophysical Apparatus, St. Petersburg, Russia

A B C D E F G H I J K L M N O P Q R S T U V W X Y Z

Stursa, J.

Paper	Title	Page
IXC-06	**Experiments on the Axial Injection System of the Cyclotron U-120M**	465

- **Z. Trejbal**, M. Krivánek, J. Kucera, V. Bejsovec, J. Stursa
  Czechoslovak Academy of Sciences, Rez, Czechoslovakia

A B C D E F G H I J K L M N O P Q R S T U V W X Y Z

Sudou, M.

Paper	Title	Page
XD-07	**Beam Transport System for the HIMAC**	625

- **K. Noda**, Y. Hirao, A. Itano, M. Kanazawa, A. Kitagawa, T. Kohno, M. Kumada, H. Ogawa, K. Sato, Y. Sato, M. Sudou, E. Takada, S. Yamada, T. Yamada
  NIRS, Chiba, Japan
- K. Endo
  KEK, Ibaraki, Japan

A B C D E F G H I J K L M N O P Q R S T U V W X Y Z

Suit, H.D.

Paper	Title	Page
VI-02	**Current and Potential Clinical Indications of Proton Irradiation (Invited Paper)**	234

- **A.F. Thornton**, H.D. Suit
  Harvard Medical School, Boston, Massachusetts, USA

A B C D E F G H I J K L M N O P Q R S T U V W X Y Z

Sura, J.

Paper	Title	Page
I-18	**Status Report on the Heavy Ion Facility at LNS**	90

- **F. Alessandria**, G. Bellomo, A. Bosotti, C. De Martinis, D. Giove, P. Michelato, C. Pagani, L. Rossi
  INFN/LASA, Segrate, Italy
- L. Calabretta, G. Ciavola, G. Cuttone, M. Di Giacomo, S. Gammino, P. Gmaj, G. Raia, D. Rifuggiato, J. Sura
  INFN/LNS, Catania, Italy

XC-06	**Material Consideration for Magnetic Channels**	589

- **J. Sura**, L. Calabretta, G. Di Biasi, P. Gmaj, D. Rifuggiato
  INFN/LNS, Catania, Italy

A B C D E F G H I J K L M N O P Q R S T U V W X Y Z

Susini, A.

Paper	Title	Page
XA-02	**The RF Coupling System of the VINCY Cyclotron**	511

- **B. Bojovic**, M. Josipovic, A. Susini
  CERN, Geneva, Switzerland

A B C D E F G H I J K L M N O P Q R S T U V W X Y Z

Syresinm, Ye.M.

Paper	Title	Page
VII-05	**Dubna Project of the Heavy Ion Storage Ring Complex K4-K10**	290

- **Yu.Ts. Oganessian**, O.N. Malyshev, G.S. Popeko, A.M. Rodin, S.I. Sidorchuk, Ye.A. Sokol, S.V. Stepantsov, G.M. Ter-Akopian, V.A. Timakov
  JINR, Dubna, Russia
- V.V. Parhomchuk, A.A. Sery, V.D. Shiltsev
  Institute for Nuclear Physics, Novosibirsk, Russia
- I.N. Meshkov, Ye.M. Syresinm
  Center for Applied Physics and Technology, Lipetsk, Russia
- V.P. Belov, A.A. Makarov, Yu.P. Severgin, I.A. Shukeylo, M.N. Tarovik
  D.V. Efremov Scientific Research Institute of Electrophysical Apparatus, St. Petersburg, Russia

A B C D E F G H I J K L M N O P Q R S T U V W X Y Z

Tachibana, M.

Paper	Title	Page
XI-04	**Control System for JAERI AVF Cyclotron**	648

- **S. Okumura**, T. Agematsu, K. Arakawa, M. Fukuda, I. Ishibori, T. Kamiya, Y. Nakamura, T. Nara, W. Yokota
  JAERI, Gunma, Japan
- K. Hoshika, K. Iso, M. Maruyama, M. Tachibana
  Sumitomo Heavy Industries, Ehime, Japan

XI-10	**Construction and System Tuning of Control System for the RCNP Ring Cyclotron and Beam Lines**	672

- **T. Yamazaki**, A. Ando, K. Hosono, T. Itahashi, M. Kibayashi, I. Miura, K. Nagayama, H. Ogata, T. Saito, A. Shimizu, K. Tamura, M. Uraki
  Osaka University, Osaka, Japan
- K. Aoki, Y. Kimura, M. Maruyama, M. Tachibana, S. Yamada
  Sumitomo Heavy Industries, Ehime, Japan
- K. Kodaira
  Sumitomo Heavy Industries Systems Engineering Laboratory, Tokyo, Japan

A B C D E F G H I J K L M N O P Q R S T U V W X Y Z

Tachikawa, T.

Paper	Title	Page
II-03	**Construction and First Year's Operation of the JAERI AVF Cyclotron**	119

- **K. Arakawa**, T. Agematsu, M. Fukuda, I. Ishibori, T. Karasawa, T. Nara, Y. Nakamura, S. Okumura, R. Tanaka, W. Yokota
  JAERI, Gunma, Japan
- A. Shimizu
  Osaka University, Osaka, Japan
- Y. Hayashi, K. Ishii, T. Satoh, T. Tachikawa
  Sumitomo Heavy Industries, Ehime, Japan

VIII-09	**Operation of Ion Sources and Beam Transport to JAERI AVF Cyclotron**	336

- **W. Yokota**, T. Agematsu, K. Arakawa, M. Fukuda, I. Ishibori, Y. Nakamura, T. Nara, S. Okumura
  JAERI, Gunma, Japan
- Y. Hayashi, K. Ishii, T. Tachikawa
  Sumitomo Heavy Industries, Ehime, Japan

XI-03	**An Operator Assistance System for the AVF Cyclotron**	644

- **T. Okamura**, T. Murakami
  Sumitomo Heavy Industries Systems Engineering Laboratory, Tokyo, Japan
- T. Tachikawa
  Sumitomo Heavy Industries, Ehime, Japan
- T. Agematsu, S. Okumura, K. Arakawa
  JAERI, Gunma, Japan

XC-04	**Performance of Beam Chopping System for JAERI AVF Cyclotron**	581

- **W. Yokota**, T. Agematsu, K. Arakawa, M. Fukuda, I. Ishibori, Y. Nakamura, T. Nara, S. Okumura
  JAERI, Gunma, Japan
- Y. Hayashi, Y. Kumata, T. Tachikawa
  Sumitomo Heavy Industries, Ehime, Japan

A B C D E F G H I J K L M N O P Q R S T U V W X Y Z

Tada, J.

Paper	Title	Page
VI-08	**A Proton Therapy Facility Plan**	258

- **S. Fukumoto**, Y. Hayakawa, T. Inada, A. Maruhashi, M. Sato, J. Tada, Y. Takada, H. Tsuji, H. Tsujii
  University of Tsukuba, Ibaraki, Japan
- K. Endo, Y. Irie, K. Muto
  KEK, Ibaraki, Japan

A B C D E F G H I J K L M N O P Q R S T U V W X Y Z

Tadokoro, M.

Paper	Title	Page
II-06	**A Newly Developed Compact Cyclotron for Neutron Therapy and Positron Nuclear Medicine**	129

- **K. Ito**, T. Ishigaki, S. Itoh, Y. Kasugai, T. Kato, T. Misawa, M. Nishino, M. Osakabe, T. Ota, S. Sakuma, M. Tadokoro, H. Yamamoto
  Nagoya University, Nagoya, Japan
- Y. Toda, Y. Yamamoto
  Japan Steel Works Ltd., Tokyo, Japan

A B C D E F G H I J K L M N O P Q R S T U V W X Y Z

Takada, E.

Paper	Title	Page
XD-07	**Beam Transport System for the HIMAC**	625

- **K. Noda**, Y. Hirao, A. Itano, M. Kanazawa, A. Kitagawa, T. Kohno, M. Kumada, H. Ogawa, K. Sato, Y. Sato, M. Sudou, E. Takada, S. Yamada, T. Yamada
  NIRS, Chiba, Japan
- K. Endo
  KEK, Ibaraki, Japan

A B C D E F G H I J K L M N O P Q R S T U V W X Y Z

Takada, Y.

Paper	Title	Page
VI-08	**A Proton Therapy Facility Plan**	258

- **S. Fukumoto**, Y. Hayakawa, T. Inada, A. Maruhashi, M. Sato, J. Tada, Y. Takada, H. Tsuji, H. Tsujii
  University of Tsukuba, Ibaraki, Japan
- K. Endo, Y. Irie, K. Muto
  KEK, Ibaraki, Japan

A B C D E F G H I J K L M N O P Q R S T U V W X Y Z

Takahashi, N.

Paper	Title	Page
VI-04	**Progress Report on the IBA-SHI Proton Therapy System**	244

- **Y. Jongen**, W. Beeckman, J.P. Dufour, A. Laisné, H. Marie, R. Verbruggen
  Ion Beam Applications, Louvain-la-Neuve, Belgium
- M. Sano, S. Satoh, N. Takahashi, T. Takayama
  Sumitomo Heavy Industries, Ehime, Japan

A B C D E F G H I J K L M N O P Q R S T U V W X Y Z

Takayama, T.

Paper	Title	Page
VI-04	**Progress Report on the IBA-SHI Proton Therapy System**	244

- **Y. Jongen**, W. Beeckman, J.P. Dufour, A. Laisné, H. Marie, R. Verbruggen
  Ion Beam Applications, Louvain-la-Neuve, Belgium
- M. Sano, S. Satoh, N. Takahashi, T. Takayama
  Sumitomo Heavy Industries, Ehime, Japan

A B C D E F G H I J K L M N O P Q R S T U V W X Y Z

Tamura, K.

Paper	Title	Page
I-01	**Commissioning of the RCNP Ring Cyclotron (Invited Paper)**	3

- **I. Miura**, A. Ando, K. Hatanaka, K. Hosono, H. Ikegami, T. Itahashi, M. Kibayashi, M. Kondo, H. Ogata, T. Saito, A. Shimizu, K. Tamura, M. Uraki, T. Yamazaki
  Osaka University, Osaka, Japan
- J. Abe
  Sumitomo Heavy Industries, Ehime, Japan

XI-10	**Construction and System Tuning of Control System for the RCNP Ring Cyclotron and Beam Lines**	672

- **T. Yamazaki**, A. Ando, K. Hosono, T. Itahashi, M. Kibayashi, I. Miura, K. Nagayama, H. Ogata, T. Saito, A. Shimizu, K. Tamura, M. Uraki
  Osaka University, Osaka, Japan
- K. Aoki, Y. Kimura, M. Maruyama, M. Tachibana, S. Yamada
  Sumitomo Heavy Industries, Ehime, Japan
- K. Kodaira
  Sumitomo Heavy Industries Systems Engineering Laboratory, Tokyo, Japan

A B C D E F G H I J K L M N O P Q R S T U V W X Y Z

Tanaka, R.

Paper	Title	Page
II-03	**Construction and First Year's Operation of the JAERI AVF Cyclotron**	119

- **K. Arakawa**, T. Agematsu, M. Fukuda, I. Ishibori, T. Karasawa, T. Nara, Y. Nakamura, S. Okumura, R. Tanaka, W. Yokota
  JAERI, Gunma, Japan
- A. Shimizu
  Osaka University, Osaka, Japan
- Y. Hayashi, K. Ishii, T. Satoh, T. Tachikawa
  Sumitomo Heavy Industries, Ehime, Japan

A B C D E F G H I J K L M N O P Q R S T U V W X Y Z

Tang, J.Y.

Paper	Title	Page
VI-05	**Recent Activities of the Cyclotron Laboratory in Nice**	248

- **P. Mandrillon**, N. Brassart, P. Chauvel, A. Courdi, F. Farley, N. Fietier, J. Herault, J.Y. Tang
  Centre Antoine Lacassagne, Nice, France

A B C D E F G H I J K L M N O P Q R S T U V W X Y Z

Tarovik, M.N.

Paper	Title	Page
VII-05	**Dubna Project of the Heavy Ion Storage Ring Complex K4-K10**	290

- **Yu.Ts. Oganessian**, O.N. Malyshev, G.S. Popeko, A.M. Rodin, S.I. Sidorchuk, Ye.A. Sokol, S.V. Stepantsov, G.M. Ter-Akopian, V.A. Timakov
  JINR, Dubna, Russia
- V.V. Parhomchuk, A.A. Sery, V.D. Shiltsev
  Institute for Nuclear Physics, Novosibirsk, Russia
- I.N. Meshkov, Ye.M. Syresinm
  Center for Applied Physics and Technology, Lipetsk, Russia
- V.P. Belov, A.A. Makarov, Yu.P. Severgin, I.A. Shukeylo, M.N. Tarovik
  D.V. Efremov Scientific Research Institute of Electrophysical Apparatus, St. Petersburg, Russia

A B C D E F G H I J K L M N O P Q R S T U V W X Y Z

Tatum, B.A.

Paper	Title	Page
XIII-07	**The ORNL Radioactive Ion Beam Project with the ORIC Accelerator**	741

- **D.K. Olsen**, G.D. Alton, C. Baktash, D.T. Dowling, J.D. Garrett, D.L. Haynes, C.M. Jones, R.C. Juras, S.N. Lane, I.Y. Lee, M.J. Meigs, G.D. Mills, S.W. Mosko, B.A. Tatum, K.S. Toth
  ORNL, Oak Ridge, Tennessee, USA
- H.K. Carter, J. Kormicki
  Associated Universities Oak Ridge, Oak Ridge, Tennessee, USA

A B C D E F G H I J K L M N O P Q R S T U V W X Y Z

Tazawa, S.

Paper	Title	Page
IV-10	**A Proposal for an Intense Cyclotron-Based Thermal Neutron Source**	191

- **S. Tazawa**
  Sumitomo Heavy Industries, Toyo-shi, Toyo-shi, Japan
- W.L. Whittemore
  General Atomics, San Diego, California, USA

A B C D E F G H I J K L M N O P Q R S T U V W X Y Z

ten Kate, H.J.H.

Paper	Title	Page
XC-05	**The AGOR Superconducting Extraction Channel EMC2**	585

- **K. Pieterman**, J.A.M. Dam
  Cryocon B.V., Amersfoort, The Netherlands
- H.J.H. ten Kate
  TU Twente, Enschede, The Netherlands
- S. Gustafsson
  IPN, Orsay, France

A B C D E F G H I J K L M N O P Q R S T U V W X Y Z

Ter-Akopian, G.M.

Paper	Title	Page
VII-05	**Dubna Project of the Heavy Ion Storage Ring Complex K4-K10**	290

- **Yu.Ts. Oganessian**, O.N. Malyshev, G.S. Popeko, A.M. Rodin, S.I. Sidorchuk, Ye.A. Sokol, S.V. Stepantsov, G.M. Ter-Akopian, V.A. Timakov
  JINR, Dubna, Russia
- V.V. Parhomchuk, A.A. Sery, V.D. Shiltsev
  Institute for Nuclear Physics, Novosibirsk, Russia
- I.N. Meshkov, Ye.M. Syresinm
  Center for Applied Physics and Technology, Lipetsk, Russia
- V.P. Belov, A.A. Makarov, Yu.P. Severgin, I.A. Shukeylo, M.N. Tarovik
  D.V. Efremov Scientific Research Institute of Electrophysical Apparatus, St. Petersburg, Russia

A B C D E F G H I J K L M N O P Q R S T U V W X Y Z

Theron, P.J.

Paper	Title	Page
XI-06	**The New Distributed Control System of the NAC**	656

- **H.F. Weehuizen**, R.K. Fisch, E.J.S. Franklin, M.E. Hogan, I.H. Kohler, J.P. Rogers, P.J. Theron
  National Accelerator Centre, Faure, Republic of South Africa

A B C D E F G H I J K L M N O P Q R S T U V W X Y Z

Thornton, A.F.

Paper	Title	Page
VI-02	**Current and Potential Clinical Indications of Proton Irradiation (Invited Paper)**	234

- **A.F. Thornton**, H.D. Suit
  Harvard Medical School, Boston, Massachusetts, USA

A B C D E F G H I J K L M N O P Q R S T U V W X Y Z

Tihomirova, S.T.

Paper	Title	Page
V-05	**Radiopharmaceutical "Thallium-201-Chloride" Production using Thallium-203 Irradiation by Helium-3 Ions**	216

- **A.A. Arzumanov**, N.K. Hamidov, A.I. Kozin, G.I. Shychikov, S.T. Tihomirova
  Kazakhstan Academy of Sciences, Alma-Ata, Republic of Kazakhstan

A B C D E F G H I J K L M N O P Q R S T U V W X Y Z

Tilbury, R.

Paper	Title	Page
V-07	**Dual Chemical Station for Cyclotron Produced ^{18}F**	222

- **M.L. Mallory**, G. Grimmett, R. Tilbury, D. Yang
  The University of Texas, Houston, Texas, USA

A B C D E F G H I J K L M N O P Q R S T U V W X Y Z

Timakov, V.A.

Paper	Title	Page
VII-05	**Dubna Project of the Heavy Ion Storage Ring Complex K4-K10**	290

- **Yu.Ts. Oganessian**, O.N. Malyshev, G.S. Popeko, A.M. Rodin, S.I. Sidorchuk, Ye.A. Sokol, S.V. Stepantsov, G.M. Ter-Akopian, V.A. Timakov
  JINR, Dubna, Russia
- V.V. Parhomchuk, A.A. Sery, V.D. Shiltsev
  Institute for Nuclear Physics, Novosibirsk, Russia
- I.N. Meshkov, Ye.M. Syresinm
  Center for Applied Physics and Technology, Lipetsk, Russia
- V.P. Belov, A.A. Makarov, Yu.P. Severgin, I.A. Shukeylo, M.N. Tarovik
  D.V. Efremov Scientific Research Institute of Electrophysical Apparatus, St. Petersburg, Russia

A B C D E F G H I J K L M N O P Q R S T U V W X Y Z

Timmermans, C.J.

Paper	Title	Page
IXA-03	**Emittance Growth in Nonlinear Beam Guiding and Focusing Elements**	384

- **W.J.G.M. Kleeven**, J.I.M. Botman, J.L. Delhez, H.L. Hagedoorn, C.J. Timmermans, G.A. Webers
  Eindhoven University of Technology, Eindhoven, The Netherlands

A B C D E F G H I J K L M N O P Q R S T U V W X Y Z

Toda, Y.

Paper	Title	Page
II-06	**A Newly Developed Compact Cyclotron for Neutron Therapy and Positron Nuclear Medicine**	129

- **K. Ito**, T. Ishigaki, S. Itoh, Y. Kasugai, T. Kato, T. Misawa, M. Nishino, M. Osakabe, T. Ota, S. Sakuma, M. Tadokoro, H. Yamamoto
  Nagoya University, Nagoya, Japan
- Y. Toda, Y. Yamamoto
  Japan Steel Works Ltd., Tokyo, Japan

A B C D E F G H I J K L M N O P Q R S T U V W X Y Z

Tomizawa, M.

Paper	Title	Page
VII-04	**Study of Beam Dynamics at Cooler Synchrotron TARN-II**	286

- **S. Watanabe**, Y. Arakaki, K. Chida, T. Katayama, M. Tomizawa, T. Watanabe, M. Yoshizawa
  University of Tokyo, Tanashi-shi, Tokyo, Japan
- K. Noda, M. Kanazawa
  NIRS, Chiba, Japan

A B C D E F G H I J K L M N O P Q R S T U V W X Y Z

Toporkov, D.

Paper	Title	Page
VII-07	**Superthin Internal Target for Storage Rings**	297

- **V. Pugatch**, A. Glushko, G. Pitatelev, G. Sivtsov
  Institute for Nuclear Research, Kiev, Ukraine
- S. Popov, D. Toporkov, B. Voitsechovsky
  Institute for Nuclear Physics, Novosibirsk, Russia

A B C D E F G H I J K L M N O P Q R S T U V W X Y Z

Toth, K.S.

Paper	Title	Page
XIII-07	**The ORNL Radioactive Ion Beam Project with the ORIC Accelerator**	741

- **D.K. Olsen**, G.D. Alton, C. Baktash, D.T. Dowling, J.D. Garrett, D.L. Haynes, C.M. Jones, R.C. Juras, S.N. Lane, I.Y. Lee, M.J. Meigs, G.D. Mills, S.W. Mosko, B.A. Tatum, K.S. Toth
  ORNL, Oak Ridge, Tennessee, USA
- H.K. Carter, J. Kormicki
  Associated Universities Oak Ridge, Oak Ridge, Tennessee, USA

A B C D E F G H I J K L M N O P Q R S T U V W X Y Z

Tran, D.

Paper	Title	Page
XC-09	**Results from the Deflector Test Stand at Texas A&M University**	602

- **D.P. May**, G. Derrig, W. Dewees, P. Smelser, D. Tran, R.C. Rogers
  Texas A&M University, College Station, Texas, USA

A B C D E F G H I J K L M N O P Q R S T U V W X Y Z

Trejbal, Z.

Paper	Title	Page
IXC-06	**Experiments on the Axial Injection System of the Cyclotron U-120M**	465

- **Z. Trejbal**, M. Krivánek, J. Kucera, V. Bejsovec, J. Stursa
  Czechoslovak Academy of Sciences, Rez, Czechoslovakia

A B C D E F G H I J K L M N O P Q R S T U V W X Y Z

Trinks, U.

Paper	Title	Page
XII-01	**The Superconducting Separated-Orbit Cyclotron Tritron (Invited Paper)**	693

- **U. Trinks**
  TU München, Garching, Germany

A B C D E F G H I J K L M N O P Q R S T U V W X Y Z

Tsuji, H.

Paper	Title	Page
VI-08	**A Proton Therapy Facility Plan**	258

- **S. Fukumoto**, Y. Hayakawa, T. Inada, A. Maruhashi, M. Sato, J. Tada, Y. Takada, H. Tsuji, H. Tsujii
  University of Tsukuba, Ibaraki, Japan
- K. Endo, Y. Irie, K. Muto
  KEK, Ibaraki, Japan

A B C D E F G H I J K L M N O P Q R S T U V W X Y Z

Tsujii, H.

Paper	Title	Page
VI-08	**A Proton Therapy Facility Plan**	258

- **S. Fukumoto**, Y. Hayakawa, T. Inada, A. Maruhashi, M. Sato, J. Tada, Y. Takada, H. Tsuji, H. Tsujii
  University of Tsukuba, Ibaraki, Japan
- K. Endo, Y. Irie, K. Muto
  KEK, Ibaraki, Japan

A B C D E F G H I J K L M N O P Q R S T U V W X Y Z

Unezhev, V.N.

Paper	Title	Page
XI-05	**Automatic Control System of Magnetic Separator for Kurchatov IAE Cyclotron**	652

- **N.I. Venikov**, V. Buranov, O. Gotovtsev, L.I. Iudin, P.Yu. Komissarov, V.N. Unezhev
  Kurchatov Institute, Moscow, Russia

A B C D E F G H I J K L M N O P Q R S T U V W X Y Z

Uraki, M.

Paper	Title	Page
I-01	**Commissioning of the RCNP Ring Cyclotron (Invited Paper)**	3

- **I. Miura**, A. Ando, K. Hatanaka, K. Hosono, H. Ikegami, T. Itahashi, M. Kibayashi, M. Kondo, H. Ogata, T. Saito, A. Shimizu, K. Tamura, M. Uraki, T. Yamazaki
  Osaka University, Osaka, Japan
- J. Abe
  Sumitomo Heavy Industries, Ehime, Japan

XA-09	**Initial Operation of the RF System for the RCNP Ring Cyclotron**	538

- **T. Saito**, I. Miura, A. Shimizu, M. Uraki
  Osaka University, Osaka, Japan

XI-10	**Construction and System Tuning of Control System for the RCNP Ring Cyclotron and Beam Lines**	672

- **T. Yamazaki**, A. Ando, K. Hosono, T. Itahashi, M. Kibayashi, I. Miura, K. Nagayama, H. Ogata, T. Saito, A. Shimizu, K. Tamura, M. Uraki
  Osaka University, Osaka, Japan
- K. Aoki, Y. Kimura, M. Maruyama, M. Tachibana, S. Yamada
  Sumitomo Heavy Industries, Ehime, Japan
- K. Kodaira
  Sumitomo Heavy Industries Systems Engineering Laboratory, Tokyo, Japan

A B C D E F G H I J K L M N O P Q R S T U V W X Y Z

Valek, A.

Paper	Title	Page
I-20	**Heavy Ion Facility in ATOMKI**	99

- **S. Biri**, J. Pálinkás, A. Valek
  Institute of Nuclear Research of the Hungarian Academy of Sciences, Debrecen, Hungary

A B C D E F G H I J K L M N O P Q R S T U V W X Y Z

Val'Kov, A.E.

Paper Title		Page
VII-06	**The New Project of INR (Kiev's) Storage-Accelerating Complex**	294

- **A.V. Dolinsky**, A.I. Papash, S.N. Pavlov, A.T. Rudchik, A.E. Val'Kov, I.N. Vishnevsky, A.V. Zhmendak
  Institute for Nuclear Research, Kiev, Ukraine
- V.P. Belov, A.M. Kokorin, A.A. Makarov, I.A. Schukeilo, Yu.P. Severgin
  D.V. Efremov Scientific Research Institute of Electrophysical Apparatus, St. Petersburg, Russia

A B C D E F G H I J K L M N O P Q R S T U V W X Y Z

van Rooyen, D.M.

Paper	Title	Page
VIII-15	**Progress with the NAC Injector Cyclotron for Heavy and Polarized Ions**	361

- **Z.B. du Toit**, S.J. Burger, P.J. Celliers, J.G. de Villiers, H.N. Jungwirth, A. Müller, P.F. Rohwer, D.M. van Rooyen
  National Accelerator Centre, Faure, Republic of South Africa

A B C D E F G H I J K L M N O P Q R S T U V W X Y Z

Varisco, G.

Paper	Title	Page
IXD-05	**High Sensitivity Electronic System for the Phase Probes of the LNS/MILANO Superconducting Cyclotron**	483

- **A. Bosotti**, D. Corti, C. Pagani, G. Varisco, F. Zibra
  INFN/LASA, Segrate, Italy
- M. Di Giacomo
  INFN/LNS, Catania, Italy

A B C D E F G H I J K L M N O P Q R S T U V W X Y Z

Vasilenko, A.

Paper	Title	Page
II-04	**20 MeV Cyclotron for Isotope Production**	123

- **A. Glazov**, Ju. Alenitskiy, A. Chesnov, S. Chesnova, V. Kochkin, D. Novikov, E. Samsonov, M. Semenov, A. Vasilenko, E. Zaplatin, N. Zaplatin
  JINR, Dubna, Russia
- I. Gulamov, O. Iljasov, A. Rykov
  Institute of Nuclear Physics, Tashkent, Republic of Uzbekistan

A B C D E F G H I J K L M N O P Q R S T U V W X Y Z

Vasiliev, A.A.

Paper	Title	Page
II-05	**Status of a Compact H^- Cyclotron at the Kurchatov Institute of Atomic Energy**	126

- **N.I. Venikov**, C.D. Burbeza, P.Yu. Komissarov, Yu.M. Krasnikov, S.T. Latushkin, V.V. Leonov, V.P. Moryakov, I.V. Naumov, A.Ya. Pisman, V.A. Rezvov, A.A. Vasiliev, V.E. Yarosh, L.I. Yudin
  Kurchatov Institute, Moscow, Russia

A B C D E F G H I J K L M N O P Q R S T U V W X Y Z

Venikov, N.I.

Paper	Title	Page
II-05	**Status of a Compact H^- Cyclotron at the Kurchatov Institute of Atomic Energy**	126

- **N.I. Venikov**, C.D. Burbeza, P.Yu. Komissarov, Yu.M. Krasnikov, S.T. Latushkin, V.V. Leonov, V.P. Moryakov, I.V. Naumov, A.Ya. Pisman, V.A. Rezvov, A.A. Vasiliev, V.E. Yarosh, L.I. Yudin
  Kurchatov Institute, Moscow, Russia

XI-05	**Automatic Control System of Magnetic Separator for Kurchatov IAE Cyclotron**	652

- **N.I. Venikov**, V. Buranov, O. Gotovtsev, L.I. Iudin, P.Yu. Komissarov, V.N. Unezhev
  Kurchatov Institute, Moscow, Russia

A B C D E F G H I J K L M N O P Q R S T U V W X Y Z

Verbruggen, R.

Paper	Title	Page
VI-04	**Progress Report on the IBA-SHI Proton Therapy System**	244

- **Y. Jongen**, W. Beeckman, J.P. Dufour, A. Laisné, H. Marie, R. Verbruggen
  Ion Beam Applications, Louvain-la-Neuve, Belgium
- M. Sano, S. Satoh, N. Takahashi, T. Takayama
  Sumitomo Heavy Industries, Ehime, Japan

A B C D E F G H I J K L M N O P Q R S T U V W X Y Z

Vienet, R.

Paper	Title	Page
IXC-01	**Commissioning of the New High Intensity Axial Injection System for GANIL**	446

- **Ch. Ricaud**, E. Baron, J. Bony, M.P. Bourgarel, B. Bru
  GANIL, Caen, France
- R. Vienet
  CEN/Saclay, Gif-sur-Yvette, France

A B C D E F G H I J K L M N O P Q R S T U V W X Y Z

Vignon, B.

Paper	Title	Page
XIII-04	**The PIAFE Project at Grenoble: Beam Transport and Acceleration**	729

- **J.L. Belmont**, J.F. Bruandet, J.M. de Conto, M. Fruneau, G. Gimond, K. Golovanivsky, E. Liatard, J.M. Loiseaux, H. Nifenecker, A. Savalle, B. Vignon
  Université Joseph Fourier, Grenoble, France
- P. Briand
  CEN-Grenoble, Grenoble, France

A B C D E F G H I J K L M N O P Q R S T U V W X Y Z

Vincent, D.

Paper	Title	Page
IXD-06	**The Diagnostics System for the AGOR Superconducting Cyclotron**	487

- **B. Launé**, P. Dambre, J.M. Kaplanski, B. Montsanglant, C. Olivetto, D. Vincent
  IPN, Orsay, France

A B C D E F G H I J K L M N O P Q R S T U V W X Y Z

Vincent, J.

Paper	Title	Page
II-07	**Performance of the Harper Hospital Cyclotron; Effect of Pulsed Radio Frequency**	133

- **H.G. Blosser**, J. Vincent
  NSCL, East Lansing, Michigan, USA
- R. Maughan
  Harper Hospital, Detroit, Michigan, USA

A B C D E F G H I J K L M N O P Q R S T U V W X Y Z

Vincent, J.S.

Paper	Title	Page
V-03	**A Facility for Radioisotope Production at TRIUMF with 70-110 MeV Protons**	209

- **D.R. Pearce**, J.S. Vincent
  TRIUMF, Vancouver, Canada

Paper	Title	Page
XIII-08	**Research and Development Studies with Radioactive Beams at TRIUMF**	745

- **J.M. D'Auria**, M. Dombsky
  Simon Fraser University, Burnaby, BC, Canada
- L. Buchmann, H. Sprenger, J.S. Vincent
  TRIUMF, Vancouver, Canada
- J. King
  University of Toronto, Toronto, Ontario, Canada
- P. McNeely, G. Roy
  University of Alberta, Edmonton, Alberta, Canada

A B C D E F G H I J K L M N O P Q R S T U V W X Y Z

Vishnevsky, I.N.

Paper	Title	Page
VII-06	**The New Project of INR (Kiev's) Storage-Accelerating Complex**	294

- **A.V. Dolinsky**, A.I. Papash, S.N. Pavlov, A.T. Rudchik, A.E. Val'Kov, I.N. Vishnevsky, A.V. Zhmendak
  Institute for Nuclear Research, Kiev, Ukraine
- V.P. Belov, A.M. Kokorin, A.A. Makarov, I.A. Schukeilo, Yu.P. Severgin
  D.V. Efremov Scientific Research Institute of Electrophysical Apparatus, St. Petersburg, Russia

A B C D E F G H I J K L M N O P Q R S T U V W X Y Z

Voitsechovsky, B.

Paper	Title	Page
VII-07	**Superthin Internal Target for Storage Rings**	297

- **V. Pugatch**, A. Glushko, G. Pitatelev, G. Sivtsov
  Institute for Nuclear Research, Kiev, Ukraine
- S. Popov, D. Toporkov, B. Voitsechovsky
  Institute for Nuclear Physics, Novosibirsk, Russia

A B C D E F G H I J K L M N O P Q R S T U V W X Y Z

Volchenkov, V.A.

Paper	Title	Page
I-10	**Gatchina Isochronous Cyclotron**	58

- **N.K. Abrosimov**, S.A. Artamonov, P.V. Chervyakov, S.P. Dmitriev, V.A. Eliseev, V.P. Fominenko, E.M. Ivanov, G.F. Mikheev, Yu.T. Mironov, A.S. Pokrovskii, G.A. Riabov, V.A. Smolin, G.L. Sokolov, V.A. Volchenkov, A.A. Vorobiev
  Petersburg Nuclear Physics Institute, Gatchina, Russia
- P.V. Bogdanov, B.D. Ershov, V.S. Kuligin, V.N. Moshkin, V.G. Mudrolyubov, Yu.I. Stogov, A.P. Strokach
  D.V. Efremov Scientific Research Institute of Electrophysical Apparatus, St. Petersburg, Russia

A B C D E F G H I J K L M N O P Q R S T U V W X Y Z

Vorobiev, A.A.

Paper	Title	Page
I-10	**Gatchina Isochronous Cyclotron**	58

- **N.K. Abrosimov**, S.A. Artamonov, P.V. Chervyakov, S.P. Dmitriev, V.A. Eliseev, V.P. Fominenko, E.M. Ivanov, G.F. Mikheev, Yu.T. Mironov, A.S. Pokrovskii, G.A. Riabov, V.A. Smolin, G.L. Sokolov, V.A. Volchenkov, A.A. Vorobiev
  Petersburg Nuclear Physics Institute, Gatchina, Russia
- P.V. Bogdanov, B.D. Ershov, V.S. Kuligin, V.N. Moshkin, V.G. Mudrolyubov, Yu.I. Stogov, A.P. Strokach
  D.V. Efremov Scientific Research Institute of Electrophysical Apparatus, St. Petersburg, Russia

A B C D E F G H I J K L M N O P Q R S T U V W X Y Z

Vorogushin, M.F.

Paper	Title	Page
I-08	**Parameters, Present State and Application Perspectives of the U-250 Cyclotron**	50

- **A.I. Muminov**
  Institute of Nuclear Physics, Tashkent, Republic of Uzbekistan
- M.F. Vorogushin
  D.V. Efremov Scientific Research Institute of Electrophysical Apparatus, St. Petersburg, Russia

A B C D E F G H I J K L M N O P Q R S T U V W X Y Z

Wagner, Jr., H.N.

Paper	Title	Page
V-01	**The New Molecular Medicine**	202

- **H.N. Wagner, Jr.**
  The Johns Hopkins University, Baltimore, Maryland, USA

A B C D E F G H I J K L M N O P Q R S T U V W X Y Z

Wang, F.

Paper	Title	Page
XD-05	**Buncher in the Beam Line from ECR to SFC**	618

- **J.Z. Jiang**, X.H. Zhou, Q. Wang, F. Wang, W.M. Jiang
  Institute of Modern Physics, Lanzhou, People's Republic of China

A B C D E F G H I J K L M N O P Q R S T U V W X Y Z

Wang, Q.

Paper	Title	Page
XD-05	**Buncher in the Beam Line from ECR to SFC**	618

- **J.Z. Jiang**, X.H. Zhou, Q. Wang, F. Wang, W.M. Jiang
  Institute of Modern Physics, Lanzhou, People's Republic of China

A B C D E F G H I J K L M N O P Q R S T U V W X Y Z

Wang, Y.

Paper	Title	Page
I-15	**Upgrading the SFC**	78

- **F. Ye**, M. Guo, Z. Ma, Q. Qiao, Y. Wang, Q. Yin, X. Zhu
  Institute of Modern Physics, Lanzhou, People's Republic of China

A B C D E F G H I J K L M N O P Q R S T U V W X Y Z

Watanabe, S.

Paper	Title	Page
VII-04	**Study of Beam Dynamics at Cooler Synchrotron TARN-II**	286

- **S. Watanabe**, Y. Arakaki, K. Chida, T. Katayama, M. Tomizawa, T. Watanabe, M. Yoshizawa
  University of Tokyo, Tanashi-shi, Tokyo, Japan
- K. Noda, M. Kanazawa
  NIRS, Chiba, Japan

A B C D E F G H I J K L M N O P Q R S T U V W X Y Z

Watanabe, T.

Paper	Title	Page
VII-04	**Study of Beam Dynamics at Cooler Synchrotron TARN-II**	286

- **S. Watanabe**, Y. Arakaki, K. Chida, T. Katayama, M. Tomizawa, T. Watanabe, M. Yoshizawa
  University of Tokyo, Tanashi-shi, Tokyo, Japan
- K. Noda, M. Kanazawa
  NIRS, Chiba, Japan

A B C D E F G H I J K L M N O P Q R S T U V W X Y Z

Webers, G.A.

Paper	Title	Page
IXA-03	**Emittance Growth in Nonlinear Beam Guiding and Focusing Elements**	384

- **W.J.G.M. Kleeven**, J.I.M. Botman, J.L. Delhez, H.L. Hagedoorn, C.J. Timmermans, G.A. Webers
  Eindhoven University of Technology, Eindhoven, The Netherlands

A B C D E F G H I J K L M N O P Q R S T U V W X Y Z

Wedberg, R.

Paper	Title	Page
VII-01	**Recent Commissioning Results at Celsius (Invited Paper)**	266

- **D. Reistad**, T. Bergmark, C. Ekström, C.-J. Fridén, K. Gajewski, L. Hermansson, P. Jahnke, A. Johansson, O. Johansson, T. Lofnes, G. Norman, R. Wedberg, L. Westerberg, J. Zlomanczuk
  Uppsala University, Uppsala, Sweden
- M.A. Raadu, M. Sedlacek
  Royal Institute of Technology, Stockholm, Sweden

A B C D E F G H I J K L M N O P Q R S T U V W X Y Z

Wedekind, M.

Paper	Title	Page
VIII-07	**Performance and Status of the IUCF High Intensity Polarized Ion Source**	330

- **V. Derenchuk**, R. Brown, T.J.P. Ellison, D.L. Friesel, J.W. Hicks, D. Jenner, A. Pei, H. Petri, P. Schwandt, J. Sowinski, M. Wedekind
  Indiana University, Bloomington, Indiana, USA

A B C D E F G H I J K L M N O P Q R S T U V W X Y Z

Weehuizen, H.F.

Paper	Title	Page
XI-06	**The New Distributed Control System of the NAC**	656

- **H.F. Weehuizen**, R.K. Fisch, E.J.S. Franklin, M.E. Hogan, I.H. Kohler, J.P. Rogers, P.J. Theron
  National Accelerator Centre, Faure, Republic of South Africa

A B C D E F G H I J K L M N O P Q R S T U V W X Y Z

Wei, B.W.

Paper	Title	Page
I-14	**Initial Operation of HIRFL**	74

- **B.W. Wei**, F. Ye
  Institute of Modern Physics, Lanzhou, People's Republic of China

VIII-11	**Study on the Magnetic Field of Caprice Type ECR Source**	344

- **B.W. Wei**, Z. Liu, Y. Ma, D. Wu, P. Yuan, W. Zhang, X. Zhang, H. Zhao
  Institute of Modern Physics, Lanzhou, People's Republic of China
- A. Efremov
  JINR, Dubna, Russia

IXD-04	**Emittance Measurements in the HIRFL Beam Line**	479

- **H. Zhao**, Z. Shen, B.W. Wei
  Institute of Modern Physics, Lanzhou, People's Republic of China

A B C D E F G H I J K L M N O P Q R S T U V W X Y Z

Wei, J.

Paper	Title	Page
VI-07	**Design Consideration of Neutron Therapy Facility Utilizing Existing Cyclotron**	255

- **H. Chang**, X. Cui, J. Wei, J. Zhang, K. Xie
  Institute of Nuclear Research, Shanghai, People's Republic of China

A B C D E F G H I J K L M N O P Q R S T U V W X Y Z

Wells, R.P.

Paper	Title	Page
XB-02	**A Permanent Magnet System for a Cyclotron Used as a Mass Spectrometer**	561

- **C.Y. Li**, M. Cooper, K. Halbach, W.B. Kunkel, K.N. Leung, R.P. Wells, A.T. Young
  LBL, Berkeley, California, USA

A B C D E F G H I J K L M N O P Q R S T U V W X Y Z

Westerberg, L.

Paper	Title	Page
VII-01	**Recent Commissioning Results at Celsius (Invited Paper)**	266

- **D. Reistad**, T. Bergmark, C. Ekström, C.-J. Fridén, K. Gajewski, L. Hermansson, P. Jahnke, A. Johansson, O. Johansson, T. Lofnes, G. Norman, R. Wedberg, L. Westerberg, J. Zlomanczuk
  Uppsala University, Uppsala, Sweden
- M.A. Raadu, M. Sedlacek
  Royal Institute of Technology, Stockholm, Sweden

A B C D E F G H I J K L M N O P Q R S T U V W X Y Z

Whittemore, W.L.

Paper	Title	Page
IV-10	**A Proposal for an Intense Cyclotron-Based Thermal Neutron Source**	191

- **S. Tazawa**
  Sumitomo Heavy Industries, Toyo-shi, Toyo-shi, Japan
- W.L. Whittemore
  General Atomics, San Diego, California, USA

A B C D E F G H I J K L M N O P Q R S T U V W X Y Z

Wilkinson, N.A.

Paper	Title	Page
XI-12	**Application of Object Oriented Techniques in the TRIUMF Beam Line 2C Control System (Invited Paper)**	681

- **N.A. Wilkinson**, E.A. Osberg, G.A. Ludgate
  TRIUMF, Vancouver, Canada

A B C D E F G H I J K L M N O P Q R S T U V W X Y Z

Winger, J.

Paper	Title	Page
I-17	**Performance of the K1200 Cyclotron at MSU**	86

- **P. Miller**, T.A. Antaya, F. Marti, D. Poe, B. Sherrill, J. Stetson, J. Winger
  NSCL, East Lansing, Michigan, USA
- J.A. Nolen
  ANL, Argonne, Illinois, USA

A B C D E F G H I J K L M N O P Q R S T U V W X Y Z

Wootton, P.

Paper	Title	Page
VI-09	**Continued Operation of the Seattle Clinical Cyclotron Facility**	262

- **R. Risler**, S. Brossard, J. Jacky, I. Kalet, P. Wootton, F. Ziai
  University of Washington, Seattle, Washington, USA

A B C D E F G H I J K L M N O P Q R S T U V W X Y Z

Wu, D.

Paper	Title	Page
VIII-11	**Study on the Magnetic Field of Caprice Type ECR Source**	344

- **B.W. Wei**, Z. Liu, Y. Ma, D. Wu, P. Yuan, W. Zhang, X. Zhang, H. Zhao
  Institute of Modern Physics, Lanzhou, People's Republic of China
- A. Efremov
  JINR, Dubna, Russia

A B C D E F G H I J K L M N O P Q R S T U V W X Y Z

Wucherer, P.

Paper	Title	Page
I-12	**Commissioning of the Injector Complex of COSY-Jülich**	67

- **W. Bräutigam**, H. Beuscher, R. Brings, H.G. Böge, R. Maier, M. Rogge, P. Wucherer
  FZJ, Jülich, Germany

A B C D E F G H I J K L M N O P Q R S T U V W X Y Z

Wüstefeld, G.

Paper	Title	Page
XII-02	**Study of an FFAG Synchrocyclotron for a Pulsed Neutron Source**	701

- **S.A. Martin**, E. Zaplatin
  FZJ, Jülich, Germany
- P.F. Meads, Jr.
  Private Address, Oakland, California, USA
- G. Wüstefeld
  BESSY, Berlin, Germany
- K. Ziegler
  HMI, Berlin, Germany

A B C D E F G H I J K L M N O P Q R S T U V W X Y Z

Xia, J.

Paper	Title	Page
IXA-06	**Nonlinear Transport of Accelerator Beam Phase Space**	396

- **X. Xie**
  Graduate School of Nuclear Industry, Beijing, People's Republic of China
- J. Xia
  Institute of Modern Physics, Lanzhou, People's Republic of China

Paper	Title	Page
IXA-07	**Deriving the General Expressions of Nonlinear Transport Coefficients of Accelerator Beam Phase Space by Artificial Intelligence**	400

- **J. Xia**
  Institute of Modern Physics, Lanzhou, People's Republic of China
- C. Liu, X. Xie
  Graduate School of Nuclear Industry, Beijing, People's Republic of China

A B C D E F G H I J K L M N O P Q R S T U V W X Y Z

Xie, K.

Paper	Title	Page
VI-07	**Design Consideration of Neutron Therapy Facility Utilizing Existing Cyclotron**	255

- **H. Chang**, X. Cui, J. Wei, J. Zhang, K. Xie
  Institute of Nuclear Research, Shanghai, People's Republic of China

Xie, X.

Paper	Title	Page
IXA-06	**Nonlinear Transport of Accelerator Beam Phase Space**	396

- **X. Xie**
  Graduate School of Nuclear Industry, Beijing, People's Republic of China
- J. Xia
  Institute of Modern Physics, Lanzhou, People's Republic of China

IXA-07	**Deriving the General Expressions of Nonlinear Transport Coefficients of Accelerator Beam Phase Space by Artificial Intelligence**	400

- **J. Xia**
  Institute of Modern Physics, Lanzhou, People's Republic of China
- C. Liu, X. Xie
  Graduate School of Nuclear Industry, Beijing, People's Republic of China

A B C D E F G H I J K L M N O P Q R S T U V W X Y Z

Xie, Z.Q.

Paper	Title	Page
VIII-02	**Performance of the LBL AECR Source at Various Frequencies**	308

- **Z.Q. Xie**, D. Collins, S.A. Lundgren, C.M. Lyneis
  LBL, Berkeley, California, USA

Paper	Title	Page
IXC-04	**Non-Linear Beam Transport Effects in Highly Charged Positive Ion Beams Extracted From ECR Ion Sources**	457

- **T.A. Antaya**
  NSCL, East Lansing, Michigan, USA
- Z.Q. Xie
  LBL, Berkeley, California, USA

A B C D E F G H I J K L M N O P Q R S T U V W X Y Z

Yamada, S.

Paper	Title	Page
XD-07	**Beam Transport System for the HIMAC**	625

- **K. Noda**, Y. Hirao, A. Itano, M. Kanazawa, A. Kitagawa, T. Kohno, M. Kumada, H. Ogawa, K. Sato, Y. Sato, M. Sudou, E. Takada, S. Yamada, T. Yamada
  NIRS, Chiba, Japan
- K. Endo
  KEK, Ibaraki, Japan

Paper	Title	Page
XI-10	**Construction and System Tuning of Control System for the RCNP Ring Cyclotron and Beam Lines**	672

- **T. Yamazaki**, A. Ando, K. Hosono, T. Itahashi, M. Kibayashi, I. Miura, K. Nagayama, H. Ogata, T. Saito, A. Shimizu, K. Tamura, M. Uraki
  Osaka University, Osaka, Japan
- K. Aoki, Y. Kimura, M. Maruyama, M. Tachibana, S. Yamada
  Sumitomo Heavy Industries, Ehime, Japan
- K. Kodaira
  Sumitomo Heavy Industries Systems Engineering Laboratory, Tokyo, Japan

A B C D E F G H I J K L M N O P Q R S T U V W X Y Z

Yamada, T.

Paper	Title	Page
VIII-06	**An ECR Ion Source for Multiply-Charged Heavy Ions at 14 GHz**	326

- **M. Sekiguchi**, M. Fujita, Y. Ohshiro, T. Yamazaki
  University of Tokyo, Tanashi-shi, Tokyo, Japan
- Y. Isoya, T. Yamada, Y. Yamashita
  Japan Steel Works Ltd., Research Center for Advanced Technologies, Chiba, Japan
- A. Kitagawa
  NIRS, Chiba, Japan

XD-07	**Beam Transport System for the HIMAC**	625

- **K. Noda**, Y. Hirao, A. Itano, M. Kanazawa, A. Kitagawa, T. Kohno, M. Kumada, H. Ogawa, K. Sato, Y. Sato, M. Sudou, E. Takada, S. Yamada, T. Yamada
  NIRS, Chiba, Japan
- K. Endo
  KEK, Ibaraki, Japan

A B C D E F G H I J K L M N O P Q R S T U V W X Y Z

Yamamoto, H.

Paper	Title	Page
II-06	**A Newly Developed Compact Cyclotron for Neutron Therapy and Positron Nuclear Medicine**	129

- **K. Ito**, T. Ishigaki, S. Itoh, Y. Kasugai, T. Kato, T. Misawa, M. Nishino, M. Osakabe, T. Ota, S. Sakuma, M. Tadokoro, H. Yamamoto
  Nagoya University, Nagoya, Japan
- Y. Toda, Y. Yamamoto
  Japan Steel Works Ltd., Tokyo, Japan

A B C D E F G H I J K L M N O P Q R S T U V W X Y Z

Yamamoto, Y.

Paper	Title	Page
II-06	**A Newly Developed Compact Cyclotron for Neutron Therapy and Positron Nuclear Medicine**	129

- **K. Ito**, T. Ishigaki, S. Itoh, Y. Kasugai, T. Kato, T. Misawa, M. Nishino, M. Osakabe, T. Ota, S. Sakuma, M. Tadokoro, H. Yamamoto
  Nagoya University, Nagoya, Japan
- Y. Toda, Y. Yamamoto
  Japan Steel Works Ltd., Tokyo, Japan

A B C D E F G H I J K L M N O P Q R S T U V W X Y Z

Yamashita, Y.

Paper	Title	Page
VIII-06	**An ECR Ion Source for Multiply-Charged Heavy Ions at 14 GHz**	326

- **M. Sekiguchi**, M. Fujita, Y. Ohshiro, T. Yamazaki
  University of Tokyo, Tanashi-shi, Tokyo, Japan
- Y. Isoya, T. Yamada, Y. Yamashita
  Japan Steel Works Ltd., Research Center for Advanced Technologies, Chiba, Japan
- A. Kitagawa
  NIRS, Chiba, Japan

A B C D E F G H I J K L M N O P Q R S T U V W X Y Z

Yamazaki, N.

Paper	Title	Page
IXC-02	**A Formulation of Spiral Inflector Design and Its Application to SF Cyclotron**	450

- **M. Sekiguchi**, M. Fujita, M. Nishiguchi, Y. Ohshiro, Y. Shida, N. Yamazaki, T. Yamazaki
  University of Tokyo, Tanashi-shi, Tokyo, Japan

A B C D E F G H I J K L M N O P Q R S T U V W X Y Z

Yamazaki, T.

Paper	Title	Page
I-01	**Commissioning of the RCNP Ring Cyclotron (Invited Paper)**	3

- **I. Miura**, A. Ando, K. Hatanaka, K. Hosono, H. Ikegami, T. Itahashi, M. Kibayashi, M. Kondo, H. Ogata, T. Saito, A. Shimizu, K. Tamura, M. Uraki, T. Yamazaki
  Osaka University, Osaka, Japan
- J. Abe
  Sumitomo Heavy Industries, Ehime, Japan

XI-10	**Construction and System Tuning of Control System for the RCNP Ring Cyclotron and Beam Lines**	672

- **T. Yamazaki**, A. Ando, K. Hosono, T. Itahashi, M. Kibayashi, I. Miura, K. Nagayama, H. Ogata, T. Saito, A. Shimizu, K. Tamura, M. Uraki
  Osaka University, Osaka, Japan
- K. Aoki, Y. Kimura, M. Maruyama, M. Tachibana, S. Yamada
  Sumitomo Heavy Industries, Ehime, Japan
- K. Kodaira
  Sumitomo Heavy Industries Systems Engineering Laboratory, Tokyo, Japan

VIII-06	**An ECR Ion Source for Multiply-Charged Heavy Ions at 14 GHz**	326

- **M. Sekiguchi**, M. Fujita, Y. Ohshiro, T. Yamazaki
  University of Tokyo, Tanashi-shi, Tokyo, Japan
- Y. Isoya, T. Yamada, Y. Yamashita
  Japan Steel Works Ltd., Research Center for Advanced Technologies, Chiba, Japan
- A. Kitagawa
  NIRS, Chiba, Japan

IXC-02	**A Formulation of Spiral Inflector Design and Its Application to SF Cyclotron**	450

- **M. Sekiguchi**, M. Fujita, M. Nishiguchi, Y. Ohshiro, Y. Shida, N. Yamazaki, T. Yamazaki
  University of Tokyo, Tanashi-shi, Tokyo, Japan

A B C D E F G H I J K L M N O P Q R S T U V W X Y Z

Yang, D.

Paper	Title	Page
V-07	**Dual Chemical Station for Cyclotron Produced ^{18}F**	222

- **M.L. Mallory**, G. Grimmett, R. Tilbury, D. Yang
  The University of Texas, Houston, Texas, USA

A B C D E F G H I J K L M N O P Q R S T U V W X Y Z

Yano, Y.

Paper	Title	Page
I-21	**Recent Achievements at the RIKEN Ring Cyclotron**	102
	• **Y. Yano** RIKEN, Saitama, Japan	
VIII-16	**Plasma Cathode Method for RIKEN ECRIS**	365
	• **T. Nakagawa**, A. Goto, T. Kageyama, M. Kase, Y. Yano RIKEN, Saitama, Japan	

A B C D E F G H I J K L M N O P Q R S T U V W X Y Z

Yarosh, V.E.

Paper	Title	Page
II-05	**Status of a Compact H^- Cyclotron at the Kurchatov Institute of Atomic Energy**	126

- **N.I. Venikov**, C.D. Burbeza, P.Yu. Komissarov, Yu.M. Krasnikov, S.T. Latushkin, V.V. Leonov, V.P. Moryakov, I.V. Naumov, A.Ya. Pisman, V.A. Rezvov, A.A. Vasiliev, V.E. Yarosh, L.I. Yudin
  Kurchatov Institute, Moscow, Russia

A B C D E F G H I J K L M N O P Q R S T U V W X Y Z

Ye, F.

Paper	Title	Page
I-14	**Initial Operation of HIRFL**	74

- **B.W. Wei**, F. Ye
  Institute of Modern Physics, Lanzhou, People's Republic of China

Paper	Title	Page
I-15	**Upgrading the SFC**	78

- **F. Ye**, M. Guo, Z. Ma, Q. Qiao, Y. Wang, Q. Yin, X. Zhu
  Institute of Modern Physics, Lanzhou, People's Republic of China

A B C D E F G H I J K L M N O P Q R S T U V W X Y Z

Yin, Q.

Paper	Title	Page
I-15	**Upgrading the SFC**	78

- **F. Ye**, M. Guo, Z. Ma, Q. Qiao, Y. Wang, Q. Yin, X. Zhu
  Institute of Modern Physics, Lanzhou, People's Republic of China

A B C D E F G H I J K L M N O P Q R S T U V W X Y Z

Yin, Y.

Paper	Title	Page
IXD-09	**A DC Current Transformer for TRIUMF**	498

- **Y. Yin**
  TRIUMF, Vancouver, Canada

A B C D E F G H I J K L M N O P Q R S T U V W X Y Z

Yokota, W.

Paper	Title	Page
II-03	**Construction and First Year's Operation of the JAERI AVF Cyclotron**	119

- **K. Arakawa**, T. Agematsu, M. Fukuda, I. Ishibori, T. Karasawa, T. Nara, Y. Nakamura, S. Okumura, R. Tanaka, W. Yokota
  JAERI, Gunma, Japan
- A. Shimizu
  Osaka University, Osaka, Japan
- Y. Hayashi, K. Ishii, T. Satoh, T. Tachikawa
  Sumitomo Heavy Industries, Ehime, Japan

VIII-09	**Operation of Ion Sources and Beam Transport to JAERI AVF Cyclotron**	336

- **W. Yokota**, T. Agematsu, K. Arakawa, M. Fukuda, I. Ishibori, Y. Nakamura, T. Nara, S. Okumura
  JAERI, Gunma, Japan
- Y. Hayashi, K. Ishii, T. Tachikawa
  Sumitomo Heavy Industries, Ehime, Japan

IXB-02	**Beam Studies of Injection to Extraction System for JAERI AVF Cyclotron**	423

- **M. Fukuda**, T. Agematsu, K. Arakawa, I. Ishibori, T. Karasawa, Y. Nakamura, T. Nara, S. Okumura, W. Yokota
  JAERI, Gunma, Japan

XC-04	**Performance of Beam Chopping System for JAERI AVF Cyclotron**	581

- **W. Yokota**, T. Agematsu, K. Arakawa, M. Fukuda, I. Ishibori, Y. Nakamura, T. Nara, S. Okumura
  JAERI, Gunma, Japan
- Y. Hayashi, Y. Kumata, T. Tachikawa
  Sumitomo Heavy Industries, Ehime, Japan

XI-04	**Control System for JAERI AVF Cyclotron**	648

- **S. Okumura**, T. Agematsu, K. Arakawa, M. Fukuda, I. Ishibori, T. Kamiya, Y. Nakamura, T. Nara, W. Yokota
  JAERI, Gunma, Japan
- K. Hoshika, K. Iso, M. Maruyama, M. Tachibana
  Sumitomo Heavy Industries, Ehime, Japan

A B C D E F G H I J K L M N O P Q R S T U V W X Y Z

Yoshizawa, M.

Paper	Title	Page
VII-04	**Study of Beam Dynamics at Cooler Synchrotron TARN-II**	286

- **S. Watanabe**, Y. Arakaki, K. Chida, T. Katayama, M. Tomizawa, T. Watanabe, M. Yoshizawa
  University of Tokyo, Tanashi-shi, Tokyo, Japan
- K. Noda, M. Kanazawa
  NIRS, Chiba, Japan

A B C D E F G H I J K L M N O P Q R S T U V W X Y Z

Young, A.T.

Paper	Title	Page
VIII-03	**Ion Sources for Cyclotron Application**	312

- **K.N. Leung**, D.A. Bachman, D.S. McDonald, A.T. Young
  LBL, Berkeley, California, USA

XB-02	**A Permanent Magnet System for a Cyclotron Used as a Mass Spectrometer**	561

- **C.Y. Li**, M. Cooper, K. Halbach, W.B. Kunkel, K.N. Leung, R.P. Wells, A.T. Young
  LBL, Berkeley, California, USA

XII-03	**Design of a Compact Permanent Magnet Cyclotron Mass Spectrometer for the Detection and Measurement of Trace Isotopes**	705

- **A.T. Young**, K.J. Bertsche, D.J. Clark, K. Halbach, W.B. Kunkel, K.N. Leung, C.Y. Li
  LBL, Berkeley, California, USA

A B C D E F G H I J K L M N O P Q R S T U V W X Y Z

Yuan, P.

Paper	Title	Page
VIII-11	**Study on the Magnetic Field of Caprice Type ECR Source**	344

- **B.W. Wei**, Z. Liu, Y. Ma, D. Wu, P. Yuan, W. Zhang, X. Zhang, H. Zhao
  Institute of Modern Physics, Lanzhou, People's Republic of China
- A. Efremov
  JINR, Dubna, Russia

A B C D E F G H I J K L M N O P Q R S T U V W X Y Z

Yudin, L.I.

Paper	Title	Page
II-05	**Status of a Compact H^- Cyclotron at the Kurchatov Institute of Atomic Energy**	126

- **N.I. Venikov**, C.D. Burbeza, P.Yu. Komissarov, Yu.M. Krasnikov, S.T. Latushkin, V.V. Leonov, V.P. Moryakov, I.V. Naumov, A.Ya. Pisman, V.A. Rezvov, A.A. Vasiliev, V.E. Yarosh, L.I. Yudin
  Kurchatov Institute, Moscow, Russia

A B C D E F G H I J K L M N O P Q R S T U V W X Y Z

Yurkon, J.

Paper	Title	Page
IXB-04	**Selection and Measurement of RF Phase Width of the K1200 Cyclotron Beam**	431

- **J. Bailey**, J. Kuchar, F. Marti, J. Yurkon
  NSCL, East Lansing, Michigan, USA
- J.A. Nolen
  ANL, Argonne, Illinois, USA
- D. Rifuggiato
  INFN/LNS, Catania, Italy

A B C D E F G H I J K L M N O P Q R S T U V W X Y Z

Zach, M.

Paper	Title	Page
XA-03	**Dual Frequency Resonator System for a Compact Cyclotron**	515

- **M. Eiche**, K.L. Erdman
  Ebco Technologies Ltd, Richmond, BC, Canada
- P. Lanz, M. Lipnicki, M. Zach
  TRIUMF, Vancouver, Canada

A B C D E F G H I J K L M N O P Q R S T U V W X Y Z

Zaika, N.I.

Paper	Title	Page
VIII-10	**Spin Dynamics and Polarized Ion Sources on Isochronous Cyclotron U-240**	340

- **N.I. Zaika**
  Institute for Nuclear Research, Kiev, Ukraine

A B C D E F G H I J K L M N O P Q R S T U V W X Y Z

Zaitseva, N.G.

Paper	Title	Page
V-04	**Possibility of Producing Some Radionuclides for Medicine Using JINR Accelerators**	213

- **S.N. Dmitriev**, G.G. Gulbekyan, V.A. Khalkin, R.Ts. Oganessian, L.M. Onishchenko, G.Ya. Starodub, N.G. Zaitseva
  JINR, Dubna, Russia

A B C D E F G H I J K L M N O P Q R S T U V W X Y Z

Zaplatin, E.

Paper	Title	Page
XA-07	**Multi-Point Cavity Excitation**	530

- **E. Zaplatin**
  FZJ, Jülich, Germany

Paper	Title	Page
XII-02	**Study of an FFAG Synchrocyclotron for a Pulsed Neutron Source**	701

- **S.A. Martin**, E. Zaplatin
  FZJ, Jülich, Germany
- P.F. Meads, Jr.
  Private Address, Oakland, California, USA
- G. Wüstefeld
  BESSY, Berlin, Germany
- K. Ziegler
  HMI, Berlin, Germany

Paper	Title	Page
II-04	**20 MeV Cyclotron for Isotope Production**	123

- **A. Glazov**, Ju. Alenitskiy, A. Chesnov, S. Chesnova, V. Kochkin, D. Novikov, E. Samsonov, M. Semenov, A. Vasilenko, E. Zaplatin, N. Zaplatin
  JINR, Dubna, Russia
- I. Gulamov, O. Iljasov, A. Rykov
  Institute of Nuclear Physics, Tashkent, Republic of Uzbekistan

A B C D E F G H I J K L M N O P Q R S T U V W X Y Z

Zaplatin, N.

Paper	Title	Page
II-04	**20 MeV Cyclotron for Isotope Production**	123

- **A. Glazov**, Ju. Alenitskiy, A. Chesnov, S. Chesnova, V. Kochkin, D. Novikov, E. Samsonov, M. Semenov, A. Vasilenko, E. Zaplatin, N. Zaplatin
  JINR, Dubna, Russia
- I. Gulamov, O. Iljasov, A. Rykov
  Institute of Nuclear Physics, Tashkent, Republic of Uzbekistan

A B C D E F G H I J K L M N O P Q R S T U V W X Y Z

Zelenskii, A.N.

Paper	Title	Page
VIII-05	**Status of the TRIUMF Optically-Pumped Polarized H^- Ion Source**	322

- **C.D.P. Levy**, K. Jayamanna, M. McDonald, R. Ruegg, P.W. Schmor
  TRIUMF, Vancouver, Canada
- A.N. Zelenskii
  Institute of Nuclear Research, Russian Academy of Sciences, Moscow, Russia

A B C D E F G H I J K L M N O P Q R S T U V W X Y Z

Zhang, J.

Paper	Title	Page
VI-07	**Design Consideration of Neutron Therapy Facility Utilizing Existing Cyclotron**	255

- **H. Chang**, X. Cui, J. Wei, J. Zhang, K. Xie
  Institute of Nuclear Research, Shanghai, People's Republic of China

A B C D E F G H I J K L M N O P Q R S T U V W X Y Z

Zhang, W.

Paper	Title	Page
VIII-11	**Study on the Magnetic Field of Caprice Type ECR Source**	344

- **B.W. Wei**, Z. Liu, Y. Ma, D. Wu, P. Yuan, W. Zhang, X. Zhang, H. Zhao
  Institute of Modern Physics, Lanzhou, People's Republic of China
- A. Efremov
  JINR, Dubna, Russia

A B C D E F G H I J K L M N O P Q R S T U V W X Y Z

Zhang, X.

Paper	Title	Page
VIII-11	**Study on the Magnetic Field of Caprice Type ECR Source**	344

- **B.W. Wei**, Z. Liu, Y. Ma, D. Wu, P. Yuan, W. Zhang, X. Zhang, H. Zhao
  Institute of Modern Physics, Lanzhou, People's Republic of China
- A. Efremov
  JINR, Dubna, Russia

A B C D E F G H I J K L M N O P Q R S T U V W X Y Z

Zhao, H.

Paper	Title	Page
VIII-11	**Study on the Magnetic Field of Caprice Type ECR Source**	344

- **B.W. Wei**, Z. Liu, Y. Ma, D. Wu, P. Yuan, W. Zhang, X. Zhang, H. Zhao
  Institute of Modern Physics, Lanzhou, People's Republic of China
- A. Efremov
  JINR, Dubna, Russia

IXD-04	**Emittance Measurements in the HIRFL Beam Line**	479

- **H. Zhao**, Z. Shen, B.W. Wei
  Institute of Modern Physics, Lanzhou, People's Republic of China

A B C D E F G H I J K L M N O P Q R S T U V W X Y Z

Zhmendak, A.V.

Paper	Title	Page
VII-06	**The New Project of INR (Kiev's) Storage-Accelerating Complex**	294

- **A.V. Dolinsky**, A.I. Papash, S.N. Pavlov, A.T. Rudchik, A.E. Val'Kov, I.N. Vishnevsky, A.V. Zhmendak
  Institute for Nuclear Research, Kiev, Ukraine
- V.P. Belov, A.M. Kokorin, A.A. Makarov, I.A. Schukeilo, Yu.P. Severgin
  D.V. Efremov Scientific Research Institute of Electrophysical Apparatus, St. Petersburg, Russia

A B C D E F G H I J K L M N O P Q R S T U V W X Y Z

Zhou, X.H.

Paper	Title	Page
XD-05	**Buncher in the Beam Line from ECR to SFC**	618

- **J.Z. Jiang**, X.H. Zhou, Q. Wang, F. Wang, W.M. Jiang
  Institute of Modern Physics, Lanzhou, People's Republic of China

A B C D E F G H I J K L M N O P Q R S T U V W X Y Z

Zhu, X.

Paper	Title	Page
I-15	**Upgrading the SFC**	78

- **F. Ye**, M. Guo, Z. Ma, Q. Qiao, Y. Wang, Q. Yin, X. Zhu
  Institute of Modern Physics, Lanzhou, People's Republic of China

A B C D E F G H I J K L M N O P Q R S T U V W X Y Z

Ziai, F.

Paper	Title	Page
VI-09	**Continued Operation of the Seattle Clinical Cyclotron Facility**	262

- **R. Risler**, S. Brossard, J. Jacky, I. Kalet, P. Wootton, F. Ziai
  University of Washington, Seattle, Washington, USA

A B C D E F G H I J K L M N O P Q R S T U V W X Y Z

Zibra, F.

Paper	Title	Page
IXD-05	**High Sensitivity Electronic System for the Phase Probes of the LNS/MILANO Superconducting Cyclotron**	483

- **A. Bosotti**, D. Corti, C. Pagani, G. Varisco, F. Zibra
  INFN/LASA, Segrate, Italy
- M. Di Giacomo
  INFN/LNS, Catania, Italy

A B C D E F G H I J K L M N O P Q R S T U V W X Y Z

Ziegler, K.

Paper	Title	Page
IV-01	**Material Research with Beams at Cyclotron Energies (Invited Paper)**	149

- **K. Ziegler**
  HMI, Berlin, Germany

XII-02	**Study of an FFAG Synchrocyclotron for a Pulsed Neutron Source**	701

- **S.A. Martin**, E. Zaplatin
  FZJ, Jülich, Germany
- P.F. Meads, Jr.
  Private Address, Oakland, California, USA
- G. Wüstefeld
  BESSY, Berlin, Germany
- K. Ziegler
  HMI, Berlin, Germany

A B C D E F G H I J K L M N O P Q R S T U V W X Y Z

Zlomanczuk, J.

Paper	Title	Page
VII-01	**Recent Commissioning Results at Celsius (Invited Paper)**	266

- **D. Reistad**, T. Bergmark, C. Ekström, C.-J. Fridén, K. Gajewski, L. Hermansson, P. Jahnke, A. Johansson, O. Johansson, T. Lofnes, G. Norman, R. Wedberg, L. Westerberg, J. Zlomanczuk
  Uppsala University, Uppsala, Sweden
- M.A. Raadu, M. Sedlacek
  Royal Institute of Technology, Stockholm, Sweden

A B C D E F H I J K L M N O P Q R S T V

acceleration

Paper	Title	Other Keywords	Page
I-01	**Commissioning of the RCNP Ring Cyclotron (Invited Paper)** • **I. Miura**, A. Ando, K. Hatanaka, K. Hosono, H. Ikegami, T. Itahashi, M. Kibayashi, M. Kondo, H. Ogata, T. Saito, A. Shimizu, K. Tamura, M. Uraki, T. Yamazaki, Osaka University, Osaka, Japan • J. Abe, Sumitomo Heavy Industries, Ehime, Japan	cyclotron, proton, cavity, injection	3
I-05	**The Commissioning of PSI Injector 2 for High Intensity, High Quality Beams** • **J. Stetson**, NSCL, East Lansing, Michigan, USA • S. Adam, M. Humbel, W. Joho, Th. Stammbach, PSI, Villigen, Switzerland	space-charge, simulation, cyclotron, bunching	36
I-21	**Recent Achievements at the RIKEN Ring Cyclotron** • **Y. Yano**, RIKEN, Saitama, Japan	ion, cyclotron, ion-source, injection	102
II-04	**20 MeV Cyclotron for Isotope Production** • **A. Glazov**, Ju. Alenitskiy, A. Chesnov, S. Chesnova, V. Kochkin, D. Novikov, E. Samsonov, M. Semenov, A. Vasilenko, E. Zaplatin, N. Zaplatin, JINR, Dubna, Russia • I. Gulamov, O. Iljasov, A. Rykov, Institute of Nuclear Physics, Tashkent, Republic of Uzbekistan	cyclotron, target, isotope-production, proton	123
VII-04	**Study of Beam Dynamics at Cooler Synchrotron TARN-II** • **S. Watanabe**, Y. Arakaki, K. Chida, T. Katayama, M. Tomizawa, T. Watanabe, M. Yoshizawa, University of Tokyo, Tanashi-shi, Tokyo, Japan • K. Noda, M. Kanazawa, NIRS, Chiba, Japan	ion, synchrotron, injection, cyclotron	286
VIII-10	**Spin Dynamics and Polarized Ion Sources on Isochronous Cyclotron U-240**	ion, resonance, cyclotron, polarization	340

- **N.I. Zaika**
  Institute for Nuclear Research, Kiev, Ukraine

IXA-04	**Ion_Tracker, a Trace Tracking Program for Cyclotron Design**	cyclotron, ion, injection, optics	388

- **M. Rinta-Nikkola**
  University of Jyväskylä, Jyväskylä, Finland

IXB-01	**Cyclotron Tuning as a Rebuncher**	extraction, cyclotron, target, emittance	419

- **D. Bibet**, M-H. Moscatello
  GANIL, Caen, France

IXC-02	**A Formulation of Spiral Inflector Design and Its Application to SF Cyclotron**	ion, cyclotron, injection, ion-source	450

- **M. Sekiguchi**, M. Fujita, M. Nishiguchi, Y. Ohshiro, Y. Shida, N. Yamazaki, T. Yamazaki
  University of Tokyo, Tanashi-shi, Tokyo, Japan

IXC-06	**Experiments on the Axial Injection System of the Cyclotron U-120M**	ion, cyclotron, injection, ion-source	465

- **Z. Trejbal**, M. Kriványek, J. Kucera, V. Bejsovec, J. Stursa
  Czechoslovak Academy of Sciences, Rez, Czechoslovakia

IXD-07	**Beam Diagnostics in the RCNP Ring Cyclotron**	cyclotron, injection, cavity, proton	491

- **T. Itahashi**, T. Saito, I. Miura
  Osaka University, Osaka, Japan
- S. Ichida
  Sumitomo Heavy Industries, Ehime, Japan

XA-09	**Initial Operation of the RF System for the RCNP Ring Cyclotron**	cavity, cyclotron, coupling, proton	538

- **T. Saito**, I. Miura, A. Shimizu, M. Uraki
  Osaka University, Osaka, Japan

XB-03	**Sector Magnet of the RCNP Ring Cyclotron and the Isochronization**	cyclotron, extraction, injection, proton	565

- **K. Hosono**, M. Kibayashi, I. Miura
  Osaka University, Osaka, Japan

XC-02	**Potential Enhancement of Magnetic Deflection in the Chalk River Superconducting Cyclotron Extraction System**	extraction, cyclotron, dipole, ion	573

- **C.R. Hoffmann**, E.H. Lindqvist
  Atomic Energy of Canada, Chalk River, Ontario, Canada

XIII-02	**A Conceptual Design for a Primary Cyclotron for the ISL Radioactive Beam Project**	extraction, cyclotron, ion, proton	721

- **D.J. Clark**
  LBL, Berkeley, California, USA

XIII-06	**Radioactive Ion Beam Production Using the Louvain-La-Neuve Cyclotrons: Present Status and Future Developments**	cyclotron, target, extraction, ECR	737

- **G. Ryckewaert**, M. Loiselet, N. Postiau
  Université Catholique de Louvain, Louvain-la-Neuve, Belgium

A B C D E F H I J K L M N O P Q R S T V

accumulation

Paper	Title	Other Keywords	Page
V-01	**The New Molecular Medicine**	radiation, site, ion, monitoring	202

- **H.N. Wagner, Jr.**
  The Johns Hopkins University, Baltimore, Maryland, USA

A B C D E F H I J K L M N O P Q R S T V

AGOR

Paper	Title	Other Keywords	Page
I-06	**AGOR: Recent Achievements (Invited Paper)** • **H.W. Schreuder** IPN, Orsay, France	cyclotron, extraction, vacuum, site	40
IXD-03	**A Beam Profile Monitor Using the Ionization of Residual Gas** • **J.M. Schippers**, H.H. Kiewiet Kernfysisch Versneller Instituut, Groningen, The Netherlands	MCP, ion, background, cyclotron	477
XB-01	**Low Temperature Tests of the AGOR Superconducting Coil System** • **K. Pieterman**, J.A.M. Dam Cryocon B.V., Amersfoort, The Netherlands • C. Commeaux IPN, Orsay, France • C. Penco Ansaldo Componenti, Genoa, Italy	cryogenics, power-supply, factory, vacuum	557
XC-05	**The AGOR Superconducting Extraction Channel EMC2** • **K. Pieterman**, J.A.M. Dam Cryocon B.V., Amersfoort, The Netherlands • H.J.H. ten Kate TU Twente, Enschede, The Netherlands • S. Gustafsson IPN, Orsay, France	cyclotron, radiation, background, extraction	585
XD-03	**Superconducting Focussing Channel for the AGOR Cyclotron** • **H.W. Schreuder**, P. Blache, C. Commeaux, S. Gustafsson, A. Lafoux, M. Mormiche, R. Panvier IPN, Orsay, France	quadrupole, shielding, dipole, cyclotron	612
XD-04	**The Beam-Guiding System of AGOR** • **J.M. Schippers**	target, controls, heavy-ion, diagnostics	615

Kernfysisch Versneller Instituut, Groningen, The Netherlands

A B C D E F H I J K L M N O P Q R S T V

ALICE

Paper	Title	Other Keywords	Page
V-05	**Radiopharmaceutical "Thallium-201-Chloride" Production using Thallium-203 Irradiation by Helium-3 Ions**	ion, target, proton, cyclotron	216

- **A.A. Arzumanov**, N.K. Hamidov, A.I. Kozin, G.I. Shychikov, S.T. Tihomirova
  Kazakhstan Academy of Sciences, Alma-Ata, Republic of Kazakhstan

A B C D E F H I J K L M N O P Q R S T V

background

Paper	Title	Other Keywords	Page
IV-07	**Neutron Productions from Carbon by Charged Particle Bombardment at Different Energies** • **M.A. Chaudhri** Austin Hospital & University of Melbourne, Melbourne, Australia	neutron, target, proton, cyclotron	178
VI-03	**Pion Therapy for Cancer - What are the Prospects?** • **G.B. Goodman** University of British Columbia, Vancouver, Canada	photon, TRIUMF, radiation, controls	242
IXD-03	**A Beam Profile Monitor Using the Ionization of Residual Gas** • **J.M. Schippers**, H.H. Kiewiet Kernfysisch Versneller Instituut, Groningen, The Netherlands	MCP, AGOR, ion, cyclotron	477
IXD-08	**Signal Processing for the Internal Phase Probe in the TRIUMF Cyclotron** • **K. Fong** TRIUMF, Vancouver, Canada	cavity, cyclotron, TRIUMF, pick-up	495
XC-05	**The AGOR Superconducting Extraction Channel EMC2** • **K. Pieterman**, J.A.M. Dam Cryocon B.V., Amersfoort, The Netherlands • H.J.H. ten Kate TU Twente, Enschede, The Netherlands • S. Gustafsson IPN, Orsay, France	cyclotron, radiation, AGOR, extraction	585

A B C D E F H I J K L M N O P Q R S T V

beam-losses

Paper	Title	Other Keywords	Page
I-04	**Experience with the High Current Operation of the PSI Cyclotron Facility (Invited Paper)** • **Th. Stammbach** PSI, Villigen, Switzerland	cyclotron, space-charge, extraction, injection	28
XA-05	**Low Frequency RF System for the Indiana University Cooler Ring** • **X. Pei**, S. Anderson, V. Derenchuk, G. East, D.L. Friesel, D. Jenner, D. McCammon, T. Sloan Indiana University, Bloomington, Indiana, USA	cavity, kicker, injection, synchrotron	523
XI-09	**Two Dimensional Scans with Adaptive Domain Control** • **S. Adam**, A.C. Mezger PSI, Villigen, Switzerland	controls, extraction, interlocks, status	668

A B C D E F H I J K L M N O P Q R S T V

beam-transport

Paper	Title	Other Keywords	Page
I-16	**Status Report of Cyclone** • **M. Loiselet**, N. Postiau, G. Ryckewaert Université Catholique de Louvain, Louvain-la-Neuve, Belgium	cyclotron, ion, target, neutron	82
IXA-06	**Nonlinear Transport of Accelerator Beam Phase Space** • **X. Xie** Graduate School of Nuclear Industry, Beijing, People's Republic of China • J. Xia Institute of Modern Physics, Lanzhou, People's Republic of China	optics	396
IXA-06	**Nonlinear Transport of Accelerator Beam Phase Space** • **X. Xie** Graduate School of Nuclear Industry, Beijing, People's Republic of China • J. Xia Institute of Modern Physics, Lanzhou, People's Republic of China	optics	396
IXA-07	**Deriving the General Expressions of Nonlinear Transport Coefficients of Accelerator Beam Phase Space by Artificial Intelligence** • **J. Xia** Institute of Modern Physics, Lanzhou, People's Republic of China • C. Liu, X. Xie Graduate School of Nuclear Industry, Beijing, People's Republic of China	cyclotron, electromagnetic-fields, optics	400
XD-01	**Some Perspectives in the Beam Transport and Analyzing System Design for the U-250 Cyclotron** • **L.E. Korolev** D.V. Efremov Scientific Research Institute of Electrophysical Apparatus, St. Petersburg, Russia	cyclotron, target, sextupole	606
XD-07	**Beam Transport System for the HIMAC**	ion, injection, optics, heavy-ion	625

- **K. Noda**, Y. Hirao, A. Itano, M. Kanazawa, A. Kitagawa, T. Kohno, M. Kumada, H. Ogawa, K. Sato, Y. Sato, M. Sudou, E. Takada, S. Yamada, T. Yamada
  NIRS, Chiba, Japan
- K. Endo
  KEK, Ibaraki, Japan

A B C D E F H I J K L M N O P Q R S T V

betatron

Paper	Title	Other Keywords	Page
IXA-02	**The Influence of Magnetic Field Imperfections on the Beam Quality in an H^- Cyclotron**	resonance, emittance, cyclotron, extraction	380

- **W.J.G.M. Kleeven**, H.L. Hagedoorn
  Eindhoven University of Technology, Eindhoven, The Netherlands
- B.F. Milton, G. Dutto
  TRIUMF, Vancouver, Canada

IXB-06	**Effect of the Main-Coil Position on the Accelerated Beam of the K500 Cyclotron**	extraction, cyclotron, vacuum, focusing	439

- **D.P. May**, G. Mouchaty
  Texas A&M University, College Station, Texas, USA

A B C D E F H I J K L M N O P Q R S T V

BNL

Paper	Title	Other Keywords	Page
IV-09	**A Simple Method for Estimating Activation Sensitivities of Different Elements / Isotopes with Cyclotron Produced Neutrons**	neutron, target, cyclotron, radiation	187

- **M.A. Chaudhri**
  Austin Hospital & University of Melbourne, Melbourne, Australia

A B C D E F H I J K L M N O P Q R S T V

booster

Paper	Title	Other Keywords	Page
III-02	**The KAON Factory at TRIUMF** • **M.K. Craddock** University of British Columbia, Vancouver, Canada	TRIUMF, kaon, lattice, factory	143
VII-06	**The New Project of INR (Kiev's) Storage-Accelerating Complex** • **A.V. Dolinsky**, A.I. Papash, S.N. Pavlov, A.T. Rudchik, A.E. Val'Kov, I.N. Vishnevsky, A.V. Zhmendak Institute for Nuclear Research, Kiev, Ukraine • V.P. Belov, A.M. Kokorin, A.A. Makarov, I.A. Schukeilo, Yu.P. Severgin D.V. Efremov Scientific Research Institute of Electrophysical Apparatus, St. Petersburg, Russia	electron, ion, target, injection	294
XA-04	**The RF-System for a VICKSI Injector Cyclotron** • **W. Pelzer** HMI, Berlin, Germany	cyclotron, ion, ECR, injection	519
XI-11	**Early Experience with DECwindows/Motif in the TRIUMF Central Control System** • **S. Kadantsev** JINR, Dubna, Russia • M. Mouat TRIUMF, Vancouver, Canada	controls, laser, TRIUMF, ion-source	676

A B C D E F H I J K L M N O P Q R S T V

bunching

Paper	Title	Other Keywords	Page
I-05	**The Commissioning of PSI Injector 2 for High Intensity, High Quality Beams** • **J. Stetson**, NSCL, East Lansing, Michigan, USA • S. Adam, M. Humbel, W. Joho, Th. Stammbach, PSI, Villigen, Switzerland	space-charge, acceleration, simulation, cyclotron	36
XD-02	**Beam Transport System for the IUCF High Intensity Polarized Ion Source** • **W.P. Jones**, M.S. Ball, J.C. Collins, D. DuPlantis, T.J.P. Ellison, D.L. Friesel, B. Hamilton, J.W. Hicks, P. Schwandt, Indiana University, Bloomington, Indiana, USA	quadrupole, cyclotron, dipole, diagnostics	609
XD-05	**Buncher in the Beam Line from ECR to SFC** • **J.Z. Jiang**, X.H. Zhou, Q. Wang, F. Wang, W.M. Jiang, Institute of Modern Physics, Lanzhou, People's Republic of China	ECR, ion, ion-source, controls	618
XD-08	**Design of a Beam Buncher Using a Half-Cosine Driving Function** • **R.C. Rogers**, Texas A&M University, College Station, Texas, USA	cyclotron, injection, ECRIS, ion	629

A B C D E F H I J K L M N O P Q R S T V

cathode

Paper	Title	Other Keywords	Page
IV-04	**^{178m2}Hf and ^{237}Pu Isotopes Production on the U-200 Cyclotron** • **S.L. Bogomolov**, S.N. Dmitriev, Yu.P. Gangrski, G.G. Gulbekyan, S.A. Karamian, V.B. Kutner, B.N. Markov, Yu.Ts. Oganessian, N.V. Pronin, G.Ya. Starodub JINR, Dubna, Russia	ion, cyclotron, target, ion-source	167
VIII-11	**Study on the Magnetic Field of Caprice Type ECR Source** • **B.W. Wei**, Z. Liu, Y. Ma, D. Wu, P. Yuan, W. Zhang, X. Zhang, H. Zhao Institute of Modern Physics, Lanzhou, People's Republic of China • A. Efremov JINR, Dubna, Russia	ion, plasma, ECR, extraction	344
VIII-16	**Plasma Cathode Method for RIKEN ECRIS** • **T. Nakagawa**, A. Goto, T. Kageyama, M. Kase, Y. Yano RIKEN, Saitama, Japan	ion, plasma, electron, ECRIS	365
XA-11	**TRIUMF Cyclotron RF System Improvements** • **G.C. Blaker**, A.K. Mitra, R.L. Poirier TRIUMF, Vancouver, Canada	impedance, TRIUMF, cyclotron, controls	545
XC-01	**The Electrostatic Deflector for the Chalk River Superconducting Cyclotron** • **W.T. Diamond**, C.R. Hoffmann, G.R. Mitchel, H. Schmeing Atomic Energy of Canada, Chalk River, Ontario, Canada	high-voltage, cyclotron, vacuum, electron	569
XC-08	**Deflector Development for the K1200 Cyclotron** • **T.Y.T. Kuo** TRIUMF, Vancouver, Canada • J.A. Nolen ANL, Argonne, Illinois, USA	electron, cyclotron, ion, site	596

A B C D E F H I J K L M N O P Q R S T V

cavity

Paper	Title	Other Keywords	Page
I-01	**Commissioning of the RCNP Ring Cyclotron (Invited Paper)** • **I. Miura**, A. Ando, K. Hatanaka, K. Hosono, H. Ikegami, T. Itahashi, M. Kibayashi, M. Kondo, H. Ogata, T. Saito, A. Shimizu, K. Tamura, M. Uraki, T. Yamazaki Osaka University, Osaka, Japan • J. Abe Sumitomo Heavy Industries, Ehime, Japan	cyclotron, proton, acceleration, injection	3
I-18	**Status Report on the Heavy Ion Facility at LNS** • **F. Alessandria**, G. Bellomo, A. Bosotti, C. De Martinis, D. Giove, P. Michelato, C. Pagani, L. Rossi INFN/LASA, Segrate, Italy • L. Calabretta, G. Ciavola, G. Cuttone, M. Di Giacomo, S. Gammino, P. Gmaj, G. Raia, D. Rifuggiato, J. Sura INFN/LNS, Catania, Italy	cyclotron, vacuum, coupling, ion	90
III-01	**The TRIUMF 520 MeV Cyclotron: Recent and Future Developments** • **G. Dutto** TRIUMF, Vancouver, Canada	TRIUMF, cyclotron, extraction, proton	138
IXB-07	**Beam Test Results Using the Auxiliary Accelerating Cavity** • **R.E. Laxdal**, G.H. Mackenzie, L. Root TRIUMF, Vancouver, Canada	simulation, cyclotron, extraction, TRIUMF	442
IXD-07	**Beam Diagnostics in the RCNP Ring Cyclotron** • **T. Itahashi**, T. Saito, I. Miura Osaka University, Osaka, Japan • S. Ichida Sumitomo Heavy Industries, Ehime, Japan	cyclotron, injection, acceleration, proton	491
IXD-08	**Signal Processing for the Internal Phase Probe in the TRIUMF Cyclotron** • **K. Fong** TRIUMF, Vancouver, Canada	background, cyclotron, TRIUMF, pick-up	495

XA-01	**Advances in RF Technology for Cyclotrons** • **C. Pagani** INFN/LASA, Segrate, Italy	cyclotron, coupling, impedance, controls	501
XA-02	**The RF Coupling System of the VINCY Cyclotron** • **B. Bojovic**, M. Josipovic, A. Susini CERN, Geneva, Switzerland	coupling, impedance, cyclotron, vacuum	511
XA-03	**Dual Frequency Resonator System for a Compact Cyclotron** • **M. Eiche**, K.L. Erdman Ebco Technologies Ltd, Richmond, BC, Canada • P. Lanz, M. Lipnicki, M. Zach TRIUMF, Vancouver, Canada	cyclotron, impedance, isotope-production, vacuum	515
XA-05	**Low Frequency RF System for the Indiana University Cooler Ring** • **X. Pei**, S. Anderson, V. Derenchuk, G. East, D.L. Friesel, D. Jenner, D. McCammon, T. Sloan Indiana University, Bloomington, Indiana, USA	kicker, injection, beam-losses, synchrotron	523
XA-06	**A Modified RF System of JAERI AVF Cyclotron** • **Y. Kumata**, Y. Fukumoto Sumitomo Heavy Industries, Ehime, Japan • K. Arakawa, M. Fukuda, T. Karasawa JAERI, Gunma, Japan • A. Shimizu Osaka University, Osaka, Japan	cyclotron, ion, proton, controls	526
XA-07	**Multi-Point Cavity Excitation** • **E. Zaplatin** FZJ, Jülich, Germany	coupling, resonance, impedance, simulation	530
XA-08	**Experience with the PSI-Cyclotron RF-System Under Heavy Beam Loading** • **P.K. Sigg**, J. Cherix, H. Frei, M. Märki PSI, Villigen, Switzerland	coupling, cyclotron, controls, impedance	534
	Initial Operation of the RF System for the RCNP Ring	acceleration,	538

XA-09	**Cyclotron**	cyclotron, coupling, proton	

- **T. Saito**, I. Miura, A. Shimizu, M. Uraki
  Osaka University, Osaka, Japan

XA-12	**Improvements to the RF Separator in the M9 Muon Channel at TRIUMF**	TRIUMF, controls, impedance, cyclotron	549

- **G.C. Blaker**, A.K. Mitra, R.L. Poirier
  TRIUMF, Vancouver, Canada

XII-01	**The Superconducting Separated-Orbit Cyclotron Tritron (Invited Paper)**	injection, proton, cyclotron, focusing	693

- **U. Trinks**
  TU München, Garching, Germany

XII-02	**Study of an FFAG Synchrocyclotron for a Pulsed Neutron Source**	injection, neutron, linac, synchrotron	701

- **S.A. Martin**, E. Zaplatin
  FZJ, Jülich, Germany
- P.F. Meads, Jr.
  Private Address, Oakland, California, USA
- G. Wüstefeld
  BESSY, Berlin, Germany
- K. Ziegler
  HMI, Berlin, Germany

A B C D E F H I J K L M N O P Q R S T V

CERN

Paper	Title	Other Keywords	Page
I-07	**Thoughts on Decommissioning the CERN Synchro Cyclotron**	vacuum, shielding, plasma, synchro-cyclotron	47

- **G. Spinney**
  CERN, Geneva, Switzerland

A B C D E F H I J K L M N O P Q R S T V

closed-orbit

Paper	Title	Other Keywords	Page
IXA-01	**Advantage of Using Differential Algebra and Lie Algebra in the Orbit Dynamics of Cyclotrons (Invited Paper)**	resonance, cyclotron, octupole, sextupole	372

- **W.G. Davies**
  Atomic Energy of Canada, Chalk River, Ontario, USA

A B C D E F H I J K L M N O P Q R S T V

controls

Paper	Title	Other Keywords	Page
I-09	**GANIL Status Report** • **M. Bajard** GANIL, Caen, France	ion, ECR, injection, emittance	54
I-12	**Commissioning of the Injector Complex of COSY-Jülich** • **W. Bräutigam**, H. Beuscher, R. Brings, H.G. Böge, R. Maier, M. Rogge, P. Wucherer FZJ, Jülich, Germany	COSY, cyclotron, ion, injection	67
II-02	**The Operation of Cyclotrons Used for Radiopharmaceutical Production** • **T. Grey-Morgan** Cyclotron Isotopes Manufacturing, Buckinghamshire, England • R.E. Hubbard Medi + Physics Inc., Arlington Heights, Illinois, USA	cyclotron, target, radiation, isotope-production	115
II-05	**Status of a Compact H^- Cyclotron at the Kurchatov Institute of Atomic Energy** • **N.I. Venikov**, C.D. Burbeza, P.Yu. Komissarov, Yu.M. Krasnikov, S.T. Latushkin, V.V. Leonov, V.P. Moryakov, I.V. Naumov, A.Ya. Pisman, V.A. Rezvov, A.A. Vasiliev, V.E. Yarosh, L.I. Yudin Kurchatov Institute, Moscow, Russia	cyclotron, ion, vacuum, ion-source	126
II-07	**Performance of the Harper Hospital Cyclotron; Effect of Pulsed Radio Frequency** • **H.G. Blosser**, J. Vincent NSCL, East Lansing, Michigan, USA • R. Maughan Harper Hospital, Detroit, Michigan, USA	cyclotron, target, neutron, ion	133
IV-12	**A Remotely Controlled Robotic Vehicle for Work Within Radioactive Environments** • **N.R. Stevenson**, P. Bloemhard, M. Brigham, J. Ko, C. LaForge, J. Orzechowski, E. Pattyn, T. Rattray TRIUMF, Vancouver, Canada	target, cyclotron, radiation, TRIUMF	198

V-03	**A Facility for Radioisotope Production at TRIUMF with 70-110 MeV Protons** • **D.R. Pearce**, J.S. Vincent TRIUMF, Vancouver, Canada	target, proton, cyclotron, TRIUMF	209
V-06	**Experiences with the Cyclone 3 Oxygen 15 Generator** • **E. Conard**, J.-L. Morelle Ion Beam Applications, Louvain-la-Neuve, Belgium • J.C. Clark, D.B. Mackay Hammersmith Hospital, London, England	cyclotron, target, ion, ion-source	218
V-07	**Dual Chemical Station for Cyclotron Produced ^{18}F** • **M.L. Mallory**, G. Grimmett, R. Tilbury, D. Yang The University of Texas, Houston, Texas, USA	cyclotron, radioactivity, diagnostics, target	222
VI-02	**Current and Potential Clinical Indications of Proton Irradiation (Invited Paper)** • **A.F. Thornton**, H.D. Suit Harvard Medical School, Boston, Massachusetts, USA	proton, photon, radiation, site	234
VI-03	**Pion Therapy for Cancer - What are the Prospects?** • **G.B. Goodman** University of British Columbia, Vancouver, Canada	photon, TRIUMF, radiation, background	242
VI-07	**Design Consideration of Neutron Therapy Facility Utilizing Existing Cyclotron** • **H. Chang**, X. Cui, J. Wei, J. Zhang, K. Xie Institute of Nuclear Research, Shanghai, People's Republic of China	target, neutron, cyclotron, proton	255
VI-09	**Continued Operation of the Seattle Clinical Cyclotron Facility** • **R. Risler**, S. Brossard, J. Jacky, I. Kalet, P. Wootton, F. Ziai University of Washington, Seattle, Washington, USA	neutron, cyclotron, target, radiation	262
IXB-05	**Internal Beam Dynamics Studies with a TV Probe** • **F. Marti**, S. Snyder NSCL, East Lansing, Michigan, USA	resonance, cyclotron, simulation, ion	435

IXC-01	**Commissioning of the New High Intensity Axial Injection System for GANIL**	injection, cyclotron, ion, emittance	446

- **Ch. Ricaud**, E. Baron, J. Bony, M.P. Bourgarel, B. Bru
  GANIL, Caen, France
- R. Vienet
  CEN/Saclay, Gif-sur-Yvette, France

IXD-01	**The New Phase Detection System of the Cosy-Injector**	pick-up, cyclotron, COSY, linac	469

- **K. Kennepohl**, W. Bräutigam, M. Herschbach, D. Maeckelburg
  FZJ, Jülich, Germany

IXD-02	**High-Sensitive Ionization Detectors of Transverse Distribution of Accelerated Particles Beam**	ion, cyclotron, electron, proton	473

- **V.G. Mikhailov**, V.A. Rezvov, A.A. Roshchin, V.I. Sklyarenko, L.I. Iudin
  Kurchatov Institute, Moscow, Russia

IXD-05	**High Sensitivity Electronic System for the Phase Probes of the LNS/MILANO Superconducting Cyclotron**	cyclotron, ion, injection, rf-amplifier	483

- **A. Bosotti**, D. Corti, C. Pagani, G. Varisco, F. Zibra
  INFN/LASA, Segrate, Italy
- M. Di Giacomo
  INFN/LNS, Catania, Italy

XA-01	**Advances in RF Technology for Cyclotrons**	cavity, cyclotron, coupling, impedance	501

- **C. Pagani**
  INFN/LASA, Segrate, Italy

XA-06	**A Modified RF System of JAERI AVF Cyclotron**	cavity, cyclotron, ion, proton	526

- **Y. Kumata**, Y. Fukumoto
  Sumitomo Heavy Industries, Ehime, Japan
- K. Arakawa, M. Fukuda, T. Karasawa
  JAERI, Gunma, Japan
- A. Shimizu
  Osaka University, Osaka, Japan

XA-08	**Experience with the PSI-Cyclotron RF-System Under Heavy Beam Loading**	cavity, coupling, cyclotron, impedance	534

- **P.K. Sigg**, J. Cherix, H. Frei, M. Märki
  PSI, Villigen, Switzerland

XA-11	**TRIUMF Cyclotron RF System Improvements**	impedance, TRIUMF, cyclotron, cathode	545

- **G.C. Blaker**, A.K. Mitra, R.L. Poirier
  TRIUMF, Vancouver, Canada

XA-12	**Improvements to the RF Separator in the M9 Muon Channel at TRIUMF**	cavity, TRIUMF, impedance, cyclotron	549

- **G.C. Blaker**, A.K. Mitra, R.L. Poirier
  TRIUMF, Vancouver, Canada

XA-13	**The RF System of the Gustaf Werner Cyclotron/Synchrocyclotron**	cyclotron, proton, synchro-cyclotron, vacuum	553

- **B. Lundström**, B. Holmgren
  Uppsala University, Uppsala, Sweden

XD-04	**The Beam-Guiding System of AGOR**	target, AGOR, heavy-ion, diagnostics	615

- **J.M. Schippers**
  Kernfysisch Versneller Instituut, Groningen, The Netherlands

XD-05	**Buncher in the Beam Line from ECR to SFC**	ECR, ion, bunching, ion-source	618

- **J.Z. Jiang**, X.H. Zhou, Q. Wang, F. Wang, W.M. Jiang
  Institute of Modern Physics, Lanzhou, People's Republic of China

XI-01	**Integrated Tools for Cyclotron Operation (Invited Paper)**	cyclotron, monitoring, TRIUMF	634

- **W. Busse**
  HMI, Berlin, Germany

XI-02	**The IUCF High Intensity Polarized Ion Source Control System**	vacuum, ion, ion-source, interlocks	641

- **T. Capshew**, J.C. Collins, D. DuPlantis, D.W. Frame, J. Graham, D.D. Reid
  Indiana University, Bloomington, Indiana, USA

XI-04	**Control System for JAERI AVF Cyclotron**	cyclotron, JAERI, injection, status	648

- **S. Okumura**, T. Agematsu, K. Arakawa, M. Fukuda, I. Ishibori, T. Kamiya, Y. Nakamura, T. Nara, W. Yokota
  JAERI, Gunma, Japan
- K. Hoshika, K. Iso, M. Maruyama, M. Tachibana
  Sumitomo Heavy Industries, Ehime, Japan

XI-05	**Automatic Control System of Magnetic Separator for**	cyclotron, ion, status,	652

	Kurchatov IAE Cyclotron	power-supply	

- **N.I. Venikov**, V. Buranov, O. Gotovtsev, L.I. Iudin, P.Yu. Komissarov, V.N. Unezhev
  Kurchatov Institute, Moscow, Russia

XI-06	**The New Distributed Control System of the NAC**	instrumentation, status, cyclotron, light-ion	656

- **H.F. Weehuizen**, R.K. Fisch, E.J.S. Franklin, M.E. Hogan, I.H. Kohler, J.P. Rogers, P.J. Theron
  National Accelerator Centre, Faure, Republic of South Africa

XI-07	**Ion Spectra Identification Software for the ECR Ion Source at NAC**	ion, ion-source, ECR, cyclotron	660

- **E.J.S. Franklin**, J.G. de Villiers
  National Accelerator Centre, Faure, Republic of South Africa

XI-08	**Micro-Controlled Vacuum Systems at NAC**	vacuum, cyclotron, instrumentation, monitoring	664

- **P.J. Celliers**, E.J.S. Franklin
  National Accelerator Centre, Faure, Republic of South Africa

XI-09	**Two Dimensional Scans with Adaptive Domain Control**	beam-losses, extraction, interlocks, status	668

- **S. Adam**, A.C. Mezger
  PSI, Villigen, Switzerland

XI-10	**Construction and System Tuning of Control System for the RCNP Ring Cyclotron and Beam Lines**	cyclotron, power-supply, status, injection	672

- **T. Yamazaki**, A. Ando, K. Hosono, T. Itahashi, M. Kibayashi, I. Miura, K. Nagayama, H. Ogata, T. Saito, A. Shimizu, K. Tamura, M. Uraki
  Osaka University, Osaka, Japan
- K. Aoki, Y. Kimura, M. Maruyama, M. Tachibana, S. Yamada
  Sumitomo Heavy Industries, Ehime, Japan
- K. Kodaira
  Sumitomo Heavy Industries Systems Engineering Laboratory, Tokyo, Japan

XI-11	**Early Experience with DECwindows/Motif in the TRIUMF Central Control System**	laser, booster, TRIUMF, ion-source	676

- **S. Kadantsev**
  JINR, Dubna, Russia

- M. Mouat
  TRIUMF, Vancouver, Canada

XI-12	**Application of Object Oriented Techniques in the TRIUMF Beam Line 2C Control System (Invited Paper)**	target, kaon, TRIUMF, factory	681

- **N.A. Wilkinson**, E.A. Osberg, G.A. Ludgate
  TRIUMF, Vancouver, Canada

XI-13	**The TR30 Control System - A Case for Off-the-Shelf Software**	vacuum, diagnostics, cyclotron, TRIUMF	685

- **R. Keitel**, D.J. Dale, B.F. Milton
  TRIUMF, Vancouver, Canada

XI-14	**Formal Specifications for a Cyclotron Control System**	cyclotron, neutron, status, radiation	689

- **J. Jacky**, R. Risler
  University of Washington, Seattle, Washington, USA

XV-01	**Proper and Improper Accelerators - In Praise of Cyclotrons and Their Builders**	cyclotron, TRIUMF, ion, synchrotron	765

- **M.K. Craddock**
  University of British Columbia, Vancouver, Canada

A B C D E F H I J K L M N O P Q R S T V

COSY

Paper	Title	Other Keywords	Page
I-12	**Commissioning of the Injector Complex of COSY-Jülich** • **W. Bräutigam**, H. Beuscher, R. Brings, H.G. Böge, R. Maier, M. Rogge, P. Wucherer FZJ, Jülich, Germany	cyclotron, ion, controls, injection	67
VII-03	**COSY-Jülich - A Synchrotron and Storage Ring for Medium Energy Physics** • **R. Maier**, U. Pfister FZJ, Jülich, Germany	quadrupole, injection, dipole, extraction	282
IXD-01	**The New Phase Detection System of the Cosy-Injector** • **K. Kennepohl**, W. Bräutigam, M. Herschbach, D. Maeckelburg FZJ, Jülich, Germany	pick-up, cyclotron, controls, linac	469

A B C D E F H I J K L M N O P Q R S T V

coupling

Paper	Title	Other Keywords	Page
I-18	**Status Report on the Heavy Ion Facility at LNS** • **F. Alessandria**, G. Bellomo, A. Bosotti, C. De Martinis, D. Giove, P. Michelato, C. Pagani, L. Rossi, INFN/LASA, Segrate, Italy • L. Calabretta, G. Ciavola, G. Cuttone, M. Di Giacomo, S. Gammino, P. Gmaj, G. Raia, D. Rifuggiato, J. Sura, INFN/LNS, Catania, Italy	cyclotron, vacuum, cavity, ion	90
IV-02	**A Cyclotron as a Mass Spectrometer** • **P. Bricault**, G. Auger, M. Bajard, E. Baron, D. Bibet, A. Chabert, J. Fermé, L. Gaudart, J. Joubert, M. Lewitowicz, W. Mittig, E. Plagnol, Ch. Ricaud, Y. Schutz, GANIL, Caen, France • G. Audi, CSNSM, Orsay, France • A. Gillibert, CEN/Saclay, Gif-sur-Yvette, France • K. Fifield, Australian National University, Canberra , Australia	cyclotron, ion, injection, target	158
IXC-03	**Preliminary Design of a New Central Region for the LNS Superconducting Cyclotron** • **M-H. Moscatello**, GANIL, Caen, France	cyclotron, injection, emittance, ion	454
IXD-04	**Emittance Measurements in the HIRFL Beam Line** • **H. Zhao**, Z. Shen, B.W. Wei, Institute of Modern Physics, Lanzhou, People's Republic of China	emittance, quadrupole, linac, optical-matching	479
XA-01	**Advances in RF Technology for Cyclotrons** • **C. Pagani**, INFN/LASA, Segrate, Italy	cavity, cyclotron, impedance, controls	501
XA-02	**The RF Coupling System of the VINCY Cyclotron**	impedance, cyclotron, vacuum, cavity	511

B. Bojovic, M. Josipovic, A. Susini
CERN, Geneva, Switzerland

XA-07	**Multi-Point Cavity Excitation**	cavity, resonance, impedance, simulation	530

- **E. Zaplatin**
FZJ, Jülich, Germany

XA-08	**Experience with the PSI-Cyclotron RF-System Under Heavy Beam Loading**	cavity, cyclotron, controls, impedance	534

- **P.K. Sigg**, J. Cherix, H. Frei, M. Märki
PSI, Villigen, Switzerland

XA-09	**Initial Operation of the RF System for the RCNP Ring Cyclotron**	cavity, acceleration, cyclotron, proton	538

- **T. Saito**, I. Miura, A. Shimizu, M. Uraki
Osaka University, Osaka, Japan

A B C D E F H I J K L M N O P Q R S T V

cryogenics

Paper	Title	Other Keywords	Page
XB-01	**Low Temperature Tests of the AGOR Superconducting Coil System**	AGOR, power-supply, factory, vacuum	557

- **K. Pieterman**, J.A.M. Dam
  Cryocon B.V., Amersfoort, The Netherlands
- C. Commeaux
  IPN, Orsay, France
- C. Penco
  Ansaldo Componenti, Genoa, Italy

A B C D E F H I J K L M N O P Q R S T V

cyclotron

Paper	Title	Other Keywords	Page
I-01	**Commissioning of the RCNP Ring Cyclotron (Invited Paper)** • **I. Miura**, A. Ando, K. Hatanaka, K. Hosono, H. Ikegami, T. Itahashi, M. Kibayashi, M. Kondo, H. Ogata, T. Saito, A. Shimizu, K. Tamura, M. Uraki, T. Yamazaki, Osaka University, Osaka, Japan • J. Abe, Sumitomo Heavy Industries, Ehime, Japan	proton, acceleration, cavity, injection	3
I-02	**New Development at the JINR Heavy Ion Cyclotron Facility (Invited Paper)** • **G.G. Gulbekyan**, V. Bekhterev, O. Borisov, B. Gikal, A. Ivanenko, I. Kolesov, V.B. Kutner, A. Morduev, Yu.Ts. Oganessian, JINR, Dubna, Russia	ion, extraction, vacuum, ECR	11
I-03	**New K130 Cyclotron at Jyväskylä (Invited Paper)** • **E. Liukkonen**, University of Jyväskylä, Jyväskylä, Finland	ion, ECR, vacuum, ion-source	22
I-04	**Experience with the High Current Operation of the PSI Cyclotron Facility (Invited Paper)** • **Th. Stammbach**, PSI, Villigen, Switzerland	space-charge, beam-losses, extraction, injection	28
I-05	**The Commissioning of PSI Injector 2 for High Intensity, High Quality Beams** • **J. Stetson**, NSCL, East Lansing, Michigan, USA • S. Adam, M. Humbel, W. Joho, Th. Stammbach, PSI, Villigen, Switzerland	space-charge, acceleration, simulation, bunching	36
I-06	**AGOR: Recent Achievements (Invited Paper)** • **H.W. Schreuder**, IPN, Orsay, France	AGOR, extraction, vacuum, site	40

I-08	**Parameters, Present State and Application Perspectives of the U-250 Cyclotron** • **A.I. Muminov** Institute of Nuclear Physics, Tashkent, Republic of Uzbekistan • M.F. Vorogushin D.V. Efremov Scientific Research Institute of Electrophysical Apparatus, St. Petersburg, Russia	ion, vacuum, heavy-ion, resonance	50
I-10	**Gatchina Isochronous Cyclotron** • **N.K. Abrosimov**, S.A. Artamonov, P.V. Chervyakov, S.P. Dmitriev, V.A. Eliseev, V.P. Fominenko, E.M. Ivanov, G.F. Mikheev, Yu.T. Mironov, A.S. Pokrovskii, G.A. Riabov, V.A. Smolin, G.L. Sokolov, V.A. Volchenkov, A.A. Vorobiev Petersburg Nuclear Physics Institute, Gatchina, Russia • P.V. Bogdanov, B.D. Ershov, V.S. Kuligin, V.N. Moshkin, V.G. Mudrolyubov, Yu.I. Stogov, A.P. Strokach D.V. Efremov Scientific Research Institute of Electrophysical Apparatus, St. Petersburg, Russia	ion, synchro-cyclotron, vacuum, injection	58
I-11	**Status Report of SARA** • **M. Fruneau**, S. Albrand, D. Barnéoud, J.L. Belmont, G. Bizouard, J.L. Bouly, G. Campillo, M. Guisset, G. Laborie Université Joseph Fourier, Grenoble, France	ion, injection, ECR, vacuum	62
I-12	**Commissioning of the Injector Complex of COSY-Jülich** • **W. Bräutigam**, H. Beuscher, R. Brings, H.G. Böge, R. Maier, M. Rogge, P. Wucherer FZJ, Jülich, Germany	COSY, ion, controls, injection	67
I-13	**Current Status and Future Project of Cyclotron Laboratory in Alma-Ata** • **A.A. Arzumanov**, V. Batischev, V. Berger, V. Gerasimov, M. Gorcovets Kazakhstan Academy of Sciences, Alma-Ata, Republic of Kazakhstan	ion, extraction, heavy-ion, emittance	71
I-16	**Status Report of Cyclone** • **M. Loiselet**, N. Postiau, G. Ryckewaert Université Catholique de Louvain, Louvain-la-Neuve, Belgium	ion, target, neutron, beam-transport	82
I-17	**Performance of the K1200 Cyclotron at MSU**	ion, target, emittance, power-supply	86

- **P. Miller**, T.A. Antaya, F. Marti, D. Poe, B. Sherrill, J. Stetson, J. Winger
  NSCL, East Lansing, Michigan, USA
- J.A. Nolen
  ANL, Argonne, Illinois, USA

I-18	**Status Report on the Heavy Ion Facility at LNS**	vacuum, cavity, coupling, ion	90

- **F. Alessandria**, G. Bellomo, A. Bosotti, C. De Martinis, D. Giove, P. Michelato, C. Pagani, L. Rossi
  INFN/LASA, Segrate, Italy
- L. Calabretta, G. Ciavola, G. Cuttone, M. Di Giacomo, S. Gammino, P. Gmaj, G. Raia, D. Rifuggiato, J. Sura
  INFN/LNS, Catania, Italy

I-19	**Development of the NAC Accelerator Facilities**	extraction, injection, ion, proton	95

- **J.L. Conradie**, A.H. Botha, P.M. Cronje, R.E.F. Fenemore, H.N. Jungwirth, J.J. Kritzinger, W.A.G. Nel, D. Reitmann, L.M.M. Roels, P.F. Rohwer, H.A. Smit
  National Accelerator Centre, Faure, Republic of South Africa

I-20	**Heavy Ion Facility in ATOMKI**	ion, ECR, heavy-ion, ion-source	99

- **S. Biri**, J. Pálinkás, A. Valek
  Institute of Nuclear Research of the Hungarian Academy of Sciences, Debrecen, Hungary

I-21	**Recent Achievements at the RIKEN Ring Cyclotron**	ion, ion-source, acceleration, injection	102

- **Y. Yano**
  RIKEN, Saitama, Japan

I-22	**Status Report on the Gustaf Werner Cyclotron in Uppsala**	ion, extraction, injection, vacuum	106

- **S. Holm**
  Uppsala University, Uppsala, Sweden

II-01	**Commercially Available Compact Cyclotrons for Isotope Production (Invited Paper)**	ion, target, ion-source, proton	110

- **V. Bechtold**
  FZK, Karlsruhe, Germany

II-02	**The Operation of Cyclotrons Used for Radiopharmaceutical Production**	target, controls, radiation, isotope-production	115

- **T. Grey-Morgan**
  Cyclotron Isotopes Manufacturing, Buckinghamshire, England
- R.E. Hubbard
  Medi + Physics Inc., Arlington Heights, Illinois, USA

II-03 **Construction and First Year's Operation of the JAERI AVF Cyclotron** ion, JAERI, extraction, proton 119

- **K. Arakawa**, T. Agematsu, M. Fukuda, I. Ishibori, T. Karasawa, T. Nara, Y. Nakamura, S. Okumura, R. Tanaka, W. Yokota
  JAERI, Gunma, Japan
- A. Shimizu
  Osaka University, Osaka, Japan
- Y. Hayashi, K. Ishii, T. Satoh, T. Tachikawa
  Sumitomo Heavy Industries, Ehime, Japan

II-04 **20 MeV Cyclotron for Isotope Production** target, acceleration, isotope-production, proton 123

- **A. Glazov**, Ju. Alenitskiy, A. Chesnov, S. Chesnova, V. Kochkin, D. Novikov, E. Samsonov, M. Semenov, A. Vasilenko, E. Zaplatin, N. Zaplatin
  JINR, Dubna, Russia
- I. Gulamov, O. Iljasov, A. Rykov
  Institute of Nuclear Physics, Tashkent, Republic of Uzbekistan

II-05 **Status of a Compact H^- Cyclotron at the Kurchatov Institute of Atomic Energy** ion, controls, vacuum, ion-source 126

- **N.I. Venikov**, C.D. Burbeza, P.Yu. Komissarov, Yu.M. Krasnikov, S.T. Latushkin, V.V. Leonov, V.P. Moryakov, I.V. Naumov, A.Ya. Pisman, V.A. Rezvov, A.A. Vasiliev, V.E. Yarosh, L.I. Yudin
  Kurchatov Institute, Moscow, Russia

II-06 **A Newly Developed Compact Cyclotron for Neutron Therapy and Positron Nuclear Medicine** neutron, target, positron, proton 129

- **K. Ito**, T. Ishigaki, S. Itoh, Y. Kasugai, T. Kato, T. Misawa, M. Nishino, M. Osakabe, T. Ota, S. Sakuma, M. Tadokoro, H. Yamamoto
  Nagoya University, Nagoya, Japan
- Y. Toda, Y. Yamamoto
  Japan Steel Works Ltd., Tokyo, Japan

II-07 **Performance of the Harper Hospital Cyclotron; Effect of Pulsed Radio Frequency** target, neutron, ion, controls 133

- **H.G. Blosser**, J. Vincent
  NSCL, East Lansing, Michigan, USA
- R. Maughan

Harper Hospital, Detroit, Michigan, USA

III-01	**The TRIUMF 520 MeV Cyclotron: Recent and Future Developments**	cavity, TRIUMF, extraction, proton	138

- **G. Dutto**
  TRIUMF, Vancouver, Canada

IV-01	**Material Research with Beams at Cyclotron Energies (Invited Paper)**	ion, radiation, proton, heavy-ion	149

- **K. Ziegler**
  HMI, Berlin, Germany

IV-02	**A Cyclotron as a Mass Spectrometer**	ion, injection, coupling, target	158

- **P. Bricault**, G. Auger, M. Bajard, E. Baron, D. Bibet, A. Chabert, J. Fermé, L. Gaudart, J. Joubert, M. Lewitowicz, W. Mittig, E. Plagnol, Ch. Ricaud, Y. Schutz
  GANIL, Caen, France
- G. Audi
  CSNSM, Orsay, France
- A. Gillibert
  CEN/Saclay, Gif-sur-Yvette, France
- K. Fifield
  Australian National University, Canberra , Australia

IV-04	**^{178m2}Hf and ^{237}Pu Isotopes Production on the U-200 Cyclotron**	ion, target, cathode, ion-source	167

- **S.L. Bogomolov**, S.N. Dmitriev, Yu.P. Gangrski, G.G. Gulbekyan, S.A. Karamian, V.B. Kutner, B.N. Markov, Yu.Ts. Oganessian, N.V. Pronin, G.Ya. Starodub
  JINR, Dubna, Russia

IV-05	**Radionuclide Technique in Mechanical Engineering (RTM)**	injection, ion, diagnostics, radiation	171

- **P. Fehsenfeld**, A. Kleinrahm
  FZK, Karlsruhe, Germany
- V. Novikov
  Kurchatov Institute, Moscow, Russia

IV-06	**A P.E.T. Study of Proton Induced Radioactivity in Different Materials**	target, proton, positron, radioactivity	175

- **J.M. Schippers**
  Kernfysisch Versneller Instituut, Groningen, The Netherlands
- A.M.J. Paans
  University Hospital, Groningen, The Netherlands

	Neutron Productions from Carbon by Charged Particle	neutron, target,	178

IV-07	**Bombardment at Different Energies** • **M.A. Chaudhri** Austin Hospital & University of Melbourne, Melbourne, Australia	proton, background	
IV-08	**Analytical Applications of Cyclotrons in Biomedical Fields - Charged Particle Activation Analysis** • **M.A. Chaudhri** Austin Hospital & University of Melbourne, Melbourne, Australia	proton, neutron, target, ion	181
IV-09	**A Simple Method for Estimating Activation Sensitivities of Different Elements / Isotopes with Cyclotron Produced Neutrons** • **M.A. Chaudhri** Austin Hospital & University of Melbourne, Melbourne, Australia	neutron, target, BNL, radiation	187
IV-10	**A Proposal for an Intense Cyclotron-Based Thermal Neutron Source** • **S. Tazawa** Sumitomo Heavy Industries, Toyo-shi, Toyo-shi, Japan • W.L. Whittemore General Atomics, San Diego, California, USA	neutron, target, proton, extraction	191
IV-11	**External High Current Targetry for Radioisotope Production** • **N.R. Stevenson**, W.Z. Gelbart TRIUMF, Vancouver, Canada	target, TRIUMF, radiation, vacuum	196
IV-12	**A Remotely Controlled Robotic Vehicle for Work Within Radioactive Environments** • **N.R. Stevenson**, P. Bloemhard, M. Brigham, J. Ko, C. LaForge, J. Orzechowski, E. Pattyn, T. Rattray TRIUMF, Vancouver, Canada	target, controls, radiation, TRIUMF	198
V-02	**The Production of Radionuclides for the Biosciences (Invited Paper)** • **T.J. Ruth** TRIUMF, Vancouver, Canada	target, ion, proton, extraction	206
V-03	**A Facility for Radioisotope Production at TRIUMF with 70-110 MeV Protons** • **D.R. Pearce**, J.S. Vincent TRIUMF, Vancouver, Canada	target, controls, proton, TRIUMF	209

V-04 **Possibility of Producing Some Radionuclides for Medicine Using JINR Accelerators** proton, electron, target, microtron 213

- **S.N. Dmitriev**, G.G. Gulbekyan, V.A. Khalkin, R.Ts. Oganessian, L.M. Onishchenko, G.Ya. Starodub, N.G. Zaitseva
  JINR, Dubna, Russia

V-05 **Radiopharmaceutical "Thallium-201-Chloride" Production using Thallium-203 Irradiation by Helium-3 Ions** ion, target, proton, ALICE 216

- **A.A. Arzumanov**, N.K. Hamidov, A.I. Kozin, G.I. Shychikov, S.T. Tihomirova
  Kazakhstan Academy of Sciences, Alma-Ata, Republic of Kazakhstan

V-06 **Experiences with the Cyclone 3 Oxygen 15 Generator** target, ion, controls, ion-source 218

- **E. Conard**, J.-L. Morelle
  Ion Beam Applications, Louvain-la-Neuve, Belgium
- J.C. Clark, D.B. Mackay
  Hammersmith Hospital, London, England

V-07 **Dual Chemical Station for Cyclotron Produced ^{18}F** radioactivity, diagnostics, target, controls 222

- **M.L. Mallory**, G. Grimmett, R. Tilbury, D. Yang
  The University of Texas, Houston, Texas, USA

VI-04 **Progress Report on the IBA-SHI Proton Therapy System** proton, extraction, scattering, emittance 244

- **Y. Jongen**, W. Beeckman, J.P. Dufour, A. Laisné, H. Marie, R. Verbruggen
  Ion Beam Applications, Louvain-la-Neuve, Belgium
- M. Sano, S. Satoh, N. Takahashi, T. Takayama
  Sumitomo Heavy Industries, Ehime, Japan

VI-05 **Recent Activities of the Cyclotron Laboratory in Nice** ion, synchrotron, proton, light-ion 248

- **P. Mandrillon**, N. Brassart, P. Chauvel, A. Courdi, F. Farley, N. Fietier, J. Herault, J.Y. Tang
  Centre Antoine Lacassagne, Nice, France

VI-06 **Health Physics Data Acquisition System at the National Medical Cyclotron** radiation, monitoring, target, neutron 252

- **B.N. Mukherjee**
  ANSTO, Menai, NSW, Australia
- D.W. Arnott

National Medical Cyclotron, Camperdown, NSW, Australia

VI-07	**Design Consideration of Neutron Therapy Facility Utilizing Existing Cyclotron**	target, neutron, controls, proton	255

- **H. Chang**, X. Cui, J. Wei, J. Zhang, K. Xie
  Institute of Nuclear Research, Shanghai, People's Republic of China

VI-08	**A Proton Therapy Facility Plan**	proton, synchrotron, radiation, electron	258

- **S. Fukumoto**, Y. Hayakawa, T. Inada, A. Maruhashi, M. Sato, J. Tada, Y. Takada, H. Tsuji, H. Tsujii
  University of Tsukuba, Ibaraki, Japan
- K. Endo, Y. Irie, K. Muto
  KEK, Ibaraki, Japan

VI-09	**Continued Operation of the Seattle Clinical Cyclotron Facility**	neutron, controls, target, radiation	262

- **R. Risler**, S. Brossard, J. Jacky, I. Kalet, P. Wootton, F. Ziai
  University of Washington, Seattle, Washington, USA

VII-04	**Study of Beam Dynamics at Cooler Synchrotron TARN-II**	acceleration, ion, synchrotron, injection	286

- **S. Watanabe**, Y. Arakaki, K. Chida, T. Katayama, M. Tomizawa, T. Watanabe, M. Yoshizawa
  University of Tokyo, Tanashi-shi, Tokyo, Japan
- K. Noda, M. Kanazawa
  NIRS, Chiba, Japan

VII-05	**Dubna Project of the Heavy Ion Storage Ring Complex K4-K10**	ion, injection, heavy-ion, target	290

- **Yu.Ts. Oganessian**, O.N. Malyshev, G.S. Popeko, A.M. Rodin, S.I. Sidorchuk, Ye.A. Sokol, S.V. Stepantsov, G.M. Ter-Akopian, V.A. Timakov
  JINR, Dubna, Russia
- V.V. Parhomchuk, A.A. Sery, V.D. Shiltsev
  Institute for Nuclear Physics, Novosibirsk, Russia
- I.N. Meshkov, Ye.M. Syresinm
  Center for Applied Physics and Technology, Lipetsk, Russia
- V.P. Belov, A.A. Makarov, Yu.P. Severgin, I.A. Shukeylo, M.N. Tarovik
  D.V. Efremov Scientific Research Institute of Electrophysical Apparatus, St. Petersburg, Russia

VIII-03	**Ion Sources for Cyclotron Application**	ion, plasma, ion-source, electron	312

- **K.N. Leung**, D.A. Bachman, D.S. McDonald, A.T. Young

LBL, Berkeley, California, USA

VIII-04	**A Review of Polarized Ion Sources for Cyclotrons (Invited Paper)**	ion, ion-source, electron, polarization	316

- **P.W. Schmor**
  TRIUMF, Vancouver, Canada

VIII-09	**Operation of Ion Sources and Beam Transport to JAERI AVF Cyclotron**	ion, ECR, ion-source, extraction	336

- **W. Yokota**, T. Agematsu, K. Arakawa, M. Fukuda, I. Ishibori, Y. Nakamura, T. Nara, S. Okumura
  JAERI, Gunma, Japan
- Y. Hayashi, K. Ishii, T. Tachikawa
  Sumitomo Heavy Industries, Ehime, Japan

VIII-10	**Spin Dynamics and Polarized Ion Sources on Isochronous Cyclotron U-240**	ion, resonance, polarization, acceleration	340

- **N.I. Zaika**
  Institute for Nuclear Research, Kiev, Ukraine

VIII-13	**Recent Development of Internal H^-/D^- Source for Compact Cyclotrons**	ion, extraction, plasma, proton	352

- **T.Y.T. Kuo**
  TRIUMF, Vancouver, Canada
- G.O. Hendry
  Cyclotron Inc., Napa, California, USA

VIII-14	**Plan for the Ion Source Emittance Measurement Under the RF Extraction**	emittance, ion, ion-source	357

- **J.W. Kim**, H.G. Blosser
  NSCL, East Lansing, Michigan, USA

VIII-15	**Progress with the NAC Injector Cyclotron for Heavy and Polarized Ions**	ion, proton, heavy-ion, diagnostics	361

- **Z.B. du Toit**, S.J. Burger, P.J. Celliers, J.G. de Villiers, H.N. Jungwirth, A. Müller, P.F. Rohwer, D.M. van Rooyen
  National Accelerator Centre, Faure, Republic of South Africa

VIII-17	**Performance of the Texas A&M ECRIS**	ECRIS, injection, ion, ion-source	369

- **G. Mouchaty**, D.P. May, R.C. Rogers, P. Smelser
  Texas A&M University, College Station, Texas, USA

IXA-	**Advantage of Using Differential Algebra and Lie Algebra in**	resonance, octupole,	372

01	**the Orbit Dynamics of Cyclotrons (Invited Paper)** • **W.G. Davies** Atomic Energy of Canada, Chalk River, Ontario, USA	sextupole, closed-orbit	
IXA-02	**The Influence of Magnetic Field Imperfections on the Beam Quality in an H^- Cyclotron** • **W.J.G.M. Kleeven**, H.L. Hagedoorn Eindhoven University of Technology, Eindhoven, The Netherlands • B.F. Milton, G. Dutto TRIUMF, Vancouver, Canada	resonance, emittance, extraction, betatron	380
IXA-04	**Ion_Tracker, a Trace Tracking Program for Cyclotron Design** • **M. Rinta-Nikkola** University of Jyväskylä, Jyväskylä, Finland	ion, injection, optics, acceleration	388
IXA-05	**Ion Optics in the Jyväskylä K130 Cyclotron** • **P. Heikkinen**, M. Rinta-Nikkola University of Jyväskylä, Jyväskylä, Finland	ion, injection, solenoid, extraction	392
IXA-07	**Deriving the General Expressions of Nonlinear Transport Coefficients of Accelerator Beam Phase Space by Artificial Intelligence** • **J. Xia** Institute of Modern Physics, Lanzhou, People's Republic of China • C. Liu, X. Xie Graduate School of Nuclear Industry, Beijing, People's Republic of China	beam-transport, electromagnetic-fields, optics	400
IXA-08	**Evaluation of Third-Harmonic Voltage Flattopping for a Superconducting Cyclotron** • **M.M. Gordon**, D. Jeon NSCL, East Lansing, Michigan, USA	extraction, ion, TRIUMF, resonance	404
IXA-09	**Crossing of Resonances** • **L.A. Sarkisyan**, A.L. Sarkisyan Moscow Institute-Internate, Moscow, Russia	resonance, synchrotron, extraction	408
IXA-10	**Increase of Beam Intensity**	injection, resonance, synchrotron, proton	409

- **L.A. Sarkisyan**, A.L. Sarkisyan
  Moscow Institute-Internate, Moscow, Russia

IXA-11	**Developments in RELAX3D, a 2D/3D Laplace and Poisson Equation Solver**	TRIUMF, electron, simulation, proton	411

- **H. Houtman**, F.W. Jones, C.J. Kost
  TRIUMF, Vancouver, Canada

IXA-12	**Beam Quality Investigations for H^- Extraction at TRIUMF**	emittance, extraction, resonance, simulation	415

- **R.E. Laxdal**, G.H. Mackenzie, J.B. Pearson, L. Root
  TRIUMF, Vancouver, Canada

IXB-01	**Cyclotron Tuning as a Rebuncher**	extraction, target, emittance, acceleration	419

- **D. Bibet**, M-H. Moscatello
  GANIL, Caen, France

IXB-02	**Beam Studies of Injection to Extraction System for JAERI AVF Cyclotron**	proton, injection, extraction, JAERI	423

- **M. Fukuda**, T. Agematsu, K. Arakawa, I. Ishibori, T. Karasawa, Y. Nakamura, T. Nara, S. Okumura, W. Yokota
  JAERI, Gunma, Japan

IXB-03	**K1200 Cyclotron Beam Development Techniques**	ion, ion-source, injection, ECR	427

- **T.A. Antaya**, D. Cole, P. Miller, D. Poe
  NSCL, East Lansing, Michigan, USA

IXB-04	**Selection and Measurement of RF Phase Width of the K1200 Cyclotron Beam**	extraction, vacuum, injection, ion	431

- **J. Bailey**, J. Kuchar, F. Marti, J. Yurkon
  NSCL, East Lansing, Michigan, USA
- J.A. Nolen
  ANL, Argonne, Illinois, USA
- D. Rifuggiato
  INFN/LNS, Catania, Italy

IXB-05	**Internal Beam Dynamics Studies with a TV Probe**	resonance, simulation, controls, ion	435

- **F. Marti**, S. Snyder
  NSCL, East Lansing, Michigan, USA

IXB-06	**Effect of the Main-Coil Position on the Accelerated Beam of the K500 Cyclotron** • **D.P. May**, G. Mouchaty Texas A&M University, College Station, Texas, USA	extraction, vacuum, focusing, betatron	439
IXB-07	**Beam Test Results Using the Auxiliary Accelerating Cavity** • **R.E. Laxdal**, G.H. Mackenzie, L. Root TRIUMF, Vancouver, Canada	cavity, simulation, extraction, TRIUMF	442
IXC-01	**Commissioning of the New High Intensity Axial Injection System for GANIL** • **Ch. Ricaud**, E. Baron, J. Bony, M.P. Bourgarel, B. Bru GANIL, Caen, France • R. Vienet CEN/Saclay, Gif-sur-Yvette, France	injection, ion, emittance, controls	446
IXC-02	**A Formulation of Spiral Inflector Design and Its Application to SF Cyclotron** • **M. Sekiguchi**, M. Fujita, M. Nishiguchi, Y. Ohshiro, Y. Shida, N. Yamazaki, T. Yamazaki University of Tokyo, Tanashi-shi, Tokyo, Japan	ion, injection, acceleration, ion-source	450
IXC-03	**Preliminary Design of a New Central Region for the LNS Superconducting Cyclotron** • **M-H. Moscatello** GANIL, Caen, France	injection, emittance, ion, coupling	454
IXC-05	**Numerical Studies for Suppression of Vertical Oscillations in the K1200 Cyclotron** • **K. Joh**, F. Marti NSCL, East Lansing, Michigan, USA • J.A. Nolen ANL, Argonne, Illinois, USA	emittance, simulation	461
IXC-06	**Experiments on the Axial Injection System of the Cyclotron U-120M** • **Z. Trejbal**, M. Kriványek, J. Kucera, V. Bejsovec, J. Stursa Czechoslovak Academy of Sciences, Rez, Czechoslovakia	ion, injection, acceleration, ion-source	465
IXD-01	**The New Phase Detection System of the Cosy-Injector**	pick-up, COSY, controls, linac	469

K. Kennepohl, W. Bräutigam, M. Herschbach, D. Maeckelburg
FZJ, Jülich, Germany

IXD-02	**High-Sensitive Ionization Detectors of Transverse Distribution of Accelerated Particles Beam**	ion, controls, electron, proton	473

- **V.G. Mikhailov**, V.A. Rezvov, A.A. Roshchin, V.I. Sklyarenko, L.I. Iudin
  Kurchatov Institute, Moscow, Russia

IXD-03	**A Beam Profile Monitor Using the Ionization of Residual Gas**	MCP, AGOR, ion, background	477

- **J.M. Schippers**, H.H. Kiewiet
  Kernfysisch Versneller Instituut, Groningen, The Netherlands

IXD-05	**High Sensitivity Electronic System for the Phase Probes of the LNS/MILANO Superconducting Cyclotron**	controls, ion, injection, rf-amplifier	483

- **A. Bosotti**, D. Corti, C. Pagani, G. Varisco, F. Zibra
  INFN/LASA, Segrate, Italy
- M. Di Giacomo
  INFN/LNS, Catania, Italy

IXD-06	**The Diagnostics System for the AGOR Superconducting Cyclotron**	extraction, diagnostics, injection, vacuum	487

- **B. Launé**, P. Dambre, J.M. Kaplanski, B. Montsanglant, C. Olivetto, D. Vincent
  IPN, Orsay, France

IXD-07	**Beam Diagnostics in the RCNP Ring Cyclotron**	injection, cavity, acceleration, proton	491

- **T. Itahashi**, T. Saito, I. Miura
  Osaka University, Osaka, Japan
- S. Ichida
  Sumitomo Heavy Industries, Ehime, Japan

IXD-08	**Signal Processing for the Internal Phase Probe in the TRIUMF Cyclotron**	cavity, background, TRIUMF, pick-up	495

- **K. Fong**
  TRIUMF, Vancouver, Canada

XA-01	**Advances in RF Technology for Cyclotrons**	cavity, coupling, impedance, controls	501

- **C. Pagani**
  INFN/LASA, Segrate, Italy

XA-02	**The RF Coupling System of the VINCY Cyclotron**	coupling, impedance, vacuum, cavity	511

- **B. Bojovic**, M. Josipovic, A. Susini
  CERN, Geneva, Switzerland

XA-03	**Dual Frequency Resonator System for a Compact Cyclotron**	impedance, cavity, isotope-production, vacuum	515

- **M. Eiche**, K.L. Erdman
  Ebco Technologies Ltd, Richmond, BC, Canada
- P. Lanz, M. Lipnicki, M. Zach
  TRIUMF, Vancouver, Canada

XA-04	**The RF-System for a VICKSI Injector Cyclotron**	ion, ECR, injection, booster	519

- **W. Pelzer**
  HMI, Berlin, Germany

XA-06	**A Modified RF System of JAERI AVF Cyclotron**	cavity, ion, proton, controls	526

- **Y. Kumata**, Y. Fukumoto
  Sumitomo Heavy Industries, Ehime, Japan
- K. Arakawa, M. Fukuda, T. Karasawa
  JAERI, Gunma, Japan
- A. Shimizu
  Osaka University, Osaka, Japan

XA-08	**Experience with the PSI-Cyclotron RF-System Under Heavy Beam Loading**	cavity, coupling, controls, impedance	534

- **P.K. Sigg**, J. Cherix, H. Frei, M. Märki
  PSI, Villigen, Switzerland

XA-09	**Initial Operation of the RF System for the RCNP Ring Cyclotron**	cavity, acceleration, coupling, proton	538

- **T. Saito**, I. Miura, A. Shimizu, M. Uraki
  Osaka University, Osaka, Japan

XA-11	**TRIUMF Cyclotron RF System Improvements**	impedance, TRIUMF, controls, cathode	545

- **G.C. Blaker**, A.K. Mitra, R.L. Poirier
  TRIUMF, Vancouver, Canada

XA-12	**Improvements to the RF Separator in the M9 Muon Channel at TRIUMF**	cavity, TRIUMF, controls, impedance	549

G.C. Blaker, A.K. Mitra, R.L. Poirier
TRIUMF, Vancouver, Canada

XA-13	**The RF System of the Gustaf Werner Cyclotron/Synchrocyclotron**	controls, proton, synchro-cyclotron, vacuum	553

- **B. Lundström**, B. Holmgren
Uppsala University, Uppsala, Sweden

XB-02	**A Permanent Magnet System for a Cyclotron Used as a Mass Spectrometer**	vacuum, injection, permanent-magnet, ion	561

- **C.Y. Li**, M. Cooper, K. Halbach, W.B. Kunkel, K.N. Leung, R.P. Wells, A.T. Young
LBL, Berkeley, California, USA

XB-03	**Sector Magnet of the RCNP Ring Cyclotron and the Isochronization**	extraction, injection, proton, acceleration	565

- **K. Hosono**, M. Kibayashi, I. Miura
Osaka University, Osaka, Japan

XC-01	**The Electrostatic Deflector for the Chalk River Superconducting Cyclotron**	high-voltage, cathode, vacuum, electron	569

- **W.T. Diamond**, C.R. Hoffmann, G.R. Mitchel, H. Schmeing
Atomic Energy of Canada, Chalk River, Ontario, Canada

XC-02	**Potential Enhancement of Magnetic Deflection in the Chalk River Superconducting Cyclotron Extraction System**	extraction, acceleration, dipole, ion	573

- **C.R. Hoffmann**, E.H. Lindqvist
Atomic Energy of Canada, Chalk River, Ontario, Canada

XC-03	**Model Study of an Electrostatic Deflector Configuration with an Intermediate Electrode**	high-voltage, vacuum, septum, power-supply	577

- **C.R. Hoffmann**, J.F. Mouris
Atomic Energy of Canada, Chalk River, Ontario, Canada

XC-04	**Performance of Beam Chopping System for JAERI AVF Cyclotron**	extraction, ion, injection, JAERI	581

- **W. Yokota**, T. Agematsu, K. Arakawa, M. Fukuda, I. Ishibori, Y. Nakamura, T. Nara, S. Okumura
JAERI, Gunma, Japan
- Y. Hayashi, Y. Kumata, T. Tachikawa
Sumitomo Heavy Industries, Ehime, Japan

XC-05	**The AGOR Superconducting Extraction Channel EMC2**	radiation, AGOR, background, extraction	585

- **K. Pieterman**, J.A.M. Dam
  Cryocon B.V., Amersfoort, The Netherlands
- H.J.H. ten Kate
  TU Twente, Enschede, The Netherlands
- S. Gustafsson
  IPN, Orsay, France

XC-06	**Material Consideration for Magnetic Channels**	extraction, simulation, synchro-cyclotron	589

- **J. Sura**, L. Calabretta, G. Di Biasi, P. Gmaj, D. Rifuggiato
  INFN/LNS, Catania, Italy

XC-07	**Design of Passive Magnetic Channels**	multipole, focusing, dipole, quadrupole	592

- **G. Bellomo**
  INFN/LASA, Segrate, Italy

XC-08	**Deflector Development for the K1200 Cyclotron**	cathode, electron, ion, site	596

- **T.Y.T. Kuo**
  TRIUMF, Vancouver, Canada
- J.A. Nolen
  ANL, Argonne, Illinois, USA

XC-09	**Results from the Deflector Test Stand at Texas A&M University**	high-voltage, power-supply, shielding, monitoring	602

- **D.P. May**, G. Derrig, W. Dewees, P. Smelser, D. Tran, R.C. Rogers
  Texas A&M University, College Station, Texas, USA

XD-01	**Some Perspectives in the Beam Transport and Analyzing System Design for the U-250 Cyclotron**	beam-transport, target, sextupole	606

- **L.E. Korolev**
  D.V. Efremov Scientific Research Institute of Electrophysical Apparatus, St. Petersburg, Russia

XD-02	**Beam Transport System for the IUCF High Intensity Polarized Ion Source**	quadrupole, bunching, dipole, diagnostics	609

- **W.P. Jones**, M.S. Ball, J.C. Collins, D. DuPlantis, T.J.P. Ellison, D.L. Friesel, B. Hamilton, J.W. Hicks, P. Schwandt
  Indiana University, Bloomington, Indiana, USA

XD-03	**Superconducting Focussing Channel for the AGOR Cyclotron**	quadrupole, AGOR, shielding, dipole	612

- **H.W. Schreuder**, P. Blache, C. Commeaux, S. Gustafsson, A. Lafoux, M. Mormiche, R. Panvier
  IPN, Orsay, France

XD-06	**Beamlines for a Second Injector Cyclotron at NAC**	ion, solenoid, dipole, ion-source	621

- **J.C. Cornell**, J.L. Conradie, D.T. Fourie
  National Accelerator Centre, Faure, Republic of South Africa

XD-08	**Design of a Beam Buncher Using a Half-Cosine Driving Function**	injection, bunching, ECRIS, ion	629

- **R.C. Rogers**
  Texas A&M University, College Station, Texas, USA

XI-01	**Integrated Tools for Cyclotron Operation (Invited Paper)**	controls, monitoring, TRIUMF	634

- **W. Busse**
  HMI, Berlin, Germany

XI-03	**An Operator Assistance System for the AVF Cyclotron**	injection, extraction, survey, status	644

- **T. Okamura**, T. Murakami
  Sumitomo Heavy Industries Systems Engineering Laboratory, Tokyo, Japan
- T. Tachikawa
  Sumitomo Heavy Industries, Ehime, Japan
- T. Agematsu, S. Okumura, K. Arakawa
  JAERI, Gunma, Japan

XI-04	**Control System for JAERI AVF Cyclotron**	controls, JAERI, injection, status	648

- **S. Okumura**, T. Agematsu, K. Arakawa, M. Fukuda, I. Ishibori, T. Kamiya, Y. Nakamura, T. Nara, W. Yokota
  JAERI, Gunma, Japan
- K. Hoshika, K. Iso, M. Maruyama, M. Tachibana
  Sumitomo Heavy Industries, Ehime, Japan

XI-05	**Automatic Control System of Magnetic Separator for Kurchatov IAE Cyclotron**	controls, ion, status, power-supply	652

- **N.I. Venikov**, V. Buranov, O. Gotovtsev, L.I. Iudin, P.Yu. Komissarov, V.N. Unezhev
  Kurchatov Institute, Moscow, Russia

		controls,	656

XI-06	**The New Distributed Control System of the NAC**	instrumentation, status, light-ion	

- **H.F. Weehuizen**, R.K. Fisch, E.J.S. Franklin, M.E. Hogan, I.H. Kohler, J.P. Rogers, P.J. Theron
  National Accelerator Centre, Faure, Republic of South Africa

XI-07	**Ion Spectra Identification Software for the ECR Ion Source at NAC**	ion, ion-source, ECR, controls	660

- **E.J.S. Franklin**, J.G. de Villiers
  National Accelerator Centre, Faure, Republic of South Africa

XI-08	**Micro-Controlled Vacuum Systems at NAC**	vacuum, controls, instrumentation, monitoring	664

- **P.J. Celliers**, E.J.S. Franklin
  National Accelerator Centre, Faure, Republic of South Africa

XI-10	**Construction and System Tuning of Control System for the RCNP Ring Cyclotron and Beam Lines**	controls, power-supply, status, injection	672

- **T. Yamazaki**, A. Ando, K. Hosono, T. Itahashi, M. Kibayashi, I. Miura, K. Nagayama, H. Ogata, T. Saito, A. Shimizu, K. Tamura, M. Uraki
  Osaka University, Osaka, Japan
- K. Aoki, Y. Kimura, M. Maruyama, M. Tachibana, S. Yamada
  Sumitomo Heavy Industries, Ehime, Japan
- K. Kodaira
  Sumitomo Heavy Industries Systems Engineering Laboratory, Tokyo, Japan

XI-13	**The TR30 Control System - A Case for Off-the-Shelf Software**	controls, vacuum, diagnostics, TRIUMF	685

- **R. Keitel**, D.J. Dale, B.F. Milton
  TRIUMF, Vancouver, Canada

XI-14	**Formal Specifications for a Cyclotron Control System**	controls, neutron, status, radiation	689

- **J. Jacky**, R. Risler
  University of Washington, Seattle, Washington, USA

XII-01	**The Superconducting Separated-Orbit Cyclotron Tritron (Invited Paper)**	cavity, injection, proton, focusing	693

- **U. Trinks**
  TU München, Garching, Germany

	Design of a Compact Permanent Magnet Cyclotron Mass	ion, ion-source,	705

XII-03	**Spectrometer for the Detection and Measurement of Trace Isotopes** • **A.T. Young**, K.J. Bertsche, D.J. Clark, K. Halbach, W.B. Kunkel, K.N. Leung, C.Y. Li LBL, Berkeley, California, USA	injection, permanent-magnet	
XII-04	**A New Design Proposal for a 200 MeV Superconducting Ring-Cyclotron Magnet** • **H.N. Jungwirth**, J.G. de Villiers National Accelerator Centre, Faure, Republic of South Africa	extraction, focusing, proton	709
XIII-01	**Accelerated Radioactive Nuclear Beams: Existing and Planned Facilities (Invited Paper)** • **J.M. Nitschke** LBL, Berkeley, California, USA	ion, target, ISOL, heavy-ion	713
XIII-02	**A Conceptual Design for a Primary Cyclotron for the ISL Radioactive Beam Project** • **D.J. Clark** LBL, Berkeley, California, USA	extraction, ion, proton, acceleration	721
XIII-04	**The PIAFE Project at Grenoble: Beam Transport and Acceleration** • **J.L. Belmont**, J.F. Bruandet, J.M. de Conto, M. Fruneau, G. Gimond, K. Golovanivsky, E. Liatard, J.M. Loiseaux, H. Nifenecker, A. Savalle, B. Vignon Université Joseph Fourier, Grenoble, France • P. Briand CEN-Grenoble, Grenoble, France	ion, quadrupole, ECRIS, extraction	729
XIII-05	**High Intensity Superconducting Cyclotron Beams for a Radioactive Ion Beam Facility** • **L. Calabretta**, D. Rifuggiato INFN/LNS, Catania, Italy	extraction, ion, focusing, emittance	733
XIII-06	**Radioactive Ion Beam Production Using the Louvain-La-Neuve Cyclotrons: Present Status and Future Developments** • **G. Ryckewaert**, M. Loiselet, N. Postiau Université Catholique de Louvain, Louvain-la-Neuve, Belgium	target, acceleration, extraction, ECR	737
XIV-04	**Conference Summary (Invited Paper)** • **D.J. Clark** LBL, Berkeley, California, USA	proton, ion, ECR, electron	758

XV-01 **Proper and Improper Accelerators - In Praise of Cyclotrons and Their Builders** TRIUMF, ion, controls, synchrotron 765

- **M.K. Craddock**
  University of British Columbia, Vancouver, Canada

A B C D E F H I J K L M N O P Q R S T V

diagnostics

Paper	Title	Other Keywords	Page
IV-05	**Radionuclide Technique in Mechanical Engineering (RTM)** • **P. Fehsenfeld**, A. Kleinrahm, FZK, Karlsruhe, Germany • V. Novikov, Kurchatov Institute, Moscow, Russia	injection, ion, cyclotron, radiation	171
V-07	**Dual Chemical Station for Cyclotron Produced ^{18}F** • **M.L. Mallory**, G. Grimmett, R. Tilbury, D. Yang, The University of Texas, Houston, Texas, USA	cyclotron, radioactivity, target, controls	222
VII-02	**Beam Diagnosis for Unmeasurably Cold Beams (Invited Paper)** • **T.J.P. Ellison**, Indiana University, Bloomington, Indiana, USA	space-charge, electron, proton, emittance	274
VIII-15	**Progress with the NAC Injector Cyclotron for Heavy and Polarized Ions** • **Z.B. du Toit**, S.J. Burger, P.J. Celliers, J.G. de Villiers, H.N. Jungwirth, A. Müller, P.F. Rohwer, D.M. van Rooyen, National Accelerator Centre, Faure, Republic of South Africa	ion, cyclotron, proton, heavy-ion	361
IXD-06	**The Diagnostics System for the AGOR Superconducting Cyclotron** • **B. Launé**, P. Dambre, J.M. Kaplanski, B. Montsanglant, C. Olivetto, D. Vincent, IPN, Orsay, France	extraction, cyclotron, injection, vacuum	487
XD-02	**Beam Transport System for the IUCF High Intensity Polarized Ion Source** • **W.P. Jones**, M.S. Ball, J.C. Collins, D. DuPlantis, T.J.P. Ellison, D.L. Friesel, B. Hamilton, J.W. Hicks, P. Schwandt, Indiana University, Bloomington, Indiana, USA	quadrupole, cyclotron, bunching, dipole	609
XD-04	**The Beam-Guiding System of AGOR**	target, AGOR, controls, heavy-ion	615

- **J.M. Schippers**
  Kernfysisch Versneller Instituut, Groningen, The Netherlands

XI-13	**The TR30 Control System - A Case for Off-the-Shelf Software**	controls, vacuum, cyclotron, TRIUMF	685

- **R. Keitel**, D.J. Dale, B.F. Milton
  TRIUMF, Vancouver, Canada

A B C D E F H I J K L M N O P Q R S T V

dipole

Paper	Title	Other Keywords	Page
VII-03	**COSY-Jülich - A Synchrotron and Storage Ring for Medium Energy Physics** • **R. Maier**, U. Pfister FZJ, Jülich, Germany	quadrupole, COSY, injection, extraction	282
IXA-03	**Emittance Growth in Nonlinear Beam Guiding and Focusing Elements** • **W.J.G.M. Kleeven**, J.I.M. Botman, J.L. Delhez, H.L. Hagedoorn, C.J. Timmermans, G.A. Webers Eindhoven University of Technology, Eindhoven, The Netherlands	emittance, octupole, sextupole, focusing	384
XC-02	**Potential Enhancement of Magnetic Deflection in the Chalk River Superconducting Cyclotron Extraction System** • **C.R. Hoffmann**, E.H. Lindqvist Atomic Energy of Canada, Chalk River, Ontario, Canada	extraction, cyclotron, acceleration, ion	573
XC-07	**Design of Passive Magnetic Channels** • **G. Bellomo** INFN/LASA, Segrate, Italy	multipole, focusing, quadrupole, cyclotron	592
XD-02	**Beam Transport System for the IUCF High Intensity Polarized Ion Source** • **W.P. Jones**, M.S. Ball, J.C. Collins, D. DuPlantis, T.J.P. Ellison, D.L. Friesel, B. Hamilton, J.W. Hicks, P. Schwandt Indiana University, Bloomington, Indiana, USA	quadrupole, cyclotron, bunching, diagnostics	609
XD-03	**Superconducting Focussing Channel for the AGOR Cyclotron** • **H.W. Schreuder**, P. Blache, C. Commeaux, S. Gustafsson, A. Lafoux, M. Mormiche, R. Panvier IPN, Orsay, France	quadrupole, AGOR, shielding, cyclotron	612
XD-06	**Beamlines for a Second Injector Cyclotron at NAC** • **J.C. Cornell**, J.L. Conradie, D.T. Fourie National Accelerator Centre, Faure, Republic of South Africa	ion, solenoid, cyclotron, ion-source	621

A B C D E F H I J K L M N O P Q R S T V

ECR

Paper	Title	Other Keywords	Page
I-02	**New Development at the JINR Heavy Ion Cyclotron Facility (Invited Paper)** • **G.G. Gulbekyan**, V. Bekhterev, O. Borisov, B. Gikal, A. Ivanenko, I. Kolesov, V.B. Kutner, A. Morduev, Yu.Ts. Oganessian JINR, Dubna, Russia	ion, cyclotron, extraction, vacuum	11
I-03	**New K130 Cyclotron at Jyväskylä (Invited Paper)** • **E. Liukkonen** University of Jyväskylä, Jyväskylä, Finland	cyclotron, ion, vacuum, ion-source	22
I-09	**GANIL Status Report** • **M. Bajard** GANIL, Caen, France	ion, controls, injection, emittance	54
I-11	**Status Report of SARA** • **M. Fruneau**, S. Albrand, D. Barnéoud, J.L. Belmont, G. Bizouard, J.L. Bouly, G. Campillo, M. Guisset, G. Laborie Université Joseph Fourier, Grenoble, France	cyclotron, ion, injection, vacuum	62
I-14	**Initial Operation of HIRFL** • **B.W. Wei**, F. Ye Institute of Modern Physics, Lanzhou, People's Republic of China	ion, ion-source, heavy-ion, vacuum	74
I-15	**Upgrading the SFC** • **F. Ye**, M. Guo, Z. Ma, Q. Qiao, Y. Wang, Q. Yin, X. Zhu Institute of Modern Physics, Lanzhou, People's Republic of China	ion, ion-source, injection, extraction	78
I-20	**Heavy Ion Facility in ATOMKI** • **S. Biri**, J. Pálinkás, A. Valek Institute of Nuclear Research of the Hungarian Academy of Sciences, Debrecen, Hungary	ion, heavy-ion, ion-source, cyclotron	99

VIII-01	**ECR Ion Sources for Accelerators (Invited Paper)**	ion, plasma, electron, ion-source	301

- **C.M. Lyneis**
  LBL, Berkeley, California, USA

VIII-02	**Performance of the LBL AECR Source at Various Frequencies**	sextupole, ion, plasma, ion-source	308

- **Z.Q. Xie**, D. Collins, S.A. Lundgren, C.M. Lyneis
  LBL, Berkeley, California, USA

VIII-06	**An ECR Ion Source for Multiply-Charged Heavy Ions at 14 GHz**	ion, plasma, ion-source, extraction	326

- **M. Sekiguchi**, M. Fujita, Y. Ohshiro, T. Yamazaki
  University of Tokyo, Tanashi-shi, Tokyo, Japan
- Y. Isoya, T. Yamada, Y. Yamashita
  Japan Steel Works Ltd., Research Center for Advanced Technologies, Chiba, Japan
- A. Kitagawa
  NIRS, Chiba, Japan

VIII-07	**Performance and Status of the IUCF High Intensity Polarized Ion Source**	ion, sextupole, ion-source, extraction	330

- **V. Derenchuk**, R. Brown, T.J.P. Ellison, D.L. Friesel, J.W. Hicks, D. Jenner, A. Pei, H. Petri, P. Schwandt, J. Sowinski, M. Wedekind
  Indiana University, Bloomington, Indiana, USA

VIII-09	**Operation of Ion Sources and Beam Transport to JAERI AVF Cyclotron**	ion, cyclotron, ion-source, extraction	336

- **W. Yokota**, T. Agematsu, K. Arakawa, M. Fukuda, I. Ishibori, Y. Nakamura, T. Nara, S. Okumura
  JAERI, Gunma, Japan
- Y. Hayashi, K. Ishii, T. Tachikawa
  Sumitomo Heavy Industries, Ehime, Japan

VIII-11	**Study on the Magnetic Field of Caprice Type ECR Source**	ion, plasma, cathode, extraction	344

- **B.W. Wei**, Z. Liu, Y. Ma, D. Wu, P. Yuan, W. Zhang, X. Zhang, H. Zhao
  Institute of Modern Physics, Lanzhou, People's Republic of China
- A. Efremov
  JINR, Dubna, Russia

IXB-03	**K1200 Cyclotron Beam Development Techniques**	ion, cyclotron, ion-source, injection	427

- **T.A. Antaya**, D. Cole, P. Miller, D. Poe

NSCL, East Lansing, Michigan, USA

IXC-04	**Non-Linear Beam Transport Effects in Highly Charged Positive Ion Beams Extracted From ECR Ion Sources**	emittance, ion, space-charge, ion-source	457

- **T.A. Antaya**
  NSCL, East Lansing, Michigan, USA
- Z.Q. Xie
  LBL, Berkeley, California, USA

XA-04	**The RF-System for a VICKSI Injector Cyclotron**	cyclotron, ion, injection, booster	519

- **W. Pelzer**
  HMI, Berlin, Germany

XA-10	**RF Transmitter for ECR Ion Sources**	ion, klystron, plasma, ion-source	542

- **R. Boux**, J.P. Ichac, M. Soudée
  Thomson Tubes Electroniques, Velizy-Villacoublay, France

XD-05	**Buncher in the Beam Line from ECR to SFC**	ion, bunching, ion-source, controls	618

- **J.Z. Jiang**, X.H. Zhou, Q. Wang, F. Wang, W.M. Jiang
  Institute of Modern Physics, Lanzhou, People's Republic of China

XI-07	**Ion Spectra Identification Software for the ECR Ion Source at NAC**	ion, ion-source, controls, cyclotron	660

- **E.J.S. Franklin**, J.G. de Villiers
  National Accelerator Centre, Faure, Republic of South Africa

XIII-03	**An On-Line Isotopic Separator Test Bench at GANIL**	ion, target, ion-source, extraction	725

- **P. Bricault**, R. Leroy, M. Lewitowicz, J.Y. Pacquet, M.G. St-Laurent, P. Sortais
  GANIL, Caen, France
- A.C. Mueller, J. Obert, J.C. Putaux
  IPN, Orsay, France
- C.F. Liang, P. Paris
  CSNSM, Orsay, France
- J.C. Steckmeyer
  LPC, Caen, France

XIII-06	**Radioactive Ion Beam Production Using the Louvain-La-Neuve Cyclotrons: Present Status and Future Developments**	cyclotron, target, acceleration, extraction	737

- **G. Ryckewaert**, M. Loiselet, N. Postiau

Université Catholique de Louvain, Louvain-la-Neuve, Belgium

XIV-04	**Conference Summary (Invited Paper)**	cyclotron, proton, ion, electron	758

- **D.J. Clark**
  LBL, Berkeley, California, USA

A B C D E F H I J K L M N O P Q R S T V

ECRIS

Paper	Title	Other Keywords	Page
VIII-12	**The Super Gas Mixing Technique for Highly Charged Uranium Ions** • **T.A. Antaya**, D. Cole NSCL, East Lansing, Michigan, USA	ion, plasma, ion-source, insertion	348
VIII-16	**Plasma Cathode Method for RIKEN ECRIS** • **T. Nakagawa**, A. Goto, T. Kageyama, M. Kase, Y. Yano RIKEN, Saitama, Japan	ion, plasma, electron, cathode	365
VIII-17	**Performance of the Texas A&M ECRIS** • **G. Mouchaty**, D.P. May, R.C. Rogers, P. Smelser Texas A&M University, College Station, Texas, USA	cyclotron, injection, ion, ion-source	369
XD-08	**Design of a Beam Buncher Using a Half-Cosine Driving Function** • **R.C. Rogers** Texas A&M University, College Station, Texas, USA	cyclotron, injection, bunching, ion	629
XIII-04	**The PIAFE Project at Grenoble: Beam Transport and Acceleration** • **J.L. Belmont**, J.F. Bruandet, J.M. de Conto, M. Fruneau, G. Gimond, K. Golovanivsky, E. Liatard, J.M. Loiseaux, H. Nifenecker, A. Savalle, B. Vignon Université Joseph Fourier, Grenoble, France • P. Briand CEN-Grenoble, Grenoble, France	ion, cyclotron, quadrupole, extraction	729

A B C D E F H I J K L M N O P Q R S T V

electromagnetic-fields

Paper	Title	Other Keywords	Page
IXA-07	**Deriving the General Expressions of Nonlinear Transport Coefficients of Accelerator Beam Phase Space by Artificial Intelligence**	beam-transport, cyclotron, optics	400

- **J. Xia**
  Institute of Modern Physics, Lanzhou, People's Republic of China
- C. Liu, X. Xie
  Graduate School of Nuclear Industry, Beijing, People's Republic of China

A B C D E F H I J K L M N O P Q R S T V

electron

Paper	Title	Other Keywords	Page
IV-03	**The Use of Heavy Ion Cyclotrons of the Flerov Laboratory of Nuclear Reactions in Condensed Matter Investigations** • **R.Ts. Oganessian**, A.Yu. Didyk JINR, Dubna, Russia	ion, radiation, heavy-ion, neutron	162
V-04	**Possibility of Producing Some Radionuclides for Medicine Using JINR Accelerators** • **S.N. Dmitriev**, G.G. Gulbekyan, V.A. Khalkin, R.Ts. Oganessian, L.M. Onishchenko, G.Ya. Starodub, N.G. Zaitseva JINR, Dubna, Russia	proton, cyclotron, target, microtron	213
VI-08	**A Proton Therapy Facility Plan** • **S. Fukumoto**, Y. Hayakawa, T. Inada, A. Maruhashi, M. Sato, J. Tada, Y. Takada, H. Tsuji, H. Tsujii University of Tsukuba, Ibaraki, Japan • K. Endo, Y. Irie, K. Muto KEK, Ibaraki, Japan	proton, cyclotron, synchrotron, radiation	258
VII-01	**Recent Commissioning Results at Celsius (Invited Paper)** • **D. Reistad**, T. Bergmark, C. Ekström, C.-J. Fridén, K. Gajewski, L. Hermansson, P. Jahnke, A. Johansson, O. Johansson, T. Lofnes, G. Norman, R. Wedberg, L. Westerberg, J. Zlomanczuk Uppsala University, Uppsala, Sweden • M.A. Raadu, M. Sedlacek Royal Institute of Technology, Stockholm, Sweden	ion, target, proton, injection	266
VII-02	**Beam Diagnosis for Unmeasurably Cold Beams (Invited Paper)** • **T.J.P. Ellison** Indiana University, Bloomington, Indiana, USA	space-charge, proton, diagnostics, emittance	274
VII-06	**The New Project of INR (Kiev's) Storage-Accelerating Complex** • **A.V. Dolinsky**, A.I. Papash, S.N. Pavlov, A.T. Rudchik, A.E. Val'Kov, I.N. Vishnevsky, A.V. Zhmendak	ion, target, booster, injection	294

Institute for Nuclear Research, Kiev, Ukraine
- V.P. Belov, A.M. Kokorin, A.A. Makarov, I.A. Schukeilo, Yu.P. Severgin
D.V. Efremov Scientific Research Institute of Electrophysical Apparatus, St. Petersburg, Russia

VII-07	**Superthin Internal Target for Storage Rings**	target, micro-particles, laser, storage-ring	297

- **V. Pugatch**, A. Glushko, G. Pitatelev, G. Sivtsov
Institute for Nuclear Research, Kiev, Ukraine
- S. Popov, D. Toporkov, B. Voitsechovsky
Institute for Nuclear Physics, Novosibirsk, Russia

VIII-01	**ECR Ion Sources for Accelerators (Invited Paper)**	ECR, ion, plasma, ion-source	301

- **C.M. Lyneis**
LBL, Berkeley, California, USA

VIII-03	**Ion Sources for Cyclotron Application**	ion, plasma, ion-source, cyclotron	312

- **K.N. Leung**, D.A. Bachman, D.S. McDonald, A.T. Young
LBL, Berkeley, California, USA

VIII-04	**A Review of Polarized Ion Sources for Cyclotrons (Invited Paper)**	ion, ion-source, polarization, cyclotron	316

- **P.W. Schmor**
TRIUMF, Vancouver, Canada

VIII-16	**Plasma Cathode Method for RIKEN ECRIS**	ion, plasma, cathode, ECRIS	365

- **T. Nakagawa**, A. Goto, T. Kageyama, M. Kase, Y. Yano
RIKEN, Saitama, Japan

IXA-11	**Developments in RELAX3D, a 2D/3D Laplace and Poisson Equation Solver**	TRIUMF, cyclotron, simulation, proton	411

- **H. Houtman**, F.W. Jones, C.J. Kost
TRIUMF, Vancouver, Canada

IXD-02	**High-Sensitive Ionization Detectors of Transverse Distribution of Accelerated Particles Beam**	ion, cyclotron, controls, proton	473

- **V.G. Mikhailov**, V.A. Rezvov, A.A. Roshchin, V.I. Sklyarenko, L.I. Iudin
Kurchatov Institute, Moscow, Russia

XC-01	**The Electrostatic Deflector for the Chalk River Superconducting Cyclotron**	high-voltage, cathode, cyclotron, vacuum	569

- **W.T. Diamond**, C.R. Hoffmann, G.R. Mitchel, H. Schmeing
  Atomic Energy of Canada, Chalk River, Ontario, Canada

XC-08	**Deflector Development for the K1200 Cyclotron**	cathode, cyclotron, ion, site	596

- **T.Y.T. Kuo**
  TRIUMF, Vancouver, Canada
- J.A. Nolen
  ANL, Argonne, Illinois, USA

XIV-03	**Physics with Storage Rings (Invited Paper)**	target, ion, storage-ring, luminosity	753

- **R.E. Pollock**
  Indiana University, Bloomington, Indiana, USA

XIV-04	**Conference Summary (Invited Paper)**	cyclotron, proton, ion, ECR	758

- **D.J. Clark**
  LBL, Berkeley, California, USA

A B C D E F H I J K L M N O P Q R S T V

emittance

Paper	Title	Other Keywords	Page
I-09	**GANIL Status Report** • **M. Bajard** GANIL, Caen, France	ion, controls, ECR, injection	54
I-13	**Current Status and Future Project of Cyclotron Laboratory in Alma-Ata** • **A.A. Arzumanov**, V. Batischev, V. Berger, V. Gerasimov, M. Gorcovets Kazakhstan Academy of Sciences, Alma-Ata, Republic of Kazakhstan	cyclotron, ion, extraction, heavy-ion	71
I-17	**Performance of the K1200 Cyclotron at MSU** • **P. Miller**, T.A. Antaya, F. Marti, D. Poe, B. Sherrill, J. Stetson, J. Winger NSCL, East Lansing, Michigan, USA • J.A. Nolen ANL, Argonne, Illinois, USA	ion, cyclotron, target, power-supply	86
VI-04	**Progress Report on the IBA-SHI Proton Therapy System** • **Y. Jongen**, W. Beeckman, J.P. Dufour, A. Laisné, H. Marie, R. Verbruggen Ion Beam Applications, Louvain-la-Neuve, Belgium • M. Sano, S. Satoh, N. Takahashi, T. Takayama Sumitomo Heavy Industries, Ehime, Japan	proton, extraction, scattering, cyclotron	244
VII-02	**Beam Diagnosis for Unmeasurably Cold Beams (Invited Paper)** • **T.J.P. Ellison** Indiana University, Bloomington, Indiana, USA	space-charge, electron, proton, diagnostics	274
VIII-14	**Plan for the Ion Source Emittance Measurement Under the RF Extraction** • **J.W. Kim**, H.G. Blosser NSCL, East Lansing, Michigan, USA	ion, cyclotron, ion-source	357
IXA-	**The Influence of Magnetic Field Imperfections on the Beam**	resonance, cyclotron,	380

02	**Quality in an H^- Cyclotron** • **W.J.G.M. Kleeven**, H.L. Hagedoorn Eindhoven University of Technology, Eindhoven, The Netherlands • B.F. Milton, G. Dutto TRIUMF, Vancouver, Canada	extraction, betatron	
IXA-03	**Emittance Growth in Nonlinear Beam Guiding and Focusing Elements** • **W.J.G.M. Kleeven**, J.I.M. Botman, J.L. Delhez, H.L. Hagedoorn, C.J. Timmermans, G.A. Webers Eindhoven University of Technology, Eindhoven, The Netherlands	octupole, sextupole, dipole, focusing	384
IXA-12	**Beam Quality Investigations for H^- Extraction at TRIUMF** • **R.E. Laxdal**, G.H. Mackenzie, J.B. Pearson, L. Root TRIUMF, Vancouver, Canada	extraction, cyclotron, resonance, simulation	415
IXB-01	**Cyclotron Tuning as a Rebuncher** • **D. Bibet**, M-H. Moscatello GANIL, Caen, France	extraction, cyclotron, target, acceleration	419
IXC-01	**Commissioning of the New High Intensity Axial Injection System for GANIL** • **Ch. Ricaud**, E. Baron, J. Bony, M.P. Bourgarel, B. Bru GANIL, Caen, France • R. Vienet CEN/Saclay, Gif-sur-Yvette, France	injection, cyclotron, ion, controls	446
IXC-03	**Preliminary Design of a New Central Region for the LNS Superconducting Cyclotron** • **M-H. Moscatello** GANIL, Caen, France	cyclotron, injection, ion, coupling	454
IXC-04	**Non-Linear Beam Transport Effects in Highly Charged Positive Ion Beams Extracted From ECR Ion Sources** • **T.A. Antaya** NSCL, East Lansing, Michigan, USA • Z.Q. Xie LBL, Berkeley, California, USA	ion, space-charge, ECR, ion-source	457
IXC-05	**Numerical Studies for Suppression of Vertical Oscillations in the K1200 Cyclotron**	cyclotron, simulation	461

- **K. Joh**, F. Marti
  NSCL, East Lansing, Michigan, USA
- J.A. Nolen
  ANL, Argonne, Illinois, USA

IXD-04	**Emittance Measurements in the HIRFL Beam Line**	quadrupole, linac, coupling, optical-matching	479

- **H. Zhao**, Z. Shen, B.W. Wei
  Institute of Modern Physics, Lanzhou, People's Republic of China

XIII-05	**High Intensity Superconducting Cyclotron Beams for a Radioactive Ion Beam Facility**	extraction, cyclotron, ion, focusing	733

- **L. Calabretta**, D. Rifuggiato
  INFN/LNS, Catania, Italy

A B C D E F H I J K L M N O P Q R S T V

extraction

Paper	Title	Other Keywords	Page
I-02	**New Development at the JINR Heavy Ion Cyclotron Facility (Invited Paper)** • **G.G. Gulbekyan**, V. Bekhterev, O. Borisov, B. Gikal, A. Ivanenko, I. Kolesov, V.B. Kutner, A. Morduev, Yu.Ts. Oganessian JINR, Dubna, Russia	ion, cyclotron, vacuum, ECR	11
I-04	**Experience with the High Current Operation of the PSI Cyclotron Facility (Invited Paper)** • **Th. Stammbach** PSI, Villigen, Switzerland	cyclotron, space-charge, beam-losses, injection	28
I-06	**AGOR: Recent Achievements (Invited Paper)** • **H.W. Schreuder** IPN, Orsay, France	AGOR, cyclotron, vacuum, site	40
I-13	**Current Status and Future Project of Cyclotron Laboratory in Alma-Ata** • **A.A. Arzumanov**, V. Batischev, V. Berger, V. Gerasimov, M. Gorcovets Kazakhstan Academy of Sciences, Alma-Ata, Republic of Kazakhstan	cyclotron, ion, heavy-ion, emittance	71
I-15	**Upgrading the SFC** • **F. Ye**, M. Guo, Z. Ma, Q. Qiao, Y. Wang, Q. Yin, X. Zhu Institute of Modern Physics, Lanzhou, People's Republic of China	ion, ECR, ion-source, injection	78
I-19	**Development of the NAC Accelerator Facilities** • **J.L. Conradie**, A.H. Botha, P.M. Cronje, R.E.F. Fenemore, H.N. Jungwirth, J.J. Kritzinger, W.A.G. Nel, D. Reitmann, L.M.M. Roels, P.F. Rohwer, H.A. Smit National Accelerator Centre, Faure, Republic of South Africa	cyclotron, injection, ion, proton	95
I-22	**Status Report on the Gustaf Werner Cyclotron in Uppsala**	ion, cyclotron, injection, vacuum	106

- **S. Holm**
  Uppsala University, Uppsala, Sweden

II-03	**Construction and First Year's Operation of the JAERI AVF Cyclotron**	cyclotron, ion, JAERI, proton	119

- **K. Arakawa**, T. Agematsu, M. Fukuda, I. Ishibori, T. Karasawa, T. Nara, Y. Nakamura, S. Okumura, R. Tanaka, W. Yokota
  JAERI, Gunma, Japan
- A. Shimizu
  Osaka University, Osaka, Japan
- Y. Hayashi, K. Ishii, T. Satoh, T. Tachikawa
  Sumitomo Heavy Industries, Ehime, Japan

III-01	**The TRIUMF 520 MeV Cyclotron: Recent and Future Developments**	cavity, TRIUMF, cyclotron, proton	138

- **G. Dutto**
  TRIUMF, Vancouver, Canada

IV-10	**A Proposal for an Intense Cyclotron-Based Thermal Neutron Source**	neutron, cyclotron, target, proton	191

- **S. Tazawa**
  Sumitomo Heavy Industries, Toyo-shi, Toyo-shi, Japan
- W.L. Whittemore
  General Atomics, San Diego, California, USA

V-02	**The Production of Radionuclides for the Biosciences (Invited Paper)**	target, cyclotron, ion, proton	206

- **T.J. Ruth**
  TRIUMF, Vancouver, Canada

VI-04	**Progress Report on the IBA-SHI Proton Therapy System**	proton, scattering, cyclotron, emittance	244

- **Y. Jongen**, W. Beeckman, J.P. Dufour, A. Laisné, H. Marie, R. Verbruggen
  Ion Beam Applications, Louvain-la-Neuve, Belgium
- M. Sano, S. Satoh, N. Takahashi, T. Takayama
  Sumitomo Heavy Industries, Ehime, Japan

VII-03	**COSY-Jülich - A Synchrotron and Storage Ring for Medium Energy Physics**	quadrupole, COSY, injection, dipole	282

- **R. Maier**, U. Pfister
  FZJ, Jülich, Germany

VIII-06	**An ECR Ion Source for Multiply-Charged Heavy Ions at 14 GHz**	ECR, ion, plasma, ion-source	326

- **M. Sekiguchi**, M. Fujita, Y. Ohshiro, T. Yamazaki

University of Tokyo, Tanashi-shi, Tokyo, Japan
- Y. Isoya, T. Yamada, Y. Yamashita
  Japan Steel Works Ltd., Research Center for Advanced Technologies, Chiba, Japan
- A. Kitagawa
  NIRS, Chiba, Japan

VIII-07	**Performance and Status of the IUCF High Intensity Polarized Ion Source**	ECR, ion, sextupole, ion-source	330

- **V. Derenchuk**, R. Brown, T.J.P. Ellison, D.L. Friesel, J.W. Hicks, D. Jenner, A. Pei, H. Petri, P. Schwandt, J. Sowinski, M. Wedekind
  Indiana University, Bloomington, Indiana, USA

VIII-09	**Operation of Ion Sources and Beam Transport to JAERI AVF Cyclotron**	ion, ECR, cyclotron, ion-source	336

- **W. Yokota**, T. Agematsu, K. Arakawa, M. Fukuda, I. Ishibori, Y. Nakamura, T. Nara, S. Okumura
  JAERI, Gunma, Japan
- Y. Hayashi, K. Ishii, T. Tachikawa
  Sumitomo Heavy Industries, Ehime, Japan

VIII-11	**Study on the Magnetic Field of Caprice Type ECR Source**	ion, plasma, cathode, ECR	344

- **B.W. Wei**, Z. Liu, Y. Ma, D. Wu, P. Yuan, W. Zhang, X. Zhang, H. Zhao
  Institute of Modern Physics, Lanzhou, People's Republic of China
- A. Efremov
  JINR, Dubna, Russia

VIII-13	**Recent Development of Internal H^-/D^- Source for Compact Cyclotrons**	cyclotron, ion, plasma, proton	352

- **T.Y.T. Kuo**
  TRIUMF, Vancouver, Canada
- G.O. Hendry
  Cyclotron Inc., Napa, California, USA

IXA-02	**The Influence of Magnetic Field Imperfections on the Beam Quality in an H^- Cyclotron**	resonance, emittance, cyclotron, betatron	380

- **W.J.G.M. Kleeven**, H.L. Hagedoorn
  Eindhoven University of Technology, Eindhoven, The Netherlands
- B.F. Milton, G. Dutto
  TRIUMF, Vancouver, Canada

IXA-05	**Ion Optics in the Jyväskylä K130 Cyclotron**	cyclotron, ion, injection, solenoid	392

- **P. Heikkinen**, M. Rinta-Nikkola
  University of Jyväskylä, Jyväskylä, Finland

IXA-08	**Evaluation of Third-Harmonic Voltage Flattopping for a Superconducting Cyclotron**	cyclotron, ion, TRIUMF, resonance	404

- **M.M. Gordon**, D. Jeon
  NSCL, East Lansing, Michigan, USA

IXA-09	**Crossing of Resonances**	resonance, cyclotron, synchrotron	408

- **L.A. Sarkisyan**, A.L. Sarkisyan
  Moscow Institute-Internate, Moscow, Russia

IXA-12	**Beam Quality Investigations for H^- Extraction at TRIUMF**	emittance, cyclotron, resonance, simulation	415

- **R.E. Laxdal**, G.H. Mackenzie, J.B. Pearson, L. Root
  TRIUMF, Vancouver, Canada

IXB-01	**Cyclotron Tuning as a Rebuncher**	cyclotron, target, emittance, acceleration	419

- **D. Bibet**, M-H. Moscatello
  GANIL, Caen, France

IXB-02	**Beam Studies of Injection to Extraction System for JAERI AVF Cyclotron**	cyclotron, proton, injection, JAERI	423

- **M. Fukuda**, T. Agematsu, K. Arakawa, I. Ishibori, T. Karasawa, Y. Nakamura, T. Nara, S. Okumura, W. Yokota
  JAERI, Gunma, Japan

IXB-04	**Selection and Measurement of RF Phase Width of the K1200 Cyclotron Beam**	cyclotron, vacuum, injection, ion	431

- **J. Bailey**, J. Kuchar, F. Marti, J. Yurkon
  NSCL, East Lansing, Michigan, USA
- J.A. Nolen
  ANL, Argonne, Illinois, USA
- D. Rifuggiato
  INFN/LNS, Catania, Italy

IXB-06	**Effect of the Main-Coil Position on the Accelerated Beam of the K500 Cyclotron**	cyclotron, vacuum, focusing, betatron	439

- **D.P. May**, G. Mouchaty
  Texas A&M University, College Station, Texas, USA

IXB-	**Beam Test Results Using the Auxiliary Accelerating Cavity**	cavity, simulation,	442

07		cyclotron, TRIUMF	

- **R.E. Laxdal**, G.H. Mackenzie, L. Root
  TRIUMF, Vancouver, Canada

IXD-06	**The Diagnostics System for the AGOR Superconducting Cyclotron**	diagnostics, cyclotron, injection, vacuum	487

- **B. Launé**, P. Dambre, J.M. Kaplanski, B. Montsanglant, C. Olivetto, D. Vincent
  IPN, Orsay, France

XB-03	**Sector Magnet of the RCNP Ring Cyclotron and the Isochronization**	cyclotron, injection, proton, acceleration	565

- **K. Hosono**, M. Kibayashi, I. Miura
  Osaka University, Osaka, Japan

XC-02	**Potential Enhancement of Magnetic Deflection in the Chalk River Superconducting Cyclotron Extraction System**	cyclotron, acceleration, dipole, ion	573

- **C.R. Hoffmann**, E.H. Lindqvist
  Atomic Energy of Canada, Chalk River, Ontario, Canada

XC-04	**Performance of Beam Chopping System for JAERI AVF Cyclotron**	cyclotron, ion, injection, JAERI	581

- **W. Yokota**, T. Agematsu, K. Arakawa, M. Fukuda, I. Ishibori, Y. Nakamura, T. Nara, S. Okumura
  JAERI, Gunma, Japan
- Y. Hayashi, Y. Kumata, T. Tachikawa
  Sumitomo Heavy Industries, Ehime, Japan

XC-05	**The AGOR Superconducting Extraction Channel EMC2**	cyclotron, radiation, AGOR, background	585

- **K. Pieterman**, J.A.M. Dam
  Cryocon B.V., Amersfoort, The Netherlands
- H.J.H. ten Kate
  TU Twente, Enschede, The Netherlands
- S. Gustafsson
  IPN, Orsay, France

XC-06	**Material Consideration for Magnetic Channels**	simulation, synchro-cyclotron, cyclotron	589

- **J. Sura**, L. Calabretta, G. Di Biasi, P. Gmaj, D. Rifuggiato
  INFN/LNS, Catania, Italy

XI-03	**An Operator Assistance System for the AVF Cyclotron**	cyclotron, injection, survey, status	644

- **T. Okamura**, T. Murakami
  Sumitomo Heavy Industries Systems Engineering Laboratory, Tokyo, Japan
- T. Tachikawa
  Sumitomo Heavy Industries, Ehime, Japan
- T. Agematsu, S. Okumura, K. Arakawa
  JAERI, Gunma, Japan

XI-09	**Two Dimensional Scans with Adaptive Domain Control**	controls, beam-losses, interlocks, status	668

- **S. Adam**, A.C. Mezger
  PSI, Villigen, Switzerland

XII-04	**A New Design Proposal for a 200 MeV Superconducting Ring-Cyclotron Magnet**	cyclotron, focusing, proton	709

- **H.N. Jungwirth**, J.G. de Villiers
  National Accelerator Centre, Faure, Republic of South Africa

XIII-02	**A Conceptual Design for a Primary Cyclotron for the ISL Radioactive Beam Project**	cyclotron, ion, proton, acceleration	721

- **D.J. Clark**
  LBL, Berkeley, California, USA

XIII-03	**An On-Line Isotopic Separator Test Bench at GANIL**	ion, target, ion-source, ECR	725

- **P. Bricault**, R. Leroy, M. Lewitowicz, J.Y. Pacquet, M.G. St-Laurent, P. Sortais
  GANIL, Caen, France
- A.C. Mueller, J. Obert, J.C. Putaux
  IPN, Orsay, France
- C.F. Liang, P. Paris
  CSNSM, Orsay, France
- J.C. Steckmeyer
  LPC, Caen, France

XIII-04	**The PIAFE Project at Grenoble: Beam Transport and Acceleration**	ion, cyclotron, quadrupole, ECRIS	729

- **J.L. Belmont**, J.F. Bruandet, J.M. de Conto, M. Fruneau, G. Gimond, K. Golovanivsky, E. Liatard, J.M. Loiseaux, H. Nifenecker, A. Savalle, B. Vignon
  Université Joseph Fourier, Grenoble, France
- P. Briand
  CEN-Grenoble, Grenoble, France

XIII-05	**High Intensity Superconducting Cyclotron Beams for a Radioactive Ion Beam Facility**	cyclotron, ion, focusing, emittance	733

- **L. Calabretta**, D. Rifuggiato
  INFN/LNS, Catania, Italy

XIII-06	**Radioactive Ion Beam Production Using the Louvain-La-Neuve Cyclotrons: Present Status and Future Developments**	cyclotron, target, acceleration, ECR	737

- **G. Ryckewaert**, M. Loiselet, N. Postiau
  Université Catholique de Louvain, Louvain-la-Neuve, Belgium

A B C D E F H I J K L M N O P Q R S T V

factory

Paper	Title	Other Keywords	Page
III-02	**The KAON Factory at TRIUMF** • **M.K. Craddock** University of British Columbia, Vancouver, Canada	booster, TRIUMF, kaon, lattice	143
XB-01	**Low Temperature Tests of the AGOR Superconducting Coil System** • **K. Pieterman**, J.A.M. Dam Cryocon B.V., Amersfoort, The Netherlands • C. Commeaux IPN, Orsay, France • C. Penco Ansaldo Componenti, Genoa, Italy	AGOR, cryogenics, power-supply, vacuum	557
XI-12	**Application of Object Oriented Techniques in the TRIUMF Beam Line 2C Control System (Invited Paper)** • **N.A. Wilkinson**, E.A. Osberg, G.A. Ludgate TRIUMF, Vancouver, Canada	controls, target, kaon, TRIUMF	681

A B C D E F H I J K L M N O P Q R S T V

feedback

Paper	Title	Other Keywords	Page
IXD-09	**A DC Current Transformer for TRIUMF**	ion, ion-source, vacuum, TRIUMF	498

- **Y. Yin**
  TRIUMF, Vancouver, Canada

A B C D E F H I J K L M N O P Q R S T V

focusing

Paper	Title	Other Keywords	Page
IXA-03	**Emittance Growth in Nonlinear Beam Guiding and Focusing Elements** • **W.J.G.M. Kleeven**, J.I.M. Botman, J.L. Delhez, H.L. Hagedoorn, C.J. Timmermans, G.A. Webers Eindhoven University of Technology, Eindhoven, The Netherlands	emittance, octupole, sextupole, dipole	384
IXB-06	**Effect of the Main-Coil Position on the Accelerated Beam of the K500 Cyclotron** • **D.P. May**, G. Mouchaty Texas A&M University, College Station, Texas, USA	extraction, cyclotron, vacuum, betatron	439
XC-07	**Design of Passive Magnetic Channels** • **G. Bellomo** INFN/LASA, Segrate, Italy	multipole, dipole, quadrupole, cyclotron	592
XII-01	**The Superconducting Separated-Orbit Cyclotron Tritron (Invited Paper)** • **U. Trinks** TU München, Garching, Germany	cavity, injection, proton, cyclotron	693
XII-04	**A New Design Proposal for a 200 MeV Superconducting Ring-Cyclotron Magnet** • **H.N. Jungwirth**, J.G. de Villiers National Accelerator Centre, Faure, Republic of South Africa	cyclotron, extraction, proton	709
XIII-05	**High Intensity Superconducting Cyclotron Beams for a Radioactive Ion Beam Facility** • **L. Calabretta**, D. Rifuggiato INFN/LNS, Catania, Italy	extraction, cyclotron, ion, emittance	733
XIII-09	**Post-Accelerator Studies for the ISOL Facility at TRIUMF** • **L. Root**, H.R. Schneider, J.S. Fraser TRIUMF, Vancouver, Canada	solenoid, rfq, linac, ion	749

A B C D E F H I J K L M N O P Q R S T V

heavy-ion

Paper	Title	Other Keywords	Page
I-08	**Parameters, Present State and Application Perspectives of the U-250 Cyclotron** • **A.I. Muminov** Institute of Nuclear Physics, Tashkent, Republic of Uzbekistan • M.F. Vorogushin D.V. Efremov Scientific Research Institute of Electrophysical Apparatus, St. Petersburg, Russia	ion, cyclotron, vacuum, resonance	50
I-13	**Current Status and Future Project of Cyclotron Laboratory in Alma-Ata** • **A.A. Arzumanov**, V. Batischev, V. Berger, V. Gerasimov, M. Gorcovets Kazakhstan Academy of Sciences, Alma-Ata, Republic of Kazakhstan	cyclotron, ion, extraction, emittance	71
I-14	**Initial Operation of HIRFL** • **B.W. Wei**, F. Ye Institute of Modern Physics, Lanzhou, People's Republic of China	ion, ion-source, ECR, vacuum	74
I-20	**Heavy Ion Facility in ATOMKI** • **S. Biri**, J. Pálinkás, A. Valek Institute of Nuclear Research of the Hungarian Academy of Sciences, Debrecen, Hungary	ion, ECR, ion-source, cyclotron	99
IV-01	**Material Research with Beams at Cyclotron Energies (Invited Paper)** • **K. Ziegler** HMI, Berlin, Germany	ion, radiation, cyclotron, proton	149
IV-03	**The Use of Heavy Ion Cyclotrons of the Flerov Laboratory of Nuclear Reactions in Condensed Matter Investigations** • **R.Ts. Oganessian**, A.Yu. Didyk JINR, Dubna, Russia	ion, radiation, neutron, electron	162
VII-05	**Dubna Project of the Heavy Ion Storage Ring Complex K4-K10** • **Yu.Ts. Oganessian**, O.N. Malyshev, G.S. Popeko, A.M. Rodin,	ion, injection, target, cyclotron	290

S.I. Sidorchuk, Ye.A. Sokol, S.V. Stepantsov, G.M. Ter-Akopian, V.A. Timakov
JINR, Dubna, Russia
- V.V. Parhomchuk, A.A. Sery, V.D. Shiltsev
Institute for Nuclear Physics, Novosibirsk, Russia
- I.N. Meshkov, Ye.M. Syresinm
Center for Applied Physics and Technology, Lipetsk, Russia
- V.P. Belov, A.A. Makarov, Yu.P. Severgin, I.A. Shukeylo, M.N. Tarovik
D.V. Efremov Scientific Research Institute of Electrophysical Apparatus, St. Petersburg, Russia

VIII-15 **Progress with the NAC Injector Cyclotron for Heavy and Polarized Ions** ion, cyclotron, proton, diagnostics 361

- **Z.B. du Toit**, S.J. Burger, P.J. Celliers, J.G. de Villiers, H.N. Jungwirth, A. Müller, P.F. Rohwer, D.M. van Rooyen
National Accelerator Centre, Faure, Republic of South Africa

XD-04 **The Beam-Guiding System of AGOR** target, AGOR, controls, diagnostics 615

- **J.M. Schippers**
Kernfysisch Versneller Instituut, Groningen, The Netherlands

XD-07 **Beam Transport System for the HIMAC** beam-transport, ion, injection, optics 625

- **K. Noda**, Y. Hirao, A. Itano, M. Kanazawa, A. Kitagawa, T. Kohno, M. Kumada, H. Ogawa, K. Sato, Y. Sato, M. Sudou, E. Takada, S. Yamada, T. Yamada
NIRS, Chiba, Japan
- K. Endo
KEK, Ibaraki, Japan

XIII-01 **Accelerated Radioactive Nuclear Beams: Existing and Planned Facilities (Invited Paper)** ion, target, cyclotron, ISOL 713

- **J.M. Nitschke**
LBL, Berkeley, California, USA

XIII-07 **The ORNL Radioactive Ion Beam Project with the ORIC Accelerator** ion, target, ion-source, tandem-accelerator 741

- **D.K. Olsen**, G.D. Alton, C. Baktash, D.T. Dowling, J.D. Garrett, D.L. Haynes, C.M. Jones, R.C. Juras, S.N. Lane, I.Y. Lee, M.J. Meigs, G.D. Mills, S.W. Mosko, B.A. Tatum, K.S. Toth
ORNL, Oak Ridge, Tennessee, USA
- H.K. Carter, J. Kormicki
Associated Universities Oak Ridge, Oak Ridge, Tennessee, USA

A B C D E F H I J K L M N O P Q R S T V

high-voltage

Paper	Title	Other Keywords	Page
XC-01	**The Electrostatic Deflector for the Chalk River Superconducting Cyclotron** • **W.T. Diamond**, C.R. Hoffmann, G.R. Mitchel, H. Schmeing Atomic Energy of Canada, Chalk River, Ontario, Canada	cathode, cyclotron, vacuum, electron	569
XC-03	**Model Study of an Electrostatic Deflector Configuration with an Intermediate Electrode** • **C.R. Hoffmann**, J.F. Mouris Atomic Energy of Canada, Chalk River, Ontario, Canada	cyclotron, vacuum, septum, power-supply	577
XC-09	**Results from the Deflector Test Stand at Texas A&M University** • **D.P. May**, G. Derrig, W. Dewees, P. Smelser, D. Tran, R.C. Rogers Texas A&M University, College Station, Texas, USA	power-supply, cyclotron, shielding, monitoring	602

A B C D E F H I J K L M N O P Q R S T V

impedance

Paper	Title	Other Keywords	Page
XA-01	**Advances in RF Technology for Cyclotrons** • **C. Pagani** INFN/LASA, Segrate, Italy	cavity, cyclotron, coupling, controls	501
XA-02	**The RF Coupling System of the VINCY Cyclotron** • **B. Bojovic**, M. Josipovic, A. Susini CERN, Geneva, Switzerland	coupling, cyclotron, vacuum, cavity	511
XA-03	**Dual Frequency Resonator System for a Compact Cyclotron** • **M. Eiche**, K.L. Erdman Ebco Technologies Ltd, Richmond, BC, Canada • P. Lanz, M. Lipnicki, M. Zach TRIUMF, Vancouver, Canada	cyclotron, cavity, isotope-production, vacuum	515
XA-07	**Multi-Point Cavity Excitation** • **E. Zaplatin** FZJ, Jülich, Germany	cavity, coupling, resonance, simulation	530
XA-08	**Experience with the PSI-Cyclotron RF-System Under Heavy Beam Loading** • **P.K. Sigg**, J. Cherix, H. Frei, M. Märki PSI, Villigen, Switzerland	cavity, coupling, cyclotron, controls	534
XA-11	**TRIUMF Cyclotron RF System Improvements** • **G.C. Blaker**, A.K. Mitra, R.L. Poirier TRIUMF, Vancouver, Canada	TRIUMF, cyclotron, controls, cathode	545
XA-12	**Improvements to the RF Separator in the M9 Muon Channel at TRIUMF** • **G.C. Blaker**, A.K. Mitra, R.L. Poirier TRIUMF, Vancouver, Canada	cavity, TRIUMF, controls, cyclotron	549

A B C D E F H I J K L M N O P Q R S T V

injection

Paper	Title	Other Keywords	Page
I-01	**Commissioning of the RCNP Ring Cyclotron (Invited Paper)** • **I. Miura**, A. Ando, K. Hatanaka, K. Hosono, H. Ikegami, T. Itahashi, M. Kibayashi, M. Kondo, H. Ogata, T. Saito, A. Shimizu, K. Tamura, M. Uraki, T. Yamazaki, Osaka University, Osaka, Japan • J. Abe, Sumitomo Heavy Industries, Ehime, Japan	cyclotron, proton, acceleration, cavity	3
I-04	**Experience with the High Current Operation of the PSI Cyclotron Facility (Invited Paper)** • **Th. Stammbach**, PSI, Villigen, Switzerland	cyclotron, space-charge, beam-losses, extraction	28
I-09	**GANIL Status Report** • **M. Bajard**, GANIL, Caen, France	ion, controls, ECR, emittance	54
I-10	**Gatchina Isochronous Cyclotron** • **N.K. Abrosimov**, S.A. Artamonov, P.V. Chervyakov, S.P. Dmitriev, V.A. Eliseev, V.P. Fominenko, E.M. Ivanov, G.F. Mikheev, Yu.T. Mironov, A.S. Pokrovskii, G.A. Riabov, V.A. Smolin, G.L. Sokolov, V.A. Volchenkov, A.A. Vorobiev, Petersburg Nuclear Physics Institute, Gatchina, Russia • P.V. Bogdanov, B.D. Ershov, V.S. Kuligin, V.N. Moshkin, V.G. Mudrolyubov, Yu.I. Stogov, A.P. Strokach, D.V. Efremov Scientific Research Institute of Electrophysical Apparatus, St. Petersburg, Russia	cyclotron, ion, synchro-cyclotron, vacuum	58
I-11	**Status Report of SARA** • **M. Fruneau**, S. Albrand, D. Barnéoud, J.L. Belmont, G. Bizouard, J.L. Bouly, G. Campillo, M. Guisset, G. Laborie, Université Joseph Fourier, Grenoble, France	cyclotron, ion, ECR, vacuum	62
I-12	**Commissioning of the Injector Complex of COSY-Jülich**	COSY, cyclotron, ion, controls	67

- **W. Bräutigam**, H. Beuscher, R. Brings, H.G. Böge, R. Maier, M. Rogge, P. Wucherer
  FZJ, Jülich, Germany

I-15	**Upgrading the SFC**	ion, ECR, ion-source, extraction	78

- **F. Ye**, M. Guo, Z. Ma, Q. Qiao, Y. Wang, Q. Yin, X. Zhu
  Institute of Modern Physics, Lanzhou, People's Republic of China

I-19	**Development of the NAC Accelerator Facilities**	cyclotron, extraction, ion, proton	95

- **J.L. Conradie**, A.H. Botha, P.M. Cronje, R.E.F. Fenemore, H.N. Jungwirth, J.J. Kritzinger, W.A.G. Nel, D. Reitmann, L.M.M. Roels, P.F. Rohwer, H.A. Smit
  National Accelerator Centre, Faure, Republic of South Africa

I-21	**Recent Achievements at the RIKEN Ring Cyclotron**	ion, cyclotron, ion-source, acceleration	102

- **Y. Yano**
  RIKEN, Saitama, Japan

I-22	**Status Report on the Gustaf Werner Cyclotron in Uppsala**	ion, extraction, cyclotron, vacuum	106

- **S. Holm**
  Uppsala University, Uppsala, Sweden

IV-02	**A Cyclotron as a Mass Spectrometer**	cyclotron, ion, coupling, target	158

- **P. Bricault**, G. Auger, M. Bajard, E. Baron, D. Bibet, A. Chabert, J. Fermé, L. Gaudart, J. Joubert, M. Lewitowicz, W. Mittig, E. Plagnol, Ch. Ricaud, Y. Schutz
  GANIL, Caen, France
- G. Audi
  CSNSM, Orsay, France
- A. Gillibert
  CEN/Saclay, Gif-sur-Yvette, France
- K. Fifield
  Australian National University, Canberra , Australia

IV-05	**Radionuclide Technique in Mechanical Engineering (RTM)**	ion, cyclotron, diagnostics, radiation	171

- **P. Fehsenfeld**, A. Kleinrahm
  FZK, Karlsruhe, Germany
- V. Novikov
  Kurchatov Institute, Moscow, Russia

VII-01	**Recent Commissioning Results at Celsius (Invited Paper)**	electron, ion, target, proton	266

- **D. Reistad**, T. Bergmark, C. Ekström, C.-J. Fridén, K. Gajewski, L. Hermansson, P. Jahnke, A. Johansson, O. Johansson, T. Lofnes, G. Norman, R. Wedberg, L. Westerberg, J. Zlomanczuk
  Uppsala University, Uppsala, Sweden
- M.A. Raadu, M. Sedlacek
  Royal Institute of Technology, Stockholm, Sweden

VII-03	**COSY-Jülich - A Synchrotron and Storage Ring for Medium Energy Physics**	quadrupole, COSY, dipole, extraction	282

- **R. Maier**, U. Pfister
  FZJ, Jülich, Germany

VII-04	**Study of Beam Dynamics at Cooler Synchrotron TARN-II**	acceleration, ion, synchrotron, cyclotron	286

- **S. Watanabe**, Y. Arakaki, K. Chida, T. Katayama, M. Tomizawa, T. Watanabe, M. Yoshizawa
  University of Tokyo, Tanashi-shi, Tokyo, Japan
- K. Noda, M. Kanazawa
  NIRS, Chiba, Japan

VII-05	**Dubna Project of the Heavy Ion Storage Ring Complex K4-K10**	ion, heavy-ion, target, cyclotron	290

- **Yu.Ts. Oganessian**, O.N. Malyshev, G.S. Popeko, A.M. Rodin, S.I. Sidorchuk, Ye.A. Sokol, S.V. Stepantsov, G.M. Ter-Akopian, V.A. Timakov
  JINR, Dubna, Russia
- V.V. Parhomchuk, A.A. Sery, V.D. Shiltsev
  Institute for Nuclear Physics, Novosibirsk, Russia
- I.N. Meshkov, Ye.M. Syresinm
  Center for Applied Physics and Technology, Lipetsk, Russia
- V.P. Belov, A.A. Makarov, Yu.P. Severgin, I.A. Shukeylo, M.N. Tarovik
  D.V. Efremov Scientific Research Institute of Electrophysical Apparatus, St. Petersburg, Russia

VII-06	**The New Project of INR (Kiev's) Storage-Accelerating Complex**	electron, ion, target, booster	294

- **A.V. Dolinsky**, A.I. Papash, S.N. Pavlov, A.T. Rudchik, A.E. Val'Kov, I.N. Vishnevsky, A.V. Zhmendak
  Institute for Nuclear Research, Kiev, Ukraine
- V.P. Belov, A.M. Kokorin, A.A. Makarov, I.A. Schukeilo, Yu.P. Severgin
  D.V. Efremov Scientific Research Institute of Electrophysical Apparatus, St. Petersburg, Russia

VIII-		cyclotron, ECRIS, ion,	369

17	**Performance of the Texas A&M ECRIS**	ion-source	

- **G. Mouchaty**, D.P. May, R.C. Rogers, P. Smelser
  Texas A&M University, College Station, Texas, USA

IXA-04	**Ion_Tracker, a Trace Tracking Program for Cyclotron Design**	cyclotron, ion, optics, acceleration	388

- **M. Rinta-Nikkola**
  University of Jyväskylä, Jyväskylä, Finland

IXA-05	**Ion Optics in the Jyväskylä K130 Cyclotron**	cyclotron, ion, solenoid, extraction	392

- **P. Heikkinen**, M. Rinta-Nikkola
  University of Jyväskylä, Jyväskylä, Finland

IXA-10	**Increase of Beam Intensity**	resonance, synchrotron, cyclotron, proton	409

- **L.A. Sarkisyan**, A.L. Sarkisyan
  Moscow Institute-Internate, Moscow, Russia

IXB-02	**Beam Studies of Injection to Extraction System for JAERI AVF Cyclotron**	cyclotron, proton, extraction, JAERI	423

- **M. Fukuda**, T. Agematsu, K. Arakawa, I. Ishibori, T. Karasawa, Y. Nakamura, T. Nara, S. Okumura, W. Yokota
  JAERI, Gunma, Japan

IXB-03	**K1200 Cyclotron Beam Development Techniques**	ion, cyclotron, ion-source, ECR	427

- **T.A. Antaya**, D. Cole, P. Miller, D. Poe
  NSCL, East Lansing, Michigan, USA

IXB-04	**Selection and Measurement of RF Phase Width of the K1200 Cyclotron Beam**	cyclotron, extraction, vacuum, ion	431

- **J. Bailey**, J. Kuchar, F. Marti, J. Yurkon
  NSCL, East Lansing, Michigan, USA
- J.A. Nolen
  ANL, Argonne, Illinois, USA
- D. Rifuggiato
  INFN/LNS, Catania, Italy

IXC-01	**Commissioning of the New High Intensity Axial Injection System for GANIL**	cyclotron, ion, emittance, controls	446

- **Ch. Ricaud**, E. Baron, J. Bony, M.P. Bourgarel, B. Bru
  GANIL, Caen, France

- R. Vienet
  CEN/Saclay, Gif-sur-Yvette, France

IXC-02 **A Formulation of Spiral Inflector Design and Its Application to SF Cyclotron** — ion, cyclotron, acceleration, ion-source — 450

- **M. Sekiguchi**, M. Fujita, M. Nishiguchi, Y. Ohshiro, Y. Shida, N. Yamazaki, T. Yamazaki
  University of Tokyo, Tanashi-shi, Tokyo, Japan

IXC-03 **Preliminary Design of a New Central Region for the LNS Superconducting Cyclotron** — cyclotron, emittance, ion, coupling — 454

- **M-H. Moscatello**
  GANIL, Caen, France

IXC-06 **Experiments on the Axial Injection System of the Cyclotron U-120M** — ion, cyclotron, acceleration, ion-source — 465

- **Z. Trejbal**, M. Krivánek, J. Kucera, V. Bejsovec, J. Stursa
  Czechoslovak Academy of Sciences, Rez, Czechoslovakia

IXD-05 **High Sensitivity Electronic System for the Phase Probes of the LNS/MILANO Superconducting Cyclotron** — cyclotron, controls, ion, rf-amplifier — 483

- **A. Bosotti**, D. Corti, C. Pagani, G. Varisco, F. Zibra
  INFN/LASA, Segrate, Italy
- M. Di Giacomo
  INFN/LNS, Catania, Italy

IXD-06 **The Diagnostics System for the AGOR Superconducting Cyclotron** — extraction, diagnostics, cyclotron, vacuum — 487

- **B. Launé**, P. Dambre, J.M. Kaplanski, B. Montsanglant, C. Olivetto, D. Vincent
  IPN, Orsay, France

IXD-07 **Beam Diagnostics in the RCNP Ring Cyclotron** — cyclotron, cavity, acceleration, proton — 491

- **T. Itahashi**, T. Saito, I. Miura
  Osaka University, Osaka, Japan
- S. Ichida
  Sumitomo Heavy Industries, Ehime, Japan

XA-04 **The RF-System for a VICKSI Injector Cyclotron** — cyclotron, ion, ECR, booster — 519

- **W. Pelzer**
  HMI, Berlin, Germany

XA-05 **Low Frequency RF System for the Indiana University Cooler Ring** — cavity, kicker, beam-losses, synchrotron — 523

- **X. Pei**, S. Anderson, V. Derenchuk, G. East, D.L. Friesel, D. Jenner, D. McCammon, T. Sloan
  Indiana University, Bloomington, Indiana, USA

XB-02 **A Permanent Magnet System for a Cyclotron Used as a Mass Spectrometer** — cyclotron, vacuum, permanent-magnet, ion — 561

- **C.Y. Li**, M. Cooper, K. Halbach, W.B. Kunkel, K.N. Leung, R.P. Wells, A.T. Young
  LBL, Berkeley, California, USA

XB-03 **Sector Magnet of the RCNP Ring Cyclotron and the Isochronization** — cyclotron, extraction, proton, acceleration — 565

- **K. Hosono**, M. Kibayashi, I. Miura
  Osaka University, Osaka, Japan

XC-04 **Performance of Beam Chopping System for JAERI AVF Cyclotron** — cyclotron, extraction, ion, JAERI — 581

- **W. Yokota**, T. Agematsu, K. Arakawa, M. Fukuda, I. Ishibori, Y. Nakamura, T. Nara, S. Okumura
  JAERI, Gunma, Japan
- Y. Hayashi, Y. Kumata, T. Tachikawa
  Sumitomo Heavy Industries, Ehime, Japan

XD-07 **Beam Transport System for the HIMAC** — beam-transport, ion, optics, heavy-ion — 625

- **K. Noda**, Y. Hirao, A. Itano, M. Kanazawa, A. Kitagawa, T. Kohno, M. Kumada, H. Ogawa, K. Sato, Y. Sato, M. Sudou, E. Takada, S. Yamada, T. Yamada
  NIRS, Chiba, Japan
- K. Endo
  KEK, Ibaraki, Japan

XD-08 **Design of a Beam Buncher Using a Half-Cosine Driving Function** — cyclotron, bunching, ECRIS, ion — 629

- **R.C. Rogers**
  Texas A&M University, College Station, Texas, USA

XI-03 **An Operator Assistance System for the AVF Cyclotron** — cyclotron, extraction, survey, status — 644

- **T. Okamura**, T. Murakami
  Sumitomo Heavy Industries Systems Engineering Laboratory, Tokyo, Japan

- T. Tachikawa
  Sumitomo Heavy Industries, Ehime, Japan
- T. Agematsu, S. Okumura, K. Arakawa
  JAERI, Gunma, Japan

XI-04 **Control System for JAERI AVF Cyclotron** — controls, cyclotron, JAERI, status — 648

- **S. Okumura**, T. Agematsu, K. Arakawa, M. Fukuda, I. Ishibori, T. Kamiya, Y. Nakamura, T. Nara, W. Yokota
  JAERI, Gunma, Japan
- K. Hoshika, K. Iso, M. Maruyama, M. Tachibana
  Sumitomo Heavy Industries, Ehime, Japan

XI-10 **Construction and System Tuning of Control System for the RCNP Ring Cyclotron and Beam Lines** — controls, cyclotron, power-supply, status — 672

- **T. Yamazaki**, A. Ando, K. Hosono, T. Itahashi, M. Kibayashi, I. Miura, K. Nagayama, H. Ogata, T. Saito, A. Shimizu, K. Tamura, M. Uraki
  Osaka University, Osaka, Japan
- K. Aoki, Y. Kimura, M. Maruyama, M. Tachibana, S. Yamada
  Sumitomo Heavy Industries, Ehime, Japan
- K. Kodaira
  Sumitomo Heavy Industries Systems Engineering Laboratory, Tokyo, Japan

XII-01 **The Superconducting Separated-Orbit Cyclotron Tritron (Invited Paper)** — cavity, proton, cyclotron, focusing — 693

- **U. Trinks**
  TU München, Garching, Germany

XII-02 **Study of an FFAG Synchrocyclotron for a Pulsed Neutron Source** — cavity, neutron, linac, synchrotron — 701

- **S.A. Martin**, E. Zaplatin
  FZJ, Jülich, Germany
- P.F. Meads, Jr.
  Private Address, Oakland, California, USA
- G. Wüstefeld
  BESSY, Berlin, Germany
- K. Ziegler
  HMI, Berlin, Germany

XII-03 **Design of a Compact Permanent Magnet Cyclotron Mass Spectrometer for the Detection and Measurement of Trace Isotopes** — ion, cyclotron, ion-source, permanent-magnet — 705

- **A.T. Young**, K.J. Bertsche, D.J. Clark, K. Halbach, W.B. Kunkel, K.N. Leung, C.Y. Li
  LBL, Berkeley, California, USA

A B C D E F H I J K L M N O P Q R S T V

insertion

Paper	Title	Other Keywords	Page
VIII-12	**The Super Gas Mixing Technique for Highly Charged Uranium Ions**	ion, plasma, ion-source, ECRIS	348

- **T.A. Antaya**, D. Cole
  NSCL, East Lansing, Michigan, USA

A B C D E F H I J K L M N O P Q R S T V

instrumentation

Paper	Title	Other Keywords	Page
XI-06	**The New Distributed Control System of the NAC** • **H.F. Weehuizen**, R.K. Fisch, E.J.S. Franklin, M.E. Hogan, I.H. Kohler, J.P. Rogers, P.J. Theron National Accelerator Centre, Faure, Republic of South Africa	controls, status, cyclotron, light-ion	656
XI-08	**Micro-Controlled Vacuum Systems at NAC** • **P.J. Celliers**, E.J.S. Franklin National Accelerator Centre, Faure, Republic of South Africa	vacuum, controls, cyclotron, monitoring	664

A B C D E F H I J K L M N O P Q R S T V

interlocks

Paper	Title	Other Keywords	Page
XI-02	**The IUCF High Intensity Polarized Ion Source Control System** • **T. Capshew**, J.C. Collins, D. DuPlantis, D.W. Frame, J. Graham, D.D. Reid Indiana University, Bloomington, Indiana, USA	controls, vacuum, ion, ion-source	641
XI-09	**Two Dimensional Scans with Adaptive Domain Control** • **S. Adam**, A.C. Mezger PSI, Villigen, Switzerland	controls, beam-losses, extraction, status	668

A B C D E F H I J K L M N O P Q R S T V

ion

Paper	Title	Other Keywords	Page
I-02	**New Development at the JINR Heavy Ion Cyclotron Facility (Invited Paper)** • **G.G. Gulbekyan**, V. Bekhterev, O. Borisov, B. Gikal, A. Ivanenko, I. Kolesov, V.B. Kutner, A. Morduev, Yu.Ts. Oganessian JINR, Dubna, Russia	cyclotron, extraction, vacuum, ECR	11
I-03	**New K130 Cyclotron at Jyväskylä (Invited Paper)** • **E. Liukkonen** University of Jyväskylä, Jyväskylä, Finland	cyclotron, ECR, vacuum, ion-source	22
I-08	**Parameters, Present State and Application Perspectives of the U-250 Cyclotron** • **A.I. Muminov** Institute of Nuclear Physics, Tashkent, Republic of Uzbekistan • M.F. Vorogushin D.V. Efremov Scientific Research Institute of Electrophysical Apparatus, St. Petersburg, Russia	cyclotron, vacuum, heavy-ion, resonance	50
I-09	**GANIL Status Report** • **M. Bajard** GANIL, Caen, France	controls, ECR, injection, emittance	54
I-10	**Gatchina Isochronous Cyclotron** • **N.K. Abrosimov**, S.A. Artamonov, P.V. Chervyakov, S.P. Dmitriev, V.A. Eliseev, V.P. Fominenko, E.M. Ivanov, G.F. Mikheev, Yu.T. Mironov, A.S. Pokrovskii, G.A. Riabov, V.A. Smolin, G.L. Sokolov, V.A. Volchenkov, A.A. Vorobiev Petersburg Nuclear Physics Institute, Gatchina, Russia • P.V. Bogdanov, B.D. Ershov, V.S. Kuligin, V.N. Moshkin, V.G. Mudrolyubov, Yu.I. Stogov, A.P. Strokach D.V. Efremov Scientific Research Institute of Electrophysical Apparatus, St. Petersburg, Russia	cyclotron, synchro-cyclotron, vacuum, injection	58
I-11	**Status Report of SARA**	cyclotron, injection, ECR, vacuum	62

M. Fruneau, S. Albrand, D. Barnéoud, J.L. Belmont, G. Bizouard, J.L. Bouly, G. Campillo, M. Guisset, G. Laborie
Université Joseph Fourier, Grenoble, France

I-12 **Commissioning of the Injector Complex of COSY-Jülich** COSY, cyclotron, controls, injection 67

- **W. Bräutigam**, H. Beuscher, R. Brings, H.G. Böge, R. Maier, M. Rogge, P. Wucherer
FZJ, Jülich, Germany

I-13 **Current Status and Future Project of Cyclotron Laboratory in Alma-Ata** cyclotron, extraction, heavy-ion, emittance 71

- **A.A. Arzumanov**, V. Batischev, V. Berger, V. Gerasimov, M. Gorcovets
Kazakhstan Academy of Sciences, Alma-Ata, Republic of Kazakhstan

I-14 **Initial Operation of HIRFL** ion-source, ECR, heavy-ion, vacuum 74

- **B.W. Wei**, F. Ye
Institute of Modern Physics, Lanzhou, People's Republic of China

I-15 **Upgrading the SFC** ECR, ion-source, injection, extraction 78

- **F. Ye**, M. Guo, Z. Ma, Q. Qiao, Y. Wang, Q. Yin, X. Zhu
Institute of Modern Physics, Lanzhou, People's Republic of China

I-16 **Status Report of Cyclone** cyclotron, target, neutron, beam-transport 82

- **M. Loiselet**, N. Postiau, G. Ryckewaert
Université Catholique de Louvain, Louvain-la-Neuve, Belgium

I-17 **Performance of the K1200 Cyclotron at MSU** cyclotron, target, emittance, power-supply 86

- **P. Miller**, T.A. Antaya, F. Marti, D. Poe, B. Sherrill, J. Stetson, J. Winger
NSCL, East Lansing, Michigan, USA
- J.A. Nolen
ANL, Argonne, Illinois, USA

I-18 **Status Report on the Heavy Ion Facility at LNS** cyclotron, vacuum, cavity, coupling 90

- **F. Alessandria**, G. Bellomo, A. Bosotti, C. De Martinis, D. Giove, P. Michelato, C. Pagani, L. Rossi

INFN/LASA, Segrate, Italy
- L. Calabretta, G. Ciavola, G. Cuttone, M. Di Giacomo, S. Gammino, P. Gmaj, G. Raia, D. Rifuggiato, J. Sura
INFN/LNS, Catania, Italy

I-19 **Development of the NAC Accelerator Facilities** cyclotron, extraction, injection, proton 95

- **J.L. Conradie**, A.H. Botha, P.M. Cronje, R.E.F. Fenemore, H.N. Jungwirth, J.J. Kritzinger, W.A.G. Nel, D. Reitmann, L.M.M. Roels, P.F. Rohwer, H.A. Smit
National Accelerator Centre, Faure, Republic of South Africa

I-20 **Heavy Ion Facility in ATOMKI** ECR, heavy-ion, ion-source, cyclotron 99

- **S. Biri**, J. Pálinkás, A. Valek
Institute of Nuclear Research of the Hungarian Academy of Sciences, Debrecen, Hungary

I-21 **Recent Achievements at the RIKEN Ring Cyclotron** cyclotron, ion-source, acceleration, injection 102

- **Y. Yano**
RIKEN, Saitama, Japan

I-22 **Status Report on the Gustaf Werner Cyclotron in Uppsala** extraction, cyclotron, injection, vacuum 106

- **S. Holm**
Uppsala University, Uppsala, Sweden

II-01 **Commercially Available Compact Cyclotrons for Isotope Production (Invited Paper)** cyclotron, target, ion-source, proton 110

- **V. Bechtold**
FZK, Karlsruhe, Germany

II-03 **Construction and First Year's Operation of the JAERI AVF Cyclotron** cyclotron, JAERI, extraction, proton 119

- **K. Arakawa**, T. Agematsu, M. Fukuda, I. Ishibori, T. Karasawa, T. Nara, Y. Nakamura, S. Okumura, R. Tanaka, W. Yokota
JAERI, Gunma, Japan
- A. Shimizu
Osaka University, Osaka, Japan
- Y. Hayashi, K. Ishii, T. Satoh, T. Tachikawa
Sumitomo Heavy Industries, Ehime, Japan

II-05 **Status of a Compact H^- Cyclotron at the Kurchatov Institute of Atomic Energy** cyclotron, controls, vacuum, ion-source 126

- **N.I. Venikov**, C.D. Burbeza, P.Yu. Komissarov, Yu.M. Krasnikov, S.T. Latushkin, V.V. Leonov, V.P. Moryakov, I.V. Naumov, A.Ya. Pisman, V.A. Rezvov, A.A. Vasiliev, V.E. Yarosh, L.I. Yudin
  Kurchatov Institute, Moscow, Russia

II-07 **Performance of the Harper Hospital Cyclotron; Effect of Pulsed Radio Frequency** — cyclotron, target, neutron, controls — 133

- **H.G. Blosser**, J. Vincent
  NSCL, East Lansing, Michigan, USA
- R. Maughan
  Harper Hospital, Detroit, Michigan, USA

IV-01 **Material Research with Beams at Cyclotron Energies (Invited Paper)** — radiation, cyclotron, proton, heavy-ion — 149

- **K. Ziegler**
  HMI, Berlin, Germany

IV-02 **A Cyclotron as a Mass Spectrometer** — cyclotron, injection, coupling, target — 158

- **P. Bricault**, G. Auger, M. Bajard, E. Baron, D. Bibet, A. Chabert, J. Fermé, L. Gaudart, J. Joubert, M. Lewitowicz, W. Mittig, E. Plagnol, Ch. Ricaud, Y. Schutz
  GANIL, Caen, France
- G. Audi
  CSNSM, Orsay, France
- A. Gillibert
  CEN/Saclay, Gif-sur-Yvette, France
- K. Fifield
  Australian National University, Canberra , Australia

IV-03 **The Use of Heavy Ion Cyclotrons of the Flerov Laboratory of Nuclear Reactions in Condensed Matter Investigations** — radiation, heavy-ion, neutron, electron — 162

- **R.Ts. Oganessian**, A.Yu. Didyk
  JINR, Dubna, Russia

IV-04 **^{178m2}Hf and ^{237}Pu Isotopes Production on the U-200 Cyclotron** — cyclotron, target, cathode, ion-source — 167

- **S.L. Bogomolov**, S.N. Dmitriev, Yu.P. Gangrski, G.G. Gulbekyan, S.A. Karamian, V.B. Kutner, B.N. Markov, Yu.Ts. Oganessian, N.V. Pronin, G.Ya. Starodub
  JINR, Dubna, Russia

IV-05 **Radionuclide Technique in Mechanical Engineering (RTM)** — injection, cyclotron, diagnostics, radiation — 171

- **P. Fehsenfeld**, A. Kleinrahm

FZK, Karlsruhe, Germany
- V. Novikov
Kurchatov Institute, Moscow, Russia

IV-08	**Analytical Applications of Cyclotrons in Biomedical Fields - Charged Particle Activation Analysis**	cyclotron, proton, neutron, target	181

- **M.A. Chaudhri**
Austin Hospital & University of Melbourne, Melbourne, Australia

V-01	**The New Molecular Medicine**	radiation, accumulation, site, monitoring	202

- **H.N. Wagner, Jr.**
The Johns Hopkins University, Baltimore, Maryland, USA

V-02	**The Production of Radionuclides for the Biosciences (Invited Paper)**	target, cyclotron, proton, extraction	206

- **T.J. Ruth**
TRIUMF, Vancouver, Canada

V-05	**Radiopharmaceutical "Thallium-201-Chloride" Production using Thallium-203 Irradiation by Helium-3 Ions**	target, proton, cyclotron, ALICE	216

- **A.A. Arzumanov**, N.K. Hamidov, A.I. Kozin, G.I. Shychikov, S.T. Tihomirova
Kazakhstan Academy of Sciences, Alma-Ata, Republic of Kazakhstan

V-06	**Experiences with the Cyclone 3 Oxygen 15 Generator**	cyclotron, target, controls, ion-source	218

- **E. Conard**, J.-L. Morelle
Ion Beam Applications, Louvain-la-Neuve, Belgium
- J.C. Clark, D.B. Mackay
Hammersmith Hospital, London, England

VI-01	**Accelerators for Charged Particle Therapy: Performance Criteria from the User Point of View (Invited Paper)**	proton, radiation, photon, target	226

- **E. Pedroni**
PSI, Villigen, Switzerland

VI-05	**Recent Activities of the Cyclotron Laboratory in Nice**	cyclotron, synchrotron, proton, light-ion	248

- **P. Mandrillon**, N. Brassart, P. Chauvel, A. Courdi, F. Farley, N. Fietier, J. Herault, J.Y. Tang
Centre Antoine Lacassagne, Nice, France

VII-01	**Recent Commissioning Results at Celsius (Invited Paper)**	electron, target, proton, injection	266

- **D. Reistad**, T. Bergmark, C. Ekström, C.-J. Fridén, K. Gajewski, L. Hermansson, P. Jahnke, A. Johansson, O. Johansson, T. Lofnes, G. Norman, R. Wedberg, L. Westerberg, J. Zlomanczuk
  Uppsala University, Uppsala, Sweden
- M.A. Raadu, M. Sedlacek
  Royal Institute of Technology, Stockholm, Sweden

VII-04	**Study of Beam Dynamics at Cooler Synchrotron TARN-II**	acceleration, synchrotron, injection, cyclotron	286

- **S. Watanabe**, Y. Arakaki, K. Chida, T. Katayama, M. Tomizawa, T. Watanabe, M. Yoshizawa
  University of Tokyo, Tanashi-shi, Tokyo, Japan
- K. Noda, M. Kanazawa
  NIRS, Chiba, Japan

VII-05	**Dubna Project of the Heavy Ion Storage Ring Complex K4-K10**	injection, heavy-ion, target, cyclotron	290

- **Yu.Ts. Oganessian**, O.N. Malyshev, G.S. Popeko, A.M. Rodin, S.I. Sidorchuk, Ye.A. Sokol, S.V. Stepantsov, G.M. Ter-Akopian, V.A. Timakov
  JINR, Dubna, Russia
- V.V. Parhomchuk, A.A. Sery, V.D. Shiltsev
  Institute for Nuclear Physics, Novosibirsk, Russia
- I.N. Meshkov, Ye.M. Syresinm
  Center for Applied Physics and Technology, Lipetsk, Russia
- V.P. Belov, A.A. Makarov, Yu.P. Severgin, I.A. Shukeylo, M.N. Tarovik
  D.V. Efremov Scientific Research Institute of Electrophysical Apparatus, St. Petersburg, Russia

VII-06	**The New Project of INR (Kiev's) Storage-Accelerating Complex**	electron, target, booster, injection	294

- **A.V. Dolinsky**, A.I. Papash, S.N. Pavlov, A.T. Rudchik, A.E. Val'Kov, I.N. Vishnevsky, A.V. Zhmendak
  Institute for Nuclear Research, Kiev, Ukraine
- V.P. Belov, A.M. Kokorin, A.A. Makarov, I.A. Schukeilo, Yu.P. Severgin
  D.V. Efremov Scientific Research Institute of Electrophysical Apparatus, St. Petersburg, Russia

VIII-01	**ECR Ion Sources for Accelerators (Invited Paper)**	ECR, plasma, electron, ion-source	301

- **C.M. Lyneis**
  LBL, Berkeley, California, USA

VIII-02	**Performance of the LBL AECR Source at Various Frequencies** • **Z.Q. Xie**, D. Collins, S.A. Lundgren, C.M. Lyneis LBL, Berkeley, California, USA	sextupole, ECR, plasma, ion-source	308
VIII-03	**Ion Sources for Cyclotron Application** • **K.N. Leung**, D.A. Bachman, D.S. McDonald, A.T. Young LBL, Berkeley, California, USA	plasma, ion-source, electron, cyclotron	312
VIII-04	**A Review of Polarized Ion Sources for Cyclotrons (Invited Paper)** • **P.W. Schmor** TRIUMF, Vancouver, Canada	ion-source, electron, polarization, cyclotron	316
VIII-05	**Status of the TRIUMF Optically-Pumped Polarized H^- Ion Source** • **C.D.P. Levy**, K. Jayamanna, M. McDonald, R. Ruegg, P.W. Schmor TRIUMF, Vancouver, Canada • A.N. Zelenskii Institute of Nuclear Research, Russian Academy of Sciences, Moscow, Russia	polarization, laser, proton, TRIUMF	322
VIII-06	**An ECR Ion Source for Multiply-Charged Heavy Ions at 14 GHz** • **M. Sekiguchi**, M. Fujita, Y. Ohshiro, T. Yamazaki University of Tokyo, Tanashi-shi, Tokyo, Japan • Y. Isoya, T. Yamada, Y. Yamashita Japan Steel Works Ltd., Research Center for Advanced Technologies, Chiba, Japan • A. Kitagawa NIRS, Chiba, Japan	ECR, plasma, ion-source, extraction	326
VIII-07	**Performance and Status of the IUCF High Intensity Polarized Ion Source** • **V. Derenchuk**, R. Brown, T.J.P. Ellison, D.L. Friesel, J.W. Hicks, D. Jenner, A. Pei, H. Petri, P. Schwandt, J. Sowinski, M. Wedekind Indiana University, Bloomington, Indiana, USA	ECR, sextupole, ion-source, extraction	330
VIII-08	**Ion Source of Discharge Type** • **I.B. Enchevich** TRIUMF, Vancouver, Canada	ion-source, plasma, vacuum, permanent-magnet	334

- S.A. Korenev
  JINR, Dubna, Russia

VIII-09	**Operation of Ion Sources and Beam Transport to JAERI AVF Cyclotron**	ECR, cyclotron, ion-source, extraction	336

- **W. Yokota**, T. Agematsu, K. Arakawa, M. Fukuda, I. Ishibori, Y. Nakamura, T. Nara, S. Okumura
  JAERI, Gunma, Japan
- Y. Hayashi, K. Ishii, T. Tachikawa
  Sumitomo Heavy Industries, Ehime, Japan

VIII-10	**Spin Dynamics and Polarized Ion Sources on Isochronous Cyclotron U-240**	resonance, cyclotron, polarization, acceleration	340

- **N.I. Zaika**
  Institute for Nuclear Research, Kiev, Ukraine

VIII-11	**Study on the Magnetic Field of Caprice Type ECR Source**	plasma, cathode, ECR, extraction	344

- **B.W. Wei**, Z. Liu, Y. Ma, D. Wu, P. Yuan, W. Zhang, X. Zhang, H. Zhao
  Institute of Modern Physics, Lanzhou, People's Republic of China
- A. Efremov
  JINR, Dubna, Russia

VIII-12	**The Super Gas Mixing Technique for Highly Charged Uranium Ions**	plasma, ion-source, insertion, ECRIS	348

- **T.A. Antaya**, D. Cole
  NSCL, East Lansing, Michigan, USA

VIII-13	**Recent Development of Internal H^-/D^- Source for Compact Cyclotrons**	cyclotron, extraction, plasma, proton	352

- **T.Y.T. Kuo**
  TRIUMF, Vancouver, Canada
- G.O. Hendry
  Cyclotron Inc., Napa, California, USA

VIII-14	**Plan for the Ion Source Emittance Measurement Under the RF Extraction**	emittance, cyclotron, ion-source	357

- **J.W. Kim**, H.G. Blosser
  NSCL, East Lansing, Michigan, USA

VIII-15	**Progress with the NAC Injector Cyclotron for Heavy and Polarized Ions**	cyclotron, proton, heavy-ion, diagnostics	361

- **Z.B. du Toit**, S.J. Burger, P.J. Celliers, J.G. de Villiers,

H.N. Jungwirth, A. Müller, P.F. Rohwer, D.M. van Rooyen
National Accelerator Centre, Faure, Republic of South Africa

VIII-16	**Plasma Cathode Method for RIKEN ECRIS**	plasma, electron, cathode, ECRIS	365

- **T. Nakagawa**, A. Goto, T. Kageyama, M. Kase, Y. Yano
RIKEN, Saitama, Japan

VIII-17	**Performance of the Texas A&M ECRIS**	cyclotron, ECRIS, injection, ion-source	369

- **G. Mouchaty**, D.P. May, R.C. Rogers, P. Smelser
Texas A&M University, College Station, Texas, USA

IXA-04	**Ion_Tracker, a Trace Tracking Program for Cyclotron Design**	cyclotron, injection, optics, acceleration	388

- **M. Rinta-Nikkola**
University of Jyväskylä, Jyväskylä, Finland

IXA-05	**Ion Optics in the Jyväskylä K130 Cyclotron**	cyclotron, injection, solenoid, extraction	392

- **P. Heikkinen**, M. Rinta-Nikkola
University of Jyväskylä, Jyväskylä, Finland

IXA-08	**Evaluation of Third-Harmonic Voltage Flattopping for a Superconducting Cyclotron**	cyclotron, extraction, TRIUMF, resonance	404

- **M.M. Gordon**, D. Jeon
NSCL, East Lansing, Michigan, USA

IXB-03	**K1200 Cyclotron Beam Development Techniques**	cyclotron, ion-source, injection, ECR	427

- **T.A. Antaya**, D. Cole, P. Miller, D. Poe
NSCL, East Lansing, Michigan, USA

IXB-04	**Selection and Measurement of RF Phase Width of the K1200 Cyclotron Beam**	cyclotron, extraction, vacuum, injection	431

- **J. Bailey**, J. Kuchar, F. Marti, J. Yurkon
NSCL, East Lansing, Michigan, USA
- J.A. Nolen
ANL, Argonne, Illinois, USA
- D. Rifuggiato
INFN/LNS, Catania, Italy

IXB-05	**Internal Beam Dynamics Studies with a TV Probe**	resonance, cyclotron, simulation, controls	435

- **F. Marti**, S. Snyder
  NSCL, East Lansing, Michigan, USA

IXC-01	**Commissioning of the New High Intensity Axial Injection System for GANIL**	injection, cyclotron, emittance, controls	446

- **Ch. Ricaud**, E. Baron, J. Bony, M.P. Bourgarel, B. Bru
  GANIL, Caen, France
- R. Vienet
  CEN/Saclay, Gif-sur-Yvette, France

IXC-02	**A Formulation of Spiral Inflector Design and Its Application to SF Cyclotron**	cyclotron, injection, acceleration, ion-source	450

- **M. Sekiguchi**, M. Fujita, M. Nishiguchi, Y. Ohshiro, Y. Shida, N. Yamazaki, T. Yamazaki
  University of Tokyo, Tanashi-shi, Tokyo, Japan

IXC-03	**Preliminary Design of a New Central Region for the LNS Superconducting Cyclotron**	cyclotron, injection, emittance, coupling	454

- **M-H. Moscatello**
  GANIL, Caen, France

IXC-04	**Non-Linear Beam Transport Effects in Highly Charged Positive Ion Beams Extracted From ECR Ion Sources**	emittance, space-charge, ECR, ion-source	457

- **T.A. Antaya**
  NSCL, East Lansing, Michigan, USA
- Z.Q. Xie
  LBL, Berkeley, California, USA

IXC-06	**Experiments on the Axial Injection System of the Cyclotron U-120M**	cyclotron, injection, acceleration, ion-source	465

- **Z. Trejbal**, M. Krivánek, J. Kucera, V. Bejsovec, J. Stursa
  Czechoslovak Academy of Sciences, Rez, Czechoslovakia

IXD-02	**High-Sensitive Ionization Detectors of Transverse Distribution of Accelerated Particles Beam**	cyclotron, controls, electron, proton	473

- **V.G. Mikhailov**, V.A. Rezvov, A.A. Roshchin, V.I. Sklyarenko, L.I. Iudin
  Kurchatov Institute, Moscow, Russia

IXD-03	**A Beam Profile Monitor Using the Ionization of Residual Gas**	MCP, AGOR, background, cyclotron	477

- **J.M. Schippers**, H.H. Kiewiet
  Kernfysisch Versneller Instituut, Groningen, The Netherlands

IXD-05	**High Sensitivity Electronic System for the Phase Probes of the LNS/MILANO Superconducting Cyclotron**	cyclotron, controls, injection, rf-amplifier	483

- **A. Bosotti**, D. Corti, C. Pagani, G. Varisco, F. Zibra
  INFN/LASA, Segrate, Italy
- M. Di Giacomo
  INFN/LNS, Catania, Italy

IXD-09	**A DC Current Transformer for TRIUMF**	ion-source, feedback, vacuum, TRIUMF	498

- **Y. Yin**
  TRIUMF, Vancouver, Canada

XA-04	**The RF-System for a VICKSI Injector Cyclotron**	cyclotron, ECR, injection, booster	519

- **W. Pelzer**
  HMI, Berlin, Germany

XA-06	**A Modified RF System of JAERI AVF Cyclotron**	cavity, cyclotron, proton, controls	526

- **Y. Kumata**, Y. Fukumoto
  Sumitomo Heavy Industries, Ehime, Japan
- K. Arakawa, M. Fukuda, T. Karasawa
  JAERI, Gunma, Japan
- A. Shimizu
  Osaka University, Osaka, Japan

XA-10	**RF Transmitter for ECR Ion Sources**	ECR, klystron, plasma, ion-source	542

- **R. Boux**, J.P. Ichac, M. Soudée
  Thomson Tubes Electroniques, Velizy-Villacoublay, France

XB-02	**A Permanent Magnet System for a Cyclotron Used as a Mass Spectrometer**	cyclotron, vacuum, injection, permanent-magnet	561

- **C.Y. Li**, M. Cooper, K. Halbach, W.B. Kunkel, K.N. Leung, R.P. Wells, A.T. Young
  LBL, Berkeley, California, USA

XC-02	**Potential Enhancement of Magnetic Deflection in the Chalk River Superconducting Cyclotron Extraction System**	extraction, cyclotron, acceleration, dipole	573

- **C.R. Hoffmann**, E.H. Lindqvist
  Atomic Energy of Canada, Chalk River, Ontario, Canada

XC-04	**Performance of Beam Chopping System for JAERI AVF**	cyclotron, extraction,	581

	Cyclotron	injection, JAERI	

- **W. Yokota**, T. Agematsu, K. Arakawa, M. Fukuda, I. Ishibori, Y. Nakamura, T. Nara, S. Okumura
  JAERI, Gunma, Japan
- Y. Hayashi, Y. Kumata, T. Tachikawa
  Sumitomo Heavy Industries, Ehime, Japan

XC-08	**Deflector Development for the K1200 Cyclotron**	cathode, electron, cyclotron, site	596

- **T.Y.T. Kuo**
  TRIUMF, Vancouver, Canada
- J.A. Nolen
  ANL, Argonne, Illinois, USA

XD-05	**Buncher in the Beam Line from ECR to SFC**	ECR, bunching, ion-source, controls	618

- **J.Z. Jiang**, X.H. Zhou, Q. Wang, F. Wang, W.M. Jiang
  Institute of Modern Physics, Lanzhou, People's Republic of China

XD-06	**Beamlines for a Second Injector Cyclotron at NAC**	solenoid, dipole, cyclotron, ion-source	621

- **J.C. Cornell**, J.L. Conradie, D.T. Fourie
  National Accelerator Centre, Faure, Republic of South Africa

XD-07	**Beam Transport System for the HIMAC**	beam-transport, injection, optics, heavy-ion	625

- **K. Noda**, Y. Hirao, A. Itano, M. Kanazawa, A. Kitagawa, T. Kohno, M. Kumada, H. Ogawa, K. Sato, Y. Sato, M. Sudou, E. Takada, S. Yamada, T. Yamada
  NIRS, Chiba, Japan
- K. Endo
  KEK, Ibaraki, Japan

XD-08	**Design of a Beam Buncher Using a Half-Cosine Driving Function**	cyclotron, injection, bunching, ECRIS	629

- **R.C. Rogers**
  Texas A&M University, College Station, Texas, USA

XI-02	**The IUCF High Intensity Polarized Ion Source Control System**	controls, vacuum, ion-source, interlocks	641

- **T. Capshew**, J.C. Collins, D. DuPlantis, D.W. Frame, J. Graham, D.D. Reid
  Indiana University, Bloomington, Indiana, USA

	Automatic Control System of Magnetic Separator for	controls, cyclotron,	652

XI-05	**Kurchatov IAE Cyclotron** • **N.I. Venikov**, V. Buranov, O. Gotovtsev, L.I. Iudin, P.Yu. Komissarov, V.N. Unezhev Kurchatov Institute, Moscow, Russia	status, power-supply	
XI-07	**Ion Spectra Identification Software for the ECR Ion Source at NAC** • **E.J.S. Franklin**, J.G. de Villiers National Accelerator Centre, Faure, Republic of South Africa	ion-source, ECR, controls, cyclotron	660
XII-03	**Design of a Compact Permanent Magnet Cyclotron Mass Spectrometer for the Detection and Measurement of Trace Isotopes** • **A.T. Young**, K.J. Bertsche, D.J. Clark, K. Halbach, W.B. Kunkel, K.N. Leung, C.Y. Li LBL, Berkeley, California, USA	cyclotron, ion-source, injection, permanent-magnet	705
XIII-01	**Accelerated Radioactive Nuclear Beams: Existing and Planned Facilities (Invited Paper)** • **J.M. Nitschke** LBL, Berkeley, California, USA	target, cyclotron, ISOL, heavy-ion	713
XIII-02	**A Conceptual Design for a Primary Cyclotron for the ISL Radioactive Beam Project** • **D.J. Clark** LBL, Berkeley, California, USA	extraction, cyclotron, proton, acceleration	721
XIII-03	**An On-Line Isotopic Separator Test Bench at GANIL** • **P. Bricault**, R. Leroy, M. Lewitowicz, J.Y. Pacquet, M.G. St-Laurent, P. Sortais GANIL, Caen, France • A.C. Mueller, J. Obert, J.C. Putaux IPN, Orsay, France • C.F. Liang, P. Paris CSNSM, Orsay, France • J.C. Steckmeyer LPC, Caen, France	target, ion-source, ECR, extraction	725
XIII-04	**The PIAFE Project at Grenoble: Beam Transport and Acceleration** • **J.L. Belmont**, J.F. Bruandet, J.M. de Conto, M. Fruneau, G. Gimond, K. Golovanivsky, E. Liatard, J.M. Loiseaux, H. Nifenecker, A. Savalle, B. Vignon Université Joseph Fourier, Grenoble, France	cyclotron, quadrupole, ECRIS, extraction	729

P. Briand
CEN-Grenoble, Grenoble, France

XIII-05	**High Intensity Superconducting Cyclotron Beams for a Radioactive Ion Beam Facility**	extraction, cyclotron, focusing, emittance	733

- **L. Calabretta**, D. Rifuggiato
  INFN/LNS, Catania, Italy

XIII-07	**The ORNL Radioactive Ion Beam Project with the ORIC Accelerator**	target, ion-source, tandem-accelerator, heavy-ion	741

- **D.K. Olsen**, G.D. Alton, C. Baktash, D.T. Dowling, J.D. Garrett, D.L. Haynes, C.M. Jones, R.C. Juras, S.N. Lane, I.Y. Lee, M.J. Meigs, G.D. Mills, S.W. Mosko, B.A. Tatum, K.S. Toth
  ORNL, Oak Ridge, Tennessee, USA
- H.K. Carter, J. Kormicki
  Associated Universities Oak Ridge, Oak Ridge, Tennessee, USA

XIII-09	**Post-Accelerator Studies for the ISOL Facility at TRIUMF**	solenoid, rfq, focusing, linac	749

- **L. Root**, H.R. Schneider, J.S. Fraser
  TRIUMF, Vancouver, Canada

XIV-03	**Physics with Storage Rings (Invited Paper)**	target, electron, storage-ring, luminosity	753

- **R.E. Pollock**
  Indiana University, Bloomington, Indiana, USA

XIV-04	**Conference Summary (Invited Paper)**	cyclotron, proton, ECR, electron	758

- **D.J. Clark**
  LBL, Berkeley, California, USA

XV-01	**Proper and Improper Accelerators - In Praise of Cyclotrons and Their Builders**	cyclotron, TRIUMF, controls, synchrotron	765

- **M.K. Craddock**
  University of British Columbia, Vancouver, Canada

A B C D E F H I J K L M N O P Q R S T V

ion-source

Paper	Title	Other Keywords	Page
I-03	**New K130 Cyclotron at Jyväskylä (Invited Paper)** • **E. Liukkonen** University of Jyväskylä, Jyväskylä, Finland	cyclotron, ion, ECR, vacuum	22
I-14	**Initial Operation of HIRFL** • **B.W. Wei**, F. Ye Institute of Modern Physics, Lanzhou, People's Republic of China	ion, ECR, heavy-ion, vacuum	74
I-15	**Upgrading the SFC** • **F. Ye**, M. Guo, Z. Ma, Q. Qiao, Y. Wang, Q. Yin, X. Zhu Institute of Modern Physics, Lanzhou, People's Republic of China	ion, ECR, injection, extraction	78
I-20	**Heavy Ion Facility in ATOMKI** • **S. Biri**, J. Pálinkás, A. Valek Institute of Nuclear Research of the Hungarian Academy of Sciences, Debrecen, Hungary	ion, ECR, heavy-ion, cyclotron	99
I-21	**Recent Achievements at the RIKEN Ring Cyclotron** • **Y. Yano** RIKEN, Saitama, Japan	ion, cyclotron, acceleration, injection	102
II-01	**Commercially Available Compact Cyclotrons for Isotope Production (Invited Paper)** • **V. Bechtold** FZK, Karlsruhe, Germany	cyclotron, ion, target, proton	110
II-05	**Status of a Compact H^- Cyclotron at the Kurchatov Institute of Atomic Energy** • **N.I. Venikov**, C.D. Burbeza, P.Yu. Komissarov, Yu.M. Krasnikov, S.T. Latushkin, V.V. Leonov, V.P. Moryakov, I.V. Naumov, A.Ya. Pisman, V.A. Rezvov, A.A. Vasiliev, V.E. Yarosh, L.I. Yudin Kurchatov Institute, Moscow, Russia	cyclotron, ion, controls, vacuum	126

IV-04	**^{178m2}Hf and ^{237}Pu Isotopes Production on the U-200 Cyclotron** • **S.L. Bogomolov**, S.N. Dmitriev, Yu.P. Gangrski, G.G. Gulbekyan, S.A. Karamian, V.B. Kutner, B.N. Markov, Yu.Ts. Oganessian, N.V. Pronin, G.Ya. Starodub JINR, Dubna, Russia	ion, cyclotron, target, cathode	167
V-06	**Experiences with the Cyclone 3 Oxygen 15 Generator** • **E. Conard**, J.-L. Morelle Ion Beam Applications, Louvain-la-Neuve, Belgium • J.C. Clark, D.B. Mackay Hammersmith Hospital, London, England	cyclotron, target, ion, controls	218
VIII-01	**ECR Ion Sources for Accelerators (Invited Paper)** • **C.M. Lyneis** LBL, Berkeley, California, USA	ECR, ion, plasma, electron	301
VIII-02	**Performance of the LBL AECR Source at Various Frequencies** • **Z.Q. Xie**, D. Collins, S.A. Lundgren, C.M. Lyneis LBL, Berkeley, California, USA	sextupole, ECR, ion, plasma	308
VIII-03	**Ion Sources for Cyclotron Application** • **K.N. Leung**, D.A. Bachman, D.S. McDonald, A.T. Young LBL, Berkeley, California, USA	ion, plasma, electron, cyclotron	312
VIII-04	**A Review of Polarized Ion Sources for Cyclotrons (Invited Paper)** • **P.W. Schmor** TRIUMF, Vancouver, Canada	ion, electron, polarization, cyclotron	316
VIII-06	**An ECR Ion Source for Multiply-Charged Heavy Ions at 14 GHz** • **M. Sekiguchi**, M. Fujita, Y. Ohshiro, T. Yamazaki University of Tokyo, Tanashi-shi, Tokyo, Japan • Y. Isoya, T. Yamada, Y. Yamashita Japan Steel Works Ltd., Research Center for Advanced Technologies, Chiba, Japan • A. Kitagawa NIRS, Chiba, Japan	ECR, ion, plasma, extraction	326
VIII-	**Performance and Status of the IUCF High Intensity Polarized**	ECR, ion, sextupole,	330

07 **Ion Source** extraction

- **V. Derenchuk**, R. Brown, T.J.P. Ellison, D.L. Friesel, J.W. Hicks, D. Jenner, A. Pei, H. Petri, P. Schwandt, J. Sowinski, M. Wedekind
  Indiana University, Bloomington, Indiana, USA

VIII-08 **Ion Source of Discharge Type** ion, plasma, vacuum, permanent-magnet 334

- **I.B. Enchevich**
  TRIUMF, Vancouver, Canada
- S.A. Korenev
  JINR, Dubna, Russia

VIII-09 **Operation of Ion Sources and Beam Transport to JAERI AVF Cyclotron** ion, ECR, cyclotron, extraction 336

- **W. Yokota**, T. Agematsu, K. Arakawa, M. Fukuda, I. Ishibori, Y. Nakamura, T. Nara, S. Okumura
  JAERI, Gunma, Japan
- Y. Hayashi, K. Ishii, T. Tachikawa
  Sumitomo Heavy Industries, Ehime, Japan

VIII-12 **The Super Gas Mixing Technique for Highly Charged Uranium Ions** ion, plasma, insertion, ECRIS 348

- **T.A. Antaya**, D. Cole
  NSCL, East Lansing, Michigan, USA

VIII-14 **Plan for the Ion Source Emittance Measurement Under the RF Extraction** emittance, ion, cyclotron 357

- **J.W. Kim**, H.G. Blosser
  NSCL, East Lansing, Michigan, USA

VIII-17 **Performance of the Texas A&M ECRIS** cyclotron, ECRIS, injection, ion 369

- **G. Mouchaty**, D.P. May, R.C. Rogers, P. Smelser
  Texas A&M University, College Station, Texas, USA

IXB-03 **K1200 Cyclotron Beam Development Techniques** ion, cyclotron, injection, ECR 427

- **T.A. Antaya**, D. Cole, P. Miller, D. Poe
  NSCL, East Lansing, Michigan, USA

IXC-02 **A Formulation of Spiral Inflector Design and Its Application to SF Cyclotron** ion, cyclotron, injection, acceleration 450

- **M. Sekiguchi**, M. Fujita, M. Nishiguchi, Y. Ohshiro, Y. Shida,

N. Yamazaki, T. Yamazaki
University of Tokyo, Tanashi-shi, Tokyo, Japan

IXC-04	**Non-Linear Beam Transport Effects in Highly Charged Positive Ion Beams Extracted From ECR Ion Sources**	emittance, ion, space-charge, ECR	457

- **T.A. Antaya**
  NSCL, East Lansing, Michigan, USA
- Z.Q. Xie
  LBL, Berkeley, California, USA

IXC-06	**Experiments on the Axial Injection System of the Cyclotron U-120M**	ion, cyclotron, injection, acceleration	465

- **Z. Trejbal**, M. Krivánek, J. Kucera, V. Bejsovec, J. Stursa
  Czechoslovak Academy of Sciences, Rez, Czechoslovakia

IXD-09	**A DC Current Transformer for TRIUMF**	ion, feedback, vacuum, TRIUMF	498

- **Y. Yin**
  TRIUMF, Vancouver, Canada

XA-10	**RF Transmitter for ECR Ion Sources**	ion, ECR, klystron, plasma	542

- **R. Boux**, J.P. Ichac, M. Soudée
  Thomson Tubes Electroniques, Velizy-Villacoublay, France

XD-05	**Buncher in the Beam Line from ECR to SFC**	ECR, ion, bunching, controls	618

- **J.Z. Jiang**, X.H. Zhou, Q. Wang, F. Wang, W.M. Jiang
  Institute of Modern Physics, Lanzhou, People's Republic of China

XD-06	**Beamlines for a Second Injector Cyclotron at NAC**	ion, solenoid, dipole, cyclotron	621

- **J.C. Cornell**, J.L. Conradie, D.T. Fourie
  National Accelerator Centre, Faure, Republic of South Africa

XI-02	**The IUCF High Intensity Polarized Ion Source Control System**	controls, vacuum, ion, interlocks	641

- **T. Capshew**, J.C. Collins, D. DuPlantis, D.W. Frame, J. Graham, D.D. Reid
  Indiana University, Bloomington, Indiana, USA

XI-07	**Ion Spectra Identification Software for the ECR Ion Source at NAC**	ion, ECR, controls, cyclotron	660

- **E.J.S. Franklin**, J.G. de Villiers

National Accelerator Centre, Faure, Republic of South Africa

XI-11	**Early Experience with DECwindows/Motif in the TRIUMF Central Control System**	controls, laser, booster, TRIUMF	676

- **S. Kadantsev**
  JINR, Dubna, Russia
- M. Mouat
  TRIUMF, Vancouver, Canada

XII-03	**Design of a Compact Permanent Magnet Cyclotron Mass Spectrometer for the Detection and Measurement of Trace Isotopes**	ion, cyclotron, injection, permanent-magnet	705

- **A.T. Young**, K.J. Bertsche, D.J. Clark, K. Halbach, W.B. Kunkel, K.N. Leung, C.Y. Li
  LBL, Berkeley, California, USA

XIII-03	**An On-Line Isotopic Separator Test Bench at GANIL**	ion, target, ECR, extraction	725

- **P. Bricault**, R. Leroy, M. Lewitowicz, J.Y. Pacquet, M.G. St-Laurent, P. Sortais
  GANIL, Caen, France
- A.C. Mueller, J. Obert, J.C. Putaux
  IPN, Orsay, France
- C.F. Liang, P. Paris
  CSNSM, Orsay, France
- J.C. Steckmeyer
  LPC, Caen, France

XIII-07	**The ORNL Radioactive Ion Beam Project with the ORIC Accelerator**	ion, target, tandem-accelerator, heavy-ion	741

- **D.K. Olsen**, G.D. Alton, C. Baktash, D.T. Dowling, J.D. Garrett, D.L. Haynes, C.M. Jones, R.C. Juras, S.N. Lane, I.Y. Lee, M.J. Meigs, G.D. Mills, S.W. Mosko, B.A. Tatum, K.S. Toth
  ORNL, Oak Ridge, Tennessee, USA
- H.K. Carter, J. Kormicki
  Associated Universities Oak Ridge, Oak Ridge, Tennessee, USA

A B C D E F H I J K L M N O P Q R S T V

ISAC

Paper	Title	Other Keywords	Page
XIII-08	**Research and Development Studies with Radioactive Beams at TRIUMF**	target, TRIUMF, kaon, proton	745

- **J.M. D'Auria**, M. Dombsky
  Simon Fraser University, Burnaby, BC, Canada
- L. Buchmann, H. Sprenger, J.S. Vincent
  TRIUMF, Vancouver, Canada
- J. King
  University of Toronto, Toronto, Ontario, Canada
- P. McNeely, G. Roy
  University of Alberta, Edmonton, Alberta, Canada

A B C D E F H I J K L M N O P Q R S T V

ISOL

Paper	Title	Other Keywords	Page
XIII-01	**Accelerated Radioactive Nuclear Beams: Existing and Planned Facilities (Invited Paper)**	ion, target, cyclotron, heavy-ion	713

- **J.M. Nitschke**
  LBL, Berkeley, California, USA

A B C D E F H I J K L M N O P Q R S T V

isotope-production

Paper	Title	Other Keywords	Page
II-02	**The Operation of Cyclotrons Used for Radiopharmaceutical Production** • **T. Grey-Morgan** Cyclotron Isotopes Manufacturing, Buckinghamshire, England • R.E. Hubbard Medi + Physics Inc., Arlington Heights, Illinois, USA	cyclotron, target, controls, radiation	115
II-04	**20 MeV Cyclotron for Isotope Production** • **A. Glazov**, Ju. Alenitskiy, A. Chesnov, S. Chesnova, V. Kochkin, D. Novikov, E. Samsonov, M. Semenov, A. Vasilenko, E. Zaplatin, N. Zaplatin JINR, Dubna, Russia • I. Gulamov, O. Iljasov, A. Rykov Institute of Nuclear Physics, Tashkent, Republic of Uzbekistan	cyclotron, target, acceleration, proton	123
XA-03	**Dual Frequency Resonator System for a Compact Cyclotron** • **M. Eiche**, K.L. Erdman Ebco Technologies Ltd, Richmond, BC, Canada • P. Lanz, M. Lipnicki, M. Zach TRIUMF, Vancouver, Canada	cyclotron, impedance, cavity, vacuum	515

A B C D E F H I J K L M N O P Q R S T V

JAERI

Paper	Title	Other Keywords	Page
II-03	**Construction and First Year's Operation of the JAERI AVF Cyclotron** • **K. Arakawa**, T. Agematsu, M. Fukuda, I. Ishibori, T. Karasawa, T. Nara, Y. Nakamura, S. Okumura, R. Tanaka, W. Yokota, JAERI, Gunma, Japan • A. Shimizu, Osaka University, Osaka, Japan • Y. Hayashi, K. Ishii, T. Satoh, T. Tachikawa, Sumitomo Heavy Industries, Ehime, Japan	cyclotron, ion, extraction, proton	119
IXB-02	**Beam Studies of Injection to Extraction System for JAERI AVF Cyclotron** • **M. Fukuda**, T. Agematsu, K. Arakawa, I. Ishibori, T. Karasawa, Y. Nakamura, T. Nara, S. Okumura, W. Yokota, JAERI, Gunma, Japan	cyclotron, proton, injection, extraction	423
XC-04	**Performance of Beam Chopping System for JAERI AVF Cyclotron** • **W. Yokota**, T. Agematsu, K. Arakawa, M. Fukuda, I. Ishibori, Y. Nakamura, T. Nara, S. Okumura, JAERI, Gunma, Japan • Y. Hayashi, Y. Kumata, T. Tachikawa, Sumitomo Heavy Industries, Ehime, Japan	cyclotron, extraction, ion, injection	581
XI-04	**Control System for JAERI AVF Cyclotron** • **S. Okumura**, T. Agematsu, K. Arakawa, M. Fukuda, I. Ishibori, T. Kamiya, Y. Nakamura, T. Nara, W. Yokota, JAERI, Gunma, Japan • K. Hoshika, K. Iso, M. Maruyama, M. Tachibana, Sumitomo Heavy Industries, Ehime, Japan	controls, cyclotron, injection, status	648

A B C D E F H I J K L M N O P Q R S T V

kaon

Paper	Title	Other Keywords	Page
III-02	**The KAON Factory at TRIUMF** • **M.K. Craddock** University of British Columbia, Vancouver, Canada	booster, TRIUMF, lattice, factory	143
XI-12	**Application of Object Oriented Techniques in the TRIUMF Beam Line 2C Control System (Invited Paper)** • **N.A. Wilkinson**, E.A. Osberg, G.A. Ludgate TRIUMF, Vancouver, Canada	controls, target, TRIUMF, factory	681
XIII-08	**Research and Development Studies with Radioactive Beams at TRIUMF** • **J.M. D'Auria**, M. Dombsky Simon Fraser University, Burnaby, BC, Canada • L. Buchmann, H. Sprenger, J.S. Vincent TRIUMF, Vancouver, Canada • J. King University of Toronto, Toronto, Ontario, Canada • P. McNeely, G. Roy University of Alberta, Edmonton, Alberta, Canada	target, TRIUMF, ISAC, proton	745

A B C D E F H I J K L M N O P Q R S T V

kicker

Paper	Title	Other Keywords	Page
XA-05	**Low Frequency RF System for the Indiana University Cooler Ring**	cavity, injection, beam-losses, synchrotron	523

- **X. Pei**, S. Anderson, V. Derenchuk, G. East, D.L. Friesel, D. Jenner, D. McCammon, T. Sloan
  Indiana University, Bloomington, Indiana, USA

A B C D E F H I J K L M N O P Q R S T V

klystron

Paper	Title	Other Keywords	Page
XA-10	**RF Transmitter for ECR Ion Sources**	ion, ECR, plasma, ion-source	542

- **R. Boux**, J.P. Ichac, M. Soudée
  Thomson Tubes Electroniques, Velizy-Villacoublay, France

A B C D E F H I J K L M N O P Q R S T V

laser

Paper	Title	Other Keywords	Page
VII-07	**Superthin Internal Target for Storage Rings** • **V. Pugatch**, A. Glushko, G. Pitatelev, G. Sivtsov Institute for Nuclear Research, Kiev, Ukraine • S. Popov, D. Toporkov, B. Voitsechovsky Institute for Nuclear Physics, Novosibirsk, Russia	target, micro-particles, electron, storage-ring	297
VIII-05	**Status of the TRIUMF Optically-Pumped Polarized H^- Ion Source** • **C.D.P. Levy**, K. Jayamanna, M. McDonald, R. Ruegg, P.W. Schmor TRIUMF, Vancouver, Canada • A.N. Zelenskii Institute of Nuclear Research, Russian Academy of Sciences, Moscow, Russia	polarization, ion, proton, TRIUMF	322
XI-11	**Early Experience with DECwindows/Motif in the TRIUMF Central Control System** • **S. Kadantsev** JINR, Dubna, Russia • M. Mouat TRIUMF, Vancouver, Canada	controls, booster, TRIUMF, ion-source	676

A B C D E F H I J K L M N O P Q R S T V

lattice

Paper	Title	Other Keywords	Page
III-02	**The KAON Factory at TRIUMF**	booster, TRIUMF, kaon, factory	143

- **M.K. Craddock**
  University of British Columbia, Vancouver, Canada

A B C D E F H I J K L M N O P Q R S T V

light-ion

Paper	Title	Other Keywords	Page
VI-05	**Recent Activities of the Cyclotron Laboratory in Nice** • **P. Mandrillon**, N. Brassart, P. Chauvel, A. Courdi, F. Farley, N. Fietier, J. Herault, J.Y. Tang Centre Antoine Lacassagne, Nice, France	cyclotron, ion, synchrotron, proton	248
XI-06	**The New Distributed Control System of the NAC** • **H.F. Weehuizen**, R.K. Fisch, E.J.S. Franklin, M.E. Hogan, I.H. Kohler, J.P. Rogers, P.J. Theron National Accelerator Centre, Faure, Republic of South Africa	controls, instrumentation, status, cyclotron	656

A B C D E F H I J K L M N O P Q R S T V

linac

Paper	Title	Other Keywords	Page
IXD-01	**The New Phase Detection System of the Cosy-Injector** • **K. Kennepohl**, W. Bräutigam, M. Herschbach, D. Maeckelburg FZJ, Jülich, Germany	pick-up, cyclotron, COSY, controls	469
IXD-04	**Emittance Measurements in the HIRFL Beam Line** • **H. Zhao**, Z. Shen, B.W. Wei Institute of Modern Physics, Lanzhou, People's Republic of China	emittance, quadrupole, coupling, optical-matching	479
XII-02	**Study of an FFAG Synchrocyclotron for a Pulsed Neutron Source** • **S.A. Martin**, E. Zaplatin FZJ, Jülich, Germany • P.F. Meads, Jr. Private Address, Oakland, California, USA • G. Wüstefeld BESSY, Berlin, Germany • K. Ziegler HMI, Berlin, Germany	injection, cavity, neutron, synchrotron	701
XIII-09	**Post-Accelerator Studies for the ISOL Facility at TRIUMF** • **L. Root**, H.R. Schneider, J.S. Fraser TRIUMF, Vancouver, Canada	solenoid, rfq, focusing, ion	749

A B C D E F H I J K L M N O P Q R S T V

luminosity

Paper	Title	Other Keywords	Page
XIV-03	**Physics with Storage Rings (Invited Paper)**	target, electron, ion, storage-ring	753

- **R.E. Pollock**
  Indiana University, Bloomington, Indiana, USA

A B C D E F H I J K L M N O P Q R S T V

MCP

Paper	Title	Other Keywords	Page
IXD-03	**A Beam Profile Monitor Using the Ionization of Residual Gas**	AGOR, ion, background, cyclotron	477

- **J.M. Schippers**, H.H. Kiewiet
  Kernfysisch Versneller Instituut, Groningen, The Netherlands

A B C D E F H I J K L M N O P Q R S T V

micro-particles

Paper	Title	Other Keywords	Page
VII-07	**Superthin Internal Target for Storage Rings**	target, electron, laser, storage-ring	297

- **V. Pugatch**, A. Glushko, G. Pitatelev, G. Sivtsov
  Institute for Nuclear Research, Kiev, Ukraine
- S. Popov, D. Toporkov, B. Voitsechovsky
  Institute for Nuclear Physics, Novosibirsk, Russia

A B C D E F H I J K L M N O P Q R S T V

microtron

Paper	Title	Other Keywords	Page
V-04	**Possibility of Producing Some Radionuclides for Medicine Using JINR Accelerators**	proton, cyclotron, electron, target	213

- **S.N. Dmitriev**, G.G. Gulbekyan, V.A. Khalkin, R.Ts. Oganessian, L.M. Onishchenko, G.Ya. Starodub, N.G. Zaitseva
  JINR, Dubna, Russia

A B C D E F H I J K L M N O P Q R S T V

monitoring

Paper	Title	Other Keywords	Page
V-01	**The New Molecular Medicine** • **H.N. Wagner, Jr.** The Johns Hopkins University, Baltimore, Maryland, USA	radiation, accumulation, site, ion	202
VI-06	**Health Physics Data Acquisition System at the National Medical Cyclotron** • **B.N. Mukherjee** ANSTO, Menai, NSW, Australia • D.W. Arnott National Medical Cyclotron, Camperdown, NSW, Australia	radiation, cyclotron, target, neutron	252
XC-09	**Results from the Deflector Test Stand at Texas A&M University** • **D.P. May**, G. Derrig, W. Dewees, P. Smelser, D. Tran, R.C. Rogers Texas A&M University, College Station, Texas, USA	high-voltage, power-supply, cyclotron, shielding	602
XI-01	**Integrated Tools for Cyclotron Operation (Invited Paper)** • **W. Busse** HMI, Berlin, Germany	controls, cyclotron, TRIUMF	634
XI-08	**Micro-Controlled Vacuum Systems at NAC** • **P.J. Celliers**, E.J.S. Franklin National Accelerator Centre, Faure, Republic of South Africa	vacuum, controls, cyclotron, instrumentation	664

A B C D E F H I J K L M N O P Q R S T V

multipole

Paper	Title	Other Keywords	Page
XC-07	**Design of Passive Magnetic Channels**	focusing, dipole, quadrupole, cyclotron	592

- **G. Bellomo**
  INFN/LASA, Segrate, Italy

A B C D E F H I J K L M N O P Q R S T V

neutron

Paper	Title	Other Keywords	Page
I-16	**Status Report of Cyclone** • **M. Loiselet**, N. Postiau, G. Ryckewaert Université Catholique de Louvain, Louvain-la-Neuve, Belgium	cyclotron, ion, target, beam-transport	82
II-06	**A Newly Developed Compact Cyclotron for Neutron Therapy and Positron Nuclear Medicine** • **K. Ito**, T. Ishigaki, S. Itoh, Y. Kasugai, T. Kato, T. Misawa, M. Nishino, M. Osakabe, T. Ota, S. Sakuma, M. Tadokoro, H. Yamamoto Nagoya University, Nagoya, Japan • Y. Toda, Y. Yamamoto Japan Steel Works Ltd., Tokyo, Japan	target, cyclotron, positron, proton	129
II-07	**Performance of the Harper Hospital Cyclotron; Effect of Pulsed Radio Frequency** • **H.G. Blosser**, J. Vincent NSCL, East Lansing, Michigan, USA • R. Maughan Harper Hospital, Detroit, Michigan, USA	cyclotron, target, ion, controls	133
IV-03	**The Use of Heavy Ion Cyclotrons of the Flerov Laboratory of Nuclear Reactions in Condensed Matter Investigations** • **R.Ts. Oganessian**, A.Yu. Didyk JINR, Dubna, Russia	ion, radiation, heavy-ion, electron	162
IV-07	**Neutron Productions from Carbon by Charged Particle Bombardment at Different Energies** • **M.A. Chaudhri** Austin Hospital & University of Melbourne, Melbourne, Australia	target, proton, background, cyclotron	178
IV-08	**Analytical Applications of Cyclotrons in Biomedical Fields - Charged Particle Activation Analysis** • **M.A. Chaudhri** Austin Hospital & University of Melbourne, Melbourne, Australia	cyclotron, proton, target, ion	181
IV-09	**A Simple Method for Estimating Activation Sensitivities of Different Elements / Isotopes with Cyclotron Produced Neutrons**	target, cyclotron, BNL, radiation	187

- **M.A. Chaudhri**
  Austin Hospital & University of Melbourne, Melbourne, Australia

IV-10	**A Proposal for an Intense Cyclotron-Based Thermal Neutron Source**	cyclotron, target, proton, extraction	191

- **S. Tazawa**
  Sumitomo Heavy Industries, Toyo-shi, Toyo-shi, Japan
- W.L. Whittemore
  General Atomics, San Diego, California, USA

VI-06	**Health Physics Data Acquisition System at the National Medical Cyclotron**	radiation, cyclotron, monitoring, target	252

- **B.N. Mukherjee**
  ANSTO, Menai, NSW, Australia
- D.W. Arnott
  National Medical Cyclotron, Camperdown, NSW, Australia

VI-07	**Design Consideration of Neutron Therapy Facility Utilizing Existing Cyclotron**	target, cyclotron, controls, proton	255

- **H. Chang**, X. Cui, J. Wei, J. Zhang, K. Xie
  Institute of Nuclear Research, Shanghai, People's Republic of China

VI-09	**Continued Operation of the Seattle Clinical Cyclotron Facility**	cyclotron, controls, target, radiation	262

- **R. Risler**, S. Brossard, J. Jacky, I. Kalet, P. Wootton, F. Ziai
  University of Washington, Seattle, Washington, USA

XI-14	**Formal Specifications for a Cyclotron Control System**	controls, cyclotron, status, radiation	689

- **J. Jacky**, R. Risler
  University of Washington, Seattle, Washington, USA

XII-02	**Study of an FFAG Synchrocyclotron for a Pulsed Neutron Source**	injection, cavity, linac, synchrotron	701

- **S.A. Martin**, E. Zaplatin
  FZJ, Jülich, Germany
- P.F. Meads, Jr.
  Private Address, Oakland, California, USA
- G. Wüstefeld
  BESSY, Berlin, Germany
- K. Ziegler
  HMI, Berlin, Germany

A B C D E F H I J K L M N O P Q R S T V

octupole

Paper	Title	Other Keywords	Page
IXA-01	**Advantage of Using Differential Algebra and Lie Algebra in the Orbit Dynamics of Cyclotrons (Invited Paper)**	resonance, cyclotron, sextupole, closed-orbit	372
	• **W.G. Davies** Atomic Energy of Canada, Chalk River, Ontario, USA		
IXA-03	**Emittance Growth in Nonlinear Beam Guiding and Focusing Elements**	emittance, sextupole, dipole, focusing	384
	• **W.J.G.M. Kleeven**, J.I.M. Botman, J.L. Delhez, H.L. Hagedoorn, C.J. Timmermans, G.A. Webers Eindhoven University of Technology, Eindhoven, The Netherlands		

A B C D E F H I J K L M N O P Q R S T V

optical-matching

Paper	Title	Other Keywords	Page
IXD-04	**Emittance Measurements in the HIRFL Beam Line**	emittance, quadrupole, linac, coupling	479

- **H. Zhao**, Z. Shen, B.W. Wei
  Institute of Modern Physics, Lanzhou, People's Republic of China

A B C D E F H I J K L M N O P Q R S T V

optics

Paper	Title	Other Keywords	Page
IXA-04	**Ion_Tracker, a Trace Tracking Program for Cyclotron Design**	cyclotron, ion, injection, acceleration	388
	• **M. Rinta-Nikkola** University of Jyväskylä, Jyväskylä, Finland		
IXA-06	**Nonlinear Transport of Accelerator Beam Phase Space**	beam-transport, beam-transport	396
	• **X. Xie** Graduate School of Nuclear Industry, Beijing, People's Republic of China • J. Xia Institute of Modern Physics, Lanzhou, People's Republic of China		
IXA-07	**Deriving the General Expressions of Nonlinear Transport Coefficients of Accelerator Beam Phase Space by Artificial Intelligence**	beam-transport, cyclotron, electromagnetic-fields	400
	• **J. Xia** Institute of Modern Physics, Lanzhou, People's Republic of China • C. Liu, X. Xie Graduate School of Nuclear Industry, Beijing, People's Republic of China		
XD-07	**Beam Transport System for the HIMAC**	beam-transport, ion, injection, heavy-ion	625
	• **K. Noda**, Y. Hirao, A. Itano, M. Kanazawa, A. Kitagawa, T. Kohno, M. Kumada, H. Ogawa, K. Sato, Y. Sato, M. Sudou, E. Takada, S. Yamada, T. Yamada NIRS, Chiba, Japan • K. Endo KEK, Ibaraki, Japan		

A B C D E F H I J K L M N O P Q R S T V

permanent-magnet

Paper	Title	Other Keywords	Page
VIII-08	**Ion Source of Discharge Type** • **I.B. Enchevich** TRIUMF, Vancouver, Canada • S.A. Korenev JINR, Dubna, Russia	ion, ion-source, plasma, vacuum	334
XB-02	**A Permanent Magnet System for a Cyclotron Used as a Mass Spectrometer** • **C.Y. Li**, M. Cooper, K. Halbach, W.B. Kunkel, K.N. Leung, R.P. Wells, A.T. Young LBL, Berkeley, California, USA	cyclotron, vacuum, injection, ion	561
XII-03	**Design of a Compact Permanent Magnet Cyclotron Mass Spectrometer for the Detection and Measurement of Trace Isotopes** • **A.T. Young**, K.J. Bertsche, D.J. Clark, K. Halbach, W.B. Kunkel, K.N. Leung, C.Y. Li LBL, Berkeley, California, USA	ion, cyclotron, ion-source, injection	705

A B C D E F H I J K L M N O P Q R S T V

photon

Paper	Title	Other Keywords	Page
VI-01	**Accelerators for Charged Particle Therapy: Performance Criteria from the User Point of View (Invited Paper)** • **E. Pedroni** PSI, Villigen, Switzerland	proton, radiation, ion, target	226
VI-02	**Current and Potential Clinical Indications of Proton Irradiation (Invited Paper)** • **A.F. Thornton**, H.D. Suit Harvard Medical School, Boston, Massachusetts, USA	proton, controls, radiation, site	234
VI-03	**Pion Therapy for Cancer - What are the Prospects?** • **G.B. Goodman** University of British Columbia, Vancouver, Canada	TRIUMF, radiation, controls, background	242

A B C D E F H I J K L M N O P Q R S T V

pick-up

Paper	Title	Other Keywords	Page
IXD-01	**The New Phase Detection System of the Cosy-Injector** • **K. Kennepohl**, W. Bräutigam, M. Herschbach, D. Maeckelburg FZJ, Jülich, Germany	cyclotron, COSY, controls, linac	469
IXD-08	**Signal Processing for the Internal Phase Probe in the TRIUMF Cyclotron** • **K. Fong** TRIUMF, Vancouver, Canada	cavity, background, cyclotron, TRIUMF	495

A B C D E F H I J K L M N O P Q R S T V

plasma

Paper	Title	Other Keywords	Page
I-07	**Thoughts on Decommissioning the CERN Synchro Cyclotron** • **G. Spinney** CERN, Geneva, Switzerland	vacuum, CERN, shielding, synchro-cyclotron	47
VIII-01	**ECR Ion Sources for Accelerators (Invited Paper)** • **C.M. Lyneis** LBL, Berkeley, California, USA	ECR, ion, electron, ion-source	301
VIII-02	**Performance of the LBL AECR Source at Various Frequencies** • **Z.Q. Xie**, D. Collins, S.A. Lundgren, C.M. Lyneis LBL, Berkeley, California, USA	sextupole, ECR, ion, ion-source	308
VIII-03	**Ion Sources for Cyclotron Application** • **K.N. Leung**, D.A. Bachman, D.S. McDonald, A.T. Young LBL, Berkeley, California, USA	ion, ion-source, electron, cyclotron	312
VIII-06	**An ECR Ion Source for Multiply-Charged Heavy Ions at 14 GHz** • **M. Sekiguchi**, M. Fujita, Y. Ohshiro, T. Yamazaki University of Tokyo, Tanashi-shi, Tokyo, Japan • Y. Isoya, T. Yamada, Y. Yamashita Japan Steel Works Ltd., Research Center for Advanced Technologies, Chiba, Japan • A. Kitagawa NIRS, Chiba, Japan	ECR, ion, ion-source, extraction	326
VIII-08	**Ion Source of Discharge Type** • **I.B. Enchevich** TRIUMF, Vancouver, Canada • S.A. Korenev JINR, Dubna, Russia	ion, ion-source, vacuum, permanent-magnet	334
VIII-	**Study on the Magnetic Field of Caprice Type ECR Source**	ion, cathode, ECR,	344

11		extraction	

- **B.W. Wei**, Z. Liu, Y. Ma, D. Wu, P. Yuan, W. Zhang, X. Zhang, H. Zhao
  Institute of Modern Physics, Lanzhou, People's Republic of China
- A. Efremov
  JINR, Dubna, Russia

VIII-12	**The Super Gas Mixing Technique for Highly Charged Uranium Ions**	ion, ion-source, insertion, ECRIS	348

- **T.A. Antaya**, D. Cole
  NSCL, East Lansing, Michigan, USA

VIII-13	**Recent Development of Internal H^-/D^- Source for Compact Cyclotrons**	cyclotron, ion, extraction, proton	352

- **T.Y.T. Kuo**
  TRIUMF, Vancouver, Canada
- G.O. Hendry
  Cyclotron Inc., Napa, California, USA

VIII-16	**Plasma Cathode Method for RIKEN ECRIS**	ion, electron, cathode, ECRIS	365

- **T. Nakagawa**, A. Goto, T. Kageyama, M. Kase, Y. Yano
  RIKEN, Saitama, Japan

XA-10	**RF Transmitter for ECR Ion Sources**	ion, ECR, klystron, ion-source	542

- **R. Boux**, J.P. Ichac, M. Soudée
  Thomson Tubes Electroniques, Velizy-Villacoublay, France

A B C D E F H I J K L M N O P Q R S T V

polarization

Paper	Title	Other Keywords	Page
VIII-04	**A Review of Polarized Ion Sources for Cyclotrons (Invited Paper)**	ion, ion-source, electron, cyclotron	316
	• **P.W. Schmor** TRIUMF, Vancouver, Canada		
VIII-05	**Status of the TRIUMF Optically-Pumped Polarized H^- Ion Source**	laser, ion, proton, TRIUMF	322
	• **C.D.P. Levy**, K. Jayamanna, M. McDonald, R. Ruegg, P.W. Schmor TRIUMF, Vancouver, Canada • A.N. Zelenskii Institute of Nuclear Research, Russian Academy of Sciences, Moscow, Russia		
VIII-10	**Spin Dynamics and Polarized Ion Sources on Isochronous Cyclotron U-240**	ion, resonance, cyclotron, acceleration	340
	• **N.I. Zaika** Institute for Nuclear Research, Kiev, Ukraine		

A B C D E F H I J K L M N O P Q R S T V

positron

Paper	Title	Other Keywords	Page
II-06	**A Newly Developed Compact Cyclotron for Neutron Therapy and Positron Nuclear Medicine** • **K. Ito**, T. Ishigaki, S. Itoh, Y. Kasugai, T. Kato, T. Misawa, M. Nishino, M. Osakabe, T. Ota, S. Sakuma, M. Tadokoro, H. Yamamoto Nagoya University, Nagoya, Japan • Y. Toda, Y. Yamamoto Japan Steel Works Ltd., Tokyo, Japan	neutron, target, cyclotron, proton	129
IV-06	**A P.E.T. Study of Proton Induced Radioactivity in Different Materials** • **J.M. Schippers** Kernfysisch Versneller Instituut, Groningen, The Netherlands • A.M.J. Paans University Hospital, Groningen, The Netherlands	target, proton, radioactivity, cyclotron	175

power-supply

Paper	Title	Other Keywords	Page
I-17	**Performance of the K1200 Cyclotron at MSU** • **P. Miller**, T.A. Antaya, F. Marti, D. Poe, B. Sherrill, J. Stetson, J. Winger NSCL, East Lansing, Michigan, USA • J.A. Nolen ANL, Argonne, Illinois, USA	ion, cyclotron, target, emittance	86
XB-01	**Low Temperature Tests of the AGOR Superconducting Coil System** • **K. Pieterman**, J.A.M. Dam Cryocon B.V., Amersfoort, The Netherlands • C. Commeaux IPN, Orsay, France • C. Penco Ansaldo Componenti, Genoa, Italy	AGOR, cryogenics, factory, vacuum	557
XC-03	**Model Study of an Electrostatic Deflector Configuration with an Intermediate Electrode** • **C.R. Hoffmann**, J.F. Mouris Atomic Energy of Canada, Chalk River, Ontario, Canada	high-voltage, cyclotron, vacuum, septum	577
XC-09	**Results from the Deflector Test Stand at Texas A&M University** • **D.P. May**, G. Derrig, W. Dewees, P. Smelser, D. Tran, R.C. Rogers Texas A&M University, College Station, Texas, USA	high-voltage, cyclotron, shielding, monitoring	602
XI-05	**Automatic Control System of Magnetic Separator for Kurchatov IAE Cyclotron** • **N.I. Venikov**, V. Buranov, O. Gotovtsev, L.I. Iudin, P.Yu. Komissarov, V.N. Unezhev Kurchatov Institute, Moscow, Russia	controls, cyclotron, ion, status	652
XI-10	**Construction and System Tuning of Control System for the RCNP Ring Cyclotron and Beam Lines** • **T. Yamazaki**, A. Ando, K. Hosono, T. Itahashi, M. Kibayashi, I. Miura, K. Nagayama, H. Ogata, T. Saito, A. Shimizu,	controls, cyclotron, status, injection	672

K. Tamura, M. Uraki
Osaka University, Osaka, Japan
- K. Aoki, Y. Kimura, M. Maruyama, M. Tachibana, S. Yamada
Sumitomo Heavy Industries, Ehime, Japan
- K. Kodaira
Sumitomo Heavy Industries Systems Engineering Laboratory, Tokyo, Japan

A B C D E F H I J K L M N O P Q R S T V

proton

Paper	Title	Other Keywords	Page
I-01	**Commissioning of the RCNP Ring Cyclotron (Invited Paper)** • **I. Miura**, A. Ando, K. Hatanaka, K. Hosono, H. Ikegami, T. Itahashi, M. Kibayashi, M. Kondo, H. Ogata, T. Saito, A. Shimizu, K. Tamura, M. Uraki, T. Yamazaki Osaka University, Osaka, Japan • J. Abe Sumitomo Heavy Industries, Ehime, Japan	cyclotron, acceleration, cavity, injection	3
I-19	**Development of the NAC Accelerator Facilities** • **J.L. Conradie**, A.H. Botha, P.M. Cronje, R.E.F. Fenemore, H.N. Jungwirth, J.J. Kritzinger, W.A.G. Nel, D. Reitmann, L.M.M. Roels, P.F. Rohwer, H.A. Smit National Accelerator Centre, Faure, Republic of South Africa	cyclotron, extraction, injection, ion	95
II-01	**Commercially Available Compact Cyclotrons for Isotope Production (Invited Paper)** • **V. Bechtold** FZK, Karlsruhe, Germany	cyclotron, ion, target, ion-source	110
II-03	**Construction and First Year's Operation of the JAERI AVF Cyclotron** • **K. Arakawa**, T. Agematsu, M. Fukuda, I. Ishibori, T. Karasawa, T. Nara, Y. Nakamura, S. Okumura, R. Tanaka, W. Yokota JAERI, Gunma, Japan • A. Shimizu Osaka University, Osaka, Japan • Y. Hayashi, K. Ishii, T. Satoh, T. Tachikawa Sumitomo Heavy Industries, Ehime, Japan	cyclotron, ion, JAERI, extraction	119
II-04	**20 MeV Cyclotron for Isotope Production** • **A. Glazov**, Ju. Alenitskiy, A. Chesnov, S. Chesnova, V. Kochkin, D. Novikov, E. Samsonov, M. Semenov, A. Vasilenko, E. Zaplatin, N. Zaplatin JINR, Dubna, Russia • I. Gulamov, O. Iljasov, A. Rykov Institute of Nuclear Physics, Tashkent, Republic of Uzbekistan	cyclotron, target, acceleration, isotope-production	123

II-06	**A Newly Developed Compact Cyclotron for Neutron Therapy and Positron Nuclear Medicine** • **K. Ito**, T. Ishigaki, S. Itoh, Y. Kasugai, T. Kato, T. Misawa, M. Nishino, M. Osakabe, T. Ota, S. Sakuma, M. Tadokoro, H. Yamamoto Nagoya University, Nagoya, Japan • Y. Toda, Y. Yamamoto Japan Steel Works Ltd., Tokyo, Japan	neutron, target, cyclotron, positron	129
III-01	**The TRIUMF 520 MeV Cyclotron: Recent and Future Developments** • **G. Dutto** TRIUMF, Vancouver, Canada	cavity, TRIUMF, cyclotron, extraction	138
IV-01	**Material Research with Beams at Cyclotron Energies (Invited Paper)** • **K. Ziegler** HMI, Berlin, Germany	ion, radiation, cyclotron, heavy-ion	149
IV-06	**A P.E.T. Study of Proton Induced Radioactivity in Different Materials** • **J.M. Schippers** Kernfysisch Versneller Instituut, Groningen, The Netherlands • A.M.J. Paans University Hospital, Groningen, The Netherlands	target, positron, radioactivity, cyclotron	175
IV-07	**Neutron Productions from Carbon by Charged Particle Bombardment at Different Energies** • **M.A. Chaudhri** Austin Hospital & University of Melbourne, Melbourne, Australia	neutron, target, background, cyclotron	178
IV-08	**Analytical Applications of Cyclotrons in Biomedical Fields - Charged Particle Activation Analysis** • **M.A. Chaudhri** Austin Hospital & University of Melbourne, Melbourne, Australia	cyclotron, neutron, target, ion	181
IV-10	**A Proposal for an Intense Cyclotron-Based Thermal Neutron Source** • **S. Tazawa** Sumitomo Heavy Industries, Toyo-shi, Toyo-shi, Japan • W.L. Whittemore General Atomics, San Diego, California, USA	neutron, cyclotron, target, extraction	191
V-02	**The Production of Radionuclides for the Biosciences (Invited Paper)**	target, cyclotron, ion, extraction	206

- **T.J. Ruth**
  TRIUMF, Vancouver, Canada

V-03 **A Facility for Radioisotope Production at TRIUMF with 70-110 MeV Protons** — target, controls, cyclotron, TRIUMF — 209

- **D.R. Pearce**, J.S. Vincent
  TRIUMF, Vancouver, Canada

V-04 **Possibility of Producing Some Radionuclides for Medicine Using JINR Accelerators** — cyclotron, electron, target, microtron — 213

- **S.N. Dmitriev**, G.G. Gulbekyan, V.A. Khalkin, R.Ts. Oganessian, L.M. Onishchenko, G.Ya. Starodub, N.G. Zaitseva
  JINR, Dubna, Russia

V-05 **Radiopharmaceutical "Thallium-201-Chloride" Production using Thallium-203 Irradiation by Helium-3 Ions** — ion, target, cyclotron, ALICE — 216

- **A.A. Arzumanov**, N.K. Hamidov, A.I. Kozin, G.I. Shychikov, S.T. Tihomirova
  Kazakhstan Academy of Sciences, Alma-Ata, Republic of Kazakhstan

VI-01 **Accelerators for Charged Particle Therapy: Performance Criteria from the User Point of View (Invited Paper)** — radiation, ion, photon, target — 226

- **E. Pedroni**
  PSI, Villigen, Switzerland

VI-02 **Current and Potential Clinical Indications of Proton Irradiation (Invited Paper)** — photon, controls, radiation, site — 234

- **A.F. Thornton**, H.D. Suit
  Harvard Medical School, Boston, Massachusetts, USA

VI-04 **Progress Report on the IBA-SHI Proton Therapy System** — extraction, scattering, cyclotron, emittance — 244

- **Y. Jongen**, W. Beeckman, J.P. Dufour, A. Laisné, H. Marie, R. Verbruggen
  Ion Beam Applications, Louvain-la-Neuve, Belgium
- M. Sano, S. Satoh, N. Takahashi, T. Takayama
  Sumitomo Heavy Industries, Ehime, Japan

VI-05 **Recent Activities of the Cyclotron Laboratory in Nice** — cyclotron, ion, synchrotron, light-ion — 248

- **P. Mandrillon**, N. Brassart, P. Chauvel, A. Courdi, F. Farley, N. Fietier, J. Herault, J.Y. Tang

Centre Antoine Lacassagne, Nice, France

VI-07	**Design Consideration of Neutron Therapy Facility Utilizing Existing Cyclotron**	target, neutron, cyclotron, controls	255

- **H. Chang**, X. Cui, J. Wei, J. Zhang, K. Xie
  Institute of Nuclear Research, Shanghai, People's Republic of China

VI-08	**A Proton Therapy Facility Plan**	cyclotron, synchrotron, radiation, electron	258

- **S. Fukumoto**, Y. Hayakawa, T. Inada, A. Maruhashi, M. Sato, J. Tada, Y. Takada, H. Tsuji, H. Tsujii
  University of Tsukuba, Ibaraki, Japan
- K. Endo, Y. Irie, K. Muto
  KEK, Ibaraki, Japan

VII-01	**Recent Commissioning Results at Celsius (Invited Paper)**	electron, ion, target, injection	266

- **D. Reistad**, T. Bergmark, C. Ekström, C.-J. Fridén, K. Gajewski, L. Hermansson, P. Jahnke, A. Johansson, O. Johansson, T. Lofnes, G. Norman, R. Wedberg, L. Westerberg, J. Zlomanczuk
  Uppsala University, Uppsala, Sweden
- M.A. Raadu, M. Sedlacek
  Royal Institute of Technology, Stockholm, Sweden

VII-02	**Beam Diagnosis for Unmeasurably Cold Beams (Invited Paper)**	space-charge, electron, diagnostics, emittance	274

- **T.J.P. Ellison**
  Indiana University, Bloomington, Indiana, USA

VIII-05	**Status of the TRIUMF Optically-Pumped Polarized H^- Ion Source**	polarization, laser, ion, TRIUMF	322

- **C.D.P. Levy**, K. Jayamanna, M. McDonald, R. Ruegg, P.W. Schmor
  TRIUMF, Vancouver, Canada
- A.N. Zelenskii
  Institute of Nuclear Research, Russian Academy of Sciences, Moscow, Russia

VIII-13	**Recent Development of Internal H^-/D^- Source for Compact Cyclotrons**	cyclotron, ion, extraction, plasma	352

- **T.Y.T. Kuo**
  TRIUMF, Vancouver, Canada
- G.O. Hendry

Cyclotron Inc., Napa, California, USA

VIII-15	**Progress with the NAC Injector Cyclotron for Heavy and Polarized Ions**	ion, cyclotron, heavy-ion, diagnostics	361

- **Z.B. du Toit**, S.J. Burger, P.J. Celliers, J.G. de Villiers, H.N. Jungwirth, A. Müller, P.F. Rohwer, D.M. van Rooyen
  National Accelerator Centre, Faure, Republic of South Africa

IXA-10	**Increase of Beam Intensity**	injection, resonance, synchrotron, cyclotron	409

- **L.A. Sarkisyan**, A.L. Sarkisyan
  Moscow Institute-Internate, Moscow, Russia

IXA-11	**Developments in RELAX3D, a 2D/3D Laplace and Poisson Equation Solver**	TRIUMF, cyclotron, electron, simulation	411

- **H. Houtman**, F.W. Jones, C.J. Kost
  TRIUMF, Vancouver, Canada

IXB-02	**Beam Studies of Injection to Extraction System for JAERI AVF Cyclotron**	cyclotron, injection, extraction, JAERI	423

- **M. Fukuda**, T. Agematsu, K. Arakawa, I. Ishibori, T. Karasawa, Y. Nakamura, T. Nara, S. Okumura, W. Yokota
  JAERI, Gunma, Japan

IXD-02	**High-Sensitive Ionization Detectors of Transverse Distribution of Accelerated Particles Beam**	ion, cyclotron, controls, electron	473

- **V.G. Mikhailov**, V.A. Rezvov, A.A. Roshchin, V.I. Sklyarenko, L.I. Iudin
  Kurchatov Institute, Moscow, Russia

IXD-07	**Beam Diagnostics in the RCNP Ring Cyclotron**	cyclotron, injection, cavity, acceleration	491

- **T. Itahashi**, T. Saito, I. Miura
  Osaka University, Osaka, Japan
- S. Ichida
  Sumitomo Heavy Industries, Ehime, Japan

XA-06	**A Modified RF System of JAERI AVF Cyclotron**	cavity, cyclotron, ion, controls	526

- **Y. Kumata**, Y. Fukumoto
  Sumitomo Heavy Industries, Ehime, Japan
- K. Arakawa, M. Fukuda, T. Karasawa
  JAERI, Gunma, Japan
- A. Shimizu
  Osaka University, Osaka, Japan

XA-09	**Initial Operation of the RF System for the RCNP Ring Cyclotron** • **T. Saito**, I. Miura, A. Shimizu, M. Uraki Osaka University, Osaka, Japan	cavity, acceleration, cyclotron, coupling	538
XA-13	**The RF System of the Gustaf Werner Cyclotron/Synchrocyclotron** • **B. Lundström**, B. Holmgren Uppsala University, Uppsala, Sweden	controls, cyclotron, synchro-cyclotron, vacuum	553
XB-03	**Sector Magnet of the RCNP Ring Cyclotron and the Isochronization** • **K. Hosono**, M. Kibayashi, I. Miura Osaka University, Osaka, Japan	cyclotron, extraction, injection, acceleration	565
XII-01	**The Superconducting Separated-Orbit Cyclotron Tritron (Invited Paper)** • **U. Trinks** TU München, Garching, Germany	cavity, injection, cyclotron, focusing	693
XII-04	**A New Design Proposal for a 200 MeV Superconducting Ring-Cyclotron Magnet** • **H.N. Jungwirth**, J.G. de Villiers National Accelerator Centre, Faure, Republic of South Africa	cyclotron, extraction, focusing	709
XIII-02	**A Conceptual Design for a Primary Cyclotron for the ISL Radioactive Beam Project** • **D.J. Clark** LBL, Berkeley, California, USA	extraction, cyclotron, ion, acceleration	721
XIII-08	**Research and Development Studies with Radioactive Beams at TRIUMF** • **J.M. D'Auria**, M. Dombsky Simon Fraser University, Burnaby, BC, Canada • L. Buchmann, H. Sprenger, J.S. Vincent TRIUMF, Vancouver, Canada • J. King University of Toronto, Toronto, Ontario, Canada • P. McNeely, G. Roy University of Alberta, Edmonton, Alberta, Canada	target, TRIUMF, ISAC, kaon	745
XIV-04	**Conference Summary (Invited Paper)**	cyclotron, ion, ECR, electron	758

- **D.J. Clark**
  LBL, Berkeley, California, USA

A B C D E F H I J K L M N O P Q R S T V

quadrupole

Paper	Title	Other Keywords	Page
VII-03	**COSY-Jülich - A Synchrotron and Storage Ring for Medium Energy Physics** • **R. Maier**, U. Pfister FZJ, Jülich, Germany	COSY, injection, dipole, extraction	282
IXD-04	**Emittance Measurements in the HIRFL Beam Line** • **H. Zhao**, Z. Shen, B.W. Wei Institute of Modern Physics, Lanzhou, People's Republic of China	emittance, linac, coupling, optical-matching	479
XC-07	**Design of Passive Magnetic Channels** • **G. Bellomo** INFN/LASA, Segrate, Italy	multipole, focusing, dipole, cyclotron	592
XD-02	**Beam Transport System for the IUCF High Intensity Polarized Ion Source** • **W.P. Jones**, M.S. Ball, J.C. Collins, D. DuPlantis, T.J.P. Ellison, D.L. Friesel, B. Hamilton, J.W. Hicks, P. Schwandt Indiana University, Bloomington, Indiana, USA	cyclotron, bunching, dipole, diagnostics	609
XD-03	**Superconducting Focussing Channel for the AGOR Cyclotron** • **H.W. Schreuder**, P. Blache, C. Commeaux, S. Gustafsson, A. Lafoux, M. Mormiche, R. Panvier IPN, Orsay, France	AGOR, shielding, dipole, cyclotron	612
XIII-04	**The PIAFE Project at Grenoble: Beam Transport and Acceleration** • **J.L. Belmont**, J.F. Bruandet, J.M. de Conto, M. Fruneau, G. Gimond, K. Golovanivsky, E. Liatard, J.M. Loiseaux, H. Nifenecker, A. Savalle, B. Vignon Université Joseph Fourier, Grenoble, France • P. Briand CEN-Grenoble, Grenoble, France	ion, cyclotron, ECRIS, extraction	729

A B C D E F H I J K L M N O P Q R S T V

radiation

Paper	Title	Other Keywords	Page
II-02	**The Operation of Cyclotrons Used for Radiopharmaceutical Production** • **T. Grey-Morgan**, Cyclotron Isotopes Manufacturing, Buckinghamshire, England • R.E. Hubbard, Medi + Physics Inc., Arlington Heights, Illinois, USA	cyclotron, target, controls, isotope-production	115
IV-01	**Material Research with Beams at Cyclotron Energies (Invited Paper)** • **K. Ziegler**, HMI, Berlin, Germany	ion, cyclotron, proton, heavy-ion	149
IV-03	**The Use of Heavy Ion Cyclotrons of the Flerov Laboratory of Nuclear Reactions in Condensed Matter Investigations** • **R.Ts. Oganessian**, A.Yu. Didyk, JINR, Dubna, Russia	ion, heavy-ion, neutron, electron	162
IV-05	**Radionuclide Technique in Mechanical Engineering (RTM)** • **P. Fehsenfeld**, A. Kleinrahm, FZK, Karlsruhe, Germany • V. Novikov, Kurchatov Institute, Moscow, Russia	injection, ion, cyclotron, diagnostics	171
IV-09	**A Simple Method for Estimating Activation Sensitivities of Different Elements / Isotopes with Cyclotron Produced Neutrons** • **M.A. Chaudhri**, Austin Hospital & University of Melbourne, Melbourne, Australia	neutron, target, cyclotron, BNL	187
IV-11	**External High Current Targetry for Radioisotope Production** • **N.R. Stevenson**, W.Z. Gelbart, TRIUMF, Vancouver, Canada	target, TRIUMF, cyclotron, vacuum	196
IV-12	**A Remotely Controlled Robotic Vehicle for Work Within Radioactive Environments** • **N.R. Stevenson**, P. Bloemhard, M. Brigham, J. Ko, C. LaForge,	target, controls, cyclotron, TRIUMF	198

J. Orzechowski, E. Pattyn, T. Rattray
TRIUMF, Vancouver, Canada

V-01	**The New Molecular Medicine**	accumulation, site, ion, monitoring	202

- **H.N. Wagner, Jr.**
  The Johns Hopkins University, Baltimore, Maryland, USA

VI-01	**Accelerators for Charged Particle Therapy: Performance Criteria from the User Point of View (Invited Paper)**	proton, ion, photon, target	226

- **E. Pedroni**
  PSI, Villigen, Switzerland

VI-02	**Current and Potential Clinical Indications of Proton Irradiation (Invited Paper)**	proton, photon, controls, site	234

- **A.F. Thornton**, H.D. Suit
  Harvard Medical School, Boston, Massachusetts, USA

VI-03	**Pion Therapy for Cancer - What are the Prospects?**	photon, TRIUMF, controls, background	242

- **G.B. Goodman**
  University of British Columbia, Vancouver, Canada

VI-06	**Health Physics Data Acquisition System at the National Medical Cyclotron**	cyclotron, monitoring, target, neutron	252

- **B.N. Mukherjee**
  ANSTO, Menai, NSW, Australia
- D.W. Arnott
  National Medical Cyclotron, Camperdown, NSW, Australia

VI-08	**A Proton Therapy Facility Plan**	proton, cyclotron, synchrotron, electron	258

- **S. Fukumoto**, Y. Hayakawa, T. Inada, A. Maruhashi, M. Sato, J. Tada, Y. Takada, H. Tsuji, H. Tsujii
  University of Tsukuba, Ibaraki, Japan
- K. Endo, Y. Irie, K. Muto
  KEK, Ibaraki, Japan

VI-09	**Continued Operation of the Seattle Clinical Cyclotron Facility**	neutron, cyclotron, controls, target	262

- **R. Risler**, S. Brossard, J. Jacky, I. Kalet, P. Wootton, F. Ziai
  University of Washington, Seattle, Washington, USA

XC-05	**The AGOR Superconducting Extraction Channel EMC2**	cyclotron, AGOR, background,	585

		extraction	

- **K. Pieterman**, J.A.M. Dam
  Cryocon B.V., Amersfoort, The Netherlands
- H.J.H. ten Kate
  TU Twente, Enschede, The Netherlands
- S. Gustafsson
  IPN, Orsay, France

XI-14	**Formal Specifications for a Cyclotron Control System**	controls, cyclotron, neutron, status	689

- **J. Jacky**, R. Risler
  University of Washington, Seattle, Washington, USA

A B C D E F H I J K L M N O P Q R S T V

radioactivity

Paper	Title	Other Keywords	Page
IV-06	**A P.E.T. Study of Proton Induced Radioactivity in Different Materials** • **J.M. Schippers** Kernfysisch Versneller Instituut, Groningen, The Netherlands • A.M.J. Paans University Hospital, Groningen, The Netherlands	target, proton, positron, cyclotron	175
V-07	**Dual Chemical Station for Cyclotron Produced ^{18}F** • **M.L. Mallory**, G. Grimmett, R. Tilbury, D. Yang The University of Texas, Houston, Texas, USA	cyclotron, diagnostics, target, controls	222

A B C D E F H I J K L M N O P Q R S T V

resonance

Paper	Title	Other Keywords	Page
I-08	**Parameters, Present State and Application Perspectives of the U-250 Cyclotron** • **A.I. Muminov** Institute of Nuclear Physics, Tashkent, Republic of Uzbekistan • M.F. Vorogushin D.V. Efremov Scientific Research Institute of Electrophysical Apparatus, St. Petersburg, Russia	ion, cyclotron, vacuum, heavy-ion	50
VIII-10	**Spin Dynamics and Polarized Ion Sources on Isochronous Cyclotron U-240** • **N.I. Zaika** Institute for Nuclear Research, Kiev, Ukraine	ion, cyclotron, polarization, acceleration	340
IXA-01	**Advantage of Using Differential Algebra and Lie Algebra in the Orbit Dynamics of Cyclotrons (Invited Paper)** • **W.G. Davies** Atomic Energy of Canada, Chalk River, Ontario, USA	cyclotron, octupole, sextupole, closed-orbit	372
IXA-02	**The Influence of Magnetic Field Imperfections on the Beam Quality in an H^- Cyclotron** • **W.J.G.M. Kleeven**, H.L. Hagedoorn Eindhoven University of Technology, Eindhoven, The Netherlands • B.F. Milton, G. Dutto TRIUMF, Vancouver, Canada	emittance, cyclotron, extraction, betatron	380
IXA-08	**Evaluation of Third-Harmonic Voltage Flattopping for a Superconducting Cyclotron** • **M.M. Gordon**, D. Jeon NSCL, East Lansing, Michigan, USA	cyclotron, extraction, ion, TRIUMF	404
IXA-09	**Crossing of Resonances** • **L.A. Sarkisyan**, A.L. Sarkisyan Moscow Institute-Internate, Moscow, Russia	cyclotron, synchrotron, extraction	408
IXA-		injection,	409

10	**Increase of Beam Intensity**	synchrotron, cyclotron, proton	

- **L.A. Sarkisyan**, A.L. Sarkisyan
  Moscow Institute-Internate, Moscow, Russia

IXA-12	**Beam Quality Investigations for H⁻ Extraction at TRIUMF**	emittance, extraction, cyclotron, simulation	415

- **R.E. Laxdal**, G.H. Mackenzie, J.B. Pearson, L. Root
  TRIUMF, Vancouver, Canada

IXB-05	**Internal Beam Dynamics Studies with a TV Probe**	cyclotron, simulation, controls, ion	435

- **F. Marti**, S. Snyder
  NSCL, East Lansing, Michigan, USA

XA-07	**Multi-Point Cavity Excitation**	cavity, coupling, impedance, simulation	530

- **E. Zaplatin**
  FZJ, Jülich, Germany

A B C D E F H I J K L M N O P Q R S T V

rf-amplifier

Paper	Title	Other Keywords	Page
IXD-05	**High Sensitivity Electronic System for the Phase Probes of the LNS/MILANO Superconducting Cyclotron**	cyclotron, controls, ion, injection	483

- **A. Bosotti**, D. Corti, C. Pagani, G. Varisco, F. Zibra
  INFN/LASA, Segrate, Italy
- M. Di Giacomo
  INFN/LNS, Catania, Italy

A B C D E F H I J K L M N O P Q R S T V

rfq

Paper	Title	Other Keywords	Page
XIII-09	**Post-Accelerator Studies for the ISOL Facility at TRIUMF**	solenoid, focusing, linac, ion	749

- **L. Root**, H.R. Schneider, J.S. Fraser
  TRIUMF, Vancouver, Canada

A B C D E F H I J K L M N O P Q R S T V

scattering

Paper	Title	Other Keywords	Page
VI-04	**Progress Report on the IBA-SHI Proton Therapy System**	proton, extraction, cyclotron, emittance	244

- **Y. Jongen**, W. Beeckman, J.P. Dufour, A. Laisné, H. Marie, R. Verbruggen
  Ion Beam Applications, Louvain-la-Neuve, Belgium
- M. Sano, S. Satoh, N. Takahashi, T. Takayama
  Sumitomo Heavy Industries, Ehime, Japan

A B C D E F H I J K L M N O P Q R S T V

septum

Paper	Title	Other Keywords	Page
XC-03	**Model Study of an Electrostatic Deflector Configuration with an Intermediate Electrode**	high-voltage, cyclotron, vacuum, power-supply	577

- **C.R. Hoffmann**, J.F. Mouris
  Atomic Energy of Canada, Chalk River, Ontario, Canada

A B C D E F H I J K L M N O P Q R S T V

sextupole

Paper	Title	Other Keywords	Page
VIII-02	**Performance of the LBL AECR Source at Various Frequencies** • **Z.Q. Xie**, D. Collins, S.A. Lundgren, C.M. Lyneis LBL, Berkeley, California, USA	ECR, ion, plasma, ion-source	308
VIII-07	**Performance and Status of the IUCF High Intensity Polarized Ion Source** • **V. Derenchuk**, R. Brown, T.J.P. Ellison, D.L. Friesel, J.W. Hicks, D. Jenner, A. Pei, H. Petri, P. Schwandt, J. Sowinski, M. Wedekind Indiana University, Bloomington, Indiana, USA	ECR, ion, ion-source, extraction	330
IXA-01	**Advantage of Using Differential Algebra and Lie Algebra in the Orbit Dynamics of Cyclotrons (Invited Paper)** • **W.G. Davies** Atomic Energy of Canada, Chalk River, Ontario, USA	resonance, cyclotron, octupole, closed-orbit	372
IXA-03	**Emittance Growth in Nonlinear Beam Guiding and Focusing Elements** • **W.J.G.M. Kleeven**, J.I.M. Botman, J.L. Delhez, H.L. Hagedoorn, C.J. Timmermans, G.A. Webers Eindhoven University of Technology, Eindhoven, The Netherlands	emittance, octupole, dipole, focusing	384
XD-01	**Some Perspectives in the Beam Transport and Analyzing System Design for the U-250 Cyclotron** • **L.E. Korolev** D.V. Efremov Scientific Research Institute of Electrophysical Apparatus, St. Petersburg, Russia	cyclotron, beam-transport, target	606

A B C D E F H I J K L M N O P Q R S T V

shielding

Paper	Title	Other Keywords	Page
I-07	**Thoughts on Decommissioning the CERN Synchro Cyclotron**	vacuum, CERN, plasma, synchro-cyclotron	47
	• **G. Spinney** CERN, Geneva, Switzerland		
XC-09	**Results from the Deflector Test Stand at Texas A&M University**	high-voltage, power-supply, cyclotron, monitoring	602
	• **D.P. May**, G. Derrig, W. Dewees, P. Smelser, D. Tran, R.C. Rogers Texas A&M University, College Station, Texas, USA		
XD-03	**Superconducting Focussing Channel for the AGOR Cyclotron**	quadrupole, AGOR, dipole, cyclotron	612
	• **H.W. Schreuder**, P. Blache, C. Commeaux, S. Gustafsson, A. Lafoux, M. Mormiche, R. Panvier IPN, Orsay, France		

simulation

Paper	Title	Other Keywords	Page
I-05	**The Commissioning of PSI Injector 2 for High Intensity, High Quality Beams**	space-charge, acceleration, cyclotron, bunching	36
	• **J. Stetson** NSCL, East Lansing, Michigan, USA • S. Adam, M. Humbel, W. Joho, Th. Stammbach PSI, Villigen, Switzerland		
IXA-11	**Developments in RELAX3D, a 2D/3D Laplace and Poisson Equation Solver**	TRIUMF, cyclotron, electron, proton	411
	• **H. Houtman**, F.W. Jones, C.J. Kost TRIUMF, Vancouver, Canada		
IXA-12	**Beam Quality Investigations for H^- Extraction at TRIUMF**	emittance, extraction, cyclotron, resonance	415
	• **R.E. Laxdal**, G.H. Mackenzie, J.B. Pearson, L. Root TRIUMF, Vancouver, Canada		
IXB-05	**Internal Beam Dynamics Studies with a TV Probe**	resonance, cyclotron, controls, ion	435
	• **F. Marti**, S. Snyder NSCL, East Lansing, Michigan, USA		
IXB-07	**Beam Test Results Using the Auxiliary Accelerating Cavity**	cavity, cyclotron, extraction, TRIUMF	442
	• **R.E. Laxdal**, G.H. Mackenzie, L. Root TRIUMF, Vancouver, Canada		
IXC-05	**Numerical Studies for Suppression of Vertical Oscillations in the K1200 Cyclotron**	cyclotron, emittance	461
	• **K. Joh**, F. Marti NSCL, East Lansing, Michigan, USA • J.A. Nolen ANL, Argonne, Illinois, USA		
XA-07	**Multi-Point Cavity Excitation**	cavity, coupling, resonance, impedance	530
	• **E. Zaplatin**		

FZJ, Jülich, Germany

XC-06	**Material Consideration for Magnetic Channels**	extraction, synchro-cyclotron, cyclotron	589

- **J. Sura**, L. Calabretta, G. Di Biasi, P. Gmaj, D. Rifuggiato
  INFN/LNS, Catania, Italy

A B C D E F H I J K L M N O P Q R S T V

site

Paper	Title	Other Keywords	Page
I-06	**AGOR: Recent Achievements (Invited Paper)** • **H.W. Schreuder** IPN, Orsay, France	AGOR, cyclotron, extraction, vacuum	40
V-01	**The New Molecular Medicine** • **H.N. Wagner, Jr.** The Johns Hopkins University, Baltimore, Maryland, USA	radiation, accumulation, ion, monitoring	202
VI-02	**Current and Potential Clinical Indications of Proton Irradiation (Invited Paper)** • **A.F. Thornton**, H.D. Suit Harvard Medical School, Boston, Massachusetts, USA	proton, photon, controls, radiation	234
XC-08	**Deflector Development for the K1200 Cyclotron** • **T.Y.T. Kuo** TRIUMF, Vancouver, Canada • J.A. Nolen ANL, Argonne, Illinois, USA	cathode, electron, cyclotron, ion	596

solenoid

Paper	Title	Other Keywords	Page
IXA-05	**Ion Optics in the Jyväskylä K130 Cyclotron** • **P. Heikkinen**, M. Rinta-Nikkola University of Jyväskylä, Jyväskylä, Finland	cyclotron, ion, injection, extraction	392
XD-06	**Beamlines for a Second Injector Cyclotron at NAC** • **J.C. Cornell**, J.L. Conradie, D.T. Fourie National Accelerator Centre, Faure, Republic of South Africa	ion, dipole, cyclotron, ion-source	621
XIII-09	**Post-Accelerator Studies for the ISOL Facility at TRIUMF** • **L. Root**, H.R. Schneider, J.S. Fraser TRIUMF, Vancouver, Canada	rfq, focusing, linac, ion	749

A B C D E F H I J K L M N O P Q R S T V

space-charge

Paper	Title	Other Keywords	Page
I-04	**Experience with the High Current Operation of the PSI Cyclotron Facility (Invited Paper)**	cyclotron, beam-losses, extraction, injection	28
	• **Th. Stammbach** PSI, Villigen, Switzerland		
I-05	**The Commissioning of PSI Injector 2 for High Intensity, High Quality Beams**	acceleration, simulation, cyclotron, bunching	36
	• **J. Stetson** NSCL, East Lansing, Michigan, USA • S. Adam, M. Humbel, W. Joho, Th. Stammbach PSI, Villigen, Switzerland		
VII-02	**Beam Diagnosis for Unmeasurably Cold Beams (Invited Paper)**	electron, proton, diagnostics, emittance	274
	• **T.J.P. Ellison** Indiana University, Bloomington, Indiana, USA		
IXC-04	**Non-Linear Beam Transport Effects in Highly Charged Positive Ion Beams Extracted From ECR Ion Sources**	emittance, ion, ECR, ion-source	457
	• **T.A. Antaya** NSCL, East Lansing, Michigan, USA • Z.Q. Xie LBL, Berkeley, California, USA		

A B C D E F H I J K L M N O P Q R S T V

status

Paper	Title	Other Keywords	Page
XI-03	**An Operator Assistance System for the AVF Cyclotron** • **T. Okamura**, T. Murakami Sumitomo Heavy Industries Systems Engineering Laboratory, Tokyo, Japan • T. Tachikawa Sumitomo Heavy Industries, Ehime, Japan • T. Agematsu, S. Okumura, K. Arakawa JAERI, Gunma, Japan	cyclotron, injection, extraction, survey	644
XI-04	**Control System for JAERI AVF Cyclotron** • **S. Okumura**, T. Agematsu, K. Arakawa, M. Fukuda, I. Ishibori, T. Kamiya, Y. Nakamura, T. Nara, W. Yokota JAERI, Gunma, Japan • K. Hoshika, K. Iso, M. Maruyama, M. Tachibana Sumitomo Heavy Industries, Ehime, Japan	controls, cyclotron, JAERI, injection	648
XI-05	**Automatic Control System of Magnetic Separator for Kurchatov IAE Cyclotron** • **N.I. Venikov**, V. Buranov, O. Gotovtsev, L.I. Iudin, P.Yu. Komissarov, V.N. Unezhev Kurchatov Institute, Moscow, Russia	controls, cyclotron, ion, power-supply	652
XI-06	**The New Distributed Control System of the NAC** • **H.F. Weehuizen**, R.K. Fisch, E.J.S. Franklin, M.E. Hogan, I.H. Kohler, J.P. Rogers, P.J. Theron National Accelerator Centre, Faure, Republic of South Africa	controls, instrumentation, cyclotron, light-ion	656
XI-09	**Two Dimensional Scans with Adaptive Domain Control** • **S. Adam**, A.C. Mezger PSI, Villigen, Switzerland	controls, beam-losses, extraction, interlocks	668
XI-10	**Construction and System Tuning of Control System for the RCNP Ring Cyclotron and Beam Lines** • **T. Yamazaki**, A. Ando, K. Hosono, T. Itahashi, M. Kibayashi,	controls, cyclotron, power-supply, injection	672

I. Miura, K. Nagayama, H. Ogata, T. Saito, A. Shimizu,
K. Tamura, M. Uraki
Osaka University, Osaka, Japan
- K. Aoki, Y. Kimura, M. Maruyama, M. Tachibana, S. Yamada
Sumitomo Heavy Industries, Ehime, Japan
- K. Kodaira
Sumitomo Heavy Industries Systems Engineering Laboratory,
Tokyo, Japan

XI-14	**Formal Specifications for a Cyclotron Control System**	controls, cyclotron, neutron, radiation	689

- **J. Jacky**, R. Risler
University of Washington, Seattle, Washington, USA

storage-ring

Paper	Title	Other Keywords	Page
VII-07	**Superthin Internal Target for Storage Rings** • **V. Pugatch**, A. Glushko, G. Pitatelev, G. Sivtsov Institute for Nuclear Research, Kiev, Ukraine • S. Popov, D. Toporkov, B. Voitsechovsky Institute for Nuclear Physics, Novosibirsk, Russia	target, micro-particles, electron, laser	297
XIV-03	**Physics with Storage Rings (Invited Paper)** • **R.E. Pollock** Indiana University, Bloomington, Indiana, USA	target, electron, ion, luminosity	753

A B C D E F H I J K L M N O P Q R S T V

survey

Paper	Title	Other Keywords	Page
XI-03	**An Operator Assistance System for the AVF Cyclotron**	cyclotron, injection, extraction, status	644

- **T. Okamura**, T. Murakami
  Sumitomo Heavy Industries Systems Engineering Laboratory, Tokyo, Japan
- T. Tachikawa
  Sumitomo Heavy Industries, Ehime, Japan
- T. Agematsu, S. Okumura, K. Arakawa
  JAERI, Gunma, Japan

A B C D E F H I J K L M N O P Q R S T V

synchro-cyclotron

Paper	Title	Other Keywords	Page
I-07	**Thoughts on Decommissioning the CERN Synchro Cyclotron** • **G. Spinney** CERN, Geneva, Switzerland	vacuum, CERN, shielding, plasma	47
I-10	**Gatchina Isochronous Cyclotron** • **N.K. Abrosimov**, S.A. Artamonov, P.V. Chervyakov, S.P. Dmitriev, V.A. Eliseev, V.P. Fominenko, E.M. Ivanov, G.F. Mikheev, Yu.T. Mironov, A.S. Pokrovskii, G.A. Riabov, V.A. Smolin, G.L. Sokolov, V.A. Volchenkov, A.A. Vorobiev Petersburg Nuclear Physics Institute, Gatchina, Russia • P.V. Bogdanov, B.D. Ershov, V.S. Kuligin, V.N. Moshkin, V.G. Mudrolyubov, Yu.I. Stogov, A.P. Strokach D.V. Efremov Scientific Research Institute of Electrophysical Apparatus, St. Petersburg, Russia	cyclotron, ion, vacuum, injection	58
XA-13	**The RF System of the Gustaf Werner Cyclotron/Synchrocyclotron** • **B. Lundström**, B. Holmgren Uppsala University, Uppsala, Sweden	controls, cyclotron, proton, vacuum	553
XC-06	**Material Consideration for Magnetic Channels** • **J. Sura**, L. Calabretta, G. Di Biasi, P. Gmaj, D. Rifuggiato INFN/LNS, Catania, Italy	extraction, simulation, cyclotron	589

A B C D E F H I J K L M N O P Q R S T V

synchrotron

Paper	Title	Other Keywords	Page
VI-05	**Recent Activities of the Cyclotron Laboratory in Nice** • **P. Mandrillon**, N. Brassart, P. Chauvel, A. Courdi, F. Farley, N. Fietier, J. Herault, J.Y. Tang Centre Antoine Lacassagne, Nice, France	cyclotron, ion, proton, light-ion	248
VI-08	**A Proton Therapy Facility Plan** • **S. Fukumoto**, Y. Hayakawa, T. Inada, A. Maruhashi, M. Sato, J. Tada, Y. Takada, H. Tsuji, H. Tsujii University of Tsukuba, Ibaraki, Japan • K. Endo, Y. Irie, K. Muto KEK, Ibaraki, Japan	proton, cyclotron, radiation, electron	258
VII-04	**Study of Beam Dynamics at Cooler Synchrotron TARN-II** • **S. Watanabe**, Y. Arakaki, K. Chida, T. Katayama, M. Tomizawa, T. Watanabe, M. Yoshizawa University of Tokyo, Tanashi-shi, Tokyo, Japan • K. Noda, M. Kanazawa NIRS, Chiba, Japan	acceleration, ion, injection, cyclotron	286
IXA-09	**Crossing of Resonances** • **L.A. Sarkisyan**, A.L. Sarkisyan Moscow Institute-Internate, Moscow, Russia	resonance, cyclotron, extraction	408
IXA-10	**Increase of Beam Intensity** • **L.A. Sarkisyan**, A.L. Sarkisyan Moscow Institute-Internate, Moscow, Russia	injection, resonance, cyclotron, proton	409
XA-05	**Low Frequency RF System for the Indiana University Cooler Ring** • **X. Pei**, S. Anderson, V. Derenchuk, G. East, D.L. Friesel, D. Jenner, D. McCammon, T. Sloan Indiana University, Bloomington, Indiana, USA	cavity, kicker, injection, beam-losses	523
XII-02	**Study of an FFAG Synchrocyclotron for a Pulsed Neutron**	injection, cavity,	701

	Source	neutron, linac	

- **S.A. Martin**, E. Zaplatin
  FZJ, Jülich, Germany
- P.F. Meads, Jr.
  Private Address, Oakland, California, USA
- G. Wüstefeld
  BESSY, Berlin, Germany
- K. Ziegler
  HMI, Berlin, Germany

XV-01	**Proper and Improper Accelerators - In Praise of Cyclotrons and Their Builders**	cyclotron, TRIUMF, ion, controls	765

- **M.K. Craddock**
  University of British Columbia, Vancouver, Canada

A B C D E F H I J K L M N O P Q R S T V

tandem-accelerator

Paper	Title	Other Keywords	Page
XIII-07	**The ORNL Radioactive Ion Beam Project with the ORIC Accelerator**	ion, target, ion-source, heavy-ion	741

- **D.K. Olsen**, G.D. Alton, C. Baktash, D.T. Dowling, J.D. Garrett, D.L. Haynes, C.M. Jones, R.C. Juras, S.N. Lane, I.Y. Lee, M.J. Meigs, G.D. Mills, S.W. Mosko, B.A. Tatum, K.S. Toth
  ORNL, Oak Ridge, Tennessee, USA
- H.K. Carter, J. Kormicki
  Associated Universities Oak Ridge, Oak Ridge, Tennessee, USA

A B C D E F H I J K L M N O P Q R S T V

target

Paper	Title	Other Keywords	Page
I-16	**Status Report of Cyclone** • **M. Loiselet**, N. Postiau, G. Ryckewaert Université Catholique de Louvain, Louvain-la-Neuve, Belgium	cyclotron, ion, neutron, beam-transport	82
I-17	**Performance of the K1200 Cyclotron at MSU** • **P. Miller**, T.A. Antaya, F. Marti, D. Poe, B. Sherrill, J. Stetson, J. Winger NSCL, East Lansing, Michigan, USA • J.A. Nolen ANL, Argonne, Illinois, USA	ion, cyclotron, emittance, power-supply	86
II-01	**Commercially Available Compact Cyclotrons for Isotope Production (Invited Paper)** • **V. Bechtold** FZK, Karlsruhe, Germany	cyclotron, ion, ion-source, proton	110
II-02	**The Operation of Cyclotrons Used for Radiopharmaceutical Production** • **T. Grey-Morgan** Cyclotron Isotopes Manufacturing, Buckinghamshire, England • R.E. Hubbard Medi + Physics Inc., Arlington Heights, Illinois, USA	cyclotron, controls, radiation, isotope-production	115
II-04	**20 MeV Cyclotron for Isotope Production** • **A. Glazov**, Ju. Alenitskiy, A. Chesnov, S. Chesnova, V. Kochkin, D. Novikov, E. Samsonov, M. Semenov, A. Vasilenko, E. Zaplatin, N. Zaplatin JINR, Dubna, Russia • I. Gulamov, O. Iljasov, A. Rykov Institute of Nuclear Physics, Tashkent, Republic of Uzbekistan	cyclotron, acceleration, isotope-production, proton	123
II-06	**A Newly Developed Compact Cyclotron for Neutron Therapy and Positron Nuclear Medicine**	neutron, cyclotron, positron, proton	129

K. Ito, T. Ishigaki, S. Itoh, Y. Kasugai, T. Kato, T. Misawa, M. Nishino, M. Osakabe, T. Ota, S. Sakuma, M. Tadokoro, H. Yamamoto
Nagoya University, Nagoya, Japan
- Y. Toda, Y. Yamamoto
Japan Steel Works Ltd., Tokyo, Japan

II-07 **Performance of the Harper Hospital Cyclotron; Effect of Pulsed Radio Frequency** — cyclotron, neutron, ion, controls — 133

- **H.G. Blosser**, J. Vincent
NSCL, East Lansing, Michigan, USA
- R. Maughan
Harper Hospital, Detroit, Michigan, USA

IV-02 **A Cyclotron as a Mass Spectrometer** — cyclotron, ion, injection, coupling — 158

- **P. Bricault**, G. Auger, M. Bajard, E. Baron, D. Bibet, A. Chabert, J. Fermé, L. Gaudart, J. Joubert, M. Lewitowicz, W. Mittig, E. Plagnol, Ch. Ricaud, Y. Schutz
GANIL, Caen, France
- G. Audi
CSNSM, Orsay, France
- A. Gillibert
CEN/Saclay, Gif-sur-Yvette, France
- K. Fifield
Australian National University, Canberra , Australia

IV-04 **^{178m2}Hf and ^{237}Pu Isotopes Production on the U-200 Cyclotron** — ion, cyclotron, cathode, ion-source — 167

- **S.L. Bogomolov**, S.N. Dmitriev, Yu.P. Gangrski, G.G. Gulbekyan, S.A. Karamian, V.B. Kutner, B.N. Markov, Yu.Ts. Oganessian, N.V. Pronin, G.Ya. Starodub
JINR, Dubna, Russia

IV-06 **A P.E.T. Study of Proton Induced Radioactivity in Different Materials** — proton, positron, radioactivity, cyclotron — 175

- **J.M. Schippers**
Kernfysisch Versneller Instituut, Groningen, The Netherlands
- A.M.J. Paans
University Hospital, Groningen, The Netherlands

IV-07 **Neutron Productions from Carbon by Charged Particle Bombardment at Different Energies** — neutron, proton, background, cyclotron — 178

- **M.A. Chaudhri**
Austin Hospital & University of Melbourne, Melbourne, Australia

IV-08 **Analytical Applications of Cyclotrons in Biomedical Fields -** — cyclotron, proton, — 181

	Charged Particle Activation Analysis	neutron, ion	

- **M.A. Chaudhri**
  Austin Hospital & University of Melbourne, Melbourne, Australia

IV-09	**A Simple Method for Estimating Activation Sensitivities of Different Elements / Isotopes with Cyclotron Produced Neutrons**	neutron, cyclotron, BNL, radiation	187

- **M.A. Chaudhri**
  Austin Hospital & University of Melbourne, Melbourne, Australia

IV-10	**A Proposal for an Intense Cyclotron-Based Thermal Neutron Source**	neutron, cyclotron, proton, extraction	191

- **S. Tazawa**
  Sumitomo Heavy Industries, Toyo-shi, Toyo-shi, Japan
- W.L. Whittemore
  General Atomics, San Diego, California, USA

IV-11	**External High Current Targetry for Radioisotope Production**	TRIUMF, cyclotron, radiation, vacuum	196

- **N.R. Stevenson**, W.Z. Gelbart
  TRIUMF, Vancouver, Canada

IV-12	**A Remotely Controlled Robotic Vehicle for Work Within Radioactive Environments**	controls, cyclotron, radiation, TRIUMF	198

- **N.R. Stevenson**, P. Bloemhard, M. Brigham, J. Ko, C. LaForge, J. Orzechowski, E. Pattyn, T. Rattray
  TRIUMF, Vancouver, Canada

V-02	**The Production of Radionuclides for the Biosciences (Invited Paper)**	cyclotron, ion, proton, extraction	206

- **T.J. Ruth**
  TRIUMF, Vancouver, Canada

V-03	**A Facility for Radioisotope Production at TRIUMF with 70-110 MeV Protons**	controls, proton, cyclotron, TRIUMF	209

- **D.R. Pearce**, J.S. Vincent
  TRIUMF, Vancouver, Canada

V-04	**Possibility of Producing Some Radionuclides for Medicine Using JINR Accelerators**	proton, cyclotron, electron, microtron	213

- **S.N. Dmitriev**, G.G. Gulbekyan, V.A. Khalkin, R.Ts. Oganessian, L.M. Onishchenko, G.Ya. Starodub, N.G. Zaitseva
  JINR, Dubna, Russia

V-05	**Radiopharmaceutical "Thallium-201-Chloride" Production using Thallium-203 Irradiation by Helium-3 Ions**	ion, proton, cyclotron, ALICE	216

- **A.A. Arzumanov**, N.K. Hamidov, A.I. Kozin, G.I. Shychikov, S.T. Tihomirova
  Kazakhstan Academy of Sciences, Alma-Ata, Republic of Kazakhstan

V-06	**Experiences with the Cyclone 3 Oxygen 15 Generator**	cyclotron, ion, controls, ion-source	218

- **E. Conard**, J.-L. Morelle
  Ion Beam Applications, Louvain-la-Neuve, Belgium
- J.C. Clark, D.B. Mackay
  Hammersmith Hospital, London, England

V-07	**Dual Chemical Station for Cyclotron Produced ^{18}F**	cyclotron, radioactivity, diagnostics, controls	222

- **M.L. Mallory**, G. Grimmett, R. Tilbury, D. Yang
  The University of Texas, Houston, Texas, USA

VI-01	**Accelerators for Charged Particle Therapy: Performance Criteria from the User Point of View (Invited Paper)**	proton, radiation, ion, photon	226

- **E. Pedroni**
  PSI, Villigen, Switzerland

VI-06	**Health Physics Data Acquisition System at the National Medical Cyclotron**	radiation, cyclotron, monitoring, neutron	252

- **B.N. Mukherjee**
  ANSTO, Menai, NSW, Australia
- D.W. Arnott
  National Medical Cyclotron, Camperdown, NSW, Australia

VI-07	**Design Consideration of Neutron Therapy Facility Utilizing Existing Cyclotron**	neutron, cyclotron, controls, proton	255

- **H. Chang**, X. Cui, J. Wei, J. Zhang, K. Xie
  Institute of Nuclear Research, Shanghai, People's Republic of China

VI-09	**Continued Operation of the Seattle Clinical Cyclotron Facility**	neutron, cyclotron, controls, radiation	262

- **R. Risler**, S. Brossard, J. Jacky, I. Kalet, P. Wootton, F. Ziai
  University of Washington, Seattle, Washington, USA

VII-01	**Recent Commissioning Results at Celsius (Invited Paper)**	electron, ion, proton, injection	266

- **D. Reistad**, T. Bergmark, C. Ekström, C.-J. Fridén, K. Gajewski, L. Hermansson, P. Jahnke, A. Johansson, O. Johansson, T. Lofnes, G. Norman, R. Wedberg, L. Westerberg, J. Zlomanczuk
  Uppsala University, Uppsala, Sweden
- M.A. Raadu, M. Sedlacek
  Royal Institute of Technology, Stockholm, Sweden

VII-05	**Dubna Project of the Heavy Ion Storage Ring Complex K4-K10**	ion, injection, heavy-ion, cyclotron	290

- **Yu.Ts. Oganessian**, O.N. Malyshev, G.S. Popeko, A.M. Rodin, S.I. Sidorchuk, Ye.A. Sokol, S.V. Stepantsov, G.M. Ter-Akopian, V.A. Timakov
  JINR, Dubna, Russia
- V.V. Parhomchuk, A.A. Sery, V.D. Shiltsev
  Institute for Nuclear Physics, Novosibirsk, Russia
- I.N. Meshkov, Ye.M. Syresinm
  Center for Applied Physics and Technology, Lipetsk, Russia
- V.P. Belov, A.A. Makarov, Yu.P. Severgin, I.A. Shukeylo, M.N. Tarovik
  D.V. Efremov Scientific Research Institute of Electrophysical Apparatus, St. Petersburg, Russia

VII-06	**The New Project of INR (Kiev's) Storage-Accelerating Complex**	electron, ion, booster, injection	294

- **A.V. Dolinsky**, A.I. Papash, S.N. Pavlov, A.T. Rudchik, A.E. Val'Kov, I.N. Vishnevsky, A.V. Zhmendak
  Institute for Nuclear Research, Kiev, Ukraine
- V.P. Belov, A.M. Kokorin, A.A. Makarov, I.A. Schukeilo, Yu.P. Severgin
  D.V. Efremov Scientific Research Institute of Electrophysical Apparatus, St. Petersburg, Russia

VII-07	**Superthin Internal Target for Storage Rings**	micro-particles, electron, laser, storage-ring	297

- **V. Pugatch**, A. Glushko, G. Pitatelev, G. Sivtsov
  Institute for Nuclear Research, Kiev, Ukraine
- S. Popov, D. Toporkov, B. Voitsechovsky
  Institute for Nuclear Physics, Novosibirsk, Russia

IXB-01	**Cyclotron Tuning as a Rebuncher**	extraction, cyclotron, emittance, acceleration	419

- **D. Bibet**, M-H. Moscatello
  GANIL, Caen, France

XD-01	**Some Perspectives in the Beam Transport and Analyzing System Design for the U-250 Cyclotron**	cyclotron, beam-transport, sextupole	606

- **L.E. Korolev**
  D.V. Efremov Scientific Research Institute of Electrophysical Apparatus, St. Petersburg, Russia

XD-04	**The Beam-Guiding System of AGOR**	AGOR, controls, heavy-ion, diagnostics	615

- **J.M. Schippers**
  Kernfysisch Versneller Instituut, Groningen, The Netherlands

XI-12	**Application of Object Oriented Techniques in the TRIUMF Beam Line 2C Control System (Invited Paper)**	controls, kaon, TRIUMF, factory	681

- **N.A. Wilkinson**, E.A. Osberg, G.A. Ludgate
  TRIUMF, Vancouver, Canada

XIII-01	**Accelerated Radioactive Nuclear Beams: Existing and Planned Facilities (Invited Paper)**	ion, cyclotron, ISOL, heavy-ion	713

- **J.M. Nitschke**
  LBL, Berkeley, California, USA

XIII-03	**An On-Line Isotopic Separator Test Bench at GANIL**	ion, ion-source, ECR, extraction	725

- **P. Bricault**, R. Leroy, M. Lewitowicz, J.Y. Pacquet, M.G. St-Laurent, P. Sortais
  GANIL, Caen, France
- A.C. Mueller, J. Obert, J.C. Putaux
  IPN, Orsay, France
- C.F. Liang, P. Paris
  CSNSM, Orsay, France
- J.C. Steckmeyer
  LPC, Caen, France

XIII-06	**Radioactive Ion Beam Production Using the Louvain-La-Neuve Cyclotrons: Present Status and Future Developments**	cyclotron, acceleration, extraction, ECR	737

- **G. Ryckewaert**, M. Loiselet, N. Postiau
  Université Catholique de Louvain, Louvain-la-Neuve, Belgium

XIII-07	**The ORNL Radioactive Ion Beam Project with the ORIC Accelerator**	ion, ion-source, tandem-accelerator, heavy-ion	741

- **D.K. Olsen**, G.D. Alton, C. Baktash, D.T. Dowling, J.D. Garrett, D.L. Haynes, C.M. Jones, R.C. Juras, S.N. Lane, I.Y. Lee, M.J. Meigs, G.D. Mills, S.W. Mosko, B.A. Tatum, K.S. Toth
  ORNL, Oak Ridge, Tennessee, USA
- H.K. Carter, J. Kormicki

Associated Universities Oak Ridge, Oak Ridge, Tennessee, USA

XIII-08	**Research and Development Studies with Radioactive Beams at TRIUMF**	TRIUMF, ISAC, kaon, proton	745

- **J.M. D'Auria**, M. Dombsky
  Simon Fraser University, Burnaby, BC, Canada
- L. Buchmann, H. Sprenger, J.S. Vincent
  TRIUMF, Vancouver, Canada
- J. King
  University of Toronto, Toronto, Ontario, Canada
- P. McNeely, G. Roy
  University of Alberta, Edmonton, Alberta, Canada

XIV-03	**Physics with Storage Rings (Invited Paper)**	electron, ion, storage-ring, luminosity	753

- **R.E. Pollock**
  Indiana University, Bloomington, Indiana, USA

A B C D E F H I J K L M N O P Q R S T V

TRIUMF

Paper	Title	Other Keywords	Page
III-01	**The TRIUMF 520 MeV Cyclotron: Recent and Future Developments** • **G. Dutto** TRIUMF, Vancouver, Canada	cavity, cyclotron, extraction, proton	138
III-02	**The KAON Factory at TRIUMF** • **M.K. Craddock** University of British Columbia, Vancouver, Canada	booster, kaon, lattice, factory	143
IV-11	**External High Current Targetry for Radioisotope Production** • **N.R. Stevenson**, W.Z. Gelbart TRIUMF, Vancouver, Canada	target, cyclotron, radiation, vacuum	196
IV-12	**A Remotely Controlled Robotic Vehicle for Work Within Radioactive Environments** • **N.R. Stevenson**, P. Bloemhard, M. Brigham, J. Ko, C. LaForge, J. Orzechowski, E. Pattyn, T. Rattray TRIUMF, Vancouver, Canada	target, controls, cyclotron, radiation	198
V-03	**A Facility for Radioisotope Production at TRIUMF with 70-110 MeV Protons** • **D.R. Pearce**, J.S. Vincent TRIUMF, Vancouver, Canada	target, controls, proton, cyclotron	209
VI-03	**Pion Therapy for Cancer - What are the Prospects?** • **G.B. Goodman** University of British Columbia, Vancouver, Canada	photon, radiation, controls, background	242
VIII-05	**Status of the TRIUMF Optically-Pumped Polarized H^- Ion Source** • **C.D.P. Levy**, K. Jayamanna, M. McDonald, R. Ruegg, P.W. Schmor TRIUMF, Vancouver, Canada • A.N. Zelenskii Institute of Nuclear Research, Russian Academy of Sciences, Moscow, Russia	polarization, laser, ion, proton	322

IXA-08	**Evaluation of Third-Harmonic Voltage Flattopping for a Superconducting Cyclotron** • **M.M. Gordon**, D. Jeon NSCL, East Lansing, Michigan, USA	cyclotron, extraction, ion, resonance	404
IXA-11	**Developments in RELAX3D, a 2D/3D Laplace and Poisson Equation Solver** • **H. Houtman**, F.W. Jones, C.J. Kost TRIUMF, Vancouver, Canada	cyclotron, electron, simulation, proton	411
IXB-07	**Beam Test Results Using the Auxiliary Accelerating Cavity** • **R.E. Laxdal**, G.H. Mackenzie, L. Root TRIUMF, Vancouver, Canada	cavity, simulation, cyclotron, extraction	442
IXD-08	**Signal Processing for the Internal Phase Probe in the TRIUMF Cyclotron** • **K. Fong** TRIUMF, Vancouver, Canada	cavity, background, cyclotron, pick-up	495
IXD-09	**A DC Current Transformer for TRIUMF** • **Y. Yin** TRIUMF, Vancouver, Canada	ion, ion-source, feedback, vacuum	498
XA-11	**TRIUMF Cyclotron RF System Improvements** • **G.C. Blaker**, A.K. Mitra, R.L. Poirier TRIUMF, Vancouver, Canada	impedance, cyclotron, controls, cathode	545
XA-12	**Improvements to the RF Separator in the M9 Muon Channel at TRIUMF** • **G.C. Blaker**, A.K. Mitra, R.L. Poirier TRIUMF, Vancouver, Canada	cavity, controls, impedance, cyclotron	549
XI-01	**Integrated Tools for Cyclotron Operation (Invited Paper)** • **W. Busse** HMI, Berlin, Germany	controls, cyclotron, monitoring	634
XI-11	**Early Experience with DECwindows/Motif in the TRIUMF Central Control System**	controls, laser, booster, ion-source	676

- **S. Kadantsev**
  JINR, Dubna, Russia
- M. Mouat
  TRIUMF, Vancouver, Canada

XI-12	**Application of Object Oriented Techniques in the TRIUMF Beam Line 2C Control System (Invited Paper)**	controls, target, kaon, factory	681

- **N.A. Wilkinson**, E.A. Osberg, G.A. Ludgate
  TRIUMF, Vancouver, Canada

XI-13	**The TR30 Control System - A Case for Off-the-Shelf Software**	controls, vacuum, diagnostics, cyclotron	685

- **R. Keitel**, D.J. Dale, B.F. Milton
  TRIUMF, Vancouver, Canada

XIII-08	**Research and Development Studies with Radioactive Beams at TRIUMF**	target, ISAC, kaon, proton	745

- **J.M. D'Auria**, M. Dombsky
  Simon Fraser University, Burnaby, BC, Canada
- L. Buchmann, H. Sprenger, J.S. Vincent
  TRIUMF, Vancouver, Canada
- J. King
  University of Toronto, Toronto, Ontario, Canada
- P. McNeely, G. Roy
  University of Alberta, Edmonton, Alberta, Canada

XV-01	**Proper and Improper Accelerators - In Praise of Cyclotrons and Their Builders**	cyclotron, ion, controls, synchrotron	765

- **M.K. Craddock**
  University of British Columbia, Vancouver, Canada

A B C D E F H I J K L M N O P Q R S T V

vacuum

Paper	Title	Other Keywords	Page
I-02	**New Development at the JINR Heavy Ion Cyclotron Facility (Invited Paper)** • **G.G. Gulbekyan**, V. Bekhterev, O. Borisov, B. Gikal, A. Ivanenko, I. Kolesov, V.B. Kutner, A. Morduev, Yu.Ts. Oganessian JINR, Dubna, Russia	ion, cyclotron, extraction, ECR	11
I-03	**New K130 Cyclotron at Jyväskylä (Invited Paper)** • **E. Liukkonen** University of Jyväskylä, Jyväskylä, Finland	cyclotron, ion, ECR, ion-source	22
I-06	**AGOR: Recent Achievements (Invited Paper)** • **H.W. Schreuder** IPN, Orsay, France	AGOR, cyclotron, extraction, site	40
I-07	**Thoughts on Decommissioning the CERN Synchro Cyclotron** • **G. Spinney** CERN, Geneva, Switzerland	CERN, shielding, plasma, synchro-cyclotron	47
I-08	**Parameters, Present State and Application Perspectives of the U-250 Cyclotron** • **A.I. Muminov** Institute of Nuclear Physics, Tashkent, Republic of Uzbekistan • M.F. Vorogushin D.V. Efremov Scientific Research Institute of Electrophysical Apparatus, St. Petersburg, Russia	ion, cyclotron, heavy-ion, resonance	50
I-10	**Gatchina Isochronous Cyclotron** • **N.K. Abrosimov**, S.A. Artamonov, P.V. Chervyakov, S.P. Dmitriev, V.A. Eliseev, V.P. Fominenko, E.M. Ivanov, G.F. Mikheev, Yu.T. Mironov, A.S. Pokrovskii, G.A. Riabov, V.A. Smolin, G.L. Sokolov, V.A. Volchenkov, A.A. Vorobiev Petersburg Nuclear Physics Institute, Gatchina, Russia • P.V. Bogdanov, B.D. Ershov, V.S. Kuligin, V.N. Moshkin,	cyclotron, ion, synchro-cyclotron, injection	58

V.G. Mudrolyubov, Yu.I. Stogov, A.P. Strokach
D.V. Efremov Scientific Research Institute of Electrophysical Apparatus, St. Petersburg, Russia

I-11	**Status Report of SARA**	cyclotron, ion, injection, ECR	62

- **M. Fruneau**, S. Albrand, D. Barnéoud, J.L. Belmont, G. Bizouard, J.L. Bouly, G. Campillo, M. Guisset, G. Laborie
Université Joseph Fourier, Grenoble, France

I-14	**Initial Operation of HIRFL**	ion, ion-source, ECR, heavy-ion	74

- **B.W. Wei**, F. Ye
Institute of Modern Physics, Lanzhou, People's Republic of China

I-18	**Status Report on the Heavy Ion Facility at LNS**	cyclotron, cavity, coupling, ion	90

- **F. Alessandria**, G. Bellomo, A. Bosotti, C. De Martinis, D. Giove, P. Michelato, C. Pagani, L. Rossi
INFN/LASA, Segrate, Italy
- L. Calabretta, G. Ciavola, G. Cuttone, M. Di Giacomo, S. Gammino, P. Gmaj, G. Raia, D. Rifuggiato, J. Sura
INFN/LNS, Catania, Italy

I-22	**Status Report on the Gustaf Werner Cyclotron in Uppsala**	ion, extraction, cyclotron, injection	106

- **S. Holm**
Uppsala University, Uppsala, Sweden

II-05	**Status of a Compact H^- Cyclotron at the Kurchatov Institute of Atomic Energy**	cyclotron, ion, controls, ion-source	126

- **N.I. Venikov**, C.D. Burbeza, P.Yu. Komissarov, Yu.M. Krasnikov, S.T. Latushkin, V.V. Leonov, V.P. Moryakov, I.V. Naumov, A.Ya. Pisman, V.A. Rezvov, A.A. Vasiliev, V.E. Yarosh, L.I. Yudin
Kurchatov Institute, Moscow, Russia

IV-11	**External High Current Targetry for Radioisotope Production**	target, TRIUMF, cyclotron, radiation	196

- **N.R. Stevenson**, W.Z. Gelbart
TRIUMF, Vancouver, Canada

VIII-08	**Ion Source of Discharge Type**	ion, ion-source, plasma, permanent-magnet	334

I.B. Enchevich
TRIUMF, Vancouver, Canada
- S.A. Korenev
JINR, Dubna, Russia

IXB-04	**Selection and Measurement of RF Phase Width of the K1200 Cyclotron Beam**	cyclotron, extraction, injection, ion	431

- **J. Bailey**, J. Kuchar, F. Marti, J. Yurkon
NSCL, East Lansing, Michigan, USA
- J.A. Nolen
ANL, Argonne, Illinois, USA
- D. Rifuggiato
INFN/LNS, Catania, Italy

IXB-06	**Effect of the Main-Coil Position on the Accelerated Beam of the K500 Cyclotron**	extraction, cyclotron, focusing, betatron	439

- **D.P. May**, G. Mouchaty
Texas A&M University, College Station, Texas, USA

IXD-06	**The Diagnostics System for the AGOR Superconducting Cyclotron**	extraction, diagnostics, cyclotron, injection	487

- **B. Launé**, P. Dambre, J.M. Kaplanski, B. Montsanglant, C. Olivetto, D. Vincent
IPN, Orsay, France

IXD-09	**A DC Current Transformer for TRIUMF**	ion, ion-source, feedback, TRIUMF	498

- **Y. Yin**
TRIUMF, Vancouver, Canada

XA-02	**The RF Coupling System of the VINCY Cyclotron**	coupling, impedance, cyclotron, cavity	511

- **B. Bojovic**, M. Josipovic, A. Susini
CERN, Geneva, Switzerland

XA-03	**Dual Frequency Resonator System for a Compact Cyclotron**	cyclotron, impedance, cavity, isotope-production	515

- **M. Eiche**, K.L. Erdman
Ebco Technologies Ltd, Richmond, BC, Canada
- P. Lanz, M. Lipnicki, M. Zach
TRIUMF, Vancouver, Canada

XA-13	**The RF System of the Gustaf Werner Cyclotron/Synchrocyclotron**	controls, cyclotron, proton, synchro-cyclotron	553

- **B. Lundström**, B. Holmgren
  Uppsala University, Uppsala, Sweden

XB-01	**Low Temperature Tests of the AGOR Superconducting Coil System**	AGOR, cryogenics, power-supply, factory	557

- **K. Pieterman**, J.A.M. Dam
  Cryocon B.V., Amersfoort, The Netherlands
- C. Commeaux
  IPN, Orsay, France
- C. Penco
  Ansaldo Componenti, Genoa, Italy

XB-02	**A Permanent Magnet System for a Cyclotron Used as a Mass Spectrometer**	cyclotron, injection, permanent-magnet, ion	561

- **C.Y. Li**, M. Cooper, K. Halbach, W.B. Kunkel, K.N. Leung, R.P. Wells, A.T. Young
  LBL, Berkeley, California, USA

XC-01	**The Electrostatic Deflector for the Chalk River Superconducting Cyclotron**	high-voltage, cathode, cyclotron, electron	569

- **W.T. Diamond**, C.R. Hoffmann, G.R. Mitchel, H. Schmeing
  Atomic Energy of Canada, Chalk River, Ontario, Canada

XC-03	**Model Study of an Electrostatic Deflector Configuration with an Intermediate Electrode**	high-voltage, cyclotron, septum, power-supply	577

- **C.R. Hoffmann**, J.F. Mouris
  Atomic Energy of Canada, Chalk River, Ontario, Canada

XI-02	**The IUCF High Intensity Polarized Ion Source Control System**	controls, ion, ion-source, interlocks	641

- **T. Capshew**, J.C. Collins, D. DuPlantis, D.W. Frame, J. Graham, D.D. Reid
  Indiana University, Bloomington, Indiana, USA

XI-08	**Micro-Controlled Vacuum Systems at NAC**	controls, cyclotron, instrumentation, monitoring	664

- **P.J. Celliers**, E.J.S. Franklin
  National Accelerator Centre, Faure, Republic of South Africa

XI-13	**The TR30 Control System - A Case for Off-the-Shelf Software**	controls, diagnostics, cyclotron, TRIUMF	685

- **R. Keitel**, D.J. Dale, B.F. Milton
  TRIUMF, Vancouver, Canada

ANL
Argonne, Illinois, USA

Author
Nolen, J.A.

ANSTO
Menai, NSW, Australia

Author
Mukherjee, B.N.

Ansaldo Componenti
Genoa, Italy

Author
Penco, C.

Associated Universities Oak Ridge
Oak Ridge, Tennessee, USA

Author

Carter, H.K.

Kormicki, J.

Atomic Energy of Canada
Chalk River, Ontario, Canada

Author

Diamond, W.T.
Hardy, J.C.
Hoffmann, C.R.
Lindqvist, E.H.
Mitchel, G.R.
Mouris, J.F.
Schmeing, H.
Davies, W.G.

Austin Hospital & University of Melbourne
Melbourne, Australia

Author
Chaudhri, M.A.

Australian National University
Canberra , Australia

Author
Fifield, K.

BESSY
Berlin, Germany

Author
Wüstefeld, G.

CEN-Grenoble
Grenoble, France

Author
Briand, P.

CEN/Saclay
Gif-sur-Yvette, France

Author
Gillibert, A.
Vienet, R.

CERN
Geneva, Switzerland

Author

Bojovic, B.
Josipovic, M.
Spinney, G.
Susini, A.

CSNSM
Orsay, France

Author

Audi, G.

Liang, C.F.

Paris, P.

Center for Applied Physics and Technology Lipetsk, Russia

Author

Meshkov, I.N.

Syresinm, Ye.M.

Centre Antoine Lacassagne
Nice, France

Author

Brassart, N.
Chauvel, P.
Courdi, A.
Farley, F.
Fietier, N.
Herault, J.
Mandrillon, P.
Tang, J.Y.

Cryocon B.V.
Amersfoort, The Netherlands

Author
Dam, J.A.M.
Pieterman, K.

Cyclotron Inc.
Napa, California, USA

Author

Hendry, G.O.

Cyclotron Isotopes Manufacturing Buckinghamshire, England

Author

Grey-Morgan, T.

Czechoslovak Academy of Sciences
Rez, Czechoslovakia

Author

Bejsovec, V.

Krivánek, M.

Kucera, J.

Stursa, J.

Trejbal, Z.

D.V. Efremov Scientific Research Institute of Electrophysical Apparatus St. Petersburg, Russia

Author

Belov, V.P.
Bogdanov, P.V.
Ershov, B.D.
Kokorin, A.M.
Korolev, L.E.
Kuligin, V.S.
Makarov, A.A.
Moshkin, V.N.
Mudrolyubov, V.G.
Schukeilo, I.A.
Severgin, Yu.P.
Shukeylo, I.A.
Stogov, Yu.I.
Strokach, A.P.
Tarovik, M.N.
Vorogushin, M.F.

Ebco Technologies Ltd
Richmond, BC, Canada

Author
Eiche, M.
Erdman, K.L.

Eindhoven University of Technology
Eindhoven, The Netherlands

Author

Botman, J.I.M.

Delhez, J.L.

Hagedoorn, H.L.

Kleeven, W.J.G.M.

Timmermans, C.J.

Webers, G.A.

FZJ
Jülich, Germany

Author

Beuscher, H.
Brings, R.
Bräutigam, W.
Böge, H.G.
Herschbach, M.
Kennepohl, K.
Maeckelburg, D.
Maier, R.
Martin, S.A.
Pfister, U.
Rogge, M.
Wucherer, P.
Zaplatin, E.

FZK
Karlsruhe, Germany

Author
Bechtold, V.
Fehsenfeld, P.
Kleinrahm, A.

GANIL
Caen, France

Author

Auger, G.
Bajard, M.
Baron, E.
Bibet, D.
Bony, J.
Bourgarel, M.P.
Bricault, P.
Bru, B.
Chabert, A.
Fermé, J.
Gaudart, L.
Joubert, J.
Leroy, R.
Lewitowicz, M.
Mittig, W.
Moscatello, M-H.
Pacquet, J.Y.
Plagnol, E.
Ricaud, Ch.
Schutz, Y.
Sortais, P.
St-Laurent, M.G.

General Atomics
San Diego, California, USA

Author
Whittemore, W.L.

Graduate School of Nuclear Industry
Beijing, People's Republic of China

Author

Liu, C.

Xie, X.

HMI
Berlin, Germany

Author

Busse, W.

Pelzer, W.

Ziegler, K.

Hammersmith Hospital
London, England

Author

Clark, J.C.

Mackay, D.B.

Harper Hospital
Detroit, Michigan, USA

Author
Maughan, R.

Harvard Medical School
Boston, Massachusetts, USA

Author
Suit, H.D.
Thornton, A.F.

INFN/LASA
Segrate, Italy

Author
Alessandria, F.
Bellomo, G.
Bosotti, A.
Corti, D.
De Martinis, C.
Giove, D.
Michelato, P.
Pagani, C.
Rossi, L.
Varisco, G.
Zibra, F.

INFN/LNS
Catania, Italy

Author

Calabretta, L.
Ciavola, G.
Cuttone, G.
Di Biasi, G.
Di Giacomo, M.
Gammino, S.
Gmaj, P.
Raia, G.
Rifuggiato, D.
Sura, J.

IPN
Orsay, France

Author

Blache, P.
Commeaux, C.
Dambre, P.
Gustafsson, S.
Kaplanski, J.M.
Lafoux, A.
Launé, B.
Montsanglant, B.
Mormiche, M.
Mueller, A.C.
Obert, J.
Olivetto, C.
Panvier, R.
Putaux, J.C.
Schreuder, H.W.
Vincent, D.

Indiana University
Bloomington, Indiana, USA

Author

Anderson, S.
Ball, M.S.
Brown, R.
Capshew, T.
Collins, J.C.
Derenchuk, V.
DuPlantis, D.
East, G.
Ellison, T.J.P.
Frame, D.W.
Friesel, D.L.
Graham, J.
Hamilton, B.
Hicks, J.W.
Jenner, D.
Jones, W.P.
McCammon, D.
Pei, A.
Pei, X.
Petri, H.
Pollock, R.E.
Reid, D.D.
Schwandt, P.
Sloan, T.
Sowinski, J.
Wedekind, M.

Institute for Nuclear Physics
Novosibirsk, Russia

Author

Parhomchuk, V.V.

Popov, S.

Sery, A.A.

Shiltsev, V.D.

Toporkov, D.

Voitsechovsky, B.

Institute for Nuclear Research
Kiev, Ukraine

Author

Dolinsky, A.V.
Glushko, A.
Papash, A.I.
Pavlov, S.N.
Pitatelev, G.
Pugatch, V.
Rudchik, A.T.
Sivtsov, G.
Val'Kov, A.E.
Vishnevsky, I.N.
Zaika, N.I.
Zhmendak, A.V.

Institute of Modern Physics
Lanzhou, People's Republic of China

Author

Guo, M.
Jiang, J.Z.
Jiang, W.M.
Liu, Z.
Ma, Y.
Ma, Z.
Qiao, Q.
Shen, Z.
Wang, F.
Wang, Q.
Wang, Y.
Wei, B.W.
Wu, D.
Xia, J.
Ye, F.
Yin, Q.
Yuan, P.
Zhang, W.
Zhang, X.
Zhao, H.
Zhou, X.H.
Zhu, X.

Institute of Nuclear Physics
Tashkent, Republic of Uzbekistan

Author

Gulamov, I.

Iljasov, O.

Muminov, A.I.

Rykov, A.

Institute of Nuclear Research of the Hungarian Academy of Sciences Debrecen, Hungary

Author

Biri, S.

Pálinkás, J.

Valek, A.

Institute of Nuclear Research
Shanghai, People's Republic of China

Author

Chang, H.

Cui, X.

Wei, J.

Xie, K.

Zhang, J.

Institute of Nuclear Research, Russian Academy of Sciences Moscow, Russia

Author

Zelenskii, A.N.

Ion Beam Applications
Louvain-la-Neuve, Belgium

Author

Beeckman, W.
Conard, E.
Dufour, J.P.
Jongen, Y.
Laisné, A.
Marie, H.
Morelle, J.-L.
Verbruggen, R.

JAERI
Gunma, Japan

Author

Agematsu, T.
Arakawa, K.
Fukuda, M.
Ishibori, I.
Kamiya, T.
Karasawa, T.
Nakamura, Y.
Nara, T.
Okumura, S.
Tanaka, R.
Yokota, W.

JINR
Dubna, Russia

Author

Alenitskiy, Ju.
Bekhterev, V.
Bogomolov, S.L.
Borisov, O.
Chesnov, A.
Chesnova, S.
Didyk, A.Yu.
Dmitriev, S.N.
Efremov, A.
Gangrski, Yu.P.
Gikal, B.
Glazov, A.
Gulbekyan, G.G.
Ivanenko, A.
Kadantsev, S.
Karamian, S.A.
Khalkin, V.A.
Kochkin, V.
Kolesov, I.
Korenev, S.A.
Kutner, V.B.
Malyshev, O.N.
Markov, B.N.
Morduev, A.
Novikov, D.
Oganessian, R.Ts.
Oganessian, Yu.Ts.
Onishchenko, L.M.
Popeko, G.S.
Pronin, N.V.
Rodin, A.M.
Samsonov, E.
Semenov, M.
Sidorchuk, S.I.
Sokol, Ye.A.
Starodub, G.Ya.
Stepantsov, S.V.

Ter-Akopian, G.M.
Timakov, V.A.
Vasilenko, A.
Zaitseva, N.G.
Zaplatin, E.
Zaplatin, N.

Japan Steel Works Ltd.
Tokyo, Japan

Author
Toda, Y.
Yamamoto, Y.

Japan Steel Works Ltd., Research Center for Advanced Technologies Chiba, Japan

Author

Isoya, Y.

Yamada, T.

Yamashita, Y.

KEK
Ibaraki, Japan

Author

Endo, K.
Irie, Y.
Muto, K.

Kazakhstan Academy of Sciences
Alma-Ata, Republic of Kazakhstan

Author

Arzumanov, A.A.
Batischev, V.
Berger, V.
Gerasimov, V.
Gorcovets, M.
Hamidov, N.K.
Kozin, A.I.
Shychikov, G.I.
Tihomirova, S.T.

Kernfysisch Versneller Instituut
Groningen, The Netherlands

Author

Kiewiet, H.H.

Schippers, J.M.

Kurchatov Institute
Moscow, Russia

Author

Buranov, V.
Burbeza, C.D.
Gotovtsev, O.
Iudin, L.I.
Komissarov, P.Yu.
Krasnikov, Yu.M.
Latushkin, S.T.
Leonov, V.V.
Mikhailov, V.G.
Moryakov, V.P.
Naumov, I.V.
Novikov, V.
Pisman, A.Ya.
Rezvov, V.A.
Roshchin, A.A.
Sklyarenko, V.I.
Unezhev, V.N.
Vasiliev, A.A.
Venikov, N.I.
Yarosh, V.E.
Yudin, L.I.

LBL
Berkeley, California, USA

Author

Bachman, D.A.
Bertsche, K.J.
Clark, D.J.
Collins, D.
Cooper, M.
Halbach, K.
Kunkel, W.B.
Leung, K.N.
Li, C.Y.
Lundgren, S.A.
Lyneis, C.M.
McDonald, D.S.
Nitschke, J.M.
Wells, R.P.
Xie, Z.Q.
Young, A.T.

LPC
Caen, France

Author
Steckmeyer, J.C.

Medi + Physics Inc.
Arlington Heights, Illinois, USA

Author
Hubbard, R.E.

Moscow Institute-Internate
Moscow, Russia

Author

Sarkisyan, A.L.

Sarkisyan, L.A.

NIRS
Chiba, Japan

Author

Hirao, Y.
Itano, A.
Kanazawa, M.
Kitagawa, A.
Kohno, T.
Kumada, M.
Noda, K.
Ogawa, H.
Sato, K.
Sato, Y.
Sudou, M.
Takada, E.
Yamada, S.
Yamada, T.

NSCL
East Lansing, Michigan, USA

Author

Antaya, T.A.
Bailey, J.
Blosser, H.G.
Cole, D.
Gordon, M.M.
Jeon, D.
Joh, K.
Kim, J.W.
Kuchar, J.
Marti, F.
Miller, P.
Poe, D.
Sherrill, B.
Snyder, S.
Stetson, J.
Vincent, J.
Winger, J.
Yurkon, J.

Nagoya University
Nagoya, Japan

Author
Ishigaki, T.
Ito, K.
Itoh, S.
Kasugai, Y.
Kato, T.
Misawa, T.
Nishino, M.
Osakabe, M.
Ota, T.
Sakuma, S.
Tadokoro, M.
Yamamoto, H.

National Accelerator Centre
Faure, Republic of South Africa

Author

Botha, A.H.
Burger, S.J.
Celliers, P.J.
Conradie, J.L.
Cornell, J.C.
Cronje, P.M.
Fenemore, R.E.F.
Fisch, R.K.
Fourie, D.T.
Franklin, E.J.S.
Hogan, M.E.
Jungwirth, H.N.
Kohler, I.H.
Kritzinger, J.J.
Müller, A.
Nel, W.A.G.
Reitmann, D.
Roels, L.M.M.
Rogers, J.P.
Rohwer, P.F.
Smit, H.A.
Theron, P.J.
Weehuizen, H.F.
de Villiers, J.G.
du Toit, Z.B.
van Rooyen, D.M.

National Medical Cyclotron
Camperdown, NSW, Australia

Author

Arnott, D.W.

ORNL
Oak Ridge, Tennessee, USA

Author

Alton, G.D.
Baktash, C.
Dowling, D.T.
Garrett, J.D.
Haynes, D.L.
Jones, C.M.
Juras, R.C.
Lane, S.N.
Lee, I.Y.
Meigs, M.J.
Mills, G.D.
Mosko, S.W.
Olsen, D.K.
Tatum, B.A.
Toth, K.S.

Osaka University
Osaka, Japan

Author

Ando, A.
Hatanaka, K.
Hosono, K.
Ikegami, H.
Itahashi, T.
Kibayashi, M.
Kondo, M.
Miura, I.
Nagayama, K.
Ogata, H.
Saito, T.
Shimizu, A.
Tamura, K.
Uraki, M.
Yamazaki, T.

PSI
Villigen, Switzerland

Author

Adam, S.
Cherix, J.
Frei, H.
Humbel, M.
Joho, W.
Mezger, A.C.
Märki, M.
Pedroni, E.
Sigg, P.K.
Stammbach, Th.

Petersburg Nuclear Physics Institute
Gatchina, Russia

Author

Abrosimov, N.K.
Artamonov, S.A.
Chervyakov, P.V.
Dmitriev, S.P.
Eliseev, V.A.
Fominenko, V.P.
Ivanov, E.M.
Mikheev, G.F.
Mironov, Yu.T.
Pokrovskii, A.S.
Riabov, G.A.
Smolin, V.A.
Sokolov, G.L.
Volchenkov, V.A.
Vorobiev, A.A.

RIKEN
Saitama, Japan

Author
Goto, A.
Kageyama, T.
Kase, M.
Nakagawa, T.
Yano, Y.

Royal Institute of Technology
Stockholm, Sweden

Author

Raadu, M.A.

Sedlacek, M.

Simon Fraser University
Burnaby, BC, Canada

Author
D'Auria, J.M.
Dombsky, M.

Sumitomo Heavy Industries Systems Engineering Laboratory Tokyo, Japan

Author

Kodaira, K.

Murakami, T.

Okamura, T.

Sumitomo Heavy Industries
Ehime, Japan

Author

Abe, J.
Aoki, K.
Fukumoto, Y.
Hayashi, Y.
Hoshika, K.
Ichida, S.
Ishii, K.
Iso, K.
Kimura, Y.
Kumata, Y.
Maruyama, M.
Sano, M.
Satoh, S.
Satoh, T.
Tachibana, M.
Tachikawa, T.
Takahashi, N.
Takayama, T.
Yamada, S.

Sumitomo Heavy Industries, Toyo-shi
Toyo-shi, Japan

Author
Tazawa, S.

TRIUMF
Vancouver, Canada

Author

Blaker, G.C.
Bloemhard, P.
Brigham, M.
Buchmann, L.
Dale, D.J.
Dutto, G.
Enchevich, I.B.
Fong, K.
Fraser, J.S.
Gelbart, W.Z.
Houtman, H.
Jayamanna, K.
Jones, F.W.
Keitel, R.
Ko, J.
Kost, C.J.
Kuo, T.Y.T.
LaForge, C.
Lanz, P.
Laxdal, R.E.
Levy, C.D.P.
Lipnicki, M.
Ludgate, G.A.
Mackenzie, G.H.
McDonald, M.
Milton, B.F.
Mitra, A.K.
Mouat, M.
Orzechowski, J.
Osberg, E.A.
Pattyn, E.
Pearce, D.R.
Pearson, J.B.
Poirier, R.L.
Rattray, T.
Root, L.
Ruegg, R.

Ruth, T.J.
Schmor, P.W.
Schneider, H.R.
Sprenger, H.
Stevenson, N.R.
Vincent, J.S.
Wilkinson, N.A.
Yin, Y.
Zach, M.

TU München
Garching, Germany

Author
Trinks, U.

TU Twente
Enschede, The Netherlands

Author
ten Kate, H.J.H.

Texas A&M University
College Station, Texas, USA

Author

Derrig, G.
Dewees, W.
May, D.P.
Mouchaty, G.
Rogers, R.C.
Smelser, P.
Tran, D.

The Johns Hopkins University
Baltimore, Maryland, USA

Author

Wagner, Jr., H.N.

The University of Texas
Houston, Texas, USA

Author

Grimmett, G.
Mallory, M.L.
Tilbury, R.
Yang, D.

Thomson Tubes Electroniques
Velizy-Villacoublay, France

Author

Boux, R.

Ichac, J.P.

Soudée, M.

Université Catholique de Louvain
Louvain-la-Neuve, Belgium

Author

Loiselet, M.

Postiau, N.

Ryckewaert, G.

Université Joseph Fourier
Grenoble, France

Author

Albrand, S.
Barnéoud, D.
Belmont, J.L.
Bizouard, G.
Bouly, J.L.
Bruandet, J.F.
Campillo, G.
Fruneau, M.
Gimond, G.
Golovanivsky, K.
Guisset, M.
Laborie, G.
Liatard, E.
Loiseaux, J.M.
Nifenecker, H.
Savalle, A.
Vignon, B.
de Conto, J.M.

University Hospital
Groningen, The Netherlands

Author
Paans, A.M.J.

University of Alberta
Edmonton, Alberta, Canada

Author
McNeely, P.
Roy, G.

University of British Columbia
Vancouver, Canada

Author

Craddock, M.K.

Goodman, G.B.

University of Jyväskylä
Jyväskylä, Finland

Author

Heikkinen, P.

Liukkonen, E.

Rinta-Nikkola, M.

University of Tokyo
Tanashi-shi, Tokyo, Japan

Author

Arakaki, Y.
Chida, K.
Fujita, M.
Katayama, T.
Nishiguchi, M.
Ohshiro, Y.
Sekiguchi, M.
Shida, Y.
Tomizawa, M.
Watanabe, S.
Watanabe, T.
Yamazaki, N.
Yamazaki, T.
Yoshizawa, M.

University of Toronto
Toronto, Ontario, Canada

Author
King, J.

University of Tsukuba
Ibaraki, Japan

Author

Fukumoto, S.
Hayakawa, Y.
Inada, T.
Maruhashi, A.
Sato, M.
Tada, J.
Takada, Y.
Tsuji, H.
Tsujii, H.

University of Washington
Seattle, Washington, USA

Author

Brossard, S.
Jacky, J.
Kalet, I.
Risler, R.
Wootton, P.
Ziai, F.

Uppsala University
Uppsala, Sweden

Author

Bergmark, T.
Ekström, C.
Fridén, C.-J.
Gajewski, K.
Hermansson, L.
Holm, S.
Holmgren, B.
Jahnke, P.
Johansson, A.
Johansson, O.
Lofnes, T.
Lundström, B.
Norman, G.
Reistad, D.
Wedberg, R.
Westerberg, L.
Zlomanczuk, J.

ENTRY NO. C1 **Date** June 1992

Name of Machine CYCLONE

Institution Université Catholique de Louvain

Address Chemin du Cyclotron, 2 B-1348 Louvain-la-Neuve Belgium

Tel +32-10-473273 **Telex** 59065 IPLB **Fax** +32-10-452183 **EMAIL** RYCKEWAERT@CYC.UCL.AC.BE

In Charge: G. RYCKEWAERT **Reported by:** M. LOISELET

HISTORY

MILESTONE DATES:
Design 1969 Model Tests 1969
Construction 1969-1971 First Beam 1972
DESIGN/CONSTRUCTION BY:
in house ... other 6 CGR-MEV ... 6
COST: Accelerator 3 x 10 US $ Facility 6.5 x 10 US $
FUNDED BY: Univ. de Louvain, IISN (State)

STATUS

STAFF: Machine
Scientists 4 Engineers 4
Technicians 11 Students ...
Research (in house/external)
Scientists ... / ... Engineers ... / ...
Technicians ... / ... Students ... / ...
BUDGET: Machine ... Funded by ...
Research ... Funded by ...
TIME DISTRIBUTION:
Basic Research (~~in house/external~~) 53 % / ... %
Applied Program (~~in house/external~~) 24 % / ... %
Development 10 % Maintenance 13 %

MAGNET

POLE PARAMETERS:
Diameter 215.6. cm $R_{extract}$ 93 cm R_{inject} ... cm
HILL PARAMETERS: Gap (min) 16.5 cm B_{max} 2.15 T
(@ 4 x 10^5 AT) Gap (max) - cm B_{min} - T
VALLEY PARAMETERS: Gap (min) 40.5 cm B_{max} 1.15 T
(@ 4 x 10^5 AT) Gap (max) - cm B_{min} - T
AVERAGE FIELD: $< B >_{min}$ 0.6 T $< B >_{max}$ 1.6 T
NUMBER OF SECTORS: compact/separated 4 / ...
sector angle variable deg. spiral (max) 53 deg.
FIELD TRIMMING: Trim Coils 12 pairs
Harmonic Coils 2 x 4 pairs
Other -
CURRENT: Main Coils 1100 Amps Stability 10^{-5}
Trim Coils 300-500-700 Amps Stability 10^{-3}
Stored Energy (cryogenic) ... MJ
WEIGHT: Iron 200 tons Conductor 6 tons
ION ENERGY: Bending Limit E/A = 115 q^2/A^2 MeV/u
Focussing Limit E/A = 95 q/A MeV/u

ACCELERATION SYSTEM

FUNDAMENTAL ACCELERATION:
Description: moving panels ; 2 dees 86 deg
No. of Gaps/turn 4 dE/dn(max) 0.200 MeV/q
Voltage(max) 0.050 MV Harmonic f_{rf}/f_{ion} 1,2,3,6
Freq 108-23 MHz Power in(max) 0.200 MW
Stability: Phase 0.1 deg. Voltage 10^{-4}
OTHER CAVITIES (Flattopping or otherwise):
Description: ...
Region of Influence: R_{min} ... cm R_{max} ... cm
No. of Gaps/turn ... dE/dn(max) ... MeV/q
Voltage(max) ... MV Harmonic f_{rf}/f_{ion} ...
Freq ... MHz Power in(max) ... MW
Stability: Phase ... Voltage ...

VACUUM SYSTEM

OPERATING PRESSURE: $2 \cdot 10^{-6}$
PUMPS: No. and type 2 oil diffusion 12.000 l/s
2 cryopumps 3.600 l/s

ION SOURCE(S)

	Type	Intensity (mA)	@	$\epsilon_n = \beta\gamma\epsilon$ (πmm mrad)	Ion Species
(a)	Livingston				p, d, α
(b)	ECR 2 stages				heavy ions
(c)	ECR 1 stage				radioactive ions
(d)					

INJECTION SYSTEM

axial injection ... Efficiency (max) 16 %

EXTRACTION SYSTEM

dc electrostatic + magn. chan. ... Efficiency (max) 80 %

CHARACTERISTIC BEAMS

	Accelerated Ions	E/A (MeV/u)	Current(part μA) Internal	External
(a)	p	85/65	...	5/25
(b)	α	115	...	15
(c)	heavy ions	115 Q^2/A	...	...
(d)	radioactive ions (^{13}N, ^{19}Ne)		...	100 ppA

	Secondary Particles	E (MeV)	part/sec
(a)	n from p + Be at 65 MeV	...	10^{11}
(b)		...	...
(c)		...	...

EXTRACTED BEAM PROPERTIES:
For 15 μA of 65 MeV/u H ions
$\Delta E/E$ 0.3 % $\Delta\phi$ ... °rf
$\epsilon_n = \beta\gamma\epsilon$ x 23 πmm mrad z 15 πmm mrad

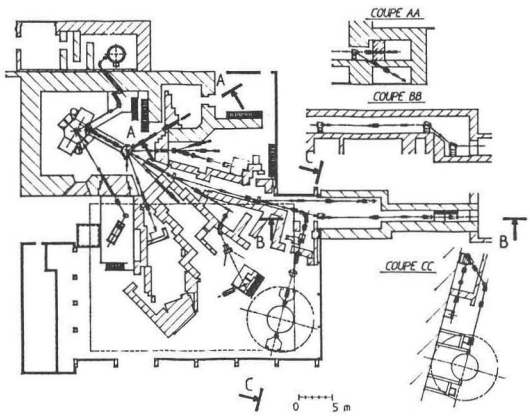
FACILITIES FOR RESEARCH

SHIELDED AREA: Fixed 490 m² Moveable 1300 m²
Target Stations: 11 No. Served At Same Time: 1
MAGNETIC SPECTROMETERS: ...
OTHER FACILITIES: hot cells - neutrontherapy (multileaves collimator) - protontherapy - on line mass separator (LISOL) - radioactive beams

REFERENCES/NOTES

(a) ...
(b) ...

PLAN VIEW OF FACILITY, COMMENTS



ENTRY NO. C2 **Date**

Name of Machine TASCC (Tandem Accelerator Superconducting Cyclotron)

Institution AECL Research

Address Chalk River Laboratories, Chalk River, Ontario, Canada K0J 1J0

Tel (613) 584-3311 Telex 053-34555 Fax (613) 584-4024 EMAIL

In Charge: J.C. Hardy Reported by: H. Schmeing

HISTORY

MILESTONE DATES:

Design 1973 Model Tests 1974-78

Construction 1978-84 First Beam Sept. 1985

DESIGN/CONSTRUCTION BY:

in house X other

COST: Accelerator Facility

FUNDED BY: AECL Research

STATUS

STAFF: Machine

~~Scientists~~ Scientists and Engineers 11

Technicians 8 ~~Students~~ Operators 15

Research (in house/external)

Scientists 15 / Engineers /

Technicians 20 / Students /

BUDGET: Machine Funded by AECL Research

Research Funded by AECL Research

TIME DISTRIBUTION:

Basic Research (in house/external) 52 % / %

Applied Program (in house/external) % / %

Development 20 % Maintenance 28 %

MAGNET

POLE PARAMETERS:

Diameter 138.6 cm $R_{extract}$ 65 cm R_{inject} 14.5 cm

HILL PARAMETERS: Gap (min) 3.7 cm B_{max} 6.0 T

(@ AT) Gap (max) cm B_{min} T

VALLEY PARAMETERS: Gap (min) cm B_{max} T

(@ AT) Gap (max) 64 cm B_{min} 4.3 T

AVERAGE FIELD: $< B >_{min}$ 2.4 T $< B >_{max}$ 5.0 T

NUMBER OF SECTORS: compact/separated 4 /

sector angle deg. spiral (max) 50 deg.

FIELD TRIMMING: Trim Coils 13 saturated rods in

Harmonic Coils each flutter pole

Other

CURRENT: Main Coils 2200 Amps Stability ±20 mA

Trim Coils Amps Stability

Stored Energy (cryogenic) 22 MJ

WEIGHT: Iron 170 tonnes Conductor NbTi

ION ENERGY: Bending Limit E/A = 520 q^2/A^2 MeV/u

Focussing Limit E/A = 100 q/A MeV/u

ACCELERATION SYSTEM

FUNDAMENTAL ACCELERATION:

Description:

No. of Gaps/turn 8 dE/dn(max) 0.8 MeV/q

Voltage(max) 0.1 MV Harmonic f_{rf}/f_{ion} 2, 4, 6

Freq 31-62 MHz Power in(max) 0.1 MW

Stability: Phase +1-1° Voltage 0.02%

OTHER CAVITIES (Flattopping or otherwise):

Description:

Region of Influence: R_{min} cm R_{max} cm

No. of Gaps/turn dE/dn(max) MeV/q

Voltage(max) MV Harmonic f_{rf}/f_{ion}

Freq MHz Power in(max) MW

Stability: Phase Voltage

VACUUM SYSTEM

OPERATING PRESSURE:

PUMPS: No. and type two cryopanels

1500 l/s each

ION SOURCE(S)

	Type	Intensity (mA)	@ $\epsilon_n = \beta\gamma\epsilon$ (πmm mrad)	Ion Species
(a)				
(b)	Beam injected from MP Tandem - 15 MV			
(c)				
(d)				

INJECTION SYSTEM

Carbon stripper after radial injection Efficiency %

EXTRACTION SYSTEM

Electrostatic deflector, superconducting magnet channel Efficiency %

CHARACTERISTIC BEAMS

	Accelerated Ions	E/A (MeV/u)	Current(part μA) Internal	External
(a)	^{6}Li	50		
(b)	C^{12}	50		$23x10^{-3}$
(c)	I^{127}	19		$1.5x10^{-3}$
(d)	U^{238}	3		$1.3x10^{-6}$

	Secondary Particles	E (MeV)	part/sec
(a)			
(b)			
(c)			

EXTRACTED BEAM PROPERTIES:

For 0.1 μA of 15 MeV/u ^{127}I ions

$\Delta E/E$ 0.3 % $\Delta\phi$ 3 °rf

$\epsilon_n = \beta\gamma\epsilon$ x 0.7 πmm mrad z 0.6 πmm mrad

FACILITIES FOR RESEARCH

SHIELDED AREA: Fixed m^2 Moveable m^2

Target Stations: 9 No. Served At Same Time: 1

MAGNETIC SPECTROMETERS: Q3D

OTHER FACILITIES: 8-pi high spin spectrometer

ISOL on-line isotope separator

Atomic physics particle physics

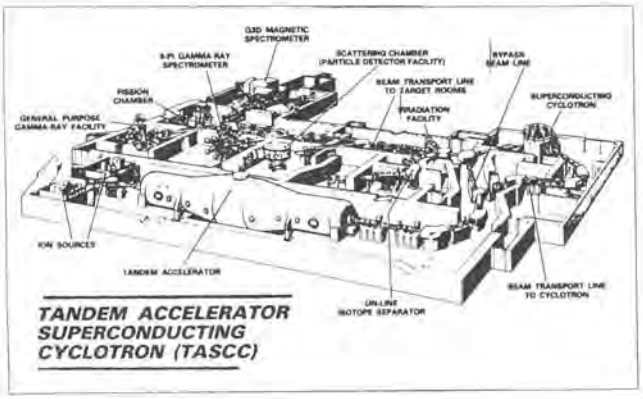
scattering chambers, AMS, SEU

REFERENCES/NOTES

(a) H. Schmeing, et al., Proc. 12th Int. Conf.

(b) on Cyclotron and their Applications, Berlin, 1989

PLAN VIEW OF FACILITY, COMMENTS



TANDEM ACCELERATOR SUPERCONDUCTING CYCLOTRON (TASCC)

ENTRY No. C3 University of Manitoba
NAME OF MACHINE Spiral Ridge Cyclotron DATE
INSTITUTION University of Manitoba Accelerator Laboratory
ADDRESS University of Manitoby, Winnipeg, Manitoba, R3T 2N2, CANADA
TEL (204) 474-9378 TELEX 07-587721
IN CHARGE J.S.C. McKee REPORTED BY S. Oh, Y. Derenchuk, J. Anderson

---

HISTORY AND STATUS
DESIGN, date 1959 Model tests 1959-1961
ENG DESIGN, date 1960-63
CONSTRUCTION, date 1960-64
FIRST BEAM, date (or goal) 1965
MAJOR ALTERATIONS 100% external injection (1965), magnetic field reshaped (1985) & a new dee system (1985).
COST, ACCELERATOR $ 600,000.00 (1960)
COST, FACILITY, total $ 1,500,000.00
FUNDED BY University of Manitoba and NSERC

ACCELERATOR STAFF, OPERATION AND DEVELOPMENT
SCIENTISTS 5 ENGINEERS 1
TECHNICIANS 3 CRAFTS 1
GRAD STUDENTS involved during year 8
OPERATED BY X Research staff or Operators
OPERATION hr/wk, On target hr/wk
TIME DISTR, in house %, Outside %
BUDGET, op & dev $ 500,000.00
FUNDED BY NSERC, University of Manitoba

RESEARCH STAFF, not included above
USERS, in house 13 outside 14
GRAD STUDENTS involved during year 12
RESEARCH BUDGET, in house
FUNDED BY NSERC

MAGNET
POLE FACE, diameter (compact) 117 cm, R extraction 30-52cm
R injection 0.8 cm
GAP, min 3.6 cm, Field 26.5 kG
max 15 cm, Field 15.5 kG } at 280,000 Ampere turns
AVERAGE FIELD at R ext 19.2-19.7 kG
B max/ <B> 1.4
NUMBER OF SECTORS { compact 4 / separated } Spiral, max 50 deg
SECTOR ANGLE (SSC) deg
TRIMMING COILS Total of 64 Invar blocks situated on the four hills+
CONDUCTOR, material and type Water cooled copper
STORED ENERGY (cryogenic) MJ
POWER : main coils 113 max, kW ; current stability $1/10^4$
trimming coils + max, kW ; current stability +
WEIGHT : Fe 38 tons ; coils 4 tons
COOLING system Demineralized water
ION ENERGY (bending limit) E/A = 50 q^2/a^2 MeV/amu
(focusing limit) E/A = q^2/a^2 MeV/amu

ACCELERATION SYSTEM
DEES, number 2 ; angle 55 deg
BEAM APERTURE 1.8 cm ; DC Bias -1 kV
TUNED by, coarse sliding short fine variable capacitor
RF 21 to 31 mHz, stable ± $1/10^6$
Orb F 15.25 to 28.3 mHz
HARMONICS, RF/Orb F, used 1 or 2
DEE - Gnd, max 42 kV, min gap 0.3 cm
STABILITY, (pk-pk noise)/(pk RF volt) $1/10^3$
ENERGY GAIN, max 80 for H 140 for D kV/turn
RF PHASE, stable to ± 10 deg
RF POWER input, max 2 x 15 kW
FREQUENCY MODULATION, rate /s
modulator, type E
beam pulse, width

VACUUM SYSTEM
OPERATING PRESSURE $15-25 \times 10^{-6}$ Torr or mbar
PUMPS, No, Type, Size 2 x 16" Balzers diffusion pumps, 1 x 6" NRC diffusion pump, 2 cryopumps on injection system

ION SOURCES
Duoplasmatron, Ehlers source for H^- & D^-, Lamb-shift nuclear spin filter source for H^- & D^- ions.

INJECTION SYSTEM
Axial injection

EXTRACTION SYSTEM
Stripping of electrons from H^- & D^- by a stripping foil

FACILITIES FOR RESEARCH
SHIELDED AREA, fixed 300 m² ; movable 20 m²
TARGET STATIONS 7 in 2 rooms
STATIONS served at same time, max 1
MAG SPECTROGRAPH, type
COMPUTER model VAX 11/750
OTHER FACILITIES PIXE, Neutral Hydrogen Beam, 10-50 MeV, Proton Microprobe, High resolution spectroscopy, Isotope production

CHARACTERISTIC BEAMS

PARTICLE	ENERGY (MeV) Goal	Achieved	CURRENT (pμA) Internal	External
P	20-50	20-50	10-1	10-1
d	10-27	11-21	5-1	5-1
H^0	10-50	23-47	4	0.25
d	10-27	11-21		12-2 nA
SECONDARY			(part/s)	
n			4×10^7 sr^{-1}	

BEAM PROPERTIES

MEASURED		CONDITIONS
PULSE WIDTH 20 RF deg	1	pμA of 20-50 MeV P. ions
PHASE EXC, max 12 RF deg		pμA of MeV P. ions
EXTRACT eff 100 %		pμA of 20-50 MeV P. ions
RESOL ΔE/E 1,2 %		pμA of MeV P. ions
EMITTANCE		
(π mm. mrad) { axial / rad }		pμA of MeV ions

OPERATING PROGRAMS, time distribution
BASIC NUCLEAR PHYSICS 40% SOLID STATES PHYSICS
BIOMEDICAL APPLICAT. 20% ISOTOPE PRODUCTIONS 5%
Applied Physics 35%

REFERENCES/NOTES
1) IEEE Trans.Nucl.Sci. NS-32, No.5 (1985) 2724
+) Invar is an alloy with temperature dependent permeability. Magnetic field is shaped by controlling the temperature of each Invar block.

PLAN VIEW OF FACILITY, NOTEWORTHY FEATURES, COMMENTS

ENTRY NO. 04 **Date** June 1/92

Name of Machine TRIUMF Cyclotron

Institution TRIUMF

Address 4004 Wesbrook Mall, Vancouver, B.C., Canada

Tel (604) 222-1047 Telex (0)4 508503 Fax (604) 222-1074 EMAIL PEARCED@TRIUMFCL

In Charge: G. Dutto Reported by: D. Pearce

HISTORY

MILESTONE DATES:

Design July 1966 Model Tests December 1966

Construction October 1968 First Beam December 1974

DESIGN/CONSTRUCTION BY:

in house yes other various engineering contracts

COST: Accelerator 12 M$ Can. Facility 50 M$ Can.

FUNDED BY: AECB, SFU, UBC, U of Victoria, U of Alberta (to 1976), NRC, Province of B.C. (since 1977)

STATUS

STAFF: Machine

Scientists 15 Engineers 26

Technicians 70 Students 2

Research (in house/external)

Scientists 47 / 150 Engineers 12 / -

Technicians 30 / - Students 30 / 64

BUDGET: Machine 26 M$ Can. Funded by NRC

Research 4.6 M$ Can. Funded by NSERC

TIME DISTRIBUTION:

Basic Research (in house/external) 10 % / 44 %

Applied Program (in house/external) 12 % / - %

Development 3 % Maintenance 31 %

MAGNET

POLE PARAMETERS:

Diameter 1717. cm $R_{extract}$ 580-760. cm R_{inject} 25 cm

HILL PARAMETERS: Gap (min) 52.8 cm B_{max} 0.58 T

(@ 720000 AT) Gap (max) 52.8 cm B_{min} 0.30 T

VALLEY PARAMETERS: Gap (min) - cm B_{max} 0.30 T

(@ 720000 AT) Gap (max) - cm B_{min} 0.12 T

AVERAGE FIELD: $< B >_{min}$ 0.30 T $< B >_{max}$ 0.46 T

NUMBER OF SECTORS: compact/separated / 6

sector angle 17.5 deg. spiral (max) 70 deg.

FIELD TRIMMING: Trim Coils 55

Harmonic Coils 13

Other

CURRENT: Main Coils 18400 Amps Stability 10 ppm

Trim Coils Amps Stability

Stored Energy (cryogenic) MJ

WEIGHT: Iron 4000 tons Conductor 170 tons

ION ENERGY: Bending Limit E/A = 520 q^2/A^2 MeV/u

Focussing Limit E/A = q/A MeV/u

ACCELERATION SYSTEM

FUNDAMENTAL ACCELERATION:

Description: 80 lambda/4 resonators, push-pull mode

No. of Gaps/turn 2 dE/dn(max) 0.34 MeV/q

Voltage(max) 0.085 MV Harmonic f_{rf}/f_{ion} 5

Freq 23.05 MHz Power in(max) 1.1 MW

Stability: Phase +-5 deg Voltage 4×10^{-4}

OTHER CAVITIES (Flattopping or otherwise):

Description: Auxiliary Acc. Cav., lambda/4

Region of Influence: R_{min} 700 cm R_{max} 775 cm

No. of Gaps/turn 2 dE/dn(max) 0.300 MeV/q

Voltage(max) 0.15 MV Harmonic f_{rf}/f_{ion} 20

Freq 92 MHz Power in(max) 0.060 MW

Stability: Phase Voltage

VACUUM SYSTEM

OPERATING PRESSURE: 5×10^{-8} Torr

PUMPS: No. and type 2 He cooled cryo-panels (2,8 m^2) 4-41 cm cryo-pumps, 1-46 cm cryo-pump, 1-25 cm turbo

ION SOURCE(S)

	Type	Intensity (mA)	@ $\epsilon_n = \beta\gamma\epsilon$ (πmm mrad)	Ion Species
(a)	Ehlers PIG	0.30	0.2 h, x, 05 v	H^-
(b)	Cusp	2	0.25 h, v	H^-
(c)	Lamb Shift	6×10^{-4}	0.35 h, v	H^- pol (80%)
(d)	Optically pumped	0.010	0.35 h, v	H^- pol (75%)

INJECTION SYSTEM

axial injection, two bunchers, spiral inflector Efficiency 65-70 %

EXTRACTION SYSTEM

Stripping in pyrolytic graphite foil Efficiency 99.95 %

CHARACTERISTIC BEAMS

	Accelerated Ions	E/A (MeV/u)	Current(part μA) Internal	External
(a)	H^-	180-520	180 H^-	180 p^+
(b)	H^-	65-100	100 H^-	100 p^+
(c)	H^- (pol)	180-520	5 H^-	5 p^+ (pol)
(d)				

	Secondary Particles	E (MeV)	part/sec
(a)	pi+	20-350	10^7-10^8
(b)	muon+	4-90	10^6-10^7
(c)			

EXTRACTED BEAM PROPERTIES:

For 160 μA of 500 MeV/u p ions

$\Delta E/E$ 0.2 % $\Delta\phi$ 35 °rf

$\epsilon_n = \beta\gamma\epsilon$ x 2 πmm mrad z 2 πmm mrad

FACILITIES FOR RESEARCH

SHIELDED AREA: Fixed 2350 m^2 Moveable m^2

Target Stations: 18 No. Served At Same Time: 10

MAGNETIC SPECTROMETERS: MRS R=2.5m, OOD R=0.6m

OTHER FACILITIES: Biomedical π^- irradiation

Thermal Neutron Source, Polarized Fast Neutron Beam

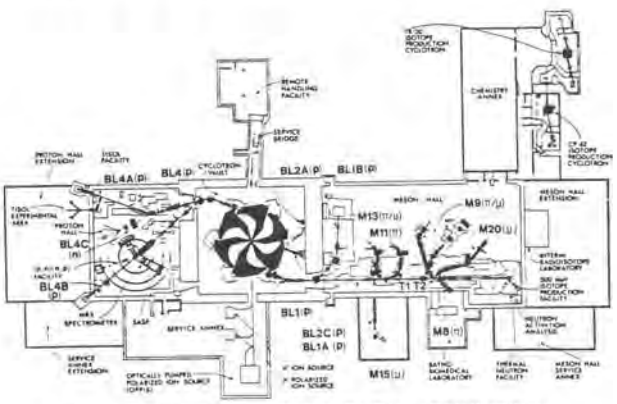
Isotope Production, on line isotope separator

REFERENCES/NOTES

(a)

(b)

PLAN VIEW OF FACILITY, COMMENTS



BEAM LINES AND EXPERIMENTAL FACILITIES
— EXISTING — PROPOSED

ENTRY No. C5

NAME OF MACHINE ELECTRON U. de CHILE DATE JUNE 1965
INSTITUTION FACULTAD DE CIENCIAS - UNIVERSIDAD DE CHILE
ADDRESS SANTIAGO, CHILE, CASILLA 653
TEL 2712865 Anexo 215 TELEX 240230 BOOTH CL NUCLEAR
IN CHARGE J.R. MORALES REPORTED BY J.R. MORALES

HISTORY AND STATUS

DESIGN, date 1960 1960 - 1964 Model tests 1962
ENG DESIGN, date
CONSTRUCTION, date 1960 - 1964
FIRST BEAM, date (or goal) 1962 (Davis) 1967 (Santiago)
MAJOR ALTERATIONS New design MS and RI

COST, ACCELERATOR $ 500,000
COST, FACILITY, total $ 300,000
FUNDED BY U. of Chile,

ACCELERATOR STAFF, OPERATION AND DEVELOPMENT

SCIENTISTS 1 ENGINEERS 1
TECHNICIANS 1 CRAFTS 1
GRAD STUDENTS involved during year
OPERATED BY 1 Research staff or 1 Operators
OPERATION 50 hr/wk On target 40 hr/wk
TIME DISTR. in house 90 %, Outside 10 %
BUDGET, op & dev US $ 10.000
FUNDED BY Univ. of Chile

RESEARCH STAFF, not included above

USERS, in house 4 outside 3
GRAD STUDENTS involved during year 2
RESEARCH BUDGET, in house non fixed, about US $ 10.000
FUNDED BY U. of Chile, CONICYT

MAGNET

POLE FACE, diameter (compact) cm, R extraction cm
R injection cm
GAP, min cm, Field kG
max 4.4 cm, Field 19.7 kG
19.7 kG
at $0.2.10^6$ Ampere turns
AVERAGE FIELD at R ext kG
B max/ <B>
NUMBER OF SECTORS compact 3 separated Spiral, max deg
SECTOR ANGLE (SSC) deg
TRIMMING COILS 1/sect.

CONDUCTOR, material and type Cu. pipes
STORED ENERGY (cryogenic) MJ
POWER: main coils 74 max, kW ; current stability 10^{-4}
trimming coils max, kW ; current stability
WEIGHT : Fe 50 tons ; coils 3 tons
COOLING system Destil. water
ION ENERGY (bending limit) E/A = q^2/a^2 MeV/amu
(focusing limit) E/A = q^2/a^2 MeV/amu

ACCELERATION SYSTEM

DEES, number 2 ; angle 100 deg
BEAM APERTURE 1.5 cm ; DC Bias kV
TUNED by, coarse MS fine
RF 15 to 30 mHz, stable ± 10^{-6}
Orb F to mHz
HARMONICS, RF/Orb F, used
DEE - Gnd, max 60kV, min gap 0.05 cm
STABILITY, (pk-pk noise)/(pk RF volt)
ENERGY GAIN, max 100 kV/turn
RF PHASE, stable to ± deg
RF POWER input, max 15 kW
FREQUENCY MODULATION, rate 500 /s
modulator, type pulsed
beam pulse, width 25-30 %

VACUUM SYSTEM

OPERATING PRESSURE 15 μ mbar
PUMPS, No, Type, Size Leybold D-250/two diffusion pumps

ION SOURCES

A "COLD-CATHODE" ion source is now being used.

INJECTION SYSTEM

EXTRACTION SYSTEM

Electrostatic

FACILITIES FOR RESEARCH

SHIELDED AREA, fixed 150 m² ; movable m²
TARGET STATIONS 3 in 2 rooms
STATIONS served at same time, max 1
MAG SPECTROGRAPH, type
COMPUTER model PC Acer 500*;
OTHER FACILITIES 19 in. ORTEC SCATT. CHAMBER

CHARACTERISTIC BEAMS

PARTICLE	ENERGY (MeV) Goal	Achieved	CURRENT (pμA) Internal	External
p	12	10	15	1.0
d	6	4.8	10	2.0
^{3}He	12	10	0.5	0.3
SECONDARY				(part/s)
0		20		10^5

BEAM PROPERTIES

	MEASURED		CONDITIONS		
PULSE WIDTH	RF deg		pμ A of	MeV	ions
PHASE EXC, max	RF deg		pμ A of	MeV	ions
EXTRACT eff	30 %	2	pμ A of	5 MeV	d ions
RESOL ΔE/E	1 %	2	pμ A of	5 MeV	d ions
EMITTANCE					
(π mm. mrad) axial / rad			pμA of	MeV	ions

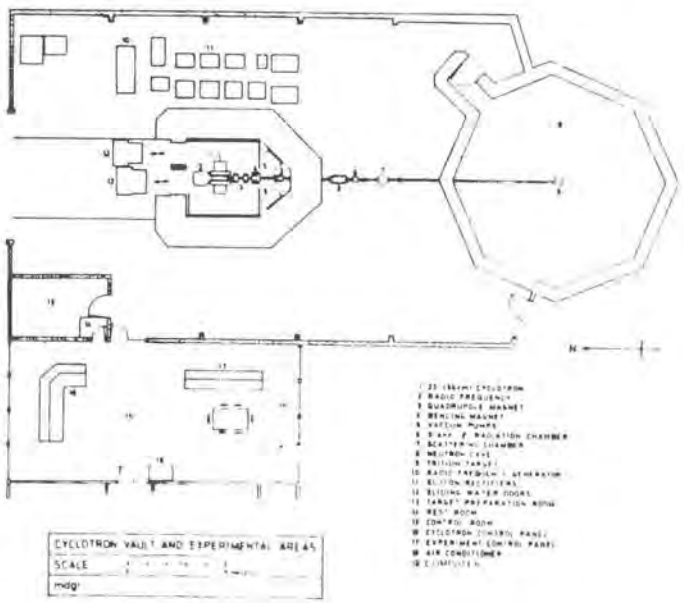
OPERATING PROGRAMS, time distribution

BASIC NUCLEAR PHYSICS 10% SOLID STATES PHYSICS
BIOMEDICAL APPLICAT. ISOTOPE PRODUCTIONS
PIXE 70%
PROTON ACTIVATION ANALYSIS 20%

REFERENCES/NOTES

(1) Nucl. Inst. Meth. 18, 19, 120-124 and 125-128.(1962)
UCD - CNL 56 Report (1970).
(2) Cyclotron transferred from UC Davis through U. Chile - U. Calif. cooperative program, financed by Ford Foundation.

PLAN VIEW OF FACILITY, NOTEWORTHY FEATURES, COMMENTS



ENTRY No. C6

NAME OF MACHINE Y-20 DATE

INSTITUTION Institute of Atomic Energy

ADDRESS Box 275, Beijing, PRC

TEL 868221 TELEX

IN CHARGE REPORTED BY

HISTORY AND STATUS

DESIGN, date Model tests

ENG DESIGN, date

CONSTRUCTION, date October 1, 1958

FIRST BEAM, date (or goal)

MAJOR ALTERATIONS

COST, ACCELERATOR 6 million yuan

COST, FACILITY, total 10 million yuan

FUNDED BY

ACCELERATOR STAFF, OPERATION AND DEVELOPMENT

SCIENTISTS ENGINEERS

TECHNICIANS CRAFTS

GRAD STUDENTS involved during year

OPERATED BY Research staff or Operators

OPERATION 120 hr/wk, On target 100 hr/wk

TIME DISTR. in house 100 %, Outside %

BUDGET, op & dev

FUNDED BY

RESEARCH STAFF, not included above

USERS, in house outside

GRAD STUDENTS involved during year

RESEARCH BUDGET, in house

FUNDED BY

MAGNET

POLE FACE, diameter (compact) 120 cm, R extraction 52.5 cm

R injection cm

GAP, min 148 cm, Field 15.95 kG
max 218 cm, Field 13.05 kG
} at 286944 Ampere turns

AVERAGE FIELD at R ext 14.50 kG

B max/ <B>

NUMBER OF SECTORS { compact / separated } Spiral, max 45 deg

SECTOR ANGLE (SSC) deg

TRIMMING COILS 7 coils

CONDUCTOR, material and type Cu

STORED ENERGY (cryogenic) MJ

POWER: main coils 130 max, kW ; current stability 2×10^{-4}
trimming coils max, kW ; current stability 1×10^{-3}

WEIGHT: Fe 120 tons ; coils 15 tons

COOLING system water

ION ENERGY (bending limit) E/A = q^2/a^2 MeV/amu
(focusing limit) E/A = q^2/a^2 MeV/amu

ACCELERATION SYSTEM

DEES, number 2 ; angle 180 deg

BEAM APERTURE 35 cm ; DC Bias kV

TUNED by, coarse fine

RF 5.9 to 19.3 mHz, stable ± 2×10^{-6}

Orb F 6 to 17.2 mHz

HARMONICS, RF/Orb F, used 1st

DEE - Gnd, max 70 kV, min gap 26.5 cm

STABILITY, (pk-pk noise)/(pk RF volt) 1×10^{-3}

ENERGY GAIN, max 200 kV/turn

RF PHASE, stable to ± 1 deg

RF POWER input, max 120 kW

FREQUENCY MODULATION, rate 300 /s

modulator, type outside modulator

beam pulse, width 2-3 ms

VACUUM SYSTEM

OPERATING PRESSURE 1×10^{-5} Torr or mbar

PUMPS, No, Type, Size

ION SOURCES

PIG type

INJECTION SYSTEM

EXTRACTION SYSTEM

Electrostatic deflector

FACILITIES FOR RESEARCH

SHIELDED AREA, fixed 150 m² ; movable m²

TARGET STATIONS 3 in 2 rooms

STATIONS served at same time, max 1

MAG SPECTROGRAPH, type

COMPUTER model

OTHER FACILITIES

CHARACTERISTIC BEAMS

PARTICLE	ENERGY (MeV) Goal	ENERGY (MeV) Achieved	CURRENT (pμA) Internal	CURRENT (pμA) External
P	3-20	6-15	200	60
D	3-15	4.5-15	200	60
Alpha	6-30	9-30	10	3
SECONDARY				(part/s)

BEAM PROPERTIES

MEASURED	CONDITIONS
PULSE WIDTH 6 RF deg	1 pμA of 12 MeV P. ions
PHASE EXC, max RF deg	pμA of MeV ions
EXTRACT eff 0.7 %	pμA of MeV ions
RESOL ΔE/E %	pμA of MeV ions
EMITTANCE (π mm. mrad) { axial / rad }	pμA of MeV ions

OPERATING PROGRAMS, time distribution

BASIC NUCLEAR PHYSICS 90% SOLID STATES PHYSICS

BIOMEDICAL APPLICAT. ISOTOPE PRODUCTIONS

REFERENCES/NOTES

PLAN VIEW OF FACILITY, NOTEWORTHY FEATURES, COMMENTS

ENTRY NO. C7 **Date** June 20/92

Name of Machine HIRFL Sector Focusing Cyclotron (Injector)

Institution Institute of Modern Physics, Chinese Academy of Sciences (IMP)

Address P.O.Box 31, Lanzhou 730000, P.R.China

Tel 28951 Telex 72153 IMPAS CN Fax 0086-931-23600 EMAIL IMP @ VX IHEP.

In Charge: B.W.Wei **Reported by:** F.Ye IHEP. CERN. CH

HISTORY

MILESTONE DATES:

Design ..... Model Tests .....

Construction ..... First Beam .....

DESIGN/CONSTRUCTION BY:

in house ..... other .....

COST: Accelerator ..... Facility .....

FUNDED BY: .....

STATUS

STAFF: Machine

Scientists 10 Engineers 10

Technicians 10 Students 3

Research (in house/external)

Scientists ... / ... Engineers ... / ...

Technicians ... / ... Students ... / ...

BUDGET: Machine ..... Funded by .....

Research ..... Funded by .....

TIME DISTRIBUTION:

Basic Research (in house/external) ..... % / ..... %

Applied Program (in house/external) ..... % / ..... %

Development ..... % Maintenance ..... %

MAGNET

POLE PARAMETERS:

Diameter 170 cm $R_{extract}$ 75 cm R_{inject} 4.5 cm

HILL PARAMETERS: Gap (min) 19 cm B_{max} 2.0 T

(@ ... AT) Gap (max) ... cm B_{min} ... T

VALLEY PARAMETERS: Gap (min) ... cm B_{max} ... T

(@ ... AT) Gap (max) 31.6 cm B_{min} 1.2 T

AVERAGE FIELD: $< B >_{min}$ 0.8 T $< B >_{max}$ 1.6 T

NUMBER OF SECTORS: compact/separated 3 / ...

sector angle ... deg. spiral (max) 33° deg.

FIELD TRIMMING: Trim Coils 12

Harmonic Coils 4 X 3

Other .....

CURRENT: Main Coils 1300 Amps Stability $1 e^{-5}$

Trim Coils 500 Amps Stability $1 e^{-4}$

Stored Energy (cryogenic) ..... MJ

WEIGHT: Iron 220 tons Conductor 16 tons

ION ENERGY: Bending Limit E/A = 69 q^2/A^2 MeV/u

Focussing Limit E/A = ... q/A MeV/u

ACCELERATION SYSTEM

FUNDAMENTAL ACCELERATION:

Description: 1/2 lambda/ 1 resonator

No. of Gaps/turn 2 dE/dn(max) 0.2 MeV/q

Voltage(max) 100 MV Harmonic f_{rf}/f_{ion} 1, 3

Freq 6-18 MHz Power in(max) 0.2 MW

Stability: Phase 1° Voltage 10^{-3}

OTHER CAVITIES (Flattopping or otherwise):

Description: .....

Region of Influence: R_{min} ... cm R_{max} ... cm

No. of Gaps/turn ... dE/dn(max) ... MeV/q

Voltage(max) ... MV Harmonic f_{rf}/f_{ion} ...

Freq ... MHz Power in(max) ... MW

Stability: Phase ... Voltage ...

VACUUM SYSTEM

OPERATING PRESSURE: 5×10^{-5} Pa

PUMPS: No. and type 2 HIRFL 800 cryo-pumps,

2 turbo-pumps, rough pumping system

ION SOURCE(S)

	Type	Intensity (mA)	@	$\epsilon_n = \beta\gamma\epsilon$ (πmm mrad)	Ion Species
(a)	ECR	0.1-0.3		200	C - Ta
(b)					
(c)					
(d)					

INJECTION SYSTEM

spiral electrostatic inflector ... Efficiency 30 %

EXTRACTION SYSTEM

electrostatic deflectors + magnetic channel Efficiency 70 %

CHARACTERISTIC BEAMS

	Accelerated Ions	E/A (MeV/u)	Current(part μA) Internal	External
(a)	C^{4+}	4.5		1
(b)	C^{4+}	6.6		1
(c)	O^{5+}	4.5		1
(d)	Ar^{8+}	2.3		0.8

	Secondary Particles	E (MeV)	part/sec
(a)			
(b)			
(c)			

EXTRACTED BEAM PROPERTIES:

For ... μA of ... MeV/u ... ions

$\Delta E/E$ ... % $\Delta\phi$ ... °rf

$\epsilon_n = \beta\gamma\epsilon$ x ... πmm mrad z ... πmm mrad

FACILITIES FOR RESEARCH

SHIELDED AREA: Fixed ... m^2 Moveable ... m^2

Target Stations: ... No. Served At Same Time: ...

MAGNETIC SPECTROMETERS: .....

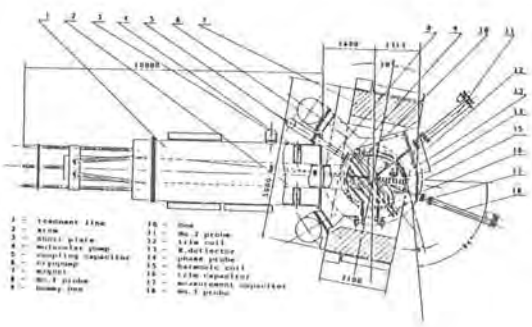
OTHER FACILITIES: .....

REFERENCES/NOTES

(a) .....

(b) .....

PLAN VIEW OF FACILITY, COMMENTS



ENTRY NO. C8 Date June 20/92

Name of Machine HIRFL Separated Sector Cyclotron (Main Accelerator)

Institution Institute of Modern Physics, Chinese Academy of Science (IMP)

Address P.O.Box 31, Lanzhou 730000, P.R.China

Tel 28951 Telex 72153 IMPAS CN Fax 0086-931-23600 EMAIL IMP @ VX IHEP

In Charge: B.W.Wei Reported by: F.Ye IHEP. CERN. CH

HISTORY

MILESTONE DATES:

Design 1976 Model Tests 1976

Construction 1978 First Beam Dec.12, 1988

DESIGN/CONSTRUCTION BY:

in house yes other engineering contracts

COST: Accelerator 100 M yuans Facility 140 M yuans

FUNDED BY: State Planning Commission, CAS

STATUS

STAFF: Machine

Scientists 40 Engineers 50

Technicians 60 Students 10

Research (in house/external)

Scientists / Engineers /

Technicians / Students /

BUDGET: Machine 10 M yuans Funded by SPC

Research 2 M yuans Funded by CAS

TIME DISTRIBUTION:

Basic Research (in house/external) 40 % / 11 %

Applied Program (in house/external) 10 % / 5 %

Development 14 % Maintenance 20 %

MAGNET

POLE PARAMETERS:

Diameter 717 cm $R_{extract}$ 321 cm R_{inject} 100 cm

HILL PARAMETERS: Gap (min) 10 cm B_{max} 16 T

(@ AT) Gap (max) 10 cm B_{min} 6 T

VALLEY PARAMETERS: Gap (min) cm B_{max} T

(@ AT) Gap (max) cm B_{min} T

AVERAGE FIELD: $< B >_{min}$ 0.35 T $< B >_{max}$ 0.92 T

NUMBER OF SECTORS: compact/separated / 4

sector angle 52° deg. spiral (max) deg.

FIELD TRIMMING: Trim Coils 36

Harmonic Coils

Other

CURRENT: Main Coils 4000 Amps Stability 5 e-6

Trim Coils 300 Amps Stability 5 e-5

Stored Energy (cryogenic) MJ

WEIGHT: Iron 2000 tons Conductor 15.6 tons

ION ENERGY: Bending Limit E/A = q^2/A^2 MeV/u

Focussing Limit E/A = q/A MeV/u

ACCELERATION SYSTEM

FUNDAMENTAL ACCELERATION:

Description: 1/2 lambda / 2 resonators

No. of Gaps/turn 4 dE/dn(max) 1.0 MeV/q

Voltage(max) 250 MV Harmonic f_{rf}/f_{ion} 2, 4, 6

Freq 6.5-14 MHz Power in(max) 0.24 MW

Stability: Phase 1° Voltage 10^{-3}

OTHER CAVITIES (Flattopping or otherwise):

Description:

Region of Influence: R_{min} cm R_{max} cm

No. of Gaps/turn dE/dn(max) MeV/q

Voltage(max) MV Harmonic f_{rf}/f_{ion}

Freq MHz Power in(max) MW

Stability: Phase Voltage

VACUUM SYSTEM

OPERATING PRESSURE: 10^{-5} Pa

PUMPS: No. and type 4 HIRFL 800 cryo-pumps with rough pumping system

ION SOURCE(S)

	Type	Intensity (mA)	@	$\epsilon_n = \beta\gamma\epsilon$ (πmm mrad)	Ion Species
(a)	ECR	0.1-0.3		200	C-Ta
(b)					
(c)					
(d)					

INJECTION SYSTEM

bending magnets + deflector + magnetic channels Efficiency 50 %

EXTRACTION SYSTEM

bump+deflector+magnetic channels+bending magnets Efficiency 50 %

CHARACTERISTIC BEAMS

	Accelerated Ions	E/A (MeV/u)	Current(part μA) Internal	External
(a)	C^{6+}	50		0.07
(b)	C^{6+}	75		0.07
(c)	O^{8+}	50		0.05
(d)	Ar^{16+}	25		

	Secondary Particles	E (MeV)	part/sec
(a)			
(b)			
(c)			

EXTRACTED BEAM PROPERTIES:

For 0.4 μA of 50 MeV/u C^{6+} ions

$\Delta E/E$ 0.3 % $\Delta\phi$ °rf

$\epsilon_n = \beta\gamma\epsilon$ x 7 πmm mrad z 7 πmm mrad

FACILITIES FOR RESEARCH

SHIELDED AREA: Fixed 1456 m² Moveable m²

Target Stations: 8 No. Served At Same Time:

MAGNETIC SPECTROMETERS:

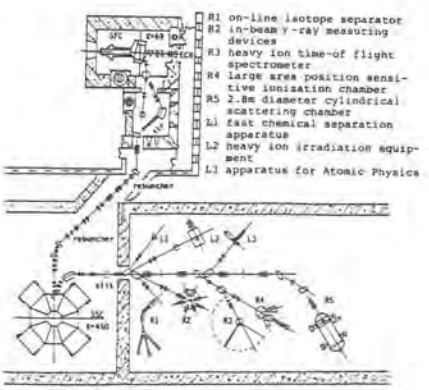
OTHER FACILITIES: Isotope Separator, In-beam γ-ray Measuring Device, Heavy Ion Telescope, Ionization Chamber, Scattering Chamber, Fast Chemistry Separation Apparatus, Material Science Terminal, Atomic Physics Terminal

REFERENCES/NOTES

(a)

(b)

PLAN VIEW OF FACILITY, COMMENTS



ENTRY NO. C9 Date

Name of Machine INR Cyclotron

Institution Institute of Nuclear Research, Academia Sinica, Shanghai

Address Shanghai, China

Tel 9530998 Telex Fax EMAIL

In Charge: Lin-xing Chen Reported by: Gen-xiang Gu

HISTORY

MILESTONE DATES:

Design 1978-1979 Model Tests

Construction 1980-1982 First Beam Nov.1983

DESIGN/CONSTRUCTION BY:

in house other

COST: Accelerator Facility

FUNDED BY: Academia Sinica

STATUS

STAFF: Machine

Scientists Engineers

Technicians Students

Research (in house/external)

Scientists / Engineers /

Technicians / Students /

BUDGET: Machine Funded by

Research Funded by

TIME DISTRIBUTION:

Basic Research (in house/external) 30 % / %

Applied Program (in house/external) 60 % / %

Development % Maintenance 10 %

MAGNET

POLE PARAMETERS:

Diameter 138 cm $R_{extract}$ 61 cm R_{inject} cm

HILL PARAMETERS: Gap (min) 14.6 cm B_{max} 17.5 T

(@ AT) Gap (max) cm B_{min} T

VALLEY PARAMETERS: Gap (min) 22.4 cm B_{max} 11.7 T

(@ AT) Gap (max) cm B_{min} T

AVERAGE FIELD: $< B >_{min}$ 14.6 T $< B >_{max}$ T

NUMBER OF SECTORS: compact/separated 3 /

sector angle deg. spiral (max) deg.

FIELD TRIMMING: Trim Coils 9

Harmonic Coils 3

Other 5

CURRENT: Main Coils 450 Amps Stability 5×10^{-4}

Trim Coils 400 Amps Stability 1×10^{-4}

Stored Energy (cryogenic) MJ

WEIGHT: Iron 120 tons Conductor

ION ENERGY: Bending Limit E/A = 32 q^2/A^2 MeV/u

Focussing Limit E/A = 30 q/A MeV/u

ACCELERATION SYSTEM

FUNDAMENTAL ACCELERATION:

Description: 1x180 Dee

No. of Gaps/turn 2 dE/dn(max) 0.140 MeV/q

Voltage(max) 0.07 MV Harmonic f_{rf}/f_{ion}

Freq 10-22 MHz Power in(max) 0.100 MW

Stability: Phase Voltage

OTHER CAVITIES (Flattopping or otherwise):

Description:

Region of Influence: R_{min} cm R_{max} cm

No. of Gaps/turn dE/dn(max) MeV/q

Voltage(max) MV Harmonic f_{rf}/f_{ion}

Freq MHz Power in(max) MW

Stability: Phase Voltage

VACUUM SYSTEM

OPERATING PRESSURE: 1.5×10^{-5} torr

PUMPS: No. and type 2x1250 l/s oil diff.

ION SOURCE(S)

	Type	Intensity (mA)	@	$\epsilon_n = \beta\gamma\epsilon$ (πmm mrad)	Ion Species
(a)	P.I.G type				p,alpha,d
(b)					
(c)					
(d)					

INJECTION SYSTEM

Efficiency %

EXTRACTION SYSTEM 2 sections of electrostatic defl.+ Foc. Mag. Channel + Mag. Weak. Channel

Efficiency %

CHARACTERISTIC BEAMS

Accelerated Ions	E/A (MeV/u)	Current(part μA) Internal	External
(a) p	10-30		30
(b) d	20-16		60
(c) alpha	32-40		15
(d)			

Secondary Particles	E (MeV)	part/sec
(a)		
(b)		
(c)		

EXTRACTED BEAM PROPERTIES:

For μA of 15-30 MeV/u p ions

$\Delta E/E$ 0.43-0.7 % $\Delta\phi$ °rf

$\epsilon_n = \beta\gamma\epsilon$ x πmm mrad z πmm mrad

FACILITIES FOR RESEARCH

SHIELDED AREA: Fixed m^2 Moveable m^2

Target Stations: No. Served At Same Time:

MAGNETIC SPECTROMETERS:

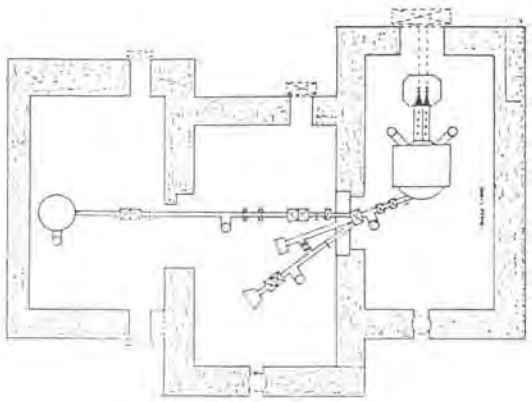
OTHER FACILITIES:

REFERENCES/NOTES

(a)

(b)

PLAN VIEW OF FACILITY, COMMENTS



ENTRY NO. C10 Date June 30 / 1992

Name of Machine U-120M

Institution Nuclear Physics Institute

Address 250 68 REZ near Prague, Czechoslovakia

Tel (+422) 6851831 Telex 122626 ujv c Fax (+422) 6857003 EMAIL UJF26@CSPGCS11

In Charge: Z.Trejbal Reported by: J.Stursa

HISTORY

MILESTONE DATES:
Design 1972 Model Tests 1975
Construction First Beam August 1977

DESIGN/CONSTRUCTION BY:
in house no other JINR Dubna Russia

COST: Accelerator 1.2 MS Facility

FUNDED BY: Czechoslovak Academy of Sciences

STATUS

STAFF: Machine
Scientists 4 Engineers 3
Technicians 15 Students 1
Research (in house/external)
Scientists 0 / 9 Engineers 0 /
Technicians 0 / Students 0 /

BUDGET: Machine Funded by
Research Funded by

TIME DISTRIBUTION:
Basic Research (in house/external) % / 40 %
Applied Program (in house/external) 1 % / 40 %
Development 5 % Maintenance 15 %

MAGNET

POLE PARAMETERS:
Diameter 120 cm $R_{extract}$ 50 cm R_{inject} 18 cm
HILL PARAMETERS: Gap (min) 8.2 cm B_{max} 1.80 T
(@ AT) Gap (max) 12.0 cm B_{min} 2.05 T
VALLEY PARAMETERS: Gap (min) 22 cm B_{max} 1.72 T
(@ AT) Gap (max) 22 cm B_{min} 1.61 T
AVERAGE FIELD: $< B >_{min}$ T $< B >_{max}$ 1.85 T
NUMBER OF SECTORS: compact/separated 4 /
sector angle deg. spiral (max) 70 deg.
FIELD TRIMMING: Trim Coils 18
Harmonic Coils 1 (first harm.)
Other
CURRENT: Main Coils 600 Amps Stability 1e-5
Trim Coils 500 Amps Stability 1e-3
Stored Energy (cryogenic) MJ
WEIGHT: Iron 110 t Conductor 11.6 t
ION ENERGY: Bending Limit E/A = 40 q^2/A^2 MeV/u
Focussing Limit E/A = q/A MeV/u

ACCELERATION SYSTEM

FUNDAMENTAL ACCELERATION:
Description: 1 dee 180°
No. of Gaps/turn 2 dE/dn(max) 0.08 MeV/q
Voltage(max) 0.04 MV Harmonic f_{rf}/f_{ion} 1
Freq 10-26 MHz Power in(max) 0.1 MW
Stability: Phase Voltage 5e-3

OTHER CAVITIES (Flattopping or otherwise):
Description:
Region of Influence: R_{min} cm R_{max} cm
No. of Gaps/turn dE/dn(max) MeV/q
Voltage(max) MV Harmonic f_{rf}/f_{ion}
Freq MHz Power in(max) MW
Stability: Phase Voltage

VACUUM SYSTEM

OPERATING PRESSURE: $6 \cdot 10^{-4}$ Pa
PUMPS: No. and type 2 x 2000 l/s diff.pumps

ION SOURCE(S)

	Type	Intensity (mA)	@	$\epsilon_n = \beta\gamma\epsilon$ (πmm mrad)	Ion Species
(a)	Inner PIG	0.6			p, d $\psi+$
(b)	Inner PIG	0.05			^3He $\psi+$, ^4He $\psi+$
(c)					
(d)					

INJECTION SYSTEM

Axial injection,spiral inflec. Efficiency 12-40 %

EXTRACTION SYSTEM

Magnetic regenerator, Efficiency 30 %
3 electrostatic defl.sections

CHARACTERISTIC BEAMS

	Accelerated Ions	E/A (MeV/u)	Current(part μA) Internal	External
(a)	p	37	100	4-10
(b)	d $\psi+$	10	100	4-10
(c)	^3He $\psi+$	18	20	2-6
(d)	^3He	10	20	2-6

	Secondary Particles	E (MeV)	part/sec
(a)	neutrons	6	10^{12}
(b)			
(c)			

EXTRACTED BEAM PROPERTIES:
For 10 μA of 30 MeV/u p ions
$\Delta E/E$ 1 % $\Delta\phi$ 40 °rf
$\epsilon_n = \beta\gamma\epsilon$ x 11 πmm mrad z 2.5 πmm mrad

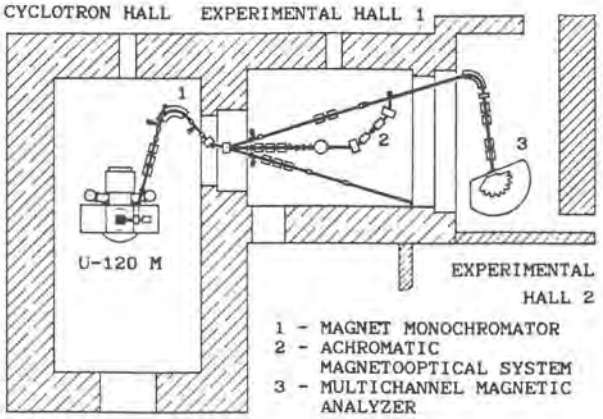
FACILITIES FOR RESEARCH

SHIELDED AREA: Fixed 265 m² Moveable 0 m²
Target Stations: 8 No. Served At Same Time: 1
MAGNETIC SPECTROMETERS: R=0.8m, 124deg, $\Delta E/E=5 \cdot 10^{-4}$
OTHER FACILITIES:
Multichannel magnetic analyzer $E/\Delta E=2500$
Achromatic magnetooptical system (AMOS) 90°,5m

REFERENCES/NOTES

(a) J.Stursa,et al., Proc.EPAC 92, Berlin
(b) V.Bejsovec,et al.,II.Int.Conf...Czechoslov., JINR,D9-89-708,Dubna 1989,pp.44-46

PLAN VIEW OF FACILITY, COMMENTS



ENTRY NO. C11 **Date** 26.6.1992

Name of Machine K130 cyclotron

Institution Department of Physics, University of Jyväskylä (JYFL)

Address P.O.Box 35, 40351 JYVÄSKYLÄ, Finland

Tel +358-41-602400 **Telex** ... **Fax** +358-41-602401 **EMAIL** ...

In Charge: E. Liukkonen **Reported by:** T. Poikolainen

HISTORY

MILESTONE DATES:
Design 1988 Model Tests None 1)
Construction 1988-90 First Beam 1992 1)
DESIGN/CONSTRUCTION BY:
in house ... other ...
COST: Accelerator ab.7 million US$ Facility ab.20 million US$
FUNDED BY: Government of Finland

STATUS

STAFF: Machine
Scientists 5 Engineers 4
Technicians 3 Students 5
Research (in house/external)
Scientists ... / ... Engineers ... / ...
Technicians ... / ... Students ... / ...
BUDGET: Machine 1million US$/year Funded by Government of Finland through Univ.
Research ... Funded by ...
TIME DISTRIBUTION:
Basic Research (in house/external) 60 % / ... %
Applied Program (in house/external) 20 % / ... %
Development 10 % Maintenance 10 %

MAGNET

POLE PARAMETERS:
Diameter 240 cm $R_{extract}$ 95 cm R_{inject} 83 cm
HILL PARAMETERS: Gap (min) 33 cm B_{max} 2.12 T
(@ 400.000 AT) Gap (max) 33 cm B_{min} ... T
VALLEY PARAMETERS: Gap (min) 17.4 cm B_{max} ... T
(@ 400.000 AT) Gap (max) 17.4 cm B_{min} 1.26 T
AVERAGE FIELD: $< B >_{min}$ 0.35 T $< B >_{max}$ 1.77 T
NUMBER OF SECTORS: compact/separated 3 / ...
sector angle 51-81 deg. spiral (max) 58 deg.
FIELD TRIMMING: Trim Coils 15
Harmonic Coils 4 sets in valleys
Other ...
CURRENT: Main Coils 1000 Amps Stability 10^{-5}
Trim Coils 70 Amps Stability ...
Stored Energy (cryogenic) ... MJ
WEIGHT: Iron 300 tons Conductor 15 tons
ION ENERGY: Bending Limit E/A = 130 q^2/A^2 MeV/u
Focussing Limit E/A = 90 q/A MeV/u

ACCELERATION SYSTEM

FUNDAMENTAL ACCELERATION:
Description: λ/4 resonator; 2 dees
No. of Gaps/turn 4 dE/dn(max) 0.195 MeV/q
Voltage(max) 0.05 MV Harmonic f_{rf}/f_{ion} 1,2,3
Freq 10-21 MHz Power in(max) 0.2 MW
Stability: Phase ... Voltage ...
OTHER CAVITIES (Flattopping or otherwise):
Description: ...
Region of Influence: R_{min} ... cm R_{max} ... cm
No. of Gaps/turn ... dE/dn(max) ... MeV/q
Voltage(max) ... MV Harmonic f_{rf}/f_{ion} ...
Freq ... MHz Power in(max) ... MW
Stability: Phase ... Voltage ...

VACUUM SYSTEM

OPERATING PRESSURE: 10^{-7}
PUMPS: No. and type 2 cryo pumps
5000 l/s (for nitrogen)

ION SOURCE(S)

	Type	Intensity (mA)	@	$\epsilon_n = \beta\gamma\epsilon$ (πmm mrad)	Ion Species
(a)					
(b)	ECR	max 1			gaseous
(c)					
(d)					

INJECTION SYSTEM

Axial, spiral inflector, buncher (1st+2nd) Efficiency ... %

EXTRACTION SYSTEM

electrostatic defl.+EMC+2 passive channels Efficiency ... %

CHARACTERISTIC BEAMS

	Accelerated Ions	E/A (MeV/u)	Current(part μA) Internal	External
(a)	p	70		
(b)	$^{40}Ar^{\alpha}$	55 MeV		
(c)		6.0		
(d)				

	Secondary Particles	E (MeV)	part/sec
(a)			
(b)			
(c)			

EXTRACTED BEAM PROPERTIES:
For ... μA of ... MeV/u ... ions
ΔE/E ... % Δφ ... °rf
$\epsilon_n = \beta\gamma\epsilon$ x ... πmm mrad z ... πmm mrad

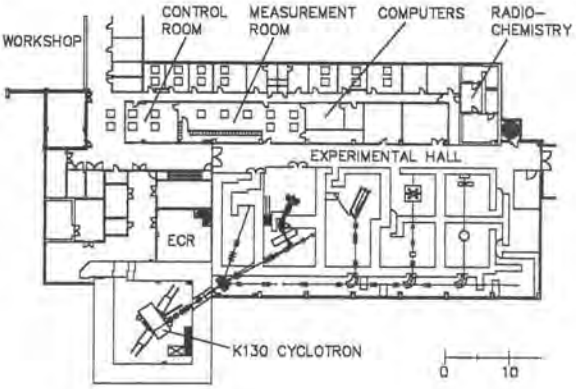
FACILITIES FOR RESEARCH

SHIELDED AREA: Fixed ... m^2 Moveable 425 m^2
Target Stations: 9 No. Served At Same Time: 1
MAGNETIC SPECTROMETERS: gas filled recoil separator
OTHER FACILITIES: on-line mass separator
gamma and electron spectrometers

REFERENCES/NOTES

(a) 1). Magnet design by JYFL; design and construction by
(b) Scanditronix AB, Sweden

PLAN VIEW OF FACILITY, COMMENTS



ENTRY NO. C12 **Date** 01/07/1992

Name of Machine GANIL C01 and C02 (Upgraded : CAE (1989) and CAI (first beam June 92) projects)

Institution GANIL

Address BP 5027 - F 14021 CAEN Cedex

Tel 31.45.46.47 Telex 170533 F Fax 31.45.46.65 EMAIL

In Charge: M. BAJARD Reported by: GANIL STAFF

HISTORY : see SSC1, 2 entry

MILESTONE DATES:

Design ..... Model Tests .....

Construction ..... First Beam .....

DESIGN/CONSTRUCTION BY:

in house ..... other .....

COST: Accelerator ..... Facility .....

FUNDED BY: .....

STATUS : see SSC1, 2 entry

STAFF: Machine

Scientists ..... Engineers .....

Technicians ..... Students .....

Research (in house/external)

Scientists ..... / ..... Engineers ..... / .....

Technicians ..... / ..... Students ..... / .....

BUDGET: Machine ..... Funded by .....

Research ..... Funded by .....

TIME DISTRIBUTION:

Basic Research (in house/external) ..... % / ..... %

Applied Program (in house/external) ..... % / ..... %

Development ..... % Maintenance ..... %

MAGNET

POLE PARAMETERS: C01 7.41

Diameter 131.6 cm $R_{extract}$ 48.825 cm R_{inject} C02 3.64 cm

HILL PARAMETERS: Gap (min) 21 cm B_{max} ..... T

(@ ..... AT) Gap (max) ..... cm B_{min} ..... T

VALLEY PARAMETERS: Gap (min) 30 cm B_{max} ..... T

(@ ..... AT) Gap (max) ..... cm B_{min} 1.565 T

AVERAGE FIELD: $< B >_{min}$ 1 T $< B >_{max}$ ..... T

NUMBER OF SECTORS: compact/separated 3 / .....

sector angle ..... deg. spiral (max) tg = 0.033r deg.

FIELD TRIMMING: Trim Coils 6 (circular)

Harmonic Coils .....

Other .....

CURRENT: Main Coils 1500 Amps Stability 10^{-5}

Trim Coils 500 Amps Stability 10^{-4}

Stored Energy (cryogenic) ..... MJ

WEIGHT: Iron ..... Conductor .....

ION ENERGY: Bending Limit E/A = 28 q^2/A^2 MeV/u

Focussing Limit E/A = ... q/A MeV/u

ACCELERATION SYSTEM

FUNDAMENTAL ACCELERATION:

Description: 180° D resonator tuned by two movable panels

No. of Gaps/turn 2 dE/dn(max) 0.18 MeV/q

Voltage(max) 0.09 MV Harmonic f_{rf}/f_{ion} 3

Freq 7 - 14 MHz Power in(max) ..... MW

Stability: Phase ± 0.1° Voltage 10^{-4}

OTHER CAVITIES (Flattopping or otherwise):

Description: .....

Region of Influence: R_{min} ..... cm R_{max} ..... cm

No. of Gaps/turn ..... dE/dn(max) ..... MeV/q

Voltage(max) ..... MV Harmonic f_{rf}/f_{ion} .....

Freq ..... MHz Power in(max) ..... MW

Stability: Phase ..... Voltage .....

VACUUM SYSTEM

OPERATING PRESSURE: $7 \cdot 10^{-6}$ Pascal

PUMPS: No. and type 1 cryo on vacuum chamber (20000 l/s)

2 cryo on HF resonator (20000 l/s)

ION SOURCE(S)

	Type	Intensity (mA)	@	$\epsilon_n = \beta\gamma\epsilon$ (πmm mrad)	Ion Species
(a)	C01 : ECR4 (14.5 GHz)				
(b)					He_3 - U_{238}
(c)	C02 : ECR3 (10 GHz)				
(d)					

INJECTION SYSTEM

C01 : 100kV injection line-spiral infl Efficiency up to 65 %

C02 : 20kV injection line-Muller infl up to 25 %

EXTRACTION SYSTEM

electrostatic deflector ..... Efficiency 100 %

+ electrostatic quadrupole

CHARACTERISTIC BEAMS

	Accelerated Ions	E/A (MeV/u)	Current(part μA) Internal	External
(a)	C01 : Ne^{+6}	1		4
(b)	Ta^{+24}	0.4		0.2
(c)	C02 : Ne^{+6}	1		1.2
(d)	U^{+24}	0.4		0.02

	Secondary Particles	E (MeV)	part/sec
(a)			
(b)			
(c)			

EXTRACTED BEAM PROPERTIES: (maximum values ful l width)

For ..... μA of ..... MeV/u ..... ions

$\Delta E/E$ 0.5 - 1.5 % $\Delta\phi$ 12 °rf

$\epsilon_n = \beta\gamma\epsilon$ x 30 - 45 πmm mrad z 45 πmm mrad

FACILITIES FOR RESEARCH : see SSC1, 2 entry

SHIELDED AREA: Fixed ..... m^2 Moveable ..... m^2

Target Stations: ..... No. Served At Same Time: .....

MAGNETIC SPECTROMETERS: .....

OTHER FACILITIES: .....

.....

.....

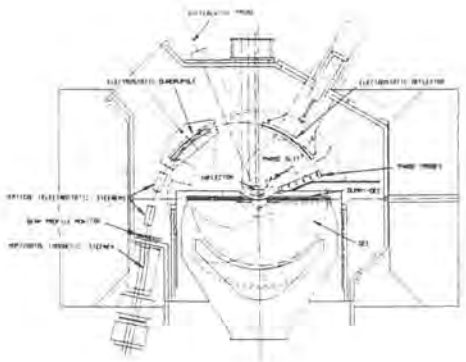
.....

REFERENCES/NOTES

(a) M.F. BOURGAREL et al. 12th Int. Conf. on cyclotron. BERLIN89

(b) C. RICAUD et al. this proceedings

PLAN VIEW OF FACILITY, COMMENTS



ENTRY NO. C13 Date 01/07/1992

Name of Machine GANIL SSC1 and SSC2 (Upgraded ; OAE (1989) and OAI (1992) projects)

Institution GANIL

Address BP 5027 F 14021 CAEN Cedex

Tel 31.45.46.47 Telex 170533 F Fax 31.45.46.65 EMAIL

In Charge: M. BAJARD Reported by: GANIL STAFF

HISTORY

MILESTONE DATES:

Design 1973-76 Model Tests 1976

Construction 1976-82 First Beam Nov. 82

DESIGN/CONSTRUCTION BY:

in house X other

COST: Accelerators 400 MF (86) Facility 750 MF (86)

FUNDED BY: CEA - CNRS

STATUS

STAFF: Machine and research

Scientists - Engineers 70

Technicians 117 Students -

Research (in house/external)

Scientists 18 / 400 Engineers - / -

Technicians / Students 10 / -

BUDGET: Machine } 50 MF (91) Funded by } CEA - CNRS

Research } Funded by }

TIME DISTRIBUTION: 5530 h (91) + 1500 h (SME 91)

Basic Research (in house/external) 66.5 % / - %

Applied Program (in house/external) 3.5 % / - %

Development 7.5 % Maintenance during shut-down %

Tunings : 22.5 %

MAGNET

POLE PARAMETERS:

Diameter - cm $R_{extract}$ 300 cm R_{inject} SSC1:81.4 SSC2:120 cm

HILL PARAMETERS: Gap (min) 10 cm B_{max} 1.65 T

(@ 190000 AT) Gap (max) - cm B_{min} 0.7 T

VALLEY PARAMETERS: Gap (min) - cm B_{max} - T

(@ - AT) Gap (max) - cm B_{min} - T

AVERAGE FIELD: $< B >_{min}$ 0.39 T $< B >_{max}$ 0.95 T

NUMBER OF SECTORS: compact/separated - / 4

sector angle 52 (straight) deg. spiral (max) - deg.

FIELD TRIMMING: Trim Coils 12 in series for isochronism

Harmonic Coils -

Other 28

CURRENT: Main Coils 950 kW-1850 Amps Stability 10^{-5}

Trim Coils 140 kW Amps Stability 10^{-4}

Stored Energy (cryogenic) - MJ

WEIGHT: Iron 1700 Tons Conductor 14 Tons

ION ENERGY: Bending Limit E/A = 380 q^2/A^2 MeV/u

Focussing Limit E/A = - q/A MeV/u

ACCELERATION SYSTEM

FUNDAMENTAL ACCELERATION:

Description: 2x34° resonators, movable panel, rotating loop

No. of Gaps/turn 4 dE/dn(max) 0.8 MeV/q

Voltage(max) 0.250 MV Harmonic f_{rf}/f_{ion} SSC1:5-SSC2:2

Freq 7 - 14 MHz Power in(max) 0.1/resonator MW

Stability: Phase ±0.1° Voltage 10^{-4}

OTHER CAVITIES (Flattopping or otherwise):

Description: -

Region of Influence: R_{min} - cm R_{max} - cm

No. of Gaps/turn - dE/dn(max) - MeV/q

Voltage(max) - MV Harmonic f_{rf}/f_{ion} -

Freq - MHz Power in(max) - MW

Stability: Phase - Voltage -

VACUUM SYSTEM

OPERATING PRESSURE: $6 \cdot 10^{-6}$ Pascal

PUMPS: No. and type 4 turbo : 3500 l/s

8 cryo : 20000 l/s

ION SOURCE(S)

	Type	Intensity (mA)	@ $\epsilon_n = \beta\gamma\epsilon$ (π mm mrad)	Ion Species
(a)	SSC1 injected by C01 or C02			
(b)	(see related entry)			Ne_3 - U_{238}
(c)	SSC2 injected by SSC1 after solid foil			
(d)	stripper (nominal stripping ratio : 2.5)			

INJECTION SYSTEM

electrostatic inflector and magnetic channel Efficiency 80-100 %

EXTRACTION SYSTEM

eleotrostatic deflector and magnetic channel Efficiency 80-100 %

CHARACTERISTIC BEAMS

Accelerated Ions	E/A (MeV/u)	Current(part μA) Internal	External
(a) SSC1-Ne^{+6}	15	1.25 10^{13}	pps
(b) U^{+24}	4	$5 \cdot 10^{10}$	pps
(c) SSC2-Ne^{+10}	95	limited to 400 W	$1.2 \cdot 10^{12}$ pps
(d) U^{+58}	25	10^9	pps

Secondary Particles	E (MeV)	part/sec
(a) RIB by fragmentation (SISSI upgrade project in progress)		
(b) Be_{11}	40 MeV/u	10^5
(c) O_{14}	70 MeV/u	$4 \cdot 10^5$

EXTRACTED BEAM PROPERTIES: (maximum values full width)

For 10^9 - 10^{12} pps A of 25-95 MeV/u C - U ions

ΔE/E 0.1-0.4 % $\Delta\phi$ SSC1:8-10, SSC2:10-15 °rf

$\epsilon_n = \beta\gamma\epsilon$ x SSC1:7 SSC2:5 π mm mrad z SSC1:7 SSC2:5 π mm mrad

FACILITIES FOR RESEARCH

SHIELDED AREA: Fixed - m^2 Moveable 4000 m^2

Target Stations: 10 No. Served At Same Time: 2

MAGNETIC SPECTROMETERS: α, SPEG, and LISE (RIB)

OTHER FACILITIES:

4π detectors (NAUTILUS-INDRA-ORION)

Industrial applications (dedicated)

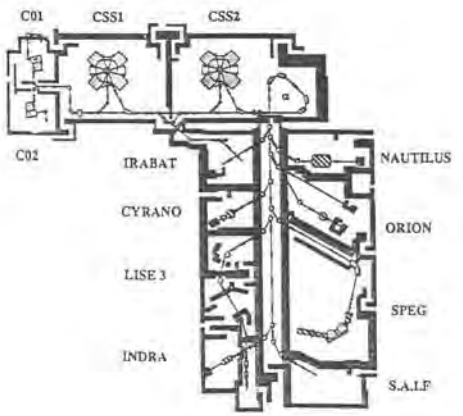
Atomic-solid state physics on a spare Q after stripping (SME)

REFERENCES/NOTES

(a)

(b)

PLAN VIEW OF FACILITY, COMMENTS



ENTRY NO. C14 **Date** June 1992

Name of Machine SARA (Injector)

Institution INSTITUT DES SCIENCES NUCLEAIRES

Address 53, avenue des Martyrs 38026 GRENOBLE Cedex France

Tel (33)76.28.40.00 Telex 320301F Fax (33)76.28.40.04 EMAIL

In Charge: D. BARNEOUD, M. FRUNEAU Reported by: M. FRUNEAU

HISTORY

MILESTONE DATES:

Design 1962 Model Tests 1963

Construction 1963-1967 First Beam 1968

DESIGN/CONSTRUCTION BY:

in house other C.S.F.

COST: Accelerator 2.10^6 $ Facility 6.10^6 $

FUNDED BY: IN2P3/CNRS

STATUS

STAFF: Machine

Scientists 1 Engineers 9

Technicians 27 Students 1

Research (in house/external)

Scientists 40 / 50 Engineers 2 / .....

Technicians 8 / ..... Students 6 / .....

BUDGET: Machine 10^6 $ Funded by IN2P3/CNRS

Research $0.5.10^6$ $ Funded by IN2P3/CNRS

TIME DISTRIBUTION:

Basic Research (in house/external) 70 % / 30 %

Applied Program (in house/external) 2 % / 6 %

Development 6 % Maintenance 7 %

MAGNET

POLE PARAMETERS:

Diameter 212 cm $R_{extract}$ 88 cm R_{inject} 2 cm

HILL PARAMETERS: Gap (min) 16 cm B_{max} 1.9 T

(@ 360.10^3 AT) Gap (max) ..... cm B_{min} ..... T

VALLEY PARAMETERS: Gap (min) 36 cm B_{max} 1.2 T

(@ 360.10^3 AT) Gap (max) ..... cm B_{min} ..... T

AVERAGE FIELD: $< B >_{min}$ 1.6 T $< B >_{max}$ 1.6 T

NUMBER OF SECTORS: compact/separated 4 / .....

sector angle ..... deg. spiral (max) 40 deg.

FIELD TRIMMING: Trim Coils 11

Harmonic Coils 4

Other .....

CURRENT: Main Coils 1100 Amps Stability 10^{-5}

Trim Coils 200 Amps Stability 10^{-4}

Stored Energy (cryogenic) ..... MJ

WEIGHT: Iron 200 t Conductor CU 13 x 18 mm

ION ENERGY: Bending Limit E/A = 90 q^2/A^2 MeV/u

Focussing Limit E/A = ... q/A MeV/u

ACCELERATION SYSTEM

FUNDAMENTAL ACCELERATION:

Description: 2 Moving pannel resonators

No. of Gaps/turn 4 dE/dn(max) ..... MeV/q

Voltage(max) 0.06 MV Harmonic f_{rf}/f_{ion} (1), 2, 3

Freq 10.5 to 16 MHz Power in(max) 0.03 MW

Stability: Phase $\pm$ 0.1° Voltage $\pm 10^{-4}$

OTHER CAVITIES (Flattopping or otherwise):

Description: .....

Region of Influence: R_{min} ..... cm R_{max} ..... cm

No. of Gaps/turn ..... dE/dn(max) ..... MeV/q

Voltage(max) ..... MV Harmonic f_{rf}/f_{ion} .....

Freq ..... MHz Power in(max) ..... MW

Stability: Phase ..... Voltage .....

VACUUM SYSTEM

OPERATING PRESSURE: 10^{-6}

PUMPS: No. and type .....

2 NRC OIL Diffusion

ION SOURCE(S)

	Type	Intensity (mA)	@	$\epsilon_n = \beta\gamma\epsilon$ (πmm mrad)	Ion Species
(a)	MINIMAFIOS	.....		150	p to Kr
(b)	CAPRICE	.....		150	p to Xe
(c)	.....	.....		.....	.....
(d)	.....	.....		.....	.....

INJECTION SYSTEM

18 m line + Belmont Inflector Efficiency 30 %

EXTRACTION SYSTEM

Electrostatic + Magnetic channels Efficiency 75 %

CHARACTERISTIC BEAMS

	Accelerated Ions	E/A (MeV/u)	Current(part μA) Internal	External
(a)	$^{20}Ne^{6+}$	5.6	.....	2 eμA
(b)	$^{28}Si^{6+}$	3.8	.....	2 eμA
(c)	$^{40}Ca^{11+}$	6.6	.....	1.5eμA
(d)	$^{84}Kr^{18+}$	4.0	.....	0.1eμA

	Secondary Particles	E (MeV)	part/sec
(a)	.....	.....	.....
(b)	.....	.....	.....
(c)	.....	.....	.....

EXTRACTED BEAM PROPERTIES:

For 1 μA of 5 MeV/u $Néon^{6+}$ ions

$\Delta E/E$ 0.4 % $\Delta\phi$ 10 °rf

$\epsilon_n = \beta\gamma\epsilon$ x 15 πmm mrad z 17 πmm mrad

FACILITIES FOR RESEARCH

SHIELDED AREA: Fixed 900 m^2 Moveable ..... m^2

Target Stations: 7 No. Served At Same Time: 1

MAGNETIC SPECTROMETERS: .....

OTHER FACILITIES: .....

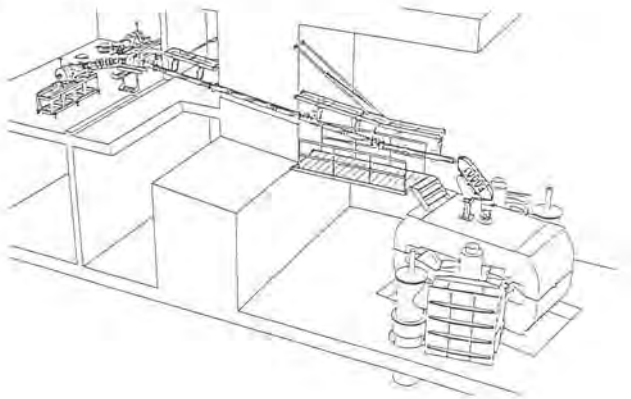
REFERENCES/NOTES

(a) Annales de radioélectricité TXXI April 1966 p.121-150

(b) New developments at SARA, These proceedings.

PLAN VIEW OF FACILITY, COMMENTS

See following entry



ENTRY NO. C15 **Date** June 1992

Name of Machine SARA (Post-Accelerator)

Institution INSTITUT DES SCIENCES NUCLEAIRES

Address 53, avenue des Martyrs 38026 GRENOBLE Cedex France

Tel (33) 76.28.40.00 **Telex** 320301F **Fax** (33) 76.28.40.04 **EMAIL**

In Charge: O. BARNEOUD, M. FRUNEAU **Reported by:** M. FRUNEAU

HISTORY

MILESTONE DATES:
Design 1976 Model Tests 1977
Construction 1978-1981 First Beam 1981

DESIGN/CONSTRUCTION BY:
in house Yes other

COST: Accelerator 1.6 10^6 $ Facility 6 10^5 $

FUNDED BY: IN2P3/CNRS

STATUS

STAFF: Machine
Scientists 1 Engineers 9
Technicians 27 Students 1
Research (in house/external)
Scientists 40 / 50 Engineers 2 /
Technicians 8 / Students 8 /

BUDGET: Machine 10^6 $ Funded by IN2P3/CNRS
Research 0.5 10^6 $ Funded by IN2P3/CNRS

TIME DISTRIBUTION:
Basic Research (in house/external) 70 % / 30 %
Applied Program (in house/external) 2 % / 6 %
Development 7 % Maintenance 6 %

MAGNET

POLE PARAMETERS:
Diameter 450 cm $R_{extract}$ 214 cm R_{inject} 90 cm

HILL PARAMETERS: Gap (min) 6 cm B_{max} 1.65 T
(@ AT) Gap (max) 6 cm B_{min} 1.65 T

VALLEY PARAMETERS: Gap (min) cm B_{max} 0 T
(@ AT) Gap (max) cm B_{min} 0 T

AVERAGE FIELD: $< B >_{min}$ 0.9 T $< B >_{max}$ 0.9 T

NUMBER OF SECTORS: compact/separated / 4
sector angle 48 deg. spiral (max) 0 deg.

FIELD TRIMMING: Trim Coils 15
Harmonic Coils 2
Other

CURRENT: Main Coils 900 Amps Stability $\pm 10^{-5}$
Trim Coils 200 Amps Stability 10^{-3}
Stored Energy (cryogenic) MJ

WEIGHT: Iron 400 t Conductor 14 x 14 mm

ION ENERGY: Bending Limit E/A = 160 q^2/A^2 MeV/u
Focussing Limit E/A = q/A MeV/u

ACCELERATION SYSTEM

FUNDAMENTAL ACCELERATION:
Description: Δ shaped dees moving pannels
No. of Gaps/turn 4 dE/dn(max) 0.2 MeV/q
Voltage(max) 0.05 MV Harmonic f_{rf}/f_{ion} 4.6
Freq 20 - 32 MHz Power in(max) 0.03 MW
Stability: Phase 0.1° Voltage 10^{-4}

OTHER CAVITIES (Flattopping or otherwise):
Description:
Region of Influence: R_{min} cm R_{max} cm
No. of Gaps/turn dE/dn(max) MeV/q
Voltage(max) MV Harmonic f_{rf}/f_{ion}
Freq MHz Power in(max) MW
Stability: Phase Voltage

VACUUM SYSTEM

OPERATING PRESSURE: 10^{-6} mbar
PUMPS: No. and type Cryogenic
6X CTI CT320

ION SOURCE(S)

	Type	Intensity (mA)	@	$\epsilon_n = \beta\gamma\epsilon$ (πmm mrad)	Ion Species
(a)					
(b)	See preceeding entry.				
(c)					
(d)					

INJECTION SYSTEM

3 magnetic +1 electrostatic channel Efficiency 75 %

EXTRACTION SYSTEM

1 electrostatic +1 electrostic channels Efficiency 75 %

CHARACTERISTIC BEAMS

	Accelerated Ions	E/A (MeV/u)	Current(part μA) Internal	External
(a)	$^{20}Ne^{10+}$	38		0.6 enA
(b)	$^{58}Ni^{13+}$	35		0.02 enA
(c)	$^{58}Ni^{24+}$	28		0.03 enA
(d)				

	Secondary Particles	E (MeV)	part/sec
(a)			
(b)			
(c)			

EXTRACTED BEAM PROPERTIES:
For 0.2 μA of 30 MeV/u $^{10+}$Neon ions
$\Delta E/E$ 0.5 % $\Delta\phi$ 20 °rf
$\epsilon_n = \beta\gamma\epsilon$ x 20 πmm mrad z 10 πmm mrad

FACILITIES FOR RESEARCH

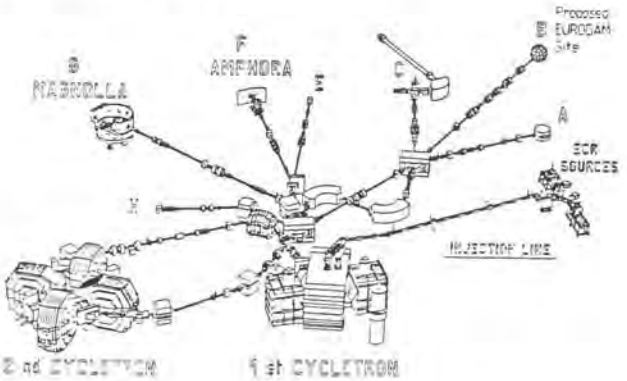
SHIELDED AREA: Fixed 900 m^2 Moveable m^2
Target Stations: 7 No. Served At Same Time: 1
MAGNETIC SPECTROMETERS:
OTHER FACILITIES:

REFERENCES/NOTES

(a) IEEE/NS-30 N° 4 August 1983
(b)

PLAN VIEW OF FACILITY, COMMENTS

See preceeding entry



ENTRY NO. C16 **Date** JULY 1992

Name of Machine MEDICYC

Institution CYCLOTRON LABORATORY, CENTRE ANTOINE LACASSAGNE

Address 227 Avenue de la Lanterne 06200 NICE (France)

Tel (33) 93 18 03 09 Telex ..... Fax (33) 93 18 04 33 EMAIL .....

In Charge: P. MANDRILLON Reported by: P.MANDRILLON

HISTORY

MILESTONE DATES:

Design 1983/1984 Model Tests .....

Construction 1984/1989 First Beam extracted in Dec.90

DESIGN/CONSTRUCTION BY:

(in house) other .....

COST: Accelerator 56 MFF Facility 120 MFF

FUNDED BY: Centre Antoine Lacassagne

STATUS

STAFF: Machine

Scientists 1 Engineers 2

Technicians 12 Students 1

Research (in house/~~outbound~~)

Scientists 1 / ..... Engineers ..... / .....

Technicians 2 / ..... Students ..... / .....

BUDGET: Machine ..... Funded by .....

Research ..... Funded by .....

TIME DISTRIBUTION:

Basic Research (in house/external) .....10 % / ..... %

Applied Program (in house/external) .....80 % / ..... %

Development .....10 % Maintenance ..... %

MAGNET

POLE PARAMETERS:

Diameter.....160 cm $R_{extract}$ ....68.8 cm R_{inject} .....2.5 cm

HILL PARAMETERS: Gap (min) .....13... cm B_{max} .....2.15 T

(@ ..... AT) Gap (max) ..... cm B_{min} ..... T

VALLEY PARAMETERS: Gap (min) ...27... cm B_{max} ....1.7. T

(@ ..... AT) Gap (max) ..... cm B_{min} ..... T

AVERAGE FIELD: $< B >_{min}$ ..... T $< B >_{max}$ ..... T

NUMBER OF SECTORS: compact/separated .....4. / .....

sector angle .....42.5 deg. spiral (max) .....60 deg.

FIELD TRIMMING: Trim Coils ..10 circular

Harmonic Coils ....4.....

Other .....

CURRENT: Main Coils ...1200..... Amps Stability ..10^{-5}.....

Trim Coils ....100..... Amps Stability ...10^{-4}.....

Stored Energy (cryogenic) ..... MJ

WEIGHT: Iron ...130 tons..... Conductor ..copper.....

ION ENERGY: Bending Limit E/A = ...70... q^2/A^2 MeV/u

Focussing Limit E/A = ... q/A MeV/u

ACCELERATION SYSTEM

FUNDAMENTAL ACCELERATION:

Description: 2 dees with 75 deg. aperture.....

No. of Gaps/turn 4..... dE/dn(max) 0.120..... MeV/q

Voltage(max) ...0.055..... MV Harmonic f_{rf}/f_{ion} 1.....

Freq .....25. MHz Power in(max) .....0.050. MW

Stability: Phase <0.5 deg..... Voltage .....10^{-5}.....

OTHER CAVITIES (Flattopping or otherwise):

Description: .....

Region of Influence: R_{min} ..... cm R_{max} ..... cm

No. of Gaps/turn ..... dE/dn(max) ..... MeV/q

Voltage(max) ..... MV Harmonic f_{rf}/f_{ion} .....

Freq ..... MHz Power in(max) ..... MW

Stability: Phase ..... Voltage .....

VACUUM SYSTEM

OPERATING PRESSURE: 10^{-7} Torr

PUMPS: No. and type ..2 turbo + 2 cryogenics.....

.....

ION SOURCE(S)

	Type	Intensity (mA)	@	$\epsilon_n = \beta\gamma\epsilon$ (πmm mrad)	Ion Species
(a)	multi cusp	1		0.15	H^-
(b)					
(c)					
(d)					

INJECTION SYSTEM

Axial with spiral inflector ..... Efficiency ..... %

EXTRACTION SYSTEM

..By stripping..... Efficiency .....100. %

CHARACTERISTIC BEAMS

	Accelerated Ions	E/A (MeV/u)	Current(part μA) Internal	External
(a)	Protons	65	20μA	20μA
(b)			/	/
(c)				
(d)				

	Secondary Particles	E (MeV)	part/sec
(a)	Neutrons $\sim$	20. average	
(b)			
(c)			

EXTRACTED BEAM PROPERTIES:

For ..... μA of ..... MeV/u ..... ions

$\Delta E/E$ .....% $\Delta\phi$ ..... °rf

$\epsilon_n = \beta\gamma\epsilon$ x ..... πmm mrad z ..... πmm mrad

FACILITIES FOR RESEARCH

SHIELDED AREA: Fixed ..... m^2 Moveable ..... m^2

Target Stations: ..... No. Served At Same Time: .....

MAGNETIC SPECTROMETERS: .....

OTHER FACILITIES: .....

.....

.....

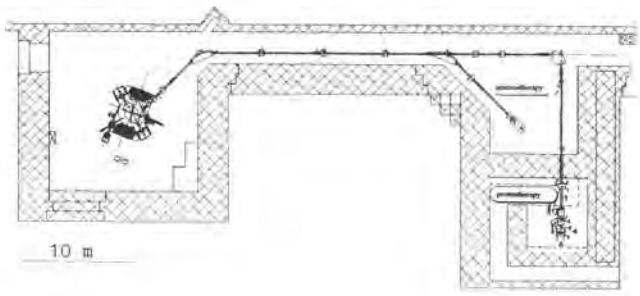
.....

REFERENCES/NOTES

(a) Proc. 10th Int. Conf. cycl. and Appli. 1984, MSU .....

(b) Proc. 12th Int. Conf. cycl. and Appli. 1989, Berlin

PLAN VIEW OF FACILITY, COMMENTS



ENTRY No. C17

NAME OF MACHINE ORLEANS ISOCHRONUS CYCLOTRON DATE JUNE 1992
INSTITUTION CENTRE NATIONAL DE LA RECHERCHE SCIENTIFIQUE
ADDRESS C.E.R.I. 3A RUE DE LA FEROLLERIE 45071 ORLEANS CEDEX 2
TEL ..... TELEX .....
IN CHARGE ..G.GOIN..... REPORTED BY ..G.GOIN.....

HISTORY AND STATUS

DESIGN, date ....1971..... Model tests ...1971.....
ENG DESIGN, date .....1971.....
CONSTRUCTION, date ....1972-1973.....
FIRST BEAM, date (or goal) .....1974.....
MAJOR ALTERATIONS .....
.....
COST, ACCELERATOR ....9.x.10^6.FF.(1970).....
COST, FACILITY, total .8.5x10^{6}FF.(1974)+.8x10^6.FF.(1980)....
FUNDED BY .C.N.R.S.....

ACCELERATOR STAFF, OPERATION AND DEVELOPMENT

SCIENTISTS ..... ENGINEERS .3.....
TECHNICIANS ..4..... CRAFTS .....
GRAD STUDENTS involved during year .....
OPERATED BY ..... Research staff or .....6.. Operators
OPERATION .....64. hr/wk, On target .....46.. hr/wk
TIME DISTR. in house ....6..... %. Outside ..... %
BUDGET, op & dev ≃ 10^6 FF (1992)
FUNDED BY CENTRE NATIONAL DE LA RECHERCHE SCIENTIFIQUE

RESEARCH STAFF, not included above

USERS, in house ....10..... outside ....6.....
GRAD STUDENTS involved during year .....
RESEARCH BUDGET, in house .....
FUNDED BY .....

MAGNET

POLE FACE, diameter (compact) 160. cm, R extraction67.5. cm
R injection ..... cm
GAP, min ..13..... cm, Field .19..... kG
max .27..... cm, Field .11..... kG
at .0,25.10^6 Ampere turns
AVERAGE FIELD at R ext .....15..... kG
B max/ <B> .....1,27.....
NUMBER OF SECTORS { compact .4... / separated ..... } Spiral, max 53 deg
SECTOR ANGLE (SSC) ..... deg
TRIMMING COILS HARMONIC COILS ..4.....
.....CIRC. COILS.....8.....
CONDUCTOR, material and type .....
STORED ENERGY (cryogenic) ..... MJ
POWER : main coils 110... max, kW ; current stability 2.10^{-5}
trimming coils ..... max, kW ; current stability 2.10^{-5}
WEIGHT : Fe .....100..... tons ; coils ..... tons
COOLING system DEMINERALISED WATER.....
ION ENERGY (bending limit) E/A = .50..... q²/a² MeV/amu
(focusing limit) E/A = .50..... q²/a² MeV/amu

ACCELERATION SYSTEM

DEES, number ...2..... ; angle .....60..... deg
BEAM APERTURE ...3..... cm ; DC Bias ..... kV
TUNED by, coarse .M-PANEL..... fine ..M-PANEL.....
RF ....20..... to ..40..... mHz, stable ± ....1.....10^{-6}
Orb F ..5..... to ..20..... mHz
HARMONICS, RF/Orb F, used .....
DEE - Gnd, max .90... kV, min gap .....3..... cm
STABILITY, (pk-pk noise)/(pk RF volt) ...5.10^{-3}.....
ENERGY GAIN, max .....132..... kV/turn
RF PHASE, stable to ± .....0,2..... deg
RF POWER input, max .....110..... kW
FREQUENCY MODULATION, rate ..... /s
modulator, type .....
beam pulse, width .....

VACUUM SYSTEM

OPERATING PRESSURE .....2.x.10^{-6}..... Torr or mbar
PUMPS, No, Type, Size .DIFFUSION PUMPS.....
.....2 x 4000 l./s.....
.....

ION SOURCES

.....INTERNAL LIVINGSTONE TYPE.....

INJECTION SYSTEM

.....

EXTRACTION SYSTEM

ELECTROSTATIC DEFLECTOR+FOCUSING MAGNET.....

FACILITIES FOR RESEARCH

SHIELDED AREA, fixed ...25..... m² ; movable .≃.225..... m²
TARGET STATIONS ..4..... in ...4..... rooms
STATIONS served at same time, max ....1.....
MAG SPECTROGRAPH, type .....
COMPUTER model .....
OTHER FACILITIES-FAST NEUTRON PRODUCTION FOR NEUTRONTHERAPY, BIOLOGY and ACTIVATION. - SHORT LIVED GAZ ISOTOPE PRODUCTION-ISOTOPE PRODUCTION.....-CHEMISTRY FACILITY.

CHARACTERISTIC BEAMS (WITH HOT CELLS)

PARTICLE	ENERGY (MeV) Goal	Achieved	CURRENT (pμA) Internal	External
P	.5-38	.5-36		55.
d	.5-24	.5-25		55.
ALPHA	.10-48	.10-50		10.

SECONDARY (part/s)
n, FROM P+Be ...FOR 10x10cm FIELD SIZE AT 135cm SSD/.....
..34 MeV... DOSE RATE: 17 CGy min⁻¹.....

BEAM PROPERTIES

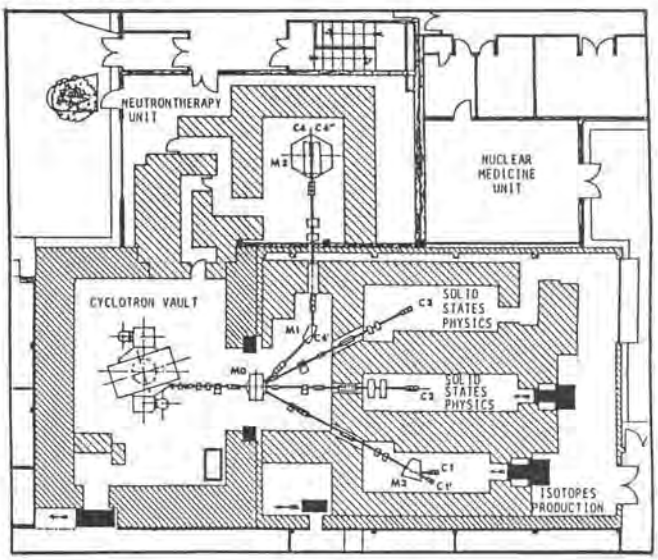
	MEASURED	CONDITIONS	
PULSE WIDTH	25-30 RF deg	5..... pμA of 25. MeV d.	ions
PHASE EXC, max	... RF deg	..... pμA of .... MeV	... ions
EXTRACT eff	.65.... %	.40.... pμA of 34. MeV p.	ions
RESOL ΔE/E	..... %	..... pμA of .... MeV	... ions
EMITTANCE (π mm. mrad)	{... axial / 40.. rad}	.3..... pμA of 45... MeV α	ions

OPERATING PROGRAMS, time distribution

BASIC NUCLEAR PHYSICS 0% SOLID STATES PHYSICS 69%
BIOMEDICAL APPLICAT. 31% ISOTOPE PRODUCTIONS 0%
.....
.....

REFERENCES/NOTES

PLAN VIEW OF FACILITY, NOTEWORTHY FEATURES. COMMENTS



ENTRY No. C18

NAME OF MACHINE ALICE DATE 25 mars 1984
INSTITUTION Institut de Physique Nucleaire
ADDRESS B.P. no 1 ORSAY FRANCE
TEL 941 73 04 TELEX
IN CHARGE Richomme REPORTED BY Richomme

HISTORY AND STATUS
DESIGN, date 1959 Model tests 1958-59
ENG DESIGN, date 1959-62
CONSTRUCTION, date 1960-64
FIRST BEAM, date (or goal) 1965 April
MAJOR ALTERATIONS Liner injector 1968
New Beams Area 1972
COST, ACCELERATOR 5 10^6 F
COST, FACILITY, total 12 10^6 F
FUNDED BY Ministère de la Recherche Scientifique

ACCELERATOR STAFF, OPERATION AND DEVELOPMENT
SCIENTISTS 0 ENGINEERS 1
TECHNICIANS 17 CRAFTS 7
GRAD STUDENTS involved during year
OPERATED BY Research staff or 8 Operators
OPERATION 120 hr/wk, On target 100 hr/wk
TIME DISTR. in house 49 %, Outside 51 %
BUDGET, op & dev 0.9 10^6 F
FUNDED BY IN2P3

RESEARCH STAFF, not included above
USERS, in house 38 outside 61
GRAD STUDENTS involved during year
RESEARCH BUDGET, in house 0.7 10^6 F
FUNDED BY IN2P3-CNRS

MAGNET
POLE FACE, diameter (compact) cm, R extraction 80 cm
R injection 20 cm
GAP, min 21 cm, Field 18 kG
max 47 cm, Field 12.4 kG
at 0.75 10^6 Ampere turns
AVERAGE FIELD at R ext 15 kG
B max/ <B> 1.2
NUMBER OF SECTORS compact 3, separated — Spiral, max deg
SECTOR ANGLE (SSC) 50 deg
TRIMMING COILS 3
CONDUCTOR, material and type Aluminium
STORED ENERGY (cryogenic) MJ
POWER : main coils 490 max, kW ; current stability 5 10^{-5}
trimming coils 72 max, kW ; current stability 5 10^{-5}
WEIGHT : Fe 260 tons ; coils 20 tons
COOLING system oil and demineralized water
ION ENERGY (bending limit) E/A = 75 q^2/a^2 MeV/amu
(focusing limit) E/A = q^2/a^2 MeV/amu

ACCELERATION SYSTEM
DEES, number 1 ; angle 180 deg
BEAM APERTURE 5 cm ; DC Bias 0 kV
TUNED by, coarse fine TRIM CAP
RF 5 to 10.2 mHz, stable ± 7 10^{-6}
Orb F to mHz
HARMONICS, RF/Orb F, used 1-3
DEE - Gnd, max 75 kV, min gap cm
STABILITY, (pk-pk noise)/(pk RF volt) 0.01
ENERGY GAIN, max 150 kV/turn
RF PHASE, stable to ± deg
RF POWER input, max 100 kW
FREQUENCY MODULATION, rate /s
modulator, type
beam pulse, width

VACUUM SYSTEM
OPERATING PRESSURE LINAC 5. 10^{-7} CEV 10^{-6} Torr or mbar
PUMPS, No, Type, Size 4 diffusion pumps one 80 cm
three 60 cm TURBO-MOLECULAR PUMPS

ION SOURCES
Internal penning and Linac with internal stripping in the cyclotron

INJECTION SYSTEM
Internal stripping in the cyclotron
EXTRACTION SYSTEM
Electrostatic deflector + 2 magnetics channel
FACILITIES FOR RESEARCH
SHIELDED AREA, fixed 290 m^3 ; movable m^3
TARGET STATIONS 9 in 2 rooms
STATIONS served at same time, max 1
MAG SPECTROGRAPH, type 1200 n=1/2
COMPUTER model IBM 360-70
OTHER FACILITIES PDP 11/05 and 11/34

CHARACTERISTIC BEAMS

PARTICLE	ENERGY (MeV) Goal	Achieved	CURRENT (pμA) Internal	External
$^{14}N^{7+}$		210		50 nA
$^{40}Ca^{15}$		400		100 nA
$^{63}Cu^{20}$		450		80 nA
$^{109}Ag^{29+}$		550		3 nA
SECONDARY				(part/s)
SINGLE LINEAR $^{131}Xe^{10+}$ 200 nA				

BEAM PROPERTIES

MEASURED	CONDITIONS
PULSE WIDTH 11. RF deg	1 pμA of MeV ions
PHASE EXC, max RF deg	pμA of MeV ions
EXTRACT eff 45. %	pμA of MeV ions
RESOL ΔE/E 1. %	pμA of MeV ions
EMITTANCE	
(π mm. mrad) .42 axial, 120 rad	pμA of MeV ions

OPERATING PROGRAMS, time distribution

BASIC NUCLEAR PHYSICS	64	SOLID STATES PHYSICS	
BIOMEDICAL APPLICAT.	3	ISOTOPE PRODUCTIONS	
Various	23		
Development	10		

REFERENCES/NOTES
Time is assigned program comittee

PLAN VIEW OF FACILITY, NOTEWORTHY FEATURES, COMMENTS

ENTRY NO. C19 **Date** June 1992
Name of Machine VICKSI (Van-de-Graaff Isochron Cyclotron Kombination für Schwere Ionen)
Institution Hahn-Meitner-Institut
Address Glienicker Straße 100, W-1000 Berlin 39, Germany
Tel 30/80 09 2415 **Telex** 01/85763 **Fax** 30/80 09 2097 **EMAIL** HOMEYER@VAX.HMI.DBP.DE
In Charge: H. Homeyer **Reported by:** W. Pelzer

HISTORY

MILESTONE DATES:
Design 1973-74 Model Tests 1973-74
Construction 1974-76 First Beam June 1977
DESIGN/CONSTRUCTION BY:
in house yes, and other like Scanditronix, Danfysik
COST: Accelerator 36 Million DM Facility 56 Million DM
FUNDED BY: FRG (90%) + Berlin (10%)

STATUS

STAFF: Machine (Cyclotron plus 2 electrostatic injectors)
Scientists 5 Engineers 7
Technicians 15 Students -
Research (in house/external)
Scientists 36 / ~120 Engineers 2 /
Technicians 7 / Students 33 / ~60
BUDGET: Machine 2.5 Million DM Funded by FRG (90%) + ...
Research 2.5 Million DM Funded by Berlin (10%)
TIME DISTRIBUTION: (100%=7000 h operating time per year)
Basic Research (in house/external) 40 % / 40 %
Applied Program (in house/external) - % / - %
Development + set up 12 % Maintenance 8 %

MAGNET

POLE PARAMETERS:
Diameter - cm $R_{extract}$ 171 cm R_{inject} 43 cm
HILL PARAMETERS: Gap (min) 6 cm B_{max} 1.57 T
(Φ AT) Gap (max) cm B_{min} T
VALLEY PARAMETERS: Gap (min) cm B_{max} T
(Φ AT) Gap (max) open cm B_{min} <0.1 T
AVERAGE FIELD: $< B >_{min}$ T $< B >_{max}$ 0.89 T
NUMBER OF SECTORS: compact/separated / 4
sector angle 50 deg. spiral (max) 0 deg.
FIELD TRIMMING: Trim Coils 12
Harmonic Coils 3 (of the 12)
Other
CURRENT: Main Coils 2000 Amps Stability 2 · 10-5
Trim Coils 150 Amps Stability
Stored Energy (cryogenic) MJ
WEIGHT: Iron 360 tons Conductor 6 tons
ION ENERGY: Bending Limit E/A = 130 q^2/A^2 MeV/u
Focussing Limit E/A = q/A MeV/u

ACCELERATION SYSTEM

FUNDAMENTAL ACCELERATION: $0^o/180^o$-operation
Description: Two λ/4-resonators in opposite magnet valleys,
No. of Gaps/turn 4 dE/dn(max) 0.56 MeV/q
Voltage(max) 0.14 MV Harmonic f_{rf}/f_{ion} 2 to 7
Freq 10 to 20 MHz Power in(max) per cavity 0.02 MW
Stability: Phase <0.05° Voltage <10-3
OTHER CAVITIES (Flattopping or otherwise):
Description: none
Region of Influence: R_{min} cm R_{max} cm
No. of Gaps/turn dE/dn(max) MeV/q
Voltage(max) MV Harmonic f_{rf}/f_{ion}
Freq MHz Power in(max) MW
Stability: Phase Voltage

VACUUM SYSTEM

OPERATING PRESSURE: 1 x 10-7 bar
PUMPS: No. and type 2 cryopumps 10000 l/sec
2 turbopumps 1450 l/sec

ION SOURCE(S)

	Type	Intensity (mA)	Φ	$\epsilon_n = \beta\gamma\epsilon$ (πmm mrad)	Ion Species
(a)	Axial Penning Source in 6 MV Van-de-Graaff				
(b)	Sputter Source for 8 MV Tandem Injector				
(c)	Stripper between injectors and cyclotron; $1 \le A \le 129$; $1 \le q/A \le 1/8$				
(d)					

INJECTION SYSTEM radial inflectors, 2 magnetic + 1 electrostatic Efficiency 70 %

EXTRACTION SYSTEM radial deflectors, 1 electrostatic, 2 magnetic channels Efficiency 100 %

CHARACTERISTIC BEAMS

	Accelerated Ions	E/A (MeV/u)	Current(part μA) Internal	External
(a)	p	50		1.0
(b)	^{12}C	4 - 32		1.0 - 0.1
(c)	^{40}Ar	1.3 - 13		1.0 - 0.001
(d)	^{58}Ni	3.4 - 14.5		0.01 - 0.001

	Secondary Particles	E (MeV)	part/sec
(a)	--	--	--
(b)			
(c)			

EXTRACTED BEAM PROPERTIES:
For 0.5 p μA of 7.5 MeV/u 20 Ne ions
ΔE/E 0.1 % Δφ ±3 (<1 ns) °rf
$\epsilon_n = \beta\gamma\epsilon$ x 6 πmm mrad z 5 πmm mrad

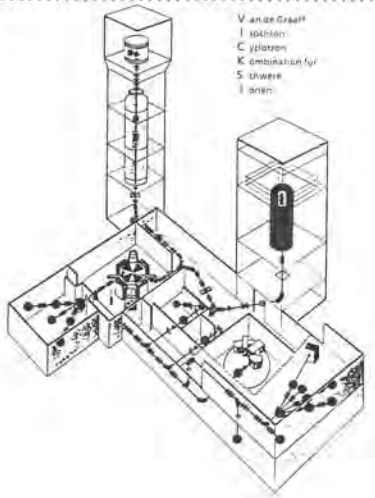
FACILITIES FOR RESEARCH

SHIELDED AREA: Fixed 800 m² Moveable - m²
Target Stations: 23 No. Served At Same Time: 2
MAGNETIC SPECTROMETERS: 03D
OTHER FACILITIES: - beams of the 6 MV Van-de-Graaff available in parallel to these of the tandem/cyclotron combination. - external pulsing gives 1 ns beam pulses with 100 ns repetition down to one shot operation.

REFERENCES/NOTES

(a) IEEE Vol.NS-26/2, 79, p.1872,2300,2209,2355,2202
(b) Proc.10th Int.Conf. on Cycl. and Appl., 1984, 230

PLAN VIEW



ENTRY NO. C20 **Date** June 92

Name of Machine Bonn Isochronous Cyclotron

Institution University of Bonn, Institut für Strahlen- und Kernphysik

Address Nußallee 14 - 16, W-5300 Bonn 1, Germany

Tel (02 28) 73-22 01 Telex ... Fax (02 28) 73 37 28 EMAIL ...

In Charge: T. Mayer-Kuckuk Reported by: H. Wahl

HISTORY

MILESTONE DATES:
Design 1965 Model Tests 1966 - 67
Construction 1967 - 69 First Beam Dec. 1968

DESIGN/CONSTRUCTION BY:
in house ~~MMK~~ and AEG

COST: Accelerator 5,000,000 DM Facility 8,000,000 DM

FUNDED BY: BMFT

STATUS

STAFF: Machine
Scientists 1 Engineers 2
Technicians 8 Students -
Research (in house/external)
Scientists 20 / 2 Engineers 1 / -
Technicians 3 / - Students 40 / 6

BUDGET: Machine 1,900,000 DM Funded by MWF
Research 600,000 DM Funded by BMFT, MWF, DFG, EG

TIME DISTRIBUTION:
Basic Research (in house/external) 70 % / 5 %
Applied Program (in house/external) 15 % / - %
Development 5 % Maintenance 5 %

MAGNET

POLE PARAMETERS:
Diameter 200 cm $R_{extract}$ 90 cm R_{inject} 3,7 cm
HILL PARAMETERS: Gap (min) 8,4 cm B_{max} 1,85 T
(Φ 1,47 e.5 AT) Gap (max) 8,6 cm B_{min} 0,64 T
VALLEY PARAMETERS: Gap (min) 24,0 cm B_{max} 0,70 T
(Φ 0,46 e.5 AT) Gap (max) 24,0 cm B_{min} 0,24 T
AVERAGE FIELD: $< B >_{min}$ 0,5 T $< B >_{max}$ 1,27 T
NUMBER OF SECTORS: compact/separated 3 / -
sector angle 40 deg. spiral (max) 0 deg.
FIELD TRIMMING: Trim Coils 7/sector
Harmonic Coils
Other
CURRENT: Main Coils 480 Amps Stability 10^{-5}
Trim Coils ± 25 Amps Stability 10
Stored Energy (cryogenic) MJ
WEIGHT: Iron 200 Conductor 8
ION ENERGY: Bending Limit E/A = 60 q^2/A^2 MeV/u
Focussing Limit E/A = 30 q/A MeV/u

ACCELERATION SYSTEM

FUNDAMENTAL ACCELERATION:
Description: 3-Dee-system
No. of Gaps/turn 6 dE/dn(max) 0,2 MeV/q
Voltage(max) 0,045 MV Harmonic f_{rf}/f_{ion} 3
Freq 20 - 29 MHz Power in(max) 0,3-4 MW
Stability: Phase 2 deg Voltage 10

OTHER CAVITIES (Flattopping or otherwise):
Description:
Region of Influence: R_{min} cm R_{max} cm
No. of Gaps/turn dE/dn(max) MeV/q
Voltage(max) MV Harmonic f_{rf}/f_{ion}
Freq MHz Power in(max) MW
Stability: Phase Voltage

VACUUM SYSTEM

OPERATING PRESSURE: $2 \cdot 10^{-6}$ mbar
PUMPS: No. and type 1 oil-diffusion, 60 cm, 12,000 l/s

ION SOURCE(S)

	Type	Intensity (mA)	$\varepsilon_n = \beta\gamma\varepsilon$ (πmm mrad)	Ion Species
(a)	ECR	0,2 - 4		up to ^{20}Ne
(b)	polarized I.S. $1 \cdot 10^{14}$			polarized p, d
(c)				
(d)				

INJECTION SYSTEM

axial hyberbolic inflector Efficiency 30 %

EXTRACTION SYSTEM

electrostat. deflector, screen, channel, foc. channel Efficiency 80 %

CHARACTERISTIC BEAMS

	Accelerated Ions	E/A (MeV/u)	Current(part μA) Internal	External
(a)	p	7 - 14	15	12
(b)	d	7 - 14	7	5
(c)	α	7 - 14	4	3
(d)	$^{12}C^{4+}$ $^{14}N^{5+}$	7	0,12	0,1
	Secondary Particles	E (MeV)	part/sec	
(a)				
(b)				
(c)				

EXTRACTED BEAM PROPERTIES:
For 10 μA of 12 MeV/u d ions
ΔE/E 0,1 % Δφ 6 - 40 °rf
$\epsilon_n = \beta\gamma\epsilon$ x 6 πmm mrad z 6 πmm mrad

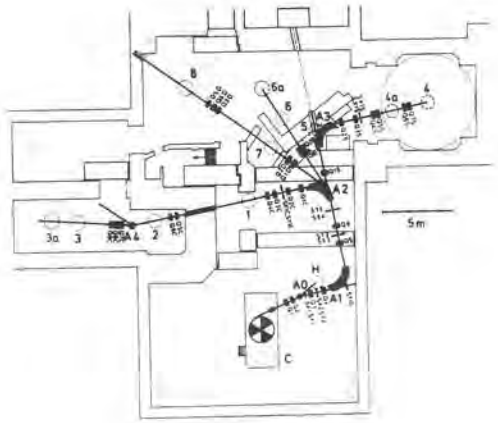
FACILITIES FOR RESEARCH

SHIELDED AREA: Fixed 415 m² Moveable - m²
Target Stations: 12 No. Served At Same Time: 1
MAGNETIC SPECTROMETERS: split pole (Scanditronix)
OTHER FACILITIES: isotope production + hot-labors, orange-spectr., off-line-mass-separator

REFERENCES/NOTES

(a) F. Hinterberger et al., Nucl.Instr. 130(1975)335+
(b) M. Agena et al., IEEE NS 26,2156, (1979)

PLAN VIEW OF FACILITY, COMMENTS



ENTRY NO. C21 Date

Name of Machine JULIC

Institution Institut für Kernphysik des Forschungszentrums Jülich GmbH (KFA)

Address Postfach 1913, D-5170 Jülich, Germany

Tel 02461/613980 Telex Fax 02461/613930 EMAIL

In Charge: R. Maier Reported by: W. Bräutigam

HISTORY

MILESTONE DATES:

Design 1963 Model Tests 1963 - 1965

Construction 1966 - 1969 First Beam int. 1968, ext. 1969

DESIGN/CONSTRUCTION BY:

in house other AEG Frankfurt

COST: Accelerator $19 \cdot 10^6$ DM Facility $29 \cdot 10^6$ DM

FUNDED BY: Kernforschungsanlage Jülich

STATUS

STAFF: Machine

Scientists (a) Engineers (a)

Technicians (a) Students (a)

Research (in house/external)

Scientists / Engineers /

Technicians / Students /

BUDGET: Machine (b) Funded by

Research (b) Funded by

TIME DISTRIBUTION:

Basic Research (in house/external) (c) % /

Applied Program (in house/external) (c) % /

Development % Maintenance %

MAGNET

POLE PARAMETERS:

Diameter 330 cm $R_{extract}$ 154 cm R_{inject} cm

HILL PARAMETERS: Gap (min) 8.4 cm B_{max} 1.92 T

(@ AT) Gap (max) cm B_{min} T

VALLEY PARAMETERS: Gap (min) 24 cm B_{max} 0.7 T

(@ AT) Gap (max) cm B_{min} T

AVERAGE FIELD: $< B >_{min}$ 0.95 T $< B >_{max}$ 1.35 T

NUMBER OF SECTORS: compact/separated 3 /

sector angle deg. spiral (max) 20 deg.

FIELD TRIMMING: Trim Coils 9

Harmonic Coils -

Other -

CURRENT: Main Coils 400 Amps Stability $2 \cdot 10^{-6}$

Trim Coils 9 Amps Stability $1 \cdot 10^{-4}$

Stored Energy (cryogenic) MJ

WEIGHT: Iron 700 tons Conductor 12 tons

ION ENERGY: Bending Limit E/A = 180 q^2/A^2 MeV/u

Focussing Limit E/A = q/A MeV/u

ACCELERATION SYSTEM

FUNDAMENTAL ACCELERATION:

Description: 3 dees, angle 40 deg

No. of Gaps/turn 6 dE/dn(max) 0.24 MeV/q

Voltage(max) 0.045 MV Harmonic f_{rf}/f_{ion} 3

Freq 20 - 30 MHz Power in(max) 0.1 MW

Stability: Phase $< \pm 0.5$ deg. Voltage $< \pm 1 \cdot 10^{-4}$

OTHER CAVITIES (Flattopping or otherwise):

Description:

Region of Influence: R_{min} cm R_{max} cm

No. of Gaps/turn dE/dn(max) MeV/q

Voltage(max) MV Harmonic f_{rf}/f_{ion}

Freq MHz Power in(max) MW

Stability: Phase Voltage

VACUUM SYSTEM

OPERATING PRESSURE: $\sim 2 \cdot 10^{-7}$ mbar

PUMPS: No. and type 3 cryo 10000 l/s each

2 turbo 2200 l/s each

ION SOURCE(S)

	Type	Intensity (mA)	@	$\epsilon_n = \beta\gamma\epsilon$ (πmm mrad)	Ion Species
(a)	ECR 14 GHz				heavy ions
(b)	ECR 2.45 GHz				H_2^+
(c)	Neg. Ion S.				H^-, D^-
(d)					

INJECTION SYSTEM

axial magn. comp. Efficiency %

EXTRACTION SYSTEM

el. static defl. screen + foc. chan. Efficiency ~60 %

CHARACTERISTIC BEAMS

Accelerated Ions	E/A (MeV/u)	Current(part μA) Internal	External
(a) H_2^+	22.5 - 45		~ 10
(b) p, d, $^3H^{2+}$	22.5 - 45		> 10
(c) N^{5+}, Ne^{8+}			
(d) S^{13+}, a.o.			

Secondary Particles	E (MeV)	part/sec
(a)		
(b)		
(c)		

EXTRACTED BEAM PROPERTIES:

For 6 μA of 38 MeV/u H_2^+ ions

$\Delta E/E$ 0.3 % $\Delta\phi$ 14 °rf

$\epsilon_n = \beta\gamma\epsilon$ x 2.5 πmm mrad z 5 πmm mrad

FACILITIES FOR RESEARCH

SHIELDED AREA: Fixed m^2 Moveable m^2

Target Stations: No. Served At Same Time:

MAGNETIC SPECTROMETERS:

OTHER FACILITIES:

The cyclotron JULIC will serve as injector for the new cooler synchrotron COSY Jülich

REFERENCES/NOTES

(a) operation by COSY operating group

(b) common budget with COSY

(c) COSY injector

PLAN VIEW OF FACILITY, COMMENTS

see

Cooler Synchrotron COSY-Jülich

ENTRY NO. C22 Date July 92

Name of Machine Karlsruher Isochronous Cyclotron (KIZ)

Institution Kernforschungszentrum Karlsruhe GmbH, Cyclotron-Laboratory

Address D-7500 Karlsruhe, Postfach 3640, Germany

Tel 07247-82-2433 Telex 17724716 Fax 07247-82-3156 EMAIL

In Charge: H. Schweickert Reported by: H. Schweickert

HISTORY

MILESTONE DATES:
Design 1958 Model Tests 1958-60
Construction 1960-62 First Beam

DESIGN/CONSTRUCTION BY:
in house other AEG

COST: Accelerator 4.6×10^6 DM Facility 20×10^6 DM

FUNDED BY: Federal Gouvernment, State of Baden-Württemberg

STATUS

STAFF: Machine
Scientists 2 Engineers 2
Technicians 10 Students 4
Research (in house/external)
Scientists 20 / 40 Engineers 10 / 20
Technicians 10 / 20 Students 5 / 10

BUDGET: Machine 2×10^6 DM Funded by Government
Research 2×10^6 DM Funded by Government

TIME DISTRIBUTION:
Basic Research (in house/external) 50 % / 50 %
Applied Program (in house/external) 80 % / 20 %
Development 5 % Maintenance 3 %

MAGNET

POLE PARAMETERS:
Diameter 225 cm $R_{extract}$ 105 cm R_{inject} 10 cm
HILL PARAMETERS: Gap (min) 8 cm B_{max} 1.95 T
(@ 0.16×10^6 AT) Gap (max) cm B_{min} T
VALLEY PARAMETERS: Gap (min) 16 cm B_{max} 0.95 T
(@ 0.16×10^6 AT) Gap (max) cm B_{min} T
AVERAGE FIELD: < B >xxx 1.43 T < B >max T
NUMBER OF SECTORS: compact/separated 3 /
sector angle deg. spiral (max) deg.
FIELD TRIMMING: Trim Coils 6 on hill sectors
Harmonic Coils 6 on hill sectors
Other
CURRENT: Main Coils 360 Amps Stability 10^{-6}
Trim Coils 10 Amps Stability 10^{-3}
Stored Energy (cryogenic) MJ
WEIGHT: Iron 280 tons Conductor 8.5 tons
ION ENERGY: Bending Limit E/A = 104 q^2/A^2 MeV/u
Focussing Limit E/A = 26 q/A MeV/u

ACCELERATION SYSTEM

FUNDAMENTAL ACCELERATION:
Description: Self exited system, 3 DEES
No. of Gaps/turn 6 dE/dn(max) 0.24 MeV/q
Voltage(max) 0.05 MV Harmonic f_{rf}/f_{ion} 3
Freq 33 MHz Power in(max) 0.05 MW
Stability: Phase ± 1 deg Voltage 10^{-3}

OTHER CAVITIES (Flattopping or otherwise):
Description:
Region of Influence: R_{min} cm R_{max} cm
No. of Gaps/turn dE/dn(max) MeV/q
Voltage(max) MV Harmonic f_{rf}/f_{ion}
Freq MHz Power in(max) MW
Stability: Phase Voltage

VACUUM SYSTEM

OPERATING PRESSURE: 2×10^{-6} torr
PUMPS: No. and type 2 diffusions pumps, 2 x 12.000 l/sec

ION SOURCE(S)

	Type	Intensity (mA)	@	$\epsilon_n = \beta\gamma\epsilon$ (πmm mrad)	Ion Species
(a)	Hot cathode penning	0.5			H_2^+, d, $^4He^{2+}$
(b)	ECR-source	0.1			$^6Li^{3+}$
(c)	Atomic beam	0.02			d
(d)					

INJECTION SYSTEM

Electrostatic, Hyperboloid Infl. Efficiency 20 %

EXTRACTION SYSTEM

Electrostatic Efficiency 70-80 %

CHARACTERISTIC BEAMS

Accelerated Ions	E/A (MeV/u)	Current(part μA) Internal	External
(a) H_2^+, d	26	300	50
(b) He^{2+}	26	100	20
(c) Li-6	26	1	0.5
(d) pol. d	26	2	1

Secondary Particles	E (MeV)	part/sec
(a)		
(b)		
(c)		

EXTRACTED BEAM PROPERTIES:
For 1 μA of MeV/u d ions
$\Delta E/E$ 0.1 % $\Delta\phi$ 5-10 °rf
$\epsilon_n = \beta\gamma\epsilon$ x 8 πmm mrad z 4 πmm mrad

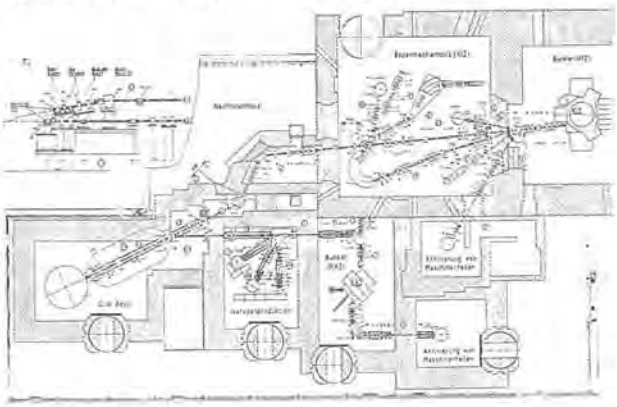
FACILITIES FOR RESEARCH

SHIELDED AREA: Fixed 350 m² Moveable m²
Target Stations: 8 No. Served At Same Time: 1
MAGNETIC SPECTROMETERS: Little John K=300
OTHER FACILITIES:
Neutron Hall with POLKA
Dual Beam Facility

REFERENCES/NOTES

(a) Proc. 7th Int. Conf. on cyclotrons, p. 496
(b) Prof. 12th Int.Conf. on cyclotrons, p. 194

PLAN VIEW OF FACILITY, COMMENTS



ENTRY No. C23

NAME OF MACHINE AEG COMPACT CYCLOTRON DATE 01 / 04 / 89
INSTITUTION PHYSICS DEPARTMENT TECHNICAL UNIVERSITY MUNICH
ADDRESS JAMES FRANCKSTR. D 8046 GARCHING
TEL 089/32092692 TELEX
IN CHARGE E. Huenges REPORTED BY

HISTORY AND STATUS

DESIGN, date 1968 Model tests 1970
ENG DESIGN, date 1970
CONSTRUCTION, date 1972
FIRST BEAM, date (or goal) 1973
MAJOR ALTERATIONS
TRITIUM ION SOURCE SYSTEM
COST, ACCELERATOR 1,5 Mill. DM
COST, FACILITY, total 3 " "
FUNDED BY Bavarian Government

ACCELERATOR STAFF, OPERATION AND DEVELOPMENT

SCIENTISTS 2 ENGINEERS 1
TECHNICIANS 3 CRAFTS 2
GRAD STUDENTS involved during year
OPERATED BY x Research staff or y Operators
OPERATION 100 hr/wk, On target 80 hr/wk
TIME DISTR. in house %, Outside %
BUDGET, op & dev 90,000.- DM
FUNDED BY Technical University

RESEARCH STAFF, not included above

USERS, in house 5 outside 10
GRAD STUDENTS involved during year
RESEARCH BUDGET, in house
FUNDED BY

MAGNET

POLE FACE, diameter (compact) 109 cm, R extraction 48 cm
R injection cm
GAP, min 5,4 cm, Field 19 kG
max 17,5 cm, Field 8 kG } at Ampere turns
AVERAGE FIELD at R ext 14 kG
B max/ <B>
NUMBER OF SECTORS { compact 4 / separated } Spiral, max deg
SECTOR ANGLE (SSC) deg
TRIMMING COILS 4 Pairs

CONDUCTOR, material and type Copper
STORED ENERGY (cryogenic) MJ
POWER : main coils 40 max, kW ; current stability 10^{-5} Ω
trimming coils 2 max, kW ; current stability "
WEIGHT : Fe 25 tons ; coils 5 tons
COOLING system Water
ION ENERGY (bending limit) E/A = 25 q^2/a^2 MeV/amu
(focusing limit) E/A = " q^2/a^2 MeV/amu

ACCELERATION SYSTEM

DEES, number 2 ; angle 63 deg
BEAM APERTURE 2,3 cm ; DC Bias kV
TUNED by, coarse Short stub fine Trim. Capacitor
RF 28 to 42,5 mHz, stable ± $2 \cdot 10^{-6}$
Orb F to mHz
HARMONICS, RF/Orb F, used 2 / 4
DEE - Gnd, max 50 kV, min gap 2,3 cm
STABILITY, (pk-pk noise)/(pk RF volt) 5×10^{-4}
ENERGY GAIN, max 150 kV/turn
RF PHASE, stable to ± deg
RF POWER input, max 40 kW
FREQUENCY MODULATION, rate /s
modulator, type
beam pulse, width

VACUUM SYSTEM

OPERATING PRESSURE 5×10^{-7} – 2×10^{-5} Torr or mbar
PUMPS, No, Type, Size 2 oil diffusion pumps
1000 l/s each

ION SOURCES

Internal Livingston Type

INJECTION SYSTEM

EXTRACTION SYSTEM

Electrostatic Septum 70 kV

FACILITIES FOR RESEARCH

SHIELDED AREA, fixed 200 m^2 ; movable m^2
TARGET STATIONS 5 In 2 rooms
STATIONS served at same time, max 1
MAG SPECTROGRAPH, type
COMPUTER model
OTHER FACILITIES

CHARACTERISTIC BEAMS

PARTICLE	ENERGY (MeV) Goal	Achieved	CURRENT (pμA) Internal	External
p		22	500	50
d		11	"	"
t		7,3	50	30
SECONDARY			(part/s)	

BEAM PROPERTIES

	MEASURED	CONDITIONS
PULSE WIDTH	20 RF deg	300. pμ A of 22. MeV H^+ Ions
PHASE EXC, max	RF deg	pμ A of MeV Ions
EXTRACT eff	40-80 %	pμ A of MeV Ions
RESOL ΔE/E	0,1 %	pμ A of MeV H^+ / Ions
EMITTANCE (π mm. mrad)	{ axial / rad }	pμA of MeV Ions

OPERATING PROGRAMS, time distribution

BASIC NUCLEAR PHYSICS 10% SOLID STATES PHYSICS
BIOMEDICAL APPLICAT. ISOTOPE PRODUCTIONS 90%

REFERENCES/NOTES

PLAN VIEW OF FACILITY, NOTEWORTHY FEATURES, COMMENTS

The compact cyclotron is an energy fixed machine with rather high beam intensities for light ions including the radioactive triton beam. It is used nearly exclusively for radioisotope production.
Very strong 57Co-sources of about 1 Curie are produced with the 500 uA proton beam on a high speed rotational target. Biological tracer isotopes, as 28Mg or 42K , are produced using the triton beam.

ENTRY No. C25

NAME OF MACHINE Zyklotron U-120 **DATE** March 1989
INSTITUTION Zentralinstitut für Kernforschung Rossendorf
ADDRESS DDR - 8051 Dresden, PF 19
TEL 5910 TELEX
IN CHARGE E. Richter **REPORTED BY** E. Richter, H. Guratzsch

---

HISTORY AND STATUS
DESIGN, date Model tests
ENG DESIGN, date
CONSTRUCTION, date 1957-1959
FIRST BEAM, date (or goal) August 1958
MAJOR ALTERATIONS see below x)

COST, ACCELERATOR
COST, FACILITY, total
FUNDED BY government

ACCELERATOR STAFF, OPERATION AND DEVELOPMENT
SCIENTISTS 4 ENGINEERS 4
TECHNICIANS 10 CRAFTS -
GRAD STUDENTS involved during year -
OPERATED BY - Research staff or 2 Operators
OPERATION 120 hr/wk, On target 110 hr/wk
TIME DISTR. in house 75 %, Outside 25 %
BUDGET, op & dev
FUNDED BY government

RESEARCH STAFF, not included above
USERS, in house outside
GRAD STUDENTS involved during year
RESEARCH BUDGET, in house
FUNDED BY

MAGNET
POLE FACE, diameter (compact) 120 cm, R extraction 52.5 cm
R injection cm
GAP, min 17 cm, Field 14.5 kG
max cm, Field kG } at 0.29×10^6 Ampere turns
AVERAGE FIELD at R ext 14.1 kG
B max/ <B>
NUMBER OF SECTORS {compact / separated} Spiral, max deg
SECTOR ANGLE (SSC) deg
TRIMMING COILS

CONDUCTOR, material and type hollow copper
STORED ENERGY (cryogenic) MJ
POWER : main coils 70 max, kW ; current stability 5×10^{-4}
trimming coils max, kW ; current stability
WEIGHT : Fe 105 tons ; coils 15 tons
COOLING system H_2O
ION ENERGY (bending limit) E/A = 27 q^2/a^2 MeV/amu
(focusing limit) E/A = q^2/a^2 MeV/amu

ACCELERATION SYSTEM
DEES, number 2 ; angle 180 deg
BEAM APERTURE 4.5 cm ; DC Bias kV
TUNED by, coarse mov. short fine trim cap.
RF 8.2 to 16.8 mHz, stable ±
Orb F 8.2 to 16.8 mHz
HARMONICS, RF/Orb F, used 1
DEE - Gnd, max 60 kV, min gap 5 cm
STABILITY, (pk-pk noise)/(pk RF volt)
ENERGY GAIN, max 240 kV/turn
RF PHASE, stable to ± deg
RF POWER input, max 120 kW
FREQUENCY MODULATION, rate /s
modulator, type
beam pulse, width

VACUUM SYSTEM
OPERATING PRESSURE 10^{-5} Torr or ~~mbar~~
PUMPS, No, Type, Size 5 oil diffusion pumps
2 2500 l/s, 3 500 l/s

ION SOURCES
PIG internal

INJECTION SYSTEM

EXTRACTION SYSTEM
electrostatic deflector 110 degr.
FACILITIES FOR RESEARCH
SHIELDED AREA, fixed 200 m² ; movable - m²
TARGET STATIONS 6 in 2 rooms
STATIONS served at same time, max 1
MAG SPECTROGRAPH, type
COMPUTER model K 1630 + PCs
OTHER FACILITIES Isotope production fac.
Neutron therapy fac.
Irradiation fac.

CHARACTERISTIC BEAMS

PARTICLE	ENERGY (MeV) Goal	Achieved	CURRENT (pμA) Internal	External
d, H_2^+		13.5		50
α		27		10
$^3He^{2+}$		31		2
$^6Li^{3+}$		42		0.05
SECONDARY				(part/s)
n				1.3×10^{12}

BEAM PROPERTIES

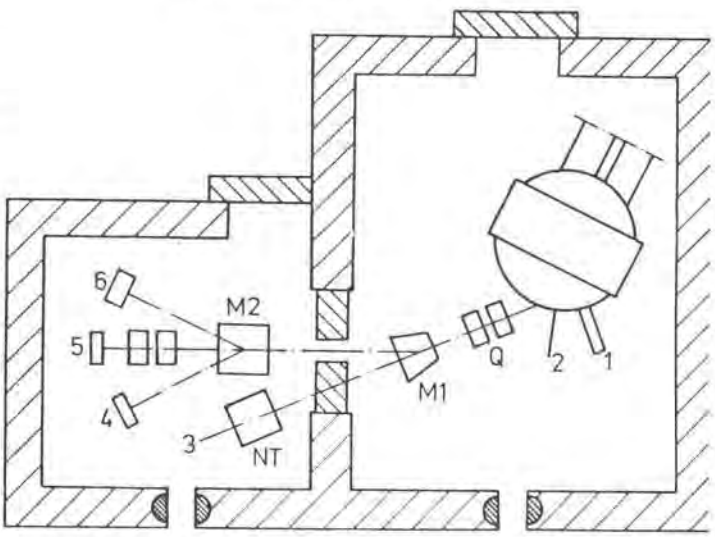
	MEASURED		CONDITIONS		
PULSE WIDTH	16 RF deg	50	pμA of 13.5	MeV	d Ions
PHASE EXC, max	RF deg		pμA of	MeV	Ions
EXTRACT eff	60 %		pμA of	MeV	Ions
RESOL ΔE/E	0.6 %		pμA of	MeV	Ions
EMITTANCE					
(π mm. mrad) {axial / rad}			pμA of	MeV	Ions

OPERATING PROGRAMS, time distribution
BASIC NUCLEAR PHYSICS 25 % SOLID STATES PHYSICS 40 %
BIOMEDICAL APPLICAT. Medicine 25 % ISOTOPE PRODUCTIONS Thin Layer Activation 10 %

REFERENCES/NOTES

1) Alekseew A.G. et. al. Kernenergie 3 (1960)456
2) 20 Jahre Rossendorfer Zyklotron, ZfK-363 (1978)

PLAN VIEW OF FACILITY, NOTEWORTHY FEATURES, COMMENTS
x) Extensionse switching magnet 1963, computer 1970, fast neutron facility 1972, ^3He 1975, ^6Li 1978, isotope production facility 1977, circ. coils 1989 (p 12 MeV).



ENTRY NO. C26 Date June 1992

Name of Machine Chandigarh Variable Energy Cyclotron

Institution Physics Department, Panjab University, Chandigarh.

Address Physics Department, Panjab University, Chandigarh-160014, INDIA

Tel (0172) 541741 Telex 395-464 RSIC IN Fax 0091-0172-43633 EMAIL

In Charge: Prof. I.M.GOVIL Reported by: Dr. I.M.Govil

HISTORY

MILESTONE DATES:

Design 1953 Model Tests *

Construction 1965-70 First Beam 1971

DESIGN/CONSTRUCTION BY:

in house other

COST: Accelerator $. 250,000 Facility 400,000

FUNDED BY: UGC, New Delhi-India and P.U, Chandigarh.

STATUS

STAFF: Machine

Scientists 4 Engineers 4

Technicians 5 Students 4

Research (in house/external)

Scientists 5 / Engineers /

Technicians / Students 2 /

BUDGET: Machine Funded by

Research Funded by

TIME DISTRIBUTION:

Basic Research (in house/external) 75 % / 25 %

Applied Program (in house/external) % / %

Development % Maintenance %

MAGNET

POLE PARAMETERS:

Diameter 66 cm $R_{extract}$ 28 cm R_{inject} 0 cm

HILL PARAMETERS: Gap (min) 16 cm B_{max} 16 T

(@ AT) Gap (max) cm B_{min} T

VALLEY PARAMETERS: Gap (min) cm B_{max} T

(@ AT) Gap (max) cm B_{min} T

AVERAGE FIELD: $< B >_{min}$ T $< B >_{max}$ T

NUMBER OF SECTORS: compact/separated /

sector angle deg. spiral (max) deg.

FIELD TRIMMING: Trim Coils

Harmonic Coils

Other

CURRENT: Main Coils 400 Amps Stability

Trim Coils Amps Stability

Stored Energy (cryogenic) MJ

WEIGHT: Iron 20 tons Conductor

ION ENERGY: Bending Limit E/A = 8 q^2/A^2 MeV/u

Focussing Limit E/A = 8 q/A MeV/u

ACCELERATION SYSTEM

FUNDAMENTAL ACCELERATION:

Description:

No. of Gaps/turn dE/dn(max) MeV/q

Voltage(max) MV Harmonic f_{rf}/f_{ion}

Freq MHz Power in(max) MW

Stability: Phase Voltage

OTHER CAVITIES (Flattopping or otherwise):

Description:

Region of Influence: R_{min} cm R_{max} cm

No. of Gaps/turn dE/dn(max) MeV/q

Voltage(max) MV Harmonic f_{rf}/f_{ion}

Freq MHz Power in(max) MW

Stability: Phase Voltage

VACUUM SYSTEM

OPERATING PRESSURE: 2.10^{-5} mm of Hg, Torr or mbar

PUMPS: No. and type 4 Diffusion Pumps (15,3 cm)

1 Diff. Pump 23 cm, 2 Kinney Rotary Pumps

ION SOURCE(S)

	Type	Intensity (mA)	@	$\epsilon_n = \beta\gamma\epsilon$ (πmm mrad)	Ion Species
(a)	Hooded Arc				
(b)					
(c)					
(d)					

INJECTION SYSTEM

Pullers attached to Dee Efficiency %

EXTRACTION SYSTEM

Electrostatic Deflector Efficiency %

CHARACTERISTIC BEAMS

	Accelerated Ions	E/A (MeV/u)	Current(part μA) Internal	External
(a)	$^{1}H^{+}$	2-7	50 μA	20 μA
(b)	$^{2}H^{+}$	4	20 μA	10 μA
(c)	$^{3}H^{++}$	4-11	7 μA	2 μA
(d)	$^{4}H^{++}$	8	7 μA	2 μA

	Secondary Particles	E (MeV)	part/sec
(a)			
(b)			
(c)			

EXTRACTED BEAM PROPERTIES:

For μA of MeV/u ions

$\Delta E/E$ % $\Delta\phi$ °rf

$\epsilon_n = \beta\gamma\epsilon$ x πmm mrad z πmm mrad

FACILITIES FOR RESEARCH

SHIELDED AREA: Fixed 300 m^2 Moveable 100 m^2

Target Stations: 2 No. Served At Same Time:

MAGNETIC SPECTROMETERS: -

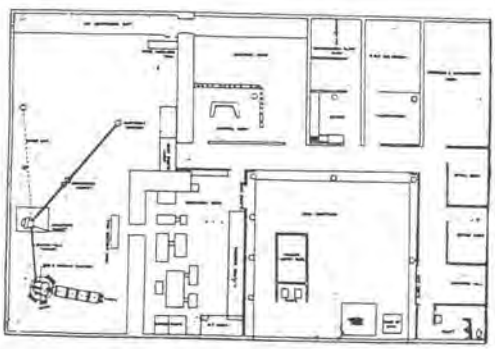
OTHER FACILITIES:

REFERENCES/NOTES

(a) *This cyclotron was built around 1953-54 at Univ.of Rochester USA. This has been shifted to modified and reinstalled at Chandigarh in 1971.

(b)

PLAN VIEW OF FACILITY, COMMENTS



ENTRY NO. C27 **Date** July 6, 1992

Name of Machine VARIABLE ENERGY CYCLOTRON

Institution VARIABLE ENERGY CYCLOTRON CENTRE

Address 1/AF, BIDHAN NAGAR, CALCUTTA-700 064, INDIA

Tel +91 33 371230(4 lines) Telex CA 4526 Fax +91 33 346871 EMAIL ..!uunet!shaktil!veccal!guest!

In Charge: BIKASH SINHA Reported by: N.K. MUKHOPADHYAY

HISTORY

MILESTONE DATES:

Design 1967 Model Tests .....

Construction 1969-77 First Beam June'77 Internal, July'78 External

DESIGN/CONSTRUCTION BY:

in house ..... other 8

COST: Accelerator $ 3 x 10^6 Facility $ 15 x 10^6

FUNDED BY: Department of Atomic Energy

STATUS

STAFF: Machine

Scientists 14 Engineers 36

Technicians 60 Students .....

Research (in house/external)

Scientists 7 Groups / 30 groups Engineers ..... / .....

Technicians ..... / ..... Students ..... / .....

BUDGET: Machine $ 2 x 10^6 Funded by DAE

Research $ 1 x 10^6 Funded by DAE

TIME DISTRIBUTION:

Basic Research (in house/external) 10 % / 43 %

Applied Program (in house/external) 10 % / 12 %

Development 5 % Maintenance 20 %

MAGNET

POLE PARAMETERS:

Diameter 224 cm $R_{extract}$ 100 cm R_{inject} ..... cm

HILL PARAMETERS: Gap (min) 19 cm B_{max} 2.1 T

(@ ..... AT) Gap (max) 19 cm B_{min} ..... T

VALLEY PARAMETERS: Gap (min) 30 cm B_{max} 1.4 T

(@ ..... AT) Gap (max) 30 cm B_{min} ..... T

AVERAGE FIELD: $< B >_{min}$ ..... T $< B >_{max}$ 1.7 T

NUMBER OF SECTORS: compact/separated Compact / 3

sector angle ..... deg. spiral (max) 55 deg.

FIELD TRIMMING: Trim Coils 17

Harmonic Coils 5

Other .....

CURRENT: Main Coils 2800 Amps Stability 1×10^{-4}

Trim Coils 2500 Amps Stability 1×10^{-3}

Stored Energy (cryogenic) ..... MJ

WEIGHT: Iron 275 Tons Conductor Cu

ION ENERGY: Bending Limit E/A = 140 q^2/A^2 MeV/u

Focussing Limit E/A = 70 q/A MeV/u

ACCELERATION SYSTEM

FUNDAMENTAL ACCELERATION:

Description: Single 180 Degree Dee

No. of Gaps/turn 2 dE/dn(max) 12 MeV/q

Voltage(max) 0.05 MV Harmonic f_{rf}/f_{ion} 1,3

Freq 5.5 - 16.5 MHz Power in(max) 0.3 MW

Stability: Phase ..... Voltage 2×10^{-3}

OTHER CAVITIES (Flattopping or otherwise):

Description: .....

Region of Influence: R_{min} ..... cm R_{max} ..... cm

No. of Gaps/turn ..... dE/dn(max) ..... MeV/q

Voltage(max) ..... MV Harmonic f_{rf}/f_{ion} .....

Freq ..... MHz Power in(max) ..... MW

Stability: Phase ..... Voltage .....

VACUUM SYSTEM

OPERATING PRESSURE: 2×10^{-6} T

PUMPS: No. and type 2 x 89 Cms. Oil Diff. Pump, 10 inch Diffstack near extraction

ION SOURCE(S)

	Type	Intensity (mA)	@	$\epsilon_n = \beta\gamma\epsilon$ (πmm mrad)	Ion Species
(a)	PIG Int	2			p, d, α
(b)	ECR	undertest			
(c)					
(d)					

INJECTION SYSTEM

Axial injection under progress, minor inflector. Efficiency ..... %

EXTRACTION SYSTEM

Electrostatic Efficiency 20 %

CHARACTERISTIC BEAMS

Accelerated Ions	E/A (MeV/u)	Current(part μA) Internal	External
(a) p	30	12	2
(b) d	12.5	100	20
(c) α	30	5	
(d) α	22	5	0.5

Secondary Particles	E (MeV)	part/sec
(a)		
(b)		
(c)		

EXTRACTED BEAM PROPERTIES:

For 5 μA of 10 MeV/u He^{++} ions

$\Delta E/E$ 0.3 % $\Delta\phi$ 30 °rf

$\epsilon_n = \beta\gamma\epsilon$ x ..... πmm mrad z ..... πmm mrad

FACILITIES FOR RESEARCH

SHIELDED AREA: Fixed 225 m² Moveable 535 m²

Target Stations: 3 No. Served At Same Time: 1

MAGNETIC SPECTROMETERS: .....

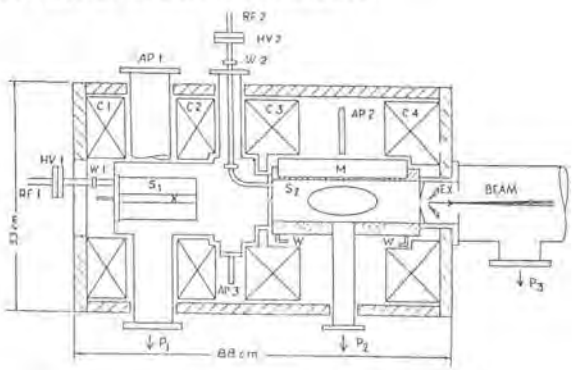
OTHER FACILITIES: 915 mm Scattering Chamber, Target detector lab., Electronic Module, Radiochemistry, Radio-Isotope Lab., ISOL System, Rabbit (under construction)

REFERENCES/NOTES

(a) Int. Cyclotron Conf. Proc. 1989, 86, 84, 78, 75, 72

(b) .....

PLAN VIEW OF FACILITY, COMMENTS



Room Temp. ECR Source Commissioned, Injection line near completion.

ENTRY NO. C28 Date JULY 1992

Name of Machine L.N.S. SUPERCONDUCTING CYCLOTRON

Institution I.N.F.N. (ISTITUTO NAZIONALE DI FISICA NUCLEARE)

Address L.N.S. V.LE A. DORIA ang. V. S. SOFIA 95123 CATANIA ITALY

Tel (95) 542111 Telex 971432 LNSI Fax (95) 7141815 EMAIL BIBLIO@.LNS.INFN.IT

In Charge: E. MIGNECO Reported by: L..CALABRETTA

HISTORY

MILESTONE DATES:

Design 1975-76 Model Tests 1977

Construction STARTED FEB. 81 First Beam GOAL 1993

DESIGN/CONSTRUCTION BY:

in house MILAN other 6

COST: Accelerator $ 7 10 Facility

FUNDED BY: I.N.F.N.

STATUS

STAFF: Machine

Scientists 14 Engineers 4

Technicians 22 Students

Research (in house/external)

Scientists / Engineers /

Technicians / Students /

BUDGET: Machine Funded by

Research Funded by

TIME DISTRIBUTION:

Basic Research (in house/external) % / %

Applied Program (in house/external) % / %

Development % Maintenance %

MAGNET

POLE PARAMETERS:

Diameter 180 cm $R_{extract}$ 86.7 cm R_{inject} 10 - 25 cm

HILL PARAMETERS: Gap (min) 8.6 cm B_{max} 5.6 T

(Φ 6.55.10 AT) Gap (max) 8.6 cm B_{min} T

VALLEY PARAMETERS: Gap (min) cm B_{max} T

(Φ 6.55.10^6 AT) Gap (max) 91.6 cm B_{min} T

AVERAGE FIELD: $< B >_{min}$ 2.2 T $< B >_{max}$ 4.8 T

NUMBER OF SECTORS: compact/separated 3 / COMPACT

sector angle deg. spiral (max) 69 2deg.

FIELD TRIMMING: Trim Coils 20-CONDUCTOR:COPPER 6X6 mm

Harmonic Coils

Other

CURRENT: Main Coils 2000 Amps Stability 10 e-5

Trim Coils 500 Amps Stability 10 e-4

Stored Energy (cryogenic) 40 MJ

WEIGHT: Iron 176 TONS Conductor 9.6 TONS

ION ENERGY: Bending Limit E/A = 800 q^2/A^2 MeV/u

Focussing Limit E/A = 200 q/A MeV/u

ACCELERATION SYSTEM

FUNDAMENTAL ACCELERATION:

Description: 3 DEES WITH ANGLE OF 58 DEG.

No. of Gaps/turn 6 dE/dn(max) 0.480 MeV/q

Voltage(max) 0.1 MV Harmonic f_{rf}/f_{ion} 1 2 3

Freq 15-49 MHz Power in(max) 0.18 MW

Stability: Phase 0.5 DEG. Voltage 10 e-4

OTHER CAVITIES (Flattopping or otherwise):

Description:

Region of Influence: R_{min} cm R_{max} cm

No. of Gaps/turn dE/dn(max) MeV/q

Voltage(max) MV Harmonic f_{rf}/f_{ion}

Freq MHz Power in(max) MW

Stability: Phase Voltage

VACUUM SYSTEM

OPERATING PRESSURE: 10 e-7 Torr

PUMPS: No. and type 4 CRYOPUMPS

ION SOURCE(S)

	Type	Intensity (mA)	Φ	$\epsilon_n = \beta\gamma\epsilon$ (πmm mrad)	Ion Species
(a)					
(b)					
(c)					
(d)					

INJECTION SYSTEM

RADIAL FROM 15 MV TANDEM AND AXIAL Efficiency %

FROM ECR SOURCE

EXTRACTION SYSTEM

ELETTROSTATIC DEFLECTOR(2) AND MAGNETIC Efficiency %

CHANNELS(7)

CHARACTERISTIC BEAMS

Accelerated Ions	E/A (MeV/u)	Current(part μA) Internal	External
(a)			
(b)			
(c)			
(d)			

Secondary Particles	E (MeV)	part/sec
(a)		
(b)		
(c)		

EXTRACTED BEAM PROPERTIES:

For μA of MeV/u ions

$\Delta E/E$ % $\Delta\phi$ °rf

$\epsilon_n = \beta\gamma\epsilon$ x πmm mrad z πmm mrad

FACILITIES FOR RESEARCH

SHIELDED AREA: Fixed 2000 m² Moveable m²

Target Stations: 6 No. Served At Same Time:

MAGNETIC SPECTROMETERS:

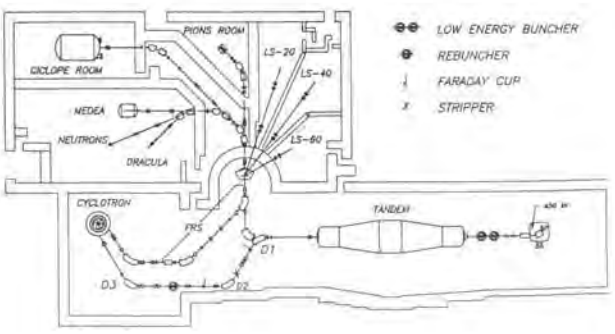
OTHER FACILITIES: Fragment Recoil Separator

REFERENCES/NOTES

(a) E.ACERBI et al., XI Int. Conf. on Cycl. 168(1986)

(b) E.ACERBI et al., XII Int. Conf. on Cycl. 26(1989)

PLAN VIEW OF FACILITY, COMMENTS



ENTRY NO. C29 Date 1st July, 1992

Name of Machine RCNP AVF cyclotron

Institution Research Center for Nuclear Physics Osaka University

Address Ibaraki, Osaka 567, JAPAN

Tel 06-877-5111 Telex 5286214 RCNPJ Fax 06-875-2920 EMAIL

In Charge: M. Kondo Reported by: T. Itahashi

HISTORY

MILESTONE DATES:

Design 1970-1972 Model Tests 1966-69

Construction 1971-1973 First Beam 1974

DESIGN/CONSTRUCTION BY:

in house design other various engineering contracts

COST: Accelerator 3.5×10^{6}(1971) Facility 9×10^{6}(1971)

FUNDED BY: Ministry of Education, Science and Culture

STATUS

STAFF: Machine

Scientists ~8 (including Ring Cyclotron) Engineers 6 (including Ring Cyclotron)

Technicians — Students —

Research (in house/external)

Scientists ~9 / Engineers 1 /

Technicians / Students 2 /

BUDGET: Machine ~3×10^{6} Ring Funded by Science and Cultures (including Ministry of Education

Research ~2×10^{6} " Funded by "

TIME DISTRIBUTION:

Basic Research (in house/external) 85 % / (inhouse & ext.) %

Applied Program (in house/external) 5 % / (") %

Development 5 % Maintenance 5 %

MAGNET

POLE PARAMETERS:

Diameter 230 cm $R_{extract}$ 100 cm R_{inject} cm

HILL PARAMETERS: Gap (min) 29.7 cm B_{max} 1.95 T

(@ AT) Gap (max) cm B_{min} T

VALLEY PARAMETERS: Gap (min) 34.7 cm B_{max} 1.2 T

(@ AT) Gap (max) cm B_{min} T

AVERAGE FIELD: $<B>_{min}$ T $<B>_{max}$ 1.6 T

NUMBER OF SECTORS: compact/separated 3 /

sector angle deg. spiral (max) 52 deg.

FIELD TRIMMING: Trim Coils 16

Harmonic Coils 5/sec

Other

CURRENT: Main Coils 6×10^{6} AT Amps Stability 3×10^{-5}

Trim Coils 4.5×10^{3} AT Amps Stability 10^{-4}

Stored Energy (cryogenic) MJ

WEIGHT: Iron 400 tons Conductor Copper, Hollow

ION ENERGY: Bending Limit E/A = 140 q^2/A^2 MeV/u

Focussing Limit E/A = 85 q/A MeV/u

ACCELERATION SYSTEM

FUNDAMENTAL ACCELERATION:

Description: Single Dee, Coaxial Resonator

No. of Gaps/turn 2 dE/dn(max) 0.16 MeV/q

Voltage(max) 0.08 MV Harmonic f_{rf}/f_{ion} 1 3

Freq 6~18 MHz Power in(max) 0.4 MW

Stability: Phase 1 deg Voltage 1×10^{-4}

OTHER CAVITIES (Flattopping or otherwise):

Description:

Region of Influence: R_{min} cm R_{max} cm

No. of Gaps/turn dE/dn(max) MeV/q

Voltage(max) MV Harmonic f_{rf}/f_{ion}

Freq MHz Power in(max) MW

Stability: Phase Voltage

VACUUM SYSTEM

OPERATING PRESSURE: 6×10^{-7}

PUMPS: No. and type 3 Diffusion pumps

(one 55cm, two 90 cm)

ION SOURCE(S)

	Type	Intensity (mA)	@	$\epsilon_n = \beta\gamma\epsilon$ (πmm mrad)	Ion Species
(a)	Internal, hoodedarc				p,d,h,α
(b)	Internal, pulsedPIG				Li, ... Ar
(c)	External, pol. atomic				p, d
(d)					

INJECTION SYSTEM

Electrstatic Focusing and dc mirror Inflector Efficiency ~10 %

EXTRACTION SYSTEM

Dc Electrostatic with Magnetic Channel Efficiency 50~100 %

CHARACTERISTIC BEAMS

Accelerated Ions	E/A (MeV/u)	Current(part μA) Internal	External
(a) p	$\leq$ 85	50	50
(b) α	$\leq$ 30	20	20
(c) $\vec{p}_{e+}$	$\leq$ 85	1	1
(d) Ne^{6+}	$\leq$ 11	0.2	0.2

Secondary Particles	E (MeV)	part/sec
(a)		
(b)		
(c)		

EXTRACTED BEAM PROPERTIES:

For 1 μA of 65 MeV/u p ions

$\Delta E/E$ 0.2 % $\Delta\phi$ 12 °rf

$\epsilon_n = \beta\gamma\epsilon$ x 6 πmm mrad z 3 πmm mrad

FACILITIES FOR RESEARCH

SHIELDED AREA: Fixed 1130 m² Moveable — m²

Target Stations: No. Served At Same Time: 1

MAGNETIC SPECTROMETERS: QDDQ(RAIDEN)

OTHER FACILITIES:

Recoil Mass Separator (CARP), Triple Focusing Electron Spectrometer (AGNES)

REFERENCES/NOTES

(a) M.Kondo, Eighth Internat. Conf on Cyclotrons and their applications, Bloomington, (1978), pp.1904-1911

(b) RCNP Annual Report (1987)

PLAN VIEW OF FACILITY, COMMENTS

1) Intensity of polarized proton and deuteron beam is increased up to 600 nA at target.
2) Horizontally polarized proton and deuteron beam are used in experiments.
3) $^{6}Li^{3+}$(E$\leq$210 MeV). $^{7}Li^{3+}$(E$\leq$180 MeV) and $^{40}Ca^{7+}$ ($\leq$147 MeV) are supplied using back bombard method with LiF and CaF_2 crystals.
4) The J-beam line is equipped with recoil mass separator (CARP).
5) The six sector ring cyclotron as a booster of the present cyclotron was completed in March 1991.

ENTRY NO. C30 **Date** June 22, 1992

Name of Machine RCNP Ring Cyclotron

Institution Research Center for Nuclear Physics, Osaka University

Address Ibaraki Osaka 567, Japan

Tel 06-877-5111 **Telex** 5286214 RCNPJ **Fax** 06-875-2920 **EMAIL**

In Charge: I. Miura **Reported by:** I. Miura

HISTORY

MILESTONE DATES:
Design 1985 Model Tests 1987
Construction Aug. 1987 First Beam Oct. 1991
DESIGN/CONSTRUCTION BY:
in house design other constructed by SHI
COST: Accelerator 3.8 B¥ Facility 1.6 B¥
FUNDED BY: Ministry of Education, Japan

STATUS SEE RCNP AVF

STAFF: Machine
Scientists ... Engineers ...
Technicians ... Students ...
Research (in house/external)
Scientists ... / ... Engineers ... / ...
Technicians ... / ... Students ... / ...
BUDGET: Machine ... Funded by ...
Research ... Funded by ...
TIME DISTRIBUTION:
Basic Research (in house/external) ... % / ... %
Applied Program (in house/external) ... % / ... %
Development ... % Maintenance ... %

MAGNET

POLE PARAMETERS:
Diameter ... cm $R_{extract}$ 400 cm R_{inject} 200 cm
HILL PARAMETERS: Gap (min) 6 cm B_{max} 1.75 T
(Φ ... AT) Gap (max) ... cm B_{min} ... T
VALLEY PARAMETERS: Gap (min) ... cm B_{max} ... T
(Φ ... AT) Gap (max) ... cm B_{min} ... T
AVERAGE FIELD: $< B >_{min}$ ... T $< B >_{max}$ 0.76 T
NUMBER OF SECTORS: compact/separated ... / 6
sector angle 22-27.5 deg. spiral (max) 30 deg.
FIELD TRIMMING: Trim Coils 36
Harmonic Coils 3
Other ...
CURRENT: Main Coils 900 Amps Stability 3x10⁻⁶
Trim Coils 500x16+350x20 Amps Stability 1x10⁻⁵
Stored Energy (cryogenic) ... MJ
WEIGHT: Iron 2200 ton Conductor 32 ton
ION ENERGY: Bending Limit E/A = 400 q^2/A^2 MeV/u
Focussing Limit E/A = >400 q/A MeV/u

ACCELERATION SYSTEM

FUNDAMENTAL ACCELERATION:
Description: Single gap type
No. of Gaps/turn 3 dE/dn(max) 1.5 MeV/q
Voltage(max) 0.5 MV Harmonic f_{rf}/f_{ion} 6,10,12,18
Freq 30~ 52 MHz Power in(max) 0.25x3 MW
Stability: Phase (0.01°) Voltage (10^{-4})
OTHER CAVITIES (Flattopping or otherwise):
Description: ...
Region of Influence: R_{min} 200 cm R_{max} 400 cm
No. of Gaps/turn 1 dE/dn(max) 0.17 MeV/q
Voltage(max) 0.17 MV Harmonic f_{rf}/f_{ion} 18,30,36,54
Freq 90~155 MHz Power in(max) 0.045 MW
Stability: Phase (0.01°) Voltage (10^{-4})

VACUUM SYSTEM

OPERATING PRESSURE: $1x10^{-7}$ Torr
PUMPS: No. and type 6 Cryo. pumps 500ø,
3 Cryo. pumps 400ø, 6 Diff. pumps 400ø

ION SOURCE(S)

	Type	Intensity (mA)	Φ	$\epsilon_n = \beta\gamma\epsilon$ (πmm mrad)	Ion Species
(a)					
(b)					
(c)					
(d)					

INJECTION SYSTEM

2 inflectors + 2 magnetic channels ... Efficiency (100) ... %

EXTRACTION SYSTEM

2 deflectors + 2 magnetic channels ... Efficiency (100) ... %

CHARACTERISTIC BEAMS

	Accelerated Ions	E/A (MeV/u)	Current(part μA) Internal	External
(a)	p	300	0.02	0.02
(b)	p	300	0.005	0.005
(c)	p	400	0.01	
(d)				

	Secondary Particles	E (MeV)	part/sec
(a)			
(b)			
(c)			

EXTRACTED BEAM PROPERTIES:
For ... μA of 300 MeV/u p ions
ΔE/E 0.1 % Δφ 10 °rf
$\epsilon_n = \beta\gamma\epsilon$ x 0.6 πmm mrad z 0.6 πmm mrad

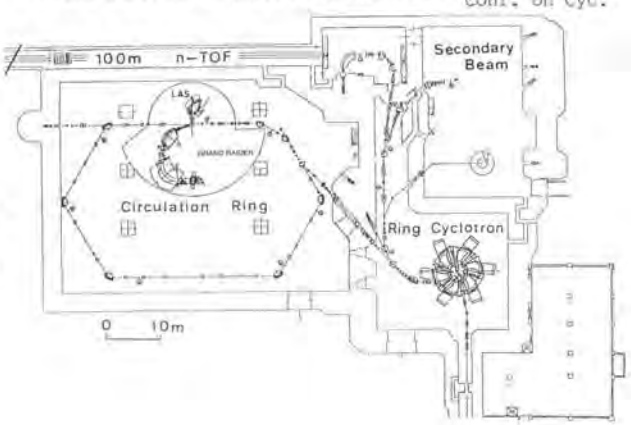
FACILITIES FOR RESEARCH

SHIELDED AREA: Fixed 3600 m² Moveable 0 m²
Target Stations: 5 No. Served At Same Time: 1
MAGNETIC SPECTROMETERS: $B\rho_{max}$=9000,54kGm+$B\rho_{max}$=5000,32kGm
OTHER FACILITIES:
100m TOF Tunnel and 0~90° Beam Swinger
Beam Circulation Ring with 200MeV H_2^+ injection
Secondary-Beam Course

REFERENCES/NOTES

(a) Commissioning of the RCNP Ring Cyclotron, Proc. of
(b) this conf.
H. Ikegami, The RCNP Ring Cyclotron Facilities, Proc. of the 12th Conf. on Cyc.

PLAN VIEW OF FACILITY, COMMENTS



ENTRY NO. C31 Date July 1, 1992

Name of Machine 715 CYCLOTRON-RIKEN

Institution The Institute of Physical and Chemical Research (RIKEN)

Address Wako-shi, Saitama 351-01, Japan

Tel 0484-62-1111 Telex 296-2818 RIKEN J Fax 0484-62-4642 EMAIL goto @ ringps.riken.go.jp

In Charge: Y. Yano Reported by: A. Goto

HISTORY

MILESTONE DATES:

Design 1985-1987 Model Tests

Construction 1987-1989 First Beam April 1989

DESIGN/CONSTRUCTION BY: Dsign RIKEN/SHI

in house other Construction SHI

COST: Accelerator ¥12x10^{9} (incl. BT) Facility

FUNDED BY: Science and Technology Agency (STA)

STATUS

STAFF: Machine Same as those of RIKEN Ring Cyclotron (RRC).

Scientists Engineers

Technicians Students

Research (in house/external)

Scientists / Engineers /

Technicians / Students /

BUDGET: Machine Funded by

Research Funded by

TIME DISTRIBUTION:

Basic Research (in house/external) % / %

Applied Program (in house/external) % / %

Development % Maintenance %

MAGNET

POLE PARAMETERS:

Diameter 172.6 cm $R_{extract}$ 71.4 cm R_{inject} 1.63 cm

HILL PARAMETERS: Gap (min) 12.8 cm B_{max} 2.02 T

(@ 320,000 AT) Gap (max) cm B_{min} T

VALLEY PARAMETERS: Gap (min) cm B_{max} T

(@ 320,000 AT) Gap (max) 30.0 cm B_{min} 1.14 T

AVERAGE FIELD: $< B >_{min}$ 0.5 T $< B >_{max}$ 1.7 T

NUMBER OF SECTORS: compact/separated 4 /

sector angle deg. spiral (max) 50 deg.

FIELD TRIMMING: Trim Coils 9 pairs

Harmonic Coils 4 pairs (in the extraction region)

Other

CURRENT: Main Coils 1113 Amps Stability ±1x10^{-5}

Trim Coils 70-300 Amps Stability ±2x10^{-4}

Stored Energy (cryogenic) MJ

WEIGHT: Iron 102 tons Conductor 5.3tons

ION ENERGY: Bending Limit E/A = 70 q^2/A^2 MeV/u

Focussing Limit E/A = q/A MeV/u

ACCELERATION SYSTEM

FUNDAMENTAL ACCELERATION:

Description: 2x85° Dees

No. of Gaps/turn 4 dE/dn(max) 0.2 MeV/q

Voltage(max) 0.05 MV Harmonic f_{rf}/f_{ion} 2

Freq 12-24 MHz Power in(max) 0.06 MW

Stability: Phase ±0.2° Voltage ±5x10^{-4}

OTHER CAVITIES (Flattopping or otherwise):

Description:

Region of Influence: R_{min} cm R_{max} cm

No. of Gaps/turn dE/dn(max) MeV/q

Voltage(max) MV Harmonic f_{rf}/f_{ion}

Freq MHz Power in(max) MW

Stability: Phase Voltage

VACUUM SYSTEM

OPERATING PRESSURE: 2x10^{-8} Torr

PUMPS: No. and type 1500 l/s TMPx1

4000 l/s CRYOx1, 6500 l/s CRYOx1

ION SOURCE(S)

	Type	Intensity (mA)	@ $\epsilon_n = \beta\gamma\epsilon$ (πmm mrad)	Ion Species
(a)	ECR	0.05-0.2		p-Ar
(b)	PIS (under construction and will be conpleted this fall)			
(c)				
(d)				

INJECTION SYSTEM

Axial, Solenoid, Spiral inflector Efficiency 20-30 %

EXTRACTION SYSTEM

Deflector, Mag.chan., Passive focusing chan. Efficiency 40-60 %

CHARACTERISTIC BEAMS

	Accelerated Ions	E/A (MeV/u)	Current(part μA) Internal	External
(a)	p/d	4-9.9/4-9.5		1-4/1-3
(b)	^{12}C, ^{14}N, ^{16}O, ^{20}Ne,	4-7		0.5-2
(c)	^{24}Mg, ^{27}Al	5.5		0.03
(d)	^{40}Ar	4.5-5.2		0.03-0.2

	Secondary Particles	E (MeV)	part/sec
(a)			
(b)			
(c)			

EXTRACTED BEAM PROPERTIES:

For μA of MeV/u ions

$\Delta E/E$ % $\Delta\phi$ °rf

$\epsilon_n = \beta\gamma\epsilon$ x πmm mrad z πmm mrad

FACILITIES FOR RESEARCH Same as those of RRC.

SHIELDED AREA: Fixed m^2 Moveable m^2

Target Stations: No. Served At Same Time:

MAGNETIC SPECTROMETERS:

OTHER FACILITIES:

REFERENCES/NOTES

(a) A.Goto et al.: Proc.12th Int.Cyclo. Conf., 51 (1989)

(b) A.Goto et al.: ibid., 439 (1989)

PLAN VIEW OF FACILITY, COMMENTS

This cyclotron has been used as an injector for RIKEN RING Cyclotron (RRC)
The stand-alone use of the 715 cyclotron will also start from this fall.

ENTRY NO. C32 Date July 1, 1992

Name of Machine RIKEN Ring Cyclotron

Institution The Institute of Physical and Chemical Research (RIKEN)

Address Wako-shi, Saitama 351-01, Japan

Tel 0484-62-1111 Telex 296-2818 RIKEN J Fax 0484-62-4642 EMAIL goto @ ringps. riken.go.jp

In Charge: Y.Yano Reported by: A.Goto

HISTORY

MILESTONE DATES:

Design 1975 Model Tests 1977

Construction 1980-1986 First Beam Dec. 16, 1986

DESIGN/CONSTRUCTION BY: Design RIKEN
Construction SHI (major)

in house ... other ...

COST: Accelerator ¥40x10^8 Facility ¥137x10^8

FUNDED BY: Science and Technology Agency (STA)

STATUS

STAFF: Machine

Scientists 6 Engineers 14

Technicians ... Students ...

Research (in house/external)

Scientists 46 / 240 Engineers 2 / ...

Technicians ... / ... Students ... / 110

BUDGET: Machine ¥4.2x10^8 Funded by STA

Research ¥4.4x10^8 Funded by STA

TIME DISTRIBUTION:

Basic Research (in house/external) 20 % / 50 %

Applied Program (in house/external) ... % / ... %

Development 10 % Maintenance 20 %

MAGNET

POLE PARAMETERS:

Diameter ... cm $R_{extract}$ 356 cm R_{inject} 89 cm

HILL PARAMETERS: Gap (min) 8 cm B_{max} 1.67 T

(@ 1.28x10^3 AT) Gap (max) 8 cm B_{min} ... T

VALLEY PARAMETERS: Gap (min) ... cm B_{max} ... T

(@ ... AT) Gap (max) ... cm B_{min} ... T

AVERAGE FIELD: $< B >_{min}$ ... T $< B >_{max}$ 0.97 T

NUMBER OF SECTORS: compact/separated ... / 4

sector angle 50 deg. spiral (max) ... deg.

FIELD TRIMMING: Trim Coils 26x4 pairs

Harmonic Coils ...

Other ...

CURRENT: Main Coils 1072 Amps Stability <5x10^{-6}

Trim Coils 230-600 Amps Stability <5x10^{-5}

Stored Energy (cryogenic) ... MJ

WEIGHT: Iron 2100 tons Conductor 16 tons

ION ENERGY: Bending Limit E/A = 540 q^2/A^2 MeV/u

Focussing Limit E/A = ... q/A MeV/u

ACCELERATION SYSTEM

FUNDAMENTAL ACCELERATION:

Description: 2x23.5° -Dees

No. of Gaps/turn 4 dE/dn(max) 1 MeV/q

Voltage(max) 0.25 MV Harmonic f_{rf}/f_{ion} 5,9,10,11

Freq 18-45 MHz Power in(max) 2x0.3 MW

Stability: Phase ±0.2° Voltage ±1.5x10^{-4}

OTHER CAVITIES (Flattopping or otherwise):

Description: ...

Region of Influence: R_{min} ... cm R_{max} ... cm

No. of Gaps/turn ... dE/dn(max) ... MeV/q

Voltage(max) ... MV Harmonic f_{rf}/f_{ion} ...

Freq ... MHz Power in(max) ... MW

Stability: Phase ... Voltage ...

VACUUM SYSTEM

OPERATING PRESSURE: <1x10^{-8} Torr

PUMPS: No. and type 5,000 l/s Cryopanels x4

10,000 l/s Cryopumps x10

ION SOURCE(S)

	Type	Intensity (mA)	@	$\epsilon_n = \beta\gamma\epsilon$ (πmm mrad)	Ion Species
(a)	External injection by use of two injectors (715 cyclotron and heavy-ion linac)				
(b)	...	...	...	...	...
(c)	...	...	...	...	...
(d)	...	...	...	...	...

INJECTION SYSTEM

Magnetic chan and electrostatic chan. ... Efficiency 70 %

EXTRACTION SYSTEM

Electrostatic chan and Magnetic chan. ... Efficiency 100 %

CHARACTERISTIC BEAMS

	Accelerated Ions	E/A (MeV/u)	Current(part μA) Internal	External
(a)	P	70-210	...	0.03-0.1
(b)	d, ^{12}C, ^{14}N, ^{16}O, ^{20}Ne,	30-135	...	0.01-0.5
(c)	^{40}Ar	7.5-95	...	0.03-0.2
(d)	$^{132,136}Xe$	7.0-26	...	0.002-0.004

	Secondary Particles	E (MeV)	part/sec
(a)	^{11}Li	910	3x10^4
(b)	^{12}Be	980	1x10^6
(c)	^{16}C	1250	1x10^7

EXTRACTED BEAM PROPERTIES:

For ... μA of ... MeV/u ... ions

$\Delta E/E$ 0.1 % $\Delta\phi$ 4 °rf

$\epsilon_n = \beta\gamma\epsilon$ x 0.7 πmm mrad z 0.7 πmm mrad

FACILITIES FOR RESEARCH

SHIELDED AREA: Fixed 4000 m^2 Moveable ... m^2

Target Stations: 14 No. Served At Same Time: 2

MAGNETIC SPECTROMETERS: QQD-QD (SMART)

OTHER FACILITIES: Projectile Fragment Separator (RIPS)

Gas-filled Recoil Isotope Separator / Ion-guided Isotope ...

Separator On-line (GARIS/IGISOL) ...

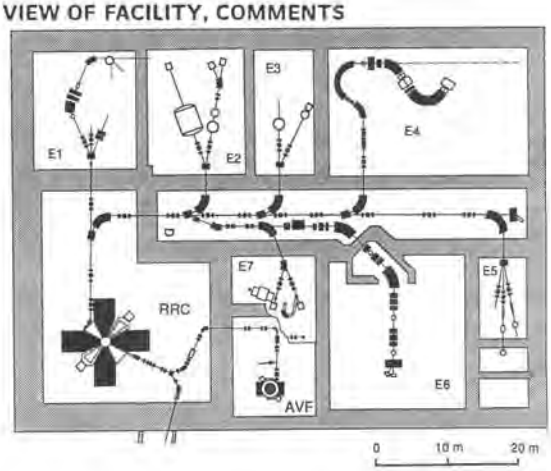
Scattering Chamber (ASCHRA), Muon Channel (Large Ω) ...

REFERENCES/NOTES

(a) Y.Yano : this conference

(b) ...

PLAN VIEW OF FACILITY, COMMENTS



ENTRY NO. ....c33..... Date ....18 June, 1992.....
Name of Machine .....JAERI AVF Cyclotron.....
Institution .Takasaki Radiation Chemistry Research Establishment,Japan Atomic Energy Research Institute.....
Address ...1233 Watanuki-cho, Takasaki, Gunma, 370-12 Japan.....
Tel .....0273(46)9636..... Telex ...J24596..... Fax ....0273(46)9690..... EMAIL .....
In Charge: .....K.Arakawa..... Reported by: ....K.Arakawa.....

HISTORY

MILESTONE DATES:
Design ..... Model Tests .....
Construction .1988-1991..... First Beam .March, 1991....
DESIGN/CONSTRUCTION BY:
in house ..... other .....
COST: Accelerator ..... Facility .....
FUNDED BY: ....The Science and Technology Agency.....

STATUS

STAFF: Machine
Scientists .....5..... Engineers .....5.....
Technicians .....8..... Students .....
Research (in house/external)
Scientists .....40... / ....80... Engineers ..... / .....
Technicians ..... / ..... Students ..... / ..20....
BUDGET: Machine ....170 MYEN.... Funded by Sci. Tec. Age.
Research ....200 MYEN.... Funded by Sci. Tec. Age.
TIME DISTRIBUTION:
Basic Research (in house/external) .....5.... % / .....5.... %
Applied Program (in house/external) ...35..... % / ....25.... %
Development .....20..... % Maintenance .....10.... %

MAGNET

POLE PARAMETERS:
Diameter..216... cm $R_{extract}$ ...92.3. cm R_{inject} ..... cm
HILL PARAMETERS: Gap (min) ...16.6.. cm B_{max} ..2.10... T
(@ ..432000. AT) Gap (max) ..... cm B_{min} ..... T
VALLEY PARAMETERS: Gap (min) .40.5.. cm B_{max} ..... T
(@ ..432000. AT) Gap (max) ..... cm B_{min} ..1.21... T
AVERAGE FIELD: $< B >_{min}$ ..1.66.... T $< B >_{max}$ ..1.69... T
NUMBER OF SECTORS: compact/separated .....4.... / .....
sector angle ..... deg. spiral (max) .....53..... deg.
FIELD TRIMMING: Trim Coils .....12 pairs.....
Harmonic Coils .....8 pairs.....
Other .....
CURRENT: Main Coils .....900.... Amps Stability .$\pm 1 \times 10^{-5}$....
Trim Coils ..... Amps Stability ....$\pm 2 \times 10^{-4}$.....
Stored Energy (cryogenic) ..... MJ
WEIGHT: Iron .....220. tons..... Conductor .....9 tons.....
ION ENERGY: Bending Limit E/A = ...110..... q^2/A^2 MeV/u
Focussing Limit E/A = ...95..... q/A MeV/u

ACCELERATION SYSTEM

FUNDAMENTAL ACCELERATION:
Description: .....
No. of Gaps/turn .....4..... dE/dn(max) ....0.16.... MeV/q
Voltage(max) .....0.06.... MV Harmonic f_{rf}/f_{ion} 1,2,3.....
Freq ..10.6-22.0.... MHz Power in(max) .....0.05....MW
Stability: Phase .....±0.5 deg. Voltage .....$\pm 1 \times 10^{-3}$.....
OTHER CAVITIES (Flattopping or otherwise):
Description: .....
Region of Influence: R_{min} ..... cm R_{max} ..... cm
No. of Gaps/turn ..... dE/dn(max) ..... MeV/q
Voltage(max) ..... MV Harmonic f_{rf}/f_{ion} .....
Freq ..... MHz Power in(max) ..... MW
Stability: Phase ..... Voltage .....

VACUUM SYSTEM

OPERATING PRESSURE: .....2×10^{-5}...pa.....
PUMPS: No. and type ...Turbo molecular pump .(2000L/s,1 set)
...Cryogenic pump .(4000L/s for N_2 , 4 sets).....

ION SOURCE(S)

	Type	Intensity (mA)	@	$\epsilon_n = \beta\gamma\epsilon$ (πmm mrad)	Ion Species
(a)	cusp	1.3		300	H^+
(b)	cusp	1.0			D^+
(c)	ECR	0.16		100	$^{40}Ar^{8+}$
(d)	ECR	0.012			$^{84}Kr^{18+}$

INJECTION SYSTEM

Axial injection,Spiral inflector.... Efficiency ..20.... %

EXTRACTION SYSTEM

Deflector, Magnetic channel ..... Efficiency ..80.... %

CHARACTERISTIC BEAMS

	Accelerated Ions	E/A (MeV/u)	Current(part μA) Internal	External
(a)	proton	90		10
(b)	deuteron	17.5		40
(c)	$^4He^{2+}$	25		10
(d)	$^{40}Ar^{8+}$	4.4		3.0

	Secondary Particles	E (MeV)	part/sec
(a)	neutron...Be(d,n).....	.....	.....
(b)	.....Be(p,n).....	.....	.....
(c)	.....	.....	.....

EXTRACTED BEAM PROPERTIES:
For .....5..... μA of ....4.4..... MeV/u .....$^{40}Ar^{8+}$..... ions
$\Delta E/E$ .....% $\Delta\phi$ ..... °rf
$\epsilon_n = \beta\gamma\epsilon$ x ...14.0..... πmm mrad z .....9.9..... πmm mrad

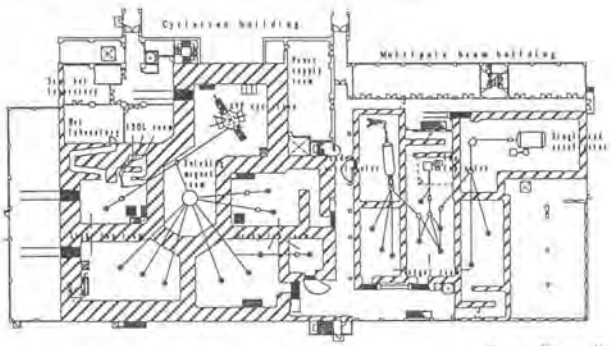
FACILITIES FOR RESEARCH

SHIELDED AREA: Fixed ..4000.... m^2 Moveable ....0..... m^2
Target Stations: ...18.... No. Served At Same Time: ..1.....
MAGNETIC SPECTROMETERS: .....
OTHER FACILITIES: .....
...On-line isotope separator,.....
...Beam chopping system, Beam scanner,.....
...Fast neutron production.....

REFERENCES/NOTES

(a) .....
(b) .....

PLAN VIEW OF FACILITY, COMMENTS



Plan of the First floor of TIARA Facilities

ENTRY NO. C34 **Date** June,1992

Name of Machine INS SF Cyclotron

Institution Institute for Nuclear Study, University of Tokyo

Address Midori-cho 3-2-1, Tanashi-shi, Tokyo Japan

Tel 0424-61-4131 Telex INSUT J34273 Fax 0424-68-5845 EMAIL

In Charge: M.Sekiguchi Reported by: M.Sekiguchi

HISTORY

MILESTONE DATES:

Design 1968 Model Tests 1968-1970

Construction 1969-1973 First Beam 1974

DESIGN/CONSTRUCTION BY:

in house yes other coustructed by Mitsbishi

COST: Accelerator ~3×10^8 yen Facility ~7×10^8 yen

FUNDED BY: Japan Ministry of Education

STATUS

STAFF: Machine

Scientists 1 Engineers 3

Technicians 3 Students 0

Research (in house/external)

Scientists 10 / 30 Engineers 5 /

Technicians 10 / Students /

BUDGET: Machine 3×10^7 yen Funded by JME

Research 5×10^7 yen Funded by JME

TIME DISTRIBUTION:

Basic Research (in house/external) 50 % / %

Applied Program (in house/external) % / 5 %

Development 5 % Maintenance 20 %

MAGNET

POLE PARAMETERS:

Diameter 168 cm $R_{extract}$ 73 cm R_{inject} cm

HILL PARAMETERS: Gap (min) 14.6 cm B_{max} T

(@ AT) Gap (max) 14.6 cm B_{min} T

VALLEY PARAMETERS: Gap (min) 22.8 cm B_{max} T

(@ AT) Gap (max) 22.8 cm B_{min} T

AVERAGE FIELD: $< B >_{min}$ T $< B >_{max}$ 1.64 T

NUMBER OF SECTORS: compact/separated 3 /

sector angle deg. spiral (max) 55 deg.

FIELD TRIMMING: Trim Coils 11

Harmonic Coils 7

Other

CURRENT: Main Coils 600 Amps Stability 10^{-5}

Trim Coils 450,250 Amps Stability 5×10^{-4}, 10^{-3}

Stored Energy (cryogenic) MJ

WEIGHT: Iron 130 tons Conductor 5 tons

ION ENERGY: Bending Limit E/A = 68 q^2/A^2 MeV/u

Focussing Limit E/A = 48 q/A MeV/u

ACCELERATION SYSTEM

FUNDAMENTAL ACCELERATION:

Description: lambda/4 resonator, MOPA

No. of Gaps/turn 2 dE/dn(max) 0.14 MeV/q

Voltage(max) 0.07 MV Harmonic f_{rf}/f_{ion} 1,3,5

Freq 7.4-22.5 MHz Power in(max) 0.15 MW

Stability: Phase +-1.0 deg. Voltage 2×10^{-4}

OTHER CAVITIES (Flattopping or otherwise):

Description:

Region of Influence: R_{min} cm R_{max} cm

No. of Gaps/turn dE/dn(max) MeV/q

Voltage(max) MV Harmonic f_{rf}/f_{ion}

Freq MHz Power in(max) MW

Stability: Phase Voltage

VACUUM SYSTEM

OPERATING PRESSURE: 2×10^{-6} Torr

PUMPS: No. and type 36 inch and 10 inch oil diffusion

ION SOURCE(S)

	Type	Intensity (mA)	@	$\epsilon_n = \beta\gamma\epsilon$ (πmm mrad)	Ion Species
(a)	internal PIG				p,d,^{3}He,α
(b)	cold cathode PIG				
(c)	ECR	0.08 Ar	$^{8+}$		Li~Ar
(d)					

INJECTION SYSTEM

axial inj(electrostatic mirror) Efficiency 15 %

EXTRACTION SYSTEM

2 channel dc deflectors Efficiency ~90 %

CHARACTERISTIC BEAMS

	Accelerated Ions	E/A (MeV/u)	Current(part μA) Internal	External
(a)	p	45		10
(b)	α	17		5
(c)	O	6.7		1.1
(d)	$^6Li^{2+}$	6.2		0.6

	Secondary Particles	E (MeV)	part/sec
(a)			
(b)			
(c)			

EXTRACTED BEAM PROPERTIES:

For 0.1 μA of 12.5 MeV/u α ions

$\Delta E/E$ 0.1 % $\Delta\phi$ 30 °rf

$\epsilon_n = \beta\gamma\epsilon$ x 18 πmm mrad z 13 πmm mrad

FACILITIES FOR RESEARCH

SHIELDED AREA: Fixed 950 m^2 Moveable m^2

Target Stations: 11 No. Served At Same Time: 1

MAGNETIC SPECTROMETERS: QDD

OTHER FACILITIES: 80 cm scatt.chamber

IGISOL,GARIS,line for channeling

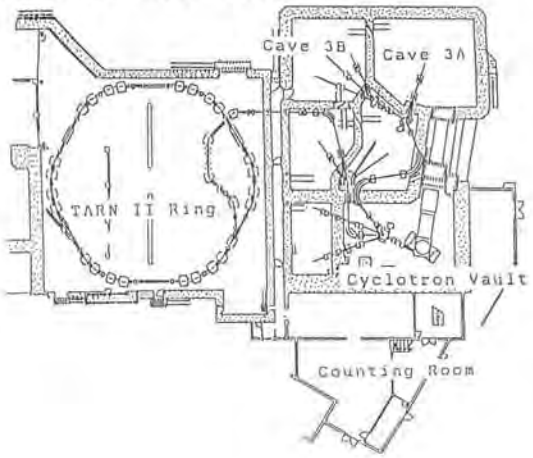
HI cooler ring TARN II

REFERENCES/NOTES

(a) proc.7th Cyclotron conf.,p.103 and 312 (1975)

(b) proc 7th Cyclotron conf.,p.1984 (1978)

PLAN VIEW OF FACILITY, COMMENTS



ENTRY NO. C35 Kazakhstan Variable Energy
NAME OF MACHINE Isochronous Cyclotron DATE July, 1981
INSTITUTION Institute of Nuclear Physics, Kazakhtan Academy of Sciences
ADDRESS Alma-Ata, 480082, USSR
TEL 690 243 TELEX
IN CHARGE A.A. Arzumanov REPORTED BY A.A. Arzumanov

HISTORY AND STATUS
DESIGN, date 1966 Model tests 1966-1968
ENG DESIGN, date 1967-1969
CONSTRUCTION, date 1970-1971
FIRST BEAM, date (or goal) September 1971
MAJOR ALTERATIONS
COST, ACCELERATOR
COST, FACILITY, total
FUNDED BY Kazakhstan Academy of Sciences

ACCELERATOR STAFF, OPERATION AND DEVELOPMENT
SCIENTISTS ENGINEERS
TECHNICIANS CRAFTS
GRAD STUDENTS involved during year
OPERATED BY Research staff or Operators
OPERATION 160 hr/wk. On target 135 hr/wk
TIME DISTR. in house 85 %, outside 15 %
BUDGET, op & dev
FUNDED BY Kazakhstan Academy of Sciences

RESEARCH STAFF, not included above
USERS, in house outside
GRAD STUDENTS involved during year
RESEARCH BUDGET, in house
FUNDED BY

MAGNET
POLE FACE, diameter (compact) 150 cm, R-extraction 66.5 cm
R injection cm
GAP, min 21 cm, Field 19.2 kG
max 35 cm, Field 12.2 kG at $5 \cdot 10^5$
AVERAGE FIELD at R ext 15.6 kG Ampere turns
B max/<B>
NUMBER OF SECTORS compact 3, separated; Spiral, max 25 deg
SECTOR ANGLE (SSC) deg
TRIMMING COILS 9 circular
2 harmonic per sector
CONDUCTOR, material and type copper
STORED ENERGY (cryogenic) MJ
POWER: main coils 275 max kW: current stability 10^{-4}
trimming coils 50 max kW: current stability 10^{-4}
WEIGHT: Fe tons: coils tons
COOLING system water
ION ENERGY (Bending limit) E/A = 50 q^2/A^2 MeV/amu
(Focusing limit) E/A = 30 q/A MeV/amu

ACCELERATION SYSTEM
DEES, number 2; angle 180 deg
BEAM APERTURE 7 cm; DC Bias kV
TUNED by, coarse mov. short fine Var. cap. auto
RF 8.5 to 19.0 MHz, stable ± 10^{-6}
Orb F 8.5 to 19.0 MHz
HARMONICS, RF/Orb F, used 1
DEE-Gnd, max 80 kV, min gap 3.9 cm
STABILITY, (pk-pk noise)/(pk RF volt) 0.01
ENERGY GAIN, max 320 kV/turn
RF PHASE, stable to ± deg
RF POWER input, max. 300 kW
FREQUENCY MODULATION, rate /s
modulator, type
beam pulse, width

VACUUM SYSTEM
OPERATING PRESSURE $8 \cdot 10^{-6}$ Torr or mbar
PUMPS, No, Type, Size diffusion pumps
(two 50 cm, five 16 cm)

ION SOURCES
Internal, hot filament, hooded

INJECTION SYSTEM

EXTRACTION SYSTEM
radially focusing dc reflector, magnetic chan.

FACILITIES FOR RESEARCH
SHIELDED AREA, fixed 132 m²; movable m²
TARGET STATIONS 2 in 2 rooms
STATIONS served at same time, max
MAG SPECTROGRAPH, type
COMPUTER model
OTHER FACILITIES

CHARACTERISTIC BEAMS

PARTICLE	ENERGY (MeV) Goal	Achieved	CURRENT (pμA) Internal	External
p		6-30	200	30
d		12-25	150	30
He-3		19-62	20	10
He-4		25-51	40	20
SECONDARY			(part/s)	

BEAM PROPERTIES

MEASURED		CONDITIONS			
PULSE WIDTH	35 RF deg	20	pμA of 30	MeV	p ions
PHASE EXC. max	RF deg		pμA of	MeV	ions
EXTRACT eff.	60 %		pμA of	MeV	ions
RESOL ΔE/E	0.6 %		pμA of	MeV	ions
EMITTANCE					
(π mm-mrad)	16 axial, 16 rad	15	pμA of 30	MeV	p

OPERATING PROGRAMS, time distribution
BASIC NUCLEAR PHYSICS 40 SOLID STATES PHYSICS 45
BIOMEDICAL APPLICAT. ISOTOPE PRODUCTIONS 10
Development 5

REFERENCES/NOTES

A.A. Arzumanov, L.M. Nemenov,
Nucl. Instr. Metho. 166 (1973) 201

PLAN VIEW OF FACILITY, COMMENTS, ETC.

Conversion of 150 cm FF machine.

^{3}He recovery system.

Radioisotope production.

ENTRY NO. C36 **Date** june 1992

Name of Machine V.U. AVF. Cyclotron

Institution Vrije Universiteit

Address De Boelelaan 1085 c 1081 HV AMSTERDAM NETHERLANDS

Tel (0)20 - 548 4707 Telex Fax (0)20 - 548 2944 EMAIL

In Charge: P.J. van der Jagt Reported by: C. Hoekstra

HISTORY

MILESTONE DATES:

Design Model Tests

Construction First Beam april 1965

DESIGN/CONSTRUCTION BY:

in house other Philips

COST: Accelerator Facility

FUNDED BY: Vrije Universiteit

STATUS

STAFF: Machine

Scientists 1 Engineers 1

Technicians 11 Students 0

Research (in house/external)

Scientists / Engineers /

Technicians / Students /

BUDGET: Machine Funded by

Research Funded by

TIME DISTRIBUTION:

Basic Research (in house/external) - % / 2 %

Applied Program (in house/external) 2 % / 80 %

Development 1 % Maintenance 15 %

MAGNET

POLE PARAMETERS:

Diameter 70 cm $R_{extract}$ 59 cm R_{inject} 2 cm

HILL PARAMETERS: Gap (min) 15 cm B_{max} 2 T

(@ 0.4e6 AT) Gap (max) 27 cm B_{min} 1 T

VALLEY PARAMETERS: Gap (min) cm B_{max} T

(@ AT) Gap (max) cm B_{min} T

AVERAGE FIELD: $< B >_{min}$ 0.3 T $< B >_{max}$ 1.5 T

NUMBER OF SECTORS: compact/separated 3 /

sector angle 65 deg. spiral (max) 37 deg.

FIELD TRIMMING: Trim Coils 10

Harmonic Coils 3

Other

CURRENT: Main Coils 450 Amps Stability

Trim Coils 150 Amps Stability

Stored Energy (cryogenic) MJ

WEIGHT: Iron 100 Conductor 20 tons

ION ENERGY: Bending Limit E/A = 30 q^2/A^2 MeV/u

Focussing Limit E/A = q/A MeV/u

ACCELERATION SYSTEM

FUNDAMENTAL ACCELERATION:

Description: Single DEE-system

No. of Gaps/turn 2 dE/dn(max) 0.05 MeV/q

Voltage(max) 0.050 MV Harmonic f_{rf}/f_{ion} 1.3

Freq 6 - 22 MHz Power in(max) 0.085 MW

Stability: Phase Voltage

OTHER CAVITIES (Flattopping or otherwise):

Description:

Region of Influence: R_{min} cm R_{max} cm

No. of Gaps/turn dE/dn(max) MeV/q

Voltage(max) MV Harmonic f_{rf}/f_{ion}

Freq MHz Power in(max) MW

Stability: Phase Voltage

VACUUM SYSTEM

OPERATING PRESSURE: 2.e-6

PUMPS: No. and type 1 oil.diff 6000 l/sec

ION SOURCE(S)

	Type	Intensity (mA)	@	$\epsilon_n = \beta\gamma\epsilon$ (πmm mrad)	Ion Species
(a)	Livingston	0.3			p,d,He3,α
(b)					
(c)					
(d)					

INJECTION SYSTEM

Efficiency %

EXTRACTION SYSTEM

Electrostatic + Magnetic Channel Efficiency 70 %

CHARACTERISTIC BEAMS

	Accelerated Ions	E/A (MeV/u)	Current(part μA) Internal	External
(a)	p	2 - 28	200	35
(b)	d	1 - 16		15
(c)	He3	6 - 45		10
(d)	α	5 - 32		10

	Secondary Particles	E (MeV)	part/sec
(a)			
(b)			
(c)			

EXTRACTED BEAM PROPERTIES:

For 30 μA of 24 MeV/u p ions

$\Delta E/E$ 0.3 % $\Delta\phi$ 40 °rf

$\epsilon_n = \beta\gamma\epsilon$ x 5 πmm mrad z 5 πmm mrad

FACILITIES FOR RESEARCH

SHIELDED AREA: Fixed m^2 Moveable m^2

Target Stations: No. Served At Same Time:

MAGNETIC SPECTROMETERS:

OTHER FACILITIES:

Internal Isotope Production

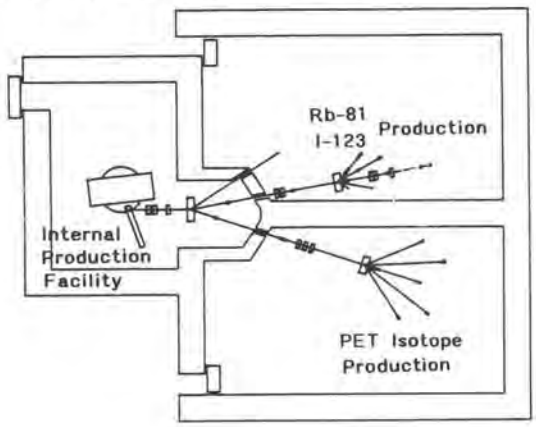
External Isotope Production

REFERENCES/NOTES

(a)

(b)

PLAN VIEW OF FACILITY, COMMENTS



ENTRY NO. C37 **Date** August 1992

Name of Machine MINI-CYCLOTRON ILEC

Institution Eindhoven University of Technology

Address Cyclotron Laboratory, EUT, P.O. Box 513, 5600 MB EINDHOVEN, The Netherlands

Tel (40) 47.40.46 **Telex** 51163 **Fax** 43.80.60 **EMAIL**

In Charge: J.A. van der Heide **Reported by:** J.A. van der Heide

HISTORY

MILESTONE DATES:
Design 1982 Model Tests 1986
Construction 1985-1988 First Beam 1989
DESIGN/CONSTRUCTION BY:
in house yes other no
COST: Accelerator DFL 400.000 Facility DFL 500.000
FUNDED BY: University

STATUS

STAFF: Machine
Scientists 1.5 Engineers 1
Technicians 1 Students 2
Research (in house/external)
Scientists / Engineers /
Technicians / Students /
BUDGET: Machine DFL 20.000 Funded by EUT
Research Funded by
TIME DISTRIBUTION:
Basic Research (in house/external) 100 % / %
Applied Program (in house/external) % / %
Development 100 % Maintenance %

MAGNET

POLE PARAMETERS:
Diameter 20 cm $R_{extract}$ 16.7 cm R_{inject} cm
HILL PARAMETERS: Gap (min) 3.3 cm B_{max} 1.8 T
(@ 50.000 AT) Gap (max) cm B_{min} T
VALLEY PARAMETERS: Gap (min) 5.0 cm B_{max} 1.2 T
(@ 50.000 AT) Gap (max) cm B_{min} T
AVERAGE FIELD: $< B >_{min}$ 1.43 T $< B >_{max}$ 1.43 T
NUMBER OF SECTORS: compact/separated 4 /
sector angle 40° hill deg. spiral (max) 0 deg.
FIELD TRIMMING: Trim Coils no circular
Harmonic Coils 4 sets
Other
CURRENT: Main Coils 140 Amps Stability 10^{-5}
Trim Coils 20 Amps Stability 10^{-4}
Stored Energy (cryogenic) MJ
WEIGHT: Iron 2.8 tons Conductor 0.25 ton
ION ENERGY: Bending Limit E/A = 3 q^2/A^2 MeV/u
Focussing Limit E/A = q/A MeV/u

ACCELERATION SYSTEM

FUNDAMENTAL ACCELERATION:
Description: 2nd harmonic dees
No. of Gaps/turn 4 dE/dn(max) 0.080 MeV/q
Voltage(max) 0.028 MV Harmonic f_{rf}/f_{ion} 2
Freq 43.5 MHz Power in(max) 0.014 MW
Stability: Phase 0.2° Voltage 10^{-4}
OTHER CAVITIES (Flattopping or otherwise):
Description: two 6th harmonic flattop dees
Region of Influence: R_{min} 5.5 cm R_{max} 16.7 cm
No. of Gaps/turn 4 dE/dn(max) 0.012 MeV/q
Voltage(max) 0.003 MV Harmonic f_{rf}/f_{ion} 6
Freq 130.5 MHz Power in(max) 0.0002 MW
Stability: Phase 0.7° Voltage 10^{-4}

VACUUM SYSTEM

OPERATING PRESSURE: 10^{-5} torr
PUMPS: No. and type 1 oil diffusion pump 3000 l/s

ION SOURCE(S)

	Type	Intensity (mA)	@	$\epsilon_n = \beta\gamma\epsilon$ (πmm mrad)	Ion Species
(a)	Internal	3			protons
(b)					
(c)					
(d)					

INJECTION SYSTEM

Efficiency %

EXTRACTION SYSTEM

electrostatic and passive magnetic Efficiency 40 %

CHARACTERISTIC BEAMS

	Accelerated Ions	E/A (MeV/u)	Current(part μA) Internal	External
(a)	protons	2.9	60	20
(b)				
(c)				
(d)				

	Secondary Particles	E (MeV)	part/sec
(a)			
(b)			
(c)			

EXTRACTED BEAM PROPERTIES:
For μA of MeV/u ions
$\Delta E/E$ % $\Delta\phi$ °rf
$\epsilon_n = \beta\gamma\epsilon$ x πmm mrad z πmm mrad

FACILITIES FOR RESEARCH

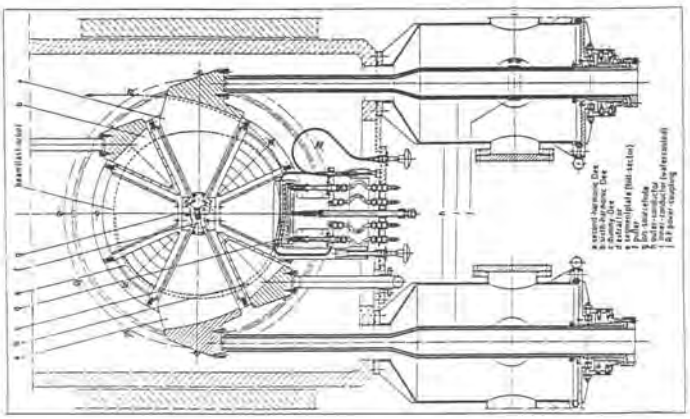
SHIELDED AREA: Fixed 30 m^2 Moveable 60 m^2
Target Stations: 3 No. Served At Same Time: 1
MAGNETIC SPECTROMETERS:
OTHER FACILITIES:

REFERENCES/NOTES

(a) J.A. van der Heide, e.a. Nucl.Instr.& Meth. A240(1985)32-35
(b) J.A. van der Heide, e.a. Nucl.Instr.& Meth. B64(1992)336-341

PLAN VIEW OF FACILITY, COMMENTS

The pole faces are copper plated to form grounded parts of the RF circuit.



ENTRY NO. C38 **Date** August 1992

Name of Machine EINDHOVEN AVF CYCLOTRON

Institution Eindhoven University of Technology

Address P.O. Box 513, 5600 MB EINDHOVEN

Tel (40) 47 40 48 Telex 51163 Fax (40) 43 80 60 EMAIL

In Charge: H.L. HAGEDOORN Reported by: J.I.M. Botman, R. Queens

HISTORY

MILESTONE DATES:

Design 1960 Model Tests 1960

Construction 1962-1963 First Beam April 1963

DESIGN/CONSTRUCTION BY:

in house other Philips

COST: Accelerator gift from Philips Facility M$3 (1968)

FUNDED BY: Eindhoven University, EUT

STATUS

STAFF: Machine

Scientists 1 Engineers 2

Technicians 3 Students 4

Research (in house/external)

Scientists 10 / 5 Engineers /

Technicians 2 / Students 20 / 5

BUDGET: Machine k$ 100 Funded by EUT

Research k$ 200 Funded by EUT

TIME DISTRIBUTION:

Basic Research (in house/external) 40 % / %

Applied Program (in house/external) % / 45 %

Development 5 % Maintenance 10 %

MAGNET

POLE PARAMETERS:

Diameter 130 cm $R_{extract}$ 52 cm R_{inject} 2 cm

HILL PARAMETERS: Gap (min) 15 cm B_{max} 2 T

(@ $4 \cdot 10^6$ AT) Gap (max) cm B_{min} T

VALLEY PARAMETERS: Gap (min) 30 cm B_{max} 1.2 T

(@ $4 \cdot 10^6$ AT) Gap (max) cm B_{min} T

AVERAGE FIELD: $< B >_{min}$ T $< B >_{max}$ 1.55 T

NUMBER OF SECTORS: compact/separated 3 /

sector angle 70 deg. spiral (max) 35 deg.

FIELD TRIMMING: Trim Coils 10

Harmonic Coils 3

Other

CURRENT: Main Coils 300 Amps Stability 10^{-5}

Trim Coils 200 Amps Stability 10^{-4}

Stored Energy (cryogenic) MJ

WEIGHT: Iron 80 ton Conductor 10 ton

ION ENERGY: Bending Limit E/A = 30 q^2/A^2 MeV/u

Focussing Limit E/A = q/A MeV/u

ACCELERATION SYSTEM

FUNDAMENTAL ACCELERATION:

Description: lambda/4 resonator

No. of Gaps/turn 2 dE/dn(max) 0.1 MeV/q

Voltage(max) 0.05 MV Harmonic f_{rf}/f_{ion} 1 or 3

Freq 5 - 23.3 MHz Power in(max) 0.1 MW

Stability: Phase 1 deg. Voltage 10^{-5}

OTHER CAVITIES (Flattopping or otherwise):

Description:

Region of Influence: R_{min} cm R_{max} cm

No. of Gaps/turn dE/dn(max) MeV/q

Voltage(max) MV Harmonic f_{rf}/f_{ion}

Freq MHz Power in(max) MW

Stability: Phase Voltage

VACUUM SYSTEM

OPERATING PRESSURE: 10^{-6} Torr

PUMPS: No. and type 1 oil diffusion 8000 l/s

ION SOURCE(S)

	Type	Intensity (mA)	@	$\epsilon_n = \beta\gamma\epsilon$ (πmm mrad)	Ion Species
(a)	interal Livingston type				
(b)					
(c)					
(d)					

INJECTION SYSTEM

Efficiency %

EXTRACTION SYSTEM

electrostatic, 80°, 60 kV/4mm Efficiency 70 %

followed by magnetic channel

CHARACTERISTIC BEAMS

	Accelerated Ions	E/A (MeV/u)	Current(part μA) Internal	External
(a)	p	2.5 - 29.5	500	100
(b)	d	3 - 15	500	100
(c)	^{4}He	6 - 30	50	30
(d)				

	Secondary Particles	E (MeV)	part/sec
(a)			
(b)			
(c)			

EXTRACTED BEAM PROPERTIES:

For 100 μA of 25 MeV/u p ions

$\Delta E/E$ 0.3 % $\Delta\phi$ 40 °rf

$\epsilon_n = \beta\gamma\epsilon$ x 6 πmm mrad z 4 πmm mrad

FACILITIES FOR RESEARCH

SHIELDED AREA: Fixed 120 m² Moveable 230 m²

Target Stations: 9 No. Served At Same Time: 1

MAGNETIC SPECTROMETERS:

OTHER FACILITIES: isotope production

PIXE facility

microbeam

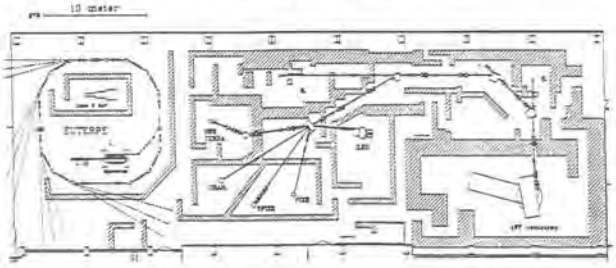
channeling facility

REFERENCES/NOTES

(a) EUT thesis Schutte (1973), Van Heusen (1976)

(b) Botman (1981)

PLAN VIEW OF FACILITY, COMMENTS



ENTRY No. C39

NAME OF MACHINE AGOR DATE June 1989
INSTITUTION Institut de Physique Nucléaire – Kernfysisch Versneller Instituut
ADDRESS 91406 Orsay, France – Zernikelaan 25, 9747 AA Groningen, The Netherlands
TEL ..... TELEX .....
IN CHARGE S. Galès REPORTED BY H.W. Schreuder

HISTORY AND STATUS
DESIGN, date 1986 Model tests .....
ENG DESIGN, date 1989
CONSTRUCTION, date 1988-1992
FIRST BEAM, date (or goal) 1992
MAJOR ALTERATIONS .....
COST, ACCELERATOR Mf1 33
COST, FACILITY, total .....
FUNDED BY .....

ACCELERATOR STAFF, OPERATION AND DEVELOPMENT
SCIENTISTS ..... ENGINEERS .....
TECHNICIANS ..... CRAFTS .....
GRAD STUDENTS involved during year .....
OPERATED BY ..... Research staff or ..... Operators
OPERATION ..... hr/wk, On target ..... hr/wk
TIME DISTR. in house ..... %, Outside ..... %
BUDGET, op & dev .....
FUNDED BY .....

RESEARCH STAFF, not included above
USERS, in house ..... outside .....
GRAD STUDENTS involved during year .....
RESEARCH BUDGET, in house .....
FUNDED BY .....

MAGNET
POLE FACE, diameter (compact) 188 cm, R extraction 91 cm
R injection 1,3-1,7 cm
GAP, min 7 cm, Field ..... kG
max ..... cm, Field ..... kG } at .....
AVERAGE FIELD at R ext 17-41 ..... kG } Ampere turns
B max/ <B> .....
NUMBER OF SECTORS { compact 3 ... / separated - ... } Spiral, max .. deg
SECTOR ANGLE (SSC) ..... deg
TRIMMING COILS 15
CONDUCTOR, material and type NbTi
STORED ENERGY (cryogenic) 57 MJ
POWER : main coils ..... max, kW ; current stability .....
trimming coils 30 max, kW ; current stability .....
WEIGHT : Fe 320 tons ; coils ..... tons
COOLING system .....
ION ENERGY (bending limit) E/A = 600 q^2/a^2 MeV/amu
(focusing limit) E/A = 200 q^2/a^2 MeV/amu

ACCELERATION SYSTEM
DEES, number 3 ; ~~xxxxx~~ in valleys ~~xxx~~
BEAM APERTURE 1,8 cm ; DC Bias ----- kV
TUNED by, coarse short fine short
RF 24 to 63 MHz, stable ± .....
Orb F 6 to 63 MHz
HARMONICS, RF/Orb F, used 2,3,4
DEE - Gnd, max 110 kV, min gap ..... cm
STABILITY, (pk-pk noise)/(pk RF volt) 10^{-4}
ENERGY GAIN, max 300 kV/turn
RF PHASE, stable to ± 0,2 deg
RF POWER input, max 3*70 kW
FREQUENCY MODULATION, rate ..... /s
modulator, type .....
beam pulse, width .....

VACUUM SYSTEM
OPERATING PRESSURE $< 10^{-7}$ Torr or mbar
PUMPS, No, Type, Size 3 cryopumps
2 turbopumps

ION SOURCES multicusp, ecr, polarized (all external)

INJECTION SYSTEM
axial

EXTRACTION SYSTEM
1.electrostatic, 2.electromagnetic

FACILITIES FOR RESEARCH
SHIELDED AREA, fixed ..... m^3 ; movable ..... m^3
TARGET STATIONS ..... in ..... rooms
STATIONS served at same time, max .....
MAG SPECTROGRAPH, type .....
COMPUTER model .....
OTHER FACILITIES .....

CHARACTERISTIC BEAMS

PARTICLE	ENERGY (MeV) Goal	Achieved	CURRENT (pμA) Internal	External
p	120-200			
α	120-380			
q/A=0,3	10- 50 MeV/A			
q/A=0,14	6- 10 "			
SECONDARY			(part/s)	

BEAM PROPERTIES
MEASURED CONDITIONS
PULSE WIDTH ..... RF deg ..... pμ A of .... MeV ... ions
PHASE EXC, max ... RF deg ..... pμ A of .... MeV ... ions
EXTRACT eff ..... % ..... pμ A of .... MeV ... ions
RESOL ΔE/E ..... % ..... pμ A of .... MeV ... ions
EMITTANCE
(π mm. mrad) { ... axial / ... rad } ..... pμA of ..... MeV ... ions

OPERATING PROGRAMS, time distribution
BASIC NUCLEAR PHYSICS .. SOLID STATES PHYSICS ....
BIOMEDICAL APPLICAT. .... ISOTOPE PRODUCTIONS ....

REFERENCES/NOTES

PLAN VIEW OF FACILITY, NOTEWORTHY FEATURES, COMMENTS

ENTRY No. C40

NAME OF MACHINE Automatic Isochronous Cyclotron(AIC-144) DATE

INSTITUTION Institute of Nuclear Physics

ADDRESS Krakow, Poland, Radzikowskiego 152

TEL 37 02 22 TELEX

IN CHARGE J. Schwabe REPORTED BY J. Schwabe

HISTORY AND STATUS

DESIGN, date 1976-78 Model tests 1977-79

ENG DESIGN, date 1979

CONSTRUCTION, date 1980-85

FIRST BEAM, date (or goal) 10.04.87

MAJOR ALTERATIONS

COST, ACCELERATOR

COST, FACILITY, total

FUNDED BY

ACCELERATOR STAFF, OPERATION AND DEVELOPMENT

SCIENTISTS 7 ENGINEERS 12

TECHNICIANS 7 CRAFTS

GRAD STUDENTS involved during year

OPERATED BY Research staff or Operators

OPERATION hr/wk, On target hr/wk

TIME DISTR. in house %, Outside %

BUDGET, op & dev

FUNDED BY

RESEARCH STAFF, not included above

USERS, in house outside

GRAD STUDENTS involved during year

RESEARCH BUDGET, in house

FUNDED BY

MAGNET

POLE FACE, diameter (compact) 144 cm, R extraction 63,5 cm

R injection 0,5-1 cm

GAP, min 11,2 cm, Field 20,5 kG
max 22 cm, Field 14,5 kG
at 710(A)x672(W) Ampere turns

AVERAGE FIELD at R ext 17,5 kG

B max/ <B> 1,17

NUMBER OF SECTORS compact 4, separated — Spiral, max 54 deg

SECTOR ANGLE (SSC) 45 deg

TRIMMING COILS circular 15
valley 8

CONDUCTOR, material and type Cu

STORED ENERGY (cryogenic) MJ

POWER: main coils 240 max, kW ; current stability 4×10^{-5}
trimming coils 120 max, kW ; current stability 10^{-5}

WEIGHT : Fe 150 tons ; coils 2 x 7,55 tons

COOLING system

ION ENERGY (bending limit) E/A = 60 (56). q^2/a^2 MeV/amu
(focusing limit) E/A = 60 (56). q^2/a^2 MeV/amu

ACCELERATION SYSTEM

DEES, number 1 ; angle 180 deg

BEAM APERTURE 16 cm ; DC Bias kV

TUNED by, coarse panels fine trimmers, capact.

RF 8 to 26 mHz, stable ± 10^{-7}

Orb F 8 to 26 mHz

HARMONICS, RF/Orb F, used 1

DEE - Gnd, max 50 kV, min gap 2,79 cm

STABILITY, (pk-pk noise)/(pk RF volt) 10^{-4}

ENERGY GAIN, max 100 kV/turn

RF PHASE, stable to ± 15 ÷ 45 deg

RF POWER input, max 150 kW

FREQUENCY MODULATION, rate 10 ÷ 1000 /s

modulator, type

beam pulse, width μ-structure; 15,6-4,8 ns; pulse: 1,25 μs

VACUUM SYSTEM

OPERATING PRESSURE $6 \cdot 10^{-6}$ Torr or mbar

PUMPS, No, Type, Size 2 diffusion oil pumps 4800 L/S

ION SOURCES

Penning Internal

INJECTION SYSTEM

Internal or external with electrostatic inflector

EXTRACTION SYSTEM

Electrostatic deflector, 3 sector

FACILITIES FOR RESEARCH

SHIELDED AREA, fixed m³ ; movable m³

TARGET STATIONS in rooms

STATIONS served at same time, max

MAG SPECTROGRAPH, type

COMPUTER model

OTHER FACILITIES

CHARACTERISTIC BEAMS

PARTICLE	ENERGY (MeV) Goal	Achieved	CURRENT (pμA) Internal	External
p	60	–		
d	30	25	> 400	
α	60	52	50	
SECONDARY				(part/s)

BEAM PROPERTIES

	MEASURED	CONDITIONS
PULSE WIDTH	35 RF deg	pμ A of 25 MeV d ions
PHASE EXC, max	RF deg	pμ A of MeV ions
EXTRACT eff	%	pμ A of MeV ions
RESOL ΔE/E	%	pμ A of MeV ions
EMITTANCE (π mm. mrad)	12 axial, 15 rad	pμA of MeV pd. ions

OPERATING PROGRAMS, time distribution

BASIC NUCLEAR PHYSICS SOLID STATES PHYSICS

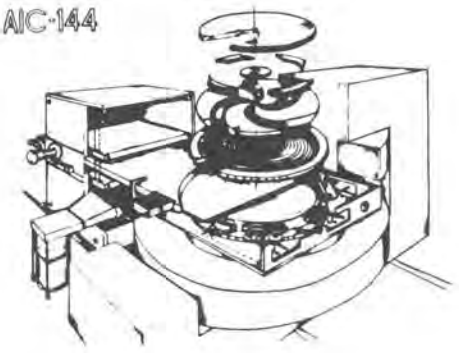
BIOMEDICAL APPLICAT. ISOTOPE PRODUCTIONS

REFERENCES/NOTES

1) International seminar on isochronous Cyclotron technique
Poland Krakow J.N.PH. 13÷18 Nov. 1978
report JFJ No. 1069/PL

PLAN VIEW OF FACILITY, NOTEWORTHY FEATURES, COMMENTS

AIC-144



ENTRY No. C41

NAME OF MACHINE C-30 DATE 04.05.89

INSTITUTION SOLTAN INSTITUTE FOR NUCLEAR STUDIES

ADDRESS 05-400 OTWOCK-SWIERK, POLAND

TEL 798138 TELEX 813244

IN CHARGE J.Sura REPORTED BY J.SURA

HISTORY AND STATUS

DESIGN, date 1983 Model tests 1983

ENG DESIGN, date 1984

CONSTRUCTION, date 1985-1987

FIRST BEAM, date (or goal) 7.02.1989

MAJOR ALTERATIONS

COST, ACCELERATOR

COST, FACILITY, total 350 Mzł

FUNDED BY Polish Atomic Agency

ACCELERATOR STAFF, OPERATION AND DEVELOPMENT

SCIENTISTS 4 ENGINEERS 5

TECHNICIANS 4 CRAFTS 2

GRAD STUDENTS involved during year

OPERATED BY Research staff or Operators

OPERATION hr/wk, On target hr/wk

TIME DISTR. in house %, Outside %

BUDGET, op & dev

FUNDED BY

RESEARCH STAFF, not included above

USERS, in house outside

GRAD STUDENTS involved during year

RESEARCH BUDGET, in house

FUNDED BY

MAGNET

POLE FACE, diameter (compact) 105 cm, R extraction 45 cm

R injection cm

GAP, min 2 cm, Field 22.5 kG
max 10 cm, Field 12.5 kG
at 164000 Ampere turns

AVERAGE FIELD at R ext 18 kG

B max/ <B> 1.25

NUMBER OF SECTORS compact 4 / separated ; Spiral, max 0 deg

SECTOR ANGLE (SSC) 45 deg

TRIMMING COILS none

CONDUCTOR, material and type copper Ø 12x2

STORED ENERGY (cryogenic) MJ

POWER : main coils 65 max, kW ; current stability 10

trimming coils max, kW ; current stability

WEIGHT : Fe 38 tons ; coils 1.38 tons

COOLING system water

ION ENERGY (bending limit) E/A = 31 q^2/a^2 MeV/amu

(focusing limit) E/A = 50 q^2/a^2 MeV/amu

ACCELERATION SYSTEM

DEES, number 2 ; angle 45 deg

BEAM APERTURE 2 cm ; DC Bias kV

TUNED by, coarse fixed fine ±0.4 MHz trimmer

RF 52.78 to mHz, stable ± 10^{-6}

Orb F 26.39 to mHz

HARMONICS, RF/Orb F, used 2

DEE - Gnd, max 50 kV, min gap 0.5 10^{-3} cm

STABILITY, (pk-pk noise)/(pk RF volt) 10^{-4}

ENERGY GAIN, max 141 kV/turn

RF PHASE, stable to ± deep bridged deg

RF POWER input, max 25 kW

FREQUENCY MODULATION, rate /s

modulator, type

beam pulse, width

VACUUM SYSTEM

OPERATING PRESSURE $5 \cdot 10^{-6}$ Torr or mbar

PUMPS, No, Type, Size oil diffusion 2x2000 l/s

ION SOURCES

cold cathode used, external during assembling

INJECTION SYSTEM

axial during assembling

EXTRACTION SYSTEM

stripping by carbon foil

FACILITIES FOR RESEARCH

SHIELDED AREA, fixed 2x60 m² ; movable m²

TARGET STATIONS 1 In 1 rooms

STATIONS served at same time, max 1

MAG SPECTROGRAPH, type

COMPUTER model

OTHER FACILITIES

CHARACTERISTIC BEAMS

PARTICLE	ENERGY (MeV) Goal	Achieved	CURRENT (pμA) Internal	External
$H^- \rightarrow p$	30	15 test		50 goal
SECONDARY				(part/s)

BEAM PROPERTIES

MEASURED	CONDITIONS
PULSE WIDTH RF deg	pμ A of MeV ions
PHASE EXC, max RF deg	pμ A of MeV ions
EXTRACT eff %	pμ A of MeV ions
RESOL ΔE/E %	pμ A of MeV ions
EMITTANCE	
(π mm. mrad) axial / rad	pμA of MeV ions

OPERATING PROGRAMS, time distribution

BASIC NUCLEAR PHYSICS SOLID STATES PHYSICS

BIOMEDICAL APPLICAT. ISOTOPE PRODUCTIONS 100%

REFERENCES/NOTES

1/ J.Sura et al., IPJ 1982, Warszawa /1983/.

2/ IEEE Trans.Nucl.Sci., Vol. NS-32,5 /1985/.

3/ 11-th Cycl.Conf., Tokyo, 76-79 /1986/.

PLAN VIEW OF FACILITY, NOTEWORTHY FEATURES, COMMENTS

ENTRY NO. C42 **Date** June 26/92

Name of Machine U-200P Cyclotron

Institution Heavy Ion Laboratory, Warsaw University

Address ul.Banacha 4, PL 02-097 Warsaw, POLAND

Tel (48-22) 222 123 Telex 817330 SLCJ PL Fax (48-2) 659 2714 EMAIL

In Charge: J. Jastrzebski Reported by: A. Śliwiński

HISTORY

MILESTONE DATES:

Design 1978 Model Tests

Construction 1989 at final site First Beam (expected)1993

DESIGN/CONSTRUCTION BY:

in house yes other JINR Dubna, INS Świerk

COST: Accelerator Facility

FUNDED BY: Univ. of Warsaw, Ministry of Education
State Committee for Scientific Research (KBN)

STATUS

STAFF: Machine

Scientists 18 Engineers 18

Technicians 21 Students

Research (in house/external)

Scientists / Engineers /

Technicians / Students /

BUDGET: Machine Total PLZ(1991) Funded by UW, MEN, KBN

Research 17.15billion Funded by

TIME DISTRIBUTION:

Basic Research (in house/external) % / %

Applied Program (in house/external) % / %

Development % Maintenance %

MAGNET

POLE PARAMETERS:

Diameter 200 cm $R_{extract}$ 85 cm R_{inject} cm

HILL PARAMETERS: Gap (min) 2.7 cm B_{max} 2.63 T

(@ 0.5x10 AT) Gap (max) 5.15 cm B_{min} 2.5 T

VALLEY PARAMETERS: Gap (min) 15.2 cm B_{max} 1.7 T

(@ 0.5x10 AT) Gap (max) 15.2 cm B_{min} 1.6 T

AVERAGE FIELD: $< B >_{min}$ 1.8 T $< B >_{max}$ 2.1 T

NUMBER OF SECTORS: compact/separated 4 /

sector angle 42 deg. spiral (max) deg.

FIELD TRIMMING: Trim Coils 10 pairs water cooled

Harmonic Coils

Other 4

CURRENT: Main Coils 1400 max Amps Stability 1/10^4

Trim Coils 450 max Amps Stability 4/10^4

Stored Energy (cryogenic) MJ

WEIGHT: Iron 240 tonnes Conductor 30 tonnes

ION ENERGY: Bending Limit E/A = 160 q^2/A^2 MeV/u

Focussing Limit E/A = 36 q/A MeV/u

ACCELERATION SYSTEM

FUNDAMENTAL ACCELERATION:

Description: two 45 deg dees with movable stem

No. of Gaps/turn 4 dE/dn(max) 0.3 MeV/q

Voltage(max) 0.075 MV Harmonic f_{rf}/f_{ion} 1,2,3,4

Freq 12-21 MHz Power in(max) 2x0.12^4 MW

Stability: Phase ±1 deg. Voltage 1/10^4

OTHER CAVITIES (Flattopping or otherwise):

Description:

Region of Influence: R_{min} cm R_{max} cm

No. of Gaps/turn dE/dn(max) MeV/q

Voltage(max) MV Harmonic f_{rf}/f_{ion}

Freq MHz Power in(max) MW

Stability: Phase Voltage

VACUUM SYSTEM

OPERATING PRESSURE: 1/10^6 Tr

PUMPS: No. and type 4 oil diffusion pumps

1700 l/s each, liquid nitrogen traps

ION SOURCE(S)

	Type	Intensity (mA)	@ $\epsilon_n = \beta\gamma\epsilon$ (πmm mrad)	Ion Species
(a)	PIG hot cath.			
(b)	ECR (under development)			
(c)				
(d)				

INJECTION SYSTEM

PIG at centre region Efficiency %

EXTRACTION SYSTEM

stripping Efficiency %

CHARACTERISTIC BEAMS

Accelerated Ions	E/A (MeV/u)	Current(part μA) Internal	External
(a)			
(b)			
(c)			
(d)			

Secondary Particles	E (MeV)	part/sec
(a)		
(b)		
(c)		

EXTRACTED BEAM PROPERTIES:

For μA of MeV/u ions

$\Delta E/E$ % $\Delta\phi$ °rf

$\epsilon_n = \beta\gamma\epsilon$ x πmm mrad z πmm mrad

FACILITIES FOR RESEARCH

SHIELDED AREA: Fixed 30 m² Moveable 1300 m²

Target Stations: 7 No. Served At Same Time: 1

MAGNETIC SPECTROMETERS:

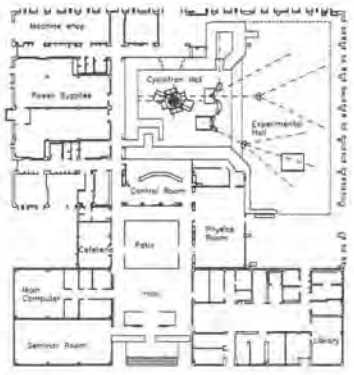
OTHER FACILITIES: Energy monochromatization by two 120 deg magnets.

REFERENCES/NOTES

(a)

(b)

PLAN VIEW OF FACILITY, COMMENTS



ENTRY No. C43

NAME OF MACHINE U-200 DATE

INSTITUTION Joint Institute for Nuclear Research

ADDRESS Dubna, USSR

TEL TELEX MSK DUBNA 9 12621

IN CHARGE Yu.Ts. Oganessian REPORTED BY G.G. Gulbekian

HISTORY AND STATUS

DESIGN, date 1966 Model tests

ENG DESIGN, date 1966-67

CONSTRUCTION, date 1966-67

FIRST BEAM, date (or goal) 1968

MAJOR ALTERATIONS

COST, ACCELERATOR

COST, FACILITY, total

FUNDED BY

ACCELERATOR STAFF, OPERATION AND DEVELOPMENT

SCIENTISTS ENGINEERS

TECHNICIANS CRAFTS

GRAD STUDENTS involved during year

OPERATED BY Research staff or Operators

OPERATION 30 hr/wk, On target 25 hr/wk

TIME DISTR. in house %, Outside %

BUDGET, op & dev

FUNDED BY

RESEARCH STAFF, not included above

USERS, in house outside

GRAD STUDENTS involved during year

RESEARCH BUDGET, in house

FUNDED BY

MAGNET

POLE FACE, diameter (compact) 200 cm, R extraction 86. cm

R injection cm

GAP, min 3 cm, Field 26 kG
max 15 cm, Field 24 kG
} at 0.59×10^6 Ampere turns

AVERAGE FIELD at R ext 20 kG

B max/ <B> 1.3

NUMBER OF SECTORS { compact 4 / separated } Spiral, max deg

SECTOR ANGLE (SSC) deg

TRIMMING COILS 7 circular
4 harmonic

CONDUCTOR, material and type Cu

STORED ENERGY (cryogenic) MJ

POWER : main coils 350 max, kW ; current stability 10^{-4}
trimming coils 20 max, kW ; current stability 10^{-3}

WEIGHT : Fe 220 tons ; coils 11.5 tons

COOLING system Demineralized water

ION ENERGY (bending limit) E/A = 145 q^2/a^2 MeV/amu
(focusing limit) E/A = 20 q^2/a^2 MeV/amu

ACCELERATION SYSTEM

DEES, number 2,4,2,9 ; angle deg

BEAM APERTURE 2.5 cm ; DC Bias 0 kV

TUNED by, coarse MS fine VC

RF 12 to 21.5 mHz, stable ± 10^{-5}

Orb F 3 to 10.7 mHz

HARMONICS, RF/Orb F, used 2,3

DEE - Gnd, max 75 kV, min gap 4 cm

STABILITY, (pk-pk noise)/(pk RF volt) 10^{-2}

ENERGY GAIN, max 275 kV/turn

RF PHASE, stable to ± 4 deg

RF POWER input, max 50 kW

FREQUENCY MODULATION, rate /s

modulator, type

beam pulse, width

VACUUM SYSTEM

OPERATING PRESSURE 2×10^{-6} Torr or mbar

PUMPS, No, Type, Size 2 oil diffusion pumps
4000 l/s each

ION SOURCES

Arc type with heated cathode

INJECTION SYSTEM

EXTRACTION SYSTEM

Stripping + magnetic channel

FACILITIES FOR RESEARCH

SHIELDED AREA, fixed 225 m² ; movable m²

TARGET STATIONS 4 in 2 rooms

STATIONS served at same time, max 1

MAG SPECTROGRAPH, type

COMPUTER model

OTHER FACILITIES

CHARACTERISTIC BEAMS

PARTICLE	ENERGY (MeV) Goal	Achieved	CURRENT (pμA) Internal	External
$^4He^{1+}$	39	37	600	60
$^{12}C^{3+}$	208	198	20	10
$^{40}Ar^{8+}$	230	220	0.012	0.006
SECONDARY				(part/s)

BEAM PROPERTIES

MEASURED	CONDITIONS
PULSE WIDTH 30. RF deg	pμ A of MeV ions
PHASE EXC, max RF deg	pμ A of MeV ions
EXTRACT eff 40-100 %	pμ A of MeV ions
RESOL ΔE/E 1. %	pμ A of MeV ions
EMITTANCE	
(π mm. mrad) { 30 axial / 70 rad }	5 pμA of 37 MeV ions

OPERATING PROGRAMS, time distribution

BASIC NUCLEAR PHYSICS 100% SOLID STATES PHYSICS

BIOMEDICAL APPLICAT. ISOTOPE PRODUCTIONS

REFERENCES/NOTES

1) Proc.of the VIth Int.Cyclotron Conf., New York;232,1972

PLAN VIEW OF FACILITY, NOTEWORTHY FEATURES, COMMENTS

ENTRY No. C44

NAME OF MACHINE U-400 M DATE
INSTITUTION Joint Institute for Nuclear Research, Laboratory of Nuclear Reactions
ADDRESS JINR, Head Post Office, P.O. Box 79, Moscow, USSR
TEL TELEX MSK Dubna 412621
IN CHARGE Yu.Ts. Oganessian REPORTED BY G.G. Gulbekian

HISTORY AND STATUS

DESIGN, date Model tests
ENG DESIGN, date 1985-1987
CONSTRUCTION, date 1987-1990
FIRST BEAM, date (or goal) 1991
MAJOR ALTERATIONS

COST, ACCELERATOR
COST, FACILITY, total
FUNDED BY

ACCELERATOR STAFF, OPERATION AND DEVELOPMENT

SCIENTISTS ENGINEERS
TECHNICIANS CRAFTS
GRAD STUDENTS involved during year
OPERATED BY Research staff or Operators
OPERATION hr/wk, On target hr/wk
TIME DISTR. in house %, Outside %
BUDGET, op & dev
FUNDED BY

RESEARCH STAFF, not included above

USERS, in house outside
GRAD STUDENTS involved during year
RESEARCH BUDGET, in house
FUNDED BY

MAGNET

POLE FACE, diameter (compact) 400 cm, R extraction 175 cm
R injection cm
GAP, min 10 cm, Field 25.5 kG
max 50 cm, Field 14 kG
at $1.26 \cdot 10^6$ Ampere turns
AVERAGE FIELD at R ext 19.5 kG
B max/ <B> 1.3
NUMBER OF SECTORS compact 4, separated — Spiral, max 40 deg
SECTOR ANGLE (SSC) 45 deg
TRIMMING COILS 15 circular
5 harmonic
CONDUCTOR, material and type Copper
STORED ENERGY (cryogenic) MJ
POWER: main coils 750 max, kW ; current stability 10^{-4}
trimming coils 120 max, kW ; current stability 10^{-3}
WEIGHT: Fe 2100 tons ; coils 115 tons
COOLING system Demineralized water
ION ENERGY (bending limit) E/A = 540 q^2/a^2 MeV/amu
(focusing limit) E/A = 120 q^2/a^2 MeV/amu

ACCELERATION SYSTEM

DEES, number 4 ; angle 45 deg
BEAM APERTURE 10 cm ; DC Bias 0 kV
TUNED by, coarse MS fine VC
RF 11.5 to 25 mHz, stable ± 10^{-5}
Orb F 5.75 to 12.5 mHz
HARMONICS, RF/Orb F, used 2
DEE - Gnd, max 150-200 V, min gap 18 cm
STABILITY, (pk-pk noise)/(pk RF volt) 10^{-3}
ENERGY GAIN, max 1200 kV/turn
RF PHASE, stable to ± deg
RF POWER input, max 4x100 kW
FREQUENCY MODULATION, rate /s
modulator, type
beam pulse, width

VACUUM SYSTEM

OPERATING PRESSURE $(0.5\text{-}1) \cdot 10^{-6}$ Torr or mbar
PUMPS, No, Type, Size 20000 l/s for N

ION SOURCES

U-400, PIG with heated cathode , ECR

INJECTION SYSTEM

Carbon stripper after radial injection

EXTRACTION SYSTEM

electrostatic deflector, magnetic channel

FACILITIES FOR RESEARCH

SHIELDED AREA, fixed 1500 m² ; movable m²
TARGET STATIONS 10 in rooms
STATIONS served at same time, max 1
MAG SPECTROGRAPH, type
COMPUTER model
OTHER FACILITIES

CHARACTERISTIC BEAMS

PARTICLE	ENERGY (MeV) Goal	Achieved	CURRENT (pμA) Internal	External
^{16}O	1920			
^{238}U	4760			
SECONDARY				(part/s)

BEAM PROPERTIES

MEASURED	CONDITIONS
PULSE WIDTH RF deg	pμ A of MeV ions
PHASE EXC, max RF deg	pμ A of MeV ions
EXTRACT eff %	pμ A of MeV ions
RESOL ΔE/E %	pμ A of MeV ions
EMITTANCE	
(π mm. mrad) axial, rad	pμA of MeV ions

OPERATING PROGRAMS, time distribution

BASIC NUCLEAR PHYSICS — SOLID STATES PHYSICS
BIOMEDICAL APPLICAT. — ISOTOPE PRODUCTIONS

REFERENCES/NOTES

1) Proc. of the X Int.Conf.on Cycl.and their Appl., 1984, East Lansing, USA, p.317

PLAN VIEW OF FACILITY, NOTEWORTHY FEATURES, COMMENTS

ENTRY No. C45

NAME OF MACHINE U-400 DATE

INSTITUTION Joint Institute for Nuclear Research

ADDRESS Dubna, USSR

TEL TELEX MSK DUBNA 412621

IN CHARGE Yu.Ts. Oganessian REPORTED BY B.N. Gikal

HISTORY AND STATUS

DESIGN, date Model tests

ENG DESIGN, date 1973-1977

CONSTRUCTION, date 1974-1978

FIRST BEAM, date (or goal) 1978

MAJOR ALTERATIONS

COST, ACCELERATOR

COST, FACILITY, total

FUNDED BY

ACCELERATOR STAFF, OPERATION AND DEVELOPMENT

SCIENTISTS ENGINEERS

TECHNICIANS CRAFTS

GRAD STUDENTS involved during year

OPERATED BY Research staff or Operators

OPERATION 80 hr/wk, On target 65 hr/wk

TIME DISTR. in house %, Outside %

BUDGET, op & dev

FUNDED BY

RESEARCH STAFF, not included above

USERS, in house outside

GRAD STUDENTS involved during year

RESEARCH BUDGET, in house

FUNDED BY

MAGNET

POLE FACE, diameter (compact) 400 cm, R extraction 172 cm

R injection cm

GAP, min 4.2 cm, Field 26 kG
max 30 cm, Field 16 kG
} at 1.26×10^6 Ampere turns

AVERAGE FIELD at R ext 21.4 kG

B max/ <B> 1.21

NUMBER OF SECTORS { compact 4 / separated } Spiral, max deg

SECTOR ANGLE (SSC) deg

TRIMMING COILS 10 circular

8 harmonic

CONDUCTOR, material and type Al

STORED ENERGY (cryogenic) MJ

POWER: main coils 850 max, kW ; current stability 10^{-4}

trimming coils 56 max, kW ; current stability 10^{-3}

WEIGHT: Fe 2000 tons ; coils tons

COOLING system Demineralized water

ION ENERGY (bending limit) E/A = 625 q^2/a^2 MeV/amu

(focusing limit) E/A = 35 q^2/a^2 MeV/amu

ACCELERATION SYSTEM

DEES, number 2.429 , angle deg

BEAM APERTURE 4.2 cm ; DC Bias 0 kV

TUNED by, coarse MS fine VC

RF 6 to 12 mHz, stable ± 10^{-5}

Orb F 1.5 to 12 mHz

HARMONICS, RF/Orb F, used 1,2,3,4

DEE - Gnd, max 100 kV, min gap 8 cm

STABILITY, (pk-pk noise)/(pk RF volt) 10^{-3}

ENERGY GAIN, max 400 kV/turn

RF PHASE, stable to ± 2 deg

RF POWER input, max 150 kW

FREQUENCY MODULATION, rate /s

modulator, type

beam pulse, width

VACUUM SYSTEM

OPERATING PRESSURE 1×10^{-6} Torr or mbar

PUMPS, No, Type, Size 5 oil diffusion pumps

4000 l s-1 each

ION SOURCES

Arc type with heated cathode

INJECTION SYSTEM

EXTRACTION SYSTEM

Stripping + magnetic channel

FACILITIES FOR RESEARCH

SHIELDED AREA, fixed 400 m² ; movable m²

TARGET STATIONS 15 in 7 rooms

STATIONS served at same time, max 1

MAG SPECTROGRAPH, type

COMPUTER model Intel-8080

OTHER FACILITIES

CHARACTERISTIC BEAMS

PARTICLE	ENERGY (MeV) Goal	Achieved	CURRENT (pμA) Internal	External
$^{14}N^{2+}$		176.	30	25.
$^{48}Ti^{5+}$		269.	7.	2.5
$^{58}Fe^{6+}$		298.	3.5	1.2
$^{76}Ge^{8+}$		400.	0.3	0.1
SECONDARY				(part/s)

BEAM PROPERTIES

MEASURED	CONDITIONS
PULSE WIDTH 30 RF deg	pμ A of MeV ions
PHASE EXC, max RF deg	pμ A of MeV ions
EXTRACT eff 30-70 %	pμ A of MeV ions
RESOL ΔE/E 1 %	pμ A of MeV ions
EMITTANCE	
(π mm. mrad) { 80 axial / 40. rad }	pμA of MeV ions

OPERATING PROGRAMS, time distribution

BASIC NUCLEAR PHYSICS 100% SOLID STATES PHYSICS

BIOMEDICAL APPLICAT. - ISOTOPE PRODUCTIONS

REFERENCES/NOTES

1) Proc.of the YIIIth All-Union Meeting on charged Particle Accelerators, Dubna, v.1, 47, 1983

PLAN VIEW OF FACILITY, NOTEWORTHY FEATURES, COMMENTS

ENTRY No. C46

NAME OF MACHINE CI-100 DATE

INSTITUTION Joint Institute for Nuclear Research, Laboratory of Nuclear Reactions

ADDRESS JINR, Head Post Office, P.O. Box 79, Moscow, USSR

TEL TELEX MSK Dubna 412621

IN CHARGE R. Ts. Oganessian REPORTED BY R. Ts. Oganessian

HISTORY AND STATUS

DESIGN, date 1974 Model tests 1984

ENG DESIGN, date 1984

CONSTRUCTION, date 1984-1985

FIRST BEAM, date (or goal) May, 1985

MAJOR ALTERATIONS

COST, ACCELERATOR

COST, FACILITY, total

FUNDED BY

ACCELERATOR STAFF, OPERATION AND DEVELOPMENT

SCIENTISTS ENGINEERS

TECHNICIANS CRAFTS

GRAD STUDENTS involved during year

OPERATED BY Research staff or Operators

OPERATION hr/wk, On target hr/wk

TIME DISTR, In house %, Outside %

BUDGET, op & dev

FUNDED BY

RESEARCH STAFF, not included above

USERS, In house outside

GRAD STUDENTS involved during year

RESEARCH BUDGET, In house

FUNDED BY

MAGNET

POLE FACE, diameter (compact) 105 cm, R extraction 46 cm

R injection cm

GAP, min 2 cm, Field 25 kG
max 11 cm, Field 11 kG
at 0.17.10^6 Ampere turns

AVERAGE FIELD at R ext 19.4 kG

B max/ <B> 1.25

NUMBER OF SECTORS compact 4
separated
Spiral, max 0. deg

SECTOR ANGLE (SSC) 66 deg

TRIMMING COILS

CONDUCTOR, material and type Copper

STORED ENERGY (cryogenic) MJ

POWER: main coils 110 max, kW ; current stability 10^{-4}
trimming coils max, kW ; current stability

WEIGHT : Fe 43 tons ; coils 0.7 tons

COOLING system Demineralized Water

ION ENERGY (bending limit) E/A = 40 q^2/a^2 MeV/amu
(focusing limit) E/A = q^2/a^2 MeV/amu

ACCELERATION SYSTEM

DEES, number 2 ; angle 34 deg

BEAM APERTURE 2 cm ; DC Bias 0 kV

TUNED by, coarse MS fine VC

RF 20.4 to 20.9 mHz, stable ± 10^{-5}

Orb F 5.1 to 5.22 mHz

HARMONICS, RF/Orb F, used 4

DEE - Gnd, max 70 kV, min gap 3.5 cm

STABILITY, (pk-pk noise)/(pk RF volt)

ENERGY GAIN, max 200 kV/turn

RF PHASE, stable to ± deg

RF POWER input, max 25 kW

FREQUENCY MODULATION, rate /s
modulator, type
beam pulse, width

VACUUM SYSTEM

OPERATING PRESSURE (5-10).10^{-6} Torr or mbar

PUMPS, No, Type, Size 3 oil diffusion pumps
one 4000 L/S, two 500 L/S (each)

ION SOURCES

Arc type with heated cathode

INJECTION SYSTEM

EXTRACTION SYSTEM

dc, electrostatic and stripping

FACILITIES FOR RESEARCH

SHIELDED AREA, fixed m^3 ; movable m^3

TARGET STATIONS In rooms

STATIONS served at same time, max 1

MAG SPECTROGRAPH, type

COMPUTER model

OTHER FACILITIES

CHARACTERISTIC BEAMS

PARTICLE	ENERGY (MeV) Goal	Achieved	CURRENT (pμA) Internal	External
$^{12}C^{2+}$		13	12	5
$^{16}O^{3+}$		20	1	1
$^{22}Ne^{4+}$		27	1	0.5
$^{40}Ar^{7+}$		46	0.5	0.25
SECONDARY			(part/s)	

BEAM PROPERTIES

MEASURED	CONDITIONS
PULSE WIDTH RF deg	pμ A of MeV ions
PHASE EXC, max 50 RF deg	pμ A of MeV ions
EXTRACT eff %	pμ A of MeV ions
RESOL ΔE/E %	pμ A of MeV ions
EMITTANCE	
(π mm. mrad) axial / rad	pμA of MeV ions

OPERATING PROGRAMS, time distribution

BASIC NUCLEAR PHYSICS SOLID STATES PHYSICS 100%

BIOMEDICAL APPLICAT. ISOTOPE PRODUCTIONS

REFERENCES/NOTES

PLAN VIEW OF FACILITY, NOTEWORTHY FEATURES, COMMENTS

ENTRY NO. C47 Date June 25/92

Name of Machine Gatchina cyclotron

Institution PNPI Russian Academy of Sciences

Address Gatchina Petersburg District 188350 Russia

Tel ..... Telex ..... Fax ..... EMAIL .....

In Charge: N.K.Abrosimov Reported by: .....

HISTORY

MILESTONE DATES:

Design 1990 - 1992 Model Tests 1991 - 1992

Construction 1992 - 1994 First Beam .....

DESIGN/CONSTRUCTION BY:

in house yes other various engineering contracts

COST: Accelerator ..... Facility .....

FUNDED BY: .....

STATUS

STAFF: Machine

Scientists ..... Engineers .....

Technicians ..... Students .....

Research (in house/external)

Scientists ..... / ..... Engineers ..... / .....

Technicians ..... / ..... Students ..... / .....

BUDGET: Machine ..... Funded by .....

Research ..... Funded by .....

TIME DISTRIBUTION:

Basic Research (in house/external) ..... % / ..... %

Applied Program (in house/external) ..... % / ..... %

Development ..... % Maintenance ..... %

MAGNET

POLE PARAMETERS:

Diameter 205 cm $R_{extract}$ 85-90 cm R_{inject} ..... cm

HILL PARAMETERS: Gap (min) 146 cm B_{max} ..... T

(@ ..... AT) Gap (max) ..... cm B_{min} ..... T

VALLEY PARAMETERS: Gap (min) 386 cm B_{max} ..... T

(@ ..... AT) Gap (max) ..... cm B_{min} ..... T

AVERAGE FIELD: $< B >_{min}$ 1.352 T $< B >_{max}$ 1.46 T

NUMBER OF SECTORS: compact/separated 4 / .....

sector angle 42,5 deg. spiral (max) 60 deg.

FIELD TRIMMING: Trim Coils .....

Harmonic Coils 4x4

Other .....

CURRENT: Main Coils 800 Amps Stability .....

Trim Coils ..... Amps Stability .....

Stored Energy (cryogenic) ..... MJ

WEIGHT: Iron 220 Conductor 16 (Cu)

ION ENERGY: Bending Limit E/A = 80 q^2/A^2 MeV/u

Focussing Limit E/A = ... q/A MeV/u

ACCELERATION SYSTEM

FUNDAMENTAL ACCELERATION:

Description: 2, Lambda/4

No. of Gaps/turn 4 dE/dn(max) 0,200 MeV/q

Voltage(max) 0,060 MV Harmonic f_{rf}/f_{ion} 2/1

Freq 41,2 MHz Power in(max) 2x0,040 MW

Stability: Phase ..... Voltage .....

OTHER CAVITIES (Flattopping or otherwise):

Description: .....

Region of Influence: R_{min} ..... cm R_{max} ..... cm

No. of Gaps/turn ..... dE/dn(max) ..... MeV/q

Voltage(max) ..... MV Harmonic f_{rf}/f_{ion} .....

Freq ..... MHz Power in(max) ..... MW

Stability: Phase ..... Voltage .....

VACUUM SYSTEM

OPERATING PRESSURE: 10^{-7} (N_2), 10^{-6} (H_2)

PUMPS: No. and type ... 2 turbo 10 m³/s

2 evapor. getter 60 m³/s (H_2), Cryopanel (N_2) - 03m²

ION SOURCE(S)

	Type	Intensity (mA)	@	$\epsilon_n = \beta\gamma\epsilon$ (πmm mrad)	Ion Species
(a)				internal	Ehlers Pig
(b)				external	Surface p.
(c)					Cusp
(d)					

INJECTION SYSTEM

axial injection ..... Efficiency ..... %

EXTRACTION SYSTEM

stripping ..... Efficiency 100 %

CHARACTERISTIC BEAMS

	Accelerated Ions	E/A (MeV/u)	Current(μA) Internal	External
(a)	H^-	45 - 80	100	p 100
(b)				
(c)				
(d)				

	Secondary Particles	E (MeV)	part/sec
(a)			
(b)			
(c)			

EXTRACTED BEAM PROPERTIES:

For ..... μA of ..... MeV/u ..... ions

$\Delta E/E$ ..... % $\Delta\phi$ ..... °rf

$\epsilon_n = \beta\gamma\epsilon$ x ..... πmm mrad z ..... πmm mrad

FACILITIES FOR RESEARCH

SHIELDED AREA: Fixed ..... m² Moveable ..... m²

Target Stations: ..... No. Served At Same Time: .....

MAGNETIC SPECTROMETERS: .....

OTHER FACILITIES: .....

REFERENCES/NOTES

(a) XIII International Cyclotron Conference,

(b) Vancouver 92

PLAN VIEW OF FACILITY, COMMENTS

ENTRY NO. C48 Date July 2, 1992

Name of Machine Kurchatov Institute of Atomic Energy

Institution Cyclotron IAE

Address 123182 Moscow, Russia

Tel ..... Telex 411594 SHUGA ..... Fax ..... EMAIL .....

In Charge: ..... Reported by: V.E.Jarosh

HISTORY

MILESTONE DATES:

Design ....date 1971-73 Model Tests ..1973-74.....

Construction .date 1976.... First Beam 1976.....

DESIGN/CONSTRUCTION BY:

in house ..... other ....

COST: Accelerator ..... Facility .....

FUNDED BY: .....

STATUS

STAFF: Machine

Scientists ..... Engineers .....

Technicians ..... Students .....

Research (in house/external)

Scientists ..... / ..... Engineers ..... / .....

Technicians ..... / ..... Students ..... / .....

BUDGET: Machine ..... Funded by .....

Research ..... Funded by .....

TIME DISTRIBUTION:

Basic Research (in house/external) ..... % / ..... %

Applied Program (in house/external) ..... % / ..... %

Development ..... % Maintenance ..... %

MAGNET

POLE PARAMETERS:

Diameter...150... cm $R_{extract}$ ...67.5.. cm R_{inject} ..... cm

HILL PARAMETERS: Gap (min) .20..... cm B_{max} ...2.1... T

(@ ..... AT) Gap (max) ..... cm B_{min} ..... T

VALLEY PARAMETERS: Gap (min) .34..... cm B_{max} ..... T

(@ ..... AT) Gap (max) ..... cm B_{min} ...1.5... T

AVERAGE FIELD: $< B >_{min}$ ..... T $< B >_{max}$ ..... T

NUMBER OF SECTORS: compact/separated ...3..... / .....

sector angle ..... deg. spiral (max) .....50..... deg.

FIELD TRIMMING: Trim Coils .....

Harmonic Coils ....3 pairs.....

Other .....concentric, 8 pairs.....

CURRENT: Main Coils ..... Amps Stability .....

Trim Coils ..... Amps Stability .....

Stored Energy (cryogenic) ..... MJ

WEIGHT: Iron ....300 tons.... Conductor ....70 tons.....

ION ENERGY: Bending Limit E/A = ... q^2/A^2 MeV/u

Focussing Limit E/A = ... q/A MeV/u

ACCELERATION SYSTEM

FUNDAMENTAL ACCELERATION:

Description: ...dees number 2,angle 180 deg,.....

No. of Gaps/turn ..... dE/dn(max) ..... MeV/q

Voltage(max) ..... MV Harmonic f_{rf}/f_{ion} .....

Freq ....6 to 20.... MHz Power in(max) .....~3..... MW

Stability: Phase ..... Voltage .....10^{-3}%.....

OTHER CAVITIES (Flattopping or otherwise):

Description: .....

Region of Influence: R_{min} ..... cm R_{max} ..... cm

No. of Gaps/turn ..... dE/dn(max) ..... MeV/q

Voltage(max) ..... MV Harmonic f_{rf}/f_{ion} .....

Freq ..... MHz Power in(max) ..... MW

Stability: Phase ..... Voltage .....

VACUUM SYSTEM

OPERATING PRESSURE: .....10^{-5} torr.....

PUMPS: No. and type .....

.....

ION SOURCE(S)

	Type	Intensity (mA)	@	$\epsilon_n = \beta\gamma\epsilon$ (πmm mrad)	Ion Species
(a)	...Penning type.....	.....		.....	.....
(b)	.....	.....		.....	.....
(c)	.....	.....		.....	.....
(d)	.....	.....		.....	.....

INJECTION SYSTEM

..... Efficiency ..... %

EXTRACTION SYSTEM

..Electrostatic defl.,mag.chanEfficiency ..... %

CHARACTERISTIC BEAMS

Accelerated Ions	E/A (MeV/u)	Current(part μA) Internal	External
(a) p, d	.....	.....	30
(b) $^{6}Li, ^{12}C$	.....	.....	7.5-1.5
(c) ^{14}N	.....	.....	7.5
(d)	.....	.....	3

	Secondary Particles	E (MeV)	part/sec
(a)	.....	.....	.....
(b)	.....	.....	.....
(c)	.....	.....	.....

EXTRACTED BEAM PROPERTIES:

For ..... μA of ..... MeV/u ..... ions

$\Delta E/E$ .....% $\Delta\phi$ ..... °rf

$\epsilon_n = \beta\gamma\epsilon$ x .....20... πmm mrad z ....30..... πmm mrad

FACILITIES FOR RESEARCH

SHIELDED AREA: Fixed ..... m^2 Moveable ..... m^2

Target Stations: ..... No. Served At Same Time: .....

MAGNETIC SPECTROMETERS: .....

OTHER FACILITIES: .....

.....

.....

.....

REFERENCES/NOTES

(a) .Venikov.N..I...e.a..LEEE.Trans..on.Nucl.....

(b) .Sci.,.v..NS-26.(1979).1996.....

PLAN VIEW OF FACILITY, COMMENTS

ENTRY NO. C49 **Date** June 15/92

Name of Machine NAC Injector Cyclotron 1

Institution National Accelerator Centre

Address P O Box 72, Faure 7131, Republic of South Africa

Tel 24-43820 Telex tex 555046 SA Fax 24-43525 EMAIL POSTMASTER@NAC.DHL.NAC.AC.ZA

In Charge: D. Reitmann Reported by: A.H. Botha

HISTORY

MILESTONE DATES:

Design 1978 Model Tests 1979 - 1980

Construction 1978 - 1983 First Beam December 1983

DESIGN/CONSTRUCTION BY:

in house yes other various engineering contractors

COST: Accelerator ..... Facility .....

FUNDED BY: .....

STATUS (See NAC Separated-Sector Cyclotron)

STAFF: Machine

Scientists ..... Engineers .....

Technicians ..... Students .....

Research (in house/external)

Scientists ..... / ..... Engineers ..... / .....

Technicians ..... / ..... Students ..... / .....

BUDGET: Machine ..... Funded by .....

Research ..... Funded by .....

TIME DISTRIBUTION:

Basic Research (in house/external) ..... % / ..... %

Applied Program (in house/external) ..... % / ..... %

Development ..... % Maintenance ..... %

MAGNET

POLE PARAMETERS:

Diameter 116 cm $R_{extract}$ 47.6 cm R_{inject} - cm

HILL PARAMETERS: Gap (min) ..... cm B_{max} ..... T

(@ ..... AT) Gap (max) 15.6 cm B_{min} 1.23 T

VALLEY PARAMETERS: Gap (min) ..... cm B_{max} ..... T

(@ ..... AT) Gap (max) 25.0 cm B_{min} 0.75 T

AVERAGE FIELD: $< B >_{min}$ 0.3 T $< B >_{max}$ 0.98 T

NUMBER OF SECTORS: compact/separated 4 / .....

sector angle 45 deg. spiral (max) - deg.

FIELD TRIMMING: Trim Coils 5

Harmonic Coils 2

Other 2 cone coils

CURRENT: Main Coils 800 Amps Stability 10^{-5}

Trim Coils 160 Amps Stability 10^{-4}

Stored Energy ~~(cryogenic)~~ 0.1 MJ

WEIGHT: Iron 54.5 tons Conductor 1.85 tons

ION ENERGY: Bending Limit E/A = 11 q^2/A^2 MeV/u

Focussing Limit E/A = - q/A MeV/u

ACCELERATION SYSTEM

FUNDAMENTAL ACCELERATION:

Description: Two λ/4 resonators with 90° dees

No. of Gaps/turn 4 dE/dn(max) 0.24 MeV/q

Voltage(max) 0.060 MV Harmonic f_{rf}/f_{ion} 2, 6

Freq 8.6 - 26 MHz Power in(max) 2 × 0.025 MW

Stability: Phase 0.1 deg Voltage 10^{-3}

OTHER CAVITIES (Flattopping or otherwise):

Description: -

Region of Influence: R_{min} ..... cm R_{max} ..... cm

No. of Gaps/turn ..... dE/dn(max) ..... MeV/q

Voltage(max) ..... MV Harmonic f_{rf}/f_{ion} .....

Freq ..... MHz Power in(max) ..... MW

Stability: Phase ..... Voltage .....

VACUUM SYSTEM

OPERATING PRESSURE: 1.5×10^{-5} mbar

PUMPS: No. and type 1 Turbo 4.8 $m^3 s^{-1}$, 1 Roots 350 $m^3 h^{-1}$, 1 Rotary Vane 60 $m^3 h^{-1}$

ION SOURCE(S)

	Type	Intensity (mA)	@ $\epsilon_n = \beta\gamma\epsilon$ (πmm mrad)	Ion Species
(a)	PIG	4		p
(b)				
(c)				
(d)				

INJECTION SYSTEM

..... Efficiency ..... %

EXTRACTION SYSTEM

Electrostatic & 2 magnetic channels Efficiency 96 %

CHARACTERISTIC BEAMS

	Accelerated Ions	E/A (MeV/u)	Current(part μA) Internal	External
(a)	p	1.4 - 8	414	323
(b)	d	0.9 - 1.9	6	3
(c)	$^4He^+$	0.62	3	3
(d)	α	1.88	5	3

	Secondary Particles	E (MeV)	part/sec
(a)			
(b)			
(c)			

EXTRACTED BEAM PROPERTIES:

For 230 μA of 3.14 MeV/u p ions

ΔE/E 0.85 % Δφ 15 °rf

$\epsilon_n = \beta\gamma\epsilon$ x 0.98 πmm mrad z 0.49 πmm mrad

FACILITIES FOR RESEARCH

SHIELDED AREA: Fixed ..... m^2 Moveable ..... m^2

Target Stations: ..... No. Served At Same Time: .....

MAGNETIC SPECTROMETERS: .....

OTHER FACILITIES: .....

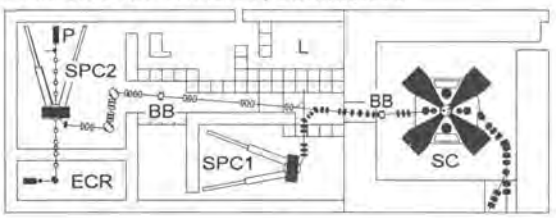
See NAC Separated-Sector Cyclotron

REFERENCES/NOTES

(a) Proc. Tenth Int. Cycl. Conf., 67, 94, 373 (1984)

(b) Proc. Eleventh Int. Cycl. Conf., 9, 109 (1986)

PLAN VIEW OF FACILITY, COMMENTS



BB	Beamline buncher
ECR	ECR ion source (basement)
L	Low energy experimental area
P	Polarized ion source (basement)
SPC1	Solid pole injector cyclotron for light ions
SPC2	Solid pole injector cyclotron for heavy or polarized ions
SC	Separated-sector cyclotron

ENTRY NO. C50 **Date** June 15/92

Name of Machine NAC Injector Cyclotron 2

Institution National Accelerator Centre

Address P O Box 72, Faure 7131, Republic of South Africa

Tel 24-43820 **Telex** tex 555046 SA **Fax** 24-43525 **EMAIL** POSTMASTER @ NAC.DHL.NAC.AC.ZA

In Charge: D. Reitmann **Reported by:** A.H. Botha

HISTORY

MILESTONE DATES:
Design 1986 - 1992 Model Tests .....
Construction 1989 - 1993 First Beam December 1993

DESIGN/CONSTRUCTION BY:
in house yes other various engineering contracts

COST: Accelerator ..... Facility .....

FUNDED BY: .....

STATUS (See NAC Separated-Sector Cyclotron)

STAFF: Machine
Scientists ..... Engineers .....
Technicians ..... Students .....
Research (in house/external)
Scientists ..... / ..... Engineers ..... / .....
Technicians ..... / ..... Students ..... / .....

BUDGET: Machine ..... Funded by .....
Research ..... Funded by .....

TIME DISTRIBUTION:
Basic Research (in house/external) ..... % / ..... %
Applied Program (in house/external) ..... % / ..... %
Development ..... % Maintenance ..... %

MAGNET

POLE PARAMETERS:
Diameter 116 cm $R_{extract}$ 47.6 cm R_{inject} ..... cm

HILL PARAMETERS: Gap (min) ..... cm B_{max} ..... T
(@ 1.55×10^5 AT) Gap (max) 15.6 cm B_{min} 1.24 T

VALLEY PARAMETERS: Gap (min) ..... cm B_{max} ..... T
(@ 1.55×10^5 AT) Gap (max) 25.0 cm B_{min} 0.75 T

AVERAGE FIELD: $< B >_{min}$ 0.3 T $< B >_{max}$ 1.0 T

NUMBER OF SECTORS: compact/separated 4 / .....
sector angle 45° deg. spiral (max) ..... deg.

FIELD TRIMMING: Trim Coils 6
Harmonic Coils 2
Other Cone coils: 2

CURRENT: Main Coils 690 Amps Stability 10^{-5}
Trim Coils 200 Amps Stability 10^{-3}
Stored Energy (cryogenic) ..... MJ

WEIGHT: Iron 54.5 tons Conductor 1.85 tons copper

ION ENERGY: Bending Limit E/A = 11 q^2/A^2 MeV/u
Focussing Limit E/A = - q/A MeV/u

ACCELERATION SYSTEM

FUNDAMENTAL ACCELERATION:
Description: Two λ/4 resonators with 90° dees
No. of Gaps/turn 4 dE/dn(max) 0.24 MeV/q
Voltage(max) 0.060 MV Harmonic f_{rf}/f_{ion} 2, 6
Freq 6 - 26 MHz Power in(max) 2 x 0.025 MW
Stability: Phase 0.1 deg Voltage 10^{-3}

OTHER CAVITIES (Flattopping or otherwise):
Description: -
Region of Influence: R_{min} ..... cm R_{max} ..... cm
No. of Gaps/turn ..... dE/dn(max) ..... MeV/q
Voltage(max) ..... MV Harmonic f_{rf}/f_{ion} .....
Freq ..... MHz Power in(max) ..... MW
Stability: Phase ..... Voltage .....

VACUUM SYSTEM

OPERATING PRESSURE: 8×10^{-5} Pa

PUMPS: No. and type 1 Turbo 2.2 m^3/s, 1 cryo 10 m^3/s and 2 LN cryo 18 m^3/s

ION SOURCE(S)

	Type	Intensity (mA)	@	$\epsilon_n = \beta\gamma\epsilon$ (πmm mrad)	Ion Species
(a)	ECR				p to Xe
(b)	Pol.Source(At.B.)	0.028		0.9	p and d
(c)					
(d)					

INJECTION SYSTEM

3 Interchangeable spiral inflectors. Efficiency ..... %

EXTRACTION SYSTEM

Electrostatic+2 magnetic channels... Efficiency ..... %

CHARACTERISTIC BEAMS

	Accelerated Ions	E/A (MeV/u)	Current(part μA) Internal	External
(a)	protons	2 - 8		
(b)	Ar	0.2 - 1.0		
(c)	Xe	0.1 - 0.25		
(d)				

	Secondary Particles	E (MeV)	part/sec
(a)			
(b)			
(c)			

EXTRACTED BEAM PROPERTIES:
For ..... μA of ..... MeV/u ..... ions
ΔE/E ..... % Δφ ..... °rf
$\epsilon_n = \beta\gamma\epsilon$ x ..... πmm mrad z ..... πmm mrad

FACILITIES FOR RESEARCH

SHIELDED AREA: Fixed ..... m^2 Moveable ..... m^2
Target Stations: ..... No. Served At Same Time: .....

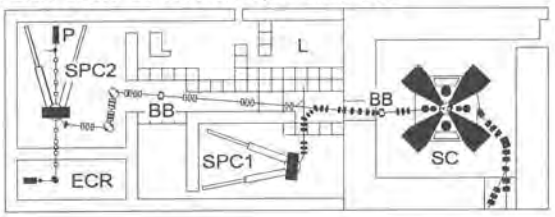
MAGNETIC SPECTROMETERS: .....

OTHER FACILITIES: .....
See NAC Separated-Sector Cyclotron

REFERENCES/NOTES

(a) Proc. Eleventh Int. Conf., 515 (1986)
(b) Proceedings of this conference

PLAN VIEW OF FACILITY, COMMENTS



BB	Beamline buncher
ECR	ECR ion source (basement)
L	Low energy experimental area
P	Polarized ion source (basement)
SPC1	Solid pole injector cyclotron for light ions
SPC2	Solid pole injector cyclotron for heavy or polarized ions
SC	Separated-sector cyclotron

ENTRY NO. C51 **Date** June 15/92

Name of Machine NAC Separated-Sector Cyclotron

Institution National Accelerator Centre

Address P O Box 72, Faure 7131, Republic of South Africa

Tel 24-43820 **Telex** tex 555 046 SA **Fax** 24-43525 **EMAIL** POSTMASTER @ NAC.DEL.NAC.AC.ZA

In Charge: D. Reitmann **Reported by:** A.H. Botha

HISTORY

MILESTONE DATES:
Design 1977 Model Tests
Construction 1979 First Beam October 1985
DESIGN/CONSTRUCTION BY:
in house yes other various engineering contractors
COST: Accelerator Facility
FUNDED BY: South African Government

STATUS

STAFF: Machine
Scientists 15 Engineers 15
Technicians 31 Students 2
Research (in house/external)
Scientists 23 / 62 Engineers - / -
Technicians 11 / 0 Students 5 / 15
BUDGET: Machine Funded by SA Government
Research Funded by SA Government
TIME DISTRIBUTION:
Basic Research (in house/external) 16 % / 26 %
Applied Program (in house/external) 3.5 % / 27 %
Development 3 % Maintenance 11.5 %

MAGNET

POLE PARAMETERS:
Diameter - cm $R_{extract}$ 443 cm R_{inject} 101 cm
HILL PARAMETERS: Gap (min) 6.6 cm B_{max} 1.27 T
(@ 1.08×10^3 AT) Gap (max) cm B_{min} T
VALLEY PARAMETERS: Gap (min) cm B_{max} T
(@ AT) Gap (max) cm B_{min} T
AVERAGE FIELD: $< B >_{min}$ T $< B >_{max}$ 0.24 T
NUMBER OF SECTORS: compact/separated / 4
sector angle 34 deg. spiral (max) 0 deg.
FIELD TRIMMING: Trim Coils 29
Harmonic Coils 0
Other 2 yoke coils on each of the 4 sectors
CURRENT: Main Coils 1600 Amps Stability 10^{-4}
Trim Coils 500 Amps Stability 10^{-4}
Stored Energy (cryogenic) 1.5 MJ
WEIGHT: Iron 1400 tons Conductor 5.8 tons
ION ENERGY: Bending Limit E/A = 220 q^2/A^2 MeV/u
Focussing Limit E/A = 220 q/A MeV/u

ACCELERATION SYSTEM

FUNDAMENTAL ACCELERATION:
Description: 2 lambda/2 resonators, push-push mode
No. of Gaps/turn 4 dE/dn(max) 1 MeV/q
Voltage(max) 0.25 MV Harmonic f_{rf}/f_{ion} 4 and 12
Freq 6 to 26 MHz Power in(max) 2 x 0.15 MW
Stability: Phase 0.1 deg Voltage 10^{-3}
OTHER CAVITIES (Flattopping or otherwise):
Description: -
Region of Influence: R_{min} cm R_{max} cm
No. of Gaps/turn dE/dn(max) MeV/q
Voltage(max) MV Harmonic f_{rf}/f_{ion}
Freq MHz Power in(max) MW
Stability: Phase Voltage

VACUUM SYSTEM

OPERATING PRESSURE: 7×10^{-7} mbar
PUMPS: No. and type 4 Rotary vane 120 $m^3 h^{-1}$, 4 Roots 350 $m^3 h^{-1}$, 6 turbo pumps 2 $m^3 s^{-1}$ and 2 cryopumps 5 $m^3 s^{-1}$

ION SOURCE(S) k=8 Injector Cyclotron

	Type	Intensity (mA)	@	$\epsilon_n = \beta\gamma\epsilon$ (πmm mrad)	Ion Species
(a)					
(b)					
(c)					
(d)					

INJECTION SYSTEM

2 dipoles and a magnetic channel Efficiency 100 %

EXTRACTION SYSTEM

1 electrostatic channel & 2 septum magnets Efficiency 100 %

CHARACTERISTIC BEAMS

	Accelerated Ions	E/A (MeV/u)	Current(part μA) Internal	External
(a)	p	27 - 220	205	200 (66 MeV)
(b)	d	35 - 40	2	2
(c)	$^4He^{++}$	10 - 12.5	2	2
(d)	$^4He^{+}$	30 - 50	2	2

	Secondary Particles	E (MeV)	part/sec
(a)			
(b)			
(c)			

EXTRACTED BEAM PROPERTIES:
For 35 μA of 66 MeV/u p ions
$\Delta E/E$ 0.4 % $\Delta\phi$ 10 °rf
$\epsilon_n = \beta\gamma\epsilon$ x 2.7 πmm mrad z 0.8 πmm mrad

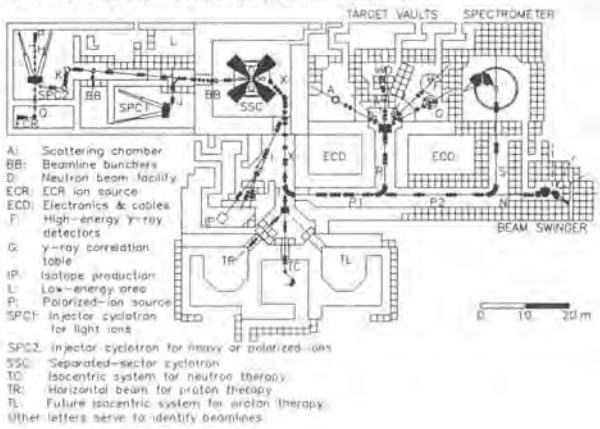
FACILITIES FOR RESEARCH

SHIELDED AREA: Fixed 700 m^2 Moveable 900 m^2
Target Stations: 7 No. Served At Same Time: 1
MAGNETIC SPECTROMETERS: k=600 QDD
OTHER FACILITIES: 66 MeV isocentric system for neutron therapy, a beam swinger for neutron time-of-flight measurements, a 1.5 m scattering chamber, a neutron time-of-flight facility, a 3-armed γ correlation table

REFERENCES/NOTES

(a) Proc. Eleventh Int. Conf., 9 (1986)
(b) Proc. Twelfth Int. Conf., 80 (1989)

PLAN VIEW OF FACILITY, COMMENTS



ENTRY NO. C52 Date 2.7.1992

Name of Machine Gustaf Werner Cyclotron

Institution The Svedberg Laboratory

Address Box 533, S-75121 Uppsala, Sweden

Tel +4618182500 Telex 76088 TSL-ISV S Fax +4618183833 EMAIL stigh@tsl.uu.se

In Charge: S. Holm Reported by: S. Holm

HISTORY

MILESTONE DATES:
Design 1946- ; 1977- Model Tests 1974 - 1978
Construction 1946-51; 1979-86 First Beam 1951, 1986, 1987ext

DESIGN/CONSTRUCTION BY:
in house 4 other

COST: Accelerator Reconstr. 25MSEK Facility 70 MSEK total

FUNDED BY: Swedish state

STATUS

STAFF: Machine
Scientists 3 Engineers 5
Technicians 7 Students
Research (in house/external)
Scientists 20 / 100 Engineers /
Technicians / Students /

BUDGET: Machine 1 MSEK Funded by Swedish state
Research 10 MSEK Funded by Swedish state

TIME DISTRIBUTION:
Basic Research (in house/external) 60 % / %
Applied Program (in house/external) 20 % / %
Development 10 % Maintenance 10 %

MAGNET

POLE PARAMETERS:
Diameter 280 cm $R_{extract}$ 120 cm R_{inject} cm

HILL PARAMETERS: Gap (min) 20 cm B_{max} 2.0 T
(Φ 0.6 MAT) Gap (max) cm B_{min} 0.8 T

VALLEY PARAMETERS: Gap (min) 36 cm B_{max} 1.3 T
(Φ 0.6 MAT) Gap (max) cm B_{min} 0.5 T

AVERAGE FIELD: $< B >_{min}$ 0.4 T $< B >_{max}$ 1.75 T

NUMBER OF SECTORS: compact/separated 3 /
sector angle deg. spiral (max) deg.

FIELD TRIMMING: Trim Coils 13 pair circular
Harmonic Coils 2 sets
Other

CURRENT: Main Coils 1000 Amps Stability 10 ppm
Trim Coils 100 Amps Stability 100 ppm
Stored Energy (cryogenic) MJ

WEIGHT: Iron 600 tons Conductor 50 tons

ION ENERGY: Bending Limit E/A = 200 q^2/A^2 MeV/u
Focussing Limit E/A = 105 q/A MeV/u

ACCELERATION SYSTEM

FUNDAMENTAL ACCELERATION:
Description: lambda-quarter cavity
No. of Gaps/turn 4 dE/dn(max) 0.20 MeV/q
Voltage(max) 0.050 MV Harmonic f_{rf}/f_{ion} 1, 2, 3
Freq 12 - 24 MHz Power in(max) 0.200 MW
Stability: Phase +-0.5 deg. Voltage +-0.1%

OTHER CAVITIES (Flattopping or otherwise):
Description:
Region of Influence: R_{min} cm R_{max} cm
No. of Gaps/turn dE/dn(max) MeV/q
Voltage(max) MV Harmonic f_{rf}/f_{ion}
Freq MHz Power in(max) MW
Stability: Phase Voltage

VACUUM SYSTEM

OPERATING PRESSURE: $5 \cdot 10^{-7}$ mbar
PUMPS: No. and type 2 oildiff. pumps, each 9000 l/sec baffled, Intermediate vacuum: < 10^{-4} mbar, 700 l/sec

ION SOURCE(S)

	Type	Intensity (mA)	Φ	$\epsilon_n = \beta\gamma\epsilon$ (πmm mrad)	Ion Species
(a)	PIG	0.1			p+, 4He++
(b)	ECR	0.050			Heavy ions
(c)	Polarized	0.050			p+, d+
(d)					

INJECTION SYSTEM

Spiral infl., extern injection Efficiency ≤5% %

EXTRACTION SYSTEM

Presessional, regenerative Efficiency 60 - 80 %

CHARACTERISTIC BEAMS

	Accelerated Ions	E/A (MeV/u)	Current(part μA) Internal	External
(a)	p+	10 - 100	100	10
(b)	p+	100 - 190		100nA
(c)	Heavy ions	5 - 50	0.1 - 100	0.05 - 0.5
(d)				

	Secondary Particles	E (MeV)	part/sec
(a)	neutrons	≤ 190	10^6 in 10 sr
(b)			
(c)			

EXTRACTED BEAM PROPERTIES:
For 0.1 μA of 50 MeV/u p+ ions
ΔE/E 0.2 % Δφ 20 °rf
$\epsilon_n = \beta\gamma\epsilon$ x 9 πmm mrad z 9 πmm mrad

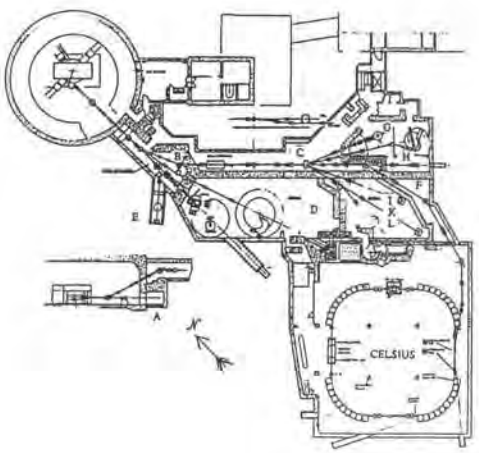
FACILITIES FOR RESEARCH

SHIELDED AREA: Fixed 600 m^2 Moveable m^2
Target Stations: 7 No. Served At Same Time:
MAGNETIC SPECTROMETERS: HESM, PACMAN, LISA
OTHER FACILITIES: Treatment bench for eye melanoma
Cave for production of isotopes
Special target system for neutron production

REFERENCES/NOTES

(a) S. Holm et al., Physica Scripta, Vol 34, 513-532, 1986
(b) C. Ekström et al, Physica Scripta, Vol T22, 256-268

PLAN VIEW OF FACILITY, COMMENTS



ENTRY NO. C53 Date July 1992

Name of Machine PSI Philips Cyclotron "Injector I"

Institution PSI, Paul Scherrer Institute

Address CH-5232 Villigen PSI, Switzerland

Tel ++41 (0)56 99 31 11 Telex 827 442 psi ch Fax ++41 (0)56 99 33 83 EMAIL

In Charge: Dr U. Schryber Reported by: Dr P.-A. Schmelzbach

HISTORY

MILESTONE DATES:

Design 1967 - 1969 Model Tests 1968 - 1971

Construction 1970 - 1973 First Beam Jan. 1st, 1974

DESIGN/CONSTRUCTION BY:

in house other Philips

COST: Accelerator 14 MSFr Facility *

FUNDED BY: Swiss Federal Government

STATUS

STAFF: Machine

Scientists 1 Engineers 1

Technicians 4 Students

Research (in house/external) VE + pol. Inj. mode

Scientists 5 / 75 Engineers /

Technicians / Students / 30

BUDGET: Machine * Funded by *

Research * Funded by *

TIME DISTRIBUTION:

Basic Research (in house/external) 3 % / 70 %

Applied Program (in house/external) 14 % / %

Development 3 % Maintenance 10 %

MAGNET

POLE PARAMETERS:

Diameter 250 cm $R_{extract}$ 105 cm R_{inject} 1.5 cm

HILL PARAMETERS: Gap (min) 24 cm B_{max} T

(Φ AT) Gap (max) cm B_{min} T

VALLEY PARAMETERS: Gap (min) 45 cm B_{max} T

(Φ AT) Gap (max) cm B_{min} T

AVERAGE FIELD: $< B >_{min}$ T $< B >_{max}$ 16.5 T

NUMBER OF SECTORS: compact/separated 4 /

sector angle deg. spiral (max) 55 deg.

FIELD TRIMMING: Trim Coils 12 concentric

Harmonic Coils 4 sets harmonic

Other

CURRENT: Main Coils ≤ 700 Amps Stability 10 E-6

Trim Coils ≤ 250 Amps Stability 10E-6

Stored Energy (cryogenic) MJ

WEIGHT: Iron 470 t Conductor 20 t Al

ION ENERGY: Bending Limit E/A = 135 q^2/A^2 MeV/u

Focussing Limit E/A = 135 q/A MeV/u

ACCELERATION SYSTEM

FUNDAMENTAL ACCELERATION:

Description: 1 Dee, 2 HF systems (VE/Inj. modes)

No. of Gaps/turn 2 dE/dn(max) 0.16 MeV/q

Voltage(max) 0.08 MV Harmonic f_{rf}/f_{ion} 1.3 / 3

Freq 4.6 to 17/50 MHz Power in(max) 0.1 MW

Stability: Phase 1 deg / 0.1 deg Voltage 10E-2 / 10E-4

OTHER CAVITIES (Flattopping or otherwise):

Description:

Region of Influence: R_{min} cm R_{max} cm

No. of Gaps/turn dE/dn(max) MeV/q

Voltage(max) MV Harmonic f_{rf}/f_{ion}

Freq MHz Power in(max) MW

Stability: Phase Voltage

VACUUM SYSTEM

OPERATING PRESSURE: without gas 10E-6 mbar

PUMPS: No. and type 20000 + 12000 l/s oil-diff. pumps (Balzers), cryogenic panel (Philips)

ION SOURCE(S)

	Type	Intensity (mA)	Φ	$\epsilon_n = \beta\gamma\epsilon$ (πmm mrad)	Ion Species
(a)	Internal Livingston				p, d
(b)					(A,Z) (14,4)
(c)	axial: atomic beam pol. source				p, d
(d)	ECR "Caprice" heavy ion source (1993)				

INJECTION SYSTEM

axial: e.m. quads, buncher, mirror. Efficiency %

EXTRACTION SYSTEM

electrostatic, electromagn., magn. Efficiency 93 %

CHARACTERISTIC BEAMS

	Accelerated Ions	E/A (MeV/u)	Current(part μA) Internal	External
(a)	p (Inj.-mode)	72	215	200
(b)	p (VE-mode)	10 - 72	≤110	≤100
(c)	N^{4+}	5 - 30	4	3 / 0.01
(d)	pol. p (d)	10 - 72	≤15	≤12

	Secondary Particles	E (MeV)	part/sec/cm²
(a)	n, pol. n	30 - 70	≤5 E-5/s/cm²
(b)	n, pol. n	200 - 580	5 E-6/s/cm² *
(c)			

EXTRACTED BEAM PROPERTIES:

For 100 μA of 72 MeV/u p ions

ΔE/E 0.5 % Δφ 15 °rf

$\epsilon_n = \beta\gamma\epsilon$ x 3 πmm mrad z 2 πmm mrad

FACILITIES FOR RESEARCH

SHIELDED AREA: Fixed m² Moveable m²

Target Stations: No. Served At Same Time:

MAGNETIC SPECTROMETERS:

OTHER FACILITIES: π-production targets, spin rotators, users owned/operated devices: crystal spectrometer, 4π-scattering chambers, double scattering, apparatus, spectrometers, biol. vertical beam (1993)

PLAN VIEW OF FACILITY, COMMENTS

* see PSI 590 MeV Ring Cyclotron (this compilation)

REFERENCES/NOTES

1) The SIN injector cyclotron (A. Baan et al.) IEEE Trans. Nucl. Sci. NS-20.3 (1973) 257
2) The axial injection system of the SIN injector cyclotron (N. Hazewindus), I. Design considerations/ II. Description and experiments, buncher, Nucl. Instr. & Meth. 129 (1975) 325/331
3) The central region of the SIN injector cyclotron (J.M. van Nieuwland et al.)Nucl. Instr. Meth. 142 (1977) 339
4) Improvements in the SIN injector RF system (P. Sigg) Nucl. Instr. & Meth. 155 (1978) 1
5) Aspects of the 100 μA operation (G. Heidenreich et al.) 9th Int. Conf. on Cyclotrons, Caen (1981) 365
6) Polarized Beams at PSI (P.-A. Schmelzbach et al.) European Particle Accelerator Conference, Rome (1988)

ENTRY NO. C54 Date July 1992
Name of Machine PSI Injector Cyclotron 2
Institution PSI, Paul Scherrer Institute
Address CH-5232 Villigen PSI, Switzerland
Tel ++41.(0)56.99.31.11. Telex 827.442 psi ch Fax ++41.(0)56.99.33.83 EMAIL
In Charge: Dr. U. Schryber Reported by: Dr. W. Joho, Dr. U. Schryber

HISTORY

MILESTONE DATES:
Design 1972 Model Tests 1973 - 1980
Construction 1978 - 1983 First Beam April 1984
DESIGN/CONSTRUCTION BY:
in house PSI other
COST: Accelerator 22 MSFr Facility 134 MSFr
FUNDED BY: Swiss Federal Government

STATUS

STAFF: Machine
Scientists ca. 15 Engineers ca. 15
Technicians 50 Students
Research (in house/external)
Scientists 40 / 300 Engineers /
Technicians / Students /
BUDGET: Machine 7 MSFr Funded by Swiss Fed. Gov.
Research Funded by
TIME DISTRIBUTION:
Basic Research (in house/external) % / %
Applied Program (in house/external) % / %
Development % Maintenance %

MAGNET

POLE PARAMETERS:
Diameter cm $R_{extract}$ 342 cm R_{inject} 46 cm
HILL PARAMETERS: Gap (min) 3.5 cm B_{max} 11.0 T
(@ AT) Gap (max) 3.5 cm B_{min} 10.5 T
VALLEY PARAMETERS: Gap (min) cm B_{max} T
(@ AT) Gap (max) cm B_{min} T
AVERAGE FIELD: $< B >_{min}$ 0.33 T $< B >_{max}$ 0.36 T
NUMBER OF SECTORS: compact/separated / 4
sector angle 27 deg. spiral (max) 0 deg.
FIELD TRIMMING: Trim Coils 11 pairs per magnet
Harmonic Coils 1
Other
CURRENT: Main Coils 400 Amps Stability 5E-6
Trim Coils $\lesssim$ 40 Amps Stability 5E-5
Stored Energy (cryogenic) MJ
WEIGHT: Iron 4 x 180 tons Conductor 4 x 0.96 tons
ION ENERGY: Bending Limit E/A = 72 q^2/A^2 MeV/u
Focussing Limit E/A = q/A MeV/u

ACCELERATION SYSTEM

FUNDAMENTAL ACCELERATION:
Description: 2 Resonators 50 MHz
No. of Gaps/turn 4 dE/dn(max) 1.0 MeV/q
Voltage(max) 0.5 MV Harmonic f_{rf}/f_{ion} 10
Freq 50.6 MHz Power in(max) 0.17 MW
Stability: Phase 0.01 deg. Voltage 0.03 %
OTHER CAVITIES (Flattopping or otherwise):
Description: 2 flattop cavities 150 MHz
Region of Influence: R_{min} 80 cm R_{max} 342 cm
No. of Gaps/turn 2 dE/dn(max) 0.1 MeV/q
Voltage(max) $\simeq$ 0.05 MV Harmonic f_{rf}/f_{ion} 30
Freq 151.8 MHz Power in(max) 0.01 MW
Stability: Phase $\lesssim$ 0.1 deg. Voltage 0.1 %

VACUUM SYSTEM

OPERATING PRESSURE: 2E-6
PUMPS: No. and type 4 x turbo molecular pumps
2200 l/s each

ION SOURCE(S)

	Type	Intensity (mA)	@	$\epsilon_n = \beta\gamma\epsilon$ (πmm mrad)	Ion Species
(a)	cusp type, in Cockcroft Walton preaccelerator				
(b)		8.0			p
(c)					
(d)					

INJECTION SYSTEM

Axial, at 870 keV magn. cone with n = 0.6 ... Efficiency 100 %

EXTRACTION SYSTEM el. stat. deflector

2 septum magnets ... Efficiency 100 %

CHARACTERISTIC BEAMS

	Accelerated Ions	E/A (MeV/u)	Current(part μA) Internal	External
(a)	p	72	1500	1500
(b)				
(c)				
(d)				

	Secondary Particles	E (MeV)	part/sec
(a)			
(b)			
(c)			

EXTRACTED BEAM PROPERTIES:
For 1500 μA of 72 MeV/u ions
$\Delta E/E$ 0.6 % $\Delta\phi$ 16 °rf
$\epsilon_n = \beta\gamma\epsilon$ x 1.5 πmm mrad, z 1.5 πmm mrad

FACILITIES FOR RESEARCH

SHIELDED AREA: Fixed m^2 Moveable m^2
Target Stations: No. Served At Same Time:
MAGNETIC SPECTROMETERS:
OTHER FACILITIES: Isotope production

see entry "PSI 590 MeV Ring Cyclotron"

REFERENCES/NOTES

(a)
(b)

PLAN VIEW OF FACILITY, COMMENTS

1) Two stage accelerator for 72 MeV protons (see Proc. 9th Int. Conf. on Cyclotrons & their Application, (1981), 43
   Stage 1: 870 keV DC preacc. (Cockcroft-Walton)
   Stage 2: Isochronous ring cyclotron
2) See PSI 590 MeV Ring Cyclotron (this compilation)
3) Special coils outside vacuum chamber for correction of isochronism
4) RF-systems: two /2-resonators (50.6 MHz) for acceleration and two flattop cavities (151.8 MHz)

ENTRY NO. C55 Date July 1992

Name of Machine PSI 590 MeV Ring Cyclotron (with Injectorcyclotron 1 and 2, see separate entries)

Institution PSI, Paul Scherrer Institute

Address CH-5232 Villigen PSI, Switzerland

Tel ++41.(0)56.99.31.11 Telex 827.442 psi.ch Fax ++41.(0)56.99.33.83 EMAIL

In Charge: Dr.U. Schryber Reported by: Dr.W. Joho and Dr.M. Olivo

HISTORY

MILESTONE DATES:

Design 1962 Model Tests 1962 - 1968

Construction 1969 - 1974 First Beam Jan. 1974

DESIGN/CONSTRUCTION BY:

in house PSI other

COST: Accelerator 35 MSFr.(1974). Facility 134 MSFr.(1975).

FUNDED BY: Swiss Federal Government

STATUS

STAFF: Machine

Scientists ca. 15 Engineers ca. 15

Technicians 50 Students

Research (in house/external)

Scientists 40. / 300 Engineers /

Technicians / Students /

BUDGET: Machine 7. MSFr. Funded by Swiss. Fed. Gov.

Research Funded by

TIME DISTRIBUTION:

Basic Research (in house/external) % / %

Applied Program (in house/external) % / %

Development % Maintenance %

MAGNET

POLE PARAMETERS:

Diameter cm $R_{extract}$ 445 cm R_{inject} 210 cm

HILL PARAMETERS: Gap (min) 5 cm B_{max} 2.09 T

(@ AT) Gap (max) 9 cm B_{min} 1.5 T

VALLEY PARAMETERS: Gap (min) 5 cm B_{max} T

(@ AT) Gap (max) cm B_{min} T

AVERAGE FIELD: $< B >_{min}$ 0.58 T $< B >_{max}$ 0.87 T

NUMBER OF SECTORS: compact/separated / 8

sector angle deg. spiral (max) 35. deg.

FIELD TRIMMING: Trim Coils 18

Harmonic Coils 5

Other

CURRENT: Main Coils 900 Amps Stability 5E-6

Trim Coils ≤120 Amps Stability 5E-4

Stored Energy (cryogenic) MJ

WEIGHT: Iron 1960 tons Conductor 28 tons

ION ENERGY: Bending Limit E/A = 590 q^2/A^2 MeV/u

Focussing Limit E/A = q/A MeV/u

ACCELERATION SYSTEM

FUNDAMENTAL ACCELERATION:

Description: 4 cavities 50 MHz (AJ)

No. of Gaps/turn 4 dE/dn(max) 2.0 MeV/q

Voltage(max) 0.5 - 0.75 MV Harmonic f_{rf}/f_{ion} 6

Freq 50.6 MHz Power in(max) 0.15 - 0.5 MW

Stability: Phase 0.01 deg. Voltage 0.03 %

OTHER CAVITIES (Flattopping or otherwise):

Description: 1 flattop cavity 150 MHz

Region of Influence: R_{min} 210 cm R_{max} 445 cm

No. of Gaps/turn 1 dE/dn(max) ≃0.3 MeV/q

Voltage(max) ≃0.3 MV Harmonic f_{rf}/f_{ion} 18

Freq 151.8 MHz Power in(max) ≃35 MW

Stability: Phase ≤0.1 deg. Voltage 0.1 %

VACUUM SYSTEM

OPERATING PRESSURE: 2E-6 mbar

PUMPS: No. and type 4 turbomol. pumps 500 l/s and 4 cryopumps and 4 Ti-sublimators 14000 l/s

ION SOURCE(S) see entry "PSI - Injector 1/2"

	Type	Intensity (mA)	@ $\epsilon_n = \beta\gamma\epsilon$ (πmm mrad)	Ion Species
(a)	4 Ti-sublimators 14000 l/s each			
(b)				
(c)				
(d)				

INJECTION SYSTEM

Magnetic and electrostatic channel... Efficiency 100 %

EXTRACTION SYSTEM

Electrostatic septum Efficiency ≃99.9 %

CHARACTERISTIC BEAMS

	Accelerated Ions	E/A (MeV/u)	Current(part μA) Internal	External
(a)	p	590	500	500
(b)				
(c)				
(d)				

	Secondary Particles	E (MeV)	part/sec
(a)		30 - 600	10E-10
(b)		5 - 125	10E-8
(c)			

EXTRACTED BEAM PROPERTIES:

For 500 μA of 590 MeV/u p ions

ΔE/E 0.1 % Δφ ≃10 °rf

$\epsilon_n = \beta\gamma\epsilon$ x ≃2 πmm mrad z ≃1.5 πmm mrad

FACILITIES FOR RESEARCH

SHIELDED AREA: Fixed m² Moveable m²

Target Stations: 2 No. Served At Same Time: 2

MAGNETIC SPECTROMETERS: 2 pion spectrometers

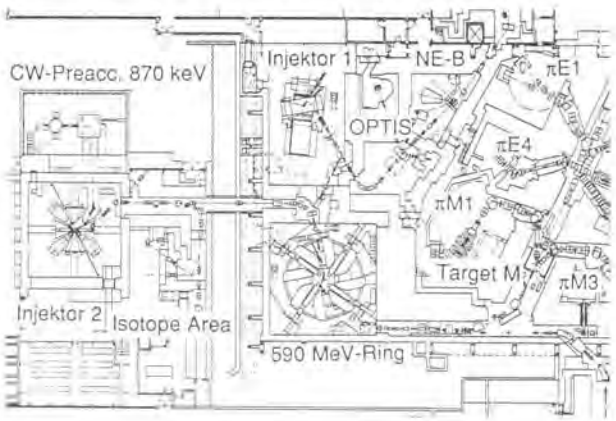
OTHER FACILITIES: 2 supercond. muon channels, detectors for the obs. of rare decays, μSR-facilities, annexes pion and proton therapy, nucleon area, material irradiation, isotope production

REFERENCES/NOTES

(a) W. Joho, M. Olivo, T. Stammbach, H. Willax; IEEE NS-24

(b) W. Joho, IEEE NS-26 (1979) 1950

PLAN VIEW OF FACILITY, COMMENTS



ENTRY NO. C56 **Date** June 1992

Name of Machine U - 240 Cyclotron

Institution Institute for the nuclear Research Ukrainian Academy of Sciences

Address Ukraine, Kiev - 252028 prospekt Nauki, 47

Tel (044) 2651456 Telex 132400 Proton Fax (044) 2654463 EMAIL

In Charge: I.N. Vishvevsky Reported by: A.I. Papash

HISTORY

MILESTONE DATES:

Design 1965 - 1970 Model Tests 1963 - 1966

Construction 1966 - 1972 First Beam March 1976

DESIGN/CONSTRUCTION BY:

in house yes other Efremov's Institute/Leningrad

COST: Accelerator Facility 50 MRb(SU)

FUNDED BY: USSR Academy of Sciences
Comittee Utilization of Atomic Energy

STATUS

STAFF: Machine

Scientists 6 Engineers 20

Technicians 60 Students 2

Research (in house/external)

Scientists 200 / Engineers /

Technicians / Students /

BUDGET: Machine 2 MRub (1990) Funded by Ukr.Ac. of Scien-ces

Research Funded by

TIME DISTRIBUTION:

Basic Research (in house/external) 50 % / %

Applied Program (in house/external) 20 % / %

Development % Maintenance 30 %

MAGNET

POLE PARAMETERS:

Diameter 240 cm $R_{extract}$ 102 cm R_{inject} 23.2 cm

HILL PARAMETERS: Gap (min) cm B_{max} 2.3 T

(@ 0.83e6 AT) Gap (max) cm B_{min} T

VALLEY PARAMETERS: Gap (min) 53.2 cm B_{max} 11.2 T

(@ AT) Gap (max) cm B_{min} T

AVERAGE FIELD: $< B >_{min}$ T $< B >_{max}$ 1.7 T

NUMBER OF SECTORS: compact/separated 3 /

sector angle deg. spiral (max) 45 deg.

FIELD TRIMMING: Trim Coils 15 circulating coils

Harmonic Coils 3 per sector

Other valley coils (1per sector)

CURRENT: Main Coils 2100 Amps Stability 2.0e-5

Trim Coils 2100 Amps Stability 1.0e-4

Stored Energy (cryogenic) MJ

WEIGHT: Iron 650 tons Conductor 84 tons

ION ENERGY: Bending Limit E/A = 140 q^2/A^2 MeV/u

Focussing Limit E/A = 80(protons). q/A MeV/u

ACCELERATION SYSTEM

FUNDAMENTAL ACCELERATION:

Description: 180° dee and dummy dee

No. of Gaps/turn 2 dE/dn(max) 0.18 MeV/q

Voltage(max) 0.09 MV Harmonic f_{rf}/f_{ion} 1.3

Freq 7 - 21 MHz Power in(max) 0.25 MW

Stability: Phase ± 20 Voltage 2.e-3

OTHER CAVITIES (Flattopping or otherwise):

Description:

Region of Influence: R_{min} cm R_{max} cm

No. of Gaps/turn dE/dn(max) MeV/q

Voltage(max) MV Harmonic f_{rf}/f_{ion}

Freq MHz Power in(max) MW

Stability: Phase Voltage

VACUUM SYSTEM

OPERATING PRESSURE: 2.0 e-6

PUMPS: No. and type 3 diffusion pumps (50 cm)

ION SOURCE(S)

	Type	Intensity (mA)	@	$\epsilon_n = \beta\gamma\epsilon$ (πmm mrad)	Ion Species
(a)	internal pig				H_2^+, D_2^+, a
(b)	with filament	2			
(c)	with indirect				C^{4+}, B^{4+}, N^{5+}, N^{+}
(d)	heated cathode	0.1-1.0			F^{+}, O^{+}, Ne^{+}, etc.

INJECTION SYSTEM

Axial injection mirror inflector Efficiency %

not in operation

EXTRACTION SYSTEM

e/s deflector, compensated magneric. Efficiency 20-50 %

channel and iron channel

CHARACTERISTIC BEAMS

	Accelerated Ions	E/A (MeV/u)	Current(part μA) Internal	External
(a)	protons	20-78	up to 200	10
(b)	D_2^+, α^{2+}	10-25	10-20	5-10
(c)	C^{3+}, O^{4+}, Ne^{5+}	5	2	0.5
(d)	N^{+}	10	1	0.3

	Secondary Particles	E (MeV)	part/sec
(a)			
(b)			
(c)			

EXTRACTED BEAM PROPERTIES:

For 5 μA of 70 MeV/u P ions

$\Delta E/E \pm 0.3$ % $\Delta\phi$ 30° °rf

$\epsilon_n = \beta\gamma\epsilon$ x 5 πmm mrad z 5 πmm mrad

FACILITIES FOR RESEARCH

SHIELDED AREA: Fixed 1000 m² Moveable 1200 m²

Target Stations: 15 No. Served At Same Time: 1

MAGNETIC SPECTROMETERS: MS 200 R=200 cm dE/E=20e-5

OTHER FACILITIES:

REFERENCES/NOTES

(a) Atomnaja Energia, 6, 1976

(b) 8. International Conference on Cyclotrons, Bloomington, September 18-21, 1976

PLAN VIEW OF FACILITY, COMMENTS

1. The polarized ion source will be installed in 1993
2. The ECR ion source in construction (collobaration with JINR, Dubna)
3. The radioactive ions seperator in design (Efremov NIIEPA - Petersburg)
4. The storage ring complex with U-240 injector under consideration.

ENTRY No. C 57

NAME OF MACHINE IM Radial Ridge DATE July 1989

INSTITUTION School of Physics & Space Research

ADDRESS University of Birmingham, P.O. Box 363, Birmingham B15 2TT, U.K.

TEL 021-414-4704 TELEX

IN CHARGE Prof. T.D.Beynon REPORTED BY R. G. Green

HISTORY AND STATUS

DESIGN, date 1957 Model tests None

ENG DESIGN, date 1957 - 63

CONSTRUCTION, date 1958 - 63

FIRST BEAM, date (or goal) Int. 1963, Ext. 1963

MAJOR ALTERATIONS --

COST, ACCELERATOR £ 30 K

COST, FACILITY, total

FUNDED BY SERC/since 1988 self funding

ACCELERATOR STAFF, OPERATION AND DEVELOPMENT

SCIENTISTS ENGINEERS 1

TECHNICIANS 2 CRAFTS 1

GRAD STUDENTS involved during year

OPERATED BY Research staff or Operators

OPERATION hr/wk, On target hr/wk

TIME DISTR. In house %, Outside %

BUDGET, op & dev £ 15 K

FUNDED BY self funded

RESEARCH STAFF, not included above

USERS, In house outside

GRAD STUDENTS involved during year

RESEARCH BUDGET, In house

FUNDED BY

MAGNET

POLE FACE, diameter (compact) 102 cm, R extraction 46. cm

R injection cm

GAP, min 7 cm, Field 19 kG } at

max 14.5 cm, Field 13 kG } Ampere turns

AVERAGE FIELD at R ext 16 kG

B max/ <B> 1.2

NUMBER OF SECTORS { compact 3 } radial
{ separated } spiral, max deg

SECTOR ANGLE (SSC) deg

TRIMMING COILS Harmonic - 2

Circular - 8

CONDUCTOR, material and type Cu. Strip

STORED ENERGY (cryogenic) MJ

POWER : main coils 40 max, kW ; current stability

trimming coils max, kW ; current stability

WEIGHT : Fe 50 tons ; coils 8 tons

COOLING system H_2O

ION ENERGY (bending limit) E/A = q^2/a^2 MeV/amu

(focusing limit) E/A = q^2/a^2 MeV/amu

ACCELERATION SYSTEM

DEES, number 1 ; angle 180 deg

BEAM APERTURE 2-3 cm ; DC Bias - kV

TUNED by, coarse M.S fine M.S

RF 12 to 16 mHz, stable ± 2/10^6

Orb F 12 to 16 mHz

HARMONICS, RF/Orb F, used 1

DEE - Gnd, max 27. kV, min gap 0.3 cm

STABILITY, (pk-pk noise)/(pk RF volt) 0.001

ENERGY GAIN, max 54 kV/turn

RF PHASE, stable to ± 3 deg

RF POWER input, max 45 kW

FREQUENCY MODULATION, rate /s

modulator, type

beam pulse, width

VACUUM SYSTEM

OPERATING PRESSURE 4×10^{-6} Torr or mbar

PUMPS, No, Type, Size 1 x 40 cm

2 x 22 cm Silicon Oil Diff.

ION SOURCES

Internal Hot Kathode, polarized external source de-commissioned

INJECTION SYSTEM

Axial

EXTRACTION SYSTEM

Mag/Elect. Regenerator & Elect Def.

FACILITIES FOR RESEARCH

SHIELDED AREA, fixed 90 m² ; movable 0 m²

TARGET STATIONS 6 , in 1 rooms

STATIONS served at same time, max 1

MAG SPECTROGRAPH, type -

COMPUTER model GEC

OTHER FACILITIES 10 Mass Ident System using counter telescopes

CHARACTERISTIC BEAMS

PARTICLE	ENERGY (MeV) Goal	Achieved	CURRENT (pμA) Internal	External
^4He		25	300	150
^3He		33	300	150
p^+		12.5	800	
P		6.5	600	

SECONDARY (part/s)

BEAM PROPERTIES

MEASURED CONDITIONS

PULSE WIDTH 30 RF deg 10 pμ A of 33 MeV ^3He Ions

PHASE EXC, max 15 RF deg 10 pμ A of MeV Ions

EXTRACT eff 60 % pμ A of MeV Ions

RESOL ΔE/E 0.4 % pμ A of MeV Ions

EMITTANCE

(π mm. mrad) { 40 axial / 40 rad } pμA of MeV Ions

OPERATING PROGRAMS, time distribution

BASIC NUCLEAR PHYSICS 30% SOLID STATES PHYSICS

BIOMEDICAL APPLICAT. 10% ISOTOPE PRODUCTIONS 60%

REFERENCES/NOTES

PLAN VIEW OF FACILITY, NOTEWORTHY FEATURES, COMMENTS

Although this machine was used in the nuclear structure field it now concentrates mainly on isotope production producing ^{81}Kr, ^{52}Fe, ^{57}Co, ^{22}Ne. Isotopes are produced internally and externally.

Polarized D^+, He^3 external source has been de-commissioned.

ENTRY No. C58

NAME OF MACHINE Nuffield 60" Cyclotron DATE

INSTITUTION Birmingham University, School of Physics and Space Research

ADDRESS P.O. Box 363, Birmingham B15 2TT

TEL 021-414-4547 TELEX

IN CHARGE Prof. T.D.Beynon REPORTED BY E.C. Cartwright

HISTORY AND STATUS

DESIGN, date 1938 Model tests

ENG DESIGN, date

CONSTRUCTION, date

FIRST BEAM, date (or goal) 1948

MAJOR ALTERATIONS New Dees and Electromagnetic Shimming of Magnei Profile for H^+ He^3

COST, ACCELERATOR

COST, FACILITY, total

FUNDED BY

ACCELERATOR STAFF, OPERATION AND DEVELOPMENT

SCIENTISTS 1 ENGINEERS --

TECHNICIANS 3 CRAFTS --

GRAD STUDENTS involved during year

OPERATED BY Research staff or 3 Operators

OPERATION 120 hr/wk, On target 140 hr/wk

TIME DISTR. in house 20 %, Outside 80 %

BUDGET, op & dev £ 25 K

FUNDED BY

RESEARCH STAFF, not included above

USERS, in house outside

GRAD STUDENTS involved during year

RESEARCH BUDGET, in house

FUNDED BY

MAGNET

POLE FACE, diameter (compact) 180 cm, R extraction 104 cm

R injection 0 cm

GAP, ~~max~~ fixed cm, Field 18 max kG } at

~~max~~ 25 cm, Field kG } Ampere turns

AVERAGE FIELD at R ext 0 13.5 kG

B max/ <B>

NUMBER OF SECTORS { compact / separated None } Plane Field / Spiral, max deg

SECTOR ANGLE (ISSC) deg

TRIMMING COILS 5 Radial 4 in Quadrature

CONDUCTOR, material and type Copper Pyrotenax

STORED ENERGY (cryogenic) None MJ

POWER: main coils 4.0 max, kW ; current stability 1 in 10^5

trimming coils 1.5 max, kW ; current stability 1 in 10^3

WEIGHT : Fe 250 tons ; coils 40 tons

COOLING system Air

ION ENERGY (bending limit) E/A = q^2/a^2 MeV/amu

(focusing limit) E/A = q^2/a^2 MeV/amu

ACCELERATION SYSTEM

DEES, number 2 ; angle Symetrical deg

BEAM APERTURE at extract cm ; DC Bias 1 kV

TUNED by, coarse fixed fine

RF to 10.5 mHz, stable ± 1 in 10^4

Orb F to mHz

HARMONICS, RF/Orb F, used

DEE - Gnd, max 90 kV, min gap 7.5 cm

STABILITY, (pk-pk noise)/(pk RF volt)

ENERGY GAIN, max kV/turn

RF PHASE, stable to ± deg

RF POWER input, max 80 kW

FREQUENCY MODULATION, rate None /s

modulator, type --

beam pulse, width --

VACUUM SYSTEM

OPERATING PRESSURE 10^{-5} Torr or mbar

PUMPS, No, Type, Size 2 x 37 cm + 22 cm Booster + Leybold Rotary + Kinney for roughing

ION SOURCES

Enclosed Graphite (Oak Ridge Variant)

INJECTION SYSTEM

NA

EXTRACTION SYSTEM

70° neg. deflector

FACILITIES FOR RESEARCH

SHIELDED AREA, fixed m² ; movable m²

TARGET STATIONS In rooms

STATIONS served at same time, max

MAG SPECTROGRAPH, type

COMPUTER model None

OTHER FACILITIES Automatic Internal Rotating Target Inserting, Extracting

CHARACTERISTIC BEAMS

PARTICLE	ENERGY (MeV) Goal	Achieved	CURRENT (pμA) Internal	External
H^+			500	100
D^+			500	100
He^4			250	50
He^3			250	60
SECONDARY			(part/s)	

BEAM PROPERTIES N/A

MEASURED CONDITIONS

PULSE WIDTH RF deg pμA of MeV ions

PHASE EXC, max RF deg pμA of MeV ions

EXTRACT eff % pμA of MeV ions

RESOL ΔE/E % pμA of MeV ions

EMITTANCE

(π mm. mrad) { axial / rad } pμA of MeV ions

OPERATING PROGRAMS, time distribution

BASIC NUCLEAR PHYSICS 5% SOLID STATES PHYSICS

BIOMEDICAL APPLICAT. 5% ISOTOPE PRODUCTIONS 95%

REFERENCES/NOTES

PLAN VIEW OF FACILITY, NOTEWORTHY FEATURES, COMMENTS

ENTRY No. C59

NAME OF MACHINE Argonne 60 Inch Cyclotron DATE July 10, 1989

INSTITUTION Argonne National Laboratory

ADDRESS 9700 South Cass Avenue - Argonne, Illinois 60439, U.S.A.

TEL 312-972-4887 TELEX

IN CHARGE Robert Atcher REPORTED BY Ed Kemereit / R. Atcher

HISTORY AND STATUS

DESIGN, date 1944-1949 Model tests

ENG DESIGN, date 1949-1951

CONSTRUCTION, date 1950-1952

FIRST BEAM, date for good, productive, operation July 10, 1952

MAJOR ALTERATIONS Modifications for He^3 - 1964

COST, ACCELERATOR $ 966,456.50

COST, FACILITY, total

FUNDED BY University of Chicago under contract U.S.A.

ACCELERATOR STAFF, OPERATION AND DEVELOPMENT

SCIENTISTS ENGINEERS 1

TECHNICIANS 0 CRAFTS 0

GRAD STUDENTS involved during year 0

OPERATED BY Research staff or 1 Operators

OPERATION 20 hr/wk, On target 20 hr/wk

TIME DISTR. in house %, Outside %

BUDGET, op & dev

FUNDED BY CHER/DOE, Work for others

RESEARCH STAFF, not included above

USERS, In house 3 outside 3

GRAD STUDENTS involved during year 1

RESEARCH BUDGET, In house

FUNDED BY ANL

MAGNET

POLE FACE, diameter (compact) 157.5 cm, R extraction 65.2 cm

R injection 0 cm

GAP, min 25.4 cm, Field 11.2 kG } He^3

max 25.4 cm, Field 15.4 kG } at d, α, P..

AVERAGE FIELD at R ext kG } Ampere turns

B max/ <B>

NUMBER OF SECTORS { compact 2 / separated } Spiral, max deg

SECTOR ANGLE (SSC) deg

TRIMMING COILS 3 pairs - Copper

CONDUCTOR, material and type Main Magnet - Aluminium

STORED ENERGY (cryogenic) MJ

POWER : main coils 65. max, kW ; current stability

trimming coils max, kW ; current stability

WEIGHT : Fe 225 tons ; coils 26 tons

COOLING system water, demineralized

ION ENERGY (bending limit) E/A = q^2/a^2 MeV/amu

(focusing limit) E/A = q^2/a^2 MeV/amu

ACCELERATION SYSTEM

DEES, number 2 ; angle deg

BEAM APERTURE cm ; DC Bias kV

TUNED by, coarse fine

RF 11.2 to 11.4 mHz, stable ± 100 Hz

Orb F 11.2 to 11.4 mHz

HARMONICS, RF/Orb F, used

DEE - GND, max 290 kV, min gap cm

STABILITY, (pk-pk noise)/(pk RF volt)

ENERGY GAIN, max kV/turn

RF PHASE, stable to ± deg

RF POWER input, max 100 kW

FREQUENCY MODULATION, rate /s

modulator, type

beam pulse, width

VACUUM SYSTEM

OPERATING PRESSURE 3 to 9 x 10^{-6} Torr or mbar

PUMPS, No, Type, Size 2 - 16 inch Diffusion Pumps

2 - Kinney Type Mech. Pumps, 100 CFM + 300 CFM

ION SOURCES

Hooded Graphite Arc Type with 1/8-inch Dia. TA Hair Pin Filament

INJECTION SYSTEM

EXTRACTION SYSTEM 75 KV D.C.

FACILITIES FOR RESEARCH

SHIELDED AREA, fixed 186. m² ; movable m²

TARGET STATIONS 3 in same rooms

STATIONS served at same time, max

MAG SPECTROGRAPH, type none

COMPUTER model

OTHER FACILITIES Senior hot cells; junior hot cells radiochemistry laboratories including glove box facilities

CHARACTERISTIC BEAMS

PARTICLE	ENERGY (MeV) Goal	Achieved	CURRENT (pμA) Internal	External
Deuterons		21.4		80
Alphas		43.0		30
H_2^+		10.2		50
He^3		33.5		30
SECONDARY				(part/s)

BEAM PROPERTIES

MEASURED CONDITIONS

PULSE WIDTH RF deg pμ A of MeV ions

PHASE EXC, max RF deg pμ A of MeV ions

EXTRACT eff % pμ A of MeV ions

RESOL ΔE/E % pμ A of MeV ions

EMITTANCE

(π mm. mrad) { axial / rad } pμA of MeV ions

OPERATING PROGRAMS, time distribution

BASIC NUCLEAR PHYSICS SOLID STATES PHYSICS

BIOMEDICAL APPLICAT. 50% ISOTOPE PRODUCTIONS 50%

REFERENCES/NOTES

PLAN VIEW OF FACILITY, NOTEWORTHY FEATURES, COMMENTS

ENTRY NO. C60 **Date** June 26, 1992

Name of Machine 88-Inch Cyclotron

Institution Lawrence Berkeley Laboratory

Address 1 Cyclotron Road, Berkeley, CA 94720 U.S.A.

Tel 510/486-5088 **Telex** 910-366-2037 **Fax** 510/486-7983 **EMAIL** CMLYNEIS@LBL.GOV

In Charge: C. M. Lyneis **Reported by:** D. J. Clark

HISTORY

MILESTONE DATES:
Design 1958 Model Tests 1958-59
Construction 1959-62 First Beam external 1962

DESIGN/CONSTRUCTION BY:
in house Yes other outside contracts

COST: Accelerator 3.5 M$ Facility 5.1 M$

FUNDED BY: U.S. D.O.E.

STATUS

STAFF: Machine
Scientists 3 Engineers 3
Technicians 12 Students
Research (in house/external)
Scientists 20 / 50 Engineers 1 /
Technicians 4 / Students 14 / 15

BUDGET: Machine Funded by D.O.E.
Research Funded by D.O.E.

TIME DISTRIBUTION:
Basic Research (in house/external) 24 % / 36 %
Applied Program (in house/external) -- % / 20 %
Development 2 % Maintenance 18 %

MAGNET

POLE PARAMETERS:
Diameter 224 cm $R_{extract}$ 99 cm R_{inject} 0 cm

HILL PARAMETERS: Gap (min) 19 cm B_{max} 2.1 T
(@ 1.6x10^6 AT) Gap (max) cm B_{min} T

VALLEY PARAMETERS: Gap (min) 30 cm B_{max} 1.5 T
(@ 1.6x10^6 AT) Gap (max) cm B_{min} T

AVERAGE FIELD: $< B >_{min}$ T $< B >_{max}$ 1.8 T

NUMBER OF SECTORS: (compact)/separated 3 /
sector angle (hill) 60 deg. spiral (max) 55 deg.

FIELD TRIMMING: Trim Coils 17 Circular
Harmonic Coils 5 valley
Other

CURRENT: Main Coils 3000 Amps Stability 10^{-5}
Trim Coils 750-2500 Amps Stability 10^{-3}
Stored Energy (cryogenic) MJ

WEIGHT: Iron 290 tons Conductor 10 tons

ION ENERGY: Bending Limit E/A = 160 q^2/A^2 MeV/u
Focussing Limit E/A = 65 q/A MeV/u

ACCELERATION SYSTEM

FUNDAMENTAL ACCELERATION:
Description: 180 degree dee
No. of Gaps/turn 2 dE/dn(max) 1 MeV/q
Voltage(max) 05 MV Harmonic f_{rf}/f_{ion} 1,3,5,7
Freq 5.5-16.2 MHz Power in(max) 3 MW
Stability: Phase Voltage 10^{-3}

OTHER CAVITIES (Flattopping or otherwise):
Description:
Region of Influence: R_{min} cm R_{max} cm
No. of Gaps/turn dE/dn(max) MeV/q
Voltage(max) MV Harmonic f_{rf}/f_{ion}
Freq MHz Power in(max) MW
Stability: Phase Voltage

VACUUM SYSTEM

OPERATING PRESSURE: $1x10^{-6}$ torr
PUMPS: No. and type 2-25 cm diff. pumps,
2-25 cm diff. pumps, 20° K cryopanel

ION SOURCE(S)

	Type	Intensity (mA)	©	$\epsilon_n = \beta\gamma\epsilon$ (πmm mrad)	Ion Species
(a)	ECR, AECR	10^{-3}-1		--	All Ions
(b)	Atomic Beam	3 x 10^{-3}		--	Pol. H, D
(c)					
(d)					

INJECTION SYSTEM

Axial injection, 90° mirror Efficiency -- %

EXTRACTION SYSTEM

Electrostatic, 3 section Efficiency 50 %

CHARACTERISTIC BEAMS

	Accelerated Ions	E/A (MeV/u)	Current(part μA) Internal	External
(a)	p	2-55	50	25-2
(b)	p(pol.)	6-50	1	.5
(c)	$^{16}O^{5+}$	9	4	2
(d)	$^{86}Kr^{29+}$	10	.004	.002

	Secondary Particles	E (MeV)	part/sec
(a)			
(b)			
(c)			

EXTRACTED BEAM PROPERTIES:
For 5 μA of 16 MeV/u $^{4}He^{2+}$ ions
$\Delta E/E$ 3 % $\Delta\phi$ °rf
$\epsilon_n = \beta\gamma\epsilon$ x 3 πmm mrad z 4 πmm mrad

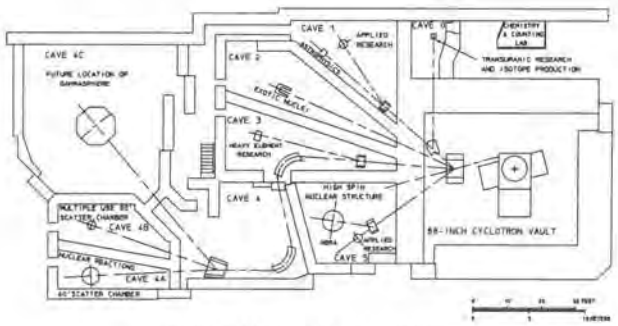
FACILITIES FOR RESEARCH

SHIELDED AREA: Fixed -- m^2 Moveable 800 m^2
Target Stations: 12 No. Served At Same Time: 1
MAGNETIC SPECTROMETERS:
OTHER FACILITIES: on-line mass separator, Transuranic chemistry, gamma ray ball, atomic physics facility

REFERENCES/NOTES

(a) R.S.I., 62 (3), Mar., 1991 (AECR) p. 775
(b) I.E.E.E. Part. Accel. Conf., May, 1991, p. 2796

PLAN VIEW OF FACILITY, COMMENTS



88-INCH CYCLOTRON FACILITY

ENTRY NO. C62 **Date** 21 JUNE 92

Name of Machine INDIANA UNIVERSITY CYCLOTRON FACILITY

Institution INDIANA UNIVERSITY

Address 2401 Milo B Sampson Lane, Bloomington, IN 47408

Tel (812) 855-9365 **Telex** 272279 INDIANA U BLOM **Fax** (812) 855-6645 **EMAIL** FRIESEL@IUCF

In Charge: JOHN CAMERON, Director **Reported by:** D. L. FRIESEL

HISTORY

MILESTONE DATES:
Design 1966 Model Tests 1967-1972
Construction 1968--1974 First Beam Sept., 1975

DESIGN/CONSTRUCTION BY:
in house yes other Various Fabrication Vendors

COST: Accelerator $5 x 10^6 Facility $11 x 10^6

FUNDED BY: NATIONAL SCIENCE FOUNDATION (NSF)

STATUS

STAFF: Machine
Scientists 14 Engineers 14
Technicians 46 Students 3
Research (in house/external)
Scientists 41 / >200 Engineers 0 / 1
Technicians 9 / -- Students 53 / 25

BUDGET: Machine $10x$10^6$ Funded by NSF
Research Funded by NSF

TIME DISTRIBUTION:
Basic Research (in house/external) 34 % / 34 %
Applied Program (in house/external) 2 % / 1 %
Development 12 % Maintenance 17 %

MAGNET

POLE PARAMETERS:
Diameter N/A cm $R_{extract}$ 330 cm R_{inject} 101 cm
HILL PARAMETERS: Gap (min) 7.6 cm B_{max} 1.65 T
(@ 150,000 AT) Gap (max) 7.6 cm B_{min} 1.65 T
VALLEY PARAMETERS: Gap (min) ∞ cm B_{max} <0.02 T
(@ 150,000 AT) Gap (max) ∞ cm B_{min} <0.02 T
AVERAGE FIELD: $< B >_{min}$ 0.058 T $< B >_{max}$ 0.64 T
NUMBER OF SECTORS: compact/separated N/A / 4
sector angle 36 deg. spiral (max) N/A deg.
FIELD TRIMMING: Trim Coils 21 Gradiant
Harmonic Coils 4 Axial, 4 Radial
Other None
CURRENT: Main Coils 1000 Amps Stability $1x10^{-6}$
Trim Coils 950 Amps Stability $1x10^{-5}$
Stored Energy (cryogenic) MJ
WEIGHT: Iron 2000 Tons Conductor 10 Tons
ION ENERGY: Bending Limit E/A = 215 q^2/A^2 MeV/u
Focussing Limit E/A = 215 q/A MeV/u

ACCELERATION SYSTEM

FUNDAMENTAL ACCELERATION:
Description: 2-1/4 Wave RF Resonators
No. of Gaps/turn 4 dE/dn(max) 0.80 MeV/q
Voltage(max) 0.2 MV Harmonic f_{rf}/f_{ion} 3-7; 11-14
Freq 25-35.5 MHz Power in(max) 150 MW
Stability: Phase 0.25 RF Degree Voltage $8 x 10^{-5}

OTHER CAVITIES (Flattopping or otherwise):
Description: NONE
Region of Influence: R_{min} cm R_{max} cm
No. of Gaps/turn dE/dn(max) MeV/q
Voltage(max) MV Harmonic f_{rf}/f_{ion}
Freq MHz Power in(max) MW
Stability: Phase Voltage

VACUUM SYSTEM

OPERATING PRESSURE: $3 x 10^{-6} Torr
PUMPS: No. and type 4 CRYOGENIC, 2 DIFFUSION PUMPS

ION SOURCE(S)

	Type	Intensity (mA)	@ $\epsilon_n = \beta\gamma\epsilon$ (πmm mrad)	Ion Species
(a)	ANAL POL.	0.008	20.0	P,d (78% Pol)
(b)	Duoplasmotron	0.300	<10.0	P,d, ^{3}He, ^{4}He
(c)	AB(ECR)PIS*	0.100	<20.0	P,d (>70% Pol)
(d)				

*Undergoing beam development presently.

INJECTION SYSTEM

Midplane Injection Radial Inflector Efficiency 75 %

EXTRACTION SYSTEM

Electrostatic & Magnetic Septums Efficiency 99 %

CHARACTERISTIC BEAMS

Accelerated Ions	E/A (MeV/u)	Current(part μA) Internal	External
(a) H^+ & Pol H^+	20-205	0.5	0.5
(b) d & Pol d	10-50	0.5	0.5
(c) ^{3}He	8-95	0.3	0.3
(d) ^{4}He	7-50	0.3	0.3

Secondary Particles	E (MeV)	part/sec
(a) n & Pol n	20-205	10^5
(b)		
(c)		

EXTRACTED BEAM PROPERTIES:
For 0.5 μA of ALL MeV/u ALL ions
$\Delta E/E$ 0.1 % $\Delta\phi$ 4.0 °rf
$\epsilon_n = \beta\gamma\epsilon$ x 1.5 πmm mrad z 1.5 πmm mrad

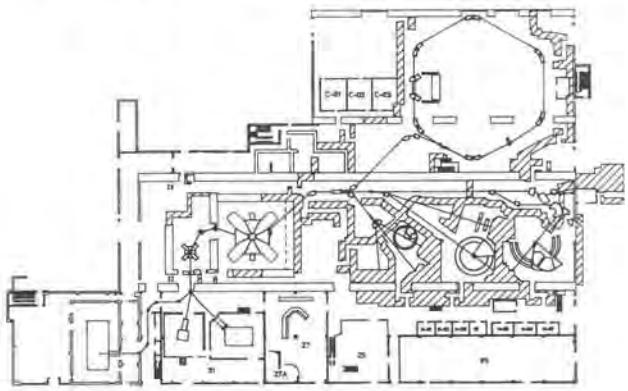
FACILITIES FOR RESEARCH

SHIELDED AREA: Fixed 4600 m^2 Moveable -- m^2
Target Stations: 8 No. Served At Same Time: 2
MAGNETIC SPECTROMETERS: K600 High Res. Spectrometer
OTHER FACILITIES: QQSP Pion Spectrometer
--3.6 Tm Synchrotron Storage Ring with Electron Cooling
--Neutron Beam Swinger & PNF TOF Facilities
--Proton Radiation Therapy Facility (under construction)

REFERENCES/NOTES

(a) --1991 IUCF Scientific and Technical Report
(b) --The IUCF Cooler, R.E. Pollock, IEEE Trans. Nucl. Sci., NS-30, No. 4, p. 2056 (1983).

PLAN VIEW OF FACILITY, COMMENTS



ENTRY No. C63

NAME OF MACHINE Cleveland Clinic Fast Neutron Therapy Facility
INSTITUTION ... National Aeronautics & Administrations Lewis Research Center
ADDRESS ..... M. S. 49-2 ....21000 Brookpark Rd. ..Cleveland, OH 44135
TEL ..(216). 433-6379..... TELEX
IN CHARGE ... James. Blue ..... REPORTED BY ... James. Blue

HISTORY AND STATUS

DESIGN, date ...Ref. 1 ..... Model tests .....
ENG DESIGN, date ..1968-69.....
CONSTRUCTION, date .....1970 .....
FIRST BEAM, date (or goal) ...1972.....
MAJOR ALTERATIONS ..Vertical and horizontal beams of fast neutrons for cancer therapy.....
COST, ACCELERATOR ..... $ 1.5 M.....
COST, FACILITY, total ..... $ 2.0 M.....
FUNDED BY .. NASA, Cleveland Clinic, NCI.....

ACCELERATOR STAFF, OPERATION AND DEVELOPMENT

SCIENTISTS .....0..... ENGINEERS ...1.....
TECHNICIANS .....1..... CRAFTS .....1.....
GRAD STUDENTS involved during year ... 0.....
OPERATED BY ..... Research staff or .....1... Operators
OPERATION ...30..... hr/wk, On target ..... hr/wk
TIME DISTR. in house .... 90..... %, Outside ...10..... %
BUDGET, op & dev .....$ 75,000.....
FUNDED BY .....NCI.....

RESEARCH STAFF, not included above

USERS, in house ....2..... outside .....10.....
GRAD STUDENTS involved during year .....0.....
RESEARCH BUDGET, in house .....$ 25,000.....
FUNDED BY .....NCI, NASA.....

MAGNET

POLE FACE, diameter (compact) 175 cm, R extraction 73.5 cm
R injection ....1.5.. cm
GAP, min ....17... cm, Field .....19.2.. kG } at .....
max ....41... cm, Field .....8.8.. kG } Ampere turns
AVERAGE FIELD at R ext ..... kG
B max/ <B> .....
NUMBER OF SECTORS { compact ...3.. / separated ..... } Spiral, max .. deg
SECTOR ANGLE (SSC) ..... deg
TRIMMING COILS ....8 pair.....
.....
CONDUCTOR, material and type ..copper-hollow H_2O cooled.
STORED ENERGY (cryogenic) ..... MJ
POWER : main coils .250.. max, kW ; current stability .10...
trimming coils ..10.. max, kW ; current stability .100..
WEIGHT : Fe ...206..... tons ; coils ....28..... tons
COOLING system ...deionized water.....
ION ENERGY (bending limit) E/A = ...55... q^2/a^2 MeV/amu
(focusing limit) E/A = ...45... q^2/a^2 MeV/amu

ACCELERATION SYSTEM

DEES, number .....2..... ; angle ....134..... deg
BEAM APERTURE ..2.5.... cm ; DC Bias ....0..... kV
TUNED by, coarse ...panels.... fine ...panels.....
RF ..13.6..... to .....23... mHz, stable ± ...10^{-8}.....
Orb F ..6.7.... to .....23... mHz
HARMONICS, RF/Orb F, used ....1 & 2.....
DEE - Gnd, max ..70.. kV, min gap .....5..... cm
STABILITY, (pk-pk noise)/(pk RF volt) .....
ENERGY GAIN, max .....220..... kV/turn
RF PHASE, stable to ± .....2..... deg
RF POWER input, max ....200..... kW
FREQUENCY MODULATION, rate ..... /s
modulator, type .....
beam pulse, width .....

VACUUM SYSTEM

OPERATING PRESSURE ....10^{-5}..... Torr or mbar
PUMPS, No, Type, Size ..two 40 cm diam. diffusion pumps.
.....with freon baffles.....
.....

ION SOURCES

.....Internal, hopped, hot filament.....

INJECTION SYSTEM

.....

EXTRACTION SYSTEM

..Electrostatic deflector and magnetic channel.....

FACILITIES FOR RESEARCH

SHIELDED AREA, fixed ..... m^3 ; movable ..... m^3
TARGET STATIONS ....3.... in ..two.... rooms
STATIONS served at same time, max .....1.....
MAG SPECTROGRAPH, type .....none.....
COMPUTER model ...two. IBM-PC .....
OTHER FACILITIES ..Cobalt-60 teletherapy unit.....
.....
.....

CHARACTERISTIC BEAMS

PARTICLE	ENERGY (MeV) Goal	Achieved	CURRENT (pμA) Internal	External
p	50	46		50
d	26	26		50
^{3}He	80	80		5
^{4}He	52	52		5

SECONDARY (part/s)
neutrons from 43 MeV p on Be yields 20 rad/min.....
125 cm .$$0.....

BEAM PROPERTIES

MEASURED	CONDITIONS
PULSE WIDTH ..... RF deg	..... pμ A of .... MeV ... ions
PHASE EXC, max ... RF deg	..... pμ A of .... MeV ... ions
EXTRACT eff ...60.. %	..30... pμ A of 43.. MeV p.. ions
RESOL ΔE/E ..... %	..... pμ A of .... MeV ... ions

EMITTANCE
(π mm. mrad) { ... axial / .... rad } ..... pμA of ..... MeV ... ions

OPERATING PROGRAMS, time distribution

BASIC NUCLEAR PHYSICS .. SOLID STATES PHYSICS ....
BIOMEDICAL APPLICAT. . 95% ISOTOPE PRODUCTIONS 1.%.
RADIATION DAMAGE .....4%.....
.....

REFERENCES/NOTES

1) Modified 60" fixed freq. cycl. to MSU magnetic field and dee design with redesigned rf system.

PLAN VIEW OF FACILITY, NOTEWORTHY FEATURES. COMMENTS

ENTRY NO. C64 **Date** June 26, 1992

Name of Machine: Texas A&M K500 Cyclotron

Institution: Texas A&M University

Address: College Station, Texas USA 77843-3366

Tel (409) 845-1411 Telex (510) 892-7689 Fax (409) 845-1899 EMAIL OFFICE@TAMCOMP

In Charge: J. B. Natowitz Reported by: R. C. Rogers

HISTORY

MILESTONE DATES:
Design 1980 Model Tests
Construction 1982-1988 First Beam June 15, 1988

DESIGN/CONSTRUCTION BY:
in house 80% other 20%

COST: Accelerator $8,500,000 Facility $36,000,000

FUNDED BY: Texas A&M University, Welch Foundation

STATUS

STAFF: Machine
Scientists 3 Engineers 5
Technicians 20 Students
Research (in house/external)
Scientists 20 / Engineers 34 /
Technicians / Students /

BUDGET: Machine $2,000,000 Funded by State of Texas, DOE
Research $1,500,000 Funded by DOE, Welch, NSF

TIME DISTRIBUTION:
Basic Research (in house/external) 90 % / 10 %
Applied Program (in house/external) % /
Development 14 % Maintenance 25 %

MAGNET

POLE PARAMETERS:
Diameter 142 cm $R_{extract}$ 67 cm R_{inject} 0.8 cm
HILL PARAMETERS: Gap (min) 6.35 cm B_{max} 5.8 T
(@ $4.7X10^6$ AT) Gap (max) -- cm B_{min} -- T
VALLEY PARAMETERS: Gap (min) 91.4 cm B_{max} 4.3 T
(@ $4.7X10^6$ AT) Gap (max) -- cm B_{min} -- T
AVERAGE FIELD: $< B >_{min}$ T $< B >_{max}$ 4.9 T
NUMBER OF SECTORS: compact/separated 3 /
sector angle 60° deg. spiral (max) 113.5 deg.
FIELD TRIMMING: Trim Coils 13
Harmonic Coils 2
Other
CURRENT: Main Coils 800 Amps Stability 2X10-5
Trim Coils 400 Amps Stability $1X10^{-4}$
Stored Energy (cryogenic) 22 MJ
WEIGHT: Iron 100 Conductor NbTi in Cu
ION ENERGY: Bending Limit E/A = 520 q^2/A^2 MeV/u
Focussing Limit E/A = 160 q/A MeV/u

ACCELERATION SYSTEM

FUNDAMENTAL ACCELERATION:
Description: 3, 53° DEES
No. of Gaps/turn 6 dE/dn(max) 0.24 MeV/q
Voltage(max) 0.08 MV Harmonic f_{rf}/f_{ion} 1,2
Freq 9-28 MHz Power in(max) 0.24 MW
Stability: Phase < 0.1 Voltage 10^{-4}

OTHER CAVITIES (Flattopping or otherwise):
Description:
Region of Influence: R_{min} cm R_{max} cm
No. of Gaps/turn dE/dn(max) MeV/q
Voltage(max) MV Harmonic f_{rf}/f_{ion}
Freq MHz Power in(max) MW
Stability: Phase Voltage

VACUUM SYSTEM

OPERATING PRESSURE: $6X10^{-8}$ to $2X10^{-7}$ Torr
PUMPS: No. and type 3 turbomolecular, 1 cryopanel,
2 cryopanels to be added late 1992

ION SOURCE(S)

	Type	Intensity (mA)	@	$\epsilon_n = \beta\gamma\epsilon$ (πmm mrad)	Ion Species
(a)	Ext RT ECR	.019		–	$^{14}N^{6+}$
(b)		.001			$^{181}Ta^{27+}$
(c)					
(d)					

INJECTION SYSTEM

Axial, Buncher, Spiral, Inflector Efficiency 4-20 %

EXTRACTION SYSTEM

Electrostatic + Magnetic Efficiency 15-50 %

CHARACTERISTIC BEAMS

Accelerated Ions	E/A (MeV/u)	Current(part μA) Internal	External
(a) D^+	65	0.06	0.015
(b) $^{12}C^{5+}$	50	0.012	0.003
(c) $^{40}Ar^{14+}$	40	0.0005	0.00025
(d) $^{181}Ta^{24+}$	6	0.004	0.001

Secondary Particles	E (MeV)	part/sec
(a)		
(b)		
(c)		

EXTRACTED BEAM PROPERTIES:
For μA of MeV/u ions
$\Delta E/E$ % $\Delta\phi$ °rf
$\epsilon_n = \beta\gamma\epsilon$ x πmm mrad z πmm mrad

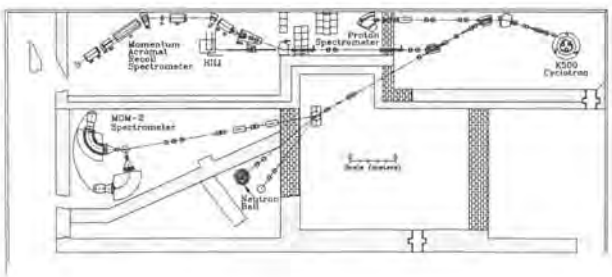
FACILITIES FOR RESEARCH

SHIELDED AREA: Fixed 720 m² Moveable m²
Target Stations: 9 No. Served At Same Time: 1
MAGNETIC SPECTROMETERS: 3
OTHER FACILITIES: Neutron Ball, 4π Charged Particle Detector (HILI+CsI Ball), BaF2 Array

REFERENCES/NOTES

(a)
(b)

PLAN VIEW OF FACILITY, COMMENTS



ENTRY NO. C65 Date

Name of Machine: University of California Davis 76" Cyclotron

Institution: Crocker Nuclear Laboratory (CNL)

Address: University of California, Crocker Nuclear Laboratory, Davis, CA, USA 95616-8569

Tel: (916) 752-1460 Telex: Fax: (916) 752-0952 EMAIL: rgflocchini@UCdavis.edu

In Charge: Dr. Robert G. Flocchini, Director Reported by: CNL Personnel

HISTORY

MILESTONE DATES:

Design: ORIC Copy Model Tests:

Construction: 1964-1966 First Beam: 1966

DESIGN/CONSTRUCTION BY:

in house: other: W.M. Brobeck & Associates

COST: Accelerator: $1,400,000. Facility: $4,500,000.

FUNDED BY: AEC

STATUS

STAFF: Machine

Scientists: 1 Engineers: None

Technicians: 8 Students: 2

Research (in house/external)

Scientists: / Engineers: /

Technicians: / Students: /

BUDGET: Machine: Funded by: Recharge

Research: Funded by: Recharge to Grant of User.

TIME DISTRIBUTION:

Basic Research (in house/external): 5 % / %

Applied Program (in house/external): 35 % / 30 %

Development: % Maintenance: 15 %

MAGNET

POLE PARAMETERS:

Diameter: 193 cm $R_{extract}$: 80 cm R_{inject}: cm

HILL PARAMETERS: Gap (min): 19 cm B_{max}: 2.27 T

(@ AT) Gap (max): cm B_{min}: T

VALLEY PARAMETERS: Gap (min): 71 cm B_{max}: T

(@ AT) Gap (max): cm B_{min}: 1.27 T

AVERAGE FIELD: $< B >_{min}$: T $< B >_{max}$: 1.75 T

NUMBER OF SECTORS: compact/separated: 3 /

sector angle: deg. spiral (max): 30 deg.

FIELD TRIMMING: Trim Coils: 10

Harmonic Coils: 3

Other: 3 Valley Coils

CURRENT: Main Coils: 4,000 Amps Stability: 5×10^{-4}

Trim Coils: 800 Amps Stability: 5×10^{-4}

Stored Energy (cryogenic): MJ

WEIGHT: Iron: 268 Conductor: 42

ION ENERGY: Bending Limit E/A = 90 q^2/A^2 MeV/u

Focussing Limit E/A = q/A MeV/u

ACCELERATION SYSTEM

FUNDAMENTAL ACCELERATION:

Description: Dee 1

No. of Gaps/turn: 2 dE/dn(max): 0.14 MeV/q

Voltage(max): 0.07 MV Harmonic f_{rf}/f_{ion}: 3:1

Freq: 7.3 to 22.5 MHz Power in(max): 0.15 MW

Stability: Phase: ± 10 Deg. Voltage: 0.005

OTHER CAVITIES (Flattopping or otherwise):

Description: None

Region of Influence: R_{min}: cm R_{max}: cm

No. of Gaps/turn: dE/dn(max): MeV/q

Voltage(max): MV Harmonic f_{rf}/f_{ion}:

Freq: MHz Power in(max): MW

Stability: Phase: Voltage:

VACUUM SYSTEM

OPERATING PRESSURE: 10^{-7} Torr

PUMPS: No. and type: 32 in., 35 in., Diffusion Pumps

Two 300 CFM Mechechanical Pumps

ION SOURCE(S)

	Type	Intensity (mA)	@	$\epsilon_n = \beta\gamma\epsilon$ (πmm mrad)	Ion Species
(a)	P.I.G. Hot Fil. 2.0ma				Positive Ion
(b)					
(c)					
(d)					

INJECTION SYSTEM

None Efficiency: %

EXTRACTION SYSTEM

Electrostatic + 2 Magnetic Efficiency: 30-90 %

CHARACTERISTIC BEAMS

	Accelerated Ions	E/A (MeV/u)	Current(part μA) Internal	External
(a)	Protons	4 - 68	60	30
(b)	Deutrons	15 - 45	60	30
(c)	Alphas	16 - 90	60	30
(d)				

	Secondary Particles	E (MeV)	part/sec
(a)	Neutron		15 - 65 x 10^6
(b)			
(c)			

EXTRACTED BEAM PROPERTIES:

For 1.0 μA of 67.5 MeV/u Proton ions

$\Delta E/E$: 0.4 % $\Delta\phi$: °rf

$\epsilon_n = \beta\gamma\epsilon$ x: πmm mrad z: πmm mrad

FACILITIES FOR RESEARCH

SHIELDED AREA: Fixed: 360 m² Moveable: None m²

Target Stations: 9 No. Served At Same Time: 1

MAGNETIC SPECTROMETERS:

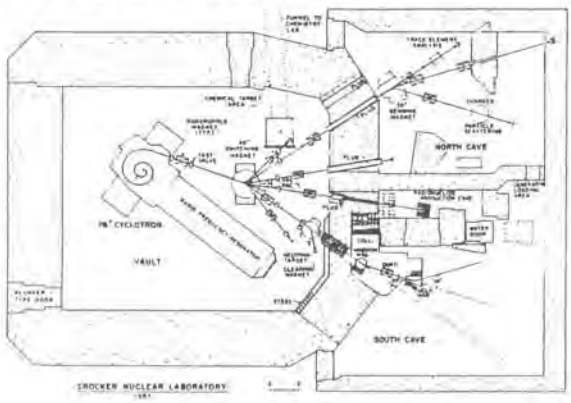
OTHER FACILITIES:

REFERENCES/NOTES

(a)

(b)

PLAN VIEW OF FACILITY, COMMENTS



ENTRY NO. C66 **Date** JULY 1992

Name of Machine HARPER HOSPITAL K100 (BUILT AT NATIONAL SUPERCONDUCTING CYCLOTRON LAB., E. LANSING)

Institution GERSHENSON RADIATION ONCOLOGY CENTER, HARPER HOSPITAL

Address 3990 JOHN R., DETROIT, MI 48201, U.S.A.

Tel (313) 745-9191 Telex — Fax (313) 745-2314 EMAIL —

In Charge: R.L. MAUGHAN Reported by: R.L. MAUGHAN

HISTORY

MILESTONE DATES:
Design 81-84 Model Tests 83-85
Construction 84-89 First Beam APRIL 1989

DESIGN/CONSTRUCTION BY:
in house NO other NSCL, MSU, E. LANSING

COST: Accelerator $2,000,000 US Facility $5,000,000 U.S.

FUNDED BY: HARPER HOSPITAL, INC.

STATUS

STAFF: Machine
Scientists 1 Engineers 2
Technicians 1 Students —
Research (in house/external)
Scientists 1 / — Engineers — / —
Technicians 1 / — Students — / —

BUDGET: Machine $400,000 US. Funded by HARPER HOSP.
Research $60,000 US. Funded by VARIOUS

TIME DISTRIBUTION:
Basic Research (in house/external) 10 % / — %
Applied Program (in house/external) 70 % / — %
Development 15 % Maintenance 5 %

MAGNET

POLE PARAMETERS:
Diameter — cm $R_{extract}$ 30 cm R_{inject} — cm
HILL PARAMETERS: Gap (min) 3.8 cm B_{max} 55.3 T
(@ — AT) Gap (max) — cm B_{min} — T
VALLEY PARAMETERS: Gap (min) 40.6 cm B_{max} 40.7 T
(@ — AT) Gap (max) — cm B_{min} — T
AVERAGE FIELD: $<B>_{min}$ — T $<B>_{max}$ — T
NUMBER OF SECTORS: compact/separated 3 / —
sector angle — deg. spiral (max) — deg.
FIELD TRIMMING: Trim Coils NONE
Harmonic Coils NONE
Other —
CURRENT: Main Coils 203 Amps Stability 5 X 10-5
Trim Coils — Amps Stability —
Stored Energy (cryogenic) 2.0 MJ
WEIGHT: Iron 24 US TONS Conductor NbTi IN CU
ION ENERGY: Bending Limit E/A = 100 q^2/A^2 MeV/u
Focussing Limit E/A = 50 q/A MeV/u

ACCELERATION SYSTEM

FUNDAMENTAL ACCELERATION:
Description: 3-DEE/6 STEM DEES GALVANICALLY COUPLED
No. of Gaps/turn 3.6 dE/dn(max) 200 MeV/q
Voltage(max) 0.033 MV Harmonic f_{rf}/f_{ion} 3
Freq 105.000.0 MHz Power in(max) 0.025 MW
Stability: Phase — Voltage —

OTHER CAVITIES (Flattopping or otherwise):
Description: NONE
Region of Influence: R_{min} — cm R_{max} — cm
No. of Gaps/turn — dE/dn(max) — MeV/q
Voltage(max) — MV Harmonic f_{rf}/f_{ion} —
Freq — MHz Power in(max) — MW
Stability: Phase — Voltage —

VACUUM SYSTEM

OPERATING PRESSURE: 1×10^{-5}
PUMPS: No. and type 2 TURBO
300 L/SEC

ION SOURCE(S)

	Type	Intensity (mA)	@	$\epsilon_n = \beta\gamma\epsilon$ (πmm mrad)	Ion Species
(a)	COLD CATHODE	—		—	d
(b)					
(c)					
(d)					

INJECTION SYSTEM

NONE Efficiency — %

EXTRACTION SYSTEM

NONE Efficiency — %

CHARACTERISTIC BEAMS

	Accelerated Ions	E/A (MeV/u)	Current(part μA) Internal	External
(a)	DEUTERON	24.25	15	—
(b)	BEAM R-F IS PULSED. 2MS ON, 8 MS OFF			
(c)	PEAK BEAM DURING PULSE 180 μA			
(d)				

	Secondary Particles	E (MeV)	part/sec
(a)	NEUTRON	(21)	48.5Gy/MIN.
(b)	(BERYLLIUM STOPPING)		FLATTENED
(c)	TARGET)		

EXTRACTED BEAM PROPERTIES:
For — μA of — MeV/u — ions
$\Delta E/E$ — % $\Delta\phi$ — °rf
$\epsilon_n = \beta\gamma\epsilon$ x — πmm mrad z — πmm mrad

FACILITIES FOR RESEARCH

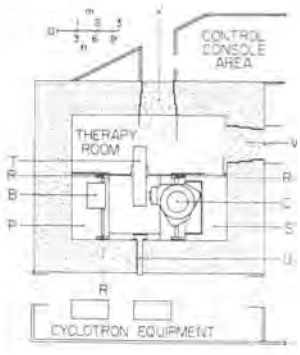
SHIELDED AREA: Fixed 47 m^2 Moveable NONE m^2
Target Stations: 1 No. Served At Same Time: 1
MAGNETIC SPECTROMETERS: NONE
OTHER FACILITIES: ISOCENTRIC GANTRY, VARIABLE MULTI-ROD COLLIMATION SYSTEM FOR NEUTRON RADIATION THERAPY

REFERENCES/NOTES

(a) IEEE TRANS. ON NUCL. SCI. NS-32 (1985) 3287
(b) H. BLOSSER, PROC. 13TH INT. CONF. ON CYC. (1992) IN PRESS.

PLAN VIEW OF FACILITY, COMMENTS

V-VERTICAL LIFT DOOR
T-THERAPY COUCH
B-COUNTERWEIGHT
R-GANTRY RINGS
C-CYCLOTRON
U-UTILITY ARM
S-SERVICE PLATFORM
P-PIT AREA



ENTRY NO. C67 **Date** July 1992

Name of Machine K500

Institution Michigan State University

Address NSCL/CYCLOTRON LABORATORY, MICHIGAN 48824-1321 USA

Tel 517-355-9671 Telex 5106019207 NATSUPCYCLAB Fax 517-353-5967 **EMAIL** BITNET:Miller@MSUNSCL

In Charge: C.K. GELBKE **Reported by:** P. MILLER

HISTORY

MILESTONE DATES:

Design 74-79 Model Tests 75-77

Construction 77-81 First Beam 8/82

DESIGN/CONSTRUCTION BY:

in house ..... other .....

COST: Accelerator $2,900,000 Facility $3,500,000

FUNDED BY: National Science Foundation

STATUS

STAFF: Machine

Scientists ..... Engineers .....

Technicians ..... Students .....

Research (in house/external)

Scientists ..... / ..... Engineers ..... / .....

Technicians ..... / ..... Students ..... / .....

BUDGET: Machine ..... Funded by .....

Research ..... Funded by .....

TIME DISTRIBUTION:

Basic Research (in house/external) ..... % / ..... %

Applied Program (in house/external) ..... % / ..... %

Development ..... % Maintenance ..... %

MAGNET

POLE PARAMETERS:

Diameter 142 cm $R_{extract}$ 67 cm R_{inject} 1 cm

HILL PARAMETERS: Gap (min) 6.35 cm B_{max} 5.8 T

(@ 4.681 MAT) Gap (max) 91.4 cm B_{min} 4.3 T

VALLEY PARAMETERS: Gap (min) ..... cm B_{max} ..... T

(@ ..... AT) Gap (max) ..... cm B_{min} ..... T

AVERAGE FIELD: $< B >_{min}$ 3.0 T $< B >_{max}$ 4.95 T

NUMBER OF SECTORS: compact/separated 3 / .....

sector angle ..... deg. spiral (max) 120 deg.

FIELD TRIMMING: Trim Coils (13x3) + 1

Harmonic Coils 2x3

Other .....

CURRENT: Main Coils 700 Amps Stability 1/10^5

Trim Coils 400 Amps Stability 6/10^4

Stored Energy (cryogenic) 18 MJ

WEIGHT: Iron 100 US ton Conductor 8 US ton

ION ENERGY: Bending Limit E/A = 520 q^2/A^2 MeV/u

Focussing Limit E/A = 160 q/A MeV/u

ACCELERATION SYSTEM

FUNDAMENTAL ACCELERATION:

Description: 3 half wavelength cavities, 120° phasing

No. of Gaps/turn 6 dE/dn(max) 0.51 MeV/q

Voltage(max) 0.1 MV Harmonic f_{rf}/f_{ion} 1,2

Freq 9-27 MHz Power in(max) 0.42 MW

Stability: Phase ..... Voltage 1/10^4

OTHER CAVITIES (Flattopping or otherwise):

Description: .....

Region of Influence: R_{min} ..... cm R_{max} ..... cm

No. of Gaps/turn ..... dE/dn(max) ..... MeV/q

Voltage(max) ..... MV Harmonic f_{rf}/f_{ion} .....

Freq ..... MHz Power in(max) ..... MW

Stability: Phase ..... Voltage .....

VACUUM SYSTEM

OPERATING PRESSURE: 3×10^{-6} Torr

PUMPS: No. and type 2 cryopanels, 7K, charcoal,

3 turbomolecular pumps

ION SOURCE(S)

	Type	Intensity (mA)	@	$\epsilon_n = \beta\gamma\epsilon$ (πmm mrad)	Ion Species
(a)	RTECR	1.0		0.1-0.2	all
(b)	CPECR	1.0		0.1-0.2	alkali metals
(c)	SCECR	3.0		0.1-0.3	all
(d)					

INJECTION SYSTEM

Buncher, spiral inflector ..... Efficiency 10 %

EXTRACTION SYSTEM

Precessional, 2 elec. defl ..... Efficiency 50 %

CHARACTERISTIC BEAMS

	Accelerated Ions	E/A (MeV/u)	Current(part μA) Internal	External
(a)	$^{4}He^{2+}$	54	1	.05
(b)	$^{14}N^{6+}$	50	.01	.007
(c)	$^{40}Ar^{12+}$	35	.004	.0002
(d)	$^{86}Kr^{19+}$	20	.00026	.0001

	Secondary Particles	E (MeV)	part/sec
(a)			
(b)			
(c)			

EXTRACTED BEAM PROPERTIES:

For ..... μA of ..... MeV/u ..... ions

$\Delta E/E$ ..... % $\Delta\phi$ ..... °rf

$\epsilon_n = \beta\gamma\epsilon$ x ..... πmm mrad z ..... πmm mrad

FACILITIES FOR RESEARCH

SHIELDED AREA: Fixed ..... m² Moveable 1300 m²

Target Stations: 6 No. Served At Same Time: 1

MAGNETIC SPECTROMETERS: S320

OTHER FACILITIES: 4 pi array, miniball, Reaction Product Mass Spectrometer, 92 inches Scattering Chamber, 7T Solenoid

REFERENCES/NOTES

(a) IEEE Trans. on Nuc. Sci. NS-26(1979)2040 3653

(b) MSU Annual Report 1974-1985

PLAN VIEW OF FACILITY, COMMENTS

ENTRY NO. C68 **Date** July 1992

Name of Machine K1200 (formerly K800)

Institution MICHIGAN STATE UNIVERSITY

Address NSCL/CYCLOTRON LABORATORY, EAST LANSING, MICHIGAN 48824-1321 USA

Tel 517-355-9671 Telex 5106019207 NATSUPCYCLAB Fax 517-353-5967 EMAIL BITNET:Miller@MSUNSCL

In Charge: C.K. GELBKE Reported by: P. MILLER

HISTORY

MILESTONE DATES:

Design 76-86 Model Tests

Construction 80-87 First Beam 6/88

DESIGN/CONSTRUCTION BY:

in house other

COST: Accelerator 7,500,000 Facility 35,000,000

FUNDED BY: DOE(1980-82), NSF(1983-present)

STATUS

STAFF: Machine

Scientists Engineers

Technicians Students

Research (in house/external)

Scientists / Engineers /

Technicians / Students /

BUDGET: Machine Funded by

Research Funded by

TIME DISTRIBUTION:

Basic Research (in house/external) % / %

Applied Program (in house/external) % / %

Development % Maintenance %

MAGNET

POLE PARAMETERS:

Diameter 219.7 cm $R_{extract}$ 103 cm R_{inject} 1 cm

HILL PARAMETERS: Gap (min) 7.6 cm B_{max} 6.2 T

(@ 7.2x10^6 AT) Gap (max) 91.4 cm B_{min} 4.5 T

VALLEY PARAMETERS: Gap (min) cm B_{max} T

(@ AT) Gap (max) cm B_{min} T

AVERAGE FIELD: $< B >_{min}$ 3.0 T $< B >_{max}$ 5.3 T

NUMBER OF SECTORS: compact/separated 3 /

sector angle deg. spiral (max) 176 deg.

FIELD TRIMMING: Trim Coils (21x3)+1

Harmonic Coils (2x3)

Other

CURRENT: Main Coils 900 Amps Stability 1/105

Trim Coils 400 Amps Stability 6/104

Stored Energy (cryogenic) 60 MJ

WEIGHT: Iron 265 US ton Conductor 22US ton

ION ENERGY: Bending Limit E/A = 1200 q^2/A^2 MeV/u

Focussing Limit E/A = 400 q/A MeV/u

ACCELERATION SYSTEM

FUNDAMENTAL ACCELERATION:

Description: 3 half wavelength cavities, 120° phasing

No. of Gaps/turn 6 dE/dn(max) 0.48 MeV/q

Voltage(max) 0.160 MV Harmonic f_{rf}/f_{ion} 1

Freq 9-27 MHz Power in(max) 0.92 MW

Stability: Phase Voltage 1/10^4

OTHER CAVITIES (Flattopping or otherwise):

Description:

Region of Influence: R_{min} cm R_{max} cm

No. of Gaps/turn dE/dn(max) MeV/q

Voltage(max) MV Harmonic f_{rf}/f_{ion}

Freq MHz Power in(max) MW

Stability: Phase Voltage

VACUUM SYSTEM

OPERATING PRESSURE: 1x10^{-6} Torr

PUMPS: No. and type 2 cryopanels, 7K, Cu

2500 l/s/panel. 3 turbomolecular pumps

ION SOURCE(S)

	Type	Intensity (mA)	@	$\epsilon_n = \beta\gamma\epsilon$ (πmm mrad)	Ion Species
(a)	RTECR	1.0		0.1-0.2	all
(b)	CPECR	1.0		0.1-0.2	alkali metals
(c)	SCECR	3.0		0.1-0.3	all
(d)					

INJECTION SYSTEM

Buncher, spiral inflector Efficiency 10 %

EXTRACTION SYSTEM

Precessional, 2 elec. defl. Efficiency 50 %

CHARACTERISTIC BEAMS

	Accelerated Ions	E/A (MeV/u)	Current(part μA) Internal	External
(a)	$^4He^{2+}$	155		3.8x10^{-3}
(b)	$^{20}Ne^{9+}$	125	1.3x10^{-3}	0.7x10^{-3}
(c)	$^{129}Xe^{31+}$	65		0.5x10^{-6}
(d)	$^{238}U^{39+}$	25	3.8x10^{-6}	0.44x10^{-6}

	Secondary Particles	E (MeV)	part/sec
(a)	^{11}Li	700	2500
(b)	^{20}Mg	1300	3.5
(c)	^{40}Cl	2200	1.6x10^6

EXTRACTED BEAM PROPERTIES:

For 0.5x10^{-3} μA of 75 MeV/u $^{40}Ar^{13+}$ ions

$\Delta E/E$ % $\Delta\phi$ °rf

$\epsilon_n = \beta\gamma\epsilon$ x 2 πmm mrad z 3 πmm mrad

FACILITIES FOR RESEARCH

SHIELDED AREA: Fixed m^2 Moveable 1300 m^2

Target Stations: 6 No. Served At Same Time: 1

MAGNETIC SPECTROMETERS: S320, S800, A1200

OTHER FACILITIES: 4 pi array, Miniball, Reaction Product Mass Spectrometer, 92 inches Scattering Chamber, 7T Solenoid

REFERENCES/NOTES

(a) MSU Reports MSUCP 29(June 80) & MSUCP 35(June 81)

(b) Proc. of 11th Int. Conf. on Cyc. (1986)157

PLAN VIEW OF FACILITY, COMMENTS

ENTRY NO. C69 Date June 26, 1992

Name of Machine Oak Ridge Isochronous Cyclotron

Institution Oak Ridge Nation Laboratory

Address P.O. Box 2008, Mail Stop 6368, Oak Ridge Tennessee 37831-6368, U.S.A.

Tel 615-574-4757 Telex 854468 Fax 615-574-1268 EMAIL

In Charge: D.K. Olsen Reported by: S.W. Mosko

HISTORY

MILESTONE DATES:

Design 1958 Model Tests 1958-59

Construction 1958-1962 First Beam 1963

DESIGN/CONSTRUCTION BY:

in house X other

COST: Accelerator $ 2.3 M Facility $ 24 M

FUNDED BY: US Department of Energy

STATUS

STAFF: Machine

Scientists 1 Engineers 3

Technicians 4 Students

Research (in house/external)

Scientists / Engineers /

Technicians / Students /

BUDGET: Machine Funded by

Research Funded by

TIME DISTRIBUTION:

Basic Research (in house/external) % / %

Applied Program (in house/external) % / %

Development % Maintenance %

MAGNET

POLE PARAMETERS:

Diameter 193 cm $R_{extract}$ 77 cm R_{inject} cm

HILL PARAMETERS: Gap (min) 19 cm B_{max} 2.37 T

(@ 16.5 / 20.5 AT) Gap (max) 71 cm B_{min} 1.40 T

VALLEY PARAMETERS: Gap (min) cm B_{max} T

(@ AT) Gap (max) cm B_{min} 1.92 T

AVERAGE FIELD: $< B >_{min}$ T $< B >_{max}$ T

NUMBER OF SECTORS: compact/separated 3 /

sector angle deg. spiral (max) 30. deg.

FIELD TRIMMING: Trim Coils 10. pairs

Harmonic Coils 4 pairs per valley

Other 5

CURRENT: Main Coils 5000 Amps Stability 2*10^{-4}

Trim Coils 800 Amps Stability 2*10^{-4}

Stored Energy (cryogenic) 3 MJ

WEIGHT: Iron 1.8*10^{6} Conductor 8.2*10^{3} kg

ION ENERGY: Bending Limit E/A = 100. q^2/A^2 MeV/u

Focussing Limit E/A = 75 q/A MeV/u

ACCELERATION SYSTEM

FUNDAMENTAL ACCELERATION:

Description: Single 180 degree dee

No. of Gaps/turn 2 dE/dn(max) 0.16 MeV/q

Voltage(max) 0.08 MV Harmonic f_{rf}/f_{ion} 1

Freq 6.7 to 20.1 MHz Power in(max) 0.20 MW

Stability: Phase ± 1 degree Voltage ± 40

OTHER CAVITIES (Flattopping or otherwise):

Description:

Region of Influence: R_{min} cm R_{max} cm

No. of Gaps/turn dE/dn(max) MeV/q

Voltage(max) MV Harmonic f_{rf}/f_{ion}

Freq MHz Power in(max) MW

Stability: Phase Voltage

VACUUM SYSTEM

OPERATING PRESSURE: 1*10^{-6} TORR

PUMPS: No. and type 2 / 80 cm oil diffusion pumps

1 / 50 cm oil diffusion pumps 1/50cm cryopump

ION SOURCE(S)

	Type	Intensity (mA)	@ $\epsilon_n = \beta\gamma\epsilon$ (πmm mrad)	Ion Species
(a)	Penning (Internal)			H^+
(b)				$^4H^+_2$
(c)				^4He
(d)	25 MV electrostatic tandem			

INJECTION SYSTEM

Radial with foil stripping Efficiency %

EXTRACTION SYSTEM

Electrostatic+2 magnetic channels. Efficiency 65 %

CHARACTERISTIC BEAMS

Accelerated Ions	E/A (MeV/u)	Current(part μA) Internal	External
(a) H^+	50		50uA
(b) Ni	17.4		0.03
(c) Sn	7.9		0.002
(d) Gd	5.6		0.001

	Secondary Particles	E (MeV)	part/sec
(a)			
(b)			
(c)			

EXTRACTED BEAM PROPERTIES:

For μA of MeV/u ions

$\Delta E/E$ % $\Delta\phi$ °rf

$\epsilon_n = \beta\gamma\epsilon$ x πmm mrad z πmm mrad

FACILITIES FOR RESEARCH

SHIELDED AREA: Fixed m² Moveable m²

Target Stations: No. Served At Same Time:

MAGNETIC SPECTROMETERS:

OTHER FACILITIES:

REFERENCES/NOTES

(a) Paper R3 in the proceedings of this conference

(b)

PLAN VIEW OF FACILITY, COMMENTS

Facility is beginning a 3 year reconfiguration program where the cyclotron will serve as the primary beam generator for the production of radioactive beams which will be accelerated in the HHIRF electrostatic tandem.

ENTRY No. C70

NAME OF MACHINE Princeton AVF Cyclotron DATE March 21, 1989
INSTITUTION PRINCETON UNIVERSITY, Department of Physics
ADDRESS Jadwin Hall, P.O. Box 708, Princeton, New Jersey 08544
TEL (609) 452-4425 TELEX 4993512/JADWIN TELEFAX: (609) 243-7300
IN CHARGE Robert A. Naumann REPORTED BY Richard T. Kouzes

HISTORY AND STATUS

DESIGN, date 1965 Model tests
ENG DESIGN, date 1966-1967
CONSTRUCTION, date 1967-1968
FIRST BEAM, date (or goal) December 1968
MAJOR ALTERATIONS None

COST, ACCELERATOR $1.45M
COST, FACILITY, total $3.0 M
FUNDED BY 70% University; 30% AEC

ACCELERATOR STAFF, OPERATION AND DEVELOPMENT

SCIENTISTS 0 ENGINEERS 1
TECHNICIANS 3 CRAFTS 0
GRAD STUDENTS involved during year 1
OPERATED BY X Research staff or Operators
OPERATION 60 hr/wk, On target 50 hr/wk
TIME DISTR. In house 75 %, Outside 25 %
BUDGET, op & dev $300K
FUNDED BY NSF

RESEARCH STAFF, not included above

USERS, In house 11 outside 34
GRAD STUDENTS involved during year 6
RESEARCH BUDGET, In house $800K
FUNDED BY NSF

MAGNET

POLE FACE, diameter (compact) 175 cm, R extraction 75 cm
R injection 2 cm
GAP, min 17 cm, Field 19.5 kG
max 50 cm, Field 8.0 kG } at .51x10^6 Ampere turns
AVERAGE FIELD at R ext 15 kG
B max/ <B> 1.3
NUMBER OF SECTORS { compact 3 / separated } Spiral, max ≤5 deg
SECTOR ANGLE (SSC) deg
TRIMMING COILS 8

CONDUCTOR, material and type Cu
STORED ENERGY (cryogenic) – MJ
POWER: main coils 175 max, kW ; current stability 10^{-5}
trimming coils 20 max, kW ; current stability 10^{-5}
WEIGHT: Fe 100 tons ; coils 16 tons
COOLING system Water
ION ENERGY (bending limit) E/A = 60 q^2/a^2 MeV/amu
(focusing limit) E/A = 60 q^2/a^2 MeV/amu

ACCELERATION SYSTEM

DEES, number 2 ; angle 134 deg
BEAM APERTURE 4.5 cm ; DC Bias 0 kV
TUNED by, coarse Movable Panels fine None
RF 14 to 23.5 mHz, stable ± 10^{-7}
Orb F 3.5 to 20.6 mHz
HARMONICS, RF/Orb F, used 1,2,4
DEE - Gnd, max 70 kV, min gap 1 cm
STABILITY, (pk-pk noise)/(pk RF volt) 0.001
ENERGY GAIN, max 250 kV/turn
RF PHASE, stable to ± 1 deg
RF POWER input, max 300 kW
FREQUENCY MODULATION, rate – /s
modulator, type –
beam pulse, width –

VACUUM SYSTEM

OPERATING PRESSURE $2.5x10^{-6}$ Torr or mbar
PUMPS, No, Type, Size 1 Diffusion 32 inch

ION SOURCES

Hooded Arc; Cold Cathode

INJECTION SYSTEM

Internal Injection

EXTRACTION SYSTEM

Electrostatic & Magnetic

FACILITIES FOR RESEARCH

SHIELDED AREA, fixed 0 m² ; movable 325 m²
TARGET STATIONS 8 In 4 rooms
STATIONS served at same time, max 1
MAG SPECTROGRAPH, type 14 msr, QDDD, p/Δp=10^4
COMPUTER model Data General MV4000, MV10000
OTHER FACILITIES Scattering Chambers 150 cm; On-Line Recirculating Gas Target; Bombardement Box, Laser Polarized Target, On-Line Isotope Separator

CHARACTERISTIC BEAMS

PARTICLE	ENERGY (MeV) Goal	Achieved	CURRENT (pμA) Internal	External
p	50	48		20
d	30	28		15
^{3}He	75	85		8
α	60	58		8
SECONDARY				(part/s)

BEAM PROPERTIES

	MEASURED	CONDITIONS
PULSE WIDTH ±1.8° RF deg	1	pμ A of .42 MeV p. Ions
PHASE EXC, max RF deg		pμ A of MeV Ions
EXTRACT eff 95 %	1	pμ A of .42 MeV p. Ions
RESOL ΔE/E .05 %	1	pμ A of .42 MeV p. Ions
EMITTANCE (π mm. mrad) { .20 axial / .3 rad }	1	pμA of .42 MeV p. Ions

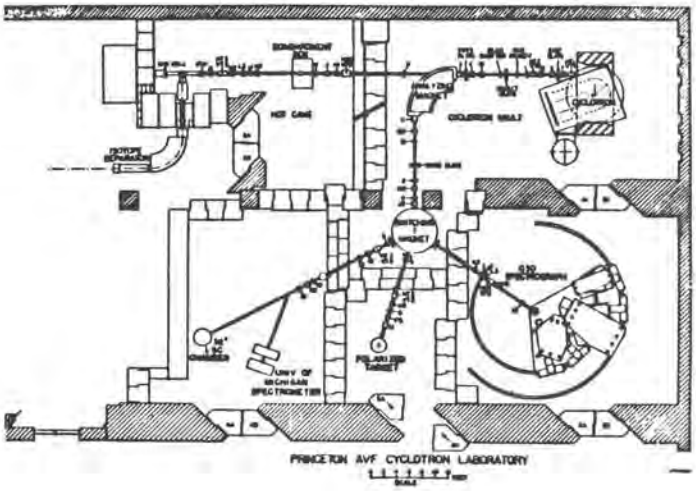
OPERATING PROGRAMS, time distribution

BASIC NUCLEAR PHYSICS 100 SOLID STATES PHYSICS 0
BIOMEDICAL APPLICAT. 0 ISOTOPE PRODUCTIONS 0

REFERENCES/NOTES

1) Pollock, R.E., Proceedings of the Fifth International Cyclotron Conference (1969), p. 120.

PLAN VIEW OF FACILITY, NOTEWORTHY FEATURES, COMMENTS



ENTRY No. C71

NAME OF MACHINE W.U.Sector Focused Cyclotron DATE 7/15/81
INSTITUTION Washington University
ADDRESS Box 1134, St. Louis, Missouri 63130, U.S.A.
TEL 314-889-6579 TELEX
IN CHARGE John T. Hood REPORTED BY John T. Hood

HISTORY AND STATUS
DESIGN, date 1960 Model tests 1961-62
ENG DESIGN, date 1961-63
CONSTRUCTION, date 1962-65
FIRST BEAM, date (or goal) 1965
MAJOR ALTERATIONS

COST, ACCELERATOR
COST, FACILITY, total
FUNDED BY AFOSR, NSF

ACCELERATOR STAFF, OPERATION AND DEVELOPMENT
SCIENTISTS ENGINEERS 1
TECHNICIANS CRAFTS 1
GRAD STUDENTS involved during year
OPERATED BY Research staff or x Operators
OPERATION 12 hr/wk, On target 10 hr/wk
TIME DISTR. in house %, Outside %
BUDGET, op & dev
FUNDED BY Washington University

RESEARCH STAFF, not included above
USERS, in house 4 outside 1
GRAD STUDENTS involved during year 6
RESEARCH BUDGET, in house
FUNDED BY

MAGNET
POLE FACE, diameter (compact) 137 cm, R extraction 54.5 cm
R injection cm
GAP, min 14.8 cm, Field 17.8 kG
max 33.8 cm, Field 10.3 kG
at 46 X 10^6 Ampere turns
AVERAGE FIELD at R ext 14 kG
B max/ <B>
NUMBER OF SECTORS compact 3 / separated; Spiral, max deg
SECTOR ANGLE (SSC) deg
TRIMMING COILS 5 pairs radial
4 pairs/sector first harmonic
CONDUCTOR, material and type copper strap
STORED ENERGY (cryogenic) MJ
POWER: main coils 120 max, kW ; current stability
trimming coils 60 max, kW ; current stability
WEIGHT: Fe 82 tons ; coils 12 tons
COOLING system oil
ION ENERGY (bending limit) E/A = q^2/a^2 MeV/amu
(focusing limit) E/A = q^2/a^2 MeV/amu

ACCELERATION SYSTEM
DEES, number 1 ; angle 180 deg
BEAM APERTURE 3.2 cm ; DC Bias 0 kV
TUNED by, coarse MS fine VC, Auto
RF 7 to 16 mHz, stable ±
Orb F 7 to 16 mHz
HARMONICS, RF/Orb F, used
DEE - Gnd, max 60 kV, min gap 1 cm
STABILITY, (pk-pk noise)/(pk RF volt)
ENERGY GAIN, max kV/turn
RF PHASE, stable to ± deg
RF POWER input, max 100 kW
FREQUENCY MODULATION, rate /s
modulator, type
beam pulse, width

VACUUM SYSTEM
OPERATING PRESSURE 20 μ Torr or mbar
PUMPS, No, Type, Size 2 - oil diffusion
Twenty and seven inch

ION SOURCES
Penning, Hot Filament

INJECTION SYSTEM

EXTRACTION SYSTEM
Electrostatic and Magnetic Channel

FACILITIES FOR RESEARCH
SHIELDED AREA, fixed 100 m^2 ; movable m^2
TARGET STATIONS 6 in 2 rooms
STATIONS served at same time, max 1
MAG SPECTROGRAPH, type
COMPUTER model
OTHER FACILITIES

CHARACTERISTIC BEAMS

PARTICLE	ENERGY (MeV) Goal	Achieved	CURRENT (pμA) Internal	External
α		12-30		10
^{3}He		9-37		20
p		12		20
d		15		20
SECONDARY			(part/s)	

BEAM PROPERTIES
MEASURED CONDITIONS
PULSE WIDTH RF deg pμ A of MeV ions
PHASE EXC, max RF deg pμ A of MeV ions
EXTRACT eff % pμ A of MeV ions
RESOL ΔE/E % pμ A of MeV ions
EMITTANCE
(π mm. mrad) axial / rad pμA of MeV ions

OPERATING PROGRAMS, time distribution
BASIC NUCLEAR PHYSICS 60% SOLID STATES PHYSICS
BIOMEDICAL APPLICAT. 20% ISOTOPE PRODUCTIONS 20%

REFERENCES/NOTES

PLAN VIEW OF FACILITY, NOTEWORTHY FEATURES, COMMENTS

ENTRY NO. C72 **Date** 25-AUG-92
Name of Machine 60" Cyclotron
Institution Brookhaven National Laboratory
Address Upton, NY 11973
Tel (516) 282-4551 Telex Fax (516) 282-7350 EMAIL schlyer@chm.chm.bnl.90
In Charge: A. P. Wolf Reported by: D. J. Schlyer

HISTORY

MILESTONE DATES:
Design 1963 Model Tests 1963
Construction 1964 First Beam 1968
DESIGN/CONSTRUCTION BY:
in house XX other
COST: Accelerator 400,000 Facility 950,000
FUNDED BY: USAEC-DOE

STATUS

STAFF: Machine
Scientists 1 Engineers
Technicians 2 Students
Research (in house/external)
Scientists 2 / 0 Engineers /
Technicians / Students /
BUDGET: Machine Funded by DOE-NIH
Research Funded by DOE-NIH
TIME DISTRIBUTION:
Basic Research (in house/external) 95 % / 5 %
Applied Program (in house/external) % / %
Development % Maintenance 5 %

MAGNET

POLE PARAMETERS:
Diameter 152 cm $R_{extract}$ 65 cm R_{inject} 0 cm
HILL PARAMETERS: Gap (min) cm B_{max} T
(@ AT) Gap (max) cm B_{min} T
VALLEY PARAMETERS: Gap (min) cm B_{max} T
(@ AT) Gap (max) cm B_{min} T
AVERAGE FIELD: $< B >_{min}$ 1 T $< B >_{max}$ 1.54 T
NUMBER OF SECTORS: compact/separated 3 /
sector angle deg. spiral (max) 50 deg.
FIELD TRIMMING: Trim Coils 8
Harmonic Coils 5
Other
CURRENT: Main Coils 1200 Amps Stability
Trim Coils 300 Amps Stability
Stored Energy (cryogenic) MJ
WEIGHT: Iron 196 Tons Conductor Cu hollow
ION ENERGY: Bending Limit E/A = q^2/A^2 MeV/u
Focussing Limit E/A = q/A MeV/u

ACCELERATION SYSTEM

FUNDAMENTAL ACCELERATION:
Description: 1 DEE, 1 DUMMY DEE @ 180°
No. of Gaps/turn 2 dE/dn(max) 0.120 MeV/q
Voltage(max) 0.060 MV Harmonic f_{rf}/f_{ion} 1.3
Freq MHz Power in(max) 0.100 MW
Stability: Phase Voltage
OTHER CAVITIES (Flattopping or otherwise):
Description:
Region of Influence: R_{min} cm R_{max} cm
No. of Gaps/turn dE/dn(max) MeV/q
Voltage(max) MV Harmonic f_{rf}/f_{ion}
Freq MHz Power in(max) MW
Stability: Phase Voltage

VACUUM SYSTEM

OPERATING PRESSURE: 1×10^{-5} Torr
PUMPS: No. and type 1 - Diffusion 24"

ION SOURCE(S)

	Type	Intensity (mA)	@	$\epsilon_n = \beta\gamma\epsilon$ (πmm mrad)	Ion Species
(a)	hot filament				H^+
(b)					
(c)					
(d)					

INJECTION SYSTEM

Efficiency %

EXTRACTION SYSTEM

Electrostatic Efficiency 10 %

CHARACTERISTIC BEAMS

	Accelerated Ions	E/A (MeV/u)	Current(part μA) Internal	External
(a)	H^+	34	300	25
(b)	D^+	23	300	20
(c)	$He\text{-}3^{++}$	56	200	10
(d)	$He\text{-}4^{++}$	46	200	10

	Secondary Particles	E (MeV)	part/sec
(a)			
(b)			
(c)			

EXTRACTED BEAM PROPERTIES:
For μA of MeV/u ions
$\Delta E/E$ % $\Delta\phi$ °rf
$\epsilon_n = \beta\gamma\epsilon$ x πmm mrad z πmm mrad

FACILITIES FOR RESEARCH

SHIELDED AREA: Fixed 100 m² Moveable m²
Target Stations: 2 No. Served At Same Time: 1
MAGNETIC SPECTROMETERS:
OTHER FACILITIES:

REFERENCES/NOTES

(a)
(b)

PLAN VIEW OF FACILITY, COMMENTS

ENTRY No. C73

NAME OF MACHINE NAVAL RESEARCH LABORATORY CYC DATE 7/24/78
INSTITUTION NAVAL RESEARCH LABORATORY, Radiation Technology Division
ADDRESS Washington, D.C. 20375, USA
TEL ..... TELEX .....
IN CHARGE Rollon O. Bondelid REPORTED BY Rollon O. Bondelid

HISTORY AND STATUS

DESIGN, date 1) Model tests 1)
ENG DESIGN, date 1963-1964
CONSTRUCTION, date 1965-1967
FIRST BEAM, date (or goal) int. 1967, ext. 1968
MAJOR ALTERATIONS 2)
COST, ACCELERATOR $ 1.8 10^6
COST, FACILITY, total $ 6.0 10^6
FUNDED BY U.S. Navy Department

ACCELERATOR STAFF, OPERATION AND DEVELOPMENT

SCIENTISTS 0 ENGINEERS 4
TECHNICIANS 6 CRAFTS 2
GRAD STUDENTS involved during year 3
OPERATED BY Research staff or Operators
OPERATION 52 hr/wk, On target 50 hr/wk
TIME DISTR. in house 60 %, Outside 40 %
BUDGET, op & dev
FUNDED BY Office of Naval Research & Users

RESEARCH STAFF, not included above

USERS, in house 11 outside 3
GRAD STUDENTS involved during year 3
RESEARCH BUDGET, in house 725 k
FUNDED BY Office of Naval Research

MAGNET

POLE FACE, diameter (compact) 19.3 , R extraction cm
R injection cm
GAP, min 19 cm, Field 22.7 kG
max 71 cm, Field 12.7 kG } at
AVERAGE FIELD at R ext 17 kG } Ampere turns
B max/ <B> 1.3
NUMBER OF SECTORS { compact 3 / separated } Spiral, max 30 deg
SECTOR ANGLE (SSC) deg
TRIMMING COILS Harmonic correction; 3/sect
10 circular coils
CONDUCTOR, material and type
STORED ENERGY (cryogenic) 6.5 MJ
POWER : main coils 800 max, kW ; current stability 5 10^-5
trimming coils 350 max, kW ; current stability
WEIGHT : Fe 250 tons ; coils 45 tons
COOLING system Demineralized water
ION ENERGY (bending limit) E/A = q²/a² MeV/amu
(focusing limit) E/A = 75 q²/a² MeV/amu

ACCELERATION SYSTEM

DEES, number 1 ; angle 180 deg
BEAM APERTURE 4.5 cm ; DC Bias 0 kV
TUNED by, coarse fine VC, auto
RF 7.5 to 22.5 mHz, stable ± 10^-6
Orb F 1.5 to 22.5 mHz
HARMONICS, RF/Orb F, used 1,3
DEE - Gnd, max 70 kV, min gap 1 cm
STABILITY, (pk-pk noise)/(pk RF volt) 0.005
ENERGY GAIN, max 100 kV/turn
RF PHASE, stable to ± 3 deg
RF POWER input, max 300 kW
FREQUENCY MODULATION, rate /s
modulator, type
beam pulse, width

VACUUM SYSTEM

OPERATING PRESSURE 10^-5 Torr or mbar
PUMPS, No, Type, Size 2 diffusion 30", 32"
(32 K & 50 kl/s)

ION SOURCES

Hot filament

INJECTION SYSTEM

EXTRACTION SYSTEM

Electrostatic with magnetic channel

FACILITIES FOR RESEARCH

SHIELDED AREA, fixed 868 m² ; movable m²
TARGET STATIONS 4 In 3 rooms
STATIONS served at same time, max 1
MAG SPECTROGRAPH, type
COMPUTER model SEL 32/55
OTHER FACILITIES Double focusing 2.75 m beam analyzing magnet; provision for 11 beam paths, 8 with analyzed beam; beam pickoff unit for T.O.F. measurements

CHARACTERISTIC BEAMS

PARTICLE	ENERGY (MeV) Goal	Achieved	CURRENT (pμA) Internal	External
p	70	52	30	10
d	40	40	30	12
α	78	78	30	10
^{3}He	120	90		
SECONDARY			(part/s)	

BEAM PROPERTIES

MEASURED	CONDITIONS
PULSE WIDTH 5 RF deg	pμ A of MeV ions
PHASE EXC, max 30 RF deg	pμ A of MeV ions
EXTRACT eff 40 %	pμ A of MeV ions
RESOL ΔE/E %	pμ A of MeV ions
EMITTANCE	
(π mm. mrad) { axial / rad }	pμA of MeV ions

OPERATING PROGRAMS, time distribution

BASIC NUCLEAR PHYSICS 0% SOLID STATES PHYSICS 40%
BIOMEDICAL APPLICAT. 60% ISOTOPE PRODUCTIONS 0%

REFERENCES/NOTES

1) Horizontal median plane version of ORIC
2) Conversion to RCA4648 power tetrode from RCA 6949 in late 1976. New computer installed July 1976

PLAN VIEW OF FACILITY, NOTEWORTHY FEATURES, COMMENTS

ENTRY NO. C74 Date July 1,1992
Name of Machine U-115T
Institution Institute of Nuclear Physics
Address 702132 Tashkent Uzbekistan
Tel ..... Telex ..... Fax ..... EMAIL .....
In Charge: A. Rylov Reported by: A. Glazov

HISTORY

MILESTONE DATES:
Design 1991 Model Tests .....
Construction 1991-92 First Beam .....
DESIGN/CONSTRUCTION BY:
in house ..... other JINR Dubna.....
COST: Accelerator ..... Facility .....
FUNDED BY: .....

STATUS

STAFF: Machine
Scientists ..... Engineers .....
Technicians ..... Students .....
Research (in house/external)
Scientists ..... / ..... Engineers ..... / .....
Technicians ..... / ..... Students ..... / .....
BUDGET: Machine ..... Funded by .....
Research ..... Funded by .....
TIME DISTRIBUTION:
Basic Research (in house/external) ..... % / ..... %
Applied Program (in house/external) ..... % / ..... %
Development ..... % Maintenance ..... %

MAGNET

POLE PARAMETERS:
Diameter 115 cm $R_{extract}$ 48 cm R_{inject} ..... cm
HILL PARAMETERS: Gap (min) 8.2 cm B_{max} 1.69 T
(@ ..... AT) Gap (max) ..... cm B_{min} ..... T
VALLEY PARAMETERS: Gap (min) 16.2 cm B_{max} 1.02 T
(@ ..... AT) Gap (max) ..... cm B_{min} ..... T
AVERAGE FIELD: $< B >_{min}$ 1.32 T $< B >_{max}$ 1.35 T
NUMBER OF SECTORS: compact/separated 4/ .....
sector angle 40-52 deg. spiral (max) 56 deg.
FIELD TRIMMING: Trim Coils .....
Harmonic Coils 2 x 4
Other .....
CURRENT: Main Coils 560 Amps Stability 10^{-4}
Trim Coils 10 Amps Stability 10^{-4}
Stored Energy (cryogenic) ..... MJ
WEIGHT: Iron 50 T Conductor Cu 0.7 T
ION ENERGY: Bending Limit E/A = ... q^2/A^2 MeV/u
Focussing Limit E/A = ... q/A MeV/u

ACCELERATION SYSTEM

FUNDAMENTAL ACCELERATION:
Description: Dee,resonant line
No. of Gaps/turn 2 dE/dn(max) 0.1 MeV/q
Voltage(max) 0.05 MV Harmonic f_{rf}/f_{ion} 1
Freq 20,2 MHz Power in(max) 0.025 MW
Stability: Phase ..... Voltage .....
OTHER CAVITIES (Flattopping or otherwise):
Description: .....
Region of Influence: R_{min} ..... cm R_{max} ..... cm
No. of Gaps/turn ..... dE/dn(max) ..... MeV/q
Voltage(max) ..... MV Harmonic f_{rf}/f_{ion} .....
Freq ..... MHz Power in(max) ..... MW
Stability: Phase ..... Voltage .....

VACUUM SYSTEM

OPERATING PRESSURE: 10^{-6}
PUMPS: No. and type 2 Oil diffusion
.....

ION SOURCE(S)

	Type	Intensity (mA)	@	$\epsilon_n = \beta\gamma\epsilon$ (πmm mrad)	Ion Species
(a)	Internal PIG	.....		.....	Protons
(b)	.....	.....		.....	.....
(c)	.....	.....		.....	.....
(d)	.....	.....		.....	.....

INJECTION SYSTEM

..... Efficiency ..... %

EXTRACTION SYSTEM

..... Efficiency ..... %

CHARACTERISTIC BEAMS

	Accelerated Ions	E/A (MeV/u)	Current(part μA) Internal	External
(a)	p	20	.....	.....
(b)	.....	.....	.....	.....
(c)	.....	.....	.....	.....
(d)	.....	.....	.....	.....

	Secondary Particles	E (MeV)	part/sec
(a)	.....	.....	.....
(b)	.....	.....	.....
(c)	.....	.....	.....

EXTRACTED BEAM PROPERTIES:
For ..... μA of ..... MeV/u ..... ions
$\Delta E/E$ ..... % $\Delta\phi$ ..... °rf
$\epsilon_n = \beta\gamma\epsilon$ x ..... πmm mrad z ..... πmm mrad

FACILITIES FOR RESEARCH

SHIELDED AREA: Fixed ..... m^2 Moveable ..... m^2
Target Stations: ..... No. Served At Same Time: .....
MAGNETIC SPECTROMETERS: .....
OTHER FACILITIES: .....
.....
.....
.....

REFERENCES/NOTES

(a) .....
(b) .....

PLAN VIEW OF FACILITY, COMMENTS

ENTRY NO. CM1 Date July 3, 1992

Machine Name CYCLONE 3
Manufacturer IBA
Address Rue J. E. Lenoir 6, 1348 Louvain-la-Neuve, Belgium
Tel 32 10 47 58 11 Telex
Fax 32 10 47 58 10 EMAIL
In Charge: Yves JONGEN Reported by: Stephane FASSIN

HISTORY AND STATUS

DATES: Design 1989 First Machine 1990
SALES: No. Sold/Operational 3 / 2 Currently Available Y
COST: Accelerator Facility

MAGNET

POLE PARAMETERS:
Diameter 50 cm $R_{extract}$ 20.5 cm R_{inject} 2 cm
HILL PARAMETERS: Gap (min) 3.4 cm B_{max} 1.95 T
(@ AT) Gap (max) cm B_{min} T
VALLEY PARAMETERS: Gap (min) 5 cm B_{max} 1.70 T
(@ AT) Gap (max) cm B_{min} T
AVERAGE FIELD: $< B >_{min}$ 1.85 T $< B >_{max}$ T
NUMBER OF SECTORS: compact/separated 4 /
sector angle 40° deg. spiral (max) deg.
FIELD TRIMMING: Trim Coils
Harmonic Coils
Other
CURRENT: Main Coils 225 Amps Stability 10^{-4}
Trim Coils +/- 5 Amps Stability 10^{-4}
Stored Energy (cryogenic) MJ
WEIGHT: Iron 5 Tons Conductor 0.5 Tons
ION ENERGY: Bending Limit E/A = 7.6 q^2/A^2 MeV/u
Focussing Limit E/A = 7.6 q/A MeV/u

ACCELERATION SYSTEM

FUNDAMENTAL ACCELERATION:
Description: 2 x 90° Dees
No. of Gaps/turn 4 dE/dn(max) 0.08 MeV/q
Voltage(max) 0.02 MV Harmonic f_{rf}/f_{ion} 2
Freq 30 MHz Power in(max) 10 kW
Stability: Phase +/- 10 % Voltage 20 kV (dee)

VACUUM SYSTEM

OPERATING PRESSURE: $8\ 10^{-5}$ mbar
PUMPS: No. and type 1 x 300 l/sec ODP

ION SOURCE(S)

	Type	Intensity (mA)	@ $\epsilon_n = \beta\gamma\epsilon$ (π mm mrad)	Ion Species
(a)	PIG cold cathode	1		deuteron
(b)				

INJECTION SYSTEM

Efficiency %

EXTRACTION SYSTEM

Deflector Efficiency 70 %

CHARACTERISTIC BEAMS

	Accelerated Ions	E/A (MeV/u)	Current(part. μA) Internal	External
(a)	deuteron	1.90	100	70
(b)				

EXTRACTED BEAM PROPERTIES:
For μA of MeV/u ions
$\Delta E/E$ % $\Delta\phi$ °rf
$\epsilon_n = \beta\gamma\epsilon$ x πmm mrad z πmm mrad

REFERENCES/NOTES

(a) EPAC 90, Y. Jongen et al., Nice 1990
(b)

ENTRY NO. CM2 Date July 3, 1992

Machine Name CYCLONE 10/5
Manufacturer IBA
Address Rue J.E. Lenoir, 6 / 1348 Louvain-la-Neuve
Tel 32 10 47 58 11 Telex Belgium
Fax 32 10 47 58 10 EMAIL
In Charge: Yves JONGEN Reported by: Stephane FASSIN

HISTORY AND STATUS

DATES: Design 1988 First Machine 1989
SALES: No. Sold/Operational 2 / 2 Currently Available Y
COST: Accelerator Facility

MAGNET

POLE PARAMETERS:
Diameter 76 cm $R_{extract}$ ~35 cm R_{inject} 2 cm
HILL PARAMETERS: Gap (min) 3 cm B_{max} 4.9 T
(@ 112.000AT) Gap (max) cm B_{min} T
VALLEY PARAMETERS: Gap (min) 80 cm B_{max} 0.4 T
(@ AT) Gap (max) cm B_{min} T
AVERAGE FIELD: $< B >_{min}$ 1.3 T $< B >_{max}$ 1.3 T
NUMBER OF SECTORS: compact/separated 4 /
sector angle 50 deg. spiral (max) 0 deg.
FIELD TRIMMING: Trim Coils None
Harmonic Coils None
Other
CURRENT: Main Coils 200 Amps Stability $5\ 10^{-5}$
Trim Coils N/A Amps Stability N/A
Stored Energy (cryogenic) N/A MJ
WEIGHT: Iron 12 Tons Conductor 1,250 Tons
ION ENERGY: Bending Limit E/A = 11 q^2/A^2 MeV/u
Focussing Limit E/A = 11 q/A MeV/u

ACCELERATION SYSTEM

FUNDAMENTAL ACCELERATION:
Description: 2 x 30° Dees on lambda/2 Helical/Vertical Stems
No. of Gaps/turn 4 dE/dn(max) 0.104 MeV/q
Voltage(max) 0.03 MV Harmonic f_{rf}/f_{ion} 2 p / 4 d
Freq 40 MHz Power in(max) 0.010 MW
Stability: Phase Voltage $2\ 10^{-3}$

VACUUM SYSTEM

OPERATING PRESSURE: $3\ 10^{-6}$
PUMPS: No. and type 2 x 2000 l/sec ODP

ION SOURCE(S)

	Type	Intensity (mA)	@ $\epsilon_n = \beta\gamma\epsilon$ (π mm mrad)	Ion Species
(a)	PIG	1 DC		H^-
(b)	PIG	1 DC		d^-

INJECTION SYSTEM

2 Internal Sources Efficiency 10 %

EXTRACTION SYSTEM

Stripping Efficiency 100 %

CHARACTERISTIC BEAMS

	Accelerated Ions	E/A (MeV/u)	Current(part. μA) Internal	External
(a)	H^-	10	100	100
(b)	d^-	2.5	50	50

EXTRACTED BEAM PROPERTIES:
For μA of MeV/u ions
$\Delta E/E$ % $\Delta\phi$ °rf
$\epsilon_n = \beta\gamma\epsilon$ x πmm mrad z πmm mrad

REFERENCES/NOTES

(a) EPAC 90, Y. Jongen et al., Nice 1990
(b)

ENTRY NO. CM1 Date July 3, 1992

Machine Name CYCLONE 3
Manufacturer IBA
Address Rue J. E. Lenoir 6, 1348 Louvain-la-Neuve, Belgium
Tel 32 10 47 58 11 Telex
Fax 32 10 47 58 10 EMAIL
In Charge: Yves JONGEN Reported by: Stephane FASSIN

HISTORY AND STATUS

DATES: Design 1989 First Machine 1990
SALES: No. Sold/Operational 3 / 2 Currently Available Y
COST: Accelerator Facility

MAGNET

POLE PARAMETERS:
Diameter 50 cm $R_{extract}$ 20.5 cm R_{inject} 2 cm
HILL PARAMETERS: Gap (min) 3.4 cm B_{max} 1.95 T
(@ AT) Gap (max) cm B_{min} T
VALLEY PARAMETERS: Gap (min) 5 cm B_{max} 1.70 T
(@ AT) Gap (max) cm B_{min} T
AVERAGE FIELD: $< B >_{min}$ 1.85 T $< B >_{max}$ T
NUMBER OF SECTORS: compact/separated 4 /
sector angle 40° deg. spiral (max) deg.
FIELD TRIMMING: Trim Coils
Harmonic Coils
Other
CURRENT: Main Coils 225 Amps Stability 10^{-4}
Trim Coils +/- 5 Amps Stability 10^{-4}
Stored Energy (cryogenic) MJ
WEIGHT: Iron 5 Tons Conductor 0.5 Tons
ION ENERGY: Bending Limit E/A = 7.6 q^2/A^2 MeV/u
Focussing Limit E/A = 7.6 q/A MeV/u

ACCELERATION SYSTEM

FUNDAMENTAL ACCELERATION:
Description: 2 x 90° Dees
No. of Gaps/turn 4 dE/dn(max) 0.08 MeV/q
Voltage(max) 0.02 MV Harmonic f_{rf}/f_{ion} 2
Freq 30 MHz Power in(max) 10 kW
Stability: Phase +/- 10 % Voltage 20 kV (dee)

VACUUM SYSTEM

OPERATING PRESSURE: $8\ 10^{-5}$ mbar
PUMPS: No. and type 1 x 300 l/sec ODP

ION SOURCE(S)

	Type	Intensity (mA)	@ $\epsilon_n = \beta\gamma\epsilon$ (π mm mrad)	Ion Species
(a)	PIG cold cathode	1		deuteron
(b)				

INJECTION SYSTEM

Efficiency %

EXTRACTION SYSTEM

Deflector Efficiency 70 %

CHARACTERISTIC BEAMS

	Accelerated Ions	E/A (MeV/u)	Current(part. μA) Internal	External
(a)	deuteron	1.90	100	70
(b)				

EXTRACTED BEAM PROPERTIES:
For μA of MeV/u ions
$\Delta E/E$ % $\Delta\phi$ °rf
$\epsilon_n = \beta\gamma\epsilon$ x πmm mrad z πmm mrad

REFERENCES/NOTES

(a) EPAC 90, Y. Jongen et al., Nice 1990
(b)

ENTRY NO. CM2 Date July 3, 1992

Machine Name CYCLONE 10/5
Manufacturer IBA
Address Rue J.E. Lenoir, 6 / 1348 Louvain-la-Neuve
Tel 32 10 47 58 11 Telex Belgium
Fax 32 10 47 58 10 EMAIL
In Charge: Yves JONGEN Reported by: Stephane FASSIN

HISTORY AND STATUS

DATES: Design 1988 First Machine 1989
SALES: No. Sold/Operational 2 / 2 Currently Available Y
COST: Accelerator Facility

MAGNET

POLE PARAMETERS:
Diameter 76 cm $R_{extract}$ ~35 cm R_{inject} 2 cm
HILL PARAMETERS: Gap (min) 3 cm B_{max} 4.9 T
(@ 112.000AT) Gap (max) cm B_{min} T
VALLEY PARAMETERS: Gap (min) 80 cm B_{max} 0.4 T
(@ AT) Gap (max) cm B_{min} T
AVERAGE FIELD: $< B >_{min}$ 1.3 T $< B >_{max}$ 1.3 T
NUMBER OF SECTORS: compact/separated 4 /
sector angle 50 deg. spiral (max) 0 deg.
FIELD TRIMMING: Trim Coils None
Harmonic Coils None
Other
CURRENT: Main Coils 200 Amps Stability $5\ 10^{-5}$
Trim Coils N/A Amps Stability N/A
Stored Energy (cryogenic) N/A MJ
WEIGHT: Iron 12 Tons Conductor 1,250 Tons
ION ENERGY: Bending Limit E/A = 11 q^2/A^2 MeV/u
Focussing Limit E/A = 11 q/A MeV/u

ACCELERATION SYSTEM

FUNDAMENTAL ACCELERATION:
Description: 2 x 30° Dees on lambda/2 Helical/Vertical Stems
No. of Gaps/turn 4 dE/dn(max) 0.104 MeV/q
Voltage(max) 0.03 MV Harmonic f_{rf}/f_{ion} 2 p / 4 d
Freq 40 MHz Power in(max) 0.010 MW
Stability: Phase Voltage $2\ 10^{-3}$

VACUUM SYSTEM

OPERATING PRESSURE: $3\ 10^{-6}$
PUMPS: No. and type 2 x 2000 l/sec ODP

ION SOURCE(S)

	Type	Intensity (mA)	@ $\epsilon_n = \beta\gamma\epsilon$ (π mm mrad)	Ion Species
(a)	PIG	1 DC		H^-
(b)	PIG	1 DC		d^-

INJECTION SYSTEM

2 Internal Sources Efficiency 10 %

EXTRACTION SYSTEM

Stripping Efficiency 100 %

CHARACTERISTIC BEAMS

	Accelerated Ions	E/A (MeV/u)	Current(part. μA) Internal	External
(a)	H^-	10	100	100
(b)	d^-	2.5	50	50

EXTRACTED BEAM PROPERTIES:
For μA of MeV/u ions
$\Delta E/E$ % $\Delta\phi$ °rf
$\epsilon_n = \beta\gamma\epsilon$ x πmm mrad z πmm mrad

REFERENCES/NOTES

(a) EPAC 90, Y. Jongen et al., Nice 1990
(b)

ENTRY NO. CM3 Date July 3, 1992
Machine Name CYCLONE 18/9
Manufacturer IBA
Address Rue J.E. Lenoir , 6 / 1348 Louvain-la-Neuve
Tel 32 10 47 58 11 Telex Belgium
Fax 32 10 47 58 10 EMAIL
In Charge: Yves JONGEN Reported by: Stephane FASSIN

HISTORY AND STATUS

DATES: Design 01/04/90 First Machine 03/92
SALES: No. Sold/Operational 5 / 2 Currently Available Y
COST: Accelerator Facility

MAGNET

POLE PARAMETERS:
Diameter 108 cm $R_{extract}$ 48 cm R_{inject} 3 cm
HILL PARAMETERS: Gap (min) 3 cm B_{max} 2.1 T
(Φ 112.000. AT) Gap (max) 3 cm B_{min} 2.1 T
VALLEY PARAMETERS: Gap (min) 67 cm B_{max} 0.6 T
(Φ - AT) Gap (max) 67 cm B_{min} 0.6 T
AVERAGE FIELD: $< B >_{min}$ 1.35 T $< B >_{max}$ 1.35 T
NUMBER OF SECTORS: compact/separated 4 /
sector angle 57° deg. spiral (max) - deg.
FIELD TRIMMING: Trim Coils None
Harmonic Coils None
Other Iron edges (movable for deuterons)
CURRENT: Main Coils 200 Amps Stability 10^{-4}
Trim Coils N/A Amps Stability N/A
Stored Energy (cryogenic) N/A MJ
WEIGHT: Iron 20 Tons Conductor copper 2 Tons
ION ENERGY: Bending Limit E/A = 20 q^2/A^2 MeV/u
Focussing Limit E/A = 20 q/A MeV/u

ACCELERATION SYSTEM

FUNDAMENTAL ACCELERATION:
Description: 2 x 30° Dees on lambda/4 straight stems
No. of Gaps/turn 4 dE/dn(max) 0.104 MeV/q
Voltage(max) 0.032 MV Harmonic f_{rf}/f_{ion} 2 p/ 4 d
Freq 42 MHz Power in(max) 0.010 MW
Stability: Phase Dees connected. Voltage 8.10^{-3}

VACUUM SYSTEM

OPERATING PRESSURE: 0.10^{-6}
PUMPS: No. and type 4 x 700 l/sec ODP

ION SOURCE(S)

	Type	Intensity (mA)	Φ	$\epsilon_n = \beta\gamma\epsilon$ (π mm mrad)	Ion Species
(a)	PIG	1 DC			H^-
(b)	PIG	1 DC			d^-

INJECTION SYSTEM

2 internal sources Efficiency 10 %

EXTRACTION SYSTEM

Carbon Stripper Efficiency 100 %

CHARACTERISTIC BEAMS

	Accelerated Ions	E/A (MeV/u)	Current(part. μA) Internal	External
(a)	H^-	18	100	100
(b)	d^-	4.5	35	35

EXTRACTED BEAM PROPERTIES:
For ... μA of ... MeV/u ... ions
ΔE/E ... % Δφ ... °rf
$\epsilon_n = \beta\gamma\epsilon$ x ... πmm mrad z ... πmm mrad

REFERENCES/NOTES

(a) EPAC 90, Y. Jongen, Nice 1990
(b)

ENTRY NO. CM4 Date July 3, 1992
Machine Name CYCLONE 30
Manufacturer IBA
Address Rue J.E. Lenoir , 6 / 1348 Louvain-la-Neuve
Tel 32 10 47 58 11 Telex Belgium
Fax 32 10 47 58 10 EMAIL
In Charge: Yves Jongen Reported by: Stephane Fassin

HISTORY AND STATUS

DATES: Design 1985 First Machine 1986
SALES: No. Sold/Operational 14 / 10 Currently Available Y
COST: Accelerator Facility

MAGNET

POLE PARAMETERS:
Diameter 160 cm $R_{extract}$ 50-75 cm R_{inject} 3 cm
HILL PARAMETERS: Gap (min) 3 cm B_{max} 1.7 T
(Φ 60.000.. AT) Gap (max) 3 cm B_{min} T
VALLEY PARAMETERS: Gap (min) 100 cm B_{max} 0.12 T
(Φ - AT) Gap (max) 100 cm B_{min} T
AVERAGE FIELD: $< B >_{min}$ 1.0 T $< B >_{max}$ 1.3 T
NUMBER OF SECTORS: compact/separated 4 /
sector angle 54-58 deg. spiral (max) 0 deg.
FIELD TRIMMING: Trim Coils None
Harmonic Coils None
Other
CURRENT: Main Coils 110 Amps Stability 5×10^{-5}
Trim Coils N/A Amps Stability N/A
Stored Energy (cryogenic) N/A MJ
WEIGHT: Iron 45 Tons Conductor 4 Tons
ION ENERGY: Bending Limit E/A = 30 q^2/A^2 MeV/u
Focussing Limit E/A = 30 q/A MeV/u

ACCELERATION SYSTEM

FUNDAMENTAL ACCELERATION:
Description: 2 x 30° Dees on lambda/2 Vertical Stems
No. of Gaps/turn 4 dE/dn(max) 0.17 MeV/q
Voltage(max) ~0.055 MV Harmonic f_{rf}/f_{ion} 4
Freq ~66 MHz Power in(max) 0.025 MW
Stability: Phase Voltage 10^{-3}

VACUUM SYSTEM

OPERATING PRESSURE: $2.5\ 10^{-7}$
PUMPS: No. and type 3 x 2,000 l/sec ODP + 2 x 1,500 l/sec (N_2) cryo's

ION SOURCE(S)

	Type	Intensity (mA)	Φ	$\epsilon_n = \beta\gamma\epsilon$ (π mm mrad)	Ion Species
(a)	Multicusp	3			H^-, d^-
(b)					

INJECTION SYSTEM

Axial Efficiency 35 %

EXTRACTION SYSTEM

Stripping Efficiency 100 %

CHARACTERISTIC BEAMS

	Accelerated Ions	E/A (MeV/u)	Current(part. μA) Internal	External
(a)	Protons (H^-)	30	500 H^-	500
(b)				

EXTRACTED BEAM PROPERTIES:
For 500 μA of 30 MeV/u Pro tons ~~ions~~
ΔE/E 1 % Δφ °rf
$\epsilon_n = \beta\gamma\epsilon$ x 10 πmm mrad z 5 πmm mrad

REFERENCES/NOTES

(a) ACC 92, Y. Jongen et al., St Petersburg 1992
(b) EPAC 1990, Y. Jongen et al., Nice 1990

ENTRY NO. CM3 Date July 3, 1992
Machine Name CYCLONE 18/9
Manufacturer IBA
Address Rue J.E. Lenoir , 6 / 1348 Louvain-la-Neuve
Tel 32 10 47 58 11 Telex Belgium
Fax 32 10 47 58 10 EMAIL
In Charge: Yves JONGEN Reported by: Stephane FASSIN

HISTORY AND STATUS

DATES: Design 01/04/90 First Machine 03/92
SALES: No. Sold/Operational 5 / 2 Currently Available Y
COST: Accelerator Facility

MAGNET

POLE PARAMETERS:
Diameter 108 cm $R_{extract}$ 48 cm R_{inject} 3 cm
HILL PARAMETERS: Gap (min) 3 cm B_{max} 2.1 T
(Φ 112.000. AT) Gap (max) 3 cm B_{min} 2.1 T
VALLEY PARAMETERS: Gap (min) 67 cm B_{max} 0.6 T
(Φ - AT) Gap (max) 67 cm B_{min} 0.6 T
AVERAGE FIELD: $< B >_{min}$ 1.35 T $< B >_{max}$ 1.35 T
NUMBER OF SECTORS: compact/separated 4 /
sector angle 57° deg. spiral (max) - deg.
FIELD TRIMMING: Trim Coils None
Harmonic Coils None
Other Iron edges (movable for deuterons)
CURRENT: Main Coils 200 Amps Stability 10^{-4}
Trim Coils N/A Amps Stability N/A
Stored Energy (cryogenic) N/A MJ
WEIGHT: Iron 20 Tons Conductor copper 2 Tons
ION ENERGY: Bending Limit E/A = 20 q^2/A^2 MeV/u
Focussing Limit E/A = 20 q/A MeV/u

ACCELERATION SYSTEM

FUNDAMENTAL ACCELERATION:
Description: 2 x 30° Dees on lambda/4 straight stems
No. of Gaps/turn 4 dE/dn(max) 0.104 MeV/q
Voltage(max) 0.032 MV Harmonic f_{rf}/f_{ion} 2 p/ 4 d
Freq 42 MHz Power in(max) 0.010 MW
Stability: Phase Dees connected. Voltage 8.10^{-3}

VACUUM SYSTEM

OPERATING PRESSURE: 0.10^{-6}
PUMPS: No. and type 4 x 700 l/sec ODP

ION SOURCE(S)

	Type	Intensity (mA)	Φ	$\epsilon_n = \beta\gamma\epsilon$ (π mm mrad)	Ion Species
(a)	PIG	1 DC			H^-
(b)	PIG	1 DC			d^-

INJECTION SYSTEM

2 internal sources Efficiency 10 %

EXTRACTION SYSTEM

Carbon Stripper Efficiency 100 %

CHARACTERISTIC BEAMS

	Accelerated Ions	E/A (MeV/u)	Current(part. μA) Internal	External
(a)	H^-	18	100	100
(b)	d^-	4.5	35	35

EXTRACTED BEAM PROPERTIES:
For ... μA of ... MeV/u ... ions
ΔE/E ... % Δφ ... °rf
$\epsilon_n = \beta\gamma\epsilon$ x ... πmm mrad z ... πmm mrad

REFERENCES/NOTES

(a) EPAC 90, Y. Jongen, Nice 1990
(b)

ENTRY NO. CM4 Date July 3, 1992
Machine Name CYCLONE 30
Manufacturer IBA
Address Rue J.E. Lenoir , 6 / 1348 Louvain-la-Neuve
Tel 32 10 47 58 11 Telex Belgium
Fax 32 10 47 58 10 EMAIL
In Charge: Yves Jongen Reported by: Stephane Fassin

HISTORY AND STATUS

DATES: Design 1985 First Machine 1986
SALES: No. Sold/Operational 14 / 10 Currently Available Y
COST: Accelerator Facility

MAGNET

POLE PARAMETERS:
Diameter 160 cm $R_{extract}$ 50-75 cm R_{inject} 3 cm
HILL PARAMETERS: Gap (min) 3 cm B_{max} 1.7 T
(Φ 60.000.. AT) Gap (max) 3 cm B_{min} T
VALLEY PARAMETERS: Gap (min) 100 cm B_{max} 0.12 T
(Φ - AT) Gap (max) 100 cm B_{min} T
AVERAGE FIELD: $< B >_{min}$ 1.0 T $< B >_{max}$ 1.3 T
NUMBER OF SECTORS: compact/separated 4 /
sector angle 54-58 deg. spiral (max) 0 deg.
FIELD TRIMMING: Trim Coils None
Harmonic Coils None
Other
CURRENT: Main Coils 110 Amps Stability 5×10^{-5}
Trim Coils N/A Amps Stability N/A
Stored Energy (cryogenic) N/A MJ
WEIGHT: Iron 45 Tons Conductor 4 Tons
ION ENERGY: Bending Limit E/A = 30 q^2/A^2 MeV/u
Focussing Limit E/A = 30 q/A MeV/u

ACCELERATION SYSTEM

FUNDAMENTAL ACCELERATION:
Description: 2 x 30° Dees on lambda/2 Vertical Stems
No. of Gaps/turn 4 dE/dn(max) 0.17 MeV/q
Voltage(max) ~0.055 MV Harmonic f_{rf}/f_{ion} 4
Freq ~66 MHz Power in(max) 0.025 MW
Stability: Phase Voltage 10^{-3}

VACUUM SYSTEM

OPERATING PRESSURE: $2.5\ 10^{-7}$
PUMPS: No. and type 3 x 2,000 l/sec ODP + 2 x 1,500 l/sec (N_2) cryo's

ION SOURCE(S)

	Type	Intensity (mA)	Φ	$\epsilon_n = \beta\gamma\epsilon$ (π mm mrad)	Ion Species
(a)	Multicusp	3			H^-, d^-
(b)					

INJECTION SYSTEM

Axial Efficiency 35 %

EXTRACTION SYSTEM

Stripping Efficiency 100 %

CHARACTERISTIC BEAMS

	Accelerated Ions	E/A (MeV/u)	Current(part. μA) Internal	External
(a)	Protons (H^-)	30	500 H^-	500
(b)				

EXTRACTED BEAM PROPERTIES:
For 500 μA of 30 MeV/u Pro tons ~~ions~~
ΔE/E 1 % Δφ °rf
$\epsilon_n = \beta\gamma\epsilon$ x 10 πmm mrad z 5 πmm mrad

REFERENCES/NOTES

(a) ACC 92, Y. Jongen et al., St Petersburg 1992
(b) EPAC 1990, Y. Jongen et al., Nice 1990

ENTRY NO. CM5 Date

Machine Name TR30

Manufacturer EBCO Technologies

Address 4004 Wesbrook Mall, Vancouver Canada V6T2A3

Tel (604)224-7090 Telex

Fax (604)228-1715 EMAIL

In Charge: Reported by: B. Milton

HISTORY AND STATUS

DATES: Design 1988-89 First Machine July 1,1990

SALES: No. Sold/Operational 2 / 1 Currently Available yes

COST: Accelerator Facility

MAGNET

POLE PARAMETERS:

Diameter 76 cm $R_{extract}$ 47-66 cm R_{inject} 2.5 cm

HILL PARAMETERS: Gap (min) 3.5 cm B_{max} 1.9 T

(@ 9 x 10^5 AT) Gap (max) 5.2 cm B_{min} 1.3 T

VALLEY PARAMETERS: Gap (min) 18 cm B_{max} 1.1 T

(@ 9 x 10^5 AT) Gap (max) 18 cm B_{min} 0.4 T

AVERAGE FIELD: $< B >_{min}$ 1.2 T $< B >_{max}$ 1.24 T

NUMBER OF SECTORS: compact/separated 4 /

sector angle 32 - 45 deg. spiral (max) none deg.

FIELD TRIMMING: Trim Coils none

Harmonic Coils none

Other

CURRENT: Main Coils 500 Amps Stability 0.01%

Trim Coils Amps Stability

Stored Energy (cryogenic) MJ

WEIGHT: Iron 45 tonnes Conductor 1 tonne

ION ENERGY: Bending Limit E/A = 30 q^2/A^2 MeV/u

Focussing Limit E/A = 30 q/A MeV/u

ACCELERATION SYSTEM

FUNDAMENTAL ACCELERATION:

Description: 2 pie shape dees with lambda/4 stems

No. of Gaps/turn 4 dE/dn(max) 0.200 MeV/q

Voltage(max) 0.050 MV Harmonic f_{rf}/f_{ion} 4

Freq 73.14 MHz Power in(max) 0.035 MW

Stability: Phase 1° Voltage 10^{-4}

VACUUM SYSTEM

OPERATING PRESSURE: 3 x 10e-7 Torr

PUMPS: No. and type 2 cryo pumps

ION SOURCE(S)

	Type	Intensity (mA)	@ $\epsilon_n = \beta\gamma\epsilon$ (π mm mrad)	Ion Species
(a)	Cusp	7	0.7	H-
(b)				

INJECTION SYSTEM

Axial - spiral Efficiency 12 %

EXTRACTION SYSTEM

Stripping Efficiency 100 %

CHARACTERISTIC BEAMS

	Accelerated Ions	E/A (MeV/u)	Current(part. μA) Internal	External
(a)	H-	30	450 H-	450 p
(b)				

EXTRACTED BEAM PROPERTIES:

For 400 μA of 30 MeV/u H+ ions

$\Delta E/E$ 1 % $\Delta\phi$ 30 °rf

$\epsilon_n = \beta\gamma\epsilon$ x 2 πmm mrad z 2 πmm mrad

REFERENCES/NOTES

(a) 12th International Cyclotron Conf. B. Milton et al

(b) PAC 1991 B. Milton et al

ENTRY NO. CM6 Date

Machine Name BC168

Manufacturer The Japan Steel Works,LTD.

Address 1-2, Yurakucho 1-chome, Chiyoda-ku, Tokyo Japan

Tel (03)3501-6111 Telex J24256 (JSW)

Fax (03)3504-0727 EMAIL

In Charge: Reported by: Y. Toda

HISTORY AND STATUS

DATES: Design 1981-1982 First Machine 1982

SALES: No. Sold/Operational 4 / 4 Currently Available yes

COST: Accelerator Facility

MAGNET

POLE PARAMETERS:

Diameter 91 cm $R_{extract}$ 38 cm R_{inject} cm

HILL PARAMETERS: Gap (min) 7 cm B_{max} T

(@ 1.2x10.^{5} AT) Gap (max) 7 cm B_{min} T

VALLEY PARAMETERS: Gap (min) 13 cm B_{max} T

(@ 1.2x10.^{5} AT) Gap (max) 13 cm B_{min} T

AVERAGE FIELD: $< B >_{min}$ 1.54 T $< B >_{max}$ 1.54 T

NUMBER OF SECTORS: compact/separated 4 /

sector angle 45 deg. spiral (max) none deg.

FIELD TRIMMING: Trim Coils 2

Harmonic Coils 2

Other

CURRENT: Main Coils 310 Amps Stability 1x10-4

Trim Coils 50 Amps Stability 1x10-4

Stored Energy (cryogenic) MJ

WEIGHT: Iron 20 ton Conductor 1 ton

ION ENERGY: Bending Limit E/A = q^2/A^2 MeV/u

Focussing Limit E/A = q/A MeV/u

ACCELERATION SYSTEM

FUNDAMENTAL ACCELERATION:

Description: 2 sets of pie/4 shape dee with lambda/4 stems

No. of Gaps/turn 4 dE/dn(max) 0.15 MeV/q

Voltage(max) 0.04 MV Harmonic f_{rf}/f_{ion} 2.4

Freq 47 MHz Power in(max) 0.02 MW

Stability: Phase 1° Voltage 1x10-4

VACUUM SYSTEM

OPERATING PRESSURE: 1x10-6 Torr

PUMPS: No. and type 1 diffusion pump

ION SOURCE(S)

	Type	Intensity (mA)	@ $\epsilon_n = \beta\gamma\epsilon$ (π mm mrad)	Ion Species
(a)	Hot Cathode PIG	1		H+
(b)				

INJECTION SYSTEM

Efficiency %

EXTRACTION SYSTEM

Electrostatic deflector Efficiency 80 %

CHARACTERISTIC BEAMS

	Accelerated Ions	E/A (MeV/u)	Current(part. μA) Internal	External
(a)	H+	16	150	70
(b)	D+	8	150	70

EXTRACTED BEAM PROPERTIES:

For 50 μA of 16 MeV/u H+ ions

$\Delta E/E$ 1 % $\Delta\phi$ °rf

$\epsilon_n = \beta\gamma\epsilon$ x 30 πmm mrad z 10 πmm mrad

REFERENCES/NOTES

(a)

(b)

ENTRY NO. CM5 Date

Machine Name TR30

Manufacturer EBCO Technologies

Address 4004 Wesbrook Mall, Vancouver Canada V6T2A3

Tel (604)224-7090 Telex

Fax (604)228-1715 EMAIL

In Charge: Reported by: B. Milton

HISTORY AND STATUS

DATES: Design 1988-89 First Machine July 1,1990

SALES: No. Sold/Operational 2 / 1 Currently Available yes

COST: Accelerator Facility

MAGNET

POLE PARAMETERS:

Diameter 76 cm $R_{extract}$ 47-66 cm R_{inject} 2.5 cm

HILL PARAMETERS: Gap (min) 3.5 cm B_{max} 1.9 T

(@ 9 x 10^5 AT) Gap (max) 5.2 cm B_{min} 1.3 T

VALLEY PARAMETERS: Gap (min) 18 cm B_{max} 1.1 T

(@ 9 x 10^5 AT) Gap (max) 18 cm B_{min} 0.4 T

AVERAGE FIELD: $< B >_{min}$ 1.2 T $< B >_{max}$ 1.24 T

NUMBER OF SECTORS: compact/separated 4 /

sector angle 32 - 45 deg. spiral (max) none deg.

FIELD TRIMMING: Trim Coils none

Harmonic Coils none

Other

CURRENT: Main Coils 500 Amps Stability 0.01%

Trim Coils Amps Stability

Stored Energy (cryogenic) MJ

WEIGHT: Iron 45 tonnes Conductor 1 tonne

ION ENERGY: Bending Limit E/A = 30 q^2/A^2 MeV/u

Focussing Limit E/A = 30 q/A MeV/u

ACCELERATION SYSTEM

FUNDAMENTAL ACCELERATION:

Description: 2 pie shape dees with lambda/4 stems

No. of Gaps/turn 4 dE/dn(max) 0.200 MeV/q

Voltage(max) 0.050 MV Harmonic f_{rf}/f_{ion} 4

Freq 73.14 MHz Power in(max) 0.035 MW

Stability: Phase 1° Voltage 10^{-4}

VACUUM SYSTEM

OPERATING PRESSURE: 3 x 10e-7 Torr

PUMPS: No. and type 2 cryo pumps

ION SOURCE(S)

	Type	Intensity (mA)	@ $\epsilon_n = \beta\gamma\epsilon$ (π mm mrad)	Ion Species
(a)	Cusp	7	0.7	H-
(b)				

INJECTION SYSTEM

Axial - spiral Efficiency 12 %

EXTRACTION SYSTEM

Stripping Efficiency 100 %

CHARACTERISTIC BEAMS

	Accelerated Ions	E/A (MeV/u)	Current(part. μA) Internal	External
(a)	H-	30	450 H-	450 p
(b)				

EXTRACTED BEAM PROPERTIES:

For 400 μA of 30 MeV/u H+ ions

$\Delta E/E$ 1 % $\Delta\phi$ 30 °rf

$\epsilon_n = \beta\gamma\epsilon$ x 2 πmm mrad z 2 πmm mrad

REFERENCES/NOTES

(a) 12th International Cyclotron Conf. B. Milton et al

(b) PAC 1991 B. Milton et al

ENTRY NO. CM6 Date

Machine Name BC168

Manufacturer The Japan Steel Works,LTD.

Address 1-2, Yurakucho 1-chome, Chiyoda-ku, Tokyo Japan

Tel (03)3501-6111 Telex J24256 (JSW)

Fax (03)3504-0727 EMAIL

In Charge: Reported by: Y. Toda

HISTORY AND STATUS

DATES: Design 1981-1982 First Machine 1982

SALES: No. Sold/Operational 4 / 4 Currently Available yes

COST: Accelerator Facility

MAGNET

POLE PARAMETERS:

Diameter 91 cm $R_{extract}$ 38 cm R_{inject} cm

HILL PARAMETERS: Gap (min) 7 cm B_{max} T

(@ 1.2x10.^{5} AT) Gap (max) 7 cm B_{min} T

VALLEY PARAMETERS: Gap (min) 13 cm B_{max} T

(@ 1.2x10.^{5} AT) Gap (max) 13 cm B_{min} T

AVERAGE FIELD: $< B >_{min}$ 1.54 T $< B >_{max}$ 1.54 T

NUMBER OF SECTORS: compact/separated 4 /

sector angle 45 deg. spiral (max) none deg.

FIELD TRIMMING: Trim Coils 2

Harmonic Coils 2

Other

CURRENT: Main Coils 310 Amps Stability 1x10-4

Trim Coils 50 Amps Stability 1x10-4

Stored Energy (cryogenic) MJ

WEIGHT: Iron 20 ton Conductor 1 ton

ION ENERGY: Bending Limit E/A = q^2/A^2 MeV/u

Focussing Limit E/A = q/A MeV/u

ACCELERATION SYSTEM

FUNDAMENTAL ACCELERATION:

Description: 2 sets of pie/4 shape dee with lambda/4 stems

No. of Gaps/turn 4 dE/dn(max) 0.15 MeV/q

Voltage(max) 0.04 MV Harmonic f_{rf}/f_{ion} 2.4

Freq 47 MHz Power in(max) 0.02 MW

Stability: Phase 1° Voltage 1x10-4

VACUUM SYSTEM

OPERATING PRESSURE: 1x10-6 Torr

PUMPS: No. and type 1 diffusion pump

ION SOURCE(S)

	Type	Intensity (mA)	@ $\epsilon_n = \beta\gamma\epsilon$ (π mm mrad)	Ion Species
(a)	Hot Cathode PIG	1		H+
(b)				

INJECTION SYSTEM

Efficiency %

EXTRACTION SYSTEM

Electrostatic deflector Efficiency 80 %

CHARACTERISTIC BEAMS

	Accelerated Ions	E/A (MeV/u)	Current(part. μA) Internal	External
(a)	H+	16	150	70
(b)	D+	8	150	70

EXTRACTED BEAM PROPERTIES:

For 50 μA of 16 MeV/u H+ ions

$\Delta E/E$ 1 % $\Delta\phi$ °rf

$\epsilon_n = \beta\gamma\epsilon$ x 30 πmm mrad z 10 πmm mrad

REFERENCES/NOTES

(a)

(b)

ENTRY NO. CM7 Date

Machine Name BC1710

Manufacturer The Japan Steel Works, LTD.

Address 1-2, Yurakucho 1-chome, Chiyoda-ku, Tokyo Japan

Tel (03)3501-6111 Telex J24256 (JSW)

Fax (03)3504-0727 EMAIL

In Charge: Reported by: Y. Toda

HISTORY AND STATUS

DATES: Design 1980-1981 First Machine 1981

SALES: No. Sold/Operational 8 / 8 Currently Available yes

COST: Accelerator Facility

MAGNET

POLE PARAMETERS:

Diameter 101 cm $R_{extract}$ 42 cm R_{inject} cm

HILL PARAMETERS: Gap (min) 7 cm B_{max} T

(@ 1.2x10⁵ AT) Gap (max) 7 cm B_{min} T

VALLEY PARAMETERS: Gap (min) 13 cm B_{max} T

(@ 1.2x10⁵ AT) Gap (max) 13 cm B_{min} T

AVERAGE FIELD: $< B >_{min}$ 1.43 T $< B >_{max}$ 1.54 T

NUMBER OF SECTORS: compact/separated 4 /

sector angle 45 deg. spiral (max) none deg.

FIELD TRIMMING: Trim Coils 3

Harmonic Coils 2

Other

CURRENT: Main Coils 380 Amps Stability ±2x10⁻⁵

Trim Coils 50 Amps Stability ±1x10⁻⁴

Stored Energy (cryogenic) MJ

WEIGHT: Iron 30 ton Conductor 1 ton

ION ENERGY: Bending Limit E/A = q^2/A^2 MeV/u

Focussing Limit E/A = q/A MeV/u

ACCELERATION SYSTEM

FUNDAMENTAL ACCELERATION:

Description: 2 sets of pie/4 shape dee with lambda/4 stems

No. of Gaps/turn 4 dE/dn(max) 0.16 MeV/q

Voltage(max) 0.04 MV Harmonic f_{rf}/f_{ion} 2.4

Freq 43.5-47 MHz Power in(max) 0.02 MW

Stability: Phase 1° Voltage 1x10⁻³

VACUUM SYSTEM

OPERATING PRESSURE: 1x10⁻⁶ Torr

PUMPS: No. and type 1 diffusion pump

ION SOURCE(S)

	Type	Intensity (mA)	@ $\epsilon_n = \beta\gamma\epsilon$ (π mm mrad)	Ion Species
(a)	Hot Cathode PIG	1		H^+
(b)				

INJECTION SYSTEM

Efficiency %

EXTRACTION SYSTEM

Electrostatic deflector Efficiency 80 %

CHARACTERISTIC BEAMS

	Accelerated Ions	E/A (MeV/u)	Current(part. μA) Internal	External
(a)	H^+	17	150	70
(b)	D^+	10	150	70

EXTRACTED BEAM PROPERTIES:

For 50 μA of 17 MeV/u H^+ ions

$\Delta E/E$ 1 % $\Delta\phi$ °rf

$\epsilon_n = \beta\gamma\epsilon$ x 30 πmm mrad z 10 πmm mrad

REFERENCES/NOTES

(a)

(b)

ENTRY NO. CM8 Date

Machine Name BC2211

Manufacturer The Japan Steel Works, LTD.

Address 1-2, Yurakucho 1-chome, Chiyoda-ku, Tokyo Japan

Tel (03)3501-6111 Telex J24256 (JSW)

Fax (03)3504-0727 EMAIL

In Charge: Reported by: Y. Toda

HISTORY AND STATUS

DATES: Design 1988-1989 First Machine 1989

SALES: No. Sold/Operational 1 / 1 Currently Available yes

COST: Accelerator Facility

MAGNET

POLE PARAMETERS:

Diameter 101 cm $R_{extract}$ 42 cm R_{inject} cm

HILL PARAMETERS: Gap (min) 7 cm B_{max} T

(@ 1.3x10⁵ AT) Gap (max) 7 cm B_{min} T

VALLEY PARAMETERS: Gap (min) 13 cm B_{max} T

(@ 1.3x10⁵ AT) Gap (max) 13 cm B_{min} T

AVERAGE FIELD: $< B >_{min}$ 1.60 T $< B >_{max}$ 1.80 T

NUMBER OF SECTORS: compact/separated 4 /

sector angle 45 deg. spiral (max) deg.

FIELD TRIMMING: Trim Coils 3

Harmonic Coils 2

Other

CURRENT: Main Coils 400 Amps Stability ±2x10⁻⁵

Trim Coils 50 Amps Stability ±1x10⁻⁴

Stored Energy (cryogenic) MJ

WEIGHT: Iron 30 ton Conductor 1 ton

ION ENERGY: Bending Limit E/A = q^2/A^2 MeV/u

Focussing Limit E/A = q/A MeV/u

ACCELERATION SYSTEM

FUNDAMENTAL ACCELERATION:

Description: 2 sets of pie/4 shape dee with lambda/4 stems

No. of Gaps/turn 4 dE/dn(max) 0.15 MeV/q

Voltage(max) 0.04 MV Harmonic f_{rf}/f_{ion} 2.4

Freq 49 MHz Power in(max) 0.02 MW

Stability: Phase 1° Voltage 1x10⁻³

VACUUM SYSTEM

OPERATING PRESSURE: 1x10⁻⁶ Torr

PUMPS: No. and type 1 diffusion pump

ION SOURCE(S)

	Type	Intensity (mA)	@ $\epsilon_n = \beta\gamma\epsilon$ (π mm mrad)	Ion Species
(a)	Hot Cathode PIG	1		H^+
(b)				

INJECTION SYSTEM

Efficiency %

EXTRACTION SYSTEM

Electrostatic deflector Efficiency 80 %

CHARACTERISTIC BEAMS

	Accelerated Ions	E/A (MeV/u)	Current(part. μA) Internal	External
(a)	H^+	22	150	70
(b)	D^+	11	150	70

EXTRACTED BEAM PROPERTIES:

For 50 μA of 22 MeV/u H^+ ions

$\Delta E/E$ 1 % $\Delta\phi$ °rf

$\epsilon_n = \beta\gamma\epsilon$ x 30 πmm mrad z 10 πmm mrad

REFERENCES/NOTES

(a)

(b)

ENTRY NO. CM7 Date

Machine Name BC1710

Manufacturer The Japan Steel Works, LTD.

Address 1-2, Yurakucho 1-chome, Chiyoda-ku, Tokyo Japan

Tel (03)3501-6111 Telex J24256 (JSW)

Fax (03)3504-0727 EMAIL

In Charge: Reported by: Y. Toda

HISTORY AND STATUS

DATES: Design 1980-1981 First Machine 1981

SALES: No. Sold/Operational 8 / 8 Currently Available yes

COST: Accelerator Facility

MAGNET

POLE PARAMETERS:

Diameter 101 cm $R_{extract}$ 42 cm R_{inject} cm

HILL PARAMETERS: Gap (min) 7 cm B_{max} T

(@ 1.2x10⁵ AT) Gap (max) 7 cm B_{min} T

VALLEY PARAMETERS: Gap (min) 13 cm B_{max} T

(@ 1.2x10⁵ AT) Gap (max) 13 cm B_{min} T

AVERAGE FIELD: $< B >_{min}$ 1.43 T $< B >_{max}$ 1.54 T

NUMBER OF SECTORS: compact/separated 4 /

sector angle 45 deg. spiral (max) none deg.

FIELD TRIMMING: Trim Coils 3

Harmonic Coils 2

Other

CURRENT: Main Coils 380 Amps Stability ±2x10⁻⁵

Trim Coils 50 Amps Stability ±1x10⁻⁴

Stored Energy (cryogenic) MJ

WEIGHT: Iron 30 ton Conductor 1 ton

ION ENERGY: Bending Limit E/A = q^2/A^2 MeV/u

Focussing Limit E/A = q/A MeV/u

ACCELERATION SYSTEM

FUNDAMENTAL ACCELERATION:

Description: 2 sets of pie/4 shape dee with lambda/4 stems

No. of Gaps/turn 4 dE/dn(max) 0.16 MeV/q

Voltage(max) 0.04 MV Harmonic f_{rf}/f_{ion} 2.4

Freq 43.5-47 MHz Power in(max) 0.02 MW

Stability: Phase 1° Voltage 1x10⁻³

VACUUM SYSTEM

OPERATING PRESSURE: 1x10⁻⁶ Torr

PUMPS: No. and type 1 diffusion pump

ION SOURCE(S)

	Type	Intensity (mA)	@ $\epsilon_n = \beta\gamma\epsilon$ (π mm mrad)	Ion Species
(a)	Hot Cathode PIG	1		H^+
(b)				

INJECTION SYSTEM

Efficiency %

EXTRACTION SYSTEM

Electrostatic deflector Efficiency 80 %

CHARACTERISTIC BEAMS

	Accelerated Ions	E/A (MeV/u)	Current(part. μA) Internal	External
(a)	H^+	17	150	70
(b)	D^+	10	150	70

EXTRACTED BEAM PROPERTIES:

For 50 μA of 17 MeV/u H^+ ions

$\Delta E/E$ 1 % $\Delta\phi$ °rf

$\epsilon_n = \beta\gamma\epsilon$ x 30 πmm mrad z 10 πmm mrad

REFERENCES/NOTES

(a)

(b)

ENTRY NO. CM8 Date

Machine Name BC2211

Manufacturer The Japan Steel Works, LTD.

Address 1-2, Yurakucho 1-chome, Chiyoda-ku, Tokyo Japan

Tel (03)3501-6111 Telex J24256 (JSW)

Fax (03)3504-0727 EMAIL

In Charge: Reported by: Y. Toda

HISTORY AND STATUS

DATES: Design 1988-1989 First Machine 1989

SALES: No. Sold/Operational 1 / 1 Currently Available yes

COST: Accelerator Facility

MAGNET

POLE PARAMETERS:

Diameter 101 cm $R_{extract}$ 42 cm R_{inject} cm

HILL PARAMETERS: Gap (min) 7 cm B_{max} T

(@ 1.3x10⁵ AT) Gap (max) 7 cm B_{min} T

VALLEY PARAMETERS: Gap (min) 13 cm B_{max} T

(@ 1.3x10⁵ AT) Gap (max) 13 cm B_{min} T

AVERAGE FIELD: $< B >_{min}$ 1.60 T $< B >_{max}$ 1.80 T

NUMBER OF SECTORS: compact/separated 4 /

sector angle 45 deg. spiral (max) deg.

FIELD TRIMMING: Trim Coils 3

Harmonic Coils 2

Other

CURRENT: Main Coils 400 Amps Stability ±2x10⁻⁵

Trim Coils 50 Amps Stability ±1x10⁻⁴

Stored Energy (cryogenic) MJ

WEIGHT: Iron 30 ton Conductor 1 ton

ION ENERGY: Bending Limit E/A = q^2/A^2 MeV/u

Focussing Limit E/A = q/A MeV/u

ACCELERATION SYSTEM

FUNDAMENTAL ACCELERATION:

Description: 2 sets of pie/4 shape dee with lambda/4 stems

No. of Gaps/turn 4 dE/dn(max) 0.15 MeV/q

Voltage(max) 0.04 MV Harmonic f_{rf}/f_{ion} 2.4

Freq 49 MHz Power in(max) 0.02 MW

Stability: Phase 1° Voltage 1x10⁻³

VACUUM SYSTEM

OPERATING PRESSURE: 1x10⁻⁶ Torr

PUMPS: No. and type 1 diffusion pump

ION SOURCE(S)

	Type	Intensity (mA)	@ $\epsilon_n = \beta\gamma\epsilon$ (π mm mrad)	Ion Species
(a)	Hot Cathode PIG	1		H^+
(b)				

INJECTION SYSTEM

Efficiency %

EXTRACTION SYSTEM

Electrostatic deflector Efficiency 80 %

CHARACTERISTIC BEAMS

	Accelerated Ions	E/A (MeV/u)	Current(part. μA) Internal	External
(a)	H^+	22	150	70
(b)	D^+	11	150	70

EXTRACTED BEAM PROPERTIES:

For 50 μA of 22 MeV/u H^+ ions

$\Delta E/E$ 1 % $\Delta\phi$ °rf

$\epsilon_n = \beta\gamma\epsilon$ x 30 πmm mrad z 10 πmm mrad

REFERENCES/NOTES

(a)

(b)

ENTRY NO. CM9 Date

Machine Name BC3015

Manufacturer The Japan Steel Works,LTD.

Address 1-2, Yurakucho 1-chome, Chiyoda-ku, Tokyo Japan

Tel (03)3501-6111 Telex J24256 (JSW)

Fax (03)3504-0727 EMAIL

In Charge: Reported by: Y. Todo

HISTORY AND STATUS

DATES: Design 1983-1985 First Machine 1985

SALES: No. Sold/Operational 1 / 1 Currently Available yes

COST: Accelerator Facility

MAGNET

POLE PARAMETERS:

Diameter 129 cm $R_{extract}$ 52 cm R_{inject} cm

HILL PARAMETERS: Gap (min) 10.7 cm B_{max} T

(@ 2.6x10³ AT) Gap (max) 10.7 cm B_{min} T

VALLEY PARAMETERS: Gap (min) 19.9 cm B_{max} T

(@ 2.6x10³ AT) Gap (max) 19.9 cm B_{min} T

AVERAGE FIELD: $< B >_{min}$ 1.54 T $< B >_{max}$ 1.54 T

NUMBER OF SECTORS: compact/separated 4 /

sector angle 45 deg. spiral (max) 90 deg.

FIELD TRIMMING: Trim Coils 6

Harmonic Coils 4

Other

CURRENT: Main Coils 450 Amps Stability ±2x10⁻⁵

Trim Coils 50 Amps Stability 1x10⁻⁴

Stored Energy (cryogenic) MJ

WEIGHT: Iron 60 ton Conductor 2 ton

ION ENERGY: Bending Limit E/A = q^2/A^2 MeV/u

Focussing Limit E/A = q/A MeV/u

ACCELERATION SYSTEM

FUNDAMENTAL ACCELERATION:

Description: 2 sets of pie/4 shape dee with 1 gap/4 steps

No. of Gaps/turn 4 dE/dn(max) 0.16 MeV/q

Voltage(max) 0.04 MV Harmonic f_{rf}/f_{ion} 2,4

Freq 47 MHz Power in(max) 0.025 MW

Stability: Phase 1° Voltage 1x10⁻³

VACUUM SYSTEM

OPERATING PRESSURE: 1x10⁻⁶ Torr

PUMPS: No. and type 2 diffusion pump

ION SOURCE(S)

	Type	Intensity (mA)	@ $\epsilon_n = \beta\gamma\epsilon$ (π mm mrad)	Ion Species
(a)	Hot Cathode PIG	1		H^+
(b)				

INJECTION SYSTEM

Efficiency %

EXTRACTION SYSTEM

Electrostatic deflector Efficiency 70 %

CHARACTERISTIC BEAMS

	Accelerated Ions	E/A (MeV/u)	Current(part. μA) Internal	External
(a)	H^+	30	150	70
(b)	D^+	15	150	70

EXTRACTED BEAM PROPERTIES:

For 50 μA of 30 MeV/u H^+ ions

$\Delta E/E$ 1 % $\Delta\phi$ °rf

$\epsilon_n = \beta\gamma\epsilon$ x 30 πmm mrad z 10 πmm mrad

REFERENCES/NOTES

(a)

(b)

ENTRY NO. CM10 Date June 19,1992

Machine Name HM-18 CYCLOTRON

Manufacturer Sumitomo Heavy Industries, Ltd.

Address 10-11, Kiba 5-chome, Koto-ku, Tokyo 135, Japan

Tel (03)3820-6588 Telex

Fax (03)3820-6452 EMAIL

In Charge: Reported by: Y.Seki

HISTORY AND STATUS

DATES: Design 1989 First Machine 1991

SALES: No. Sold/Operational 2 / 1 Currently Available yes

COST: Accelerator Facility

MAGNET

POLE PARAMETERS:

Diameter 104 cm $R_{extract}$ 43.46 cm R_{inject} — cm

HILL PARAMETERS: Gap (min) 3.6 cm B_{max} 2.1 T

(@ 9.7x10⁴ AT) Gap (max) cm B_{min} T

VALLEY PARAMETERS: Gap (min) 15.4 cm B_{max} 7.2 T

(@ 9.7x10⁴ AT) Gap (max) cm B_{min} T

AVERAGE FIELD: $< B >_{min}$ 1.51 T $< B >_{max}$ 1.56 T

NUMBER OF SECTORS: compact/separated 4 /

sector angle 50 deg. spiral (max) no deg.

FIELD TRIMMING: Trim Coils 4 pairs

Harmonic Coils

Other

CURRENT: Main Coils 180 Amps Stability 0.01 %

Trim Coils 30,30,60,80 Amps Stability 0.1 %

Stored Energy (cryogenic) MJ

WEIGHT: Iron 26 tons Conductor 0.7 tons

ION ENERGY: Bending Limit E/A = q^2/A^2 MeV/u

Focussing Limit E/A = q/A MeV/u

ACCELERATION SYSTEM

FUNDAMENTAL ACCELERATION:

Description: 2 dees (λ/4 cavities)

No. of Gaps/turn 4 dE/dn(max) 0.12 MeV/q

Voltage(max) 0.035 MV Harmonic f_{rf}/f_{ion} 2(H^-),4(D^-)

Freq 45 MHz Power in(max) 0.015 MW

Stability: Phase ±0.5° Voltage 1x10⁻³

VACUUM SYSTEM

OPERATING PRESSURE: 7 x 10⁻⁸ Torr

PUMPS: No. and type 2 oil-diffusion pumps

ION SOURCE(S)

	Type	Intensity (mA)	@ $\epsilon_n = \beta\gamma\epsilon$ (π mm mrad)	Ion Species
(a)	PIG(internal)	—	—	H^-, D^-
(b)				

INJECTION SYSTEM

No Efficiency %

EXTRACTION SYSTEM

Stripping Efficiency 100 %

CHARACTERISTIC BEAMS

	Accelerated Ions	E/A (MeV/u)	Current(part. μA) Internal	External
(a)	H^-	18		70
(b)	D^-	10		50

EXTRACTED BEAM PROPERTIES:

For μA of MeV/u ions

$\Delta E/E$ % $\Delta\phi$ °rf

$\epsilon_n = \beta\gamma\epsilon$ x πmm mrad z πmm mrad

REFERENCES/NOTES

(a)

(b)

ENTRY NO. CM9 Date

Machine Name BC3015

Manufacturer The Japan Steel Works,LTD.

Address 1-2, Yurakucho 1-chome, Chiyoda-ku, Tokyo Japan

Tel (03)3501-6111 Telex J24256 (JSW)

Fax (03)3504-0727 EMAIL

In Charge: Reported by: Y. Todo

HISTORY AND STATUS

DATES: Design 1983-1985 First Machine 1985

SALES: No. Sold/Operational 1 / 1 Currently Available yes

COST: Accelerator Facility

MAGNET

POLE PARAMETERS:

Diameter 129 cm $R_{extract}$ 52 cm R_{inject} cm

HILL PARAMETERS: Gap (min) 10.7 cm B_{max} T

(@ 2.6x10³ AT) Gap (max) 10.7 cm B_{min} T

VALLEY PARAMETERS: Gap (min) 19.9 cm B_{max} T

(@ 2.6x10³ AT) Gap (max) 19.9 cm B_{min} T

AVERAGE FIELD: $< B >_{min}$ 1.54 T $< B >_{max}$ 1.54 T

NUMBER OF SECTORS: compact/separated 4 /

sector angle 45 deg. spiral (max) 90 deg.

FIELD TRIMMING: Trim Coils 6

Harmonic Coils 4

Other

CURRENT: Main Coils 450 Amps Stability ±2x10⁻⁵

Trim Coils 50 Amps Stability 1x10⁻⁴

Stored Energy (cryogenic) MJ

WEIGHT: Iron 60 ton Conductor 2 ton

ION ENERGY: Bending Limit E/A = q^2/A^2 MeV/u

Focussing Limit E/A = q/A MeV/u

ACCELERATION SYSTEM

FUNDAMENTAL ACCELERATION:

Description: 2 sets of pie/4 shape dee with 1 gap/4 steps

No. of Gaps/turn 4 dE/dn(max) 0.16 MeV/q

Voltage(max) 0.04 MV Harmonic f_{rf}/f_{ion} 2,4

Freq 47 MHz Power in(max) 0.025 MW

Stability: Phase 1° Voltage 1x10⁻³

VACUUM SYSTEM

OPERATING PRESSURE: 1x10⁻⁶ Torr

PUMPS: No. and type 2 diffusion pump

ION SOURCE(S)

	Type	Intensity (mA)	@ $\epsilon_n = \beta\gamma\epsilon$ (π mm mrad)	Ion Species
(a)	Hot Cathode PIG	1		H^+
(b)				

INJECTION SYSTEM

Efficiency %

EXTRACTION SYSTEM

Electrostatic deflector Efficiency 70 %

CHARACTERISTIC BEAMS

	Accelerated Ions	E/A (MeV/u)	Current(part. μA) Internal	External
(a)	H^+	30	150	70
(b)	D^+	15	150	70

EXTRACTED BEAM PROPERTIES:

For 50 μA of 30 MeV/u H^+ ions

$\Delta E/E$ 1 % $\Delta\phi$ °rf

$\epsilon_n = \beta\gamma\epsilon$ x 30 πmm mrad z 10 πmm mrad

REFERENCES/NOTES

(a)

(b)

ENTRY NO. CM10 Date June 19,1992

Machine Name HM-18 CYCLOTRON

Manufacturer Sumitomo Heavy Industries, Ltd.

Address 10-11, Kiba 5-chome, Koto-ku, Tokyo 135, Japan

Tel (03)3820-6588 Telex

Fax (03)3820-6452 EMAIL

In Charge: Reported by: Y.Seki

HISTORY AND STATUS

DATES: Design 1989 First Machine 1991

SALES: No. Sold/Operational 2 / 1 Currently Available yes

COST: Accelerator Facility

MAGNET

POLE PARAMETERS:

Diameter 104 cm $R_{extract}$ 43.46 cm R_{inject} — cm

HILL PARAMETERS: Gap (min) 3.6 cm B_{max} 2.1 T

(@ 9.7x10⁴ AT) Gap (max) cm B_{min} T

VALLEY PARAMETERS: Gap (min) 15.4 cm B_{max} 7.2 T

(@ 9.7x10⁴ AT) Gap (max) cm B_{min} T

AVERAGE FIELD: $< B >_{min}$ 1.51 T $< B >_{max}$ 1.56 T

NUMBER OF SECTORS: compact/separated 4 /

sector angle 50 deg. spiral (max) no deg.

FIELD TRIMMING: Trim Coils 4 pairs

Harmonic Coils

Other

CURRENT: Main Coils 180 Amps Stability 0.01 %

Trim Coils 30,30,60,80 Amps Stability 0.1 %

Stored Energy (cryogenic) MJ

WEIGHT: Iron 26 tons Conductor 0.7 tons

ION ENERGY: Bending Limit E/A = q^2/A^2 MeV/u

Focussing Limit E/A = q/A MeV/u

ACCELERATION SYSTEM

FUNDAMENTAL ACCELERATION:

Description: 2 dees (λ/4 cavities)

No. of Gaps/turn 4 dE/dn(max) 0.12 MeV/q

Voltage(max) 0.035 MV Harmonic f_{rf}/f_{ion} 2(H^-),4(D^-)

Freq 45 MHz Power in(max) 0.015 MW

Stability: Phase ±0.5° Voltage 1x10⁻³

VACUUM SYSTEM

OPERATING PRESSURE: 7 x 10⁻⁸ Torr

PUMPS: No. and type 2 oil-diffusion pumps

ION SOURCE(S)

	Type	Intensity (mA)	@ $\epsilon_n = \beta\gamma\epsilon$ (π mm mrad)	Ion Species
(a)	PIG(internal)	—	—	H^-, D^-
(b)				

INJECTION SYSTEM

No Efficiency %

EXTRACTION SYSTEM

Stripping Efficiency 100 %

CHARACTERISTIC BEAMS

	Accelerated Ions	E/A (MeV/u)	Current(part. μA) Internal	External
(a)	H^-	18		70
(b)	D^-	10		50

EXTRACTED BEAM PROPERTIES:

For μA of MeV/u ions

$\Delta E/E$ % $\Delta\phi$ °rf

$\epsilon_n = \beta\gamma\epsilon$ x πmm mrad z πmm mrad

REFERENCES/NOTES

(a)

(b)

ENTRY NO. CM11 Date July 9,1992
Machine Name 480 AVF CYCLOTRON
Manufacturer Sumitomo Heavy Industries, Ltd.
Address 10-11, Kiba 5-chome, Koto-ku, Tokyo 135, Japan
Tel (03)3820-6588 Telex
Fax (03)3820-6452 EMAIL
In Charge: Reported by: T.Tachikawa

HISTORY AND STATUS

DATES: Design First Machine June '85
SALES: No. Sold/Operational 1 / 1 Currently Available yes
COST: Accelerator Facility

MAGNET

POLE PARAMETERS:
Diameter 115 cm $R_{extract}$ 48 cm R_{inject} cm
HILL PARAMETERS: Gap (min) cm B_{max} 2.0 T
(@ 171,200 AT) Gap (max) 8.6 cm B_{min} T
VALLEY PARAMETERS: Gap (min) cm B_{max} 1.57 T
(@ 171,200 AT) Gap (max) 14.1 cm B_{min} T
AVERAGE FIELD: $< B >_{min}$ T $< B >_{max}$ 1.66 T
NUMBER OF SECTORS: compact/separated 4 /
sector angle deg spiral (max) deg.
FIELD TRIMMING: Trim Coils 6 pairs
Harmonic Coils 4 pairs
Other
CURRENT: Main Coils Amps Stability 2×10^{-5}
Trim Coils Amps Stability 5×10^{-4}
Stored Energy (cryogenic) MJ
WEIGHT: Iron 28 tons Conductor 1 tons
ION ENERGY: Bending Limit E/A = q^2/A^2 MeV/u
Focussing Limit E/A = q/A MeV/u

ACCELERATION SYSTEM

FUNDAMENTAL ACCELERATION:
Description: 2-90° dees with $\lambda/4$ cavities
No. of Gaps/turn dE/dn(max) 0.099 MeV/q
Voltage(max) 0.040 MV Harmonic f_{rf}/f_{ion} 1
Freq 20.4 MHz Power in(max) 0.065 MW
Stability: Phase $\pm1\times10^{-7}$ Voltage $\pm1\times10^{-5}$

VACUUM SYSTEM

OPERATING PRESSURE: 2×10^{-5} Torr
PUMPS: No. and type 2000 l/s D.P.

ION SOURCE(S)

	Type	Intensity (mA)	@ $\epsilon_n = \beta\gamma\epsilon$ (π mm mrad)	Ion Species
(a)	Livingston			H^+
(b)				

INJECTION SYSTEM

Efficiency %

EXTRACTION SYSTEM

Electrostatic + Magnetic Efficiency 75 %

CHARACTERISTIC BEAMS

	Accelerated Ions	E/A (MeV/u)	Current(part. μA) Internal	External
(a)	H^+	30	200	80
(b)				

EXTRACTED BEAM PROPERTIES:
For μA of MeV/u ions
$\Delta E/E$ % $\Delta\phi$ °rf
$\epsilon_n = \beta\gamma\epsilon$ x πmm mrad z πmm mrad

REFERENCES/NOTES

(a)
(b)

ENTRY NO. CM12 Date July 9,1992
Machine Name 750 AVF CYCLOTRON
Manufacturer Sumitomo Heavy Industries, Ltd.
Address 10-11, Kiba 5-chome, Koto-ku, Tokyo 135, Japan
Tel (03)3820-6588 Telex
Fax (03)3820-6452 EMAIL
In Charge: Reported by: T.Tachikawa

HISTORY AND STATUS

DATES: Design First Machine Feb. '85
SALES: No. Sold/Operational 2 / 2 Currently Available yes
COST: Accelerator Facility

MAGNET

POLE PARAMETERS:
Diameter 180 cm $R_{extract}$ 75 cm R_{inject} cm
HILL PARAMETERS: Gap (min) cm B_{max} 2.0 T
(@ 263,000 AT) Gap (max) 13.9 cm B_{min} T
VALLEY PARAMETERS: Gap (min) cm B_{max} 1.57 T
(@ 263,000 AT) Gap (max) 31.5 cm B_{min} T
AVERAGE FIELD: $< B >_{min}$ T $< B >_{max}$ 1.64 T
NUMBER OF SECTORS: compact/separated 4 /
sector angle deg spiral (max) deg.
FIELD TRIMMING: Trim Coils 10 pairs
Harmonic Coils 4 pairs
Other
CURRENT: Main Coils Amps Stability 2×10^{-5}
Trim Coils Amps Stability 5×10^{-4}
Stored Energy (cryogenic) MJ
WEIGHT: Iron 120 tons Conductor 6 tons
ION ENERGY: Bending Limit E/A = q^2/A^2 MeV/u
Focussing Limit E/A = q/A MeV/u

ACCELERATION SYSTEM

FUNDAMENTAL ACCELERATION:
Description: 90°-2 dees with $\lambda/4$ cavities
No. of Gaps/turn dE/dn(max) 0.127 MeV/q
Voltage(max) 0.050 MV Harmonic f_{rf}/f_{ion} 1
Freq 13-25 MHz Power in(max) 80 MW
Stability: Phase $\pm1\times10^{-7}$ Voltage $\pm1\times10^{-5}$

VACUUM SYSTEM

OPERATING PRESSURE: 2×10^{-5} Torr
PUMPS: No. and type 2000 l/s D.P. x2

ION SOURCE(S)

	Type	Intensity (mA)	@ $\epsilon_n = \beta\gamma\epsilon$ (π mm mrad)	Ion Species
(a)	Livingston			H^+
(b)				

INJECTION SYSTEM

Efficiency %

EXTRACTION SYSTEM

Electrostatic + Magnetic Efficiency 80 %

CHARACTERISTIC BEAMS

	Accelerated Ions	E/A (MeV/u)	Current(part. μA) Internal	External
(a)	H^+	70	200	55
(b)	H^+	25	200	100

EXTRACTED BEAM PROPERTIES:
For μA of MeV/u ions
$\Delta E/E$ % $\Delta\phi$ °rf
$\epsilon_n = \beta\gamma\epsilon$ x πmm mrad z πmm mrad

REFERENCES/NOTES

(a)
(b)

ENTRY NO. CM11 Date July 9,1992
Machine Name 480 AVF CYCLOTRON
Manufacturer Sumitomo Heavy Industries, Ltd.
Address 10-11, Kiba 5-chome, Koto-ku, Tokyo 135, Japan
Tel (03)3820-6588 Telex
Fax (03)3820-6452 EMAIL
In Charge: Reported by: T.Tachikawa

HISTORY AND STATUS

DATES: Design First Machine June '85
SALES: No. Sold/Operational 1 / 1 Currently Available yes
COST: Accelerator Facility

MAGNET

POLE PARAMETERS:
Diameter 115 cm $R_{extract}$ 48 cm R_{inject} cm
HILL PARAMETERS: Gap (min) cm B_{max} 2.0 T
(@ 171,200 AT) Gap (max) 8.6 cm B_{min} T
VALLEY PARAMETERS: Gap (min) cm B_{max} 1.57 T
(@ 171,200 AT) Gap (max) 14.1 cm B_{min} T
AVERAGE FIELD: $< B >_{min}$ T $< B >_{max}$ 1.66 T
NUMBER OF SECTORS: compact/separated 4 /
sector angle deg spiral (max) deg.
FIELD TRIMMING: Trim Coils 6 pairs
Harmonic Coils 4 pairs
Other
CURRENT: Main Coils Amps Stability 2×10^{-5}
Trim Coils Amps Stability 5×10^{-4}
Stored Energy (cryogenic) MJ
WEIGHT: Iron 28 tons Conductor 1 tons
ION ENERGY: Bending Limit E/A = q^2/A^2 MeV/u
Focussing Limit E/A = q/A MeV/u

ACCELERATION SYSTEM

FUNDAMENTAL ACCELERATION:
Description: 2-90° dees with $\lambda/4$ cavities
No. of Gaps/turn dE/dn(max) 0.099 MeV/q
Voltage(max) 0.040 MV Harmonic f_{rf}/f_{ion} 1
Freq 20.4 MHz Power in(max) 0.065 MW
Stability: Phase $\pm1\times10^{-7}$ Voltage $\pm1\times10^{-5}$

VACUUM SYSTEM

OPERATING PRESSURE: 2×10^{-5} Torr
PUMPS: No. and type 2000 l/s D.P.

ION SOURCE(S)

	Type	Intensity (mA)	@ $\epsilon_n = \beta\gamma\epsilon$ (π mm mrad)	Ion Species
(a)	Livingston			H^+
(b)				

INJECTION SYSTEM

Efficiency %

EXTRACTION SYSTEM

Electrostatic + Magnetic Efficiency 75 %

CHARACTERISTIC BEAMS

	Accelerated Ions	E/A (MeV/u)	Current(part. μA) Internal	External
(a)	H^+	30	200	80
(b)				

EXTRACTED BEAM PROPERTIES:
For μA of MeV/u ions
$\Delta E/E$ % $\Delta\phi$ °rf
$\epsilon_n = \beta\gamma\epsilon$ x πmm mrad z πmm mrad

REFERENCES/NOTES

(a)
(b)

ENTRY NO. CM12 Date July 9,1992
Machine Name 750 AVF CYCLOTRON
Manufacturer Sumitomo Heavy Industries, Ltd.
Address 10-11, Kiba 5-chome, Koto-ku, Tokyo 135, Japan
Tel (03)3820-6588 Telex
Fax (03)3820-6452 EMAIL
In Charge: Reported by: T.Tachikawa

HISTORY AND STATUS

DATES: Design First Machine Feb. '85
SALES: No. Sold/Operational 2 / 2 Currently Available yes
COST: Accelerator Facility

MAGNET

POLE PARAMETERS:
Diameter 180 cm $R_{extract}$ 75 cm R_{inject} cm
HILL PARAMETERS: Gap (min) cm B_{max} 2.0 T
(@ 263,000 AT) Gap (max) 13.9 cm B_{min} T
VALLEY PARAMETERS: Gap (min) cm B_{max} 1.57 T
(@ 263,000 AT) Gap (max) 31.5 cm B_{min} T
AVERAGE FIELD: $< B >_{min}$ T $< B >_{max}$ 1.64 T
NUMBER OF SECTORS: compact/separated 4 /
sector angle deg spiral (max) deg.
FIELD TRIMMING: Trim Coils 10 pairs
Harmonic Coils 4 pairs
Other
CURRENT: Main Coils Amps Stability 2×10^{-5}
Trim Coils Amps Stability 5×10^{-4}
Stored Energy (cryogenic) MJ
WEIGHT: Iron 120 tons Conductor 6 tons
ION ENERGY: Bending Limit E/A = q^2/A^2 MeV/u
Focussing Limit E/A = q/A MeV/u

ACCELERATION SYSTEM

FUNDAMENTAL ACCELERATION:
Description: 90°-2 dees with $\lambda/4$ cavities
No. of Gaps/turn dE/dn(max) 0.127 MeV/q
Voltage(max) 0.050 MV Harmonic f_{rf}/f_{ion} 1
Freq 13-25 MHz Power in(max) 80 MW
Stability: Phase $\pm1\times10^{-7}$ Voltage $\pm1\times10^{-5}$

VACUUM SYSTEM

OPERATING PRESSURE: 2×10^{-5} Torr
PUMPS: No. and type 2000 l/s D.P. x2

ION SOURCE(S)

	Type	Intensity (mA)	@ $\epsilon_n = \beta\gamma\epsilon$ (π mm mrad)	Ion Species
(a)	Livingston			H^+
(b)				

INJECTION SYSTEM

Efficiency %

EXTRACTION SYSTEM

Electrostatic + Magnetic Efficiency 80 %

CHARACTERISTIC BEAMS

	Accelerated Ions	E/A (MeV/u)	Current(part. μA) Internal	External
(a)	H^+	70	200	55
(b)	H^+	25	200	100

EXTRACTED BEAM PROPERTIES:
For μA of MeV/u ions
$\Delta E/E$ % $\Delta\phi$ °rf
$\epsilon_n = \beta\gamma\epsilon$ x πmm mrad z πmm mrad

REFERENCES/NOTES

(a)
(b)

ENTRY NO. CM13 Date June 19,1992
Machine Name 930 AVF CYCLOTRON
Manufacturer Sumitomo Heavy Industries, Ltd.
Address 10-11, Kiba 5-chome, Koto-ku, Tokyo 135, Japan
Tel (03)3820-6588 Telex
Fax (03)3820-6452 EMAIL
In Charge: Reported by: T.Tachikawa

HISTORY AND STATUS

DATES: Design First Machine
SALES: No. Sold/Operational 5 / 5 Currently Available yes
COST: Accelerator Facility

MAGNET

POLE PARAMETERS:
Diameter 215.6 cm $R_{extract}$ 92.3 cm R_{inject} cm
HILL PARAMETERS: Gap (min) cm B_{max} 1.96 T
(@ 408.000 AT) Gap (max) 16.6 cm B_{min} T
VALLEY PARAMETERS: Gap (min) cm B_{max} 1.13 T
(@ 408.000 AT) Gap (max) 40.5 cm B_{min} T
AVERAGE FIELD: $< B >_{min}$ T $< B >_{max}$ 1.64 T
NUMBER OF SECTORS: compact/separated 4 /
sector angle deg. spiral (max) 53 deg.
FIELD TRIMMING: Trim Coils 12 pairs
Harmonic Coils 4 pairs
Other
CURRENT: Main Coils 900 Amps Stability $\pm 1x10^{-5}$
Trim Coils 100-800 Amps Stability $\pm 2x10^{-4}$
Stored Energy (cryogenic) MJ
WEIGHT: Iron 220 tons Conductor 9 tons
ION ENERGY: Bending Limit E/A = 110 q^2/A^2 MeV/u
Focussing Limit E/A = 95 q/A MeV/u

ACCELERATION SYSTEM

FUNDAMENTAL ACCELERATION:
Description: 2-90° dees with 2/4 cavities
No. of Gaps/turn 4 dE/dn(max) 0.17 MeV/q
Voltage(max) 0.060 MV Harmonic f_{rf}/f_{ion} 1, 2, 3
Freq 10.6 - 22.0 MHz Power in(max) 2 x 0.07 MW
Stability: Phase ±0.5 deg. Voltage $\pm 1x10^{-3}$

VACUUM SYSTEM

OPERATING PRESSURE: 5x10⁻⁷ Torr
PUMPS: No. and type 4 cryo pumps + 1 turbo pump

ION SOURCE(S)

	Type	Intensity (mA)	@ $\epsilon_n = \beta\gamma\epsilon$ (π mm mrad)	Ion Species
(a)	No standard source			
(b)	Both heavy and light ion sources are available			

INJECTION SYSTEM

Axial injection, Spiral inflector, Efficiency 10 - 20 %

EXTRACTION SYSTEM

Electrostatic + Magnetic Efficiency 60 - 70 %

CHARACTERISTIC BEAMS

	Accelerated Ions	E/A (MeV/u)	Current(part. μA) Internal	External
(a)	H^+	90	25	10
(b)	D^+	35	68	41

EXTRACTED BEAM PROPERTIES:
For 3 μA of 44 MeV/u Ar^{8+} ions
$\Delta E/E$ % $\Delta\phi$ °rf
$\epsilon_n = \beta\gamma\epsilon$ x 1.4 πmm mrad z 1.0 πmm mrad

REFERENCES/NOTES

(a) Proc. of the Int. Conf. on Evolution in Beam Applications
(b) Takasaki, Japan, 1991, P270 - 274

ENTRY NO. CM14 Date 30.06.92
Machine Name PIC-10
Manufacturer D.V.Efremov Institute
Address 189631 St.Petersburg, Russia
Tel (812) 2655682 Telex
Fax (812) 2657880 EMAIL
In Charge: Reported by: Vorogushin

HISTORY AND STATUS

DATES: Design 1991 First Machine 1993
SALES: No. Sold/Operational / Currently Available
COST: Accelerator Facility

MAGNET

POLE PARAMETERS:
Diameter 73 cm $R_{extract}$ 32,5 cm R_{inject} cm
HILL PARAMETERS: Gap (min) 5,0 cm B_{max} 1,70 T
(@ AT) Gap (max) 5,0 cm B_{min} T
VALLEY PARAMETERS: Gap (min) 10,0 cm B_{max} 1,20 T
(@ 10,0 AT) Gap (max) cm B_{min} T
AVERAGE FIELD: $< B >_{min}$ 1,48 T $< B >_{max}$ 1,48 T
NUMBER OF SECTORS: compact/separated 4 /
sector angle deg. spiral (max) 0 deg.
FIELD TRIMMING: Trim Coils none
Harmonic Coils none
Other
CURRENT: Main Coils 380 Amps Stability 0,01%
Trim Coils Amps Stability
Stored Energy (cryogenic) MJ
WEIGHT: Iron 7,5 t Conductor 1,05 t
ION ENERGY: Bending Limit E/A = q^2/A^2 MeV/u
Focussing Limit E/A = q/A MeV/u

ACCELERATION SYSTEM

FUNDAMENTAL ACCELERATION:
Description: 2 dees 45 deg
No. of Gaps/turn 4 dE/dn(max) 0,10 MeV/q
Voltage(max) 0,035 MV Harmonic f_{rf}/f_{ion} 2
Freq 45 + - MHz Power in(max) 0,009 MW
Stability: Phase ± 5 deg Voltage 0,1%

VACUUM SYSTEM

OPERATING PRESSURE: $5,10^{-6}$
PUMPS: No. and type 2 diffusion pumps

ION SOURCE(S)

	Type	Intensity (mA)	@ $\epsilon_n = \beta\gamma\epsilon$ (π mm mrad)	Ion Species
(a)	PIG	H		
(b)				

INJECTION SYSTEM

Efficiency %

EXTRACTION SYSTEM

charge exchange foil Efficiency 100 %

CHARACTERISTIC BEAMS

	Accelerated Ions	E/A (MeV/u)	Current(part. μA) Internal	External
(a)	H	11	50 H	50 p
(b)				

EXTRACTED BEAM PROPERTIES:
For μA of MeV/u ions
$\Delta E/E$ % $\Delta\phi$ °rf
$\epsilon_n = \beta\gamma\epsilon$ x πmm mrad z πmm mrad

REFERENCES/NOTES

(a)
(b)

ENTRY NO. CM13 Date June 19,1992
Machine Name 930 AVF CYCLOTRON
Manufacturer Sumitomo Heavy Industries, Ltd.
Address 10-11, Kiba 5-chome, Koto-ku, Tokyo 135, Japan
Tel (03)3820-6588 Telex
Fax (03)3820-6452 EMAIL
In Charge: Reported by: T.Tachikawa

HISTORY AND STATUS

DATES: Design First Machine
SALES: No. Sold/Operational 5 / 5 Currently Available yes
COST: Accelerator Facility

MAGNET

POLE PARAMETERS:
Diameter 215.6 cm $R_{extract}$ 92.3 cm R_{inject} cm
HILL PARAMETERS: Gap (min) cm B_{max} 1.96 T
(@ 408.000 AT) Gap (max) 16.6 cm B_{min} T
VALLEY PARAMETERS: Gap (min) cm B_{max} 1.13 T
(@ 408.000 AT) Gap (max) 40.5 cm B_{min} T
AVERAGE FIELD: $< B >_{min}$ T $< B >_{max}$ 1.64 T
NUMBER OF SECTORS: compact/separated 4 /
sector angle deg. spiral (max) 53 deg.
FIELD TRIMMING: Trim Coils 12 pairs
Harmonic Coils 4 pairs
Other
CURRENT: Main Coils 900 Amps Stability $\pm 1x10^{-5}$
Trim Coils 100-800 Amps Stability $\pm 2x10^{-4}$
Stored Energy (cryogenic) MJ
WEIGHT: Iron 220 tons Conductor 9 tons
ION ENERGY: Bending Limit E/A = 110 q^2/A^2 MeV/u
Focussing Limit E/A = 95 q/A MeV/u

ACCELERATION SYSTEM

FUNDAMENTAL ACCELERATION:
Description: 2-90° dees with 2/4 cavities
No. of Gaps/turn 4 dE/dn(max) 0.17 MeV/q
Voltage(max) 0.060 MV Harmonic f_{rf}/f_{ion} 1, 2, 3
Freq 10.6 - 22.0 MHz Power in(max) 2 x 0.07 MW
Stability: Phase ±0.5 deg. Voltage $\pm 1x10^{-3}$

VACUUM SYSTEM

OPERATING PRESSURE: 5x10⁻⁷ Torr
PUMPS: No. and type 4 cryo pumps + 1 turbo pump

ION SOURCE(S)

	Type	Intensity (mA)	@ $\epsilon_n = \beta\gamma\epsilon$ (π mm mrad)	Ion Species
(a)	No standard source			
(b)	Both heavy and light ion sources are available			

INJECTION SYSTEM

Axial injection, Spiral inflector, Efficiency 10 - 20 %

EXTRACTION SYSTEM

Electrostatic + Magnetic Efficiency 60 - 70 %

CHARACTERISTIC BEAMS

	Accelerated Ions	E/A (MeV/u)	Current(part. μA) Internal	External
(a)	H^+	90	25	10
(b)	D^+	35	68	41

EXTRACTED BEAM PROPERTIES:
For 3 μA of 44 MeV/u Ar^{8+} ions
$\Delta E/E$ % $\Delta\phi$ °rf
$\epsilon_n = \beta\gamma\epsilon$ x 1.4 πmm mrad z 1.0 πmm mrad

REFERENCES/NOTES

(a) Proc. of the Int. Conf. on Evolution in Beam Applications
(b) Takasaki, Japan, 1991, P270 - 274

ENTRY NO. CM14 Date 30.06.92
Machine Name PIC-10
Manufacturer D.V.Efremov Institute
Address 189631 St.Petersburg, Russia
Tel (812) 2655682 Telex
Fax (812) 2657880 EMAIL
In Charge: Reported by: Vorogushin

HISTORY AND STATUS

DATES: Design 1991 First Machine 1993
SALES: No. Sold/Operational / Currently Available
COST: Accelerator Facility

MAGNET

POLE PARAMETERS:
Diameter 73 cm $R_{extract}$ 32,5 cm R_{inject} cm
HILL PARAMETERS: Gap (min) 5,0 cm B_{max} 1,70 T
(@ AT) Gap (max) 5,0 cm B_{min} T
VALLEY PARAMETERS: Gap (min) 10,0 cm B_{max} 1,20 T
(@ 10,0 AT) Gap (max) cm B_{min} T
AVERAGE FIELD: $< B >_{min}$ 1,48 T $< B >_{max}$ 1,48 T
NUMBER OF SECTORS: compact/separated 4 /
sector angle deg. spiral (max) 0 deg.
FIELD TRIMMING: Trim Coils none
Harmonic Coils none
Other
CURRENT: Main Coils 380 Amps Stability 0,01%
Trim Coils Amps Stability
Stored Energy (cryogenic) MJ
WEIGHT: Iron 7,5 t Conductor 1,05 t
ION ENERGY: Bending Limit E/A = q^2/A^2 MeV/u
Focussing Limit E/A = q/A MeV/u

ACCELERATION SYSTEM

FUNDAMENTAL ACCELERATION:
Description: 2 dees 45 deg
No. of Gaps/turn 4 dE/dn(max) 0,10 MeV/q
Voltage(max) 0,035 MV Harmonic f_{rf}/f_{ion} 2
Freq 45 + - MHz Power in(max) 0,009 MW
Stability: Phase ± 5 deg Voltage 0,1%

VACUUM SYSTEM

OPERATING PRESSURE: $5,10^{-6}$
PUMPS: No. and type 2 diffusion pumps

ION SOURCE(S)

	Type	Intensity (mA)	@ $\epsilon_n = \beta\gamma\epsilon$ (π mm mrad)	Ion Species
(a)	PIG	H		
(b)				

INJECTION SYSTEM

Efficiency %

EXTRACTION SYSTEM

charge exchange foil Efficiency 100 %

CHARACTERISTIC BEAMS

	Accelerated Ions	E/A (MeV/u)	Current(part. μA) Internal	External
(a)	H	11	50 H	50 p
(b)				

EXTRACTED BEAM PROPERTIES:
For μA of MeV/u ions
$\Delta E/E$ % $\Delta\phi$ °rf
$\epsilon_n = \beta\gamma\epsilon$ x πmm mrad z πmm mrad

REFERENCES/NOTES

(a)
(b)

ENTRY NO. CM15 Date 30.06.92
Machine Name MGO-20
Manufacturer D.V.Efremov Institute
Address 189631 St.-Petersburg, Russia
Tel (812) 2655682 Telex
Fax (812) 2657880 EMAIL
In Charge: Reported by: Vorogushin

HISTORY AND STATUS
DATES: Design 1970 First Machine 1974
SALES: No. Sold/Operational / Currently Available
COST: Accelerator Facility

MAGNET
POLE PARAMETERS:
Diameter 103 cm $R_{extract}$ 45 cm R_{inject} cm
HILL PARAMETERS: Gap (min) 7.2 cm B_{max} 1.62 T
(@ 1,2,10^{5}AT) Gap (max) 7.2 cm B_{min} T
VALLEY PARAMETERS: Gap (min) 12.0 cm B_{max} 1.02 T
(@ 1,2,10^{5}AT) Gap (max) 12.0 cm B_{min} T
AVERAGE FIELD: $< B >_{min}$ 0.65 T $< B >_{max}$ 1.48 T
NUMBER OF SECTORS: compact/separated 3 /
sector angle deg. spiral (max) 35 deg.
FIELD TRIMMING: Trim Coils 4 pairs
Harmonic Coils 2 sets
Other
CURRENT: Main Coils 420 Amps Stability 0.01%
Trim Coils 15 Amps Stability 0.1%
Stored Energy (cryogenic) MJ
WEIGHT: Iron 24 t Conductor 1.2 t
ION ENERGY: Bending Limit E/A = q^2/A^2 MeV/u
Focussing Limit E/A = q/A MeV/u

ACCELERATION SYSTEM
FUNDAMENTAL ACCELERATION:
Description: 2 dees 180-140 deg
No. of Gaps/turn 2 dE/dn(max) 0.12 MeV/q
Voltage(max) 0.030 MV Harmonic f_{rf}/f_{ion} 1.3
Freq 8-24 MHz Power in(max) 0.05 MW
Stability: Phase $\pm$ 5 deg Voltage 0.1%

VACUUM SYSTEM
OPERATING PRESSURE: 10^{-5}
PUMPS: No. and type 3 deffusion pumps

ION SOURCE(S)

	Type	Intensity (mA)	@ $\epsilon_n = \beta\gamma\epsilon$ (π mm mrad)	Ion Species
(a)	hot filament Levingstone p.s.,			He$^-$3(++)
(b)				

INJECTION SYSTEM
Efficiency %

EXTRACTION SYSTEM
electrostatic deflection Efficiency 50 %

CHARACTERISTIC BEAMS

Accelerated Ions	E/A (MeV/u)	Current(part. μA) Internal	External
(a) p, d,	18 5	200	500
(b) He$^-$3(++)	5.8	50	25

EXTRACTED BEAM PROPERTIES:
For 50 μA of 18 MeV/u P ions
$\Delta E/E$ 0.3 % $\Delta\phi$ °rf
$\epsilon_n = \beta\gamma\epsilon$ x 50 πmm mrad z 15 πmm mrad

REFERENCES/NOTES
(a)
(b)

ENTRY NO. CM16 Date July 6, 1992
Machine Name U-250
Manufacturer D.V. Efremov Institute
Address 189631 St. Petersburg, Russia
Tel (812) 2655682 Telex
Fax (812) 2657880 EMAIL
In Charge: V. Glukhikh Reported by: Vorogushin/Muminov

HISTORY AND STATUS
DATES: Design 1991 First Machine 1994
SALES: No. Sold/Operational / Currently Available
COST: Accelerator Facility

MAGNET
POLE PARAMETERS:
Diameter 250 cm $R_{extract}$ cm R_{inject} cm
HILL PARAMETERS: Gap (min) 2.6 cm B_{max} 2.4 T
(@ AT) Gap (max) 4.5 cm B_{min} T
VALLEY PARAMETERS: Gap (min) 15 cm B_{max} T
(@ AT) Gap (max) 15 cm B_{min} 1.4 T
AVERAGE FIELD: $< B >_{min}$ 1.6 T $< B >_{max}$ 1.9 T
NUMBER OF SECTORS: compact/separated 4 /
sector angle 45 deg. spiral (max) - deg
FIELD TRIMMING: Trim Coils 7 x 4
Harmonic Coils
Other
CURRENT: Main Coils 900 Amps Stability 10^{-5}
Trim Coils 20 Amps Stability 0.01
Stored Energy (cryogenic) MJ
WEIGHT: Iron 385t Conductor 5.4t
ION ENERGY: Bending Limit E/A = 204 q^2/A^2 MeV/u
Focussing Limit E/A = q/A MeV/u

ACCELERATION SYSTEM
FUNDAMENTAL ACCELERATION:
Description: 2 dees 42 deg
No. of Gaps/turn dE/dn(max) MeV/q
Voltage(max) 0.075 MV Harmonic f_{rf}/f_{ion} 1,2,3,4
Freq 8-19 MHz Power in(max) 0.150 MW
Stability: Phase $\pm$ 1 deg Voltage 0.1%

VACUUM SYSTEM
OPERATING PRESSURE: 10^{-6}
PUMPS: No. and type 3
2 diff. pumps 10m/sec

ION SOURCE(S)

	Type	Intensity (mA)	@ $\epsilon_n = \beta\gamma\epsilon$ (π mm mrad)	Ion Species
(a)	pig	600	30	^{2}H$^+$
(b)	heavy ions		to 84Kr^{+8}	

INJECTION SYSTEM
axial inter injection Efficiency %

EXTRACTION SYSTEM
stripping foil, electrostatic DEFL Efficiency 50-95 %

CHARACTERISTIC BEAMS

Accelerated Ions	E/A (MeV/u)	Current(part. μA) Internal	External
(a) ^{2}H$^+$, d, ^{3}H$^+$, ^{4}H^{++}	40-12.5	500	
(b) ^{12}C^{+3}, 84Kr^{+8}	12.5-1.9	5-100	

EXTRACTED BEAM PROPERTIES:
For 500 μA of 40 MeV/u ^{2}H$^+$ ions
$\Delta E/E$ 0.1-1 % $\Delta\phi$ °rf
$\epsilon_n = \beta\gamma\epsilon$ x 50 πmm mrad z 20 πmm mrad

REFERENCES/NOTES
(a)
(b)

ENTRY NO. CM15 Date 30.06.92
Machine Name MGO-20
Manufacturer D.V.Efremov Institute
Address 189631 St.-Petersburg, Russia
Tel (812) 2655682 Telex
Fax (812) 2657880 EMAIL
In Charge: Reported by: Vorogushin

HISTORY AND STATUS
DATES: Design 1970 First Machine 1974
SALES: No. Sold/Operational / Currently Available
COST: Accelerator Facility

MAGNET
POLE PARAMETERS:
Diameter 103 cm $R_{extract}$ 45 cm R_{inject} cm
HILL PARAMETERS: Gap (min) 7.2 cm B_{max} 1.62 T
(@ 1,2,10^{5}AT) Gap (max) 7.2 cm B_{min} T
VALLEY PARAMETERS: Gap (min) 12.0 cm B_{max} 1.02 T
(@ 1,2,10^{5}AT) Gap (max) 12.0 cm B_{min} T
AVERAGE FIELD: $< B >_{min}$ 0.65 T $< B >_{max}$ 1.48 T
NUMBER OF SECTORS: compact/separated 3 /
sector angle deg. spiral (max) 35 deg.
FIELD TRIMMING: Trim Coils 4 pairs
Harmonic Coils 2 sets
Other
CURRENT: Main Coils 420 Amps Stability 0.01%
Trim Coils 15 Amps Stability 0.1%
Stored Energy (cryogenic) MJ
WEIGHT: Iron 24 t Conductor 1.2 t
ION ENERGY: Bending Limit E/A = q^2/A^2 MeV/u
Focussing Limit E/A = q/A MeV/u

ACCELERATION SYSTEM
FUNDAMENTAL ACCELERATION:
Description: 2 dees 180-140 deg
No. of Gaps/turn 2 dE/dn(max) 0.12 MeV/q
Voltage(max) 0.030 MV Harmonic f_{rf}/f_{ion} 1.3
Freq 8-24 MHz Power in(max) 0.05 MW
Stability: Phase $\pm$ 5 deg Voltage 0.1%

VACUUM SYSTEM
OPERATING PRESSURE: 10^{-5}
PUMPS: No. and type 3 deffusion pumps

ION SOURCE(S)

	Type	Intensity (mA)	@ $\epsilon_n = \beta\gamma\epsilon$ (π mm mrad)	Ion Species
(a)	hot filament Levingstone p.s.,			He$^-$3(++)
(b)				

INJECTION SYSTEM
Efficiency %

EXTRACTION SYSTEM
electrostatic deflection Efficiency 50 %

CHARACTERISTIC BEAMS

Accelerated Ions	E/A (MeV/u)	Current(part. μA) Internal	External
(a) p, d,	18 5	200	500
(b) He$^-$3(++)	5.8	50	25

EXTRACTED BEAM PROPERTIES:
For 50 μA of 18 MeV/u P ions
$\Delta E/E$ 0.3 % $\Delta\phi$ °rf
$\epsilon_n = \beta\gamma\epsilon$ x 50 πmm mrad z 15 πmm mrad

REFERENCES/NOTES
(a)
(b)

ENTRY NO. CM16 Date July 6, 1992
Machine Name U-250
Manufacturer D.V. Efremov Institute
Address 189631 St. Petersburg, Russia
Tel (812) 2655682 Telex
Fax (812) 2657880 EMAIL
In Charge: V. Glukhikh Reported by: Vorogushin/Muminov

HISTORY AND STATUS
DATES: Design 1991 First Machine 1994
SALES: No. Sold/Operational / Currently Available
COST: Accelerator Facility

MAGNET
POLE PARAMETERS:
Diameter 250 cm $R_{extract}$ cm R_{inject} cm
HILL PARAMETERS: Gap (min) 2.6 cm B_{max} 2.4 T
(@ AT) Gap (max) 4.5 cm B_{min} T
VALLEY PARAMETERS: Gap (min) 15 cm B_{max} T
(@ AT) Gap (max) 15 cm B_{min} 1.4 T
AVERAGE FIELD: $< B >_{min}$ 1.6 T $< B >_{max}$ 1.9 T
NUMBER OF SECTORS: compact/separated 4 /
sector angle 45 deg. spiral (max) - deg
FIELD TRIMMING: Trim Coils 7 x 4
Harmonic Coils
Other
CURRENT: Main Coils 900 Amps Stability 10^{-5}
Trim Coils 20 Amps Stability 0.01
Stored Energy (cryogenic) MJ
WEIGHT: Iron 385t Conductor 5.4t
ION ENERGY: Bending Limit E/A = 204 q^2/A^2 MeV/u
Focussing Limit E/A = q/A MeV/u

ACCELERATION SYSTEM
FUNDAMENTAL ACCELERATION:
Description: 2 dees 42 deg
No. of Gaps/turn dE/dn(max) MeV/q
Voltage(max) 0.075 MV Harmonic f_{rf}/f_{ion} 1,2,3,4
Freq 8-19 MHz Power in(max) 0.150 MW
Stability: Phase $\pm$ 1 deg Voltage 0.1%

VACUUM SYSTEM
OPERATING PRESSURE: 10^{-6}
PUMPS: No. and type 3
2 diff. pumps 10m/sec

ION SOURCE(S)

	Type	Intensity (mA)	@ $\epsilon_n = \beta\gamma\epsilon$ (π mm mrad)	Ion Species
(a)	pig	600	30	^{2}H$^+$
(b)	heavy ions		to 84Kr^{+8}	

INJECTION SYSTEM
axial inter injection Efficiency %

EXTRACTION SYSTEM
stripping foil, electrostatic DEFL Efficiency 50-95 %

CHARACTERISTIC BEAMS

Accelerated Ions	E/A (MeV/u)	Current(part. μA) Internal	External
(a) ^{2}H$^+$, d, ^{3}H$^+$, ^{4}H^{++}	40-12.5	500	
(b) ^{12}C^{+3}, 84Kr^{+8}	12.5-1.9	5-100	

EXTRACTED BEAM PROPERTIES:
For 500 μA of 40 MeV/u ^{2}H$^+$ ions
$\Delta E/E$ 0.1-1 % $\Delta\phi$ °rf
$\epsilon_n = \beta\gamma\epsilon$ x 50 πmm mrad z 20 πmm mrad

REFERENCES/NOTES
(a)
(b)

ENTRY NO. CM18 Date

Machine Name MC30 p. fixed Energy

Manufacturer Scanditronix

Address Husyborg, S752 29 Uppsala, Sweden

Tel 46 18 18 0700 Telex

Fax 46 18 53 7276 EMAIL

In Charge: Reported by: Jonas Modéer

HISTORY AND STATUS

DATES: Design 1987 First Machine 1988

SALES: No. Sold/Operational 1 / 1 Currently Available Y

COST: Accelerator Facility

MAGNET

POLE PARAMETERS:

Diameter 130 cm $R_{extract}$ cm R_{inject} cm

HILL PARAMETERS: Gap (min) 10 cm B_{max} T

(@ AT) Gap (max) cm B_{min} T

VALLEY PARAMETERS: Gap (min) 18 cm B_{max} T

(@ AT) Gap (max) cm B_{min} T

AVERAGE FIELD: $< B >_{min}$ 1.4 T $< B >_{max}$ T

NUMBER OF SECTORS: compact/separated 3 /

sector angle deg. spiral (max) 50 deg.

FIELD TRIMMING: Trim Coils 5

Harmonic Coils 2

Other 5

CURRENT: Main Coils 600 Amps Stability 10

Trim Coils Amps Stability

Stored Energy (cryogenic) MJ

WEIGHT: Iron 69,000 kg Conductor

ION ENERGY: Bending Limit E/A = q^2/A^2 MeV/u

Focussing Limit E/A = q/A MeV/u

ACCELERATION SYSTEM

FUNDAMENTAL ACCELERATION:

Description: Driven System

No. of Gaps/turn 4 dE/dn(max) 0.1 MeV/q

Voltage(max) 0.035 MV Harmonic f_{rf}/f_{ion} 1

Freq MHz Power in(max) MW

Stability: Phase Voltage

VACUUM SYSTEM

OPERATING PRESSURE: 10^{-5} – 10^{-6}

PUMPS: No. and type 2 x 4000 ℓ/sec Diff pump

ION SOURCE(S)

	Type	Intensity (mA)	@	$\epsilon_n = \beta\gamma\epsilon$ (π mm mrad)	Ion Species
(a)	Hot filament	0.3			P
(b)					

INJECTION SYSTEM

Efficiency –

EXTRACTION SYSTEM

Efficiency –

CHARACTERISTIC BEAMS

	Accelerated Ions	E/A (MeV/u)	Current(part. μA) Internal	External
(a)	P	30	500	–
(b)				

EXTRACTED BEAM PROPERTIES:

For μA of MeV/u ions

$\Delta E/E$ % $\Delta\phi$ °rf

$\epsilon_n = \beta\gamma\epsilon$ x πmm mrad z πmm mrad

REFERENCES/NOTES

(a)

(b)

ENTRY NO. CM19 Date

Machine Name MC 32 NI

Manufacturer Scanditronix

Address Husyborg, S752 29 Uppsala Sweden

Tel 46 18 18 0700 Telex

Fax 46 18 18 7276 EMAIL

In Charge: Reported by: Jonas Modéer

HISTORY AND STATUS

DATES: Design 90 First Machine 90

SALES: No. Sold/Operational 2 / 2 Currently Available Y

COST: Accelerator Facility

MAGNET

POLE PARAMETERS:

Diameter 130 cm $R_{extract}$ 47 cm R_{inject} cm

HILL PARAMETERS: Gap (min) cm B_{max} T

(@ AT) Gap (max) cm B_{min} T

VALLEY PARAMETERS: Gap (min) cm B_{max} T

(@ AT) Gap (max) cm B_{min} T

AVERAGE FIELD: $< B >_{min}$ 1.59 T $< B >_{max}$ T

NUMBER OF SECTORS: compact/separated 4 /

sector angle deg. spiral (max) deg.

FIELD TRIMMING: Trim Coils 3

Harmonic Coils 2

Other

CURRENT: Main Coils 700 Amps Stability

Trim Coils Amps Stability

Stored Energy (cryogenic) MJ

WEIGHT: Iron Conductor

ION ENERGY: Bending Limit E/A = q^2/A^2 MeV/u

Focussing Limit E/A = q/A MeV/u

ACCELERATION SYSTEM

FUNDAMENTAL ACCELERATION:

Description:

No. of Gaps/turn 4 dE/dn(max) 0.1 MeV/q

Voltage(max) 0.035 MV Harmonic f_{rf}/f_{ion} 1

Freq 24 MHz Power in(max) 0.05 MW

Stability: Phase Voltage

VACUUM SYSTEM

OPERATING PRESSURE: $< 10^{-6}$

PUMPS: No. and type 2 x 4000 ℓ/sec diff pump

ION SOURCE(S)

	Type	Intensity (mA)	@	$\epsilon_n = \beta\gamma\epsilon$ (π mm mrad)	Ion Species
(a)	PIG	0.1			H^-, D^-
(b)					

INJECTION SYSTEM

Efficiency %

EXTRACTION SYSTEM

Stripping foils Efficiency %

CHARACTERISTIC BEAMS

	Accelerated Ions	E/A (MeV/u)	Current(part. μA) Internal	External
(a)	H^-	32	60	60
(b)	D^-	16	60	60

EXTRACTED BEAM PROPERTIES:

For μA of MeV/u ions

$\Delta E/E$ % $\Delta\phi$ °rf

$\epsilon_n = \beta\gamma\epsilon$ x πmm mrad z πmm mrad

REFERENCES/NOTES

(a)

(b)

ENTRY NO. CM18 Date

Machine Name MC30 p. fixed Energy

Manufacturer Scanditronix

Address Husyborg, S752 29 Uppsala, Sweden

Tel 46 18 18 0700 Telex

Fax 46 18 53 7276 EMAIL

In Charge: Reported by: Jonas Modéer

HISTORY AND STATUS

DATES: Design 1987 First Machine 1988

SALES: No. Sold/Operational 1 / 1 Currently Available Y

COST: Accelerator Facility

MAGNET

POLE PARAMETERS:

Diameter 130 cm $R_{extract}$ cm R_{inject} cm

HILL PARAMETERS: Gap (min) 10 cm B_{max} T

(@ AT) Gap (max) cm B_{min} T

VALLEY PARAMETERS: Gap (min) 18 cm B_{max} T

(@ AT) Gap (max) cm B_{min} T

AVERAGE FIELD: $< B >_{min}$ 1.4 T $< B >_{max}$ T

NUMBER OF SECTORS: compact/separated 3 /

sector angle deg. spiral (max) 50 deg.

FIELD TRIMMING: Trim Coils 5

Harmonic Coils 2

Other 5

CURRENT: Main Coils 600 Amps Stability 10

Trim Coils Amps Stability

Stored Energy (cryogenic) MJ

WEIGHT: Iron 69,000 kg Conductor

ION ENERGY: Bending Limit E/A = q^2/A^2 MeV/u

Focussing Limit E/A = q/A MeV/u

ACCELERATION SYSTEM

FUNDAMENTAL ACCELERATION:

Description: Driven System

No. of Gaps/turn 4 dE/dn(max) 0.1 MeV/q

Voltage(max) 0.035 MV Harmonic f_{rf}/f_{ion} 1

Freq MHz Power in(max) MW

Stability: Phase Voltage

VACUUM SYSTEM

OPERATING PRESSURE: 10^{-5} – 10^{-6}

PUMPS: No. and type 2 x 4000 ℓ/sec Diff pump

ION SOURCE(S)

	Type	Intensity (mA)	@	$\epsilon_n = \beta\gamma\epsilon$ (π mm mrad)	Ion Species
(a)	Hot filament	0.3			P
(b)					

INJECTION SYSTEM

Efficiency –

EXTRACTION SYSTEM

Efficiency –

CHARACTERISTIC BEAMS

	Accelerated Ions	E/A (MeV/u)	Current(part. μA) Internal	External
(a)	P	30	500	–
(b)				

EXTRACTED BEAM PROPERTIES:

For μA of MeV/u ions

$\Delta E/E$ % $\Delta\phi$ °rf

$\epsilon_n = \beta\gamma\epsilon$ x πmm mrad z πmm mrad

REFERENCES/NOTES

(a)

(b)

ENTRY NO. CM19 Date

Machine Name MC 32 NI

Manufacturer Scanditronix

Address Husyborg, S752 29 Uppsala Sweden

Tel 46 18 18 0700 Telex

Fax 46 18 18 7276 EMAIL

In Charge: Reported by: Jonas Modéer

HISTORY AND STATUS

DATES: Design 90 First Machine 90

SALES: No. Sold/Operational 2 / 2 Currently Available Y

COST: Accelerator Facility

MAGNET

POLE PARAMETERS:

Diameter 130 cm $R_{extract}$ 47 cm R_{inject} cm

HILL PARAMETERS: Gap (min) cm B_{max} T

(@ AT) Gap (max) cm B_{min} T

VALLEY PARAMETERS: Gap (min) cm B_{max} T

(@ AT) Gap (max) cm B_{min} T

AVERAGE FIELD: $< B >_{min}$ 1.59 T $< B >_{max}$ T

NUMBER OF SECTORS: compact/separated 4 /

sector angle deg. spiral (max) deg.

FIELD TRIMMING: Trim Coils 3

Harmonic Coils 2

Other

CURRENT: Main Coils 700 Amps Stability

Trim Coils Amps Stability

Stored Energy (cryogenic) MJ

WEIGHT: Iron Conductor

ION ENERGY: Bending Limit E/A = q^2/A^2 MeV/u

Focussing Limit E/A = q/A MeV/u

ACCELERATION SYSTEM

FUNDAMENTAL ACCELERATION:

Description:

No. of Gaps/turn 4 dE/dn(max) 0.1 MeV/q

Voltage(max) 0.035 MV Harmonic f_{rf}/f_{ion} 1

Freq 24 MHz Power in(max) 0.05 MW

Stability: Phase Voltage

VACUUM SYSTEM

OPERATING PRESSURE: $< 10^{-6}$

PUMPS: No. and type 2 x 4000 ℓ/sec diff pump

ION SOURCE(S)

	Type	Intensity (mA)	@	$\epsilon_n = \beta\gamma\epsilon$ (π mm mrad)	Ion Species
(a)	PIG	0.1			H^-, D^-
(b)					

INJECTION SYSTEM

Efficiency %

EXTRACTION SYSTEM

Stripping foils Efficiency %

CHARACTERISTIC BEAMS

	Accelerated Ions	E/A (MeV/u)	Current(part. μA) Internal	External
(a)	H^-	32	60	60
(b)	D^-	16	60	60

EXTRACTED BEAM PROPERTIES:

For μA of MeV/u ions

$\Delta E/E$ % $\Delta\phi$ °rf

$\epsilon_n = \beta\gamma\epsilon$ x πmm mrad z πmm mrad

REFERENCES/NOTES

(a)

(b)

ENTRY NO. CM20 Date

Machine Name MC35, 40

Manufacturer Scanditronix

Address Husyborg, S75229, Uppsala, Sweden

Tel 46 18 18 07 00 Telex

Fax 46 18 53 72 76 EMAIL

In Charge: Reported by: Jonas Hodéer

HISTORY AND STATUS

DATES: Design 1976-78 First Machine 1979

SALES: No. Sold/Operational 12 / 11 Currently Available Y

COST: Accelerator Facility

MAGNET

POLE PARAMETERS:

Diameter 130 cm $R_{extract}$ 48 cm R_{inject} cm

HILL PARAMETERS: Gap (min) 10 cm B_{max} T

(@ AT) Gap (max) cm B_{min} T

VALLEY PARAMETERS: Gap (min) 18 cm B_{max} T

(@ AT) Gap (max) cm B_{min} T

AVERAGE FIELD: $< B >_{min}$ 0.85 T $< B >_{max}$ 1.78 T

NUMBER OF SECTORS: compact/separated 3 /

sector angle deg. spiral (max) 50 deg.

FIELD TRIMMING: Trim Coils 8

Harmonic Coils 4

Other -5

CURRENT: Main Coils 900 Amps Stability 10

Trim Coils Amps Stability

Stored Energy (cryogenic) MJ

WEIGHT: Iron 69,000 kg. Conductor

ION ENERGY: Bending Limit E/A = q^2/A^2 MeV/u

Focussing Limit E/A = q/A MeV/u

ACCELERATION SYSTEM

FUNDAMENTAL ACCELERATION:

Description: Driven System

No. of Gaps/turn 4 dE/dn(max) 0.1 MeV/q

Voltage(max) 0.035 MV Harmonic f_{rf}/f_{ion} 1,2

Freq 14 - 26.5 MHz Power in(max) 0.060 MW

Stability: Phase Voltage

VACUUM SYSTEM

OPERATING PRESSURE: 10^{-5}, 10^{-6}

PUMPS: No. and type 2 x 4000 ℓ/sec diff pump

ION SOURCE(S)

	Type	Intensity (mA)	@	$\epsilon_n = \beta\gamma\epsilon$ (π mm mrad)	Ion Species
(a)	Hot filament	0.2 - 0.5			p,d,He^3,α
(b)					

INJECTION SYSTEM

Efficiency %

EXTRACTION SYSTEM

Efficiency 60-85 %

CHARACTERISTIC BEAMS

Accelerated Ions	E/A (MeV/u)	Current(part. μA) Internal	External
(a) p,d	10-40,5-20	300	75
(b) He^3,α	13-53,10-40	150	65

EXTRACTED BEAM PROPERTIES:

For μA of MeV/u ions

$\Delta E/E$ % $\Delta\phi$ °rf

$\epsilon_n = \beta\gamma\epsilon$ x πmm mrad z πmm mrad

REFERENCES/NOTES

(a)

(b)

ENTRY NO. CM21 Date

Machine Name MC50

Manufacturer Scanditronix

Address Husyborg, S75229 Uppsala, Sweden

Tel 46 18 18 07 00 Telex

Fax 46 18 53 72 76 EMAIL

In Charge: Reported by: Jonas Hodeer

HISTORY AND STATUS

DATES: Design 83 First Machine 89

SALES: No. Sold/Operational 2 / 2 Currently Available Y

COST: Accelerator Facility

MAGNET

POLE PARAMETERS:

Diameter 143 cm $R_{extract}$ 58 cm R_{inject} cm

HILL PARAMETERS: Gap (min) 11 cm B_{max} 2.05 T

(@ AT) Gap (max) cm B_{min} T

VALLEY PARAMETERS: Gap (min) cm B_{max} T

(@ AT) Gap (max) 20 cm B_{min} T

AVERAGE FIELD: $< B >_{min}$ 1.05 T $< B >_{max}$ 1.75 T

NUMBER OF SECTORS: compact/separated 3 /

sector angle deg. spiral (max) 55 deg.

FIELD TRIMMING: Trim Coils 10

Harmonic Coils 4

Other -3

CURRENT: Main Coils 900 Amps Stability 10

Trim Coils Amps Stability

Stored Energy (cryogenic) MJ

WEIGHT: Iron 93,000 kg. Conductor

ION ENERGY: Bending Limit E/A = q^2/A^2 MeV/u

Focussing Limit E/A = q/A MeV/u

ACCELERATION SYSTEM

FUNDAMENTAL ACCELERATION:

Description: Driven system

No. of Gaps/turn 4 dE/dn(max) 0.1 MeV/q

Voltage(max) 0.035 MV Harmonic f_{rf}/f_{ion} 1,2

Freq 15-27 MHz Power in(max) 0.06 MW

Stability: Phase Voltage

VACUUM SYSTEM

OPERATING PRESSURE: 10^{-5}, 10^{-6}

PUMPS: No. and type 2 x 4000 ℓ/sec diff. pump

ION SOURCE(S)

	Type	Intensity (mA)	@	$\epsilon_n = \beta\gamma\epsilon$ (π mm mrad)	Ion Species
(a)	PIG	0.1			p,d,He^3,α
(b)					

INJECTION SYSTEM

Efficiency %

EXTRACTION SYSTEM

Efficiency 60-85 %

CHARACTERISTIC BEAMS

Accelerated Ions	E/A (MeV/u)	Current(part. μA) Internal	External
(a) p,d	18-50,9-25	> 200	50
(b) He^3,α	24-66,18-50	60	30

EXTRACTED BEAM PROPERTIES:

For μA of MeV/u ions

$\Delta E/E$ % $\Delta\phi$ °rf

$\epsilon_n = \beta\gamma\epsilon$ x πmm mrad z πmm mrad

REFERENCES/NOTES

(a)

(b)

ENTRY NO. CM20 Date

Machine Name MC35, 40

Manufacturer Scanditronix

Address Husyborg, S75229, Uppsala, Sweden

Tel 46 18 18 07 00 Telex

Fax 46 18 53 72 76 EMAIL

In Charge: Reported by: Jonas Hodéer

HISTORY AND STATUS

DATES: Design 1976-78 First Machine 1979

SALES: No. Sold/Operational 12 / 11 Currently Available Y

COST: Accelerator Facility

MAGNET

POLE PARAMETERS:

Diameter 130 cm $R_{extract}$ 48 cm R_{inject} cm

HILL PARAMETERS: Gap (min) 10 cm B_{max} T

(@ AT) Gap (max) cm B_{min} T

VALLEY PARAMETERS: Gap (min) 18 cm B_{max} T

(@ AT) Gap (max) cm B_{min} T

AVERAGE FIELD: $< B >_{min}$ 0.85 T $< B >_{max}$ 1.78 T

NUMBER OF SECTORS: compact/separated 3 /

sector angle deg. spiral (max) 50 deg.

FIELD TRIMMING: Trim Coils 8

Harmonic Coils 4

Other -5

CURRENT: Main Coils 900 Amps Stability 10

Trim Coils Amps Stability

Stored Energy (cryogenic) MJ

WEIGHT: Iron 69,000 kg. Conductor

ION ENERGY: Bending Limit E/A = q^2/A^2 MeV/u

Focussing Limit E/A = q/A MeV/u

ACCELERATION SYSTEM

FUNDAMENTAL ACCELERATION:

Description: Driven System

No. of Gaps/turn 4 dE/dn(max) 0.1 MeV/q

Voltage(max) 0.035 MV Harmonic f_{rf}/f_{ion} 1,2

Freq 14 - 26.5 MHz Power in(max) 0.060 MW

Stability: Phase Voltage

VACUUM SYSTEM

OPERATING PRESSURE: 10^{-5}, 10^{-6}

PUMPS: No. and type 2 x 4000 ℓ/sec diff pump

ION SOURCE(S)

	Type	Intensity (mA)	@	$\epsilon_n = \beta\gamma\epsilon$ (π mm mrad)	Ion Species
(a)	Hot filament	0.2 - 0.5			p,d,He^3,α
(b)					

INJECTION SYSTEM

Efficiency %

EXTRACTION SYSTEM

Efficiency 60-85 %

CHARACTERISTIC BEAMS

Accelerated Ions	E/A (MeV/u)	Current(part. μA) Internal	External
(a) p,d	10-40,5-20	300	75
(b) He^3,α	13-53,10-40	150	65

EXTRACTED BEAM PROPERTIES:

For μA of MeV/u ions

$\Delta E/E$ % $\Delta\phi$ °rf

$\epsilon_n = \beta\gamma\epsilon$ x πmm mrad z πmm mrad

REFERENCES/NOTES

(a)

(b)

ENTRY NO. CM21 Date

Machine Name MC50

Manufacturer Scanditronix

Address Husyborg, S75229 Uppsala, Sweden

Tel 46 18 18 07 00 Telex

Fax 46 18 53 72 76 EMAIL

In Charge: Reported by: Jonas Hodeer

HISTORY AND STATUS

DATES: Design 83 First Machine 89

SALES: No. Sold/Operational 2 / 2 Currently Available Y

COST: Accelerator Facility

MAGNET

POLE PARAMETERS:

Diameter 143 cm $R_{extract}$ 58 cm R_{inject} cm

HILL PARAMETERS: Gap (min) 11 cm B_{max} 2.05 T

(@ AT) Gap (max) cm B_{min} T

VALLEY PARAMETERS: Gap (min) cm B_{max} T

(@ AT) Gap (max) 20 cm B_{min} T

AVERAGE FIELD: $< B >_{min}$ 1.05 T $< B >_{max}$ 1.75 T

NUMBER OF SECTORS: compact/separated 3 /

sector angle deg. spiral (max) 55 deg.

FIELD TRIMMING: Trim Coils 10

Harmonic Coils 4

Other -3

CURRENT: Main Coils 900 Amps Stability 10

Trim Coils Amps Stability

Stored Energy (cryogenic) MJ

WEIGHT: Iron 93,000 kg. Conductor

ION ENERGY: Bending Limit E/A = q^2/A^2 MeV/u

Focussing Limit E/A = q/A MeV/u

ACCELERATION SYSTEM

FUNDAMENTAL ACCELERATION:

Description: Driven system

No. of Gaps/turn 4 dE/dn(max) 0.1 MeV/q

Voltage(max) 0.035 MV Harmonic f_{rf}/f_{ion} 1,2

Freq 15-27 MHz Power in(max) 0.06 MW

Stability: Phase Voltage

VACUUM SYSTEM

OPERATING PRESSURE: 10^{-5}, 10^{-6}

PUMPS: No. and type 2 x 4000 ℓ/sec diff. pump

ION SOURCE(S)

	Type	Intensity (mA)	@	$\epsilon_n = \beta\gamma\epsilon$ (π mm mrad)	Ion Species
(a)	PIG	0.1			p,d,He^3,α
(b)					

INJECTION SYSTEM

Efficiency %

EXTRACTION SYSTEM

Efficiency 60-85 %

CHARACTERISTIC BEAMS

Accelerated Ions	E/A (MeV/u)	Current(part. μA) Internal	External
(a) p,d	18-50,9-25	> 200	50
(b) He^3,α	24-66,18-50	60	30

EXTRACTED BEAM PROPERTIES:

For μA of MeV/u ions

$\Delta E/E$ % $\Delta\phi$ °rf

$\epsilon_n = \beta\gamma\epsilon$ x πmm mrad z πmm mrad

REFERENCES/NOTES

(a)

(b)

ENTRY NO. CM22 Date

Machine Name MC60 PF

Manufacturer Scanditronix

Address Husyborg, S75229, Uppsala, Sweden

Tel 46.18.18.07.00 Telex

Fax 46.18.53.72.76 EMAIL

In Charge: Reported by: Jonas Hodéer

HISTORY AND STATUS

DATES: Design 83 First Machine 84

SALES: No. Sold/Operational 1 / 1 Currently Available Y

COST: Accelerator Facility

MAGNET

POLE PARAMETERS:

Diameter 160 cm $R_{extract}$ 65 cm R_{inject} cm

HILL PARAMETERS: Gap (min) cm B_{max} 2.05 T

(@ AT) Gap (max) cm B_{min} T

VALLEY PARAMETERS: Gap (min) cm B_{max} T

(@ AT) Gap (max) cm B_{min} T

AVERAGE FIELD: $< B >_{min}$ T $< B >_{max}$ 1.75 T

NUMBER OF SECTORS: compact/separated 3 /

sector angle deg. spiral (max) 60 deg.

FIELD TRIMMING: Trim Coils 2

Harmonic Coils 4

Other

CURRENT: Main Coils 900 Amps Stability

Trim Coils Amps Stability

Stored Energy (cryogenic) MJ

WEIGHT: Iron 120,000 kg Conductor

ION ENERGY: Bending Limit E/A = q^2/A^2 MeV/u

Focussing Limit E/A = q/A MeV/u

ACCELERATION SYSTEM

FUNDAMENTAL ACCELERATION:

Description: Driven System

No. of Gaps/turn 4 dE/dn(max) 0.1 MeV/q

Voltage(max) 0.04 MV Harmonic f_{rf}/f_{ion} 1

Freq 25 MHz Power in(max) 0.05 MW

Stability: Phase Voltage

VACUUM SYSTEM

OPERATING PRESSURE: 10^{-5}, 10^{-6}

PUMPS: No. and type 2 x 4000 l/sec diff. pump

ION SOURCE(S)

	Type	Intensity (mA)	@ $\epsilon_n = \beta\gamma\epsilon$ (π mm mrad)	Ion Species
(a)	PIG	0.1		
(b)				

INJECTION SYSTEM

Efficiency %

EXTRACTION SYSTEM

Efficiency 80 %

CHARACTERISTIC BEAMS

	Accelerated Ions	E/A (MeV/u)	Current(part. μA) Internal	External
(a)	p	60	100	35
(b)				

EXTRACTED BEAM PROPERTIES:

For μA of MeV/u ions

$\Delta E/E$ % $\Delta\phi$ °rf

$\epsilon_n = \beta\gamma\epsilon$ x πmm mrad z πmm mrad

REFERENCES/NOTES

(a)

(b)

ENTRY NO. CM23 Date 2/7/92

Machine Name OSCAR

Manufacturer OXFORD INSTRUMENTS

Address OSNEY MEAD

Tel 44 865 269500 Telex

Fax 269690 EMAIL

In Charge: Reported by: M KRUIP

HISTORY AND STATUS

DATES: Design 86-88 First Machine 90

SALES: No. Sold/Operational 3 / Currently Available YES

COST: Accelerator Facility

MAGNET

POLE PARAMETERS:

Diameter 50 cm $R_{extract}$ 21 cm R_{inject} 13 cm

HILL PARAMETERS: Gap (min) 2.9 cm B_{max} 3.1 T

(@ 7.6x10 AT) Gap (max) cm B_{min} T

VALLEY PARAMETERS: Gap (min) / cm B_{max} 1.7 T

(@ AT) Gap (max) cm B_{min} T

AVERAGE FIELD: $< B >_{min}$ 2.36 T $< B >_{max}$ T

NUMBER OF SECTORS: compact/separated 3 /

sector angle 54 deg. spiral (max) / deg.

FIELD TRIMMING: Trim Coils /

Harmonic Coils /

Other /

CURRENT: Main Coils 360 Amps Stability (PERSISTENT MODES)

Trim Coils / Amps Stability

Stored Energy (cryogenic) 0.55 MJ

WEIGHT: Iron 1.5 TON Conductor NbTi, 250 KG

ION ENERGY: Bending Limit E/A = 12 q^2/A^2 MeV/u

Focussing Limit E/A = / q/A MeV/u

ACCELERATION SYSTEM

FUNDAMENTAL ACCELERATION:

Description: 3 x 60°, AXIAL $\lambda/4$ STEMS

No. of Gaps/turn 6 dE/dn(max) 0.2 MeV/q

Voltage(max) 0.033 MV Harmonic f_{rf}/f_{ion} 3

Freq 108 MHz Power in(max) 0.01 MW

Stability: Phase 1° Voltage 10^{-3}

VACUUM SYSTEM

OPERATING PRESSURE: 5×10^{-7} mbar

PUMPS: No. and type 2 TURBO

ION SOURCE(S)

	Type	Intensity (mA)	@ $\epsilon_n = \beta\gamma\epsilon$ (π mm mrad)	Ion Species
(a)	MULTICUSP	1	0.16	H^-
(b)				

INJECTION SYSTEM

AXIAL, SPIRAL Efficiency ~10 %

EXTRACTION SYSTEM

STRIPPING Efficiency ~100 %

CHARACTERISTIC BEAMS

	Accelerated Ions	E/A (MeV/u)	Current(part. μA) Internal	External
(a)	H^-	12	100	100
(b)				

EXTRACTED BEAM PROPERTIES:

For 50 μA of 12 MeV/u H^+ ions

$\Delta E/E$ % $\Delta\phi$ °rf

$\epsilon_n = \beta\gamma\epsilon$ x 1.5 πmm mrad z 3 πmm mrad

REFERENCES/NOTES

(a)

(b)

ENTRY NO. CM22 Date

Machine Name MC60 PF

Manufacturer Scanditronix

Address Husyborg, S75229, Uppsala, Sweden

Tel 46.18.18.07.00 Telex

Fax 46.18.53.72.76 EMAIL

In Charge: Reported by: Jonas Hodéer

HISTORY AND STATUS

DATES: Design 83 First Machine 84

SALES: No. Sold/Operational 1 / 1 Currently Available Y

COST: Accelerator Facility

MAGNET

POLE PARAMETERS:

Diameter 160 cm $R_{extract}$ 65 cm R_{inject} cm

HILL PARAMETERS: Gap (min) cm B_{max} 2.05 T

(@ AT) Gap (max) cm B_{min} T

VALLEY PARAMETERS: Gap (min) cm B_{max} T

(@ AT) Gap (max) cm B_{min} T

AVERAGE FIELD: $< B >_{min}$ T $< B >_{max}$ 1.75 T

NUMBER OF SECTORS: compact/separated 3 /

sector angle deg. spiral (max) 60 deg.

FIELD TRIMMING: Trim Coils 2

Harmonic Coils 4

Other

CURRENT: Main Coils 900 Amps Stability

Trim Coils Amps Stability

Stored Energy (cryogenic) MJ

WEIGHT: Iron 120,000 kg Conductor

ION ENERGY: Bending Limit E/A = q^2/A^2 MeV/u

Focussing Limit E/A = q/A MeV/u

ACCELERATION SYSTEM

FUNDAMENTAL ACCELERATION:

Description: Driven System

No. of Gaps/turn 4 dE/dn(max) 0.1 MeV/q

Voltage(max) 0.04 MV Harmonic f_{rf}/f_{ion} 1

Freq 25 MHz Power in(max) 0.05 MW

Stability: Phase Voltage

VACUUM SYSTEM

OPERATING PRESSURE: 10^{-5}, 10^{-6}

PUMPS: No. and type 2 x 4000 l/sec diff. pump

ION SOURCE(S)

	Type	Intensity (mA)	@ $\epsilon_n = \beta\gamma\epsilon$ (π mm mrad)	Ion Species
(a)	PIG	0.1		
(b)				

INJECTION SYSTEM

Efficiency %

EXTRACTION SYSTEM

Efficiency 80 %

CHARACTERISTIC BEAMS

	Accelerated Ions	E/A (MeV/u)	Current(part. μA) Internal	External
(a)	p	60	100	35
(b)				

EXTRACTED BEAM PROPERTIES:

For μA of MeV/u ions

$\Delta E/E$ % $\Delta\phi$ °rf

$\epsilon_n = \beta\gamma\epsilon$ x πmm mrad z πmm mrad

REFERENCES/NOTES

(a)

(b)

ENTRY NO. CM23 Date 2/7/92

Machine Name OSCAR

Manufacturer OXFORD INSTRUMENTS

Address OSNEY MEAD

Tel 44 865 269500 Telex

Fax 269690 EMAIL

In Charge: Reported by: M KRUIP

HISTORY AND STATUS

DATES: Design 86-88 First Machine 90

SALES: No. Sold/Operational 3 / Currently Available YES

COST: Accelerator Facility

MAGNET

POLE PARAMETERS:

Diameter 50 cm $R_{extract}$ 21 cm R_{inject} 13 cm

HILL PARAMETERS: Gap (min) 2.9 cm B_{max} 3.1 T

(@ 7.6x10 AT) Gap (max) cm B_{min} T

VALLEY PARAMETERS: Gap (min) / cm B_{max} 1.7 T

(@ AT) Gap (max) cm B_{min} T

AVERAGE FIELD: $< B >_{min}$ 2.36 T $< B >_{max}$ T

NUMBER OF SECTORS: compact/separated 3 /

sector angle 54 deg. spiral (max) / deg.

FIELD TRIMMING: Trim Coils /

Harmonic Coils /

Other /

CURRENT: Main Coils 360 Amps Stability (PERSISTENT MODES)

Trim Coils / Amps Stability

Stored Energy (cryogenic) 0.55 MJ

WEIGHT: Iron 1.5 TON Conductor NbTi, 250 KG

ION ENERGY: Bending Limit E/A = 12 q^2/A^2 MeV/u

Focussing Limit E/A = / q/A MeV/u

ACCELERATION SYSTEM

FUNDAMENTAL ACCELERATION:

Description: 3 x 60°, AXIAL $\lambda/4$ STEMS

No. of Gaps/turn 6 dE/dn(max) 0.2 MeV/q

Voltage(max) 0.033 MV Harmonic f_{rf}/f_{ion} 3

Freq 108 MHz Power in(max) 0.01 MW

Stability: Phase 1° Voltage 10^{-3}

VACUUM SYSTEM

OPERATING PRESSURE: 5×10^{-7} mbar

PUMPS: No. and type 2 TURBO

ION SOURCE(S)

	Type	Intensity (mA)	@ $\epsilon_n = \beta\gamma\epsilon$ (π mm mrad)	Ion Species
(a)	MULTICUSP	1	0.16	H^-
(b)				

INJECTION SYSTEM

AXIAL, SPIRAL Efficiency ~10 %

EXTRACTION SYSTEM

STRIPPING Efficiency ~100 %

CHARACTERISTIC BEAMS

	Accelerated Ions	E/A (MeV/u)	Current(part. μA) Internal	External
(a)	H^-	12	100	100
(b)				

EXTRACTED BEAM PROPERTIES:

For 50 μA of 12 MeV/u H^+ ions

$\Delta E/E$ % $\Delta\phi$ °rf

$\epsilon_n = \beta\gamma\epsilon$ x 1.5 πmm mrad z 3 πmm mrad

REFERENCES/NOTES

(a)

(b)

ENTRY NO. CM24 Date

Machine Name CS-15

Manufacturer The Cyclotron Corporation (a)

Address 950 Gilman Street, Berkeley, CA 94710 USA

Tel (510) 524-8844 Telex 910-366-7116

Fax (510) 527-9336 EMAIL

In Charge: n/a Reported by: F.A. Ramsey

HISTORY AND STATUS

DATES: Design 1965 First Machine OCT 1967

SALES: No. Sold/Operational 3 / 3 Currently Available no

COST: Accelerator Facility

MAGNET

POLE PARAMETERS:

Diameter 81 cm $R_{extract}$ 35 cm R_{inject} cm

HILL PARAMETERS: Gap (min) 5 cm B_{max} 20 T

(@ AT) Gap (max) cm B_{min} T

VALLEY PARAMETERS: Gap (min) cm B_{max} T

(@ AT) Gap (max) 10 cm B_{min} 12 T

AVERAGE FIELD: $< B >_{min}$ T $< B >_{max}$ T

NUMBER OF SECTORS: compact/separated 3 /

sector angle deg. spiral (max) deg.

FIELD TRIMMING: Trim Coils none

Harmonic Coils One set - outer

Other

CURRENT: Main Coils 250 Amps Stability 0.01%

Trim Coils Amps Stability

Stored Energy (cryogenic) MJ

WEIGHT: Iron 22,000 kg TOTAL Conductor

ION ENERGY: Bending Limit E/A = q^2/A^2 MeV/u

Focussing Limit E/A = q/A MeV/u

ACCELERATION SYSTEM

FUNDAMENTAL ACCELERATION:

Description: Two 120° dees

No. of Gaps/turn 4 dE/dn(max) MeV/q

Voltage(max) 0.025 MV Harmonic f_{rf}/f_{ion}

Freq 12.5 - 25 MHz Power in(max) 0.030 MW

Stability: Phase Voltage

VACUUM SYSTEM

OPERATING PRESSURE: 10^{-5} torr

PUMPS: No. and type One oil diffusion pump

ION SOURCE(S)

	Type	Intensity (mA)	@ $\epsilon_n = \beta\gamma\epsilon$ (π mm mrad)	Ion Species
(a)	Penning		not available	H^+/D^+
(b)	"		"	$^3He^{++}/^4He^{++}$

INJECTION SYSTEM

Radial Efficiency 10-12 %

EXTRACTION SYSTEM

Electrostatic deflector and septum Efficiency 70 %

CHARACTERISTIC BEAMS

	Accelerated Ions	E/A (MeV/u)	Current(part. μA) Internal	External
(a)	H^+/D^+	15/8	200/300	60/100
(b)	$^3He^{++}/^4He^{++}$	20/16	135/90	60/40

EXTRACTED BEAM PROPERTIES:

For μA of MeV/u ions

$\Delta E/E$ 1 % $\Delta\phi$ °rf

$\epsilon_n = \beta\gamma\epsilon$ x πmm mrad z πmm mrad

REFERENCES/NOTES

(a) CTI Cyclotron Systems, 950 Gilman St., Berkeley, CA

(b)

ENTRY NO. CM25 Date

Machine Name CS-22

Manufacturer The Cyclotron Corporation (a)

Address 950 Gilman Street, Berkeley, CA 94710 USA

Tel (510) 524-8844 Telex 910-366-7116

Fax (510) 527-9336 EMAIL

In Charge: n/a Reported by: F.A. Ramsey

HISTORY AND STATUS

DATES: Design 1969 First Machine SEPT. 1970

SALES: No. Sold/Operational 4 / 3 Currently Available no.

COST: Accelerator Facility

MAGNET

POLE PARAMETERS:

Diameter 96 cm $R_{extract}$ 42 cm R_{inject} cm

HILL PARAMETERS: Gap (min) 5 cm B_{max} 20 T

(@ AT) Gap (max) cm B_{min} T

VALLEY PARAMETERS: Gap (min) cm B_{max} T

(@ AT) Gap (max) 10 cm B_{min} 12 T

AVERAGE FIELD: $< B >_{min}$ T $< B >_{max}$ T

NUMBER OF SECTORS: compact/separated 3 /

sector angle deg. spiral (max) deg.

FIELD TRIMMING: Trim Coils none

Harmonic Coils One set - outer

Other

CURRENT: Main Coils 250 Amps Stability 0.01%

Trim Coils Amps Stability

Stored Energy (cryogenic) MJ

WEIGHT: Iron 23,000 kg TOTAL Conductor

ION ENERGY: Bending Limit E/A = q^2/A^2 MeV/u

Focussing Limit E/A = q/A MeV/u

ACCELERATION SYSTEM

FUNDAMENTAL ACCELERATION:

Description: Two 90° dees

No. of Gaps/turn 4 dE/dn(max) MeV/q

Voltage(max) 0.025 MV Harmonic f_{rf}/f_{ion}

Freq 13 - 25 MHz Power in(max) 0.060 MW

Stability: Phase Voltage

VACUUM SYSTEM

OPERATING PRESSURE: 10^{-5} torr

PUMPS: No. and type One oil diffusion pump

ION SOURCE(S)

	Type	Intensity (mA)	@ $\epsilon_n = \beta\gamma\epsilon$ (π mm mrad)	Ion Species
(a)	Penning		not available	H^+/D^+
(b)	"		"	$^3He^{++}/^4He^{++}$

INJECTION SYSTEM

Radial Efficiency 10-12 %

EXTRACTION SYSTEM

Electrostatic deflector and septum Efficiency 70 %

CHARACTERISTIC BEAMS

	Accelerated Ions	E/A (MeV/u)	Current(part. μA) Internal	External
(a)	H^+/D^+	22/12	200/300	50/50
(b)	$^3He^{++}/^4He^{++}$	32/24	135/90	50/50

EXTRACTED BEAM PROPERTIES:

For μA of MeV/u ions

$\Delta E/E$ 1 % $\Delta\phi$ °rf

$\epsilon_n = \beta\gamma\epsilon$ x πmm mrad z πmm mrad

REFERENCES/NOTES

(a) CTI Cyclotron Systems, 950 Gilman St., Berkeley, CA

(b)

ENTRY NO. CM24 Date

Machine Name CS-15

Manufacturer The Cyclotron Corporation (a)

Address 950 Gilman Street, Berkeley, CA 94710 USA

Tel (510) 524-8844 Telex 910-366-7116

Fax (510) 527-9336 EMAIL

In Charge: n/a Reported by: F.A. Ramsey

HISTORY AND STATUS

DATES: Design 1965 First Machine OCT 1967

SALES: No. Sold/Operational 3 / 3 Currently Available no

COST: Accelerator Facility

MAGNET

POLE PARAMETERS:

Diameter 81 cm $R_{extract}$ 35 cm R_{inject} cm

HILL PARAMETERS: Gap (min) 5 cm B_{max} 20 T

(@ AT) Gap (max) cm B_{min} T

VALLEY PARAMETERS: Gap (min) cm B_{max} T

(@ AT) Gap (max) 10 cm B_{min} 12 T

AVERAGE FIELD: $< B >_{min}$ T $< B >_{max}$ T

NUMBER OF SECTORS: compact/separated 3 /

sector angle deg. spiral (max) deg.

FIELD TRIMMING: Trim Coils none

Harmonic Coils One set - outer

Other

CURRENT: Main Coils 250 Amps Stability 0.01%

Trim Coils Amps Stability

Stored Energy (cryogenic) MJ

WEIGHT: Iron 22,000 kg TOTAL Conductor

ION ENERGY: Bending Limit E/A = q^2/A^2 MeV/u

Focussing Limit E/A = q/A MeV/u

ACCELERATION SYSTEM

FUNDAMENTAL ACCELERATION:

Description: Two 120° dees

No. of Gaps/turn 4 dE/dn(max) MeV/q

Voltage(max) 0.025 MV Harmonic f_{rf}/f_{ion}

Freq 12.5 - 25 MHz Power in(max) 0.030 MW

Stability: Phase Voltage

VACUUM SYSTEM

OPERATING PRESSURE: 10^{-5} torr

PUMPS: No. and type One oil diffusion pump

ION SOURCE(S)

	Type	Intensity (mA)	@ $\epsilon_n = \beta\gamma\epsilon$ (π mm mrad)	Ion Species
(a)	Penning		not available	H^+/D^+
(b)	"		"	$^3He^{++}/^4He^{++}$

INJECTION SYSTEM

Radial Efficiency 10-12 %

EXTRACTION SYSTEM

Electrostatic deflector and septum Efficiency 70 %

CHARACTERISTIC BEAMS

	Accelerated Ions	E/A (MeV/u)	Current(part. μA) Internal	External
(a)	H^+/D^+	15/8	200/300	60/100
(b)	$^3He^{++}/^4He^{++}$	20/16	135/90	60/40

EXTRACTED BEAM PROPERTIES:

For μA of MeV/u ions

$\Delta E/E$ 1 % $\Delta\phi$ °rf

$\epsilon_n = \beta\gamma\epsilon$ x πmm mrad z πmm mrad

REFERENCES/NOTES

(a) CTI Cyclotron Systems, 950 Gilman St., Berkeley, CA

(b)

ENTRY NO. CM25 Date

Machine Name CS-22

Manufacturer The Cyclotron Corporation (a)

Address 950 Gilman Street, Berkeley, CA 94710 USA

Tel (510) 524-8844 Telex 910-366-7116

Fax (510) 527-9336 EMAIL

In Charge: n/a Reported by: F.A. Ramsey

HISTORY AND STATUS

DATES: Design 1969 First Machine SEPT. 1970

SALES: No. Sold/Operational 4 / 3 Currently Available no.

COST: Accelerator Facility

MAGNET

POLE PARAMETERS:

Diameter 96 cm $R_{extract}$ 42 cm R_{inject} cm

HILL PARAMETERS: Gap (min) 5 cm B_{max} 20 T

(@ AT) Gap (max) cm B_{min} T

VALLEY PARAMETERS: Gap (min) cm B_{max} T

(@ AT) Gap (max) 10 cm B_{min} 12 T

AVERAGE FIELD: $< B >_{min}$ T $< B >_{max}$ T

NUMBER OF SECTORS: compact/separated 3 /

sector angle deg. spiral (max) deg.

FIELD TRIMMING: Trim Coils none

Harmonic Coils One set - outer

Other

CURRENT: Main Coils 250 Amps Stability 0.01%

Trim Coils Amps Stability

Stored Energy (cryogenic) MJ

WEIGHT: Iron 23,000 kg TOTAL Conductor

ION ENERGY: Bending Limit E/A = q^2/A^2 MeV/u

Focussing Limit E/A = q/A MeV/u

ACCELERATION SYSTEM

FUNDAMENTAL ACCELERATION:

Description: Two 90° dees

No. of Gaps/turn 4 dE/dn(max) MeV/q

Voltage(max) 0.025 MV Harmonic f_{rf}/f_{ion}

Freq 13 - 25 MHz Power in(max) 0.060 MW

Stability: Phase Voltage

VACUUM SYSTEM

OPERATING PRESSURE: 10^{-5} torr

PUMPS: No. and type One oil diffusion pump

ION SOURCE(S)

	Type	Intensity (mA)	@ $\epsilon_n = \beta\gamma\epsilon$ (π mm mrad)	Ion Species
(a)	Penning		not available	H^+/D^+
(b)	"		"	$^3He^{++}/^4He^{++}$

INJECTION SYSTEM

Radial Efficiency 10-12 %

EXTRACTION SYSTEM

Electrostatic deflector and septum Efficiency 70 %

CHARACTERISTIC BEAMS

	Accelerated Ions	E/A (MeV/u)	Current(part. μA) Internal	External
(a)	H^+/D^+	22/12	200/300	50/50
(b)	$^3He^{++}/^4He^{++}$	32/24	135/90	50/50

EXTRACTED BEAM PROPERTIES:

For μA of MeV/u ions

$\Delta E/E$ 1 % $\Delta\phi$ °rf

$\epsilon_n = \beta\gamma\epsilon$ x πmm mrad z πmm mrad

REFERENCES/NOTES

(a) CTI Cyclotron Systems, 950 Gilman St., Berkeley, CA

(b)

ENTRY NO. CM26 Date

Machine Name CV-28

Manufacturer The Cyclotron Corporation (a)

Address 950 Gilman Street, Berkeley, CA 94710 USA

Tel (510) 524-8844 Telex 910-366-7116

Fax (510) 527-9336 EMAIL

In Charge: n/a Reported by: F.A. Ramsey

HISTORY AND STATUS

DATES: Design 1972-1973 First Machine 1974

SALES: No. Sold/Operational 5 / 5 Currently Available no

COST: Accelerator Facility

MAGNET

POLE PARAMETERS:

Diameter 96.5 cm $R_{extract}$ 42 cm R_{inject} cm

HILL PARAMETERS: Gap (min) 5 cm B_{max} 20 T

(Ø AT) Gap (max) cm B_{min} T

VALLEY PARAMETERS: Gap (min) cm B_{max} T

(Ø AT) Gap (max) 10 cm B_{min} 14 T

AVERAGE FIELD: $< B >_{min}$ T $< B >_{max}$ T

NUMBER OF SECTORS: compact/separated 3 /

sector angle deg. spiral (max) deg.

FIELD TRIMMING: Trim Coils 4

Harmonic Coils Two sets: inner/outer @ 13/38 cm.

Other

CURRENT: Main Coils 500 Amps Stability 0.01%

Trim Coils Amps Stability

Stored Energy (cryogenic) MJ

WEIGHT: Iron 30,164 kg TOTAL Conductor

ION ENERGY: Bending Limit E/A = q^2/A^2 MeV/u

Focussing Limit E/A = q/A MeV/u

ACCELERATION SYSTEM

FUNDAMENTAL ACCELERATION:

Description: Two 90° dees

No. of Gaps/turn 4 dE/dn(max) 0.08 MeV/q

Voltage(max) 0.030 MV Harmonic f_{rf}/f_{ion} 1

Freq 7.5-25.5 MHz Power in(max) 0.060 MW

Stability: Phase Voltage

VACUUM SYSTEM

OPERATING PRESSURE: 10^{-5} torr

PUMPS: No. and type One oil diffusion pump

ION SOURCE(S)

	Type	Intensity (mA)	Ø	$\epsilon_n = \beta\gamma\epsilon$ (π mm mrad)	Ion Species
(a)	Penning			not available	H^+/D^+
	"			"	$^3He^{++}/^4He^{++}$
(b)					

INJECTION SYSTEM

Radial Efficiency 10-12 %

EXTRACTION SYSTEM

Electrostatic deflector and septum Efficiency 70 %

CHARACTERISTIC BEAMS

		Current(part. μA)	
Accelerated Ions	E/A (MeV/u)	Internal	External
(a) H^+/D^+	2-24/4-14	200/300	60/100
(b) $^3He^{++}/^4He^{++}$	6-36/8-28	135/90	5-50/8-40

EXTRACTED BEAM PROPERTIES:

For μA of MeV/u ions

$\Delta E/E$ % $\Delta\phi$ °rf

$\epsilon_n = \beta\gamma\epsilon$ x πmm mrad z πmm mrad

REFERENCES/NOTES

(a) CTI Cyclotron Systems, 950 Gilman St., Berkeley, CA

(b)

ENTRY NO. CM27 Date

Machine Name CS-30

Manufacturer The Cyclotron Corporation (a)

Address 950 Gilman Street, Berkeley, CA 94710 USA

Tel (510) 524-8844 Telex 910-366-7116

Fax (510) 527-9336 EMAIL

In Charge: n/a Reported by: F.A. Ramsey

HISTORY AND STATUS

DATES: Design 1969-1970 First Machine FEB. 1973

SALES: No. Sold/Operational 15 / 16(b) Currently Available yes

COST: Accelerator Facility

MAGNET

POLE PARAMETERS:

Diameter 96.5 cm $R_{extract}$ 42 cm R_{inject} cm

HILL PARAMETERS: Gap (min) 5.08 cm B_{max} 22.5 T

(Ø AT) Gap (max) cm B_{min} T

VALLEY PARAMETERS: Gap (min) cm B_{max} T

(Ø AT) Gap (max) 11.68 cm B_{min} 14.4 T

AVERAGE FIELD: $< B >_{min}$ T $< B >_{max}$ T

NUMBER OF SECTORS: compact/separated 3 /

sector angle deg. spiral (max) deg.

FIELD TRIMMING: Trim Coils none

Harmonic Coils Two sets: inner/outer @ 13/38 cm.

Other

CURRENT: Main Coils 500 Amps Stability 0.01%

Trim Coils Amps Stability

Stored Energy (cryogenic) MJ

WEIGHT: Iron 28,803 kg TOTAL Conductor

ION ENERGY: Bending Limit E/A = q^2/A^2 MeV/u

Focussing Limit E/A = q/A MeV/u

ACCELERATION SYSTEM

FUNDAMENTAL ACCELERATION:

Description: Two 90° dees

No. of Gaps/turn 4 dE/dn(max) MeV/q

Voltage(max) 0.028 MV Harmonic f_{rf}/f_{ion}

Freq 14.2-26.5 MHz Power in(max) 0.060 MW

Stability: Phase Voltage

VACUUM SYSTEM

OPERATING PRESSURE: 10^{-5} torr

PUMPS: No. and type One oil diffusion pump

ION SOURCE(S)

	Type	Intensity (mA)	Ø	$\epsilon_n = \beta\gamma\epsilon$ (π mm mrad)	Ion Species
(a)	Penning			not available	H^+/D^+
	"			"	$^3He^{++}/^4He^{++}$
(b)					

INJECTION SYSTEM

Radial Efficiency 10-12 %

EXTRACTION SYSTEM

Electrostatic deflector and septum Efficiency 70 %

CHARACTERISTIC BEAMS

		Current(part. μA)	
Accelerated Ions	E/A (MeV/u)	Internal	External
(a) H^+/D^+	26/15	200/300	60/100
(b) $^3He^{++}/^4He^{++}$	38/30	135/90	60/40

EXTRACTED BEAM PROPERTIES:

For μA of MeV/u ions

$\Delta E/E$ 1 % $\Delta\phi$ °rf

$\epsilon_n = \beta\gamma\epsilon$ x πmm mrad z πmm mrad

REFERENCES/NOTES

(a) CTI Cyclotron Systems, 950 Gilman St., Berkeley, CA

(b) A CNI-30 was converted to a CS-30

ENTRY NO. CM26 Date

Machine Name CV-28

Manufacturer The Cyclotron Corporation (a)

Address 950 Gilman Street, Berkeley, CA 94710 USA

Tel (510) 524-8844 Telex 910-366-7116

Fax (510) 527-9336 EMAIL

In Charge: n/a Reported by: F.A. Ramsey

HISTORY AND STATUS

DATES: Design 1972-1973 First Machine 1974

SALES: No. Sold/Operational 5 / 5 Currently Available no

COST: Accelerator Facility

MAGNET

POLE PARAMETERS:

Diameter 96.5 cm $R_{extract}$ 42 cm R_{inject} cm

HILL PARAMETERS: Gap (min) 5 cm B_{max} 20 T

(Ø AT) Gap (max) cm B_{min} T

VALLEY PARAMETERS: Gap (min) cm B_{max} T

(Ø AT) Gap (max) 10 cm B_{min} 14 T

AVERAGE FIELD: $< B >_{min}$ T $< B >_{max}$ T

NUMBER OF SECTORS: compact/separated 3 /

sector angle deg. spiral (max) deg.

FIELD TRIMMING: Trim Coils 4

Harmonic Coils Two sets: inner/outer @ 13/38 cm.

Other

CURRENT: Main Coils 500 Amps Stability 0.01%

Trim Coils Amps Stability

Stored Energy (cryogenic) MJ

WEIGHT: Iron 30,164 kg TOTAL Conductor

ION ENERGY: Bending Limit E/A = q^2/A^2 MeV/u

Focussing Limit E/A = q/A MeV/u

ACCELERATION SYSTEM

FUNDAMENTAL ACCELERATION:

Description: Two 90° dees

No. of Gaps/turn 4 dE/dn(max) 0.08 MeV/q

Voltage(max) 0.030 MV Harmonic f_{rf}/f_{ion} 1

Freq 7.5-25.5 MHz Power in(max) 0.060 MW

Stability: Phase Voltage

VACUUM SYSTEM

OPERATING PRESSURE: 10^{-5} torr

PUMPS: No. and type One oil diffusion pump

ION SOURCE(S)

	Type	Intensity (mA)	Ø	$\epsilon_n = \beta\gamma\epsilon$ (π mm mrad)	Ion Species
(a)	Penning			not available	H^+/D^+
	"			"	$^3He^{++}/^4He^{++}$
(b)					

INJECTION SYSTEM

Radial Efficiency 10-12 %

EXTRACTION SYSTEM

Electrostatic deflector and septum Efficiency 70 %

CHARACTERISTIC BEAMS

		Current(part. μA)	
Accelerated Ions	E/A (MeV/u)	Internal	External
(a) H^+/D^+	2-24/4-14	200/300	60/100
(b) $^3He^{++}/^4He^{++}$	6-36/8-28	135/90	5-50/8-40

EXTRACTED BEAM PROPERTIES:

For μA of MeV/u ions

$\Delta E/E$ % $\Delta\phi$ °rf

$\epsilon_n = \beta\gamma\epsilon$ x πmm mrad z πmm mrad

REFERENCES/NOTES

(a) CTI Cyclotron Systems, 950 Gilman St., Berkeley, CA

(b)

ENTRY NO. CM27 Date

Machine Name CS-30

Manufacturer The Cyclotron Corporation (a)

Address 950 Gilman Street, Berkeley, CA 94710 USA

Tel (510) 524-8844 Telex 910-366-7116

Fax (510) 527-9336 EMAIL

In Charge: n/a Reported by: F.A. Ramsey

HISTORY AND STATUS

DATES: Design 1969-1970 First Machine FEB. 1973

SALES: No. Sold/Operational 15 / 16(b) Currently Available yes

COST: Accelerator Facility

MAGNET

POLE PARAMETERS:

Diameter 96.5 cm $R_{extract}$ 42 cm R_{inject} cm

HILL PARAMETERS: Gap (min) 5.08 cm B_{max} 22.5 T

(Ø AT) Gap (max) cm B_{min} T

VALLEY PARAMETERS: Gap (min) cm B_{max} T

(Ø AT) Gap (max) 11.68 cm B_{min} 14.4 T

AVERAGE FIELD: $< B >_{min}$ T $< B >_{max}$ T

NUMBER OF SECTORS: compact/separated 3 /

sector angle deg. spiral (max) deg.

FIELD TRIMMING: Trim Coils none

Harmonic Coils Two sets: inner/outer @ 13/38 cm.

Other

CURRENT: Main Coils 500 Amps Stability 0.01%

Trim Coils Amps Stability

Stored Energy (cryogenic) MJ

WEIGHT: Iron 28,803 kg TOTAL Conductor

ION ENERGY: Bending Limit E/A = q^2/A^2 MeV/u

Focussing Limit E/A = q/A MeV/u

ACCELERATION SYSTEM

FUNDAMENTAL ACCELERATION:

Description: Two 90° dees

No. of Gaps/turn 4 dE/dn(max) MeV/q

Voltage(max) 0.028 MV Harmonic f_{rf}/f_{ion}

Freq 14.2-26.5 MHz Power in(max) 0.060 MW

Stability: Phase Voltage

VACUUM SYSTEM

OPERATING PRESSURE: 10^{-5} torr

PUMPS: No. and type One oil diffusion pump

ION SOURCE(S)

	Type	Intensity (mA)	Ø	$\epsilon_n = \beta\gamma\epsilon$ (π mm mrad)	Ion Species
(a)	Penning			not available	H^+/D^+
	"			"	$^3He^{++}/^4He^{++}$
(b)					

INJECTION SYSTEM

Radial Efficiency 10-12 %

EXTRACTION SYSTEM

Electrostatic deflector and septum Efficiency 70 %

CHARACTERISTIC BEAMS

		Current(part. μA)	
Accelerated Ions	E/A (MeV/u)	Internal	External
(a) H^+/D^+	26/15	200/300	60/100
(b) $^3He^{++}/^4He^{++}$	38/30	135/90	60/40

EXTRACTED BEAM PROPERTIES:

For μA of MeV/u ions

$\Delta E/E$ 1 % $\Delta\phi$ °rf

$\epsilon_n = \beta\gamma\epsilon$ x πmm mrad z πmm mrad

REFERENCES/NOTES

(a) CTI Cyclotron Systems, 950 Gilman St., Berkeley, CA

(b) A CNI-30 was converted to a CS-30

ENTRY NO. CM28 Date

Machine Name: CP-42

Manufacturer: The Cyclotron Corporation (a)

Address: 950 Gilman St., Berkeley, CA 94710 USA

Tel: (510) 524-8844 Telex: 910-366-7116

Fax: (510) 527-9336 EMAIL:

In Charge: n/a Reported by: F. Ramsey

HISTORY AND STATUS

DATES: Design 1978 First Machine 1980

SALES: No. Sold/Operational 5 / 4(b) Currently Available no

COST: Accelerator Facility

MAGNET

POLE PARAMETERS:

Diameter 120 cm $R_{extract}$ 28-52 cm R_{inject} cm

HILL PARAMETERS: Gap (min) 5 cm B_{max} 24 T

(@ AT) Gap (max) cm B_{min} T

VALLEY PARAMETERS: Gap (min) 11.4 cm B_{max} 16 T

(@ AT) Gap (max) cm B_{min} T

AVERAGE FIELD: $< B >_{min}$ 14 T $< B >_{max}$ 22 T

NUMBER OF SECTORS: compact/separated 3 /

sector angle deg. spiral (max) 64 deg.

FIELD TRIMMING: Trim Coils

Harmonic Coils 2 sets: inner and outer

Other

CURRENT: Main Coils 350 Amps Stability 1 x 10(-5)

Trim Coils n/a Amps Stability

Stored Energy (cryogenic) MJ

WEIGHT: Iron 35 tons Conductor 3 tons

ION ENERGY: Bending Limit E/A = q^2/A^2 MeV/u

Focussing Limit E/A = q/A MeV/u

ACCELERATION SYSTEM

FUNDAMENTAL ACCELERATION:

Description: Two 90° dees

No. of Gaps/turn 4 dE/dn(max) MeV/q

Voltage(max) 0.035 MV Harmonic f_{rf}/f_{ion}

Freq MHz Power in(max) 0.090 MW

Stability: Phase Voltage

VACUUM SYSTEM

OPERATING PRESSURE: 6 x 10(-6)

PUMPS: No. and type Four oil diffusion pumps

ION SOURCE(S)

	Type	Intensity (mA)	@ $\epsilon_n = \beta\gamma\epsilon$ (π mm mrad)	Ion Species
(a)	Penning		not available	H^-
(b)				

INJECTION SYSTEM

Radial Efficiency %

EXTRACTION SYSTEM

H^- stripping foil Efficiency 100 %

CHARACTERISTIC BEAMS

	Accelerated Ions	E/A (MeV/u)	Current(part. μA) Internal	External
(a)	H^-	11-42	200	200 (H^+)
(b)				

EXTRACTED BEAM PROPERTIES:

For μA of MeV/u ions

$\Delta E/E$ % $\Delta\phi$ °rf

$\epsilon_n = \beta\gamma\epsilon$ x πmm mrad z πmm mrad

REFERENCES/NOTES

(a) CTI Cyclotron Systems, 950 Gilman St, Berkeley CA 94710

(b) Status of machine #5 unknown, presumed functional

ENTRY NO. CM29 Date

Machine Name: RDS-112

Manufacturer: CTI PET Systems/Siemens

Address: 810 Innovation Drive, Knoxville, TN. 37932 USA

Tel: (615) 966-7539 Telex:

Fax: (615) 966-8955 EMAIL:

In Charge: Dr. T. Douglass Reported by: F.A. Ramsey

HISTORY AND STATUS

DATES: Design 1985-1986 First Machine 1987

SALES: No. Sold/Operational 21 / 21 Currently Available yes

COST: Accelerator Facility

MAGNET

POLE PARAMETERS:

Diameter 72 cm $R_{extract}$ 27 cm R_{inject} cm

HILL PARAMETERS: Gap (min) 6 cm B_{max} 2.5 T

(@ AT) Gap (max) cm B_{min} T

VALLEY PARAMETERS: Gap (min) cm B_{max} T

(@ AT) Gap (max) cm B_{min} T

AVERAGE FIELD: $< B >_{min}$ 1.8 T $< B >_{max}$ T

NUMBER OF SECTORS: compact/separated 3 /

sector angle deg. spiral (max) deg.

FIELD TRIMMING: Trim Coils n/a

Harmonic Coils none

Other

CURRENT: Main Coils 270 Amps Stability 1 x 10(-5)

Trim Coils n/a Amps Stability

Stored Energy (cryogenic) MJ

WEIGHT: Iron 20 tonnes TOTAL Conductor

ION ENERGY: Bending Limit E/A = q^2/A^2 MeV/u

Focussing Limit E/A = q/A MeV/u

ACCELERATION SYSTEM

FUNDAMENTAL ACCELERATION:

Description: 2 dees

No. of Gaps/turn 4 dE/dn(max) 0.100 MeV/q

Voltage(max) 0.035 MV Harmonic f_{rf}/f_{ion} 1

Freq 27 MHz Power in(max) 0.030 MW

Stability: Phase Voltage

VACUUM SYSTEM

OPERATING PRESSURE: 3 x 10(-6) torr

PUMPS: No. and type Two oil diffusion pumps

ION SOURCE(S)

	Type	Intensity (mA)	@ $\epsilon_n = \beta\gamma\epsilon$ (π mm mrad)	Ion Species
(a)	Penning	0.250	not available	H^-
(b)				

INJECTION SYSTEM

Radial Efficiency %

EXTRACTION SYSTEM

Carbon foil Efficiency 100 %

CHARACTERISTIC BEAMS

	Accelerated Ions	E/A (MeV/u)	Current(part. μA) Internal	External
(a)	H^-	11		100 (H^+)
(b)				

EXTRACTED BEAM PROPERTIES:

For μA of MeV/u ions

$\Delta E/E$ % $\Delta\phi$ °rf

$\epsilon_n = \beta\gamma\epsilon$ x 50 πmm mrad z 50 πmm mrad

REFERENCES/NOTES

(a)

(b)

ENTRY NO. CM28 Date

Machine Name: CP-42

Manufacturer: The Cyclotron Corporation (a)

Address: 950 Gilman St., Berkeley, CA 94710 USA

Tel: (510) 524-8844 Telex: 910-366-7116

Fax: (510) 527-9336 EMAIL:

In Charge: n/a Reported by: F. Ramsey

HISTORY AND STATUS

DATES: Design 1978 First Machine 1980

SALES: No. Sold/Operational 5 / 4(b) Currently Available no

COST: Accelerator Facility

MAGNET

POLE PARAMETERS:

Diameter 120 cm $R_{extract}$ 28-52 cm R_{inject} cm

HILL PARAMETERS: Gap (min) 5 cm B_{max} 24 T

(@ AT) Gap (max) cm B_{min} T

VALLEY PARAMETERS: Gap (min) 11.4 cm B_{max} 16 T

(@ AT) Gap (max) cm B_{min} T

AVERAGE FIELD: $< B >_{min}$ 14 T $< B >_{max}$ 22 T

NUMBER OF SECTORS: compact/separated 3 /

sector angle deg. spiral (max) 64 deg.

FIELD TRIMMING: Trim Coils

Harmonic Coils 2 sets: inner and outer

Other

CURRENT: Main Coils 350 Amps Stability 1 x 10(-5)

Trim Coils n/a Amps Stability

Stored Energy (cryogenic) MJ

WEIGHT: Iron 35 tons Conductor 3 tons

ION ENERGY: Bending Limit E/A = q^2/A^2 MeV/u

Focussing Limit E/A = q/A MeV/u

ACCELERATION SYSTEM

FUNDAMENTAL ACCELERATION:

Description: Two 90° dees

No. of Gaps/turn 4 dE/dn(max) MeV/q

Voltage(max) 0.035 MV Harmonic f_{rf}/f_{ion}

Freq MHz Power in(max) 0.090 MW

Stability: Phase Voltage

VACUUM SYSTEM

OPERATING PRESSURE: 6 x 10(-6)

PUMPS: No. and type Four oil diffusion pumps

ION SOURCE(S)

	Type	Intensity (mA)	@ $\epsilon_n = \beta\gamma\epsilon$ (π mm mrad)	Ion Species
(a)	Penning		not available	H^-
(b)				

INJECTION SYSTEM

Radial Efficiency %

EXTRACTION SYSTEM

H^- stripping foil Efficiency 100 %

CHARACTERISTIC BEAMS

	Accelerated Ions	E/A (MeV/u)	Current(part. μA) Internal	External
(a)	H^-	11-42	200	200 (H^+)
(b)				

EXTRACTED BEAM PROPERTIES:

For μA of MeV/u ions

$\Delta E/E$ % $\Delta\phi$ °rf

$\epsilon_n = \beta\gamma\epsilon$ x πmm mrad z πmm mrad

REFERENCES/NOTES

(a) CTI Cyclotron Systems, 950 Gilman St, Berkeley CA 94710

(b) Status of machine #5 unknown, presumed functional

ENTRY NO. CM29 Date

Machine Name: RDS-112

Manufacturer: CTI PET Systems/Siemens

Address: 810 Innovation Drive, Knoxville, TN. 37932 USA

Tel: (615) 966-7539 Telex:

Fax: (615) 966-8955 EMAIL:

In Charge: Dr. T. Douglass Reported by: F.A. Ramsey

HISTORY AND STATUS

DATES: Design 1985-1986 First Machine 1987

SALES: No. Sold/Operational 21 / 21 Currently Available yes

COST: Accelerator Facility

MAGNET

POLE PARAMETERS:

Diameter 72 cm $R_{extract}$ 27 cm R_{inject} cm

HILL PARAMETERS: Gap (min) 6 cm B_{max} 2.5 T

(@ AT) Gap (max) cm B_{min} T

VALLEY PARAMETERS: Gap (min) cm B_{max} T

(@ AT) Gap (max) cm B_{min} T

AVERAGE FIELD: $< B >_{min}$ 1.8 T $< B >_{max}$ T

NUMBER OF SECTORS: compact/separated 3 /

sector angle deg. spiral (max) deg.

FIELD TRIMMING: Trim Coils n/a

Harmonic Coils none

Other

CURRENT: Main Coils 270 Amps Stability 1 x 10(-5)

Trim Coils n/a Amps Stability

Stored Energy (cryogenic) MJ

WEIGHT: Iron 20 tonnes TOTAL Conductor

ION ENERGY: Bending Limit E/A = q^2/A^2 MeV/u

Focussing Limit E/A = q/A MeV/u

ACCELERATION SYSTEM

FUNDAMENTAL ACCELERATION:

Description: 2 dees

No. of Gaps/turn 4 dE/dn(max) 0.100 MeV/q

Voltage(max) 0.035 MV Harmonic f_{rf}/f_{ion} 1

Freq 27 MHz Power in(max) 0.030 MW

Stability: Phase Voltage

VACUUM SYSTEM

OPERATING PRESSURE: 3 x 10(-6) torr

PUMPS: No. and type Two oil diffusion pumps

ION SOURCE(S)

	Type	Intensity (mA)	@ $\epsilon_n = \beta\gamma\epsilon$ (π mm mrad)	Ion Species
(a)	Penning	0.250	not available	H^-
(b)				

INJECTION SYSTEM

Radial Efficiency %

EXTRACTION SYSTEM

Carbon foil Efficiency 100 %

CHARACTERISTIC BEAMS

	Accelerated Ions	E/A (MeV/u)	Current(part. μA) Internal	External
(a)	H^-	11		100 (H^+)
(b)				

EXTRACTED BEAM PROPERTIES:

For μA of MeV/u ions

$\Delta E/E$ % $\Delta\phi$ °rf

$\epsilon_n = \beta\gamma\epsilon$ x 50 πmm mrad z 50 πmm mrad

REFERENCES/NOTES

(a)

(b)

ENTRY NO. CU2 Date 19/06/92

Cyclotron Model ION BEAM APPLICATIONS CYCLONE 30

Institution NATIONAL MEDICAL CYCLOTRON (ANSTO/RPAH)

Address GROSE ST., CAMPERDOWN, NSW. 2050, AUSTRALIA

Tel 02 565 7600 Telex -

Fax 02 565 7676 EMAIL -

In Charge: R E BOYD Reported by: D W ARNOTT/ B MUKHERJEE

HISTORY

MILESTONE DATES:

Installation 09/04/91 First Beam 09/07/91

DESIGN/CONSTRUCTION BY: IBA (ION BEAM APPLICATIONS)

COST: Accelerator $4.3M Facility $20.5M

FUNDED BY: ANSTO-RPAH

STATUS

STAFF: Operators 3 Technicians 8

BUDGET: Machine $3M Funded by ANSTO

TIME DISTRIBUTION: (e.g. basic research, isotope production, maintenance, etc.)

(a) PET RADIOISOTOPES 88 %

(b) SPECT RADIOISOTOPES 88 %

(c) MAINTENANCE 10 %

(d) BASIC RESEARCH (HEALTH PHYSICS) 2+ %

(e) %

CHARACTERISTIC BEAMS

	Accelerated Ions	E/A (MeV/u)	Current(part μA) Internal	External
(a)	H^-	15-30MeV	15-200uA	
(b)				

1991 μA-hours on target: 10,000uAhr

FACILITIES

SHIELDED AREA: Fixed 168 m² Moveable - m²

Target Stations: 6 No. Served At Same Time: 2

OTHER FACILITIES:

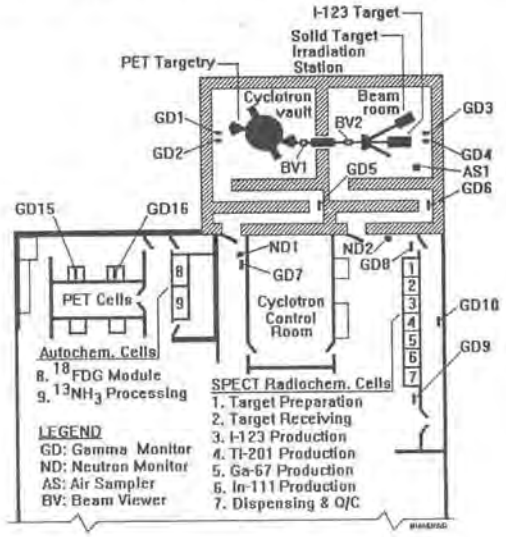
REFERENCES/NOTES

(a)

(b)

PLAN VIEW OF FACILITY, COMMENTS

Facility provides dual PET/SPECT simultaneous production. Shielding wall made of 2.3m thick low sodium content concrete.



ENTRY NO. CU5 Date June 19, 1992

Cyclotron Model IBA CYCLONE 30

Institution Nordion Europe S.A.

Address B-6220 FLEURUS (Belgium)

Tel 32-71-829211 Telex -

Fax 32-71-829221 EMAIL -

In Charge: C. PIRART Reported by: C. PIRART

HISTORY

MILESTONE DATES:

Installation January 1992 First Beam March 1992

DESIGN/CONSTRUCTION BY: Ion Beam Applications S.A.

COST: Accelerator 4 M US$ Facility 8 M US$

FUNDED BY: NORDION EUROPE S.A.

STATUS

STAFF: Operators 4 Technicians 6

BUDGET: Machine - Funded by -

TIME DISTRIBUTION: (e.g. basic research, isotope production, maintenance, etc.)

(a) Isotope production 100 %

(b) %

(c) %

(d) %

(e) %

CHARACTERISTIC BEAMS

	Accelerated Ions	E/A (MeV/u)	Current(part μA) Internal	External
(a)	H	15-30	-	2x200 μA
(b)				

1991 μA-hours on target:

FACILITIES

SHIELDED AREA: Fixed 80 m² Moveable - m²

Target Stations: 4 No. Served At Same Time: 2

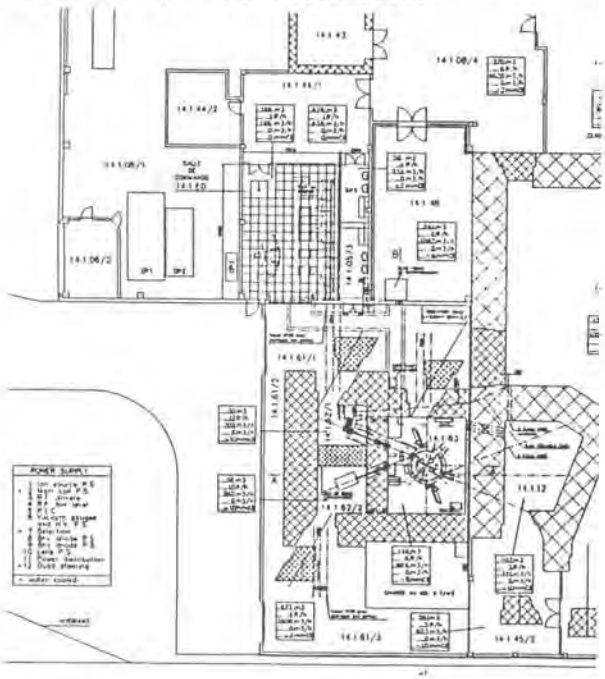
OTHER FACILITIES:

REFERENCES/NOTES

(a)

(b)

PLAN VIEW OF FACILITY, COMMENTS



ENTRY NO. CU2 Date 19/06/92

Cyclotron Model ION BEAM APPLICATIONS CYCLONE 30

Institution NATIONAL MEDICAL CYCLOTRON (ANSTO/RPAH)

Address GROSE ST., CAMPERDOWN, NSW. 2050, AUSTRALIA

Tel 02 565 7600 Telex -

Fax 02 565 7676 EMAIL -

In Charge: R E BOYD Reported by: D W ARNOTT/ B MUKHERJEE

HISTORY

MILESTONE DATES:

Installation 09/04/91 First Beam 09/07/91

DESIGN/CONSTRUCTION BY: IBA (ION BEAM APPLICATIONS)

COST: Accelerator $4.3M Facility $20.5M

FUNDED BY: ANSTO-RPAH

STATUS

STAFF: Operators 3 Technicians 8

BUDGET: Machine $3M Funded by ANSTO

TIME DISTRIBUTION: (e.g. basic research, isotope production, maintenance, etc.)

(a) PET RADIOISOTOPES 88 %

(b) SPECT RADIOISOTOPES 88 %

(c) MAINTENANCE 10 %

(d) BASIC RESEARCH (HEALTH PHYSICS) 2+ %

(e) %

CHARACTERISTIC BEAMS

	Accelerated Ions	E/A (MeV/u)	Current(part μA) Internal	External
(a)	H^-	15-30MeV	15-200uA	
(b)				

1991 μA-hours on target: 10,000uAhr

FACILITIES

SHIELDED AREA: Fixed 168 m² Moveable - m²

Target Stations: 6 No. Served At Same Time: 2

OTHER FACILITIES:

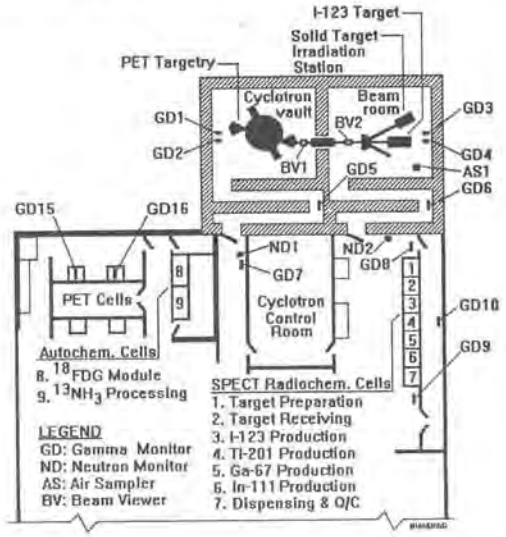
REFERENCES/NOTES

(a)

(b)

PLAN VIEW OF FACILITY, COMMENTS

Facility provides dual PET/SPECT simultaneous production. Shielding wall made of 2.3m thick low sodium content concrete.



ENTRY NO. CU5 Date June 19, 1992

Cyclotron Model IBA CYCLONE 30

Institution Nordion Europe S.A.

Address B-6220 FLEURUS (Belgium)

Tel 32-71-829211 Telex -

Fax 32-71-829221 EMAIL -

In Charge: C. PIRART Reported by: C. PIRART

HISTORY

MILESTONE DATES:

Installation January 1992 First Beam March 1992

DESIGN/CONSTRUCTION BY: Ion Beam Applications S.A.

COST: Accelerator 4 M US$ Facility 8 M US$

FUNDED BY: NORDION EUROPE S.A.

STATUS

STAFF: Operators 4 Technicians 6

BUDGET: Machine - Funded by -

TIME DISTRIBUTION: (e.g. basic research, isotope production, maintenance, etc.)

(a) Isotope production 100 %

(b) %

(c) %

(d) %

(e) %

CHARACTERISTIC BEAMS

	Accelerated Ions	E/A (MeV/u)	Current(part μA) Internal	External
(a)	H	15-30	-	2x200 μA
(b)				

1991 μA-hours on target:

FACILITIES

SHIELDED AREA: Fixed 80 m² Moveable - m²

Target Stations: 4 No. Served At Same Time: 2

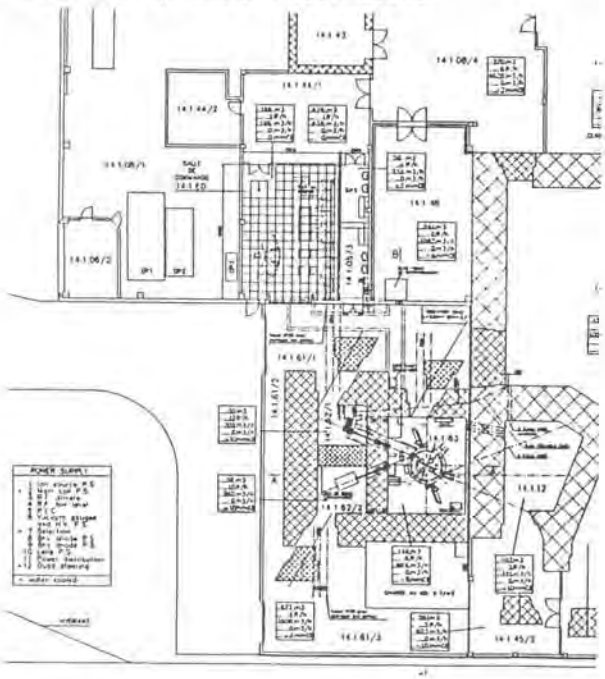
OTHER FACILITIES:

REFERENCES/NOTES

(a)

(b)

PLAN VIEW OF FACILITY, COMMENTS



ENTRY NO. CU6 Date June 19, 1992

Name of Machine CGR-MeV 930S

Institution NORDION EUROPE S.A.

Address B-6220 FLEURUS (Belgium)

Tel 32-71-829211 Telex Fax 32-71-829221 EMAIL

In Charge: C. PIRART Reported by: C. PIRART

HISTORY

MILESTONE DATES:

Design 1980 Model Tests

Construction 1981-1983 First Beam 1983

DESIGN/CONSTRUCTION BY:

in house other

COST: Accelerator 6 M US$ Facility 12 M US$

FUNDED BY:

STATUS

STAFF: Machine

Scientists Engineers

Technicians 5 Students

Research (in house/external)

Scientists / Engineers /

Technicians / Students /

BUDGET: Machine Funded by

Research Funded by

TIME DISTRIBUTION:

Basic Research (in house/external) % /

Applied Program (in house/external) 100 % / %

Development % Maintenance %

MAGNET

POLE PARAMETERS:

Diameter 215.6 cm $R_{extract}$ 92.4 cm R_{inject} cm

HILL PARAMETERS: Gap (min) 16.6 cm B_{max} 2.15 T

(@ AT) Gap (max) 40.5 cm B_{min} 1.15 T

VALLEY PARAMETERS: Gap (min) cm B_{max} T

(@ AT) Gap (max) cm B_{min} T

AVERAGE FIELD: $< B >_{min}$ T $< B >_{max}$ T

NUMBER OF SECTORS: compact/separated 4 /

sector angle deg. spiral (max) 53 deg.

FIELD TRIMMING: Trim Coils 12 pairs

Harmonic Coils centering 4 pairs Ext. 4 pairs

Other 5

CURRENT: Main Coils 1100 Amps Stability 10

Trim Coils 300 Amps Stability 10-3

Stored Energy (cryogenic) MJ

WEIGHT: Iron 200 T Conductor Cu

ION ENERGY: Bending Limit E/A = 110 q^2/A^2 MeV/u

Focussing Limit E/A = 80 q/A MeV/u

ACCELERATION SYSTEM

FUNDAMENTAL ACCELERATION:

Description:

No. of Gaps/turn 4 dE/dn(max) 0.15 MeV/q

Voltage(max) 0.05 MV Harmonic f_{rf}/f_{ion} 1 , II

Freq 10.6-23 MHz Power in(max) 0.14 MW

Stability: Phase 0.1° Voltage < 10-3

OTHER CAVITIES (Flattopping or otherwise):

Description:

Region of Influence: R_{min} cm R_{max} cm

No. of Gaps/turn dE/dn(max) MeV/q

Voltage(max) MV Harmonic f_{rf}/f_{ion}

Freq MHz Power in(max) MW

Stability: Phase Voltage

VACUUM SYSTEM

OPERATING PRESSURE: 2.10-6

PUMPS: No. and type 2 x OIL DIF. 12000 l/s

ION SOURCE(S)

	Type	Intensity (mA)	@	$\epsilon_n = \beta\gamma\epsilon$ (πmm mrad)	Ion Species
(a)	LIV-JONES				p,d,α
(b)					
(c)					
(d)					

INJECTION SYSTEM

Efficiency %

EXTRACTION SYSTEM

DC electrost. + act. magn. channel Efficiency 60 %

CHARACTERISTIC BEAMS

	Accelerated Ions	E/A (MeV/u)	Current(part μA) Internal	External
(a)	p	80	700	50
(b)				
(c)				
(d)				

	Secondary Particles	E (MeV)	part/sec
(a)			
(b)			
(c)			

EXTRACTED BEAM PROPERTIES:

For μA of MeV/u ions

$\Delta E/E$ % $\Delta\phi$ °rf

$\epsilon_n = \beta\gamma\epsilon$ x πmm mrad z πmm mrad

FACILITIES FOR RESEARCH

SHIELDED AREA: Fixed m² Moveable m²

Target Stations: 4 No. Served At Same Time: 1

MAGNETIC SPECTROMETERS:

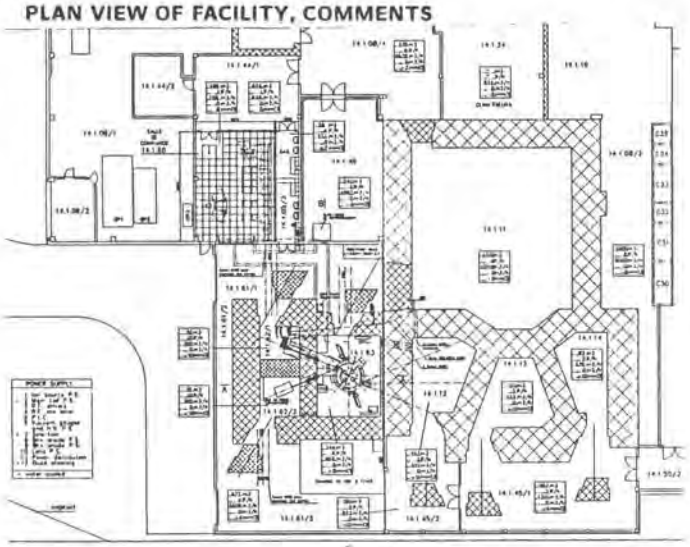
OTHER FACILITIES:

REFERENCES/NOTES

(a)

(b)

PLAN VIEW OF FACILITY, COMMENTS



ENTRY NO. CU7 **Date** June 16, 1992

Cyclotron Model : CGR-MeV 520
Institution Lab. Anal. Chem. - Inst. Nucl. Sc. - Universiteit Gent
Address Proeftuinstraat 86, B-9000 Gent, Belgium
Tel +32 91/64 66 16 Telex
Fax +32 91/64 66 99 EMAIL STRYKMAN@INWCHEM.RUG.AC.BE
In Charge: Dr. K. Strijckmans Reported by: Dr. K. Strijckmans
Prof. Dr. R. Dams (Director)

HISTORY

MILESTONE DATES:
Installation 1976 First Beam 1977
DESIGN/CONSTRUCTION BY: CGR-MeV
COST: Accelerator 5 MECU Facility 5 MECU
FUNDED BY: NFWO Nat. Fund for Scientific Research (Belgium) RUG University Gent

STATUS

STAFF: Operators 1 full-time Technicians 2 part-time
BUDGET: Machine 50 000 ECU/y Funded by IIKW [a]
TIME DISTRIBUTION: (e.g. basic research, isotope production, maintenance, etc.)

(a)	isotope production for PET	50 %
(b)	charged particle and neutron activation anal.	20 %
(c)	proton induced X-ray emission (PIXE) analysis	20 %
(d)	neutron therapy	5 %
(e)	thin layer activation	5 %

CHARACTERISTIC BEAMS

	Accelerated Ions	E/A (MeV/u)	Current(part μA) Internal	External
(a)	p	2.5 - 24		100
(b)	d	1.5 - 7.3		100
	^{3}He	2 - 10.7		60
	^{4}a	2.5 - 7.3		60

1991 μA-hours on target: $\sim 10^4$

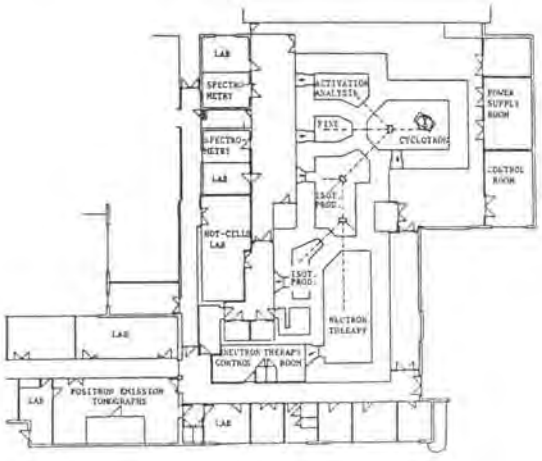
FACILITIES

SHIELDED AREA: Fixed 200 m^2 Moveable m^2
Target Stations: 7 No. Served At Same Time: 1
OTHER FACILITIES: 2 positron emission tomographs, 6 hot-cells, radiochemistry labs, 2 HPGe spectrometers, 1 γ-γ coincidence set-up, 1 well type ion chamber, n-dosimetry

REFERENCES/NOTES

(a) IIKW = Inter-University Institute Nuclear Sciences.
(b) A biannual report, describing the research activities (cyclotron applications a.o.) can be requested to the director

PLAN VIEW OF FACILITY, COMMENTS



ENTRY NO. CU8 **Date** 1989

Cyclotron Model : CGR-MeV 520
Institution Université de Liège
Address Centre de Recherches du Cyclotron
Tel 32 41 56 36 87 Telex
Fax 32 41 56 29 46 EMAIL
In Charge: D. LaMotte Reported by: D. LaMotte

HISTORY

MILESTONE DATES:
Installation First Beam 1975
DESIGN/CONSTRUCTION BY: CGR-MeV
COST: Accelerator Facility
FUNDED BY:

STATUS

STAFF: Operators 5 Technicians 5
BUDGET: Machine Funded by
TIME DISTRIBUTION: (e.g. basic research, isotope production, maintenance, etc.)

(a)	Solid State Physics	30 %
(b)	Bio-Medical Application	40 %
(c)	Isotope Production	30 %
(d)		%
(e)		%

CHARACTERISTIC BEAMS

	Accelerated Ions	E/A (MeV/u)	Current(part μA) Internal	External
(a)	p	2.5-24	300	100
(b)	d	2-7	500	100
	^{3}He, ^{4}He			

1991 μA-hours on target: -

FACILITIES

SHIELDED AREA: Fixed 700 m^2 Moveable m^2
Target Stations: 7 No. Served At Same Time: 1
OTHER FACILITIES: radiochemistry (automated production of labelled compounds), medical unit (positron scanners), radio pharmacy, biological laboratories

REFERENCES/NOTES

(a)
(b)

PLAN VIEW OF FACILITY, COMMENTS

ENTRY NO. CU7 **Date** June 16, 1992

Cyclotron Model : CGR-MeV 520
Institution Lab. Anal. Chem. - Inst. Nucl. Sc. - Universiteit Gent
Address Proeftuinstraat 86, B-9000 Gent, Belgium
Tel +32 91/64 66 16 Telex
Fax +32 91/64 66 99 EMAIL STRYKMAN@INWCHEM.RUG.AC.BE
In Charge: Dr. K. Strijckmans Reported by: Dr. K. Strijckmans
Prof. Dr. R. Dams (Director)

HISTORY

MILESTONE DATES:
Installation 1976 First Beam 1977
DESIGN/CONSTRUCTION BY: CGR-MeV
COST: Accelerator 5 MECU Facility 5 MECU
FUNDED BY: NFWO Nat. Fund for Scientific Research (Belgium) RUG University Gent

STATUS

STAFF: Operators 1 full-time Technicians 2 part-time
BUDGET: Machine 50 000 ECU/y Funded by IIKW [a]
TIME DISTRIBUTION: (e.g. basic research, isotope production, maintenance, etc.)

(a)	isotope production for PET	50 %
(b)	charged particle and neutron activation anal.	20 %
(c)	proton induced X-ray emission (PIXE) analysis	20 %
(d)	neutron therapy	5 %
(e)	thin layer activation	5 %

CHARACTERISTIC BEAMS

	Accelerated Ions	E/A (MeV/u)	Current(part μA) Internal	External
(a)	p	2.5 - 24		100
(b)	d	1.5 - 7.3		100
	^{3}He	2 - 10.7		60
	^{4}a	2.5 - 7.3		60

1991 μA-hours on target: $\sim 10^4$

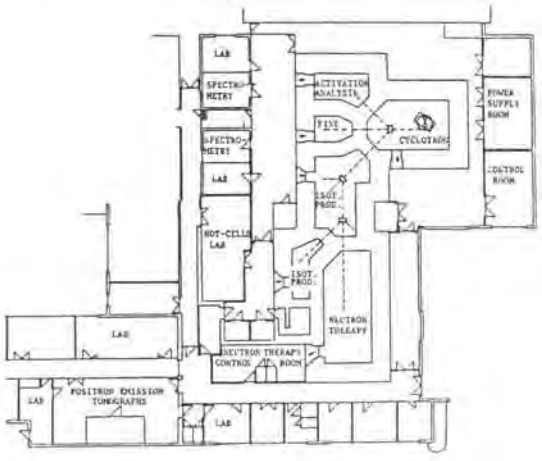
FACILITIES

SHIELDED AREA: Fixed 200 m^2 Moveable m^2
Target Stations: 7 No. Served At Same Time: 1
OTHER FACILITIES: 2 positron emission tomographs, 6 hot-cells, radiochemistry labs, 2 HPGe spectrometers, 1 γ-γ coincidence set-up, 1 well type ion chamber, n-dosimetry

REFERENCES/NOTES

(a) IIKW = Inter-University Institute Nuclear Sciences.
(b) A biannual report, describing the research activities (cyclotron applications a.o.) can be requested to the director

PLAN VIEW OF FACILITY, COMMENTS



ENTRY NO. CU8 **Date** 1989

Cyclotron Model : CGR-MeV 520
Institution Université de Liège
Address Centre de Recherches du Cyclotron
Tel 32 41 56 36 87 Telex
Fax 32 41 56 29 46 EMAIL
In Charge: D. LaMotte Reported by: D. LaMotte

HISTORY

MILESTONE DATES:
Installation First Beam 1975
DESIGN/CONSTRUCTION BY: CGR-MeV
COST: Accelerator Facility
FUNDED BY:

STATUS

STAFF: Operators 5 Technicians 5
BUDGET: Machine Funded by
TIME DISTRIBUTION: (e.g. basic research, isotope production, maintenance, etc.)

(a)	Solid State Physics	30 %
(b)	Bio-Medical Application	40 %
(c)	Isotope Production	30 %
(d)		%
(e)		%

CHARACTERISTIC BEAMS

	Accelerated Ions	E/A (MeV/u)	Current(part μA) Internal	External
(a)	p	2.5-24	300	100
(b)	d	2-7	500	100
	^{3}He, ^{4}He			

1991 μA-hours on target: -

FACILITIES

SHIELDED AREA: Fixed 700 m^2 Moveable m^2
Target Stations: 7 No. Served At Same Time: 1
OTHER FACILITIES: radiochemistry (automated production of labelled compounds), medical unit (positron scanners), radio pharmacy, biological laboratories

REFERENCES/NOTES

(a)
(b)

PLAN VIEW OF FACILITY, COMMENTS

ENTRY NO. CU11 **Date** 1989

Cyclotron Model: TCC CV-28

Institution: Instituto de Egenharia Nuclear/CNEN

Address: Caixa Postal 2186, Rio de Janeiro, Brazil

Tel: (021) 280 3113 Telex: 02121112

Fax: EMAIL:

In Charge: A.G. DaSilva Reported by: Jose A.D.Furlanetto

HISTORY

MILESTONE DATES:

Installation: First Beam: Dec. 1974

DESIGN/CONSTRUCTION BY: TCC

COST: Accelerator: 0.5M US$ Facility: 1.2M US$

FUNDED BY: CNEN-Brazil, FINEP-Brazil

STATUS

STAFF: Operators: Technicians: 6

BUDGET: Machine: 80K US$ Funded by: CNEN-Brazil

TIME DISTRIBUTION: (e.g. basic research, isotope production, maintenance, etc.)

(a) Basic Nuclear Physics 40 %

(b) Isotope Production 40 %

(c) %

(d) %

(e) %

CHARACTERISTIC BEAMS

Accelerated Ions	E/A (MeV/u)	Current(part μA) Internal	External
(a) p	24	100	70
(b) d, ^{3}He, α	7	140	100

1991 μA-hours on target:

FACILITIES

SHIELDED AREA: Fixed: 50 m² Moveable: 250 m²

Target Stations: 5 No. Served At Same Time: 1

OTHER FACILITIES: 2 scattering chambers, He jet transport system, neutron production and spect. station, radio-isotope production and separation cells, ion implantation station

REFERENCES/NOTES

(a) A.G. da Silva et al, NIM A264 (1988) 381

(b)

PLAN VIEW OF FACILITY, COMMENTS

ENTRY NO. CU12 **Date** 1986

Cyclotron Model: TCC CV-28

Institution: Inst. de Pesquises Ener e Nucl. - CNEN/SP

Address: C.P. 11049 Cidade Univ., Sao Paulo, Brazil

Tel: 211-6011 Telex: (011) 23592

Fax: EMAIL:

In Charge: G. Lucki Reported by: G. Lucki

HISTORY

MILESTONE DATES:

Installation: First Beam: 1981

DESIGN/CONSTRUCTION BY: TCC

COST: Accelerator: 1M US$ Facility: 2M US$

FUNDED BY: Brazil Government

STATUS

STAFF: Operators: 5 Technicians: 2

BUDGET: Machine: 0.1M US$ Funded by: Brazil Govt.

TIME DISTRIBUTION: (e.g. basic research, isotope production, maintenance, etc.)

(a) Isotope Production 100 %

(b) %

(c) %

(d) %

(e) %

CHARACTERISTIC BEAMS

Accelerated Ions	E/A (MeV/u)	Current(part μA) Internal	External
(a) P	24	300	40
(b) α, ^{3}He, d	14	50	25

1991 μA-hours on target:

FACILITIES

SHIELDED AREA: Fixed: 80 m² Moveable: 180 m²

Target Stations: 2 No. Served At Same Time: 1

OTHER FACILITIES:

REFERENCES/NOTES

(a) G. Lucki et al, 4th Japan-Brazil Symposium on

(b) Science and Technology-Sao Paulto Aug. 1984

PLAN VIEW OF FACILITY, COMMENTS

ENTRY NO. CU11 **Date** 1989

Cyclotron Model: TCC CV-28

Institution: Instituto de Egenharia Nuclear/CNEN

Address: Caixa Postal 2186, Rio de Janeiro, Brazil

Tel: (021) 280 3113 Telex: 02121112

Fax: EMAIL:

In Charge: A.G. DaSilva Reported by: Jose A.D.Furlanetto

HISTORY

MILESTONE DATES:

Installation: First Beam: Dec. 1974

DESIGN/CONSTRUCTION BY: TCC

COST: Accelerator: 0.5M US$ Facility: 1.2M US$

FUNDED BY: CNEN-Brazil, FINEP-Brazil

STATUS

STAFF: Operators: Technicians: 6

BUDGET: Machine: 80K US$ Funded by: CNEN-Brazil

TIME DISTRIBUTION: (e.g. basic research, isotope production, maintenance, etc.)

(a) Basic Nuclear Physics 40 %

(b) Isotope Production 40 %

(c) %

(d) %

(e) %

CHARACTERISTIC BEAMS

Accelerated Ions	E/A (MeV/u)	Current(part μA) Internal	External
(a) p	24	100	70
(b) d, ^{3}He, α	7	140	100

1991 μA-hours on target:

FACILITIES

SHIELDED AREA: Fixed: 50 m² Moveable: 250 m²

Target Stations: 5 No. Served At Same Time: 1

OTHER FACILITIES: 2 scattering chambers, He jet transport system, neutron production and spect. station, radio-isotope production and separation cells, ion implantation station

REFERENCES/NOTES

(a) A.G. da Silva et al, NIM A264 (1988) 381

(b)

PLAN VIEW OF FACILITY, COMMENTS

ENTRY NO. CU12 **Date** 1986

Cyclotron Model: TCC CV-28

Institution: Inst. de Pesquises Ener e Nucl. - CNEN/SP

Address: C.P. 11049 Cidade Univ., Sao Paulo, Brazil

Tel: 211-6011 Telex: (011) 23592

Fax: EMAIL:

In Charge: G. Lucki Reported by: G. Lucki

HISTORY

MILESTONE DATES:

Installation: First Beam: 1981

DESIGN/CONSTRUCTION BY: TCC

COST: Accelerator: 1M US$ Facility: 2M US$

FUNDED BY: Brazil Government

STATUS

STAFF: Operators: 5 Technicians: 2

BUDGET: Machine: 0.1M US$ Funded by: Brazil Govt.

TIME DISTRIBUTION: (e.g. basic research, isotope production, maintenance, etc.)

(a) Isotope Production 100 %

(b) %

(c) %

(d) %

(e) %

CHARACTERISTIC BEAMS

Accelerated Ions	E/A (MeV/u)	Current(part μA) Internal	External
(a) P	24	300	40
(b) α, ^{3}He, d	14	50	25

1991 μA-hours on target:

FACILITIES

SHIELDED AREA: Fixed: 80 m² Moveable: 180 m²

Target Stations: 2 No. Served At Same Time: 1

OTHER FACILITIES:

REFERENCES/NOTES

(a) G. Lucki et al, 4th Japan-Brazil Symposium on

(b) Science and Technology-Sao Paulto Aug. 1984

PLAN VIEW OF FACILITY, COMMENTS

ENTRY NO. CU13 **Date**

Cyclotron Model RDS-112

Institution McMaster University, Faculty of Health Sciences

Address 1200 Main Street West, Hamilton, Ontario

Tel (416) 521 2100, ext5671 Telex

Fax (416) 546 1125 EMAIL

In Charge: Dr. Günter Firnau Reported by: Dr. Günter Firnau

HISTORY

MILESTONE DATES:

Installation Sept-Nov 1989 First Beam 6 December 1989

DESIGN/CONSTRUCTION BY: Siemens-CTI

COST: Accelerator appr. 2M Facility 5M

FUNDED BY: Ontario Ministry of Health

STATUS

STAFF: Operators 0 ~~Technicians~~ Chemists 2

BUDGET: Machine none Funded by MRC, NSERC + other foundations

TIME DISTRIBUTION: (e.g. basic research, isotope production, maintenance, etc.)

(a) Isotope production 95 %

(b) Maintenance 5 %

(c) %

(d) %

(e) %

CHARACTERISTIC BEAMS

	Accelerated Ions	E/A (MeV/u)	Current(part μA) Internal	External
(a)	H⁻ only	10.5MeV	100	100
(b)				

1991 μA-hours on target: 3245

FACILITIES

SHIELDED AREA: Fixed m² Moveable m²

Target Stations: 4 No. Served At Same Time: 2

OTHER FACILITIES:

REFERENCES/NOTES

(a) none

(b)

PLAN VIEW OF FACILITY, COMMENTS

ENTRY NO. CU15 **Date** 1986

Cyclotron Model JSW BC - 107

Institution Montreal Neurological Instr., McGill University

Address 3801 University St., Montreal, PQ, Canada

Tel 514 284 4675 Telex

Fax EMAIL

In Charge: Dr. M. Diksic Reported by: Dr. M. Diksic

HISTORY

MILESTONE DATES:

Installation First Beam

DESIGN/CONSTRUCTION BY:

COST: Accelerator 0.6M US$ Facility 15M Can$

FUNDED BY:

STATUS

STAFF: Operators Technicians

BUDGET: Machine Funded by

TIME DISTRIBUTION: (e.g. basic research, isotope production, maintenance, etc.)

(a) %

(b) %

(c) %

(d) %

(e) %

CHARACTERISTIC BEAMS

	Accelerated Ions	E/A (MeV/u)	Current(part μA) Internal	External
(a)	p	10	150	50
(b)	d	35	145	50

1991 μA-hours on target:

FACILITIES

SHIELDED AREA: Fixed 20 m² Moveable m²

Target Stations: No. Served At Same Time:

OTHER FACILITIES:

REFERENCES/NOTES

(a)

(b)

PLAN VIEW OF FACILITY, COMMENTS

ENTRY NO. CU13 **Date**

Cyclotron Model RDS-112

Institution McMaster University, Faculty of Health Sciences

Address 1200 Main Street West, Hamilton, Ontario

Tel (416) 521 2100, ext5671 Telex

Fax (416) 546 1125 EMAIL

In Charge: Dr. Günter Firnau Reported by: Dr. Günter Firnau

HISTORY

MILESTONE DATES:

Installation Sept-Nov 1989 First Beam 6 December 1989

DESIGN/CONSTRUCTION BY: Siemens-CTI

COST: Accelerator appr. 2M Facility 5M

FUNDED BY: Ontario Ministry of Health

STATUS

STAFF: Operators 0 ~~Technicians~~ Chemists 2

BUDGET: Machine none Funded by MRC, NSERC + other foundations

TIME DISTRIBUTION: (e.g. basic research, isotope production, maintenance, etc.)

(a) Isotope production 95 %

(b) Maintenance 5 %

(c) %

(d) %

(e) %

CHARACTERISTIC BEAMS

	Accelerated Ions	E/A (MeV/u)	Current(part μA) Internal	External
(a)	H⁻ only	10.5MeV	100	100
(b)				

1991 μA-hours on target: 3245

FACILITIES

SHIELDED AREA: Fixed m² Moveable m²

Target Stations: 4 No. Served At Same Time: 2

OTHER FACILITIES:

REFERENCES/NOTES

(a) none

(b)

PLAN VIEW OF FACILITY, COMMENTS

ENTRY NO. CU15 **Date** 1986

Cyclotron Model JSW BC - 107

Institution Montreal Neurological Instr., McGill University

Address 3801 University St., Montreal, PQ, Canada

Tel 514 284 4675 Telex

Fax EMAIL

In Charge: Dr. M. Diksic Reported by: Dr. M. Diksic

HISTORY

MILESTONE DATES:

Installation First Beam

DESIGN/CONSTRUCTION BY:

COST: Accelerator 0.6M US$ Facility 15M Can$

FUNDED BY:

STATUS

STAFF: Operators Technicians

BUDGET: Machine Funded by

TIME DISTRIBUTION: (e.g. basic research, isotope production, maintenance, etc.)

(a) %

(b) %

(c) %

(d) %

(e) %

CHARACTERISTIC BEAMS

	Accelerated Ions	E/A (MeV/u)	Current(part μA) Internal	External
(a)	p	10	150	50
(b)	d	35	145	50

1991 μA-hours on target:

FACILITIES

SHIELDED AREA: Fixed 20 m² Moveable m²

Target Stations: No. Served At Same Time:

OTHER FACILITIES:

REFERENCES/NOTES

(a)

(b)

PLAN VIEW OF FACILITY, COMMENTS

ENTRY NO. CU16 **Date** June 29/1992

Cyclotron Model Scanditronix MC17

Institution PET Centre, Clarke Institute of Psychiatry

Address 250 College Street, Toronto, Canada M5T 1R8

Tel (416) 979 4650 Telex

Fax (416) 979 4656 EMAIL

In Charge: S. Houle Reported by: S. Houle

HISTORY

MILESTONE DATES:

Installation June 91- April 92 First Beam May 1992

DESIGN/CONSTRUCTION BY: CIP & Scanditronix

COST: Accelerator Facility

FUNDED BY: Government of Ontario

STATUS

STAFF: Operators Technicians

BUDGET: Machine Funded by

TIME DISTRIBUTION: (e.g. basic research, isotope production, maintenance, etc.)

(a) PET Research 85 %

(b) PET Clinical 10. %

(c) Maintenance 5. %

(d) %

(e) %

CHARACTERISTIC BEAMS

	Accelerated Ions	E/A (MeV/u)	Current(part μA) Internal	External
(a)	p^+	17	75	60
(b)	d^+	8.5		

1991 μA-hours on target:

FACILITIES

SHIELDED AREA: Fixed 50 m² Moveable m²

Target Stations: 1 No. Served At Same Time: 1

OTHER FACILITIES:

REFERENCES/NOTES

(a)

(b)

PLAN VIEW OF FACILITY, COMMENTS

ENTRY NO. CU17 **Date**

Cyclotron Model TR 30

Institution TRIUMF

Address 4004 Wesbrook Mall, Vancouver BC, Canada V6T 2A3

Tel (604) 222-1047 Telex (0) 4508503

Fax (604) 222-1074 EMAIL NIGEL@TRIUMFCL

In Charge: N.R. Stevenson Reported by: N.R. Stevenson

HISTORY

MILESTONE DATES:

Installation Jun.89 - Jun.90. First Beam July 1990

DESIGN/CONSTRUCTION BY: TRIUMF/EBCO

COST: Accelerator $3,500,000 Facility $10,000,000

FUNDED BY: Nordion International Inc.

STATUS

STAFF: Operators 10 Technicians 5

BUDGET: Machine $800,000 Funded by Nordion Int.Inc.

TIME DISTRIBUTION: (e.g. basic research, isotope production, maintenance, etc.)

(a) Isotope Production 95 %

(b) Maintenance 5 %

(c) %

(d) %

(e) %

CHARACTERISTIC BEAMS

	Accelerated Ions	E/A (MeV/u)	Current(part μA) Internal	External
(a)	H^-	15-30	420 H^-	420 p
(b)				

1991 μA-hours on target: 1.84 x 10e6

FACILITIES

SHIELDED AREA: Fixed 100 m² Moveable m²

Target Stations: 3 No. Served At Same Time: 2

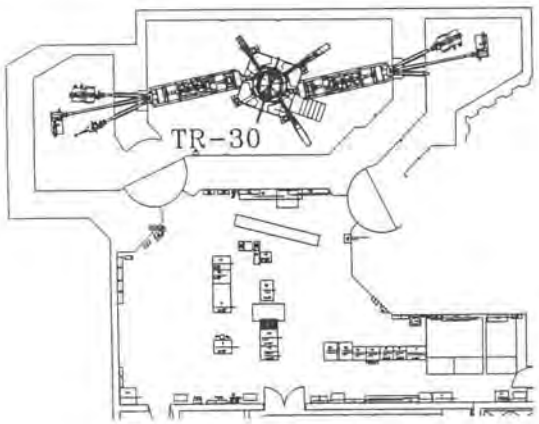
OTHER FACILITIES:

REFERENCES/NOTES

(a) B.F. Milton et al, Particle Accelerator Conf, 1991

(b) IEEE p.65

PLAN VIEW OF FACILITY, COMMENTS



ENTRY NO. CU16 **Date** June 29/1992

Cyclotron Model Scanditronix MC17

Institution PET Centre, Clarke Institute of Psychiatry

Address 250 College Street, Toronto, Canada M5T 1R8

Tel (416) 979 4650 Telex

Fax (416) 979 4656 EMAIL

In Charge: S. Houle Reported by: S. Houle

HISTORY

MILESTONE DATES:

Installation June 91- April 92 First Beam May 1992

DESIGN/CONSTRUCTION BY: CIP & Scanditronix

COST: Accelerator Facility

FUNDED BY: Government of Ontario

STATUS

STAFF: Operators Technicians

BUDGET: Machine Funded by

TIME DISTRIBUTION: (e.g. basic research, isotope production, maintenance, etc.)

(a) PET Research 85 %

(b) PET Clinical 10. %

(c) Maintenance 5. %

(d) %

(e) %

CHARACTERISTIC BEAMS

	Accelerated Ions	E/A (MeV/u)	Current(part μA) Internal	External
(a)	p^+	17	75	60
(b)	d^+	8.5		

1991 μA-hours on target:

FACILITIES

SHIELDED AREA: Fixed 50 m² Moveable m²

Target Stations: 1 No. Served At Same Time: 1

OTHER FACILITIES:

REFERENCES/NOTES

(a)

(b)

PLAN VIEW OF FACILITY, COMMENTS

ENTRY NO. CU17 **Date**

Cyclotron Model TR 30

Institution TRIUMF

Address 4004 Wesbrook Mall, Vancouver BC, Canada V6T 2A3

Tel (604) 222-1047 Telex (0) 4508503

Fax (604) 222-1074 EMAIL NIGEL@TRIUMFCL

In Charge: N.R. Stevenson Reported by: N.R. Stevenson

HISTORY

MILESTONE DATES:

Installation Jun.89 - Jun.90. First Beam July 1990

DESIGN/CONSTRUCTION BY: TRIUMF/EBCO

COST: Accelerator $3,500,000 Facility $10,000,000

FUNDED BY: Nordion International Inc.

STATUS

STAFF: Operators 10 Technicians 5

BUDGET: Machine $800,000 Funded by Nordion Int.Inc.

TIME DISTRIBUTION: (e.g. basic research, isotope production, maintenance, etc.)

(a) Isotope Production 95 %

(b) Maintenance 5 %

(c) %

(d) %

(e) %

CHARACTERISTIC BEAMS

	Accelerated Ions	E/A (MeV/u)	Current(part μA) Internal	External
(a)	H^-	15-30	420 H^-	420 p
(b)				

1991 μA-hours on target: 1.84 x 10e6

FACILITIES

SHIELDED AREA: Fixed 100 m² Moveable m²

Target Stations: 3 No. Served At Same Time: 2

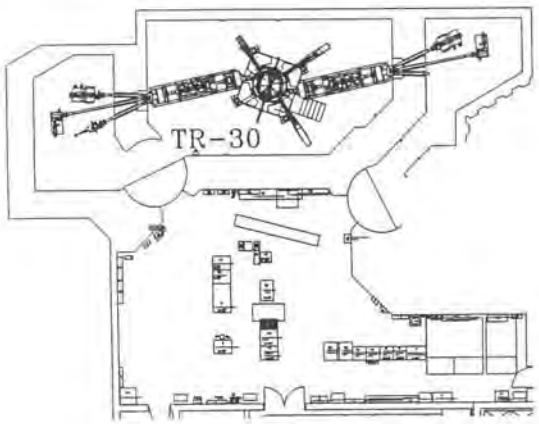
OTHER FACILITIES:

REFERENCES/NOTES

(a) B.F. Milton et al, Particle Accelerator Conf, 1991

(b) IEEE p.65

PLAN VIEW OF FACILITY, COMMENTS



ENTRY NO. CU18 **Date**

Cyclotron Model THE CYCLOTRON CORPORATION CP42
Institution TRIUMF
Address 4004 Wesbrook Mall, Vancouver, B.C. V6T 2A3
Tel 604 222 1047 Telex 04508503
Fax 604 222 1074 EMAIL NIGEL@TRIUMFCL
In Charge: N.R. STEVENSON Reported by: N.R. STEVENSON

HISTORY

MILESTONE DATES:
Installation September 1978 First Beam July 1979
DESIGN/CONSTRUCTION BY: THE CYCLOTRON CORPORATION
COST: Accelerator Facility
FUNDED BY: Atomic Energy of Canada Ltd., Radiochemical Co.

STATUS

STAFF: Operators 10 Technicians 5
BUDGET: Machine $800,000 Funded by Nordion Int.
TIME DISTRIBUTION: (e.g. basic research, isotope production, maintenance, etc.)

(a) Isotope Production 85 %
(b) PET and other research 7 %
(c) Maintenance 8% %
(d) %
(e) %

CHARACTERISTIC BEAMS

	Accelerated Ions	E/A (MeV/u)	Current(part μA) Internal	External
(a)	H⁻	11-42	200	
(b)	p	11-42		200

1991 μA-hours on target: 8.1×10^5

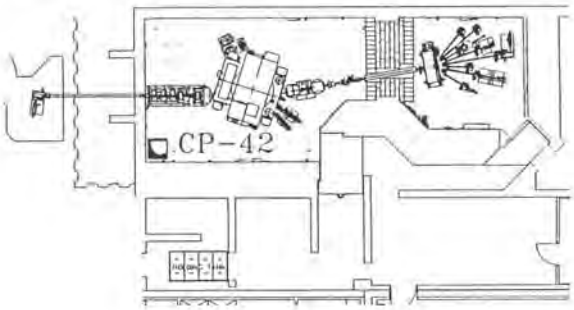
FACILITIES

SHIELDED AREA: Fixed 100 m² Moveable m²
Target Stations: 7 No. Served At Same Time: 1
OTHER FACILITIES:

REFERENCES/NOTES

(a) G.O. Hendry et al., "Design and performance of a compact H⁻ cyclotron", Proc. 9th Int. Conf. on Cyclotrons, p.125 (1981)

PLAN VIEW OF FACILITY, COMMENTS



ENTRY NO. CU20 **Date** 27 June 1992

Cyclotron Model MC 32 NI/NE
Institution Rigshospitalet (University Hospital)
Address Blegdamsvej 9, DK 2100 CPH DENMARK
Tel + 45-35453896 Telex
Fax + 45-35453898 EMAIL
In Charge: Mikael Jensen Reported by: Mikael Jensen

HISTORY

MILESTONE DATES:
Installation Dec. 1991 First Beam 02/19/1992
DESIGN/CONSTRUCTION BY: Scanditronix
COST: Accelerator 21 M.SKr Facility 16 M.SKr
FUNDED BY: Meyer Foundation / Danish State

STATUS

STAFF: Operators 1 Technicians 1
BUDGET: Machine Funded by
TIME DISTRIBUTION: (e.g. basic research, isotope production, maintenance, etc.)

(a) PET Isotopes 50 %
(b) other Isotopes 50 %
(c) %
(d) %
(e) %

CHARACTERISTIC BEAMS

	Accelerated Ions	E/A (MeV/u)	Current(part μA) Internal	External
(a)	H⁻	32 MeV		60
(b)	D⁻	16 MeV		60

1991 μA-hours on target: -

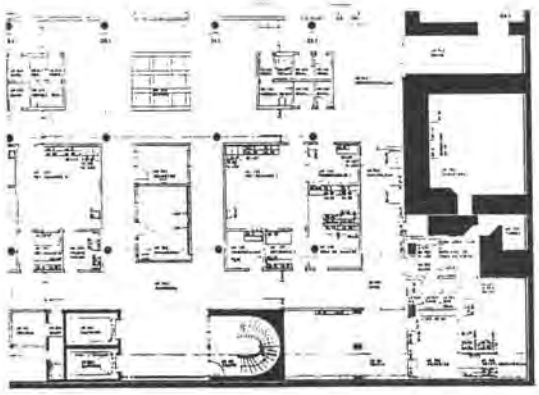
FACILITIES

SHIELDED AREA: Fixed 50 m² Moveable m²
Target Stations: 2 No. Served At Same Time: 2
OTHER FACILITIES:

REFERENCES/NOTES

(a) External Ion Source
(b) to be installed

PLAN VIEW OF FACILITY, COMMENTS



ENTRY NO. CU18 **Date**

Cyclotron Model THE CYCLOTRON CORPORATION CP42
Institution TRIUMF
Address 4004 Wesbrook Mall, Vancouver, B.C. V6T 2A3
Tel 604 222 1047 Telex 04508503
Fax 604 222 1074 EMAIL NIGEL@TRIUMFCL
In Charge: N.R. STEVENSON Reported by: N.R. STEVENSON

HISTORY

MILESTONE DATES:
Installation September 1978 First Beam July 1979
DESIGN/CONSTRUCTION BY: THE CYCLOTRON CORPORATION
COST: Accelerator Facility
FUNDED BY: Atomic Energy of Canada Ltd., Radiochemical Co.

STATUS

STAFF: Operators 10 Technicians 5
BUDGET: Machine $800,000 Funded by Nordion Int.
TIME DISTRIBUTION: (e.g. basic research, isotope production, maintenance, etc.)

(a) Isotope Production 85 %
(b) PET and other research 7 %
(c) Maintenance 8% %
(d) %
(e) %

CHARACTERISTIC BEAMS

	Accelerated Ions	E/A (MeV/u)	Current(part μA) Internal	External
(a)	H⁻	11-42	200	
(b)	p	11-42		200

1991 μA-hours on target: 8.1×10^5

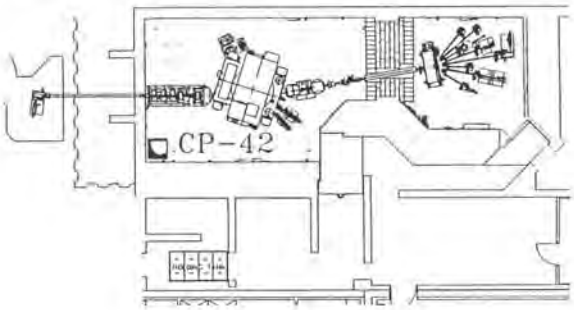
FACILITIES

SHIELDED AREA: Fixed 100 m² Moveable m²
Target Stations: 7 No. Served At Same Time: 1
OTHER FACILITIES:

REFERENCES/NOTES

(a) G.O. Hendry et al., "Design and performance of a compact H⁻ cyclotron", Proc. 9th Int. Conf. on Cyclotrons, p.125 (1981)

PLAN VIEW OF FACILITY, COMMENTS



ENTRY NO. CU20 **Date** 27 June 1992

Cyclotron Model MC 32 NI/NE
Institution Rigshospitalet (University Hospital)
Address Blegdamsvej 9, DK 2100 CPH DENMARK
Tel + 45-35453896 Telex
Fax + 45-35453898 EMAIL
In Charge: Mikael Jensen Reported by: Mikael Jensen

HISTORY

MILESTONE DATES:
Installation Dec. 1991 First Beam 02/19/1992
DESIGN/CONSTRUCTION BY: Scanditronix
COST: Accelerator 21 M.SKr Facility 16 M.SKr
FUNDED BY: Meyer Foundation / Danish State

STATUS

STAFF: Operators 1 Technicians 1
BUDGET: Machine Funded by
TIME DISTRIBUTION: (e.g. basic research, isotope production, maintenance, etc.)

(a) PET Isotopes 50 %
(b) other Isotopes 50 %
(c) %
(d) %
(e) %

CHARACTERISTIC BEAMS

	Accelerated Ions	E/A (MeV/u)	Current(part μA) Internal	External
(a)	H⁻	32 MeV		60
(b)	D⁻	16 MeV		60

1991 μA-hours on target: -

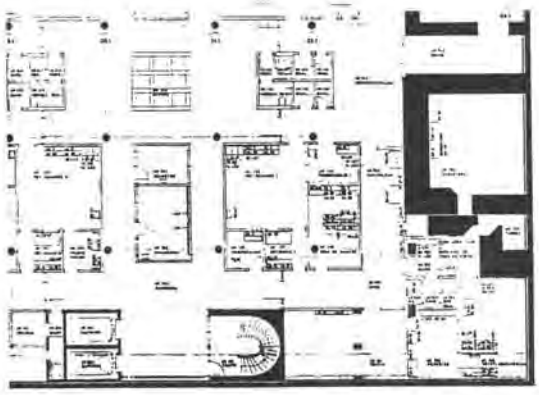
FACILITIES

SHIELDED AREA: Fixed 50 m² Moveable m²
Target Stations: 2 No. Served At Same Time: 2
OTHER FACILITIES:

REFERENCES/NOTES

(a) External Ion Source
(b) to be installed

PLAN VIEW OF FACILITY, COMMENTS



ENTRY NO. C021 Date August 18, 1992

Name of Machine MGC-20

Institution Accelerator Laboratory, Åbo Akademi University

Address Porthansg. 3, SF-20500 Turku, FINLAND

Tel +358.21.654.311 Telex 62301 aabib sf Fax +358.21.654.776 EMAIL kschalien@finabo.fi

In Charge: Sven-Johan Heselius Reported by: Sven-Johan Heselius and Stefan Johansson

HISTORY

MILESTONE DATES:

Design ..... Model Tests .....

Construction Dec 73 - Oct 74 First Beam July 1974

DESIGN/CONSTRUCTION BY: D. V. Efremov Institute of

in house ..... other ... Electrophysical Apparatus

COST: Accelerator ..... Facility 4 MFIM

FUNDED BY: Finnish Government

STATUS

STAFF: Machine

Scientists 3 Engineers 1

Technicians 2 Students 5 student operators

Research (in house/external)

Scientists 5 / 7 Engineers 1 / .....

Technicians 2 / 1 Students 5 / .....

BUDGET: Machine 0.7 MFIM Funded by Åbo Akademi

Research ..... Funded by .....

TIME DISTRIBUTION:

Basic Research (in house/external) 17 % / 10 %

Applied Program (in house/external) 18 % / 35 %

Development 5 % Maintenance 15 %

MAGNET

POLE PARAMETERS:

Diameter 103 cm $R_{extract}$ 45 cm R_{inject} ..... cm

HILL PARAMETERS: Gap (min) 7.2 cm B_{max} 1.65 T

(@ ..... AT) Gap (max) ..... cm B_{min} ..... T

VALLEY PARAMETERS: Gap (min) ..... cm B_{max} ..... T

(@ ..... AT) Gap (max) 12 cm B_{min} 1.25 T

AVERAGE FIELD: $< B >_{min}$ ..... T $< B >_{max}$ 1.45 T

NUMBER OF SECTORS: compact/separated 3 / .....

sector angle ..... deg. spiral (max) 35 deg.

FIELD TRIMMING: Trim Coils 4 pairs of concentric

Harmonic Coils 2 sets

Other .....

CURRENT: Main Coils 410 Amps Stability 0.01 %

Trim Coils ± 10 Amps Stability 0.1 %

Stored Energy (cryogenic) ..... MJ

WEIGHT: Iron 24 tons Conductor 1.2 tons

ION ENERGY: Bending Limit E/A = ... q^2/A^2 MeV/u

Focussing Limit E/A = ... q/A MeV/u

ACCELERATION SYSTEM

FUNDAMENTAL ACCELERATION:

Description: 2 x lambda/4 resonators, push-pull mode

No. of Gaps/turn 2 dE/dn(max) ..... MeV/q

Voltage(max) 0.03 MV Harmonic f_{rf}/f_{ion} .....

Freq 8.5 - 25.5 MHz Power in(max) 0.05 MW

Stability: Phase ± 10 ppm Voltage .....

OTHER CAVITIES (Flattopping or otherwise):

Description: .....

Region of Influence: R_{min} ..... cm R_{max} ..... cm

No. of Gaps/turn ..... dE/dn(max) ..... MeV/q

Voltage(max) ..... MV Harmonic f_{rf}/f_{ion} .....

Freq ..... MHz Power in(max) ..... MW

Stability: Phase ..... Voltage .....

VACUUM SYSTEM

OPERATING PRESSURE: 5×10^{-4} Pa

PUMPS: No. and type 2 diffusion pumps, 1600 l/s,

with baffles

ION SOURCE(S)

	Type	Intensity (mA)	@	$\epsilon_n = \beta\gamma\epsilon$ (πmm mrad)	Ion Species
(a)	Livingston hot filament				
(b)					
(c)					
(d)					

INJECTION SYSTEM

..... Efficiency ..... %

EXTRACTION SYSTEM

Electrostatic deflector + magnetic channel Efficiency 50 %

CHARACTERISTIC BEAMS

	Accelerated Ions	E/A (MeV/u)	Current(part μA) Internal	External
(a)	p	19 MeV	300	50
(b)	d	10.5 MeV	300	50
(c)	alpha	21 MeV	100	40
(d)	^{3}He	29 MeV	90	40

	Secondary Particles	E (MeV)	part/sec
(a)			
(b)			
(c)			

EXTRACTED BEAM PROPERTIES:

For 0.4 μA of 18 MeV/u protons ions

$\Delta E/E$ 0.3 % $\Delta\phi$ ..... °rf

$\epsilon_n = \beta\gamma\epsilon$ x ..... πmm mrad z ..... πmm mrad

FACILITIES FOR RESEARCH

SHIELDED AREA: Fixed 174 m^2 Moveable ..... m^2

Target Stations: 5 No. Served At Same Time: 1

MAGNETIC SPECTROMETERS: .....

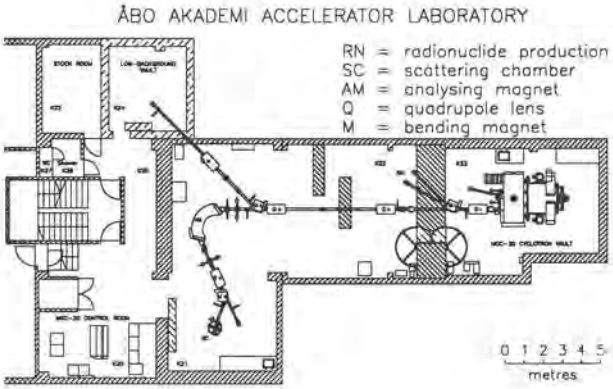
OTHER FACILITIES: Scattering chamber facilities for radionuclide production and equipment for PIXE-analysis

REFERENCES/NOTES

(a) Basargin et al.: Proc. 6th Int. Cycl. Conference

(b) .....

PLAN VIEW OF FACILITY, COMMENTS



ENTRY NO. CU22 Date January 1, 1992
Cyclotron Model Cyclone 3
Institution Turku Medical Cyclotron - PET Center
Address Turku University Central Hospital
Tel 358-21-611611 Telex SF 20520 Turku, Finland
Fax 358-21-318191 EMAIL
In Charge: Hannu Sipila Reported by: Hannu Sipila

HISTORY

MILESTONE DATES:
Installation January 7, 1992 First Beam April 15, 1992
DESIGN/CONSTRUCTION BY: Ion Beam Applications
COST: Accelerator 2400000 FIM Facility 700000 FIM
FUNDED BY: Turku University Central Hospital (TUCH)

STATUS

STAFF: Operators 2 Technicians 1
BUDGET: Machine ? Funded by TUCH
TIME DISTRIBUTION: (e.g. basic research, isotope production, maintenance, etc.)
(a) Isotope Production 95 %
(b) Maintenance 5 %
(c) %
(d) %
(e) %

CHARACTERISTIC BEAMS

Accelerated Ions	E/A (MeV/u)	Current(part μA) Internal	External
(a) Deuterons	3.85	100	70
(b)			

1991 μA-hours on target:

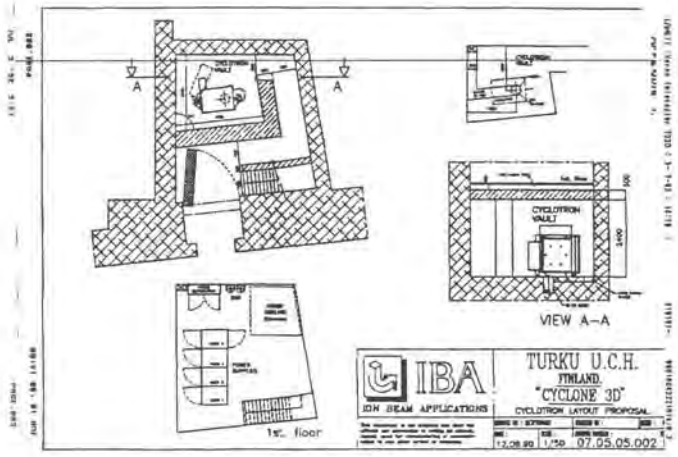
FACILITIES

SHIELDED AREA: Fixed 8 m^2 Moveable - m^2
Target Stations: 1 No. Served At Same Time: -
OTHER FACILITIES:

REFERENCES/NOTES

(a)
(b)

PLAN VIEW OF FACILITY, COMMENTS



ENTRY NO. CU23 Date 15 juin 1992
Cyclotron Model 520 CGR MEV
Institution CEA/DRIPP - Service Hospitalier Frédéric Joliot
Address 91406 ORSAY FRANCE
Tel 69.86.77.04 Telex
Fax 69.86.77.68 EMAIL
In Charge: C. CROUZEL Reported by: C. CROUZEL

HISTORY

MILESTONE DATES:
Installation 1975 First Beam May 1975
DESIGN/CONSTRUCTION BY: CGR - MEV
COST: Accelerator Facility
FUNDED BY: CEA

STATUS

STAFF: Operators Technicians
BUDGET: Machine Funded by
TIME DISTRIBUTION: (e.g. basic research, isotope production, maintenance, etc.)
(a) Isotopes production ^{11}C, ^{18}F, ^{15}O, ^{76}Br 100 %
(b) %
(c) %
(d) %
(e) %

CHARACTERISTIC BEAMS

Accelerated Ions	E/A (MeV/u)	Current(part μA) Internal	External
(a) Proton		200	70
(b) Deutron		200	70
Helium -3		100	50

1991 μA-hours on target: 30 μA

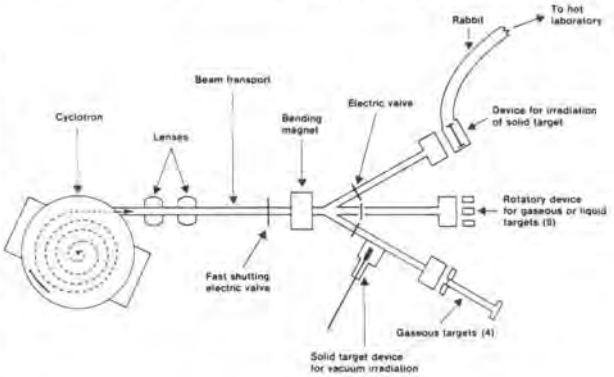
FACILITIES

SHIELDED AREA: Fixed m^2 Moveable m^2
Target Stations: 3 No. Served At Same Time: 1
OTHER FACILITIES:

REFERENCES/NOTES

(a)
(b)

PLAN VIEW OF FACILITY, COMMENTS



Plan of irradiation devices at the SHFJ Cyclotron

ENTRY NO. CU22 Date January 1, 1992
Cyclotron Model Cyclone 3
Institution Turku Medical Cyclotron - PET Center
Address Turku University Central Hospital
Tel 358-21-611611 Telex SF 20520 Turku, Finland
Fax 358-21-318191 EMAIL
In Charge: Hannu Sipila Reported by: Hannu Sipila

HISTORY

MILESTONE DATES:
Installation January 7, 1992 First Beam April 15, 1992
DESIGN/CONSTRUCTION BY: Ion Beam Applications
COST: Accelerator 2400000 FIM Facility 700000 FIM
FUNDED BY: Turku University Central Hospital (TUCH)

STATUS

STAFF: Operators 2 Technicians 1
BUDGET: Machine ? Funded by TUCH
TIME DISTRIBUTION: (e.g. basic research, isotope production, maintenance, etc.)
(a) Isotope Production 95 %
(b) Maintenance 5 %
(c) %
(d) %
(e) %

CHARACTERISTIC BEAMS

Accelerated Ions	E/A (MeV/u)	Current(part μA) Internal	External
(a) Deuterons	3.85	100	70
(b)			

1991 μA-hours on target:

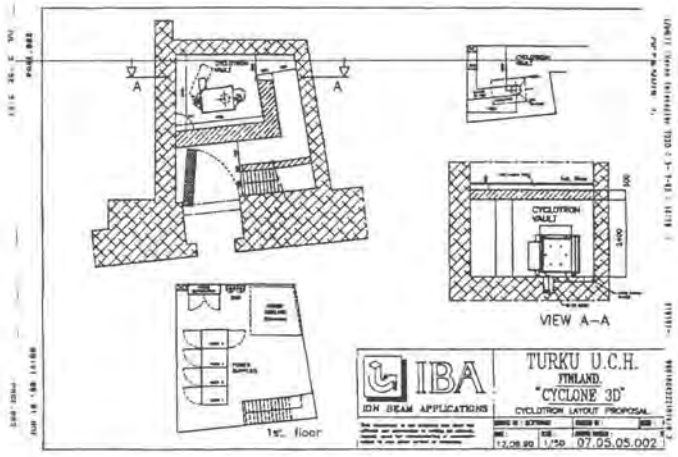
FACILITIES

SHIELDED AREA: Fixed 8 m^2 Moveable - m^2
Target Stations: 1 No. Served At Same Time: -
OTHER FACILITIES:

REFERENCES/NOTES

(a)
(b)

PLAN VIEW OF FACILITY, COMMENTS



ENTRY NO. CU23 Date 15 juin 1992
Cyclotron Model 520 CGR MEV
Institution CEA/DRIPP - Service Hospitalier Frédéric Joliot
Address 91406 ORSAY FRANCE
Tel 69.86.77.04 Telex
Fax 69.86.77.68 EMAIL
In Charge: C. CROUZEL Reported by: C. CROUZEL

HISTORY

MILESTONE DATES:
Installation 1975 First Beam May 1975
DESIGN/CONSTRUCTION BY: CGR - MEV
COST: Accelerator Facility
FUNDED BY: CEA

STATUS

STAFF: Operators Technicians
BUDGET: Machine Funded by
TIME DISTRIBUTION: (e.g. basic research, isotope production, maintenance, etc.)
(a) Isotopes production ^{11}C, ^{18}F, ^{15}O, ^{76}Br 100 %
(b) %
(c) %
(d) %
(e) %

CHARACTERISTIC BEAMS

Accelerated Ions	E/A (MeV/u)	Current(part μA) Internal	External
(a) Proton		200	70
(b) Deutron		200	70
Helium -3		100	50

1991 μA-hours on target: 30 μA

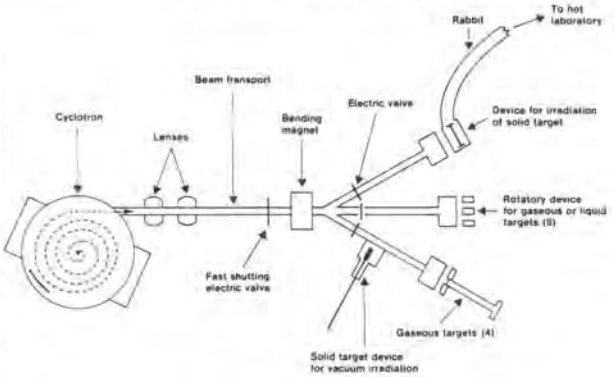
FACILITIES

SHIELDED AREA: Fixed m^2 Moveable m^2
Target Stations: 3 No. Served At Same Time: 1
OTHER FACILITIES:

REFERENCES/NOTES

(a)
(b)

PLAN VIEW OF FACILITY, COMMENTS



Plan of irradiation devices at the SHFJ Cyclotron

ENTRY NO. CU24 **Date**
Cyclotron Model CYPRIS 325
Institution CERMEP
Address 59 Bd Pinel, 69003 LYON (France)
Tel 33/72.33.00.07 Telex
Fax 33/78.53.31.12 EMAIL
In Charge: D. LE BARS Reported by: D. LE BARS

HISTORY

MILESTONE DATES:
Installation Sept-Dec 1987 First Beam Jan 1988
DESIGN/CONSTRUCTION BY: CGR Mev
COST: Accelerator 15 MF Facility 60 MF
FUNDED BY: INSERM/CNRS/HOSPITAL/UNIVERSITIES

STATUS

STAFF: Operators 1 Technicians
BUDGET: Machine 500 000 F Funded by CERMEP
TIME DISTRIBUTION: (e.g. basic research, isotope production, maintenance, etc.)
(a) Isotope production 95 %
(b) Maintenance 5 %
(c) %
(d) %
(e) %

CHARACTERISTIC BEAMS

	Accelerated Ions	E/A (MeV/u)	Current(part μA) Internal	External
(a)	H^+	16 Mev		50 μA
(b)	D^+	8 Mev		50 μA

1991 μA-hours on target: ≃ 2 000

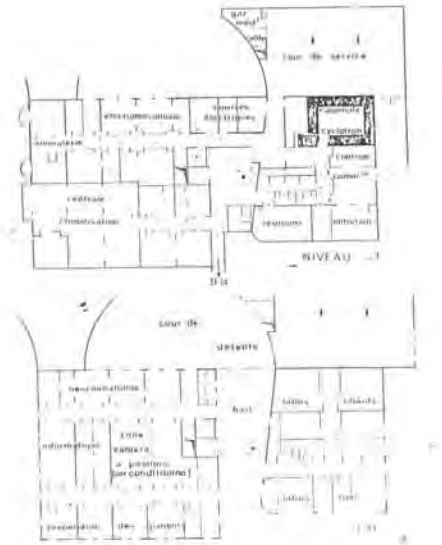
FACILITIES

SHIELDED AREA: Fixed 30 m² Moveable m²
Target Stations: No. Served At Same Time:
OTHER FACILITIES: 4 hot cells
Automated chemistry (Developped on-site)

REFERENCES/NOTES

(a)
(b)

PLAN VIEW OF FACILITY, COMMENTS



ENTRY NO. CU25 **Date**
Cyclotron Model CV 28
Institution Physikalisch-Technische Bundesanstalt
Address Bundesallee 100, W-3300 Braunschweig, FRG
Tel 0531-592.7121 Telex 952822.ptb.d
Fax 0531-592 4006 EMAIL
In Charge: R. Böttger Reported by: R. Böttger

HISTORY

MILESTONE DATES:
Installation 1972-1973 First Beam 1973
DESIGN/CONSTRUCTION BY: The Cyclotron Corporation
COST: Accelerator $3 \cdot 10^6$ DM Facility $25 \cdot 10^6$ DM
FUNDED BY: Federal Republic of Germany

STATUS

STAFF: Operators 4 Technicians 2
BUDGET: Machine $2 \cdot 10^6$ DM Funded by FRG
TIME DISTRIBUTION: (e.g. basic research, isotope production, maintenance, etc.)
(a) Nuclear data (neutron physics) 30 %
(b) Calibration (n+γ) 30 %
(c) Dosimetry 40 %
(d) %
(e) %

CHARACTERISTIC BEAMS

	Accelerated Ions	E/A (MeV/u)	Current(part μA) Internal	External
(a)	p	max. 24	> 350	70-100
(b)	d	max. 7	> 300	100

1991 μA-hours on target: 2000

FACILITIES

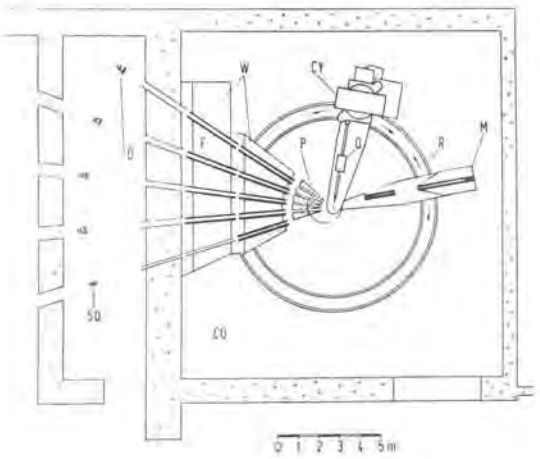
SHIELDED AREA: Fixed 850 m² Moveable – m²
Target Stations: 5 No. Served At Same Time: 2
OTHER FACILITIES: Time of flight facility for fast neutrons; standard neutron field for therapy and radiobiology

REFERENCES/NOTES

(a) Nucl. Instrum. Meth., 169 (1980) 349 - 358
(b) Nucl. Instrum. Meth., 193 (1982) 635 - 644

PLAN VIEW OF FACILITY, COMMENTS

Movable cyclotron arrangement with ns-pulsing system especially designed for neutron scattering experiments.



ENTRY NO. CU24 **Date**
Cyclotron Model CYPRIS 325
Institution CERMEP
Address 59 Bd Pinel, 69003 LYON (France)
Tel 33/72.33.00.07 Telex
Fax 33/78.53.31.12 EMAIL
In Charge: D. LE BARS Reported by: D. LE BARS

HISTORY

MILESTONE DATES:
Installation Sept-Dec 1987 First Beam Jan 1988
DESIGN/CONSTRUCTION BY: CGR Mev
COST: Accelerator 15 MF Facility 60 MF
FUNDED BY: INSERM/CNRS/HOSPITAL/UNIVERSITIES

STATUS

STAFF: Operators 1 Technicians
BUDGET: Machine 500 000 F Funded by CERMEP
TIME DISTRIBUTION: (e.g. basic research, isotope production, maintenance, etc.)
(a) Isotope production 95 %
(b) Maintenance 5 %
(c) %
(d) %
(e) %

CHARACTERISTIC BEAMS

	Accelerated Ions	E/A (MeV/u)	Current(part μA) Internal	External
(a)	H^+	16 Mev		50 μA
(b)	D^+	8 Mev		50 μA

1991 μA-hours on target: ≃ 2 000

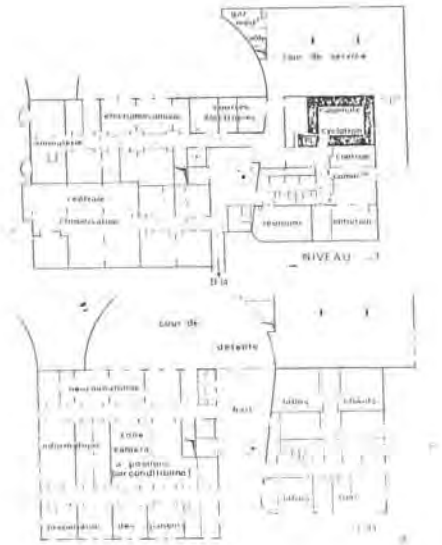
FACILITIES

SHIELDED AREA: Fixed 30 m² Moveable m²
Target Stations: No. Served At Same Time:
OTHER FACILITIES: 4 hot cells
Automated chemistry (Developped on-site)

REFERENCES/NOTES

(a)
(b)

PLAN VIEW OF FACILITY, COMMENTS



ENTRY NO. CU25 **Date**
Cyclotron Model CV 28
Institution Physikalisch-Technische Bundesanstalt
Address Bundesallee 100, W-3300 Braunschweig, FRG
Tel 0531-592.7121 Telex 952822.ptb.d
Fax 0531-592 4006 EMAIL
In Charge: R. Böttger Reported by: R. Böttger

HISTORY

MILESTONE DATES:
Installation 1972-1973 First Beam 1973
DESIGN/CONSTRUCTION BY: The Cyclotron Corporation
COST: Accelerator $3 \cdot 10^6$ DM Facility $25 \cdot 10^6$ DM
FUNDED BY: Federal Republic of Germany

STATUS

STAFF: Operators 4 Technicians 2
BUDGET: Machine $2 \cdot 10^6$ DM Funded by FRG
TIME DISTRIBUTION: (e.g. basic research, isotope production, maintenance, etc.)
(a) Nuclear data (neutron physics) 30 %
(b) Calibration (n+γ) 30 %
(c) Dosimetry 40 %
(d) %
(e) %

CHARACTERISTIC BEAMS

	Accelerated Ions	E/A (MeV/u)	Current(part μA) Internal	External
(a)	p	max. 24	> 350	70-100
(b)	d	max. 7	> 300	100

1991 μA-hours on target: 2000

FACILITIES

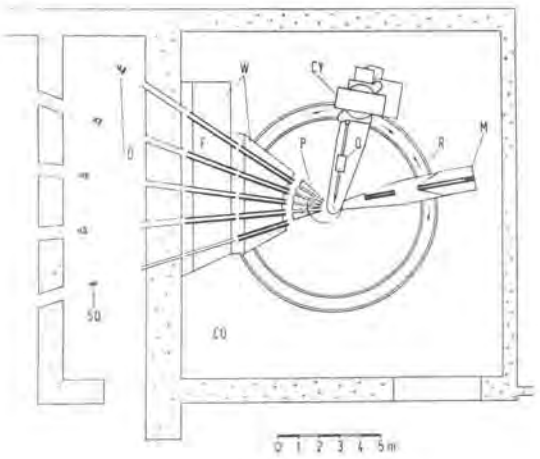
SHIELDED AREA: Fixed 850 m² Moveable – m²
Target Stations: 5 No. Served At Same Time: 2
OTHER FACILITIES: Time of flight facility for fast neutrons; standard neutron field for therapy and radiobiology

REFERENCES/NOTES

(a) Nucl. Instrum. Meth., 169 (1980) 349 - 358
(b) Nucl. Instrum. Meth., 193 (1982) 635 - 644

PLAN VIEW OF FACILITY, COMMENTS

Movable cyclotron arrangement with ns-pulsing system especially designed for neutron scattering experiments.



ENTRY No. CU26

NAME OF MACHINE Isochronous variable energy DATE CV 28 TCC Berkeley Sept. 1981

INSTITUTION Institut Medizinische Strahlenphysik und Strahlenbiologie, Universitätsklinikum Essen

ADDRESS ...Hufelandstr. 55, D 4300 Essen, W-Germany

TEL ..0201/723 2171 .... TELEX ...857 9573 klies d

IN CHARGE .Prof.. Dr. J. Rassow. REPORTED BY ..Rassow

HISTORY AND STATUS

DESIGN, date ...1973..... Model tests .....1974.....

ENG DESIGN, date ....1972.....

CONSTRUCTION, date ....1974.....

FIRST BEAM, date (or goal) ....Sept. 1975 (Essen).....

MAJOR ALTERATIONS .....

.....

COST, ACCELERATOR ...so.9.....10^6.....

COST, FACILITY, total ...s1.6.....10^6.....

FUNDED BY Land Nordrhein-Westfalen (University).....

ACCELERATOR STAFF, OPERATION AND DEVELOPMENT

SCIENTISTS .....7..... ENGINEERS .....4.....

TECHNICIANS .....3..... CRAFTS .....2.....

GRAD STUDENTS involved during year .....

OPERATED BY ..... Research staff or ..2..... Operators

OPERATION ...50..... hr/wk, On target 45 ..... hr/wk

TIME DISTR. in house ..... %, Outside ..... %

BUDGET, op & dev .....

FUNDED BY .....

RESEARCH STAFF, not included above

USERS, in house .....3..... outside .....

GRAD STUDENTS involved during year .....

RESEARCH BUDGET, in house .....

FUNDED BY .....

MAGNET

POLE FACE, diameter (compact) ..96.. cm, R extraction ..42.. cm

R injection ..... cm

GAP, min ..5.0.... cm, Field ..14..... kG
max ..10.1... cm, Field ..20..... kG
} at 0.25 10^6 Ampere turns

AVERAGE FIELD at R ext .....17..... kG

B max/ <B> .....

NUMBER OF SECTORS { compact ... / separated ...3... } Spiral, max 47 deg

SECTOR ANGLE (SSC) ....120..... deg

TRIMMING COILS .3 pairs inner and outer harmonic coils

.....each 4 pairs profile coils .....

CONDUCTOR, material and type ..Cu tubes.....

STORED ENERGY (cryogenic) ..... MJ

POWER : main coils ..70.. max, kW ; current stability $2 \cdot 10^{-6}$

trimming coils ..20.. max, kW ; current stability $2 \cdot 10^{-5}$

WEIGHT : Fe ..21..... tons ; coils ....1.8..... tons

COOLING system ....demineralized water.....

ION ENERGY (bending limit) E/A = .28(H^+24 q^2/a^2 MeV/amu

(focusing limit) E/A = .28..... q^2/a^2 MeV/amu

ACCELERATION SYSTEM

DEES, number .....2... ; angle .....90..... deg

BEAM APERTURE ..2.0.... cm ; DC Bias ..1..... kV

TUNED by, coarse Short Plane, fine Trim Capacitor.....

RF .....6.5.. to ...25.5... mHz, stable ± 100 Hz

Orb F ....6.5.. to ..26.5... mHz

HARMONICS, RF/Orb F, used ..fundamental.....

DEE - Gnd, max .30... kV, min gap ..1.3..... cm

STABILITY, (pk-pk noise)/(pk RF volt) .....

ENERGY GAIN, max .....60..... kV/turn

RF PHASE, stable to ± ..... deg

RF POWER input, max .....40..... kW

FREQUENCY MODULATION, rate .....0..... /s

modulator, type .....

beam pulse, width .....

VACUUM SYSTEM

OPERATING PRESSURE .< 5×10^{-5} Torr..... Torr or mbar

PUMPS, No, Type, Size ..NEC 1x25 cm .....

.....Oil diffusion pump .....

.....

ION SOURCES

.....penning ion source.....

INJECTION SYSTEM

.....

EXTRACTION SYSTEM

.electrostatic deflector magnet channel.....

FACILITIES FOR RESEARCH

SHIELDED AREA, fixed ..138..... m^2 ; movable ..... m^2

TARGET STATIONS .....8. in ....4.... rooms

STATIONS served at same time, max ..1.....

MAG SPECTROGRAPH, type .....

COMPUTER model .....

OTHER FACILITIES .isocentric neutron therapy facility..

6 external and 1 internal target stations.....

1 neutron activation station., PET facility (Siemens)..

CHARACTERISTIC BEAMS

PARTICLE	ENERGY (MeV) Goal	Achieved	CURRENT (pμA) Internal	External
proton	2.24	2.24	300	85
deuterons	3.14	3.14	400	120
Helium 3++	5.36	5.37	150	80
Helium 4++	6.28	6.28	100	50
SECONDARY				(part/s)

BEAM PROPERTIES

MEASURED		CONDITIONS	
PULSE WIDTH	RF deg	pμ A of	MeV ... ions
PHASE EXC, max	RF deg	pμ A of	MeV ... ions
EXTRACT eff ...70..	%	.100.. pμ A of 14.	MeV d^+ .. ions
RESOL ΔE/E ..0.5..	%	..50.. pμ A of 28.	MeV He^{++} ions

EMITTANCE

(π mm. mrad) { 250 axial / 250. rad } .100.. pμA of .14. MeV d^+ ions

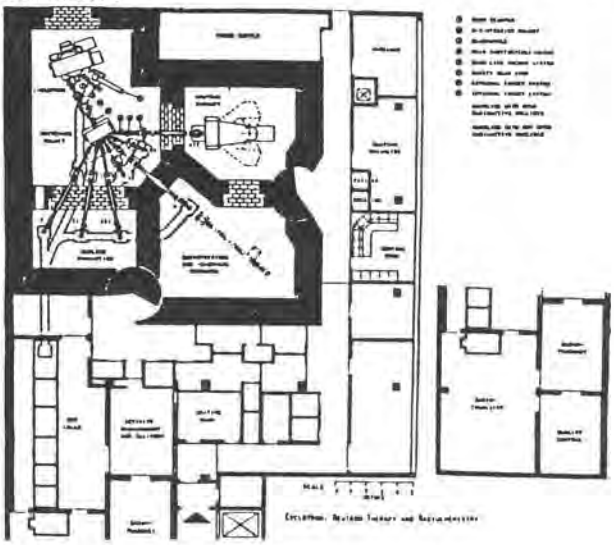
OPERATING PROGRAMS, time distribution

BASIC NUCLEAR PHYSICS		SOLID STATES PHYSICS	
BIOMEDICAL APPLICAT.	10%	ISOTOPE PRODUCTIONS	10%
Neutron therapy	42%	Safety tests, maintenance	17%
Radiation physics	18%	Dead time	1%

REFERENCES/NOTES

Rassow, J., Hudepohl, G., Maier, E., Meissner, P.:
CIRCE-Cyclotron Isocentric Neutron Therapy Facility. In:
Burger, G., Ebert, H.G.: Proceedings Third Symposium on
Neutron Dosimetry, Munich 1977, EURATOM EUR 5848/DE/EN/FR 1978

PLAN VIEW OF FACILITY, NOTEWORTHY FEATURES, COMMENTS



ENTRY NO. CU27 Date June 22nd, 1992

Name of Machine MC 32 NI

Institution German Cancer Research Center/Deutsches Krebsforschungszentrum Heidelberg, DKFZ

Address Im Neuenheimer Feld 280 / P. O. Box 10 19 49

Tel +6221 - 422681 Telex Fax +6221 - 411 307 EMAIL

In Charge: Dr. Gerd Wolber Reported by: Dr. Gerd Wolber

HISTORY

MILESTONE DATES:
Design 1989/90 Model Tests 1991-92
Construction 1989-91 First Beam April 1991

DESIGN/CONSTRUCTION BY:
in house other SCANDITRONIX AB

COST: Accelerator 5MDM(3.2M$) Facility

FUNDED BY: DKFZ

STATUS

STAFF: Machine
Scientists 1 Engineers 1
Technicians 3 Students
Research (in house/external)
Scientists 5 / 2 Engineers * /
Technicians 4 / 3 Students * /

BUDGET: Machine 100 K$ Funded by DKFZ
Research 200 K $ Funded by DKFZ+others

TIME DISTRIBUTION:
Basic Research (in house/external) 50 % / * %
Applied Program (in house/external) 50 % / * %
Development % Maintenance %

MAGNET

POLE PARAMETERS:
Diameter 135 cm $R_{extract}$ 48.6 cm R_{inject} cm
HILL PARAMETERS: Gap (min) 10 cm B_{max} 1.95 T
(@ AT) Gap (max) 18 cm B_{min} T
VALLEY PARAMETERS: Gap (min) 18 cm B_{max} T
(@ AT) Gap (max) 18 cm B_{min} T
AVERAGE FIELD: $< B >_{min}$ 1.615 T $< B >_{max}$ 1.655 T
NUMBER OF SECTORS: compact/separated 4 /
sector angle 40 deg. spiral (max) 75 deg.
FIELD TRIMMING: Trim Coils 3
Harmonic Coils 2
Other 5
CURRENT: Main Coils 520 Amps Stability 1x10^{-5}
Trim Coils 5/10/15 Amps Stability
Stored Energy (cryogenic) MJ
WEIGHT: Iron 53 000 kg Conductor 3 023 kg
ION ENERGY: Bending Limit E/A = 34 q^2/A^2 MeV/u
Focussing Limit E/A = q/A MeV/u

ACCELERATION SYSTEM

FUNDAMENTAL ACCELERATION:
Description: 2 master oscillators + power amplif.
No. of Gaps/turn 2 dE/dn(max) 0.06 MeV/q
Voltage(max) 0.03 MV Harmonic f_{rf}/f_{ion}
Freq 24.3 MHz Power in(max) MW
Stability: Phase Voltage

OTHER CAVITIES (Flattopping or otherwise):
Description:
Region of Influence: R_{min} cm R_{max} cm
No. of Gaps/turn dE/dn(max) MeV/q
Voltage(max) MV Harmonic f_{rf}/f_{ion}
Freq MHz Power in(max) MW
Stability: Phase Voltage

VACUUM SYSTEM

OPERATING PRESSURE: 2x10^{-7} mbar
PUMPS: No. and type 2 oil diff. p. 4000 l/sec
1 roots p. 250 cbm/h, 1 backing p. 30 cbm/h

ION SOURCE(S)

	Type	Intensity (mA)	@	$\epsilon_n = \beta\gamma\epsilon$ (πmm mrad)	Ion Species
(a)	dual cold cathode	1300 max.			H^- / D^-
(b)					
(c)					
(d)					

INJECTION SYSTEM

Efficiency %

EXTRACTION SYSTEM

stripper foil Efficiency ≥ 95 %

CHARACTERISTIC BEAMS

	Accelerated Ions	E/A (MeV/u)	Current(part μA) Internal	External
(a)	H^-	32		60 (guar.)
(b)	D^-	75		60 (")
(c)				
(d)				

	Secondary Particles	E (MeV)	part/sec
(a)	n (p → Be.)	$E_n \sim 14$	*
(b)			
(c)			

EXTRACTED BEAM PROPERTIES:
For 1 μA of 32 MeV/u H ions
$\Delta E/E$ % $\Delta\phi$ °rf
$\epsilon_n = \beta\gamma\epsilon$ x 9 πmm mrad z 8 πmm mrad

FACILITIES FOR RESEARCH

SHIELDED AREA: Fixed 18x20 m² Moveable m²
Target Stations: max. 9 No. Served At Same Time: 1
MAGNETIC SPECTROMETERS:
OTHER FACILITIES:
targets for radionuclide production
Be-targets for fast neutron production
(scheduled for Oct. 1991)

REFERENCES/NOTES

(a)
(b)

PLAN VIEW OF FACILITY, COMMENTS

The MC 32 NI is able to accelerate H^- as well as D^- ions.
Acceptance test is scheduled for Sept. 92
Routine operation has not started yet.

---

* will be cleared up in 1 to 2 years

ENTRY NO. CU28 **Date** 22.06.92

Cyclotron Model MC 35

Institution Medizinische Hochschule Hannover

Address Konstanty-Gutschow-Str. 8 D-3000 Hannover 61

Tel 0511/5321 Telex

Fax 0511/5322315 EMAIL

In Charge: Dr. Junker Reported by: Dr. Helmeke

HISTORY

MILESTONE DATES:

Installation 1976/77 First Beam 21.01.1977

DESIGN/CONSTRUCTION BY: Scanditronix

COST: Accelerator Facility

FUNDED BY:

STATUS

STAFF: Operators 1 ~~Technicians~~ Engineers 1

BUDGET: Machine Funded by

TIME DISTRIBUTION: (e.g. basic research, isotope production, maintenance, etc.)

(a) isotope production 90 %

(b) maintenance 7 %

(c) tests (cyclotron, targets) 3 %

(d) %

(e) %

CHARACTERISTIC BEAMS

Accelerated Ions	E/A (MeV/u)	Current(part μA) Internal	External
(a) Protons	35		65
(b) deuterons	18		65

1991 μA-hours on target: 205

FACILITIES

SHIELDED AREA: Fixed ~ 100 m² Moveable m²

Target Stations: 2 No. Served At Same Time: 1

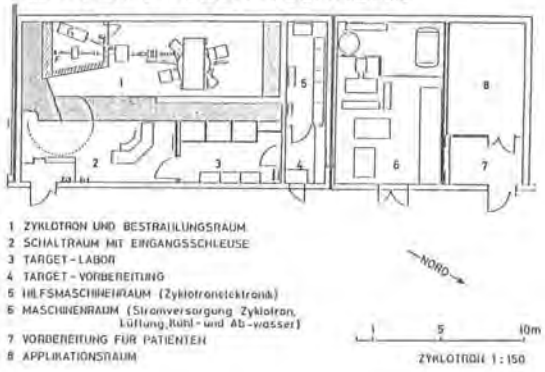
OTHER FACILITIES:

REFERENCES/NOTES

(a) target stations:solids-3 positions/Gas-6 positions

(b) He - 3 and He 4 beam is available too

PLAN VIEW OF FACILITY, COMMENTS



ENTRY NO. CU29 **Date**

Cyclotron Model BC 1710

Institution Institute of Nuclear Chemistry, KFA Jülich

Address 5170 Jülich, Germany

Tel 2461-614141 Telex 833556 KFA D

Fax 2461-612535 EMAIL

In Charge: Prof. G. Stöcklin Reported by: Dr. S.M. Qaim

HISTORY

MILESTONE DATES:

Installation January 1987 First Beam April 1987

DESIGN/CONSTRUCTION BY: Japan Steel Works

COST: Accelerator DM 3.3 M Facility DM 1.5 M (both 1987 values)

FUNDED BY: Federal Government

STATUS

STAFF: Operators 2 Technicians

BUDGET: Machine DM 50.000 Funded by Federal Govt. (running costs)

TIME DISTRIBUTION: (e.g. basic research, isotope production, maintenance, etc.)

(a) Isotope production 100 %

(b) %

(c) %

(d) %

(e) %

CHARACTERISTIC BEAMS

Accelerated Ions	E/A (MeV/u)	Current(part μA) Internal	External
(a) Protons	17		50
(b) Deuterons	10		40

1991 μA-hours on target: 8200

FACILITIES

SHIELDED AREA: Fixed ca. 350 m² Moveable m²

Target Stations: 1 No. Served At Same Time:

OTHER FACILITIES: 6 Hot cells

Radiochemical and Radiopharmaceutical laboratories;

PET; SPECT; Radioagronomy laboratories

REFERENCES/NOTES

(a)

(b)

PLAN VIEW OF FACILITY, COMMENTS

ENTRY NO. CU28 **Date** 22.06.92

Cyclotron Model MC 35

Institution Medizinische Hochschule Hannover

Address Konstanty-Gutschow-Str. 8 D-3000 Hannover 61

Tel 0511/5321 Telex

Fax 0511/5322315 EMAIL

In Charge: Dr. Junker Reported by: Dr. Helmeke

HISTORY

MILESTONE DATES:

Installation 1976/77 First Beam 21.01.1977

DESIGN/CONSTRUCTION BY: Scanditronix

COST: Accelerator Facility

FUNDED BY:

STATUS

STAFF: Operators 1 ~~Technicians~~ Engineers 1

BUDGET: Machine Funded by

TIME DISTRIBUTION: (e.g. basic research, isotope production, maintenance, etc.)

(a) isotope production 90 %

(b) maintenance 7 %

(c) tests (cyclotron, targets) 3 %

(d) %

(e) %

CHARACTERISTIC BEAMS

Accelerated Ions	E/A (MeV/u)	Current(part μA) Internal	External
(a) Protons	35		65
(b) deuterons	18		65

1991 μA-hours on target: 205

FACILITIES

SHIELDED AREA: Fixed ~ 100 m² Moveable m²

Target Stations: 2 No. Served At Same Time: 1

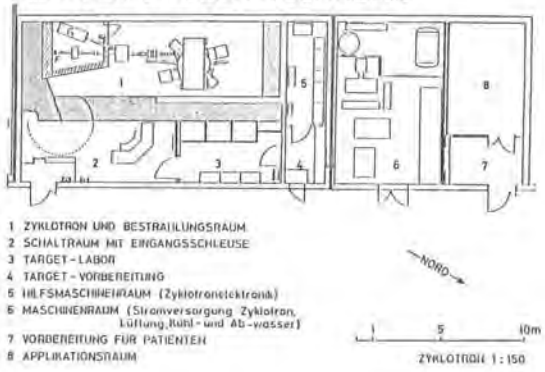
OTHER FACILITIES:

REFERENCES/NOTES

(a) target stations:solids-3 positions/Gas-6 positions

(b) He - 3 and He 4 beam is available too

PLAN VIEW OF FACILITY, COMMENTS



ENTRY NO. CU29 **Date**

Cyclotron Model BC 1710

Institution Institute of Nuclear Chemistry, KFA Jülich

Address 5170 Jülich, Germany

Tel 2461-614141 Telex 833556 KFA D

Fax 2461-612535 EMAIL

In Charge: Prof. G. Stöcklin Reported by: Dr. S.M. Qaim

HISTORY

MILESTONE DATES:

Installation January 1987 First Beam April 1987

DESIGN/CONSTRUCTION BY: Japan Steel Works

COST: Accelerator DM 3.3 M Facility DM 1.5 M (both 1987 values)

FUNDED BY: Federal Government

STATUS

STAFF: Operators 2 Technicians

BUDGET: Machine DM 50.000 Funded by Federal Govt. (running costs)

TIME DISTRIBUTION: (e.g. basic research, isotope production, maintenance, etc.)

(a) Isotope production 100 %

(b) %

(c) %

(d) %

(e) %

CHARACTERISTIC BEAMS

Accelerated Ions	E/A (MeV/u)	Current(part μA) Internal	External
(a) Protons	17		50
(b) Deuterons	10		40

1991 μA-hours on target: 8200

FACILITIES

SHIELDED AREA: Fixed ca. 350 m² Moveable m²

Target Stations: 1 No. Served At Same Time:

OTHER FACILITIES: 6 Hot cells

Radiochemical and Radiopharmaceutical laboratories;

PET; SPECT; Radioagronomy laboratories

REFERENCES/NOTES

(a)

(b)

PLAN VIEW OF FACILITY, COMMENTS

ENTRY No. CU30

NAME OF MACHINE Jülich Compact Cycl. (CV28) DATE SEPT. 81
INSTITUTION Kernforschungsanlage Juelich - IFF
ADDRESS Postfach 1913, D-5170 Juelich, Germany
TEL ..... TELEX .....
IN CHARGE R. Holzle, W. Kogler REPORTED BY R. Holzle

HISTORY AND STATUS

DESIGN, date 1969 Model tests 1973
ENG DESIGN, date 1970
CONSTRUCTION, date 1973-1975
FIRST BEAM, date (or goal) Oct. 1975
MAJOR ALTERATIONS
COST, ACCELERATOR $ 1 Mio
COST, FACILITY, total $ 2 Mio
FUNDED BY German Government

ACCELERATOR STAFF, OPERATION AND DEVELOPMENT

SCIENTISTS -- ENGINEERS 2
TECHNICIANS 4 CRAFTS
GRAD STUDENTS involved during year 4
OPERATED BY -- Research staff or 4 Operators
OPERATION 80 hr/wk, On target 72 hr/wk
TIME DISTR. in house 40 %, Outside 80 %
BUDGET, op & dev 100 000 per year
FUNDED BY German Government

RESEARCH STAFF, not included above

USERS, In house 6 outside 20
GRAD STUDENTS involved during year
RESEARCH BUDGET, In house
FUNDED BY

MAGNET

POLE FACE, diameter (compact) 96 cm, R extraction 42 cm
R injection cm
GAP, min 5 cm, Field kG
max 10 cm, Field kG } at 2×10^6 Ampere turns
AVERAGE FIELD at R ext 18.5 kG
B max/ <B>
NUMBER OF SECTORS { compact 3 / separated } Spiral, max 60 deg
SECTOR ANGLE (ISSC) deg
TRIMMING COILS
CONDUCTOR, material and type Copper
STORED ENERGY (cryogenic) MJ
POWER: main coils 60 max, kW ; current stability 5×10^{-6}
trimming coils 50 max, kW ; current stability
WEIGHT : Fe total 23 tons ; coils tons
COOLING system Demineralized water
ION ENERGY (bending limit) E/A = 28 q^2/a^2 MeV/amu
(focusing limit) E/A = q^2/a^2 MeV/amu

ACCELERATION SYSTEM

DEES, number 2 ; angle 90 deg
BEAM APERTURE 2,5 cm ; DC Bias 0.5-2 kV
TUNED by, coarse short plane fine Var. cap
RF 6 to 26 mHz, stable ± 1/10^6
Orb F to mHz
HARMONICS, RF/Orb F, used fundamental
DEE - Gnd, max kV, min gap 1.27 cm
STABILITY, (pk-pk noise)/(pk RF volt) 1×10^{-3}
ENERGY GAIN, max kV/turn
RF PHASE, stable to ± deg
RF POWER input, max 75 kW
FREQUENCY MODULATION, rate /s
modulator, type
beam pulse, width

VACUUM SYSTEM

OPERATING PRESSURE 5×10^{-5} Torr or mbar
PUMPS, No, Type, Size
2 x 1500 l/s Turbo

ION SOURCES

"cold cathode" Penning or thermionic

INJECTION SYSTEM

--

EXTRACTION SYSTEM

dc. electrostatic + mag. channel

FACILITIES FOR RESEARCH

SHIELDED AREA, fixed 200. m² ; movable -- m²
TARGET STATIONS 8 In 4 rooms
STATIONS served at same time, max 1
MAG SPECTROGRAPH, type none
COMPUTER model PDP 11-40 (1981)
OTHER FACILITIES Pneumatic transfer for internal and external target

CHARACTERISTIC BEAMS

PARTICLE	ENERGY (MeV) Goal	Achieved	CURRENT (pμA) Internal	External
p	2-24	2-24	500	70
d	3-14	3-14	500	100
$^3He^{++}$	5-36	5-36	100	70
α	6-28	6-28	100	50
SECONDARY			(part/s)	
n			3×10^{12}	

BEAM PROPERTIES

	MEASURED	CONDITIONS
PULSE WIDTH	RF deg	pμA of MeV ions
PHASE EXC, max	RF deg	pμA of MeV ions
EXTRACT eff	%	pμA of MeV ions
RESOL ΔE/E	%	pμA of MeV ions
EMITTANCE (π mm. mrad)	.15 axial / .15. rad	.5 pμA of .24 MeV P. Ions

OPERATING PROGRAMS, time distribution

BASIC NUCLEAR PHYSICS .. SOLID STATES PHYSICS 40.
BIOMEDICAL APPLICAT. 20. ISOTOPE PRODUCTIONS 40.

REFERENCES/NOTES

J. Hemmerich, R. Holzle, W. Kogler,
Kerntechnik 19 (1977)

PLAN VIEW OF FACILITY, NOTEWORTHY FEATURES, COMMENTS

ENTRY NO. CU31 **Date** July 92

Cyclotron Model CP42 H (KAZ)
Institution Kernforschungszentrum Karlsruhe GmbH, Cyclotron-Lab
Address D-7500 Karlsruhe, P.O. Box 3640, Germany
Tel 07247-82-2433 Telex 17724714
Fax 07247-82-3156 EMAIL
In Charge: H. Schweickert Reported by: H. Schweickert

HISTORY

MILESTONE DATES:
Installation 1983 First Beam 1983
DESIGN/CONSTRUCTION BY: TCC
COST: Accelerator $ 2.000.000 Facility $ 8. 000.000
FUNDED BY: Federal Government + State of Bad. Württ.

STATUS

STAFF: Operators 6 Technicians 4
BUDGET: Machine $ 2.000.000 Funded by Income
TIME DISTRIBUTION: (e.g. basic research, isotope production, maintenance, etc)

(a)	Isotope Production	40 %
(b)	Irradiation of Maschine Parts	30 %
(c)	Materials Research	20 %
(d)	Others	20 %
(e)		%

CHARACTERISTIC BEAMS

Accelerated Ions	E/A (MeV/u)	Current(part μA) Internal	External
(a) H^-	15-42	200	200
(b)			

1991 μA-hours on target:

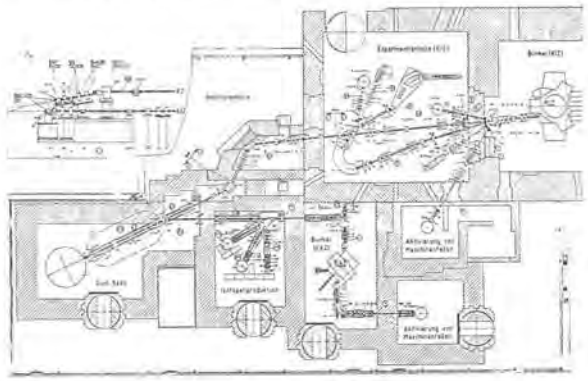
FACILITIES

SHIELDED AREA: Fixed 200 m² Moveable m²
Target Stations: 8 No. Served At Same Time: 2
OTHER FACILITIES:
Dual Beam-Facility for Materials Research
Irradiation Facility for Machine Parts

REFERENCES/NOTES

(a) Proc. 9th Int. Conf. on Cyclotrons, p. 125
(b)

PLAN VIEW OF FACILITY, COMMENTS



ENTRY NO. CU32 **Date**

Cyclotron Model MC 17
Institution Max-Planck-Institut für neurologische Forschung
Address Gleueler Str. 50, D-5000 Köln 41, Germany
Tel 0221-478-6066 Telex
Fax 0221-4726-298 EMAIL
In Charge: K. Wienhard Reported by: K. Wienhard

HISTORY

MILESTONE DATES:
Installation 1987 First Beam June 1987
DESIGN/CONSTRUCTION BY: Scanditronix
COST: Accelerator DM 3.000.000 Facility
FUNDED BY:

STATUS

STAFF: Operators 1 Technicians 1
BUDGET: Machine Funded by
TIME DISTRIBUTION: (e.g. basic research, isotope production, maintenance, etc.)

(a)	isotope production	90 %
(b)	maintenance	10 %
(c)		%
(d)		%
(e)		%

CHARACTERISTIC BEAMS

Accelerated Ions	E/A (MeV/u)	Current(part μA) Internal	External
(a) P	17		20
(b) d	17		20

1991 μA-hours on target: 1,2 x 10 e 4

FACILITIES

SHIELDED AREA: Fixed 40 m² Moveable m²
Target Stations: 1 No. Served At Same Time:
OTHER FACILITIES:

REFERENCES/NOTES

(a)
(b)

PLAN VIEW OF FACILITY, COMMENTS

ENTRY NO. CU31 **Date** July 92

Cyclotron Model CP42 H (KAZ)
Institution Kernforschungszentrum Karlsruhe GmbH, Cyclotron-Lab
Address D-7500 Karlsruhe, P.O. Box 3640, Germany
Tel 07247-82-2433 Telex 17724714
Fax 07247-82-3156 EMAIL
In Charge: H. Schweickert Reported by: H. Schweickert

HISTORY

MILESTONE DATES:
Installation 1983 First Beam 1983
DESIGN/CONSTRUCTION BY: TCC
COST: Accelerator $ 2.000.000 Facility $ 8. 000.000
FUNDED BY: Federal Government + State of Bad. Württ.

STATUS

STAFF: Operators 6 Technicians 4
BUDGET: Machine $ 2.000.000 Funded by Income
TIME DISTRIBUTION: (e.g. basic research, isotope production, maintenance, etc)

(a)	Isotope Production	40 %
(b)	Irradiation of Maschine Parts	30 %
(c)	Materials Research	20 %
(d)	Others	20 %
(e)		%

CHARACTERISTIC BEAMS

Accelerated Ions	E/A (MeV/u)	Current(part μA) Internal	External
(a) H^-	15-42	200	200
(b)			

1991 μA-hours on target:

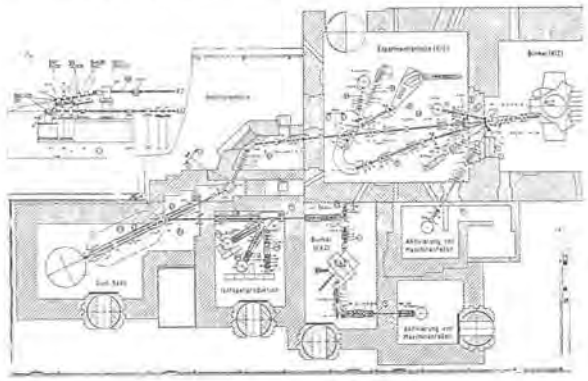
FACILITIES

SHIELDED AREA: Fixed 200 m² Moveable m²
Target Stations: 8 No. Served At Same Time: 2
OTHER FACILITIES:
Dual Beam-Facility for Materials Research
Irradiation Facility for Machine Parts

REFERENCES/NOTES

(a) Proc. 9th Int. Conf. on Cyclotrons, p. 125
(b)

PLAN VIEW OF FACILITY, COMMENTS



ENTRY NO. CU32 **Date**

Cyclotron Model MC 17
Institution Max-Planck-Institut für neurologische Forschung
Address Gleueler Str. 50, D-5000 Köln 41, Germany
Tel 0221-478-6066 Telex
Fax 0221-4726-298 EMAIL
In Charge: K. Wienhard Reported by: K. Wienhard

HISTORY

MILESTONE DATES:
Installation 1987 First Beam June 1987
DESIGN/CONSTRUCTION BY: Scanditronix
COST: Accelerator DM 3.000.000 Facility
FUNDED BY:

STATUS

STAFF: Operators 1 Technicians 1
BUDGET: Machine Funded by
TIME DISTRIBUTION: (e.g. basic research, isotope production, maintenance, etc.)

(a)	isotope production	90 %
(b)	maintenance	10 %
(c)		%
(d)		%
(e)		%

CHARACTERISTIC BEAMS

Accelerated Ions	E/A (MeV/u)	Current(part μA) Internal	External
(a) P	17		20
(b) d	17		20

1991 μA-hours on target: 1,2 x 10 e 4

FACILITIES

SHIELDED AREA: Fixed 40 m² Moveable m²
Target Stations: 1 No. Served At Same Time:
OTHER FACILITIES:

REFERENCES/NOTES

(a)
(b)

PLAN VIEW OF FACILITY, COMMENTS

ENTRY NO. CU33 Date June 30/92

Name of Machine MGC-20 Cyclotron

Institution ATOMKI

Address Bem tér 18/c, Debrecen, Hungary

Tel (52) 17-266 Telex (52) 72-210 Fax (52) 16-181 EMAIL h5159val@ella.hu

In Charge: A. Valek Reported by: A. Valek

HISTORY

MILESTONE DATES:

Design ..... Model Tests .....

Construction 1982-84 First Beam August 1985

DESIGN/CONSTRUCTION BY:

in house ..... other SRIEA,St.Petersburg,CIS

COST: Accelerator 80 MHUF Facility 250 MHUF

FUNDED BY: Hungarian Academy of Sciences

STATUS

STAFF: Machine

Scientists 1 Engineers 2

Technicians 6 Students .....

Research (in house/external)

Scientists 25 / 10 Engineers ..... / .....

Technicians 4 / 4 Students 2 / .....

BUDGET: Machine 7.5 MHUF Funded by ATOMKI

Research 20 MHUF Funded by var.sources

TIME DISTRIBUTION:

Basic Research (in house/external) 25 % / 12 %

Applied Program (in house/external) 17 % / 23 %

Development 2 % Maintenance 21 %

MAGNET

POLE PARAMETERS:

Diameter 103 cm $R_{extract}$ 45 cm R_{inject} ..... cm

HILL PARAMETERS: Gap (min) 7.2 cm B_{max} 1.8 T

(@ 0.12e6 AT) Gap (max) 7.2 cm B_{min} ..... T

VALLEY PARAMETERS: Gap (min) 12 cm B_{max} ..... T

(@ ..... AT) Gap (max) 12 cm B_{min} 0.4 T

AVERAGE FIELD: $< B >_{min}$ 0.5 T $< B >_{max}$ 1.45 T

NUMBER OF SECTORS: compact/separated 3 / .....

sector angle 89 deg. spiral (max) 35 deg.

FIELD TRIMMING: Trim Coils 4

Harmonic Coils 6

Other .....

CURRENT: Main Coils 400 Amps Stability 1e-4

Trim Coils 10 Amps Stability 1e-4

Stored Energy (cryogenic) ..... MJ

WEIGHT: Iron 24 tons Conductor 1.2 tons

ION ENERGY: Bending Limit E/A = 20 q^2/A^2 MeV/u

Focussing Limit E/A = ... q/A MeV/u

ACCELERATION SYSTEM

FUNDAMENTAL ACCELERATION:

Description: moving panels, push-pull mode

No. of Gaps/turn 2 dE/dn(max) 0.12 MeV/q

Voltage(max) 0.035 MV Harmonic f_{rf}/f_{ion} 1,3

Freq 8-24 MHz Power in(max) 0.14 MW

Stability: Phase ..... Voltage 1e-4

OTHER CAVITIES (Flattopping or otherwise):

Description: .....

Region of Influence: R_{min} ..... cm R_{max} ..... cm

No. of Gaps/turn ..... dE/dn(max) ..... MeV/q

Voltage(max) ..... MV Harmonic f_{rf}/f_{ion} .....

Freq ..... MHz Power in(max) ..... MW

Stability: Phase ..... Voltage .....

VACUUM SYSTEM

OPERATING PRESSURE: 1x10^{-3} Pa

PUMPS: No. and type 3 oil diffusion

.....

ION SOURCE(S)

	Type	Intensity (mA)	@	$\epsilon_n = \beta\gamma\epsilon$ (πmm mrad)	Ion Species
(a)	Penning	0.6			p,d
(b)					
(c)					
(d)					

INJECTION SYSTEM

..... Efficiency ..... %

EXTRACTION SYSTEM

electrostatic deflector Efficiency 40-60 %

CHARACTERISTIC BEAMS

Accelerated Ions	E/A (MeV/u)	Current(part μA) Internal	External
(a) p	3,5-20	100	50
(b) d	2 -10	100	50
(c) alpha	5 -20	40	20
(d) $^3He^{++}$	6 -27	30	15

Secondary Particles	E (MeV)	part/sec
(a)		
(b)		
(c)		

EXTRACTED BEAM PROPERTIES:

For 35 μA of 18 MeV/u p ions

$\Delta E/E$ 0.3 % $\Delta\phi$ 40 °rf

$\epsilon_n = \beta\gamma\epsilon$ x 15 πmm mrad z ..... πmm mrad

FACILITIES FOR RESEARCH

SHIELDED AREA: Fixed ..... m² Moveable 550 m²

Target Stations: 10 No. Served At Same Time: 1

MAGNETIC SPECTROMETERS: .....

OTHER FACILITIES: Isotope production,

Be neutron source

.....

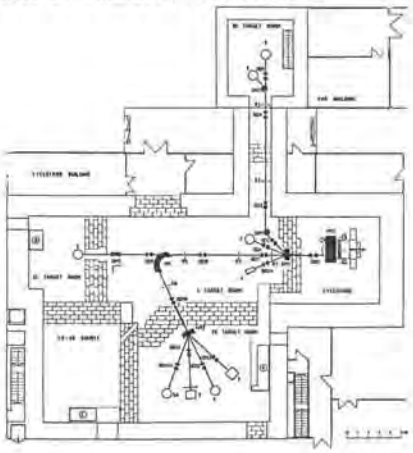
.....

REFERENCES/NOTES

(a) .....

(b) .....

PLAN VIEW OF FACILITY, COMMENTS



ENTRY No. CU34

NAME OF MACHINE . ISPRA .CYCLOTRON..... DATE .....
INSTITUTION . JOINT. RESEARCH. CENTRE .-. ADVANCED .MATERIALS .INSTITUTE.....
ADDRESS ....21020 ISPRA. (VA). ITALY.....
TEL .. 0039 .332. 789895 ... TELEX ... 380042 .-. 380058. EUR .1.....
IN CHARGE ... CASTIGLIONI, M. .... REPORTED BY . CASTIGLIONI, M. .....

HISTORY AND STATUS
DESIGN, date ..... Model tests .....
ENG DESIGN, date .. MC-40 .SCANDITRONIX.....
CONSTRUCTION, date .....
FIRST BEAM, date (or goal) ..1982.....
MAJOR ALTERATIONS .....
.....6.....
COST, ACCELERATOR ..9x10^6. SKR .....
COST, FACILITY, total ...1.1x10^7. SKR .(EXCL.. BLD.) .....
FUNDED BY ....E.E.C.....

ACCELERATOR STAFF, OPERATION AND DEVELOPMENT
SCIENTISTS ....1..... ENGINEERS ...2.....
TECHNICIANS ...1..... CRAFTS .....2.....
GRAD STUDENTS involved during year .....
OPERATED BY ..... Research staff or ...5..... Operators
OPERATION .....55.... hr/wk, On target ....44..... hr/wk
TIME DISTR. In house .....70%, Outside 30%
BUDGET, op & dev ...2.0x10^5. ECU .....
FUNDED BY ...E.E.C.....

RESEARCH STAFF, not included above
USERS, In house ....6..... outside .....6.....
GRAD STUDENTS involved during year .....
RESEARCH BUDGET, In house ..... 4.5x10^5. ECU.....
FUNDED BY ..E.E.C.....

MAGNET
POLE FACE, diameter (compact) 135. cm, R extraction 50 . cm
R injection ..... cm
GAP, min ....10.. cm, Field .....21.2.. kG } at 241,000..
max ....18.. cm, Field .....13.3.. kG } Ampere turns
AVERAGE FIELD at R ext .....17.9.. kG
B max/ <B> ....1.19.....
NUMBER OF SECTORS { compact ...3.. / separated ..... } Spiral, max 45 deg
SECTOR ANGLE (SSC) ..... deg
TRIMMING COILS . 8 .CIRCULAR. COILS .....
..... 4 .SETS .OF. HARMONIC .COILS.....
CONDUCTOR, material and type ... Cu .....
STORED ENERGY (cryogenic) ..... MJ
POWER : main coils ..100. max, kW ; current stability .10^{-5}
trimming coils ...10. max, kW ; current stability .10^{-4}
WEIGHT : Fe ....67..... tons ; coils ....2.4..... tons
COOLING system . DEMINERALIZED .WATER.....
ION ENERGY (bending limit) E/A = ...40... q^2/a^2 MeV/amu
(focusing limit) E/A = ... q^2/a^2 MeV/amu

ACCELERATION SYSTEM
DEES, number ....2..... ; angle .....90..... deg
BEAM APERTURE ....2..... cm ; DC Bias ...0..... kV
TUNED by, coarse ...MOV. SHORT fine . VAR. CAPACITOR .....
RF ...12.5 ... to ....27.... mHz, stable ± 10^{-6} .....
Orb F ...6.25 ... to ....27.... mHz
HARMONICS, RF/Orb F, used .... 1 .AND .2.....
DEE - Gnd, max . 44.. kV, min gap ..... cm
STABILITY, (pk-pk noise)/(pk RF volt) .....10^{-3}.....
ENERGY GAIN, max .....176..... kV/turn
RF PHASE, stable to ± ....0.5..... deg
RF POWER input, max .... 60..... kW
FREQUENCY MODULATION, rate ..... /s
modulator, type .....
beam pulse, width ....15 .- 20.. deg .....

VACUUM SYSTEM
OPERATING PRESSURE ...2x10^{-6} ..... Torr or mbar
PUMPS, No, Type, Size ....2 .TURBO. MOLECULAR.....
.LEYBOLD HERAEUS. TYPE .3500.....
.....

ION SOURCES
.INTERNAL .COLD .CATHODE .AXIALLY .MOUNTED .....

INJECTION SYSTEM
.....

EXTRACTION SYSTEM
ELECTROSTATIC .DEFLECTOR, .MAGNETIC. CHANNEL.....

FACILITIES FOR RESEARCH
SHIELDED AREA, fixed ..280..... m^2 ; movable ..... m^2
TARGET STATIONS .....6. In ..3..... rooms
STATIONS served at same time, max .1.....
MAG SPECTROGRAPH, type .....
COMPUTER model .....
OTHER FACILITIES .HELIUM. JET .COOLING .SYSTEM .FOR .TARGET..
.....
.....

CHARACTERISTIC BEAMS

PARTICLE	ENERGY (MeV) Goal	Achieved	CURRENT (pμA) Internal	External
. PROTONS ..	....38....		...100.....	....65.....
. DEUTERONS	....19....		...100.....	....65.....
. ALPHAS...	....38....		....60.....	....30.....
.....	.....		.....	.....
SECONDARY				(part/s)
.....	.....		.....	.....
.....	.....		.....	.....

BEAM PROPERTIES

	MEASURED		CONDITIONS		
PULSE WIDTH	RF deg	pμ A of	MeV ...	Ions
PHASE EXC, max ...	RF deg	pμ A of	MeV ...	Ions
EXTRACT eff	%	pμ A of	MeV ...	Ions
RESOL ΔE/E	%	pμ A of	MeV ...	Ions

EMITTANCE
(π mm. mrad) { ... axial / .... rad } ..... pμA of ..... MeV ... Ions

OPERATING PROGRAMS, time distribution
BASIC NUCLEAR PHYSICS .. SOLID STATES PHYSICS ....
BIOMEDICAL APPLICAT. 5% . ISOTOPE PRODUCTIONS 10%
.RADIATION. DAMAGE .AND. ALPHA .IMPLANTATION .IN .FUSION.....
.REACTOR. MATERIALS .85%.....

REFERENCES/NOTES

PLAN VIEW OF FACILITY, NOTEWORTHY FEATURES, COMMENTS

ENTRY NO. CU35 Date 22/06/1992

Cyclotron Model MC 17 F

Institution ISTITUTO NAZIONALE DEI TUMORI - DIV. MED. NUCL

Address V. VENEZIAN, 1 - 20133 MILANO - ITALY

Tel (02) 2390220 Telex (02) 333290 TUMIST I

Fax (02) 2367874 EMAIL

In Charge: PROF. G.L. BURAGGI Reported by: G.L. BURAGGI

HISTORY

MILESTONE DATES:

Installation APRIL 92-JUNE 93 First Beam

DESIGN/CONSTRUCTION BY: SCANDITRONIX

COST: Accelerator $2.180.000 Facility $5.820.000

FUNDED BY: NATIONALHEALTH SERVICE - LOCAL COMMITTEE OF CONTROL (REGIONE LOMBARDIA)

STATUS

STAFF: Operators 1 Technicians 1

BUDGET: Machine Funded by

TIME DISTRIBUTION: (e.g. basic research, isotope production, maintenance, etc.)

(a) ISOTOPE PRODUCTION 80 %

(b) MAINTENANCE 20 %

(c) %

(d) %

(e) %

CHARACTERISTIC BEAMS

Accelerated Ions	E/A (MeV/u)	Current(part μA) Internal	External
(a) H^+	17,2	100	65
(b) D^+	8,6	100	65

1991 μA-hours on target:

FACILITIES

SHIELDED AREA: Fixed 35,4 m² Moveable m²

Target Stations: 8 No. Served At Same Time: 1

OTHER FACILITIES:

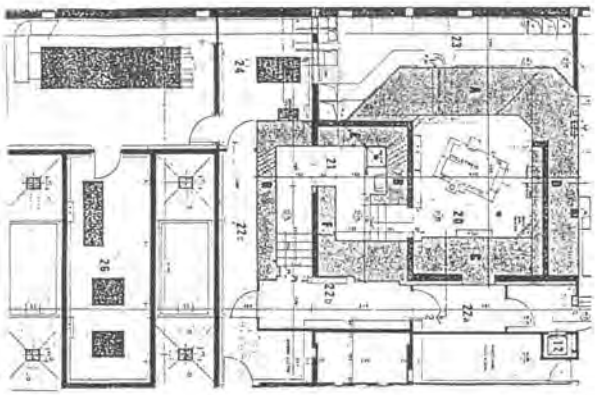
REFERENCES/NOTES

(a)

(b)

PLAN VIEW OF FACILITY, COMMENTS

CYCLOTRON AND TARGETS, BOTH PLACED IN A BUNKER, ARE AT B3. LABORATORIES AND PET-CAMERA ARE AT B2.



ENTRY NO. CU36 Date 25/6/92

Cyclotron Model SCANDITRONIX MC17

Institution FONDAZIONE SENATORE PASCALE

Address VIA MARIANO SEMMOLA NAPOLI

Tel 39-81-5452455 Telex

Fax 39-81-5461688 EMAIL

In Charge: Reported by:

HISTORY

MILESTONE DATES:

Installation 1991 First Beam 1991 - MAY

DESIGN/CONSTRUCTION BY: SCANDITRONIX

COST: Accelerator Facility 600.000 $

FUNDED BY: MEDICAL SCHOOL AND FONDAZIONE PASCALE

STATUS

STAFF: Operators 3 Technicians 1

BUDGET: Machine Funded by PASCALE

TIME DISTRIBUTION: (e.g. basic research, isotope production, maintenance, etc.)

(a) ISOTOPE PRODUCTION 80 %

(b) MAINTENANCE 20 %

(c) %

(d) %

(e) %

CHARACTERISTIC BEAMS

Accelerated Ions	E/A (MeV/u)	Current(part μA) Internal	External
(a) PROTONS	17	23	21
(b) DEUTERONS	8,5	40	30

1991 μA-hours on target: 300 (INSTALLATION)

FACILITIES

SHIELDED AREA: Fixed 35 m² Moveable / m²

Target Stations: 5 No. Served At Same Time: 1

OTHER FACILITIES: RADIOISOTOPES AUTOMATIC TRANSPORTATION TO HOT CELLS. AUTOMATIC SINTESIS BY MEANS OF ROBOT

REFERENCES/NOTES

(a)

(b)

PLAN VIEW OF FACILITY, COMMENTS

ENTRY NO. CU35 Date 22/06/1992

Cyclotron Model MC 17 F

Institution ISTITUTO NAZIONALE DEI TUMORI - DIV. MED. NUCL

Address V. VENEZIAN, 1 - 20133 MILANO - ITALY

Tel (02) 2390220 Telex (02) 333290 TUMIST I

Fax (02) 2367874 EMAIL

In Charge: PROF. G.L. BURAGGI Reported by: G.L. BURAGGI

HISTORY

MILESTONE DATES:

Installation APRIL 92-JUNE 93 First Beam

DESIGN/CONSTRUCTION BY: SCANDITRONIX

COST: Accelerator $2.180.000 Facility $5.820.000

FUNDED BY: NATIONALHEALTH SERVICE - LOCAL COMMITTEE OF CONTROL (REGIONE LOMBARDIA)

STATUS

STAFF: Operators 1 Technicians 1

BUDGET: Machine Funded by

TIME DISTRIBUTION: (e.g. basic research, isotope production, maintenance, etc.)

(a) ISOTOPE PRODUCTION 80 %

(b) MAINTENANCE 20 %

(c) %

(d) %

(e) %

CHARACTERISTIC BEAMS

Accelerated Ions	E/A (MeV/u)	Current(part μA) Internal	External
(a) H^+	17,2	100	65
(b) D^+	8,6	100	65

1991 μA-hours on target:

FACILITIES

SHIELDED AREA: Fixed 35,4 m² Moveable m²

Target Stations: 8 No. Served At Same Time: 1

OTHER FACILITIES:

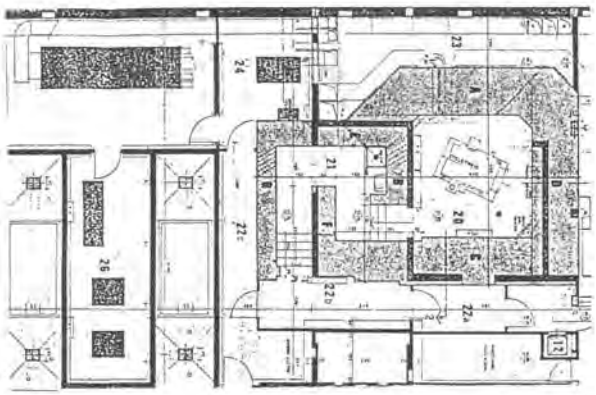
REFERENCES/NOTES

(a)

(b)

PLAN VIEW OF FACILITY, COMMENTS

CYCLOTRON AND TARGETS, BOTH PLACED IN A BUNKER, ARE AT B3. LABORATORIES AND PET-CAMERA ARE AT B2.



ENTRY NO. CU36 Date 25/6/92

Cyclotron Model SCANDITRONIX MC17

Institution FONDAZIONE SENATORE PASCALE

Address VIA MARIANO SEMMOLA NAPOLI

Tel 39-81-5452455 Telex

Fax 39-81-5461688 EMAIL

In Charge: Reported by:

HISTORY

MILESTONE DATES:

Installation 1991 First Beam 1991 - MAY

DESIGN/CONSTRUCTION BY: SCANDITRONIX

COST: Accelerator Facility 600.000 $

FUNDED BY: MEDICAL SCHOOL AND FONDAZIONE PASCALE

STATUS

STAFF: Operators 3 Technicians 1

BUDGET: Machine Funded by PASCALE

TIME DISTRIBUTION: (e.g. basic research, isotope production, maintenance, etc.)

(a) ISOTOPE PRODUCTION 80 %

(b) MAINTENANCE 20 %

(c) %

(d) %

(e) %

CHARACTERISTIC BEAMS

Accelerated Ions	E/A (MeV/u)	Current(part μA) Internal	External
(a) PROTONS	17	23	21
(b) DEUTERONS	8,5	40	30

1991 μA-hours on target: 300 (INSTALLATION)

FACILITIES

SHIELDED AREA: Fixed 35 m² Moveable / m²

Target Stations: 5 No. Served At Same Time: 1

OTHER FACILITIES: RADIOISOTOPES AUTOMATIC TRANSPORTATION TO HOT CELLS. AUTOMATIC SINTESIS BY MEANS OF ROBOT

REFERENCES/NOTES

(a)

(b)

PLAN VIEW OF FACILITY, COMMENTS

ENTRY NO. CU37 Date

Cyclotron Model CGR-MEV CYPRIS 325
Institution CNR INSTITUTE OF CLINICAL PHYSIOLOGY
Address VIA SAVI 8 56100 PISA ITALY
Tel +39.50.583254 Telex 590549 IFC I
Fax +39.50.553461 EMAIL
In Charge: P. SALVADORI Reported by: P. SALVADORI

HISTORY

MILESTONE DATES:
Installation 1985 First Beam 1986
DESIGN/CONSTRUCTION BY: CGR MEV - FRANCE
COST: Accelerator 900,000 USD Facility 1,100,000 USD
FUNDED BY: NATIONAL COUNCIL OF RESEARCH (CNR)

STATUS

STAFF: Operators 1 Technicians 2
BUDGET: Machine 400,000 Funded by CNR
TIME DISTRIBUTION: (e.g. basic research, isotope production, maintenance, etc.)
(a) isotope production 80 %
(b) basic research 16 %
(c) maintenance 5 %
(d) %
(e) %

CHARACTERISTIC BEAMS

Accelerated Ions	E/A (MeV/u)	Current(part μA) Internal	External
(a) p	16	80	40
(b) d	4	50	30

1991 μA-hours on target:

FACILITIES

SHIELDED AREA: Fixed 50 m² Moveable m²
Target Stations: 1 No. Served At Same Time: 1
OTHER FACILITIES:

REFERENCES/NOTES

(a)
(b)

PLAN VIEW OF FACILITY, COMMENTS



ENTRY NO. CU39 Date

Cyclotron Model JSW BC-168
Institution Research Inst. for Brain & Blood Vessels-AKITA
Address 6-10 Senshu-Kubota machi, Akita city, Akita 010, JAPAN
Tel Jpn:188-33-0115 Telex
Fax Jpn:188-33-2104 EMAIL
In Charge: Kazuo Uemura Reported by: Matsutaro Murakami

HISTORY

MILESTONE DATES:
Installation Oct.1982-Apr.1983 First Beam Feb.1983
DESIGN/CONSTRUCTION BY:
COST: Accelerator ¥ 300,000,000 Facility
FUNDED BY: Akita Prefecture

STATUS

STAFF: Operators 3 Technicians 1
BUDGET: Machine ¥ 15,000,000 Funded by Akita Prefecture
TIME DISTRIBUTION: (e.g. basic research, isotope production, maintenance, etc.)
(a) Isotope production for clinical use 80 %
(b) Isotope Production for basic research 10 %
(c) Maintenance 10 %
(d) %
(e) %

CHARACTERISTIC BEAMS

Accelerated Ions	E/A (MeV/u)	Current(part μA) Internal	External
(a) H+	16 - 50	8.5 H+	5.7 H+
(b) D+	8 - 50	7.2 H+	4.6 H+

1991 μA-hours on target: 4.2 x 10e4

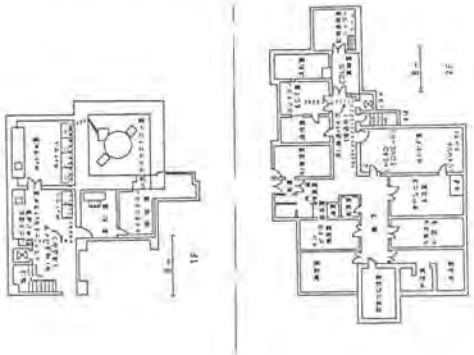
FACILITIES

SHIELDED AREA: Fixed 22.5 m² Moveable m²
Target Stations: 5 No. Served At Same Time: 1
OTHER FACILITIES:

REFERENCES/NOTES

(a)
(b)

PLAN VIEW OF FACILITY, COMMENTS



ENTRY NO. CU37 Date

Cyclotron Model CGR-MEV CYPRIS 325
Institution CNR INSTITUTE OF CLINICAL PHYSIOLOGY
Address VIA SAVI 8 56100 PISA ITALY
Tel +39.50.583254 Telex 590549 IFC I
Fax +39.50.553461 EMAIL
In Charge: P. SALVADORI Reported by: P. SALVADORI

HISTORY

MILESTONE DATES:
Installation 1985 First Beam 1986
DESIGN/CONSTRUCTION BY: CGR MEV - FRANCE
COST: Accelerator 900,000 USD Facility 1,100,000 USD
FUNDED BY: NATIONAL COUNCIL OF RESEARCH (CNR)

STATUS

STAFF: Operators 1 Technicians 2
BUDGET: Machine 400,000 Funded by CNR
TIME DISTRIBUTION: (e.g. basic research, isotope production, maintenance, etc.)
(a) isotope production 80 %
(b) basic research 16 %
(c) maintenance 5 %
(d) %
(e) %

CHARACTERISTIC BEAMS

Accelerated Ions	E/A (MeV/u)	Current(part μA) Internal	External
(a) p	16	80	40
(b) d	4	50	30

1991 μA-hours on target:

FACILITIES

SHIELDED AREA: Fixed 50 m² Moveable m²
Target Stations: 1 No. Served At Same Time: 1
OTHER FACILITIES:

REFERENCES/NOTES

(a)
(b)

PLAN VIEW OF FACILITY, COMMENTS



ENTRY NO. CU39 Date

Cyclotron Model JSW BC-168
Institution Research Inst. for Brain & Blood Vessels-AKITA
Address 6-10 Senshu-Kubota machi, Akita city, Akita 010, JAPAN
Tel Jpn:188-33-0115 Telex
Fax Jpn:188-33-2104 EMAIL
In Charge: Kazuo Uemura Reported by: Matsutaro Murakami

HISTORY

MILESTONE DATES:
Installation Oct.1982-Apr.1983 First Beam Feb.1983
DESIGN/CONSTRUCTION BY:
COST: Accelerator ¥ 300,000,000 Facility
FUNDED BY: Akita Prefecture

STATUS

STAFF: Operators 3 Technicians 1
BUDGET: Machine ¥ 15,000,000 Funded by Akita Prefecture
TIME DISTRIBUTION: (e.g. basic research, isotope production, maintenance, etc.)
(a) Isotope production for clinical use 80 %
(b) Isotope Production for basic research 10 %
(c) Maintenance 10 %
(d) %
(e) %

CHARACTERISTIC BEAMS

Accelerated Ions	E/A (MeV/u)	Current(part μA) Internal	External
(a) H+	16 - 50	8.5 H+	5.7 H+
(b) D+	8 - 50	7.2 H+	4.6 H+

1991 μA-hours on target: 4.2 x 10e4

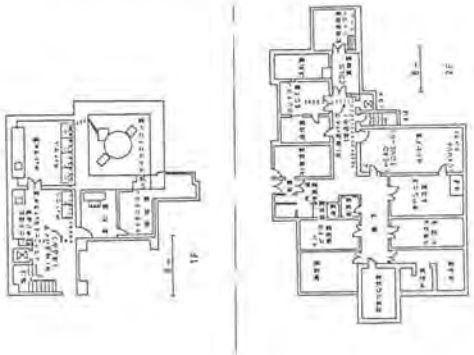
FACILITIES

SHIELDED AREA: Fixed 22.5 m² Moveable m²
Target Stations: 5 No. Served At Same Time: 1
OTHER FACILITIES:

REFERENCES/NOTES

(a)
(b)

PLAN VIEW OF FACILITY, COMMENTS



ENTRY No. CU40

NAME OF MACHINE . Model 370 (Sumitomo-CGRMeV) DATE ....June 14, 1989
INSTITUTION . Chiba Medical School Hospital
ADDRESS ....1-8-1 Inohana Chiba City, Chiba 280, Japan
TEL 0472-22-7171 ..... TELEX . 0472-24-3834
IN CHARGE . S. Yematsu ..... REPORTED BY .. Y... Itoh

HISTORY AND STATUS
DESIGN, date ..... Model tests .....
ENG DESIGN, date .....
CONSTRUCTION, date ..... 1985 .....
FIRST BEAM, date (or goal) ... Sept. 1985 .....
MAJOR ALTERATIONS .....
.....
COST, ACCELERATOR .....
COST, FACILITY, total .....
FUNDED BY .....

ACCELERATOR STAFF, OPERATION AND DEVELOPMENT
SCIENTISTS ..... ENGINEERS .....
TECHNICIANS ....2..... CRAFTS .....
GRAD STUDENTS involved during year .....
OPERATED BY ..... Research staff or ..... Operators
OPERATION ..... 30 ... hr/wk, On target .... 9 ..... hr/wk
TIME DISTR. in house ..... %, Outside ..... %
BUDGET, op & dev .....
FUNDED BY .....

RESEARCH STAFF, not included above
USERS, in house .....8..... outside .....
GRAD STUDENTS involved during year .....
RESEARCH BUDGET, in house .....
FUNDED BY .....

MAGNET
POLE FACE, diameter (compact) . 88 cm, R extraction .. 37 cm
R injection ..... cm
GAP, min ....7.... cm, Field ..... kG
max .. 12 .... cm, Field ..... kG } at 1.66x10^5
AVERAGE FIELD at R ext ..... 17.7 ..... kG } Ampere turns
B max/ <B> .....
NUMBER OF SECTORS { compact ... 4.. / separated ..... } Spiral, max .. deg
SECTOR ANGLE (SSC) ..... deg
TRIMMING COILS .. Harmonic ... 4 pairs .....
..... Circular ... 4 pairs .....
CONDUCTOR, material and type .. Copper Hollow .....
STORED ENERGY (cryogenic) ..... MJ
POWER : main coils . 78 ... max, kW ; current stability ..... 2x10^-6
trimming coils .. 3 ... max, kW ; current stability .....
WEIGHT : Fe ... 16 ..... tons ; coils .... 1 ..... tons
COOLING system . . . Demineralized Water .....
ION ENERGY (bending limit) E/A = ... q^2/a^2 MeV/amu
(focusing limit) E/A = ... q^2/a^2 MeV/amu

ACCELERATION SYSTEM
DEES, number .....1..... ; angle .....180..... deg
BEAM APERTURE ..1.8..... cm ; DC Bias ..... kV
TUNED by, coarse ..... fine .....
RF .....25..... to .....40..... mHz, stable ± .....
Orb F ..25..... to .....13.3..... mHz
HARMONICS, RF/Orb F, used ...1, 3 .....
DEE - Gnd, max . 40 .. kV, min gap ....1.2..... cm
STABILITY, (pk-pk noise)/(pk RF volt) ...1 x 10^-3 .....
ENERGY GAIN, max ....80..... kV/turn
RF PHASE, stable to ± ..... deg
RF POWER input, max ....25..... kW
FREQUENCY MODULATION, rate ..... /s
modulator, type .....
beam pulse, width .....

VACUUM SYSTEM
OPERATING PRESSURE ..4 x 10^-5 ..... Torr ~~mbar~~
PUMPS, No, Type, Size 1 Diffusion pump 1300 l/sec .....
.....
.....

ION SOURCES
.....Livingstone-Jones type.....

INJECTION SYSTEM
.....

EXTRACTION SYSTEM
Electrostatic deflector and magnetic channel (static) ..

FACILITIES FOR RESEARCH
SHIELDED AREA, fixed ....41..... m² ; movable ..... m²
TARGET STATIONS ..1..... in ..... rooms
STATIONS served at same time, max .....
MAG SPECTROGRAPH, type .....
COMPUTER model .....
OTHER FACILITIES .....
.....
.....

CHARACTERISTIC BEAMS

PARTICLE	ENERGY (MeV) Goal	Achieved	CURRENT (pμA) Internal	External
....p.....	.....	....18....	.....	....50.....
....d.....	.....	....10....	.....	....50.....
.....	.....	.....	.....	.....
.....	.....	.....	.....	.....
SECONDARY				(part/s)
.....	.....	.....	.....	.....
.....	.....	.....	.....	.....

BEAM PROPERTIES

MEASURED	CONDITIONS
PULSE WIDTH ..... RF deg	pμ A of .... MeV ... ions
PHASE EXC, max ... RF deg	pμ A of .... MeV ... ions
EXTRACT eff ..... %	pμ A of .... MeV ... ions
RESOL ΔE/E ..... %	pμ A of .... MeV ... ions

EMITTANCE
(π mm. mrad) { ... axial / .... rad } ..... pμA of ..... MeV ... Ions

OPERATING PROGRAMS, time distribution

BASIC NUCLEAR PHYSICS ..	SOLID STATES PHYSICS ....
BIOMEDICAL APPLICAT. 100%	ISOTOPE PRODUCTIONS ....

.....
.....

REFERENCES/NOTES

PLAN VIEW OF FACILITY, NOTEWORTHY FEATURES, COMMENTS

ENTRY No. CU41

NAME OF MACHINE NIRS-Chiba Cyclotron ... DATE Jan. 1989
INSTITUTION National Institute of Radiological Sciences
ADDRESS 9-1, Anagawa-4-chome, Chiba-shi, 260 Japan
TEL 0472(51)2111 ... TELEX 3722205 NIRS J
IN CHARGE T. Kondo ... REPORTED BY T. Yamada

HISTORY AND STATUS CGR-MeV Model 930
DESIGN, date ... Model tests
ENG DESIGN, date
CONSTRUCTION, date 1972 – 1973
FIRST BEAM, date (or goal) Dec. 1973
MAJOR ALTERATIONS

COST, ACCELERATOR
COST, FACILITY, total
FUNDED BY

ACCELERATOR STAFF, OPERATION AND DEVELOPMENT
SCIENTISTS 4 ... ENGINEERS
TECHNICIANS 4 ... CRAFTS
GRAD STUDENTS involved during year
OPERATED BY ... Research staff or 4 ... Operators
OPERATION 38 ... hr/wk, On target ... hr/wk
TIME DISTR. In house 100 ... %, Outside ... %
BUDGET, op & dev
FUNDED BY

RESEARCH STAFF, not included above
USERS, In house ... outside
GRAD STUDENTS involved during year
RESEARCH BUDGET, In house
FUNDED BY

MAGNET
POLE FACE, diameter (compact) ... cm, R extraction ... cm
R injection ... cm
GAP, min 16.6 ... cm, Field 20.1 ... kG
max 40.5 ... cm, Field 11.7 ... kG
at 0.36×10^6 Ampere turns
AVERAGE FIELD at R ext 16.4 ... kG
B max/ <B>
NUMBER OF SECTORS { compact 4 ... / separated ... } Spiral, max 53 deg
SECTOR ANGLE (SSC) ... deg
TRIMMING COILS 12 Circular Coils
2 per sector (Hermonic)
CONDUCTOR, material and type Cu, hollow
STORED ENERGY (cryogenic) ... MJ
POWER: main coils 360 ... max, kW ; current stability $\pm 2 \times 10^{-5}$
trimming coils 75 ... max, kW ; current stability $\pm 1 \times 10^{-4}$
WEIGHT: Fe 200 ... tons ; coils 6 ... tons
COOLING system Demineralized water
ION ENERGY (bending limit) E/A = ≃110 q^2/a^2 MeV/amu
(focusing limit) E/A = ≃93 q^2/a^2 MeV/amu

ACCELERATION SYSTEM
DEES, number 2 ... ; angle 86 ... deg
BEAM APERTURE 3.8 ... cm ; DC Bias 0 ... kV
TUNED by, coarse MP ... fine MP Auto
RF 10.6 to 22.0 ... mHz, stable $\pm < 1 \times 10^{-6}$
Orb F 5.3 to 21.14 ... mHz
HARMONICS, RF/Orb F, used 1, 2
DEE - Gnd, max 50 kV, min gap 4 ... cm
STABILITY, (pk-pk noise)/(pk RF volt) ... $< 1 \times 10^{-3}$
ENERGY GAIN, max 200 ... kV/turn
RF PHASE, stable to ± ≤0.5 ... deg
RF POWER input, max 160 ... kW
FREQUENCY MODULATION, rate ... /s
modulator, type
beam pulse, width

VACUUM SYSTEM
OPERATING PRESSURE 2×10^{-6} ... Torr or mbar
PUMPS, No, Type, Size
6x2000 l/s turbo-molecular pumps

ION SOURCES
Hot filament for light ions and penning for heavy ions.

INJECTION SYSTEM

EXTRACTION SYSTEM Electrostatic deflector and magnetic channels (Active and Passive)

FACILITIES FOR RESEARCH
SHIELDED AREA, fixed 376 ... m^2 ; movable ... m^2
TARGET STATIONS 8 ... in 4 ... rooms
STATIONS served at same time, max 1
MAG SPECTROGRAPH, type
COMPUTER model
OTHER FACILITIES Radiotherapies Facility
Radiopharmaceuticals production, and Nuclear Medical diagnosis Facilities

CHARACTERISTIC BEAMS

PARTICLE	ENERGY (MeV) Goal	Achieved	CURRENT (pμA) Internal	External
P		8 -89		20
d		10-52.5		40
^{3}He		24-140		15
^{4}He		20-105		10
SECONDARY			(part/s)	

BEAM PROPERTIES

	MEASURED		CONDITIONS		
PULSE WIDTH	2.5 ... RF deg	20 ...	pμA of 30 ...	MeV	d ... Ions
PHASE EXC, max	... RF deg	...	pμA of ...	MeV	... Ions
EXTRACT eff	80 ... %	35 ...	pμA of 30 ...	MeV	d ... Ions
RESOL ΔE/E	... %	...	pμA of ...	MeV	... Ions
EMITTANCE					
(π mm. mrad) { ... axial / ... rad }		...	pμA of ...	MeV	... Ions

OPERATING PROGRAMS, time distribution
BASIC NUCLEAR PHYSICS ... SOLID STATES PHYSICS ...
BIOMEDICAL APPLICAT. 68% ... ISOTOPE PRODUCTIONS 32%

REFERENCES/NOTES

1] Y. Sato et al, Proc. of 9th Int. Conf. on Cyclotrons (1981) 597.
2] T. Yamada et al, Proc. of 11th Int. Conf. on Cyclotrons (1986) 61

PLAN VIEW OF FACILITY, NOTEWORTHY FEATURES, COMMENTS

ENTRY NO. CU45 **Date** June 17, 1992

Name of Machine Mini cyclotron Model-325 (Sumitomo Heavy Industry)

Institution Kyoto University Hospital

Address 54, Shogoin-Kawahara-cho, Sakyo-ku, Kyoto 606, JAPAN

Tel 81-75-751-3306 Telex Fax 81-75-751-3217 EMAIL

In Charge: Junji Konishi, MD Reported by: Yasuhiro Magata, PhD

HISTORY

MILESTONE DATES:

Design Model Tests

Construction 1982 First Beam Aug 1982

DESIGN/CONSTRUCTION BY:

in house other Sumitomo-CGR MeV

COST: Accelerator Facility

FUNDED BY: Ministry of Education, Japan

STATUS

STAFF: Machine

Scientists Engineers

Technicians 1 Students

Research (in house/external)

Scientists 1 / Engineers /

Technicians / Students /

BUDGET: Machine $200,000 Funded by Japan Ministry of

Research $35,000 Funded by Education, etc.

TIME DISTRIBUTION:

Basic Research (in house/external) 20 % /

Applied Program (in house/external) 70 % /

Development % Maintenance 10 %

MAGNET

POLE PARAMETERS:

Diameter 81 cm $R_{extract}$ 32.5 cm R_{inject} cm

HILL PARAMETERS: Gap (min) 7 cm B_{max} T

(@ AT) Gap (max) cm B_{min} T

VALLEY PARAMETERS: Gap (min) 12 cm B_{max} T

(@ AT) Gap (max) cm B_{min} T

AVERAGE FIELD: $< B >_{min}$ 1.76 T $< B >_{max}$ T

NUMBER OF SECTORS: compact/separated 4 /

sector angle deg. spiral (max) deg.

FIELD TRIMMING: Trim Coils

Harmonic Coils 4 pairs

Other

CURRENT: Main Coils 2450 Amps Stability

Trim Coils Amps Stability

Stored Energy (cryogenic) MJ

WEIGHT: Iron 13 tons Conductor 1 tons

ION ENERGY: Bending Limit E/A = q^2/A^2 MeV/u

Focussing Limit E/A = q/A MeV/u

ACCELERATION SYSTEM

FUNDAMENTAL ACCELERATION:

Description: AVF

No. of Gaps/turn dE/dn(max) MeV/q

Voltage(max) 27.50 kV ~~MV~~ Harmonic f_{rf}/f_{ion}

Freq .p. 26, d. 40 MHz Power in(max) MW

Stability: Phase Voltage

OTHER CAVITIES (Flattopping or otherwise):

Description:

Region of Influence: R_{min} cm R_{max} cm

No. of Gaps/turn dE/dn(max) MeV/q

Voltage(max) MV Harmonic f_{rf}/f_{ion}

Freq MHz Power in(max) MW

Stability: Phase Voltage

VACUUM SYSTEM

OPERATING PRESSURE: 2×10^{-5} torr

PUMPS: No. and type

1, diffusion pump 1300 l/sec

ION SOURCE(S)

	Type	Intensity (mA)	@	$\epsilon_n = \beta\gamma\epsilon$ (πmm mrad)	Ion Species
(a)	Livingstone-Jones				H_2^+, D_2^+
(b)					
(c)					
(d)					

INJECTION SYSTEM

Efficiency %

EXTRACTION SYSTEM

Efficiency %

CHARACTERISTIC BEAMS

	Accelerated Ions	E/A (MeV/u)	Current(part μA) Internal	External
(a)	p	15 MeV		50
(b)	d	8 MeV		50
(c)				
(d)				

	Secondary Particles	E (MeV)	part/sec
(a)			
(b)			
(c)			

EXTRACTED BEAM PROPERTIES:

For μA of MeV/u ions

$\Delta E/E$ % $\Delta\phi$ °rf

$\epsilon_n = \beta\gamma\epsilon$ x πmm mrad z πmm mrad

FACILITIES FOR RESEARCH

SHIELDED AREA: Fixed 110 m^2 Moveable m^2

Target Stations: 1 No. Served At Same Time: 1

MAGNETIC SPECTROMETERS:

OTHER FACILITIES:

REFERENCES/NOTES

(a)

(b)

PLAN VIEW OF FACILITY, COMMENTS

ENTRY NO. CU48 Date

Cyclotron Model CYCLONE-30

Institution DIICHI RADIOISOTOPE LABS. LTD

Address 453-1 SHIMOOKURA MATSUOMACHI SANBUGUN CHIBA

Tel 0479-86-4721 Telex DISOTOPE J28747

Fax 0479-86-5111 EMAIL

In Charge: Dr.K.NITTA Reported by:

HISTORY

MILESTONE DATES:

Installation 1990.11 First Beam 1991.3

DESIGN/CONSTRUCTION BY: I.B.A.

COST: Accelerator Facility

FUNDED BY:

STATUS

STAFF: Operators Technicians

BUDGET: Machine Funded by

TIME DISTRIBUTION: (e.g. basic research, isotope production, maintenance, etc.)

(a) IOSTOPE PRODUCTION 100 %

(b) %

(c) %

(d) %

(e) %

CHARACTERISTIC BEAMS

	Accelerated Ions	E/A (MeV/u)	Current(part μA) Internal	External
(a)	H^-	30		350
(b)				

1991 μA-hours on target: 1200000

FACILITIES

SHIELDED AREA: Fixed m^2 Moveable m^2

Target Stations: 4 No. Served At Same Time:

OTHER FACILITIES:

REFERENCES/NOTES

(a)

(b)

PLAN VIEW OF FACILITY, COMMENTS

ENTRY NO. CU49 Date

Cyclotron Model MC-40

Institution DIICHI RADIOISOTOPE LABS. LTD

Address 453-1 SHIMOOKURA MATSUOMACHI SANBUGUN CHIBA

Tel 0479-86-4721 Telex DISOTOPE J28747

Fax 0479-86-5111 EMAIL

In Charge: Dr.K.NITTA Reported by:

HISTORY

MILESTONE DATES:

Installation 1984.8 First Beam 1984.12

DESIGN/CONSTRUCTION BY: SCANDITRONIX

COST: Accelerator Facility

FUNDED BY:

STATUS

STAFF: Operators Technicians

BUDGET: Machine Funded by

TIME DISTRIBUTION: (e.g. basic research, isotope production, maintenance, etc.)

(a) IOSTOPE PRODUCTION 100 %

(b) %

(c) %

(d) %

(e) %

CHARACTERISTIC BEAMS

	Accelerated Ions	E/A (MeV/u)	Current(part μA) Internal	External
(a)	P	30	180	
(b)				

1991 μA-hours on target: 1080000

FACILITIES

SHIELDED AREA: Fixed m^2 Moveable m^2

Target Stations: 1 No. Served At Same Time:

OTHER FACILITIES:

REFERENCES/NOTES

(a)

(b)

PLAN VIEW OF FACILITY, COMMENTS

ENTRY NO. CU48 Date

Cyclotron Model CYCLONE-30

Institution DIICHI RADIOISOTOPE LABS. LTD

Address 453-1 SHIMOOKURA MATSUOMACHI SANBUGUN CHIBA

Tel 0479-86-4721 Telex DISOTOPE J28747

Fax 0479-86-5111 EMAIL

In Charge: Dr.K.NITTA Reported by:

HISTORY

MILESTONE DATES:

Installation 1990.11 First Beam 1991.3

DESIGN/CONSTRUCTION BY: I.B.A.

COST: Accelerator Facility

FUNDED BY:

STATUS

STAFF: Operators Technicians

BUDGET: Machine Funded by

TIME DISTRIBUTION: (e.g. basic research, isotope production, maintenance, etc.)

(a) IOSTOPE PRODUCTION 100 %

(b) %

(c) %

(d) %

(e) %

CHARACTERISTIC BEAMS

	Accelerated Ions	E/A (MeV/u)	Current(part μA) Internal	External
(a)	H^-	30		350
(b)				

1991 μA-hours on target: 1200000

FACILITIES

SHIELDED AREA: Fixed m^2 Moveable m^2

Target Stations: 4 No. Served At Same Time:

OTHER FACILITIES:

REFERENCES/NOTES

(a)

(b)

PLAN VIEW OF FACILITY, COMMENTS

ENTRY NO. CU49 Date

Cyclotron Model MC-40

Institution DIICHI RADIOISOTOPE LABS. LTD

Address 453-1 SHIMOOKURA MATSUOMACHI SANBUGUN CHIBA

Tel 0479-86-4721 Telex DISOTOPE J28747

Fax 0479-86-5111 EMAIL

In Charge: Dr.K.NITTA Reported by:

HISTORY

MILESTONE DATES:

Installation 1984.8 First Beam 1984.12

DESIGN/CONSTRUCTION BY: SCANDITRONIX

COST: Accelerator Facility

FUNDED BY:

STATUS

STAFF: Operators Technicians

BUDGET: Machine Funded by

TIME DISTRIBUTION: (e.g. basic research, isotope production, maintenance, etc.)

(a) IOSTOPE PRODUCTION 100 %

(b) %

(c) %

(d) %

(e) %

CHARACTERISTIC BEAMS

	Accelerated Ions	E/A (MeV/u)	Current(part μA) Internal	External
(a)	P	30	180	
(b)				

1991 μA-hours on target: 1080000

FACILITIES

SHIELDED AREA: Fixed m^2 Moveable m^2

Target Stations: 1 No. Served At Same Time:

OTHER FACILITIES:

REFERENCES/NOTES

(a)

(b)

PLAN VIEW OF FACILITY, COMMENTS

ENTRY NO. CU50 Date July 2/92

Cyclotron Model Cyclone 30

Institution Nihon Medi-Physics Co., Ltd. Hyogo Facility

Address 9-1, Techno Park, Sanda City, Hyogo Pref. Japan

Tel (0795)68-4771 Telex

Fax (0795)68-3071 EMAIL

In Charge: Y. Mori Reported by: Y. Mori

HISTORY

MILESTONE DATES:

Installation May 90 - Dec. 90 First Beam August 90

DESIGN/CONSTRUCTION BY: Ion Beam Applications

COST: Accelerator Facility $100M

FUNDED BY: Own company

STATUS

STAFF: Operators 10 Technicians 5

BUDGET: Machine Funded by

TIME DISTRIBUTION: (e.g. basic research, isotope production, maintenance, etc.)

(a) Isotope Production 85 %

(b) Maintenance 10 %

(c) Development 5 %

(d) %

(e) %

CHARACTERISTIC BEAMS

	Accelerated Ions	E/A (MeV/u)	Current(part μA) Internal	External
(a)	H^-	15-30	350 H^-	350P
(b)				

1991 μA-hours on target: 4.72×10^5

FACILITIES

SHIELDED AREA: Fixed 190 m² Moveable m²

Target Stations: 4 No. Served At Same Time: 2

OTHER FACILITIES:

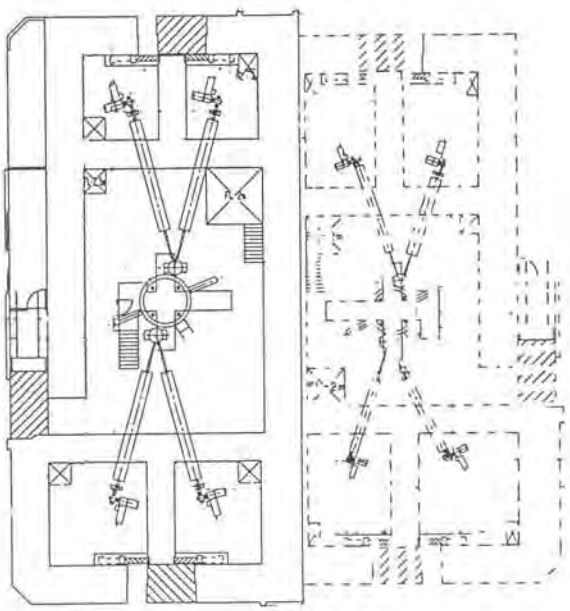
Production Area of Radiopharmaceuticals

REFERENCES/NOTES

(a)

(b)

PLAN VIEW OF FACILITY, COMMENTS



ENTRY NO. CU51 Date July 2/92

Cyclotron Model Cyclone 30

Institution Nihon Medi-Physics Co., Ltd. Hyogo Facility

Address 9-1, Techno Park, Sanda City, Hyogo Pref. Japan

Tel (0795)68-4771 Telex

Fax (0795)68-3071 EMAIL

In Charge: Y. Mori Reported by: Y. Mori

HISTORY

MILESTONE DATES:

Installation March 92 - Aug. 92 First Beam

DESIGN/CONSTRUCTION BY: Ion Beam Applications

COST: Accelerator Facility $100M

FUNDED BY: Own company

STATUS

STAFF: Operators Technicians

BUDGET: Machine Funded by

TIME DISTRIBUTION: (e.g. basic research, isotope production, maintenance, etc.)

(a) %

(b) %

(c) %

(d) %

(e) %

CHARACTERISTIC BEAMS

	Accelerated Ions	E/A (MeV/u)	Current(part μA) Internal	External
(a)	H^-	15-30	350 H^-	350P
(b)				

1991 μA-hours on target:

FACILITIES

SHIELDED AREA: Fixed 170 m² Moveable m²

Target Stations: 4 No. Served At Same Time: 2

OTHER FACILITIES:

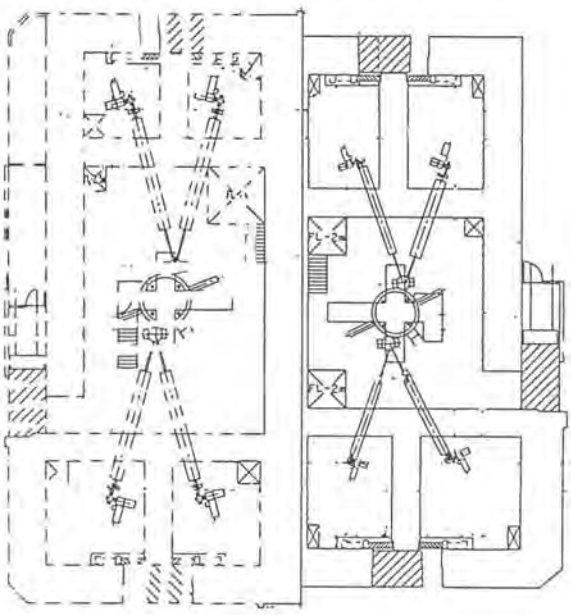
Production Area of Radiopharmaceuticals

REFERENCES/NOTES

(a)

(b)

PLAN VIEW OF FACILITY, COMMENTS



ENTRY NO. CU50 Date July 2/92

Cyclotron Model Cyclone 30

Institution Nihon Medi-Physics Co., Ltd. Hyogo Facility

Address 9-1, Techno Park, Sanda City, Hyogo Pref. Japan

Tel (0795)68-4771 Telex

Fax (0795)68-3071 EMAIL

In Charge: Y. Mori Reported by: Y. Mori

HISTORY

MILESTONE DATES:

Installation May 90 - Dec. 90 First Beam August 90

DESIGN/CONSTRUCTION BY: Ion Beam Applications

COST: Accelerator Facility $100M

FUNDED BY: Own company

STATUS

STAFF: Operators 10 Technicians 5

BUDGET: Machine Funded by

TIME DISTRIBUTION: (e.g. basic research, isotope production, maintenance, etc.)

(a) Isotope Production 85 %

(b) Maintenance 10 %

(c) Development 5 %

(d) %

(e) %

CHARACTERISTIC BEAMS

	Accelerated Ions	E/A (MeV/u)	Current(part μA) Internal	External
(a)	H^-	15-30	350 H^-	350P
(b)				

1991 μA-hours on target: 4.72×10^5

FACILITIES

SHIELDED AREA: Fixed 190 m² Moveable m²

Target Stations: 4 No. Served At Same Time: 2

OTHER FACILITIES:

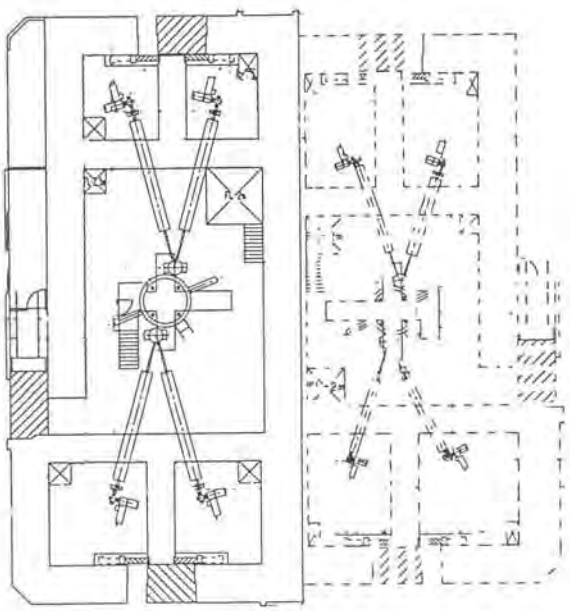
Production Area of Radiopharmaceuticals

REFERENCES/NOTES

(a)

(b)

PLAN VIEW OF FACILITY, COMMENTS



ENTRY NO. CU51 Date July 2/92

Cyclotron Model Cyclone 30

Institution Nihon Medi-Physics Co., Ltd. Hyogo Facility

Address 9-1, Techno Park, Sanda City, Hyogo Pref. Japan

Tel (0795)68-4771 Telex

Fax (0795)68-3071 EMAIL

In Charge: Y. Mori Reported by: Y. Mori

HISTORY

MILESTONE DATES:

Installation March 92 - Aug. 92 First Beam

DESIGN/CONSTRUCTION BY: Ion Beam Applications

COST: Accelerator Facility $100M

FUNDED BY: Own company

STATUS

STAFF: Operators Technicians

BUDGET: Machine Funded by

TIME DISTRIBUTION: (e.g. basic research, isotope production, maintenance, etc.)

(a) %

(b) %

(c) %

(d) %

(e) %

CHARACTERISTIC BEAMS

	Accelerated Ions	E/A (MeV/u)	Current(part μA) Internal	External
(a)	H^-	15-30	350 H^-	350P
(b)				

1991 μA-hours on target:

FACILITIES

SHIELDED AREA: Fixed 170 m² Moveable m²

Target Stations: 4 No. Served At Same Time: 2

OTHER FACILITIES:

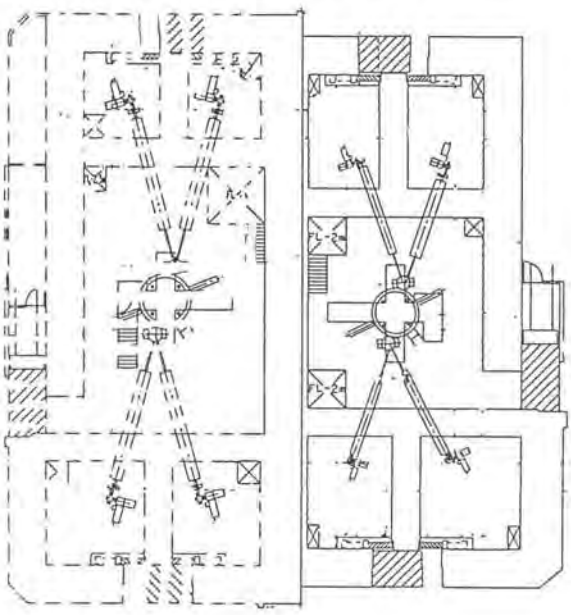
Production Area of Radiopharmaceuticals

REFERENCES/NOTES

(a)

(b)

PLAN VIEW OF FACILITY, COMMENTS



ENTRY NO. CU52 Date

Name of Machine Tohoku University Cyclotron

Institution Cyclotron and Radioisotope Center, Tohoku University

Address Aramaki-Aoba, 980 Sendai, Japan

Tel 022-263-5360 Telex 852246 THUCOM J Fax 022-263-5358 EMAIL SHINO (at) JPNTUVMϕ

In Charge: M. Fujioka Reported by: T. Shinozuka

HISTORY (CGR-MeV Model 680)

MILESTONE DATES:

Design ... Model Tests ...

Construction 1975-1977 First Beam December, 1977

DESIGN/CONSTRUCTION BY:

in house ... other ...CGR-MeV & SUMITOMO...

COST: Accelerator ... Facility 14 × 10^6

FUNDED BY: Japan Ministry of Education

STATUS

STAFF: Machine

Scientists 4 Engineers 1

Technicians 4 Students ...

Research (in house/external)

Scientists 11 / ~60 Engineers ... / ...

Technicians ... / ... Students ... / ...

BUDGET: Machine } 0.3 × 10^6 Funded by Japan Ministry

Research } ... Funded by ... of Education

TIME DISTRIBUTION:

Basic Research (in house/external) 10 % / 30 %

Applied Program (in house/external) 10 % / 30 %

Development 10 % Maintenance 10 %

MAGNET

POLE PARAMETERS:

Diameter 160 cm $R_{extract}$ 68 cm R_{inject} ... cm

HILL PARAMETERS: Gap (min) 13 cm B_{max} 1.9 T

(@ 0.26 × 10^6 AT) Gap (max) ... cm B_{min} ... T

VALLEY PARAMETERS: Gap (min) ... cm B_{max} 1.07 T

(@ ... AT) Gap (max) 28 cm B_{min} 1.07 T

AVERAGE FIELD: $< B >_{min}$ ... T $< B >_{max}$ 1.56 T

NUMBER OF SECTORS: compact/separated 4 / ...

sector angle ... deg. spiral (max) 50 deg.

FIELD TRIMMING: Trim Coils 8 circular

Harmonic Coils 2 pairs

Other ...

CURRENT: Main Coils 1000 Amps Stability 2×10^{-5}

Trim Coils 200 Amps Stability 2×10^{-5}

Stored Energy (cryogenic) ... MJ

WEIGHT: Iron 100 tons Conductor ...

ION ENERGY: Bending Limit E/A = 50 q^2/A^2 MeV/u

Focussing Limit E/A = ... q/A MeV/u

ACCELERATION SYSTEM

FUNDAMENTAL ACCELERATION:

Description: 2 Dees and 60 deg.

No. of Gaps/turn 4 dE/dn(max) 0.2 MeV/q

Voltage(max) 0.05 MV Harmonic f_{rf}/f_{ion} 2-4

Freq 20 ~ 40 MHz Power in(max) 0.12 MW

Stability: Phase ... Voltage 10^{-3}

OTHER CAVITIES (Flattopping or otherwise):

Description: ...

Region of Influence: R_{min} ... cm R_{max} ... cm

No. of Gaps/turn ... dE/dn(max) ... MeV/q

Voltage(max) ... MV Harmonic f_{rf}/f_{ion} ...

Freq ... MHz Power in(max) ... MW

Stability: Phase ... Voltage ...

VACUUM SYSTEM

OPERATING PRESSURE: 1×10^{-6} Torr

PUMPS: No. and type 2 × 8000 l/s Oil diffusion pumps

ION SOURCE(S)

	Type	Intensity (mA)	@	$\epsilon_n = \beta\gamma\epsilon$ (πmm mrad)	Ion Species
(a)	PIG(Hot)	0.1			P, d, ^{4}He, ^{3}He
(b)	PIG(Cold)				C, N, O
(c)					
(d)					

INJECTION SYSTEM

... Efficiency ... %

EXTRACTION SYSTEM

Detector: two magnetic channe Efficiency ~70 %

CHARACTERISTIC BEAMS

	Accelerated Ions	E/A (MeV/u)	Current(part μA) Internal	External
(a)	P(d)	3(5) ~ 40(25)	...	100
(b)	^{3}He	7 ~ 65	...	60
(c)	^{4}He	10 ~ 50	...	40
(d)	^{14}N	50 ~ 84	...	1

	Secondary Particles	E (MeV)	part/sec
(a)			
(b)			
(c)			

EXTRACTED BEAM PROPERTIES:

For 20 μA of 35 MeV/u P ions

ΔE/E 0.5 % Δφ ... °rf

$\epsilon_n = \beta\gamma\epsilon$ x 3.0 πmm mrad z 2.1 πmm mrad

FACILITIES FOR RESEARCH

SHIELDED AREA: Fixed 800 m^2 Moveable ... m^2

Target Stations: 10 No. Served At Same Time: 1

MAGNETIC SPECTROMETERS: ...

OTHER FACILITIES: Isotope Production positron tomograph, neutron TOF, On-line mass separator, beam choppers

REFERENCES/NOTES

(a) S.Morita et al., IEEE Trans.N.S. NS-26(1979)1930

(b) T.Shinozuka et al., Proc. Cys. Cont. (Caen) (1981) 117

PLAN VIEW OF FACILITY, COMMENTS

ENTRY NO. CU53 Date July 1/92
Cyclotron Model 480pF
Institution Nihon Medi-Physics Co.,Ltd. Chiba Facility
Address 3-1 Kitasode Sodegaura-shi, Japan
Tel (438)63-4771 Telex
Fax (438)63-3306 EMAIL 299-02
In Charge: Masaji Takahashi Reported by: Masaji Takahashi

HISTORY

MILESTONE DATES:
Installation Nov. 1984 First Beam June 1985
DESIGN/CONSTRUCTION BY: Sumitomo, CGR-MeV
COST: Accelerator Facility $60M
FUNDED BY:

STATUS

STAFF: Operators Technicians 16
BUDGET: Machine Funded by
TIME DISTRIBUTION: (e.g. basic research, isotope production, maintenance, etc.)
(a) Isotope Production 90 %
(b) Maintenance 10 %
(c) %
(d) %
(e) %

CHARACTERISTIC BEAMS

	Accelerated Ions	E/A (MeV/u)	Current(part μA) Internal	External
(a)	p	28	150	60
(b)				

1991 μA-hours on target: 3x10e5

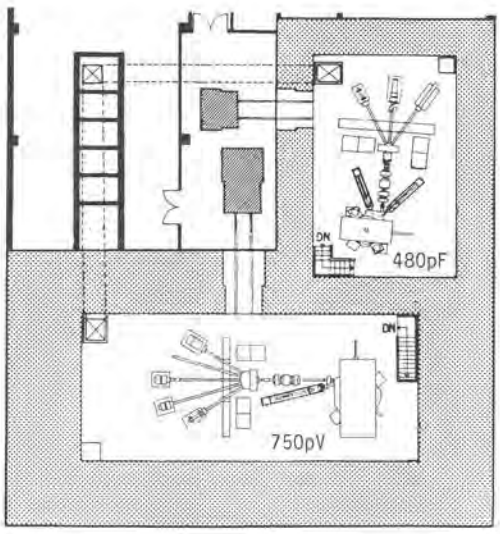
FACILITIES

SHIELDED AREA: Fixed 90 m^2 Moveable m^2
Target Stations: 5 No. Served At Same Time: 1
OTHER FACILITIES:

REFERENCES/NOTES

(a)
(b)

PLAN VIEW OF FACILITY, COMMENTS



ENTRY NO. CU54 Date July 1/92
Cyclotron Model 750pV
Institution Nihon Medi-Physics Co.,Ltd. Chiba Facility
Address 3-1 kitasode Sodegaura-shi, Japan
Tel (438)63-4771 Telex
Fax (438)63-3306 EMAIL 299-02
In Charge: Masaji Takahashi Reported by: Masaji Takahashi

HISTORY

MILESTONE DATES:
Installation Sep. 1985 First Beam June 1986
DESIGN/CONSTRUCTION BY: Sumitomo, CGR-MeV
COST: Accelerator Facility $60M
FUNDED BY:

STATUS

STAFF: Operators Technicians 16
BUDGET: Machine Funded by
TIME DISTRIBUTION: (e.g. basic research, isotope production, maintenance, etc.)
(a) Isotope Production 90 %
(b) Maintenance 10 %
(c) %
(d) %
(e) %

CHARACTERISTIC BEAMS

	Accelerated Ions	E/A (MeV/u)	Current(part μA) Internal	External
(a)	p	32	150	60
(b)	p	70		50

1991 μA-hours on target: 3x10e5

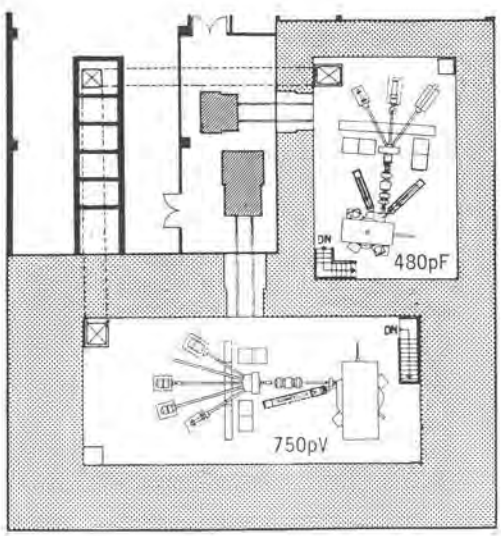
FACILITIES

SHIELDED AREA: Fixed 140 m^2 Moveable m^2
Target Stations: 6 No. Served At Same Time: 1
OTHER FACILITIES:

REFERENCES/NOTES

(a)
(b)

PLAN VIEW OF FACILITY, COMMENTS



ENTRY NO. CU53 Date July 1/92
Cyclotron Model 480pF
Institution Nihon Medi-Physics Co.,Ltd. Chiba Facility
Address 3-1 Kitasode Sodegaura-shi, Japan
Tel (438)63-4771 Telex
Fax (438)63-3306 EMAIL 299-02
In Charge: Masaji Takahashi Reported by: Masaji Takahashi

HISTORY

MILESTONE DATES:
Installation Nov. 1984 First Beam June 1985
DESIGN/CONSTRUCTION BY: Sumitomo, CGR-MeV
COST: Accelerator Facility $60M
FUNDED BY:

STATUS

STAFF: Operators Technicians 16
BUDGET: Machine Funded by
TIME DISTRIBUTION: (e.g. basic research, isotope production, maintenance, etc.)
(a) Isotope Production 90 %
(b) Maintenance 10 %
(c) %
(d) %
(e) %

CHARACTERISTIC BEAMS

	Accelerated Ions	E/A (MeV/u)	Current(part μA) Internal	External
(a)	p	28	150	60
(b)				

1991 μA-hours on target: 3x10e5

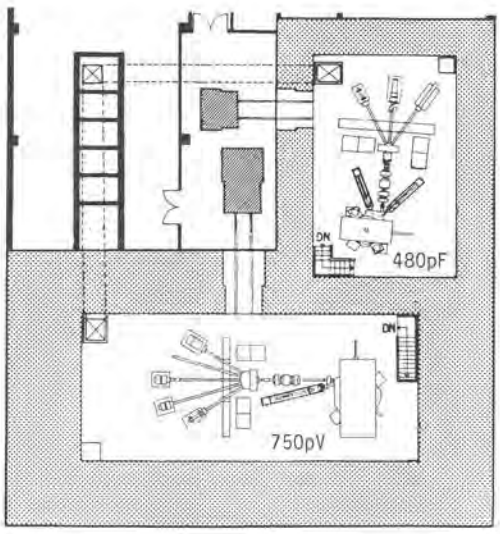
FACILITIES

SHIELDED AREA: Fixed 90 m^2 Moveable m^2
Target Stations: 5 No. Served At Same Time: 1
OTHER FACILITIES:

REFERENCES/NOTES

(a)
(b)

PLAN VIEW OF FACILITY, COMMENTS



ENTRY NO. CU54 Date July 1/92
Cyclotron Model 750pV
Institution Nihon Medi-Physics Co.,Ltd. Chiba Facility
Address 3-1 kitasode Sodegaura-shi, Japan
Tel (438)63-4771 Telex
Fax (438)63-3306 EMAIL 299-02
In Charge: Masaji Takahashi Reported by: Masaji Takahashi

HISTORY

MILESTONE DATES:
Installation Sep. 1985 First Beam June 1986
DESIGN/CONSTRUCTION BY: Sumitomo, CGR-MeV
COST: Accelerator Facility $60M
FUNDED BY:

STATUS

STAFF: Operators Technicians 16
BUDGET: Machine Funded by
TIME DISTRIBUTION: (e.g. basic research, isotope production, maintenance, etc.)
(a) Isotope Production 90 %
(b) Maintenance 10 %
(c) %
(d) %
(e) %

CHARACTERISTIC BEAMS

	Accelerated Ions	E/A (MeV/u)	Current(part μA) Internal	External
(a)	p	32	150	60
(b)	p	70		50

1991 μA-hours on target: 3x10e5

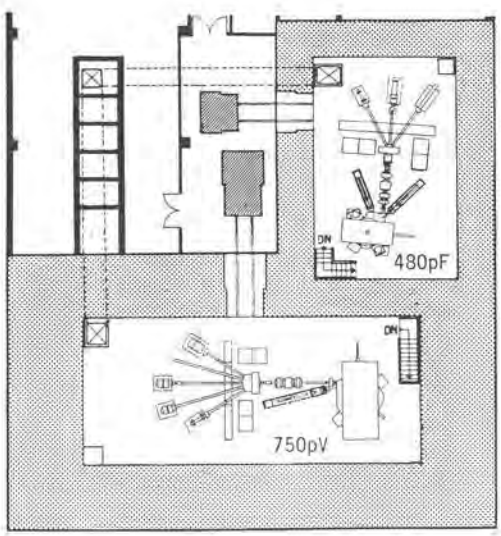
FACILITIES

SHIELDED AREA: Fixed 140 m^2 Moveable m^2
Target Stations: 6 No. Served At Same Time: 1
OTHER FACILITIES:

REFERENCES/NOTES

(a)
(b)

PLAN VIEW OF FACILITY, COMMENTS



ENTRY No. CU55

NAME OF MACHINE Meditron DATE June 1989

INSTITUTION Nihon Medi-Physics Co., Ltd. Takarazuka Facility

ADDRESS 4-2-1, Takatsukasa, Takarazuka, Hyogo, JAPAN 665

TEL 0797-71-4771 TELEX 5645669 NMP J

IN CHARGE H. Tobiki REPORTED BY Y. Tanaka

HISTORY AND STATUS

DESIGN, date ..... Model tests TCC CS-30

ENG DESIGN, date .....

CONSTRUCTION, date Aug.-Nov., 1974

FIRST BEAM, date (or goal) Nov., 1974

MAJOR ALTERATIONS Addition of Yoke Iron

New Magnet PS

COST, ACCELERATOR .....

COST, FACILITY, total .....

FUNDED BY Nihon Medi-Physics Co., Ltd.

ACCELERATOR STAFF, OPERATION AND DEVELOPMENT

SCIENTISTS ..... ENGINEERS 5

TECHNICIANS 7 CRAFTS .....

GRAD STUDENTS involved during year .....

OPERATED BY ..... Research staff or ..... Operators

OPERATION ..... hr/wk, On target ..... hr/wk

TIME DISTR. in house 100 %, Outside ..... %

BUDGET, op & dev .....

FUNDED BY .....

RESEARCH STAFF, not included above

USERS, in house ..... outside .....

GRAD STUDENTS involved during year .....

RESEARCH BUDGET, in house .....

FUNDED BY .....

MAGNET

POLE FACE, diameter (compact) 96. cm, R extraction 42. cm

R injection ..... cm

GAP, min ..... cm, Field ..... kG
max ..... cm, Field ..... kG } at .....

AVERAGE FIELD at R ext 17.5 kG } Ampere turns

B max/ <B> .....

NUMBER OF SECTORS { compact ..... / separated ..... } Spiral, max .. deg

SECTOR ANGLE (SSC) ..... deg

TRIMMING COILS .....

.....

CONDUCTOR, material and type .....

STORED ENERGY (cryogenic) ..... MJ

POWER : main coils 50 max, kW ; current stability 10-5

trimming coils ..... max, kW ; current stability .....

WEIGHT : Fe 20 tons ; coils ..... tons

COOLING system .....

ION ENERGY (bending limit) E/A = ... q^2/a^2 MeV/amu

(focusing limit) E/A = ... q^2/a^2 MeV/amu

ACCELERATION SYSTEM

DEES, number 2 ; angle 90 deg

BEAM APERTURE ..... cm ; DC Bias 1.5 kV

TUNED by, coarse ..... fine .....

RF ..... to ..... mHz, stable ± .....

Orb F ..... to ..... mHz

HARMONICS, RF/Orb F, used .....

DEE - Gnd, max ..... kV, min gap ..... cm

STABILITY, (pk-pk noise)/(pk RF volt) .....

ENERGY GAIN, max ..... kV/turn

RF PHASE, stable to ± ..... deg

RF POWER input, max ..... kW

FREQUENCY MODULATION, rate ..... /s

modulator, type .....

beam pulse, width .....

VACUUM SYSTEM

OPERATING PRESSURE 5×10^{-6} Torr or mbar

PUMPS, No, Type, Size 1 x 10" D.P.

1 x 4" D.P.

.....

ION SOURCES

PIG type

INJECTION SYSTEM

.....

EXTRACTION SYSTEM

.....

FACILITIES FOR RESEARCH

SHIELDED AREA, fixed 3 m² ; movable ..... m²

TARGET STATIONS 3 in 1 rooms

STATIONS served at same time, max .....

MAG SPECTROGRAPH, type .....

COMPUTER model .....

OTHER FACILITIES .....

.....

.....

CHARACTERISTIC BEAMS

PARTICLE	ENERGY (MeV) Goal	Achieved	CURRENT (pμA) Internal	External
proton	26	26	200	50
SECONDARY				(part/s)

BEAM PROPERTIES

	MEASURED		CONDITIONS
PULSE WIDTH	..... RF deg	..... pμA of .... MeV ... ions	
PHASE EXC, max	... RF deg	..... pμA of .... MeV ... ions	
EXTRACT eff	..... %	..... pμA of .... MeV ... ions	
RESOL ΔE/E	..... %	..... pμA of .... MeV ... ions	
EMITTANCE			
(π mm. mrad) { ... axial / ... rad }		..... pμA of ..... MeV ... ions	

OPERATING PROGRAMS, time distribution

BASIC NUCLEAR PHYSICS .. SOLID STATES PHYSICS ....

BIOMEDICAL APPLICAT. .... ISOTOPE PRODUCTIONS ....

.....

.....

REFERENCES/NOTES

PLAN VIEW OF FACILITY, NOTEWORTHY FEATURES, COMMENTS

ENTRY No. CU56

NAME OF MACHINE Physitron DATE June 1989

INSTITUTION Nihon Medi-Physics Co., Ltd, Takarazuka Facility

ADDRESS 4-2-1, Takatsukasa, Takarazuka, Hyogo, JAPAN 665

TEL 0797-71-4771 TELEX 5645669 NMP J

IN CHARGE H. Tobiki REPORTED BY Y. Tanaka

HISTORY AND STATUS

DESIGN, date ..... Model tests TCC CS-30

ENG DESIGN, date .....

CONSTRUCTION, date Jun.-Nov., 1981

FIRST BEAM, date (or goal) Dec., 1981

MAJOR ALTERATIONS Addition of Yoke Iron. Negative (P^-) Acceleration to Positive (P^+).

COST, ACCELERATOR .....

COST, FACILITY, total .....

FUNDED BY Nihon Medi-Physics Co., Ltd.

ACCELERATOR STAFF, OPERATION AND DEVELOPMENT

SCIENTISTS ..... ENGINEERS 5

TECHNICIANS 7 CRAFTS .....

GRAD STUDENTS involved during year .....

OPERATED BY ..... Research staff or ..... Operators

OPERATION ..... hr/wk, On target ..... hr/wk

TIME DISTR. in house 100 %, Outside ..... %

BUDGET, op & dev .....

FUNDED BY .....

RESEARCH STAFF, not included above

USERS, in house ..... outside .....

GRAD STUDENTS involved during year .....

RESEARCH BUDGET, in house .....

FUNDED BY .....

MAGNET

POLE FACE, diameter (compact) 96. cm, R extraction 42. cm

R injection ..... cm

GAP, min ..... cm, Field ..... kG
max ..... cm, Field ..... kG } at .....

AVERAGE FIELD at R ext 17.5 kG } Ampere turns

B max/ <B> .....

NUMBER OF SECTORS { compact ..... / separated ..... } Spiral, max .. deg

SECTOR ANGLE (SSC) ..... deg

TRIMMING COILS .....

.....

CONDUCTOR, material and type .....

STORED ENERGY (cryogenic) ..... MJ

POWER : main coils ..... max, kW ; current stability .....
trimming coils ..... max, kW ; current stability .....

WEIGHT : Fe ..... tons ; coils ..... tons

COOLING system .....

ION ENERGY (bending limit) E/A = ... q^2/a^2 MeV/amu
(focusing limit) E/A = ... q^2/a^2 MeV/amu

ACCELERATION SYSTEM

DEES, number 2 ; angle 90 deg

BEAM APERTURE ..... cm ; DC Bias 1.5 kV

TUNED by, coarse ..... fine .....

RF ..... to ..... mHz, stable ± .....

Orb F ..... to ..... mHz

HARMONICS, RF/Orb F, used .....

DEE - Gnd, max ..... kV, min gap ..... cm

STABILITY, (pk-pk noise)/(pk RF volt) .....

ENERGY GAIN, max ..... kV/turn

RF PHASE, stable to ± ..... deg

RF POWER input, max ..... kW

FREQUENCY MODULATION, rate ..... /s

modulator, type .....

beam pulse, width .....

VACUUM SYSTEM

OPERATING PRESSURE 5×10^{-6} Torr or mbar

PUMPS, No, Type, Size 1 x 10" D.P. (Aux. 1 x 10" D.P.)
1 x 4" D.P.

.....

ION SOURCES

PIG type

.....

INJECTION SYSTEM

.....

EXTRACTION SYSTEM

Deflector & Magnetic Channel

FACILITIES FOR RESEARCH

SHIELDED AREA, fixed ..... m^2 ; movable ..... m^2

TARGET STATIONS 3 in 1 rooms

STATIONS served at same time, max .....

MAG SPECTROGRAPH, type .....

COMPUTER model .....

OTHER FACILITIES .....

.....

.....

CHARACTERISTIC BEAMS

PARTICLE	ENERGY (MeV) Goal	Achieved	CURRENT (pμA) Internal	External
proton	26	26	200	50
SECONDARY				(part/s)

BEAM PROPERTIES

MEASURED	CONDITIONS
PULSE WIDTH ..... RF deg	..... pμ A of .... MeV ... ions
PHASE EXC, max ... RF deg	..... pμ A of .... MeV ... ions
EXTRACT eff ..... %	..... pμ A of .... MeV ... ions
RESOL ΔE/E ..... %	..... pμ A of .... MeV ... ions
EMITTANCE	
(π mm. mrad) { ... axial / .... rad }	..... pμA of ..... MeV ... ions

OPERATING PROGRAMS, time distribution

BASIC NUCLEAR PHYSICS .. SOLID STATES PHYSICS ....

BIOMEDICAL APPLICAT. .... ISOTOPE PRODUCTIONS ....

.....

.....

REFERENCES/NOTES

PLAN VIEW OF FACILITY, NOTEWORTHY FEATURES, COMMENTS

ENTRY No. CU59

NAME OF MACHINE IMS(IKAKEN) Cyclotron DATE 6-MAR-1989
INSTITUTION The Institute of Medical Science, The University of Tokyo
ADDRESS 4-6-1 Shirokanedai, Minato-ku, Tokyo 108, Japan
TEL 03 (446) 6771 TELEX
IN CHARGE Akira ITO REPORTED BY Akira ITO

HISTORY AND STATUS

DESIGN, date Model tests
ENG DESIGN, date TCC model CS-30
CONSTRUCTION, date 1971-1973
FIRST BEAM, date (or goal) Aug., 1973
MAJOR ALTERATIONS replacement of magnet coil (1976)
COST, ACCELERATOR about $1M(1973)
COST, FACILITY, total about $1M(1973)
FUNDED BY Japanese Government

ACCELERATOR STAFF, OPERATION AND DEVELOPMENT

SCIENTISTS 1 ENGINEERS
TECHNICIANS 3 CRAFTS
GRAD STUDENTS involved during year
OPERATED BY Research staff or Operators
OPERATION 50 hr/wk, On target 40 hr/wk
TIME DISTR. in house 90 %, Outside 10 %
BUDGET, op & dev $0.14M(1986)
FUNDED BY Japanese Government

RESEARCH STAFF, not included above

USERS, in house 6 outside 10
GRAD STUDENTS involved during year 0
RESEARCH BUDGET, in house
FUNDED BY

MAGNET

POLE FACE, diameter (compact) 96 cm, R extraction 42 cm
R injection cm
GAP, min 5 cm, Field 20 kG
max 10 cm, Field 12 kG
at 0.2×10^6 Ampere turns
AVERAGE FIELD at R ext 16 kG
B max/ <B> 1.25
NUMBER OF SECTORS compact 3 / separated — Spiral, max 60 deg
SECTOR ANGLE (SSC) deg
TRIMMING COILS 2 (inner & outer) /sec
CONDUCTOR, material and type
STORED ENERGY (cryogenic) MJ
POWER: main coils 60 max, kW ; current stability 10^{-5}
trimming coils max, kW ; current stability
WEIGHT: Fe 23 tons ; coils 1 tons
COOLING system demineralized water
ION ENERGY (bending limit) E/A = q^2/a^2 MeV/amu
(focusing limit) E/A = 30 q^2/a^2 MeV/amu

ACCELERATION SYSTEM

DEES, number 2 ; angle 90 deg
BEAM APERTURE 4 cm ; DC Bias -1.5 kV
TUNED by, coarse short bar fine V.C.
RF 14 to 26 mHz, stable ± $10/10^6$
Orb F to mHz
HARMONICS, RF/Orb F, used
DEE - Gnd, max 30 kV, min gap 1 cm
STABILITY, (pk-pk noise)/(pk RF volt) 0.1%
ENERGY GAIN, max kV/turn
RF PHASE, stable to ± 5 deg
RF POWER input, max 75 kW
FREQUENCY MODULATION, rate /s
modulator, type
beam pulse, width

VACUUM SYSTEM

OPERATING PRESSURE less than 10^{-5} Torr or mbar
PUMPS, No, Type, Size One diffusion pomp (30 cm dia)

ION SOURCES

PIG type

INJECTION SYSTEM

Internal only

EXTRACTION SYSTEM

DC deflector + mag-channel

FACILITIES FOR RESEARCH

SHIELDED AREA, fixed 330 m² ; movable 0 m²
TARGET STATIONS 6 in 4 rooms
STATIONS served at same time, max 1
MAG SPECTROGRAPH, type
COMPUTER model VAX 11/750, PDP-11/34 & Lecroy 3500
OTHER FACILITIES Isotopes production
Neutron therapy
PIXE & Proton CT / Microbeam

CHARACTERISTIC BEAMS

PARTICLE	ENERGY (MeV) Goal	Achieved	CURRENT (pμA) Internal	External
P		26		70
d		14		150
^{3}He		38		70
α		28		50

SECONDARY Be (d,n) (part/s) $\bar{E}n$=6 MeV

BEAM PROPERTIES

	MEASURED		CONDITIONS
PULSE WIDTH	10	RF deg	1 pμA of 28 MeV α ions
PHASE EXC, max		RF deg	pμA of MeV ions
EXTRACT eff	60	%	100 pμA of 14 MeV d ions
RESOL ΔE/E	1	%	1 pμA of 14 MeV d ions

EMITTANCE (π mm. mrad) {10. axial / 14. rad} 1 pμA of 18 MeV d ions

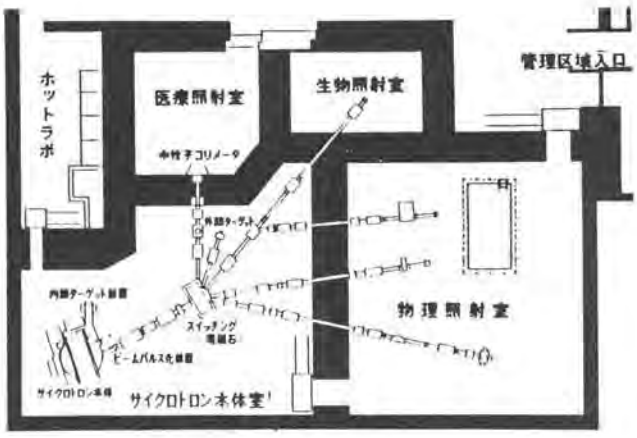
OPERATING PROGRAMS, time distribution

BASIC NUCLEAR PHYSICS SOLID STATES PHYSICS 10%
BIOMEDICAL APPLICAT. 60% ISOTOPE PRODUCTIONS 20%
Development 10%

REFERENCES/NOTES

1) Y. Yoshida et al. Nucl. Instr. & Meth., vol. 138, pp.579-788 (1976).

PLAN VIEW OF FACILITY, NOTEWORTHY FEATURES, COMMENTS



ENTRY NO. CU61 Date

Cyclotron Model: HC 168 Nippon Telegraph & Telephone Co.
Institution: Electrical Communications Laboratories
Address: Tokai, Ibaraki 319-11, Japan
Tel: +81 292 87 7586 Telex: 3632650 IECL J
Fax: +81 292 87 7875 EMAIL:
In Charge: T. Shigematsu Reported by: H. Yonezawa

HISTORY

MILESTONE DATES:
Installation: Oct. 1984 First Beam: Oct. 1984
DESIGN/CONSTRUCTION BY: NTT Electrical Communications Labs
COST: Accelerator: Facility:
FUNDED BY:

STATUS

STAFF: Operators: Technicians:
BUDGET: Machine: Funded by:
TIME DISTRIBUTION: (e.g. basic research, isotope production, maintenance, etc.)

(a)	CPAA	50 %
(b)	RBS, PIXE	40 %
(c)	Micro-beam	10 %
(d)		%
(e)		%

CHARACTERISTIC BEAMS

	Accelerated Ions	E/A (MeV/u)	Current(part μA) Internal	External
(a)	p, d	1.8-16, 3.6-8	50,	20
(b)	^{3}He, ^{4}He	5.4-21, 6.6-16	10,	10

1991 μA-hours on target:

FACILITIES

SHIELDED AREA: Fixed 70 m² Moveable m²
Target Stations: No. Served At Same Time:
OTHER FACILITIES:

REFERENCES/NOTES

(a) H. Yonezawa, 11th Cyclotron Conf., 1986 p.646
(b)

PLAN VIEW OF FACILITY, COMMENTS

ENTRY NO. CU62 Date

Cyclotron Model: JSW 1710
Institution: NRIM (National Research Inst. Metals)
Address: 1-2-1 Sengen, Tsukuba, Ibaraki 305, JAPAN
Tel: (0298) 51-6311 Telex:
Fax: (0298) 51-4556 EMAIL:
In Charge: J. Nagakawa Reported by: J. Nagakawa

HISTORY

MILESTONE DATES:
Installation: April 85 - June 86 First Beam: June 1986
DESIGN/CONSTRUCTION BY: JSW/JSW
COST: Accelerator: $1 750 000 Facility: $750 000
FUNDED BY: Science and Tchnology Agency, JPN Gov.

STATUS

STAFF: Operators: 0 Technicians: 0
BUDGET: Machine: $200 000 Funded by: STA
TIME DISTRIBUTION: (e.g. basic research, isotope production, maintenance, etc.)

(a)	Basic Research (Materials Science)	80 %
(b)	Maintenance	20 %
(c)		%
(d)		%
(e)		%

CHARACTERISTIC BEAMS

	Accelerated Ions	E/A (MeV/u)	Current(part μA) Internal	External
(a)	p/d	17/10	50 p/d	50 p/d
(b)	He-3/He-4	26/20	20	20

1991 μA-hours on target: 1.75 x 10e3

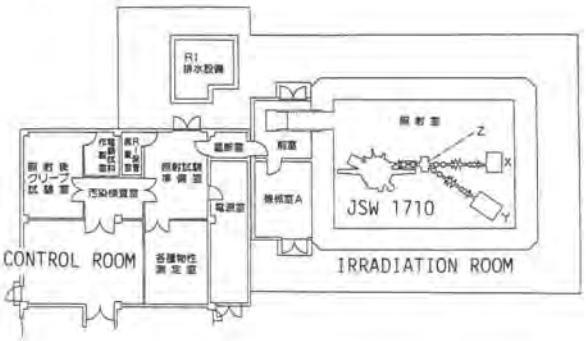
FACILITIES

SHIELDED AREA: Fixed 90 m² Moveable 0 m²
Target Stations: 1 No. Served At Same Time: 1
OTHER FACILITIES:

REFERENCES/NOTES

(a) Proc. 11th Int'l. Conf. on Cyclotron, 1986, p.571
(b) (H. Shiraishi et al.)

PLAN VIEW OF FACILITY, COMMENTS



ENTRY NO. CU61 Date

Cyclotron Model: HC 168 Nippon Telegraph & Telephone Co.
Institution: Electrical Communications Laboratories
Address: Tokai, Ibaraki 319-11, Japan
Tel: +81 292 87 7586 Telex: 3632650 IECL J
Fax: +81 292 87 7875 EMAIL:
In Charge: T. Shigematsu Reported by: H. Yonezawa

HISTORY

MILESTONE DATES:
Installation: Oct. 1984 First Beam: Oct. 1984
DESIGN/CONSTRUCTION BY: NTT Electrical Communications Labs
COST: Accelerator: Facility:
FUNDED BY:

STATUS

STAFF: Operators: Technicians:
BUDGET: Machine: Funded by:
TIME DISTRIBUTION: (e.g. basic research, isotope production, maintenance, etc.)

(a)	CPAA	50 %
(b)	RBS, PIXE	40 %
(c)	Micro-beam	10 %
(d)		%
(e)		%

CHARACTERISTIC BEAMS

	Accelerated Ions	E/A (MeV/u)	Current(part μA) Internal	External
(a)	p, d	1.8-16, 3.6-8	50,	20
(b)	^{3}He, ^{4}He	5.4-21, 6.6-16	10,	10

1991 μA-hours on target:

FACILITIES

SHIELDED AREA: Fixed 70 m² Moveable m²
Target Stations: No. Served At Same Time:
OTHER FACILITIES:

REFERENCES/NOTES

(a) H. Yonezawa, 11th Cyclotron Conf., 1986 p.646
(b)

PLAN VIEW OF FACILITY, COMMENTS

ENTRY NO. CU62 Date

Cyclotron Model: JSW 1710
Institution: NRIM (National Research Inst. Metals)
Address: 1-2-1 Sengen, Tsukuba, Ibaraki 305, JAPAN
Tel: (0298) 51-6311 Telex:
Fax: (0298) 51-4556 EMAIL:
In Charge: J. Nagakawa Reported by: J. Nagakawa

HISTORY

MILESTONE DATES:
Installation: April 85 - June 86 First Beam: June 1986
DESIGN/CONSTRUCTION BY: JSW/JSW
COST: Accelerator: $1 750 000 Facility: $750 000
FUNDED BY: Science and Tchnology Agency, JPN Gov.

STATUS

STAFF: Operators: 0 Technicians: 0
BUDGET: Machine: $200 000 Funded by: STA
TIME DISTRIBUTION: (e.g. basic research, isotope production, maintenance, etc.)

(a)	Basic Research (Materials Science)	80 %
(b)	Maintenance	20 %
(c)		%
(d)		%
(e)		%

CHARACTERISTIC BEAMS

	Accelerated Ions	E/A (MeV/u)	Current(part μA) Internal	External
(a)	p/d	17/10	50 p/d	50 p/d
(b)	He-3/He-4	26/20	20	20

1991 μA-hours on target: 1.75 x 10e3

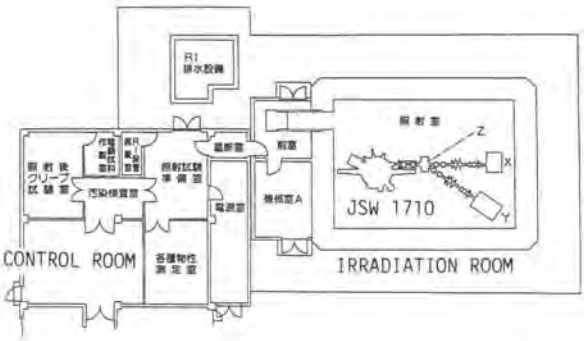
FACILITIES

SHIELDED AREA: Fixed 90 m² Moveable 0 m²
Target Stations: 1 No. Served At Same Time: 1
OTHER FACILITIES:

REFERENCES/NOTES

(a) Proc. 11th Int'l. Conf. on Cyclotron, 1986, p.571
(b) (H. Shiraishi et al.)

PLAN VIEW OF FACILITY, COMMENTS



ENTRY NO. CU63 Date 23/7/92

Cyclotron Model OSCAR

Institution NKK Corporation

Address 2-1 SUEHIRO-CHO, TSURUMI-KU, YOKOHAMA 230 JAPAN

Tel 81-45-505-7537 Telex

Fax 81-45-505-7553 EMAIL

In Charge: Reported by: MICHIO SHIMIZU

HISTORY

MILESTONE DATES:

Installation JUNE 1991 First Beam JULY 1991

DESIGN/CONSTRUCTION BY: OXFORD INSTRUMENTS

COST: Accelerator Facility

FUNDED BY:

STATUS

STAFF: Operators 5 Technicians 3

BUDGET: Machine Funded by

TIME DISTRIBUTION: (e.g. basic research, isotope production, maintenance, etc.)

(a) Development of PET chemistry modules 90 %

(b) Neutron radio graphy (1993 -) 0 %

(c) Maintenance 10 %

(d) %

(e) %

CHARACTERISTIC BEAMS

Accelerated Ions	E/A (MeV/u)	Current(part μA) Internal	External
(a) H	12	100	100
(b)			

1991 μA-hours on target: 10,000

FACILITIES

SHIELDED AREA: Fixed 72 m² Moveable - m²

Target Stations: 1 No. Served At Same Time: 1

OTHER FACILITIES: 2

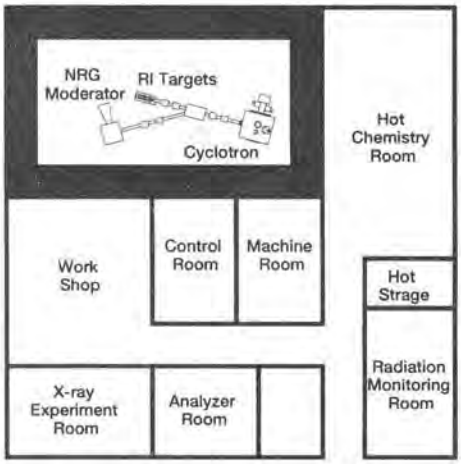
Hot chemistry room 80 m

REFERENCES/NOTES

(a)

(b)

PLAN VIEW OF FACILITY, COMMENTS



ENTRY NO. CU64 Date June 12, 1992

Cyclotron Model Scanditronix MC17F

Institution PET-Center, University Hospital

Address Oostersingel 59 NL-9713 EZ Groningen, Netherlands

Tel +.31.50.61.3311 Telex 53942 azgn NL

Fax +.31.50.696619 EMAIL CIL @ KVI.NL

In Charge: W. Vaalburg Reported by: A.M.J. Paans

HISTORY

MILESTONE DATES:

Installation 1991 First Beam March 1991

DESIGN/CONSTRUCTION BY: Scanditronix AB

COST: Accelerator 4 MDEL Facility 12 MDEL

FUNDED BY: University Hospital + University of Groningen

STATUS

STAFF: Operators Technicians

BUDGET: Machine Funded by

TIME DISTRIBUTION: (e.g. basic research, isotope production, maintenance, etc.)

(a) Isotope production (11C, 13N, 15O, 18F) 100 %

(b) %

(c) %

(d) %

(e) %

CHARACTERISTIC BEAMS

Accelerated Ions	E/A (MeV/u)	Current(part μA) Internal	External
(a) p	17 MeV	74	65
(b) d	8,5 MeV	78	50

1991 μA-hours on target: 4100 μAh

FACILITIES

SHIELDED AREA: Fixed 55 m² Moveable m²

Target Stations: 1 No. Served At Same Time: 1

OTHER FACILITIES: 1 target station with 8 target exchanger

Radiochemical Laboratory

Siemens ECAT 951/31 Positron camera

REFERENCES/NOTES

(a)

(b)

PLAN VIEW OF FACILITY, COMMENTS

ENTRY NO. CU63 Date 23/7/92

Cyclotron Model OSCAR

Institution NKK Corporation

Address 2-1 SUEHIRO-CHO, TSURUMI-KU, YOKOHAMA 230 JAPAN

Tel 81-45-505-7537 Telex

Fax 81-45-505-7553 EMAIL

In Charge: Reported by: MICHIO SHIMIZU

HISTORY

MILESTONE DATES:

Installation JUNE 1991 First Beam JULY 1991

DESIGN/CONSTRUCTION BY: OXFORD INSTRUMENTS

COST: Accelerator Facility

FUNDED BY:

STATUS

STAFF: Operators 5 Technicians 3

BUDGET: Machine Funded by

TIME DISTRIBUTION: (e.g. basic research, isotope production, maintenance, etc.)

(a) Development of PET chemistry modules 90 %

(b) Neutron radio graphy (1993 -) 0 %

(c) Maintenance 10 %

(d) %

(e) %

CHARACTERISTIC BEAMS

Accelerated Ions	E/A (MeV/u)	Current(part μA) Internal	External
(a) H	12	100	100
(b)			

1991 μA-hours on target: 10,000

FACILITIES

SHIELDED AREA: Fixed 72 m² Moveable - m²

Target Stations: 1 No. Served At Same Time: 1

OTHER FACILITIES: 2

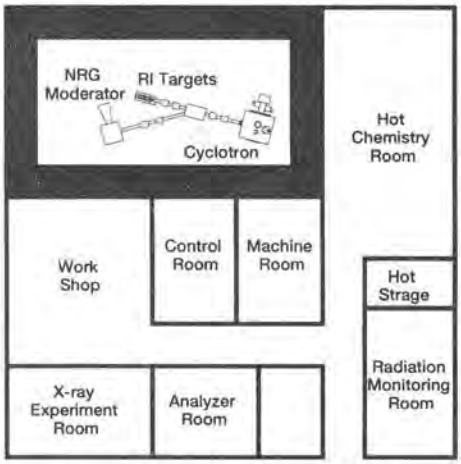
Hot chemistry room 80 m

REFERENCES/NOTES

(a)

(b)

PLAN VIEW OF FACILITY, COMMENTS



ENTRY NO. CU64 Date June 12, 1992

Cyclotron Model Scanditronix MC17F

Institution PET-Center, University Hospital

Address Oostersingel 59 NL-9713 EZ Groningen, Netherlands

Tel +.31.50.61.3311 Telex 53942 azgn NL

Fax +.31.50.696619 EMAIL CIL @ KVI.NL

In Charge: W. Vaalburg Reported by: A.M.J. Paans

HISTORY

MILESTONE DATES:

Installation 1991 First Beam March 1991

DESIGN/CONSTRUCTION BY: Scanditronix AB

COST: Accelerator 4 MDEL Facility 12 MDEL

FUNDED BY: University Hospital + University of Groningen

STATUS

STAFF: Operators Technicians

BUDGET: Machine Funded by

TIME DISTRIBUTION: (e.g. basic research, isotope production, maintenance, etc.)

(a) Isotope production (11C, 13N, 15O, 18F) 100 %

(b) %

(c) %

(d) %

(e) %

CHARACTERISTIC BEAMS

Accelerated Ions	E/A (MeV/u)	Current(part μA) Internal	External
(a) p	17 MeV	74	65
(b) d	8,5 MeV	78	50

1991 μA-hours on target: 4100 μAh

FACILITIES

SHIELDED AREA: Fixed 55 m² Moveable m²

Target Stations: 1 No. Served At Same Time: 1

OTHER FACILITIES: 1 target station with 8 target exchanger

Radiochemical Laboratory

Siemens ECAT 951/31 Positron camera

REFERENCES/NOTES

(a)

(b)

PLAN VIEW OF FACILITY, COMMENTS

ENTRY No. CU65

NAME OF MACHINE ---- DATE September 1986

INSTITUTION Mallinckrodt Diagnostics (Holland) B.V. (until Jan. 1979 Philips Duphar B.V.)

ADDRESS P.O. Box 3 1755 ZG Petten NETHERLANDS

TEL 31(0)2246-7010 TELEX 57326 CILPN nl TELEFAX 31(0)2246 7008

IN CHARGE B. Reiff REPORTED BY J.G. van der Baan

HISTORY AND STATUS

DESIGN, date Model tests

ENG DESIGN, date

CONSTRUCTION, date 1963-1964

FIRST BEAM, date (or goal) protons, June 1964

MAJOR ALTERATIONS 1966

multi particle, machine

COST, ACCELERATOR $ 1. x 10^6

COST, FACILITY, total

FUNDED BY privately Philips Duphar B.V.

ACCELERATOR STAFF, OPERATION AND DEVELOPMENT

SCIENTISTS 1 ENGINEERS 1

TECHNICIANS 5 CRAFTS 10

GRAD STUDENTS involved during year -

OPERATED BY - Research staff or 10 Operators

OPERATION 132 hr/wk, On target 130 hr/wk

TIME DISTR. in house 100 %, Outside - %

BUDGET, op & dev -

FUNDED BY privately

RESEARCH STAFF, not included above

USERS, in house - outside -

GRAD STUDENTS involved during year -

RESEARCH BUDGET, in house -

FUNDED BY -

MAGNET

POLE FACE, diameter (compact) 140 cm, R extraction 57. cm

R injection - cm

GAP, min 16. cm, Field kG
max 30. cm, Field kG
at 0.503 10^6 Ampere turns

AVERAGE FIELD at R ext 15.3 kG

B max/ <B>

NUMBER OF SECTORS compact 3 / separated - Spiral, max 48 deg

SECTOR ANGLE (SSC) deg

TRIMMING COILS

CONDUCTOR, material and type Al

STORED ENERGY (cryogenic) MJ

POWER : main coils 160 max, kW ; current stability

trimming coils max, kW ; current stability

WEIGHT : Fe 100 tons ; coils tons

COOLING system closed circuit dem water

ION ENERGY (bending limit) E/A = 30 q^2/a^2 MeV/amu

(focusing limit) E/A = q^2/a^2 MeV/amu

ACCELERATION SYSTEM

DEES, number 1 ; angle 180 deg

BEAM APERTURE 3.5 cm ; DC Bias 0.75 kV

TUNED by, coarse MS fine trim cap

RF 10 to 21 mHz, stable ± 5×10^{-6}

Orb F 7. to 21 mHz

HARMONICS, RF/Orb F, used 1st or 3rd

DEE - Gnd, max 50 kV, min gap cm

STABILITY, (pk-pk noise)/(pk RF volt) 10^{-3}

ENERGY GAIN, max 100 kV/turn

RF PHASE, stable to ± deg

RF POWER input, max 90 kW

FREQUENCY MODULATION, rate /s

modulator, type

beam pulse, width

VACUUM SYSTEM

OPERATING PRESSURE 5-10 Torr or mbar

PUMPS, No, Type, Size 1 Oil diff.-pump 12000 l/s

ION SOURCES

INTERVAL. PIG, 800V, 8A

Filament 8 V, 1000 A

INJECTION SYSTEM

EXTRACTION SYSTEM

none

FACILITIES FOR RESEARCH

SHIELDED AREA, fixed - m^3 ; movable - m^3

TARGET STATIONS - in - rooms -

STATIONS served at same time, max -

MAG SPECTROGRAPH, type -

COMPUTER model -

OTHER FACILITIES none

CHARACTERISTIC BEAMS

PARTICLE	ENERGY (MeV) Goal	Achieved	CURRENT (pμA) Internal	External
H 1	28	30	400	
H 2	15	16	400	
He3	45	48	-	-
He4	30	32	200	-
SECONDARY			(part/s)	

BEAM PROPERTIES

	MEASURED	CONDITIONS
PULSE WIDTH	RF deg	pμ A of MeV ions
PHASE EXC, max	RF deg	pμ A of MeV ions
EXTRACT eff	%	pμ A of MeV ions
RESOL ΔE/E	%	pμ A of MeV ions
EMITTANCE		
(π mm. mrad) axial / rad		pμA of MeV ions

OPERATING PROGRAMS, time distribution

BASIC NUCLEAR PHYSICS ..

SOLID STATES PHYSICS ...

BIOMEDICAL APPLICAT. ....

ISOTOPE PRODUCTIONS 99%.

Development 1%

REFERENCES/NOTES

Hagedoorn, H.L. and Verster, M.F.C.
CERN report 63-19(1963) pp 286-290

PLAN VIEW OF FACILITY, NOTEWORTHY FEATURES, COMMENTS

Accelerator exclusively used for radionuclide production with protons.

ENTRY NO. CU67 Date

Cyclotron Model MC 35

Institution Dept Phys. Univ. of Oslo

Address Blindern, Norway

Tel 02 856428 Telex

Fax 02 856422 EMAIL sveinm@fys.uio.no

In Charge: S. Messelt Reported by: S. Messelt

HISTORY

MILESTONE DATES:

Installation 1978 First Beam 1979

DESIGN/CONSTRUCTION BY: Scanditronix

COST: Accelerator 6 M NOK Facility 5 M NOK

FUNDED BY: University and Research Council

STATUS

STAFF: Operators 2 Technicians 2

BUDGET: Machine 1 M NOK Funded by Univ. Res.Coun.

TIME DISTRIBUTION: (e.g. basic research, isotope production, maintenance, etc.)

(a) Basic research 70 %

(b) Isotope prod. 20 %

(c) Maintenance 10 %

(d) %

(e) %

CHARACTERISTIC BEAMS

	Accelerated Ions	E/A (MeV/u)	Current(part μA) Internal	External
(a)	p	10-35		
(b)	d, 3He, 4He			

1991 μA-hours on target: 2200

FACILITIES

SHIELDED AREA: Fixed 150 m² Moveable m²

Target Stations: 4 No. Served At Same Time: 1

OTHER FACILITIES:

REFERENCES/NOTES

(a) Annual Report, Nucl. Phys. Group, 1991

(b)

PLAN VIEW OF FACILITY, COMMENTS

ENTRY NO. CU69 Date

Cyclotron Model TCC Model CS-30

Institution King Faisal Specialist Hospital & Research Centre

Address P.O. Box 3354, Riyadh 11211, Saudi Arabia

Tel 464-7272 Ext. 1770 Telex 401050 RYSPEC SJ

Fax 0-966-1-441-4839 EMAIL

In Charge: Edward D. Carroll Reported by: Salman Miliebari

HISTORY

MILESTONE DATES:

Installation Factory Test/1977 First Beam March October 1981

DESIGN/CONSTRUCTION BY: The Cyclotron Corporation

COST: Accelerator - Facility -

FUNDED BY: Government of Saudi Arabia

STATUS

STAFF: Operators 4 Technicians 1

BUDGET: Machine - Funded by -

TIME DISTRIBUTION: (e.g. basic research, isotope production, maintenance, etc.)

(a) Isotope Production 75 %

(b) Neutron Therapy 20 %

(c) Maintenance 5 %

(d) %

(e) %

CHARACTERISTIC BEAMS

	Accelerated Ions	E/A (MeV/u)	Current(part μA) Internal	External
(a)	P	26	200	60
(b)	d	7	300	100
	3He	13	135	60
	4He	7	90	50

1991 μA-hours on target:

FACILITIES

SHIELDED AREA: Fixed 190 m² Moveable 0 m²

Target Stations: 9 No. Served At Same Time: 1

OTHER FACILITIES:

Isotope production

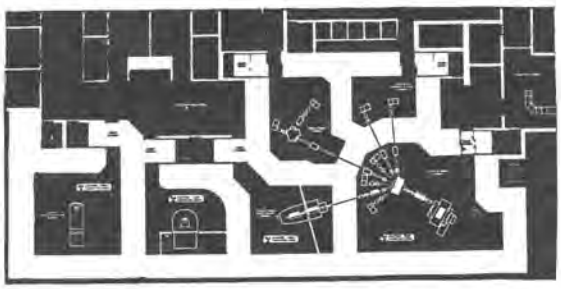
Isocentric neutron production

REFERENCES/NOTES

(a) IEEE Trans Nucl. Sci. NS-14, 70-71 (1967)

(b) " " " " NS-16, 500-503 (1969)

PLAN VIEW OF FACILITY, COMMENTS



ENTRY NO. CU67 Date

Cyclotron Model MC 35

Institution Dept Phys. Univ. of Oslo

Address Blindern, Norway

Tel 02 856428 Telex

Fax 02 856422 EMAIL sveinm@fys.uio.no

In Charge: S. Messelt Reported by: S. Messelt

HISTORY

MILESTONE DATES:

Installation 1978 First Beam 1979

DESIGN/CONSTRUCTION BY: Scanditronix

COST: Accelerator 6 M NOK Facility 5 M NOK

FUNDED BY: University and Research Council

STATUS

STAFF: Operators 2 Technicians 2

BUDGET: Machine 1 M NOK Funded by Univ. Res.Coun.

TIME DISTRIBUTION: (e.g. basic research, isotope production, maintenance, etc.)

(a) Basic research 70 %

(b) Isotope prod. 20 %

(c) Maintenance 10 %

(d) %

(e) %

CHARACTERISTIC BEAMS

	Accelerated Ions	E/A (MeV/u)	Current(part μA) Internal	External
(a)	p	10-35		
(b)	d, 3He, 4He			

1991 μA-hours on target: 2200

FACILITIES

SHIELDED AREA: Fixed 150 m² Moveable m²

Target Stations: 4 No. Served At Same Time: 1

OTHER FACILITIES:

REFERENCES/NOTES

(a) Annual Report, Nucl. Phys. Group, 1991

(b)

PLAN VIEW OF FACILITY, COMMENTS

ENTRY NO. CU69 Date

Cyclotron Model TCC Model CS-30

Institution King Faisal Specialist Hospital & Research Centre

Address P.O. Box 3354, Riyadh 11211, Saudi Arabia

Tel 464-7272 Ext. 1770 Telex 401050 RYSPEC SJ

Fax 0-966-1-441-4839 EMAIL

In Charge: Edward D. Carroll Reported by: Salman Miliebari

HISTORY

MILESTONE DATES:

Installation Factory Test/1977 First Beam March October 1981

DESIGN/CONSTRUCTION BY: The Cyclotron Corporation

COST: Accelerator - Facility -

FUNDED BY: Government of Saudi Arabia

STATUS

STAFF: Operators 4 Technicians 1

BUDGET: Machine - Funded by -

TIME DISTRIBUTION: (e.g. basic research, isotope production, maintenance, etc.)

(a) Isotope Production 75 %

(b) Neutron Therapy 20 %

(c) Maintenance 5 %

(d) %

(e) %

CHARACTERISTIC BEAMS

	Accelerated Ions	E/A (MeV/u)	Current(part μA) Internal	External
(a)	P	26	200	60
(b)	d	7	300	100
	3He	13	135	60
	4He	7	90	50

1991 μA-hours on target:

FACILITIES

SHIELDED AREA: Fixed 190 m² Moveable 0 m²

Target Stations: 9 No. Served At Same Time: 1

OTHER FACILITIES:

Isotope production

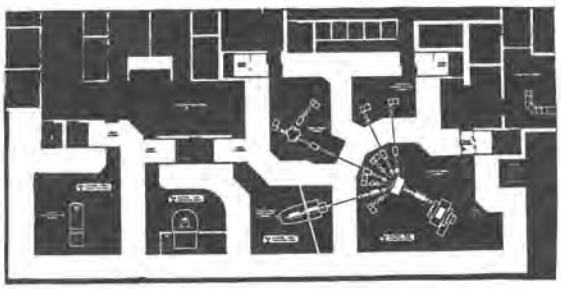
Isocentric neutron production

REFERENCES/NOTES

(a) IEEE Trans Nucl. Sci. NS-14, 70-71 (1967)

(b) " " " " NS-16, 500-503 (1969)

PLAN VIEW OF FACILITY, COMMENTS



ENTRY No. CU70

NAME OF MACHINE ..KCCH-CYCLOTRON..... DATE .....
INSTITUTION .....KOREA CANCER CENTER HOSPITAL, KAERI.....
ADDRESS .....215-4 GONGNEUNG-DONG DOBONG-KU, SEOUL.....
TEL ..974-2501..... TELEX ...KCCHOSP K27764.....
IN CHARGE ..... REPORTED BY ..CYCLOTRON LAB., KCCH.....

HISTORY AND STATUS

DESIGN, date ..'82. 4..... Model tests .....
ENG DESIGN, date ...'83. 1.....
CONSTRUCTION, date ..'84. 5.....
FIRST BEAM, date (or goal) .....'86. 1. 25.....
MAJOR ALTERATIONS .....
.....
COST, ACCELERATOR ....3,280,000 US $.....
COST, FACILITY, total ..... about 8,000,000 US $.....
FUNDED BY ..KOREA CANCER CENTER HOSPITAL.....

ACCELERATOR STAFF, OPERATION AND DEVELOPMENT

SCIENTISTS .....2..... ENGINEERS ....3.....
TECHNICIANS ....3..... CRAFTS .....
GRAD STUDENTS involved during year .....
OPERATED BY ..... Research staff or .....6.... Operators
OPERATION ...50..... hr/wk, On target ...18..... hr/wk
TIME DISTR. in house .....100... %, Outside ..... %
BUDGET, op & dev ...200,000 $/yr.....
FUNDED BY ...KOREA CANCER CENTER HOSPITAL.....

RESEARCH STAFF, not included above

USERS, in house .....2..... outside .....
GRAD STUDENTS involved during year .....
RESEARCH BUDGET, in house .....NOT DECIDED.....
FUNDED BY .....

MAGNET

POLE FACE, diameter (compact) 143 cm, R extraction .57. cm
R injection ..... cm
GAP, min ...11... cm, Field .....20.5.. kG } at 2.88x10^5
max ...19.7. cm, Field ..... kG } Ampere turns
AVERAGE FIELD at R ext .....17.6.. kG
B max/ <B> ...1.18.....
NUMBER OF SECTORS { compact ..3... / separated ..... } Spiral, max 55 deg
SECTOR ANGLE (SSC) ..... deg
TRIMMING COILS .....10 pairs.....
.....
CONDUCTOR, material and type .....Hollow Cu.....
STORED ENERGY (cryogenic) ..... MJ
POWER : main coils ..126. max, kW ; current stability 1x10^-5
trimming coils ...10. max, kW ; current stability 1x10^-5
WEIGHT : Fe ....88.2..... tons ; coils ....3.8..... tons
COOLING system . 90 L/min T=18-20°C.....
ION ENERGY (bending limit) E/A = ..50.... q²/a² MeV/amu
(focusing limit) E/A = ... q²/a² MeV/amu

ACCELERATION SYSTEM

DEES, number .....2..... ; angle .....90..... deg
BEAM APERTURE .....2.... cm ; DC Bias ....10..... kV
TUNED by, coarse coaxial stem fine movable flap.....
RF ....15.5.... to ....26.8.. mHz, stable ± .....
Orb F ..7.75... to ....26.8.. mHz
HARMONICS, RF/Orb F, used .....1,2.....
DEE - Gnd, max ..40.. kV, min gap .....2..... cm
STABILITY, (pk-pk noise)/(pk RF volt) ..10^-3.....
ENERGY GAIN, max .....160..... kV/turn
RF PHASE, stable to ± .....1°..... deg
RF POWER input, max .....60..... kW
FREQUENCY MODULATION, rate ..... /s
modulator, type .....
beam pulse, width .....

VACUUM SYSTEM

OPERATING PRESSURE .....5x10^-6..... Torr or mbar
PUMPS, No, Type, Size .....
....Diffusion pump, 2 , DIFF400 (BALZERS).....
....4000 L/sec.....

ION SOURCES

....P. I. G., COLD CATHODE.....

INJECTION SYSTEM

.....

EXTRACTION SYSTEM

.Electrostatic Deflector + Electromagnetic Channel.....

FACILITIES FOR RESEARCH

SHIELDED AREA, fixed ...180 .... m² ; movable ....25.... m²
TARGET STATIONS ....4... in .....2.. rooms
STATIONS served at same time, max .....
MAG SPECTROGRAPH, type .....
COMPUTER model ..... PDP 11/23+.....
OTHER FACILITIES .....
.NEUTRON THERAPY (NT-50).....
.MECICAL MICROTRON (MM-22).....

CHARACTERISTIC BEAMS

PARTICLE	ENERGY (MeV) Goal	Achieved	CURRENT (pμA) Internal	External
.Protron ..	50	50.5	130	85 μA
.Deutron ..				
.He-3	not tested yet			
.He-4	48	48	60	35 μA
SECONDARY			(part/s)	

BEAM PROPERTIES

MEASURED	CONDITIONS	
PULSE WIDTH ..... RF deg	pμA of .... MeV ... ions	not
PHASE EXC, max ... RF deg	pμA of .... MeV ... ions	measured
EXTRACT eff ....65. %	..70... pμA of 50.5 MeV H+. ions	yet
RESOL ΔE/E ...<1. %	..70... pμA of 50.5 MeV H+. ions	
EMITTANCE		
(π mm. mrad) { .13 axial / .14 rad }	...10.. pμA of .50.5 MeV proton ... ions	

OPERATING PROGRAMS, time distribution

BASIC NUCLEAR PHYSICS .. SOLID STATES PHYSICS ....
BIOMEDICAL APPLICAT. .... ISOTOPE PRODUCTIONS 2hr/day
NEUTRON THERAPY .....8hr/day.....
.....

REFERENCES/NOTES

1) KAERI/RR-495/85
2) SCANDITRONIX TECHANICAL SPECIFICATION NOTE

PLAN VIEW OF FACILITY, NOTEWORTHY FEATURES, COMMENTS

ENTRY NO. CU71 Date

Cyclotron Model SCANDITRONIX MC17
Institution KAROLINSKA HOSPITAL, DEP. CLIN. NEUROFYS
Address BOX 60500; S-104 01 STOCKHOLM, SWEDEN
Tel (8) 729 5590 Telex
Fax (8) 33 99 53 EMAIL
In Charge: G. PRINTZ Reported by: G. PRINTZ

HISTORY

MILESTONE DATES:
Installation JUN 81- DEC 81 First Beam DEC 1981
DESIGN/CONSTRUCTION BY: SCANDITRONIX AB
COST: Accelerator Facility
FUNDED BY: RESEARCH GRANTS

STATUS

STAFF: Operators Technicians 2
BUDGET: Machine 40 000 USD Funded by HOSPITAL
TIME DISTRIBUTION: (e.g. basic research, isotope production, maintenance, etc.)

(a)	MAINTENCE	10-15 %
(b)	ISOTOPE PRODUCTION	85-90 %
(c)		%
(d)		%
(e)		%

CHARACTERISTIC BEAMS

Accelerated Ions	E/A (MeV/u)	Current(part μA) Internal	External
(a) p	17	>50 uA	50 uA
(b) d	8.5	>25 uA	25 uA

1991 μA-hours on target:

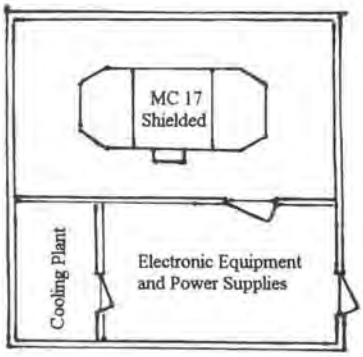
FACILITIES

SHIELDED AREA: ~~Fixed~~ m² ~~Moveable~~ m² SELFSHIELDED CYKLOTRON
Target Stations: 1 No. Served At Same Time: 1
OTHER FACILITIES: PET RADIOCHEMISTRY LAB + 2 PET CAMERAS

REFERENCES/NOTES

(a)
(b)

PLAN VIEW OF FACILITY, COMMENTS



To Control room and Radiochemistry lab.

ENTRY NO. CU72 Date

Cyclotron Model MC17
Institution Uppsala University PET-Centre
Address Akademiska Sjukhuset, 751 85 Uppsala
Tel (46) 18 18 33 81 Telex
Fax (46) 18 18 33 90 EMAIL
In Charge: Bengt Långström Reported by: Robert Reineck

HISTORY

MILESTONE DATES:
Installation dec 90 - may 91 First Beam may 91
DESIGN/CONSTRUCTION BY: Scanditronix AB
COST: Accelerator 13 000 000 SKr Facility 104 000 000 SKr
FUNDED BY: Various Funds

STATUS

STAFF: Operators 6 Technicians 1
BUDGET: Machine 1.3 MSKr Funded by PET-Centre
TIME DISTRIBUTION: (e.g. basic research, isotope production, maintenance, etc.)

(a)	Isotope production	93 %
(b)	Maintenance	7 %
(c)		%
(d)		%
(e)		%

CHARACTERISTIC BEAMS

Accelerated Ions	E/A (MeV/u)	Current(part μA) Internal	External
(a) H+	17	80	65
(b) D+	8.5	80	50

1991 μA-hours on target: 10 000

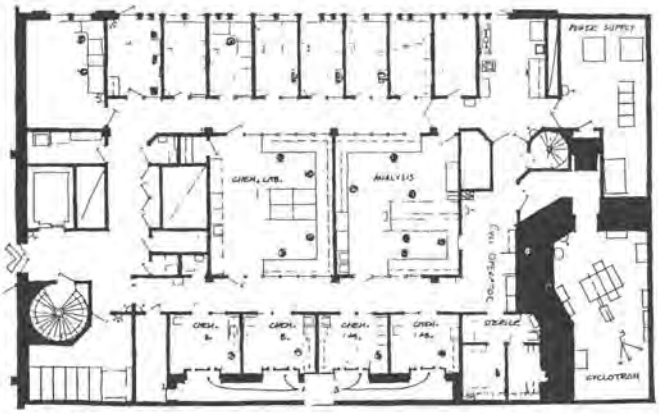
FACILITIES

SHIELDED AREA: Fixed 40 m² Moveable m²
Target Stations: 1 No. Served At Same Time:
OTHER FACILITIES:

REFERENCES/NOTES

(a)
(b)

PLAN VIEW OF FACILITY, COMMENTS



ENTRY NO. CU71 Date

Cyclotron Model SCANDITRONIX MC17
Institution KAROLINSKA HOSPITAL, DEP. CLIN. NEUROFYS
Address BOX 60500; S-104 01 STOCKHOLM, SWEDEN
Tel (8) 729 5590 Telex
Fax (8) 33 99 53 EMAIL
In Charge: G. PRINTZ Reported by: G. PRINTZ

HISTORY

MILESTONE DATES:
Installation JUN 81- DEC 81 First Beam DEC 1981
DESIGN/CONSTRUCTION BY: SCANDITRONIX AB
COST: Accelerator Facility
FUNDED BY: RESEARCH GRANTS

STATUS

STAFF: Operators Technicians 2
BUDGET: Machine 40 000 USD Funded by HOSPITAL
TIME DISTRIBUTION: (e.g. basic research, isotope production, maintenance, etc.)

(a)	MAINTENCE	10-15 %
(b)	ISOTOPE PRODUCTION	85-90 %
(c)		%
(d)		%
(e)		%

CHARACTERISTIC BEAMS

Accelerated Ions	E/A (MeV/u)	Current(part μA) Internal	External
(a) p	17	>50 uA	50 uA
(b) d	8.5	>25 uA	25 uA

1991 μA-hours on target:

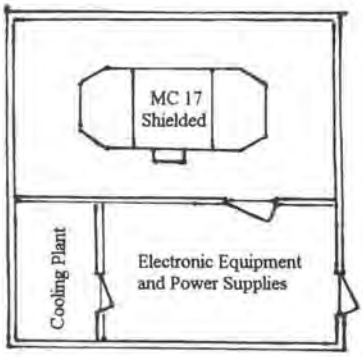
FACILITIES

SHIELDED AREA: ~~Fixed~~ m² ~~Moveable~~ m² SELFSHIELDED CYKLOTRON
Target Stations: 1 No. Served At Same Time: 1
OTHER FACILITIES: PET RADIOCHEMISTRY LAB + 2 PET CAMERAS

REFERENCES/NOTES

(a)
(b)

PLAN VIEW OF FACILITY, COMMENTS



To Control room and Radiochemistry lab.

ENTRY NO. CU72 Date

Cyclotron Model MC17
Institution Uppsala University PET-Centre
Address Akademiska Sjukhuset, 751 85 Uppsala
Tel (46) 18 18 33 81 Telex
Fax (46) 18 18 33 90 EMAIL
In Charge: Bengt Långström Reported by: Robert Reineck

HISTORY

MILESTONE DATES:
Installation dec 90 - may 91 First Beam may 91
DESIGN/CONSTRUCTION BY: Scanditronix AB
COST: Accelerator 13 000 000 SKr Facility 104 000 000 SKr
FUNDED BY: Various Funds

STATUS

STAFF: Operators 6 Technicians 1
BUDGET: Machine 1.3 MSKr Funded by PET-Centre
TIME DISTRIBUTION: (e.g. basic research, isotope production, maintenance, etc.)

(a)	Isotope production	93 %
(b)	Maintenance	7 %
(c)		%
(d)		%
(e)		%

CHARACTERISTIC BEAMS

Accelerated Ions	E/A (MeV/u)	Current(part μA) Internal	External
(a) H+	17	80	65
(b) D+	8.5	80	50

1991 μA-hours on target: 10 000

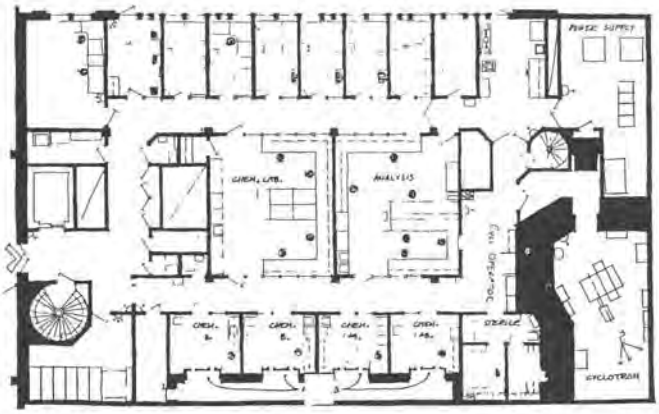
FACILITIES

SHIELDED AREA: Fixed 40 m² Moveable m²
Target Stations: 1 No. Served At Same Time:
OTHER FACILITIES:

REFERENCES/NOTES

(a)
(b)

PLAN VIEW OF FACILITY, COMMENTS



ENTRY NO. CU74 Date Jun. 92

Cyclotron Model TR30/15

Institution Institute of Nuclear Energy Research

Address 1000 Wen-Hua Rd. Lung-Tan 325, Taiwan, Rep. of China

Tel 886-2-3651717 Ex. 2701 Telex

Fax 886-2-3811542 EMAIL

In Charge: G. Ting Reported by: P.S. Song

HISTORY

MILESTONE DATES:

Installation Jan.93-Mar.93 First Beam Apr. 93

DESIGN/CONSTRUCTION BY: TRIUMF/EBCO

COST: Accelerator ——— Facility

FUNDED BY: Government of Rep. of China

STATUS

STAFF: Operators 4 Technicians 4

BUDGET: Machine Funded by

TIME DISTRIBUTION: (e.g. basic research, isotope production, maintenance, etc.)

(a) Isotope Production ~70 %

(b) Engineering Application ~15 %

(c) Other ~15 %

(d) %

(e) %

CHARACTERISTIC BEAMS

	Accelerated Ions	E/A (MeV/u)	Current(part μA) Internal	External
(a)	H^-	15-30	350 H^-	350p
(b)	D^-	8-15 (MeV)	150 D^-	150d

1991 μA-hours on target:

FACILITIES

SHIELDED AREA: Fixed 207 m² Moveable m²

Target Stations: 5 No. Served At Same Time: 2

OTHER FACILITIES:

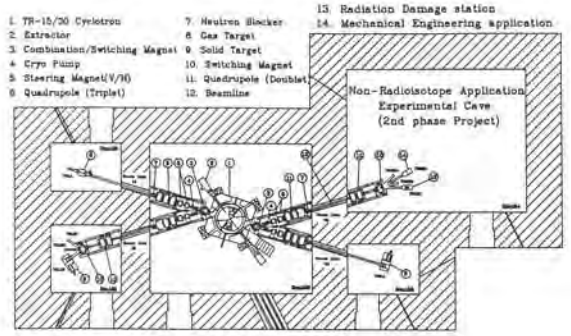
Radiochemical & Radiopharmaceutical production facilities including hot cell, lead-shielding aseptic glove box, aseptic rooms.

REFERENCES/NOTES

(a) This cyclotron machine with 3 isotope production

(b) stations will be established completely in June 1993.

PLAN VIEW OF FACILITY, COMMENTS



ENTRY NO. CU76 Date 10 July 1992

Cyclotron Model PHILIPS

Institution AMERSHAM INTERNATIONAL PLC

Address AMERSHAM LABORATORIES, WHITE LION ROAD, AMERSHAM, BUCKS.

Tel (0)494-54-3550 Telex ACTIVLG

Fax (0)494-54-3674 EMAIL

In Charge: TIM GREY-MORGAN Reported by: DEWI M LEWIS

HISTORY

MILESTONE DATES:

Installation 1963-65 First Beam 1966

DESIGN/CONSTRUCTION BY: PHILIPS

COST: Accelerator £0.35M Facility £0.30M

FUNDED BY: UK ATOMIC ENERGY AUTHORITY

STATUS

STAFF: Operators 6 Technicians 4

BUDGET: Machine Funded by Commercial

TIME DISTRIBUTION: (e.g. basic research, isotope production, maintenance, etc.)

(a) ISOTOPE PRODUCTION 70 %

(b) MAINTENANCE 30 %

(c) %

(d) %

(e) %

CHARACTERISTIC BEAMS

	Accelerated Ions	E/A (MeV/u)	Current(part μA) Internal	External	
(a)	p	27	600		max
(b)	d	16	1600		

1991 μA-hours on target:

FACILITIES

SHIELDED AREA: Fixed m² Moveable m²

Target Stations: 1 No. Served At Same Time: 1

OTHER FACILITIES:

REMOTE CONTROL TARGET

NON OPERATOR COMPUTER CONTROL

NON OPERATOR TARGET CHANGING

REFERENCES/NOTES

(a)

(b)

PLAN VIEW OF FACILITY, COMMENTS

ENTRY NO. CU74 Date Jun. 92

Cyclotron Model TR30/15

Institution Institute of Nuclear Energy Research

Address 1000 Wen-Hua Rd. Lung-Tan 325, Taiwan, Rep. of China

Tel 886-2-3651717 Ex. 2701 Telex

Fax 886-2-3811542 EMAIL

In Charge: G. Ting Reported by: P.S. Song

HISTORY

MILESTONE DATES:

Installation Jan.93-Mar.93 First Beam Apr. 93

DESIGN/CONSTRUCTION BY: TRIUMF/EBCO

COST: Accelerator ——— Facility

FUNDED BY: Government of Rep. of China

STATUS

STAFF: Operators 4 Technicians 4

BUDGET: Machine Funded by

TIME DISTRIBUTION: (e.g. basic research, isotope production, maintenance, etc.)

(a) Isotope Production ~70 %

(b) Engineering Application ~15 %

(c) Other ~15 %

(d) %

(e) %

CHARACTERISTIC BEAMS

	Accelerated Ions	E/A (MeV/u)	Current(part μA) Internal	External
(a)	H^-	15-30	350 H^-	350p
(b)	D^-	8-15 (MeV)	150 D^-	150d

1991 μA-hours on target:

FACILITIES

SHIELDED AREA: Fixed 207 m² Moveable m²

Target Stations: 5 No. Served At Same Time: 2

OTHER FACILITIES:

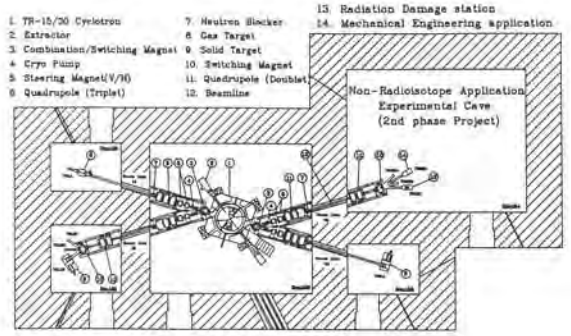
Radiochemical & Radiopharmaceutical production facilities including hot cell, lead-shielding aseptic glove box, aseptic rooms.

REFERENCES/NOTES

(a) This cyclotron machine with 3 isotope production

(b) stations will be established completely in June 1993.

PLAN VIEW OF FACILITY, COMMENTS



ENTRY NO. CU76 Date 10 July 1992

Cyclotron Model PHILIPS

Institution AMERSHAM INTERNATIONAL PLC

Address AMERSHAM LABORATORIES, WHITE LION ROAD, AMERSHAM, BUCKS.

Tel (0)494-54-3550 Telex ACTIVLG

Fax (0)494-54-3674 EMAIL

In Charge: TIM GREY-MORGAN Reported by: DEWI M LEWIS

HISTORY

MILESTONE DATES:

Installation 1963-65 First Beam 1966

DESIGN/CONSTRUCTION BY: PHILIPS

COST: Accelerator £0.35M Facility £0.30M

FUNDED BY: UK ATOMIC ENERGY AUTHORITY

STATUS

STAFF: Operators 6 Technicians 4

BUDGET: Machine Funded by Commercial

TIME DISTRIBUTION: (e.g. basic research, isotope production, maintenance, etc.)

(a) ISOTOPE PRODUCTION 70 %

(b) MAINTENANCE 30 %

(c) %

(d) %

(e) %

CHARACTERISTIC BEAMS

	Accelerated Ions	E/A (MeV/u)	Current(part μA) Internal	External	
(a)	p	27	600		max
(b)	d	16	1600		

1991 μA-hours on target:

FACILITIES

SHIELDED AREA: Fixed m² Moveable m²

Target Stations: 1 No. Served At Same Time: 1

OTHER FACILITIES:

REMOTE CONTROL TARGET

NON OPERATOR COMPUTER CONTROL

NON OPERATOR TARGET CHANGING

REFERENCES/NOTES

(a)

(b)

PLAN VIEW OF FACILITY, COMMENTS

ENTRY NO. CU77 Date 10 July 1992

Cyclotron Model CP-42

Institution AMERSHAM INTERNATIONAL PLC

Address AMERSHAM LABORATORIES, WHITE LION ROAD, AMERSHAM,

Tel (0)494-3550 Telex ACTIVLG BUCKS

Fax (0)494-3674 EMAIL

In Charge: TIM GREY-MORGAN Reported by: DEWI M LEWIS

HISTORY

MILESTONE DATES:

Installation 1980 First Beam 1981

DESIGN/CONSTRUCTION BY: CYCLOTRON CORP.

COST: Accelerator US$ 2M Facility

FUNDED BY: UK ATOMIC ENERGY AUTHORITY

STATUS

STAFF: Operators 6 Technicians 4

BUDGET: Machine Funded by Commercial

TIME DISTRIBUTION: (e.g. basic research, isotope production, maintenance, etc.)

(a) ISOTOPE PRODUCTION 70 %

(b) MAINTENANCE 30 %

(c) %

(d) %

(e) %

CHARACTERISTIC BEAMS

	Accelerated Ions	E/A (MeV/u)	Current(part μA) Internal	External
(a)	p	42	260	250 max
(b)	p	30	340	320 max
	p	11	150	

1991 μA-hours on target:

FACILITIES

SHIELDED AREA: Fixed m² Moveable m²

Target Stations: 2 No. Served At Same Time: 1

OTHER FACILITIES:

REMOTE CONTROLLED TARGETS

COMPUTER AUTOMATED TOTAL SYSTEM

REFERENCES/NOTES

(a)

(b)

PLAN VIEW OF FACILITY, COMMENTS

ENTRY NO. CU78 Date 10 JULY 1992

Cyclotron Model MC-40 Mk2

Institution AMERSHAM INTERNATIONAL PLC

Address AMERSHAM LABORATORIES, WHITE LION ROAD, AMERSHAM,

Tel (0)494-54-3550 Telex ACTIVLG BUCKS

Fax (0)494-54-3674 EMAIL

In Charge: TIM GREY-MORGAN Reported by: DEWI M LEWIS

HISTORY

MILESTONE DATES:

Installation 1986 First Beam 1986

DESIGN/CONSTRUCTION BY: SCANDITRONIX AB

COST: Accelerator approx £1.5M Facility

FUNDED BY: Commercial

STATUS

STAFF: Operators 6 Technicians 4

BUDGET: Machine Funded by

TIME DISTRIBUTION: (e.g. basic research, isotope production, maintenance, etc.)

(a) ISOTOPE PRODUCTION 70 %

(b) MAINTENANCE 30 %

(c) %

(d) %

(e) %

CHARACTERISTIC BEAMS

	Accelerated Ions	E/A (MeV/u)	Current(part μA) Internal	External
(a)	p	11 - 35.5		
(b)		33.5	250	max

1991 μA-hours on target:

FACILITIES

SHIELDED AREA: Fixed m² Moveable m²

Target Stations: 2 No. Served At Same Time: 1

OTHER FACILITIES:

AUTOMATED CYCLOTRON

REMOTE CONTROL TARGETS

REFERENCES/NOTES

(a)

(b)

PLAN VIEW OF FACILITY, COMMENTS

ENTRY NO. CU77 Date 10 July 1992

Cyclotron Model CP-42

Institution AMERSHAM INTERNATIONAL PLC

Address AMERSHAM LABORATORIES, WHITE LION ROAD, AMERSHAM,

Tel (0)494-3550 Telex ACTIVLG BUCKS

Fax (0)494-3674 EMAIL

In Charge: TIM GREY-MORGAN Reported by: DEWI M LEWIS

HISTORY

MILESTONE DATES:

Installation 1980 First Beam 1981

DESIGN/CONSTRUCTION BY: CYCLOTRON CORP.

COST: Accelerator US$ 2M Facility

FUNDED BY: UK ATOMIC ENERGY AUTHORITY

STATUS

STAFF: Operators 6 Technicians 4

BUDGET: Machine Funded by Commercial

TIME DISTRIBUTION: (e.g. basic research, isotope production, maintenance, etc.)

(a) ISOTOPE PRODUCTION 70 %

(b) MAINTENANCE 30 %

(c) %

(d) %

(e) %

CHARACTERISTIC BEAMS

	Accelerated Ions	E/A (MeV/u)	Current(part μA) Internal	External
(a)	p	42	260	250 max
(b)	p	30	340	320 max
	p	11	150	

1991 μA-hours on target:

FACILITIES

SHIELDED AREA: Fixed m² Moveable m²

Target Stations: 2 No. Served At Same Time: 1

OTHER FACILITIES:

REMOTE CONTROLLED TARGETS

COMPUTER AUTOMATED TOTAL SYSTEM

REFERENCES/NOTES

(a)

(b)

PLAN VIEW OF FACILITY, COMMENTS

ENTRY NO. CU78 Date 10 JULY 1992

Cyclotron Model MC-40 Mk2

Institution AMERSHAM INTERNATIONAL PLC

Address AMERSHAM LABORATORIES, WHITE LION ROAD, AMERSHAM,

Tel (0)494-54-3550 Telex ACTIVLG BUCKS

Fax (0)494-54-3674 EMAIL

In Charge: TIM GREY-MORGAN Reported by: DEWI M LEWIS

HISTORY

MILESTONE DATES:

Installation 1986 First Beam 1986

DESIGN/CONSTRUCTION BY: SCANDITRONIX AB

COST: Accelerator approx £1.5M Facility

FUNDED BY: Commercial

STATUS

STAFF: Operators 6 Technicians 4

BUDGET: Machine Funded by

TIME DISTRIBUTION: (e.g. basic research, isotope production, maintenance, etc.)

(a) ISOTOPE PRODUCTION 70 %

(b) MAINTENANCE 30 %

(c) %

(d) %

(e) %

CHARACTERISTIC BEAMS

	Accelerated Ions	E/A (MeV/u)	Current(part μA) Internal	External
(a)	p	11 - 35.5		
(b)		33.5	250	max

1991 μA-hours on target:

FACILITIES

SHIELDED AREA: Fixed m² Moveable m²

Target Stations: 2 No. Served At Same Time: 1

OTHER FACILITIES:

AUTOMATED CYCLOTRON

REMOTE CONTROL TARGETS

REFERENCES/NOTES

(a)

(b)

PLAN VIEW OF FACILITY, COMMENTS

ENTRY No. CU79

NAME OF MACHINE CLATTERBRIDGE CYCLOTRON DATE 8TH MAY, 1989

INSTITUTION MEDICAL RESEARCH COUNCIL

ADDRESS DOUGLAS CYCLOTRON CENTRE, CLATTERBRIDGE HOSPITAL, BEBINGTON, WIRRAL, MERSEYSIDE, L63 4JY, UK

TEL 051-334 6366 TELEX 627035 TELEFAX 051-334 2845

IN CHARGE T.E. SAXTON REPORTED BY T.E. SAXTON

HISTORY AND STATUS

DESIGN, date 1981/82 Model tests

ENG DESIGN, date 1981/82

CONSTRUCTION, date 1982/83

FIRST BEAM, date (or goal) FACTORY 1983, SITE 1984

MAJOR ALTERATIONS ADDITION OF PROTON THERAPY FACILITY, 1988

COST, ACCELERATOR £1.5M

COST, FACILITY, total £4.5M

FUNDED BY U.K. CANCER CHARITIES

ACCELERATOR STAFF, OPERATION AND DEVELOPMENT

SCIENTISTS 2 ENGINEERS 3

TECHNICIANS 2 CRAFTS 1

GRAD STUDENTS involved during year

OPERATED BY Reesearch staff or Operators

OPERATION hr/wk, On target hr/wk

TIME DISTR. In house %, Outside %

BUDGET, op & dev

FUNDED BY MEDICAL RESEARCH COUNCIL

RESEARCH STAFF, not included above

USERS, In house 3 outside

GRAD STUDENTS involved during year

RESEARCH BUDGET, In house

FUNDED BY IMPERIAL CANCER RESEARCH FUND

MAGNET

POLE FACE, diameter (compact) 160 cm, R extraction 64 cm

R injection cm

GAP, min 12.3 cm, Field 20.7 kG
max 22.1 cm, Field 13.0 kG
at 280,000 Ampere turns

AVERAGE FIELD at R ext 17.7 kG

B max/ <B> 1.19

NUMBER OF SECTORS { compact 3 / separated } Spiral, max 55 deg

SECTOR ANGLE (SSC) deg

TRIMMING COILS 4 SETS HARMONIC COILS
6 SETS CIRCULAR GRADIENT COILS

CONDUCTOR, material and type HOLLOW COPPER

STORED ENERGY (cryogenic) MJ

POWER: main coils 110 max, kW ; current stability 1×10^{-5}
trimming coils 5 max, kW ; current stability 1×10^{-4}

WEIGHT : Fe 120 tons ; coils 4.4 tons

COOLING system

ION ENERGY (bending limit) E/A = 62 q^2/a^2 MeV/amu
(focusing limit) E/A = q^2/a^2 MeV/amu

ACCELERATION SYSTEM

DEES, number 2 ; angle 80 deg

BEAM APERTURE 2.5 cm ; DC Bias kV

TUNED by, coarse fine

RF 25 to mHz, stable ± 1×10^{-6}

Orb F 25 to mHz

HARMONICS, RF/Orb F, used 1

DEE - Gnd, max 40 kV, min gap cm

STABILITY, (pk-pk noise)/(pk RF volt) $\leq10^{-3}$

ENERGY GAIN, max 100 kV/turn

RF PHASE, stable to ± 0.5 deg

RF POWER input, max 60 kW

FREQUENCY MODULATION, rate /s
modulator, type
beam pulse, width

VACUUM SYSTEM

OPERATING PRESSURE $\leq10^{-5}$ Torr or mbar

PUMPS, No, Type, Size
2 x 4000 L/SEC OIL DIFFUSION PUMP
100 m^3/HR+BOOSTER, 20 m^3/HR MECHANICAL BACKING

ION SOURCES

INTERNAL, COLD CATHODE

INJECTION SYSTEM

ELECTROSTATIC+ELECTROMAGNETIC+FOCUSSING CHANNEL

EXTRACTION SYSTEM

FACILITIES FOR RESEARCH

SHIELDED AREA, fixed m² ; movable m²

TARGET STATIONS In rooms

STATIONS served at same time, max

MAG SPECTROGRAPH, type

COMPUTER model

OTHER FACILITIES

CHARACTERISTIC BEAMS

PARTICLE	ENERGY (MeV) Goal	ENERGY (MeV) Achieved	CURRENT (pμA) Internal	CURRENT (pμA) External
P	60	62.5	>100	50

SECONDARY

(part/s)

P 50 RAD/MIN @ 150CM FROM TARGET AFTER FILTERING

BEAM PROPERTIES

MEASURED		CONDITIONS
PULSE WIDTH	RF deg	pμ A of MeV Ions
PHASE EXC, max	RF deg	pμ A of MeV Ions
EXTRACT eff	%	pμ A of MeV Ions
RESOL ΔE/E	%	pμ A of MeV Ions

EMITTANCE

(π mm. mrad) { axial / rad } pμA of MeV Ions

OPERATING PROGRAMS, time distribution

BASIC NUCLEAR PHYSICS SOLID STATES PHYSICS

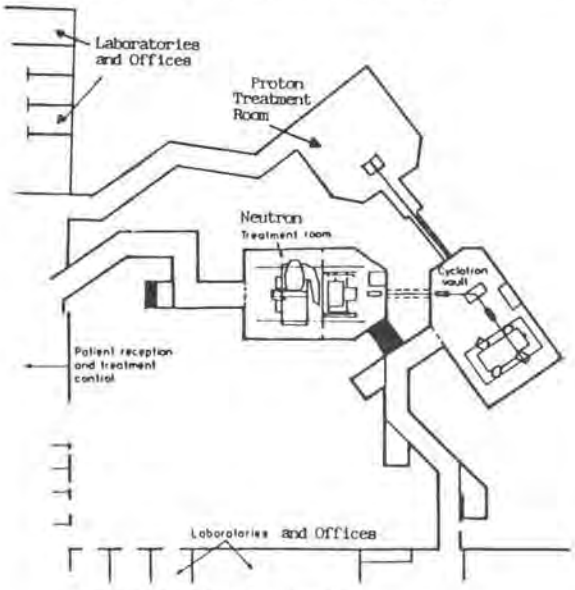
BIOMEDICAL APPLICAT. 100% ISOTOPE PRODUCTIONS

REFERENCES/NOTES

1) SCANDITRONIX MC60PP

PLAN VIEW OF FACILITY, NOTEWORTHY FEATURES, COMMENTS

ACCELERATOR USED WITH SCANDITEM HIGH ENERGY NEUTRON THERAPY UNIT. CONTROLLED BY PDP11-23.



Plan view of Clatterbridge high energy neutron therapy facility.

ENTRY NO. CU80 Date 22.6.92
Cyclotron Model Scanditronix MC40 Mark II
Institution Medical Research Council Cyclotron Unit
Address Hammersmith Hospital, Du Cane Road, London
Tel 081 740 3162 Telex W12 0HS
Fax 081 743 3987 EMAIL
In Charge: M L RENTON Reported by: D B MACKAY

HISTORY

MILESTONE DATES:
Installation 1985 First Beam March 1986
DESIGN/CONSTRUCTION BY: Scanditronix and MRC
COST: Accelerator £1 M Facility £3 M
FUNDED BY: Medical Research Council

STATUS

STAFF: Operators 8 Technicians 4
BUDGET: Machine £50K Funded by MRC
TIME DISTRIBUTION: (e.g. basic research, isotope production, maintenance, etc.)
(a) PET tracers 65 %
(b) Off-site medical isotope production 25 %
(c) Maintenance/development 10 %
(d) %
(e) %

CHARACTERISTIC BEAMS

	Accelerated Ions	E/A (MeV/u)	Current(part μA) Internal	External
(a)	PROTONS	40	300	100
(b)	DEUTERONS/ALPHA	10	300,150	100,65
(c)	^{3}He	17	150	70

1991 μA-hours on target: 80,000

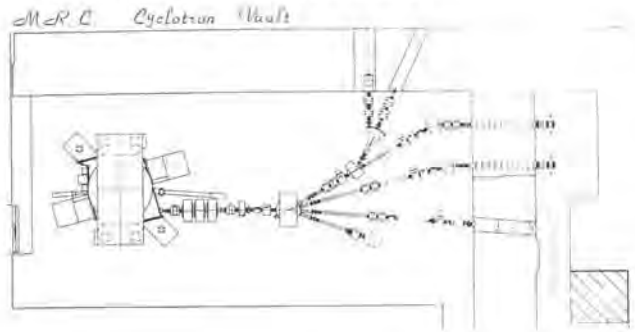
FACILITIES

SHIELDED AREA: Fixed 80 m² Moveable m²
Target Stations: 5 No. Served At Same Time: 1
OTHER FACILITIES: 2 x PET Scanner (Siemens - CTI)
1 x CYCLONE 3 OXYGEN GENERATOR (IBA) - see separate entry

REFERENCES/NOTES

(a)
(b)

PLAN VIEW OF FACILITY, COMMENTS



ENTRY NO. CU81 Date 22.6.92
Cyclotron Model CYCLONE 3 (IBA)
Institution Medical Research Council Cyclotron Unit
Address Hammersmith Hospital, Du Cane Road, London
Tel 081.740.3162 Telex W12 0HS
Fax 081.743.3987 EMAIL
In Charge: M.L.RENTON Reported by: D B MACKAY

HISTORY

MILESTONE DATES:
Installation Feb. 91 First Beam Mar 91
DESIGN/CONSTRUCTION BY: IBA
COST: Accelerator Facility conversion
FUNDED BY: Royal Postgraduate Medical School

STATUS

STAFF: Operators - Technicians -
BUDGET: Machine - Funded by
TIME DISTRIBUTION: (e.g. basic research, isotope production, maintenance, etc.)
(a) OXYGEN 15 PRODUCTION 30 HOURS/WK 95 %
(b) MAINTENANCE = 2 HOURS/WK 5 %
(c) %
(d) %
(e) %

CHARACTERISTIC BEAMS

	Accelerated Ions	E/A (MeV/u)	Current(part μA) Internal	External
(a)	DEUTERONS	1.8	120	50
(b)				

1991 μA-hours on target:

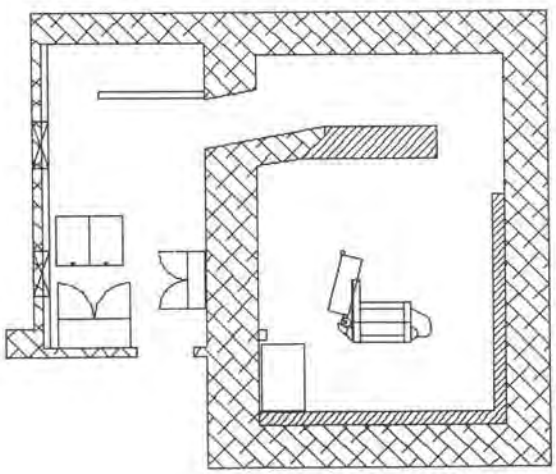
FACILITIES

SHIELDED AREA: Fixed 25 m² Moveable m²
Target Stations: 1 No. Served At Same Time:
OTHER FACILITIES:
SEE OTHER ENTRY FOR MAIN FACILITIES

REFERENCES/NOTES

(a)
(b)

PLAN VIEW OF FACILITY, COMMENTS



ENTRY NO. CU80 Date 22.6.92
Cyclotron Model Scanditronix MC40 Mark II
Institution Medical Research Council Cyclotron Unit
Address Hammersmith Hospital, Du Cane Road, London
Tel 081 740 3162 Telex W12 0HS
Fax 081 743 3987 EMAIL
In Charge: M L RENTON Reported by: D B MACKAY

HISTORY

MILESTONE DATES:
Installation 1985 First Beam March 1986
DESIGN/CONSTRUCTION BY: Scanditronix and MRC
COST: Accelerator £1 M Facility £3 M
FUNDED BY: Medical Research Council

STATUS

STAFF: Operators 8 Technicians 4
BUDGET: Machine £50K Funded by MRC
TIME DISTRIBUTION: (e.g. basic research, isotope production, maintenance, etc.)
(a) PET tracers 65 %
(b) Off-site medical isotope production 25 %
(c) Maintenance/development 10 %
(d) %
(e) %

CHARACTERISTIC BEAMS

	Accelerated Ions	E/A (MeV/u)	Current(part μA) Internal	External
(a)	PROTONS	40	300	100
(b)	DEUTERONS/ALPHA	10	300,150	100,65
(c)	^{3}He	17	150	70

1991 μA-hours on target: 80,000

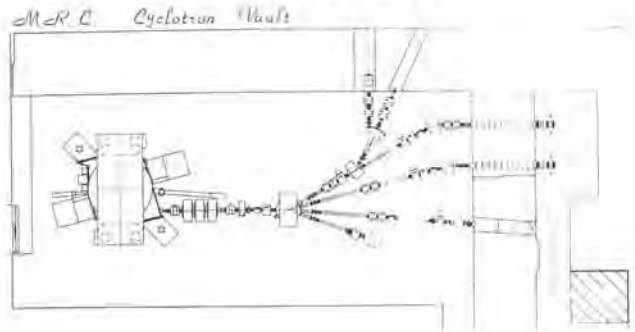
FACILITIES

SHIELDED AREA: Fixed 80 m² Moveable m²
Target Stations: 5 No. Served At Same Time: 1
OTHER FACILITIES: 2 x PET Scanner (Siemens - CTI)
1 x CYCLONE 3 OXYGEN GENERATOR (IBA) - see separate entry

REFERENCES/NOTES

(a)
(b)

PLAN VIEW OF FACILITY, COMMENTS



ENTRY NO. CU81 Date 22.6.92
Cyclotron Model CYCLONE 3 (IBA)
Institution Medical Research Council Cyclotron Unit
Address Hammersmith Hospital, Du Cane Road, London
Tel 081.740.3162 Telex W12 0HS
Fax 081.743.3987 EMAIL
In Charge: M.L.RENTON Reported by: D B MACKAY

HISTORY

MILESTONE DATES:
Installation Feb. 91 First Beam Mar 91
DESIGN/CONSTRUCTION BY: IBA
COST: Accelerator Facility conversion
FUNDED BY: Royal Postgraduate Medical School

STATUS

STAFF: Operators - Technicians -
BUDGET: Machine - Funded by
TIME DISTRIBUTION: (e.g. basic research, isotope production, maintenance, etc.)
(a) OXYGEN 15 PRODUCTION 30 HOURS/WK 95 %
(b) MAINTENANCE = 2 HOURS/WK 5 %
(c) %
(d) %
(e) %

CHARACTERISTIC BEAMS

	Accelerated Ions	E/A (MeV/u)	Current(part μA) Internal	External
(a)	DEUTERONS	1.8	120	50
(b)				

1991 μA-hours on target:

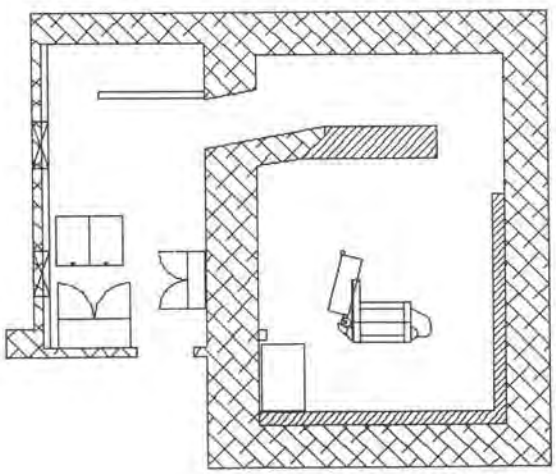
FACILITIES

SHIELDED AREA: Fixed 25 m² Moveable m²
Target Stations: 1 No. Served At Same Time:
OTHER FACILITIES:
SEE OTHER ENTRY FOR MAIN FACILITIES

REFERENCES/NOTES

(a)
(b)

PLAN VIEW OF FACILITY, COMMENTS



ENTRY NO. CU82 Date

Cyclotron Model CS-30 The Cyclotron Corp (TCC)
Institution University of Michigan Medical School
Address 3480 Kresge III, Ann Arbor, MI 48109-0552
Tel 313-936-1186 Telex None
Fax 313-764-0288 EMAIL D.Evans @UMICH.EDU
In Charge: Dr. David E. Kuhl Reported by: R. Lininger

HISTORY

MILESTONE DATES:
Installation Feb '82-Nov '82 First Beam Apr '82
DESIGN/CONSTRUCTION BY: The Cyclotron Corporation
COST: Accelerator $1.6 Million Facility $6.5 Million
FUNDED BY: NIH, Kresge Foundation, and Medical School

STATUS

STAFF: Operators 2 Technicians 1
BUDGET: Machine Not Available Funded by Grants
TIME DISTRIBUTION: (e.g. basic research, isotope production, maintenance, etc.)

(a)	Isotope Production	90%
(b)	Maintenance	10%
(c)		%
(d)		%
(e)		%

CHARACTERISTIC BEAMS

	Accelerated Ions	E/A (MeV/μ)	Current(part μA) Internal	External
(a)	p+	26		20
(b)	d+	16		20

1991 μA-hours on target: 4646

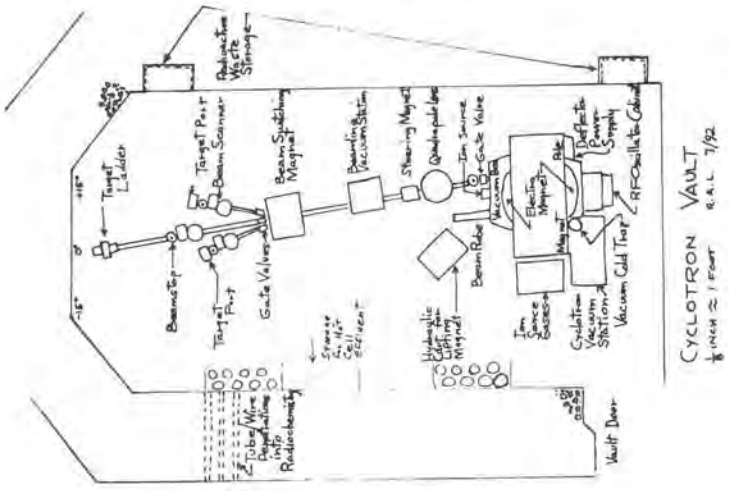
FACILITIES

SHIELDED AREA: Fixed 75 m^2 Moveable ____ m^2
Target Stations: 1 No. Served At Same Time: 1
OTHER FACILITIES:

REFERENCES/NOTES

(a)
(b)

PLAN VIEW OF FACILITY, COMMENTS



ENTRY NO. CU 83 Date

Cyclotron Model MC-40
Institution Medi-Physics, Inc.
Address 3350 N. Ridge, Arlington HEights, IL 60004
Tel (708)398-8400 Telex
Fax EMAIL
In Charge: R. Hubbard Reported by: B. Carus

HISTORY

MILESTONE DATES:
Installation 1978 First Beam February 1979
DESIGN/CONSTRUCTION BY: Scanditronix
COST: Accelerator Facility
FUNDED BY:

STATUS

STAFF: Operators 0 Technicians 4
BUDGET: Machine Funded by
TIME DISTRIBUTION: (e.g. basic research, isotope production, maintenance, etc.)

(a)	Isotope Production	80 %
(b)	Maintenance	20 %
(c)		%
(d)		%
(e)		%

CHARACTERISTIC BEAMS

	Accelerated Ions	E/A (MeV/u)	Current(part μA) Internal	External
(a)	H^+	18 - 40	200	75
(b)				

1991 μA-hours on target: 7×10^5

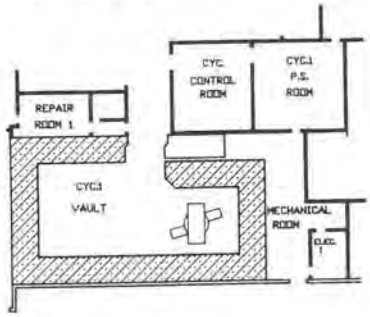
FACILITIES

SHIELDED AREA: Fixed 140 m^2 Moveable 0 m^2
Target Stations: 2 No. Served At Same Time: 1
OTHER FACILITIES:

REFERENCES/NOTES

(a)
(b)

PLAN VIEW OF FACILITY, COMMENTS



ENTRY NO. CU82 Date

Cyclotron Model CS-30 The Cyclotron Corp (TCC)
Institution University of Michigan Medical School
Address 3480 Kresge III, Ann Arbor, MI 48109-0552
Tel 313-936-1186 Telex None
Fax 313-764-0288 EMAIL D.Evans @UMICH.EDU
In Charge: Dr. David E. Kuhl Reported by: R. Lininger

HISTORY

MILESTONE DATES:
Installation Feb '82-Nov '82 First Beam Apr '82
DESIGN/CONSTRUCTION BY: The Cyclotron Corporation
COST: Accelerator $1.6 Million Facility $6.5 Million
FUNDED BY: NIH, Kresge Foundation, and Medical School

STATUS

STAFF: Operators 2 Technicians 1
BUDGET: Machine Not Available Funded by Grants
TIME DISTRIBUTION: (e.g. basic research, isotope production, maintenance, etc.)

(a)	Isotope Production	90%
(b)	Maintenance	10%
(c)		%
(d)		%
(e)		%

CHARACTERISTIC BEAMS

	Accelerated Ions	E/A (MeV/μ)	Current(part μA) Internal	External
(a)	p+	26		20
(b)	d+	16		20

1991 μA-hours on target: 4646

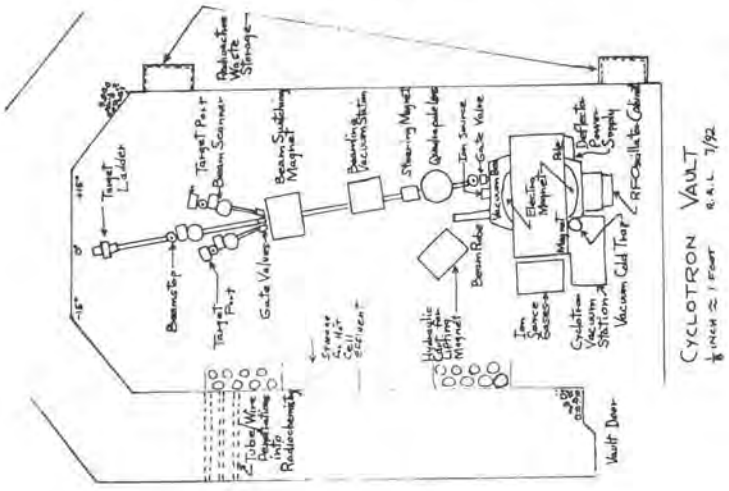
FACILITIES

SHIELDED AREA: Fixed 75 m^2 Moveable ____ m^2
Target Stations: 1 No. Served At Same Time: 1
OTHER FACILITIES:

REFERENCES/NOTES

(a)
(b)

PLAN VIEW OF FACILITY, COMMENTS



ENTRY NO. CU 83 Date

Cyclotron Model MC-40
Institution Medi-Physics, Inc.
Address 3350 N. Ridge, Arlington HEights, IL 60004
Tel (708)398-8400 Telex
Fax EMAIL
In Charge: R. Hubbard Reported by: B. Carus

HISTORY

MILESTONE DATES:
Installation 1978 First Beam February 1979
DESIGN/CONSTRUCTION BY: Scanditronix
COST: Accelerator Facility
FUNDED BY:

STATUS

STAFF: Operators 0 Technicians 4
BUDGET: Machine Funded by
TIME DISTRIBUTION: (e.g. basic research, isotope production, maintenance, etc.)

(a)	Isotope Production	80 %
(b)	Maintenance	20 %
(c)		%
(d)		%
(e)		%

CHARACTERISTIC BEAMS

	Accelerated Ions	E/A (MeV/u)	Current(part μA) Internal	External
(a)	H^+	18 - 40	200	75
(b)				

1991 μA-hours on target: 7×10^5

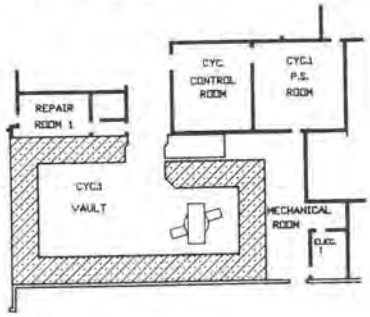
FACILITIES

SHIELDED AREA: Fixed 140 m^2 Moveable 0 m^2
Target Stations: 2 No. Served At Same Time: 1
OTHER FACILITIES:

REFERENCES/NOTES

(a)
(b)

PLAN VIEW OF FACILITY, COMMENTS



ENTRY NO. CU84 Date

Cyclotron Model MC-40
Institution Medi-Physics, Inc.
Address 3350 N. Ridge, Arlington Heights, IL 60004
Tel (708)398-8400 Telex
Fax EMAIL
In Charge: R. Hubbard Reported by: D. Bolenbaugh

HISTORY

MILESTONE DATES:
Installation 1981 First Beam May 1982
DESIGN/CONSTRUCTION BY: Scanditronix
COST: Accelerator Facility
FUNDED BY:

STATUS

STAFF: Operators 0 Technicians 4
BUDGET: Machine Funded by
TIME DISTRIBUTION: (e.g. basic research, isotope production, maintenance, etc.)

(a) Isotope Production 80 %
(b) Maintenance 20 %
(c) %
(d) %
(e) %

CHARACTERISTIC BEAMS

Accelerated Ions	E/A (MeV/u)	Current(part μA) Internal	External
(a) H^+	18 - 40	200	75
(b)			

1991 μA-hours on target: 7×10^5

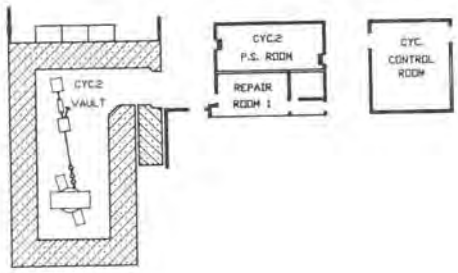
FACILITIES

SHIELDED AREA: Fixed 115 m^2 Moveable 0 m^2
Target Stations: 3 No. Served At Same Time: 1
OTHER FACILITIES:

REFERENCES/NOTES

(a)
(b)

PLAN VIEW OF FACILITY, COMMENTS



ENTRY NO. CU85 Date

Cyclotron Model PV-750
Institution Amersham - Medi-Physics, Inc.
Address 3350 N. Ridge Ave., Arlington Hgts, IL 60004
Tel 708-398-8400 Telex
Fax 708-398-8413 EMAIL
In Charge: R. Hubbard Reported by: D. Bolenbaugh

HISTORY

MILESTONE DATES:
Installation Aug. '85 First Beam May 1986
DESIGN/CONSTRUCTION BY: CGR-MEV/Sumitomo
COST: Accelerator Facility
FUNDED BY:

STATUS

STAFF: Operators 0 Technicians 4
BUDGET: Machine Funded by
TIME DISTRIBUTION: (e.g. basic research, isotope production, maintenance, etc.)

(a) Isotope Production 80 %
(b) Maintenance 20 %
(c) %
(d) %
(e) %

CHARACTERISTIC BEAMS

Accelerated Ions	E/A (MeV/u)	Current(part μA) Internal	External
(a) H^+	25-70	200	100
(b)			

1991 μA-hours on target: 7×10^5

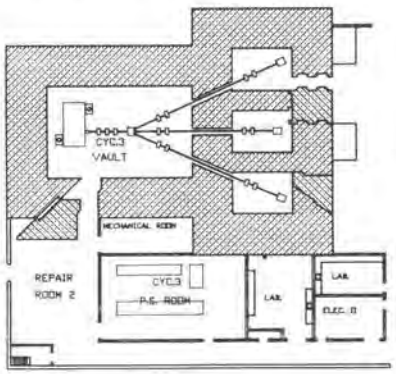
FACILITIES

SHIELDED AREA: Fixed 175 m^2 Moveable 0 m^2
Target Stations: 5 No. Served At Same Time: 1
OTHER FACILITIES:

REFERENCES/NOTES

(a)
(b)

PLAN VIEW OF FACILITY, COMMENTS



ENTRY NO. CU84 Date

Cyclotron Model MC-40
Institution Medi-Physics, Inc.
Address 3350 N. Ridge, Arlington Heights, IL 60004
Tel (708)398-8400 Telex
Fax EMAIL
In Charge: R. Hubbard Reported by: D. Bolenbaugh

HISTORY

MILESTONE DATES:
Installation 1981 First Beam May 1982
DESIGN/CONSTRUCTION BY: Scanditronix
COST: Accelerator Facility
FUNDED BY:

STATUS

STAFF: Operators 0 Technicians 4
BUDGET: Machine Funded by
TIME DISTRIBUTION: (e.g. basic research, isotope production, maintenance, etc.)

(a) Isotope Production 80 %
(b) Maintenance 20 %
(c) %
(d) %
(e) %

CHARACTERISTIC BEAMS

Accelerated Ions	E/A (MeV/u)	Current(part μA) Internal	External
(a) H^+	18 - 40	200	75
(b)			

1991 μA-hours on target: 7×10^5

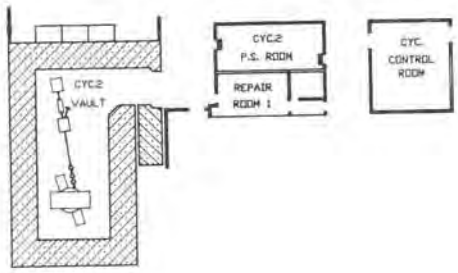
FACILITIES

SHIELDED AREA: Fixed 115 m^2 Moveable 0 m^2
Target Stations: 3 No. Served At Same Time: 1
OTHER FACILITIES:

REFERENCES/NOTES

(a)
(b)

PLAN VIEW OF FACILITY, COMMENTS



ENTRY NO. CU85 Date

Cyclotron Model PV-750
Institution Amersham - Medi-Physics, Inc.
Address 3350 N. Ridge Ave., Arlington Hgts, IL 60004
Tel 708-398-8400 Telex
Fax 708-398-8413 EMAIL
In Charge: R. Hubbard Reported by: D. Bolenbaugh

HISTORY

MILESTONE DATES:
Installation Aug. '85 First Beam May 1986
DESIGN/CONSTRUCTION BY: CGR-MEV/Sumitomo
COST: Accelerator Facility
FUNDED BY:

STATUS

STAFF: Operators 0 Technicians 4
BUDGET: Machine Funded by
TIME DISTRIBUTION: (e.g. basic research, isotope production, maintenance, etc.)

(a) Isotope Production 80 %
(b) Maintenance 20 %
(c) %
(d) %
(e) %

CHARACTERISTIC BEAMS

Accelerated Ions	E/A (MeV/u)	Current(part μA) Internal	External
(a) H^+	25-70	200	100
(b)			

1991 μA-hours on target: 7×10^5

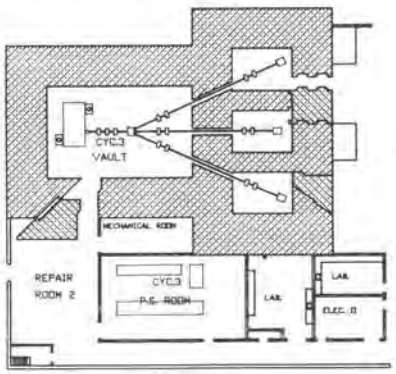
FACILITIES

SHIELDED AREA: Fixed 175 m^2 Moveable 0 m^2
Target Stations: 5 No. Served At Same Time: 1
OTHER FACILITIES:

REFERENCES/NOTES

(a)
(b)

PLAN VIEW OF FACILITY, COMMENTS



ENTRY NO. CU86 **Date**

Cyclotron Model: Scanditronix MC-16F
Institution: Johns Hopkins University
Address: Nuclear Medicine
Tel: 410-955-2916 Telex:
Fax: 410-955-0691 EMAIL:
In Charge: R.F. Dannals Reported by: R.F. Dannals

HISTORY

MILESTONE DATES:
Installation: 2/82 First Beam: 4/82
DESIGN/CONSTRUCTION BY: Scanditronix
COST: Accelerator: $1 M Facility: --
FUNDED BY: NINDS

STATUS

STAFF: Operators: 3 Technicians: --
BUDGET: Machine: $1 M Funded by: NIH
TIME DISTRIBUTION: (e.g. basic research, isotope production, maintenance, etc.)

(a)	Research - PET	95 %
(b)	Maintenance	5 %
(c)		%
(d)		%
(e)		%

CHARACTERISTIC BEAMS

	Accelerated Ions	E/A (MeV/u)	Current(part μA) Internal	External
(a)	Proton	16	75	50
(b)	Devteron	8	75	50

1991 μA-hours on target: 780

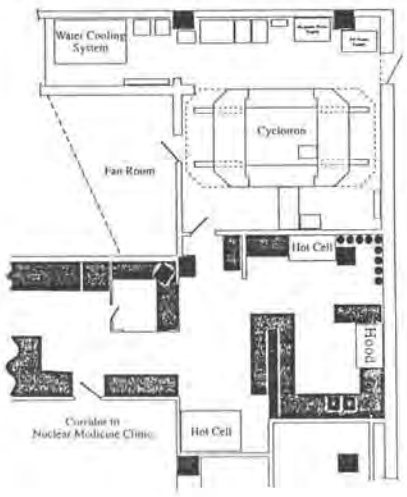
FACILITIES

SHIELDED AREA: Fixed 4 m² Moveable 10 m²
Target Stations: 4 No. Served At Same Time: 1
OTHER FACILITIES:

REFERENCES/NOTES

(a)
(b)

PLAN VIEW OF FACILITY, COMMENTS



ENTRY NO. CU88 **Date** June 1992

Cyclotron Model: JSW 1710
Institution: NIH Clinical Center
Address: Bldg. 10, Rm. 1C401, Bethesda, MD 20892
Tel: (301) 496-0345 Telex: 89422
Fax: (301) 496-0114 EMAIL: PAUL@NMDHST.CC.NIH.GOV
In Charge: W. C. Eckelman Reported by: P. S. Plasciak

HISTORY

MILESTONE DATES:
Installation: June 1985 First Beam: September 1985
DESIGN/CONSTRUCTION BY: Japan Steel Works Ltd.
COST: Accelerator: Facility:
FUNDED BY: National Institutes of Health

STATUS

STAFF: Operators: 3 Technicians:
BUDGET: Machine: $100K Funded by: NIH
TIME DISTRIBUTION: (e.g. basic research, isotope production, maintenance, etc.)

(a)	Isotope Production	85 %
(b)	Research & Development	10 %
(c)	Maintenance	5 %
(d)		%
(e)		%

CHARACTERISTIC BEAMS

	Accelerated Ions	E/A (MeV/u)	Current(part μA) Internal	External
(a)	H+	17		50
(b)	d+	10		50

1991 μA-hours on target: 15000

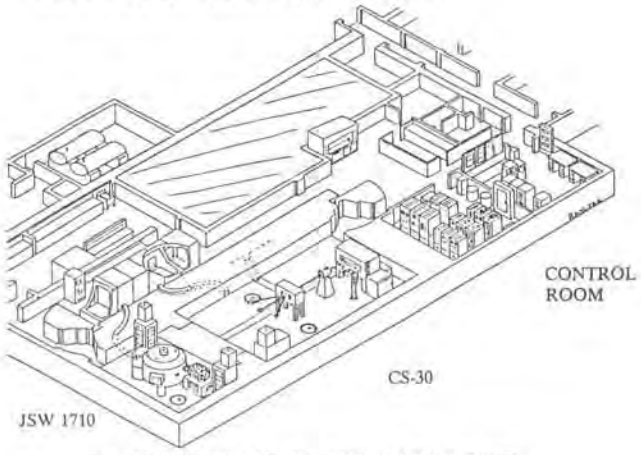
FACILITIES

SHIELDED AREA: Fixed 34 m² Moveable 6 m²
Target Stations: 1 No. Served At Same Time: 1
OTHER FACILITIES:
Target Changer
Hot Cells

REFERENCES/NOTES

(a) The Operational Status of the National Institutes
(b) of Health Cyclotron Complex, P. Plascjak, et al, Eleventh Int. Conf. on Cyclotrons and Applications, Ionics Publ., Tokyo (1987).

PLAN VIEW OF FACILITY, COMMENTS



NIH CYCLOTRON FACILITY B3 LEVEL

ENTRY NO. CU86 **Date**

Cyclotron Model: Scanditronix MC-16F
Institution: Johns Hopkins University
Address: Nuclear Medicine
Tel: 410-955-2916 Telex:
Fax: 410-955-0691 EMAIL:
In Charge: R.F. Dannals Reported by: R.F. Dannals

HISTORY

MILESTONE DATES:
Installation: 2/82 First Beam: 4/82
DESIGN/CONSTRUCTION BY: Scanditronix
COST: Accelerator: $1 M Facility: --
FUNDED BY: NINDS

STATUS

STAFF: Operators: 3 Technicians: --
BUDGET: Machine: $1 M Funded by: NIH
TIME DISTRIBUTION: (e.g. basic research, isotope production, maintenance, etc.)

(a)	Research - PET	95 %
(b)	Maintenance	5 %
(c)		%
(d)		%
(e)		%

CHARACTERISTIC BEAMS

	Accelerated Ions	E/A (MeV/u)	Current(part μA) Internal	External
(a)	Proton	16	75	50
(b)	Devteron	8	75	50

1991 μA-hours on target: 780

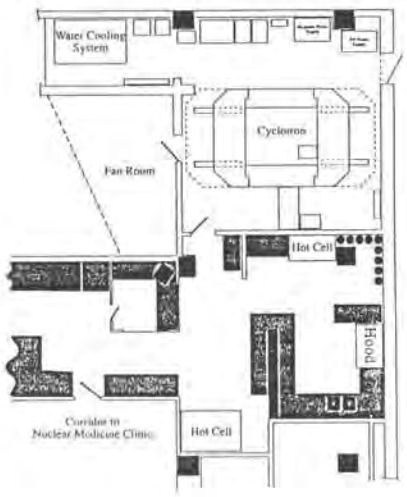
FACILITIES

SHIELDED AREA: Fixed 4 m² Moveable 10 m²
Target Stations: 4 No. Served At Same Time: 1
OTHER FACILITIES:

REFERENCES/NOTES

(a)
(b)

PLAN VIEW OF FACILITY, COMMENTS



ENTRY NO. CU88 **Date** June 1992

Cyclotron Model: JSW 1710
Institution: NIH Clinical Center
Address: Bldg. 10, Rm. 1C401, Bethesda, MD 20892
Tel: (301) 496-0345 Telex: 89422
Fax: (301) 496-0114 EMAIL: PAUL@NMDHST.CC.NIH.GOV
In Charge: W. C. Eckelman Reported by: P. S. Plasciak

HISTORY

MILESTONE DATES:
Installation: June 1985 First Beam: September 1985
DESIGN/CONSTRUCTION BY: Japan Steel Works Ltd.
COST: Accelerator: Facility:
FUNDED BY: National Institutes of Health

STATUS

STAFF: Operators: 3 Technicians:
BUDGET: Machine: $100K Funded by: NIH
TIME DISTRIBUTION: (e.g. basic research, isotope production, maintenance, etc.)

(a)	Isotope Production	85 %
(b)	Research & Development	10 %
(c)	Maintenance	5 %
(d)		%
(e)		%

CHARACTERISTIC BEAMS

	Accelerated Ions	E/A (MeV/u)	Current(part μA) Internal	External
(a)	H+	17		50
(b)	d+	10		50

1991 μA-hours on target: 15000

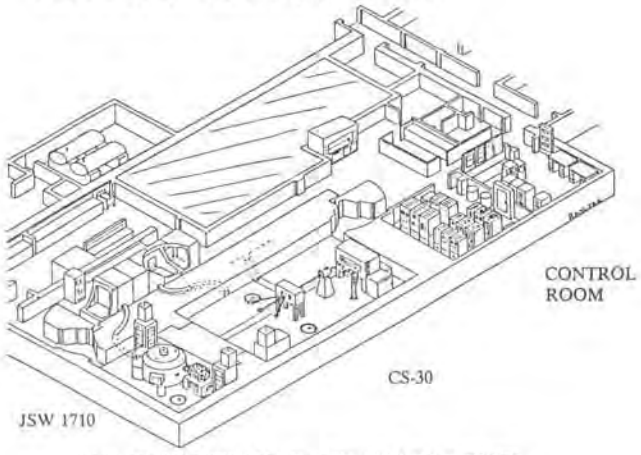
FACILITIES

SHIELDED AREA: Fixed 34 m² Moveable 6 m²
Target Stations: 1 No. Served At Same Time: 1
OTHER FACILITIES:
Target Changer
Hot Cells

REFERENCES/NOTES

(a) The Operational Status of the National Institutes
(b) of Health Cyclotron Complex, P. Plascjak, et al, Eleventh Int. Conf. on Cyclotrons and Applications, Ionics Publ., Tokyo (1987).

PLAN VIEW OF FACILITY, COMMENTS



NIH CYCLOTRON FACILITY B3 LEVEL

ENTRY NO. CU89 Date June 1992
Cyclotron Model TCC CS-30
Institution NIH Clinical Center
Address Bldg. 10, Rm. 1C401, Bethesda, MD 20892
Tel (301) 496-0345 Telex 89422
Fax (301) 496-0114 EMAIL PAUL@NMDHST.CC.NIH.GOV
In Charge: W. C. Eckelman Reported by: P. S. Plascjak

HISTORY

MILESTONE DATES:
Installation June 1985 First Beam Nov. 1985
DESIGN/CONSTRUCTION BY: The Cyclotron Corporation
COST: Accelerator Facility
FUNDED BY: National Institutes of Health

STATUS

STAFF: Operators 3 Technicians
BUDGET: Machine $100K Funded by NIH
TIME DISTRIBUTION: (e.g. basic research, isotope production, maintenance, etc.)
(a) Isotope Production 75 %
(b) Research & Development 20 %
(c) Maintenance 5 %
(d) %
(e) %

CHARACTERISTIC BEAMS

	Accelerated Ions	E/A (MeV/u)	Current(part μA) Internal	External
(a)	H+	26.5	200	60
(b)	d+, 3-He, 4-He			

1991 μA-hours on target: 8500

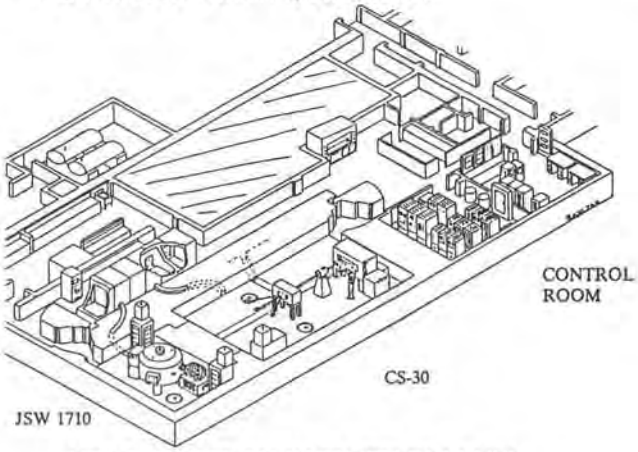
FACILITIES

SHIELDED AREA: Fixed 90 m² Moveable 6 m²
Target Stations: 7 No. Served At Same Time: 1
OTHER FACILITIES:
Target Changer
Hot Cells

REFERENCES/NOTES

(a) The Operational Status of the National Institutes
(b) of Health Cyclotron Complex, P. Plascjak, et al, Eleventh Int. Conf. on Cyclotrons and Applications, Ionics Publ., Tokyo (1987).

PLAN VIEW OF FACILITY, COMMENTS



NIH CYCLOTRON FACILITY B3 LEVEL

ENTRY NO. CU90 Date
Cyclotron Model NEN Cyclotron 1
Institution DuPont Merck Pharmaceutical Co.
Address 331 Treble Cove Rd. Billerica, MA 01862
Tel (508) 671-8012 Telex
Fax EMAIL
In Charge: Peter Holton Reported by: Frank Buck

HISTORY

MILESTONE DATES:
Installation 3/70 First Beam 7/70
DESIGN/CONSTRUCTION BY: Cyclotron Corp. CS-22
COST: Accelerator Facility
FUNDED BY: E.I. DuPont

STATUS

STAFF: Operators Technicians
BUDGET: Machine Funded by
TIME DISTRIBUTION: (e.g. basic research, isotope production, maintenance, etc.)
(a) Isotope Production 100 %
(b) %
(c) %
(d) %
(e) %

CHARACTERISTIC BEAMS

	Accelerated Ions	E/A (MeV/u)	Current(part μA) Internal	External
(a)	Protons	22	200	
(b)				

1991 μA-hours on target:

FACILITIES

SHIELDED AREA: Fixed 60 m² Moveable m²
Target Stations: 1 No. Served At Same Time:
OTHER FACILITIES:

REFERENCES/NOTES

(a)
(b)

PLAN VIEW OF FACILITY, COMMENTS

ENTRY NO. CU89 Date June 1992
Cyclotron Model TCC CS-30
Institution NIH Clinical Center
Address Bldg. 10, Rm. 1C401, Bethesda, MD 20892
Tel (301) 496-0345 Telex 89422
Fax (301) 496-0114 EMAIL PAUL@NMDHST.CC.NIH.GOV
In Charge: W. C. Eckelman Reported by: P. S. Plascjak

HISTORY

MILESTONE DATES:
Installation June 1985 First Beam Nov. 1985
DESIGN/CONSTRUCTION BY: The Cyclotron Corporation
COST: Accelerator Facility
FUNDED BY: National Institutes of Health

STATUS

STAFF: Operators 3 Technicians
BUDGET: Machine $100K Funded by NIH
TIME DISTRIBUTION: (e.g. basic research, isotope production, maintenance, etc.)
(a) Isotope Production 75 %
(b) Research & Development 20 %
(c) Maintenance 5 %
(d) %
(e) %

CHARACTERISTIC BEAMS

	Accelerated Ions	E/A (MeV/u)	Current(part μA) Internal	External
(a)	H+	26.5	200	60
(b)	d+, 3-He, 4-He			

1991 μA-hours on target: 8500

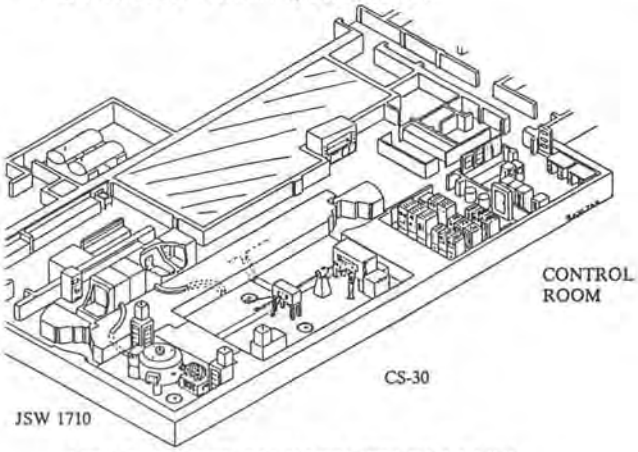
FACILITIES

SHIELDED AREA: Fixed 90 m² Moveable 6 m²
Target Stations: 7 No. Served At Same Time: 1
OTHER FACILITIES:
Target Changer
Hot Cells

REFERENCES/NOTES

(a) The Operational Status of the National Institutes
(b) of Health Cyclotron Complex, P. Plascjak, et al, Eleventh Int. Conf. on Cyclotrons and Applications, Ionics Publ., Tokyo (1987).

PLAN VIEW OF FACILITY, COMMENTS



NIH CYCLOTRON FACILITY B3 LEVEL

ENTRY NO. CU90 Date
Cyclotron Model NEN Cyclotron 1
Institution DuPont Merck Pharmaceutical Co.
Address 331 Treble Cove Rd. Billerica, MA 01862
Tel (508) 671-8012 Telex
Fax EMAIL
In Charge: Peter Holton Reported by: Frank Buck

HISTORY

MILESTONE DATES:
Installation 3/70 First Beam 7/70
DESIGN/CONSTRUCTION BY: Cyclotron Corp. CS-22
COST: Accelerator Facility
FUNDED BY: E.I. DuPont

STATUS

STAFF: Operators Technicians
BUDGET: Machine Funded by
TIME DISTRIBUTION: (e.g. basic research, isotope production, maintenance, etc.)
(a) Isotope Production 100 %
(b) %
(c) %
(d) %
(e) %

CHARACTERISTIC BEAMS

	Accelerated Ions	E/A (MeV/u)	Current(part μA) Internal	External
(a)	Protons	22	200	
(b)				

1991 μA-hours on target:

FACILITIES

SHIELDED AREA: Fixed 60 m² Moveable m²
Target Stations: 1 No. Served At Same Time:
OTHER FACILITIES:

REFERENCES/NOTES

(a)
(b)

PLAN VIEW OF FACILITY, COMMENTS

ENTRY NO. CU91 Date

Cyclotron Model NEN Cyclotron 2

Institution DuPont Merck Pharmaceutical Co.

Address 331 Treble Cove Rd. Billerica, MA 01862

Tel (508) 671-8012 Telex

Fax EMAIL

In Charge: Peter Holton Reported by: Frank Buck

HISTORY

MILESTONE DATES:

Installation 8/76 First Beam 11/76

DESIGN/CONSTRUCTION BY: Cyclotron Corp. CS-30

COST: Accelerator Facility

FUNDED BY: E.I. DuPont

STATUS

STAFF: Operators Technicians

BUDGET: Machine Funded by

TIME DISTRIBUTION: (e.g. basic research, isotope production, maintenance, etc.)

(a) Isotope Production 100 %

(b) %

(c) %

(d) %

(e) %

CHARACTERISTIC BEAMS

Accelerated Ions	E/A (MeV/u)	Current(part μA) Internal	External
(a) Protons	26	200	
(b)			

1991 μA-hours on target:

FACILITIES

SHIELDED AREA: Fixed 50 m^2 Moveable m^2

Target Stations: 1 No. Served At Same Time:

OTHER FACILITIES:

REFERENCES/NOTES

(a)

(b)

PLAN VIEW OF FACILITY, COMMENTS

ENTRY NO. CU92 Date

Cyclotron Model NEN Cyclotron 3

Institution DuPont Merck Pharmaceutical Co.

Address 331 Treble Cove Rd. Billerica, MA 01862

Tel (508) 671-8012 Telex

Fax EMAIL

In Charge: Peter Holton Reported by: Frank Buck

HISTORY

MILESTONE DATES:

Installation 5/78 First Beam 8/78

DESIGN/CONSTRUCTION BY: TME Cyclotron Corp. CS-30

COST: Accelerator Facility

FUNDED BY:

STATUS

STAFF: Operators Technicians

BUDGET: Machine Funded by

TIME DISTRIBUTION: (e.g. basic research, isotope production, maintenance, etc.)

(a) Isotope Production 100 %

(b) %

(c) %

(d) %

(e) %

CHARACTERISTIC BEAMS

Accelerated Ions	E/A (MeV/u)	Current(part μA) Internal	External
(a) Protons	26	200	
(b)			

1991 μA-hours on target:

FACILITIES

SHIELDED AREA: Fixed 50 m^2 Moveable m^2

Target Stations: 1 No. Served At Same Time:

OTHER FACILITIES:

REFERENCES/NOTES

(a)

(b)

PLAN VIEW OF FACILITY, COMMENTS

ENTRY NO. CU91 Date

Cyclotron Model NEN Cyclotron 2

Institution DuPont Merck Pharmaceutical Co.

Address 331 Treble Cove Rd. Billerica, MA 01862

Tel (508) 671-8012 Telex

Fax EMAIL

In Charge: Peter Holton Reported by: Frank Buck

HISTORY

MILESTONE DATES:

Installation 8/76 First Beam 11/76

DESIGN/CONSTRUCTION BY: Cyclotron Corp. CS-30

COST: Accelerator Facility

FUNDED BY: E.I. DuPont

STATUS

STAFF: Operators Technicians

BUDGET: Machine Funded by

TIME DISTRIBUTION: (e.g. basic research, isotope production, maintenance, etc.)

(a) Isotope Production 100 %

(b) %

(c) %

(d) %

(e) %

CHARACTERISTIC BEAMS

Accelerated Ions	E/A (MeV/u)	Current(part μA) Internal	External
(a) Protons	26	200	
(b)			

1991 μA-hours on target:

FACILITIES

SHIELDED AREA: Fixed 50 m^2 Moveable m^2

Target Stations: 1 No. Served At Same Time:

OTHER FACILITIES:

REFERENCES/NOTES

(a)

(b)

PLAN VIEW OF FACILITY, COMMENTS

ENTRY NO. CU92 Date

Cyclotron Model NEN Cyclotron 3

Institution DuPont Merck Pharmaceutical Co.

Address 331 Treble Cove Rd. Billerica, MA 01862

Tel (508) 671-8012 Telex

Fax EMAIL

In Charge: Peter Holton Reported by: Frank Buck

HISTORY

MILESTONE DATES:

Installation 5/78 First Beam 8/78

DESIGN/CONSTRUCTION BY: TME Cyclotron Corp. CS-30

COST: Accelerator Facility

FUNDED BY:

STATUS

STAFF: Operators Technicians

BUDGET: Machine Funded by

TIME DISTRIBUTION: (e.g. basic research, isotope production, maintenance, etc.)

(a) Isotope Production 100 %

(b) %

(c) %

(d) %

(e) %

CHARACTERISTIC BEAMS

Accelerated Ions	E/A (MeV/u)	Current(part μA) Internal	External
(a) Protons	26	200	
(b)			

1991 μA-hours on target:

FACILITIES

SHIELDED AREA: Fixed 50 m^2 Moveable m^2

Target Stations: 1 No. Served At Same Time:

OTHER FACILITIES:

REFERENCES/NOTES

(a)

(b)

PLAN VIEW OF FACILITY, COMMENTS

ENTRY NO. CU93 Date

Cyclotron Model NEN Cyclotron 4

Institution DuPont Merck Pharmaceutical Co.

Address 331 Treble Cove Rd. Billerica, MA 01862

Tel (508) 671-8012 Telex

Fax EMAIL

In Charge: Peter Holton Reported by: Frank Buck

HISTORY

MILESTONE DATES:

Installation 12/79 First Beam 7/80

DESIGN/CONSTRUCTION BY: Cyclotron Corp. CS-30

COST: Accelerator Facility

FUNDED BY: E.I. DuPont

STATUS

STAFF: Operators Technicians

BUDGET: Machine Funded by

TIME DISTRIBUTION: (e.g. basic research, isotope production, maintenance, etc.)

(a) Isotope Production 100 %

(b) %

(c) %

(d) %

(e) %

CHARACTERISTIC BEAMS

	Accelerated Ions	E/A (MeV/u)	Current(part μA) Internal	External
(a)	Protons	26	200	
(b)				

1991 μA-hours on target:

FACILITIES

SHIELDED AREA: Fixed 50 m² Moveable m²

Target Stations: 1 No. Served At Same Time:

OTHER FACILITIES:

REFERENCES/NOTES

(a)

(b)

PLAN VIEW OF FACILITY, COMMENTS

ENTRY NO. CU94 Date

Cyclotron Model NEN Cyclotron 5

Institution DuPont Merck Pharmaceutical Co.

Address 331 Treble Cove Rd. Billerica, MA 01862

Tel (508) 671-8012 Telex

Fax EMAIL

In Charge: Peter Holton Reported by: Frank Buck

HISTORY

MILESTONE DATES:

Installation 12/88 First Beam 1/89

DESIGN/CONSTRUCTION BY: SCANDITRONIX

COST: Accelerator Facility

FUNDED BY: E.I. DuPont

STATUS

STAFF: Operators Technicians

BUDGET: Machine Funded by

TIME DISTRIBUTION: (e.g. basic research, isotope production, maintenance, etc.)

(a) Isotpoe Production 100 %

(b) %

(c) %

(d) %

(e) %

CHARACTERISTIC BEAMS

	Accelerated Ions	E/A (MeV/u)	Current(part μA) Internal	External
(a)	Protons	30	200	
(b)				

1991 μA-hours on target:

FACILITIES

SHIELDED AREA: Fixed 90 m² Moveable 1 m²

Target Stations: 2 No. Served At Same Time: 1

OTHER FACILITIES:

REFERENCES/NOTES

(a)

(b)

PLAN VIEW OF FACILITY, COMMENTS

ENTRY NO. CU93 Date

Cyclotron Model NEN Cyclotron 4

Institution DuPont Merck Pharmaceutical Co.

Address 331 Treble Cove Rd. Billerica, MA 01862

Tel (508) 671-8012 Telex

Fax EMAIL

In Charge: Peter Holton Reported by: Frank Buck

HISTORY

MILESTONE DATES:

Installation 12/79 First Beam 7/80

DESIGN/CONSTRUCTION BY: Cyclotron Corp. CS-30

COST: Accelerator Facility

FUNDED BY: E.I. DuPont

STATUS

STAFF: Operators Technicians

BUDGET: Machine Funded by

TIME DISTRIBUTION: (e.g. basic research, isotope production, maintenance, etc.)

(a) Isotope Production 100 %

(b) %

(c) %

(d) %

(e) %

CHARACTERISTIC BEAMS

	Accelerated Ions	E/A (MeV/u)	Current(part μA) Internal	External
(a)	Protons	26	200	
(b)				

1991 μA-hours on target:

FACILITIES

SHIELDED AREA: Fixed 50 m² Moveable m²

Target Stations: 1 No. Served At Same Time:

OTHER FACILITIES:

REFERENCES/NOTES

(a)

(b)

PLAN VIEW OF FACILITY, COMMENTS

ENTRY NO. CU94 Date

Cyclotron Model NEN Cyclotron 5

Institution DuPont Merck Pharmaceutical Co.

Address 331 Treble Cove Rd. Billerica, MA 01862

Tel (508) 671-8012 Telex

Fax EMAIL

In Charge: Peter Holton Reported by: Frank Buck

HISTORY

MILESTONE DATES:

Installation 12/88 First Beam 1/89

DESIGN/CONSTRUCTION BY: SCANDITRONIX

COST: Accelerator Facility

FUNDED BY: E.I. DuPont

STATUS

STAFF: Operators Technicians

BUDGET: Machine Funded by

TIME DISTRIBUTION: (e.g. basic research, isotope production, maintenance, etc.)

(a) Isotpoe Production 100 %

(b) %

(c) %

(d) %

(e) %

CHARACTERISTIC BEAMS

	Accelerated Ions	E/A (MeV/u)	Current(part μA) Internal	External
(a)	Protons	30	200	
(b)				

1991 μA-hours on target:

FACILITIES

SHIELDED AREA: Fixed 90 m² Moveable 1 m²

Target Stations: 2 No. Served At Same Time: 1

OTHER FACILITIES:

REFERENCES/NOTES

(a)

(b)

PLAN VIEW OF FACILITY, COMMENTS

ENTRY NO. CU95 Date

Cyclotron Model NEN Cyclotron 6

Institution DuPont Merck Pharmaceutical Co.

Address 331 Treble Cove Rd. Billerica, MA 01862

Tel (508) 671-8012 Telex

Fax EMAIL

In Charge: Peter Holton Reported by: Frank Buck

HISTORY

MILESTONE DATES:

Installation 6/90 First Beam 11/90

DESIGN/CONSTRUCTION BY: IBA

COST: Accelerator Facility

FUNDED BY: E.I. DuPont

STATUS

STAFF: Operators Technicians

BUDGET: Machine Funded by

TIME DISTRIBUTION: (e.g. basic research, isotope production, maintenance, etc.)

(a) Isotope Production 100 %

(b) %

(c) %

(d) %

(e) %

CHARACTERISTIC BEAMS

	Accelerated Ions	E/A (MeV/u)	Current(part μA) Internal	External
(a)	H-	30	-	200
(b)				

1991 μA-hours on target:

FACILITIES

SHIELDED AREA: Fixed 200 m² Moveable m²

Target Stations: 3 No. Served At Same Time: 1

OTHER FACILITIES:

REFERENCES/NOTES

(a)

(b)

PLAN VIEW OF FACILITY, COMMENTS

ENTRY NO. CU97 Date 7/5/1992

Cyclotron Model IBA Cyclone 30

Institution State U. of N.Y. Nuclear Med.

Address 105 Parker Hall 3435 Main St. Buffalo NY, 14214

Tel 716 838 5889 Telex

Fax 716 838 4918 EMAIL NRCFREDC@UBVMS.CC.BUFF

In Charge: Dr. Ackerhalt Reported by: Philip Orlosky

HISTORY

MILESTONE DATES:

Installation 8/92 First Beam 12/92

DESIGN/CONSTRUCTION BY: Wendel Eng./Le Chase Const.

COST: Accelerator 2,800,000 Facility 3,800,000

FUNDED BY: State U. of NY Buffalo and Veterans Adm. Hosp

STATUS

STAFF: Operators Technicians

BUDGET: Machine Funded by

TIME DISTRIBUTION: (e.g. basic research, isotope production, maintenance, etc.)

(a) PET Targets (Anticipated) 25 %

(b) Research " 25 %

(c) Maintenance " 15 %

(d) Isotope Production " 35 %

(e) %

CHARACTERISTIC BEAMS

	Accelerated Ions	E/A (MeV/u)	Current(part μA) Internal	External
(a)	H	30	350	350
(b)				

1991 μA-hours on target: 0

FACILITIES

SHIELDED AREA: Fixed 55 m² Moveable 0 m²

Target Stations: 10 No. Served At Same Time: 2

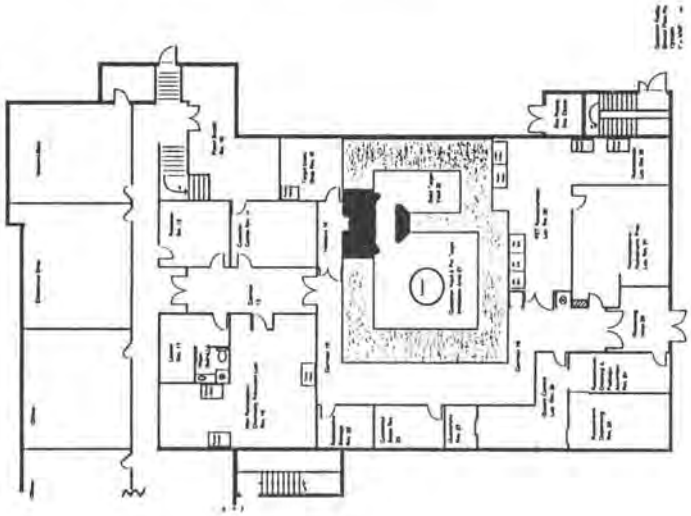
OTHER FACILITIES:

REFERENCES/NOTES

(a)

(b)

PLAN VIEW OF FACILITY, COMMENTS



ENTRY NO. CU95 Date

Cyclotron Model NEN Cyclotron 6

Institution DuPont Merck Pharmaceutical Co.

Address 331 Treble Cove Rd. Billerica, MA 01862

Tel (508) 671-8012 Telex

Fax EMAIL

In Charge: Peter Holton Reported by: Frank Buck

HISTORY

MILESTONE DATES:

Installation 6/90 First Beam 11/90

DESIGN/CONSTRUCTION BY: IBA

COST: Accelerator Facility

FUNDED BY: E.I. DuPont

STATUS

STAFF: Operators Technicians

BUDGET: Machine Funded by

TIME DISTRIBUTION: (e.g. basic research, isotope production, maintenance, etc.)

(a) Isotope Production 100 %

(b) %

(c) %

(d) %

(e) %

CHARACTERISTIC BEAMS

	Accelerated Ions	E/A (MeV/u)	Current(part μA) Internal	External
(a)	H-	30	-	200
(b)				

1991 μA-hours on target:

FACILITIES

SHIELDED AREA: Fixed 200 m² Moveable m²

Target Stations: 3 No. Served At Same Time: 1

OTHER FACILITIES:

REFERENCES/NOTES

(a)

(b)

PLAN VIEW OF FACILITY, COMMENTS

ENTRY NO. CU97 Date 7/5/1992

Cyclotron Model IBA Cyclone 30

Institution State U. of N.Y. Nuclear Med.

Address 105 Parker Hall 3435 Main St. Buffalo NY, 14214

Tel 716 838 5889 Telex

Fax 716 838 4918 EMAIL NRCFREDC@UBVMS.CC.BUFF

In Charge: Dr. Ackerhalt Reported by: Philip Orlosky

HISTORY

MILESTONE DATES:

Installation 8/92 First Beam 12/92

DESIGN/CONSTRUCTION BY: Wendel Eng./Le Chase Const.

COST: Accelerator 2,800,000 Facility 3,800,000

FUNDED BY: State U. of NY Buffalo and Veterans Adm. Hosp

STATUS

STAFF: Operators Technicians

BUDGET: Machine Funded by

TIME DISTRIBUTION: (e.g. basic research, isotope production, maintenance, etc.)

(a) PET Targets (Anticipated) 25 %

(b) Research " 25 %

(c) Maintenance " 15 %

(d) Isotope Production " 35 %

(e) %

CHARACTERISTIC BEAMS

	Accelerated Ions	E/A (MeV/u)	Current(part μA) Internal	External
(a)	H	30	350	350
(b)				

1991 μA-hours on target: 0

FACILITIES

SHIELDED AREA: Fixed 55 m² Moveable 0 m²

Target Stations: 10 No. Served At Same Time: 2

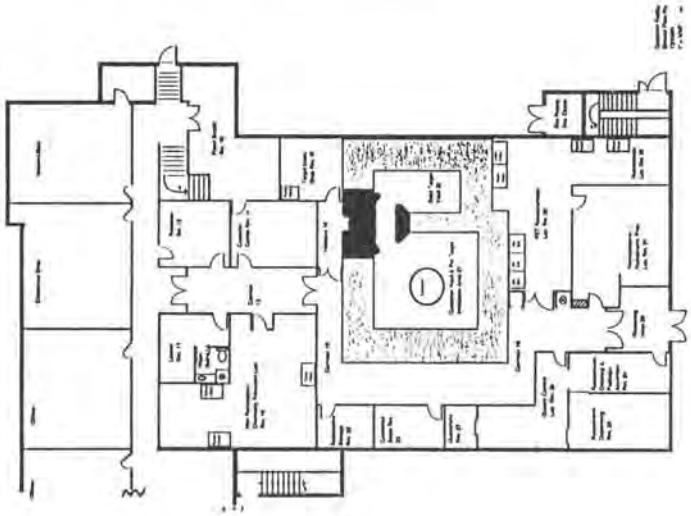
OTHER FACILITIES:

REFERENCES/NOTES

(a)

(b)

PLAN VIEW OF FACILITY, COMMENTS



ENTRY NO. CU98
NAME OF MACHINE FMI CYCLOTRON
INSTITUTION Franklin McLean Memorial Research Institute
ADDRESS 5841 S. Maryland Avenue, Chicago, Illinois 60637
TEL TELEX
IN CHARGE S. J. Gatley REPORTED BY A. J. Creer/N. Odeh

HISTORY AND STATUS
DESIGN, date 1965 Model tests 1967
ENG DESIGN, date 1965-67
CONSTRUCTION, date 1969
FIRST BEAM, date (or goal) July, 1969
MAJOR ALTERATIONS Deflector

COST, ACCELERATOR 240,000
COST, FACILITY, total 600K
FUNDED BY Department of Energy

ACCELERATOR STAFF, OPERATION AND DEVELOPMENT
SCIENTISTS 5 ENGINEERS 1
TECHNICIANS 4 CRAFTS 1
GRAD STUDENTS involved during year -
OPERATED BY X Research staff or Operators
OPERATION 15 hr/wk On target 10 hr/wk
TIME DISTR. in house 100 % outside - %
BUDGET, op & dev
FUNDED BY

RESEARCH STAFF, not included above
USERS, in house Yes outside -
GRAD STUDENTS involved during year 4
RESEARCH BUDGET, in house
FUNDED BY

MAGNET
POLE FACE, diameter (compact) 81 cm, R-extraction 35 cm
R injection cm
GAP, min 5 cm, Field 20 kG
max 10 cm, Field 12 kG at .2 x 10^5 Ampere turns
AVERAGE FIELD at R ext 16 kG
B max/<B> 1.25
NUMBER OF SECTORS {compact / separated} Spiral, max deg
SECTOR ANGLE (SSC) deg
TRIMMING COILS 3 ea. 8 Turns 100A max.

CONDUCTOR, material and type AL Foil 1 mm
STORED ENERGY (cryogenic) MJ
POWER: main coils 58 max kW, current stability 5 x 10^{-4}
trimming coils max kW, current stability
WEIGHT Fe 14 tons, coils tons
COOLING system Water
ION ENERGY (Bending limit) E/A = q^2/A^2 MeV/amu
(Focusing limit) E/A = q/A MeV/amu

ACCELERATION SYSTEM
DEES, number 2 angle deg
BEAM APERTURE 2 cm, DC Bias 1.5 KV kV
TUNED by, coarse MS fine VC Trimmer
RF 12 to 25 MHz, stable ± 1 x 10^{-4}
Orb F 12 to 25 MHz
HARMONICS, RF/Orb F, used
DEE–Gnd, max 30 kV, min gap cm
STABILITY, (pk-pk noise)/(pk RF volt)
ENERGY GAIN, max 60 max kV/turn
RF PHASE, stable to ± deg
RF POWER input, max. 29 kW
FREQUENCY MODULATION, rate /s
modulator, type
beam pulse, width

VACUUM SYSTEM
OPERATING PRESSURE 1 x 10^{-5} Torr or mbar
PUMPS, No, Type, Size 1 ea. 10" Oil Diffusion,
1 ea. 21 CFM Mechanical

ION SOURCES
Ion Heated Pig

INJECTION SYSTEM
None

EXTRACTION SYSTEM
Electrostatic Channel with Compensated Iron Chann

FACILITIES FOR RESEARCH
SHIELDED AREA, fixed 62 m^2, movable -- m^2
TARGET STATIONS 2 in 2 rooms
STATIONS served at same time, max 1
MAG SPECTROGRAPH, type --
COMPUTER model --
OTHER FACILITIES

CHARACTERISTIC BEAMS

PARTICLE	ENERGY (MeV) Goal	Achieved	CURRENT (μA) Internal	External
Proton	15	14.8	110	55
Deut.	8	8.3	400	270
He 3^{++}	20	20.3	120	53
He 4^{++}	15	15	80	40
SECONDARY			(part/s)	

BEAM PROPERTIES

	MEASURED		CONDITIONS		
PULSE WIDTH	RF deg		pμA of	MeV	ions
PHASE EXC. max	RF deg		pμA of	MeV	ions
EXTRACT eff.	55 %	270	pμA of	8 MeV	D ions
RESOL ΔE/E	1 %		pμA of	MeV	ions
EMITTANCE					
(π mm-mrad)	50 axial, 50 rad	90	pμA of	MeV	

OPERATING PROGRAMS, time distribution
BASIC NUCLEAR PHYSICS SOLID STATES PHYSICS
BIOMEDICAL APPLICAT 100% ISOTOPE PRODUCTIONS

REFERENCES/NOTES In AIP Conference Proceedings, #9, 1
1)Compact Cyclotron Engg. G.O. Hendry
2)ACRH Cyclotron, P.V. Harper
3) Design of Neutron Therapy Facility, F.T. Kuchnier

PLAN VIEW OF FACILITY, COMMENTS, ETC.

1. ^3He recovery system for economical $^3He^{++}$ operation
2. Particle changes are made in 30 minutes
3. Targets may be irradiated internally or externally
4. Two external target stations; one for isotope, the other for neutron production
5. External beams transport system includes two quadrupole doublets, one steering magnet, one switching magnet, and four collimators

ENTRY No. CU99

NAME OF MACHINE Medi-Physics Cyclotron DATE

INSTITUTION Medi-Physics, Inc.

ADDRESS 5855 Christie Ave., Emeryville, CA 94608 - USA

TEL TELEX

IN CHARGE E.R. Russell REPORTED BY E.R. Russell

HISTORY AND STATUS

DESIGN, date Model tests

ENG DESIGN, date

CONSTRUCTION, date

FIRST BEAM, date (or goal) Accepted 12/70

MAJOR ALTERATIONS None

COST, ACCELERATOR

COST, FACILITY, total

FUNDED BY Medi-Physics, Inc.

ACCELERATOR STAFF, OPERATION AND DEVELOPMENT

SCIENTISTS 1 ENGINEERS

TECHNICIANS 5 CRAFTS

GRAD STUDENTS involved during year

OPERATED BY Research staff or Operators

OPERATION 168 hr/wk, On target 120 hr/wk

TIME DISTR. In house 99 %, Outside 1 %

BUDGET, op & dev

FUNDED BY Medi-Physics, Inc.

RESEARCH STAFF, not included above

USERS, In house outside

GRAD STUDENTS involved during year

RESEARCH BUDGET, In house

FUNDED BY

MAGNET

POLE FACE, diameter (compact) 97 cm, R extraction 42 cm

R injection cm

GAP, min 5 cm, Field 21 kG
max 10 cm, Field 13.5 kG
at 2×10^6 Ampere turns

AVERAGE FIELD at R ext 16.5 kG

B max/ <B> 1.22

NUMBER OF SECTORS compact / separated Spiral, max deg

SECTOR ANGLE (SSC) deg

TRIMMING COILS Harmonic correction 1

CONDUCTOR, material and type

STORED ENERGY (cryogenic) MJ

POWER : main coils max, kW ; current stability 3×10^{-5}
trimming coils max, kW ; current stability

WEIGHT : Fe 19.5 tons ; coils tons

COOLING system

ION ENERGY (bending limit) E/A = q^2/a^2 MeV/amu
(focusing limit) E/A = q^2/a^2 MeV/amu

ACCELERATION SYSTEM

DEES, number 2 ; angle 90 deg

BEAM APERTURE 2 cm ; DC Bias 1.5 kV

TUNED by, coarse straps fine panel

RF 12 to 25 mHz, stable ±

Orb F to mHz

HARMONICS, RF/Orb F, used

DEE - Gnd, max 30 kV, min gap cm

STABILITY, (pk-pk noise)/(pk RF volt)

ENERGY GAIN, max 100 kV/turn

RF PHASE, stable to ± deg

RF POWER input, max 70 kW

FREQUENCY MODULATION, rate /s
modulator, type
beam pulse, width

VACUUM SYSTEM

OPERATING PRESSURE Torr or mbar

PUMPS, No, Type, Size

ION SOURCES

Internal cold cathode[1)]

INJECTION SYSTEM

EXTRACTION SYSTEM

Electrostatic and magnetic channel

FACILITIES FOR RESEARCH

SHIELDED AREA, fixed 100 m² ; movable m²

TARGET STATIONS 8 In 1 rooms

STATIONS served at same time, max 1

MAG SPECTROGRAPH, type None

COMPUTER model None

OTHER FACILITIES

CHARACTERISTIC BEAMS

PARTICLE	ENERGY (MeV) Goal	Achieved	CURRENT (pμA) Internal	External
p		22	400	60
d		12	400	100
^{3}He		32	100	50
SECONDARY				(part/s)

BEAM PROPERTIES

MEASURED		CONDITIONS
PULSE WIDTH	RF deg	pμ A of MeV ions
PHASE EXC, max	RF deg	pμ A of MeV ions
EXTRACT eff	%	pμ A of MeV ions
RESOL ΔE/E	%	pμ A of MeV ions
EMITTANCE		
(π mm. mrad)	axial / rad	pμA of MeV ions

OPERATING PROGRAMS, time distribution

BASIC NUCLEAR PHYSICS .. SOLID STATES PHYSICS ....

BIOMEDICAL APPLICAT. .... ISOTOPE PRODUCTIONS 100.

REFERENCES/NOTES

1) IEEE Trans. Nucl. Sci. NS-14, 70-71 (1967)
2) IEEE Trans. Nucl. Sci. NS-16, 500-503 (1969)

PLAN VIEW OF FACILITY, NOTEWORTHY FEATURES. COMMENTS

Designed by the Cyclotron Corporation.

* Data confirmed October, 1981.

ENTRY NO. CU100 **Date**
Cyclotron Model RDS 112
Institution The Christ Hospital
Address 2139 Auburn Ave. Cincinnati, OH 45219
Tel (513)369-8833 Telex
Fax (513)369-8835 EMAIL USR1436A@TSO.UC.EDU
In Charge: Tom Kemme Reported by: Danny Bingham

HISTORY

MILESTONE DATES:
Installation 8/5-10/24/91 First Beam 9/5/91
DESIGN/CONSTRUCTION BY: CTI/CTI
COST: Accelerator Facility
FUNDED BY:

STATUS

STAFF: Operators 3 Technicians 2
BUDGET: Machine Funded by
TIME DISTRIBUTION: (e.g. basic research, isotope production, maintenance, etc.)
(a) Isotope Production 95 %
(b) Maintenance 5 %
(c) %
(d) %
(e) %

CHARACTERISTIC BEAMS

Accelerated Ions	E/A (MeV/u)	Current(part μA) Internal	External
(a) H^-	11 MeV	300 uA H^-	100 uA H^+
(b)			

1991 μA-hours on target: 4100

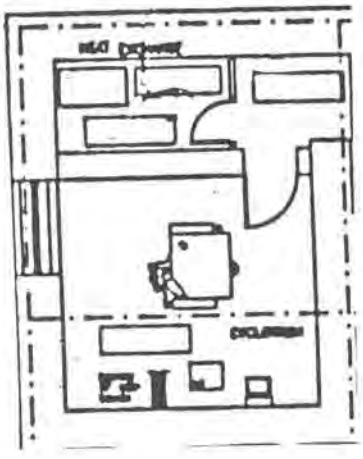
FACILITIES

SHIELDED AREA: Fixed 100 m^2 Moveable m^2
Target Stations: 4 No. Served At Same Time: 2
OTHER FACILITIES:

REFERENCES/NOTES

(a)
(b)

PLAN VIEW OF FACILITY, COMMENTS



ENTRY NO. CU102 **Date** 6/22/92
Cyclotron Model CP-42
Institution University of Texas - M.D. Anderson
Address 1515 Holcombe Blvd., Houston, TX 77030
Tel (713) 792-3238 Telex
Fax (713) 792-3642 EMAIL MALLORY @ UTMDAPHY
In Charge: M. Mallory Reported by: M. Mallory

HISTORY

MILESTONE DATES:
Installation 1980 First Beam 1981
DESIGN/CONSTRUCTION BY: The Cyclotron Corporation
COST: Accelerator Facility
FUNDED BY:

STATUS

STAFF: Operators 5 Technicians
BUDGET: Machine Funded by
TIME DISTRIBUTION: (e.g. basic research, isotope production, maintenance, etc.)
(a) Neutron Therapy 41 %
(b) PET Isotopes 53 %
(c) Research 6 %
(d) %
(e) %

CHARACTERISTIC BEAMS

Accelerated Ions	E/A (MeV/u)	Current(part μA) Internal	External
(a) H^-	30 - 42	50	50*
(b)			

1991 Number of patients served. 250

FACILITIES

SHIELDED AREA: Fixed 133.6 m^2 Moveable m^2
Target Stations: 4 No. Served At Same Time: 1
OTHER FACILITIES:
New construction to start 1993

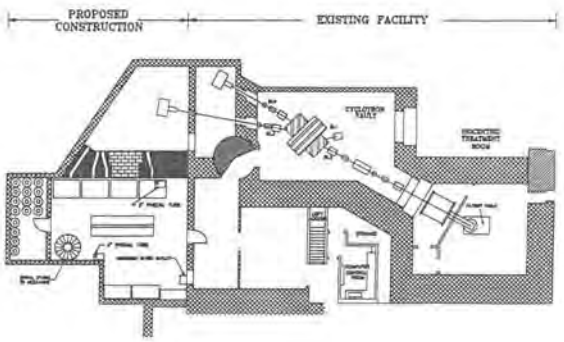
REFERENCES/NOTES

(a)
(b)
*Target Limit

PLAN VIEW OF FACILITY, COMMENTS



THE UNIVERSITY OF TEXAS
M.D. ANDERSON CANCER CENTER
EXISTING & PROPOSED LAYOUT
FOR CYCLOTRON FACILITY



ENTRY NO. CU100 **Date**
Cyclotron Model RDS 112
Institution The Christ Hospital
Address 2139 Auburn Ave. Cincinnati, OH 45219
Tel (513)369-8833 Telex
Fax (513)369-8835 EMAIL USR1436A@TSO.UC.EDU
In Charge: Tom Kemme Reported by: Danny Bingham

HISTORY

MILESTONE DATES:
Installation 8/5-10/24/91 First Beam 9/5/91
DESIGN/CONSTRUCTION BY: CTI/CTI
COST: Accelerator Facility
FUNDED BY:

STATUS

STAFF: Operators 3 Technicians 2
BUDGET: Machine Funded by
TIME DISTRIBUTION: (e.g. basic research, isotope production, maintenance, etc.)
(a) Isotope Production 95 %
(b) Maintenance 5 %
(c) %
(d) %
(e) %

CHARACTERISTIC BEAMS

Accelerated Ions	E/A (MeV/u)	Current(part μA) Internal	External
(a) H^-	11 MeV	300 uA H^-	100 uA H^+
(b)			

1991 μA-hours on target: 4100

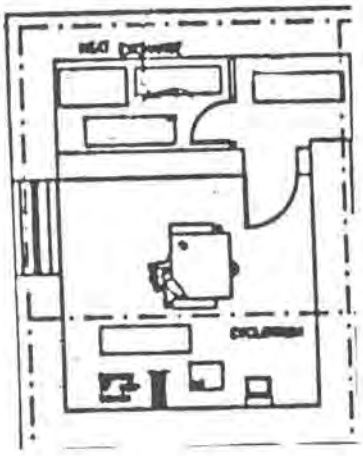
FACILITIES

SHIELDED AREA: Fixed 100 m^2 Moveable m^2
Target Stations: 4 No. Served At Same Time: 2
OTHER FACILITIES:

REFERENCES/NOTES

(a)
(b)

PLAN VIEW OF FACILITY, COMMENTS



ENTRY NO. CU102 **Date** 6/22/92
Cyclotron Model CP-42
Institution University of Texas - M.D. Anderson
Address 1515 Holcombe Blvd., Houston, TX 77030
Tel (713) 792-3238 Telex
Fax (713) 792-3642 EMAIL MALLORY @ UTMDAPHY
In Charge: M. Mallory Reported by: M. Mallory

HISTORY

MILESTONE DATES:
Installation 1980 First Beam 1981
DESIGN/CONSTRUCTION BY: The Cyclotron Corporation
COST: Accelerator Facility
FUNDED BY:

STATUS

STAFF: Operators 5 Technicians
BUDGET: Machine Funded by
TIME DISTRIBUTION: (e.g. basic research, isotope production, maintenance, etc.)
(a) Neutron Therapy 41 %
(b) PET Isotopes 53 %
(c) Research 6 %
(d) %
(e) %

CHARACTERISTIC BEAMS

Accelerated Ions	E/A (MeV/u)	Current(part μA) Internal	External
(a) H^-	30 - 42	50	50*
(b)			

1991 Number of patients served. 250

FACILITIES

SHIELDED AREA: Fixed 133.6 m^2 Moveable m^2
Target Stations: 4 No. Served At Same Time: 1
OTHER FACILITIES:
New construction to start 1993

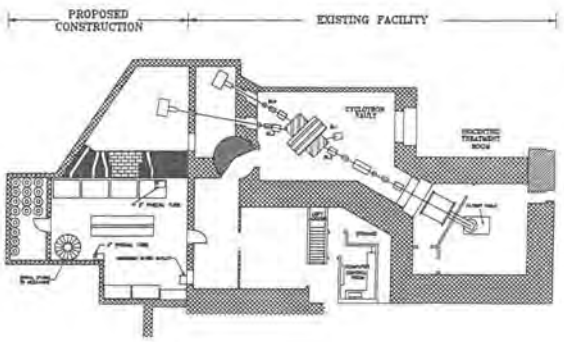
REFERENCES/NOTES

(a)
(b)
*Target Limit

PLAN VIEW OF FACILITY, COMMENTS



THE UNIVERSITY OF TEXAS
M.D. ANDERSON CANCER CENTER
EXISTING & PROPOSED LAYOUT
FOR CYCLOTRON FACILITY



ENTRY No. CU106

NAME OF MACHINE Biomedical cyclotron DATE 7/10/78
INSTITUTION University of California - Center for the Health Sciences
ADDRESS Los Angeles, CA 80024 - USA
TEL TELEX
IN CHARGE N.S. Mac Donald Ph-D REPORTED BY N. S. Mac Donald Ph-D

HISTORY AND STATUS CS-22
DESIGN, date Cyclotron Corp. Model tests 1970
ENG DESIGN, date
CONSTRUCTION, date
FIRST BEAM, date (or goal) 3/15/71
MAJOR ALTERATIONS

COST, ACCELERATOR
COST, FACILITY, total $ 700,000
FUNDED BY AEC, University

ACCELERATOR STAFF, OPERATION AND DEVELOPMENT
SCIENTISTS 1 ENGINEERS 2
TECHNICIANS 2 CRAFTS
GRAD STUDENTS involved during year 1
OPERATED BY x Research staff or Operators
OPERATION 50 hr/wk, On target 24 hr/wk
TIME DISTR. In house 100 %, Outside %
BUDGET, op & dev
FUNDED BY

RESEARCH STAFF, not included above
USERS, In house 3 outside 2
GRAD STUDENTS involved during year 1
RESEARCH BUDGET, In house
FUNDED BY D.O.E.

MAGNET
POLE FACE, diameter (compact) 97 cm, R extraction 40.5 cm
R injection cm
GAP, min 5 cm, Field 20 kG
max 10 cm, Field 12 kG } at 2.10^5 Ampere turns
AVERAGE FIELD at R ext 16 kG
B max/ <B> 1.25
NUMBER OF SECTORS { compact 3 / separated } Spiral, max deg
SECTOR ANGLE (SSC) deg
TRIMMING COILS 3/sect

CONDUCTOR, material and type
STORED ENERGY (cryogenic) MJ
POWER: main coils 30 max, kW ; current stability 3.10^-5
trimming coils max, kW ; current stability
WEIGHT : Fe 24 tons ; coils tons
COOLING system
ION ENERGY (bending limit) E/A = q²/a² MeV/amu
(focusing limit) E/A = q²/a² MeV/amu

ACCELERATION SYSTEM
DEES, number 2 ; angle 180 deg
BEAM APERTURE 4 cm ; DC Bias 2.5 kV
TUNED by, coarse straps fine VC, auto
RF 12 to 25 mHz, stable ± 10^-5
Orb F to mHz
HARMONICS, RF/Orb F, used
DEE - Gnd, max 25 kV, min gap 1 cm
STABILITY, (pk-pk noise)/(pk RF volt) 17/12 kV
ENERGY GAIN, max kV/turn
RF PHASE, stable to ± deg
RF POWER input, max 150 kW
FREQUENCY MODULATION, rate /s
modulator, type
beam pulse, width

VACUUM SYSTEM
OPERATING PRESSURE Torr or mbar
PUMPS, No, Type, Size

ION SOURCES
Penning, cold cathode

INJECTION SYSTEM

EXTRACTION SYSTEM
DC electrostatic, mag. channel

FACILITIES FOR RESEARCH
SHIELDED AREA, fixed m² ; movable m²
TARGET STATIONS 1 in 1 rooms
STATIONS served at same time, max 1
MAG SPECTROGRAPH, type
COMPUTER model
OTHER FACILITIES Isotope production
Irradiation, solid state

CHARACTERISTIC BEAMS

PARTICLE	ENERGY (MeV) Goal	Achieved	CURRENT (pμA) Internal	External
p	22.1	22.1	100	52
d	12.2	12.2	750	75
^{3}He	31.6	31.6	90	50
α			95	55
SECONDARY				(part/s)

BEAM PROPERTIES

MEASURED		CONDITIONS
PULSE WIDTH	RF deg	pμ A of MeV ions
PHASE EXC, max	RF deg	pμ A of MeV ions
EXTRACT eff 60-70	% 100	pμ A of 22 MeV p ions
RESOL ΔE/E	%	pμ A of MeV ions

EMITTANCE
(π mm. mrad) { axial / rad } pμA of MeV ions

OPERATING PROGRAMS, time distribution
BASIC NUCLEAR PHYSICS
SOLID STATES PHYSICS
BIOMEDICAL APPLICAT.
ISOTOPE PRODUCTIONS

REFERENCES/NOTES

PLAN VIEW OF FACILITY, NOTEWORTHY FEATURES, COMMENTS

- Prinicpal use: preparing radionuclides for the nuclear medicine clinic of the hospital and for research in biology and medicine.
- Quantitative analysis of ^{18}O in small water samples of biological origin by proton activation to ^{18}F are routine.

ENTRY NO. CU108 **Date**
Cyclotron Model RDS 11 MeV Siemens
Institution USC / SYNCOR
Address 2250 Alcazar St., Los Angeles CA 90033
Tel 213 225 0195 Telex
Fax 213 225 0198 EMAIL
In Charge: Ben Trickey Reported by: Gerald Kuhs /Diana Tribbey

HISTORY

MILESTONE DATES:
Installation Sept. 91 First Beam Jan. 92
DESIGN/CONSTRUCTION BY: Laffin-Lietz Architect, Kemp
COST: Accelerator Facility
FUNDED BY: USC / SYNCOR

STATUS

STAFF: Operators 2 Technicians 1
BUDGET: Machine Funded by SYNCOR
TIME DISTRIBUTION: (e.g. basic research, isotope production, maintenance, etc.)
(a) PET clinical 90 %
(b) PET research 10 %
(c) %
(d) %
(e) %

CHARACTERISTIC BEAMS

	Accelerated Ions	E/A (MeV/u)	Current(part μA) Internal	External
(a)	H^-	11 MeV		
(b)				

1991 μA-hours on target:

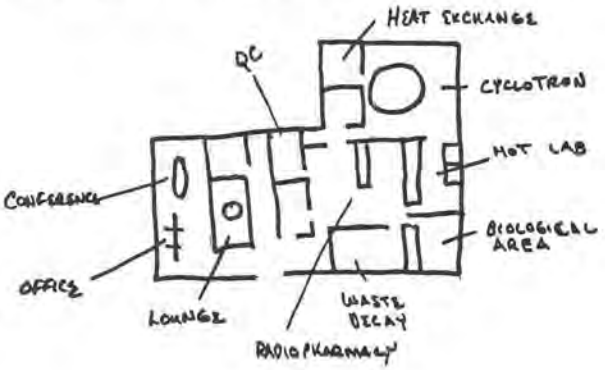
FACILITIES

SELFSHIELDED
SHIELDED AREA: Fixed m² Moveable m²
Target Stations: 4 No. Served At Same Time: 2
OTHER FACILITIES:
On Site Radiopharmacy
Regional Distribution Center

REFERENCES/NOTES

(a)
(b)

PLAN VIEW OF FACILITY, COMMENTS



ENTRY NO. CU109 **Date** 9/8/92
Cyclotron Model CTI RDS, Fe I (first one)
Institution University of Wisconsin
Address 1530 Medical Science Center, 1300 Univ. Ave. Madison
Tel 608 262 2170 Telex
Fax 608 262 2413 EMAIL
In Charge: R.J. Moddes Reported by: R.J. Moddes

HISTORY

MILESTONE DATES:
Installation May 1986 First Beam 18 days after arr.
DESIGN/CONSTRUCTION BY: CTI Inc.
COST: Accelerator $499,322 Facility $55,000
FUNDED BY: Intramural Sources (UW)

STATUS

STAFF: Operators 5 Technicians 0
BUDGET: Machine 30K Funded by UW
TIME DISTRIBUTION: (e.g. basic research, isotope production, maintenance, etc.)
(a) Basic Research 30 %
(b) Isotope Production 65 %
(c) Maintenance <5 %
(d) %
(e) %

CHARACTERISTIC BEAMS

	Accelerated Ions	E/A (MeV/u)	Current(part μA) Internal	External
(a)	protons	11.4	<60	<50
(b)				

1991 μA-hours on target: 1400 hours since 1986/300 hrs in 91

FACILITIES

SHIELDED AREA: Fixed 400 m² Moveable m²
Target Stations: 4 No. Served At Same Time: 2
OTHER FACILITIES: vertical switching magnet for a downward directed beam for molten targets, 12 interchangable targets, mach detector development

REFERENCES/NOTES

(a)
(b)

PLAN VIEW OF FACILITY, COMMENTS

ENTRY NO. CU108 **Date**
Cyclotron Model RDS 11 MeV Siemens
Institution USC / SYNCOR
Address 2250 Alcazar St., Los Angeles CA 90033
Tel 213 225 0195 Telex
Fax 213 225 0198 EMAIL
In Charge: Ben Trickey Reported by: Gerald Kuhs /Diana Tribbey

HISTORY

MILESTONE DATES:
Installation Sept. 91 First Beam Jan. 92
DESIGN/CONSTRUCTION BY: Laffin-Lietz Architect, Kemp
COST: Accelerator Facility
FUNDED BY: USC / SYNCOR

STATUS

STAFF: Operators 2 Technicians 1
BUDGET: Machine Funded by SYNCOR
TIME DISTRIBUTION: (e.g. basic research, isotope production, maintenance, etc.)
(a) PET clinical 90 %
(b) PET research 10 %
(c) %
(d) %
(e) %

CHARACTERISTIC BEAMS

	Accelerated Ions	E/A (MeV/u)	Current(part μA) Internal	External
(a)	H^-	11 MeV		
(b)				

1991 μA-hours on target:

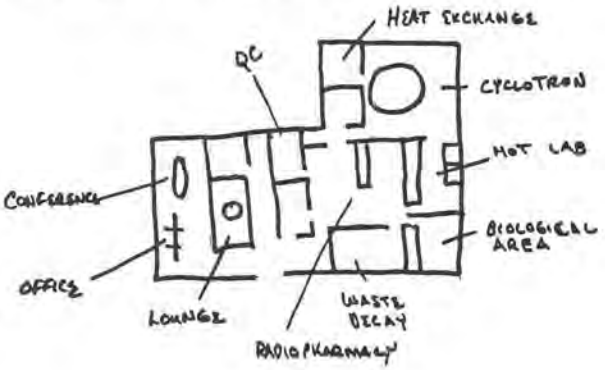
FACILITIES

SELFSHIELDED
SHIELDED AREA: Fixed m² Moveable m²
Target Stations: 4 No. Served At Same Time: 2
OTHER FACILITIES:
On Site Radiopharmacy
Regional Distribution Center

REFERENCES/NOTES

(a)
(b)

PLAN VIEW OF FACILITY, COMMENTS



ENTRY NO. CU109 **Date** 9/8/92
Cyclotron Model CTI RDS, Fe I (first one)
Institution University of Wisconsin
Address 1530 Medical Science Center, 1300 Univ. Ave. Madison
Tel 608 262 2170 Telex
Fax 608 262 2413 EMAIL
In Charge: R.J. Moddes Reported by: R.J. Moddes

HISTORY

MILESTONE DATES:
Installation May 1986 First Beam 18 days after arr.
DESIGN/CONSTRUCTION BY: CTI Inc.
COST: Accelerator $499,322 Facility $55,000
FUNDED BY: Intramural Sources (UW)

STATUS

STAFF: Operators 5 Technicians 0
BUDGET: Machine 30K Funded by UW
TIME DISTRIBUTION: (e.g. basic research, isotope production, maintenance, etc.)
(a) Basic Research 30 %
(b) Isotope Production 65 %
(c) Maintenance <5 %
(d) %
(e) %

CHARACTERISTIC BEAMS

	Accelerated Ions	E/A (MeV/u)	Current(part μA) Internal	External
(a)	protons	11.4	<60	<50
(b)				

1991 μA-hours on target: 1400 hours since 1986/300 hrs in 91

FACILITIES

SHIELDED AREA: Fixed 400 m² Moveable m²
Target Stations: 4 No. Served At Same Time: 2
OTHER FACILITIES: vertical switching magnet for a downward directed beam for molten targets, 12 interchangable targets, mach detector development

REFERENCES/NOTES

(a)
(b)

PLAN VIEW OF FACILITY, COMMENTS

ENTRY NO. CU111 Date July 15, 1992
Cyclotron Model CS-30
Institution Mount Sinai Medical Center
Address 4300 Alton Road, Miami Beach, Florida 33140
Tel (305)674-2465 Telex
Fax (305)674-2996 EMAIL
In Charge: Thomas Boothe Reported by: Thomas Boothe

HISTORY

MILESTONE DATES:
Installation 1971 First Beam 1972
DESIGN/CONSTRUCTION BY: The Cyclotron Corporation
COST: Accelerator 1M Facility 2.5M
FUNDED BY: Mount Sinai/private funding

STATUS

STAFF: Operators 5 Technicians
BUDGET: Machine Funded by Commercial production
TIME DISTRIBUTION: (e.g. basic research, isotope production, maintenance, etc.)
(a) Isotope production 85 %
(b) R&D 10 %
(c) Maintenance 5 %
(d) %
(e) %

CHARACTERISTIC BEAMS

	Accelerated Ions	E/A (MeV/u)	Current(part μA) Internal	External
(a)	p^+	26.5	130	20
(b)				

1991 μA-hours on target: 291,250

FACILITIES

SHIELDED AREA: Fixed m² Moveable m²
Target Stations: 7 No. Served At Same Time: 1
OTHER FACILITIES: seven external target stations
most targets internal

REFERENCES/NOTES

(a)
(b)

PLAN VIEW OF FACILITY, COMMENTS

13 total staff; 5 operators/engineers;
6 chemists, 1 nuclear pharmacist
1 physicist

ENTRY NO. CU113 Date 7-92
Cyclotron Model SIEMENS/CTI MODEL 112
Institution VANDERBILT UNIVERSITY MEDICAL CENTER
Address 2222 PIERCE AVE., PET FACILITY, 125 MRB,
Tel (615) 343-7511 Nashville, TN 37232-6315
Fax (615) 343-6531 EMAIL
In Charge: RON MANNING Reported by: RON MANNING

HISTORY

MILESTONE DATES:
Installation 1989 First Beam 1989
DESIGN/CONSTRUCTION BY: CTI
COST: Accelerator $1,500,000 Facility $2,600,000
FUNDED BY: VANDERBILT

STATUS

STAFF: Operators 1 Technicians 0
BUDGET: Machine $300,000 Funded by VANDERBILT
TIME DISTRIBUTION: (e.g. basic research, isotope production, maintenance, etc.)
(a) ISOTOPE PRODUCTION 95 %
(b) MAINTENANCE 5 %
(c) %
(d) %
(e) %

CHARACTERISTIC BEAMS

	Accelerated Ions	E/A (MeV/u)	Current(part μA) Internal	External
(a)	H^-	11		
(b)				

1991 μA-hours on target:

FACILITIES

SHIELDED AREA: Fixed m² Moveable m²
Target Stations: 4 No. Served At Same Time: 2
OTHER FACILITIES: RADIOCHEMISTRY LABORATORIES

REFERENCES/NOTES

(a) J. NUCL. MED. TECH. 19(1)5-19 (1991)
(b)

PLAN VIEW OF FACILITY, COMMENTS

ENTRY NO. CU111 Date July 15, 1992
Cyclotron Model CS-30
Institution Mount Sinai Medical Center
Address 4300 Alton Road, Miami Beach, Florida 33140
Tel (305)674-2465 Telex
Fax (305)674-2996 EMAIL
In Charge: Thomas Boothe Reported by: Thomas Boothe

HISTORY

MILESTONE DATES:
Installation 1971 First Beam 1972
DESIGN/CONSTRUCTION BY: The Cyclotron Corporation
COST: Accelerator 1M Facility 2.5M
FUNDED BY: Mount Sinai/private funding

STATUS

STAFF: Operators 5 Technicians
BUDGET: Machine Funded by Commercial production
TIME DISTRIBUTION: (e.g. basic research, isotope production, maintenance, etc.)
(a) Isotope production 85 %
(b) R&D 10 %
(c) Maintenance 5 %
(d) %
(e) %

CHARACTERISTIC BEAMS

	Accelerated Ions	E/A (MeV/u)	Current(part μA) Internal	External
(a)	p^+	26.5	130	20
(b)				

1991 μA-hours on target: 291,250

FACILITIES

SHIELDED AREA: Fixed m² Moveable m²
Target Stations: 7 No. Served At Same Time: 1
OTHER FACILITIES: seven external target stations
most targets internal

REFERENCES/NOTES

(a)
(b)

PLAN VIEW OF FACILITY, COMMENTS

13 total staff; 5 operators/engineers;
6 chemists, 1 nuclear pharmacist
1 physicist

ENTRY NO. CU113 Date 7-92
Cyclotron Model SIEMENS/CTI MODEL 112
Institution VANDERBILT UNIVERSITY MEDICAL CENTER
Address 2222 PIERCE AVE., PET FACILITY, 125 MRB,
Tel (615) 343-7511 Nashville, TN 37232-6315
Fax (615) 343-6531 EMAIL
In Charge: RON MANNING Reported by: RON MANNING

HISTORY

MILESTONE DATES:
Installation 1989 First Beam 1989
DESIGN/CONSTRUCTION BY: CTI
COST: Accelerator $1,500,000 Facility $2,600,000
FUNDED BY: VANDERBILT

STATUS

STAFF: Operators 1 Technicians 0
BUDGET: Machine $300,000 Funded by VANDERBILT
TIME DISTRIBUTION: (e.g. basic research, isotope production, maintenance, etc.)
(a) ISOTOPE PRODUCTION 95 %
(b) MAINTENANCE 5 %
(c) %
(d) %
(e) %

CHARACTERISTIC BEAMS

	Accelerated Ions	E/A (MeV/u)	Current(part μA) Internal	External
(a)	H^-	11		
(b)				

1991 μA-hours on target:

FACILITIES

SHIELDED AREA: Fixed m² Moveable m²
Target Stations: 4 No. Served At Same Time: 2
OTHER FACILITIES: RADIOCHEMISTRY LABORATORIES

REFERENCES/NOTES

(a) J. NUCL. MED. TECH. 19(1)5-19 (1991)
(b)

PLAN VIEW OF FACILITY, COMMENTS

ENTRY NO. CU114 Date

Cyclotron Model CTI RDS 112

Institution The Methodist Medical Center of Illinois

Address Peoria, IL USA

Tel (309)671-2738 Telex –

Fax (309)671-5185 EMAIL –

In Charge: S. Zigler Reported by: S. Zigler

HISTORY

MILESTONE DATES:

Installation Dec 1990 First Beam Jan-Feb 1991

DESIGN/CONSTRUCTION BY: Philip Swager Assoc

COST: Accelerator – Facility –

FUNDED BY: Internally

STATUS

STAFF: Operators 1 Technicians 0

BUDGET: Machine – Funded by Internally

TIME DISTRIBUTION: (e.g. basic research, isotope production, maintenance, etc.)

(a) Clinical Isotope Production 95 %

(b) Maintenance (Preventative and Service) 5 %

(c) %

(d) %

(e) %

CHARACTERISTIC BEAMS

	Accelerated Ions	E/A (MeV/u)	Current(part μA) Internal	External
(a)	H–	11	200(H–)	100(p)
(b)				

1991 μA-hours on target: 2250

FACILITIES

Standard Shields

SHIELDED AREA: Fixed – m² Moveable – m²

Target Stations: 4 No. Served At Same Time: 2

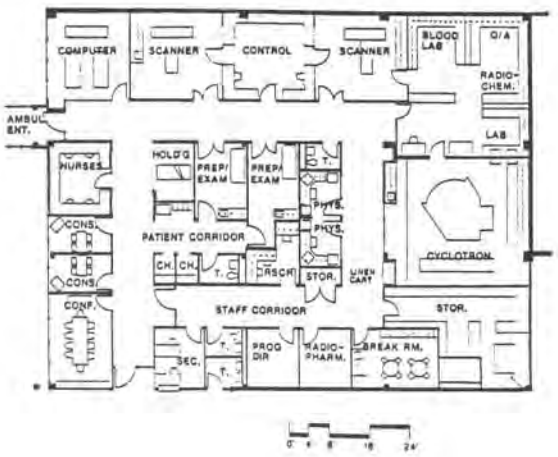
OTHER FACILITIES:

REFERENCES/NOTES

(a)

(b)

PLAN VIEW OF FACILITY, COMMENTS



ENTRY NO. CU116 Date

Cyclotron Model SIEMENS/CTI RDS 112

Institution N. CALIF. PET IMAGING CENTER

Address 3195 FOLSOM BLVD, SACRAMENTO, CA 95816

Tel 916-737-3200 Telex

Fax 916-737-6203 EMAIL

In Charge: H.C. PADGETT Reported by: H.C. PADGETT

HISTORY

MILESTONE DATES:

Installation MAY 1992 First Beam JUNE 1992

DESIGN/CONSTRUCTION BY: CTI CYCLOTRON SYSTEMS

COST: Accelerator $1,000,000 Facility $500,000

FUNDED BY: PRIVATE

STATUS

STAFF: Operators 2 Technicians 1

BUDGET: Machine – Funded by –

TIME DISTRIBUTION: (e.g. basic research, isotope production, maintenance, etc.)

(a) CLINICAL ISOTOPE PROD, IN-HOUSE 90 %

(b) CLINICAL ISOTOPE PROD, DISTRIBUTION 10 %

(c) %

(d) %

(e) %

CHARACTERISTIC BEAMS

	Accelerated Ions	E/A (MeV/u)	Current(part μA) Internal	External
(a)	H–	11	100	100
(b)				

1991 μA-hours on target: –

FACILITIES

SHIELDED AREA: Fixed 0 m² Moveable 0 m²

Target Stations: 4 No. Served At Same Time: 2

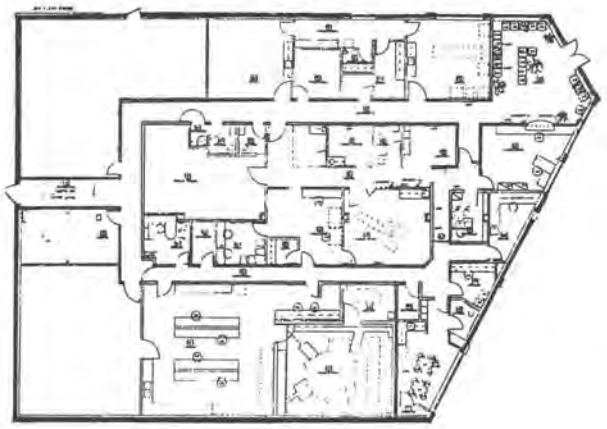
OTHER FACILITIES: CLINICAL MEDICAL IMAGING: SIEMENS 921 SCANNER

REFERENCES/NOTES

(a)

(b)

PLAN VIEW OF FACILITY, COMMENTS



ENTRY NO. CU114 Date

Cyclotron Model CTI RDS 112

Institution The Methodist Medical Center of Illinois

Address Peoria, IL USA

Tel (309)671-2738 Telex –

Fax (309)671-5185 EMAIL –

In Charge: S. Zigler Reported by: S. Zigler

HISTORY

MILESTONE DATES:

Installation Dec 1990 First Beam Jan-Feb 1991

DESIGN/CONSTRUCTION BY: Philip Swager Assoc

COST: Accelerator – Facility –

FUNDED BY: Internally

STATUS

STAFF: Operators 1 Technicians 0

BUDGET: Machine – Funded by Internally

TIME DISTRIBUTION: (e.g. basic research, isotope production, maintenance, etc.)

(a) Clinical Isotope Production 95 %

(b) Maintenance (Preventative and Service) 5 %

(c) %

(d) %

(e) %

CHARACTERISTIC BEAMS

	Accelerated Ions	E/A (MeV/u)	Current(part μA) Internal	External
(a)	H–	11	200(H–)	100(p)
(b)				

1991 μA-hours on target: 2250

FACILITIES

Standard Shields

SHIELDED AREA: Fixed – m² Moveable – m²

Target Stations: 4 No. Served At Same Time: 2

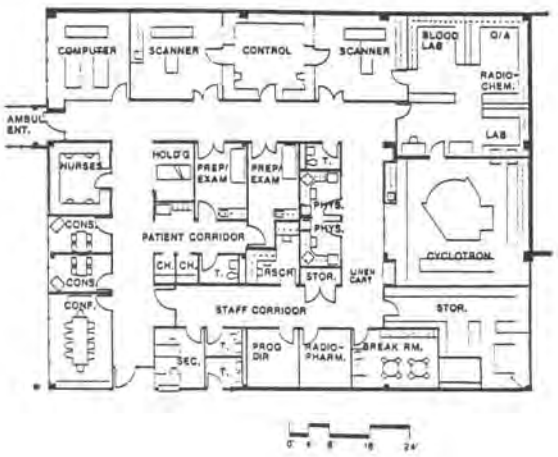
OTHER FACILITIES:

REFERENCES/NOTES

(a)

(b)

PLAN VIEW OF FACILITY, COMMENTS



ENTRY NO. CU116 Date

Cyclotron Model SIEMENS/CTI RDS 112

Institution N. CALIF. PET IMAGING CENTER

Address 3195 FOLSOM BLVD, SACRAMENTO, CA 95816

Tel 916-737-3200 Telex

Fax 916-737-6203 EMAIL

In Charge: H.C. PADGETT Reported by: H.C. PADGETT

HISTORY

MILESTONE DATES:

Installation MAY 1992 First Beam JUNE 1992

DESIGN/CONSTRUCTION BY: CTI CYCLOTRON SYSTEMS

COST: Accelerator $1,000,000 Facility $500,000

FUNDED BY: PRIVATE

STATUS

STAFF: Operators 2 Technicians 1

BUDGET: Machine – Funded by –

TIME DISTRIBUTION: (e.g. basic research, isotope production, maintenance, etc.)

(a) CLINICAL ISOTOPE PROD, IN-HOUSE 90 %

(b) CLINICAL ISOTOPE PROD, DISTRIBUTION 10 %

(c) %

(d) %

(e) %

CHARACTERISTIC BEAMS

	Accelerated Ions	E/A (MeV/u)	Current(part μA) Internal	External
(a)	H–	11	100	100
(b)				

1991 μA-hours on target: –

FACILITIES

SHIELDED AREA: Fixed 0 m² Moveable 0 m²

Target Stations: 4 No. Served At Same Time: 2

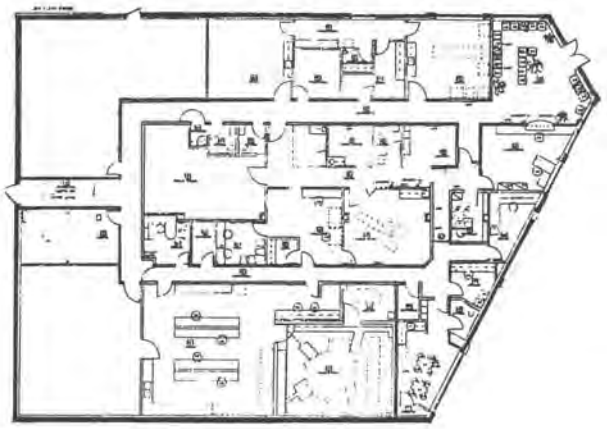
OTHER FACILITIES: CLINICAL MEDICAL IMAGING: SIEMENS 921 SCANNER

REFERENCES/NOTES

(a)

(b)

PLAN VIEW OF FACILITY, COMMENTS



ENTRY No. CU119

NAME OF MACHINE W.U. Med School Cyclotron I DATE 5/10/89
INSTITUTION Washington University Medical School, Barnard Hospital
ADDRESS St. Louis, MO 63110 USA
TEL 314-454-3596 TELEX
IN CHARGE JT Hood, Director REPORTED BY John T. Hood
MM Ter-Pogossian, Professor of Radiation Sciences

HISTORY AND STATUS

DESIGN, date 1962 Model tests
ENG DESIGN, date 1963
CONSTRUCTION, date 1963-64 Allis-Chalmers
FIRST BEAM, date (or goal) 1964
MAJOR ALTERATIONS

COST, ACCELERATOR $120,000
COST, FACILITY, total $190,000
FUNDED BY NIH

ACCELERATOR STAFF, OPERATION AND DEVELOPMENT

SCIENTISTS 2 ENGINEERS 1
TECHNICIANS 2 CRAFTS 2
GRAD STUDENTS involved during year
OPERATED BY Research staff or X Operators
OPERATION hr/wk, On target hr/wk
TIME DISTR. In house %, Outside %
BUDGET, op & dev
FUNDED BY NIH

RESEARCH STAFF, not included above

USERS, In house 6 outside
GRAD STUDENTS involved during year 2
RESEARCH BUDGET, In house
FUNDED BY NIH

MAGNET

POLE FACE, diameter (compact) 81 cm, R extraction 33 cm
R injection cm
GAP, min cm, Field kG
max cm, Field kG } at
AVERAGE FIELD at R ext 15 kG } Ampere turns
B max/ <B>
NUMBER OF SECTORS { compact / separated } Spiral, max deg
SECTOR ANGLE (SSC) deg
TRIMMING COILS

CONDUCTOR, material and type Copper, Hollow Conductor
STORED ENERGY (cryogenic) MJ
POWER: main coils 40 max, kW ; current stability
trimming coils max, kW ; current stability
WEIGHT: Fe tons ; coils tons
COOLING system water
ION ENERGY (bending limit) E/A = q²/a² MeV/amu
(focusing limit) E/A = q²/a² MeV/amu

ACCELERATION SYSTEM

DEES, number 1 ; angle 180 deg
BEAM APERTURE 2.5 cm ; DC Bias 0 kV
TUNED by, coarse fine
RF 11.4 to mHz, stable ±
Orb F to mHz
HARMONICS, RF/Orb F, used
DEE - Gnd, max kV, min gap cm
STABILITY, (pk-pk noise)/(pk RF volt)
ENERGY GAIN, max kV/turn
RF PHASE, stable to ± deg
RF POWER input, max 25 kW
FREQUENCY MODULATION, rate /s
modulator, type
beam pulse, width

VACUUM SYSTEM

OPERATING PRESSURE 20 μ Torr or mbar
PUMPS, No, Type, Size 2 - oil diffusion
Seven inch

ION SOURCES

Hot filament

INJECTION SYSTEM

EXTRACTION SYSTEM

Electrostatic and Magnetic Channel

FACILITIES FOR RESEARCH

SHIELDED AREA, fixed m² ; movable m²
TARGET STATIONS 1 in 1 rooms
STATIONS served at same time, max
MAG SPECTROGRAPH, type
COMPUTER model
OTHER FACILITIES

CHARACTERISTIC BEAMS

PARTICLE	ENERGY (MeV) Goal	Achieved	CURRENT (pμA) Internal	External
d		6.8		80
SECONDARY				(part/s)

BEAM PROPERTIES

MEASURED CONDITIONS

PULSE WIDTH RF deg pμ A of MeV ions
PHASE EXC, max RF deg pμ A of MeV ions
EXTRACT eff % pμ A of MeV ions
RESOL ΔE/E % pμ A of MeV ions
EMITTANCE
(π mm. mrad) { axial / rad } pμA of MeV ions

OPERATING PROGRAMS, time distribution

BASIC NUCLEAR PHYSICS
BIOMEDICAL APPLICAT. 100%
SOLID STATES PHYSICS
ISOTOPE PRODUCTIONS

REFERENCES/NOTES

PLAN VIEW OF FACILITY, NOTEWORTHY FEATURES, COMMENTS

ENTRY No. CU120

NAME OF MACHINE W.U. Med School Cyclotron II DATE 5/10/89
INSTITUTION Washington University Medical School, Barnard Hospital
ADDRESS St. Louis, MO 63110 USA
TEL 314-454-3596 TELEX
IN CHARGE JT Hood, Director REPORTED BY Jobo T. Hood
M.M. Ter-Pogossian, Professor of Radiation Sciences

HISTORY AND STATUS

DESIGN, date Model tests
ENG DESIGN, date Cyc Corp. CS-15
CONSTRUCTION, date
FIRST BEAM, date (or goal) June, 1978
MAJOR ALTERATIONS

COST, ACCELERATOR $650,000
COST, FACILITY, total $900,000
FUNDED BY NIH (Heart and Lung)

ACCELERATOR STAFF, OPERATION AND DEVELOPMENT

SCIENTISTS 2 ENGINEERS 1
TECHNICIANS 2 CRAFTS 2
GRAD STUDENTS involved during year
OPERATED BY Research staff or X Operators
OPERATION hr/wk, On target hr/wk
TIME DISTR. in house %, Outside %
BUDGET, op & dev
FUNDED BY NIH

RESEARCH STAFF, not included above

USERS, in house 6 outside
GRAD STUDENTS involved during year 2
RESEARCH BUDGET, in house
FUNDED BY NIH

MAGNET

POLE FACE, diameter (compact) 81 cm, R extraction 35 cm
R injection cm
GAP, min cm, Field kG
max cm, Field kG
at Ampere turns
AVERAGE FIELD at R ext 16.5 kG
B max/ <B>
NUMBER OF SECTORS compact 3, separated; Spiral, max deg
SECTOR ANGLE (SSC) deg
TRIMMING COILS

CONDUCTOR, material and type Aluminum ribbon
STORED ENERGY (cryogenic) MJ
POWER: main coils 60 max, kW ; current stability
trimming coils max, kW ; current stability
WEIGHT: Fe tons ; coils tons
COOLING system water
ION ENERGY (bending limit) E/A = q^2/a^2 MeV/amu
(focusing limit) E/A = q^2/a^2 MeV/amu

ACCELERATION SYSTEM

DEES, number 2 ; angle 120 deg
BEAM APERTURE cm ; DC Bias kV
TUNED by, coarse short fine
RF 12 to 25 mHz, stable ±
Orb F to mHz
HARMONICS, RF/Orb F, used
DEE - Gnd, max kV, min gap cm
STABILITY, (pk-pk noise)/(pk RF volt)
ENERGY GAIN, max kV/turn
RF PHASE, stable to ± deg
RF POWER input, max kW
FREQUENCY MODULATION, rate /s
modulator, type
beam pulse, width

VACUUM SYSTEM

OPERATING PRESSURE 10 μ Torr or mbar
PUMPS, No, Type, Size 1 - Oil diffusion
ten inch

ION SOURCES

Penning

INJECTION SYSTEM

EXTRACTION SYSTEM

Electrostatic and Magnetic Channel

FACILITIES FOR RESEARCH

SHIELDED AREA, fixed m^2 ; movable m^2
TARGET STATIONS 3 in 1 rooms
STATIONS served at same time, max
MAG SPECTROGRAPH, type
COMPUTER model
OTHER FACILITIES

CHARACTERISTIC BEAMS

PARTICLE	ENERGY (MeV) Goal	Achieved	CURRENT (pμA) Internal	External
p		15		50
d		8		75
α		16		
^{3}He		20		50
SECONDARY				(part/s)

BEAM PROPERTIES

MEASURED		CONDITIONS			
PULSE WIDTH	RF deg	pμ A of	MeV	Ions	
PHASE EXC, max	RF deg	pμ A of	MeV	Ions	
EXTRACT eff %		pμ A of	MeV	Ions	
RESOL ΔE/E 1 %		pμ A of	MeV	Ions	
EMITTANCE (π mm. mrad) .50 axial, .50 rad		pμA of	MeV	Ions	

OPERATING PROGRAMS, time distribution

BASIC NUCLEAR PHYSICS
BIOMEDICAL APPLICAT. 100%
SOLID STATES PHYSICS
ISOTOPE PRODUCTIONS

REFERENCES/NOTES

PLAN VIEW OF FACILITY, NOTEWORTHY FEATURES, COMMENTS

ENTRY NO. CU121 **Date** July 1992

Name of Machine: Clinical Cyclotron

Institution: University of Washington Medical Center

Address: Department of Radiation Oncology, RC-08, Seattle WA 98195 USA

Tel (206) 548-4112 Telex 4740096 UW UI Fax (206) 548-6218 EMAIL RISLER@RADONC.WASHINGTON.EDU

In Charge: R. Risler Reported by: R. Risler

HISTORY

MILESTONE DATES:
Design 1980 Model Tests 1980
Construction 1981-1984 First Beam Factory JUN 82
Facility JUN 83
DESIGN/CONSTRUCTION BY:
in house ... other ... Scanditronix AB Uppsala
COST: Accelerator 4.2 mio USD Facility 7.0 mio USD
FUNDED BY: US National Cancer Institute

STATUS

STAFF: Machine
Scientists - Engineers 2
Technicians 3 Students -
Research (in house/external)
Scientists 2 / - Engineers - / -
Technicians - / - Students - / -
BUDGET: Machine 360000 USD Funded by Hospital, some
Research excl. staff Funded by grants
TIME DISTRIBUTION:
Basic Research (in house/external) 5 % / %
Applied Program (in house/external) 85 % / %
Development 5 % Maintenance 5 %

MAGNET

POLE PARAMETERS:
Diameter 155 cm $R_{extract}$ 57 cm R_{inject} - cm
HILL PARAMETERS: Gap (min) 11.5 cm B_{max} 2.05 T
(¢ AT) Gap (max) 11.5 cm B_{min} T
VALLEY PARAMETERS: Gap (min) 20.5 cm B_{max} T
(¢ AT) Gap (max) 20.5 cm B_{min} T
AVERAGE FIELD: $< B >_{min}$ T $< B >_{max}$ 1.75 T
NUMBER OF SECTORS: compact/separated 3 /
sector angle deg. spiral (max) 55 deg.
FIELD TRIMMING: Trim Coils 10
Harmonic Coils 4 sets
Other
CURRENT: Main Coils 900 A max. Amps Stability 10^{-5}
Trim Coils 50-80 A max. Amps Stability 10^{-3}
Stored Energy (cryogenic) MJ
WEIGHT: Iron 90000 kg Conductor 3800 kg
ION ENERGY: Bending Limit E/A = 51 q^2/A^2 MeV/u
Focussing Limit E/A = q/A MeV/u

ACCELERATION SYSTEM

FUNDAMENTAL ACCELERATION:
Description: two 90 deg. Dees
No. of Gaps/turn 4 dE/dn(max) 0.160 MeV/q
Voltage(max) 0.040 MV Harmonic f_{rf}/f_{ion} 1,2
Freq 19.5 - 26 MHz Power in(max) 0.060 MW
Stability: Phase +/- 1deg Voltage 10^{-3}
OTHER CAVITIES (Flattopping or otherwise):
Description: -
Region of Influence: R_{min} cm R_{max} cm
No. of Gaps/turn dE/dn(max) MeV/q
Voltage(max) MV Harmonic f_{rf}/f_{ion}
Freq MHz Power in(max) MW
Stability: Phase Voltage

VACUUM SYSTEM

OPERATING PRESSURE: 10^{-6} mbar
PUMPS: No. and type 2 oil diffusion pumps (Edwards L9 fluid), total capacity 8500 liters/sec

ION SOURCE(S)

	Type	Intensity (mA)	¢	$\epsilon_n = \beta\gamma\epsilon$ (πmm mrad)	Ion Species
(a)	Internal Cold Cathode PIG				p,d,3He,4He
(b)	with dual chimney				
(c)					
(d)					

INJECTION SYSTEM

- Efficiency %

EXTRACTION SYSTEM

Electrostat. Def., EMC, 2passive foc. ch. Efficiency 75-85 %

CHARACTERISTIC BEAMS

	Accelerated Ions	E/A (MeV/u)	Current(part μA) Internal	External
(a)	p	28 - 50.5	90	70
(b)	d	15 - 24	65	50
(c)	3He++	21 - 35	3	2.2
(d)	4He++	30 - 48	1	0.75

	Secondary Particles	E (MeV)	part/sec
(a)	-		
(b)			
(c)			

EXTRACTED BEAM PROPERTIES:
For 1 μA of 50.5 MeV/u p ions
$\Delta E/E$ % $\Delta\phi$ °rf
$\epsilon_n = \beta\gamma\epsilon$ x 12 πmm mrad z 14 πmm mrad

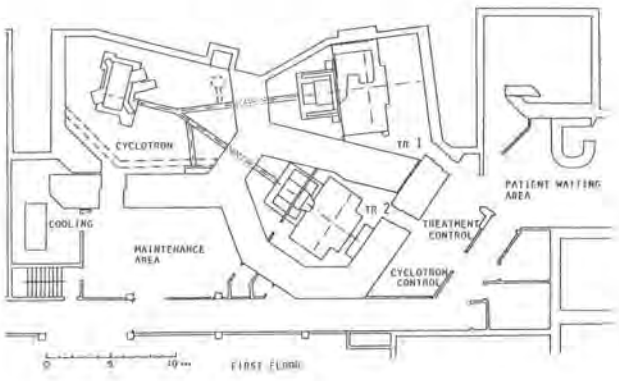
FACILITIES FOR RESEARCH

SHIELDED AREA: Fixed 265 m² Moveable 0 m²
Target Stations: 3 No. Served At Same Time: 1
MAGNETIC SPECTROMETERS: -
OTHER FACILITIES: Isocentric Neutron Therapy Room
Fixed Beam Neutron Therapy Room
Isotope Production Station in Cyclotron Vault (PET)

REFERENCES/NOTES

(a) R. Risler et al., CONTINUED OPERATION OF THE SEATTLE
(b) CLINICAL CYCLOTRON FACILITY (this conference)

PLAN VIEW OF FACILITY, COMMENTS



ENTRY NO. CU122 Date

Cyclotron Model CS-22

Institution Amersham - Medi-Physics, Inc.

Address 900 Durham Ave., South Plainfield NJ 07080

Tel 908-757-0500 Telex

Fax EMAIL

In Charge: R. Hubbard Reported by: W. Buela

HISTORY

MILESTONE DATES:

Installation July 1972 First Beam January 1973

DESIGN/CONSTRUCTION BY: The Cyclotron Corp.

COST: Accelerator Facility

FUNDED BY:

STATUS

STAFF: Operators 0 Technicians 4

BUDGET: Machine Funded by

TIME DISTRIBUTION: (e.g. basic research, isotope production, maintenance, etc.)

(a) Isotope Production 80 %

(b) Maintenance 20 %

(c) %

(d) %

(e) %

CHARACTERISTIC BEAMS

	Accelerated Ions	E/A (MeV/u)	Current(part μA) Internal	External
(a)	H^+	22	200	100
(b)				

1991 μA-hours on target: 7×10^5

FACILITIES

SHIELDED AREA: Fixed 85 m^2 Moveable 0 m^2

Target Stations: 2 No. Served At Same Time: 1

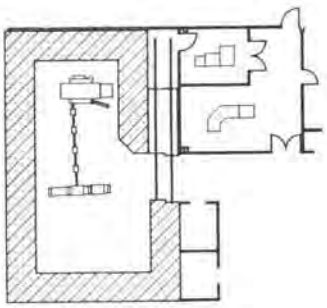
OTHER FACILITIES:

REFERENCES/NOTES

(a)

(b)

PLAN VIEW OF FACILITY, COMMENTS



ENTRY NO. CU123 Date

Cyclotron Model Cyclone 30

Institution Amersham - Medi-Physics, Inc.

Address 900 Durham Ave., South Plainfield, NJ 07080

Tel 908-757-0500 Telex

Fax EMAIL

In Charge: R. Hubbard Reported by: W. Buela

HISTORY

MILESTONE DATES:

Installation April 1989 First Beam Aug. 1989

DESIGN/CONSTRUCTION BY: ION Beam Applications

COST: Accelerator Facility

FUNDED BY:

STATUS

STAFF: Operators 0 Technicians 5

BUDGET: Machine Funded by

TIME DISTRIBUTION: (e.g. basic research, isotope production, maintenance, etc.)

(a) Isotope Production 80 %

(b) Maintenance 20 %

(c) %

(d) %

(e) %

CHARACTERISTIC BEAMS

	Accelerated Ions	E/A (MeV/u)	Current(part μA) Internal	External
(a)	H^-	30	500	2x250
(b)				

1991 μA-hours on target: 2×10^6

FACILITIES

SHIELDED AREA: Fixed 130 m^2 Moveable 0 m^2

Target Stations: 4 No. Served At Same Time: 2

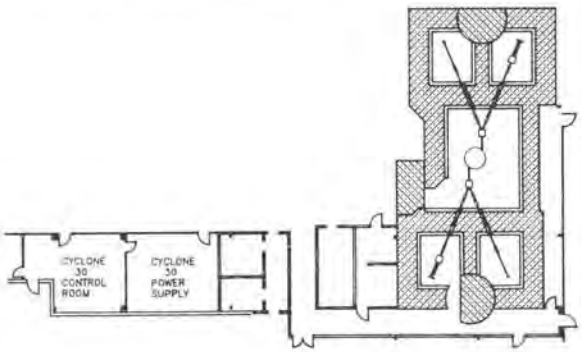
OTHER FACILITIES:

REFERENCES/NOTES

(a)

(b)

PLAN VIEW OF FACILITY, COMMENTS



ENTRY NO. CU122 Date

Cyclotron Model CS-22

Institution Amersham - Medi-Physics, Inc.

Address 900 Durham Ave., South Plainfield NJ 07080

Tel 908-757-0500 Telex

Fax EMAIL

In Charge: R. Hubbard Reported by: W. Buela

HISTORY

MILESTONE DATES:

Installation July 1972 First Beam January 1973

DESIGN/CONSTRUCTION BY: The Cyclotron Corp.

COST: Accelerator Facility

FUNDED BY:

STATUS

STAFF: Operators 0 Technicians 4

BUDGET: Machine Funded by

TIME DISTRIBUTION: (e.g. basic research, isotope production, maintenance, etc.)

(a) Isotope Production 80 %

(b) Maintenance 20 %

(c) %

(d) %

(e) %

CHARACTERISTIC BEAMS

	Accelerated Ions	E/A (MeV/u)	Current(part μA) Internal	External
(a)	H^+	22	200	100
(b)				

1991 μA-hours on target: 7×10^5

FACILITIES

SHIELDED AREA: Fixed 85 m^2 Moveable 0 m^2

Target Stations: 2 No. Served At Same Time: 1

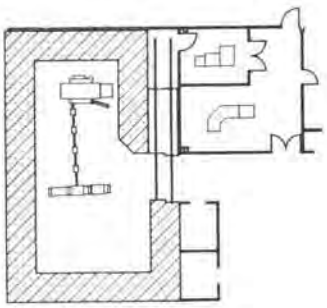
OTHER FACILITIES:

REFERENCES/NOTES

(a)

(b)

PLAN VIEW OF FACILITY, COMMENTS



ENTRY NO. CU123 Date

Cyclotron Model Cyclone 30

Institution Amersham - Medi-Physics, Inc.

Address 900 Durham Ave., South Plainfield, NJ 07080

Tel 908-757-0500 Telex

Fax EMAIL

In Charge: R. Hubbard Reported by: W. Buela

HISTORY

MILESTONE DATES:

Installation April 1989 First Beam Aug. 1989

DESIGN/CONSTRUCTION BY: ION Beam Applications

COST: Accelerator Facility

FUNDED BY:

STATUS

STAFF: Operators 0 Technicians 5

BUDGET: Machine Funded by

TIME DISTRIBUTION: (e.g. basic research, isotope production, maintenance, etc.)

(a) Isotope Production 80 %

(b) Maintenance 20 %

(c) %

(d) %

(e) %

CHARACTERISTIC BEAMS

	Accelerated Ions	E/A (MeV/u)	Current(part μA) Internal	External
(a)	H^-	30	500	2x250
(b)				

1991 μA-hours on target: 2×10^6

FACILITIES

SHIELDED AREA: Fixed 130 m^2 Moveable 0 m^2

Target Stations: 4 No. Served At Same Time: 2

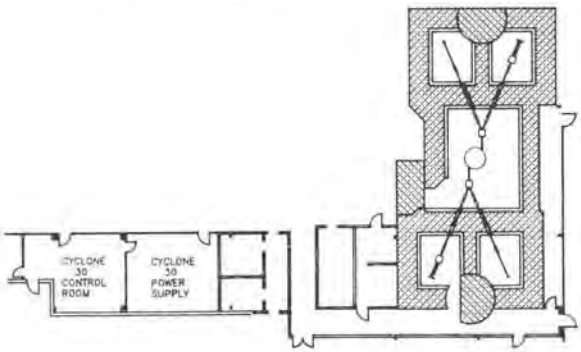
OTHER FACILITIES:

REFERENCES/NOTES

(a)

(b)

PLAN VIEW OF FACILITY, COMMENTS



ENTRY NO. CU124 **Date** 25-AUG-92

Name of Machine JSW 1710 (Japan Steel Works)

Institution Brookhaven National Laboratory

Address Upton, NY 11973

Tel (516) 282-4551 Telex Fax (516) 282-7350 EMAIL schlyer@chm.chm.bnl.90

In Charge: A. P. Wolf Reported by: D. J. Schlyer

HISTORY

MILESTONE DATES:
Design 1981 Model Tests 1981
Construction 1981 First Beam 1982

DESIGN/CONSTRUCTION BY:
in house other Japan Steel Works

COST: Accelerator 860,000 Facility 1,100,000

FUNDED BY: DOE

STATUS

STAFF: Machine
Scientists 1 Engineers
Technicians 2 Students
Research (in house/external)
Scientists / Engineers /
Technicians / Students /

BUDGET: Machine Funded by
Research Funded by

TIME DISTRIBUTION:
Basic Research (in house/external) 100 % / %
Applied Program (in house/external) 100 % / 0 %
Development % Maintenance %

MAGNET

POLE PARAMETERS:
Diameter 105 cm $R_{extract}$ 42 cm R_{inject} 0 cm

HILL PARAMETERS: Gap (min) cm B_{max} T
(ℓ AT) Gap (max) cm B_{min} T

VALLEY PARAMETERS: Gap (min) cm B_{max} T
(ℓ AT) Gap (max) cm B_{min} T

AVERAGE FIELD: $< B >_{min}$ T $< B >_{max}$ T

NUMBER OF SECTORS: compact/separated 4 / 0
sector angle deg. spiral (max) deg.

FIELD TRIMMING: Trim Coils 3
Harmonic Coils
Other

CURRENT: Main Coils Amps Stability
Trim Coils Amps Stability
Stored Energy (cryogenic) MJ

WEIGHT: Iron 35 Tons Conductor Cu hollow

ION ENERGY: Bending Limit E/A = q^2/A^2 MeV/u
Focussing Limit E/A = q/A MeV/u

ACCELERATION SYSTEM

FUNDAMENTAL ACCELERATION:
Description: 2 Dees @ 45°
No. of Gaps/turn dE/dn(max) 0,180 MeV/q
Voltage(max) MV Harmonic f_{rf}/f_{ion}
Freq 43.5 - 47 MHz Power in(max) MW
Stability: Phase Voltage

OTHER CAVITIES (Flattopping or otherwise):
Description:
Region of Influence: R_{min} cm R_{max} cm
No. of Gaps/turn dE/dn(max) MeV/q
Voltage(max) MV Harmonic f_{rf}/f_{ion}
Freq MHz Power in(max) MW
Stability: Phase Voltage

VACUUM SYSTEM

OPERATING PRESSURE: 5×10^{-6}
PUMPS: No. and type Diffusion 8"

ION SOURCE(S)

	Type	Intensity (mA)	ℓ	$\epsilon_n = \beta\gamma\epsilon$ (πmm mrad)	Ion Species
(a)					
(b)					
(c)					
(d)					

INJECTION SYSTEM

Hot Cathode Axial Source Efficiency %

EXTRACTION SYSTEM

Electrostatic Efficiency 40 %

CHARACTERISTIC BEAMS

	Accelerated Ions	E/A (MeV/u)	Current(part μA) Internal	External
(a)	H^+	17	60	40
(b)	p^+	10	50	30
(c)				
(d)				

	Secondary Particles	E (MeV)	part/sec
(a)			
(b)			
(c)			

EXTRACTED BEAM PROPERTIES:
For μA of MeV/u ions
$\Delta E/E$ % $\Delta\phi$ °rf
$\epsilon_n = \beta\gamma\epsilon$ x πmm mrad z πmm mrad

FACILITIES FOR RESEARCH

SHIELDED AREA: Fixed 60 m^2 Moveable 0 m^2
Target Stations: 1 No. Served At Same Time: 1
MAGNETIC SPECTROMETERS:
OTHER FACILITIES:

REFERENCES/NOTES

(a)
(b)

PLAN VIEW OF FACILITY, COMMENTS

ENTRY No. FM1 McGill Synchrocyclotron April 19, 1989
NAME OF MACHINE ..... DATE .....
INSTITUTION McGill University
ADDRESS 3610 University Street, Montréal, Québec H3A 2B2 CANADA
TEL (514)398-7030 TELEX 05-268510
IN CHARGE Prof. Jean Barrette REPORTED BY Mr. Leo Nikkinen

HISTORY AND STATUS
DESIGN, date 1945 Model tests -
ENG DESIGN, date -
CONSTRUCTION, date 1945 - 1946
FIRST BEAM, date (or goal) June 1949
MAJOR ALTERATIONS External Beam Hall added in 1963
External Beam Area Relocated in 1983
COST, ACCELERATOR $200K
COST, FACILITY, total $2 Million
FUNDED BY -

ACCELERATOR STAFF, OPERATION AND DEVELOPMENT
SCIENTISTS 1 ENGINEERS 1
TECHNICIANS - CRAFTS -
GRAD STUDENTS involved during year -
OPERATED BY X Research staff or Operators
OPERATION - hr/wk, On target - hr/wk
TIME DISTR. in house - %, Outside - %
BUDGET, op & dev -
FUNDED BY -

RESEARCH STAFF, not included above
USERS, In house - outside -
GRAD STUDENTS involved during year -
RESEARCH BUDGET, In house $200,000
FUNDED BY -

MAGNET
POLE FACE, diameter (compact) 90 cm, R extraction 90 cm
R injection 0 cm
GAP, min 15 cm, Field 16.1 kG
max 19 cm, Field 15.1 kG at 5.3×10^5 Ampere turns
AVERAGE FIELD at R ext 15.9 kG
B max/ <B> 1.01
NUMBER OF SECTORS compact -, separated - Spiral, max - deg
SECTOR ANGLE (SSC) - deg
TRIMMING COILS -
CONDUCTOR, material and type Aluminum, 6x1 cm
STORED ENERGY (cryogenic) - MJ
POWER: main coils 150 max, kW; current stability 10^{-5}
trimming coils - max, kW; current stability -
WEIGHT: Fe 273 tons; coils 11 tons
COOLING system De-ionized water
ION ENERGY (bending limit) E/A = 100 q^2/a^2 MeV/amu
(focusing limit) E/A = - q^2/a^2 MeV/amu

ACCELERATION SYSTEM
DEES, number 1; angle 180 deg
BEAM APERTURE 1 cm; DC Bias 0-3 kV
TUNED by, coarse - fine -
RF 30 to 6 mHz, stable ± -
Orb F 26 to 22.3 mHz (protons)
HARMONICS, RF/Orb F, used -
DEE - Gnd, max 10 kV, min gap 5 cm
STABILITY, (pk-pk noise)/(pk RF volt) -
ENERGY GAIN, max 20 kV/turn
RF PHASE, stable to ± - deg
RF POWER input, max 40 (avg.), 200 (pk) kW
FREQUENCY MODULATION, rate 4000 /s
modulator, type Swept Oscillator
beam pulse, width 20 μsec

VACUUM SYSTEM
OPERATING PRESSURE 10^{-5} Torr or mbar
PUMPS, No, Type, Size 2x16" Oil Diffusion Pump
10,000 l/sec each

ION SOURCES
Cold Cathode PIG

INJECTION SYSTEM
Radial Extraction Ion-Source

EXTRACTION SYSTEM
Regeneration Deflection

FACILITIES FOR RESEARCH
SHIELDED AREA, fixed 125 m^2; movable - m^2
TARGET STATIONS 1 In rooms
STATIONS served at same time, max -
MAG SPECTROGRAPH, type -
COMPUTER model
OTHER FACILITIES Internal Bombardment Probes

CHARACTERISTIC BEAMS

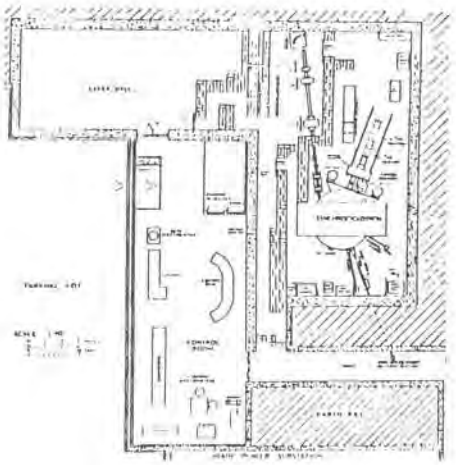
PARTICLE	ENERGY (MeV) Goal	Achieved	CURRENT (μA) Internal	External
p	100	100	2	0.3
d	50	50	2	0.3
He-3	133	133	1	0.1
He-4	100	100	0.8	0.08
SECONDARY				(part/s)

BEAM PROPERTIES
MEASURED CONDITIONS
PULSE WIDTH RF deg μA of MeV ions
PHASE EXC, max RF deg μA of MeV ions
EXTRACT eff 10-15 % μA of MeV ions
RESOL ΔE/E % μA of MeV ions
EMITTANCE
(π mm. mrad) 15 axial, 20 rad μA of MeV ions

OPERATING PROGRAMS, time distribution
BASIC NUCLEAR PHYSICS SOLID STATES PHYSICS
BIOMEDICAL APPLICAT. ISOTOPE PRODUCTIONS

REFERENCES/NOTES

PLAN VIEW OF FACILITY, NOTEWORTHY FEATURES, COMMENTS



ENTRY No. FM2

NAME OF MACHINE Synchro-Cyclotron Lyon ..... DATE ..... 3 avril 1989

INSTITUTION ..... Service Commun du Synchro-Cyclotron

ADDRESS ..... Université Claude Bernard Lyon-1 - 43, Bd du 11 Novembre 1918 - 69622 Villeurbanne Cedex (France)

TEL 78.89.81.24 ..... TELEX ..... 380273F ..... FAX 78.89.19.02

IN CHARGE Prof. B.E. Lahneche .. REPORTED BY ..G. HADINGER

HISTORY AND STATUS

DESIGN, date ..... Model tests .....
ENG DESIGN, date ..... 1956 .....
CONSTRUCTION, date ..... 1962 .....
FIRST BEAM, date (or goal) ..... 1963 .....
MAJOR ALTERATIONS ..... 1965 .....
.....
COST, ACCELERATOR ..... 2,7 MF .....
COST, FACILITY, total ..... 7,5 MF .....
FUNDED BY Ministère de l'Education Nationale .....

ACCELERATOR STAFF, OPERATION AND DEVELOPMENT

SCIENTISTS ..... 1 ..... ENGINEERS ..... 1 .....
TECHNICIANS ..... 1 ..... CRAFTS .....
GRAD STUDENTS involved during year .....
OPERATED BY ..... Research staff or ..... 1 ..... Operators
OPERATION ..... hr/wk, On target ..... hr/wk
TIME DISTR. in house ..... %, Outside ..... %
BUDGET, op & dev .....
FUNDED BY .....

RESEARCH STAFF, not included above

USERS, in house ..... outside .....
GRAD STUDENTS involved during year .....
RESEARCH BUDGET, in house .....
FUNDED BY .....

MAGNET

POLE FACE, diameter (compact) 180 cm, R extraction ..75 cm
R injection ..... cm
GAP, min ... 35 ... cm, Field ... 14.7 ..... kG
max ... 35 ... cm, Field ... 14.7 ..... kG
at .. 0.61.10^6 Ampere turns
AVERAGE FIELD at R ext ..... kG
B max/ <B> .....
NUMBER OF SECTORS { compact ..... / separated ..... } Spiral, max .. deg
SECTOR ANGLE (SSC) ..... deg
TRIMMING COILS .....
.....
CONDUCTOR, material and type ..... Aluminium .....
STORED ENERGY (cryogenic) ..... ≃ 1 ..... MJ
POWER : main coils ..... max, kW ; current stability .....
trimming coils ..... max, kW ; current stability .....
WEIGHT : Fe ≃ 200 ..... tons ; coils ..... tons
COOLING system .....
ION ENERGY (bending limit) E/A = ... q^2/a^2 MeV/amu
(focusing limit) E/A = ... q^2/a^2 MeV/amu

ACCELERATION SYSTEM

DEES, number ..... 2 ..... ; angle .. 180 ..... deg
BEAM APERTURE ... 18.5 ... cm ; DC Bias .... 0,2 ..... kV
TUNED by, coarse ..... fine .....
RF ... 10.4 ..... to ..... 11.0 mHz, stable ± .....
Orb F ..... to ..... mHz
HARMONICS, RF/Orb F, used .....
DEE - Gnd, max .. 22 .. kV, min gap ..... cm
STABILITY, (pk-pk noise)/(pk RF volt) .....
ENERGY GAIN, max ..... kV/turn
RF PHASE, stable to ± ..... deg
RF POWER input, max .... 23 ..... kW
FREQUENCY MODULATION, rate ..... /s
modulator, type ..... Rotating capacitor .....
beam pulse, width .... 40 µsec macrocycle .....

VACUUM SYSTEM

OPERATING PRESSURE ..... 8×10^{-6} ..... Torr or mbar
PUMPS, No, Type, Size .. 1 Diffusion pump .....
..... 50cm diamètre .....
.....

ION SOURCES

..... OPEN ION SOURCE .....

INJECTION SYSTEM

.....

EXTRACTION SYSTEM

..... Magnetic regenerative .....

FACILITIES FOR RESEARCH

SHIELDED AREA, fixed ..... 160 .. m² ; movable ..... m²
TARGET STATIONS ..... 2 .. in ... 2 ..... rooms
STATIONS served at same time, max .....
MAG SPECTROGRAPH, type .....
COMPUTER model .....
OTHER FACILITIES .....
.....
.....

CHARACTERISTIC BEAMS

PARTICLE	ENERGY (MeV) Goal	ENERGY (MeV) Achieved	CURRENT (pµA) Internal	CURRENT (pµA) External
.. d	.....	.... 28	.... 30	.... 1.5 .....
.. alpha ...	.....	.... 56	.... 10	.....
.....	.....	.....	.....	.....
.....	.....	.....	.....	.....
SECONDARY				(part/s)
.....	.....	.....	.....	.....
.....	.....	.....	.....	.....

BEAM PROPERTIES

MEASURED	CONDITIONS
PULSE WIDTH ..... RF deg	pµ A of .... MeV ... Ions
PHASE EXC, max ... RF deg	pµ A of .... MeV ... Ions
EXTRACT eff ..... %	..... pµ A of .... MeV ... Ions
RESOL ΔE/E .2-2.5 . %	..... pµ A of .... MeV ... Ions
EMITTANCE	
(π mm. mrad) { 40. axial / 40. rad }	..... pµA of ..... MeV ... Ions

OPERATING PROGRAMS, time distribution

BASIC NUCLEAR PHYSICS .. SOLID STATES PHYSICS ....
BIOMEDICAL APPLICAT. .70% ISOTOPE PRODUCTIONS 30%
.....
.....

REFERENCES/NOTES

PLAN VIEW OF FACILITY, NOTEWORTHY FEATURES, COMMENTS

ENTRY No. FM3

NAME OF MACHINE SYNCHROCYCLOTRON 200 MeV protons (S.C. 200) DATE April 1989

INSTITUTION Institut de Physique Nucléaire (I.P.N.)

ADDRESS 91406 ORSAY CEDEX - FRANCE

TEL 69.41.71.65 TELEX IPNORS 602606 F

IN CHARGE Mr J. GUILLOT REPORTED BY Mr M. LOUIS

HISTORY AND STATUS

DESIGN, date 1972 Model tests

ENG DESIGN, date 1973

CONSTRUCTION, date september 1975

FIRST BEAM, date (or goal) 20.06.1977

MAJOR ALTERATIONS

COST, ACCELERATOR about 10 MF) 1975

COST, FACILITY, total about 20 MF)

FUNDED BY Institut de Physique Nucléaire & Phy. Particules

ACCELERATOR STAFF, OPERATION AND DEVELOPMENT

SCIENTISTS 1 ENGINEERS 1

TECHNICIANS 18 CRAFTS

GRAD STUDENTS involved during year

OPERATED BY Research staff or 8 Operators

OPERATION 104 hr/wk, On target 200 hr/wk

TIME DISTR. In house 90 %, Outside 10 %

BUDGET, op & dev 570 KF (1989)

FUNDED BY

RESEARCH STAFF, not included above

USERS, In house 50 outside 20

GRAD STUDENTS involved during year

RESEARCH BUDGET, In house

FUNDED BY C.N.R.S. - I.N.2.P.3.

MAGNET

POLE FACE, diameter (compact) 320 cm, R extraction 140 cm

R injection 1. cm 16.07 to 14.8

GAP, min 40. cm, Field 15.4 14.1 kG

max cm, Field 15.4 14.1 kG } at 6.3 à 5.x.10⁶

AVERAGE FIELD at R ext kG } Ampere turns

B max/ <B>

NUMBER OF SECTORS { compact / separated } Spiral, max deg

SECTOR ANGLE (ISSC) no. deg

TRIMMING COILS yes

CONDUCTOR, material and type copper

STORED ENERGY (cryogenic) MJ

POWER : main coils 350 max, kW ; current stability $\pm 3 \cdot 10^{-5}$

trimming coils max, kW ; current stability $\pm 3 \cdot 10^{-5}$

WEIGHT : Fe 900 tons ; coils 22 tons

COOLING system De-ionized water

ION ENERGY (bending limit) E/A = .223 q^2/a^2 MeV/amu

(focusing limit) E/A = q^2/a^2 MeV/amu

ACCELERATION SYSTEM

DEES, number 1 ; angle 180 deg

BEAM APERTURE 6 cm ; DC Bias 1. kV

TUNED by, coarse fine

RF 25 to 10 mHz, stable ±

Orb F 25 to 10 mHz

HARMONICS, RF/Orb F, used

DEE - Gnd, max 20 kV, min gap 0.4 cm

STABILITY, (pk-pk noise)/(pk RF volt)

ENERGY GAIN, max 20 kV/turn

RF PHASE, stable to ± deg

RF POWER input, max 30 kW

FREQUENCY MODULATION, rate 440 anc. 700 new /s

modulator, type rotating condenser

beam pulse, width 50-100 micro-second

VACUUM SYSTEM

OPERATING PRESSURE Torr or mbar

PUMPS, No, Type, Size oil diffusion Galileo

16.000 l/s

ION SOURCES

Pig Hot Filament

INJECTION SYSTEM

Internal ion source

EXTRACTION SYSTEM

Electromagnetic and magnetostatic channels

FACILITIES FOR RESEARCH

SHIELDED AREA, fixed 500 m² ; movable m²

TARGET STATIONS 3 In rooms

STATIONS served at same time, max

MAG SPECTROGRAPH, type 102°N =1/2

COMPUTER model micro-processors

OTHER FACILITIES one-line Mass Snectrometer

ISOCELE II

CHARACTERISTIC BEAMS

PARTICLE	ENERGY (MeV) Goal	Achieved	CURRENT (pμA) Internal	External
P	168	to 201	4	3
d	83	to 107	9	7
^{3}He++	233	to 281	3.2	2.5
^{4}He++	166	to 216	3.2	2.5
SECONDARY				(part/s)

BEAM PROPERTIES

MEASURED	CONDITIONS
PULSE WIDTH RF deg	pμ A of MeV Ions
PHASE EXC, max RF deg	pμ A of MeV Ions
EXTRACT eff 80 %	4 pμ A of 201 MeV P. Ions
RESOL ΔE/E 0.7 %	4 pμ A of 201 MeV P. Ions
EMITTANCE	
(π mm. mrad) { 9 axial / 19 rad }	4 pμA of 201 MeV P Ions

OPERATING PROGRAMS, time distribution

BASIC NUCLEAR PHYSICS 90 % SOLID STATES PHYSICS

BIOMEDICAL APPLICAT. 10 % ISOTOPE PRODUCTIONS

Protontherapy

REFERENCES/NOTES

In project, 100 % Protontherapy programs

PLAN VIEW OF FACILITY, NOTEWORTHY FEATURES, COMMENTS

ENTRY NO. FM4 **Date** August 14, 1992

Name of Machine Göttingen Synchrocyclotron

Institution University of Göttingen, II. Physikalisches Institut

Address Bunsenstr. 7-9, D-3400 Gottingen, F.R.G.

Tel 0049-(0)551-397632 Telex Fax 0049-(0)551-394493 EMAIL "SCHMIDT_OTT@GUP2001.DNET-GWDG.DE"

In Charge: Prof. Schmidt-Ott Reported by:

HISTORY

MILESTONE DATES:

Design 1958 Model Tests

Construction 1960 First Beam 1962

DESIGN/CONSTRUCTION BY:

in house other Philips, Eindhoven

COST: Accelerator 4.2x10^6 DM Facility 5.9x10^6 DM

FUNDED BY: F.R.G. + Land Niedersachsen

STATUS

STAFF: Machine

Scientists 1 Engineers 1

Technicians 2 Students

Research (in house/external)

Scientists 3 / Engineers /

Technicians / Students 3 /

BUDGET: Machine Funded by Land Niedersachsen

Research Funded by Land Niedersachsen

TIME DISTRIBUTION:

Basic Research (in house/external) 80 % / 10 %

Applied Program (in house/external) % / %

Development % Maintenance 10 %

MAGNET

POLE PARAMETERS:

Diameter 180 cm $R_{extract}$ 75 cm R_{inject} 0 cm

HILL PARAMETERS: Gap (min) 35 cm B_{max} 1.45 T

(@ AT) Gap (max) cm B_{min} 1.42 T

VALLEY PARAMETERS: Gap (min) cm B_{max} T

(@ AT) Gap (max) cm B_{min} T

AVERAGE FIELD: $< B >_{min}$ T $< B >_{max}$ T

NUMBER OF SECTORS: compact/separated /

sector angle deg. spiral (max) deg.

FIELD TRIMMING: Trim Coils

Harmonic Coils

Other

CURRENT: Main Coils 500 Amps Stability 3x10^-4

Trim Coils Amps Stability

Stored Energy (cryogenic) 5 MJ

WEIGHT: Iron 250 tons Conductor aluminium 2 tons

ION ENERGY: Bending Limit E/A = 13.9 q^2/A^2 MeV/u

Focussing Limit E/A = q/A MeV/u

ACCELERATION SYSTEM

FUNDAMENTAL ACCELERATION:

Description: Dee+Dummy Dee, 7cm gap, freq. modulation

No. of Gaps/turn 2 dE/dn(max) 13 MeV/q

Voltage(max) 20 MV Harmonic f_{rf}/f_{ion} 1

Freq 10.6-11.1 MHz Power in(max) 0.18 MW

Stability: Phase Voltage

OTHER CAVITIES (Flattopping or otherwise):

Description:

Region of Influence: R_{min} cm R_{max} cm

No. of Gaps/turn dE/dn(max) MeV/q

Voltage(max) MV Harmonic f_{rf}/f_{ion}

Freq MHz Power in(max) MW

Stability: Phase Voltage

VACUUM SYSTEM

OPERATING PRESSURE: 10^{-6} mbar

PUMPS: No. and type 6000 l/s + 1000 l/s diffusion

ION SOURCE(S)

	Type	Intensity (mA)	@	$\epsilon_n = \beta\gamma\epsilon$ (πmm mrad)	Ion Species
(a)	gas discharge				a, d
(b)					
(c)					
(d)					

INJECTION SYSTEM

Efficiency %

EXTRACTION SYSTEM

magn. channel (Le Couteur) Efficiency 5 %

CHARACTERISTIC BEAMS

	Accelerated Ions	E/A (MeV/u)	Current(part μA) Internal	External
(a)	a	13.5	0.3	
(b)	d	13.5	8	0.4
(c)				
(d)				

	Secondary Particles	E (MeV)	part/sec
(a)			
(b)			
(c)			

EXTRACTED BEAM PROPERTIES:

For 0.4 μA of 13.5 MeV/u d ions

$\Delta E/E$ < 0.1 % $\Delta\phi$ °rf

$\epsilon_n = \beta\gamma\epsilon$ x 100 πmm mrad z 100 πmm mrad

FACILITIES FOR RESEARCH

SHIELDED AREA: Fixed 160 m² Moveable m²

Target Stations: 1 No. Served At Same Time: 1

MAGNETIC SPECTROMETERS:

OTHER FACILITIES: gas transport, cooled internal target

REFERENCES/NOTES

(a) Philips Techn. Rev. Vol. 12, No. 3

(b) CERN Report 63-19, 80

PLAN VIEW OF FACILITY, COMMENTS

ENTRY NO. FM5 Date

Name of Machine JINR PHASOTRON

Institution Joint Institute for Nuclear Research, Laboratory of Nuclear Problems

Address Head Post Office, P.O. Box 79, 101000 Moscow, Russia

Tel 926-22-20 Telex 911621 OUBNA SU Fax EMAIL

In Charge: Is. Vylov Reported by: L. Onischenko

HISTORY

MILESTONE DATES:

Design 1967 Model Tests 1968-74

Construction 1979-84 First Beam 1984

DESIGN/CONSTRUCTION BY:

in house other

COST: Accelerator Facility $18 \cdot 10^6$ roubles

FUNDED BY: JINR

STATUS

STAFF: Machine

Scientists Engineers

Technicians Students

Research (in house/external)

Scientists / Engineers /

Technicians / Students /

BUDGET: Machine Funded by

Research Funded by

TIME DISTRIBUTION:

Basic Research (in house/external) % /

Applied Program (in house/external) % /

Development % Maintenance %

MAGNET

POLE PARAMETERS:

Diameter 600 cm $R_{extract}$ 270 cm R_{inject} cm

HILL PARAMETERS: Gap (min) 15 cm B_{max} 1.8 T

(@ AT) Gap (max) 30 cm B_{min} T

VALLEY PARAMETERS: Gap (min) cm B_{max} 1.2 T

(@ AT) Gap (max) cm B_{min} T

AVERAGE FIELD: $< B >_{min}$ 1.2 T $< B >_{max}$ 1.63 T

NUMBER OF SECTORS: compact/separated 4 /

sector angle deg. spiral (max) 77 deg.

FIELD TRIMMING: Trim Coils 3

Harmonic Coils

Other 4

CURRENT: Main Coils 4000 Amps Stability $2 \cdot 10^{-4}$

Trim Coils Amps Stability

Stored Energy (cryogenic) MJ

WEIGHT: Iron 7000 tons Conductor 165 tons

ION ENERGY: Bending Limit E/A = q^2/A^2 MeV/u

Focussing Limit E/A = q/A MeV/u

ACCELERATION SYSTEM

FUNDAMENTAL ACCELERATION:

Description:

No. of Gaps/turn 2 dE/dn(max) MeV/q

Voltage(max) 0.04 MV Harmonic f_{rf}/f_{ion} 1

Freq 18.6-14.4 MHz Power in(max) 0.3 MW

Stability: Phase Voltage

OTHER CAVITIES (Flattopping or otherwise):

Description:

Region of Influence: R_{min} cm R_{max} cm

No. of Gaps/turn dE/dn(max) MeV/q

Voltage(max) MV Harmonic f_{rf}/f_{ion}

Freq MHz Power in(max) MW

Stability: Phase Voltage

VACUUM SYSTEM

OPERATING PRESSURE: $2 \cdot 10^{-6}$ Torr

PUMPS: No. and type 5 diffusion pumps with nitrogen baffles

ION SOURCE(S)

	Type	Intensity (mA)	@	$\epsilon_n = \beta\gamma\epsilon$ (πmm mrad)	Ion Species
(a)	Pig type				
(b)					
(c)					
(d)					

INJECTION SYSTEM

Efficiency %

EXTRACTION SYSTEM

Regenerative extraction Efficiency 50 %

Iron-current channel

CHARACTERISTIC BEAMS

	Accelerated Ions	E/A (MeV/u)	Current(part μA) Internal	External
(a)	p	680	7	3.5
(b)				
(c)				
(d)				

	Secondary Particles	E (MeV)	part/sec
(a)	μ^+		$3 \cdot 10^5$ /μA·s
(b)	μ^-		$1 \cdot 10^5$ /μA·s
(c)			

EXTRACTED BEAM PROPERTIES:

For μA of MeV/u ions

$\Delta E/E$ 1.5 % $\Delta\phi$ °rf

$\epsilon_n = \beta\gamma\epsilon$ x 5.1 πmm mrad z 3.4 πmm mrad

FACILITIES FOR RESEARCH

SHIELDED AREA: Fixed 1500 m² Moveable m²

Target Stations: 4-7 No. Served At Same Time: 2-3

MAGNETIC SPECTROMETERS:

OTHER FACILITIES: Medico-Biological Complex

YASNAPP (ISOL)

REFERENCES/NOTES

(a)

(b)

PLAN VIEW OF FACILITY, COMMENTS

ENTRY NO. FM6 Date June 25/92

Name of Machine Synchrocyclotron on 1 Gev.

Institution PNPI, Russian academy of Sciences

Address Gatchina, Petersburg District, 188350, Russia

Tel ..... Telex ..... Fax ..... EMAIL .....

In Charge: N.K.Abrosimov Reported by: .....

HISTORY

MILESTONE DATES:

Design ..... Model Tests .....

Construction 1967 ..... First Beam Nov. 1967

DESIGN/CONSTRUCTION BY:

in house ..... other .....

COST: Accelerator ..... Facility .....

FUNDED BY: .....

STATUS

STAFF: Machine

Scientists ..... Engineers .....

Technicians ..... Students .....

Research (in house/external)

Scientists ..... / ..... Engineers ..... / .....

Technicians ..... / ..... Students ..... / .....

BUDGET: Machine ..... Funded by .....

Research ..... Funded by .....

TIME DISTRIBUTION:

Basic Research (in house/external) ..... % / ..... %

Applied Program (in house/external) ..... % / ..... %

Development ..... % Maintenance ..... %

MAGNET

POLE PARAMETERS:

Diameter 685 ... cm $R_{extract}$ 315 cm R_{inject} ..... cm

HILL PARAMETERS: Gap (min) 39 cm B_{max} 1.93 T

(@ ..... AT) Gap (max) 50 cm B_{min} ..... T

VALLEY PARAMETERS: Gap (min) ..... cm B_{max} ..... T

(@ ..... AT) Gap (max) ..... cm B_{min} ..... T

AVERAGE FIELD: $< B >_{min}$ ..... T $< B >_{max}$ 1.9 T

NUMBER OF SECTORS: compact/separated ..... / .....

sector angle ..... deg. spiral (max) ..... deg.

FIELD TRIMMING: Trim Coils .....

Harmonic Coils .....

Other .....

CURRENT: Main Coils 4800 Amps Stability $2 \cdot 10^{-5}$

Trim Coils ..... Amps Stability .....

Stored Energy (cryogenic) ..... MJ

WEIGHT: Iron 7800 t Conductor 174 (Al)

ION ENERGY: Bending Limit E/A = 1000 q^2/A^2 MeV/u

Focussing Limit E/A = ... q/A MeV/u

ACCELERATION SYSTEM

FUNDAMENTAL ACCELERATION:

Description: Lambda/2 one dee with rotating capasitor

No. of Gaps/turn 2 dE/dn(max) ..... MeV/q

Voltage(max) 0.010 MV Harmonic f_{rf}/f_{ion} 1

Freq 29-13.3 MHz Power in(max) 0.2 MW

Stability: Phase ..... Voltage .....

OTHER CAVITIES (Flattopping or otherwise):

Description: C-electrode for slow extraction

Region of Influence: R_{min} 295 cm R_{max} 320 cm

No. of Gaps/turn 2 dE/dn(max) ..... MeV/q

Voltage(max) 0.003 MV Harmonic f_{rf}/f_{ion} 1

Freq ~13.3 MHz Power in(max) 0.002 MW

Stability: Phase ..... Voltage .....

VACUUM SYSTEM

OPERATING PRESSURE: $2 \cdot 10^{-6}$

PUMPS: No. and type 2 diffusion pumps on

40000 l/s

ION SOURCE(S)

	Type	Intensity (mA)	@	$\epsilon_n = \beta\gamma\epsilon$ (πmm mrad)	Ion Species
(a)	open with cold cathod				
(b)					
(c)					
(d)					

INJECTION SYSTEM

..... Efficiency ..... %

EXTRACTION SYSTEM

non liner regenerative system Efficiency 30 %

CHARACTERISTIC BEAMS

	Accelerated Ions	E/A (MeV/u)	Current(part μA) Internal	External
(a)	P	1000	3	1
(b)				
(c)				
(d)				

	Secondary Particles	E (MeV)	part/sec
(a)	+	150	$1.6 \cdot 10^{7}$
(b)	-	150	$5 \cdot 10^{6}$
(c)	+	4	$3 \cdot 10^{4}$

EXTRACTED BEAM PROPERTIES:

For ..... μA of ..... MeV/u ..... ions

$\Delta E/E$ ..... % $\Delta\phi$ ..... °rf

$\epsilon_n = \beta\gamma\epsilon$ x ..... πmm mrad z ..... πmm mrad

FACILITIES FOR RESEARCH

SHIELDED AREA: Fixed ..... m^2 Moveable ..... m^2

Target Stations: ..... No. Served At Same Time: .....

MAGNETIC SPECTROMETERS: .....

OTHER FACILITIES: Protontherapy, Isotope Production, Pi-Mu channel, SR, Time of Flight Neutron Spectrometer, IRIS - facility for investigation isotops far from stability region

REFERENCES/NOTES

(a) Proc. of the VII All-Union Conference on

(b) Charged Particle Accel., v2, p75 (1980)

PLAN VIEW OF FACILITY, COMMENTS

ENTRY NO. FM7 **Date** 13 August 1992

Name of Machine 160 MeV synchrocyclotron

Institution Harvard Cyclotron Laboratory, Harvard University

Address 44 Oxford St., Cambridge, MA 02138, USA

Tel (617) 495 2885 Telex Fax (617) 495 8054 EMAIL SISTERSON@ HUHEPL

In Charge: A.M. Koehler Reported by: B. Gottschalk

HISTORY

MILESTONE DATES:

Design ----- Model Tests -----

Construction 1946 First Beam 1949

DESIGN/CONSTRUCTION BY:

in house X other

COST: Accelerator $1 million Facility $ 0.7 million

FUNDED BY: Office of Naval Research 1946 - 1967

STATUS

STAFF: Machine Other 5

Scientists 2 Engineers 1

Technicians 7 Students 0

Research (in house/external)

Scientists 2 / Engineers /

Technicians / Students 1 /

BUDGET: Machine $1 million Funded by fees and

Research Funded by subcontract

TIME DISTRIBUTION:

Basic Research (in house/external) % /

Applied Program (in house/external) 90 % /

Development 5 % Maintenance 5 %

MAGNET

POLE PARAMETERS:

Diameter 241 cm $R_{extract}$ 105 cm R_{inject} 0 cm

HILL PARAMETERS: Gap (min) 29.6 cm B_{max} 1.83 T

(@ 600 000 AT) Gap (max) 30.5 cm B_{min} 1.90 T

VALLEY PARAMETERS: Gap (min) cm B_{max} T

(@ AT) Gap (max) cm B_{min} T

AVERAGE FIELD: $< B >_{min}$ T $< B >_{max}$ T

NUMBER OF SECTORS: compact/separated /

sector angle deg. spiral (max) deg.

FIELD TRIMMING: Trim Coils

Harmonic Coils

Other

CURRENT: Main Coils 160 KW Amps Stability 0.1 %

Trim Coils Amps Stability

Stored Energy (cryogenic) MJ

WEIGHT: Iron 641 tons Conductor 74 tons

ION ENERGY: Bending Limit E/A = q^2/A^2 MeV/u

Focussing Limit E/A = q/A MeV/u

ACCELERATION SYSTEM

FUNDAMENTAL ACCELERATION:

Description: 3CW40,000H3 , rotating condenser

No. of Gaps/turn 2 dE/dn(max) MeV/q

Voltage(max) .012 MV Harmonic f_{rf}/f_{ion} 1

Freq 30 - 24 MHz Power in(max) .010 MW

Stability: Phase Voltage

OTHER CAVITIES (Flattopping or otherwise):

Description: cee for stochastic extraction

Region of Influence: R_{min} cm R_{max} cm

No. of Gaps/turn dE/dn(max) MeV/q

Voltage(max) MV Harmonic f_{rf}/f_{ion}

Freq MHz Power in(max) MW

Stability: Phase Voltage

VACUUM SYSTEM

OPERATING PRESSURE: 3×10^{-6} (3×10^{-7} base)

PUMPS: No. and type 4 x NRC 6" oil diffusion

ION SOURCE(S)

	Type	Intensity (mA)	@ $\epsilon_n = \beta\gamma\epsilon$ (πmm mrad)	Ion Species
(a)	hot filament pulsed arc "volcano"			
(b)				
(c)				
(d)				

INJECTION SYSTEM

Efficiency %

EXTRACTION SYSTEM

passive regenerator and channel Efficiency ca. 3 %

CHARACTERISTIC BEAMS

Accelerated Ions	E/A (MeV/u)	Current(part μA) Internal	External
(a) protons	158.6 MeV	ca. 1 muA	ca. 10 nA
(b)			
(c)			
(d)			

Secondary Particles	E (MeV)	part/sec
(a)		
(b)		
(c)		

EXTRACTED BEAM PROPERTIES:

For μA of MeV/u ions

$\Delta E/E$ % $\Delta\phi$ °rf

$\epsilon_n = \beta\gamma\epsilon$ x πmm mrad z πmm mrad

FACILITIES FOR RESEARCH

SHIELDED AREA: Fixed m^2 Moveable m^2

Target Stations: No. Served At Same Time:

MAGNETIC SPECTROMETERS: none

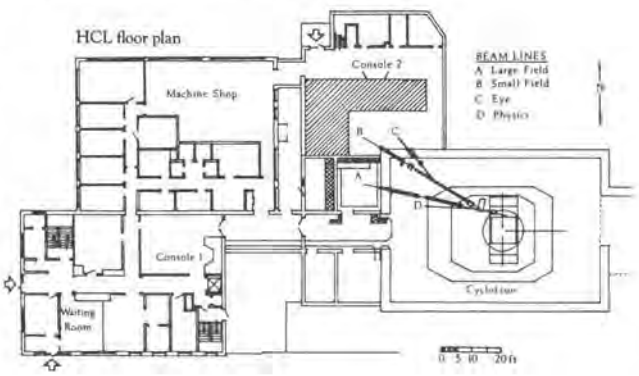
OTHER FACILITIES: Since 1967 we have operated on a fee for service basis, mostly for treating patients. The current hourly fee is $300 . As of 7/92 we have treated 5600 patients. Current rate is 300/year. The equipment and techniques developed here for irradiating patients have proved convenient for radiation damage studies often related to satellites and space probes. A fourth beamline is under construction to facilitate such studies.

REFERENCES/NOTES

(a)

(b)

PLAN VIEW OF FACILITY, COMMENTS



ENTRY NO. CB1 Date

Name of Machine Cooler Synchrotron COSY-Jülich

Institution Forschungszentrum Jülich GmbH (KFA)

Address Postfach 1913, D-5170 Jülich, Germany

Tel +49 2461 613980 Telex 833 556 kf d Fax +49 2461 613930 EMAIL rudolf@.cecs.cc.kfa-juelich.de

In Charge: Reported by: R. Maier

HISTORY

MILESTONE DATES:

Design 1985 Model Tests 1990 - 1992

Construction 1987 - 1992 First Beam

DESIGN/CONSTRUCTION BY:

in house other

COST: Accelerator Facility

FUNDED BY:

STATUS

STAFF: Machine

Scientists Engineers

Technicians Students

Research (in house/external)

Scientists / Engineers /

Technicians / Students /

BUDGET: Machine Funded by

Research Funded by

TIME DISTRIBUTION:

Basic Research (in house/external) % /

Applied Program (in house/external) % /

Maintenance % Development %

MAIN PARAMETERS

MACHINE TYPE: Synchrotron and Storage ring

ION TYPES: p ENERGY: 40-2500 MeV/u

RING: Geometry racetrack 6 fold syn Circumference 184 m

INJECTED BEAM CHARACTERISTICS

PARAMETERS: Injected Ions H_2^+

Energy 40 MeV/u Ions/bunch $7.5 \cdot 10^5$

EMITTANCE: h 2.5 πmm mrad v 5 πmm mrad

ΔE/E % Bunch length nsec

TIMING: Bunch freq MHz Filling Time sec

INJECTION METHOD: Stripping injection

MAGNET SYSTEM

LATTICE: Focusing Type separeted function

Focusing Order FDDF or DFFD

Betatron Freq: ν_h 3.38 ν_v 3.38

No. Short Straight Sections - Length m

No. Long Straight Sections 2 Length 40 m

BENDING MAGNETS: No. 24 Length(ea) 1.755 m

Field: max 1.58 T

QUADRUPOLES: No. 56 Length(ea) 0.3/0.57 m

Gradient: max 7.6 T/m

OTHER MAGNETS: 18 sextupoles 30 T/m²

RF SYSTEM

CAVITIES: No. 1 Type symmetric re-entrant

RF FREQ. 0.462-1.572 MHz HARMONIC f_{rf}/f_{rev} 1

VOLTS/CAV(max) at 100% duty cycle $5 \cdot 10^{-3}$ MV

POWER/CAV(max) $56 \cdot 10^{-3}$ MW

VACUUM SYSTEM

VACUUM CHAMBER: Material stainless steel

Aperture 15 x 6 cm²

PUMPS:(No.,Type,Speed) 80 120 l/s ions

120 1500 l/s sublimation

PRESSURE: 10^{-10} - 10^{-11} Torr

EXTRACTION SYSTEM

TYPE: (a) third order resonance

(b) with ultra slow extraction system

(c)

LENGTH OF SPILL: (a) 0.01 - 10 sec

(b) 5 - 1000 sec

(c) sec

CHARACTERISTIC BEAMS

	Ion	E/A (MeV/u)	Ions/pulse	ΔE/E (%)
(a)	p	≤2500	$\leq 2 \cdot 10^{11}$	$1 \cdot 10^{-3}$
(b)				
(c)				
(d)				

EXTRACTED BEAM PROPERTIES:

Rep. Rate (pulse/sec) ≤ 0.3

$\epsilon_n = \beta\gamma\epsilon$ h 8.8 πmm mrad for .... μA of 2500 MeV/u p... ions

v 8.8 πmm mrad for .... μA of 2500 MeV/u p... ions

FACILITIES FOR RESEARCH

SHIELDED AREA: Fixed m² Moveable m²

Target Stations: No. Served At Same Time:

MAGNETIC SPECTROMETERS:

OTHER FACILITIES:

magnetic spectrometer BIG KARL, time of flight spectrometer TOF, three internal target areas (TP1-TP3)

REFERENCES/NOTES

(a)

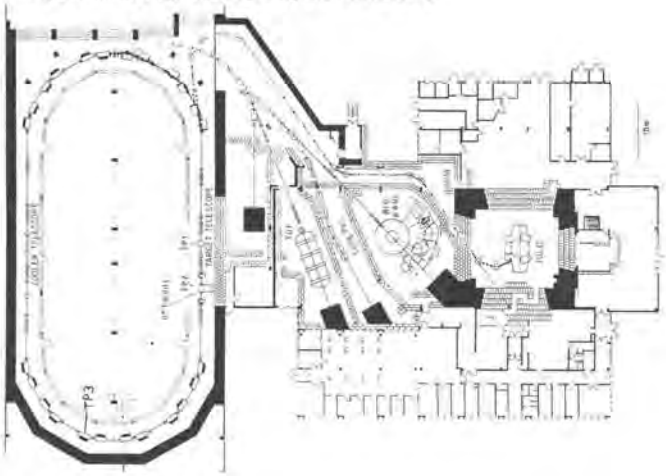
(b)

OTHER RELEVANT PARAMETERS, RECENT IMPROVEMENTS, ETC.

Electron cooling up to 200 MeV/u

Stochastic cooling at energies between 1000 and 2500 MeV/u.

PLAN VIEW OF FACILITY, COMMENTS



ENTRY NO. CB2 Date July 1/1992

Name of Machine TARN II

Institution INSTITUTE FOR NUCLEAR STUDY, Univ. of Tokyo

Address 3-2-1 MIDORICHO TANASHI Tokyo 188 JAPAN

Tel 0424-61-4131 Telex Fax 0424-68-5845 EMAIL KATAYAMA@IPNUTINS

In Charge: Reported by: T.Katayama

HISTORY

MILESTONE DATES:

Design 1984-1985 Model Tests

Construction 1985-1989 First Beam 1989

DESIGN/CONSTRUCTION BY:

in house other

COST: Accelerator 13M$(Total) Facility

FUNDED BY: MINISTRY OF Education, Science and Culture

STATUS

STAFF: Machine

Scientists 5 Engineers 5

Technicians Students 1

Research (in house/external)

Scientists / Engineers /

Technicians / Students /

BUDGET: Machine ~1 M$/year Funded by Ministry of Education

Research Funded by

TIME DISTRIBUTION:

Basic Research (in house/external) % / %

Applied Program (in house/external) % / %

Maintenance % Development %

MAIN PARAMETERS

MACHINE TYPE: Cooler Synchrotron

ION TYPES: Light Ions ENERGY: 370(q/A=0.5), 1100(p MeV/u

RING: Geometry circular, 6 fold sym Circumference 78 m

INJECTED BEAM CHARACTERISTICS

PARAMETERS: Injected Ions $P, d, \alpha, H_2, {}^3He, N, C$, etc.

Energy 5~20 MeV/u Ions/bunch

EMITTANCE: h 15 πmm mrad v 15 πmm mrad

$\Delta E/E$ 0.1 % Bunch length nsec

TIMING: Bunch freq MHz Filling Time sec

INJECTION METHOD: Multi-turn Injection Cooling Stacking

MAGNET SYSTEM

LATTICE: Focusing Type Separated function

Focusing Order FBBDBBFO

Betatron Freq: ν_h 1.706 ν_v 1.725

No. Short Straight Sections 6 Length 4 m

No. Long Straight Sections Length m

BENDING MAGNETS: No. 24 Length(ea) 1.0 m

Field: max 1.5 T

QUADRUPOLES: No. 18 Length(ea) 0.2 m

Gradient: max 7.0 T/m

OTHER MAGNETS: Sextupole Magnet for slow Extraction

RF SYSTEM

CAVITIES: No. 1 Type 2xλ/4 re-entrant

RF FREQ. 0.62~7.50 MHz HARMONIC f_{rf}/f_{ion} 2

VOLTS/CAV(max) 0.002 MV

POWER/CAV(max) 0.005 MW

VACUUM SYSTEM

VACUUM CHAMBER: Material Stainless steel

Aperture 5 x 20 cm²

PUMPS:(No.,Type,Speed) TGP:26(1500ℓ/sx8, 1000ℓ/sx3, 700ℓ/sx4 400ℓ/sx11), SIP:17(800ℓ/sx6, 400ℓ/sx5, 160ℓ/sx6),

PRESSURE: 5x10⁻¹¹ Torr

EXTRACTION SYSTEM

TYPE: (a) Slow Extraction (1/3 resonance)

(b)

(c)

LENGTH OF SPILL: (a) 1~800 sec

(b) sec

(c) sec

CHARACTERISTIC BEAMS

	Ion	E/A (MeV/u)	Ions/pulse	ΔE/E (%)
(a)	α	220	10^7	0.5
(b)				
(c)				
(d)				

EXTRACTED BEAM PROPERTIES:

Rep. Rate (pulse/sec)

$\epsilon_n = \beta\gamma\epsilon$ h .... πmm mrad for .... μA of .... MeV/u .... ions

v .... πmm mrad for .... μA of .... MeV/u .... ions

FACILITIES FOR RESEARCH

SHIELDED AREA: Fixed 650 m² Moveable m²

Target Stations: No. Served At Same Time:

MAGNETIC SPECTROMETERS:

OTHER FACILITIES:

Electron Cooler, 120 kV, 5A

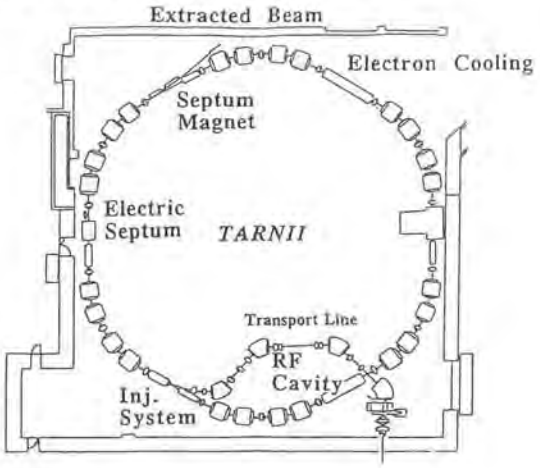
REFERENCES/NOTES

(a) T.Katayama et al., Particle Acc. Vols. 37~37 (1992)

(b) T.Tanabe et al., N.I.M. A307 (1991)

OTHER RELEVANT PARAMETERS, RECENT IMPROVEMENTS, ETC.

PLAN VIEW OF FACILITY, COMMENTS



ENTRY NO. CB3 Date 16 JULY 1992

Name of Machine CELSIUS

Institution The Svedberg Laboratory

Address Box 533, 75121 UPPSALA, Sweden

Tel +46 18 183177 Telex 76088 TSLISW Fax +46 18 183833 EMAIL REISTAD@TSL.UU.SE

In Charge: A. Johansson Reported by: D. Reistad

HISTORY

MILESTONE DATES:

Design 1984-1988 Model Tests

Construction 1984-1988 First Beam 1988

DESIGN/CONSTRUCTION BY:

in house yes other

COST: Accelerator SEK 45E6 Facility

FUNDED BY: Swedish Government

STATUS

STAFF: Machine

Scientists 2 Engineers 6

Technicians 1 Students 2

Research (in house/external)

Scientists / Engineers /

Technicians / Students /

BUDGET: Machine 300,000 SEK Funded by Swedish Govt.

Research Funded by

TIME DISTRIBUTION:

Basic Research (in house/external) - % / 25 %

Applied Program (in house/external) - % / - %

Maintenance 18 % Development 7 %

MAIN PARAMETERS

MACHINE TYPE: Storage Ring

ION TYPES: Light/Heavy Ions ENERGY: MeV/u

RING: Geometry Circumference 82 m

INJECTED BEAM CHARACTERISTICS

PARAMETERS: Injected Ions From Gustav Werner Cyclotron

Energy 12-180 MeV/u Ions/bunch

EMITTANCE: h πmm mrad v πmm mrad

ΔE/E % Bunch length nsec

TIMING: Bunch freq MHz Filling Time sec

INJECTION METHOD: Stripping and Multiturn

MAGNET SYSTEM

LATTICE: Focusing Type Combined function & separate quads

Focusing Order FDDFDFDDFD σ_x σ_D

Betatron Freq: ν_h 1.63 ν_v 1.83

No. Short Straight Sections 2 Length 9.3 m

No. Long Straight Sections 2 Length 9.6 m

BENDING MAGNETS: No. 40 Length(ea) 1.1 m

Field: max 1.0 T

QUADRUPOLES: No. 8 Length(ea) 0.44 m

Gradient: max 12.25 T/m

OTHER MAGNETS:

RF SYSTEM

CAVITIES: No. 1 Type Ferrite Tuned

RF FREQ. 0.4-3.3 MHz HARMONIC f_{rf}/f_{ion} 1

VOLTS/CAV(max) 0.0015 MV

POWER/CAV(max) 0.0015 MW

VACUUM SYSTEM

VACUUM CHAMBER: Material Stainless steel AISI316LN

Aperture x cm²

PUMPS:(No.,Type,Speed) 36 Sputter-ion, 5300 l/s

36 Titanium sublimation, 24,000 l/s

PRESSURE: Presently 2 x 10e-9 Torr

EXTRACTION SYSTEM

TYPE: (a) Ring intended for physics with very thin

(b) internal targets. No beam extraction is

(c) foreseen.

LENGTH OF SPILL: (a) sec

(b) sec

(c) sec

CHARACTERISTIC BEAMS

	Ion	E/A (MeV/u)	Ions/pulse	ΔE/E (%)
(a)	protons	48-1300	10e11	0.01-0.1
(b)	deuterons	12-480	2x10e10	0.01-0.1
(c)	α-particles	12-480	10e10	0.01-0.1
(d)	^{16}O ions	12-480	10e8	0.01-0.1

EXTRACTED BEAM PROPERTIES:

Rep. Rate (pulse/sec)

$\epsilon_n = \beta\gamma\epsilon$ h .... πmm mrad for .... μA of .... MeV/u .... ions

v .... πmm mrad for .... μA of .... MeV/u .... ions

FACILITIES FOR RESEARCH

SHIELDED AREA: Fixed 900 m² Moveable - m²

Target Stations: 2 No. Served At Same Time: 1

MAGNETIC SPECTROMETERS:

OTHER FACILITIES:

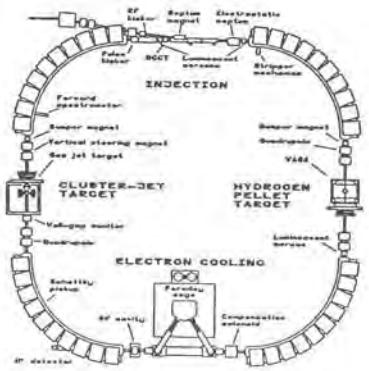
REFERENCES/NOTES

(a) Reistad et al, these proceedings

(b)

OTHER RELEVANT PARAMETERS, RECENT IMPROVEMENTS, ETC.

PLAN VIEW OF FACILITY, COMMENTS



ENTRY NO. CB4 Date 21 JUNE 92

Name of Machine INDIANA UNIVERSITY COOLER RING

Institution INDIANA UNIVERSITY CYCLOTRON FACILITY

Address 2401 Milo B. Sampson Lane Bloomington, IN 47408

Tel (812) 855-9365 Telex 272279 INDIANA U BLOM. Fax (812) 855-6544 EMAIL FRIESEL@IUCF

In Charge: JOHN CAMERON, Director Reported by: D. L. FRIESEL

HISTORY

MILESTONE DATES:

Design 1981-1983 Model Tests 1982-1986

Construction 1983-1987 First Beam 1987

DESIGN/CONSTRUCTION BY:

in house YES other Various Fabrication Vendors

COST: Accelerator $6.8 x 10^6 Facility .9 x 10^5

FUNDED BY: NATIONAL SCIENCE FOUNDATION (NSF)

STATUS

STAFF: Machine

Scientists 14 Engineers 14

Technicians 46 Students 3

Research (in house/external)

Scientists 41 / >250 Engineers -- / --

Technicians 9 / -- Students 53 / 25

BUDGET: Machine $10-x 10^6 Funded by NSF

Research Funded by

TIME DISTRIBUTION:

Basic Research (in house/external) 20 % / 20 %

Applied Program (in house/external) 0 % / 0 %

Maintenance 50 % Development 10 %

MAIN PARAMETERS

MACHINE TYPE: Synchrotron/Storage Ring

ION TYPES: P, $\bar{P}$, d, $\bar{d}$, ^{3}He, ^{4}He ENERGY: 3.6 Tm MeV/u

RING: Geometry Irregular Hexagon Circumference 86.83 m

INJECTED BEAM CHARACTERISTICS

PARAMETERS: Injected Ions P, $\bar{P}$, d, $\bar{d}$, ^{3}He, ^{4}He

Energy 200 MeV/u Ions/bunch 10^6

EMITTANCE: h 1.5 πmm mrad v 1.5 πmm mrad

$\Delta E/E$ 0.1 % Bunch length 1.0 - 0.6 nsec

TIMING: Bunch freq 60-90 MHz Filling Time 10^3-10 sec

INJECTION METHOD: Stripping Inj. & Kick Accumulation

MAGNET SYSTEM

LATTICE: Focusing Type Separated Function

Focusing Order FODO

Betatron Freq: ν_h 3.85 ν_v 4.85

No. Short Straight Sections 3 Length 10.0 m

No. Long Straight Sections 3 Length 12.5 m

BENDING MAGNETS: No. 8 + 4 Length(ea) 1.24&1.12 m

Field: max 1.53 T

QUADRUPOLES: No. 18 + 18 Length(ea) 2.3 & 3.8 m

Gradient: max 15 T/m

OTHER MAGNETS: 16 Sextupoles

RF SYSTEM

CAVITIES: No. 2 Type Coaxial Lamda/4

RF FREQ 0.5-16 MHz HARMONIC f_{rf}/f_{ion} 1-9

VOLTS/CAV(max) $3 x 10^{-3}$ (h=1) and $5 x 10^{-3}$ (PPA) MV

POWER/CAV(max) $1 x 10^{-3}$ (h=1) and $5 x 10^{-4}$ (PPA) MW

VACUUM SYSTEM

VACUUM CHAMBER: Material Stainless Steel

Aperture <5> x <5> cm^2

PUMPS:(No.,Type,Speed) 7 ION @ 220 l/s, 8 Ti Sublimation @ 900 l/s & 14 Getter @ 750 l/s

PRESSURE: $1 x 10^{-9}$ Torr

EXTRACTION SYSTEM

TYPE: (a) No external beam

(b) Internal target experiments

(c)

LENGTH OF SPILL: (a) sec

(b) sec

(c) sec

CHARACTERISTIC BEAMS (Internal Beams)

	Ion	E/A (MeV/u)	Ions/pulse	ΔE/E (%)
(a)	P, $\bar{P}$	500	$1x10^9$	0.01 Cooled
(b)	d, $\bar{d}$	150	$1x10^9$	0.01 Cooled
(c)	^{3}He	250	$1x10^9$	0.01 Cooled
(d)	^{4}He	150	$1x10^9$	

EXTRACTED BEAM PROPERTIES:

Rep. Rate (pulse/sec) N/A

$\epsilon_n = \beta\gamma\epsilon$ h .... πmm mrad for .... μA of .... MeV/u .... ions

v .... πmm mrad for .... μA of .... MeV/u .... ions

FACILITIES FOR RESEARCH

SHIELDED AREA: Fixed 2000 m^2 Moveable -- m^2

Target Stations: 4 No. Served At Same Time: 1

MAGNETIC SPECTROMETERS: None

OTHER FACILITIES: Pol. ^{3}He & Proton Targets, Scrapper and Gas Jet Targets, Siberian Snake, Electron Cooling System

REFERENCES/NOTES

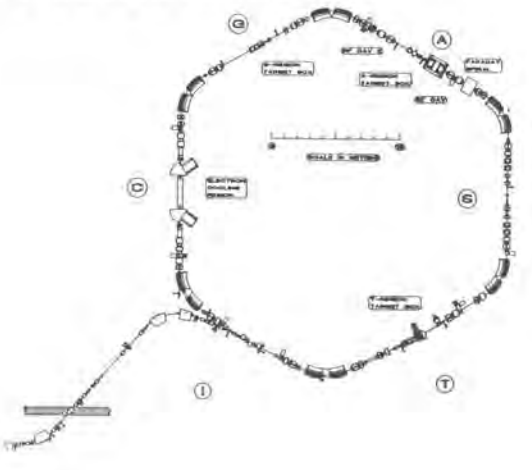
(a) 1991 IUCF Scientific & Technical Report

(b) The Indiana Cooler Project, R.E. Pollock, Proc. 11th Intl. Cyclotron Conf., Tokyo, Japan, p. 123 (1986).

OTHER RELEVANT PARAMETERS, RECENT IMPROVEMENTS, ETC.

Operating mode is to use thin internal targets (<100 ngm/cm^2) with circulating electron cooled ion beams to perform high Resolution Intermediate Energy Physics Research ($\Delta E/E = 0.01\%$)

PLAN VIEW OF FACILITY, COMMENTS



COMMISSIONING OF THE RCNP RING CYCLOTRON

I. Miura, T. Yamazaki, A. Shimizu, K. Hosono, T. Itahashi, T. Saito, A. Ando, K. Tamura,
K. Hatanaka, M. Kibayashi, M. Uraki, H. Ogata, M. Kondo and H. Ikegami
Research Center for Nuclear Physics, Osaka University,
Mihogaoka 10-1, Ibaraki, Osaka 567, Japan

and

J. Abe
Quantum Equipment Division, Sumitomo Heavy Industries, Ltd.,
Soubiraki 5-2, Niihama, Ehime 792, Japan

ABSTRACT

The construction of the ring cyclotron was started in August 1987. On October 12th 1991 the first beam was injected into the ring cyclotron. Many improvements were made for the initial trouble of operation. On December 20th the first extracted beam of 300 MeV protons was obtained. Various test experiments were done with 300 MeV polarized proton beam for a high precision magnetic spectrograph and a neutron TOF facility.

1. INTRODUCTION

The Research Center for Nuclear Physics was funded in 1971, as a national user facility. A K=140 AVF cyclotron[1] and precise experimental apparatus were used during a decade by many researchers in Japan and abroad. After intensive design study of new facility, "RCNP Cyclotron Cascade Project"[2,3] was proposed in 1985, to extend the high precision studies into energy region above threshold energy of pion production. The main components

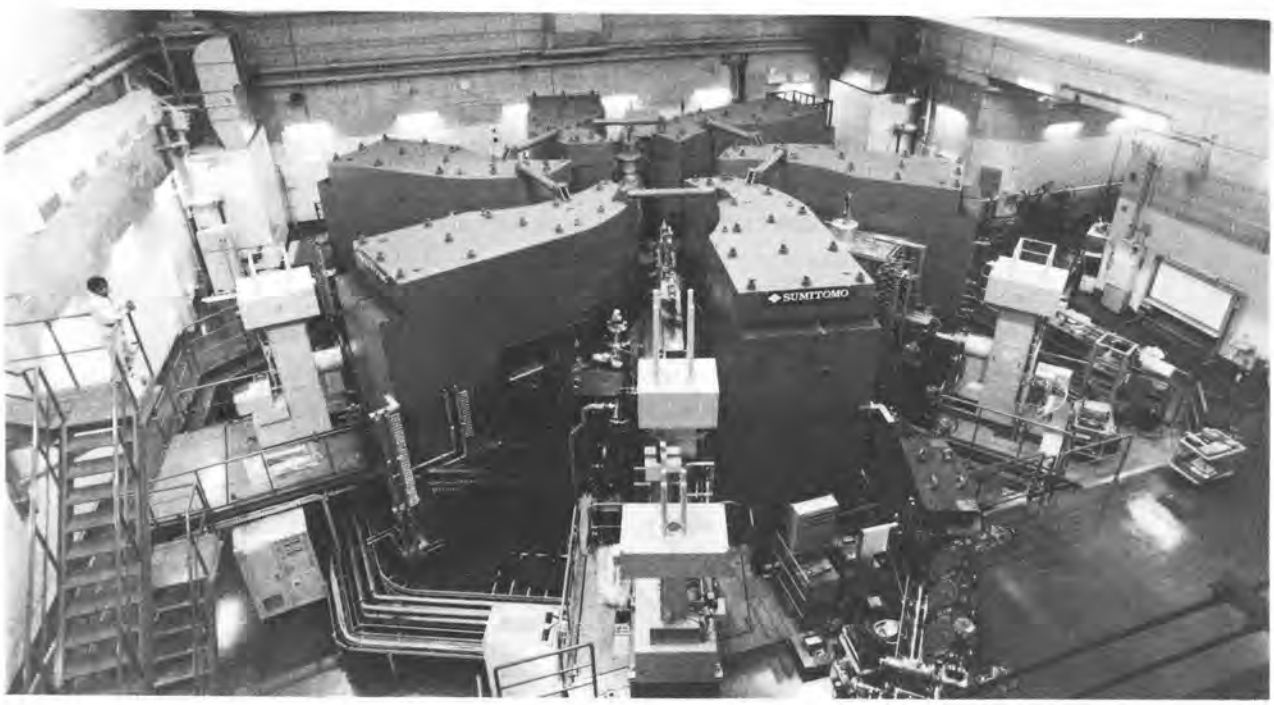


Fig. 1. Photograph of the RCNP ring cyclotron.

of the new facility are a six separated spiral sector cyclotron (ring cyclotron) and beam circulation ring linked to high precision dual magnetic spectrograph, a neutron TOF facility with a 100 m neutron flight tunnel and a heavy ion secondary beam facility.

In 1986 the proposal was accepted and the four years cyclotron construction contract was made with manufacturer in August 1987. Installation of the ring cyclotron was started in February 1990, immediately after finish of the Ring Cyclotron Hall. Figure 1 shows the photograph of the ring cyclotron. On December 20th the first extracted beam of 300 MeV protons was obtained. The chronology of construction and commissioning is shown in Table 1. Experimental study with the AVF cyclotron was continued during the construction and the commissioning. Now main effort for experimental study is made with new facility.

Table 1
Chronology of construction and commissioning

Aug.	1987	The cyclotron construction contract was made.
Nov.	1987	Readjustment of the land for the ring cyclotron building was started.
Feb.	1990	Installation of the ring cyclotron was started.
Aug.	1990	Utilities of the new facility was finished.
Apr.	1991	Accumulation of the magnetic field data of the ring cyclotron during 4 months was performed.
Sept.	1991	New beam injection line, beam buncher and beam pulser were tested. Vacuum leak-test of the ring cyclotron was finished.
Oct.	1991	The first beam was injected into the ring cyclotron and successfully pass through the injection elements to beam stopper following the flat-topping cavity.
Nov.	1991	Acceleration cavity voltage of 400 kV was achieved and proton beam accelerated up to 300 MeV.
Dec.	1991	New signal amplifier was developed for the phase probe. Correction on the deflector position drive system was made. The first extracted beam of 300 MeV proton was transported to the beam dump of TOF facility and one of the high precision spectrograph.
Mar.	1992	Acceleration cavity voltage of 510 kV was achieved for 400 MeV proton beam acceleration. Proton beam accelerated up to 400 MeV. Preliminary experimental studies were started with 300 MeV proton beams.
Apr.	1992	Polarized proton beam was transported for the experimental study. Single turn extraction was achieved by using beam buncher and flat-topping cavity.
May	1992	A 500p sec time resolution was obtained for the polarized proton beam of 300 MeV with a 1/4 pulsing of injection beam.

The new systems of the ring cyclotron had been tested and many improvements were made for the initial trouble of operation. Improvement of capability on the high voltage vacuum feed-through of deflectors and the power supply of second magnetic inflection channel will be made by replacement in August. The magnet system, the RF system, the vacuum system, the beam diagnostic system and the computer control system are reported elsewhere in these proceedings. These systems work well now and efforts being continued to improve beam quality, intensity and stability of the ring cyclotron.

The ring cyclotron is energy quadrupler of the RCNP AVF cyclotron. Protons and alpha particles can be accelerated up to 400 MeV. The K value for light-heavy ions acceleration is 400. Plan view of the ring cyclotron is shown in Fig. 2. Three single gap acceleration cavities are used in the ring cyclotron. Frequency range of the cavity is 30~52 MHz and harmonic numbers of acceleration is 6, 10, 12 and 18. An additional single gap cavity is used for flat-topping with 3rd harmonic of acceleration frequency to get good energy resolution and wide phase acceptance. The phase acceptance is 20° for

A 180°-single-dee acceleration cavity is used in the RCNP AVF cyclotron. The frequency range of the cavity is 5.5~19.5 MHz, and fundamental and

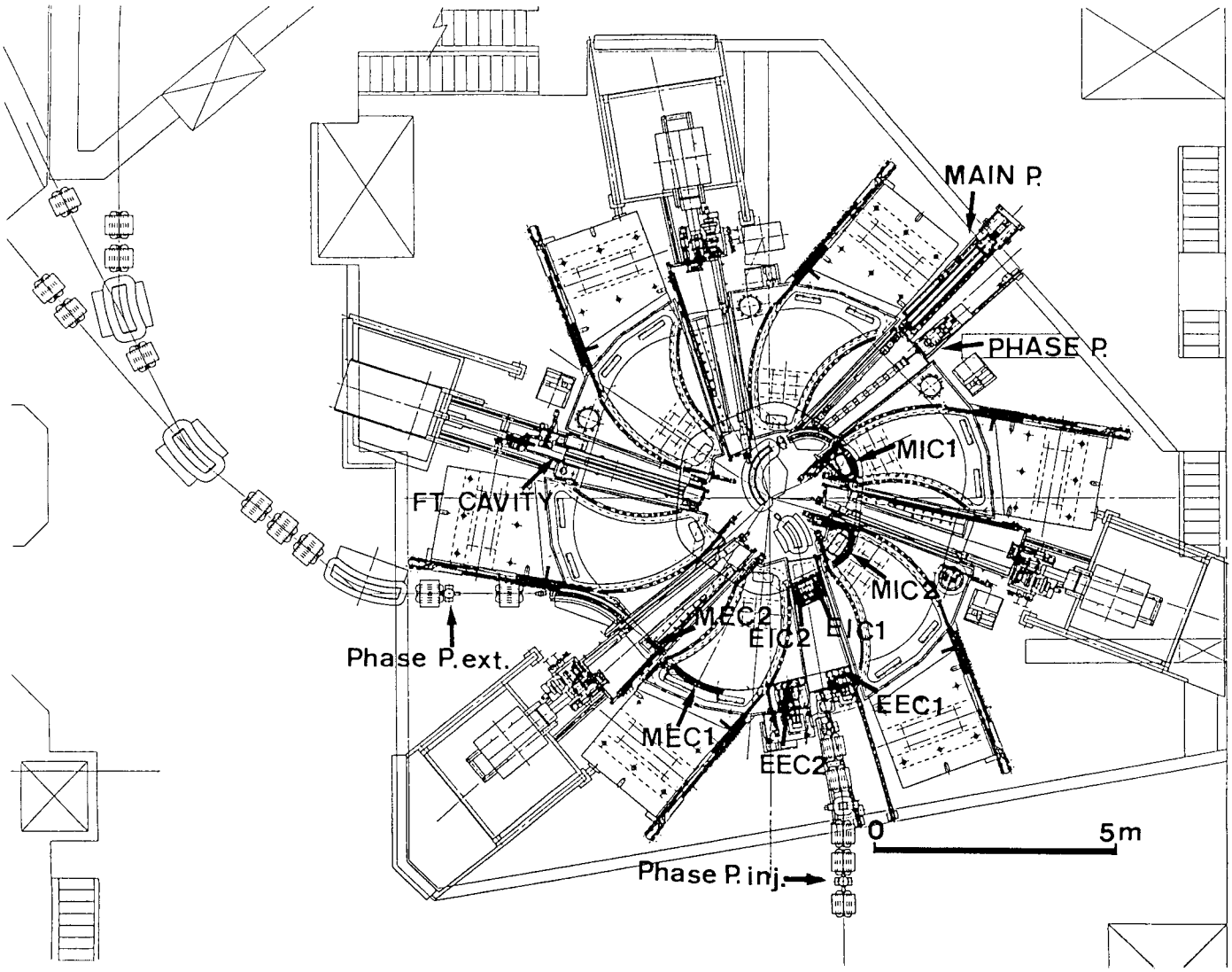


Fig. 2. Plan view of the ring cyclotron.

3rd harmonic acceleration modes are used. Figure 3 shows relation between orbital frequencies and acceleration frequencies in the AVF cyclotron and the ring cyclotron for various ions and energies.

The phase acceptance of the ring cyclotron on the acceleration frequency of the AVF cyclotron is 7° and 4°, since the ratio of acceleration frequency of the ring cyclotron to that of the AVF cyclotron is 3 and 5 for proton and alpha, respectively. The characteristics of the cyclotrons are given in Table 2.

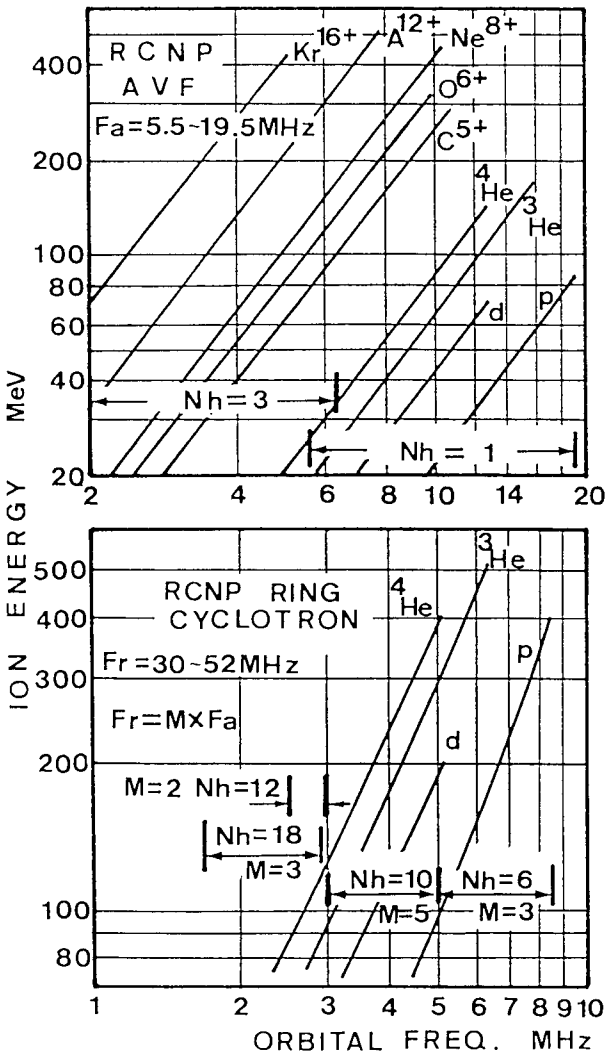


Fig. 3. Orbital frequencies, acceleration frequencies (Fa& Fr) and harmonic numbers of acceleration (Nh) in the RCNP AVF cyclotron and the RCNP ring cyclotron for various ions and energies. M is ratio of the acceleration frequency of the ring cyclotron to the AVF cyclotron.

Table 2

Characteristics of cyclotrons

	Injector Cyclotron	Ring Cyclotron
No. of sector magnets	3	6
Sector angle	max 52°	22~27.5°
Injection radius(cm)		200
Extraction radius(cm)	100	404
Magnet gap(cm)	20.7 min	6.0
Max. Mag. field(kG)	19.5	17.5
Proton max.(MeV)	84	400
Alpha max.(MeV)	130	400
^{3}He max.(MeV)	160	510
Weight of magnet(ton)	400	2100
Main coil magnet(kW)	450	440
No. of trim coils	16	36
Trim coil power(kW)	265	350
No. of cavities	1	3(Acc.)
		1(FT)
RF frequency(MHz)	5.5~19.5	30~52
		90~155
RF power(kW)	120	250×3
		45

2. ACCELERATED BEAMS

300 MeV polarized and unpolarized proton beams are used for preliminary experiments with a high precision magnetic spectrograph and a neutron TOF facility. These beams are extracted with single turn extraction mode with flat-topping. The typical characteristics of the beam used for the experiments are shown in Table 3.

400 MeV protons, 400 MeV alpha particles and 200 MeV deuterons can not be injected properly now, depending insufficient performance of the deflector feed-through and the power supply of second magnetic inflection channel.

Proton beam was accelerated up to 400 MeV using abnormal setting of the injection elements. However the proton beam can not be extracted.

Table 3
Typical characteristics of the beam

Injection beam	
Beam energy	53 MeV
Energy spread	~100 keV
Bunch length	20°(1000 ps)
Rad. emit.	2πmm mrad
Vert. emit.	2πmm mrad
Beam on target	
Beam energy	300 MeV
Energy spread	300 keV
Bunch length	10° (500 ps)
Rad. emit.	0.6π mm mrad
Vert. emit.	0.6π mm mrad
Unpolarized proton	20 nA
Polarized proton	5 nA

3. MAGNETS OF THE RING

The magnet of the six spiral sector ring cyclotron was designed by using computer code FIGER and the results of model magnet study of the previous proposal.[4] Figure 4 shows calculated field distribution with the code. The sector magnets are designed isochronous for 200 MeV proton acceleration without trim coil current. The measured magnetic field distribution are quite satisfactory.[5] Figure 5 shows comparison between betatron frequencies calculated from the measured magnetic field and the designed one. Figure 6 shows measured beam phase on predicted trim coil currents and optimized one for 300 MeV proton acceleration.

4. VACUUM SYSTEM

The vacuum chamber of the ring cyclotron consists of six magnet chambers, three acceleration cavity chambers, a flat-topping cavity chamber and two valley chambers as shown in Fig. 2. The gaps between these chambers are sealed by pneumatic expansion seals. These seals are working quite well.[6] The ring cyclotron is evacuated down to 1×10^{-7} Torr by six diffusion pumps with double chevron baffles (2,500ℓ/sec each eq.), three 16 inch cryopumps (6,500ℓ/sec each) with gate value and six 20 inch cryopumps (10,000ℓ/sec each).

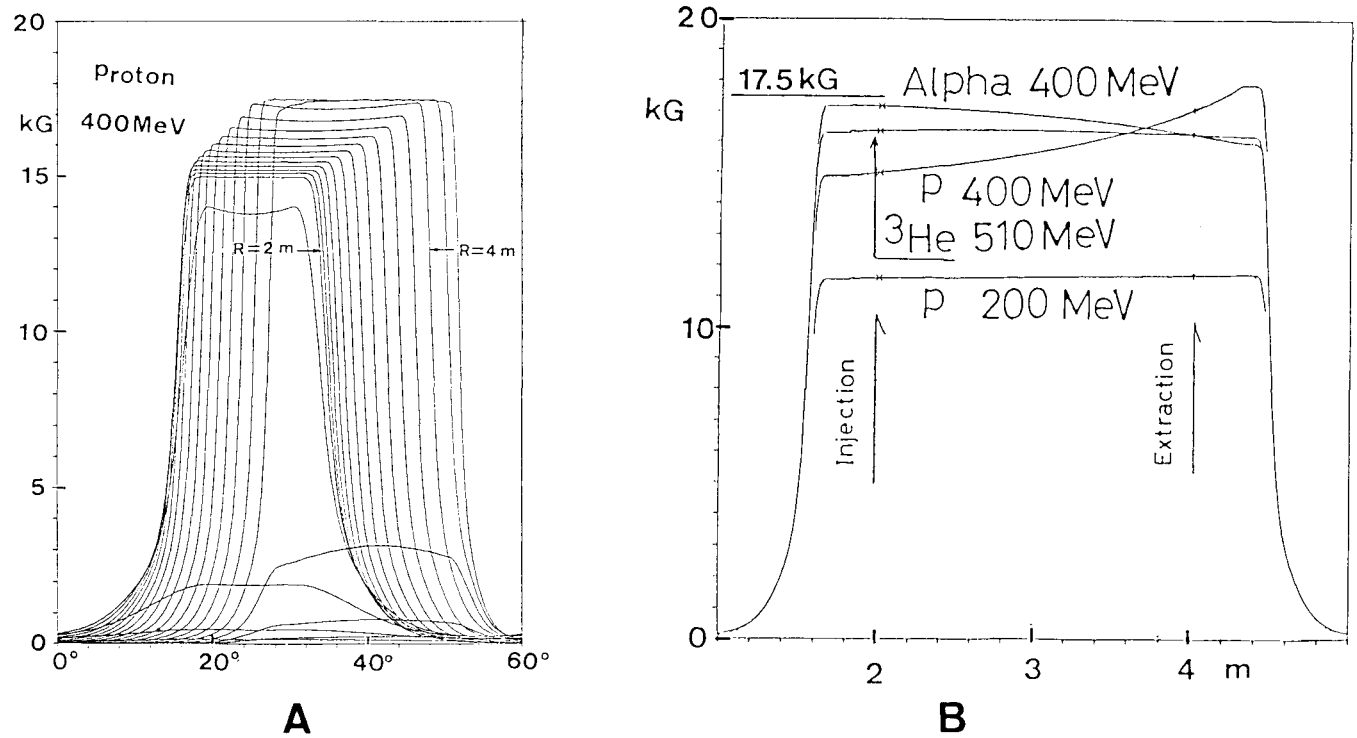


Fig. 4. A: Designed field distribution for 400 MeV proton.
B: Designed isochronous fields on hill center for various ions.

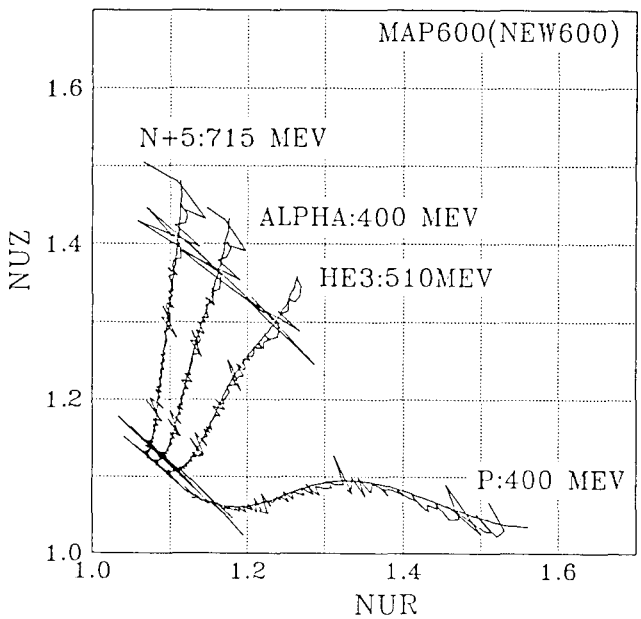


Fig. 5. Comparison between betatron frequencies calculated from the measured field and the designed one.

5. INJECTION AND EXTRACTION SYSTEM

The maximum designed parameters of the injection and extraction system are shown in Table 4. The injection and extraction system[7] worked satisfactory as designed, for 300 MeV proton. However, voltage-holding capability of deflector feedthrough is not enough for 400 MeV proton acceleration. For acceleration of 400 MeV alpha particle, present 500A DC power supply of second magnetic inflection channel must be replaced by one of 700A.

Table 4. Parameters for 400 MeV beam

		Proton	α
Extraction	MeV	400.8	401.2
Injection	MeV	63.6	86.3
Rev. frequency	MHz	8.421	5.071
MIC1 ΔB	Gauss	+1730	+1889.3
MIC2 ΔB	Gauss	+550	+551.1
EIC1/EIC2	kV/cm	80	59.1
EEC1/EEC2	kV/cm	70	38
Electrode gap	cm	1	1
MEC1 ΔB	Gauss	-900	-759.3
MEC2 B	kGauss	10	9.187

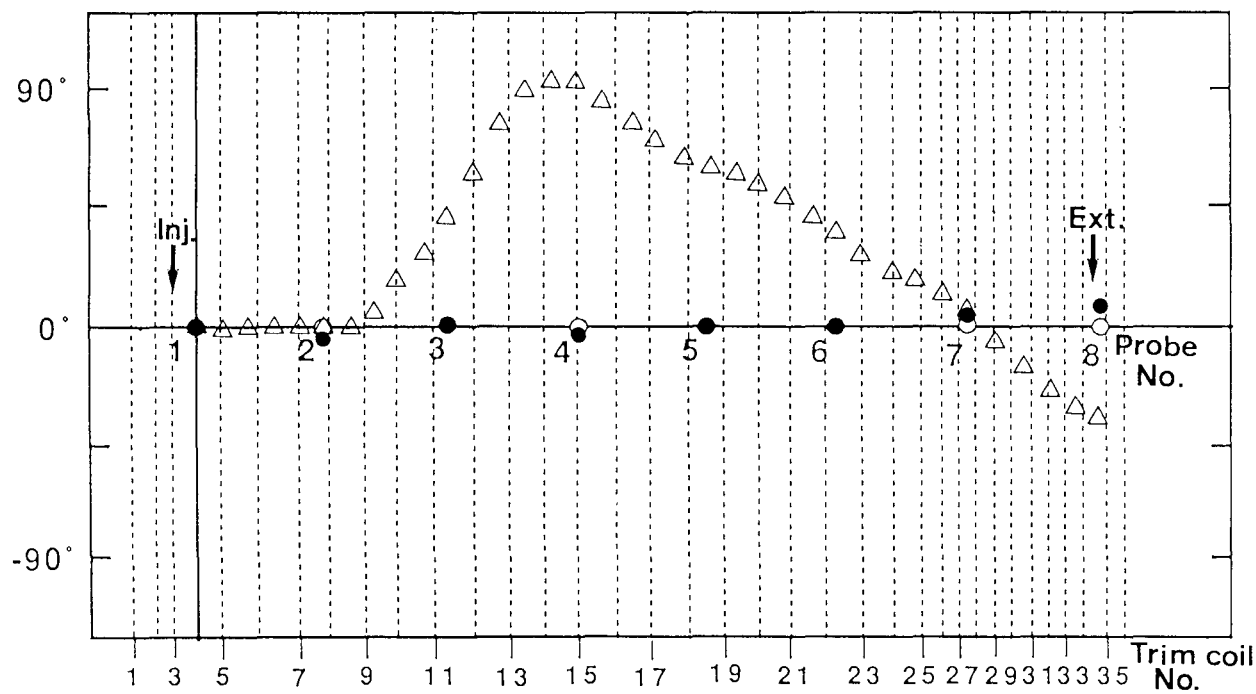


Fig. 6. Measured beam phase on predicted trim coil currents and optimized isochronous field, for 300 MeV proton acceleration.

6. ACCELERATION SYSTEM

The acceleration cavities, the flat-topping cavity and their RF power amplifiers were tested individually in 1990. The side walls of the cavity chamber can not withstand atmospheric pressure under evacuation, so these walls are supported by the magnet chambers. After full assembly of the ring cyclotron, full power test of the RF system and baking of the cavities were started.[8] The variable frequency acceleration cavity is tuned with a pair of rotatable plates. The resonant current on the rotatable plates flow through current-carrying hinges of thin copper plate and finger contact. The every finger-contact was replaced by newly designed one after initial trouble.

The RF power of the flat-topping cavity leaks easily to outside, for asymmetric setting of the sliding shorts. RF shields of trim coil feed-through were set on the both side of the flat-topping cavity.

Heterodyne method is used for the RF phase control system. Digital phase shifters, 0.03°/step, are working well on 455 kHz intermediate frequency. Stability of the acceleration voltage and phase will be improved in August.

7. AVF CYCLOTRON

Improvement of the injection beam of the ring cyclotron is also very important. A new beam phase selector for axial injection mode was developed as shown in Fig. 7. Efficient phase selection was made down to about 7°.

Upgrade of the injection beam characteristics, by using high intensity ion sources NEOMAFIOS and ECR ionizer, is expected in next year.

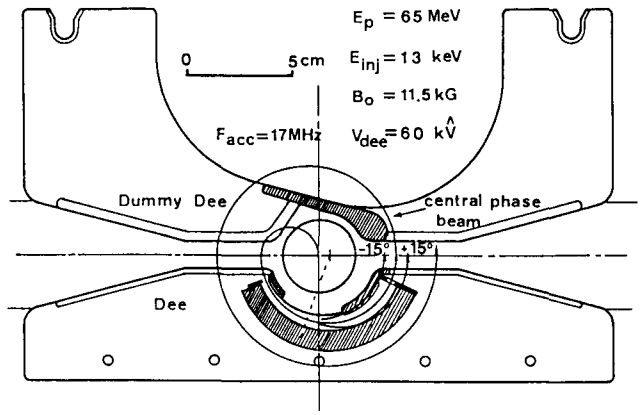


Fig. 7. Beam phase selector for axial injection mode of the AVF cyclotron.

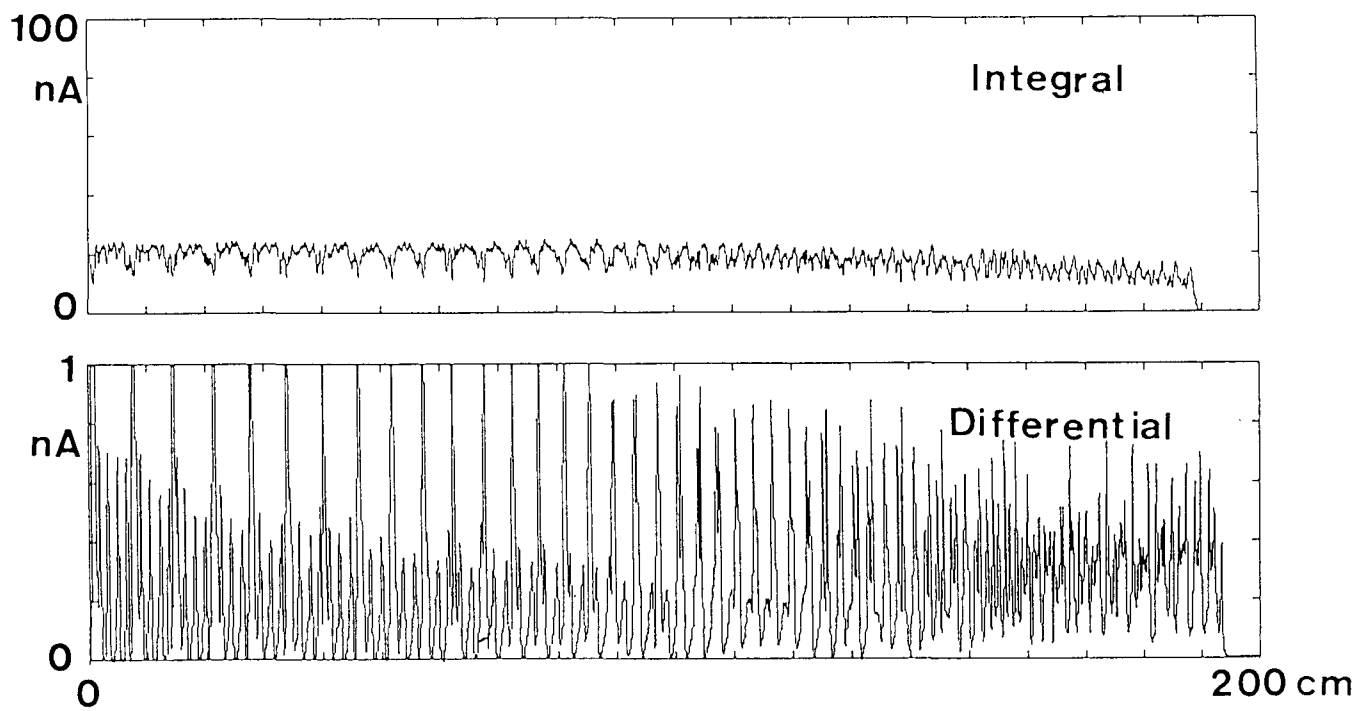


Fig. 8. Turn pattern measured by a main probe.

8. BEAM DIAGNOSTIC SYSTEM

The commissioning of the ring cyclotron is being made with various kind of beam diagnostic elements.[9] Efforts to get good S/N ratio for weak beam down to 1nA are being made. A 30 Hz 5th order (30dB/Oct) low pass filter is used for beam current measurement. Attenuation of 30dB for 60 Hz was achieved by using an integrated circuit of switched capacitor filter LTC1062. Figure 8 shows turn pattern measured by a main probe.

For beam phase measurement, noise-free phase signal amplifier for acceleration frequency was used. 5/3 and 8/5 multiple of the acceleration frequency are used for phase measurement of proton and alpha, respectively. A crystal filter is used in IF amplifier of the phase signal amplifier to reduce noise. The output signals are averaged by a digital oscilloscope to reduce thermal noise. Relative phase between beams can be measured with this phase probe for beam current down to 1nA, as shown in Fig. 9.

9. CONTROL SYSTEM

The old control system of the AVF cyclotron is used without any modification. New computer control system of the ring cyclotron was used throughout commissioning of the ring cyclotron.[10] The software of this control system performs almost satisfactory.

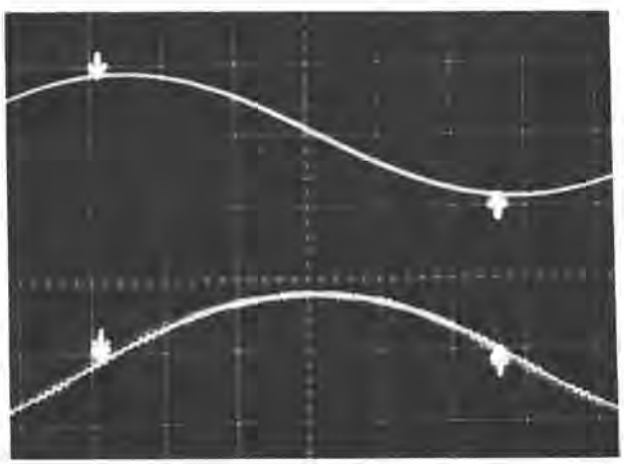


Fig. 9. Relative beam phase for few nA beams. Upper and lower correspond to pre-injection beam and pre-extraction beam, respectively. The IF phase signals are averaged by digital oscilloscope. 20°/div.

10. REFERENCES

1) M. Kondo, "Recent Developements at the Osaka RCNP 230-cm Cyclotron and a Proposal for a New Ring Accelerator", IEEE Trans NS-26, 2, 1904-1911.
2) I. Miura, et al., "Proposal for Cyclotron Cascade Project", Proc. of the 11th Conf. on Cyc. and Their Appl., Tokyo (Japan) 1986, p.207, "The RCNP Ring Cyclotron", Proc. of the Third Japan-China Joint Symposium on Accelerators for Nuclear Science and Their Appl., RIKEN (Japan) 1987, p.13.
3) H. Ikegami, "The RCNP Ring Cyclotron Facilities", Proc. of the 12th Conf. on Cyc. and Their Appl., Berlin (Germany) 1989, p.30.
4) I. Miura, et al., "A Computer Code FIGER", Proc. of the 4th Symposium on Acc. Science and Technology, RIKEN (Japan) 1982, p.97, K. Hosono et al., Spiral Sector Magnet of RCNP Ring Cyclotron Project, RCNP Annual Report 1984.
5) K. Hosono, et al., "Sector Magnet of the RCNP Ring Cyclotron and the Isochronization", Presented at this conference.
6) A. Shimizu, et al., Vacuum System of the RCNP Ring Cyclotron, RCNP Annual Report 1990.
7) A. Ando, et al., "Injection and Extraction System of the RCNP Ring Cyclotron", Proc. of the 12th Conf. on Cyc. and Their Appl., Berlin (Germany) 1989, p.346.
8) T. Saito, et al., "Initial Operation of the RF System for the RCNP Ring Cyclotron", Presented at this conference.
9) T. Itahashi, et al., "Beam Diagnostics in the RCNP Ring Cyclotron", Presented at this conference.
10) T. Yamazaki, et al., "Construction and System Tuning of Control System for the RCNP Ring Cyclotron and Beam Lines", Presented at this conference.

NEW DEVELOPMENT AT THE JINR HEAVY ION CYCLOTRON FACILITY

G.Gulbekyan, Yu.Oganessian, I.Kolesov, B.Gikal, A.Morduev,
O.Borisov, A.Ivanenko, V.Kutner, V.Bekhterev
Flerov Laboratory of Nuclear Reactions,
Joint Institute for Nuclear Research,
Dubna, Moscow reg., 141980, Russia

ABSTRACT

The Heavy Ion Cyclotron Facility of the Flerov Laboratory of Nuclear Reactions is designed for the acceleration of ions from H to U with the energies ranging from 20 up to 100 MeV/nucleon.[?)] The facility consists of 2 compact cyclotrons i.e. U-400 and U-400M, the age of the first one is about 14 years. The U-400M cyclotron can be used as a post-accelerator or as the one with independent PIG or ECR ion sources. Its construction was started in 1989. In May 1991 we got the first internal beam of $^{4}He^{1}$ with the energy of 30 MeV/n and the intensity of 10^{14}pps on the U-400M with the PIG ion source. At present we have got internal beams of light ions up to Ne and the energies up to 53 MeV/n. In 1992 we are going to realize the extraction system, the beam lines and the beam commissioning for the first experiment. We are planning to use the U-400 as an injector in 1993.

1. INTRODUCTION

The lay-out of the JINR U-400–U-400M Heavy Ion Cyclotron Facility is presented in Fig.1. Table 1 presents the characteristics of the U-400 injector-cyclotron operating since 1978. At present the cyclotron is used for the purposes of nuclear physics and applied researches, for the production of nuclear filters, for radiation study of materials. The cyclotron is equipped with 12 beam channels.

Every month we have about 20 changes of the type of ion used. The tuning time is 4 hrs. Annually the cyclotron is operated for about 5000 hrs.

At present the beam is extracted by the charge exchange on the graphite foil with the charge exchange ratio $\frac{Z_2}{Z_1}$ from 2 to 5. In 1992 there will be realized the electrostatic extraction of a low-energy beam with the energy ranging from 0.5 to 2.8 MeV/n for the injection into the U-400M cyclotron. The line for the beam transportation from the U-400 to the U-400M is basically ready. Fig.2 presents the dependence of the U-400 beam intensity on the ion mass.

Table 1.

Magnet weight	2100 t
K-factor	625
Pole diameter	4 m
Gap in the valley	30 cm
Gap on the hill	7 cm
Average magnetic field	1.93÷2.14 T
Number of sectors	4
Spiral angle	0
Number of dees	2
RF range	5.6÷12 MHz
RF harmonics	2, 4, 6
Voltage on the dees	80÷100 kV
$\frac{Z}{A}$ range	0.2÷0.028
Ion energies	22÷0.4 MeV/n
Source	PIG
Beam extraction	-via charge exchange(1978) -by electrostatic deflector(1992)
Vacuum	7 x 10^{-7}torr
Power input	1 MW

The U-400M compact cyclotron is built basing on the magnet of the classical cyclotron of ions U-300 which worked at the laboratory from 1959 to 1989. The characteristics of the U-400M cyclotron are presented in Table 2.

Fig.3 presents a scheme of the U-400 beam injection into the U-400M cyclotron.The movable stripping foil is installed on the equilibrium radius.

The internal beam parameters of the U-400M + PIG are presented in Table 3.

The goal for 1992 is to obtain maximum intensities on the extracted beams of $^{22}Ne^{6+}$ and $^{18}O^{5+}$ for the purposes of the first experiments.

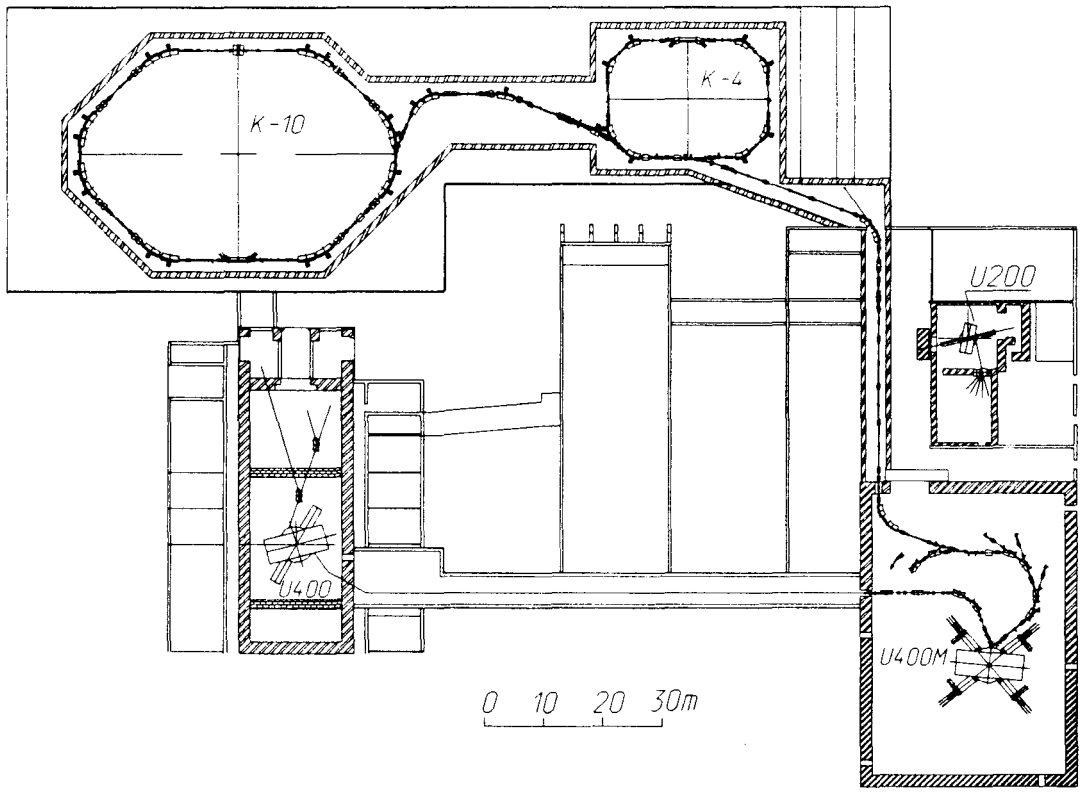


Fig.1. The lay-out of the cyclotron complex

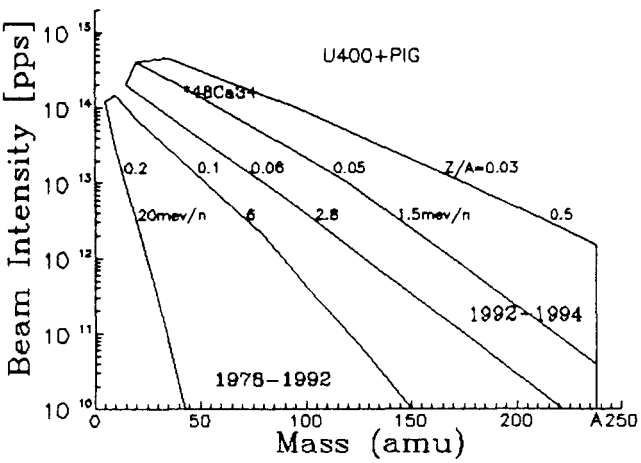


Fig.2. The dependence of the U-400 external beam intensities on the ion masses and energies.

2. MAGNETIC FIELD OF THE U-400M CYCLOTRON

The magnetic core cross section was increased by 10% and the excitation of the magnet was increased to 1.16 x 10^6A. The isochronous shape of the average magnetic field is determined by the thickness of the sectors

Table 2.

Magnet weight	2300 t
Pole diameter	4 m
Gap in the valley	50 cm
Gap on the hill	10 cm
Average magnetic field	1.5÷1.93 T
Number of sectors	4
Spiral angle	40°
Number of dees	4
Frequency range	11.5÷24.5 MHz
RF harmonics	2, 3, 4,
Voltage on the dees	130÷200 kV
$\frac{Z}{A}$ range	0.5÷0.1
Ion energies	100÷6 MeV/n
Source	PIG (1991) ECR (1994)
Beam extraction	-via charge exchange(1992) -by magnetic deflectors(1992)
Power input	1 MW

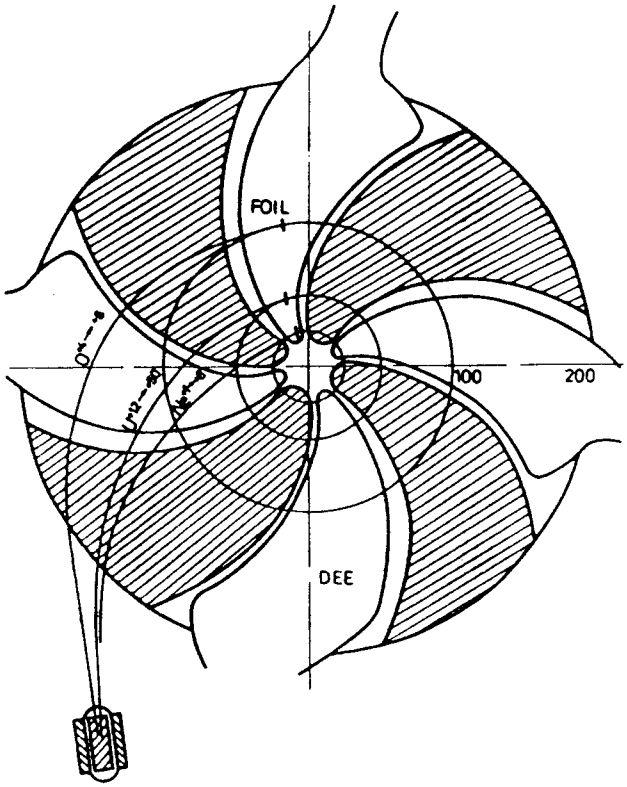


Fig.3. The scheme of the injection into the U-400M.

Table 3. Status for June 1992

Ion	Energy(MeV/n)	Intensity(pps)
$^{4}He^{1+}$	30	10^{14}
$^{12}C^{3+}$	30	2 x 10^{13}
$^{14}N^{3+}$	26	2 x 10^{13}
$^{14}N^{4+}$	40	2 x 10^{12}
$^{16}O^{3+}$	15	2 x 10^{13}
$^{16}O^{4+}$	30	3 x 10^{12}
$^{16}O^{5+}$	48	2 x 10^{12}
$^{20}Ne^{2+}$	6	5 x 10^{13}
$^{20}Ne^{4+}$	20	5 x 10^{12}
$^{20}Ne^{5+}$	30	3 x 10^{12}
$^{20}Ne^{6+}$	46	10^{12}
$^{40}Ar^{4+}$	6	2 x 10^{13}
$^{40}Ar^{5+}$	10	10^{13}

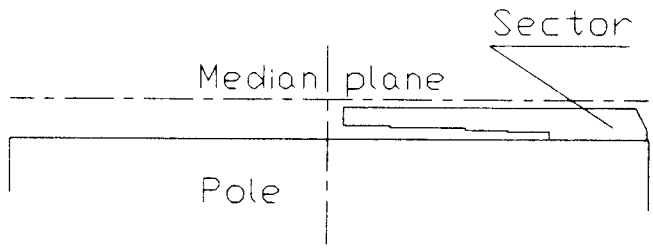


Fig.4. The lay-out of the U-400M magnetic gaps with sectors.

which grows over the radius with the machining of the sector thickness performed from the pole side to decrease the influence of the machining depth step and to increase the flutter. (Fig.4). At the 1.5 T level of the average magnetic field in the center of the cyclotron the machining of the sector thicknesses ensures the isochronous radial growth of the magnetic field for ions with the energy of 100 MeV/n.

At the increase of the average magnetic field caused by the increase of the value of current in the main coil the radial growth of the magnetic field decreases at the rate of $0.26\frac{T}{T}$. In this case the isochronous radial dependence of the average magnetic field is preserved with the accuracy of up to 0.01 T.Fig.5. Thus, the change of the magnetic field level in the cyclotron center from 1.5 T to 1.95 T ensures the isochronous acceleration of ions with $\frac{Z}{A}$ from 0.5 to 0.1 with the energy ranging from 100 to 6 MeV/nucleon with the minimum correction by the correcting coils (Fig.6).

In 1990 a full scale survey of the U-400M magnetic field was carried out. The measuring system moves in the polar coordinates. There are 14 InSb Hall probes on the block and 384 (0.9375) azimuthal and 8 (2 cm) radial steps for each Hall probe. We use usually as the radial coordinate the equilibrium orbit coordinate in the sector center, since the correcting shims and the trim coils are situated on the sector.

Fig.7 presents the flutter radial dependencies for ions with $\frac{Z}{A}$ =0.5 (100 MeV/n) and $\frac{Z}{A}$ =0:2 (22 MeV/n).

3. CORRECTING COILS

The U-400M correcting coils are used for the fine correction of the average magnetic field and of the radial gradients (10), for the correction of the median plane (3) and of the first harmonic(3). Hermetic blocks made of an aluminium alloy with 16 sector-type correcting coils are located on the surface of the sectors from the side of the median plane. The block has an autonomous vacuum pumping system. The block height is 28 mm. Multiturn coils are used. Each coil numbers from 20 to 30 turns. The cross section of the flat copper conductor is 6÷10 mm^2. The input current is reaching 30 A, i.e. the number of the ampere-turns in each coil is 400 ÷ 600 at the current density of 3 A/mm^2. The conductor has a min-

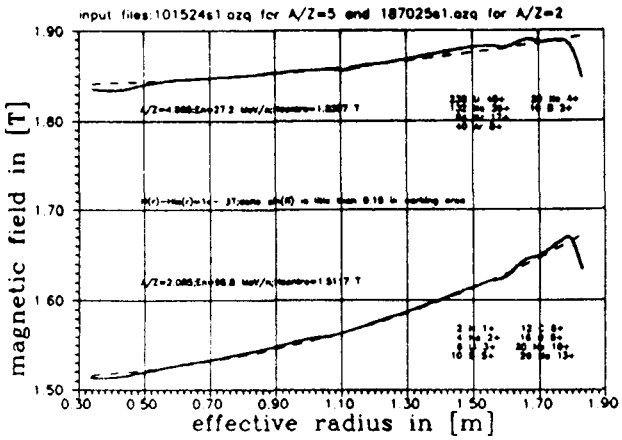


Fig.5. Radial dependence of the effective magnetic field on level of the average magnetic field.

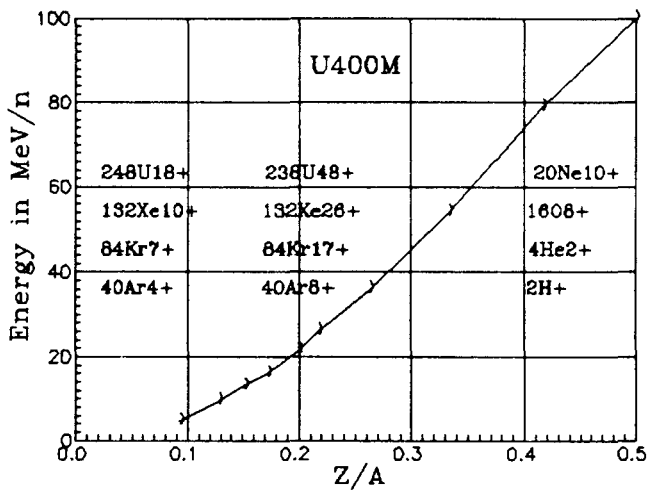


Fig.6. The dependence of the U-400M ion energies on the $\frac{Z}{A}$ ratio.

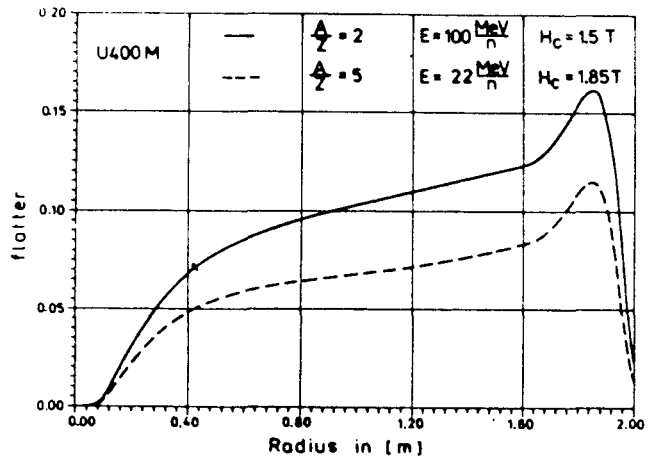


Fig.7. The radial dependence of the flutter for $\frac{Z}{A}$= 0.5 (100 MeV/n) and $\frac{Z}{A}$= 0.2 (22 MeV/n).

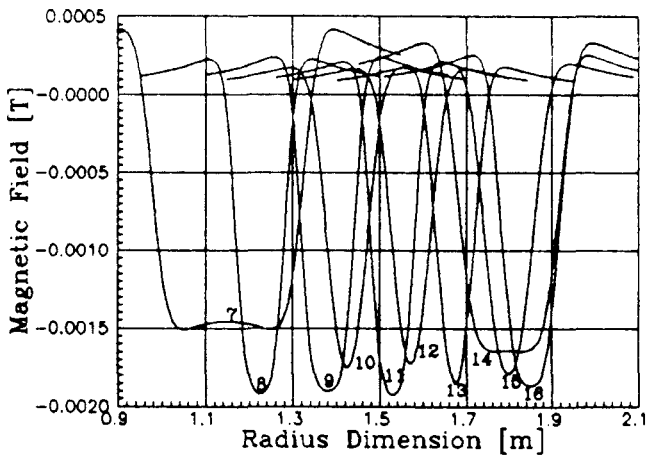


Fig.8. The form-factor of 8 correcting coils at 100 ampere-turns in each.

eral and an epoxy insulation. The coils in each block are positioned consecutively over the radius one by one and in two layers. The upper layer is shifted versus the lower one to decrease the probability of dead zones apparition. The total dissipated power in the block is reaching 1 kW. The coils are glued and pressed to the internal surface of the aluminium blocks. All the coils of the same block use the same cooling circuit mounted over the block perimeter. The total power input of the correcting coils is 8 kW. The outputs are of a compact design. Fig.8 presents the form-factor for 8 correcting coils.

Fig.9 presents the effective magnetic field distinction from the isochronous one depending on the radius for ions with $\frac{Z}{A}$ = 0.5 and of the energy of 100 MeV/n before and after the correction.

Fig.10 demonstrates the radial dependence of the

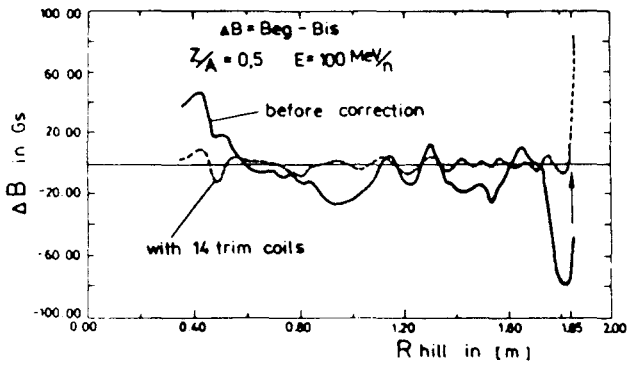


Fig.9. The distinction of the effective magnetic field from the isochronous one for ions with $\frac{Z}{A}$= 0.5 (100 MeV/n) before and after the correction.

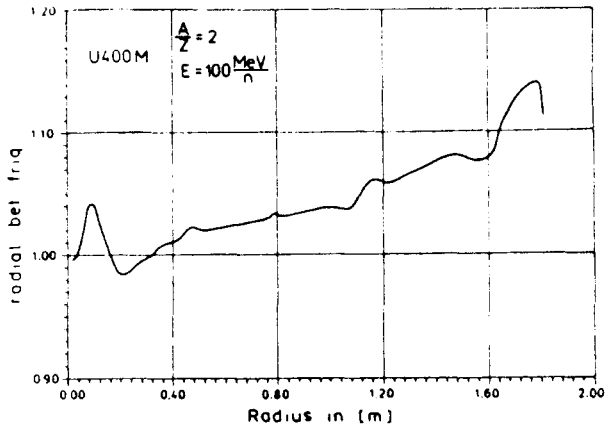


Fig.11. Radial dependence of the radial oscillations frequency for $\frac{Z}{A}$= 0.5 (100 Mev/n).

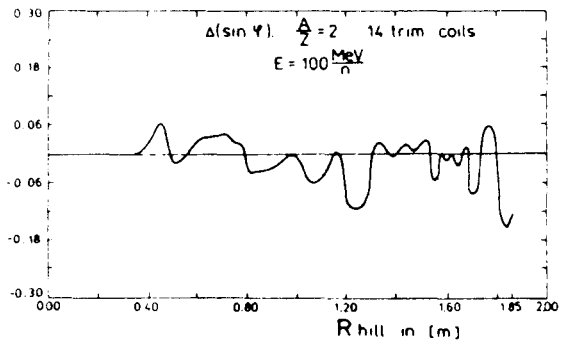


Fig.12. Phase motion of ions with $\frac{Z}{A}$= 0.5 and with the energy of 100 MeV/n.

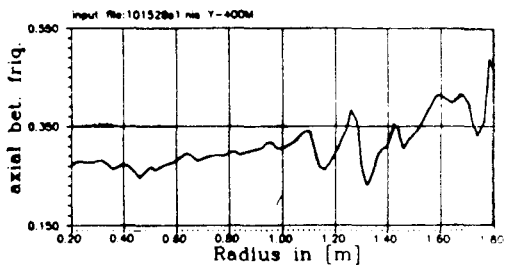


Fig.10. Radial dependence of the axial oscillations frequency for ions with $\frac{Z}{A}$ = 0.5 (100 MeV/n).

axial oscillation frequency on the radius for the same ions and Fig.11 shows the radial dependencies of the radial oscillations frequency. Fig.12 presents the phase motion of these ions with the radius.

4. RF SYSTEM

The choice of a 4-dee system has been predetermined by the necessity to ensure the acceleration rate in the central region, the optimization of the phase motion through the increase of the orbits separation before the deflector. The U-400M acceleration system consists of 4 quarter-wave radial type coaxial resonators with the dee voltage of 200 kV. A dee with the angular length of 40° and the height of 100 mm is positioned in the valley and is installed in the machine by the radial movement of the resonance tank. The resonance tank of 1.34 m diameter and 3.5 m length and the stem of 0.68 m diameter form the induction part of the resonator with the wave impedance of 40 Ohm. Fig.13 presents a scheme of the U-400M resonator.

The dee has an aluminium frame. The reducing

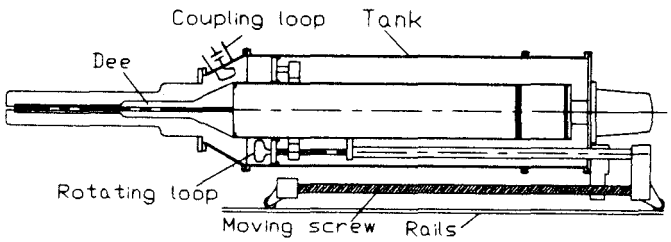


Fig.13. Lay-out of the U-400M resonator.

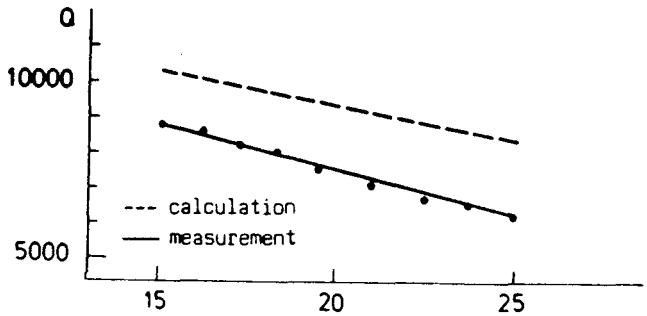


Fig.15. Dependence of the resonator quality on frequency.

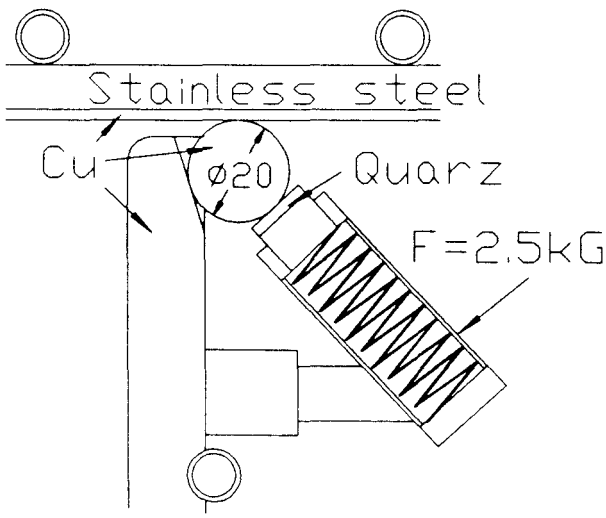


Fig.14. Scheme of the sliding contacts design.

pipe is made of copper-plated stainless steel by the explosion technology in Byelorussia. The resonance tank and the stem are made of copper-plated stainless steel by the diffusion technology with the subsequent machining in Russia. The cooling circuits are welded to the stainless steel from the outside at a step of 10÷20 cm. Chromium-plated stainless steel rails are mounted inside the tank. A short-circuiting plate installed on a carriage moves by them. The accuracy of mounting is 0.1 mm which corresponds to the values ranging from 0.4 to 1 kHz. The short-circuiting plate is actuated by the rod through the back flange by means of a screw located under the tank outside. A short-circuited rotational fine-tuning loop with the area of 400 cm^2 is mounted on the short-circuiting plate and moves together with it. The loop ensures the 80÷120 kHz range of fine frequency tuning. Sliding contacts are made of balls with the diameter of 20 mm and of hard oxy copper with a thermal quarz insulation and with the slamping force of 2.5 kg. The lay-out of the assembly operated for 1 year already on the U-400M with the current density up to 30 A/ball is presented in Fig.14.

This design is being operated on the CI-100 implanter for 4 years already with the current density of up to 300 A/ball. The reducing pipe homes a rotation connecting loop with the area of 300 cm^2 which is connected with the 60 Ohm feeder through a retunable compensation capacitor. Fig.15 presents the dependence of the resonator quality on frequency. Fig.16 presents the dependence of the voltage distribution over the dee radius for different frequencies.

For the case of radio frequencies at a voltage reaching 200 kV and for the second harmonic the effective accelerating voltage is only 750 kV per turn. Four RF generators with the power of 20 kW are situated in a separate room and provide the dees with the voltage of 140-100 kV in the frequency range of 11.5÷24.5 MHz. The start-up of the machine was performed by these generators. In 1992 the power of the generators will be increased to 80 kW and the dee voltage — to 200 kV. The voltage phase free drift on the dees is about 20° per hour because of a low current density and big gaps. The electron system ensures the phase control with the accu-

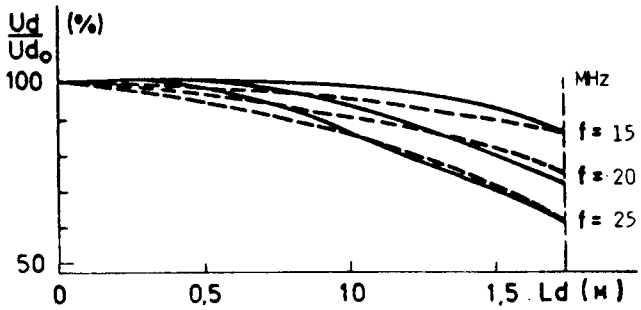


Fig.16. Radial distribution of the RF voltage of the U-400M cyclotron dee.

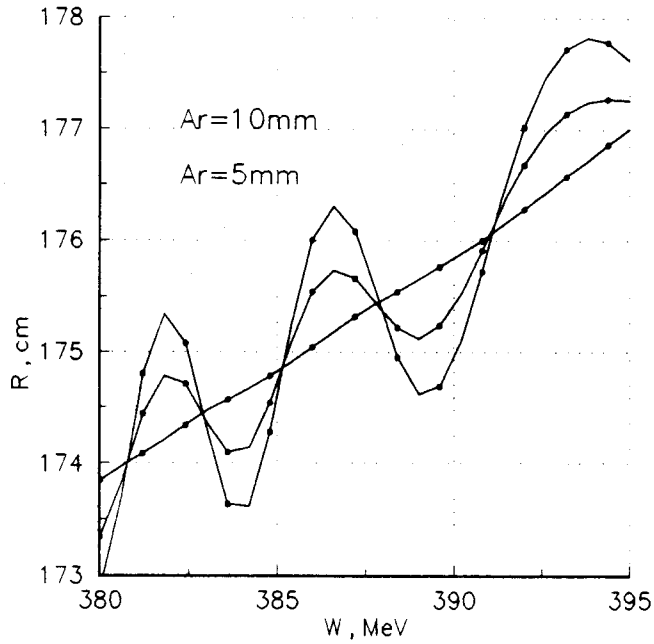


Fig.18. Radial oscillation of the beam with $\frac{Z}{A} = 0.5$ around the equilibrium orbit and the effect of orbits separation growth.

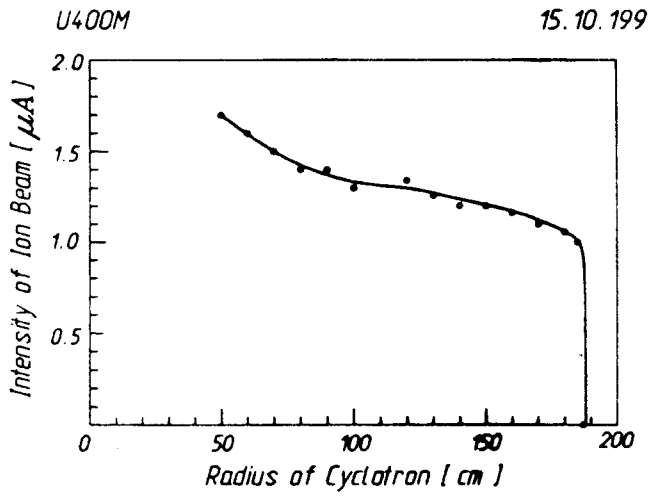


Fig.17. Radial distribution of the $^{12}C^{3+}$ beam intensity.

racy of 1° as well as the amplitude stabilization with the accuracy of 10^{-3} and is presently in the operating adjustment stage. The machine was started-up under strong multipacturing especially during the optimization of the feeder connection with the load caused by high quality, the presence of SiO_2 coming from the construction work and from the copper machining and by a low-level RF leak against the background of the generator start-up. At present the phenomenon of the resonance discharge is very seldom met.

5. THE U-400M VACUUM SYSTEM

The dismountable vacuum chamber of the U-400M consists of the cyclotron poles with octagonal aluminium alloy washers tightened around it. Racks are mounted at the corners of the polygon and the ladder-shaped seal for rectangular flanges and resonators are mounted along the perimeter. The pumping is performed by 6 diffusion pumps with LN_2 screens at the rate of 24000 l/sec. The volume of the vacuum chamber is 35 m^3. The surface area is 375 m^2. The pressure in the chamber 3 x 10^{-7}torr. The vacuum load is about 4 x 10^{-3}torr.l/sec. When a PIG-type internal source is used the process vacuum is 10^{-6}torr and the loss of the light ion beam is 50%. Fig.17 presents the radial distribution of the $^{12}C^{3+}$ beam intensity.

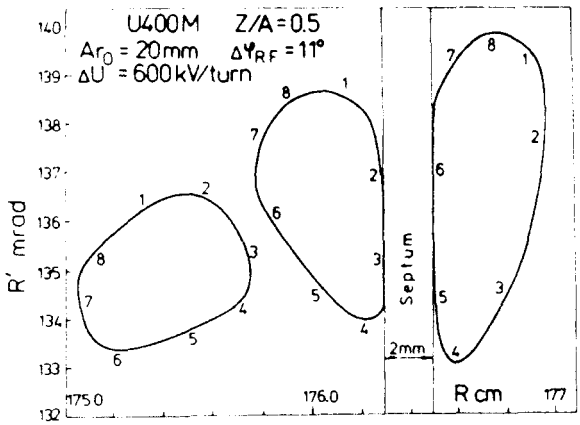


Fig.19. Transformation of the beam with $\frac{Z}{A} = 0.5$ phase portraits at the entrance into the sector during the last turns.

6. BEAM EXTRACTION SYSTEMS

The dees are installed in all the 4 valleys of the U-400M cyclotron. The gap in the sectors is 44 mm. Three electrostatic deflectors may be placed in the dees, but in this case the electric field intensity up to 140 kV/cm is to be used. On the other hand the energy separation of the orbits of the ions with $\frac{Z}{A}$ =0.5 (100 MeV/n) makes 2.7 mm at the radial oscillation frequency of υ_r =1.15. At the controlled amplitude and coherent oscillation phase the separation of orbits will be up to 10 mm. Fig.18 presents the radial oscillation of the beam with $\frac{Z}{A}$ =0.5 around the equilibrium orbit.

For ions with the energy of 22 MeV/n ($\frac{Z}{A}$ = 0.2) just the energy separation of orbits will make 9 mm. Fig.19 presents the transformation of phase portraits at the sector entrance during the last turns of the beam with the energy of 100 MeV/n, RF phase width of 11° and the coherent oscillation amplitude of 20 mm. The beam emittance at the deflector entrance will be about 20 mm.mrad at the energy spread of 5 x 10^{-3}. The beam extraction will be carried out by 4 magnetic deflectors with the 2 mm thickness of the magnetic septum. The lay-out of the extraction system is presented in Fig.20.

Deflectors I and III are purely current ones without iron and the channels II and IV are of iron. The magnetic channels characteristics are presented in Table 4. The radial and axial envelope of the beam with the energy of 100 MeV/n ($\frac{Z}{A}$ = 0.5) is shown in Fig.21.

The cross section of the first magnetic channel is presented in Fig.22.

The magnetic field distribution at the input current of 2500 A and the current density of up to 50 A/mm^2 are shown in Fig.23.

The second magnetic channel is placed into the dee and is equipped with the "wings" to compensate the dissipated field (Fig.24).

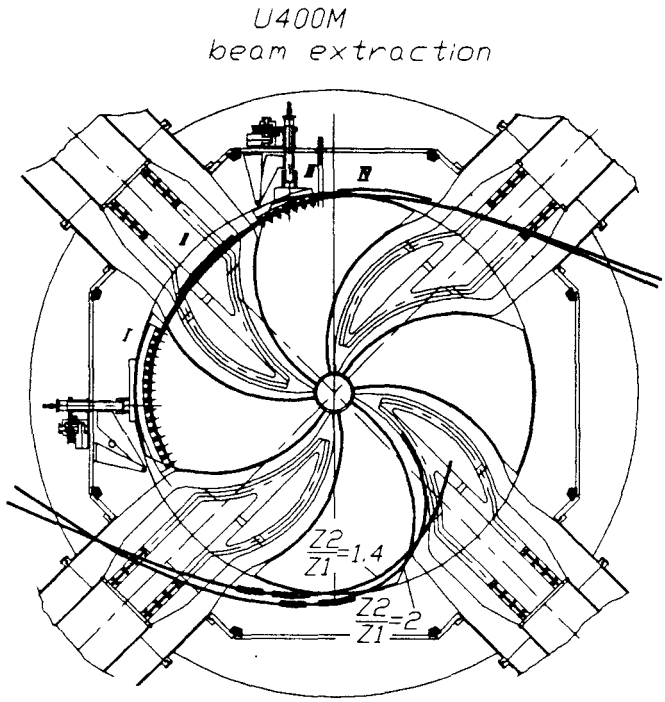


Fig.20. Lay-out of the U-400M beam outputs.

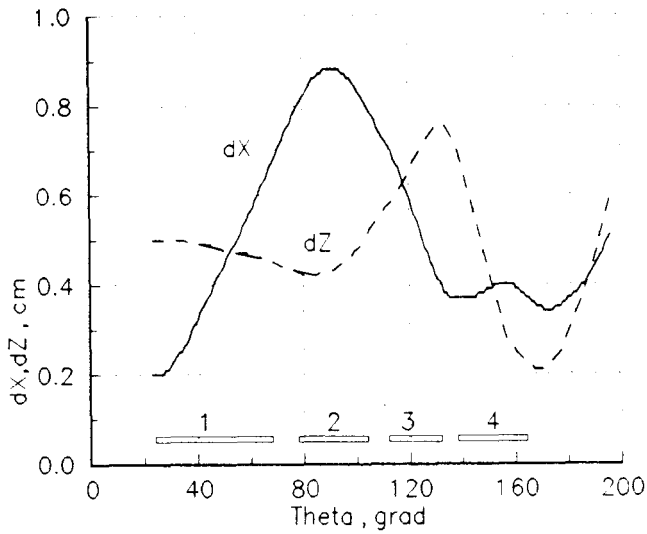


Fig.21. The radial and axial envelope of the beam.

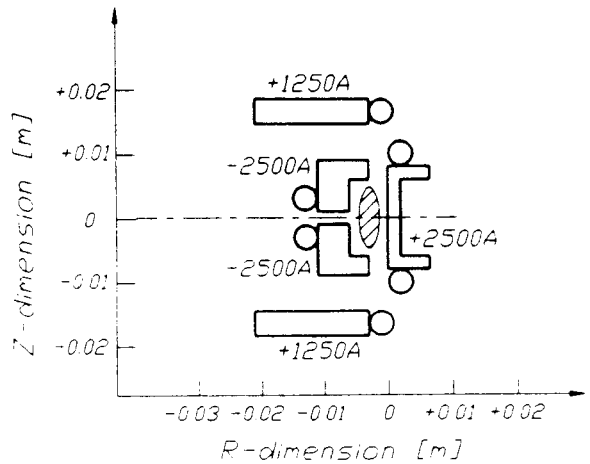


Fig.22. Cross section of the first channel.

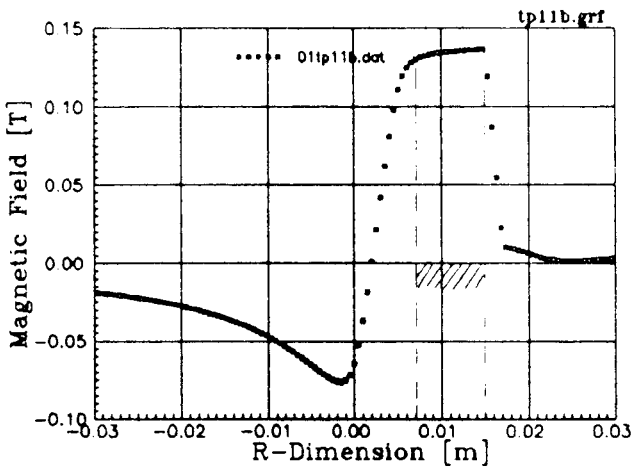


Fig.23. Distribution of the first channel magnetic field.

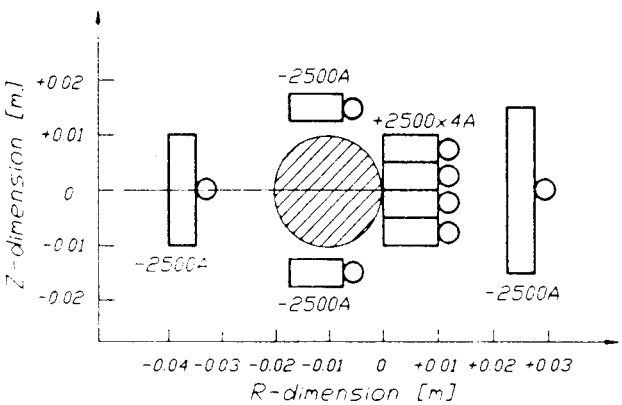


Fig.24. Cross section of the 3-d channel.

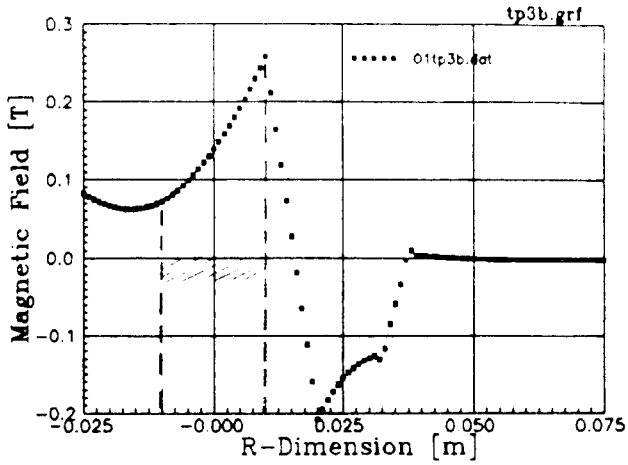


Fig.25. Distribution of the 3-d channel magnetic field.

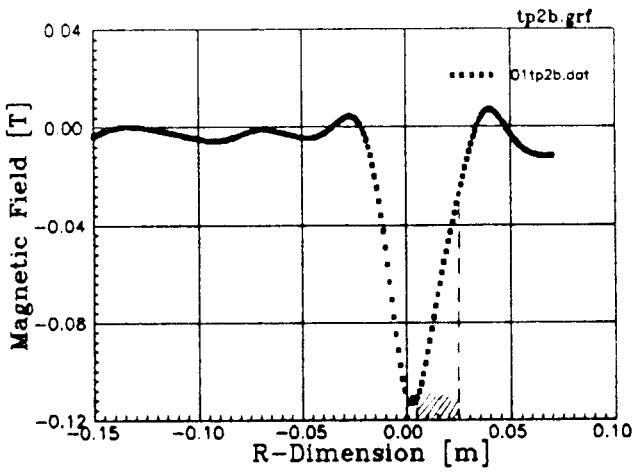


Fig.26. Distribution of the 2-nd channel magnetic field.

The cross section of the 3-d magnetic channel (Fig.25) and the magnetic field distribution are presented in Fig.26.

The beam extraction will be carried out in 1992.

7. BEAM EXTRACTION FROM THE U-400M BY THE CHARGE EXCHANGE

Beam extraction by the charge exchange on a thin graphite foil is the only one used on the FLNR U-200 and U-400 cyclotrons. This most convenient and flexible method allows to extract the beams with the RF phase range up to 40° without the emittance collimation by the deflectors apertures. The charge exchange ratio $\frac{Z_2}{Z_1}$ on the U-200 and U-400 cyclotrons is from 2 to 5. The radial beam drift based on the strong first harmonic of the magnetic field. The harmonic appears on the sector–valley boundary after the charge exchange is used. The separation of orbits is from 10 to 30 cm. On the U-400M cyclotron the characteristic range for the charge exchange ratio $\frac{Z_2}{Z_1}$ is from 1.1 to 2 and it appears impos-

Table 4.

Channel No	ΔB (T)		G (T/cm)	
	$\frac{Z}{A}=0.5$	$\frac{Z}{A}=0.2$	$\frac{Z}{A}=0.5$	$\frac{Z}{A}=0.2$
1	-0.060	-0.12	0	0
2	-0.045	-0.06	0.03	0.04
3	-0.100	-0.15	0.05	0.07
4	0.0	0.0	0.08	0.08

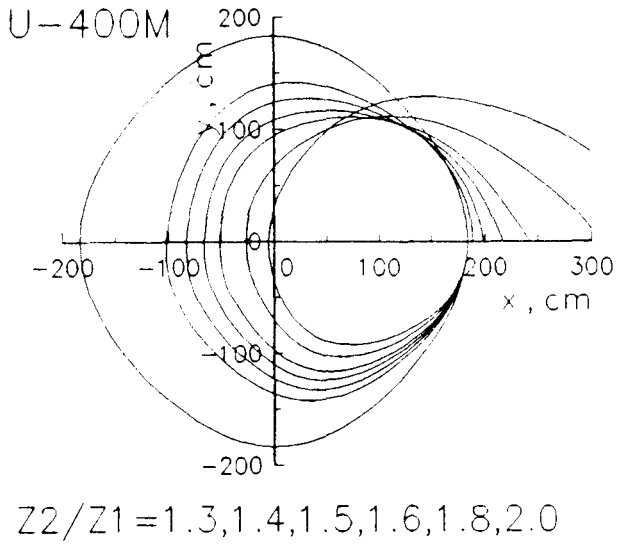


Fig.27. Simulation of the motion of ions with the charge exchange ratios from 1.3 to 2 without changing the foil position.

sible to use the first harmonic of the magnetic field in the sector-valley region. The ion motion has been simulated. It is well seen from Fig.27 that there is a possibility of extracting the beam within the charge exchange ratio range of 1.3–2.

Ions in the range from 1.4 to 2 can leave freely the cyclotron vacuum chamber. The possibility of focussing the trajectories into one point at the transportation channel entrance due to the weak radial and azimuthal motion of the foil has been studied. Fig.28.

The calculated envelope function of the beam with the emittance of 10π mm-mrad when using two focussing channels is shown in Fig.29.

The beam extraction by the charge exchange will be used on the U-400M in the direction which is opposite to the deflectors output and will be used for the production of secondary beams of exotic nuclei on a thick target. The energies of ions extracted by the charge exchange are from 30 MeV/n ($^{12}C^{3} \rightarrow ^{12}C^{6}$) to 60 MeV/n ($^{14}N^{5} \rightarrow ^{14}N^{7}$). The dispersion over charges

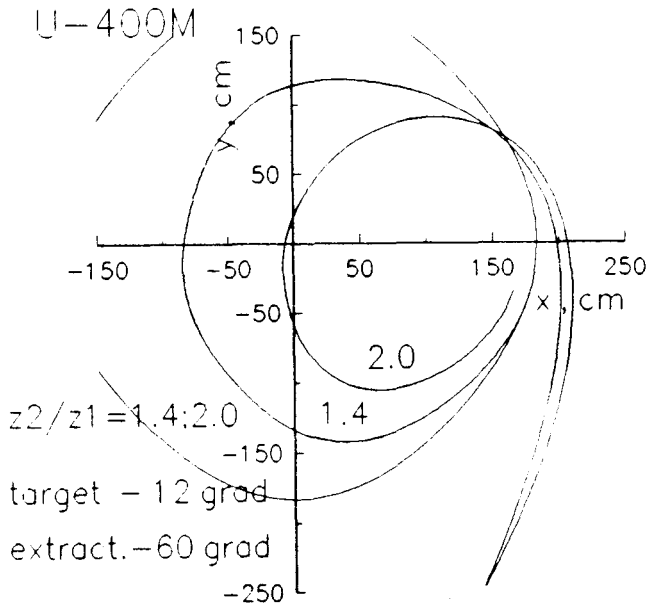


Fig.28. Focussing of the trajectories of ions with the charge exchange ratios from 1.4 to 2 onto the entrance into the transportation channel.

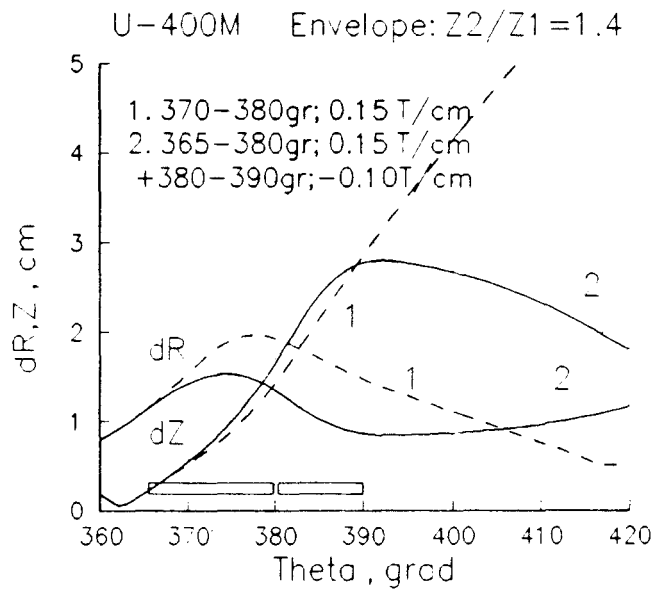


Fig.29. Beam envelope along the trajectory of extraction by charge exchange.

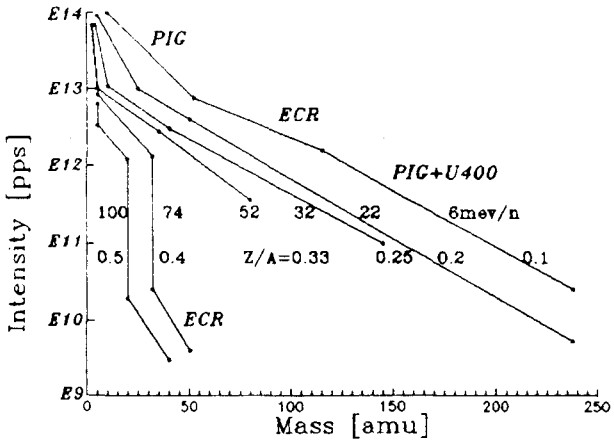


Fig.30. Intensities of the U-400+U-400M beams for different energies.

until medium mass ions (Ar, Ca, Fe, Ni) is insignificant. The life-time of foils is about 1 week at the beam intensity of 6 x 10^{12}pps. The beam extraction by the charge exchange will be performed in 1992.

The U-400M cyclotron can be used together with its own ion source as a post-accelerator after the U-400 and with independent PIG (1991) or ECR (1994) sources. The estimated beam intensities of the cyclotron complex for different energies are presented in Fig.30.

8. TRANSPORTATION CHANNELS

The lay-out of the U-400M cyclotron beams is presented in Fig.31. In 1992 it will be built of the elements manufactured in Romania, Russia and Estonia.

9. CONTROL SYSTEM

The control system is being developed on the basis of the CAMAC electronics and the IBM PC computers, connected into a local net. At present subsystems of control are built for the U-400M cyclotron itself.

10. CONCLUSION

The creation of the U-400M with a PIG-source will allow to start the experiments with fragmentation reactions and secondary beam generation reactions as early as in the beginning of 1993. Afterwards, new ion sources for the U-400M—U-400 and ECR will be eventually used. The U-400M is also the basic injector for the two-cooler project K4-K10 (Fig.1).

11. REFERENCES

1) Flerov, G.N. et al., Preprint 9-84-555, Dubna, 1984.

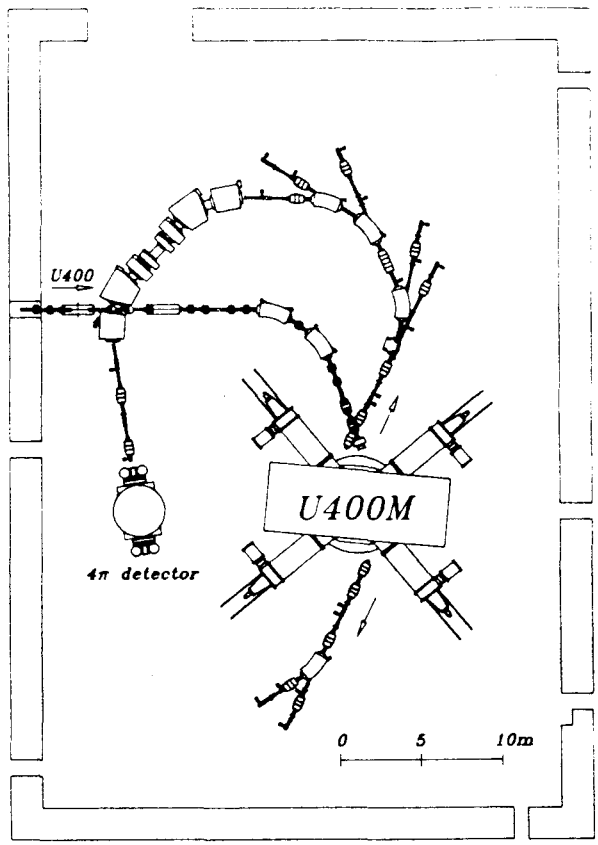


Fig.31. Lay-out of the U-400M beam channels.

NEW K130 CYCLOTRON AT JYVÄSKYLÄ

Esko Liukkonen
Accelerator Laboratory, University of Jyväskylä, P.O. Box 35, SF-40351 Jyväskylä, Finland

ABSTRACT

Installation of the K130 cyclotron and its ECR ion source was completed during 1990–91. The first plasma in the ECR was produced in May 1991. The first experiment using the ECR beam was carried out in September 1991 when 50 keV $^{40}Ar^{5+}$ was used to bombard a Cu sample for a material-physics experiment. The beam was injected for the first time into the cyclotron in December 1991. The first beam was extracted on January 28, 1992. The beam was 6.0 MeV/u $^{4}He^{1+}$. During the spring 1992 also a heavy-ion beam of $^{40}Ar^{10+}$ was successfully accelerated. The construction of the experimental hall was completed in June 1992.

1. BACKGROUND

The earlier history of the Jyväskylä cyclotron project can be found in the proceedings of the Berlin-89 cyclotron conference.[1)]

The K130 cyclotron project was started in September 1986 with the appropriation of about 7 million USD in the Finnish state budget for the years 1987–91. The funding included the K130 cyclotron, the ECR ion source and the injection line. Funding for the building was secured only afterward, which resulted in unnecessary delay. No beam-transport system nor any experimental equipment were included in the initial funding decision. They will be funded through the annual budgets of the University in 1992–96.

In order to keep costs and own man power to a minimum, commercial manufacturers were used as much as possible. The main parts of the K130 cyclotron were manufactured and delivered by the Swedish company Scanditronix AB. Scanditronix also delivered the vacuum chamber, extraction and RF systems and most of the power supplies. The Department of Physics was responsible for the rest of the facility, including the control system, installation and testing. The ECR ion source and injection line were also built locally.

Figure 1 shows a general view of the cyclotron in its bunker, the injection line and the ECR ion source. The main parameters of the K130 cyclotron are given in Table 1.



Fig. 1. Three-dimensional sketch of the K130 cyclotron with the ECR ion source and injection line.

2. MAGNET AND RF

The K130 cyclotron has three 58° spiral sectors, 15 circular correction coils and four sets of harmonic coils. The bending limit of the magnet is 130 MeV and the focusing limit is about 90 MeV. The magnet was computer designed by the Department of Physics and built without a model magnet.[2)]

The magnet was assembled by Scanditronix in Uppsala, Sweden, in January 1989. The pole configuration and shimming were confirmed during the spring 1989. The liners with the circular trim coils were installed in August–September 1989. The field mapping of the magnet was completed by Scanditronix in October 1989. Analysis of field-mapping data showed unacceptably large measuring errors. Therefore some fields were remapped in April 1990.

The RF system is of the resonator type and comprises two identical 78° dees, with associated dee stems and power amplifiers located on opposite sides of the

cyclotron magnet. Both systems are driven by a common frequency synthesizer. The maximum dee voltage is 50 kV. The dees and dummy dees can be seen in Fig. 2.

Table 1. Parameters of the K130 Cyclotron

MAGNET			
pole diameter		2.4	m
pole gap, max.		0.33	m
min.		0.174	m
number of sectors		3	
spiral angle		max. 58	degr.
weight		308	tons
trimming coils,	circular	15	
	harmonic	4	sets
conductor		hollow Cu	
power, main coils		150	kW
trim coils		35	kW
field at 400 000 At,	hill	2.1	T
	valley	1.3	T
	average	1.76	T
extraction radius		0.95	m
bending limit		130	MeV
focusing limit		90	MeV
ACCELERATION SYSTEM			
number of dees		2	
dee angle		78	degr.
beam aperture		3.0	cm
RF frequency		10–21	MHz
harmonic number		1, 2, 3	
max. dee voltage		50	kV
VACUUM			
2 cryo pumps	each	5000	l/s
operating pressure		10^{-7}	mbar
ION SOURCE + INJECTION			
external ECR			
axial + spiral inflector			
EXTRACTION			
dc electrostatic + EMC + 2 passive channels			
PARTICLE ENERGIES			
protons		6–90	MeV
other ions	$(0.2-1.0)\times 130\ q^2/A$		MeV

The RF power supplies, driven amplifiers and the control system are located in the power supply room. The entire RF system is remotely operated either from the panels in the power supply room or from the control system.

Each of the two RF cavities consists of a quarter-wavelength stem capacitively loaded by the dee at the high-voltage end. The stems enter the vacuum chamber via ceramic vacuum feedthroughs. Outside the chamber, each cavity consists of a horizontal coaxial stem with a movable grounding plate that provides coarse tuning within the 10–21 MHz range. Each system is fine tuned by a motor-driven capacitor facing the dee. The interdee phase can be set at any value (normally 180° or 0° degrees).



Fig. 2. Accelerator chamber of the K130 cyclotron. The extractor is in front. The phase probes and the central region were not installed in this photo.

The power amplifiers and the cavities for the two RF systems were completed and assembled in the autumn of 1989. The first RF tests were started in December 1989. The full power RF tests were successfully carried out in February–March 1990.

After the final factory acceptance tests in Sweden in April 1990, the cyclotron magnet was disassembled and packed for transportation. It arrived in Jyväskylä by rail in May 1990. The yoke with coils was reassembled in June 1990. The RF system arrived in Jyväskylä in June 1990.

The mounting of the cyclotron components and the cabling of its electronics were accomplished largely during 1990, but work on the smaller details continued through 1991.

3. VACUUM

The vacuum chamber is made of stainless steel and sealed against the poles with Viton O-rings. The accelerator chamber is pumped with two cryo pumps (5000 l/s each). The specified vacuum in the accelerator chamber was 10^{-5} Pa (10^{-7} mbar). The volume below the liners containing the pole, correction and harmonic coils is pumped by a small Roots pump. Outgassing from mild steel and epoxy is thereby excluded from the main vacuum. All feedthroughs for the correction coils are also kept outside the main vacuum. There are two types of safety valves between the high vacuum and the liner vacuum. Two of them work on gravity and six use thin foils with punctuation needles on both sides of the foil.

The vacuum chamber arrived from a subcontractor to the Scanditronix factory in August 1989. The first high-vacuum tests were carried out in November 1989.

A vacuum level of 10^{-4} Pa (10^{-6} mbar) was obtained with one cryo pump. However, the specified vacuum level could not be achieved until June 1990.

The vacuum chamber and liners were scheduled to be in Jyväskylä in the middle of June, but delivery was delayed by three weeks due to a fire on the train in Sweden. After difficulties with obtaining Viton O-rings of good quality, the vacuum chamber was pumped down for the first time in Jyväskylä in the middle of September 1990 using the same interim pumping system as in Uppsala.

The final vacuum tests were postponed until January 1991 when both cryo pumps were installed. A vacuum level of 1×10^{-5} Pa (1×10^{-7} mbar) was obtained after about 100 h of pumping. After a short venting with nitrogen, a vacuum level of 10^{-4} Pa (10^{-6} mbar) could be pumped in two hours. The ultimate vacuum of 3×10^{-6} Pa (3×10^{-8} mbar) was achieved after three months of continuous pumping later in 1991. This vacuum level is regarded as satisfactory. The last serious obstacle to fulfilling Scanditronix's specifications was thus removed.

The Scanditronix delivery was formally accepted on May 23, 1991 when the cyclotron group celebrated its first anniversary at the new laboratory.

4. EXTRACTION SYSTEM

An extraction system was manufactured by Scanditronix according to our calculations. The system consists of one electrostatic deflector (40°, 50 kV), one electromagnetic channel (EMC, 28°), two passive magnetic focusing channels, and one internal horizontal steering magnet for small directional corrections at the beam exit port. There is also a current probe between the deflector exit and the EMC entrance. The whole extraction system is placed on sliding arms so that it can be removed quickly from the cyclotron and transported to the shielded service area outside the cyclotron vault.

5. DIANOSTICS

In addition to the current probe in extraction, the K130 cyclotron uses one main radial current probe. This probe covers the whole acceleration range from the minimum radius of 14 cm. It can be brought completely outside the vacuum chamber and isolated with a valve. The main probe was constructed in our workshop.

In order to measure the phase history of particles during the acceleration, a phase-probe system was constructed in collaboration with Tampere Technical University. It consists of ten pairs of capacitive pickup plates mounted above and below the median plane of the cyclotron on radial supports. The pickup plates are multiplexed to a heterodyne system which makes use of a mixing technique across the 10 to 21 MHz band. With this technique, two fixed high-frequency signals are derived and fed to a phase-detecting circuit. Using compensation of RF disturbances, the system is able to determine the phase even at low beam currents. To achieve a good signal-to-noise ratio, the second harmonic is used. The phase-measuring system is controlled by the control system of the accelerator.

The phase-measuring system was completed in April 1992, and it has proved to be a very useful tool in cyclotron tuning.

6. ECR ION SOURCE

So far the only ion source for the K130 cyclotron is an ECR ion source. It was built in our workshop and it is similar to the RT-ECRIS at MSU[3] with some modifications and improvements. It is a vertical ion source with an iron yoke. One 6.4 GHz microwave transmitter with a power divider is used for two stages. The axial magnetic field is produced by nine circular coils using four power supplies. The radial magnetic field is created by strong NdFeB (Neo) permanent magnets.

A more detailed description of the Jyväskylä ECR ion source can be found in reference 3.

Figure 3 shows a photo of the ECR ion source surrounded by a high-voltage fence. Table 2 gives the essential parameters of the Jyväskylä ECR ion source.



Fig. 3. Photo of the ECR ion source inside the HV protection fence.

Two ECR sources were made during 1987–91. The first one was for the Uppsala accelerator facility, where it has delivered heavy-ion beams to the Gustaf Werner cyclotron since November 1990.

The installation of the ECR ion source was completed in the winter 1990–91, but the testing could not be started before the water cooling system was ready in April 1991. The first plasma was produced in May 1991. The development of ion beams had to be halted for July and August 1991 when rock was being blasted behind the wall on the construction site of the experimental hall. The first beams (Ar^{5+} and Ar^{7+}) were delivered for an

experiment in solid-state physics in mid-September 1991. Since September 1991 the ECR ion source has been used continuously, either to inject ion beams to the cyclotron or for solid-state physics. The remaining time has been used for developing new beams. As an example Fig. 4 shows a typical charge-state distribution of argon ions.

Table 2. Parameters of the ECR ion source

MAIN STAGE	
Lenght (adjustable)	40-50 cm
Diameter	14 cm
AXIAL MAGNETIC FIELD	
9 circular coils	
R=14.3 cm, ΔR=12.5 cm, Δz=4.0 cm	
3 double pancakes	
Conductor 0.64 × 0.64 cm^2	
Power consumption	35 kW
Maximum B on axis	0.38 T
Mirror ratio range	1.2 - 2.2
HEXAPOLE MAGNETIC FIELD	
Neo (B_r=1.15 T)	
Inner diameter	15.2 cm
Pole width	5.1 cm
Pole hight	3.8 cm
Pole length	76.5 cm
Max. field in plasma chamber	
Hexapole bar center	0.34 T
Hexapole gap center	0.27 T
MICROWAVE	
Frequency	6.4 GHz
Power, max.	3.3 kW
HIGH VOLTAGE	
Main	30 kV/10 mA
Extraction	-15 kV/20 mA
VACUUM SYSTEM	
2 turbo molecular pumps	
Injection chamber	330 l/s
Extraction chamber	500 l/s
Basic vacuum level	10^{-8} mbar

7. INJECTION LINE

The first focusing element in the injection line after the ECR source is a 40 cm long solenoid. It forms a waist at the object point of the double-focusing 90° analyzing magnet; its analyzing power is about 1/100 in mass with slits 1.0 cm wide. The analyzing magnet can be rotated around its vertical axis in order to send the beam either to the cyclotron or to solid-state experiments.

The horizontal transfer line consists of four evenly spaced 40 cm solenoids and a matching unit of four quadrupoles. A second 90° dipole bends the beam upward to the cyclotron axis, through which the beam is focused by two solenoids. The last yokeless solenoid is inside the cyclotron pole piece. Four small xy magnets are placed along the injection line. All magnets for the injection line were in place before the end of 1990.

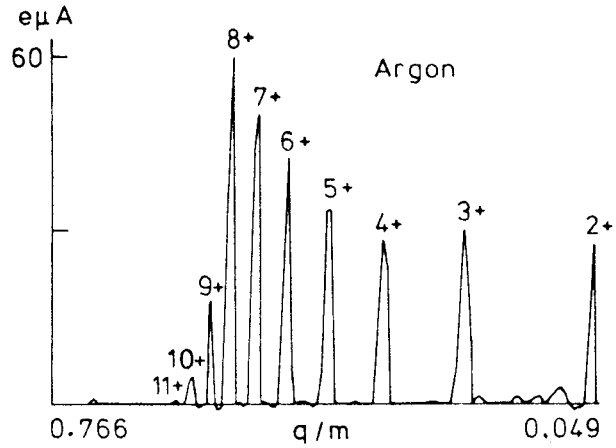


Fig. 4. Charge-state distribution of argon extracted at 10 kV. Microwave input power: 1st stage 16 W, 2nd stage 62 W.

Diagnostic equipment consisting of slits, Faraday cups and TV monitors was designed in our laboratory and produced partly by local subcontractors, partly in our workshop.

TV pictures are digitized using the same frame-grabber technique as at MSU.[5] It gives a two-dimensional current-density picture instead of the more limited x and y projections. When ordinary phosphors, e.g. Al_2O_3:Cr, are used in low-energy heavy-ion beams, they get rapidly damaged; in typical cases they last only a few seconds. After testing different phosphors, it was found that pure KBr is highly resistive to the ion beams and gives a strong light for many hours in the beam. The TV technique, in conjunction with slits and pepperpot plates, is also used to measure the emittance of the ECR ion source.

A buncher is placed into the last section of the injection line. We built it together with Tampere Technical University, which was responsible for the high-power sawtooth generator and related electronics. The generator contains electronics for phase and amplitude controls and measurement, a 2×300 W power amplifier, a high-impedance matching unit for the buncher grids and two dummy loads. The buncher is remotely controlled by the control system of the K130 cyclotron. The control system is also used to compute and lock the phases in the buncher. The buncher was installed in May 1992, but its testing is not yet completed.

The vacuum pumping in the injection line is done by turbomolecular and ion pumps which can produce an operating pressure of 5 × 10^{-6} Pa (5 × 10^{-8} mbar).

8. SPIRAL INFLECTOR

The shapes of the spiral inflectors for the $h = 1$ and $h = 2$ modes of operation were determined from analytical formulae. RELAX3D[6] was used to calculate the electric field for the ion-tracking program. The electrodes of the spirals were machined in our workshop by a numerically controlled milling machine.

The spiral deflector is lowered through the hole in the upper yoke by a lifting mechanism. When lowered, the position of the inflector is fixed in the hole of the central region without any mechanical adjustments. Figure 5 shows the central region with short aluminum arms where the dummy dees can be mounted.



Fig. 5. Photo of the central region.

9. CONTROL SYSTEM

The control system of the Jyväskylä accelerator facility has been previously described in the proceedings of the Berlin-89 cyclotron conference.[7]

The control system is based on ALCONT II hardware from the Finnish company Ahlstrom Automation Ltd (recently sold to the Honeywell Co.). It is a commercial industrial control system based on distributed microcomputers. This system is widely used in process industry (mainly paper and pulp) in Finland. The selection of this particular control system was based on economic and manpower considerations. Only two manyears were needed for programming.

The system has two display units with touch-sensitive 19" screens in the main control room and one in the ECR room.

All software development and system configuring is done with standard 386-based PCs. The PCs are also used for system software loading, backup copying and diagnostics. The ability to load and update application software on-line to the running system has proved to be extremely useful in this kind of application.

The control system hardware was installed in 1990. The final cabling and device connections were made mainly during 1991 parallel with the software development and testing.

10. THE FIRST BEAMS

When the lifting mechanism for the spiral inflector was completed by the workshop in October 1991, everything was ready for the first injected beam in the K130 cyclotron. Then it was decided to improve the water cooling system of the laboratory, which had suffered from many malfunctions and flaws during the first few months of operation. The one-week break promised lasted five weeks in practice.

The first beam was injected into the K130 cyclotron in December 1991 and detected in the main probe in its innermost position. That time there was not enough radiation shielding toward the construction site of the adjacent experimental hall. Further acceleration was therefore not permitted. In the middle of January 1992 this restriction was removed. On January 28, 1992 the 6.0 MeV/u $^4He^{1+}$ beam was extracted from the K130 cyclotron for the first time. The extracted current was 120 nA. After a few hours of tuning the extracted current had increased to 330 nA, which gave an extraction efficiency of 55% from a 600 nA internal beam. The transmission through the inflector was 7% from a DC beam, which is only slightly below the theoretical maximum (limited by phase acceptance in the central region).

Beam development has been continued during the spring 1992. In most cases, the $^4He^{1+}$ beam has been used for testing. Also a $^{40}Ar^{10+}$ beam at 6.0 MeV/u has been successfully accelerated. In all tests the $h = 2$ mode of operation was used. In June 1992 a spiral inflector for the $h = 1$ mode of operation was available, and during the last days of June of 1992, a 70 MeV proton beam was accelerated up to the full radius.

The first physics experiment using the K130 cyclotron was carried out in June 1992. Positron emitters were then produced with a 55 MeV α-beam in a provisional chamber installed a few meters beyond the cyclotron exit port.

11. LABORATORY BUILDING

The new cyclotron required a new laboratory building. It was built in two phases on a beautiful lake-shore site about two kilometers from the old laboratory. The first phase was started in June 1989 and only included the cyclotron bunker and areas for the ECR ion source, power supplies and the cooling and ventilation systems. It was completed, together with the adjacent workshop and library building, in December 1990. Unfortunately the subcontractor responsible for the water cooling system was badly behind the schedule, so that all cyclotron tests had to be postponed until April 1991.

The accelerator group moved to the new laboratory in February 1991. More than 50 staff members are still waiting for new premises for the Department of Physics, which are expected to be ready in 1994. The quality of life at the site was further upgraded by the opening of a new beautiful bridge connecting the old and new campus areas in summer 1991.

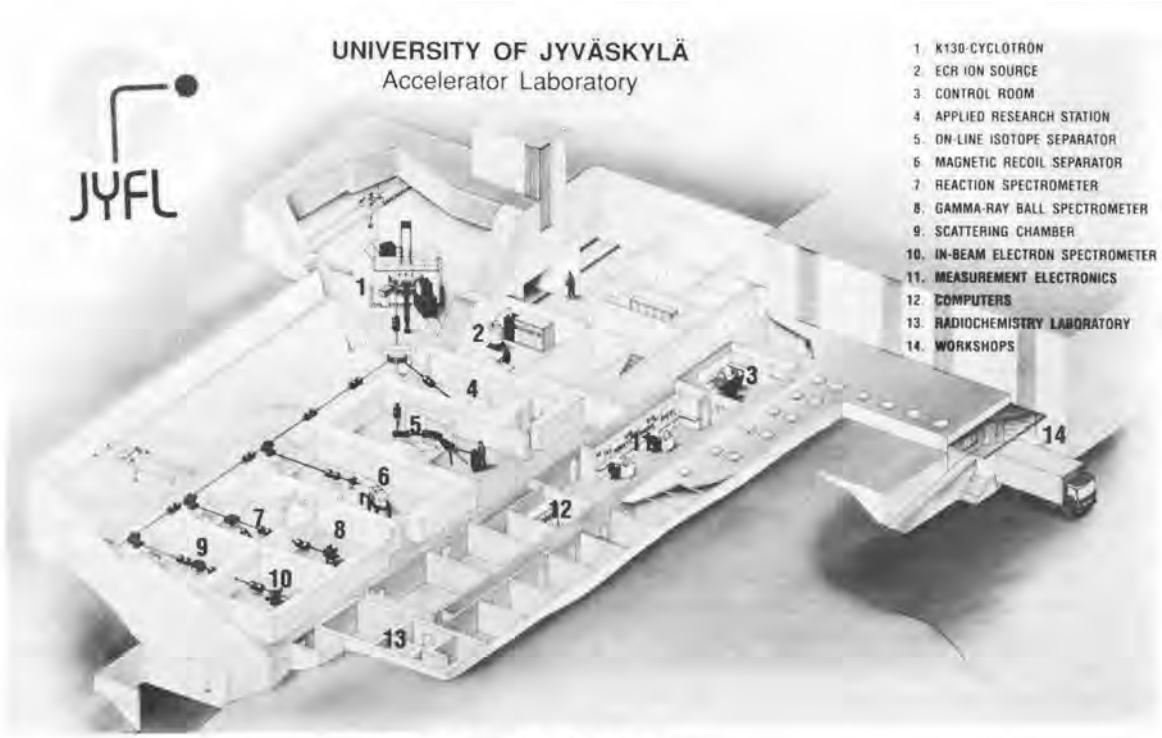


Fig. 6. Lay-out of the laboratory.

The new campus has turned out to be a popular tourist attraction. About 1200 visitors came to see the new accelerator and laboratory in 1991, and about 1800 in the first half of 1992.

The construction of the second phase of the building, which houses the experimental hall, was completed in June 1992. Concrete blocks for radiation shielding in the experimental hall were provided and installed by the construction company. The magnets for the beam lines and the new gas-filled recoil spectrometer were delivered by the Danish company Danfysik A/S in June 1992. The vacuum pumps and other vacuum components for the beam lines were also delivered. Therefore it will be possible to complete the first beam lines and experimental setups in the fall of 1992. The first experiments using the new facility could be run before the end of 1992.

Figure 6 shows the general layout of the new laboratory.

12. REFERENCES

1) Liukkonen E., The Jyväskylä K130 Cyclotron Project, in **Proceedings on the 12th International Conference on Cyclotrons and their Applications**, Berlin 1989 (World Scientific, Singapore, 1991) pp. 40–42.
2) Heikkinen P., A Semi-3D Method of Calculating the Magnetic Field in a Conventional Sector-Focused Cyclotron, Nucl. Instr. and Meth. **A301**, 417(1991).
3) Antaya T. A. and Xie Z. Q., in **Proceedings of the 7th Workshop on ECR Ion Sources**, Jül-Conf-57, ISSN 0344-5798, KFA Jülich GmbH (1986) 72.
4) Ärje J., Nieminen V., Choinski J. and Antaya T. A., in **Proceedings of the 10th Workshop on ECR Ion Sources**, Oak Ridge National Laboratories, Knoxville, (1990) 343.
5) Marti F., Blue R. A., Johnson J., Kuchar J., Nolen J. A., Rutt P., Sherrill B. and Yurkon J., Beam Diagnostic Developments at MSU, in **Proceedings on the 12th International Conference on Cyclotrons and their Applications**, Berlin 1989 (World Scientific, Singapore, 1991) pp. 268–277.
6) Houtman H. and Kost C. J., A Fortran Program (RELAX3D) to Solve the 3-Dimensional Poisson (Laplace) Equation, Computing in Accelerator Design and Operation, **Europhys. Conf. Abstracts**, vol.**74** (1983) Berlin.
7) Taskinen P., Lampinen J. and Loberg K., The Control System of Jyväskylä K130 Cyclotron, in **Proceedings on the 12th International Conference on Cyclotrons and their Applications**, Berlin 1989 (World Scientific, Singapore, 1991) pp. 240–243.

EXPERIENCE WITH THE HIGH CURRENT OPERATION OF THE PSI CYCLOTRON FACILITY

Th. Stammbach,
Paul Scherrer Institute,
CH-5232 Villigen, Switzerland

ABSTRACT

The PSI two stage accelerator facility is at present being upgraded to higher beam intensities. In view of the spallation neutron source under construction, beam currents of about 1.5 mA at an energy of 590 MeV are anticipated. The status of the upgrading program is summarized and operational experience with increased beam intensities is reported. At the 72 MeV injection energy the design goal could be reached. Making use of strong bunching a stable beam of 1.5 mA could be extracted from the 'Injector 2' cyclotron. The behaviour of strongly bunched beams and the effect of space charge forces are discussed. In the partially upgraded 590 MeV Ring cyclotron and at the reconstructed target station and beam dump area, the beam intensity could be increased to 0.5 mA, at present limited by the available RF-power. Beam loss, beam quality and possible limits are discussed.

1. INTRODUCTION

The cyclotron facility at PSI (Paul Scherrer Institute) is one of the three existing meson factories in the world. A high current proton beam at an energy of 590 MeV is used for the production of intense secondary beams of pions and muons. The main accelerator is a separated sector 'Ring cyclotron' specially designed for the acceleration of high intensity beams with a 72 MeV cyclotron as injector. Until 1985 the facility was operated with beam intensities up to 200 μA using the Philips cyclotron as injector and is now stepwise being upgraded to increase the available beam currents at 590 MeV from the previous level to an expected 1.5 mA. The goal of this upgrade is to provide more intense meson beams for the next generation of precise experiments in medium energy particle physics, especially rare decays, and to produce enough beam power for a spallation neutron source (SINQ) presently under construction at PSI. Several important steps of this upgrade program could be realized in the preceding years:

- 1985: upgrade of the first of the two meson production targets by reconstruction according to design criteria adapted to beam currents of 1.5 mA, to higher beam losses, and hence elevated levels of radiation and activation,
- 1985: start of beam production with Injector 2, a new dedicated injector cyclotron for 72 MeV protons built by PSI and especially designed for high beam intensities,
- 1990: commissioning of a new 500 kW 50 MHz-amplifier designed by PSI as an essential step towards an upgraded RF system capable to deliver the necessary RF power to the Ring cyclotron and installation of the first of four units at the Ring cyclotron,
- 1990/91: reconstruction of the second meson production target station, upgrade of the beam dump area and preparation work for the connection of the future spallation neutron source, again according to design criteria adapted to the anticipated beam intensities.

Details of the upgrading program have been given in earlier publications.[1-3] This publication reports on the present status of the upgrade and on initial operational experience with increased beam intensities from Injector 2 and in the Ring cyclotron. An 18 month shutdown for the reconstruction work in the beam dump area and for installations in view of the upgrade of RF systems in the Ring cyclotron was used to demonstrate the high current capability of Injector 2 and to investigate the behaviour of the beam. Making use of a highly bunched beam the design goal could be reached and a stable beam of 1.5 mA was extracted. In the partially upgraded Ring cyclotron a beam of 500μA could be accelerated. Separate contributions to this conference deal with investigations on strongly bunched beams in the Injector 2 cyclotron combining simulations and beam tests[4] and with the status of the upgrade of the RF systems to the demand of the high intensity beams.[5]

The problems and limits with the high intensity operation of the cyclotrons at PSI have been summarized in several papers by W.Joho and U.Schryber.[6,7,1] They concluded that the key point is the RF-system and an accelerator design that allows high accelerating voltage and well separated turns. The RF-system has to not only deliver the necessary power to the beam, but also to fulfil high standards in stability under extreme beam loading conditions. The effect of space charge forces have been investigated by S.Adam.[8] The beam current is expected to be an important parameter that affects the setting of components and can have dramatic influence on the beam quality. This then interferes with the goal to keep beam losses at extraction around 0.1%, i.e. 99.9% extraction efficiency, to keep the activation of components at acceptable levels and to protect them from damage.

2. INJECTOR 2

2.1. Design criteria

The new injector cyclotron is built by PSI and is described in detail in ref.9. Its main features are a large orbit radius and good turn separation to allow extraction virtually free of beam loss. This is realized with large separated magnets leaving space for large accelerating structures with a high energy gain. The consequence is operation at a high harmonic number (h=10). The ion source is external and mounted in the dome of an 870 keV Cockcroft - Walton preinjector[10] which is normally operated with an 8 to 10 mA proton beam. The beam is injected axially with two vertical 90° bends.

The final energy of 72 MeV is reached after about 100 revolutions. The turns remain well separated and the turn separation at extraction is still as large as 20 mm. Extraction losses can therefore be kept very low, and restricted to particles travelling far away from the equilibrium orbit as a result of coupling effects, aberrations or space charge forces. Two flattop resonators operating at the third harmonic of the main accelerating RF are installed to reduce the effect of phase width and field errors on the energy spread of the beam.

2.2. Commissioning to beam currents above 1 mA

Since commissioning of the Injector 2 cyclotron in 1985 several attempts to extract beam currents above 1mA were undertaken. In all cases a degradation of the beam with increasing beam current was observed. The following cases were investigated:

- Injection of an unbunched beam with 8 to 10 mA beam current. Above 0.8 mA the phase width of the beam exceeded the acceptance of the cyclotron of ± 20 deg.
- Injection of a weakly bunched beam. This resulted in a reduced phase width but introduced additional energy dispersion into the centre region that could not be properly matched to the corresponding equilibrium orbit.
- Use of a more intense beam from the ion source. A beam current of up to 16 mA could be transported and injected into the cyclotron, but the handling in the injection beam line was very difficult and the gain from the correspondingly reduced phase width was cancelled by drastically increased beam losses at extraction, probably due to a degradation of beam quality introduced by space charge forces in the injection beam line.
- Pulsed beams. Extraction in a 1 out of 3 pulsed mode was expected to be a fair test of space charge effects, since the charge in the individual bunches remains unchanged, while problems related to high beam power, as operation of RF systems close to power limits, stability of RF systems and excessive beam loss at collimators and in the extraction system could be avoided.
- The highest beam currents could be extracted making use of strongly bunched beams, improved collimation in the centre region and with a special effort to match the vertical dispersion at the injection into the cyclotron.

The result of these experiments is summarized in fig. 1. Two probes that scan the beam over several turns before extraction were used to get a quick estimate of the beam quality at this point. The width of the beam averaged over the last turns before extraction for well optimized cases is plotted as a function of the beam current. In all cases the width of the beam increases steadily with increasing beam current. Several facts make the average width of the beam depend upon beam intensity. Since the beam intensity is adjusted by the position of a phase defining collimator on the first orbit, the phase space volume occupied by the beam grows at low intensities first radially, and then in phase. Finally, at higher beam currents space charge forces add to the energy dispersion in the beam.

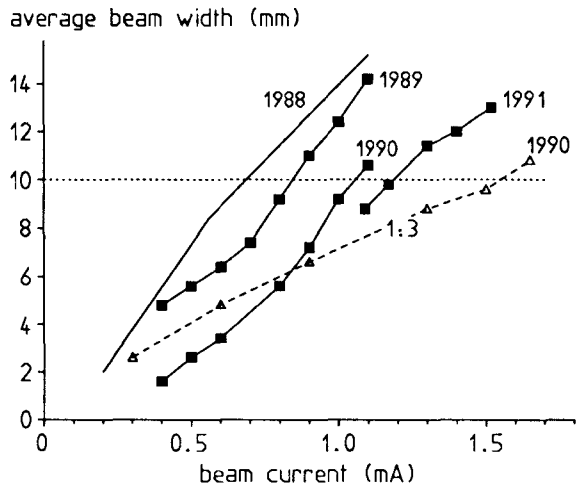


Fig. 1. Average width of the beam on the last turns before extraction from Injector 2 as a function of the beam current. It shows the degradation of the beam quality observed in several experiments to accelerate elevated beam currents. Best results were found making use of strongly bunched beams (1990/91). Beams with widths below 10 mm can be accelerated in the 590 MeV Ring cyclotron without excessive losses.

2.3. Longitudinal space charge forces

Theoretical investigations on the effect of space charge forces in the PSI cyclotron have been performed by S. Adam and W. Joho.[8,6,7] Their results are summarized in fig. 2. In an isochronous cyclotron the longitudinal space charge effects dominate. They manifest themselves threefold, in a tilt or rotation of the bunch in phase and radius, in a deformation of the bunch, and a vortex motion of the particles.[11-13] Leading particles gain additional energy and drift adiabatically to the corresponding equilibrium orbit with larger radius, thus producing the tilt. The forces that generate the tilt, however, are not linear with the phase of individual particles in the bunch, but depend on the shape of the distribution function and lead to the typical 'butchers hook' deformation

of the bunch as shown in fig. 2a. Due to the coupling of radial and longitudinal motion, finally, the radial deplacement of the particles and radial space charge forces introduce a longitudinal motion as well. This generates the vortex motion or in extreme cases the spiraling of the bunch as shown in fig. 2b.

The tilt of the bunch in phase against radius can be compensated by detuning of the phase between the flattop and the accelerating resonators. A change of 1 degree in the flattop phase produces an energy variation of .034% per degree phase width in the beam. An example of this compensating effect is given in fig. 3 for the case of a 1 mA beam extracted from Injector 2.

In order to observe the deformation of the bunch in phase and radius a system to measure the time structure of the beam with high radial resolution has been installed on the last turn in the Injector 2 cyclotron. The predicted deformation of the bunch in phase and radius and its vortex motion is barely observed in the measured time structure. An example is given in fig. 4a, but in most cases the resolution of the measuring system is not sufficient and the structure disappears in the general degradation of the beam. This is particularly the case with strongly bunched beams in which the phase width of the beam is reduced to just a few degrees.

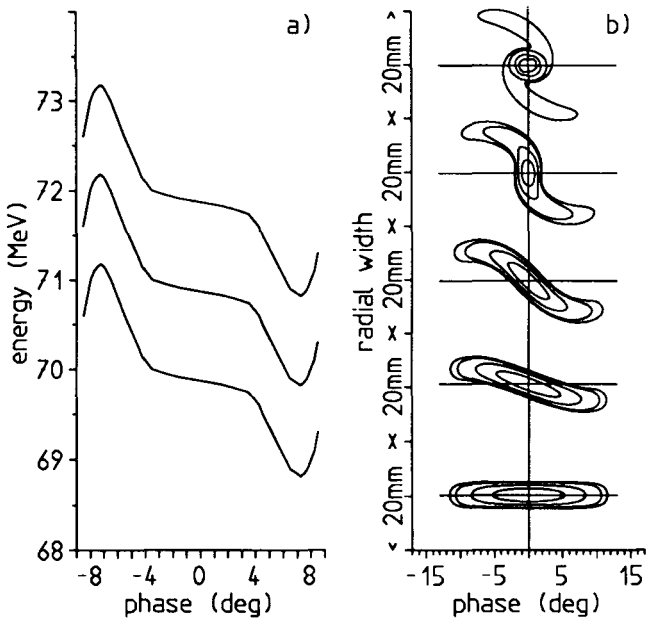


Fig. 2 Calculated deformation of the bunches under the influence of longitudinal space charge forces taken from ref.8. The left side (a) shows the tilt of the bunch in energy vs. phase on the last turns of Injector 2 at a beam current of 1 mA within 30 deg at injection. The phase width is reduced by phase compression during acceleration. The effect of stronger space charge forces result in a vortex motion as shown on the right side (b) for the case of a 3 MeV beam with a current of 1.5 mA within 20 deg coasting over eight revolutions, every second turn is shown.

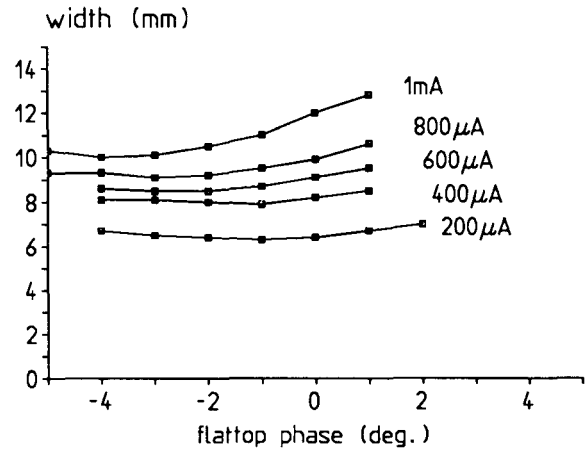


Fig. 3. Dependence of the average beam width at extraction from Injector 2 on beam intensity and flattop phase. It demonstrates that an enegy spread builds up. It is introduced by longitudinal space charge forces and is proportional to the beam current. This effect can be partially compensated by adjustment of the flattop phase.

2.4. Strongly bunched beams

Investigations on the properties and behaviour of strongly bunched beams in the injection beamline and on the first few orbits of the Injector 2 cyclotron are presented in detail in a separate contribution to this conference.[4] The results can be summarized as follows. With beam currents of several mA at the injection energy of 870 keV, the debunching effect of space charge forces can not be neglected. The action of these forces, however, can be very favorable if the beam current is adjusted such that the debunching from the space charge forces compensates the energy modulation introduced by the buncher. A prerequisite for the compensation is a beam transport with minimal dispersion. Because Injector 2 works with axial injection, the debunching would otherwise result in a distortion of the beam in the vertical phase space. The beam is expected to be bunched into about 14 degrees phase width with a bunching factor around 3. In addititon the calculation showed that the beam enters over a phase range of about 40 degrees on the same radius into the cyclotron and that the phase acceptance is extended to late particles too far out in phase. To remove these phase tails from the beam an additional cleaning collimator was added in the calculations and installed in the cyclotron a quarter of a turn behind the phase defining collimator. According to the calculations 43% of the incoming dc beam would be accepted on the first orbit, but 8% would have to be cut off in the cleaning collimator and 35% would be accelerated within a phase range of ± 20 degrees and within 4 mm radial spread, which would be a perfect beam for a cyclotron equipped with a flattop system. Space charge effects in the cyclotron could not be taken into account in these calculations. Table 1 gives selected results from the calculations.

The data show the improvement of the beam quality by the cleaning collimator. This allows to accept more beam by repositioning of the phase defining collimator.

Table 1: Calculated effect of the buncher and the cleaning collimator on the beam injected into the Injector 2 for the case of a 10 mA dc beam.

buncher voltage	0 kV	4 kV	7 kV
without cleaning collimator			
average width	5 mm	11 mm	13 mm
phase range	42 deg	52 deg	38 deg
acceptable beam	1.0 mA	1.9 mA	1.1 mA
with cleaning collimator			
average width	4 mm	4 mm	4 mm
phase range	42 deg	44 deg	36 deg
acceptable beam	1.1 mA	2.0 mA	3.5 mA

It was difficult to predict how such a beam would be affected by the longitudinal space charge forces in the cyclotron. Since the vortex motion in the plane defined by phase and radius increases with the third power of the inverse phase width, the limit of the "spiraling instability" predicted by S.Adam[8] would certainly be crossed. Experiments with such a beam in the cyclotron gave good results and did not show the drastic increase of the energy spread expected from space charge simulations. Several observations give evidence of a "soliton-like", well compacted beam in radius and phase, and with no visible structure or filamentation within the resolution of the available beam diagnostic systems.

2.5. Observations with the 1.5 mA beam

As seen in fig. 1, injection of a strongly bunched beam gave the best beam quality at the extraction energy of 72 MeV. After tuning to minimize beam losses measured by ionization monitors and on collimators in the extraction system, the current could be raised to more than 1.5 mA. The extraction rate was around 99.9%, the measured beam losses 1.3 μA. The beam was stable and could be kept at this level over days. Some of the results are given in fig. 4c, fig. 5 and in table 4. The orbits are slightly off centre by a coherent betatron oscillation of 2 mm to improve turn separation at the electrostatic and electromagnetic deflectors. Beam collimation in the centre region was important as predicted from the buncher and centre region calculations.[4] With a dc beam current of 8.0 mA in the injection beam line, 3.0 mA were accepted into the first orbit, but only half of it could be used for acceleration. 600 μA were cut away in the vertical slit, 800 μA in the cleaning collimator and 100 μA in the slit on the fourth turn. The percentage of the beam cut off by the cleaning collimator agrees well with the 25% predicted.[4] The fact that the beam is improved by cutting with the vertical slit, however, was not expected. It gives evidence that

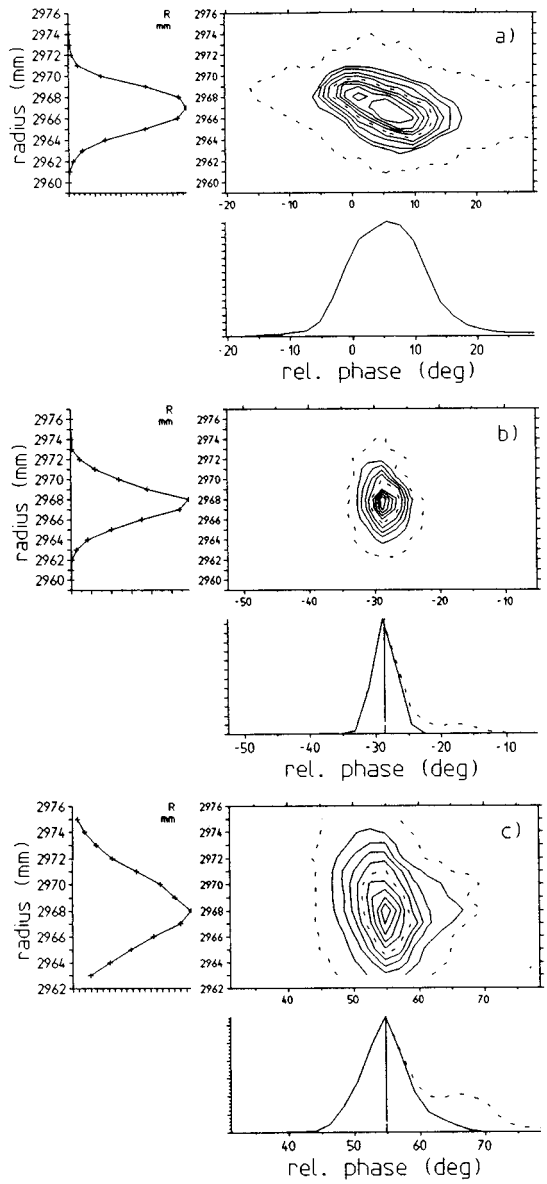


Fig. 4. Improvement in the longitudinal phase space of the beam on the last turn before extraction from Injector 2: a) a 300 μA beam in 1989 before optimization of bunching, b) typical production run at 360 μA using a strongly bunched beam with proper dispersion matching and with a cleaning collimator added 90 deg behind the phase defining collimator, c) the 1.5 mA beam extracted in 1991. Shown are the intensity distribution (1%, 10%,....90%) projected onto the plane defined by radius and phase as well as the radial and longitudinal profiles. The measurement is made with a time of flight analysis of protons scattered from a thin carbon fibre as a function of its radial position. The dashed lines in the phase profile show the raw data before application of a correction for pileup in the photomultiplier at elevated beam intensity.

vertical distortion from the debunching described above either makes beam quality worse or is used to improve the phase cut.

The phase width of the beam remains uncertain. The time structure measurement (fig. 4), based on a time of flight analysis of protons scattered from a thin carbon fibre (30 μm) in function of the radial position of the fibre, gave a phase width of 16 deg (full width for 96% of the beam) at 1.5 mA. This is in accordance with the width of 11 deg expected for a bunching factor of 3 for a perfectly cut square distribution, if the phase compression by a factor of 2 is accounted for. On the other hand, the buncher calculations predict a phase width of only a few degrees which is supported by the results of several experiments described below. The small phase width demonstrates in any case that the bunching and the phase cut were indeed very effective. It was, however, a surprise that the influence of longitudinal space charge forces did obviously not destroy the beam. As shown in fig. 1, the radial width of the beam did only moderately increase with beam current and as seen in fig. 4c and in fig. 5 the phase space volume remained compact. The phase width and the radial width of the beam were observed to grow roughly by the same amount and in parallel and it seems that the vortex motion in the plane defined by radius and phase keeps the beam together and leads to a compact

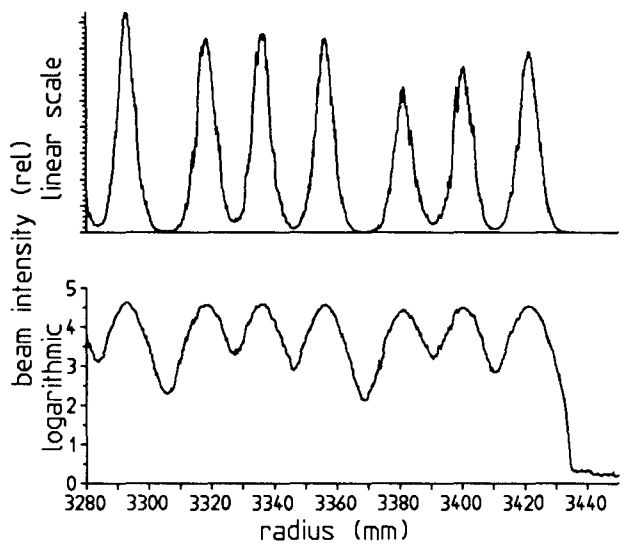


Fig. 5. Beam profile of the last seven turns in the Injector 2 cyclotron measured at a beam current of 1.5 mA. In order to see space charge induced broadening of the beam such measurements must be made at full beam current. Only a probe equipped with a thin Carbon wire (about 50 microns diameter) can withstand the high power density of this beam. The profiles are also shown in a logarithmic scale to give information on beam losses to be expected from beam tails or from the halo of particles extending into the valleys between the orbits.

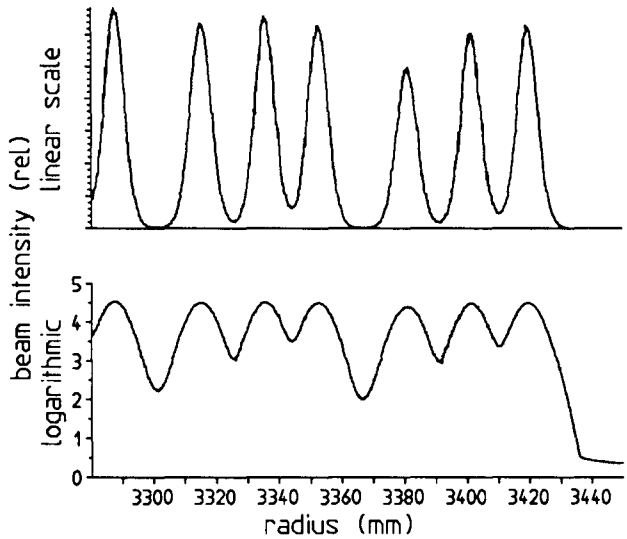


Fig. 6. The same measurement as in fig. 5 for the case of 1.3 mA extracted with the flattop resonators turned off. Despite space charge forces and the fact that acceleration is no longer independent on phase, the turns remain separated and compact.

ball of charges growing with increasing beam current, a situation already predicted in early publications on space charge effects in cyclotrons.[12] Recently, several experiments with the flattop resonators turned off also gave surprising results which support this interpretation. A beam of up to 1.3 mA could be extracted in this mode with still well separated, compact turns (fig. 6) while a phase width above 10 deg should result in a complete overlap of the turns. Similar inconsistencies are observed if the magnetic field setting is varied or if the flattop resonators are used to introduce a phase dependent acceleration. Further investigations are necessary to understand the combined effects of vortex motion and phase compression on the beam during acceleration.

3. RING CYCLOTRON

3.1. The Upgrade program in the Ring cyclotron

The 590 MeV Ring cyclotron was designed two decades ago by PSI (formerly SIN) according to identical design criteria as later copied for Injector 2: a large structure with separated magnets and hence operation in a high harmonic number (h=6). This gives enough room for injection and extraction elements and for four powerful acceleration cavities with a high energy gain of about 2 MeV/turn. The Ring cyclotron is also equipped with a flattop cavity operated at the third harmonic of the accelerating voltage. The turn separation at extraction is 4.5 mm for a well centered beam, but it is generally expanded to about 8 mm by off-centre injection, in order to achieve full extraction. The original design goal was a beam current of 100 to 300 μA, but the first

Table 2: RF power requirements in the Ring cyclotron

proton current	(mA)	0.25	1.5
beam power	(kW)	150	900
50 MHz RF systems			
cavity voltage	(kV)	520	730
beam power per cavity	(kW)	37	220
dissipation per cavity	(kW)	150	300
total power	(kW)	187	520
150 MHz flattop system			
beam power deposited	(kW)	15	90
dissipation in cavity	(kW)	50	100
dynamic range	(kW)	50 - 35	100 - 10

years of routine operation showed that up to 200 μA beam losses were still extremely low. After installation of the flattop cavity, an extraction rate of better than 99.98% could be reported. In a pulsed mode, where two out of three pulses were suppressed, beam losses could be held below the given limits up to beam currents of 250 μA. Based on this, one could expect that in an unpulsed mode it would be possible to extract beam currents up to 750 μA. The intensity, however, was limited by the power that could be deposited in the beam dump and by the power available from the RF systems.

The requirements on the RF systems given by 1.5 mA beam intensity in the Ring cyclotron are summarized in table 2 taken from ref.3. A new 50 MHz power amplifier based on the Siemens Tetrode RS2074 had to be developed by PSI. It delivered a maximum of 850 kW into a resistive load and up to 400 kW into the cavity (300 kW to the walls and 100 kW to the beam). Routine operation is restricted to lower power levels due to problems with the coupling loop (overheating and deposit of sputtered material on ceramic insulators) at increased voltage levels. With one of the RF systems equipped with the new amplifier stage, the power is sufficient for the acceleration of beam currents up to 500 μA. As seen from table 2, a special challenge comes from the decelerating flattop system which was equipped with a new, more powerful 150 MHz amplifier in January 1992. It has to operate at decreasing power with increasing beam intensity, under stringent specifications in phase and amplitude stability. In order to reduce effects from beam loading, the flattop cavity has to be artificially loaded. Even if the power dissipation in the loaded cavity is doubled an extreme dynamic range of 100 to 10 results, if the beam intensity is raised to 1.5 mA. Operational experience and details of the upgrade program on the RF systems are given in a separate contribution to this conference.[5)]

In the years 1992/94 the remaining three 50 MHz RF systems will be equipped with the new amplifier stage. With all RF systems upgraded, the acceleration voltage can be increased and the energy gain be raised from 2.0 to 2.8 MeV per turn. This improves the extraction in two ways. It enhances the turn separation and it diminishes the number of turns which reduces the effect of longitudinal space charge forces. The upgrade program for the Ring cyclotron also includes the replacement of all the injection and extraction elements. The new generation will be equipped with improved local shielding and it will be adapted for easier handling at the higher activation levels to be expected.

3.2. Upgrade of the beam facilities

As with the Ring cyclotron, the original beam facilities were designed for beam currents of up to 200 μA and had to be replaced. The first of the two meson production target stations was rebuilt in 1985. The reconstruction of the second meson production target station, of the beam dump area and the preparation work for the connection of the future spallation neutron source were a major task accomplished in an 18 month shutdown in the years 1990/1991. A special challenge was the dismantling of the old target and beam dump, which had served for 15 years at beam currents of 100 to 200 μA with a total charge of 6.6Ah deposited. 500 t of activated material with a total activity of 10^{15} Bq had to be removed. About two thirds of this material could be reused and the rest was enclosed in concrete boxes and reinstalled as shielding. Local dose rates were as high as 400 Sv/h and the contamination levels were locally a factor 10^4 above tolerance level. Nevertheless incorporation could be avoided and the highest personal dose was about 20 mSv. The total dose received by 200 persons was 470 mSv.

The new beam dump and meson production target station are designed for a beam intensity of up to 2 mA. At the anticipated intensity of 1.5 mA, a beam power of almost 900 kW has to be handled. The beam loss and power balance for this case is summarized in table 3. The design accounts for the fact that one third of the power escapes as radiation of secondary particles and has to be absorbed in water cooled shielding. Therefore the structure is strictly separated into an inner part optimized to handle the thermal problems and an outer mechanical part that is protected from heat and radiation. The inner part is a closed shell of heavy radiation shields around the collimators and the beam dump, all water cooled and generally made out of copper. All sensitive mechanical parts such as vacuum chambers, the seals and the support structures are outside of this shielding and hence protected against heat induced deformations. To ensure easy handling at the activation levels to be expected, all parts are vertically mounted and removable by crane. Their supports are self centering pins without additional fastening, vacuum seals are all metal inflatable elements that do not require any clamping and all the power-, cooling- and signal connections are brought up through the shielding to an accessible platform 2.5 m above the beamline.

3.3. Operational experience with a beam of 500 μA

Operation of the facility after the extended reconstruction work could be resumed in June 1991. The beam intensity through the Ring cyclotron and onto the rebuilt pion

Table 3: Beam loss and power balance in the upgraded target station and beam dump

	beam loss	power
incoming beam (1.5 mA, 590 MeV)		885 kW
pion production target (C12, 10gr/cm^2)	18%	45 kW
particle radiation from target		140 kW
primary beam in shaping collimators	22%	145 kW
neutron radiation from shaping coll.		50 kW
primary beam into beam dump	60%	380 kW
neutron radiation from beam dump		125 kW

production target could be continuously increased and a stable beam of 500 μA at 590 MeV was finally reached in December 1991. New protection systems against beam loss and against deviation from full beam transmission were installed and tested. Initially these systems were the source of a large number of false alarms and interruptions in the beam production. The handling of the beam is supported by beam loss monitors (simple air filled ionization chambers) distributed all along the beam line and in the Ring cyclotron and by computer controlled on-line centering of the beam in the transport system.

The beam losses, as measured on collimators of the extractor and in the beam loss monitor system, were around .1% at an extracted beam current of 500 μA, but in further production runs in 1992, the losses could be reduced to about .01% at an extracted beam current of 400 μA (see fig. 7). Data on the beam quality are summarized in table 4 in comparison to values of the beam from Injector 2. Horizontal and vertical emittance areas could be deduced from the width of profiles in the beam transport system. The dispersive resolution, however, was not sufficient to accurately separate the effects of energy spread from the horizontal emittance. The phase width of the 590 MeV beam could not be measured, but was calculated from the result of the time structure measurement in Injector 2 and the known phase compression in the Ring cyclotron. The question of space charge limits is still open. At a beam current of 500 μA, the beam quality seems to deteriorate and beam losses do increase with increasing beam intensity, but higher beam currents or better diagnostics would be needed to clearly attribute these effects to space charge forces. It is expected, however, that at the full beam intensity of 1.5 mA, the space charge forces will manifest themselves very strongly and that the voltage on the cavities has to be increased as indicated in table 2 to reduce their effect. Observed intensity limits from the operation at reduced voltage (e.g. with only three cavities in operation, case b in fig. 7) scale well with the prediction, but the data are too uncertain to allow a positive statement on the limit imposed by space charge forces.

With increasing beam intensity, a detailed analysis of the beam becomes more and more difficult. While beam diagnostic should be done at the full beam current, the use

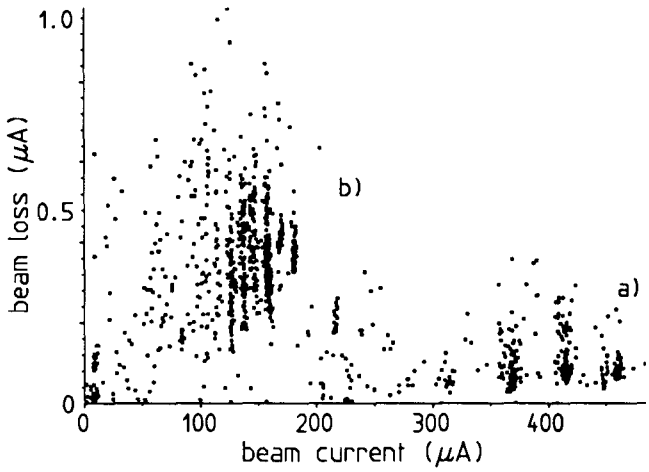


Fig. 7. Beam loss in the Ring cyclotron in correlation to the beam current for a normal production run (a) and for reduced acceleration voltage (b). It demonstrates that beam loss can be kept below 0.1%, if the acceleration voltage is sufficiently high. The beam loss is measured in an air filled ionization chamber. The data are taken by a logging program that reads all cyclotron parameters every 15 minutes and stores them on disc for later analysis.

Table 4: Quality of the beams in the PSI facility

energy	beam	emitt. area (2σ)		energy	phase
	current	horiz.	vert.	spread	width
(MeV)	(mA)	(mm mr)	(mm mr)	(%)	(deg)
Cockcroft - Walton preinjector:					
0.87	8.0	8. π	8. π		dc
Injector 2:					
72	0.5	2. π	2. π	0.4	$<12.$
	1.5	3. π	3. π	0.6	$<16.$
Ring cyclotron:					
590	0.5	1.5 π	1.5 π	$\sim$0.2	$<10.$

of most of the probes is restricted to low intensities where the properties of the beam are substantially different. Beam profile monitors that can be operated at full current, produce beam spill that exceeds the protection levels. A beam probe that can withstand the full beam is planned, but not yet installed. Under these conditions, new diagnostic methods have to be employed. Two examples are given in fig. 7 and 8. The first is statistical information from a data logging program that reads all cyclotron parameters every 15 minutes and stores the data on disc for later analysis. Apart from error detection, it can be used to find correlations between values and parameters of interest. The second example is a result from a two parameter scan that can be used under operational conditions. This scanning program changes two

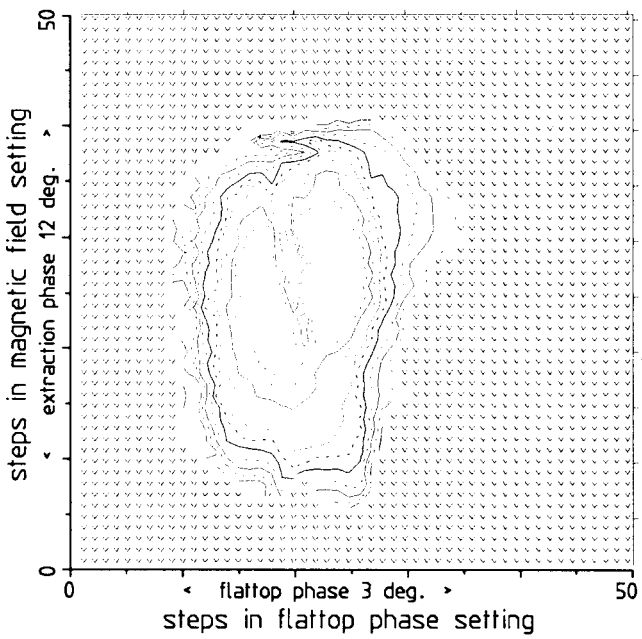


Fig. 8. An example of the complicated structure of the low level beam losses of interest in high current operation, here the beam loss in the Ring cyclotron as a function of the magnetic field setting and of the phase between flattop and accelerating voltage. Shown is the output of an automatic scanning routine, that has been developed to support accelerator tuning under running conditions at high beam currents. It starts from the actual value and automatically avoids the marked region (v) where interlock situations are encountered.

parameters in a specified range, but automatically restricts the range to parameter values where beam loss does not exceed given limits. The value that is recorded in the scan can be any passive parameter related to beam quality. Details on this program are presented in a separate contribution to this conference.[14)]

The setup for a beam with high current and minimal losses proceeds in steps. At first all parameters are adjusted to optimize the beam quality based on measurable properties, partially at low beam intensity. In general, when the beam current is increased also the RF amplifiers have to be adjusted in order to deliver the necessary power with good stability. In a final fine-tuning the beam losses as measured in collimators and in the ionization chambers are minimized. This last step is always based on experience, takes plenty of time (days or even weeks) and does not follow strict recipes. Particles far out in phase space follow other tracks than the main beam, they can have different source points (e.g. collimators) and their phase space coordinates often show strong coupling between horizontal, vertical and longitudinal planes (e.g. aberrations, space charge effects). Once optimized, the beam is very stable and needs little adjustment. Beam losses at extraction do not depend strongly upon magnetic field tuning, but are sensitive to certain parameters in the injector cyclotron like instabilities in the buncher phase, setting of trimcoils in the centre region, ion source parameters and beam position in collimators.

4. ACKNOWLEDGEMENT

This report summarizes the work and effort of a very large number of persons, be it responsible for the design, involved in the upgrade and reconstruction work, or last but not least being patiently engaged in the tuning of the beams. It is absolutely impossible to honor individual contributions to the achievements, but this is a welcome opportunity to express thanks to everybody who has been involved.

5. REFERENCES

1) U. Schryber, "Upgrading the SIN facilities to higher intensities", **Proceedings of the 10th Int. Cycl. Conf.& their Appl.**, East Lansing 1984, p.195
2) W.Joho, "Upgrading the PSI cyclotrons for research at high beam intensities", presented at the **Int. Symp. on new trends and facilities in intermediate energy Nucl.Phys.**, Osaka 1991
3) U. Schryber et al., "Upgrading the PSI accelerator facility for high intensity operation", presented at the **3rd Europ. Acc. Conf**, Berlin, March 1992
4) J. Stetson et al., "The commissioning of PSI Injector2 for high intensity, high quality beams", presented at this conference
5) P. Sigg et al., "Experience with the PSI-cyclotron RF-system under heavy beam loading", presented at this conference
6) W. Joho, "High intensity problems in cyclotrons", **Proceedings of the 9th Int. Conf. on Cycl. & their Appl.**, Caen 1981, p.337 and **Proceedings of the 11th Int. Conf. on Cycl. & their Appl.**, Tokyo 1986, p.31
7) W. Joho "Space charge effects in cyclotrons", presented at the **Int. Acc. School**, Dubna 1988
8) S. Adam, "Calculations of space charge effects in isochronous cyclotrons", **IEEE NS-32** (1985) 2507 and **thesis 7694** ETH Zurich, 1985
9) U. Schryber et al., "Status report on the new Injector at SIN", **Proceedings of the 9th Int. Conf. on Cycl. & their Appl.**, Caen 1981, p.43
10) M. Olivo, **Proceedings of the 11th Int. Conf. on Cycl. & their Appl.**, Tokyo 1986, p.519
11) M. M. Gordon, "The longitudinal space charge effect and energy resolution", **Proceedings of the 5th Int. Conf. on Cycl. & their Appl.**, Oxford 1969, p.305
12) A .Chabert et al., "Beam dynamics in separate sector cyclotrons", **Proceedings of the 7th Int. Conf. on Cycl. & their Appl.**, Zürich 1975, p.245
13) E. Baron et al., "High intensity and space charge problems at GANIL", **Proceedings of the 11th Int. Cycl. Conf. & their Appl.**, Tokyo 1986, p.234
14) S. Adam, "Twodimensional scans with adaptive domain control", presented at this conference

THE COMMISSIONING OF PSI INJECTOR 2 FOR HIGH INTENSITY, HIGH QUALITY BEAMS

J. Stetson,
National Superconducting Cyclotron Laboratory,
East Lansing, MI 48823, USA

and

S. Adam, M. Humbel, W. Joho, Th. Stammbach,
Paul Scherrer Institute (PSI),
5232 Villigen, Switzerland

ABSTRACT

Since 1984 injector 2 is producing beams of 72 MeV protons for injection into the 590 MeV ring cyclotron of PSI. The RF-system of this ring is not yet able to accelerate beams above 0.6 mA, but the injector 2 has been commissioned to produce beams with intensities of up to 1.5 mA. Theoretical investigations done in parallel with beam experiments have helped to increase maximum extracted beam intensities and, to simultaneously improve beam quality at these higher currents. Simulations of bunching effects under space charge conditions predicted a high intensity kernel in the injected beam with minimal energy spread. Studies of the phase selection mechanism in the cyclotron center aimed at selecting this beam part for acceleration. As a result of these studies, an additional phase cutting collimator was installed, the buncher voltage was increased and its phase was stabilized.

1. LAYOUT

The following discussion principally concerns the PSI 72 MeV injector 2 and associated 870 keV proton injection beam line.

The acceleration process begins with protons extracted at 60 kV from a multi-cusp type ion source. This first beam is focused into the 810 keV acceleration tube of the Cockroft Walton DC accelerator. The 870 keV beam line, located on a level of 3 meters above the cyclotron midplane, leads the protons towards the cyclotron center. Two 90 degree bending magnets guide the beam vertically down and back horizontally into the midplane of injector 2. An Alvarez-type buncher is located near the end of the horizontal section, shortly before the downward bend. Injection, acceleration and phase selection of the 870 keV beam in the center region is shown in fig. 1.

Acceleration in the cyclotron is done by two 50 Mhz delta-shaped (two-gap) resonators with a voltage per gap that rises radially from 125 to 250 kV. Flattopping over about ± 20 RF degrees is achieved by two third-harmonic (one gap) cavities beginning on the fifth orbit. Extraction at a radius of 3 meters occurs after $\approx$102 turns. The limits of extracted beam current are set in an absolute sense by the losses allowable in the extraction system (a total of about 3 μA) and by the goal of having beam of sufficient quality for transmission and acceleration in the 590 MeV ring cyclotron.

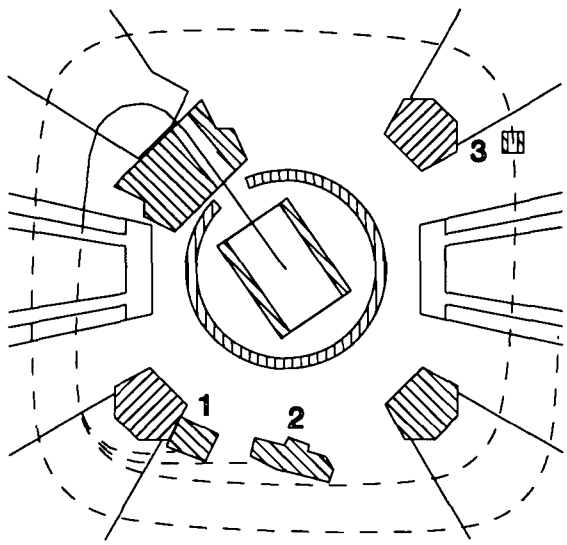


Fig. 1. **Midplane section of the center region of injector 2.** The beam starts in the center, bending from the vertical into the horizontal plane. After the 135° bend in the tip of the first sector magnet, the beam crosses a pair of acceleration gaps. Acceleration or deceleration depends on phase and produces a fan-out of the particles after sector magnet 2. The initial phase (and intensity) selection is made with collimators KIP1, KIP2(1,2). The additional collimator RIL2 (3) improves the phase selection.

2. MOTIVATION

Various upgrade programs underway at PSI will require beam intensities of 1 to 1.5 mA at 590 MeV.[1)2)] In the first years of operation 870 keV DC beams of 8

to 10 mA were used in the center region of injector 2 to get intensities of 0.8 to 1 mA extracted. With flat-topping extending over 10% of the RF phase, a corresponding fraction of the DC beam was expected to be usable for acceleration. However, while 1 mA extraction was achieved by 1985, beams above 0.5 mA were not of a quality good enough for the 590 MeV ring.

Improving the beam quality at high currents became the primary goal, with the two possible approaches being an increase of the DC beam current or use of a buncher. As bad beam quality could be partially due to the wide phase acceptance needed to produce high intensity beams, these two methods to enhance the local current density were tried early on in the attempt to improve extracted beam quality. Increasing ion source output current above 10 mA was found not to be possible without worsening beam quality in the center region. This, in turn, ruined phase selection and therefore canceled any advantages of a potentially narrower half-maximum phase width. Initial experience with bunching showed minimal or negative results. This inspired an extensive model- and experimental- based examination of bunching under space-charge conditions and of the phase selection mechanism acting on the resulting bunched beam.

3. BUNCHING MODEL RESULTS

Two different levels of buncher modeling were used. One was a simple linear model which assumes no space charge forces; only the momentum variation from the buncher acts on longitudinal motion. A more realistic model written by Rick Baartman[3)] was used to treat the "one-dimensional" space charge case. In this model, energy variations and the resulting longitudinal motion of particles in a beam line are simulated by calculating space charge forces as a function of average beam diameter, beam tube diameter and of the longitudinal density distribution.

Figure 2 shows the simulated effect of a buncher in a diagram plotting momentum deviation vs. phase for four different cases: with and without space charge forces and for 4 kV and 7 kV amplitudes on the double gap buncher. The intensity distribution can be derived from dot spacing, which corresponds to an initial phase separation of 3.6 degrees at the buncher (1% of DC beam). In all of the cases shown, the limit to acceptance is not due to the restricted phase width of the acceptance window, but to the small acceptance in momentum spread of about ±0.15%, imposed by the requirement for high beam quality at extraction.

In the 4 kV, "mild" bunching case of the simple linear model, the phase × momentum spread window can accept only 10% of the initial DC beam, the same fraction as can be accepted without bunching. With space-charge effects, momentum spread is reduced, allowing 16% of the DC beam into the window.

Assuming a buncher at 7 kV, the situation is dramatically different. Without space-charge, acceptance is minimal, due to the large momentum spread. However, with space-charge effects included, the model shows that the resultant momentum damping allows 25% acceptance into the same window. This quite different behaviour in the space-charge case is due to the fact that over a ±6 degree range, space-charge momentum "braking" results in a virtually mono-energetic beam of high intensity. We call this situation "space-charge-limit bunching" (SCL bunching).

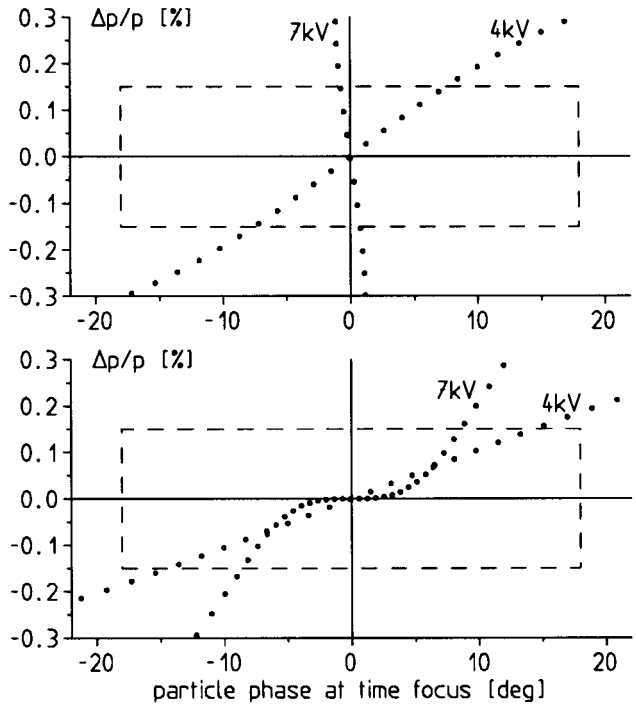


Fig. 2. **Momentum variation vs. phase at time focus** for a linear buncher model (above) and a buncher model with longitudinal space-charge forces (below). For both models, two cases, for voltages of 4 kV and 7 kV, are drawn. The effect of space-charge forces is to produce a highly monoenergetic kernel of intense beam.

As a first step in examining the applicability of a SCL bunched beam in injector 2, plots such as those in fig. 3 were generated by a simple phase selection model which adds the momentum spread from the buncher simulation to the energy gain of the beam in the first acceleration cavity and follows the drift for a distance equal to that from the acceleration gaps to KIP2, the main phase selecting collimator. In fig. 3a, the case of "mildly" bunched beam, one sees the energy vs. phase relation at the location of KIP2 as a slightly distorted cosine peak, 3 degrees phase-delayed. In the case of SCL bunched beam, as shown in fig. 3b, the cosine becomes extremely distorted. The sharp rise in the momentum of trailing particles compensates for the fall-off in the resonator voltage! The phase width over which the SCL bunched beam has near-zero momentum spread is effectively doubled. The results of this simple model stimulated a more

detailed examination of the phase selection mechanism.

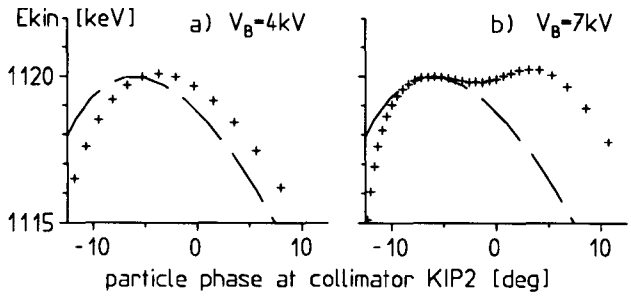


Fig. 3. **Particle energy as a function of phase at KIP2** (after half a turn). Energy values result from adding 870 keV to the buncher simulation results (including longitudinal space charge forces) and to the phase-dependent energy gain of the first accelerating cavity.

4. INJECTOR MODEL RESULTS

Injector 2 beam dynamics are modelled by a simulation called MATADOR. (MAtrix Techniques for Acceleration studies and Display of ORbits).[4] In this program the positions in radius and phase of up to several hundred particles are calculated during acceleration process. To speed up the simulation, transfer matrices are used to calculate the change of particle positions from one azimuth to the next, stepping over large sections of a turn in one operation. Beam simulations with MATADOR initially used a uniform-density, mono-energetic column of particles, using the centerline of resonator 1 as the starting point for particle tracking. In order to investigate the implications of SCL bunched beam, MATADOR was modified to allow input of beams with correlations between radial position, momentum, and phase, as well as non-uniform intensity distributions. Additionally, radial cutting of beams by collimators was entered into the simulation. Including the dispersive effects of the 135° bend in the tip of sector magnet 1, phase and momentum information from the buncher model was used to generate a more realistic sample input beginning at the first acceleration gap of resonator 1.

Important results from simulations for SCL bunching are given in fig. 4. Figure 4a shows a "snapshot" of the beam (from above) at the azimuth of KIP2 (Θ=135°) on the first orbit. If KIP2 is placed at the radial location indicated by the horizontal broken line, the beam at Θ = 235° (at the second gap of Resonator 3) is as shown in fig. 4b (faint and solid lines). Notice the asymmetrical nature of the initial phase cut. The phase tails of this beam, when tracked to full radius will spread over such a large phase space volume that clean extraction becomes impossible. However, if a second cut is made using the new collimator RIL2, the simulation shows a well-defined pattern at extraction with a net acceptance of about 35% of the DC beam.

The effect that KIP2 only makes a clean cut for the leading phase edge and generates long tails for the lagging phases, occurs for DC beams and "mildly" bunched beams as well. Based on these results, a second phase cutting collimator was installed in injector 2. A quick solution was to mount a collimator block on an already-installed radial probe mechanism, labelled RIL2 in fig. 1.

Located at an azimuth of 250° it was near enough to a 90° betatron phase advance downstream from KIP2 to have the desired effects. Plenty of cooling power is required for RIL2; the simulations predict that for optimal phase selection the intensity cut away by RIL2 is approximately 1/3 of the extracted beam intensity.

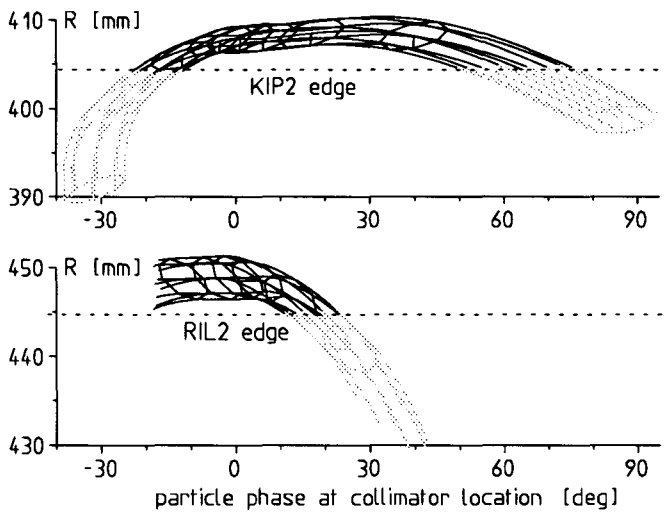


Fig. 4. **Phasespace cutting by the radial collimators KIP2 and RIL2 for a SCL bunched beam.** The radial and phase distribution of a simulated beam before (faint lines) and after (solid lines) being cut by KIP2 (135°) and by the new collimator RIL2 (235°).

5. RESULTS AND CONFIRMATION OF PREDICTIONS

Most of the beam measurements made to compare the simulations to the real beam behaviour showed a good agreement between measurements and simulations. The agreement was even better than could be expected taking into account the substantial simplifications used in the models. A critical point of the setup that had been predicted by the MATADOR runs was the radial focusing of the 870 keV beam in the first resonator and at the collimator KIP2. The beam optical behaviour of the 870 keV beamline was therefore analyzed in detail to establish the proper settings of optical elements. In this analysis the need to set the optics in a vertically dispersionless mode was detected. It can not be simulated by the one-dimensional buncher model, but is intuitively clear that if leading and lagging parts of a SCL bunched beam are bent onto different vertical positions the "braking" force is no longer acting in the longitudinal direction.

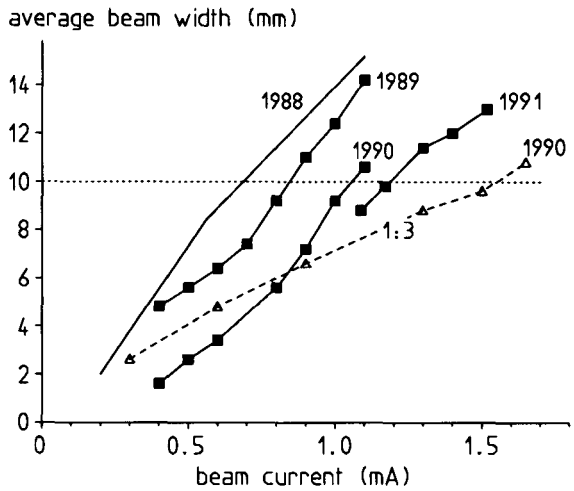


Fig. 5. **Average radial beam width at extraction vs. beam intensity.** The "wavefronts" progressing downwards and to the right indicate the best beam settings that could be achieved in terms of the high intensity and small beam width. The dashed curve (marked 1:3) represents equivalent intensities of beams where only one out of three pulses is accelerated. The critical value of 10 mm for the beam width marks the beam quality required for acceleration in the 590 MeV ring cyclotron.

An excellent overall test of the validity of these investigations is shown in fig. 5. Each line gives the correlation between the smallest beam width and the extracted beam intensity defined by a series of best beam setups in a particular period. The progress from 1988 to 1989 can mainly be assigned to the usage of the buncher with settings based upon simulations, but without the new collimator RIL2. The installation of RIL2 brought along the big progress from 1989 to 1990, where for the first time a beam of 1 mA was produced with sufficient quality for the ring cyclotron. Stabilizing the buncher phase, as well as the RF voltage and phase at high currents, gave another substantial improvement and enabled the extraction of 1.5 mA in 1991, again using a strongly bunched beam.

A direct measurement of a SCL beam, compared to an unbunched beam at the same high intensity is shown in fig. 6. Time structure information is obtained from counting protons elastically scattered on a thin carbon fibre placed in the beam. Several of these measurements taken for different radial positions of the fibre are combined to give a "top view" and a phase profile of the beam at extraction. The beam obtained with SCL bunching really shows a very narrow phase width beam of extremely high local current density.

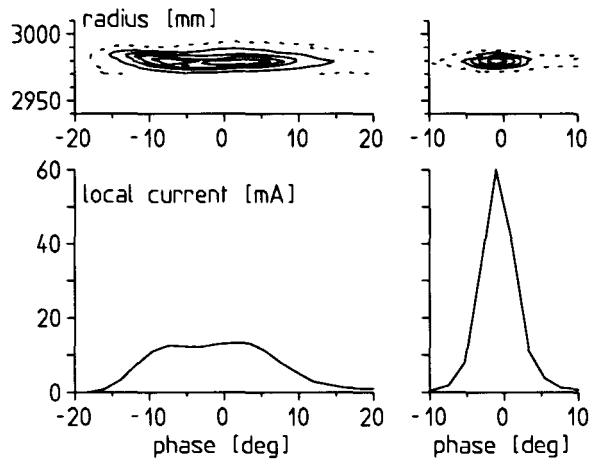


Fig. 6. **Measured phase width of two different beams at extraction.** Comparing the results of the radial and time structure measurements for an unbunched beam to the results for a SCL bunched beam show the high intensity narrow phase beam obtained with bunching. In both cases, the extracted intensity is 0.9 mA.

6. CONCLUSIONS

All of the above results support the conclusion that "space-charge-limit bunching" (SCL bunching) is in fact occurring in a manner substantially as discussed above and is a useful approach to increasing intensity without decreasing beam quality. Proper dispersion matching in the injection line and careful phase selection are necessary conditions for applying this technique. It is quite surprising that a such simple bunching model can give such good results. A full 6 dimensional simulation of this phenomenon may yield further useful predictions. The survival of such an intense beam, approaching 60 mA DC equivalent, through injector 2, challenges previous notions and simulations of space-charge effects under such conditions and warrants further investigation.

7. REFERENCES

1) Schryber, Urs, "Upgrading the PSI Accelerator Facility for High Intensity Operation." 3rd European Accelerator Conf., Berlin, 1992
2) Stammbach, Th., "Experience with the High Current Operation of the PSI Cyclotron Facility." this conference.
3) Baartmann, R., "SPUNCH - A Space Charge Bunching Computer Code." Proc. 11th. Conf. on Cyclotrons Tokyo, Japan. 1987, p. 283.
4) Adam, S., "Calculation of Space Charge Effects in Isochronous Cyclotrons." IEEE NS-32, 2506 (1985) and Thesis 7694 ETH Zurich. 1985.

AGOR : RECENT ACHIEVEMENTS

H.W.Schreuder *(for the AGOR staff)
Institut de Physique Nucléaire, 91406 Orsay, France†

ABSTRACT

The AGOR cyclotron, in construction since 1987, is now in the phase of field mapping and final assembly. The first results of the field mapping campaign are available. The construction of the RF resonators is nearly completed and the extraction channels will soon be ready for mounting in the machine. All subsystems are controlled by their dedicated section of the control system, the software for the central control consoles is being written.

1. INTRODUCTION

The major design parameters of the AGOR cyclotron, allowing acceleration of protons as well as heavy ions, have been presented previously.[1,2] Here, only the most salient design features will be briefly recalled. The two superconducting main coils produce the required level and gradient of the main field, without requiring polarity reversal. The main cryostat is designed to have a nearly unobstructed median plane, allowing radial insertion of the extraction channels. The RF resonators have no insulator and can therefore reach the frequency of 62 MHz, required for the acceleration of 200 MeV protons. The absence of an insulator implies that the resonators are placed in the machine vacuum. Beam extraction is done with an electrostatic deflector, followed by a room-temperature and a superconducting electromagnetic channel. A channel with superconducting quadrupoles provides focussing in the final traversal of the magnet yoke. A recent picture of the machine is shown in fig.1.

2. MAGNET AND CORRECTION COILS.

The magnet is constructed as a circular yoke consisting of 6 rings, in which upper and lower pole plugs are

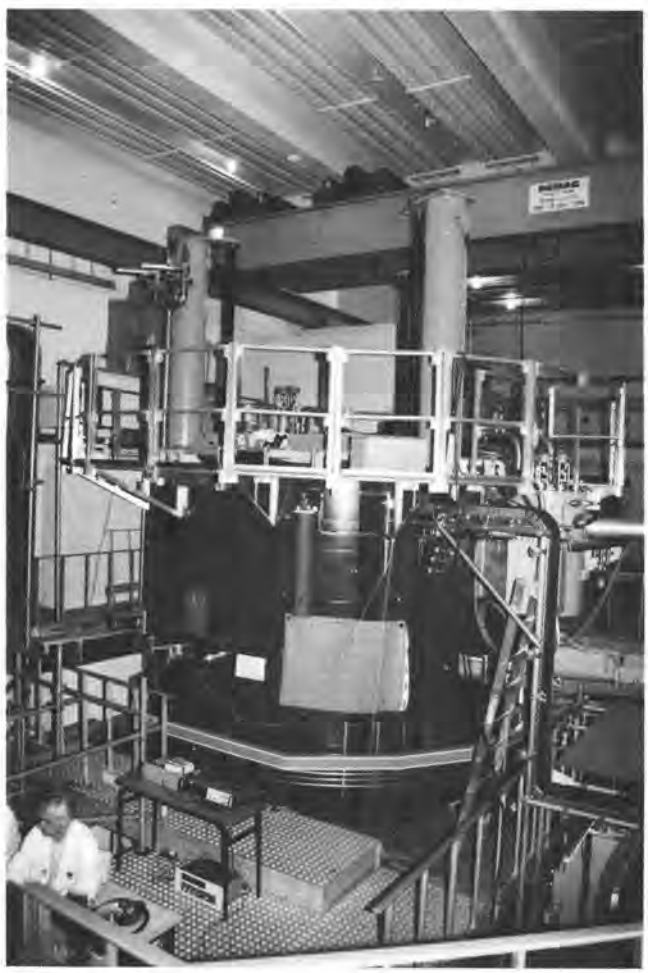


Figure 1. The AGOR cyclotron at the start of the field mapping campaign.

*permanent address: Kernfysisch Versneller Instituut, Zernikelaan 25, 9747 AA Groningen, Netherlands.
†Work jointly supported by the Institut de Physique Nucl'eaire et de Physique des Particules (IN2P3), France and by the Stichting voor Fundamenteel Onderzoek der Materie (FOM), Netherlands

inserted vertically. On the top and the bottom of the yoke lift mechanisms are permanently mounted. They are equipped with three motor-driven spindles for inserting and removing the poles from the yoke. The top pole can then directly be taken by the overhead cranes, the bottom pole lowers onto a rail-guided carriage, allowing sideways movement away from the yoke. When mounted, the position of the poles with respect to the yoke is defined by means of precision pins. Their coaxiality has been verified to be reproducible within approximately 0.01 mm after a significant number of removals and insertions. In the assembly hall, a motorized 'pole rotator' is used to select the proper up/down orientation of the poles for assembly operations.

The 15 correction coils are wound on the upper parts of the hill sectors and are made of water-cooled copper conductors, insulated with epoxy impregnated glass cloth. Figure 2 shows the lower pole, mounted in the yoke, equipped with correction coils. The radial arm of the field mapper is also shown. The power supplies for the correction coils have been installed and complete system tests have been performed in 1990.

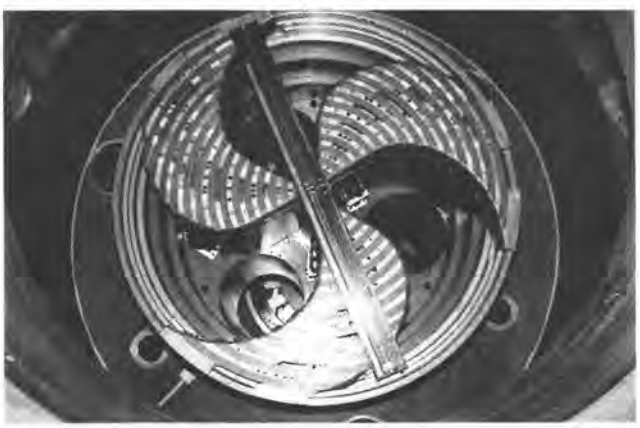


Figure 2. The lower pole with correction coils and field mapper.

3. MAIN COILS AND CRYOGENICS

The assembly of the main coils in their cryostat at the manufacturer Ansaldo (Genova, Italy) was completed in October 1991. Cooldown of the coils required 4 weeks, in agreement with expectations. The cooling rate was controlled for limiting the temperature difference between the warmest and the coldest coil to a maximum of 40 K in order to reduce stress in the coil impregnation due to shrinkage.

Factory acceptance tests were done in the first week of December when the heat input and the coplanarity and coaxiality of the two coil pairs were determined. The measured heat losses at 4 K and 80 K were 18 W and 70 W respectively and should be compared to the specified values of 12 W and 190 W. The coil position measurements were done with the coils at 50% of their maximum currents. In the absence of the magnet yoke, this excitation produces the maximum design value for the attractive force between the coils of 4.5 MN. The coplanarity and the coaxiality were found to be better than 0.1 mm each. Although the heat loss at 4 K is higher than specified, the cryostat and croils were provisionally accepted, after agreement had been obtained on improvements.

The system was finally delivered at the Orsay construction site on February 14, 1992, approximately 18 months later than the date foreseen in the contract.

Leak testing, assembly in the magnet yoke, cabling and cooldown proceeded without major difficulties, thanks to the dexterity of the assembly crew. Figure 3 shows the cryostat in the lower half of the magnet. Clearance between cryostat and yoke does not exceed 5 mm in any direction. The coils reached their operating temperature on May 12.



Figure 3. The cryostat, placed in the lower half of the yoke.

The liquid helium plant, centered around a TCF50 machine by Sulzer, has passed its final acceptance tests in 1991. Its nominal capacity is 600 W at 80 K, 50 W at 4 K while maintaining a helium liquefaction rate of

15 l/h. The installation is controlled through a PLC in which all standard operating procedures are programmed so that human intervention is not required for day-to-day operation of the cryostat and coils.

More details on the low-temperature tests on the coils are presented elsewhere in this Conference.[3)]

4. FIELD MAPPING

The field mapping operations will be performed in a number of sequential phases. In the first phase, the median plane field is mapped at 4 different field levels in order to determine the shimming required to optimize the currents in the correction coils. In a second phase, after completion of the shimming operations, the median plane field will be mapped for 25 sets of currents in the two main coils of the cyclotron. In this phase the field maps of the correction coils will also be taken. At the end of this phase the field produced by the extraction channel EMC-1 will be mapped, with special attention to its stray field in the region of circulating beam. Finally, in a third phase, the field along the injection axis will be mapped.

The design of the mapper for the median plane field has been inspired by the radial mapper used for measuring the field of the MSU K1200 cyclotron,[4)] and uses a radially moving search coil on a rotating arm. The height of the radial arm is only 16 mm, allowing field maps to be taken with the RF electrodes in place (of which only the central region noses have to be dismounted). This feature is important for the future transfer to the KVI: it will not be necessary to remove the resonators from the poles for allowing verification field maps to be taken after reassembly of the magnet.

The data acquisition software provides on-line error checking of the data in each radial series using polynomial functions in a sliding 5 cm interval around each measuring point. Tests using calculated field maps indicated that single errors of 2 mT can easily be detected and this is confirmed by experience gained with measured data. A suite of off-line data analysis routines has been readied well in advance. It allows spectral analysis, the production of contour plots, creation of difference maps, centering analysis etc.

As an example, fig.4 represents a spectral analysis of one of the first maps, taken at a central field of 2.2 T, at a radius of 0.8 m. Although erroneous data have not been corrected, the noise level is less than 1 mT.

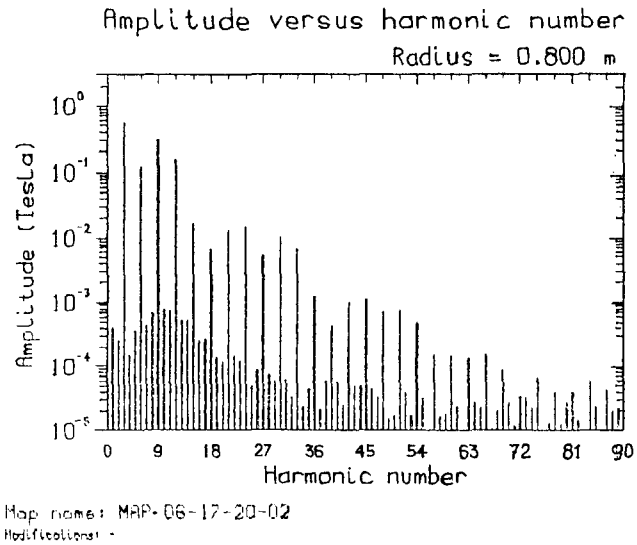


Fig.4. Measured field at $B_0 = 2.2\ T$: spectral analysis at r=0.8 m.

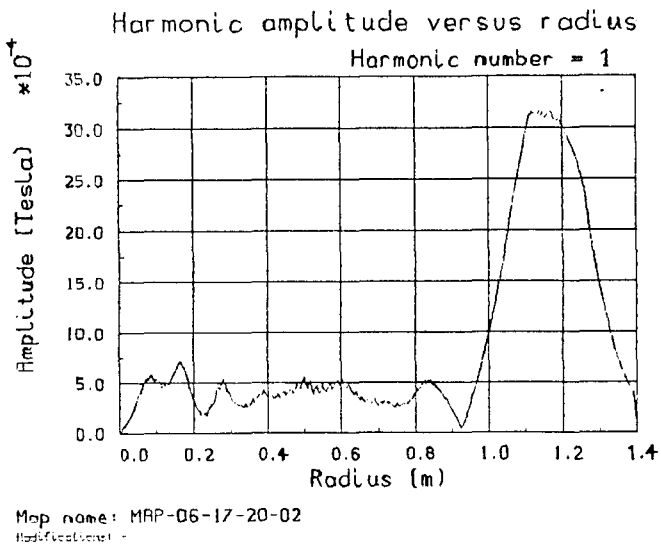


Fig.5. Measured field at $B_0 = 2.2\ T$: first harmonic amplitude as a function of radius.

Figure 5 shows the first harmonic amplitude as a function of radius derived from the same uncorrected data. The large peak at 1.2 m radius is caused by an as yet uncorrected centering error of the main coils of approximately 0.5 mm.

5. RF SYSTEM

The electrical design of the RF resonator system for the AGOR cyclotron and the building blocks for the stabilization of amplitude and phase have been described at a previous conference.[5)] Since then, the mechanical

design of the resonators and the RF liners - which are also vacuum lids covering the magnet poles - has been completed and their construction is now nearly complete. Figure 6 shows one of the vacuum lids (or RF liners) after final cleaning at the factory. The design required machining of electron-beam welds. This has resulted in a number of vacuum leaks that have been difficult to repair. The lids are fixed to the hill sectors by means of 13 BeCu bolts per sector, each, of course, having a vacuum cover. The picture also shows dust covers on the apertures for the phase probes. Near the centre the mounting holes for the three centring probes[6] are visible.



Fig.6. AGOR vacuum lid and RF liner.

The accelerating electrodes have been completed and have been fixed to the central conductors of the coaxial resonators. Figure 7 shows an interior view of one half electrode with its supporting frame and the mounting flange for a cryopump.[7]

The outer conductors and the positioning mechanisms for the short circuits have all been delivered on site. The drive mechanism for short-circuit positioning has been tested for reproducibility and position resolution. The results, better than 0.01 mm in both cases, were significantly better than the 0.04 mm specified contractually.

The three RF power amplifiers have been accepted after extensive tests at nominal power output. The regulation electronics for the three resonators have been built, as well as for the buncher in the injection beam line. Complete system tests have been performed on all regulation systems, using one of the power amplifiers and a test resonator. The measured amplitude stability was 1.2 10^{-4} and the phase was stable within 0.2 deg. The tests of the sliding RF contacts were satisfactory: the temperature rise at nominal current and at 60 MHz agreed with calculations as well as with extrapolations based on measurements at lower frequencies.

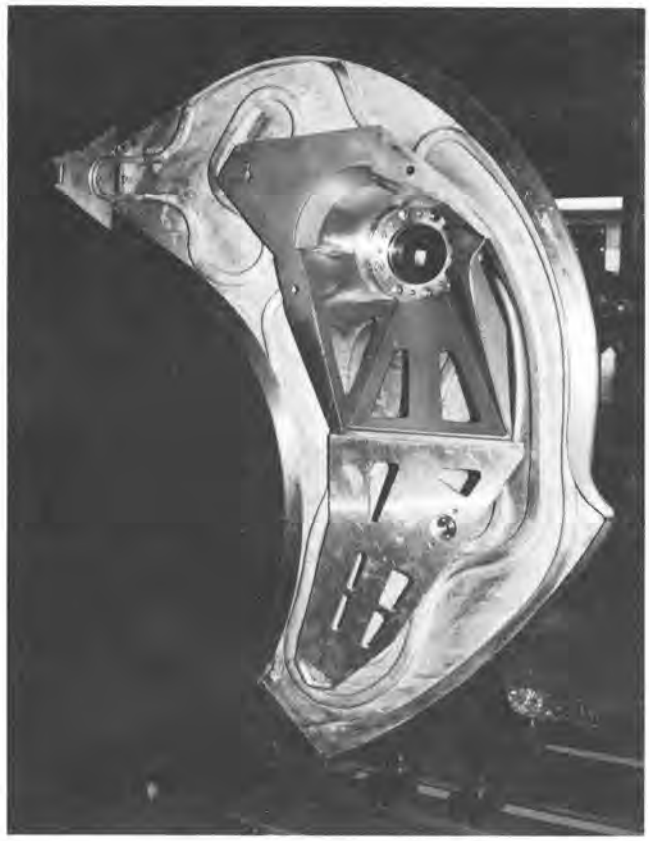


Fig.7. Interior view of acceleration electrode.

6. EXTRACTION

6.1. Overview

Beam extraction in the AGOR cyclotron is done via three deflectors and a focussing channel, shown in overview in figure 8. Beam deflection is achieved with an electrostatic deflector, an electromagnetic channel with water-cooled copper coils and an electromagnetic channel with superconducting coils. The two electromagnetic channels are provided with gradient coils for focussing. The quadrupole channel provides focussing and beam steering facilities before the beam enters the external beam line. All deflectors are inserted in the machine through radial apertures in the magnet yoke in the median plane. The machine vacuum is sealed with elastomer seals on one of the three large flanges in the median plane section of the cryostat.

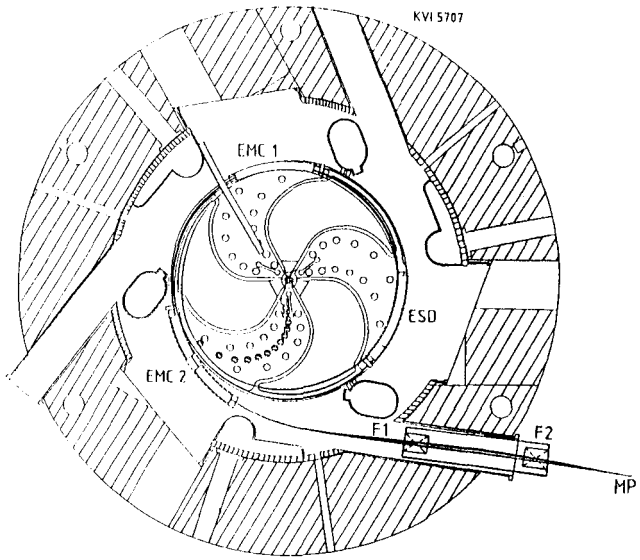


Fig.8. Midplane section of AGOR, showing location of the extraction channels.

When the channel is in place, a large fraction of the aperture in the yoke is closed with a wedge-shaped block of iron, in order to limit the reduction in yoke reluctance associated with the large radial hole. The blocks are moved into and from the magnet using a chariot on a set of rails. The same equipment is used for removing and inserting the channel.

6.2. Electrostatic Deflector

The electrostatic deflector* has two hinges, allowing adaptation of its shape to the variations of orbit scalloping with magnet excitation. The radial positions of the entrance, the exit and the two hinges can be adjusted through motor driven positioning mechanisms. Read back of the actual positions is done by means of potentiometers attached to the driven object itself, in vacuum. Similarly, hermetically sealed limit switches are attached to the moving parts in the machine vacuum. The field strength does not exceed 105 kV/cm over a 7 mm gap. Although these values are rather conservative, tests have been made to ascertain voltage holding capabilities. The high voltage feed-through , equipped with an internal damping resistor, was successfully tested in a set-up in a 0.4 T magnet. The same set-up was used to test the high voltage insulators. Finally, a short section, including a hinge, of the channel in its final transverse geometry was successfully tried, including hinge movement under full voltage. The channel is is construction at the IPN, Orsay and will be completed in September.

*the collaboration of R.Dubois (CERN) in the design is gratefully acknowledged

6.3. First Electromagnetic Channel EMC-1

The electromagnetic extraction channel EMC-1[2] has four water-cooled copper coil sets. Two of the coils are used to produce the deflecting field of up to 0.2 T and the focussing gradient of 13 T/m, the other two coils are used for long range and short range compensation of the stray field in the region of circulating beam. An optimisation code is used to calculate the currents in the two sets of correction coils in order to minimize the stray field at the radius of $\nu_r - 1$. Figure 9 shows an example of the median plane field obtained in this way. The field inside the channel as well as the stray field in the region of the circulating beam will be mapped.

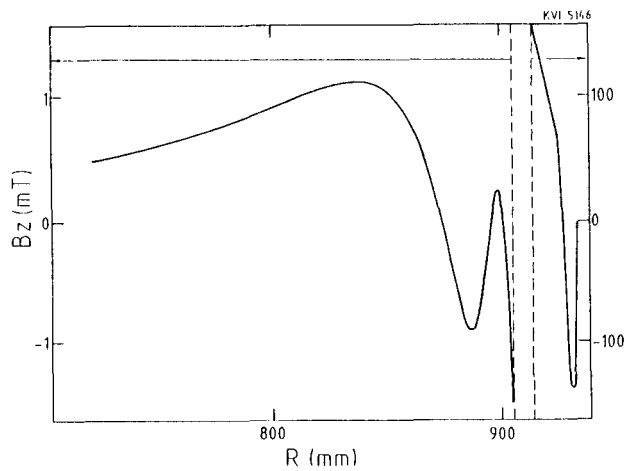


Fig.9. The radial field profile produced by EMC-1.

Since the available space is very limited, the available cross-sections for copper and for the hole for passage of the coolant are small. The smallest conductor has a size of 4×3 mm with a central hole of 2 mm diameter. The resulting current densities in the conductors are rather high: up to 144 A/mm^2 and the total power dissipation in the channel is 100 kW. Careful calculations have therefore been made on the cooling circuits, numbering 18 and mounted in parallel on single inlet and outlet manifolds, in order to have correct predictions for the water flow and the required water inlet pressure. The necessary flow can be obtained with a pressure drop of 22 Bar, produced by an additional high-pressure pump. The water velocity is in the range 8-11 m/s. The risk of cavitation occurring at these velocities was studied theoretically and experimentally[8] using the cavitation coefficient S as a parameter. This coefficient is given by the expression $S = 2(P - P_s)/v^2 \times r$ in which P denotes the local pressure, P_s the saturation pressure of the vapour, v the velocity of the flow and r the density of the fluid. Measurements, using a microphone to detect the noise of cavitation, have shown that cavitation occurs for $S < 8$. It was therefore decided to adjust the pressure drop in each of the hydraulic circuits by means of inserts at the outlet, raising the water pressure inside the channel. The resulting safety margin in the parameter S is

at least a factor 2 for all circuits. The channel has been completed and is illustrated in fig.10 and fig.11, showing the complexity and the density of conductors and water tubes.



Fig.10. EMC-1: Overview of the completed channel.

Because of the high power dissipation, the time available for reacting to a sudden loss of coolant is limited to approximately 0.5 s. Apart from standard securities such as flow switches, pressure surveillance and thermal switches in the water outlets, two additional interlocks have been introduced. An analog temperature measurement using thermistors provides a continuous surveillance of the water outlet temperature, and creates an interlock signal when a predetermined limit is exceeded. In addition, the power supplies have an internal interlock based on measurement of the load resistance.



Fig.11. EMC-1: Detail of conductor lay-out at the channel exit.

6.4. Second Electromagnetic Channel EMC-2

The design of AGOR's second electromagnetic channel EMC-2 has been described at a previous conference,[9,10] and a detailed description of its construction is presented elsewhere in this Conference.[11] The channel is built in two hinged sections, having identical conductor geometries. The optical axis are circular arcs with lengths of 17.5 degrees and having slightly different radii. The beam aperture is 16×12 mm. There are three coils: the first produces a field drop of up to 0.4 T, the second produces a focussing gradient of up to 22 T/m and the third produces a compensatory field at the location of the circulating beam. Positioning of the channel is done by three motor driven rods located at the entrance, at the swivel joint and at the exit of the channel. Inside the channel bore, a shielding tube intercepts beam particles that would otherwise be lost on the 4 K winding mandrel of the coils. This tube is cooled with gaseous helium to a temperature of approximately 10 K, at least 10 W of beam power can be dissipated without the superconducting coils going normal. The channel is surrounded by a thermal shield, nominally at a temperature of 80 K. The channel is situated in the machine vacuum so that no superinsulation could not used. The thermal losses are estimated to be 3 W at 4 K and 10 W at 80 K, apart from possible beam loss. The superconductor is NbTi in copper and is used at up to 40% of the critical current. The coil mandrels and the superconducting coils are nearing completion at the Low-Temperature group at the University of Twente (Netherlands), assembly with the support structure and the positioning mechanisms as well as cryogenic and vacuum tests will be done by Leybold (Netherlands), who are expected to deliver the channel at the Orsay site in September 1992.

6.5. Focussing Channel

The focussing channel[12] is the final element of the AGOR extraction system. It consists of two focussing elements equipped with superconducting coils, located in the tangential hole in the magnet yoke for passage of the extracted beam. Their maximum gradient is 36 T/m over an effective length of 0.20 m. The conductor configuration is shown in fig.12, which also shows the soft iron tube shielding the extracted beams from the magnetic field, which reaches 0.22 T at the maximum central field of 4.05 T.

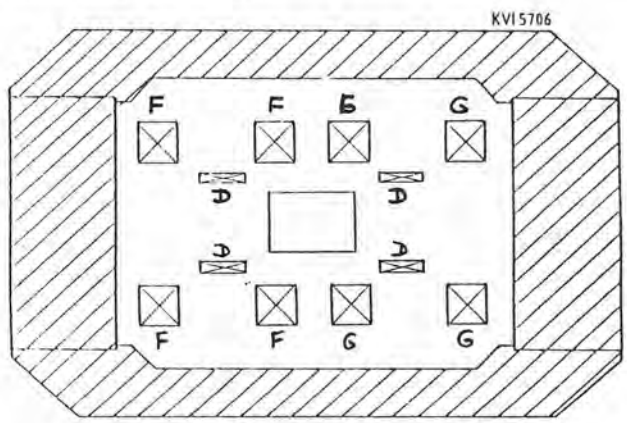


Fig.12. Cross-section of the focussing channel at the location of the first active element. F and G are gradient coils, D indicates dipole coils

The first lens has an additional dipole coil for horizontal beam steering. In both lenses, 2.5 mrad of vertical steering can be obtained by disequilibrating the currents in the upper and lower coils. Beam profiling harps at the entrance and exit provide positioning and steering information.

7. PROJECT STATUS

Important delays in the construction of two major subsystems, the superconducting coils and cryostat and the RF resonators, have retarded the initial project schedule by approximately one year. However, field mapping is now foreseen to be completed in September and assembly of the RF resonators on the magnet poles will then start. Next on the main line of our planning are vacuum installation and tests and RF measurements and tests. We hope to be able to start beam tests at Orsay in June 1993. In the mean time, the K160 cyclotron, in regular operation at the KVI since 1972, has been decommissioned on January 24 and is being dismantled. The beamlines and the experimental equipment have been taken away and the shielding in the experimental hall is being rearranged and reinforced. Installation of the AGOR beam lines, described elsewhere in this Conference,[13] and experimental set-ups will start this fall. Disassembly of AGOR will start on completion of the beam tests in Orsay, in mid-1993. The interleaving of this operation with transport to Groningen and reassembly is intricate, since we do not have a large area for intermediate storage. In any case, the parts last to be disassembled will be the first to be required on the assembly site. This is painfully true for the overhead cranes. The entire operation of moving the cyclotron is scheduled to be completed in 16 months.

8. REFERENCES

1) S.Gales, "AGOR, a Superconducting Cyclotron for light and heavy Ions," in **Proceedings of the 11-th International Conference on Cyclotrons and their Applications** (Ionics, Tokyo, 1987) p.184.
2) H.W.Schreuder, "The AGOR Cyclotron past the half-way mark" **Proceedings of the 12-th International Conference on Cyclotrons and their Applications** (World Scientific, Berlin, 1989) p.21.
3) K.Pieterman et al, "Low-temperature Tests of the AGOR Cryostat and Coils" in these Proceedings.
4) L.H.Harwood, J.A.Nolen, "Plans for Magnetic Mapping of the NSCL K800 Cyclotron Magnet. " in **Proceedings of the 10-th International Conference on Cyclotrons and their Applications** (IEEE, East Lansing, 1984) p.101.
5) S.Brandenburg et al., "The RF System of the Superconducting Cyclotron AGOR" in **Proceedings of the 12-th International Conference on Cyclotrons and their Applications** (World Scientific, Berlin, 1989) p.197.
6) B.Laune et al., "The diagnostics system for the AGOR superconducting Cyclotron" in these Proceedings.
7) S.Bühler, A.Horbowa, "The AGOR Cryopumps" in **Proceedings of the 12-th International Conference on Cyclotrons and their Applications** (World Scientific, Berlin, 1989) p. 224.
8) E.Martin et al. "Etude technologique de l'ensemble canal electromagnetique d'extraction EMC1 du cyclotron AGOR" **AGOR technical note NT/EXT/01/10/91** (in french).
9) S.Gustafsson, "A Superconducting Extraction Channel for AGOR" in **Proceedings of the 12-th International Conference on Cyclotrons and their Applications** (World Scientific, Berlin, 1989) p.354
10) K.Pieterman et al., "A Design Study for a superconducting Extraction Element for AGOR" in **Proceedings of the 12-th International Conference on Cyclotrons and their Applications** (World Scientific, Berlin, 1989) p.358
11) K.Pieterman et al., "The AGOR Superconducting Extraction Channel EMC-2," in these Proceedings.
12) H.W.Schreuder et al. "Superconducting quadrupole channel for the AGOR Cyclotron" in these Proceedings.
13) J.M.Schippers, "The Beam-Guiding System of AGOR." in these Proceedings.

THOUGHTS ON DECOMMISSIONING THE CERN SYNCHRO CYCLOTRON

Glen Spinney

European Organization for Nuclear Research,
1211 Geneva, 23, Switzerland

ABSTRACT

Solutions proposed on the decommissioning of the CERN Synchro-Cyclotron and thoughts on the construction of future accelerators which in use will become radio-active and which eventually will need to be dismantled to enable their disposal according to the prevailing safety requirements.

1. GENERAL

After 33 years of loyal and active service the 600 MeV CERN Synchrocyclotron (S.C.) was closed down at the end of 1991. Discussions took place concerning the decommissioning and initially it was hoped to start towards the end of 1991 or early 1992, but due to financial restraints it has only been possible to remove the beam lines, including the trolleys upon which they have been built, from the neutron side of the machine. However, in carrying out this work, one of the principal radioactive hot-spots, the electro-mechanical channel has been removed

2. DESCRIPTION

The S.C. machine consists of a conventional 2500 tonnes magnet assembly encompassing a large stainless steel vacuum tank welded to the pole pieces of the magnet. Inside the vacuum tank are the beam control, measurement and beam extraction units : kim coil, regenerator, magnetic channel, electromagnetic channel probe target, diagnostic targets, internal targets, small dees and the accelerating electrode (dee) of the RF system.

External to the vacuum chamber is the vacuum pumping system, the ion source and beam limiter mechanisms. Running on rails between the S.C., and the neutron room were three beam lines (the 125 MeV, 70 MeV and muon) and the electromagnetic channel. It is these latter which have been removed.

3. CONSIDERATIONS

The S.C. was not constructed to be readily dismantled the vacuum tank being welded to the magnet pole pieces and there are also several highly radioactive areas which need special consideration.

It was essential that a decommissioning programme be prepared and in doing so several problems that had not been considered during the construction and exploitation of the S.C. were encountered, to which solutions must be found. The disposal of radioactive waste also needed careful attention.

The two main problems are the induced radiation and/or contamination of major parts of the installation and the need to physically seperate the vacuum tank from the magnet assembly. A subsidiary problem is that all the large steel blocks forming the magnet yoke are tack welded together as well as being bolted.

3.1 Induced radiation

The possibilities for the disposal of radioactive items are governed by the level of the induced activity. At CERN anything below 2 Bq/g is considered non active, between 2 and 40 Bq/g slightly active, between 40 and 400 Bq/g active and over 400 Bq/g highly active. Non-active in this context means that a single piece shall nowhere exceed 2Bq/g and is the limit accepted by the Swiss Authorities for the unrestricted release of scrap. Slightly active items would normally be stored locally until they decay to less than 2Bq/g or be reused. Recently, an alternative possibility, available in France and Germany, is the controlled melting of slightly active steel scrap of less than 74 Bq/g allowing its conversion into shielding blocks at a cost of 4-5 SF/kg. Ref. 1.

Both active and highly active items may be reused in controlled radioactive areas or reduced to a convenient size and placed in concrete containers acceptable to the appropriate Swiss Authorities before they can be considered for disposal at the radioactive waste depository in Switzerland.

The problem of induced radioactivity is created by the presence of long lived radionuclides. The majority of which have half-lives of several years. It has been estimated that one would have to wait until the year 2079 before the specific activity falls below 2 Bq/g. The dose rates inside the vacuum tank and in other areas preclude their dismantling other than by remote procedures.

3.2 Vacuum tank removal

The second problem is the removal of the vacuum chamber, welded to the pole pieces. Should one remove this weld it would still not be possible to withdraw the vacuum chamber in one piece, as the highly active pole pieces protrude inside the vacuum tank. It is therefore necessary to cut up the vacuum chamber in sufficiently small pieces to facilitate their removal and at the same time be small enough to be accepted in the concrete radioactive waste disposal containers. It is a process which

will have to be carried our remotely and as some of the walls of the vacuum chamber are 60 mm thick investigations have been carried out on suitable cutting techniques. Methods investigated have been flame cutting, oxy-arc cutting, arc water jet, arc saw cutting, plasma arc cutting, laser cutting and abrasive water jet cutting.

3.2.1 Flame cutting

A burning process consisting of a torch assembly using a mixture of oxygen and usually acetylene gas. The workpiece is preheated by the acetylene flame and when the oxygen is turned on, the metal is burnt away. Cutting ferrous metals presents no specific problem but for non-ferrous metals such as stainless steel, a special technique is necessary. When cutting stainless steel, refractory oxides, with melting points higher than the torch temperature, are formed. However, iron or iron/aluminium in a flowing mixture can be introduced at the torch nozzle to increase the flame temperature enough to melt the refractory oxides and permit the cutting of the stainless steel. The cutting speed is high, even for thick metals, and the torch has a long life; a disadvantage is that the distance from the nozzle to the workpiece is relatively precise.

3.2.2 Oxy-arc cutting

This process uses a hollow rod electrode and an oxygen jet supply. After touching the workpiece, an electric arc is established, the material melts and the kinetic energy of the oxygen jet removes the melted material. It is a simple and cheap process which suffers from the fact that the electrode has to be changed rather frequently.

3.2.3 Arc saw cutting

This is a circular toothless metallic blade which can be used to cut any conducting material without touching the workpiece. The blade rotates at between 300 and 1800 revolutions per minute facilitating the cooling of the blade and the removal of the molten material. The cutting action is obtained by means of an electric arc between the rotating blade and the material being cut. Thick sections can be cut at high speed but as the blade is normally of the order of 1 meter in diameter, it is extremely heavy and cumbersome and very expensive.

3.2.4 Arc water jet

This consists of a consumable electrode surrounded by a water jet. The electrode touches the workpiece and melts the material and the water jet removes the molten material. It is a relatively cheap and efficient method and can handle large thicknesses but suffers from the fact that the electrodes have to be changed regularly and provision has to be made for water recuperation, which could possibly be radio-active.

3.2.5 Plasma arc cutting

A gas, which is introduced into an electric arc and is constricted by a thermal and magnetic pinch, produces a plasma at approximately 8000°C. The material melts and the kinetic energy of the gas removes the molten metal. It is possible to cut thin sections at high speed but will not handle thick sections.

3.2.6 Plasma arc saw

This process is being developed by the German Government. Several plasma torches are fixed on the periphery of a rotating disc and are oriented in slightly different directions. The blade is rotated at low speed permitting the cutting of very thick metal up to 300 mm. Ref. 2.

3.2.7 Laser cutting

Lasers have been used, especially underwater, to cut extremely thick sections (at least, 1 meter) but they are too bulky and expensive.

3.2.8 Abrasive water jet

A small diameter high velocity water jet and a stream of solid abrasives are introduced into a specially shaped abrasive jet nozzle from seperate entries. Part of the water jet momentum is transferred to the abrasives, whose velocity increases rapidly. This equipment can be used to cut both metal and concrete but is is extremely expensive and the water/abrasive mixture has to be recuperated. It also has a short nozzle life.

3.2.9 Recommendation

After careful consideration, it has been recommended that flame cutting will be used to cut up the CERN vacuum tank and special equipment will need to be designed to retain the torch at an optimum distance from the workpiece.

3.3

Other problems, not without their own importance, are the lack of up-to-date drawings concerning the mechanical assembly of the machine and the fact that equipment used to assemble the S.C. after its reconstruction about 15 years ago, has been destroyed in the interim period. This includes a moving overhead crane in the S.C. building which was dismantled some years ago to facilitate handling in the machine vault - one crane still remains but two are essential for removal of the heavy and cumbersome elements. The grinding away of the yoke element welds will be time consuming and dirty work in a radio-active environment.

4. REFLECTIONS

Finding solutions for these problems at the decommissioning stage tends to be rather more difficult than if, at the design stage, more thought had gone into some of what are typical pit falls.

A safety series published by the International Atomic Energy Agency lays down guide lines concerning all aspects of the decommissioning procedure. Ref. 3.

Every installation one day reaches the end of its useful life and its ultimate fate is either demolition or leaving it to decay (in the radioactive sense). the responsibility rests with the owner for its demolition but more and more Local Authorities and Central Government are insisting that appropriate provision for an orderly and controlled demolition be included in the initial design before allowing planning consent. This particularly applies to electrical power station construction but one can imagine that before long it will become the routine for all similar installations.

In most cases what is needed for efficient demolition is the preservation of adequate information of the original design and its subsequent history. It is also adviseable, even at the design stage to involve a reputable company (or in-house service if available) versed in industrial demolition and decommissioning..It is absolutely essential that the decommissioning operation be planned in outline in advance so that it can be integrated in a way which optimises both safety and costs. Although such a programme could well enhance its selling possibilities in a commercial organisation, it must be remembered that deconstruction is hardly ever the simple reverse of construction.

Not only are complete records of the construction require, supplemented by copious photographs taken during the construction and afterwards, covering every detail required, but also full listings of the isotopic composition of all materials used in the radioactive zones are necessary. All these records must be in a permanent form, since they may remain unused for often 30 years , but they must also be correctly archived and catalogued.

As the timing for the decommissioning cannot be determined at the design stage, it is necessary to think in terms of durable building construction, reliable ventilation, heating, protection systems etc... even if more expensive at the outset, as after the installation has been shut down, the period between this time and decommissioning could be of the order of several tens of years and maintenance must be reduced to a minimum over such a long period.

In the case of shielding, there is a clear case for trying to maximise the amount of mobile shielding used around a machine. One reason is that it gives more flexibility for modifications to machine or beam line layouts during the normal operation of the machine and secondly at the decommissioning stage, it facilitates the removal of the maximum amount of shielding, without the use of pneumatic hammers, and in doing so reduces the amount of exposure time for personnel in radioactive zones. Consideration should be given to the provision of shielding on the outside of a building, allowing more internal space. Care, however, should be taken to ensure that the seismic design requirements are achieved.

Prestressed concrete is often impossible to distinguish, visually, from ordinary reinforced concrete. It is not unusal to stress up horizontal beams in two seperate stages. The first degree of prestress is applied to the tensile side of the beam to enable it to carry part of its load. As the construction proceeds and the load on the beam increases, the pre-stress is correspondingly increased. Accidents have occured during demolition whereby beams have suddenly and unexpectedly failed upwards, to the great danger of the demolition workers. A much more common accident is the unexpected effect of attempting to cut up a pre-stressed concrete beam believing it to be ordinary concrete . It is thus absolutely necessary that permanent records be kept of this type of construction.

5. CONCLUSION

5.1 Decommissioning a radioactive apparatus should start at the design stage.

5.2 Special attention should be taken in the initial design to try to facilitate the ease by which such a construction can be dismantled.

5.3 Adequate permanent records should be kept up to date concerning all aspects of the construction, including the building.

6. REFERENCES

1. The decommissioning of the CERN synchro-cyclotron. A preliminary report.
B. Allardyce, G.F. Spinney and J.W.N. Tuyn. CERN TIS/RP/TM/90-22, PS 90-57 (S.C.)

2. Cutting techniques Developments Friedrich-Wilhem Bach University of Hanover. Decommissioning of Nuclear Installations edited by Pflugrad. Bisci Huber and Skupinski published by Elsener Applied Science London.

3. The regulatory Process for the decommissioning of Nuclear Facilities published by the International Atomic Energy Agency Vienna 1990

PARAMETERS, PRESENT STATE AND APPLICATION PERSPECTIVES OF THE U-250 CYCLOTRON

A.I. Muminov
Institute of Nuclear Physics, Tashkent, Republic of Uzbekistan

and

M.F. Vorogushin
D.V. Efremov Scientific Research Institute, St. Petersburg, Russia

ABSTRACT

Design features of the basic elements of the U-250 multipurpose isochronous cyclotron – magnetic structure, ion source, vacuum and RF systems, beam extraction and beam transport systems – are described.

Possibilities for further sophistication of cyclotron design and those for further extension of mass over charge state ratio range of accelerated ions along with increasing their attainable energies using new type ion sources have been analysed.

1. INTRODUCTION

Modern cyclotrons, first of all isochronous ones, enable beams of accelerated ions to be obtained in a wide range of atomic masses and energies. In constructing the multipurpose U-250 cyclotron the most optimal approaches have been used which stemmed from experience gained at the Laboratory of Nuclear Reactions of JINR in designing, manufacturing and heavy ion accelerating on the U-200 and U-400 cyclotrons.

Designing and manufacturing of the U-250 cyclotron is carried out at the NIIEFA. The isochronous cyclotron U-250 is intended for accelerating ions with $A/Z = 2 \div 6$ to the energy over Coulomb barrier and those with $A/Z \leq 10$ to energies 1 to 2 MeV/amu. Maximum attainable energy of accelerated ions will comprise 204 Z^2/A. Beam energies and intensities for the U-250 are presented in Table 1. This cyclotron is planned to be installed at the Institute of Nuclear Physics in Tashkent (Republic of Uzbekistan). Given below is a description of the U-250 design features and a review of the scope of the applied and fundamental research planned.

2. DESIGN FEATURES OF THE U-250

The main problems related to the development of heavy ion cyclotrons are: necessity of controlled field – frequency variation in a wide range, utilization of acceleration modes based on integer harmonics keeping acceleration conditions and orbit centering satisfied for all the set of ion species; obtaining and maintaining of operational vacuum in the particle acceleration zone.

Configuration of the accelerator has been chosen to be typical for cyclotrons developed at the NIIEFA: H-shaped electromagnet, vacuum chamber between poles is to be constituent part of the magnetic structure; double Δ shaped resonance system with panel frequency tuning, axial introduction of the internal ion source.

The main parameters of the U-250 are given in Table 2, the lay-out of the cyclotron facility equipment is shown in Fig. 1.

3. MAGNETIC STRUCTURE

Magnetic structure of the cyclotron involves H-shaped electromagnet, two 100 mm thick pole disks which are parts of the vacuum chamber lids, four pairs of pole sectors, two main magnetizing coils and correcting windings.

Electromagnet consisting of upper and lower girders, two uprights and two conical cores made of armco-type steel, girders and uprights being of welded structure made of 30 mm thick sheets, and core's disks and sectors being made of forged pieces.

The heaviest bulk unit of the electromagnet weighs not more than 30 tonnes. Sectors providing magnetic field azimuthal variation have straight edges and angular extension of 45°.

With two main magnetizing coils of 170 turns each the current is 900 A, cooling water consumption flux is 60 litres/min. Seven groups of correcting coils positioned in the valleys are intended for correction azimuthal magnetic field lower harmonics and regulation of the radial field profile for obtaining isochronic dependence.

4. VACUUM

Vacuum chamber of dismountable structure consists of two soldered hexagonal covers and six uprights between the latters. Side walls of the chamber made of non-ferric steel have holes for joining resonance system, vacuum pumps, three diagnostic probes and beam extraction system. Internal surface of the chamber at points where piston rods and resonance system dees are

mounted are plated with copper sheets with water cooling tubes soldered to them.

Total volume of the chamber and both resonance systems amounts to 8.5 m^3, total released gas flux involving properties of used construction materials being estimated to be $5 \cdot 10^{-4}$ m^3 Pa/sec. (It does not include the ion source gas flux.)

Taking into account heavy ion charge exchange cross section in the residual gas, operational pressure in acceleration area is estimated to be in the $(5 \div 10) \cdot 10^{-5}$ Pa limits depending on the type of ions accelerated.

Calculation of spatial pressure distribution was carried out under the assumption that incoming gas flux from the source of light ions comprised 3 cm^3/min with that for heavy ions 0.3 cm^3/min, pumping out rate for all the system being assumed to be 12 m^3/sec. Under these assumptions acceleration of light ions will occur practically without losses and those for 8-fold charged state argon and krypton will amount up to 35% and 60%, respectively. The above pumping out rate can be provided by commercial diffusion oil pumps. Two pumps of 5 m^3/sec pumping speed connected directly to the vacuum chamber and two pumps of 1 m^3/sec pumping speed connected to resonance system. Two additional "getter" pumps of 2 m^3/sec pumping speed can be installed on the vacuum chamber by design in order to pump out active gas.

It should be noted that the small gaps of the electromagnet and the use of internal source with gas release can cause serious difficulties in obtaining proper vacuum.

5. ACCELERATION AND RF SYSTEM

Acceleration of a given set of ion species on the U-250 requires controlled variation of the accelerating frequency within 8 to 19 MHz range. In the cyclotron an acceleration system has been designed which involves two identical resonance systems with 42° angular extension dees positioned in diametrically opposite valleys. Each resonance system consists of the resonator tank, dee rod frequency tuning panel operating automatically, adjusting device and an automatically frequency tuning trimmer. The whole resonance system is mounted on a movable cart on rails providing convenience for dismounting, repairing and assembling.

Resonator tank has 1.5 × 1.2 m rectangular cross section and length of 2 m. It is made of bimetal steel-copper that simplifies the construction and reduces gas releasing surface area. Stiffening hollow ribs are soldered to the external sides of the tank's wall which serve at the same time as channels for cooling water. The hole in the side wall of the tank covered with removable copper bars is intended for panel mounting followed by joining vacuum pump.

One end of the dee rod of rectangular cross section is attached to the movable flank of adjusting device placed at the rear wall of resonator tank, the other end being attached to the dee.

Possibility of dee tuning relative to both dee rods and (together with dee rod) resonance system tank is provided.

Frequency variation is accomplished by changing the gap between dee rod and movable panels. Each panel consists of three parts attached to the tank and linked with each other with flexible copper contacts. Each link consists of stiffened soldered carcas and cooled copper cladding. The estimated RF losses at dee voltage amplitude of 75 kV and frequency of 19 MHz amount to 73 kW, maximum linear current density on contacts not exceeding 60 A/cm.

Autonomically excited RF generator is assembled by conventional configuration: commercial frequency synthesizer-aperiodic amplifier of 40 W, power-amplifier with distributed parameters of 2.5 kW power on each of the two tracts and 2 final cascades with maximum power of 100 kW each.

Final stage of the generator is located closely to the resonator tank; RF power supply is accomplished by means of conductive connection mode.

6. ION SOURCE

In order to obtain a set of ion species required two types of ion sources are assumed to be used. For acceleration of H, D and helium ions an ordinary conventional source with (pening) discharge will be used and for injection of heavy ions a compact multicharge-state ion source will be installed which is similar to that developed at the LNR of JINR with arc discharge and open magnetic trap.

For centering initial orbits and attaining required ion beam intensities puller will be able to be shifted on the pulling out dee and on the ion source tip. Shifting will be accomplished remotely without damaging vacuum.

Note that today's progress in generation of multicharged ions based on RF heating, ECR, laser sputtering of the working agent allows hope for obtaining highly charged ions and arranging external injection of particles into the U-250.

7. BEAM EXTRACTION SYSTEM

Beam extraction from the U-250 cyclotron will be mainly accomplished by their stripping on the carbon foils. This method is the most effective for relatively light ions (extraction coefficient is close to 100%) since it enables one to decrease considerably induced activity level inside the accelerator thus essentially improving its operation reliability and maintenance conditions. Along with stripping, the method of electrostatic deflector and passive magnetic channel are presumed in those modes of heavy ion acceleration when stripping method cannot provide high extraction efficiency and quality of the extracted beam.

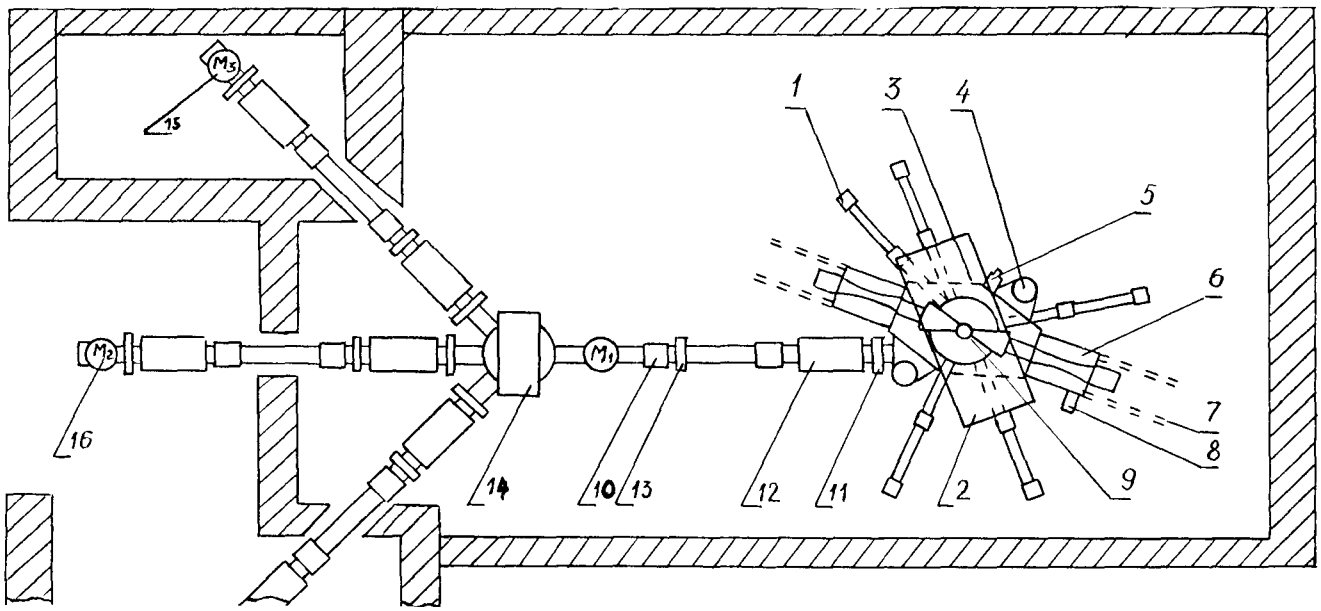


Fig. 1. Lay-out of the cyclotron facilities: 1 – probes; 2 – main magnet; 3 – vacuum chamber; 4 – deflector; 5 – chamber pumps; 6 – resonance system; 7 – final cascade of the RF generator; 8 – ion source; 9 – correcting magnet; 10 – electromagnetic lenses; 11 – diagnostic system; 12 – beam port pumps; 13 – chamber for isotope production; 14 – bending magnet; 15 – chamber for basic research; 16 – chamber for applied researches.

Table 1. Beam parameters of the U-250

Type of ions	Energy, $\frac{\text{Mev}}{\text{nucl}}$	Total energy, Mev	Beam current, μA	Extraction efficiency, %
Protons p (under acceleration of $^2H^{1+}$)	41.5	41.5	800	100
Deutrons d (under acceleration of $^2D^{1+}$	12.5	25	500	100
Deutrons d (under acceleration of DH^{1+}	22.5	45	500	100
$^4He^{1+}$	12.5	50	500	100
$^3He^{1+}$	22.5	68	500	100
$^{12}C^{3+}$	12.5	152	50–70	100
$^{14}N^{3+}$	9.4	132	70–100	80
$^{16}O^{4+}$	12.5	203	50–60	100
$^{20}Ne^{5+}$	12.5	254	10–20	60
$^{40}Ar^{7+}$	6.2	248	5–10	50
$^{40}Ar^{8+}$	8.2	328	1–2	60–65
$^{48}Ca^{8+}$	5.7	340	1	40
$^{56}Fe^{6+}$	2.3	131	10	30
$^{58}Ni^{6+}$	2.2	127	10	30
$^{84}Kr^{8+}$	1.9	155	4–6	25

Table 2. The main parameters of the U-250.

1. Magnetic structure	
Diameter of the main magnet	
yoke, cm	270
pole, cm	250
average field strength, T	1.9
gaps between poles	
between hills, mm	26–46
between valleys, mm	150
Power:	
main coil, kW	165
additional coil, kW	35
Weight (steel), tons	385
Weight (aluminium coil), tons	5.4
2. RF system	
Number of dees	2
Dee angular extension, °	42
Beam-limiting aperture, cm	2.5
Frequency range, MHz	8–19
Operation harmonics	1, 2, 3, 4
Dee voltage, kV	75
RF power, kW	150
3. Cyclotron	
Total dimensions, m	7×10×4
Total weight, tons	420
Total power, kW	800

8. BEAM TRANSPORT SYSTEM

The lay-out of the main technological areas of the cyclotron facility is shown in Fig. 1. The beam of accelerated ions is ejected into beam port through a 130 mm aperture and focused by a pair of quadrupole lenses and enters either the target chamber M1 or the tuning magnet. After the magnet the beam is transported to experimental chambers M2, M3. Conventional quadrupole lenses are used as focusing elements in the beam line. For extracted beam tuning standard type magnets are utilized.

Beam tuning and transporting system enables one without noticeable losses in intensity to have accelerated ion beam currents at the target site up to several hundred microamperes, angular divergence and energy spread not exeeding 0.3 and 1%, respectively. Beam parameter control is carried out by beam profile transducer.

In a working state vacuum (up to 10^{-4} Pa) in the beam port is provided by vacuum pumps with polyfenilethyr for oil-free pumping out.

The main chamber (M1) and chambers M2 and M3 (for fundamental research in nuclear physics and research in applied nuclear physics, respectively) are heavily shielded to provide radiation protection of the personnel when experiments are carried out with light ions at beam current values up to 800 μA. The experimental areas have been laid out in such a way that there is always possibility to carry out maintenance, check-up and adjusting operations at any experimental site.

Isotope production on an external beam considerably simplifies a number of problems related to target cooling in the main chamber.

At present works on production isotopes, such as ^{131}I and ^{57}Co, for example, are carried out at INP using the research reactor and the U-150 cyclotron.

With the U-250 accelerator put into operation it becomes possible to produce short-lived ^{123}I. ^{123}I has considerable advantages: it gives less patient radioactivity dose and provides better contrastivity of the radiograms.

Preliminary estimates suggest that using the U-250 cyclotron facilities such large amount of ^{123}I can be obtained which is enough for medical examination of several thousand patients yearly. ^{123}I is also applicable for examining kidneys, thyroid glands, for diagnosing cancer at its initial stage, for examining risk (suspected) groups. Using the same facilities ^{201}Tl isotope which nowadays is succesfully applied for early diagnostics of infarcts and for other medical purposes can also be produced.

Besides isotope production, the U-250 accelerator facilities allow us to carry out neutron activation analysis, study the effect of neutron irradiation on materials, simulate radiation produced defects in solids used in nuclear power plants, monitor new technological processes in electronic industry, conduct research in metallurgy, etc.

In addition to applied research listed above, the very same facilities open new vistas for developing research in nuclear physics in the following lines:

Nuclear structure studies using in-beam nuclear spectroscopy methods. Accelerated heavy ions are a unique means for populating highly excited high spin states of nuclei – residual reaction products – which, as a rule, lie far away from β-stability line.

The determination of spin-parities of nuclear excited states, their maximum energies and spin values along with transition probabilities can elucidate behaviour of the nucleus at high rotation rates which attained in heavy ion induced reactions, in particular, the changes of its shape, moment of inertia and other parameters caused by the response of nuclear matter to the extreme external perturbation exerted by heavy projectile.

Nuclear reaction mechanism studies. The distinctive feature of heavy ion induced reaction is its new mechanism called deep inelastic process. It is intermediate between reaction proceeding through compound nucleus stage and that of direct interaction. Deep inelastic processes are specified by the formation of binuclear systems, by intensive kinetic energy dissipation over different degrees of freedom. Multinucleon transfer reaction is of similar nature. Nuclear reaction time delay studies along with those of reaction product angular distributions can yield detailed information on the reaction mechanism and the behaviour of nuclear matter in such strong perturbations.

Studies of atomic phenomena in heavy ion collisions. Time-dependent Coulomb field of colliding ions causes an essential shift of atomic levels and restructuring of electronic configurations from states in isolated atoms to those of molecular orbitals. Dynamical Coulomb field induced restructuring of electrons is accompanied by mutual inner shells ionization of colliding ions, the ionization probability being dependent on the combination of atomic numbers and on the energy of collision. The determination of ionization probabilities gives information on the average field value at any moment, the latter quantity being significant for studies of ions collision dynamics. Results of this kind of experiment are widely used in studying reaction time delays, ion interaction with matter, activation analysis, etc.

As mentioned above, the project can be subjected to further upgrading in respect to expanding the range of atomic masses of accelerated ions and attainable energies of acceleration ion using new types of ion sources.

But solving these problems requires great technical and intellectual efforts and proper high expenditures. The way out of the situation could be found in collaboration – pulling efforts of all groups interested in the project.

9. REFERENCES

1) Oganessyan, R.Ts. *et al.*, "The multi-purpose isochronous cyclotron U-250", Communication of the JINR, N9-12855, Dubna 1979.

2) Malychev, I.E. *et al.*, "General purpose heavy ions U-250 cyclotron", in **Proc. 8th All Union Conf. on Charged Particle Accelerators** (Dubna, 1983) v.1, pp.80-87.

GANIL STATUS REPORT

M. BAJARD and the GANIL Group

GANIL - B.P. 5027 - F-14021 Caen Cedex

ABSTRACT

Following the OAE (augmentation of energy) modification[1] and the installation of the SME[2] (medium energy facility) the accelerator has been operating for three years with the new ECR source (CAPRICE IIB at 10 GHz). Results obtained with new beams, metallic beams and the first tests with the new injector[3] system using an ECR source installed on a 100 kV platform are given.

1. INTRODUCTION

The GANIL (Grand Accélérateur National d'Ions Lourds) has been operating at Caen since 1983. This national facility is widely opened to the International Nuclear Physics Community.

The accelerating system provides the physicists with ion beams from carbon (E_{max} = 100 MeV/u) up to uranium (E_{max} = 25 MeV/u). The intensity varies from 1.5 x 10^{12} pps for carbon to 1 x 10^{9} pps for uranium (see below).

2. STATISTICS OF OPERATION

The OAE increased the energy of the ion beam as well as its intensity. A new ECR source called ECR3 has been operating since 1989.

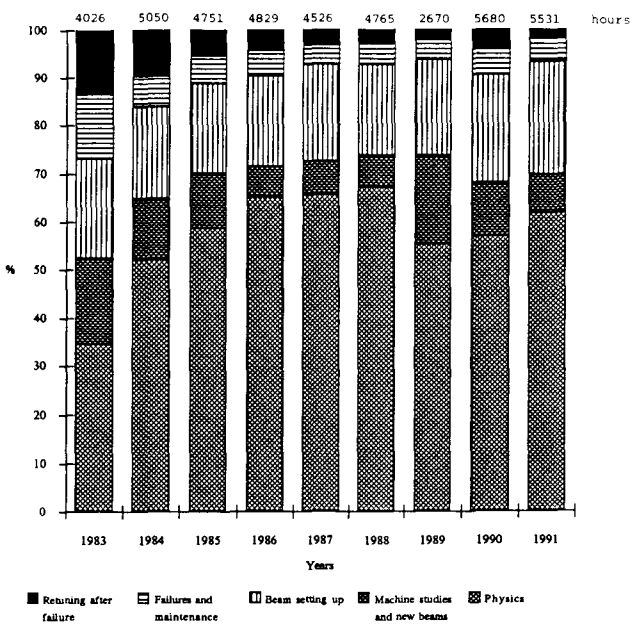


Figure 1

Figure 1 shows how the total running time (41 828 hours) has been shared for 9 years between physics, industrial applications, machine and new beam studies, initial settings and beam tunings, failures and maintenance during operation, and retuning.

Out of a total time of 41828 hours, 28614 hours were available (24284 were effectively used on target and 4 330 hours for machine studies and new beam developments), 2169 hours were used for beam retunings and 2467 hours in equipment failures.

The operation efficiency during experiments has grown regularly up to 90%.

The number of metallic ions to be tuned has increased, during the last three years. Fifty experiments have been performed at high energy in 1991. Fig 2 and 3 show the experimental caves time sharing.

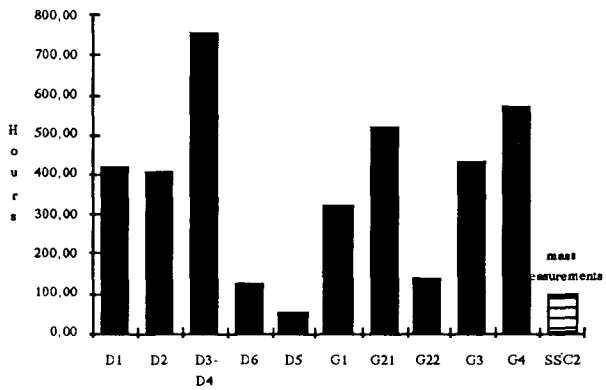


Figure 2

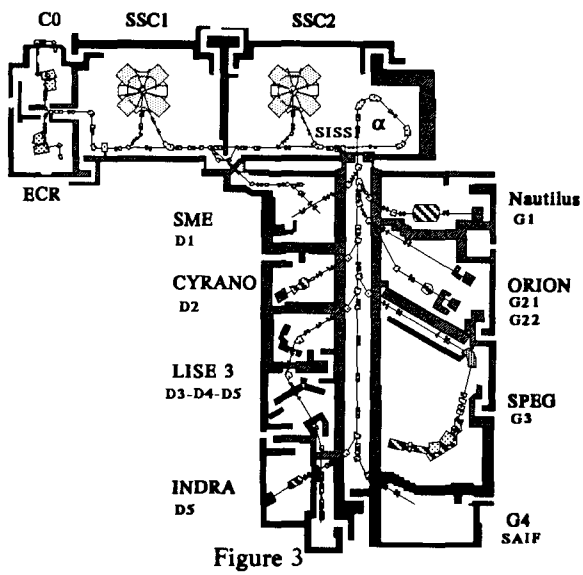


Figure 3

3. BEAM CHARACTERISTICS

Table 1 shows the ion beams and their characteristics accelerated up to June, 1992. They were produced with the ECR3 source (10 GHz), except tantalum which was produced with the ECR4 source (14.5 GHz).

All ion beams from SSC1 are available for the SME with energy ranging from 4 to 13 MeV/nucleon.

Beam intensities shown are those adjusted on target according to the experiment requirements.

The power of the ion beam at the output of the SSC2 is, for the time being, deliberately limited to 400 Watts, to ensure the safety of the equipment.

Other beam energies have been obtained by decreasing the velocity after the SSC2.

Exotic ion beams of ^{14}O at 70 MeV/u and ^{12}N at 65 MeV/u were produced by fragmentation of the primary ion beam in front of the high energy spectrometer.

Light ion beams (p, d, α) as well as exotic ion beams can be produced at various energies for detector calibration purpose.

Other ion beams have been tuned without changing the magnetic field up to the stripper.

Pencil beams with a diameter less than 0.5 mm on target are available.

Parallel ion beams for channelling are also available, with a diameter of 3 mm and a divergence smaller than 0.1 mrad.

The time structure of the beam[4] can be reduced by tuning SSC2 as a rebuncher. The method consists in increasing the magnetic field over the last 50 turns, with one or two trim-coils.

Mass of elements can be measured with a high level of resolution, using the GANIL cyclotron SSC2 as an Accelerator-Mass Spectrometer System[5].

ION/M	Charge state before and after stripping	RF Frequency (MHz)	Maximum energy (MeV per nucleon)	Maximum intensity on target (6) (measured)		Beam characteristics (measured)		
				pps x 10^{11}	enA	± ΔW/W half height (10^{-3})	Bunch timing half height ns	Intensity enA
C 12	3/6	13.45	96.3	20.5	2000	0.30	-	173
N 14	3/7	13.45	95	18.75	2100			
O 16	4/8	13.45	95	15.6	2000			
(5)O 17	4/8	12.75	84	9.8	1250			
(1)O 18	4/8	12.2	76	16.4	2100	0.64	0.2	6
Ne 20	3/10	9.893	48	21.87	3500	0.32		
(4)Mg 24	7/12	13.45	95	1.88	360			
(1)Ar 36	10/18	13.45	95	2.8	800		0.3	10
Ar 40	7/17	11.77	70	3.67	1000	0.79	0.5	340
Ca 40	6/19	10.1347	50.4	1	300			
(2)Ca 48	8/19	11	60.3	2.78	800		0.3	360
Ni 58	10/26	11.651	68.5	1.92	800		< 1	180
(5)Ni 64	10/26	11.061	61	0.72	300			
(4)Zn 64	11/29	12.42	79	0.2	100		< 0.8	10
(3)Kr 84	14/33	11	60	2.8	1500	0.59	0.6	900
(1)Kr 86	14/34	11	60	1.10	600			
(4)Nb 93	14/33	8.075	31	0.53	280		1.8	250
(4)Ag 107	18/38	8.71	36.4	0.2	120			
(4)Ag 109	18/38	8.55	35	0.2	120		1.5	80
(5)Te 125	17/38	7.55	27	0.03	16			
(2)Xe 129	18/44	9.52	44	1.09	800	0.90	0.2	18
(2)Xe 132	18/45	9.649	45.4	0.61	440	0.6		
(4)Gd 155	19/47	8.672	36.1	0.05	40	0.5		
(4)Gd 157	19/47	8.562	35.1	0.03	25	0.5		
(4)Ta181[a]	24/55	8.66	36	0.34	300			
(4)Pb 208	23/56	7.82	29	0.049	45	0.61	< 1.9	30
(4)U 238	24/58	7.13	24	0.01	10	0.32	1	5

(1) enriched 99% ; (2) enriched 70% ; (3) enriched 90% ; (4) natural ; (5) enriched 50% ; (6) for light ion beams. the intensity is voluntarily reduced according to the radiation level

Table 1

$^{238}U^{24/58+}$ was accelerated in October 1991 for the first time for experiments. The beam characteristics are presented below :

ECR3 source (CAPRICE IIB)	Material UO_2 Gas : neon
Intensity before analysis in axial injection	2.6 eμA U^{24+}
SSC1 output energy	3.72 MeV/u
Charge state in SSC2	58+
Carbon stripper	100 μg/cm^2
SSC2 output intensity	1 x 10^9 pps
Half bunch length	less than 1 ns

4. MEDIUM-ENERGY BEAM FACILITY (SME)

An unused charge state of the beam stripped between SSC1 and SSC2 can be sent into a new experiment room dedicated to atomic and solid state physics.

In 1991 approximately 1500 hours of beam have been delivered consisting of :
$^{14}N^{6+}$, $^{16}O^{7+}$, $^{16}O^{8+}$, $^{24}Mg^{11+}$, $^{20}Ne^{9+}$, $^{36}Ar^{17+}$, $^{40}Ar^{14+}$, $^{40}Ca^{18+}$, $^{48}Ca^{18+}$, $^{58\text{-}64}Ni^{25+}$, $^{64}Zn^{27+}$, $^{84\text{-}86}Kr^{32+}$, $^{93}Nb^{31+}$, $^{107}Ag^{36+}$, $^{129\text{-}132}Xe^{42+}$, $^{155}Gd^{45+}$, $^{181}Ta^{55+}$, $^{208}Pb^{53+}$, $^{238}U^{55+}$.
energy range : 3.5 to 13.5 MeV/u
emittance : 10π.mm.mrad in both planes
number of experiments : 50
for example : intensity of $^{208}Pb^{53+}$ was 2.4 10^{10} pps at 4.4 MeV/u.

5. MACHINE AND TECHNICAL STUDIES

The topics recently investigated were :

- charge distribution after stripping in order to increase the intensity of Ar^{16+}, Ar^{17+}, Ar^{18+} as a function of the carbon foil thickness,
- beam transmission through vacuum,
- longitudinal emittance measurements at the ouput of SSC1 or SSC2,
- reduction of the time structure of the beam,
- supervision of the temperature and voltage measurements of the RF cavities,
- supervision of the programmable logic sequencer controlling the vacuum between the SSC2 and the experimental areas,
- operation logs and statistics viewing. This application read the INGRES database by means of the graphic query language (GQL) to feed an EXCEL application,
- acceleration of light ions at high intensity.

Two tests have been carried out with a $^{20}Ne^{6+}$ beam which was produced by the ECR4 source installed on a 100 kV platform, driven into the new axial injection and accelerated by the C01 cyclotron.

Results are presented here after :

- Source analysis

. 65 to 95% of the analysed beam was concentrated, depending on the platform voltage, within a transverse emittance of 60 π.mm.mrad which corresponds to the admittance of the C01 injection system.

- Beam intensity

	Injected into C01	Extracted from C01
$^{20}Ne^{6+}$	36 eμA(3.75 10^{13}pps)	24 eμA(2.5 10^{13} pps)

NB : 60 to 70% of the extracted beam is within the acceptance of the SSC1.

In June 1992 this beam was accelerated by SSC1 and ejected at maximum energy. The power of this beam accelerated by SSC2 would exceed by 5 times the maximum value permitted by the safety of the equipment.

6. NEW BEAM DEVELOPMENTS

They are essentially related to ions produced from solid materials. The ECR source is operated both by a sputtering and by an electrically heated oven methods. The second one allows us to obtain stable intensity of Zn, Nb, Mg, Cr, Ca, Ag, Pb ions. Now the Lu ion production is under development.

7. OPERATION WITH THE NEW INJECTOR

The new injector of the GANIL facility[6] (new ECR source operating at 14.5 GHz installed on a 100 kV platform, new axial injection and modified C01 cyclotron) is now running for the operation.

The $^{181}Ta^{24/57+}$ was accelerated at the energy of 36 MeV/nucleon. The availability of the beam for experiments was 100% :

ECR4 source (14.5 GHz) $^{181}Ta^{24+}$	Material tantalum Gas : oxygen
Intensity after analysis in axial injection	8 eμA (60 π x 60π mm.mrad)
C01 output intensity	5 eμA
SSC1 input intensity	2.2 eμA (40 π x 40π mm.mrad) and $\frac{\Delta W}{W} = \pm 5\%$
SSC1 output intensity	1.8 eμA (24+)
Carbon foil	180 μg/cm^2
SSC2 output intensity for the users	0.3 eμA (55+)

8. REJUVENATION OF THE COMPUTER CONTROL SYSTEM[7]

Rejuvenation of the control system of GANIL is under way to fulfil the increasing requirements of the accelerator operation which aims at providing the physicists with a wider range of ion beams under flexible and reliable conditions. The distributed architecture adopted exhibits

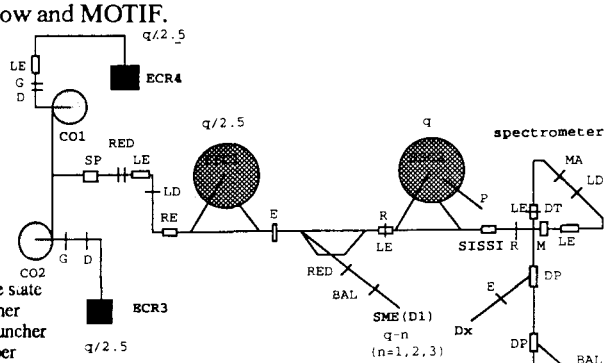
three functional levels federated by an Ethernet local area network (LAN) :

- The Host Level provides a general purpose and powerful environment for software developments, off-line calculations, database management, and simulation. It relies on a VAX6000-410 computer, linked to video terminals, and workstations VS4000 for colour graphics displays. Connection to other facilities of the GANIL and to remote laboratories via wide area networks (WAN) are available.

- The Realtime Control Level is devoted to human interface for accelerator controls. Man-machine interaction is accomplished via operator consoles, supervision systems, and graphic field terminals. This level is based on a μVax 3800 cluster, workstations VS4000 and Xterminals to benefit from the enhanced graphic capabilities.

- The Equipment Level performs low level controls. It makes use of -Front end controllers : CAMAC controllers (K.3968 from KINETIC SYSTEMS) and VME controllers (VME300 from AEON) to run applications under the VAXELN O.S. - Programmable logic controllers (PCL) : S5-135U from SIEMENS, and PB400 from APRIL. CAMAC and VME front end controllers, as well as the SIEMENS PLC are directly linked to the controls Ethernet.

To achieve productive and dependable software, VMS for VAX processors and VAXELN for real time controls are chosen. ADA (as major programming language), Fortran and C are adopted. Assembly language is relinquished. In addition to the VMS environment and LAN softwares, important packages are used : - The INGRES RDBMS from ASK/INGRES which complies with the SQL standard and encompasses the W4GL 4th generation language for NON-realtime database management (realtime database being hosted in the μVAX3800 and fragmented into dedicated live database to be down loaded into the front end controllers), - the IMAGIN family from SFERCA for PLC supervision, - Xwindow and MOTIF.



q : charge state
G : buncher
RE : rebuncher
E : stripper
MA : periodic beam stop
D : beam chopper to stop periodically the beam from experimental areas
SP : bunch suppressor to select one or several RF bunches (1/10 max)
R : energy degrader to slow down the beam, change the final charge state and produce secondary beams
M : intensity modulator (ratio up to 100) when the beam is time shared between two experiments
DP : pulsed dipole to establish the beam in 0.5 sec
RED : intensity reduction grid to reduce intensity by 5 or 25 while conserving emittance
BAL : beam sweeping from 4 Hz to 7 Hz
LD : energy spread limitation
LE : emittance limitation (down to 0.05 π.mm.mrad in both plans H and V)
Δt : time structure measurement
SME : medium energy beam facility with two beam lines in room D1 at SSC1 energy

A specific software layer was designed to match the accelerator environment and to support its controls. This so called GANICIEL layer is quite transparent to the users and is built upon the industry softwares. It makes widely use of the client-server model and takes into consideration the distributed architecture.

Main effort is, by the time being, mainly devoted to coding the GANICIEL and user software. The future control system is planned to be operational by spring 1993.

9. SISSI PROJECT[8]

The aim of this project is to increase the transmission of the secondary beams by a factor of 50 with respect to the present set-up; the main component is a pair of high magnetic field solenoids (11 T) providing a large angular acceptance (80 mrad). Both the SPEG and LISEIII spectrometers should take advantage of this improvement (better mass resolution). It should be completed in 1993.

10. CONCLUSION

After three years of operation with high energies and high intensities the demand is still strong both for light and heavy ions like C, N, O... Ta, PB, U. The demand is increasing for metallic ions Mg, Ni, Nb, Ag, Te, Lu, Gd, Ta, Pb, U.

The new high intensity injector system is operating since June 1992. The completion of the high resolution 4 π detector for light charged particles and nuclei detection INDRA[9] is scheduled for the end of 1992.

Medium-energy beams, diverted after the stripper have been permanently available (1500 hours a year) for non-nuclear physics since December 1989.

A study group is now investigating the spallation production of secondary beams by heavy ions.

11 REFERENCES

[1] J. Fermé "Project OAE at GANIL", 11th Int. Conf. on Cycl. and their Applications, Tokyo, 1986

[2] R. Beck and SME Group, "Medium Energy Beam Facility at GANIL", 12th Int. Conf. on Cycl. and their Applications, Berlin, 1989

[3] M.P. Bourgarel, E. Baron et al "Modifications of the GANIL Injectors" same Conf. as [2]

[4] D. Bibet, M.H. Moscatello to be published

[5] G. Auger et al, "Mass Measurements with the GANIL Cyclotrons", "Les Nouvelles du GANIL n° 37", 1991

[6] Ch. Ricaud et al."Commissioning of the new high Intensity axial injection system for GANIL" this Conf.

[7] T.T.Luong, L.David, E.Lécorché, M.Ulrich "The Next Generation Control System of GANIL'Int. Conf. on Accelerator and Large Experimental Physics Control Systems (ICALEPCS'91), Tsukuba, Japan November 1991

[8] A. Joubert et al, "The SISSI project" European Particle Accelerator Conf., Nice, June 1990.

[9] INDRA, GANIL internal report October 1989.

GATCHINA ISOCHRONOUS CYCLOTRON

N.K.Abrosimov, S.A.Artamonov, P.V.Bogdanov*, V.A.Volchenkov, A.A.Vorobiev, S.P.Dmitriev, V.A.Eliseev, B.D.Ershov*, V.S.Kuligin*, E.M.Ivanov, Yu.T.Mironov, G.F.Mikheev, V.N.Moshkin*, V.G.Mudrolyubov*, A.S.Pokrovskii, G.A.Riabov, V.A.Smolin, G.L.Sokolov, Yu.I.Stogov*, A.P.Strokach*, V.P.Fominenko, P.V.Chervyakov
Petersburg Nuclear Physics Institute, Gatchina, Russia

ABSTRACT

A design and construction of a $75-80\,MeV\,H-$ ion cyclotron with intensity of $100\mu A$ is in progress in Petersburg Nuclear Physics Institute. The cyclotron is to be used both for medical purposes (radio pharmaceuticals production) and for the investigations in nuclear physics, solid state physics, etc. To decrease the expenditures the iron yoke of the 1 *Gev* synchrocyclotron magnet model is utilized for a cyclotron magnet system. The accelerator itself is installed in the building of the operated synchrocyclotron and uses the existing electric power and water cooling systems. We assume the design of the cyclotron main systems to be completed this year, the building reconstruction has been finished, magnet assembly is in progress now.

1. INTRODUCTION

In Petersburg Nuclear Physics Institute up to now is in operation synchrocyclotron that accelerates protons up to 1 GeV at beam intensity 1 μA.[1)] The accelerator is applied for studies in physics of elementary particles, nuclear physics as well as for proton therapy and radioisotope production for medicine, etc. For increasing radioisotope production, for organization of the ocular melonome irradiation facility as well as for extending the traditional studies of short-lived isotopes it was decided to build a $75-80\,Mev\,H-$ ion accelerator with beam current $100\,\mu A$.

2. GENERAL DESCRIPTION

To minimize the expenditures while designing the cyclotron an attempt was made to use at most the existing synchrocyclotron infrastructure, i.e. the building, the bridge crane for 30 tones, the electric power , water cooling, ventilation systems, etc. The iron yoke of the existing synchrocyclotron magnet model is used for a magnet system. Such an approach provides saving of the resources at the cost of the restriction in the variety of design solutions.

Tab. 1 and Fig. 1 show the main cyclotron parameters and the plain view of its arrangement is given in Fig. 2. Probably,the energy of $75-80\,MeV$ is nearly the maximum possible one for an $H-$isochronouse cyclotron with the magnet pole diameter of $2m$. The $75-80\,MeV$ energy and the possibility to regulate it are necessary for isotope production using some reactions unattainable at lower energies. The $H-$ ions acceleration enables to perform smooth energy regulation of the extracted beam. The intensity of 100 μA is necessary for isotope production and is limited both with an ion source and the chamber activation.

The vertical focusing at the final radii has been achieved due to 60° spirals. Another way, e.g. the flatter enlargement at a given average field, would lead to a hill field growth and $H-$ ion losses in the result of $H-$ dissociation in magnetic field.

The chamber has an unusual design . The magnet pole tips and the harmonic coils are located outside the vacuum chamber. The chamber from stainless steel having relatively thin lids and being large in size is mechanically attached to a pole tips that provides relative rigidity under the action of atmospheric pressure.

3. MAGNET AND MAGNETIC FIELD STRUCTURE

The cyclotron magnet was designed in such a way that the iron of the existing synchrocyclotron model to be used for it. Design of the magnet was done with the aid of the $2D$ magnetic field code $POISSON$. Magnet of the model was completely reconstructed. The new $2m$ diameter poles were manufactured, the side yoke height was made $500\,mm$ lower, the support plates for the lower and upper yoke bars were introduced, the holes were drilled to inject the beam vertically, newly insulated coils were manufactured. To have an access inside the chamber the upper magnet bar with a pole and the chamber lid can be lifted on $450\,mm$ using four hydraulic jacks.

*The D.V.Efremov Scientific Research Institute of Electrophysical Apparatus (St.Petersburg, Russia)

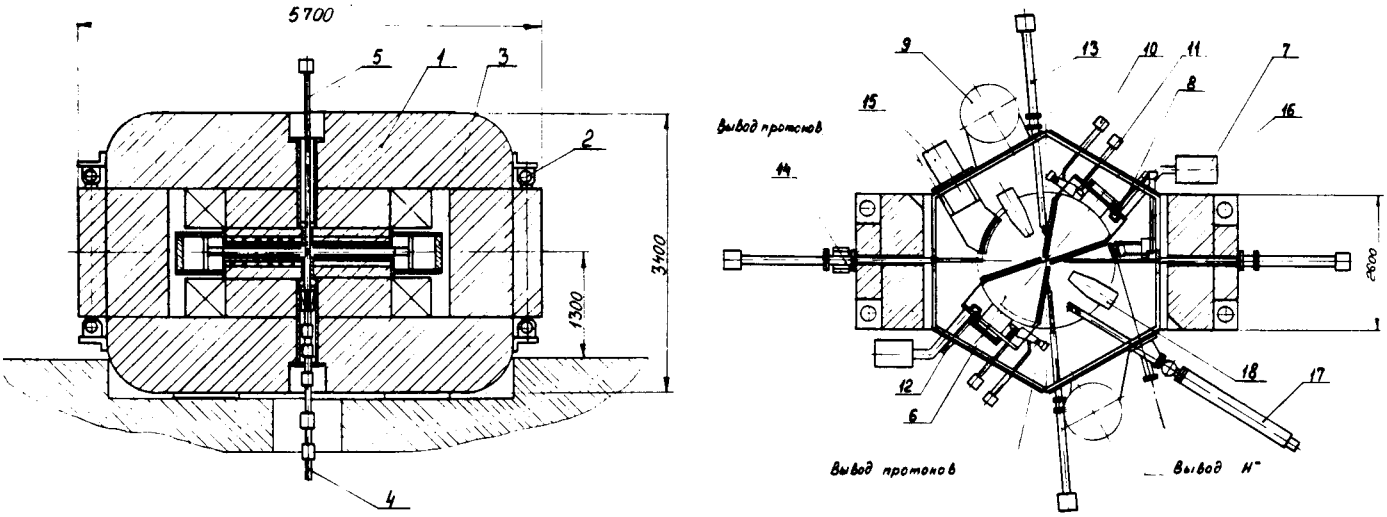


Fig. 1. General view of cyclotron. 1 - Electromagnet, 2 - Hydraulic jack, 3 - Vacuum chamber, 4 - External injection system, 5 - Axial injection deflector, 6 - Resonance system (dee), 7 - Final cascade of RF generator, 8 - RF power input, 9 - Vacuum pump, 10 - Tuning condenser, 11 - Trimmer of automatic frequency tuning, 12 - RF probe, 13 - Diagnostics probe, 14 - Septum protection foil, 15 - Extraction system deflector, 16 - Magnetic channel, 17 - Stripping device, 18 - Cryopanel.

The magnetic field structure was chosen to be a 4– sector one the maximum flatter value of 0.04 and the maximum spiral of 60°. Under such conditions and at 1.352 T field in the center the $H-$ losses make $3-5\%$ due to dissociation. Azimuth variation of the magnetic field that is the hill and valley gaps, the flatter and spiral were simulated using the magnet model before its reconstruction at 1 : 1.3 scale. The magnetic field isochronism and flatter is planned to be corrected using a set of sector ring iron shims while making magnetic measurements. To regulate the first harmonic the valley coils were installed. They are subdivided into four groups along the radius.

4. ACCELERATING SYSTEM

The cyclotron accelerating system is composed of two identical 1/4– wave dee subsystems excited at a fixed frequency of 41.2 MHz (second harmonic of ion revolution). Two 60° dees are conductivily coupled in the center and together with the resonance tanks form a uniform 1/2– wave system with a maximum voltage in the center and 17% voltage drop at the final radius. At 60 kV the accelerating system provides 200 keV energy gain per turn. The dee plates thickness is 15 mm, the dee aperture is 30 mm, the gap between a dee and a ground plaque is 33 mm.

The excitation generator has a common pre-amplifier of power up to 15 kW. The output of this pre-amplifier via two fidder lines is switched onto two final cascades 40 kW each placed in the chamber vicinity. Each of the resonance subsystems is inductively coupled via loop with the output cascade anodes, thus forming their resonance anode contours. The power supply rectifier is of 10 kV and 160 kW. The automatic amplitude, frequency and phase control systems are envisaged.

5. CHAMBER AND VACUUM SYSTEM

The chamber frame of hexagonal shape is welded of nonmagnetic steel. The chamber walls are of duralumin. The two of them that face the side yoke are undetachable. The chamber lid is welded of a bimetal sheet, i.e. nonmagnetic steel and copper. The copper lid surfaces serve as ground plaques for the resonance system. The steel lid sheets have the channels to let the cooling water through. The application of bimetal sheets enable approximately by 3 times to decrease the out gassing surface and to diminish the load on vacuum pumping means.

Due to the large recharge cross-sections on the residual gas molecules at $H-$ ions acceleration a high oil-free vacuum is required. The maximum load on the pumping means originates from an inner source and gas desorption from the surface. The estimations show that to reach 10^{-7} $Torr$ for air and 10^{-6} $Torr$ for hydrogen it is necessary to provide the following pumping speeds: with an internal source 100 $m^3/s(H_2)$, 25 $m^3/s(H_2O)$, 10 $m^3/s\,(CO_2 and N_2)$ and 5 m^3/s (hydrocarbon). The necessary pumping speed of hydrogen drops abruptly

MAGNET	Pole diameter	$2.05\,m$
	Valley gap (max.)	$386\,mm$
	Hill (min.)	$146\,mm$
	Number of sectors	4
	Spiral angle (max.)	60°
	Field in center	$1.352\,T$
	Flatter (max.)	0.04
	Extraction radius	$0.85 - 0.90\,m$
	Ampere-turns	$3.4 * 10^5$
	Power	$120\,kWA$
	Weight	$250\,tones$
RF SYSTEM	Frequency	$41.2\,MHZ$
	Voltage	$60\,kV$
	Harmonic	2
	RF Power	$2 * 40\,kVA$
VACUUM	Pressure	$10^{-7}(N_2), 10^{-6}\,Torr(H_2)$
	Turbomolecular pumps	$2 * 10\,m^3/s$
	Evaporation getter pumps	$2 * 60\,m^3/s(H_2)$
	Cryopanels, two , N_2	$S = 0.3\,m^2$
H- SOURCES	Internal Ehlers Pig	
	External:	
	surface plasma, pulsed	
	surface plasma, stationary	
	multi pole source	
	voltage	$20\,kV$
EXTRACTION	Energy	$45 - 80\,MeV$
	Method	Stripping

Tab. 1. Gatchina cyclotron parameters.

down to $10\,m^3/s$ for an external source. Based on the above estimations the vacuum system was composed of two turbomolecular pumps $TMNG - 10000$ with the pumping speed of $10000\,l/s$ each, two evaporation getter pumps $NDMA - 20$ with $60000\,l/s(H_2)$ pumping speed each and of $0.3\,m^2$ cryopanels. The estimations show that the beam losses due to the residual gas make 10% at an internal source and 5% at the external injection.

6. SOURCES AND INJECTION

The cyclotron design envisages the application of internal and external sources. An internal source (Penning type with a filament thermal cathode, an anode and a cathode reflector) is considered to be a source for the accelerator operation at initial stage.

An external source has a number of advantages. Primarily, there is no gas leakage into chamber and there is a decrease of $H-$ ion losses. Several types of external sources have been considered. The most well developed in Russia source is a surface-plasma one designed in Novosibirsk and applied at Moscow Meson Factory.[2] The source operates in a pulse mode with a single pulse duration of $1\,ms$, duty factor of 10 and a pulse current up to $10\,mA$. But, the pulsed mode of its operation does not correspond to the continuous mode of cyclotron operation. A version of a surface plasma source with continuous operation is under consideration.

To inject $H-$ ions into the cyclotron an axial injection channel has been designed. This channel happens to be a universal one for various types of sources. and is composed of two magnetic lenses, a focusing solenoid and two quadruples. The transition from one type of a source to another one is done by changing the switching mode of the channel optic elements. A type of channel with a $SmCo_5DC$ magnet is under study. An electrostatic mirror and a spiral deflector are considered to be a deflector. A testing stand is now built to experiment with an axial injection system.

7. BEAM EXTRACTION

The main means of extraction is the $H-$ stripping on a thin carbon foil. The stripping probe with a magazine of 4 foils moves along the radius from $750\,mm$ to $900\,mm$ and over 30° angle along azimuth providing beam energy variation from $45\,MeV$ to $80\,MeV$. In case of a necessity to extract $H-$ ions (e.g. for injection into a storage, etc.) there is a place envisaged for a system of $H-$ ions extraction using a processional or regeneration mechanism of beam injection into an electrostatic or high frequency deflector with a septum protection by means a recharged foil, as it was proposed in $TRIUMF$ cyclotron.[3] However, this system at present is on paper

and, thus, is a system of the second order.

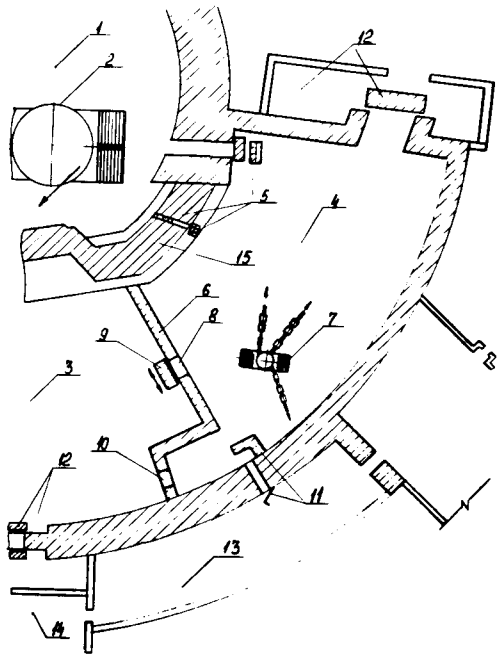


Fig. 2. Scheme of cyclotron arrangement. 1 - Hall of synchrocyclotron, 2 - Synchrocyclotron, 3 - Experimental hall, 4 - Cyclotron hall, 5 - Additional shielding, 6 - Wall separating the cyclotron hall, 7 - Cyclotron, 8 - Opening for crane passage closed by a wheeled block, 9 - Crane cargo opening, 10 - Cyclotron hall entrance, 12 - Shielding doors, 13 - Control hall, 14 - Laboratories, 15 - Shielding wall from iron block.

8. RADIATION ASPECTS AND SHIELDING

The aspects of induced activity are of great importance during a cyclotron design. To reduce an induced activity and to catch an H^o particles beam formed during $H-$ ions decomposition all the chamber elements are shielded along the perimeter with graphite screens made of $50 * 50$ *mm bars*. The screens are attached to easily detachable aluminum panels fixed to the chamber. The screen application reduces the dose power by 2 times when the chamber walls are made of Al and by 5 times when they are of SS. The estimations show that at 10% $(10\ \mu A)$ beam losses the dose power of $\gamma-$ irradiation of an induced radioactivity in one hour after switching off the accelerator at 1 m distance will not exceed 0.1 rad/hr after a long time operation. At the maintenance time the screens are taken out of the chamber to reduce additionally the personnel irradiation. To protect against an H^o particles beam all the chamber mechanisms are located, if possible, outside the median plane. The magnet coils insulation provides a 10 year operation and the rubber vacuum gaskets are meant for one year service approximately.

The biological shielding against the irradiation of an active cyclotron is solved by installing it in the experimental hall of the existing synchrocyclotron. The 4 m thick walls are made of heavy concrete. For the protection of the personnel assembling the cyclotron against the secondary particles beam of the synchrocyclotron a $1.2m$ thick and $4.8m$ high protective wall has been built. It protects personnel against meson beams (but not full proton beam) extracted into another area of the hall. The aspects of shielding of personnel that works in the synchrocyclotron hall will be considered and solved later on during the new accelerator commissioning by means of local shielding and beam traps.

9. PRESENT STATUS

The main cyclotron systems design is planned to be finished this year. The cyclotron magnet has been almost finished and the manufacturing of its spiral sectors is coming to an end. The shielding wall and the basement construction has been accomplished and the magnet assembly started. An automated system for magnet measurements based on the Hall probes is finished to be built.

A high frequency system is being simulated on models $1:2$ and $1:1$, the $41.2\ MHz$ $15\ kW$ generator was put into operation and the design of $40\ kW$ final cascades of the generator has been finished.

The internal $H-$ ion source design is now being checked at a stand, as well as, the evaporation getter pumps of $NDMA-20$ type are under testing. A pulse external $H-$ ion source and the power supply system have been manufactured. An axial injection model construction has been started.

Provided the financing be substantial, the first cyclotron beam could be generated in two years.

10. REFERENCES

1) Abrosimov, N.K., et al., "Present Status of 1 GeV Synchrocyclotron in Gatchina," in **Proceedings of the 7th All-Union Conference on Charged Particles Accelerators** (Dubna, October 14-16, 1980), v.2, p.75.
2) Belchenko, Yu.I., et al., "Study of Surface Plasma Sources of Active Ions in Novosibirsk," in **Proceedings of the 13th International Conference on High Energy Particle Accelerators** ("Nauka", Novosibirsk, August 7-11, 1986), v.2, p. 276.
3) Mackenzie, G.H., et al., "Plans for the Extraction of Intense Beams of $H-$ Ions from the TRIUMF Cyclotron," in **Proceedings of the 10th International Cyclotron Conference** (Michigan, USA, 1984), p.233.

STATUS REPORT OF SARA

S. Albrand, D. Barnéoud, J.L. Belmont, G. Bizouard, J.L. Bouly, G. Campillo, M. Fruneau, M. Guisset, G. Laborie
Institut des Sciences Nucléaires - IN2P3 - Université Joseph Fourier
53, avenue des Martyrs 38026 Grenoble Cedex, France

ABSTRACT

Recent improvements to SARA are described. Three years operation with two ECR sources and their developments are presented. Differences between flux measurements of the 4 sectors of the second cyclotron show the need to uncouple the trim coils currents of the sectors.

1 - INTRODUCTION

S.A.R.A. (Système-Accélérateur Rhône-Alpes)[1-2] is a two cyclotron accelerator designed to accelerate heavy ions up to 40 MeV/u up to calcium, the maximum energy decreasing to 10 MeV/u for xenon. The first cyclotron with a K of 84MeV, originally devoted to light ions was rebuilt in 1987 for heavy ions. After stripping the beam is injected into a separated sector cyclotron of K = 160 MeV.

2 - OPERATION

Table I presents the statistics of operation for the last two years. 96 beams have been delivered in 1990 and 130 in 1991. Typical total setting up times for a new beam are four hours for one cyclotron and nine hours for the two machines.

In 1991, the breakdown time increased sharply because of a field dependent vacuum leak on the lower pole D_1 of the post-accelerator. Limitation of the magnetic field and injection of a sealing compound on the O ring allowed limited operation till the winter shutdown. A complete dismantling showed noticeable vertical movements of the yokes attributed to displacements of the concrete floor of the vault and a deep crack in the O ring.

Precise levelling of the yokes has been achieved for the whole machine and optical markers have been added to critical points of the poles for precise control.

Year		Total time	Tuning	On target	Develo-pment	Break-down
1990	hours	3632	438	2651	200	343
	%	100	12	73	5,5	9,4
1991	hours	4352	392	2912	312	736
	%	100	9	67	7	17

Table 1 - Operation of SARA

3 - AXIAL INJECTION LINE

Since 1989, an axial injection line for two ECR sources equips SARA. This 18 m long line has an 11 m long section in which a periodic focusing is ensured by 13 lattices of electrostatic lenses[3]. The rather low voltage (-8 to -15 KV) on these electrodes and the good cryogenic vacuum (2.10^{-9} torr) were important factors in maintaining high reliability over the last three years.

The overall transmission from the source to the center of the cyclotron is of the order of 75 %, the losses are due to some mismatching between the first 8 m straight section and the 3 m section leading to the yoke. The decentring of the central trajectory is attributed to the mechanical misalignement of the electrostatic lenses[4]. This causes oscillations of the trajectories that may subsequently cross regions of the lenses where aberrations are no longer negligible.

The possibility of rapid commutation of the two sources is very useful for simultaneous development on the source not used in injection, for quick change in case of failure, and also for preparing one source before changing the accelerated beam.

4 - ECR SOURCES

SARA was one of the first cyclotrons equipped with ECR ion sources . MINIMAFIOS built by R. GELLER[5] has been operating at SARA since 1983. In 1989, FERROMAFIOS was installed together with the new injection line. In 1991, it has been replaced by CAPRICE[6]. Table 2 and 3 show the ion yields of these sources.

Charge state	5	6	7	8	9	10	11	12	13	14	15	Feed
^{19}F	*7*	*0,3*										SF_6
^{20}Ne	*80*	*24*	*11*									Ne
^{27}Al	*3*	*2,5*	*6,3*	*9,3*								Al_2O_3
^{28}Si			*11*	*9*	*2,5*							SiH_4
^{32}S	*21*	*10*		*20*	*7*							SH_2
^{35}Cl				*23*	*11*	*1,1*	*0,3*					CCl_4
^{40}Ar			*20*	*22*	*13*	*10*	*2,5*					Ar
^{40}Ca				*8,5*	*10*	*12*	*15*	*2*	*0,6*			Ca
^{48}Ti						*10*	*8*		*1,8*			Ti
^{56}Fe							*5,5*	*2,4*	*2,6*			Fe
^{58}Ni							*2*		*3,2*	*4*	*0,8*	NiO
^{84}Kr							*8*	*5*	*4*	*1*		Kr

Table 2 - Intensities from MINIMAFIOS (electrical µA)

Charge state	9	10	11	12	13	14	15	16	17	18	Feed
^{32}S	*15*	*7*									SH_2
^{40}Ar			*8*	*3,6*							Ar
^{40}Ca			*20*	*3*							Ca
^{63}Cu		*12*	*9*								Cu
^{80}Se						*1,6*	*1,3*	*1*			SeH_2
^{84}Kr					*5,7*	*10*	*8,6*	*6,8*	*3,3*	*1,1*	Kr
^{86}Kr					*1,3*	*2,5*					Kr

Table 3 - Intensities from CAPRICE (electrical μA)

Metallic ions

MINIMAFIOS has been used for metallic ions with the insertion method, and a lot of long runs (two weeks) have been completed with calcium and aluminium. The sample (pure metal or oxide) is introduced close to the ECR surface and is driven by a stepping motor for precise control of its position and its advance rate. In our case, introduction 4 mm off-axis gives better results. With this method, the position of the sample and its speed are strongly coupled with the currents in the confinement coils that define the ECR surface, and to the microware power, all these parameters modify the temperature of the sample and its vaporization rate.

Some control is obtained by modifying heat exchanges with the supporting rod. Low vaporization temperature samples like calcium need to be supported on rather good heat conductors and refractory samples (Al_2O_3, NiO,...) have to be held with smaller diameter supports.

The pollution of the chamber by metal evaporated in excess is important, it reduces the efficiency of the source for subsequent runs and renders careful cleaning of the source indispensable.

Metallic ion development has begun on CAPRICE, using a small oven similar to that of GANIL[7]. First results on calcium at 800° C show the advantages over the insertion technique : ion yields are greater, the sample consumption is of the order of a few tenths mg per hour, the stability is good and the tuning is easier because the temperature of the sample is controlled independently of its position and of the magnetic confinement. Copper and nickel are currently under development.

5 - INCREASING THE TIME BETWEEN BEAM BURSTS

The radio frequency range of the first cyclotron is 10.5 to 16.5 MHz and the harmonic numbers are 2 and 3, the second cyclotron runs at twice this frequency and the harmonic numbers are 4 and 6 respectively. Time separation between these bursts corresponds to the first acceleration frequency and lies in the range from 60 to 100 ns and this time is too short for precise time-of-flight measurements.

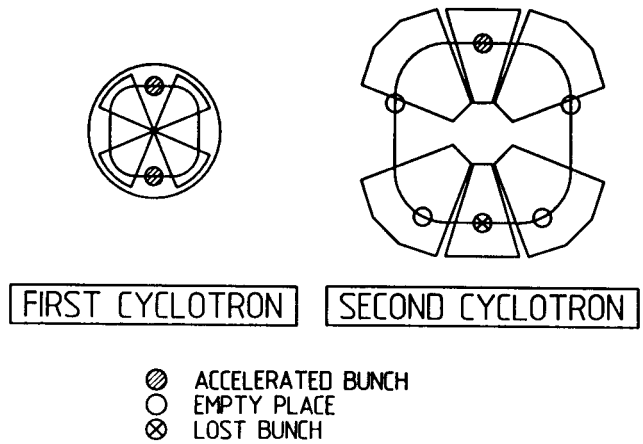


Figure 1 - Schematic view of the beam bursts with the 1st cyclotron in harmonic 2 and the 2nd in harmonic 5 for Neon 6^+ at 30 MeV/u.

When the first cyclotron is running in harmonic number 2, two beam bursts lie on the same turn, 180° apart. The second cyclotron RF is twice that frequency, in harmonic 4, four possible places are available for acceleration on each turn, only two of which are occupied by bursts, each 180° apart. By running the post-accelerator at different harmonic numbers, it is possible to extend time separation up to 300 ns.

If the harmonic number becomes 5, it would be possible to accelerate five bursts, but just one of the two injected bursts is accelerated, the other falls just between two places and is lost (Fig. 1). So one burst remains per turn ; beam burst separation has doubled. In the same way, with the first cyclotron in harmonic 3, and the second in harmonic 5 or 7, according to the frequency, one burst out of three is kept, original separation is multiplied by three. In this way, time separation between bursts ranges from 160 to 280 ns.

6 - MAGNETIC FLUX MEASUREMENTS

6.1 - Motivation and method

The orbits in the second cyclotron are frequently off-centred at intermediate radii even when the early orbits are well centred. This would seem to indicate that the magnetic fields in the four sectors are unequal. Individual adjustement of the field of each sector was not sufficient and indicated that the shapes of the field maps were different. Moreover the influence of the injection magnets in the center region is not known precisely. Hence it was decided to undertake magnetic measurements of the four sectors with the machine

nearly completely assembled (without the resonators) to obtain more accurate information on their differences.

The measurement of a field map point by point posed too many practical problems. A global method was more appropriate in our case, so we chose the measurement of variations of magnetic flux generated by the poles when a large coil, in the form of boomerang, moves by defined steps along the sector radius (Fig. 2).

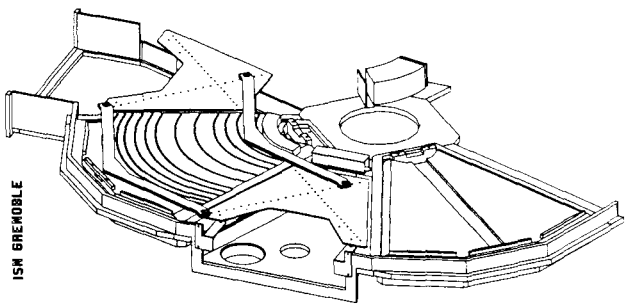


Figure 2 - Magnetic flux measurements. The coil is shown in two extreme positions on the pole of sector D_2.

Integrating the voltage of the coil gives the measurement of the flux variation between two positions.

$$\int_{t_1}^{t_2} V_{coil}(t)\, dt = -\Delta\phi_{i,\, i+1}$$

if the coil is moved from radial position i at time t_1 to i+1 at time t_2.

The coil was wound on a glass fiber epoxy material core form that was placed in a box of the same material

The angle betwen the two straight parts of the 1600 turn coil was a compromise chosen to cover no more than two trim coils from the center to outer radius (close to the trajectories). The coil was radially displaced in 60 mm radial steps between holes precisely drilled on templates previously centered on the magnetic structure, 23 holes defined 22 measurements. The radial extent of the coil is also close to 60 mm. Each step corresponds to a variation of 27 cm^2 in the surface of the poles seen by the coil so a nearly constant flux variation had to be integrated for each field level, improving the precision of measurements.

The displacement of the coil was manual ; one person at each extremity slid it on a teflon plate between 2 radial positions. Precise positionning at the drilled holes was obtained by dowel pins with compensation for backlash. Each movement was made in a period slightly less than the 20 s integration time, and these measurements of $\Delta\phi$ were sandwiched between dummy measurements which were used to correct for drifts in the integrator and to detect eventual parasites.

The apparatus used was a Metrolab PDI 5025 integrating voltmeter connected to a PC for logging and sequencing of the operations.

Measurements were made on each pole at 4 field levels and NMR probes in regions of "flat" magnetic field normalized the measurements and compensated drifts of the four sectors (Fig. 3).

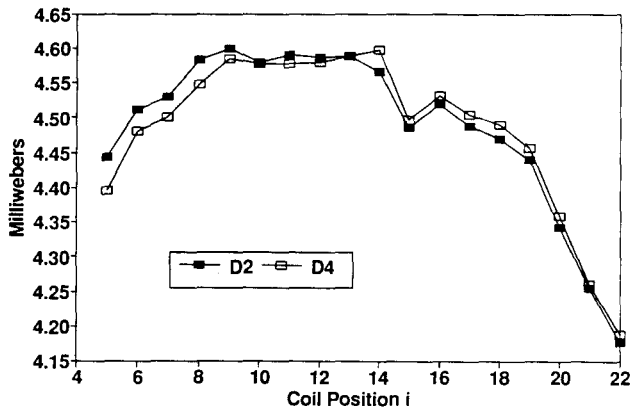


Figure 3 - Magnetic flux variation when the coil is moved from position i to i+1, for sectors D_2 and D_4 at a nominal field of 1.0 T.

It was difficult to maintain the coil at a constant temperature, but a rough stabilization of the cyclotron vault was installed, giving a variation of ± 0.4° C. Since the surface thermal expansion of glass fiber of the support is 8.10^{-5} per degree, this led to an error of $\pm\ 3.10^{-5}$ on the flux.

Tests of the measurements showed that after cycling the magnetic field and reinstalling the coil in a sector, a reproducibility of $\pm\ 3.10^{-4}$ was obtained ; this figure is limited by mechanical problems.

6.2 - The exploitation of the measurements

The field maps of the sector D_4, previously measured with Hall probes, were used as references to calculate the flux seen by the coil in each of its 23 positions. This calculation was done by summing the elementary fluxes at each point of the field map, no interpolations were used.

Using the experimental measurements of the variations of flux of each sector with respect to those of D_4 we calculate a small correction for each of the coil positions. For instance, for the sector D_2

$$\delta_i = \Delta\phi^{exp}_{i,\, i+1}(D_3) - \Delta\phi^{exp}_{i,\, i+1}(D_4) \qquad (1)$$

where $\Delta\phi^{exp}_{i,\, i+1}$ is the variation in magnetic flux measured when the coil is moved from position i to position i+1, defined above.

Our first aim is to produce a field map which represents the sector D_3. The first step is to use these values of δ_i (of the order of 10^{-5} Weber) to estimate the effective magnetic flux in D_2.

Since no absolute measurements of flux were made we suppose that there is one point where the actual flux is equal to the flux calculated in our reference field map. We call this point p the pivot.

$$\phi_p = \phi_p^{calc} \tag{2}$$

We can consider that for positions p + j, j = 1, ... (23 - p), the flux through the coil i :

$$\phi_{p+j} = \phi_{p+j}^{calc} + \sum_{i=0}^{i=j-1} \delta_{p+i} \tag{3}$$

Whereas for positions p - j, j = 1, ... p - 1

$$\phi_{p-j} = \phi_{p-j}^{calc} - \sum_{i=1}^{i=j} \delta_{p-i} \tag{4}$$

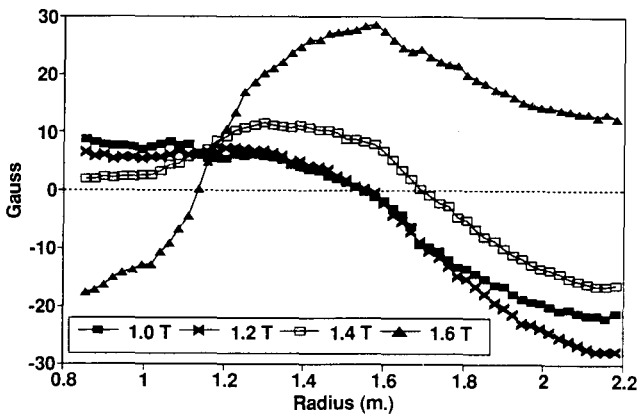


Figure 4 - Differences between mean magnetic fields of sectors D_2 and D_4, at four levels.

Thus to obtain the map for D_2, all the points in the reference field map $B(\theta,r)$ of the D_4 sector which lie under the coil in position i must be corrected by a factor.

$$F_i = \frac{\phi_i}{\phi_i^{calc}}$$

where ϕ_i is given by equation (3) or equation (4) (Fig. 4). D1 and D_3 are treated in the same way.

Our final aim is to obtain three sectors identical to D_4. Standard calculations of the trim coils, comparing these corrected maps to that of D_4, determine the currents needed to obtain identical magnetic fields in the four magnets. The 15 trim coils of the four sectors that are at presently serially fed will have to be decoupled. Further studies will indicate the number of individual coils to be fed separately or corrected either by an electronic shunt or by a power supply connected in parallel.

7 - VACUUM SYSTEM

7.1 - The automation of the vacuum system

The automation of the vacuum system that began with the injection line has been completed.The pumps, valves and pressure gauges of the entire machine, from the ions sources to the target chambers, are interfaced to several industrial programmable controllers. These controllers are ideal for surveillance, and can also supervise a sequence of operations following a single command. They are connected to a P.C. by a serial bus (RS485).

The application interface consists of 8 pages of synoptics which are colour graphics representing the geographic position and state of each element (Fig. 5). The operator interacts with the system uniquely with the mouse, by "clicking" on a virtual button. All commands and changes of state are logged on an on-line printer.

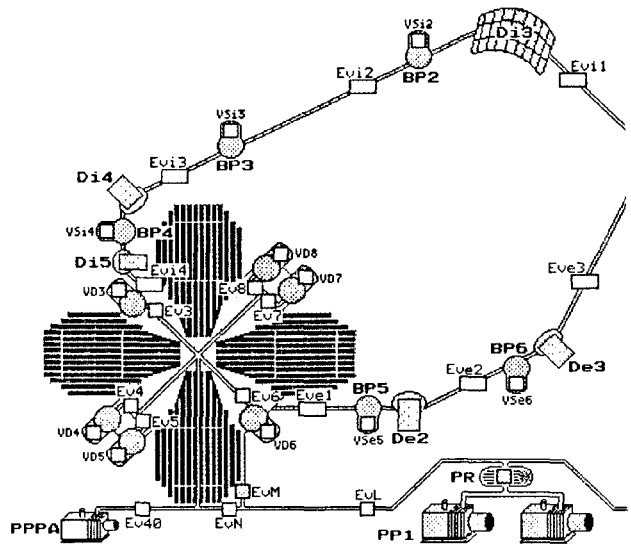


Figure 5 - Partial view of the synoptic of the vacuum system.

This system is proving to be reliable, flexible, and "user-friendly".

7.2 - Cryogenic pumping

Pumping the 3.5 m^3 vacuum chamber of the second cyclotron was ensured by 6 oil diffusion pumps with cold traps, 2 pumps being placed in each resonator, and one in the free sector.

Eight years experience showed that undetected failures in the cooling of the cold traps and troubles in the old control system led to important oil pollutions of the resonators. This reduced the maximum dee voltage and polluted the electrostatic inflectors, particularly at the extraction, that had to be frequently removed for cleaning.

Six cryogenic pumps (CTI, CT 320) with a pumping speed of 3000 l/s for air have replaced the oil diffusion pumps and are controlled by the automation system described above. RF voltages of 60 KV have been quickly obtained after cleaning the resonators.The large pumping speed for water vapor insures short pumping times after opening the chamber and quick resuming of the operation.

8 - FUTURE DEVELOPMENT

The project PIAFE[4] of accelerating fission products coming from the I.L.L. high flux reactor requires the transport of singly charged radioactive ions, injection into an ECR source for multiple ionization to typical q/m of 0.15 and acceleration by S.A.R.A. Extraction at a continuously variable radius in the second cyclotron could permit variation of energy from 4 to 10 MeV/u.

9 - ACKNOWLEGMENTS

We are greathly, indebted to Mrs TKATCHENKO (CEN Saclay) for helful discussion about field measurements.

10 - REFERENCES

1) M. Lieuvin, "SARA a low cost heavy ion accelerator for 10 to 40 MeV/A", IEEE Trans. Nucl. Sci. **NS-30**, n° 4 (1983), p. 2072.

2) M. Lieuvin, "SARA-GRENOBLE Status Report", 12th International Conference on Cyclotrons and their Applications CAEN (1981), pp. 81-88.

3) J.L. Belmont, M. Fruneau, P. Martin and the SARA Staff, "New developments at SARA", proceedings of the 12th International Conference on Cyclotrons and their applications, Berlin (1989), pp. 116-120, (World Scientific).

4) J.L. Belmont et al. "The PIAFE Project at Grenoble", This Conference.

5) R. Geller, B. Jacquot and Pauthenet, Rev. Phys. Appl. **15**, (1980), p. 995.

6) F. Bourg, R. Geller, B. Jacquot, "Source d'Ions Lourds Multichargés CAPRICE 10 GHz", NIM **A254**, (1987), pp. 13-21.

7) M.P. Bourgarel, M. Bisch, P. Leherissier, J.Y. Paquet and J.P. Rataud, "Development of metallic ions in the ECR sources" Rev. Sci. Instrum., Vol. **63**, n° 4 (1992), pp. 2854-2856.

COMMISSIONING OF THE INJECTOR COMPLEX OF COSY-JÜLICH

W. Bräutigam, H. Beuscher, R. Brings, H.G. Böge, R. Maier, M. Rogge, P. Wucherer
Institut für Kernphysik, Forschungszentrum Jülich (KFA) GmbH,
Postfach 1913, 5170 Jülich, Germany

ABSTRACT

The Isochronous Cyclotron JULIC was upgraded over the last years to serve as injection machine for the new Cooler Synchrotron COSY-Jülich[1]: A new RF system replaces the former self oscillating unit to achieve more power, better stability of frequency/phase and amplitude and easier operation. Mineral insulated trim coils with modified winding patterns replace the old set of coils, which suffered severely from radiation damage. Several especially adapted ion sources provide the H_2^+- and H^--beams for the injection into COSY. The injector was extensively equipped with new instrumentation and computer control for compatibility with the COSY control system. An entirely new transfer beamline between the injector and COSY-ring is finished and ready for use. The cyclotron is back in operation since February 1992.
This paper gives a brief description of some modified subsystems, focuses on the commissioning procedure and reports first results.

1. INTRODUCTION

JULIC was originally conceived for the acceleration of light ions (p, d, $^3H^{2+}$,α) in the energy range of 22.5 to 45 MeV/A. After about 15 years of more or less continuous operation the machine was upgraded for the acceleration of light and medium heavy ions. So since 1987 a spectrum of additional ions was available. In September 1989 after more than 100000 h of operation the cyclotron was finally switched off as accelerator for experiments mainly in nuclear physics but also in life sciences, material investigation and others. - In order to serve as injector for COSY-Jülich the cyclotron complex (ion sources, accelerator, beam lines, technical infrastructure) needed extensive technical upgrading[2]. Emphasis was given to the development of H_2^+-beams, which are needed for the injection into COSY with first priority, but also to H^--beams as precursor for polarized particles. The optimization of beam parameters defines stability factors for magnetic field, RF amplitude and phase, which could only be achieved by new installations. To improve reliability, the trim coil system and parts of the technical infrastructure had to be rebuilt. The extensive upgrading of diagnostics equipment[8], general instrumentation and computer control was necessary, to simplify operation and to provide the basis for compatibility with the COSY computer control system. An entirely new transfer beamline was built between cyclotron and the COSY ring.

2. ION SOURCES

Four ion sources will be available for the different particles to be accelerated in COSY[3]. The types of sources are mainly determined by the fact, that the injection into the cooler synchrotron is performed by stripping. First COSY beams will be delivered by a H_2^+ source, which can be easily replaced by a H^-/D^- source. The main reason for this negative ion source is to study the injection, acceleration and extraction of negative ions in the cyclotron, which is of major importance for the future use of polarized particles. A H^-/D^- polarized source provides the only possibility to inject such ions into the ring by stripping.
The transmission through the source beam-line and the cyclotron can be remarkably increased by reducing the beam emittance much below the expected acceptance of the cyclotron. Experimental results imply, that a source with low emittance ($< 35\ \pi\cdot$mm$\cdot$mrad at 8.2 keV) and medium high currents ($> 100\ \mu$A) to avoid space charge effects would probably be the best choice. For injection into COSY H_2^+ beams of 80 MeV and currents above 10 μA are requested at the exit of the cyclotron.
A well adapted H_2^+ source was developped with the additional condition to maintain the advantage of an ECR source without any wearout components (see Fig. 1). Since the emittance of ECR sources increase with the axial magnetic field in the extraction region, it is reasonable to use low microwave frequencies like 2.45 GHz and lower the field in the extraction as much as possible. The best results have been achieved with a source consisting of a permanent magnetic multipole with zero axial magnetic field at the extraction and only one mirror coil at the opposite side as shown in Fig.1. By tuning the source parameters (solenoid field, microwave power, gas pressure and puller voltage) H_2^+ beams of about 100 μA with emittances in the range of 25 to 40 $\pi\cdot$mm$\cdot$mrad could be obtained.

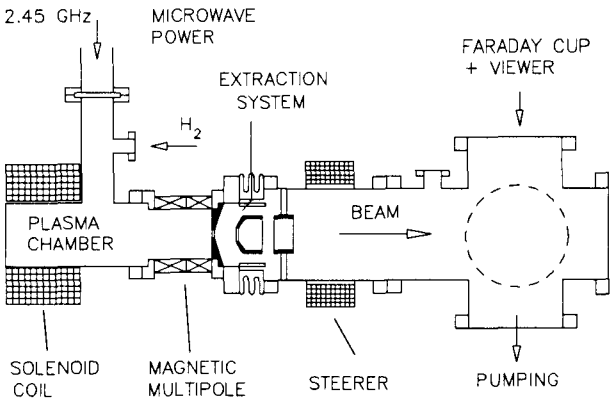


Fig. 1. H_2^+-ion source

The H^-/D^- source bought from IBA company was originally designed for extraction voltages of 25 to 30 kV. When only 4.5 kV is applied, which is needed in our case, the large divergence of the low energy beam resulted in an incomplete matching between the source and the existing beam line. The situation could be remarkably improved by introducing two additional electrostatic electrodes behind the puller.

The big superconducting 14 GHz ECR source, which had been developped for heavy ion acceleration with the cyclotron, was frequently used since shutdown of JULIC in 1989 for atomic physics experiments. In connection with COSY it is supposed to deliver heavy ion beams for medical applications in a somewhat later stage of operation. - The polarized ion source is realized in form of a collaboration of the universities of Bonn, Köln and Erlangen. It is going to be assembled at its final location by the end of the year.

3. TRIM COILS

At JULIC the tuning of the isochronous field is performed by three pairs of trim coil arrangements (plates) mounted on the hill sectors of the pole tips inside the vacuum chamber. The new design was necessary because of severe radiation damage of the old units, where extensive use had been made of epoxy resin for insulation as well as for the mechanical fixing of the structure. The new coils were optimized in respect to radiation damage and from vacuum point of view. Mineral insulated cable material was used, made by Pyrotenax Ltd., Canada. The square shaped coaxial copper cable with an outer dimension of 6.35 mm and a MgO-powder insulation of 0.5 mm allows an effective (indirect) cooling of the conductor. In total 9 coils of four windings each are combined with 5 water pipes for cooling. The coil/cooling channel configuration was inserted into a solid copper plate with precisely milled grooves and then soft-soldered at a time in a vacuum environment.

Trim coils have to correct the variation of relativistic mass increase, saturation effects in the iron of the hill sectors and local field errors. Concentric sector coils are well suited to cover the first two items, but local field errors can only be corrected by adequate field differences of subsequent coils. Accurate field measurements[4] had to make the basis for the precalculation of trim coil current sets before the beam could be accelerated, but also for the interactive optimization during operation. Since JULIC has a 3-fold symmetry it is sufficient to do field mapping for a sector of 120°. Figure 2 shows one trim coil mounted on the hill sector together with the strongly simplified field mapping equipment. The hall probe of a high precision

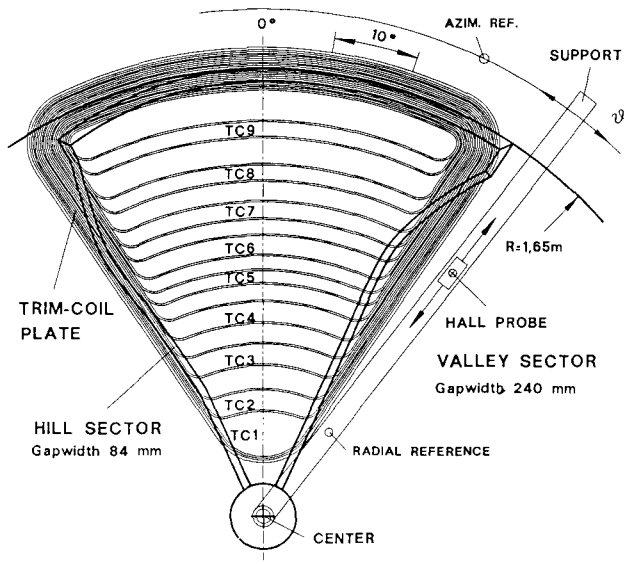


Fig. 2. Trim coil with field mapping unit

field measuring unit could be positionned by DC motors azimuthally over ± 60° from the center line of the hill sector and radially up to $R_{max} \approx 1.6$m. The integral field on an orbit has to be measured with an accuracy of $1 \cdot 10^{-3}$. Due to field gradients of up to 0.25 T/cm in the hill-valley region, the precision for positioning the probe must be 0.1 mm or 0.005°. A PC based system was used to perform field mapping, i.e. to control the motion of the probe and to do the corresponding data acquisition. The main field was measured for H_2^+ ions of 80 MeV, which corresponds to a level of 0.65 T in the valley region. Then with the main field switched on the trim coil fields were subsequently measured with maximum positive as well as negative excitation, to improve accuracy.

4. RF SYSTEM

A new system for rf power generation and control replaces the former self oscillating unit[1,5]. This modification was done in close cooperation with the industry in such a way, that a contract with HERFURTH GmbH, Hamburg, covered the new RF power generator and most of the low level subsystems like signal generation, frequency tuning, regulation and control, while the cyclotron group was responsible for all installations in the vacuum chamber like frequency tuning elements, coupling loops inclusive feedthrus, pick ups for phase, amplitude etc.

Figure 4 is a simplified schematic of the system. Operation of the rf is controlled by a special dedicated micro-computer, which controles more than 20 tuning elements and monitors the proper operation of signal detection and conditioning, regulation loops etc. The frequency is generated in a synthesizer, which was selected for a very good short term stability. Power amplification is achieved in a two stage setup. Two solid state wideband amplifiers of 1 kW each in parallel serve as preamplifier for a power stage equipped with the SIEMENS tetrode RS 2058 CJ. The nominal output power is 100 kW in the frequency range of 20 to 30 MHz.

The rf power is transfered to the cyclotron via a 6 1/8" coax-line over a distance of about 21 m. After passing a tuned impedance transforming network, the power is coupled inductively into one accelerating sector. Multiple loop control was necessary for amplitude and phase regulation, to achieve the specified long and short term stability. The resonance frequency of the accelerating system is preset within the operating range by motor driven panels in the dees. Simultaneously also the adjustable coax line on top of the machine is pretuned. The coax line is terminated with two watercooled variable vacuum capacitors in parallel, which are the active elements of the resonance frequency fine tuning loop arranged around the resonator. Amplitude regulation is performed by two superposed control loops (Fig. 3). A fast inner loop stabilizes the amplification factor between power splitter 2 and directional coupler 1, hence suppressing amplitude modulation contents introduced by the non ideal power amplifier. The amplitude setting is achieved by use of an overall regulation loop, which also defines long term stability. It is appearent, that for a long term stability of $<1 \cdot 10^{-4}$ the characteristics of demodulator 4 is of prime importance. - The regulation scheme is completed by an overall phase regulation loop.

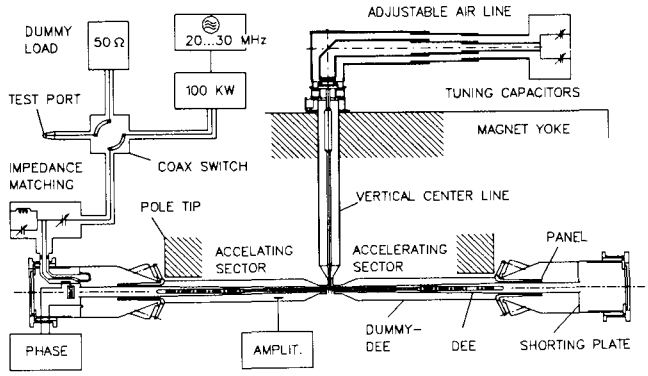


Fig. 4. Simplified schematic of the rf system

Figure 3 shows the situation in normal mode operation. Because of the influence of the multipactor effect, the switching on procedure requires a modified

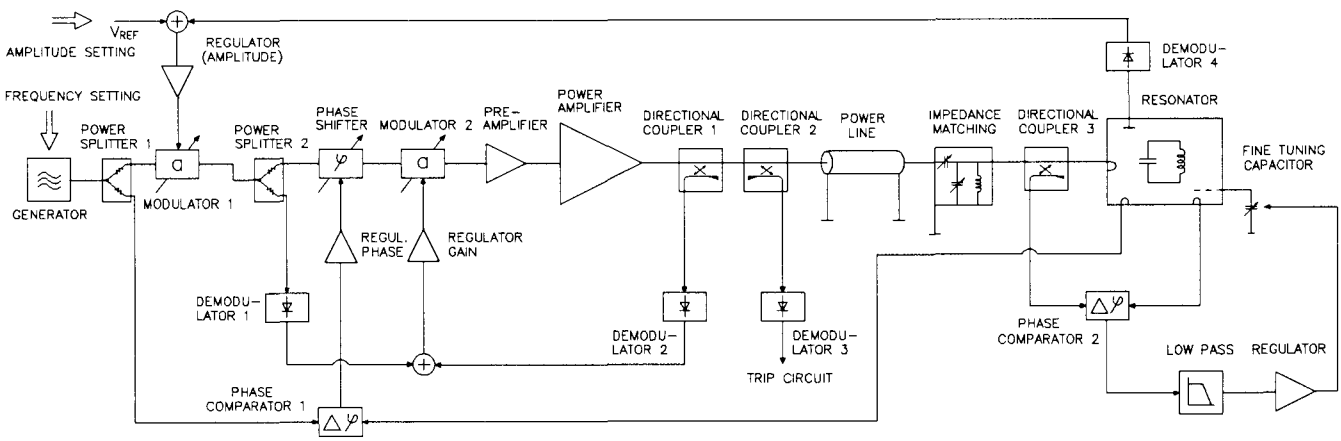


Fig. 3. Circuit diagram of the rf-system (normal mode operation)

system configuration. In this case trip- and safety-circuits as well as part of the regulating loops are switched to an inactive state by the control computer. Amplification factors for signal conditioning etc. are adapted, to respond on the very low levels during start up. After presetting all tuning elements in the system, rf power of maximum only 1 Watt is applied to the resonator, to be safely free from multipactoring. When the resonator has been precisely tuned in closed loop mode to the operating frequency, then for start up a rf burst is generated. For approximately 10 μs the maximum available rf power is applied to the system, in order to increase the voltage in the resonator with a slope of $> 1 kV/\mu s$, which is necessary to overcome the multipactor effect. After 500 μs the system is switched to normal mode operation.
As the improvement in stability of amplitude and frequency/phase had been a first order argument for the new rf system, these figures were checked carefully during the acceptance tests and the first time of operation with beam. Short term amplitude stability in normal operation, refered to the maximum accelerating voltage of $\hat{u}_{max} = 45$ kV in our cyclotron was well below the specified figure of $\hat{u}/\hat{u}_{max} < \pm 1 \cdot 10^{-4}$ for all settings of voltage and frequency in the tuning range. Phase stability refered to the output of the master oszillator proved to be $\Delta\varphi < \pm 0.3°$.
$\hat{u}_{max} = 45$ kV is needed in JULIC, which correspond to rf power of only 45 kW. But the above described switching on procedure is significantly simplified with the extra power of up to 100 kW.

5. TRANSFER BEAMLINE

The H_2^+ or H^-/D^- particles of about 40 MeV/A must be transfered from the cyclotron over a distance of about 100 m to the COSY ring, which is to be filled with protons by stripping injection[6]. The transfer beamline was constructed by a department of the SIEMENS company[7]. All the 57 magnets of the beamline connected to 19 computer controlled power supplies are now running with the proper B[I]-curves. The vacuum system is also fully accepted and provides a pressure of $p < 1 \cdot 10^{-7}$ mbar, dropping to $p < 1 \cdot 10^{-10}$ mbar near the COSY ring. The beamline was tested section by section with a H_2^+ beam of 76 MeV and intensities of about 4 μA. The first section, which matches the cyclotron beam with an emittance of 6 $\pi \cdot$mm$\cdot$mrad to the subsequent FODO structures and achromatic sections, produced the designed beam waist at its end. Most of the magnets can be set to the calculated field levels within a tolerance of 2%. Without the limitations by beam slits about 97% of the beam current can be transported to section I6. Even if the beam at the entrance of the beamline is misadjusted by ± 1 mrad in horizontal or vertical plane, losses do not exceed 10%. The local distribution of the full intensity beam is measured at 7 positions along the beamline by grids of 30 wires (wire diameter 0.1 mm, distance 1.5 mm). As the H_2^+ particles, hitting the wires, are stripped to protons, the shadow of the wires can be observed in the H_2^+ beam for detailed diagnostics. The protons appear as bright lines on the scintillator screen with half the rigidity of the H_2^+ ions. - The acceptance tests for the last two beamline sections have to be done in September, when the COSY ring is ready to accept the first ions by stripping injection.

6. CONCLUSION

Because of severe interaction between the various tasks at the COSY injector complex, the modification took a relative long time. The cyclotron was back in operation with internal H_2^+ beam in November 1991 and with extracted beam in February 1992. New instrumentation and especially the new computer control, which was available in a preliminary version only, caused a series of difficulties. As the beam was urgently needed for the commissioning and acceptance tests of the transfer beamline, debugging is not yet completely finished. - Up now H_2^+ beams of up to 8.5 μA could be extracted from the cyclotron.

7. REFERENCES

1) Maier, R., Pfister, U., "COSY-Jülich, a Synchrotron and Storage Ring for Medium Energy Physics," This conference.
2) Bräutigam, W., Beuscher, H., Brings, R., Böge, H.G., Wucherer, P., "Upgrading JULIC as Injector for COSY," EPAC, Rome, 1988, pp. 317-319.
3) Beuscher, H., "Ion Sources at the Cooler Synchrotron COSY," Rev. Sci. Instr. 63/1992, p. 2847.
4) Wucherer, P., et al., "Measurement of the Magnetic Field of the Cyclotron for H_2^+ Beam," IKP Annual Report 1991, pp. 259-261, Jül-2590.
5) Bräutigam, W., Brings, R., Rotert, N., "Commissioning of the new RF-System at the Cyclotron," IKP Annual Report 1991, pp. 256-258, Jül-2590.
6) Rogge, M., et al., "Stripping Injection of H_2^+ and H^- into COSY," PAC 1989, Chicago, pp. 417-419.
7) Anton, F., et al., "Beam Transfer and Matching between the Cyclotron JULIC and the Cooler Synchrotron COSY," EPAC, Berlin 1992.
8) Kennepohl, K., Herschbach, M., Maeckelburg, D., Bräutigam, W., "The new Phase Detection System of the COSY-Injector," This conference.

CURRENT STATUS AND FUTURE PROJECT OF CYCLOTRON LABORATORY IN ALMA-ATA

A.Arzumanov, V.Batischev, V.Berger, V.Gerasimov, M.Gorcovets
Institute of Nuclear Physics, Kazakhstan Academy of Sciences
Alma-Ata, 480082, Republic of Kazakhstan

ABSTRACT

The present paper describes the results of improvements performed at the cyclotron facility in Alma-Ata during last years. Among them are increasing the efficiency of beam extraction system and opportunity of increasing time range between two successive beam pulses by RF-beam pulser. Future plans on the K=600 heavy ions separated sector cyclotron are also presented.

1. INTRODUCTION

The main trend of the Cyclotron laboratory in the INP in Alma-Ata is the improvement of the accelerated particles beam parameters and isochronous cyclotron systems to meet the increasing demands of nuclear physics experiments and commercial applications of the cyclotron[1]. Since commissioning the isochronous cyclotron in 1972[2] the beam transport system, ion source, vacuum system were modernized and RF voltage was stabilized. The present paper describes further modernization of the beam extraction system including remote controllable electrostatic deflector located inside the dee. The installation of an additional external deflector for ion bunches selection is also considered.

Another trend of the Cyclotron laboratory research was development of the project of accelerator installation the main part of which is the separated sector cyclotron with K=600. Some results of the model magnet magnetic field measurements are presented.

2. ADJUSTABLE DEFLECTOR

The main feature of the Alma-Ata cyclotron is the accelerating system, consisting of two 180° dees. This system affords the large energy gain per turn thus decreasing influence of magnetic field disturbances and enlarging the turn separation at extraction radius. At the same time the necessity of placing the deflector inside the dee complicates substantially it's design.

The high effective and reliable extraction system must meet the needs of necessary deflection and focusing of the beam and to be reliable under large heat load. At changing magnetic field in the wide range it is necessary also to take into account the changing of the shape of the orbit at extraction radius. For this reason a new electrostatic deflector with nonuniform electric field and with precise replacing of it's parts without switching off high voltage potential was designed. This deflector located inside the dee is shown schematically in Fig. 1, the angular coordinates (15°, 55°, 125°) of three movable parts of the deflector are depicted.

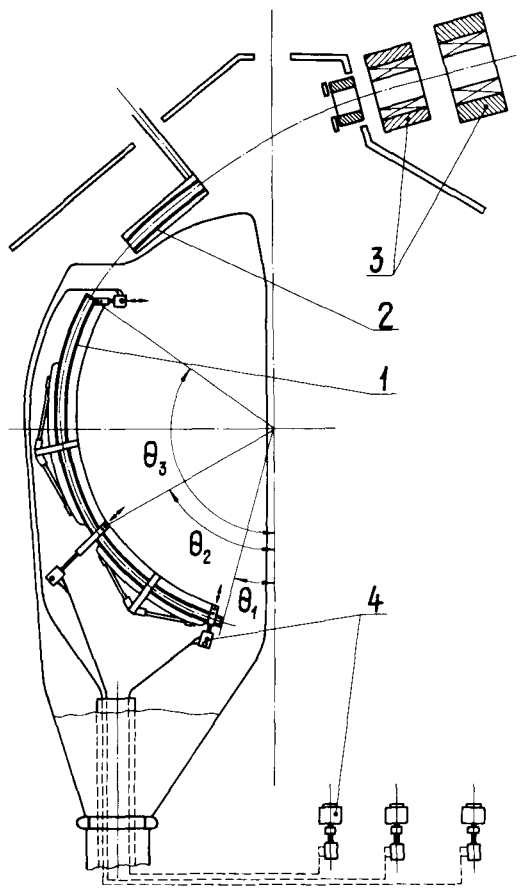


Fig. 1. The beam extraction system: 1-adjustable deflector, 2-additional deflector, 3-steering magnets, 4-hydraulic cylinders.

The fine displacement of these parts of the deflector may be made in the range of ± 7 mm with accuracy of 0,1 mm and be produced remotely from the main control panel with three pairs of hydraulic cylinders. General view of the deflector is shown in Fig. 2. This device is very effective in adjusting the acceptance of the deflector to the emittance of the internal beam.



Fig. 2. General view of the adjustable deflector.

3. THE SYSTEM FOR REDUCTION OF PARTICLE BUNCHES REPETITION RATES

This system is designed for increasing the resolution of a neutron spectrometer based on time-of-flight measurements by reducing the beam repetition rate. Using a selection slit, three successive accelerated particles bunches of every four ones are stopped at a collimator after sweeping off by high-voltage RF deflector. Only the bunches which see a zero resulting electric field between the electrodes of the deflector are able to pass the selection slit. Usually as a bunch selector a deflector with flat electrodes and sinusoidally varying potential difference between them is used[3,4].

An effective sweeping off system assumes absence of beam losses, minimum deflecting voltage, reliable design, simple tuning and easy running. To meet these needs a deflection system was developed which is located in the fringing magnetic field of the cyclotron immediately after the main deflector. Such a system gives substantial reduction of deflection potential in comparison with ordinary one located in nonuniform magnetic field free space. The deflection system is shown in Fig. 1. An additional deflector (pulser) is located inside the accelerator chamber and outside the dee (θ=142°-162°), where the beam size is sufficiently small yet.

The deflector is composed of a pair of plates 30 cm long and separated by 3 cm, in cross section they have hyperbolic profile for increasing radial focusing of the beam. The results of the numerical calculations of the beam envelopes in the horizontal plane for different potentials at the deflector are shown in Fig. 3. The experimentally measured beam emittance and ion transit time in the deflector have been taken into account. The minimum potential for 30 MeV protons burst separation is 15 kV.

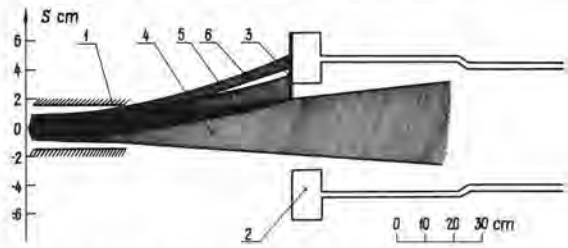


Fig. 3. Particles bursts sweeping off system and beam envelopes: 1-RF selector, 2-beamline, 3-collimator, 4,5,6-beams at potential difference of 0, 15 kV and 30 kV.

The power-supply electrical circuit is analogous to those of [3,4] and is shown in Fig. 4.

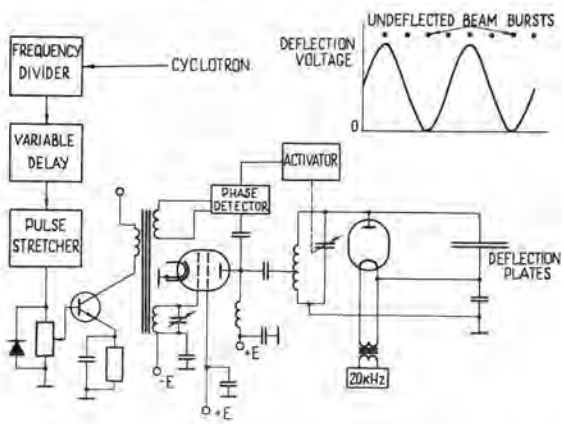


Fig. 4. Simplified scheme of particles bursts selection system.

The final section is a resonant LC circuit in which the selector is a capacitive element. In this circuit a sinusoidal voltage is excited. The frequency varies from 2-4,5 MHz. The final amplifier stage consists of a power tetrode run in class AB with a total power of 0,8-1,0 kW. The resulting potential difference generated between the electrodes of the selector varies sinusoidally from zero to the peak value. This signal is phased with the particles bunches, so that the interesting bunch passes through the deflector when the potential across the electrodes V is

zero and dV/dt is zero also.

4. CYCLOTRON PROJECT WITH K=600

In order to develop accelerator-assisted scientific research in the Republic of Kazakhstan after 20 years of intensive use of 150-cm isochronous cyclotron in Alma-Ata it was decided to carry out preliminary accelerator science research on new K=600 cyclotron facility, for these research necessary financies were allowed. The facility consists of a separated sector cyclotron and injector cyclotron with K=100. The ion species and energy range are considered to be from 200 MeV protons to very heavy ions with A 200 and energy as high as possible. Up to this time magnetic field mapping on the model magnet were carried out and orbit characteristics were investigated numerically and analitically. The schematic plan of the four sector cyclotron is shown in Fig. 5. The 1/20 scale model of the sector magnet is shown in Fig. 6.

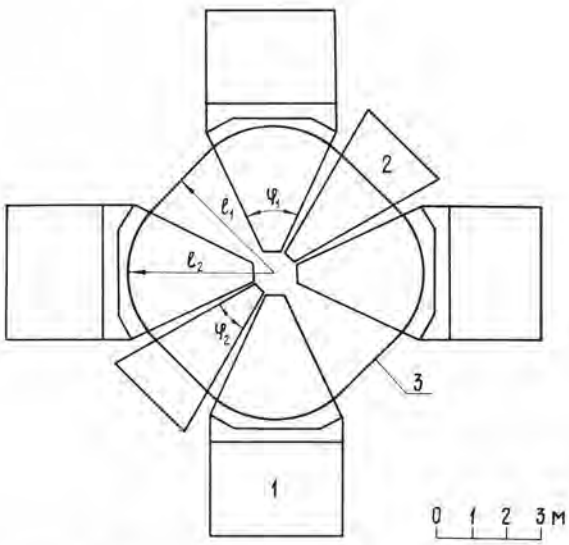


Fig. 5. Simplified scheme of separated sector cyclotron: 1-sector, φ_1=50°, 2-dee, φ_2=30°, 3-equilibrium orbit.



Fig. 6. Model magnet.

Magnetic field mapping was carried out at the full range of radii and angles for different levels of magnetic field density. Tipical azimuthal distribution of magnetic field is shown in Fig. 7.

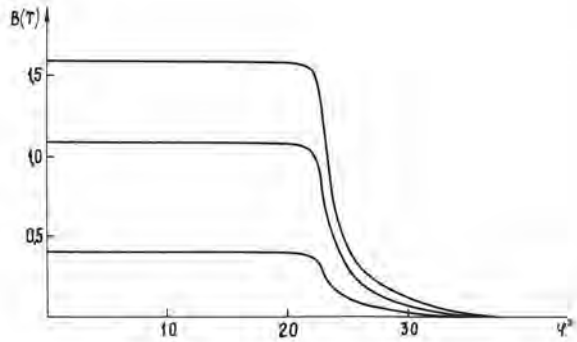


Fig. 7. Azimuthal distribution of magnetic field in the median plane.

The choice of general scheme of the main cyclotron, determination of injection and extraction radii at this stage were carried out at the simplifying assumption of sharp end fringing field. Accurate calculations of equilibrium orbits, betatron frequences and isochronous magnetic fields were performed using different computer programes. The frequency band of the RF system is from 6 to 29 MHz, the orbital frequency band is from 2 to 7,3 MHz. Detailed design of different elements of the facility is now in progress but the future development of the project is not yet approved by the Kazakhstan government.

5. REFERENCES

1) A.A.Arzumanov, V.N.Batischev et al., "Medical Radioisotopes Production at the Isochronous Cyclotron in Alma-Ata" in Proceedings of the EPAC-88 (World Sci., Rome, 1988), pp. 1454-1455.
2) A.A.Arzumanov, L.M.Nemenov, "Kazakhstan Variable Energy Isochronous Cyclotron", Nucl.Instr.Meth., v.106, pp. 201-202 (1973).
3) C.Roulet, G.Albouy et al., "A device for in-beam G-factor measurements for isomeric states in the range of a few hundred nanoseconds", Nucl.Instr.Meth. v. 125, pp. 29-40 (1975).
4) H.H.Wieman and L.A.Erb, "A high voltage RF deflector for reduction of cyclotron beam repetition rates", Nucl.Instr.Meth., v.142, 573-576 (1977)

INITIAL OPERATION OF HIRFL

B.W.Wei, F.Ye
Institute of Modern Physics, Chinese Academy of Sciences P.O.Box 31, Lanzhou 730000, P.R.China

ABSTRACT

HIRFL consisting of a main accelerator K450 separated sector cyclotron (SSC) and an injector K69 sector focusing cyclotron (SFC) was commissioned on December 12,1988. Since then, five kinds of ion species have been provided for testing of terminal equipments and experiments of nuclear physics, atomic physics, nuclear chemistry, material science and radiobiology. High quality beams with transverse emittance less than 8π mm mrad, energy spread of about 0.3% and beam intensity ranging from 10^{11} to 10^{12} pps were extracted.

A 10 GHz ECR heavy ion source, CAPRICE with the 8m beam transfer line and the axial injection system from the bottom of injector SFC have got into operation this year and have achieved convenient performance.

The initial three year operation and the present status of HIRFL are presented in this report.

1. INTRODUCTION

Table 1. The mile stone for construction of HIRFL

	SSC
Nov.,1976	Project approval
1978	Earth broken
1976-1980	Theoretical study
	Model test
	Technical design
1980-1986	Construction
1987	Assembling
	Magnetic field measurement
1988	Vacuum pumping
	Rf conditioning
	Beam tuning
Dec.12,1988	First beam ($^{12}C^{6+}$ 50 MeV/N)
	SFC
1984	Shut down for conversion
May.17.1987	First beam
1992	Operation of ECR ion source

On December 12, 1988, the first beam of $^{12}C^{6+}$ 50 MeV/N was successfully extracted from the main accelerator SSC coupled with the injector SFC. It had taken approximately 10 years since the construction of SSC started in 1978. Table 1 gives the mile stone for construction of HIRFL.

The scheme and parameter of HIRFL and the commissioning result have been described in previous publications[1-2]. Figure 1 recalls the general layout of HIRFL.

During the year 1989, the trial operation of HIRFL only delivered 50 MeV/N $^{12}C^{6+}$ beam. From 1990 to 1991, another two kinds of ion species, $^{16}O^{8+}$ 50 MeV/N and $^{12}C^{6+}$ 75 MeV/N have been provided for users according to the experimental requirement. After putting into operation of the ECR heavy ion source as an external ion source of SFC with the 8m beam transfer line and the axial injection system from the bottom of SFC, the ions of $^{20}Ne^{8+}$ 25 MeV/N and $^{40}Ar^{16+}$ 25 MeV/N have been accelerated. We are planning to get the designed top energy of HIRFL, 100 MeV/N $^{12}C^{6+}$ in the autumn this year. Table 2 lists the accelerated beams and the operated parameters of HIRFL.

Table 2. The accelerated beams and the operated parameters of HIRFL

	Z	RF (MHz)	h	E (MeV/N)	I (μA)
			SFC		
^{12}C	4	6.26	1	4.5	5.0
^{12}C	4	7.53	1	6.6	5.0
^{16}O	5	6.26	1	4.5	5.0
^{20}Ne	4	13.54	3	2.3	1.0
^{40}Ar	8	13.54	3	2.3	1.0
			SSC		
^{12}C	6	9.39	2	50.0	0.4
^{12}C	6	11.29	2	75.0	0.4
^{16}O	8	9.39	2	50.0	0.4
^{20}Ne	8	13.54	4	25.0	
^{40}Ar	16	13.54	4	25.0	

High quality beams with transverse emittance less than 8π mm mrad, energy spread of about 0.3% and beam intensity ranging from 10^{11} to 10^{12} pps have been obtained. Roughly say, half of the beam time was used

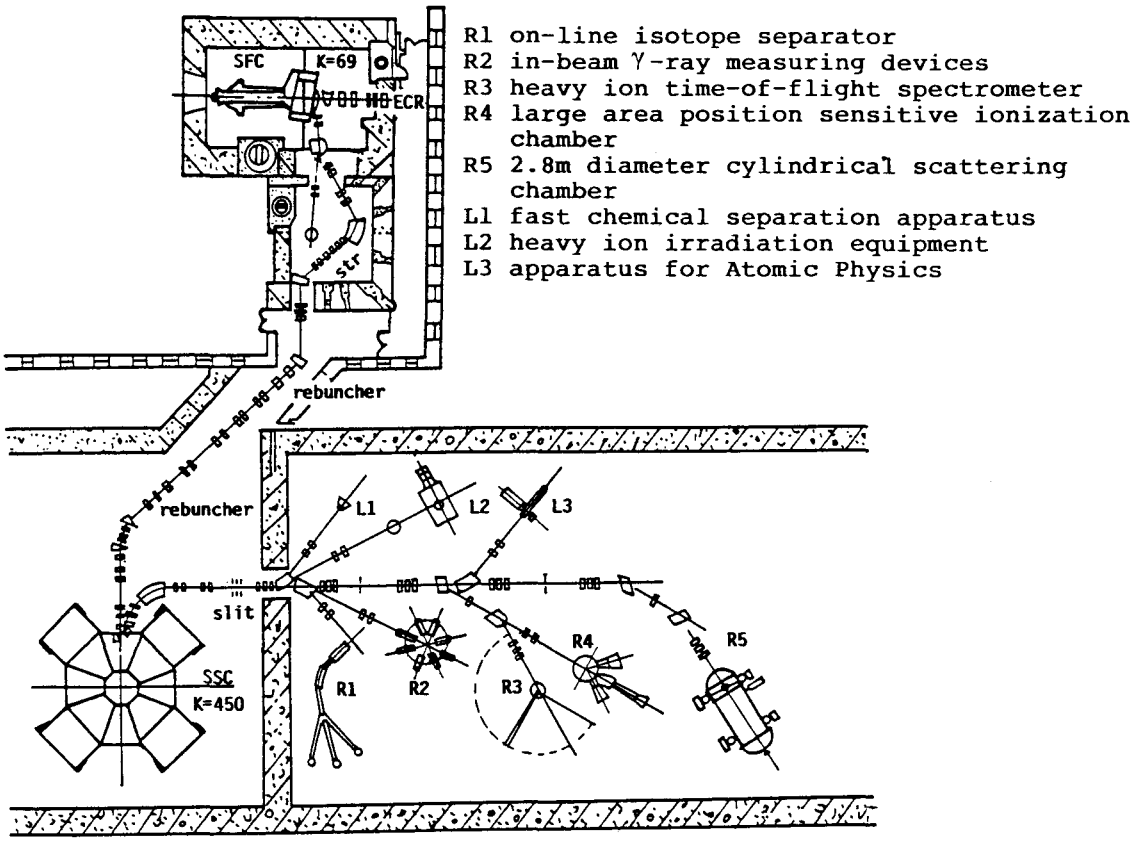


Fig.1. The general layout of HIRFL. R1- Isotope Separator, R2- In Beam Gamma-ray Measuring Device, R3- Heavy Ion Telescope, R4- Large Area Position Sensitive Ionization Chamber, R5- Heavy Ion Scattering Chamber, L1- Fast Chemical Separation Apparatus, L2- Irradiation Terminal, L3- Atomic Physics Terminal.

for machine tuning and testings of the terminal equipments and the rest was used for experiments. The beam time used for experiments was about 3500 hrs from 1989 to May of 1991. Among them, 70 percent was used for nuclear physics and nuclear chemistry and 30 percent was used for atomic physics, material science and radio biology.

The initial three year operation and the present status of HIRFL are presented in this report.

2. OPERATION STATUS

2.1. ECR Ion Source

The CAPRICE type ECR ion source made in Grenoble has achieved convenient performance in IMP. It has been not only used for the injector SFC as an external ion source but also for the atomic physics experiments.

The improvement to CAPRICE has been done recently by adding a conical iron ring to the end of the injection stage to make the first magnetic field mirror peak of the ECR stage more narrow. It could facilitate the plasma diffusion from the first stage to the second as the distance between the stages is smaller than before. As a result, the higher beam current more than 250μa both for $^{20}Ne^{4+}$ and $^{40}Ar^{8+}$ has been extracted from the CAPRICE ion source under the condition of extraction voltage and plasma electrode hole being 15kV and 6mm respectively[3]. The main parameters of CAPRICE is given in table 3.

Table 3. Main parameters of CAPRICE

Microwave generator	
frequency	10 GHz
output max.	2.5 kW
power consumption	10 kW
Magnetic field	
B max.	0.9 T
B min	0.3 T
power consumption	35 kW
hexapole	$SmCo_5$
B at cavity wall	0.4 T
Vacuum	10 torr
first stage	10 torr
second stage	10 torr
Pumping speed	
first stage	50 1/s
second stage	450 1/s
Extraction geometry	
electrode hole	6 mm
puller hole	16 mm
gap	33 mm

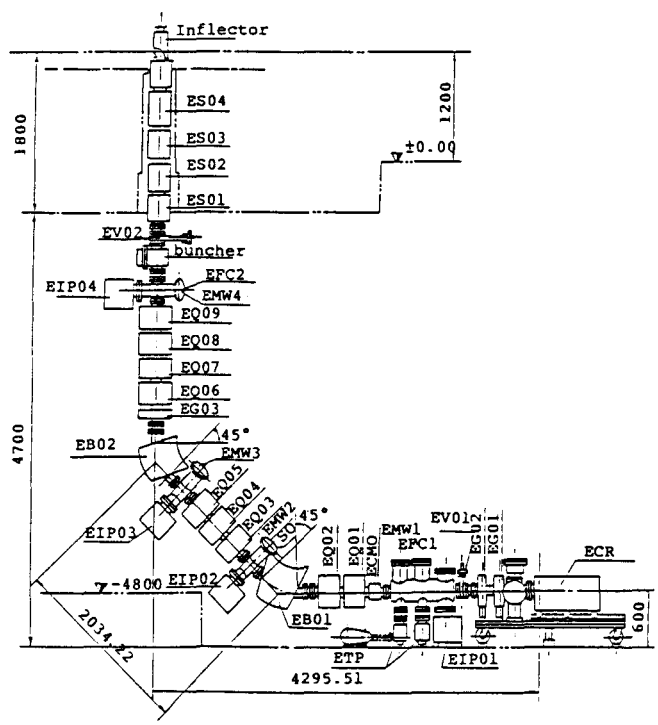


Fig.2. The beam transfer line from ECR ion source to the center of SFC

2.2. SFC

Figure 2 shows the beam transfer line from ECR ion source to the center of SFC. Two Glasser type lenses focus the beam from ECR ion source into waists at the diagnostics position. The other two match the beam to the 90° achromatic deflection section which consists of two 45° dipoles and three quadrupoles. This section also provides charge state selection with the charge state resolution of 1/20°which is only enough for ions up to Ta. 4 quadrupole lenses are placed subsequently to match the phase spaces. At the entrance of yoke hole a buncher consisting of two parallel mesh plates forming a single gap and excited by an rf power supply with sawtooth shape voltage is placed, and then four solenoid lenses focus the beam to the spiral electrostatic inflector which is located at the center of SFC. The inflector bends the beam direction by 90° and brings the ion trajectories on to the median plane of SFC. Table 4 gives the main parameters of the spiral electrostatic inflector. The steering magnets are

Table 4. The main parameters of the spiral electrostatic inflector

Electric radius (Re)	6.0 cm
Magnetic radius (Rm)	2.5 cm
k (Re/2Rm)	1.2
Distance between electrodes	0.8 cm
Width of electrode	2.0 cm
Injection radius of SFC	4.5 cm
Extraction voltage of ECR ion source max.	20 kV

arranged along the beam line for adjusting the optical axis. The preliminary results show that the beam transfer efficiency from ECR ion source to inflector is about 60%, and the vacuum pressure is about 10^{-5} pa. in the beam line tube.

After installing of the axial injection system, the magnetic field in the centre region of SFC should be re-measured. We decided to map all the required magnetic field from the center of SFC to outmost radius for ten magnetic field levels up to 16 kG. The isochronous field accuracy obtained by directly exciting the main coil and coaxial coils is about 10^{-3} which is good enough for guarantee the primary accelerating procedure and easy for isochronous optimization by using the center phase probes.

Besides of remapping the magnetic field, some other improvements to SFC had been done. The Dee box was rebuilt to meet the axial injection system requirement, the main coil was rebuilt also as it had been used 30 years

and its power supply, the DC generator was replaced by a silicon rectifier set. In order to eliminate oil backstreaming and to improve the vacuum, we substituted two cryopumps combined with turbomolecular pumping units for original diffusion pumps. 5×10^{-5} pa pressure was obtained for the $15m^3$ vacuum chamber of SFC with an effective pumping speed of about 30000 $1/s^{4-5)}$.

2.3. SSC

The operation of SSC is quite satisfactory. The beam emittance was measured by using three multiwire profilers located along the distribution beam line near the exit of SSC and the beam emittance less than 8π mm mrad was obtained. The energy spread was measured by using the ^{197}Au target elastic scattering method and the energy spread better than 3×10^{-3} was obtained.

Owing to large consumption of liquid nitrogen, the Balzers cryopump of RKP 800 with a combined pumping speed of about 14000 l/s was replaced by the HIRFL 800 cryopump without using liquid nitrogen. All of the helium compressor of HIRFL 800 cryopumps is installed on a non-radiation area outside the SSC hall. An expander is connected to a compressor with 60 m stainless steel tube which is easy to operate, monitor and maintain. The pumping speed of HIRFL 800 cryopump has been tested at a standard test dome to be 25000 and 27000 1/s for nitrogen and hydrogen respectively in the molecular flow region. The auxiliary pumping system consisting of four turbo-molecular pumps of type TPH 5000 manufactured by Pfeiffer has been suspended as the new powerful cryopump could put into operation at the pressure as high as 10 pa. By using the pumping system, after one hour pumping the pressure is reduced to about 10 pa in the SSC vacuum chamber. Then four HIRFL 800 cryopumps can be started. Within 6 hours cool down, the pressure of 10^{-5} pa could be obtained$^{6-7)}$.

3. FUTURE PROGRAM

A by-pass beam transfer line guiding the beam from SFC to the terminal equipments at the experimental hall directly is under constructing. It will be completed next year. By using the existing beam distribution line, from the slit position to R3, the heavy ion telescope terminal, a second emission beam line has been planned(Fig.1). The optical design has been completed and the technical design is now under progress.

4. REFERENCE

1) B.W.Wei, "Results from Lanzhou K450 heavy ion cyclotron," Proc. 1989 IEEE Particle Acc. Conf. (Chicago, 1989), Vol.1, pp.29.

2) B.W.Wei, "Commissioning of HIRFL, Proc. 12th Inter. Conf. on Cyclotrons and Their Applications," Berlin, 1989, (World Scientific, Singapore, 1989), pp.9.

3) B.W.Wei, Z.W.Liu, etc.,"Study on the magnetic field of CAPRICE type ECR ion source," this conference.

4) F.Ye, Z.R.Ma, etc.,"Upgrading the SFC," this conference.

5) J.Z.Jiang, X.H.Zhou, etc.,"Buncher in the beam line from ECR to SFC," this conference.

6) H.W.Zhao, Z.Q.Shen, etc., "Emittance measurements in HIRFL beam line," this conference.

7) S.X.Zhang, "Improvements of the vacuum system for HIRFL," Proc. China-Japan joint Symposium on Accelerators for Nuclear Science and Their Applications, Beijing, 1990, pp.213.

UPGRADING THE SFC

Ye Feng, Ma Zhongren, Yin Quanmin
Zhu Xuezhen, Qiao Qingwen,
Guo Minyan, Wang Yifang
Institute of Modern Physics, Academia Sinica, P.O. Box 31, Lanzhou, 730000, China

ABSTRACT

The ECR ion source,the beam line from ECR to SFC and the electrostatic inflector have been designed and installed to increase the ion species and the beam intensity.The working points are mainly located in the third harmonic accelerating region.The central region was studied carefully and the Dee, dummy Dee were rebuilt to match the external injection system.Other improvements were made to improve the the SFC performance and the operation efficiency.The commissioning of the upgraded SFC is also described.

1. INTRODUCTION

The injector of HIRFL is a 1.7m sector focusing cyclotron (SFC k=69) converted from a 1.5m classical cyclotron.In May 1987 the C^{4+} and O^{5+} beams were extracted from SFC using the internal PIG ion source. To increase the beam intensity and the ion species and improve the beam performances, an ECR external ion injection system was constructed and put into operation this year. Some other improvements were also finished to match the external injection system and to improve operation efficiency. The design, test and commissining of SFC are presented.

2. ECR ION SOURCE AND BEAM LINE

The ECR ion source named Caprice purchased from CENG Lab, and the beam line from the ECR ion source to the SFC have been installed. To meet the need for ions of heavier elements, some possible modifications at the first stage of the ECR ion source had been tried. As shown in Fig.1, component 15, a conical iron ring plays an important role in the formation of the first mirror peak. The position of the ring can be adjusted along the axis to meet the optimum for each ion species. But this movement can only change the position of the mirror peak not its shape. When we cut the ring shorter and made the cone sharper, the shape of the peak become narrow (Fig.2.). As a result, the distance between the two stages becomes smaller[1].

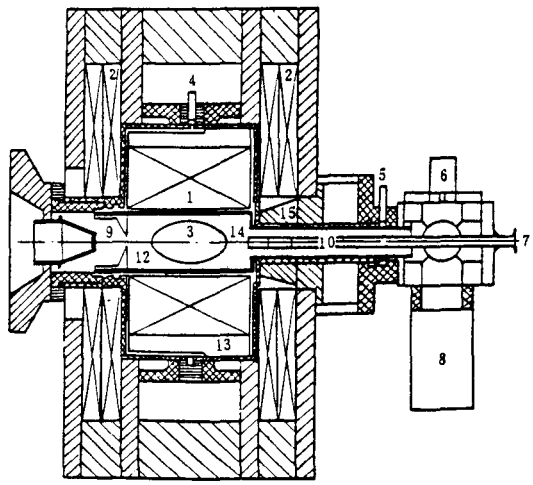


Fig.1. ECR ion source,Caprice.

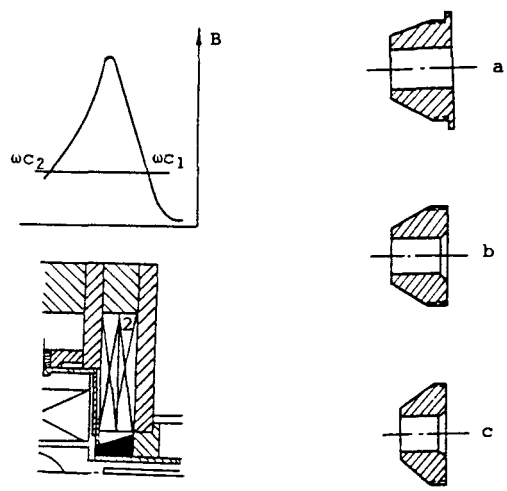


Fig.2. Conical iron ring and the axial field distribution.

It facilitates the plasma diffusion from the first stage to the second one. Figure 3 shows the ion-spectra optimized for Ar^{8+} with He as a mixing gas. It is worth notice that the benefit is based mainly on the improvement of charge state distribution in the plasma at the second stage. This probably implies that by shortening the distance between the two stages the second stage can obtain more preliminary ionized plasma than the neutral working gas from the first stage. In table 1 the results with the new ring are given. For comparision, the results obtained with the original ring are also specified on the left top of each figure. It is very clear that a considerable increase in ion current with a factor of about 1.5 to 2 is gotten for Ne and Ar respectively.

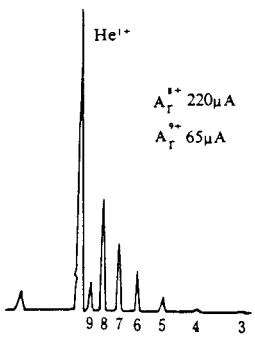


Fig.3. Ar^{8+} ion - spectrum with He as amixing gas.

Table 1. Beam current with the modificated ring

	O	Ne	Ar	Xe
3	315/390			
4		124/300		
5	220/220			
6	206/205	100/155		
7		25.4/35	108/183	
8			110/220	
9			56/105	
11			8.2/15	
15				22/25

The beam is injected from the bottom of the cyclotron SFC. The limited space of the basement brought a lot of trouble to the design and installation of the beam line from ECR to the SFC which is shown in Fig.4. The beam line was designed by using the TRANSPORT code. Only magnetic elements have been used. Two Glasser type lenses focus the beam to the vertical 90° achromatic deflection section, which consists of two 45° dipoles and triple quatrupoles. This section also provides charge state selection with resolution $Q/\triangle Q = 20$. The four quatrupoles EQ06–EQ09 are placed subsequently used to match the phase spaces. The ES01–ES04 are used to match the injection beam to the SFC acceptance. A sprial inflector was adopted to bend and place the beam on orbit .

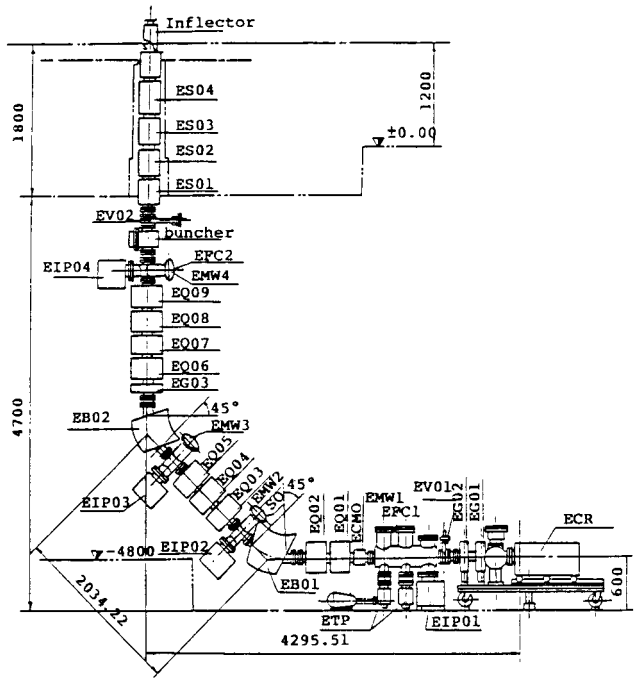


Fig.4 Beam line from ECR ion source to the inflector.

At the entrance of yoke hole a buncher is placed for bunching of the DC beams from ECR ion source. The buncher consists of two parallel mesh plates forming a single accelerating gap, and it is excited by an RF power supply with sawtooth shape voltage. The sawtooth-like waveform voltage is obtained directly from the sine waves by using a waveform converter, not from the combining RF sine waves with fundamental, second and third harmonic frequencies[2].

3. DESIGN OF THE CENTRAL REGION AND THE INFLECTOR

The main parameters of SFC are given in table 2. According to our condition we used CO to calculate the center region of SFC, and used CENTOM and CENTER, writen by GANIL and RCNP respectively, to check the calculated data. Figure 5 shows the opration diagram of SFC for particles with diffirent charge to mass ratios. Because the extraction voltage is limited by the isolation cover of ECR ion source, the voltage value is lower than 20 KV. So we chose the typical particle at point A to design our injection system.

Table 2. Main parameters of SFC

number of sector	3
spiral angle	33°
pole diameter	170 cm
extraction radius	75 cm
mean magnet field	1.6 T
circular coil	12 pairs
valley coil	4 × 3 pairs
dee number	1
dee angle	180°
frequency range	6 - 18 MHz
peak voltage	100 KV
RF power	200 KW
vacuum	5×10^{-5} Pa

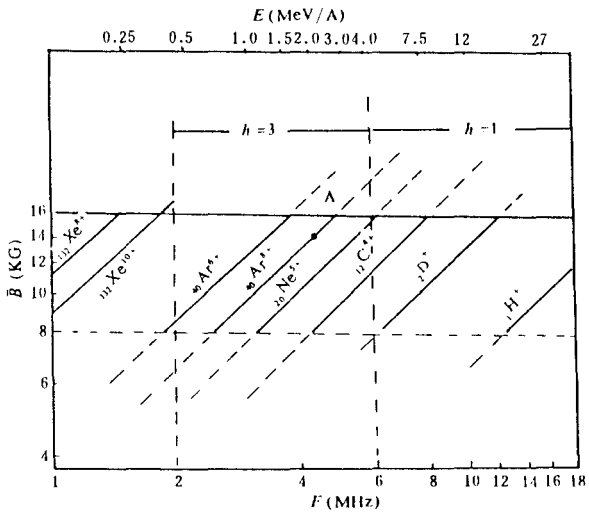


Fig.5 Operation diagram of SFC

To meet the requirement of the installation and adjustment of the inflector, and to calculate the ion trajectories, the electric field was calculated by numerical methods (3D code) and an electrolytic tank was used to measure the electric potential to check the calculated data. The design of the center region is shown in Fig.6.

The inflector is one of the key devices in the axial injection scheme. A spiral electrostatic inflector has been adopted to bend the beam direction by 90° and bring the ion trajectories onto the median plane. Following the used generally design principles and the equations of motion for the central trajectories an unslanted inflector had been designed and fabricated[3]. Its main parameters are listed in table 3.

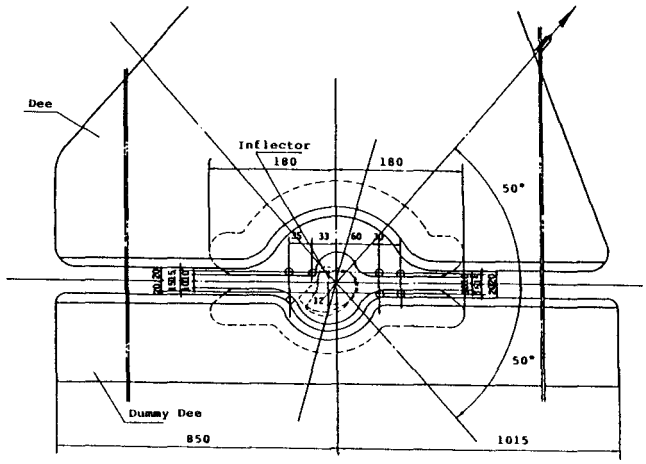


Fig.6 Design of the center region of SFC.

Table 3. Main parameters of the inflector

ECR extraction voltage (max.)	20 KV
Electric radius	
(height of the inflector)	6 cm
Magnetic radius	2.5 cm
k	1.2
β	0
Distance between electrodes	0.8 cm
Side width of the electrodes	2.0 cm
Dee voltage	60 KV
Injection radius	4.5 cm

4. STUDY OF CENTRAL TRAJECTORIES

The equation of the charged particle motion in the central region had been integrated analytically and the satisfactory results was obtained by using SCDD method. Firstly the displacement of the centres of rotation during the acceleration at third harmonic was obtained and the acceleration can be centred of the machine in several minimeters. Secondly the phase drift caused by the accelerated particles across the gap between Dee and dummy Dee can be controlled into ±5°. To give as large as possible space available for the center region and to improve the vertical electric focusing, the large gain in energy passage through a narrow gap at the first time was chosen. To select an optimum initial phase and to match the optic requirement of the inflector, a pump magnet field introduced by the plug at the region of 10cm has been adopted. The dependence of trajectories in the central region on the injection phase is shown in Fig.7.

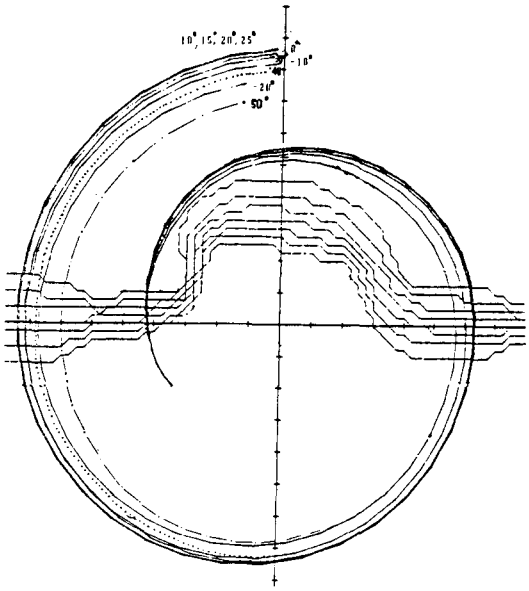


Fig.7 Dependence of trajectories on the injection phase.

Meanwhile to study the beam behaviour in the cyclotron in detail, acceleration simulation was done. Figure 8 shows the acceptance of SFC centre region.

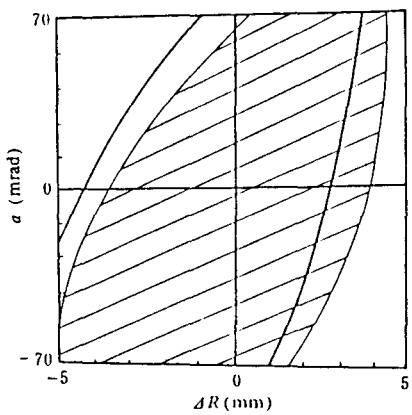


Fig.8 Acceptance of SFC center region.

5. MAGNET FIELD MAPPING AND OTHER IMPROVEMENTS

Because the new main coils took the place of the original one which was used for about 30 years and the external injection system has been adopted , the magnet field must be mapped again. The measurement was performed in case that the vacuume chamber had been installed. All measurements had been done by using the same excitation procedure for the main coils. The field distributions along the radius were mapped at 10 field levels at the excitation current of 300, 400, 500, 600, 700, 800, 900, 1000, 1100 and 1200 A. And at same field levels the contribution of the trim coils were measured. Especially we made efforts for measuring the contribution of plug at some magenet field levels and tried to obtain the optimum value. The measurement accuracies is ±2 Gauss. The deviation between the required isochronous field distribution along the radius of $Ar^{8+} - 2.345 MeV/A$ and measured one is 5×10^{-4}. We measured the three-dimensions field distribution at the center region from 0 to 45 cm along radius and along axis by using 10 pieces of hall probe at field levels of 800 A. The magnet field distribution in the hole of yoke along axis had been measured at field levels of 300, 800 and 1100 A. The edge magnet field distribution along exraction direcion at some field levels also had been measured.

At same time the Dee and dummy Dee was rebuilt to match the external injection system. The electrostatic deflector was replaced by new one to increase extraction efficiency. Two HIRFL-800 cryopumps took the place of two oil diffusion pumps. And the microcomputer-CAMAC system is used to control the SFC and the beam line.

6. COMMISSIONING

The commissioning was started in May. $Ar^{8+} - 2.345 MeV/A$ was accelerated at 3rd harmonic. ECR ion source worked stably. The transportation efficiency of beam line from ECR ion source to the inflector is better than 60%. When the main magnet field of 50 Gauss was decreased and the angle of 2° of inflector was tuned, the beam reached the extraction radius. The extraction efficiency of electrostatic deflector is better than 60%. Then Ne^{4+} was accelerated smoothly. These are just initial results.

7. REFERENCE

1) B.W.Wei, Z.W.Liu, etc.,"Study on the magnetic field of CAPRICE type ECR ion source," this conference.

2) J.Z.Jiang, X.H.Zhou, etc.,"Buncher in the beam line from ECR to SFC," this conference.

3) J. Belmont, "Axial injection and central region of the AVF cyclotron," **Lecture Notes of 1986 RCNP KIKUCHI Summer School on accelerator Tech.**,1986.

STATUS REPORT OF CYCLONE

M. Loiselet, N.Postiau and G. Ryckewaert,
Centre de Recherches du Cyclotron,
Université Catholique de Louvain,
2, Chemin du Cyclotron,
B 1348 Louvain-la-Neuve, Belgium

ABSTRACT

Although the main effort of the cyclotron group during the last years was devoted to the production of radioactive ion beams, several other major developments have been undertaken. The experimental hall has been rearranged to accomodate a large neutron multidetector (DEMON) for the study of nuclear reaction mechanisms with heavy ions. A new beam transport line has been designed and built to bring the heavy ion beams to this experiment. To improve the possibilities for time-of-flight experiments, a beam chopper has been constructed. The neutrontherapy unit has been equipped with an in-house built multileaf variable collimator.

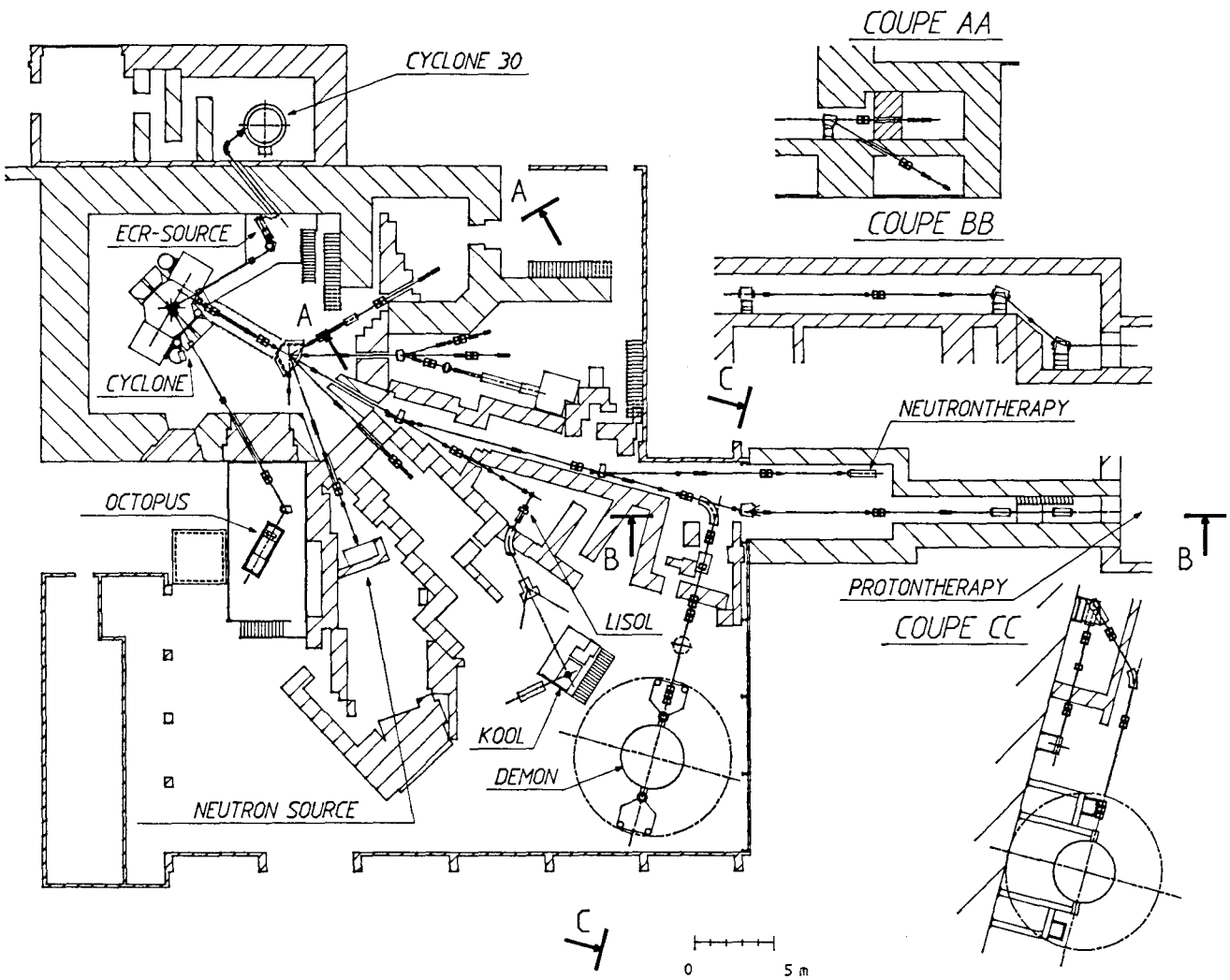


Figure 1. Layout of the Louvain-la-Neuve facility.

1. INTRODUCTION

After 20 years of operation, CYCLONE still delivers beams, of a greater variety than ever, to a multidisciplinary users community. This is illustrated e.g. by the beam time allocation in 1991, given in Table 1.

		HOURS	%
PHYSICS using		2843	52.9
light ions	1206 h		
heavy ions	1093 h		
radioactive ions	544 h		
ISOTOPE PRODUCTION		320	6.0
PROTON- AND NEUTRONTHERAPY		767	14.3
TECHNOLOGICAL APPLICATIONS		220	4.1
MAINTENANCE AND BEAM DEVELOPMENT		1223	22.7

Table 1 : Beam time distribution in 1991.

During the last years, a large effort was devoted to improve and extend the acceleration of radioactive ion beams mainly for nuclear astrophysics experiments.[1] In the following paragraphs other developments for the nuclear physics and medical users of the cyclotron are described. Figure 1 shows an actual layout of the facility at Louvain-la-Neuve.

2. BEAM TRANSPORT TO "DEMON"

The beam transport between the cyclotron exit and the target in the centre of DEMON, a large neutron multidetector, can be followed on Fig.1. Note that the centre of the sphere is situated 5 metres above ground, far from large volumes of solid material, to avoid rebounding neutrons. Part of the beam transport uses existing lines. One of the requirements for the design of the new section was that existing lines would not (or very little) have to be modified and that, as much as possible, existing beam line elements, recuperated from the former installation, would be used. The final choice uses a doubly focusing 90° bending magnet which can be tilted up around its incoming axis to an angle of 45 degrees. When the beam reaches the height of 5 metres, it is bent back in the horizontal plane by a 45°

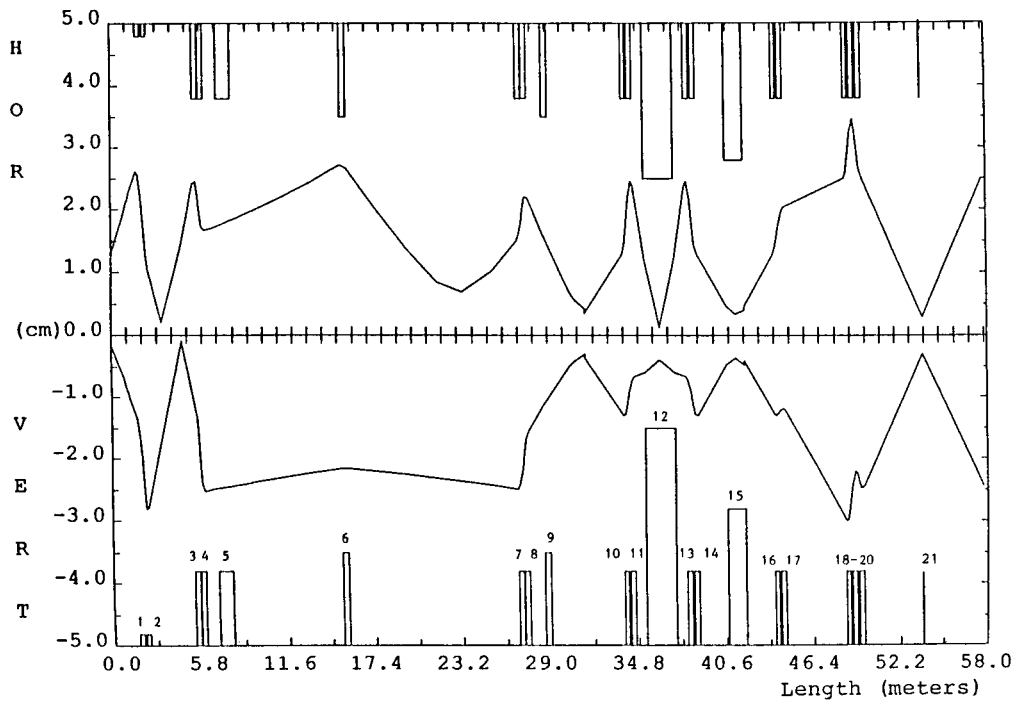


Figure 2. Beam envelopes along the transport line between the cyclotron and DEMON.
1, 3, 8, 11, 13, 17, 19 : horizontally focusing quadrupoles ;
2, 4, 10, 14, 16, 18, 20 : vertically focusing quadrupoles ;
6, 12, 15 : bending magnets ; 21 : target.

magnet. Underneath this line, another experimental set-up is installed which can be connected to the rest of the beam transport system by lowering the 90° magnet to its horizontal position when DEMON is not used. Other goals set for the design of these new lines were: a) minimise dispersion at the target location. b) keep the spot size on target within a 6 mm diameter. c) assure 100 % transmission. d) minimize the cost of the 90° magnet (small gap, optics rather unsensitive to small deviations from nominal values of its characteristics). The beam envelopes for a monoenergetic beam obtained with the TRANSPORT code are shown in Fig. 2. Table 2 shows the effect of energy dispersion on the beam characteristics at the target.

Beam characteristics	$\frac{\Delta E}{E} = 0$	$\frac{\Delta E}{E} = 0.3\ \%$
x/2	0,289 cm	0,290 cm
θ/2	6,191 mrad	6,261 mrad
y/2	0,296 cm	0,296 cm
ϕ/2	6,052 mrad	6,480 mrad
l/2	0,820 cm	0,821 cm

Table 2 : Spot size on target in DEMON with 0 and 0.3 % energy dispersion.

3. EXTERNAL BEAM CHOPPER

Several experiments using time-of-flight methods request longer times between beam pulses than the cyclotron normally provides. Since single turn extraction is not practicable with CYCLONE,[2] it was decided to build an external chopper to be placed in the main beamline between the cyclotron and the switching magnet. The beam chopper consists of two pairs of electrodes of respectively 60 cm and 28 cm length. The gap between electrodes is adjustable but nominally set to 35 mm. The first set is tuned around 1 MHz at a variable subharmonic of the cyclotron frequency. The second one works at the third harmonic. This way, the time between pulses is fixed in the range of 500 ± 50 ns. Peak voltage on the electrodes is 30 kV. Figure 3 shows a view of the electrode system and Fig.4 shows the block diagram.

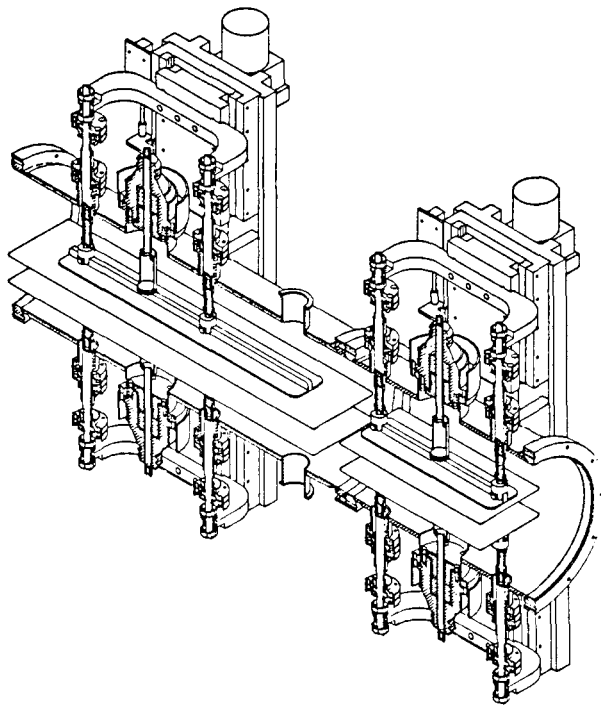


Fig. 3. View of the beam chopper.

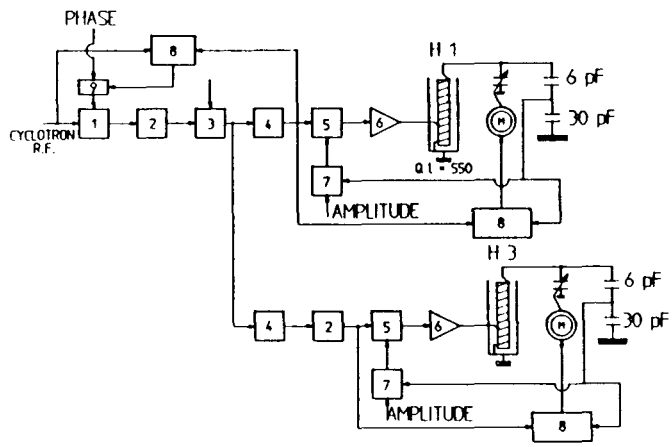


Fig. 4. Block diagramme of the chopper electronics : 1 : phase modulator; 2 : delay line ; 3 : programmable frequency divider ; 4: filter ; 5 : amplitude modulator ; 6 : power amplifier ; 7 : amplitude regulation ; 8 : phase discriminator.

4. MULTILEAF VARIABLE COLLIMATOR FOR NEUTRONTHERAPY

For more than ten years, a fixed collimator with variable inserts of various sizes has been used to define the irradiated field at the level of the patient. In order to be able to generate in all cases an optimally defined neutron field, a multileaf collimator, of SCANDITRONIX design was constructed and put into operation in 1992. The main part consists of two sets (left and right) of 22 leaves of 92 centimeters long. Each leaf can be positioned independently. A maximum field of 30*30 cm at the patient can be obtained. The leaves, made of soft iron with borated polyester disks imbedded, have been optimized to minimize the neutron leakage flux. Figure 5 shows a section through the new collimator.

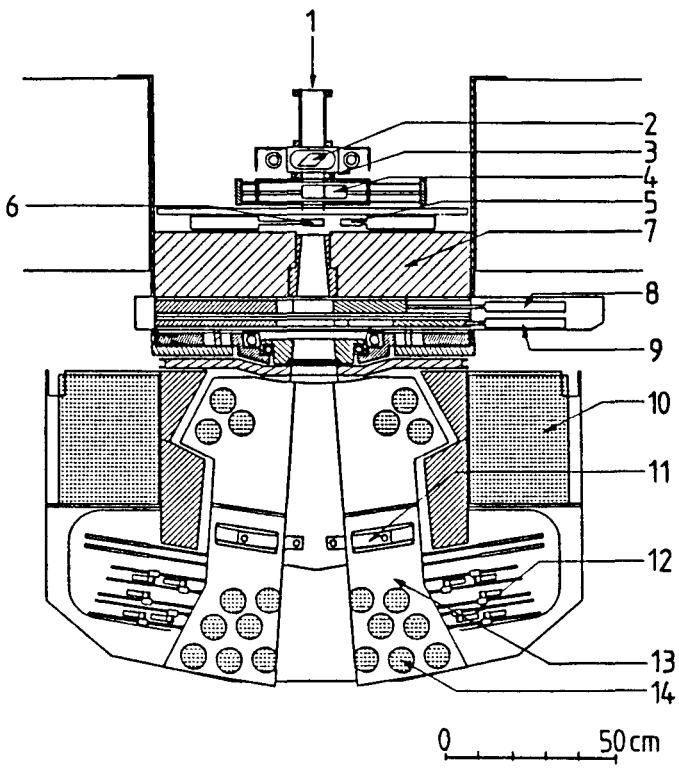


Figure 5. Section view of the multileaf neutron collimator.
1 : 65 MeV Protons (15 μA) ; 2 : Alumina ; 3 : Collimator ; 4 : Beryllium target ; 5 : Filter ; 6 : Light source ; 7 : Iron-precollimator ; 8 : Transmission chamber ; 9 : Filter ; 10 : Borated paraffin ; 11 : Slide ; 12 : Motor + potentiometer ; 13 : Iron leaf ; 14 : Borated polyester.

5. REFERENCES

1) Ryckewaert, G., Loiselet, M. and Postiau, N., "Radioactive ion beam production using the Louvain-la-Neuve cyclotrons : present status and future developments," Proceedings of this Conference.
2) Yokota,W., et al., "Design of beam chopping system for JAERI AVF cyclotron," Proceedings 12th Int. Conf. on Cyclotrons and their Applications (World Scientific, Singapore,1991) pp. 388-391.

PERFORMANCE OF THE K1200 CYCLOTRON AT MSU

P. Miller, T. Antaya, F. Marti, D. Poe, B. Sherrill, J. Stetson, J. Winger*
NSCL, Michigan State University,E. Lansing,
MI 48824 U.S.A.

and

J. Nolen
Physics Divison, Argonne National Lab., Argonne,
Illinois 60439 U.S.A.

ABSTRACT

The current performance of the K1200 cyclotron, the primary accelerator in the National Superconducting Cyclotron Laboratory, is reported and results of development projects are summarized.

1. RELIABILITY

The initial reliability of the cyclotron system, as evidenced by statistics of equipment breakdown, was not acceptable. Breakdowns occurred in many different systems. Improvements of deflectors, rf power supply and rf voltage holding are outlined below. Efforts to improve reliability of the overall facility were successful and are continuing.

Running statistics are shown in Figures 1 and 2.

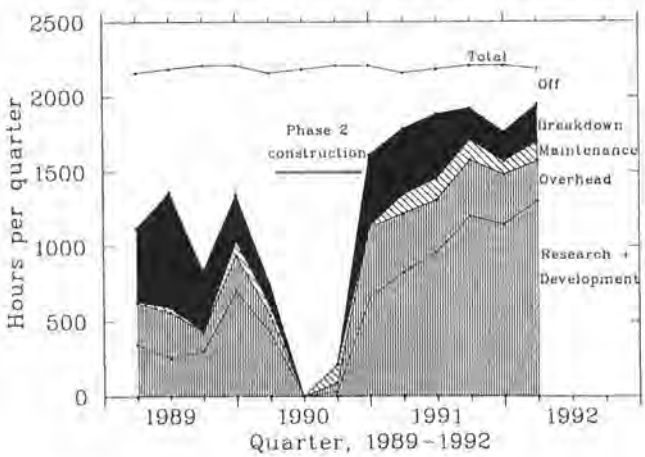


Fig. 1. K1200 operating time distribution.

Displayed in Fig. 1 is the distribution of the total time in each 3 month period among the following categories: operation (total of research, development and overhead), breakdown, maintenance and scheduled down time. In Figure 2 the reliability ratio, operation time

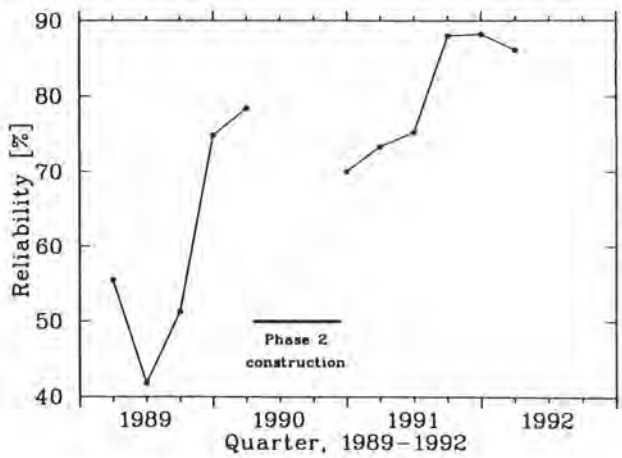


Fig. 2. Reliability, measured as the ratio of operating time to time scheduled for operation.

divided by operation plus breakdown time, is plotted for the same period, 1989 to the present. From February to September 1990 the K1200 was shut down for construction of the A1200 fragment separator and completion of the Phase 2 beam lines.

1.1. Deflectors

The voltage that electrostatic deflector E1 will sustain with beam present has increased from 45 kV on 7 mm gap in 1988[1] to 60 kV on 6 mm gap at present. The second deflector, E2, being shorter and having no hinges, operates reliably up to 80 kV (6 mm). Advances in voltage holding performance have resulted from the following developments[2] :

- ceramic glass/ metal vacuum feedthrough with internal cable and current limiting resistor
- suppression of electron emission current by an insulating coating on the cathode

*This work is supported in part by the National Science Foundation under Grant No. PHY-8913815.

- ceramic glass insulator material and terminations which resist arcing breakdown
- conditioning procedures that avoid large dark currents and sparks, which are detrimental to electrodes
- stainless steel anode plates, which seem to remain cleaner and smoother than tungsten or molybdenum plates during operation

In anticipation of increased beam current, a water cooled section of E1 with copper anodes has been installed. Performance with low beam power (<5 W) has been similar to the standard deflector.

1.2. Rf transmitter anode power supplies

The anode power supply consists of a power distribution section, with crowbar unit and controls, and a separate power transformer and rectifier. Due to its high reliability the 400 kW transformer and rectifier from the K500 cyclotron has been used for approximately 95% of the operating time of the K1200 in 1991 and the first half of 1992.

The large (1200 kW) transformer is required to run beam energies above a threshold that depends on the charge/mass of the ion and is in the range 80 to 140 MeV/u. The 1200 kW subsystem has experienced failures in the transformer, filter choke and rectifiers. The major cause of these failures has been transient current and voltage swings associated with triggering the crowbar circuit. The large magnetic forces resulting from the short circuit current during a crowbar event exceeded the capabilities of the windings in the original transformers and the filter choke. The transformer, choke and rectifier have been redesigned and new units ordered. Besides being more rugged, the new rectifier and choke will be more accessible for maintenance, as they are not immersed in oil. The modifications will be finished in summer 1992.

1.3. Reduced dee voltage

The dee voltage in the K1200 is set for each beam in such a way that the design ray follows the same path through the cyclotron central region for all beams. The voltage requirements thus depend on the charge to mass ratio and the final velocity. The central region was designed originally for a maximum dee voltage of 200 kV. The cyclotron was operated with this central region until March 1991. During this period we discovered that the resonators would spark across the dee stem support insulators on the atmosphere side when the voltage at the insulator reached 80 kV. Due to the variation of the voltage at the insulator with frequency, this effect restricted the range of charge/mass for energies between 30 and 100 MeV/nucleon. Therefore, a new central region was designed and installed which allows a dee voltage reduction of 20%. This change has eliminated the problem at the cost of a small increase in phase slip. The absolute value of $\sin(\phi)$ remains less than 0.50. The required input power to the rf amplifiers at maximum energy (200 MeV/u) is reduced to 920 kW by this modification.

2. IMPROVEMENTS IN HIGH ENERGY BEAM LINE TUNING

A systematic program to improve beam line tuning was begun and partially implemented in 1991 with goals of reducing tuning time, increasing reproducibility, and improving the beam on target. Tuning is complicated by the use of inherently large emittance secondary beams and the desire to make clean, low cross section measurements at very forward angles.

Key to this effort is the use of TRANSPORT code predictions for each set-up. Initial attempts to do so gave poor correspondence between predicted and measured beam envelopes. All beam transport lines were physically measured, dimensioned in the CAD layout drawings, and the TRANSPORT input decks altered to reflect the corrected distances. Inter-element distances and effective lengths of the super- conducting quad doublets were revised to reflect the dimensions of the magnets in their cold state. Current calibrations were checked and higher resolution DACs were fitted to quads and bending magnets. With these changes, correspondence was improved significantly and is now of sufficient quality to allow reasonably accurate pre-run estimates of the actual beam envelope and magnet settings.

Development and testing of a complete set of predicted values for beam line magnets on each of the five vaults was begun and partially completed. Beams are assumed to be of three general types: primary (x and y emittance of 3 π mm-mr),[3] medium acceptance (30 π mm-mr) and high acceptance (x=50 π mm-mr, y=80 π mm-mr).

Operational experience has been important in determining the choice of optical conditions to be fitted by TRANSPORT. Primary beam experiments with the 4π array in the N2 vault indicated that the 5 cm dipole gaps impose significant restrictions on desireable optical solutions. When predictions gave a vertical beam height of more than about 2 cm in this gap, runs using such predictions had substantially increased noise due to particles hitting the target frame (presumably from halo scattering from the pole faces) as compared to optical solutions giving a smaller beam height in the dipole.

Additionally it was noted that while the spot size and shape at the object point for the beam transport system remains relatively constant for different beams and energies, the primary beam emittance, hence divergence, could vary by a factor of 2 or more.

These two considerations, together with desire to transmit high-emittance secondary beams with maximum efficiency, led to abandoning the technique of point-to-point transfer of the beam from the A1200 to target with multiple foci, in favor of no intermediate imaging and reduced divergences until the final spot on target.

Rules for generating beam line optics have been developed. This program has already resulted in performance improvements that meet its three general goals.

3. ENERGY RANGE

The maximum energy per nucleon of ions from the K1200 cyclotron was envisioned to vary with mass number as shown by the curve in Fig. 3. The points plotted on the graph show examples of beams obtained. The energy goal for mass 208 has been exceeded (mass 238); that for mass 129 has been reached. Progress toward the goals for lighter ions can be seen from the graph.

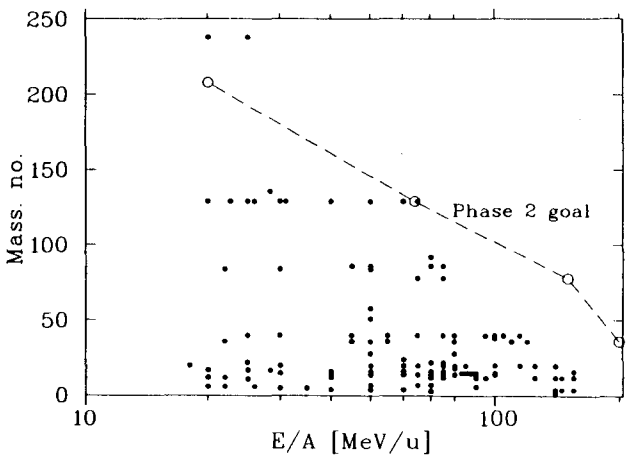


Fig. 3. Mass number vs. beam energy: actual performance (solid points) and goal (open circles).

4. ENERGY AND ION VARIABILITY

For schedule planning purposes the time allowed for changing beams is 8 hours. Many experiments are scheduled to run 2 or 3 different beams (ion-energy combinations). In the year Jan.-Dec. 1991 a total of 72 beams were produced by the K1200 for experiments and development. There were 134 beam changes made in the year, i.e. an average of 1 change every 2.1 days, during the 6877 hr. that the cyclotron was scheduled for operation. In this same period 31 nuclear science experiments were performed. Not included in the energy change figures are so-called cocktail beams which have become increasingly in demand for calibration of detector energy response. For example, the following series of ions, all with charge/mass approximately 0.2, were run in a 6 hour period: $^{129}Xe^{26+}$, $^{84}Kr^{17+}$, $^{65}Cu^{13+}$, $^{55}Mn^{11+}$, $^{50}Cr^{10+}$, and $^{15}N^{3+}$. The frequency was shifted by the small amount corresponding to the difference in charge/mass to select the ion to be accelerated, but all magnet currents remained constant.

Table 1 contains examples of energies and intensities obtained for some respresentative ions produced by the ECR ion sources and accelerated.[4] Molecular beams are a useful option. Compared to atomic ions in the K1200, molecular ions containing hydrogen and helium allow lower energy helium and deuterium beams than otherwise available, and they allow acceleration of protons. In addition, the $(H\text{-}He)^+$ ion has been used to excite and study forces produced by electron wake distributions in a target.

Table 2 lists a few secondary beams produced in the A1200 separator and used for physics experiments. Primary beam intensity is in the range 10-50 pnA.

Table 1. Examples of beams extracted from the K1200.

Ion	E/A [MeV/u]	Intensity [part. nA]	Source feed
$^{11}B^{2+}$	25	15	solid
$^{51}V^{13+}$	50	1	"
$^{58}Ni^{15+}$	70	2.4	"
$^{92}Mo^{25+}$	70	0.024	"
$^{238}U^{39+}$	25	0.0004	"
$^{6}Li^{2+}$	90	25	oven
$^{40}Ca^{11+}$	55	3.2	"
$^{12}C^{6+}$	155	0.1	gas
$^{18}O^{6+}$	80	53	"
$^{20}Ne^{9+}$	125	0.27	"
$^{20}Ne^{10+}$	140	0.008	"
$^{28}Si^{8+}$	50	5	"
$^{78}Kr^{22+}$	75	0.30	"
$^{129}Xe^{31+}$	65	0.0005	"
Molecular ions:			
$(D\text{-}H)^+$	70	25	gas
$(H\text{-}He)^+$	35	6	"
$(D\text{-}He)^+$	26	1.5	"

Table 2. Examples of radioactive beams.

Ion	E/A	Intensity p/s/pnA	accept. mode	primary beam
^{11}Li	64	50	high	^{18}O, 80 MeV/u
	35	20	"	"
^{20}Mg	65	0.35	high	^{36}Ar, 80 MeV/u
^{40}Cl	55	200000	med.	^{40}Ar, 80 MeV/u

5. TIME STRUCTURE

The cyclotron central region accepts injected beam in a time interval of 40 degrees.[5] The time distribution of the beam is cut by the loss of beam on the deflector septum and possibly by other contraints placed by the extraction process. The time structure of the external beam has several peaks distributed over a portion of the

acceptance interval (see Fig. 4a).

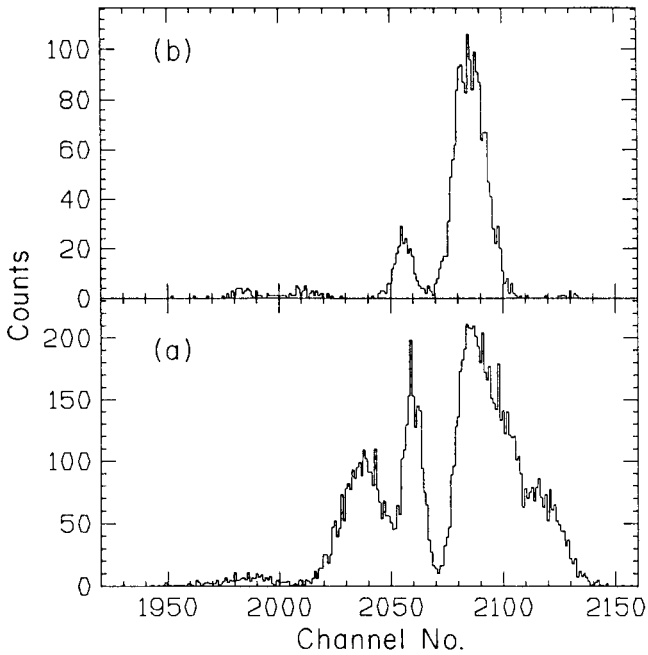


Fig. 4. (a) Time of flight spectrum obtained from a solid state detector in the focal plane of the A1200 separator detecting the primary beam, 60 MeV/u 24 Mg 7+. The stop signal for the time converter is derived from the dee voltage. The rf period is 61.7 ns, and 1 ns corresponds to 40.8 channels. The base width of the distribution is 3.1 ns (18 degrees). (b) As above except phase slits are inserted into the beam. The primary peak centered at channel 2085 has a full width at half maximum of 0.44 ns (2.6 degrees). The beam intensity is reduced X 0.25 by the phase slits.

The phase slit system narrows this time distribution. It is similar to the one used in the K500 cyclotron[6)7)] . Two independently movable pins are inserted into the beam at a radius near 7 inches. The time spectrum in Fig. 4b is an example of the results. The performance of the phase slits is being studied and the operator interface is being developed for routine beam diagnostic use.[8)]

6. BEAM DIAGNOSTICS

A probe shaft with a thin scintillator mounted on the tip and viewed by a miniature TV camera 10 cm from the scintillator is used to display the internal beam spot as a function of position in the median plane.[9)] This probe enables the operator to directly see effects of parameter adjustments on the radial and axial betatron oscillations. It is therefore useful for detecting and correcting centering errors, especially with beams which are sensitive to centering because they remain near a resonance for a long time during acceleration.

A computer program is used to automatically center the beam. This program controls the TV probe drive, a frame grabber to digitize the picture of the beam spot and the centering coil power supplies. It measures the horizontal size of the beam spot as a function of radius and determines the betatron oscillation amplitude. Repeating this for different centering coil currents, it finds settings that minimize this amplitude. The search takes approximately 15 minutes.

A second hill probe was built in access port A5, and is presently used to measure current.

7. CONCLUSIONS

The K1200 cyclotron with the ECR ion source has met the energy goals for Xe and heavier ions. Improvements to the deflectors and the rf system are being made to increase the energy for light ions. The reliability has remained consistently good in the past year. A great variety of ions and energies is available and transitions between different beams occur rapidly. The laboratory produces many secondary beams by projectile fragmentation.

8. REFERENCES

1) Nolen, J.A., Antaya, T.A., Kuo, T.S., Marti, F., Sherrill, B.M., Zeller,A.F. and Blosser,H.G. in **Proc. 12th Int. Conf. on Cyclotrons and their Applications** (World Scientific, Singapore 1989) p. 5.
2) Kuo, T.,"Deflector Development for the K1200 Cyclotron", paper PA30 at this conference.
3) Marti, F., Blue, R.A., Johnson, J., Kuchar,J., Nolen, J.A., Rutt,P., Sherrill, B. and Yurkon, J., in **Proc. 12th Int. Conf. on Cyclotrons and their Applications** (World Scientific, Singapore, 1989) p. 268.
4) Antaya, T. A., "Space Charge Effects in Highly Charged Positive Ion Beams Extracted from ECR Ion Sources", paper BD2 at this conference and Antaya, T. A. "Super Gas Mixing Technique for Highly Charged Uranium Ions" paper PC9 at this conference.
5) Marti, F.and Gavalya, A. , in **Proc. 11th Int. Conf. on Cyclotrons and their Applications** (Ionics, Tokyo, 1987) p. 484.
6) Milton, B.F., Fowler, M. J., Kuchar, J. and Ronningen, R.M., in**Proc. 10th Int. Conf. on Cyclotrons and their Applications**,(IEEE, New York, 1984) p. 55.
7) Milton,B. F. **Phase Selection in the K500 Cyclotron and the Development of a Non-linear Transfer Matrix Program**, (Ph.D Thesis, MSU, 1986).
8) Bailey,J.D. , "Selection and Measurement of RF Phase Width of the K1200 Cyclotron Beam" paper PA34 at this conference.
9) Marti, F. and Snyder, S. "Internal Beam Dynamics Studies with a TV Probe", paper BD5 at this conference.

STATUS REPORT ON THE HEAVY ION FACILITY AT LNS

F. Alessandria, G. Bellomo, A. Bosotti, C. De Martinis
D. Giove, P. Michelato, C. Pagani, L. Rossi
INFN - Sezione di Milano, Università degli studi di Milano
Laboratorio LASA, Via F.lli Cervi 201, Segrate (MI),20090,Italy

and

L. Calabretta, G. Ciavola, G. Cuttone, M. Di Giacomo, S. Gammino
P. Gmaj, G. Raia, D. Rifuggiato, J. Sura
L.N.S. - INFN, V.le A. Doria ang. S.Sofia, Catania, 95125,Italy

ABSTRACT

The Milan superconducting cyclotron has been transferred and assembled in Catania. The status of the main components and the results of the tests performed along the radial injection line are here presented.

1. INTRODUCTION

The superconducting cyclotron, which will be commissioned at L.N.S., was moved to Catania after the first cool-down and the preliminary magnetic measurements done in Milan.[1,2] Now the assembling of the cryostat and of the other main components of the machine, which are here described, is completed, Fig. 1.

To save time between the next campaign of magnetic measurement and the tests of RF and acceleration, the cyclotron cryostat was assembled together with the RF liner. The final magnetic measurements will be carried out by a new field mapping system able to fit the small gap of the liner. At the beginning, the beam accelerated by the Tandem will be radially injected in the median plane of the Cyclotron, where it will be stripped by a carbon foil placed near the center. Tests on the beam transfer line, charge state distributions measurements before and after the cyclotron stripper, and on the bunching system were done and are here presented. In Fig. 2 the lay-out of the LNS facility is shown, including the accelerator rooms, the Tandem-Cyclotron coupling line and the experimental rooms.

2. CRYOSTAT AND CRYOGENIC PLANT

At the end of 1990 the assembling of the cryostat started in Catania. We took 16 months to assemble the cryostat with the final vacuum chamber complete of all the radial penetrations for the injection and extraction lines, the electrostatic deflectors, the magnetic channels and the current probe. In May 1992 the cryostat was put in the magnetic yoke in its final position. In the first magnetic measurements done in Milan a first harmonic contribution due to the inner vacuum chamber of the cryostat was detected; now in order to reduce this effect, the center position of the vacuum chamber with respect to the center of the pole has been measured with great accuracy. The position of the center has been extracted by Fourier analysis of the values of the distance between the vacuum chamber and the pole center. After some trials the centre of the vacuum chamber was nominally placed at 0.01 mm from the centre of the poles. Because of unknown possible errors and due to the difficulties to



Fig. 1. View of the Cyclotron assembled with the cryostat inside and the upper and lower RF cavities installed.

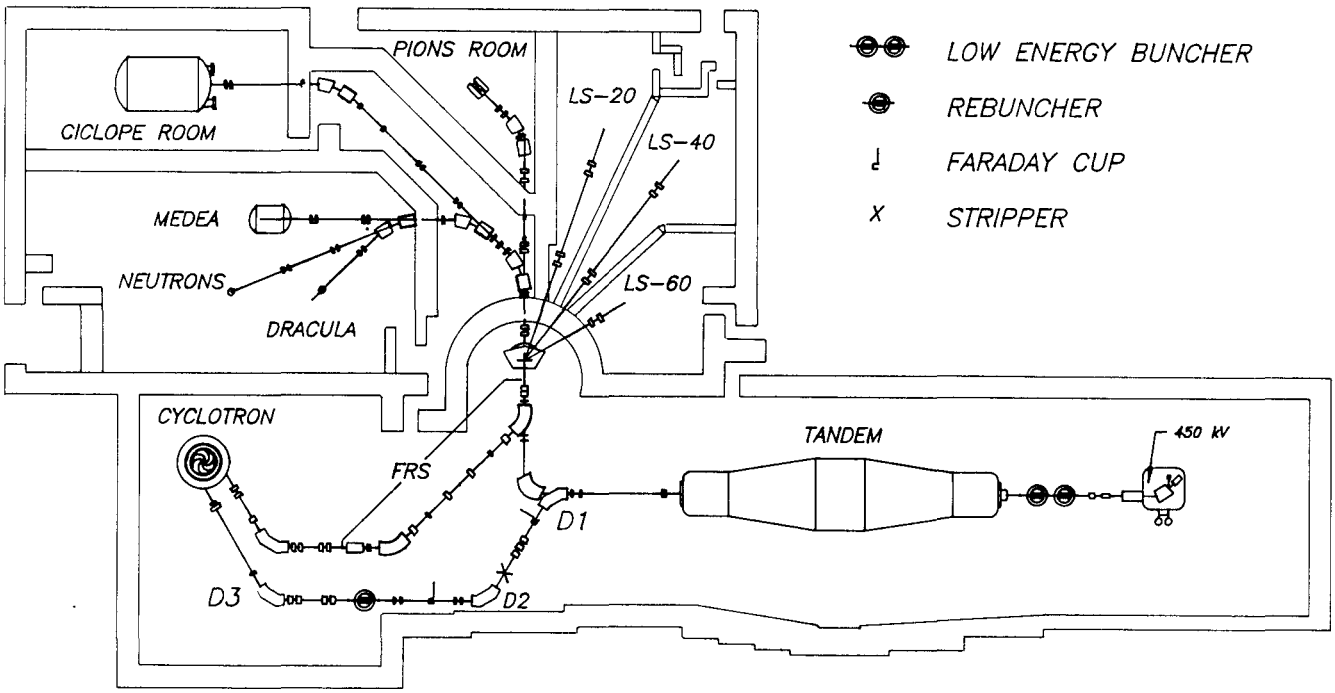


Fig. 2. Layout of the LNS facility.

measure the positions of the poles, covered by the liner, and of the vacuum chamber, we can not rely completely on this result. The final check on the exact position of the cryostat will be possible by magnetic measurements. The cryostat has been vacuum tested before the installation inside the magnet yoke. Two small leakages lower than 10^{-5}mbar·l/sec have been detected, one inside the injection channel, the second inside the channel of a compensation bar. The two leaks have also been measured after the assembling of the cryostat in its final position and no variation has been monitored. We decided that it is not necessary to attempt to perform any repair because of the acceptable low values of the leakages and of their stability.

All the equipments needed for the refrigeration of the cryostat have been installed and separately tested. At present we are carrying out the connection of the cryogenic transfer lines and the tests on the measurement and control systems. The cryogenic circuit is based on a Helial refrigerator delivering 180 W or 53 l/h of LHe at 4.3 K without LN precooling and about 100 l/h with precooling. The refrigerator is equipped with an internal purifier to avoid the treatment of the recovered helium and the risk of valve clogging. Two ejectors, one on the warm line coming from the current leads,the other into the cold box on the cold line from the cryostat, make the operating pressure of the cryostat indipendent of the compressor low pressure. During the normal operation the refrigerator supplies a 1000 l. reservoir from which the LHe is transferred to the cryostat; a regulating valve on the transfer line keeps the level constant and independent of the production and consumption fluctuations. The LN, required for the cooling of the 80^0 K shields (~10 l/h) is drawn in turn from two 10.000 l. tanks and arrives at the cryostat via a multilayer insulated transfer line and phase separator. During the warm up of the cryostat the gaseus helium is recovered in a 20 m^3 balloon and compressed to 220 bar in large high pressure cilinders (1700 l) by a 50 m^3/h compressor. The storage capacity is ~3000 std m^3 of He.

3. RF SYSTEM

The cavity resonators and the trimming capacitors are already mounted in their permanent positions and the connession to the ancillary equipment and to the electronics are in progress. The transmission coaxial lines connecting the RF amplifiers to the coupler capacitors have been installed too. The trimming and coupling capacitors, the lower and upper stubs of the resonant cavities have also been vacuum tested. During the assembling of the cryostat a lot of work has been done to complete the lower and upper parts of the RF liner. The liner, sealed to the cryostat inner wall constitutes the vacuum chamber of the accelerator.

The copper liner presents a large surface exposed to vacuum in the acceleration chamber and therefore an efficient cleaning procedure of this part is of vital importance on the vacuum conditions of the machine. The liner was first degreased (locally) with acetone for a rough removing of the oils used in the machining. After-

wards the liner was ultrasonic cleaned (fully immersed) in a hot alkaline detergent solution to remove fats; a hot acid detergent solution was then used to deoxidize copper. Thereafter the liner was dried with ethanol after a long rinsing (about 1 hour) with room temperature demineralized water. The liner is now completely installed in the magnet.

4. EXTRACTION

The construction of the magnetic channels and their actuators is completed and they have been already installed in the cyclotron. The construction of the two electrostatic deflectors, Fig. 3. is underway and they will be ready for testing and installation by the end of September. The deflectors have been designed with a gap of 8 mm. This will limit the maximum sustainable field to around 100 kV/cm, whereas the peak design value was 140 kV/cm. After the beam size measurement in the extraction region, we shall evaluate the possibility of turning to a 6 mm gap, which has proved to work satisfactory up to 135 kV/cm on the deflector prototype. A test bench with a 1 Tesla magnetic field has been installed at LNS for further deflector development.

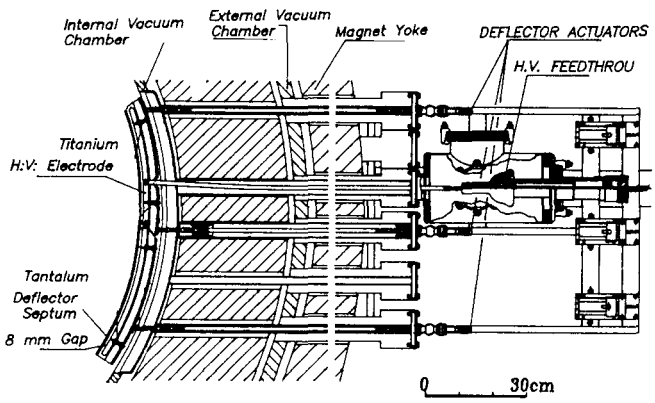


Fig. 3. Design of the electrostatic deflector

5. MAGNETIC MEASUREMENT SYSTEM

The description of the new field mapping system and its test were published elsewhere,[3] therefore herein we will mention only its general concepts and features. Due to the small gap accessible in the median plane of the cyclotron and the great number of field maps to be measured the search coil technique was chosen as a basis of the system. It provides both small vertical size and high speed properties. The system is made up of a coil put on a motorized cart together with an optical encoder sensing the actual probe position by means of a stripped tape fixed to a guiding carbon-fiber bar. The 1800 mm long bar is settled on the motorized axis which ensure an azimuthal positioning accuracy of 10^{-3} deg. The cart controller triggers by means of encoder pulses a digital integrator (PDI5025-Metrolab), which sums up the frequency of an ADC and stores the result each time a preprogrammed number of trigger signals is counted. When calibrated this system gives the field variation from a reference point. The absolute value of the field is read by the NMR probe placed on the symmetry axis of the cyclotron. Another NMR probe is placed in one of the RF holes to allow an on-place calibration of the coil. The misalignment of the coil plane with respect to the symmetry plane of the cyclotron of .8 deg leads to a systematic error of the order of 10^{-4}. For this reason the possibility of calibration inside the cyclotron is important. The whole system is controlled via GPIB bus by a PC386. The PC performs data aquisition, *on line* calculations of average field and harmonics with appropriate graphs. The computer analyzes *on line* the measurement performance and in case of a failure cased by an overrange error or an encoder counter error repeats automatically erroneous azimuthal step.

The main problem encountered during the tests of the system was a nonlinearity of the integrator drift as well as a noise generated probably by the digitization process. It is very difficult to get rid of the last error since it depends not only on a trigger number and temperature but a part of it seems to be clearly casual. Thus the system parameters (coil sensitivity, cart velocity, integrator amplifier gain) was chosen to diminish a casual error. For the best balanced gain value (G=10) and high coil sensitivity (0.13 m^2) the cart velocity is limited by the highest field gradient expected (15 T/m) to 0.2 m/s. To reduce the measurement time and the probability of the casual drift error, the cart starts with the maximal velocity (0.5 m/s) and it automatically moderates only in the region where the gradient is high. This property ensures the measurement accuracy within 10^{-4} for an individual measurement point and better then 3×10^{-5} for average field and harmonic amplitudes.

The system will be tested inside the cyclotron the next weeks and the magnetic field measurements are planned to begin this summer.

6. COMPUTER CONTROL

The establishment of accepted general rules for the lower levels of the control system and the importance of the operator interface in the management of the experiment have stimulated a lot of work in the design of new approaches to man machine interaction tools. The console has been redesigned as an Ethernet segment with a distributed software running on the computers connected to it. The most relevant challenge has been the development of GIULIA,[4] a dedicated package running on top of X-Windows on VMS Based worksations. GIULIA isa modular, object oriented code which provides a set of tools for the management of a plant or of an experiment. The operator is driven,through windows based dialog paths, to the handling of all parameters of concern. There is the possibility to work with predefined

tools or with run time user defined tools. Alarm handling, logging monitor capabilities and the management of a database for the different parameters are included. The experience gained using GIULIA during the final assembling of the machine has shown that the package fits all the requirements arised during the first cool-down and excitation operations.

7. BEAM LINE TESTS

The coupling beam line between the Tandem and the Cyclotron has been tested. The lay-out of the line is shown in Fig. 2, where the diagnostic elements, the Faraday cups (FC), are represented too. Each Faraday cup is accompanied by a Beam Profile Monitor[5] The aims of these tests are:

- to verify the agreement of the experimental setting with the theoretical values;
- to estimate the transfer efficiency of the line;
- to evaluate the intensity of the charge state to be injected into the Cyclotron;
- to evaluate the stripping efficiency for the charge state to be accelerated in the Cyclotron after stripping.

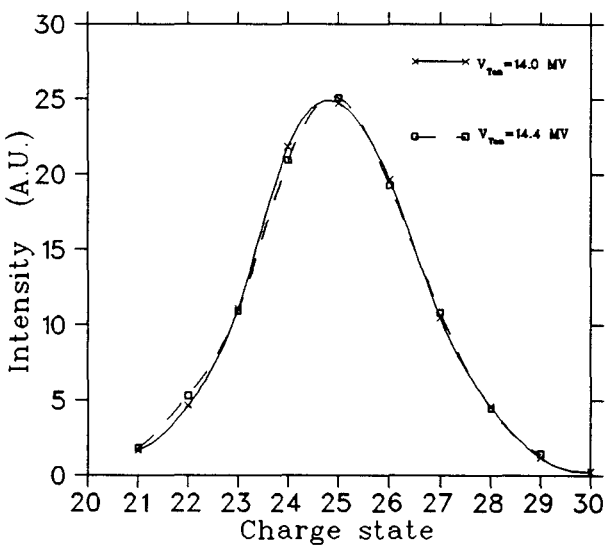


Fig. 4. Charge states distribution after the second solid stripper.

The beam line tests were performed with ^{16}O and ^{127}I, employing a N_2 gas stripper at the Tandem H.V. terminal. They proved that the theoretical setting of the quadrupoles agrees with the experimental one within a few %. A $^{16}O^{2+}$ beam, accelerated with V_{Tandem}=10 MV, was transported until the Rebuncher position (Fig. 2), where a double waist is created, and the transfer efficiency resulted to be ~100% for an intensity in the order of 120-140 enA. The most interesting feature of these tests is the easiness of the setting procedure. At 14 MV, injecting a current of 600 nA in the Tandem and extracting a current More extensive tests were done with ^{127}I. of 5000 enA, the current of the 7^+ charge state measured on the FC after the dipole D1 was ~560 enA. In order to simulate the Cyclotron stripper, a foil stripper system was installed in the coupling line in front of the dipole D2. In Fig. 4 the charge state distribution measured on the FC after the dipole D2 is shown. The intensity for each charge state is calculated with respect to the total current measured. The incoming beam was I^{7+}, with energies 112 and 115.2 MeV respectively. The most probable charge state appears to be 25^+.

Considering the results obtained, the commissioning of the Cyclotron is feasible with the injection of a $^{127}I^{7+}$ beam; the acceleration of a $^{127}I^{28+}$ beam is planned.

8. THE BUNCHING SYSTEM

The coupling between the two accelerators requires that the beams coming from the Tandem have to be bunched at the same frequency of the C.S. radiofrequency system, i.e. 15-48 MHz. The goal for the temporal bunch length at the cyclotron stripper is $\pm 1.5^o$ RF, corresponding to Δt=170-560 psec., shorter than the $\pm 3^o$ RF necessary to reduce the energy spread at the extraction and make feasible the single turn extraction. This task is accomplished by a so called Low Energy Buncher (L.E.B.), located just in front of the Tandem and by the Rebuncher, placed between the Tandem and the Cyclotron, Fig. 2. In Table 1 the main parameters of the cavities of the bunching sytem are presented. A complete description of the pulsing system has been presented elsewhere.[6] To test the first stage of bunching system an oxygen ion beam was used. The L.E.B. was driven at frequencies of 17.1, 24.7 and 33 MHz. To measure the length of the bunches delivered by the L.E.B. a μ-channel plate has been used. The μ-channel plate gives a timing signal for each ion that strikes a thin wire placed to cross the beam. The time between the μ-channel plate signals and the R.F. generator signals has been measured by a Time Amplitude Converter and monitored on a multichannel analyzer Fig. 5.

Table 1: Main parameters of the bunching system

	Buncher Cavity 1	Buncher Cavity 2	Rebuncher
Frequency	15-48 MHz	30-96 MHz	60-192 MHz
Peak volt.	1500 V	600 V	30 KV
In. Diam.	66 mm	66 mm	60 mm
Out. Diam.	238 mm	238 mm	255 mm
Cooling	air	air	water
Z_{sh} ($K\Omega$)	45-180	70-180	280-380
Q factor	560-2300	900-2300	3300-4400
Refl. power	~5%	~5%	

Temporal lengths as short as 1.32÷1.6 nsec. FWHM, and efficiencies in the order of 55÷65%, have been recorded. The efficiencies here reported are the ratio between the number of event in the area of the peak and the total event recorded during the period of the R.F., corrected for background noise. The results are satisfactory and in good agreement with the theoretical simulations. As foreseen by the calculations for heavyer ions like iodine we observed only small temporal structures on a continuous beam because of the poor uniformity of the electric field in the gaps when the $\beta\lambda$ of the beam is short. To counterbalance this effect, it is planned to put grids on the electrodes.

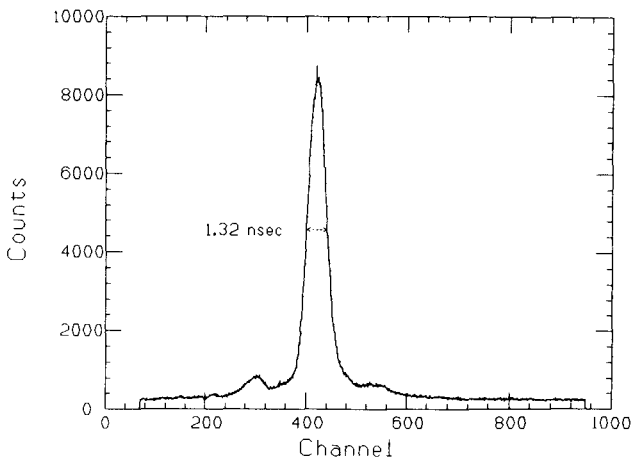


Fig. 5. A typical time spectrum for O^{5+}

9. CONCLUSIONS

The Superconducting Cyclotron was successfully moved from Milan to Catania without any damage. After a long time required to perform the welding of the radial penetrations in the cryostat and the assembling in the new site, we are now ready to restart the cool-down of the machine and to perform in the next months the final field mapping.

10. REFERENCES

1) Acerbi, E., et al., "Progress report on the Milan Superconducting Cyclotron," **ICCA** 26 (1989).
2) Acerbi, E., et al., "Progress report on the heavy ion facility at LNS," **IIndEPAC** 425 (1990).
3) Gmaj, P., et al., "Test and calibration of the magnetic measurement system for the Superconducting Cyclotron at LNS,Catania", Proc. of the **IIIrd EPAC**, Berlin, March 1992.
4) Giove, D. and Cuttone, G.,"Man machine interaction tools based on X-windows", in Proc. of E.P.A.C., Nice, France, 1990
5) Calabretta L., et al., "Beam diagnostic elements at the Laboratorio Nazionale del Sud", Nucl. Instr. and Method P.R. A268(1988)496
6) Calabretta, L. et al., presented at the VI Int. Conf. on Electrostatic Accelerators and Associated Boosters, Montegrotto Terme (Padova), Italy, 1992

DEVELOPMENT OF THE NAC ACCELERATOR FACILITIES

J.L. Conradie, A.H. Botha, J.J. Kritzinger, R.E.F. Fenemore, L.M.M. Roels, D. Reitmann, P.M. Cronje
P.F. Rohwer, W.A.G. Nel, H.A.Smit, H.N. Jungwirth

National Accelerator Centre, P. O. Box 72, Faure, 7131, Republic of South Africa

ABSTRACT

Improvements to the injection and extraction systems of the separated-sector cyclotron are in progress. A flat-top acceleration system, making use of the existing dees, for the light-ion injector cyclotron, is being tested. A bi-directional beam sweeping system for the isotope production targets has been designed and built.

1. INTRODUCTION

The 200 MeV separated-sector cyclotron[1)] and the 8 MeV light ion injector cyclotron at the NAC have been in operation since the beginning of 1987. Beam time is allocated to physical sciences (49%), neutron therapy (14%), radiobiology and biophysics (8%) and isotope production (26%). An injector cyclotron for polarized and heavy ions is scheduled for completion in December 1993. The ECR and polarized ion sources are operational. A beamline and facilities for proton therapy are under construction and will be completed later this year. The K600 spectrometer has been commissioned. The final detector is now being constructed. A number of improvements to the existing facilities are discussed below.

2. BEAM CENTERING IN THE SEPARATED-SECTOR CYCLOTRON

To center a beam the change in the centering error for increments in the currents of each of the injection elements is measured at a given turn. By using linear combinations of these increments for any pair of injection elements, the centering error can be adjusted to the required value. With this procedure the centering error is typically reduced by a factor of six in a single step.

Owing to the lower than expected dee voltage at injection in the 200 MeV separated-sector cyclotron, proton beams with energies above 120 MeV could not be centered with the injection system as it was originally designed. During beam centering studies it was noticed that when the injection system is set up for total transmission through the magnetic inflection channel, the centering error can be adjusted to only an angular error on the third or fourth turn, depending on the injection energy. To center the beam at energies above 120 MeV, it is therefore only necessary to change the beam angle, on the third or fourth turn, with a short electrostatic injection channel (EIC). The available space in the cyclotron allows a maximum channel length of 190 mm. The maximum angular error on the third turn is 25 mrad. The maximum required field strength in the channel is 23.5 kV/cm. A cross-sectional view of the EIC is shown in Fig. 1. A grounded shield screens the first few orbits from the electrical field around the deflector. Figure 2 shows the orbit pattern for 200 MeV protons at injection. On the first two turns the beam is not centered but from the third turn onward the centering error is only 3 mm. In practice the beam is centered by first obtaining only an angular centering error at the EIC, through adjustment of the first few injection elements. The beam angle is then corrected by applying the calculated voltage for a properly centered beam to the channel. During operation the beam center is adjusted to give the maximum orbit

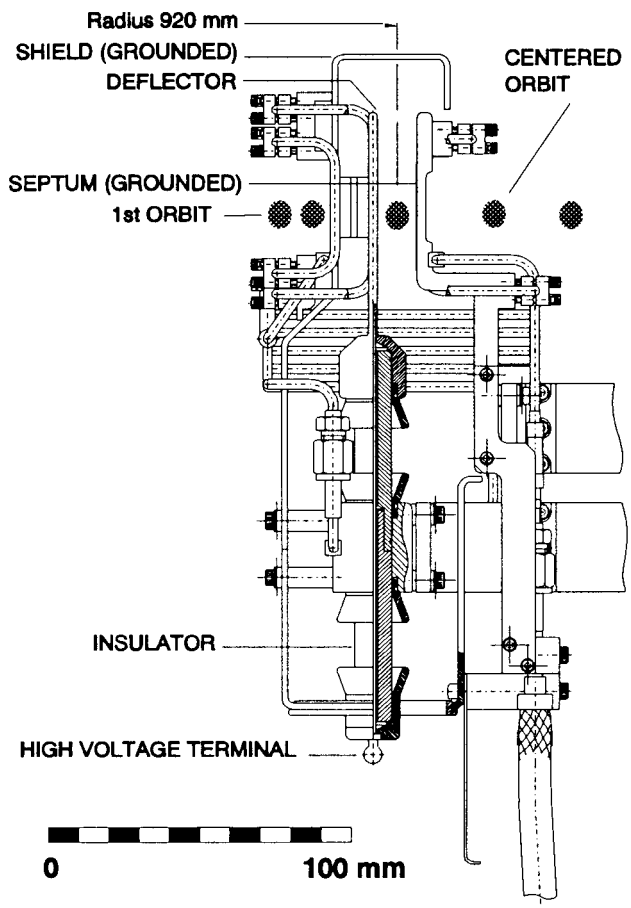


Fig. 1. A cross-sectional view of the EIC.

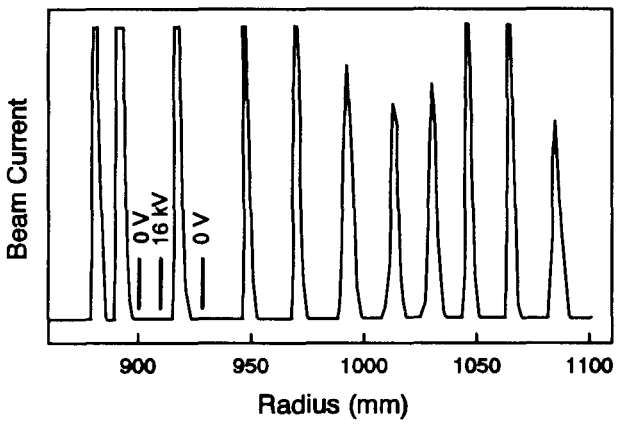


Fig. 2. Beam centering in the separated-sector cyclotron with an additional electrostatic inflection channel (EIC) at injection for 200 MeV protons. The EIC electrodes at the third turn are indicated. From the third turn onward the centering error is 3 mm.

separation at the first extraction element, for a given centering error. It is now possible to work with a much smaller centering error at 200 MeV and still get the same orbit separation at extraction.

At present the extraction system consists of an electrostatic channel (EEC) and two septum magnets (SPM1 and SPM2), as shown in Fig. 3. When the beam is centered and the EEC is used, the orbit separation at SPM1 is 12 mm. Because $\nu_x = 1.5$ at extraction for 200 MeV protons, it is possible to obtain double the normal orbit separation of 6 mm at the septum magnet SPM1, by making use of a centering error. Under these conditions the EEC cannot be

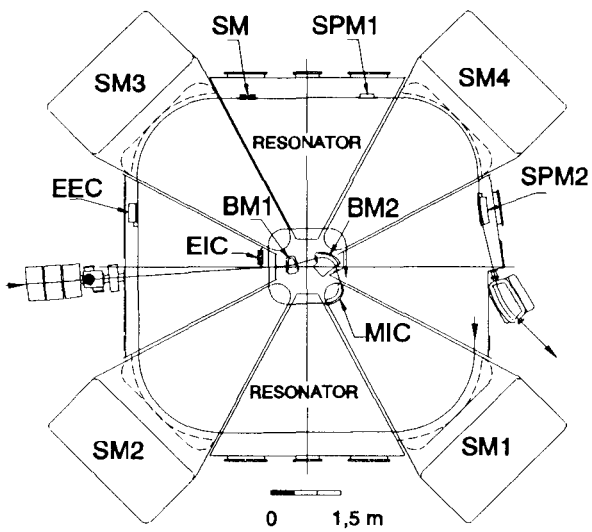


Fig. 3. Layout of the separated-sector cyclotron showing the positions of the the new electrostatic channel (EIC) at injection and the magnetic channel (SM) at extraction.

used because the outer orbit at the EEC swings in to pass SPM1 on the inside due to radial focusing in sector magnet three. To improve the extraction efficiency for 200 MeV protons, a further septum magnet SM is required at the position shown in Fig. 3, in which the position of the EIC is also indicated. At the entrance of the new septum magnet the orbit separation is 24 mm with a field strength of 60 kV/cm in the EEC and with a centering error of 6 mm. Due to the centering error the orbit separation at the EEC is 10 mm. The new septum magnet which is presently being planned will be similar to SPM1.

3. A FLAT-TOP SYSTEM FOR SPC1

The extraction efficiency of the separated-sector cyclotron for a 66 MeV proton beam, which is used for isotope production and neutron therapy, decreases sharply for beam currents above 120 μA. In order to increase the extraction efficiency for this beam and also for proton beams in the energy range 120 to 200 MeV, where the orbit separation is small, a flat-top acceleration system for the separated-sector cyclotron has been considered. Such a system is, however, at present too expensive. A flat-top system for SPC1 can be made more cheaply, especially if the existing resonators could be used for this purpose. It was thought that with such a system the energy spread in the beam extracted from SPC1 would be much lower and the beam could be bunched to shorter pulse lengths in the separated-sector cyclotron than before. The energy spread of beams in the separated-sector cyclotron will therefore be smaller and the extraction efficiency should improve. With shorter pulse lengths higher beam currents for a given beam loss in the separated-sector cyclotron will be available, and a larger percentage of the beam extracted from SPC1 could be injected into the separated-sector cyclotron. Longitudinal space charge forces in the separated-sector cyclotron, however, restrict the pulse lengths which can be used.

The next resonance frequency, above the main resonance frequency, of the SPC1 resonators does not occur at an harmonic of the main frequency. To adjust the second resonance frequency to coincide with an harmonic of the main frequency, two systems were considered. In the first case a loop, tuned to a frequency close to the desired harmonic frequency, is coupled inductively to a main resonator. In the second case an additional co-axial transmission line resonator, also tuned to a frequency close to the desired harmonic frequency, is coupled capacitively to a main resonator.

A computer program was developed to calculate the characteristics of the SPC1 resonators. Because of the calculated high power dissipation at the third harmonic in both the loops and additional resonators, it was decided to design the flat-top system to operate at the fifth harmonic

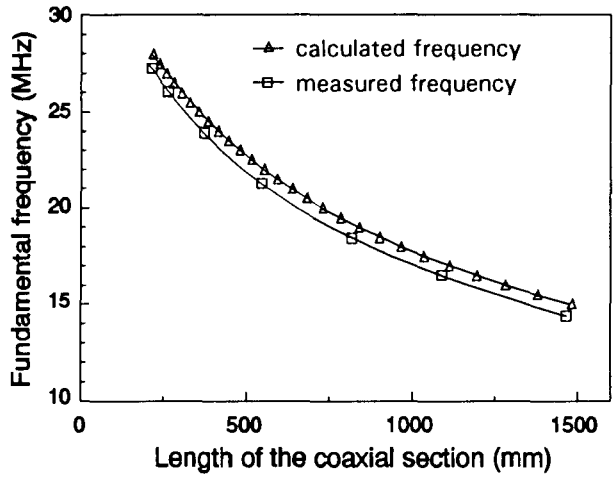


Fig. 4. Calculated and measured main resonance frequencies of an SPC1 resonator vs. the length of the co-axial section of the resonator.

of the main frequency. The calculated and measured main resonance frequencies, as a function of the length of the co-axial section of the SPC1 resonators, are shown in Fig. 4. The measured and calculated second resonance frequencies of the resonator, as a function of the main frequency, are shown in Fig. 5. Calculations have shown that the current in the loop and the voltage across the loop capacitor will be too high. The optimum position for the loop is also occupied by existing cyclotron components.

It was therefore decided to use the additional transmission line resonators with adjustable short-circuit plates to tune the main resonators to the fifth harmonic frequency. The additional resonators are coupled through series capacitors to the main resonators as shown in Fig. 6. The resonators are 1.2 m long and the diameters of the inner and outer conductors are 40 mm and 120 mm, respectively. The largest part of an additional resonator, including the

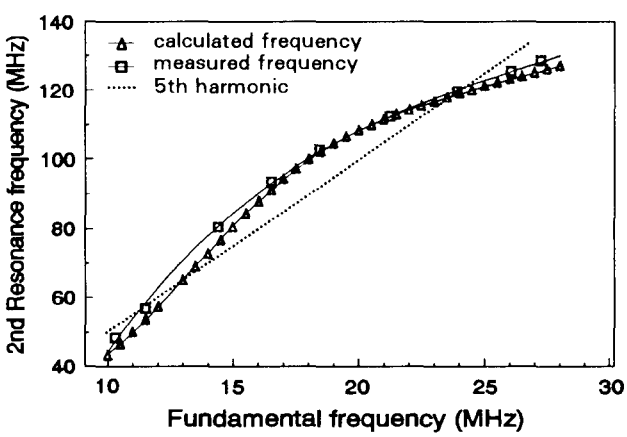


Fig. 5. Calculated and measured second resonance frequencies of an SPC1 resonator vs. the main resonance frequency.

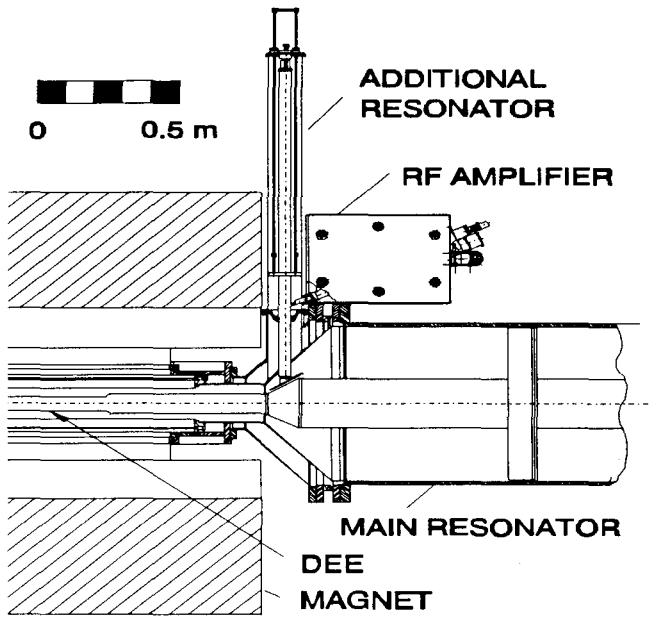


Fig. 6. An additional transmission line resonator coupled capacitively to an SPC1 main resonator to obtain a flat-top dee voltage.

short-circuit plate and the coupling system to the amplifier, is at atmospheric pressure and does not require vacuum feedthroughs. The series capacitor and the short-circuit plate have to be adjusted to obtain the harmonic frequency.

Calculations and measurements on the system have shown that the SPC1 main resonators can be tuned to the main and fifth harmonic frequencies over the main frequency range 10 MHz to 26 MHz. The maximum calculated power dissipation of 380 W at 130 MHz, i.e. the 5th harmonic of 26 MHz, is small compared to the maximum power dissipation at the main frequency. The harmonic voltage on the anode of the main amplifier is less than 1400 V, whereas the main voltage at the anode of the harmonic amplifier is 130 V. The tolerances on the amplitude and phase of the main dee voltage are 0.3% and 0.3°, respectively. For the harmonic voltage the corresponding tolerances are 7.5% and 1.5°, respectively.

To determine the influence of a flat-top system in SPC1 on the beam quality, an orbit code OCEM was used. This program was modified to take the harmonic dee voltage and its radial distribution into account. There is no noticeable change in the vertical focusing when the harmonic voltage is included in the calculation. With the flat-top system the beam separation increased from 1 mm to 8 mm at the extraction radius for a beam pulse length of 30°.

The two systems have been operated simultaneously at a main frequency of 16.3 MHz and a flat-top frequency of 81.5 MHz with beam.

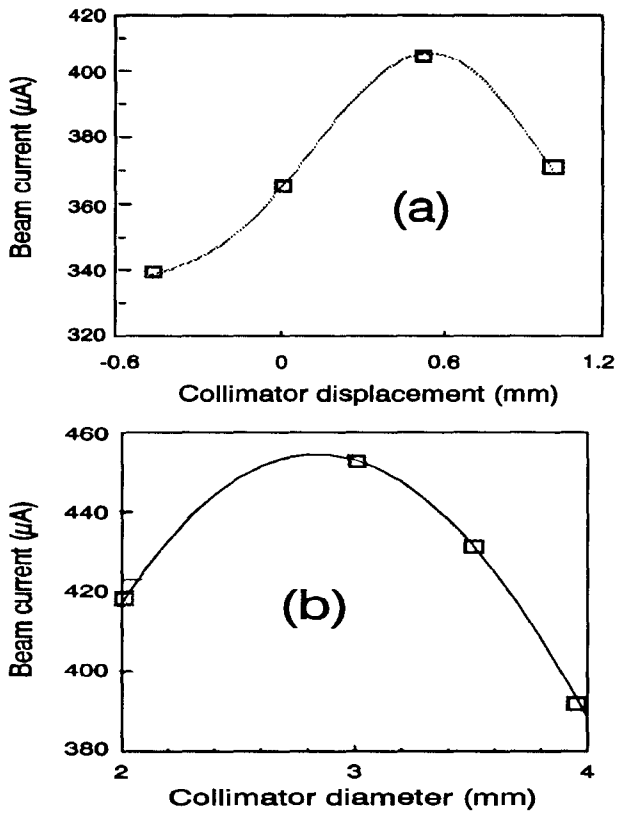


Fig. 7. Beam current vs. collimator position (a) and diameter (b) of the PIG ion source in the light-ion injector cyclotron.

4. OPTIMIZATION OF THE PIG ION SOURCE

A PIG ion source is used in the central region of the light-ion injector cyclotron. To optimize the source for high beam intensities, experiments in which the diameter and position of the collimators for the electron beam have been varied, were carried out. Figure 7 shows the internal beam intensity vs. these two parameters. Another parameter which was varied is the thickness of the extraction slit. The beam intensity has been increased by a factor of 2 by the optimization of these three parameters.

5. A BEAM SWEEPING SYSTEM

Radioisotopes are produced with a 65 μA proton beam of 66 MeV on a circular water-cooled target with a diameter of 18 mm. In order to limit the rise in the target temperature, a 450 Hz beam sweeper is used in the isotope production line. The sweeper consists of two 200 mm long dipole magnets, made from 0.3 mm thick laminations, mounted around the stainless steel beam pipe. Each magnet has two coils consisting of 640 turns each. The reactance of the two coils, which are connected in series, is 1261 ohm. The resistance is 2.7 ohm. To limit the voltage across the supply to the coils they are connected in series with a 280 nF capacitor to form a series resonance circuit. Two 400 W commercial audio power amplifiers are connected to the magnets through transformers to obtain a field strength of 6 mT. The currents through the coils of the two magnets are 90° out of phase, and can be varied independently to obtain circular or elliptical beam profiles with a maximum diameter of 10 mm.

6. ACCELERATOR OPERATION

Table 1 shows the beam statistics for the past three years of operation. More than 50% of the unscheduled interruptions for 1991 originated from the injector cyclotron and are mainly due to the ion source.

Table 1. Distribution of scheduled time

	1989	1990	1991
Scheduled time as % of calendar time	82.8%	85.1%	86.4%
Scheduled time (normalized to 100%)	7251h 100%	7453h 100%	7567h 100%
Interruptions	4.3%	6.9%	3.9%
Beam retuning after power dip or failure	2.5%	0.6%	0.8%
Beam development	4.7%	3.6%	2.2%
Energy change and beam tuning	7.8%	6.3%	6.3%
Beam time	80.6%	82.5%	86.8%
Average no of 8 hour shifts per month	61.0	64.1	68.4

7. ACKNOWLEDGEMENTS

The authors would like to thank the staff of the electronics and mechanical engineering divisions as well as the operating staff for their enthusiastic participation in the development and operation of the NAC facilities.

8. REFERENCES

1) Botha, A.H., Conradie, J.L., et al., "Operation and Development of the NAC Accelerator Facilities", in **Proceedings of the Twelfth International Conference on Cyclotrons and their Applications** (World Scientific, Singapore, 1989) pp. 80-83.

HEAVY ION FACILITY IN ATOMKI

S. Biri, J. Pálinkás, A. Valek
Institute of Nuclear Research of the Hungarian Academy of Sciences (ATOMKI)
4001 Debrecen, Pf. 51., Hungary

ABSTRACT

A plan of a heavy ion facility based on ECR ion source, compact cyclotron and electrostatic acceleretor is presented. The project is partly funded and the development of the ECR ion source is in progress.

1. INTRODUCTION

Experimental atomic and nuclear physics research in ATOMKI are based on the particle accelerators of the institute. During the 38-years history of the institute the beam power of the accelerators was increased continuously: 0.8 MV Cockroft-Walton generator (1962), 1 MV Van de Graaff generator (1969), 5 MV Van de Graaff generator (1971), K=20 variable energy cyclotron (1985).

The latest trend of accelerator based atomic and nuclear physics research is undoubtedly heavy ion collision physics. Our participation in front line research programmes requires the extension of our atomic and nuclear physics studies into this direction.

To facilitate heavy ion collision research in atomic and nuclear physics a decision has been made to establish a heavy ion physics facility, based on an electron cyclotron resonance (ECR) ion source .

Beside an ECR ion source, which can be used alone (low energies up to 10 keV/amu), or can be coupled to an electrostatic accelerator (medium energies) or to the cyclotron (higher energies), one gets a special heavy ion facility not available in Central- and East-European countries, and it makes possible a variety of research programs. The scheme of the planned facility can be seen in Fig.1.

2. THE ECR ION SOURCE

The basic element of the proposed facility is an ECR-type ion source. Although ECR ion sources are commercially available, because of the limited financial support we plan to manufacture it in ATOMKI, buying only the main units and using the experiences of other laboratories.

After making a detailed survey on working and planned sources,[1] we restricted our interest to room-temperature ECR-s. Examining the cost/power ratio, knowing the $A/Q \leq 4$ condition for the cyclotron and studying the world-wide trends in ECR developments, a 14 GHz ECR source seems to be the optimum choice for us.

For these type of ion sources one of the most critical point is the structure of the magnetic field. In order to prepare the design, the measurement and the final formation of the magnetic field of the ECR source, preliminary model computations and instrumental developments were carried out.

1. Using a simple interactive PC computer code the axial magnetic field and the parameters of the coils, creating this field, can be determined. In Fig.2 the result of such a calculation is given for a 2-stages, 14 GHz source. The calculation of the total magnetic field, which is a superposition of the magnetic field of a hexapole (radial) and the coils (axial), is also possible.

2. To measure the magnetic field inside the coils and/or the hexapole, a PC-controlled Gauss-meter was developed.[2] With a small modification it can be used for measuring the magnetic field in the hole of the cyclotron yoke, as well.

3. The results of magnetic field measurements can be transformed to any required text or graphics form, and axial, radial or azimuthal magnetic fields and two-dimensional field maps can be obtained. A Fourier-analyzis of the B_r(phi) or B_{phi}(phi) field components is also possible (Fig.3).

3. THE ELECTROSTATIC ACCELERATOR

To cover the energy gap between extraction energy (5-10 keV/amu) of the ECR source and energies after the acceleration by cyclotron (MeV/amu), a 500 kV electrostatic accelerator was proposed (Fig.1). Technical details are being continuously worked out. According to our present concept the accelerator will be similar to the 350 kV PIIECR facility of the Argonne National Laboratory .[3] During the operation of the ECR source at

the cyclotron, a hollow-cathode type ion source will be used[4] to produce single charged ions for the users.

4. THE CYCLOTRON

The existing MGC-20 cyclotron was designed to accelerate protons, deuterons, $^3He^{2+}$ ions and alpha particles in an energy range determined by the K value of 5-20.[5] Mainly the first harmonic mode of operation is used, but low energy alpha particle and deuterons beams are accelerated on the third harmonics of the revolution frequency.

Because of the increasing interest in the heavy ion beams, which have a higher mass to charge ratio and they should be accelerated in the third harmonic mode of operation, an extensive study of that mode was carried out.[6] At first the formation of the isochronous field, the radial stability of the beam and the orbit centring in the central region were investigated using the measured value of the magnetic field of the cyclotron, then with runs of $^3He^+$ and $^4He^+$ ions the results of the calculations were experimentally tested. The conclusions of these study are the followings: the MGC-20 cyclotron is capable of accelerating heavier ions with a mass to charge ratio up to 4; the magnet yokes have suitable axial holes for injection of a low energy beam from an external ion source; there is a serious beam loss during the acceleration at pressures of $(0.8\text{-}1.2)10^{-3}$ Pa due to the stripping on the residual gas atoms.

To couple the ECR ion source to the cyclotron studies begin in the near future to work out the method of injection, the beam transport system and to improve the vacuum system of the cyclotron. The external ion sources (ECR and duoplasmatron for protons and deuterons) could be roomed on the underground floor near to the cyclotron.

5. PLANNED RESEARCH

The research activity at the proposed heavy ion facility will include investigations with a variety of ion beams at low and medium energies in atomic physics, solid state and plasma physics, while in the high energy range atomic physics, nuclear spectroscopy and applications will be the main topics.

Atomic physics. Atomic physics investigations with multiple charged heavy ions are performed with beams of high-power ion sources (ECR, IBIS) or with high-energy heavy ion accelerators; the range between them has not been covered. If after the ECR source an electrostatic or linear accelerator would be applied, a new experimental area would be opened, covering partly the gap between the energy of the ECR's (<10 keV/amu) and high energy ion accelerators (>500 keV/amu). The most interesting fields to study are: charge exchange processes, molecular mechanism, direct ionization, ion-solid state interaction, quantum electrodynamical effects.

Nuclear physics, nuclear spectroscopy. One of the most important direction of progress in nuclear physics is heavy ion physics. In large nuclear physics research centres heavy ion physics is the main field of research, and smaller laboratories in the neighbouring countries (Krakow, Warsaw, Prague, Bucharest, Kiev etc.) do significant efforts to establish heavy ion accelerators. Some proposed experiments with heavy ions are: determine new level parameters by (heavy ion,xn) reactions, study of the structure of high-spin levels (rotational bands, back-bending, yrast-levels), proton-neutron multiple high-spin states of the odd-odd nucleus, Coulomb excitation.

Applications. Among the many industrial, medical etc. applications we plan to deal with production of nuclear filters, investigation of the radiation damage in various materials, materials sciences.

6. REALIZATION IN THE ATOMKI

A design study has been made to reveal the possibilities of establishing the proposed facility in ATOMKI.[7] In this study we worked out the specifications of the units (ECR source, injection into the cyclotron, electrostatic accelerator), finance, the necessary manpower, time schedule.

The realization of the facility is suggested in two steps. First the ion source and the electrostatic accelerator will be built in the rooms used formerly by the Cockroft-Walton generator and they will be applied for atomic physics investigations. In the second step the ECR source will be coupled to the cyclotron, and further on, it will be used alternately in the low and high energy ranges.

At present the financial resources seem to cover only the development costs of the ECR ion source. This work starts in the very near future, and we continue our efforts to get the necessary funds for the injection system and the electrostatic accelerator, as well.

7. REFERENCES

1) Proc. 10th workshop on ECR sources, Knoxville, USA, 1990. Proc. 4th Int. Conf. on Ion Sources, Bensheim, Germany, 1991. Rev.Sci.Instr. **63**, Number 4, Part II, (1992).
2) Biri, S., Efremov, A.A., Behterev, V.V. and Molnár, J., presented at XII. All-Union Conf. Charged Part. Accel., Moscow, USSR, 1990. (in Russian)
3) Pardo, R., Nucl.Instr.Meth. **B40/41**, 1014 (1989).
4) Biri, S., Pálinkás, J. and Báder A., ATOMKI Ann. Rep. 143 (1991).
5) Galchuk, A.V., Koroljev, L.E., Stepanov, A.V., Kormány, Z. and Valek, A., in **Proc. IX. All-Union Conf. Charged Part. Accel.** (JINR,Dubna, USSR, 1984) p.40. (in Russian)
6) Kormány, Z., Szucs, I., Valek, A. and Vámosi, J., Acta Phys. Hung. **65**, 359 (1989).
7) The heavy ion physics program of the ATOMKI. Non- published. ATOMKI, Debrecen, Hungary, 1991. (in Hungarian)

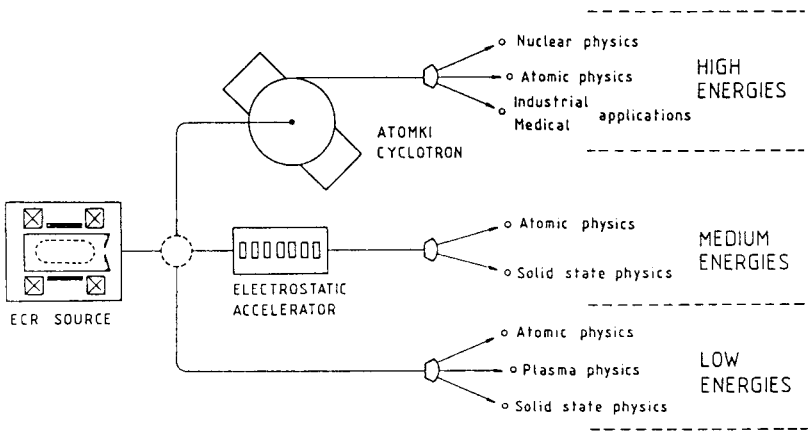
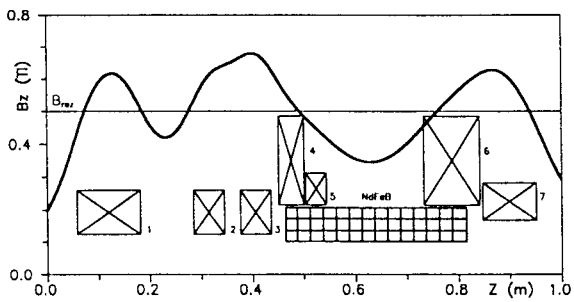


Fig.1. The scheme of the proposed heavy ion facility.



Num	R-in(m)	R-out(m)	Leng(m)	Dist(m)	Turns	Current(A)
1	0.050	0.140	0.124	0.120	120	800
2	0.050	0.140	0.060	0.315	60	800
3	0.050	0.140	0.060	0.406	60	800
4	0.110	0.290	0.050	0.476	60	800
5	0.110	0.175	0.040	0.524	28	900
6	0.110	0.290	0.107	0.787	120	900
7	0.080	0.155	0.104	0.899	80	900

dz(m)=0.001

Fig.2. Axial magnetic field on the axis of the ECR ion source and coil parameters.

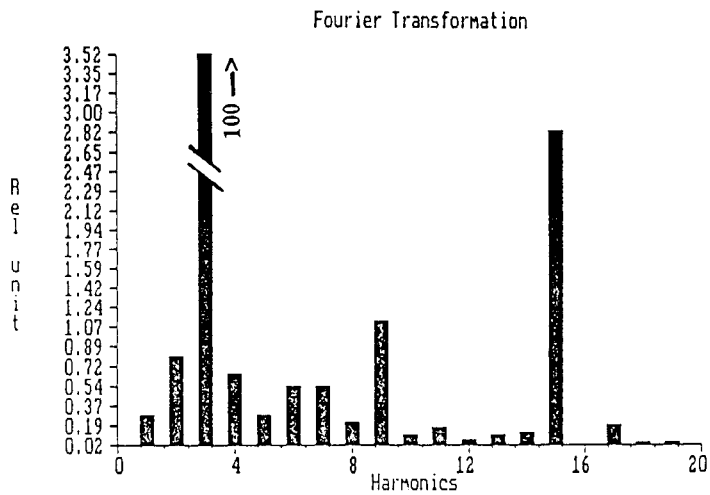


Fig.3. The Fourier-spectra of the radial field component at a given axial position inside a NdFeB hexapole magnet (region: 0-360°, R=33 mm).

RECENT ACHIEVEMENTS AT THE RIKEN RING CYCLOTRON

Yasushige Yano
RIKEN
Wako-shi, Saitama 351-01, Japan

ABSTRACT

In April 1987 the K540 RIKEN ring cyclotron went into operation with the RILAC as an injector; another injector of a K70 AVF cyclotron was installed in April 1989 to upgrade the acceleration performance for light ions.

So far 210 MeV protons and twenty kinds of heavy ions ranging from deuteron through erbium with energies of 7 - 135 MeV/nucleon have been delivered for a wide variety of experiments of nuclear physics, atomic physics, nuclear chemistry, material science and radiobiology.

The current status of this accelerator complex is described with an emphasis on recent improvements and developments.

1. GENERAL DESCRIPTION OF RIKEN ACCELERATOR RESEARCH FACILITY

The fourteen-year project of constructing the RIKEN Accelerator Research Facility (RARF)[1] was carried to completion in 1989 FY. This facility houses a main accelerator of a K540 ring cyclotron (RIKEN Ring Cyclotron, RRC) and its two types of injectors of a heavy-ion linac (RIKEN Heavy-Ion Linac, RILAC) and a K70 AVF cyclotron. This accelerator system delivers various kinds of heavy-ion beams with a mass range from A=1 to A=209. Maximum energies of protons and helium-3 particles are 210 MeV and 185 MeV/nucleon, respectively. Energy range of heavy-ion beams extends from 7 MeV/nucleon to 135 MeV/nucleon for light lions and to about 20 MeV/nucleon for very heavy ions.

The milestones so far read as follows: the RILAC was completed in 1981, and subsequently construction of the RRC was started. In December 1986, the RRC coupled with the RILAC was commissioned. The routine operation of this accelerator complex began in April 1987. In 1987 - 1989, construction of the injector AVF cyclotron and its ECR ion source, fabrication of various experimental apparatus, and extension of beam distribution lines were conducted. Due to this work beam services were sometimes interrupted. In July 1989 a 135 MeV/nucleon nitrogen beam was successfully extracted from the RRC in the AVF injection. This beam has the largest magnetic rigidity that the RRC is capable of providing. Owing to the installation of the AVF injector, the design goal of light-ion acceleration has been achieved. Since September 1989, experimental programs have been carried out by using both RILAC and AVF injected beams. In late 1990 an ECR ion source named NEOMAFIOS[2], developed and manufactured by C.E.N.-G., France, was newly installed on a high voltage injector of the RILAC, being substituted for an old PIG ion source. Thanks to this installation, the RILAC performance has been greatly improved, and consequently the RRC performance for heavy-ion acceleration has been upgraded.

Up to the present, the RRC has provided 210 MeV protons and twenty kinds of heavy-ion beams ranging from deuteron through erbium with energies of 7.0 - 135 MeV/nucleon for experiments of nuclear physics, atomic physics, nuclear chemistry, material science and radiobiology. High quality beams with transverse emittances as small as 10 mm•mrad, an energy spread of approximately 0.1 % and a pulse width shorter than 300 psec have been used.

1.1. Statistics of Operation

Figure 1 summarizes the change in yearly operation hours of the RRC from 1987 to 1991. Since 1990 a routine machine-time schedule for the year has almost established, because there have been no interruptions due to construction works. In these two years an extensive improvements have been made for the whole parts of the machine; this work was very effective in quick starting up, stable operation, and easy maintenance. Thereby hours for tuning and breakdown have been cut back so that total effective hours for users reached nearly 5000 hours in 1991. These hours have been dovoted to proceed nuclear (70 % in portion) and non-nuclear (30 % in portion) experiments. The AVF-injected beam time exceeded the RILAC-injected beam time in a ratio of 7 to 3. Regular long-term overhauls were carried out for 3 weeks in the winter and 6 weeks in the summer.

2. RECENT IMPROVEMENTS AND OPERATION PERFORMANCE

2.1. Ring Cyclotron, RRC

The RRC consists of four straight-edge separate sector magnets and two rf dees. A sector angle of the magnet is 50 degrees; a maximum magnetic field 16.7 kG. Isochronous fields are created by main coils and 26 pairs of trim coils mounted on the pole surfaces. A couple of delta-shaped rf resonators are placed at opposite sides to each other in the magnet valleys. Frequency range of 18 - 45 MHz is tuned

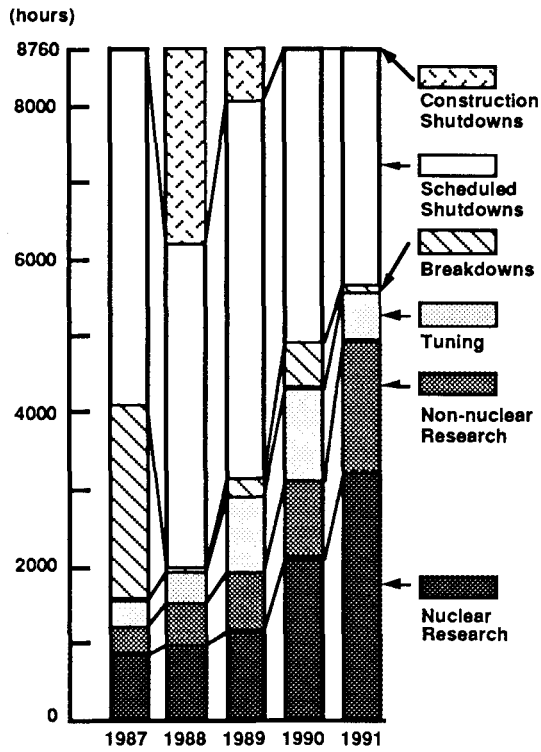


Fig.1. Statistics of the RRC operation from 1987 to 1991.

coarsely by moving boxes housed inside the resonator, which is our original mechanism for changing a resonant rf frequency. An rf power is fed to the resonator through a 50 ohm coaxial line by a final amplifier composed of a 300 kW max. tetrode (SIEMENS 2042SK). At present an rf voltage of 275 kV is generated by a 200 kW power between 10 cm dee gaps at 32.6 MHz, corresponding to 135 MeV/nucleon. An acceleration harmonic number of 5 is used for the AVF injection, while 9 - 11 for the RILAC injection. The RILAC works at the same frequency as the RRC, while the AVF at half of RRC frequency. The large vacuum chamber of 30 m^3 in volume is evacuated by means of fourteen cryopumps of 1.2×10^5 l/sec in total speed to maintain a pressure as good as 10^{-8} Torr. Mean injection and extraction radii are 0.89 m and 3.56 m, respectively; thus a final velocity becomes four times an incident velocity.

An off-centered acceleration technique to facilitate single turn extraction has been established. Such off-centering can be easily obtained by changing a beam inflection voltage at the injection, as illustrated in Fig. 2. It is noticed that each peak appearing in the pattern (c) contains overlapped three turns, resulting from $\nu_r \cong 1.3$. The minimum point between the last two neighbouring peaks is carefully positioned at a 0.5-mm-thick copper septum of an electrostatic extraction deflector. This is done by adjusting an rf voltage slightly. In this way we can get nearly 100 % extraction efficiency and high beam quality, even for a top energy beam. Beam transmission efficiency over 70 % is obtained throughout the RRC. The major beam

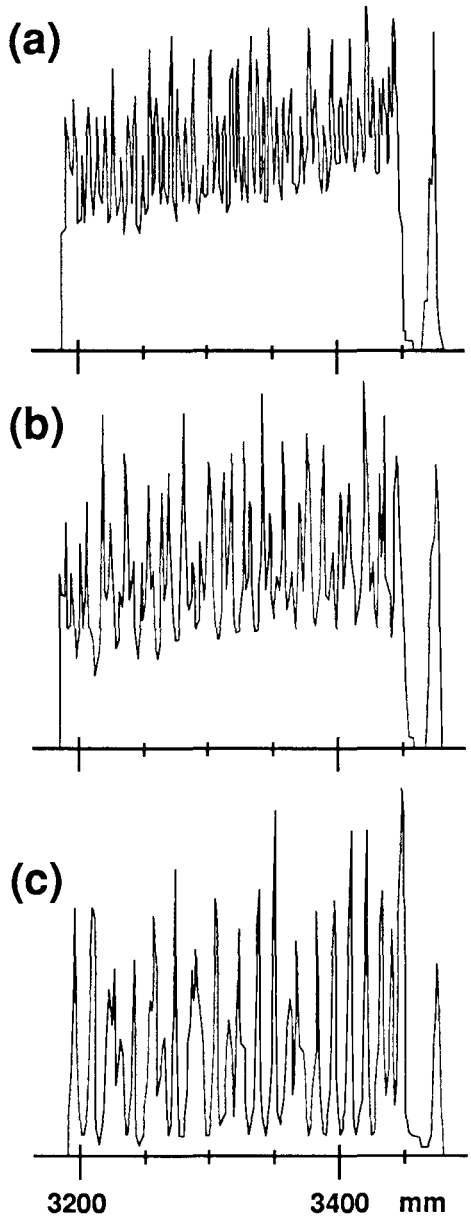


Fig.2. Turn patterns in the extraction region taken with the radial differential probe for a 135 MeV/nucleon nitrogen beam. The last peak appearing at 3475 mm has passed through the electrostatic deflector. (a) a well-centered turn pattern with an average turn spacing of 5.7 mm which is nearly equal to the estimated value; (b) off-centering is driven only by a change of the inflector voltage at injection; (c) the further voltage change followed by a fine adjust of the injection rf phase finally leads clear turn spacings of 15 mm on average.

loss is considered to occur in the course of injection due to emittance mismatching or bad quality of an injected beam.

An rf oscillator system has been improved to work stably at 18 MHz which is lowered from a nominal value of

20 MHz; thus the lowest beam energy of 7 MeV/nucleon has been available in the acceleration harmonics of 11.

Trim-coil power supplies have potentiality to create an isochronous field for a 270 MeV proton beam, while according to calculations a vertical betatron frequency crosses the dangerous resonace $\nu_z = 0.5$ at 212 MeV and decreases down to 0.2 at the final energy. In order to study the resonance-crossing phenomena, we tried to accelerate protons up to 270 MeV. In this trial, protons were

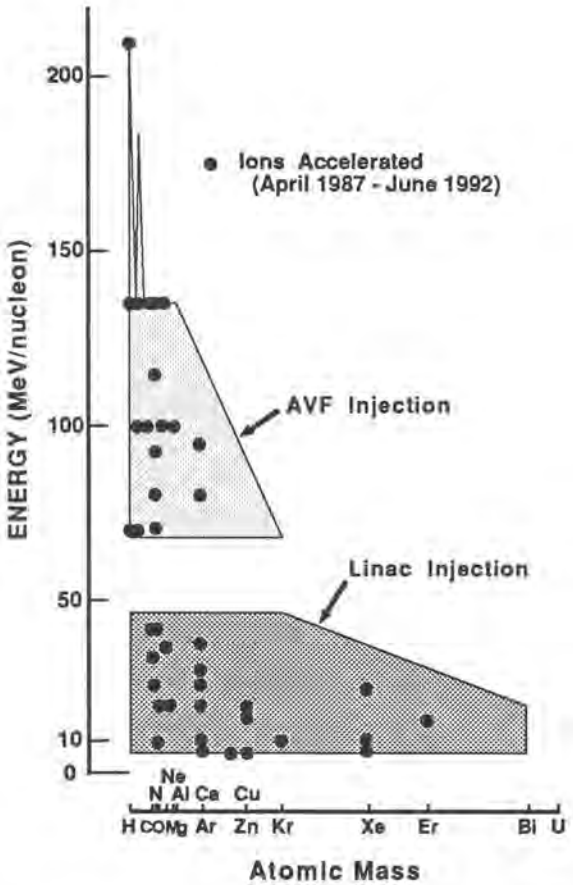


Fig. 3. Energy-Mass curve for the RRC; beams delivered for users are plotted.

successfully accelerated up to the final energy inside the RRC, but some part of the beam was lost near the resonance-crossing radius, where abrupt vertical shift of central particles was observed. These phenomena will be investigated in further detail.

Figure 3 shows plots of ions accelerated so far on an energy-mass space where the RARF accelerator complex can stably provide beams. The energy gap between 45 MeV/nucleon and 67 MeV/nucleon is due to an operational instability of the RILAC rf system at frequencies of 39 MHz - 45 MHz.

Beam intensities have been greatly upgraded: e.g. those of 135 MeV/nucleon light-ions and 95 MeV/nucleon ^{40}Ar ions have reached 500 pnA and 50 pnA, respectively.

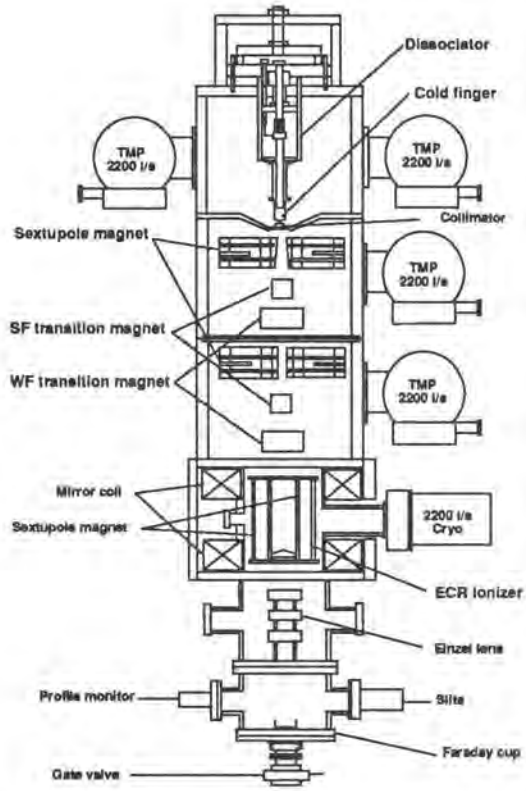


Fig.4. Schematic side view of the polarized ion source.

2.2. Injector AVF Cyclotron

The K70 AVF cyclotron has four spiral sectors and two rf dees with an angle of 85 degrees. Its mean extraction radius of 71.4 cm is four-fifth the mean injection radius of RRC. An rf frequency is tunable from 12 to 24 MHz, and a harmonic number of 2 is used for acceleration. A maximum average field is 17.0 kG. This cyclotron accelerates ions having a mass-to-charge ratio smaller than 4.2 in energy range of 3.8 - 14.5 MeV/nucleon.

The ECR ion source is placed on the floor above the cyclotron vault. The beam is injected axially into the AVF cyclotron through a spiral inflector. A beam buncher generating a sawtooth-like wave-form rf voltage in a single gap between a couple of mesh plates is placed 2 m upstream from the inflector. A beam transmission efficiency between before injection and after extraction is improved significantly by the use of this buncher which gives a phase compression of a factor of 5 - 6; it amounts up to 10 - 15 %. Single turn extraction can be achieved by a carefull tuning, which is indispensable to obtain better beam transmission through the RRC.

This ECR ion source is basically similar in structure to the LBL's[3]. It is of a two-stage configuration and 10 GHz microwaves are supplied to both stages. When metallic ions are produced, a ceramic rod made of their oxide is inserted radially onto a second-stage ECR plasma boundary.

We have studied several methods to upgrade the beam intensity of highly-charged ions. In this improvement works it was found that applying a negative voltage to an electrode housed in a first-stage chamber as well as coating aluminum and magnesium oxide on a second-stage plasma chamber wall enhance the high-charge state performance.[4-5] By these means 35 eμA of $^{40}Ar^{12+}$ and 6 eμA of $^{84}Kr^{20+}$ have been obtained, which allows the RRC to deliver 110 MeV/nucleon ^{40}Ar and 70 MeV/nucleon ^{84}Kr beams with intensities of approximately 2pnA. Recently we have tested "plasma cathode method" by which 80 eμA of $^{40}Ar^{11+}$ could be much stably obtained without any mixing gas.[6] This method has a distinct advantage of very long lifetime and very small gass consumption.

This ECR source is utilized by itself for atomic physics experiments as well.

In May 1992 a polarized proton/deuteron ion source of an atomic beam type was assembled about 8 m directly above the AVF cyclotron center. This source modelled on that of TUNL[7]. Figure.4 shows the schematic side view of the source which consists of a dissociator with a cooled nozzle (~30 K), a pair of sextupole magnets, a pair of weak and strong rf transition units and a 2.45 GHz ECR ionizer. In June the first acceleration test for 14 MeV polarized deuterons were carried out by the AVF cyclotron. A pure vector polarization of 20 % with 30 enA was obtained, which is basically limited to 67%(2/3). An effort is being made to upgrade intensity and polarization.

2.3. RILAC

The RILAC consists of a Cockcroft-Walton injector and six acceleration tanks of the Wideroe type. An rf frequecy is variable for a coupled operation with the RRC. Its range covers 17 - 43 MHz. A maximum effective rf voltage remains constant at 16 MV in the frequency range up to 34 MHz, but it gradually decreases down to 11 MV at 43 MHz. The RILAC is able to accelerate ions having a mass-to-charge ratio smaller than 24 in energy range of 0.7 - 3.7 MeV/nucleon.

At a fixed rf frequency, the RILAC beam energy can be lowered by switching off the last one or two acceleration tanks. Accordingly, an output beam energy of the RRC can be lowered below the nominal value obtained in the fundamental acceleration harmonics of 9; the acceleration harmonics of 10 and 11 are used for this purpose.

The NEOMAFIOS is operated at 8 GHz and generates a mirror magnetic field by permanent magnets. It is compact and consumes less electric power than 20 kW. It is, therefore, suitable for use at the 500 kV injector platform. There have been steady improvements in production of a wide variety of ions and high charge states. So far 8 kinds of gaseous ions, helium through xenon, and 30 kinds of solid ions, magnesium through bismuth have been produced. The higher charge states obtained have roughly doubled the acceleration performance for heavy ions in comparison with the PIG ion source. This high-charge-state performance has also enabled us to increase the RRC beam energies and intensities for heavy ions. In addition, when we accelerate ions of mass-to-charge ratio less than 8.1 up to the RRC minimum energy of 7 MeV/nucleon, no charge stripping is preferable owing to the high intensity for the high charge states. Here the RRC has the K-value of 460 MeV for such a low velocity beam. We applied this acceleration scheme to 7 MeV/nucleon $^{58}Ni^{8+}$ and $^{65}Cu^{8+}$, and 7.5 MeV/nucleon $^{40}Ar^{5+}$ beams; the intensities obtainable have been significantly increased by a factor of 5 as a result of no beam loss due to the stripping process.

An additional beam buncher will be installed on the injection beam line. It will be operated in a second-harmonic mode to an existing beam buncher. This two-buncher system will enhance a phase compression power so that the beam transmission efficiency through the RILAC is expected to increase by a factor of 2.

Although the NEOMAFIOS suits the use inside the high voltage terminal, its performance is much lowered as compared with the 10 GHz AVF ECR ion source. Thus, as the next project, we have decided to construct a new injector consisting of an over 10 GHz ECR ion source and RFQ linac in order to upgrade beam intensity for heavy ions by one or two order of magnitude. Here it is crucial for us to develop a frequency-tunable RFQ. The extreme case required for the RFQ corresponds to the maximum energy 90 keV/nucleon of ions having a mass-to-charge ratio of 5 at 40 MHz. This project is scheduled to complete within two years.

3. References

1) Yano,Y., "Status Report on RIKEN Ring Cyclotron," in **Proceedings of 12th Int. Conf. on Cyclotrons and their Applications** (World Scientific, Berlin, 1989) pp. 13-16.
2) Melin, G. et al., in **Proceedings of Int. Conf. on Physics of Multiply Charged Ions and Int. Workshop on ECR Ion Sources** (Grenoble, 1988) p.673.
3) Lyneis, C.M., in **Proceedings of 7th Workshop ECR Ion Source** (1986) p.1.
4) Nakagawa, T.,"Effect of Coating on the Plasma Chamber Wall in RIKEN Electron Cyclotron Resonance Ion Source," **Jpn. J. Appl. Phys. 30,** L930 (1991).
5) Nakagawa, T. and Kageyama, T.,"The Effect of an Electrode in the First Stage of RIKEN Electron Cyclotron Resonace Ion Source (ECRIS)," **Jpn. J. Appl. Phys. 30,** L1588 (1991).
6) Nakagawa, T. et al.,"Plasma Cathode Method for RIKEN 10 GHzECRIS,": **this proceedings.**
7) Clegg, T.B., in **Proceedings of AIP Conf. 187,** 1227 (1989).

STATUS REPORT ON THE GUSTAF WERNER CYCLOTRON IN UPPSALA

S. Holm
The Svedberg Laboratory, Box 533, S-75121 Uppsala, Sweden

ABSTRACT

The reconstructed Gustaf Werner synchrocyclotron has now been in operation with external beam since May 29, 1987. Until May 1991 it was operating only in the isochronous mode accelerating protons to about 100 MeV and heavier ions to energies corresponding to 200 q^2/A. The main use of the cyclotron has been for physics experiments, proton therapy of malignant melanoma in the eye and arterio-venous malformations (AVM) in the brain, production of isotopes and injection into the CELSIUS ring. In May 31, 1991 a proton beam of 180 MeV was extracted for the first time using frequency modulation but no beam stretching was used. In the beginning of October 1991 work was done to stretch the beam and the results showed that a duty cycle of more than 50 % can be obtained with full repetition rate. The performance of the cyclotron and the obtained results will be described.

1. GENERAL CHARACTERISTICS

The synchrocyclotron was shut down in 1977 for the present reconstruction from cylindrical poles to 3-fold sector geometry. The original ideas were to operate only with frequency modulation using broad band amplifiers. Model measurements, which were started in 1974, showed however that frequency modulation could be restricted to protons above 100 MeV and Helium-3 above 240 MeV. All other ions could be accelerated with fixed frequency. With the sector shape chosen the band-width is about 10 % for the highest energy protons, about 190 MeV.

After installation of the new pole-gap geometry in 1979 the field measurements were started in 1980. The fields were mapped over the useful range, 0.25 to 1.73 T. Vertical focussing is maintained with fields having gradients smaller than 0.2 T/m. The high effect tests of the highfrequency system were started in June 1984 and the field measuring programme finished in June 1985. In December 1985 high vacuum pumping started and in January 1986 high frequency tests of the rf system began. On November 6, 1986 the first internal beam of $^4He^{2+}$ was accelerated and on May 29, 1987 the $^4He^{2+}$ beam was extracted for the first time. About two months were used to optimize the extraction process using a $^4He^{2+}$ beam of 110 MeV accelerated on harmonic 2 and a proton beam of 72 MeV accelerated on harmonic 1. The measured optimum transmission through the electrostatic channel was found to be over 80 % in both modes of acceleration and the total extraction efficiency about 65 %.

After installation of a pair of slits on the first and second turn on the harmonic 1 orbit at the centre of the cyclotron the transmission through the electrostatic deflector increased to nearly 100 % and the total extraction efficiency to over 80 %.

On November 6, 1987 nuclear physics experiments were started and the first eye melanoma treatments were made on April 11, 1989 and presently 20 patients have been treated for eye melanoma and 7 patients for AVM in the brain.

For acceleration of heavy ions an internal ion source was used from the beginning. After installation of the ECR-source, the first alpha beam from the ECR-source was accelerated to the experimental hall on November 20, 1990 and later on the same week a beam of $^{16}O^{5+}$ was accelerated to the same experimental hall for testing of a detector system.

The first extracted beam in the synchrocyclotron mode using regenerative extraction was obtained on May 31,1991, when a beam of 70 nA was extracted using a repetition rate of 70 Hz. The beam was extracted during 7 μsec, which gives a peak current of 140 μA. A special frequency program is used to stretch the beam to prolonge the extracted beam pulse. Calculations have shown that a duty cycle of 40 % can be obtained if the time derivative of the accelerating frequency is changed from 1.6 to 0.03 MHz/msec just before extraction. The beam is then spilled out during 1.3 msec out of a total accelerating time of 3.2 msec. It is also foreseen to increase the repetition rate to 300 Hz which will give an extracted beam of about 0.3 μA.

The first test with slow extraction started the second week of October 1991. The length of the stretched beam was successively increased by lowering the sweep rate at extraction from 0.03 to 0.012 MHz/msec. With a sweep length of 4.2 msec this corresponds to a duty cycle of 52 %.

A problem which has appeared when using high rf-voltage is a vacuum leak to the intermediate vacuum system caused by expansion of the vacuum chamber. To prevent this leak to appear, conical pressure plates have been mounted during August 1991, in order to keep the oring seals under pressure even if the vacuum chamber expands. Tests made at the end of October 1991 with a dee-voltage of 50 kV and a frequency of 24 MHz showed that the leak no longer appears. The RF system is described in a separate paper.

2. ION SOURCES AND BEAM INJECTION

The cyclotron has initially been been equipped with an internal ion source of the cold cathode type. In the c.w. mode, due to the high voltage available, up to 50 kV, the source has a double-arc anode, which permits operation in both first and second harmonic mode without changing the the position of the source. Fig.1 shows the initial medianplane orbits in this case.

In the FM case the highest voltage is 16 kV, which gives sufficient turn separation to clear a closed internal source. A separate geometry is used in this case. By using a special jigg it is possible to change the geometries without breaking the vacuum.Table 1 presents a summary of particles and energies tested so far and available on target.

The external ion source of the ECR-type was buildt in collaboration with the Department of Physics of the University of Jyväskylä in Finland and it is of the same type as the room temparature ECR source at NSCL, East Lancing, USA. The source is vertically mounted and has a plasma chamber of 14 cm diameter and a total length of 82 cm, surrounded by a sextupole of NdFeB permanent magnets giving 0.27 T at the edge of the plasma chamber. An axial field of maximum 0.52 T on the axis of the plasma chamber is obtained by 9 circular coils excited by four 250 A, 60 V and 80 V magnet power supplies. To increase the flexibility in magnetic field variations, additional power supplies will be added to the coils. The original two-stage source has been rebuildt to a one-stage version with an axial injection of the 6.4 GHz micro-wave power. The gas supply to the ion source is provided through a line connected to the main gas bottles and regulated by two stepmotor-driven needle valves. The gases are chosen from a manifold of small gas bottles placed close to the source. The ion source has been tested with the noble gases helium, neon, argon and xenon and with nitrogen and oxygen. An example of charge state distribution of argon

TABLE 1

Ion	Harm	Energy(MeV)	Current (max. extr)
p^+	1	50,55,60,72, 87,94,99,103	10 μA
	2	41, 45	10 μA
H^{2+}	1	100	50 μA pulse
d^+	2	40	1 μA
$^4He^{2+}$	2	50,68,75,113, 120,185	10 eμA
	1	200	1 "
$^{12}C^{4+}$	2	155, 260	200 enA
$^{12}C^{5+}$	2	380	100 enA
$^{14}N^{5+}$	2	340	100 enA
$^{14}N^{6+}$	2	480	60 enA
$^{16}O^{4+}$	3	120	400 enA
$^{16}O^{5+}$	2	300	100 enA
$^{16}O^{6+}$	2	355	60 enA
p^+	1	180, FM 70 Hz	70 nA

ions, analyzed in a 90^0 magnet, is shown in fig. 2. The mixing gas was in this case nitrogen. The data were obtained with a slit opening of 15 mm after the bending magnet. In the case of xenon and a slit opening of 3 mm, the resolution is very much improved with a clear isotope separation within the different charge states.

The ECR source is located in a separate house close to the cyclotron hall and connected to the cyclotron through a 25 m long beam line. A photo of the ECR source is shown at the end of this report. Fig.4 shows the lay-out of the injection beam line. The vertical part of the beam line contains solenoids and steering magnets and a 90^0 bending magnet. In the horizontal part of the beam line quadrupoles and electrostatic lenses are used for focussing and also special iron shieldings to minimize the steering effect of the stray field from the cyclotron magnet. The ion beam is deflected 90^0 down axially through the upper yoke of the cyclotron and finally focussed on a spiral inflector in the median plane using a combination of the field from Glaser lenses and the field in the vertical hole in the magnet yoke.

The spiral inflector is constructed with a ratio of 2.6 between the electric radius, which is the same as the height of the spiral, and the magnetic radius. The highest injection voltage is 20 kV for protons in the CW mode harmonic 1 accerated to 100 Mev, and 12.5 kV for heavy ions accelerated to 50 MeV/nucleon. The central geometry for harmonic 2 and 3 is shown in Fig. 3. When changing from harmonic 2 and 3 to harmonic 1 the spiral inflector is turned 55^0 and a prolonged tip of the dee is installed. In FM mode the highest injection voltage is 6.6 kV and a spiral inflector and a central region of smaller dimensions are used. To increase the intensity accepted by the cyclotron a special bunching system has been buildt. Recent tests have shown that the intensity can be increased by a factor of nearly 5 by using this system. The control of the ECR source and the beam transport system to the cyclotron is made either locally or remotely from the cyclotron control room using a programmable logic controler and a PC system.

A commercially manufactured source for polarized protons and deuterons is installed as shown in Fig. 4. It is specified to deliver beams with up to 20 keV energy with an emittance of 55 mm-mrad$[MeV]^{1/2}$ and a figure of merit $p^2I >$ 41 μA for protons and $p^2I >$ 18 μA for deuterons, where p is the polarization and I the intensity.

3. BEAM EXTRACTION

For extracting the beam two different methods are used:

- In CW mode, when the accelerating voltage is sufficiently high, precessional extraction is used.
- In FM mode regenerative extraction is used.

The main deflecting elements are an electrostatic deflector (ESC) and an electromagnetic channel (EMC). The beam enters first the deflector which has a carbon septum with a thickness of 0.5 mm. Here the beam gets a radial deflection by the electric field between the septum and the high voltage electrode, which causes it to jump the 5 mm thick current septum of the EMC, which is placed 20 degrees from the exit of the ESC. In the EMC the field is reduced by up to 0.25 T. The increased orbit curvature inside the channel directs the beam through the fringe field of the magnet. Before leaving the magnet, the beam passes a radially focussing, passive channel and a radial steering magnet, which is used to align the beam along the axis of the beam transport system.

When precessional extraction is used, a small first harmonic component of the field is used to displace the orbit centre of the beam as it passes the radial resonance $Q_r = 1$ close to extraction. As Q_r decreases when the beam is accelerated into the fringe field, the beam starts to precess, which creates a turn separation of the orbits, propotional to the displacement of the orbit centre and the precession frequency. Due to the fall-off of the magnetic field, the whole procedure is accompanied by a slip of phase, which sets a lower limit to the dee voltage which can be used for this mode of extraction. Another important factor is the presence of the Walkinshaw resonance ($Q_r = 2Q_z$), a coupling resonance between the radial and the vertical motion, which can cause a vertical blow-up of the beam if it is too much off centre. Special harmonic coils are used to eliminate the unwanted first harmonic component in the field and to add the wanted one.

When regenerative extraction is used the extraction point lies at a smaller radius where the phase shifts are unimportant. Therefore this method is suitable in the FM mode where the energy gain approaches zero for some particles. Two more magnetic elements have then to be inserted before and after the EMC: a "peeler" (P) and a "regenerator" (R). The peeler gives a negative gradient of max 250 G/cm and the regenerator a positive gradient of max 300 G/cm. If certain conditions are fulfilled concerning the azimuthal width and the strength of the peeler and the regenerator gradients, the radial oscillation frequency, Q_r, is locked to 1 when the beam is accelerated into these field gradients. As the energy increases, the beam approaches an unstable fixpoint in the radial phase plane, becomes radially unstable and the turn separation starts to grow approximately exponentially, while the vertical motion is kept stable. The calculation shows that this type of extraction gives a smaller emittance but a somewhat increased energy spread.

4. VACUUM SYSTEM

The pumping system for high vacuum consists of two baffled diffusion pumps each giving with the baffles 9000 l/s and for the intermediate vacuum, where the trimcoils are located, a diffusion pump of 700 l/s. They are backed by a Roots-pump of 1000 m^3/h. The pumping is fully automized by means of an industrial programmable controller of type Modicon 484.

5. DIAGNOSTIC SYSTEM

The diagnostic system consists of two radially moving probes, placed at opposite sides of the cyclotron and are used to measure the beam intensity at different radii. One of them is located after the electrostatic deflector to allow measurements of the extraction efficiency and to control the transmission of the beam through the electromagnetic channel and the focussing channel to the external beam. Before and after the electromagnetic channel secondary emission foils are placed for alignment purposes. Four-sector probes are placed on the entrance to the focussing channel and at the beam exit. They are normally not hit by the beam, but used in the procedure of optimizing the setting of the deflecting elements.

6. CONTROL SYSTEM

The control system is based on the use of distributed microprocessors arranged at three levels, the lowest being integrated in the equipment and the middle taking care of whole subsystems such as magnets, rf-system, diagnostics etc. The main computer is connected to the control console and takes care of setting and reading parameters via a database. The safety system is based on industrial programmable controllers. Via a special bus system the computer can read on-off status and registers in the controllers and also set special status bits. A separate computer system is used for the radiation protection and the interlock system.

7. EXPERIMENTAL FACILITIES

Fig. 5 shows a view of the entire experimental area which is used for experiments with the beam from the cyclotron. A specification of the beam lines to different experimental halls is given in table 2. Each beam line contains scanners or viewers to be used for beam diagnostics and Faraday cups which can be inserted at strategic positions for measuring the beam intensity. Heavy radiation shielding between the halls permits access to halls adjecent to beam holding areas.

Beam line A

The irradiation facilities in the Crypt consist of a system containing a viewer plate, which is moved into the position where the target will be placed and used for controlling and trimming the beam position and size. When this in done the target is moved into place for irradiation. A rabbit system is connected to the target mechanism, by means of which the irradiated target can be transported to a nearby placed hot cell. Special water tanks are placed on both sides of the target to moderate the neutron flux from the target.

Beam line B

Beam line B brings the beam by a 30 degree bend up to the level of the experimental halls: Blue Hall, Bio-Medical Hall and the Gamma Hall. The Marble Room is used as a switch-yard for the beam to different experiments such as (n,p) to study isovector multipole resonances with the spectrometer LISA. The pair spectrometer PACMAN, in which intermediate energy photons are produced in the target by the reaction $^{11}B(p, gamma)^{12}C$, features large solid angle, wide momentum bite, excellent energy and angular resolution and efficient background rejection to enable measurements of cross sections of a few nb/sr.

TABLE 2

Beam line	Area	Activity
A	Crypt	Irradiation facilities
B	Marble Room	Neutron production Switchyard
	Blue Hall	PACMAN, LISA spectrometers
C	Beam corridor:	Beam transport to: Bio-medical experimental areas, Gamma hall, CELSIUS
D	Blue Hall	Spectrometer physics
E	Beam Dump	Irradiation Facility
F	Beam corridor	Injection line for CELSIUS
G,H	Bio-Medical	Bio-Medical Experiments Hall
I,K,L	Gamma Hall	Heavy Ion Experiments
Y	C-hall, Ion-source room	Injection of heavy ions and polarized particles

Beam line C

Beam line C is used for transporting the beam to the Bio-Medical areas, to the Gamma Hall and to the injection line for CELSIUS.

Beam line D

The beam line D is used for spectrometer physics with the renovated High Energy Spectrometer Magnet(HESM)

Beam line E

The beam line E takes care of remaining charged particles after the beam has passed through the neutron target. In addition to the beam dump, a facility for irradiation of materials
is planned.

Beam line F

The beam line F starts in the beam corridor by a downward bend to a 0.74 m lower level. It is bent 90 degrees by means of three 30 degree magnets to enter the CELSIUS hall, leaving space for experimental equipment in the gamma hall.

Beam lines G, H and I, K, L

A switching magnet in the beam corridor is used to direct the beam to the beam lines G and H, which are used for radio-therapy with narrow and broad beams and to the beam lines I, K and L which are used for experiments with heavy ions.

Beam line Y

The beam line Y is from the external sources. Special iron hubs are used to screen off the stray magnetic field from the cyclotron magnet.

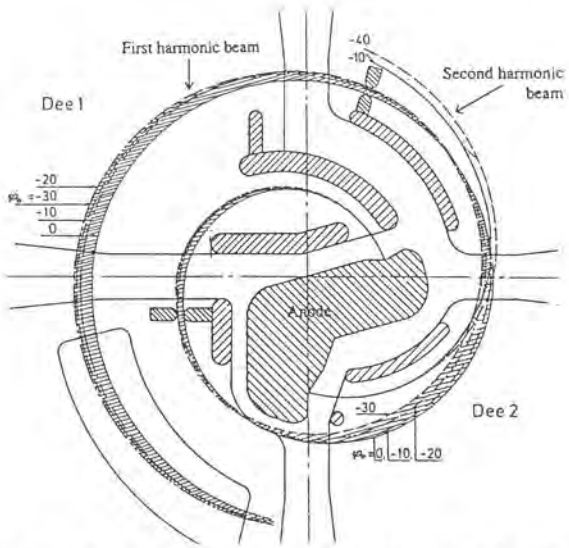


Fig. 1. Central region in the CW case with internal ion source. Double arc anode permits operation both with first and second harmonic.

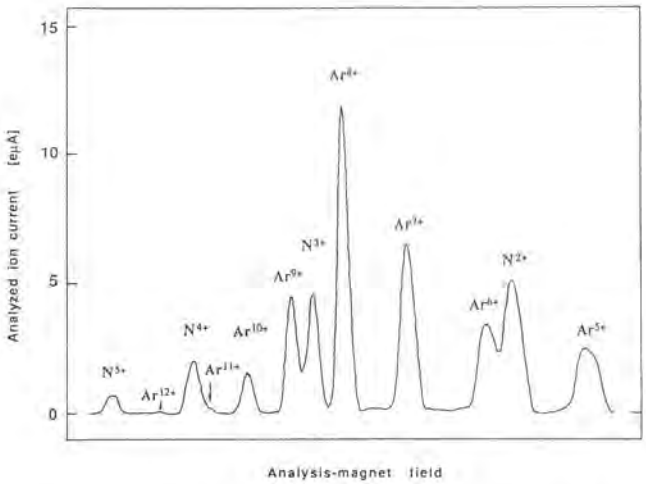


Fig. 2. Charge state distribution of argon ions analyzed with a 90-degree magnet.

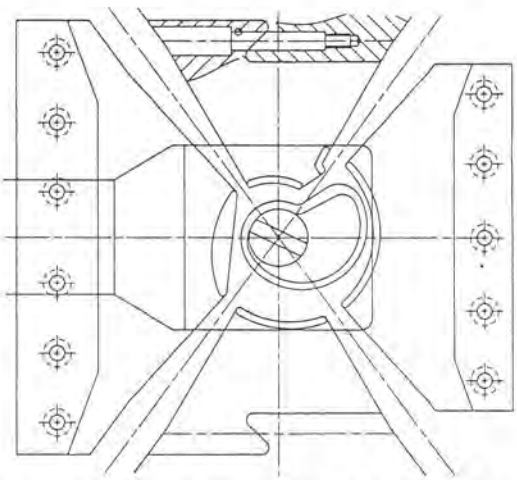


Fig. 3. Central region for harmonic 2 and 3 with external injection.

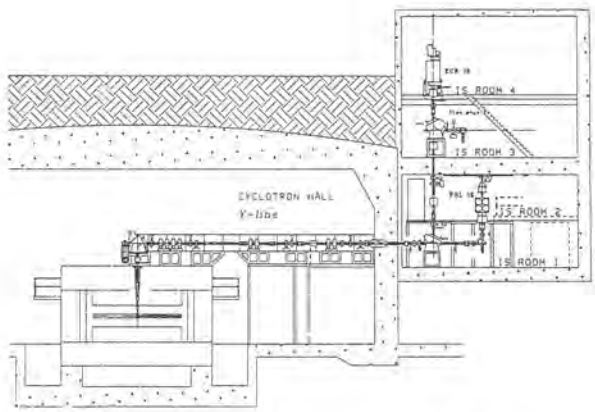


Fig. 4. Lay-out of the external beam line

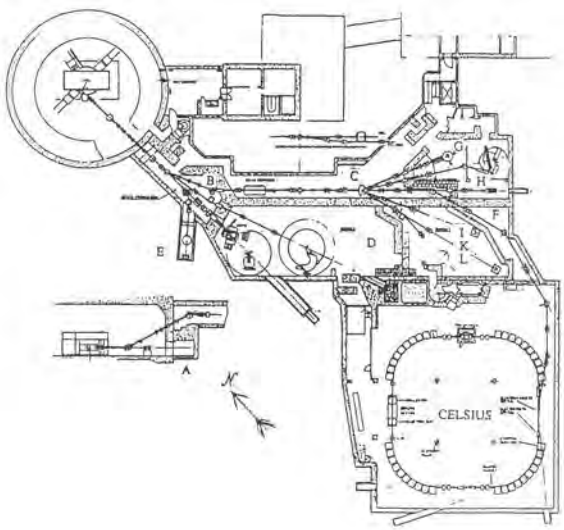


Fig. 5. View of the accelerators and the experimental areas as described in table 2.



Fig. 6. Photo of the ECR source

Commercially Available Compact Cyclotrons for Isotope Production

V. Bechtold
Kernforschungszentrum Karlsruhe GmbH, Hauptabteilung Zyklotron
Postfach 3640, D-7500 Karlsruhe, Germany

Abstract

A variety of different compact cyclotrons are nowadays commercially available The energy ranges from a few MeV to 40 MeV, with beam currents up to 500 microamperes. This overview will cover positive ion machines as well as negative ion machines. It will describe the main specifications, special features and the dominant applications of these modern cyclotrons in research, hospitals and industry.

1. Introduction

Since the last decade the number of compact cyclotrons dedicated to applications has steadily increased from 22 in 1982 to 43 in 1992 (fig. 1).

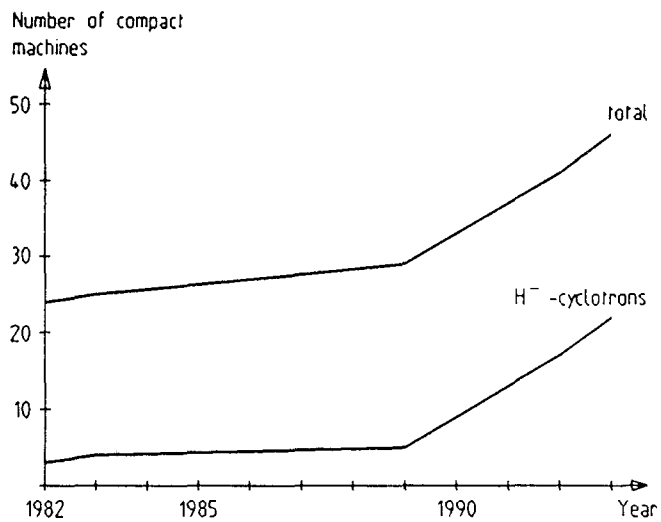


Fig. 1 : Compact cyclotrons for applications in medicine and engineering

These cyclotrons are mostly used for the commercial production of radioisotopes for medical diagnosis like Thallium-201, Iodine-123, Indium-111, Gallium-68, Gallium-67, Rubidium-81 and Fluorine-18. Some institutions are using these cyclotrons for the activation of machine parts for wear studies and for applied research, but they are rarely used for basic nuclear research.

2. Requirements for compact cyclotrons

Modern compact cyclotrons for isotope production should meet the following requirements:

2.1 High beam current > 300 µA

To ensure a high productivity in isotope production the available beam current should be at least 300 µA Higher currents would be desirable but so far appropriate targets are difficult to construct. There are some developments under way e.g. improving the high-power-target design and enhancing the cooling efficiency but these new developments have not proven to be reliable for routine use.

In compact positive ion machines the extraction process limits the availbility of high external currents. As a consequence most isotope productions were done with internal targets (restricted for metallic targets only). This internal irradiations on the other hand are causing also a number of disadvantages:

- complex target transport via air-lock from and to cyclotron vacuum chamber,
- beam handling on target not adjustable,
- beam diagnostic difficult,
- activation of cyclotron components around the target is very high.

The latter restricts the access to the machine for regular maintenance, due to exposure of high level of radiation to personnel.

In contrary a negative ion cyclotron delivers very high external beam currents due to the injection of negative hydrogen ions from an external ion source and the 100 % extraction efficiency via double charge exchange in a thin carbon foil. This type of cyclotron however, is limited to proton and deuteron beams only. But almost all major radioisotopes for medical applications can be produced via (p,xn) reactions (table 1). The advantages of using a negative ion machine are:

- external target located remotely from the cyclotron
- beam handling on target is very flexible
- on-line beam diagnostic during irradiation
- simultaneous extraction of two beams provides more flexibility in the production, splits high current beams on two targets hence reduces beam power on target surface.
- production of two (even different) isotopes at the same time
- activation of cyclotron components very low; access to the machine without high radiation levels within one hour after switching off the cyclotron.

Radioisotope	Half-life	Nuclear Reaction	Bombarding Energy
Gallium-67	78.3 h	Zn-68(p,2n)Ga-67	25 MeV
Gallium-68	1.1 h	Ga-69 (p,2n)Ge-68 Ge-68 → Ga-68	35 MeV
Bromine-77	57 h	Kr-78(p,2n)Rb-77 Rb-77→Kr-77→Br-77	30 MeV
Rubidium-81	4.6 h	Kr-82(p,2n)Rb-81	30 MeV
Indium-111	67.2 h	Cd-112(p,2n)In-111	22 MeV
Iodine-123	13.2 h	Xe-124(p,2n)Cs-123 Cs-123→Xe-123→ I-123	30 MeV
Thallium-201	73.5 h	Tl-203(p,3n)Pb-201 Pb-201→ Tl-201	29 MeV
Fluorine-18	1.8 h	O-18(p,n)F-18	18 MeV

Table 1: Most common cyclotron produced radioisotopes for medical diagnostic

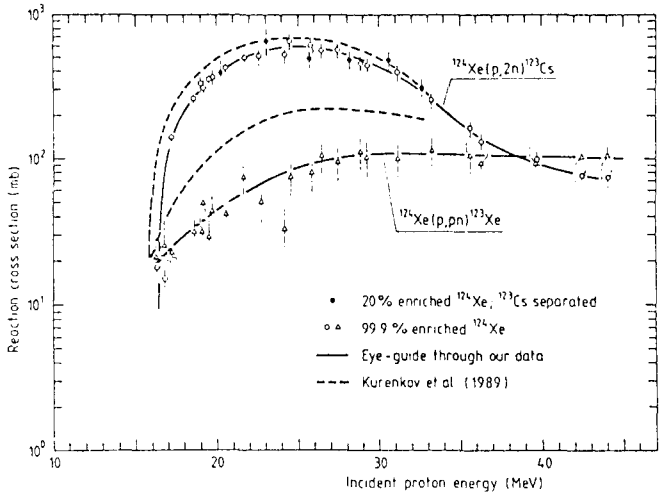


Fig. 2 : Cross section for I-123 via Xe-124(p,2n) taken from ref. 1

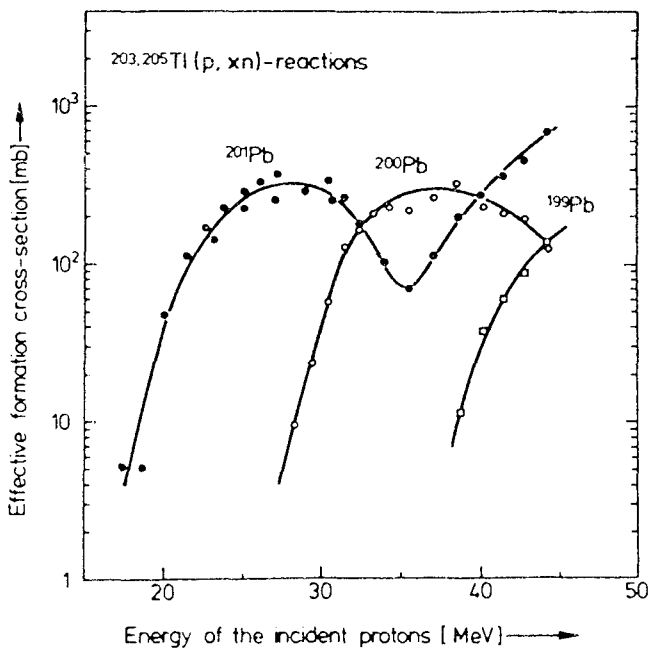


Fig. 3 : Cross section for the nuclear reaction Tl-203(p,3n) taken from ref. 2

2.2 Energy 30 MeV

Most of the machines used so far for routine production have energies between 24 MeV and 26 MeV (e.g. CU-28, CS-30) which are too low. Fig. 2 and Fig. 3 show typical cross section for nuclear reactions in radioisotope production. It can be seen that 30 MeV proton energy is sufficently high for these reactions. For technical reasons some production processes (like in gas- or liquid targets) are using thin metal foils as entrance windows for the beam. While passing the metal foil the beam looses about 1 MeV, but 30 MeV initial beam energy is still sufficient to get maximum production yields. Much higher proton energy than 40 MeV is also not advisable since it will not increase the productivity but only contributes to higher investement- and operational costs.

2.3 Low power consumption

Cyclotrons in the past used typically a few hundred's of kilowatt electrical power while producing less than 10 kW of beam. This energy conversion effi-

ciency (ratio of beam power to electrical power) was only a few (1-3) percent. Due to special magnet design (e.g. four sector compact design with small hill gap) modern compact machines could demonstrate an energy conversion efficiency as high as 15 percent. The total electrical power required should not exceed 150 kW. This keeps operational costs down and makes the radioisotope production more economical.

2.4 Safe and easy operation

For a routinely operated cyclotron in commercial isotope production the use of a fully integrated computer control system is absolutely necessary. It has to be user friendly and should allow the operator to control and monitor every aspect of operation. However, during normal production runs it should not require any operator at all. The software should enable an automatic start-up routine, a safety control for unattended runs and a complete cyclotron trouble shooting to provide an easy, safe and reliable operation.

2.5 Maintenance

The design of the machine has to be very simple and robust to make the operation reliable and to keep the down-time small. Taking into consideration the following subjects the maintenance should require as little time as possible.

- The upper half of the cyclotron magnet can be lifted with jacks sufficiently high for good access to the center of the machine. When opening the cyclotron all components are installed in such a way that there is no need to break any connections. This makes reassembling more save, fast and reliable.

- Activation of cyclotron components and vacuum chamber should be very low. This was feasible since beam losses are kept small due to the axial injection of negative ions from an external ion source, the differential pumping and the highly efficient extraction process via stripping.

- Generally, components are constructed for long life time and the material choosen is radiation resistent or/and gets less activated.

- Components which require a regular service can be isolated by vacuum valves (e.g. ion source, filament, stripper foils)

3. Manufacturers and their compact cyclotrons

The following is a brief description in alphabetic order of the cyclotron manufacturers and their modern compact machines.

- EBCO[3] was established in 1956 as a high tech company. Since 1989 in the cyclotron business based on an TRIUMF-EBCO technology transfer agreement.

- IBA[4] since 1986 established as a Societe Anonyme (SA) with key-experts from the cyclotron department of the University Louvain-la-Neuve.

- NIIEFA[5] is the leading accelerator (cyclotrons and linacs) manufacturer in former USSR since 1952.

- SCX[6] more than 20 years world wide reputation as a cyclotron producer.

- SHI[7] since 1974 producing cyclotrons for research and application in medicine and industry.

Table 2 lists the main specifications of the available cylotrons. Two machines (MC 40 from SCX and 480 from SHI (Fig. 4)) are positive ion cyclotrons with the potential to provide α-particles in addition to hydrogen beams. The available external beam current for protons is limited to 100 μA.



Fig. 4 : 480 from Sumitomo

In commercial isotope production these latter machines are therefore mostly used for internal irradiations.

3.1 Common features

Some common features for these negative ion machines are:

- compact magnet design
- fixed magnet field
- fixed frequency
- variable energy between 15 MeV and 30 MeV
- extraction via stripping
- simultaneous extraction of two beams at different currents and different energies
- external ion source (CUSP-type)
- high extracted beam intensities > 350 µA
- low power consumption < 130 kW
- Vacuum provided by a combination of diffusion pumps and cryopumps
- Controlsystem with commercial PLC's
- D⁻-option

3.2 The differences

In all machines the rf-amplifier is installed very close to the cyclotron and the power is directly coupled to the cavity. Only the TR 30 (Fig. 5) from EBCO uses a coaxial transmission line between the cavity and the power amplifier.

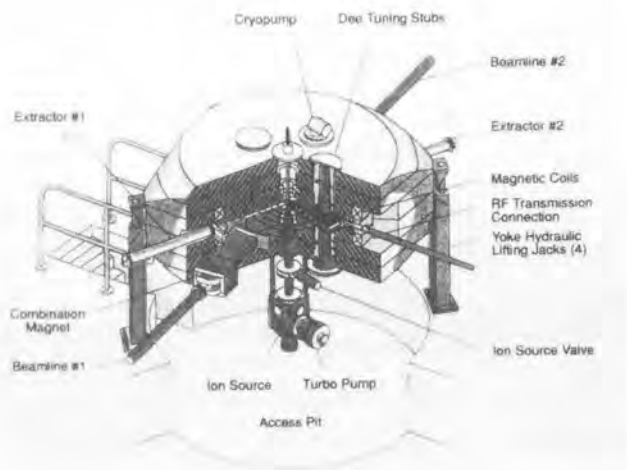


Fig. 5 : TR 30 from EBCO

The external ion source is either installed on top of the cyclotron (Cyclone 30, (Fig. 6) MC 32 NE, Fig. 7)) or in a pit below the machine (TR 30, RIC 35, (Fig. 8)). The TR 30 uses a negative ion source of the CUSP-type with a very high brightness (10 mA dc H beam at 0.44 π mm-mrad).

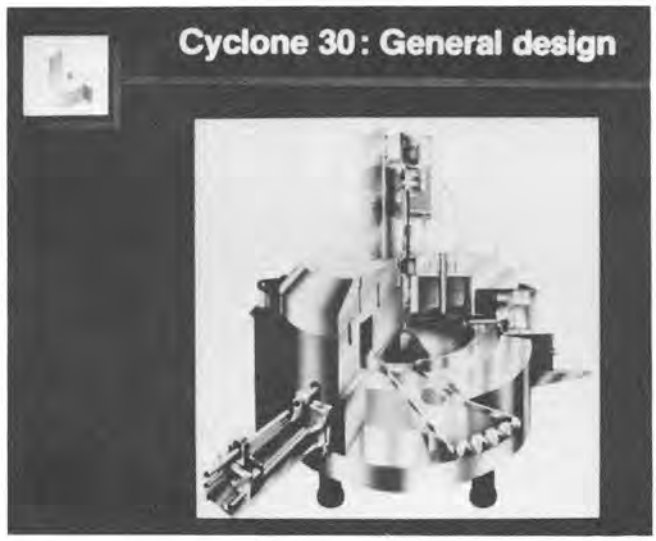


Fig. 6 : Cyclone 30 from IBA

The injection is done with a buncher in the Cyclone 30 and without bunching system in the TR 30, RIC 35 and MC 32 NE.

For the vacuum system of the main vacuum chamber the MC 32 NE uses only diffusion pumps, the RIC 35 and Cyclone 30 have installed diffusions

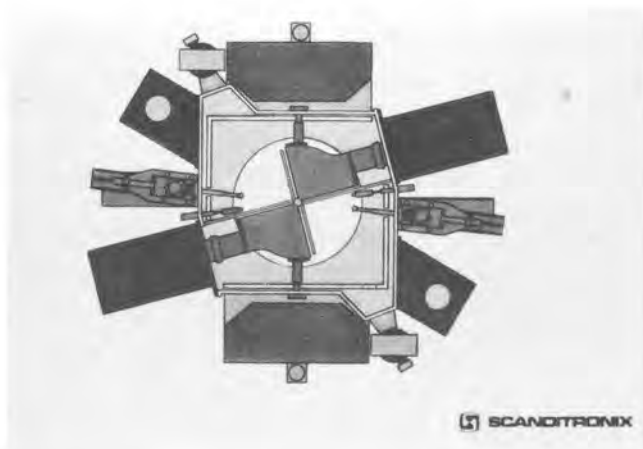


Fig. 7 : MC 32 NE from Scanditronix

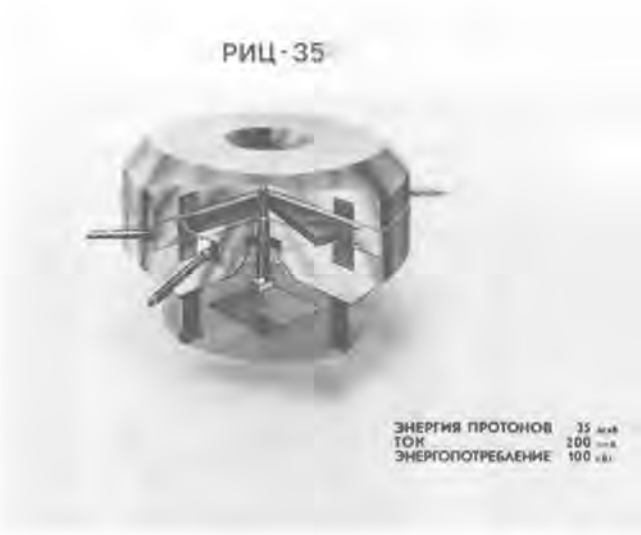


Fig. 8 : RIC-35 from NIIEFA

pump and cryopumps whereas the TR 30 uses cryopumps only.

The beam is generally extracted into two beamlines at 180° except for RIC 35. In this machine there are two beams at 60° available. The Cyclone 30 in addition provides in each opposite exit port a "selection magnet" integrated in the yoke which directs the beam into one of the two possible beam lines.

The maximum beam energy for protons is 30 MeV in the TR 30, 32 MeV in Cyclone 30 and MC 32 NE and 35 MeV in the RIC 35.

For completness it should be mentioned that the above listed manufactures are also offering small negative ion cyclotrons dedicated for PET isotope production. For these applications there is no need for high intensity, hence these machines are all equipped with an internal ion source which makes the cyclotron even more simple. The energy ranges from 10 MeV to 18 MeV with beam intensities up to 100 μA.

4. Conclusion

A variety of compact cyclotrons for isotope production in medicine and industry is commercially available. The presented machines slightly differ in the use and arrangement of external components. The feasibility of providing a high-current, highly power-efficient and fully automated cyclotron for radioisotope production could be shown by the manufactures.

5. Acknowledgment

It is a pleasure to express my appreciation to the cyclotron manufactures who have provided a lot of useful information for this paper. I am also indepted to H. Schweickert for his valuable suggestions and helpful discussions.

6. References

1) F. Tarkanyi, S.M. Qaim, G. Stöcklin, M. Sajjad, R.M. Lambrecht and H. Schweickert, Excitation function of (p,2n) and (p,pn) reactions and differential and integral yield of J-123 in proton-induced nuclear reactions on highly enriched XE-124, Appl. Radiat. Isot. Vol. 42, No. 3, pp. 221-228, 1991, Int. J. Radiat. Appl. Instrum. Part A

2) S.M. Raim, R. Weinreich and H. Ollig, Production of Tl-201 and Pb-203 via proton-induced nuclear reactions on natural thallium, Int. J. Appl. Radiat. Isot. 30, 85-95 (1979)

3) EBCO Technologies Inc. 7851 Alderbridge Way Richmond, B.C., Canada V6X2A4

4) IBA, Ion Beam Applications S.A., Chemin du Cyclotron, 2, B-1348 Louvain-la-Neuve, Belgium

5) NIIEFA, D.V. Efremov Scientific Research Institute of Electrophysical Apparatus, Russia

6) SCX, Scanditronix AB Husbyborg S-75229 Uppsala, Sweden

7) SHI, Sumitomo Heavy Industries, LTD 5-2 Sobiraki-cho, Niihama-shi, EHIME 792, Japan

THE OPERATION OF CYCLOTRONS USED FOR RADIOPHARMACEUTICAL PRODUCTION

T Grey-Morgan
Cyclotron Isotopes Manufacturing, Amersham International plc,
White Lion Road, Amersham, Buckinghamshire, HP7 9LL, England

and

RE Hubbard
Medi+Physics Inc, 3350 North Ridge Avenue,
Arlington Heights, Illinois 60004, USA

ABSTRACT

Amersham International and Medi+Physics have been involved in the use of cyclotrons for licensed radiopharmaceutical production for over a quarter of a century. Amersham was the first company to purchase a cyclotron for commercial radioisotope production and it is still operational after 27 years. The latest cyclotron was commissioned 2 years ago. A wealth of experience has been accumulated both on the practical aspects of cyclotron operation for the high current irradiation of targets and the associated support functions. This paper discusses the operation and scheduling of the cyclotrons for the many isotopes produced as well as our progress on machine reliability and operator dose reduction.

1. INTRODUCTION

Two years ago Amersham acquired the North American operation of Medi+Physics and now combined they operate eight cyclotrons at three sites, Amersham (UK), North Arlington Heights IL. and South Plainfield NJ. In total there are 150 people employed directly in the production of the radiopharmaceuticals. The cyclotrons operated are listed in Table 1.

Name	Installed	Energy MeV	Target
Philips	1966	25	Internal
CS22	1972	22	Internal/External
MC40-1	1979	20 - 40	Internal/External
MC40-2	1981	20 - 40	Internal/External
CP42	1984	20 - 42	External
PV70	1985	25 - 70	Internal/External
MC40-3	1986	20 - 40	Internal
Cyclone-30	1989	15 - 30	External

Table 1.

All of these machines were purchased from dedicated cyclotron manufacturers and then customized for intensive machine operation by the addition of targetry systems which differ for the various applications.

A variety of different targets are irradiated. These include:

Reaction	Uses
$^{203}Tl(p,3n)^{201}Pb \rightarrow ^{201}Tl$	Myocardial scintigraphy (Heart)
$^{112}Cd(p,2n)^{111}In$	Monoclonal antibody studies and cistern/ventriculography
$^{124}Te(p,2n)^{123}I$	} Thyroid studies
$^{127}I(p,5n)^{123}Xe \rightarrow ^{123}I$	} Thyroid studies
$^{124}Xe(p,2n)^{123}Cs \rightarrow ^{123}Xe \rightarrow ^{123}I$	} Thyroid studies
$^{68}Zn(p,2n)^{67}Ga$	Tumour location
$^{82}Kr(p,2n)^{81}Rb \rightarrow ^{81m}Kr$	Lung function studies

To be successful in the commercial production of radiopharmaceuticals, it is important to be able to deliver the product to the customer reliably day after day, all year long. The products produced have half-lives in the range of 4.8 hours (Kr) to 73 hours (Ga), and therefore it is not possible to stock these isotopes for more than a few days at most. To comply with the expiry date requirements of licensed radiopharmaceuticals the shorter lived isotopes are made to order on a daily basis, thus customer service levels are critically dependent on cyclotron reliability. To support this requirement there is a significant organizational challenge, in co-ordinating the demands of production, maintenance, development and best radiological practice.

2. ISOTOPE IRRADIATION

In order to maximize reliable isotope production sophisticated target systems are required. These systems are constrained by a number of parameters. These include the

method of positioning the target reproducibly, beam spot size on target, the requirement to dissipate several kilowatts of heat and the minimization of operator dose uptake and isotope usage. The magnitude of beam that can be used is target material dependent and requires a consistent high quality of target plating to ensure reproducible production rates. To control the usage of the enriched isotope the solid targets are normally electroplated. Current prices are \$6.15/mg for ^{68}Zn, \$3.10/mg for ^{203}Tl and \$4.35/mg for ^{112}Cd[1] making the recycling of unused material a necessity.

Irradiation performance of targets internal to the cyclotron is complicated because the vapour pressure of the solid target is decreased by several orders of magnitude by having to operate in the cyclotron tank at a pressure of about 5 microtorr. This means that short duration pulses of high intensity beam, due perhaps to ion source instability, can evaporate target material. The original cyclotron designers expertise in producing beams of low emittance further complicate the process giving high power densities (a few kilowatts/cm^2) which have to be dissipated. The size of the target is limited by the physical constraints of the vacuum tank ports but is optimized by allowing the beam to hit the target at grazing incidence, paying particular attention to the water cooling of the target backing. It is necessary to ensure there is no air in the water and that turbulent flow conditions are maintained at all times to maximise heat transfer. Increased power dissipation can be achieved by rotating the target but this complicates the design of the target handling mechanism. The opportunity for beam diagnostics is limited on internal beam machines making production control more difficult. The beam size is particularly susceptible to machine parameters such as dee phase, harmonic coil and gradient coil settings. These parameters may be detuned purposely sacrificing ion source/machine efficiency for increases in isotope productivity. The design of internal targets are often unique to each commercial cyclotron model but isotope production remains target limited.

On external beam machines the control over the irradiation is enhanced by the diagnostic techniques available in the beamlines such as slits and collimators, phosphor screens or flying wires used to determine the position of the beam. The beam shape can be optimized by steering and focusing magnets making it largely independent of tuning parameters internal to the cyclotron. Again the power dissipation requirements are satisfied by inclining the target, water cooling and occasionally rotation. Another significant advantage of external beam cyclotrons is that it is possible to irradiate the target at atmospheric pressure by passing the beam through a very thin titanium or Havar foil which is force cooled with a jet of inert gas[2]. External targets can dissipate between 50-100 % more power than internal targets and thus isotope production is beam current limited.

For both internal and external target types it is useful to monitor the proton/neutron ratio during irradiation as this can aid machine diagnostics and tuning.

3. TARGET HANDLING

A number of different target handling systems are installed at our facilities. The prime function of these systems is to place the target reproducibly for irradiation by remote control minimizing the dose uptake to the operator. Conveyor systems are used to move the target through the shielding walls of the cyclotron vault. After testing for vacuum and coolant integrity the targets are mounted in their irradiation position either by the use of through-the-wall manipulators, robots or by electromechanical methods. Programmable logic controllers are used for this repetitive operation which may be automated so that unattended target changes are possible. These handling systems have to be reliable with complete backup if a full production capability is to be maintained. This is particularly important when dealing with short half-life isotopes such as ^{201}Pb that require immediate processing. This may involve the use of battery operated recovery methods or emergency generator systems for critical circuitry.

4. SCHEDULING

Scheduling the cyclotrons is a compromise between machine maintenance and production requirements. The cyclotrons are able to run unattended 24 hours/day every day of the year. A variety of shift patterns are worked by the staff so that the appropriate people are available at the required time for operational duties eg maintenance, breakdown cover, chemical processing. When scheduling irradiations the usual starting parameter is the amount of activity that is required by the customer base at a specific time. From this information it is possible to calculate when the activity must be generated allowing for chemical processing, dispensing, quality assurance, shipment and decay. As it is possible to produce several isotopes on each cyclotron a sophisticated software package has been developed to optimize the multi-isotope, multi-cyclotron utilization schedule. By iterative refinement and rapid feedback of actual yield rates dynamic scheduling is possible. A typical weekly irradiation schedule for one of our cyclotrons is shown in Fig 1.

Of particular interest are the periods during the week when the cyclotron is available but not used for production (shaded areas in Fig 1.). This reflects a high degree of efficiency so that the correct amount of radioactivity is made at the correct time. The short periods (Monday evening, Friday evening) can be used for instrumentation/calibration checks outside the vault. The longer periods of available time (Saturday) reflect production capacity that can either be exploited for development, additional production or used to

	0000	0200	0400	0600	0800	1000	1200	1400	1600	1800	2000	2200	0000
Sunday	→	I				Tl				Xe		I	→
Monday	→	I				Tl						I	→
Tuesday	→	I				In						I	→
Wednesday	→	I				Tl							
Thursday						MAINTENANCE						Tl	→
Friday	→		Tl				Tl					Tl	→
Saturday	→		Tl									I	→

Fig. 1. A typical weekly irradiation schedule

create a longer maintenance period on one of the other machines.

The production schedule sometimes requires that irradiation of short half-life isotopes ends before order acceptance stops that day eg the overnight iodine runs. It is vitally important that the yield information is fed-back into the scheduler to optimise the following night's production.

5. MAINTENANCE

In a multiple cyclotron operation, each machine becomes an integral part of an overall operating plan. Operations are scheduled in an eight part scenario that includes the requirements of production and maintenance on two continents.

It is easy in this industry to operate the machines until they break down and then effect emergency repairs. This is a short-sighted approach which results in increased down time, increased operator dose and low reliability. A rigorous maintenance policy supported fully by senior management is required to achieve the reliability necessary to produce short-lived radiopharmaceuticals.

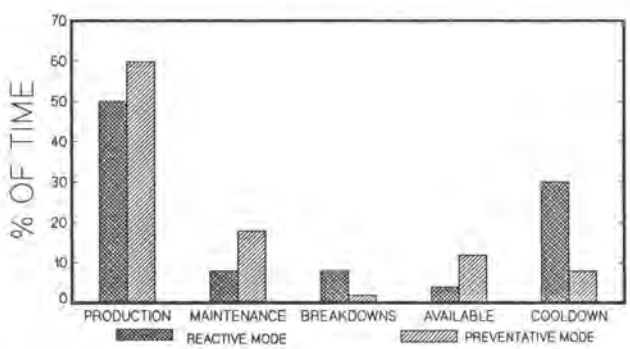


Fig. 2. Comparison of cyclotron utilization in breakdown and preventative modes

Over the last few years operations have moved gradually from the reactive to the pro-active mode. Accumulation of data during this period has enabled the step from breakdown maintenance to systematic preventative maintenance to be made. Recently it has been possible to take the next step to predictive maintenance. Figure 2. shows the utilization of the eight cyclotrons. It is clear that the reactive maintenance regime is significantly less productive requiring more unusable time as the radiation levels in the vault reduce to acceptable levels.

In the move from breakdown maintenance to predictive maintenance, it has been possible to halve operator exposures whilst experiencing an eightfold increase in machine activation due to product volume increases. Additionally, the unplanned breakdown time has been reduced from an average of 8 percent to less than 2 percent.

The Preventative Maintenance program relies on a sophisticated commercial software package[3]. This software maintains a large data base of machine maintenance and breakdown information. Additionally, it maintains an inventory of all spare parts. This, coupled with a bar-code system of inventory management, ensures that adequate stocks of critical spares are maintained. As spares are used, the inventory is updated and at determined levels purchase orders are produced automatically.

The powerful and flexible report writing facility of the software tracks the work orders and work completed including important task/dose information. It is possible to produce reports which indicate the maintenance by specific system allowing the determination of which systems are most liable to failure. This allows management to make informed decisions on where to invest funds for maximum benefit in reliability and safety.

6. DOSE CONTROL

Regulatory control of radiation exposure is always an important issue in a production operation. Permissible dose levels are continuously being revised downwards. In the UK the Company limit is 15mSv/year, in the US it is 25mSv/year (these limits will be reduced to 10mSv/year and 15mSv/year respectively in 1994). A benefit of the Preventive Maintenance program is that adherence to these limitations is achieved without compromising production primarily because we are able to benefit from planned machine cooldowns. It has been possible to identify those areas generating the highest dose uptake prompting engineered improvements or modification of working practises.

Figure 3. shows the total dose uptake by cyclotron operators at our UK and US facilities over the last 5 years.

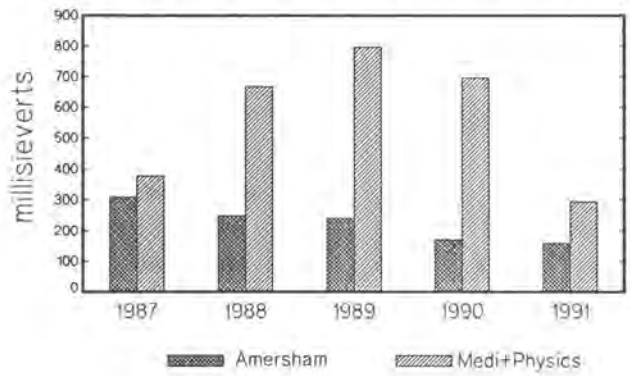


Fig. 3. Cyclotron Group Dose Uptake 1987-1991

Practical methods employed to reduce dose uptake include accurate in-vault and in-tank surveys to identify hotspots which may have dose rates of several hundred millisieverts/hour. Using this information and historic data it is possible to predict accurately the dose uptake for particular procedures. Other methods include the use of remote controlled TV cameras in the vaults to aid fault diagnosis or monitor staff; laser pointers are used to indicate equipment requiring attention without needing to enter beyond the vault door area; video recordings and photographs are used to train new operators in routine procedures without any radiation exposure. Major rebuilds are also recorded so that the information can be shared with our other facilities.

7. QUALITY

Quality, in its broadest sense, is critical to the radio-pharmaceutical business; both in terms of the efficient utilisation of expensive capital equipment and the statutory requirements of Good Manufacturing Practise (GMP)[4].

In-process control is used at all stages of production. This starts with the definition of performance criteria for the cyclotrons and the adherence to calibrated standards. Each target is checked for weight and condition prior to acceptance for bombardment. During bombardment all cyclotron operating parameters are automatically checked to be within the acceptable range. The integrated beam current, length of run and prior yield values are used to calculate the predicted yield. This is then compared with the actual yield and fed back into the scheduling program and used as a performance measure for that machine. Isotopic abundance analysis of the product is used to check that the energy of the beam was correct during irradiation. For instance, on an internal ^{203}Tl target a radial position increase of 0.5mm will increase the beam energy sufficiently to cause a non-compliance with the pharmaceutical licence due to increased ^{200}Tl content in the product.

8. CONCLUSION

Producers of licensed radiopharmaceuticals are subject to stringent controls both in terms of the regulatory compliance of the product and the legislation governing the radiation dose received by staff. Conformance with these requirements is essential for the long term viability of suppliers in this business. Operating cyclotrons is capital intensive, demanding the best possible use of the resources available. The initiatives outlined in this paper are part of an ongoing improvement programme which addresses these requirements thus ensuring reliable supplies of radiopharmaceuticals both now and in the future. This will benefit everyone in the supplier/customer chain.

REFERENCES

1) Oak Ridge National Laboratory, "Electromagnetically Separated Stable Isotopes," (Rev 5.1.90)
2) Votaw J.R. & Nickles R.J., NIM A281 (1989) 216
3) Ounce of Prevention System (OOPS), Peregrine Systems Inc. Pittsburgh Penn.15237
4) European Communities Commission, "The rules governing medicinal products in the European Community" Vol IV (1989) ISBN 92-825-9572-2

CONSTRUCTION AND FIRST YEAR'S OPERATION OF THE JAERI AVF CYCLOTRON

K. Arakawa, Y. Nakamura, W. Yokota, M. Fukuda, T. Nara,
T. Agematsu, S. Okumura, I. Ishibori, T. Karasawa and R. Tanaka
Takasaki Radiation Chemistry Research Establishment,
Japan Atomic Energy Research Institute,
1233, Watanuki-cho, Takasaki, Gunma 370-12, Japan,

A. Shimizu
Research Center for Nuclear Physics, Osaka University,
10-1, Mihogaoka, Ibaraki, Osaka 567, Japan

and

T. Tachikawa, Y. Hayashi, K. Ishii and T. Satoh
Quantum Equipment Division, Sumitomo Heavy Industries, Ltd.
5-2, Sobiraki-cho, Niihama, Ehime 792, Japan

ABSTRACT

The construction of the JAERI AVF cyclotron was started in 1988. The first beam, 50 MeV $^4He^{2+}$ ion, was extracted from the cyclotron in March, 1991! The performance of the cyclotron has been tested with several kinds of ions in a wide energy range. The present report outlines the cyclotron system and shows major results in the first year's operation.

1. INTRODUCTION

Takasaki Ion Accelerators for Advanced Radiation Applications (TIARA) including an AVF cyclotron have been constructed at the Takasaki Radiation Chemistry Research Establishment of the Japan Atomic Energy Research Institute (JAERI).[1] The Advanced Radiation Technology (ART) project is intended to make effective use of the characteristics of ion beams and their interactions with matter for R & D on materials for space environment and nuclear fusion reactors, and for research on biotechnology and new functional materials.

The JAERI AVF cyclotron is of the model 930 of Sumitomo Heavy Industries, Ltd. (SHI), the same model as the CYCLONE (Université Catholique de Louvain, Belgium), the IRE cyclotron (Institut National des Radioelements, Belgium) and the NIRS-Chiba cyclotron (National Institute of Radiological Sciences, Japan). The latter three cyclotrons have movable panel type resonators with a peak RF voltage of 50 kV. The movable-panel type one originally proposed was replaced by the coaxial type resonator in order to make allowance for generating a higher maximum dee voltage of 60 kV, which is required for accelerating 90 MeV protons. In order to meet technical requirements in the research plan of the ART project, we modified or improved the design of the accelerator system as follows; (1) The system is equipped with two external ion sources, an ECR source for generating heavy ions and a multicusp source for generating light ions.[2] (2) The system is equipped with a beam chopping system[3] for pulsed beam operation and beam scanning systems for uniform irradiation to the wide area of target samples. (3) A distributed computer control system is introduced for rapid and reliable control of operation parameters.[4] (4) In order to reduce the radiation exposure of operators, the cyclotron is equipped with automatic changing systems for inflector and puller electrodes. A remote controlled conveying system makes a deflector remove from the cyclotron and guide to a cooling room.

The construction of the cyclotron was started in 1988. The field mapping for the main magnet was carried out from December, 1988 to March, 1989 and the performance of the RF system was tested from October, 1989 to March, 1990 at the Niihama works of SHI. The cyclotron was installed at JAERI, Takasaki, in July, 1990. The beam generation test has been started from March 1991. The cyclotron has been used for experiments since January 1992.

2. OUTLINE OF JAERI AVF CYCLOTRON

Figure 1 shows a photograph of the cyclotron. A schematic drawing of the cyclotron is shown in Fig.2 and the major characteristics of the JAERI AVF cyclotron are shown in Table 1.

The cyclotron is a 4-sectored variable-energy AVF machine with an extraction radius of 923 mm. The acceleration electrodes consist of a couple of 86-degree dees, each connected with a resonant cavity. Beams of protons, deuterons and helium ions are available with maximum energies of 90, 53 and 108 MeV, respectively. Heavy ion beams can be accelerated to an energy range of $(2.5\times M)$ MeV to $(110\times Z^2/M)$ MeV, where M is mass number and Z is charge state. Acceleration harmonic numbers of 1, 2 and 3 are available.

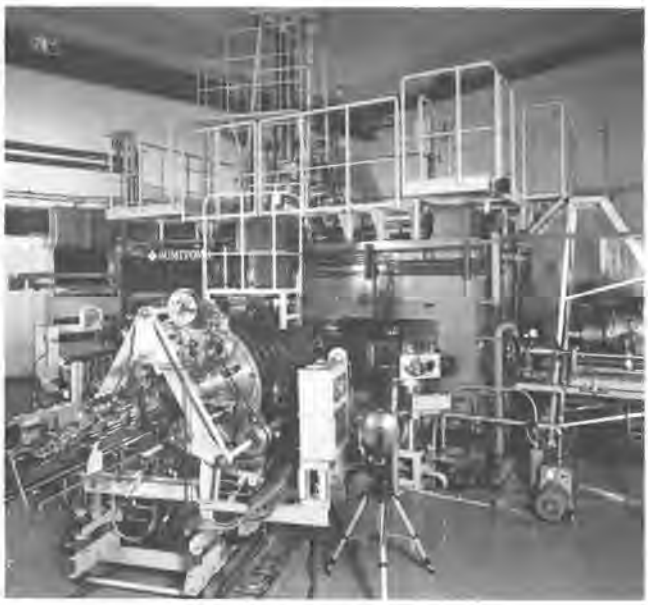


Fig. 1. Photo of the JAERI AVF cyclotron.

2.1. Magnet

The cyclotron magnet consists of a H-type with a pole diameter of 2156 mm and four spiral sectors. Twelve pairs of circular trim coils are wound concentrically on the sectors. Four pairs of harmonic coils are placed in the central region for centering the off-centered beam. Another four pairs of harmonic coils are placed in the extraction region for fine adjustment of turn separation. The field mapping on the median plane in the cyclotron was done in polar coordinates of (r,θ). A Hall probe was moved by 2 cm steps in r and 1.8 degree steps in θ.

The maximum field strength at the extraction radius is 16.7 kG, which is high enough to produce the isochronous field for heavy ions with high energy. The strength of the first harmonic field was less than 4G within the extraction radius, which can be corrected by optimizing the harmonic coil field.

Two pairs of the harmonic coils were excited at a maximum current with opposite polarity. The maximum first harmonic amplitudes at r=200 mm and r=860 mm at a base field of 850A are 17G and 27G, respectively. The isochronous field for light to heavy ions can be produced accurately based on the measured field of main and trim coils. The isochronous field is reproducible within a precision of 4×10^{-4}.

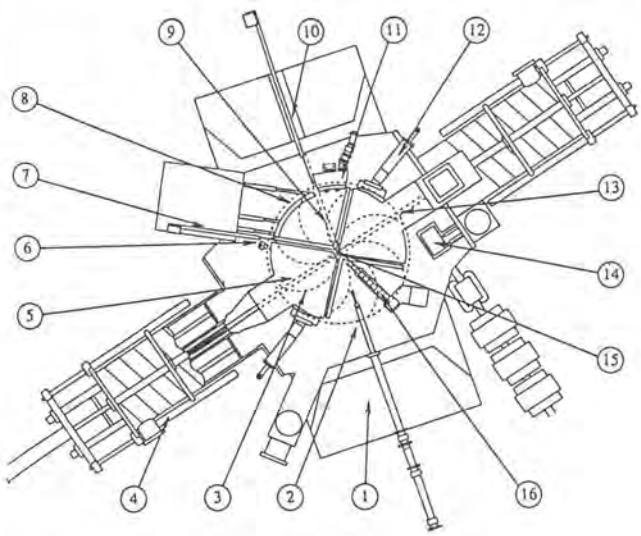
2.2. RF System

A maximum dee voltage of 60 kV was required to realize a constant orbit of harmonic 1 acceleration for 90 MeV protons. The power loss on the stem in the movable panel type resonator makes it difficult to generate the dee voltage of 60 kV. The asymmetrical structure of the cavity results in partial increment of a current density on the stem facing the tuning panel, causing thermal damage due to the local power loss. The final amplifier with large output power above 80 kW is required to generate 60 kV for movable-panel type resonator.

In consideration of the difficulty, the $\lambda/4$ coaxial type resonator with a movable shorting plate was adopted for JAERI AVF cyclotron. The coaxial type one has a higher Q-value because of the symmetrical current density distribution, allowing relatively low output power within 30 kW for the final amplifier. The resonant frequency ranges from 10.6 to 22.0 MHz, and is finely tunable within a relative frequency $\Delta f/f$ of 1.6 %. The maximum peak dee voltage of 60 kV at 21.14 MHz is generated within a stability of $\pm1\times10^{-3}$. The details of the RF system are reported in a separate paper at this conference.[5)]

2.3. Injection, Central Region, Extraction

Low-energy beams from the ion sources, located in the basement, are axially injected into the median plane of the cyclotron upwards through the hole of the bottom yoke. Four Glazer lenses and a steerer are placed inside the hole. The injected beam is guided to the median plane through a spiral inflector and a puller, which are prepared separately for each acceleration harmonic number from 1 to 3. The inflector is inserted downwards through the hole of the upper yoke. The layout of the central region is shown in Fig.3. Two movable phase defining slits are set inside the dee and the dummy



(1) Yoke, (2) Main probe, (3) Dee, (4) Resonator, (5) Puller, (6) Dee voltage pickup, (7) Deflector probe, (8) Deflector, (9) Phase slit(II), (10) Magnetic channel probe, (11) Magnetic channel, (12) Capacitive frequency tuner, (13) Phase slit(I), (14) Gradient corrector, (15) Inflector, (16) Phase probe

Fig. 2. Schematic drawing of the AVF cyclotron.

Table 1. Characteristics of JAERI AVF cyclotron

CYCLOTRON		
Number of sectors		4
Sector gap		166 mm
Pole gap		405 mm
Pole diameter		2156 mm
Spiral angle		53 degrees
Extraction radius		923 mm
Max. average field		16.7 kG
Circular trimming coils		12 pairs
Harmonic coils		8 pairs
Magnet weight		206 tons
Bending limit		110 MeV
Focusing limit		95 MeV
Number of dees		2
Dee angle		86 degrees
Frequency		10.6 - 22 MHz
Max. dee voltage		60 kV
Max. RF power		50 kW x 2
Resonator		movable short plate (mode λ /4)
Harmonic number		1,2,3
Main vacuum pump		Cryogenic (4000 L/s, 4 sets)
Range of M/Z (M:mass, Z:charge state)		1 ~ 6.5
RANGE OF ACCELERATION ENERGY		
Light ions	H^+	5 ~ 90 MeV
	D^+	5 ~ 53 MeV
	$^4He^{2+}$	10 ~ 108 MeV
Heavy ions		2.5 x M ~ 110xZ^2/M MeV

dee within the first turn.
The beam extraction system consists of an electrostatic deflector and a magnetic channel and also of a gradient corrector to focus the beam horizontally. For the purpose of minimizing the deflector voltage to extract 90 MeV protons, the maximum field of magnetic channel was improved from 3.5 kG to 4.3 kG by adding a chilling unit in the water cooling system.

2.4. Beam Diagnostics

A main radial probe, a deflector probe, a magnetic channel probe and a set of phase probes are placed inside of the acceleration chamber of the cyclotron for beam diagnostics. The main probe is inserted through a hole of the side yoke and its stroke covers 1150 mm (r=40~1190 mm). The main radial probe head provides three finger-like electrodes to measure the beam current differentially and integrally. The phase probes consist of ten pairs of rectangular pickup electrodes of copper to measure the relative phase of beams on different turns (r=236~893 mm). The amount of field correction necessary for the outer 10 circular coils is calculated using the phase differences measured by this probe.

A baffle slit system consisting of four leaves is placed just before the entrance of the inflector. Other baffle slit systems are placed at the entrance of the magnetic channel and the gradient corrector. Another baffle slit system is also placed at the extraction hole of the acceleration chamber.

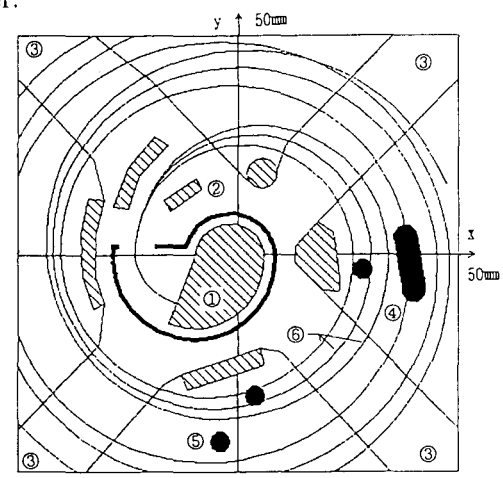


Fig. 3. Schematic drawing of the central region of the cyclotron. (1) Inflector, (2) Puller, (3) Dee gap, (4) Phase slit(II), (5) Phase slit(I), (6) Beam trajectories (dee voltage 40,50 and 60kV)

3. RESULTS OF FIRST YEAR'S OPERATION

3.1. Extraction Current and Transmission

The first beam, 50 MeV $^4He^{2+}$, was extracted from the cyclotron in March, 1991. The beam acceleration tests have been conducted for H^+(10, 45, 70 and 90 MeV), D^+(10, 35 and 50 MeV), $^4He^{2+}$(20, 50 and 100 MeV), $^{40}Ar^{8+}$(175 MeV), $^{40}Ar^{13+}$(460 MeV) and $^{84}Kr^{20+}$(520 MeV). The results of the beam acceleration test are summarized in Table 2. Protons and deuterons are generated by the multicusp ion source, and other ions by the ECR ion source.

The 90 MeV protons were successfully extracted with a beam current of 10 μA. The stability of extracted beam for light ions is typically $\pm$5%. The overall transmission from ion source analyzing magnet to cyclotron external beam is typically 4~5%. The extraction efficiency is the intensity ratio of main probe at r=900 mm to magnetic channel probe (just after deflector). The best transmission and extraction efficiency are 15% ($^4He^{2+}$ 50 MeV) and 89% (H^+ 70 MeV), respectively! The phase slit I on the opposite side of the puller is effective to optimize the extraction efficiency through the deflector. The transmission from cyclotron entrance to r=200 mm is about 20%. This is limited by mainly the RF phase acceptance and the efficiency of a beam buncher installed just at the entrance of the cyclotron. Measured bunching efficiency is about 2.5. The estimated transmission is 2.5$\times$30/360 = 21% assuming that the phase acceptance is 30 degrees.

Table 2. Results of extracted intensity and transmission.

Ion	Energy (MeV)	Harmonic No.	Frequency (MHz)	Injection Voltage (kV)	Extracted Intensity (e μ A)	Extraction Efficiency (%)	Overall Transmission (%)
H^+	10	2	14.97	3.10	10	54	3.8
	45	1	15.46	8.64	30	85*	4.0
	70	1	18.92	12.47		89*	4.0
D^+	90	1	21.14	16.11	10	53*	2.0
	10	2	10.63	3.10	11	45	3.7
	35	2	19.70	11.00	41	71*	4.6
$^4He^{2+}$	50	1	11.76	9.53	21	64*	7.2
	20	2	10.67	3.40	5.7	55	11
	50	2	16.77	8.53	20	82*	15
$^{40}Ar^{8+}$	100	1	11.81	10.15	10	51	6.4
$^{40}Ar^{13+}$	175	3	15.14	10.06	3.0	60	5.7
$^{84}Kr^{20+}$	460	2	16.24	11.71	0.011	26	2.8
	520	2	11.98	8.81	0.004	17	1.0

* Phase slit 1 is inserted.

3.2. Correction of Isochronous Field by Phase Probe

Deviation of magnetic field from the isochronous one can be corrected using the phase probe. The typical pickup signal induced by ion beams is shown in Fig.4. The signal voltage is adjusted by a variable attenuator and a 40 dB fast amplifier. The amount of correction to reduce the deviation for 10 outer circular coils is calculated by the least squares method. After corrections repeated a few times, the phase difference becomes negligibly small.

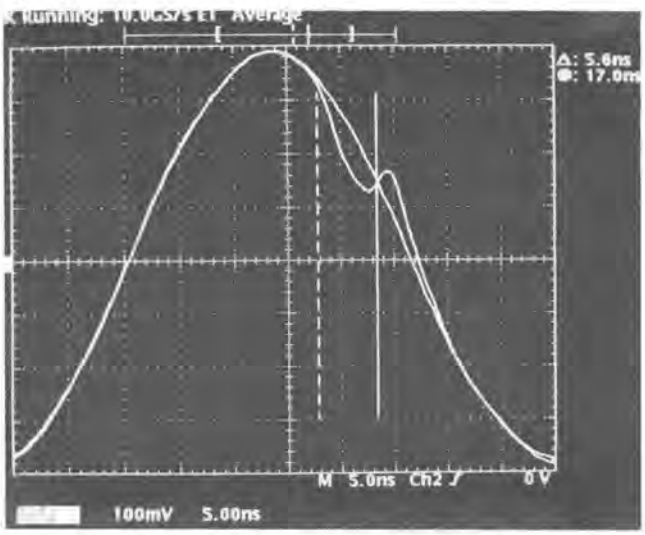


Fig. 4. Typical beam signals measured by the phase probe(CH10) in case of 70 MeV protons.

3.3. Emittance

The phase space configuration of extracted beams can be measured by an emittance monitor at the exit of cyclotron. The horizontal and vertical emittance for $^{40}Ar^{8+}$ 175 MeV are 14.0 πmm·mrad and 9.9 πmm·mrad, respectively.

4. REFERENCES

1) Tanaka, R., Arakawa, K., Yokota, W., Nakamura, Y., Kamiya, T., Fukuda, M., Agematsu, T., Watanabe, H.,
Akiyama, N., Tanaka, S., Nara, T., Hagiwara, M.,
Okada, S. and Maruyama, M., "JAERI AVF cyclotron for research of advanced radiation technology," presented at the Conference on Cyclotrons and Their Applications, Berlin, Germany, May 8-12, 1989.
2) Yokota, W., Arakawa, K., Nakamura, Y., Nara, T., Fukuda, M., Agematsu, T., Okumura, S., Ishibori, I., Tachikawa, T., Hayashi, Y. and Ishii, K., "Operation of ion sources and beam transport to JAERI AVF cyclotron," presented at this conference.
3) Yokota, W., Arakawa, K., Fukuda, M., Tachikawa, T., Hayashi, Y., Kumata, Y., "Performance of beam chopping system for JAERI AVF cyclotron," presented at this conference.
4) Okumura, S., Agematsu, T., Yokota, W., Kamiya, T., Fukuda, M., Nakamura, Y., Nara, T., Ishibori, I., Arakawa, K., Maruyama, M., Iso, K., Hoshika, K. and Tachibana, M., "Control system for JAERI AVF cyclotron," presented at this conference.
5) Kumata, Y., Fukumoto, Y., Fukuda, M., Arakawa, K., Karasawa, T. and Shimizu, A., "Modified RF system for JAERI AVF cyclotron," presented at this conference.

20 MEV CYCLOTRON FOR ISOTOPE PRODUCTION.

A.Glazov, Ju.Alenitskiy, S.Chesnova, A.Chesnov, V.Kochkin, D.Novikov,
E.Samsonov, M.Semenov, A.Vasilenko, E.Zaplatin, N.Zaplatin
Joint Institute for Nuclear Research,
Head Post Office, P.O. Box 79, 101000 Moscow, Russia
and
I.Gulamov, O.Iljasov, A.Rylov.
Institute of Nuclear Physics, 702132 Tashkent, Uzbekistan

ABSTRACT

The $20MeV$ fixed-energy proton cyclotron was constructed based on the conventional magnet with pole diameter $115cm$, which is the standard equipment of physical laboratories in Russia. It is proposed to use an internal target for isotope production. A special two-element magnetic system to increase the size of the beam on the target in the axial and radial directions will be used. The cyclotron was designed and constructed at the JINR (Dubna), but will be used at the INP (Tashkent)

1. BASIS CHARACTERISTICS OF THE ACCELERATOR

The cyclotron is intended for acceleration of protons to fixed energy 20 MeV with current up to $400\mu A$. The design and construction of the accelerator were started simultaneously at the beginning of 1991, and from May 1992 commissioning period began. The cyclotron was designed based on a conventional magnet with dimensions : $3 \times 1.5m^2$ in plane and $2.12m$ high (weight $48T$). The necessary magnetic rigidity and focusing conditions are reached in the magnetic structure with fourfold symmetry and $8.2cm$ gap in the hill of spiral shims. The maximum working radius is $48cm$, the maximum magnetic field is $1.35T$. This structure was chosen not only to solve the main problem, but to be a model for reconstruction of the cyclotron U-150 at INP, Tashkent.[1]

The leading idea in designing the accelerator was to decrease the cost of the production and to simplify and make cheaper the exploitation. So we chosen a standard magnet, forming the magnetic field by iron shims, a self-excited single-tube oscillator to generate rf power, an internal ion source, an internal target for isotope production and a passive magnetic regenerative system to decrease the density of the beam on the target.

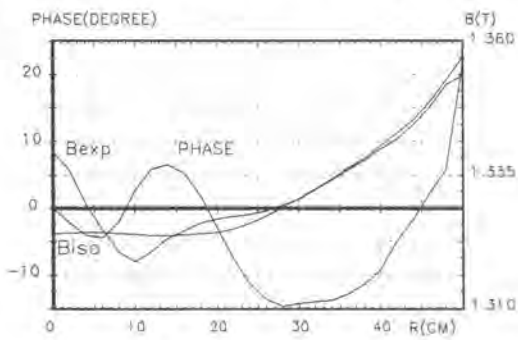


Figure 1: Radial dependence of the isochronous field (Biso), measured average field (Bexp) and phase motion of the beam

2. MAGNETIC SYSTEM

An isochronous magnetic field of the cyclotron is formed with the help of four pairs of spiral and sector shims. For simplicity and precision in production, the edges of the spiral shims are arcs of circumference. The spiral angle varies from 10 to 50 degrees. An increase of the magnetic field along the radius is produced by increasing the azimuthal length of spiral shims and the thickness of the sector ones placed in valleys starting from the radius $18cm$. The radial dependence of the isochronous field, measured average field, and the phase motion of the beam are shown in Fig. 1.

The focusing properties of the magnetic field are illustrated in Fig. 2. The values obtained for frequencies of free oscillations correspond to stability of the particle motion. The low harmonics of

the magnetic field amplitudes are quite small. In the central region ($R < 30cm$) the amplitude of the first harmonic is less then $0.3mT$, on the radii $30-45cm \sim 0.7mT$. To regulate their value, if necessary, in the central region ($4cm \leq R \leq 14cm$) and at the periphery ($32cm \leq R \leq 46cm$) there are four pairs of harmonic coils placed in the valleys.

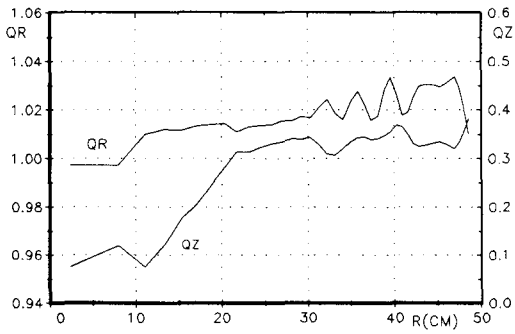


Figure 2: Frequencies of free oscillations

3. ACCELERATION SYSTEM

In a formed magnetic field the revolution frequency for protons is $20.2MHz$. A conventional scheme with one 180° dee and a quarter -wavelength resonant line on the revolution frequency was chosen for the acceleration. Dee aperture is $20mm$. To increase the mean axial gap between the dee and the chamber the cooling tubes were soldered outside the aperture. The minimal gap is $22mm$, the accelerating voltage is $50kV$.

Dee and resonant line were made flat rectangular in plane like it is proposed for convertion of Tashkent cyclotron.[1] The vertical distance "d" between inner and external electrode resonant line outside the magnet were chosen as compromise between convenience for installation of vacuum pumps and rf power consumption .

The calculation of parameters was made by conventional formula for the resonance line. The expression for the wave impedance was taken from.[2] The experimental value of the resonant frequency became 5% less than a calculated one. The rf losses are $12kW$ at the accelerating voltage $50kV$. For generation rf power a triode oscillator with the selective feedback circuit is used. There is a possibility of pulse work of the oscillator by means of a grid modulation. Initial coarse tuning of the resonator is made by changing the distance d in some limits. For fine automatic tuning two trimmer capacitors on both sides of the dee are used.

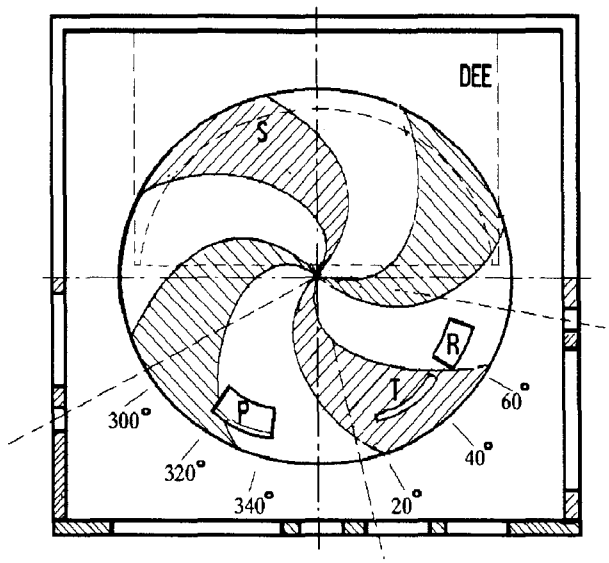


Figure 3: Beam spread system : P-peeler, R-regenerator, T-target

4. THE TARGET AND THE BEAM SPREAD SYSTEM

For isotope production internal target with dimension $2cm$ in the axial direction and $17cm$ in the azimuthal one will be used. The surface of the target has an inclination 6° to the beam orbit. The internal water-cooled side was made with ribs to increase the possible power dissipation up to $10kW$.

The beam spread system must produce the radial deflection of the beam by $1.5cm$ and the extension of its axial dimension up to $1.5-2cm$. For this purpose it was decided to use a passive regenerative system.[3] It consists of two ferromagnetic elements: a peeler with the gradient $-5T/m$ and a regenerator with the gradient $2T/m$. The position of the elements in the accelerating chamber is shown on fig 3. The field disturbance on the working radii ($35-45cm$) is less then $0.5mT$ (first harmonic).

The results of computation of the beam behavior in the regenerating system are shown in fig 4. Approximately at 20 turns the turn separation increases from 0.1 to $1.5cm$ at the azimuth of the target. In computation it is also seen that the amplitude of the axial oscillation increases by a factor of ~ 2.

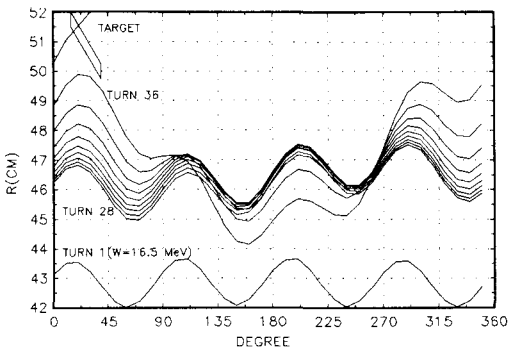


Figure 4: Turns separation in the regenerative system

5. THE BEAM GENERATION AND DIAGNOSTIC ELEMENTS

For ion production an internal ion source of the Penning type with a hot cathode and an insulated anticathode is used. The extraction and selection of the beam on the first turn is realized by means of a puller, turned at the angle 16° to dee edge.

There are three water-cooled probes to control the beam. One of them goes through the dee along the axis. When adjusting the accelerator, low current multielectrode targets on the probes can be installed. The accelerating voltage is measured by means of capacitive probes.

6. STATUS

At present time the cyclotron was assembled at the test stand at the JINR (Dubna). Most systems and devices were tuned independently and ready to work. Two weeks ago we began the vacuum pumping of the accelerator and the struggle with leaks. Soon we plan to study the beam behavior in the central region. The full-scale experiments will be possible only in Tashkent where a proper radiation shielding is provided.

7. REFERENCES

1) Alenitskij Yu.G et al., **"Convertion Project of the AS Uzbekistan Cyclotron"**, JINR, P9-91-82, Dubna, 1991
2) Glazov A.A. et al.,**"Study acceleration system of U-200T isocchronous cyclotron"**, JINR, P9-91-84, Dubna, 1991
3) Dmitriewskij W.P. et al., **"The choise of system for beam deflection on the inside target of syclotron U-120"**, JINR, P9-91-480, Dubna, 1991

STATUS OF A COMPACT H^- CYCLOTRON AT THE KURCHATOV INSTITUTE OF ATOMIC ENERGY

C. D. Burbeza, A. A. Vasiliev, N. I. Venikov, P. Yu. Komissarov, Yu. M. Krasnikov, S. T. Latushkin, V. V. Leonov, V. P. Moryakov, I. V. Naumov, A. Ya. Pisman, V. A. Rezvov, L. I. Yudin, V. E. Yarosh
Kurchatov Institute of Atomic Energy, Moscow, 123182, Russia

ABSTRACT

A compact isochronous cyclotron MPC-10[1] is currently being constructed at the Kurchatov Institute. The main parameters and status of all systems of MPC-10 are discussed.

1. INTRODUCTION

The MPC-10 is compact isochronous cyclotron intended for operating as a component part of a positron emission tomography research center and will be used for producing ultrashort-lived radionuclides ^{11}C, ^{13}N, ^{15}O, and ^{18}F. The main parameters of the cyclotron are given in Table 1.

Table 1 - Main cyclotron parameters

1. Beam		
Type of ion	- accelerated	H^-
	- extracted	H^+
Maximum energy	- guaranteed	10 MeV
	- expected	12 MeV
Intensity		50 μA
Number of extracted beams		2
2. Magnetic system		
Pole diameter		80 cm
Number of sectors		3
Average field		1.55 T
Coil power consumption		33 kW
Weight	- iron	17.5 tons
	- copper	1.5 tons
3. RF system		
Number of dees		2
Dee angle		90 deg
Harmonic mode		1
Dee voltage		40 kV
Operating frequency (fixed)		23.5 MHz
Dissipated power		17 kW
4. Ion source		
Type of source		"Cold cathode", internal, Penning, of thermionic mode
Insertion		radial
Arc power		1 kW
Gas flow		5 - 10 ccm
5. External dimensions		2.5*2*1.5 m*m*m

Cyclotron parameters selection are dictated by the requirement to provide the negative ions acceleration and also by a compromise between the requirements on magnetic and RF systems and the power of their power supply systems, taking into account the requirements on vacuum and reduction in weiht and dimensions. Accelerated ions are extracted by stripping electrons at 1mm thick graphite stripper.

The possibility of accelerating D^- ions is also under investigation. It is suggested that D^- ions will accelerate till the energy value totals ~6Mev at the second accelerating voltage harmonic.

2. MAGNETIC SYSTEM

The cyclotron magnetic system[2] consists of a yoke, poles, exciting coil and a structure shaping an isochronous magnetic field (Fig.1 and Fig.2).



Fig. 1. Magnet structure and main coils.



Fig. 2. Yoke and poles of MPC-10 magnetic system.

The magnet structure geometry was found by applying a technique which combined experimental studies on a magnet mock-up made on a 1:4.57 scale and computer simulation according to a code computing 3-D magnetic fields in a uniform magnetization approximation. Gaps in the structure hill and valley are 80 and 126 mm respectively, a sector angle increases with the radius from 60° to 75°. This provides the possibility to form a magnetic field at the level of 1.55 T capable of accelerating both H^- and D^- ions with acceptable phase shifts, and also provides a flutter required for vertical focusing.

At present the most parts of magnetic system are produced. An automated magnetic field-measuring system intended for a final field shaping directly at the cyclotron magnet is constructed too.

The power supply for a magnet main coil provides the current up to 400 A at the stability of 10^{-4} and at the voltage of 100 V. The power supply is installed in the production area and tested for dummy load (Fig.3).



Fig. 3. Magnet main coil power supply (on the left) and RF oscillator (on the right).

3. RF SYSTEM

A resonance circuit[2] is a two-conductor quarter-wave line ($\rho \sim$ 100 Ohm) in a common rectangular chamber loaded with capacity of 90° dees (C ~ 140 pF) at its end. An operating frequency is 23.5 MHz. The commercial transmitter PKM-20 (power of up to 25 kW) will be used as an RF oscillator. At present the oscillator is installed in the production area and adjusted for dummy load (Fig.3). Frequency tuning within 1.5MHz is provided which is achieved by changing the dee area. There are trimmer capacitors for tuning (the tuning range is 0.5 to 0.6 MHz), an inductive loop and capacitor for coupling to an RF oscillator, a facility for controlling a dee position involving TV monitoring of a shift of laser beam reflected by mirror fixed on a dee.

The equipment includes also a master oscillator; facilities of resonator frequency stabilization based on a phase detector and transistor transformer with pulse modulation for trimmers drive control; a facility for accelerating voltage amplitude stabilization; synchronizer for pulsed modulation of RF voltage during while; in the process of tuning and training, providing also the protection under breakdown.

4. ION SOURCE

An internal ion source of PIG-type with cathode self-warming and radial insertion has been chosen for the MPC-cyclotron. The design of this source has been developed and optimized for intensity at the test bench. At present the work aimed at increasing ion current and the source lifetime is beeing conducted.

The ion source, providing the possibility to change ion acceleration regimes (from H^- to D^-) in the minimal time-period without violating the vacuum, is beeing developed. At the same time the research work aimed at the determination of central area optimal geometry, which will make it possible to combine the above-mentioned acceleration regimes, is conducted.

5. VACUUM SYSTEM

The cyclotron vacuum chamber[2] consists of a body and two covers, produced of stainless steel. The chamber is gasketed with rubber seals in its grooves. The copper clad is fixed to the inner chamber surfase by diffuse welding and cooled by the water sirculating in the tubes sutuated between the clad and the body. The chamber is pumped hard by means of two diffuse pumps with a pumping velocity over

hydrogen of~10^{4} l/s. The fine vacuum of $8 \cdot 10^{-7}$ torr was obtained after the elimination of vacuum leaks during the chamber test (Fig. 4).



Fig. 4. Vacuum tests of the cyclotron chamber.

6. BEAM DIAGNOSTIC

The system of integral and differential probes, Faraday cups, luminescence screens with TV recording of an optical image of a cross-section is provided for monitoring the intensity and position of both internal and extracted beam. An ionization detector of a beam cross-section is provided for monitoring the beam intensity and size during target irradiation. The accuracy of current measurement is ~10% at the intensity in excess of 1 mA, a spatial resolution in each coordinate is ~1 mm.

7. CONTROL AUTOMATION AND CYCLOTRON PARAMETERS MONITORING

Automatic Control System development is based on the components and experience gained when operating the control and monitoring system intended for the cyclotron at the Kurchatov Institute. IBM PC/AT is used for control. As a basic control and monitoring complex the equipment in a CAMAC standard is taken .Transmission-reception facilities of analogue and discrete data involving fiber-optics communication lines are used to achieve connections between CAMAC-units with objects, control and monitoring. Application of these data communication facilities simplifies cable mounting, provides electric isolation of control units from objects under control, enhance noise immunity, simplifies the composition of CAMAC equipment.

The hard- and software are adjusted and tested while operating separate cyclotron functional systems.

8. REFERENCES

1) C.D.Burbeza et al., "Status of a compact cyclotron for PET at IAE", in Proc. 2 th International Meeting on Cyclotrons and Their Applications, L9-89-708, Dubna, 1989, pp.107-114.

2). N.S.Artemov et al.,"Designs of magnetic and resonance systems for a special medical cyclotron MPC-10". IAE-5004/14, Moscow, 1990 (in Russian).

A Newly Developed Compact Cyclotron for Neutron Therapy and Positron Nuclear Medicine

KENGO ITO, SADAYUKI SAKUMA, TAKASHI KATO, MASANORI TADOKORO,
TOYOHIRO OTA, MASANARI NISHINO, TAKEO ISHIGAKI
Department of Radiology School of Medicine Nagoya University,
65 Tsuruma, Showa-ku, Nagoya, 466 Japan
YOSHIMI KASUGAI, HIROSHI YAMAMOTO, MASAKI OSAKABE,
TSUYOSHI MISAWA, SHIKOH ITOH
Department of Nuclear Engineering Faculty of Engineering Nagoya University
Furo-cho, Chikusa-ku, Nagoya, 464-01 Japan
and
YOJIRO TODA, YASUO YAMASHITA
The Japan Steel Works Ltd.
1-1-2 Yuuraku-cho, Chiyaoda-ku, Tokyo 100 Japan

ABSTRACT

In order to demonstrate effective use of small cyclotron , we have developed a new compact cyclotron (BC2211) which enables neutron therapy and positron nuclear medicine. The energies available for proton and deuteron beams are 22 and 11 MeV respectively. Whereas maximum external current is obtainable 60mA. After a half life irradiation, sufficient activities of positron emitters are obtained. ^{11}C:77.7 GBq. ^{13}N:24.1 GBq. ^{15}O:42.6GBq. ^{18}F:27.8 GBq. A basic experiment for neutron therapy was performed using the ^{10}Be(p,n)^{10}Bo reaction at Ep=22MeV. The obtained neutron flux was 7.5×10^{9}/cm^{2}sec (fast neutrons) and 4.0×10^{8}/cm^{2}sec (thermal neutrons) on target. The neutron spectrum depicted maximum and mean energies of 21 and 11 Mev respectively. The absorbed dose was 0.14 Gy/min at 125 cm from the target and not sufficient. The target is now under reconstruction to obtain the more refined neutron flux and spectrum.

1. INTRODUCTION

Recently many PET (positron emission tomography) centers have been established round the world. Such centers utilize small cyclotrons only for the synthesis of positron emitters, and substantial machine time of the cyclotron is left unused.From this view point , it is indeed very important to ensure the optimal utilization of unused time for the purposes of producing fast neutrons presently effectively used for various malignant conditions such as cancer of salivary gland , prostatic cancer and sarcoma of bone [1)-2)].

The present study focussed on the developing of a new compact cyclotron for neutron therapy and positron nuclear medicine and evaluate its basic characteristics for neutron therapy.

2. MATERIALS AND METHOD

2.1. Specifications of BC2211

The specifications of BC2211 are shown in Table 1. The geometorical size is almost same as that of BC1710 (p: 17MeV, d: 10MeV) previously developed. The increase in energies of proton and deuteron was achieved by the increase of magnetic field. A diagram of cyclotron and beam transport for neutron therapy is shown in Fig. 1. The details of Be target are also shown in Fig. 2.

Table 1(A). Main specification of BC2211.

ITEM	proton	deuteron
beam ehergy (MeV)	22	11
beam current (μA)	60	60
magnetic field (T)	1.6	
radio frequency (MHz)	49.0	
extraction radius (mm)	420	
magnet size	Φ2150x1500 mm	

Table 1(B) Radionuclide and yield (BC2211)

Nuclides	Chemical Form	Irradiation Time (T 1/2)(min)	Recoverd Activity E.O.B. (GBq)
^{11}C	$^{11}CO_2$	20	77.7
	^{11}CO	20	68.5
^{13}N	$^{13}NO_x$ in water	10	24.1
^{15}O	^{15}O	2	42.6
	$C^{15}O_2$	2	40.7
	C^{15}O	2	21.5
^{18}F	$^{18}F_2$	110	27.8 (from Ne)
	^{18}F$^-$	110	40.7 (from $H_2{}^{18}O$)

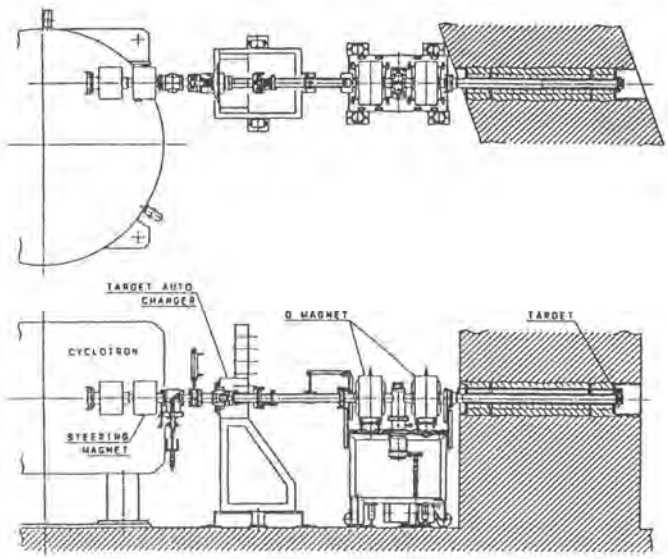


Fig. 1. A diagram of cyclotron and beam transport for neutron therapy.

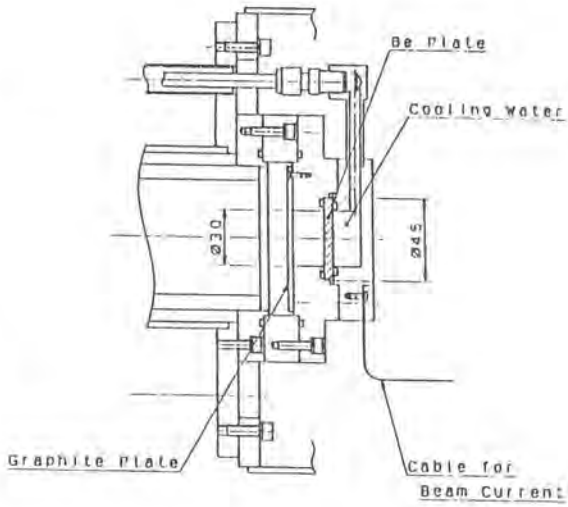


Fig.2. The details of Be target.

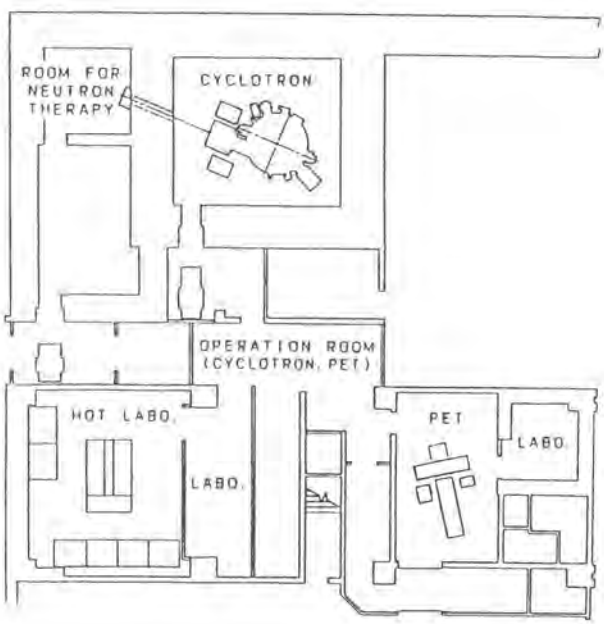


Fig.3. A diagram of our PET center.

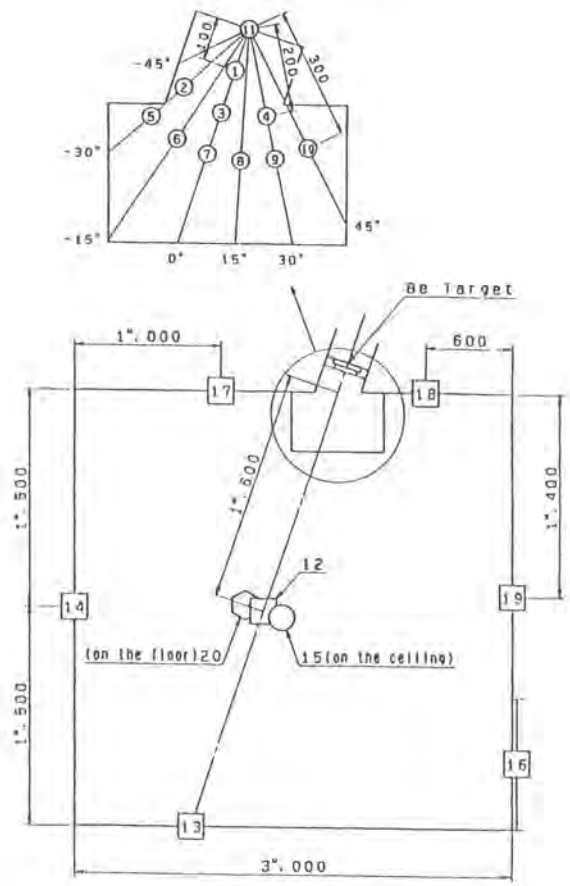


Fig.4. Setting of samples for the measurement of neutron flux.

2.2. PET center of Nagoya university

Our PET center is shown diagrammatically in Fig.3 . The room for neutron therapy is located next to the cyclotron room, whereas Be target exists in the wall.

2.3.Meaurement of neutron flux and energy spectrum

2.3.1.Measurement of neutron flux

Neutrons were produced by bombarding Be target with the proton beam (Ep: 22MeV, external current: 20μA) for a period of 1 hour. The direction and central axis distribution of neutron were measured using radioactivation method. The involved reactions were $^{27}Al(n,a)^{24}Na$, $^{58}Ni(n,2n)^{57}N$, and $^{197}Au(n,g)^{198}Au$. One sample consisted of packed slices of Al x 2, Ni x 2 and Au x 1. Many samples were set in the room for neutron therapy as shown in Fig. 4. After the irradiation, activities of samples were measured with Ge detector and subsequently the activity was converted into the neutron flux.

2.3.2.Measurement of neutron energy spectrum

As already described neutrons were produced by bombarding Be target with the proton beam (Ep: 22MeV, external current: 0.1μA) for 5373 and 3671 sec. A simple collimator was used to direct the neutron beam and reduce the scatter. A collimator is shown in Fig.5.

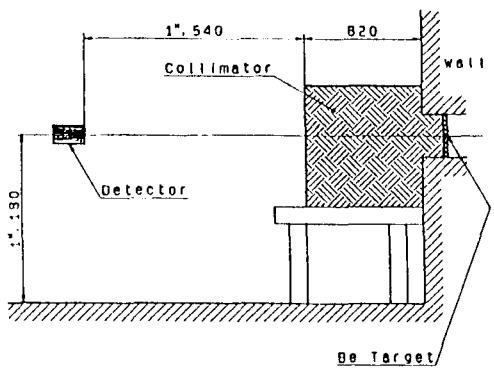


Fig. 5. The diagram of apparatus for the measurement of neutron energy spectrum.

The neutron energy spectrum was measured by proton recoilling method using a organic liquid scintillator (NE213). The measurement was done for two times. Second measurement was done with shadow-bar to evaluate the scattered neutrons. Shadow-bar was made of paraffin and a mixture of Li_2CO_3.

3. RESULTS

3.1. Measurement of neutron flux

Direction distribution of neutrons is shown in Fig. 6. Fast neutrons were measured by $^{27}Al(n,a)^{24}Na$ (En >5 Mev) and $^{58}Ni(n,2n)^{57}Ni$(En >13MeV) reactions. Fast neutrons showed a significant direction dependence. In particular high energy fast neutrons (En >13MeV) showed a sharp distribution. Thermal neutrons were measured by $^{197}Au(n,g)^{198}Au$ reaction and their distribution did not reveal any direction dependence . The neutron flux was observed to be $7.5x10^9/cm^2sec$ (fast neutrons En >5 MeV), $3.5x10^9/cm^2$ (fast neutrons En >13 MeV)and $4.0x10^8/cm^2sec$ (thermal neutrons) on target. Fast neutrons decreased according to inverse square law on the central axis (Fig. 7).

3.2. Measurement of neutron energy spectrum

The energy spectrum of neutrons is shown in Fig. 8. The energy spectrum thus obtained by us resembled with one obtained by Lone et al[3] further confirming the methodological precision and accuracy of measurement. The maximum and mean energy of neutrons were found to be 21 and 11 Mev respectively.

4. DISCUSSION

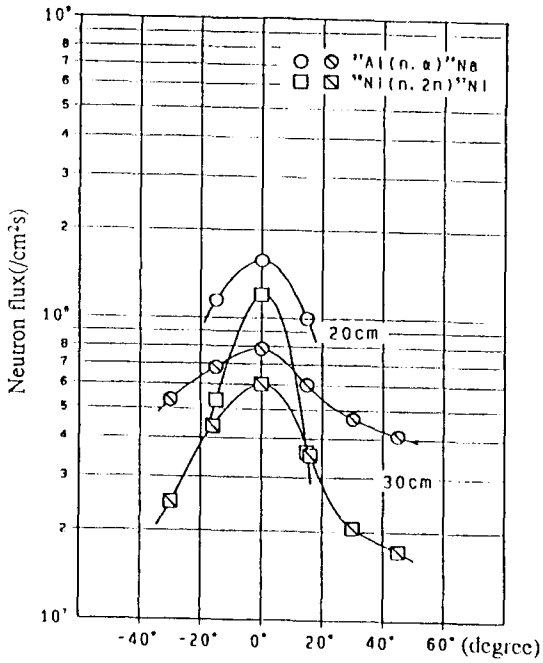
The cyclotron currently used at our center is considered to be rather underutilized even though it is used for routine production of positron emitters for PET studies. In view of this the basic experiments related to neutron flux and energy measurements were performed to explore the feasibility of using neutron beams for therapy of malignant disorders.However, neutron flux and energy spectrum were not enough for the practice of neutron therapy. The calculated absorbed dose using the results of this study is about 0.14 Gy/min at 125 cm from the target (external current : 60 μA). This absorbed dose is not sufficient and hence the target is now under reconstruction to obtain the more refined neutron flux and spectrum. After the target reconstruction a practical collimetor will be planned. Furthermore the low energy neutron shows a high RBE. Therefore the effect on normal tissue should be evaluated before clinical use.

5. REFERENCES

1) Battermann, J.J. & Breur, K.: Results of fast neutron teletherapy for locally advanced head and neck tumors. Int J. Radiat. Oncol. Biol.Phys. 7:1045 (1981)

2)Tatezaki, S.: Systemic multimodal treatment of osteosarcoma, with special reference to the role of fast neutron radiotherapy. J. Jpn.Orthop. Ass.53:831 (1979)

3)M.A. Lone et al., : Thick Target Neutron Yields and Spectral Distributions from the $^7Li(d,n)^7Li(p,n)$, $^9Be(d,n)$ and $^9Be(p,n)$ reactions. Nucl. Inssstr. Meth. 143:33(1977)



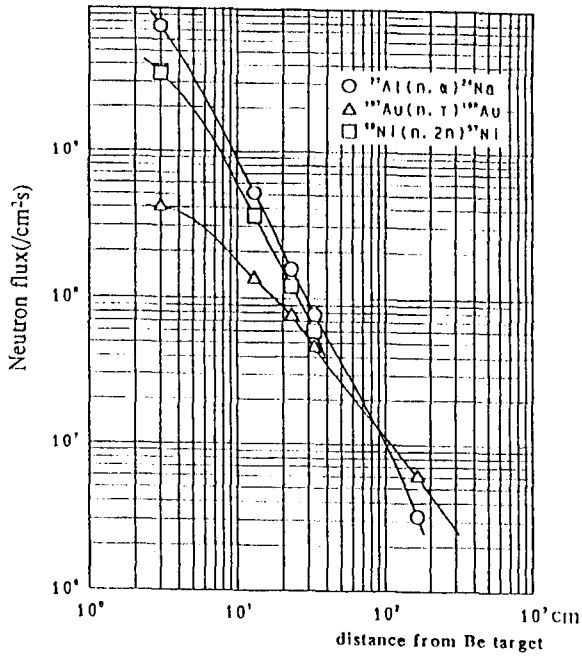


Fig. 7 Axial distribution of neutrons.

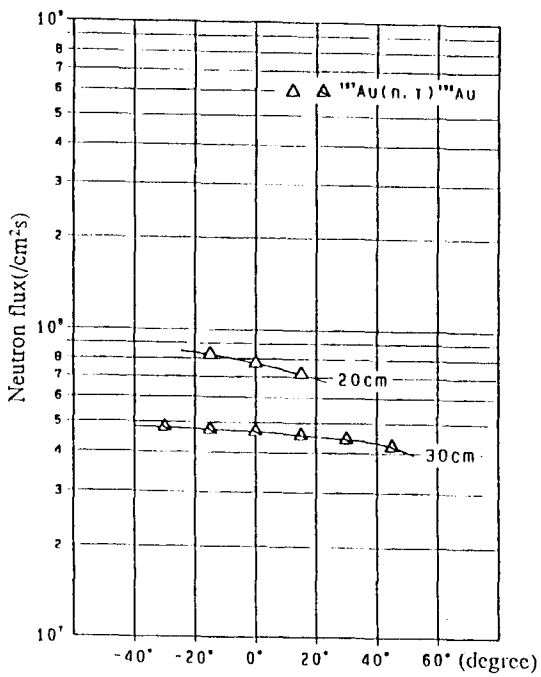


Fig.6 Direction distribution of neutrons.

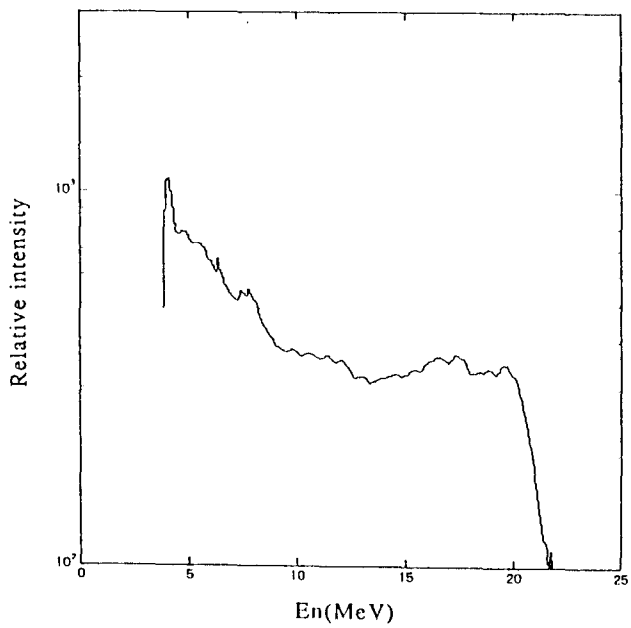


Fig.8 The energy spectrum of neutrons.

PERFORMANCE OF THE HARPER HOSPITAL CYCLOTRON; EFFECT OF PULSED RADIO FREQUENCY*

H. Blosser, J. Vincent
NSCL, Michigan State University
East Lansing, MI 48824-1321, USA

and

Richard Maughan
Gershenson Radiation Oncology Center, Harper Hospital
3990 John R., Detroit, MI, 48201-2097, USA

ABSTRACT

In the years 1984-1990, the National Superconducting Cyclotron Laboratory constructed and tested a K100 superconducting cyclotron to provide neutrons for cancer therapy; this cyclotron was installed in the Gershenson Radiation Oncology Center of Detroit's Harper Hospital in July 1990 and is now in routine use providing intense neutron beams for radiation therapy. In the process of starting up the cyclotron, a 1 in 5 pulsed operation mode was introduced to limit the beam current to levels required by target power limits – this pulsed mode easily provides beam currents at the 10 microamp design level (corresponding to approximately 1 rad/sec at the system isocenter and 2 minute treatment times). Moreover, radio frequency power used by the system is reduced to about one fourth of its unpulsed level, and cyclotron operation is exceedingly stable; this pulsed mode has therefore been adopted as the standard operating mode for the cyclotron. In the pulsed mode, beam power during the pulse is comparable to the resistive power loss in the rf cavity, and interesting new accelerator physics phenomena show up in the instantaneous time dependance of the beam during the 2 millisecond "beam-on" pulses.

1. INTRODUCTION

The K100 superconducting cyclotron for neutron therapy has been described in a number of earlier papers[1] including a report at the last Cyclotron Conference.[2] At the time of the report at the previous Conference, the cyclotron had just started up, and reliable measurements of beam current were not available. Operation was also severely handicapped by the absence of shielding which caused radiation protection trips to occur almost immediately. In following months shielding was installed around the cyclotron and beam current monitors were calibrated.

In the first months of operation with this improved configuration, beam currents were low compared to the specification and changes in the ion source and in the central region were introduced to correct this difficulty. The most important changes were: 1) reducing the clearance between ion source and dee to 3 mm, 2) reprogramming the central region slit system to correspond to a dee voltage of 33 kv rather than the 40 originally contemplated, and 3) changing the design of the cathode assembly in the ion source. With these changes, beam currents shifted from being too low to being too large – currents of 50 microamps were common and Beryllium targets melted on two occasions (overcurrent interlocks were enforced by a computer control system which had a two second cycle time – too slow to fully protect the target – much faster hard wired interlocks have since been installed). Efforts to achieve a smoothly adjustable operating current by turning down the rf voltage or by turning down the ion source arc current were overly sensitive and/or unstable and a circuit for lowering beam current by operating in a pulsed rf mode was next introduced. This last change was strikingly successful in both its current control aspect and in several unexpected other aspects – operation overall became extremely stable, rf power levels dropped to approximately one quarter of the unpulsed level, and tuning and other parameters were much less sensitive to thermal shifts. Given this ensemble of very helpful improvements, the pulsing circuit was adopted as a permanent part of the cyclotron system and operation since that time has been extremely smooth and reliable.

2. ACCELERATOR DESCRIPTION

The neutron therapy cyclotron, as described at the previous conference,[2] has the unusual feature of rotating on a full 360 degree vertical arc relative to a patient positioned at the center of this arc. If the patient is positioned to put the tumor at the center of this arc, the "isocenter" of the system, the neutron beam from every cyclotron orientation intersects the tumor whereas surrounding normal tissue is significantly exposed only when it is on the side of the patient facing the cyclotron and is therefore protected (when all treatment directions are summed) relative to the lethal doses administered at the tumor site.

The rotation system for the cyclotron consists of

two large (4.27 m dia) steel rings which support the cyclotron and an opposing counterweight; these rings are supported by, and turn, on four large roller assemblies as indicated schematically in Fig. 1 and photographically in Fig. 2, (with H. Blosser and W. Powers standing on the cyclotron). On July 9, 1990 the cyclotron and support ring system were taken by motor-truck to Detroit and installed in an already prepared room in the Gershenson Radiation Oncology Center of Harper Hospital. Figure 3 is a photo showing the cyclotron as it was being lowered into the therapy room and Fig. 4 is a photo showing the cyclotron as it now appears to a patient entering the treatment room.



Figure 1. Schematic view of the Harper Hospital neutron therapy system showing the cyclotron mounted between two large rings which move it on a veritcal arc about the patient.

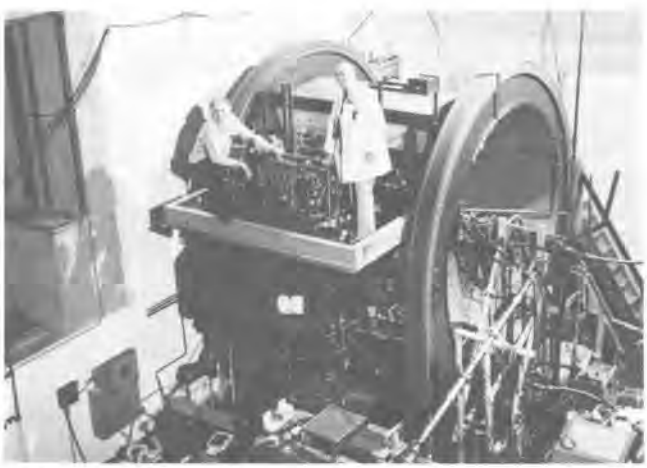


Figure 2. View of the Harper cyclotron and support ring system at NSCL with H. Blosser (left) and W. Powers.

In routine operation, the cyclotron is filled with liquid helium early each morning and the magnet is ramped to its operating current. Filaments in the final stage tube of the rf amplifier are also turned on at this point and, like the magnet, are left on for the day. Ion source arc

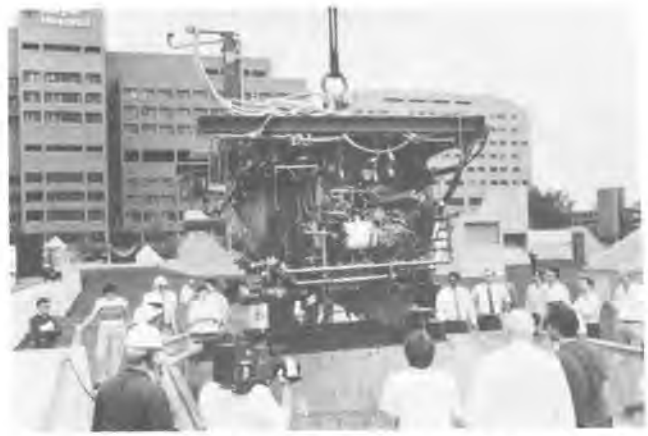


Figure 3. View of the K100 cyclotron being lowered through the roof of the Harper Hospital Oncology Center.

current and rf drive are turned on and off at the beginning and end of each treatment, the pair of systems being used to provide turn-off redundancy.

At present (June 1992) an accelerator technician or a physicist is usually present during a treatment run and also customarily starts up the machine at the beginning of each day. A typical treatment run consists of aligning the patient relative to markers established in the treatment planning sequence, checking and closing radiation areas, pre-setting the dose monitor system to turn off the cyclotron when the stipulated dose has been delivered (or when the time interval allowed for the treatment has expired), and setting a keyed interlock which enables the cyclotron to turn on. The cyclotron beam is then brought on by pressing "ion source on" and "rf on" buttons in sequence (normally no other control action is required to activate the beam). When the stipulated dose has been delivered (or when the preset time has elapsed) the source and rf are turned off by a "treatment complete" interlock and cannot again be turned on until the dose control system is reset and the key control again activated to authorize further operation.

Since normal cyclotron beam turn-on has been found to consist of simply pressing the "on" buttons for source and rf, modifications to the control system are in process to have the key switch on the therapy console automatically initiate the "on" condition in the ion source and rf circuits; the therapy technician will then be in complete control of the treatment in the same fashion as is customary on X-ray units and the cyclotron technician or physicists will only be summoned in the event of difficulty. A major virtue of this operating mode (associated with the operating stability provided by the pulsed rf) is that a cyclotron operator is clearly not needed which is an important saving in operating costs.



Figure 4. The Harper Cyclotron as it appears to a patient arriving for therapy. The large object above the patient table is the neutron collimator consisting of 12,000 adjustable 3 mm dia. Tungsten rods.

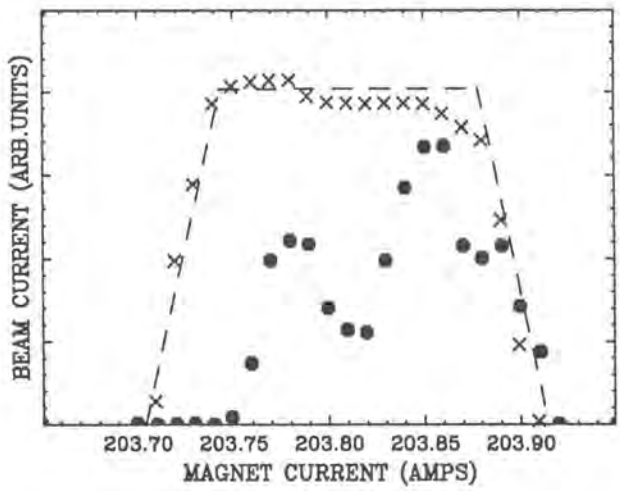


Figure 5. Plot of target current vs. magnet current with target at 286 millimeter for the x data and 298 millimeters for the circle data. The dashed line is the expected 286 millimeter curve.

3. BEAM CHARACTERISTICS WITH PULSED RF

The first hint of unusual beam phenomena associated with the rf pulsing mode came from magnet tuning curves, i.e. graphs of beam current vs. magnet current. Figure 5 shows two such curves, one with the main target at a radius of 286 mm, the other with the target at 298 mm. (The nominal full energy target radius is 305 mm.) The 286 mm curve has the dominantly trapezoidal shape which one expects from such tuning curves, the flat top of the curve indicating the "phase window" available for deviations from isochronism with the given rf voltage and the linear edge indicating the "phase width" of the beam relative to the rf. (The curve provides the data to compute the phase of the beam relative to the rf at any magnetic field setting using the formalism of Garren and Smith.[3]) In contrast with the 286 mm curve, the 298 mm results show strong "pathological features", i.e. peaks, valleys, plateaus, etc. – structure which should not be possible if a single ion species is being accelerated in a normal cyclotron.

A number of possible explanations of the strange 298 mm pattern have been considered. One hypothesis for explaining the strange struture is that the beam consists of several Q/A components, a situation which is easily possible at Q/A = 1/2; radiation monitors, however, showed no change in neutron production per microcoulomb at various points on the 298 curve, indicating that the entire structure was dominantly due to deuterons, any other ion being at least x5 less effective than the deuteron in neutrons per microcoulomb. The relatively sudden appearance of the structure in a radius interval of only 12 mm is also quanitatively inconsistent with Q/A groups seperating due to differences in phase slip. A number of other beam dynamics explanations have also been explored but no phenomena in reasonable correspondence with the Fig. 5 data has come up.

Searching for other measureable aspects of the pulsed beam brought up the idea of looking at the time dependance of the beam on the target, which turned out to be quite surprising. Figure 6, for example, shows a pair of scope traces on a 2 milli-sec/cm scale, the upper trace giving the rf on a dee stem pickup loop and the lower giving the beam current on the target. The rf trace shows the programmed 2 milli-sec "on", 8 milli-sec "off" pattern of the pulsing, whereas the lower trace shows for each rf pulse the surprising pattern of a large target current component at the beginning of the rf pulse, followed by an interval of zero current, followed by a second, smaller target current pulse. The instantaneous current in the target pusles is quite large; the time average beam on this run was 12μa, indicating that the large peak is at about 170μa. Beam power in this time interval is then about 8 kw, a level of the same order as the nominal 25 kw rf drive provided by the main power amplifier.

The rf trace in Fig. 6 shows a considerable "droop" with time and the possibility that the beam was passing first inside and then outside of some central region obstruction came to mind as a possible cause of the observed double peak structure. This hypothesis however had difficulty with another observed aspect of the phenomena, namely that very small changes in either the dee fine tuner or in the magnetic field would cause the time structure to shift relative to the rf pulse as indicated in Figs. 7 and 8. (The horizontal scale has been expanded in these Figs. relative to the scale for Fig. 6 to better show the pulse.) Changes in the magnet current of a few parts in 10,000 were sufficient to shift the pulses from

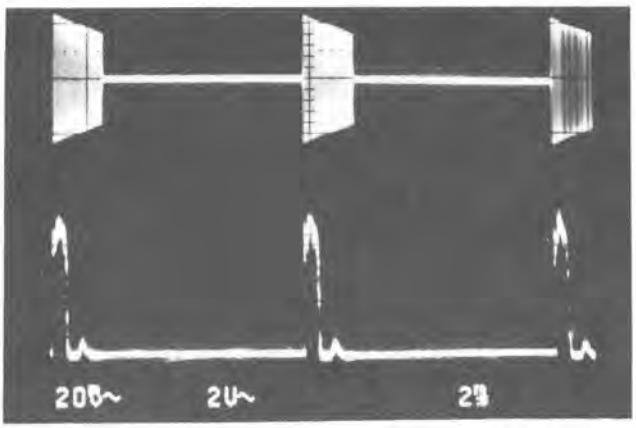


Figure 6. Dual beam scope trace from an rf pickup loop (top) and from the full energy target (bottom) showing three 2 millisecond 100 Herz pulses on a 2 ms/cm time scale. Time average beam 12μa.

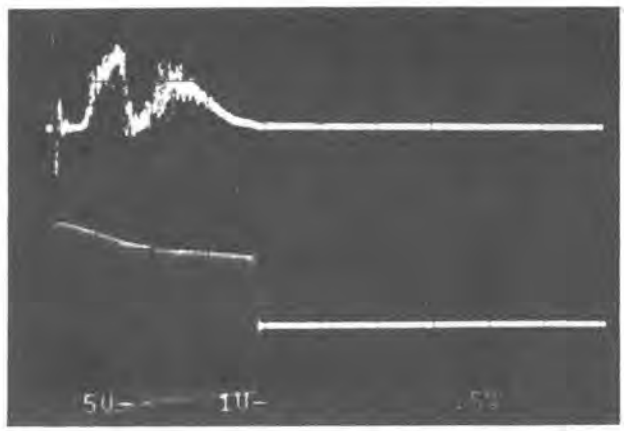


Figure 8. Scope trace similar to Fig. 7 except a further adjustment of the dee fine tuner has moved the first target current peak away from the origin and changed the time average beam current to 8.4μa.

the Fig. 6 pattern to that of Figs. 7 or 8 and it seems quite unlikely that the transverse phase space could be so sharp that such a time shift could happen due to the microscopic movement of the early turns caused by a 1 in 10,000 magnetic field shift. Two other aspects of the observations are difficult to reconcile with this hypothesis namely: 1) raising and lowering the rf voltage changed the amplitude of the pulses, but did not cause their time position to shift and 2) the sharp on/off/on structure shown in Figs. 7 and 8 never appears on a plunging target at 200 mm radius, whereas it would be expected to show on this target in the same way if the phenomena is due to some aspect of the cyclotron's central region.

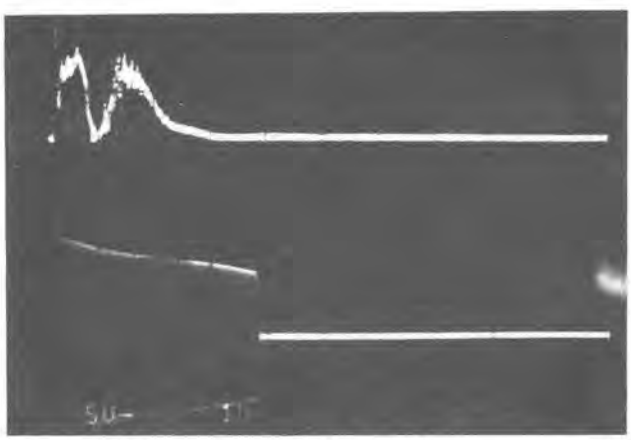


Figure 7. Target current and dee volts on an expanded time scale (0.5 ms/cm) with the dee fine tuner shifted slightly relative to Fig. 6 and with the target trace on the upper scale. This setting reduced the beam current to 9.2μa and changed the two target current peaks to approximately equal magnitude.

Another conjecture as to the origin of the pulsing phenomena is that the beam is exciting an unusual rf mode which could actually be at a much higher frequency. (The beam pulse is quite narrow in time, as indicated by the edges of the 286 mm trapezoid in Fig. 6, and its Fourier components thus include strong harmonics well into the Ghz range.) A survey of possible higher modes was made in the computer using a transmission line representation of the cyclotron resonator. Several modes showed up in the computer search near harmonics of the main frequency and with waveforms such as push-pull-pull, etc. which would be expected to mainly disturb the beam at large radii. Noting these results, actual modes in the cyclotron were checked experimentally by coupling a frequency synthesizer into the main rf drive line of the cyclotron (replacing the main power amplifier) and using a spectrum analyzer to observe the response in a dee stem pick up loop. Table I gives a partial presentation of the wealth of peaks found in this search, with "height" (of the line on the spectrum analyzer) as an indication of the coupling effectiveness and/or the "Q" of the particular mode. The right hand column of Table I shows an expanded search in the vicinity of the second, fourth, fifth, and ninth harmonics of the main rf drive frequency (210, 420, 525 and 945 Mhz). A relatively weak mode shows at 420 Mhz i.e. at the exact fourth harmonic frequency to within measurement error, and stronger modes occur nearby at 439 and 442 Mhz. Similarly near the fifth harmonic, several modes which the beam could excite are found near the harmonic frequency, and likewise for the ninth harmonic.

These higher order modes if excited could deaccelerate the beam by simply absorbing energy from the beam or could throw the beam off center in the case of push-pull-pull configurations or could disturb the axial motion in the circumstance of modes which are anti-symmetric relative to the median plane. Many of the higher or-

Table 1. Harper cyclotron rf modes (exicted through coupler). "Height" on 10db/cm scale. "Fine Scan" near 2, 4, 5, and 9th harmonics of 105 Mhz.

	Course Scan		Fine Scan	
mode	freq. Mhz	height (cm)	freq. Mhz	height (cm)
1	105	5.6	207.8	1.0
2	146	3.6	227.1	1.1
3	158	3.6		
4	177	2.6	420	1.1
5	207	2.4	439.44	4.4
6	219	3.0	442.11	4.6
7	229	2.1		
8	240	3.9	508.75	3.1
9	271	3.0	513.0	2.0
10	355	3.6	525	2.0
11	365	4.2	529	3.6
12	386	4.6	542	4.2
13	439	4.2		
14	453	3.5	941	2.0
15	465	4.0	942	2.8
16	482	5.7	943.06	2.0
	peaks above 3.5 only		944	1.6
17	511	4.0	944.5	1.6
18	536	4.8	945.0	2.0
19	619	3.6	945.37	2.4
20	923	3.7	946.8	1.1
21	938	3.3		
22	943	4.0		

der modes have a voltage null near or at the center of the cyclotron and peak at the outer edges of the dee (like a half-wave open ended line); such modes would be preferentially excited by the large radius beam and be consistent with the pulsing phenomena not appearing on the 200 mm target. The sensitivity of the pulse pattern to small changes in the magnetic field and to fine tuning of the rf cavity are also plausibly consistent with this explanation, the shift with magnetic field shifting the beam rotation frequency slightly and possibly moving the frequency across the response curve of a very high Q mode, and the shift with fine tuning possibly preferentially shifting the mode frequency of a higher order mode so that the mode sweeps through the beam rotation frequency.

An experiment to directly observe a possible higher order mode was attempted with a null result, namely to introduce a special triggering circuit for the spectrum analyzer which would trigger the analyzer at any desired point in the beam pulse structure. If a higher order mode appeared in correlation with triggering at null points of the beam current, the higher mode hypothesis would have been strongly supported. The experiment, however, showed no such modes detectable above the background. This could mean that the dee stem pick up loop to which the analyzer was coupled was at a null current point of the desired mode, and a second search with a capacitive pick up probe near a dee would give a very different view of possible modes, but this is rather difficult to implement from the hardware aspect, the necessary changes leading to excessive interference with the ongoing medical program. It then seems likely to the authors that the interesting time structure of the Harper cyclotron beam is due to excitation of higher modes in the cavity by the beam, but experiments to fully confirm this hypothesis are not likely at the present time.

4. SUMMARY

The superconducting K100 medical cyclotron is in routine use for treatment of cancer patients and performs with superb stability and reliability. Control systems are being modified so that the cyclotron can be turned on and off with a key switch on the therapy console with no operator present at the cyclotron console. An interesting time dependence of the beam structure is perhaps due to excitation of higher order modes by the very intense beam which is circulating in the cyclotron during the pulses. This hypothesis has not been rigorously confirmed.

5. REFERENCES

1) H. Blosser, J. Bailey, R. Burleigh, D. Johnson, E. Kashy, T. Kuo, F. Marti, J. Vincent, A. Zeller, E. Blosser, G. Blosser, R. Maughan, W. Powers & J. Wagner, IEEE Trans. on Magnetics **25**(1989)1746 and R. Maughan, G. Blosser, E. Blosser, H. Blosser & W. Powers, Radiotherapy and Oncology **15**(1989)125.
2) H. Blosser, Twelth International Conference on Cyclotrons and their Applications, World Scientific, Editors B. Martin and K. Ziegler(1989)p. 137.
3) A. Garren & L. Smith, International Conference on Sector-Focused Cyclotrons & Meson Factories, Cern Report **63–19**(1963)18.

*Work supported by Harper Hospital. Use of NSCL facilities through National Science Foundation and Michigan State University approval.

THE TRIUMF 520 MeV CYCLOTRON: RECENT AND FUTURE DEVELOPMENTS

Gerardo Dutto
TRIUMF, 4004 Wesbrook Mall, Vancouver,
British Columbia, V6T 2A3

ABSTRACT

The TRIUMF cyclotron is now routinely producing 150 μA protons at 500 MeV for meson production with a maximum available current of 200 μA and beam availability of 90%. A successful resonator upgrade program, the recent commissioning of a new 92 MHz rf booster cavity and a new compact CUSP ion source will allow the current to be increased to 225 μA routinely and 300 μA maximum, once an upgrade of the high radiation target areas is completed. Furthermore, the 300 μA maximum H^- internal current will allow, in parallel with 100~200 μA for meson production, the simultaneous extraction of 50-100 μA for a radioactive beam facility and of 50-100 μA for isotope production at 70-100 MeV. A proton therapy facility is also proposed. A new optically pumped H^- polarized source will allow a highly stable and reproducible 5 μA beam at ~75% polarization to be extracted. The feasibility of the extraction of an H^- beam with electrostatic and magnetic channels has also been demonstrated. Problems and plans for the extraction of 150 μA H^- for KAON will be discussed.

1. INTRODUCTION

The TRIUMF cyclotron has now been operating since 1975. The design goal of 100 μA proton beam extracted at energies between 200 and 500 MeV was achieved at the end of 1977. It is only since 1984 however, that the present level of high intensity beam production, based on routine extracted currents between 140 μA and 200 μA, for a total yearly integrated charge of about 300 mAh, has been attained. Beam availability has been maintained, over these last years, above 85%, with >90% achieved during 1991. A typical yearly schedule includes two shutdowns of six to eight weeks each, for maintenance and development; two periods of six to seven weeks of polarized beam before the shutdowns; and two periods of 12 to 13 weeks of high intensity beam after shutdowns. Typical simultaneously extracted beams during high intensity operation are: 140 μA at 500 MeV down BL1A, 40 to 50 μA at energies between 70 and 110 MeV down BL2C and up to 10 μA down beam line 4A or 1 to 100 nA down BL4B with variable energy between 180 and 520 MeV (Fig. 1).

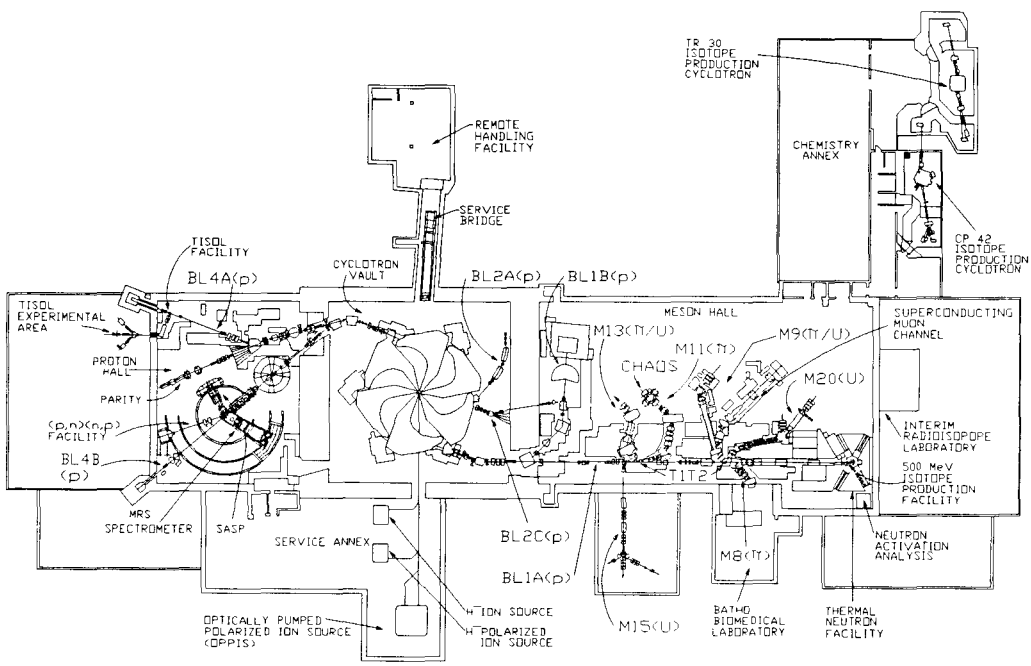


Fig 1. Layout of TRIUMF facility.

2. THE RESONATOR IMPROVEMENT PROGRAM FOR RELIABILITY AND BEAM STABILITY

Although all systems have been improved and made more reliable over the last ten years, the system which originally caused greatest concern and therefore received greater attention was the rf cavity. Conceptually, the system is simple. It can be seen as made of two 1/4 wavelength coaxial stubs face to face and flattened to fit in the 16m diameter, 0.4m high, stainless steel vacuum chamber to form the two 180 ° dees of the accelerating structure.[1)]

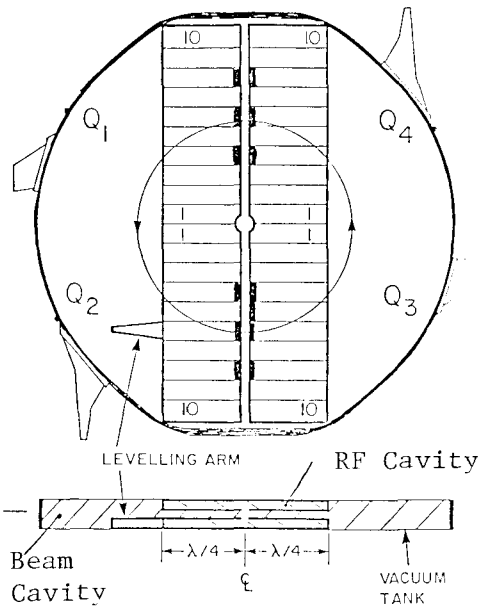


Fig. 2. Schematic view of main resonator cavity.

Mechanically, the system is made of eighty segments (Fig. 2), 10 upper and 10 lower segments in each quadrant. Mechanical tolerances for the 3m long cantilevered panels are very stringent: maximum deviation from the reference plane ±0.5mm and tip vibrations below ± 25 μm for a rf voltage stability in the order of ~10^{-4}. The original resonator panels were composed essentially of water-cooled copper panels facing the rf cavity with non-cooled aluminum strong-backs facing the beam. Soon after initial operation, it was found that small vertical electrical asymmetries in the cavity will excite substantial TM_{310} and TM_{410} parasitic modes in the beam volume.[2)] Voltage differences, between upper and lower strong-backs, exceeding a few hundred volts resulted in multipactoring currents, transferring rf power to the non-cooled aluminum structures. Thermal deflections and serious panel distortions occurred, with structural rf damage. The problem has now been cured. Voltage probe and thermocouple diagnostics have been installed to allow monitoring, reduction and control of parasitic voltages and temperatures.

To reduce parasitic amplitudes, hot arm to ground arm distances are adjusted at the tip of strategic segments with the intent of providing better electrical alignment and inducing additional perturbations of opposite sign to partially suppress in amplitude and phase the pre-existing perturbations. Reduction of stray voltages below multipactoring levels can normally be achieved over most of the volume. New type, more rigid, resonator segments with cooled copper surfaces on both sides of the aluminum strong-back have been constructed and installed in strategic positions (segments 4, 6, and 8) to bring tip alignment closer to the required tolerance and within tuning range. A factor of 2.5 improvement of the voltage stability was recently achieved with voltage stability better than 4 x 10^{-4}.

3. INTENSITY UPGRADE

Plans toward upgrading the intensity of the TRIUMF cyclotron to 500 μA extracted at 500 MeV, have been previously reported.[3)] In brief, they are based on the optimization and installation of a high brightness, more stable H^- Cusp source in the 300 kV terminal and on the addition, inside the existing vacuum chamber, of one or two fourth harmonic frequency Auxiliary Accelerating Cavities (AAC) to double or triple the energy gain per turn in the region between 400 and 500 MeV.[4)] Electromagnetic stripping of the accelerated H^- ions is significant (8%) in this region and can be reduced by reducing the number of turns i.e. flight time of the ions through this region. Losses produced by residual gas in the 2~3 x 10^{-8} Torr environment of the cryogenically pumped chamber are of minor significance compared with electromagnetic stripping losses.

The Cusp source which will be installed in the operational 300 kV terminal is a 10 cm diameter, 15 cm long copper cylinder volume source with its plasma contained by a system of $SmCo_5$ permanent magnets distributed around the volume.[5)] Total extraction voltage across a well optimized system of electrodes is 25 keV. The normalized emittance of the beam is 0.12 π mm mrad for 1 mA current from the source. This current is adequate for 500 μA extracted since a combination of fundamental plus second harmonic buncher in the injection line provides a cyclotron acceptance of ≥ 50% at these current levels.

Beam bunching will introduce energy spread and emittance distortions causing beam halos which, if not skimmed in the centre region through slits, will cause vertical losses at higher energies. Ideally one would like to operate without bunching, and with higher injection intensity, up to ~7 mA, so that ~500 μA can be

transmitted say in a ~25 ° cyclotron phase acceptance. However, the normalized injected beam emittance for a 7 mA beam is higher, ~0.35 π mm mrad in both directions, and the advantage of avoiding bunchers is therefore questionable, specifically in light of the non-trivial problem of dissipating several kW of beam power through the beam defining central region electrodes.

4. AUXILIARY ACCELERATING CAVITY

Schematically, the cavity is made of two trapezoidal structures, placed symmetrically above and below the mid-plane, vertically separated by a 64 mm horizontal gap (Fig. 3). Hot arms and ground arms define electric accelerating fields at the periphery of the structure. The cavity operates at the fourth harmonic (92.24 MHz) of the main rf frequency and is $\lambda/4$ long radially, $\beta\lambda/2$ wide azimuthally so that orbiting ions can receive acceleration impulses both entering and exiting the cavity. The peak accelerating voltage rises sinusoidally with radius, covering the energy range from 370 to 520 MeV. Operational voltages of 150~160 kV have been achieved with 50~60 kW of power up to routine high intensity beam current. When tested during beam production the cavity behaved well for an extensive period of time and the corresponding new extracted beam characteristics were acceptable to experimenters. Beam intensity from cavity off to cavity on increased by 4%, a substantial fraction of the ~10% beam loss at high energy. The observed phase compression of the extracted beam (slightly less than a factor two) is shown in another paper to this conference; Ref. 6, Fig. 4. The same paper shows, Fig. 10, the longitudinal beam splitting phenomena which can be produced by using the cavity with opposite phase to locally reduce the total energy gain per turn to zero. Possible uses of this cavity are discussed in Ref. 6-7.)

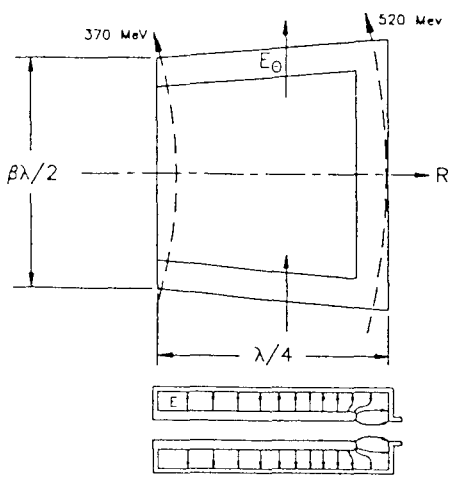


Fig. 3. Schematic view of auxiliary accelerating cavity.

The implementation of new levels of high intensity beam production on a continuous basis requires an upgrade of diagnostics and of the corresponding remote handling systems around the thin (1 cm C) and thick (10 cm Be) meson production targets. This has been delayed pending the decision for KAON, since in the latter case most beam would be extracted down BL2A and the present 200 μA limit in 1A would be adequate. Operation with AAC cavities will still be important, however, because of the reduction in tank activation for the remaining 500 MeV experimental program and the improvement of beam quality H^- extraction from 4th harmonic flattopping.[7)]

5. EXPERIMENTAL FACILITIES

In the meson area, six secondary channels have been organized to collect pions and muons for experiments. On the M8 channel π^- are collected and transported to the medical cancer treatment area, where so far about 300 patients have been treated mostly for brain tumours or for deep-seated pelvic tumours. Results to date have been very encouraging. A clinical randomized trial is underway to establish through statistical analysis the effectiveness of the method. Results will be presented to this conference by Dr. George Goodman.[8)]

Recent secondary lines include M15 for high quality, polarized surface muons, with two high gradient electrostatic separators with compensating magnets providing the capability of transverse spin directions. The second arm of M9 operates with a large solid angle acceptance superconducting muon channel delivering an intensity of negative muons of ~5 x 10^5 at 40 MeV/C.

A large angular spectrometer, called CHAOS, is being constructed for pion physics. This will detect pions within ± 8 ° of the horizontal plane, over an angular range approaching 360 °. Four concentric wire chambers and a ring of scintillators and Cerenkov counters will be used for trajectory measurement and particle identification. The purpose is to study low energy pion-pion and pion-nucleon scattering at M11 and M13.

In the proton area on BL4B, a Medium Resolution Spectrometer (MRS, 1 MeV resolution) of the qqd type is being joined by a Second Arm Spectrometer (SASP), designed to have a much larger angular acceptance. Improved energy resolutions (250 keV) are envisaged.

A facility of interest to this conference is the TISOL facility on BL4A. Here a thick target station is connected to an ECR source producing a wide range of radioisotopic ion beams. A 90° mass analyzing magnet is followed by an electrostatic transport line bringing the low energy (20 keV) radio-isotopes to an experimental area at

ground level. This installation is important since it is the prototype of the front end of the 10 MeV/n ISAC facility, being proposed for radioactive beam studies at TRIUMF.[9]

The polarized beam has recently been upgraded to satisfy the demands for several experiments including π production from polarized neutrons on a proton target, charge symmetry breaking and parity violation. The new optically pumped H^- polarized source has been upgraded with more powerful titanium sapphire lasers for optical pumping of Rubidium instead of Sodium vapour in the polarized cell. Intensities of 2 μA with 78% polarization have been extracted at several energies from the cyclotron. It is believed that 5 μA extracted with 78% polarization is within reach with further source optimization.[10] For the experiments above, both source and cyclotron have to satisfy very stringent requirements: short pulse time structure (<500 ps), 10^{-3} polarization stability during spin reversal, $<10^{-4}$ (or better) intensity or energy variation between spin up and down and other challenging features. The optically pumped source is believed to be superior in this regard compared with atomic or Lamb-shift sources.

The low energy beams of beam line 2C are used for isotope research and production. Recently a metallic rubidium target has been tested which can safely be operated at 50 to 100 μA current without reduction in yield. Rubidium targets producing 2 Ci of ^{82}Sr have been realized. Two papers to this conference describe BL2C and its control.[11-12]

Finally, a proton therapy facility is being planned in the BL1B area. Two beam lines will be used: BL2C for eye melanoma with available proton energies between 60 and 100 MeV, and the existing BL1B (180 to 520 MeV) or a proposed BL2B (140 to 280 MeV) for brain tumours or other deep seated tumours and AVMs treatment. A scheme providing room for a gantry system and involving substantial building modifications is also being considered. A treatment facility plan has now been prepared by the B.C. Cancer Agency and has been submitted for funding.

6. H^- EXTRACTION FOR KAON

The scheme for direct extraction of an H^- beam (Fig. 4) has been reported previously.[13] A 11.5 MHz rf cavity (RFD) oscillating at 1/2 the fundamental rf frequency generates a radial coherent oscillation downstream of $\nu_r \sim 3/2$ at 428 MeV. In one of the minima of the precession pattern (see Fig. 6 in Ref. 6), where the radial beam density has been reduced by a factor of 5, a 1 mm wide stripping foil is used to extract about 10% of the internal circulating H^- beam through an existing port into one of the existing beam lines. This will create a gap in the radial beam density at the location of the septum of the first electrostatic deflector. The other 90% of beam will then be extracted through the first and second electrostatic deflectors and through the five following magnetic channels. The first two channels, of moderate strength around 85 mTm, are iron free. The three channels downstream have iron cores. A separate iron free quadrupole and a gradient on channel five will provide vertical and radial beam focussing. The magnetic channels have to be designed so that the perturbations in the radial field gradient dB_z/dr in the region of the internal beam are kept below a maximum of 0.15 G/cm, on average over one turn.

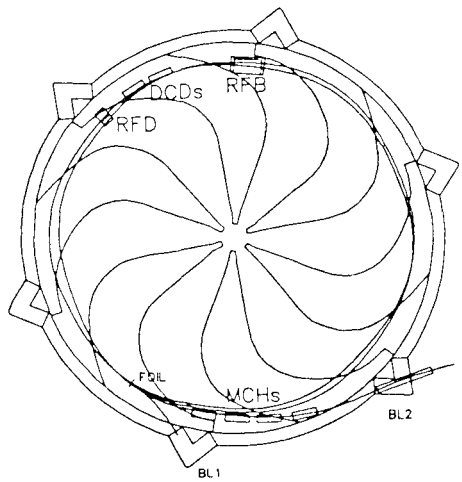


Fig. 4. H^- extraction layout
RFB - auxiliary accelerating cavity; RFD - rf deflector; DCDs - electrostatic deflectors; MCHs - magnetic channels.

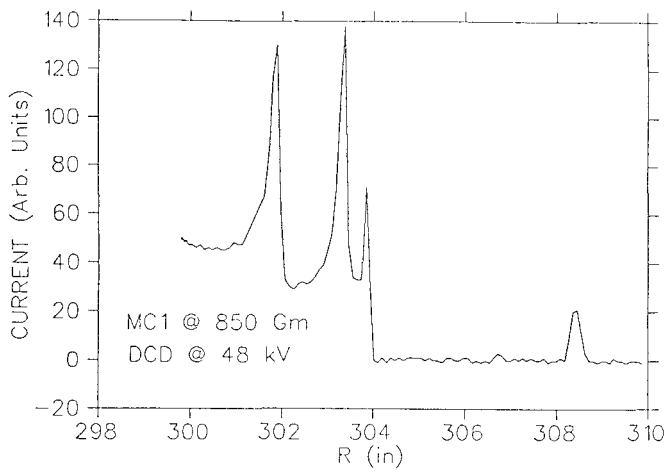


Fig 5. Radial H^- beam profile showing deflected 90% beam 6 m downstream magnetic channel 1.

A prototype of channel 1 was tested on the cyclotron with beam. Figure 5 shows the profile of the H^- beam radially separated by 10 cm from the internal cyclotron beam, 6 m downstream the channel: no beam losses on the magnetic channel were observed. The cross-section of the iron core current compensated channel to be used for channel 3 is given in Fig. 6. The channel has been designed so that it will produce a field reduction of 540 mT over a distance of 0.9 m with a useful aperture of 3.8 cm high by 3.0 cm wide. Model measurements in a rather uniform 4 Tesla test magnet show good agreement between calculated and measured field inside and outside the channel. However, beam measurements with a prototype channel installed in the highly non-uniform field of the cyclotron are planned for verification.

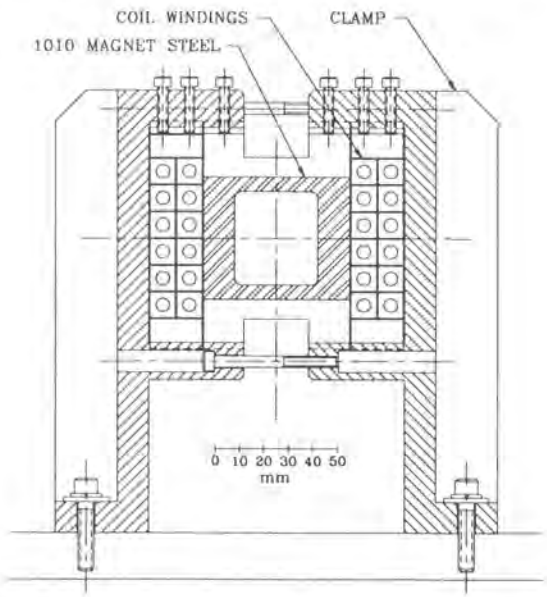


Fig. 6. Schematic section of magnetic channel 3.

The DCD has been shown to hold 80 kV positive voltage at low extraction intensities. However, during recent tests, voltage holding became marginal at extracted currents of approximately 30 μA, 25% duty cycle. The reason for this is attributed to a larger than expected vertical beam size at extraction caused, inter alia, by emittance growth in the region of the rf deflector. In addition, the beam was vertically misaligned, with respect to the median plane of the electrostatic channel, by approximately 1.5 cm, thereby occupying a channel region where electric field gradients start being significant. Finally, the larger vertical emittance and halo distortions caused problems with spills down beam line 1 where the 30 μA beam was being channelled.

Obtaining and maintaining a high quality, stable beam at extraction is therefore essential at high intensity, even if the traditional requirement of separated turns is in our case not necessary because of the septum prestripper protection. Beam studies with simulations and measurements are being carried out to achieve the necessary quality and stability. It has been found that phase dependent vertical emittance stretching occurring at $\nu_z = 0.25$ due to gradients in the RFD field, could result in 50% vertical emittance growth. The Auxiliary Accelerating Cavity (AAC) can be used to locally flattop the accelerating voltage during the precession so that all particles spend the same time between the start of the precession and extraction and phase dependence is cancelled.[7)]

7. REFERENCES

1) Warren, J., "The TRIUMF project", in **Proceedings of the 5th International Cyclotron Conference, Oxford, 1969** (Butterworth, London, 1971) p. 73.
2) Dohan, D., Fong, K., and Pacak, V.,"Control of RF leakage in the TRIUMF cyclotron", in **Proceedings of the 11th International Conference on Cyclotrons and Their Applications** (IPC, Tokyo, 1987) p. 345.
3) Dutto, G. et al, "The upgrading of the TRIUMF facility to 500 μA operation", in **Proceedings of the 1st EPAC,** (World Scientific, Singapore, 1989) p. 326.
4) Laxdal, R.E. et al, "Initial operating experience with the auxiliary accelerating cavity for the TRIUMF cyclotron", in **Proceedings of the 1991 IEEE Particle AcceleratorConference,**(IEEE,NewYork,1991)p.810.
5) Jayamanna, K. et al, "The TRIUMF compact DC H^-/D^- ion source", in **Proceedings of EPAC 90, Nice** (Frontières,Gif-sur-Yvette, 1991) p. 647.
6) Laxdal, R.E., Mackenzie, G.H., Root, L., "Beam test results using the auxiliary accelerating cavity", these proceedings.
7) Laxdal, R.E., Mackenzie, G.H., Root, L., "Beam quality investigations for H^- extraction at TRIUMF", these proceedings.
8) Goodman, G., "Pion therapy for cancer - what are the prospects?", these proceedings.
9) D'Auria, J., "Research and development studies with radioactive beams at TRIUMF", these proceedings.
10) Levy, C.D.P. et al, "Status of the optically pumped H^- ion source at TRIUMF", these proceedings.
11) Pearce, D. and Vincent, J., "A facility for radioisotope production at TRIUMF with 70-110 MeV protons", these proceedings.
12) Wilkinson, N.A. and Ludgate, G., "Experience with the application of object oriented techniques in the TRIUMF beam line 2C control", these proceedings.
13) Zach, M. et al, "Status of the H^- extraction program at TRIUMF", in **Proceedings of the 12th Cyclotron Conference,** (World Scientific, Singapore, 1991) p. 368.

THE KAON FACTORY AT TRIUMF

M.K. Craddock
Physics Department, University of British Columbia, Vancouver, B.C., V6T 1Z1
and
TRIUMF, 4004 Wesbrook Mall, Vancouver, B.C., V6T 2A3

ABSTRACT

The TRIUMF KAON Factory is designed to produce beams of kaons, antiprotons, other hadrons and neutrinos 100 times more intense, or cleaner, than are available now, for a broad range of particle and nuclear physics experiments. This will require a 100 μA beam of 30 GeV protons, to be produced by an interleaved sequence of two fast-cycling synchrotrons and three storage rings, with the existing TRIUMF H^- cyclotron as injector. An $11-million preconstruction study has enabled the overall design to be reviewed and prototypes of various components to be built and evaluated – fast-cycling dipole and quadrupole magnets, a dual-frequency magnet power supply, ceramic beam pipes with internal rf shields, an rf cavity (using perpendicular bias), an extraction kicker, an rf beam chopper, and production targets. Environmental, industrial and economic impact studies have also been completed and the cost estimates and schedule updated. The total cost of $708 million (Canadian) will be shared equally between Canada, British Columbia and international contributors; the first two-thirds of this sum have already been approved and negotiations for the remainder are under way.

1. INTRODUCTION

The TRIUMF Kaon-Antiproton-Otherhadron-Neutrino Factory is described in full in the original proposal[1] and in the revised version[2–4] issued in 1990. The basic aim is to accelerate a 100 μA beam of protons to 30 GeV, roughly 100 times the intensity available now. This would provide correspondingly more intense – or pure – beams of secondary particles (kaons, pions, muons, antinucleons, hyperons and neutrinos) for particle and nuclear physics studies on the "precision frontier", complementary to the "energy frontier". Major areas of investigation would be

- rare decay modes of kaons and hyperons
- CP violation
- meson and baryon spectroscopy
- meson and baryon interactions
- neutrino scattering and oscillations
- quark structure of nuclei
- properties of hypernuclei
- K^+ and $\overline{p}$ scattering from nuclei.

The physics case for K factories is fully described in the proposals[1,4] and in the proceedings of ten specialized workshops sponsored by TRIUMF in Germany, Italy, Japan and Canada during 1988-89. The strong international interest was confirmed by the attendance of 257 prospective users at a general workshop on "Science at the KAON Factory" held in Vancouver in July 1990 to initiate experimental collaborations.[5]

From 1988 to 1990 the project was the subject of an $11-million pre-construction Engineering Design and Impact Study funded jointly by the governments of Canada and British Columbia. This comprehensive study was designed to provide all the information needed for the governments to take a funding decision. The topics covered include:

- review of the scientific justification
- accelerator and experimental facilities designs
- construction of prototype components
- design of buildings and tunnels
- review of cost estimates and schedule
- study of Canadian industrial capability
- environmental, legal and economic impact studies
- international consultations on funding.

This paper will review the results of these studies, and of the ongoing R&D, except for work on extracting H^- ions intact from the TRIUMF cyclotron, which is discussed in detail by Dutto[6] and by Laxdal *et al.*[7]

2. ACCELERATOR DESIGN

The TRIUMF H^- cyclotron, which routinely delivers 150 μA beams at 500 MeV, provides a ready-made and reliable injector. It would be followed by two fast-cycling synchrotrons, interleaved with 3 storage rings, as follows:

A	Accumulator:	accumulates cw 450 MeV beam from the cyclotron over 20 ms periods
B	Booster:	50 Hz synchrotron; accelerates beam to 3 GeV; circumference 216 m
C	Collector:	collects 5 Booster pulses and manipulates longitudinal emittance
D	Driver:	10 Hz synchrotron; accelerates to 30 GeV; circumference 1078 m
E	Extender:	30 GeV stretcher for slow extraction for coincidence experiments

This arrangement allows the B and D rings to run continuous acceleration cycles without flat bottoms or flat tops, as shown in the energy-time plot (Fig. 1). The use of a Booster permits a smaller normalized emittance and hence reduces the aperture and cost of the Driver magnets for a given space-charge tune shift. The use of a Booster also simplifies the rf design by separating the requirements for large frequency swing and high voltage (33% and 750 kV respectively for the Booster, and 3% and 2550 kV for the Driver). These high rf voltages are associated with the high cycling rates; the use of an asymmetric magnet cycle with a rise 3 times longer than the fall in the Driver reduces the voltage required by one-third, and the number of cavities in proportion. In the Booster the saving is less because more voltage is needed for bucket creation.

Figure 2 shows the proposed layout together with the tunnel cross sections. The Accumulator will be mounted above the Booster in the small tunnel and the Collector above the Driver in the main tunnel. The Extender will be installed towards the outer wall of the tunnel, separated by ~4 m horizontally from the Driver. Similar lattices and tunes are used for the rings in each tunnel. This is a natural choice providing structural simplicity, similar magnet apertures and straightforward matching for beam transfer.

Separated-function magnet lattices are used with the dispersion modulated so as to lower its mean value and keep transition above top energy in all rings. This avoids transition-crossing problems such as emittance mismatch and change of rf phase under high beam loading. Racetrack lattices have been adopted for the C, D and E rings, and are being studied for the smaller rings;

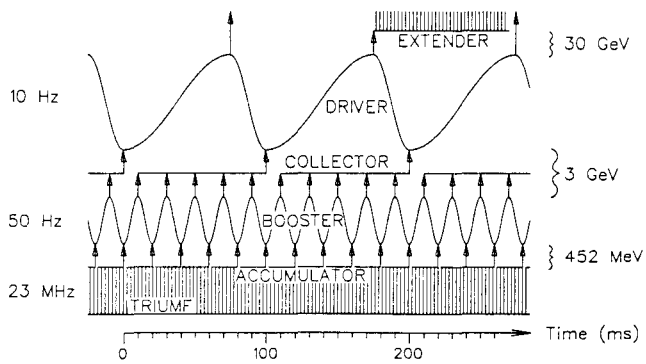


Fig. 1. Energy-time plot showing the progress of the beam through the five rings.

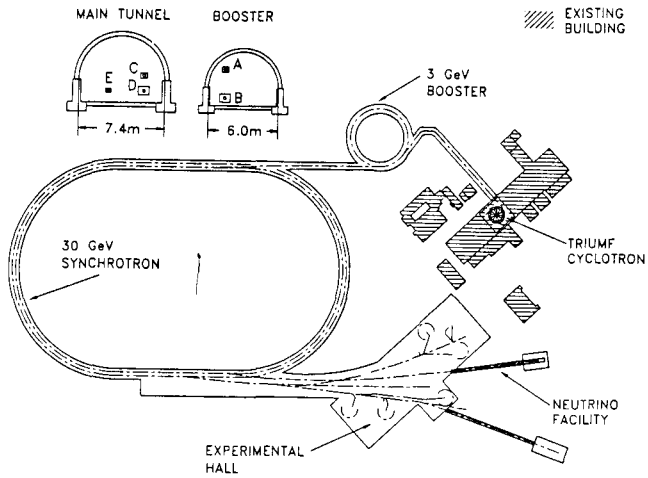


Fig. 2. Proposed layout of the accelerators and cross sections through the tunnels.

but the reference designs for the latter are almost circular, with superperiodicity 6 for the Booster and 3 for the Accumulator.

Injection into the Accumulator is achieved by stripping the H^- beam from the cyclotron, enabling many turns to be injected into the same area of phase space. The small emittance H^- beam is in fact "painted' over the much larger three-dimensional acceptance of the Accumulator to limit the space-charge tune shift. Painting also enables the optimum density profile to be obtained and the number of passages through the stripping foil to be limited.

3. BEAM DYNAMICS

In order to cut beam loss during slow extraction well below the usual 1%, racetrack lattices have been adopted for the C,D and E rings. These provide long straights with high β (100 m) at the septa and room for an additional pre-septum and for collimators downstream. Tracking simulations, which include power supply noise effects, suggest that the beam loss can be kept below 0.2%. The loss on the extraction elements amounts to 0.005%. The 180° arcs contain 24 cells, and are second-order achromats, normally tuned to $5 \times 2\pi$. The tune for the whole ring may be varied by ± 1 in each plane independently. A half-integer resonance may be used for extraction, to simplify the collimation process. Such a racetrack lattice is also convenient for the Driver synchrotron, allowing either for the insertion of Siberian snakes, or for tuning for low depolarization without snakes, using high-periodicity arcs and spin-transparent straight sections. Quadrupole matching sections for the Siberian snake have now been designed with very smooth excitation cycles.

Tracking studies show that the dynamic aperture of the lattice is as large as for the old circular design. Various measures have been taken to speed up the tracking. The first has been to vectorize and streamline the DIMAD code, resulting in six times faster operation. The

second has been to use differential and Lie algebra techniques to produce higher order maps directly. A new tracking code DIMFAST, able to transfer maps with DIMAD, COSY∞ and DALIE, is now in use.[8)]

The Booster reference lattice has 24 FODO cells with 6 OBOBBOBO missing-magnet superperiods. An alternative 3-cell superperiod (OBBBBO), derived from that proposed for the Moscow kaon factory booster[9)] and providing larger dynamic aperture and dispersionless straight sections, is under study.[10)] Such a lattice would require a larger circumference or, less favourably, a lower top energy for the Booster.[11)] Wienands *et al.*[12)] use a similar structure for the Low Energy Booster of the SSC. For both machines the new code package has enabled sextupole resonance correction schemes to be determined. Simulation studies of collimator arrangements for the Booster have shown that 80% collection efficiences can be achieved with copper and 90% with tungsten.

Longitudinal effects of importance include synchro-betatron resonances and coupled-bunch instabilities. Recent studies on these topics include the discovery of a rather tight tolerance (0.1%) on the vertical asymmetry in accelerating gap voltage[13)] and the determination of stationary phase-space distributions in the presence of space charge.[14)] A test stand has been set up for accurate measurement of the longitudinal impedance of components of the rings, using the TSD-calibration method.

To synchronize each of the five pulse trains from the Booster to about 1 ns, for transfer to the Collector, a feedback scheme has been devised, based on heterodyning the Booster's revolution frequency with an ideal frequency.[15)] A scheme has also been devised for shortening the base length of the extracted proton bunches from 3 ns to 0.5 ns, for better timing in experiments.

4. MAGNETS AND POWER SUPPLIES

A prototype Booster dipole magnet has been built and its field measured.[16)] The magnet is 3 m long with a pole gap of 10.7 cm and is designed to cycle at 50 Hz between 0.27 T and 1.12 T with a field uniformity $< \pm 2 \times 10^{-4}$ over ± 5 cm. The prototype is constructed from 26-gauge laminations of M17 (non-grain oriented) steel. The dc field surveys showed the field uniformity to be within specifications; ac surveys have also been made. A prototype quadrupole for the Booster has been built using indirectly cooled coils and its field measured. Initial reference designs have been made for the various other magnets needed, to establish dimensions, material requirements and costs.

The test stand used previously to investigate the dual-frequency excitation of a NINA synchrotron magnet has been reconfigured (Fig. 3) for testing the Booster dipole.[17)] Four NINA magnets are wired in parallel to act as the dc bypass choke and there are new capacitor banks and power supplies. Both dipole and quadrupole have been tested at full power in ac tests with dc bias.

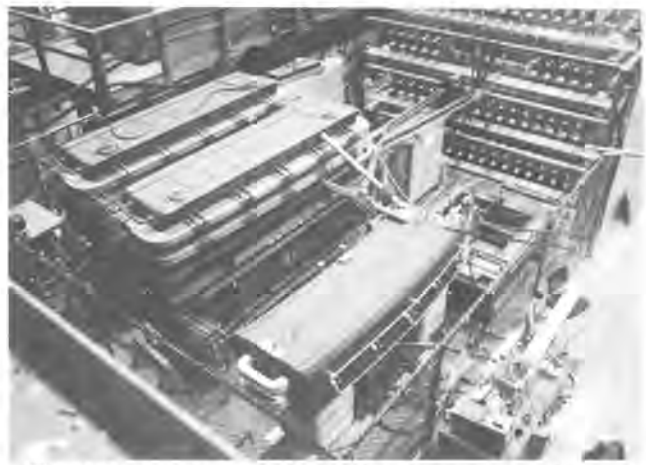


Fig. 3. Magnet test stand, showing the prototype Booster dipole (front), choke magnets (left) and capacitor bank (behind, right).

5. KICKERS AND CHOPPER

A prototype kicker of the transmission-line type has been built for Booster extraction – the most challenging case – based on CERN PS designs. A pulse generator and pulse forming network were obtained on loan from CERN and successfully modified to increase the cycling rate from 1 Hz to 50 Hz. Sufficiently flat 40 kV pulses were obtained, 600 ns long and with 5% –95% rise and fall times better than 30 ns.[18)] Simulations show that pre- and post-pulse kicks can be suppressed using ferrite saturating inductors, bringing the entire 1% – 99% region within 30 ns.[19)]

A prototype has also been built of the 1 MHz chopper[20)] (Fig. 4) required in the transfer line from the cyclotron to create the 110 ns beam gap needed for kicker rise and fall. The stripline deflector plates must provide 38 kV-m with rise and fall <35 ns. Energy storage and power saving are provided by a 150-m (0.5-μs)-long coaxial delay-line cable 10 cm in diameter. Initial tests of this novel concept have been promising, 11 kV pulses being produced with rise and fall times of 22 ns, meeting the specification.

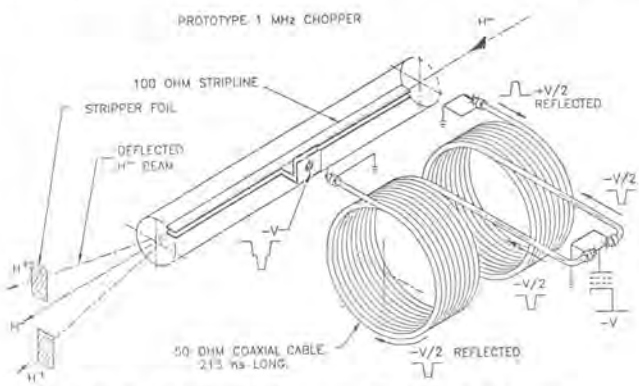


Fig. 4. Schematic diagram of rf beam chopper.

6. RADIO-FREQUENCY SYSTEMS

Recent work has concentrated exclusively on the full-scale prototype booster cavity built at LAMPF using perpendicularly-biased microwave ferrite.[21] Under dc bias at Los Alamos it produced relatively high voltages (over 100 kV), potentially reducing the number of cavities required and also the impedance presented to the beam and the likelihood of inducing coupled-bunch instabilities. The tuner has now been completely reconstructed at TRIUMF to permit ac operation, with stranded cable, a laminated yoke and improved cooling. The first high-power tests were successfully completed in 1991, demonstrating 50 Hz operation over the full 46–61 MHz range with the required maximum gap voltage of 65 kV (Fig. 5). This is believed to be the first full-scale demonstration of the superior capabilities of perpendicularly-biassed ferrite tuners.

Work is now proceeding on feedback control of the cavity. The fast feedback loop and a bias tuning loop around the amplifier chain have been successfully closed under dc biased conditions. Design of the rf control loops for ac biasing is underway, based on measurements of the frequency response of the tuner. The ac magnetic field of the tuner has also been measured.[22]

A new initiative is the testing on this cavity of a varactor, a magnetron-like capacitative tuning device, in collaboration with INR and RTI, Moscow.[9] This would avoid the magnetic field and eddy current problems associated with ferrite tuners.

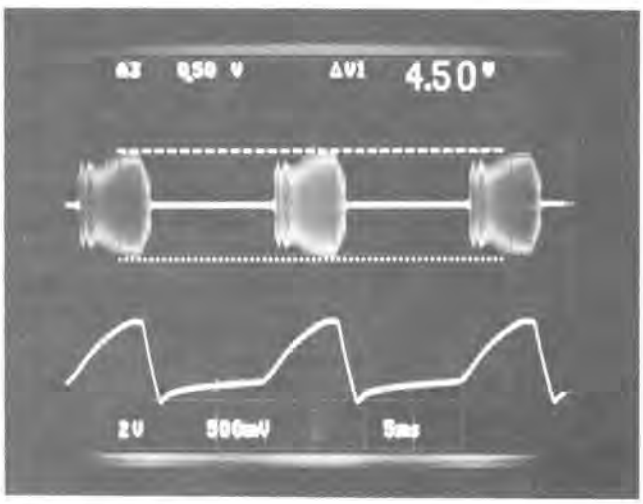


Fig. 5. High power operation of rf cavity using perpendicularly biassed ferrite. The top trace shows voltage at the accelerating gap (dashed lines indicate 65 kV), the lower trace the bias power supply current.

7. BEAM PIPE AND VACUUM

The high circulating beam current makes beam-induced multipactoring and ion desorption from the walls the most critical processes for the vacuum system. A hydrocarbon-free system is required with all metal elements pre-baked to 300°C, and pumps spaced no more than 5 m apart, an arrangement that will ensure a vacuum better than 10^{-8} Torr. An additional concern in the Extender ring, where the beam may be debunched, is the possibility of electron-proton oscillations; electrostatic collector plates will be needed to suppress these.

Ceramic chambers must be used within the fast-cycling magnets but must contain a conducting shield to provide a low impedance path for the image currents. Two shielding schemes are being considered and for each a 4-m-long prototype chamber is being constructed for the Booster dipoles.[23] That from RAL (UK), incorporating a separate wire cage, as used in the ISIS synchrotron, has been delivered (Fig. 6) and has successfully undergone vacuum tests; bakeout at 100 C appears to be essential for a quick pumpdown. RAL has subsequently doubled the length of the pipe segments to 50 cm and simplified the supports for the cage. That from SAIC (San Diego) has longitudinal silver stripes laid down directly in internal grooves in the pipe; three 1.3 m-long curved sections have now been completed and joined by glazing to form a single 3.9 m pipe. Recent vacuum tests achieved 2×10^{-9} Torr after 24 h bakeout at 100° C.

Short sections of pipe have also been produced with the stripes specially configured to form beam position and higher-order moment monitors. Tests with the 500 MeV cyclotron beam confirmed the expected position sensitivity, while lab tests have shown that quadrupole moments can be measured quite accurately.[24]



Fig. 6. Ceramic pipe and wire shield (RAL design).

8. COMPUTER CONTROL SYSTEM

The system architecture will be based on a general-purpose local area network, interconnecting the operator consoles (workstations), the microprocessor-based equipment controllers, the database management system, and the software development facilities. Object-oriented techniques have been used to specify a logical

model of the entire control system organized in a hierarchical structure.

Two prototype development projects are under way to evaluate the design methodology. One project, to upgrade a PDP-11 based radio-isotope production control system on beam line 2C, has succeeded in replacing the PDP-11 hardware and software with less than 1 man-year of effort. New software now runs on VAX stations and employs a commercial graphical user-interface package. A second project is under way to control an auxiliary rf cavity in the cyclotron.[25)]

9. EXPERIMENTAL AREAS AND TARGETS

The slow extracted proton beam will be shared between two lines each with two production targets. Each target will feed at least two forward K and $\overline{p}$ channels, and in some cases backward μ channels. The six charged kaon channels will have maximum momenta of 0.55, 0.8, 1.5, 2.5, 6 and 21 GeV/c. With solid angle and momentum acceptances ranging from 8 msr × 6% for the lowest momentum channel to 0.1 msr × 1% for the highest, the maximum fluxes range from 0.6 to 3.7 × 10^8 K^+/s and from 0.7 to 11 × 10^7 $\overline{p}$/s. The 0.8 GeV design has been used for the new LESB3 channel at Brookhaven. Initial commissioning runs this summer have achieved fluxes of 3×10^6 $K^+/\mu C$ protons, with K^+/π^+ ratios up to 5:1, an order of magnitude improvement over LESB1.[26)]

A dedicated line and area is provided for polarized proton beams. The neutrino production target, fed by the fast extracted beam, is located in the main experimental hall for good crane access, but the neutrino experimental area is in a separate building. Target development has included both modification of an existing rotating graphite target (driven and cooled by water) from graphite to tungsten, and the construction of a prototype target rotated by a flexible cooling line. Successful tests have also been carried out on remote welding of aluminum flanges for high-radiation areas.

10. IMPACT STUDIES

The industrial capability study showed that nearly 200 Canadian firms are capable of being key contractors for high technology components worth $316 million. Over 85% of these components are accorded high priority in such areas as robotics, microelectronics and software.

The environmental impact study identified various concerns: ground water changes or contamination, noise, effects on trees and wildlife, cooling tower vapour, energy consumption, electromagnetic radiation from power lines, and public access to a nearby park. Following two public meetings, none of these was judged serious enough to require reconsideration of the project.

The economic impact study assessed the total industrial activity and employment that would be created during construction and operation. Even without counting the benefits from applications and spin-offs, it was concluded that nearly 80% of the project costs would eventually be recovered by the government in taxes and other revenues.

11. INTERNATIONAL PARTICIPATION

Funding for the project is being sought along the same lines as for HERA, where a number of countries have contributed accelerator components. To assess the prospects, a Canadian delegation visited several countries during 1989 under the auspices of the Department of External Affairs. In the US the NSAC Long Range Planning Committee recommended $75 million (US) for KAON construction and an additional $30 million for experimental equipment. The construction money has been included in DOE budget planning and was confirmed in the base budget recommended by the Schiffer subcommittee in April 1992. Germany, France and Italy have also promised support, proportional to the number of their potential users. Participation is also expected from Japan, where there is a large potential user community, a history of collaboration with TRIUMF, and strong support from the Nuclear and High Energy Physics Committees and from the Science Council of Japan. A number of other countries – Israel, PR China, South Korea, UK and Russia – will contribute manpower towards design and construction and equipment for experiments. Altogether the delegation estimated that the total foreign contribution to construction would be close to $200 million.

12. PRESENT STATUS OF THE PROJECT

The reports of the various studies, amounting to about 2800 pages altogether, were formally submitted to the governments of Canada and British Columbia in May 1990. The cost of the project is of course of major interest to government. With a six-year construction period, the total cost was estimated to be $708 million in 1989 Canadian dollars; the operating cost would $90 million per year. In September 1990 the province of British Columbia announced that it would increase its support from one-sixth to one-third of the total, or $236 million. In September 1991 the Government of Canada followed suit, offering a second $236 million. In October, however, an election and change of government in B.C. delayed progress while the new party settled into office. In May they renewed a pledge by the previous B.C. government to contribute to the operating costs. Canada responded by appointing the previous provincial minister and KAON champion, Stan Hagen, as leader of negotiations with other countries to confirm their pledges towards the remaining one-third of capital costs. These are scheduled to begin in August and be complete within a few months, enabling construction to begin in 1993.

13. ACKNOWLEDGEMENTS

It is a pleasure to acknowledge the efforts of all those who have contributed to the work reported here and especially to those who have read and corrected drafts of

this paper. Contributions and advice from our colleagues at other laboratories have been very valuable. The author is particularly grateful to Jana Thomson for her efficiency in putting this paper together.

14. REFERENCES

1) KAON Factory Proposal, TRIUMF (1985)
2) KAON Factory Engineering Design and Impact Study – Report of the Steering Committee, TRIUMF (1990)
3) KAON Factory Study – Accelerator Design Report, TRIUMF (1990)
4) KAON Factory Study – Science and Experimental Facilities, TRIUMF (1990)
5) **Proc. Workshop on Science at the KAON Factory**, Vancouver, ed. D.R. Gill, TRIUMF (1990)
6) G. Dutto, "The TRIUMF 520 MeV Cyclotron ..." (these proceedings).
7) R.E. Laxdal *et al.*, "Beam quality investigations for H^- extraction at TRIUMF" *ibid.*
8) R.V. Servranckx, **Proc. Int. Workshop on Nonlinear Problems in Accelerator Physics**, Gosen, March 1992 (IOP, in press).
9) V.V. Balandin *et al.*, **Proc. 1991 PAC** (IEEE, New York, 1991), 2823.
10) U. Wienands *et al.*, "A racetrack lattice ..." **Proc. XV Intern. Conf. on High Energy Accelerators** (Hamburg, 1992, in press).
11) R. Baartman, "New Booster Scenarios", TRIUMF Report TRI-DN-92-K200 (1992)
12) U. Wienands *et al.*, "The high-γ_t lattice ..." **Proc. XV Intern. Conf. on High Energy Accelerators**, (Hamburg, 1992, in press).
13) R. Baartman, "Synchro-betatron resonance due to gap-voltage asymmetry", *ibid.*
14) M. D'yachkov & R. Baartman, "Methods for finding stationary longitudinal phase space distributions", *ibid.*
15) S.R. Koscielniak, "Continuous synchronization ...", *ibid.*
16) A.J. Otter, P.A. Reeve, Proc. 1991 PAC (IEEE, New York, 1991), p. 2363
17) K.W. Reiniger, Proc. 1991 PAC (IEEE, New York, 1991), p. 920
18) M.J. Barnes & G. Wait, "Kickers for the KAON Factory", **Proc. XV Intern. Conf. on High Energy Accelerators**, (Hamburg, 1992, in press).
19) M.J. Barnes, G. Wait & D.C. Fiander, "Improving the performance of kicker magnet systems", *ibid.*
20) G.D. Wait & M.J. Barnes, "Results for the 75 kW prototype 1 MHz chopper ...", *ibid.*
21) R.L. Poirier *et al.*, "Performance of the ac perpendicular-biased ferrite-tuned cavity ...", *ibid.*
22) I.B. Enchevich & R.L. Poirier, "Magnetic field measurements ...", *ibid.*
23) T. Hodges *et al.*, "Deposition of metallic rf shield stripes ...", *ibid.*
24) Y. Yin, "A multistrip beam profile high order moment monitor", *ibid.*
25) G.A. Ludgate, Proc. 1991 PAC (IEEE, New York, 1991), p. 1350.
26) E787 Collaboration (private communication).

MATERIAL RESEARCH WITH BEAMS AT CYCLOTRON ENERGIES

Klaus Ziegler

Hahn Meitner Institut Berlin GmbH
Glienicker Strasse 100
D-1000 Berlin 39
Germany

ABSTRACT

The use of cyclotron beams for material research covers a wide range from analytical research to radiation damage, materials modification and to solid state physics. The application of particle beams in these different areas will be described, and examples for these applications will be given. Up to now very few facilities are equipped to fully supply all the needs material scientists have. The requirements for cyclotron facilities catering to material science, solid state physics and ion beam applications are given.

1. INTRODUCTION

The use of particle beams in material research is on a steady increase, as the response to a survey at cyclotron facilities indicates. This type of research can be classified into the following areas:

-Analysis, used to determine material composition, impurities and depth-distributions of either unwanted impurities or of atoms, which have been introduced especially to change the properties of the original material.

-Investigation of radiation damage to materials, with the aim to understand the mechanism of damage and thus hopefully provide a means to design materials with better radiation resistance.

-Modification of materials by use of particle beams to find ways to create materials with new properties which could not be obtained by any other way, or to improve on already existing properties of the material under investigation.

-Investigations in solid state physics providing information on internal properties of solids, or on internal defects and helping us to understand the solid state of materials better. This type of research is often referred to as "nuclear solid state physics".[1)]

So far only a few facilities exist, which provide the necessary equipment for some of the investigations discussed. Generally the material research experiments are being done as a side line at facilities which have been built mainly for the use in nuclear physics, and we cyclotron builders need to become aware of the different requirements for the experimental equipment as well as for beam properties needed for material research. The only exception is Japan,[2)] where a facility is being built solely for the use in material research, with all the required ancillary equipment, to perform the full width of investigations described.

In the following I want to describe the different types of research with particle beams in material science in more detail, and give examples of work which is going on at different cyclotrons laboratories.

2. MATERIAL ANALYSIS WITH PARTICLE BEAMS

To analyze materials, and to determine amount and distribution of impurities, several different methods are being applied. A short description of these methods and of their applications will be given.

2.1 Charged Particle Activation Analysis (CPAA)

The method of charged particle activation analysis is based on the use of nuclear reactions to determine the presence of certain atoms in a material. It is therefore also often referred to as "nuclear reaction analysis" (NRA). This method is used primarily to determine low concentrations of impurities. This is especially important for the development of semiconductor devices, where the type and amount of impurities need to be monitored and controlled to concentrations down as low as possible. Other applications are metallurgy, biology and medicine, archeology and environmental technology. In general CPAA is rather complex and therefore not useful for routine applications. Its high sensitivity however makes this method very important for the development of procedures in the manufacturing of high purity materials. The sensitivity of this method reaches down to concentrations as low as 1 to 10 ng/g. A relatively recent account of this method has been given by Strijckmans et.al.[3)] The group in FZR Rossendorf near Dresden have used this method also and reached sensitivities as low as given above.[4)]

2.1.1. Thin layer activation (TLA)

A special case of CPAA is the method of thin layer activation. It was first developed by Schatz et. al.[5] and is now used as a research tool to help in the design of automotive parts and machine tools and to measure erosion and corrosion on pipes etc.. The method uses nuclear reactions of light and medium heavy ions to produce trace quantities of radioisotopes with well defined depth distributions near the surface of the parts, which one wants to monitor or improve. This way for instance the wear on motor parts can be observed in actual operating conditions by simply monitoring the activity in the motor oil with a simple radiation detector. This method is now in use in the automobile industry in Germany, the United States, Great Britain and Japan.[6] Also at VEC in Calcutta TLA - studies for motor parts have been performed.[7]
Originally the method of TLA was mainly used for metallic surfaces, where the particle beam could be directly applied to the surfaces to be studied. For nonmetallic, insulating or composite materials no nuclear reactions are available to use the direct beam on the material. In these applications the use of ^{7}Be has become the probe of choice, and developments at several laboratories are under way to produce ^{7}Be via the ^{7}Li(p,n)^{7}Be reaction and simultaneously recoil implant the probe nucleus into the sample for TLA investigations. At NSCL in East Lansing[8][9] the production of ^{7}Be via a spallation process and successive acceleration has been successfully demonstrated. KFK Karlsruhe[10], in a cooperation with the Kurchatov Institute, is using the reaction mentioned above to produce the ^{7}Be and recoil implant it into the sample. These two institutions also are developing a Be ion source with the aim to produce eventually an accelerated beam of ^{7}Be ions.

2.2 Neutron Radiography (NR)

Neutron radiography[11] has long been a method of choice in material research, often applied in investigations of paintings etc..
In the past mostly reactors have been used. However there is now a proposal in Japan[12] to produce neutrons for radiography with an intense cyclotron beam.

2.3 Rutherford Back Scattering (RBS)

This is probably the oldest ion beam method. It is based on the elastic back scattering of ions from the surface or the bulk of a material and it was used around 1910 by Rutherford in the first investigation of atomic structure. This method gives information about the different atoms in the material hit by the beam simultaneously, but often the peaks overlap with a continuum, due to signals from the bulk and the energy loss of the scattered particle in the material. This leads to an ambiguity which presents the main limitation to the use of this technique. Nevertheless this method is very useful in routine applications, especially when samples are compared relatively to each other. The typical sensitivity of RBS is about 0.1 atomic % with a depth resolution of 10 nm at a penetration of about 1 µm.[13]

2.4 Elastic Recoil Detection Analysis (ERDA)

The ERDA-method is closely related to the RBS-method. Here one does look at the elastic recoil atoms coming from the sample instead of the beam particles scattered from the sample as in RBS. Due to the kinematics one preferably uses a heavy ion beam for ERDA, looking at all the lighter recoils coming from the sample, because the energy transfer to the recoiling ion is optimized this way. With ERDA one can measure simultaneously several different ions and their depth profiles, provided one determines the mass and energy of all the recoiling ions separately. In order to avoid nuclear reactions in the sample one tries to stay with the beam energy below the Coulomb barrier. This way the sample will not be activated at all and it can be handled after the ERDA analysis immediately. At VICKSI a high energy ERDA facility is being installed, using an ^{129}I beam of about 360 MeV. In Fig. 1. a sketch of the experimental setup

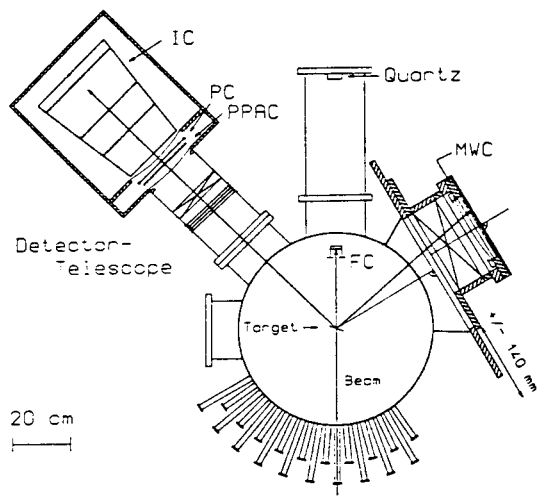


Figure 1 Sketch of the experimental ERDA setup. The scattering chamber is mounted on a rotatable support, with two large-area detectors attached.

is depicted. The detector telescope consists of a parallel plate avallange counter (PPAC), a proportional counter (PC) and an ionisation chamber (IC).The second detector is a low-pressure multiwire chamber (MWC). Tests have shown the great power of this method especially when combined with detectors and detection methods used for nuclear physics.[14]

At the TU Eindhoven Rijken et. al.[15] using high energy α-particles, coincidence and pulse shape discrimination have also developed this method to obtain background free spectra and a depth resolution of 5 nm. In Brazil da Silva et al.[16] have recently used ERDA for Hydrogen profiling in surfaces of metallic materials.

2.5 Particle Induced X-ray Emission (PIXE)

The PIXE-method is mostly used with a relatively low energy proton beam. Often this beam is transferred out of the vacuum of the accelerator and furthermore used in conjunction with a microbeam. The method is based on the use of a beam particle to kick an electron out of the inner shell of a sample atom, and then to look at the characteristic X-rays coming from the sample with an appropriate detector. Practically all elements can be detected this way simultaneously. The absorption of the characteristic X-ray in the material surrounding the detector determines the limit for the lighter elements, so that in general elements lighter than sodium (Z = 11) can not be detected this way. The PIXE-method is in wide use at many places for all kinds of measurements pertaining to environment, health, biology, archeology and others.

3. RADIATION DAMAGE STUDIES

The studies of radiation damage in materials was one of the first applications of particle beams. Besides reactors, particle accelerators provided a means to determine the effect of radiation on materials used in the construction of equipment for a radiation environment. The studies today include tests of structural materials, of semiconductor devices, used in satellites or high flying airplanes and of metals, metal alloys and of insulators.

3.1 Radiation Effects in Metallic Materials

3.1.1 Search for first wall materials for fusion reactors

The investigation of materials which might be used in the first wall of a fusion reactor is of great interest and studied at many places. The simulation of the effect of 14 MeV neutrons, produced in the tritium-deuterium fusion reaction, on materials is needed to determine, if a specific material can be considered as first wall material. At PSI[17] a proton irradiation experimental area (PIREX) is set up especially to look at effects of protons on prospective materials. The proton beam in this area is degraded to 300 MeV and it can be degraded further in steps of 2.3 MeV to an energy as low as desired. The Institute for Advanced Materials of the European Communities in ISPRA is investigating materials for the first wall under irradiation and mechanical stress.[18][19] Similar experiments are also performed at VEC in Calcutta[20] and at the HIRFL in Lanzhou.[21] At KfK Karlsruhe a recently installed universal testing machine at their "dual beam facility" allows to

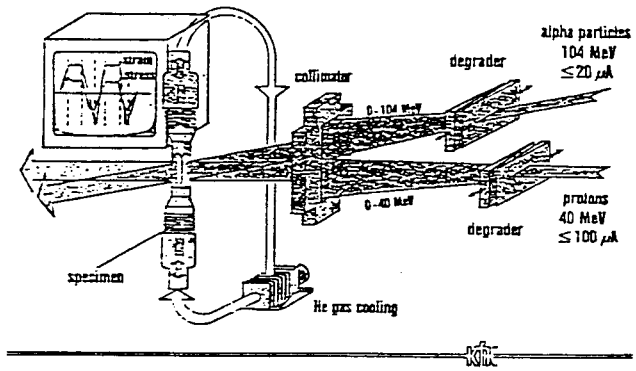


Figure 2 Scheme of the Karlsruhe dual beam facility.

investigate various static and dynamic loadings in terms of stresses and strains like push-pull fatigue, creep or creep-fatigue during irradiation in a vacuum chamber[22] (Fig. 2).

3.1.2 Radiation effects on permanent magnets and amorphous metallic alloys

The effect of radiation on permanent magnets is looked into at NSCL in East Lansing[23] and at the cyclotron in Jyväskylä.[24][25] In both places a reduction of the magnetic field was observed.

The investigation of amorphous metallic glasses was pioneered by Klaumünzer et al.[26][27] and extended to higher energy beams by the group at GANIL lead by Jousset.[28] The original hope was to find a particular radiation resistant material. To the great surprise however a makroscopic growth of amorphous metals was observed under particle irradiation. The CIRIL group at GANIL has performed extensive studies of radiation effects on materials[29] over a wide range of energies available at the GANIL facility.

3.2 Radiation Effects on Semiconductor Devices

The effect of radiation on the performance and lifetime of semiconductor devices is of obvious importance for satellites and space probes. Accordingly experiments to simulate the radiation in space are done at many places, and test facilities to routinely check all devices are needed. One Single-Event-Upset (SEU) test facility is in operation at the tandem accelerator in Brookhaven,[30] and there are discussions about setting up a similar facility at VICKSI. At the Philips injector at PSI in Zürich an interesting simulation was caried out[31]: on the ESA Earth Resource Satellite

ERS-1 an instrument had failed after five days of operation. Immediately before the failure a transient overcurrent had been measured. Using the data of the on-board telemetry record, one could deduct, that a proton induced latch-up might have occured in a CMOS device. The tests at the OPTIS facility at PSI with a 60 MeV proton beam verified this conclusion beautifully.

3.3 Radiation Effects on optical Glasses

At INS Tokyo [32] the effect of proton irradiation on glasses was investigated, especially with the objective to determine the possibility to use these glasses for optical systems in a satellite. The transmission curves for optical glasses before and after 40 MeV proton irradiation are shown in Fig. 3. At

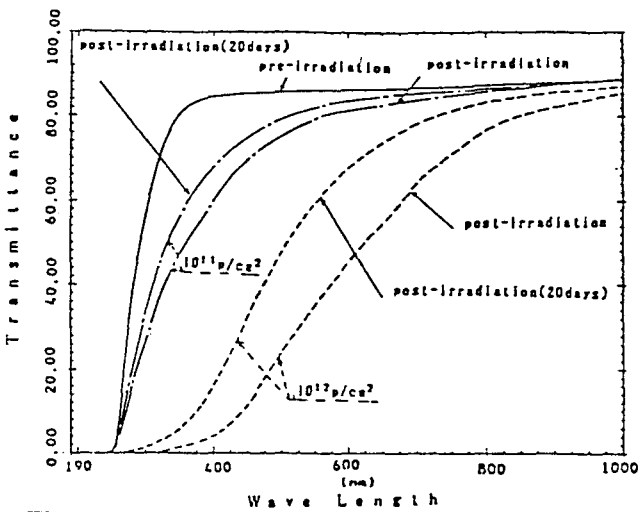


Figure 3 Transmission curves of optical glass before and after 40 MeV proton irradiation.

shorter wavelength the transmission is reduced considerably at proton fluxes above $10^{10}cm^{-2}$, but a significant recovery can be observed 20 days after the irradiation, indicating a self healing effect of the glasses. This might be similar to the production and bleaching out of "colour-centers" in alkali halides[33] which occurs especially at elevated temperatures. This effect is also important for glassfiber cables in a radiation environment as for instance accelerator tunnels.

4. BASIC RESEARCH IN SOLID STATE PHYSICS WITH PARTICLE BEAMS

The use of particle beams in solid state physics and in applied physics becomes more and more common. At VICKSI presently more than half of the beam time is used for experiments in these fields, with increasing demand. The purpose of the condensed matter studies is to get a better understanding of local properties like the magnetic behaviour of isolated atoms in metals depending on lattice sites or the dynamics of implanted atoms in solids. With the ion beam one produces shortlived radioactive isotopes and uses their recoil momentum to implant them into solids. The experimental setup for recoil implantation is shown in Fig. 4. In the upper part of the figur the primary ion beam will pass through the sample, while in the arrangement shown in the lower part the passage of primary ions through the sample is avoided. In the solid the nuclear moment of the recoil nucleus will interact with either the internal or an externally applied magnetic field, or the electric field gradient of the solid at the respective lattice site. These interactions can be observed by nuclear methods like the "Perturbed Angular Distribution Method" (PAD) or "In Beam Mössbauer spectroscopy". In the following these methods shall be given as examples.

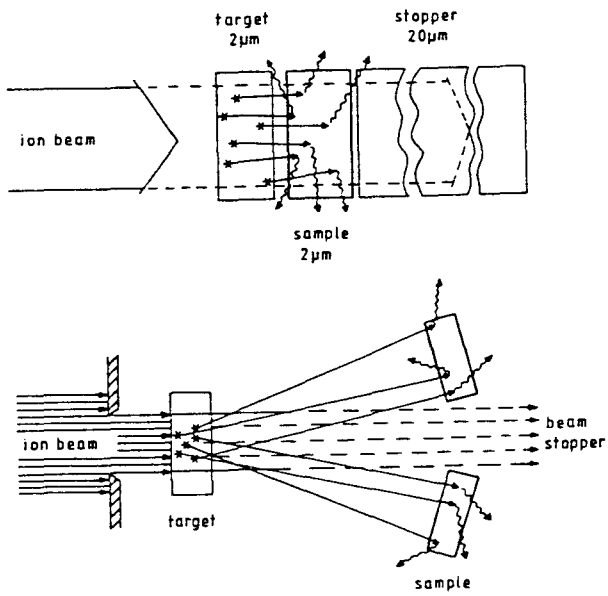


Figure 4 Experimental arrangements for recoil implantation.

4.1 Perturbed Angular Distribution

The measurement of the perturbed angular distribution is based on the fact, that the γ-ray emission of the recoil implanted radioactive isotope is modified by the interaction between the nuclear moment of the probe nucleus and magnetic fields or electric fieldgradients present at its location in the sample. The spin of the probe nucleus makes a Larmor-precession, and this precession is observed as a modulation of the γ-ray intensity in time. The period of this modulation gives information about the field or field gradients, provided one knows the magnetic moment of the probe nucleus.[34]

4.2 In Beam Mössbauer Spectroscopy

While the standard Mössbauer spectroscopy uses a long lived parent radioisotope, the in-beam method[35] uses a particle beam to excite the Mössbauer isotope via Coulomb excitation to the Mössbauer level. A ^{57}Fe target is bombarded with an ^{40}Ar beam at an energy well below the Coulomb barrier. This way any background from nuclear reactions is avoided. The Fe atoms are excited to the 14.3 keV Mössbauer level and simultaneously recoiled out of the target. The angular distribution of the recoils peaks between 20° and 70° with respect to the beam axis. So the probes can easily be implanted into the sample material avoiding that the beam strikes the sample. A sketch of an experimental

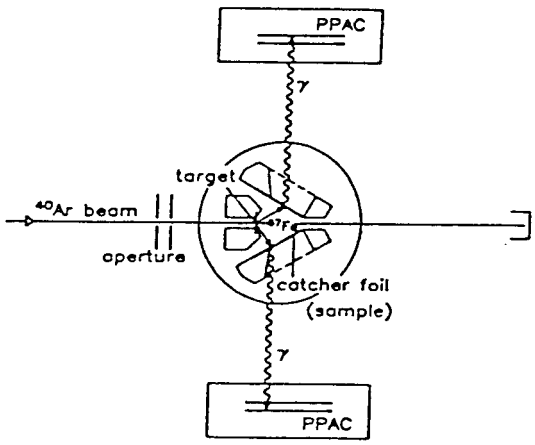


Figure 5 Sketch of the experimental setup for "in beam Mössbauer spectroscopy". PPAC stands for parallel plate avalanche counter.

setup for in-beam Mössbauer spectroscopy is shown in Fig. 5.

The actual measurements are taken between the cyclotron beam pulses, contrary to on-line Mössbauer spectroscopy, where a macropulsing of the cyclotron is required.

5. MATERIAL MODIFICATION WITH ION BEAMS

5.1 High Energy Implantation

While in the past implantation was performed at energies below about 500 keV, in recent years implantations at energies as high as several 100 MeV have been reported.[36] Low energy implantations have been used extensively to improve the surface behaviour of materials, reducing wear, friction, oxidation and corrosion,[37][38] or to produce radiation enhanced cohesion[39]. Implantations at high energies can be used to produce burried layers of ions in a solid, to produce insulating layers for instance in silicon by implanting with oxygen or nitrogen or to introduce doping atoms into semiconductor wafers. The applications are manyfold, but, to my knowledge, so far only used in experimental studies and not yet in industrial applications. This is partly due to the fact that high energy accelerators are not so easily accessible as low energy implanters but also because the users and operators of high energy facilities have not made much of an effort to introduce industry to the possibilities of their facilities.

5.2 Production of New Material Properties with Ion Beams

5.2.1 Microfilters

The production of microfilters with ion beams developed by Spohr and Fischer[40]is since being pursued at many different laboratories. Besides GSI in Germany, Riken in Japan,[41]also JAERI in Takasaki is producing these filters.[42] FZR Rossendorf[43][44] has also produced and marketed microfilters used in the food and beverage industry. They used a 30 MeV chlorine beam from their tandem accelerator. A particularly interesting development is

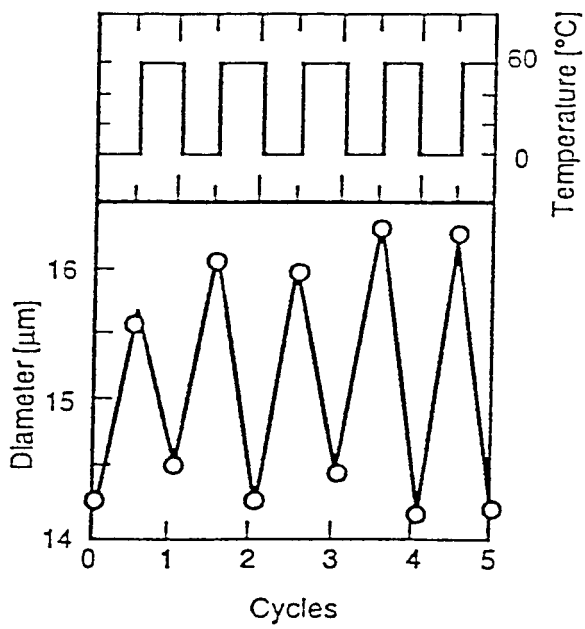


Figure 6 Change in size of pores formed in a thermally responsive film when cycled between 0°C and 60°C.

reported by Tamada et al..[45] They produced a foil, which depending on the temperature was swelling or deswelling. When micropores were introduced into this foil, using heavy ion beams, the pore diameter could be varied between about 14 µ and 16 µ, depending on the temperature of the water

the foil was immersed in. Fig. 6 shows how the pore size varies with temperature cycling. This is the first porous film, where pore size can be controlled by such an environmental condition as temperature. The filter is expected to separate various substances by changing the ambient temperature.

5.3 Influence of Radiation on High T_c Superconductor Properties

Very soon after the discovery of the high T_c superconducting ceramics the effect of radiation on the properties of these ceramics were studied.[46] The properties of the high T_c materials are affected by intrinsic defects and the structure-related anisotropy. The introduction of artificial defects by radiation can then be used to obtain a better understanding of the structural parameters and the related super- and normal-conducting properties of these materials. In general irradiation of high T_c materials lowers the critical temperature T_c. Therefore on first sight it appears, that radiation is harmfull for these materials. However extensive studies[47] using different projectiles have revealed, that the projectiles and the direction of the particle track with respect to the crystal axes can also have a positive effect on the superconducting properties.

5.3.1 Enhancement of critical current density J_c

High energy heavy ion irradiation using a 580 MeV $^{116}Sn^{16+}$ beam at the Holifield Facility in Oak Ridge has been shown to increase the critical current density J_c significantly.[48] Irradiations with protons or very light ions, which produce only point defects are not very effective in this respect. Irradiations with 770 MeV ^{129}Xe and 560 MeV ^{16}O done at the Texas A & M Cyclotron[49] and with 500 MeV ^{129}I at VICKSI[50] produced columnar defects which acted as flux pinning centers, and increased the critical current to values of 10^5 A/cm^2.

5.3.2 Radiation induced improvement of persistent field magnets using high T_c materials

At the Institute for Beam Particle Dynamics and the Texas Center for Superconductivity in Houston R. Weinstein et al. have produced permanent magnets by trapping magnetic fields in high T_c superconductors.[51] By irradiating the superconductors with protons at the Harvard Cyclotron, and with ^{3}He-ions at the Indiana University Cyclotron facility they could increase the trapped fields by almost a factor of four[52](see Fig. 7). Again this effect is caused by flux pinning. Using heavier ions and higher energies the trapped fields should increase even more. Persistent magnets with fields of 1.4 T have been produced and it is expected to reach 3 T this year and 6 T in the course of the next year. The possible applications of these magnets are manifold and very exciting: the production of external beam line magnets is in progress, a small motor using these magnets has been produced and the construction of a generator is being tested. Another application is the production of levitated bearings.

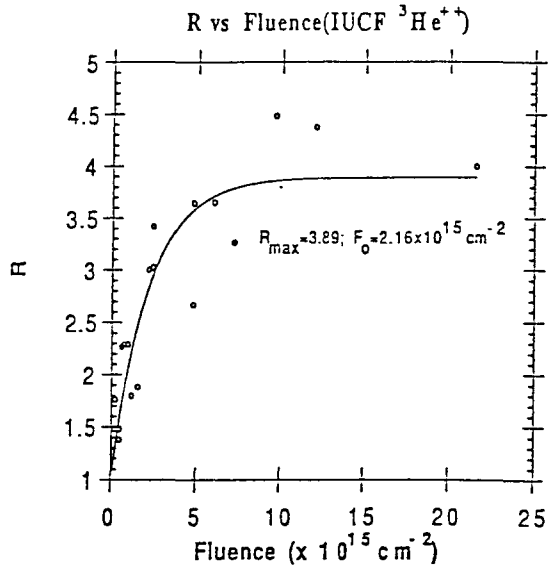


Figure 7 Ratio R of trapped field after to trapped field before irradiation versus particle fluence.

Many other applications are also considered. A very interesting application is the production of so called "replica" magnets.[53] Due to the pinning centers present in the superconductor the magnetic field is not expelled (Meissner-effect), but rather trapped. So superconductors with trapped field behave like metallic permanent magnets, except that they copy, essentially precisely, the fields which are used to activate them. So with one very precise prototype magnet one could reproduce identical magnets at will. The mechanical shape of the superconductor would not have to be precise at all, but nevertheless the field of the prototype magnet will be reproduced accurately. So far two technical problems have to be overcome: 1) It is still not easy to produce large volume high T_c material and 2) the trapped field magnets show a certain "creep", but there already exist ways to reduce this to only a few % per year and further improvements are certainly possible.

6. REQUIREMENTS FOR CYCLOTRON FACILITIES USED FOR MATERIALS RESEARCH

In the past most cyclotron facilities have been designed and built for the use in nuclear physics research. For material research however new requirements for beams and experimental equipment do become important.

6.1 Beam Properties

While for nuclear physics experiments small beam spots and a small emittance were the main requirements, in material research these beam properties might not be requested very often. At VICKSI we had situations where a 4" wafer needed to be homogeneously implanted with boron ions, and simple changes in the focussing did not produce a beam suitable for the given requirement. Ideally the experimenters would have liked four steering magnets to sweep the beam horizontally and vertically, and to ensure that the beam impinges on the surface perpendicularly. For implantations very high and constant intensities are required to be able to implant 10^{16} or 10^{17}ions/cm^3 in a reasonable time and with a high accuracy. For channeling experiments we were presented with the request to produce a parallel beam with a divergence of less than 0.01 mrad. Fortunately we have the space and a flexible enough beam optic system to produce this beam.
As the experiments in material research generally do not require very long times, quick energy- and ion-changes become important, and a special effort needs to be made to try to change the energy or the ion in a time small compared to the average irradiation time of a material research experiment.

6.2 Experimental Facilities

For surface investigations, implantations and analytical investigations often a very clean and good vacuum is required. Therefore ultrahigh vacuum chambers are needed. Often also vacuum manipulators are requested for the experiments. The control of the sample temperature from 4°K to as high as 1300°K is needed to perform the experiments in solid state physics. For the production of short lived PAC (perturbed angular correlation)-sources, which are recoil-implanted into the sample, remote handling and temperature control is needed to anneal the sample and eliminate the irradiation-produced defects. It is an interesting learning process which nuclear physicists and accelerator physicists have to go through, to understand all the requirements and experimental facilities which are necessary to perform high quality research in material science and in applications. It is obvious therefore, that considerable effort and money is necessary to supply all the required facilities. At VICKSI we are presently working on a proposal to provide an ion beam user-facility for solid state physics, material science and applications. One idea was to use an ECR-ion source injecting into a small cyclotron[54], which then injects into the existing VICKSI-cyclotron. With no stripping between the source and the injector-cyclotron and the two cyclotrons, the intensity of VICKSI will increase significantly. Recently the development of frequency variable RFQ's[55] has stimulated the idea to use one or two RFQ-accelerators instead of a small cyclotron. This would again give a large increase in intensity but a limited energy variation due to the restricted frequency variability of the RFQ's. Presently a layout which would give energies out of the cyclotron between 2 MeV/u and 6 MeV/u is being considered. This energy range is quite suitable for most "high energy" applications. The use of RFQ accelerators as injectors for VICKSI would hopefully furthermore decrease the required set-up time for a new beam.

7. ACKNOWLEDGEMENTS

I gratefully acknowledge the support I received from the cyclotron community. Over 90% of the laboratories I have addressed have responded and provided information about the research performed at their facilities. I am sorry that I was not able to use all the data I have been provided with, but time and space available made it necessary to make a selection which necessarily is biased by my personal preference. I apologize to all colleagues who might feel I have wrongly neglected their information. I am especially gratefull to all colleagues, who have granted permission to use their data in some cases even before publication. Finally I would like to thank the organizers of the Cyclotron Conference for giving me the opportunity to collect these data and present them at this Conference. I am sure I benefitted the most from it, and I am especially grateful for this.

8. REFERENCES

1) Schatz, G. and Weidinger, A., Nukleare Festkörperphysik (Teubner Studienbücher Physik, Stuttgart, 1992).
2) Sato, S., "The Advanced Radiation Technology Project Using Ion-beams in JAERI-Takasaki", Proc. of the Conf. on Evolution in Beam Applications, Takasaki, Japan, Nov. 1991 (to be published).
3) Strijckmans, K. and Vandecasteele, C., "Activation Analysis with Charged Particles", Analytica Chimica Acta, **195**, pp. 141-152 (1987).
4) Böttger, M. L., Birnstein, D., Helbig, W. and Niese, S., "Removal of Disturbances in Carbon Determination by Activation Analysis for lowering the Detection Limit", Journal of Radioanalytical Chemistry, Vol. 58, 173 (1980).
5) Gerve,A. and Schatz, G.,"Applications of Cyclotrons in Technical and Analytical Studies," Proc. 7th Int. Conf. on Cyclotrons and their Appl., (Birkhäuser, Basel, 1975) pp. 496-502.

6) Tazawa,S. and Kataoka,S.,"Light Element Analysis of Semiconductors through CPAA and Radio-Nuclide Technique for Machine Wear," in Proceedings of the 1st workshop on Beam Engineering of Advanced Materials, Tokyo, Nov. (1990).
7) Choudhury, D. P., Choudhury, J., Raju, V.S., Das, S.K., Bhattarcharjee, B.B. and Gangadharan, S.,"Study of wear between piston ring and cylinder housing of an internal combustion engine by thin layer activation technique," Nucl. Instr. and Meth. B42, 375 (1989).
8) Mallory, M.L., Ronningen, R.M., McHarris, Wm.C., Sherrill, B. and Dardenne, Y.X.,"Tribology Studies: ^{7}Be Implantation in a Ceramic Sample by Means of fragmented high Energy ^{14}N Beam," Nucl. Instr. and Meth. B40/41, 579 (1989).
9) McHarris, Wm.C., Mallory, M.L., Ronningen, R.M. and Dardenne, Y.X., "Gamma-Ray Spectroscopy of implanted ^{7}Be and ^{22}Na for tribology Studies," Nucl. Instr. and Meth. A299, 593 (1990).
10) Fehsenfeld, P., KfK Karlsruhe, private Communication June (1992).
11) Fujine, S., Kanda, K., Matsumoto, G.-I. and Barton, J.P., "Neutron Radiography (3)," Proc. of the 3rd World Conference, Osaka, Japan, May 14-18, 1989 (Kluwer Academic Publishers, Dordrecht/Boston/London).
12) Tazawa,S.[a] and Whittemore,W.L.[b], "A Proposal of Intense Cyclotron-Based thermal Neutron Source," Contribution A2C to this Conference. [a]Sumitomo Heavy Ind. Toyo-Shi, 799-13 Japan, [b]General Atomics, San Diego, CA 92138, U.S.A.
13) Conlon, T. W., "Nuclear Physics for Materials Technology: Accelerator based Methods", Contemp. Phys. 26, 521 (1985).
14) Goppelt, P., Gebauer, B., Fink, D., Wilpert, M., Wilpert, Th., Bohne, W., "High Energy ERDA with very heavy Ions using Mass and Energy dispersive Spectrometry", Nucl. Instr. Meth. B68, 235 (1992).
15) Rijken, H.A., Klein, S.S., Van Ijzendoorn, L.J., Van Dijk, P.W.L. and De Voigt, M.J.A., "Materials Analysis With High-Energy Nuclear Scattering," in Proceedings of the Int. Conf. Appl. Nucl. Techn., Myconos, June 7-13 (1992).
16) Bott, A.H., Suita, J.C., da Silva, A.G. and de Miranda, P.E.V.,"Surface Hydrogen profiling in metallic Materials by the elastic-recoil Detection Technique," presented at "Advances in Corrosion and Protection Conference," Manchester, England, June 28th - July 3rd, 1992.
17) Schryber, U., PSI, CH-5234 Villigen, private communication, April (1992).
18) Institute for Advanced Materials, Joint Research Center, Commission of the European Communities, Annual Report (1990).
19) Fenici, P. and Suolang, S., "Fatigue Crack Growth in 316 Type Stainless Steel at Temperatures and Displacement Damage Rates representative for the NET first Wall Loading," to be published in the proceedings of the "5th Int. Conf. Fusion Reactor Materials" held in Nov. 1991.
20) Mukhopadhyay, G., Das, D., Majumdar, C.K. and Sen, P., "Isochronal Annealing Studies on Alpha-Irradiated SS 302," Rad. Eff. Exp., 1, 141 (1987).
21) Mingdong, H., "An Outline of Application Research on the Irradiation Equipment of HIRFL," Internal Report, Institute of Modern Physics, Academia Sinica, Lanzhou 730000, China.
22) Möslang, A., Baumgärtner, S., Bürkle, G.,Lindau, R., Przykutta, G. and Ehrlich, K., "In-Situ Fatigue Experiments at the Karlsruhe dual Beam Facility: Capabilities and first Results," to be presented at the 17th Symposium on Fusion Technology (SOFT), Sept. 14-18, 1992.
23) Zeller, F.A., "Radiation Damage Mechanism in NdFeB," in Proc. 11th Int. Workshop on Rare-Earth Magnets and their Applications (Carnegie Mellon University, Pittsburg, PA 15213, USA) p. 258.
24) Kähkönen, O.-P., Mäkinen, S. Talvitie, M. Rajainmäki, H. and Manninen, M., "Temperature Dependence of Irradiation-Induced Magnetic Flux Loss in $Nd_2Fe_{14}B$ Permanent Magnets," Europhys. Lett., 12(5), 413 (1990).
25) Kähkönen, O-P., Mäkinen, S., Talvitie, M. and Manninen, M., "Radiation Damage in Nd-Fe-B Magnets: Temperature and Shape Effects," J. Phys. Condens. Matter 4, 1007 (1992).
26) Klaumünzer, S., Schumacher, G., Rentzsch, S. and Vogl, G., "Severe Radiation Damage by heavy Ions in glassy $Pd_{80}Si_{20}$," Acta. Met. 30, 1493 (1982).
27) Klaumünzer, S., Mingdong Hou, Schumacher, G., "Coulomb Explosion in a metallic Glass due to the Passage of fast heavy Ions ?," Phys. Rev. Let. 57, 850 (1986).
28) Audouard, A., Balanzat, E., Fuchs, G., Jousset, J.C., Lesueur, D. and Thome. L., "High-energy heavy Ion Irradiation of $Fe_{85}B_{15}$ amorphous alloy: Evidence for electronic Energy Loss Effect," Europhys. Lett. 3, 327 (1987).
29) Rapport d'activite Scientifique 1987-1988-1989, CIRIL Laboratoire mixte CEA-CNRS.
30) "Heavy Ion R and D Opportunities at the BNL Tandem Facility," Brookhaven National Laboratory, Upton, Long Island, New York 11973.
31) Adams, L., Daly, E.J., Harboe-Sorensen, R., Nickson, R. and Haines,J., ESA-ESTEC, Noordwijk, Netherlands, Schafer, W., Conrad, M., Griech, H., Merkel, J. and Schwall, T., University of Stuttgart, Inst. of Navigation, Stuttgart, Germany, Henneck, R., Paul Scherrer Institute, Villigen, Switzerland,"The first verified proton induced

latch-up in space," presented at the IEEE/NSREC Conference, New Orleans, LA, USA, July 13 - 17, 1992.
32) Morimoto, Y., Ishito, S., Ueda, M., Sakamato, M., Asami, T., Numazaki, K., Miyano, E., Muira, S., Shibuya, M., Saito, M., Hayashida, B., Sasayama, S., Shibata, T., Uwamino, Y., Ohkubo, T. and Sato, S., "Proton Irradiation Damage in Optical Materials," Annual Report 1990, Institute of Nuclear Study, University Tokyo, Tanashi, Tokyo 188, Japan.
33) Seitz, F.,"Colour centers in alkali halide crystals," Rev. Mod. Phys. 18, 384 (1946).
34) Mahnke, H.E., "Application of heavy Ion Beams to condensed Matter Studies," in Proc. of 12th Int. Conf. on Cycl. and their Appl. (World Scientific, Singapore, 1991) pp. 587-593.
35) Sielemann, R. and Yoshida, Y., "In Beam Mössbauer Spectroscopy at heavy Ion Accelerators," Hyperfine Interactions 68, 119 (1991).
36) Fahrner, W.R., Laschinski, J.R. and Bräunig, D., "Application of high Energy Implantation in Semiconductors," Nucl. Instr. and Meth. A268, 579 (1988).
37) Dearnaley,G.,"The Modification of Materials by Ion Implantation," Phys. Technol., 14, 225 (1983).
38) Picraux,S.T.,"Ion Implantation in Metals," Ann. Rev. Mater. Sci., 14, 335 (1984).
39) Baglin, J.E.E., "Ion beam enhancement of metal-insulator adhesion," Nucl. Instr. Meth. B65, 119 (1992).
40) Fischer, B.E. and Spohr, R., "Production of Microstructures by heavy Ions," in Proc. of 12th Int. Conference on Cycl. and their Appl. (World Scientific, Singapore, 1991) pp. 555-565.
41) Nakanishi,N., Nakajima,S. and Wakasa,S.,"Development of Nuclear Track Microfilters," RIKEN Accel. Progr. Rep., 24, 63 (1990).
42) See Ref. 2).
43) Matthes, H., Pfestorf, W. and Seidel, M., "Eine Bestrahlungsanlage für Folienmaterial," Jahresbericht des ZfK-Rossendorf, ZfK-530 (1983).
44) Lück, H.B., Gemende,B., Heinrich, B., Matthes, H., Pfestorf, W., Seidel, W., Turuc, S., "Production of particle track membranes by means of the 5MV tandem accelerator," Jahresbericht des ZfK-Rossendorf, ZfK-731 (1989).
45) Tamada, M., Yoshida, M., Asano, M., Omichi, H., Stejny, J., Katakai, R., Spohr, R. and Vetter, J., "Intelligent porous Membranes prepared by Ion Beam Irradiation," in Proc. of the Int. Conf. on Intelligent Materials, March 23-25, Japan (1992) to be published.
46) Barreto, J., Mattievich, R., Pereira, R., Da Silveira, M.F., Goncalves, Z.C., Dos Santos G.R., "Charged particle damage studies of $YBa_2Cu_3O_7$," Journ. of Mat. Sci. Lett. 8, 689 (1989).
47) Kraus, M., van Haßelt, P., Ströbel, J.P., Peehs, S., Leghissa, M., Kreiselmeyer, G., Holzapfel, B., Gerhäuser, W., Hensel, B., Bouffard, S., Klaumünzer, S. and Saemann-Ischenko, G., "Heavy Ion Irradiation of High-Temperature-Superconductors: Material Modifications and Influence on Pinning Mechanisms," Conference contribution to SHIM 92, May 1992, Bensheim (Darmstadt), to be published in Rad. Eff. and Def. in Solids.
48) Civale, L., Marvick, A.D., Worthington, T.K., Kirk, M.A., Thompson, J.R., Krusin-Elbaum, L., Sun, Y., Clem, J.R. and Holtzberg,F., "Vortex Confinement by Columnar Defects in $YBa_2Cu_3O_7$ Crystals: Enhanced Pinning at High Fields and Temperatures," Phys. Rev. Lett. 67,648 (1991).
49) Bechtold, J., Jin, X.C., Xue, Y.Y., Rusakova, I.A., Hungerford, E.V., Feng, H., Hor, P.H. and Chu, C.W., "AC Permeability Measurements in 770 Mev $^{129}Xe^{17+}$and 560 MeV $^{16}O^{6+}$ Irradiated $YBa_2Cu_3O_7$," Preprint, Texas Center of Superconductivity, Univ. of Houston, Houston, TX 77204-5932.
50) Gerhäuser, W., Ries, G., Neumüller, H.W., Schmidt, W., Eibl, O., Saemann-Ischenko, G. and Klaumünzer, S., "Flux Line Pinning in Bi-2212 Crystals - Interplay of Intrinsic 2D Behaviour and Irradiation Induced Columnar Defects," Phys. Rev. Lett. 568, 879 (1992).
51) Weinstein, R., In-Gann Chen, Liu, J., Parks, D., Selvamanickam, V. and Salama, K., "Persistant magnetic fields trapped in high T_c superconductor," Appl. Phys. Lett. 56(15), 1475 (1990).
52) Weinstein, R. and In-Gann Chen, "Persistent Field: Techniques for Improvement and Applications," Preprint presented at TCSUH Workshop on "HTS Materials, Bulk Processing, and Bulk Applications," Houston Feb. 1992.
53) Weinstein, R., In-Gann Chen, and Liu, J., "Magnetic Replicas composed of high T_c Superconductors," Proc. of the Second Int. World Conf. on Superconductivity, Houston, 1991.
54) Pelzer, W., "The RF-system for the proposed VICKSI injector cyclotron," Contribution PC29 to this Conference, HMI Berlin GmbH, Glienicker Strasse 100, D-1000 Berlin 39, Germany.
55) Schempp, A., Inst. für Angewandte Physik der Universität Frankfurt, Robert-Mayer-Strasse 2-4, D-6000 Frankfurt/Main 11, private communication, Feb. (1992).

A CYCLOTRON AS A MASS SPECTROMETER

P. Bricault, G. Auger, M. Bajard, E. Baron, D. Bibet, A. Chabert, J. Fermé, L. Gaudart, J. Joubert, M. Lewitowicz, W. Mittig, E. Plagnol, C. Ricaud, Y. Schutz

Ganil, BP 5027, 14021 Caen, Cedex, France,

G. Audi

CSNSM, 91940 ORSAY, France

A. Gillibert

CEN Saclay, 91191 Gif sur Yvette, Cedex, France

K. Fifield

Australia National University, GPO box 4, Camberra act 2601,Australia

ABSTRACT

Taking advantage of the system of coupled cyclotrons at GANIL, we have developed a method for mass measurements with a cyclotron. The secondary nuclei are produced in a target located between the two separated sector cyclotrons by the interaction of a beam coming from the first cyclotron. They are subsequently accelerated in the second cyclotron. The prior tuning of this cyclotron for those very low intensity is accomplished using a beam having the same q/A ratio at the right velocity. For fine tuning, we have developed a probe inside one sector of the cyclotron. This new probe is described and first results will be presented.

1. INTRODUCTION

Mass measurements provide information on one of the most fundamental properties of the nuclide, its atomic mass. Number of techniques have been used for such measurements. Masses of radioactive nuclides are traditionally determined through reaction Q-value measurements, or through measurements of the energy released in α or β decays. Direct mass measurements of nuclides far from stability are available by coupling a high resolution spectrometer to a production facility for radioactive isotopes[1,2,3]. More recently mass measurements of radioactive nuclides have been done using recoil mass spectrometers, SPEG[4] at GANIL and TOFI[5] at LAMPF. Precision of 100-500 keV has been achieved. The cyclotron resonance mass spectrometer at CERN[6,7] has the potential of mass measurement of 1 keV level. We have developed at GANIL a new method for mass measurement using a cyclotron as mass spectrometer. The present paper describes the technique used for this measurement and gives some of the results obtained.

2. PRINCIPLE OF THE METHOD

GANIL consists of a system of three coupled cyclotrons (fig. 1). Highly stripped ions from the ECR ion source are accelerated by a compact cyclotron, k=30 (C0) before being injected in the first of two identical separated sector cyclotrons (CSS1 and CSS2). In normal operating mode, the accelerated ions emerging from CSS1 are stripped of electrons in a thin carbon foil before being injected into CSS2 for their final acceleration. If the stripper foil is replaced with a thicker target, then secondary ions produced in this target, rather than the ions of the primary beam, may be accelerated in CSS2.

2.1. Coupling relation between two cyclotrons

In the following the index 1 and 2 will refer to CSS1 and CSS2 respectively.

The fundamental relation for the cyclotron is,

$$B\,q = m\,\omega/h \qquad 1)$$

where B is the magnetic field, q the charge, m the mass of the ion, ω the radio frequency and h the radio frequency harmonic.

Since the two cyclotrons are operated at the same radio frequency, we obtain easily the relation governing the coupling between two cyclotrons,

$$\omega = \left(\frac{q_1}{m_1}\right) B_1 h_1 = \left(\frac{q_2}{m_2}\right) B_2 h_2 \qquad 2)$$

The velocity can also be expressed in term of the frequency ω and the mean radius of curvature, so we have the following relation,

$$\omega = \left(\frac{v_1}{\rho_1}\right) h_1 = \left(\frac{v_2}{\rho_2}\right) h_2 \qquad 3)$$

where v_1 and v_2 are the velocity at the ejection of CSS1 and at the injection of CSS2, ρ_1 and ρ_2 are the ejection and injection radius, h_1 and h_2 are the harmonic number of CSS1 and CSS2 respectively.

The ratio ρ_1/ρ_2 of the GANIL cyclotrons is 2.5 and since the velocity in normal use is the same between the ejection of CSS1 and the injection of CSS2 then the harmonic number ratio must be equal at 5/2. And since $h_1 = 5$, in normal operating mode, then h_2 must be equal 2.

Given that the production of secondary nuclei by nuclear reaction, between CSS1 and CSS2, will invariably be associated with a velocity loss, we must consider other solutions for which $v_2 < v_1$. The most favorable case is $h_2=3$, for which $v_2/v_1=2/3$. Other combination are of course possible as long as h_1 and h_2 are integer numbers.

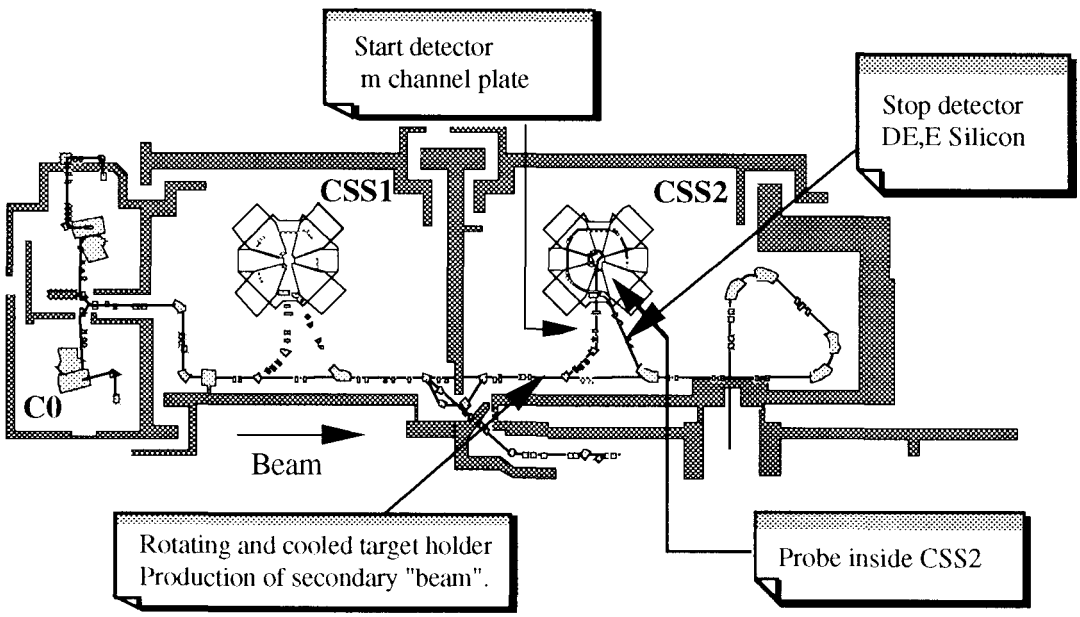


Fig. 1 Schematic view of the GANIL cyclotron facility. The principal component locations used for the mass measurements are indicated.

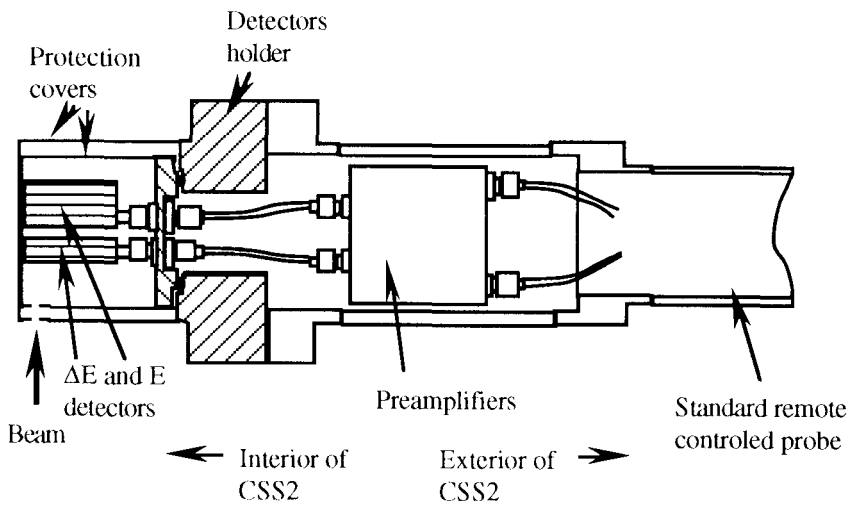


Fig. 2 Schematic of the probe installed in one sector of the CSS2.

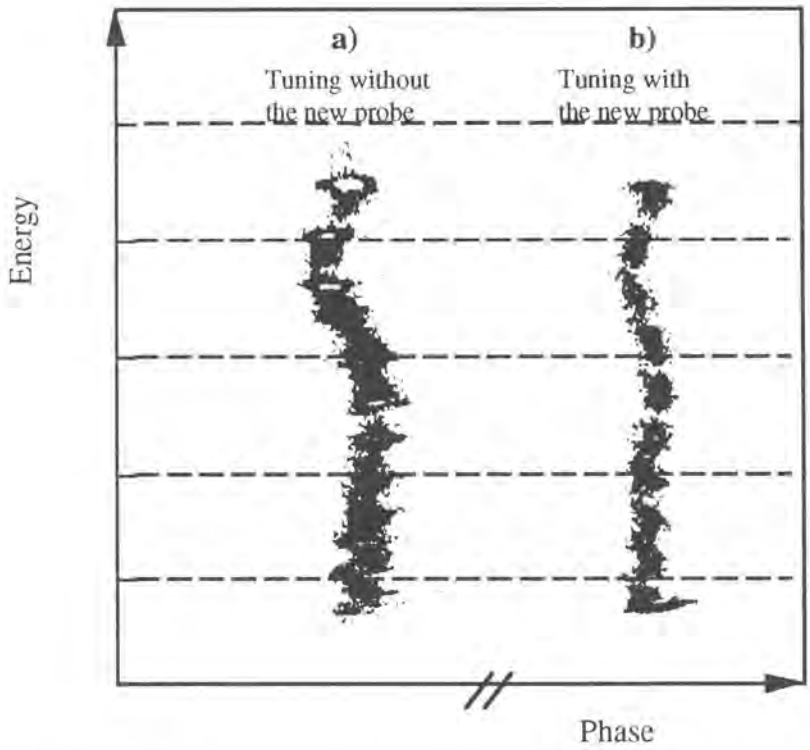


Fig. 3 Phase space diagram of the particles in the cyclotron. Fig. 3a shows the phase space obtained just after the prior tuning using a particle having the same A/q ratio as the nuclei of interest. Fig. 3b shows the final phase space using this detector for the fine tuning of the magnetic field.

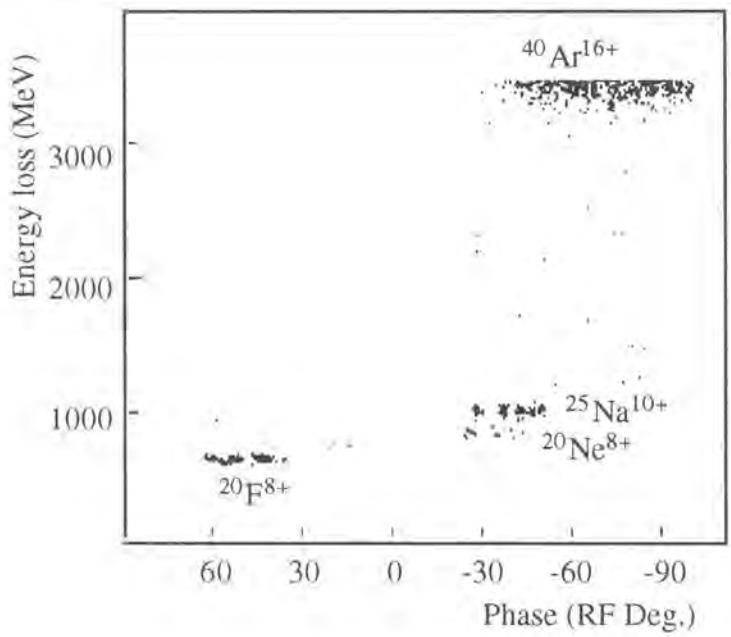


Fig. 4 Two-dimensional spectrum of data from the silicon showing both $^{40}Ar^{16+}$ ions and accelerated secondary ions produced between the two cyclotrons.

2.2. PRECISION OF THE METHOD

Consider two nuclei with slightly different masses, m and m+δm. During the acceleration process the heavier of the two will lag behind the other.

From the expression 1 we easily obtain

$$\frac{\Delta m}{m} = \frac{\Delta B}{B} - \frac{\Delta \phi}{\phi} . \qquad 4)$$

We can neglect the variation of the magnetic field during the time of measurement. Thus, we obtain the simple relation,

$$\frac{\Delta m}{m} = \frac{\Delta \phi}{\phi} . \qquad 5)$$

After N turns at harmonic h the total phase is

$$\phi_{total} = 360\ h\ N. \qquad 6)$$

Taking typical values of h = 3 and N = 250 we obtain,

$$\frac{\Delta m}{m} = \frac{\Delta \phi}{\phi_{total}} = 3.7\ 10^{-6}\ \Delta\phi . \qquad 7)$$

A timing resolution of 250 ps is readily attainable and corresponds to a resolution of 1.2° in the phase difference at ω = 13.MHz. Hence the mass resolution attainable is

$$\frac{\Delta m}{m} = 5\ 10^{-6} . \qquad 9)$$

3. TUNING THE CYCLOTRON

In the case of an arbitrary m_2/m_1 there is no simple general method for the prior tuning of CSS2. Since secondary beam intensity are very low compared to those of stable beams, standard diagnosis are not useable for the tuning. However, in the special case where a charge state of the incident beam leading to the same value of A/q exists, this charge state can be used to tune the magnetic field in the cyclotron using standard beam tuning diagnosis within the cyclotron.

But, often it is not possible to achieve the tuning as precisely as desired, because the mass difference between the tuning mass and the mass of interest is too large. So, it is useful to tune the magnetic field and the injection system using a tuning mass having the same magnetic rigidity.

For the fine tuning it is necessary to use an apparatus able to detect very low intensity, typically from 10 to 10000 pps. Also, this detector must give the following informations: total kinetic energy, atomic number and have a very good timing. A telescope composed of silicon detectors can fulfill these specifications. We have developed and installed such a detector in one magnetic sector of the cyclotron.

4 DESCRIPTION OF THE PROBE

Silicon telescope detectors have been mounted on the normal remote control probe inside one sector of the cyclotron. It can be moved along a radius in the median plane. Fig. 2 shows a schematic view of this probe, it is composed of a ΔE of 300 μm and a E detector of 3.6 mm tick.

Two shielding protect the silicon detectors from the rf and other perturbations. This has the effect that there is a dead zone where no particle are detected for a given radial position. The width of this dead zone is about 2 mm and has no importance since the radial dimension of a pulse in CSS2 is between 5 mm and 10 mm.

In a cyclotron the energy is a function of the radius, $E(r) = dE_0 N_t$, where dE_0 is the energy gain per turn and N_t is the number of turns. Fig 3. shows the difference in the phase space of the particles in the isochronous field obtained without this new probe and using it. Fig. 3a shows the phase space obtained just after the prior tuning using a particle having the same A/q ratio as the nucleus of interest. Fig. 3b shows the final phase space using this detector for the fine tuning of the magnetic field.

The precession effect of the beam in the cyclotron combined with the motion of the probe leads to discontinuous spectrum in energy. This effect can be observed in the phase space spectrum of the fig. 3. At given energy there is no count.

5. ESTIMATION OF MASSES

Despite the complexity of the spectra of the secondary ions, they are sufficiently similar from one species to the another that, using one as a calibration, it is possible to estimate the masses of the others. This is clearly visible in fig. 4. Assuming the mass of one nuclei as the reference we are able to derive the masses of the others.

6. REFERENCES.

1) C. Thibault et al., Phys. Rev. C12, 644 (1975).
2) M. Epherre et al., Phys. Rev. C19, 1504 (1979).
3) F. Kern et al., Proc. 5th Int. Conf. on Nuclei far from Stability, Rousseau Lake, Ontario,Canada 1987, AIP Conf. Proc.164, 22 (1988).
4) A. Gillibert et al., Phys. Lett. B192, 39 (1987).
5) D.J. Viera et al., Phys. Rev. Lett. 57, 3253 (1986).
6) F. Kern et al , Proc. 5th Int. Conf. on Nuclei far from Stability, Rousseau Lake, Ontario,Canada 1987, AIP Conf. Proc. 164, 22 (1988).
7) H.J. Kluge, "Ion Traps - Recent Applications and Developments" EMIS12, Sendai, Japan.

THE USE OF HEAVY ION CYCLOTRONS OF THE FLEROV LABORATORY OF NUCLEAR REACTIONS IN CONDENSED MATTER INVESTIGATIONS

R.Ts. Oganessian, A.Yu Didyk
Flerov Laboratory of Nuclear Reaction, Joint Institute of Nuclear Research, Head Post Office, P.O. Box 79, Moscow, 101000 Russia

ABSTRACT

The goal of the present work is the presentation of separate reseach directions in radiation physics of condensed media and the results obtained while carrying out these works at present at FLNR.

1. INTRODUCTION

With the development of accelerating technique and as a result the emergence of power radiation sources, one of the reseach directions besides the intensive growth of nuclear and atomic physics is radiation solid state physics (of condensed metter). This direction is rapidly grown in a member of leading centres of the developed contries.

The creation of heavy ion accelerators with high intensities of ion beam (F) and energies (E) exceeding $1MeV/a.m.u.$ essentially expands the leading investigations both for the development of general concepts of radiation damage physics and for the materials modification for the purpose of radiative-stimulated change of their properties and new technologies creation in semiconductor technique.

2. EXPERIMENTAL PROCEDURE AND RESULTS

2.1. IRRADIATION CONDITIONS

Samples irradiation of different materials is realized on U-400, U-200 and U-100 heavy ion accelerators FLNR both in vacuum and on ion beams extracted into the air or atmosphere of other gases (e.g.inert gases).

Irradiation temperature can be varied from the temperature of liquid nitrogen (T=77K) up to 1000°C depending on required irradiation conditions. Ion flux density (F) is varied from 10^2 up to 10^{12} ion $/cm^2$s. The irradiation is carried out by ions from He to Xe with energies from $1MeV/a.m.u.$ up to $10MeV/a.m.u.$

If it is necessary ion beam can move on the plane of irradiation along horizontal by 15 cm and along vertical by 5 cm towards both sides from ionowire axis that allows the uniformily of irradiated square $30 \times 10cm^2$ to be not worth than 5%. The studing of peculiarities of the point defects accumulation in samples irradiated by heavy ions is realized by different nuclear physical and other methods. Such methods are: electron scanning and transmission microscopy, x-ray structural analysis, methods of positron-electron annihilation (by positron lifetime and angular correlation of annihilation γ -quanta), methodics of measurements of samples electroresistance, methodics of determination of mechanical properties changes (methods of microhadness and measurement of yield point and other characteristics by means of tensile testing machines of the "INSTRON" type), methods of photo-, cathode- and ionolumenescence, methods by spectra of light absorption and etc.

2.2. INVESTIGATION OF RADIATION EFFECTS IN METALS AND ALLOYS

One of the most important effects by neutron irradiation in reactors resulted in their structural materials is swelling and radiation hardening. In the work[1] there was studied radiation copper swelling by irradiation of inert gas ions Xe and Cu ions with the energies of $1MeV/a.m.u.$. There were obtain dose and temperature dependensies of swelling value and shown that by ions Xe irradiation there is an anomalous temperature shift of swelling maximum in comparison with Cu ions irradiation which can be explained by different behaviour of implanted ion interaction with vacancy complexes.

The cycle of works on studying of radiation hardness of a number of pure metals (Al,V,Ni,Cu,Zr),[2-4,6] radiation annealing hardness of vanadium alloys series with Al, Fe, Nb, Ti, Y[5] and also stainless steel Cr18Ni10Ti and etc. In Fig.1 there is shown the change of Cr18Ni10Ti steel microhardness from fluence for three ions: B (13 MeV), Ne (27 MeV) and Ar (46 MeV)- curves 1,2 and 3 respectively (annealed samples with low dislocation density), and also B and Ar- curves 4,5 respectively (cold-deformed samples with high dislocation density).

As seen, in all cases one observes the saturation of radiation hardness with fluence. Saturation level value depends on mass of irradiating ion, it increases together with ion mass increasing. This is connected with the differencies in defect structure, produced by ions of different masses. The degree of hardness is higher for cold-

deformed samples in comparison with annealed ones.

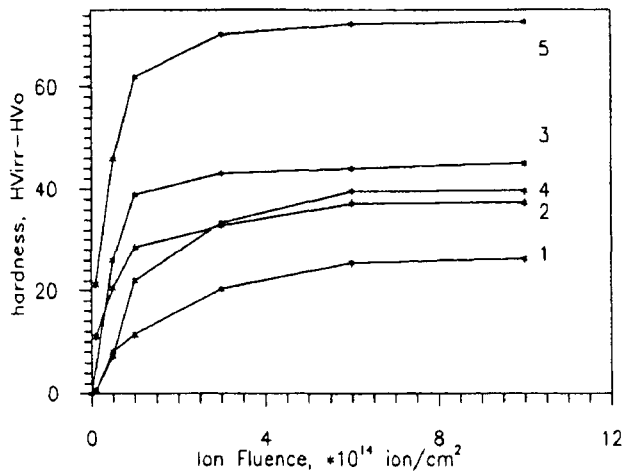


Fig. 1. Fig.1. The hardness of Cr18Ni10Ti stell versus ions fluence.

By anology of effects of radiation influence from neutron and heavy ion irradiation there was studied the effect of radiation annealing hardness of a number of vanadium alloys.

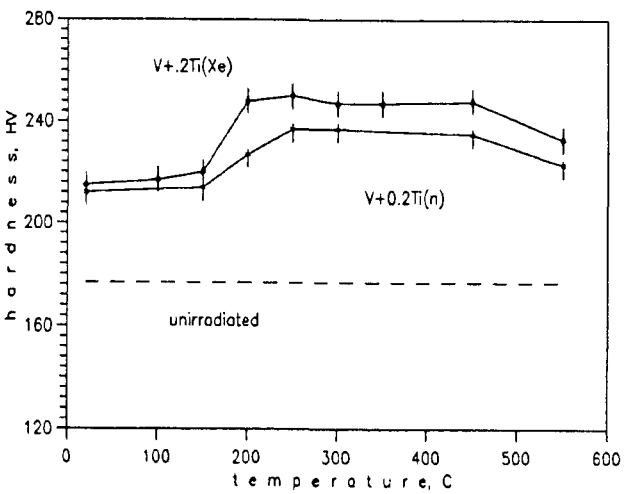


Fig.2. The change of V+0,2%Ti alloy microhardnes versus temperature of post-radiation annealing.

In Fig.2 the change of V+0,2%Ti alloy microhardness from temperature of post-radiation annealing is shown. The curve 1 is irradiation by Xe ions with the energy of 124 MeV ($D = 6,5 \times 10^{-3} dpa$), curve 2 - irradiation by fast neutrons ($D = 9 \times 10^{-4} dpa$). It is seen, that maximum radiation annealing hardness takes place at temperature $200°C$, and the behaviour of annealing curve change for ions and neutrons is similar qualitatively. This fast allows to draw a conclusion about the legitimacy of effects simulation of radiation annealing hardness from neutrons by heavy ions.

2.3. PROJECTIVE RANGE OF HIGH ENERGETIC HEAVY IONS ($1-6 MeV/a.m.u.$) IN SEMICONDUCTOR AND DIELECTRIC MARERIALS

Space positions of radiation damage's maximumes resulting from implantations of high energetic ($1 - 6 MeV/a.m.u.$) B, O, Ne, Ar, Kr, Xe, Pb ions into practically used semi conductors were measured with an optical and scanning microscopy techniques. The monocrystals of Si, Ge, GaAs and a model ionic crystal of LiF were used as targets. The experimental data were compared with the same values and projected ranges, calculated with the TRIM-89[7] and E-DEP-1[8] computer programs. High energy ion implantation is mainly used in the case, when the inelastic stopping power determines ion's losses of energy. The adequacy of the description by modern theoretical models of ionization energy's losses in a wide band of energies and atomic numbers was investigated. The ratios of experimental to theoretical ranges is represented in Fig.3 and shown the goodness of the theory for velocities of ions exceeding $v_o Z_1^{2/3}$, where v_o is the Bohr velocity and Z_1 is the ion's atomic number (that is for Bethe-Bloch theory case).

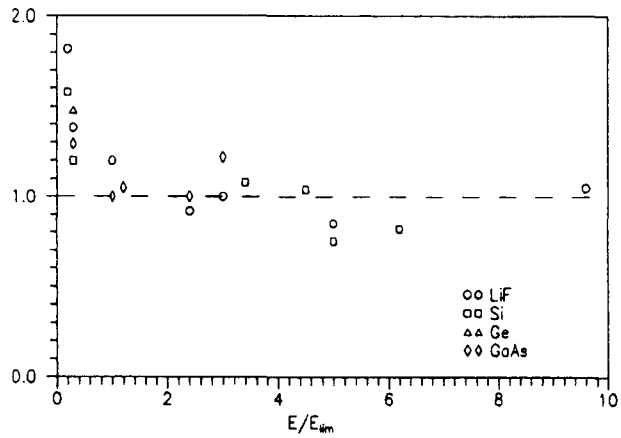


Fig.3.Comparison of experimental and theoretically calculated range's values of ions in different targets (□ - Si, △- Ge, ◇- GaAs, ○- LiF). $\delta = R^{exp}/R_c$ and $E_{lim} = A_2 v_o^2 Z_1^{4/3}$

It was shown, that at the same time the TRIM program gave an essential discrepancy with the experiment, especially for big atomic numbers, when ion's velocity below or equal to that parameter.

2.4. RADIATION EFFECTS IN SEMICONDUCTOR AND DIELECTRIC SINGLE CRYSTALS

The high energy ion implantation into the semiconductor materials, with high energies at $(dE/dx)_{inel}$. $(dE/dx)_{el}$ has a member of essential poculiarities in comparison with low-energy one. In connection with high

specific ion losses the local region heating-up near projective ion range - "ion track" takes place that causes the enhancement of point defects-i.e. intersticials and vacancies and moreover recrystallization of destruction region even in such high-melting monocrystal as diamond.[9)]

The investigations on production of defects in monocrystals Si, GaAs and a member of others were carried out by the methods of infrared absorption, x-ray structural analyses, secondary masses of ion spectroscopy, measurement of electroresistance etc. In Fig.3 there is the dependence of point defects concentration irradiated by the ions of Ar with the energy of 46 MeV up to fluence $Ft = 7 \times 10^{14} cm^{-2}$ of Si sample on the depth by ions range. The curve is obtained by using the x-ray analysis (from data of measurement of lattice parameters. The curve 1- experiment, and curve 2- the calculated dependence by means of the TRIM-89 program.

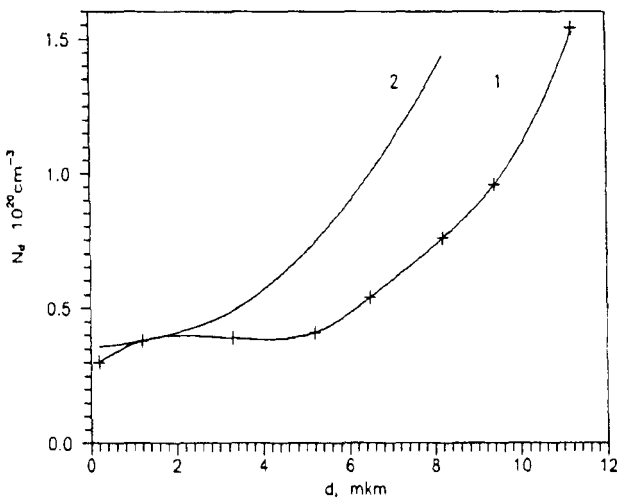


Fig.4. Profile of distribution of defects concentration (1- experimental, 2- calculated) from the depth in monocrystal Si irradiated by the Ar ions.

It is seen that the calculated profile is essentially differs from the measured one, it denotes that while accumulation of point defects there simultaneously occur the intensive processes of their munual annihilation at the same time the more is the contribution of these processes the more is the concentration of point defects.

In Fig.5 the dependencies of the relative reflection coefficient of the light with wavelength $\lambda = 650nm$ - $k = \Delta R/R\%$ for Si irradiated by B (E=14 MeV, $Ft = 8 \times 10^{14}\ cm^{-2}$)- curve 1 and by the Ar (E=46 MeV, $Ft = 8 \times 10^{14} cm^{-2}$)- curve 2 are presented.

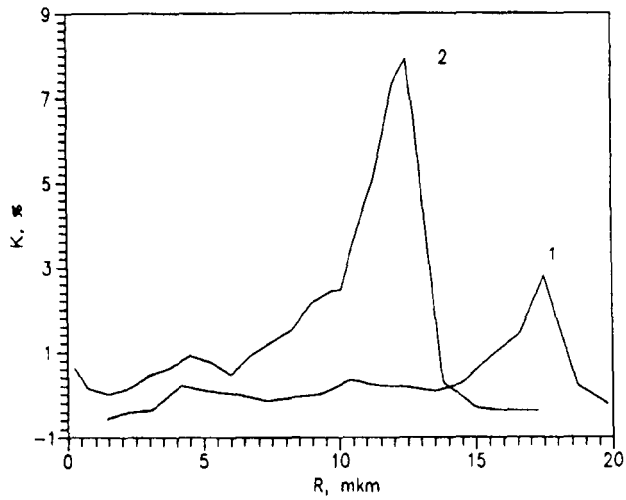


Fig.5. The distribution of the relative change of reflection coefficient k of Si samples by the ion range (curve 1- B and curve 2- Ar).

One can see that in regions from 15μ to 20μ and from 6μ up to 14μ there are peaks with maxima at $R = 17.5\mu$ and $R = 12.5\mu$. These peaks are caused by the elastic losses of the ions energy of B and Ar and are connected with partial amorphization of these regions that leds to the change of reflection coefficient. It is shown that the amorphization degree for the Ar ions is essentially higher with a less fluence than for B. This is connected with differencies in production defect cross-section.

For the investigation of the role of elastic and inelastic energy losses the structural and mechanical properties of the model ionic crystal LiF, irradiated with ions Xe (118 MeV), Ar (225 MeV and 46 MeV), Ne (113 MeV) and Ne (27 Mev) at 10^{10}- $10^{14} cm^{-2}$ dose range were stidied by using spectrophotometric and microhardness technique.[10)] The comparison of the total number of anion vacancies from absorption spectra by using the Smakula equation with the data obtained from the E-DEP1 program, it was shown that the total number of anion vacancies is determined generally by the total ionization energy losses of heavy ions. The observed differences in dose dependences of point defect concentrations for Xe, Ar, Ne beginning after a certain dose may be explained as a result of the ion track overlapping. It's increases the annealling of point defects in track's region taking into account the high value of electronic stopping power for heavy ions with $1 MeV/a.m.u.$ energy.

The change of mechanical properties of LiF crystals as shown is determined by the radiation damages caused by the elastic collisions of bombarded ions with the lattice atoms.

2.5. THE LUMINESCENCE OF CRYSTALS IRRADIATED WITH $1 MeV/a.m.u.$ HEAVY IONS

In distinction from the traditional methods of luminescence the high energy ion beams induced luminescence can allow to study the structure of materials during the formation and further evolution of radiation damages. In this case the radiation damages are created by elastic losses $(dE/dx)_{el}$ and the excitation of the luminescence centres - by electronic losses of ion energy $(dE/dx)_{inel}$.[11] The luminescence spectra of an unalloyed LiF single crystal during Ar (46 MeV) bombardment at various fluence are shown in Fig.6.

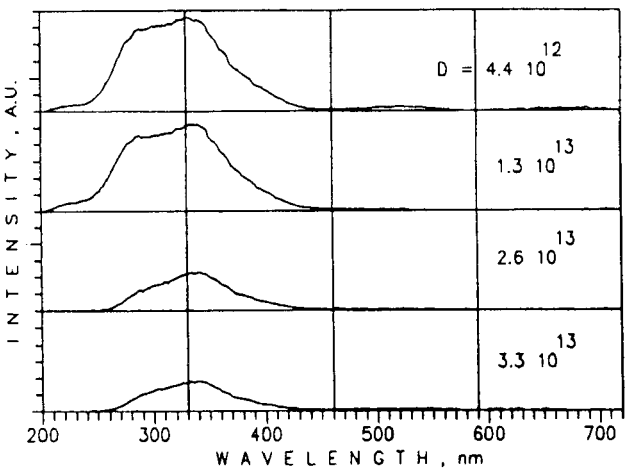


Fig.6.The intensity/wave length dependence of LiF luminescence during Ar bombardment.

In this spectra a series of width bands are seen. The intensity of this bands strongly depends from ion fluence and decrease to phone values for a long-wave band ($\lambda_{max} = 670nm$), which occurs by the F2-centres. This band isn't observed in ealier investigations by using low energy ions excitation. Luminescence yield in the bands with $\lambda_{max} = 335$ and 515 nm is a result of a recombination of V_k and V_F centres with free electrons and electron F-centres arising during ion bombardment. Also, the difference in temperature dependences of luminescence intensity between low and high energy ion bombardment is observed.

2.6. THE RADIATION STABILITY OF SEMICONDUCTOR DEVICES

The electron devices being a long period of time in the field of ionizing radiations are subjected to significant radiation loads leading to their breakdown or impossibility of realization of their functional tasks. This concerns both devices acting in reactors and semiconductor devices operating in cosmic space.

Application of heavy ion accelerators for spectra simulating of cosmic radiation, influence of neutrons and other types of radiation seems to be a promissing one.

The ion beams of the most different energies and masses provide wide possibilities to carry out such investigations. In this paper we consider one of the examples of such works, notably, the investigation of errors accumulation of time and energy dependences of the microcircuit memory cells of operative memory while irradiation by the ions B, O and Ne with the energy of $1 MeV/a.m.u.$.[12] To decrease the density of ion flux there was applied a scattering chamber, in which the ions were being scattered on thin gold foil and reached the integral microcircuit and semiconductor detecter positioned at angles of 30° to the beam axis. In Fig.7 there is the dependence of errors member on time while irradiation of memory cell, by capacity 4098, ions O and Ne with the energies of 19 MeV and 27 MeV, respectively. The transition of memory cell from state "1" into state "0" is considered as an error.

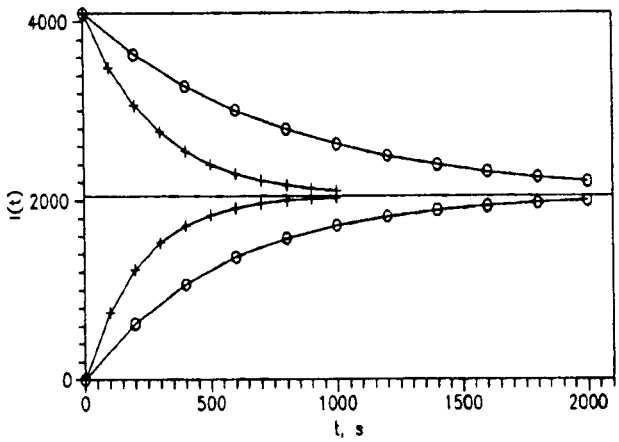


Fig.7. The errors member versus time for null and unit back ground state of memory cells for O (+) and Ne (o).

As seen, the effect manifestation has a nature close to exponential one and is approximated by the following expressions: $L(t) = A(1 \pm exp(-FSt))$, where sign "-" relates to the null background state and sign "+" - to unit one, A= 2048, S- effective square of memory cell, and F- density of ion flux.

2.7. RADIATION RESEARCHES OF POLYMERIC MATERIALS. TRACK MEMBRANES

By creation of detectors of heavy charged particles (fragments of nuclei fission) in which tracks manifested themselves by the following chemical etching there has been appeared a new direction namely the production of track membranes from different polymers with the use both the products of uranium nuclei fission (reactor method of membrane production) and on heavy ion accelerators.[13] The main advantage of this method is the energy homogeneity of ion beams that provides a possibility to have relatively low dispersion by pore diameters

of track membranes ($\gamma = \Delta d/d$) and a wide choice of ions of different energies for polymeric materials irradiation from 10μ to 100μ of thickness.

In FLNR for irradiation of polymeric materials there are used heavy ions beams Kr with energies up to 300 MeV and in prospect (by putting the accelerator complex U-400+U-400M in operation) up to U.

The applications for track membranes production from chemically and radiative stable ion polymers with high specific ionizing energy losses (by performing the conditions of $(dE/dx)_{inel} \geq (dE/dx)_{lim}$ - registration threshold of the given particle in polymer) allow one to produce, first, pores with small sizes ($d < 0.1\mu$) and, secondly, with a low value of dispersion of pore diameters ($\gamma < 0.05$).

2.8. CONCLUSION

In the given review there are presented only partial directions of investigations on heavy ion beams with the energies exceeding 1 MeV/a.m.u. At the same time it is seen that "professions" of heavy ions are enough extended and regions of their application are various.

On the whole it is worth to mention that heavy ion accelerators are a good instrument in the investigations of condensed metter and radiation solid state physics.

3. REFERENCES

1) S.P.Vagin, A.Yu.Didyk, V.F.Reutov, V.A.Skuratov. "Pe- culiarity of Copper Radiation Swelling Irradiated by Xenon and Copper Ions with Energy 1 MeV/a.m.u. "Preprint JINR R14-88-440, 1988, Dubna.
2) A.Yu.Didyk, V.R.Regel, V.A.Skuratov, N.Yu.Mikhailova. "Radiation hardening of metals irradiated with heavy ions". Journal of Technical Phys., 1989, **59**, N5, p.107-111.
3) A.Bermudes, A.Yu.Didyk, V.N.Chernikov, V.A.Skuratov. "New cross-section method for investigation of heavy ion irradiation effects." In.: Abstracts of International Conference on Physics of Irradiation Effects in Metals, Hungary, 1991, p.W-12.
4) L.I.Gomozov, A.Yu.Didyk, T.N.Zvereva, I.L.Sashin, V.A.Skuratov. "Radiative-annealing hardening of vanadium. Phys. Metals and Metallovedenie", 1990, N7, p.160-168.
5) L.I.Gomozov, S.N.Votinov, A.Yu.Didyk et al. "Heavy Ion and Neutron Irradiation Effects on Vanadium Alloy Behaviour at post Radiative Annealing." Preprint JINR 14-86-409, 1986, Dubna.
6) A.Bermudes, A.Yu.Didyk, V.A.Skuratov. "Structure and Mechanical Properties of Metals Irradiated with $1 - 1.2 MeV/a.m.u.$" In.: Abstracts of International Conference on Physics of Irradiation Effects in Metals, Hungary, 1991, p.W-3.
7) J.F.Ziegler, J.P.Biersack, U.Littmark. "The stopping power, and range of the ions in solids", **1**, Pergamon Press, New, Jork, 1984.
8) C.M.Davisson and I.Manning. Adaptation of the program for, depth distribution of energy deposition by ion bombardment:, better stopping powers.- Comp.Phys.Comm., 1986, **42**, p.137-147.
9) A.Yu.Didyk,A.M.Zaitsev,S.A.Karamian. "Shift Ar^{40} and Xe^{129} on the Diamond Monocrystal". JINR Rapid Comm., N 4/37/-1989.
10) A.Yu.Didyk, R.Ts.Oganessian, V.R.Regel, V.A.Skuratov. "Influence of nuclear and ionization energy losses on damage production in crystals". Phys.Tverd.Tela, 1989, **31**, p.17-21.
11) D.V.Akinshin, A.Yu.Didyk, V.A.Skuratov. "The luminescence of crystals irradiated by 1 MeV/a.m.u. heavy ions". JINR Rapid Communication, 4/43/-90, 1990,p.48-55.
12) D.V.Akinshin, M.N.Borisova, N.G.Goleminov et al. "Use of MOS RAM for control of heavy ions flux". Device and technique of experiments, 1990, N 6, p.49-50.
13) G.N.Flerov, P.Yu.Apel, A.Yu.Didyk et al. "The use of heavy ion accelerators for the production of nuclear track membranes," Atomic energy, 1989, **67**, p.274-280.

^{178m2}Hf AND ^{237}Pu ISOTOPES PRODUCTION ON THE U-200 CYCLOTRON

S.L.Bogomolov, Yu.P.Gangrski, G.G.Gulbekian,
S.N.Dmitriev, S.A.Karamian, V.B.Kutner, B.N.Markov,
Yu.Ts.Oganessian, N.V.Pronin, G.Ya.Starodub
Flerov Laboratory of Nuclear Reactions
Joint Institute for Nuclear Research
101000, Moscow, Head Post Office, P.O. Box 79, Russia

ABSTRACT

The results of producing a high current He ion beam on the U-200 cyclotron for isotope production are presented. The paper presents also the results of experiments on the production of the ^{178m2}Hf isotope in the reaction ^{176}Yb(^{4}He,2n) and of the ^{237}Pu isotope in the reaction ^{235}U(^{4}He,2n). The target assembly is described.

1. U-200 CYCLOTRON

The two meter cyclotron U-200[1)] is a sector focussing machine with four straight sectors for acceleration of heavy ions with the charge to mass ratio within the range $0.14 \leq q/A \leq 0.36$. The maximal energy is determined by K = 145.

The ions with $q/A \leq 0.263$ are extracted from the cyclotron by a stripping carbon foil, installed at the boundary valley - hill[2)]. After stripping the ion motion becomes radially unstable due to the difference of the magnetic fields in the valley and on the hill, and ions are extracted from the vacuum chamber. Depending on the ratio of ion charges before and after stripping and on the position of the stripping foil ions can be extracted from the vacuum chamber on making one, two or more turns in the magnetic field.

At the U-200 cyclotron the one turn extraction of ions with the charge increased by the factor of two is used. A mechanical assembly for moving the stripping foil in the radial and azimuthal directions allows to regulate the energy of the extracted beam within 35% below the maximum. The extracted beam has the horizontal emittance of 30π mm·mrad, the vertical - 10π mm·mrad, the energy spread ~1%.

Last years the mode of long time operation with an intense ($\geq$100 eμA, 36 MeV) He ion beam was investigated for the production of isotopes for fundamental and applied research.

For the production of the He^{1+} ion beam the gas discharge ion source with a directly heated cathode was used[3)]. The head of the source and the diagram of the power supply circuit are shown in Fig.1 and Fig.2.

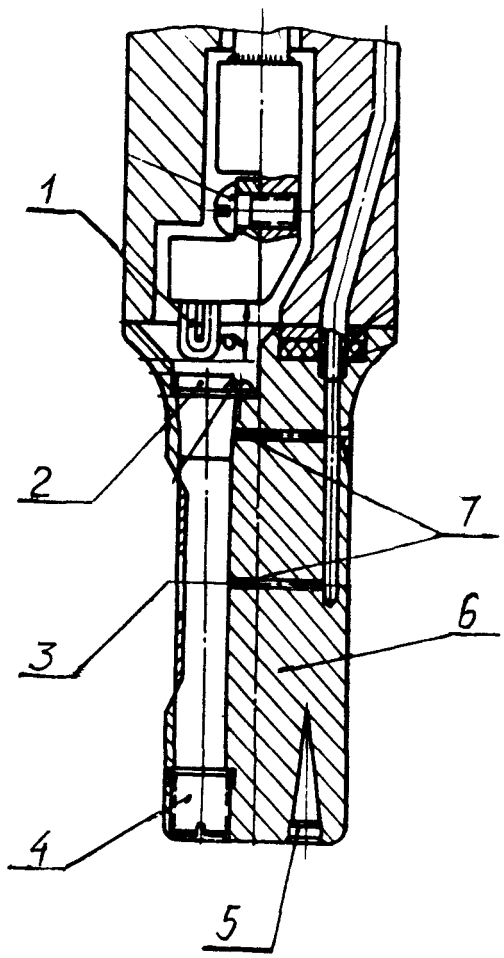


Fig. 1. The head of the ion source:
1-cathode, 2-diaphragm, 3-emission slit,
4-anticathode, 5-cooling, 6-chamber body
(anode), 7-gas inlet.

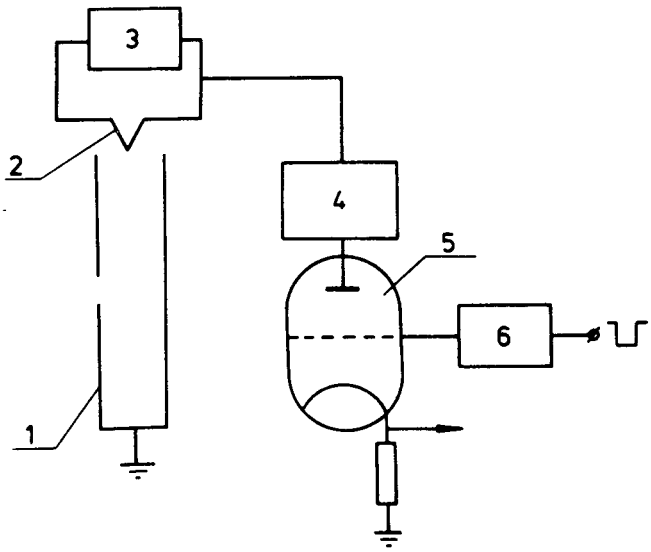


Fig. 2. The power supply circuit of the ion source: 1-discharge chamber (anode), 2-cathode, 3-cathode power supply, 4-discharge power supply, 5-modulating valve, 6-amplifier.

It was necessary to find the optimal from the point of view of source service life and the beam intensity mode of the source operation because the ion source head is activated due to vacuum losses of accelerated ions. The estimations show that at the operating pressure of $\sim 10^{-5}$ Torr the level of vacuum losses is about 50%.

The ion source operated in the pulsed mode with the repetition rate of 150 Hz and the pulse length of 2–3 ms. For the production of 100 eμA of He ions at the physical target one needs the following mode of operation: the discharge current of 2.5–3 A, the disharge voltage of ~200 V, the consumption of He ~2 cm^3/min.

The ion source service life is mainly determined by the sputtering rate of the directly heated cathode. Different cathodes were investigated. Except for the sputtering the cathode is affected by the Lorentz force in the sections where the direction of the current is perpendicular to the direction of the cyclotron magnetic field. The cathodes, prepared from the Ta and W rods with the diameters within the range 2–4 mm were tested. For heating the Ta cathode to the temperature of thermo-emission one needs a lower current that allows to use a larger diameter of the rod, but the service life of Ta cathodes never exceeds 10 hours with the subsequent break-up of the cathode. It seems that it is caused by the loss of the mechanical strength of Ta at the temperatures of termo-emission.

The most optimal one is a W cathode with 2.5 mm diameter. For the ignition of the discharge the heating current 280–290 A is necessary, which should be reduced during the operation of the source because the cathode diameter is decreased due to sputtering. It means that the source service life depends also from the skill of the operator. The average service life of the ion source is about 16 hours, the best result for the time being is 40 hours.

The other systems of the cyclotron showed stable operation during the acceleration of a high current beam.

Since the level of neutron radiation was relatively high the cyclotron operated in the high current mode only in the evening and at night. Figure 3 represents the record of target current during one of the such periods of irradiation for production ^{178m2}Hf isotope (see section 2).

The experience shows that the cyclotron can provide an integral number of He ions of about $\sim 10^{20}$ per month.

Now we are studying the possibilities to improve the vacuum inside the cyclotron and to develop an ion source with an increased service life.

2. LONG LIVED ^{178m2}HF ISOTOPE PRODUCTION

The ^{178m2}Hf isomer has unique properties due to its high spin $I^\pi = 16^+$, relatively low excitation energy $E^* = 2.447$ MeV and half-life $T_{1/2} = 31$ years.

At first the long-lived ^{178m2}Hf isomer was produced the in reaction of thermal neutron radiation capture with a very low yield[4]. The isomeric ratio for this reaction is $5 \cdot 10^{-10}$. The total amount of ^{178m2}Hf $\sim 10^{15}$ nuclei could provide a possibility to measure with a high accuracy the magnetic dipole and the electric quadrupole moments of the isomer, to define the changes of the rms radius of nuclei in the ground and isomeric states by the methods of nuclear orientation and laser spectroscopy. The use of this isomer as a target provides a possibility to define the influence of the isomeric state spin value in the reactions of sythesis and fission, to perform experiments on the Coulomb excitation of ^{178m2}Hf with mass-separation of ^{178}Hf isotopes[5,6].

For the optimal choice of the reaction for the accumulation of a microweight quantity of ^{178m2}Hf the experiments on light and heavy ion interactions with different targets were performed at FLNR, JINR. It turned that the optimal reaction is a ^{176}Yb(^{4}He,2n). The isomeric ratio for this reaction equals 0.05.

During the 1990–1991 the irradiations of enriched ^{176}Yb target (96% enrichment) by the He beam with the energy of 36 MeV and intensity of more than 100 eμA were fulfilled at the U-200 cyclotron. An inclined ($\sin\alpha$=0.2–0.3) water-cooled target was used. The target is situated in a closed metal collector with the entrance hole of 30 mm diameter for the ion beam. The cover of the collector is made of aluminum. Before the entrance of the collector a copper diaphragm for the limitation of the beam size is situated. The target material (Yb_2O_3 powder) was pressed on the 3 mm thickness aluminum substrate. The effective thickness of the target equals 80 mg/cm^2.

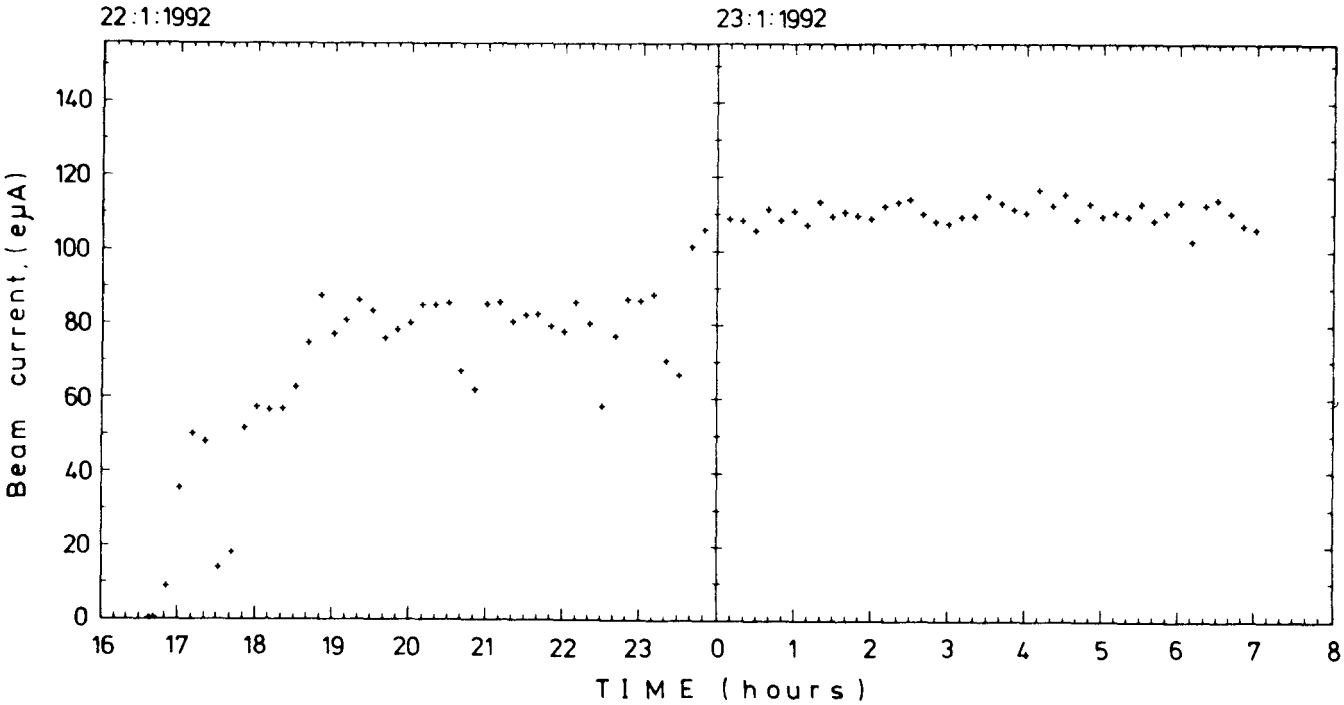


Fig. 3 The record of a target current during irradiation.

During the first series of irradiations of the enriched ^{176}Yb target, about $3 \cdot 10^{14}$ atoms of ^{178m2}Hf were accumulated. The identifications of Hf isotopes and the control of their yield were performed by measuring γ-spectrums with a Ge(Li) detector. The method of chemical isolation of Hf from the irradiated target material is described in reference[6].

The target prepared from the super enriched (99.998%) ^{176}Yb was also irradiated. Such super enrichment was fulfilled at PARIS[6] mass-separator in CSNSM (Orsay) for the reduction of the admixture of Hf isomer yield. About $3 \cdot 10^{14}$ atoms of ^{178m2}Hf were accumulated with a sharp decrease of other Hf isomer yields.

The experience of such irradiations and the results of ^{178m2}Hf isotope yield measurements show, that with a steady operation of the U-200 cyclotron one can expect the yield of 10^{15} atoms of ^{178m2}Hf in a month of irradiation with a current $\geq$100 eμA.

3. PRODUCTION OF THE ^{237}Pu ISOTOPE

Due to its nuclear-physical properties (T=45.2 days, EC=99.99%) ^{237}Pu is the only plutonium isotope which is sutable, according to modern medical concepts, for studying the plutonium metabolism *in vivo*. The content of neughboring isotopes of ^{236}Pu and ^{238}Pu which are the α-emitters in such a sample should not exceed 10^{-7} Bq/Bq.

The most suitable reaction for the production of ^{237}Pu is the ^{235}U(^{4}He,2n) reaction[7]. But it is practically impossible to provide the necessary purity of the sample produced in such a reaction due to covering the excitation function of the reactions ^{235}U(^{4}He,n) and ^{235}U(^{4}He,3n). Therefore it was suggested to make an additional purification of the produced sample of ^{237}Pu at an electromagnetic mass-separator.

The highly enriched (99.99%) ^{235}U isotope was used as the target material. The irradiations were fulfilled at the internal beam of the U-200 cyclotron in the energy range from 22 up to 26 MeV. The yield of ^{237}Pu isotope in this energy range is 0.2 kBq$\cdot\mu$A$^{-1}\cdot$h$^{-1}\cdot$mg^{-1} and the relative content of plutonium isotopes ^{236}Pu/^{237}Pu/^{238}Pu=$2.2 \cdot 10^{-4}/1/1.5 \cdot 10^{-4}$.

On the basis of this results the experiments on the production of the ^{237}Pu sample sufficient for the mass separation and subsequent use in a metabolism study were fulfilled. The target with the thickness of 10 mg/cm^{-2} was irradiated by He ions with the energy of 25 MeV during 20 hours. The activity of the ^{237}Pu sample after radiochemical isolation and purification from the substrate material and products of nuclear reactions is 1.5 MBq. The relative content of the plutonium isotopes ^{236}Pu/^{237}Pu/^{238}Pu=$1.6 \cdot 10^{-4}/1/1.5 \cdot 10^{-4}$.

Such a sample was purified at the mass separator YaSNAPP-2 of the Laboratory of Nuclear Problems, JINR. The yield of ^{237}Pu after separation is about 40%. The relative activity of plutonium isotopes after separation is ^{236}Pu/^{237}Pu/^{238}Pu=$2 \cdot 10^{-7}/1/\leq 3 \cdot 10^{-7}$ Bq/Bq.

The prepared sample is radiochemically and isotopically ultrapure and is practically safe for use in the research of plutonium metabolism *in vivo*.

4. REFERENCES

1) Gikal B.N. et al. "The experience of Operating and Improving the U-200 Cyclotron" JINR Communication 9-83-311, Dubna, 1983.(in Russian)
2) Oganessian Yu.Ts. et al. "Extraction of Heavy Ions from Sector Focussing Cyclotron by the Recharge Method" JINR Preprint 9-11993, Dubna, 1978. (in Russian)
3) Tauth Th. et al. "The Light Ion Source for the U-200 Cyclotron" JINR Communication 9-4368, Dubna, 1969. (in Russian)
4) Helmer R.G. and Reich C.W. "Half-life of ^{178m2}Hf and its Neutron Capture Production" Nucl.Phys. **A211**,1 (1973)
5) Oganessian Yu.Ts. "Possibilities of Production and Investigation of Long-Lived Isomer^{178m2}Hf" in **Proceedings of the Workshop on Application of Lasers in Atomic Nuclei Research** (JINR D15-91-410, Dubna, 1991) pp.55–59.
6) Oganessian Yu.Ts. et al. "Production, Chemical and Isotopic Separation of the Long-lived isomer ^{178m2}Hf ($T_{1/2}$ = 31 years)" J.Phys. G: Nucl.Part. Phys. **18**, 393 (1992).
7) Pelevin L.A. et al. "Production of Isotopically Pure ^{237}Pu and its Application for Study of Processes of Plutonium Isolation from Environmental Samples" Radiokhimia **6**, 806, (1988). (in Russian)

RADIONUCLIDE TECHNIQUE IN MECHANICAL ENGINEERING (RTM)

P.Fehsenfeld, A.Kleinrahm, V. Novikov *)
Kernforschungszentrum Karlsruhe GmbH, Hauptabteilung Zyklotron
Postfach 3640, D-7500 Karlsruhe, Germany

Abstract

New developments at KfK Cyclotron in the field of the thin-layer activation technique for modern engineering materials, the various measurement methods and the wear measurement device will be presented. A sophisticated method for the radioactive surface labelling of modern synthetic materials such as plastics, polymers and rubber has been established in a fruitful cooperation with the Kurchatov Institute, Moscow. First results of the application of this technique to measurements of machine parts will be reported. The outstanding properties of the RTM on-line wear diagnostics shall be demonstrated by the results of dedicated measurements performed last time at the KfK facilities.

1. INTRODUCTION

A subject of increasing application of cyclotron machines is RTM, the measuring system that enables wear and corrosion diagnostics of components of operating machines, apparatus or processing plants. The three components of the system, the thin layer activation at the cyclotron, the measuring methods and the measuring instruments for application in industry have already been presented in detail on the last International Conference on Cyclotrons [1]. So this contribution deals with recent development work in RTM at the Cyclotron Laboratory of KfK. [2)-5)]

2. DEVELOPMENT WORK

Beside the work in activation service, supplying irradiated parts to the industry and the efforts in know how transfer within the frame of cooperation contracts, nearly 40% of the total man power of the RTM-Group is engaged in development work to the subjects activation technique, irradiation equipment, measurement methods and device to new areas of application, new components and new materials coming into use in industry. All developments are performed in cooperation with a representative industrial company to ensure that the actual requirements of the industry are fulfilled and the results of the developments can be used directly and profitably by the industry. A typical example of development work is the running project for the contruction of a test bench for refrigerating machines, based on RTM. Such test benches are required by industry for the urgent development of advanced refrigerators, free of Chloro-Fluoro-Carbons (C-F-C), because of the well - known environmental impact of C-F-C.

This project is performed in a cooperation with the industrial manufacturer of refrigerating machines, dkk-Scharfenstein, and a working group of the Institute For Surface Modification, Leipzig, specialized on wear problems of compressors.A prototype of a suitable test bench has been established. The optimizing work on this is going on.

Since the successful development of thin layer activation technique for the application to ceramic materials [1)] we concentrated on the radioactive labelling of synthetic materials, all kinds of polymers, elastomers, rubber. The interest in this is mainly coming from the car, engine and gearing manufacturer. The replacement of iron parts by parts of synthetic materials in mechanical systems is reducing the weight of such devices at least by a factor three.

All irradiation tests using the conventional thin layer activation method via nuclear reaction in the synthetic materials failed because of the high sensitivity of these materials to the applied particle irradiation at the KfK-Cyclotron. So, in cooperation with the Kurchatov Institute, Moscow, a project for the development of surface labelling by directed implantation of radioactive ions of Be-7 ($T_{1/2}$ = 53 d, $E\gamma$ = 478 keV) has been started. This method of labelling promises by a factor of 10^5 less radiation effects in the sensitive material, compared to the conventional activation method. The principle of Be-7 recoil implantation, based on the nuclear reaction B -10 (p,α) Be-7, is well known and is illustrated in Fig. 1. The external beam of B-10 ions (6 - 10 MeV/nucleon) from the cyclotron is producing in the hydrogen converter Be-7 ions with a recoil energy in direction of the primary beam. The absorber behind

*)Kurchatov Institute, Moscow

the converter is stopping the B-10 ions of the primary beam, which passed the converter without any reaction. The pure Be-7 beam is hiting the machine part to be labelled.

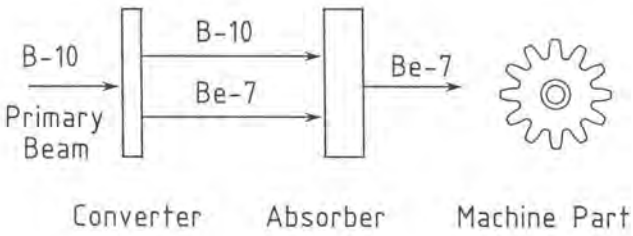


Fig. 1: The principle of Be-7 recoil implantation for the radioactive surface labelling of synthetic materials. The external beam of B-10 ions from the cyclotron is producing Be-7 ions, according to the reaction B-10(p,α) Be-7, with a recoil energy of the Be-7 ions in primary beam direction.The absorber is stopping the B-10 ions which passed the converter without any reaction.The pure Be-7 beam is hiting the machine part to be labelled.

After some improvements of the converter-absorber system the material investigations of Be-7 implanted samples of Polyamid, Elastomer (Viton) and synthetic rubber did not show any defects from the radioactive labelling. The material tests have been performed by KfK as well as by a private material test institute [6] specialized on synthetic materials.

The quality of the Be-7 labelling is demonstrated in Fig. 2 by the activity versus depth profile in special Polyamid (EPM),. The linear region of the total activity over the depth of 20 µm near the surface is suitable for precise wear measurements.

In cooperation with the company Audi A.G.and the material test institute Firma Heß, Ingolstadt [6] in situ wear measurements of engine parts, of a Polyamid gear and of a Viton crankshaft seal have been performed on an engine test bench, Fig.3. The results of the demonstration measurements are illustrated by Fig. 4 and Fig. 5.

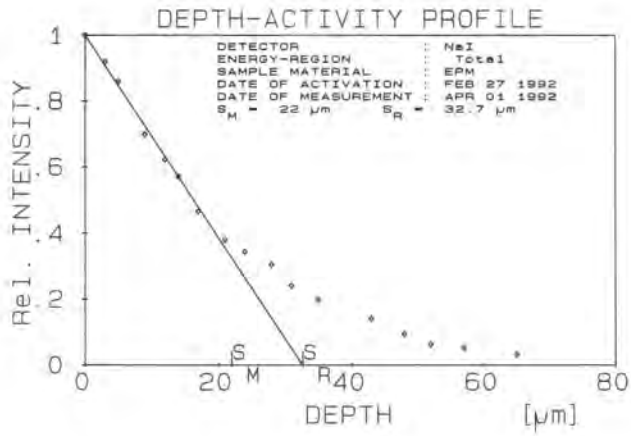


Fig. 2: The activity over depth distribution of implanted Be-7 in EPM-Polyamid is demonstrating the quality of the radioactive labelling by the linear region of 20 µm near the surface suitable for wear measurements.



Fig. 3: The wear behavior of Be-7 labelled parts, a gear of Polyamid and a crankshaft seal of Viton (Elastomer), have been measured under real operation conditions in a high-powered engine of Audi on a test bench at the Fa. Heß, as illustrated by the picture. Demonstration measurements and material testing have been performed in cooperation with the Company Audi and Fa. Heß, Ingolstadt.

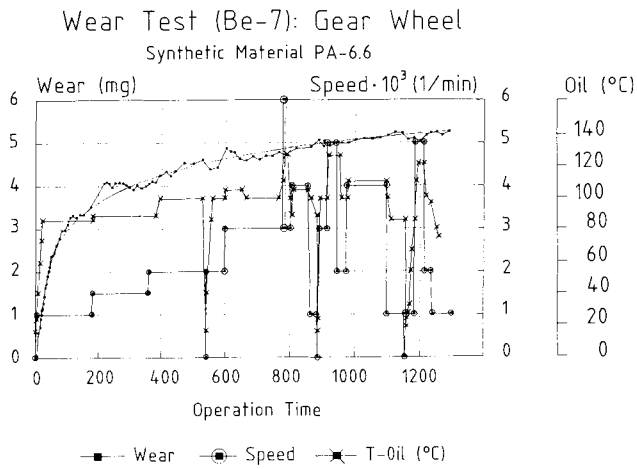


Fig. 4 : The wear behavior of the Polyamid gear over operation time at variated speed and oil temperature in an Audi engine is demonstrating the advantage of RTM on-line wear diagnosis. After the running-in phase the wear of the synthetic gear is undependent of speed and oil temperature. A result of a 24 h RTM wear test, that could not be established by conventional tests over several months.

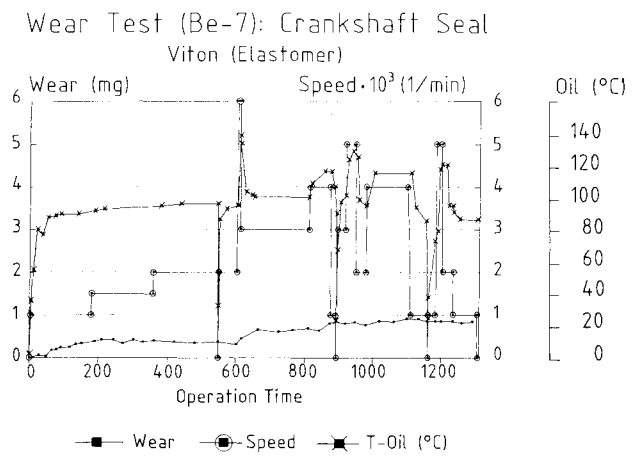


Fig. 5 : .The wear behavior of the Be-7 labelled Viton (Elastomer) seal of the crankshaft in an engine (Audi V 6, 24 Valves) at different speed and oil temperature, was measured in a 24 h wear test and is demonstrating the effectiveness of RTM application.

3. SENSITIVITY AND REACTIVITY OF RTM WEAR DIAGNOSTICS

The experimental investigation of reliability, sensitivity and reactivity in RTM wear diagnostics was performed recently at a typical example of application, the engine wear measurement with the concentration measurement method.

In the running engine (1.6 Liter Diesel engine of 5 Liter oil volume) on the KfK test bench, a suddenly occuring wear was simulated by the injection of a definite liquid activity (Co-56) -, corresponding to a wear mass of 25µg resp.30µg, - in the engine. The concentration wear measurement device was connected to the oil sump, as usual, and was recording continuously the concentration of wear in the oil of the engine. The measurement results for the injection in the oil sump and in the cylinder head, displayed in Fig. 6 resp. Fig. 7, are demonstrating a sufficient reactivity of 120 sec delay at maximum from the occurence of wear (point of injection) to full height of the measurement signal. A wear mass of the minuteness 10µg - corresponding usually to a linear wear of several nanometers - can clearly be resolved by this technique. The reproducibility and reliability is demonstrated by the constant values for wear concentration before and after the injections, as delineated in Fig. 6 and Fig. 7.

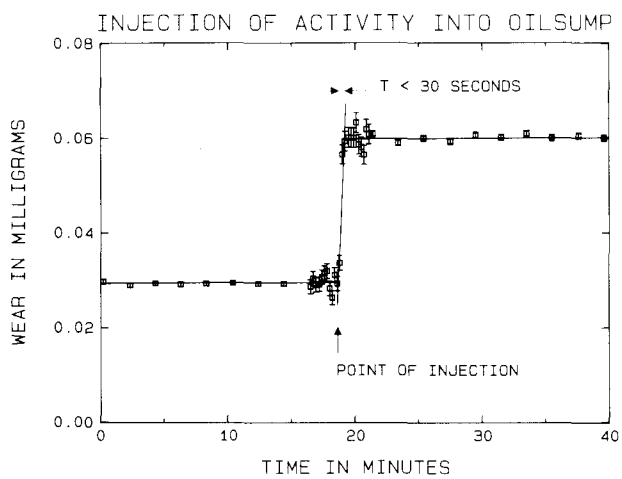


Fig. 6 :.For the demonstration of the sensivity and reactivity of RTM wear diagnosis a definite activity - representing 30 µg wear mass - was injected in the oil sump of the operated engine on the KfK test bench. The applied concentration measurement device registered the full wear mass 30 sec after the injection. A wear mass down to 10 µg - corresponding to a linear wear of several nanometers - can distinctly be resolved.

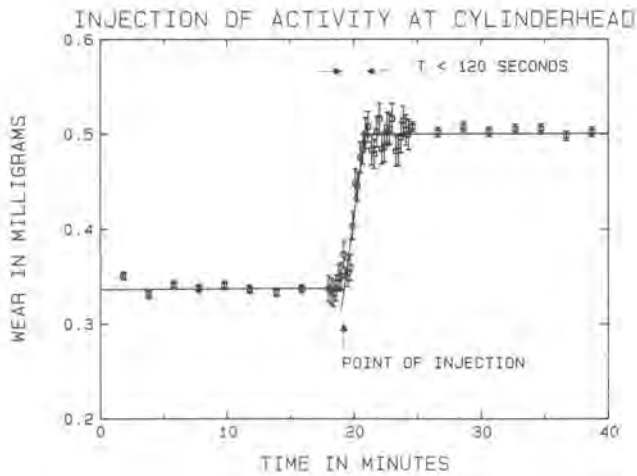


Fig. 7: In case of the activity injection into the cylinder head of the running engine, simulating wear occuring at the camshaft, the reactivity decreased to 120 sec..

4. REFERENCES

1) P.Fehsenfeld, A.Kleinrahm, "Radionuclide Technique in Mechanical Engineering", Proc. Twelfth Int. Conf. on Cyclotrons and Their Applications, Berlin, ed. K. Ziegler, 577 (1989)

2) D.Stegemann, "Wear measurements of a crankshaft bearing in a 4-cylinder Diesel engine with radio-isotopes," MTZ-Motortechn.Zeitschrift, 24,3 (1963).

3) A.Gervé, G.Katzenmeier, "Relationship Between Oil Film Thickness and Wear of Journal Bearings" SAE-Paper 700717 (1970).

4) G.Essig, P.Fehsenfeld, "Thin Layer Activation Technique and Wear Measurements in Mechanical Engineering," Nuclear Physics Methods in Materials Research, K.Bethge ed., 70 (1980).

5) M.A. Balnaves, E.W.Schneider, "Effect of Speed and Power Output on Piston Ring Wear in a Diesel Engine," SAE-Paper 880672 (1988)

6. Firma G.Hess GmbH Ziegeleistr. 42 D-8070 Ingolstadt

A P.E.T. STUDY OF PROTON INDUCED RADIOACTIVITY IN DIFFERENT MATERIALS

J.M. Schippers
Kernfysisch Versneller Instituut
Zernikelaan 25, 9747 AA Groningen
the Netherlands

and

A.M.J. Paans
PET-Center
University Hospital
Oostersingel 59, 9713 EZ Groningen
the Netherlands

ABSTRACT

A possible application of the Positron Emission Tomography (PET) technique as a tool for in situ dosimetry during radio therapy with protons is investigated. Measurements have been performed on activation induced by 55 MeV protons in two different materials. The calculated dose distribution is compared with model calculations and 3-dimensional measurements with PET of the induced activity.

1. INTRODUCTION

If a patient or a material is irradiated with particles of sufficiently high energy, radioactive nuclei will be created along the trajectory of the particle beam. In target materials containing ^{12}C, ^{16}O or ^{14}N, the positron emitters ^{11}C ($T_{1/2}$=20 min) and ^{13}N ($T_{1/2}$=10 min) will be created. Using a PET scanner, the distribution of the activity can be measured in three dimensions and as a function of time. Of course, the PET scan has to be made very shortly after the irradiation, or even better: during the irradiation. As a pilot experiment for studying the feasibility of this technique we have performed a PET-measurement of the induced activity by protons in Melamine and Poly-ethylene-glycol.

2. EXPERIMENTAL TECHNIQUE

In Groningen we have benefitted from the convenient situation that the PET Center of the University Hospital is only 7 km from the KVI-cyclotron. The last experiment performed with the Philips cyclotron at KVI was an irradiation with 55 MeV protons of two target materials with different composition:

I) Poly-ethylene-glycol, mass composition:
54.3% C, 9.1% H and 36.6% O.

II) Melamine, mass composition:
28.6% C, 4.8% H and 66.6% N.

These materials have been selected because of the resemblance of their nuclear composition with tissue, but also to limit the possible amount of reaction types.

The beam was collimated to 4 mm diameter and each target was irradiated for 1 minute with a beam intensity of 10 nA. Current measurement during irradiation was done by integrating the current on the targets, which were isolated from ground. Since the range of 55 MeV protons in the target materials is approx. 22 mm, the 33 J deposited in each target is equivalent to an average dose of about 90×10^3 Gy, which is about 3000 times a typical dose delivered to a patient during a treatment.

After the irradiation the targets were quickly transported to the PET scanner, a Siemens ECAT 951/31, calibrated in absolute terms with ^{68}Ga and ^{18}F sources. The axial range of the tomograph is divided in 31 image planes with a slice thickness of 3.375 mm. The position resolution of the scanner is 6 mm FWHM.

In Fig. 1 a measured activity distribution, projected on a horizontal plane, along the image planes is shown. The plane nr. indicates the axial position.

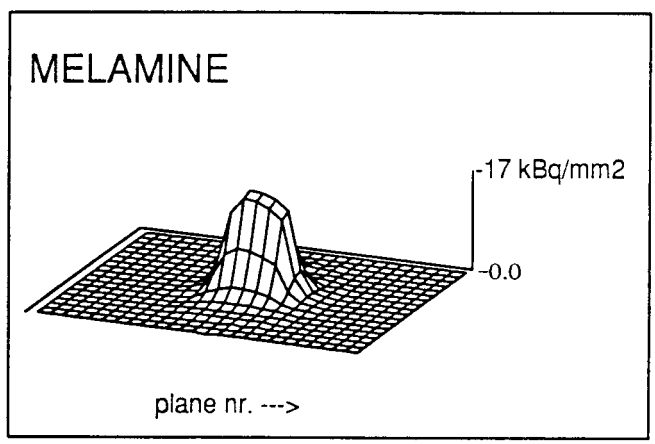


Fig.1. Distribution of proton induced activity in Melamine, in axial (=plane nr) and lateral direction. The vertical scale indicates 17 kBq/mm^2.

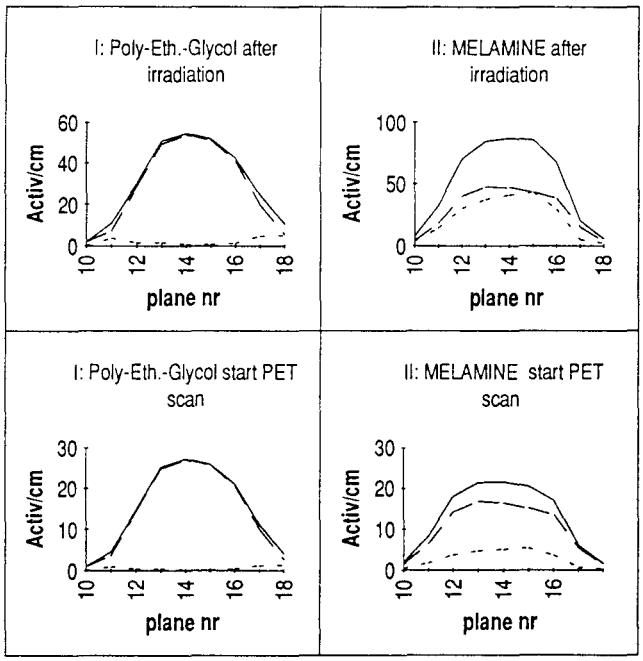


Fig. 2. Measured ^{11}C (dashed lines) and ^{13}N activity (dotted lines) as function of plane nr, at the beginning of the PET scan (bottom) and immediatly after irradiation (top).

The measurement of the activity distribution in target I started 20 min. after the irradiation and for target II 30 min. after irradiation. During 30 minutes, for every plane, 30 time intervals of 1 minute were measured and the measured intensity was corrected for ^{11}C-decay. At the beginning of the scan the coincidence count-rate from target I was 22×10^3 s^{-1} and from target II: 18×10^3 s^{-1}.

3. ANALYSIS

By measuring the lateral width of the activity distribution in each plane the spreading of the beam has been examined. No significant increase of the beam dimension has been detected.

By following the count rate as a function of time, the total activity can be separated in the contributions of ^{11}C and ^{13}N. This has been done for each image plane. In Fig. 2 these contributions and the total activity are shown as they were at the beginning of the PET scan (bottom) and extrapolated to the end of the irradiation (top).

As can be seen in Fig. 2, the contribution of ^{13}N has quickly vanished. This also results in a change of the shape of the total intensity versus plane nr. Although the ^{13}N-production in target I is almost negligible, the two reaction channels (i.e. the $^{16}O(p,2p2n)$ and $^{16}O(p,\alpha)$ reactions) show up clearly as the two little peaks at plane 11 and plane 17+18.

The integrated total activity at the beginning of the PET scan was:
target I : 5.1 MBq (5.0 MBq ^{11}C + 0.1 MBq ^{13}N)
target II: 4.1 MBq (3.4 MBq ^{11}C + 0.7 MBq ^{13}N)

Correcting for the different life times, this yields immediatly after a real treatment with 55 MeV protons the following coincidence count-rates:

Dose=30 Gy: Target I: 15 s^{-1} and Target II: 25 s^{-1}.

In a low background situation, as is the case for these PET studies, these count rates can be sufficient to be used for on-line analysis of the beam position.

4. MODEL CALCULATIONS

Energy dependent cross sections of the possible reactions producing ^{11}C and ^{13}N have been obtained from refs.[1-4]. Taking into account the energy loss of the protons along their trajectory an estimation of the activity as a function of plane nr. (z) can be made. In Fig. 3 the calculated activities and the doses are shown as a function of z for the two targets. A Gaussian shaped position-resolution function has been folded into the calculated activity curves. The curves shown in Fig. 3 are calculated for the moment where the PET scan starts, where the difference in half-lifes has been taken into account.

Since the Bragg peak in the dose distibution cannot coincide with a large cross section for nuclear reactions, this part of the trajectory cannot be mapped with this method. However, for energies larger than the reaction threshold (approx. 10 MeV in Melamine and 15 MeV in Poly-ethylene-glycol, the cross sections show a rather flat continuum, and so does the activity distribution for low z.

It can be seen, however, that there is a strong disagreement between the calculated and measured activity at the end of the trajectory in Melamine. Due to the large values of the cross sections of the $^{14}N(p,\alpha)^{11}C$ reaction below 20 MeV, according to ref.,[2] the calculation shows an increase of activity at high z, while Fig. 2, shows a decrease at high plane nr. However, for the lower plane nrs the overall shape of the ^{11}C and ^{13}N activities is in agreement with the data.

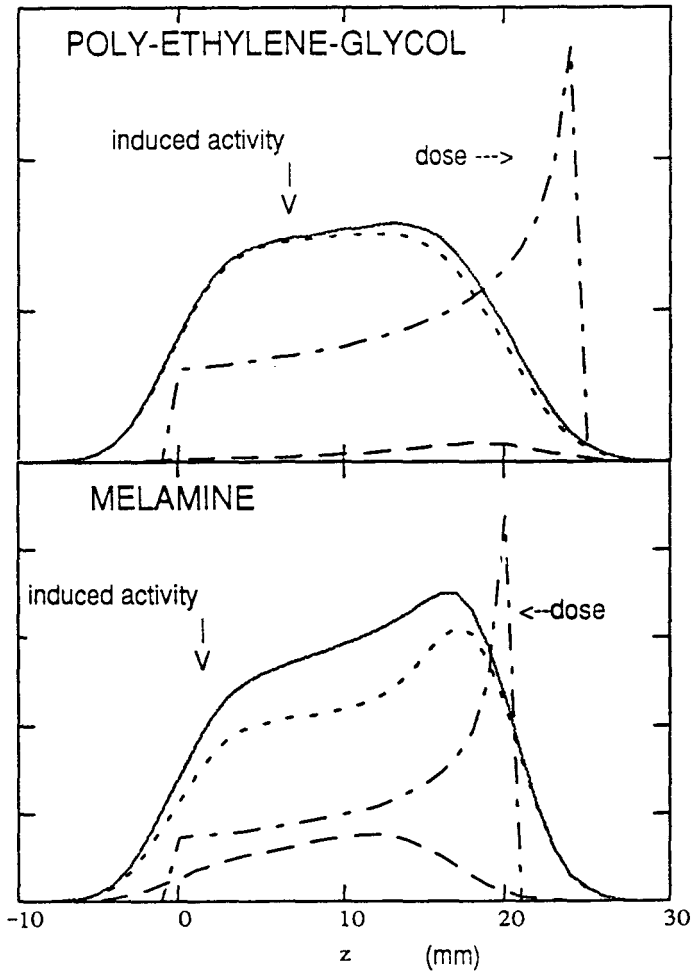


Fig.3. Calculated activity distributions in Polyethylene-glycol (top) and Melamine (bottom). ^{11}C: ...., ^{13}N: - - - and total activity:——. The dose, indicated with – – – –, is also shown in the figure.

Integration of the total induced activity as calculated, gives at the start of the scan:
target I : 6.2 MBq (5.9 MBq ^{11}C + 0.3 MBq ^{13}N)
target II: 6.4 MBq (5.3 MBq ^{11}C + 1.1 MBq ^{13}N)
Considering the uncertainties in the cross sections, these calculations are in rather good agreement with the data.

5. CONCLUSIONS

The radioactivity induced by proton beams in tissue-like (=consisting mainly of C, N and O) materials can be measured accurately by means of PET. It is expected that also the rather low amount of activity created during a therapy treatment can be detected with sufficient accuracy. Especially the region preceeding the Bragg peak in the dose distribution can be monitored quite well with this method. However, for the determination of an accurate Activity-Dose relation more data on the reaction cross-sections below 25 MeV is necessary.

We found that the calculated total amount of activity is in rather good agreement with the data.

We have shown that a dynamic PET study gives an accurate insight in the concentrations of the different types of positron emitters.

This work was performed as part of the research program of the "Stichting voor Fundamenteel Onderzoek der Materie" (FOM) with financial support from the "Nederlandse Organisatie voor Wetenschappelijk Onderzoek" (NWO).

6. REFERENCES

1) L. Valentin, Nucl. Phys. 62(1965)81
2) M. Epherre and C. Seide, Phys. Rev. 3C(1971)2167
3) D.F. Measday et al., Nucl. Phys. 78(1966)476
4) G. Albouy at al., Phys. Lett. 2(1962)306

NEUTRON PRODUCTIONS FROM CARBON BY CHARGED PARTICLE BOMBARDMENT AT DIFFERENT ENERGIES

M. Anwar Chaudhri

Department of Medical Physics, Austin Hospital,

Melbourne and University of Melbourne,

Vic. 3084, Australia

ABSTRACT

By making use of the published cross section data and the range-energy tabulations, we have calculated neutron yields from carbon under bombardment with protons, deuterons and alphas of up to about 23 MeV. This data would help in estimating the neutron background/contamination when carbon is used as a backing/dumping material in cyclotrons while producing fast neutrons for therapy or other applications.

1. INTRODUCTION

Due to its extraordinary stability (temperature, nuclear, etc) carbon is an excellent material for "target-backings", "beam-dumps" and collimators for neutron producing reactions in cyclotrons at high beam intensities. However, for utilising the full potential of carbon in the aforementioned applications it is important to estimate the neutron productions from carbon under bombardment with charged particles of different energies. This information is not conveniently available from the literature.

In our programme on neutron production from different elements under charged particle bombardment we have already estimated the neutron output from all the elements with Z = 20 to Z = 92.[1] This data is now being extended to lower Z elements. In this paper we are presenting the neutron output from carbon under bombardment with protons, deuterons and alphas of up to 12, 20 and 23 MeV respectively.

2. THEORY AND METHOD

As shown by Chaudhri et al,[2] the neutron output from a thick target under bombardment with a beam of charged particles of atomic number z and energy E (MeV) is given by

$$A = f\ (N_A/W)\ .\ (6.25/z)\ 10^{12} I \qquad \sigma_E(-dE/dx)^{-1}dE$$

where

- f = the abundance of the isotope in the target which is undergoing nuclear transformation to produce neutrons
- N_A = the Avagadro's number
- W = the atomic weight of the target nuclide producing neutrons
- E_i = the incident energy of the charged particle beam
- E_O = the lowest energy for which any appreciable number of neutrons would be produced
- I = the current in microamperes of the incident charged particles beam falling on the target.
- σ_E = Cross sections of the neutron producing nuclear reaction at energy E.
- $\frac{dE}{dx}$ = Stopping power of the target for the charged particle beam.

To evaluate the neutron yield equation the cross section and the stopping power data is required. The cross sections at different energies are obtained from the literature and the stopping powers for different elements from the tabulations of Williamson et al.[3] The cross sections for deuterons is taken from Brill and Sumin,[5] and for alphas from Black et al.[6] Due to non-availability of proton cross sections the neutron yields from Bair et al have been modified.[6]

3. RESULTS AND DISCUSSION

a) Protons on Carbon

Total neutron yield obtained by bombarding an "infinitely" thick target of high purity natural carbon, with protons from 4 - 12 MeV, is shown in Fig.1. This curve is produced by slightly modifying the neutron yield data of Bair et al, [6] as the c(p, n) cross section is not conveniently

available. Since the $^{12}C(p, n)$ threshold is above 12 MeV, ^{12}C does not contribute to the neutron yield and most of the neutrons are produced by ^{13}C present in natural carbon. To estimate neutrons at o degree or in any given direction, on could assume an isotopic angular distribution, and calculate the desired yield as an approximation.

b) Deuterons on Carbon

Total numbers (4π) of neutrons produced from a "thick" ^{12}C-target under bombardment with deuterons of up to 20 MeV as shown in Fig.2. As mentioned already the cross section data for this curve has been taken from Brill et al,[5]. From this yield curve the total thick target neutron yield at any desired deuteron energy can be directly read. This curve can also be applied to estimate the neutron output from "semi-thick" targets of known thickness in the following way. The total neutron yield at the energies, at which the deuteron beam enters and leaves the "semi-thick" target are read from the yield curve. The difference between the two values is the neutron output from the "semi-thick" carbon target. Here again, if one wants to estimate the 0-degree yield, or yield at any other desired angle, one has to assume an isotropic distribution to get approximate estimates of neutrons in that direction. Please note that unlike the Carbon plus proton data, all the data in Fig.2 refers to ^{12}C and not a natural Carbon target. Moreover, the neutron yield is given for a 10μA deuteron beam. As is expected the deuteron beam produces many more neutrons from ^{12}C target than a proton beam of similar energy would produce even from a natural carbon target.

c) Alphas on Carbon

Total (4π) neutron yield produced from a "thick" target of 100% ^{12}C, under bombardment with alphas of up to 23 MeV are shown in Fig.3. The cross section for this yield curve has been taken from the data of Black et al.[6] The neutron yield is given for a 10μA alpha beam.

4. SUMMARY

Total neutron yields from thick Carbon targets (natural carbon for protons but 100% ^{12}C for deuterons and alphas) under bombardment with protons, deuterons and alphas of up to 12, 20 and 23 MeV respectively are presented. From these total yield curves neutron yield in any desired direction can be approximately estimated. Moreover, the thick target yield curves are also suitable for estimating yields from "semi-thick" targets. This information would be helpful when estimating the neutron background contamination from Carbon backings of neutron producing targets, Carbon collimators and Carbon beam dumps.

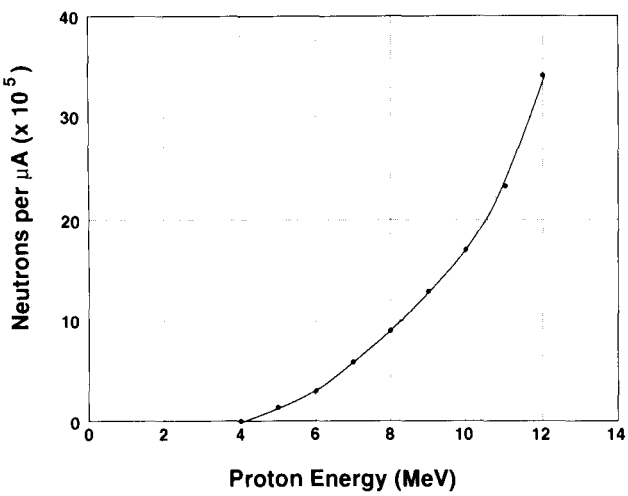


Fig. 1. Total neutron yield from the bombardment of a thick natural Carbon target with protons.

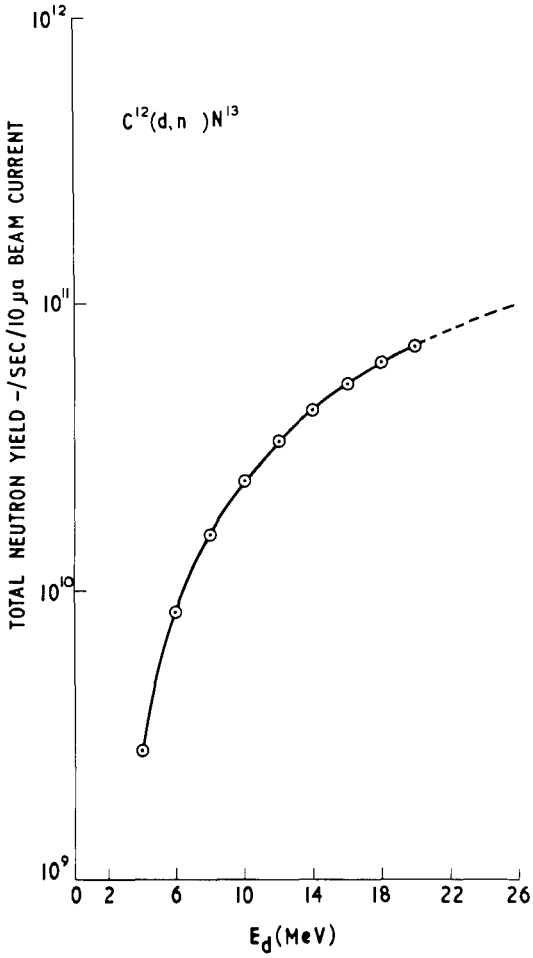


Fig.2. Total neutron yield from a C - 12 target under bombardment with deuterons of different energies

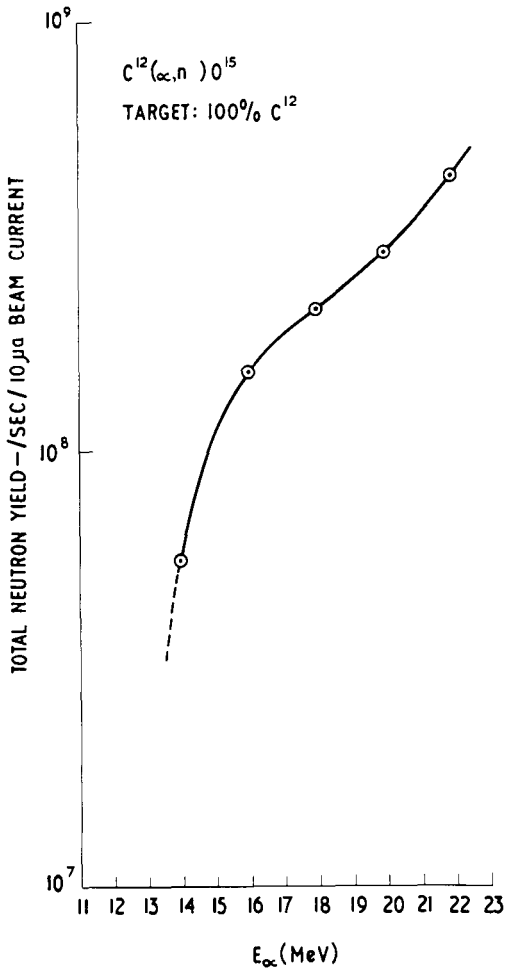


Fig.3. Total neutron yield from a "thick" C - 12 target under bombardment with alphas of different energies

5. REFERENCES

1. Chaudhri, M.A. "Neutron production from all the elements with Z = 20 - Z = 92 under bombardment with protons, deuterons and alphas of up to 35 MeV", to be published.
2. Chaudhri, M.A., Burns, G., Reen, E., Rouse, J.L. and Spicer, B.M.,"A method for charged particle activation and its application to fluorine determination by the $^{19}F(p, \alpha\gamma)^{16}O$ reaction"J. Radioanal. Chem. **37**, 243(1977).
3. Williamson, C.F., Boujot, J.P. and Picard, J. Tables of Range and Stopping Powers of Chemical elements for Charged particles of energy 0.05 - 500 MeV. CEA Rapport R 3042, Saclay(1966).
4. Brill, O.D. and Sumin, L.V. "Excitation curves for the reaction $^{11}B(d,2n)^{11}C$, $^{9}Be(\alpha,2n)^{11}$, $^{10}B(d,n)^{11}C$ and $^{12}C(d,n)^{13}N$", Atom. Energiye **7**,377(1959).
5. Black, J.L., Kuan, H.M., Gruhle, W., Suffert, M. and Latshaw, G.L., "Reactions $^{12}C(\alpha,n)$ ^{15}O and $^{12}C(\alpha,p)$ ^{13}N", Nucl.Phys. A **155**, 683(1968).
6. Bair, J.K., Miller, P.D. and Wieland, B.W., "Neutron Yields from the 4 - 12 MeV proton bombardment of ^{11}B, ^{13}C and ^{18}O as related to the production of ^{11}C, ^{13}N and ^{18}F," Int. J. Appl.Rad. and Isotopes **32**,389(1981).

ANALYTICAL APPLICATIONS OF CYCLOTRONS IN BIOMEDICAL FIELDS - CHARGED PARTICLE ACTIVATION ANALYSIS

M. Anwar Chaudhri
Department of Medical Physics, Austin Hospital,
Melbourne and University of Melbourne,
Vic. 3084, Australia

ABSTRACT

Activation analysis of biomedical materials is another important and useful application of modern cyclotrons. Various methods and theories of charged particle activation analysis are discussed and some practical examples are given. Activation sensitivity curves, for one-particle-emission reactions through proton, deuteron and alpha bombardment of any element with Z=20 to Z=92 in a tissue matrix are given for bombarding energies of up to 35 MeV.

1. INTRODUCTION

Production of short-lived neutron deficient radio-isotopes for diagnostic studies is by far the most commonly used application of medical cyclotrons, and almost all such cyclotrons are engaged in this activity. However, there are other important applications of cyclotrons in medicine and biology which are also being pursued successfully in many cyclotron establishments around the world. These are production of fast neutrons for therapy, and activation and reaction analyses using accelerated charged particles and neutrons. The neutron therapy aspects of cyclotron applications has been recently described by Chaudhri [1]. In this paper, we are presenting some of the analytical applications of cyclotrons - that is the elemental analysis of biological materials with cyclotron produced beams of charged-particles. Activation analysis of biomedical material with cyclotron produced fast neutrons is described in another paper of the Proceedings.

Particle induced X-ray emission analysis (PIXE) is another accelerator based analytical technique which is commonly used for trace element analysis. However, small accelerators (Van de Graaffs, etc), rather than cyclotrons, are generally used for PIXE. With this method most elements heavier than F can be conveniently determined with detection limits of a few ppm. The sample preparation for PIXE analysis is relatively simple and small quantities of the sample are required. A great deal of useful work on the analysis of biomedical samples can be carried out, and in fact has been carried out, with PIXE. However, there are many elements of interest in biomedical fields which cannot be conveniently, or at all, determined by PIXE as it is not sensitive enough. Furthermore, for elements lighter than F, PIXE is not practical.

Charged particle activation analysis (CPA), using modern cyclotrons, tend to overcome the shortcomings of PIXE. With CPA not only elements lighter than F can be determined but also sensitivities of as low as ppb can be achieved in favourable circumstances. Furthermore, certain elements, such as Al, Si, Ti, Cd, Tl, Pb, Bi, etc., which cannot be conveniently or at all determined with slow neutron activation analysis (by far the most commonly used nuclear analytical method) can also be measured with CPA. In this paper the technique of charged particle activation analysis of biomedical materials, using cyclotrons, is described. Different theories of CPA and some examples, where this method has been successfully applied, are presented. The Activation Sensitivity Curves, for the detection of most elements with atomic numbers between 20 and 90 in a tissue matrix, when activated with proton, deuterons and alphas of up to 35 MeV and one-particle emission reactions, are presented in graphical form. Full comprehensive data, including two and three particle emission reactions, would be published elsewhere.[3]

Although there are many papers in the literature on CPA, including a recent book by Vandecasteele,[4] most of the authors deal with metals and semiconductors and not with biomedical samples. In fact, Vandecasteele devotes only a few lines in his book on CPA as applied to biomedicine.[4]

2. CHARGED PARTICLE ACTIVATION ANALYSIS

As already mentioned CPA using a cyclotron offers many possibilities for carrying our trace elements determination in biomedical material. Up until now mostly protons have been used for CPA, though other projectiles, such as deuterons, He-3 and He-4 particles, offer a great deal of potential too. However, unlike neutron activation analysis, there are a number of practical difficulties in CPA which has to be overcome. These are:

i. Energy loss and heat generation: The charged particles lose their energy rapidly in the biological material thus generating a great deal of heat in a small volume and damage the sample. This effect/damage can be minimized by cooling the sample,[5] and or by mixing the sample (usually dried and powered) with analytical grade graphite powder to conduct away heat.

ii. Simultaneous or controlled similar irradiation of the sample (to be analysed) and the "standard" (with known trace elements composition) is required. This can generally be achieved by keeping the irradiation conditions (energy, current, etc) stable during irradiation and monitoring the beam carefully. Simultaneous irradiation of the "standard" and sample can also be accomplished by mounting the two on a special holder and rotating the holder at a constant speed during irradiation. In this way both the standard and sample are bombarded with identical amount of charged particles.

iii. The trace element which is being determined has to be ;uniformly distributed in the sample to be analysed. This condition is generally met in biological fluids while for organs the sample is freeze dried and/or ashed, and then homogenized.

iv. A knowledge of the major constituents of the matrices of the sample and the 'standard' is required in order to calculate the range of charged particles in them for estimating the activation depths.

As shown by Chaudhri et al,[6] the induced activity at saturation A, in an element/isotope Y, uniformly distributed in a thick sample X, after irradiations with a beam of charged particles of atomic number z and energy E(MeV), is given by the activation equations:

$$A = cf\,(N_A/W)\,.\,(6.25/z)\;10^{12}\;I\int_{E_o}^{E_i}\sigma_E(-dE/dx)^{-1}dE \qquad (1)$$

where c = the concentration of Y in X (in ppm or ppb)

f = the natural abundance of the isotope in nuclide Y undergoing nuclear transformation

N_A = the Avegadoo's number

W = the atomic weight of Y

E_i = the incident energy of the projectiles

E_o = the lowest energy for which an appreciable amount of activity in Y would be produced.

I = the current in microamperes of the incident charged particle beam falling on the target/sample.

σ = activation cross section for the element/isotope Y

dE/dx = the stopping power of the incident charged particles in the matrix X.

The Eq.1 can be written as

$$A = CKIF \qquad (2)$$

where $K = f\,(N_A/W) \times (6.25 \times 10^{12})/z$

and $F = \int_{E_o}^{E_i}\sigma_E\,(-dE/dx)^{-1}dE$

The induced activity for any given irradiation time t is given

$$A_t = CKIF\,(1-e^{-\lambda t})$$

where λ is the decay constant of the activity being induced in Y.

In order to obtain the values of A for different bombarding energies F has to be evaluated at these energies. This cannot be done by exact integration as neither the σ nor dE/dx have simple and useful analytical forms. Therefore this integral has to be calculated by numerical integration. The values of σ-, the reaction cross section, at different bombardment energies can be taken from the known excitation functions and those of the stopping powers from the tabulations of Andersen and Zigler[7] Zeigler[8]. If A is measured experimentally under known bombarding and measuring conditions then using eqn.U, the value of c the concentration of Y in X can be calculated.However, in practice it is generally more convenient to use the "comparator method" for activation analysis with charged particles as is the case of neutrons.In this method a standard thick sample Xs is irradiated simultaneously or under similar (identical if possible) conditions as the unknown sample X containing an unknown concentration c of Y. The induced activity in the two cases A_s and A can be related by Eq. 2 as

$$A_s/A = C_s I_s F_s/CIF \qquad (3)$$

which can also be written as

$$A_S/A = C_S Q_S F_S / CQF \qquad (4)$$

where Qs and Q are the beam charges collected at the Standard and sample respectively during irradiation at identical or similar beam currents.

In order to make use of Eq. 4) the integrals F_s and F have to be calculated for the standard and the sample matrices, which is a relatively laborious and complex task. To simplify this Chaudhri et al[6] used some approximations and presented a modified equation

$$\frac{A_S}{A} = \frac{C_S Q_S \ (dE/dx)}{CQ \ (dE/dx)_S} \qquad (5)$$

where (dE/dx)s and (dE/dx) are the stopping power values for the standard and the sample at the mean energy (Ei + Eo)/2.

They showed, though extensive calculations, that more accurate results could be obtained with Eqr.5 than with previous approximations.[9]

Using Eq.1, we have calculated the activation sensitivities of all the elements with atomic numbers between 20 and 90 assumed to be uniformly distributed in a tissue matrix, by bombardment with protons deuterons and alphas of up to 34 MeV. The results for a "thick" biological sample (tissue matrix) and for one particle emission - reactions are shown in Fig.1 and 2. The results for 2 and 3 particle emission reactions and for other matrices would be published elsewhere.[3]

Thick target activation sensitivities can be read directly from the "Activation Curves" at given irradiation conditions. These curves can also be applied to thin samples of known thickness simply be taking the difference between activation sensitivities at the energies at which the charged particle beam enters and leaves the target sample.

As already mentioned only a limited number of papers have been published on CPA of biomedical samples. Most of the studies are confined to the analysis of standard reference materials, calculating the minimum detection limits and pointing out the potential of this method rather than its application to particular biomedical problem. [10-14]

By using protons of 10-13 MeV at 500nA - 1uA intensity and irradiation of up to 1 - 2 hours, detection limits of as low as a few ppb to many ppm were obtained for many elements.

Most of the authors have used protons for activation analysis. But with modern cyclotrons which are equally capable of providing beams of deuterons, He3 and He-4 particles, activation with these particles can also be carried out. However, again as is the case for proton activation analysis, there are very few papers in the literature on the applications of these particles on the activation analysis of biomedical materials. Deuterons and He-3 particles, which are both loosely bound would induce many nuclear reactions in most elements throughout the periodic table and therefore should be quite useful for the purpose of activation analysis. However, in practice this is not the case and relatively fewer (compared to protons) activation analyses have been carried out with d + He-3. Perhaps, one of the main reasons could be that these particles produce positron activities from many elements/isotopes, thus involving the complex task of separating a number of exponentials with different half lives, if radiochemical separation was to be avoided.

As early as the mid sixties Ricci and Hahn [9] promoted the idea of activation analysis with 18MeV He-3 particles. For a number of elements they determined the sensitivities of detection, both experimentally and theoretically, with good agreement between the two methods. Sastri et al [15] used 14 MeV He-3 beams for activation analysis of a number of elements with Z between 12 and 47. For irradiation time of 1 hour or 1 half life of the product nuclides (which ever is shorter), at 2μA they calculated the detection limits to be

1 - 50 ppb for Al, Ti, V, Mn, Ni, Zn and Nb,

50 - 100ppb for Mo,

100 - 500ppb for Mg, Cr, Fe, Zr, Ag.

Kosmali and Schweihart[16] compared the potential of 20MeV protons and deuterons with 40MeV alphas and He-3 particles for activation analysis of medium Z elements. Only those product nuclides with half lives between 10 min and 3 days were considered. They concluded that the protons provided an optimum compromise between sensitivity and selectivity.

Recently we have developed a new method for the determination of carbon in dental hard tissue by activation analysis with He-3 beams and applied it to study the role of carbon in tooth decay.[17]

3. SAMPLE HANDLING AND TREATMENT

As already mentioned, unlike neutron activation, in CPA a large amount of energy is deposited in a small volume in the sample. Therefore, biological material, which are predominantly organic, are liable to decompose unless appropriate steps are taken to avoid it. Chaudhri et al[5] pelleted the sample, covered it with a thin Al-foil, mounted it on a Cu-holder and cooled the sample holder and thus the sample with liquid nitrogen. In this way they observed that even after 1 hour of irradiation with 8.5 MeV protons at up to 1uA intensity, there was no decomposition and/or deterioration of the sample material.

The specially designed container could hold enough nitrogen to last for more than a couple of hours.

Zikovsky et al[10] mixed freeze dried biological materials, standard reference materials, (SRM) with nuclear grade graphite, pressed into pellets and wrapped them in Al-foils. They showed that this sort of set up could withstand 12 MeV protons at 0.6 uA for 1 hour. Cantone et al[12] pressed freeze dried serum a 0.7 mn thick pellet, sandwiched it in a 6um Mylar and an aluminized Mylar foil of 30um thickness, and cooled the samples to -5°C with freon. They demonstrated that such a system could withstand irradiation with 23 MeV proton at 300nA for 3 hour. Bonardi et al[11] successfully used high purity graphite container in which various SRM's were pressed, cooled it with freon, in order to determine Pb by using 31 MeV protons at 0.5 - 0.6 uA. Besides cooling, and mixing the freeze dried biological samples with a heat conducting material such as graphite[10] in order to avoid the damage to the sample under irradiation, one can also use an internal standard in order to compensate for the loss of the sample material[13].

However, generally speaking it is advantageous to mineralize the biological sample either by LTA (low temperature ashing) or by careful incineration at 400 - 450° Naturally some volatile elements, such as Br, Se, Hg, etc., would be partly lost, but a considerable increase in the sensitivity of detections would also be obtained.

For example the residual ash is only about 1% referred to the original liquid and about 10% referred to the freeze dried sample.

4. CONCLUSIONS

It has been pointed out that CPA of biological materials, using cyclotrons, is a practical and worthwhile analytical method. It has certain difficulties, such as the excessive heating of the samples during the irradiation. However, as demonstrated it can easily be overcome by mixing the samples with graphite and/or cooling the sample holder. Good sensitivities of detections for many elements (e.g. as low as a few ppb in favourable circumstances) can be obtained. Up until now about 15 elements have been determined in biological materials, mostly by proton activation and instrumental analyses. This method is specially useful for the determination of those elements which can not be detected at all, or with sufficient sensitivities with fast neutron activation analysis.

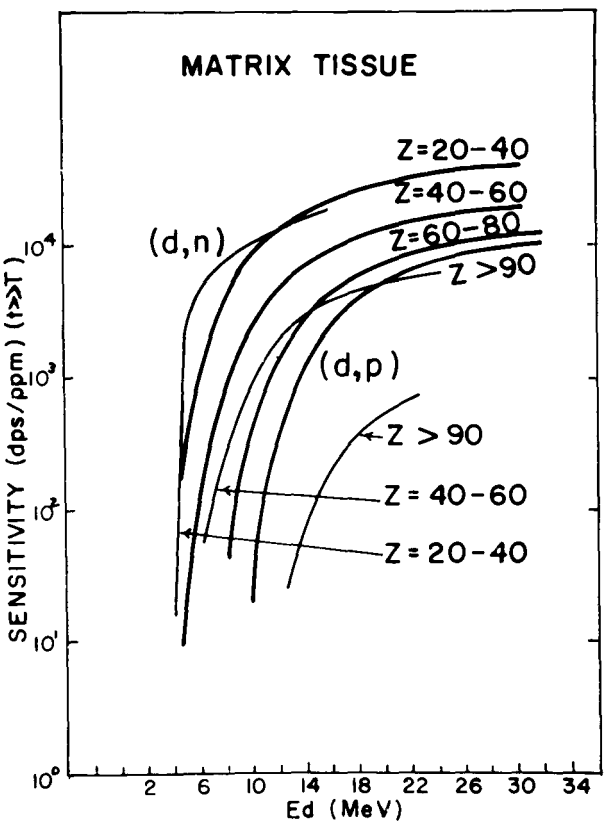


Fig. 1. The sensitivity curves at saturation for all the elements with atomic numbers from 20 to greater than 90 activated by protons and alphas of different energies through the (p,n) and (α,n) reactions.

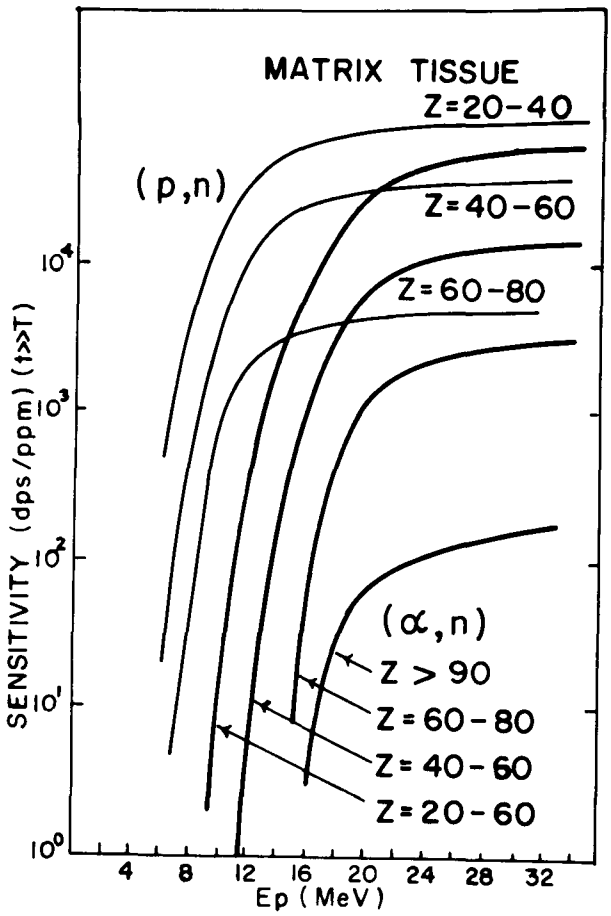


Fig. 2. The sensitivity curves at saturation for all the elements with atomic numbers from 20 to greater than 90 activated by deuterons of different energies through the (d,n) and (d,p) reactions.

5. REFERENCES

1. Chaudhri, M.A., "Cyclotron production of neutrons for therapy - Historical development and current status". Acta Radiologica, Supplementum **376**,53(1991)

2. Chaudhri, M.A., "A simple method for estimating activation sensitivities of different elements/isotopes with cyclotron produced neutrons", Proc. XIII Int. Conf. on Cyclotrons and their Applications.

3. Chaudhri, M.A., "Activation sensitivities of all the elements with Z from 20 to 90, in different matrices, activated with protons, deuterons and alphas of up to 34 MeV. To be published.

4. Vandacasteele, C., Activation Analysis with charged particles (Ellis Horwood Ltd., Chichester, 1988).

5. Chaudhri, M.A. and Lee, M., "Trace elements determination in blank Polystyrene air filters by charged particle activation analysis with a cyclotron" in Proceedings of the Twelfth International Conference on Cyclotrons and their Applications (World Scientific, Singapore, 1991)pp.612.

6. Chaudhri, M.A., Burns, G., Reen, E., Rouse, J.L. and Spicer, B.M., "A method for charged particle activation and its application to fluorine determination in biological materials", J.Radioanal. Chem. **37**,243(1976)

7. Andersen, H.H. and Ziegler, J.F., Hydrogen Stopping Powers and Ranges in all Elements (Pergamon Press, New York, 1977).

8. Ziegler, J.F., Helium Stopping Powers and Ranges in all Elemental Matter (Pergamon Press, New York, 1977).

9. Ricci, E. and Hahn, R.L., "Theory and Experiment in rapid, sensitive He-3 activation analysis", Anal.Chem. **37**,742(1965)

10. Zikovsky, L. and Schweikert, E.A. "Comparison of non destructive proton and neutron activation analysis: The case of biological samples", J.Radioanal. Chem., **37**,550(1977)

11. Bonardi, M., Birattari, C., Gilardi, H.C., Pierta, R. and Sabbioni, E., "Development of proton activation analysis for the determination of heavy metals in biological matrices: excitation functions, irradiation system and selective radiochemical separations", J.Radioanal .Chem **70**,337(1982)

12. Cantone, M.C., Molho, N. and Pirola, L., "cadmium and titanium in human serum determined by proton nuclear activation", J.Radioanal. Chem. **91**,197(1985)

13. Masumoto, K. and Yagi, M., "Simultaneous determinations of P, Cl, K and Ca in several control serums by alpha particle activation analysis using the internal standard method, J.Radioanal. Nucl. Chem. **109**,449(1987).

14. Yagi, M. and Masumoto, K. "Instrumental charged particle activation analysis of several selected elements in biological materials using the internal standard method", J.Radioanal. Nucl. Chem. **111**,359(1987)

15. Sastri, C.S., Petri, H. and Erdtmann, G., "Determination of 13 elements with atomic number between 12 and 47 by 14MeV He-3 activations analysis", Anal. Chem. **49**,1510(1977)

16. Kormali, S.M. and Schweikert, E.A., "Charged particle activation of medium Z elements", J.Radioanal., Chem. **31**,413(1976)

17. Chaudhri, M.A. and Crawford, A.C., "Carbon determination in human teeth by activation with He-3 ions", Nuclear Analytical Methods in the Life Sciences, Ed. Zeisler, R. and Guinn, V.P. (Humana Press, Clifton, N.J. 1990)521

A SIMPLE METHOD FOR ESTIMATING ACTIVATION SENSITIVITIES OF DIFFERENT ELEMENTS/ISOTOPES WITH CYCLOTRON PRODUCED NEUTRONS

M. Anwar Chaudhri

Department of Medical Physics, Austin Hospital,

Melbourne and University of Melbourne,

Vic. 3084, Australia

ABSTRACT

A simple method for estimating the activation sensitivity of an element/isotope, activated with Cyclotron produced neutrons, has been developed. It uses the measured neutron spectra produced by bombarding a thick Be target with deuterons of different energies (15-54 Mev) and the measured/estimated neutron cross sections for the particular nuclear reaction. This method is applicable to all sorts of neutron spectra and all the elements/isotopes whose cross sections/excitation functions in the relevant energy ranges are available. We have applied this method to estimate the activation sensitivities of a number of lighter elements of biomedical interest. It is pointed out that this simple method is much cheaper, more convenient and quicker in estimating the activation sensitivities than experimental measurements - of course as long as the appropriate excitation functions are available.

1. INTRODUCTION

Fast neutron activation analysis is specially suited to low z elements and to those elements which are difficult or impossible to determine by slow neutron activation analysis, such as Al, Si, V, Cr, Ni, Cd, Sn, Tl, Pb, etc. Before choosing a particular fast neutron induced reaction for the determination of a given element/isotope it is helpful to estimate the activation/detection sensitivity obtainable with the neutron beam being used. The activation/detection sensitivities of most of the elements/isotopes bombarded by neutrons from d-T generators have been calculated and/or experimentally measured. In this case all neutrons are monoenergetic (around 15Mev) and it is simple to calculate the activation sensitivity. However, the d-T neutrons are not useful for the detection of these elements/isotopes where the thresholds of corresponding nuclear reactions are higher than 15MeV. Furthermore, the total neutron output from such generators is normally around 10^9 - 10^{10}n/sec, which limits the activation sensitivities. Moreover, the life of tritium target is limited to some tens of hours only, which means regular expensive replacements of the target if such generators are used for activation analysis over long periods.

The aforementioned short-comings of d-T generators for activation analysis can be overcome by using fast neutrons produced in a cyclotron. Depending upon the cyclotron size and the mode of neutron productions, those elements/isotopes, which have greater than 15MeV threshold energy for activation, can also be determined. Moreover, neutron fluxes of around 10^{12}n/sec and higher can be obtained in a cyclotron. Also the target life is much longer and cost a lot less than that of a tritium target. However, the neutrons produced are not monoenergetic and therefore the sensitivities of activation cannot be calculated so simply. A number of groups have experimentally determined activation/detection sensitivities of many elements by using neutrons produced with cyclotrons of different sizes. [1-4]

In this paper we describe a simple method which helps in calculating the activation sensitivity of any element/isotope for any known fast neutron beam. Using this method, and fast neutrons produced by deuterons of different energies on thick Be targets, the results for the determination of some light elements of biological interest (e.g. C, N, O, Na, P, Cl, etc) are presented.

2. METHOD

Neutrons considered in this paper are those produced by thick Be-targets under the bombardment of 100uA deuteron beams of 15, 20, 24, 40 and 54 MeV energies respectively, through the Be(d,xn) reactions. The spectra, measured by different authors but summarized by Schmidt and Muenzel,[5] are shown in Fig.1.

A suitable fast neutron induced nuclear reaction, in the element/isotope whose activation sensitivity is to be determined, is selected. The threshold energy of this reaction is noted and marked on the neutron spectrum.

Then as shown in Fig.2 the "effective neutron spectrum and flux" are determined. From the "effective neutron spectrum" the "effective mean or average energy" E_n is calculated with the following Eqn.

$$E_n = E_n(N_E)dE/N_E dE$$

At the "effective mean energy", the "effective average cross section" of the particular nuclear reaction is noted from the neutron cross section/excitation function data. [6-7]

In a similar way the "effective neutron flux" and "average cross section" of the nuclear reaction is evaluated for all the neutron spectra given in Fig.1. From the values the activation sensitivity A, can be simply calculated for each of the neutron spectra using the following Eqn.

$$A = N k \sigma S T$$

Where
- A = Induced Activity - Disintegrations per sec per gm
- N = Number of atoms of the element/isotope per gm
- K = Abundance of the isotope in the element undergoing transformation
- σ = Effective average cross section
- F = Effective neutron flux n/sec/cm^2
- T = Duration of irradiation
- S = Saturation factor - which approaches unity if the time of irradiation is greater than 4-5 times the half life of the activity being induced. For shorter irradiation time 't'
- S = $(1-e^{-\lambda t})$

where λ = The decay constant of the induced activity

3. RESULTS AND DISCUSSION

The results on the induced activity calculations in some light elements of biomedical interest are given in Tables 1-6. The tables are self explanatory. However, it must be kept in mind that the induced activity figures are the total 4π activity produced, and must be modified for the detector solid angle and efficiency when comparing with experimental results.

NUC. REACTION $^{12}C(n,2n)^{11}C$

Abundance 98.892%

Half life 20.5 Min.

Threshold Energy 20MeV

Incident Energy (MeV)	Effective Flux (n/sec/cm^2)	Average energy of effective spectrum (MeV)	σ (m.b)	Induced activity at saturation (d.p.s.μg^{-1})
24	77 x 10^9	21.4	1	.04 x 10^2
40	1304.0 x 10^9	25.9	9.5	6.19 x 10^2
53.8	3406.4 x 10^9	25.7	8.5	1.45 x 10^3

TABLE 1

NUC. REACTION $^{14}N(n,2n)^{13}N$

Abundance 99.635%

Half life 10 Min.

Threshold Energy 12 MeV

Incident Energy (MeV)	Effective Flux (n/sec/cm^2)	Average energy of effective spectrum (MeV)	σ (m.b)	Induced activity at saturation (d.p.s.μg^{-1})
20	573.5 x 10^9	13.3	3.1	7.61 x 10^1
24	945 x 10^9	15.2	9	3.64 x 10^2
40	3462.7 x 10^9	20.4	11.2	1.66 x 10^3
53.8	5385.2 x 10^9	23.3	11.3	5.37x 10^3

TABLE 2

NUC. REACTION	^{16}O (n, ρ) ^{16}N
Abundance	99.759%
Half Life	7.35 sec.
Threshold Energy	10.25 MeV

Incident Energy (MeV)	Effective Flux (n/sec/cm^2)	Average energy of effective spectrum (MeV)	σ (m.b)	Induced activity at saturation (d.p.s.μg^{-1})
15MeV	293.3x 10^9	11.8	84	9.24 x 10^2
20 MeV	1081.4x 10^9	12.2	26	1.05 x 10^3
24 MeV	2294.5 x 10^9	13.7	45	3.87 x 10^3
40 MeV	3933.9 x 10^9	19.6	24	3.54 x 10^3
53.8 MeV	5350.1 x 10^9	22.8	--	----

TABLE 3

NUC. REACTION	$^{23}Na(n,p)^{23}Ne$
Abundance	100%
Half Life	38 sec.
Threshold Energy	4 MeV

Incident Energy (MeV)	Effective Flux (n/sec/cm^2)	Average energy of effective spectrum (MeV)	σ (m.b)	Induced activity at saturation (d.p.s.μg^{-1})
15	1671.7x 10^9	7.5	31	1.35 x 10^3
20	2762.6x 10^9	9.8	50	3.61 x 10^3
24	3124.3 x 10^9	10.2	20	1.63 x 10^3
40	3930.8 x 10^9	17.4	22.5	2.31 x 10^3
53.8	6358.6 x 10^9	21	5	2.3 x 10^3

TABLE 4

NUC. REACTION	^{31}P (n, 2n)^{30}P
Abundance	100%
Half Life	2.6 Min.
Threshold Energy	12.5 MeV

Incident Energy (MeV)	Effective Flux (n/sec/cm^2)	Average energy of effective spectrum (MeV)	σ (m.b)	Induced activity at saturation (d.p.s.μg^{-1})
20	413.8x 10^9	13.5	6	0.48 x 10^2
24	683.6 x 10^9	15	36	4.77 x 10^2
40	3205.0 x 10^9	20.6	--	----
53.8	5130 x 10^9	23.5	--	----

TABLE 5

NUC. REACTION	$^{35}Cl(n,2n)^{34m}Cl$
Abundance	75.53%
Half Life	32.4 Min
Threshold Energy	15 MeV

Incident Energy (MeV)	Effective Flux (n/sec/cm^2)	Average energy of effective spectrum (MeV)	σ (m.b)	Induced activity at saturation (d.p.s.μg^{-1})
15	14.8x 10^9	15.5	7	0.01 x 10^2
20	193.8x 10^9	14.4	6	0.15 x 10^2
24	235.6 x 10^9	17.6	14	0.42 x 10^2
40	2649.4 x 10^9	22.9	--	----
53.8	4687.7 x 10^9	22.6	--	----

TABLE 6

4. SUMMARY

A simple method for estimating the activation sensitivity of an element/isotope, activated with any given neutron spectrum is presented. This method is applicable for the detection of any element/isotope, with any neutron beam, as long as the respective neutron cross section is available in the literature. As fast neutrons cross sections on most of the elements/isotopes are available it is suggested that this method should be used to estimate the activation sensitivities of different nuclides rather than experimental measurements which are more time consuming and expensive.

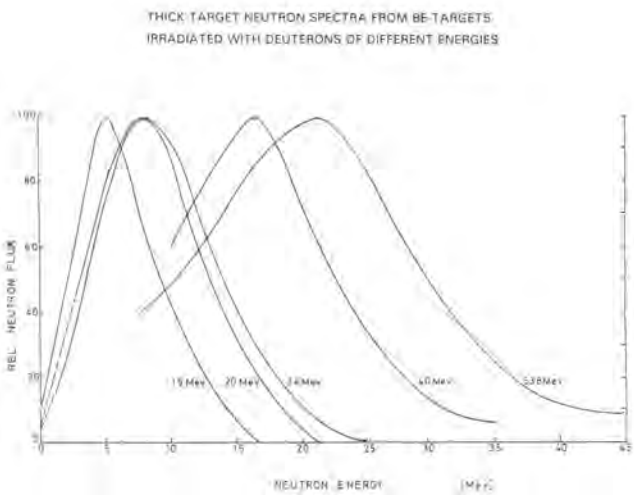


Fig. 1. Thick-target neutron spectra for Be at 15, 20, 24, 40 and 53.8 MeV deuteron energies.

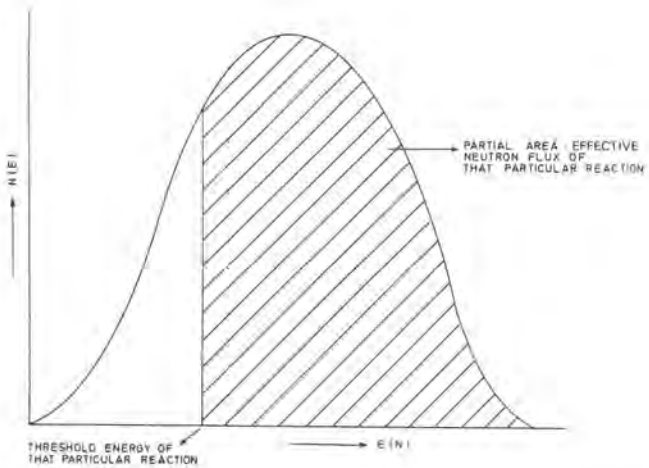


Fig. 2. The concept of "Effective Spectrum" and "Effective Flux"-shaded area

5. REFERENCES

1. Muenzel, H., Michel, F., Coetzee, P.P. and Krivan, V., "Utilization of cyclotron produced fast neutrons in the activation analysis for oxygen.", J.Radioanal.Chem 37,267(1977)
2. Espirit, M., Vandecasteele, C. and Hoste, J., "Sensitivities and interferences in activation with cyclotron produced fast neutrons," J. Radioanal. and Nuclear Chem., Articles 88/1, 31(1983)
3. Randall, K., Haken Ten., Awschalom, M. and Rosenberg, I., "Activation of the major constituents of tissue and air by fast neutron radiation therapy beam," Med.Phys 10(5),636(1983)
4. Olmez, I., Kowalezyk, G.S. and Harrison, G.H., "Use of cyclotron produced neutrons in activation analysis," J.Radioanal, Nucl. Chem., Letters 94/6/, 391(1985)
5. Schmidt, K. and Muenzel, H. Erzeugung von Neutronen durch Bestrahlung dicker Berylliiumtargets mit Deuteroneu in Energie - breich von 15 bis 55 MeV. Report No. KFK-1288(Karlsrule,1970)
6. Hughes, D.J. and Schwartz, R.B. (Eds.) Neutron Cross sections BNL 325, Supplement No. 2, Vol. 1, Vol. 2 and Vol. 3 (Brookhaven National Laboratory, and Associated Universities, Inc., Upton, N.Y., 1965)
7. Schwartz, R.B., Schrack, R.A. and Heaton, H.T. (Eds.) MeV Total Neutron Cross Sections, NBS Monograph 138(US Dept. of Commerce, National Bureau of Standards, Washington D.C., 1974)

A PROPOSAL FOR AN INTENSE CYCLOTRON-BASED THERMAL NEUTRON SOURCE

S. Tazawa
Sumitomo Heavy Industries, Ltd., Toyo-shi, 799-13 Japan

and

W.L. Whittemore
General Atomics, San Diego, California 92138, U.S.A.

ABSTRACT

A cyclotron-based thermal neutron source using the Be(p, n) reaction is summarized, with particular regard to basic parameters affecting source intensity and characteristics such as bombarding energy, current, moderation of fast neutrons and thermal neutron flux, based mainly on the experimental results from an existing cyclotron of proton energy 18 MeV. The thermal neutron flux intensity is estimated based on the commercially available high intensity current from an H^- cyclotron and compared with common neutron sources including nuclear reactors. Also, amplification of these thermal neutrons using U-235 bundles is estimated.

1. INTRODUCTION

One of the practical applications of neutrons is N-ray radiography, which is a non-destructive tool used to detect the presence and/or structural nature of materials opaque to neutrons. This technique is similar to X-ray radiography in that radiation is passed through an object being inspected and an image is recorded on photographic film or through real-time imaging on such memory devices as magnetic tape, floppy disks or laser disks.

Neutron radiography differs from X-ray radiography in that, unlike X-rays, which are increasingly absorbed by materials of increasing atomic number, neutrons are absorbed selectively by various elements depending on the characteristics of the nucleus.

As a result, neutrons of the correct energy, unlike X-rays, can penetrate heavy metals like steel and lead and be scattered by hydrogen-bearing materials like plastics or absorbed by specific elements like Gd, Cd, of Boron. This technique was initially developed using highly intense thermal neutron fluxes obtained from a nuclear reactor. Its applicability has been tested in aviation, defense and nuclear industries for pyrotechnic components, composite material, nuclear spent fuel and corrosion detection of airplane wings (Table 1).

Table 1. Example of Neutron Radiography

	Film Method
Pyrotechnics	: Detonating cord, igniter plug, fusing device
Composite Materials	: ERP, FRM, Honeycomb Structure
Turbine Engine	: Residual core detection of turbine blade
Electrical Components	: Electrical contact point, potting of resin
Ceramics	: Green body
Nuclear fuel	: Spent fuel detection R-T Imaging
Aluminum Structure	: Corrosion and moisture detection in wing
Flow visualization	: Plastic extruder, Heated water
Two phase flow	NH_3 in heat pipe, Freon in refrigerator
& Streak line	Streak line of Pb-Bi eutectic metal

2. CHARACTERISTICS OF A CYCLOTRON-BASED NEUTRON RADIOGRAPHY (NR) SYSTEM

Cyclotron-based neutron sources are not only used for fast neutron therapy, but also as practical thermal neutron sources for NR. An actual cyclotron system is routinely operational at Toyo Works[1] of SHI for charged particle activation analysis (CPAA) of light elements like B, C, N and O, thin layer activation (TLA) for machine wear measurement with joint collaboration of KfK, and irradiation for power transistor and switching devices like GTOs, IGBTs, power diodes and thyristors. The basic principle of a cyclotron-based neutron radiography system is to bombard a beryllium target with a proton beam of 18 MeV at a current of 50 μA, producing fast neutrons of 3.4 MeV through the ^{9}Be$(p, n)^9$B reaction.[2]

A special feature of this cyclotron-based system is that it can produce a much larger fast neutron yield than the ordinary rather low energy electrostatic accelerator systems like a Van de Graaff system[3] using ^{9}Be$(d, n)^{10}$B reaction with an energy range of a few MeV, or a tritium neutron generator using T$(d, n)^4$He with a 100 kV range.

This situation is shown in Fig. 1 which presents the relation between fast neutron yield and bombarding energy specially for the compact cyclotron energy region with Be(p,n) and Be(d,n). Much more needs to be said here about the various energies of fast neutrons from these accelerators and the ability to moderate them, as the neutron energy of most interest is in the thermal region of 0.025 eV, in order to obtain good contrast in the radiograph images. Also, most elements have a maximum scattering cross section which serves to enhance the contrast for different elements in the actual object.

Thermalisation is achieved in this system by elastic and inelastic scattering processes with hydrogen atoms contained in the moderator, which in this system is constituted from polyethylene. This moderation process is similar to that in a nuclear reactor, but the small size of the neutron source requires special consideration. The thermalized neutrons are extracted from the moderator with some beams lacking definition, which causes poor edge definition due to penumbral shadow. The neutron current is required to be nearly parallel for use with thick specimens. The neutrons are collimated by passing them through a divergent type of collimator characterized by L/D where L is the length and D the entrance diameter of the collimator.

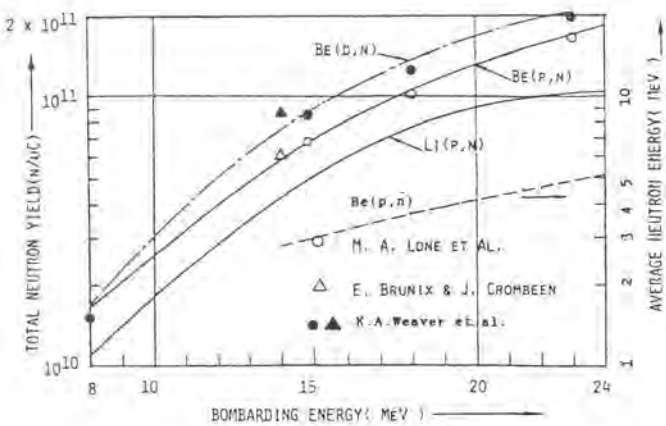


Fig. 1. Fast neutron yield from thick Be and Li targets bombarded by protons and deuterons versus average energy for Be(p,n).

When one requires a small penumbral shadow, its width is related to the height of the object (h) by Eq. 1:

$$w = h/(L/D) \tag{1}$$

Larger L/D is realized at the sacrifice of the neutron flux current (J), which is shown generally to vary as the inverse square of L/D (Eq. 2).

$$J/J_i = 1/16(L/D)^2 \tag{2}$$

Then the use of a collimator with large L/D requires long exposure time and is not practical in actual operation. So, optimization for good images and shorter exposure times is very important for the design of the system. The neutrons incident on the object and passing through it, impinge on a converter screen and are converted to another form of radiation such as photons for a fluorescent converter or electrons for a Gd film converter, which then exposes a silver halide film. Usually it requires a large fluence for the Gd converter, plasma sputtered on an aluminum film, but excellent image quality can be obtained. With a small neutron beam current, a long exposure is usually required. Fluorescent converters like LiF-ZnS,[4] activated with Ag or GdO_2S (Tb) are mostly used for real-time imaging coupled with a nocturnal TV camera. In Fig. 2 the sensitivity of various types of converter is shown using a film exposure method for the film density versus the neutron fluence.

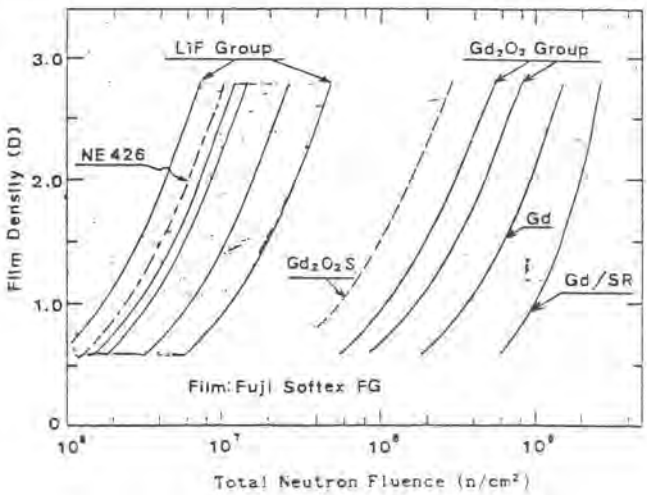


Fig. 2. Sensitivity of several neutron converters using either the Li(n,α) or the Gd(n,γ) reaction emitting 70 keV internal conversion electrons.

Table 2. Characteristics of the Cyclotron-based NR Facility at SHI

Cyclotron	: Model 370
Particle & Energy	: proton 18 MeV, deuteron 10 MeV, ^{3}He 24 MeV
Current(max)	: 50 μA
Nuclear Reaction	: ^{9}Be(p,n)^{9}B
Moderator	: High density polyethylene at inside
Dimension	: 700 mm cube(400 mm cube)
Collimator	: Borated polyethylene(B_2O_3:10%)
Extraction	: Downward and horizontal direction
L/D	: 32, 44(32), 74 , Field size : 14" x 17"
Neutron flux	Horizontal Vertical
at L/D = 44	: 1.7×10^6 1.0×10^6 n/cm^2/sec
Cd ratio	: 4.2 n/γ ratio : 1.5×10^5 n/cm^2/mR
Neutron Component by ASTM 545-81 Beam Purity Indicator	
Thermal neutron content(%)	: 65.3 (48.1), Horizontal(Vertical)
Scatter " (%)	: 0.5 (8.1)
γ ray content (%)	: 3.7 (1.3)
Pair creation (%)	: 3.2 (1.9)

*( ) is obtained from the umbra shadow method of ASTM E803-81.
*Film : Kodak SR with 25 μ Gd converter

2.1. Cyclotron-based Neutron Radiography Facility

A typical example of a cyclotron-based neutron radiography facility is shown in Fig. 3. In this facility two neutron radiography ports are provided for efficient beam utilization. The neutron beams emerging from the target are directed mostly forward so that vertical beams are collected from the beams directed downwards from the stochastic collisions of the thermalisation process. Therefore the vertical beam port provides more thermal neutrons than the horizontal port. In practice, handling the object material is more convenient for the vertical port, as the objects are simply placed on a film cassette.

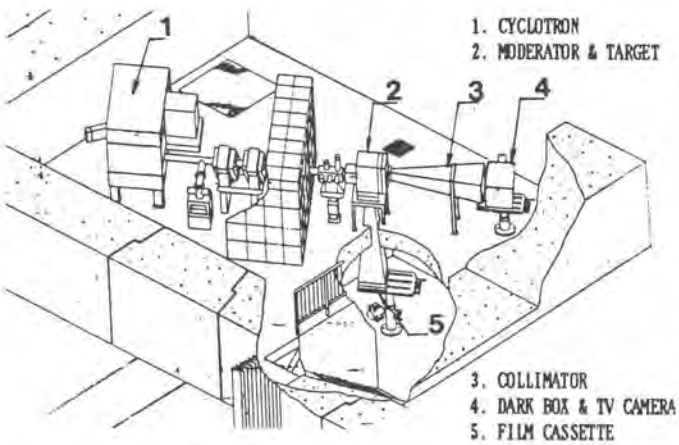


Fig. 3. NR Facility at Toyo Works of SHI.

2.2. Thermal Neutron Enhancement in the Moderation Process

The typical flux obtained is shown in Table 3, where we compare several cases of our improvements to the moderation process by decreasing the target diameter from ϕ120 mm to 60 mm and changing the moderator material from normal to high density polyethylene, where the hydrogen content was 8.0 and 8.3 $\times$ 10^{22} per cc. The smaller target space contributes a large flux increase of 110% and the use of high density polyethylene gives 36%, resulting in an overall improvement by a factor 2.8; but vertical extraction is 62% of horizontal extraction and further improvement is necessary.

Table 3. Thermal Neutron Flux Ratios (%) for $L/D = 44$

Collimator End Direction	Horizontal	Vertical
High/Normal Polyethylene	136%	120%
Target ϕ60/120 mm	210%	145%

Also, this targetry and moderator system was initially tested with 17 MeV and 30 MeV protons at Tohoku University.[5] The thermalization efficiency for each system is compared where the thermalization factor is defined as the ratio of source yield (neutrons/sec) to the peak thermal flux (neutron /cm^2.s) in a given moderator. A typical example[6] gives a value of 40 for Be(p, n) with 2.8 MeV protons and 300 for Be(d, n) with 2.8 MeV deuterons, as summarized in Table 4.

Table 4. Example of Thermalisation Factor for Be(p, n) and Be(d, n)

Energy (MeV)	Source S_0(n/μC)	Thermalisation Factor	Remarks: Target diameter + Materials
p 3.2	10^{11}	40	M.R.Hawkesworth[6]
d 3.2		300	"
p 17	0.93×10^{11}	~940	ϕ120+Normal Poly.
p 18	1.06×10^{11}	1040	"
"	"	1040	"
"	"	880	"
"	"	660	ϕ60+Normal Poly.
"	"	590	ϕ60+High Density Poly.
p 30	3.26	~990	ϕ120+N

3. THE IMAGING SYSTEM AND ITS QUALITY

For real-time imaging the neutron radiography image is converted to a TV signal and digital imaging processing can then be used for construction of the final image. One example of imaging is shown in Fig. 4a and 4b, where a single TV frame with a real time of 1/30 second, and its image integration over 256 frames, are presented, respectively.

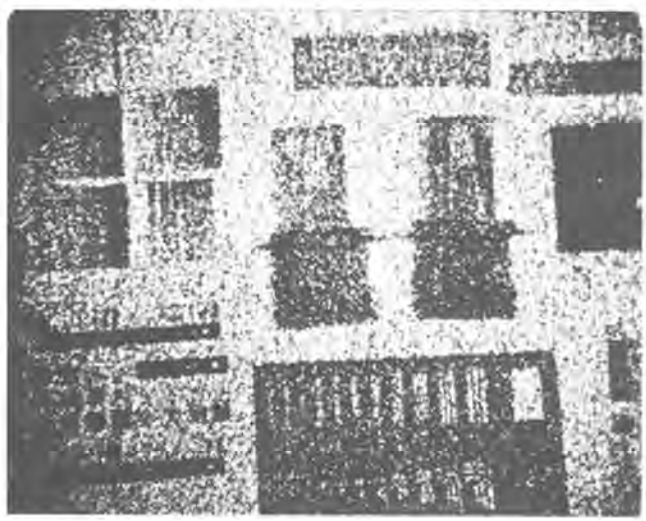


Fig. 4a. One TV frame image of real-time neutron radiograph of turbine blade at neutron flux of 1.1×10^6n/cm^2/sec, with LiF-ZnS converter (A4 Kasei Opto. Inc.) and SIT TV camera (Tokyo Electric Co.) with RCA 4804 SIT tube.

From Fig. 4a the neutron radiographic image looks as if it is composed from dot points and requires great neutron flux density for noise suppression; actually, as shown in Fig. 4b, with 256 frames of image integration, a digital image of 512 $\times$ 512 pixels can be achieved with 8-bit gray levels. A single pixel corresponds to 0.38 $\times$ 0.33 mm^2 in Fig. 4. If the neutron flux is 10^6 n/cm^2/sec,

one pixel receives only 42 neutrons for one NTSC system frame of 33 msec. Statistical analysis of the gray level for a definite domain of pixels showed that the noise appearing in the raw image of Fig. 4a can be explained well by neutron fluctuations due to Poisson statistics.[7] If one integrates 256 frames, the fluctuation decreases to 1% as shown in Fig. 4b, corresponding approximately to 8×10^6 n/cm^2 fluence. This value gives a film density of 3 in Fig. 2 for the fluence versus film density curve for the LiF-ZnS converter that was used for this R-T imaging. Here we can conclude that 10^7n/cm^2 fluence is a criterion for obtaining good neutron radiography images, but images with a few 10^6 n/cm^2 fluence level can be reconstructed by digital local filtering techniques like median, contrast stretching, fast Fourier method etc.

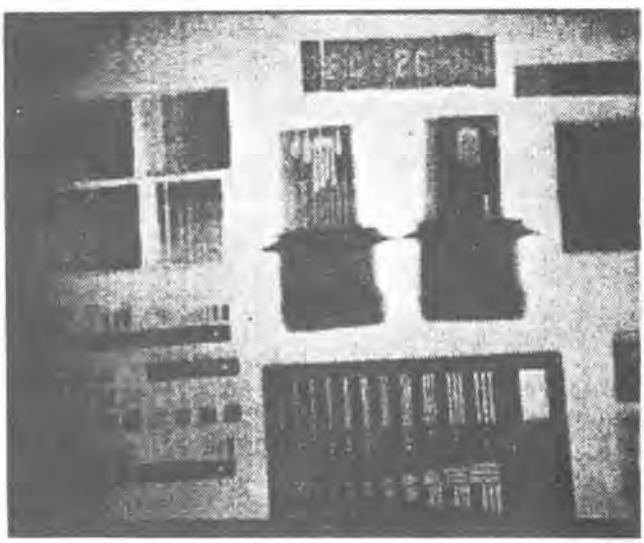


Fig. 4b. Image integration of 256 frames of Fig 4a.

4. NEUTRON RADIOGRAPHY EXAMPLE

We have conducted many real-time imaging experiments on flow visualization as shown in Table 1. One of the real-time NR applications is the visualization of streak lines in liquid metal, as used for the coolants of highly dense heat sources like fast fusion reactors, nuclear fusion reactors, etc. Here we applied real-time NR imaging for visualization of Pb-Bi eutectic metal using a Cd-Au tracer and a Cd dye method. This eutectic metal target is considered as one of the candidates for a neutron spallation target where the cooling is designed to occur by natural convective flow.[8,9] As this target is intended for use with a highly intense 1 mA beam of 590 MeV protons, any turbulence or dead space in the flow may be crucial for the cooling. Observation of the streak line is difficult except by NR, as light and X-rays are not opaque for the metal. A neutron radiograph of the Cd-Au tracer is shown in Fig. 5a, where we made a forced flow of the Pb-Bi, melted at 125°C, from the upper of wall (left) to the center of the hill, in a two-dimensional model of the target, simulating the convective flow of the actual target, where the beams hit the bottom from the down to the up direction. The tracer is prepared with 82.6% gold content to be the same density as the Pb-Bi (10.5) with a shape of few mm length. The arrow lines show the tracers of Au-Cd. Figure 5b shows the streak-lines drawn by tracing the video-tapes of every movement of the tracers by the use of two gray levels of image processing.

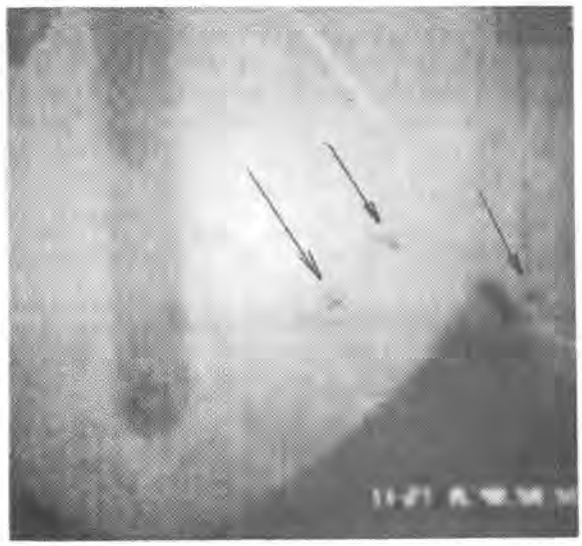


Fig. 5a. Visualization of tracers of Au_3Cd in liquid Pb-Bi eutectic metal.

5. CONCLUSION AND FURTHER POSSIBILITY FOR AN ACCELERATOR SOURCE

We have described a cyclotron-based thermal neutron source using the (p, n) reaction on a beryllium target, together with some examples of NR imaging. H^- cyclotrons have been recognized for their production of high-current proton beams up to the 1 mA level while maintaining stable operation. For efficient moderation of fast neutrons the energy of an H^- cyclotron should be in the 22 MeV energy range. Here we simply extend our 18 MeV cyclotron-based source to 22 MeV by estimating the target yield from Fig. 1 and assuming the same thermalization factor of 600 as at 18 MeV (Table 4). If we can design a target resisting 22 kW heat loss, the thermal neutron flux will reach that from a small reactor – 5×10^6n/cm^2/sec with a L/D=100 collimator. Also, the neutron flux with a subcritical multiplier, fueled with U-235, gave a multiplication factor of five in the previous study.[1] If we use this multiplier for the cyclotron source, the thermal neutron fluxes are at the same level or exceed those from the TRIGA reactor. The conceptual arrangement of the target, moderator and the uranium bundles is shown in Fig. 6. We summarize these results in Table 5 for comparison with another type of intense neutron source.

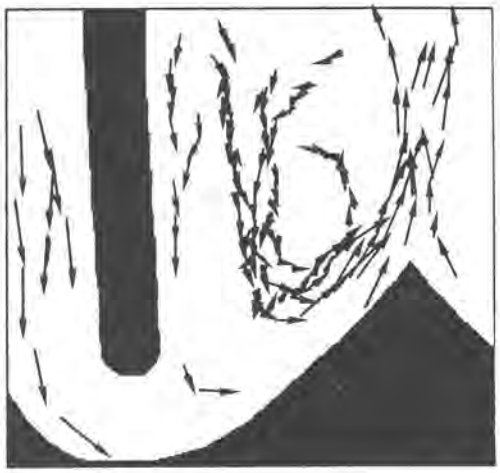


Fig. 5b. Streak lines drawn by movement tracers of Au_3Cd in Pb-Bi eutectic metal in a forced flow from the left of the upper wall to the center of the target.

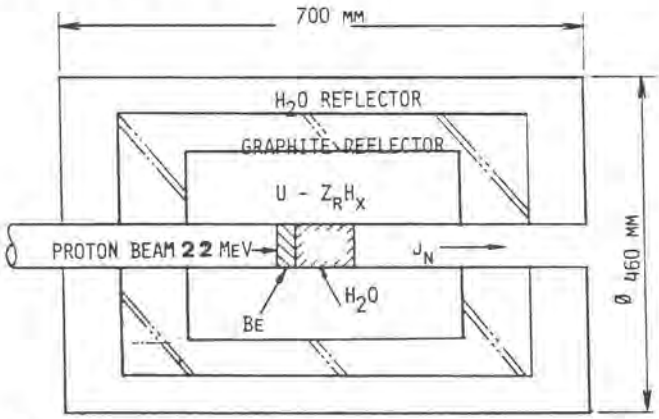


Fig. 6. Concept of amplification of neutrons using uranium bundles and a target.

Table 5. Comparison of typical thermal neutron source

Source	Characteristics	L/D	Source Flux (n/sec)	Output Flux ($n/cm^2/sec$)	Remarks
D-T Sealed Tube	225 kV	12	4×10^{11}	2.5×10^{5}	10)
RFQ Linac	p 3.9 MeV, 1 mA	24	1.3×10^{12}	3×10^{6}	AccSys Catalog
Van de Graaff	d 3MeV, 300 μA	30	2.6×10^{9}	3×10^{5}	3)
TRIGA Reactor	250 kW	100	10^{13}	1×10^{7}	
			($n/cm^2/sec$)		
Cyclotron	p 18 MeV, 50 μA	32	5.3×10^{12}	1.7×10^{6}	H^+ extraction
	p 22 MeV, 1 MA	100	1.6×10^{14}	5×10^{6}	H^- "
	"	100	"	2×10^{7}	U multiplier[2]*

*Assuming a factor five multiplication with water moderator, presuming the normal polyethylene and water are equivalent for thermalization factor.

6. ACKNOWLEDGEMENT

We appreciate Prof. A. Ono, Dr. N. Takenaka, Dr. K. Sonoda of Kobe Univ. group for R-T imaging and the analysis. We would thank Dr. Y. Takeda of PSI for suggesting the liquid metal visualization and offering the model targets.

7. REFERENCES

1) S. Tazawa and T. Nakanii, "Present status of the cyclotron-based neutron radiography" **Proc. 3rd WCNR** (Kluwer, Osaka, 1989) pp.213-220.
2) S. Tazawa and W.L. Whittemore, "Thermal neutron intensity in cyclotron-based neutron radiography systems" *ibid.*, pp.221-229.
3) Jin-Si Kwon and W.L. Whittemore, **Proc. 2nd WCNR** (Reidel, Paris, 1986) pp.231.
4) Y. Suzuki, E. Hiraoka, S. Tazawa *et al.*, "Development of imaging converter", **Proc. 3rd WCNR** (Kluwer, Osaka, 1989) pp.277-279.
5) S. Tazawa and T. Nakanii *et al.*, "Cyclotron-based neutron radiography cacility", **Proc. 2nd WCNR** (Reidel, Paris, 1986) pp.231-238.
6) M.R. Hawkesworth, Atomic Energy Rev. **15**, No.2, pp.169 (1977).
7) R. Taniguchi, A. Ono, S. Tazawa *et al.*, "Statistical properties of R-T neutron radiography image", **Proc. 2nd WCNR** (Reidel, Paris, 1986) pp.555-562.
8) N. Takenaka, A. Ono, S. Tazawa *et al.*, "Visualization of streak lines in liquid metal by neutron radiography", presented at the 4th WCNR, San Francisco, May 10-14, 1992.
9) F. Atchison, W.E. Fischer, M. Pepin and Y. Takeda, "Spallation neutron source", **Proc. on Neutron Scattering in the 'Nineties** (IAEA, Jülich, 1985) pp.171-177.
10) S. Cluzeau *et al.*, "Thermal neutron source using a neutron sealed tube", presented at the 4th WCNR, San Francisco, May 10-14, 1992.

EXTERNAL HIGH CURRENT TARGETRY FOR RADIOISOTOPE PRODUCTION

N.R. Stevenson and W.Z. Gelbart
TRIUMF, 4004 Wesbrook Mall, Vancouver,
B.C., V6T 2A3, Canada

ABSTRACT

A prototype high current 12 kW (400 μA at 30 MeV) solid target system for radioisotope production has been constructed for use with the new TRIUMF/EBCO TR30 cyclotron. Improvements in target body design and construction allow a surface area of 43mm×100mm for plating target materials which are kept below 160°C during the irradiation process. The existing 6kW system employing pneumatic transfer and remote controlled manipulation of the target and shuttle requires very few changes to incorporate this upgrade. With such increases in target current limits the potential of the new breed of cyclotrons, such as the TR30, can be more fully utilized.

1. SOLID TARGET SYSTEMS AT TRIUMF

Two commercial compact cyclotrons exist at TRIUMF for the production of radioisotopes, PET research, etc. A large part of this production proceeds on "Solid Target Systems" (STS). These systems irradiate plated materials on a water cooled target body (for more details of the technology involved see Ref. [1,2]).

The traditional targets used for the STS are shown in Fig. 1. The beam is deliberately diffused over the active surface area (~30×70 mm) by a combination of magnetic defocusing and by aligning the horizontal axis of the target at 7° to the beam to produce a 1:8 magnification factor. Under these conditions the targets are capable of accepting a proton beam up to 200 μA at 30 MeV (6 kW). Water cooled collimation systems, placed immediately before the target, are responsible for the well defined edges of the irradiated plate surface. Under this arrangement, these targets routinely receive almost 200 μA while spilling less than 40 μA on the collimators. The surface temperature of the targets stays below 140° if sufficient water flow (15 litres per minute) is maintained.

The targets are transferred to the target stations from the hot cells along pneumatic transport systems. Targets are briefly placed within carriers ("rabbits") for the journey. At each target station, a manipulation system removes the target and places it in a vacuum box connected to the beamline. Cooling water is connected to the target through the manipulator arm which holds the target securely in place during the irradiation process. An O-ring, placed around the body of the target, seals against a flange on the vacuum box. After the the pump-down procedure (typically taking 10-15 mins) the main beamline valve is opened to the target station and the irradiation can proceed. This procedure is reversed to return the irradiated targets to the hot cells for processing. Complete remote operation of the system is achieved with a programmable logic controller.

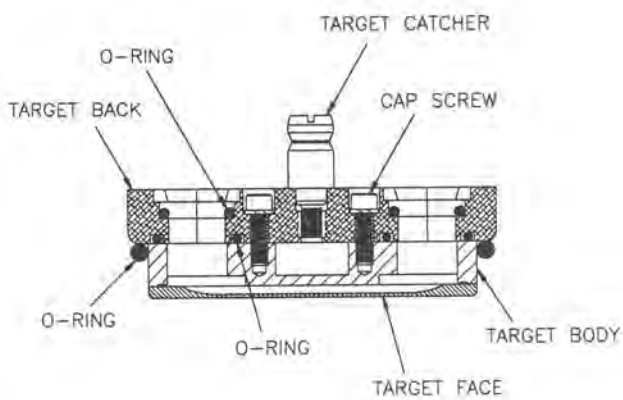


Fig. 1. A 200μA target used on the TRIUMF STS.

Over the years minor improvements to this system have been made. Choices of materials and electrical com-

ponents that are more radiation resistant have reduced the repair/maintenance requirements. Shortcomings, inherent to the original system, have been ironed out one-by-one. For example, the original design incorporated O-rings for sealing the cooling water *on the manipulator head.* This necessitated a routine replacement every two weeks since these items were very susceptible to radiation damage at this location. New targets now incorporate these O-rings on the targets and are changed routinely during the target preparation.

While work continues towards ever improving this target system it became obvious to us that an absolute limit had been reached with regard to beam current on these targets. Because of the thin silver face of the target, necessary to conduct heat efficiently, the water pressure has to be kept at no more than 6 bars to prevent any bulging of the material. Cooling power and beam currents are therefore limited to about 6kW or 200 μA at 30 MeV on these targets. Since modern cyclotron systems can deliver much more than this it is highly desirable to have targetry that can accept these higher powers.

2. HIGHER CURRENT TARGETRY

Methods of increasing the power rating of targets include moving the beam over surfaces or having rotating targets. A much simpler method, in principle, is simply to increase the target surface area and water cooling requirements. For our system this has the advantage of minimizing the changes required to the existing hardware (only three components have to be modified – and these can all be accomplished in situ).

Figure 2 shows the prototype 12kW solid target assembly [3]. Here we have maximized the target surface area available for irradiation (43×100 mm) while keeping the target body still within the geometrical limitations of the present rabbit system for transportation. Water cooling requirements have been doubled to allow correspondingly higher power levels. The beam incident on the target face is diffused to twice the area thereby keeping the collimator to target ratio the same. The power density remains the same at the centre of the target.

Another specific improvement is to the target body material which we have constructed from aluminum (rather than the traditional copper) so that the new targets are in fact lighter (500 g) than before and are not a problem for the pneumatic transfer system. Aluminum is also a better choice of material in terms of residual radiation after radioisotopes have been produced. The aluminum is soft soldered to the silver target face after the aluminum body is copper plated. A central rib is connected between the target silver face and the body. This gives added strength and an additional route for cooling to the target.

The remote manipulation of the target on the 6kW targets involves grasping and locking onto a target "nipple". Due to the geometrical limitations of the new target design, the nipple has been replaced by an insert as shown in Fig. 2 with the corresponding changes to the manipulator head.

Tests with modified 6kW targets show that this styl of target performs equally well as the traditional (copper bodied) targets.

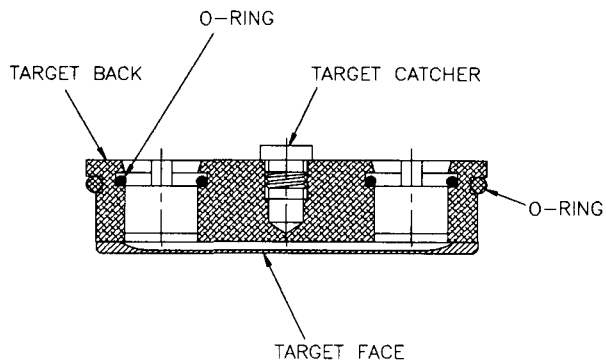


Fig. 2. Higher current (12kW) solid target.

3. CONCLUSION

To address the increasing requirements for radioisotope production on external targetry the TRIUMF TR30/CP42 solid target system is being upgraded to 12 kW (400 μA at 30 MeV protons). This is being achieved primarily by a corresponding increase in surface area and water cooling and is designed such as to utilize most of the existing STS hardware. The first complete prototype will be installed later this year on the TR30 system.

4. REFERENCES

1) Pinto, G., *et al.*, "Target Systems for Radioisotope Production," in **Proceedings of the 7th Conf. on the Applications of Accelerators in Research and Industry**, Denton, Texas, 1982.
2) Burgerjon, J.J., *et al.*, "A High Power Target System for Radioisotope Production," in **Proceedings of the 11th Conference on Cyclotrons and their Applications,** Tokyo, 1986.
3) Gelbart, W.Z. and Stevenson, N.R., "High Current Targetry for Radioisotope Production," in **Proceedings of the Fourth Int. Workshop on Targetry and Target Chemistry**, Villigen, Switzerland, 1991.

A REMOTELY CONTROLLED ROBOTIC VEHICLE FOR WORK WITHIN RADIOACTIVE ENVIRONMENTS

N.R. Stevenson, P. Bloemhard, M. Brigham, J. Ko, C. LaForge, J. Orzechowski, E. Pattyn, and T. Rattray
TRIUMF, 4004 Wesbrook Mall, Vancouver,
B.C., V6T 2A3, Canada

ABSTRACT

A remotely controlled manipulator arm mounted on a miniature vehicle, originally designed for explosives ordinance disposal, has been modified for use in remote handling and inspection within the TRIUMF CP42/TR30 facility. Use of several cameras and accessories enables the detailed inspection of cyclotron and targetry systems at close range in high radiation environments. A modified manipulator enables the performance of simple tasks thereby saving personnel dose and (cooldown) time. The system is general enough for application in any cyclotron or radiation environment.

1. INTRODUCTION

1.1. Objectives

Radioisotope production facilities, such as the CP42 and TR30 cyclotrons at TRIUMF, use high intensity (several hundred μA) beams in the irradiation process. The resulting residual fields, particularly in target caves, can be quite high (~10 mSv/h) depending on the extent and nature of the irradiation. The drive to ever increasing currents and higher running efficiencies can be hindered or limited by several factors such as maintenance and repair requirements which increase with the load put on the system. To some extent this limits the efficiency of operation. Longer cooldown times are required for personnel access after particularly intense or long running periods. By prudent choices of materials and careful design the need for repairs and maintenance can be reduced.

The Isotope Production Group at TRIUMF is responsible for operation, maintenance, and improvements to the CP42 and TR30 systems. Experience has shown relatively simple tasks such as hot target retrieval and viewing target stations, beamlines, cyclotron systems etc., contribute several 10s of mSv to the overall group radiation dose each year. In addition, work is often hurried, shortcuts taken, etc. due to the awareness of the environment in which the person is working. This unfortunately can result in the need to redo the work or the problem reoccurring later thus compounding the radiation dose problem in the long run.

While the majority of work done in the radioactive environments is highly skilled and requires the versatility and adaptability that can only be provided by human workers there are some simple (yet potentially dose intensive) tasks, such as hot target retrieval and inspection work, that potentially could be undertaken by automated methods. We investigated various means of achieving this with the result that the most comprehensive solution was determined to be a system based on a remote controlled robotic vehicle.

1.2. Basic Robotic Vehicle

The prototype of a miniature remote vehicle (MRV) was purchased from Hovey Industries Ltd. This vehicle, shown in Fig. 1, was designed originally for explosives ordinance disposal (EOD). Basically, MRV contains three major sections : the drive, manipulator, and control systems.

The drive system is based on high efficiency permanent magnetic motors driving cleated tracks. The design gives high forward and reverse traction but low turning resistance. Full speed right angle and zero radius full circle turns are possible without losing the track. It can laterally traverse 30° slopes in addition to climbing stairs and slopes up to 45°.

The manipulator consists of an turret, boom, and arm systems on which a claw type hand is mounted. A particular feature of this vehicle system is its tremendous dexterity as demonstrated in Fig. 1. It has the ability to reach just about anything within a 2m radius of the boom base even within a confined area. It has the capability to lift objects up to 7 kg. A mount for a camera and other accessories was provided.

The control of the system is based on a microprocessor that processes audio, video, and data signals. Either a co-axial or radio link is available with a system incorporated to prevent cross talk from noisy environments. The control console is ergonomically designed to accentuate ease of operator control and monitoring. In particular,

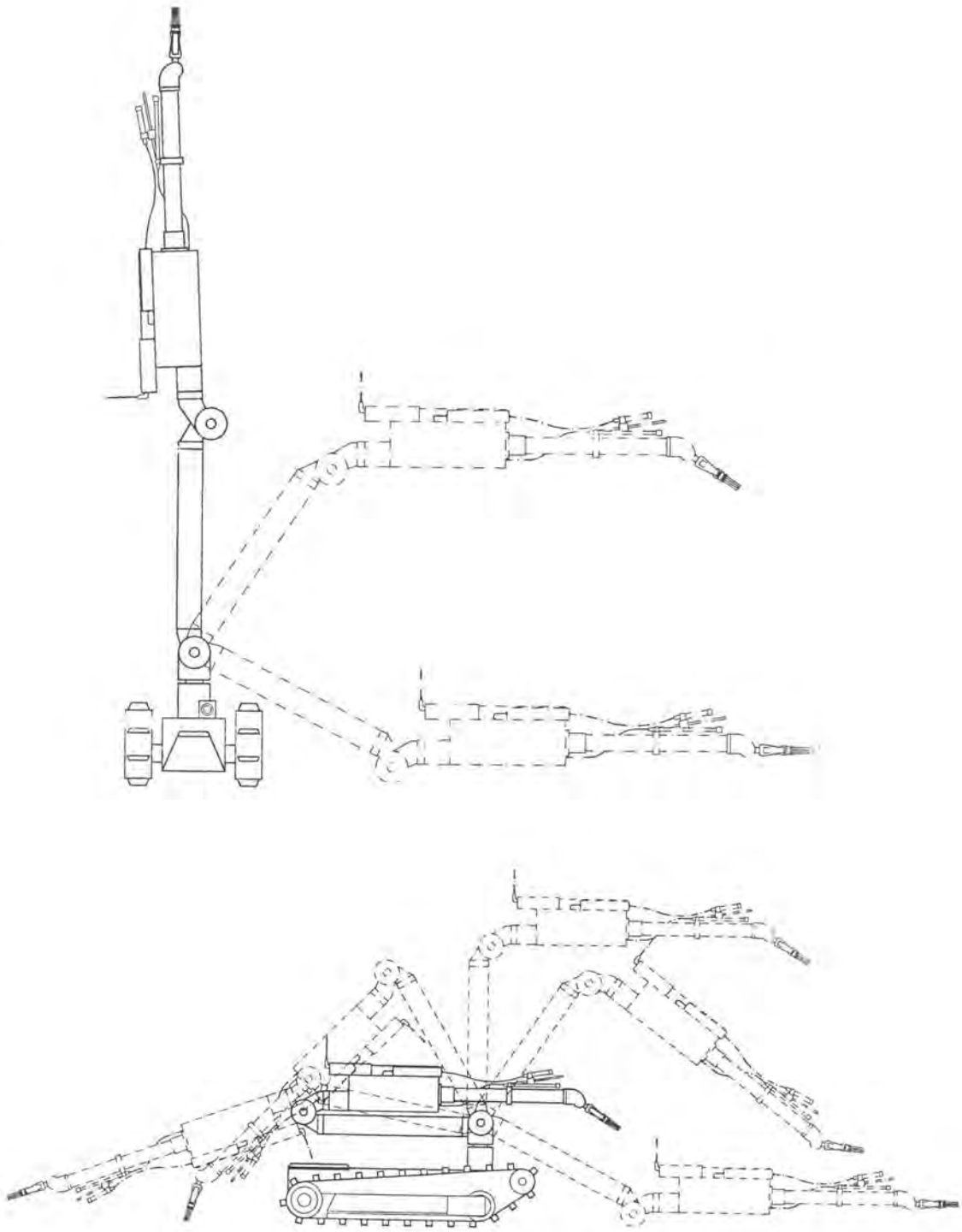


Fig. 1. The basic MRV model demonstrating its dexterity and reach capabilities.

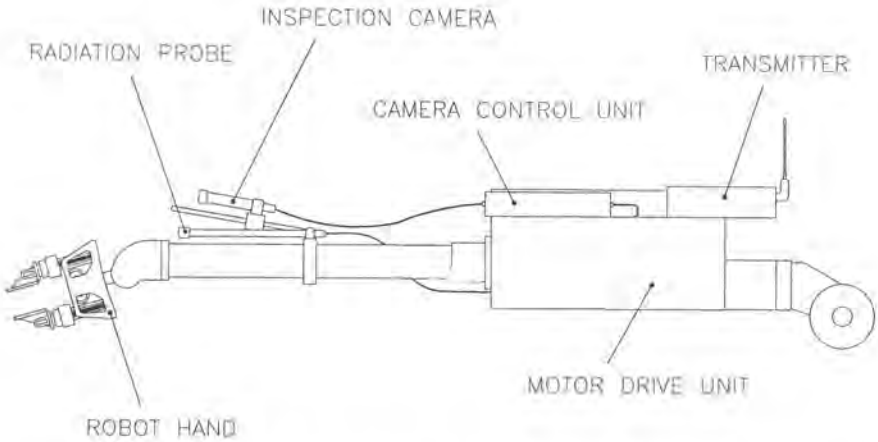


Fig. 2. The new manipulator arm designed to pick up hot targets and other small objects.

multi-function joy sticks give proportional control over drive and manipulator functions.

2. IMPROVEMENTS AND ADAPTATIONS

2.1. Manipulator Arm

Tasks that could be undertaken by the MRV are numerous. While hot target retrieval is no longer undertaken frequently it is a good example of a high dose simple task that should be possible with the MRV. Therefore, one of our primary goals was to design a suitable manipulator hand that could be attached to the present arm replacing the claw mechanism that was designed for EOD work. A schematic of the prototype hand is shown in Fig. 2. This hand is a modification of the present manipulator system currently being used in the hot cells for processing radioisotopes, handling targets, chemicals etc. Since the system works well in the hot cells for preparing targets it is also well suited for the task of hot target retrieval.

2.2. Vision and Monitoring System

Areas in which cyclotrons and target stations are situated are often confined and contain delicate equipment. To negotiate a path through this maze and perform the task under consideration requires an operator who is skilled at controlling the MRV. Obviously, the operators requires sufficiently good visual information to perform this correctly. Some areas may have wide angle or panning camera systems that can be of great assistance. In general, though, the best solution lies in on-board cameras.

The MRV came with the provision for two cameras. A navigation camera is mounted on the chassis. The second camera, which was mounted on the back of the manipulator arm, has been replaced with a miniature camera on the wrist of the new manipulator hand for close-up viewing of local objects.

Radiation monitoring is performed by using a monitor attachment near the manipulator hand with information being fed to an LED display in the direct view of the navigation camera.

3. FUTURE PLANS

Future plans for this device include the following :

- Improve the precision of motion through the use of anti-backlash gears on the arm, boom, and turret.
- Drive train operation will be smoothed out by improvements to the track slides and idlers.
- A wheeled version of the drive system may work better on certain surfaces.
- The communications will be upgraded to use commercially available components (e.g., PLCs) and include such things as control feedback for positional information and allow proximity, radiation, and temperature information to be read at the control console.
- The versatility of the navigation camera would be increased if it were mounted on a separate boom with zoom, pan, and tilt capabilities.
- The arm motor drive has the provision to allow for rotational motion. Having a selection of different end-effectors (i.e., the manipulator hand, claw, grappling hook etc.) would accentuate this degree of freedom for certain types of work.

4. CONCLUSION

A remotely controlled robotic vehicle with a mounted manipulator hand has been adapted for viewing and performing simple tasks in the CP42 and TR30 radioisotope production facilities at TRIUMF. Changes to the manipulator hand and the vision/monitoring systems enable it to do hot target and similar basic tasks in addition to inspecting target stations at very close

range. Little or no cooldown is required thereby saving production time and also personnel dose. The system is robust and resilient enough to be used in other radioactive environments (e.g., other cyclotrons, irradiators, nuclear reactors etc.). Other potential uses include waste management in chemically hazardous/toxic environments and explosives ordinance disposal (its original purpose).

THE NEW MOLECULAR MEDICINE

Henry N. Wagner, Jr. M.D.
Division of Radiation Health Sciences, The Johns Hopkins University, School of Hygiene and Public Health,
615 North Wolfe Street, Baltimore, MD 21205-2179, USA

Nuclear medicine is based on the concept that diseases can be characterized by in situ molecular abnormalities. Advances in our understanding of intra- and intercellular communication are revolutionizing the practice of medicine. In the future, diagnosis, treatment and the monitoring of the response to treatment will be molecular. NanoDx probes will search out molecular abnormalities within different organs and parts of organs. NanoRx probes will correct them.

Modern scientific medicine is moving away from an organ orientation, and is advancing by leaps and bounds through a holistic approach to disease, exemplified by revolutionary advances in human genetics, immunology, oncology, endocrinology, neuropsychiatry, and molecular biology, all of which are holistic approaches to disease. The new, integrated, global approach of nuclear medicine goes beyond anatomy and gross pathology to physiology and molecular medicine. In the future, localized diseases are likely to become the exclusive domain of surgeons, a field in which an anatomical orientation will continue to advance dramatically through advances in anatomical and pathological imaging.

In the practice of molecular medicine, patients' problems can be viewed as molecular dysfunction, not structural abnormalities (structure and function converge at the molecular level). Molecular "slices of life" provided by nuclear medicine will join histopathology as a way to characterize disease.

The practice of medicine remains strongly influenced by a concept described 150 years ago by the great physiologist, Claude Bernard – the concept of the extracellular fluid as the milieu interieur, or internal environment – which maintains a constancy which buffers the cells of the body from the changes that occur constantly in the external environment. Examination of the constituents of blood and urine, commonplace in medical practice today, reflects Bernard's concepts. Nuclear medicine extends Bernard's concepts by making it possible to study the cells themselves, including their importantant interface with the extracellular fluid that surrounds them. Radioactive tracers make it possible to examine regional blood flow, cellular bioenergetics and intercellular communication, the latter involving membrane and intracellular receptors, enzymes and substrate transport systems.

Although the number of radiotracers has expanded greatly, the principles of "molecular nuclear medicine" remain the same as when the first studies of the thyroid were carried out half a century ago. By studying the accumulation of radioactive iodine by the thyroid gland, it was possible to examine the accumulation of environmental iodine and track the formation of thyroxine and other thyroid hormones. The first study in which I was involved in nuclear medicine was the mapping of the accumulation of radioiodine in thyroid nodules with a hand held Geiger tube positioned at 1 cm intervals over the neck in order to determine whether a nodule of the thyroid gland was functional, that is, accumulating radioactive iodine. This laborious, time-consuming task was simplified by the invention of Benedict Cassen, who in 1951 invented the rectilinear scanner in which a crystal radiation detector was automatically moved back and forth over the neck for the portrayal of regional thyroidal function. Its commercial development occurred in the late 1950's.

In 1960, the radionuclide, technetium 99-m/molybdenum generator was developed by Stang and Richards, and advertised for sale by the Brookhaven National Laboratory at a time when no one had any idea of how the technetium-99m would be used. In 1963, Paul Harper at the University of Chicago recognized the technetium-99m's emission of 140 keV photons, decay by isomeric transition, and 6 hour half life were ideal for use in nuclear medicine.

In 1958, Hal Anger described the first scintillation camera at the meeting of the Society of Nuclear Medicine in the United States, but his exhibit drew little interest. Nevertheless, the combination of technetium 99-m and Anger's scintillation camera, and the movement of industry into the field led to a logarithmic phase of growth that continued until the 1970's, at which time a plateau was reached, related chiefly to the development of computed tomography (CT). This brought about a great decrease in nuclear brain scanning, and the first exodus from nu-

clear medicine. The development of positron emission tomography (PET) by TerPogossian, Phelps and Hoffman at Washington University moved nuclear medicine into a new logarithmic growth phase, and encouraged industry to develop single photon emission computed tomography (SPECT) to facilitate the extension of PET successes into more widespread clinical use. TerPogossian had been among the first to recognize the potential of the cyclotron for producing short-lived radiotracers, such as oxygen-15, carbon-11 and fluorine-18.

Whitehead has written: "It is a well-founded historical generalization that the last thing to be discovered in any science is what the science is really about. Men go on groping, guided merely by a dim instinct and a puzzled curiosity until at last some great truth is loosened." Nuclear medicine has become molecular medicine. Its images are concerned with the temporal as well as spatial distribution of the molecules of the living human body. Health requires the proper integration of hundreds of billions of chemical reactions. Proper functions require proper chemistry, and diseases can be defined at the molecular as well as cellular level, often before structural changes have occurred.

Nuclear medicine has the technology that can extend to medical practice the enormous advances in molecular biology and genetics. Two principles of genetics are of special relevance to nuclear medicine: pleotropism and genetic heterogeneity. Pleotropism is the condition in which a single gene defect does not affect a single tissue or organ, or even a single organ system, but can lead to many different manifestations of disease. Genetic heterogeneity describes the fact that abnormalities in different genes can result in the same clinical syndrome. Thus, it is necessary to examine molecular phenotypes as well as genotypes – if one is to see the whole picture. Genes are blueprints for molecules. Genes don't cause disease directly. They express themselves through molecules. The genome is the map; nuclear medicine images the territory.

The microscope revealed the neuron as the fundamental unit of the nervous system. PET/SPECT and more simple radiation detectors make it possible to examine molecular intercellular communication – to examine how neurons (and other cells) "talk" to each other. Electrical "action potentials" transmit information along axons, and there is some electrical neuron-to-neuron communication, but most is by molecular "messengers", carrying information among the 1,000 to 10,000 synapses that connect hundreds of billions of neurons in the human brain. Membrane receptors are involved in the recognition and transfer of information between presynaptic neurons and second and subsequent "messengers", including channels through which sodium, calcium and potassium ions travel. Energy-carrying molecules, such as adenosine tri-phosphate (ATP), modulate the over-all activity of the neurons. With evolution, the increasing complexity of the nervous systems does not seem to have resulted in the development of new neurotransmitters, but rather in the development of incredibly more complex circuitry of neuronal connections, most of which involve molecules, including biopolymers, which "recognize" specific "messenger" molecules that are released locally or circulate through the body until they encounter the appropriate biopolymer on the surface of neurons or other cells which fit their specific configuration. The neurotransmitters have the right shape, charge, and other physicochemical properties to bind to the receptor biopolymers. The patterns and quantities of these "recognition sites" integrate individual cells of the body to make the person a unique, whole individual. "Disintegration" results in disease or death. In the brain, neurotransmitters and receptors affect how we think, feel and act. Molecules are the words that make up the story of our lives – past and present.

The maintenance of life requires intercellular communication, which in turn requires energy, that needed to generate the ion gradients that produce electrical "action potentials" and that needed to synthesize transmitters and receptors. The rate of consumption of the principle source of energy – glucose – can be measured by positron emission tomography.

Since the 1950's, more than 100 neurotransmitters, or "chemical messengers", such as serotonin and dopamine, have been discovered. Many single neurotransmitters, such as acetyl choline, dopamine or serotonin, have different effects on different receptors. For example, acetyl choline stimulates skeletal muscle cells to contract, but causes heart muscles to relax. Muscarinic acetyl choline receptors are excitatory; nicotinic acetyl choline receptors are inhibitory.

The production of the molecules of life is directed by the desoxyribose nucleic acids (DNA) within each cell – including somatic cells – that serve as blueprints for the growth, development, and repair of the molecules that make up our bodies. Molecules must repair themselves when injured, and reproduce themselves when they wear out. When the processes stop, we age or die. Wrinkled skin, poor healing of wounds, and poor memory reflect damaged molecules that accumulate with aging. Antibiotic molecules may be needed to selectively overcome the effects of invading microorganisms. Other molecules may be needed to stimulate or inhibit defective chemical reactions. Many drugs act by stimulating or blocking "recognition sites" on the surface of cells, such as cimetidine that blocks histamine receptors, propranolol that blocks nor-epinephrine receptors, and haloperidol that blocks dopamine receptors. One of the characteristics of chemical receptors, such as those on post-synaptic neurons, is their exceedingly low concentrations, in the range of picomoles/gram. The great sensitivity with which radioactivity can be measured is needed in order to measure receptor concentrations in different parts of the body, such as the brain.

Not only administered drugs, but naturally-occurring neurotransmitter molecules, affect intercellular communication. These include amines, such as nore-

pinephrine, dopamine and serotonin; amino acides, such as gamma-aminobutyric acid (GABA), glutamic acid, aspartic acid, and glycine, and peptides, such as endogenous enkephalins. Neurotransmitters are secreted in varying amounts depending on the number and rate of electrical impuses traveling down the axon of the presynaptic neuron from which the neurotransmitter is secreted. Neurotransmitters bind to enzymes that degrade the unbound neurotransmitter.

In addition to involvement in neuron-to-neuron information transfer, neurotransmitters, including enkephalins, act as modulators of regional neuronal activity. Some chemical "messengers" act within fractions of a second while others have an effect over hours or even days. Thousands of synapses connecting with a single post-synaptic neuron are integrated and determine whether the post-synaptic neuron fires an action potential. The availability of 20 different amino acids means that a vast number of different combinations are possible, and can encode a large amount of information.

Each cell of the body contains billions of molecules of thousands of different types. At birth, molecular blueprints are encoded in the inherited DNA within each cell of the body, making up the "genome" or "genotype", which determine cell structure and, eventually, function. The location of over 1,800 genes on specific chromosomal regions is known. As a result of the "human genome" project, established in the United States in 1988, eventually all 50,000 or more genes will have been assigned locations on chromosomes. Approximately 4,000 human diseases are believed to be genetic in orgin.

The human genome initiative is a joint effort sponsored by the National Institutes of Health (NIH) and the Department of Energy (DOE). The proposal for the project was made originally by the DOE in order to study the genetic effects of radiation on DNA. The NIH was included because of the potential impact on health care. According to Victor A. McKusick: "What Vesalius' anatomy text of 1543 was to medicine in the past, the anatomy of the human genome is to medicine today – a body of knowledge that will inform all future clinical practice."

Where does nuclear medicine fit into the picture? Genes direct the production of molecules that make up the structure of the body, provide energy or carry information. Genetic mutations result in biochemical abnormalities, such as enzyme deficiencies. For example, an abnormality in the gene that signals the development of the pigment melanin results in the phenotype called albinism. Such molecular abnormalities have been identified in about 430 disorders out of the over 1 million classifiable human diseases. Mutations occur in human being at a rate of about one in one hundred thousand cell divisions and affect about one in a million genes per generation. Thus, there is approximately one mutation per 20 persons per generation. Approximately 2,000 specific mutations have brought about identifiable human diseases. About 300 of these affect the brain.

Radioactive tracers make it possible to detect and quantify the molecular abnormalities that the genes bring about. The molecular studies are needed because (as described above), abnormality of a single gene may produce several different types of diseases, or phenotypes. One can illustrate the role of nuclear medicine in the field of cancer. Multiple genes are involved, some resulting in the excessive production of growth factors, and other involving deficient production of growth suppressor molecules, such as somatostatin.

Cancer is the result of genetic and environmental factors. For example, in small cell cancer of the lung, a genetic defect sets the stage for an environmental factor, such as smoking, that finally results in the disease. Many types of cancer, including carcinoid, neuroendocrine cancers, and almost half of the cancers of the breast contain increased concentrations of somatostatin receptors. The increase in somatostatin receptors suggests that a deficiency in the growth-suppressor somatostatin may be the cause of the increase – "up-regulation" – of somatostatin receptors.

Geneticists search for genetic abnormalities in patients with specific syndromes. Another approach, called "reverse genetics", is to search for manifestations of disease when abnormal genes are found. Initially, the search is for an abnormal protein, such as an enzyme. Then the search is for a clinical disorder.

In the 1950's and 60's, inborn errors of metabolism could be detected by amino acid analysis, spectroscopy, spectrophotometry, and the use of newly available radioisotopes. Abnormalities of proteins included enzymes, receptors, and structural proteins. In some cases, a predisposition to disease can be identified by finding an abnormal gene locus even before birth, while the fetus is still in utero. Nuclear medicine makes it possible to extend the search to the molecules involved in intercellular communication.

As described above, there is not a one-to-one relationship between a gene and a disease. As McKusick has written, "it would be ludicrous to conclude that when we have determined the last nucleotide in the human genome, we will know all it means to be human." Radioactive tracers play a major role in trying to connect the genome to human disease. Nuclear medicine can be defined as "in vivo molecular medicine".

Molecular nuclear medicine not only makes it possible to classify disease biochemically, it also provides a new approach to the design and development of drugs. One can determine the relationship between a specific molecular configuration and the in vivo biochemical effects of a drug. The effects of drugs on energy metabolism, synthetic processes, communication and regulatory mechanisms can be expressed in molecular terms. Such knowledge not only provides a more homogeneous selection of patients, but also a way to plan and monitor drug treatment. In the past, pharmacological research consisted of an alliance between organic chemists to make new compounds and pharmacolo-

gists to screen them for possible effectiveness in animals. Molecular nuclear medicine is now involved in drug design, development, evaluation, and monitoring in human beings, as well as animals.

Nuclear medicine techniques can be used to assess the effectiveness of surgery or radiation therapy, and can document the extent of tumors, and progression or regression in response to different forms of treatment. Such data permit modifications of the treatment plan sooner than can be determined by the clinical response of the patients or changes in the size of the lesions. Thus, treatment need no longer be based solely on clinical response, gross morphology or the lesions and histopathological examination of biopsies.

An important characteristic of neoplastic tissue is its increased rate of cell division. In general, accumulation of thymidine into neoplasms is increased in the presence of increased DNA synthesis. Amino acid transport across tumor cell membranes has also been found to differentiate many malignant from non-malignant tumors. Not only membrane transport, but also protein synthesis can be examined if suitable mathematical modeling is used in data anlysis. The accumulation of fluoro-deoxyglucose can be used to measure both aerobic and anerobic regional glucose utilization. Many malignant tumors have accelerated glycolysis compared to surrounding tissues.

In addition to measuring blood flow to tumors, blood volume, substrate incorporation or DNA synthesis, PET and SPECT can be used to measure the number and affinity of hormone receptors which characterize certain tumors. Estrogen receptors are increased in many breast tumors, in both the primary and metastatic sites. Dopamine receptors are often increased in pituitary adenomas.

Fluorine-18 estradiol accumulation as determined by PET makes it possible to tailor the treatment of a specific patient on the basis of the number of estrogen receptors. A tumor containing estrogen receptors is more likely to be treated successfully with estrogen-receptor blocking drugs, such as Tamoxifin, than cancers which do not contain estrogen receptors. The presence of progesterone receptors as well as estrogen receptors is the best prognostic sign. Radioactive tracers that bind to estrogen receptors make it possible to assess the status of the primary breast cancer and regional metastatic deposits. Histopathology alone need no longer be the only criterion for diagnosis, prognosis and therapy.

Receptors are also found on pituitary tumors. Using the depamine receptor binding agent (11-C)-N-methylspiperone, it has been possible to classify pituitary adenomas according to whether they possess dopamine receptors. If the tumors contain such receptors, they can be treated chemically rather than surgically, that is, by administering the dopamine receptor agonist, bromocryptine.

After treatment, measurement of the metabolic activity of the tumor makes it possible to detect persistence or recurrence of the tumor and damage to normal brain tissue, such as that resulting from radiation. For example, (11-C)-methionine is useful for delineating the boundaries of brain tumors, providing information of value in the planning and performance of brain surgery, by permitting differentiation of the metabolizing brain tumor from simple disruption of the blood brain barrier.

THE PRODUCTION OF RADIONUCLIDES FOR THE BIOSCIENCES

Thomas J. Ruth
UBC/TRIUMF PET Program, 2211 Wesbrook Mall, Vancouver, B.C., Canada V6T 1Z3

ABSTRACT

The use of cyclotrons for the production of radioisotopes used in the biosciences has experienced a renaissance during the last 20 years. A major factor for this renewed interest has been the development of the negative ion cyclotron permitting multiple simultaneous beams with differing energies and intensities. With these new cyclotrons, the commercial suppliers of radioisotopes could greatly expand their production capabilities with a single cyclotron. A look at future needs as expressed by the proposal by the United States Department of Energy to build a National Biomedical Tracer Facility are addressed.

In order to appreciate the issues surrounding radionuclide production one must first understand the *tracer principle* which is the basis for the use of these radioisotopes. The tracer principle requires that the tracer behave in a similar manner to the components of the system to be probed, that the tracer does not alter the system in any measurable fashion and that the tracer itself can be measured.

In assessing the radioisotopes that can be used to probe biological systems, there are but a few that have the requisite physical properties that enable them to be used in situations requiring external detection. Table 1 provides some examples. Included are the theoretical specific activities, a measure of the quantity of material that would be introduced into the system to be probed. It is evident that the higher the specific activity the greater the chance that the system will not be perturbed by the introduction of the tracer. For this reason, short-lived radionuclides are often the choice for the tracer.

The advantages associated with short-lived radioisotopes are the low radiation dose to personnel preparing the tracer and subject receiving the tracer, often serial studies can be performed on the same day, and there is little if any waste disposal problem. The disadvantages, on the other hand include the requirement of having an on-site accelerator such as a cyclotron and the burden of

Table 1. Radioisotopes Used as Tracers

Radioisotope	$T_{1/2}$	Theoretical Sp. Act. (Ci/mmol)
^{3}H	12.4 y	29
^{14}C	5730 y	0.62
^{11}C	20.3 min	9.3×10^{6}
^{18}F	110 min	1.7×10^{6}
^{13}N	9.97 min	1.9×10^{7}

- 1 mCi $^{14}C = 9.6 \times 10^{18}$ atoms = 0.22 milligrams
- 1 mCi $^{11}C = 6.5 \times 10^{10}$ atoms = 1.5 picograms

rapid chemistry in order to provide the radionuclide in a usable biochemically active form.

In order to provide a radionuclide for use as a tracer there are a number of production considerations that need to be addressed as outlined below.

1. Energy required to initiate the reaction.
2. Energy where maximum cross section occurs.
3. Chemical form of the target nucleus.
4. Physical form of the target nuclei.
5. Chemical form of the product.
6. Physical form of the product.
7. Ease of separation of the product from the target.

As an example, the production of ^{18}F will be addressed using the above criteria.

Table 2 illustrates the possible reactions one can use to produce ^{18}F. Depending upon what type of accelerator is being used there are a number of reaction processes requiring different bombarding particles and energies.

The target materials cover the full spectrum including cryogenically frozen water targets. The chemical

Table 2. ^{18}F Production

Possible Reactions:

Reaction	E_{th}(MeV)	E_{max}(MeV)
^{18}O(p,n)	2.6	6.0
^{20}Ne(d,α)	0	5.5
^{16}O(^{3}He,p)	3.8	7
^{16}O(α,pn)	23.2	37
^{nat}Ne(p,X)	26	45

forms include elemental and simple compounds of oxygen as well as neon gas. The product is in two basic chemical states, either as aqueous fluoride or as fluorine gas. The ease of separation of product from target depends on the physical/chemical forms of the two. In the case of the neon, the target material is chemically inert and does not participate in any subsequent reactions. For the water targets, the fluoride ion is usually trapped to separate from the target material and then taken up in a non-protic solvent. The F_2/O_2 system is still under investigation but shows promise for use in a number of situations.

For many target configurations there is still controversy as to the target chamber materials that should be used. For the case of water targets, the choices include silver, titanium and nickel with silver or titanium being preferred. For gaseous fluorine it was long felt that the target chamber must be constructed of nickel or nickel alloys. Recent results indicate that aluminum may be just as useful.

The expected yield from a reaction is determined by integrating the cross section over the energy range of the bombarding particles. The yield also depends upon the particle flux and bombarding time. For short-lived radioisotopes the yield is adjusted by the saturation factor, $(1\text{-}e^{-\lambda t})$ to account for the fact that as the nuclei are produced these same nuclei are decaying.

Quite often the yield from a particular reaction does not equal the calculated yield. Possible causes include the following:

- Wall interactions (low recovery).
- Target gas density reduction in beam path, also cavitation in liquid targets (low production).
- Bombarding energy not optimized (low production).
- Contaminates in the target mixture (low recovery).

In spite of these difficulties, a well designed target can produce yields that approach the theoretical maximum, even at high beam current. In using gas targets, the designs require the use of high gas pressure which presents its own problems, especially with respect to the thin target isolation foils. The construction of gas targets requires a good understanding of heat transfer and material sciences.

Table 3 gives the estimated use, in curies, for a variety of radionuclides used in nuclear medicine over the past decade. Beside the obvious conclusion that the ^{99}Mo/^{99m}Tc generator system dominates nuclear medicine usage, is the fact that there has been a tremendous growth in the use of ^{201}Tl and ^{123}I.

This increase in availability of radioisotopes has resulted from the manufacture of a new generation of cyclotron designed explicitly for radionuclide production. Up until the last 15 years or so most of the cyclotrons that were used as *medical* cyclotrons were multi-particle physics machines with fixed energy electrostatic deflection. For high current operation internal targets were utilized. In the late 1970's, The Cyclotron Corporation introduced the first commercially available negative ion cyclotron.

The negative ion cyclotrons accelerate H^- ions which makes it possible to extract the beam of protons at any energy and to also extract multiple beams simultaneously. These features have the advantage of simplicity of extraction with a thin graphite foil which is extremely efficient, nearly quantitative. And by placing the foil extraction system at various radii, the energy can be varied. With more than one extraction system multiple beams can be extracted simultaneously. Thus, a 30 MeV negative ion cyclotron becomes a highly efficient machine for producing radionuclides. Most of the major radiopharmaceutical companies now own at least one of these cyclotrons.

A less obvious trend is that the use of the chemically inert xenon continues to grow. In spite of the better decay properties of ^{127}Xe in comparison to ^{133}Xe, the latter still dominates in usage. The reason for this is the requirement for a high energy accelerator for producing ^{127}Xe (around 100 MeV). At the present time the only sources for ^{127}Xe are the large accelerators at the national labs in the U.S. and facilities like TRIUMF. Because these facilities use machines designed for physics programs the schedules preclude the routine, reliable production of medical radioisotopes.

Table 3. Estimated Usage of Selected Radioisotopes by Year (curies)

Nuclide	$t_{1/2}$	Retail Consumption 1982	Retail Consumption 1987	Retail Consumption 1990
^{99}Mo/^{99m}Tc	66 h/6 h	100,000 (^{99}Mo)	120,000	150,000
^{111}In	68 h	150	160	185
^{123}I	13.2 h	75	1,250	3100
^{127}Xe	36.4 d	100	100	100
^{133}Xe	5.2 d	25,000	25,000	45,000
^{201}Tl	73 h	500	2,500	6,000

In addition there are a number of other radioisotopes that are not readily available through the commercial route which have the potential of having importance in medical research as diagnostic or theraputic agents. The U.S. Department of Energy at the urging of the Society of Nuclear Medicine has organized a number of workshops to address ways these radioisotopes can be made available. At the most recent workshop at Purdue University, a draft mission statement was formulated which included the following aims.

- Production of research radionuclides
- Research – production, separation and purification of radionuclides
- Education and training
- Research in basic radiopharmaceutical chemistry
- Production of commercial radionuclides

In order to meet the mission the accelerator was to have the following design features:

- Proton beams
  - 30 - 100 MeV, variable to 1 MeV increments.
  - >750 μA.
- 2 High intensity beam lines
- 2 Low intensity beam lines
- Any 2 operational simultaneously
- Operation -
  - 24 hours/day
  - 7 days/week
  - Minimum of 46 weeks/year

The outcome of this movement awaits Congressional action.

This presentation began as a retrospective look at the roots of radionuclide production. If we are to be more than simple historians we need to examine the basis of this evolution and try and learn from the experience. Thus it seems fitting to speculate on the future of cyclotrons, as seen by this author and in doing so we can look forward to seeing cyclotrons in the following areas.

- (>100) Small cyclotrons (3–18 MeV) located at regional centres and large research hospitals.
- (10-20) Production cyclotrons (30 MeV) operated for commercial production and distribution of radionuclides.
- (1 or 2) High energy cyclotrons (100 MeV) located at national research centres.

So it is with these predictions that designers of cyclotrons are challenged to find ways to make this a reality so that biomedical research can continue to grow to the benefit of all.

A FACILITY FOR RADIOISOTOPE PRODUCTION AT TRIUMF WITH 70-110 MeV PROTONS

D.R. Pearce and J.S. Vincent
TRIUMF, 4004 Wesbrook Mall, Vancouver, B.C., Canada, V6T 2A3

ABSTRACT

A radioisotope production facility using protons between 70 and 110 MEV and currents in excess of 70 μA has been operating for several years at TRIUMF. This beam operates simultaneously with two other research beams from the 500 MeV cyclotron. 10 curies of ^{82}Sr were produced for commercial sales with 53.8 mAh of production in 92 days. The beamline is radiation hardened, modular and pre-aligned for ease of remote handling. Four production targets are accessible to the beam from a multiport switching magnet. These targets can also be handled remotely. The target control system uses CAMAC and a commercial, object oriented program which operates from a stored data base. Recent improvements and current applications of the production facility will be discussed.

1. INTRODUCTION

A dedicated radioisotope production facility is located adjacent to the TRIUMF 500 MeV H^- cyclotron. It consists of beamline 2C (BL2C) that can extract protons from 65 to 120 MeV with beam intensities up to 100 μA and four target stations that are mounted in the cyclotron vault wall (fig. 1). A fifth station in an adjacent area is planned for proton therapy. A switching magnet with seven ports delivers the beam to the selected branch line 2C1-7. The target station on line 2C4 is a solid target facility (STF) that is currently being used for production of ^{82}Sr and for the development of several other isotopes. Preliminary measurements for proton therapy have been made on 2C1. The lithium bromide target on 2C2, the sodium iodine target on 2C3 and the molten cesium target on 2C5 are uncommissioned. There is a Faraday cup on 2C6 for calibrations and one unused beam port, 2C7. All of the targets were designed for rapid removal into a shielded transfer flask and for repair in a remote hot cell.

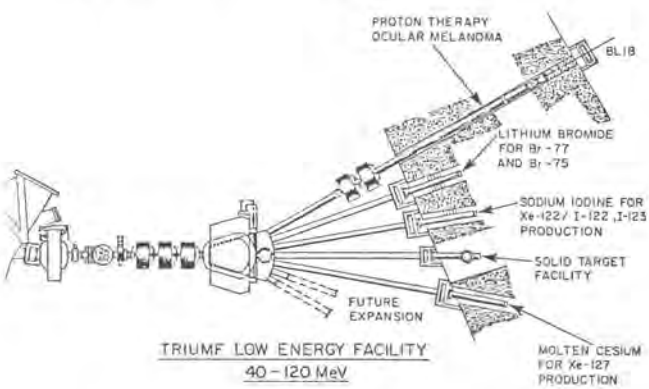


Fig.1. Beam line 2C (BL2C) and the four target stations used for radioisotope production.

The purpose of this facility is to develop isotope production technology at 65-110 MeV up to high intensity levels for medical research and future commercial exploitation. A major advantage is that isotope production on BL2C is done with almost no impact on the other beam operations at TRIUMF. Typical high circulating beam currents in the cyclotron for multiple simultaneous extractions are BL2C extracting 40 μA at 85 MeV, BL4B extracting 100 nA at 350 MeV and BL1A extracting 140 μA at 500 MeV. However, it is often necessary that the ratio of beam intensities (split ratio) in these beamlines vary by 10^4 depending on the application.

2. RECENT IMPROVEMENTS

Recent improvements in beam extraction, diagnostics and controls have resulted in regular production of ^{82}Sr for supply to North American market. A change in the target capacity of the STF was also made to increase the production rate of ^{82}Sr. The following sections describe these recent additions.

2.1. BL2C extraction mechanism

It is necessary to select the optimum incident and exit proton energies for production targets to maximize the yield of desired isotope species while minimizing the yields of undesired species. This requires that beam can be extracted over the complete energy range of the production facility. Furthermore, it is necessary to have a selection of foils available in the extraction mechanism for remote replacement when damaged by intense beams and also to alter the split ratio as mentioned above. The original 2C extraction mechanism used four single foil mechanisms positioned for discrete energies. Another undesirable feature of this mechanism was that the stripping foils were rotated into the beam which caused unnecessary beam steering as a function of the intensity split ratio. The new extraction probe described here corrects this problem and satisfies all of the requirements noted above. It was installed in the fall of 1990 after extensive testing in the laboratory. It has three orthogonal

foil positioning mechanisms which are accurate to 0.1 mm. This allows continuous operation over the energy range of 65 to 120 MeV. The energy spread is 0.5 MeV due to overlapping orbits in the cyclotron. The beam intensity can be varied over a range of 10^4. Six different, reusable graphite foils (pyrolytic) are available from a carousel attached to the probe positioning mechanism, (figure 2). The carousel is designed for quick replacement. During normal operating periods, 8-12 weeks, 30 mAh of beam charge is extracted with intensities up to 45 μA. In this period two or three of the foils, 2.5-4.0 mm wide, are typically damaged. A range of foil widths from 0.1 mm to 8.0 mm is required to obtain the split ratio variation noted above. The stripper mechanism employs three DC motors with absolute shaft encoders for positioning and it is controlled by a microprocessor that communicates with cyclotron control system via the CAMAC highway. The entire mechanism is mounted on a frame which is attached to the tank lid and can be installed or removed by standard, in-tank remote handling equipment.



Fig. 2 . An extraction foil deployed from the foil carousel.

2.2. Diagnostics

For successful operation of the facility it is necessary to monitor beam loss to less than 0.1 μA out of 50 μA, to maximize isotope production and to minimize beamline activation. This is achieved by accurate total current measurement, by accurate beam profile measurement and by target protection. The original nonintercepting total current monitor had been sync6hronized with the time of flight signal so that whenever the extraction energy was changed the electronics required retuning. The electronics were changed to incorporate a 1 KHz digital comb filter that is synchronized to the RF fundamental frequency. On the STF, a prototype scanning wire monitor has been installed and the target protect monitor has been redesigned. The scanning wire monitor is a pneumatically driven, single stroke cross which passes through the beam at 45°. The cross is made of molybdenum strips which are 0.05 mm wide and 3 mm deep with respect to the beam. The monitor gives good beam profiles from 50 nA-50 μA without causing significant beam losses. It was installed in the 90 fall shutdown. The redesigned halo monitor was installed in June, 91 following the beam destruction of the original which inaccurately measured beam losses. The target protect monitor measures the beam halo using secondary emission foils. The new monitor incorporates a thermocouple in a graphite shielding ring upstream of the monitor and the halo foils have been moved away from the high intensity beam but out of the beam shadow of the graphite ring. This improved halo monitor design is being used in the other 2C lines.

2.3. Controls

The 2C targets control system must monitor all of the targets parameters and take the necessary actions. Space restrictions in cyclotron control console meant the 2C targets must be controlled through a single terminal that could be configured to an individual operator's needs with multiple, responsive displays. The 2C control system that ran on a PDP11 was replaced in 1990 with VISTA™, a current value database programme using a graphical, user interface that runs in a microVAX II. This programme allows icon displays and mouse control as well as on-line editing on sections of the 2C controls. VISTA recently underwent several upgrades along with terminal improvements in the main control console so that multiple displays with 1 sec. response are available and programme crashes are less frequent. Initially the displays would only control a single action such as starting a pump or opening a valve and would read back monitoring devices such as thermocouples, flow meters and pressure transducers. In the STF, targets are lowered into the beam by a water system that is isolated from the target cooling water. To insert, remove, or cool a target, a sequence must be followed that depends on various conditions in the STF. To automate these operations and reduce the chance of operator error, process controls have been developed for the STF using VISTA and will be used in the other target controls[1]. Figure 3 show a typical terminal screen with a display indicating the state of the individual components including the halo monitor, a display for setting the process and several icon displays. The STF has been set to *TUNE* which means the cooling water system is running to act as a beam dump but the target is not inserted.

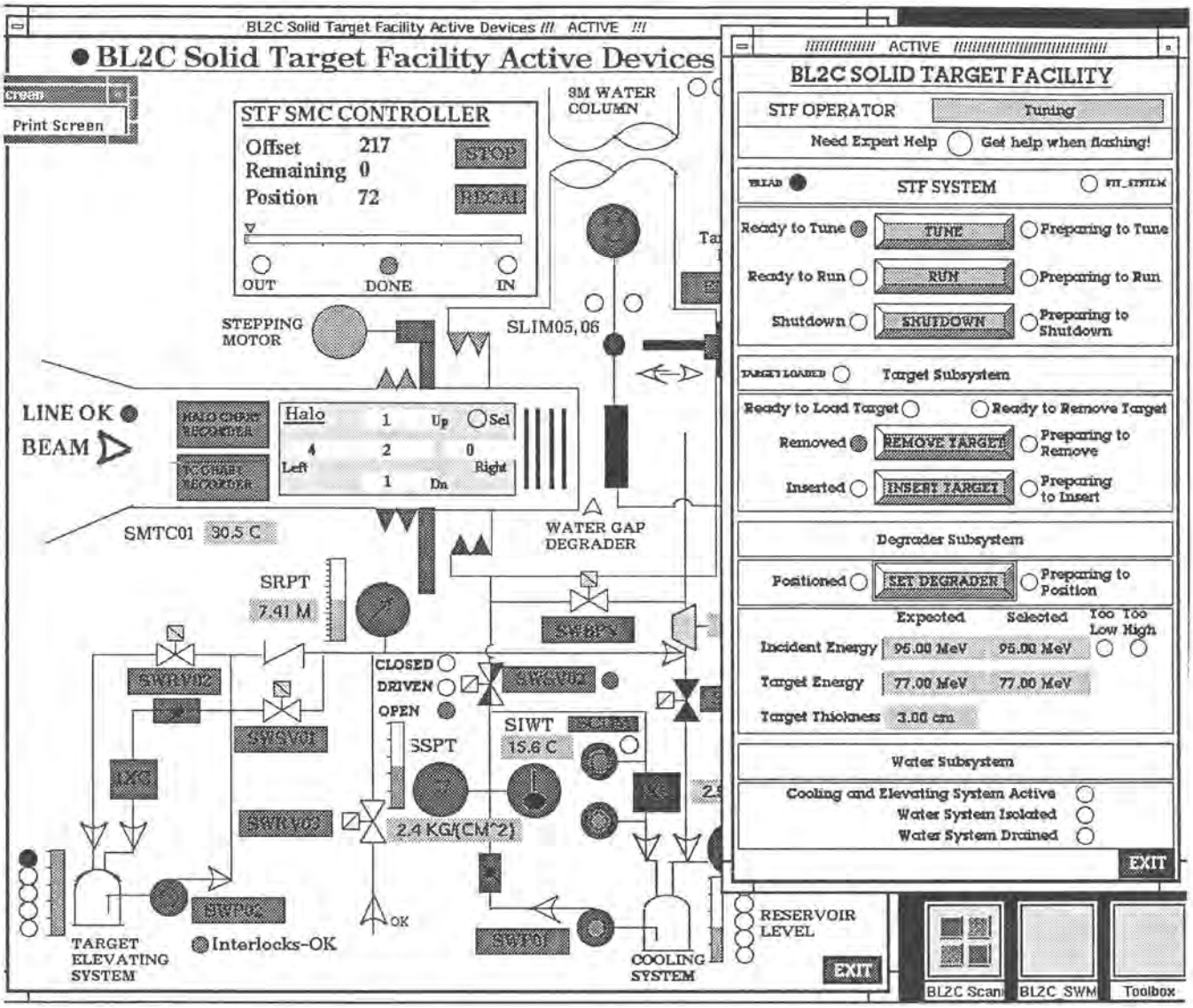


Fig. 3. A typical terminal screen with two displays and several display icons.

2.4 Enlarged target capacity of the solid target facility

The original solid target facility had been designed for targets thinner than 8 mm and densities greater than 3 g/cm^3. However, in the case of metallic rubidium the density is only 1.5 g/cm^3 and improved yields of ^{82}Sr can be obtained by increasing target thickness and incident beam energy in correlation. In the spring of this year, it was decided to remove the solid target facility and rebuild the target receiver to accommodate 30 mm steel cassettes, 4 g/cm^2. To accomplish this activity, it was necessary to remove the bottom section of the facility to a hot cell where it was remotely disassembled and the new receiver was installed. In more than five years operation, this was the first instance where the remote handling devices and special facility design for remote service has been exercised. Radiation fields of about 10 R/h were measured inside the STF target cave. The activity was satisfactorily completed in 30 man days with an accumulated dose of 0.6 man-rem distributed among 4 persons. The improved performance is described in the following section.

3. RECENT OPERATIONS AND APPLICATIONS

During the last year, 1991 and the first half of 1992, about half of the available operating time has been devoted to high level production of ^{82}Sr and the improvement of production and processing technologies

developed earlier. Metallic rubidium targets, 1.8 g/cm^2, have been bombarded with 62 MeV protons as shown in the following table. The average beam current noted includes an average of 1.2 days per week where there was no beam due to cyclotron maintenance activities. The beam is normally 30 to 45 μA during bombardment and one target was run at 70 μA for a test of the cooling system. The short run ^{82}Sr production rate, i.e. neglecting decay, is 0.22 mCi/μAh. Currently, 4 g/cm^2, rubidium metal targets are being tested with 76 MeV protons up to 100 μA in a effort to shorten the batch production time from three weeks to one.

RADIOISOTOPE PRODUCTION ON BEAMLINE 2C, 1991
All rubidium targets, 1.8 g/cm^2
61 MeV incedent proton energy

TARGET #	mAh	Ci@EOB
A3	7437	1.40
A6	6230	1.70
A5	5880	1.30
A10	4531	0.93
A12	4400	0.92
A17	1599	0.37
A16	8140	1.60
A15	15603	2.60
TOTAL	53880	10.3

The new BL2C stripper allowed operation of the cyclotron at high currents when the primary high current beamline, BL1A, was unable to accept beam because of target problems. 30 μA, 95% of the circulating beam, was extracted by 2C for the irradiation of target A16 with the remainder of the beam passing on to the beamline 4 stripper. This operating mode eliminates the irradiation caused by electromagnetic stripping since most of the beam is extracted at 85 MeV and is an acceptable alternative to production with shared beam when minimum activation of the cyclotron is desired before a cyclotron maintenance. A full 100 μA test is planned in the near future but regular operation at this level waits for an improvement in the ion source and injection system.

4. FUTURE DEVELOPMENT

Other beamline activities center on the search for production schemes of possible therapeutic isotopes, ^{97}Ru, ^{178}W and ^{188}Pt. There are several production schemes for these species and cross sections have been measured for rhodium, tantalum and iridium targets respectively, but the overall viability depends also on the development of efficient and easy radiochemical procedures for separating the desired species from its production target. These procedures are now being investigated. Also there has been a request for ^{122}Xe which is used as a generator of ^{122}I for PET. This requires commissioning of the molten sodium iodide on branch line 2C3. No radio-chemistry is required here as the xenon parent is easily trapped on most surfaces at 77 °K. This target can supply one Curie of ^{122}Xe or ^{123}I in a few hours at 20 μA of 86 or 70 MeV protons. In the next year, beam time will be shared with developments in the external beam area (1B) for proton therapy.

5. CONCLUSION

The radioisotope facility at TRIUMF has successfully demonstrated new techniques for commercial isotope production at high intensities. The recent improvements have allowed the facility to operate smoothly with almost no impact on other TRIUMF operations. Through careful planning and design, the upgrades and operation of the facility have had a minimal impact on the dose budget at TRIUMF.

6. REFERENCES

[1] Wilkinson, N.A. and Ludgate, G.A., "Application of Object Oriented Techniques in the TRIUMF Beam Line 2C Control System". p. 681 of this proceedings.

POSSIBILITY OF PRODUCING SOME RADIONUCLIDES FOR MEDICINE USING JINR ACCELERATORS

S.N.Dmitriev, V.A.Khalkin, R.Ts.Oganessian, G.G.Gulbekyan,
L.M.Onishchenko, G.Ya.Starodub, N.G.Zaitseva
Joint Institute for Nuclear Research, Dubna, Moscow reg., 141980, Russia

ABSTRACT

Prospects of using the JINR accelerators (the microtron MT–25, the cyclotron U–200 and the phasotron) for the production of some medical radioisotopes from various targets at different energies of accelerated ions are considered. Methods of producing the high-purity ^{123}I on the MT–25 and the isotopically ultra pure ^{237}Pu on the U–200 are described. A project of a proton cyclotron dedicated to the production of radioisotopes is discussed.

1. INTRODUCTION

The application of radionuclides for the diagnostics of different diseases and, to a lesser extent, for the radiotherapy has a tendency to growth. A significant part of radionuclides for nuclear medicine are obtained in the nuclear reactions with accelerated ions. The widely used radionuclides are:

1. The gamma-emitters used in cardiology, oncology, pulmonology: ^{67}Ga, ^{111}In, ^{123}I, ^{127}Xe, ^{201}Tl.
2. The short-lived β^+ emitters for PET:^{11}C, ^{13}N, ^{15}O, ^{18}F.
3. Generator isotopes including: the gamma-emitters ^{81}Rb–^{81m}Kr, ^{195m}Hg–^{195m}Au and β^+ emitters ^{68}Ge–^{68}Ga, ^{82}Sr–^{82}Rb, etc.
4. The potentially important nuclides investigated with the aim of introducing them for regular application: ^{52}Fe, ^{73}Se, ^{75}Br, ^{97}Ru, ^{178}Ta, ^{211}At, etc.

The greatest volumes of production and application characterize such nuclides as ^{67}Ga, ^{111}In, ^{123}I, ^{201}Ta, the generators ^{81}Rb–^{81m}Kr, ^{82}Sr–^{82}Rb.

Along with the progress in the creation and wide application in the clinical practice of new efficient electron devices (scintillation chambers, tomographs and etc.) which recreate quickly and in detail the picture of radionuclides distribution in the body, there goes on continuously the search for new promising radiopharmaceuticals.

Active investigations are going on with such radionuclides as ^{97}Ru, ^{211}At, ^{237}Pu, the generators ^{68}Ge–^{68}Ga, ^{178}W–^{178}Ta for which methods of producing the amount required for the routine work are studied. Thus, the ^{97}Ru is regarded as a nuclide possessing greater diagnostic potential than ^{99m}Tc and also as a chemical therapeutic agent for oncology.[1] The ^{68}Ge–^{68}Ga generator is an extremely convenient source for a positron emitter and ^{68}Ga has the same importance for the PET investigations as ^{99m}Tc in gamma-chamber research.[2] The ^{178}Ta becomes important both for the radionuclidic angiography using low energy detectors and for the PET investigations.[1]

2. PRODUCTION OF RADIONUCLIDES AT THE JINR

The possibility of obtaining a number of radionuclides for nuclear medicine on the accelerators of the JINR such as the U–200 cyclotron, the MT–25 microtron, the phasotron and a special high current proton accelerator which can be specially created (U-120I)[3] is considered in the Table. It contains the data referring to the production mode, estimates of the expected yields and of the probable volumes of radionuclides which could be obtained.

The data presented in the Table demonstrate that a large scale production of ^{97}Ru, ^{68}Ge and ^{178}W may be organized on the U–120I proton accelerator (in case it is built).

The table presents methods of producing radionuclides which are most widely used in medicine. There is also a possibility to produce on the JINR accelerators sufficient quantities of other more rare but not less important radionuclides for nuclear-medical investigations such as, ^{26}Al, ^{143}Pm, ^{144}Pm, ^{145}Pm, ^{175}Hf.

As an example, the tecnique of producing isotopically ultra-pure plutonium-237 (for metabolic research *in vivo*) on the U–200 accelerator and short-lived iodine-123 on the MT–25 microtron is described in brief below.

TABLE

JINR Accelerators and production of some radionuclides

A — the U–200 cyclotron, 36 MeV, ^{4}He, 100 μA; FLNR
B — the phasotron, 660 ÷ 20 MeV, proton, 6 μA (internal beam)*; LNP
C — the U–120I proton cyclotron, 35–40 MeV, 100 μA (projected)[3)]
D — the MT–25 microtron, 25 MeV e^{-}, 20 μA; FLNR

nuclide ($T_{1/2}$)	accele-rator	nuclear reaction	energy range, MeV	yield(EOB) mCi/μA-hr	exposi-tion, hr	production yield, mCi
^{68}Ge–^{68}Ga	A	^{66,67}Zn(^{4}He,xn)	35–15	0,001	200	20
(288d/68m)	B	^{nat}Ga(p,xn)	60–15	0,057	100	35
	C	^{69}Ga(p,2n)	35–15	0,044	100	440
^{81}Rb–^{81m}Kr	C	^{82}Kr(p,2n)	35–15	6,5	5	2750
(4,6h/13s)						
^{82}Sr–^{82}Rb	B	^{85}Rb(p,4n)	60–30	0,4	100	220
(25d/78s)						
^{97}Ru (2,9d)	A	^{nat}Mo(^{4}He,xn)	36–14	0,1	20	180
	B	^{99}Tc(p,3n)	50–20	7,0	20	760
	C	^{99}Tc(p,3n)	35–20	3,7	20	6700
^{111}In(2,83d)	A	^{109}Ag(^{4}He,2n)	35–10	0,7	20	1280
	C	^{112}Cd(p,2n)	30–20	6,0	20	10900
	C	^{113}Cd(p,3n)	35–25	9,45	20	17000
^{123}I(13,3h)	C	^{124}Xe(p,2n)+(p,pn)	30–25	10	4(+7)**	4000
	D	^{124}Xe(γ,n)	25	0,1/1g^{124}Xe	10(+2)	200
^{127}Xe(36,4d)	B	^{133}Cs(p,7n)	100–60	0,47	50	140
	C	^{127}I(p,n)	35–10	0,015	100	145
^{178}W–^{178}Ta	A	^{176,177}Hf(^{4}He,xn)	35–18	0,07	100	625
(22d/9,3m)	B	^{181}Ta(p,4n)	60–30	1,3	50	370
	C	^{181}Ta(p,4n)	35–30	0,3	20	580
^{195m}Hg–^{195m}Au	B	^{197}Au(p,3n)	50–20	10	5	290
(40h/30s)	C	^{197}Au(p,3n)	35–20	6	10	5600
^{201}Tl(3,06d)	C	^{203}Tl(p,3n)	30–22	0,7	10(+32)	700
^{211}At(7,2h)	A	^{209}Bi(^{4}He,2n)	30–10	0,5	10	335
^{237}Pu(45,3d)	A	^{235}U(^{4}He,2n)	32–21	0,0003	100	3
			25–24	0,00005	100	0,5***

* practically, only 70% of the proton beam intensity are used;
** decay time;
*** isotopically ultra-pure ^{237}Pu for the metabolism research *in vivo*.

3. PRODUCTION OF I–123 ON THE MT–25 ELECTRON BEAM

The method of producing ^{123}I in photonuclear reactions from enriched ^{124}Xe(γ,n)^{123}Xe$\longrightarrow$^{123}I using a small size electron accelerator was suggested and developed at the FLNR, JINR.[4–6] Though in this case the yield of ^{123}I is lower as compared with that of the proton irradiated ^{124}Xe, compact electron accelerators can complete with more expensive cyclotrons. An important advantage of this method is the possibility of creating a wide enough net of regional centers producing ^{123}I on these facilities. The researches carried out on the microtron MT–22, MT–25[5–7] and including the designing of a target assembly and of the radiochemical procedure have allowed to suggest a method of producing a high-purity ^{123}I preparation with the following characteristics: specific activity ~200 mCi/ml (~7.4 GBq/ml), radionuclidic admixtures $<10^{-6}$(Bq/Bq), content of I^- $\geq$95%, pH of the solution 7—9, admixtures of stable elements <0.05 μg/ml.

At the corresponding organization of the work on the MT–25 microtron there could be produced during a year at the irradiation of ^{124}Xe weighting 10 g (250 runs of 10 hr each) up to 50 Ci of iodine-123.

4. PRODUCTION OF ISOTOPICALLY ULTRA PURE ^{237}Pu

The ^{237}Pu ($T_{1/2}$=45,3 d, EC 99,9%) is the only Pu isotope which answers the medical requirements to metabolism research *in vivo*. However, a ^{237}Pu preparation used for injection to humans must be nearly free from α-emitting Pu isotopes. The method of producing isotopically ultra pure ^{237}Pu was developed.[7] Plutonium-237 was obtained in the reaction ^{235}U(^{4}He,2n) on the U–200 cyclotron of the FLNR. ^{235}U of 99,99% isotopic purity was used as a target. The dependence of the yields of ^{237}Pu, ^{236}Pu and ^{238}Pu on the energy of the ion beam was studied. Plutonium was separated from uranium and fission products (after dissolving the irradiated target in nitric acid) by using the anion exchange chromatography. An additional isotopic enrichment of ^{237}Pu was carried out with the electromagnetic mass-separator of the YASNAPP–facility. The preparation obtained with the ^{236}Pu:^{237}Pu:^{238}Pu ratio equal to 2.10^{-7}:1:$\leq 3.10^{-7}$ (Bq/Bq) is the purest among the preparations reported to date by different laboratories.

5. REFERENCES

1) Proc. 33th Annual Meeting Soc. Nucl. Med., Washington 1986, J. Nucl. Med.**27**, Abstr. 142, 687, 691, pp.911, 1043, 1044(1986).
2) Guillaume,M. and Brihaye,C.,"Generators of ultrashort lived radionuclides for routine clinical aplications,"Radiochim. Acta **41**,119(1987).
3) Glazov, A.A., Denisov, Yu.N., Dmitrievskij, V.P. et al. "Cyclotron for medical isotopes production (U–120I)," 2nd Int. Conf. on Cycl. and their Appl., Bechine ČSSR 1989 (JINR, Dubna 1989), D9-89-708, pp.87-95.
4) Zvara,I.,"Possibility of ^{123}I production for radiodiagnostics using electron accelerators," Comm. JINR 18-82-20, Dubna 1982.
5) Flerov,G.N., Oganessian,Yu.Ts., Belov,A.G., Starodub,G.Ja., "Production of short-lived ^{123}I isotope at the microtron MT–25," Preprint JINR 18-85-75, Dubna 1 1985.
6) Oganessian, Yu.Ts., Starodub, G.Ja., Buklanov, G.V., Korotkin, Yu.S., Belov, A.G.,"Production of ^{123}I radiobiological specimen on 25 MeV electron beam," Preprint JINR 18-88-758, Dubna 1988.
7) Dmitriev, S.N., Oganessian, Yu.Ts., Buklanov, G.V. et al., "Production of radiochemically ultra pure Plutonium-237 for metabolism research in human body," presented at the 3rd Int.Conf. on Nuclear and Radiochemistry, Vienna, Austr.,Sept.1992.

RADIOPHARMACEUTICAL "THALLIUM-201-CHLORIDE" PRODUCTION USING THALLIUM-203 IRRADIATION BY HELIUM-3 IONS

A.A. Arzumanov, A.I. Kozin, G.I. Shychikov, S.T. Tihomirova, N.K. Hamidov
Institute of Nuclear Physics, Kazakhstan Academy of Sciences,
Alma-Ata, 480082, Republic of Kazakhstan

ABSTRACT

A method of radiopharmaceutical "thallium-201 chloride" production has been developed on the basis of experimental and calculated data on the excitation functions and nuclear reaction yields in thallium-203 targets irradiated by helium-3 ions. The calculated and experimental results allow us to determine the reaction channel priorities in thallium-203 (^{3}He,5n) bismuth-201 → lead-201 → thallium-201 formation.

1. INTRODUCTION

Thallium-201 radiopharmaceuticals are widely used in medical practice for early diagnosis of heart diseases. Thallium-201's main characteristics are radionuclide purity and low chemical contamination content and depend on the complex conditions of the radioactive isotope production.

At the Institute of Nuclear Physics of the Kazakhstan Academy of Sciences regular production of a "thallium-201 chloride" radiopharmaceutical using radiochemical treatment of a thallium-203 target irradiated by 29 MeV protons began in 1986. One of the possible ways of continuing this radiopharmaceutical production all the year round is to use not only protons but other ions also, especially after development of helium-3 ion acceleration using a high efficiency recovery system.[1)]

2. EXPERIMENTAL RESULTS

Irradiating thallium-203 by helium-3 ions, the radionuclide thallium-201 can be produced through the following reactions:

^{203}Tl(^{3}He,5n)^{201}Bi → ^{201}Pb → ^{201}Tl
^{203}Tl(^{3}He, p 4n)^{201}Pb → ^{201}Tl
^{205}Tl(^{3}He,7n)^{201}Bi → ^{201}Pb → ^{201}Tl
^{205}Tl(^{3}He, p 6n)^{201}Pb → ^{201}Tl

It was necessary to obtain experimental data on excitation functions of these nuclear reactions, and also on competitive ones in which contaminant radionuclides are formed, to choose the optimum irradiation conditions for the thallium-203 targets.

Unfortunately, the available experimental data on such excitation functions are not enough for solving this problem. So it was necessary to use model calculations.

Such calculations have been carried out using a statistical model of the compound nucleus decay with the program ALICE modified for helium-3 ions in the entry channel.[2)]

The nuclear masses, the binding energies and the energy effect of the reactions were calculated with the liquid drop model using Mayers-Swyatetckey parameters.[3)] Also the data from the tables of Ref.[4)] were used.

Figures 1 and 2 show the calculated excitation functions of the nuclear reactions of thallium-203 with helium-3 ions leading to the formation of Pb and Bi radionuclides with A=200-202. The curves obtained predict considerable cross sections for the formation of Bi

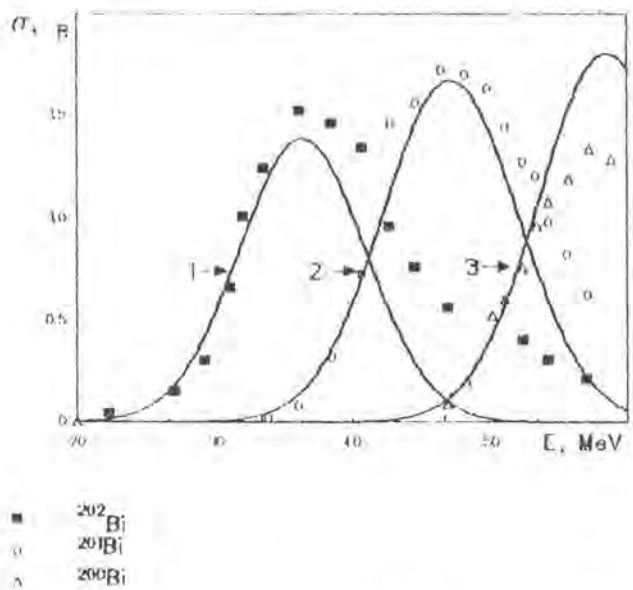


Fig. 1. The excitation functions of the reactions thallium-203 (helium-3,xn) with radionuclide formation. Continuous curves – the results of calculation, the points – experiment: 1 – bismuth-202, 2 – bismuth-201, 3 – bismuth-200.

radionuclides. At the same time experiments like the ones in Ref.[5] were performed.

The experimental results are shown on Fig. 1 as points. The experimental excitation functions of the evaporation reactions agree satisfactorily with calculated ones.

Some excess of the experimental values over the theoretical ones in the high energy "tails" of the excitation functions is explained by insufficient account being taken of pre-equilibrium processes. The part played by such processes for high-energy bombarding particles is essential and it leads to higher cross section values in comparison with calculated ones.

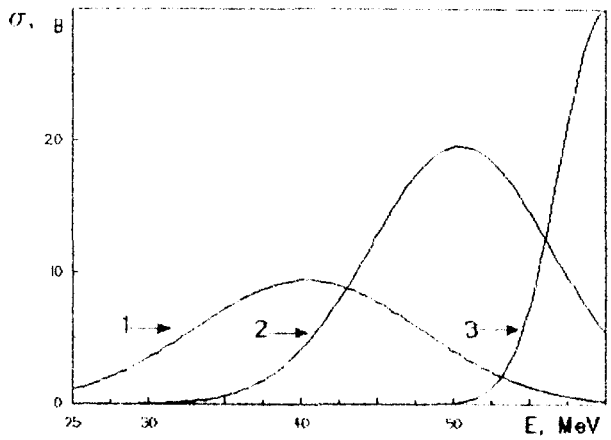


Fig. 2. Calculated excitation functions of the reactions thallium-203 (helium-3,p xn) with radionuclide formation.

The systematic overestimate of the calculated excitation function for bismuth-200 can be explained by the fact that the gamma-lines are not known with enough accuracy.[6–8]

The physical yield of Bi radionuclide as a function of the energy of the helium-3 ions was calculated by numerical integration of the experimental excitation functions for a flux of 3.12×10^6 part/sec for irradiation per hour by the formula

$$Y = 3.12 \cdot 10^6 \cdot n \cdot \lambda \int_o^{x_s} \sigma(x)dx$$

where Y – physical yield, MBr/μAh; n – number of nuclei in one milligram of target substance; x – distance travelled by the particle in the target.

For estimation of the reliability of the obtained results irradiation of "thick" thallium targets has been carried out over two energy ranges 43–33 MeV and 44.5–33 MeV. After one hour's irradiation with 1 mA of beam current each target was dissolved in nitric acid and then the gamma-radiation spectra of these samples were measured from the solution obtained.

The measurement was carried out in 2 and 35 hours. The accumulated thallium radionuclide activities after 2 hours' exposure were subtracted from the corresponding ones after 35 hours' exposure, taking into account the nuclides' decay. Such an approach gives the possibility of realizing the thallium-201 production method on condition of keeping the technology of the radiochemical treatment. The results are presented in Table 1.

Table 1. The experimental functions and the yields of bismuth and lead isotopes in bombarding thallium-203 with helium-3 ions.

N	E_{in} MeV	E_{out} MeV	Yield ^{201}Tl MB/μAh	Contaminant, % ^{200}Tl	^{202}Tl
1	47.0	33	11.9*	8.0	<0.1
	47.0	33	12.4**	7.0	<0.1
2	44.5	33	8.6*	1.9	<0.1
	44.5	33	9.13**	1.5	<0.1
3	43.1	33	4.5***	0.5	<0.1
4	45.0	33	3.0***	3.0	0.2

* – physical yield,
** – calculated data,
*** – yield after radiochemical treatment.

3. CONCLUSION

On the basis of the results obtained it can be concluded that the bismuth radionuclide yield is the main fraction for thallium-201 production from the "thick" targets (enriched with thallium-203) and that for the required isotope purity an accurate energy range must be kept. Thus, the method developed for production of the radiopharmaceutical "thallium-201 chloride" by irradiating a thallium-203 target with helium-3 ions is suitable for practical use, although it gives less yield in comparison with proton irradiation.[9]

4. REFERENCES

1) Arzumanov, A.A., Batishev, N.N., *et al.*, "Performance report on the Kazakhstan Variable Energy Isochronous Cyclotron", in **Proceedings of the 7th Int. Conf. Cyclotrons and Their Applications** (Birkhäuser, Basel, 1975).
2) Blann, M., Bishlinghoff, J., "Corrections to OVERLAID ALICE", preprint COO-3494-27, 1975.
3) Myers, W.D., Swiatecki, W.J., "Nuclear masses and deformation", Ark. Physik, **36**, 593 (1967).
4) Wapstra, A.H., Bosk, K., "Atomic data and nuclear data tables", **19**, 185 (1977).
5) Haustov, I.N., Tichomirova, S.T., Beizin, S.D., "Receipt thallium-201 using helium-3 ions", Izv. Akad. Nauk Kaz. SSR, Ser. Fiz.-Mat. **N2**, 3 (1990).
6) Shmorak, M.R., Nuclear data sheets **49**, N4 (1986).
7) Shmorak, M.R., *ibid.*, **50**, N4 (1987).
8) Shmorak, M.R., *ibid.*, **51**, N4 (1987).
9) Lebowtz, E., Greene, M.W., *et al.*, "Thallium-201 for medical use", J. Nucl. Med. **16**, 151 (1975).

EXPERIENCES WITH THE CYCLONE 3 OXYGEN 15 GENERATOR

E Conard, J-L Morelle,
IBA, Chemin du Cyclotron 2, 1348 Louvain la Neuve, Belgium

J C Clark, D B Mackay,
MRC Cyclotron Unit, Hammersmith Hospital, Du Cane Road, London W12 OHS England.

ABSTRACT

The Cyclone 3 is a simple compact low energy cyclotron operated via keyboard. It generates a 50 μA beam of 3.6 MeV deuterons which strike a nitrogen gas target to produce oxygen 15 via the $^{14}N(d,n)^{15}O$ reaction. The oxygen 15 is piped 80m to a novel bedside infuser which produces ^{15}O water without the disadvantages of earlier techniques. 25 μA of beam provides an adequate supply of ^{15}O water for patient blood flow studies. The availability of ^{15}O water "on tap" is of great assistance in running the extremely full clinical research schedule at Hammersmith.

This technique has enormous potential in clinical PET programmes.

Specification

A collaborative programme was drawn up with IBA. A performance specification was agreed that would meet the current demands for ^{15}O products to support the Hammersmith PET programme.

$^{15}O_2$	30	mCi/min
C $^{15}O_2$	80	mCi/min
C ^{15}O	40	mCi/min

all of the above were for a delivery flow rate of 500 ml/min, measured 80m from the cyclotron. All products were produced in excess of specification during the factory acceptance tests in Jan 91 and the cyclone 3 shipped to Hammersmith in February of that year.

The cyclotron

The cyclone 3 was originally conceived as a classical cyclotron with plane pole faces. The pole faces were later modified to incorporate sector focussing. It was intended to have a simple 'push -button' operating system.

The plane of acceleration is vertical with the target at the bottom. The magnet yoke is hinged to allow access for servicing (Fig. 1). The weight of the cyclotron is approx 5 tonnes.

The rf system is a free-running oscillator which operates in first harmonic mode at 14.4 MHz. The dees, which are fabricated from flat copper plate are uncooled except at the dee stems. Additional rigidity is provided by dee support insulators mounted on the sides of the vacuum box. The D^+ ions are produced in a standard P.I.G. source.

A diagnostic probe measures beam intensity at extraction radius. Extraction is via an electrostatic deflector which achieves 40% efficiency.

Overall power consumption of the cyclotron is 40 KVA

Improvements to the prototype Cyclone 3

The rf system has now been redesigned by IBA to eliminate the dee support insulators . This design of rf system operates in 2nd harmonic mode and has been used in the 2nd cyclone 3 (delivered to Turku, Finland) and is to be retro-fitted in the Hammersmith machine during August '92. The redesigned rf system runs at 30 MH_z. The main magnet field has been increased also, resulting in a deuteron energy of 3.8 MeV. This increased deuteron energy has significantly increased the yield of ^{15}O from the target. The Turku machine has passed its acceptance tests at the end of June.

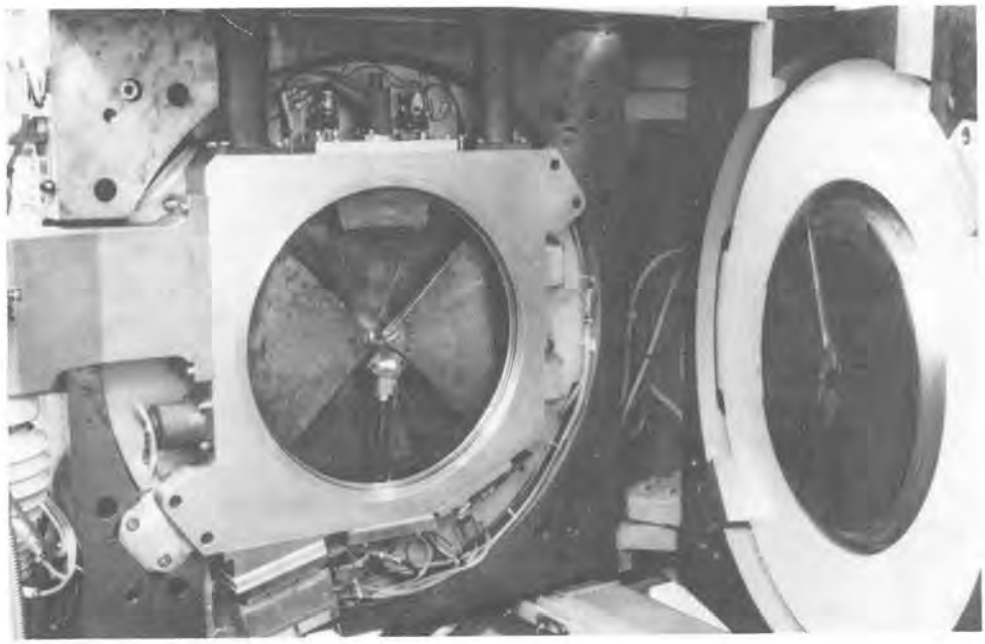
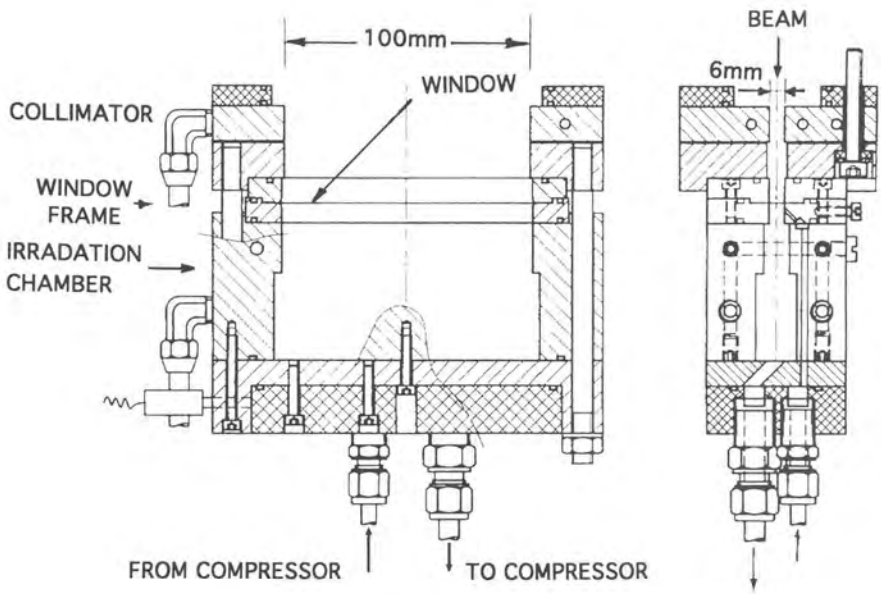


Fig 1. THE CYCLONE-3 Pole face diameter approx 480 mm

The target

The target construction is shown in Fig. 2. The target gas is dry nitrogen mixed with 1% 0_2 or 1% CO_2 at an absolute pressure of approx 1.5 bar. The cyclotron beam, having been defocussed in traversing the fringe field of the main magnet enters the target through a single thin window (currently 7.6 micron Titanium). The target gas is recirculated at 15 l/min by a ss. bellows compressor. Jets of target gas are directed on to the window, providing cooling.



^{15}O TARGET FOR CYCLONE-3

Fig. 2

The main use of the cyclone 3 so far has been to make ^{15}O water. This is done at the bedside using a novel water generator infuser.[7] A schematic of the water generator is shown in Fig. 3.

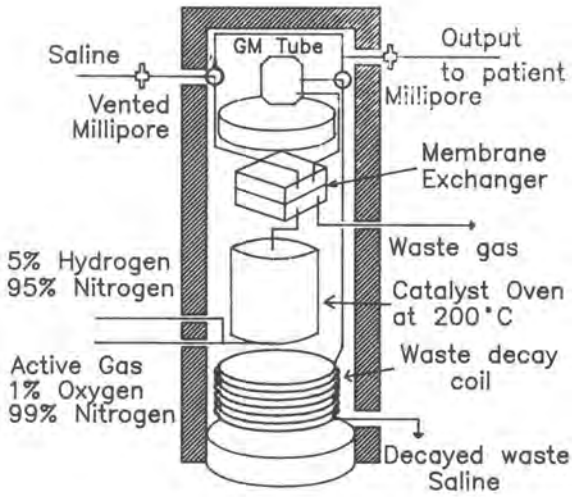


Fig. 3

The key component of the water generator is a semi-permeable membrane exchanger which introduces $H_2{}^{15}O$ into a normal saline (0.9% NaCl) infusate. (Fig. 4)



Fig. 4

$H_2{}^{15}O$ is synthesised in the gas phase by the Palladium catalysed reaction of $^{15}O_2$ with H_2 (5% in N_2)

$$^{15}O_2 + 2H_2 \xrightarrow[150°C]{Pd} 2H_2{}^{15}O$$

As the device is closely connected to the patient all the electrical controls are extra low voltage (24 volt) and isolated to comply with electromedical safety requirements.

Operation and Reliability

At high beam intensities, 50μA, the prototype cyclone 3 has continuing problems with breakage of the dee support insulators. Apart from one major water leak into the cyclotron tank, the cyclotron has run reliably at modest beam currents up to 30 μA for approx 25 hours/wk during 1992. Target window lifetime estimated to be 80 hours. Ion source service interval > 100 hours. The cyclone 3 is operated via a lap-top portable computer. Some operator intervention is required to tune in the magnet as the cyclotron warms up.In practice $H_2{}^{15}O$ water output is controlled by adjustment of cyclotron beam by altering the ion source arc conditions. Residual radioactivity in the cyclotron tank after beam off is higher than expected but not a problem.

Use of Cyclone 3 in the Hammersmith clinical programme

^{15}O water is used to carry out an average of 6 PET brain blood flow studies per week. 25 μA of beam current produces an adequate supply of ^{15}O water for these studies. The machine plays an important role in releasing the more flexible multi-particle 40 MeV cyclotron to be applied more efficiently to ^{11}C and ^{18}F PET radiopharmaceutical production.

Potential in clinical applications

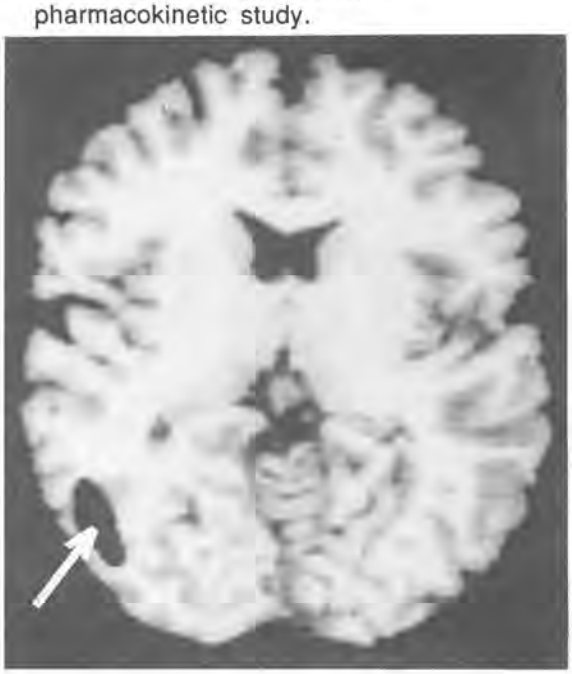
The combination of the new generation of high sensitivity "septa less" PET scanners[1] and the bedside $H_2{}^{15}O$ infusion device fed with $^{15}O_2$ from the Cyclone-3[2] has provided an extremely versatile research platform for the study of small transient blood flow changes[3] in the brain of man

blood flow changes[3] in the brain of man when stimulated with a wide range of paradigms with acceptably small doses of radiation. These paradigms when carefully designed can elicit focal responses in the brain which when quantified lead to a wider understanding of normal and abnormal brain function. These "activation" paradigms range through visual (Fig.5), sound, speech, smell, movement, breathing control and cognitive processes (memory) are seen to be contributing valuable data in the "Decade of the Brain" 1990 - 2000.

$^{15}O_2$ which may be used to study tissue oxygen utilization is converted to $H_2^{15}O$ in vivo and the measurement of this metabolic water signal can be related to oxidative metabolism in tissue.

$C^{15}O_2$ when breathed in air is converted to $H_2^{15}O$ in the lung.[4,5] It has recently been demonstrated that this water can be exploited in the assessment of myocardial viability by providing a measure of regional tissue perfusion index.[6] This technique should have significant routine clinical applicability.

$C^{15}O$ binds to haemoglobin in red blood cells and thus provides a method of measuring the blood volume of organs and tissue capillaries which is often necessary as part of a PET quantitative pharmacokinetic study.



REFERENCES

1) Townsend, D., GeissbüHler, A., Defrise, M., Hoffman, E.J., Spinks, J., Bailey, D., Gilardi, M.C and Jones, T. Fully three dimensional reconstruction for a PET camera with retractable septa. IEEE Trans Nucl Sci: NS-38 (1991).

2) Jongen, Y. The Cyclone-3D. Proceedings of 3rd International Workshop on Targetry and Target Chemistry. Vancouver 19-23 June (1989).

3) Lueck, C.J., Zeki, S., Friston, K.J., Deiber, M-P., Cope, P., Cunningham, V.J., Lammertsma, A.A., Kennard, C., Frackowiak, R.S.J. The colour centre in the cerebral cortex of man. Nature: 340; 386-389 (1989).

4) Lenzi, G.L., Jones, T., McKenzie, C.G., Buckingham, P.D., Clark, J.C and Moss, S. Study of Radioanal Cerebral Metabolism and blood flow relationships in man using the method of continuously inhaling oxygen-15 and oxygen-15 labelled carbon dioxide. J Neurol Neurosurg Psychiat, 41, 1-10 (1978).

5) Ter-Pogossian, M.M and Herscovich, P. Radioactive oxygen in the study of cerebral blood flow, blood volume and oxygen metabolism. Seminars in Nuclear Medicine, 15, 4, 377-394 (1985).

6) Yamamoto, Y., De Silva R., Rhodes, C.G., Araujo, L.I., Iida, H, Rechavia, E., Nihoyannopoulos, P., Hackett, D., Galassi, A.R., Taylor, C.J.V., Lammertsma, A.A., Jones, T and Maseri, A. A new strategy for the assessment of viable myocardium and regional myocardial blood flow using ^{15}O-water and dynamic positron emission tomography. Circulation, Vol 86. (1992).

7) Clark, J.C and Tochon-Danguy, H. R2D2 A Bedside $H_2^{15}O$ Infuser. Proceedings of 4th International Workshop on Targetry and Target Chemistry, Paul Scherrer Institute, Switzerland, 9-12 September (1991).

Fig.5 Co-registered PET/MRI Images MRI Transaxial scan slices with statistically significant increases in blood flow measured using Positron Emission Tomography (PET) and Oxygen-15 labelled water (arrowed).

DUAL CHEMICAL STATION FOR CYCLOTRON PRODUCED ^{18}F

M.L. Mallory, G. Grimmett, D. Yang and R. Tilbury
The University of Texas, M.D. Anderson
Cancer Center, 1515 Holcombe Blvd.,
Houston, TX 77030

ABSTRACT

The demands for large quantities of 2[18F] fluoro-2-deoxy-D-glucose (FDG) for cancer diagnostics and the desire for 100% product delivery reliability has led us to develop a dual chemistry station. The irradiated target water (18O enriched) is transmitted to a counting vial located in the chemistry station hot cell and then is transmitted to either side of the dual chemistry processing station. The two stations are cleaned in the morning, when radioactivity has decayed from the previous day's runs, and then loaded for either two runs of FDG and/or one run of FDG and one run of another 18F-labeled compound. This station has over forty remotely operating valves. All gases from the chemical reactions are collected in a retaining bag and radioactive products are allowed to decay 24 hours. We have successfully achieved essentially zero radioactivity release. All operations are remote and little personnel radiation exposure is obtained. Since implementation of this dual station, we have greatly reduced failures due to chemistry station malfunction.

1. INTRODUCTION

PET (Positron Emission Tomography) has been used for medical purposes for many years. For example, D.K. Bewley's presentation at the Ninth[1] International Conference on Cyclotrons and Their Application, discussed the early uses of cyclotron produced PET isotopes. In our facility, a cancer hospital, PET imaging studies of tumors has existed for about three years. Recently (1991), the in house production of cyclotron produced PET isotopes has become available and the ready supply of these isotopes in large quantities has seen a tremendous increase in their use for medical diagnostic purposes. In particular, PET scans are now being offered for any part of the body. The medical findings at our institution are that PET does have a contribution to make in supplementing the other standard diagnostic modalities in the detection of cancer and also in the surveillance of the treatment progress of cancerous tumors.

The technical success of PET for cancer diagnostis depends on some type of differentiation in the biologic activity between cancer and noncancerous cells. This difference is not usually exploited by other diagnostic techniques. Figures 1 and 2 are diagnostic scans from two different techniques of the same breast tumor and illustrate the value of PET scans. Figure 1 is a standard mammogram and a possible neoplasm can be detected by the physicians. Figure 2, is a scan from a PET procedure and the cancerous tumor is readily apparent in the computer reconstructed image as indicated by the two dark spots. The success of these initial experimental PET scans at M.D. Anderson has put a demand upon the reliability of the cyclotron PET isotope production program and the conversion of the PET isotopes into the desired drug. Efforts at increasing the redundancy for failure items or a fast turn around after a failure have been implemented on the cyclotron, beam line and the target. In this paper, the efforts at increasing the redunancy in the PET chemistry station, where the desired drug produced is FDG, is reported in the following section.

2. FDG CHEMISTRY STATION

The process of making FDG in our chemistry station is the method first introduced by Hamacher.[2] This process involves, heating, cooling vacuum pumping, filtration and addition of chemicals, all done remotely in an enclosed hot cell. This process of producing FDG requires many operations and failures have occurred in various stages of this procedure, thus usually causing a total failure for that days production. To avoid this kind of failure, a dual station has been

built. Figure 3 is a schematic valve layout of this dual chemical station and it contains over forty valves. Figure 4 is a picture of the hardware (valves, test tubes, filter) all mounted on a rack inside the hot cell. The two stations are mounted side by side. The control panel for this process is depicted in fig. 5, where the valves are positioned on a graphic representation of the chemical process. A master valve switching the routing of the chemicals to either station is located at the top of the panel. The first step in either side of the process is a measurement of the radioactive yield of the target. This data is a check on the cyclotron and target performance and is also used in measuring the chemistry station efficiency.

A particular difficult problem has been sealing the chemical station against vacuum leaks. Our normal procedure is to test the system for leaks after cleaning and loading the chemicals for the days run. However, we still have on occasion, air leaks. These leaks interfere in the successful transfer of product thru the chemistry station, which is usually done by pressurizing the appropriate test tube. As a backup, we have found that applying vacuum in the appropriate areas can also cause the radioactive chemicals to be transferred and this option has been added.

It is well known that the process of making[3] FDG, gives off volatile radioactive gases that are not trapped out by standard air filters. Figure 6 is a graph of the detection of radioactivity being released from our air stack monitors. We have found that this activity can range up to 100 mCi of product. We now operate our system with total capture of all discharged gases into a bag. We have successfully contained all radioactivity for the FDG and also for all other PET radiopharmacutial production. The stack radioactive monitors are an excellent detection device for air leaks within our chemical station system and these leaks also interfere in the efficient production of FDG.

A potential problem in capturing the gas in our bag system is the buildup of pressure on the discharge side of our chemical operation. To avoid transfer of liquids due to this pressure buildup, we have built traps into the discharge lines.

With so many valves in the system, it is to be expected that we have experienced valve failures. Initially, we used 30 psi valves in the system. We have determined that on occasion the pressure can exceed this value. We are retrofitting the valves to 100 psi. Our second concern is that some of the valves must operate for time period of 1-2 hours. The high power applied to the valves' control solenoid causes them to become thermally hot in this time period. We are implementing an electronic circuit that reduces the power to these valves after initial opening.

3. CONCLUSION

The redundant chemistry station has been utilized 4 times since the first of the year (~ 6 months) hence, providing a greater reliability in PET drug product delivery for our patients. In the process of making our chemistry station perform, we have encountered some interesting technical problems, but have devised solutions. We are most encouraged that we can make PET isotope drugs without releasing any radioactivity to the environment during a normal production run.

4. ACKNOWLEDGMENT

We acknowledge the dedicated work of the cyclotron staff in designing, construction and debugging this apparatus. We acknowledge the funding by the Division of Diagnostic Imaging. We thank B. Taylor, and V. Forward for their help in producing this manuscript.

5. REFERENCES

1) Bewley, D.K., "Medical Uses of Cyclotrons: Treatment and Diagnosis," in Proceeding Ninth International Conference on Cyclotrons and Their Applications" (les editions de physique, Caen, France, Sept. 7-10th, 1981) pp 653-660.

2) Hamacher, K., Coenen, H.H. and Stocklin, G., "Efficient Stereospecfic synthesis of no-carrier-added 2 - [18F] fluoro-2-deoxy-D-glucose using

aminopolyether supported nucleophilic substitution," J. Nucl. Med. 27, 235, (1986).

3) Kleck, J.H., Benedict, S.H., Cook, J.S., Birdsall, R.L., Satyamurthy, N., "Assessment of 18F Gaseous Releases During the Production of 18F-Fluorodeoxyglucose," Health Physics 60, No5, pp. 657-660, (1991).



Fig. 1. A standard mammogram of a breast cancer patient is shown. This diagnostic method depends upon a density difference between cancer and noncancerous tissue. A trained expert could detect a potential problem with this patient.

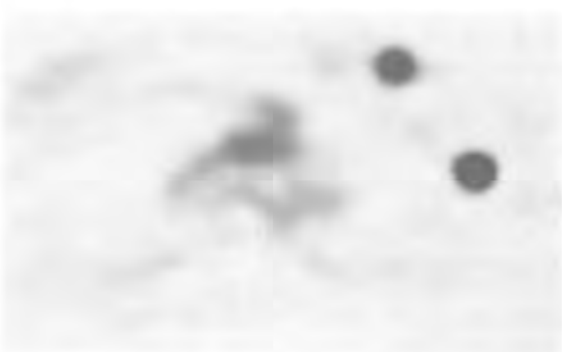


Fig. 2. PET scan of the same patient shown in fig. 1 is displayed. The two dark spots located in the patient right breast areas where 18F has accumulated, are diagnosed as cancerous cells and were later verified by needle biopsy and pathology. This remarkable clarity in diagnosing breast cancer with PET scans have in part motivated the subject of this paper, increased reliability in the production of FDG by a dual redundant chemistry station.

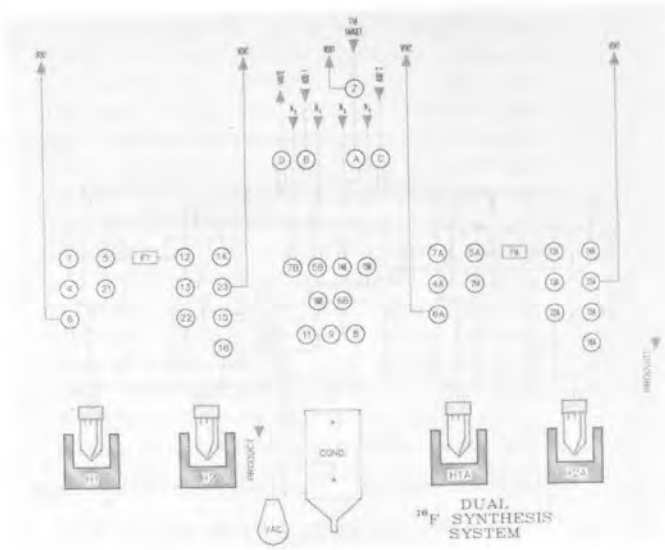


Fig. 3. A schematic drawing of the FDG dual processing chemistry station showing over forty Teflon valves. The first step in this process is to measure the radioactivity from the target.

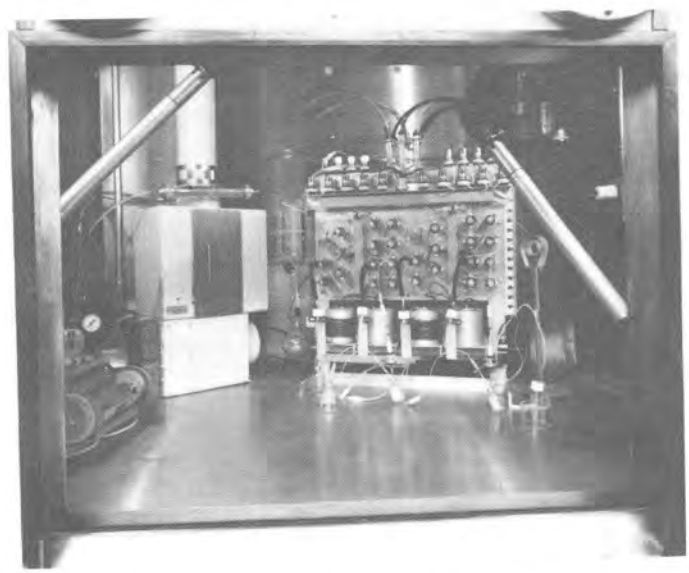


Fig. 4. A picture of the chemistry station mounted on a rack inside the hot cell. The two chemistry station are mounted side by side. The stations are cleaned and loaded with chemicals before the processing start each morning.

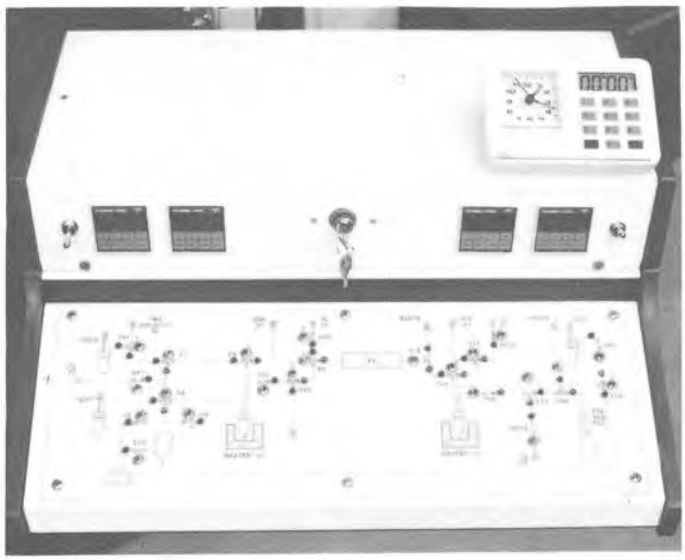


Fig. 5. The chemistry control panel is depicted in the following photo. Only one side of the chemistry station is shown. The switches are located on a graphical layout of the process. A master switch for either side is located at the top of the panel.



Fig. 6. The radioactivity of two peaks of 15O released up the stacks of the cyclotron hot cells are shown. The radioactivity takes approximately one minute from release to detection by the stack monitors. The stack monitors are G.M. detectors. All gas released from the chemistry station hot cell is now bagged and allowed to decay for 24 hours, hence decreasing our released radioactivity to essentially zero.

ACCELERATORS FOR CHARGED PARTICLE THERAPY: PERFORMANCE CRITERIA FROM THE USER POINT OF VIEW

E.Pedroni
Department of Radiation Medicine, Paul Scherrer Institute
CH-5232 Villigen PSI, Switzerland

ABSTRACT

The introduction of charged particle therapy in the hospitals could provide substantial improvements to external radiation therapy for cancer treatment. Many different types of accelerators have been proposed for installation in the hospitals, all with their own merits and disadvantages. In this report we discuss the requirements posed by charged particle therapy on the quality of the beam delivered by the accelerator (variable or fixed energy, beam duty factor, beam intensity, etc.). **Special emphasis is given to items** like dynamic beam scanning, gantry design and proton radiography and tomography, **which are not well established yet** in this field but **which could eventually have a strong impact on the choice of the accelerator** for charged particle therapy in the future.

1. INTRODUCTION

About 2/3 of all cancer patients receive radiation therapy in the course of the disease (alone or in combination with other therapy modalities, with curative intent or for palliation only). Radiation therapy continues therefore to be one of the most used weapons in the fight against cancer, a disease which nowadays statistically hits (over lifetime) about one individual out of four of the population of the industrial countries.
It is the opinion of many experts working in the field, that improvements in the techniques of radiation therapy, especially concerning **treatment precision**, is needed to improve local control of the primary tumour. Better radiation therapy with curative, instead of palliative intent, will be also probably needed in a rather immediate future in combination and as a complement to new systemic treatments, like immunotherapy and chemotherapy, which hopefully will be able to cope with the problem of the spread of microscopic distant metastasis.
A possible significant improvement in external radiation therapy can be expected from the use of **heavy charged particle beams** (heavier than electrons).

Despite the size and costs of the accelerators and beam transport systems involved, the interest for the introduction of protons (and eventually of heavier ions) in the clinics is steadily increasing in the oncological community. This is certainly also a consequence of the very remarkable event, that in 1991 the first **hospital-based proton facility** of the world has been successfully put into operation in **Loma Linda**, California.
The commitment to further develop radiation therapy with charged particles is also a tradition of PSI, where this goal is being actively pursued since about 10 years, first by the introduction of pion therapy in 1981 and second with the introduction in Europe of the treatment of uveal melanomas with a 70 MeV proton beam. A new beam line dedicated to proton therapy has been assembled this year at PSI. Next year we will install at PSI a compact gantry in the new beam line and we expect to be able to start patient treatments of deep seated tumours with the gantry in 1994.
The experience gained at PSI with proton treatments should encourage the introduction of hospital-based proton machines in our country. This is the reason for our interest in all questions regarding the choice of the accelerator type to be used in a hospital environment.
In this report we focus our attention mainly on the different factors affecting charged particle radiation therapy, with special emphasis on their relationship with the properties of the different proposed accelerators.

2. CHARGED PARTICLES FOR RADIATION THERAPY

We discuss briefly the utilization of **protons, neutrons, pions and heavy ions** as possible alternatives to conventional therapy with **electrons and photons**.

2.1. Comparison of Charged Particles: Classification Criteria

2.1.1. Dose distribution precision

The precision of the dose distribution continues to be a major key for improvements in radiation therapy.

This has been undoubtedly demonstrated in the past by the successes of the introduction of high energy photon machines in the hospitals (megavoltage therapy). This is also documented by the numerous present activities to improve conventional therapy, like the development of 3D treatment planning, dose conformation techniques with multileaf collimators and "inverse" dose algorithms for treatment planning.
The goal to confine the dose to the target volume is the basic requirement of radiation therapy. The therapist is very often faced with contradictory requirements, dictated by practical technical limitations of the dose application system. On one side one needs to increase the dose in the target volume (in order to improve the probability of tumour control) and on the other side it is necessary to reduce the radiation burden on healthy sensitive organs surrounding the tumour (in order to avoid treatment complications). The utilization of the **superior ballistic properties of protons and heavier ions** is expected to be very helpful in all situations, where a better confinement of the dose to the target volume is required.

2.1.2. High and low LET radiation

The Linear Energy Transfer (LET) is a physical quantity describing the density of ionisation events at a microscopic level. Depending on the amount of LET the radiobiological effect of radiation on living cells can be quite different.
a) With **low LET radiation** at low dose rate (factors dose and time) a significant portion of the radiation damages can be repaired by the cells themselves (mainly single DNA strand break repairs). The repair mechanisms are important in the context of fractionated treatments. The fractionation of the dose is used to enhance the differential cell sensitivity between healthy and malignant cells. Most successes of radiation therapy are based on the fact that malignant cells are usually more sensitive to radiation than healthy cells ("positive" therapeutic ratio). **Fractionated low LET radiation** is therefore especially successfull for the treatment of **radiosensitive tumours**.
b) With **high LET** the capability of the cells to repair radiation damages is strongly depleted (the densely ionising radiation produces multiple DNA strand breaks, which are difficult to repair or which are repaired with a high probability of errors). A general reduction of any differential cell sensitivity is usually observed with high LET radiation. This should be an advantage in the case of very **radioresistant tumours** (the reduction, due to the high LET, of the "negative" therapeutic ratio between healthy and cancer cells could provide an improvement of the chances of cure in this case).
High LET radiation is, in other words, a more efficient (with higher relative biological efficiency, RBE), but also less selective method to provide cell killing. Late complications are observed unfortunately more often with this kind of radiation than with low LET.
A very important feature of high LET, which has paved the way to the introduction of neutron and pion therapy in many research centers around the world in the seventies, is the reduction, due to high LET, of the so called Oxygen Enhancement Ratio (OER). Living cells with poor content of oxygen are usually more resistant to radiation than cells in contact with intact blood supply. Since tumours generally have a rather poor vascularization, the oxygen effect is considered to be a possible cause of treatment failure in conventional therapy (cells close to necrotic regions, are poorly oxygenated, are more radioresistant and are therefore likely candidates for tumour regrowth). With high LET the cells at risk should be more efficiently destroyed.
The results of the experience with high LET gained in the last 15 years from neutron, heavy ions and pion treatments seem to indicate that high LET radiation could be advantageous for at most 10 to 15% of all patients. For all the other patients low LET radiation seems to be more appropriate.

2.1.3. The costs for charged particle therapy

The costs for a treatment course of conventional radiation therapy (around 5000$ depending on the country) are usually less than for comparable techniques, like surgery or chemotherapy. Compared with very advanced techniques like heart or bone marrow transplantations, the costs are indeed very low.
If we perform a very rough estimate and we assume the extra investments necessary for installing a proton facility to be about 25 M$ (the money exceeding the costs of an equivalent conventional facility), to be amortized over a period of 10 years and financed with an interest rate of 10%, we end up with additional expenses in the order of 5 M$ per year. If the facility is optimized to treat around 1000 patients per year, the additional costs distributed over individual patients should be in the order of 5000$ per patient. If the proton treatments could be limited only to those cases, where better clinical results are expected, for example in the form of avoiding additional surgical interventions or medical care or to permit the reinsertion of the patient into the work cycle, this amount of money would be immediately justified also from an economical point of view.
In other words: if the results are sufficiently promising and the treatment technique is sufficiently efficient, any of the proposed particle therapy facilities can be justified in the industrial countries also from the economical point of view.
The facility costs clearly remain an important parameter for the comparison of particle accelerators for therapy.

2.2. Comparison of Particles for External Radiation Therapy

Figure 1 shows in a very qualitative picture a personal judgement on the merits of the different particles:

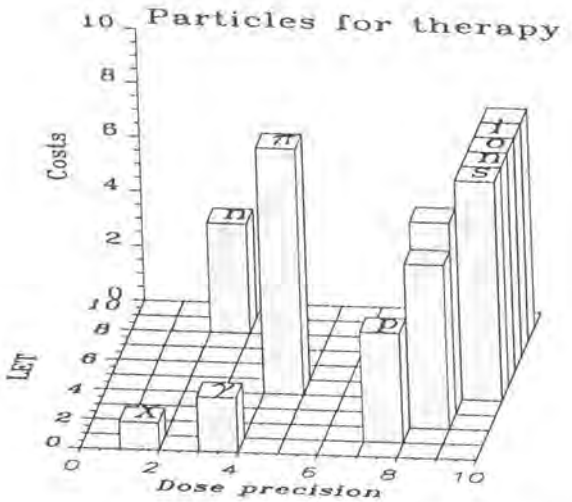


Fig. 1. Qualitative comparison of the different types of particles used for external radiation therapy. The discussion of the judgement criteria is given in the text. The numbers on the scales are arbitrary units.

a) **Photons**
The merits of megavoltage photons in providing a cheap, quite precise low LET radiation source are undiscutable. Photons and electrons will continue to cover the needs of the majority of the cancer patients.

b) **Neutrons**
Neutrons are the cheapest in the class of particles with high LET and are already available since a decade at few selected therapy centers. From the point of view of dose precision they are similar to X-rays and MeV photons. Concerning dose shaping capability they are less precise than pions and heavier ions. Because of their more immediate availability neutrons will continue to be the major source of high LET radiation. The practical impact of neutrons in the hospital environment seems however to be less important than anticipated and hoped for in the seventies.

c) **Pions**
Pions are very expensive, have less precision than ions and have, as secondary particles, very stringent practical dose rate limitations. Pions are probably nowadays the particles which have the least chances for introduction in a hospital environment (heavy ions are probably a better choice in the same range of costs).

d) **Light and heavier ions (from Helium to Neon)**
A very appealing feature of ion accelerators is the flexibility to produce beams of different ion types. In this way it is possible to provide low and high LET with the same radiation source. This flexibility is extremely attractive for facilities planned with strong **research interests**.
Another appealing feature is given by the possibility to use radioactive beams.
Concerning the precision of treatment heavier ions have, at least in theory, the best ballistic properties. In practice the advantages of ions over protons are partly destroyed by the **fragmentation of the ions** and by the complications given by the **variation of RBE and LET** with position inside the dose field.

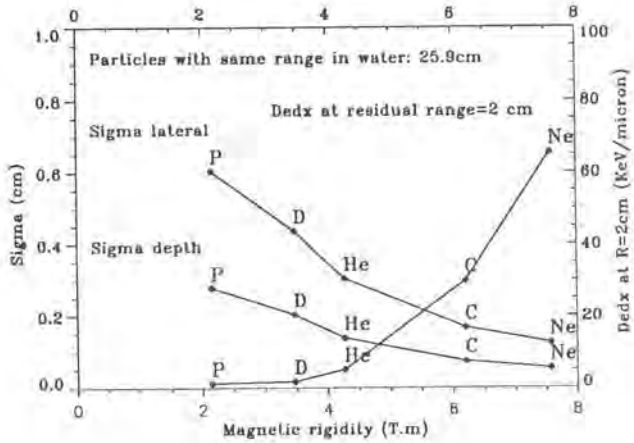


Fig. 2. Dedx, lateral and distal beam width as a function of the magnetic rigidity for different ion types (for the same range of penetration).

Figure 2 shows the calculated lateral (multiple scattering) and distal (range straggling) beam width σ of the dose of a pencil beam for different types of ions (see also section 3.1). The heavier the ion, the better the sharpness of the beam and the higher the LET. The beam width is plotted as a function of the magnetic rigidity of the particles, with the beam energy chosen to provide the same range of penetration of the particles into the patient. The factor of 3 higher magnetic rigidity of the carbon ions compared with protons scales linearly into the dimensions of the accelerator and beam transport system and therefore more than linearly into the costs needed for a facility for ion therapy. Ion therapy is expected to be much more expensive than proton therapy, as it can be argued from a comparison of the costs of the Himac facility in Japan (300 M$) with the costs of the Loma Linda proton facility (60 M$) in the USA.
The higher costs of ion therapy can be justified only in two ways: I) by the need of high LET together with good dose precision (a subclass of the neutron indications?) or II) by the need of extreme dose precision (a subclass of the proton indications?).
How does the extreme precision of the ions compare with other sources of errors, like variations of patient anatomy, organ movements and similar uncertainties?
It is the task of the new ion facility in Chiba, the first in the world dedicated exclusively to ion therapy (and expected to become operational in 1994), to provide the answers to these questions.
Berkeley is at the moment the only place in the world, where ion therapy is performed on patients.

e)**Protons**
Proton therapy is expected to bring significant improvements concerning the quality of the dose distribution at

relatively moderate costs (a doubling of the costs over conventional therapy is a generally accepted estimate). From the radiobiological point of view, protons can be considered to be a low LET radiation. Since for most of the patients low LET seems to be a better choice, protons represent the next immediate alternative to photons for introduction in the hospitals on a large scale.
In the following we will follow our preferences and we will discuss only proton therapy.

3. PROTON THERAPY

3.1. Physical Characteristics Relevant for Therapy

Figure 3 shows, as an example, the dose distribution of a proton pencil beam, measured with a degraded beam at PSI.

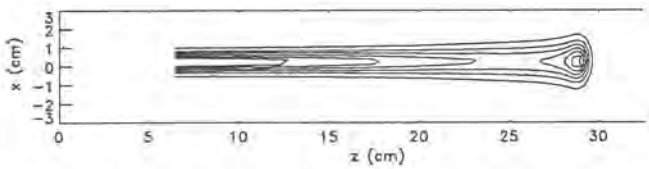


Fig. 3. Dose distribution of a proton pencil beam.

Charged particles, when they penetrate matter, lose energy by collision with atomic electrons. The range of penetration of protons is extremely well defined with a range straggling of about 1% (standard deviation). As the particles approach the position where they stop, they lose more and more energy giving rise to the well known characteristic **Bragg peak**. The dose precision at the distal edge of the field is governed by the range straggling process.
The other major factor affecting the precision of the dose distribution is **multiple Coulomb scattering** (collisions of the projectile with the charge of the nuclei). This affects the precision of the dose in the direction transverse to the beam. Nuclear collisions represent an additional nuisance, since they produce some degree of attenuation of the beam (10-30% depending on the range). The phase space of the beam delivered by a dedicated proton accelerator should be chosen to be smaller than the contributions from range straggling and multiple scattering at the Bragg peak position.
The precision of the dose fall-off at the edge of the field depends directly on the choice of the **beam energy**. To a good approximation the dose fall-off can be considered to vary linearly with the energy of the beam. The possibility to choose a variable beam energy in the range between 70 and 220 MeV (270 MeV if proton radiography must be supported) is a generally accepted requirement for proton therapy machines for the hospitals.
An ultimate precision in the order of few mm for the confinement of the dose at the edge of the dose distribution and a dose homogeneity of few % inside a 3D shaped target volume is a performance achievable with proton therapy.

3.2. Indications for Proton Therapy

The main strategies to be used to exploit the possible advantages of proton therapy over conventional photon therapy, can be summarized in the following way:
a) **The dose beyond the Bragg peak is essentially zero**. This should be used in all situations, where the tumour is surrounded by sentivitive structures and where stopping the beam exactly in front of healthy, very sensitive structures behind the target volume, brings a significant reduction of treatment complications. This is actually the speciality developed mainly at Harvard, with the treatments of tumours close to the base of the skull (chordomas and chondrosarcomas) or close to the spinal chord. Together with the eye treatments, these very impressive indications represent now the **"classical" proton indications**, those which have attracted the interest of the oncologists on proton therapy worldwide.

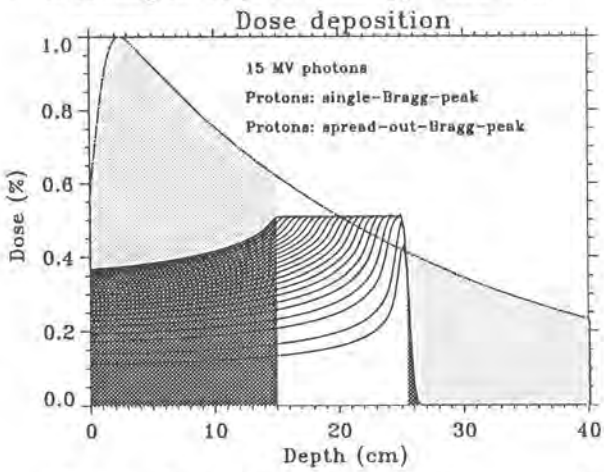


Fig. 4. Depth dose distribution comparison of photons and protons. The shaded areas represent the amount of undesired dose outside a 10 cm target volume located on the axis of a "patient" of 40 cm diameter.

b) **Low integral dose outside of the target volume**. This can be seen from Fig. 4, where the dose distribution of photons and of Spread-Out-Bragg-Peak (SOBP) protons are compared. The light and dark+light shaded area in the picture represent the undesired dose deposited outside the target volume for protons and photons respectively. The situation in the picture is more favourable to protons by about a factor of 3. This advantage is maintained for multiple fields, provided that the same number of fields can be used with protons as with photons (Fig. 5). The reduction of integral dose could prove to be very effective for the treatment of **large target volumes**, where the dose outside the target volume is the limiting factor. These indications require however the installation of **isocentric gantries for proton**

therapy, similar to those used in conventional therapy. Up to now protons have been used only on horizontal beam lines, without isocentric gantries (and sometime with other limitations like insufficient beam energy). This is probably the reason, why up to now protons have been used mainly for treatments of rather small target volumes. Since fall 1991 the door for a completely new class of indications, namely **large target volumes**, has been opened in Loma Linda with the installation of the first proton therapy facility of the world with isocentric gantries.

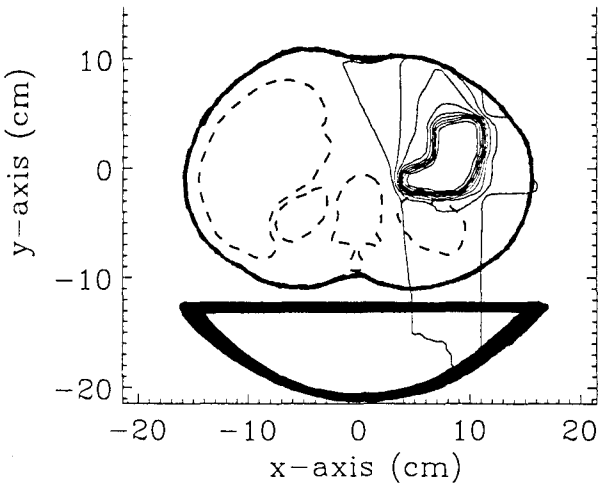


Fig.5. Example of a dose distribution to be achieved using the spot scanning technique: the isodose lines are 10%, 20%, 30%, ..., 90% respectively.

c) **Protons are ideal particles for dose conformation.**
This for two reasons. The first reason is that protons are **charged particles**. They can be transported, focussed and deflected at wish with magnetic devices, giving unpaired flexibility to manipulate the distribution of the dose under **complete computer control**, the rationale for the introduction of the so called **spot scanning technique**.
The second reason is, that protons are **well localized in all three dimensions already as an elementary pencil beam**, as opposed to the photons, which acquire 3D dose localisation only through the overlapping of convergent collimated beams. For these reasons **dose conformation** is expected to be **more precise and easier** to perform **with protons** than with photons.
A true 3D dose conformation with protons, using a spot scanning method is still a novelty to be realized in this field. This is together with the design of a compact gantry dedicated to beam scanning, one of the key points of the developments for proton therapy at PSI. These developments should open the door to a third class of indications for proton therapy, namely **tumours with complex shape** to be treated with a routine automated conformal method.

3.3. Proton Therapy: Factors Affecting the Accelerator Choice

3.3.1. Proton application techniques: scatter foil technique and spot scan technique

The traditional technique used up to now for proton therapy, is based on the spreading of the beam in the transversal direction using **scatter foils** (or similar devices). The lateral shaping of the dose field is performed using **collimators**. The spreading of the beam in depth is performed using **rotating wheels** with variable thickness or **ridge filter systems**. The SOBP function is chosen to produce a dose flat top with constant length equal to the maximal thickness of the target volume in depth. The dose conformation to the target volume is not performed in depth, only the position of the distal edge of the dose field is usually adjusted in depth using **compensator** boluses. Through overlapping of multiple fields excellent 3D-shaped dose distributions can be however achieved with this technique. The advantages of the scatter foil technique are given by its reliability and safety.
An alternative technique is to use the undisturbed focussed beam and to scan the beam in three dimensions. **Magnetic deflections** (and/or patient translations) are used for the positioning of the spot in the lateral direction. For positioning the Bragg peak in depth **range shifting material** is inserted in front of the patient or the **energy of the beam** is changed directly in the accelerator, if this option is available. At PSI we are developing a **discrete spot scanning** technique. The dose is applied statically at each spot position by switching on and off the beam with a **kicker magnet** and by measuring the spot dose with a fast beam monitor system. This simplifies the control system at the expenses of some dead time for the application method.
The spot scanning technique is expected to be superior to the scatter foil method, because of its full flexibility, since it allows a true 3D conformation of the dose (4D conformation -non homogeneous dose distributions- is in principle also readily available) and permits complete computer control with minimal patient individualized hardware. The full beam is dumped (most of the time and in a controlled way) in the patient and is not lost in the equipment, reducing the requirements on beam intensity for the accelerator and reducing the activation problems of all components of the facility.
The spot scanning can be integrated in the optics of the beam transport system of the isocentric gantry, thus permitting a reduction of the gantry diameter.
A possible problem faced by the spot scanning technique is the problem of organ movements during scanning, with possible interferences between scanning of the beam and motion of the patients.
Since the flexibility of the scanning method is achieved by performing dose spot applications sequentially as a function of time, a good **beam duty factor** is required in this case from the accelerator.

We assume here, as a typical example of scanning performance, the irradiation in 2 minutes of a 1 liter (complex shaped) target volume, with scanning on a regular mesh with 5mm distance from spot to spot (positioning of the dose field edge better than ± 2.5mm). This requires about 10000 spot applications in 2 minutes, with a mean spot irradiation time of about 10 ms (100Hz). We don't assume here any particular **stability of the beam**. The PSI scanning method is supposed to be able to cope with beam fluctuations in the order of 100% of the mean intensity. The spot dose is chosen individually for each spot in the treatment planning system. If the dose of each spot has to be controlled with a precison of 1% of its mean value, we must measure it and, when the required amount of dose has been deposited, immediately switch off the beam with a typical reaction time of 100μs (10KHz). These are typical requirements for a fast spot scanning with a DC-like beam (beam of a cyclotron or slow extraction from a synchrotron). Other similar schemes of dynamic scanning have been proposed for example by IBA(Belgium), ITEP Moscow(Russia), Uppsala(Sweden) or under development in Berkeley(USA) and Darmstadt(Germany).[1)]

3.3.2. Isocentric gantries for proton therapy

The major problem encountered in the construction of an isocentric gantry for proton therapy is the high magnetic rigidity of the protons used for therapy (with conventional bending magnets the bending radius can not be chosen smaller than about 1.3 m) For this reason an isocentric gantry for proton therapy is larger and more massive than a conventional gantry for photons.
The only existing gantries of the world are the three "cork-screw" gantries of Loma Linda, which span a diameter of 12 m and have a weight of about 90 tons each. In the "cork-screw" design (first proposed at Harvard) the beam is bent first by 90^0 away from the axis and then is bent back on axis by a 270^0 bending in the plane transverse to the axis of the gantry. The Loma Linda gantry is designed to support both application methods, the spot scan method and the scatter foil technique (the last requiring a large distance between last bending magnet and patient).
The proton gantry to be realized next in the world, should be the gantry for PSI, commissioned for installation in 1993. The diameter of the PSI gantry has been reduced down below 4 m in diameter, by combining the spot scanning technique into the optics of the beam transport system and by mounting the patient transporter excentrically on the gantry. In this way the space in the radial direction is occupied only by the 90^0 magnet and by the patient transporter system respectively. The PSI gantry does not support the scatter foil technique. If the Loma Linda gantry looks like a large disk, the PSI gantry looks like a smaller but longer cylinder. Since the beam used at PSI is a degraded beam (energy degradation from 590 MeV down to 100-260 MeV) the phase space of the beam used at PSI is large and the magnets are correspondingly very massive. The gantry of PSI is heavier (120 tons) than the Loma Linda gantries despite the facts, that less total bending is applied on the beam. This is not a problem of the gantry design itself, but is a problem related to the proton source used at PSI (fixed beam energy and degradation of the beam). A PSI gantry design adapted to a dedicated accelerator with a beam with small phase space and variable energy, would be much less massive than the present prototype. For other gantry designs (IBA (Belgium), Uppsala (Sweden), Moscow (Russia), MSU East Lansing (USA), ACCTEK (USA)) or other solutions with combined fixed horizontal and vertical beams (Tsukuba and Chiba (Japan)) we have to refer here to the literature.[1)]
The performance of isocentric gantries does not depend much on the accelerator type, except for the two factors already mentioned:
a)Depending on the quality of the beam delivered by the accelerator (degraded or direct beam) the gantry magnets can be very massive or not.
b)The gantry dimensions depend partly on the application technique chosen for the gantry, and consequently the feasibility of the gantry depends indirectly on the duty factor of the beam delivered by the accelerator.

3.3.3. Proton radiography and Proton Tomography

The intensity of the proton beam must be attenuated down to a proton rate which permits the use of Multiwire Proportional Chambers (MWPC). The energy is chosen such that the protons barely pierce through the patient and exit on the other side with low energy. The entrance and exit coordinates of each proton are measured with MWPC and the residual energy is measured with a scintillating crystal (or the residual range with a stack of plastic scintillators). The measurement in coincidence of entrance and exit proton coordinates permits to reduce the position resolution error due to multiple Coulomb scattering by about a factor of 4 (position resolution in the order of few mm instead of around 1 cm). Since protons have a well defined penetration range, very few protons give already a very precise information on the integral electron density of the patient along the proton path. Proton radiography is therefore very sensitive to small density variations.
Proton radiography realized in the context of proton therapy could prove to be very appealing for the following reasons:
a) Proton radiography could be used to control the positioning of the patient in the beam directly on the gantry (substitution of the position verification usually performed by X-rays projections).
b) "Absolutely calibrated" proton radiography images contain precious additional information on the exact penetration depth of protons into the patient. Penetration errors due to organ misalignments or wrong calibration of CT data used for treatment planning, could be directly detected with digitized proton radiography images taken

directly **on line** before starting treatment. The quantitative verification by means of absolute **proton radiography** measurements, of the correctness of the residual range values calculated by the treatment planning system for the **passing-through particles**, should give confidence in the correctness of the corresponding calculations for the **stopping protons** for **therapy**. Proton radiography is therefore a very interesting tool to check the penetration depth of the beam into the patient together with the control of the correct positioning of the patient in the beam.
c) Proton radiography has excellent density resolution characteristics. A factor of 10 or 20 less dose is necessary for proton radiography to provide the same density resolution as with X-rays. Proton radiography could eventually prove to be a new interesting diagnostics tool, more sensitive to soft tissue differences.
e)Proton tomography, if possible to realize in practice on the gantry, should give access in theory to the ideal data base for treatment planning, since it would provide directly electron densities without the need of doubtful calibrations of Hounsfield numbers (without beam hardening artefacts like for X-rays).
We plan at PSI to test these ideas in the new beam line dedicated to proton therapy, in order to learn about their practical importance.
For the point of view of the requirements on the accelerator type, proton radiography and tomography require a very high rate of data taking, with individual events resolved by coincidence measurements in time. The duty factor of the beam is a crucial parameter for the acquisition time of the radiographic images.

3.3.4. Synchronisation with breathing

If dynamic scanning with conformation of the dose and/or proton radiography are performed together with the synchronization of breathing of the patient, the requirements on beam duty factor are even more important.

4. ACCELERATOR REQUIREMENTS

In this section we summarize the requirements on accelerators for proton therapy in the prospective of the future developments described in the previous sections:
a) **Maximum beam energy**.
For therapy 220 MeV energy seems to be adequate, but 260-280 MeV energy (40-45 cm range) is necessary for the feasibility of proton radiography in the body.
b) **Fixed beam energy and beam degradation**.
A fixed energy of the beam (cyclotron and synchrocyclotron) could prove to be an acceptable solution for the hospital, for reasons of simplicity and reliability.
The option to choose a variable energy (in steps or continously) is however the solution preferred by most of the proton therapy experts. A possible compromise for fixed energy machines is to use degraded beams, realized with variable thickness absorbers placed in the beam line possibly at an intermediate double focus . The scattered beam must be analyzed in momentum and phase space in the subsequent beam line, which could be the gantry itself. If the degradation of the beam is performed from 260 MeV (needed for proton radiography) down to 70 MeV, the intensity of the analyzed beam is expected to change with energy as much as a factor of 20.
The disadvantges of the degradation are given by the large variation (with all related safety problems) of beam intensity (needed in the accelerator to obtain a constant intensity of the degraded beam), by the increased activation of beam line elements in the region around and before the degrader and by the large phase space of the extracted beam, which requires massive magnets on the gantry.
c) **Variable energy**
directly from the accelerator (continuously from the synchrotron and in steps from a proton linac) is certainly a better solution, if available.
In the case of the synchrotron, the possibility to change beam energy from pulse to pulse is very appealing, since it should permit to control the deposition of the beam without range shifter systems (only the patient body contributes to the scattering of the beam), which is a necessary condition to achieve the ultimate precision possible with proton therapy. This requires however the simultaneous tuning, pulse by pulse, of all magnetic elements in the beam transport system, which could prove to be very difficult to obtain with sufficient beam position stability.
d)**Beam intensity**.
The required beam intensity depends on the application technique used. For tumours treatments with the spot scanning method a few nA proton current should be sufficient. For the scatter foil technique the generally accepted requirement is 10-20 nA.
e) **The duty factor of the beam**.
A good duty factor could prove to be, in the long range, equally important for proton therapy as it has been in the past for physics experiments in the same energy range.
The cyclotron provides the best possible time structure of the beam. This is indicated for beam dynamic scanning and for the data taking for proton radiography and tomography.
The slow extraction from a synchrotron is an acceptable alternative solution, which is however often criticized as a technical complex solution (?).
The other pulsed machines (linac and synchrocyclotron) should provide at least 100 Hz together with some method of control of the beam intensity from pulse to pulse at the ion source (or a 10kHz pulsed beam) in order to remain competitive for dynamic scanning methods (see section 3.3.1). For coincidence measurements with MWPCs for proton radiography a pulsed machine is always less efficient.
f) A **fast beam shutter**, to switch quickly the beam on and off, is a necessary device for the **discrete beam scanning technique**, which is more interesting than a

continuous scan, because of its simplicity and reliability. The switching can be realized with a **kicker magnet** mounted in the high energy proton beam line. For accelerators without ramping of the magnetic field (with sufficiently short transport time from the ion source to the patient) the switching of the beam should be performed more easily at the **ion source**.

g) **Superconducting accelerators and superconducting beam transport systems.**

These developments are very important, since they should provide a true miniaturisation of the proton facility, down to sizes comparable with those used for conventional therapy, up to the point even to envisage the rotation of the accelerator system itself around the patient (proposed MSU facility, East Lansing, USA).[1)]

Superconducting technology should also help to reduce the dimensions of gantries. The problems still to solve are the reliability (long repair time for the cooling down of the cryogenic parts) and the complexity (design, beam optics and wiring) of superconducting bending magnets with small bending radius.

h) **Acceleration of H^- ions.**

This solution can be used to provide a very simple and very reliable slow extraction of the beam from a synchrotron (charge exchange extraction with stripping foils). The phase space of the beam can be chosen to be very small, thus permitting to construct gantry systems with very small magnets (Moscow gantry).[1)] The price to pay for this solution is given by the large dimensions of the accelerator ring (around 15 m diameter) and by the need of ultrahigh vacuum (both requirements are necessary to avoid ion stripping). The large size of the accelerator ring can be compensated by designing the facility to be very compact, with short beam lines connecting the ring with the treatment rooms, aligned on a circle around the accelerator.

i)The **reliability and simplicity of operation** (which does not exclude a priori very advanced technologies, if they are well automatized) of the proposed solutions is probably the most important parameter for the success of the introduction of proton accelerators in the hospital environment.

5. CONCLUSIONS

What we need just now are more hospital-based proton therapy facilities in the world, in order to improve our clinical and technical experience on this subject.

Which is the most optimal technical solution for the clinics is not completely clear yet. The Loma Linda synchrotron represents a well optimized solution, which satisfies the needs of the techniques presently available (scatter foil method on a cork screw gantry) and at the same time permits future developments (slow extraction, variation of the energy pulse by pulse, dynamic scanning, etc.). The practical relative importance of the different performance parameters (like size, costs, patients throughput, simplicity of operation, safety) and the future development of new technical issues (like automated spot scanning, proton radiography and tomography, superconducting accelerators and gantries) could however change the conclusions in favour of other accelerator solutions.

6. ACKNOWLEDGMENTS

In this report we have discussed, for reasons of space, mainly those items, like dynamic scanning, compact gantries, proton radiography and tomography, which are now not well established in the field of charged particles, but which have good chances to become more popular in the case of the spreading of proton therapy facilities. This should not in any case diminish the importance of the more traditional techniques developed in the last decades by the centers pioneering charged particle therapy like Berkeley, Uppsala, Harvard, Dubna, Moscow , Leningrad, Chiba, Triumf, PSI, Tsukuba, Clatterbridge, Loma Linda, Louvain, Nice, Orsay, ...

Many of the ideas discussed in this paper refer indirectly to propositions originating from and presented and discussed in more details at PTCOG (Proton Therapy Co-Operative Group) meetings. I would like to thank all members of the PTCOG community for their help and for the very open and friendly atmosphere, which is much profitable for the promotion of charged particle therapy.

7. REFERENCES

1) The list of contributions of relevance in the context of this paper would be too long to be presented here without important omissions. We refer therefore to the specialized literature. The different charged particle facilities discussed in this paper have been presented at several conferences and the contributions are collected in several proceedings, for example in:

A)Proceedings of the NIRS International Workshop on Heavy Charged Particle Therapy and related subjects, (NIRS-M-81, Chiba, JAPAN, 1991).

B)Proceedings of the Proton Radiotherapy Workshop held at PSI, (Paul Scherrer Institute, CH-5232 Villigen, 1991).

C)Proceedings of the International Heavy Particle Therapy Workshop (PTCOG/EORTC/ECNEU) held at PSI, (Paul Scherrer Institute, CH-5232 Villigen, 1989).

D)Proceedings of the 2nd European Particle Accelerator Conference in Nice, (Ed. Frontieres, 91192 Gif-sur-Yvette Cedex, France, 1990).

E)Extended Abstracts of The fourth Workshop on Heavy Charged Particles in Biology and Medicine in Darmstadt, (GSI-91-29, D-6100 Darmstadt, 1991).

F)Proceedings of the Twelfth International Conference on Cyclotrons and their Applications in Berlin (World Scientific, Singapore, 1989).

CURRENT AND POTENTIAL CLINICAL INDICATIONS OF PROTON IRRADIATION

ALLAN F. THORNTON and HERMAN D. SUIT

Department of Radiation Oncology
Massachusetts General Hospital
Harvard Medical School
Harvard Cyclotron Laboratory
Boston, MA., USA

ABSTRACT

Over the past 2 decades of clinical development, proton irradiation has become the standard of care for selected tumor sites, e.g. ocular melanoma and skull base sarcomas (chordomas/chondrosarcomas). Proton therapy has made possible tumor dose escalation with maintenance of normal tissue dose constraints, increasing local control rates by over 30% in these tumors. The 3-dimensional planning tools developed specifically for proton treatment design have recently been emulated in several advanced 3-D photon planning algorithms, narrowing the dosimetric advantage afforded by proton therapy. However, the precise beam range modulation has been demonstrated to be of continued potential advantage in other clinical sites - specifically, advanced nasopharynx, paranasal sinus, oropharyngeal, nervous system, and prostate neoplasia. Reviews of the current tumor indications and control rates, Proton Radiation Oncology Group (PROG) clinical trials, and future applications are presented.

INTRODUCTION

Radiation oncology represents a discipline of medicine with the mandate of maximizing the local control of malignant disease. Although the spectrum of human neoplasia is broad and includes tumors whose natural behavior may be so aggressive as to be metastatic at first clinical presentation, many tumors remain locally confined for a significant period before dissemination. Such tumors range from slow-growing sarcomas of the skull base and ocular melanomas, to more histologically aggressive prostate carcinoma and squamous cell tumors of the head and neck. Recent statistical analyses of patterns of failure suggest that the ability to obtain local control of a tumor does, indeed, translate into decreased rates of metastases and, ultimately, into increased survivals.[1)]

Proton therapy represents one therapeutic modality within the armamentarium of irradiation possessing unique dosimetric qualities.[2)] The particle nature of proton irradiation results in extremely rapid dose fall-off at the distal range of the absorption - a phenomenon recognized as the "Bragg Peak". Unlike photon irradiation, the positive charge of protons results in slowing of the particles by attraction of electrons in tissue, as well as deflection and repulsion from nuclei. These magnetic characteristics result in a finite range of the proton as it traverses through tissue medium. Furthermore, this range is energy dependent and may be controlled by "range modulation". Additionally, dose profiles of protons in tissue equivalent phantom materials suggest a constant loss of energy across a range, resulting in a "flat" dose distribution across a useful depth of tissue. However, such a distribution comes at the expense of the well-recognized "skin-sparing" provided by higher energy photon beams. Because entrance doses for proton beams may vary as high as 70-100%, clinical therapy dictates either multiple entrance sites (i.e., multiple proton portals) or some mixture of photon and proton irradiation in order to lessen skin toxicity. The effective absence of exit dose beyond the range of proton irradiation also results in a lack of useful energy with which to image treatment volumes; therefore, diagnostic photon energy must be used to generate treatment portal verification films.

The sharp distal edge to the proton beam, combined with the ability to contour its width profile through the use of tissue compensation designed, not only to replace missing tissue, but also to correct for tissue inhomogeneities, both result in a facile method for tightly conformal therapy design. Such conformal therapy results in significant savings to "normal" non-target tissues during the irradiation of adjacent tumors. It is this ability to shape, or contour, the dose profile about the target volume that distinguishes proton irradiation - no radiobiological advantage is recognized for proton radiation per se. Relative Biologic Effectiveness (RBE) values have been repeatedly measured for proton therapy and are recognized to approximate 1.1; that is a coefficient multiplier of 1.1 will translate proton absorbed dose into photon, "Cobalt Gray Equivalent = CGE", dose. Therefore, only through target dose escalation made possible by conformal proton irradiation will local control of tumors be increased.

Tumor Control Probability (TCP) and Normal Tissue Complication Probability (NTCP) curves both assume sigmoidal shapes, paralleling each other. Over the dose range resulting in significant incremental increases in tumor kill, i.e., over the range of the sigmoidal curve with the greatest slope, there exists a relatively small dose difference between curves reflecting damage to tumor and normal tissue. Scattered and "exit" radiation, such as exists in conventional photon therapy, results in dose to normal tissues, reducing the dose available to treat tumorous tissues. Partial organ tolerances, for the most part, have been poorly described in conventional photon literature. Proton therapy makes restriction of treated volumes possible and also allows treatment of only partial volumes of normal structures. One important result of proton therapy trials is the recognition of partial organ tolerances, some of which are currently being reported.[3)]

Three-dimensional treatment planning is a requirement of proton radiotherapy. Accurate predictions of scatter from surrounding tissue in all planes can only be made with the use of dose algorithms capable of 3-dimensional calculations. Equally important is the ability to represent the tumor and surrounding normal structures in such a fashion as to allow arbitrary viewing from any projection angle. The capacity to generate isodose surfaces, correlate these surfaces with CT and MR-defined anatomy, and to view the relationships of these surfaces and anatomy from any "Beam's Eye View" angle brings interactive 3-dimensional treatment planning to reality. Such software was originally developed for proton therapy and has been emulated by several photon algorithms.[4)] The volumetrics associated with the 3-dimensional surfacing implicit in this software makes it now possible to quantitatively compare volumes irradiated, patterns of recurrence relative to volumes irradiated, and normal tissue complications relative to volumes of normal tissues treated.

The development of powerful software tools capable of 3-dimensional treatment planning for both proton and now, photon, therapy has narrowed the dosimetric advantage gap between proton and photon treatments. Conformal photon irradiation is now possible for a number of disease sites, significantly improving the potential therapeutic ratio. However, the presence of a photon exit dose dictates the use of many beams in order to average the integral dose to normal tissue over as great a volume as possible. The ultimate expression of this integral dose averaging lies in dynamic therapy - conformal shaping of photon fields dynamically changing with rotation about the patient. Dynamic therapy has yet to become a practical reality, thwarted by the practicality of dose and conformal shielding verification. Proton therapy does not require such dose averaging to normal tissues - precise modulation of the distal edge depth and effective compensation across field dimensions obviate the need for more than a few static beams to achieve conformal therapy distributions. Nonetheless, optimal radiation planning may ultimately require both modalities: proton therapy for restricted, conformal boost irradiation and dynamic photon therapy for irradiation of surrounding tissues at risk for subclinical disease.

CURRENT CLINICAL EFFORTS

Proton therapy commenced at the Lawrence Berkeley Laboratory in 1955 for patients with benign arteriovenous malformations and pituitary neoplasia. Since that inception, worldwide interest has increased markedly, most recently due to the availability of practical software planning tools and to the decreased cost of cyclotron construction. It is estimated that over 12,000 patients have received proton irradiation, the majority for small intracranial lesions and for tumors of the eye. The recent formation of the ACR (American College of Radiology) sponsored Proton Radiation Oncology Group (PROG) represents a significant clinical focus designed to test the relative efficacy of proton therapy in well-designed trials. Several on-going Phase III trials, as well as recently commenced Phase I-II efforts, will be described.

Phase III trials

Uveal melanoma

As of June, 1992, 1764 patients have received radical irradiation therapy for choroidal melanomas utilizing protons delivered by the Harvard Cyclotron Laboratory (HCL). It is estimated that over 3000 melanoma patients have been treated worldwide.

Alternative therapies for choroidal melanoma include either enucleation or radioactive plaque therapy. Survival rates have been demonstrated to be fully comparable to those realized with enucleation, suggesting that dissemination of tumor cells during treatment localization, delivery, or follow-up is not occurring.[5] Plaque therapy is also being tested in a nationwide randomized trial against enucleation and appears to offer another alternative.[6]

Analysis of greater than 1000 proton patients at the HCL suggests local control rates within the globe to exceed 96% with control within the high-dose region exceeding 99%.[7] Ten-year survivals have remained in excess of 80% across all participating centers. With the excellent local control and equivalent survival rates to enucleation and plaque therapy, proton therapy for uveal melanoma appears to be most suited for 1) Posterior lesions close to the fovea where plaque placement is difficult and 2) Larger lesions with ultrasound measured height >/= 8mm which are not homogeneously treated with plaque therapy. Anterior lesions are more readily suited to plaque therapy due to facile placement.

We are currently testing the hypothesis that lower proton dose levels are possible while maintaining control rates and decreasing toxicity to the disc and fovea. The current Phase III dose trial randomly compares 5 x 10 CGE to our historical 5 x 14 CGE dose level for patients with tumors proximal to the disc and fovea. Eligibility criteria have remained constant throughout this trial and include tumors of </=15 mm diameter and </= 5mm height + located within 4 disc diameters of the optic disc/fovea + no evidence of distant disease + vision of counting fingers or better. Clinical results thus far have remained excellent, with no evidence of local failures. Therefore, the trial will continue with current acceptance parameters. An anticipated 176 patients are expected to be entered into the trial.

An additional phase III trial is underway testing the efficacy of DTIC chemotherapy and BCG immunotherapy in preventing the spread of disease for patients with larger choroidal melanomas and higher risks of metastatic spread. These established agents for the treatment of cutaneous melanomas are tested for patients with ocular melanomas >/= 15 mm in diameter and >/= 8 mm in height with no evidence of metastases. The radiation therapy will remain at the higher level (our historical control) of 70 CGE over 5 treatments.

Skull base sarcomas

Sarcomas of the skull base represent rare, difficult neoplasms to treat with conventional means of surgery and photon irradiation. Consisting primarily of chordomas and

chondrosarcomas, these tumors are usually not accessible to complete surgical removal, manifest relentless local invasive behavior, and are juxtaposed to critical structures (brainstem and chiasm) that effectively prevent the delivery of photon doses greater than 55.8 Gy. Austin-Seymour reviewed the historical control rates for this site with conventional treatment and reported local control rates at 3.5 years not to exceed 36%.[8)]

Proton therapy results have been previously reviewed and found to offer clear advantages over conventional photon treatment.[9-10)] Since 1974, over 200 patients with chordomas or low-grade chondrosarcomas of the base of skull have been treated with combined, fractionated proton and photon irradiation at the MGH/HCL facility. Greater than 70% of the dose was given with proton radiation, allowing significantly increased doses to be delivered, while respecting tolerance doses to adjacent critical structures (brainstem, chiasm). All planning has been performed with the aid of 3-dimensional planning techniques, optimizing the delivery of irradiation. Median dose delivered was 68 CGE. Outcome has been assessed in terms of local recurrence-free survival (LRFS) and overall survival. Local failure, defined as a definite increase on CT or MR imaging, occurred in 18% of patients, while metastases was documented in 4%. Median follow-up at time of last analysis is 37 months. LRFS at 36 and 84 months is 84% and 65% respectively, while overall survival is 94% and 77%. Significant prognostic variables include sex (males significantly better than females); histology (chondrosarcoma better than chordoma); location (base of skull better than cervical spine); and age (younger better). Currently, RTOG 86-25, a randomized dose protocol between 66.6 and 72 CGE for skull base sarcomas employing combined proton and photon irradiation, is being examined.

Advanced prostatic carcinoma

As of June, 1992, 192 patients have been entered onto a MGH/HCL study of dose escalation for advanced carcinoma of the prostate.[11)] Designed for T3-4 disease with N0-2 nodal status, the trial randomly compares 68.4 G to 75.6 CGE using conformal proton therapy. A total of 200 patients are planned to be treated before conclusion of the study. The acceptable tolerances of the rectum and bladder to the higher dose of irradiation suggests that proton beam therapy may realize significant increases in local control. Results from the trial will only be available after accrual completion and adequate follow-up time has occurred; however, toxicity results suggest the higher proton dose to be well-tolerated.

Phase II Clinical Trials

Recently, expanding clinical focus has resulted in the development and implementation of new protocols for the treatment of tumors of the paranasal sinus, oropharynx, benign intracranial meningioma, and astrocytomas at the HCL. These new efforts have required renewed attention to the details of facile, precise immobilization, as well as the incorporation of permanently implanted fiducial markers.[12)] Used in concert with repositioning software, these markers allow corrections of cranial position to be made to the sub-millimeter level in a reasonable treatment period of time, usually 20-30 minutes per patient.

It is noteworthy to indicate a change in emphasis in clinical trials towards the therapy of more rapidly growing, locally aggressive tumors. Whereas the period from surgical resection to irradiation for skull base sarcomas often exceeds several months, every effort is made to follow surgery with post-operative irradiation within 3-6 weeks for the squamous cell tumors of the paranasal sinus and oropharynx. Additionally, the astrocytoma treatment regimens demand a similar time schedule, including aggressive steroid management during therapy for intracranial swelling. Such new time constraints dictate close coordination with referring surgeons, rapid and interactive treatment planning, and close follow-up of these tumors.

Paranasal sinus

A hyperfractionated, accelerated combined photon and proton trial is currently in progress for patients with advanced malignancies of the paranasal sinuses. This aggressive regimen builds on the MGH experience of hyperfractionation to include the increased targeting accuracy of proton therapy, hoping to spare patients morbid, extensive surgical resections of the orbital contents and premaxillary area.[13] Tumors of this anatomical area have a relatively sparse lymphatic drainage pattern; therefore, they represent a category of head and neck tumors for whom increased local control may translate into increased survival.[14] Statistical predictions based upon dose-response data from pharyngeal wall tumors (similar in metastatic rate and growth patterns) suggest that a dose increase from current standards of 65 Gy to 75 Gy may result in as much as a 35% increase in local control.[15]

This program has accrued 10 patients thus far, including 2 currently under treatment. Despite the complexity of treatment planning involved, we have been able to maintain the same timetable for post-operative treatment as for conventional planning, i.e., commencing irradiation within 4 weeks following limited surgery. Permanently implanted cranial fiducials, in concert with improved cranial immobilization, have resulted in daily positioning inaccuracies of less than 0.5 mm. Because of this patient set-up accuracy, we have been able to treat tumors in close approximation to the visual system (optic nerves and chiasm) to radical (curative) doses.

Astrocytoma

Treatment of patients with high-grade astrocytomas of the brain has seen little improvement in local control over the past two decades, despite increasingly aggressive surgery and sophisticated imaging. Irradiation techniques have previously been constrained from delivering higher doses due to dose-volume tolerances of the brain. However, restricted volumes of the brain seem to be able to tolerate high levels of radiation from stereotactic interstitial techniques.[16]

A protocol has been developed, and is presently accruing the third patient, designed to deliver 90 CGE to restricted volumes of brain for patients with glioblastoma multiforme, totally resected. Fields are designed to conformally irradiate MR and CT-planned volumes, sparing the maximal amount of "normal" brain surrounding enhancing target volumes. Fractionation involves twice-daily irradiation - 1.8 Gy photon in the morning followed by 1.8 CGE proton treatment in the afternoon, at least 7 hours later. 50.4 CGE is delivered to the CT enhancing volume + 3 cm; 60 CGE to the CT enhancing volume + 2 cm; and 90 CGE to the enhancing volume alone. In such a manner, a dose gradient is delivered to the tumor isocenter that parallels the tumor cell densities at radial distances about the center of the tumor.

Maximal surgical extirpation will be required prior to irradiation in order to relieve edema effects of radiotherapy. Our previous pilot study of 9 patients indicated that edema resulting either from tumor expansion or acute radiation cerebral swelling is a major untoward effect of high dose irradiation and must be relieved by maximal resection when possible. The patients in the previous pilot study who received maximal resection are the only patients still alive and free of evidence of tumor.

Future protocols for low and intermediate-high grade astrocytomas (Grades II and III) are planned, building on our current study. These efforts will maintain the tightly conformal therapy possible with proton therapy, although total dose will be reduced, reflecting the earlier tumor stage.

Benign intracranial meningioma

A randomized, prospective, trial is currently underway to examine the additional efficacy afforded by 63.0 CGE versus conventional 55.8 CGE for recurrent, or

incompletely excised, benign intracranial meningiomas. These tumors account for 20% of intracranial neoplasms and, although histologically benign, account for significant morbidity due to their frequent proximity to the visual system. Tumors of the sphenoid ridge, parasellar area, and posterior fossa represent particularly difficult areas where detection is often late and complete surgical resection rates are low. Although a dose response relationship has not been established, data from University of California at San Francisco would suggest that 5 and 10 year local control is significantly improved when post-operative radiotherapy is delivered.[17] Nonetheless, 10-year local control rates remain as low as 50% following combined therapy with conventional irradiation doses of 55.8 Gy.

This trial employs the precise dose delivery of proton irradiation to ensure marginal coverage of resected meningiomas - marginal coverage which is difficult to ensure with conventional therapy because of close proximity to eyes, chiasm, and brainstem. Additionally, the dose escalation arm will seek to establish a dose response relationship for the treatment of benign meningiomas. To demonstrate an increase in local control rate of 13% at 5-years (80% to 93%) in this group of patients, 110 patients will be needed. Prior experience at MGH, LBL, and Loma Linda suggest that combined accrual rates dictate 5 year completion dates for the study. Thus far at the MGH, 6 patients have been randomized to the study this year. No acute complications have been realized from the treatment of this initial patient group.

Carcinoma of oropharynx

The Loma Linda proton facility has introduced to PROG a phase II protocol for oropharyngeal squamous carcinoma involving the delivery of concomitant proton boost irradiation during the last 3 weeks of photon treatment. This focussed "field-in-field" proton irradiation is intended to deliver a total of 3.3 CGE of daily treatment to sites of gross disease during the final, most radioresistant phase of a conventional course of therapy. Intended for tumors of the tonsil and base of tongue, both sites where local control is poor (<40%) and morbidity of surgical resection is high (total glossectomy/laryngectomy), this application of proton therapy seeks to emulate a non-invasive brachytherapeutic boost to sites of palpable, gross disease. However, unlike implant therapy, no requisite interval will be needed after conventional photon therapy for mucositis to heal. M.D. Anderson experience suggests that concomitant boost therapy results in superior local control for photon therapy, and should be delivered at the conclusion of the course of irradiation.[18] This protocol seeks to improve on the results of the M.D. Anderson group by targeting the tumor more precisely during this boost period, reducing morbidity and allowing an increased dose to be delivered.

Accordingly, 75.6 CGE will be prescribed to all sites of visible tumor at the time of initial endoscopic evaluation. This volume will not include nodal disease - such residual disease following irradiation to 50.4 CGE will be resected with modified neck dissection. All effort will be made to confine the proton boost most effectively in order to spare contralateral parotid and preserve pharyngeal wall constrictor function. Two patients have been entered on this protocol thus far - one each at the Loma Linda and MGH facilities. It is expected that this effort will be a major clinical endeavor due to the large numbers of patients with suitable tumors.

FUTURE CLINICAL EFFORTS

Extrasellar and recurrent pituitary neoplasia

Patients with recurrent (after transphenoidal surgery) pituitary disease, as well as those patients presenting with bulky, suprasellar and extrasellar disease not manageable with surgery, will be offered a tightly conformal, MRI-planned, fractionated irradiation course to elevated doses of 55.8 CGE. Normal tissue constraints to the hypothalamus and optic chiasm will be

maintained, if possible. This protocol will examine if the precise dose localization of proton therapy may offer these patients improved marginal control of pituitary adenomas, while minimizing untoward effects to the hypothalamus and medial temporal lobes.

Acoustic neuromas

Patients with unresectable or incompletely resected acoustic neuromas, for whom observation alone is inappropriate, either because of aggressive growth rates or critical tumor location, will be offered a fractionated, conformal proton therapy designed to deliver 35 CGE to the tumor + 0.5 cm while maintaining normal tissue constraints to the brain stem and temporal lobes. Developed in concert with the Department of Neurosurgery at MGH, this protocol will offer distinct dosimetric advantages over conventional photon "wedged-pair" therapy or "gamma-knife" stereotactic treatments in the reduction of dose inhomogeneities to surrounding structures. Larger fraction sizes will be employed in order to effect a greater therapeutic ratio, taking advantage of the dosimetry of proton therapy.

Advanced nasopharynx

Patients with advanced nasopharyngeal tumors (T3 and T4) will be offered a proton boost designed to ensure uniform delivery of 72 CGE to the base of skull. The cranial foramen are common routes of direct extension of these larger nasopharyngeal tumors, accounting for a significant proportion of the local failure rate (>40%) for advanced disease. Conventional therapy is constrained from uniform delivery of dose through the base of skull because of adjacent brainstem and cerebral tolerances. Proton therapy experience with skull base sarcomas will be applied directly to these tumors and should result in an increased cure rate as a result of improved local control.

SUMMARY

Although proton therapy is well-established for the treatment of ocular melanomas and skull base sarcomas, the dosimetric advantages of this particle therapy should also be of benefit to patients with other malignancies, specifically those of the paranasal sinuses, nasopharynx, brain, and prostate. However, in order to statistically demonstrate the advantages of proton therapy in local control of these tumors, cooperative trials must be completed with consistent protocol guidelines. The Proton Radiation Oncology Group represents an important collaboration towards achieving this protocol cooperation. Even within the short period since its inception, PROG has designed and implemented a number of challenging, new clinical efforts in order to test proton therapy. This next period of protocol accrual and completion will be an important one in the effort to make proton therapy a practical reality to the radiation oncology community at large.

REFERENCES

1) Fuks, Z., Leibel, S.A., Wallner, K.E., et al., "The effect of local control on metastatic dissemination in carcinoma of the prostate: long-term results in patients treated with 125I implantation", Int J Radiat Oncol Biol Phys 21(3), 537-47, 1991.

2) Suit, H.D., Goitein, M., Tepper, J.E., et al., "Clinical experience and expectation with protons and heavy ions", Int J Radiat Oncol Biol Phys 3, 115-125, 1977.

3) Urie, M., Fullerton, B., Tatsuzaki, H., et al., "A dose response analysis of injury to cranial nerves and/or nuclei following proton beam radiation therapy", Int J Radiat Oncol Biol Phys. 23(1), 27-39, 1992.

4) Fraass, B.A., McShan, D.L., **The Use of Computers in Radiation Therapy** (Elsevier Science Publishers B.V., North-Holland, 1987), Overview of a Clinical Planning System: 3-D Treatment planning, pp.273-276.

5) Seddon, J.M., Gragoudas, E.S., Egan, K.M., et al., "Relative survival rates after alternative therapies for uveal melanoma", Ophthalmol 94, 354-361, 1987.

6) Cruess, A.F., Augsburger, J.J., Shields, J.A., et al., "Visual results following cobalt plaque radiotherapy for posterior uveal melanomas", Ophthalmol 91, 131-136, 1984.

7) Munzenrider, J.E., Verhey, L.J., Gragoudas, E.S., et al., "Conservative treatment of uveal melanoma: local recurrence after proton beam therapy", Int J Radiat Oncol Biol Phys., 1992 (in press).

8) Austin-Seymour, M., Munzenrider, J.E., Goitein, M., et al., "Progress in low-LET heavy particle therapy: intracranial and paracranial tumors and uveal melanomas", Radiat Res 104, 219-226, 1985.

9) Austin-Seymour, M., Munzenrider, J.E., Goitein, M., et al., "Fractionated proton radiation therapy of chordoma and low-grade chondrosarcoma of the base of skull", J Neurosurg 70, 13-17, 1989.

10) Berson, A.M., Castro, J.R., Petti, P., et al., "Charged particle irradiation of chordoma and chondrosarcoma of the base of skull and cervical spine", Int J Radiat Oncol Biol Phys 15, 559-565, 1988.

11) Shipley, W.U., Tepper, J.E., Prout, G.R., et al., "Proton radiation as boost therapy for localized prostatic carcinoma", JAMA 241, 1912-1915, 1979.

12) Rosenthal, S.J., Thornton, A.F., Gall, K., "An improved cranial immobilization device for combined photon and proton therapy of advanced paranasal sinus tumors", abstract to be presented at the annual meeting of American Association of Physicists in Medicine, Calgary, 1992.

13) Wang, C.C., Blitzer, P.H., Suit, H.D., "Twice-a-day radiation therapy for cancer of the head and neck", Cancer 55, 2100-2104, 1985.

14) Parsons, J.T., Mendenhall, W.M., Mancuso, A.A., et al., "Malignant tumors of the nasal cavity and ethmoid and sphenoid sinuses", Int J Radiat Oncol Biol Phys 14(1), 11-22, 1988.

15) Thornton, A.F., Ten Haken, R.K., McLaughlin, W.C., et. al., "Contributions of 3-dimensional volumetrics and treatment planning to irradiation of advanced paranasal sinus tumors", Int J Radiat Oncol Biol Phys, manuscript in preparation.

16) Gutin, P.H., Leibel, S.A., Wara, W.M., et al., "Recurrent malignant gliomas: survival following interstitial brachytherapy with high-activity iodine-125 sources", J Neurosurg 67, 864-873, 1987.

17) Wara, W.M., Sheline, G.E., Newman, H.J., et al., "Radiation therapy of meningiomas", Am J Roentgenol Rad Ther Nuc Med 123, 453-458, 1975.

18) Peters, L.J., Ang, K.K., Thames, H.D., "Accelerated fractionation in the treatment of head and neck cancer: a critical comparison of strategies", Acta Radiol, 1992 (in press).

PION THERAPY FOR CANCER - WHAT ARE THE PROSPECTS?

George B.Goodman, FRCPC, FRCR, FACR, FRCP(Ed.)
Clinical Professor Emeritus Surgery, University of British Columbia
Honorary Medical Staff, B.C.Cancer Agency, 600 West 10th Ave.
Vancouver, B.C., V5Z 4E6, Canada

ABSTRACT

Promising results in uncontrolled trials from pion radiotherapy at TRIUMF in the treatment of high grade astrocytoma and cancer of the prostate gland indicate their potential for therapeutic gain. Prospectively designed randomized trials comparing pions and photons have begun for scientific evaluation under rigorously controlled conditions.

1. INTRODUCTION

We are conducting two randomized clinical trials at TRIUMF comparing pimeson (pion) against photon therapy in cancer. The studies involve malignant astrocytomas of the brain and locally advanced cancer of the prostate gland. The trials were prospectively designed and are strictly controlled for critical assessment of the encouraging results of pion therapy observed in our initial studies.

2. BRAIN

2.1. Background Review of Initial Studies

53 patients with grade 3 & 4 astrocytomas were treated from 1982-85 inclusive in a dose escalation study using pions.[1] It was found that survival was significantly improved with pions in a dose above 30 π-Gy compared with a mixed schedule using whole brain photon radiation with a pion boost. At 36 π-Gy survival worsened and one patient showed cortical brain necrosis and demyelination. This indicated dose had exceeded tolerance of normal brain tissue. Optimal dose for pion therapy appeared to be between 33 and 36 π-Gy.

Our preliminary studies indicated a gain for pion therapy compared retrospectively with our photon experience in Vancouver using Cobalt 60 to a total dose of 50 Gy. Results showed a doubling of median survival from about 200 days to over 400 days, and, with long term survivals from pions approximately 20% at 4.5 years of follow up.[2] A controlled trial was considered essential for critical evaluation of pion therapy and its design was finalized and approved in 1988.

2.1.1. Prospective comparative trial of pions versus photons

This study compares normal tissue tolerance doses of pions and photons in the treatment of high grade 3 and grade 4 astrocytoma (glioblastoma multiforme). The pion doses were estimated at 34.5 π-Gy and 33 π-Gy in 15 daily fractions for treatment volumes less than 500 ccs, and between 500 and 850 ccs respectively. The empirically determined best standard photon dose was estimated at 60 Gy in 30 fractions using 4-10 MeV x-rays. Stratification of prognostic factors significant in determining treatment outcomes ensured their equal distribution between the pion and photon arms. So equal numbers of patients would be treated by age (less, equal to 49 years, or, 50 years and over) by Karnofsky performance score (less, equal to 69, or 70 and over) by extent of prior surgery (biopsy only or debulking, excisional procedure). A block method, determined by and known only to our biostatisticians, was used for randomization. The patient registrations and treatment allocations are done by a clinical trials secretary.

The principal end point is survival. A successful outcome for pion therapy demands "worthwhile survival (median survival of 500 days)" over "just worthwhile survival (median survival of 250 days)" from photons. Using a power factor of 80% and a significance level of 0.05 it was estimated that a total accrual of 82 patients would be required to show this difference.

Patients eligible for study are between 18 and 70 years of age and with histology assessed by our review pathologists as high grade 3 or grade 4 astrocytoma. Patients must be fit enough for radical radiotherapy (Karnofsky score equal to or greater than 50) and capable minimally of self-care with aid. The lesions must be unifocal and the treatment volume less than 850 ccs. Treatments must start within 30 days of surgery. Patients with another malignancy within previous 5 years are excluded (except common skin cancer). All patients must sign informed consent.

As at August 1992 a total of 57 patients has been entered into the trial, 30 patients to pions and 27 to photons. Accrual is slower than was anticipated because of the strict entry requirements which reduced the "pool of available patients", the scheduling at TRIUMF controlling beam access, and other factors viz. nursing strikes, mechanical failures etc.

3. PROSTATE

3.1. Background Review of Initial Studies

45 patients with advanced pelvic tumours (colo-rectal 8, prostate 20, bladder 7) were irradiated with pions in dose escalation and site selection studies (1982-87). Pion dose was escalated to 37.5 Gy at 2.5 Gy per fraction. Results showed that local tumour control was better with total dose greater than 30π-Gy while prostate cancer responded best.[3] By 1990, 49 patients

with prostate cancer had been treated.[4] Most had inoperable, large primary tumours spreading extracapsularly (T3-15) or invading adjacent pelvic organs (T4-32). 43% showed lymph node or distant metastases at treatment. The acute and late morbidity (mild & severe) for pions was similar to that from photon therapy reported in published series. The actuarial cumulative late toxicity rates to 87 months follow up remained constant from 24 months onward. Pion doses of 37.5 Gy, corresponding to estimated photon dose-equivalents of 56 Gy in 15 fractions or 78 Gy in 39 fractions at 2 Gy/fraction, were safely delivered.

I was satisfied that the severity and duration of reactions at the 37.5 Gy π- dose level were comparable to those from my experience of photon therapy using 15 daily fractions and that they approached the threshold of clinical tolerance. Local tumour response rates appeared to be similar to those recorded for photons at 2 years.

Because high LET was reported superior to photons for prostate cancer[5], a trial for pions was designed, approved and launched in 1990.

3.1.1. Prospective comparative trial of pions versus photons in prostate cancer

This randomized trial compares pions against photons in the treatment of patients with inoperable, locally advanced cancer of the prostate gland (clinical stages T_{3-4}, N_{0-x}, M_0).

Eligible patients were staged clinically while those staged surgically were excluded. Adenocarcinoma of the prostate histologically verified by review pathologists, an E.C.O.G. 0-2 rating attesting fitness for radical treatment, as well as signed informed consent were mandatory. Enrolment also required discontinuance of any hormone therapy for the month antecedent to randomization, together with a serum testosterone level reverted to normal. Patients with another malignancy in the previous 5 years were excluded (except common skin cancers).

The pion and photon doses used for treatments were: (1) for pions - 37.5 π-Gy and 36 π-Gy in 15 fractions for treatment volumes less or greater than 500 ccs respectively and, (2) for photons using 10-25 MeV x-rays - 66, 64, 60 Gy in a dose/fraction of 2 Gy for treatment volumes less than 500 ccs, greater than 500 but less than 750 ccs, and greater than 750 ccs respectively. This was considered to be an accepted best standard therapy in North America.

Again, the randomization, decided by our biostatisticians, was by block method, was unknown to clinicians and the registration and treatment allocations was implemented through a clinical trials secretary.

Prognostic factors used for stratification purposes were the extent of local disease (T_3 or T_4), the tumour differentiation (well and moderately differentiated versus poorly differentiated) and the prostatic specific antigen level at the time of treatment (less or equal to 49 μg/L versus equal to or greater than 50 μg/L).

The principal end point of this study required demonstration of an increased local control of 20% (from 60-80%) and, a 15% increase of crude survival (from 65-80%) at 5 years for pions over photons. Statistically a sample size of about 100 patients per treatment arm was estimated as necessary to demonstrate this difference (using a 1-sided test, a significance level of 0.05 and an 80% power factor).

Accrual to August 1992 shows a total enrolment of 112 patients, with 65 allocated to pions and 47 to photons. Accrual rates appear to be in accord with predictions.

4. WHAT ARE THE PROSPECTS?

The clinical trials reported here are the only prospective, comparative, randomized trials of pions versus photons in the world. The prospects are good that accruals will be complete in about 2 years.

PSI discontinued pion irradiation for high grade astrocytomas in 1988 stating results did not show a therapeutic gain compared with conventional treatment.[6] Yet, none of the PSI studies involved prospective comparative controlled trials of pions versus photons. Had we at TRIUMF judged outcome of pion therapy on the basis of retrospective comparisons we would have concluded that pions were twice as good as photons for glioblastoma. Clearly meaningful scientific assessment of the value of new treatments can only be effected by prospective, controlled, randomized trials.

5. BIBLIOGRAPHY

1) Goodman, G.B., Skarsgard, L.D., Thompson, G.B. et al, "Pion Therapy at TRIUMF: Treatment Results for Astrocytoma Grades 3 & 4: A Pilot Study", **Radiotherapy and Oncology, 17**, pp.21-28, 1990. Elsevier.

2) Goodman, G.B., Bowen, J.L., et al, "Pimeson Radiotherapy at TRIUMF". **The Journal of J.A.S.T.R.O. VOL.2, NO.2,** pp.85-99, 1990.

3) Goodman, G.B., Harrison, R., Kornelsen, R.O., et al, "Clinical Evaluation of Pimeson Radiotherapy at TRIUMF." **Radiation Research Proceedings of 8th International Congress of Radiation Research in Edinburgh 19-24 July 1987. Vol.2.** Fielden, E.M., Fowler, J.E., Hendy,J.H., Scott, D.(Ed). Taylor & Francis (Publisher), pp.928-933. 1987.

4) Pickles, T., Bowen, J., et al. "Pions-The Potential for Therapeutic Gain in Locally Advanced Prostate Cancer: Dose Escalation and Toxicity Studies". **Int.J.Rad.Oncol.Biol.Phys.Vo.21.** pp.1005-1011. 1991.

5) Laramore, G., Krall, J., et al. "Fast neutron radiotherapy for locally advanced prostate cancer: results of an RTOG randomised trial". **Int.J.Rad.Oncol.Biol.Phys.11.** pp.1621-1627. 1985.

6) Munkel, G., Greimer, R., et al. "Pion Radiotherapy". **PSI Life Sciences Newsletter 1989/90.** pp.3. Annex II. Annual Report 1989.

PROGRESS REPORT ON THE IBA-SHI PROTON THERAPY SYSTEM

Y.Jongen, A.Laisné, W.Beeckman, J.P.Dufour, H.Marie, R.Verbruggen
Ion Beam Applications, Chemin du Cyclotron 2
B-1348 Louvain-la-Neuve, Belgium

and

N.Takahashi, S.Satoh, M.Sano, T.Takayama
Sumitomo Heavy Industries
Niihama-city, Japan

ABSTRACT

The current status of the proton therapy facility developed by IBA and SHI is presented. This includes general aspects of the machine already presented in previous papers as well as more recent features such as the closed gap, the extraction device and the central magnetic field. Two types of isocentric gantries, one for scanning and one for scattering are at the design stage.

1. INTRODUCTION

A proton therapy facility using a compact, high-field non superconducting cyclotron was first presented by Ion Beam Applications (IBA) at the Proton Therapy Cooperative Group (PTCOG) meeting held in Loma Linda in June 1990. In December 1990, funding was secured to start the design of a prototype at IBA. In October 1991 a collaboration agreement was signed between IBA and Sumitomo Heavy Industries (SHI).

The main features of this accelerator were presented elsewhere[1-3] and are summarized and updated where necessary in table 1. A general view of the accelerator is presented in Fig.1.

Table 1 **Magnet system**

number of sectors	4	
sector angle at r=150 mm	36	°
sector angle at extraction	57	°
maximum gap heigth	48	mm
maximum hill field	2.9	T
minimum valley field	0.9	T
average field at extraction	2.165	T
average field at center	1.74	T
Spiral angle at the center	0	°
at extraction radius	~60	°
magnetic induction	$5.324\ 10^5$	A.t
apparent current density in coils	155	A/cm^2
actual current density in coils	200	A/cm^2
power per coil	87.5	kW
total copper weight (2 coils)	20.8	tons
weight of the iron	190	tons

R.F. System

resonating system	2 dees in opposite valleys	
harmonic mode	H = 4	
dee voltage	100	kV
frequency	106.11	MHz
length of resonator	60	cm
estimated capacitance per resonator	58	pF
estimated RF power for 100 kV	65	kW

Miscellaneous

operation vacuum	$5\ 10^{-6}$	mbar
source type	hot filament PIG	
source turn on/off time	15	µs
extracted intensity	1...100	nA
output vertical emittance	1...2	π mm.mrad
output horizontal emittance	1...2	π mm.mrad

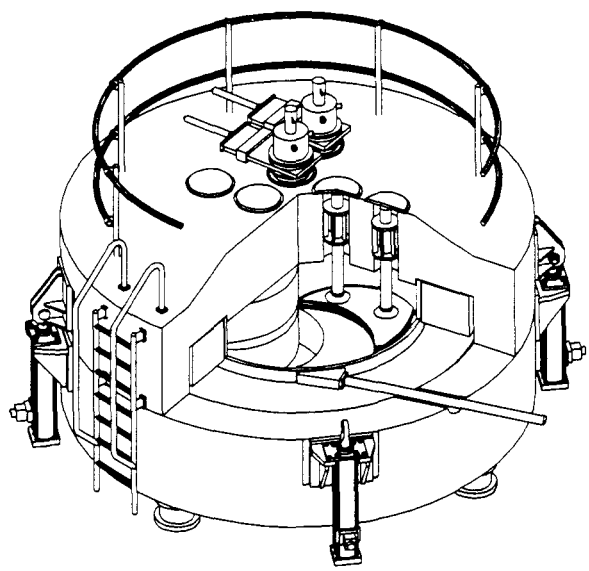


Figure 1 General view of the proton therapy cyclotron

The induction profile in the vicinity of the extraction radius was improved by the introduction of a magnetic shunt resulting in a completely closed gap at the median plane. The extraction system is also described in this paper.

First calculations on the central region were performed with the PE2D code using a simplified 2-D model with stacking factors in order to describe its actual 3-D geometry.

Two types of isocentric gantries namely a scanning gantry as initially proposed by IBA and a scattering gantry are currently designed. Their status is also presented in this paper.

2. NEW FEATURES IN THE CYCLOTRON DESIGN

2.1. Magnetic Shunt

As mentioned earlier[1-4], the hill gap profile is elliptical. The two main advantages of this design is the fact that the iron contribution to the field is uniform within the hills or valleys and that the induction radial gradient only depends on the coil field. The other advantage is the steep induction decrease outside the pole which allows an extremely easy extraction.

The ideal fied profile obtained with an elliptical shaped magnet gap is somewhat distorted if one opens the ellipsoid in the median plane in order to allow the beam extraction. Indeed, instead of the steep field decrease outside the pole, the maximum of the radial field profile flattens and is moved towards the inside of the machine (fig. 2a).

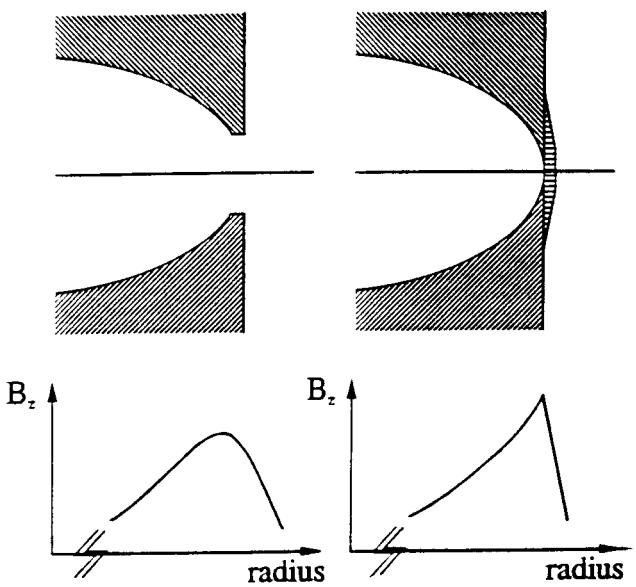


Figure 2 Behaviour of the magnetic field with gap opening and with a magnetic shunt

This prevents the use of the isochronous field up to the maximum radius of the pole . This decreases the maximum energy of the machine and also increases the distance between the last accelerated trajectory and the extracted trajectory, complicating therefore the extraction.

To avoid this problem, we found convenient to use a magnetic shunt that completely closes the median plane and whose thickness, height and shape allows a very accurate control of the bypassed flux (fig. 2b).

Both 2-D (PE2D*) and 3-D (TOSCA*) codes were used to compute the best dimensions for this shunt. The accuracy of the field in that region is very important as there are many turns in that area. The shunt thickness at the median plane is 6 mm and has a triangular profile for a height of 60 mm from the median plane.

From a mechanical standpoint, this part is intended to be removable from the main pole in order to allow an easy adjustement of the shunt during the field mapping/shimming phase.

2.2. Extraction System

The radial betatron frequency ν_r is about 1.3 in the extraction region. With this ν_r value one can expect some precessional extraction contribution induced by an off-centering of 1...3 millimeters. Such an amount of uncentering is practically unavoidable due to small central region errors and to the residual first harmonic in the field

The field gradient just outside the pole amounts to 0.3 Tesla per mm. This very steep decrease shortens the path from the pole region to the field-free region to only 250 mm ie 13° instead of a large fraction of a turn as in other cyclotrons of this energy.

An in-valley electrostatic deflector 570 mm long, 5 mm wide with a 0.1 mm thick septum deviates the beam to a specific window managed through the magnetic shunt. After passing the high gradient region, the beam enters a magnetostatic iron bar channel intended to compensate the quadrupole component of the fringe field.

The extraction efficiency without any precessional contribution is above 62%, and could be close to 100% with the precession.

2.3. Central Region

We performed a PE2D study of the central region. Its main goal was to provide access for an axially introduced ion source radially adjustable, and to provide a magnetic fied bump at the centre in order to produce weak focusing at radii where the flutter is insufficient.

A central plug with two symmetrical holes 180° apart was designed to obtain a 0.1 Tesla field bump at the centre. The field reaches back its normal isochronous value at a radius about three times the plug radius.

*Trademarks of Vector Fields Limited
24 Bankside, Kidlington,Oxford OX5 1JE England

3. THE DOSE DELIVERY SYSTEM

3.1. Main Energy Degrader

In order to uncouple the gantry optics and the upstream transport optics, the main energy degrader has been placed at the entrance point of the gantry. Unlike previous gantry designs, the resulting emittance degradation is not a major problem but is rather used as a means to obtain quasi-identical emittance ellipses in both planes at the entrance point of the gantry. Similar scattering angles are obtained for different output energies using different degrader materials (lead above 200 MeV, diamond below 150 MeV and copper in between).

3.2. Scanning Gantry

The basic design of the scanning gantry proposed by IBA[5-6] remains unchanged but some points were revised to address different concerns.

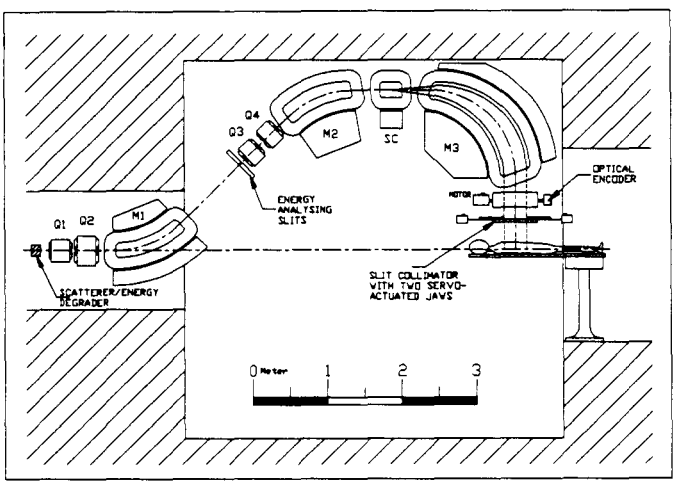


Figure 3 The scanning gantry

In order to address the problem of possible dose errors at the voxels boundary a large amount of voxel overlapping is included in the design. To achieve this, the pencil beam size is increased and a slit shaped collimator is introduced to maintain a very sharp lateral fall-off.

The gantry optics is designed with a large admittance of 70 π mm.mrad. This allows handling of large beam emittances from the energy degrader with an intensity reduction factor of 3...5, depending on the final energy, instead of a factor of 2...50 in the previous design.

The distal fall-off degradation created by the absorber is corrected by an analyzing section which allows an energy selection of ±2% and thus a distal fall-off only sligthly larger than that of a monochromatic beam.

3.3. Scattering Gantry

Though attractive in principle, the safety, complexity and even usefulness of the scanning method are still beeing debated. As a consequence, many proton therapy teams still prefer the classical scattering method.

A large, uniform beam is produced by a combination of scatterers and patient-specific collimators and bolus.

To meet the needs of these groups, IBA designed a 2.8 m radius compact isocentric gantry[7] allowing for large field irradiation (35 x 20 cm) using the double scattering method proposed by Gottschalk[8].

The first scatterer is placed at the entrance point of the gantry (see above) and the second one before the last analyzing section ie last quadrupole and last 90° magnet. This second scatterer is a sandwich of high and low Z materials whose thicknesses are patterned to provide a radially non uniform scattering effect but a constant energy loss. The radially dependent scattering is optimized to give a flat intensity profile at the patient location.

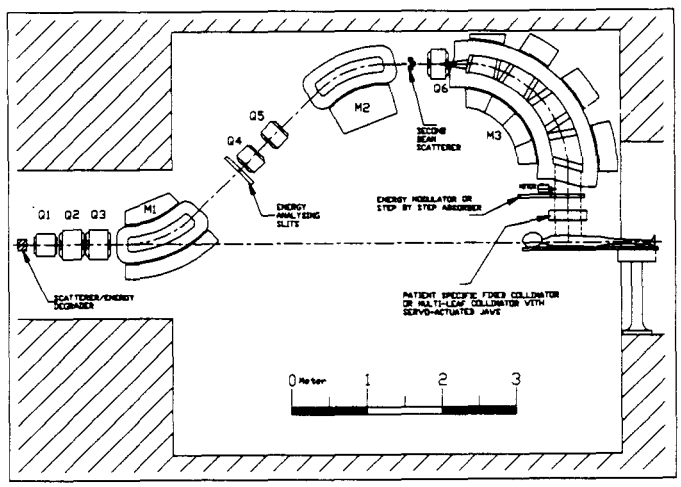


Figure 4 The scattering gantry

The magnifying properties of the last analyzing section allow to achieve a large field size with a divergence of only 22 mrad at the second scatterer exit thus a mere energy loss of 2.5 MeV at 220 MeV.

4. REFERENCES

1) W.Beeckman, Y.Jongen, A.Laisné, G.Lannoye, "Preliminary design of a reduced cost proton facility using a compact, high field isochronous cyclotron" Nucl.Inst.Meth. B56/57, 1201 (1991)

2) Y.Jongen, W.Beeckman, A.Laisné, "Development of a low-cost compact cyclotron system for proton therapy" presented at NIRS International Workshop on Heavy Charged Particle Therapy and Related Subjects, Chiba, Japan, July 4-5, 1991

3) Y.Jongen, "Status report of IBA's proton therapy program" presented at the Proton Radiotherapy Workshop, Villingen, Switzerland, February 28-March 1, 1991

3) A.Laisné, "IPN Orsay Project - First Machine Design Studies" in Proceedings of the 9th Conference on Cyclotrons and their Applications, Caen, France, 1981, p.203

4) W.Beeckman, Y.Jongen, "Intensity losses resulting from emittance and energy dispersion limits for an energy degraded proton beam" presented at the XIII PTCOG meeting, Berkeley, USA, November 1-2, 1990

5) Y.Jongen, G.Lannoye, "A new concept of isocentric gantry for proton therapy" presented at the XII PTCOG meeting, Loma Linda, USA, May 6-9, 1990

6) Y.Jongen, "An improved isocentric gantry with reduced diameter for proton therapy by scanned beam" presented at the XVI PTCOG meeting, Vancouver B.C., Canada, March 30-31, 1992

7) Y.Jongen, "An isocentric gantry of reduced diameter using the large field, beam scattering method for proton therapy" presented at the XVI PTCOG meeting, Vancouver B.C., Canada, March 30-31, 1992

8) B.Gottschalk, A.M.Koehler, J.M.Sisterson, M.S.Wagner, "The case for passive beam spreading" presented at the Proton Radiotherapy Workshop, Villingen, Switzerland, February 28-March 1, 1991

RECENT ACTIVITIES OF THE CYCLOTRON LABORATORY IN NICE

P. Mandrillon, N. Brassart, A. Courdi, P. Chauvel, F. Farley,
N. Fietier , J. Herault, J.Y. Tang

Laboratoire du cyclotron, Centre Antoine Lacassagne
227 Avenue de la Lanterne, 06200 - Nice - France

ABSTRACT

This paper presents the results of the first year of operation of the MEDICYC cyclotron in Nice and the medical programme of the laboratory. It outlines also the involvement of the laboratory in the 2 year work of the EULIMA feasibility study group and future projects.

1. INTRODUCTION

The Centre Antoine Lacassagne in Nice is one of the 20 cancer centers in France. Considering the frequency with which various types of cancer treatment were applied in the 80's in the french cancer centers, it appeared that radiotherapy was used in 66.3% of treatment including 24.1% in association with other forms of therapy. This high frequency determined the need expressed by the radiotherapists to develop their techniques and the MEDICYC programme based on a compact 65 Mev H^- cyclotron was initiated [1]. The cyclotron is presently used for protontherapy and radiobiology, in the coming months neutrontherapy will start. In the near future, the negative ion design of the cyclotron will allow for simultaneous production of F^{18} for PET scanning for various medical teams. The general layout of the facility is shown on the Fig1.

MEDICYC is used by a wide collaboration with several cancer centers and university hospital in France extended also to Barcelona (Spain) Genova and Sienna (Italy), Essen (Germany). A communication and data exchange network is being implemented.

2. PROTONTHERAPY

The low intensity beam for protontherapy is left to spread out at the exit of the last 90 degrees horizontal bending magnet, then diffused through a 50 nm tantalum foil and collimated to 35 mm before entering the treatment room. The characteristics of a standard proton beam are listed in the table 1.

Table 1

Maximum range measured on the 90 % distal isodose	32.2 mm
Bragg peak thickness on the 50 % isodose	3 mm
Lateral penumbra between 90 and 10 % isodoses	1.7 mm
Rotating plexiglass modulator	2000 rpm
Dose homogeneity in the plateau	± 1 %

By July 1st, a total number of 103 patients have completed their treatment.

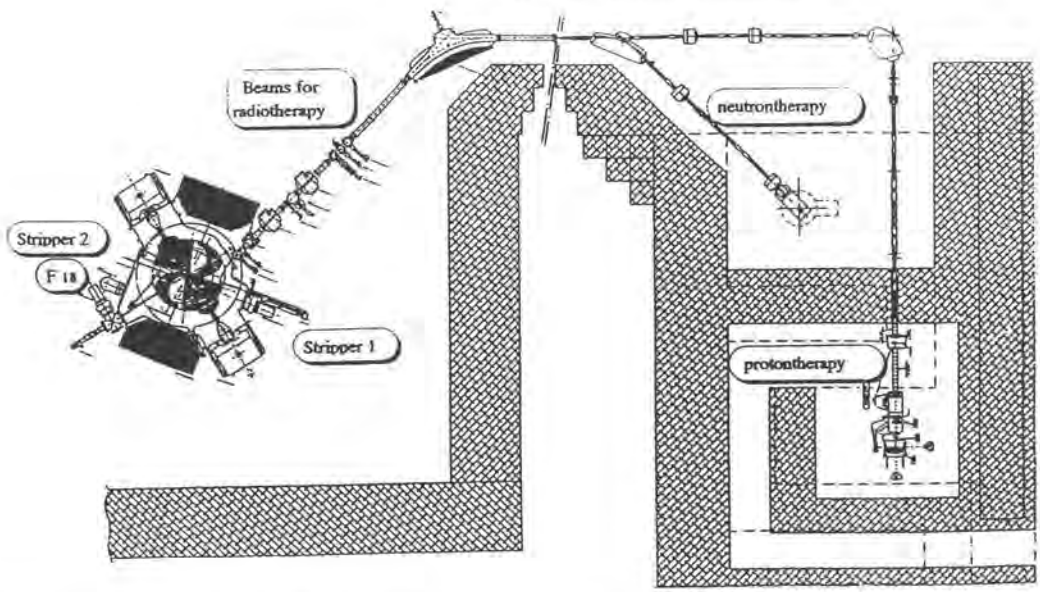


Fig 1 : MEDICYC 65 MEV H^- cyclotron for neutrontherapy, low energy protontherapy and F^{18} production.

3. RADIOBIOLOGY

The RBE of the 65 MeV protons, measured on the 15 cm spread out Bragg peak, of a human melanoma cell line, has been recently published by A. Courdi[2]. Figure 2 presents the survival curve of this cell line for proton and cobalt irradiation. A slightly decreasing value of the RBE versus the delivered dose has been found, from 1.15 at 2 Gray to 1.12 at 10 Gray. Therefore a provisional clinical value of 1.1 has been adopted for the treatment. Further experiments on different cell lines are in progress.

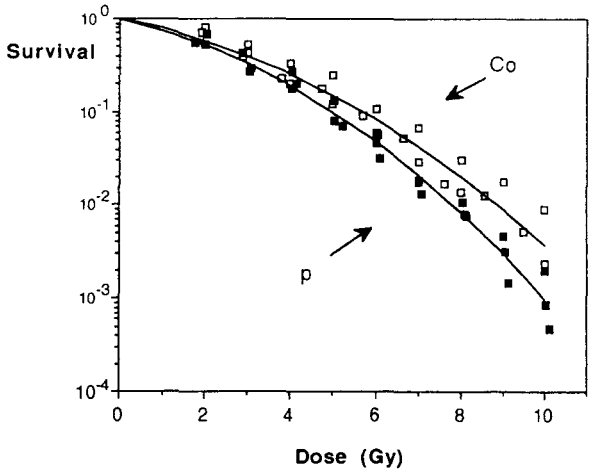


Fig 2 : Survival curve of human melanoma cell lines after proton and cobalt irradiation.

4. NEUTRONTHERAPY

The neutrontherapy room is located under the deflection area. Neutrons are produced in a Beryllium target which is retractable at the end of each treatment, avoiding unnecessary irradiation of the staff. The intensity of proton beam on target is around 15 μA. The emerging neutron beam is defined to obtain maximum fields up to 20 x 20 cm at 170 cm from the target. A continuously adjustable multileaf collimator of the Scanditronix design, modified for 65 MeV p/Be neutrons has been constructed by the "Cyclotron Research Center" in Louvain-La-Neuve. This multileaf collimator consists in 44 independent steel leaves placed in 2 groups of 22 parallel and opposed leaves. Each leaf can reach and pass over the beam axis to obtain complex field shapes avoiding interposition of heavy metallic shielding blocks in the beam.

A system which permits a 290 deg rotation of the collimator around the vertical axis has been recently installed.

The early control sequence for achieving the collimator setting for a specific field was performed through an analogic system which gave positioning errors of the leaves which were not acceptable. Therefore a new system was developed using a PC giving the obvious advantage of a easy access to the desired field and to the best reproducibility of the settings during the treatment course.

The following Fig 3 shows the layout of the treatment rooms.

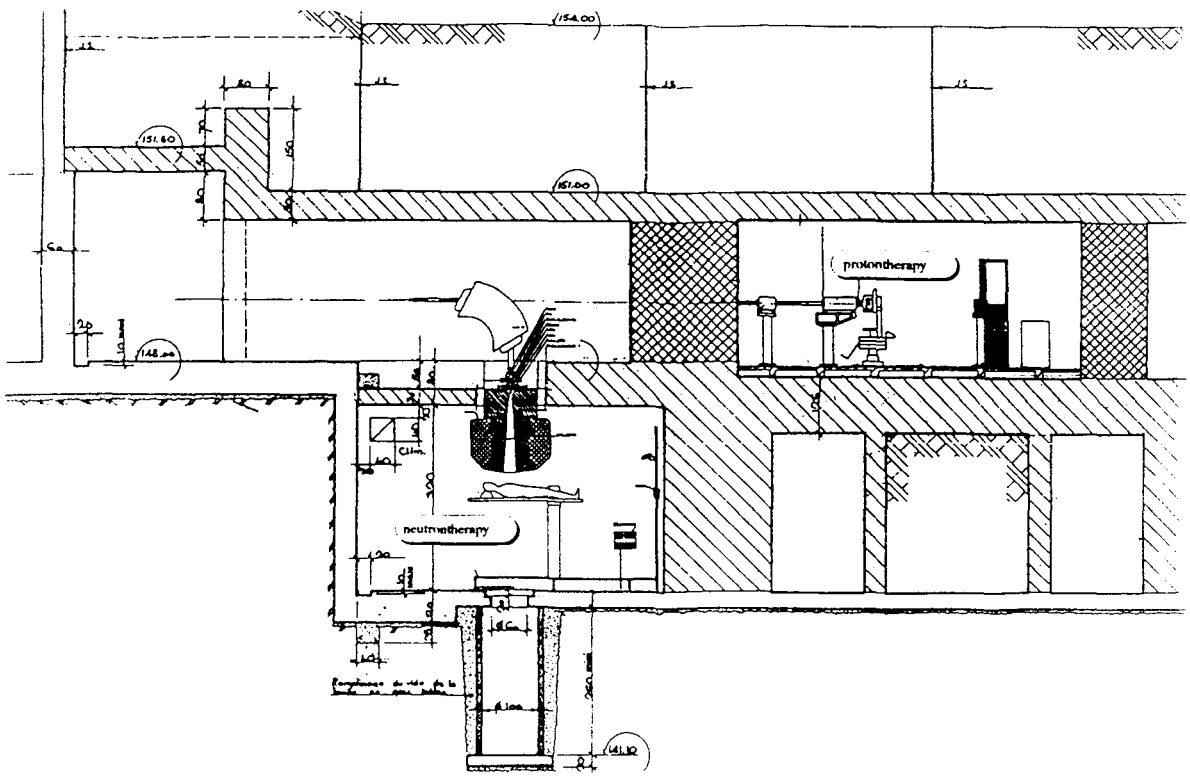


Fig 3 : Layout of the treatment rooms

5. F^{18} -DEOXYGLUCOSE PRODUCTION

A group of physicians from various medical disciplines such as neurology, oncology, cardiology and psychiatry have recently set-up a group of users of the MEDICYC facility for the production of F^{18} -DG. In order to avoid any interference with the radiotherapy schedule it was proposed to investigate the possibility of a beam sharing system based on a simultaneous extraction of two beams using two strippers at different azimuth. Figure 4 presents the two symetric simultaneous extracted beams.

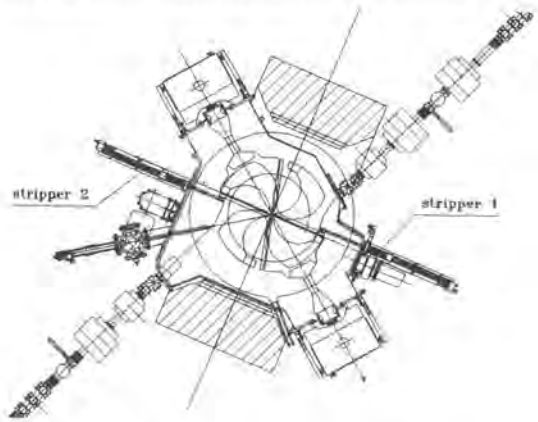


Fig 4 : Simultaneous extracted beams

6. EULIMA COLLABORATION

The Cyclotron laboratory was also involved with several european institutes in the feasibility studies of the EUropean Light Ion Medical Accelerator (EULIMA) project[2] which were partly funded by the Commission of the European Communities and by the Conseil Général des Alpes Maritimes (Nice, France).

Two approaches to a 400 MeV/nucleon machine design have been investigated, namely a superconducting cyclotron and a synchrotron. The Cyclotron laboratory together with the CRC Louvain-la-Neuve which investigated ECR source performances and the possibility to produce radioactive light ions (C^{11},O^{15},Ne^{19}) for postacceleration[2], contributed significantly to the technical (mechanical studies and construction of wooden and copper half scale model of the RF cavity) and theoretical (axial injection and central region) studies of the superconducting cyclotron option. Being partly hosted by CERN, Geneva, the feasibility studies profited from the CERN technical expertise in superconducting magnets and cryogenics for the cyclotron, and conceptual and technical studies for the synchrotron.

6.1 Superconducting cyclotron

A fixed-frequency super-conducting cyclotron design was investigated, and a solution comprising a single superconducting coil (external radius ; 2.32 m) and moderately spiralled sectors was found to be feasible.

Numerical calculations to assess the general strength of the magnet structure assuming a cylindrical vacuum chamber have shown that this solution fulfils the mechanical requirements.

Accelerating peak voltages on the 2 cavities are increasing from 100 kV at injection up to 250 kV at extraction. The total RF power losses are about 150 kW per cavity.

Light ion beams to be injected into the cyclotron are produced in an Electron Cyclotron Resonance Source (ECRIS), which in its latest version delivers intensities of completely stripped Carbon, Nitrogen, Oxygen and Neon ions, several orders of magnitude above what is needed for treatment. An axial injection scheme using a spiral inflector was foreseen. A preliminary layout of the beam extraction system consisting of two electrostatic deflectors and one electromagnetic channel was analysed.

For the coil and cryostat design a solution in which the coils are wound in the double-layer pancake technique, and are cooled in direct contact at 4.2°K in a liquid helium bath at atmospheric pressure, was studied.

6.2 Synchrotron

The great advantage of this type of accelerator is the possibility to vary the energy covering the interval from 100 to 400 MeV/n. This energy range is very similar to the LEAR accelerator at CERN, and several technical concepts developed for this machine could be used. Two possibilities to design a more compact machine have been investigated : a separate function machine (SFM) of 59 m of circumference, more flexible for developments, and a combined function machine (CFM), if space is crucial. In this case a further reduction in size can be achieved.

A classical injection scheme has been designed, with an ion source of Electron Cyclotron Resonance type (ECR) feeding a small Radio Frequency linac (RFQ) followed by a conventional linac (5 MeV/n) with a repetition rate of about 1Hz. This basic design could be developed to include better monitoring of the extracted beam, and a storage and cooling facility[3].

6.3 Accelerator choice

The continuous and highly intense output beam of the cyclotron permits simultaneous treatment in different rooms by splitting the beam. Moreover, the operation of such a fixed frequency accelerator is very simple. The drawback is the fixed energy, so to change the range in tissue the energy of the ions must be degraded to the value corresponding to the deepest range for a given tumour. Nevertheless such a high energy cyclotron is more of a new design : in order to avoid a large number of RF periods

high dee voltages should be used and the magnetic field should be accurately shaped. The magnet is heavy and if faults develop, access to the interior will be time consuming.

On the other hand, the synchrotron requires costly injectors and sophisticated controls devices to take profit of the inherent flexibility in energy, but has the following advantages :

- short repair time, i.e. repairs within 6 hours.
- possibility for further increase of intensity through beam cooling. Hence, modulation of the beam intensity and programming of dose across the irradiation volume could become possible.
- well known techniques, important for the reliability of a medical accelerator, which should reduce the construction time and the running-in time.

Based on these arguments, the project management board has recommended the synchrotron option but funding is not available.

7. FUTURE PLANS

Evidence is progressively established that high-LET radiations (the cheapest are of course neutrons with physical properties reaching nearly the same level as the modern medical linac) will play a role in radiotherapy for some well defined patient series. In order to take the full benefit of neutrontherapy, physicians are asking for variable incidence beams. Therefore an isocentric gantry will be investigated. The other promising way in radiotherapy is to develop low LET radiations with high physical selectivity and reflexions towards an high energy protontherapy programme have started. Of course, the MEDICYC cyclotron which is fully dedicated to medical applications, should also continue to develop beam lines for the production of the most commonly used radioisotopes.

8 . ACKNOWLEDGEMENTS

The authors are very grateful to the MEDICYC staff for their enthusiastic involvement in operating and improving the facility. They are also indebted to CERN for advices and stimulating discussions during the EULIMA feasibility studies.

9 . REFERENCES

[1] P.Mandrillon et al. "Commissioning and implementation of the MEDICYC cyclotron programme", Proceedings of the 12th International Conference on cyclotrons and their applications, Berlin, May 1989.

[2] A. Courdi et al. Efficacité biologique relative des protons de MEDICYC sur une lignée de mélanomes humains, Bulletin du cancer, 1992,79,613, Elsevier, Paris.

[3] G. Berger and al. "Radioactive ions beams : results and perspectives for light ion therapy and diagnostic purposes. Proceedings of the EPAC90, Nice, June 1990.

[4] G. Cesari, P. Lefèvre and D. Vandeplassche, "Feasibility study of a synchrotron for the European Light Ion Medical Accelerator", Proceedings of the EPAC92, Berlin, March 1992.

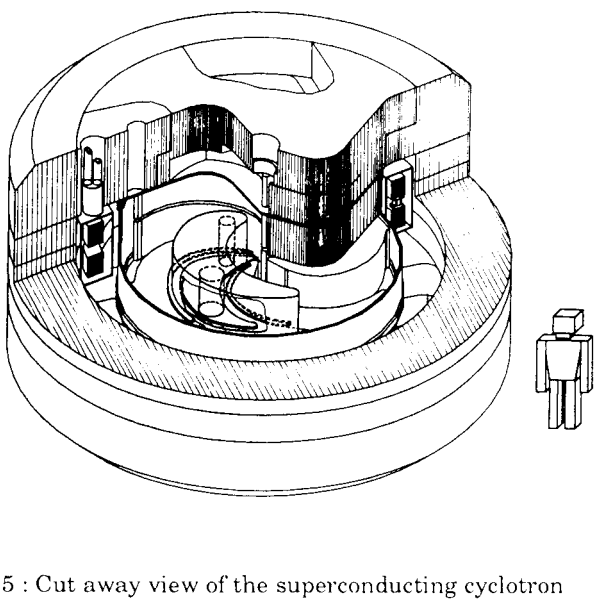


Fig 5 : Cut away view of the superconducting cyclotron and general layout of the SFM synchrotron proposed for EULIMA.

HEALTH PHYSICS DATA ACQUISITION SYSTEM AT THE NATIONAL MEDICAL CYCLOTRON

B. Mukherjee[1] and D.W. Arnott[2]

1) Occupational Health and Safety Program
ANSTO, PMB-1, Menai, NSW 2234
AUSTRALIA

2) National Medical Cyclotron
Grose Street, Camperdown, NSW 2050
AUSTRALIA

ABSTRACT

A data acquisition system for health physics radiation monitoring instruments at the National Medical Cyclotron Facility has been developed. Analogue outputs from the radiation monitors, placed at various locations within the facility are connected to an industrial datalogger with RF shielded, twisted pair cables. A driver software has been written for the presentation of various real time mimics and trend graphs, automatic sequential data storage in a 600 Mega Byte optical disk and for the delivery of digital alarm outputs for safety interlock circuitry.

1. INTRODUCTION

The National Medical Cyclotron (NMC) located at Sydney Australia, has been operating since July 1991. The NMC is a variable energy cyclotron, accelerating negative hydrogen ions (H^-) up to 30 MeV. It has a dual beam capability for simultaneous production of PET (^{18}F,^{13}N, ^{15}O, ^{13}C) and SPECT (^{67}Ga, ^{111}In and ^{201}Tl) isotopes and ^{123}I for domestic use and for the export to neighbouring countries.

During the routine operation of the cyclotron, the solid targets are bombarded with an intense proton beam of up to 130 μA and strong gamma and neutron radiation fields are produced. Therefore, radiological shielding comprising a 2.3 metre thick low sodium content concrete wall for the cyclotron vault and the beam room[1] and a reliable radiation surveillance system have been developed in order to reduce the radiation exposure to the cyclotron workers and the members of the public.

2. LAYOUT OF THE MONITORING SYSTEM

The radiation monitoring system at the NMC has been structured into three sections.

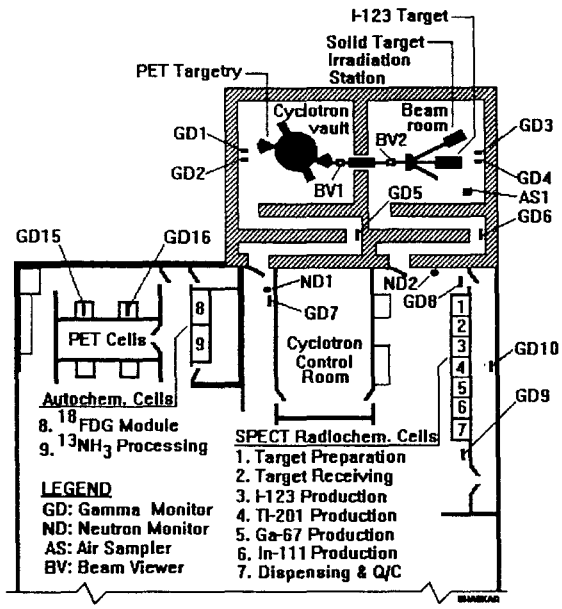


Fig. 1. Schematic diagram of the Australian National Medical Cyclotron Facility showing the Cyclotron vault, Beam room, Radiochemical Hot-Cells, Automatic Chemistry modules, PET Research Cells and the Targets.

2.1) Cyclotron vault, Beam room and Hot cell Monitoring

Gamma and neutron monitors are placed at various locations near the targets, maze and entrance door as shown in Figure 1. The local door interlock relays are connected to the monitors.

2.2) Stack Monitoring

Gamma detectors are fixed near the high efficiency particulate (HEPA) and iodine filters. Additionally, a noble gas monitor, developed by the Occupational Health and Safety Program of ANSTO is connected directly to the stack for a continuous assessment of radioactive ^{41}Ar produced in the target room due to the neutron activation of stable ^{40}Ar present in air[2] and is shown in Figure 2.

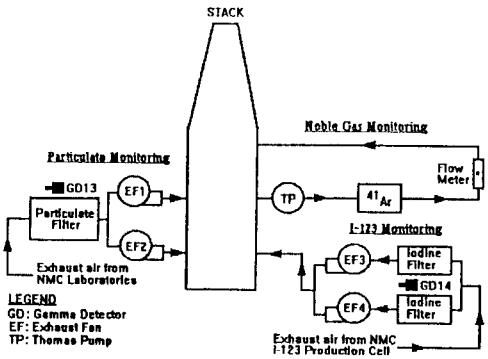


Fig. 2. Schematic Diagram of the Stack monitoring system showing the Filters, Radiation monitors and Pumps.

2.3) Liquid Waste Monitoring

Gamma monitors are fixed at the critical delay tanks, located in the basement of the facility as shown in Figure 3. All monitors are connected to the central health physics data acquisition system.

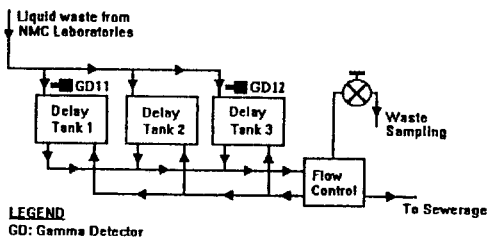


Fig. 3. Schematic Diagram of the Liquid Waste Monitoring System showing the delay tanks, Gamma monitors and Flow control unit.

3. HARDWARE CONFIGURATION

The NMC radiation monitoring system is basically comprised of two types of hardware.

3.1) Radiation Monitor

Gamma ray monitors using energy compensated Geiger-Mueller counters with the following specifications have been chosen (Fig. 4):

(a) Wide range dose measurement
(b) Local alarm contact with preset threshold
(c) Visual and audible alarm
(d) Preset local alarm contacts
(e) Large analogue display
(f) Analogue voltage output (0-5V)
(g) Built in low activity check source
(h) Uninterrupted power supply (240V, 50 Hz)

The neutron detectors with polyethylene moderated BF_3 tubes are connected to a similar type of monitoring instrument.

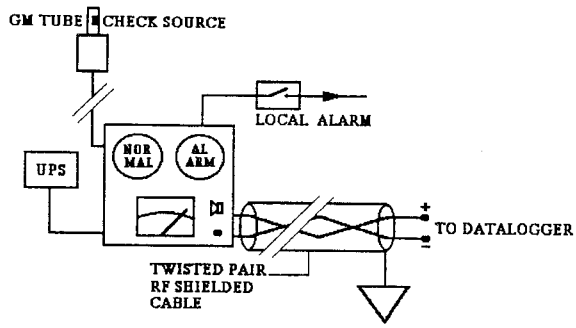


Fig. 4. Schematic Diagram of the basic Radiation Monitoring unit with its various components and Data and Alarm pathways.

3.2) Datalogger

A robust industrial standard datalogger (Australian made) of 15 bit resolution and with the following specifications has been chosen:

(a) 25 differential analogue input channels
(b) 21 digital I/O channels
(c) 8 high power (solid state relay) digital output channels
(d) Internal NiCad battery buffered power supply
(e) RS232 serial interface with a Personal Computer.

3.3) Personal Computer

An IBM compatible PC (386SX) with 6 MB RAM, a 80 MB hard disk and a 600 MB optical WORM drive has been used with a 24 pin dot matrix printer.

4. DATA ACQUISITION SYSTEM

Dataloggers have already been used for low level radiation monitoring around high energy particle accelerators[3]. Commercially available PLC based centralised radiation data acquisition systems are suitable for large complexes like nuclear research centres and nuclear power stations[4]. The present system, on the other hand, uses a datalogger in conjunction with inexpensive radiation monitors having analogue signal outputs and a supervisory control and acquisition software, developed specially for high current compact medical cyclotrons located in urban hospitals.

4.1) Software Description

Supervisory Control and Data Acquisition (SCADA) software developed by an Australian company with the following features was used as the host software:

(a) Bi-directional communication with the external datalogger
(b) High resolution mimic and graphics generation
(c) Statistical data base and data analysis capability
(d) Production of reports and print-outs
(e) Data archive in optical WORM drive
(f) File transfer capability to Lotus 1-2-3
(g) Remote data transfer capability via modem or LAN
(h) Password protection

4.2) System Description

The cyclotron health physics data acquisition (driver) software (TLCYCLO) has been written within the host software package with the following unique characteristics:

(a) Real time data acquisition
(b) Automatic calibration of the radiation monitors
(c) Linearisation of the outputs with multi-order polynomials
(d) Tamperproof alarm set up capability with pass word
(e) Delivery of remote alarms
(f) Delivery of start-up signal to cyclotron interlock PLC
(g) Display of the high resolution mimic of the facility
(h) Password protection upto 3 different priority levels

The schematic diagram of the NMC radiation monitoring system is shown in Figure 5.

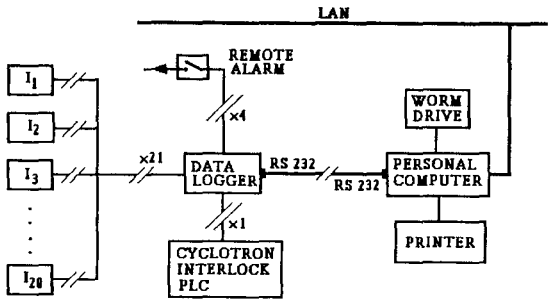


Fig. 5. Schematic Diagram of the Radiation Monitoring System showing the various Radiation monitors (I_1, I_2....I_{20}), Dataloger, Remote alarms (x4), Cyclotron interlock PLC (x1) and the Computer system.

5. ACKNOWLEDGMENT

The principal author wishes to thank Mr. J. Grey, the Director of Occupational Health and Safety (OHS) Program of Australian Nuclear Science and Technology Organisation (ANSTO), for his continued encouragement and support and Mr. G. Wignall, Senior Health Physics Technician for the calibration of the radiation monitors.

6. REFERENCES

1) Mukherjee, B. et al., Assessment of the shielding facility of the National Medical Cyclotron, OHS Internal Report (Unpublished), 1989.

2) Ishikawa, T. et al., Thermalisation of Accelerator-Produced Neutrons in a Concrete Room, Health Phys. **60(2)**, 209 (1991).

3) Jianping, L. et al., An Intelligent Environmental Neutron and Gamma Monitoring System, in Proc. of Europhysics Conf. on Control Systems for Experimental Physics, Villars-sur-Ollon, Switzerland, September 28 - October 2, 1987.

4) Hartman & Braun , Technical Brochure on Digital Nuclear Radiation Measuring System TK 250, Frankfurt on Main, Germany, 1987.

DESIGN CONSIDERATION OF NEUTRON THERAPY FACILITY UTILIZING EXISTING CYCLOTRON

Chang Hongjun Cui Xingtian Wei Jing
Zhang Jian Xie Kuanshong
Institute of Nuclear Research, Academia Sinica
P.O.Box.800-204 Shanghai 201800 China

ABSTRACT

A facility for testing the effectiveness of fast neutrons for the treatment of malignant tumors will be constructed at the Institute ofNuclear Research, Academia Sinica. Neutrons are produced by the bombardment of 30 Mev protons on a semithick beryttium target. The design consideration of the collimation system, target assembly, dosimetry and beam control aregiven.

1. INTRODUCTION

The use of cyclotrons for radiotherapy purposes is not new. In fact, fast neutrons has been used to treat human cancers on a continuing basis since 1966 when the MRC cyclotron was made available for radiotherpy at the Mammersmith Hospital in London. Since then, various centers throughout the world have also begun clinical trials with fast noutrons. The usefulness of these studies has been to show that neutron therapy can be carried out with optimstic results.[1] Nation wide there are four cyclotros in operation, and most of these machines are used for isotope production or basic research only. With the installation of the neutron therapy facility, the INR cyclotron will be mainly used for production of radioactive isotopes and for generation of neutrons for treating cancer patients.

2. COLLIMATION SYSTEM

Available funds and limited room condition do not permit either a isocentric or a verticalneutron therapy beam, and decision was taken to use, at the initial stage, a fixed horizontal beam. The collimation system, Fig.1, consists of sheilding and collimators. The area around the target and the ionization chamber is covered with a cyclindrical shielding constructed from 20cm thick pure iron and 25cm thick borated wax, which is 60cm long. The primary collimatormade of pure iron is position ed immediately beyond the target to delimitate the largest available field size(20×20cm), which is 8cm long.

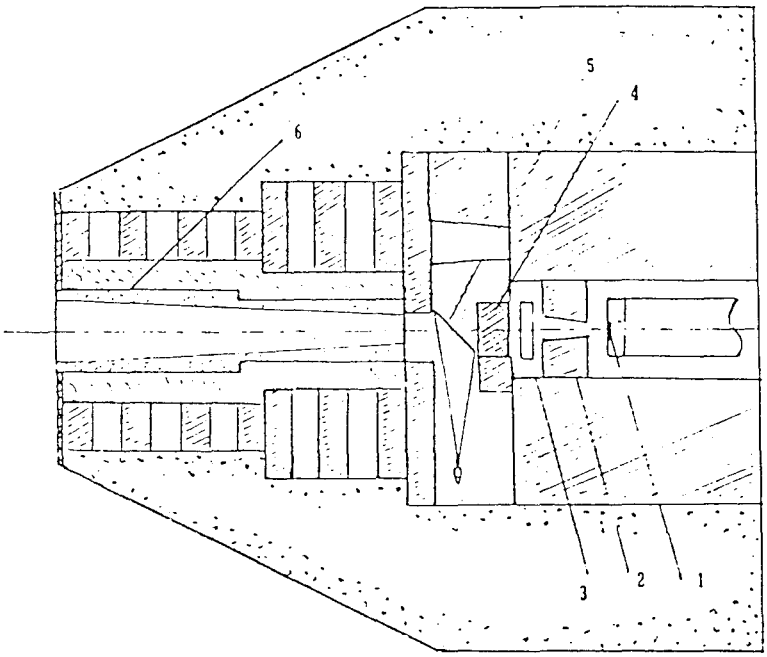
Following the cyclindrical Shielding a shielding in cone shape is provided. The inner parts, i. e. secondary collimators, which is adjacent to its axial aperture into which the interchangeable polyethylene concrete collimator is inserted are constructed from high density(1. 4 g cm^{-3}) borated wood. To achieve therequired attenuation, each collimators is 60cm long. The field sizes (5×5-20×20 cm) are defined with these collimators. The collimator system will allow remote motor driven angulation of the collimator.

The outer parts consist of alternate layers of borated polyethene and pure iron. The total length of the layers is 58 cm, 3/5 of them are iron, having outer diameter of 44-50 cm. The remainder surrounding the layers is filled with borated wax in cone shape.

The system is designed at 125 cm SAD with distance from the end of the collimator to the surface of the patient being 32 cm.

In addition, a gamma radiation shutter made of lead, 5 cm thick, is supplied, which located in the front of collimators in order to reduce activities in and around the target. one mirror with lamp is used for the field illumination.

As the beam is fixed horizontal, the treatment coach is designed to move on multiple axes, rotate and tilt in order that the patient may be adjusted to the beam.



Pure iron
Borated polyethene
Borated high density wood
Lead
Borax + wax
Concrete + polyethene + borax

1. Target
2. Primary collimator
3. Ionization chamber
4. Shutter
5. Mirror
6. Secondary collimator

Fig.1 The collimation system.

3. TARGET ASSEMBLY

Neutrons are produced by bombarding a semithik beryllium(Be content over 99%) target with 30 Mev protons. The target housed in a water cooled aluminum holder consists of 0.4 cm in thickness, 2.5 cm in diameter of beryllium backed by 0.17cm graphite." For the 30 Mev, 50μa proton beam current, a dose rate of 28 rads minute with a depth for 50% dose of 10.5 cm is expected.

The position of the beam on the target is monitored by a graphite defining iris consisting of four insulated quadrants, from each of which the current can be monitored separatedly. A electron suppressor is supplied.

In selecting the materials for manufacturing the target assembly care must be taken to minimize the induced activities produced by neutrons. The titanium is preferable to aluminum and steel.

4. BEAM CONTROL

A semiautomatic set up system of fast neutron therapy is considered. In the design, care is taken account of safety in beam hadling. The relevant parameters monitored in the console located in the control room are the integrated and instantaneous beam current on the target, integrated ionization current form the transmitted ionization chamber, instantaneous beam current on the beam defining iris and the etapse time. Also one beam stoppers located before the target and the gamma radiation shutter are controled from the console.

A microcomputer is applied to verify the patients setting up, to store the patients records and relevant cyclotron parameters. For each treatment program, the dose to be delivered are preset prior to patient treament in the primary beam. In addition, a talkphone is provided to communicate with the cyclotron control room and the treatment room.

5. DOSIMETRY

Neutrons emitted form the target are then detected with a transmitted ionization chamber located behind primary collimator. Two electrodes mounted in the chamber, each of which collects ionization charge from two air filled cavities, are connected to an independent dose monitor system.

The chamber must be callibrated with

standardized one prior to treatment of patients.

Extensive radiation dosimetry measurements should be carried out to evaluate the neutron beam characteristics including central axis depth dose, off axis ratios and dose buildup, etc.

6. REFERENCES

1) T. W. Griffin, "Hight LET, Heavy particle trials" , Int.J.Radiation Oncology Bio. Phys., Vol.14. pp. s83-92 (1988).

2) Miguel Awschalom and Ivan Rosenberg, "The influence of target thickness and backstop material on proton-produced neutron beams for radiotherapy" Med, Phys. 7(5), Sept. /Oct. pp.495-502 (1980)

A PROTON THERAPY FACILITY PLAN

S. Fukumoto, H. Tsujii, T. Inada, A. Maruhashi, Y. Takada, Y. Hayakawa, J. Tada, H. Tsuji, M. Sato
Proton Medical Research Center, University of Tsukuba (PMRC)
Tsukuba-shi, Ibaraki-ken, 305 Japan

and

K. Endo, Y. Irie, K. Muto
National Laboratory for High Energy Physics (KEK)
Tsukuba-shi, Ibaraki-ken, 305 Japan

ABSTRACT

A dedicated proton beam therapy facility has being designed. Its first plan was made in 1988 with a synchrotron as its main accelerator. A new plan based on the small SHI-IBA cyclotron is being made. It has two treatment rooms, one is equipped with a rotating gantry, the other with horizontal and vertical fixed beams. Specifications for proton beams were reexamined based on the energy and field size statistics of PMRC clinical trials. Former design goals of 230 MeV and 20 nA are supported. A double scatterer system, in which the second scatterer consists of a central disk and a peripheral ring, will give flat proton distributions in a region of 20 cm in diameter. Efforts are being made to keep the cyclotron building wall 2 m thick.

1. INTRODUCTION

To improve conventional radiation therapy with photons and electrons, several modalities have been investigated. They are divided into two categories, low LET radiation and high LET one. Neutrons, heavy ions and π^- are high LET radiations which have larger biological effects than low LET ones. Proton beams are much different from photons and electrons in point view of physics research, however, they are classified to low LET's as well as photons and electrons in radiation biology. However, they have a big advantage over photons or electrons in clinical purposes. Dose of photons or electrons decreases almost monotonically when they penetrate in human body. Dose distribution of high energy proton beams in water and also in tissue is characterized with plateau and Bragg peak. Almost constant low ionization occurs in plateau for high energy protons whereas sudden high dose appears at the end of proton range as shown in Fig. 1. This is a favorable property for deep-seated cancer therapy [1] because of sufficient dose for cancer with lower dose in normal tissue between body surface to the cancer and with no dose in normal tissue behind the cancer. The low LET characteristic was thought to be a disadvantage of proton beams at the beginning of new modality search because of high OER (oxygen enhancement ratio), but it ensured their quick recognition as a new radiation therapy modality because their acute and late effects are easily estimated with huge amount of experiences on conventional radiotherapy. Recent development of diagnostics and modern treatment planning with computer prepared practical use of

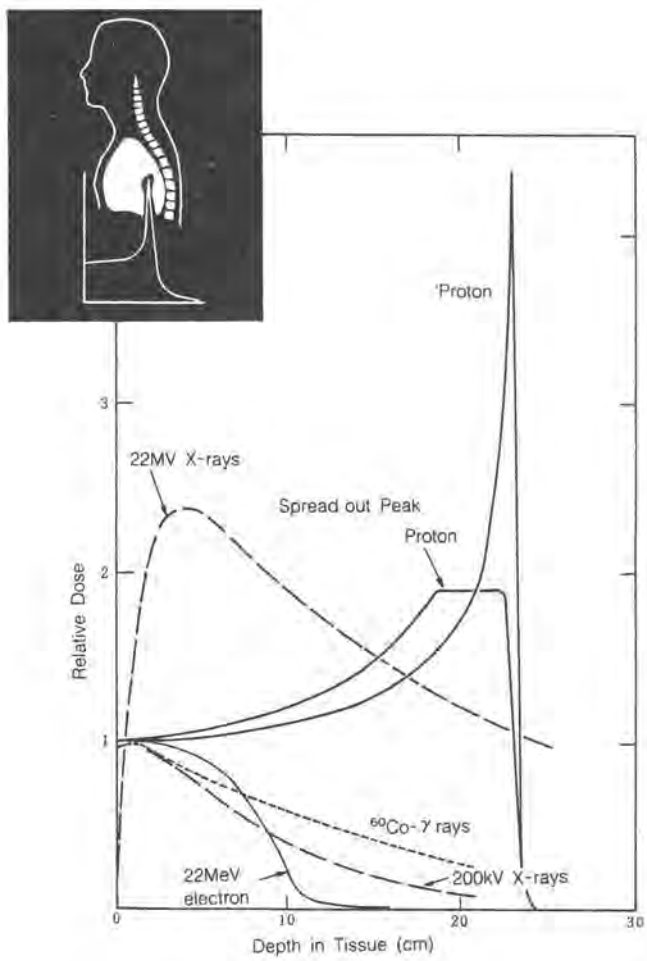


Fig. 1 Comparison of depth-dose distribution.

proton beams.

To confirm the potentiality of proton beams, a clinical therapy facility, PARMS (Particle Radiation Medical Science Center) was built and clinical trials were started at Tsukuba in 1983. The fast-extracted 500 MeV Booster beam of KEK Proton Synchrotron Complex is degraded to 250 MeV with a graphite degrader and guided to treatment areas [2]. Because the clinical results are so promising, a dedicated proton beam therapy facility plan has been made since 1988. Its design goal of proton energy and intensity were 230 MeV and 20 nA and these will be reviewed later. The facility will be built next to the conventional radiation therapy building of the University Hospital. A linear accelerator, a cyclotron or a synchrotron can be used for the beam specifications.

A synchrotron was chosen as the main accelerator in the first plan [3,4]. Many high energy synchrotrons have been built so that little R&D is required for the dedicated machine. The proton energy can be variable and protons can be extracted either in fast-extraction or slow-extraction modes.The protons are potentially extracted without loss in the fast-extraction mode and with around 90% efficiency in the slow-extraction mode. The former provides a possible way of detecting Bragg peak in the body during irradiation [5] and the latter is needed for advanced raster scan of the beam in the future. Total weight of the magnets is much less than 100 tons. In fall of 1991, SHI Japan and IBA Bergium jointly disclosed a commercially available small cyclotron for proton beam therapy in a hospital. A new plan based on this cyclotron is being made.

2. PROTON BEAM THERAPY FACILITY PLAN

No dose-rate effect for therapy is expected to appear between CW beams and fast-extracted beams of a synchrotron. Thus the time structure of the beam is selected by an accelerator, a beam delivery system or other factors such as Bragg peak detection mentioned above. The SHI-IBA cyclotron is 4.3 m in outer diameter and 2.1 m high [6]. Its accelerator room is smaller than that of the synchrotron, and this make the cyclotron attractive with a simple magnet power supply for hospital use. A cyclotron delivers usually CW beams. They will be suitable for advanced 3D beam scan in the future if they are switched on and off quickly or their intensity is regulated properly with a modern external ion source. At the present, the beam is spread by a scatterer of 6 mm thick Pb plate and shaped by a multi-leaf slit made of 5 mm thick brass plates in transverse plane at PMRC which succeeds PARMS. Its Bragg peak is spread out by a ridge filter and distal peak is shaped by a bolus. Although this passive method needs to make a bolus for each direction of irradiation of each patient, it has no preference for beam time structure.

In the new facility, a rotating gantry will be installed in one treatment room, while the other room will be equipped with two isocentric fixed beams, one is horizontal and the other is vertical. Passive beam delivery system is assumed because of its dependability. To reduce the rotating gantry size, "ex-centric" system is being studied, where a patient and a beam delivery system with some magnets rotate simultaneously around an axis.[7,8] If necessary space was assumed for patient setting by MDs and/or therapeutists, the rotating gantry did not reduce as expected before. Tentative facility layout is shown in Fig. 2. An alternative is an isocentric gantry with a smaller field size, which is not necessary to be same as that of

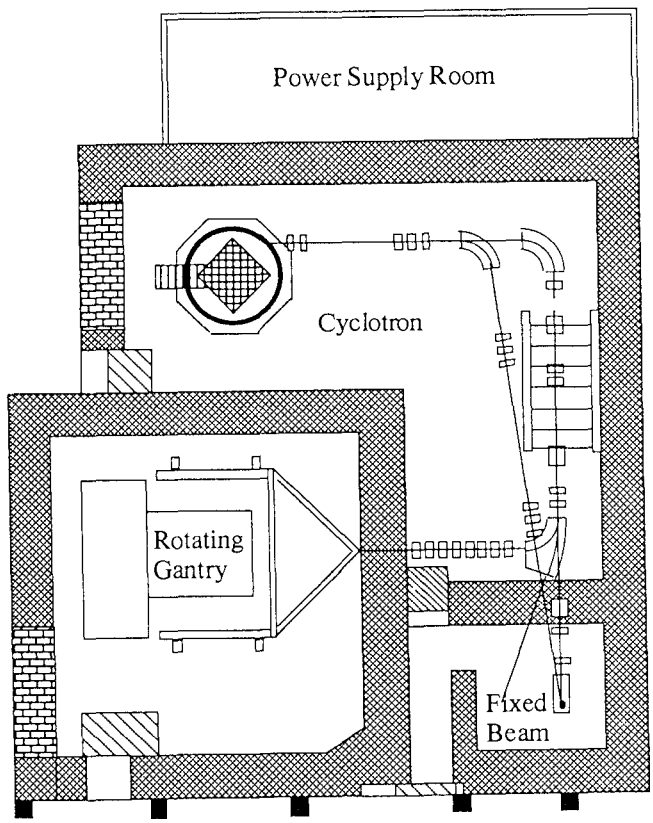


Fig. 2. Preliminary layout of proton beam therapy facility with a 230 MeV cyclotron as the main accelerator.

the fixed beams. Field sizes and other properties used for therapy at PMRC in 1991 are surveyed to design the proper field size.

3. FIELD SIZES, ENERGIES AND SOBP USED IN 1991

50 patients of liver, lung and other cancers were treated with proton beams in 1991 at PMRC. There are horizontal and vertical irradiation ports. The totals of port selection are 121, in which 56 are horizontal and 65 are vertical. Patients are irradiated 10-30 times with every selected port (fractionation). The maximum field size and the integrated port selection

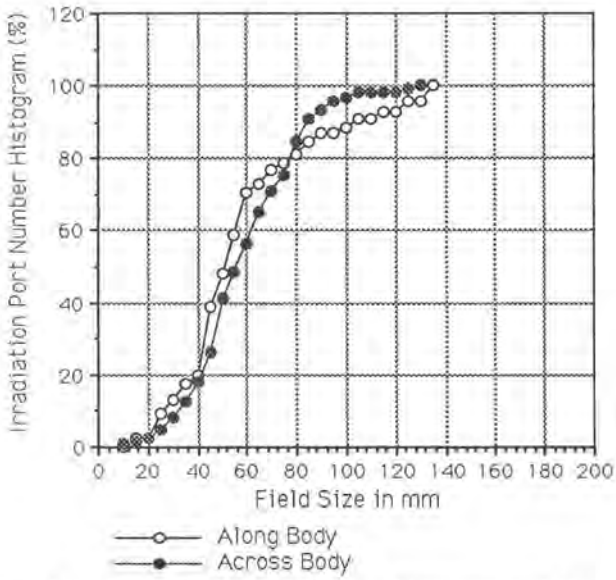


Fig. 3 Irradiation port selection histogram to different field sizes for 50 patients treated in 1991. The totals are 121.

number are shown in Fig. 3. Breath-synchronized irradiation was applied when it was effective.The port selection numbers are summed up separately for along body and across body, but no big difference between them. It is found that all patients were treated with field sizes of less than 14 cm and 90% were treated with field sizes of less than 10 cm. If the beam is spread axial-symmetrically, a 20-cm diameter field covers all these sizes.

The maximum proton energies on patients and retated SOBP (Spread-out Bragg Peak) are plotted in Fig. 4. The

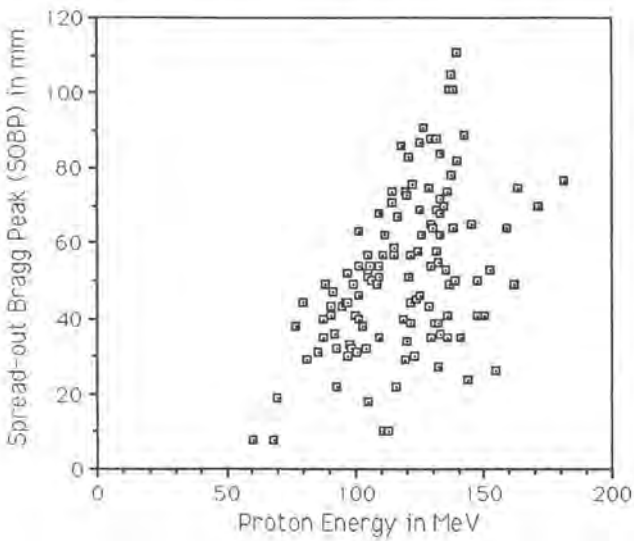


Fig. 4. Maximum proton energies on patients and Spread-out Bragg Peak depths.

energies are distributed in a region from 60 MeV to 182 MeV which correspond to ranges of 3 cm and 22 cm in water. The design energy of 230 MeV will be sufficient even if scatterers are used for beam spreading where 10-20 MeV energy is lost in scatterers. The SOBP spread in a wide range from 0.8 cm to 11 cm. Several ridge filters were prepared for covering the range. Some are made of copper, others are of brass or aluminum.

4. DOUBLE SCATTERER BEAM SPREADING

Field shaping with a double scatterer system is investigated to get good flatness as well as high efficiency. The first scatterer is made of a high-Z material such as Pb. The second one consists of a high-Z material disk surrounded by an annular low-Z material plate. Both the disk and the plate have equal energy loss for penetrating protons. Calculation is made for the 2 mm thick first scatterer with the second one of a 4 mm thick, 23.8 mm in radius Pb disk with 10.9 mm Al annular

Configuration of Dual-Ring Scatterer Method for Beam Spreading

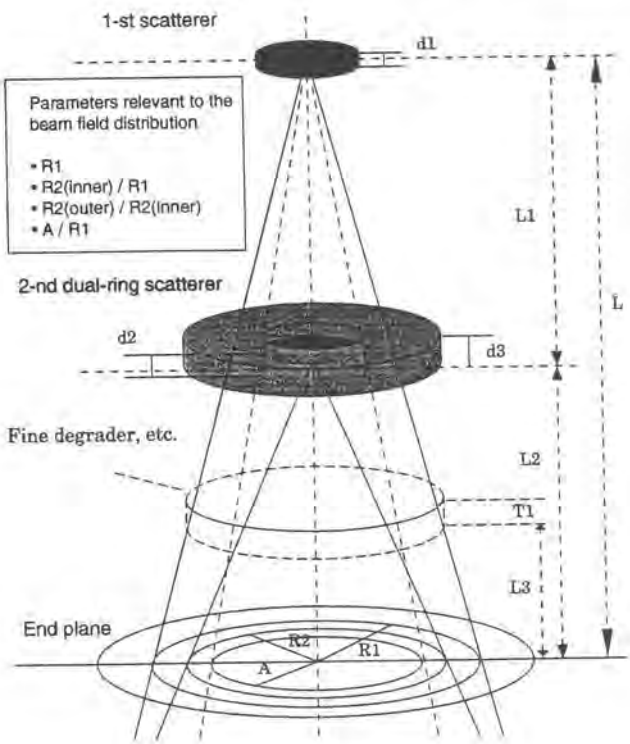


Fig. 5. Double scatterer system with a dual-ring scatterer.

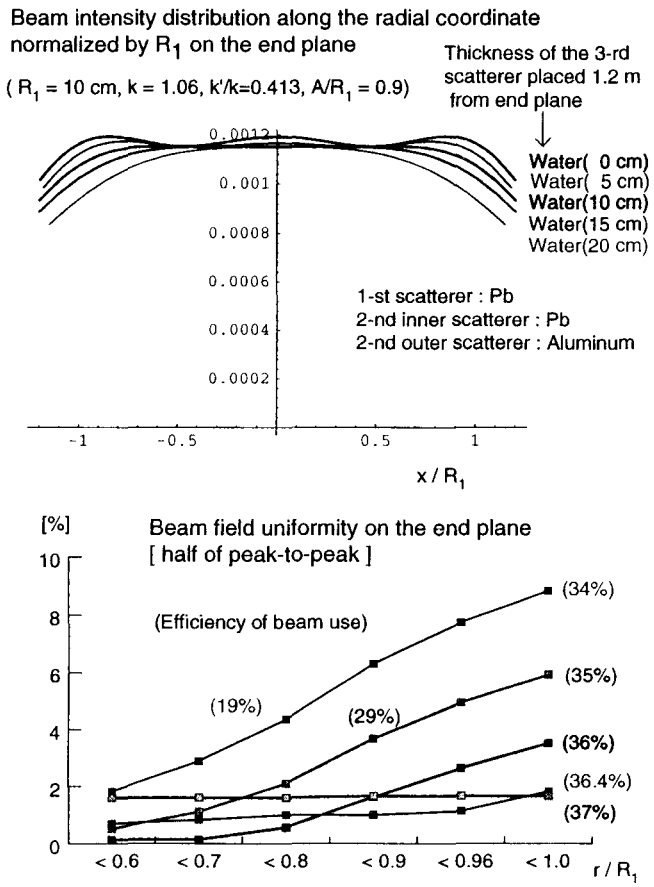


Fig. 6. Beam intensity distribution along the radial coordinate and percentages of proton beam inside specific radii for different thickness of water fine degrader

plate. The distance between the first one and the second is 87.4 cm (Fig. 5). If the incident beam angle deviation is less than 1 mrad, the beam uniformities within 20 cm diameter region are excellent as shown in Fig. 6 for different fine degrader thickness with a distance of 3.3 m from the first scatterer to the target. 37 % of incident protons to the first scatter will enter into the 20 cm diameter region for the highest energy and 34% for a degraded energy with 20 cm thick water fine degrader. Combining these with the field sizes above mentioned, the rotating gantry will be redesigned.

5. RADIATION SHIELDING

Since 50% extraction efficiency of the cyclotron is guaranteed by SHI, a design goal of 2 m thick wall is set for accelerator and treatment rooms. If thicker wall were needed, the cyclotron would lose its advantage to a great extent for hospital use. Following simple estimation is made for setting the intensity design goal. At the present time, 250 MeV proton beams are supplied to the fixed beam delivery systems at PMRC. They are scattered by a scatterer, pass through a fine energy degrader and a ridge filter, then they are shaped with a slit and a bolus as mentioned above. This method is assumed at the beginning operation of the new facility for 230 MeV incident beams. The beam intensity to the scatterer is 10 nA now and patients are ordinarily irradiated in two to three minutes. When breath-synchronized irradiation is applied, it takes two times longer or more. Therefore the design goal of 20 nA at the first scatterer is chosen for the new facility, and the design goal of the wall thickness is hoped to be attained. Apparently higher beam utilization efficiency is expected with future 3D beam delivery system.

ACKNOWLEDGEMENT

The authors would like to thank Dr. E. Toyota of SHI and his division members for technical information on the cyclotron.

REFERENCES

1) Wilson, R. R., "Radiological Use of Fast Protons," Radiology **47**, 487 (1946).
2) Fukumoto, S. et al., "Present Status and Future of University of Tsukuba Proton Medical Research Center," in Proceedings of the NIRS International Workshop on Heavy Charged Particle Therapy and Related Subjects (National Institute of Radiological Science, Chiba, 1991) pp. 6-12
3) Endo, K. et al., "Medical Synchrotron for Proton Therapy," in Proceedings of the European Particle Accelerator Conference (World Scientific Publishers Co. 1988) pp. 1459-1561
4) Fukumoto, S. et al., "Proton Synchrotron for Cancer Therapy and its Breath-Synchronized Operation," in Proceedings of the 8th Symposium on Accelerator Science and Technology (Ionics Publishing Company, Tokyo, 1991) pp. 456-458.
5) Tada, J. et al., "Time Resolved Properties of Acoustic Pulses Generated in Water and in Soft Tissue by Pulsed Proton Beam Irradiation — A Possibility of Doses Distribution Monitoring in Proton Radiation Therapy," Medical Physics, **18**, 1100 (1991).
6) Takayama, T., et al., "Compact Cyclotron for Proton Therapy," in Proceedings of the 8th Symposium on Accelerator Science and Technology (Ionics Publishing Company, Tokyo, 1991) pp. 380-382.
7) Japanese Patent No.1358145.
8) Pedroni, E., et al., "Voxel Scanning for Proton Therapy," in Proceedings of the NIRS International Workshop on Heavy Charged Particle Therapy and Related Subjects (National Institute of Radiological Science, Chiba, 1991) pp.94-109.

CONTINUED OPERATION OF THE SEATTLE CLINICAL CYCLOTRON FACILITY

R. Risler, P. Wootton, F. Ziai, J. Jacky,
S. Brossard and I. Kalet

Department of Radiation Oncology,
University of Washington,
Seattle,WA 98195, USA

ABSTRACT

The clinical cyclotron continues to be used for routine neutron therapy, and over 1100 patients have been treated over the past 7-3/4 years. Clinical results continue to be positive for certain tumor systems. PET isotopes are produced between patient runs.

System reliability has improved further and over the past 3 years less than 2% of the scheduled treatments had to be rescheduled for machine related reasons. Additional beams have been developed and used besides the routine 50.5 MeV proton beam. These include deuterons, $^3He^{++}$, and $^4He^{++}$ at several energies.

Slow neutrons are produced in a phantom or patient by moderation of the fast neutron beam. The potential use of these neutrons using Boron Neutron Capture (BNC) to enhance the present therapy beam is being explored. System improvements to allow more sophisticated treatment modes like conformal therapy are in progress.

1. INTRODUCTION

The clinical cyclotron facility at the University of Washington in Seattle is based on a Scanditronix built MC50 cyclotron with an isocentric neutron therapy gantry with leaf collimator. It has been in routine operation since 1984.[1] The original mission of the system was to conduct clinical trials comparing fast neutron therapy to other treatment modalities. This phase has been completed and at present no further trials have been funded. The clinical neutron therapy system continues to treat patients on a routine basis, concentrating on tumor systems which have shown promising results in the clinical trials.

Radionuclide production, primarily of short lived PET isotopes has been in operation since 1985 and the cyclotron use is expected to increase with the installation of a second PET scanner early next year.

The third use of the cyclotron beam is for experimental work to explore additional neutron therapy modalities, other radionuclide production schemes and some experiments by external users.

2. DAY TO DAY OPERATION

The original treatment schedule for fast neutron therapy has been changed from three treatments per week to four, with the same total treatment time of four weeks. Patients are now treated with 16 fractions instead of the original 12. This was done to reduce accute complications. As a result of this change the availability of the machine for other uses has been reduced. Mondays are now shared between experiments and maintenance. Tuesdays through Fridays are therapy days. Apart from major overhauls no weekend operations are scheduled, primarily for manpower reasons.

Radionuclide production continues as before with batch runs before the start of therapy and short runs between patients during the day on three to four days per week.

Apart from the increased demand because of the changed fractionation scheme, the beam use for therapy and radionuclide production has stayed fairly steady over the years. The number of patients treated continues to be determined by patient referral numbers and not by the availability of the system.

3. NEUTRON THERAPY

Neutron therapy has been proven to be superior to other treatment modalities in the case of salivary gland tumors.[2] Other tumors with positive results from clinical trials are locally advanced prostate cancer[3] and non-small cell lung carcinoma.[4] These tumors account presently for about 60% of the patient treatments performed with the neutron therapy unit (Table 1).

In order to keep normal tissue complication rates to a minimum, extensive shaping of the treatment fields to match the target volume is essential. The multi-leaf col-

Table 1. Treatment Sites Treated with Neutrons in 1991

Site	Patients Treated
Lung and Bronchus	31
Prostate Gland	28
Major Salivary Glands	20
Connective Tissue and Soft Tissue	7
Nasal Cavity and Sinus	6
Skin, Melanoma	6
Kidney	5
Brain	5
Leukemia	4
Nasopharynx	3
Others	18
Total	**133**

limator has proven to be very effective for this purpose. For the same reason multiple beam directions must be available, such as is possible with a rotating gantry.

4. OPERATIONAL STATISTICS

The operational statistics for the facility are summarized in Table 2. Rescheduled sessions are counted when they are rescheduled for a subsequent day. Minor delays during the day are not counted. Downtime is counted when the system is unavailable for technical reasons during the 10-hour operating days . The isotope production time reflects actual beam on target time for the production of radionuclides. Beamline switching time and tuning time is not counted.

Table 2 only shows the statistics for the standard operation with the 50.5 MeV proton beam for neutron therapy and PET radionuclide production. In addition, $^3He^{++}$ and $^4He^{++}$ beams have been developed at several energies for experimental production of radiosotopes. The internal PIG source is not very suited for this application and the beam intensity at the machine exit was limited to less than 5 μA with only 1 to 2 μA at the production station. If requests for Helium beams become more serious a new source will have to be acquired.

Also not shown are beam runs for quality assurance for the neutron therapy beam, for BNC experimental runs and some beam time for outside users.

5. EQUIPMENT PERFORMANCE

From Table 2 it can be seen that only very few patient sessions had to be rescheduled for equipment reasons during the past few years. This has been achieved by systematic improvements to the systems causing major interruptions and by building an extensive stock of spare parts.

The Anode Power Supply which used to cause major blocks of downtime has been improved with an upgrade kit from the manufacturer and has since run without problem.

The leaf collimator continues to operate reliably. The most major problem was a sticking leaf which was traced to a broken internal pin. It is not clear what caused the pin to break, one possibility is the original transport to Seattle. The collimator downtime reported is largely caused by bad cable connections. This is true also for failures in other systems such as the RF controls or power supply controls. We have started to replace or upgrade many of the connectors.

The new Beryllium target design reported at the last Cyclotron Conference[1] has worked well. The first prototype target lasted for 7100 therapy fields. It failed because of minute cracks in the copper beam stop which caused a vacuum leak from the cooling water. The leak developed slowly over a time period of about two weeks. The second target has now reached 8200 fields and is still in routine operation at 3kW of beam power.

A RTD thermometer probe was installed at the ion chamber location in the treatment head. It is used for the daily pressure/temperature correction of the dosimetry system. The daily variations of the built-in dosimetry system in comparison to an external standard is less than 0.5%.

6. TECHNOLOGISTS' EXPOSURE

Unlike standard radiation therapy with electrons and X-rays the technologists who set up the neutron patients are exposed to residual gamma radiation from the therapy equipment and the treatment room. In order to reduce the individual exposure, the technologists are rotated between neutron therapy and the other treatment machines in the department. The total dose for all technologists has been added each month and divided by the number of fields treated.

Year 6 (10/89 to 9/90): 5.1 ± 1.5 μSv per field
Year 7 (10/90 to 9/91): 3.9 ± 1.3 μSv per field

The variation shown is the standard deviation for the monthly exposure data. It is not known whether the difference between the two years is significant or not. The exposure per field is typically shared between two technologists.

This data can be compared to a similar study which was conducted for the first 18 months of operation.[5] At that time the technologists' exposure was 7.5 ± 1.9 μSv per field. The decreased exposure since then can be attributed to changes in working practices by the technologists and to more efficient set-up procedures as they became more familiar and confident with the equipment.

Comparisons with other similar facilities show that

the Seattle exposures are somewhat lower, possibly because of the leaf collimator which requires no set-up time for blocking of irregular fields. Clatterbridge has reported 5.1 ± 1.8 μSv per field and technologist,[6] the NAC facility in South Africa 4.1 ± 1.5 μSv.[7]

7. PLANS FOR FUTURE IMPROVEMENTS

At present there are several projects in progress which will make the facility more reliable and easier to use:

1. Operation without the permanent presence of a cyclotron operator. After the start-up in the morning when the beam is tuned from the accelerator to the therapy target and a check of the proper operation of the dosimetry system is performed, the cyclotron operator so far was required to stay at the console to be able to respond to beam problems such as septum overtemperature, overcurrents on stray beam detectors because of magnet drifts and technical problems with the therapy equipment. As the stability of the system has improved, this permanent presence of the operator is no longer required and the person in charge of the machine can be on call somewhere else in the facility. We are at present experimenting with this new mode of operation.

2. Additional production station for ^{15}O. One of the major reasons for having an operator permanently stationed at the control console is his coordination function between neutron therapy and short ^{15}O runs between patients. The operator switches the beam line and coordinates the timing. Plans are being made to install a pop-up target in the beam line to the isocentric therapy unit. Such a system will allow a very rapid changeover from therapy to isotope production and back. As long as no therapy run is immediately ready or in progress, the group responsible for the PET isotope production will be free to insert their target at any time to produce ^{15}O.

3. Moving Floor Controls. A moving floor covers the 3m deep pit which allows the therapy gantry to rotate underneath the patient support assembly. The floor was delivered as part of the building and its automatic controls never worked. It has been run manually by the technologists. This is not very satisfactory and a new control system has been developed and is at present being installed.

4. Leaf Collimator Controller. The leaf collimator controller is at present the least reliable subsystem and work on a new controller has started.

5. Computer Control System. The PDP11/23 based control system is not very sophisticated and very difficult to maintain. Plans for a replacement system have progressed and are being reported separately.[8] A more elaborate control system is also needed for conformal therapy where the number of fields in a given treatment session is substantially increased and automatic remotely controlled patient set-up will be used.

Since the beginning of operation all major scheduled maintenance work has occurred over weekends, including Monday. On only two occasions has a therapy day been cancelled to gain an extra day for a scheduled modification. It is planned to continue with no scheduled downtime periods in order to minimize interruptions of the clinical operation.

8. BORON NEUTRON CAPTURE ENHANCEMENT OF FAST NEUTRON THERAPY

Thermal or epithermal neutrons can be used to deliver dose to cancerous tissue if a suitable substance with high neutron capture cross section can be selectively accumulated in the tumor.[9] 10-Boron is the most widely used target nucleus used so far. While the Seattle fast neutron beam has practically no intrinsic thermal component, some of the fast neutrons are moderated by the patient's tissue and a thermal energy component is added to the beam. Experimental investigations have shown that these slow neutrons can potentially be used to increase the dose to the tumor without affecting the surrounding tissue, if a suitable boron-10 carrier can be found.[10] During the past few years a series of experiments has been carried out to determine to what extent the fast neutron beam can be modified in order to enhance the BNC effect without losing the fast neutron beam characteristics. These experiments have taken advantage of the existing fixed beam room, which is not used for therapy. The fixed beam unit has a therapy head identical to the isocentric gantry, but has no leaf collimator. This arrangement allows to make modifications to the target and collimation system without interfering with the ongoing therapy. Further efforts to establish a basis for clinical applications of boron neutron capture are continuing.

9. CONCLUSION

The Clinical Cyclotron at the University of Washington Medical Center in Seattle has now been in successful operation for nearly eight years. It is used for routine fast neutron therapy and production of PET radionuclides. New medical applications, in particular boron neutron capture enhancement of fast neutron therapy may play a role in the future.

Table 2: OPERATING STATISTICS

YEAR	SCHEDULED TREATMENT SESSIONS	PERFORMED TREATMENT SESSIONS	RESCHEDULED SESSIONS PATIENT CAUSED	MACHINE CAUSED	DOWNTIME [HOURS]	FIELDS TREATED	PATIENTS STARTED	ISOTOPE PRODUCTION [HOURS]
OCT 84 SEP 85	1806	1430	27 (1.5%)	349 (19.3)		2954	142	0.0
OCT 85 SEP 86	1937	1623	83 (4.3%)	231 (11.9%)		3574	152	17.4
OCT 86 SEP 87	2235	1968	145 (6.5%)	122 (5.5%)		4016	160	68.6
OCT 87 SEP 88	1919	1630	173 (9.0%)	116 (6.0%)	143.0	3645	142	100.5
OCT 88 SEP 89	1812	1589	201 (11.1%)	22 (1.2%)	73.3	3455	157	69.8
OCT 89 SEP 90	1919	1575	273 (14.2%)	71 (3.7%)	87.3	3506	140	85.4
OCT 90 SEP 91	2239	1947	277 (12.4%)	15 (0.7%)	38.7	4360	133	62.6
OCT 91 JUN 92	1718	1569	129 (7.5%)	20 (1.2%)	28.2	3729	102	44.8
TOTAL	**15585 (100%)**	**13331 (85.5%)**	**1308 (8.4%)**	**946 (6.1%)**		**29239**	**1128**	**449.1**

10. REFERENCES

1) R. Risler, S. Brossard, J. Eenmaa, J. Jacky, I. Kalet, A. Rask, and P. Wootton. Routine operation of the Seattle cyclotron facility. In *Proceedings of the Twelfth International Conference on Cyclotrons and Their Applications*, 1989.
2) T. W. Griffin. Optimal treatment for salivary gland tumors. *Int. J. Radiation Oncology Biol. Phys.*, 857, 1991.
3) K. J. Russell, G. E. Laramore, T. W. Griffin, R. G. Parker, M. H. Maor, L. W. Davis, and J. M. Krall. Fast neutron radiotherapy in the treatment of locally advanced adenocarcinoma of the prostate. *Am J Clin. Oncol. (CCT)*, 12(4):307, 1989.
4) G. Stewart, T. W. Griffin, B. R. Griffin, G. E. Laramore, K. J. Russell, R. G. Parker, M. N. Maor, and L. W. Davis. Neutron radiation therapy for unresectable non-small-cell carcinoma of the lung. *American Journal of Clinical Oncology (CCT)*, 12:290–294, 1989.
5) J. Eenmaa, P. Wootton, and R. Risler. Technologists exposures and radiation protection aspects of the clinical neutron therapy facility in Seattle. *British Journal of Radiology*, 60:310, 1987.
6) J. Finch and D. E. Bonnet. An investigation of the dose equivalent to radiographers from a high-energy neutron therapy facility. *British Journal of Radiology*, 65:327, 1992.
7) NAC annual report. National Accelerator Center, PO Box 72 Faure, 7131 South Africa, March 1991. (Data from p. 75).
8) J. Jacky and R. Risler. Formal specifications for a cyclotron control system. (in the proceedings of this conference).
9) R. F. Barth, A. H. Soloway, and R. G. Fairchild. Boron neutron capture therapy of cancer. *Cancer Research*, 50:1061, 1990.
10) P. Wootton, R. Risler, J. Livesey, S. Brossard, G. Laramore, and T. Griffin. Boron neutron capture enhancement of the tumor dose in fast neutron therapy beams. In *Proceedings of the 4th International Symposium on Neutron Capture Therapy for Cancer*, pages 195 – 198, Plenum Press, New York, 1992.

RECENT COMMISSIONING RESULTS AT CELSIUS

D. Reistad, T. Bergmark, C. Ekström, C.-J. Fridén, K. Gajewski, L. Hermansson, P. Jahnke, A. Johansson, O. Johansson, T. Lofnes, G. Norman, R. Wedberg, L. Westerberg, J. Zlomanczuk
The Svedberg Laboratory, Uppsala University, S-751 21 Uppsala, Sweden

M.A. Raadu, M. Sedlaček
Alfvén Laboratory, Royal Institute of Technology, S-100 44 Stockholm, Sweden

ABSTRACT

The CELSIUS storage ring, which is fed from the Gustaf Werner Cyclotron in Uppsala, has been brought into operation for physics. Protons, deuterons, α-particles, and oxygen ions have been stored, accelerated, and exposed to internal targets. These are a cluster-jet target with hydrogen, deuterium, argon, or nitrogen, and a carbon fibre target. The carbon fibre has been used to estimate beam profiles. The electron cooling system, which is on the ring, still gives an unexplained effect, sometimes heating rather than cooling the stored ion beam. A system of radiation detectors has been mounted around the ring to help to adjust the machine parameters for minimum background. A transverse feed-back system has been tested.

Some parameters of the CELSIUS ring	
Circumference	82 m
Max. magnetic field	1.0 T (1.2 T planned)
Max. momentum	2.1×Z GeV/c (at present)
Max. energy ($Z/A = 1/2$)	470×A MeV (at present)
Q_x, Q_y	1.63, 1.83
β_x, β_y at internal targets	1.4 m, 1.5 m
Electron beam voltage	5-300 kV
Electron beam current	0-3 A
Electron beam diameter	2 cm
Achieved intensities	
Proton intensity	2×10^{11}
Deuteron intensity	4×10^{10}
α-particle intensity	1×10^{10}
^{16}O intensity	3×10^{8}
Internal targets	
Cluster jet target	hydrogen 3×10^{14} atoms/cm^2 nitrogen 4×10^{13} atoms/cm^2 argon 2×10^{13} atoms/cm^2
Fibre target	7 μm carbon filaments
Pellet target[1]	20 μm hydrogen pellets

[1]Under development

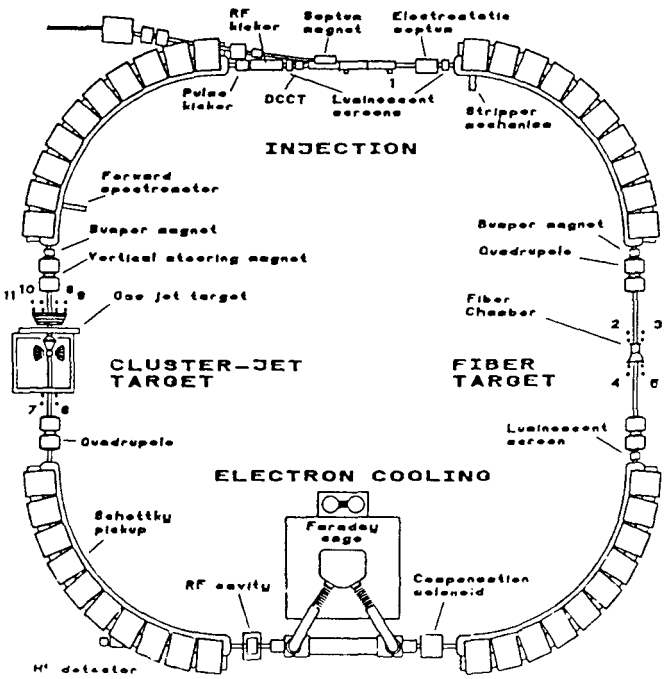


Fig. 1. Present layout of CELSIUS. The numbered dots represent radiation detector pairs, which are discussed in section 6 below.

1. INTRODUCTION

The CELSIUS ring has been described at the previous Cyclotron Conference [1], and other conferences [2-3]. A more complete description is available in the recent Progress Report from The Svedberg Laboratory [4]. The ring consists of four 90° arcs and four straight sections, see fig. 1, which shows the present layout.

One straight section is used for injection [5].

The hydrogen pellet target [6] and the WASA detector [7] are planned to be installed on the second straight section. They will then replace the fibre target scattering chamber, which is presently mounted there.

The third straight section holds the electron cooler [8] and a radio frequency cavity [9].

The fourth straight section holds the cluster-jet target [10], which is being used in the present physics experiments.

2. INJECTION

The ions that are injected into CELSIUS come from the Gustaf Werner Cyclotron [11-12], in which they usually have been brought to the maximum energy, $192 \times Q^2/A$ MeV.

The injection system of the ring must be versatile enough to cope with a variety of conditions. Therefore, both "multiturn injection" (without charge exchange) and "stripping injection" schemes are implemented [5].

The injection elements of the CELSIUS ring consist of electromagnetic and electrostatic septa, and a thin stripper foil, mounted on a mechanism in the first bending magnet of the ring. The present foil is of carbon with thickness 30 $\mu g/cm^2$.

Two bumper magnets displace the closed orbit during injection towards the septum foil and stripper foil, i.e., towards the outside of the ring. Both during "multiturn injection" and "stripping injection" the injection process takes place during an exponential decrease of the magnetic field in the bumper magnets.

During "multiturn injection," the electrostatic septum is used to separate the paths of the injected beam and the circulating beam. It was the first injection method to be tried in CELSIUS, in 1988. The cyclotron beam current was 30 μA. About 2×10^8 protons were stored. This is almost one order of magnitude less than what ought to be possible according to calculations [5]. The reason for the discrepancy could be inadequate matching between the transverse phase space occupied by the incoming beam and the transverse acceptance of the ring.

Stripping injection allows by far the best ratio between the stored beam current and the incoming beam current for light and moderately heavy ions, and is the preferred method to inject protons (using 96 MeV H_2^+ ions), deuterons (using 48 MeV D_2^+ ions), α-particles (using 48 MeV He^+ ions), and other ions up to Ar. This is even though the energy of the injected protons, deuterons, and α-particles is only 1/4 of the energy that could be available from the cyclotron, if the ions were accelerated in their naked states, and the energies of heavier ions is also always lower than for naked ions.

Achieved intensities are, for 48 MeV protons, 2×10^{11}, for 24 MeV deuterons, 4×10^{10}, and for 48 MeV α-particles, 1×10^{10}.

Electron cooling can be used in order to build up the intensity in cases when what is achieved with a single ordinary injection is much less than what corresponds to the stability limit of the ring [13-15]. Both multiturn injection and stripping injection can be combined with such accumulation with electron cooling. Once the cooling has shrunk the transverse beam dimensions, the bumper magnets can be activated again in order to displace the closed orbit, and another pulse train from the cyclotron can be injected, without that the stored beam is lost, provided that the stored beam is not displaced into the septum foil or stripper foil. Using this method in combination with stripping injection we have stored 2×10^7 of O^{8+}, starting with a cyclotron current of 6×10^{10} s^{-1}. The ion source in the cyclotron was pulsed with 1 ms pulse length and repetition rate of 4 Hz.

Another way to do stripping injection has been found. This is without using any time-varying elements in the ring at all, but by making use of the electron cooling system. A small fraction of the beam is hitting the stripper foil at a position in transverse phase space, which is so close to the acceptance, that the electron cooling system brings the ions into the acceptance fast enough that they never cross the foil again. Thus, this is an injection method with a very low efficiency, but with which large stored beam currents can be achieved by injecting for long enough. 3×10^8 oxygen ions were injected with this method by injecting 6×10^{10} s^{-1} during 20 s.

3. MODES OF OPERATION

CELSIUS can be operated in static mode or in cycles. In the static mode the machine parameters have constant values, and the energy of the stored beam remains at the value at injection. The static mode of operation is used only for machine development or accelerator physics purposes. During operation in the cyclic mode, the beam is accelerated to the energy, which is required for the experiment. Usually, the beam is brought into collision with the target only after that it has reached its final energy, but sometimes the physicists have found it useful to make use of the acceleration part of the cycle, to calibrate their detectors.

3.1. Acceleration

The variation of the magnetic field during a typical cycle is illustrated in fig. 2.

Since the dipole magnets of CELSIUS are not laminated [16], the acceleration is performed slowly; the standard period used for acceleration is 22 s so far. This is consistent with the use of the ring for experiments with ultra-thin internal targets; even though the overhead time per machine cycle typically totals 60 s the duty factor is acceptable, 50 % in two-minute cycles and 80 % in five-minute cycles.

So far cycles have been developed for acceleration of protons to several final energies between 200 MeV and 1300 MeV, and for experimental situations where a slow ramping of the proton energy is performed during the "flat" top. Examples of such slow ramps are from 270 to 310 MeV (π^0 threshold in $p+p$ reactions) and from 1230 to 1300 MeV (η threshold in $p+p$ reactions). The maximum intensity after

acceleration obtained so far is 5×10^{10} protons at 1150 MeV and 1×10^{10} protons at 1300 MeV. α-particles have been accelerated to 600 MeV, and deuterons to several final energies up to 783 MeV where they (1×10^{10}) have also been cooled (measured $\Delta p/p = 3\times10^{-5}$). Oxygen ions, which were injected without using the bumper magnets as described above, have been accelerated to 1600 MeV.

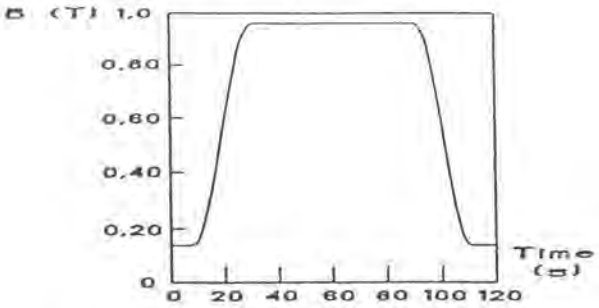


Fig. 2. Variation of the main magnetic field in CELSIUS during a cycle with acceleration of protons to 1.3 GeV.

Recent software developments allow us to prolong a cycle, which has been developed, by extending the flat top. We can also stop the function generators at any time in the cycle. This has been used to create machine cycles which are as long as 10 minutes.

3.2 Other manipulations

Several groups are going to make use of a part or all of the magnets in the quadrant of the ring which follows the target as a magnetic spectrometer [17].

Moving detectors, placed either inside of the quadrant as shown in fig. 3 or on the injection straight section, will detect reaction products. In order to protect the detectors from un-necessary irradiation, they are moved away from the beam during injection and acceleration, and moved into position at the beginning of the flat top.

One example of an experiment that makes use of the quadrant of the ring which follows the target is the study of giant resonances in heavy nuclei through inelastic scattering of heavy ions at several hundred MeV/nucleon. In this case the whole quadrant is required to distinguish the inelastically scattered heavy ions from the elastically scattered ones and from the beam. For this experiment a system of moveable detectors will be mounted on the injection straight section.

Then it is optimal to have 180° betatron phase shift between the target and the detectors, preferably in both planes. With the position of the detectors which was chosen, this implies the working point $Q_x = 1.80$, $Q_y = 1.85$. We have found that it is quite inefficient to inject with this working point. On the other hand, we have found that it is possible to let the working point jump after acceleration from the usual to this point with beam losses that do not exceed 20-30 %.

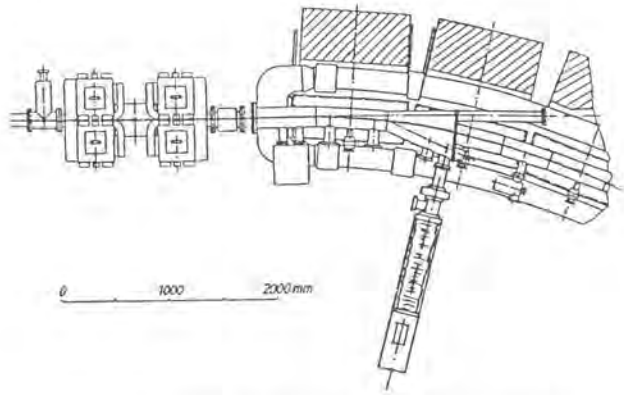


Fig. 3. Moveable detector arrangement to make use of the first magnets in quadrant 4 of CELSIUS as a spectrometer.

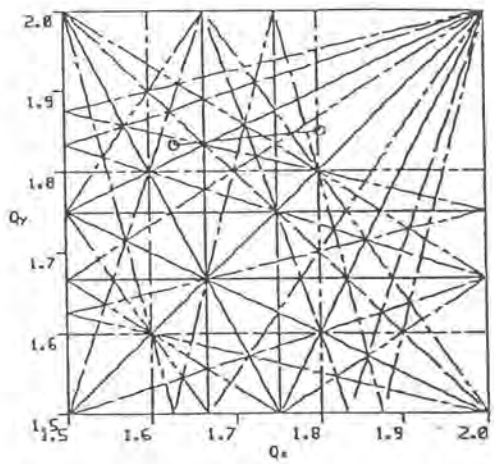


Fig. 4. Jump of working point to obtain required focusing for experiment, which uses quadrant 4 as a spectrometer.

4. ELECTRON COOLING

Fig. 5 shows a cross section of the electron cooling system. The electron gun launches a 20 mm diameter electron beam from a dispenser cathode. The cathode and the whole beam path are fully immersed in a homogeneous longitudinal magnetic field of 0.1 - 0.15 T.

The electrons are accelerated in an electrostatic column to a maximum energy of 300 keV. For energies above 70 keV the beam current can amount to 3 A. At the collector side the electron beam is decelerated in another electrostatic column. After passing through a hole in the collector anode, which is at a potential of 0.1 - 0.4 kV above the cathode potential, the beam is again accelerated, and reaches the collector with a kinetic energy of 5 keV.

Electron cooling has been studied at the injection energies (using stripping injection) of protons (48 MeV),

deuterons (24 MeV), oxygen ions (292 MeV), as well as after acceleration with 275 MeV protons and with 390 MeV, 600 MeV, and 783 MeV deuterons.

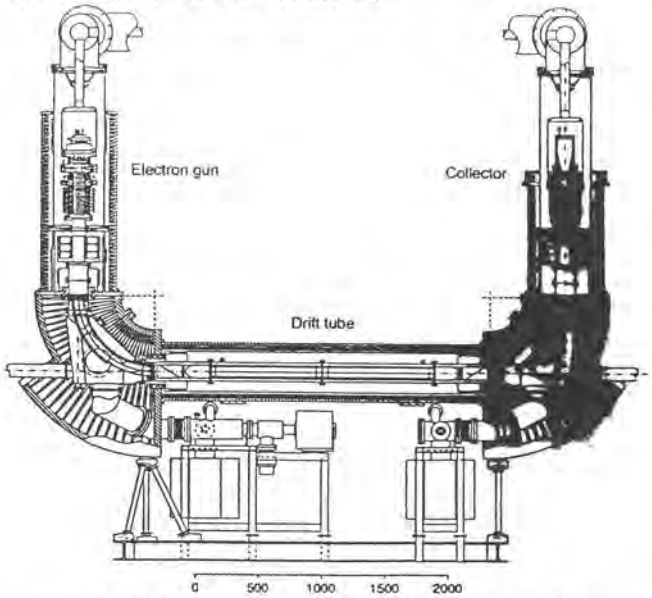


Fig. 5. Cross section of CELSIUS electron cooler.

Measurements of the longitudinal cooling time have been performed with bunched beams, where the momentum spread is proportional to the time spread in the bunch (unless space charge effects are important). The result of one such measurement is illustrated in fig. 6

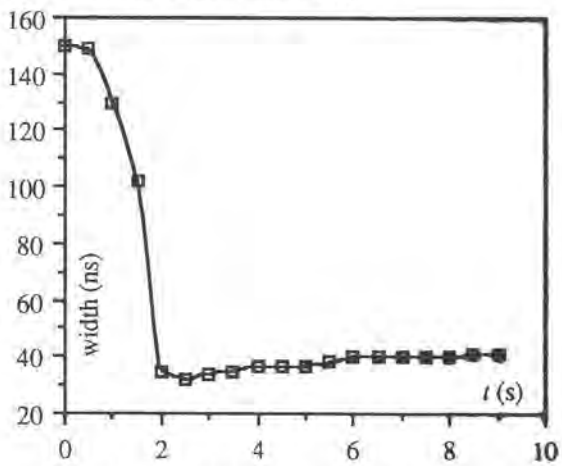


Fig. 6. Measured FWHM time spread of a bunch of 275 MeV protons during cooling with 410 mA of electrons.

The longitudinal drag rate has been measured with coasting beams of protons, deuterons, and oxygen ions with several energies. The measurement technique has been to step the output voltage from the electron cooler high voltage power supply, and to measure how the revolution frequency of the ions changes as a function of time after the step. Fig. 7 shows several measured scaled drag rates for 783 MeV deuterons and a single measured point for 296 MeV oxygen ions together with measured scaled drag rates from several other laboratories [15,18].

The drag rates measured at CELSIUS do not yet seem to be quite competitive with the best drag rates measured elsewhere. This may have to do with a disturbing phenomenon, which is not yet understood. There is an apparent "heating" of the stored ion beam by the electron beam as soon as the electron beam is put together with the ion beam. This heating causes a dramatic drop in lifetime of the stored ion beam, particularly when the ion beam has a low energy.

With no electrons present, the 48 MeV (injection energy) proton beam lifetime is typically 50 s.

An example of a measurement of the lifetime of a 48 MeV proton beam as a function of the electron current is shown in fig. 8.

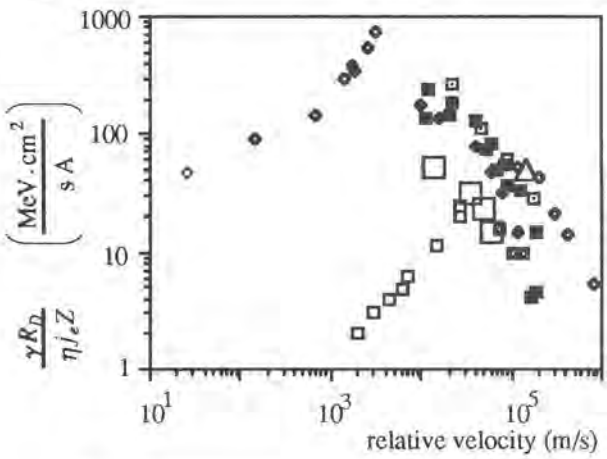


Fig. 7. Comparison between measured drag rates at NAP-M (65 MEV p)●, ICE (47 MeV p) □, FNAL (203 MEV p) ■, LEAR (49 MeV p)⊡, IUCF (45 MeV p)◆, INS (20 MeV p) ■, and CELSIUS with 783 MeV deuterons □, and 296 MeV oxygen ions △.

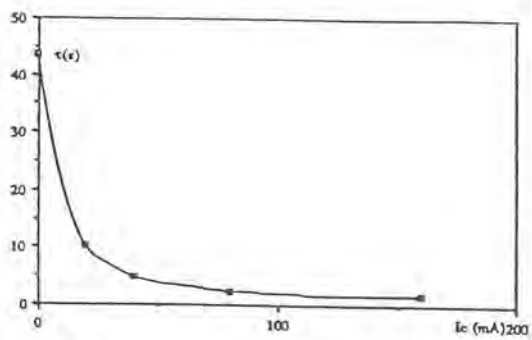


Fig. 8. Measurement of lifetime of a 48 MeV proton beam as a function of electron current.

As seen in fig. 8, the proton beam lifetime is approximately inversely proportional to the electron intensity. On

the other hand, the proton beam lifetime does not depend on the proton intensity.

Similar effects were observed already with the electron cooler at the NAP-M ring at Novosibirsk, Russia [19]. There, the effect was attributed to slow electrons, which accumulated inside the electron beam. Neutrals were created in integrated sputter-ion pumps, which were operating in the longitudinal magnetic field of the electron cooler. These neutrals were ionized in the electron beam. The ions left the beam, but the slow electrons were left behind, trapped by the longitudinal magnetic field and the decelerating electric fields of the gun and the collector. In their paper [19] the Russians conclude, that a transverse electric field may be formed. The field is determined by the equilibrium between ionization and electrons leaving across the field lines or by recombination with ions. This field can be of the order of $W_i/e\rho_0$, where W_i is the ion energy (given by the sputter-ion pump voltage) and ρ_0 is the electron beam radius.

We have however measured the tune shifts, which are induced on the ion beam by the electron beam, and found that they are rather close to the predicted values, see fig. 9. We can therefore conclude that no large un-expected and un-compensated charge is stored inside the electron beam.

Similar effects have also been observed at the TARN II ring in Tokyo, Japan [15], and (to a less disturbing degree) at the Indiana Cooler in Bloomington, Indiana [20]. In Tokyo, a drastic change of the working point improved the stored beam lifetime. On the other hand, such effects have not been observed at the LEAR ring at CERN [21], nor at the TSR ring at Heidelberg [22], the ESR ring at Darmstadt [22], or the CRYRING in Stockholm [23].

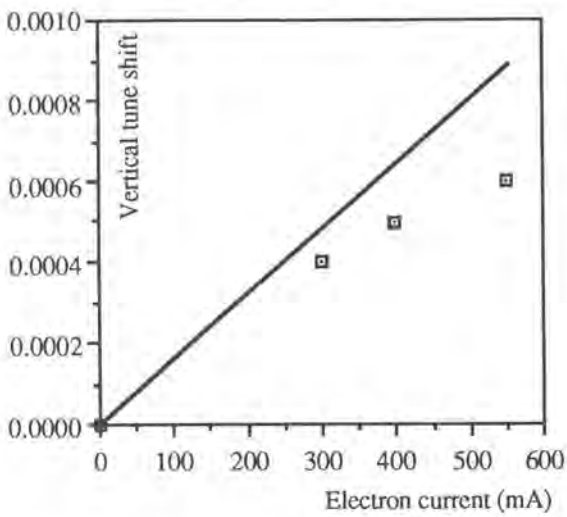


Fig. 9. Measured tune shift as a function of electron current. The measurement was done with 275 MeV protons. The calculated slope of the tune shift is also shown as a straight line.

It seems to be the electron coolers that have the best degree of vacuum, which are spared the effects of "electron heating."

The "heating" is present also when the beams have large relative velocity. From this we conclude that the problem is not simply due to drag force; i.e. that the electron beam is forcing the momentum of the stored ion beam outside the acceptance.

This "electron heating" effect is quite disturbing, because it makes it more complicated to operate the electron cooling system. When we want to cool the beam before and after acceleration, for example, then we have turn the electron current to zero during the acceleration in order not to get beam loss due to the electron heating effect.

Even more important, although the "electron heating" is compensated by the electron cooling when the electron and ion velocities are well enough matched, it seems that the heating is disturbing the electron cooling, so that the results obtained are not as good as they should be.

We have observed rf. signals at the Δ-outputs from the horizontal and vertical beam position monitors in the electron cooler. A typical spectrum as measured by a spectrum analyzer is shown in fig. 10.

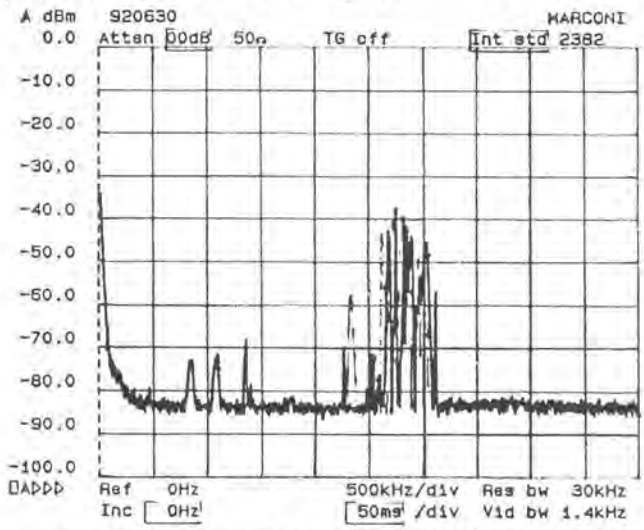


Fig. 10. Spectrum analyzer measurement of signal at Δ output from beam position monitor in electron cooler. The signals are essentially the same in both the horizontal and vertical planes, and the same at the monitor which is near the gun as at the one which is near the collector. The electron current was 300 mA and the voltage was 26 kV. The magnetic field was 0.1 T and the pressure in the cooler was 6×10^{-8} Pa.

There are no signals at the same frequency at the corresponding Σ-output from the beam position monitors.

These signals indicate the presence of transverse motions of the electron beam, of about the same amplitude in both transverse planes.

For a longitudinal magnetic field of 1.0 T the central frequency is about 2.5 MHz. It varies as $1/B$ and has a very small positive derivative with respect to electron beam voltage, and small positive derivatives with respect to electron beam current and rest gas pressure.

If these signals indicate the presence of coherent transverse motions of the electron beam, then the amplitude of these motions varies randomly between about 3 and 15 μm.

The frequency band observed includes the eigenfrequencies $4-Q_y \approx 2.4$ MHz and $4-Q_x \approx 2.7$ MHz.

It is therefore our present hypothesis, that the electron beam for some reason is oscillating in both transverse planes, and that the resulting electrical field is exciting the stored beam at one or several of its betatron eigenfrequencies (rf. knockout).

5. THE CLUSTER-JET TARGET SYSTEM.

The cluster-jet target system [10] has been in operation for experiments since 1989 using target beams of hydrogen, deuterium, nitrogen, and argon. The target thicknesses are 3×10^{14} atoms/cm^2 for hydrogen and deuterium, 4×10^{13} atoms/cm^2 for nitrogen, and 2×10^{13} atoms/cm^2 for argon. When the system is running with these target thicknesses the pressure in the scattering chamber becomes 2×10^{-5} Pa.

In order to increase the solid angle that is available for the nuclear reaction products, a new central scattering chamber for the cluster-jet target has been constructed [10]. A schematic view of the new scattering chamber is shown in fig. 11.

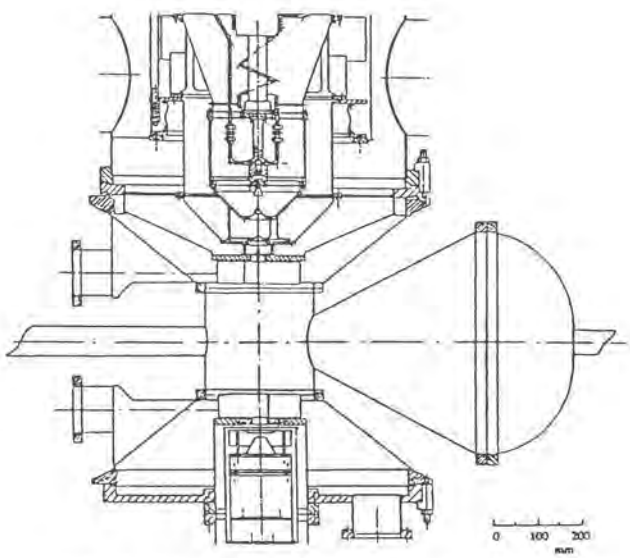


Fig. 11. Schematic view of the new scattering chamber connected to the cluster-jet target.

The new chamber consists of three parts, two permanent chambers including the valves towards the target beam source and the beam dump, and an exchangeable central chamber.

The new central chamber allows a large fraction of the horizontal plane and ±35° vertically to be covered by external detectors outside the thin-walled central cylinder, and between 3° and 25° for external forward detection by using a thin-walled forward window [24].

6. STRAY RADIATION DETECTORS

Many experiments to be carried out at the CELSIUS ring are devoted to studies of reactions with small cross sections. Such measurements require careful tuning of the accelerator in order to minimize the background count rate (as the background we consider particles emerging from interactions between the beam particles and the vacuum chamber and all other objects in the ring except the target).

In order to guide the operator while tuning the ring, we have built a system to monitor the beam losses. This consists of 11 pairs of plastic scintillator counters placed around the ring. The detectors are rectangular with dimensions $5\times50\times40$ mm^3. The detectors pairs are put in the median plane of the ring, at distances ranging between 60 mm and 250 mm from the beam. The positions of the detector pairs are indicated with dots in fig. 1. The numbering of the detectors is also shown in fig. 1.

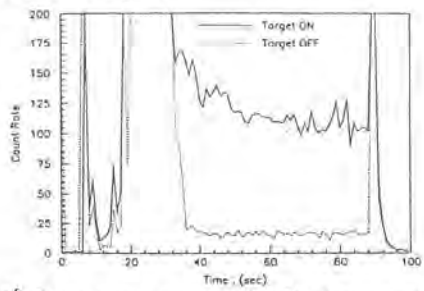


Fig. 11. Count rates, measured with detector pair #9, in cycle with acceleration of protons to 1150 MeV, with and without hydrogen target.

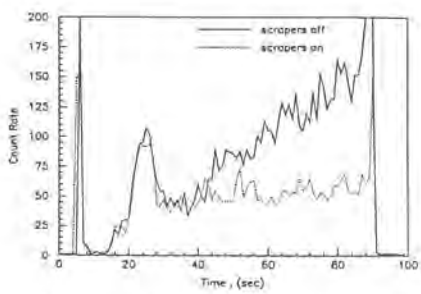


Fig. 12. Count rates, measured with detector pair #8, in cycle with acceleration of protons to 500 MeV, with and without using the scrapers.

As examples of measurements made with this system, we show in fig. 11 measured count rates during a cycle with acceleration to 1150 MeV at detector pair #9 with and without the hydrogen target, and in fig. 12 measured count rates during a cycle with acceleration to 500 MeV with and without using the horizontal scrapers, which are located on the second straight section. We see that the background is high during the acceleration, which is finished at $t = 30$ s. Then the synchronism between magnetic field and rf. frequency is less good than during the flat top, which lasts from 30 s to 90 s. At 90 s the beam is dumped, resulting in a peak in the background.

We observe that the background gets reduced when using the scrapers. On the other hand we have not yet observed any general decrease in background when using the electron cooling system. This may have to do with the unexplained effects of "electron heating" discussed in section 4 above.

7. Beam Profile Measurements

The radiation monitor pair #4 has also been used to estimate the horizontal beam profile. The 7 μm carbon fibre was moved through the beam with a velocity of 50 mm/s. It moved twice through the beam, in opposite directions, at cycle times $t \approx 40$ s and $t \approx 70$ s. In fig. 13 is shown how the count rate at the detector pair #4 varied as a function of time when the fibre moved through the beam. The beam size appears much larger when the detector is moved "inwards," than when it is moved "outwards". During this measurement the rf. system of the ring was turned off. The protons are decelerated during the traversal through the fibre. Since the dispersion at the target is positive, the fibre will repeatedly "see" protons which it has previously decelerated when it moves inwards. On the other hand, when it moves outwards, it will only see each proton once, and a true beam profile measurement is obtained.

8. Transverse Feed-back System

The phase space density limit that is first met in small cooler rings is that of transverse instabilities. Therefore, feed-back systems to damp transverse instabilities have been developed at several laboratories [25-28].

Such a system has also been constructed for CELSIUS. It is essentially a copy of the feed-back system built for LEAR, and uses circuit boards built for CELSIUS by members of the PS Division at CERN. It is now being tested on the CELSIUS ring. A block diagram of the feed-back system is shown in fig. 14.

Transverse oscillations of the beam are measured with a beam position monitor, and corrected by a kicker located at a position that is approximately an odd number of quarter wavelengths of betatron oscillations away from the monitor.

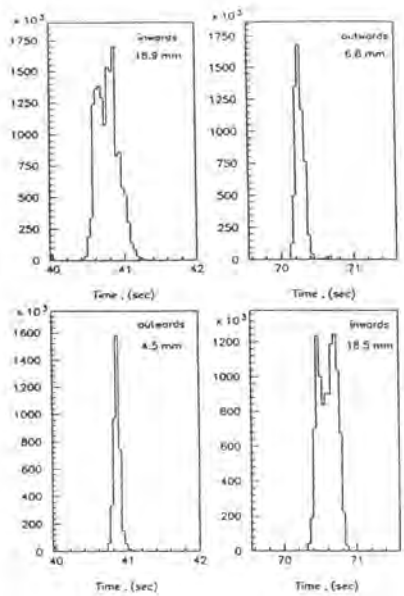


Fig. 13. Measurement of beam profile of 500 MeV proton beam with carbon fibre.

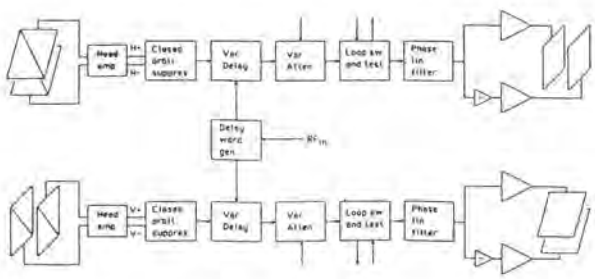


Fig. 14. The Transverse Feed-back System.

The "Closed Orbit Suppressor" shown in the block diagram in fig. 14 suppresses the signal from the closed orbit position error at the beam position monitor by a technique that virtually moves the centre of the monitor towards the closed orbit position. Thus only the deviations due to instabilities are measured. This is done electronically by giving the two pick-up electrodes of the beam position monitor a different weight, calculated from the closed orbit position measurement. The closed orbit component of the signal is normally, by far, the largest one. The "Closed Orbit Suppressor" therefore makes it possible to increase the loop gain without increasing the power of the amplifier. A good degree of suppression is hence important.A variable delay is achieved by switching in or out different delay cables, with propagation times in binary progression. The delay is controlled from the revolution frequency, by a "Delay Word

Generator." This makes it possible to use the feed-back system during acceleration. At the "Loop Switch and Test Unit" test signals can be added and the response checked with the loop open as well as closed.

The "Phase Linear Filter" keeps the phase linear up to a frequency where the gain has dropped by 40 dB. This is important, since otherwise high frequency oscillations could be amplified rather than damped.

Tests of the transverse feed-back system have been performed since November 1991. These tests have shown that the system can eliminate particle losses, that otherwise take place during electron cooling, and that it also can eliminate losses that may take place during acceleration if the working point is not controlled carefully enough.

9. CONCLUSIONS

The CELSIUS ring has been brought into operation for nuclear and particle physics with internal targets. High intensities of protons, deuterons and α-particles have been stored by stripping injection and accelerated to various energies (up to 1300 MeV for protons).

The intensities achieved with "multi-turn" injection (without charge exchange) are lower than expected.

An unexplained effect, causing "electron heating" makes the operation of the electron cooler difficult, and less beneficial. This effect is under investigation.

10. REFERENCES

[1] D. Reistad, "Status of the CELSIUS Cooler-Storage Ring Project." Proc. 12th Int. Conf. on Cyclotrons and their Applications, Berlin, Germany, May 8-12, 1989, p. 62.

[2] A. Johansson, D. Reistad, "Present Status of CELSIUS", Proc. 19th INS Symposium on Cooler Rings and their Applications, Tokyo, Japan, November 5-8, 1990, p. 15.

[3] T. Bergmark et al., "Operations with Internal Targets and Electron Cooling at CELSIUS." To be published in Proc. 3rd European Particle Accelerator Conference, Berlin, Germany, March 24-28, 1992.

[4] A. Ingemarsson (ed.), "TSL Progress Report July 1987 - December 1991." The Svedberg Laboratory, Uppsala, 1992.

[5] K. Hedblom et al., "Calculations on Multiturn and Stripping Injection in CELSIUS." To be published in Proc. 3rd European Particle Accelerator Conference, Berlin, Germany, March 24-28, 1992.

[6] B. Trostell, F. Kullander, "Hydrogen Pellet Target Developments for CELSIUS," Proc. 2nd European Particle Accelerator Conference, Nice, France, June 12-16, 1990, p. 1306.

[7] H. Calén et al., "Particle Physics at CELSIUS," Proc. 19th INS Symposium on Cooler Rings and their Applications, Tokyo, Japan, November 5-8, 1990, p. 166.

[8] M. Sedlacek et al., to be published.

[9] T. Lofnes, "RF and Beam Control System for CELSIUS," Proc. 2nd European Particle Accelerator Conference, Nice, France, June 12-16, 1990, p. 946.

[10] C. Ekström, "Internal Targets at the CELSIUS Storage Ring," Proc. 19th INS Symposium on Cooler Rings and their Applications, Tokyo, Japan, November 5-8, 1990, p. 228.

[11] S. Holm, these proceedings.

[12] B. Lundström, B. Holmgren, these proceedings.

[13] M. Grieser et al., "Advanced Stacking Methods Using Electron Cooling at the TSR Heidelberg," Proc IEEE Particle Accelerator Conference, San Francisco, California, May 6-9, 1991, p. 2817.

[14] T.J.P Ellison et al., "Progress in Commissioning the IUCF Cooler," Proc IEEE Particle Accelerator Conference, Chicago, Illinois, March 20-23, 1989, p. 1608.

[15] T. Tanabe et al., "Electron Cooling Experiments at INS," Nucl. Instr. and Meth. in Phys. Res. **A307** (1991) 7.

[16] G. Norman et al., "Accelerating with Solid Core Magnets," Proc. 2nd European Particle Accelerator Conference, Nice, France, June 12-16, 1990, p. 881.

[17] L. Nilsson, "The CELSIUS Storage Ring - Present Status and Future Experiments." To be published in Proc. Int. Symp. on New Trends and Facilities for Intermediate-Energy Nuclear Physics, RCNP, Osaka, Japan, November 14-15, 1991.

[18] T.J.P. Ellison, "Electron Cooling at IUCF — 0.3 MeV in 1988, 9 MeV in 1998?" Proc. Workshop on Electron Cooling and New Cooling Techniques, Legnaro, Italy, May 15-17, 1990. p. 29.

[19] G.I. Budker et al., "Experimental Studies on Electron Cooling." Particle Accelerators, 7, 197 (1976).

[20] T.J.P. Ellison, private communication.

[21] M. Chanel, private communication.

[22] M. Steck, private communications.

[23] H. Danared, private communication.

[24] F. Bertinelli, C. Ekström, "A transparent ultra high vacuum window for external detection at CELSIUS." To be published in Proc. 15th Int. Conf. on High Energy Accelerators, Hamburg, Germany, July 20-24, 1992.

[25] C. Carter et al., "The Transverse Feedback System for the CERN PS Booster." Proc. 1981 Particle Accelerator Conference, Washington, D.C., March 11-13, 1981, IEEE Trans. Nucl. Sci. **NS-28**, 2270.

[26] J. Bosser et al., "Operational Aspects of Electron Cooling at the Low Energy Antiproton Ring (LEAR)". Proc. 1991 IEEE Particle Accelerator Conference, San Francisco, California, May 6-9, 1991, p. 2832, and M. Chanel, private communication.

[27] U. Schaaf, "Schotty-Diagnose und BTF-Messungen an gekühlten Strahlen im Schwerionen-Speicherring ESR." GSI-91-22, Gesellschaft für Schwerionenforschung mbH, Darmstadt, 1991.

[28] T.J.P. Ellison, private communication.

BEAM DIAGNOSIS FOR UNMEASURABLY COLD BEAMS
-- OR -- "HOW COLD IS IT, AND DOES THE OPERATOR KNOW OR CARE?"

Tim Ellison*

The Indiana University Cyclotron Facility
2401 Milo Sampson Lane; Bloomington, IN 47405 USA

ABSTRACT

In the first part of this paper, the most unique property of a proton beam in an electron-cooled storage ring is discussed: namely, its extremely small relative momentum spread ($\Delta p/p$, FWHM) and emittance (ϵ, non-normalized, rms). In most cases, due to the very low values of these parameters, their measurement is extremely difficult to perform and interpret; these small values also lead to very low space charge current limitations and threshold currents for instabilities. On the other hand, these same beam properties make the ring an ideal laboratory for studying nonlinear beam dynamics and beam instabilities. A model is conjectured which predicts a suppression of synchrotron oscillations within the bunch leading to a much smaller momentum spread than one would expect when interpreting measurements using the standard independent particle model for the beam.

In the last part of this paper the practical application of beam diagnostics is discussed, and our ambitious plans to make a self-tuning accelerator are outlined.

I. EQUILIBRIUM BEAM PROPERTIES OF AN ELECTRON COOLED PROTON BEAM

I.A. Equilibrium momentum spread

In the absence of intrabeam scattering and space charge effects, the rest frame longitudinal proton beam energy spread is expected to be[1] on the order of $k(T_{e\perp}T_{e\parallel})^{1/2}$, where k is the Boltzmann constant; $T_{e\perp}$ the electron beam transverse temperature, $\approx$ 1300 K or 0.12 eV/k (due to the cathode temperature); and $T_{e\parallel}$ is the longitudinal electron beam temperature, $\approx 2 \times 10^{-04}$ eV/k (determined by longitudinal-longitudinal and longitudinal-transverse electron beam intrabeam scattering)[2]. The lab frame $\Delta p/p$ (FWHM) is $\approx 2.35 \cdot [k(T_{e\perp}T_{e\parallel})^{1/2}/M\beta^2c^2]^{1/2}$ $\approx 2 \times 10^{-05}$ ($\beta = 0.3$, see Eq.(5)). Magnetized cooling effects are theorized[1] to possibly lead to ever smaller proton beam longitudinal temperatures, on the order of $T_{e\parallel}$. However, for currents above a few μA, proton beam intrabeam scattering is expected to determine the equilibrium momentum spread; indeed, systematic measurements of the coasting beam momentum spread as a function of current appear to show the expected $I_p^{2/5}$ scaling[3].

The coasting beam momentum spread can be measured using Schottky signals, though for currents above a few tens of μA, where the beam has exceeded the Keil-Schnell stability limit, the interpretation is nontrivial[4,5]. Even for lower currents, due to the time involved in the measurement process, one can only measure the time-averaged momentum spread rather than the instantaneous momentum spread. The lowest measured momentum spreads[3] are typically a few $\times 10^{-05}$, with the exception of measurements at Novosibirsk which were as low as a few $\times 10^{-06}$, and which interpreted using a different model.

Measurement of the bunched beam momentum spread, on the other hand, at first glance seems quite straightforward: since there is a simple relation between the momentum and phase spreads of a bunch in an rf bucket, it seems that one need only to measure the beam time spread using a high bandwidth longitudinal pickup. Using this technique at face value, we typically measure bunched beam relative momentum spreads of about 1×10^{-04}; however, as discussed below in the section concerning space charge limits, these measurements indicate that the rest frame electrostatic potential energy across the bunch is much greater than the rest frame kinetic energy spread for beam currents in excess of a few μA; consequently this simple-minded interpretation is probably not correct.

I.B. Equilibrium emittance

The expected proton beam transverse temperature is $\frac{1}{2}kT_e$ when the proton beam is in equilibrium between cooling and diffusion from the electron beam[6,7]. For typical beta functions of 5 m, the equilibrium emittance would be $\approx$ 0.005 $\pi\mu$m. Emittances about a factor of 4 times smaller are expected in the magnetized cooling regime[8]. Two attempts[9,10] to measure the emittance at IUCF have resulted in measurements of our detector resolution ($\leq$ 0.05 and $\leq$ 0.02 $\pi\mu$m). We are presently building a single pass flying wire scanner to measure the profiles of a 2 A, 2 MeV electron beam[11]. This scanner will first be installed in the cooling ring for tests and may be able to resolve the beam emittance.

*This work is supported in part by a grant from the National Science Foundation (Grant No. NSF PHY 90-15957).

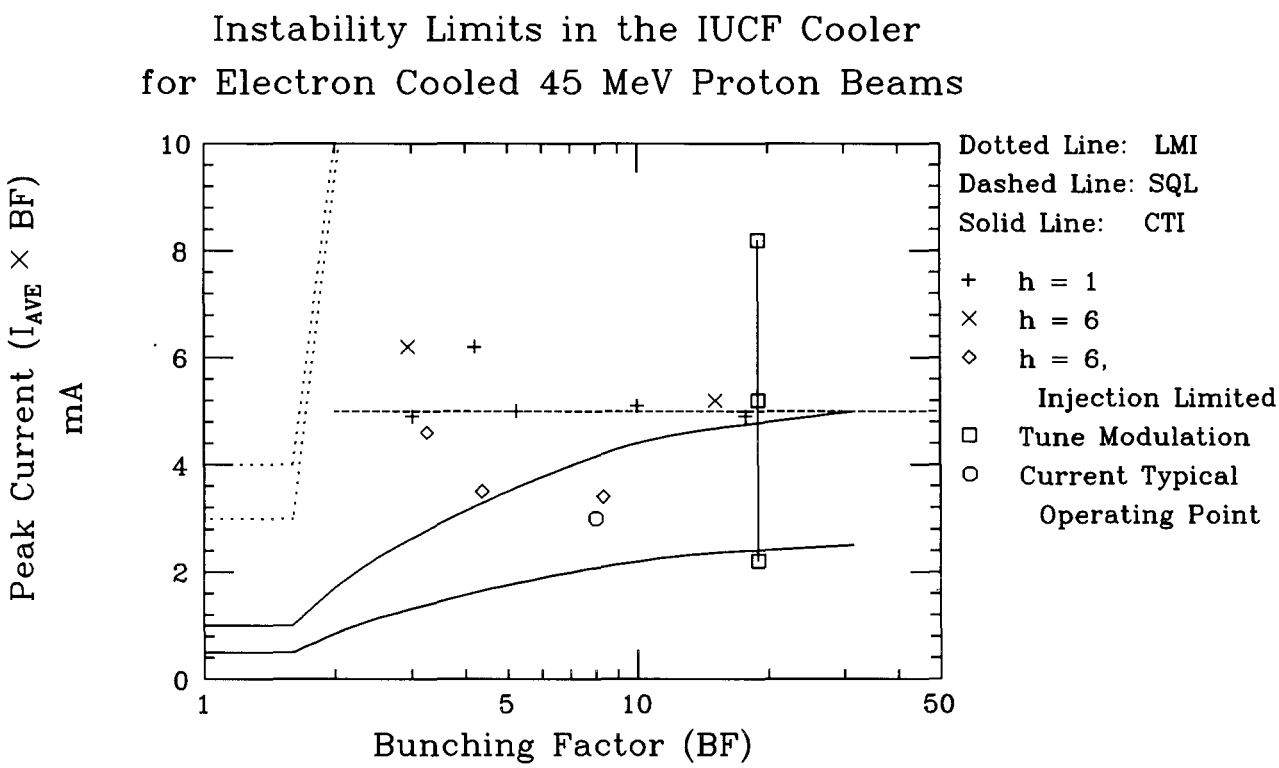


Figure 1. Threshold currents for various instabilities for electron cooled beams in the IUCF Cooler. These curves are based upon measurements and extrapolated according to theory.

The interpretation of these profiles may not, however, be so straightforward: as discussed below in the section concerning space charge limitations, taken at face value these profiles indicate that the particle rms electrostatic potential energy spread is a significant fraction of the rms transverse kinetic energy.

I.C. Intensity limits due to the very cold beams

These cold beams occupy ≈ 2% of the accelerator momentum aperture, and ≈ 0.1% of the transverse acceptance in each plane. This very high phase space density leads to severe limits on the beam intensity: the longitudinal instability threshold current scales as $(\Delta p/p)^2$; the transverse instability threshold current scales as $(\Delta p/p)$; and the space charge current limit scales as ϵ.

In Figure 1 the peak threshold currents (the DC beam current times the bunching factor, B_F (i.e. $B_F = I_{peak}/I_{average}$)) for various current limitations are plotted as a function of B_F for electron cooled 45 MeV protons in the IUCF cooler[12]. The intensity limitations are a function of B_F since as B_F increases from 1 to about 50, the beam momentum spread typically increases roughly a factor 5. The dotted line shows the threshold peak currents for longitudinal microwave instabilities (LMI); the solid curves show the range of threshold peak currents for coherent transverse instabilities (CTI), and the dashed line shows the peak current limitation due to what are presumably space charge effects (SQL).

The transverse instability limit has been removed with a damping system, so apparently a single limitation remains for $B_F > 2$: that due to space charge. This appears to be a "soft" limit: beam is lost at the same rate at which it is added to the ring; no "catastrophic" beam losses, such as occur with transverse instabilities, are observed. Similar "soft" limits seen in electron-positron colliders are tentatively attributed to the beam-beam tune shift[13].

The IUCF system of cyclotrons, with its relatively poor transmission efficiencies, cannot inject enough *uncooled* beam into the ring to reach the *cooled* beam intensity limits. Cooling is then used to accumulate beam until these limits are reached. These limits, as mentioned above, appear to be one or two orders of magnitude lower than the limits would otherwise be for uncooled beam.

Consequently, the technique (electron cooling accumulation) which allows beam accumulation, also precipitates the limitations which prevent the further beam accumulation. We are presently experimenting with methods of transverse beam "heating" to increase the space charge limits. This is a bit more difficult than it sounds since the effects which heat the beam also limit our ability to accumulate beam.

II. THE BEAM SPACE CHARGE

II.A. An interesting variety of ways in which to express the beam space charge tune shift

II.A.1. The space charge tune shift model

It is well known that the large space charge defocussing forces of high intensity, low energy beams significantly affect beam optics. Ion source and electron beam designers routinely calculate the required lens strengths and optics as a function of beam current. Synchrotron people, who generally work with high energy beams having much smaller space charge effects (which scale as $I/(\beta\gamma)^3$ for a constant ϵ, where I is the beam current), refer to these "small" effects as the space charge tune shift, i.e., the small decrease in the transverse oscillation frequency of a particle in the machine. The betatron tune value, Q, (the number of transverse oscillations per revolution in the machine) typically scales as $\approx \gamma^{1/2}$, with low energy machines ($\gamma \approx 1$) exceeding this scaling ratio by about a factor of $\approx 2 - 5$ (the machine tune stays fixed though the beam energy changes). One considers a space charge tune shift, ΔQ_{SC}, of 0.3 to be very large, and the limit at which a machine should be designed to operate.

Although the mechanism of emittance blow up due to high space charge tune shifts is better known empirically than theoretically, the common intuitive model is that when the tune shift is large, particles will be shifted down onto strong (integer or half-integer Q) resonance lines, or that the nonlinear defocussing fields can drive a variety of higher order nonlinear resonances.

The space charge tune shift for a beam with a Gaussian transverse distribution may be expressed as[14]:

$$\Delta Q_{SC} = \frac{-B_F I R r_p}{2ec\beta^3\gamma^3\epsilon} \qquad (1)$$

where R is the effective machine radius, r_p the classical proton radius, e the proton charge, c the speed of light, and β and γ are the usual relativistic parameters.

II.A.2. Ratio of the rest frame potential to transverse kinetic energy of a particle in the beam

Another way to view the effect of space charge is to compare the ratio of the rest frame potential energy difference, PE^*, between a particle on axis and at the beam rms radius due to the beam space charge to the rest frame kinetic energy amplitude, KE^*, of a particle with action ϵ. This ratio can be expressed in terms of ΔQ_{SC}, again for a Gaussian distribution, (to within 10%) as:

$$\frac{PE^*}{KE^*} = 2\frac{\Delta Q_{SC}}{Q} \qquad (2)$$

In the IUCF Cooler where the transverse tunes are about 3.7 and 4.7, the ratio of the electrostatic potential energy to transverse kinetic energy is about 0.15 for $\Delta Q_{SC} = 0.3$ using the "average" value of the beta function (R/Q); however, locally in regions where the beta functions are more than an order of magnitude higher than "average", this ratio exceeds unity.

I.A.3. Ratio of the beam plasma frequency to the betatron oscillation frequency

It is also interesting to compare the beam plasma frequency, f_p, (i.e., the frequency at which the beam envelope will oscillate if disturbed) with the beam betatron frequency, $f_\beta = Qf_0$, where f_0 is the beam revolution frequency. Expressing this ratio in terms of the ΔQ_{SC}, on axis for a Gaussian distribution we have:

$$\frac{f_p}{f_\beta} \approx 2\sqrt{\frac{\Delta Q_{SC}}{Q}} \qquad (3)$$

This ratio is typically ½ in most machines operating with large space charge tune shifts. In weak focussing machines with low Q-values (i.e. $Q = 1.2$) this ratio can equal unity for a space charge tune shift of 0.3. (When this ratio is unity, $<PE^*>/<KE^*> = ½$). I would not be surprised to find an instability associated with this condition.

II.B. Longitudinal space charge effects

Since the typical energy spread of a bunched 45 MeV proton beam is on the order of 10 keV, and the total space charge depression across the beam on the order of 0.5 eV, one might naively expect that the space charge has a negligible effect upon the longitudinal beam dynamics. This, however, is not the case. The rest frame electrostatic potential difference between the tails and center of a bunch, PE^*_{TOTAL}, is given approximately by:

$$PE^*_{TOTAL} \approx \frac{2B_F I r_p}{ec}\frac{Mc^2}{\beta\gamma}\left(\left[\frac{1}{2} + \ln\frac{r_v}{r_b}\right] \approx 5\right) \qquad (4)$$

where M is the proton mass, r_v the vacuum chamber radius, and r_b the beam radius. Eq. (4) is correct to within 1% for a Gaussian transverse distribution with $r_v \gg r_b$ if the ½ is neglected and σ is used for r_b.

This potential energy difference is the same for nonrelativistic beams whether measured in the moving or rest frames. The beam kinetic energy spread, however, is *much* less in the moving frame than in the lab frame. In the moving frame, the beam kinetic energy spread, ΔE^*, in terms of the lab frame energy spread, ΔE, is given by:

$$\Delta E^* = \frac{\Delta E^2}{4W}, \quad \text{(nonrelativistic)}$$
$$= \tfrac{1}{2} Mc^2 \beta^2 \left(\frac{\Delta p}{p}\right)^2, \quad \text{(relativistic)} \qquad (5)$$

where W is the beam kinetic energy.

In the IUCF cooler, for a modest beam current of 100 μA, B_F = 15, W = 45 MeV, and ΔE equal to 10 keV, the ratio $PE^*_{TOTAL}/\Delta E^* > 5$. Consequently we cannot, as mentioned above, trivially discern the beam momentum spread from its phase spread. This effect is elaborated upon in the following two sections.

III. Nonlinear Beam Dynamics Studies

These beam properties which are a bane for the accelerator physicist trying to maximize the stored beam intensity, are a boon for the accelerator physicist wishing to study nonlinear beam dynamics. The very low beam momentum spread and emittance allow the mapping of nonlinear phase space with high resolution and provide relatively large decoherence times for both longitudinal and transverse induced coherent oscillations. In other words, the beam bunch behaves very much like a single macro particle. An example of a transverse phase space map[15], i.e., a turn by turn mapping of the beam bunch in phase space, is shown in Figure 2.

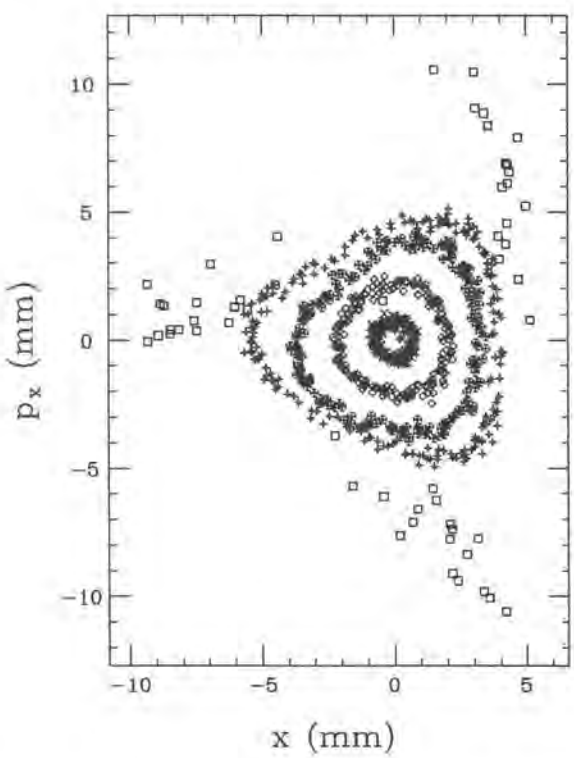


Figure 2. Poincaré map for motion near the 3rd integer resonance.

In the most simple-minded model one expects transverse oscillations to principally decohere due to the machine chromaticity, $\xi = (\Delta Q/Q)/(\Delta p/p)$; though there is also decoherence from the effect of octupolar fields which cause the tune to vary linearly (quadratically) with the betatron amplitude (action). In our machine, the first effect should dominate. The natural chromaticity for a machine is typically about - 1.3. Consequently, with a momentum spread of about 1×10^{-04} and $Q \approx 4.75$, we expect significant decoherence in less than 10^3 turns. If the synchrotron period (longitudinal oscillation period) is much shorter than this, and if we only consider linear chromaticity, the coherence time should be extremely long. This is not the case in our machine, yet it is not unusual to observe coherence for 10^4 or more turns!

Similar effects have been observed in longitudinal phase space. Artificially-excited longitudinal oscillations have been observed to stay coherent for 1 or 2 orders of magnitude longer than a single-independent particle model would predict given the beam time spread and consequently synchrotron tune spread.

Consequently, the electron-cooled beam bunches behave even more ideally than we ever expected; this is good news, but the question remains, why does the electron-cooled beam behave orders of magnitude more like a single particle than an ensemble? Here I conjecture the unexpectedly-long decoherence times are due to the longitudinal space charge effects mentioned earlier. Due to the high ratio of the rest frame particle electrostatic potential energy to kinetic energy, particles are not freely rotating in the bucket (i.e., the expected phase focussing); instead, the conservative electrostatic forces which are trying to make the beam expand, are in equilibrium with the conservative force from the rf cavity. This behavior in longitudinal phase space can also explain the unexpectedly large transverse decoherence times as well, since the beam momentum spread may be significantly lower than what we simplistically infer from a measurement of the beam time spread. In the following section I model this conjecture quantitatively.

IV. Theory of a Stable Bunch With No Decoherence

IV.A. Model development

Let us conjecture that the equilibrium proton beam momentum spread is essentially zero; let us further conjecture that the bunch will coherently oscillate at the nominal synchrotron oscillation frequency, but particles within the bunch will not due to the space charge forces: in other words, the space charge forces trying to expand the bunch are exactly balanced by the forces exerted upon the beam by the rf cavity which is trying to compress the beam. Starting with this conjecture we can solve for the equilibrium beam distribution.

Since the typical bunch length, a few meters, is so much greater than the vacuum chamber radius, $r_v \approx 0.04$ m, we can easily find the longitudinal force exerted on the particle by the beam electromagnetic forces: it is merely the derivative of the potential energy of a particle on axis with respect to the longitudinal coordinate, s. (Note: as in Eq. (4), the logarithmic term is an order of magnitude larger than the constant term, ½, for a well cooled beam so the spread in potential energy across the beam transverse dimension is neglected; here, I use $\ln(r_v/r_b) = 5$.) In the laboratory frame we can express this force, $F_\parallel$, as:

$$F_\parallel(s) = \frac{-10Mc^2 r_p}{ec\beta\gamma^2}\frac{dI(s)}{ds} \qquad (6)$$

where $I(s)$ is $\beta c\rho_l(s)$, with $\rho_l(s)$ the beam linear charge density. Noting that $F^*_\parallel = \gamma F_\parallel$, and $f^*_0 = \gamma f_0$, the change in rest frame momentum per turn in the machine, Δp^*_{SC}, for particles as a function of s due to the beam space charge is:

$$\Delta p^*_{SC} = \frac{4\pi\ln(r_v/r_b)}{\beta^2\gamma^2}\frac{Rr_pM}{e}\frac{dI(s)}{ds} \qquad (7)$$

The particle rest frame momentum change per turn, Δp^*_{rf}, due to the rf system operating with a waveform $V_o\sin(sh/R)$, on the other hand, is given by (using Eq. (5)):

$$\Delta p^*_{rf} = \frac{heV_o}{\beta\gamma c}\frac{s}{R} \qquad (8)$$

where V_o is the rf amplitude, and h is the harmonic number. We have assumed short bunches (i.e. $hs/R \ll 1$).

We can then, following our assumption of a stationary bunch, set $\Delta p^*_{SC} + p^*_{rf} = 0$ and solve for $dI(s)/ds$:

$$\frac{dI(s)}{ds} = \frac{\beta\gamma h}{4\pi\ln(r_v/r_b)}\frac{eV_o}{Mc^2}\frac{ec}{R^2r_p}s \qquad (9)$$

Equation (9) can then be integrated to yield the parabolic current distribution, $I(s)$:

$$I(s) = \frac{\beta\gamma h}{8\pi\ln(r_v/r_b)}\frac{eV_o}{Mc^2}\frac{ec}{r_p}\frac{L_B^2 - s^2}{R^2}, \quad |s| < L_B$$
$$= 0, \quad |s| > L_B \qquad (10)$$

where L_B is the full bunch half width, and we have used the constant of integration to set the beam current to zero at the end of the bunch.

Consequently, a parabolic beam distribution could possibly be stable. We also note that the central portion of a Gaussian distribution is parabolic.

To see whether this model is at all sensible, we integrate the current distribution to find the total current and a relation between the average current and the bunching factor:

$$I_{DC} = \frac{h}{\pi R}\int_0^{L_B} I(s)\,ds$$
$$= \frac{9\pi\beta\gamma}{32h\ln(r_v/r_b)}\frac{eV_o}{Mc^2}\frac{ec}{r_p}B_F^{-3} \qquad (11)$$
$$\text{where } B_F \equiv \frac{3\pi R}{2hL_B}$$

We note that the bunching factor, B_F, (see section I.C) is equal to the FWHM time spread divided by the rf period to within 10% for either a Gaussian or parabolic distribution.

VI.B. Numerical example and discussion

For an example we take a 100 μA, 45 MeV proton beam bunched on the first harmonic with an rf amplitude of 50 V in the IUCF Cooler which has a circumference of 87 m. Eq. (11) predicts an equilibrium bunching factor of 9.2 for $\ln(r_v/r_b) = 5$. A rough measurement of the bunching factor for these parameters yielded a value of 12.9. In general, rough measurements of the bunching factor agree with this model to about 20%.

At this point these ideas are still pure conjecture. However, the fact that the predictions are so close to what is observed sparks some interest. The discrepancies

between the measurement and model may be accounted for by differences in the actual and assumed values for $\ln(r_v/r_b)$. This model also provides a mechanism to explain why we do not observe the expected decoherence of longitudinal oscillations in the ring (i.e., the bunch is stationary), as well as an explanation for the long decoherence time of transverse oscillations (i.e. the beam momentum spread may be significantly lower than we have estimated in the past).

Even if this model is not exactly correct, some similar model is necessary in order to account for the large ratio of beam rest frame potential energy to *apparent* longitudinal kinetic energy, and the ratio of space charge force to rf force. Other, less probable, explanations for the long decoherence times being explored include effects arising from intrabeam scattering or the excitation of high frequency cavity structures in the ring by the beam.

In some future beam development period we will make careful measurements of both the beam bunch shape and bunching factor as a function of intensity and rf voltage while operating in the mode where no decoherence of large amplitude longitudinal oscillations are observed. The bunch length should oscillate about the stable beam size. It should be possible to induce these oscillations by stepping or modulating the rf amplitude; these oscillations can be measured as a test of this model.

This model is of course only applicable to high intensity electron cooled beams.

V. The Usefulness of Beam Diagnostic Systems

V.A. Editorial comments

The usefulness of a beam diagnostic system for an accelerator operator does not increase linearly with the effort put into it. My impressions of this phenomenon are summarized in Table I. For example, let us suppose we install a wire scanner at the output of the cyclotron preceding a complex beamline. A beam physicist might use this device during a study period and, per chance, find something interesting which could lead to an improvement in operations. The second step would be to install a convenient operator interface. Then its usefulness at least triples: the operators will learn how the beam looks when things are "good" and use this diagnostic as feedback to help achieve this "good" state; operations will certainly benefit. One could then take the final significant step: why not have the computer automatically scan a preceding quadrupole, measure the beam emittance, and then adjust upstream quadrupoles so that the beam emittance entering the line is just as it ought to be?

Table I. Percentage of the potential usefulness of a beam diagnostic system which is achieved as a function effort.

Diagnostic System Components		
	Work	Usefulness
Hardware	45%	10%
User Interface	15%	30%
Expert System	40%	100%

In many respects, at IUCF we are still in stages I and II:

--We have a system which allows the tracking of a single beam bunch in 6 dimensional phase space, yet the operator doesn't know what the tune is, let alone have a system to automatically measure and correct the tune during a ramp.

--We can measure and display the beam position in the Cooler with a precision of 50 μm and bandwidth of 100 kHz, yet the operator does not have a fool-proof user-friendly method of correcting the closed orbit.

On the other hand, we are beginning to make the first steps to create a self-tuning accelerator system. In the following two sections I summarize some of these activities.

V.B. Recent and future hardware developments

Some of the work completed since the last cyclotron conference includes:

--The addition of gridded klystron pre-bunchers to both ion source high voltage terminals. The rf systems for these bunchers are phase-locked to the beam. The use of these systems has increased the beam transmission efficiency through the cyclotrons from a nominal value of about 1.5% to as high as 9%, as shown in Figure 3.

--An rf phase feedback system has been installed in the Cooler. This system allows nearly perfect transmission efficiency. Without this system, acceleration is nearly impossible.

--A transverse beam damping system has enabled a 4 fold increase in the amount of coasting beam which can be stored in the cooler.

The these projects, which have all enhanced operations, share one common feature: feedback from the beam to control a device. We are now trying to use diagnostic systems for feedback on a much broader scale.

Another project under development is a digital signal processor system which takes data from the phase space tracking system and calculates the tune. A phase-locked loop, locked to the beam, will allow the digitizing system to accurately sample the beam even for currents as low as a few tens of nA even during acceleration. This system will give the operators an online-tune measurement, and allow tracking of the tune up the ramp: a measurement which has not been made in several years. Of course, the

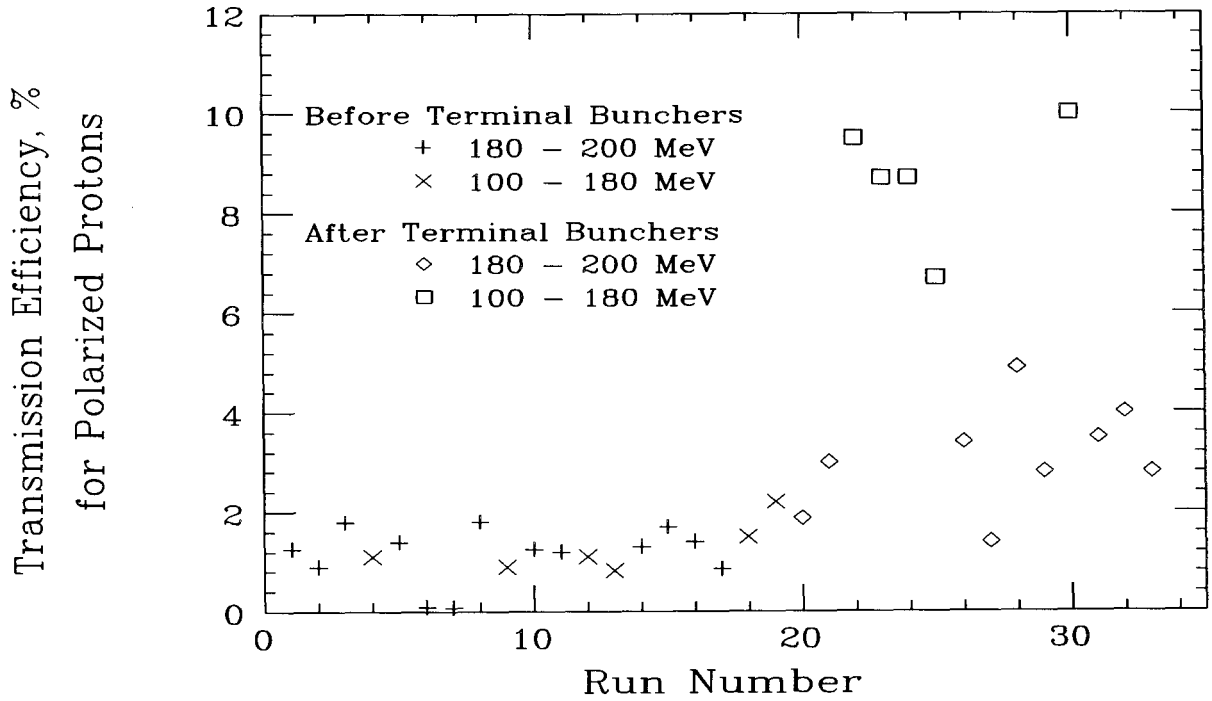


Figure 3. Effect of terminal bunchers. The numbers are from the operations logbook, not "typical" results obtained during beam studies.

next step will be to have the computer correct the tune the tune during the ramp using this system.

Also in the Cooler a system is being developed to automatically measure the influence matrix: the effect each steerer has upon each BPM. This matrix will be inverted (or used in a multi-linear regression, or chi-squared minimization program) to correct the beam closed orbit.

V.C. Diagnostic feedback systems for a new beam transport line

A new 30 m beamline is under construction to transport a 0.6 MeV beam from the new high intensity polarized ion source[16] to the cyclotrons. The beam diagnostic systems for this line is our most ambitious project yet: beam feedback will be used to provide a unique error signal for *every* device in the beamline. This includes all quadrupoles, dipoles, steerers, and buncher amplitudes and phases. Here I briefly outline this system; a more thorough report can be found elsewhere in these proceedings[17].

V.C.1. Transverse beam diagnostic feedback systems

The basis of this system will be a new beam position monitor (BPM) system. The hardware, all contained on a single 4-layer board, will accept signals from 4 electrodes and calculate the beam horizontal and vertical position, intensity, and quadrupole moment at 100 kHz rates.

An automatic emittance measurement system will measure the beam phase space ellipse at the entrance to the line. A beam scanning system will then sweep the beam centroid along an ellipse of the same shape but reduced area. Consequently, the BPM system can monitor the beam envelope[18]. Linear combinations and ratios of the beam envelope at various BPM locations will provide polar-error signals for linear combinations of quadrupoles. There will be similar systems for automatic steering and dispersion correction. We also hope to implement an automated "pencil" beam scanning system to map the acceptance of the injector cyclotron.

V.C.2. Longitudinal beam feedback systems

The new wideband ramp-waveform terminal buncher and resonant beamline bunchers will be phase-locked to beam. Their amplitudes will be set using a Bunching Factor Diagnostic (BFD) to optimize the bunching factor. A feedforward system, using a nonintercepting beam intensity monitor (BIM), will adjust the buncher amplitude to compensate for space charge effects. We are also exploring installing amplitude and phase modulators with synchronous detectors using the BFD and BIM, respectively, to set the quiescent phases and amplitudes.

ACKNOWLEDGEMENTS

The beam diagnostic system hardware design and construction discussed in this paper is being principally performed by Mark Ball and Brett Hamilton in the IUCF Beam Dynamics Group. I look forward to them reporting on the success of their efforts at the next cyclotron conference.

IUCF has a noble tradition for accomplishing great things with little more than a single Simpson meter as a beam diagnostic system; consequently, we are warily treading on new ground. The impetus for creating an expert system approach has resulted from discussions with Derek DuPlantis, John Collins, Bill Jones and Dennis Friesel. To accomplish our goals we will be relying heavily on the entire IUCF technical staff.

Many thanks to Dave Caussyn for enjoyable discussions, and for his comments on this paper. I am also grateful to Peter Schwandt for his editorial comments.

ADDENDUM

Note: a number a minor misprints in the preprint were corrected in this final version, though none affect the conclusions. It was also pointed out to me at the Cyclotron Conference by Dag Reistad (Uppsala) that the dependence of the beam bunch-width on beam current is discussed in an Appendix to a preprint submitted for publication[19].

REFERENCES

1. Ya. S. Derbenev and A.N. Skrinsky, "The effect of an accompanying magnetic field on electron cooling", *Particle Accelerators*, **8** (1978) 235-243.

2. A.V. Alesandrov, N.S. Dikansky, N.Ch. Kot, V.I. Kudelainen, V.A. Lebedev, P.V. Logachov, "Temperature relaxation and adiabatic acceleration at magnetized electron flux", *Proc. Workshop on Electron Cooling and New Cooling Techniques* (15-17 May 1990, Padova-Italy, World Scientific, ed. by R. Calabrese and L. Tecchio) 279-291.

3. Helmut Poth, "Electron cooling, Theory, experiment, application", Phys. Reports **196**(3) (1990) 135.

4. V.V. Parkhomchuk and D.V. Pestrikov, "Thermal noise in an intense beam in a storage ring", Sov. Phys. Tech. Phys. **25**(7) (July 1980) 818-822.

5. I. Hoffman, et al, "Diagnostics and instabilities of cooled ion beams", Proc. EPAC 1990.

6. Ya. S. Derbenev and A.N. Skrinsky, "The kinetics of electron cooling of beams in heavy particle storage rings", Particle Accelerators **8** (1977) 1-20.

7. Allan H. Sørensen and Ejvind Bonderup, "Electron cooling", NIM **215** (1983) 27-54.

8. N.S. Dikansky, V.I. Kudelainen, V.A. Lebedev, I.N. Meshkov, V.V. Parkhomchuk, A.A. Sery, A.N. Skrinsky, V.N. Sukhina, "Ultimate possibilities of electron cooling", preprint 88-61, Inst. of Nuc. Phys., 630090, Novosibirsk 90, CIS.

9. Tim Ellison, "Electron Cooling", thesis Indiana University (1990).

10. M. Ball, D. Caussyn, S. Curtis, M. Ellison, T. Ellison, J. Frey, B. Hamilton, J. Frey, B. Lozowski, C. Merton, T. Rinckel, B. Jones, P. Dittner, "Measurement of the equilibrium emittance of an electron-cooled 45 MeV proton beam", IUCF Newsletter No. 49 (4 September 1991, internal report, in print).

11. D.R. Anderson, M.S. Ball, D. Caussyn, M.J. Ellison, T.J.P. Ellison, W. Fox, D. Friesel, B. Hamilton, S.Y. Lee, S. Nagaitsev, P. Schwandt, J. Adney, J. Ferry, M. Sundquist, D. Reistad, M. Sedlacek, "Design of a 6 MeV electron cooling system for the SSC Medium Energy Booster", *Proc. EPAC 92* (Tech. U. of Berlin-Germany, 24-28 March 1992).

12. Mark Ball, Dave Caussyn, Tim Ellison, Brett Hamilton, and S.Y. Lee, "Cooler intensity limitations", IUCF Newsletter No. 49 (4 September 1991, internal report, in print).

13. Maury Tigner, Cornell, private communication, 1992.

14. B. Zotter, "Betatron frequency shifts due to image and self field", in *CERN Accelerator School, General Accelerator Physics*, eds. P. Bryant, S. Turner, CERN 85−19, p. 253.

15. D.D. Caussyn, M. Ball, B. Brabson, J. Collins, S.A. Curtis, V. Derenchuck, D. DuPlantis, G. East, M. Ellison, T. Ellison, D. Friesel, B. Hamilton, W.P. Jones, W. Lamble, S.Y. Lee, D. Li, M.G. Minty, T. Sloan, G. Xu, A.W. Chao, S. Tepikian, K.Y. Ng, "Experimental beam dynamics at the third order resonance", *Proc. EPAC 92* (Tech. U. of Berlin-Germany, 24-28 March 1992).

16. V. Derenchuk, M. Wedekind, R. Brown, T. Ellison, D. Friesel, J. Hicks, D. Jenner, A. Pei, H. Petri, P Schwandt, J. Sowinski, "Performance and status of the IUCF high intensity polarized ion source", these proceedings.

17. W.P. Jones, T.J.P. Ellison, M.S. Ball, J.C. Collins, D. DuPlantis, D.L. Friesel, B. Hamilton, J.W. Hicks, and P. Schwandt, "Beam transport system for the IUCF high intensity polarized ion source", these proceedings.

18. Though, as noted by Jeff Stetson at the Cyclotron Conference (private communication), this system will not show any beam envelope changes due to the beam space charge.

19. Yu. Ts. Oganessian, O.N. Malyshev, I.N. Meshkov, V.V. Parkhomchuk, P. Pokorny, A.A. Sery, S.V. Stepantsov, Ye.A. Syresin, G.M. Ter-Akopian and V.A. Timakov, "The project of the heavy ion storage ring complex K4-K10 and possibilities of producing, storing and cooling radioactive ion beams" (submitted to T. Phys. A).

COSY-JÜLICH A SYNCHROTRON AND STORAGE RING FOR MEDIUM ENERGY PHYSICS

R. Maier, U. Pfister for the COSY-Team,
Forschungszentrum Jülich (KFA) GmbH, Postfach 1913, 5170 Jülich, Germany

ABSTRACT

At present the cooler synchrotron COSY a synchrotron and storage ring for medium high energy physics is being built at Jülich. The cooler ring will deliver protons in the momentum range from 270 to 3300 MeV/c and has the option to accelerate $^{3}He^{2+}$, $^{12}C^{6+}$, $^{16}O^{8+}$ and $^{20}N^{10+}$ ions. The maximal number of stored protons will be $2 \cdot 10^{11}$. The phase space density of the circulating protons will be increased with electron cooling between the injection level and 600 MeV/c. The stochastic cooling system is designed to cool protons in the momentum range between 1500 and 3300 MeV/c. For external experiments averaged intensities up to $\simeq 2 \cdot 10^{8}$ cooled protons per second are expected with a duty cycle of $\simeq$ 50% on quite narrow target spots. High luminosities can be achieved with solid targets in the internal beam.

The lattice parameters to match the different ion optical requirements for electron and stochastic cooling, acceleration, internal experiments and slow extraction are discussed. An overview of the ion sources, the injector cyclotron, the injection and extraction beamlines is given. Field measurements on the dipol and quadrupol magnets are reported. The results of the commissioning of the power converters and of the accelerating cavity are shown. The results on the sensitivity measurements of the beam position monitors are explained.

1 INTRODUCTION

The COSY facility consists of different ion sources, the cyclotron JULIC as injector, the injection beamline with a length of 100 m, the ring with a circumference of 184 m and the extraction beamlines to the external experimental areas. The high resolution beamline to the magnetic spectrometer BIG KARL, the beamline to the Time of Flight spectrometer (TOF) and the beamline for medical therapy application[1] are under construction. In a later stage a fourth beamline will be added for polarization measurements. The layout of the COSY facility is shown in Fig. 1.

The lattice of the COSY ring consists of two 52 m long 180^{0} bending sections, which are separated by two 40 m long straight sections. The straights are designed as telescopic systems with a 1:1 image from the beginning to the end with a phase advance either π or 2π. Bridged by four optical triplets one straight section is dedicated to two internal target places TP 1 and TP2. The opposite straight section provides free space for the rf cavity, the electron cooler[2], scrapers, Schottky pick-ups and current monitors.

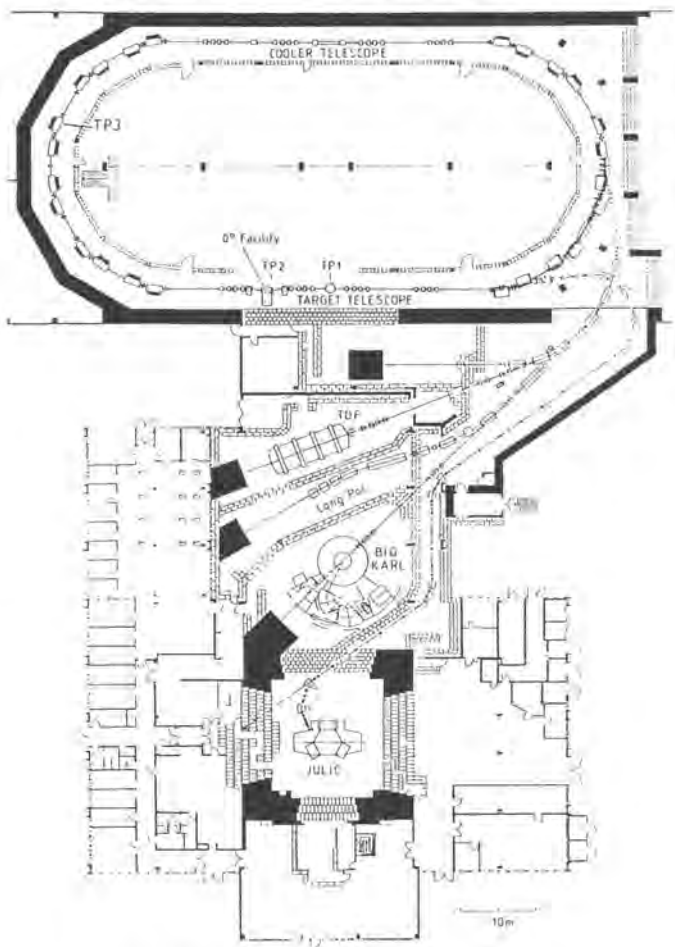


Fig. 1. Layout of the COSY facility.

The two arcs are composed of six mechanically identical periods. Each of the mirror symmetric half cells is given a QF-bend-QD-bend structure leading

to a six-fold symmetry of the total magnetic lattice. By interchanging the focussing and defocussing properties additional flexibility for adjusting the tune is achieved.

One of the bending arcs houses the injection and extraction devices, the stripping target, the magnet septum and bumper magnets for injection as well as the electrostatic and magnetic septa for extraction. The other arc offers space for a third internal target area TP3, which will make use of one of the ring magnets to separate 0^0 ejectiles, the diagnostic kicker and the elements for the ultra-slow extraction. At the intersection between straight sections and arcs the stochastic cooling pick-ups and kickers[3] will be installed. The basic machine parameters are summarized in Table 1.

Table I
COSY Basic Parameters

Vacuum system	
pressure	10^{-10}-10^{-11} mbar
in the arcs	rectangular 150·60 mm²
in the straights	circular, ϕ 150 mm
RF system	
cavity type/ acceleration structure	symmetric re-entrant ferrite loaded
frequency range (h=1)	0.462-1.572 MHz
quality factor (at frequency)	8(400 kHz), 40(2 MHz)
max. rate of frequency increase	4 MHz/s
gap voltage (at duty cycle)	5 kV (100%), 8 kV (50%)
gap voltage dynamic range	55 dB
nominal/actual rf power	56/16 kW in push-pull
bending magnets	
number	24
radius	7 m
angle	15⁰
field range	0.23-1.585 T
quadrupole magnets in the arcs	
number	24
no. of families	6
eff. length	0.3 m
aperture radius	85 mm
max. gradient	7.5 T/m
quadrupole magnets in the telescopes	
number	32
no. of families	8
eff. length	0.55 m
aperture radius	85 mm
max. gradient	7.5 T/m
sextupole magnets	
number	18
no. of families	7
eff. length	0.3/0.2/0.1 m
aperture radius	85 mm
max. strength	30 T/m²

The magnetic lattice of the ring has to match different ion optical conditions:

(i) the internal targets require low betatron functions and low dispersion

(ii) the slow extraction needs the horizontal tune near a third order resonance

(iii) the stochastic cooling demands a phase advance close to $(2n+1)\cdot\pi/2$ between the pick- up and kicker location for both planes

(iv) the electron cooler prefers low betatron amplitudes

These requirements can be fulfilled with the chosen working point. The beam and optical properties are listed in Table 2.

Table II
Beam and Optical Properties of COSY

momentum range	270-3300 MeV/c		
max. no. of stored protons	$2\cdot10^{11}$		
horizontal/vertical tune	3.38/3.38		
transition momentum	1860 MeV/c		
geometrical acceptance	horizontal: 130 π mm mrad vertical: 35 π mm mrad Δp/p: ± 0.5%		
nat. chromaticity hor./vert.	- 5.2/- 4.5		
lattice function at	β_{hor}	β_{vert}	dispersion
TP1:	5.6 m	5.9 m	0 m
TP2:	1.6 m	5.1 m	0 m
TP3:	6.0 m	22.2 m	10.1 m

radii and divergences for an extracted emittance of 2.5 π mm mrad and Δp/p of $1\cdot10^{-3}$ at

	x/mm	x'/mrad	z/mm	z'/mrad
medical therapy area	3.25	1.34	1.88	1.24
Time of Flight	0.56	4.90	0.72	3.47
BIG KARL	0.45	7.14	0.43	6.92

2. ACCELERATOR COMPONENTS

2.1. Field Measurements of the Bending and the Quadrupole Magnets

The measurements of the bending magnets were done with sets of long coils, covering the whole beam field region. Seen in beam direction there are a long coil, two short coils located in the homogeneous part of the field and a second long coil. The coils are imbedded in a rod made from carbon fibre to be mechanically rigid. This coil support is driven across aperture of the magnet. Voltage induced in the coils are integrated. The reproducibility of the $\int$Bdl measurement is in the order of 10^{-5}.

Figure 2 shows after shimming the relative deviation of $\int$Bdl of the individual magnets from the mean value of $\int$Bdl of all dipole magnets. The identity of the individual 24 dipole magnets is better than $2\cdot10^{-4}$.

The field components of the quadrupole magnets are determined on a measuring bench with slowly rotating coils. The quadrupole as well as the dipole component are compensated by a bucking coil, with

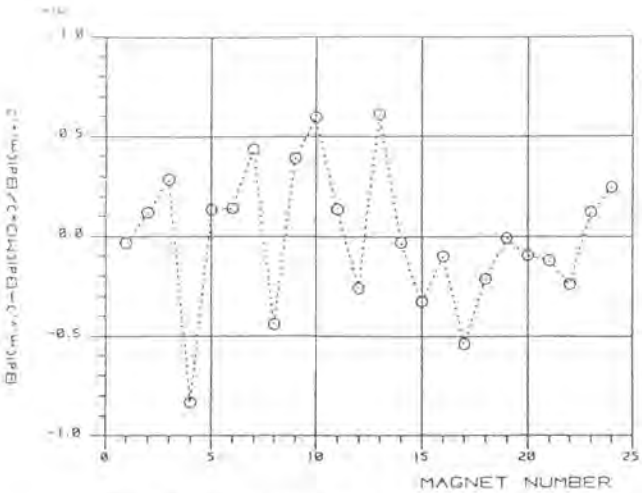


Fig. 2. Relative deviation of $\int$Bdl of the individual dipole magnets with respect to the mean value of $\int$Bdl of all the dipole magnets.

maximum sensitivity for harmonics n $\geq$ 3. The achieved supression of the quadrupole term was $\sim 10^{-3}$. The measuring probe consists of 3 sets of compensated coils. One long set integrates over the whole length of the magnets, the other two are integrating at the entrance and the exit sides of the quadrupole from inside the magnet to the field free region. After aligning the quadrupole on the measuring bench the excitation curve, the harmonic content as well as the gradient are measured for a number of currents. The gradient is deduced from the difference between the long coil and the two short coils. The relative deviation of $\int$gdl of the individual quadrupole magnet with respect to the mean values of $\int$gdl of all quadrupole magnets is shown in Fig. 3. Besides the quadrupole No. 1 which is the prototyp, the identity is better than $4 \cdot 10^{-3}$.

2.2. Power Converter

Only one power converter feeds 25 dipole magnets connected in series via a busbar system. Due to iron saturation the inductance decreases at max. current of 5000 A from 300 mH to about 100 mH. The load is changing its characteristic from a power consuming to a generating device at a current value of about 2600 A. This requires for proper operation two set values, the current set value and the set value for the output voltage. Figure 4 shows the actual current during ramping of the dipole magnet together with the difference signal of the actual current and the demanded current. During the ramping of the dipole the relative accuracy is better than $2 \cdot 10^{-5}$.

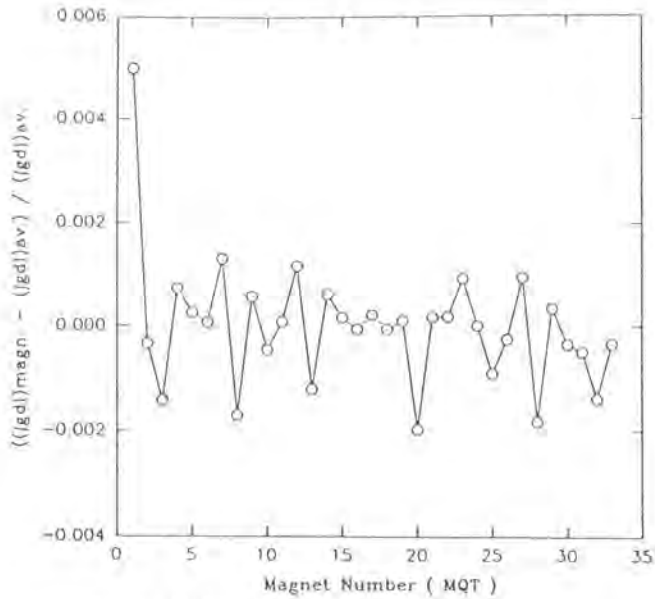


Fig. 3. Relative deviation of $\int$gdl of the individual quadrupole magnets MQT with respect to the mean value of $\int$gdl of all the quadrupole magnets MQT.

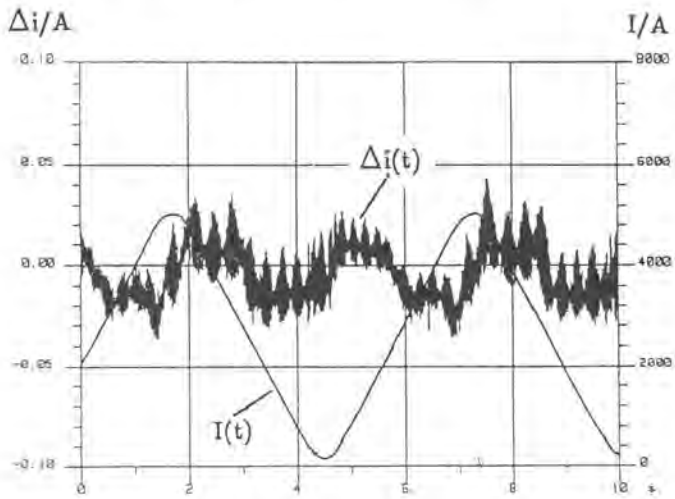


Fig. 4. Actual current I(t) during ramping and the differences Δi(t) of the actual current and the demanded current over the time t.

2.3. Accelerator System H = 1

The 50 kW rf acceleration system based on a ferrite-loaded coaxial cavitiy, has been developed in close cooperation with the Laboratoire National SATURNE and Thomson Tubes Electroniques. The accelerating system has been installed after measuring the rf properties with the extremely agile rf signal synthesizer for the control of the low level acceleration

signals. With this synthesizer the rf phase can be changed instantaneously. This rapid change of the acceleration phase of about 180^0 is necessary to pass through γ transition. Figure 5 shows the waveforms of the amplifier input and the resulting gap voltage during the phase switching procedure. The quality factor Q can directly be determined from the time of zero crossing of the envelope of the gap voltage. The relatively high Q factor of about 38 allows the realisation of a rapid phase switch.

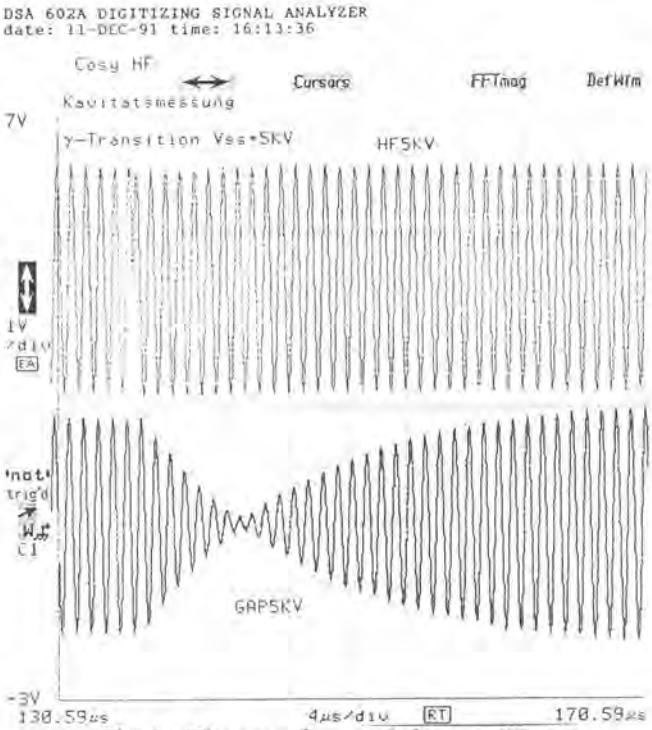


Fig. 5 The waveforms of the amplifier input and the resulting gap voltage during the phase switching procedure.

2.4. Beam Position Monitors

For measurement of the transverse sensitivity of the beam position monitors (BPM) a test bench was installed. A 2 MHz-signal was injected to simulate the bunch current. The quantity difference $\Delta(x)$ over the sum Σ of the electrode signals was measured in dependence of the position x. A linear dependend holds almost over the total BPM-aperture. This leads to a position sensitivity of 10^{-2} mm^{-1} in both planes of the cylindrical BPM. This value is in good agreement with the theoretical predictions. The position sensitivities of the rectangular BPM are $7.5 \cdot 10^{-3}$ and $2 \cdot 10^{-2}$ mm^{-1} in the horizontal and vertical plane, respectively. The amplitude sensitivity or transfer impedance of the cylindrical BPM was measured in a 50 Ω matched coaxial system.

The set up allows to inject a well defined signal for beam current simulation in a large frequency range. In the case of high impedances ($\geq$ 500 kΩ input impedance of the BPM preamplifiers) the transfer response is nearly constant in the frequency range 0.01-100 MHz. The transfer impedance of one electrode results to about 3 Ω in this frequency range. This agrees with the theoretical values for the transfer impedance of a particle, which moves with the speed of light.

3. SUMMARY

All magnetic elements for the ring, injection and extraction beam line have been installed in the final position. Measurements on stability, dynamic behaviour of the power converters with the final set ups of the magnetic elements are being completed. The commissioning of the injector cyclotron and parts of the injection beam line together with careful radiation protection measurement have been finished. The upgrade of the high resolution spectrograph BIG KARL is in progress. First injection into the cooler synchrotron and the commissioning are scheduled to start in autumn 1992. Start of users operation is aimed at April 1993.

4. ACKNOWLEDGEMENT

We would like to express our sincere thanks to our colleagues from accelerator laboratories around the world. We are indepted to the members of the machine advisory committee for their advice. We are grateful to the CANU members for stimulating discussions.

5. REFERENCES

1) Linz, U. and Maier, R., "A First Concept to Use the Cooler Synchrotron COSY-Jülich for Cancer Therapy," European Particle Accelerator Conference (EPAC), Berlin, March 1992.

2) Derissen, W., Maier, R., Pfister, U., Prasuhn, D., Sauer, M., Schwab, W., Schwarz, U., Sedlacek, M., Stein, H.J., Wimmer, J., Witt, J.D., and Zumloh, A., "Status of the COSY Electron Cooler," European Particle Accelerator Conference (EPAC), Berlin, March 1992.

3) Brittner, P., Hacker, H.U., Maier, R., Pfister, U., Prasuhn, D., Schug, G., Singer, H., Spieß, W., Stassen, R., Stockhorst, H. and Zumloh, A., "The Stochastic-Cooling System of COSY," European Particle Accelerator Conference (EPAC), Berlin, March 1992.

STUDY OF BEAM DYNAMICS AT COOLER SYNCHROTRON TARN-II

S. Watanabe, T. Katayama, T. Watanabe, M. Yoshizawa, M. Tomizawa, K. Chida,
Y. Arakaki, K. Noda * and M. Kanazawa*

Institute for Nuclear Study, University of Tokyo, 3-2-1 Midori-cho, Tanashi,
Tokyo 188, Japan

*National Institute for Radiological Sciences, 4-9-1 Anagawa , Inage-ku,
Chiba-shi 263, Japan

ABSTRACT

Several kinds of beam diagnostic instruments, have been developed at cooler-synchrotron TARN-II. These are intended to study beam dynamics at low beam current of several microamperes and then have high sensitivity of good S/N ratio. In addition, the acceleration system, especially low level RF system, has been improved to attain the maximum beam energy. With the successful performance of these instrumentations, the study of beam dynamics are presently being carried out. For example, the synchrotron acceleration of the light ions was achieved up to 220 MeV/u without any beam loss.

1. INTRODUCTION

TARN-II is a cooler-synchrotron with a maximum magnetic rigidity of 5.8 Tm, corresponding to 1.1 GeV for protons and 0.37 GeV/u for ions of charge-to-mass ratio of 1/2.[1] The ring has a circumference of 78 m and FBDBFO magnetic structure with a superperiodicity of 6. An injector is a sector-focusing cyclotron with K number of 68 which can accelerate a variety of ion beams supplied by ECR or PIG ion sources. Normally the intensity from the cyclotron is as low as several microamperes for light ions and almost two order smaller for heavy ions. To handle such a low current beam in the ring, we have developed several kinds of beam monitors[2] for the detection of beam positions, beam phase , DC beam current and Schottky signals. With the successful performance of these diagnostic instrumentations, the synchrotron acceleration, for example, was achieved up to 220 MeV/u without any beam loss. The vacuum, ion source and control system have been improved to perform an extended study of beam dynamics. The present paper summarizes the recent experimental results of beam dynamics studies at cooler-synchrotron TARN-II.

2. BEAM DIAGNOSTIC INSTRUMENTS

A permalloy core monitor, a travelling wave monitor, a DC beam monitor and electrostatic beam monitors, are used to measure the beam dynamics during injection, accumulation and acceleration batch. The layout of beam diagnostic instruments is given in Fig. 1.

The permalloy core monitor is placed at the straight section, S5. It comprises laminated permalloy tape of the average diameter of 210 mm with the initial permeability of around 10000. The sensitivity and time constant of the electronics system attached to the permalloy core, can be varied according to the beam conditioning. The typical sensitivity and the time constant are 0.2 microampere and 5 seconds, respectively.

The travelling wave monitor is placed at the straight section, S5 just upstream the permalloy core monitor. This is used for the detection of Schottky signals from the circulating beam. The structure of inner conductor is a helical type, of which the pitch is adjusted to equal to the beam velocity. The coherent beam signals from the bunched beam, such as the synchrotron oscillation frequency, can be detected with this monitor. The sensitivity for the coasting beam is around 1 microampere at a window frequency of 15 MHz with the signal averaging by the spectrum analyzer.

The DC beam monitor based on the magnetic modulation method has been constructed. It is placed at the straight section, S5 just behind the travelling wave monitor.

The DC beam monitor comprises the laminated amorphous cores with the average diameter of 230 mm. The record of the sensitivity is 0.5 microamperes at the time constant of low pass filter, 1 second.

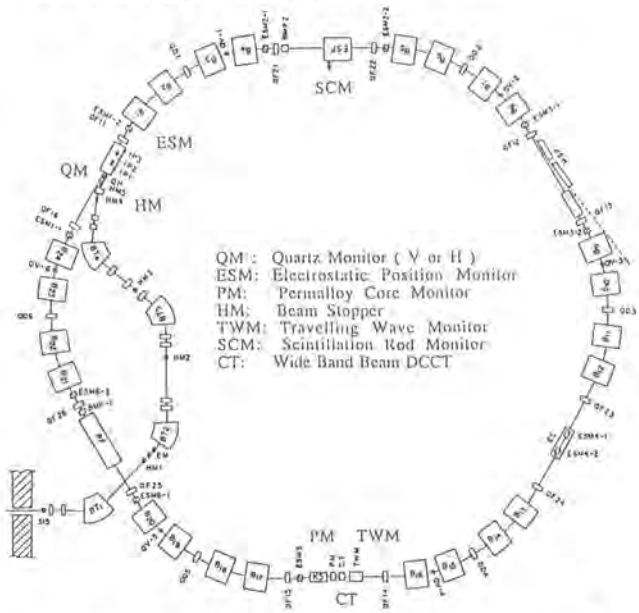


Fig. 1. Layout of beam diagnostic instruments at TARN-II.

To measure the bunched beam positions in horizontal plane, 8 sets of electrostatic monitors are installed at the straight sections, S1 to S6. Each electrostatic monitor comprises a pair of metal plates with a diagonal cut. Details of position monitors are given in the section 3. 2.

3. BEAM DYNAMICS STUDY

3.1 Beam Transport and Multiturn Injection

The ion source of injector cyclotron, is operated under a pulsing mode to increase an output current of the cyclotron. A repetition rate and a pulse width of the output current are 30 Hz and 3 ms, respectively.

The cyclotron and TARN-II is coupled with a beam transport line in 60 m length. A momentum spread and emittance of the injection beam are 0.1 % and 15π (mm.mrad), respectively. Transmission efficiency of the beam was measured as a function of the emittance and distance from the cyclotron. The measured results show that transmission of the 40 MeV α beam of 15π (mm.mrad) is about 45% at an entrance of the ring. The transmission of 13 MeV $^3He^1$ beam of 35π (mm.mrad) was about 15%.

The transported beam is injected into the ring with an electrostatic inflector at the straight section, S1. Optical elements of the ring and transport line, are to be matched to accumulate the beam as much as possible. The injected beam is accumulated into a transverse phase space of the ring by the multiturn injection method. The multiturn injection is performed by using a gradually decreased bump orbit generated by two pulse magnets at the straight sections, S2 and S6. The horizontal acceptance of the ring is designed to be 300π(mm.mrad). The maximum number of multiturn injection is then estimated at 17 turns.

3.2 Closed Orbit Measurement

The horizontal closed orbit around the ring, was measured with use of eight Δ–type electrostatic pickups, each connected by the head-and post-amplifiers. The capacitance between the inner pickup and the earth cover, is measured at typically 65 pF within the deviation of ±2%. The head amplifier, gain of 20 dB, is a low noise type and the measured noise level is as low as 1.7 nV/ √Hz. The amplified beam signals from right (R) and left (L) pickups are sent to a control room and analyzed with two spectrum analyzers of averaging fuction. The beam position are obtained by the relation, $\Delta R=K\cdot(V_R-V_L)/(V_R+V_L)$ where K is a constant determined by test bench experiments. A typical example of closed orbit is shown in Fig. 2 where the deviations of a closed orbit distortion (COD) are around ten mm's.

The correction of COD is performed using six correction coils, each wound on a bending magnet in a sextunt in the ring. The current in each correction coil is calculated so that the COD is to be minimized.

Machine parameters, such as the transition γ, local dispersion functions η, can be experimentally obtained by the closed orbit shift (ΔR) versus RF frequency (Δf) and the field strength of bending magnet (B). The measured values

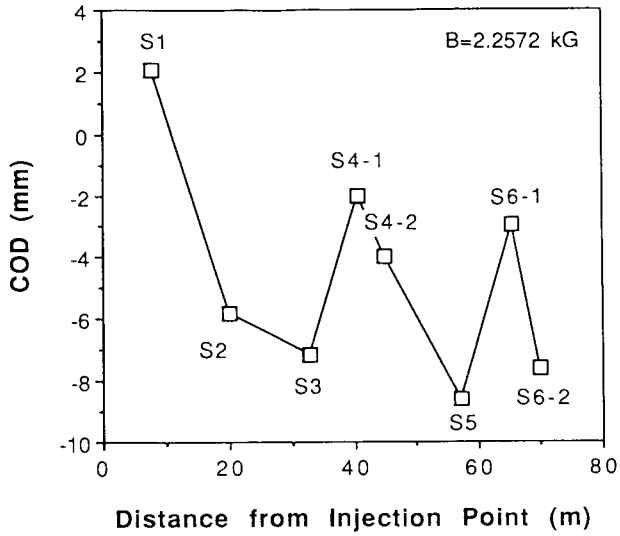


Fig. 2. Closed orbit distortion around the ring.

of ΔR/Δf and ΔR/ΔB are typically 5.62 (mm / kHz) and -2.70 (mm / Gauss), respectively which are around 20 % different from the calculated values by the computer code "MAGIC".

The vertical COD's are not yet measured. The COD calculation with MAD program shows that the maximum COD would be as large as 15 mm due to the rotation of bending magnets and the deviation of central axis of Q magnets. Therefore the vertical correction coils are prepared and the measuring system for vertical COD are now being constructed to improve the vertical ring acceptance.

3.3 Chromaticity Measurement

The horizontal and vertical betatron tunes ν_x, ν_y were measured as a function of beam momentum, and they were corrected with use of a sextupole magnet located just downstream a focusing quadrupole magnet at the straight section No. 5. The experimental procedure was as follows;

Injected beam was firstly captured by the RF field and was accelerated up to the required beam momentum, holding the magnetic field constant. Then the tune values were measured with the RF knockout method. The maximum fractional momentum variation Δp/p was around 1 %, corresponding to the horizontal movement of beam position 44.8 mm when the RF frequency was varied from 1.117 to 1.125 MHz. A current of sextupole magnet was adjusted to correct the horizontal tune values. In Fig. 3, the measured results are given as a function of fractional momentum change Δp/p. The horizontal tune ν_x is constant, chromaticity corrected, in the case that the current of sextupole magnet is 35A. On the other hand, the natural chromaticities, $\xi = (\Delta\nu/\nu)/(\Delta p/p)$ at Isextupole = 0, were measured at $\xi_x = -1.83$ and $\xi_y = 2.13$, respectively.

3.4 Beam Transfer Function

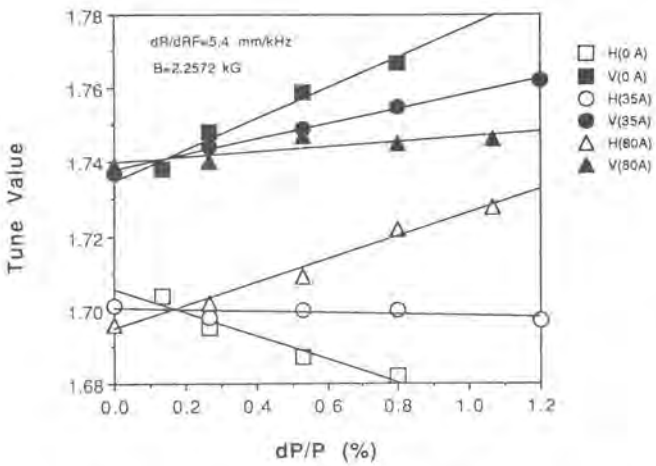


Fig. 3. Horizontal and vertical tunes vs. beam momentum.

A tracking generator, an analog spectrum analyzer, transverse and longitudinal Schottky signal detectors, a wideband power amplifier with the max. power of 60 watt, and a kicker are used for the measurement of beam transfer function. The kicker is composed of two sets of parallel plates, one is for the horizontal and the other for the vertical. The RF signals from the tracking generator are amplified and fed to the kicker. The longitudinal or transverse Schottky signals are detected by the electrostatic pickup, 1/6 circumference downstream the kicker. Schottky signals are observed on the spectrum analyzer with co-use of tracking generator. The strong signals are corresponding to coherent longitudinal beam oscillations, integer times the revolution frequency, whereas the non-coherent signals, two side band signals neighbouring the coherent signals, could be observed. They represents the betatron motions with the frequencies given by the following relation;

$$\omega_{x,y} = (m \pm \nu_{x,y}) \omega_{rev} ,$$

where m is an integer and ω_{rev} is a revolution frequency around the ring. Thus the precise values of betatron tunes

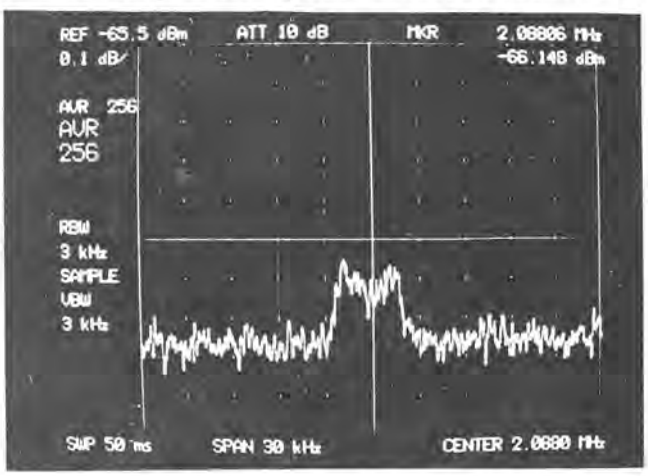


Fig. 4. Schottky signals of betatron sideband.

can be determined by the BTF measurement instead of RF knockout method. The observed ω_x has a finite spread as in Fig. 4 where the width of frequency Δf is 4.3 kHz, corresponding to m=2 and ν_x=1.7487, respectively . Normally this spread is due to the momentum spread of circulating beam and to the finite chromaticity , and is represented by the following formulation;

$$\Delta\omega_x = (\xi_x + (m \pm \nu_x) \eta) \cdot \Delta p/p \cdot \omega_{rev} ,$$

where η is the dipersion function defined by $\eta=\gamma^{-2}-\gamma_t^{-2}$.

The closer observation shows that the shape of the frequency spreads of sideband, has two peaks. The separation of two peaks becomes smaller when the RF voltage is put off. The analysis of these phenomena is now in progress.

3.5 Beam Life Time

The life time of the stored beam is determined by several factors in the cooler ring. The life of the heavy ions with atomic electrons, is determined by the rate of electron capture at e-cool section. For the molecules, such as H_2^+ or H_3^+, the dissociation due to the residual gas, play a key role. For the completely stripped light and heavy ions, the multiple scattering with residual gas in the vacuum chamber, is a leading factor. In any cases, the operation points, ν_x and ν_y values, should be selected so as to avoid the resonance lines, at least up to 5th orders. Otherwise beam would be lost due to the emittance growth by the resonance effects.

Here the experimental results of 40 MeV α beam, are explained . The average vacuum pressure at TARN II ring is presently ~ 2×10^{-10} Torr, measured by the B-A gauges. The beam currents are measured by the parmalloy core monitors. We measured the e-folding beam life time for two cases, the one the RF voltage of 500 Volt was applied and the other the RF was put off. In the former case, the life time was 100 seconds whereas it was 400 seconds in the latter case. Short life time in the presence of RF field, could be explained by the following considerations; The betatron operation points extended over the resonance lines due to the finite chromaticity and large momentum spread with the phase oscillations . In the present case, the tune spreads $\Delta\nu$ are evaluated at ~ 3×10^{-2} and then the operation lines did cross or touch the stop band of resonance lines of 5th orders. Precise chromaticity corrections of both the horizontal and vertical directions, would be necessary to obtain the long life time in the presence of RF field.

Another example is the ionization energy loss of the circulating beam due to the collision with residual gas. The 40 MeV α beam was stored in the ring and Schottky signals was observed. The shift of the central frequency of the spectrum, 360 seconds after the beam injection, was Δf = 7.5 kHz at the 35th harmonics of revolution frequency (Fig. 5), which corresponds to the energy loss of 44 keV and the horizontal beam position movement of 2 mm.

By using the data of residual gas analysis and this ionization loss, the average vacuum pressure, N_2 equivalent, was determined 7×10^{-11}, roughly two times better than the value obtained by B-A gauges.

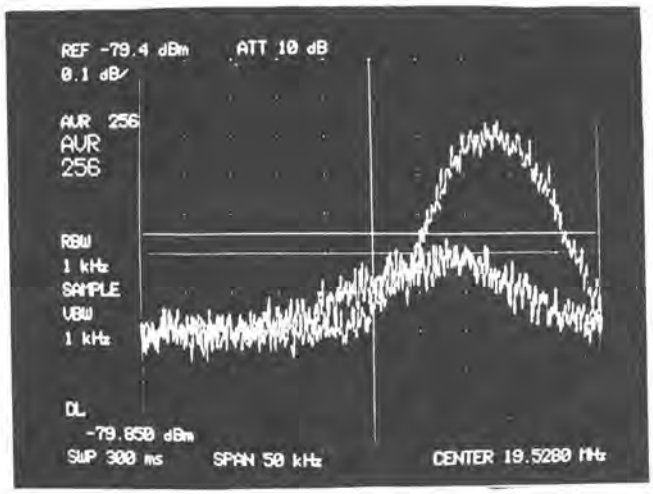


Fig. 5. Longitudinal Schottky signals at the injection and at 360 sec after the injection.

4. ACCELERATION

The synchrotron acceleration system was completed to the designed maximum energy 370 MeV/u for light ions. However, due to the limitation of the electric power station in the campus, the presently available energy is 220 MeV/u. The detailed descriptions of the RF system are given elsewhere[3], and in this chapter, two subjects concerning the RF acceleration are presented.

4.1 Tracking Error Correction

Four magnet power supplies, one for bending magnet and 3 for Q magnets, should be excited synchronously with a finite tracking error. From the experiences at DC operation of the ring, the permissible tracking error was estimated at 0.2 %. For this purpose, the self learning correction system for tracking error was built with a microcomputer system, PSC 1000, consisting 5 sets of computer boards and I/O interface boards.

At each power supply, Digital to Analog (DA) and Analog to Digital (AD) converters are equipped for the current control. The 1st approximation pattern data, caculated from the ideal reference pattern data, are sent firstly to each power supply via DA converter, then the excitation currents of power supplies are measured with DC current transformer. Then the measured results are compared with a reference ideal value. At this first trial, the tracking error was as much as 5% due to the non-linearity and delay of the circuits. The 2nd approximation data, is then corrected to advance the readout time for the compensation of delay components. Afterthat the self-learning correction is performed to correct the nonlinear term.

Iteration of the self-learning was finished after 6 or 7 repeating this procedure. The tracking errors between , one dipole magnet and three quadrupole magnets, were finally obtained within 0.2%.

4.2 Beam Acceleration

The beam acceleration is performed by the following procedures: The injected beam is captured adiabatically by the RF bucket within the period 6 ms. In this period, the capture frequency is controlled by a fixed frequency generator to track the twice of revolution frequency of the injected beam. After the adiabatic capture process, the bucket which is controlled by a phase locked loop, takes over the captured beam. The frequency of voltage controlled oscillator, a part of phase locked loop, is regulated by a B-dot generator, position and phase feedback system. The voltage at an acceleration gap of RF cavity is controlled by a AGC system during the whole acceleration period. For example, the injected 10 MeV/u α beam was accelerated up to 220 MeV/u. The field excitation and beam position signals are given in Fig. 6. During the acceleration, the beam position was kept almost constant in the ring. The dB/dt is chosen at 0.37 Tesla/sec.

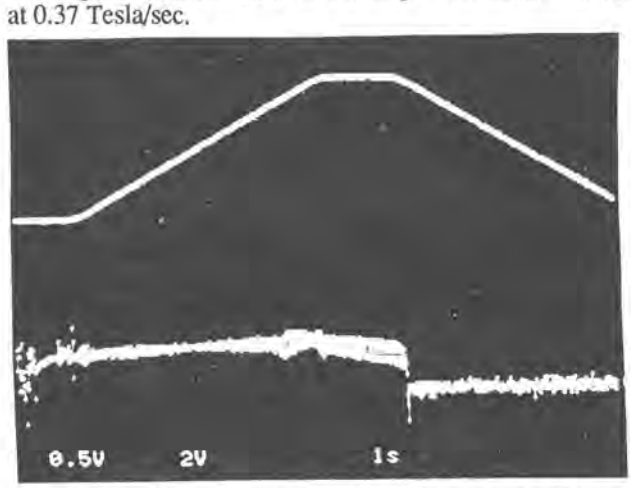


Fig. 6. Excitation pattern of magnetic field and the horizontal beam orbit during the acceleration.

5. ACKNOWLEDGEMENT

The authors would like to express their thanks to Mr. T. Honnma, Mrs. R. Nagai, Mr. J. Yoshizawa and the crew of SF cyclotron for the collaboration on the cyclotron operation and beam transport. Pofs. T. Tanabe and I. Katayama are acknowledge for the useful discussions during the experiments.

6. REFERENCES

1) T.Katayama et al., "Cooler Synchrotron TARN II", Paticle Accelerators, Vol. 32 (1990).
2) S.Watanabe "Beam Diagnostic Instruments of TARN II", presented at the Workshop on Advanced Beam Instrumentation, KEK, April 1991.
3) T.Katayama et al., "Beam Acceleration at Cooler Synchrotron TARN II", presented at 3rd EPAC, Berlin, 23-28 March(1992).
4) S.Watanabe, "Synchrotron Power Supply of TARN-II", INS-T-504, July 1991.

DUBNA PROJECT OF THE HEAVY ION STORAGE RING COMPLEX K4-K10

Yu.Ts.Oganesian, O.N.Malyshev, G.S.Popeko, A.M.Rodin, S.I.Sidorchuk, Ye.A.Sokol, S.V.Stepantsov, G.M.Ter-Akopian, V.A.Timakov
JINR, P. O. Box 79, SU-101000 Moscow, Dubna, Russia

V.V.Parhomchuk, A.A.Sery, V.D.Shiltsev
INP, Novosibirsk, Russia

I.N.Meshkov, Ye.M.Syresinm
CAPT, Lipetsk, Russia

and

V.P.Belov, A.A.Makarov, I.A.Shukeylo, Yu.P.Severgin, M.N.Tarovik
Yefremov Institute, St.Petersburg, Russia

ABSTRACT

The project consists of two cooler rings (4 and 10 $T \times m$) connected by the fragment separator.[1)] The JINR U400M cyclotron will be the injector for the K4 ring.The cooled primary beams obtained as short (20ns) bunches after the fast extraction from the K4 are focused onto a small target.This reduces considerably the transverse and longitudinal emittances of the produced secondary exotic beams,thus facilitating their cooling after injection into the K10 ring.The K4 - K10 complex will provide the luminosity values on internal targets of 10^{24} - $10^{28} cm^{-2} s^{-1}$ with beams of such ions as $^{6}He, ^{8}He, ^{11}Be, ^{16}C, ^{38}Ar$ etc. having lifetimes $> 0.1s$.

We specify the main purpose of the project by dedicating it to the producing of high precision Exotic Ion Beams (EIB's) with $A < 100$. Production of EIB's imposes specific requirements on such a heavy ion complex.

The layout of the storage ring complex K4-K10 is shown in Fig 1 together with the one of the heavy ion cyclotrons of the JINR (Dubna). The project includes two rings, K4 and K10. The beam channels related to this project are also shown in Fig. 1. These are the channel guiding from the U400M[2)] cyclotron to the injection section of the ring K4 and the fast beam extraction line of the K4 ring followed by a fragment separation channel allowing the injection of EIB's into the K10 ring. The fast and slow extraction beam lines from the K10 ring are envisaged as well.

Two long straight sections of the K4 ring and one long straight section of the K10 ring are reserved for experiments employing internal targets.

Basic parameters of the rings are listed in Table 1.

We are intended to provide the highest possible electron beam density in the coolers of both the rings in order to reduce the cooling time. For the same reason, we optimized the ring structures in a way allowing relatively high values of amplitude functions at the cooler section straights. The reduction of the cooling time in both rings is essential for the production rates of beams of short lived exotic nuclei.

Rather powerful RF-systems are planned for the rings especially for the ring K10. This provides necessary conditions for generating short bunches before beam extraction from the K4 ring. In the case of the K10 ring we need a high RF amplitude to manipulate the large momentum spread EIB's injected on the ring orbit.

Fragmentation reactions of medium energy heavy ions with mass numbers $A < 100$ will be used for producing the EIB's. Primary heavy ion beams ($\epsilon_{\perp} = 15\pi mm \times mrad$, $\Delta p/p = 0.15\%$) will first be accelerated by the U400M cyclotron and then injected into the ring K4. Cooled and additionally accelerated in this ring the ion beam, after the fast extraction in the form of a short, about 20 ns bunch, will be focused on the production target of less than 1 mm in its diameter. This causes the reduction of both the transverse and longitudinal emittances of secondary EIB's produced on this target and greatly facilitates the reduction of the EIB cooling time on the orbit of the ring K10.

The primary ion accumulation time in the K4 ring will be rather short ($= 60ms$) in the case of the stripping injection of light ions ($A < 20$). For heavier ions the multiple single turn injection is proposed. This method of accumulation employs the beam emittance contraction due to electron cooling to open the space for successive events. Single-turn injection is prefered due to the capability to retain the quality of the injected beam. In addition, by keeping the cooling electron velocity equal to the mean velocity of the injected ions one minimizes the beam cooling time. For the case of the single turn injection of the $^{48}Ca^{10+}$ beam extracted from the U400M

Ring		K4	K10
$B\rho_{max}/B\rho_{min}$	(T·m)	4.0/0.7	10.0/0.7
Circumference	(m)	83.12	146.24
Acceptance			
$\varepsilon_{\perp}$	(π mm*mrad)	50	25
$\Delta p/p$	(%)	1.0	2.0
Electron cooling section			
$E_{e\ max}$	(keV)	100	250
Length	(m)	3	3
$I_{e\ max}$	(A)	1.0	3.0
Cathode diameter	(cm)	3	3
β_h/β_v	(m)	10.9/6.3	5.6/5.8
RF-system			
f_{max}/f_{min}	(MHz)	3.6/0.4	2.09/0.25
harmonic number		1	1
number of stations and RF amplitude	(n·kV)	1·14	4·14

TABLE 1 Basic parameters of the rings K4 and K10.

cyclotron and stripped before the injection into the K4 ring to the charge state 20+ the value of the injection and cooling time of about 200 ms is evaluated for 10^9 ions stored on the ring orbit.

Fast extraction from the K4 ring should routinely provide beams with momentum spread and bunch length of about $\pm 0.2\%$ and 20 ns correspondingly. The beam momentum spread of $\pm 0.2\%$ is still tolerable from point of view of focussing onto a small target.

The momentum loss achromat technique is utilized in the design of this separator channel.[3] It is designed to transmit EIB's with the value of emittance $\epsilon_{\perp} = 25\pi mm \times mrad$ and momentum spread of $\pm 0.5\%$.

The design of the K10 ring provides the possibility to keep simultaneously two beams on the orbit, i.e. the newly injected beam with mean momentum p_{inj} and another one corresponding to the momentum shifted by about 1.5% from p_{inj}. We suppose that the newly injected EIB beam bunch is immediately captured within a stationary RF bucket in such a way that this bunch occupies a phase interval of about 7° being $\pm 0.5\%$ in its value of momentum spread. We take the height of the separatrix two times larger than the minimum value U_{RFmin} needed for the capture of the full size injected bunch. Such a value of U_{RF} prevents the injected beam bunch from serious filamentation during the quarter period of the synchrotron oscillation. After completion of the quarter period of synchrotron oscillation, two ways of the ring operation are possible.

For those short-lived ($T_{1/2} < 1s$) EIB's for which the accumulation on the ring orbit has no sense a specific ring operation mode is of interest. In this case, the RF is switched off just after completion of the quarter period of synchrotron oscillation. The electron cooling system matched to p_{inj} cools the beam both longitudinally and transversely within a time interval of $< 100ms$. This cooled beam is used immediately for experiments on an internal target.

For long-lived EIB's ($T_{1/2} > 1s$) for which accumulation is reasonable the RF stacking procedure[4] should be applied. The RF matching of the EIB bunch should be performed just after injection. As the first stage, the RF matching implies a quarter period synchrotron oscillation. After the RF matching the beam acceleration towards the working orbit takes place. We assume

Primary beam	EIB	$T_{1/2}$, s	N	L, $cm^{-2}s^{-1}$ (injection energy)	E_{max} (MeV/nucl.)	L, $cm^{-2}s^{-1}$ (maximum energy)
^{7}Li	^{6}He	0.8	$3\ 10^{7}$	$2\ 10^{27}$	430	$1\ 10^{27}$
^{18}O	^{8}He	0.122	20	$2\ 10^{21}$	260	$1\ 10^{20}$
	^{11}Be	13.8	$4\ 10^{7}$	$4\ 10^{27}$	500	$2\ 10^{27}$
	^{15}C	2.45	$3\ 10^{7}$	$2\ 10^{27}$	580	$1\ 10^{27}$
	^{16}C	0.747	$2\ 10^{6}$	$2\ 10^{26}$	520	$1\ 10^{26}$
^{48}Ca	^{44}Ar	720	$3\ 10^{7}$	$2\ 10^{27}$	600	$1\ 10^{27}$
	^{46}Ar	7.8	$4\ 10^{4}$	$3\ 10^{24}$	560	$2\ 10^{24}$
	^{47}K	17.5	$5\ 10^{7}$	$6\ 10^{27}$	590	$3\ 10^{27}$
	^{38}S	$1\ 10^{4}$	$2\ 10^{8}$	$2\ 10^{28}$	630	$1\ 10^{28}$
^{18}O	^{8}He	0.122	$1 \cdot 10^{4}$	10^{24}		
	^{11}Li	0.009	$1.2 \cdot 10^{3}$	$1.2 \cdot 10^{23}$		

TABLE 2 Estimations of numbers of some exotic ions and the relevant luminosities available on the orbit of the ring K10. The given values are calculated for the internal target of $10^{14} cm^{-2}$.

that the beam accumulated on the working orbit is used in experiments with an internal target. This beam is permanently cooled and new beam portions approaching, due to RF stacking, the working orbit are left free at some distance from it. We count on the electron cooler which will cool new beam portions thus equating their momentum with the beam momentum on the working orbit. Cooling time of about one second can be reached in this case. Some results of calculations for the luminosity values which can be achieved with different EIB's in experiments making use of internal targets in the K10 ring are presented in Table 2.

The K4-K10 project is the subject of considerations by the JINR scientific community as a major facility planned for construction within next five years. Proceeding from the general policy of the JINR, we want to make the new heavy ion complex open for research groups coming from the JINR member states as well as from any other research centers. This imposes on us the responsibility for providing the necessary performance features of the complex.

We used in this paper results of the Technical Proposal[5] prepared by the K4-K10 design group.

REFERENCES

1) Yu.Ts. Oganesian et. al., Z. Phys.A - Hadrons and Nuclei 341, 217-222 (1992).
2) G.N. Flerov et. al. JINR Preprint 9-84-555, Dubna, 1984.
3) B.M.Sherill In: Second Int. Conf. on Radioactive Nuclear Beams, Louvain-la-Neuve, Belgium, 1991, Th.Delbar, Ed., Adam Hilger, Bristol, Philadelphia, New-York, 1992, p.3.
4) E. Caiapala: CAS CERN Accelerator School. General Accelerator Physics. Gif-sur-Yvette,Paris, France 1984. Report CERN 85-19, 1985, v.1, p. 195.
5) G.M. Ter-Akopian, Ed., Heavy Ion Storage Rings K4-K10, A technical proposal, JINR E5-92-15, Dubna, 1992.

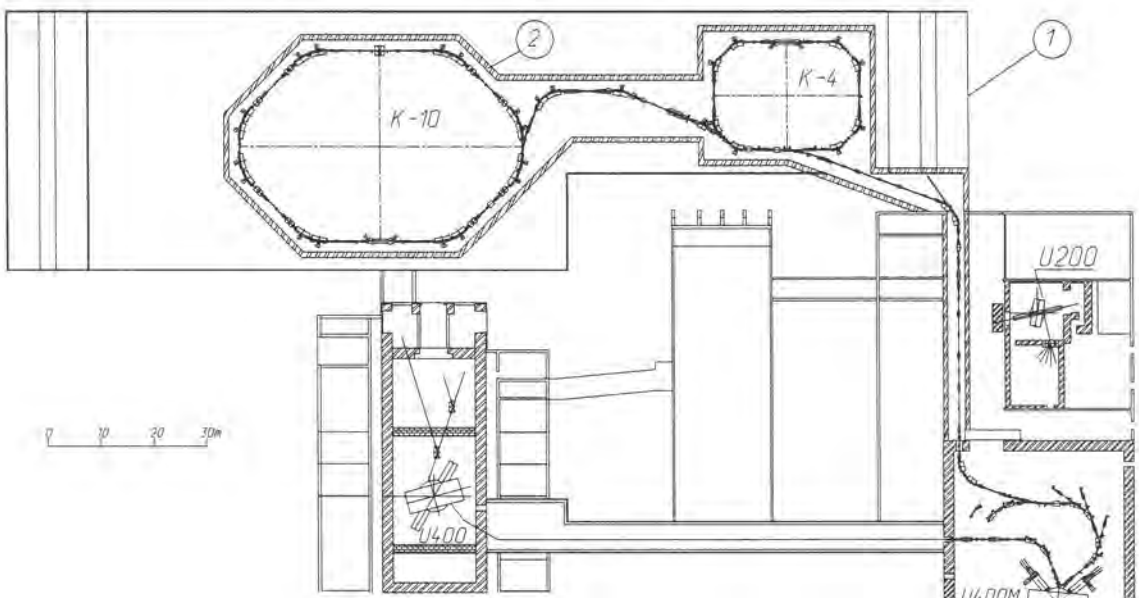


Fig. 1 Diagram of the JINR heavy ion cyclotron complex with the heavy ion storage ring complex K4-K10. Two cyclotrons, U400 and U400M, coupled in a tandem as well as the U200 cyclotron are shown. A curved arrow at the U400M main beam line shows the direction to U400M experimental set-ups. Just at the right side of this arrow the beam splitting system is installed and the beam transport channel to the K4-ring starts. 1-perimeter of a building projected for the K4-K10 complex, 2-concrete shielding of projected rings and beam lines.

THE NEW PROJECT OF INR (KIEV'S) STORAGE-ACCELERATING COMPLEX

A.V.DOLINSKY, A.I.PAPASH, S.N.PAVLOV, A.T.RUDCHIK,
A.E.VAL'KOV, I.N.VISHNEVSKY, A.V.ZHMENDAK
Institute for Nuclear Research, Kiev, 252028, Ukraine,
and
V.P.BELOV, A.M.KOKORIN, A.A.MAKAROV,
Yu.P.SEVERGIN, I.A.SCHUKEILO
Efremov's Scientific Research Institute for Electric Physical Equipment, Sankt-Peterburg, 189631, Russia

Abstract

The new project of Ion Storage Ring (ISR) complex of Institute for Nuclear Research (INR) of Ukrainian Academy of Sciences is presented. The INR ISR complex consists of the U-240 isochronous cyclotron, the ISR with the Electron Cooling (EC) and intermediate Fast Booster (FB). The INR ISR complex will provide ion beams of wide mass range (from protons to xenon) including radioactive ion beams with the energies up to 300 MeV/u at A/Z=2.

1. Introduction

In 1989 the Institute for Nuclear Physics (INP, Novosibirsk, Russia) and INR (Kiev, Ukraine) created the project of the Ion Storage Ring for INR, allowing to provide the experiments with light and middle nuclei up to Neon [1]. In 1991 Efremov's Institute, INR and INP prepared the essentially improved new project of ISR based on the INR U-240 isochronous cyclotron.

The ISR complex of INR is planned to be built in two stages. First, the main ISR with electron cooling will be built for storage of light ions up to neon at injection energies 5-10 MeV/u to have ion beams with energies up to 300 MeV/u. At the second stage the intermediate fast booster (FB) with a multiple charge exchange of ions will be created to have possibility to accelerate ions heavier than neon in order to store them in the main ISR. The storage and cooling of nuclei at physical experiment take place in the main ring (fig.1). The main parameters of the ISR complex are presented in Table 1.

Table 1.

Circumference, m:	
Storage Ring	100
Booster	54
Mass range	1-130
Max.energy, MeV/u:	
protons	900
ions with A/Z=2	300
ions with A/Z=3	200
Magnetic field, T	1.5
Magnetic Rigidity,T·m:	
Booster	4.3
Storage Ring	5.4
Injector	U-240
A/Z	1-3
Injection energy,MeV/u:	
light ions(p,d,a)	25-70
C - Ar	5-10
Kr - Xe	3
Electron cooling energy, kev	2-100
Vacuum, torr	10^{-11}

2. The beam parameters

The average current of U-240 cyclotron ion beams changes from 0.2 μA for the Neon up to 10 μA for protons. When the Electron Cyclotron Resonance (ECR) source will be put into operation then all ions up to Xenon can be accelerated on U-240.

The ISR operation cycle is the following:

1. Injection (duration is 2-40 μsec). Single turn injection for the completely stripped ions is carried out, multiturn charge- exchange injection of heavy ions is prosecuted /2/.

2.RF stecking (duration is 10-20 msec) with increasing of the injected beam energy on 2.1% . RF stecking used for elimination of the cooled beam passing through the stripping foil

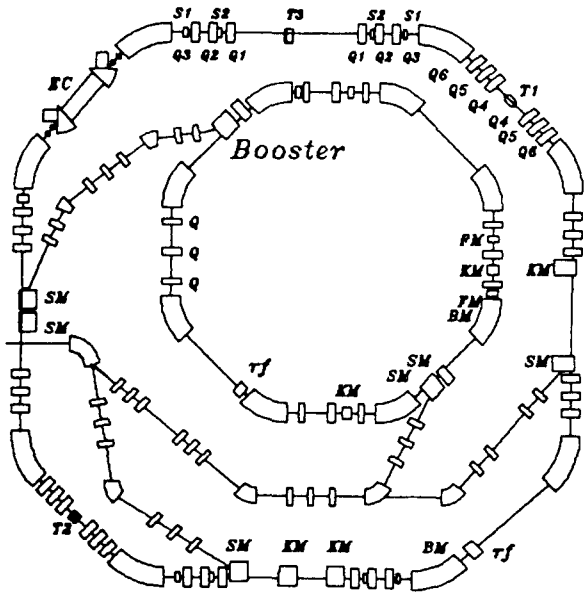


Fig.1. Magnetic structure of Ion Storage Ring and Fast Booster:
BM - bending magnets, Q_i- quadrupoles, T_i- targets, EC - electron cooling, KM - kicker magnets, SM - septum magnets, FM - fast (bump) magnets, rf - RF cavity.

or the injection kicker magnet during following injection cycles.

3. Electron cooling: during the 40-1400 msec the beam is cooled and then another injection cycle follows.

4. Storage:the above mentioned cycles are repeated many times (up to 10 sec or more).

5. Acceleration - during 1 sec the ions are accelerated.

6. Physical experiment (up to 10 sec or more) with electron cooling on high energy.

7. New cycle preparation is 1 sec.

The storage of ions heavier than the Ne ions is impossible at U-240 cyclotron injection energies, because total ion life-times are less than 1 sec. All elements up to Xe can be stored in the main ring if the preliminary acceleration in Fast Booster is used (total storage time can be reached 46 sec for the Kr ions and 20 sec for the Xe ions). The pressure in the ring must be better than 10^{-10}Torr.

When the internal target is switch on, the ion life-time is defined by the single scattering on the target and electron capture by the target atoms since multiply processes are suppressed by electron cooling. The calculations shown that the typical ion life-time is about 20 sec for the heavy ions and the Pb target.

The target thickness should not exceed $2.6\cdot10^{16}/Z_t$ cm^{-2} to compensate the energy losses in the target by means of electron cooling during one ion turn.

The ISR beam parameters estimates are: cooled beam emittance is 2.4 π mm mr for protons ($N=10^{11}$) and 0.2 the Ne ions ($N=10^{9}$), cooled beam cross-section diameter on the target is 2.8 mm for the protons and 0.6 mm for the Ne ions.

3.Magnetic structure of storage ring and fast booster

Designing ISR magnetic structure it was taken into consideration of such requirements:

1) to have the straight sections (with length 7 m) for electron cooling system with zero dispersion (ψ=0) and to obtain the symmetrical beam sizes, i.e. beta-functions with $\beta_x = \beta_z = 4$ m.

2) to also have the straight sections (with length more than 6 m) in which the dispersions function must be constant (ψ=3 m); these sections will be used for the radial multiturn charge-exchange and single-turn injections;

3) to have straight sections for the internal targets and coordinate triplets which must assure small beam size on the target (i.e. ψ = 0, $\beta_x$and β_z- functions less than 1m).

4) to have straight section for the radial injection from FB to ISR.

5) to provide, for all regimes, the constant position of working point of betatron oscillations to prevent the crossing of resonance lines.

To carry out the aforementioned requirements the octupole magnetic structure with triplets is most convenient (fig.1).

The ion storage ring is the zero gradient synchrophasotron which includes eight 45° bending magnets and 36 quadrupole lenses. The

ISR magnetic structure consists of the two superperiods. Beta- functions and dispersion for the ring one-quarter are shown in fig.2.

Two symmetrical triplets $Q_4Q_5Q_6$ provide the beam focusing on the target. When coordinate triplets $Q_4Q_5Q_6$ are switched on the β-functions do not change throughout except in the experimental section where β-function is minimized (dashed lines in fig.2). For the experiments which don't require zero dispersion there is the 6 m section where T_3 target can be installed.

Betatron tune values for ISR are: for synchrotron mode ν_x=3.16, ν_z=2.43, for low β-mode ν_x=3.63, ν_z=3.12.

For the chromatic corrections will be used 8 sextupoles installed between main quadrupole lenses.

The booster magnetic structure is more simple. Betatron tune values for FB are: ν_x=1.61, ν_z=1.27.

The bending magnets of ISR and FB have frame shape.

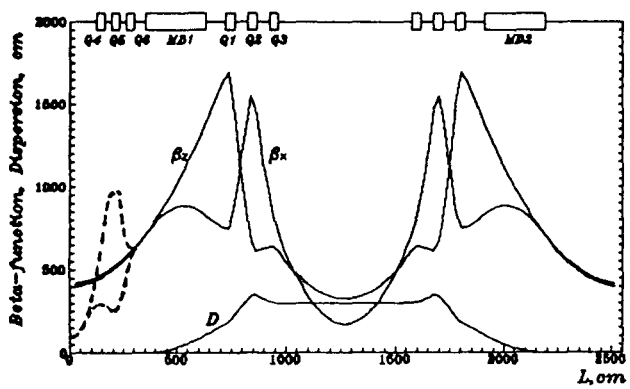


Fig.2.Beta-functions and dispersions on one-quarter of SR:
solid lines - synchrotron mode ($Q_{4,5,6}$-switch off), dashed lines - low β-mode ($Q_{4,5,6}$ - switch on).

4. Electron cooling system

In the electron cooling system the solenoids with the magnetic inhomogeneity $B_\perp/B_\parallel = 3\cdot10^{-5}$ are used. The electron beam is formed by the two-electrodes gun with a smooth optics. The cathode is immersed into the longitudinal magnetic field. The pair of correction magnets with effective length of 20 cm are situated in the entrance and exit of cooler to compensate a negative influence of toroidal magnets on the ion beam. [3,4].

5. Injection system

The single-turn injection into the ISR was designed for the light ions. The such injection system is also used for the ion beams transmitted from U-240 cyclotron into FB and from FB to ISR.

The multi-turn radial injection system with the ion stripping on the foil was designed for the incompletely stripped ions with A/Z = 3-5. During injection the ions with A/Z = 4 and A/Z = 2 fall simultaneously on the stripping foil just where the tangencies come together.

To inject a new beam portion in the ISR the circulating cooled beam must been shifted to the outer orbit on 5-6 cm with increasing of beam energy on 2.1% by auxiliary RF cavity. All injection elements are located in one of the straight sections.

6. Conclusions

The experimental luminosity is expected to be 10^{29}-10^{30} $cm^{-2}\cdot sec^{-1}$ and the ion beam life-time from several tens to hundred seconds. The Storage - Accelerating Complex is planed to use for the studies of nuclear reactions in the wide energy range, nuclear spectroscopy, nuclear structure etc.

References

1. A.V.Dolinsky, A.I.Papash, S.N.Pavlov, A.T. Rudchik et.Cooler Rings and Their Applications (Proceedings of the 19th INS Symposium, Tokyo, 1990, Ed. T.Katayama, A.Noda), World Scientific, Singapore, N.J., L.,H.K., 1991, p.48.
2. A.S.Schlachter,J.W.Stears,W.G.Graham, Phys. Rev. A27 (1983) 3372.
3. G.I.Budker, A.N.Scrinsky, Uspekhi Fiz. Nauk 124 (1978) 561.
4. N.S.Dikansky, V.I.Kudelainen, D.V.Pestrikov et al, Limit Capabilities of Electron Cooling. Preprint No 88-61, INP, Novosibirsk, 1988.

SUPERTHIN INTERNAL TARGET FOR STORAGE RINGS

V.Pugatch, G.Sivtsov, A.Glushko, G.Pitatelev
Institute for Nuclear Research, Kiev-28, Ukraine

and

S.Popov, B.Voitsechovsky, D.Toporkov
Institute for Nuclear Physics, Novosibirsk-90, Russia

ABSTRACT

The construction, operation of the superthin micropowder spray target for storage rings as well as testing results are presented. The "dust beam" is created by a gas-particle mixture flowing through a capillary into a vacuum. The profile and density of the microparticle beam as well as velocity of microparticles is measured by a diagnostic system based on He-Ne laser with splitted light beams. The target thickness (7,0 10^{14}atoms/cm^2) has been determined by weighting procedure. The scheme of other target design are presented.

1. INTRODUCTION

The development of accelerating storage rings with internal targets offers a number of experimental benefits. Among the main advantages are increasing of variety of interacting pairs, high efficiency of a beam utilization, fine energy resolution, lowest detection thresholds for heavy charged products of nuclear reactions. To realize these benefits one obviously should use the regime of the superthin internal target [1-9]. The allowable range of thickness of internal targets depends on some conditions, but it is roughly between 10^{14}-10^{16} atoms/cm^2[3]. This thickness is some orders of magnitude lower than commonly used in one-pas experiments. This constraint rules out self supporting foil targets. Gas targets in the desired thickness range are easily realized [6], but this is not the fact for solid state materials. Several approaches are known for inhomogeneous targets in form of fibers, pellets and microparticle dust [10]. The present paper is concerned with the construction and operation of two types of superthin micropowder spray targets designed as internal targets for the electron storage ring of the Novosibirsk Institute for Nuclear Physics.

2. EXPERIMENTAL SET-UP

2.1. Spray micropowder internal target (SMIT)

The schematic view of the first target-design (SMIT) is shown in Fig.1. The micropowder in amounts of 5-7 grams is loaded into a generator-mixer "G" via the hole "H" while the carrier-gas is supplied via the needle-valve "V". The sound generator "D" is used to excite the 20-200 Hz vibrations of the electromagnet connected with the bottom of a mixer cavity. The resonance frequency depends on the amount of a micropowder and should be tuned during the experiment. The flow of carrier-gas involves microparticles by a dragging force into movement along

the flowing direction, while the Bernoulle force concentrates them close to the capillary "K" axis. Inside the long (~ 500 mm) and narrow (diameterr 0.2-0.4mm) stainless capillary the micron - size (0.2 - 2.0 μm) microparticles attain velocities up to 300 m/s.

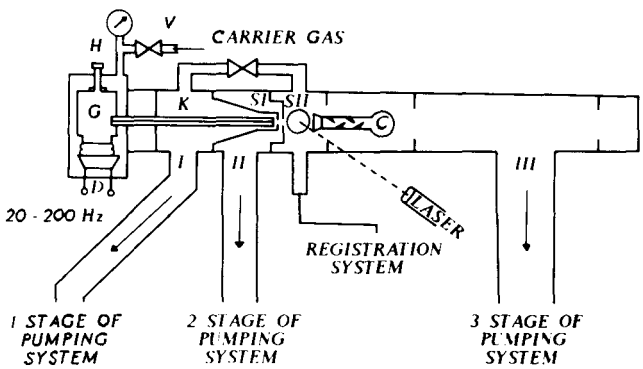


Fig. 1. The schematic view of the first target design (SMIT).

At the exit of the capillary the gas diffuses, but particles, due to their inertia continue to move and arrive to the intersection region with the circulated electron beam. The dust beam is then collected in a catcher "C".

To provide a high vacuum requirement inside the storage ring and to have appropriate acceleration of microparticles which depends on the pressure difference between mixer and vacuum chambers we have used the differential pumping system consisted of three stages with two skimmers "S1","S2" (diameter 2 mm and 4mm respectively). The 1,2,3 stage was pumped up to 10^{-1} Torr, 10^{-3} Torr and 10^{-6} Torr respectively. The pressure inside the generator-mixer cavity - 200 - 400 Torr.

To control density and velocity distributions as well as a profile of the microparticle beam we utilized a laser diagnostic system similar to one described in detail elsewhere [10]. The Mie scattering of laser photons has been focused onto a photomultiplier mounted in horizontal plane at 0° to the laser and microparticles beam axez. We used He-Ne laser at a 2 mW power. This technique allows to count microparticles crossing the laser beam as well as to measure the microparticle beam profile by scanning procedure. For homogeneous microparticles it was possible to measure the velocity distribution as well. For that purpose the time-of-flight technique was employed to measure time difference between the microparticle crossings of two narrow laser beams. In practice the He-Ne laser beam was splitted into two parallel beams 4 mm apart and 150 μm wide. The measurements have shown that commercially available micropowder is rather inhomogeneous and we have used so-called gravitational filter to separate microparticles of different size [3]. We have also investigated the monitoring system based on discharge pulses occurred at the catcher region when the microparticle beam interacted with a lexan foil. We have checked the target operation for C,Ni,W,Mo,Ti elements. The target thickness has been measured by means of weighting. The measured target thickness (W, diameter of microparticles 1-2 μm, N_2 carrier - gas) for the microparticle beam diameter 4 mm was estimated as 7.0 10^{14} atoms/cm^2.

2.2. Electrodynamic micropowder target (EMT)

Recently we have tested another method of introducing microparticles into circulating electron beam. It is so-called Electrodynamic Micropowder Target (EMT). A schematic diagram of a target is shown in Fig.2. The principle of operation is similar to the described

elsewhere [8] and based on a contact-charging of dust particles in electric field on metal surfaces of preparing (1) and injecting (2) chambers.

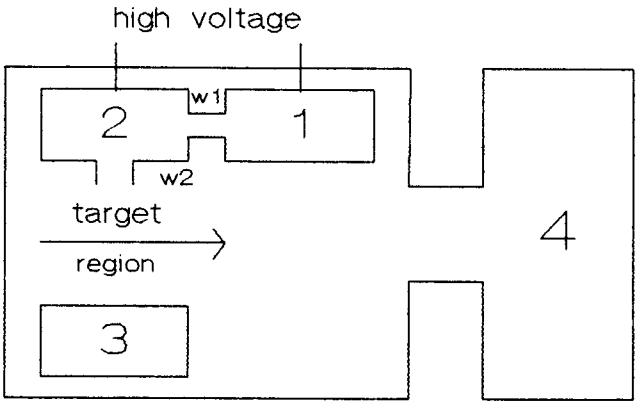


Fig. 2. The schematic diagram of a target (EMT).

The chamber (1) is connected with chamber (2) by window (W1). The density of dust cloud in injection chamber is regulated by variable window (W1) dimension. Moving microparticles are extracted from injection chamber through the hole (W2) (diameter 4 mm) in a lower electrode to the target region. After crossing target region microparticles are collected in the catcher (3). The electric field applied between electrodes chamber (1),(2) ranged 10^5-10^6 V/m. In that case target thickness was in the range of 10^{16} atoms/cm^2. The pumping system provides vacuum up to 10^{-7} Torr (4). The laser diagnostic system described above has been used for the microparticle beam monitoring.

3. EXPERIMENTAL RESULTS

The first construction of the micropowder spray target described above has been installed in the straight section of the electron storage ring at Novosibirsk [3]. The Ni-micropowder particles with a diameter close to several micrometers were brought into reaction area, by CO_2-carrier gas. The short (50 mm) glass capillary with an exit diameter of 100 micrometers linked the mixer-cavity-gravitational filter region with a vacuum chamber of the storage ring via two-stage differential pumping system. The two criopanels effectively pumped the CO_2-carrier-gas so that at ~ 5 l*Torr/s gas flow the contribution of carbon and oxygen nuclei into measured spectra was not detectable (less 2%). The Ni-micropowder beam density measured by weighting procedure as well as calculated from electron elastic scattering data was in the range of 10^{15}atoms/cm^2. The example of electron spectrum obtained at electron energy 122 MeV by means of the magnetic spectrometer at $\theta=56^0$ is shown in Fig.3.

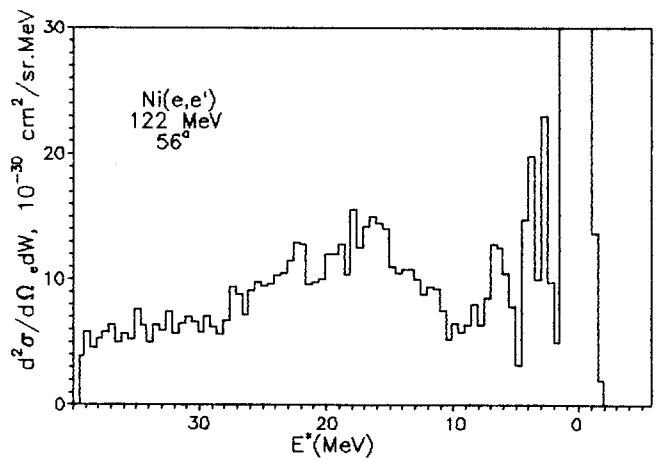


Fig. 3. The electron spectrum obtained at electron energu 122 MeV.

Besides the sharp discrete peaks corresponding to the ground state and low-lying levels of Ni the broad structure at excitation energy ~15 MeV as well as at ~ 35 MeV were clearly seen and identified as contribution from 1^-, 2^+ and presumably from 2^- giant resonances of ^{58}Ni.

The more sophisticated installation (SMIT) has been constructed for the new electron storage ring NEP-220 in Novosibirsk. The parameters of the

NEP-220 beam make limits for target thickness 10^{14} - 10^{17} atoms/cm^2 for different elements (luminosity 10^{31} - 10^{34} cm^{-2}s^{-1}), respectively.

It is worthwile to point out that a micropowder of other elements such as B, Al, Co, Cu, Re and combinations: Ti, Si, B carbides; Al, Ti, Si nitrides; Al, Zr, Y, Hf oxides; Zr, Ti, Al borides were produced for operation with internal target.

REFFERENCES

1) S.T.Belyaev, G.I.Budker, S.G.Popov. Proceed. III Intern. Conf. High Energy Physics and Nuclear Structure, (New York, 1969, Plenum Press, 1970) p.606.

2) S.G.Popov, Proceed. Workshop on the use of electron rings for nuclear physics, (Lund, Oct.5-7, 1982) v.2, p.150.

3) B.B. Wojtsekhowski,et al., Proceed. 35-th Workshop on Nuclear Spectroscopy and Structure of Atomic Nuclei (in Russian), (Leningrad, Nauka, 1985) p.367.

4) H.O.Meyer, CEBAF Workshop, Newport News, U.S.A., 1985.

5) Workshop on Internal Targets for COSY, KFA, (Julich, 1987) Jul-Spez - 409.

6) C.Ekstrom. CERN Accelerator School, Third Advanced Accelerator Physics Cours, (Uppsala, Sweden, 1989).

7) Topical Conference on Electronuclear Physics with Internal Targets SLAC, (Stanford, California, 1989).

8) T.Tanabe, I.Sugai, M.Yasue. Nucl. Instr. and Meth. A265, (1987) 439.

9) A.Berdoz et al., Nucl. Instr. and Meth. B40/41, (1989) 455.

10) H.O. Meyer et al., Nucl. Instr. and Meth. 295, (1990) 53.

11) B.B. Wojtsekhowski et al., Sov. J. Nucl. Phys.(in Russian), 52, (1988) 907.

12) G.I. Budker, A.P. Onuchin et al. Sov. J Nucl. Phys.(in Russian), 6 (1967), 775.

13) N.S. Korobeinikov, L.M. Kurdadze et al., ibid, p.84.

ECR ION SOURCES FOR ACCELERATORS

C. Lyneis
Nuclear Science Division, Lawrence Berkeley Laboratory, Berkeley
CA, 94720, USA

ABSTRACT

ECR ion sources have become the most frequently used heavy-ion source for cyclotrons. They are also being used with heavy-ion linacs, synchrotrons, and radioactive beam accelerators. Although almost 20 years have gone by since the first high charge state ions were extracted from an ECR source, the efforts to improve their performance and simplify their construction and operation seem to be expanding. Recent developments include new high frequency sources, electron injection, and superconducting magnet ECR sources. This paper surveys the application of ECR sources to accelerators, discusses recent innovations and the results of experimental studies, reviews current thinking on how they operate, and looks at potential directions for future improvement.

1. Introduction

The number of Electron Cyclotron Resonance (ECR) ion sources used for the production of high charge state ions continues to expand with more than 40 now in operation. The majority of the sources have been built for use with accelerators with the remainder being utilized for atomic physics research. The desirable characteristics of ECR sources for accelerator applications include high charge state production, high intensity, stability, wide range of ion species, reliability, longevity, and ease of operation. This has made them the source of choice for heavy-ion cyclotrons. ECR sources are also now used with heavy-ion linacs, synchrotrons, storage rings, and in a radioactive beam accelerator. Table 1 summarizes the ECR sources being used at accelerators and illustrates that they have found application in many laboratories and different countries. Much of the incentive and effort to develop better ECR sources has come from the accelerator community. The Grenoble group, which developed the first high charge state ECR source in 1974[1] and remains very active in source development, is an exception in that it is not directly associated with an accelerator facility. However, they have supplied ECR sources to many accelerators as evidenced by the number of their sources listed in Table 1 (Minimafios, Neo-Mafios, and CAPRICE).

2. ECR Source Design and Performance

Even though it has been 18 years since the first source produced high charge states, ECR source development remains very active. The development continues in spite of or perhaps because source design and performance has not yet been reduced to a known set of scaling laws. In Section 3 we discuss some aspects of ECR physics, but in this section we describe the present state of the art and summarize present performance standards.

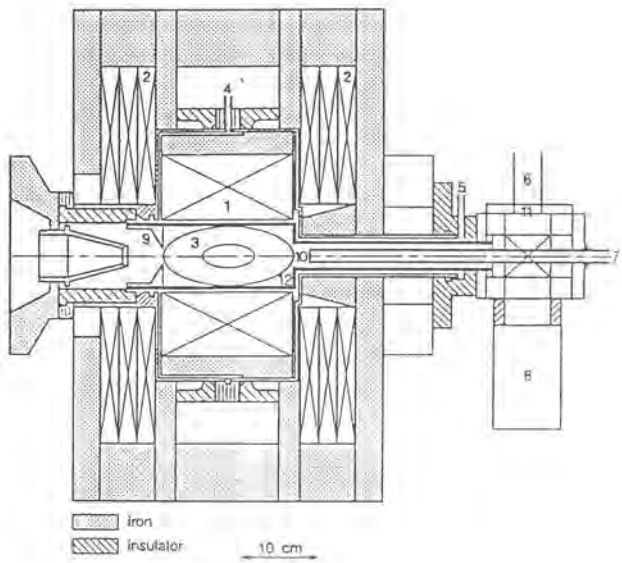


Fig. 1. Elevation view of the CAPRICE-2ω_{ce} source. (1) shows the sextupole magnet. (2) shows the solenoid magnets. (3) shows a inner elipse where the ECR resonance condition is met. On the outer elipse the magnetic field is twice as great. (6) shows RF waveguide which feeds into a transition section. (10) shows the end of the coaxial coupling.

Figure 1 illustrates the main features of the CAPRICE source from Grenoble.[2] The 10 GHz version of this source called CAPRICE-2ω_{ce} produces very large currents of intermediate charge state ions such as O^{6+}, Ar^{11+}, and Kr^{17+}. It is compact in size with a plasma chamber 16 cm long and 6.6 cm in diameter, simple in design, and has excellent stability. Three features make this source different from other 10 GHz sources. First, it operates with a very high axial mirror field of about 1 T. Second, the radial field is also very strong with a value at the wall of 0.8 T, more than twice that need to maintain a closed ECR zone at 10 GHz. Third, the microwave power is coupled into the plasma chamber through a coaxial feed, while most other sources

Table 1

Applications of high charge state ECR sources with accelerators. OP indicates the source is operational with the accelerator. TE indicates the source is being tested. PR indicates the project is in the proposal stage.

Lab Name	Country	Status	Source Name,Type or Comments
	Cyclotrons		
Louvain-la-Neuve	Belgium	OP	OCTOPUS (8.5 GHz)
Lanzhou	China	OP	CAPRICE (10GHz)
Jyväskyla	Finland	OP	Derived from RT-ECR at MSU(6.4GHz)
Ganil	France	OP	ECR3, ECR4 (14 GHz)
SARA	France	OP	Minimafios, CAPRICE
Jülich	Germany	OP	ISIS, (14 GHz) superconducting
Karlsruhe	Germany	OP	LISKA, lithium source
VECC	India	TE	Derived from CP-ECR at MSU
Catania	Italy	PR	Plans for superconducting ECR
RIKEN	Japan	OP	RIKEN ECRIS (10GHz)
INS	Japan	OP	SF-ECR (10 GHz)
JAERI,Takaski	Japan	OP	OCTOPUS
KVI, Groningen	The Netherlands	OP	Minimafios, KVI-ECRIS-2
NAC	S. Africa	TE	Minimafios (10GHz)
Uppsala	Sweden	OP	Derived from RT-ECR at MSU
PSI	Switzerland		To operate in 1993
LBL	USA	OP	LBL-ECR (6.4 GHz), AECR (14 GHz)
MSU	USA	OP	CP-ECR,RT-ECR, SC-ECR
Texas A&M	USA	OP	6.4 GHz
Dubna	Russia	TE	
	Heavy-ion Linacs		
GSI	Germany	OP	CAPRICE
Argonne	USA	OP	PI-ECR (10 GHz)
Legnaro	Italy	TE	Alice(14 GHz)
RIKEN	Japan	OP	Neomafios (8GHz)
	Synchrotrons		
NIRS-HIMAC	Japan		Medical Acc., NIRS-ECR(10GHz)
GSI	Germany	OP	CAPRICE (14GHz)
CERN	Switzerland	OP	Minimafios (14 GHz)
	Storage Rings		
Uppsala	Sweden	OP	Derived from RT-ECR at MSU(6.4GHz)
INS-TARN2	Japan		
GSI	Germany	OP	CAPRICE
	Radioactive Beam		
TRIUMPH	Canada	TE	TISOL, Isotope Separator
ISN, Grenoble	France	PR	ERIC, Reactor to Cyclotron
Louvain-la-Neuve	Belgium	OP	6.4 GHz

launch the RF from a rectangular or circular waveguide. Pumping is provided by a small turbomolecular pump in the injection region. A 14 GHz version of CAPRICE has recently been installed at GSI. Another 14 GHz source called ECR4 has been built at GANIL,[3] which differs in engineering design, but follows the general features of CAPRICE.

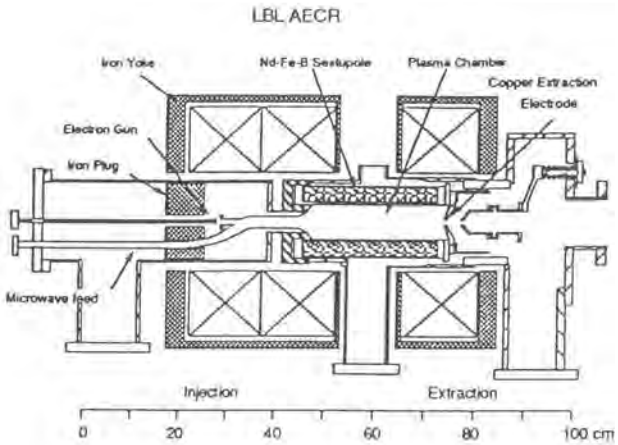


Fig. 2. Elevation view of the LBL AECR. This Nd-Fe-B sextupole has radial slots for pumping the plasma chamber. RF power is fed by a transition from rectangular to round waveguide.

Figure 2 illustrates the design of the AECR built at Berkeley.[4] This source operates at 14 GHz and differs in design from CAPRICE in several features. The plasma chamber is 30 cm in length and 7 cm in diameter. In place of an RF driven first stage, the AECR has an electron gun which can inject up to 100 ma of electrons into the plasma chamber. It also has 6 radial slots in the plasma chamber to provide pumping to the second stage. This also allows solid materials to be injected from ovens located radially. The main drawback is that the sextupole strength at the wall is only 0.6 T because the radial slots limit the achievable field. The peak performance of this source is high, but it has proved difficult to maintain the performance for the long periods required for operation with the cyclotron.

The SC-ECR built at Michigan State University is the newest ECR to use superconducting coils to produce the magnetic field.[5] The only other superconducting ECR source still in operation is ISIS at Jülich.[6] The plasma chamber of the SC-ECR is relatively large with a length of 45 cm and a diameter of 15 cm, which is characteristic of superconducting sources. The superconducting coils are designed to reach fields sufficient for the source to operate up to 35 GHz. The sextupole magnet can be adjusted independently, which allows the detailed study of how radial field strength affects source performance. The source has been operated at 6.4 GHz and performs better than the MSU RT-ECR. Extensive testing at 14 GHz is planned for the near future.[7]

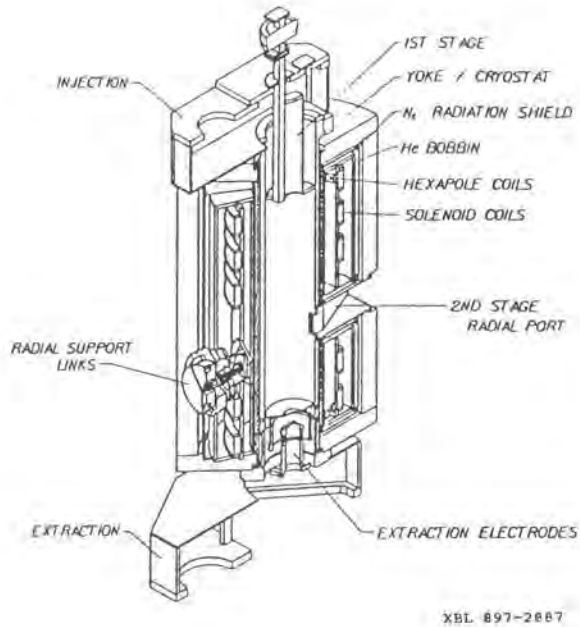


Fig. 3. Cutaway view of the MUS SC-ECR. This source operates in the vertical position. An iron yoke strengthens and confines the magnetic field produced by superconducting coils.

In Tables 2a and 2b, the current performance of ECR sources is summarized for elements as light as oxygen and heavy as uranium. These tables are not meant to be all inclusive since the field of ECR sources is so large and diverse and data was selected from published results only. It does illustrate how ECR sources perform for various ions at frequency from 6 to 18 GHz and in two modes: (CW) continuous operating and (AG) a pulse mode using the plasma after glow. For lighter elements we have quoted the performance for gases only, while the very heavy elements are by necessity produced from solids. The performance of ECR sources with metal ions and the techniques for their production was recently reviewed[14] and will not be repeated here. If we compare the values in the tables to those produced a decade earlier it is clear how much progress has been made. For example, O^{6+} is up from 15 to 800 eμA, Ar^{12+} is up from 0.3 to 80 eμA, and instead of 0.1 eμA of Kr^{16+} 1.0 eμA of Kr^{26+} can now be produced.

Table 2a
Representative beams for various ECR sources for oxygen to krypton . CW indicates continuous power. All currents in eμA.

ION	6.4 GHz (CW)	10 GHz (CW)	14 GHz (CW)	18 GHz (CW)
O^{6+}	82^{8}	385^{2}	475^{10}	800^{12}
O^{7+}	20^{9}	45^{2}	131^{10}	180^{12}
Ar^{8+}	106^{8}	500^{2}	500^{11}	
Ar^{9+}	72^{8}	260^{2}	300^{11}	
Ar^{11+}	18^{8}	60^{2}	141^{10}	130^{13}
Ar^{12+}	13^{8}	32^{2}	78^{10}	80^{13}
Ar^{13+}	5^{8}	11^{2}	34^{10}	45^{13}
Ar^{14+}	1.4^{8}	4^{2}	17^{10}	20^{12}
Ar^{16+}			1.4^{10}	1.4^{13}
Kr^{13+}	21^{8}		115^{11}	
Kr^{15+}	16^{8}		90^{11}	
Kr^{17+}	7^{8}	42^{2}	50^{11}	
Kr^{19+}	2^{8}		36^{10}	
Kr^{21+}		7^{2}	13^{10}	
Kr^{23+}		1.9^{2}	6.8^{10}	
Kr^{24+}		1^{2}	4^{10}	
Kr^{25+}			2.2^{10}	
Kr^{26+}			1^{10}	

Table 2b
Representative beams for various ECR sources for xenon to uranium. CW indicates continuous power. AG indicates the RF power is pulsed and the current is measured during a short pulse produced in the plasma afterglow. All currents in eμA.

ION	6.4 GHz (CW)	10 GHz (CW)	14 GHz (CW)	14 GHz (A. G.)	18 GHz (A. G.)
Xe^{22+}	3^{8}	34^{2}	30^{11}		
Xe^{25+}	2^{8}	25^{2}	17^{11}		
Xe^{27+}		8.4^{2}	12^{10}		
Xe^{29+}		1.9^{2}	3^{11}		
Xe^{31+}			1^{10}		
Pb^{25+}		16^{2}	30^{11}	70^{3}	
Pb^{27+}		10.5^{2}	25^{11}	90^{3}	
Pb^{31+}		2.2^{2}	8^{11}	75^{3}	
Pb^{32+}		1.1^{2}		55^{3}	
Bi^{23+}	3.1^{8}				
Bi^{25+}	3.6^{8}		3.8^{10}		80^{13}
Bi^{27+}	3^{8}		5.5^{10}		85^{13}
Bi^{29+}	1.6^{8}		5.7^{10}		90^{13}
Bi^{31+}			4.5^{10}		85^{13}
Bi^{34+}			1.5^{10}		30^{13}
Bi^{36+}					15^{13}
U^{21+}		28^{2}			
U^{23+}		21^{2}	22^{11}		
U^{25+}		14^{2}	18^{11}		
U^{27+}		8^{2}	10^{11}		
U^{29+}		3.5^{2}			
U^{31+}		1^{2}			

Some general characteristics of ECR source performance can be observed in the tables. First the intensity for high charge state ions improves as the source frequency is increased. The results for Minimafios-18GHz are particularly impressive.[12, 13] However, as discussed below, frequency is only one of many factors which determine source performance and at a given frequency there is a wide range of source performance. Second, even though uranium has 92 electrons and xenon only 54, the intensities of U^{29+} and U^{31+} are not higher than those for Xe^{29+} and Xe^{31+}. While this is in part due to the increased difficulty in producing uranium beams since it is a solid, it also indicates the maximum charge state attainable increases very slowly with increasing atomic number for very heavy elements.

3. ECR Physics and Source Design

The basic concepts for high charge state production in ECR sources are relatively straight forward. Electrons are heated by microwave power on a surface defined by the ECR resonance condition

$$\omega_{RF} = eB/m_e \qquad \text{Eq (1)}$$

where B is the magnitude of the magnetic field, e the electron charge and m_e the mass of the electron. The ionization is produced largely by stepwise electron impact ionization and the degree of ionization is determined by $n_e\tau_i$, where n_e is the density of hot electrons and τ_i is the ion confinement time. Computer codes based on these concepts have been developed which incorporate the cross sections for ionization, charge exchange and other atomic physics processes involved.[15,16] These models usually require that the plasma density, neutral density, confinement time, and electron temperatures be specified. With a reasonable set of parameters these codes can reproduce measured charge state distributions. From these models it is clear that for high charge states the sources should run at low neutral pressures, high plasma densities, with sufficiently high electron temperatures, and long ion confinement times.

The challenge in understanding, predicting, or improving ECR performance comes from the tenuous connection between the set of internal variables discussed above and the external variables of ECR sources. The external variables available in the design stage include size, shape and strength of the magnetic field, microwave frequency and power, microwave coupling, plasma chamber dimensions, and pumping. Once the source is built the adjustable variables are axial magnetic field, gas flow, and microwave power. During the last decade many ideas to improve the source performance have been proposed and tried. To increase τ_i some sources were made large. This was not successful and the trend is to small compact sources such as CAPRICE. To reduce the neutral pressure increased pumping to the plasma chamber has been used. While this

may help when producing low density high charge state plasmas, it conflicts with the need to increase the radial magnetic field described below.

To increase the plasma density, sources have been built to operate at higher frequencies. The idea is that the ECR sources must operate below the critical density and since it scales as f^2, higher densities should be achieved at higher frequencies.[17] In order to increase frequency, the ECR resonance condition given by Eq. 1 requires the magnetic field must also be increased proportionally. While increasing the frequency has resulted in improved performance as shown in Table 2a and 2b, the improved performance is not as great as would be expected if the plasma density was increasing as f^2.[13] Another approach has been to increase the magnetic field of both the sextupole and axial mirrors as with the CAPRICE source. This was based on a prediction of improved microwave to coupling.[2] This approach has produced very good performance as shown in Tables 2a and 2b for the 10 GHz Caprice source. Tests with the MSU SC-ECR, on which the radial field strength can be independently adjusted, also indicated that increasing the radial field strength enhanced high charge state production.[7] So it appears that both higher frequency and stronger magnetic fields improve performance although the connection to internal variables remains unclear. The fact that the plasma density increases more slowly than f^2 indicates some other mechanism may be limiting it. This indicates there is still the possibility for much better performance if this limitation can be overcome.[13]

One external variable which has been largely overlooked, is the coupling of microwave power into the plasma. This is a complex question since most ECR sources operate in multimode configuration. That is the microwave modes of the plasma chamber are spaced close together and depending on their loaded Q (Q_L) several modes may be excited at one time. In addition, the dielectric constant for the plasma depends on the density so the cavity modes are shifted in frequency roughly as

$$\omega^2 = \omega_o^2 + \omega_p^2 \qquad \text{Eq (2)}$$

where ω_o is the mode frequency in vacuum and ω_p is the plasma frequency given by

$$\omega_p^2 = 4\pi e^2 n_e/m_e \qquad \text{Eq (3)}$$

The typical loaded Q's for ECR plasma chambers are also not known. While the cavity Q_o can be estimated for any single mode, it is difficult to measure or calculate the plasma loading. Measurements in Grenoble indicated that in a stainless steel cavity only 20% of the microwave power was coupled into the plasma.[18] While the question is complex, there is considerable evidence that microwave cavity modes play an important role in the coupling to the plasma. Much of the tuning done with ECR sources involves making small changes in the magnetic field and microwave power. Small changes in magnetic field can result in large changes in high charge state production, total extracted current, and bremsstrahlung radiation from the source. Other evidence includes instabilities where the plasma jumps back and forth between two states, suggesting the microwave field in the chamber shifts between two modes. Finally, a hysteresis is sometimes observed when a source is carefully tuned to peak at high output and then jumps back to a very different state. To recover it is sometimes necessary to reset the source parameters and work the output back up.

Table 3

Calculated frequencies in GHz for all modes in vacuum between 9.5 and 10.5 GHz for a cylindrical cavity 16.28 cm in length and 6.6 cm in diameter.

Mode	Frequency		Mode	Frequency
TE 3,1,8	9.55394		TE 2,2,3	10.0888
TE 1,1,10	9.59107		TM 1,2,0	10.1513
TM 3,1,3	9.63604		TM 1,2,1	10.1930
TE 5,1,3	9.68456		TE 0,2,1	10.1930
TM 2,1,6	9.71339		TE 2,1,10	10.2185
TE 2,2,1	9.74641		TM 2,1,7	10.2657
TM 0,1,10	9.84895		TE 3,1,9	10.2815
TE 2,2,2	9.87620		TM 3,1,5	10.3167
TM 3,1,4	9.93960		TM 1,2,2	10.3172
TM 1,1,9	9.97518		TE 0,2,2	10.3172
TE 0,1,9	9.97518		TE 5,1,5	10.3621
TE 5,1,4	9.98665		TE 2,2,4	10.3791
TE 4,1,7	10.0400		TE 1,1,11	10.4793
TE 1,2,7	10.0556			

If we accept for the moment this picture of cavity modes, then can techniques be developed to determine which modes couple efficiently to the plasma at the ECR surface and then control those modes? For a simple cylindrical cavity it is easy to calculate the distribution of modes without plasma. In Table 3 a set of modes are listed for a CAPRICE size cavity operating at 10 GHz. The average mode spacing is 37 MHz not counting mode degeneracies. The half power points for cavity modes are given by

$$\Delta f/f = 1/Q_L \qquad \text{Eq (4)}$$

Substituting the average mode spacing into this equation gives Q_L of 270. So if the cavity modes have Q's significantly higher that this they will not necessarily overlap, while if the Q's are lower then there would be a significant overlap. It remains to be experimentally or theoretically determined what the typical Q's are for ECR

sources. To determine if a cavity mode will couple well to the plasma, calculations could be made to evaluate the coupling of the RF electric fields to the transverse energy of the electrons. By integrating this over the ECR surface the relative coupling strength could be determined. These calculations could indicate whether it is advantageous to excite TE or TM type modes. Some modes will couple only weakly to the electrons because their electric field patterns don't overlap the ECR surface strongly. Techniques to experimentally control the modes include using coupling schemes which preferentially excite one type of mode, selectively loading unfavorable modes, using adjustable coupling, or even dynamically tunable cavities. The coaxial coupling developed for CAPRICE has an adjustable tuning short in the waveguide to coaxial transition section, which may allow some mode control.[19] Some of these techniques have been used for low charge state ECR sources for commercial applications. In these sources, they adjust both the cavity frequency and the coupling strength and report significant improvements in the transfer of microwave energy to the plasma.[20]

4. Special Techniques

There are several special techniques which have been developed recently to boost ECR source performance. Surface coatings with high secondary emission coefficients such as SiO_2, Mb, Ca and Th have been applied to the walls of ECR plasma chambers.[17,21] Very recently Al_2O_3 has also been shown to be very effective in enhancing high charge state production.[22] Direct injection of electrons into the plasma chamber was developed with the LBL AECR and it can result in an increase of 2 or more in extracted intensities.[4] A similar technique using a bias disk to intercept plasma and feed electrons back in has also proved effective.[23,24] The optimum bias voltages and currents for the disks are similar in magnitude to those for the electron gun. Short intense pulses suitable for synchrotrons have been developed by utilizing the beams extracted during the plasma afterglow.[3,13] Some data is given in Table 2b for afterglow currents and it appears that for heavier elements this can produce much higher intensities than continuous operation. The typical pulse lengths are on the order of 1 ms.

5. Conclusion

As we have indicated, the field of ECR sources continues to grow and diversify. New applications such as radioactive beam accelerators are appearing. With ECR sources now operating in 14 countries, the effort has truly become international. It is difficult to predict where the next major step will come from. It could come from higher frequencies, stronger magnetic fields, better coupling systems, or specialized techniques. However there are ample indications that there is still room for better performance from ECR sources.

6. Acknowledgment

The author gratefully acknowledges the great number of preprints and personal communications sent by the ECR source and accelerator community. This was a great help in preparing this paper. Zuqi Xie helped summarize current performance levels and helped clarify many of the concepts presented here.

This work was supported by the Director, Office of Energy Research, Division of Nuclear Physics of the Office of High Energy and Nuclear Physics of the U.S. Department of Energy under Contract DE ACO3-76SF00098.

7. References

1) Geller, R., " Electron Cyclotron Resonance Multiply Charged Ion Sources," IEEE Trans. Nucl. Sci. NS-**23**, 904 (1976).
2) Jaquot, B. and Pontonnier, M, "The New CAPRICE source-Magnetic Structures and Performances," in **Proceedings of the 10th International Workshop on ECR Ion Sources** (Oakridge National Laboratory, Knoxville, 1990) pp. 133-155.
3) Sortais, P., "Pulsed ECR Ion Source Using The Afterglow Mode," Rev. Sci. Instrum. **63** (4), 2801 (1992).
4) Xie, Z., Lyneis, C.M., Lam, R.S., and Lundgren, S.A., "Enhanced ECR Ion Source Performance With An Electron Gun," Rev. Sci. Instrum. **62**, 775 (1991).
5) Antaya, T.A., "A Review of Studies For a Variable Frequency Superconducting ECR Ion Source at MSU," J. Phys. (Paris) Colloq **50**, cl 707 (1989).
6) Beuscher, H., "Status of the ISIS-ECR-Source and its Operation at the Cyclotron," in **Proceedings of the International Conference on ECR Ion Sources and their Applications** (NSCL Report#MSUCP-47, East Lansing, 1987) pp. 33-41.
7) Antaya, T.A. (Private Communication).
8) Lyneis, C.M., "Operating Experience with the LBL ECR Source and their Applications," in **Proceedings of the International Conference on ECR Ion Sources and their Applications** (NSCL Report #MSUCP-47, East Lansing, 1987) pp. 42-56.
9) Lyneis, C.M., "High Performance Single Stage Operation of the LBL ECR and the Design of an Advanced ECR Ion Source," J. Phys. (Paris) Colloq. **50**, cl 689 (1989).
10) Lyneis, C.M., Xie, Zuqi, Clark, D.J., Lam, R.S. , Lundgren, S.A., "Preliminary Performance of the LBL AECR," in **Proceedings of the Workshop on the 10th International ECR Ion Sources** (Oakridge National Laboratory, Knoxville, 1990) pp. 47-62.
11) Sortais, P. Attal, Bisch, M., Bourgarel, M.P., Cornen, P.M., Leherissier, J.Y., Rataud, G. Schmiechen, "Results of the New "ECR 4" 14.5 GHz ECRIS, at GANIL," in **Proceedings of the Workshop on the 10th International ECR Ion Sources** (Oakridge National Laboratory, Knoxville, 1990) pp. 36-46.

12) Barue, C., et al, "Hot Electron studies in the minimafios ECR Ion Source," Rev. Sci. Instrum. **63** (4), 2801 (1992).
13) Melin, G., Hitz, C., Barue, C., Bourg, F., Briand, P., Delaunay, M., Geller, R., Girad, A., Jaquot, B., Ludwig, P., Pontonnier, M., "Electron Cyclotron Resonance Sources of Multicharged Ions: State of the Art, Recent Developments and Prospects," in **Proceedings of EPAC 92**, Berlin (1992) (To be published).
14) Geller, R., Ludwig, P. and Melin, G., "Metal Ion Production in ECRIS," Rev. Sci. Instrum. **63**, 2795 (1992).
15) Jongen, Y., "E.C.R. Electron Acceleration," **in Proceedings of the Workshop on the sixth International ECR Ion Source** (Lawrence Berkeley Laboratory, Berkeley, 1985) pp. 238-255.
16) West, H.I. Jr., "Calculation of Ion Charge-State Distribution in ECR Ion Source," (**UCRL-53391, LLNL,** 1982).
17) Geller, R., et al, "The Grenoble ECRIS Status 1987 and Proposals for ECRIS Scalings," in **Proceedings of the International Conference on ECR Ion Sources and their Applications** (NSCL Report#MSUCP-47, East Lansing, 1987) pp. 1-32.
18) Melin, G., et al, "Some Particular Aspects of the Physics of ECR sources for Multicharged Ions," Rev. Sci. Instrum. **61**, 236 (1990).
19) Delaunay, M., Jacquot, B. and Pontonnier, M., "Exploration axiale du plasma RCE d'une source d'ions multicharges CAPRICE," Nucl. Instru. and Math. **A305,** 223 (1991).
20) Asmussen, J., Hopwood, J. and Size, F.C., "A 915 MHz/2.45 GHz ECR Plasma Source for Large Area Ion Beam and Plasma Processing, "Rev. Sci Instrum. **61** (1), 250 (1990) and Amussen, J. (private communication).
21) Lyneis, C.M., "Operation Experience with the LBL ECR Source," in **Proceedings of the International Conference on ECR Ion Sources and their Applications** (NSCL Report#MSUCP-47, East Lansing, 1987) pp. 42-56.
22) Nakagawa, T., "Effect on Coating on the Plasma Chamber Wall in RIKEN Electron Cyclotron Resonance Ion Source," Japanese Journal of Applied Physics Vol **30**, 930 (1991).
23) Melin, G., et al., "Recent Developments and Future projects on ECR Ion Sources at Grenoble" in **Proceedings of the 10th International Workshop on ECR Ion Sources** (Oakridge National Laboratory, Knoxville, 1990) pp. 1-15.
24) Gammino, S., Sijbring, J. and Drentje, A.G., "Experiment with a Biased Disk at the K.V.I. ECRIS," Rev. Sci. Instrum. **63** (4), 2872 (1992).

PERFORMANCE OF THE LBL AECR SOURCE AT VARIOUS FREQUENCIES

Z. Q. Xie, C.M. Lyneis, S.A. Lundgren and D. Collins
Nuclear Science Division, Lawrence Berkeley Laboratory, Berkeley
CA, 94702, USA

ABSTRACT

To study the effects of frequency on an electron cyclotron resonance (ECR) ion source, the LBL Advanced ECR ion source (designed to operate at 14 GHz) has been tested at 6.4, 10, and 14 GHz with one plasma chamber (ID = 6.0 cm), a permanent sextupole magnet ("closed sextupole") with a field strength of 0.84 Tesla at the chamber wall, and no radial vacuum pumping. Pure oxygen was used as the running gas for a fair comparison. The source was tested as a single stage, as well as with cold electron injection using an electron gun in place of a conventional microwave-driven first stage. Higher frequency, with a higher axial magnetic field to ensure a closed ECR zone for electron heating, does give better performance. As demonstrated before, at each frequency electron injection led to about a factor of two increase in the high charge state oxygen beam intensity. The 14 GHz performance of the AECR source with the closed sextupole magnet was compared to the "slotted sextupole" (a plasma chamber with radial pumping slots of 7.0-cm dia and a weaker magnet of 0.64 Tesla at the chamber wall). Results show that a stronger sextupole magnet alone does not automatically improve the source performance.

1. INTRODUCTION

Development of Electron Cyclotron Resonance sources for production of high intensity and high charge state ion beams began in the early '70s.[1] The detailed operation of ECR sources involves control of many parameters including frequency,[2] magnetic field profile and strength, gas mixing,[3] plasma confinement, and microwave heating. How these parameters affect performance is still being studied. Frequency scaling in ECR sources was first predicted and then demonstrated on various ECR sources by Geller, et al.[2] Scaling predicts that the plasma density in ECR sources should increase as the square of frequency just as the plasma critical density does. Thus, by running at a higher frequency the ECR source should produce higher charge state ion beams with higher intensities. In the past few years ECR development has been centered on higher frequency and higher magnetic fields.[4] ECR sources around the world operate at frequencies between 2.5 and 18 GHz. Sources at 35 GHz and higher have been proposed.[5,6] In general, sources operating at higher frequencies with higher axial and radial magnetic fields work better. However, the CAPRICE ECR[7] ion source, which operates at 10 GHz, has produced results comparable to 14 GHz sources. CAPRICE has a microwave coaxial feed mechanism and very strong mirror and sextupole magnetic fields. It has also shown very good long-term stability. Therefore the question of whether the frequency or magnetic field, either axial or radial, enhances ECR performance the most, is still open.

The ECR Group from Michigan State University reported the NSCL (National Superconducting Cyclotron Laboratory) superconducting ECR ion source running at 6.4 GHz, with a sextupole magnetic field strong enough for running at 14 GHz, can produce good stability at about the same beam intensity as it has at 14 GHz.[8] Can higher sextupole magnetic fields alone improve the source performance on every ECR ion source? If so, new ion sources could be built with strong sextupole fields and operated at lower frequencies and reduced costs. Clarifying the effect of the sextupole magnetic field on the ECR source performance would give better understanding of the physics process involved in ECR ion sources.

2. DESCRIPTION OF THE AECR

Tests at 6.4, 10, and 14 GHz were carried out on the LBL Advanced ECR (AECR) ion source, which is designed to operate at 14 GHz. Figure 1 illustrates the design of the AECR. A detailed description of this source can be found elsewhere.[9,10] Microwaves are launched on axis by making a transition, from a rectangular waveguide to a circular waveguide, inside the injection region. An iron plug added to the injection region increases peak axial field to more than 1 Tesla. The sextupole field is produced by a Nd-Fe-B multipole magnet. Pumping for the copper plasma chamber and the extraction region is provided by a 240 and a 500 l/s turbomolecular pumps, respectively. A lanthanum hexaboride (LaB_6) electron gun is installed at the location of a conventional microwave-driven first stage as indicated in Fig. 1. It injects cold electrons axially into the plasma chamber.[10]

The sextupole magnet was originally designed as a slotted sextupole, to accommodate radial vacuum pumping, oven access, and solid material insertion. This limited the field strength to 0.64 Tesla at the plasma chamber wall as shown in Fig. 2. The internal diameter and the length of the plasma chamber are 7.0 cm and 30 cm, respectively. During the initial tests, using the electron gun, the AECR ion source has produced intense, high charge state ion beams.[10] For example, 131 eμA of O^{7+} and 475 eμA of O^{6+} were

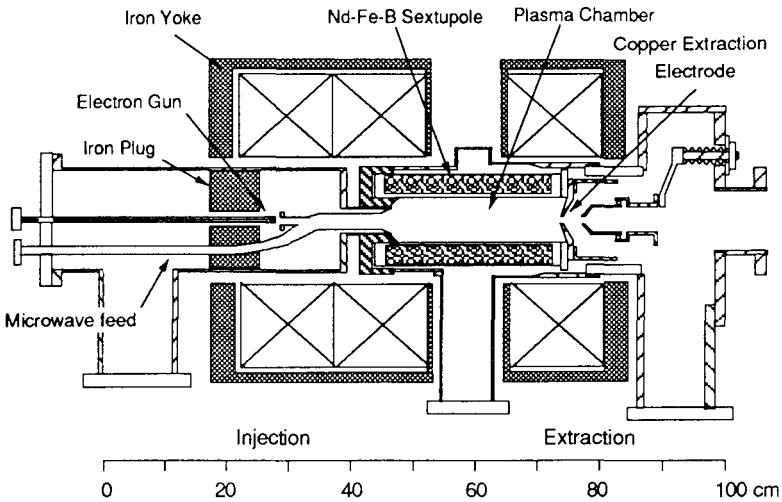


Fig. 1. Schematic drawing of the AECR. The magnetic field is produced by copper coils in an iron yoke. The iron plug on the injection side was added to increase the axial magnetic field. Electrons from a LaB_6 filament flow along the axial magnetic field lines into the plasma chamber.

produced. Typically, the gun was biased at 50 to 150 V and produced bias currents of 20 to 100 mA. The source showed very good short-term stability, but its long-term stability was not sufficient for regular operation with the 88-Inch Cyclotron at Lawrence Berkeley Laboratory. Based on the reports mentioned in the introduction, we suspected that the reduced long-term stability was caused by a weak sextupole field. Thus, a modified plasma chamber was built. It eliminated the pumping slots and reduced the chamber ID from 7.0 to 6.0 cm. This "closed sextupole" design has increased the sextupole field at the plasma chamber wall from 0.64 to 0.84 Tesla, a 30 percent increase over the field strength shown in Fig. 2.

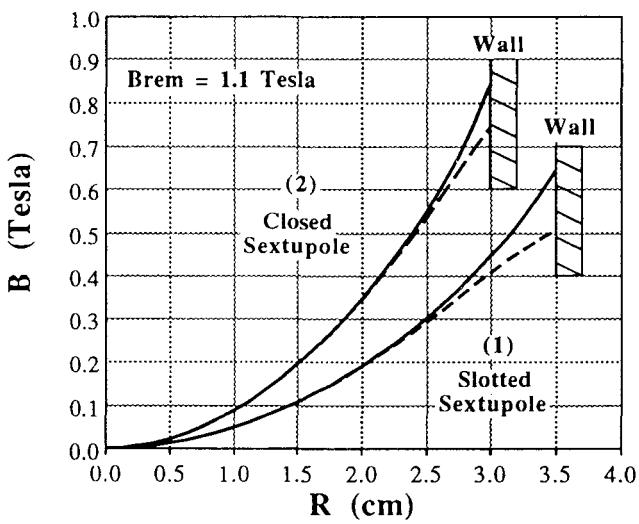


Fig. 2. Two radial field profiles are shown for the AECR. The solid lines show the pole field strength and the dashed lines show the gap field intensity between two adjacent sextupole bars. (1) indicates the case of the plasma chamber with an ID = 7.0 cm (slotted sextupole) and a maximum field of 0.64 Tesla at the chamber wall. (2) illustrates the case of the smaller chamber of ID = 6.0 cm (closed sextupole) and the maximum field strength is increased to 0.84 Tesla.

3. PERFORMANCE AT VARIOUS FREQUENCIES

Performance of the AECR at 6.4, 10, and 14 GHz with pure oxygen gas for the two mode operations is presented below. First, with the electron gun injecting cold electrons axially into the plasma chamber; second, the source was run as a single stage source.

Results with the closed sextupole are shown in Fig. 3 for the cold electron injection and Fig. 4 for the single stage mode operation. The source was tuned to optimize the O^{6+} and O^{7+} ion beam currents. During the tests, the axial magnetic field was scaled in proportion to each frequency to ensure a closed ECR surface for electron heating. At 14 GHz and with cold electron injection, no improvement in output was observed for the closed sextupole compared to the slotted sextupole. Comparison to the initial tests[10] with the slotted sextupole shows the output intensities for O^{7+} and O^{6+} actually were down by factors of 5 and 3, respectively.

At lower frequencies, the source produced lower outputs as can be clearly seen in Fig. 3 and Fig. 4. At 6.4 GHz and single stage mode operation, the source produced virtually no x-rays and the output intensities for O^{6+} and O^{7+} were down by factors of 20 and 100, respectively, compared to the 6.4 GHz LBL ECR.[11] The explanation for reduced output may be that the microwave power was not efficiently coupled to the plasma thus the electron density and temperature were low. At 6.4 GHz, tests were also done to raise the axial field to construct a very high mirror field configuration (like the CAPRICE source at 10 GHz), but no enhanced beam output was observed. Plasma died out as soon as the fundamental ECR zone was eliminated. At 10

GHz, the output for O^{6+} and O^{7+} increased, as shown in Fig. 4, by factors of 5 and 10 respectively. The x-ray level also increased. Such outputs are still lower than other 10 GHz ECR sources.[7] At each frequency with cold electron injection, compared to the single stage mode operation, the high charge state oxygen ions increased a factor of two or higher as demonstrated previously at 14 GHz.[10]

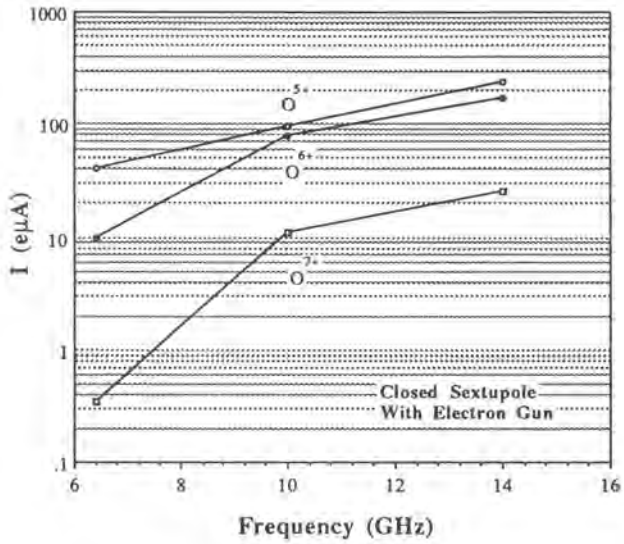


Fig. 3. High charge state oxygen ions produced by the AECR with the closed sextupole magnet and cold electron injection at 6.4, 10, and 14 GHz.

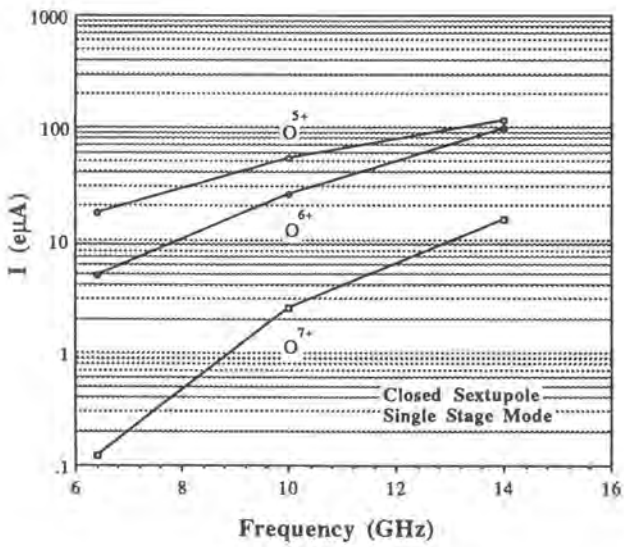


Fig. 4. High charge state oxygen ions produced by the AECR with the closed sextupole magnet operated at a single stage mode at 6.4, 10, and 14 GHz.

Tests at these three frequencies have shown the source tuning parameters were still very critical to the source output. A change less than half percent of the microwave power, axial magnetic field, or neutral gas input can cause the source become unstable. One could at times tune the source into a very quiet mode with above indicated output for a period of a few hours. Then, the source would jump spontaneously to an unstable mode with very low output and a higher x-ray level. In a comparison between the original sextupole and the stronger sextupole at 14 GHz, the source long-term stability is just slightly improved and still not sufficiently stable for regular operation with the cyclotron.

4. DISCUSSIONS AND CONCLUSIONS

The motivation for building a stronger sextupole magnet is to maintain or enhance the source output and improve its long-term stability. As these tests have shown, the AECR ion source operating at 6.4, 10, and 14 GHz with the stronger sextupole magnet, only minor improvement of long-term source stability has been observed. In this study, the output of O^{7+} ions is better when the source is operating at higher frequency. Maximum beam output of O^{7+} with the stronger sextupole actually dropped a factor of 5 compared to the AECR performance with the slotted sextupole. Such reduced output indicates that the source is running at low plasma density. The low density plasma is thought to be due to poor microwave coupling, since the plasma chamber size has been changed (the cavity r-f operating mode could have changed). When the ion source is running at low plasma density with no radial vacuum pumping, neutral gas pumping is not sufficient .

The criticality of the source tuning parameters may be caused by the high Q of the plasma chamber. It is made from copper and the resonances allowed in the cavity may not overlap each other. Jumping between r-f modes is likely to happen as plasma is produced. The estimated power absorbed in the plasma is about 20 percent of the input microwave power.[12] This won't load down the cavity enough to lower the Q. A lower Q test was carried out by inserting a stainless steel liner into the copper chamber to reduce the chamber Q by a factor of ~7. At 14 GHz the source produces about the same output as the copper chamber, but the long-term stability is dramatically improved, as is the source tunability. The output intensity is linear with the axial magnetic field over a few percent of field change and, to a great extent, to the input microwave power. This could indicate that the ECR source should not be operated with a very high Q chamber unless all the allowed cavity modes overlap each other. The best Q value for an ECR ion source at a specific configuration should be given further and more detailed study in future.

We have concluded from this study that a high sextupole magnetic field along does not automatically improve the source performance. Source performance can benefit from a strong sextupole field if the microwave power can be efficiently coupled to the plasma, as does the CAPRICE source. For the same strong sextupole field, a

higher frequency and a higher axial magnetic field, the ECR source can produce more beam output. This is consistent with frequency scaling. AECR source long-term stability may ultimately depend upon the optimum Q value of the plasma chamber.

The authors wish to thank the mechanical and electronic engineering groups and shops of the LBL 88-inch Cyclotron for their great support on this study. This work was supported by the Director, Office of Energy Research, Division of Nuclear Physics of the Office of High Energy and Nuclear Physics of the U.S. Department of Energy under Contract DE ACO3-76SF00098.

5. REFERENCES

1) Geller, R., "New high intensity ion source with very low extraction voltage," Appl.. Phys. Lett. **16**, No **10**, 401 (1970).
2) Geller, R., Jacquot, B. and Sortais, P., "The upgrading of the multiply charged heavy-ion source MINIMAFIOS," Nucl. Instrum. Methods Phys. Res. A **243**, 244 (1986).
3) Drentje, A.G., "Recent developments with the KVI ECR-source," in **Proceedings of the Workshop on the Sixth International ECR Ion Source** (Lawrence Berkeley Laboratory, Berkeley, 1985) pp.73-82.
4) Lyneis, C.M. and Antaya, T.A., "ECR sources for the production of highly charged ions," Rev. Sci. Instrum. **61**, 21 (1990).
5) Antaya, T.A., "A review of studies for the variable frequency superconducting ECR ion source project at MSU," J. Phys. (Paris) Colloq. **50**, Cl 707 (1989).
6) Halverson, W., et al, "Gyrotron-driven ECR ion source scaling, design, and experiments," J. Phys. (Paris) Colloq. **50**, Cl 751 (1989).
7) Jacquot, B., Geller, R. and Drf-Padsi, "CAPRICE 10 GHz - New 2 Ω_{ce} Radial B Field," in **Proceedings of the International Conference on ECR Ion Sources and their applications** (NSCL Report #MSUCP-47, East Lansing, 1987) pp. 254-278.
8) Antaya, T.A., presented at the 10th International Workshop on ECR Ion Sources Knoxville, Tennessee, Nov. 1-2, 1990.
9) Lyneis, C.M., "High Performance Single Stage Operation of the LBL ECR and the Design of an Advanced ECR Ion Source," J. Phys. (Paris) Colloq. **50**, Cl 689 (1989).
10) Xie, Zuqi, Lyneis, C.M., Lam, R.S. and Lundgren, S.A., "Enhanced ECR ion source performance with an electron gun," Rev. Sci. Instrum. **62**, 775 (1991).
11) Lyneis, C.M., "Operating Experience with the LBL ECR Source," in **Proceedings of the International Conference on ECR Ion Sources and their applications** (NSCL Report #MSUCP-47, East Lansing, 1987) pp. 42-56.
12) Melin, G., et al, "Some particular aspects of the physics of the ECR sources for multicharged ions," Rev. Sci. Instrum. **61**, 236 (1990).

ION SOURCES FOR CYCLOTRON APPLICATIONS

K. N. Leung, D. A. Bachman, D. S. McDonald, and A. T. Young
Lawrence Berkeley Laboratory
University of California
Berkeley, CA 94720, USA

ABSTRACT

The use of a multicusp plasma generator as an ion source has many advantages. The development of both positive and negative ion beams based on the multicusp source geometry is presented. It is shown that these sources can be operated at steady state or cw mode. As a result they are very suitable for cyclotron operations.

1. INTRODUCTION

The Magnetic Fusion Energy (MFE) Group at the Lawrence Berkeley Laboratory (LBL) has been engaged in the development of neutral beam systems for fusion applications for the last twenty years. Large area positive hydrogen or deuterium ion sources designed at LBL have been selected and employed by various fusion research facilities in the US. In the next generation tokamak fusion reactors, high energy neutral beams will be needed for plasma heating and for current drive. In order to meet these future demands, negative hydrogen ion sources are also being developed by the MFE Group. These sources must generate amperes of H^-/D^- beams for steady-state operations.

The research on ion sources for fusion applications has led to the development of other types of ion sources, such as radio-frequency (RF) driven ion sources, high charge state ion sources, and multicusp sources capable of delivering almost pure H^+, N^+ or O^+ ions. Most of these ion sources can be operated in steady-state or cw mode. Therefore, they are also useful for most cyclotron applications.

2. HIGH CONCENTRATION H^+ ION SOURCES

Multicusp plasma generators have been used as ion sources for the production of positive and negative ion beams. These ion sources are capable of producing large volumes of uniform and quiescent plasma with densities exceeding 10^{12} ion/cm^3. For this reason, there was a great interest in the early 1980s in applying such devices as ion sources for neutral beam injection systems. To increase plasma penetration by a neutral beam, a high percentage of H^+ or D^+ ions is required. We had investigated the hydrogen ion species composition in a multicusp source with different magnet configurations. Experimental results indicated that the presence of primary ionizing electrons in the vicinity of the plasma electrode increased the percentage of the H_2^+ ions in the extracted beam.

To take advantage of this observation, a magnetic filter was incorporated into the multicusp ion source.[1] This filter, generated either by inserting small magnets into the source chamber or by installing a pair of dipole magnets on the external surface of the source chamber, provides a limited region of transverse B-field which is strong enough to deflect away high energy electrons but allow the plasma to diffuse into the extraction region. The absence of energetic electrons will prevent the formation of H_2^+ or D_2^+ in the extraction region and thus enhance the atomic ion species percentage in the extracted beam. It has been demonstrated that atomic species higher than 85% can be obtained routinely if a multicusp ion source is operated with a magnetic filter.

3. RF-DRIVEN POSITIVE ION SOURCES

A multicusp source can be operated with RF induction discharge to generate positive ion beams. There are several advantages of the RF driven plasma over the dc filament discharge plasma: (1) the RF discharge can be operated with all gases (including oxygen, which can easily poison tungsten filament cathodes); (2) power for heating the cathode is avoided; (3) there are no short life components in the source; (4) a clean plasma free from contamination from the cathode material can be maintained; and (5) the RF power supplies operate conveniently at ground potential.

At LBL, an RF driven multicusp source has been operated in both cw and pulsed modes to generate various positive ion beams. A schematic diagram of a 10-cm-diam RF ion source is shown in Fig. 1. The

RF antenna is fabricated from 4.7-mm-diam copper tubing and is coated with a thin layer of hard porcelain material. The thin coating is slightly flexible and resistant to cracking. It has maintained a clean plasma in cw operation for periods of a week or more; the antenna life expectancy has not yet been determined.

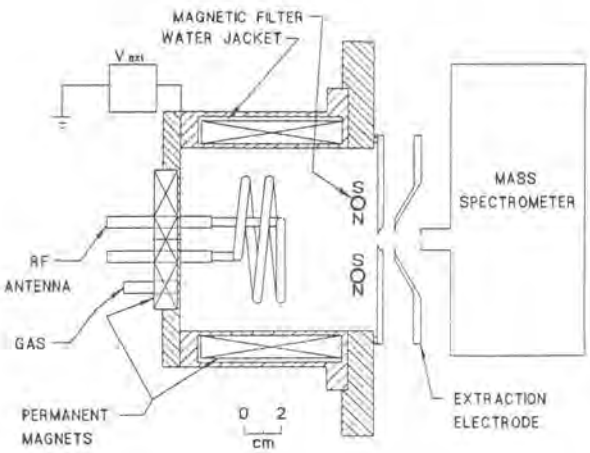


Fig. 1 Schematic diagram of the RF multicusp ion source.

The RF multicusp source has been tested with inert gas plasmas such as He, Ne, Ar, Kr and Xe. Figure 2 shows the extractable positive ion current (and current density) as a function of RF power when the filter rods are removed. The optimum source pressure is typically below 1 mTorr. It can be seen that the output currents increase almost linearly with RF input power. In most cases, the extractable ion current density can be as high as 1 A/cm^2.

We have investigated the hydrogen ion species composition in the RF driven source with and without the magnetic filter. Figure 3 shows the hydrogen ion species distribution as a function of RF power when the filter is in place. The H^+ ion concentration increases from 80 to 97% as the RF power is varied from 12 to 30 kW. The highest current density achieved is about 1.5 A/cm^2.

We have operated the RF driven source with a nitrogen plasma. Similar to the hydrogen discharge, the atomic ion concentration increases with the RF input power. A nearly pure (>98%) N^+ ion beam with current densities in excess of 500 mA/cm^2 has been obtained when the magnetic filter is employed.

In addition to hydrogen and nitrogen, we have also operated this ion source with other diatomic gases such as oxygen. Oxygen plasmas are usually produced by either RF or microwave discharges. It is difficult to use a dc discharge with tungsten filaments because electron emission deteriorates very fast when oxygen is present. The porcelain-coated antenna has been operated very successfully with an oxygen plasma both in pulsed and cw modes. Atomic ion concentration higher than 93% can be achieved with approximately 16 kW of RF power. The extractable ion current density is found to be greater than 500 mA/cm^2.

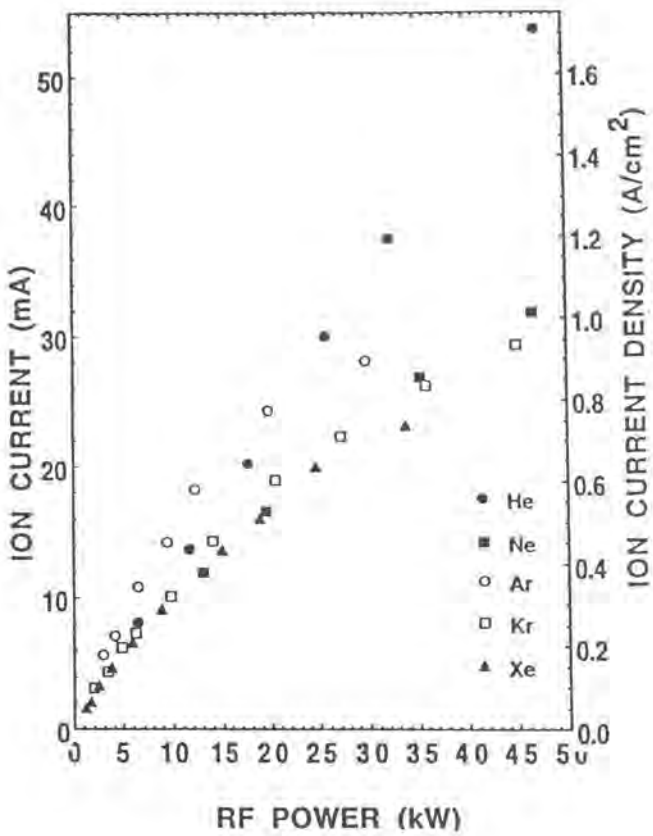


Fig. 2 Extracted beam current and density as a function of RF power for various inert gas plasmas.

4. NEGATIVE ION SOURCES

H^- ions are used extensively in particle accelerators such as cyclotrons, tandem accelerators and proton storage rings. In order to heat plasmas and to drive currents in future tokamak fusion reactors, multiamperes of very high energy neutral beams will be required. The high neutralization efficiency of H^- or D^- ions enables them to form atomic beams with energies in excess of 200 keV. At LBL, two different types of H^- ion sources have been investigated and developed by the MFE Group.

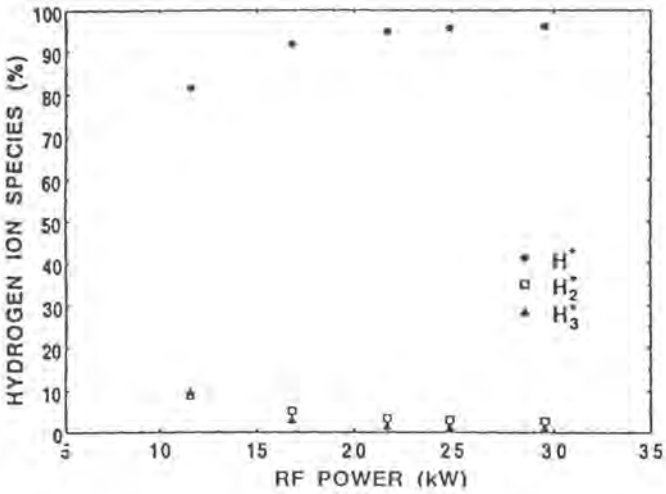


Fig. 3 Hydrogen ion species as a function of RF power when the source is operated with the filter.

4.1 Surface Conversion Negative Sources

Figure 4 shows a LBL type surface conversion source. In this ion source, a water-cooled molybdenum converter is inserted into the multicusp plasma generator. By biasing the converter negatively with respect to the plasma, positive ions are accelerated across the sheath and impinge on the converter surface. H^- (or other negative ions) that are

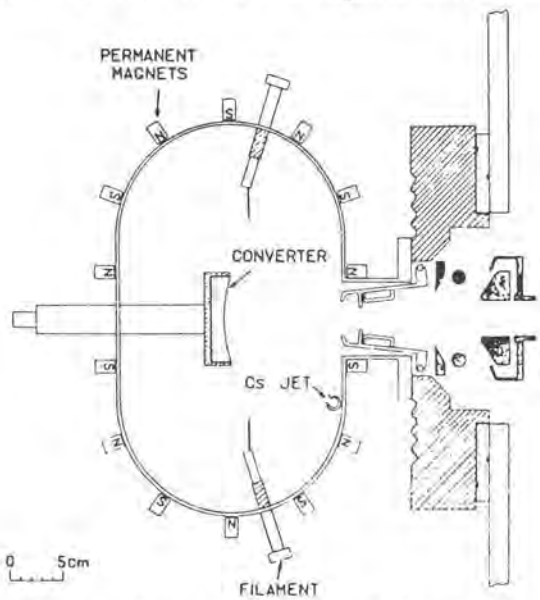


Fig. 4 A schematic diagram of the multicusp surface conversion negative ion source.

formed at the converter are then accelerated back through the sheath by the same potential. The bias voltage on the converter thus becomes the negative ion extraction potential. The converter surface is normally curved to geometrically focus the negative ions through the plasma to the exit aperture.

The advantages of the surface conversion source are low source operating pressure and very small electron content in the self-extracted negative ion beam. The source can be operated either in steady-state or pulsed mode. However, source operation always requires the presence of cesium which can cause voltage breakdown in the accelerator column. Nevertheless, steady-state H^- beams with currents greater than 1 A have been generated by this type of surface conversion source.[2] Production of other negative ions (such as Au^-) by this type of source have been reported by Mori and Alton.[3]

4.2 Volume Production Negative Ion Sources

A hydrogen plasma contains not only positive ions and electrons, but also H^- ions. In 1983, a novel method of extracting volume-produced H^- directly from a multicusp source was reported by Leung et al.[4] In this H^- source, a magnetic filter divides the source chamber into a discharge and an extraction region. Excitation and ionization of the gas molecules are performed by primary electrons in the discharge region. In the extraction region, the low electron temperature makes it favorable for the production and survival of H^- ions.

It was demonstrated in 1984 that the filter-equipped multicusp source could provide high quality H^- beams with current densities ~38 mA/cm^2.[5] In 1988, a small 7.5-cm-diam multicusp source has been operated successfully to generate H^- ions in a pulsed mode. From this compact volume source, an H^- current density greater than 250 mA/cm^2 has been extracted.[6] In order to improve the lifetime of the volume source, RF induction discharge has been employed in a manner described in section 3. To date, an H^- current of ~40 mA can be obtained from a 5.6-mm-diam aperture with the source operated at a pressure of about 12 mTorr and 50 kW of RF power.[7]

The multicusp source has also been employed to generate volume-produced C^- ions for Cyclotron Mass Spectrometry (CMS) applications. In this case, the C^- ions are extracted directly from a CO or CO_2 discharge plasma. Thus, the tedious graphitization process in a surface conversion source is avoided. Figure 5 shows the mass spectrum of the accelerated beam when CO_2 is used in the discharge. Work is now in progress to incorporate this new volume-production C^- source into the compact permanent magnet cyclotron spectrometer.

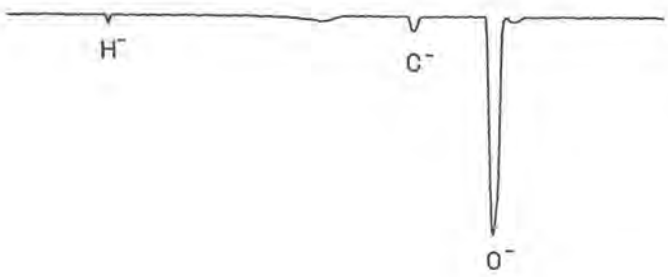


Fig. 5 Negative ion species from a CO_2 gas filament discharge.

5. HIGH CHARGE STATE MULTICUSP SOURCE

Multicusp generators can confine primary electrons very efficiently. Since the magnetic fields are localized near the chamber wall, large volumes of uniform and high density plasmas can be obtained at low pressure, conditions which favor the formation of high charge state ions. Attempts have been made at LBL to generate multiply charged ion beams by employing a modified multicusp source. Experimental results demonstrate that charge state as high as +7 can be obtained with argon or xenon plasmas.[8] Total ion current densities higher than 63 mA/cm^2 have been achieved with a discharge voltage of 400 V and a discharge current of 100 A. However, additional work is needed in order to extend the charge state to values higher than +7. If this is successful, the multicusp source will become very useful for accelerator and high energy ion implantation applications.

6. METALLIC ION BEAM GENERATION

We have operated a multicusp source to generate positive copper ion beams by using a background DC filament argon discharge. The plasma electrode was made of copper and biased at approximately 200 volts negative with respect to the anode allowing the neutral copper atoms to be sputtered from the plasma electrode. These copper atoms are subsequently ionized in the plasma and become positive copper ions. These positive copper ions will fall back towards the extraction aperture and be accelerated. Figure 6 shows an extracted beam spectrum which contains the background argon ions as well as the copper ions. With a total filament discharge power of 80 volts at 5 amperes, 120 microamperes of positive ion current was extracted. The beam was composed of 57% argon ions and 43% copper ions, giving a total copper beam current of 51 microamperes. Extracted through a 1.0mm diameter hole, the copper ion current density was 10 mA/cm^2.

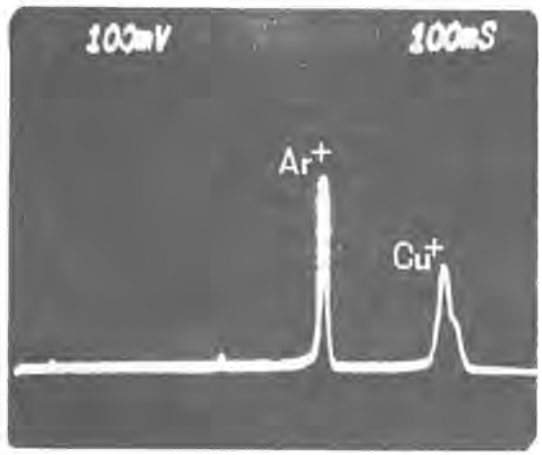


Fig. 6 Spectrum of Cu^+ from a small multicusp source.

ACKNOWLEDGMENT

This work is supported by the U.S. Dept. of Energy, Division of Advanced Energy Projects, Office of Basic Energy Sciences under Contract No. DE-AC03-76SF00098.

REFERENCES

1. K. W. Ehlers and K. N. Leung, Rev. Sci. Instrum., 52, 1452 (1981).
2. K. N. Leung and K. W. Ehlers, Rev. Sci. Instrum., 53, 803 (1982); and J. W. Kwan et al., Rev. Sci. Instrum., 57, 831 (1986).
3. Y. Mori, G. D. Alton, A. Takagi, A. Ueno, and S. Fukumoto, Nucl. Instrum. Meth. A 273, 5 (1988).
4. K. N. Leung, K. W. Ehlers, and M. Bacal, Rev. Sci. Instrum., 54, 56 (1983).
5. R. L. York, Ralph R. Stevens, Jr., K. N. Leung, and K. W. Ehlers, Rev. Sci. Instrum., 55, 681 (1984).
6. K. N. Leung, K. W. Ehlers, C. A. Hauck, W. B. Kunkel, and A. F. Lietzke, Rev. Sci. Instrum., 59, 453 (1988).
7. K. N. Leung, D. A. Bachman and D. S. McDonald, Pro. 1992 European Particle Accelerator, Berlin, Germany (March, 1992).
8. K. N. Leung and R. Keller, Rev. Sci. Instrum., 61, 333 (1990).

A Review of Polarized Ion Sources for Cyclotrons

P.W. SCHMOR
TRIUMF, 4004 Wesbrook Mall, Vancouver, B.C., V6T 2A3

Abstract

Polarized nuclei have become an important nuclear physics probe. Present day experiments are often precision experiments measuring rare processes. These experiments require that the polarized ion source provide beams with high polarization, high beam current, exceptional beam quality and long term reliability. The three types of polarized ion sources in use on cyclotrons are; a) the Lamb Shift source, b) the Atomic Beam (ground state) source and c) the Optically Pumped source. Each type can provide intense beams of nuclearly polarized light ions which are either positively or negatively charged. Heavy ion polarized ion sources for cyclotrons are being developed. The ideal choice for a particular cyclotron depends on the precise experimental requirements. This review article presents a brief description of each of these sources, outlining the current capabilities and the future prospects.

1. INTRODUCTION

Although polarized ion sources have been in use for more than 30 years, their performance continues to improve to meet the changing demands of current experiments. Present day experiments are often precision experiments measuring rare processes and require intense, stable beams within a small emittance. For example, the measurement of the parity violation amplitude in *pp* scattering at TRIUMF requires a modest polarized current of only 0.5 μA at 230 MeV but with a challenging spin-flip coherent current modulation less than 1 part in 10^5 at a spin flip rate of approximately 100 Hz. Another experiment examining pion production in *np* scattering used cyclotron slits to reduce, substantially, the cyclotron emittance and even though the experiment required only 0.5 μA at 475 MeV, it was necessary for the ion source to provide more than 8 μA of polarized H^-.

There are a number of factors which must be taken into account in deciding the best polarized source for an accelerator. The experimental programme defines parameters such as current, polarization, spatial polarization uniformity, stability requirements, spin-flip criteria and polarized species. The accelerator defines the allowed beam emittance, the overall source size and the required ion charge state. The administration is concerned with the cost and risk. The risk is often minimized by purchasing an ion source from a commercial company in order to minimize the research and development required to meet the experimental requirements.

Polarized ions are generally produced in an ion source comprised of three distinct stages. The three components are shown schematically in figure 1. The first step is to produce an intense high quality atomic beam. Next this atomic beam is electronically polarized in a magnetic field by selecting the hyperfine states of one of the Zeeman levels. Nuclear polarization is achieved by inducing transitions from selected remaining hyperfine states (of an undesired nuclear spin direction) to the unoccupied hyperfine states (of correct nuclear spin). Finally the remaining beam which is now nuclearly polarized is ionized in the presence of a magnetic field to preserve the polarization. The strength of the magnetic field depends on the particular hyperfine states being ionized.

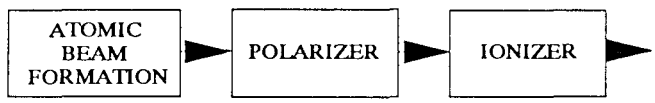


Fig. 1. A schematic representation of the three distinct processes involved in making a polarized ion beam.

2. LAMB-SHIFT POLARIZED ION SOURCE

A comprehensive review of Lamb-shift sources, published six years ago, is still valid.[1] The basic techniques used in the Lamb-Shift source (LSPIS) to obtain a polarized beam are shown schematically in figure 2. Protons at an energy of about 550 eV (or ^2H, ^3H, ^3He at the same velocity) are directed through a cesium vapour target where a large fraction of the ions are neutralized. Many of the atoms in the beam emerging from the cesium target are in the metastable 2S states. Unwanted hyperfine states are quenched to the ground states within the magnetic field of a solenoid either by a static electric field (which removes, from the four metastable hyperfine states, the two states with similar electron spin orientation) or by an rf field (spin filter) which allows only one of the four metastable hyperfine states to transit the region of the rf field without quenching. If two of the hyperfine states are used it is necessary to follow the solenoid by a Sona type transition to transform from the two states with similar electron polarization to two states with similar nuclear polarization.[2] Selective ionization of the metastable atoms occurs in a magnetic field (to preserve the spin direction). The polarized atoms in are selectively (compared to the unpolarized atoms in the ground states) ionized either to positive ions in an iodine vapour or to negative ions in an argon vapour.

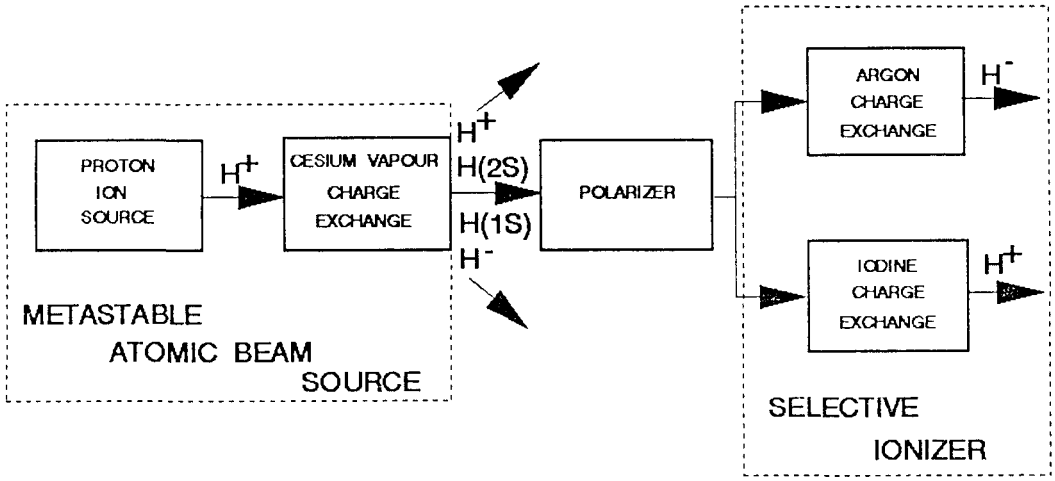


Fig. 2. A schematic of a Lamb-shift type polarized ion source. Two ionizing options are shown.

Frequently the selectivity of ions originating from metastable atoms (over those from atoms in the unpolarized ground states) is enhanced with the use of an emittance defining aperture.

The current from a LSPIS is limited to about 1 μA per hyperfine state by space charge forces. The beam leaving the cesium charge exchange target contains un-neutralized ions. These ions give rise to an electric field which quenches and limits the flux of metastable atoms.[3] The polarization depends somewhat on the current but is generally in the range of 0.8 to 0.85. The LSPIS is an economical and reliable choice for a cyclotron with its relatively small acceptance. However the restriction in maximum current limits the source's usefulness for many of the present-day precise experiments.

3. *ATOMIC BEAM POLARIZED SOURCES*

Figure 3 depicts schematically the elements of an atomic beam ion source (ABIS). H (or ^{2}H) atoms are generated in a dissociator by a radio-frequency discharge and then formed into a low velocity atomic beam with the aid of a cooled nozzle and a system of skimmers. Tapered sextupole magnets are used to separate (Stern-Gerlach technique) one set of hyperfine states (with the electron spin aligned to the magnetic field) from the other set (with the electron spin aligned in the opposite direction). Hyperfine transitions, to convert the separated atomic states which now have a similar electron spin direction (electron polarization) to states of similar nuclear polarization, are induced by

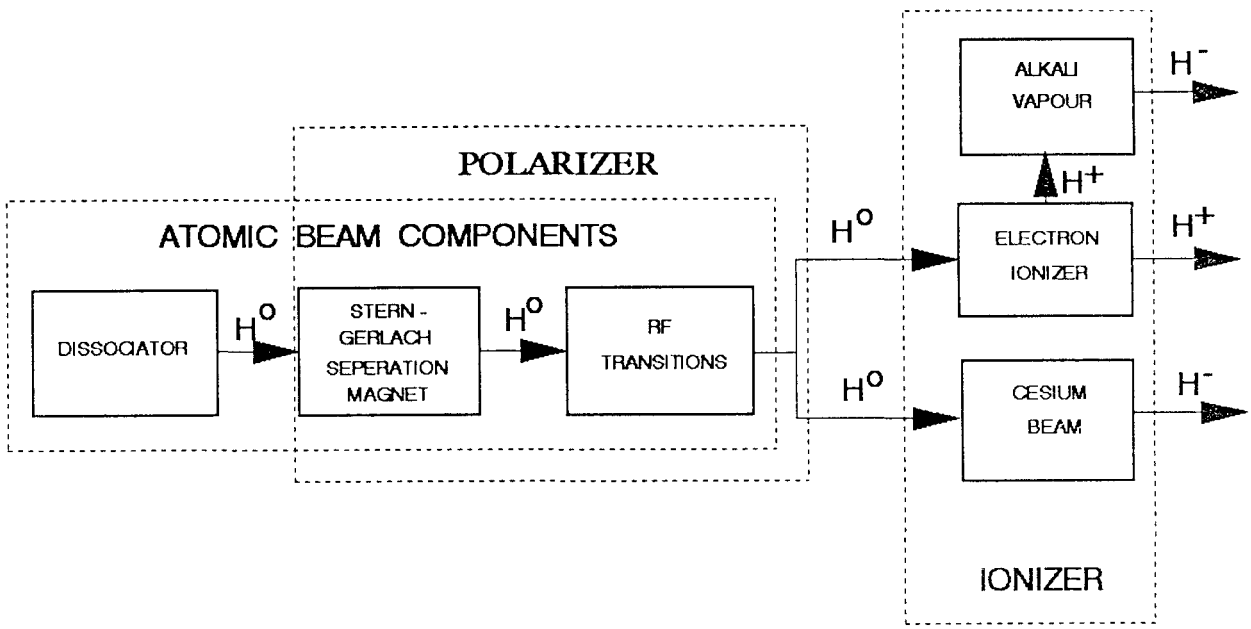


Fig. 3. Schematic of an Atomic Beam Polarized Ion Source showing several ionizing options.

applying the appropriate radio-frequency field. The interested reader can find more detailed descriptions in the literature.[4]

There are a number of approaches being used to ionize the nuclearly-polarized, neutral, atomic beam. To produce positively charged ions, an electron impact ionizer is used. This is achieved either by producing an intense electron beam with a hot filament in a solenoid magnet or by using the electrons generated in an electron-cyclotron-resonance (ECR) heated plasma. Space charge forces within the intense electron beam give rise to an energy spread in the polarized ions which limits the amount of polarized beam which can be matched into a cyclotron. The ECR ionizer avoids the space charge problems of the intense electron beam by using the electrons in a quasi neutral plasma and the resulting polarized beam is considerably brighter (more current within a given emittance). However, experience has shown that the polarization is slightly degraded ($\sim 5\%$) by the ECR ionizer. The PSI source, for example, produces about 150 μA of positive beam with about 79% polarization within a normalized emittance of less than 1.2π mm-mrad. The ETH group has reported positive currents as high as 400 μA.[5] To produce negatively charged ions, the positively charged ions are accelerated to about 5 keV prior to being directed through an alkali vapour target where about 7% of the positive ions are converted to negative ions by double charge exchange. An alternate approach to producing the negative ion beam has been to use charge exchange directly between the slow moving polarized, neutral atomic beam and a counter-flowing, coaxial, neutral beam of cesium atoms at 40 keV. This approach provides a highly polarized beam ($>95\%$) of excellent emittance ($\sim 0.35\ \pi$ mm-mrad normalized by $\beta\gamma$). At the INR in Moscow, very high currents (~ 6 mA) have been achieved (albeit with 30 μS long pulses at a 1 Hz repetition rate within a normalized emittance of 2π) by making use of the larger charge exchange cross-sections of $^2H^+$ (compared to electrons) in a plasma to ionize directly the polarized atoms.[6] A similar arrangement to the INR scheme with the exception that the source be designed to make use of charge exchange with $^2H^-$ (instead of $^2H^+$) has been proposed for producing negatively charged hydrogen ions.

4. OPTICALLY PUMPED SOURCES

A review of the status of optically pumped polarized ion sources in 1990 has been given by York.[7] The current status of the TRIUMF source can be found elsewhere in these proceedings.[8] The optically pumped polarized ion source (OPPIS) is based on a proposal by Anderson.[9] A schematic of an OPPIS using charge exchange is shown in figure 4. Lasers are used to achieve electronic spin alignment in an alkali vapour. Initially, as proposed by Anderson, sodium was pumped with dye lasers tuned to the D1 transition at 596 nm, but more recently titanium sapphire lasers are being used to pump rubidium (or potassium) vapour at 795 (770) nm. Protons are directed at an energy of about 2 to 5 keV through the polarized vapour where by charge exchange they can pick up a spin aligned electron. The charge exchange process must take place in a large magnetic field ($\sim$ 2.5 T) in order to preserve the spin alignment. After removing any un-neutralized particles by means of transverse electric fields , the beam emerging from the alkali vapour is a neutral atomic hydrogen beam with two hyperfine states (of similar electronic spin) predominately occupied. A Sona type transition is then used, as in the Lamb-shift source to transform the electron alignment to a nuclear alignment prior to ionization. The nuclearly polarized atomic beam is ionized in either an alkali to form negative ions or in helium to form positive ions.

The OPPIS has limitations on the output brightness (current\emittance^2) as a result of the large magnetic field required to preserve (decouple **L** & **S**) the electron polarization during charge transfer. It has been proposed to avoid this problem by using spin exchange with a neutral hydrogen beam instead of charge exchange with a proton beam.

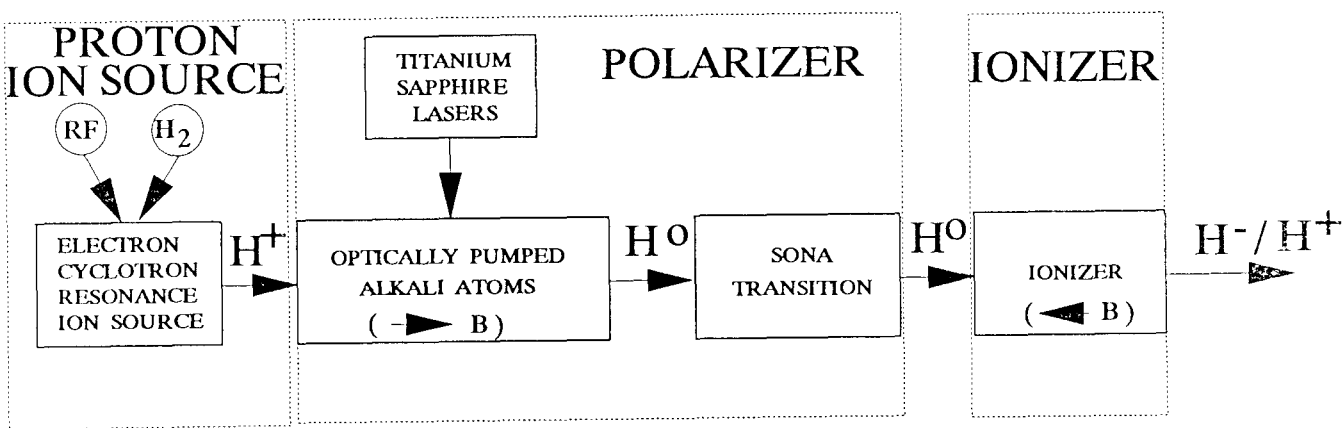


Fig. 4. A schematic of an optically pumped polarized ion source.

The performance figures of an OPPIS depend on the emittance and duty cycle of the ion beam. The current can be increased by opening apertures until the ion source emittance matches the accelerator acceptance. The efficiency for ionization to protons is about a factor of ten larger than the efficiency for ionization to H^- with the result that negative currents from the source are about a factor of ten less than positive currents. Both the current and the polarization also depend on the thickness of alkali vapour that can be polarized. The alkali thickness that can be polarized, in turn, depends on the power available from the lasers. Peak power from lasers can be substantially increased through pulsing. Thus for an accelerator (or for a particular experiment) requiring a pulsed polarized beam it is possible, under some conditions, to provide higher peak currents by matching the laser repetition rate to that of the accelerator (or experiment). For a given laser power, higher currents at lower polarization result from an increase in alkali thickness. With the TRIUMF source operating in a dc mode the measured nuclear polarization is about 61% @ 20 μA of H^-, 75% @ 10 μA, 78% @ 5 μA and 80% for low currents. These currents are for a normalized emittance estimated to be less than 0.7 π mm-mrad.

5. POLARIZED HEAVY ION SOURCES

An ion source for polarized beams of ^{6}Li, ^{7}Li and ^{23}Na was developed and used at Heidelberg.[10,11] An electron polarized beam was achieved by passing an unpolarized atomic beam through a Stern-Gerlach separation magnet (quadrupole). Subsequently, three sets of rf transitions were used to populate appropriate hyperfine states and provide various different vector and tensor nuclear polarizations. Positive ionization was achieved through surface ionization. These positive ions were converted to negative ions in a cesium vapour. With the use of lasers it is possible to pump alkali hyperfine states directly. This technique has yielded currents in the range of 2 to 6 μA and polarizations of about 80% for beams of ^{7}Li and ^{23}Na. Heavy ion polarized ion sources for cyclotrons are under development at the Institute for Nuclear Research in Kiev and at RCNP in Osaka.[12,13] The INR source is designed to provide polarized alkalies and is similar to the Heidelberg design. The RCNP source is of the OPPIS design and will be used initially to produce beams of polarized ^{3}He.

6. LOW ENERGY POLARIMETERS

In order to optimize a polarized ion source, efficiently, it is essential to have a dedicated on-line low energy polarimeter near the ion source. There is, in general, too much competition for accelerator time to allow adequate scheduling of the accelerator and its polarimeters for ion source optimization. Moreover, experience at TRIUMF has shown that the overhead, in terms of time and manpower, in preparing the cyclotron and high energy polarimeters is a significant fraction of the optimization process. At TRIUMF two different low energy polarimeters have been extremely useful. The first, a Lyman-α polarimeter, yields the polarization of protons in the energy range of 1 to 10 keV.[14] This polarimeter measures the asymmetric Lyman-α emission of photons by selective quenching of polarized hydrogen atoms excited to the 2S metastable states. Count rates are of the order of 0.5 MHz. This type of polarimeter is, in principle, suitable for deuterium beams. The second is a nuclear polarimeter based on the ^{6}Li(p,^{3}He)α reaction.[15] The analyzing power for detecting ^{3}He at 130° is approximately 0.21 at 300 keV. For deuterons the ^{3}H(^{2}H,n)^{4}He reaction has been used for energies around 100 keV.

7. CONCLUSION

Table I outlines the main performance characteristics of polarized sources which are either in use, suitable for use or being developed for use on cyclotrons. Caution must be exercised in interpreting the table as the best characteristics from a particular source are not necessarily all achievable simultaneously. The sources are frequently optimized to meet the needs of a particular accelerator or experiment and as such the emittance, polarization and/or resulting current may be different if the same source were optimized for a different accelerator. Much of the recent work on polarized internal targets overlaps and complements the work being done with sources. Two recent review papers provide an excellent overview of polarized ion source and related polarized target development.[16,17]

In summary, polarized ion source development remains a very active research endeavour and large improvements in source performance are still being realized.

8. REFERENCES

1) P. Schiemenz, Helv. Phys. Acta **59**, 620 (1986)
2) P. G. Sona, Energy Nucl. **14**, 295 (1967)
3) J. Benage, LANL report **LA-UR-85-4463**
4) W. Haeberli, Helv. Phys. Acta **59**, 513 (1986)
5) W. Greubler, KEK Report **90-15**, 56 (1990)
6) A. S. Belov *et al.*, KEK Report **90-15**, 69 (1990)
7) R. L. York, KEK Report **90-15**, 142 (1990)
8) C. D. P. Levy *et al.*, these proceedings
9) L. W. Anderson, Nucl. Instrum. Methods **167**, 363 (1979)
10) E. Steffans *et al.*, Nucl. Instrum. Methods **124**, 601 (1975)
11) D. Krämer *et al.*, Nucl. Instrum. Methods **220**, 123 (1984)
12) N. I. Zaika, these proceedings
13) M. Tanaka *et al.*, KEK Report **90-15**, 288 (1990)

Table I. A COMPARISON OF POLARIZED ION SOURCE PARAMETERS

PARAMETERS / SOURCES		LAMB-SHIFT	ATOMIC		OPPIS (CHARGE EXCHANGE)		OPPIS DIRECT
POLARIZATION (%)	H^+	85	80[c]		≈ H^-		
	H^-	85[a]	80	95[d]	75[a]	61[a]	
CURRENT	H^+	1	150[c]		≈ 10 * H^- current		
(DC μA)	H^-	1[a]	16	3[d]	10[a]	22[a]	
NORMALIZED EMITTANCE	H^+	0.3	< 1.2[c]		≈ H^-		
(π mm-mrad)	H^-	0.3[a]		0.35[d]	< 0.7[a]		
TENSOR POLARIZATION (% of maximum for D^+/D^-)		70[b]	85[c]	95[d]	not suitable		
ONLINE POL'N ESTIMATE		yes	no		yes		
PARTICLES	H^+/H^-	yes	yes		yes		no
	D^+/D^-	yes	yes		vector only		no
	$^3H^+/^3H^-$	yes	yes		yes		no
	$^3He^+$	yes	yes		yes		yes
	HEAVY IONS	no	yes		yes		alakalis
COHERENT INT. MODUL'N (%)			≈ $5 \cdot 10^{-5}$		≤ $5 \cdot 10^{-5}$ [a]		
P^2I (μA)	H^+	0.7	96		≈ 56.	≈ 80.	
	H^-	0.7	10	3	5.6	8.	
COMMERCIAL SUPPLIER		no	yes		no		no
RELATIVE COST		1	7 - 9		8		

[a] TRIUMF [b] Munich [c] PSI [d] Wisconsin

14) A. N. Zelenskii *et al.*, Nucl. Instrum. Methods **A245**, 223 (1986)
15) L. Buchmann, Nucl. Instrum. Methods **A301**, 383 (1991)
16) P. Schiemenz, Rev. Sci. Instrum. **63 (4)**, 2519 (1992)
17) T. B. Clegg, Conference Recored of the 1991 IEEE Particl Accelerator Conference, **Vol. 4**, 2083 (1991)

STATUS OF THE TRIUMF OPTICALLY-PUMPED POLARIZED H⁻ ION SOURCE

C.D.P. Levy, K. Jayamanna, M. McDonald, R. Ruegg, and P.W. Schmor
TRIUMF, 4004 Wesbrook Mall, Vancouver, B.C., Canada V6T 2A3

and

A.N. Zelenskii
Institute of Nuclear Research, Russian Academy of Sciences, Moscow

ABSTRACT

The TRIUMF polarized H⁻ ion source, based on optical pumping of Rb vapour, produces up to 10 μA of 75% polarized H⁻ beam at 300 keV. A 1–10 keV polarimeter, based on the detection of Lyman-α photons from metastable H(2S) atoms, has been used to study source parameters affecting polarization, which is up to 80% at low current. Preliminary measurements of beam intensity variations correlated with the Rb polarization show that they are likely within the requirements of an upcoming parity violation experiment.

1. INTRODUCTION

The optically pumped polarized ion source (OPPIS) at TRIUMF has been described previously.[1,2] It now produces up to 10 μA of 75% polarized H⁻ beam at 300 keV, half of which is accelerated to high energy by the TRIUMF cyclotron. Figure 1 is a schematic drawing of OPPIS. Figure 2 shows the downstream section of OPPIS, containing beam transport optics and a low-energy (1–10 keV) polarimeter. Bender plates divert polarized protons produced (with about 10% of the polarized H⁻ intensity) by the source into the polarimeter, where they are neutralized in a Na cell. Electron-spin-down H(2S) metastables are quenched in a spin filter (as in the Lamb-shift source), and Lyman-α photons emitted by the remaining metastables after quenching in an electric field are counted. The proton polarization is calculated from the asymmetry in photon counts between the polarized (lasers on) and unpolarized (lasers off) cases.[3] Count rates are of the order of 500,000/s.

Many factors affect the polarization, and only small improvements are possible from each, given that the polarization is already quite high. The Lyman-α polarimeter has allowed us to measure small changes in the polarization and to begin a program of further improvement in polarization.

Our other interest is the application of the source to parity violation experiments. The measurement of the parity violation amplitude in pp scattering requires

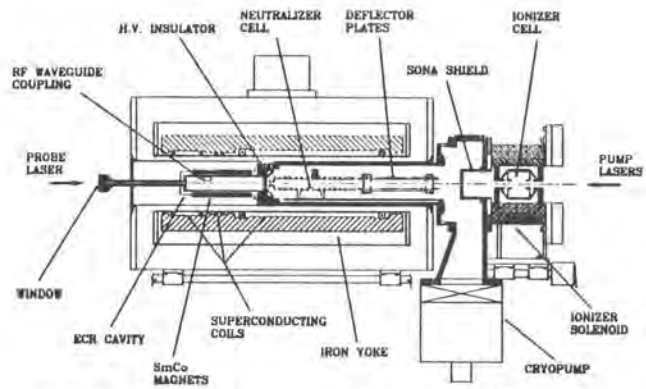


Fig. 1. Schematic diagram of the TRIUMF optically-pumped polarized H⁻ ion source.

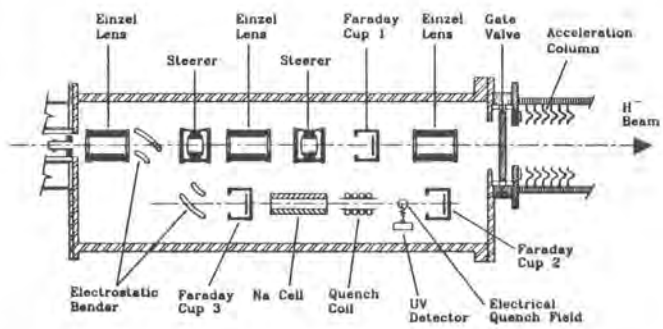


Fig. 2. Schematic diagram of the beam transport optics downstream of the ion source, and the Lyman-α polarimeter contained within the same chamber. During normal source operation the H⁻ beam passes through a 2.0 cm diameter aperture in the first electrostatic bender. During polarimeter operation deflecting voltages are applied to the benders. Faraday Cups 1 and 3 can be moved out of the beam axis. The UV detector is a dual microchannel plate protected by a LiF window.

extremely high beam stability, especially with respect to current modulation (CM) correlated with spin helicity. Spin reversal is achieved by reversing the circular polarization of the pump laser light and adjusting the laser frequency to allow for the Zeeman shift of $\sim$ 85 GHz in the Rb neutralizer target, which is immersed in a high magnetic field of $\sim$ 23 kG. At least two properties of optical pumping of alkali vapour are known that affect the polarized ion current. The best understood is the dependence of the neutral beam emitted by the Rb cell on the Rb polarization.[4] Some neutrals undergo a second charge exchange reaction in the Rb to become H^-. Since H^- has a single bound state $^1S_0$, it cannot be formed by a polarized hydrogen atom picking up an electron from Rb polarized in the same direction. The H^- yield in the Rb is given by

$$I_- \sim I_0 \sigma_{o-} nl(1 - TP^2)C \qquad (1)$$

where I_0 is the H^0 yield in the Rb, $\sigma_{o-} \sim 3 \times 10^{-16}$ cm^2 is the cross section for H^- production, $nl \sim 5 \times 10^{13}$ atoms cm^{-2} is the Rb thickness, P is the Rb polarization, $T \sim 1$ is the polarization tranfer ratio between Rb and H^0, and $C \sim 0.5$ is a correction factor accounting for integration of H^- production along the length of the cell. All the I_- is swept out of the beam by deflection plates between the Rb cell and the Na negative ionizer cell (see Fig. 1), giving rise to a dependence of the ultimate polarized H^- source current on P. For Rb polarizations $P_{\rm up}$ and $P_{\rm down}$, and ultimate H^- currents $I_{\rm up}$, $I_{\rm down}$, and $I_{\rm unpolarized}$, the following is true:

$$\frac{I_{\rm up} - I_{\rm down}}{I_{\rm unpolarized}} \sim \sigma_{o-} nl\{P_{\rm up}^2 - P_{\rm down}^2\}TC \qquad (2)$$

For useful parity violation measurements, the asymmetry in polarized current is required to be of the order of 10^{-5}. The above equation implies that the upper limit on Rb polarization asymmetry is about 10^{-3}, thus requiring a thin Rb target with highly saturated polarization.

A second physical process producing CM is the ionization of Rb vapour by resonant D1 line laser light. CM due to this effect was first seen at INR, Moscow.[5] A reduction in current of close to 100% was observed when the Na density was more than 10^{13} atoms cm^{-3} and high pulsed laser power was used. The ionization is caused by a process involving collisions between excited state atoms, and is highly non-linear with respect to both laser power and vapour density. Direct measurements of alkali ion production under the action of resonant light were first carried out in 1983.[6] Since the ionization process decreases the vapour density and hence the final beam current, this modulation is opposite in sign to the double charge exchange process.

2. POLARIZATION RESULTS

A light chopper modulated the laser beams at 100 Hz, and photon counting was gated with the lasers on and off. The gate lengths were identical for both laser states and shorter than the laser modulation times so that the Rb polarization had time to reach equilibrium. Two Ti:sapphire lasers each pumped by a 20 W argon ion laser produced up to 9 W of 795 nm light for optical pumping of Rb. Because the polarimeter measures proton polarization, it underestimates the H^- polarization by a few percent, since the proton beam is more affected by the unpolarized residual gas background.

Figure 3 shows the proton polarization and H^- current as functions of Rb thickness.[7] The Rb cell was designed to produce a smooth Rb-density distribution close to the extraction electrodes. This minimizes the effect of background hydrogen gas near the electrodes, and allows us to achieve relatively high beam polarization for very thin targets. The smooth distribution of Rb prevents the premature reduction of polarization by radiation trapping.[8,9] Figure 3 also shows the Rb polarization and the efficiency with which it is transferred to the ion beam, after correcting for unpolarized background beam seen at zero Rb thickness.

Polarization has also been measured as a function of laser frequency (see Fig. 4). In principle, the Lyman-α polarimeter is superior to the Faraday rotation method for optimizing the laser frequency. The polarimeter gives a direct measure of ion beam polarization and is averaged over the whole beam, rather than just sampling the Rb polarization along the small interaction volume of a probe laser.

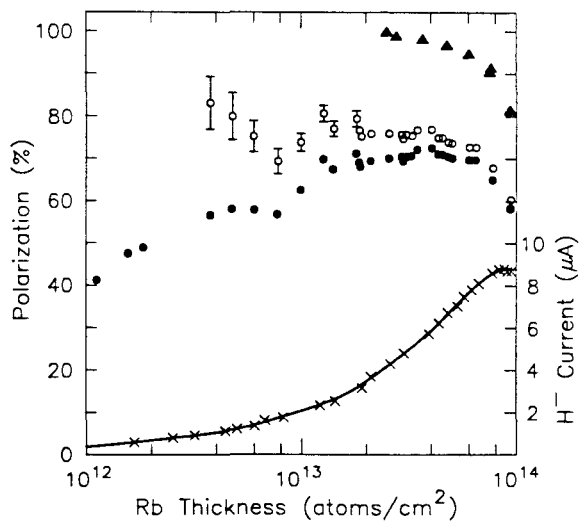


Fig. 3. Polarization, and H^- current measured at Faraday Cup 3, as functions of Rb thickness. Triangles; Rb polarization measured with the ion beam on. Solid circles; proton polarization measured in the Lyman-α polarimeter. Open circles; calculated proton polarization if the effect of unpolarized background current is removed. Crosses; H^- current, which had a background value of (0.32 $\pm$ 0.03) μA when the Rb cell was cold. The proton polarization was measured down to $\sim$30%, at a Rb thickness smaller than the estimated error of $\pm 5 \times 10^{11}$ atoms cm^{-2}.

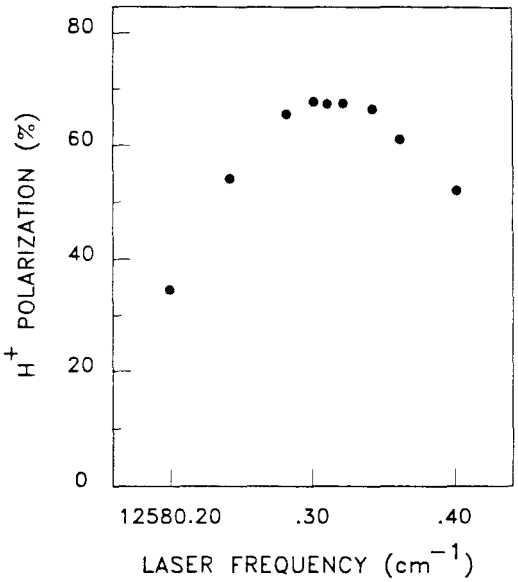


Fig. 4. Proton polarization as a function of pump laser frequency, for a single 5 W laser having a bandwidth (FWHM) of 0.1 cm^{-1}. The laser frequency was measured with a Burleigh WA-10 wavemeter.

Figure 5 shows the dependence of proton polarization on the magnetic field in the Rb cell. We observe that contrary to spin-orbit depolarization calculations,[10] the polarization is still rising significantly above 22 kG. Further study is required to decide if T is increasing at the highest fields, or if other factors are at play.

Figure 6 shows the polarization as a function of magnetic field in the ionizer cell. The theoretical difference in polarization between 1.5 and 2.0 kG is 1%, whereas we observe 2.5–3%. This is because the ionizer magnetic field drops at the edges of the Na vapour-density distribution, and the H^- ions produced there lose more polarization. The ionizer solenoid is being lengthened by 8 cm to improve the field uniformity.

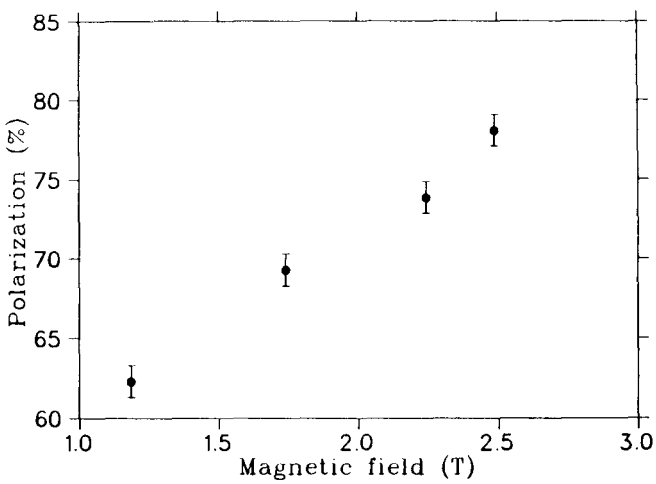


Fig. 5. Proton polarization as a function of magnetic field in the Rb cell.

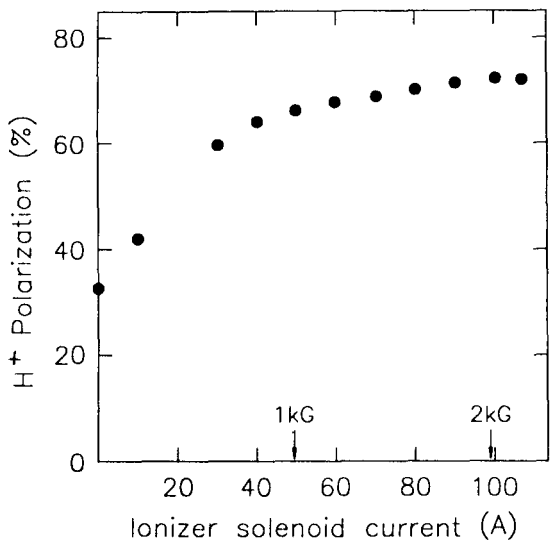


Fig. 6. Proton polarization dependence on ionizer-cell magnetic field.

Polarization was also studied as functions of hydrogen gas flow rate, beam energy and trim coil current (controlling the magnetic field gradient in the Sona transition region). At 25 kG in the Rb cell and 2.3 kG in the ionizer cell, at a beam energy of 2.8 keV, the highest proton polarization measured with the Lyman-α polarimeter was (80.1 ± 0.5)%, after optimizing all source parameters for polarization only.

3. CM RESULTS

When measuring CM, the voltage on the bender plates is reversed so that H^- beam enters the polarimeter. Current is measured either with Faraday Cup 3, or with Faraday Cup 2 (see Fig. 2). In the latter case CM can be measured simultaneously with polarization, while the current signal is applied as a normalizing correction to the polarimeter counts. The current signals were measured with a 4 MHz linear current digitizer and gated with the laser modulation as described above.

The results of CM measurements as a function of Rb thickness are shown in Fig. 7, where the CM is defined as

$$\frac{I_{\text{laser on}} - I_{\text{laser off}}}{I_{\text{laser off}}} \qquad (3)$$

Over the thickness range 3–8 × 10^{13} atoms cm^{-2} the CM rises linearly as expected for the double charge exchange process and shows quantitative agreement with the estimates above. At higher thickness the modulation of opposite sign is observed and at a thickness of 9 × 10^{13} atoms cm^{-2} has a maximum magnitude of about 1%. The sudden change from one dominant process to the other is surprising, as is complicated behaviour below 3 × 10^{13} atoms cm^{-2}.

In practice, one is interested in the difference of current between opposite spin states. We cannot measure such modulation directly, since the fast 100 Hz spin reversal system suitable for parity violation experiments has not yet been completed. We measured CM separately for up and down helicities. Figure 8 shows CM as a function of Rb polarization. A least squares quadratic fit shows that the CM is symmetric with helicity, as implied by Eq. 2, within an error of $\pm 1.0 \times 10^{-4} P^2$. Further measurements will be required to test this down to the 10^{-5} level.

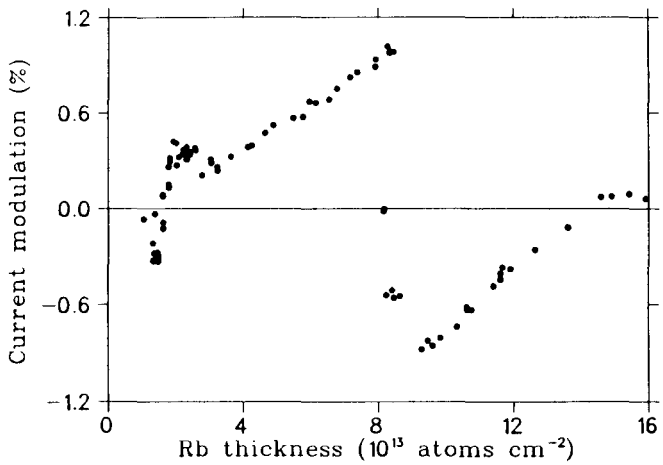


Fig. 7. Modulation of H^- source current between unpolarized and polarized conditions, as a function of Rb thickness.

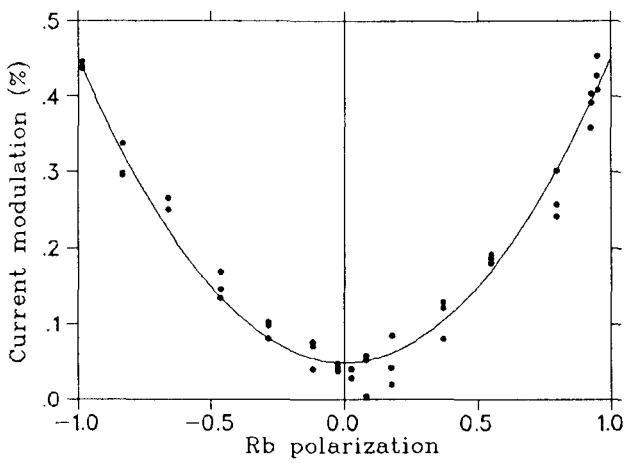


Fig. 8. Modulation of H^- current between polarized and unpolarized conditions, as a function of Rb polarization. The data were taken at a Rb thickness of 4×10^{13} atoms cm^{-2}. The polarization was varied by adjusting the frequency tune of the pumping lasers. The curve is a least squares fit to the data of $CM = a + bP^2$, where a and b are adjustable parameters. The standard error of b is $\pm$ 1.0 $\times 10^{-4}$.

4. CONCLUSION

The TRIUMF optically pumped H^- source has become a reliable producer of microamps of 75% polarized beam. The construction of a low-energy polarimeter allows us to further optimize and study OPPIS in an accurate and efficient way, showing that 80% polarization or more is within reach. Preliminary results on the modulation of ion current with spin helicity show that OPPIS is promising for use in parity violation measurements requiring modulation at or below the 10^{-5} level.

5. REFERENCES

1) C.D.P. Levy *et al.*, **Proc. Fourth Int. Conf. Ion Sources (Bensheim)**, Rev. Sci. Instrum. **63**, 2625 (1992).
2) L. Buchmann *et al.*, Nucl. Instrum. Meth. **A306**, 413 (1991).
3) A.N. Zelenskii *et al.*, Nucl. Instrum. Meth. **A245**, 223 (1986).
4) W.D. Cornelius, ANL-84-50, 385 (1984).
5) A.N. Zelenskii *et al.*, JETP Lett. **44**, 24 (1986).
6) B. Carre *et al.*, J. Phys. **B14**, 4271 (1985).
7) Rb thickness and polarization are measured using constants calculated using Program Faraday by M. Dulick, LANL. The probe laser light frequency was 12808.0 cm^{-1}. One version of the Faraday rotation technique is described in: Y. Mori *et al.*, Nucl. Instrum. Meth. **220**, 264 (1984).
8) D. Tupa *et al.*, Phys. Rev. **A33**, 1045 (1986).
9) Y. Mori *et al.*, Nucl. Instrum. Meth. **A268**, 270 (1988).
10) E.A. Hinds *et al.*, Nucl. Instrum. Meth. **189**, 599 (1981).

AN ECR ION SOURCE FOR MULTIPLY-CHARGED HEAVY IONS AT 14 GHz

M. Sekiguchi, Y. Ohshiro, M. Fujita, T. Yamazaki
Institute for Nuclear Study, University of Tokyo, 3-2-1 Midori-cho, Tanashi-shi, Tokyo, 188, Japan

Y. Yamashita, Y. Isoya, T. Yamada
Research Center for Advanced Technologies, the Japan Steel Works, Ltd., 1-3 Takanodai, Yotsukaido-shi, Chiba, 284, Japan

and

A. Kitagawa
National Institute of Radiological Sciences, 4-9-1 Anagawa, Inage-ku, Chiba-shi, Chiba, 263, Japan

ABSTRACT

An ECR ion source for multiply-charged heavy ions was designed and constructed by using a 14.25-GHz microwave power source based on our experiences obtained by development efforts on other sources. In addition to the high frequency, it has high axial and radial magnetic field strengths over 10 kG. The diameter of the plasma chamber is 50 mm and the diameter and length of the ECR zone is 30 mm and 70 mm, respectively. Preliminary tests show good performance. The ion yield turned out to be 36 eμA for O^{7+}, 1.5 eμA for Ne^{9+}, 350 eμA and 190 eμA for Ar^{8+} and Ar^{9+}, respectively, without using special technique such as electron injection or electron repeller. This paper describes the design concept and preliminary performance.

1. INTRODUCTION

Many ECR sources for multiply-charged heavy ions have been constructed and are working at various heavy-ion accelerators. The basic structure has been developed by R. Geller and his collaborators at Grenoble.[1] Among them, one of the best performance has been attained, to the authors' knowledge, by the CAPRICE[2] and its modifications.[3]

At the Institute for Nuclear Study, University of Tokyo, we developed four sets of ECR ion sources in these five years. The first was SF-ECR for the SF cyclotron of our institute working at 6.1 GHz microwave frequency, now serving for experiments.[4] The second was a test machine developed in collaboration with Tokyo Institute of Technology, named HiECR, without its own microwave and coil power supplies.[5,6] The third one is a 10-GHz source for heavy-ion medical accelerator complex at the National Institute of Radiological Sciences(NIRS). This source was designed at NIRS and tested at our institute according to a collaboration program between the two institutes.[7]

The source reported in this paper is the fourth one developed at our institute, named HyperECR. This was designed, constructed and tested in collaboration with the Research Center for Advanced Technologies, the Japan Steel Works, Ltd..

According to the experiences based on the development of the above mentioned sources, ECR sources of any design can surely produce beams, but we are not certain why one source works well and another not. Moreover, we can not predict how much beam a source of a certain design can produce before testing it. In the design of the present source, we have made efforts to make the design principle as clear as possible so as to evaluate each item after testing. The primary aim is to construct a compact and powerful source at low cost.

2. DESIGN AND CONSTRUCTION

We started our design based on an existing microwave amplifier purchased from a Japanese company, which has a frequency of 14.25 GHz and a maximum output power of 2.0 kW. According to the Geller's scaling law,[1] the higher the frequency is, the better the performance. In addition, we assumed that both axial and radial magnetic field should be as high as possible at a given frequency in order to make the confinement of the plasma better.

Since the frequency is rather high and, consequently, the ECR field is high, the diameter of the plasma chamber was chosen to be 50 mm in order to produce a high sextupole field by using permanent magnet material commercially available. We adopted Nd-Fe-B alloy with a trade name NEOMAX35, whose maximum BH product is about 280 kJ/m^3. This diameter is one of the smallest one ever used in ECR sources but still more than twice of the wavelength of the microwave.

From our experience concerning other ECR sources,[5-7] the ECR surface was designed to be 10 mm apart from the wall of the plasma chamber. We searched for a magnetic configuration which makes the diameter of the ECR surface less than 30 mm. The distance between the two coils was determined mainly from this requirement. The ampere-turns of the coils were determined to produce as high peak fields as possible on the axis with sizable coils and power supplies.

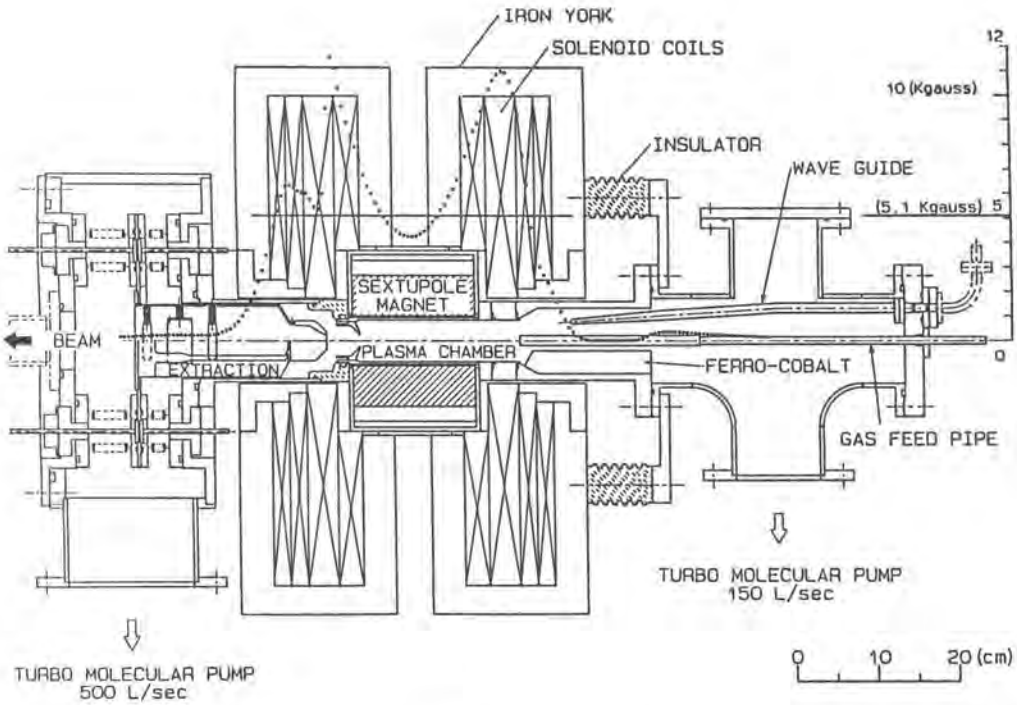


Fig. 1. Schematic drawing of the HyperECR and the measured axial-field distribution on the axis.

In order to increase the field on the axis, *pole tips* are used near the axis to guide the lines of force of the magnetic field. Various shapes of magnetic material can be inserted at both ends of the plasma chamber to tune the axial field distribution. In addition, the vacuum chambers outside the sextupole magnet and extending the plasma chamber into both directions are made of iron, while the plasma chamber itself is made of copper. These iron chambers also contribute to collect the magnetic lines of force on the axis.

Taking into account that at a high magnetic field above 10 kG iron might saturate locally and could not produce the field shape intended, the return yokes for the mirror coils were made from pure iron 4 cm thick. A ferro-cobalt alloy was used as the material of the *pole tips* where the lines of force concentrate.

Magnetic material such as yokes and *pole tips* inserted near the axis to increase the axial field reduces the conductance of the pumping. We assumed that the working pressure in the plasma chamber should be less than 1.0×10^{-6} Torr. The conductance for pumping was made as large as the above-mentioned conditions permit; for example, the *pole tips* were made axially asymmetric in order to provide space for pumping, and for inserting a wave guide and a gas feed pipe. In this context, we did not employ the axial injection of microwave power as is done in CAPRICE: the microwave power is led into the plasma chamber through an ordinary wave guide set a little off-axis.

The effective pumping speed for the plasma chamber is estimated to be about 10 l/s although two turbomolecular pumps evacuate the chamber from its both ends and some efforts are paid to make the conductance large.

The resultant size of the expected ECR zone turned out to have a diameter of less than 30 mm and length of 50 mm, as shown in Table 1. In addition, the mirror ratio has been made variable by varying the distance of the two mirror coils, reaching a value of about 3 at the largest.

Field measurements after assembling the parts have proved that field calculations with the computer code PANDIRA predicted well the strengths of the fields, although some difference has been found concerning the details, because some local saturation points appear due to the sharp edges of the ferromagnetic material, which the calculations could not predict accurately; further, the program cannot calculate the axially asymmetric field.

We can approximate the strength of the mirror field near the axis in the center of the two coils as

$$B_z = B_0 + az^2,$$

where B_0 is the minimum field, z is the length along the axis and a is a constant. The sextupole field can also be approximated as

$$B_r = br^2,$$

where b is the field gradient and r is the radius. The length (L) and the diameter (D) of the ECR zone can

Table 1. Design and measured values of the ECR zone parameters.

	Designed	Measured
min. field B_0(kG)	4.21	4.13
mirr. field grad. a(kG/cm^2)	0.129	0.074
sex. field grad. b(kG/cm^2)	1.34	1.30
length of ECR zone L(cm)	5.34	7.35
dia. of ECR zone D(cm)	2.96	3.00

be expressed as

$$L = 2\sqrt{\frac{B_{ECR} - B_0}{a}}$$

and

$$D = 2\left(\frac{B_{ECR}^2 - B_0^2}{b^2}\right)^{1/4}$$

respectively, where B_{ECR} is the ECR field for 14.25 GHz.

The design and measured values of these parameters are summarized in Table 1. The design values were calculated by the program PANDIRA and the measured values were taken from one of the configurations in which the beam intensity was optimized. It should be noted that the design value of the diameter agrees very well with the measured one, while the agreement for the length does not have much meaning since the mirror ratio is adjustable.

An example of the measured field distributions is shown in Fig. 1 and the main parameters of this source are summarized in Table 2. The field distribution on the axis has a sharp peak between the anode and the extraction electrode. This is a result that the extraction electrode is made of soft iron. In the design stage, we tried to set the position of this peak just on the anode, but it was unsuccessful. This may be due to the iron configuration near the axis. An additional peak in the extraction electrode is also a result of using iron for this electrode and we don't believe it plays any essential role on the performance.

It should be remarked that the surface field strength of the NEOMAX was measured to be 11.8 kG on the average when it was virgin; after putting it in the mirror field of about 12 kG, however, the strength was reduced to 10.6 kG on the average, resulting in about a 10 % reduction. It is supposed to be one of the initial effects, because no remarkable reduction has been noticed ever since.

The two coils, the plasma chamber and a vacuum box containing the extraction electrode and an einzel lens are mounted on an accurate common rail, so that the position adjustment of these components along the axis can be easily made. The axial position of the extraction electrode is adjustable without breaking the vacuum. All components of this source, namely, the plasma chamber, the vacuum chamber on both sides of the plasma chamber, the coils, the extraction electrodes and sextupole magnet, can be easily disassembled and replaced to make the system highly flexible for future modification.

Table 2. Main parameters of HyperECR.

Microwave power source	
frequency	14.25 GHz
max.power	2.0 kW
Plasma chamber	
diameter	50 mm
length	190 mm
Multipole magnet	
multipolarity	Sextupole
Field strength on the surface	10.6 kG
material	Nd-Fe-B
inner diameter	57 mm
length	150 mm
Mirror field	
Max.field strength on axis	12 kG
max.Current	600 A
max.Power	72 kW
Turbomolecular pumps	500 l/sec
	150 l/sec

3. PRELIMINARY PERFORMANCE

The beam test started in February, 1992. Argon ions were chosen as a target at first; we have obtained so far 350 eμA of Ar^{8+} and 190 eμA of Ar^{9+}, for example, with 20 kV extraction voltage without such special technique as electron injection[8] and electron repeller.[9]

Some different behaviours have been found on this source from those of other sources we have tested. Firstly, the best performance is obtained when the diameters of the anode hole and the extraction electrode are 18 mm and 14 mm, respectively. These are larger than those of other sources(10mm to 12 mm). This may be related with the field distribution on the axis: the peak of the mirror field is just between these two electrodes.

Since a large extraction hole usually results in a large emittance of the beam, we tried to estimate it by measuring the beam spread after a thin slit. The width of the beam 30 cm downstream of a 2-mm slit was found to be about 2 cm. Although this measurement is rough, we can say that the emittance is not worse than other sources.

Secondly, the gas flow rate required for the best performance is very small: it is of the order of 0.001 atm·cc/min. This is consistent with the value estimated from the observation that the gas flow increases the vacuum pressure by about 5×10^{-7} Torr and the estimated pumping speed of about 10 l/s. The gas flow rate affects

Table 3. Examples of ion yield.

	4	5	6	7	8	9	10	11	12	13	14
N	315	300	57								
O	480	330	245	36							
Ne	240	195	115	65	32	1.5					
Ar					351	195	-	43	13	11	2.2

the beam intensity so much that its control is very difficult with our present regulator. The third point is that this source can produce large drain current: it sometimes reaches more than 5 mA while others do not exceed 2 mA. The third one may also be related to the large holes mentioned above.

The fourth point of the difference is that the gap between the anode and the extraction electrode for optimum operation is smaller than our other sources: it is about 30 mm while it is more than 40 mm in other sources. The best axial position of the anode was searched and found to yield larger drain current exceeding 6 mA and higher ion yields at an inner position than the designed. The best performance has not been attained, however, due to the limited current capacity of our present high-voltage power supply.

The axial field near the design value turned out to give the best performance although some fine adjustment was needed, but the distance between the two coils seems to be larger for better performance. This fact suggests that a longer ECR zone is better.

A list of ion yield obtained in the preliminary survey is shown in Table 3.

4. DISCUSSIONS

The HyperECR ion source has been proved to have a high performance, although the results are still preliminary and the emittance has not been measured accurately. One of the reasons of this good performance is certainly attributed to the higher frequency of the microwave and the higher axial and radial magnetic fields. Various efforts to make them high resulted in a sharp peaks and valley of the axial field distribution keeping the diameter of the ECR zone within the reasonable size. In addition, this valley allows us to use an 18 GHz microwave frequency without changing the magnetic configuration, because the length and the diameter of the ECR zone are estimated to be 11.2 cm and 3.9 cm, respectively, according to the formulae in section 2.

The high peak axial field around the extraction seems to have effects on the ion yield. Rather large drain current is apparently inconsistent with the low gas flow rate: if all of the gas input of 0.001 atm·cc/min were to be ionized and extracted from the source, the drain current would be about 70 pμA. We must assume that a large amount of electrons should be injected into the high voltage side from the extraction electrode. If most of the electrons pass through the anode hole and get into the plasma since the diameter of our anode hole is large, we are injecting electrons effectively without any special device for it. It is interesting to see if the electron injection improves the ion yield as reported in refs.[8,9] in our source.

Emittance measurement, metallic ion production, electron injection, injection of low-charge-state ions from another ion source and pulse operation to produce afterglow[3] are being prepared as well as searching for better working parameters.

5. REFERENCES

1) Geller, R., "ECRIS:The Electron Cyclotron Resonance Ion Sources," Ann.Rev.Nucl.Sci.**40**, 15(1990).
2) Jacquot, B. and Pontonnier, M., "La source Caprice ..," Nucl.Instrum.Meth.**A287**, 341(1990); ibid **A295**, 5(1990).
3) Sortais, P., "Pulsed ECR Ion Source using the Afterglow Mode," Rev.Sci.Instrum.**63**, 2801(1992).
4) Sekiguchhi, M.*et al.*, "Design of the INS ECR Ion Source," in **Proc. Int. Conf. on ECR Ion Sources and their Applications** (NSCL Report #MSUP-47, 1987) pp.323-333.
5) Hattori, T. *et al.*, "Development of Higher Order Mode ECR (HiECR) Ion Source (Test of 6GHz Operation)," in **Proc. 7th Symp. on Accelerator Science and Technology** (Ionics, Tokyo, 1989), pp.71-85.
6) Sekiguchi, M. *et al.*, "INS ECR Sources for Accelerators," in **Proc. 12th Symp. on ISIAT'89** (Ionics, Tokyo, 1989), pp.187-194.
7) Kitagawa, A. *et al.*, "Development of ECR Ion Source for the HIMAC Medical Accelerator," in **Proc. 8th Symp. on Accelerator Science and Technology** (Ionics, Tokyo, 1991), pp.58-60.
8) Xie, Q., Lyneis, C.M., Lam, R.S. and Lundgren, S. A., "Enhanced ECR Ion Source Performance with an Electron Gun," Rev.Sci.Instrum.**62**, 775(1991).
9) Nakagawa, T. and Kageyama, T., "The Effect of an Electrode in the First Stage of RIKEN Electron Cyclotron Resonance Ion Source(ECRIS)," Jpn.J.Appl.Phys.**30**, L1588(1991).

PERFORMANCE AND STATUS OF THE IUCF HIGH INTENSITY POLARIZED ION SOURCE

V. Derenchuk, M. Wedekind, R. Brown, T. Ellison, D. Friesel, J. Hicks,
D. Jenner, A. Pei, H. Petri, P. Schwandt, J. Sowinski
Indiana University Cyclotron Facility
2401 Milo B. Sampson Lane
Bloomington, IN 47408-0768

ABSTRACT

The IUCF High Intensity Polarized Ion Source has been completed and is being tested before its installation in a new terminal scheduled for September of this year. The design is based on the source in operation at TUNL, which employs cold (~30 K) atomic beam technology and an electron cyclotron resonance ionizer. It is expected to produce 100μA DC $\vec{H}^+$ and $\vec{D}^+$ ion beams with a polarization of 75% or greater. Coupled with a wideband and resonant bunching system and a high-transmission beam line into the injector cyclotron, the source should allow 10^{10} protons to be stored in the electron cooled storage ring in a few seconds. Results from operation of the source and studies of atomic beam properties will be described.

1. INTRODUCTION

A major fraction of the experimental program at the Indiana University Cyclotron Facility (IUCF) has always concentrated on studies of spin degrees of freedom. Most recently, the first data with low intensity polarized beam on an internal polarized $^3\vec{He}$ target has been taken with the IUCF Cooler ring[1]. To further enhance the unique opportunities in spin physics research using the Cooler ring, circulating beam intensities near the limit of ring operation, 10^{16} particles/sec, are required because target densities and/or reaction cross sections are very low.

In order to meet these experimental requirements a modern, high intensity source of polarized ions has been constructed. The source, which will be coupled by a high-

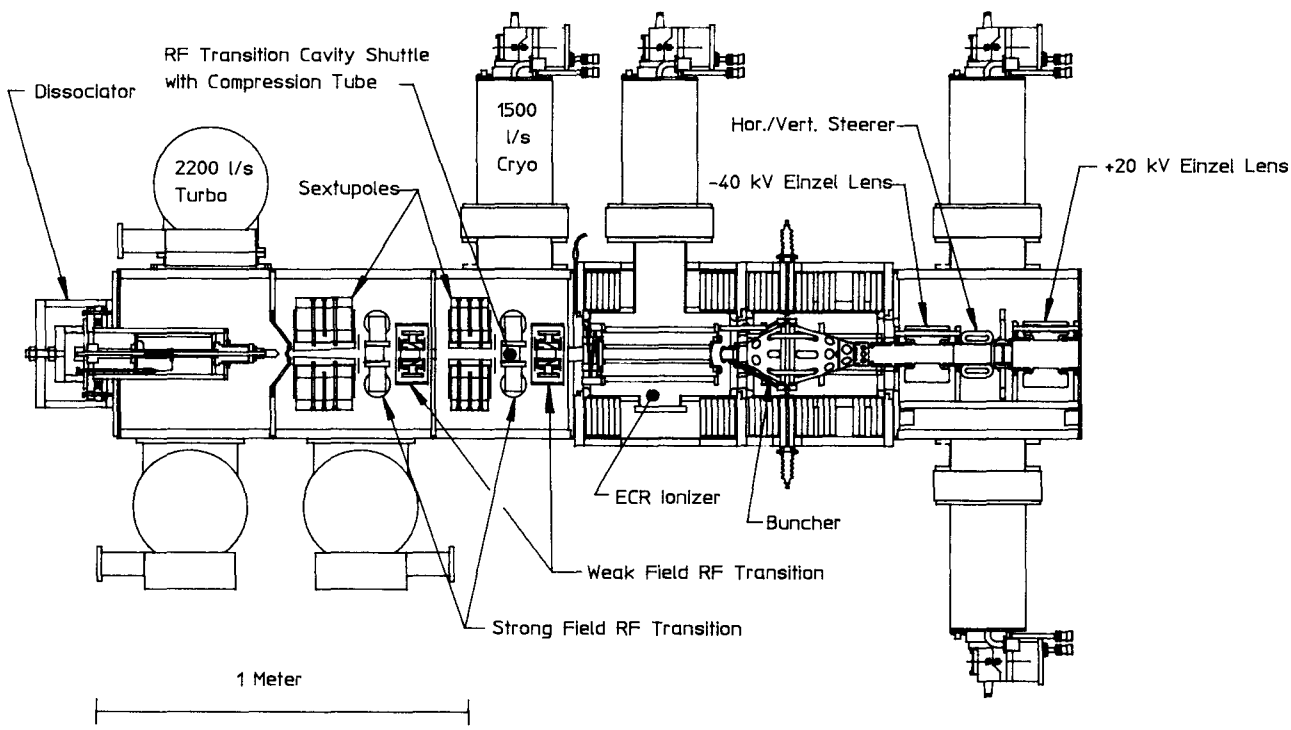


Fig. 1 General layout of the IUCF High Intensity Polarized Ion Source showing the atomic beam section, ECR ionizer and the low energy, high efficiency bunching system. The source is now complete as shown and is being commissioned off line.

efficiency bunching system and a high-transmission beam line[2] to the first cyclotron, should allow 10^{10} protons to be stored in the Cooler ring in a few seconds.

The High Intensity Polarized Ion Source (HIPIOS)[3] built at IUCF is illustrated in Fig. 1. It is similar to the system recently built and brought into successful operation at TUNL by T.B. Clegg and associates.[4] Based on TUNL's experience, HIPIOS should produce in excess of 100 μA DC, $\vec{H}^+$ and $\vec{D}^+$ ion beams. The atomic beam section, which employs cold (~30 K) atomic beam technology, is a close copy of the TUNL design. The ionizer is an electron cyclotron resonance (ECR) device similar to those used at TUNL, PSI and Bonn for ionization of polarized atomic beam.

This paper describes the recent operating experience with the completed ion source and the status of the ion source installation in the new high voltage terminal.

2. OPERATION OF THE ATOMIC BEAM SECTION

2.1. Velocity Measurements

Measurements of atomic and molecular beam velocities with W. Gruebler's (ETH) atomic beam chopper allowed us to gain considerable experience during the initial operation of the dissociator. The beam velocity distribution was measured while operating the dissociator using different nozzle temperatures, flow rates, RF power levels and types of gas. This data[5] is consistent with the velocities measured by W. Gruebler et al. when different dissociator operating conditions are taken into account. Figure 2 shows plots for atomic hydrogen for different nozzle temperatures.

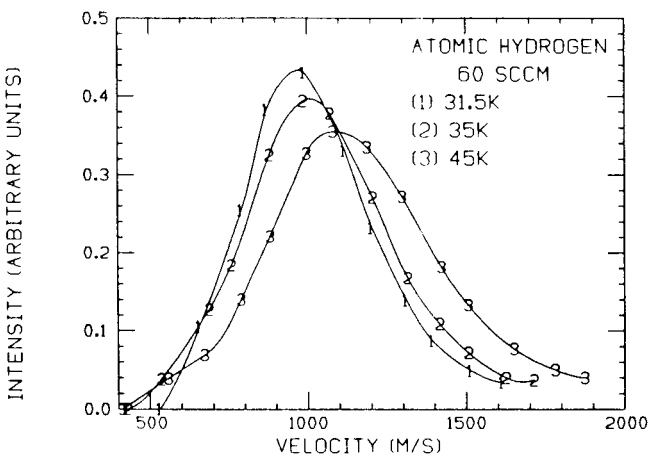


Fig. 2 Velocity distributions for atomic hydrogen for different nozzle temperatures. Relative beam intensities between distributions is arbitrary and not a true comparison.

2.2. Flux Measurements

For measuring the atomic beam flux from the dissociator, the TUNL design for a compression tube was used with changes suggested by W. Haeberli et al. The Bayard-Alpert gauge previously used to measure pressure changes in the compression tube was replaced with a cold cathode gauge in order to eliminate systematic changes dependent on exposure to H_2.

Beam fluxes from $3x10^{14}$ to $1.5x10^{15}$ atoms/sec were measured at the end of the second sextupole chamber with both sextupole chambers empty. A range of flow rates and nozzle temperatures were investigated. These measurements when compared with those with the sextupoles installed, showed little evidence of beam attenuation due to their aperture. The peak intensity was observed with 210 Amps applied to sextupole #1, which corresponds to an integrated pole tip field of 108 kG-cm. The integrated pole tip field in sextupole #2 with 200 Amps applied is 60 kG-cm. Maximum beam intensity observed was on the order of $1.0x10^{16}$ sec^{-1}.

A smaller compression tube has been added to the sextupole #2 chamber RF transition shuttle in order to allow for atomic beam measurements with the source in operation. This tube has not been calibrated, but the relative pressure differential is extremely useful for optimizing the atomic beam flux density in the ECR ionizer. The maximum ΔP observed to date is $8.0x10^{-6}$ Torr, corresponding to a sextupole power of 12 for atomic beam measured with sextupoles on versus sextupoles off.

2.3. Operating Experience and Improvements

Temperature of the cold nozzle is regulated by a heater mounted on the clamp that holds the nozzle in place against the accomodator. A copper braid leads from this clamp to the He refrigerator cold head. Modifying the heater mount in order to more evenly heat the nozzle has improved temperature stability and reproducibility of atomic beam output.

A drop in atomic beam intensity with time of 30% in the first 3 hours and 60% in 24 hours has been observed and is concluded to be due to the coating of the cold nozzle with a white powdery substance analyzed to be SiO_2. Several groups that have long term operating experience with RF dissociators with cold nozzles report varying degrees of accumulation of white powder correlated to the time integral of the RF discharge power.[6-8] It is clear that the SiO_2 is being eroded from the glass dissociator tube. We have tried a quartz tube and an alumina tube in place of the standard Pyrex one. The quartz showed little change in accumulation of white powder whereas the alumina tube would operate for less than an hour before the H_2 discharge became unstable. At the suggestion of T. Clegg

(TUNL), we also extended the Pyrex tube through the MACOR accomodator into the copper nozzle so that the atomic beam does not come into contact with the MACOR. We are continuing to determine optimum parameters for the most reliable long term operation of the dissociator.

3. ECR IONIZER

3.1. ECR Operation

The ECR ionizer (Fig. 3) was installed and ready for testing in early November of 1991 and beam was extracted shortly thereafter. The ECR sextupole magnet structure is biased at a high positive DC voltage for ion extraction. During initial operation of the ECR it was noted that the proton beam output increased as the plasma volume was increased. Current draw on the extraction supply also increased with plasma volume as did the pressure in the ECR. When the source was disassembled, there was evidence of ion beam incident on the RF transition units upstream of the ECR. Evidently, ions were being extracted from the plasma axially in the upstream direction, as well as radially through the gaps in the permanent magnet sextupole. In order to decrease the extraction current on the ECR, a cylindrical copper screen was installed around the permanent magnet sextupole and a cone inserted at the entrance to the ECR, both of which operate at a few hundred volts above the sextupole potential. This produces a potential barrier to eliminate extraction of the ion beam radially and axially upstream of the ECR. The original RF horn was substituted with a design using a microwave choke flange which can be floated at the sextupole potential and therefore come into contact with the magnets eliminating ion extraction through the horn. The choke flange horn design also is about twice as efficient in directing power into the plasma region of the ECR as measured by the temperature rise of a water sample in air.

Operation above 15 kV ECR bias has not yet been achieved due to current limitations of the power supplies. This problem is attributed to ions extracted from ECR onto the buncher electrodes through areas other than the extraction electrode. To eliminate this excess current draw, these areas will be covered. A quartz tube liner for the inside of the ECR sextupole also will be tested, which may eliminate the need for the screen and further reduce the current draw on the ECR, but at the cost of reduced radial pumping of the plasma region.

3.2. Ion Extraction

Beam has been successfully extracted from the ECR at the design energy of 2 keV which is intended to be accomplished by operating the ECR sextupole at 20 kV and the buncher electrodes at 18 kV. A second acceleration gap after the buncher provides the source output energy of 20 keV. To date, best beam extracted from the ECR was observed with the sextupole operating at 10 kV and an extraction potential of 3.5 kV.

The ECR was first operated with the atomic beam valve closed and gas injected directly into the ECR vacuum chamber. Introduction of hydrogen gas produced about 100 μA of proton current. With helium as an injection gas 25 μA of doubly charged and 200 μA of singly charged beam has been extracted and measured after mass analysis. The ECR ionizer will replace an arc source when doubly charged He beams are required.

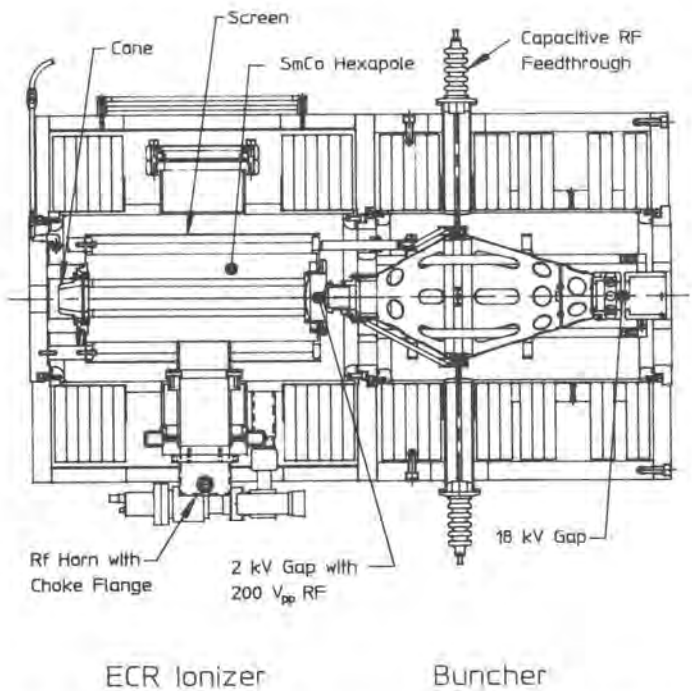


Fig. 3 ECR Ionizer and buncher assembly showing RF horn with choke flange, biased screen, entrance electrode cone and low energy (2keV) buncher.

3.3. Performance with Atomic Beam

With atomic beam injected into the ECR, over 90 μA of proton current was measured downstream of a 90° mass analysis magnet. The best 'real' beam to background ratio was observed with 68 μA of total proton current and 6 μA of background current measured by turning the focussing sextupoles off. After 18 hours of operation the total current drops to 35 μA with 8 μA of background. The drop in intensity is due to a deterioration of the performance of the dissociator while the increase in background is from loading of the sextupole #2 chamber and ECR cryopumps with hydrogen.

4. IN-TERMINAL BEAM TRANSPORT

4.1. Beam Bunching and Acceleration

The energy of the beam extracted from the ECR is relatively low (2 keV) to permit efficient prebunching before leaving the ion source. The ECR solenoidal magnetic field is continued through the buncher section following the ECR (Fig. 3) to avoid the large emittance increase that would be associated with passage of such a low-energy ion beam through a termination of the ECR solenoidal field. Immediately after extraction from the ECR, the beam passes through the short, gridded RF gap of the buncher. RF power from a 500 W wide-band amplifier, fed through a 20 kV DC capacitive RF feed-through, provides the 200 Vpp linear sawtooth bunching waveform. The conical geometry of the buncher electrode effectively results in a single gap nonresonant buncher. The energy modulated beam drifts in the uniform solenoid field of the buncher section for ~35 cm to achieve bunch formation at an acceleration gap where the beam energy is raised to 20 keV just prior to exiting the solenoid field. The strength of the solenoid field is chosen to provide focussing of the proton beam at this acceleration gap while unfocussed nitrogen ions from the N_2 plasma buffer gas are intercepted, allowing for early rejection of much of the sizeable nitrogen component extracted from the ECR.

4.2. Beam Transport System

The 20 keV ion beam emerging from the buncher section is focussed and steered in the source exit section into the 4 m long beam transfer line to the 600 kV terminal acceleration column entrance. Aside from the usual electrostatic focussing, magnetic steering, and beam diagnostic elements, this beam transport line (Fig. 4)

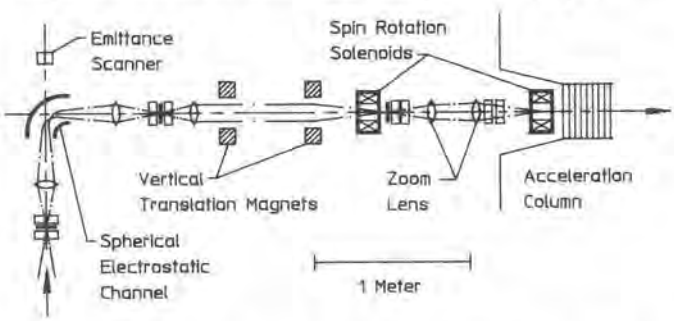


Fig. 4 In-terminal beam transport line showing the features described in the text.

incorporates three principal systems of note. A combination of a 90° bend, spherical electrostatic channel and a pair of spin-rotation solenoids placed at beam waists, is used to change the spin alignment axis of the polarized beam from axial orientation at the source exit to vertical at the end of the transfer line. A doubly focussing, doubly achromatic magnetic beam translation system produces a 0.5 m vertical parallel drop of the ion beam in the terminal to match source beam height to the acceleration column. A unit magnification electrostatic zoom lens system matches the fixed transfer line optics to the variable acceleration column optics to provide controlled ground potential beam line injection over a wide range of terminal voltages.

5. PROJECT STATUS

The ion source is complete up to the transfer beam line and is now in the testing stages. The controls system using HP workstations and X-windows software, interfaced to a VME and a PLC, is partially implemented.[9] The buncher hardware and RF drive system is ready to be tested with beam. Fabrication of all transfer beam line elements is nearly complete. Installation of the source in the new terminal will take place in September of 1992. The 600 keV beam transport line[2] will begin to be installed during a 6 week shutdown and first beam transported to the Injector Cyclotron is expected to take place in late spring of 1993.

6. ACKNOWLEDGMENTS

The authors express their appreciation to Tom Clegg and to the entire technical staff at IUCF. This work has been supported by NSF Grant PHY-891440.

7. REFERENCES

1) C.E.Jones, the CE-25 collaboration at IUCF, private communication.
2) W.P.Jones et al., "Beam Transport System for the IUCF High Intensity Polarized Ion Source," these proceedings.
3) M.Wedekind et al., "IUCF High Intensity Polarized Ion Source," in **Proceedings of IEEE Particle Accelerator Conference,** (IEEE, San Francisco, 1991) pp.1922-1924.
4) T.B.Clegg, "Polarized H^- and D^- Source Development at the Triangle Universities Nuclear Lab," in **Proc. of the High Energy Spin Physics 8th Intl. Symp.**, Minneapolis, MN, ed. K.J. Heller, A.I.P., New York, 1989, Vol. 187, 1227.
5) V.Derenchuk, R.Brown, H.Petri and M.Wedekind, "HIPIOS Beam Development", in **IUCF Annual Report 1991-1992,** (internal publication) in print.
6) L.Young, private communication.
7) A.Belov, private communication.
8) P.Schmelzbach, private communication.
9) D.W.Frame et al.,"The IUCF High Intensity Polarized Ion Source Control System", these proceedings.

ION SOURCE OF DISCHARGE TYPE

Ivan B. Enchevich
Cyclotron Division, TRIUMF, 4004 Wesbrook Mall, Vancouver,
B.C., V6T 2A3, Canada

and

Sergei A. Korenev
Super High Energy Physics Laboratory, JINR, Dubna,
Moscow District, 141980, Russia

Abstract

A new scheme of ion source based on a dielectric surface sliding discharge is described. The conditions to form this type of discharge are analyzed and experimental results are shown. The main parameters of this ion source are: accelerating voltage $U = 1 - 20$ kV; continuous extracted ion beam; current density $j = 0.01 - 0.5$ A/cm^2; ions of Cl, F, C, H; residual gas pressure $P = 10^{-6}$ Torr. A magnetic system is used to separate the different types of ions. The dielectric material in the discharge circuit (anode plasma emitter) defines the type of ions. The emission characteristics of plasma emitter and the discharge parameters are presented. The ion current yield satisfies the Child-Langmuir law.

1 INTRODUCTION

The development of different kind ion sources is going intensively nowadays. It is connected with a number of problems concerning the forming of the plasma - the ion emitter in known ion sources. Discharge schemes based on gas discharges are used to get continuous ion beams. Many difficulties exist in the production of the ions of the dielectric materials due on the demand to form a plasma which components are the ions of needed kind. In this article it is suggested to use a sliding discharge [1] on the dielectric surface for receiving of continuous ion beams of: carbon, chlorine, fluorine, hydrogen etc. from different dielectric materials

2 CONSTRUCTION AND SCHEMATICS

The ion source, shown schematically in Fig. 1, consists of two main blocks. The first one is the discharge block, formed by dielectric body 1, with a dielectric ring 2 connected to the body 1. On the surface of ring the 2 sliding non-finished discharge is ignited by the voltage, applied to the grid electrode 3. The second block is for extraction of the ion beam. It consists of a ring-shaped isolator 4 and high voltage electrode 5. The voltages igniting the discharge and extracting the ion beam are fed through vacuum sealed connectors 6 of the flange 7. The whole construction is enclosed in a vacuum chamber which may be connected to an external system by a flange. The main(principal) element of the discharge device is the dielectric ring. From the opposite to the grid electrode 3 side of the ring there is a contact electrode from copper or other conductive material. This contact electrode, as well as the grid electrode, may be attached to the dielectric surface of the ring by evaporation or other electro-chemical technique. For dielectric surface discharge stabilization an external magnetic field, produced by a permanent magnet, is applied. The ion charge/mass state separation is fulfilled also by the magnetic field of permanent magnets, changing appropriately the distance between the magnets by a mechanical device. The ion source may be powered by one of the next supply schematics, shown on Fig. 2. Residual gas pressure in the source is $10^{-6} \div 10^{-5}$ Torr. The ion source is not complicated . It may be produced and assembled easily and may be tuned quite fast.

3 PRINCIPLE OF OPERATION

The ion source principle of operation may be described as follows: by applying a voltage from the power supply to the discharge block a sliding discharge is formed on the dielectric surface between the contact and the grid electrode over the grid cells. This discharge becomes plasma ion emitter. The discharge forming depends on the electric field strength in this interval which by residual gas pressure in the above mentioned limits is 2×10^6 V/cm in average. Further processes in the plasma discharge consist in primary dusting and further disintegration of the dielectric material in the needed plasma components to reach the required current density. The upper level of the density is limited by the resource of the stable glowing of the discharge, connected to the dielectric erosion and the instability of

the plasma discharge between the cells of the grid electrode.The experiments show, that for stable discharge, supported by discharge block voltage between 4 and 15 kV, best results are received with grid cell size from 1 × 1 to 2.5 × 2.5 mm × mm. The dielectric ring material determines ions type.To receive ions of fluorine the best is to use foil-covered teflon, of chlorine - vinyplast,of carbon or hydrogen -polyethylen,etc. Ion extraction is provided by electric field, formed in the ion beam extraction block, fed by dc high voltage supply source. The needed voltage is from 1 to 20 KV.

4 RESULTS

The emission characteristics of the described ion source show that the value of the extracted ion beam for different ion sort satisfies the Child- Langmuir law. By the above mentioned voltages on the extraction block the value of the current in the continuous extracted ion beam is from 0.01 to 0.5 A. The value of the ion current strongly depends on ion mass accordingly to the Child-Langmuir law.The measurements of the formed ions charge state in the source showed that it is equal to 1. At present study and work to increase the charge state are carried out.The source life time is limited by the time of stable discharge forming and reaches 6 hours in the best cases. Additional research and development work is needed to increase the ion source life time. This concerns first of all the dielectric ring parameters and the search for its most suitable components.

5 CONCLUSIONS

The presented source works on a new principle and allows the receiving of continuous ion beams from solid state dielectric materials with any wanted form of the beam cross-section. Additional work is needed to increase its life time and to determine its emittance parameters.

References

[1] Korenev S. A., Diode with a plasma cathode, based on sliding discharge, Print 9-82-758, JINR, Dubna, 1982

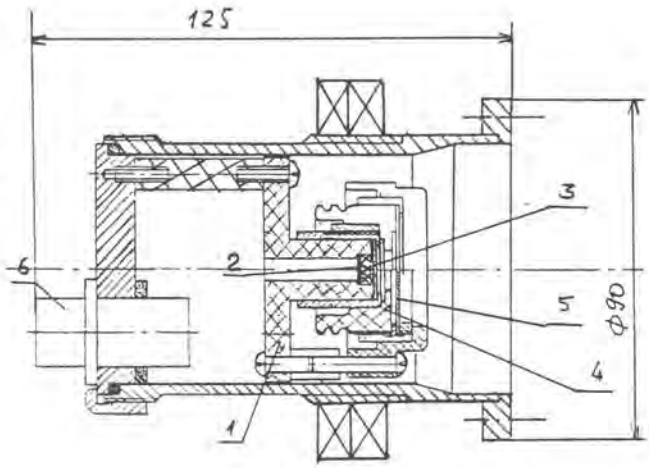


Figure 1: Ion source section

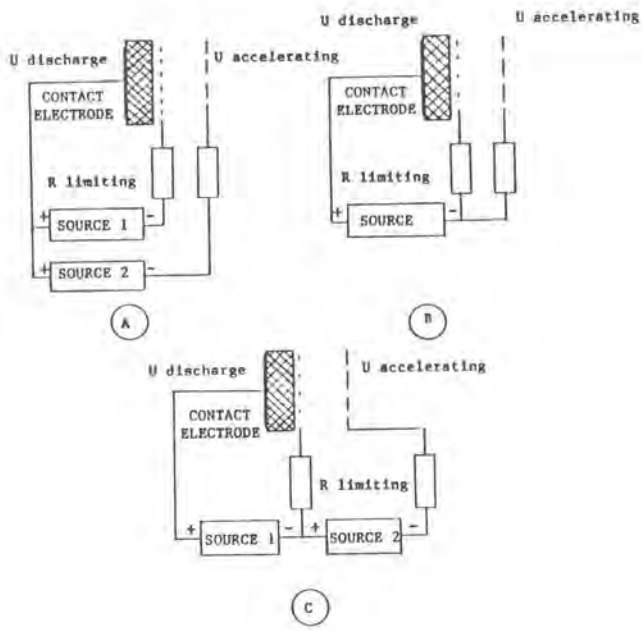


Figure 2: Power supply schematics

OPERATION OF ION SOURCES AND BEAM TRANSPORT TO JAERI AVF CYCLOTRON

W. Yokota, T. Nara, K. Arakawa, Y. Nakamura, M. Fukuda, T. Agematsu, S. Okumura, I. Ishibori
Japan Atomic Energy Research Institute,
1233, Watanuki, Takasaki, Gunma, 370-12, Japan

and

T. Tachikawa, Y. Hayashi, K. Ishii
Sumitomo Heavy Industries, Ltd.,
5-2, Sobiraki, Niihama, Ehime, 792, Japan

ABSTRACT

Two ion sources, a multi-cusp ion source for light ions and an ECR ion source for heavy ions, were installed for the JAERI AVF cyclotron. Operation of the sources at JAERI started in February 1991. The ability of ion generation required for beam injection into the cyclotron has been attained. Some characteristics, test generation of metal ions and results of beam transport to the cyclotron are described.

1. INTRODUCTION

A multi-cusp and an ECR (OCTOPUS) ion source manufactured at Ion Beam Applications s.a. in Belgium were tested and connected with the computer control system at the Niihama Works of Sumitomo Heavy Industries, Ltd. in 1990.

The sources and the cyclotron were installed at JAERI in early 1991. The beam generation tests of the sources, acceleration by the cyclotron and transport of beams to the end of beam lines have been conducted. In these days, the sources supply ion beams mainly for beam study of the cyclotron and some experiments at beam course ends.[1,2] Improvements and developments have also been carried out mainly for higher beam transmission to the cyclotron and metal ion generation. Emittance of Ar beam from an ECR ion source was measured in detail.

2. ECR ION SOURCE OPERATION

The ion generation test at JAERI has been made for O^{6+}, Ar^{8+}, Ar^{13+} and Kr^{20+} to ensure that beam currents more than 1 eμA were generated, and the test was successful for every ion species.

The beams except for O^{6+} were injected into the cyclotron, and acceleration and beam extraction tests have been carried out. The currents measured at beam course ends also satisfied those expected. The He^{2+} beam was also produced by the JAERI ECR source and was supplied for the cyclotron. The results were reported for ion beam generation from gaseous materials by the JAERI ECR source elsewhere.[3]

2.1. Metal Ion Generation

We tried to generate metal ions of Al, Mo and B by direct insertion of a rod into plasma. Rods of Al_2O_3, Mo_2C and BN were inserted radially into the 2nd stage plasma by remotely controlled motor drive and could be positioned by 50 μm steps. Though the insertion depth has not been optimized, we observed these ion beam currents as listed in Table 1 enough for acceleration by the cyclotron. Beam currents of Al ions were stable and the maximum currents were easily attained. The Mo ion beam currents were less stable and the total currents of all the isotopes were similar to the Al ion beam currents. Ion beam of B was unstable and small compared with the other two metal ions in spite of low charge state. The averaged beam currents are listed in Table 1. The performance on metal ion generation and beam stability appear to depend on physical and chemical characteristics of rod materials.

2.2. Charge State Distribution and Main Gas Feeding

The JAERI ECR source had been operated by feeding main and support gases into the 1st stage chamber. We examined the difference of charge state distribution of Ar ions by feeding Ar gas into the 1st and the 2nd stage. We used O_2 as the support gas and fed it into the 1st stage in all cases. When feeding into the 2nd stage, the beam current sensitively depended on the operating parameters, such as mirror coil current, microwave power, etc., and the plasma fired in narrower range of mirror coil current at the 2nd stage. The gas flow range of Ar reduced down to one tenth. These indicate that the plasma condition is different between the fed chambers of the 1st and the 2nd stage. Further experiments and data are necessary to assign the cause of the difference. However, it may come from the change of pressure distribution of Ar gas with feeding position, for example. The difference of the plasma condition clearly appeared in

Table 1. Maximum beam currents of metal ions.

material	support gas	ion	current(eμA)
Al_2O_3	O_2	Al^{8+}	5
		Al^{6+}	17
		Al^{4+}	43
		Al^{3+}	62
Mo_2C	N_2	$^{98}Mo^{17+}$*	5
		$^{98}Mo^{15+}$	6
		$^{98}Mo^{13+}$	7
		$^{98}Mo^{11+}$	2
		$^{98}Mo^{10+}$	4
		$^{98}Mo^{9+}$	4
BN	N_2	$^{11}B^{3+}$	5
		$^{11}B^{2+}$	5

* natural abundance of ^{98}Mo is 24%.

the charge state distribution of Ar. Figure 1 shows that beam currrents are lower for the 2nd stage feed than for the 1st stage one. On the other hand, decrease of currents at high charge state is smaller for the 2nd stage feed. We expect from the data that feeding into the 2nd stage provides higher performance in generation of high charge state ions. The contribution of the performance will be significant in generation of heavier ions.

2.3. Emittance of Ar Ion Beam

Measurement of emittance for 80% current density of Ar ion beam was carried out at an extraction voltage of 10 kV in a wide range of mirror coil current. It was measured by an emittance monitoring system at a diagnosis chamber (ES2, see Fig. 3), consisting of a pair of a slit and a multi-wire detector. When Ar gas was fed into the 1st stage, the horizontal emittance of Ar^{8+} beam varied from 100 πmm·mrad to 170 πmm·mrad, while the vertical emittance was almost constant at 100 πmm·mrad. The horizontal and the vertical emittance must be equal, since the ECR ion source and the beam extraction system is cylindrically symmetric. It may be only a reason for the observed phenomenon that emittance growth comes out in horizontal direction at the analyzing magnet due to momentum spread of ions. It is generally said that the momentum spread of ions from an ECR ion source is small because ion temperature is very low in ECR plasma. However, if extraction voltage flutters by hundreds of volts, growth of the horizontal emittance at the analyzing magnet is not negligible. We observed that extraction voltage fluttered by a few hundreds of volts when the plasma was very unstable. This result supports the above assumption. It is necessary to investigate the relation between fluctuation of the extraction voltage and the emittance.

When Ar gas was fed into the 2nd stage, the horizontal emittance was almost equal to the vertical one

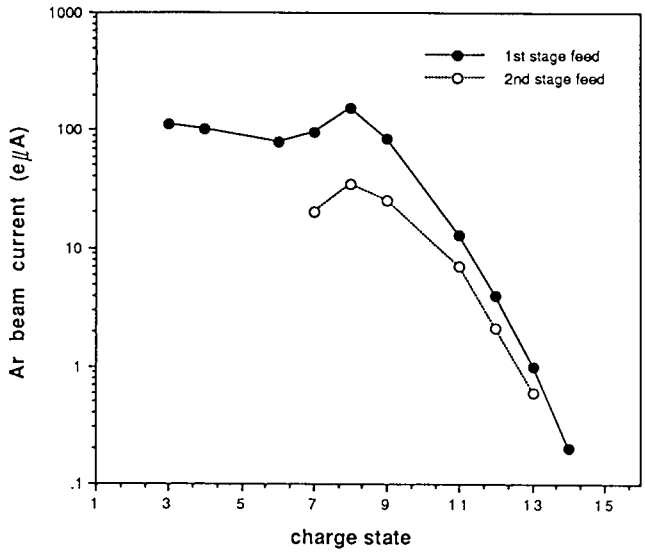


Fig. 1 Charge distribution of Ar ions, comparing 1st and 2nd stage feeding of Ar gas.

about 100 πmm·mrad, and was independent of the mirror coil currents. This also suggests that the condition of the plasma depends on the location of the inlet to feed Ar gas. The dependence of the beam emittance on charge state was not observed clearly.

It is found as a result that the emittance of beam from the JAERI ECR source depends on mirror coil currents and is a quarter to half of the beam acceptance of the injection line.

3. MULTI-CUSP ION SOURCE OPERATION

The multi-cusp ion source is of the same type as that installed at Orsay.[4] The side view of the source and specifications are shown in Fig. 2 and Table 2, respectively. The cylindrical source chamber, 15 cm in

Table 2. Specifications of Multi-cusp source.

Chamber diameter	10 cm
length	15 cm
Parmanent magnet	SmCo 46 pieces
Filament voltage	0 to 15 V
current	0 to 100 A
Arc voltage	0 to 400 V
current	0 to 15 A
Extraction voltage	3 to 20 kV
Puller voltage	0 to -3 kV
H^+ beam current	1.3 mA (maximum)
D^+ beam current	1.0 mA (maximum)

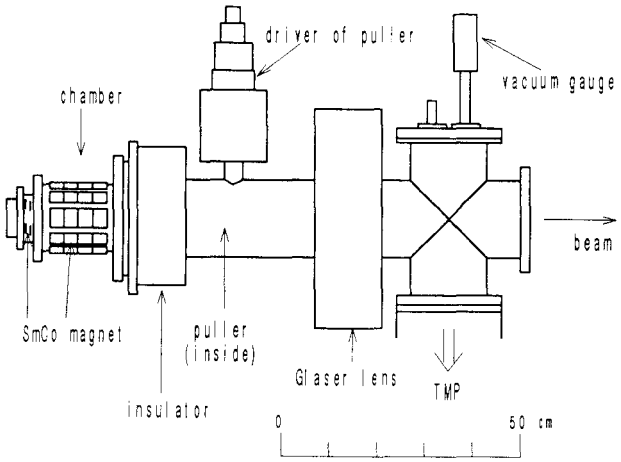


Fig. 2 Side view of the multi-cusp ion source.

length, 10 cm in diameter, is made of copper. A tungsten filament, 15 cm in length, is set along the central axis in the chamber. The arc plasma is confined by four rows of ten SmCo magnets mounted on the outer side of the chamber and six SmCo magnets at the end of the chamber. The beam extraction system consists of an extraction and movable puller electrodes, between which the gap is variable. The extracted beam is focused by a Glaser lens. The source can be simply operated mainly by arc voltage, arc current, gas flow, puller voltage and position.

The extraction voltage of the source is designed to cover a wide range of 3 kV to 20 kV to meet a wide acceleration energy range of the cyclotron. When the original extraction and puller electrodes with a single hole of 6.5 mm diameter were used, sufficient beam current was not obtained from the source at low extraction voltages. Plenty of beam current was lost around the puller electrode because of a large divergence of the extracted beam. To reduce the divergence by using a smaller aspect ratio of the diameters to the gap between the extraction and the puller electrodes, they were replaced by multi-hole type electrodes with nineteen holes of 1.8 mm diameter. This increased beam current by ten times at 3 kV extraction voltage. The maximum beam currents of H^+ (1.3 emA) and D^+ (1.0 emA) were stably extracted, in which the short term flutter was less than 5% by peak-to-peak.

However, the multi-hole puller electrode is damaged by spattering of beams. The effect of spattering turned out to be serious when high current of He^{2+} beam was extracted, and partition of holes got thin and melting also occured. Therefore we now generate He^{2+} beam usually by the JAERI ECR source.

Table 3. Beam transmission along the injection line. Beam currents are normalized by that measured at ES2. See Fig. 2.

a) JAERI ECR source

ion	Vex(kV)	ES2	IS1	IS3	IS5	I*)
Ar^{8+}	10.0	1.00	0.91	0.83	0.78	58
He^{2+}	8.5	1.00	0.94	0.92	0.84	255
He^{2+}	8.5	1.00	0.91	0.91	0.86	22

*)Beam currents at ES2 (eμA).

b) Multi-cusp source

ion	Vex(kV)	IS1	IS3	IS5	I*)	Vac**)
H^+	12.5	1.00	0.99	0.96	16	$2.8\cdot10^{-4}$
H^+	8.7	1.00	1.00	0.94	1.6	$6.3\cdot10^{-5}$
H^+	8.7	1.00	0.84	0.58	760	$6.8\cdot10^{-4}$
H^+	3.1	1.00	0.79	0.68	96	$2.0\cdot10^{-4}$
H^+	3.1	1.00	0.60	0.48	500	$9.2\cdot10^{-4}$

*)Beam currents at IS1 (eμA).
**)Pressure measured at a diagnosis chamber MS1 (Pa).

4. BEAM TRANSMISSION TO CYCLOTRON

A schemetic layout of the ion sources and injection line to the cyclotron is shown in Fig. 3. It consists of a 90 degree analyzing magnet (EAM) for the JAERI ECR source, an inflection magnet (IIM) as an analyzer for the multi-cusp source, a 90 degree bending magnet for vertical injection into the cyclotron and eight solenoid lenses. Eight chambers, each of which are equipped with a Faraday cup, X-Y slits and a beam profile monitor, were installed for beam diagnosis. The beam acceptance of the line is designed at 400 πmm·mrad to maximize the transmission of large emittance from the ECR source.[5)]

The beam transmission to the cyclotron has been improved by careful optimization of beam transport. An example of the transmission is listed in Table 3. As described above, emittance (80%) of the JAERI ECR source beam is a quarter to half of the acceptance and expected to be improved up to 95%, which is estimated to be a limitation by collision with residual gases in the line.

The transmission of the beam from the multi-cusp source is strongly dependent on the extraction voltage and beam current. The transmission is quite satisfactory for low beam current and at high extraction voltage. The transmission is very low along all the injection line when extraction voltage is low and/or beam current is high. This is attributed to large beam divergence beyond the beam acceptance of the line. Space charge in the extraction region also may have considerable effect on beam divergence. In addition, contribution of gas pressure after extraction may not negligible. When we extract high

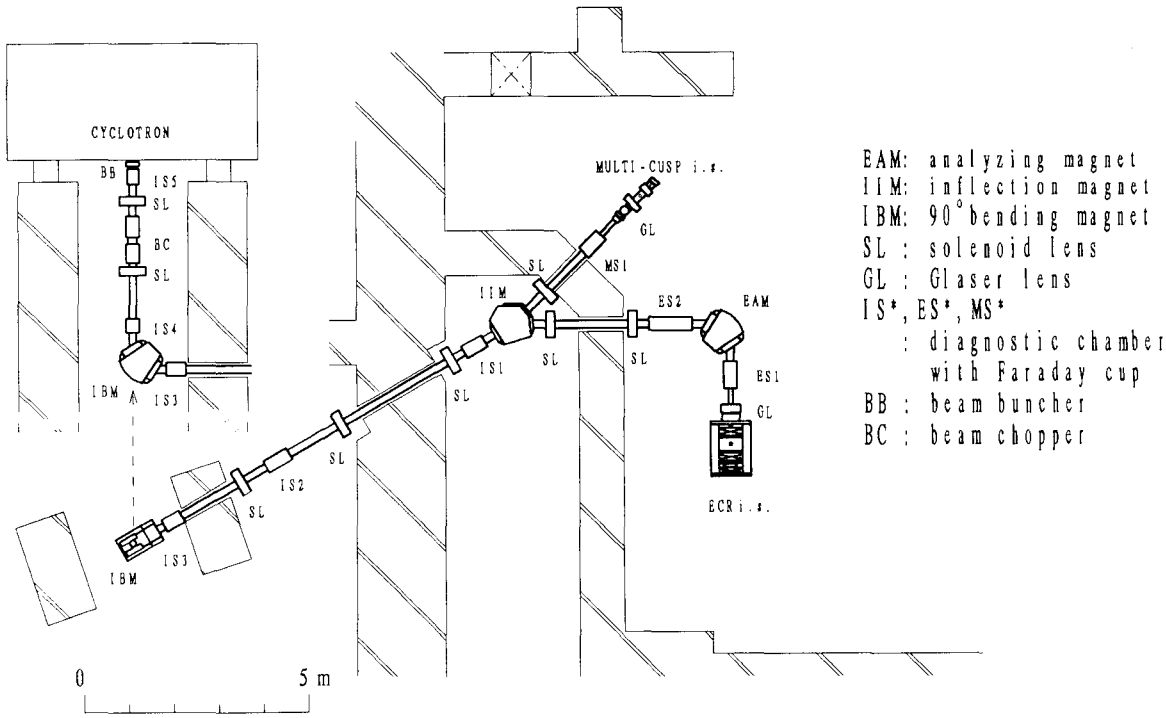


Fig. 3 Schematic layout of the ion sources and the injection line.

current beam from the source, gas is fed into the source at high flow rate, and gas pressure around the extract region increases; it is assumed to be much larger than monitored value measured at a diagnosis chamber MS1 (see Fig. 3). This contributes to growth of beam divergence through collision with the gases. In the case of the JAERI ECR source, gas pressure at extraction is about $5 \cdot 10^{-5}$ Pa, and at high current of He^{2+}, lowering of transmission was not observed at all as shown in Table 3.

5. SUMMARY

Three years have passed since the JAERI ECR and the multi-cusp sources started ion beam generation. The performance of the sources has been improved by several minor changes. Beam transmission also has been improved step by step for many ion species. For the ECR ion source, metal ion has been successfully generated by direct insertion of a rod into the plasma. We are planning to diversify metal ion species. For the multi-cusp source, further improvement will be necessary for transmission at low extraction voltage and high beam current.

Further data collection and investigation should be continued to improve performance and solve remaining problems of the sources and the injection line.

We would like to thank M. Ide of Denki Kagaku Kogyo Co. for preparing the rods for metal ion generation in the ECR ion source.

6. REFERENCES

1) Arakawa, K., Nakamura, Y., Yokota, Y., Fukuda, M., Nara, T., Agematsu, T., Okumura, S., Ishibori, I., Karasawa, T., Tanaka, R., Shimizu, A., Tachikawa, T., Hayashi, Y., Ishii, K., Satoh, T., "Construction and first year's operation of the JAERI AVF cyclotron", presented at this Conference.
2) Fukuda, M., Arakawa, K., Nakamura, Y., Yokota, Y., Nara, T., Agematsu, T., Okumura, S., Ishibori, I., Karasawa, T., Tachikawa, T., Hayashi, Y., Ishii, K., Satoh, T., "Orbit studies for JAERI AVF cyclotron", presented at this Conference.
3) Dupont, C., Jongen, Y., Arakawa, K., Yokota, W., Satoh, T., Tachikawa, T., "Result of a new 'OCTOPUS' ECR ion source at 6.4 GHz", Rev. Sci. Instr. **61**, 265 (1989).
4) Marad, M., Serafini, A., Hablot, L., Schapira, J.P., Gustafsson, S., "AGOR axial injection, using a positive light ion multicusp source", in Proceedings of the Twelfth International Conference on Cyclotrons and their Applications (World Scientific, Singapore, 1991) pp.182-185.
5) Kamiya, T., Yokota, W., Arakawa, K., Minahara, E., "Design of ECR ion source injection system for JAERI cyclotron", in the Proceedings of the 6th Symposium on Accelerator Science and Technology (Ionics, Tokyo, 1987) pp.281-283.

SPIN DYNAMICS AND POLARIZED ION SOURCES ON ISOCHRONOUS CYCLOTRON U-240

Zaika N.I.

Institute for Nuclear Research, Academy of Science of Ukraine, Kiev, 252028, Ukraine.

ABSTRACT

A matrix method approach to treat spin dynamics in electromagnetic fields of a beam line is developed and some results of calculation for Kiev's isochronous cyclotron U-240 are presented. Spin depolarization resonance conditions of various polarized ion acceleration at this cyclotron are analyzed. Polarized light and heavy ion sources for the cyclotron are discussed shortly.

1. INTRODUCTION

A great progress in development of isochronous cyclotrons, external injection systems and polarized ion sources caused applications of these accelerators for the mean energy polarized beam production to investigate various polarization phenomena in the field of nuclear physics. Contemporary high requirements to a precision of such investigations, particularly at symmetry laws studying, a necessity to have different spin states of the beam on a target, and perspectives to use isochronous cyclotron as first stage of facilities producing intermediate and high energy polarized beams, stimulate to study ion beam spin dynamics and depolarization from a source to a target. In present work the results of investigations and elaborations for production, acceleration and transportation of various polarized beams (p, $^{1}H^{-}$, d, $^{2}H^{-}$, t, $^{3}H^{-}$, $^{3}He^{2+}$, $^{6,7}Li^{3+}$, $^{14}N^{5+,7+}$, $^{23}Na^{9+}$) with energy 120 q^2/A^2 MeV/u at the isochronous cyclotron U-240 of Institute for Nuclear Research in Kiev are discussed.

2. SPIN DYNAMICS IN BEAM TRANSPORT LINE

A spin precession of polarized ions at passing through electromagnetic fields results on final spin orientation. Because of different ion trajectories and different magnetic field component directions, the movement through such fields affects an absolute value of the beam polarization, and during acceleration the beam may be fully depolarized if corresponding resonance conditions take place. For spin dynamics calculation of the ions passing through transportation system units a matrix method was used with following expression of a rotation matrix (α,β,γ are Euler's angles)

$$R=\begin{vmatrix} \cos\alpha\cos\beta\cos\gamma-\sin\alpha\sin\gamma & -(\cos\alpha\cos\beta\sin\gamma+\sin\alpha\cos\gamma) & \cos\alpha\sin\gamma \\ \sin\alpha\cos\beta\cos\gamma+\cos\alpha\sin\gamma & -\sin\alpha\cos\beta\sin\gamma+\cos\alpha\cos\gamma & \sin\alpha\sin\beta \\ -\sin\beta\cos\gamma & \sin\beta\sin\gamma & \cos\beta \end{vmatrix} \qquad (1)$$

The matrix elements are essentially simplified at decreasing of the Euler's angle number. Such simplifications are accomplished for consideration of spin dynamics in right-hand frame with $z \parallel \bar{k}$ and vertical axis y, what is convenient for an accelerator and transport line with horizontal symmetry plane.

A final spin state $\bar{S}_n(S_x,S_y,S_z)$ is a result of successive actions of the type (1) matrices R_i, inherent to each of transport line units:

$$\bar{S}(S_x,S_y,S_z)=R_nR_{n-1}\cdots R_2R_1\bar{S}(S_{x_o}S_{y_o}S_{z_o}) \qquad (2)$$

One unit may be represented by several matrices in accordance with peculiarities of the magnetic field (for example, input, central and output parts of a dipole magnet). There are among R_i matrices free path matrices and matrices needed at a plane change of the initial beam line. Thus one has opportunity to calculate spin dynamics in the transport line with any number of units and any trajectory in accordance with a specially developed TRANSPIN program. The angular (x',y') and spatial (x,y) trajectory parameters one takes from corresponding transport line calculations on the base of TRANSPORT program. A knowledge of the angles of spin axis orientations permits to determine ion polarization component values t_{kg} what is realized in TRANSPIN using appropriate formulas of work [1] for spins 1/2 and 1. The expression of Euler's angles for some typical magnetic units of a transport line as the functions of ion properties (g,A,q,v), unit parameters (B,L,ε,ρ) and trajectory parameters (x,y,θ_o,θ) are demonstrated in Table 1. Formulas for other possible units and their detailed treatment are considered in references [2,3]. Analysis of the Table 1 expressions shows that edge fields of transport line units do not affect on ion polarization values only for the central trajectory ($\theta_o=\theta=0$, $x=y=0$). The ions moving on side trajectories get spin precession around field components which do not coincide with main field direction. The difference in precession angles finally causes the beam depolarization. Calculation data for different transport lines always show decreasing of the depolarization effects at even crossovers independently on a unit set. The same takes place at decreasing of the beam emittance.

3. DEPOLARIZING RESONANCES IN THE CYCLOTRON

The second cause affecting on the ion beam depolarization is the horizontal component of magnetic field in the acceleration region. A periodical

Table 1.

№	Unit	α	β
1	Dipole magnet(DM)	-	$\beta_q(gA/2q-1)\pm(\theta-\theta_o)gA/2q$
2	Input of DM	$ygA\cos(\varepsilon)/2\rho q$	$ygA\sin(\varepsilon)2\rho q$
3	Output of DM	$ygA\cos(\varepsilon)/2\rho q$	$ygA\sin(\varepsilon)2\rho q$
4	Quadrupole lens (F)	-	$\pm(\theta-\theta_o)gA/2q$
5	Quadrupole lens (D)	-	$\pm(\theta-\theta_o)gA/2q$
6	Wien filter (WF)	-	$g\mu_oBL/hv+(\theta-\theta_o)gA/2q$
7	Input of WF	$yg\mu_oB/hv$	-
8	Output of WF	$yg\mu_oB/hv$	-

Notes: g-factor, atomic weight (A), charge (q), velocity (v) of ion; magnetic induction (B), length of unit (L), angle between normal to magnet edge and system axis (ε), trajectory radius (ρ); trajectory coordinates (x,y), input and output angles between central and treated trajectory, correspondingly (θ_o,θ).

structure of the isochronous cyclotron U-240 magnetic field (3 sectors) is a rotating field in particle bound frame. Such field may induce transition between spin substates m and m' with probability $P_{mm'}$, which is described by Majorana's formula [4]. It gives opportunity to determine a transition probability for the particles of any spin value taking into account the probability for spin I=1/2 particles $P_{1/2-1/2}$ at the same gyromagnetic ratio. Unhomogeneous magnetic field of the cyclotron in the right-hand frame (z is vertical, y∥k) has components B_x and B_y in horizontal plane. They deviate ion spins from vertical direction because of precession around horizontal components.

Owing to distortion of ion orbits depolarization resonance conditions may appear which in general relativistic case are determined by an equation

$$\gamma G = \pm k \pm m\nu_z \pm n\nu_r \qquad (3)$$

where k, m, n - are integers including 0, ν_z, ν_r are numbers of horizontal and vertical vibrations per one turn, correspondingly, $\gamma = E_k/E_0 = 1 + E_k/E_0$ with $E_0 = mc^2$, G is Larmor to cyclotron frequency ratio $G = \nu_l/\nu_c = gA/2q - 1$.

An application of the equation (3) to the isochronous cyclotron U-240 shows existence of several resonance conditions at acceleration of each of the above mentioned polarized ion types. The most important cases are shown in the Fig.1 where full lines represent solutions of the equation (3) for ν_z; points are experimental data for different field levels of the cyclotron U-240 as the functions of orbit radius (ion energy).

An influence of resonance conditions on the ion polarization depends on resonance width Γ and a strength ω. It may be shown following the works [5,6], that after passing of resonance the ion polarization P_z will be

$$P_z' = P_z\left[2\exp\left(-\frac{\pi\omega^2}{2\Gamma}\right) - 1\right] = P_z(1 - 2P_{1/2-1/2}),$$
$$P_{1/2-1/2} = 1 - \exp\left(-\frac{\pi\omega^2}{2\Gamma}\right). \qquad (4)$$

As it is obvious from (4), at $\omega^2/\Gamma \ll 1$ resonance is weak and $P_z' = P_z$, at $\omega^2/\Gamma \gg 1$ it is strong and $P_z' = -P_z$, at intermediate conditions the depolarization takes place. As in general form

$$\omega^2/\Gamma = \frac{(1+G\gamma)^2}{Gd\gamma/d\theta}(B_r/B_0)^2 \qquad (5)$$

besides the individual properties of the ion type G, acceleration rate $d\gamma/d\theta$ and magnetic field level B_0, the resonance strength depends on horizontal component

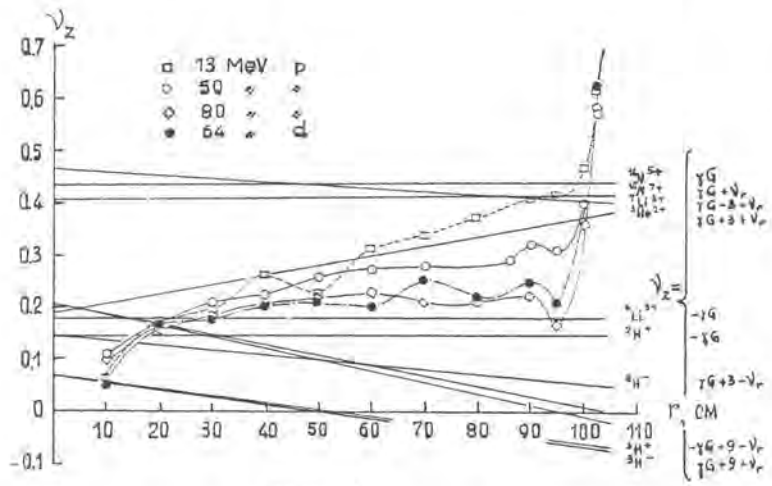


Fig. 1.

of the field in the resonance B_r

$$B_r=(B_x^2+B_y^2)^{1/2} \quad |B_x|,|B_y| \le B_r \le |B_x|+|B_y| \quad (6)$$

To determine B_r values in different resonances, the harmonic analysis of the magnetic field was carried out like reference [6], taking into account experimental data of the magnetic measurements for cyclotron U-240 and radial dependence of the field harmonics (details will be published elsewhere).

Upper and lower limits of B_r/B_o were determined from expression (5) for all ion types at the assumption that the resonances did not affect polarization if $\omega^2/\Gamma<1/3$ or $\omega^2/\Gamma>3$. Although values of these limits depending from G and γ can differ by an order for various ion types, at $B_r/B_o<0.43\ 10^{-3}$ the resonance is weak and at $B_r/B_o>1.25\cdot10^{-2}$ it is strong for all mentioned ions. The field expansion coefficients, their derivatives and the B_r/B_o limits permit to neglect all resonances of the $\gamma G=\pm\nu_z\pm\nu_r$ type, B_x components for k=6, 9 resonances, and all k=1, 2, 4, 5 resonances due to small contributions of these harmonics in the real magnetic field of the accelerator. This approach proves the absence of dangerous resonances for $^{23}Na^{9+}$. Comparisons of real field B_r/B_o ratios and their limits for every ion type in details testify that, excluding $^3He^{2+}$ ions, resonances shown in Fig.1 are also not dangerous. Therefore it is possible to produce almost all polarized ion beams without resonance depolarization at the accelerator.

4. POLARIZED ION SOURCES

To accelerate polarized ions at cyclotron U-240, ion sources of stable hydrogen isotopes and ^6Li were elaborated, using classical method of polarization [7,8]. Last years a new atomic beam unit including two sextupole magnets and a cooled nozzle for the polarized proton source, a new alkali atom source and diagnostic devices are developed.

5. REFERENCES

1)Zaika N.I., Shmarin P.L., Mochnach A.V., Fizika i technika polarizovannich puchkov ionov. Naukova Dumka, Kiev, 1987, 283 p.

2)Zaika N.I., Magal M.I., Preprint KIYaI -91-27, 1992, 19 p.

3)Zaika N.I., Magal M.I.,Trudi 11 Vsesoyuznoho soveschaniya po uskoritelyam zariadzenikh chastits. Dubna, 1989, V1,p.464.

4)Ramsey N.F. Molecuar beams. Oxford, Clarendon Press 1956, 460 p.

5)Froissart M., Stora S. Nucl. Instr. Meth. 7, 293 (1960).

6)Kim H., Burchan W.E., Nucl. Instr. Meth. 27, 211 (1964).

7)Aleshin V.A., Zaika N.I, Shmarin .L., et al. J. Phys. Soc Japan.Suppl. 55, 1063 (1986)

8)Aushev V.E., Zaika N.I., Kibkalo Yu.V., ibid 1074.

STUDY ON THE MAGNETIC FIELD OF CAPRICE TYPE ECR SOURCE

Wei Baowen, Liu Zhanwen, Zhang Wen, Wu Dezhong,
Zhao hongwei, Yuan Ping, Zhang Xuezhen , Ma Yingjie
Institute of Modern Physics, Academia Sinica,P.O.Box 31, Lanzhou 730000, P.R.China

and

A. Efremov
LNR,Joint Institute for Nuclear Research, Dubna,P.O.BOX 79, Moscow 101000, RUSSIA

ABSTRACT

The magnetic field modification and source test are presented. A preliminary test on a cold cathode used for the second stage of CAPRICE is reported.

1. INTRODUCTION

The HIRFL injector cyclotron SFC is a K69 energy variable multiparticle one-Dee machine.Originally,a radially inserted PIG source was used as its internal source. To increase significantly beam energy ,variety of ion species, operation efficiency and reliability,an ECR source has been coupled to SFC as an external source. HIRFL then will be able to accelerate ions from C to Ta upto energy of about 120 and 7.5 MeV/A respectively. The ECR source is a CAPRICE type introduced from CENG.Lab. France in 1988. Over the next year the source worked on IMP test bench.During this time a test on the magnetic field modification was carried out. In 1990 an atomic physics experiment using the high Z ions from CAPRICE was performed [1]. At the end of 1991 CAPRICE was coupled to SFC by a injection beam line. Some more tests on the source were done also. Recently,another CAPRICE -like source was designed and machined. Now it is assembled and ready for tuning.

2. CAPRICE ION SOURCE

The 10GHz ECR source CAPRICE is a very compact source suitable for producing high Z ions of gaseous and solid elements [2-3]. As it is shown in Fig.1,only one microwave generator is used for both first and second stages. The microwave is fed from waveguide 6, passing through microwave window 11, the coaxial line around the first stage,and finally is fed into the multimode cavity 12. A cold dense plasma is ignited inside the quartz tube 14 ,then diffuses into the second stage,where the working gas pressure is much lower and a good magnetic confinement is produced by the combination of the axial field and the hexapole field.Even more,a closed ECR surface can promotes to produce plasma electrons of Kev energies. The main features of CAPRICE source are:

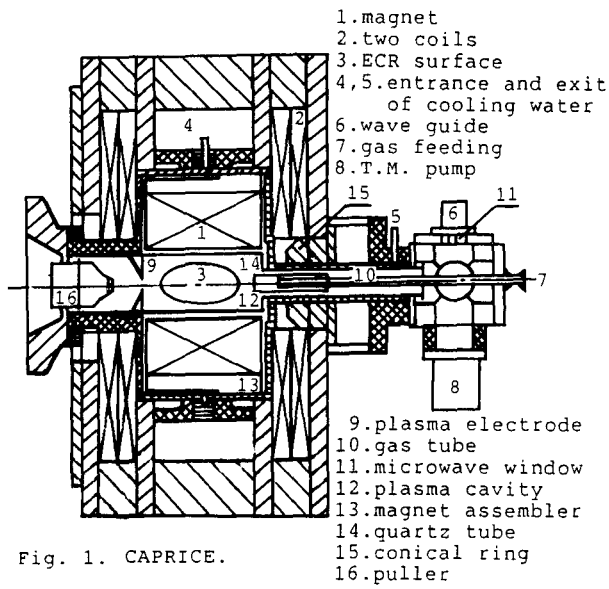


Fig. 1. CAPRICE.

(1) The solenoids are shielded with iron flanges on both sides and the hexapole is surrounded by an iron cylinder, which are helpful to decrease the electric power consumption in the mirror solenoids.
(2) Some iron parts are used to form the needed magnetic field. This makes the source compact,especial short distance between the two stages and between the ECR zone and extraction hole. As a result, a better diffusion of plasma from first stage to second stage and high extraction current are achieved.
(3) There are no pumps, no microwave window in the main stage. The plasma cavity is all in one piece for both stages. It is easy to be assembled and disassembled. These features make CAPRICE source convenient for operation, tuning and maintenance.

3. SOURCE STUDY ON TEST BENCH

CAPRICE had been well tuned at CENG. Lab.typically for oxygen ions with excellent result,and then was also tuned on IMP test bench. The result showed the extracted ion currents were essential the same as got in CENG. This implied the good reproducibility of the source and that the supplementary equipments disposed in our Lab. worked normally.

To satisfy the needed ion yields for heavy elements, we tried a possible modification of the source. As we can see in Fig.1,a conical iron ring 15 plays an important role for the formation of first magnetic mirror peak. The position of this ring can be adjusted along the axis and optimized for each ion species. Based on the magnetic field calculation,a more suitable ring shape was found out. Figure 2 shows the original iron ring and new one,while in Fig.3 the magnetic field B on the source axis is given for these two cases. It can be seen that this new ring provides a higher peak value and narrower width. The results of ion yields for Ne,Ar and Xe for both the original and new shaped conical ring are presented in Tab.1. A considerable increasing in extracted currents with factors of about 1.5 and 2 is got for Ne and Ar ions respectively. Figure 4 shows the ion-spectrum optimized for Ar^{8+} with He as a supporting gas. It is worth notice that the benefit is mainly based on the improvement of the CSD (charge state distribution) in plasma.

Table 1. Beam current with the modificated ring

	O	Ne	Ar	Xe
3	315/390			
4		124/300		
5	220/220			
6	206/205	100/155		
7		25.4/35	108/183	
8			110/220	
9			56/105	
11			8.2/15	
15				22/25

* Data on left-top are for original ring

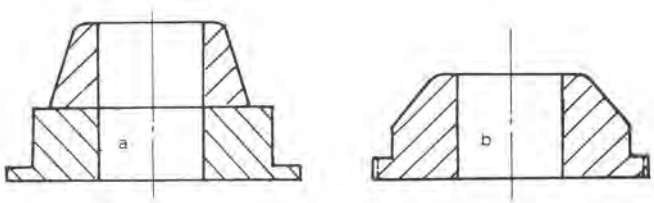


Fig.2. The shape of original ring (a) and new ring (b)

As it is shown in Fig.3,the new iron ring makes the mirror peak a little narrow,and so the first resonance point closer to the second stage. In this case a certain increment of the injected plasma from first stage is got. This plasma contains mainly low Z ions. It is helpful in igniting and sustaining plasma in second stage at a lowest possible neutral gas density. Therefore, the loss rate from charge exchange,especially for higher Z ions,is reduced, and better CSD can be expected. On the other hand, this new mirror peak with higher peak value may drive the plasma in second stage to be concentrated into the area near extraction hole.

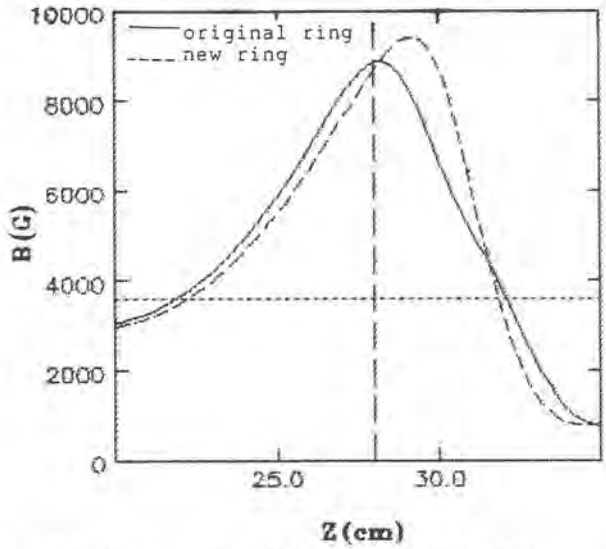


Fig.3. Magnetic field B along source axis. Coil current $I_1 = 1120A, I_2 = 1110A$.

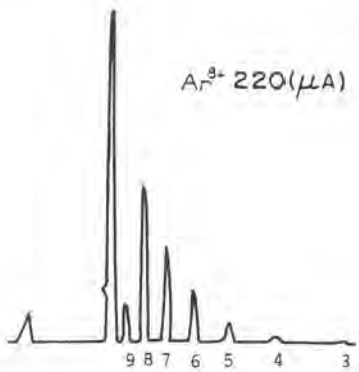


Fig.4. Ion spectrum optimized for Ar^{8+}

4. SOURCE OPERATION WITH INJECTION BEAM LINE

When CAPRICE was coupled to the injection beam line of SFC,the source had to share high pressure cooling water with other elements of the beam line.It proved that the cooling water pressure for solenoids of CAPRICE is lower than it should be.Meanwhile,the coil currents for solenoids usually exceeded 1100 A, and these were very near to the upper limit of the power supplies.The only

feasible solution is to decrease the electric power consumpion in the solenoids without any losses in the extracted beam. After the calculation of the magnetic field distribution inside soft-iron elements of the source, we found that some of them were saturated very much. In this case three options have been taken.

(1) Changing the material of the conical ring from soft iron to cobalt-steel with much higher saturation magnetization. Figure 5 shows the cross section of the new ring. It is expected to increase the first mirror peak by this change.

(2) Putting a soft-iron flange attached to the end flange at source extraction side. It should be responsible for the increasing of the second peak value.

(3) Using a puller with a special structur as shown in Fig.6. It consists of two parts,stainless-steel and soft-iron for each. Figure 7,8 show the magnetic field B distributions,especially in the extraction side, for the original stainless-steel puller and the new one with optimized coil currents for both solenoid groups.

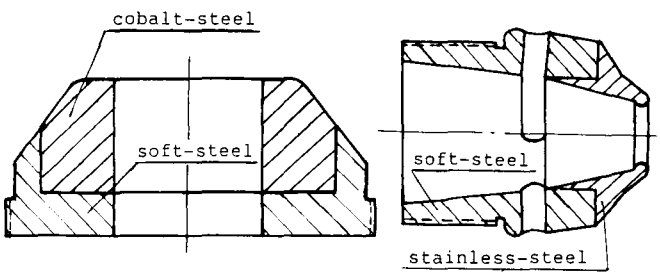


Fig.5. New conical ring with cobalt-steel.
Fig.6. New puller with two kinds of material.

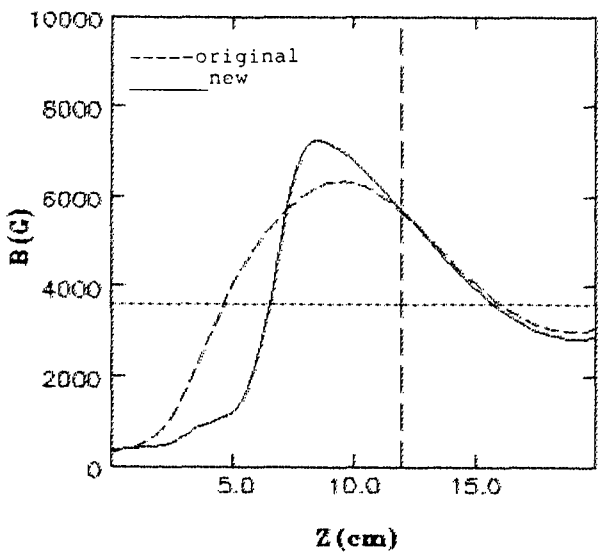


Fig.7. Axis magnetic field near the extraction. Original: $I_1 = 1120A, I_2 = 1110A$. New: $I_1 = 1062A, I_2 = 974A$

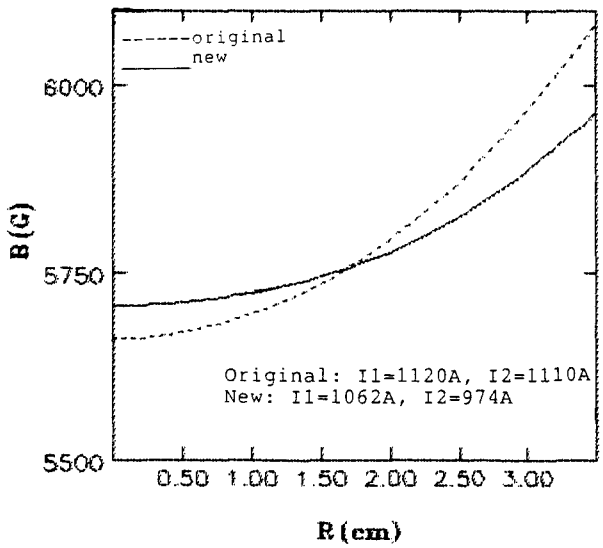


Fig.8. Magnetic field vs radius near the extraction.

In Fig.7 the curve is refered to B data along source axis. while Fig.8 is for the total mirror B data along a radius at the axial position of a few mm before the extraction hole. It can be seen that new puller gives a better field configuration with magnetic fields appropriately increased both on the source axis and on the large radius at the extraction region.

After all these changes, the magnetic field B on the source axis is shown in Fig.9. The source is then operated with a satisfactory result. The average electric power consumption for solenoids is decreased by 10% for the injection side and more than 20% for the extraction side. In addition,the gas feeding is decreased remarkably. The benefit in Ar^{8+} beam current of approximate 20% is achieved.

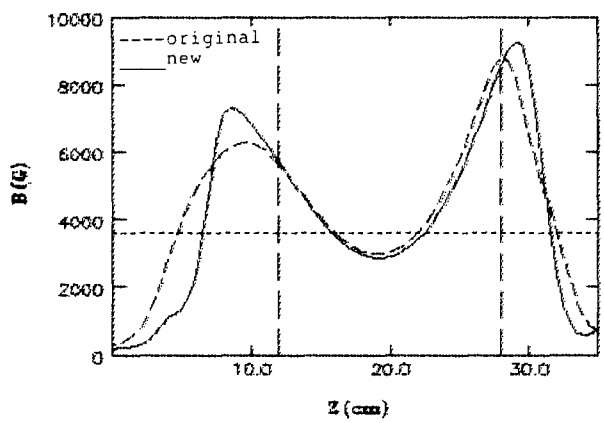


Fig.9. The final B along source axis after change. Original: $I_1 = 1120A, I_2 = 1110A$. New: $I_1 = 1062A, I_2 = 974A$

5. PRELIMINARY TEST ON A COLD CATHODE FOR ECR SOURCE

Under the inspiration of using a electron gun for ECR at LBL [4],a study on the use of a cold cathode for CAPRICE type source has been carried out. Figure 10 shows the schematic drawing with a cold cathode of position-adjusted along the axis by a piece of permanent magnet.

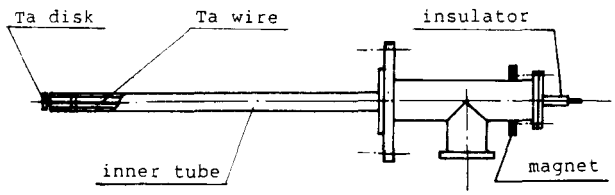


Fig.10. The cold cathode for CAPRICE.

Using this method only Ar^{8+} was tested for the ready optimum parameters of the beam line from CAPRICE to SFC. All the data quoted below for beam current are in microampere and measured at the third faraday cup, which is located in the position about 1 meter before the bottom of SFC and about 6 meters from the source.

The source was operated in the following cases:
(1) The source worked in the ordinary fashion with two stages. Beam current was about 140.
(2) Using single stage mode and extending the inner coaxial tube into the second stage. Beam current decreased to 70.
(3) The source was operated in the fashion similar to that as shown in Fig.10,but without the Ta disk. In this case,Ta wire of 1mm in diameter was used. Beam current came up gradually until 135 when the negative voltage increased upto 800 volts.
(4) Using the cold cathode as shown in Fig.10. When the biased negative voltage was only put to about 10 volts, beam current increased considerably and then reached to saturation condition. Beam current could get the maximum of 240 when the biased voltage was about 50 volts negative. That meant about 70% increasing of beam current in this case than the usual case 1. The operation parameters of the source were changed much. The optimum microwave power was decreased from the ordinary value of 500 watts to 360 watts. The gas feeding was critical and decreased obviously.

The increasing of ion current is attributed to the extra directional electron emission from the Ta cathode. These primary directional electrons from the disk are mainly concentrated around the source axis. This makes a favourite increase of the plasma density around the axis. In this case,as it is pointed out [4], an additional electrostatic trap may be got.

In principle, the emission area of the cathode is important. From the results of case 3 and case 4, we may deduce that with proper increasing of the emission area of the cathode, a more benefit could be got.

In addition, for the single stage operation mode the magnetic field configuration must be slightly changed. To reach the maximum magnetic field near the end of coaxial feeder, the conical iron was found 10mm into the source body by calculation and experimentally.

Until now, we have not yet made the source to produce metallic ions. According to the test in the case 3, it may propose a possible method of metallic material feeding for metallic ion production. In this case,instead of sample position adjusting by a mechanical way,a biased voltage adjusting is possible for tuning the sample feeding in a accurate way.

6. CONCLUSION

During our tests and operation with beam line, we found CAPRICE is an efficient source,though our source has only a 0.4 T permanent hexapole. Based on the magnetic field calculation we have made some magnetic structure innovations for CAPRICE. At the moment the maximum Ar^{8+} ion current extracted from the source is estimated to be 350 microampere or more when a cold cathode is used.

7. REFERENCES

1) Pan Guangyan, Yang Fang, Li Dawan, "Hydrogen-like nitrogen ions collision with helium into excited states," in **proceeding of 17th Int. conf. on The physics of electronic and atomic collisions** (Brisbane,Australia,1991) p462.

2) Jacquot,B., Briand,P., Bourg,F., et Geller,R., "Soure D'ions Lourds CAPRICE 10GHz $2\omega_{ce}$," N.I.M.**A269**.

3) Geller,R.,"Source of high charged ions," European particle accelerators conf. (1988), p88.

4) Xie Zuqi, Lyneis,C.M., Lam,R.S. and Lundgren,S.A., "Enhanced ECR ion source performance with an electron gun," Rev. Sci. Instrum. **62 (3)**, p775 (1991).

THE SUPER GAS MIXING TECHNIQUE FOR HIGHLY CHARGED URANIUM IONS

Timothy A Antaya

and

Dallas Cole
National Superconducting Cyclotron Laboratory, Michigan State University, East Lansing, MI 48824-1321
USA

ABSTRACT

Producing uranium ions in an ECR ion source is problematic. Uranium hexafluoride is highly corrosive and hard to handle. It also poisons the ion source. Metallic uranium has a low vapor pressure versus temperature profile— with direct insertion into the plasma, it melts before adequate vapor is produced. Uranium oxide is more refractory, aiding direct insertion vaporization, but the position sensitivity is sharp—either too much or too little uranium is produced. We have found a new technique that is based on the insertion of uranium metal powder into a high pressure oxygen plasma. The uranium concentration is low, hence the moniker 'super gas mixing', but the uranium charge state distribution is peaked around 30+ in a 6.4 GHz ECR source. The uranium consumption rate is a low 100–250 $\mu gms/hr$, and no source poisoning is observed. This technique has general applicability—we have tried it for magnesium, vanadium, nickel and molybdenum with equal success. Since small quantities of powdered metal are consumed, enriched isotopes, most generally available in powdered form, require no special handling.

1. Super Gas Mixing Technique

The origin of this technique was not actually the production of a uranium beam but rather a request to make an intense $^{92}Mo^{25+}$ beam for an isotope search experiment at the K1200 cyclotron[1]. The natural abundance of ^{92}Mo is 15%. Our starting point therefore was 100% enriched ^{92}Mo metal powder. We tried various techniques to turn this powder into a metallic fluke for direct plasma insertion, but had trouble either with material consumption (too high), or the charge state distribution (too low). We did find that powder would stick to the end of a small diameter (4mm) alumina rod. This alumina rod could be directly inserted into the oxygen plasma in the RTECR main stage with very good results, if the oxygen plasma is set up in the following manner:

1. The RTECR is initially tuned on Xe + O_2 to optimize the high charge state Xenon ions (27-31+).
2. The Xenon gas feed is shut off
3. The oxygen feed is raised above that of the $O_2 + Xe$ mixture, until the pressure has risen approximately $\frac{1}{2}$ order of magnitude above the optimum value for the high charge state Xenon tune.
4. The microwave power is approximately doubled, but the magnetic field of the ion source is held constant.
5. An alumina rod is coated with approximately 10mg of ^{92}Mo powder, then inserted radially into the RTECR, just until molybdenum ions are observed in the plasma.

With this technique, one has a relatively uncritical oxygen plasma. The details of the sample radial insertion scheme are shown in Figure 1. The resulting charge state RTECR distribution is shown in Figure 1. (In this case, the mixing gas is 90% enriched ^{18}O). As the upper spectrum shows, on the

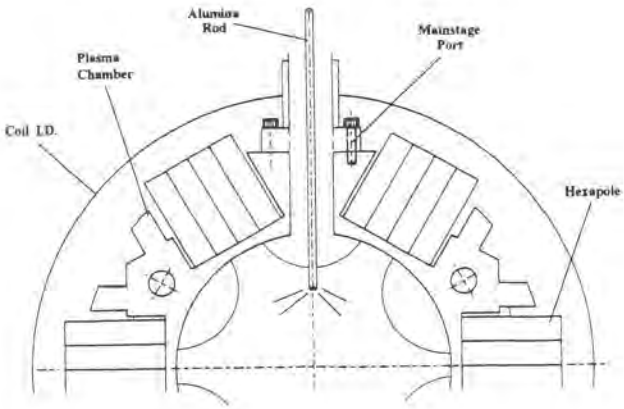


Figure 1. The metal powder doped alumina feed rod is inserted radially into the main stage plasma.

intensity scale of the oxygen ions, the molybdenum ion peaks appear as impurities. But with the scale expanded, in the lower spectrum, highly charged molybdenum ions are observed. One sees also that the oxygen charge distribution is rather poor.

We have now used this technique for V, Ni, Mo, and U ion production. When applied to ^{238}U ion production, we obtain the spectrum shown in Figure 3. To see the significance of this technique, the U ion performance of the 18 Hz ECRIS in Grenoble is also shown in Fig. 3 [2]. One can see that the RTECR actually exceeds the 18 GHz source performance for the highest charges.

Enriched isotope materials are used in powdered form with no special handling. Material consumption is low, with an upper limit of about $2\mu gm/min$ for uranium and other materials have rates of $2-5\mu gm/min$. With such small material consumption rates, source poisoning is not an issue, and metallic species chemistry hardly plays a role in the behavior of the plasma. The plasma appears to be an uncritical, high pressure oxygen plasma with a poor oxygen charge state distribution. However, the charge state distribution of the heavier metallic species comes automatically peaked at highly charged ions with very little tuning. The sample is not generally moved after initial contact with the plasma, and only the tip of the alumina rod is observed to be running hot.

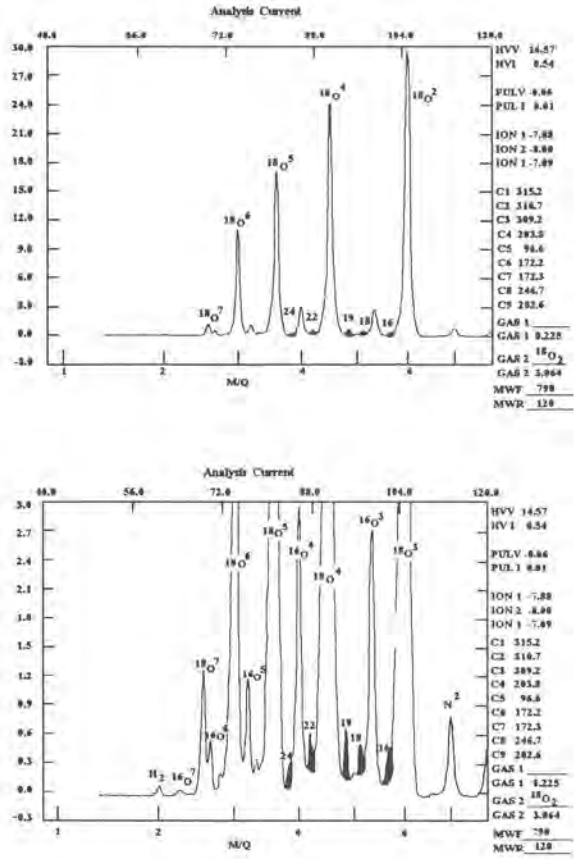


Figure 2. An $^{18}O+^{92}Mo$ spectrum for a 'super gas mixing' tune of the RTECR is shown, normal scale and expanded to show the molybdenum charge state distribution.

2. RTECR Overall Performance

The other curious feature of this tune is that the metallic ion performance for highly charged ions is the same as nearby gaseous feed species, including the noble gases. Further, as Figure 4 illustrates, the $1e\mu A$ output level of the RTECR is regular and smooth from Nitrogen to Uranium, and appears to be predictable on the basis of the ionization potential, which for all of these ions is approximately $1keV$.

3. Ionization Difficulty

The smooth performance of the RTECR has lead to a model for the ionization difficulty in the plasma. The mechanism for the production of

highly charged ions is Successive Impact Ionization

$$X^{i+} + e \rightarrow X^{(i+1)+} + 2e \quad (1)$$

The ionization rate $\nu_{i,i+1}$ for a single step is

$$\nu_{i,i+1} = n_e(E_e)\sigma_{i,i+1}(E_e)v_e \ (\sec^{-1}) \quad (2)$$

therefore, the step ionization time $\tau_{i,i+1}$ is

$$\tau_{i,i+1} = \frac{1}{\nu_{i,i+1}} = (n_e\sigma_{i,i+1}v_e)^{-1} \ (\sec) \quad (3)$$

If we take

$$\xi_{i,i+1} = < \sigma_{i,i+1}(E_e)v_e >_{T_e} \quad (4)$$

Then the ionization step time averaged over the electron distribution would be

$$\overline{\tau}_{i,i+1} = \frac{1}{n_e\xi_{i,i+1}} \quad (5)$$

Suppose $\overline{\tau}$ is the average ion lifetime in the plasma. We then make the assertion that, for the step $i \rightarrow i+1$ to be feasible, we should have

$$\overline{\tau} > \overline{\tau}_{i,i+1} \quad (6)$$

Then we have finally

$$n_e\overline{\tau}_{i,i+1} \geq \xi^{-1}_{i,i+1} \quad (7)$$

If we choose optimum conditions for a particular ion, Eq.(7) can be solved for the optimum charged state of other species that would be produced under equivalent conditions. Table 1 shows such a calculation for the noble gas charge states that would be produced when conditions are optimum for N^{7+} orNe^{10+}. Table 1 also includes the actual performance achieved with the RTECR (in $p\mu A$). Hence on the basis of purely ionization rate considerations, the N^{7+} performance is a good predictor of the RTECR performance for other species, as was shown in Fig. 4. As Table 1 shows, this scaling breaks down somewhat as a predictor of heavy ion species having ionization difficulty equal to that of Ne^{10+}. However, at present this model only includes ion production, and the inclusion of ion loss mechanisms in this calculation, particularly charge transfer processes, will correct the inherent over estimation of very highly charged ions as shown for Ne^{10+}.

Table 1. RTECR Performance vs. Theory

Opt. Ion	Te^{opt}	Ne	Ar	Kr	Xe	U
N^{7+}	3.8 keV	9	14	20	28	34
RTECR	$0.1p\mu A$	9	14	19	26	28
Ne^{10+}	7 keV		16	26	35	47
RTECR	$0.01p\mu A$		16	22	29	35

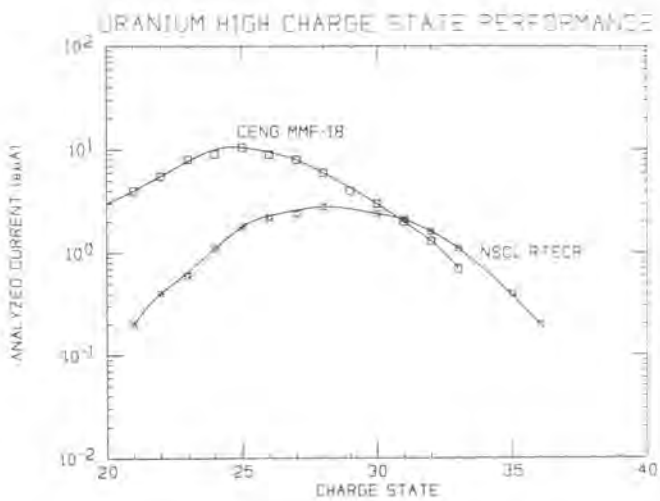


Figure 3. A comparison of uranium charge state distributions for the 18 GHz minimafios ECRIS in Grenoble [2], and the RTECR tuned via the super gas mixing technique.

4. 14.5 GHz Metallic Ion ECRIS

For the super gas mixing technique, the ion source mode is simple—a high power, high pressure oxygen plasma with little or no magnetic field tuning. Since tuning is so simple, the source design can be simplified as well. This design simplicity would then allow more operational flexibility. A projection of this technique to 14.5 GHz is shown in Figure 5. The estimated cost of hardware (sans transmitter) is 100k$. The main difference in this design is that the metallic sample is fed into the main stage through a microwave coax. Why 14.5 GHz? A further improvement in intensity and ionization efficiency would be expected on the basis of improved confinement at the higher operating frequency, at least for intermediate charge ions.

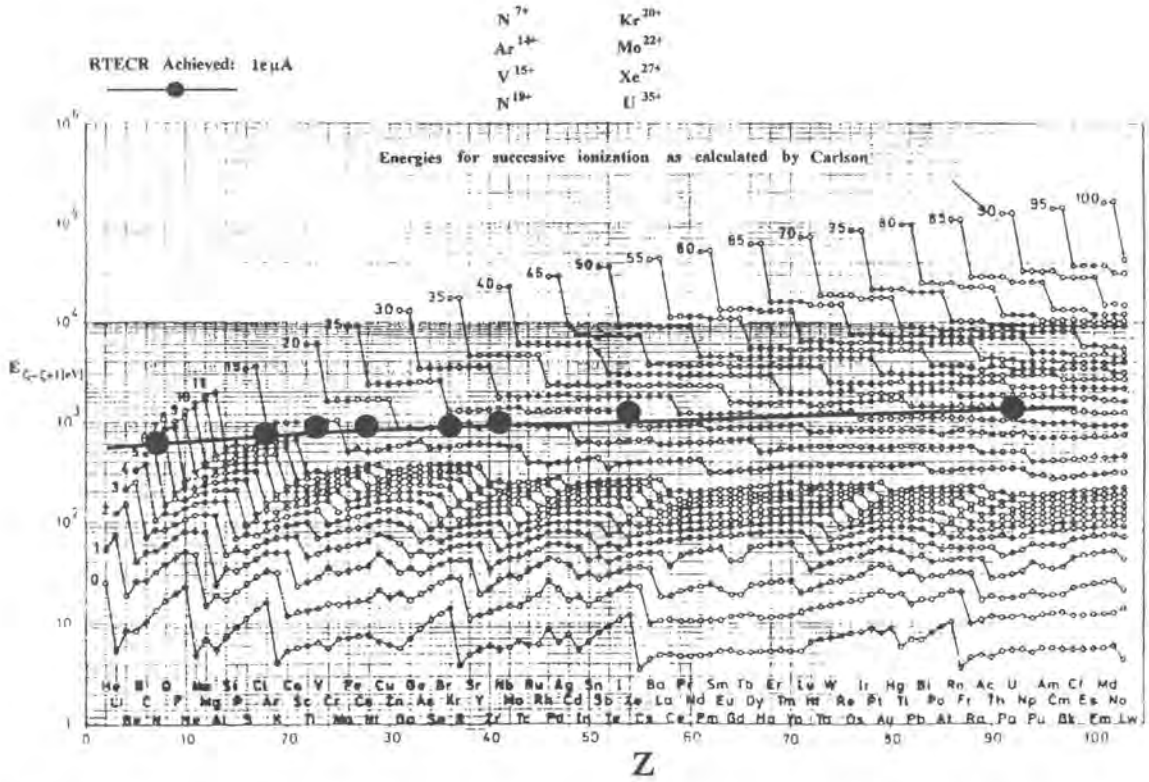


Figure 4. The $1e\mu A$ extracted charge state of various ions extracted from the RTECR are marked on this familiar plot of step ionization potential versus z from ref [3].

5. REFERENCES

1) Yennello, et.al., Phy.Rev.C, to be published, (1992).
2) Melin, G., private communication, (1991).
3) Carlson, T.A., et.al., ORNL-4562, (1970).

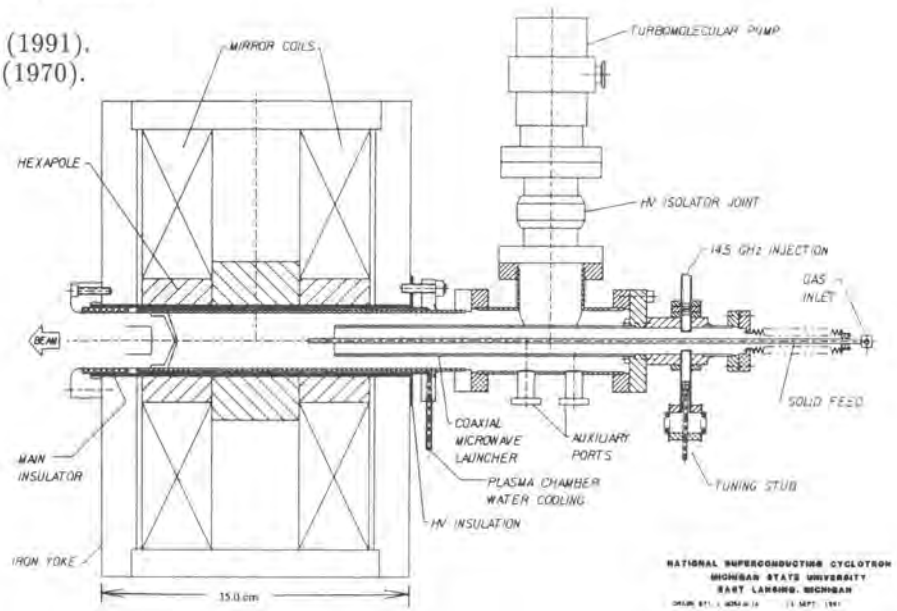


Figure 5. A 14.5 GHz RTECR source design based on the super gas mixing technique.

RECENT DEVELOPMENT OF INTERNAL H^-/D^- SOURCE FOR COMPACT CYCLOTRONS

Thomas Y.T. Kuo
TRIUMF, 4004 Wesbrook Mall, Vancouver,
B.C., V6T 2A3, Canada

and

George O. Hendry
Cyclotron Inc., 3104 Redwood Road, Napa,
California, 94558, USA

ABSTRACT

Small internal H^-/D^- sources based on Ehler's PIG source[1] design have been used in recent years for a number of compact cyclotrons of various sizes needing only 50-200 μA external beams. Source performance has been optimized in terms of H^-/D^- production and survival geometry, gas efficiency, arc requirement, mechanical tolerance and thermal stability. Data were obtained with RF extraction method using the central region of several cyclotrons as test facilities. The DC equivalent output was deduced from the information of RF phase width and the vacuum characteristics. The compact source technology has been transferred to several cyclotron manufacturers and about 30 H^- or H^-/D^- cyclotrons using compact internal source are in service today worldwide.

1. INTRODUCTION

In 1965 Ehler described the performance of his H^- PIG source with a plasma expansion gap using DC extraction. Since then several H^- cyclotrons used his source for external injection, among them the TRIUMF's H^- ion source and injection system (ISIS) is the most advanced and most successful.[2] In 1976, it was discovered that the plasma expansion gap can be generated by a special rotation of a compact internal *positive* PIG source.[3] The method allows the cyclotron to be operated in proton mode or in H^- mode without changing the ion source. Likewise, a source with an anode designed for H^- production can also be used as a proton source. Variations in anode design coupled with the rotational control provide a large range of proton/H^- ratio. High current irradiation on internal targets can be done by protons or by H^-s, while the irradiation on external targets can be done by 100% extraction of H^- using charge exchange, provided that the cyclotron vacuum capability is suitable for H^- operation. Similar statements apply to d/D^- production. In short, it is possible to have a single source which can supply protons, deuterons, H^-s and D^-s with compatible intensity.

In this report we shall concentrate on the optimization of the performance of a compact internal H^-/D^- source which leads to the development of a series of compact H^-/D^- cyclotrons using this source. While the option of external H^-/D^- cusp source[4][5] provides much higher beam currents with minimal stripping loss[6][7][8] the compact internal source does find their usefulness in many medical cyclotrons needing only 50-200 μA of external beams. The following sections describe the basic test facility and parameter optimization. A summary of source performance is also presented.

2. TEST FACILITY

2.1. Source Structure and H^- Formation

The compact internal H^-/D^- source is identical to a postive cold cathode PIG source used for protons, deuterons, He^{1+} and He^{2+} productions, except that a plasma expansion gap is added between the arc column and the extraction slit. This design was suggested by Ehler to facilitate the production and survival of the H^- ions from the reaction:

$$e + H_2 \rightarrow H^+ + H^- + e.$$

The arc column is the intense electron source but no H^- survive within the column. The collisions of the low energy electrons with the molecules of H_2 gas on the surface of the arc column produce the H^-. Only those ions created behind the anode slit are available for extraction. The molecular density of the hydrogen gas and the density of low energy electrons in the gap region are two basic variables which control the H^- production. However, the production probability and the extraction capability behind the slit are related strongly as we shall see the section of parameter studies.

2.2. RF Extraction

A DC test stand was originally planned for the source development but later the central region of several cyclotrons were used. If the RF phase width can be measured using Smith-Garren method and the stripping loss can be deduced, the DC equivalent output may be

inferred with reasonable confidence. In order to optimize the transmission efficiency from the first extraction to the beam current probe, sufficient electric and magnetic focusing are provided. The vertical dee alignment is also very important. A set of inner harmonic coils is used for beam centering and the adjustable source-puller gap can compensate the ion flight-time problem for the second or fourth harmonic operation.

2.3. Gas Stripping

When the internal source performance is monitored by the negative beams which have completed several tens of turns in a cyclotron central region, the knowledge of gas stripping loss becomes important. While the details of gas stripping calculation will be presented in a future publication, a very brief mentioning here should be helpful. If the relativistic and the radial dependence effects are neglected, it can be shown that the H^-/D^- beam current ratio between two radii is of a simple exponential form:

$$I(r_1)/I(r_2) = \exp(- F \cdot P_{eff} \cdot (1/\Delta E) \cdot (r_2 - r_1))$$

where F is the simplified stripping coefficient containing gas stripping cross-section and all other constants, ΔE is the energy gain per turn, P_{eff} is the effective pressure. For r in cm, ΔE in KeV and P in 10^{-6} torr, the empirical value of F for H_2 gas is 0.054. The effective pressure is given by

$$P_{eff} = P(H_2) + P(H_2O)\cdot 5 + P(O_2)\cdot 8 + P(N_2)\cdot 7 + \cdots$$

where the partial pressures are calibrated values from a gas analyser. One notes that the pressure is not a static parameter because gas composition might change between arc off and arc on; gas outgassing from the target probe and many other effects. Nonetheless this approximation is useful in obtaining the stripping loss expeditiously.

3. PARAMETER STUDIES

3.1. Plasma Expansion Gap

In order to investigate how critical an effect on H^- production and survival in the plasma expansion gap, a mechanism to rotate the source anode orientation is installed, as shown in Fig. 1. The axial angle of the anode with respect to the main magnetic field is adjustable for $\pm 5°$. When the angle is deviated from 0°, the arc column moves away from the extraction slit and the gap width is varied.

The effect of the gap width is illustrated in Fig. 2. On the left is the source with a positive beam anode (gap=0 at 0°). At 0°, the H^- beam is about 0 but gradually climbs to a maximum at about $\pm 2.5°$. Larger gap results in lesser beam current.

We used this $\pm 2.5°$ to measure the optimal gap, which turned out to be about 1 mm. Then we fabricated a negative beam anode which provided a 1 mm gap at 0°. As we can see, interesting results appear. The peak currents for both H^-/D^- occur at 0° and falls off at either directions of rotation. The D^- beam is less sensitive to the rotation and the nature of the higher peak at 4.5° is not quite understood. In the event that the initial source installation does not get the gap at its optimal value, this rotational drive can be used to make corrections.

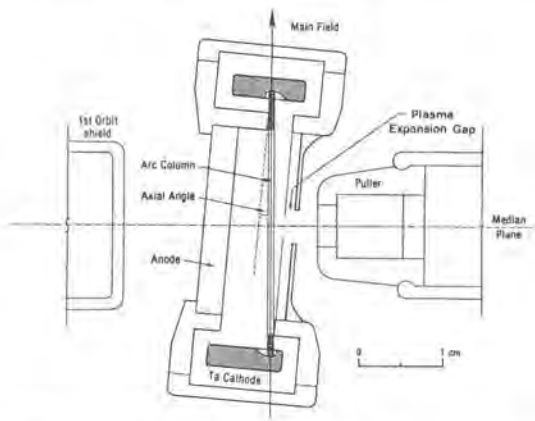


Fig. 1. A rotation mechanism to adjust the value of the expansion gap.

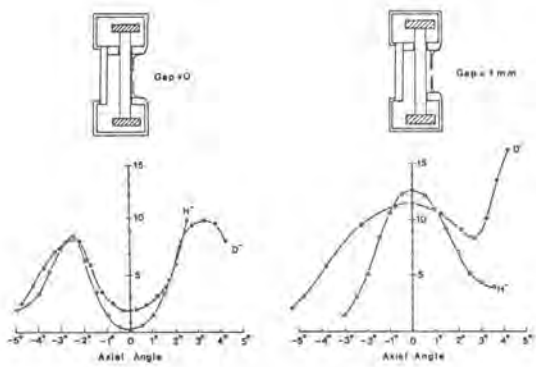


Fig. 2. H^-/D^- output measured as a function of axial angle

3.2. Chimney Slit Opening

One of the more complex source parameters is the Slit Opening, which faces the extractor. For a higher H^-/D^- current, one would like to have a wider opening for a larger ion emission area and a deeper electric field penetration. As the first result, the extracted electron current increases as well in a much higher electron to negative ion ratio because the molecular density behind the slit decreases. The arc column would have to be placed further from the slit in order to make this ratio manageable, i.e., without overloading the extraction circuit. If not so, the extractor would have to be moved

away from the slit to avoid the excess of electrons, or the space charge loading effectively decreases the electric field between the source and the puller. Thus, the gain of the total H^-/D^- emission area is somewhat cancelled by the drop of electric field.

In addition, the gas pressure inside the discharge volume drops accordingly, resulting in a decrease of negative ion production. One can step up the gas flow to compensate this drop, but the extra gas increase the vacuum chamber pressure which in turn decreases the final beam by the extra stripping loss. If one chooses to elongate the vertical slit length to increase the emission area the constraints are mainly the allowable vertical beam size developed later in the acceleration process and the maximum stripping loss permitted.

For a cyclotron system having 10^4 l/s effective pumping speed, 30% stripping loss at extraction, the slit size optimized is about 0.6 mm × 4 mm while the plasma expansion gap is set at 0.6 mm.

3.3. Geometry Optimization

After the critical plasma expansion gap has been established, we also searched for the optimum relationship between the inner anode wall and the arc column. Fig. 3 shows some of the representative geometry tested. The diameter of the inner anode wall is fixed at 6.3 mm, while the diameter of the arc column varies from 3 mm to 5 mm. In all cases from [A] to [G], the H^-/D^- output is best with gap dimensions about equal to the slit width. For an arc column length (cathode to cathode) of 30 mm and a permissible gas flow up to 7 sccm, the H^-/D^- output is best with an arc column diameter of 4.25±0.25 mm.

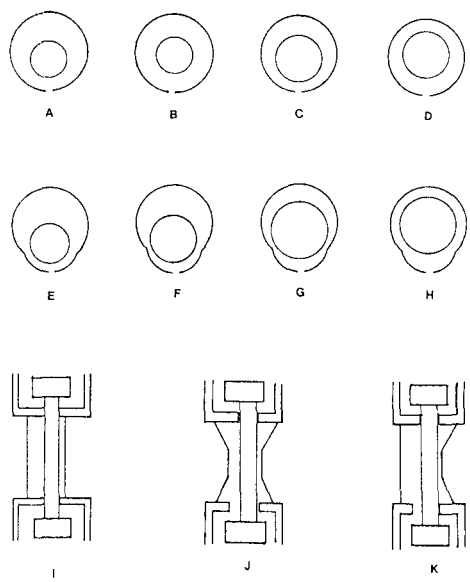


Fig. 3. Examples of arc column geometry optimization

For the cases of E, F, G, J, and K, the anode inner structure is less straightforward. Such design favors the electron flow near the extraction slit thus improving the arc current efficiency. We found that the combination of F and J is the best, while K is used if the fabrication of J is not feasible. Cases B, D, and H were expected to give less output but were explored as well for the purpose of completeness.

3.4. Gas Passage

There has been suggestion that gas efficiency can be improved if the H_2/D_2 gas is sent directly into the chimney near the extraction slit. An alternative passage, where the gas is passed through the larger opening of the bottom cathode chamber, is also used (as shown in J or K). We compared these two methods by providing two gas lines with valves controllable externally. One can choose either gas line or an adjustable combination of these two gas passages. However, for a given gas flow, we did not detect any differences in H^- output. On the other hand, when the opening of the lower cathode chamber is closed down to the same size as that of the upper chamber, all gas molecules must pass through the hot plasma if this route is taken. The H^- beam output drops about 15% to 20%. The vacuum gauge also reads lower when the arc is turned on and set at higher arc currents.

When gas molecules flow out of the internal source slit, they immediately become destructive. Thus gas utilization must be optimized and any leakage other than slit opening *must be* sealed off.

4. SOURCE PERFORMANCE

4.1. Gas Flow and Arc Current

With the parameters optimized as described in the previous sections, the H^- ions achievable measured at r=15 cm (~ 3.0 MeV) with a 32 kV RF dee voltage and a 0.6 mm × 4 mm slit opening is plotted as a function of gas flow and arc current. This is shown in Fig. 4. The plot is organized either by fixing the arc current while adjusting the gas flow or vice versa. It is interesting to point out that with the angular position set at the easiest arc generating orientation (about 0°), the beam current is continuously adjustable from picoamp range to several hundred microamps by a current regulated power supply.

Please note the H^- beam rises rapidly as the arc current increases at the low end and gradually saturates at high arc currents in all cases except for the very high gas flow. Also note that at arc currents below 0.5 A, the H^- goes through a maximum, then decreases as the gas flow increases. As an example, if one wants only 30 μA of H^-, one could use only 1.5 sccm gas flow with 0.2 A arc rather than 7 sccm at 0.2 A. Likewise for a 160 μA H^-, one could choose 4 sccm instead of 7 sccm. For a 300 μA demand, one has to use 6-7 sccm at 1.5 A or higher.

The behavior of these gas flow and arc current interdependence can be understood if one realizes that the

production and the neutralization of H^- ions takes place simultaneously in the same environment by different reaction mechanisms. Take the case of 0.2 A arc, for example. The maximum H^- production is reached at 3 sccm. Beyond that, the electrons having suitable energy for production are exhausted and the high gas pressure inside the source decreases the survival of the H^- already produced. The increase of stripping loss before reaching 15 cm also contributes to the trend of decrease, but only about a 10% drop from 3 sccm to 7 sccm. For each gas flow, the saturation at higher arc current might be due to the insufficient supply of gas molecules, the increased percentage of neutral gas being positively ionized, the over supply of electrons with destructive energy and greater H^- neutralization rate in the vicinity of a hotter plasma.

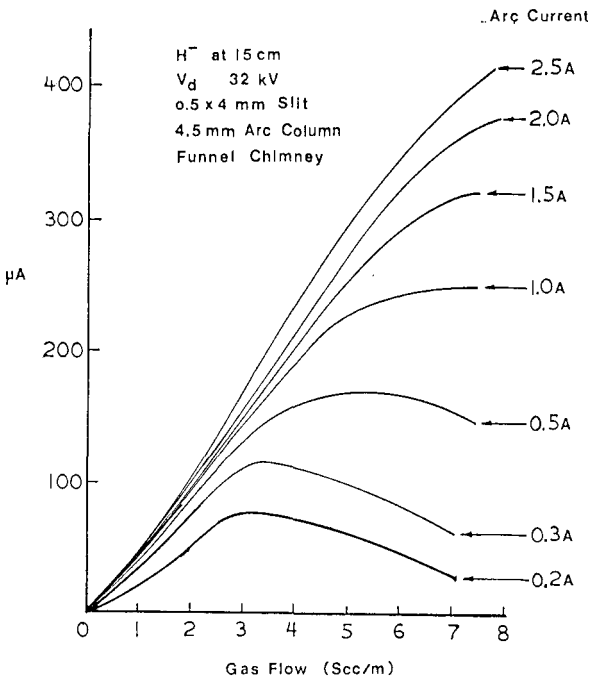


Fig. 4. H^- output as functions of gas flow and arc current.

The H^- beam dependence on gas flow and arc current is also tune dependent. The plot obtained in Fig. 4 is the result of a high arc current tune. The ion source is fed with high gas flow first and set at 1.5 A arc. The H^- beam is optimized with adjustments of ion source positions. At this tune mode the source slit to puller gap is larger (~3.0 mm) than that from a lower current tune mode (H^- beam is optimized with lower gas flow at 0.3 A arc). The high current tune mode already includes the space charge effect. The low current tune mode would suffer the space charge effect when the arc current is ramped up. The high or low current tune also affects the gas pressure behind the slit because of the restriction of gas passage between the source and puller.

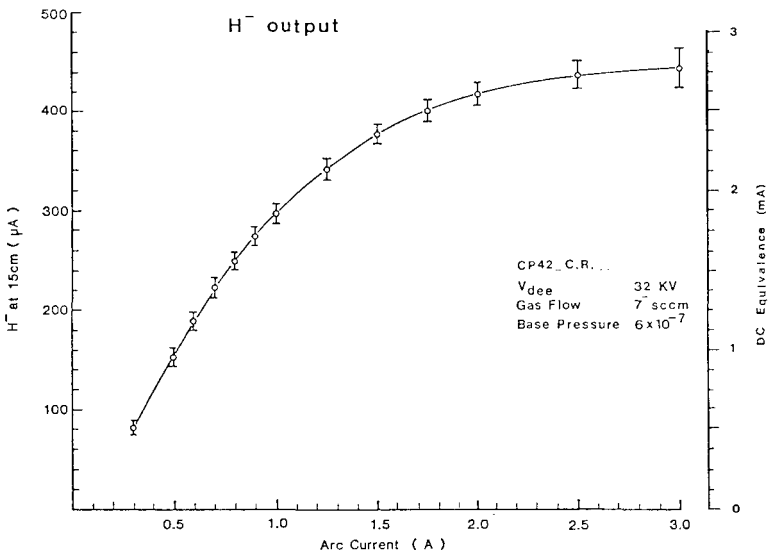


Fig. 5. H^- output as a function of arc current. The beam is adjustable from a fraction of a μA to a few hundred μA.

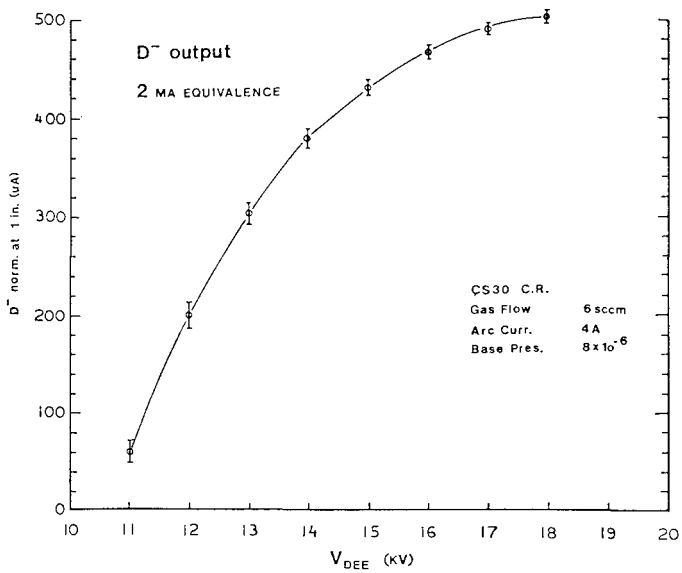


Fig. 6. D^- output as a function of dee voltage or RF phase width. Note that the result was obtained with a discrete current P.S.

4.2. DC Equivalent H^-/D^- Output

Figure 5 shows another H^- output curve as a function of arc current with a fixed gas flow of 7 sccm. The beam available at the cyclotron center is traced back to be ~ 500 μA. The RF phase width is calculated to be ~ 64°. Since the negative ions extractable are emission limited at rather low voltage, the ion density per unit phase is considered constant. The DC equivalent output is then inferred to be 2.8 mA, the current density is 144 mA/cm^2.

Figure 6 shows the D^- output traced back to the cyclotron center as a function of dee voltage. The DC equivalent is already fixed but the beam available is RF phase width dependent. The inferred DC D^- output is about 2 mA.

4.3. Source Reproducibility

The source head assembly tolerance has been within 0.1 mm in critical area. Gas leakage in the head was to be checked by means of pressure bubbling in an alcolhol bath. The cooling path should take into account of differential thermal expansion such that the source dimension and position will remain constant and independent of arc power and RF power used. The cathode stems must be cooled to maintain accurate arc column and expansion gap relationship. Using a precision central region position calibration fixture and four dimensional ion source position drives, the beam current output reproducibility has been excellent. For a properly assembled source we have not yet encountered the situation of beam fall-off phenomenon, short term or long term at high or low beam currents.

5. SOURCE TECHNOLOGY TRANSFER

Several commercial cyclotron producers have adapted the internal source technology just described through the authors of this report.

- CP-42 series cyclotrons: uses H^- only. The routine extractable external proton beam has been in excess of 200 μA at 30 MeV. 300 μA at 30 MeV on external target has also been achieved.[9)]

- An 11 MeV H^- cyclotron: uses a miniture source with 4 dimensional position controls. Peak proton beam on target is 100 μA. An axial source geometry has also been developed for a four sector version.

- A 10 MeV H^-/5 MeV D^- cyclotron: adopts a 2-source central region which accepts H^- source on one side of the dee center linkage and the D^- source on the other. Initial orbits must clear both sources and the central region. The sources are not movable and the pumping speed is limited thus the source performance has been compromized.[10)]

- An 18 MeV H^-/9MeV D^- cyclotron: an extension of the 10/5 cyclotron, but two dimensional source drives are added.

- A 16.5 MeV H^-/8.5 MeV D^- cyclotron: also 2-source central region. The source structure has been simplified to eliminate cathode stems. The source output from a test stand is strong and the RF extraction output is more than adequate for 50 μA on target.[11)]

6. REFERENCES

1) Ehler, K.W., "Design consideration for high intensity negative ion source," Nuc.Instr. & Method, 32, (1965)p.811.
2) Baartman, R., "The H^- source for high intensity beam at TRIUMF," Proceedings of the 9th Int. Conf. on Cyc., Cean, Sept.7-10 (1981)p.289.
3) Kuo, T.Y.T., and Laughlin, J.S., "Initial experiment in ion production using an ultra high power density method," Proceedings of the 7th Int. Conf. on Cyc., 1975, p.381.
4) Schmor, P.W., Baartman, R., Yuan, D.H., McDonald, M., Kendall, K.R., Jayamanna, K., Proceedings of the 4th, 5th Int. Symposium on Production and Neutralization of Negative Ions and Beams. 1986,1990.
5) Leung, N.K., Ehler, K.W., Proceedings of the 3rd, 4th, 5th Int. Symposium on Production and Neutralization of Negative Ions and Beams. 1983,1986 1990.
6) Milton, B.F., et.al., " A 30 MeV H− cyclotron for isotope production," Proceedings of the 12th Int. Conf. on Cyc., 1989, p.145.
7) Schneider, H.R., et.al., "A compact H^- cyclotron for isotope production," Proceedings of the 1st EPAC, Rome, June 7-11, 1988, p.1502.
8) Bol, J-L, et.al., "Operational experience with the 500 μA H^- isotope production cyclotron," Proceedings of the 1st EPAC, Rome, June 7-11, 1988, p.1488.
9) Hendry, G.O., and Kuo, T., "Design and performance of a compact H^- cyclotron," Proceedings of the 9th Int. Conf. on Cyc., 1981, p.125.
10) Laycock, S., et.al., "New development on ion source at IBA," Presented at the 2nd EPAC, Nice, June 12-16, 1990.
11) Lindback, S., "A new cyclotron for PET," Presented at the 13th Int. Conf. on Cyc., Vancouver, July 6-10, 1992.

Plan for the Ion Source Emittance Measurement Under the RF Extraction

J.W. Kim and H.G. Blosser*
Cyclotron Laboratory, Michigan State University, East Lansing
MI, 48824, USA

ABSTRACT

An experiment is planned to measure the emittance of a cyclotron ion source under rf extraction and in magnetic field up to 8 Tesla. Preparing for that, computations have been done to choose the slit locations and the shape of the extraction electrode. Computer simulation of many particles produces current distributions for various slit positions, which can be compared with experimental results. The sensitivity of the experiment may not be sharp due to tight requirements(8 Tesla, D^+, 50kV rf), but a careful experiment will apparently measure emittance as a function of rf time.

1. INTRODUCTION

Initial conditions of ions from the internal source in the cyclotron needed for computer studies of orbits have usually come from emittance measurements under dc extraction; possible effects of the oscillating radio frequency extraction voltage on the source emittance have been neglected, which is likely to be a significant error. Using an appropriate slit system, it appears that rf phase can be selected within some degrees, and the emittance measured as a function of rf phase directly inside of the magnet after extraction by the rf electric field. This method requires orbit calculations to interpret the results since an emittance effect on the orbits must be separated from the spread by phase, and a special central region design with ion source and slits is needed to meet this purpose. Three slits are employed to separate the three coordinates, phase, and emittance, i.e., including one more slit than the usual two slit method.

Another way of measuring the rf phase dependence of the emittance would be to observe the time dependence of current as a function of rf time, but this would be difficult due to the rf noise picked up with the current signal which has the same frequency. A PIG source(cold cathode) shown at Fig. 1 similar to one being used at Harper cyclotron[1] will be built. Measurements will be made for different plasma conditions controlled by arc current, gas flow, etc., and magnetic fields up to 8 Tesla, which will be provided by the test magnet under construction.[2]

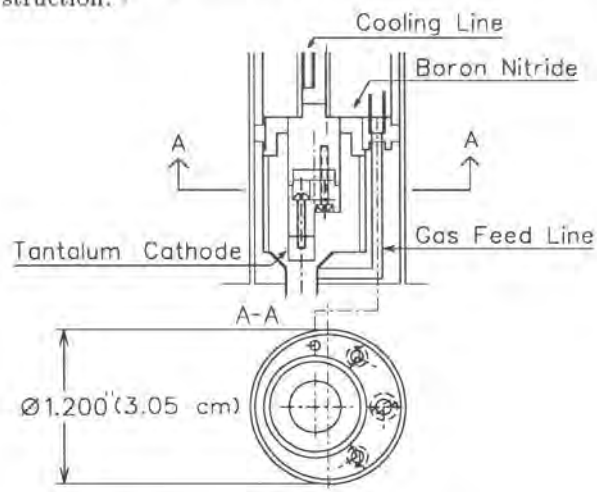


Fig. 1. PIG source designed to fit on the central hole of 8-Tesla magnet

2. CENTRAL REGION DESIGN AND CALCULATION RESULTS

The design of the central region for the emittance studies, including PIG source, puller, and ground plate, is done with an aim of spreading the beams having different rf starting time so that the emittance can be compared for different rf ranges selected by a phase slit. The general arrangement of central region electrodes in the test apparatus is shown in Fig. 2. The rf provides a two gap acceleration with a flight path of about 90° between the two gaps so that orbits with different initial phase are sharply spread. Three slits(S1,S2, and S3) approximately equally spaced, are located on the grounded dummy dee side of the system which allows easy control. The motions of slits are limited as the beam stopping area in slit touches the wall, so different slits with aperture close to the end have to be used for rf phase below 200°. The proposed extraction voltage of 50 kV

*Work supported by the U.S. National Science Foundation.

and peak electric field of 200 (kV/cm) at 5 - 8 Tesla magnetic fields come from previous experience[1] at 4.6 Tesla. For exploratory calculations initial total energy(E_t) and incident angle(α) from the PIG source as initial conditions of design calculation are inferred from dc emittance results.[3] Several such orbits are shown in Fig. 2 for different rf starting time using deuterons(D^+) as a test particle with 250 eV initial energy and 8 tesla flat magnetic field.

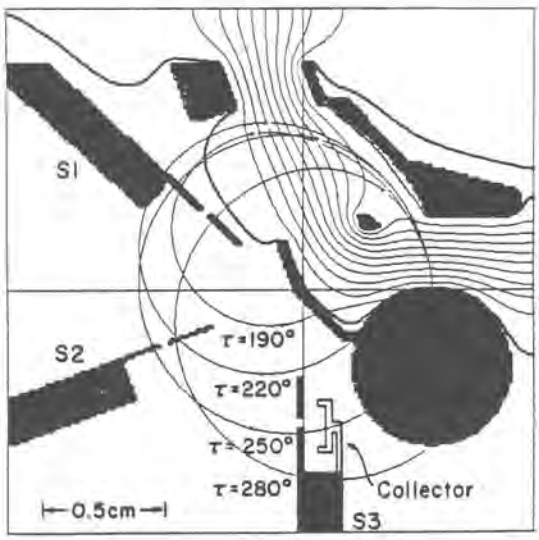


Fig. 2. The orbits on the schematic view are shown, calculated for 4 different rf phases (270° is peak voltage on the first gap). The initial energy of D^+ is 250 eV, and ions are started at the center of the source with zero divergence angle.

As we study the emittance, rather than a few particles, part I of CYCLONE program[4] is modified to handle many particles effectively and to include the slit actions. Since transmission will be measured in slit coordinate space, we need to compute the relationships between two spaces to obtain the emittance. The boundary of a rectangular shape in source phase space for different emittances described at Table 1 is projected into the slit coordinate space in Fig. 3. The spread by larger emittance appears to include smaller ones in a defined manner as the boundaries in two spaces are qualitatively related as shown in Fig. 4. The ions having different rf starting times go to fully separated regions in the slit space for starting time intervals differing by 10 degrees, i.e. rf time is well separated at slit S3. The resolution of the measurement depends on the area occupied by the beam in the slit space. In this sense the slit S2 has less orthogonality relative to S1 and S3 than might be desired. An increase in the S1, S2 spacing might be helpful and will be investigated. The actions of each slit are described, even though all three slits together select the rf phase space and the emittance coordinates.

Table 1. The initial conditions used for orbit calculations in figures 3,6, and 7. source opening size, and normalized emittances($\epsilon_o\beta\gamma$)(mm·mrad)

$E_t(eV)$	α	Opening	ϵ_n	Fig.3
250	±22°	0.381 mm	0.15	solid
250	±22°	0.762 mm	0.30	dash
250	±44°	0.762 mm	0.60	dot

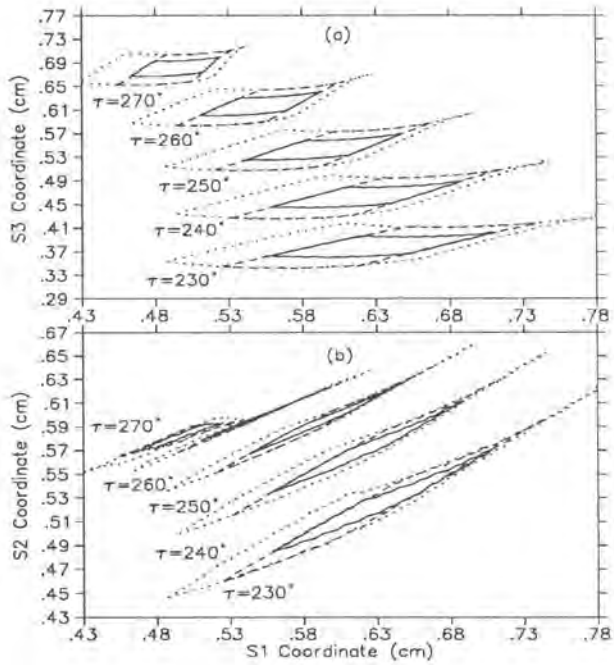


Fig. 3. The projection of the rectangular initial phase space into the slit coordinate space for five different rf starting time in the interval of 10 degrees. The dashed line is for a larger source width, and the dotted line is for an increased divergence angle, which are described in Table 1. The area occupied in the slit coordinate space shrinks for the same emittance as the rf starting time rises.

The slit S1 makes a cut angled in phase space because the rectangular source emittance is deformed to a parallelogram in the slit coordinate (Figs. 3,4). The emittance with rf phase selected by slit S3 spreads well along S1 axis allowing relatively fine selections. The slit S2 selects emittance in a very close angle to the selection by S1. The dashed and dotted lines in Fig. 4 roughly shows the selection angles by two slits.

The slit S3 functions similar to the 180° slit(S2 in Fig. 5) of the dc measurement, since the S3 coordinate is a combination of transverse position in the emittance rectangle and rf phase, but is not sensitive to initial divergence, as seen from Fig. 3 (a).

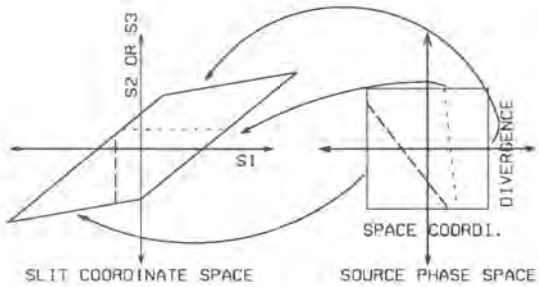


Fig. 4. Sketch of the transformation of boundaries from source emittance to slit coordinate space, The rectangular shape is deformed to a parallelogram.

To simulate the current distributions which will be actually measured in the experiment, a group of rays having uniform distribution in a rectangular phase space has been computed. The current distributions in Fig. 6 are obtained using the initial conditions in the second and third lines of Table 1 and actual slits of finite width. The phase slit S3 of 0.254mm wide is assumed fixed for both figures, and the scanning of slit S2 generates individual curves for a given S1 position. In Fig. 6 each point is the current measured at particular S2 position, and points are connected by straight lines (solid or dashed to reduce visual confusion).

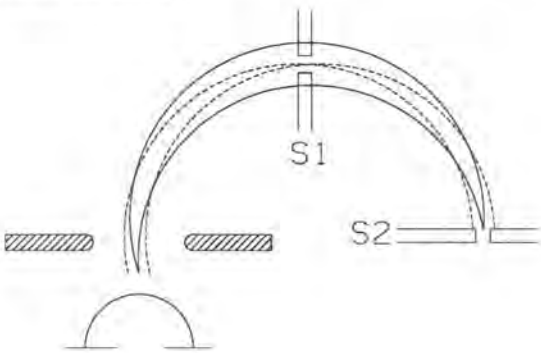


Fig. 5. The usual two slit method in the dc experiment.[3] The slit S1 selects the divergence, and the slit S2 scans the beam size. The S3 in our central region functions similar to S2 as initial divergence becomes less sensitive, while the beam spreads well by phase difference.

The distribution for the higher emittance(Fig. 6 , (b)) broadens along the S1 and S2 coordinates as expected from Fig. 3. The selections by slit S1 and S2 of 0.05 mm wide is demonstrated in Fig. 7 showing angled cuts in the source emittance, which is originated from the deformed transformation to the slit coordinate space. The selection by slit S2 is not as sharp as S1 as mentioned. The combined selections by two slits is sketched in (c) of Fig. 7.

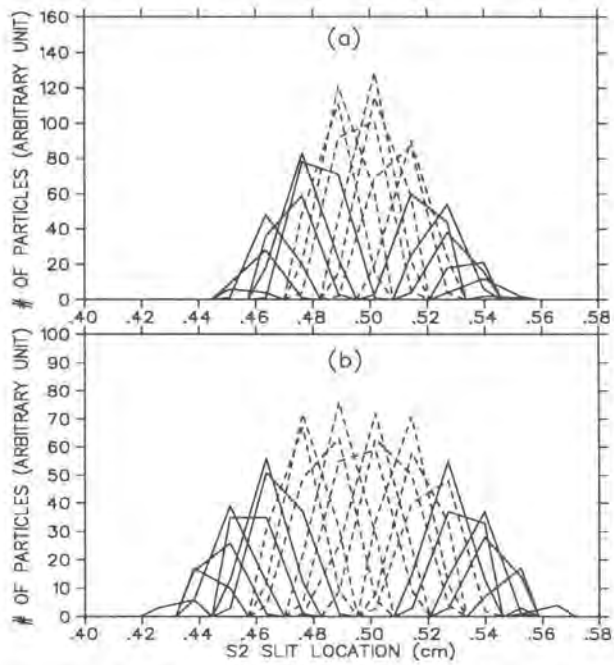


Fig. 6. The current distributions simulating the measurement are calculated for the initial conditions in the second and third lines of Table 1. The individual curves are obtained at different S1 locations as slit S2 is scanned. (a) has 19 curves(0.191 cm wide spread in S1 coordinate) , while (b) has 24 curves(0.267 cm wide spread).

The current and three slit locations measured in the experiment are the data to trace back to the corresponding emittance phase space and rf time. A large rectangular emittance which can cover the measurement and with a half degree step of rf phase, for instance, can be transformed to the slit coordinate, so the 3 dimensional meshes in slit coordinates will have the emittance and rf phase space range selected. (All calculations presented here are done at 8 tesla field which asks the most restricted design.)

3. DIFFICULTIES OF EXPERIMENTS

Since the planned magnetic field range is high(5-8 Tesla), and many ions do not clear the ion source, all dimensions in design are very tight. The difficulties anticipated in the experiments are;

1)The phase space coupling of radial and vertical motion may be a problem. We will try to minimize axial field in the central region by using structures which are

high compared to the beam height.

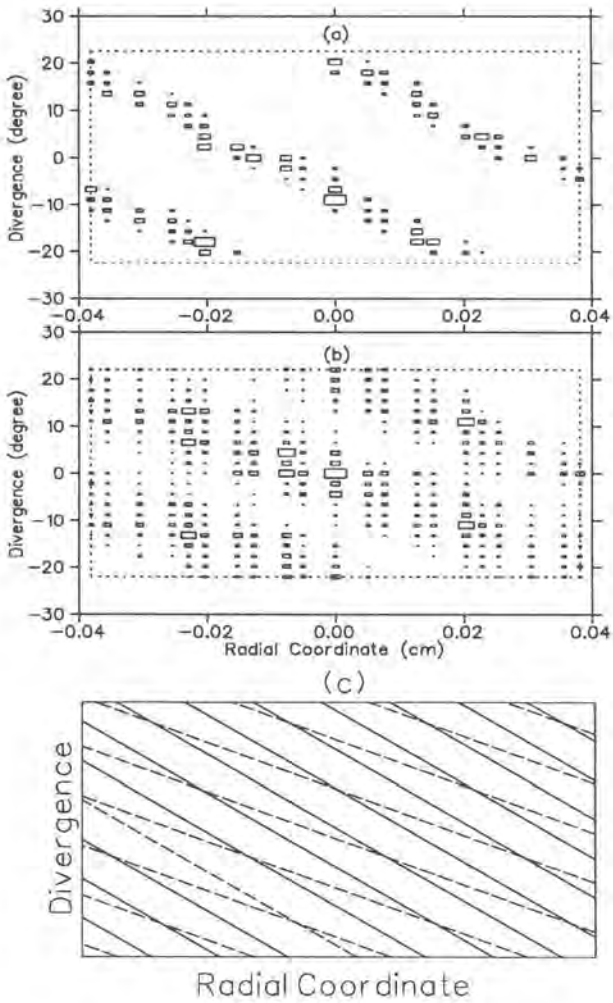


Fig. 7. The source phase space selected by slit S1 and S2 of 0.05 mm wide. The initial condition is same as the second line of Table 1 and with S3 fixed selecting τ around 215° - 225°. The three separated regions in each figure correspond to three different locations of S1 in (a), and S2 in (b) with the other slit scanned, respectively. (c) shows the sketch of pixels selected by both slits.

2)The space charge effect is not considered in present calculations, so the emittance measured includes the distortions which the space charge induces. (The rms source emittance usually appears worse than it is due to this effect.)

3)The deuteron used for calculations will contain molecules and other species in the real source; relative intensity is a function of plasma condition, and can be made small. We will check this with a dc measurement and tune the source to minimize other ions.

4. CONCLUSION

This study has the objective of measuring the time dependence of the characteristics of the ion source and the central region of the cyclotron. The central region of the study apparatus is designed to spread the beam by both emittance and phase. The radial source emittance (r,p_r) can be projected for the selected rf starting time by connecting the slit coordinates and the rf phase with a calculated map. The resolution of this method is limited by the available physical space at 8 tesla field, and as the rf starting time becomes late, the resolution decreases since the area occupied in the slit space shrinks. The selection angles by slits S1 and S2 are not orthogonal, and S2 doesn't separate the emittance space sharply. As a result the ideal resolving power is not achieved. In the situation of 8 tesla field and 50 kV maximum RF voltage, the present central region is believed to be an optimized one (even though further study may show other possibilities). In conclusion the three slit method works in calculation, but the actual resolution will depend on the slit size and an overall stability of the apparatus. We acknowledge the discussion with Dr. D.J. Clark(LBL) about the three slit system in the beginning of this project.

5. REFERENCES

1) H. Blosser, et al. "Superconducting Cyclotron for Medical Application", IEEE Trans. on Mag. **25**, No.2, 1746 (1988)

2) J. Kim, et al. "Progress on the 8-Tesla Magnet", NSCL Ann. Report 215 (1990).

3) M.L. Mallory and H.G. Blosser, "Phase Space Density Studies on Cyclotron Ion Sources" IEEE Trans. on Nucl. Sci. **NS-13**, No 4, 163 (1966)
M. Toman and M. Reiser, "Emittance Measurement for N^+ and N^{2+} in an Ion Beam from a Cyclotron Ion Source. IEEE Trans. on Nucl. Sci. **NS-19**, No.2, 80, (1972)

4) F. Marti et al., "Design Calculations for the Central Region of the NSCL 500 MeV Superconducting Cyclotron" **9th International Conference on Cyclotron and Their Applications** 484 (1981)

PROGRESS WITH THE NAC INJECTOR CYCLOTRON FOR HEAVY AND POLARIZED IONS

Z.B. du Toit, S.J. Burger, P.J. Celliers, J.G. de Villiers, H.N. Jungwirth, A. Müller, P. Rohwer, and D.M. van Rooyen

National Accelerator Centre, P.O. Box 72, FAURE, 7131 Republic of South Africa.

ABSTRACT

The k=11 MeV injector cyclotron under construction at the NAC will produce beams of light and medium heavy ions. Both the ECR source and the atomic beam source for polarized protons and deuterons are now in operation. Magnetic field mapping has been completed and the data processed. The central region of SPC2 has a fixed geometry for the three constant orbit patterns required for acceleration of ions with orbital frequencies between 1 MHz and 13 MHz. Harmonic numbers 2 and 6 will be used. Diagnostic equipment includes 2 differential probes, 2 sets of radial and axial slits, a movable harp, a phase probe and a quartz viewer plate with a TV camera. A versatile vacuum pumping system will allow pressures down to the 10^{-5} Pa range.

1. INTRODUCTION

The second injector facility for the 200 MeV separated-sector cyclotron at the NAC consists of a k=11 MeV solid-pole cyclotron, an ECR source for the production of light and medium-heavy ions and an atomic beam source for polarized protons and deuterons (Fig. 1). The cyclotron itself is very similar to the existing injector cyclotron for light ions, SPC1[1]. Major deviations from the SPC1 design are an axial inflection system, a vacuum system designed for the lower pressures required for the acceleration of heavy ions, modifications to the rf-system to decrease the low frequency limit from 8.6 MHz to 6 MHz and improved beam diagnostics.

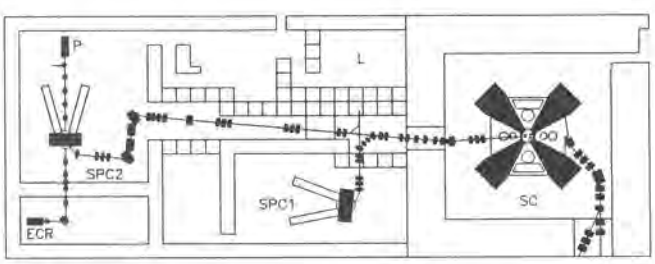


Fig. 1. Layout of the cyclotron vaults showing the second injector SPC2 and its ion sources.

Tables 1 and 2 show typical beams and intensities which should be available once the injector is in operation in December 1993.

Table 1. Beam energies and intensities expected from the 200 MeV separated-sector cyclotron with SPC2 as injector.

Element	Energy (MeV/nucleon)		Intensity (pnA)
	Min.	Max.	
^{1}H	30	200	5000
			500
		66	30000
^{4}He	40	220	500
^{15}N	2.6	32.7	>1
^{40}Ar	2.0	19.8	>1
^{84}Kr	2.0	11.25	>1
^{129}Xe	2.0	4.76	>1

Table 2. Available polarization states for proton and deuteron beams.

	protons	deuterons					
p_z	±1	-2/3	2/3	0	0	1	-1
p_{zz}		0	0	-2	1	-1	1

2. ION SOURCES

The 10 GHz minimafios ECR source is performing well. Minor modifications were implemented and, apart from the vacuum pumps and valves, it can now be operated via the accelerator control system.

Computer software and hardware were also developed for quick identification of ion spectra behind the analysing magnet, tuning of the source to the requested beam specifications, monitoring and recording

of the beam stability, and to keep a database for all the important parameters[2].

The ion source for polarized protons and deuterons is of the atomic beam type. Six 1500 ℓ/s fomblin lubricated turbopumps are used for differential pumping. The atomic beam is formed by a 25 mm long sapphire nozzle which is cooled to 30 °K. Two sextupole magnets are used for deflection of unwanted electron spin components and for beam focusing. The rf-units used to induce transitions between different spin states are located between the sextupoles and/or behind the second sextupole. Table 2 shows the various polarization states that can be obtained. The ionizer is of the well-known ANAC-CERN design.

During the acceptance tests in December 1990 a 28 μA proton beam with an emittance of 135π mm mrad was measured behind the analysing magnet. The polarization of the beam could not be measured as yet. However, the electron polarization is between 80% and 90%.

3. MAGNET

The main magnet of SPC2 is almost identical to that of SPC1[3]. The modifications to allow for the stronger magnetic fields have been described before[4].

Small modifications to the field measuring equipment[5] used for SPC1 were necessary. A new PC-based program has been implemented to make the system more reliable and user-friendly and to improve the protection of the system and the accumulated data.

The following field-setting procedure, which ensures stationary fields before the start of the measurements and reproducibility of the fields in future runs, was used: starting from any value the excitation current is first set to -800 A for 6 min to eliminate remnant fields; then the final current is set via an overshoot of 6 min duration for critical damping of eddy currents.

Field maps, each consisting of 7381 points in the median plane, were measured for 12 values of the main coil excitation current. This covered an average field range at extraction from about 0.3 tesla to 1.1 tesla. In addition, fields were also measured for each of the 8 pole-gap coils (6 trim-coils and 2 cone-coils) at two excitation currents. In total 138 fields were measured.

As a final test, we compiled fields for the reference particles (3.15 MeV protons representing the beams for neutron therapy, 8 MeV protons i.e. maximum energy protons and 47 MeV krypton ions representing the heavy ion beams). The SPC2 power supplies were then set according to the predicted currents for each reference particle and the corresponding fields were measured.

The calculated rf-phase excursions of the reference particles in these fields from injection to extraction do not deviate by more than 2 degrees, indicating good agreement between the requested and the measured fields. The vertical betatron frequencies for these particles are shown vs. the orbital radius in Fig. 2.

Although there is adequate focusing, we found that small deviations from the calculated current settings in the outer trim-coils could cause axial defocusing near the extraction radius.

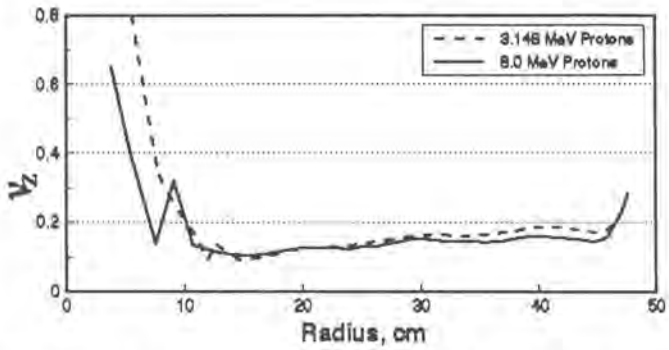


Fig. 2. Graphs showing ν_z vs. orbital radius for 3.148 MeV and 8 MeV protons respectively.

4. CENTRAL REGION

The central region (Fig. 3) has been designed for the acceleration of protons and heavier ions up to xenon. The cyclotron will be operated in constant orbit geometry mode. Three orbit patterns are used, namely 34 turns for protons, 17 turns for the lower-energy proton beams (e.g. beams for neutron therapy and radioisotope production) and for the higher energies of ions such as argon and krypton, and 9-turns for the heaviest ions (i.e. xenon) as well as for the lower energies of the lighter ions. Other design requirements were an acceptance of at least 200π mm.mrad, a vertical betatron frequency ν_z of at least 0.1 and a maximum dee voltage of 60 kV.

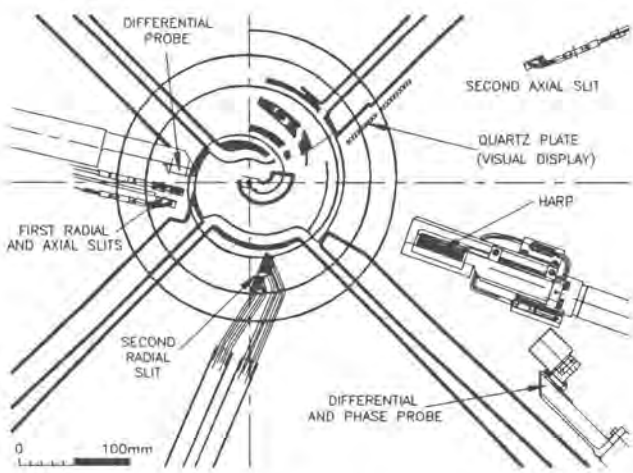


Fig. 3. Layout of the central region of SPC2 showing the first two turns of the 34-turn orbit pattern and the various slits and beam diagnostic equipment.

Switching between orbit modes can be accomplished without ventilating the cyclotron. The entrance slits in the first dee are fixed and the spiral inflectors can be exchanged or serviced in a parking chamber. Those components that have to be adjusted (i.e. diagnostic slits in the central region and extraction elements) are remotely controlled.

The preliminary orbit calculations were carried out using the measured magnetic and electric fields of the first injector cyclotron. From these orbits a model of the central region was designed for measurements in the electrolytic tank[6]. The measured electric and magnetic fields were then used to refine the calculations and obtain the final design orbits. The design particles used for the 34-, 17- and 9-turn orbit patterns were 8 MeV protons, 3.15 MeV protons and 49 MeV Kr^{16+} ions respectively.

The final design orbits were found with the requirement that in the field-free region of the inflector housing, the ion energy must match the injection energy concomitant with the dee potential. Studies of the electrical focusing at the first few gaps showed acceptable results for the 17- and 9-turn orbits, but the re-entry of the 34-turn orbit into the housing proved to be defocusing. The geometry at this crossing was changed so that the condition $\nu_z > 0.1$ was met. The acceptance of the design, excluding the inflector, was determined and proved to be adequate.

The inflectors decided on are of the spiral type. The first designs were studied using the analytic model. The physical limitation imposed by the pole gap necessitated tilting of the inflector electrodes. Form factors for the electric field seen by the design particle were evaluated by means of the code RELAX3D[7]. This field was then used by the code SPICE to calculate the orbit for a specific set of inflector parameters. The program uses either the steepest descent or the Broyden algorithm to optimize the fit of the inflector design orbit to the cyclotron design orbit. The program requires the inflector to inject the ion in the median plane of the cyclotron with no vertical component of momentum and with a radius of curvature matching that of the cyclotron design orbit. The inflector parameters allowed to vary are the inflector electrical radius, the electrical field strength, and the electrode tilt. The resultant design is then rotated to match the centres of curvature, and the parameters found are inspected to verify that they are physical acceptable. The electrode surfaces are approximated by a set of ruling lines. These can be visually inspected on the microcomputer screen.

5. RF-SYSTEM

Most components of the SPC2 rf-system, including the phase and amplitude stabilization systems and the control system, are similar to those of SPC1. The two power amplifiers have been redesigned to cover the frequency range from 6 to 26 MHz. Two ports were provided on each resonator for the additional stub lines[4] required for covering the 6 to 8.6 MHz range in two steps. This results in lower current densities compared to the use of a single stub line.

6. DIAGNOSTICS

All the diagnostic equipment installed in SPC1, i.e two differential probes, two radial slits and two axial slits as well as various collimators and insulated components on the extraction channels, are duplicated in SPC2[1,3]. However, some modifications to the original designs, as well as additional diagnostic equipment were required. The second differential probe, with current measurement on three fingers and the body itself, was modified to include a phase probe head on the tip of the probe (Fig. 3) and the indirectly water-cooled second radial slit situated in the second dee is replaced by a directly water-cooled slit.

The additional diagnostic equipment is a stepping motor driven harp consisting of 47 vertically mounted wires, spaced 1 mm apart, which will enable us to determine the horizontal beam profile and position of the orbits from a radius of about 200 mm right up to the extracted orbit in front of the second extraction channel. A quartz plate situated in the central region, viewed through a TV camera and pivoted into the beam plane will provide this information on the first turns.

A four-segmented aperture will be installed in front of the inflector to restrict the beam size and provide limited position information. We also intend to install a four-segmented capacitive pick-up probe in the magnet pole which will be used as a non-invasive beam position and intensity probe.

7. VACUUM SYSTEM

Detailed calculations were made in an attempt to improve the efficiency of the SPC2 vacuum system[4]. Pressures in the 10^{-5} Pa range will only be needed occasionally for the acceleration of highly charged heavy ions and an expensive pumping system cannot be justified for this purpose. The pressure distribution for the previously proposed system was first re-calculated, using more realistic values for the conductance, aperture and applied pumping speed. This result was compared with pressures computed for a new system consisting of one 2.2 m^3/s turbopump, a 10 m^3/s cryopump and a liquid nitrogen (LN_2) cryopump with a pumping speed of 18 m^3/s for water vapour at the far end of each resonator. It shows that a negligible increase in the pressure at the cyclotron centre will result from using a

10 m^3/s cryopump on the main vacuum chamber instead of the 18 m^3/s cryopump specified previously. Secondly, a more significant reduction in the pressure is predicted if the two 2.2 m^3/s turbopumps at the resonator ends are replaced by two LN_2 cryopumps.

Figure 4 depicts results of calculations for both systems. The effect of three different pump combinations on the pressure distribution for the new system is also shown. A pressure of 6.3×10^{-4} Pa will be obtained in the beam region using only the 2.2 m^3/s turbopump. This pressure will suffice for acceleration of protons. With the help of the 10 m^3/s cryopump the pressure will be reduced to 2.9×10^{-4} Pa, for the acceleration of light heavy ions. Adding also the LN_2 cryopumps will result in the lowest operational pressure of 8×10^{-5} Pa. This pressure is necessary for adequate transmission of heavy ions. For the LN_2 cryopump option, two additional inexpensive pumps which have a high pumping speed for air are required. Oil-diffusion pumps with a pumping speed of 1.75 m^3/s should be adequate for this purpose.

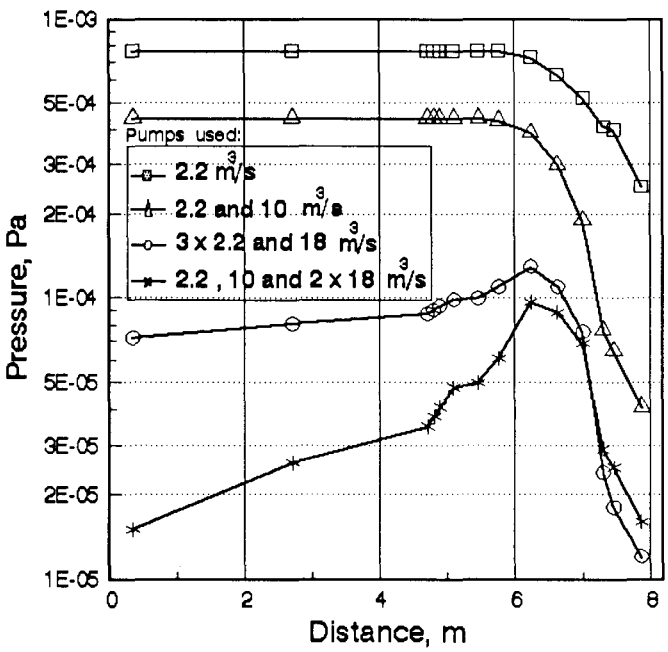


Fig. 4. Calculated pressure distribution in SPC2 for various pumping combinations. The zero length indicates the position of the resonator far end.

8. ACKNOWLEDGEMENTS

The authors would like to thank L.H.O. Schülein and J.G. de Villiers of the NAC Magnet Division and J.L.G. Delsink of the NAC mechanical workshop for their assistance.

9. REFERENCES

1) du Toit, Z.B. *et al.*, "Operating Experience with the Light-ion Injector of the NAC", in **Proceedings of the Eleventh Int. Conf. on Cyclotrons and their Application** (Ionics Publishing Company, Ltd., Tokyo, 1986) pp. 109-112.

2) Franklin, E.J.S. and de Villiers, J.G., "Ion Spectra Identification Software for ECR Source at NAC", (paper at this conference).

3) du Toit, Z.B. *et. al.*, "Aspects of the Design of an 8 MeV Cyclotron as an Injector for a 200 MeV Separated Sector Cyclotron", in **Proceedings of the Ninth Int. Conf. on Cyclotrons and their Applications** (Les Editions des Physique, Caen, 1981) pp. 129-131.

4) Botha, A.H. *et. al.*, "An Injector Cyclotron for Acceleration of Polarized and Heavy Ions at the NAC", in **Proceedings of the Eleventh Int. Conf. on Cyclotrons and their Applications** (Ionics Publishing Company, Ltd., Tokyo, 1986) pp. 515-518.

5) du Toit, Z.B. *et. al.*, "Calculated and measured magnetic fields for the Injector Cyclotron at the NAC", in **Proceedings of the Tenth Int. Conf. on Cyclotrons and their Applications** (IEEE, East Lansing, 1984) pp. 94-97.

6) Burger, S.J. *et. al.*, "The Electrolytic Tank Facility at the NAC", in **Proceedings of the Tenth Int. Conf. on Cyclotrons and their Applications** (IEEE, East Lansing, 1984) pp. 63-66.

7) Kost C.J. and Jones F.W., TRIUMF Computing Document (TRI-CD-88-01, 1988).

PLASMA CATHODE METHOD FOR RIKEN ECRIS

T. Nakagawa, T. Kageyama, M. Kase, A. Goto, and Y. Yano
The Institute of Physical and Chemical Research (RIKEN), Hirosawa 2-1, Wako-shi, Saitama 351-01, Japan

Abstract

A negatively biased electrode was set in the first-stage chamber of the RIKEN 10 GHz ECR (electron cyclotron resonance) ion source. By use of this electrode, the beam intensities of highly charged ions have been markedly increased. We studied the mechanism of this phenomenon, investigating the dependence of highly charged ion intensity upon the electrode bias voltage and current as well as the gas pressure of the first-stage chamber. Based on the results of this method, we changed the structure of the first stage. The first stage was isolated from the second stage electrically and negative bias was supplied to the first stage(plasma cathode method). We also observed that the beam intensity of highly charged ions was enhanced by using this method.

1. Introduction

In the last decade, ECRISs (electron cyclotron resonance ion sources) have been developed from a complex type into a compact and high performance ion source for accelerators and atomic physics experimental apparatus. The coupling of the ECRIS to heavy ion accelerator, in particular, has brought about a significant upgrade of their performance in energy, intensity and variety of ions.

Many laboratories have made an effort to upgrade the beam intensity of highly charged ions produced by ECRISs, using several methods. [1-6] In order to increase the electron density in the plasma, the Lawrence Berkeley Laboratory group has used an electron gun to supply electrons to the plasma of advanced ECRIS[2]. On the other hand, the Grenoble group has put a negatively biased probe near the gas injection of MINIMAFIOS to push electrons into second stage plasma. [4] The latter method is very useful for an ECRIS which consists of two stages, such as the RIKEN ECRIS.[7]

In the previous study on the RIKEN 10GHz ECRIS, we examined a method on setting up negatively biased electrode placed in the first stage.[5] This method has allowed us to significantly upgrade the beam intensity of highly charged ions: 160eμA $^{14}N^{5+}$, 150eμA $^{16,18}O^{6+}$, 60eμA $^{40}Ar^{11+}$ and 6eμA $^{84}Kr^{20+}$ have been successfully obtained. We have thus been supplying experimentalists with intense intermediate-energy heavy-ion beams from the AVF-Ring cyclotron complex.[8,9] In this paper, we present the mechanism of the phenomenon mentioned above, investigating the dependence of the output intensity of highly charged ions upon the electrode bias voltage and current as well as the pressure of the first stage chamber. Based on these results, we tried to change the structure of the first stage itself as an electron source (plasma cathode method). We also present this method and results in detail.

2. Negatively biased electrode

We measured the dependence of intensity of highly charged ions upon the bias voltage of the electrode , gas pressure and electrode current. The experimental set up is the same as described in Ref. 5. Figure 1 shows the schematic drawing of the first stage. The electrode is made of copper . The diameter and thickness are 10 and 2 mm, respectively.

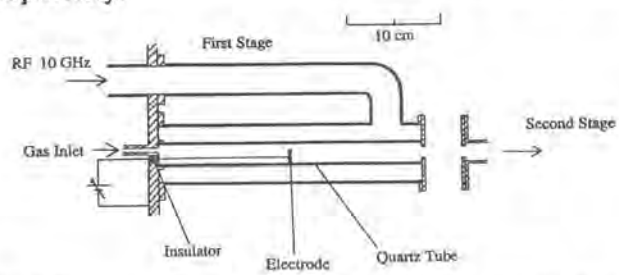


Fig.1 Schematic drawing of the electrode placed in the first stage

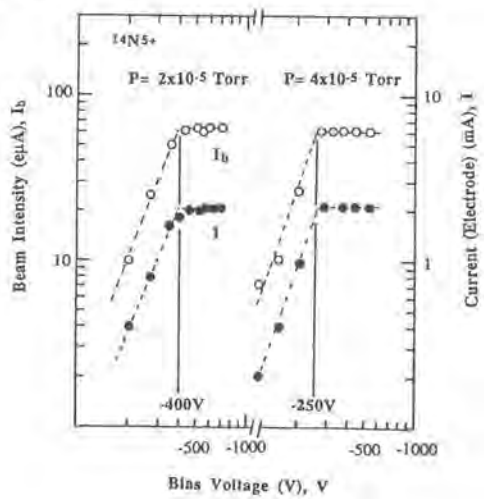


Fig. 2. Output intensity, I_b ,of $^{14}N^{5+}$ (open circles) and electrode current, I ,(closed circles) measured as a function of bias voltage, V ,at different pressures of 2 and 4×10^{-5} Torr in the first stage.

Figure 2 shows the beam intensity (I_b)of $^{14}N^{5+}$ and electrode current(I) as a function of the bias voltage (V). To clarify the dependence of the gas pressure of the first stage, only N_2 gas was fed into without any mixing gas; the other parameters such as microwave powers to the first stage and second stage and mirror magnetic fields were kept constant. I_b shows the same tendency as I. I_b saturates at -400V at a gas pressure of 2×10^{-5}Torr in the first stage, while the saturation occurs at -250V at a pressure of 4×10^{-5} Torr. In order to investigate this correlation of I_b vs I systematically, we examined several gaseous elements such as He, CO_2, N_2, O_2, and Ar. In this study, gas mixing was used, because it is very effective to obtain a higher intensity of highly charged ions for elements heavier than carbon. The optimum mixing ratio of the main gas to the auxiliary gas was nearly 1:5. the measurements were made at the pressure between $2\text{-}4\times10^{-5}$ Torr in the first stage. Figure 3 shows the beam intensity as a function of electrode current, where the highest intensities are saturated ones. Almost the same correlation has been observed for these ions except $^4He^{2+}$.

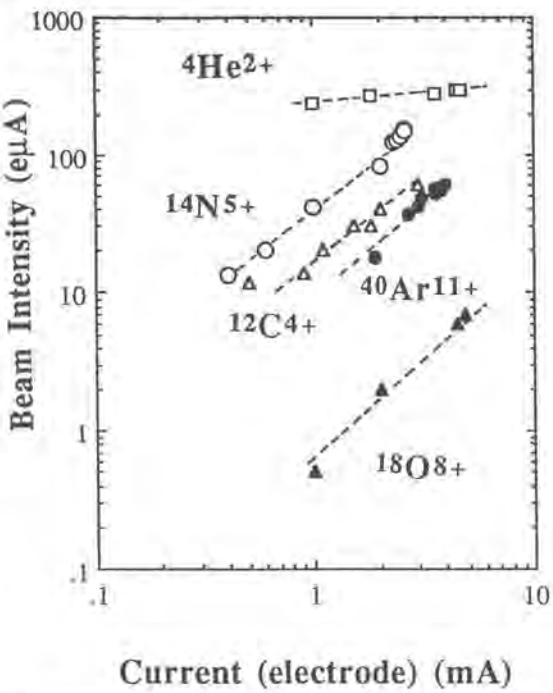


Fig. 3. Correlation between I_b and I observed for typical high-charge states of different ions. Highest intensities correspond to saturated ones. Dashed lines are guidelines.

The interpretation of the experimental results is illustrated by a schematical diagram shown in Fig. 4. It is well known that highly charged ions are produced in the successive ionization process. The production probability is assumed to be proportional to the product of $T_e \cdot \tau_i \cdot n_e$, where T_e, τ_i, and n_e are the electron temperature, ion confinement time and electron density in the second-stage plasma, respectively. Since the microwave power, gas pressure and gas mixing ratio were kept constant in the second stage, T_e and τ_i were considered to be constant. Thus $I_b \propto n_e$. The density n_e is expressed by $n_e = n_e^0 + \Delta n_e$, where n_e^0 is the density of electrons generated in the second stage and Δn_e is that of electrons (I_e') entering over the mirror field barrier in the first stage. Figure 2 shows that when $V \rightarrow 0$ V, I_b decreases to a faint intensity. This indicates that $n_e \cong \Delta n_e$, and thus $I_b \propto n_e \cong \Delta n_e \propto I_e'$.

On the other hand, the relationship observed between I and V inheres in the so-called Langmuir probe. If I_i and I_e are the currents of ions and electrons plunging into the electrode, then $I = I_i - I_e$. When the microwave power and the pressure, P ,in the first stage are kept constant, the ion density remains the same, and accordingly I_i is constant. As V increases, I_e decreases to zero, because I_e is the current of electrons plunging over the repulsive potential wall, and then I saturates to the constant value of I_i. The P-dependence on the saturation bias voltage seen in Fig. 2 implies that with increasing P the electron temperature in the first stage drops.

Since the plasma is always electrically neutral, I is proportional to the current of electrons escaping from the plasma. These electrons partially enter the second stage over the mirror field barrier, which leads to $I_e' \propto I$. Thus, $I_b \propto I_e' \propto I$. This consequence contradicts the experimental results of $I_b \propto I^k$ (k= 1.2 ~ 1.3). To explain the contradiction, we should assume that the production probability of high-charge states in the successive ionization process is proportional to the product of $T_e \cdot \tau_i \cdot n_e^k$ except for $^4He^{2+}$, but further investigation of this is beyond the aim of the present study.

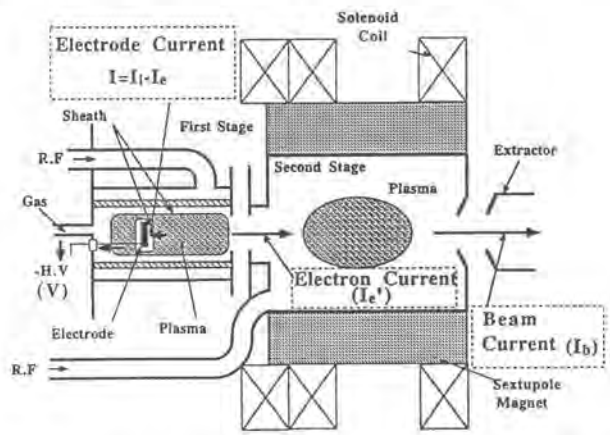


Fig. 4. Schematic diagram of the RIKEN 10 GHz ECR ion source equipped with a negatively biased electrode in its first stage, the electrode serving as the so-called Langmuir probe. Details are given in the text.

3. Plasma cathode method

If we make the potential difference between the first stage and second stage, we do not need the biased electrode in the first stage, because it is the same condition as that of negatively biased electrode method. In order to

make this condition, we have changed the structure of the first stage for the plasma cathode method as shown in Fig.5. The first stage is isolated electrically from the second stage by the insulator. The negative bias is supplied to the first stage. The aperture plate placed in front of the first stage is isolated from the first stage electrically and connected to the second stage.

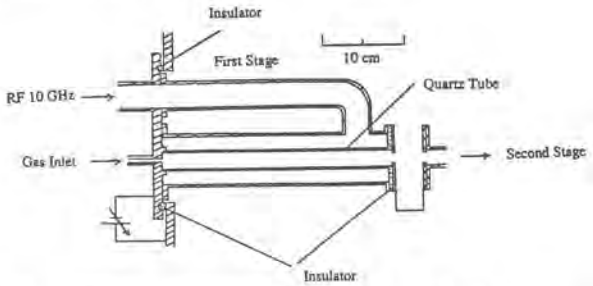


Fig.5. Schematic drawing of the first stage for plasma cathode method.

We investigated the beam intensity of $^{40}Ar^{11+}$ ions upon the bias voltage. The current increased very steeply between 0 to -100 V , whereas between -100 to -200 V the increase is about 20 % and then above -200 V the beam intensity is constant. Figure 5 shows the beam intensity as a function of current of the first stage. The intensity increases with increasing the current of the first stage. This tendency is the same as that observed when we used the negatively biased electrode.

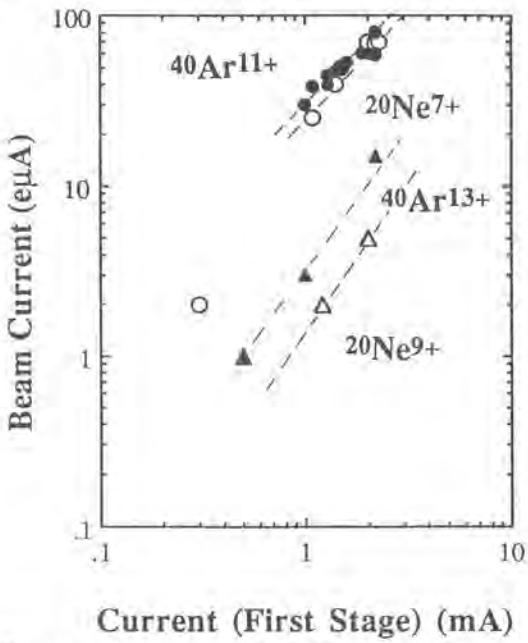


Fig.6Beam intensity measured as a function of current of the first stage

Figure 7 shows the charge state distribution of argon ions as a function of the analyzing magnet current. The source was tuned to maximize the beam intensity of $^{40}Ar^{11+}$. Usually the best beam intensity can be obtained by using the gas mixing method. To produce the Ar-ion , for example, the intensity is enhanced by using oxygen gas as a mixing gas. When we used the plasma cathode method, however, we needed no oxygen gas as a mixing to obtain the best result of 80 eμA. Another advantage of the plasma cathode method is the low consumption rate of gas. In order to obtain the best results for $^{40}Ar^{11+}$, the pressure of the first stage had to be 4-6x10^{-6} Torr using this method (Before using the plasma cathode method the optimum gas pressure was 2-3x10^{-5} Torr).

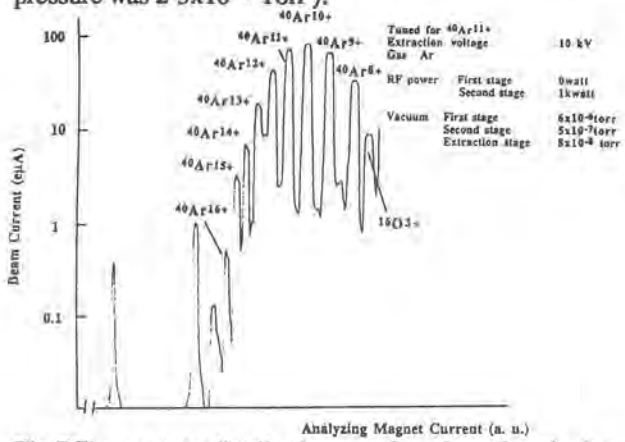


Fig.7Charge state distribution as a function of analyzing magnet current.

Figure 8 shows the beam intensities of Ar and Ne ions as a function of charge state. Open and closed circles are without and with using the plasma cathode method, respectively. It is clear that the highly charged ions are strongly enhanced by using this method.

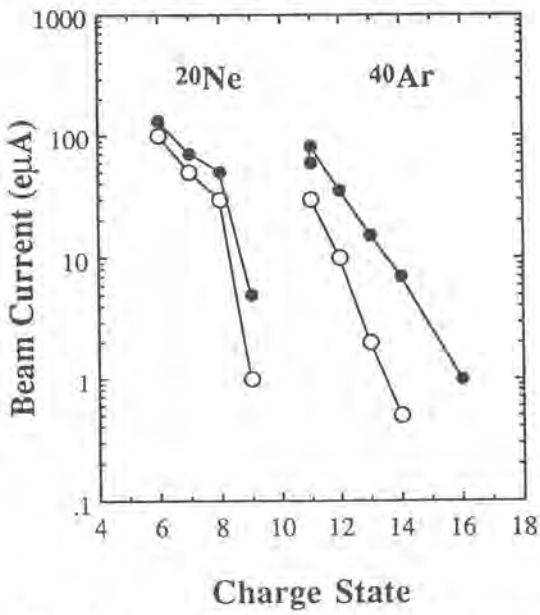


Fig. 8. Beam intensity of Ar and Ne ions as a function of charge state.

The plasma cathode method has several advantages. In principle, the plasma cathode method plays the same role as that of the biased electrode method. The first stage supply the second stage with electrons in the first stage

plasma. One advantage of the plasma cathode method is its long lifetime compared to the biased electrode method. The lifetime of the electrode is about 2 months in routine operation. This is due to the sputtering of the electrode by the ion impact. In the case of the plasma cathode method, there is no such a limitation. Furthermore, as we mentioned above, plasma cathode method has other two advantages: low consumption rate of the main gas and no gas mixing. However, the reason for last two phenomena is not yet solved.

4. Conclusion

We measured the correlation of the beam intensity of highly charged ions with the electrode current, gas pressure, and bias voltage. This work led us to conclude that the beam intensity, I_b, of highly charged ions obtainable by use of the electrode is bound by the amount of electrode current I produced by the ECR discharge in the first-stage.

Based on the results of method of negatively biased electrode we change the structure of the first stage (plasma cathode method) and tested it . The tendency of beam intensity as a function of current of the electrode is the same as that by using the biased electrode. We could obtain the best result of 80 eμA for $^{40}Ar^{11+}$ ion without gas mixing method. It also has two other advantages: long lifetime and low consumption rate of gas.

References

1)R. Geller : Annu. Rev. Nucl. Part. Sci. 40(1990)15
2)Z. Q. Xie, C. M. Lyneis, R. S. Lam and S. A. Lundgren: Rev. Sci. Instrum. 62(1991)775
3)T. Nakagawa: Jpn. J. Appl. Phys. 30(1991)L930
4)G. Melin et al. : Proc. 10th Int. Workshop on ECR Ion Source, Knoxville, 1990(Oak Ridge National Laboratory, knoxville, 1991)p.1.
5)T. Nakagawa and T. Kageyama: Jpn. J. Appl. Phys. 30(1991)L1588.
6)T. Nakagawa, T. Kageyama, M. Kase, A. Goto and Y. Yano: Jpn. j. Appl. Phys. Letter in press
7) K. Hatanaka and H. Nonaka: Proc. Int. Conf. the Physics of Multiply Charged Ions and Int. Workshop of ECR Ion Sources, Grenoble, 1988, J. Phy. C-1(1989)821
8)A. Goto, K. Hatanaka, M. Kase, Y. Yano, T. Kageyama, S. Kohara, N. Nagase, H. Takebe, K. Ikegami, M. Saito, N. Nakanishi, Y. Kumata and T. Tachikawa: Proc. 7th Symp. Accelerator Science and Techinology, Osaka, 1989(Osaka Univ. Osaka, 1990)p51
9)Y. Yano : these proceedings

PERFORMANCE OF THE TEXAS A&M ECRIS

G.Mouchaty, R.C.Rogers, P.Smelser and D.P.May
Cyclotron Institute, Texas A&M University, College Station
Texas, 77843-3366, U. S. A.

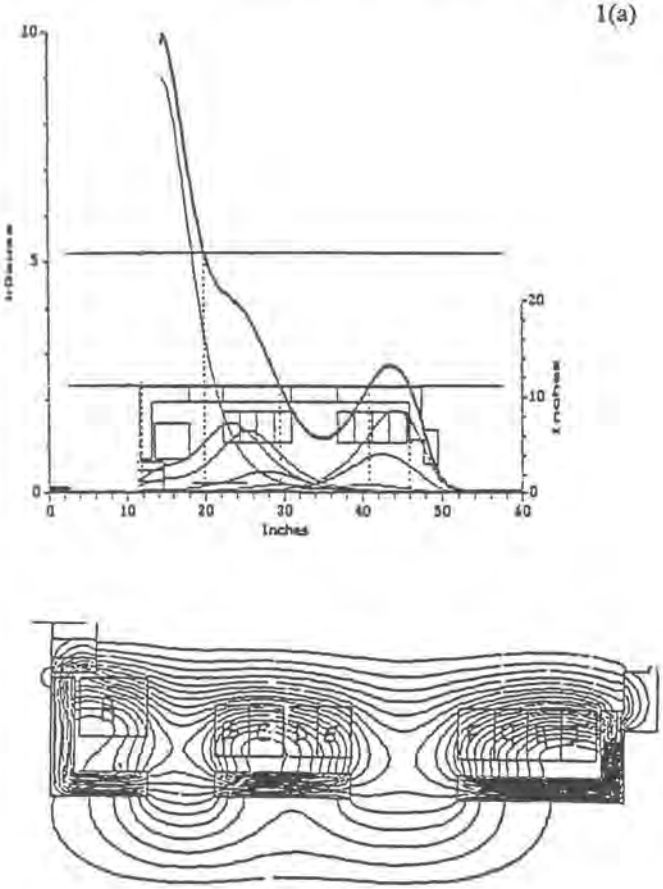
ABSTRACT

The Texas A&M ECRIS (Electron Cyclotron Resonance Ion Source) is a two stage, 14.5-6.4 GHz, source in operation since August of 1989. Injection in the K500 cyclotron was accomplished 3 months later. Since then minimal development time has been available and only essential modifications have been made. The source has produced beams as diverse as H-He+ molecules to $^{181}Ta^{24+}$ for acceleration by the cyclotron. After a brief description of the source and the injection line we report on their performance. Our plans and their development are then discussed.

1. DESCRIPTION OF THE SOURCE

The Texas A&M ECRIS is a production source. It was conceived[1] as such and built[2,3] at the Cyclotron Institute for injection into the K500 cyclotron. Figure 1 shows a sketch of the principal elements of the magnetic structure and the associated field profiles. The microwaves are provided by a 14.5 GHz transmitter for the first stage and a 6.4 GHz transmitter for second stage, thus the magnetic bottle is inherently tilted. Both stages are injected at the high field side and extraction is done through a Pierce system.[4] The minimum B configuration is achieved by the superposition of a permanent magnetic hexapole field made from Sm-Co, [Cf. Fig 1(b)], onto a mirror field produced by 9 coils separately adjustable [A to I in Fig. 1(a)]. This allows ample tuning capacity and provides reasonable margin to upgrade the source and test new ideas. The radius of the plasma chamber is 2.5 inches.

1(a)



2. OPERATION AND PERFORMANCE OF THE SOURCE

In day-to-day operations, the best solution for the mirror field is always very close to the one shown in Fig. 1(a). Minor adjustments for different beams usually result in a better production and higher stability. In Fig. 1(a), the mirror ratio on axis is approximately 2.1, and the total dissipated power is about 69 KW.

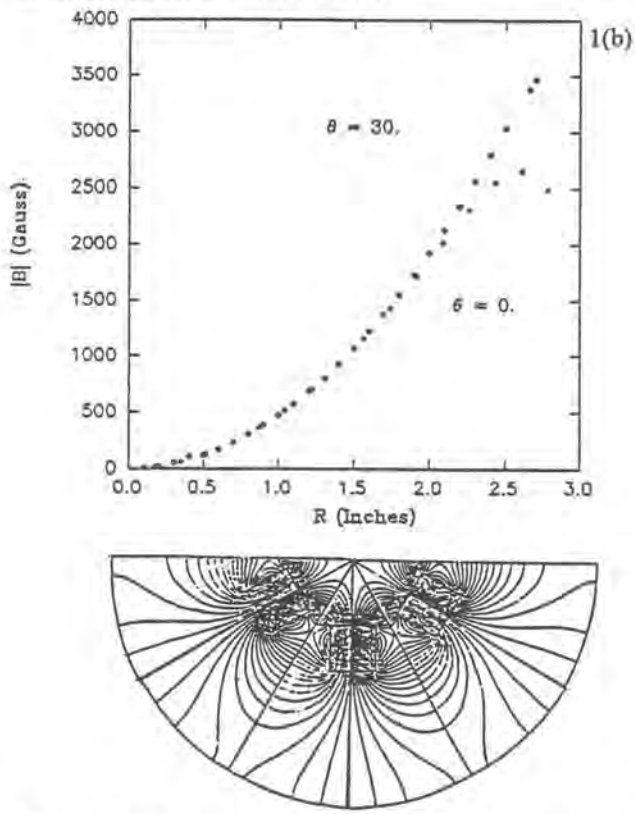


Fig. 1. A sketch of the principal elements of the magnetic structure and the associated field profiles. (a) The mirror field. (b) The hexapole field. The radius of the plasma chamber is at 2.5".

Figure 2 shows typical extracted currents for several ions ranging from $^{14}N^{5+}$ to $^{Nat}Pb^{33+}$. Keeping in mind the scaling laws of ECRIS[5] one can compare this source to

other 6.4 GHz ECRIS. (e.g. Refs. 6, 7, 8). It is clear that the orthodoxy observed in the design of this source[1] paid off. The data in Fig. 2 show a very good production capacity. As for its stability, once this source has been tuned, it usually stays stable until the injected gas pressure drops significantly.

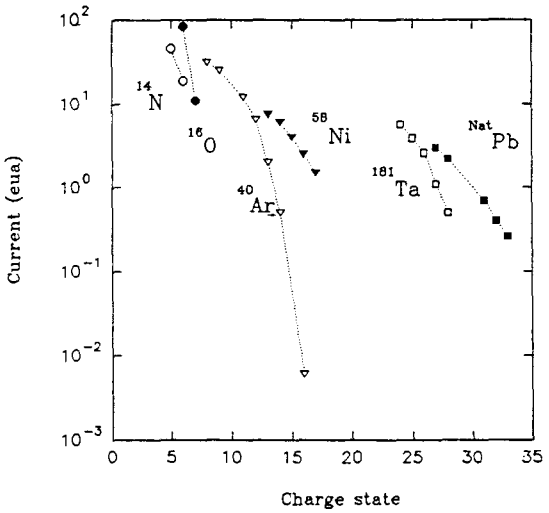


Fig. 2. Typical extracted currents for several ions ranging from $^{14}N^{5+}$ to $^{Nat}Pb^{33+}$ measured on a plate intercepting the beam after the analysis magnet (ILC02).

3. DESCRIPTION OF THE INJECTION LINE

As shown in Fig. 3, the output of the source is analyzed in a 90° magnet. A small bend (marked BM15-H in Fig. 3), allows for injection of another source into the cyclotron. The second 90° magnet bends the beam into the vertical part of the beam line which ends in a spiral inflector. The exit of the latter is in the median plane of the cyclotron. The beam size along the injection line is controlled by five solenoids with the last two being

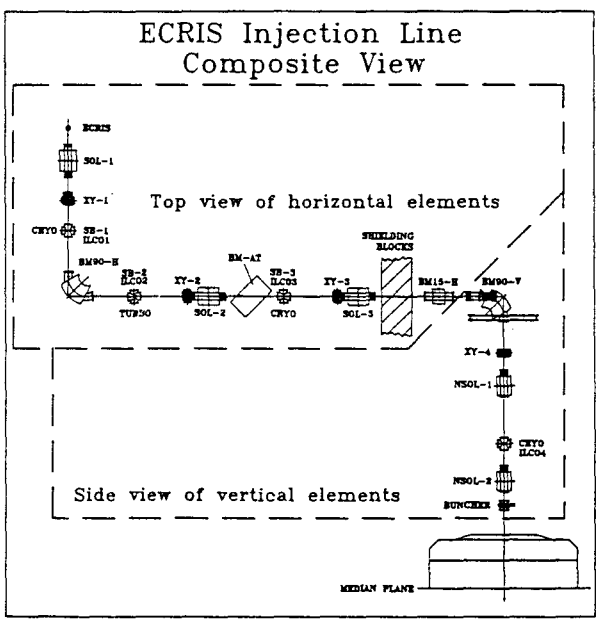


Fig. 3. The injection line components.

naked. Another 90° magnet (marked BM-AT) can bend the beam to be used before acceleration. It is usually used for atomic physics experiments.[9]

4. TRANSMISSION

Since the plate ILC04 is in the fringe field of the cyclotron, one expects to read less current on ILC04 than on ILC02 even for 100% transmission. The ratio of these two currents is shown in Fig. 4 for different beams accelerated since August of 1991 (solid circles). The ratio of the beam measured at the extraction radius of the cyclotron to that measured at ILC04 is indicated by open circles. And finally, the ratio of the beam extracted from the cyclotron to that measured at the extraction radius is shown by solid squares. We use data since August 1991 because the buncher was mounted on the injection line at that time. Also, the last time the main coil was moved was in July of 1991. Although the position of the main coil has been optimized for better extraction, one can see the dependence of the ratio of extracted beam to internal beam on gamma (E/E0) (solid squares). (*)

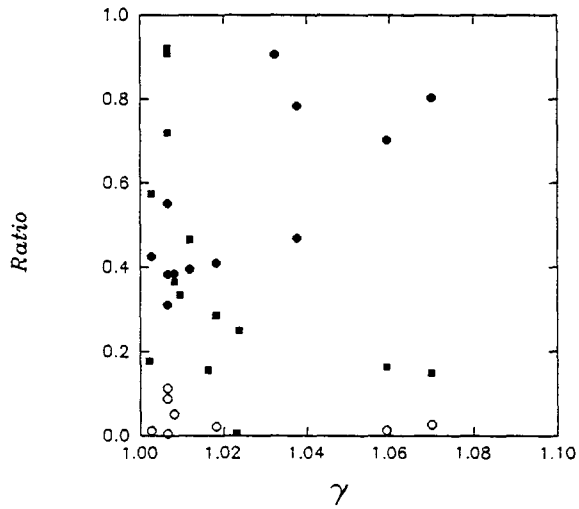


Fig. 4. The ratio of the current measured on the plate ILC04 to that measured on ILC02 (solid circles). The ratio of the beam measured at 26.5" to that measured on ILC04 (open circles). The ratio of the beam extracted from the cyclotron to that measured at the cyclotron extraction radius (solid squares). (Cf. paragraph 4)

5. PLANS

Since 1986, when this source was designed,[1] several significant developments happened in the ECRIS field, two of which have direct bearing on our plans.

5.1. Permanent magnet material

NdFeB is now widely used and has proved to be at least as safe as the Sm-Co. Since it can be magnetized to much higher values than Sm-Co, the space needed to fit a hexapole of a given strength is smaller and so is the inner radius of the coils. This point is among (if not the) most important point to be considered in any attempt to design a better source (whether for production or stability).

5.2. First stage

Among several questions that have to be addressed when upgrading our source, is the necessity of the first stage and, if at all, what should replace it. Experiments with biased plates[10,11] and with an electron gun[12] have shown substantial increase of the output of the source when these devices are used with a main stage only. We have tested a 3.5 cm diameter copper plate in our source and found very encouraging results.[13] In Table 1 the results obtained with the plate and the main stage are compared to those obtained with both stages. An effort is under way to compare the usage of an electron gun to that of a plate.[14]

(*) Depending on the charge state and the beam velocity the vacuum in the cyclotron can become another major source for beam loss.

Table 1

	with first stage	with plate
$^{20}Ne^{8+}$	12.0 μa	17.5 μa
$^{20}Ne^{9+}$	0.75 μa	1.1 μa
$^{40}Ar^{11+}$	5.1 μa	18.0 μa

6. REFERENCES

1) G. Mouchaty: The Texas A&M E.C.R.I.S. Design and justification. Unpublished report (1986). See also G.Mouchaty The Texas A&M E.C.R.I.S. an alternative first stage. Unpublished report, (1986).

2) W. H. Peeler, et al. **Progress in Research, 1988-1989**, Cyclotron Institute, Texas A&M University, p. 114.

3) R. C. Rogers, **Progress in Research, 1988-1989**, Cyclotron Institute, Texas A&M University, p. 117.

4) J. R. Pierce, J. App. Phys. 11, 548 (1940).

5) R. Geller, et al., **International Conference on ECR Ion Sources and Their Applications**, East Lansing, Michigan (1987), p. 1.

6) M. Oyazu, et al., **10th International Workshop on ECRIS**, Oak Ridge, Tennessee, Nov. 1-2 1990, p. 25.

7) C. M. Lyneis., **International Conference on ECRIS and Their Applications**, East Lansing, Michigan (1987), p. 42.

8) T.A.Antaya, et al. **International Conference On ECRIS and Their Applications**, East Lansing, Michigan (1987), p. 86.

9) R. L. Watson, D. A. Church, R. E. Tribble, L. Yang, B. B. Bandong, and T.Lotze, NIM B56/57 (1991) 223-226.

10) S. Gammino, et al., **4th International Conference on Ion Sources, ICIS 91**, Bensheim, Germany (1991).

11) G. Melin, et al., **10th International Workshop on ECR Ion Sources**, Oak Ridge, Tennessee (1990), p. 17.

12) C.Lyneis, et al., **10th International Workshop on ECR Ion Sources**, Oak Ridge, Tennessee (1990), p. 47.

13) G.Mouchaty, et al. **Progress in Research, 1991-1992**, Cyclotron Institute, Texas A&M University. In press.

14) G. Mouchaty. To be published.

ADVANTAGES OF USING DIFFERENTIAL ALGEBRA AND LIE ALGEBRA IN THE ORBIT DYNAMICS OF CYCLOTRONS

Walter G. Davies
AECL Research, Chalk River Laboratories, Chalk River Ontario, K0J 1J0.

ABSTRACT

There have been significant developments during the past few years in both numerical and analytic tools for computing and understanding the orbit dynamics of accelerators. In particular, differential-algebraic techniques can result in unprecedented accuracy in computing the nonlinear behaviour of accelerators. In addition, Lie-algebraic techniques provide powerful methods of simplifying and understanding this behaviour. The application of these techniques to the design and analysis of cyclotrons should improve their quality, predictability and ease of operation.

1. INTRODUCTION — THE TRADITIONAL METHOD

Traditionally, calculations of the orbit dynamics of cyclotrons have been done by numerically integrating the relativistic equation[1)]

$$\mathbf{F} = \frac{d}{dt}\frac{m\mathbf{v}}{\sqrt{1-\beta^2}}; \quad \beta = \frac{|\mathbf{v}|}{c} \tag{1}$$

with a Runge-Kutta integrator, where the Lorentz force is $\mathbf{F} = q(\mathbf{E} + \mathbf{v} \times \mathbf{B})$; here $\mathbf{E}$ is the electric field, $\mathbf{B}$ the magnetic field, c is the speed of light and q, m, and $\mathbf{v}$ are the charge, the mass and the velocity of the particle, respectively. Also, the usual practice is to interpolate the measured midplane field component, B_z, by, for example, Aitken's method or some combination of Fourier analysis and interpolation; we shall see that such interpolation schemes restrict both the order and the accuracy of higher derivatives of the field, which are explicitly and/or implicitly required for the analysis of the nonlinear behaviour and resonances. Finally, extrapolation of the magnetic field off the midplane is achieved by expanding B_z in a Taylor series and using Maxwell's equations plus midplane symmetry to determine the coefficients as follows: assume $\mathbf{B}$ may be derived from a magnetic scalar potential $\Phi(r,\theta,z)$ *via* $\mathbf{B} = -\nabla\Phi$; from $\nabla \cdot \mathbf{B} = 0$ we see that Φ satisfies Laplace's equation, $\nabla^2\Phi = 0$. In cylindrical coordinates, the Laplacian may be split into "transverse" and z-pieces, $\nabla^2 = \left[\nabla_\perp^2 + \partial_z^2\right]$ where $\nabla_\perp$ and ∂_z commute. Since $B_z = \partial_z\Phi$, it therefore follows that $\nabla^2 B_z = 0$ also. Assuming midplane symmetry, we expand B_z about the midplane as a Taylor series in z,

$$B_z(r,\theta,z) = \sum_m \frac{1}{(2m)!} B_{2m}(r,\theta)\, z^{2m}. \tag{2}$$

The B_{2m} may be determined by substituting Eq. 2 into Laplace's equation and setting like powers of z to zero. We find that $B_2 = -\nabla_\perp^2 B_z|_{z=0}$, $B_4 = +\nabla_\perp^4 B_z|_{z=0}$, *etc.*; in other words, we must take high-order derivatives of the interpolated midplane field B_z. Since differentiation of interpolated data rapidly results in total loss of numerical significance, we are in practice limited to $m = 0, 1$, *i.e.*, expansion of the field only to sextupole order. Furthermore, we see why we must require midplane symmetry: it is impossible to infer $\partial_z B_z|_{z=0}$ if given only B_z on the single plane $z = 0$.

With this approach, it is very difficult to analyse resonances with much accuracy. Typically, the determinant of the 1st order transfer matrix obtained by differencing the principal rays is only accurate to about 5%, and higher order maps will be much less accurate. Thus the *symplectic condition* is violated, and hence *Liouville's theorem* is not satisfied and phase-space is not preserved.

2. DIFFERENTIAL ALGEBRA — THE NEW METHOD

The limitations discussed above can be overcome with the use of *differential algebra* (DA)[2)], which allows us to accurately calculate the high order behaviour. The advantage of DA is that it automatically generates a Taylor series expansion of Eq. 1, or the Hamiltonian of the system, about any point in space. The derivatives in the expansion are computed to *machine precision*; there is no *truncation error*. Also, an arbitrary number of variables with derivatives to arbitrary order can be accommodated.

However, for DA to be used, the electromagnetic fields must be expressed in terms of analytic functions. This has pros and cons. Extrapolation of an interpolated magnetic field off the midplane does not allow us to accurately calculate high order effects in any case, so a better approach is needed even without DA. Unfortunately, a realistic and analytic magnetic (and RF) field model is in general difficult to achieve and will be much more computationally intensive than the traditional approach. Fortunately, use of a Bulirsch-Stoer[3)] integrator wins back much of this 'lost time' plus the bonus of much greater numerical accuracy than can be achieved with the

traditional Runge-Kutta integrator.* At Chalk River, we have developed accurate 3-dimensional models of the magnetic and RF fields[4] for the TASCC superconducting cyclotron, which do not require midplane symmetry; the midplane field data is only needed to fix parameters of the model.

2.1. How *DA* Works

DA[2] is a special algebra that replaces ordinary multiplication with a new kind of vector multiplication designed to achieve automatic differentiation. Space does not permit an extensive exposition of *DA*, so the rudiments will be illustrated by the following example; the interested reader is referred to ref. 2 for details. A *DA* of order n in v variables is denoted ${}_nD_v$ and the *DA* vector $Df = (f_0, f_1, f_2, \cdots f_n)$, where f_0 denotes the scalar value of $f = f(\mathbf{x})$ at $\mathbf{x} = \mathbf{x}_0, (\mathbf{x} \in \mathbf{R}^v)$. The $f_1, f_2, \cdots f_n$ are themselves sub-vectors containing the $1^{st}, 2^{nd}$, and n^{th} order derivatives of f, respectively. The *unit element* of the algebra is $(1, 0, \cdots, 0)$ and the *unit differentials* are $d_i = (0, \delta_i^1, \delta_i^2, \cdots, 0)$ where $i = 1 \cdots v$ and δ_i^v is the Kronecker δ. For 2nd derivatives of functions of one variable, ${}_2D_1$, the rules of the algebra are:

$$A + B = (A_0 + B_0, A_1 + B_1, A_2 + B_2) \tag{3}$$

$$A*B = (A_0B_0, A_0B_1+B_0A_1, A_0B_2+A_1B_1+A_2B_0). \tag{4}$$

We see that $d = (0,1,0)$, $d^2 = (0,1,0) * (0,1,0) = (0,0,1)$ and $d^3 = (0,1,0) * (0,1,0) * (0,1,0) = (0,0,0)$; *i.e.* the algebra is *nilpotent* at order n. Thus if $f(x) = x^2$ at $x = 5$, we obtain $(5,1,0) * (5,1,0) = (25,\ 5{\cdot}1 + 1{\cdot}5,\ 5{\cdot}0 + 1{\cdot}1 + 0{\cdot}5) = (25, 10, 1)$, but

$$Df = (25, 10, 1) \equiv \left(f(x), \frac{df(x)}{dx}, \frac{1}{2}\frac{d^2 f(x)}{dx^2} \right)_{x=5} \tag{5}$$

which are the coefficients of a Taylor series to 2nd order about $x = 5$. Note: only one function evaluation was needed.

2.2. Application of *DA* to Cyclotrons

As we wish to preserve the symplectic condition, canonical coordinates must be used, and it is convenient to use the Hamiltonian formulation. The relativistic Hamiltonian in cylindrical coordinates, the "natural" coordinate system for cyclotrons, is[5]

$$H = -erA_\theta - r\left\{ \left(\frac{p_0 + \varphi}{c} \right)^2 - m^2c^2 - [\mathbf{P}_\perp - \mathbf{A}_\perp]^2 \right\}^{1/2} \tag{6}$$

*In our tests Bulirsch-Stoer was from 3 to 5 times faster than Runge-Kutta and 10^6 times more accurate. *B-S* is ideal for integrating *DA* problems because all the functions are analytic.

where H is the momentum in the azimuthal direction, θ is the independent variable, r is the radius of curvature, p_0 is the total energy, φ is the electromagnetic scalar potential, and $\mathbf{P}_\perp$ and $\mathbf{A}_\perp$, are the transverse components of the momentum and the electromagnetic vector potential, respectively; A_θ is the azimuthal component of the vector potential. We make a *DA* expansion of the Hamiltonian

$$H \Rightarrow (H, H_r, H_{P_r}, H_Z, H_{P_Z}, \cdots) = \sum_{s=0}^{N} \frac{1}{s!} \frac{\partial^{|s|} H}{\partial q^s} dq^s \tag{7}$$

where $q^s = r^i P_r^j Z^k P_Z^l T^m P_T^n$, $|s| = i+j+k+l+m+n$ and $s! = i!j!k!l!m!n!$. In this expansion, the derivatives are with respect to the canonical coordinates, $\mathcal{Z} = (r, P_r, Z, P_Z, T, P_T)$, of the fundamental cylindrical coordinate system. The differential quantities dq^s are monomials of the *DA* basis vectors which represent the monomials ζ^s appearing in the usual expansion of the Hamiltonian (see Eq. 10), where $\zeta = (x, p_x, z, p_z, t, p_t)$ are the familiar differential canonical coordinates. Hamilton's equations in Poisson bracket form are

$$\mathcal{Z}' = -[H, \mathcal{Z}] \tag{8}$$

where the '$\prime$' denotes differentiation with respect to θ. The usual form of Hamilton's equations are readily obtained from Eq. 8. The *DA* expansion of Hamilton's equations have the form

$$r' = \frac{\partial}{\partial P_r}(H, H_r, H_{P_r}, H_Z, H_{P_Z}, H_T, H_{P_T} \cdots)$$
$$= (H_{P_r}, H_{P_r r}, H_{P_r P_r}, H_{P_r Z}, H_{P_r P_Z}, H_{P_r T}, H_{P_r P_T} \cdots) \tag{9}$$

for the r' equation and similarly for the other coordinates. The straightforward method of obtaining Eq. 9 is to differentiate the Hamiltonian "by hand" and evaluate the "right-hand-side" of Hamilton's equations in *DA*. The resulting *DA* vectors are integrated numerically. The result is the reference trajectory, along with the usual Taylor series map, or aberration expansion,

$$\zeta_i^{FIN} = R_{ij}\zeta_j^{IN} + T_{ijk}\zeta_j^{IN}\zeta_k^{IN} + U_{ijkm}\zeta_j^{IN}\zeta_k^{IN}\zeta_m^{IN} + \cdots; \tag{10}$$

repeated indices are summed. The superscripts, IN and FIN, refer to the initial and final coordinates connected by the map. Since *DA* can expand functions to arbitrarily high order, unlike conventional "transfer-matrix" codes the order of the Taylor-expanded map Eq. 10 is not fixed, but may be freely chosen at run-time.

One might naively assume that it is easy to use *DA* to take the derivatives of the *DA*-Hamiltonian, Eq. 7, but this is not the case, because the ∂-operator in *DA* maps ${}_nD_v$ onto ${}_{n-1}D_v$, so that expansion of the Hamiltonian to order n results in an expansion of Hamilton's

equations only to order $n-1$. Thus the nth order terms will be in error after the first integration step, the $n-1$ order terms are in error after the second step and so on. However, it can be shown (see Eq. 7 and 4) that if the first derivatives of H are zero then the problem is circumvented and we have a consistent algebra. We can make the derivatives zero by explicitly making the canonical transformation to the reference trajectory.[9)]

A further problem (and difference between DA and ordinary calculus) is that the ∂-operator in DA gives the *values* of the derivatives with respect to the expansion variables whereas the usual ∂-operator generates a *function* of the phase space variables at a general point. Because in our case the expansion variables are the phase space variables at the initial azimuth θ_0, we do not directly obtain the derivatives needed for the standard form of Hamilton's equations. The Poisson bracket form, Eq. 8 allows us to circumvent this problem, because the map from initial to final phase-space variables is a canonical transformation, and the Poisson bracket is invariant under canonical transformations. Thus the penalty for generating Hamilton's equation with DA is that we must evaluate H to one order higher than the desired map, plus we must make a canonical transformation at each step, both of which increase the computation time.

Eq. 10 plus the reference trajectory are sufficient if we are interested only in the behavior of the reference trajectory, tunes or phase-space plots. For the study of the non-linear behavior, especially resonances, it is helpful to transform to a Lie-algebraic representation, which by presenting the dynamics in a simpler and more compact form greatly facilitates understanding. Furthermore, many powerful and elegant theorems of Lie algebras, symplectic groups and symplectic geometry[10)] are immediately applicable, aiding in the simplification, analysis and understanding of the problems under study.

3. LIE-ALGEBRAIC ANALYSIS

The Poisson bracket $[H, \mathcal{Z}]$ in Hamilton's equations, Eq. 8, satisfies the requirements of a Lie algebra, namely, the commutation relation

$$A * B = (A, B) = AB - BA \tag{11}$$

and the Jacobi identity

$$(A,(B,C)) + (B,(C,A)) + (C,(A,B)) = 0. \tag{12}$$

Note: This algebra is *neither commutative nor associative.*

The Taylor series map Eq. 10, written as $\zeta^{FIN} = \mathcal{M}\zeta^{IN}$, can be transformed[6)] with the help of DA into an equivalent Lie-map

$$\mathcal{M} \Rightarrow \mathcal{M}_f, \quad \mathcal{M}_f = e^{:f:}; \quad :f:g = [f,g] \tag{13}$$

where

$$e^{:f:} \stackrel{\text{def}}{=} \sum_{n=0}^{\infty} \frac{:f:^n}{n!}; \quad :f:^0 = \mathcal{I} = \{\text{identity map}\}, \tag{14}$$

and $[\cdot,\cdot]$ is the Poisson bracket[7)] with respect to the canonical coordinates (x, p_x, z, p_z, t, p_t). The Lie-map, $\mathcal{M}_f$, can be factored[6)] into

$$\mathcal{M}_f = \mathcal{M}_1\mathcal{M}_2\mathcal{M}_3\mathcal{M}_4 \ldots = e^{:f_1:}e^{:f_2:}e^{:f_3:}e^{:f_4:}\ldots \tag{15}$$

where $\mathcal{M}_f$ and $\mathcal{M}_n$ are *symplectic maps* and f_n are homogeneous polynomials of degree n.

In a circular accelerator, it is desirable that the reference orbit be a closed orbit (*i.e.* a "*fixed point*" of the one-turn map); this is, in fact, necessary for the transformation to normal form. If the reference trajectory is not a closed orbit, the map, $\mathcal{M}_f$, will have an $\mathcal{M}_1$ factor. The closed orbit can be found from the map by solving for the fixed point given by the relation $\zeta_* = \mathcal{M}_f\zeta_*$. If the non-linearities are small and/or the initial conditions are not too far from the fixed point, the problem converges in one iteration. However, if the non-linearities in the map are large and we truncate the map (which we must invariably do), then the solution of the fixed point equation will not be exact, and the process must be repeated until convergence is obtained. Once the fixed point has been found, the map can be transformed by a canonical change of variables $\bar{\zeta} = \mathcal{A}\zeta$, such that $\bar{\zeta}_* = \mathcal{A}\zeta_* = 0 \Rightarrow \bar{\zeta}_* = \mathcal{A}\mathcal{M}_f\mathcal{A}^{-1}\bar{\zeta}_* = \bar{\mathcal{M}}_f\bar{\zeta}_* = 0$ *i.e.* $\bar{\mathcal{M}}_f$ maps the origin onto itself.

The Lie-polynomials provide a much more compact representation of the map than Eq. 10, and preserve the symplectic nature of the map, $\mathcal{M}$, exactly, which Eq. 10, when truncated, does not do. With the help of DA, Eq. 15 can be transformed into *normal form*[6)] which provides a very powerful method for identifying and analysing non-linear behaviour and resonances in particle accelerators.

3.1. Normal Form

The normal form is the transformation $\mathcal{N} = \mathcal{A}\mathcal{M}\mathcal{A}^{-1}$ such that $\mathcal{N}$ is in its *"simplest"* form; $\mathcal{M}$ must be expanded about a "closed orbit" *i.e.* no H_1 terms in H, which implies no $\mathcal{M}_1$ terms in $\mathcal{M}$. The symplectic map $\mathcal{A}$ is an nth order canonical transformation that *isolates* the *tune shifts* and *resonances* to n^{th} order. Using the factored map or alternatively the Taylor map and DA, we can normalize $\mathcal{M}$ order by order to obtain[6)]

$$\mathcal{N} = \mathcal{A}_n \cdots \mathcal{A}_4 \left\{\mathcal{A}_3\left\{\mathcal{A}_2\mathcal{M}\mathcal{A}_2^{-1}\right\}\mathcal{A}_3^{-1}\right\}\mathcal{A}_4^{-1}\cdots\mathcal{A}_n^{-1} \tag{16}$$

We proceed as follows: From the eigenvectors (they must be distinct) of R, Eq. 10, we get a canonical transformation that *rescales and block diagonalizes* R;†

$$\mathcal{R} = \mathcal{A}_2 R \mathcal{A}_2^{-1} \Rightarrow \mathcal{R} = \begin{pmatrix} \mathcal{R}_1 & & 0 \\ & \mathcal{R}_2 & \\ 0 & & \mathcal{R}_3 \end{pmatrix} \qquad (17)$$

where

$$\mathcal{R}_i = \begin{pmatrix} \cos(\mu_i) & \sin(\mu_i) \\ -\sin(\mu_i) & \cos(\mu_i) \end{pmatrix}, \begin{pmatrix} 1 & L_i \\ 0 & 1 \end{pmatrix}, \text{ or } \begin{pmatrix} 1 & 0 \\ a_i & 1 \end{pmatrix}.$$

Next, we normalize $\mathcal{M}_3$

$$\mathcal{N} = \mathcal{A}_3 \mathcal{A}_2 R e^{:f_3:} \cdots \mathcal{A}_2^{-1} \mathcal{A}_3^{-1} = e^{:G_3:} \mathcal{R} e^{:g_3:} \cdots e^{-:G_3:}$$

$$= \mathcal{R} \exp\left\{ : -(\mathcal{I} - \mathcal{R}^{-1}) G_3 + g_3 : \right\} \cdots . \qquad (18)$$

A further simplification results if we expand $(\mathcal{I} - \mathcal{R}^{-1})$, and g_3 in a complex or 'resonance' basis as follows: $h_\pm = x \pm i p_x, v_\pm = z \pm i p_z$. Hence,

$$(\mathcal{I} - \mathcal{R}^{-1}) \mid \mathbf{n}, \mathbf{m}> = \left[1 - \sum_{\mathbf{n}+\mathbf{m}=3} e^{i(\mathbf{n}-\mathbf{m})\cdot\mu} \right] |\mathbf{n}, \mathbf{m}>, \qquad (19)$$

and

$$g_3 = \sum_{\mathbf{n}+\mathbf{m}=3} A_{\mathbf{nm}} |\mathbf{n}, \mathbf{m}>, \quad |\mathbf{n}, \mathbf{m}> = h_+^{n_1} h_-^{m_1} v_+^{n_2} v_-^{m_2}; \qquad (20)$$

$\mathbf{n}, \mathbf{m}, \mu$ are vectors with components (n_1, n_2) etc. Substituting Eq. 19 and Eq. 20 into Eq. 18 and solving for G_3, we obtain

$$G_3 = \sum_{\mathbf{n}+\mathbf{m}=3} \frac{A_{\mathbf{nm}}}{\{1 - \exp[\, i(\mathbf{n}-\mathbf{m})\cdot\mu\,]\}}. \qquad (21)$$

All terms in g_3 can be incorporated into G_3 except when $\mathbf{n} - \mathbf{m} = 0$, or $(\mathbf{n} - \mathbf{m}) \cdot \mu = 2\pi\ell$, ℓ = integer; *i.e.* $(n_1 - m_1)\mu_x + (n_2 - m_2)\mu_z = 2\pi\ell$; $\ell = 0, \pm 1, \pm 2 \cdots$. The integer ℓ characterizes the resonance. In a similar fashion, we could proceed to find G_4 etc.

†The matrix R is the evaluated representation of the Lie-map $e^{:f_2:}$. As is common in the literature we will use R to represent both the Lie-map and the matrix itself, the choice being determined from the context. In fact, if canonical coordinates are used, the matrix R obtained from the Lie-map is always identical with that obtained from the Taylor-series, Eq. 10, and satisfies the symplectic condition exactly (*i.e.* $det|R| = 1$).

A further transformation to *action-angle* variables, $h_\pm = \sqrt{2J_x} e^{\mp i\varphi_x}$, $v_\pm = \sqrt{2J_z} e^{\mp i\varphi_z}$, leads to

$$\mathcal{N} = \exp : \Big\{ (\mu_x + \mu_x' p_t + \mu_x'' p_t^2 \cdots) J_x + (\mu_z + \cdots) J_z + a_x J_x^2 + a_z J_z^2 + \cdots \Big\} : \qquad (22)$$

where we have assumed no acceleration and no explicit resonances; J_x and J_z are the *action invariants* with associated angles φ_x and φ_z, μ are the *phase advances*, μ' *etc.* are the *chromaticities*, and all terms proportional to J^n are non-linear *tune shifts*. That we can incorporate all the other non-linearities into $\mathcal{A}$ and "get rid of them" makes the analysis of the tune-shifts and resonances much easier! If explicit resonances occur with $(\mathbf{n}-\mathbf{m})\cdot\mu = 2\pi\ell$; $\mathbf{n}, \mathbf{m}, \ell$ = integers, these must be added to Eq. 22. Because $[J_i^n, J_j^m] = 0$, that is all powers of the actions commute, the transformation from factored to single-exponent form is straightforward in Eq. 22. However, if there are resonances in the system, the *Campbell-Baker-Hausdorff* formula[7] or *DA* must be used to convert to single exponent form. Finally, the *normal form* has the remarkable property that

$$\mathcal{M}^n = \mathcal{A}^{-1} \mathcal{N}^n \mathcal{A} \qquad (23)$$

where n is the number of times the map is concatenated with itself. Use of Eq. 23 results in an enormous saving of work when applicable.

4. EXAMPLES AND DISCUSSION

Cyclotrons are only quasi-periodic and one should ideally work with accelerated maps, which our *DA* approach allows us to do. However, the dominant features of resonance topology can be studied using a simplified autonomous (θ-independent) Hamiltonian.

In isochronous cyclotrons, $\nu_x \simeq 1$, and the azimuthally averaged ("bulk") field $B_z \propto \gamma = (1 - \beta^2)^{-1/2}$ can be approximated as a constant plus a term proportional to r^2; this generates radially increasing bulk-quadrupole and bulk-sextupole terms when the field is expanded about the reference trajectory. The bulk quadrupole term is defocusing in the z-plane and is overcome by increasing the spiral angle of the hills, which produces additional local quadrupole and sextupole terms near the hill edges ("edge" fields) which approximately compensate the defocusing effect of the bulk field radial variation. Expanded through 3rd order about the reference trajectory, the combined effects of the bulk and edge fields can be modelled by the vector potential

$$A_\theta = -\frac{x + r_0}{2} B_0 - \frac{1}{r_0}\Big\{ Q_x x^2 + Q_z z^2 \Big\} - \frac{S_x}{r_0}\Big\{ \frac{x^3}{3} - x z^2 \Big\} \qquad (24)$$

where Q_x, Q_z, S_x, are the effective quadrupole and sextupole strengths, respectively. Inserting this vector potential into the Hamiltonian, Eq. 6, we will investigate the leading order nonlinearities and outline the analysis of the Walkinshaw or $\nu_x = 2\nu_z$ coupling resonance, which occurs near extraction in many cyclotrons. As a final illustration of the power of this type of analysis, we will show the effect of an octupole field on the orbits in the vicinity of the "one-third integer" sextupole resonance in a 3-fold symmetric cyclotron.

Because Eq. 24 is independent of θ, the Hamiltonian Eq. 6 has the solution

$$\mathcal{M}(\theta) = e^{-\theta:H:} \tag{25}$$

which can be factored into the form of Eq. 15. As we are neglecting acceleration, the energy of each particle is conserved and $p_t = (E_0 - E)/P_0 c$, where E is the particle energy, and E_0 and P_0 are the energy and momentum of the central trajectory, respectively.

4.1. Non-resonant Non-linear Behaviour

We will now apply the normalization procedure described in section 3.1 to the map given by Eq. 25. Since we assume no explicit resonances, the normal form contains $g_2 = -[\mu_x J_x + \mu_z J_z]$, the Lie-generator of the "rotation matrix" $\mathcal{R}$, Eq. 17, and

$$\begin{aligned} g_3 \;=\; & \frac{(1-\nu_x)}{4\nu_x\beta}\, J_x p_t + \frac{(1-\nu_z)}{4\nu_z\beta}\, J_z p_t \\ & + \pi S_x \frac{k_x^2}{\nu_x\beta}\, J_x p_t - \pi S_x \frac{k_x k_z}{\nu_x\beta}\, J_z p_t \\ & + \pi k_x \frac{1-\beta^2}{\nu_x\beta}\, p_t^3 + \pi S_x \frac{2k_x^3}{3\nu_x^3\beta^3}\, p_t^3 \end{aligned} \tag{26}$$

Eq. 26 has four *chromaticity* terms proportional to p_t and two time-of-flight aberration terms proportional to p_t^3. Here $k_x = r_0/\nu_x$, $k_z = r_0/\nu_z$.

If, for the moment, we make $\nu_x = 1$ (*i.e.* the system is resonant in the radial plane) then the first term in Eq. 26 vanishes. If we also adjust the spiral such that $S_x = 0$ then all the *chromaticity* terms vanish except the second one involving $(1-\nu_z)$. Under these circumstances $\mathcal{R}_1 = \mathcal{R}_x = \mathcal{I}_x$, $\mathcal{R}_2 = \mathcal{R}_z$, and we find that

$$\begin{aligned} \mathcal{M} &= \left\{\mathcal{A}_3^{-1}\mathcal{A}_2^{-1}\mathcal{N}\mathcal{A}_2\mathcal{A}_3\right\} = \left\{\mathcal{A}_3^{-1}\mathcal{I}_x\mathcal{R}_z e^{:g_3:}\mathcal{A}_3\right\} \\ &= \hat{\mathcal{A}}_3^{-1}\mathcal{R}_z e^{:\hat{g}_3:}\hat{\mathcal{A}}_3 \end{aligned} \tag{27}$$

where

$$\hat{g}_3 = \frac{(1-\nu_z)}{4\nu_z\beta}\, J_z p_t + \pi k_x \frac{1-\beta^2}{\nu_x\beta}\, p_t^3$$

and the $\hat{\mathcal{A}}$ now contain only terms involving z; *i.e.* all the non-linearities involving only the x coordinate cancel!

In reality , $\nu_x \simeq 1$, $S_x \simeq 0$ (at least on the average but not necessarily locally) and $\nu_z \ll 1$ over most of the accelerating region. Hence there is a large vertical chromaticity term in the map as is well known, but all the radial plane nonlinearities will be small through 3rd order. What happens at 4th order is another story! However, as we pass (adiabatically) through the resonances in the horizontal and vertical plane, this cancellation will be punctuated by terms with small denominators which must be retained (locally) in the normal map. In particular, in a 3-sector cyclotron, the residual sextupole can excite the "one-third integer resonance" in the radial plane (see section 4.3). Similarly, a one-forth integer resonance can be excited by the octupole field in a 4-sector cyclotron, but this is usually much weaker. This analysis demonstrates why a 4-sector cyclotron is less affected by non-linearities than a 3-sector machine.

4.2. Walkinshaw Resonance

In the fringe-field region near the extraction radius, we have large sextupole and octupole strengths and the magnetic field is no longer isochronous. We will ignore the octupole component for the purposes of this discussion, but it can have a profound effect on the stability of the orbits. At the Walkinshaw resonance, where $\nu_x = 2\nu_z$ (*i.e.* $(\mathbf{n}-\mathbf{m})\cdot\mu = 2\pi\ell$ with $\ell = 0$), we have a vanishing denominator in Eq. 21. This resonant term must be retained in the normal map. We can write the normal map, which now includes the resonance term, in factored form as follows:

$$\mathcal{N} = e^{:g_2:}e^{:g_3:}e^{:\propto p_t^3:} = e^{:g_2:}e^{:g_3':}e^{:\hat{g}_3:}e^{:\propto p_t^3:} \tag{28}$$

where $g_2 = -\mu\cdot J = -[\mu_x J_x + \mu_z J_z]$ and $g_3' = \mu_x' p_t J_x + \mu_z' p_t J_z$, the chromaticities, Eq. 26. The factorization of $e^{:g_3:}$ into $e^{:g_3':}e^{:g_3:}$ can be done trivially because we restrict ourselves to 3rd order in the map. Because $[J_i^n, J_j^m] = 0$, we can easily combine g_2 and g_3' into a single exponent as $-\hat{\mu}\cdot J = -\mu\cdot J + p_t\mu'\cdot J$ where $\hat{\mu} = \mu - p_t\mu'$, *i.e.* the new tune is energy dependent. The tune-shifted resonance occurs when $(\mathbf{n}-\mathbf{m})\cdot\hat{\mu} = 0$. The sextupole driving term, $\hat{g}_3$ is given by

$$\begin{aligned} \hat{g}_3 \;=\; & -S_x\pi\frac{\sqrt{2k_x}}{4}k_z J_x^{1/2}\left[e^{i\varphi_x} + e^{-i\varphi_x}\right]\times \\ & J_z\left[e^{2i\varphi_z} + e^{-2i\varphi_z}\right]. \end{aligned} \tag{29}$$

In order to understand the topology of this resonance it is convenient to transform to the "co-moving" frame[8]. This transformation is defined by the expression

$$\phi_1 = \mathbf{k}\cdot\varphi; \quad (\mathbf{n}-\mathbf{m}) = \lambda\mathbf{k}, \quad \lambda = \text{integer} \tag{30}$$

and

$$K_1 = \frac{\mathbf{k}\cdot J}{\|\,\mathbf{k}\,\|^2}, \quad K_2 = \frac{\mathbf{a}\cdot J}{\|\,\mathbf{a}\,\|^2} \tag{31}$$

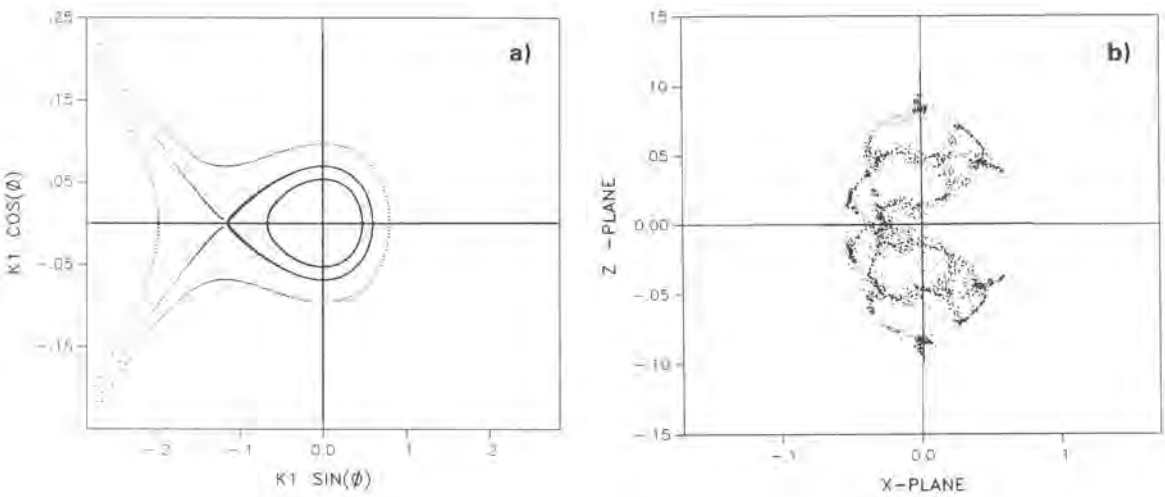


Figure 1. Phase-space plots for the $\nu_x = 2\nu_z$ resonance where $\hat{\nu}_x = 1.195$, $\hat{\nu}_z = 0.6025$ and the normalized sextupole strength is 1.700 units; $J_x = 0.0004$, $J_z = 0.0025$. a) shows the position of the fixed point at $\phi_1 = \pi$, the separatrix, and trajectories inside and outside the separatrix in order to illustrated the topology. b) x *vs* z projection in the original space. The parameters place the orbits very close to the separatrix.

where $\mathbf{a}$ is orthogonal to $\mathbf{k}$, $(\mathbf{k}\cdot\mathbf{a} = 0)$. In our case $\lambda = 1$. Hence,

$$\phi_1 = \varphi_x - 2\varphi_z \text{ and } \phi_2 = 2\varphi_x + \varphi_z \tag{32}$$

where $\mathbf{k} = (1, -2)$ and $\mathbf{a} = (2, 1)$. Thus,

$$K_1 = \frac{J_x - 2J_z}{5}, \quad K_2 = \frac{2J_x + J_z}{5}. \tag{33}$$

The transformation to the co-moving frame is effected by the transformation[8)]

$$\mathcal{N}_c = e^{:2\pi\ell K_1:}\mathcal{N} = e^{:2\pi\ell K_1:}e^{:-\vec{\mu}\cdot\vec{J}:}e^{:\tilde{g}_3:}e^{:\propto p_t^3:} \tag{34}$$

where $2\pi\ell = \mathbf{k}\cdot\mu$. In our case $\ell = 0$, and the transformation is the identity map. We want to expand about the resonance, that is we assume that we are not quite on resonance, and write $\mathbf{k}\cdot\mu = 2\pi(\nu_x - 2\nu_z) = \delta$. Hence

$$\mathcal{N}_c = e^{:-\delta K_1 - \mu\cdot a\, K_2:}e^{:\tilde{g}_3:}e^{:\propto p_t^3:} \tag{35}$$

where $\tilde{g}_3$ is in the co-moving coordinates;

$$\begin{aligned}\tilde{g}_3 \;=\; & -S_x\pi k_z\frac{\sqrt{2k_x}}{2}\left[K_1 + 2K_2\right]^{1/2} \times \\ & \left[K_2 - 2K_1\right]\left[e^{i\phi_1} + e^{-i\phi_1}\right].\end{aligned} \tag{36}$$

We note that there is no ϕ_2 dependence. Thus we have reduced the apparently two-dimensional resonance into a one-dimensional form with parameter K_2. If we combine exponents in Eq. 34 so that

$$\mathcal{N}_c = e^{:-\delta K_1 - \mu\cdot a\, K_2:}e^{:\tilde{g}_3:}e^{:\propto p_t^3:} = e^{:h:}e^{:\propto p_t^3:} \tag{37}$$

we obtain the "pseudo-Hamiltonian" h. The fixed points of the resonance can be found in the usual way by setting $\zeta = \mathcal{M}\zeta$, which reduces to

$$\frac{\partial h}{\partial K_1} = 0 \text{ and } \frac{\partial h}{\partial \phi_1} = 0, \tag{38}$$

the usual condition for a fixed point if h were the real Hamiltonian. This leads to[‡]

$$\tan(\phi_1) = -\frac{1-\cos(\delta)}{\sin(\delta)} \simeq \frac{1}{2}\delta \ll 1 \tag{39}$$

and

$$\frac{2\pi k_z\sqrt{2k_x}S_x[6K_1 + 7K_2] - \delta\sqrt{K_1 + 2K_2}}{\sqrt{K_1 + 2K_2}} = 0 \tag{40}$$

which has the solutions

$$\phi_1 = \{0, \pi\} \quad \text{and} \quad K_1 = \pm\frac{\delta\sqrt{15K_2}}{72\pi k_z\sqrt{k_x}S_x} - \frac{7K_2}{6} \tag{41}$$

where we have neglected terms of order δ^2 in the expansion of the trigonometric functions. The topology of this resonance is rather complicated, being a function of δ, S_x, and K_2. The *level sets* of the pseudo-Hamiltonian

[‡]In the non-Lie-algebraic treatment one usually obtains a sine rather than a tangent; since δ is assumed small the two results are equivalent to first order.

define the contours of normalized phase space and the level set that passes through the hyperbolic fixed point defines the *separatrix* of the resonance.

A phase-space plot for the $\nu_x = 2\nu_z$ resonance where $\hat{\nu}_x = 1.195$, $\hat{\nu}_z = 0.6025$ is shown in Fig. 1; $\hat{\nu}$ is the tune associated with the chromaticity-shifted phase advance $\hat{\mu}$. Fig. 1 shows the position of the fixed point at $\phi_1 = \pi$ and the separatrix, along with trajectories inside and outside the separatrix in order to illustrate the topology. Here we are working in the Cartesian equivalent of K_1, ϕ_1 space. This plot was generated by iterating the map, $\mathcal{M}$, 3000 times, which is approximately equivalent to Eq. 23,

$$\mathcal{M}^n = \mathcal{A}^{-1}\mathcal{N}^n\mathcal{A} = \mathcal{A}^{-1}e^{:nh:}\mathcal{A} \qquad (42)$$

except that the iterated map generates higher order non-linearities by "feed-up" which Eq. 42 does not do.

4.3. One-third Integer Resonance

In a 3-sector cyclotron, we have 3-fold symmetry in the magnetic field. Since $\nu_x \simeq 1$, the radial phase advance per cell is $\mu_x \simeq 2\pi/3$ and we see from Eq. 21 that if $n_1 - m_1 = 3$, we will have a resonant condition. For the purposes of this discussion, we will treat the θ-dependence of the sextupole and octupole fields in the "*kick*" approximation. In this approximation, the map for 1/3 of a turn can be written immediately in factored form as

$$\mathcal{M}(2\pi/3) = e^{:f_2:}e^{:f_3:}e^{:f_4:} \qquad (43)$$

where

$$f_3 = \frac{S_x x^3}{3r_0} \quad \text{and} \quad f_4 = \frac{O_x x^4}{6r_0},$$

and O_x is the octupole strength; we assume that $z = 0$. If we transform $\mathcal{M}(2\pi/3)$ into normal form, we obtain

$$\begin{aligned} g_3 &= S_x\frac{\sqrt{2}}{4}J_x^{3/2}\left[e^{3i\varphi_x} + e^{-3i\varphi_x}\right] \\ g_4 &= 4\left[O_x + \kappa S_x^2\right]J_x^2 \end{aligned} \qquad (44)$$

where κ is a factor that comes from "feed-up" from the iterated sextupole field (*i.e.* the generation of higher order non-linearities or aberrations from the repeated passage through lower order non-linear elements). The octupole component has no resonant term for a 3-fold symmetric machine, but does generate a tune-shift term. Note also that the "feed-up" term is of order S_x^2. If we neglect the g_4 component for the moment, and carry through the transformation to the co-moving frame as was done in section 4.2, we obtain the pseudo-Hamiltonian and the equations for the fixed points of the one-third integer resonance,

$$h \simeq \delta J_x - S_x\delta\frac{3\sqrt{2}}{4}\frac{\cos(3\varphi_x)\sin(3\delta)}{1-\cos(3\delta)} + \mathcal{O}(S_x^2), \qquad (45)$$

$$\begin{aligned} \frac{\partial h}{\partial \varphi_x} &\simeq \sin(3\varphi_x) = 0, \\ \frac{\partial h}{\partial J_x} &\simeq 1 - S_x\frac{9\sqrt{2J_x}}{8}\frac{\cos(3\varphi_x)\sin(3\delta)}{1-\cos(3\delta)} = 0 \end{aligned} \qquad (46)$$

where $\delta = 2\pi\ell - \mathbf{k}\cdot\mu$ with $\mathbf{k} = (3,0)$, and $\ell = 1$. (Here, $K_1 = J_x$ and $\phi_1 = 3\varphi_x$, but it is convenient to work with the original variables) This has the well-known solutions

$$\varphi_x = \{\pi/3, 2\pi/3, 5\pi/3\}, \quad J_x = \left[\frac{2\sqrt{2}\delta}{3S_x}\right]^2. \qquad (47)$$

A phase space plot for the one-third integer resonance is shown in Fig. 2a, where we have truncated the map to third order, *i.e.* only the g_3 term is included. Addition of the octupole component just adds the term $a_x J_x^2 = 4[O_x + \kappa S_x^2]J_x^2$ to the pseudo-Hamiltonian, h, Eq. 45. This term is a "tune-shift with amplitude" term (see Eq. 22) and as can be seen from Fig. 2b has a profound effect on the stability of the orbits in this example. (The strength of the octupole was chosen to be very large in the example so as to clearly illustrate the effect.) It is clear from Eq. 46 that the angles of the fixed points are unchanged by addition of the octupole, but their actions are altered. The latter are given by

$$J_x = \frac{9S_x^2 + 32a_x\delta^2 - 3\mid S_x\mid\sqrt{9S_x^2 + 64a_x\delta^2}}{64a_x^2\delta^2}. \qquad (48)$$

Equation 48 reduces to Eq. 47 as $a_x \to 0$. Although there are two solutions to the fixed point equation, Eq. 38, only one of them is physically meaningful.

In this section, we have used simplified models of the magnetic field of a cyclotron in order to illustrate the power of the Lie-algebraic method. In a real cyclotron, A_θ is a complicated function of θ, r and z. However with DA, we can accurately calculate the non-linear behaviour to high order, and transform the Taylor series into normal form in the Lie-algebraic representation; this gives us precise values for the tune shifts and resonance driving terms. These terms along with the type of analysis discussed above allows us to analyse and understand the effects of the non-linearities on the orbit dynamics of the machine in a very sophisticated manner.

5. CONCLUSIONS

In conclusion, we believe that the symbiosis of differential algebra and the Lie-algebraic methods provides a box of very powerful tools for analyzing and understanding the orbit dynamics of cyclotrons up to very

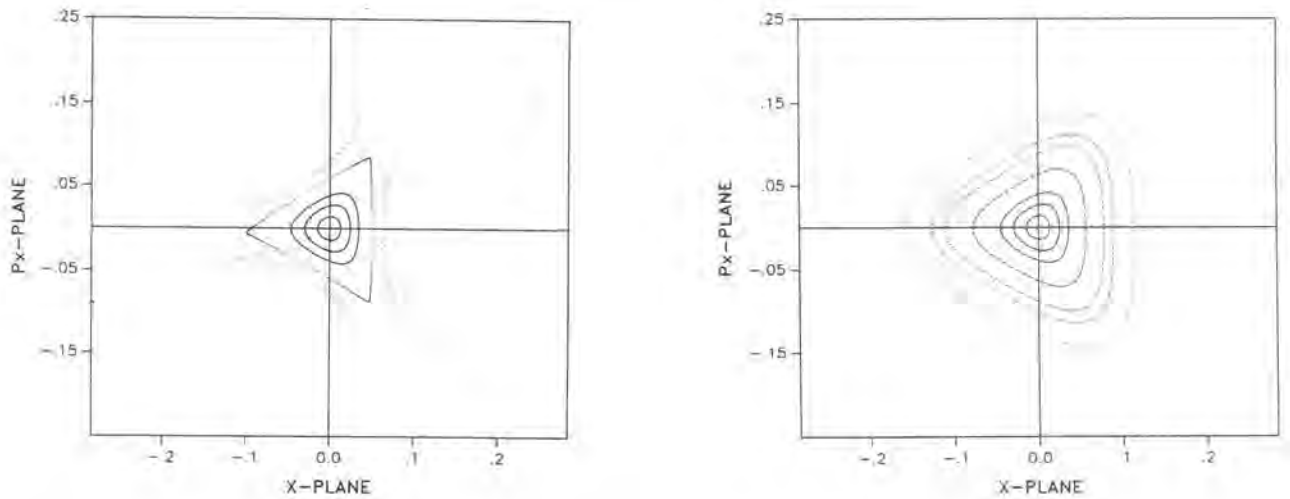


Figure 2. Phase-space plots for the "*one-third integer*" resonace where $\nu_x = 1.014$ $(\mu_x = 0.338(2\pi))$ for various values of the initial action, J_x. a) normalized sextupole strength $S_x = -0.372$, and octupole strength $O_x = 0$. b) $S_x = -0.372$,, and $O_x = -2.0$.

high orders. Although cyclotrons are only quasi-periodic devices, *maps* still provide significant advantages over tracking in terms of speed, accuracy, and the ability to analyse many orbit-dynamical properties and in particular resonances. The analysis of resonances is accomplished very elegantly by the normal form transformations. Differential algebra is essential for the efficient computation of the maps and of the normal form transformation.

6. ACKNOWLEDGEMENTS

It is a pleasure to acknowledge many fruitful discussions with Stephen Douglas and Gordon Pusch. Thanks also to Margaret Carey and Gordon Pusch for their assistance in preparing and typesetting this manuscript using LaTeX.

7. REFERENCES

1) Heighway, E.A. & Hoffmann, C.R., "Supergoblin — The Accelerated Orbit Code in use for the Chalk River Superconducting Cyclotron", IEEE Trans. on Nucl. Sci. **NS-32**, 2522 (1885).

2) Berz, M., "Differential Algebraic Description of Beam Dynamics to Very High Order," Part. Accel **24** 109 (1989); Douglas, S.R. "Automatic Differentiation of Functions," (AECL report AECL-10139, 1990); Pusch, G.D., "Theory and Application of Differential Algebra," (TASCC-P-92-6, unpublished); Rvachev, V.L., Man'ko, G.P. & Fed'ko, V.V., "Technology of Differentiating Functions of Many Variables on an Electronic Computer," Kibernetika, **5**, 31 (1983).

3) Press, W.H. *et al*, **Numerical Recipes** (Cambridge Univ. Press, Cambridge, 1986), Ch. 15.

4) Davies, W.G., Douglas, S.R., Pusch, G.D., Lee-Whiting, G.E., "The Chalk River Differential Algebra Code 'DACYC' and the Role of Differential and Lie Algebras in Understanding the Orbit Dynamics of Cyclotrons," **Proc. of the Inter. Workshop on Nonlinear Prob. in Accel. Phys.**, Berlin, (Adam Hilger, Bristol, (to be published)) Davies, W.G., Douglas, W.R., Pusch, G.D., Lee-Whiting, G.E., "Application of Differential-and-Lie-Algebraic Techniques to the Orbit Dynamics of Cyclotrons," IEEE Part. Acc. Conf. 91CH3038-7, 303–5 (1991).

5) Davies, W.G., "Useful Forms of the Hamiltonian for Ion-Optical Systems," (AECL report AECL-10364, 1991).

6) Forest, É., Berz, M. & Irwin, J., "Normal Form Methods for Complicated Periodic Systems," Part. Acc. **24**, 91 (1989).

7) Dragt, A.J., Neri, F., Rangarajan, G., Douglas, D., Healy, L.M., & Ryne, R.D., "Lie Algebraic Treatment of linear and Nonlinear Beam Dynamics," Ann. Rev. Nucl. Part. Sci. **38**, 455 (1988).

8) Forest, É. & Irwin, J., "Single Resonance Theory with Maps," **Proceedings of the workshop on Non-Linear Problems in Future Part. Acc.**, Capri, Italy, 1990.

9) Pusch, G.D. (private communication). An analogous problem is treated in Pusch, G.D. "Differential Algebraic Methods for Obtaining Approximate Numerical Solutions to the Hamilton-Jacobi Equation" (Ph.D. Dissert., 1990)

10) Arnol'd V.I., **Mathematical Methods of Classical Mechanics**, (Springer-Verlag, New York, 1989) Ch. 8.

THE INFLUENCE OF MAGNETIC FIELD IMPERFECTIONS ON THE BEAM QUALITY IN AN H⁻ CYCLOTRON

W.J.G.M. Kleeven and H.L. Hagedoorn
Eindhoven Univ. of Technology, Cyclotron Lab., P.O. Box 513, 5600 MB Eindhoven, Netherlands
B.F. Milton and G. Dutto
TRIUMF, 4004 Wesbrook Mall, Vancouver, B.C., Canada, V6T 2A3

ABSTRACT

The Hamiltonian formalism is used to derive tolerances for the magnetic field errors in an H⁻ cyclotron in order that emittance growth due to precessional mixing or vertical amplitude growth stay below specified limits. The resonances $\nu_r = 1$, $2\nu_r = 2$, $2\nu_z = 1$, $\nu_r = 2\nu_z$ and $\nu_r + 2\nu_z = 2$ are considered. Emittance growth mainly results from the $\nu_r = 1$ and $2\nu_r = 2$ resonances. The other resonances may cause vertical beam blow up. The 30 MeV isotope production cyclotron TR30[1] is used as an example. All resonances studied have in common that $\nu_r \approx 1$ and $\nu_z \approx 0.5$ as is the case for all the important resonances in TR30.[2] The resonances are driven by errors in the vertical field. Besides that, the effect of radial field errors in the median plane on emittance is considered.

1. INTRODUCTION

Magnetic field errors in a cyclotron excite coherent oscillations of the beam because they displace the central orbit or they distort the transverse phase space. The total phase advance of these oscillations at extraction will differ for different turn numbers. In an H⁻ cyclotron, because of rf phase spread, there usually are a number of different turns in the extracted beam and therefore the coherent oscillations cause an apparent increase of the emittance (precessional mixing or betatron phase mixing). This is of importance also because a larger emittance gives a larger energy spread in the extracted beam. The effect does not only depend on the magnitude of the field errors but also on the radial area in which they occur.

2. THE $\nu_r = 1$ RESONANCE

The $\nu_r = 1$ is a one-dimensional resonance that is driven by a first harmonic field error. The Hamiltonian describing this resonance is given by[3]

$$H = (\nu_r - 1)I + \tfrac{1}{2}\sqrt{2I}(A_1 \cos\phi + B_1 \sin\phi), \qquad (1)$$

where the azimuth θ is the independent variable, the action variable I is the generalized coordinate, the angle variable ϕ is the generalized momentum, $A_1 = C_1 \cos\psi_1$, and $B_1 = C_1 \sin\psi_1$ are the relative first harmonic field components and ν_r is the radial oscillation frequency. In most important order the radial phase space coordinates x, p_x and the orbit centre coordinates x_c, y_c are related to the action-angle variables by

$$x = r_0\sqrt{2I}\cos(\phi - \theta) \quad , \quad p_x = \sqrt{2I}\sin(\phi - \theta),$$

$$x_c = r_0\sqrt{2I}\cos\phi \quad , \quad y_c = r_0\sqrt{2I}\sin\phi.$$

From Eq. (1) it follows that the first harmonic excites a coherent oscillation with an amplitude

$$\Delta x_e = \tfrac{1}{2} r_0 C_1 / |\nu_r - 1|. \qquad (2)$$

The phase advance per turn of this oscillation is $\Delta\phi = 2\pi(\nu_r - 1)$, so for a turn spread at extraction of $\Delta n = 1/(\nu_r - 1)$ there is complete mixing ($\Delta\phi = 2\pi$). If the beam is initially matched and ϵ is the initial emittance, then the circulating emittance after complete mixing is (see Fig. 1)

$$\epsilon_c = \epsilon(1 + \Delta x_e / x_0)^2,$$

where x_0 is the initial beam size, related to the normal-

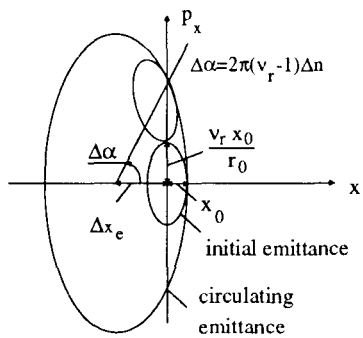


Figure 1. *Emittance growth due to a first harmonic perturbation*

ized injected emittance $\epsilon_n = \beta\gamma\epsilon$ as

$$x_0 = \left(\frac{r_0\epsilon_n}{\pi\nu_r\beta\gamma}\right)^{\frac{1}{2}} = \left(\frac{\lambda\epsilon_n}{\pi\nu_r}\right)^{\frac{1}{2}},$$

where $\lambda = m_0 c/qB_0$. If the maximum allowed emittance growth factor is denoted by $f_m = (\epsilon_c/\epsilon)_{max}$ then the maximum allowable beam shift is

$$\Delta x_e \le (f_m^{\frac{1}{2}} - 1)\left(\frac{\lambda\epsilon_n}{\pi\nu_r}\right)^{\frac{1}{2}}. \qquad (3)$$

This formula together with Eq. (2) gives an upper limit for the first harmonic amplitude, assuming a coasting beam.

If the beam is not coasting but accelerated to an outer radius then the field properties may change with

radius. In order to take this effect into account the orbit centre equations are derived with turn number n as independent variable. These are given by

$$\frac{dx_c}{dn} = \eta y_c + \pi r_0 B_1 \ , \quad \frac{dy_c}{dn} = -\eta x_c - \pi r_0 A_1 ,$$

where $\eta = 2\pi(\nu_r - 1)$. Assuming smooth acceleration[4] and an isochronous magnetic field, n and r_0 are related as follows

$$n = \alpha r_0^2, \quad \text{with} \quad \alpha = \tfrac{1}{2} q^2 \bar{B}^2/(m_0 \Delta E_{turn}), \qquad (4)$$

where $\bar{B}$ is the average magnetic field and ΔE_{turn} is the energy gain per turn. Note that ΔE_{turn} still depends on the rf phase of the particle. The orbit centre equations can be integrated for arbitrary radius dependence of ν_r, A_1 and B_1. Assuming an initially centered beam ($x_c(0) = y_c(0) = 0$), the orbit centre at radius r_0 is

$$x_c = -2\pi\alpha \int_0^{r_0} \bar{r}^2 C_1(\bar{r}) \sin\left[\Delta\phi(r_0) - \Delta\phi(\bar{r}) - \psi_1(\bar{r})\right] d\bar{r},$$

$$y_c = -2\pi\alpha \int_0^{r_0} \bar{r}^2 C_1(\bar{r}) \cos\left[\Delta\phi(r_0) - \Delta\phi(\bar{r}) - \psi_1(\bar{r})\right] d\bar{r},$$

where $\Delta\phi(r_0)$ is the total phase advance of the betatron oscillation between $r = 0$ and r_0

$$\Delta\phi(r_0) = 4\pi\alpha \int_0^{r_0} \bar{r}(\nu_r(\bar{r}) - 1) d\bar{r} = \int_0^n \eta(\bar{n}) d\bar{n}.$$

The distance at radius r_0 of the orbit centre to the origin is given by

$$R = 2\pi\alpha\Big[\Big(\int_0^{r_0} \bar{r}^2 C_1(\bar{r}) \sin(\Delta\phi(\bar{r}) - \psi_1(\bar{r})) d\bar{r}\Big)^2 + \Big(\int_0^{r_0} \bar{r}^2 C_1(\bar{r}) \cos(\Delta\phi(\bar{r}) - \psi_1(\bar{r})) d\bar{r}\Big)^2\Big]^{\frac{1}{2}}. \qquad (5)$$

This represents a circle in orbit centre space which is covered with beam, if we assume complete mixing. The quantity R is equivalent with Δx_e used in Eqs. (2) and (3) but it will give a more accurate result. From Eqs. (3) and (5) it followed for TR30 that a constant first harmonic of 2 gauss would give a total emittance growth in the order of 50%.[2]

3. THE $2\nu_r = 2$ RESONANCE

The $2\nu_r = 2$ is a linear one-dimensional resonance that is driven by a second harmonic field error and its gradient. The Hamiltonian describing this resonance is[3]

$$H = I[(\nu_r - 1) + (\tfrac{1}{2} A_2 + \tfrac{1}{4} A_2') \cos 2\phi + (\tfrac{1}{2} B_2 + \tfrac{1}{4} B_2') \sin 2\phi],$$

where the prime denotes rd/dr and with I and ϕ defined in the previous section. It is convenient to put $B_2 \equiv 0$. The equations of motion for the orbit centre are given by

$$\frac{dx_c}{d\theta} = (C_0 - C_2) y_c, \quad \frac{dy_c}{d\theta} = -(C_0 + C_2) x_c,$$

where $C_0 = \nu_r - 1$ and $C_2 = \frac{1}{2} A_2 + \frac{1}{4} A_2'$. Thus, the frequency of the perturbed motion in orbit-centre space is given by

$$\nu_c = (C_0^2 - C_2^2)^{\frac{1}{2}}.$$

The motion becomes unstable if $|C_2| > |C_0|$. For TR30 the resonance is not crossed and therefore this instability is not expected to occur.

A more important effect is the distortion of the phase space. In the ideal case the orbit centre trajectories are circles, but with a second harmonic field error these become ellipses with aspect ratio $y_0/x_0 = ((C_0 + C_2)/(C_0 - C_2))^{\frac{1}{2}}$. To obtain a worst-case estimate of the emittance growth assume that at injection the beam is matched and there is no field error. The beam is accelerated through a region where there is a finite error and then again enters into an error free region. Assuming complete mixing the emittance growth becomes (see Fig. 2)

$$f = \frac{\epsilon_c}{\epsilon} = \frac{\pi y_0^2}{\pi x_0^2} = \frac{C_0 + C_2}{C_0 - C_2}.$$

For TR30 it followed that, for the emittance growth to be smaller than 100%, the second harmonic should be less than 50 gauss and the gradient less than 10 gauss/cm everywhere in the cyclotron.

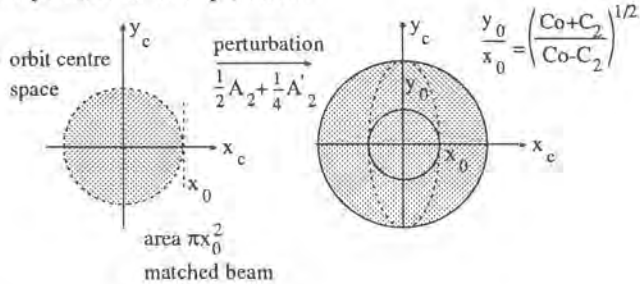


Figure 2. *Emittance growth due to a second harmonic perturbation*

4. THE $2\nu_z = 1$ RESONANCE

The $2\nu_z = 1$ is a linear resonance that is driven by the gradient of a first harmonic field error. Close to the median plane such a gradient produces a radial field component which is proportional to z. This component combines with the azimuthal velocity to give a vertical force that drives the Hill equation for z. The Hamiltonian for this resonance is

$$H = G[(\nu_z - \tfrac{1}{2}) - \frac{A_1'}{4\nu_z} \cos 2\psi - \frac{B_1'}{4\nu_z} \sin 2\psi]. \qquad (6)$$

The vertical phase space coordinates z, p_z are related to the action angle variables G, ψ as

$$z = r_0 \sqrt{2G/\nu_z} \cos(\psi - \tfrac{1}{2}\theta), \quad p_z = \sqrt{2G\nu_z} \sin(\psi - \tfrac{1}{2}\theta).$$

The Hamiltonian is a constant of motion. The curves H=constant describe the flowlines in phase space. For

$$|\nu_z - \tfrac{1}{2}| < \frac{1}{4\nu_z}\left(A_1'^2 + B_1'^2\right)^{\frac{1}{2}},$$

the flowlines are hyperbolas and the motion is unstable. The width Δr of the radial area that corresponds with this stopband of the resonance is given by

$$\Delta r = \left[\frac{2}{4\nu_z}\frac{(A_1'^2 + B_1'^2)^{\frac{1}{2}}}{d\nu_z/dr}\right]_{\nu_z=\frac{1}{2}}.$$

The number of turns in the resonance is $\Delta n = 2\alpha r \Delta r$ with α defined in Eq. (4). The amplitude of the vertical oscillation is $A_z = r_0\sqrt{2G/\nu_z}$. The amplitude growth per turn in the stopband is therefore determined by the Hamiltonian equation of motion for G. From this it follows that

$$\frac{1}{A_z}\frac{dA_z}{dn} = -\frac{\pi C}{2\nu_z}\sin(2\psi - \alpha_1),$$

where we introduced $A_1' = C\cos\alpha_1$, and $B_1' = C\sin\alpha_1$. For a worst-case estimate we can put $\sin(2\psi - \alpha_1) = -1$. Then

$$A_z = A_{z0}\exp(\tfrac{1}{2}\pi C\Delta n/\nu_z) \approx A_{z0}(1 + \pi C\Delta n),$$

with Δn the number of turns in the resonance. If one allows a maximum amplitude growth $a_m = (\Delta A_z/A_{z0})_{max}$ then this determines an upper limit for C which is given by

$$C < \sqrt{\frac{1}{r}\frac{d\nu_z}{dr}\frac{a_m}{2\pi\alpha}},$$

at the radius where $\nu_z = 0.5$. For TR30 the resonance is crossed at 30 cm with Δr=6.5 cm and Δn=15 turns; for an amplitude growth less than 50%, the gradient of the first harmonic at 30 cm should be less than 5 gauss/cm. At larger radii ν_z stays above but rather close to 0.5. Therefore there will again be emittance growth due to precessional mixing. Since $\nu_z \approx 0.5$, the Hamiltonian H as given in Eq. (6) can be used to study this effect. This Hamiltonian has exactly the same shape as the Hamiltonian for the $2\nu_r = 2$ resonance and therefore the same analysis as given in section 3 applies.

5. THE $\nu_r = 2\nu_z$ RESONANCE[5,6]

The $\nu_r = 2\nu_z$ is a two-dimensional nonlinear resonance that is driven by radial derivatives of the main field. The resonance does not cause instability but it exchanges energy between the horizontal and vertical betatron oscillations. Therefore, it may become dangerous if the horizontal beam quality is bad. In that case the vertical oscillation amplitude can become large and beam can be lost at the dees. If both $\nu_r \approx 1$ and $\nu_z \approx 0.5$ then the Hamiltonian for the resonance is

$$H = (\nu_r - 1)I + (\nu_z - \tfrac{1}{2})G - \frac{g''}{\nu_z}G\sqrt{2I}\cos(\phi - 2\psi),$$

where I, ϕ and G, ψ are the action-angle variables for the horizontal and vertical motion respectively, as defined in the previous sections. The quantity g'' is defined by

$$g'' = \frac{1}{4}(\bar{\mu}' + \bar{\mu}'' + \nu_z^2), \quad \bar{\mu}' = \frac{r}{\bar{B}}\frac{d\bar{B}}{dr}, \quad \bar{\mu}'' = \frac{r^2}{\bar{B}}\frac{d^2\bar{B}}{dr^2},$$

where $\bar{B}$ is the average magnetic field.

The quantity $2I$+G is a constant of motion. To show this, introduce new variables via the canonical transformation

$$\tilde{I} = I, \quad \tilde{\phi} = \phi - 2\psi, \quad \tilde{G} = 2I + G, \quad \tilde{\psi} = \psi.$$

The new Hamiltonian is given by

$$\tilde{H} = \Delta\nu\tilde{I} + (\nu_z - \tfrac{1}{2})\tilde{G} - g''\frac{(\tilde{G} - 2\tilde{I})\sqrt{2\tilde{I}}}{\nu_z}\cos\tilde{\phi},$$

where $\Delta\nu = \nu_r - 2\nu_z$. This Hamiltonian does not depend on $\tilde{\psi}$ and therefore $\tilde{G}$ is a constant of motion

$$2I + G = \frac{1}{r_0^2}(x_0^2 + \frac{\nu_z}{2}z_0^2) = J_0 = \text{constant} > 0, \qquad (7)$$

where x_0 and z_0 are the amplitudes of the betatron oscillations. It is convenient to scale the action variable $\tilde{I}$ as follows

$$\rho = \frac{2\tilde{I}}{J_0} = \frac{(x_0/r_0)^2}{J_0}, \quad (0 < \rho < 1).$$

Then, for a given value of $\tilde{G} = J_0$ the scaled Hamiltonian for ρ and $\tilde{\phi}$ becomes

$$K = \frac{2\tilde{H}}{J_0} = \Delta\nu\rho - \kappa\sqrt{\rho}(1 - \rho)\cos\tilde{\phi}, \qquad (8)$$

where the parameter $\kappa = 2g''\sqrt{J_0}/\nu_z$ is the excitation width of the resonance. It is related to the radial width of the stopband by

$$\Delta r = \frac{2\kappa}{d(\Delta\nu)/dr} = 2\kappa/(\frac{d\nu_r}{dr} - 2\frac{d\nu_z}{dr}).$$

The number of turns in the resonance is $\Delta n = 2\alpha r\Delta r$ with α defined in Eq. (4). The amplitude growth per turn in the stopband is determined by the Hamiltonian equation for ρ. From Eqs. (7) and (8) we obtain

$$\frac{dx_0}{dn} = \pi g''\frac{z_0^2}{r_0}\sin\tilde{\phi}, \quad \frac{dz_0}{dn} = -\frac{2\pi g''}{\nu_z}\frac{x_0 z_0}{r_0}\sin\tilde{\phi}.$$

The worst case estimate is obtained if the right-hand-sides of these equations are at maximum. This gives with $\nu_z = 0.5$

$$\left(\frac{dx_0}{dn}\right)_{max} = \left(\frac{dy_0}{dn}\right)_{max} = 4\pi g'' r_0 J_0.$$

From the previous analysis it is clear that the properties of the resonance depend on the beam sizes. For the initial design of TR30 the resonance would be crossed at 62.5 cm. For an estimated initial horizontal betatron amplitude of x_0=5 mm and a vertical amplitude z_0=3 mm the maximum vertical beam size after crossing the resonance (as obtained with Eq. (7)) would be z_{max}=10 mm, i.e. a maximum vertical blow-up with a factor three. Since the resonance was not in the fringe field, the value of g'' was relatively small ($g'' \approx 0.4$). This resulted in an excitation width $\kappa \approx 1.5 \times 10^{-2}$ a stopband-width of 3 cm, 13 turns in the stopband and a maximum amplitude growth per turn of 0.25 mm. Although the resonance did not seem to be too dangerous, it nevertheless was decided to avoid it by lowering the vertical tune.

6. THE $\nu_r+2\nu_z= 2$ RESONANCE

The $\nu_r + 2\nu_z = 2$ is a two-dimensional nonlinear resonance which is driven by a second harmonic field error and its gradients. If $\nu_r \approx 1$ and $\nu_z \approx 0.5$ then the resonance is described by the Hamiltonian

$$H = (\nu_r - 1)I + (\nu_z - \tfrac{1}{2})G - a''G\sqrt{2I}\cos(2\psi + \phi - \alpha),$$

where a'' and α are defined by

$$a'' \cos\alpha = \frac{A_2'' + A_2' - 2A_2}{8\nu_z}, \quad a'' \sin\alpha = \frac{B_2'' + B_2' - 2B_2}{8\nu_z}.$$

The treatment is similar as for the $\nu_r = 2\nu_z$ resonance. Now, the quantity $J = 2I - G$ is a constant of motion. The resonance is a sum resonance and therefore the motion can become unstable (i.e. unbounded). For TR30 it was not considered a dangerous resonance because it is not driven by the main field but by perturbations so that a'' is small. Assuming the same initial beam sizes as for the $\nu_r = 2\nu_z$ resonance and $a'' < 0.1$, then is $\Delta r < 2$ cm, $\Delta n < 4$ turns and $\Delta z_0 < 0.06$ mm/turn.

7. RADIAL FIELD COMPONENTS IN THE MEDIAN PLANE

A radial component of the magnetic field in the median plane combines with the azimuthal velocity to give a force in the vertical direction. The kth cosine component $B_{r,k}$ in the Fourier expansion of the radial median plane field drives the Hill equation for z as follows

$$\frac{d^2z}{d\theta^2} + \nu_z^2 z = \frac{r_0}{\bar{B}} B_{r,k} \cos k\theta, \qquad (9)$$

where r_0 is the radius in the cyclotron and $\bar{B}$ is the average magnetic field. The solution of Eq. (9) for a beam that initially is in the median plane ($z(0) = \dot{z}(0) = 0$) is given by

$$z(\theta) = \frac{r_0 B_{r,k}}{\bar{B}(\nu_z^2 - k^2)} (\cos k\theta - \cos \nu_z\theta). \qquad (10)$$

Thus, the radial field perturbation induces a vertical coherent oscillation. If ν_z approaches an integer ($\nu_z \approx k$), then a resonance can be excited. For TR30 this is not the case since $\nu_z \approx 0.5$ everywhere in the cyclotron. However, emittance growth due to precessional mixing once more is of importance. Since $\nu_z \approx 0.5$ only a few turns in the extracted beam will already give complete mixing. The phase advance of the $\cos k\theta$ term in Eq. (10) is equal for different turns and therefore this term can be ignored. The phase advance of the second term $\cos \nu_z\theta$ in Eq. (10) depends on turn number. The same analysis as given in section 2 for the horizontal motion applies for the vertical motion. Thus, if the maximum allowed emittance growth factor is $f_m = (\epsilon_c/\epsilon)_{max}$ then the allowable vertical beam shift is

$$\Delta z = \frac{r_0 B_{r,k}}{\bar{B}(\nu_z^2 - k^2)} < (f_m^{\frac{1}{2}} - 1)\left(\frac{\lambda\epsilon_n}{\pi\nu_z}\right)^{\frac{1}{2}}.$$

The effect of the perturbation rapidly drops with increasing k. For TR30 only the cases $k = 0$ (an average radial field component) and $k = 1$ (a first harmonic radial field component) are important. Allowing 50% emittance growth the average radial field value at extraction (where the effect is most pronounced) should be less than 5 gauss and the first harmonic less than 12 gauss.

8. REFERENCES

1) Milton, B.F., et. al., "First beam in a new compact intense 30 MeV H$^-$ cyclotron for isotope production", 2nd Europ. Part. Acc. Conf., p. 1812, Rome (1990).
2) Kleeven, W.J.G.M., "The influence of magnetic field imperfections on the transverse orbit behaviour in the TR30 H$^-$ cyclotron", TRIUMF Design Note TR30-DN-15 (1988).
3) Hagedoorn, H.L. and Verster, N.F., "Orbits in an AVF cyclotron", Nucl. Instr. Meth. **18,19**, 201 (1962).
4) Nieuwland, J.M. van, "First and second harmonic extraction", Proc. 5th. Int. Cycl. Conf., Oxford 1969, p. 215.
5) Hagedoorn, H.L. and Kramer, P., "Extraction studies in an AVF cyclotron", Int. Conf. Isochronous Cyclotrons, Gatlinburg, Tennessee, 1966, p. 64.
6) Joho, W., "Extraction of a 590 MeV proton beam from the SIN Ring Cyclotron", thesis, SIN report TM-11-8, 1970.

EMITTANCE GROWTH IN NONLINEAR BEAM GUIDING AND FOCUSING ELEMENTS

W.J.G.M. Kleeven, J.L. Delhez, J.I.M. Botman, G.A. Webers, C.J. Timmermans and H.L. Hagedoorn
Eindhoven Univ. of Technology, Cyclotron Lab., P.O. Box 513, 5600 MB Eindhoven, Netherlands

ABSTRACT

An analytical calculation is presented of rms emittance growth. The main assumption made is, that the beam divergence is small so that a thin lense approximation can be used when integrating the beam through the optical element. General results are obtained for an optical element with dipole, quadrupole, sextupole and octupole field components. Even higher order multipoles can easily be included. The effect of momentum spread in the beam on emittance is also considered. The results are applicable to all kinds of beam guiding systems, including cyclotron injection lines. As an example, a special azimuthally varying racetrack microtron dipole magnet is considered.

1. INTRODUCTION

It is well known that the emittance of a beam, defined as the phase space area divided by π, is conserved. However, when the phase space deviates considerably from an elliptical shape, then the phase space area is not such a useful quantity to express the quality of the beam. A more practical quantity is the so-called root-mean-square (rms) emittance. The rms emittance is not always conserved. We will consider two sources of rms emittance growth namely nonlinearities in the beam guiding system and momentum spread in the beam. In the first case the emittance growth is caused by a nonlinear deformation of the phase space due to the fact that the transverse kick experienced by a particle is not proportional to its transverse position. In the second case the emittance growth is due to the fact that an off-momentum particle experiences a deviating bending angle and/or focusing force as compared to the reference momentum. The different sources of emittance increase are illustrated in Fig. 1.

2. ROOT MEAN SQUARE PROPERTIES OF THE BEAM

We consider the transverse phase space of the beam with the variables $\boldsymbol{x} = (x, p_x, y, p_y)$, where x and y are the spatial coordinates and p_x and p_y the divergences, i.e. the transverse kinetic momenta, scaled with respect to the total kinetic momentum of the particle. The rms sizes $\widetilde{x}$ and $\widetilde{y}$ of the beam are defined by $\widetilde{x} = \langle x^2 \rangle^{1/2}$ and $\widetilde{y} = \langle y^2 \rangle^{1/2}$ where the brackets denote averaging over the phase space. Note that for an unbunched beam with uniform elliptical cross-section the actual beam size is twice the rms value. The rms emittance in the x-p_x phase plane is defined as

$$\varepsilon_x = \left(\langle x^2 \rangle \langle p_x^2 \rangle - \langle x p_x \rangle^2 \right)^{1/2}. \qquad (1)$$

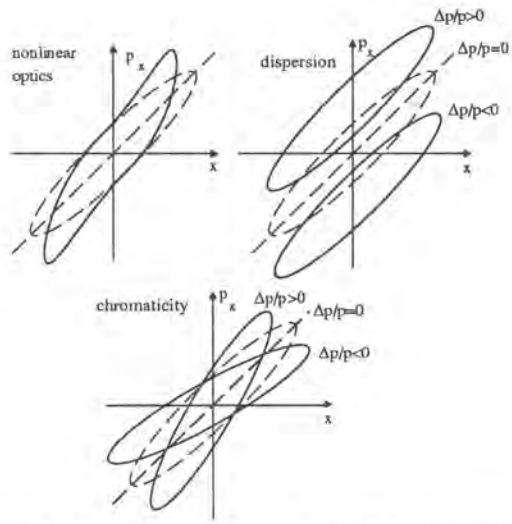


Figure 1. *A graphical illustration of three causes for emittance growth*

A similar definition holds for the y-p_y phase plane. To relate this definition with the phase space area occupied by the beam, we assume that the projected distributions have elliptical symmetry. For example in the x-p_x phase plane

$$f(x, p_x) = f(U) \quad \text{where} \quad U = cx^2 + 2axp_x + bp_x^2, \qquad (2)$$

with a, b and c arbitrary constants. For such an elliptical distribution, the number of particles $\overline{N}$ that is enclosed by an ellips with area $A = 4\pi\varepsilon_x$, is given by

$$\frac{\overline{N}}{N} = \int_0^{\lambda_{max}} f(\lambda) d\lambda \quad \text{with} \quad \lambda_{max} = 2 \int_0^{\infty} \lambda f(\lambda) d\lambda, \qquad (3)$$

where N is the total number of particles and where the normalization $\int_0^\infty f(\lambda)d\lambda = 1$ is assumed. In Table 1 the values of $\overline{N}/N$ are given for five distributions. A definition of these distributions has been given by Sacherer.[1)] For a uniform elliptical phase space distribution the actual area is 4π times the rms emittance. Therefore, the 'ordinary' emittance is approximately four times the rms emittance.

The beam envelopes $\widetilde{x}$ and $\widetilde{y}$ involve second order spatial moments of the beam. One can also define higher order spatial moments like $\langle x^4 \rangle$, $\langle x^2 y^2 \rangle$, $\langle x^6 \rangle$ etc. If the beam density profile is symmetric with respect to x and y, then the spatial moments odd in x or y are zero. The even spatial moments can be expressed in terms of the

Table 1. parameters $\overline{N}/N$, ξ_1 and ξ_2 as defined in Eqs. (3), and (6), respectively, for five distributions.

distribution	$\overline{N}/N$	ξ_1	ξ_2
uniform	1	1	1
linear	0.889	1.13	1.35
parabolic	0.914	1.07	1.19
gaussian	0.889	1.18	1.57
hollow	0.983	0.884	0.785

beam envelopes $\widetilde{x}$ and $\widetilde{y}$. For later use we calculate the spatial moments up to sixth order. For a beam profile with elliptical symmetry these are

$$\langle x^4\rangle = 2\xi_1\widetilde{x}^4, \quad \langle x^2y^2\rangle = \tfrac{2}{3}\xi_1\widetilde{x}^2\widetilde{y}^2, \tag{4}$$

$$\langle x^6\rangle = 5\xi_2\widetilde{x}^6, \quad \langle x^4y^2\rangle = \xi_2\widetilde{x}^4\widetilde{y}^2, \tag{5}$$

with ξ_1 and ξ_2 given by

$$\xi_1 = \frac{3}{4}\frac{\int_0^\infty \lambda^2 n(\lambda)d\lambda}{\left(\int_0^\infty \lambda n(\lambda)d\lambda\right)^2}, \quad \xi_2 = \frac{1}{2}\frac{\int_0^\infty \lambda^3 n(\lambda)d\lambda}{\left(\int_0^\infty \lambda n(\lambda)d\lambda\right)^3}, \tag{6}$$

and where n represents the beam density profile with $\int_0^\infty n(\lambda)d\lambda = 1$. The values of ξ_1 and ξ_2 for five profiles are given in Table 1. We note that the moments $\langle y^4\rangle$, $\langle x^2y^4\rangle$ and $\langle y^6\rangle$ are easily obtained from Eqs. (4) and (5) using symmetry considerations.

3. EMITTANCE GROWTH DUE TO NONLINEAR OPTICS

To calculate the emittance growth of the beam we treat the optical element as a nonlinear thin lense. In this assumption the transverse coordinates stay constant when the beam passes through the element and the divergences change by an amount that only depends on the initial transverse displacements. In most cases this approximation is accurate if $L\varepsilon_x/\widetilde{x} \ll \widetilde{x}$, where L is the length of the optical element. The left-hand-side of this unequality represents the transverse displacement of a particle with divergence $\varepsilon_x/\widetilde{x}$, after passing a drift of length L. This displacement must be small compared to the beam size.

Within the thin lense approximation the transformation of the phase space through the optical element can be written as

$$\overline{x} = x, \quad \overline{p}_x = p_x + g(x,y), \tag{7}$$

$$\overline{y} = y, \quad \overline{p}_y = p_y + h(x,y), \tag{8}$$

where x, p_x, y, p_y are the initial variables and $\overline{x}, \overline{p}_x, \overline{y}, \overline{p}_y$ the final variables. If the initial and final variables are canonical variables (which is the case for example if the entrance and exit are in a field-free region) then the Jacobian of the transformation must be a symplectic matrix. This then puts the condition $\partial g/\partial y = \partial h/\partial x$ on the functions g and h.

We can calculate the new emittance $\overline{\varepsilon}_x$ in the x-p_x plane by substitutings Eqs. (7) into Eq. (1). This gives

$$\overline{\varepsilon}_x^2 - \varepsilon_x^2 = \langle x^2\rangle\langle g^2\rangle - \langle xg\rangle^2 + 2\langle x^2\rangle\langle p_x g\rangle - 2\langle xp_x\rangle\langle xg\rangle. \tag{9}$$

This expression simplifies if the initial phase space distribution function (written in terms of the variables x and $p_x - \eta x$) possesses the following symmetry property

$$f(x, p_x - \eta x, y, p_y) = f(x, -p_x + \eta x, y, p_y), \tag{10}$$

where η is an arbitrary parameter. This symmetry property is illustrated graphically in Fig. 2. Note that the elliptically symmetric distribution given in Eq. (2) obeys Eq. (10) by choosing $\eta = -a/b$. For distributions obeying Eq. (10), the terms involving p_x in Eq. (9) cancel and the expression for emittance growth becomes

$$\overline{\varepsilon}_x^2 - \varepsilon_x^2 = \langle x^2\rangle\langle g^2\rangle - \langle gx\rangle^2. \tag{11}$$

A similar expression holds for the y-p_y phase plane. Since the function g depends on spatial coordinates, the right-hand-side of Eq. (11) only involves spatial moments. These are determined by the density profile of the beam.

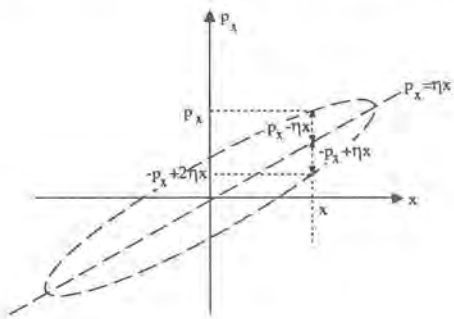


Figure 2. *Graphical illustration of the symmetry property of the phase space distribution function as assumed in the calculation of emittance growth.*

As an example, we calculate the emittance growth for an optical element that has the $y = 0$ plane as a symmetry plane. Then the function g must be even in y and the function h must be odd in y. These functions are expanded into a power series with respect to x and y. The most general expansion upto third degree is

$$g(x,y) = Ax + Bx^2 + Cy^2 + Dx^3 + Exy^2, \tag{12}$$

$$h(x,y) = Fy + Gxy + Hy^3 + Ix^2y, \tag{13}$$

where the quantities $A, B, \ldots, I$ are arbitrary constants. For a symplectic map they must obey the conditions $G = 2C$ and $I = E$. We insert Eq. (12) into Eq. (11)

and assume that the beam density profile has elliptical symmetry so that Eqs. (4) and (5) apply. The emittance growth formula then becomes

$$\begin{aligned}\overline{\varepsilon}_x^2 - \varepsilon_x^2 &= 2\xi_1[B^2\widetilde{x}^6 + \tfrac{2}{3}BC\widetilde{x}^4\widetilde{y}^2 + C^2\widetilde{x}^2\widetilde{y}^4] + \\ &+ (5\xi_2 - 4\xi_1^2)D^2\widetilde{x}^8 + 2(\xi_2 - \tfrac{4}{3}\xi_1^2)DE\widetilde{x}^6\widetilde{y}^2 + \\ &+ (\xi_2 - \tfrac{4}{9}\xi_1^2)E^2\widetilde{x}^4\widetilde{y}^4, \qquad (14)\end{aligned}$$

with the parameters ξ_1 and ξ_2 defined in Eqs. (6). As can be seen from this expression the emittance growth only depends on the nonlinear parts in the function g. This is true in general as can easily be shown from Eq. (11). Further note that there are no cross-correlations between sextupoles and octupoles. It can be shown in general that for an expansion upto arbitrary degree, there are no correlations between odd and even multipoles. The emittance growth in the y-direction is calculated in the same way as in the x-direction. For this we find

$$\begin{aligned}\overline{\varepsilon}_y^2 - \varepsilon_y^2 &= \tfrac{2}{3}\xi_1 G^2\widetilde{x}^2\widetilde{y}^4 + (\xi_2 - \tfrac{4}{9}\xi_1^2)I^2\widetilde{x}^4\widetilde{y}^4 \qquad (15)\\ &+ 2(\xi_2 - \tfrac{4}{3}\xi_1^2)HI\widetilde{x}^2\widetilde{y}^6 + (5\xi_2 - 4\xi_1^2)H^2\widetilde{y}^8.\end{aligned}$$

The results obtained so far will now be further specified for a nonlinear bending magnet.

4. EMITTANCE GROWTH IN A BENDING MAGNET

We use the Hamilton formalism to solve the equations of motion for a non-linear bending magnet within the thin-lense approximation. The transverse motion of a particle with respect to reference trajectory lying in the symmetry plane $y = 0$ is described by the Hamiltonian

$$\begin{aligned}H &= -(1+\frac{x}{\rho})\sqrt{P^2 - (P_x - qA_x)^2 - (P_y - qA_y)^2} \\ &\quad -q(1+\frac{x}{\rho})A_s, \qquad (16)\end{aligned}$$

where ρ is the radius of curvature of the reference trajectory, P is the kinetic momentum of the particle, P_x and P_y are the transverse canonical momenta and A_x, A_y, A_s are the components of the magnetic vector potential. The independent variable s is the distance along the reference trajectory. The scaled kinetic momenta p_x, p_y as introduced in section 2 are related to the canonical momenta P_x, P_y by the equations

$$p_x = \frac{P_x - qA_x}{P}, \qquad p_y = \frac{P_y - qA_y}{P}. \qquad (17)$$

In order to obtain equations of motion for the divergences p_x and p_y we first derive the canonical equations of motion from the Hamiltonian given in Eq. (16). The right-hand-sides of the canonical equations for P_x and P_y still contain the canonical momenta. These are eliminated in favour of dx/ds and dy/ds by using the canonical equations for x and y. Then the equations for dp_x/ds and dp_y/ds are obtained by differentiating Eqs. (17) with respect to s. The resulting equations express dp_x/ds and dp_y/ds in terms of x, y, dx/ds and dy/ds. Since in the thin-lense approximation the transverse coordinates stay constant, we can insert into these equations $dx/ds = 0$ and $dy/ds = 0$. The final result is then

$$\frac{dp_x}{ds} = \frac{1}{\rho} + \frac{q}{P}\left[\frac{A_s}{\rho} - \frac{\partial A_x}{\partial s} + (1+\frac{x}{\rho})\frac{\partial A_s}{\partial x}\right], \qquad (18)$$

$$\frac{dp_y}{ds} = \frac{q}{P}(1+\frac{x}{\rho})\frac{\partial A_s}{\partial y}. \qquad (19)$$

Expansions of the magnetic vector potential upto fourth degree have been given by Corsten.[2] The phase space map is obtained by inserting these expansions into Eqs. (18) and (19) and then integrating the particle through the magnet. Assuming that the entrance and exit are in a field-free region we get *

$$\begin{aligned}\overline{p}_x &= p_x - (\alpha+\overline{\alpha})x - \tfrac{1}{2}(\beta+2\overline{\beta})x^2 + \tfrac{1}{2}(\beta+\overline{\beta})y^2 \\ &- \tfrac{1}{6}(\gamma+\tfrac{5}{2}\overline{\gamma}+\tfrac{1}{2}\overline{\delta})x^3 + \tfrac{1}{2}(\gamma+\tfrac{3}{2}\overline{\gamma}+\tfrac{1}{2}\overline{\delta})xy^2, \qquad (20)\\ \overline{p}_y &= p_y + \alpha y + (\beta+\overline{\beta})xy - \tfrac{1}{6}(\gamma+\tfrac{1}{2}\overline{\gamma}-\tfrac{1}{2}\overline{\delta})y^3 \\ &+ \tfrac{1}{2}(\gamma+\tfrac{3}{2}\overline{\gamma}+\tfrac{1}{2}\overline{\delta})x^2y, \qquad (21)\end{aligned}$$

with the definitions

$$\begin{aligned}\alpha &= \frac{q}{P}\int\left(\frac{\partial B_y}{\partial x}\right)_0 ds, \quad \overline{\alpha} = \frac{q}{P}\int\frac{B_0}{\rho}ds,\\ \beta &= \frac{q}{P}\int\left(\frac{\partial^2 B_y}{\partial x^2}\right)_0 ds, \quad \overline{\beta} = \frac{q}{P}\int\frac{1}{\rho}\left(\frac{\partial B_y}{\partial x}\right)_0 ds,\\ \gamma &= \frac{q}{P}\int\left(\frac{\partial^3 B_y}{\partial x^3}\right)_0 ds, \quad \overline{\gamma} = \frac{q}{P}\int\frac{1}{\rho}\left(\frac{\partial^2 B_y}{\partial x^2}\right)_0 ds,\\ \overline{\delta} &= \frac{q}{P}\int\left(\frac{B_0''}{\rho} + \frac{1}{\rho^2}\left(\frac{\partial B_y}{\partial x}\right)_0\right)ds, \qquad (22)\end{aligned}$$

where the integration runs from the entrance to the exit of the magnet and where the prime denotes differentiation with respect to s. The quantity B_0 is defined as $B_0 = B_y(x = y = 0)$. The map through the magnet is symplectic. A comparison of Eqs. (20) and (21) with Eqs. (12) and (13) gives the relations between the parameters $A, B, \ldots, I$ as introduced in section 3 and the field quantities $\alpha, \beta, \ldots, \overline{\delta}$.

For a pure sextupole (only $\beta \neq 0$) and a round input beam ($\widetilde{x} = \widetilde{y}$) the emittance growth is given by

$$\overline{\varepsilon}_x^2 - \varepsilon_x^2 = \overline{\varepsilon}_y^2 - \varepsilon_y^2 = \tfrac{2}{3}\xi_1\beta^2\widetilde{x}^6. \qquad (23)$$

So, in order that the effects are small we must have $\beta \ll \varepsilon/\widetilde{x}^3$. If the input emittances are upright then this can be written as $\beta \ll \widetilde{p}_x/\widetilde{x}^2$ where $\widetilde{p}_x = \langle p_x^2\rangle^{1/2}$ is the rms divergence of the beam. For a pure octupole (only $\gamma \neq 0$) and a round input beam the emittance growth is given by

$$\overline{\varepsilon}_x^2 - \varepsilon_x^2 = \overline{\varepsilon}_y^2 - \varepsilon_y^2 = \tfrac{2}{9}\xi_2\gamma^2\widetilde{x}^8. \qquad (24)$$

*A sufficient assumption would be that at the entrance and exit first order derivatives of the field quantities with respect to s are zero, as is the case for example in a symmetry point of the magnet.

5. THE INFLUENCE OF MOMENTUM SPREAD

So far, a mono-energetic input beam was assumed. Momentum spread gives additional emittance growth, even if the optics in the bending magnet is linear. If the deviating momentum is $\delta = \Delta P/P$, then the functions g and h defined by Eqs. (7), (8), (20) and (21) should be replaced by functions $\overline{g}$ and $\overline{h}$ as follows:

$$\overline{g} = \frac{\delta\Delta\phi + g}{1+\delta}, \quad \overline{h} = \frac{h}{1+\delta}, \tag{25}$$

where $\Delta\phi$ is the total bending angle of the reference particle. To calculate the additional emittance growth it is convenient to assume that the distribution functions for the momentum spread and the transverse phase space are uncorrelated. Furthermore, since δ is small, only the most significant terms in δ and only the linear parts of the functions g and h are taken into account. Then the additional emittance growth due to momentum spread is

$$\overline{\varepsilon}_x^2 - \varepsilon_x^2 = \widetilde{\delta}^2\widetilde{x}^2[\Delta\phi^2 + (\alpha+\overline{\alpha})^2\widetilde{x}^2], \quad \overline{\varepsilon}_y^2 - \varepsilon_y^2 = \alpha^2\widetilde{\delta}^2\widetilde{y}^4, \tag{26}$$

where $\widetilde{\delta} = \langle\delta^2\rangle^{1/2}$ is the rms momentum spread and with α and $\overline{\alpha}$ defined in Eqs. (22).

6. AN EXAMPLE

As an application we consider the case of a racetrack microtron dipole magnet with an azimuthally varying median plane field. A microtron with such magnets is currently under construction in our laboratory.[3] In general, we may write the field map of such a magnet in polar coordinates (r,θ) as follows:

$$B_y(r,\theta) = \widehat{B}_y[1 + f(\theta)], \quad 0 \le \theta \le \tfrac{1}{2}\pi, \tag{27}$$

with $\widehat{B}_y$ the nominal field strength and $f(\theta)$ defining the (small) perturbing field profile. The orbits through this magnet start at $r = \theta = 0$ and it is assumed that the deviating field still provides for a 180° bend.

The Hamilton formalism has been applied to obtain an expression for the reference orbit through the above field map. From this we can derive expressions for the field gradients as a function of orbit length s. Since $f(\theta)$ is assumed to be small, all calculations are done first order in f. The coefficients $\alpha, \beta, \ldots, \overline{\delta}$ are calculated using Eq. (22). From these, the parameters $A, B, \ldots, I$ can be found and hence the emittance growth as described by the Eqs. (14) and (15). For a round beam we may write

$$\overline{\varepsilon}_x^2 - \varepsilon_x^2 = S_x\widetilde{x}^6 + O_x\widetilde{x}^8, \quad \overline{\varepsilon}_y^2 - \varepsilon_y^2 = S_y\widetilde{x}^6 + O_y\widetilde{x}^8, \tag{28}$$

where S_x, O_x, S_y, O_y define the sextupole and octupole contributions to the emittance growth in the x and y directions. As an example, we take the field profile

$$f(\theta) = \widehat{f}\sin^{10}(2\theta), \tag{29}$$

describing a smooth hill or valley, centered around $\theta = \frac{1}{4}\pi$ with a height or depth determined by $\widehat{f}$. Assuming a uniform distribution ($\xi_1 = \xi_2 = 1$), we get

$$S_x \approx 9\widehat{f}^2/R^4, \quad O_x \approx 900\widehat{f}^2/R^6, \tag{30}$$

where $R = P/(q\widehat{B}_y)$. The values for the y direction are of the same order of magnitude, so we will only consider the x direction. First of all, we note that the octupole component becomes significant when $\widetilde{x} \approx \sqrt{S_x/O_x} \approx 0.1R$. From this it may be concluded that in practical cases the octupole term can be neglected. Assuming that the emittance growth is small with respect to the initial emittance, we may rewrite Eq. (28) as follows

$$\frac{\Delta\varepsilon_x}{\varepsilon_x} \approx \frac{S_x\widetilde{x}^6}{2\varepsilon_x^2} = \frac{9\widehat{f}^2R^2}{2\varepsilon_x^2}\left(\frac{\widetilde{x}}{R}\right)^6, \tag{31}$$

expressing the relative change of the emittance as caused by the sextupole component only. For a numerical example, we choose values appropriate for our own microtron at injection energy, viz. $\varepsilon_x = 6$ mmmrad, $R = 0.10$ m, and $\widehat{f} = 0.5$. The result is plotted in Fig. 3. As can be

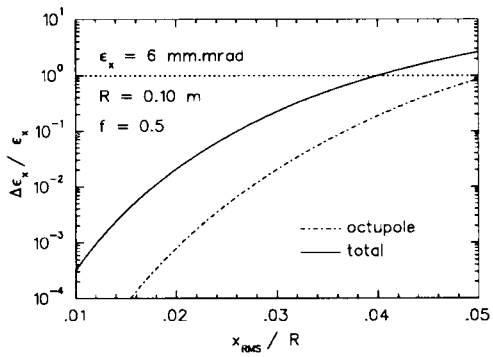


Figure 3. *Relative change of emittance in the x-direction as a function of scaled rms beam radius for a smooth hill or valley field profile.*

seen, the change of emittance is small for $\widetilde{x}/R < 0.02$, or a beam diameter of less than 8 mm. For completeness, the octupole term has been drawn as well, which has an effect that is approximately an order of magnitude smaller.

7. REFERENCES

1) Sacherer, F.J., "RMS envelope equations with space charge," IEEE Trans. Nucl. Sci. **NS-18**, 1105 (1971).
2) Corsten, C.J.A., "Resonance and coupling effects in circular accelerators," thesis, Eindhoven University of Technology, Eindhoven (1982).
3) Delhez, J.L., et al., "Electron beam focusing in a racetrack microtron by means of rotated two-sector dipole magnets," Nucl. Instr. Meth. in Phys. Res. **B68** (1992) 96-100.

ION_TRACKER, A TRACE TRACKING PROGRAM FOR CYCLOTRON DESIGN

Matti Rinta-Nikkola
Accelerator Laboratory, University of Jyväskylä,
P.O.Box 35, 40351 Jyväskylä, Finland

ABSTRACT

ION_TRACKER is an interactive program for the design of axial injection and central region of cyclotron. The ions can be tracked from the beginning of the cyclotron axis through a single gap buncher and an inflector, and then inside the cyclotron until to extractor. Tracking can be done separately in every part or through the whole system at once. It uses the predictor-corrector method to solve equation of motion of charged particle in a cyclotron. We shall introduce restrictions of the program and show some examples of its use.

1. INTRODUCTION

As is well known to cyclotron builders, numerical orbit studies are an important step in cyclotron construction. In fact, orbit studies serve initially as the basis of the design of central region and extraction elements. Furthermore, the support from the numerical orbit studies to the beam development work during the machine operation helps to guide over the possible problems considering about beam optics.

The beam optics of central region and axial injection of the K130 cyclotron have been extensively studied numerically[1] for the purpose of design and understanding of the beam injection. For the numerical calculations we have used a self written program ION_TRACKER.

In this report, we present the program ION_TRACKER which has been developed during the design of the K130 cyclotron. We shall introduce the method to solve the equation of motion of a charged particle in the electromagnetic field of a cyclotron. In particular, we draw attention to the macro programming feature of the program.

2. INTEGRATION METHOD AND FIELD CALCULATION

ION_TRACKER integrates numerically the equation $\vec{F} = q(\vec{E} + \vec{v} \times \vec{B})$ using a cartesian coordinates with a time as independent variable. Used integration method is a predictor-corrector method of order h^5. Integration method provides one measure of the error being made at each step and it is used to control the step size employed in the integration. Another attractive feature of this integration method is that only two evaluations of the force $\vec{F}$ need to be computed at each integration step. More details about predictor-corrector methods see for example R.W. Hamming, "Numerical Methods for Scientists and Engineers".[2]

Ions can be tracked all the way from the beginning of the axial injection line to the extractor of the cyclotron. Magnetic and electric fields of the cyclotron are given to the ION_TRACKER in field maps. Using predictor-corrector method with variable integration time step we need to have a method to calculate the fields at arbitrary point. Fields and their first derivative, at locations lying between the given data points, are obtained through a double three-point Lagrange interpolation.[3] This interpolation scheme provides that the fields as well as their first derivative will be continuous.

Since ION_TRACKER has been developed for the beam optics study of the K130 cyclotron it has some "machine dependent" restrictions which will be outlined below. Some attempts has been paid to make the code, especially for field calculations part of it, so that it is easy to modify if needed.

2.1. Axial Injection Line

The axial injection line may be consist of axially symmetric magnetic fields, like axial magnetic field of the cyclotron and solenoids, and a single acceleration gap buncher. The buncher can be excited by combining an rf sine wave and its second harmonic.

The electric field of the buncher is obtained by using a hard edge approximation. Electric field is assumed to be zero outside of the gap, and inside to have only axial component which is calculated from the formula $E_z = V_i/d$, where d is the gap length and V_i is the voltage of the i:th harmonic.

The axial magnetic field is given along the magnetic axis of cyclotron and it can be combined from three subfields. The subfields, for example the axial magnetic field

of the cyclotron and two solenoids, can be replaced and rescaled interactively while running the program. Outside of the axis of the cyclotron the magnetic field will be calculated from field expansions, which are derived using Maxwell's equations and assuming the perfect axial field symmetry. We shall get the expansions

$$\begin{aligned} B_r(r,z) &= \sum_{n=0}^{\infty} \frac{(-1)^{n+1}}{n!(n+1)!} B^{(2n+1)}(z)(\frac{r}{2})^{2n+1} \\ B_\theta(r,z) &= 0 \\ B_z(r,z) &= \sum_{n=0}^{\infty} \frac{(-1)^n}{n!^2} B^{(2n)}(z)(\frac{r}{2})^{2n}. \end{aligned}$$

ION_TRACKER uses the axial magnetic field and its first three derivatives to calculate magnetic field outside of the symmetry axis.

2.2. Spiral Inflector

The electric field of the spiral inflector is computed from an electric potential map. We have used RELAX3D[4] to calculate the potential map. Our RELAX3D calculations are done with the aid of an unnamed program which prescribes to RELAX3D the inflector electrode locations around an analytical central ray. The assumption of the hard edge field has been used in solving the shape of inflector electrodes. Since a real inflector will have fringe fields, which increase its effective length, we have included to the program the possibility to shorten the electrodes.

The magnetic field is calculated in the same way as in axial injection line.

2.3. Cyclotron

ION_TRACKER is limited to use of two rf systems with straight dees and the acceleration gaps have to be in constant azimuth angles. The electric field produced by the dees in the median plane of the cyclotron is calculated in two different ways. In the central region the electric field is obtained from a three dimensional rectangular potential map which can be calculated by using RELAX3D. Outside of this region the field will be calculated from a gaussian approximation.[5] In Fig. 1 are shown the electric field components calculated in both methods along the ion path for one gap crossing.

In order to describe the gaussian approximation we shall define the right handed cartesian coordinate system, which has its origin at the middle of the straight accelerating gap. The X and Y axis will lay on the median plane of the cyclotron and the Z axis is oriented axially. X axis is parallel and Y axis is normal to the gap.

The normal field component in the median plane is obtained from the gaussian function

$$E_y(y) = E_{max} e^{-1/2(y/\Delta y)^2},$$

where the width Δy is related experimentally to the gap width W and the dee-aperture H by

$$\Delta y = 0.2H + 0.4W.$$

Assuming the perfect median plane symmetry the axial field component can be calculated from the formula

$$E_z(y,z) = E_y(y)\frac{yz}{\Delta y^2}.$$

The parallel field component is assumed to be zero.

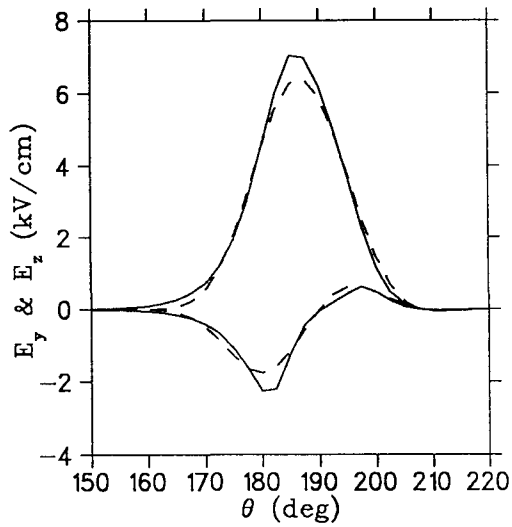


Fig. 1. Electric field components with time modulation along the ion path for one gap crossing. In solid line are drawn the field components obtained from potential map data and in dashed line from gaussian approximation.

The cyclotron magnetic field is given on the median plane in a polar map. Outside of the median plane the magnetic field will be calculated from field expansions. Using Maxwell's equations and the assumption of the median plane symmetry we shall get the expansions

$$\begin{aligned} B_r(r,\theta,z) &= \sum_{n=0}^{\infty} \frac{(-1)^n}{(2n+1)!} \frac{\partial B^{(n)}(r,\theta)}{\partial r} z^{2n+1} \\ B_\theta(r,\theta,z) &= \sum_{n=0}^{\infty} \frac{(-1)^n}{(2n+1)!} \frac{\partial B^{(n)}(r,\theta)}{\partial \theta} z^{2n+1} \\ B_z(r,\theta,z) &= \sum_{n=0}^{\infty} \frac{(-1)^n}{(2n)!} B^{(n)}(r,\theta) z^{2n}, \end{aligned}$$

where $B^{(0)}(r,\theta) = B(r,\theta)$, $B^{(1)}(r,\theta) = \nabla^2 B(r,\theta)$, $B^{(2)} = \nabla^2 B^{(1)}(r,\theta)$ and so on.

In ION_TRACKER the magnetic field off the median plane can be obtained correctly to first or fourth order in z. For the fourth order calculation in addition to the median plane magnetic field map $B(r,\theta)$ the corresponding maps for $B^{(1)}(r,\theta)$ and $B^{(2)}(r,\theta)$ are required.

These maps must be calculated and stored in advance. Since the maps $B^{(1)}$ and $B^{(2)}$ contain high derivatives of the B, they exhibit much more noise than the original field data. Even though the integration routine will act as averaging process in filtering out the high frequency components of the noise some caution is required.

We should note that for the fourth order calculation the used field expansions are the same as in code SPIRAL GAP.[6)]

3. PROGRAM INPUT AND OUTPUT

ION_TRACKER is a command driven program. The terminal interface routine, that closely mimics the DCL command recall facility, as well as many other general purpose routines, has been taken from TRIUMF libraries. For this reason the program has a lot of common features with the graphic code PLOTDATA.[7)] Some examples of the features provided by ION_TRACKER:

- basic mathematical functions
- expression evaluation
- allow scalar variables (100)
- dynamic and static 20 line input recall buffers
- macro capability with parameter passing
- looping, branching and conditional statements in macros
- create your own commands by "aliasing"
- allow you to define keypad keys

All input is fed to ION_TRACKER by commands. Field maps and other long input like equilibrium orbit and central region geometry data are read from files. The commands can be entered from three sources:

1. interactively via the terminal keyboard
2. non-interactively via a DCL command file
3. non-interactively via an ION_TRACKER command macro file

In interactive mode the status of the input of ION_TRACKER can be displayed on terminal screen when desired.

An important part of the beam optics calculation is the graphical visualization of the numerical data. ION_TRACKER itself has no graphics but it writes an input file for PLOTDATA. The absence of the graphics is not a real disadvantage: the orbit data can be read and drawn in PLOTDATA easily and fast.

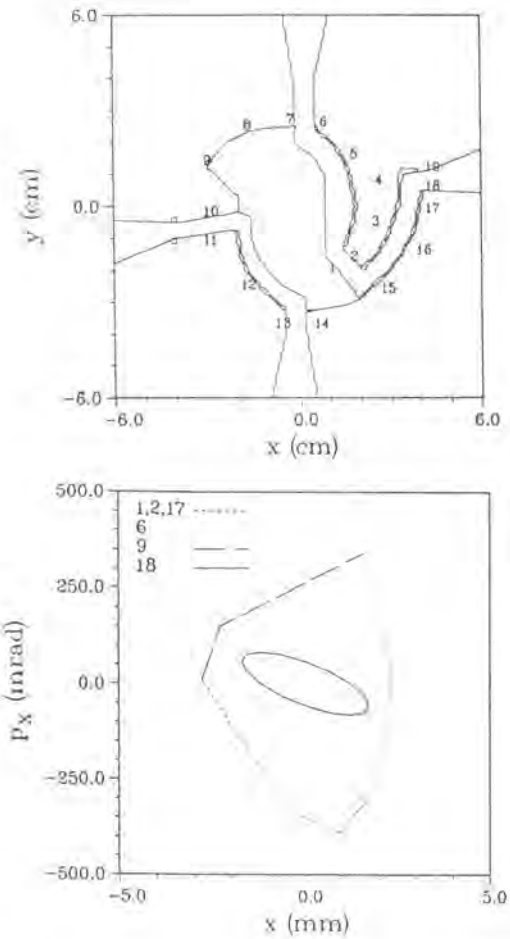


Fig. 2. In the upper picture is shown the layout of the central region. The obstacles on the central region are specified in places numbered in the picture. In the first harmonic acceleration mode the puller electrode is the dee with a 45 degrees nose. In the lower picture is shown the result of the acceptance calculation. The different line types indicate the limiting places in the central region. The matched beam, $\epsilon = 100\pi$ mm×mrad, is drawn in solid line.

4. EXAMPLES

4.1. Acceptance Calculation

ION_TRACKER can calculate transverse acceptances of the central region. Radial and axial acceptances are calculated independently and they are determined by calculating a group of ion trajectories starting from the boundary of the acceptance. In radial acceptance calculation the central region geometry is given as input. The obstacles on the central region are specified in azimuth angles θ_i. When the ion reaches the angle θ_i it will be checked if it passes the obstacle or not. Into the

output file ION_TRACKER writes the starting values of the ions which have been able to go through the central region and in radial case also the place where the "near-by" ion has been lost. In Fig. 2 we have an example of the result of a radial acceptance calculation of the first harmonic acceleration mode in the K130 cyclotron.

4.2. Macro Programming

Especially macro programming feature makes ION_TRACKER powerfull and fast to solve various kind of problems. Macros can be applied for example to generate different kind of beams, to search accelerated equilibrium orbits, to calculate spiral acceptance and to tune cyclotron parameters.

ION_TRACKER can utilize calculated orbit data. Orbit data is not stored in a memory while tracking the ions but it can be read from the output file of ION_TRACKER. From the orbit data several statistics can be calculated. In addition to the one variable statistical computation, you can do a fit of regression line and ellipse to the given data. The results of the computations will be assigned to the specified variables.

Calculated orbit data can be made use of a feedback to tune cyclotron parameters like strengths of the axial solenoids, buncher parameters, spiral voltage and rf-frequency. It is essential that those parameters are well tuned when studing the beam dynamics in the cyclotron. The tuning is straight forward but it can be time consuming and tedious work. If macros are applied to do the tuning, then it can be done by entering a single command.

As an example of beam simulation we shall present the part of macro program which generates realistic dc-beam and track it through the axial injection line into the cyclotron. Results of this calculation are presented elsewhere in this Proceedings.[1)] The beam has been generated and tracked by executing following macro loop:

```
DO I=1,1000
   EXE BEAM.TCOM 100 2.5 0.25 100 2.5 0.25
   TAU = RAN*360
   LOCATION X Y -160.0
   TRANSVER XP YP
   LONGITUD 9.7E-3 TAU
   RUN AIC
ENDDO
```

The command macro file BEAM.TCOM is executed on the first line of the loop. In this macro one point (X,XP,Y,YP) is picked randomly from a four dimensional gaussian distributed phase space. The macro has six parameters which defines the Twiss' parameters of the uncorreleted subspaces (X,XP) and (Y,YP). In this specific case both subspaces have the same Twiss' parameters: $\epsilon = 100\pi$ mm×mrad, $\beta = 2.5$ mm/mrad and $\alpha = 0.25$. On the second line of the loop a random number from the interval $0 - 360$ is assigned to the variable TAU. RAN is a random number function which will get a value from 0 to 1. In the following three lines the starting values which have been calculated on the previous lines will be set to the ion. Starting location is 160 cm from the median plane of the cyclotron, injection energy is 9.7 keV and phase is TAU. The tracking will be done on the last line of the loop. The parameter AIC (Axial Inflector Cyclotron) of the command RUN specifies the tracking area.

5. FUTURE DEVELOPMENTS

We have been planning to implement also electrostatic deflector, electromagnetic channel and focussing bars to our code. If we succeed in that we shall have a single code which can handle all the beam dynamics from the beginning of the axial injection line to out of the cyclotron.

Another aim is to make better documents and user guide to the program. Up to now we have just up dated our command reference manual and made sufficent comments in the code.

6. ACKNOWLEDGEMENTS

The author would like to thank Computing Services Group at TRIUMF for making available their codes.

7. REFERENCES

1) Heikkinen, P. and Rinta-Nikkola, M. "Ion optics in the K130 cyclotron" in this Proceedings.
2) Hamming, R.W., **Numerical Methods for Scientists and Egineers** (McGraw-Hill Book Company, Inc. 1962), Ch.15.
3) Berg, R.E., "Precise Methods for Pre-Calculation of Cyclotron Control Settings", Ph.D. Thesis, Michigan State Univ., East Lansing, 1966, p.43.
4) Houtman, H. and Cost, C.J., "A Fortran Program (RELAX3D) to Solve the Three Dimensional Poisson (Laplace) Equation.", Proc EPS Conference on "Computing in Accelerator Design and Operation" Berlin, Sebtember 1983, p.98.
5) Hazewindus, N., van Nieuwland, J.M., Faber, J. and Leistra, L., "The magnetic analogue method as used in the study of a cyclotron central region", Nucl. Instr. Meth. **118** (1974) 125-134.
6) Gordon, M.M., "Effects of spiral electric gaps in superconducting cyclotrons", Nucl. Instr. and Meth. **169** (1980) 327-336.
7) Chuma, J. "PLOTDATA Reference Manual", TRIUMF internal report, TRI-CD-87-03.

ION OPTICS IN THE JYVÄSKYLÄ K130 CYCLOTRON

Pauli Heikkinen

and

Matti Rinta-Nikkola
Accelerator Laboratory, University of Jyväskylä
P.O.Box 35, SF–40351 Jyväskylä, Finland

ABSTRACT

Beam behavior in the K130 cyclotron and in the injection line has been studied numerically. Beam formation in the ECR ion source with space charge was calculated using a 3D code in order to re-design the puller electrode. The code TRANSPORT was used in the injection line. From the axial injection to extraction the code ION_TRACKER[1] was used.

In this paper, results from the ion optical studies from the ion source to extraction will be presented.

1. INTRODUCTION

The Jyväskylä K130 cyclotron[2] was built to accelerate mainly heavy ions from an ECR ion source for nuclear physics experiments. Part of the beam time will be used for radio isotope production. The assembly of the cyclotron started in May, 1990, and the first beam extraction took place in January 28, 1992.

2. INJECTION LINE

The injection line from the ECR ion source to the K130 cyclotron is based on solenoids. The beam line elements to the last Faraday cup before the axial part of the line are shown in Fig. 1. The solenoids S2–S5 between the two double focusing 90 degree dipoles were originally planned to be used as two telescopes. In the example shown in Fig. 1 solenoids S3 and S4 act as a telescope while S2 and S5 are stronger. This setup is a result of manual optimization of the beam current in the spiral inflector. The initial divergences in Fig. 1 roughly correspond to the acceptance of the line with the specific setup.

Numerical studies with a 3D tracking code of the beam formation in the ECR ion source with tranverse space charge forces predict larger divergences. The longitudinal space charge forces were not included. The treatment of space charge effects is similar to that by Xie at MSU.[3] Experiments also indicate that we lose beam before the first solenoid which is located 88 cm after the ECR extraction hole. We have therefore planned to add some extra focusing after the extraction electrodes – possibly an Einzel lens.

The original 45 degree puller electrode of the ECR ion source has been replaced with a Pierce puller in order to improve the beam quality from the source.

The quadrupoles Q1–Q4 are used for emittance matching.

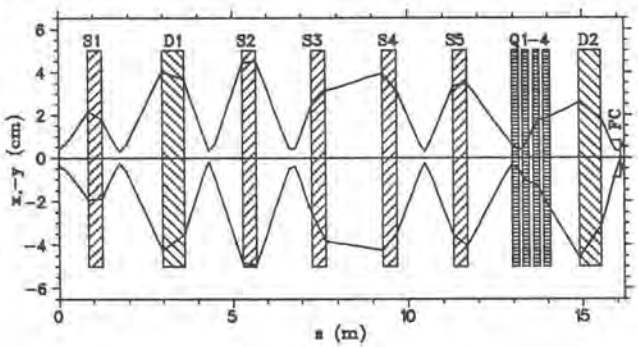


Fig. 1. The injection line elements and beam envelopes.

For the first couple of months of running the injection line we had severe problems with aligning the beam until we found out that the missing iron in the solenoid endplates (about 10 cm wide sector for current leads) caused a dipole component to the fringing field. Hence, changing the focusing strength of a solenoid resulted to a different dipole component in the field. The effect was also highly non-linear, and that disturbed the transverse phase space so that the beam had a crescent shape in the (x, y) space. Now the non-symmetric endplates of three solenoids have been removed, and the tuning of the injection line is much easier.

3. AXIAL INJECTION

There are two solenoids on the cyclotron axis, the first being outside the yoke and the second as close as possible to the median plane (23–63 cm from the median plane). The axial hole starts as a 474 mm × 474

mm rectangular hole, reducing to a 300 mm × 300 mm rectangular hole in the return yoke. In the pole piece (76 cm from the median plane) the hole is round with a diameter of 200 mm until the center plug which has a 40 mm diameter hole. The strengths of the solenoids are determined by tracking particles backwards from a 100 π mm mrad phase space ellipse that fits into the inflector acceptance to the Faraday cup which is located after the second dipole (D2). The optimum condition has been found to be such that the beam size is big between the last solenoids (almost parallel beam). A typical case of axial injection is shown in Fig. 2 where also the corresponding axial field has been plotted.

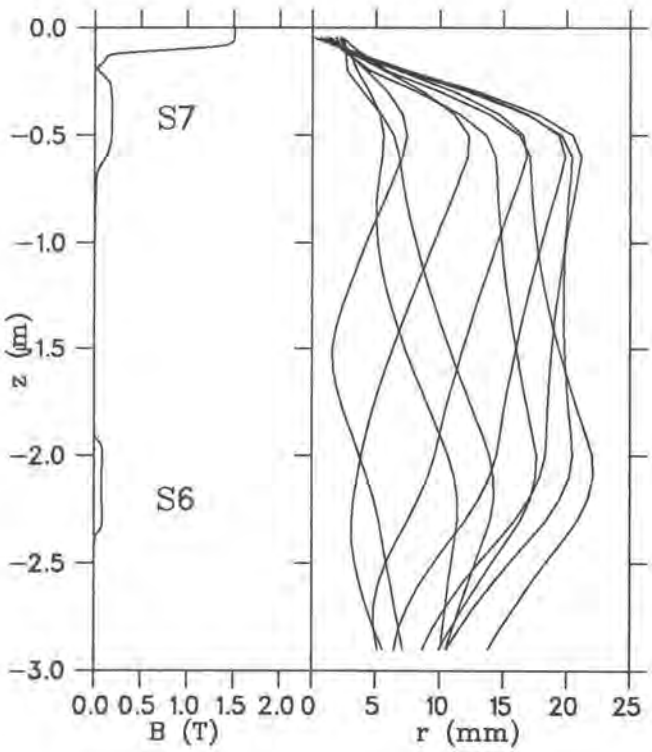


Fig. 2. Tracked beam in the axial hole of the K130 cyclotron and the corresponding axial magnetic field with solenoids S6 and S7.

3.1. Buncher

A buncher has been installed in the vertical hole of the cyclotron yoke, 145 cm from the median plane. It uses both first and second harmonic RF frequencies. The mechanical design has been adapted from MSU with minor modifications. Some parts of the electronics are still under construction. Numerical studies with ION_TRACKER have shown a beam intensity increase with a factor of 4 using only the first harmonic frequency. An example of such calculation is shown in Fig. 3 where only the first harmonic frequency has been used. The figures below show the effect of the spiral inflector to the longitudinal phase space.

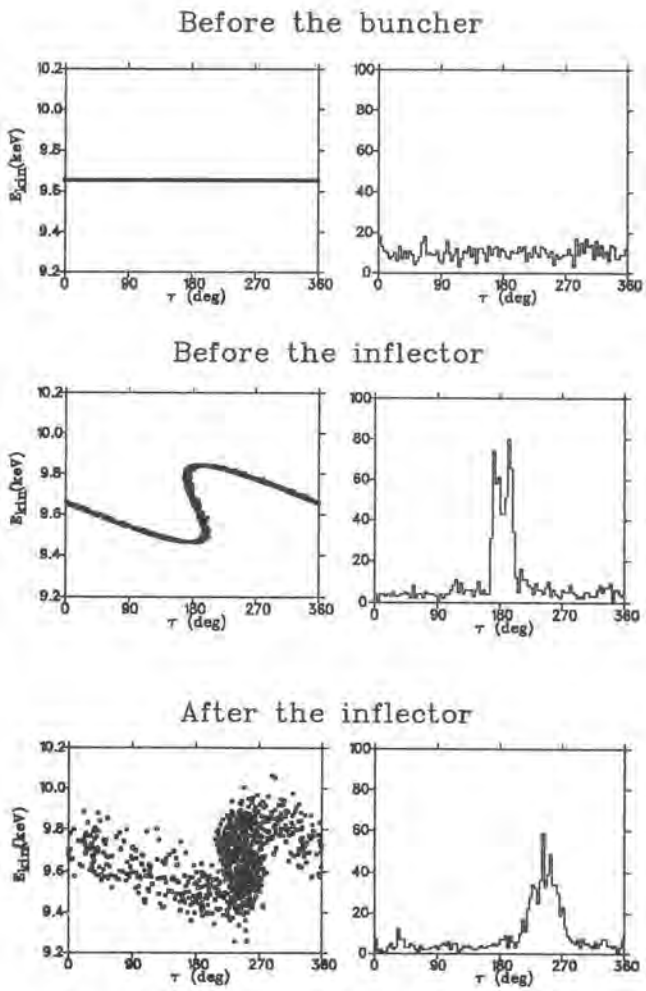


Fig. 3. Beam simulation with the buncher, before the buncher (above), before the inflector (middle) and after the inflector (below).

3.2. Spiral Inflector

The spiral inflectors for the three different harmonic modes were designed using analytic formulae and the electric fields for ION_TRACKER were calculated with RELAX3D.[4] The acceptances of the inflectors have been determined both using linear transfer matrices and tracking particles using 3D fields. The transfer matrices were determined tracking four different particles through the inflector with moderate amplitudes (each component of the four dimensional phase space non-zero at the time). The results from these calculations for the second harmonic inflector are shown in Fig. 4. The acceptances correspond to non-correlated beams in the (h, u) space in the entrance of the spiral inflector. The horizontal phase space in the frame of the inflector gap is (h, hp) and the vertical one (u, up).

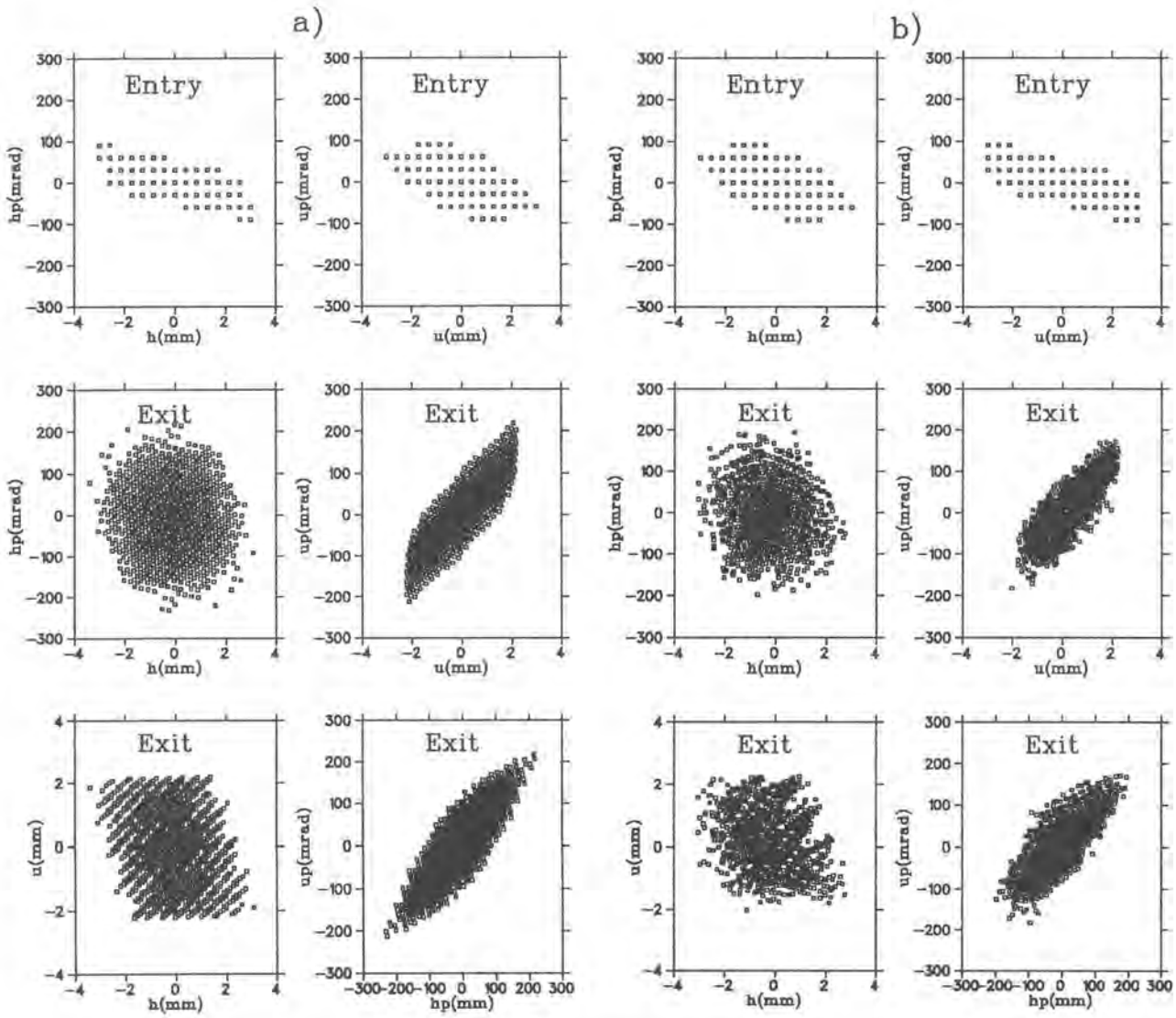


Fig. 4. The transverse acceptances (entry) of the second harmonic inflector using a) transfer matrices, and b) tracking particles with ION_TRACKER. Each point in the entry sub phase space contains several particles: same (h, hp) but different (u, up) and vice-versa.

The effective length of each spiral was determined with RELAX3D fields in ION_TRACKER so that the central ray leaves the inflector with zero axial velocity on the median plane. For example, the mechanical length of the second harmonic inflector is about 2 % shorter than that of a hard edged analytical spiral.

4. CENTRAL REGION

The central region has been designed so that only the inflector has to be changed when switching from one harmonic mode to another. This has lead to a tilted gap in the second harmonic inflector, the tilt parameter k' being 0.19 which corresponds to a final angle of 10.76 degrees. Also the maximum injection voltage must be limited in the first and third harmonic mode. The spiral inflector parameters are listed in Table 1.

Table 1. The spiral inflector parameters.

Harmonic mode	1	2	3
Max injection voltage (kV)	15.0	20.0	13.3
Spiral height (mm)	30.0	30.0	29.0
Gap height (mm)	5.0	5.0	5.0
Gap width (mm)	10.0	10.0	10.0
k'	0.00	0.19	0.00
Injection radius (mm)	13.1	18.8	18.8
Max spiral voltage (kV)	±2.5	±3.3	±2.3

The longitudinal phase acceptances for the central region are of the order of ±20 degrees in the second and

third harmonic modes and somewhat less for the first harmonic mode. The transverse phase space acceptances have been found to be larger than 100 π mm mrad for the inflector and the central region.

The simulated transmission from a DC beam through the spiral inflector and the central region is about 8 %, and the largest observed one has been about 7 %.

5. ACCELERATION

5.1. Trim Coil Settings

The trim coil settings have been determined with a slightly modified version of FIELDER.[5] A constraint not to allow big changes in currents between two subsequent trim coils was added. This leads to a "smooth" behavior of the trim coil currents when increasing the beam energy. Originally, FIELDER runs result to many discontinuities in trim coil currents as a function of beam energy when it tries to add a small local bump to the field with currents of opposite sign in two neighboring coils.

5.2. Extraction

The extraction consists of an electrostatic deflector, an electromagnetic channel EMC and two passive focusing channels. Precessional extraction method is used. Figure 5 shows the increase of turn separation for He^{1+} beam at 6 MeV/u.

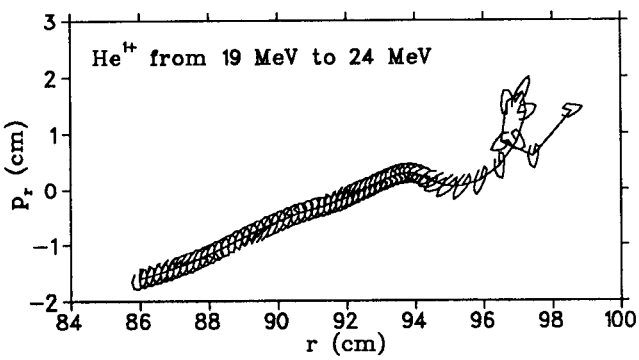


Fig. 5. Radial phase space of a He^{1+} beam prior to extraction at θ = 280 deg. The tracked particles started at an energy of 10 MeV and at the same RF phase (0 deg) on an eigen ellipse.

Beam trajectories through the deflector, EMC and the passive focusing channels were tracked with the MSU Z^4 orbit code.[6] In the MSU code, the focusing bars are assumed to be saturated. In our version, the magnetization of the iron bars depend on the main field at the trajectory so that they get saturated at 1.07 T (round iron bars). Since the main field changes along one channel the magnetization in the code changes linearily with the main field. This assumption was used in the channel design. Field measurements showed that the magnetization differed somewhat from the assumption but the field gradient can be set to the design value by changing the radial distance of the bars. The observed beam shape after the cyclotron is horizontally wide which is also the result from orbit calculations where the focusing channel fields have been corrected to the measured values.

The experimental transmission through the extraction system shortly after the first extracted beam was 55 %, the transmission through the deflector being 74 %. This can be increased with proper centering of the accelerated beam and the transmission through the rest of the extraction system will be increased after correcting the focusing channel geometries.

6. DISCUSSION

Numerical ion optical studies have served as a tool to design some essential parts of the K130 cyclotron facility. The problems in the injection line originated from non-symmetrical endplates in the solenoids. In the axial injection line as well as in the inflector, in the central region and in the acceleration, the pre-calculated values for the settings have proven to coincide fairly well with those that have resulted to highest beam currents. Some small adjustments for the pre-calculated focusing bar geometries have to be done.

7. REFERENCES

1) Rinta-Nikkola, M., "ION_TRACKER, a trace tracking program for cyclotron design," presented at the Thirteenth International Conference on Cyclotrons and their Applications, Vancouver, July 6–10, 1992.
2) Liukkonen, E., "The Jyväskylä K130 Cyclotron Project,"in **Proceedings of the Twelfth International Conference on Cyclotrons and their Applications**, Berlin, Germany, 1989 (World Scientific, Singapore, 1991) pp.40–42.
3) Xie, Z.Q., "The Effect of Space Charge Force on Beams Extracted from ECR Ion Sources," Ph.D. Dissertation, **MSUCP-60**, 1989.
4) Houtman, H. and Kost, C.J., "A Fortran Program (RELAX3D) to Solve the Three Dimensional Poisson (Laplace) Equation," The EPS Conference on Computing in Accelerator Design and Operation, Berlin, 1983, 98.
5) Gordon, M.M. and Johnson, D.A., "Application of a new field trimming program to the MSU cyclotron," in **Proceedings of the Sixth International Cyclotron Conference** (Am. Inst. Phys., New York, 1972) 298.
6) Gordon, M.M. and Taivassalo, V., "The Z^4 Orbit Code and the Focusing Bar Fields Used in Beam Extraction Calculations for Superconducting Cyclotrons,"Nucl. Instr. Meth. **A247**, 423–430(1986).

NONLINEAR TRANSPORT OF ACCELERATOR BEAM PHASE SPACE

Xie Xi
Graduate School of Nuclear Industry, P.O. Box 1477, Beijing, 102413, China

and

Xia Jiawen
Institute of Modern Physics, Academia Sinica, P.O. Box 31, Lanzhou, 730000, China

ABSTRACT

Accelerator beam is a nonlinear dynamic system, and the phase space transport of it means the variation of the phase space shape from the initial state $X_0 = X(t_0)$ to the final state $X_f = X(t)$. Mathematically, this variation is the transform from the initial boundary equation of phase space $F(X_0) = 0$ to the final equation $F(X_0(X_f, t)) = f(X_f, t) = 0$. This transform is nonlinear. The any order analytical solution for the motion differential equation of a general nonlinear dynamic system has been derived out[1], namely, the function relation $X(t) = X_f(X_0, t)$ was given. Based on the result, the inverse transform of the any order solution of the motion differential equation was completed in this paper, and the function relation $X(t_0) = X_0(X_f, t)$ was obtained, thus realizing theoretically the nonlinear transport for the phase space of nonlinear dynamic system.

1. INTRODUCTION

With the development of modern science, more and more science areas have broken through the linear category and involved the studies of nonlinear category. The phase space transport of nonlinear dynamic systems is a general nonlinear problem. At the initial state $X_0 = X(t_0)$, if the boundary equation of the phase space is

$$F(X_0) = 0 \quad . \tag{1}$$

then, at the final state $X_f = X(t)$, the boundary equation of the phase space becomes

$$F[X_0(X_f, t)] = f(X_f, t) = 0 \quad . \tag{2}$$

the process between the initial phase space Eq.1 and the finial one Eq.2 is the very phase space transport of the nonlinear dynamic system considered. Mathematically, this physical process is the nonlinear transformation from the given initial Eq.1 to the finial Eq.2. For a general nonlinear dynamic system, reference 1) gives the phase point $X(t) = [x_t^1, x_t^2, \cdots, x_t^N]^T = X_f(X_0, t)$ at the time t as the funtion of the initial phase point $X_0 = [x_0^1, x_0^2, \cdots, x_0^N]^T$ and the time t. So, our task is to find out its inverse transformation, i.e. the initial phase point $X(t_0) = X_0(X_f, t)$ as the funtion of the phase point X_f and the time t. Then, substitution of the inverse transform $X(t_0) = X_0(X_f, t)$ into the initial Eq.1 yields directly the final state Eq.2.

2. DERIVING THE INVERSE TRANSFORMATION OF $X(t) = X_f(X_0, t)$

In N-dimension phase space, the motion differential equation of a general nonlinear dynamic system is

$$\begin{aligned} \dot{x}_t^i = \; & \alpha_{j_1}^i(t) x_t^{j_1} + \alpha_{j_1 j_2}^i(t) x_t^{j_1} x_t^{j_2} \\ & + \alpha_{j_1 j_2 j_3}^i(t) x_t^{j_1} x_t^{j_2} x_t^{j_3} \\ & + \cdots \\ & + \alpha_{j_1 j_2 \cdots j_n}^i(t) x_t^{j_1} x_t^{j_2} \cdots x_t^{j_n} \\ & + \cdots \quad . \end{aligned} \tag{3}$$

where, i = 1, 2, ..., N, and the any order analytical solution[1)] of the above equation with initial phase point X_0^i is

$$\begin{aligned} x_t^i = \; & T_{j_1}^i(t) x_0^{j_1} + T_{j_1 j_2}^i(t) x_0^{j_1} x_0^{j_2} \\ & + T_{j_1 j_2 j_3}^i(t) x_0^{j_1} x_0^{j_2} x_0^{j_3} \\ & + \cdots \\ & + T_{j_1 j_2 \cdots j_n}^i(t) x_0^{j_1} x_0^{j_2} \cdots x_0^{j_n} \\ & + \cdots \quad . \end{aligned} \tag{4}$$

Express the inverse transform of Eq.4 in series:

$$\begin{aligned} x_0^j = \; & S_{i_1}^j(t)x_t^{i_1} + S_{i_1 i_2}^j(t)x_t^{i_1}x_t^{i_2} \\ & + S_{i_1 i_2 i_3}^j(t)x_t^{i_1}x_t^{i_2}x_t^{i_3} \\ & + \cdots \\ & + S_{i_1 i_2 \ldots i_n}^j(t)x_t^{i_1}x_t^{i_2}\ldots x_t^{i_n} \\ & + \cdots \; , \end{aligned} \tag{5}$$

or:

$$\left\{ \begin{aligned} x_0^{j_1} = \; & S_{i_1}^{j_1}(t)x_t^{i_1} + S_{i_1 i_2}^{j_1}(t)x_t^{i_1}x_t^{i_2} \\ & + S_{i_1 i_2 i_3}^{j_1}(t)x_t^{i_1}x_t^{i_2}x_t^{i_3} \\ & + \cdots \\ & + S_{i_1 i_2 \ldots i_n}^{j_1}(t)x_t^{i_1}x_t^{i_2}\ldots x_t^{i_n} \\ & + \cdots \\ x_0^{j_2} = \; & S_{i_1}^{j_2}(t)x_t^{i_1} + S_{i_1 i_2}^{j_2}(t)x_t^{i_1}x_t^{i_2} \\ & + S_{i_1 i_2 i_3}^{j_2}(t)x_t^{i_1}x_t^{i_2}x_t^{i_3} \\ & + \cdots \\ & + S_{i_1 i_2 \ldots i_n}^{j_2}(t)x_t^{i_1}x_t^{i_2}\ldots x_t^{i_n} \\ & + \cdots \\ x_0^{j_3} = \; & S_{i_1}^{j_3}(t)x_t^{i_1} + S_{i_1 i_2}^{j_3}(t)x_t^{i_1}x_t^{i_2} \\ & + S_{i_1 i_2 i_3}^{j_3}(t)x_t^{i_1}x_t^{i_2}x_t^{i_3} + \cdots \\ & + S_{i_1 i_2 \ldots i_n}^{j_3}(t)x_t^{i_1}x_t^{i_2}\ldots x_t^{i_n} \\ & + \cdots \\ \ldots\ldots & \\ x_0^{j_n} = \; & S_{i_1}^{j_n}(t)x_t^{i_1} + S_{i_1 i_2}^{j_n}(t)x_t^{i_1}x_t^{i_2} \\ & + S_{i_1 i_2 i_3}^{j_n}(t)x_t^{i_1}x_t^{i_2}x_t^{i_3} + \cdots \\ & + S_{i_1 i_2 \ldots i_n}^{j_n}(t)x_t^{i_1}x_t^{i_2}\ldots x_t^{i_n} \\ & + \cdots \\ \ldots\ldots & \; . \end{aligned} \right. \tag{6}$$

giving the fundamental terms:

$$\begin{aligned} & x_0^{j_1}x_0^{j_2} \\ & \quad = S_{i_1}^{j_1}(t)S_{i_2}^{j_2}(t)x_t^{i_1}x_t^{i_2} \\ & \qquad + \{S_{i_1}^{j_1}(t)S_{i_2 i_3}^{j_2}(t) \\ & \qquad + S_{i_1 i_2}^{j_1}(t)S_{i_3}^{j_2}(t)\}x_t^{i_1}x_t^{i_2}x_t^{i_3} \\ & \qquad + \cdots \\ & \qquad + \{S_{i_1}^{j_1}(t)S_{i_2 i_3 \ldots i_n}^{j_2}(t) \\ & \qquad + S_{i_1 i_2}^{j_1}(t)S_{i_3 i_4 \ldots i_n}^{j_2}(t) \\ & \qquad + \cdots \\ & \qquad + S_{i_1 i_2 \ldots i_{n-2}}^{j_1}(t)S_{i_{n-1} i_n}^{j_2}(t) \\ & \qquad + S_{i_1 i_2 \ldots i_{n-1}}^{j_1}(t)S_{i_n}^{j_2}(t)\}x_t^{i_1}x_t^{i_2}\ldots x_t^{i_n} \\ & \qquad + \cdots \\ & \quad = G_{i_1 i_2}^{j_1 j_2}(t)x_t^{i_1}x_t^{i_2} \\ & \qquad + G_{i_1 i_2 i_3}^{j_1 j_2}(t)x_t^{i_1}x_t^{i_2}x_t^{i_3} \\ & \qquad + \cdots \\ & \qquad + G_{i_1 i_2 \ldots i_n}^{j_1 j_2}(t)x_t^{i_1}x_t^{i_2}\ldots x_t^{i_n} \\ & \qquad + \cdots \end{aligned} \tag{7-1}$$

$$\begin{aligned} x_0^{j_1}x_0^{j_2}x_0^{j_3} = \; & (x_0^{j_1}x_0^{j_2})x_0^{j_3} \\ = \; & \{G_{i_1 i_2}^{j_1 j_2}(t)x_t^{i_1}x_t^{i_2} + G_{i_1 i_2 i_3}^{j_1 j_2}(t)x_t^{i_1}x_t^{i_2}x_t^{i_3} \\ & + \cdots + G_{i_1 i_2 \ldots i_n}^{j_1 j_2}(t)x_t^{i_1}x_t^{i_2}\ldots x_t^{i_n} \\ & + \cdots\}\{S_{i_1}^{j_3}(t)x_t^{i_1} + S_{i_1 i_2}^{j_3}(t)x_t^{i_1}x_t^{i_2} \\ & + S_{i_1 i_2 i_3}^{j_3}(t)x_t^{i_1}x_t^{i_2}x_t^{i_3} + \cdots \\ & + S_{i_1 i_2 \ldots i_n}^{j_3}(t)x_t^{i_1}x_t^{i_2}\ldots x_t^{i_n} + \cdots\} \\ = \; & G_{i_1 i_2}^{j_1 j_2}(t)S_{i_3}^{j_3}(t)x_t^{i_1}x_t^{i_2}x_t^{i_3} + \cdots \\ & + \{G_{i_1 i_2 \ldots i_{n-1}}^{j_1 j_2}(t)S_{i_n}^{j_3}(t) \\ & + G_{i_1 i_2 \ldots i_{n-2}}^{j_1 j_2}(t)S_{i_{n-1} i_n}^{j_3}(t) + \ldots \\ & + G_{i_1 i_2}^{j_1 j_2}(t)S_{i_3 i_4 \ldots i_n}^{j_3}(t)\}x_t^{i_1}x_t^{i_2}\ldots x_t^{i_n} \\ & + \cdots \\ = \; & G_{i_1 i_2 i_3}^{j_1 j_2 j_3}(t)x_t^{i_1}x_t^{i_2}x_t^{i_3} + \cdots \\ & + G_{i_1 i_2 \ldots i_n}^{j_1 j_2 j_3}(t)x_t^{i_1}x_t^{i_2}\ldots x_t^{i_n} \\ & + \cdots \end{aligned} \tag{7-2}$$

$\ldots\ldots$

$$\begin{aligned} & x_0^{j_1}x_0^{j_2}\ldots x_0^{j_{n-1}}x_0^{j_n} \\ & \quad = (x_0^{j_1}x_0^{j_2}\ldots x_0^{j_{n-1}})x_0^{j_n} \\ & \quad = \{G_{i_1 i_2 \ldots i_{n-1}}^{j_1 j_2 \ldots j_{n-1}}(t)x_t^{i_1}x_t^{i_2}\ldots x_t^{i_{n-1}} \\ & \qquad + G_{i_1 i_2 \ldots i_n}^{j_1 j_2 \ldots j_{n-1}}(t)x_t^{i_1}x_t^{i_2}\ldots x_t^{i_n} + \cdots\} \\ & \qquad \{S_{i_1}^{j_n}(t)x_t^{i_1} + S_{i_1 i_2}^{j_n}(t)x_t^{i_1}x_t^{i_2} \\ & \qquad + S_{i_1 i_2 i_3}^{j_n}(t)x_t^{i_1}x_t^{i_2}x_t^{i_3} + \cdots \\ & \qquad + S_{i_1 i_2 \ldots i_n}^{j_n}(t)x_t^{i_1}x_t^{i_2}\ldots x_t^{i_n} + \cdots\} \\ & \quad = G_{i_1 i_2 \ldots i_{n-1}}^{j_1 j_2 \ldots j_{n-1}}(t)S_{i_n}^{j_n}(t)x_t^{i_1}x_t^{i_2}\ldots x_t^{i_n} \\ & \qquad + \cdots \\ & \quad = G_{i_1 i_2 \ldots i_n}^{j_1 j_2 \ldots j_n}(t)x_t^{i_1}x_t^{i_2}\ldots x_t^{i_n} \\ & \qquad + \cdots \end{aligned} \tag{7-3}$$

$\ldots\ldots$,

where, the coefficients $G_{i_1 i_2 \ldots i_n}^{j_1 j_2 \ldots j_m}(t)$ with $m \leq n$ are of the following form:

$$\left\{ \begin{aligned} G_{i_1 i_2 \ldots i_n}^{j_1 j_2}(t) = \; & S_{i_1}^{j_1}(t)S_{i_2 i_3 \ldots i_n}^{j_2}(t) \\ & + S_{i_1 i_2}^{j_1}(t)S_{i_3 i_4 \ldots i_n}^{j_2}(t) + \cdots \\ & + S_{i_1 i_2 \ldots i_{n-2}}^{j_1}(t)S_{i_{n-1} i_n}^{j_2}(t) \\ & + S_{i_1 i_2 \ldots i_{n-1}}^{j_1}(t)S_{i_n}^{j_2}(t) \\ G_{i_1 i_2 \ldots i_n}^{j_1 j_2 j_3}(t) = \; & G_{i_1 i_2 \ldots i_{n-1}}^{j_1 j_2}(t)S_{i_n}^{j_3}(t) \\ & + G_{i_1 i_2 \ldots i_{n-2}}^{j_1 j_2}(t)S_{i_{n-1} i_n}^{j_3}(t) + \cdots \\ & + G_{i_1 i_2}^{j_1 j_2}(t)S_{i_3 i_4 \ldots i_n}^{j_3}(t) \\ \ldots\ldots & \\ G_{i_1 i_2 \ldots i_n}^{j_1 j_2 \ldots j_{n-1}}(t) = \; & G_{i_1 i_2 \ldots i_{n-1}}^{j_1 j_2 \ldots j_{n-2}}(t)S_{i_n}^{j_{n-1}}(t) \\ & + G_{i_1 i_2 \ldots i_{n-2}}^{j_1 j_2 \ldots j_{n-2}}(t)S_{i_{n-1} i_n}^{j_{n-1}}(t) \\ G_{i_1 i_2 \ldots i_n}^{j_1 j_2 \ldots j_n}(t) = \; & G_{i_1 i_2 \ldots i_{n-1}}^{j_1 j_2 \ldots j_{n-1}}(t)S_{i_n}^{j_n}(t) \; . \end{aligned} \right. \tag{8}$$

Substitution of Eqs. 7-1, Eq. 7-2 and Eq. 7-3 into Eq. 4 gives

$$\begin{aligned} x_t^i &= \delta_{i_1}^i x_t^{i_1} \\ &= T_{j_1}^i(t)\{S_{i_1}^{j_1}(t)x_t^{i_1} + S_{i_1 i_2}^{j_1}(t)x_t^{i_1}x_t^{i_2} \\ &\quad + S_{i_1 i_2 i_3}^{j_1}(t)x_t^{i_1}x_t^{i_2}x_t^{i_3} + \cdots \\ &\quad + S_{i_1 i_2 \ldots i_n}^{j_1}(t)x_t^{i_1}x_t^{i_2}\ldots x_t^{i_n} + \cdots\} \\ &\quad + T_{j_1 j_2}^i(t)\{G_{i_1 i_2}^{j_1 j_2}(t)x_t^{i_1}x_t^{i_2} \\ &\quad + G_{i_1 i_2 i_3}^{j_1 j_2}(t)x_t^{i_1}x_t^{i_2}x_t^{i_3} + \cdots \\ &\quad + G_{i_1 i_2 \ldots i_n}^{j_1 j_2}(t)x_t^{i_1}x_t^{i_2}\ldots x_t^{i_n} + \cdots\} \\ &\quad + \cdots\cdots \\ &\quad + T_{j_1 j_2 \ldots j_n}^i(t)\{G_{i_1 i_2 \ldots i_n}^{j_1 j_2 \ldots j_n}(t)x_t^{i_1}x_t^{i_2}\ldots x_t^{i_n} \\ &\quad + \cdots\} \\ &\quad + \cdots\cdots . \end{aligned} \tag{9}$$

Combination and comparision of the coefficients in Eq.9 yield the following coefficient equations:

$$\left\{ \begin{array}{ll} T_{j_1}^i(t)S_{i_1}^{j_1}(t) = \delta_{i_1}^i \\ T_{j_1}^i(t)S_{i_1 i_2}^{j_1}(t) + T_{j_1 j_2}^i(t)G_{i_1 i_2}^{j_1 j_2}(t) = 0 \\ \cdots\cdots \\ T_{j_1}^i(t)S_{i_1 i_2 \ldots i_n}^{j_1}(t) + T_{j_1 j_2}^i(t)G_{i_1 i_2 \ldots i_n}^{j_1 j_2}(t) \\ \quad + T_{j_1 j_2 j_3}^i(t)G_{i_1 i_2 \ldots i_n}^{j_1 j_2 j_3}(t) + \cdots \\ \quad + T_{j_1 j_2 \ldots j_{n-2}}^i(t)G_{i_1 i_2 \ldots i_n}^{j_1 j_2 \ldots j_{n-2}}(t) \\ \quad + T_{j_1 j_2 \ldots j_{n-1}}^i(t)G_{i_1 i_2 \ldots i_n}^{j_1 j_2 \ldots j_{n-1}}(t) \\ \quad + T_{j_1 j_2 \ldots j_n}^i(t)G_{i_1 i_2 \ldots i_n}^{j_1 j_2 \ldots j_n}(t) = 0 \\ \cdots\cdots . \end{array} \right. \tag{10}$$

which, in turn, yield the coefficients of the inverse transform Eq.5:

$$\left\{ \begin{array}{l} S_{i_1}^j(t) = [T^{-1}(t)]_i^j \delta_{i_1}^i \\ S_{i_1 i_2}^j(t) = -[T^{-1}(t)]_i^j T_{j_1 j_2}^i(t)G_{i_1 i_2}^{j_1 j_2}(t) \\ \cdots\cdots \\ S_{i_1 i_2 \ldots i_n}^j(t) = -[T^{-1}(t)]_i^j\{T_{j_1 j_2}^i(t)G_{i_1 i_2 \ldots i_n}^{j_1 j_2}(t) \\ \qquad + T_{j_1 j_2 j_3}^i(t)G_{i_1 i_2 \ldots i_n}^{j_1 j_2 j_3}(t) + \cdots \\ \qquad + T_{j_1 j_2 \ldots j_{n-2}}^i(t)G_{i_1 i_2 \ldots i_n}^{j_1 j_2 \ldots j_{n-2}}(t) \\ \qquad + T_{j_1 j_2 \ldots j_{n-1}}^i(t)G_{i_1 i_2 \ldots i_n}^{j_1 j_2 \ldots j_{n-1}}(t) \\ \qquad + T_{j_1 j_2 \ldots j_n}^i(t)G_{i_1 i_2 \ldots i_n}^{j_1 j_2 \ldots j_n}(t)\} \\ \cdots\cdots . \end{array} \right. \tag{11}$$

Arranging above equation with Eq.8, obtain the coefficients of Eq.5 as the following formulae:

$$S_{i_1}^j(t) = [T^{-1}(t)]_{i_1}^j \tag{12-1}$$

$$\begin{aligned} S_{i_1 i_2}^j(t) &= -[T^{-1}(t)]_i^j \\ &\quad T_{j_1 j_2}^i(t)S_{i_1}^{j_1}(t)S_{i_2}^{j_2}(t) \end{aligned} \tag{12-2}$$

$$\begin{aligned} S_{i_1 i_2 i_3}^j(t) &= -[T^{-1}(t)]_i^j \\ &\quad \{2T_{j_1 j_2}^i(t)S_{i_1}^{j_1}(t)S_{i_2 i_3}^{j_2}(t) \\ &\quad + T_{j_1 j_2 j_3}^i(t)S_{i_1}^{j_1}(t)S_{i_2}^{j_2}(t)S_{i_3}^{j_3}(t)\} \end{aligned} \tag{12-3}$$

$$\begin{aligned} &S_{i_1 i_2 i_3 i_4}^j(t) \\ &\quad = -[T^{-1}(t)]_i^j\{2T_{j_1 j_2}^i(t) \\ &\quad [S_{i_1}^{j_1}(t)S_{i_2 i_3 i_4}^{j_2}(t) + \tfrac{1}{2}S_{i_1 i_2}^{j_1}(t)S_{i_3 i_4}^{j_2}(t)] \\ &\quad + 3T_{j_1 j_2 j_3}^i(t)S_{i_1}^{j_1}(t)S_{i_2}^{j_2}(t)S_{i_3 i_4}^{j_3}(t) \\ &\quad + T_{j_1 j_2 j_3 j_4}^i(t)S_{i_1}^{j_1}(t)S_{i_2}^{j_2}(t)S_{i_3}^{j_3}(t)S_{i_4}^{j_4}(t)\} \end{aligned} \tag{12-4}$$

$$\begin{aligned} &S_{i_1 i_2 i_3 i_4 i_5}^j(t) = \\ &\quad -[T^{-1}(t)]_i^j\{2T_{j_1 j_2}^i(t) \\ &\quad [S_{i_1}^{j_1}(t)S_{i_2 i_3 i_4 i_5}^{j_2}(t) + S_{i_1 i_2}^{j_1}(t)S_{i_3 i_4 i_5}^{j_2}(t)] \\ &\quad + 3T_{j_1 j_2 j_3}^i(t)[S_{i_1}^{j_1}(t)S_{i_2}^{j_2}(t)S_{i_3 i_4 i_5}^{j_3}(t) \\ &\quad + S_{i_1}^{j_1}(t)S_{i_2 i_3}^{j_2}(t)S_{i_4 i_5}^{j_3}(t)] \\ &\quad + 4T_{j_1 j_2 j_3 j_4}^i(t)S_{i_1}^{j_1}(t)S_{i_2}^{j_2}(t)S_{i_3}^{j_3}(t)S_{i_4 i_5}^{j_4}(t) \\ &\quad + T_{j_1 j_2 j_3 j_4 j_5}^i(t)S_{i_1}^{j_1}(t)S_{i_2}^{j_2}(t)S_{i_3}^{j_3}(t) \\ &\qquad S_{i_4}^{j_4}(t)S_{i_5}^{j_5}(t)\} \end{aligned} \tag{12-5}$$

$\cdots\cdots$.

Carrying out the recursive process, the coefficients in the inverse transform Eq.5 are finally expressed in terms of those in the system solution Eq.4:

$$S_{i_1}^j(t) = [T^{-1}(t)]_{i_1}^j \tag{13-1}$$

$$\begin{aligned} S_{i_1 i_2}^j(t) &= -[T^{-1}(t)]_i^j \\ &\quad T_{j_1 j_2}^i(t)[T^{-1}(t)]_{i_1}^{j_1}[T^{-1}(t)]_{i_2}^{j_2} \end{aligned} \tag{13-2}$$

$$\begin{aligned} S_{i_1 i_2 i_3}^j(t) &= -[T^{-1}(t)]_i^j\{-2T_{j_1 j_2}^i(t) \\ &\quad [T^{-1}(t)]_{i_1}^{j_1}[T^{-1}(t)]_{i_2'}^{j_2} \\ &\quad T_{j_1' j_2'}^{i_2'}[T^{-1}(t)]_{i_2}^{j_2'}[T^{-1}(t)]_{i_3}^{j_2'}] \\ &\quad + T_{j_1 j_2 j_3}^i(t) \\ &\quad [T^{-1}(t)]_{i_1}^{j_1}[T^{-1}(t)]_{i_2}^{j_2}[T^{-1}(t)]_{i_3}^{j_3}\} \end{aligned} \tag{13-3}$$

$$\begin{aligned} &S_{i_1 i_2 i_3 i_4}^j(t) \\ &\quad = -[T^{-1}(t)]_i^j\{-2T_{j_1 j_2}^i(t) \\ &\quad [[T^{-1}(t)]_{i_1}^{j_1}[T^{-1}(t)]_{i_2'}^{j_2} \\ &\quad (-2T_{j_1' j_2'}^{i_2'}(t)[T_{i_2}^{j_1'}[T^{-1}(t)]_{i_3'}^{j_2'} \\ &\quad T_{k_1 k_2}^{i_3'}(t)[T^{-1}(t)]_{i_3}^{k_1}T^{-1}(t)]_{i_4}^{k_2} \\ &\quad + T_{j_1' j_2' j_3'}^{i_2'}(t)[T^{-1}(t)]_{i_2}^{j_1'}[T^{-1}(t)]_{i_3}^{j_2'}[T^{-1}(t)]_{i_4}^{j_3'}) \\ &\quad + \tfrac{1}{2}[T^{-1}(t)]_{i_1'}^{j_1}T_{j_1' j_2'}^{i_1'}(t)[T^{-1}(t)]_{i_1}^{j_1'}[T^{-1}(t)]_{i_2}^{j_2'} \\ &\quad [T^{-1}(t)]_{i_3'}^{j_2}T_{j_3' j_4'}^{i_3'}(t)[T^{-1}(t)]_{i_3}^{j_3'}[T^{-1}(t)]_{i_4}^{j_4'}] \\ &\quad - 3T_{j_1 j_2 j_3}^i(t)[T^{-1}(t)]_{i_1}^{j_1}[T^{-1}(t)]_{i_2}^{j_2}[T^{-1}(t)]_{i_3'}^{j_3} \\ &\quad T_{j_1' j_2'}^{i_3'}(t)[T^{-1}(t)]_{i_3}^{j_1'}[T^{-1}(t)]_{i_4}^{j_2'} \\ &\quad + T_{j_1 j_2 j_3 j_4}^i(t)[T^{-1}(t)]_{i_1}^{j_1}[T^{-1}(t)]_{i_2}^{j_2} \\ &\quad [T^{-1}(t)]_{i_3}^{j_3}[T^{-1}(t)]_{i_4}^{j_4}\} \end{aligned} \tag{13-4}$$

$$
\begin{aligned}
S^{j}_{i_1 i_2 i_3 i_4 i_5}(t) = & -[T^{-1}(t)]^{j}_{i} \\
& \{-2T^{i}_{j_1 j_2}(t)\{[T^{-1}(t)]^{j_1}_{i_1}[T^{-1}(t)]^{j_2}_{i_2} \\
& \{-2T^{j'_2}_{j'_1 j'_2}(t)[[T^{-1}(t)]^{j'_1}_{i_2}[T^{-1}(t)]^{j'_2}_{i_3} \\
& \quad (-2T^{i'_3}_{k'_1 k'_2}(t)[T^{-1}(t)]^{k'_1}_{i_3}[T^{-1}(t)]^{k'_2}_{i_4} \\
& \quad\quad T^{i'_4}_{k'_1 k'_2}(t)[T^{-1}(t)]^{k'_1}_{i_4}[T^{-1}(t)]^{k'_2}_{i_5} \\
& \quad +T^{i'_3}_{k_1 k_2 k_3}(t)[T^{-1}(t)]^{k_1}_{i_3}[T^{-1}(t)]^{k_2}_{i_4}[T^{-1}(t)]^{k_3}_{i_5}) \\
& \quad +\tfrac{1}{2}[T^{-1}(t)]^{j'_1}_{i'_2}T^{i'_2}_{k'_1 k'_2}(t)[T^{-1}(t)]^{k'_1}_{i'_2}[T^{-1}(t)]^{k'_2}_{i'_3} \\
& \quad [T^{-1}(t)]^{j'_2}_{i'_4}T^{i'_4}_{k'_1 k'_2}(t)[T^{-1}(t)]^{k'_1}_{i'_4}[T^{-1}(t)]^{k'_2}_{i'_5}] \\
& \quad -3T^{i'_2}_{j'_1 j'_2 j'_3}(t)[T^{-1}(t)]^{j'_1}_{i'_2}[T^{-1}(t)]^{j'_2}_{i'_3}[T^{-1}(t)]^{j'_3}_{i'_4} \\
& \quad\quad T^{i'_4}_{k_1 k_2}(t)[T^{-1}(t)]^{k_1}_{i_4}[T^{-1}(t)]^{k_2}_{i_5} \\
& \quad +T^{i'_2}_{j'_1 j'_2 j'_3 j'_4}(t)[T^{-1}(t)]^{j'_1}_{i'_2}[T^{-1}(t)]^{j'_2}_{i'_3} \\
& \quad\quad [T^{-1}(t)]^{j'_3}_{i'_4}[T^{-1}(t)]^{j'_4}_{i'_5}\} \\
& \quad +[T^{-1}(t)]^{j_1}_{i_1}T^{i'_1}_{j'_1 j'_2}(t)[T^{-1}(t)]^{j'_1}_{i_1}[T^{-1}(t)]^{j'_2}_{i_2} \\
& \quad [T^{-1}(t)]^{j_2}_{i'_3}[-2T^{i'_3}_{j'_1 j'_2}(t)[T^{-1}(t)]^{j'_1}_{i'_3}[T^{-1}(t)]^{j'_2}_{i'_4} \\
& \quad\quad T^{i'_4}_{k_1 k_2}(t)[T^{-1}(t)]^{k_1}_{i'_4}[T^{-1}(t)]^{k_2}_{i'_5} \\
& \quad\quad +T^{i'_3}_{j'_1 j'_2 j'_3}(t)[T^{-1}(t)]^{j'_1}_{i'_3}[T^{-1}(t)]^{j'_2}_{i'_4}[T^{-1}(t)]^{j'_3}_{i'_5}]\} \\
& \quad -3T^{i}_{j_1 j_2 j_3}(t)\{[T^{-1}(t)]^{j_1}_{i_1}[T^{-1}(t)]^{j_2}_{i_2}[T^{-1}(t)]^{j_3}_{i'_3} \\
& \quad\quad [-2T^{i'_3}_{j'_1 j'_2}(t)[T^{-1}(t)]^{j'_1}_{i'_3}[T^{-1}(t)]^{j'_2}_{i'_4} \\
& \quad\quad T^{i'_4}_{k_1 k_2}(t)[T^{-1}(t)]^{k_1}_{i'_4}[T^{-1}(t)]^{k_2}_{i'_5} \\
& \quad\quad +T^{i'_3}_{j'_1 j'_2 j'_3}(t)[T^{-1}(t)]^{j'_1}_{i'_3}[T^{-1}(t)]^{j'_2}_{i'_4}[T^{-1}(t)]^{j'_3}_{i'_5}] \\
& \quad +[T^{-1}(t)]^{j_1}_{i_1}[T^{-1}(t)]^{j_2}_{i'_2}T^{i'_2}_{j'_1 j'_2}(t) \\
& \quad\quad [T^{-1}(t)]^{j'_1}_{i'_2}[T^{-1}(t)]^{j'_2}_{i'_3} \\
& \quad\quad [T^{-1}(t)]^{j_3}_{i'_4}T^{i'_4}_{j'_1 j'_2}(t)[T^{-1}(t)]^{j'_1}_{i'_4}[T^{-1}(t)]^{j'_2}_{i'_5}\} \\
& \quad -4T^{i}_{j_1 j_2 j_3 j_4}(t)[T^{-1}(t)]^{j_1}_{i_1}[T^{-1}(t)]^{j_2}_{i_2}[T^{-1}(t)]^{j_3}_{i_3} \\
& \quad\quad [T^{-1}(t)]^{j_4}_{i'_4}T^{i'_4}_{j'_1 j'_2}(t)[T^{-1}(t)]^{j'_1}_{i'_4}[T^{-1}(t)]^{j'_2}_{i'_5} \\
& \quad +T^{i}_{j_1 j_2 j_3 j_4 j_5}(t)[T^{-1}(t)]^{j_1}_{i_1}[T^{-1}(t)]^{j_2}_{i_2}[T^{-1}(t)]^{j_3}_{i_3} \\
& \quad\quad [T^{-1}(t)]^{j_4}_{i_4}[T^{-1}(t)]^{j_5}_{i_5}\}
\end{aligned}
\qquad (13-5)
$$

..... .

3. NONLINEAR TRANSPORT FOR THE PHASE SPACE OF DYNAMIC SYSTEMS

Substitution of the inverse transform Eq.5 into the boundary Eq.1 at the initial state $X_0 = X(t_0)$ to get the boundary Eq.2 at the final state $X_t = X(t)$ completes theoretically the nonlinear transport for the phase space of a general nonlinear dynamic system. As both the system solution Eq.4 $X(t) = X_t(X_0.t)$ and its inverse transform Eq.5 $X(t_0) = X_0(X_t, t)$ are nonlinear, the phase space transport of a general nonlinear dynamic system is a nonlinear process.

As a typical example, in accelerator, the nonlinear beam phase space transport reveals essential differences from the traditional linear beam phase space transport. In Hamiltonian linear transport system, if the initial boundary equation of the accelerator beam phase space is an ellipse[2]:

$$X_0^T \sigma_0^{-1} X_0 = 1 \ . \qquad (14)$$

then, it evolves through any time still to an ellipse with its area unchanged:

$$X_t^T \sigma_t^{-1} X_t = 1 \ . \qquad (15)$$

where, $|\sigma_t| = |\sigma_0|$.

But in Hamiltonian nonlinear transport system, the substitution of Eq.5 into Eq.14 gives a equation with infinite number of power terms, showing that the beam phase space boundary is sophistically distorted but still with its volume conserved through Hamiltonian nonlinear transport system.

4. DISCUSSION

Based on the above developed theory, an expert system can be implemented on IBM 286 to output automatically the analytical expressions of any order coefficients of the inverse transform Eq.5 for a general dynamic system Eq.(3), as well as the numerical formulation of any order coeffients of the inverse transform Eq.5 for a concrete given nonlinear dynamic system. Finally the expert system demonstrates the evolution process of the phase space boundary from a given initial state to the final state at any time through a given Hamiltonian nonlinear transport system. All these works will be published in other articles.

5. REFERENCES

1) Xie Xi and Liu Chunliang, "Any order approximate analytical solution of nonlinear dynamic syetem equation for accelerators," Chinese, Journal of Nuclear physics, **Vol.12 No.3**, 1991, pp.283–286.

2) Kar L. Brown, **A first and second order matrix theory for the design of beam transport systems and charged partical spectrometers**, SLAC-75, 1971, pp.104-114.

DERIVING THE GENERAL EXPRESSIONS OF NONLINEAR TRANSPORT COEFFICIENTS OF ACCELERATOR BEAM PHASE SPACE BY ARTIFICIAL INTELLIGENCE

Xia Jiawen
Institute of Mordern Physics, Academia Sinica, P.O. Box 31, Lanzhou, 730000, China

and

Xie Xi , Liu Chunliang
Graduate School of Nuclear Industry, P.O. Box 1477, Beijing, 102413, China

ABSTRACT

The transport of accelerator beam phase space is a nonlinear theoretical problem. Recently, a new theory for the nonlinear transport of accelerator beam phase space has been developed, and a mathematical model of the nonlinear beam transport was provided. It is difficult to establish the model because of considerable and complex symbol calculations. In this paper a computer program in the logic programming language of artificial intelligence Arity/Prolog was made on IBM-PC 286 or 386 machine to derive automatically the general expressions of any order phase space transport coefficients. By this method, the concrete mathematical model of beam transport was established easily from the nonlinear transport theory. The prospect of the application of artificial intelligence can be seen, people will be further saved out from the chore of symbol calculation. Finally, the ninth order transport coefficient was given as a typical example of high order result obtained from machine.

1. INTRODUCTION

The phase space transport of accelerator beam is a nonlinear dynamic theoretical problem. Recently, a new theory has been developed for the nonlinear phase space transport. By using this new theory, the concrete mathematical model can be established for the nonlinear transport of beam phase space, but it is very difficult to establish the model by manual deriving because the mathematical derivation is a very complex work and needs a unusual carefulness and much more time. The main work of the calculation is deriving the general expressions of nonlinear transport coefficients. Now, many new techniques of artificial intelligence have been developed, symbol calculations can be done by computers with logic programming languages, such as, Lisp, Prolog etc. So, the complex manual work of mathematical calculations can become a simple computer process by using artificial intelligence, thus relieving scientists from the chore of symbol calculation. In this paper a computer program in the artificial intelligence language Arity/Prolog was made on IBM-PC 286 or 386 computer to derive automatically the general expressions of any order phase space transport coefficients.

2. MATHEMATICAL THOUGHT OF DERIVING ANY ORDER TRANSPORT COEFFICIENTS BY ARTIFICIAL INTELLIGENCE

In the new theory, the phase space transport of nonlinear dynamic system is such a mathematical process that the initial state equation of the system phase space boundary $F(X_0) = 0$ transforms to the final state boundary equation $F[X_0(X_t, t)] = f(X_t, t) = 0$. Where, the initial phase point of dynamic system $X_0 = [x_0^1, x_0^2, \ldots, x_0^N]^T$ is related with the final phase point $X_t = [x_t^1, x_t^2, \ldots, x_t^N]^T$ by the motion differential equation[1] of the system in N-dimension phase space. The solution[1] of the differential equation is

$$\begin{aligned} x_t^i = \; & R_j^i(t)[\delta_{j_1}^j x_0^{j_1} + \beta_{j_1 j_2}^j(t) x_0^{j_1} x_0^{j_2} \\ & + \beta_{j_1 j_2 j_3}^j(t) x_0^{j_1} x_0^{j_2} x_0^{j_3} + \cdots \\ & + \beta_{j_1 j_2 \ldots j_n}^j(t) x_0^{j_1} x_0^{j_2} \ldots x_0^{j_n} + \cdots] \quad . \end{aligned} \tag{1}$$

then, the inverse transform of Eq.1 can be expressed as following :

$$\begin{aligned} x_0^j = \; & S_{i_1}^j(t) x_t^{i_1} + S_{i_1 i_2}^j(t) x_t^{i_1} x_t^{i_2} + \cdots \\ & + S_{i_1 i_2 i_3}^j(t) x_t^{i_1} x_t^{i_2} x_t^{i_3} + \cdots \\ & + S_{i_1 i_2 \ldots i_n}^j(t) x_t^{i_1} x_t^{i_2} \ldots x_t^{i_n} + \cdots \quad , \end{aligned} \tag{2}$$

here, $i, i_1, i_2, \ldots, i_n; j, j_1, j_2, \ldots, j_n = 1, 2, \ldots, N$. The any order aberration coefficients $R_j^i(t)\beta_{j_1 j_2 \ldots j_n}^j(t)$ had been obtained [1] from the motion differential equa-

tion. Here, deriving the any order transport coefficients $S^j_{i_1 i_2 \ldots i_n}(t)$ is the work of this paper by artificial intelligence. The following is the mathematical thought of deriving the transport coefficients by computers.

Rewrite Eq.1 :

$$\begin{aligned} x^j_0 = \; & [R^{-1}(t)]^j_{i_1} x^{i_1}_t - \beta^j_{j_1 j_2}(t) x^{j_1}_0 x^{j_2}_0 - \cdots \\ & - \beta^j_{j_1 j_2 j_3}(t) x^{j_1}_0 x^{j_2}_0 x^{j_3}_0 - \cdots \\ & - \beta^j_{j_1 j_2 \ldots j_n}(t) x^{j_1}_0 x^{j_2}_0 \ldots x^{j_n}_0 - \cdots \quad , \end{aligned} \tag{3}$$

where, the sum calculating of tensor is used:

$$\left\{ \begin{aligned} x^j_0 = \; & \delta^j_{j_1} x^{j_1}_0 \\ [R^{-1}(t)]^j_i x^i_t = \; & [R^{-1}(t)]^j_{i_1} x^{i_1}_t \\ = \; & [R^{-1}(t)]^i_t \delta^t_{i_1} x^{i_1}_t \quad . \end{aligned} \right. \tag{4}$$

Substituting Eq.2 in the left of Eq.3 and eliminating the first order terms in two sides of the equation, Eq.3 becomes:

$$\begin{aligned} & S^j_{i_1 i_2}(t) x^{i_1}_t x^{i_2}_t + S^j_{i_1 i_2 i_3}(t) x^{i_1}_t x^{i_2}_t x^{i_3}_t + \cdots \\ & \quad + S^j_{i_1 i_2 \ldots i_n}(t) x^{i_1}_t x^{i_2}_t \ldots x^{i_n}_t + \cdots \\ & = -\beta^j_{j_1 j_2}(t) x^{j_1}_0 x^{j_2}_0 - \beta^j_{j_1 j_2 j_3}(t) x^{j_1}_0 x^{j_2}_0 x^{j_3}_0 - \cdots \\ & \quad - \beta^j_{j_1 j_2 \ldots j_n}(t) x^{j_1}_0 x^{j_2}_0 \ldots x^{j_n}_0 - \cdots \quad , \end{aligned} \tag{5}$$

the coefficients of the first order term $x^{i_1}_t$ is

$$S^j_{i_1}(t) = [R^{-1}(t)]^j_{i_1} \quad . \tag{6}$$

With replacing the up-mark j by up-marks $j_1, j_2, \ldots, j_n$ respectively, substituting Eq.2 into the right of Eq.5; then arranging the right; finally, comparing the coefficient of every order term at left with that of the same order term at right, so, the expression can be obtained of any order transport coefficiects. The obtained expressions are recursion formulae, that is, if these coefficients from first-order $S^j_{i_1}(t)$ to the (n-1)th-order $S^j_{i_1 i_2 \ldots i_{n-1}}(t)$ are known, the (n)th-order coefficient $S^j_{i_1 i_2 \ldots i_n}(t)$ can be obtained. Above three procedures, namely, substituting; arranging and comparing are the logistic thought of deriving transport coefficients by artificial intelligence. Where, the arranging is the most difficult and important procedure of computer derivation. The mathematical methods of this procedure are as follows:

(a), making maltinomial multiplications in every order terms of the right of Eq.5 become the multiplication of two multinomials, namely:

$$x^{j_1}_0 x^{j_2}_0 \rightarrow x^{j_1}_0 (x^{j_2}_0) \quad ,$$

the 2th order term is the multiplying of two multinomials $x^{j_1}_0$ and $x^{j_2}_0$;

$$x^{j_1}_0 x^{j_2}_0 x^{j_3}_0 \rightarrow (x^{j_1}_0 x^{j_2}_0) x^{j_3}_0 \quad ,$$

the 3th order term is the multiplying of two multinomials $(x^{j_1}_0 x^{j_2}_0)$ and $x^{j_3}_0$, where, the first multinomial $(x^{j_1}_0 x^{j_2}_0)$ is the multiplying result of the 2th order term;

..... ;

$$x^{j_1}_0 x^{j_2}_0 \ldots x^{j_{n-1}}_0 x^{j_n}_0 \rightarrow (x^{j_1}_0 x^{j_2}_0 \ldots x^{j_{n-1}}_0) x^{j_n}_0 \quad ,$$

the (n)th order term is the multiplying of two multinomials $(x^{j_1}_0 x^{j_2}_0 \ldots x^{j_{n-1}}_0)$ and $x^{j_n}_0$, where, the first multinomial $(x^{j_1}_0 x^{j_2}_0 \ldots x^{j_{n-1}}_0)$ is the multiplying result of the (n-1)th order term;

..... .

(b), After every multiplying of two multinomials, combining the same terms and the symmetrical terms.

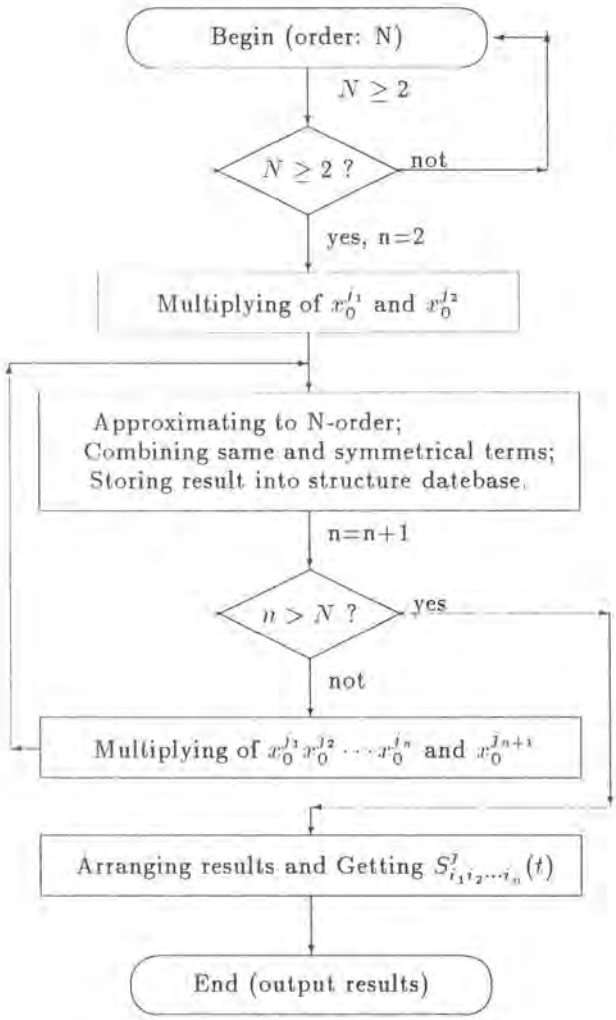
To summarize , above two procedures are such a process of processing every order terms of the right of Eq.5 one by one, and in every processing, the two mathematical procedures (a),(b) are done.

(c), After all multinomial multiplications in the right of Eq.5, combining same order terms.

In conclusion, the three procedures (a),(b),(c) are the main mathematical thoughts of deriving any order transport coefficients by artificial intelligence.

3. DERIVING ANY ORDER TRANSPORT COEFFICIENTS BY ARTIFICIAL INTELLIGENCE

Prolog is a logic programming language of intelligence. By using it, a practical artificial intelligence system can be established facilitately. In this paper, a computer program in Arity/Prolog was made which derive automatically the general expressions of any order phase space transport coefficients. With the supporting of Arity/Prolog interpreter or Arity/Prolog compiler, this program can be operated on IBM PC 286 or 386 machines. The following is the block diagram of the program structure.



Block diagram of the program structure

As the block diagram shows, the mathematical thought of deriving any order tramsport coefficients is comprised in the infereme procedure of this program.

With the using of many programming techniques[2], such as backtracking, structure database, etc., this deriving program with a tight structure can be read easily. The key technique of replacing recursion with interation broke through the 640k RAM limit and realized the practical operating of the program on IBM-PC 286 or 386 computer. By using this intelligent system, any order transport coefficints can be derived out automatically and fastly. The following are 2th,3th,4th,5th and 9th order transport coefficints output directly from a computer, and where, the results of 2th,3th,4th and 5th order are showing no difference with those by manual doing. The symbol corresponding relations between computer output and mathematical formulae are:

$$S\langle j; i(1), i(2), \cdots, i(n)\rangle \Longleftrightarrow S^j_{i_1 i_2 \ldots i_n}(t)$$
$$beta\langle j; j(1), j(2), \cdots, j(n)\rangle \Longleftrightarrow \beta^j_{j_1 j_2 \ldots j_n}(t).$$

```
N = 2
S<j;i(1),i(2)>=
  -beta<j;j(1),j(2)>
      *[S<j(1);i(1)>*S<j(2);i(2)>]
N = 3
S<j;i(1),i(2),i(3)> =
  -beta<j;j(1),j(2)>*[2*S<j(1);i(1)>
      *S<j(2);i(2),i(3)>]
  -beta<j;j(1),j(2),j(3)>*[S<j(1);i(1)>
      *S<j(2);i(2)>*S<j(3);i(3)>]
N = 4
S<j;i(1),i(2),i(3),i(4)> =
  -beta<j;j(1),j(2)>*[S<j(1);i(1),i(2)>
      *S<j(2);i(3),i(4)>+2*S<j(1);i(1)>
      *S<j(2);i(2),i(3),i(4)>]
  -beta<j;j(1),j(2),j(3)>*[3*S<j(1);i(1)>
      *S<j(2);i(2)>*S<j(3);i(3),i(4)>]
  -beta<j;j(1),j(2),j(3),j(4)>*[S<j(1);i(1)>
      *S<j(2);i(2)>*S<j(3);i(3)>*S<j(4);i(4)>]
N = 5
S<j;i(1),i(2),i(3),i(4),i(5)> =
  -beta<j;j(1),j(2)>*[2*S<j(1);i(1),i(2)>
      *S<j(2);i(3),i(4),i(5)>+2*S<j(1);i(1)>
      *S<j(2);i(2),i(3),i(4),i(5)>]
  -beta<j;j(1),j(2),j(3)>*[3*S<j(1);i(1)>
      *S<j(2);i(2),i(3)>*S<j(3);i(4),i(5)>
      +3*S<j(1);i(1)>*S<j(2);i(2)>
      *S<j(3);i(3),i(4),i(5)>]
  -beta<j;j(1),j(2),j(3),j(4)>*[4*S<j(1);i(1)>
      *S<j(2);i(2)>*S<j(3);i(3)>
      *S<j(4);i(4),i(5)>]
  -beta<j;j(1),j(2),j(3),j(4),j(5)>
      *[S<j(1);i(1)>*S<j(2);i(2)>*S<j(3);i(3)>
      *S<j(4);i(4)>*S<j(5);i(5)>]

N = 9
S<j;i(1),i(2),i(3),i(4),
                  i(5),i(6),i(7),i(8),i(9)> =
  -beta<j;j(1),j(2)>
      *[2*S<j(1);i(1),i(2),i(3),i(4)>
      *S<j(2);i(5),i(6),i(7),i(8),i(9)>
      +2*S<j(1);i(1),i(2),i(3)>
      *S<j(2);i(4),i(5),i(6),i(7),i(8),i(9)>
      +2*S<j(1);i(1),i(2)>
      *S<j(2);i(3),i(4),i(5),
                  i(6),i(7),i(8),i(9)>
      +2*S<j(1);i(1)>
      *S<j(2);i(2),i(3),i(4),i(5),
                  i(6),i(7),i(8),i(9)>]
  -beta<j;j(1),j(2),j(3)>
```

```
    *[S<j(1);i(1),i(2),i(3)>
    *S<j(2);i(4),i(5),i(6)>
    *S<j(3);i(7),i(8),i(9)>
    +6*S<j(1);i(1),i(2)>
    *S<j(2);i(3),i(4),i(5)>
    *S<j(3);i(6),i(7),i(8),i(9)>
    +3*S<j(1);i(1)>
    *S<j(2);i(2),i(3),i(4),i(5)>
    *S<j(3);i(6),i(7),i(8),i(9)>
    +3*S<j(1);i(1),i(2)>*S<j(2);i(3),i(4)>
    *S<j(3);i(5),i(6),i(7),i(8),i(9)>
    +6*S<j(1);i(1)>*S<j(2);i(2),i(3),i(4)>
    *S<j(3);i(5),i(6),i(7),i(8),i(9)>
    +6*S<j(1);i(1)>*S<j(2);i(2),i(3)>
    *S<j(3);i(4),i(5),i(6),i(7),i(8),i(9)>
    +3*S<j(1);i(1)>*S<j(2);i(2)>
    *S<j(3);i(3),i(4),i(5),
                i(6),i(7),i(8),i(9)>]
-beta<j;j(1),j(2),j(3),j(4)>
    *[4*S<j(1);i(1),i(2)>
    *S<j(2);i(3),i(4)>*S<j(3);i(5),i(6)>
    *S<j(4);i(7),i(8),i(9)>+12*S<j(1);i(1)>
    *S<j(2);i(2),i(3)>
    *S<j(3);i(4),i(5),i(6)>
    *S<j(4);i(7),i(8),i(9)>+12*S<j(1);i(1)>
    *S<j(2);i(2),i(3)>*S<j(3);i(4),i(5)>
    *S<j(4);i(6),i(7),i(8),i(9)>
    +12*S<j(1);i(1)>*S<j(2);i(2)>
    *S<j(3);i(3),i(4),i(5)>
    *S<j(4);i(6),i(7),i(8),i(9)>
    +12*S<j(1);i(1)>*S<j(2);i(2)>
    *S<j(3);i(3),i(4)>
    *S<j(4);i(5),i(6),i(7),i(8),i(9)>
    +4*S<j(1);i(1)>
    *S<j(2);i(2)>*S<j(3);i(3)>
    *S<j(4);i(4),i(5),i(6),i(7),i(8),i(9)>]
-beta<j;j(1),j(2),j(3),j(4),j(5)>
    *[5*S<j(1);i(1)>*S<j(2);i(2),i(3)>
    *S<j(3);i(4),i(5)>*S<j(4);i(6),i(7)>
    *S<j(5);i(8),i(9)>+30*S<j(1);i(1)>
    *S<j(2);i(2)>*S<j(3);i(3),i(4)>
    *S<j(4);i(5),i(6)>
    *S<j(5);i(7),i(8),i(9)>
    +10*S<j(1);i(1)>*S<j(2);i(2)>
    *S<j(3);i(3)>*S<j(4);i(4),i(5),i(6)>
    *S<j(5);i(7),i(8),i(9)>+20*S<j(1);i(1)>
    *S<j(2);i(2)>*S<j(3);i(3)>
    *S<j(4);i(4),i(5)>
    *S<j(5);i(6),i(7),i(8),i(9)>
    +5*S<j(1);i(1)>*S<j(2);i(2)>
    *S<j(3);i(3)>*S<j(4);i(4)>
    *S<j(5);i(5),i(6),i(7),i(8),i(9)>]
-beta<j;j(1),j(2),j(3),j(4),j(5),j(6)>
    *[20*S<j(1);i(1)>*S<j(2);i(2)>
    *S<j(3);i(3)>*S<j(4);i(4),i(5)>
    *S<j(5);i(6),i(7)>*S<j(6);i(8),i(9)>
    +30*S<j(1);i(1)>*S<j(2);i(2)>
    *S<j(3);i(3)>*S<j(4);i(4)>
    *S<j(5);i(5),i(6)
    *S<j(6);i(7),i(8),i(9)>
    +6*S<j(1);i(1)>*S<j(2);i(2)>
    *S<j(3);i(3)>*S<j(4);i(4)>*S<j(5);i(5)>
    *S<j(6);i(6),i(7),i(8),i(9)>]
-beta<j;j(1),j(2),j(3),j(4),j(5),j(6),j(7)>
    *[21*S<j(1);i(1)>*S<j(2);i(2)>
    *S<j(3);i(3)>*S<j(4);i(4)>*S<j(5);i(5)>
    *S<j(6);i(6),i(7)>*S<j(7);i(8),i(9)>
    +7*S<j(1);i(1)>*S<j(2);i(2)>
    *S<j(3);i(3)>*S<j(4);i(4)>*S<j(5);i(5)>
    *S<j(6);i(6)>*S<j(7);i(7),i(8),i(9)>]
-beta<j;j(1),j(2),j(3),j(4),j(5),
                j(6),j(7),j(8)>
    *[8*S<j(1);i(1)>*S<j(2);i(2)>
    *S<j(3);i(3)>*S<j(4);i(4)>*S<j(5);i(5)>
    *S<j(6);i(6)>*S<j(7);i(7)>
    *S<j(8);i(8),i(9)>]
-beta<j;j(1),j(2),j(3),j(4),j(5),
                j(6),j(7),j(8),j(9)>
    *[S<j(1);i(1)>*S<j(2);i(2)>*S<j(3);i(3)>
    *S<j(4);i(4)>*S<j(5);i(5)>*S<j(6);i(6)>
    *S<j(7);i(7)>*S<j(8);i(8)>*S<j(9);i(9)>]
```

4. DISCUSSION

By using the artificial intelligence, any high order transport coefficients can be obtained fastly and accurately. Obviously, with this new method man's brain will be extended and more time can be saved for many physicists.

Based on the transport coefficient expressions obtained from machines, a numerical calculating program can be generated and will be applied in the practical beam transport.

5. REFERENCES

1) Xie Xi and Liu Chunliang, "Any order approximate analytical solution of nonlinear dynamic system equation for accelerators," Chinese, Journal of Nuclear Physics, **Vol.12 No.3**, 1991, pp.283-286.

2) L. Sterling and E. Shapiro, **The Art of Prolog Advanced Programming Techniques**, the MIT Press, Cambridge Massachusetss, England, 1986.

Evaluation of Third-Harmonic Voltage Flattopping for a Superconducting Cyclotron*

M.M. Gordon and Dong-o Jeon
National Superconducting Cyclotron Laboratory
Michigan State University
East Lansing, MI48824-1321,U.S.A.

ABSTRACT

As demonstrated in the PSI-SIN 600 MeV cyclotron, third harmonic voltage flattopping can lead to great improvements in the phase width and energy homogeneity of the beam. The field of that cyclotron is, however, almost perfectly isochronous, and to determine whether this condition is a prerequisite for flattopping, we have investigated whether similar results could be obtained for superconducting cyclotrons like ours where the phase deviations can become quite large in the nonisochronous extraction region. Our calculations show that for phase deviations up to 30°, the beam improvements are quite comparable to those obtained for a perfectly isochronous field provided the third harmonic amplitude can be increased by about 25%. However, the benefits of flattopping decrease significantly and the third harmonic amplitude increases rapidly as the maximum phase deviations rise to about 60°.

1. Introduction

Among cyclotron designers who aim at single turn extraction, the use of third harmonic voltage flattopping has long been recognized as a valuable tool for achieving higher beam currents while fulfilling the requirement of energy homogeneity within the extracted beam.[1] A very successful application of this technique has been achieved in the 600 MeV cyclotron at PSI(SIN) near Zurich.[2] More recently, experimental results have been reported on the use of a fourth harmonic voltage at the TRIUMF cyclotron.[3]

The K500 and K1200 superconducting cyclotrons at our laboratory have three magnet sectors with three dees in the intervening valleys. The interiors of two of these dees are occupied by cryopanels, while the remaining dee is vacant so that this space could be used to house a smaller dee that would provide a third harmonic voltage. The calculations reported here were designed to determine whether this project might be worth pursuing.

We used the simple differential equations for the longitudinal motion to find the energy E and the phase ϕ as a function of turn number from given starting conditions. We then determined the range of initial phases ϕ_i for which the energy values on the final turn exceed the maximum energy of the previous turn. Within this phase range, the functional dependence of the final energy on the initial phase was optimized by adjusting the three available parameters: the amplitude and the relative phase of the third harmonic voltage , and the fundamental RF frequency. The availability of three parameters (rather than one) enables one to overcome the difficulties arising from the nonisochronous character of the magnetic field.

The electrode structures at the center of our cyclotrons are designed using the CYCLONE program which integrates orbits starting from the source (or inflector) using realistic electric fields. This process is based on the concept of a"central ray". That is, the central ray orbit is the one having the particular starting time which leads to the best overall energy-gain and which ends up with optimum centering. We assume that the current density as a function of starting time is symmetric about this value, and that the peak current density is associated with the central ray. When we compared the actual phase versus energy curve obtained from the CYCLONE program with curves obtained from the longitudinal motion equations for different starting phases, we found that the best match occured for an assumed central ray starting phase $\phi_{ci} = -10°$. The calculations reported here therefore assumed this value. We also carried out calculations using $\phi_{ci} = 0°$, but the results were not significantly different.

2. Procedure

The deviation of the magnetic field from isochronism, as determined from the equilibrium orbit code, is specified by the frequency error:

$$\Delta(E) = \omega_0/\omega - 1 = \nu_0\tau(E) - 1, \qquad (1)$$

*Work supported by the National Science Foundation under Grant No. 89-13815

where $\nu_0 = \omega_0/2\pi$ is a given reference frequency, and $\tau(E) = 2\pi/\omega$ is the orbit period for a given energy. Figure 1 shows a plot of this function as derived from the K1200 field data for two cases:

$$E_f/A = 40 \text{ MeV} \text{ with } q/A = 0.25, \text{ and}$$

$$E_f/A = 200 \text{ MeV} \text{ with } q/A = 0.5,$$

where E_f is the final energy, qe is the ion's charge, and A is its mass number. These curves show especially large values of $\Delta(E)$ near $E = E_f$ which result from the ions being accelerated out into the non-isochronous edge region of the field during the pre-extraction process. Such curves can, of course, be shifted up or down by changing the reference frequency ν_0.

During cyclotron operation, the RF frequency is adjusted as part of the optimization of the extracted beam current. We therefore set

$$\nu_{rf} = h(1+\epsilon)\nu_0, \tag{2}$$

where h is the harmonic number and ϵ is an adjustable parameter. Note that ϵ values are generally very small and are given below in parts per million(ppm). Although we assume that the magnetic field is fixed, one could choose instead to make such adjustments by shifting the central field level.

The nonzero values of $\Delta(E)$ and ϵ produce a phase change per turn given by

$$\begin{aligned} \frac{d\phi}{dn} &= \omega_{rf}\tau(E) - 2\pi h \\ &= 2\pi h\left[(1+\epsilon)\,\Delta(E) + \epsilon\right]. \end{aligned} \tag{3}$$

This equation would have an additional term if the dee voltage depended on the energy (or radius),[4] but we decided to ignore this effect for the present. Also note that $h = 1$ for the cases considered here.

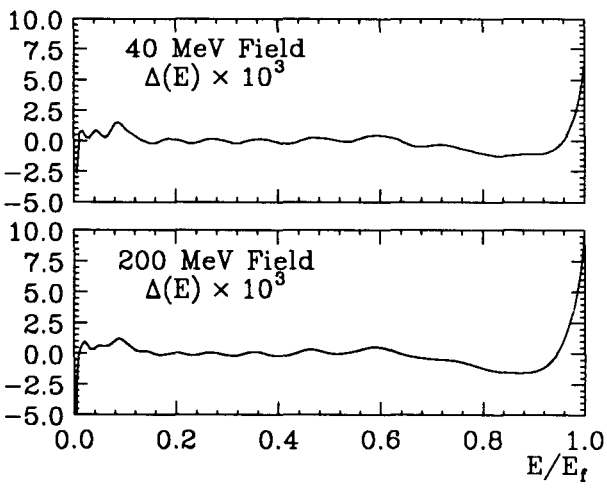


Fig. 1. Plots of the frequency error $\Delta = \omega_0/\omega - 1$ as a function of energy for two fields used to produce ions having the following final energies and charges: E_f/A=40 MeV with q/A=0.25(top), and E_f/A=200 MeV with q/A=0.5(bottom). The 200 MeV field is the least isochronous of all our fields.

When the effect of a third harmonic voltage is included, the increase in energy per turn is given by

$$\frac{dE}{dn} = qV_1\left[\cos\phi - \lambda\cos(3\phi - \psi)\right], \tag{4}$$

where V_1 is the peak voltage gain per turn produced by the first harmonic, $\lambda = V_3/V_1$ is the voltage ratio of the third to the first harmonic, and ψ is the relative phase. Because of the electrode structures in the center of the cyclotron, the turn pattern is approximately fixed. We therefore set

$$qV_1 = E_f/n_0, \tag{5}$$

where n_0 is the nominal turn number. For the present calculations, we chose both $n_0 = 500$ and $n_0 = 800$, which are approximately the values appropriate for the K500 and K1200 cyclotrons. Also, changing n_0 from 500 to 800 allowed us to investigate the effect of increasing the phase deviations without changing the magnetic field.

The above differential equations for ϕ and E were integrated starting from $n = 0$ with $E = 0$ and initial phase values ϕ_i which were distributed symmetrically about the central ray value ϕ_{ci}. For any parameter set $(\lambda, \psi, \epsilon)$, the integration proceeds until the central ray energy exactly matches the given final energy(e.g., 40 MeV), and this determines the final turn number n_f. The energy values for $n = n_f$ and different ϕ_i values are then examined to see if they meet certain criteria, and if not, a linear projection technique is used to obtain an improved parameter set. The entire process is iterated until the desired results are obtained.

For the special case $\lambda = 0$ where the third harmonic is completely absent, only the frequency parameter ϵ is available, and this is adjusted so that the central ray has the maximum energy on the final turn. This condition has long been recognized as providing the best situation for single turn extraction.[5]

As λ increases above zero, the curve showing the final turn energy as a function of ϕ_i becomes broader and flatter, and when λ exceeds a critical value λ_c, this curve exhibits two peaks rather than one. In this case, the parameters ψ and ϵ are chosen so that the two peaks have the same height with the central ray in the valley midway between them. These conditions are consistent with our previously noted assumption concerning the symmetry of the current density as a function of starting time.

Finally, when λ increases to λ_{max}, the central ray's final energy declines enough to reach the maximum energy on the previous turn. At this point, the calculation stops. Although results were obtained over the complete range of λ values, only those of particular interest will be discussed below.

3. Results

Single turn extraction requires turn separation only at the final energy where the ions must clear the septum and enter the extraction channel. This radial separation

of the turns at the final energy can be obtained provided the ion bunches are clearly separated in energy. That is, even if these bunches overlap spatially because of the radial oscillations, they can in principle be separated by a suitable dispersive process. In our cyclotrons as in many others, turn separation is generated by passage through the $\nu_r = 1$ resonance, and the amount of this separation is restricted by vertical stability requirements. This process has therefore limited dispersion.

In presenting our results here, we shall assume an energy spread within the bunch on the final turn, δE, which is just one-half of the peak energy gain on this turn. In this case, the energy gap between successive bunches is equal to δE.

Consider first the results obtained when the third harmonic is absent, i.e., $\lambda = 0$. For an isochronous field and a central phase $\phi_c \equiv 0$, one finds that the acceptable initial phase width is given by

$$\delta\phi_i = 2/\sqrt{n_0} \text{ (in radians)}, \qquad (6)$$

where n_0 is defined in Eq. 5 above. For the two cases considered here, $n_0 = 500$ and $n_0 = 800$, this yields 5.1° and 4.1°, respectively.

The corresponding results were computed for the 40 MeV and the 200 MeV fields whose deviations from isochronism are shown in Fig. 1. For $n_0 = 500$, we found $\delta\phi_i = 4.8°$ and 4.7° for the 40 MeV and 200 MeV cases, while for $n_0 = 800$, we obtained $\delta\phi_i = 3.2°$ and 2.8° for the same two cases. Considering how small these values are, and considering also that the beam current is roughly proportional to $\delta\phi_i$, one can easily recognize the potential value of flattopping.

The greatest amplification of $\delta\phi_i$ is obtained for values of λ in the range $\lambda_c < \lambda < \lambda_{max}$ where the curve showing the final energy as a function of ϕ_i has two peaks. Following the procedure described near the end of the last section, and imposing the condition discussed above on the energy spread δE within the bunch, we found the results that are summarized in the tables below, one for $n_0 = 500$ and the other for $n_0 = 800$. In each table, data are presented for the two fields (40 MeV and 200 MeV) described in Fig. 1, and as a reference, for an isochronous field ($\Delta \equiv 0$).

Note that the actual final turn number n_f exceeds n_0 as λ increases, mainly because the energy gain per turn is roughly proportional to $qV_1(1 - \lambda)$. Following n_f in the tables are the values of λ, the fractional third harmonic voltage parameter, and the relative phase ψ of the third harmonic. These are followed by the values of ϵ, the fractional change in the main RF frequency. The next row lists the resultant values of $\delta E/qV_1$, where δE is the energy spread within the final bunch as well as the energy gap between bunches, and qV_1 is the peak energy gain per turn produced by the main harmonic. Finally, the values of $\delta\phi_i$ are given.

The values of λ given in the tables show that the required percentage of third harmonic voltage rises from 12 for the isochronous field up to 14 or 15 for the two other fields when $n_0 = 500$. For $n_0 = 800$, however, this percentage rises from 12 up to between 18 and 20 in the same cases. These differences are quite significant when one considers the RF power requirement, and are due mainly to differences in the phase deviations. That is, the central phase ϕ_c ranges from −10° to +10° for the isochronous field, and from about −30° to +20° for the two nonisochronous fields when $n_0 = 500$. For $n_0 = 800$, on the other hand, the values of ϕ_c range from about −50° to +30° for the latter two fields.

Table 1 Results for $n_0 = 500$

Field	Isoc	40 MeV	200 MeV
n_f	570.1	579.1	582.3
λ	0.123	0.140	0.146
ψ(deg)	0.0	2.0	2.9
ϵ(ppm)	97.5	91.6	101.3
$\delta E/qV_1$	0.438	0.430	0.430
$\delta\phi_i$(deg)	35.4	34.2	33.5

Table 2 Results for $n_0 = 800$

Field	Isoc	40 MeV	200 MeV
n_f	910.5	962.0	980.4
λ	0.122	0.180	0.201
ψ(deg)	31.4	24.9	22.8
ϵ(ppm)	61.1	66.5	85.9
$\delta E/qV_1$	0.439	0.421	0.397
$\delta\phi_i$(deg)	31.4	24.9	22.8

The most impressive numbers in these tables are the values of $\delta\phi_i$. For $n_0 = 500$, the values for the two nonisochronous fields are less than 2° below the $\delta\phi_i$ for the isochronous field, and for all three fields, the values are about seven times larger than those given above for $\lambda = 0$. On the other hand, for $n_0 = 800$, there are significant differences between the $\delta\phi_i$ values for the isochronous and nonisochronous fields. One finds nevertheless that all these values are roughly eight times larger than those cited above for $\lambda = 0$ in the corresponding cases.

To illuminate the results further, plots of the final energy versus the initial phase are shown in Fig. 2 for all three fields when $n_0 = 800$. These curves show the two peaks of equal height with the central ray point ($\phi_{ci} = -10°$) in the valley midway between them. A horizontal broken line divides the full height into two equal halves each of height δE, as defined above. That is, the top half represents orbits within the final bunch while the bottom half shows the gap between successive bunches. The width of the curve where the straight line crosses it then defines $\delta\phi_i$, the acceptable initial phase width given in Table 2. Including the central ray itself, we therefore find three orbits which end up at $n = n_f$ with exactly the same energy.

Plots of the phase ϕ as a function of energy from $E = 0$ to $E = E_f$ are shown in Fig. 3 for the same three cases used in Fig. 2. The three solid curves correspond to the three orbits just mentioned which end up with the

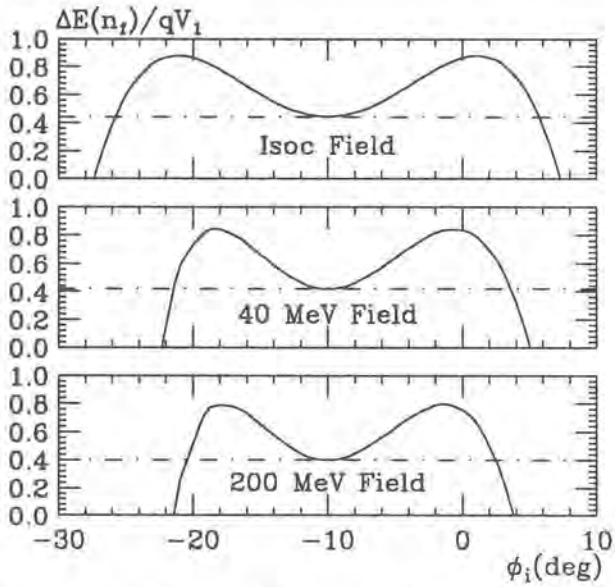


Fig. 2. Plots of the final energy as a function of the initial phase ϕ_i obtained under optimized conditions using the RF parameters given in Table 2 for three different fields: isochronous(top), 40 MeV(center), and 200 MeV(bottom). Here ΔE is the difference between the energy on the final turn and the maximum energy on the previous turn, and $qV_1 = E_f/n_0$ with $n_0 = 800$.

same final energy. The two intervening broken curves correspond to the orbits that end up with the peak energy. These sets of curves show in detail the evolution of the phase deviations mentioned above. Curves similar to those shown in Fig. 2 and Fig. 3 were obtained for $n_0 = 500$, but these are less dramatic and are omitted here to save space.

4. Conclusions

While the K1200 cyclotron is fully occupied at present with carrying out nuclear physics experiments, the K500 cyclotron is available and could be used to test the effect of a third harmonic voltage on beam properties. As noted above, this cyclotron is characterized by a $n_0 = 500$ turn geometry and would, according to Table 1, require a third harmonic voltage which is about 14% of the first harmonic. Since only one of the three dees is available for the third harmonic voltage, this percentage rises to 42%. The design of a possible RF system is now under way.

We are indebted to H. Blosser and F. Marti for many useful discussions and to the latter for assistance with the field data. We should also acknowledge that somewhat similar calculations were carried out for the TRIUMF cyclotron by C. Kost as reported by M. Craddock.[6]

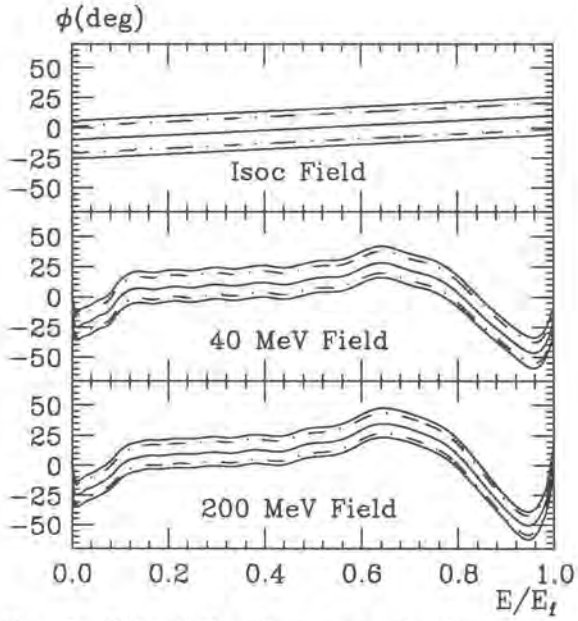


Fig. 3. Plots of the phase ϕ as a function of energy obtained for the same fields and RF parameters as those used for Fig. 2. The three solid curves all lead to the same final energy as defined by the horizontal broken line in Fig. 2, and the two broken curves lead to the two energy peaks in Fig. 2.

5. REFERENCES

1) M.M. Gordon, Nucl. Instr. & Meth. **58**, 245(1968).
2) S. Adam, et al, IEEE Trans. **NS-28**, 2721(1981); W. Joho, **Proc. Ninth Int'l. Cyclotron Conf. at Caen** (Les Editions de Physique, Paris, 1981)337.
3) R.E. Laxdal et al, Conf. Record of the 1991 Particle Accelerator Conf. (IEEE 91 CH3038-7)810.
4) W. Joho, Particle Accel. **6**, 41(1974).
5) M.M. Gordon, IEEE Trans. Nucl. Sci. **NS-13**, 48(1966).
6) M. Craddock, **Proc. Fifth All-Union Nat'l. Conf. on Particle Accel.**, Dubna, Oct. 1976.

CROSSING OF RESONANCES

L.A. Sarkisyan and A.L. Sarkisyan
Moscow Institute-Internate, 107150, Moscow, Russia

ABSTRACT

The equations for particle motion in accelerators are considered, taking into account energy gain per turn, for the investigation of integer and half-integer resonance crossing. Formulas are presented estimating amplitude behaviour when crossing resonances.

A correct analysis of integer resonance crossing in cyclotron or synchrotron accelerators leads to equations for the radial and vertical oscillations of the form[1,2)]

$$r'' + Q_r^2 r + \frac{\gamma eV}{\overline{H}\sqrt{\gamma^2-1}} r' = -R\epsilon_{zs} \sin S\psi \,,$$

$$z'' + Q_z^2 z + \frac{\gamma eV}{\overline{H}\sqrt{\gamma^2-1}} z' = -R\epsilon_{rs} \sin S\psi \,, \qquad (1)$$

where r and z – radial and vertical coordinates of the particle, $r' = dr/d\psi$, $z' = dz/d\psi$, ψ – azimuthal coordinate, γ – relativistic factor, eV – energy gain per turn, $\overline{H}$ – the mean magnetic field at radius R, ϵ_{zs}, ϵ_{rs} – relative values of the Sth harmonic vertical and radial magnetic field components respectively.

In contrast to the shortened equations, equations (1) have a term of the form $\delta = \gamma eV/[\overline{H}\sqrt{\gamma^2-1}]$, which is a friction term ("electromagnetic" friction) and is caused by energy gain per turn in explicit form.[1,2)]

The amplitudes of the oscillations excited when crossing the integer resonance are of the form[1,2)]

$$r, z = \frac{R\epsilon_{z,r,s}}{\sqrt{(Q_{r,z}^2 - S^2)^2 + \delta^2 Q_{r,z}^2}} \,. \qquad (2)$$

In the case of a half-integer resonance crossing the equations for radial and vertical oscillations are of the form[1,2)]

$$r'' + Q_r^2 r + \delta r' = -r_o \epsilon_{zs} \sin S\psi \,,$$

$$z'' + Q_z^2 z + \delta z' = -z_o \epsilon_{rs} \sin S\psi \,, \qquad (3)$$

where r_o and z_o are the initial radial and vertical coordinates.

Insofar as the half-integer resonance is far less hazardous than the integer one, shortened equations without the friction term can be used to calculate to a first approximation. In this case the maximum value of the amplitude excited in the half-integer resonance zone is approximately in explicit form[1,2)]

$$y \approx 1.2 y_o \frac{\pi H_s}{\overline{H}_s} \left(\frac{E_o}{2eV}\right)^{1/2} \,,$$

$$y = r \,, z \qquad (4)$$

where $H_s = H_{zs}$ is the amplitude of the Sth harmonic of the vertical magnetic field component in the case of radial movement and $H_s = H_{rs}$ is the amplitude of the Sth harmonic of the radial magnetic field component in the case of vertical movement; E_o is the particle rest energy.

Knowledge of the particle resonance crossing mechanism allows the particle energy in cyclotrons to be increased above E_o, the integer resonance to be used as the basis for resonant beam extraction, and the injected beam intensity to be increased.[3)]

REFERENCES

1) L.A. Sarkisyan, **The Relativistic Cyclotron** (Moscow University Press, Moscow, 1990).
2) L.A. Sarkisyan and A.L. Sarkisyan, **Nonstationary Forced Oscillations** (Chuvash University Press, Cheboksari, 1991).
3) L.A. Sarkisyan and A.L. Sarkisyan, "Increase of Beam Intensity", these proceedings.

INCREASE OF BEAM INTENSITY

L.A. Sarkisyan and A.L. Sarkisyan
Moscow Institute-Internate, 107150, Moscow, Russia

ABSTRACT

A method of particle injection into ring accelerators (cyclotrons, synchrotrons) with strong focusing is given and analytically substantiated. The given method ensures about three fold increase as compared with existing ones.

The maximum mean beam current in ring accelerators (cyclotrons, synchrotrons) determined by the decrease in free vertical oscillation frequency under the influence of space charge is calculated from the formula[1,2]

$$I = 3.2 \times 10^{-19} \frac{\pi Q_{zo} \Delta Q_z \beta^2 \gamma^3 a^2 B m F f}{R r_o}, \qquad (1)$$

where Q_{zo} is the frequency of free vertical oscillations with the mean beam current $I(A) = 0$, ΔQ_z is the shift in free vertical oscillation frequency produced by the beam current, β – relative particle speed, γ – relativistic factor, a – beam radius (cm), $f = f_o q$ – operating frequency (MHz), f_o – – rotation frequency, q – harmonic number, B – bunching factor, m – number of bunches on the orbit, F – the factor regarding beam image on vertical conducting walls of accelerator, R – accelerator radius (cm), r_o – classical particle radius (cm).

When substituting Q_{zo} and ΔQ_z by Q_{ro} and ΔQ_r in formula (1) it is possible to calculate the maximum beam current in the radial direction.

One usually chooses the initial frequency value in the range between the resonance frequency values (integer or half-integer or vice versa) with a permissible frequency shift of about 0.15–0.2. This conclusion was drawn when estimating shortened equations of motion in explicit form disregarding the energy gain per turn.[1,2]

As has been discussed in papers[2,3] in the case of the integer resonance $Q = S$ dynamic crossing the amplitude of vertical particle oscillations is

$$z = \frac{R\epsilon_s}{\sqrt{(Q_z^2 - S^2)^2 + \delta^2 Q_z^2}}, \qquad (2)$$

where $\delta = \gamma eV/[\overline{H}\sqrt{\gamma^2 - 1}]$ is the coefficient of friction ("electromagnetic" friction), eV – energy gain per turn (MeV/turn), $\epsilon_s = H_{rs}/\overline{H}$ – relative value of the Sth harmonic of the radial magnetic field component H_r, $\overline{H}$ – the mean magnetic field at radius R (cm).

The half-integer resonance is less hazardous compared with the integer one. As a first approximation regardless of the coefficient of friction, the maximum amplitude in the half-integer resonance zone is calculated from the formula[2,3]

$$z \approx 1.2 z_o \frac{\pi H_{rs}}{\overline{H} S} \left(\frac{E_o}{2eV}\right)^{1/2}, \qquad (3)$$

where E_o is the particle rest energy. The amplitude excited in the resonance zone will be considerably smaller depending on the coefficient of friction.

In ring accelerators the injection of considerable beam current is possible if the frequency shift is increased from 0.15–0.2 up to 0.6. Let us consider this method of particle injection for use in cyclotrons and synchrotrons with strong focusing.

In ring cyclotrons the orbit radius is continuously increasing during injection. Calculations for the PSI ring cyclotron with proton energy 590 MeV at the injection energy 72 MeV, R=200 cm, $\overline{H}$ = 5940 G, $Q_{zo} = 0.95$, eV = 2.4 MeV/turn[4] in the case of $Q = 0.5$, $H_{rs} = 0.5$ G show that the value of the incoherent vertical amplitude $z = 0.007\ z_o$ cm, which is insufficient. As formula (1) shows, the frequency shift decreases in a cyclotron when the beam current is conserved and the particle energy increases, through the factor $\beta^2\gamma^3$. Because of this the growing frequency Q will cross the half-integer resonance of 0.5 for the second time, but the amplitude increase will be less compared with the first crossing. The injected beam current is increased by a factor of 2 for a permissible frequency shift of 0.5 instead of 0.25.

During injection the frequency decrease caused by the beam load is partially compensated by the frequency increase for the particles with amplitude different from zero.

Injection into a synchrotron (proton, electron) is quite different due to the fact that at a constant value of magnetic field the particles in the dynamic regime will

have a bigger radius after the first turn. This method allows the energy to be decreased by the value of energy gain per turn, leading to a little bit smaller radius. The radius increases after one turn. Then the magnetic field increases over the period in which the particles are accelerated up to the full energy.

So, in the case of a proton synchrotron – the TRIUMF KAON Factory booster project with injection energy 450 MeV ($\beta = 0.737$, $\gamma_0 = 1.48$), $R = 348$ cm, $Q_{zo} = 7.22$, $eV = 0.21$ MeV/turn[5]) calculation from formula (2) with $Q_z = S = 7$, $H_{rs} = 0.5$ G shows the value of the excited vertical amplitude $z = 0.86$ cm. When the energy increases, the frequency also increases and will cross the integer resonance for the second time, but the amplitude increase will be less compared with the first crossing. When the booster is at the full proton energy of 3 GeV, ($\beta = 0.971$, $\gamma = 4.8$) the frequency shift will decrease to 0.01 and the coherent amplitude of forced oscillations will be 0.17 cm. Assuming a frequency shift of 0.6 instead of 0.15 one has a four-fold increase in the injected beam current.

In the case of the IHEP booster proton synchrotron with a proton energy of 1.5 GeV at the injection energy of 30 MeV ($\gamma = 1.03$), $R = 1600$ cm, $\overline{H} = 500$ G, $Q_{zo} = 3.8$, $eV = 0.043$ MeV/turn[6]) calculations from formula (3) with $Q_z = 3.5$ and $H_{rs} = 0.5$ G show the value of the incoherent amplitude $z = 0.77\ z_o$ cm. With a permissible frequency shift of 0.6 instead of 0.2 the beam current can increase by a factor of three at injection.

Figure 1 shows the change of Q_z frequency at injection and as the kinetic energy W of the particles increases in the PSI, TRIUMF and IHEP accelerators.

1. CONCLUSIONS

An injection method for accelerators is suggested and analytically substantiated. The method is as follows. In the dynamic regime the initial frequency of free vertical oscillations placed between integer and half-integer resonances or vice versa, decreases with beam intensity increase during injection, crossing the resonance, but increases with subsequent acceleration, crossing the resonance for a second time and approaching the initial frequency value at the full particle energy in the accelerator. The given maximum increase over the space charge in an accelerator can be used at initial frequency values Q_z and $Q_r > 0.5$. This method allows the beam intensity of operating accelerators to be increased several-fold. The method can be used in storage rings when some acceleration of the particles takes place.

2. REFERENCES

1) H. Bruck, **Accélérateurs circulaires de particules** (INSTN/Presse Universitaires, Paris, 1966).
2) L.A. Sarkisyan, **The Relativistic Cyclotron** (Moscow University Press, Moscow, 1990).
3) L.A. Sarkisyan and A.L. Sarkisyan, **Nonstationary Forced Oscillations** (Chuvash University Press, Cheboksari, 1991).
4) G. Dutto, "Recent Developments of the TRIUMF Cyclotron as an H^- Injector for the KAON Factory", in **Proc. of XIII Int. Conf. on High Energy Accelerators** (Novosibirsk, 1987) pp.270-276.
5) V.L. Bruck *et al.*, "The Dynamic Characteristics of the IHEP Fast-Cycling Injector-Synchrotron", in **Proc. of XIII Int. Conf. on High Energy Accelerators** (Novosibirsk, 1987) pp.284-287.
6) W. Joho, "Interfacing the SIN Ring Cyclotron to a Rapid Cycling Synchrotron with an Acceleration and Storage Ring ASTOR", in **Proc. X Int. Conf. on Cyclotrons and their Applications** (IEEE, 1984) pp.611-614.

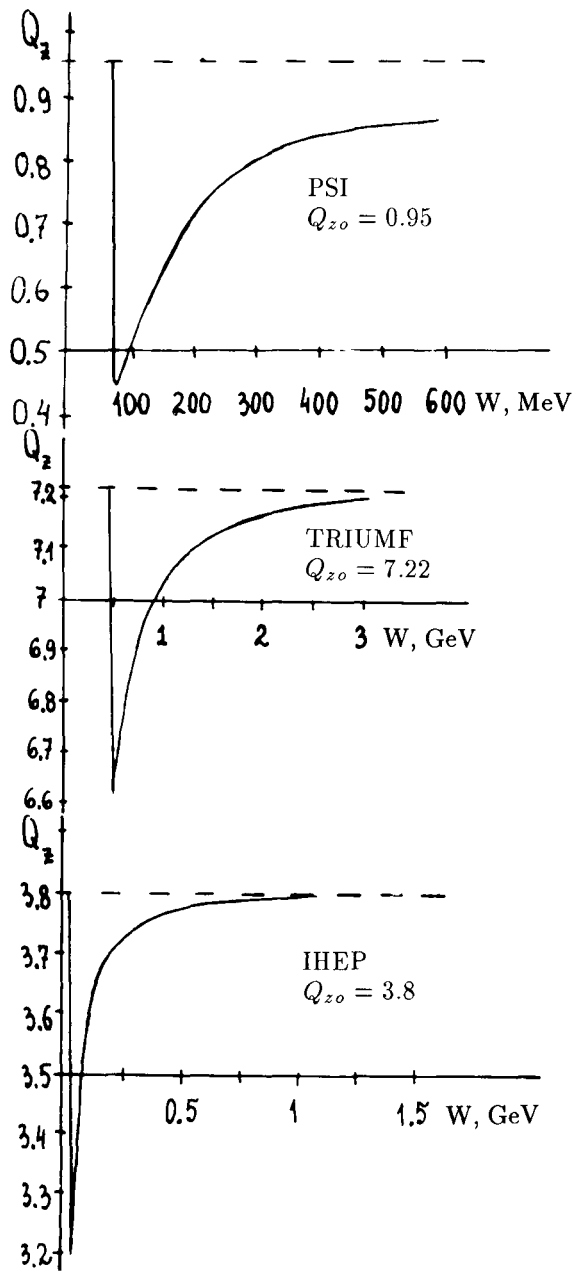


Fig. 1.

DEVELOPMENTS IN RELAX3D, A 2D/3D LAPLACE AND POISSON EQUATION SOLVER

H. Houtman, F.W. Jones, and C.J. Kost
TRIUMF, 4004 Wesbrook Mall, Vancouver,
British Columbia, Canada V6T 2A3

ABSTRACT

The widely used program RELAX3D, in continual development at TRIUMF since its inception in 1973,[1] employs the finite-difference algorithm known as symmetric successive over-relaxation (SSOR) to solve the three-dimensional second-order elliptic partial differential equation $\nabla^2 V(x,y,z) = F(x,y,z)$, which includes the Laplace ($F \equiv 0$) and Poisson ($F \neq 0$) equations. After a brief review of other solution techniques, the program is described and a variety of sample usages is given. Recent enhancements were made in the use of various grid stencils (molecules), graphics facilities, and portability to UNIX systems. The dependence of errors on grid spacing, stencils, and machine precision are presented. The investigation of higher-order relaxation formulae (stencils) has shown promising results. Using a 27-point stencil, the solution accuracy can be dramatically improved with only a modest increase in execution time.

1. INTRODUCTION

The solution of Laplace's equation has been provided in the past by a variety of techniques[2,3] such as curvilinear squares, resistor networks, conducting paper, electrolytic tank, magnetic analog, separation of variables, conformal transformation, and a wide variety of numerical methods (especially finite-difference and finite-element techniques). Some of these techniques are applicable also to Poisson's equation. These equations arise in steady state electric fields, heat flow, laminar flow in fluids, and certain magnetic field problems.

RELAX3D[4-7] solves for the potential V on a regular grid, approximating the differential equation by a finite-difference equation, defined for each grid point in terms of its neighbours. This set of equations is solved using the iterative method of successive over-relaxation. Boundary potentials of arbitrary shape, and the arbitrary function F (representing charge density, heat sources, etc.) are supplied by a user-coded subroutine. Various other options and features are provided, making the program convenient, flexible, and easy to use. Table 1 shows the current scope of the program.

Table 1. Problem types solved by RELAX3D

PROBLEM TYPE	DIMENSION	COORDINATES
Laplace and Poisson Equation	2D	Cartesian
	3D	Cartesian
	2D	Polar
	2D*	Cylindrical
	3D	Cylindrical
Laplace Equation (multi-dielectric)	2D	Cartesian
	2D*	Cylindrical

*Assumes cylindrical symmetry.

2. RELAXATION ALGORITHM

Once the initial values of F and the boundary values have been specified, RELAX3D performs the relaxation algorithm (SSOR) in which the potential V_0 at the center of the N-point stencil (molecule) is discarded, and replaced by an appropriately weighted average V_0^* of $N-1$ neighbouring potentials V_{ijk} according to

$$V_0 \longrightarrow V_0 + \omega(V_0^* - \frac{h^2}{6} F_0 - V_0), \qquad (1)$$

where F_0 is the value of the function F at the center of the stencil, and ω is the relaxation factor.[3,8] Each problem type in Table 1 has a different formula, each of which has been derived individually from Taylor series expansions.[3,7,8] For example, for the 3D Cartesian 7-point stencil shown in Fig. 1(a) we have

$$V_0^* = \sum_{d=h} \frac{V_{ijk}}{6}, \qquad (2)$$

which is simply the average of the potential at the six nearest neighbours to the central point of the stencil, all of which are at a distance h from the central point.

The relaxation subroutine sweeps the entire grid in this manner until the residuals (changes in the potentials) are within a user-specified tolerance, typically 1

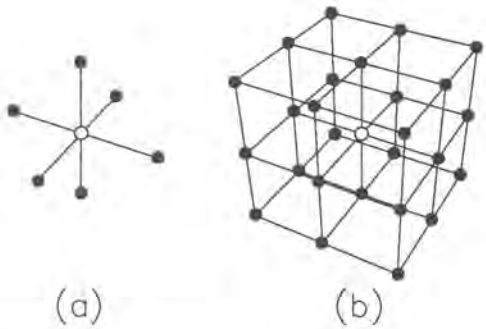


Fig. 1. Three dimensional shapes for (a) 7-point stencil and (b) 27-point stencil.

part in 10^6 or 10^7. The values stored in the 3D arrays for V and F are addressed using an efficient addressing technique,[1,7] without the use of compiler-based 3D addressing. This 1-dimensional addressing technique needs only one addition per address, and detailed tests have shown that the program execution is considerably faster than with the standard "(I,J,K)" technique, although recent FORTRAN compilers are closing the gap.

3. RELAX3D APPLICATIONS

Center regions of cyclotrons,[1,9,10] cyclotron magnets[11] and racetrack microtrons for free-electron lasers[12] have been designed with the aid of RELAX3D solutions. Cyclotron inflectors, detectors, cyclotron RF systems, Einzel lenses, electric and magnetic quadrupole lenses, corona rings, coaxial transmission line terminations and ultra-violet triggered spark gaps have been modelled and designed using RELAX3D.[7] As an example, in Fig. 2 is shown a typical slice through a $121 \times 61 \times 33 = 243573$ point solution of the TRIUMF center region; this run took 600 iterations, and 660 seconds of CPU time on a DecStation 3100.

4. STEADY-STATE HEAT CONDUCTION

There are two classes of problems that RELAX3D can deal with for steady state heat conduction.

One, in which the thermal conductivity k is constant throughout the volume, represented by the Poisson equation,[13]

$$\frac{\partial^2 t}{\partial x^2} + \frac{\partial^2 t}{\partial y^2} + \frac{\partial^2 t}{\partial z^2} = -\frac{q'''(x,y,z)}{k}, \qquad (3)$$

where $t(x,y,z)$ is the temperature and $q'''(x,y,z)$ represents any heat sources or sinks in the volume with typical units for q''' and k of W/m^3 and W/(m°K) respectively.

Two, which solves cases involving no heat sources or sinks but where regions with different thermal conductivities k are allowed (assuming there is no interface resistance). The boundary conditions between these regions are treated analogously to those between regions of different permittivity ε.

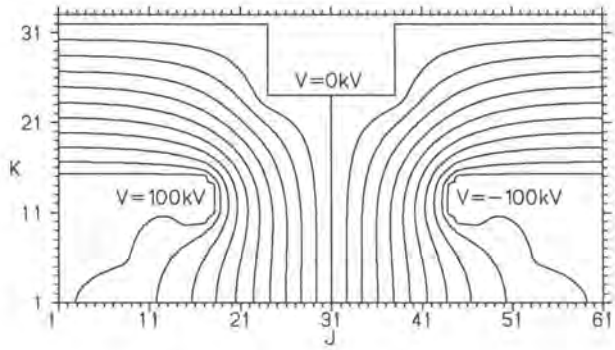


Fig. 2. RELAX3D contour plot at $l = 118$ (radius 90cm) of 121×61×33 run for TRIUMF center region, showing electric lens formed by cyclotron dees.

As an example of the first case we discuss a simulation based on a report[14] dealing with proton beam heating of a copper, water-cooled beam probe. In this simulation, in addition to taking account of the variation with depth of the proton beam energy loss (assuming a negligible energy loss in the water cooling ducts) and the resulting proton beam radial spread, we allowed for non-uniform beam profiles (using a binomial distribution[15]) as well as the variation of thermal conductivity k with temperature t.

Fig. 3 shows the results of such a 3D simulation for a 100μA beam on a copper probe with cooling ducts at 100°C and the beam density $\rho(x,z)$ assumed to be rotationally symmetric of the form:

$$\rho(x,z) = \frac{m}{\pi}(1-(r/r_l)^2)^{m-1} \qquad (4)$$

where $r^2 = x^2 + z^2$ and r_l is the limiting beam radius given by $r_l = r_b\sqrt{(m+1)/2}$ and r_b is the 2σ nominal beam radius.

5. MAGNITUDE OF ERRORS

The 7-point relaxation formula for Laplace's equation is formed from a sum of Taylor series expansions for the potentials V of the six points at distance h from the central point. In this sum all odd-order terms cancel and the second-order term $h^2\nabla^2 V$ is either zero (Laplace's equation), or $h^2 F$ (Poisson's equation), leading to a net truncation error of order h^4. However, when one considers that the potentials at the six outer points will also be subject to such a truncation error, it is seen[8] that the solution values of the entire system of equations will have a total error of order h^2.

We have demonstrated this h^2 error propagation effect by comparing RELAX3D solutions to the exact, analytical solution of the following problem: a unit box $(0 \le x,y,z \le 1)$ has the bottom and four sides held at

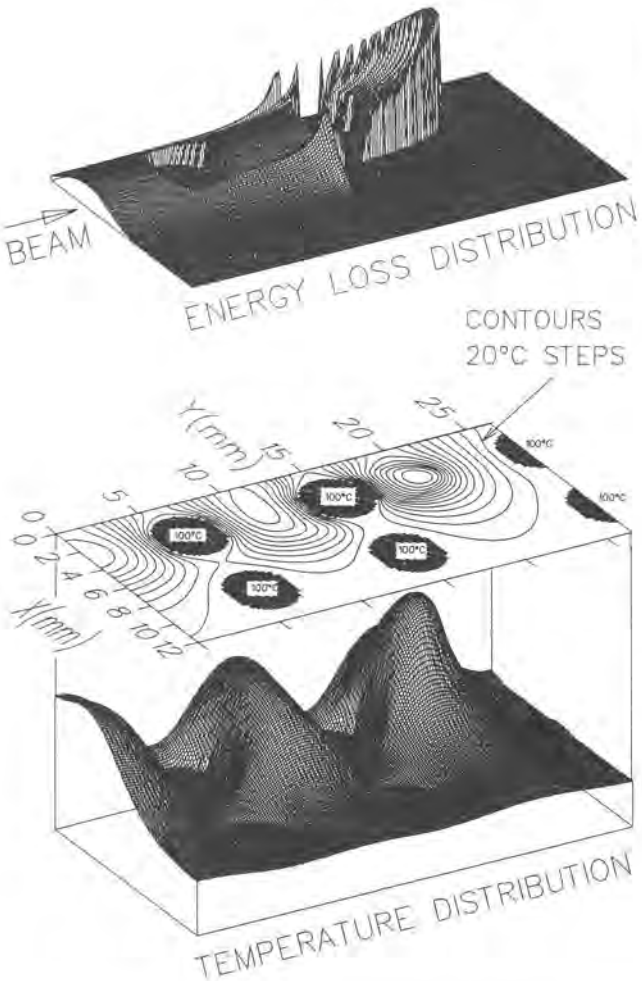


Fig. 3. Energy loss and temperature distributions in median plane (m=4.).

potential $V = 0$, while the top has a sinusoidal potential

$$V(x, y, 1) = \sin(\pi x)\sin(\pi y). \qquad (5)$$

Inside the box, the exact solution to Laplace's equation is[16]

$$V(x, y, z) = \sin(\pi x)\sin(\pi y)\frac{\sinh(\sqrt{2}\pi z)}{\sinh(\sqrt{2}\pi)}. \qquad (6)$$

We compared the exact solution at the center of the box to RELAX3D solutions for a series of progressively finer grids, ranging from $h = 1/2$ ($n^3 = 27$ points) to $h = 1/96$ ($n^3 = 912673$ points). In each case the iteration was carried out until zero residual was reached, i.e. the system of equations was satisfied exactly in the context of the finite precision of the computed potentials.

Fitting a power law to the solution errors resulted in a clear h^2 dependence, as shown by curve (1) of Fig. 4. However, as the grid is refined there is an additional effect due to machine precision and round-off. By fitting an additional term for the bottom of the error curve, we found that the total error was of the form $Ah^2 + Bh^{-1}$. Tests at other points in the solution domain also revealed the same error trend, although the coefficients A and B depend on the location in the grid.

6. HIGHER-ORDER STENCILS

The 3D relaxation "stencil" described above incorporates the six nearest neighbours to the central point. By including additional neighbouring points and forming additional Taylor expansions at these points, one can derive relaxation formulae that are more accurate, due to strategic cancellation of higher-order terms in the series. Numerous 2D examples of these larger stencils are treated in the literature, but the 3D counterparts are rarely dealt with.

One possible extension of the 7-point stencil is to include the next-nearest neighbours along each axis, the 6 points at distance $2h$ from the central point, to give a 13-point stencil. The truncation error for this stencil is of order h^6. For our investigations, however, we considered a more complex stencil consisting of all points whose array indices differ from those of the central point by at most ± 1. This includes the central point, 6 points at distance h, 12 points at distance $\sqrt{2}h$ and 8 points at distance $\sqrt{3}h$, resulting in a stencil with 27 points as shown in Fig. 1(b). This stencil was implemented as a special option for the Laplace equation in RELAX3D.

Deriving the relaxation formula for such a stencil is a non-trivial task. For example, while a detailed derivation of the relaxation formula for the 2D, 9-point (square) stencil is given in one recent book,[3] the 3D, 27-point stencil is considered only in passing.

Using the program *Mathematica*, R. Balden[17] has studied this type of problem and has recently found the optimum relaxation formula for the 3D, 27-point stencil of Fig. 1(b) which has a truncation error of $\mathcal{O}(h^8)$:

$$V_0^* = \frac{21}{32}\sum_{d=h}\frac{V_{ijk}}{6} + \frac{9}{32}\sum_{d=\sqrt{2}h}\frac{V_{ijk}}{12} + \frac{2}{32}\sum_{d=\sqrt{3}h}\frac{V_{ijk}}{8} + \mathcal{O}(h^8)$$

where V_0^* is the potential at the central point and the averages are taken over the points at distance h, $\sqrt{2}h$, and $\sqrt{3}h$ from it.

By an argument similar to that for the 7-point case, one can surmise from the $\mathcal{O}(h^8)$ truncation error that the net error in the solution values would be $\mathcal{O}(h^6)$. To confirm this, we again performed runs for the sinusoidal potential problem described in the previous section. As shown by curve (2) of Fig. 4, the error decreases as h^6 until the effects of machine precision (32 bits) cause an increasing trend as in curve (1). Fitting an additional term for these effects revealed a $1/h^2$ dependence instead of the $1/h$ dependence seen with the 7-point stencil. Also shown in this figure are the results of the same 27-point computations done in double precision (64 bits), which effectively eliminates the precision component of the er-

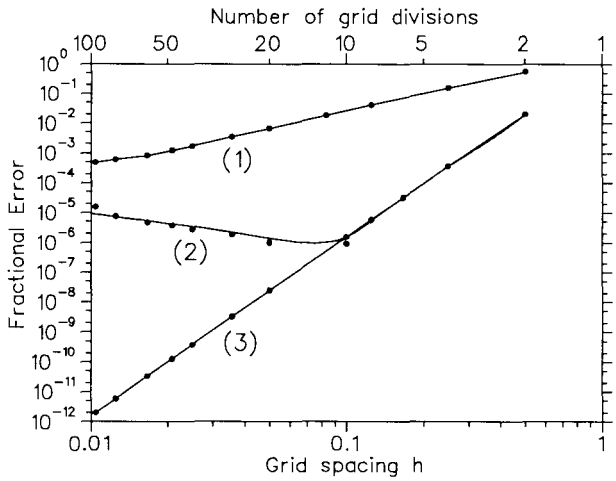


Fig. 4. Error in solution using different stencils: (1) 7-point, (2) 27-point, (3) 27-point double precision.

ror and illustrates the extremely high accuracy that can be obtained with this stencil.

Even in single precision, it is seen that for a given grid spacing one can achieve a significant improvement in accuracy by using the 27-point stencil. Of course, the larger stencil requires more cpu time per iteration, but the presence of the additional neighbouring points in the calculation tends to accelerate the convergence process. For the example shown in Fig. 4, we compared the net cpu time required to achieve a fully-converged solution (zero residual) at various grid spacings, and found that the 27-point stencil requires only about 50% more cpu time than the 7-point stencil on the same grid.

7. CONCLUSION

RELAX3D continues to be a useful and effective program for a variety of problems, of which some examples have been shown. Tests of the program show that the errors in the solution exhibit the expected trends as the grid is refined, and that errors can be reduced to negligible proportions by the use of higher-order stencils coupled with higher machine precision.

Recent upgrades to the program include the addition of polar grids and support for new graphics output devices including X Window displays and PostScript printers. The code, formerly available only on VAX/VMS systems, has been ported to DECStations running ULTRIX, allowing one to take advantage of the high performance of these RISC systems. Now that the code has been adapted to one UNIX environment, implementing it on other UNIX-based platforms should be straightforward. The continuing trend of faster, more affordable computing hardware is expected to assure RELAX3D's future and even widen its scope of applicability.

8. REFERENCES

1) H. Houtman, "RELX," TRIUMF Design Note TRI-DN-73-22 and Addendum, 17 May 1973; H. Houtman, "RELAX-INTEGER*2," TRIUMF Design Note TRI-DN-92-9, June 1992.
2) T.J. Gallagher and A.J. Pearmain, **High Voltage Measurement, Testing and Design** (Wiley, New York, 1983).
3) M. Szilagyi, **Electron and Ion Optics** (Plenum, New York, 1988).
4) H. Houtman and C.J. Kost, "A FORTRAN Program (RELAX3D) to solve the 3 Dimensional Poisson (Laplace) Equation," in **Computing in Accelerator Design and Operation**, Berlin, 20-23 September 1983, ed. W. Busse and R. Zelazny (Springer-Verlag, Berlin, 1984) pp. 98–103.
5) H. Houtman, F.W. Jones and C.J. Kost, "RELAX3D," in **Computer Codes for Particle Accelerator Design and Analysis: A Compendium**, 2nd ed., ed. H.S. Deaven and K.C.D. Chan, Los Alamos National Laboratory Report LA-UR-90-1766 (May 1990) p. 174.
6) C.J. Kost and F.W. Jones, "RELAX3D User's Guide and Reference Manual," TRIUMF Computing Document TRI-CD-88-01 (rev. 1992).
7) H. Houtman, F.W. Jones and C.J. Kost, "Laplace and Poisson Equation Solution by RELAX3D" (to be published).
8) C. Weber, "Numerical solution of Laplace's and Poisson's equations and the calculation of electron trajectories and electron beams," in **Focussing of Charged Particles** Volume II, ed. A. Septier (Academic Press, New York, 1967).
9) G. Dutto, C. Kost, G.H. MacKenzie and M.K. Craddock, Sixth Int. Cyclotron Conference, Vancouver, Canada, 18-21 July 1972, pp.340-350; H. Houtman, TRIUMF Design Note TRI-DN-92-10, June 1992.
10) E. Liukkonen, Twelfth Int. Conf. on Cyclotrons and Their Applications, Berlin, 8-12 May 1989, pp. 40-42.
11) P. Heikkinen, Nucl. Instr. and Meth. **A301**, 417 (1991).
12) J.I.M. Botman et al., Nucl. Instr. and Meth. **A304**, 192 (1991).
13) P.J. Schneider, "Conduction," in **Handbook of Heat Transfer**, ed. W.M. Rohsenow and J.P. Hartnett (McGraw-Hill, New York, 1973).
14) G.S.Z. Guasco, "Cooling calculations for the modified multi head probe (MHP), beam stop (BS), and electrostatic extraction channel (EEC) collimators," NAC Internal Report NAC/I/86-02 (1986).
15) W. Joho, "Representation of Beam Ellipses for Transport Calculations," SIN-REPORT TM-11-14, 8.5.1980.
16) J.D. Jackson, **Classical Electrodynamics**, 2nd ed. (Wiley, New York, 1975).
17) R. Balden, "Symbolic Mathematical Computation Using Mathematica: Formal Series Expansions and the Derivation of Optimal Relaxation Stencils," TRIUMF Design Note TRI-DN-92-02 (1992).

BEAM QUALITY INVESTIGATIONS FOR H⁻ EXTRACTION AT TRIUMF

R.E. Laxdal, G.H. Mackenzie, J.B. Pearson, L. Root
TRIUMF, 4004 Wesbrook Mall, Vancouver, B.C., Canada V6T 2A3

Abstract

The direct extraction of high intensities of H⁻ ions from the TRIUMF cyclotron and their injection into an accumulator ring will impose demands on beam quality and thereby on the fields of the added extraction hardware and on the operation of the cyclotron. The fields of each of the extraction devices have been simulated in computer codes to estimate their influence on the final extracted emittance. Parameters controlling vertical emittance have been experimentally investigated to devise an optimum tuning procedure. Results of both computer simulations and experimental beam tests will be given.

I. Introduction

The proposed TRIUMF KAON Factory [1] requires that the cyclotron deliver 150 μA of H⁻ ions within a longitudinal emittance of 0.003 eV-s ($\pm 10°$,± 0.6 MeV) and transverse emittances of $3.5\pi\mu$m radially and $2\pi\mu$m vertically. A larger emittance will reduce the efficiency of the injection process leading to greater beam loss in the accumulator and subsequent rings.

The cyclotron must accelerate at least 165 μA to achieve the required intensity. Space charge at the cyclotron center limits the current to about 10 μA/° rf [2]. Measurements show that the majority of particles in a well tuned beam lie within $1\pi\mu$m normalized emittance in both transverse planes. Hence the cyclotron capabilities and KAON requirements are matched but there is little margin. In particular current routine operation demonstrates drifts and jitter in the phase of the extracted beam of $\pm 7.5°$ at frequencies slower than the 50 Hz accumulator cycle and $\pm 5°$ at frequencies faster than 50 Hz. The former can be tracked by the accumulator rf but may present problems to the H⁻ extraction system while the latter require stabilization both for cyclotron extraction and KAON injection.

The changeover from extraction by stripping to direct extraction has been discussed elsewhere [3]. In summary nine new pieces of hardware are required, including two electrostatic deflectors (DCD), six channels (MC) and an rf deflecting device (RFD) to generate the large coherent radial oscillation required for precessional extraction. An auxiliary accelerating cavity (AAC) operating at 92 MHz is not strictly necessary for extraction but is available to modify beam behaviour.

II. Computer Simulations

Ensembles of particles have been tracked using the linear motion code COMA. Single particle motion was studied with the ray-tracing program GOBLIN. In COMA transverse emittances of $1\pi\mu$m and a longitudinal emittance of (ΔE,$\Delta\phi$)=$\pm 0.2\%$,20° were specified at 380 MeV, well before the extraction resonance at ν_r=3/2 (E=428 MeV). The extraction process was simulated by intercepting those particles with radial positions beyond the septum radius (~452 MeV) at the azimuth of the first DCD and recording their positions in transverse and longitudinal phase space. Transverse extracted emittances were determined by fitting ellipses enclosing 99% of the particles in the $x - p_x$, $z - p_z$ distributions. These circumscribing ellipses do not necessarily match the cyclotron acceptance. In both codes extraction devices were modelled by including in the calculation either a measured, calculated or analytic representation of the fields.

III. Multi-Turn Extraction

In the TRIUMF cyclotron at peak intensity separated turns are lost within the first few MeV as the large phase band generates energy spread in the turns. At energies above 100 MeV the incoherent radial width $2A_i$ exceeds the radius gain per turn (dR/dn) and turns composed of particles of the same phase (single phase condition) overlap. A wide stripping foil or septum extracts all beam accelerated to its radius with different phases requiring different numbers of turns during acceleration, and extraction of any single phase occuring over two or more turns. A well centred beam matched to the cyclotron acceptance will give an extracted beam whose vertical emittance is that of the circulating beam and whose radial emittance depends largely on A_i and the radius gain per turn (dR/dn). Fluctuations in turn number have little effect.

To improve the efficiency of H⁻ extraction a large coherent radial oscillation (amplitude A_c) can be introduced. The ensemble of particles is displaced in phase space from the equilibrium orbit (AEO) and precesses about it, increasing dR/dn (often beyond $2A_i$) at the septum. Even though certain ideal phases can be extracted in a single turn other phases with slightly different initial positions entering the resonance region will be split by the septum and require two passes. Particles with phases further removed take up to three passes. The extracted radial emittance of any one phase depends on A_i, the values of dR/dn and dP_r/dn (which are increased due to A_c) and the number of passes necessary for extraction. The extracted vertical emittance is largely the circulating emittance provided the ensemble is centered and matched with respect to the cyclotron acceptance. For any one phase a centred but mismatched ensemble will produce a larger extracted emittance due to rotation between turns.

Both the magnitude of A_c and the rate of motion of the precession center (AEO) can be phase-dependent causing phase-dependence both in the precession paths in radial phase space and in the numbers of turns between resonance and extraction. The former results in an increase in the extracted radial emittance since different phases end up in different regions of phase space. The latter increases the variation in orientation of a stretched ellipse at extraction hence the extracted emittance (see Fig. 4(a)).

IV. RF Deflector

A. Radial Growth

The RFD produces a radial electric rf field at the ν_r = 3/2 resonance. The frequency is 11.5 MHz, 5/2 the particle rotation frequency, so that the radial deflections alternate in sign for successive turns adding to produce the large coherent oscillation (amplitude 5 cm for a field of 110 V/mm·m) required for extraction. The amplitude gained is proportional to the product of the average radial kick and the number of turns in the resonance; this varies as $\cos(\phi/2)/\cos\phi$ while the rate of radial advance of the center of precession (AEO) varies as $\cos\phi$. The phase-dependent precession leads to growth in the extracted ra-

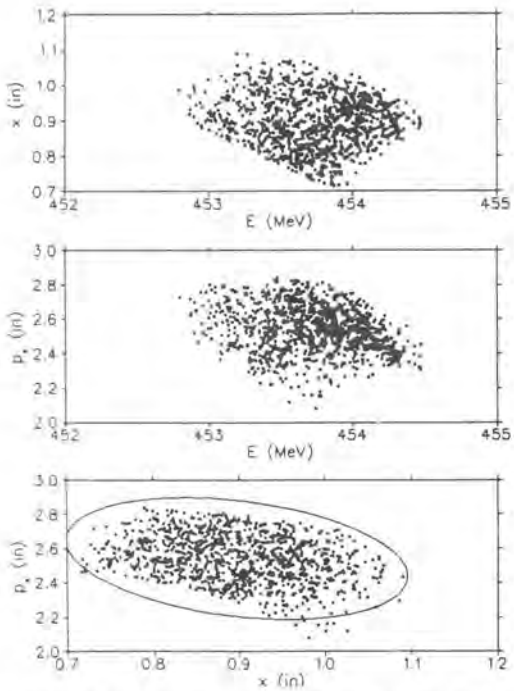


Figure 1: COMA simulation result showing the final position of particles in $E-x$, $E-p_x$ and $x-p_x$ phase spaces for a beam with circulating radial emittance of $1\pi\mu$m, phase band of 40°, and RFD voltage of 110 V/mm·m. An ellipse of $4\pi\mu$m encloses 99% of the extracted particles.

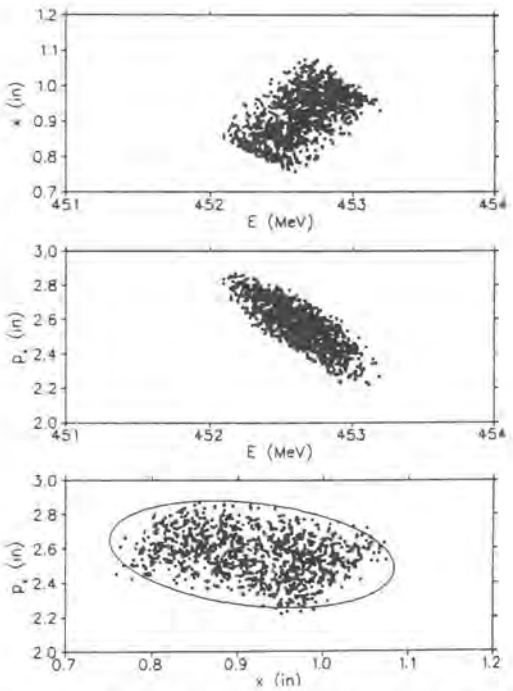


Figure 2: COMA simulation same as for study summarized in Fig. 1 only with flattopping cavity powered (18 kV) to reduce phase dependent effects. An ellipse of $3\pi\mu$m encloses 99% of the extracted particles.

dial emittance as outlined above. COMA simulations indicate that for a 40° phase band[1] the extracted emittance will be 2.5 to 4 times that of the circulating emittance for moderate to high RFD voltages respectively. Fig. 1 summarizes one such simulation showing $E-x$, $E-p_x$ and $x-p_x$ distributions of the extracted particles.

The 4th harmonic accelerating cavity (AAC) installed in the TRIUMF cyclotron reduces stripping losses in the radial range corresponding to 370-520 MeV but its performance as a flattopping cavity has also been demonstrated [4]. Simulations show that when the cavity is powered, at low voltage, the phase-dependent emittance broadening can be almost eliminated. The study summarized in Fig. 1 was repeated for an AAC voltage of 18 kV and the extracted radial emittance and energy spread were found to be reduced from $4\pi\mu$m and 1.5 MeV to $3\pi\mu$m and 1 MeV (Fig. 2). In addition, the resulting strong correlation between E and p_x may possibly be used to advantage in the accumulation process.

B. *Vertical Growth*

GOBLIN studies indicate that an initially matched ensemble in vertical phase space is stretched when traversing the RFD, increasing the vertical extent of the beam envelope (Fig. 3). The growth occurs due to vertical fields $\mathcal{E}_{z1}$ associated with the $d\mathcal{E}_r/dr$ gradient in the RFD field. These alternate in sign each turn and drive the ν_z=0.25 resonance at 419 MeV. The magnitude of the stretching is proportional to the RFD strength. Increases in the extracted vertical emittance due to phase-dependent mixing of the elongated ensemble were calculated with COMA. For an RFD voltage of 110 V/mm·m the extracted vertical emittance of a 40° band is three times that of a 5° band, Fig. 4(a). This is primarily due to differences in rotation in phase space between RFD and extraction since $\nu_z \sim 0.25$ once again at extraction, hence only every second turn is extracted ($\nu_r \approx 1.5$) and the ellipse precesses relatively slowly. In this situation flattopping should reduce the emittance growth. This is shown in Fig. 4(b), where the extracted emittance is very nearly the circulating emittance, but, because of stretching at 419 MeV the vertical size of the beam is larger. The ellipse orientation, hence the beam size in the channels, depends on the number of turns made between 419 and 452 MeV and, should it not be possible to redesign the RFD to reduce stretching, the size could be controlled by altering the energy gain/turn.

[1]KAON requirement with allowance for jitter and tuning

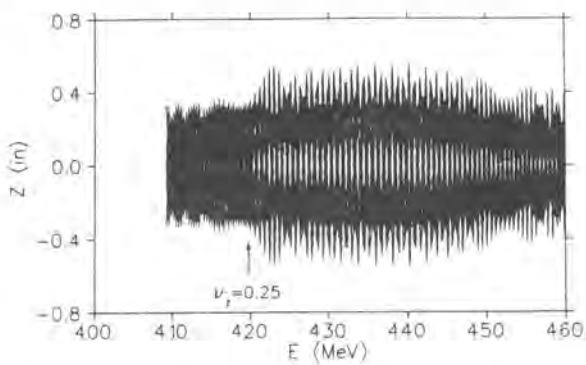


Figure 3: Result of GOBLIN simulation showing the vertical beam envelope at one azimuth while accelerating through the RFD. A growth of 50% occurs as the RFD is entered for an RFD strength of 110 V/mm·m.

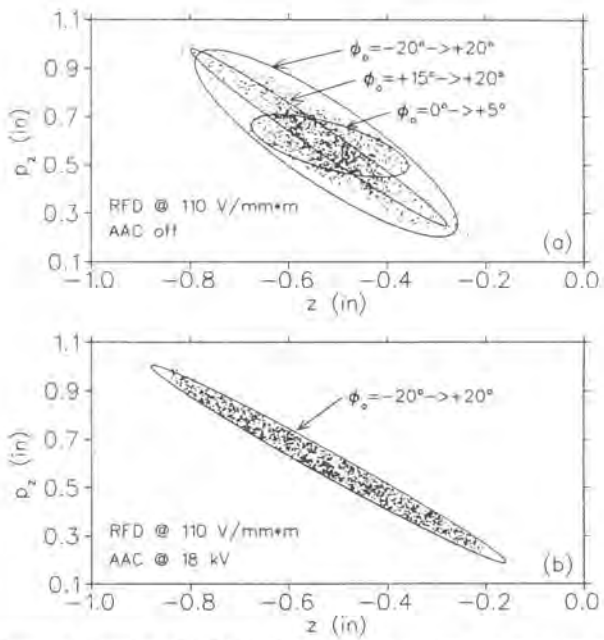


Figure 4: Results of COMA simulations showing the position of extracted particles in vertical phase space for a circulating emittance of $1\pi\mu$m and a phase band of 40°. In both cases the RFD is at 110 V/mm·m but in case (b) a flattopping cavity has been turned on at 18 kV. In (a) phases near 0° and near 20° are grouped separately in the smaller ellipses to show how the phase dependent mismatch increases the extracted emittance.

V. Electrostatic Deflector (DCD)

Two electrostatic deflectors, each contributing 40 kV/cm·m of radial deflection, are required to generate an adequate separation at the first magnetic channel (MC1). Relaxation calculations show a negligible fringe field extending between septum strips into the circulating beam. However the aperture field has non-radial components off the median plane. To avoid vertical distortion the beam must pass within the uniform region which, for an anti-septum of 5 cm full height, is ±1.3 cm from the midplane.

VI. Magnetic Channels

A. *Radial Growth*

A radial gradient in the third harmonic component of B_z will stretch the enfolding ellipse in radial phase space at the ν_r=3/2 resonance. The aperture centers of magnetic channels MC1 and MC2 are only 12.5 and 14 cm respectively from resonances at 419 and 428 MeV. Consequently their fringe fields extend through the resonance region. The channels further downstream are sufficiently distant from the resonance that their fringe fields are of less concern. COMA simulations show that at the azimuth of MC1 and MC2 negative gradients act in phase and augment the existing 3rd harmonic imperfection gradient producing an increase in the extracted radial emittance. Integrated gradients of −0.33 G/cm·m in both MC1 and MC2 yield a 30% increase in the extracted emittance, compared with the gradients off case, for a 20° wide phase band and the RFD powered at moderate strength. Since the gradients cause stretching, the phase-dependent emittance growth at extraction could be reduced or eliminated by applying a small flattop correction; no simulations have been done to date to verify this, however. A conceptual design for additional harmonic gradient coils has been completed should it be necessary to compensate the perturbation.

B. *Vertical Growth*

In general a circulating beam of matched vertical emittance will remain matched when the beam encounters an added gradient as long as the process is adiabatic. If the added gradient is defocussing ν_z will be reduced by an amount proportional to the square root of the gradient change. The vertical width will scale as $1/\sqrt{\nu_z}$. The TRIUMF cyclotron is weakly focussing vertically so that any changes in the vertical focussing by the addition of extra radial field gradients could cause a large proportional change in ν_z and hence a large change in the vertical width of the beam. In the region of interest near 450 MeV ν_z averages 0.24 over the last few turns. To limit the vertical width increase to <15% the existing radial gradient can be reduced by no more than 0.15 G/cm corresponding to $\int dB_z/dr \cdot dl < 7$ G/cm·m for the channels.

We have tested MC1 *insitu*. Three-dimensional field calculations during design gave the maximum integrated gradient in the circulating beam region to be $\int dB_z/dr \cdot dl \leq$ 1.8 G/cm·m [5]. A direct measurement of ν_z was obtained by introducing a broad ΔB_r bump using 10 trim coils and measuring the resulting average vertical shift in the beam ($\Delta z(R)$) with a 5 finger vertical probe. The value of ν_z can be deduced from

$$\nu_z \simeq \sqrt{\frac{\overline{R}}{\overline{B_z}} \frac{\overline{\Delta B_r}}{\overline{\Delta z}}}.$$

Measurements showed that ν_z was reduced from 0.24 to 0.22 with the channel powered as designed and from 0.24 to 0.15 with the coils powered to increase the gradient by a factor of 4, corresponding to integrated gradients of 2.5 G/cm·m and 10. G/cm·m respectively. Measurements of vertical width using a foil-dip technique (see next section) showed no measurable width increase in the first case and a 30% increase in the second, as predicted.

VII. Cyclotron Tune for KAON

A. *Selection of Longitudinal Phase Band*

Beam pulses of ~4 nsec (35°) are accelerated in the TRIUMF cyclotron to achieve a typical high intensity current of 150 μA with a transmission of ~60%. More intensity is available from the source at the cost of increasing the transverse emittance. In future a CUSP source already developed could be used to achieve brighter beams. With the present source we have achieved an extracted beam of 28μA at 25% duty factor (112 μA equivalent) with 90% of the extracted beam within the required 2.4 nsec (20°). The phase selection was achieved using a radial flag on the centerpost to intercept the more positive phases on the first turn and a radial slit on the 10th turn to trim the tails of the phase band. An overall transmission from injection to extraction of 30% was achieved.

B. *Vertical Emittance*

Beam measurements indicate that the horizontal emittance of the circulating beam is well behaved but the vertical emittance entering the RFD is tune dependent and is larger than at injection. This has hampered extraction tests with the DCD since the resulting large vertical beam size is defocussed in the DCD (Sect. V). A series of experiments were organized to determine the cause of the vertical emittance growth.

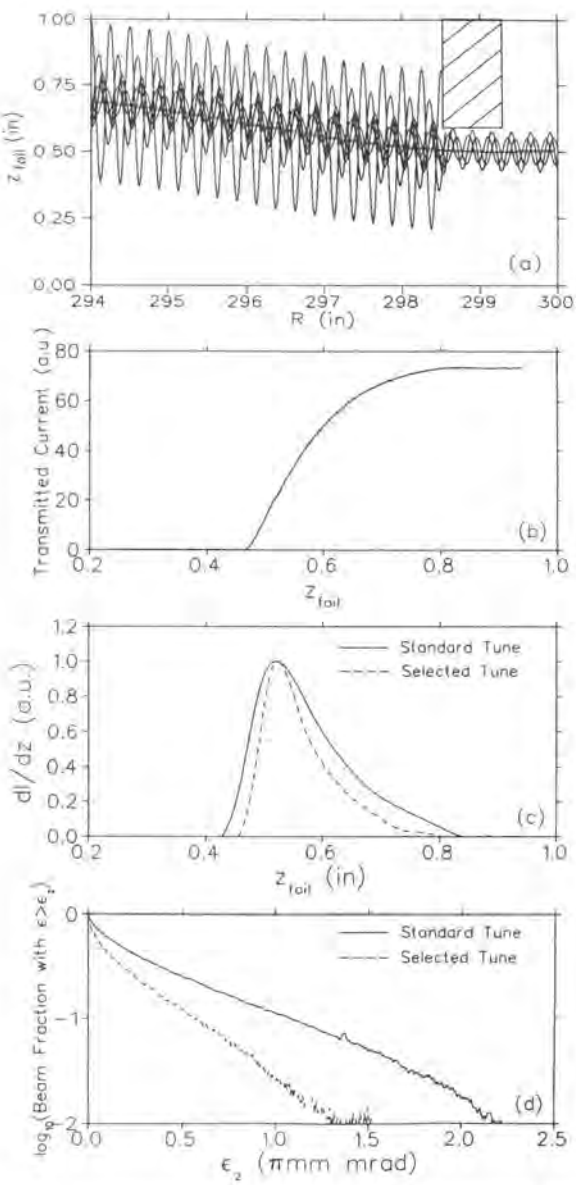


Figure 5: A schematic summarizing the foil dip method for determining vertical beam width and emittance. The beam transmitted (a) past the foil of height z is measured (b) and the result can be differentiated to produce the vertical half width (c) or plotted on a log scale to show the fraction of the beam lying outside a given emittance (d).

Vertical beam widths and emittances were determined by measuring the beam transmission as a function of foil height for a wide totalling intercepting foil. As long as the foil is wider than $\frac{dR}{dn} \cdot 1/\nu_z$, and $1/\nu_z$ is not an integer, and coherent oscillations are small compared to incoherent then the foil will intercept all particles when it has dipped to the center of the beam. Fig. 5 summarizes the foil dip method. The measured beam (b) can be differentiated to produce the vertical half width (c) or plotted on a log scale to show the fraction of the beam lying outside a given emittance (d). This last plot is useful for displaying halos in the vertical distribution [6]. The emittance is calculated from the vertical width using the relation $z_{\frac{1}{2}} = \sqrt{\epsilon_z \beta}$. The calculation assumes a properly matched centered beam. A stretched or off-centered beam may give misleading emittance results. Off-centered cases are typified by a more symmetric rounded vertical width plot as compared to the asymmetric width plots shown in Fig. 5(c).

All vertical width measurements were taken at the extraction energy of 452 MeV using a 1.9 cm wide by 2.5 cm long foil. In general a narrow phase band was selected in the center region using a first turn radial flag and a radial slit on the 10th turn to decouple phase dependent effects from the results. The central phase of the narrow band was altered by adjusting the slit radius. Phase variations at extraction were achieved by adjusting the rf frequency. Vertical and radial centering errors were either canceled or forced by adjusting vertical deflecting plates and a B_z harmonic coil in the center region while monitoring the oscillation amplitude at 80 MeV where the turns are still monotonic.

Phases between 10-15° gave a slightly smaller vertical emittance at extraction consistent with stronger focussing in the first turns for these phases [7]. A low to moderate buncher setting gave smaller emittances than bunching for optimum intensity. Increasing the source intensity by 50% above the standard increased the emittance proportionally. Forced vertical centering errors of ±3 mm at 80 MeV increased the emittance by 50%. Forced horizontal centering errors of ±3 mm coupled vertically at the $\nu_r - \nu_z = 1$ resonance at 165 MeV to increase the vertical emittance by 80%. Vertical growth due to RFD excitation was observed consistent with growth at the ν_z=0.25 resonance. Since the distribution in phase space is stretched the vertical width cannot be used to calculate the emittance. Flattopping coincident with RFD use has been done but only to stabilize the precessional radial density pattern [4]. A comparison of the vertical width measurement for the standard high intensity beam and for a phase selected optimized beam is shown in Fig. 5(c,d). The optimized result corresponds to an intensity equivalent to 60 μA at full duty cycle. The future work will involve achieving the lower emittance result at the required intensity.

VIII. Conclusion

Once beyond the center of the cyclotron almost all emittance stretching effects can be prevented at the point of origin. Magnetic imperfections can be compensated by harmonic coils, vertical stretching at $\nu_z = 0.25$ may be reduced by a redesigned RFD. The coherent radial oscillation, however, is a fundamental feature, nevertheless emittance broadening can be reduced by using the AAC to approach more closely single phase conditions.

IX. References

[1] M.K. Craddock, "The TRIUMF KAON Factory", these proceedings.

[2] R. Baartman, private communication

[3] M. Zach, *et al.*, *Proc. 12th Int. Conf. on Cyc. and Their Applic.*, Berlin, 1989 (World Scientific, 1990) p.368.

[4] R.E. Laxdal, *et al.*, "Beam Test Results using the Auxiliary Accelerating Cavity", these proceedings.

[5] J.B. Pearson, TRIUMF report, TRI-DN-91-K180.

[6] W. Joho, PSI report, SIN-TM-11-14, 1980.

[7] G. Dutto, *et al.*, *Proc. 6th Conf. on Cyc. and Their Applic.*, Vancouver, 1972 (AIP, 1972) p.340.

CYCLOTRON TUNING AS A REBUNCHER

D. Bibet, M.H. Moscatello
GANIL, B.P. 5027, F-14021, Caen Cedex, France

Abstract

A new method is being developed at GANIL to reduce the length of the beam bunches. It consists in tuning a SSC as a rebuncher by increasing the magnetic field over the last accelerated turns. This method has been applied on the SSC2 to reduce the time length of the bunches delivered to the experimental room. Encouraging results has led us to apply the same method on the first SSC in order to reduce the phase extension of the beam injected in the second SSC and subsequently minimize energy spread of the ejected beam. Procedure is described and results presented.

Physicists' wishes

In most experiments the time at which the nuclear reaction occurs is an important information. Mainly for the time of flight measurements, which gives the velocity of the particles produced, the time resolution is crucial. Present detectors have a time resolution of 0.1 to 1.0 ns typically. The most convenient and efficient method to measure the time of flight is to determine the time of arrival in the detector with respect to the rf beam pulse. Therefore, the timespread of the beam pulse should be minimized, and should be ideally shorter that the time resolution of the detector.

1. PRINCIPLE

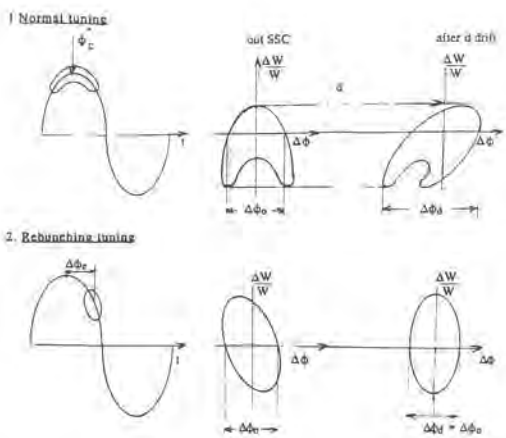


Figure 1

The phase ϕ_i of the particle i after d meters drift is :

$$\phi_i = \phi_{oi} + \frac{180}{2\pi\bar{r}} \times \frac{h}{\gamma^2} \times \frac{\Delta W_i}{W_o} \times d$$

and the central beam shift is :

$$\Delta\Phi_c = -2\pi \cdot \frac{h \cdot N}{\gamma i \cdot \gamma f} \cdot \frac{\Delta B}{B}$$

$\Delta\phi_o$: phase extension at the central momentum
$\Delta\phi_d$: total phase extension after d meters drift
$\Delta\Phi_c$: central beam phase shift for the last turn after a $\Delta B/B$ perturbation on the last N turns
h : rf harmonic
γi, γf : relativistic factor respective to radius ri, rf
$\Delta B/B$: magnetic perturbation applied between the ri and rf radius

from the reference 1 we know that
. the d length drift giving the minimal phase extension is

$$d = -\gamma 2 \frac{\sigma 43}{\sigma 44} \qquad (1)$$

. and the l length pulse at the d distance is

$$l = \sqrt{\sigma 33 + (d\sigma 43/\gamma^2)} \qquad (2)$$

where σij are the matrix elements of the beam matrix σ at the extraction of the cyclotron[1)]

2 SIMULATION [2)]

A simulation has been computed for the SSC2 using the computer code EJEC51[1)]
beam characteristics of the $^{132}Xe^{44+}$ are :
. extracted energy = 43.5 MeV/nucleon
. rf frequency = 9.38 MHz harmonic h = 2
. radial and transverse emittance = 5 π mm.mrad

. without perturbation
beam characteristics at the ejection point are :
pulse length $l = 0.142$ m
momentum spread $\Delta p/p = 0.846\ 10^{-3}$

. with a constant field gradient perturbation
of $+0.2\ 10^{-4}$ T/m extended on the 16 last centimeters of the acceleration path ; we get at the extraction point
pulse length $l = 0.140$ m
momentum spread $\Delta p/p = 1.1\ 10^{-3}$
central beam shift $\Delta\Phi_c = -37$ ° RF
the longitudinal waist point given by equations (1) and (2) :
is located at d = 108.9 m downsteam
and pulse length l = 0.088 m
effective gain for the physicist would be more if we consider the increasing phase drift it would have had without rebunching effect.

3. TUNING PROCEDURE

. firstly we do the standard tuning of the cyclotron and single turn extraction is verified with a time structure detector

. then field perturbation is applied using the last isochronism trim coils.

- the rf phase cavities must not be changed
- isochronous field pattern has to be corrected in front of the perturbation because of the return field effect of the trim coil change
- voltage acceleration is increased to compensate the lost of gain per turn due to the shift of the central phase on the last turns. It is adjusted to get the same extracted turn
- energy spread and time pulse length are measured at a given distance

. pulse length on the target is whether estimated or measured and magnitude perturbation can be adjusted

3.1 Limitation

. single turn extraction is a necessary condition
. field gradient has to be limited to respect of the matching conditions
. increasing of the energy spread induce by acceleration on the non-isochronous turns limit the turn separation extraction

3.2 Advantages and inconveniences

. tuning procedure is a little more complicated and the tuning time machine takes more time

. if the rf phase value is lost it is difficult to refine the optimum value because turn separation at extraction is not yet the best test

. increased energy spread

. bunch length reduction can be optimized for a dedicated room experiment

. bunch length reduction is achieved without or a very little lost beam intensity

. test experiments have shown a more stable beam time structure than the previous method using slits and less sensitive to any rf voltage or magnetic fluctuations.

4. RESULTS ON SSC2

Fig. 2 shows some results obtained on the SSC2 for the ^{132}Xe beam. The standard tuning gave 1.15 ns (half height) length time bunches after 40 m drift, then with +80 A applied on the last trimcoil we got bunches reduce to 0.215 ns on the target experimental room D3 located 100 m downstream SSC2.

For the ^{181}Ta beam it has been necessary to applied +120 A to get a factor 2 of reduction (see Fig.3).

Pictures 4 and 5 show a scanning of the longitudinal emittance of the ^{208}Pb beam. For the standard tuning we can see that bunches are well placed on the top of the sinusoid. With only a +90 A perturbation, bunches are not sufficiently shifted on the sinusoid as shown Fig. 5. We tried to apply a bigger perturbation (+150 A) but we got two turns extracted.

Fig. 6 gives the perturbation obtained on the axis of the four sectors magnet.

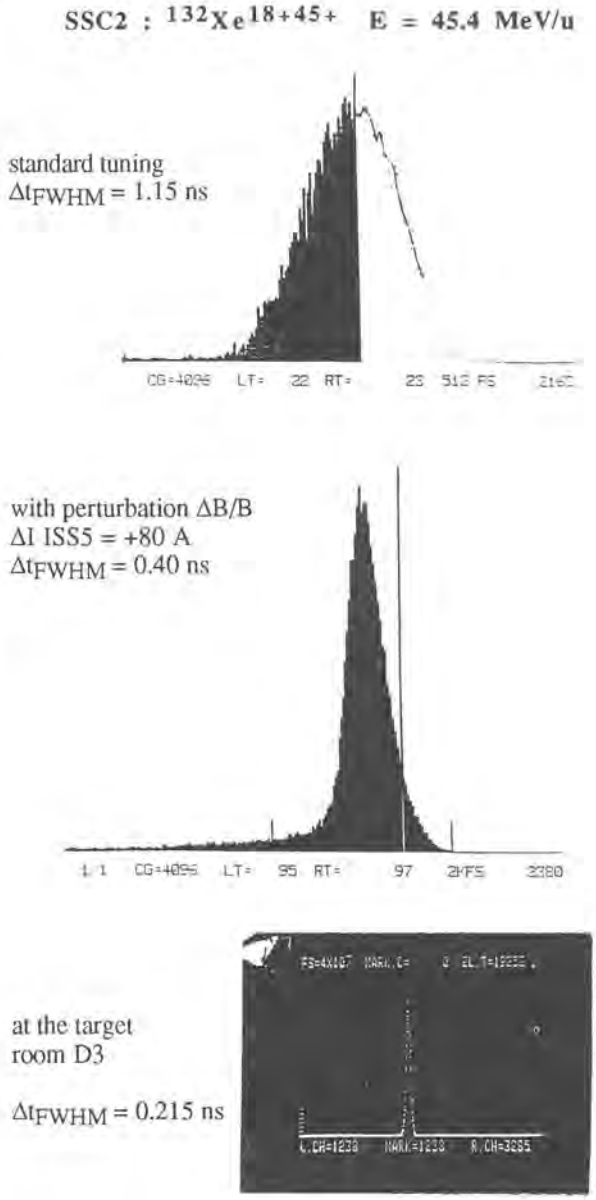
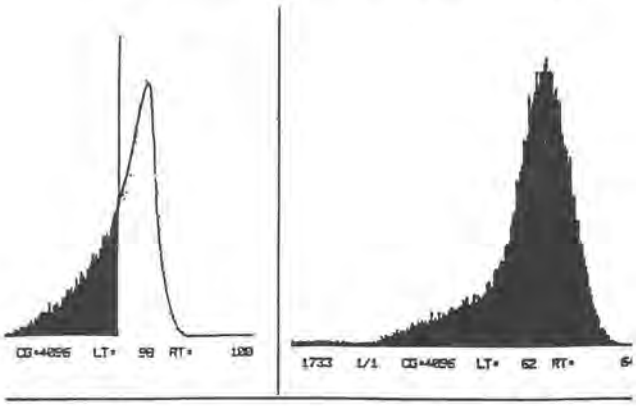


Figure 2



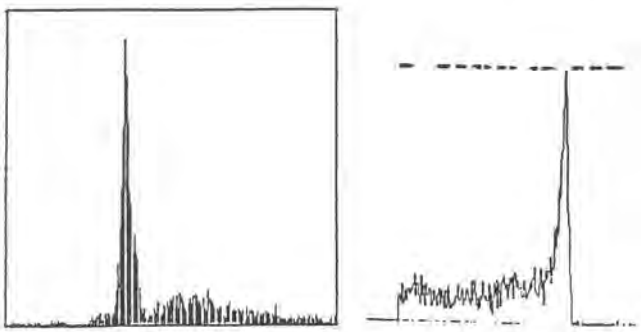


Figure 3

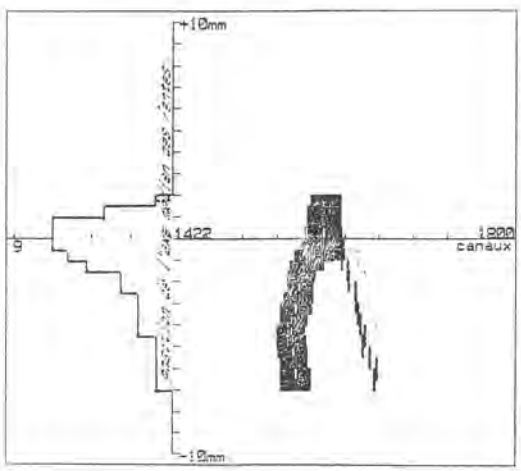


Figure 4

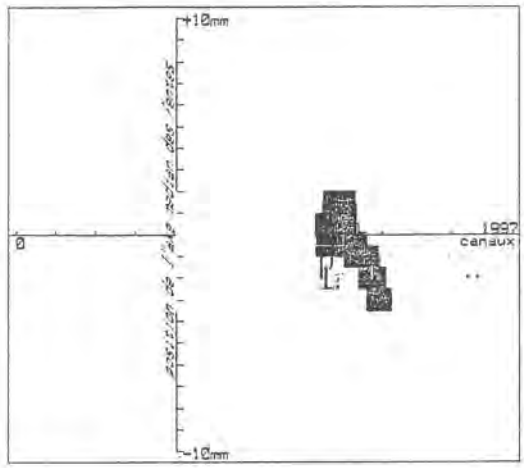


Figure 5

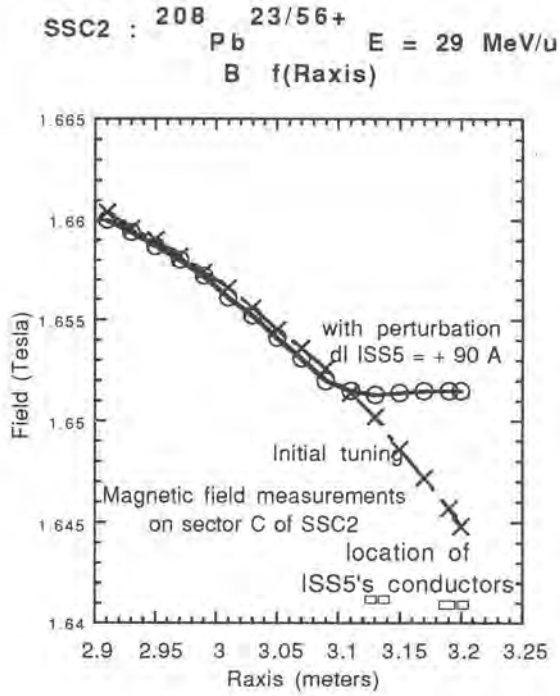


Figure 6

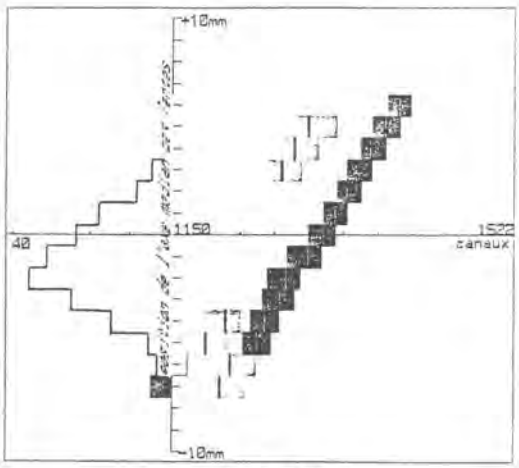
5. RESULTS OF SSC1

Encouraging results obtained on SSC2 led us to test this method on SSC1 in order to reduce the phase extension of the beam injected in SSC2.

If we got satisfying result with ^{36}Ar beam with a transparency of SSC2 near 100% ; it has been very different with ^{238}U beam. Between the two SSC, beam is passing through a stripper foil which produces a large energy spread and straggling giving a corresponding increase of the space phase volume. In this case objet point for the ($\Delta W/W$, $\Delta\phi$) phase space is still the stripper and the resulting effect of SSC1 perturbation turns out be very small. Nevertheless we have observed a small reduction of the longitudinal emittance given by a reduction of $\Delta\phi$ at the stripper. So we are still interested in another test with lighter ions, which stripper effect is smaller.

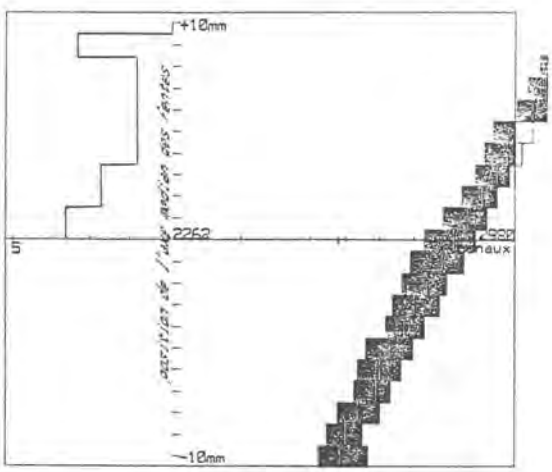
The following pictures show the different results for $^{238}U^{24/58+}$ E = 24 MeV/u obtained with non stripped and stripped beam.

SSC1 : initial tuning non stripped beam



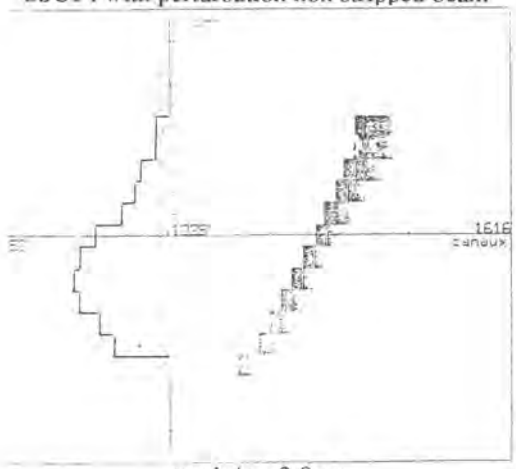
total Δt : 2.3 ns

SSC1 : initial tunning beam stripped



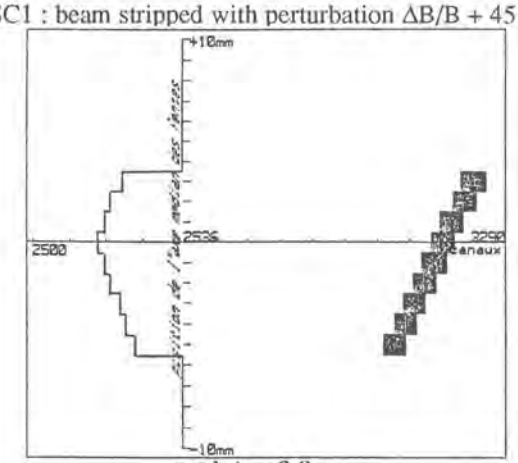
total Δt : 4.3 ns

SSC1 : with perturbation non stripped beam



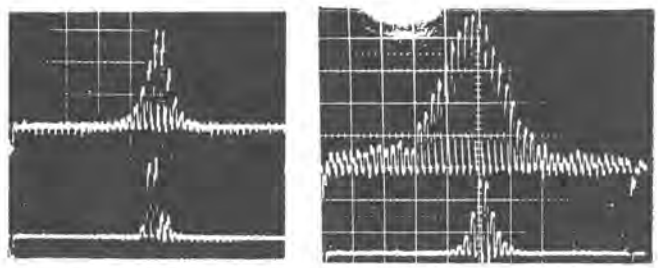
total Δt : 2.0 ns

SSC1 : beam stripped with perturbation $\Delta B/B + 45$ A



total Δt : 3.8 ns

Energy spread



non stripped beam
$\Delta W/W = \pm 0.5\ 10^{-3}$

stripped beam
$\Delta W/W = \pm 1.6\ 10^{-3}$

REFERENCES

[1] J. Fermé, "Calcul au premier ordre des termes de couplage et de la matrice faisceau adaptée dans le cas général d'un cyclotron isochrone" report GANIL R89-03

[2] M.H. Moscatello, "Diminution de la longueur en phase des pulses par réglage d'un cyclotron en regroupeur" report GANIL 561.91/ml

BEAM STUDIES OF INJECTION TO EXTRACTION SYSTEM FOR JAERI AVF CYCLOTRON

M. Fukuda, K. Arakawa, Y. Nakamura, W. Yokota, T. Nara,
T. Agematsu, S. Okumura, I. Ishibori and T. Karasawa
Japan Atomic Energy Research Institute, 1233 Watanuki, Takasaki,
Gunma, 370-12, Japan

ABSTRACT

The JAERI AVF cyclotron has distinctive features as a multi-particle, variable-energy cyclotron. Harmonic numbers of 1, 2 and 3 are available for acceleration in a wide range of energy. Beam studies have been carried out to study beam behavior in the cyclotron. Isochronous fields has been generated easily by phase measurements and cross-checked by phase measurements for small amounts of positive and negative changes of rf frequency. The relation between an electric field of a deflector and $mv^2/2q$ is surveyed for several ions accelerated in practical operation.

1. INTRODUCTION

The JAERI AVF cyclotron[1,2](K-number=110) is of the model 930 of Sumitomo Heavy Industries, Ltd. The cyclotron is basically the same model as the CYCLONE (Université Catholique de Louvain). The original design of an rf cavity, an inflector and the deflector was modified in order to make allowance for accelerating 90 MeV protons. A movable-panel type resonator originally proposed was replaced by a $\lambda/4$ coaxial type resonator[3] with a movable shorting plate for generating a maximum acceleration voltage of 60 kV. Maximum currents of circular trimming coils were also modified for generating isochronous field for 90 MeV protons. An phase probe was additionally installed for measuring relative beam phases.

In general orbit analysis using ideal isochronous field is carried out in designing the cyclotron. Beam behavior in practical operation, however, is less understood because the actual magnetic field doesn't always correspond to the ideal isochronous field. Some beam diagnostics probes in an acceleration region provide us with rough information on the beam behavior. More precise analysis of beam dynamics is required for understanding the beam behavior and operating the cyclotron. We are now developing an operation assist system[4] for easy and reliable operation of the cyclotron. The system is expected to be a base system for automatic operation in future. The system consists of a knowledge-based expert system and a beam trajectory simulation system. The results of the orbit analysis are utilized for developing the system.

In this work the orbit studies are focused on beam characteristics in a central region, generation of the isochronous field and the correlation of the electric field with mv^2/q and the entrance position of the deflector. Validity of the orbit calculation depends on reproducibility of the actual magnetic field. The calculated field is composed by using measured field maps. Accuracy of the field reconstruction is around 1×10^{-3} for main coil currents between 150 A and 550 A, and is better than 1×10^{-3} above 585 A. The circular trimming coil field is strongly dependent on the base field in the former current region. Measured maps of the trimming coil field are not sufficient for composing an actual magnetic field in the region. Beam studies of the central region to the extraction region were carried out for 70 MeV protons in order to reliably analyze the beam analysis, since the main coil current is 552.59 A. Calculated beam phase shifts for 70 MeV protons correspond to measured ones.

2. CENTRAL REGION

A schematic drawing of the central to the extraction regions is shown in Fig. 1. An inflector of the spiral type and a puller are designed for each harmonic mode. Two sets of phase slits are installed in the central region for defining beam phases. Both of the slits are movable and have enough stroke to define the beam phases for the first turn. Trajectories of central particles simulated by a computer code for 70 MeV protons with injection phases of 0°, ±10°, ±20° and ±30° are shown in Fig. 2. Without the phase defining slits, the central particles within an injection phase of ±30° can reach the entrance of the deflector. Turn numbers for the central particles with injection phases of −20° and −30° are, however, more than those with the other phases by 100~200 turns. Figure 3 shows trajectories of the particles lying in orthogonal positions on the phase ellipse of which the area is 4 mm×50 mrad×π with injection phases of 0°, +15° and −15°.

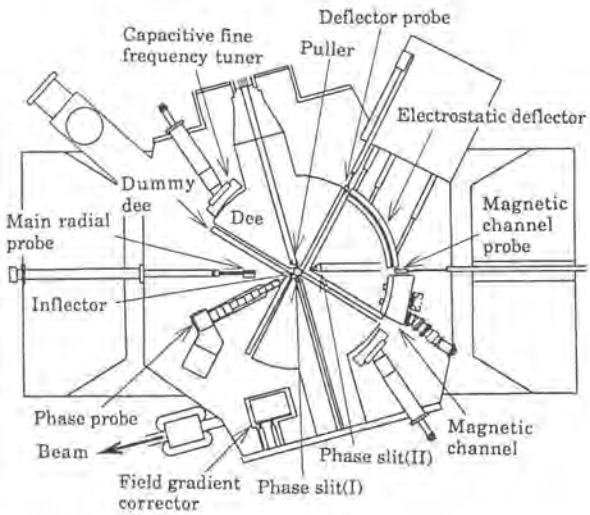


Fig. 1. Layout of the injection to extraction system of the JAERI AVF cyclotron.

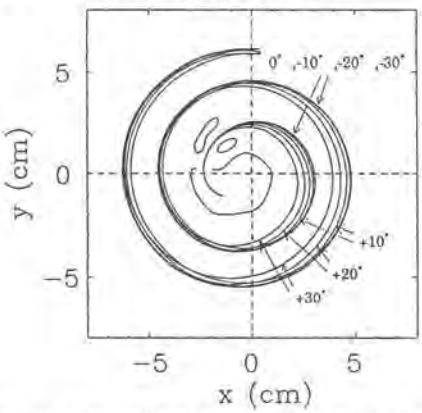


Fig. 2. Central trajectories of 70 MeV protons with injection phases of 0°, ±10°, ±20° and ±30°.

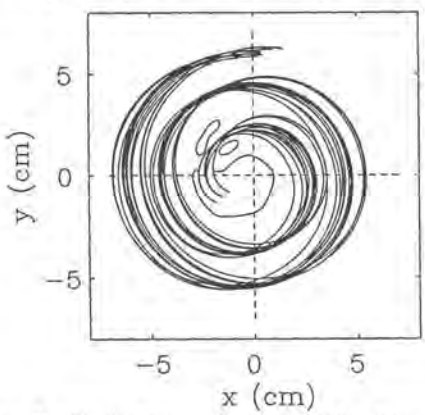


Fig. 3. Trajectories of the particles lying in orthogonal positions on the phase ellipse whose area is 4 mm×50 mrad×π with injection phases of 0°, +15° and −15°.

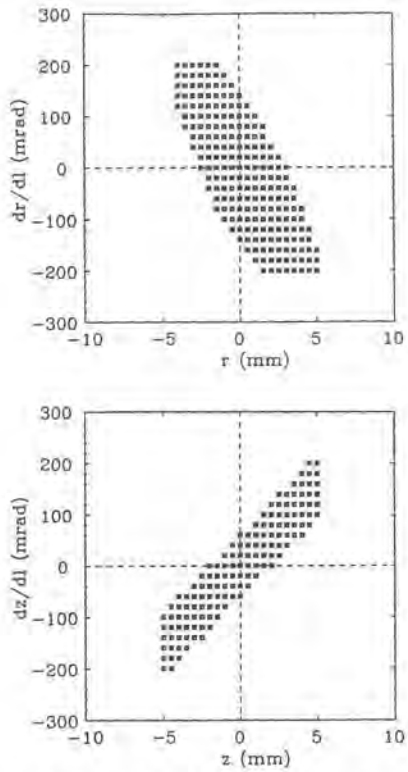


Fig. 4. Horizontal and vertical acceptances of the cyclotron for the injection phases of 0°.

The beams are horizontally focussed at the slit (I) position. An effective phase acceptance for the slit (I) gap of 6 mm is ±15°.

Horizontal and vertical acceptances of the cyclotron for the injection phases of 0° are shown in Fig. 4. The acceptances in both directions are more than 300π mm·mrad, which covers injection beam emittances[5] of 100π to 200π mm·mrad in horizontal direction and 100π mm·mrad in vertical direction. The calculated acceptances are defined as follows; horizontal and vertical deviations of particles are within the distance of ±10mm from the central particle up to a radius of 25 cm where the isochronous field starts.

3. GENERATION OF ISOCHRONOUS FIELDS

An acceleration dee voltage for the cyclotron is determined by a constant orbit method. A standard condition of the constant orbit method is 90 MeV protons for the harmonic number h=1 with a dee voltage of 60 kV, 460 MeV $^{40}Ar^{13+}$ for h=2 with 34 kV and 175 MeV $^{40}Ar^{8+}$ for h=3 with 34 kV. The beam phase is quite sensitive to field perturbation because turn number amounts to 550 for h=1, 265 for h=2 and 210 for h=3. If a base field level increases or decreases equally by $\Delta B/B=1\times10^{-4}$ from the isochronous field, the beam phase drifts away by 20° in the extraction region. Thus careful fine tuning of the coil currents is required for generating the isochronous field for each ion and energy.

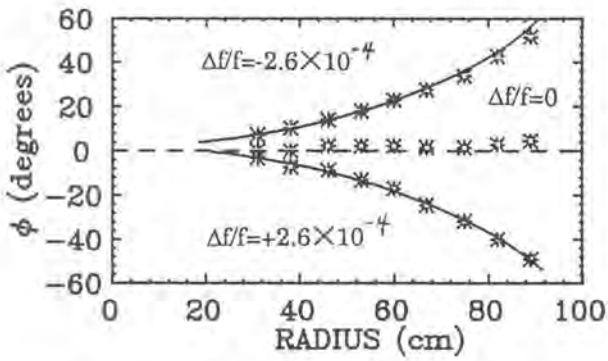


Fig. 5. Phase drifts for 45 MeV protons due to the positive and negative radio-frequency change of $\Delta f/f = \pm 2.6 \times 10^{-4}$. Measured and calculated phases are indicated by stars and solid lines, respectively.

Main coil and circular-trimming-coil currents for generating the isochronous field are calculated by using an optimization code based on measured field maps. Relative phases of beam particles are measured by the phase probe consisting of ten pairs of rectangular pickup electrodes. The electrodes are installed in radial direction as shown in Fig. 1. The electrodes are made of 2.5 mm thick oxygen free copper. The electrodes are radially 58 mm long and azimuthally 40 mm wide for the inner threes, 60 mm for the middle fours and 93 mm for the outer threes. Relative phase differences from the pickup signal of the second electrode are detected by a digital storage oscilloscope. The length of signal cables of the phase probe was made uniform within a variation of 4 mm, so that an error due to the variation is within 0.02 nsec. Current corrections of each circular trimming coil are made by a least-squares fitting code for deducing the currents so as to minimize the field deviation from the isochronous field. The phase deviations can be finally reduced within ±5° after a few iterative corrections.

The pickup signal of the phase probe is produced by the particles passing through the electrode covering a radial range of 58 mm. The phase corresponds to the radially averaged phase. The isochronous field was cross-checked by small amounts of radio-frequency shifts of $\Delta f/f = 2 \times 10^{-4}$ to 5×10^{-4} in order to reduce ambiguity of the phase measurement due to the wide sensitive area. If the isochronous field is generated ideally, the same amount of positive and negative rf shifts should result in the same amount of negative and positive phase drifts. The rf shifts are equivalent to a small change of a base field level. It is difficult to estimate exactly the change of the base field for fine tuning of the coil currents due to magnetic hysteresis. On the contrary, the radio-frequency can be set precisely at a resolution of 10 Hz. Phase drifts caused by the rf change of 2.6×10^{-4} for 45 MeV protons are shown in Fig. 5. Phase drifts are calculated on the assumption that the isochronous field starts at a radius of 20 cm and no central field bump is concerned. The measured phases are consistent with the calculated ones. The calculated phases for an initial rf phase shift of 2° are fitted well with the measured ones. The cause of the shift is under investigation. The fields generated in practical operation were found to agree with the ideal isochronous fields within 1 gauss.

4. ELECTRIC FIELD OF DEFLECTOR

Extraction system consists of an electrostatic deflector, a magnetic channel and a field gradient corrector. Analysis of beam behavior in the extraction region is much more complicated because the magnetic field remarkably varies in the radial direction. Electric field distribution of the deflector is not simple due to a complex change of a mechanical gap depending on the positions of septum and high voltage electrodes. Furthermore it is hard to define particle condition at the entrance of the deflector owing to the difficulty of orbit computation up to extraction.

The electric field of the deflector is represented by equivalent field reduction[6]:

$$\Delta B = \frac{\varepsilon}{300 \times \beta}, \tag{1}$$

where ΔB is in kG, ε is the electric field of the deflector in kV/cm and β is v/c. The electric field is given by;

$$\varepsilon = \frac{10^3}{c\rho_0} \times \frac{mv^2}{q} \times \frac{\Delta B}{B_0} \tag{2}$$

at around the entrance of the deflector, where B_0 is magnetic field averaged azimuthally at a curvature of ρ_0 at the entrance of the deflector. If the field reduction ratio $\Delta B/B_0$ and the curvature are approximately constant, the electric field is proportional to mv^2/q. Dependence of the electric field at the entrance of the deflector on mv^2/q obtained in practical operation is shown in Fig. 6 and Table 1. The electric fields are approximately proportional to mv^2/q. The electric fields are not corrected for positional dependence of the deflector on the magnetic field. The dashed line represents the calculated electric field obtained by a linear fitting for the ions. There is the upper limit of the electric field in actual use in the cyclotron. The maximum electric field is required for extracting 90 MeV protons. The entrance of the deflector for 90 MeV protons should be located at outer position in order to reduce the electric field. Actually the position for 90 MeV protons is outer than that for the other ions. We have extracted 90 MeV protons with the electric field of 140 kV/cm which is 70% of the predicted ones.

Dependence of the electric field on the entrance position of the deflector for 70 MeV protons by preliminary analysis is shown in Fig. 7. The electric fields are obtained by averaging the field at the entrance, mid and exit positions. The calculated electric fields are determined as follows; 1) Positions and momentums at the

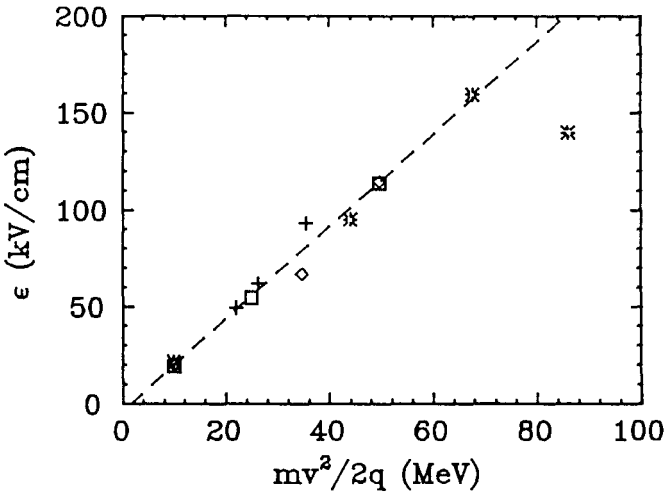


Fig. 6. Dependence of the electric field at the entrance of the deflector on mv^2/q obtained in practical operation. The measured electric fields are indicated by stars for 10 MeV, 45 MeV, 70 MeV and 90 MeV protons, diamonds for 10 MeV, 35 MeV, and 50 MeV deuterons, squares for 20 MeV, 50 MeV and 100 MeV $^4He^{2+}$ and crosses for 175 MeV $^{40}Ar^{8+}$, 460 MeV $^{40}Ar^{13+}$ and 520 MeV $^{84}Kr^{20+}$. The electric fields obtained by a linear fitting for all but 90 MeV protons are represented by a dashed line.

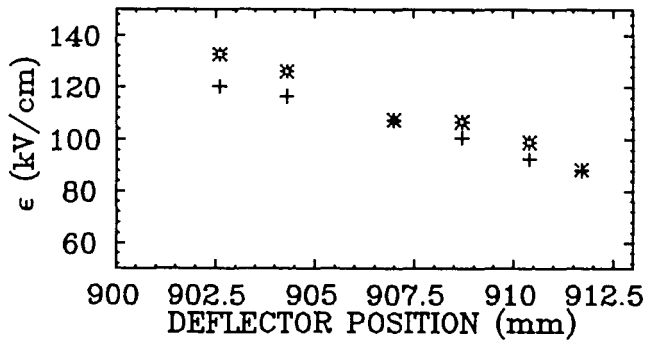


Fig. 7. Dependence of the mean electric field on the entrance position of the deflector for 70 MeV protons by preliminary analysis. The actual and calculated fields are indicated by crosses and stars, respectively.

Table 1. Dependence of the electric field at the entrance of the deflector on mv^2/q obtained in practical operation.

ε(kV/cm)	ion	$mv^2/2$(MeV)	q	B(kG)	h
19	He	20	2	5	2
20	D	10	1	7	2
21	H	10	1	5	2
49	Ar	175	8	16	3
54	He	50	2	11	2
62	Kr	520	20	16	2
67	D	35	1	13	2
93	Ar	460	13	16	2
95	H	45	1	11	1
114	He	100	2	16	1
115	D	50	1	16	1
140	H	90	1	15	1
160	H	70	1	13	1

entrance of the deflector are obtained by tracing a central particle from the exit of the inflector. 2) The gap and position of the electrodes are fixed to the actual ones. 3) The electric fields are determined so that the particle should reach the center position of the exit gap. The position dependence of the calculated electric field is consistent with the actual dependence. The calculated fields are, however, higher by around 5% than the actual ones. Precise analysis for the position dependence of the electric field is required.

5. SUMMARY

Beam studies for study of beam behavior in the central and extraction regions have been carried out for the JAERI AVF cyclotron. The cyclotron has more phase acceptance than that of the injection beams. Isochronous fields were generated in practical operation with an accuracy of 1 gauss by using the phase probe. Generation of the isochronous field is cross-checked by small changes of rf of $\Delta f/f = 2 \times 10^{-4}$ to 5×10^{-4}. The phase probe is quite useful for generation of the isochronous field. The actual electric fields of the deflector are approximately proportional to mv^2/q except for 90 MeV protons. Dependence of the field on the entrance position of the deflector was surveyed by the computer code.

6. REFERENCES

1) Tanaka, R. et al., "JAERI AVF cyclotron for research of advanced radiation technology," presented at the Conference on Cyclotrons and Their Applications, Berlin, Germany, May 8-12, 1989.
2) Arakawa, K. et al. "Construction and first year's operation of the JAERI AVF cyclotron," presented at this conference.
3) Kumata, Y. et al. "A modified rf system of JAERI AVF cyclotron," presented at this conference
4) Okamura, T. et al., "An operator assistance system for AVF cyclotron," presented at this conference.
5) Yokota, W. et al., "Operation of ion sources and beam transport to JAERI AVF cyclotron," presented at this conference.
6) Richardson, J.R.,"Sector focusing cyclotrons," Progress in Nuclear Techniques and Instrumentation (North-Holland Physics Publishing, 1965), vol.1, pp. 75-85.

K1200 CYCLOTRON BEAM DEVELOPMENT TECHNIQUES

Timothy A. Antaya, Dallas Cole, Peter Miller, David Poe

National Superconducting Cyclotron Laboratory, Michigan State University, East Lansing, MI 48824-1321 USA

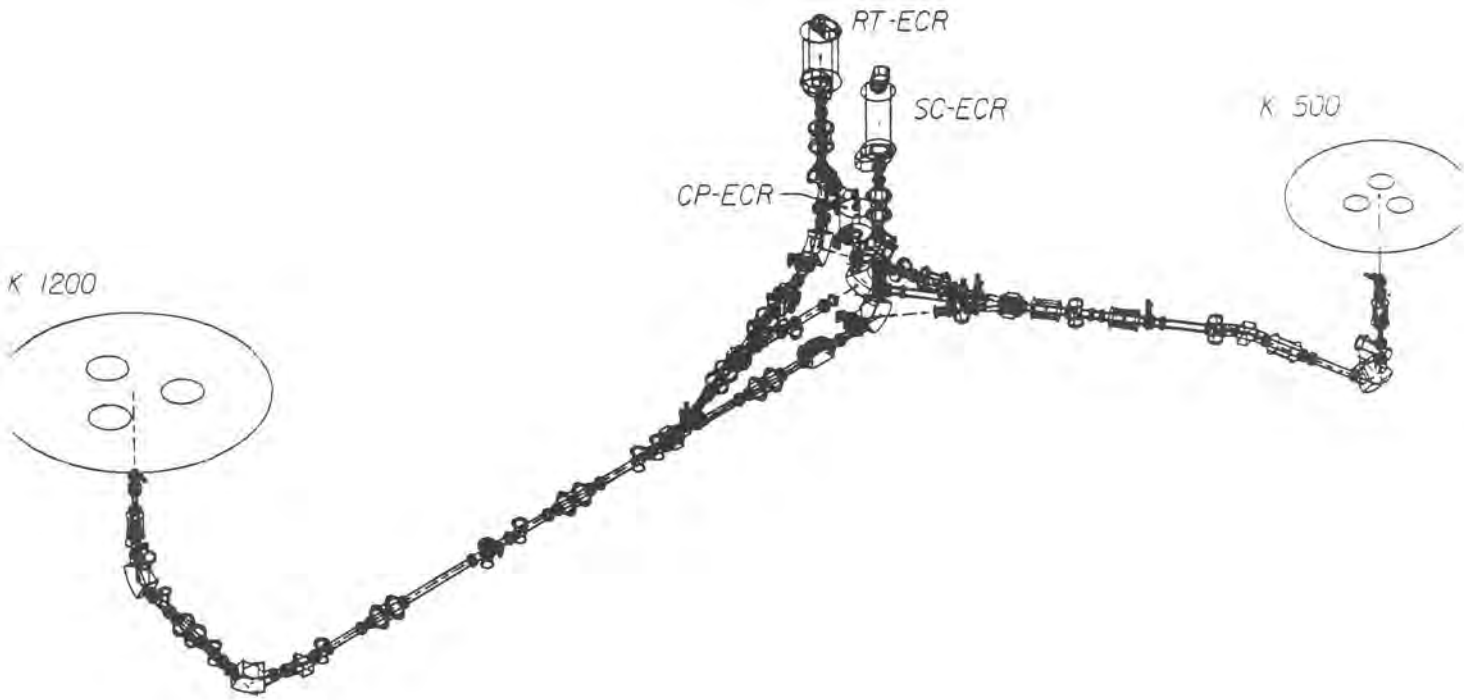


Figure 1. The beam development system at NSCL consists of ECR sources, injections and the superconducting cyclotrons.

1. Introduction

We now accelerate ions from hydrogen to uranium in the K1200 cyclotron at NSCL. There are several classes of problems associated with producing these beams: source tuning, beam transport and injection, and cyclotron tuning. The development of a particular beam can be critical in more than one of these areas. For example, uranium 35–39+ ions are not fully resolved from mixing gases at the ion source, the cyclotron fringe field is high, and an analog beam must be used to tune the cyclotron. Still, uranium beams at 20 and 25 MeV/n using 35+ and 39+ respectively, have been produced. Atomic hydrogen cannot be accelerated directly in the K1200, and H_2^+ ions are only useful for high energy hydrogen beams. For low energy hydrogen beams, HeH+ molecules are produced in an ECR source, injected, and then stripped after acceleration. We also accelerate series of ions simultaneously at fixed q/m ratios: 1/5, 1/4, 1/3, 1/2, using multiple species

and/or ion sources.

The full facility for production of heavy ion beams at NSCL is shown in Figure 1. It consists of three ECR ion sources, a switchyard to connect any ion source to either cyclotron, the two superconducting cyclotrons and their main injection lines. In this paper, we will focus on beam development techniques for stand alone operation of the K1200 cyclotron, since that is also the main facility emphasis at the present time.

2. Ion Sources and Switchyard

Ion beams injected into the K1200 cyclotron come from one of three electron resonance sources, as shown in Fig. 1. The RTECR, commissioned in 1985, and operating more than 6000 hours every year since 1986, is the basis for most K1200 cyclotron beams. Recent performance at the RTECR is summarized in Figure 2. This ion source has served both as a production ion source and development platform for new concepts, and is perhaps the most optimized of all ECR source designs. Gaseous ion production is based on a reduced first stage, single microwave feed, high injection magnetic field, SiO_2 coated plasma chamber walls and low operating pressure [1]. Metallic ion production is now based on the super gas mixing technique for highly charged metallic ions [2], but the RTECR can use (and has used) a number of different techniques for metallic ion beams.

The CPECR has two modes of operation. With the oven stage installed , it produces stable beams of alkali metals, particularly $^{6,7}Li^{2+,3+}$ [3]. The key to long stable lithium runs is a heated stainless steel liner in the main stage operating at about 400°C. The heated liner allows for enhanced recirculation of lithium into the main stage plasma. In order to accommodate oven conditioning and operation, the CPECR can be operated at pressures as high as $1 \bullet 10^{-4}$Torr, without microwave vacuum feedthru or extraction insulator failures. At such high pressures, intense beams of low binding energy molecules can be produced in the CPECR, when the oven stage is replaced by a gaseous feed first stage. The most unusual of these molecules is HeH^+, shown in Figure 3, which permits low energy H+ beam production in the K1200 thru post-accelerator stripping of the helium 'anchor weight'.

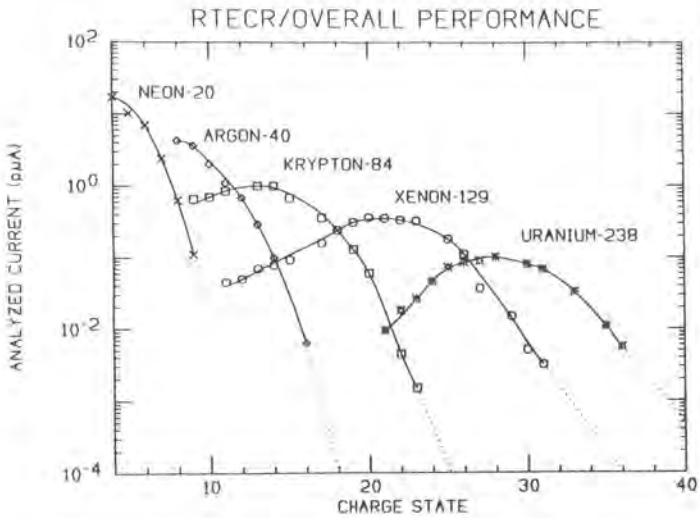


Figure 2. The optimized performance of the RTECR is smooth in Q and Z.

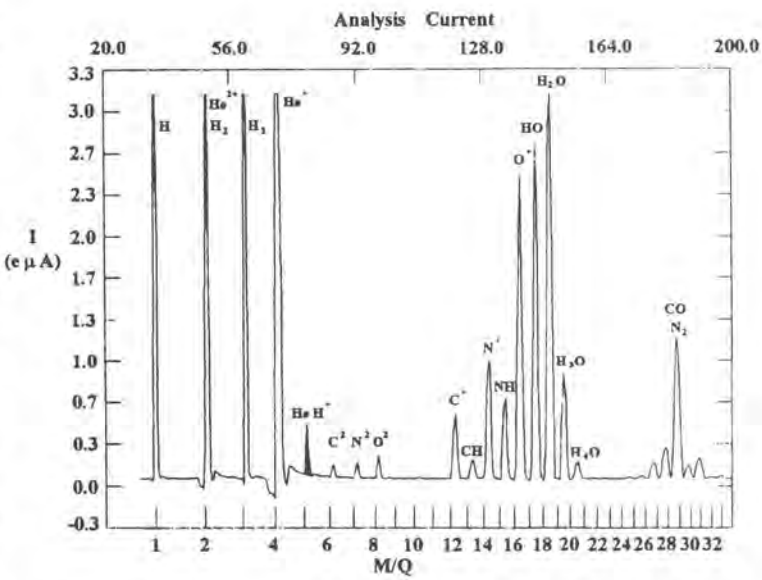


Figure 3. The He+H charge state distribution of the CPECR, showing the presence of the HeH+ molecule, used to produce low energy H beams in the K1200 cyclotron.

The multi-frequency high field SCECR now in development, is the third ECR ion source built at NSCL. The SCECR ion source structures are equivalent to the RTECR, but the magnet field is produced by a full set of superconducting coils [4]. This coil set is not operated in persistent mode, as have previous superconducting ECR designs [5,6,7], so source tuning over a wide dynamic range of magnet settings is possible. The source has available 6.4 and 14.5 GHz microwave feeds. Early experience has shown that 6.4 GHz operation at high magnetic field is equivalent to 14.5 GHz of a nominal magnetic field. Figure 4 shows a comparison of oxygen ion performance of the RTECR and SCECR at 6.4 GHz. We note that the SCECR performance in Fig. 4 comes without use of gas mixing or wall coatings, and requires 1/10 as much microwave power as the RTECR tune.

Each ion source can be connected to either main injection line (K500 or K1200) via a switchyard beamline. Switching is accomplished by breaking a beamline joint and rotating the analysis dipole to the new line. The RTECR and SCECR remain insolated and under vacuum during this process. The CPECR does not have such an insolation gate valve and must be vented. The process takes typically 2-4 hours, and is limited mainly by the need to attain high vacuum ($\leq 10^{-7}$Torr) in the beamline before operating the sources. Controls and interlocks are automatically switched to the new beamline by the PLC.

Since the K500 cyclotron is generally not operated, the full ion source set can be directed to K1200 cyclotron operations and beam development, giving unparalleled capabilities and flexibility.

3. Injection Lines

The K1200 cyclotron injection line is simply a longer version of the K500 injection line. Both were described at the Tokyo Cyclotron Conference [8]. Matching ECR beams to these injection lines has been extensively studied [9]. We find that the emittance is dominated by the fact that the ions originate in a magnetic field, but the beam transport is dominated by space charge forces. Features of this injection design that aid development include the use of solenoid lenses for focusing, the large bore beam pipes (6" ID solenoids, 4" ID dipoles), and the

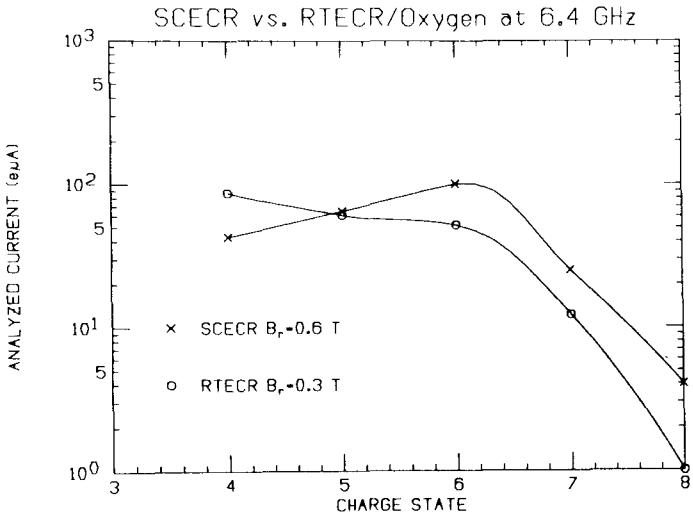


Figure 4. A comparison of the oxygen ion production of the RTECR and SCECR ion sources operated at 6.4 GHz. See text for details.

generally linear response of the system to changes in beam rigidity. However, the source operating voltage is set by injection criteria, so it is not always possible to use the optimum ion source extraction conditions.

The typical transmission from source analyzed beam current to K1200 spiral inflector is 30%. Major losses occur primarily in two areas: the transition from the switchyard to the main injection line, and the vertical beamline under the K1200 cyclotron. The losses associated with the transition from the switchyard to the main injection line occur mainly for the two room temperature ECR sources, and appear to be due to transit path differences and non-linear beam distortions in the short 'merging' dipole. On the axis of the K1200 cyclotron, there is a mis- match between the final beam emittance and the acceptance of the spiral inflector. Just above the last bend, beam profiles are elongated with a central core and high divergence tails. Part of this beam distortion is due to the cyclotron fringe field– the 'cyclotron off' transmission from the RTECR to the K1200 cyclotron axis is about 70% or higher. Space charge is also important, as the distorted beam shape is sensitive to beam current. The lowest injection transmission, about 10%, occurs for high $K_{bending}$ operation with

low Q/M ions, and is attributable to both using low velocity ions and high fringe field injection.

4. K1200 Cyclotron Characteristics

The general characteristics of the K1200 cyclotron have been summarized well at this conference [10]. We would also echo the emphasis in that paper on the excellent ion and energy variability of the K1200. Of course, these high energy beams are provided by a *single accelerator*, injected by ECR sources, rather than a set of accelerators. Specifically with regard to beam development, one should also note that there is a very good correspondence between calculated K1200 parameter settings and actual operating settings, both for internal parameters and extraction elements. The main magnet is set by calculations [11], and the resulting operating frequency is accurate to better than a few kilohertz. Therefore analog beam tuning for difficult beams is a very effective technique–both the absolute frequency of the analog and calculated frequency shift to the desired species are dependable. Once tuned, the K1200 cyclotron parameters are found to be stable and reproduceable.

5. REFERENCES

1) Antaya, T.A. to be published.
2) Antaya, T.A. et.al, "The Super Gas Mixing Technique for Highly Charged Uranium Ions," presented at the XIII International Conference on Cyclotrons and Their Applications, Vancouver B.C., July 8, 1992.
3) Sanderson, D.P., Antaya, T.A. and Xie, Z.Q., "A High Temperature Oven Stage for ECR Ion Sources," in **International Conference on ECR Ion Sources and Their Applications** (MSUCP-47, East Lansing, 1987) 300.
4) Antaya, T.A., "A Review of Studies for the Variable Frequency Superconducting ECR Ion Source Project at MSU," Journal De Physique **50**, C1-707 (1989).
5) Brautigam, W., Beuscher, H., Mathews, H.G., Reich, J. and Wucherer, P., "ECR Sources and Multiharmonic Mode Operation at Julich," in **Tenth International Conference on Cyclotrons and Their Applications** (IEEE, East Lansing, 1984) 122.
6) Bechtold, V., Friedrich, L. and Schulz, F., "External Ion Sources at the Karlsruhe Cyclotron," in **Tenth International Conference on Cyclotrons and Their Applications** (IEEE, East Lansing, 1984) 118.
7) Jongen, Y. and Ryckewaert, G., "Initial Operation of ECR Ion Sources with CYCLONE," in **1983 Particle Accelerator Conference** (IEEE, Santa Fe, 1983) 2685.
8) Harwood, L., Nolen, J.A., Tanaka, S. and Zeller, A.F., "Analysis and Transport of Beams from the ECR Ion Source to the NSCL K500 and K800 Cyclotrons," in **Eleventh International Conference on Cyclotrons and Their Applications** (Ionics, Tokyo, 1986) 488.
9) Antaya, T.A., et.al., "Space Charge Effects in Highly Charged Positive Ion Beams Extracted From ECR Ion Sources," presented at the XIII International Conference on Cyclotrons and Their Applications, Vancouver, B.C., July 9, 1992.
10) Miller, P., "Performance of the K1200 Cyclotron at MSU," presented at the XIII International Conference on Cyclotrons and Their Applications, Vancouver, B.C., July 6, 1992.
11) Johnson, D., Kuo, T., Marti, F., Nolen, J.A., Sherrill, B. and Zeller, A., "Magnetic Field of the K800 Cyclotron," in **European Particle Accelerator Conference** (World Scientific Pub., Rome, June 7-11, 1988) 1261.

SELECTION AND MEASUREMENT OF RF PHASE WIDTH OF THE K1200 CYCLOTRON BEAM

J. Bailey, J. Kuchar, F. Marti, and J. Yurkon*
NSCL, MSU, East Lansing, MI, 48824, USA

and

J. Nolen
Physics Division, Argonne National Lab., Argonne, IL, 60439,USA

and

D. Rifuggiatto
INFN, Catania, Italy

ABSTRACT

Reductions to 4° FWHM in RF phase width of the K1200 extracted beam have been achieved with the use of internal radial slits. Beam losses using the phase slits have been minimized to 70%. Rapid measurements of the time structure of the extracted beam have been obtained using a silicon detector placed in the beam shortly after extraction, with attenuators in the injection beam line. An internal timing probe using a silicon detector has been designed, and is under construction.

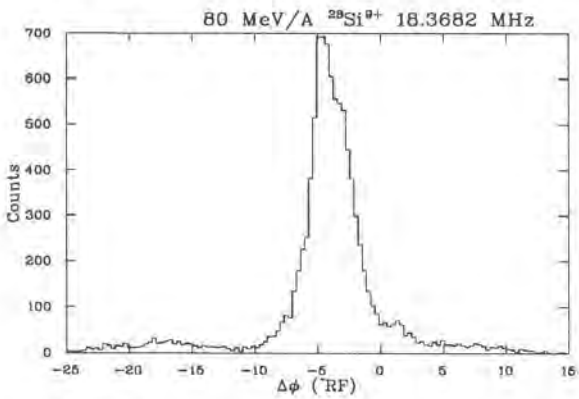


Figure 1. The best extracted beam phase width to date. The FWHM is 3.6° RF, or .55 ns at this frequency. Lower widths in the main peak have been achieved, but with larger shoulders and satellites.

1. INTRODUCTION

The RF phase acceptance determined by the central region of the K1200 cyclotron is 40° RF.[1,2] The use of a buncher to further restrict the RF phase at injection, with just first, or both first and second harmonics, is limited by debunching in time during traversal of the yoke and spiral inflector.[2] The first harmonic buncher calculations show enhancement over the entire acceptance range with a preferential enhancement of a narrower range. Multi-turn extraction adds further complications, but Fig. 2. shows that this effect can be seen after extraction.

*Work supported by the U.S. National Science Foundation.

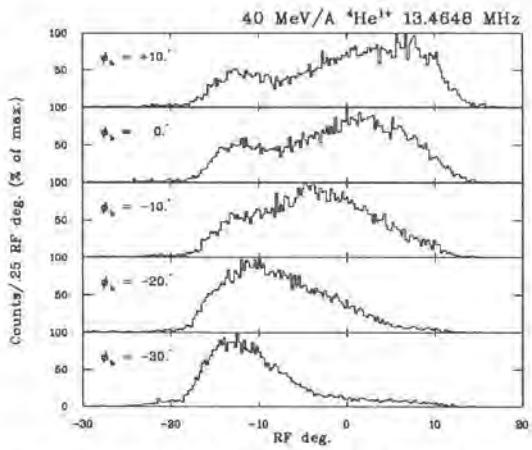


Figure 2. Measured time structure of the beam after extraction for buncher phase $\phi_b = -30°$ to $+10°$. Note the broad base even when the buncher is well tuned. Also, all phases measured to date have been relative, the zeros are not absolute.

2. PHASE SLIT DESIGN

Further reductions in transmission of RF phase can be obtained with internal cuts. Holes through the yoke, hill, and liner at 7 in. radius permit access to a region of the cyclotron where the turns are separated, and the beam energy is low, $\sim 1/40$th of the energy at extraction. At this radius correlations between RF phase and radius can exist due to differences in centering errors, and/or a phase dependent difference in energy, which to first order is $\Delta E(\phi) = -\Delta\phi \int \sin(\phi) dE$.[3]

2.1. Mechanical Design

The slits are a modified version of those used by B. Milton in the K500 cyclotron.[3,4] They are tungsten pins with a diameter of 0.094 in. Since $\nu_r \simeq 1$, the particles rotate in (r, p_r) phase space approximately once per

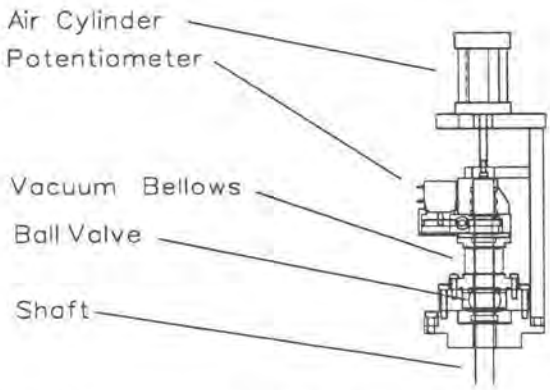


Figure 3. Part of the Phase Slit Drive. Shown are the shaft, potentiometer, air cylinder and vacuum bellows for insertion, and ball valve used to maintain vacuum when changing tips.

complete revolution in the machine. Thus a pin placed between turns will make radial cuts similar to those of radial slits about the second turn being cut. Slits separated by 120°, make cuts in (r, p_r) phase space that are rotated by $\sim 120°$ (see Fig. 4.), if, between the slits, there are zero or two orbit crossovers, of the central phase being transmitted and the phase being cut. Each orbit crossover inverts the $r-\phi$ correlation, switching the side of the pin that makes the cut. Thus the cut makes an additional 180° rotation in (r, p_r) phase space per orbit crossover. We are currently using two slits 120° apart.

Other features include remotely controlled insertion, retraction, and rotation (see Fig. 3.) The pin is mounted slightly off-center, so rotating it adjusts its radius. Electric motors mounted 8 ft. above the cap, protected with 1/2 in. cold-rolled steel shielding, drive the rotation with a stainless steel drive shaft and turn a potentiometer used for position readout. Compressed air is used for insertion and retraction. The slits are water cooled, and have interchangeable tips. Closing a ball valve after partially removing the phase slit shaft, protects the vacuum while removing the shaft to change pin sizes.

2.2. Phase Selection Calculations

Central ray orbits for 40 Mev/A $^4He^{1+}$ were obtained with the program CYCLONE[5] for RF starting times of $\tau_0 = 210° - 236°$ every 2°, where $\tau_0 = 270°$ is the peak voltage on the dee. The magnetic field and central region electric field were obtained with MONSTER[6] and RELAX3D[7] respectively. A first harmonic magnetic bump was used in CYCLONE to center $\tau_0 = 220°$ at 80 turns. SOMA[3,8] was then run to accelerate uniformly populated eigen-ellipses in (r, p_r) phase space of area 100π mm-mrad about each central ray. The slit's diameter and radius were selected to pass $\tau_0 = 220°$, cutting all other times that make it through the central region. All rays that intercepted the slits were removed. The resulting transmission for two slits is a nearly triangular shape with a FWHM of 7° in τ_0 (see Fig. 5.) Three slits gave a FWHM of 5°.

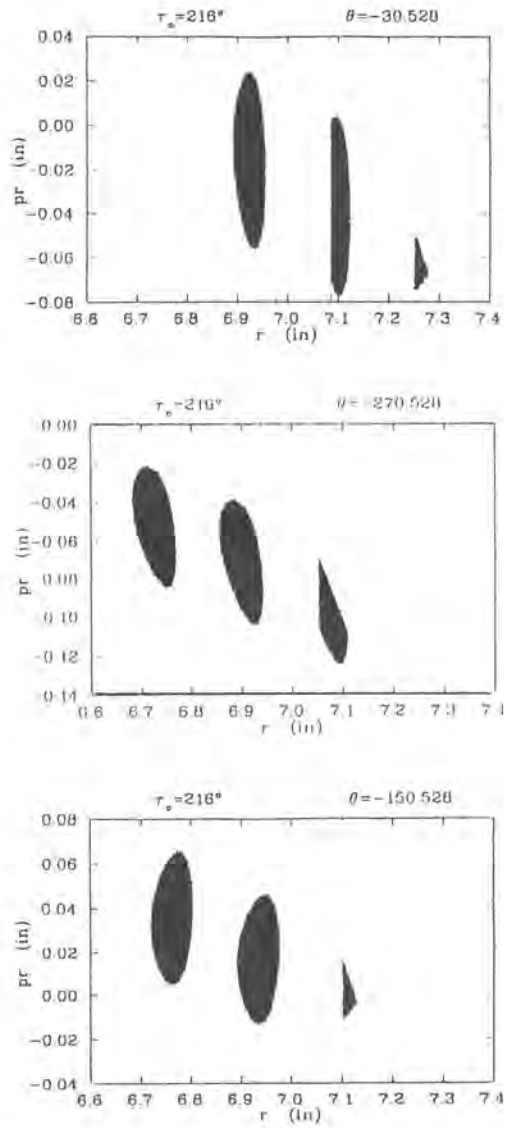


Figure 4. Snap shots, calculated with SOMA, of the (r, p_r) phase space, showing the cuts made by the pins on turns 17 and 18, for $\tau_0 = 216°$. The pins transmit all of $\tau_0 = 220°$. Note the $\sim 120°$ rotation in the (r, p_r) plane as the beam traverses 120° in the machine. At this radius $\tau_0 = 216°$ trails $\tau_0 = 220°$ in energy gain, so the innermost edge is cut by the pin. Starting times that lead $\tau_0 = 220°$ in energy gain have the outermost edge cut. Here, differences in centering errors are small enough to be a perturbation in the $r-\phi$ correlation of the phases of interest.

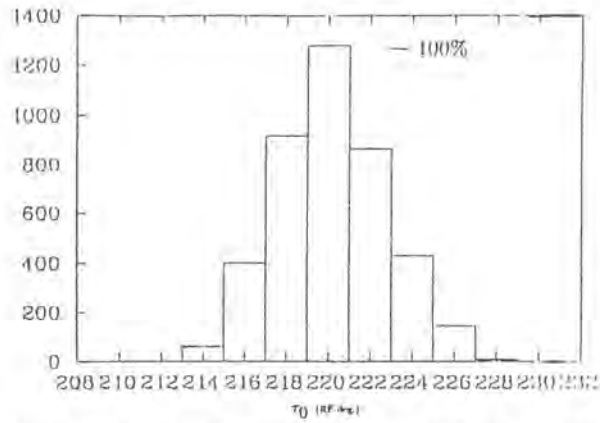


Figure 5. Calculated transmission through the phase slits, for two slits spaced 120° apart. The scale in x is starting time in RF degrees of each eigen-ellipse. Up to this point, there has been RF phase focussing, reducing the RF phase spread by 25%.

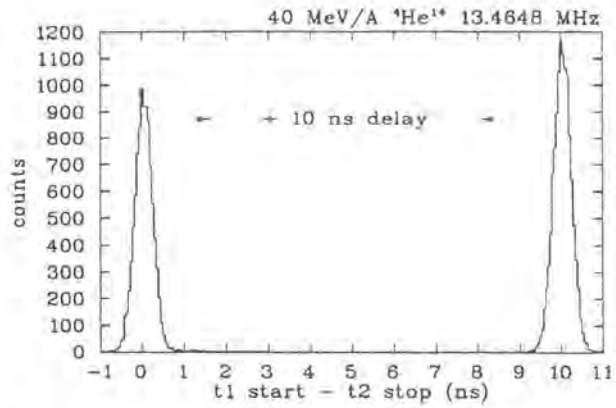


Figure 6. Time resolution of two Si PIN diodes. The second peak was obtained with an extra 10 ns delay to calibrate the TDC. FWHM is .48 ns, giving a resolution of .34 ns in each detector.

3. EXTERNAL PHASE MEASUREMENTS

Attenuators in use in the injection line of the K1200[9] can reduce the beam down to a factor of 3×10^{-7}. This reduction is such that a Si detector, placed to intercept the entire beam, can be used to measure the time of incidence of each beam particle relative to a stop signal generated by the RF. These signals are digitized, then stored in our VAX system, where they can be displayed and saved, via a CAMAC interface. Thus a short integration of counts can give a rapid measurement of the beam's relative distribution in time.

3.1. Measuring Apparatus

The detectors are two 300μ thick 18 x 18mm^2 Si PIN diodes mounted back to back in a beam diagnostic chamber 10 ft. from the cyclotron. They are mounted on a two position drive, with the first position scintillating plate mounted 45° to the vertical. A CCD camera focused on the scintillator gives the feedback necessary to tune the beam envelope onto the detector, using the first three beamline quadrupoles.

An LBL Time Pickoff obtains a fast time signal by inductively coupling a pre-amp to the transmission line between an over depleted diode and its charge sensitive pre-amp. Fast signals from each diode are amplified then input into a constant fraction discriminator. The forward diode's CFD output is used to start the time to digital converter. The TDC stops are from a zero crossing discriminator reading an inductive loop in one of the dee stems, and from the TDC of the second detector.

The detector to detector time resolution measured with a 40 MeV/A ^{4}He incident beam is shown in Fig. 6. The wide range of beam energies and atomic charges that the K1200 is capable of providing[10] result in a wide variation in signal strength (< 1 MeV to several GeV.) The above beam deposits $\simeq$ 1 MeV in each detector. This close to the cyclotron, the RF noise is a significant problem, and ions with greater signal strength are easier to detect. In the stability measurements, one narrow peak was measured at .34 ns FWHM.

3.2. Phase Selection Measurements

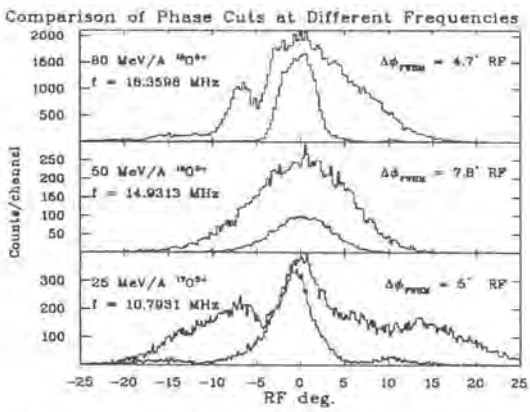


Figure 7. A comparison of extracted beam time structure at different frequencies. Each graph has been scaled so that the ratio of areas under the curves corresponds to the ratio of the measured intensities. The cuts made by the phase slits appear to be independent of frequency.

The phase slits have been fully operational since Jan. '92. In tuning the slits, it is easiest to individually scan each slit through the beam, noting the minima and maxima in transmitted intensity associated with turn structure. Then starting with the slits in convenient minima, adjust them to select some favorable portion of the uncut distribution. This procedure helps in maximizing transmission through the slits.

Table 1. shows that cuts from 4° to 8° FWHM have been consistently achieved, with transmission of $\sim$ 25 – 30% of the uncut beam. Figure 7. shows that the cuts seem to be independent of operating frequency. This is possible, because the operating parameters for

Table 1. Phase cuts and transmission.

Ion	Energy (MeV/A)	ϕ_{FWHM} uncut	ϕ_{FWHM} cut	I_{cut}/I_0
$^{17}O^{3+}$	25	15.°RF	5.7°RF	.33
$^{16}O^{5+}$	50	12.7°RF	7.8°RF	.24
			6.6°RF	—
$^{24}Mg^{7+10)}$	60	11.°RF	2.6°RF	.25
$^{18}O^{6+}$	80	14.5°RF	4.7°RF	.30
$^{28}Si^{9+}$	80	12.°RF	4.6°RF	.23
			3.6°RF	—

each beam are set to give the same path through the fixed central region.

3.3. Phase Stability Measurement

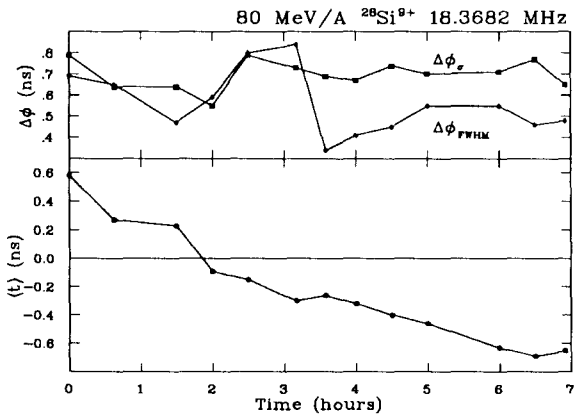


Figure 8. Tracking, over time, of the extracted beam time structure transmitted through the phase slits. Presented are the first and second moments, and the FWHM of the main peak. The cyclotron was not retuned during this time. The centroid drifted, and the structure fluctuated.

The stability of the phase reductions in the extracted beam was monitored over a seven hour period. During this time, the operators did not readjust the cyclotron settings. Figure 8. shows the time centroid of the beam drifting with respect to the RF stop signal at an almost constant rate. It was found that the uncut beam had shifted the same amount during this measurement. The source of this shift is not known, but it is a change of 2 parts in 10^5 of the $\sim$ 800 turns inside the machine. The need to periodically retune the cyclotron, and the variation in time structure shown in Fig. 8., together with this drift show a need for continual monitoring of this time structure.

4. INTERNAL PHASE PROBE

An internal timing probe for the K1200 is being made. It will be interchangeable with the radial current and scintillator probes now in use.[11] A significant problem is the tight turn spacing in the outer radius of the machine. To extend the active area of the detector to it's edge, detectors have been developed that are cut along the inner guard ring.[12]

This probe will enable us to separate the effects of extraction from those of the probe. It will be used to study beam dynamics during extraction, and measure the outer part of the phase curve inside the machine. There are also plans to use it in tuning the cyclotron at extreme lows in intensity.

5. REFERENCES

1) Nolen, J., et al., "Commissioning Experience with the NSCL K1200 Superconducting Cyclotron," in **Proc. of the 12th Int. Conf. on Cyclotrons and Their Applications** (World Scientific, Singapore, 1991) p.6.
2) Marti, F., and Gavalya, A., "Axial Injection in the K500 Superconducting Cyclotron," in **Proc. of the 11th Int. Conf. on Cyclotrons and Their Applications** (Ionics, Tokyo, 1987) pp.484–487.
3) Milton, B., "Phase Selection in the K500 Cyclotron and the Development of a Non-Linear Transfer Matrix Program," Ph. D. Thesis, Michigan State University, 1986.
4) Milton, B., et al., "Design of a Beam Phase Measurement and Selection System for the M.S.U. K500 Cyclotron," in **Proc. of the 10th Int. Conf. on Cyclotrons and Their Applications** (IEEE, New York, 1984) pp.55–58.
5) Marti, F., et al., "Design Calculation for the Central Region of the NSCL 500 MeV Superconducting Cyclotron," in **Proc. of the 9th Int. Conf. on Cyclotrons and Their Applications** (les Éditions de Physique, Caen, 1981) pp.465–468.
6) Harwood, L., "Status of Integrated Software Project for Cyclotron Design," MSU National Superconducting Cyclotron Laboratory Annual Report (1986) pp.147–148.
7) Houtman, H., and Kost, C., "Design Calculation for the Central Region of the NSCL 500 MeV Superconducting Cyclotron," in **Proc. of the Europhysics Conference on Computing in Accelerator Design and Operation** (Springer-Verlag, Berlin, 1983) pp.98–103.
8) Milton, B., "A Cyclotron Orbit Code Using Second Order Transfer Matrices," in **Proc. of the 11th Int. Conf. on Cyclotrons and Their Applications** (Ionics, Tokyo, 1987) pp.240–243.
9) Cole, D., et al., "ECR Operation Summary," MSU National Superconducting Cyclotron Laboratory Annual Report (1990) pp.147–148.
10) Miller, P., et al., "Performance of the K1200 Cyclotron at MSU," these Proceedings.
11) Marti, F., "Internal Beam Dynamics with a TV Probe," these Proceedings.
12) Evensen, L., Private communication, Senter for Industriforskning, Norway, 1992.

INTERNAL BEAM DYNAMICS STUDIES WITH A TV PROBE

F. Marti and S. Snyder*
NSCL, MSU, East Lansing, MI, 48824, USA

ABSTRACT

We have developed an internal probe for the K1200 Superconducting Cyclotron based on a TV camera and scintillator. This probe provides a detailed picture of the internal beam with a resolution of 0.05 mm. The low intensity sensitivity of this probe (1 epA) has helped in the tuning of low intensity beams. The processing of the TV signal with a digital frame grabber allows a real time pseudocolor display and a fast quantitative analysis. We have studied several beam dynamics problems (resonance traversal, radial and vertical beam centering, etc.) and simulated them with particle orbit integration codes and transfer matrix codes. Comparisons with tape recorded pictures that show extremely intricate behavior are presented.

1. INTRODUCTION

Our laboratory has successfully used scintillators and a frame grabber to tune and study external beams.[1] This experience convinced us to look into the possibility of building a beam probe physically compatible with the present current probe (utilizing the same drive) that could include a TV camera to look at a phosphor covered plate. This new kind of internal beam probe was then developed for the K1200 cyclotron.[2] It consists of a small TV camera that looks at the image produced by the beam hitting a phosphor covered plate. The small size of the camera allows it to be placed close to the screen. The image gives a detailed view of the current density in r and z, with position resolution of about 0.05 mm. Total beam currents below one electrical pA are easily analyzed. This new probe has been in use for more than a year, giving a very satisfactory performance, and allowing us to measure beam parameters that were unavailable before its commissioning. After the publication of the report previously mentioned[2] we learned of the previous use of a TV camera in a separated sector cyclotron.[3]

*Work supported by the U.S. National Science Foundation under Grant No. PHY89-13815.

2. PROBE DESIGN

One of the major difficulties in designing a median plane probe for a superconducting cyclotron like ours is the small space available in the penetrations through the coil cryostat. This space is limited to a tube of 1.25 inches diameter that is inserted in the median plane between the two sections of the superconducting coil. Figure 1 shows a sketch of the probe head showing the scintillating plate, viewing window and TV camera. The scintillating surface is obtained by spraying ZnS on an aluminum plate. This plate slides between two clips that allow for its fast replacement. Figure 2 shows a close up of the probe head before assembly.

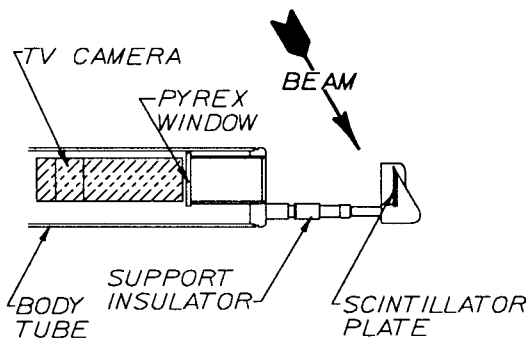


Figure 1. Sketch showing the head of the TV probe. The angle the beam makes with the scintillating plate changes between 35 and 65 degrees.

Two major concerns were the possibility of radiation damage to the camera and the high magnetic field (6 T) in which the camera must work. The simplification offered by inserting the camera close to the scintillating plate, compared to using an optical system with its associated loses, induced us to design the TV probe in its present configuration. We chose an ELMO 102BW camera, after testing it in a magnetic field, because of its small size and excellent image quality.

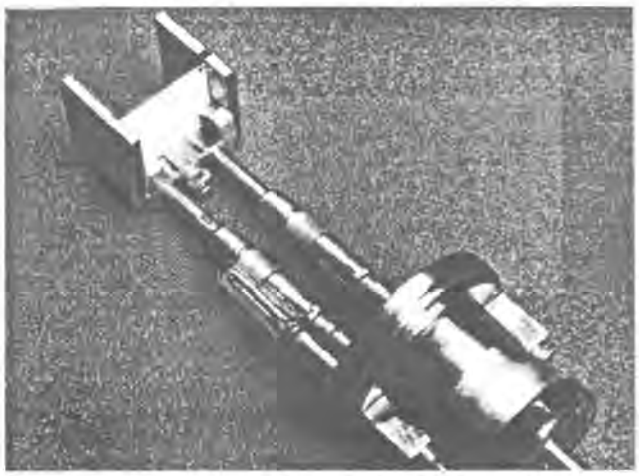


Figure 2. Close up view of the probe head before welding to the vacuum tube. The support for the scintillating plate is seen on the upper left. The plate is held in a groove by springs. The two supports are the electrical connection to the beam current monitors.

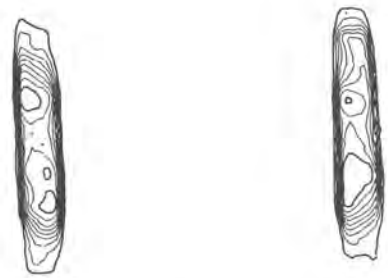


Figure 3. These two beam snapshots were taken at a radius of 0.51 m (left) and 0.52 m. The total vertical height as determined by the lowest contour line is 8.5 mm. It clearly shows the vertical oscillation of the beam and the radius gain of the beam between turns, for example on the left contour plot. The left edge of each contour plot corresponds to the edge of the scintillating plate, while the right edge is determined by the radius gain per turn and centering error.

3. MAIN APPLICATIONS

3.1. Correction of Vertical Oscillations

The first observation made with the probe showed us that the beam was not on the median plane but oscillating around it by as much as 2 mm. Considering that the beam size was close to 1 mm the oscillation was an important part of the effective beam size. Since then we have introduced an asymmetric current supply to the top and bottom trim coil 0, that together with a variable vertical positioning of the inflector allows us to correct this vertical oscillation. The original current probe did not have enough resolution to detect this error. Figure 3 shows an example of a beam off the median plane.

3.2. Radial Centering

If the beam is centered, the width of the beam trace seen on the probe should be equal to the radius gain per turn and approximately constant in a small region of radii. If instead the beam is off-centered, the beam width will appear to fluctuate when moving the probe radially. We have written a program to use the TV probe to center the beam automatically. The program searches in the phase and amplitude of the first harmonic bump used to center the beam until the beam width observed in a radius range is constant. The program has control of the probe and the harmonic coils. The process takes approximately 12 minutes and converges in most cases. It must check that the beam does not disappear because of RF sparks or similar problems.

3.3. Detailed Beam Dynamics

For the first time we could obtain really detailed information on current density as a function of r and z, much more than any differential probe could give us before. The quality of the beam and halo formation can be studied during the acceleration process. We found that one of the most interesting phenomena was the crossing of the $\nu_r = 2\nu_z$ resonance. This study will be the topic of the next section.

4. OBSERVATIONS OF THE RESONANCE CROSSING

The K1200 cyclotron beams cross the $\nu_r = 2\nu_z$ resonance between 0.65 cm and the extraction radius of 1.00 m, depending on the ion energy and Q/u. The losses are minimized by crossing the resonance with the beam centered. This is normally possible unless the resonance crossing occurs after the $\nu_r = 1$ resonance, just before extraction.

The photographs of the TV probe scintillator shown here were obtained during a run of $^4He^{1+}$ 40 MeV/u. The calculations described later were performed for the same ion and energy conditions.

Figure 4 shows two snapshots of the TV screen that displays the TV probe signal. We combine the video signal from the probe with computer generated text. The computer displays the radius that the probe is at on the lower left (in inches) and up to three parameters and their names on the upper left. These parameters can be selected from the whole data base available to the control system. In the pictures displayed we are showing the magnitude and phase of the centering bump provided by trim coil 1. The normal beam size is smaller than what is displayed on the left portion of the figure. The beam has been off-centered on purpose to show the effect of



Figure 4. Two snapshots of the TV screen showing the beam spot during the crossing of the $\nu_r = 2\nu_z$ resonance. The height of the beam spot on the left is approximately 13 mm. See text for more explanations.

the resonance. The beam height of the left picture is 13 mm.

The most surprising observation, when looking at the probe move out in radius, is the formation of arcs like the one observed on the picture on the left, and the jets observed on the picture on the right in Fig. 4. We decided to simulate the orbit dynamics and probe interception of the beam to verify that those structures could be predicted by our orbit codes.

5. SIMULATIONS OF THE RESONANCE CROSSING

The simulation of the TV probe observations involved several steps. First we used our code Z3CYCLONE[4] to track five different central rays from the inflector to a radius of about 10 cm. In this code the electric field is calculated in a 3D grid from potential data calculated with the relaxation code RELAX3D.[5] The five different rays were spaced 8 degrees in RF time between them to simulate the phase acceptance of the central region. A first harmonic imperfection was introduced as generated by trim coil 1. From a radius of 10 cm to approximately 70 cm the central rays were tracked with the code SPIRAL GAP that uses a delta function approximation for the energy gain at each gap on the six spirals.

At a radius of 70 cm (just before the resonance) we started the tracking with SOMA,[6] a second order matrix code, populating with 2000 particles an elliptical (eigenellipse) phase space around each central ray in (r, p_r) and in (z, p_z) for a total of 10000 particles. We selected a gaussian distribution, relatively flat, where the edge density was 70% of the central density. The central rays have centering errors from 2 to 7 mm.

We modified SOMA to give us the (r, z) intersection with the path of the TV probe. This data file giving the intersection of each particle in each turn with the probe path is analyzed later with another program that keeps track of the intersections with the probe to check that a hit is the first one or if a previous turn already was intercepted (and consequently lost).

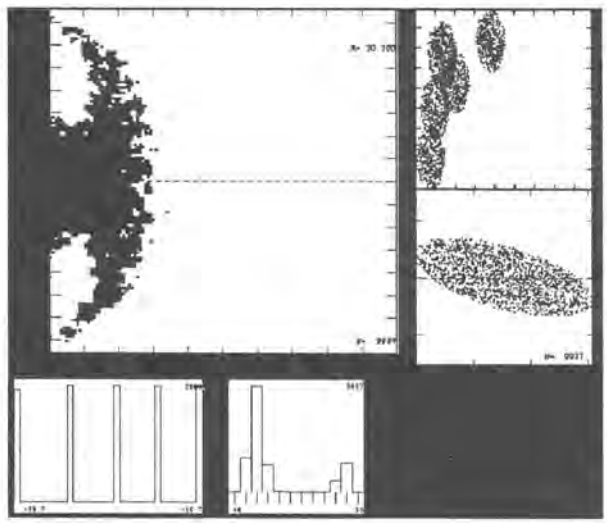


Figure 5. Snapshots of the computer screen showing the display of the probe simulation with characteristics similar to the picture observed on the left of Fig. 4. See text.

Figure 5 shows a black and white snapshot of the computer screen where the large graph on the upper left represents the (r, z) diagram of where the beam hits the scintillator at a given radius. The sharp edge on the left represents the edge of the scintillator. We can see the similarity between this simulation and the observation on the left section of Fig. 4. The graph on the upper right shows the population at the start of the SOMA calculation in (r, p_r) and in (z, p_z) under it. The two graphs at the bottom show the phase distribution (five equal bars in the histogram) and a histogram with the turn number (from the beginning of the SOMA calculation) when the particle strikes the phosphor screen. The two groups of turns agree with a ν_r value close to 1.10.

The program allows us to select an area on the screen, see Fig. 6 (area fenced in by the dashed polygon), and then gives us the initial conditions, phase and turn distribution of that group of particles. As we can see the bulk of the particles in the fenced area forming the large circular arc away from the median plane come from the ellipses with larger centering error.

Figure 7 show a different radius plot where we have selected to show only the particles that populated the ellipse around the central ray with larger centering error (compare with the initial (r, p_r) distribution of Fig. 5). The (r, z) plot shows the jet structure observed on the right hand side picture of Fig. 4.

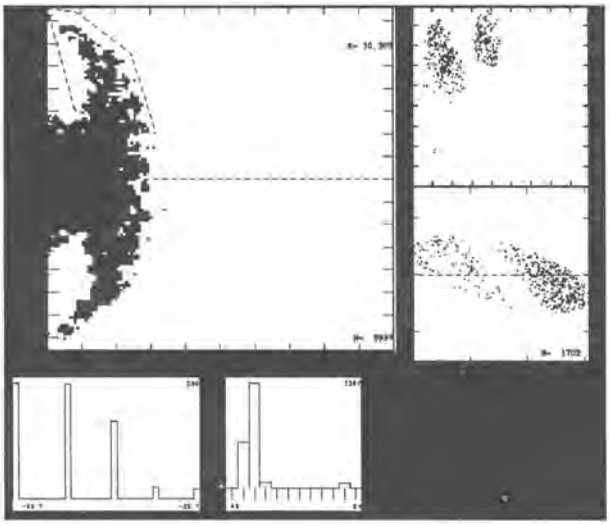


Figure 6. Snapshots of the computer screen showing a fenced area (dashed polygon) and the initial conditions and turn distribution of the selected particles.

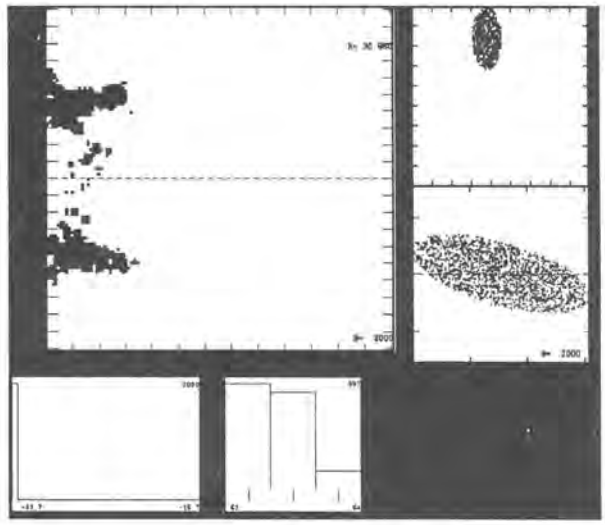


Figure 7. Snapshots of the computer screen showing the jet structure similar to the observed on the right picture of Fig. 4.

6. CONCLUSIONS

We have shown some of the applications we have found for a TV based internal beam probe in our K1200 superconducting cyclotron. Centering of the beam in both vertical and radial direction is now possible with great accuracy. The study of resonance crossing and comparison with simulated probe traces shows very good agreement on the structures observed.

7. REFERENCES

1) Marti, F., Blue, R.A., Johnson, J., Kuchar,J., Nolen, J.A., Rutt,P., Sherrill, B. and Yurkon, J., in **Proc. 12th Int. Conf. on Cyclotrons and their Applications** (World Scientific, Sin 1989) p. 268.
2) Marti, F., Blue, R.A., Kuchar,J., Nolen, J.A., Sherrill, B. and Yurkon, J., in **Conference record of the 1991 Particle Accelerator Conference**,(IEEE, New York, 1991) p. 1163.
3) Friesel, D. L., I.U.C.F., personal communication, 1991.
4) "Z3CYCLONE, Instruction Manual," MSU NSCL Accelerator Group, 1992.
5) Houtman, H. and Kost, C.J., "A Fortran Program (RELAX3D) to solve the 3-D Poisson (Laplace) Equation," in **Proc. of the Europhysics Conference, Computing in Accelerator Design and Operation** (Springer Verlag, Lect. Notes in Physics 215, Berlin, 1983) pp. 98-103.
6) Milton,B. F. **Phase Selection in the K500 Cyclotron and the Development of a Non-linear Transfer Matrix Program**, (Ph.D Thesis, MSU, 1986).

EFFECT OF THE MAIN-COIL POSITION ON THE ACCELERATED BEAM OF THE K500 CYCLOTRON

D. P. May and G. Mouchaty
Cyclotron Institute, Texas A&M University, College Station
Texas, 77843-3366, U. S. A.

ABSTRACT

As a consequence of the failure of the development of several beams by the Texas A&M superconducting cyclotron, a program was initiated to find the cause. It was found that the vertical position of the main superconducting coil was the culprit. The vertical position has been substantially changed, and the operation of the cyclotron has improved dramatically.

1. INTRODUCTION

Soon after the first beams were accelerated by the Texas A&M K500 superconducting cyclotron in 1988, it was noticed that several of the beams had problems as they approached extraction. For example, when a reasonable phase function was used to calculate the trim-coil settings for 35 MeV/amu $^{14}N^{5+}$, the beam would fail to accelerate past a radius of 24.5 in., extraction radius being 26.5 in. The attenuation of the beam was fairly sharp, with a majority of the beam disappearing within 0.25 cm. Other beams, for example 30 MeV/amu $^{14}N^{5+}$, exhibited a sharp drop at the same radius, but with some of the beam surviving to extraction. In both cases, most of the beam could be brought to extraction radius by changing the outermost trim-coil, trim-coil 13. The current in this coil was changed in such a manner that it produced a large negative magnetic field gradient around R=24.5 in. Maximum extracted beam occurred for an intermediate value of trim-coil 13 with some of the beam still being lost at R=24.5 in.

With the installation of the ECR ion source in November of 1989, beam diagnostics became considerably easier, and a quick survey of beams became possible. Beams of 30 MeV/amu $^{16}O^{6+}$, $^{14}N^{5+}$, and $^{12}C^{4+}$ (Q/A = .375, .357, and .333, respectively) were developed, but a beam of 30 MeV/amu $^{16}O^{5+}$ (Q/A = .312) would not accelerate past R=24.5 in. even by changing the current in trim coil 13. A development attempt with 35 MeV/amu $^{40}Ar^{13+}$ (Q/A=.325) failed with the beam not accelerating past R=20 in. although 35 MeV/amu $^{14}N^{5+}$ (Q/A = .357) had been developed earlier. A beam of 53 MeV/amu alphas could be accelerated to extraction radius by changing trim coil 13, but with a large intensity drop at the outer radii, and the beam could not be extracted.

In general, the beams that could be extracted were confined to the lower left-hand side of the operating diagram shown in Fig. 1. The higher field, higher frequency (high γ) beams were inaccessible. To attack this problem, the field maps were re-examined and refined, the phase of the internal beam with respect to the rf voltage was measured for several beams, all the trim-coil connections were checked (each of the 13 coils has 12 separate leads external to the cyclotron) and even the elevations of the outer-radius steel were re-measured. Nothing of significance was found.

The first hint of what the problem might be came from examining plots of the intensity of the beam hitting

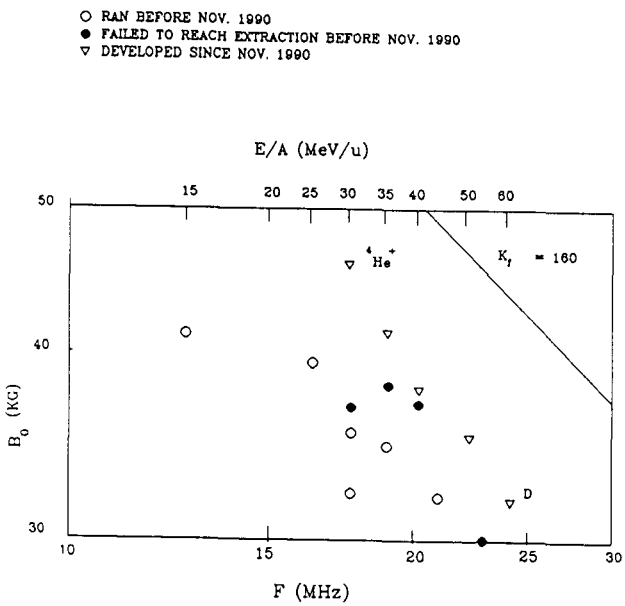


Fig. 1. Operating region for the K500. The positions of the higher-frequency, higher field beams are indicated. The line labeled Kf=160 represents the focusing limit (80 MeV/amu for Q/A=0.5).

the three-finger probe versus radius (I vs R). The three fingers of the beam probe are arrayed vertically, with each finger 5.7 mm high, separated by two 0.76 mm gaps. The data showed that for 30 MeV/amu $^{14}N^{5+}$, for example, all of the beam was intercepted either by the middle or by the bottom probe finger (Fig. 2). No beam was hitting the top finger of the probe from R=13 cm to R=67 cm except in the last 3 mm of the probe travel before the beam encounters the extraction system. This could be explained by an offset in the positioning of the probe tip which is not visible when the K500 is closed for operation. The probe is centered by the trim-coil covers, and such a light-weight device could easily be moved in the act of lowering the upper pole cap. In fact, the probe tip position is different depending upon whether the probe is moving towards or away from the center as shown by the difference between the I vs. R plots.

A difference in I vs. R plots was also noticed when examining a plot made for a 30 MeV/amu $^{14}N^{5+}$ beam after raising the superconducting main coil approximately 0.75 mm above the median plane nominal position. The coil can be raised and lowered by means of tightening and loosening nuts on the six vertical links, and this had been done to examine the effect on the vertical behavior of the extracted beam. The ratio of beam intercepted by the bottom probe finger to beam intercepted by the middle finger increased slightly by elevating the coil, so it was decided to lower the coil and examine the plots. The coil was first lowered by approximately 0.75 mm, and it was directly confirmed by plots taken under the same

conditions of beam tuning that a slightly greater percentage of the beam was intercepting the middle finger. More dramatically a beam with a trim-coil solution calculated with a standard phase history was able to bring more of the internal beam to extraction radius, and as the coil was lowered further, even more beam came to extraction radius.

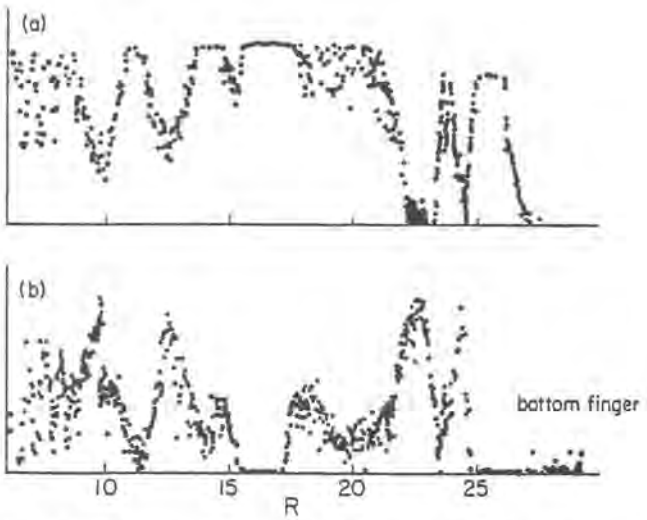


Fig. 2. Intensity versus radius for the top (a) and bottom (b) fingers of the beam probe. The main coil position was 0.8 mm below the position for which the magnetic fields were mapped.

To date, the main coil has been lowered by approximately 3.4 mm (0.135 in.) in 0.2 mm increments. After lowering the coil by 1.6 mm, a 30 MeV/amu $^{16}O^{5+}$ beam came to extraction with a standard phase solution. After lowering the coil another 0.4 mm, a 53 MeV/amu alpha beam could be extracted. With the coil lowered by 2.7 mm a 60 MeV/amu alpha beam could not be extracted. After lowering the coil by another 0.4 mm the beam was extracted. After the last lowering, a 65 MeV/amu alpha beam was extracted. Figure 1 indicates the beams developed after the lowering process began.

2. MECHANICS OF COIL LOWERING

The coil was lowered to its present position over a nine month period. Changing the coil position is fairly simple to accomplish, but it must be done with caution. The horizontal centering of the coil can give rise to large unstable horizontal forces when the field is high.[1] As described in Ref. [2], the K500 coil is an array of four coils wound on a single stainless steel bobbin. An outer stainless steel jacket is welded to the bobbin to form the liquid helium vessel. This vessel is suspended in a vacuum vessel by means of links which include low heat conductance fiberglass straps. There are no coil windings at the median-plane level, and the whole coil-cryostat assembly is penetrated at this level by a number of channels for the insertion of the extraction system devices and beam probes. If the coil is centered about these channels, there is at most 6.3 mm of vertical space above and below the channels into which the coil can be either lowered or raised. It is imperative that these channels, which are formed by tubes welded to the vacuum vessel walls, not support any of the weight of the coil. After lowering the coil by each 0.2 mm increment, the link strains were checked to make sure the links were still supporting the entire weight. The first indication of the coil approaching the channels might be excessive LHe consumption by the cryostat as the super-insulation between the coil and the channels is crushed, causing a heat leak. After each 0.8 mm increment, the coil was run at full field and the horizontal links were adjusted to balance their strains. No cold spots have been observed on the outer cryostat wall, and the LHe consumption has remained low.

3. RESULTS AND ANALYSIS

Since the performance of the cyclotron has improved with each incremental lowering of the main coil, the observation is that the magnetic mid-plane of the coil must have been at least 3.4 mm above the magnetic mid-plane of the steel poles. In this case there is a sufficient downward force on the beam at many radii to move it to the level of the lower probe finger. This force is due to the off-mid-plane, radial component of the coil magnetic field. The radial component of the coil field and the radial field components of the pole fields tend to cancel one another at a vertical displacement from the pole mid-plane of

$$Z = -\frac{R}{B_T}\frac{\partial B_c/\partial r}{\nu_z^2}\delta \qquad (1)$$

Here R is the radius, B_T is the total field strength at R, $\partial Be/\partial r$ is the radial gradient of the mid-plane magnetic field of the coil, ν_z is the vertical betatron frequency, and δ is the vertical distance the coil is offset from the steel. The quantity Z/δ is plotted vs. R in Fig. 3, along with ν_z and the phase of the beam for the 30 MeV/amu $^{14}N^{5+}$ beam.

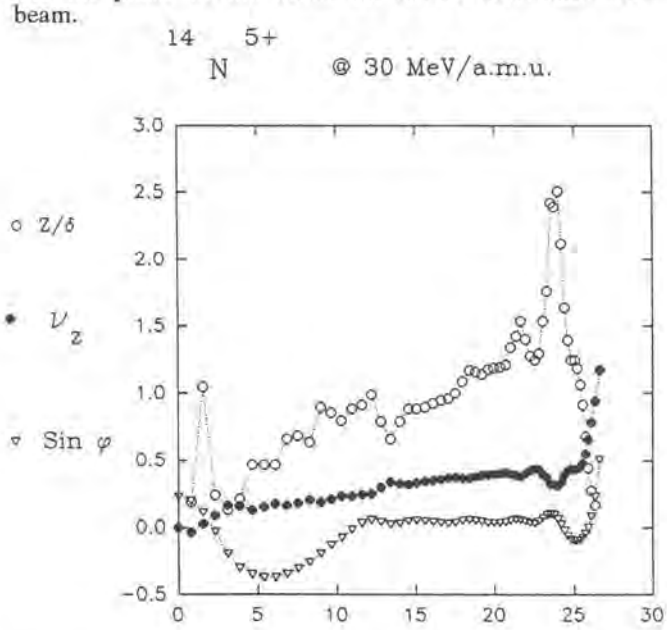


Fig. 3. Beam properties for a 30 MeV/amu $^{14}N^{5+}$ beam. Using field maps the vertical betatron frequency (ν_z) and the vertical median plane offset (Z/δ) are calculated using the sine of the beam phase ($\sin\phi$) as input.

The sudden increase in Z/δ near R=24 in. matches well with the abrupt disappearance of the beam near the same radius. For beams with higher fields ν_z decreases as the hill-to-valley field difference decreases. Thus Z/δ increases for both higher γ and for higher B_T. Near R=24.5 cm, ν_z experiences a decrease for all beams since at this radius a gap occurs between the hill steel and its continuation in the inner cryostat wall.

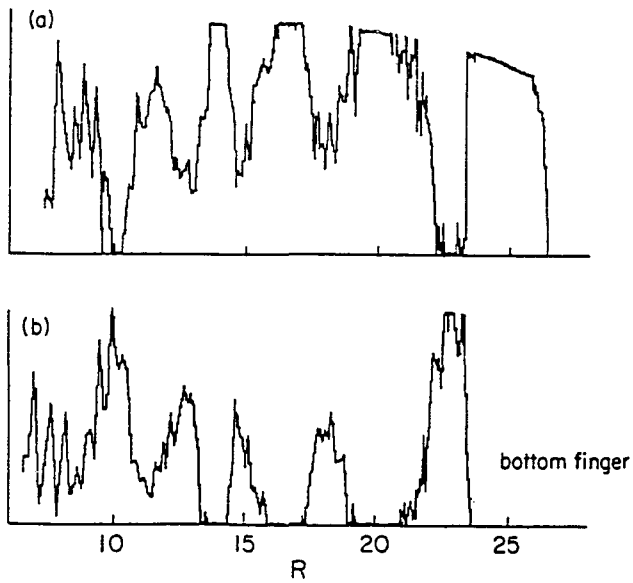


Fig. 4. Intensity versus radius for the top (a) and bottom (b) fingers of the beam probe. The main coil position was 2.7 mm below the position for which the magnetic fields were mapped.

Figure 4 shows plots of I vs. R taken with the three-finger probe for the preceding beam after the coil had been lowered by approximately 2.7 mm. The appearance of the beam on the bottom finger can be roughly, but not entirely, correlated with Z/δ. The large amount of beam hitting the bottom probe finger at R=23 in. corresponds to a local increase in Z/δ, but the beam is seen to hit the bottom finger at R=24.5 in. only for a much higher coil position.

Another effect observed with the coil lowering is the lowering of the deflector voltage required to extract such beams as 35 MeV/amu $^{14}N^{5+}$. Originally, a first deflector voltage of 65-67 kV was necessary. At present, the voltage is approximately 10% lower since the deflector is able to be positioned at a larger radius and at a less steep angle. The field maps have been largely unaffected, and indeed are more predictive now that the beam is closer to the median plane. Overall, the coil lowering has been a major success with the subsequent development of beams such as 65 MeV/amu deuterons, 50 MeV/amu $^{12}C^{5+}$ and 40 MeV/amu $^{63}Cu^{21+}$, and it has represented a major step in approaching the 80 MeV/amu focusing limit of the Texas A&M K500.

4. REFERENCES

1) Blosser, H. G., **Proceedings of the Eight International Conference on Cyclotrons and Their Applications** (IEEE, Bloomington, 1978), p. 2040.
2) Miller, P., **Proceedings of the Tenth International Conference on Cyclotrons and Their Applications** (IEEE, East Lansing, 1984), p. 11.

BEAM TEST RESULTS USING THE AUXILIARY ACCELERATING CAVITY

R.E. Laxdal, G.H. Mackenzie, L. Root
TRIUMF, 4004 Wesbrook Mall, Vancouver, B.C., Canada V6T 2A3

Abstract

A $\lambda/4$, 92 MHz cavity is now operating in the TRIUMF cyclotron. The device, when operating at 50 kW and at a peak voltage of 140 kV, increases the energy gain per turn from 0.32 MeV to a maximum of 0.60 MeV in the 370-520 MeV range. This reduces electro-magnetic stripping losses from 8% to 5% and lowers the beam induced tank activation by ~1/3. The cavity allows other modes of operation. In particular the cavity has been phased to oppose the fundamental rf to produce a localized flattop in the energy gain, stabilizing the precession pattern during resonant extraction. When the power is increased in flattop mode the corresponding strong phase expansion has been observed to split the longitudinal phase band into two bunches. In principle, additional cavities could further sub-divide the extracted beam time structures.

I. Introduction

The auxiliary accelerating cavity (AAC) has been described elsewhere [1] [2]. The cavity operates at the fourth harmonic (92.24 MHz) of the main rf frequency and consists of a trapezoid of dimension $\lambda/4$ radially and $\beta\lambda/2$ azimuthally, so that the orbiting ion receives two acceleration impulses on each passage (Fig. 1). The peak accelerating voltage rises sinusoidally with radius, covering the energy range from 370-520 MeV. When operated at 140 kV the energy gain per turn increases from the present 320 keV to a maximum of 600 keV.

The 500 MeV TRIUMF cyclotron routinely accelerates 150 μA of H^- ions. Electro-magnetic (e-m) stripping losses rise rapidly from 0 to 8% in the region from 400-500 MeV. Gas-stripping losses total ~5% for a typical tank pressure of 5×10^{-8} torr and are spread roughly uniformly throughout the machine with stripping cross-sections scaling as $1/\beta^2$ and the orbit length per energy increment scaling as β. Scraping of vertical haloes on foils defining the vertical aperture occurs at various radii through the cyclotron and account for a further ~3% of the total circulating current. Since activation scales roughly with particle energy, the electro-magnetic losses account for ~2/3 of the total tank activation. The cavity was originally conceived [3] to improve extraction efficiency for H^- extraction. However the addition of an extra higher harmonic cavity in the outer radial region to reduce losses and/or modify beam behaviour was sufficient reason to proceed with manufacture and installation after it was decided to use precessional extraction to improve extraction efficiency. [4]

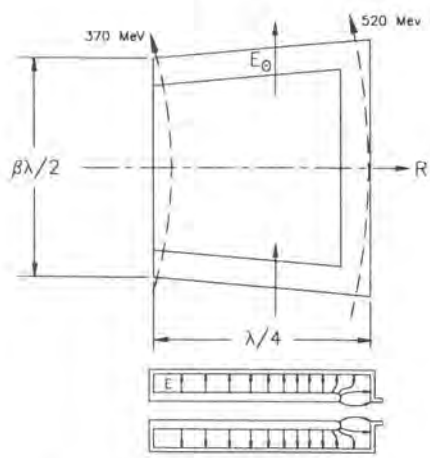


Figure 1: Schematic view of the cavity.

II. Acceleration Mode

The optimum phase of the cavity is set empirically using the time-of-flight (TOF) through the cyclotron as the main diagnostic. At the normal operating voltage, 140 kV, the TOF is reduced from 329 μsec to 303 μsec, corresponding to a reduction of 120 in the total number of turns. Even though the cavity operates at the 4th harmonic of the fundamental rf, phase stability is not a problem since phase compression tends to stabilize and damp phase wander. Computer simulations prior to cavity testing predicted the total losses from gas and e-m stripping as a function of particle phase in the region from 350-500 MeV for a tank pressure of 1×10^{-7} torr (Fig. 2). Results for cavity voltages of 0, 90 kV and 150 kV are plotted. When the cavity is powered a reduction in beam loss is predicted over a full 40° of phase.

Loss reduction measurements are shown in Fig. 3 for a standard high intensity beam (148 μA equivalent at a duty factor of 80% and 35° phase width). Plotted are the

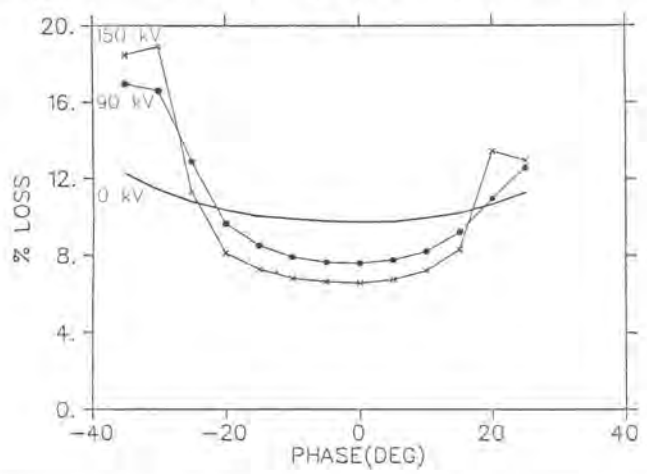


Figure 2: Results of computer simulations showing expected beam loss from gas and electro-magnetic stripping as a function of initial particle phase in the region from 350-500 MeV. Losses for cavity voltages of 0, 90 kV and 150 kV are plotted. The gas-pressure was 1×10^{-7} torr.

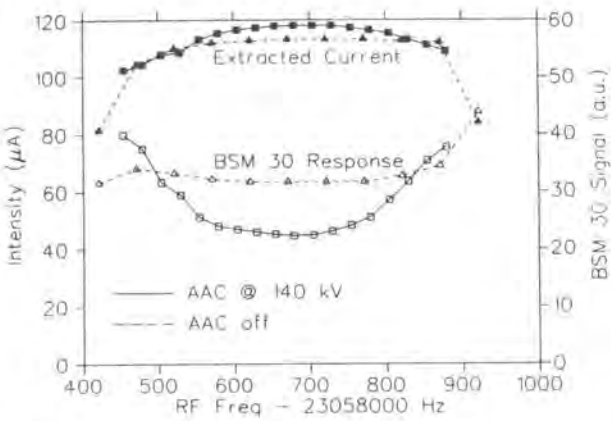


Figure 3: Experimental result showing extracted current and signal from a beam spill monitor external to the cyclotron for cavity off and for the cavity on at 140 kV. The longitudinal phase of the accelerated phase band was varied with respect to the cavity rf phase by altering the main frequency (100 Hz≃12°).

extracted current and the response from a beam spill monitor external to the cyclotron as a function of the rf frequency for the AAC off and powered (140 kV). The monitor is positioned to be selectively sensitive to e-m losses. The rf frequency is varied to scan the longitudinal phase band in the cavity region (100 Hz≃12°). As predicted the cavity reduces losses over a phase interval of ~40°. At the optimum phase the beam loss signal was reduced by 40% and the overall transmission was increased by 4%. This represents a decrease in total losses from 16% to 12% and losses weighted for energy from 12% to 8%. This reduction would allow a 33% reduction in tank activation for the same μA-hours or an equivalent increase in the μA-hours to maintain existing activation levels.

The time spectrum of the extracted beam is shown in Fig. 4. Phase compression forces from the cavity have reduced the total phase band of the extracted beam from 32° to 18° measured at 10% of the distribution maximum. This result compares well with the expected reduction given by [5]

$$E_{G1}(R_o)\sin\phi_o = E_{G1}(R_f)\sin\phi_f + \frac{E_{Gm}(R_f)}{m}\sin m(\phi_f - \phi_m) \quad (1)$$

where E_{G1} and E_{Gm} correspond to the peak energy gain per turn from the fundamental and the cavity ($m = 4$) respectively (0.32 MeV and 0.28 MeV in this case), ϕ_0 and ϕ_f correspond to the initial and final phases with respect to the fundamental and ϕ_m is the relative phase between the cavity and the fundamental (for acceleration $\phi_m = 0$).

III. Flattop Mode

In general all higher harmonic cavities can combine with the fundamental to flattop the energy gain, however as the harmonic increases the useful phase width of the flattop is reduced. The AAC can serve two functions as a flattopping cavity. Firstly the cavity can be run at relatively high voltages to flattop the number of turns (TOF) through the whole cyclotron to achieve more mono-energetic turns. The number of turns through the cavity determines the cavity voltage necessary to compensate the $\cos\phi$ dependence in the TOF. Secondly, at a somewhat lower voltage the cavity can flattop the local energy gain per turn. This is useful to control phase-dependent stretching or coherent growth at resonances or increases of the extracted emittance due to phase-dependent precession of a stretched emittance.

To test the first case the longitudinal phase width of the beam was reduced from the standard 35° used for high current operation, to 5° by phase selection in the centre region. The phase band was scanned with respect to the accelerating field by varying the rf frequency, and the TOF was recorded. In this case the phase change varies in proportion to the turn number N yielding a TOF that varies with frequency as

$$TOF \propto \frac{d\phi}{dn}/sin(N\cdot\frac{d\phi}{dn}) \quad \text{where} \quad \frac{d\phi}{dn} = 2\pi h\frac{\Delta f}{f}. \quad (2)$$

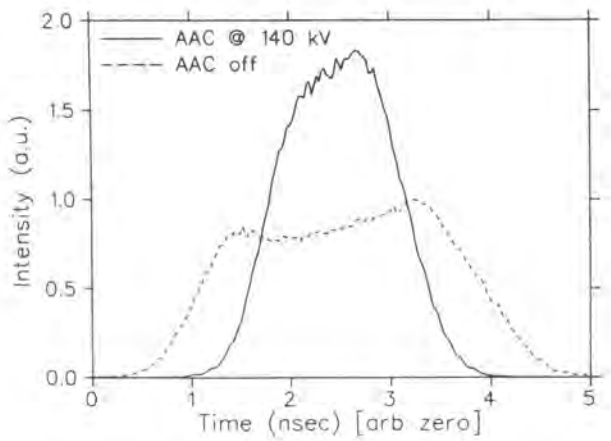


Figure 4: Time structure of the extracted beam with AAC off and AAC powered at 140 kV. Phase compression forces from the cavity have reduced the extracted phase band from 32° to 18° measured at 10% of the peak (1 nsec=8.3°).

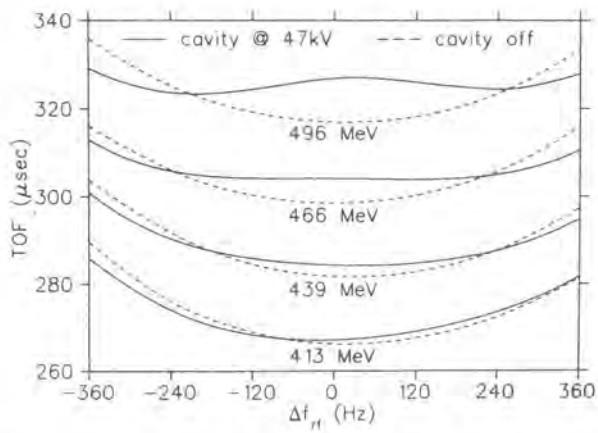


Figure 5: Measured TOF curves, after smoothing, for four different energies as a function of rf frequency for *cavity off* dashed curve) and *cavity on* at 47 kV (solid curve). The cavity was phased to give the best flattop at 466 MeV.

The AAC was powered to flattop the phase dependence of the TOF. Fig. 5 shows the measured TOF response at various radii within the AAC for the cavity @ 47 kV (solid lines) and off (dotted lines). The cumulative effects of the opposing cavity field produce flattening of the response curve at only one energy. The variations in the phase of the minimum TOF for each curve are due to radial variations in the cyclotron isochronism.

The second type of flattopping was tested with the 11.5 MHz rf deflector (RFD) being used to drive a coherent radial oscillation at ν_r=3/2 to initiate precessional extraction [4]. The coherent amplitude gained is proportional to the average radial kick and the number of turns in the resonance region and varies with particle phase as $\cos(\phi/2)/\cos\phi$, while the rate of radial advance of the centre of precession (AEO) varies as $\cos\phi$. Flattopping of the local energy gain per turn can be used to equalize both the number of turns from the ν_r=3/2 resonance to extraction and the coherent amplitude growth for a finite phase band. The advantages of this equalization are explored in another paper in these proceedings [6].

The precession of the coherent oscillation can be measured by observing the radial beam density on a differential probe. Peaks in the density plot occur at a position where the maximum radial advance for one precession cycle has lead to a build up of turns. An experimental radial scan is shown in (Fig. 6) for a narrow phase band (ϕ_o=0) and for the same phase band shifted by 24°. Such density scans were taken for various rf frequencies corresponding to different central phases and were repeated with the cavity flattopping at 15 and 30 kV. Stability of the precession pattern was characterized by measuring the position of the 4th precession peak for each case(Fig. 7). The stability of the peak of a 40° phase band improves by more than a factor of two when the flattoping voltage is 15 kV. Local optimization of the AAC phase should lead to further improvements. Computer simulations show that when properly phased the cavity should virtually eliminate phase-dependent variations in the precession pattern for the ±20° bunch required by the KAON Factory [6].

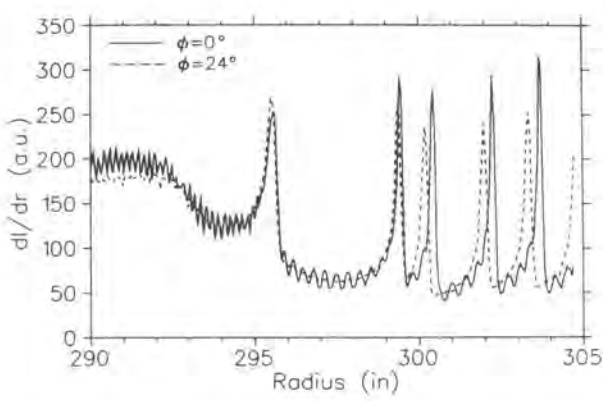


Figure 6: Radial scans using a differential probe showing the beam density pattern produced by the RFD for an optimized phase band and for a phase band off-set by 24°. Phase dependent amplitude growth at the ν_r=3/2 resonance and a $\cos\phi$ dependence in the rate of advance of the precession center account for the difference.

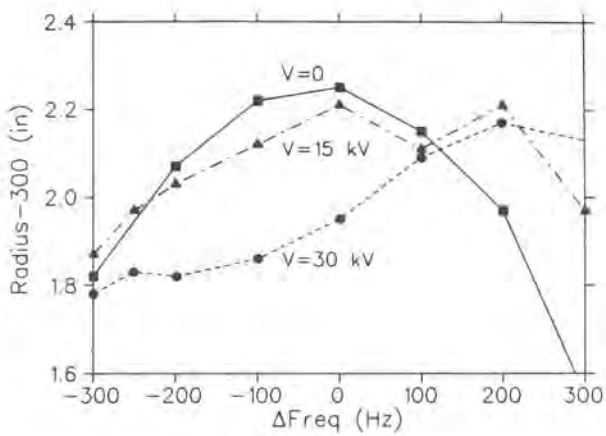


Figure 7: Position of the 4th peak of the RFD induced beam density modulation as a function of rf frequency (beam phase) and cavity flattopping voltage.

IV. Phase-Splitting Mode

A cavity operating at the mth harmonic and phased to oppose the fundamental ($m\phi_m = 180°$) will expand the longitudinal phase band according to Eq. 1. For cases where the peak energy gain from the cavity exceeds that from the fundamental an unstable fixed point occurs in phase space at the energy at which $E_{Gm}(E) = E_{G1}(E)$ and phase ϕ=0. Particles slightly off-phase skirt around a forbidden region defined by

$$\frac{m \cdot \sin\phi}{\sin m\phi} = \frac{E_{Gm}(E)}{E_{G1}(E)}. \qquad (3)$$

In this case the longitudinal bunch could be split into two without loss of beam intensity. This idea could be used to further split the bunches with additional cavities at still higher harmonics, leading to a time structure at extraction compatible with a much higher frequency than the fundamental accelerating frequency [7]. In this study we present the results of an experiment demonstrating the proof of principle.

At the maximum voltage of 140 kV the cavity energy gain is less than that from the fundamental (E_{G4}/E_{G1} = 0.88). To produce the phase-splitting effect the isochronism was shifted from the ideal so that over the radial range of the AAC the effective energy gain from the fundamental was reduced while the AAC was phased to oppose the circulating beam. The simulation results shown in Fig. 8 illustrate how the *phase-slipping* of the fundamental rf can produce phase-splitting. In Fig. 9 we present an experimental result mirroring the simulation of Fig. 8. The phase shift of the beam with respect to the fundamental is accomplished by adjusting the rf frequency. A final time spectrum of the resulting extracted beam compared to the time structure with the cavity off is shown in Fig. 10. Complete phase-splitting is evident with the two sub-bunches separated by 7.6 nsec.

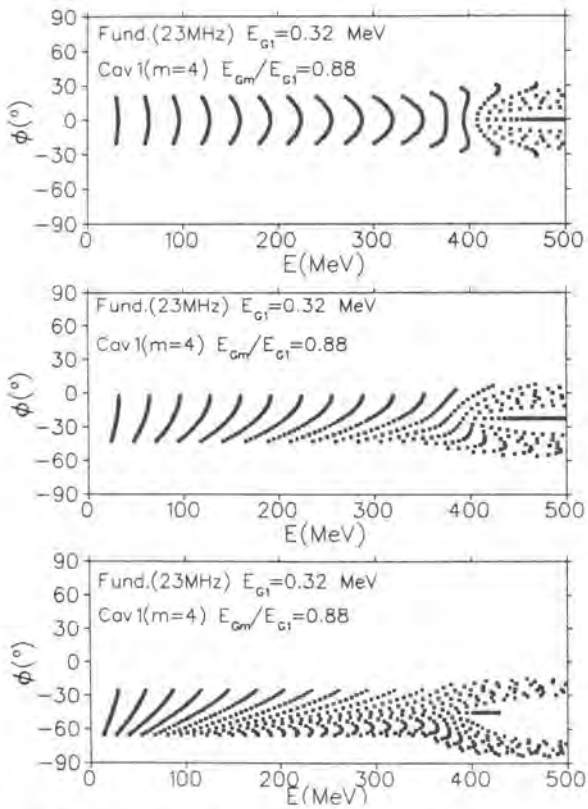


Figure 8: Simulation showing how phase-splitting can occur even when $E_{G1} > E_{G4}$. From top to bottom, the beam is progressively slipped in phase with respect to the fundamental rf prior to the cavity. In each case the phase of the 4th harmonic cavity is adjusted to oppose the beam. In the bottom plot the bunch has slipped to a point where the AAC field can overcome the energy gain from the fundamental rf and splitting results. See Fig. 9 for an experimental demonstration of these simulations.

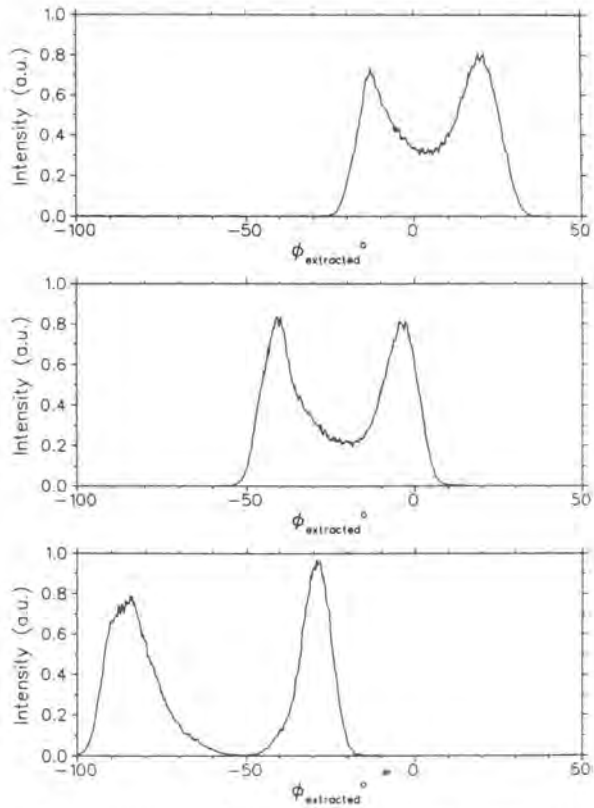


Figure 9: An experimental result mirroring the simulation result of Fig. 8. Shown are the distribution of the beam in longitudinal phase space at three different rf frequencies with the phase of the AAC adjusted to oppose the beam. From top to bottom, the beam is progressively slipped in phase with respect to the fundamental rf. In the bottom plot the bunch has slipped to a point where the AAC field can overcome the energy gain from the fundamental rf and splitting results.

V. References

[1] M. Zach, *et al.*, *Proc. European Part. Accel. Conf.*, p. 973, Nice, 1990.

[2] R.E. Laxdal, *et al.*, *Proc. IEEE Part. Accel. Conf.*, San Francisco, 1991, p. 810.

[3] J.R. Richardson, TRIUMF report TRI-DN-83-42, 1983.

[4] G.H. Mackenzie, *Proc. 11th Intl. Conf. on Cyc. and their Applic.*, Tokyo, 1986, p. 222.

[5] W. Joho, Particle Accelerators, 1974, Vol. 6, p.41.

[6] R.E. Laxdal *et al.*, "Beam Quality Investigations for H^- Extraction at TRIUMF", these proceedings.

[7] R.E. Laxdal and W. Joho, *Proc. European Part. Acc. Conf.*, "Longitudinal Splitting of Bunches in a Cyclotron by Superposition of RF Harmonics", Berlin, 1992 (to be published).

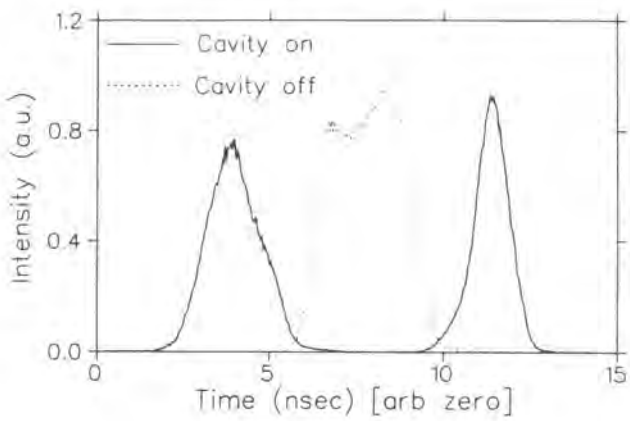


Figure 10: Experimental result showing the time spectrum of the extracted beam with the AAC ($E_{G4}(R_f)/E_{G1}(R_f)$=0.88) phased to oppose the circulating beam (solid line) and with the cavity off (dotted line).

COMMISSIONING OF THE NEW HIGH INTENSITY AXIAL INJECTION SYSTEM FOR GANIL

Ch. RICAUD, E. BARON, J. BONY, M.P. BOURGAREL, B. BRU
GANIL - B.P. 5027 - F-14021 Caen

and

R. VIENET
L.N.S. CEN/Saclay - F-91191 Gif/Yvette-Cedex

ABSTRACT

The "O.A.I." project, now completed, was undertaken at GANIL in order to obtain a better transmission efficiency and to control the space charge effect with an ECR source installed on a high voltage platform. The first measurements made with various sorts of ions show that a 40% to 50% transmission is routinely achieved through the injector cyclotron CO1. From now on, these results will be used for the heaviest ions (Pb, Ta, U) for which the stripper efficiency is weak.
The goal is now the production of exotic nuclei with light ion beams (C, O, Ne, Ar), but the full intensity will be only allowed when safe operation of the other parts of the machine is achieved.

INTRODUCTION

This paper is devoted to the commissioning of the very high efficiency axial injection system of the compact injector cyclotron NCO1.

Figure 1 shows the schematic layout of GANIL. A description of their design and construction has already been reported [1,2,3,4].

The first operation (called O.A.E.) was achieved in July 89, allowing to increase the energy, the range of masses and the intensities (by a factor of 5 to 10), with the injector NCO2, equipped with its classical axial beam transport and a 10 GHz Caprice source.

The goal of the second step (called O.A.I.), completed in June 91 and commissioned in June 92, was to improve the transmission efficiency of the injection system of the second compact injector NCO1, and to obtain beam intensities suited to exotic beam production [5,6].

The main characteristics of the new injection system, are the following :

- A 14.5 GHz ECR ion source [7] has been installed. It is the first of a series of three ECRIS already constructed at GANIL, the others having been built for HMI and CERN.

Increasing the frequency gives a global shift toward higher charge states, and a factor of 2 to 3 on the extracted currents is obtained (for instance, 300 eμA Ar^{9+}, 35 eμA Ta^{22+} have been achieved).

- The injection energy has been increased (50 - 100 kV) in order to control the space charge effects.
- A beam transport system from the platform to NCO1 allows for the 6 dimensional matching of the beam taking into account the space charge effects and the different couplings between phase planes.

1. BRIEF DESCRIPTION OF THE INSTALLATION

The details of the installation were given in ref. 3, and we will only recall its principles.

The beam extracted from the ion source is accelerated through a DC, 4-electrode column providing directly the required injection energy.

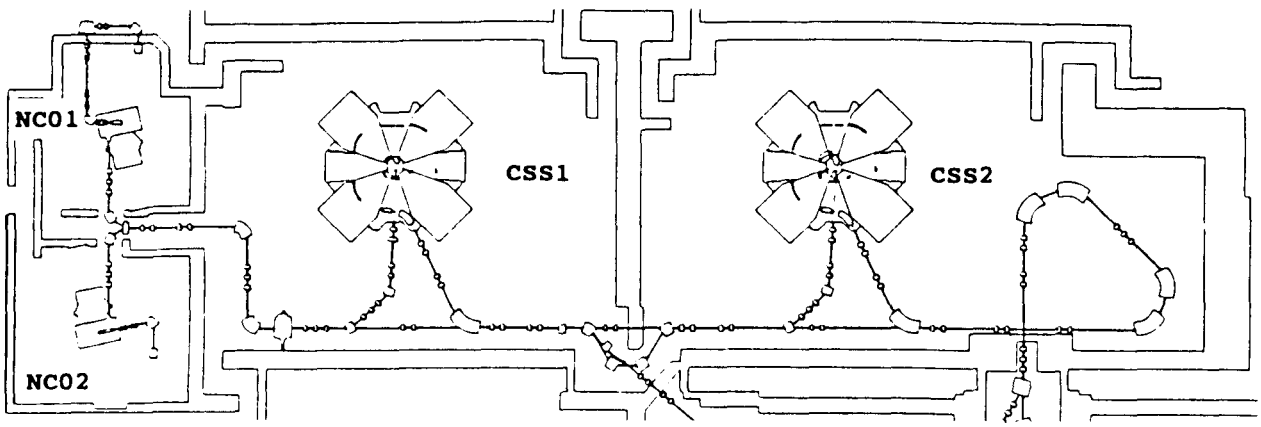


Figure 1 : Schematic layout of GANIL

The beam line between the HV platform and the NCO1 cyclotron is divided in six sections as shown on figure 2. Two main optical functions are carried out :

- The first one, performed in sections 1 and 3, concerns the mass selection (1/250) and the homothetical matching of the beam to a transverse focus which is the object point for the second part (point O). At this location, a system of 3 slits in each plane allows to define the downstream beam emittance.

- The second one, performed in sections 4, 5 and 6, allows to control the couplings introduced by the spiral inflector [6] and to match the beam at the injection point inside the cyclotron.

Between the inflector and the first accelerating gap, an electrostatic quadrupole completes the vertical matching (figure 3).

The bunching is obtained using a "double-drift two harmonic buncher"; its two elements are placed on each side of point O.

We chose to accelerate the total beam and to put the analyzing section at the ground potential, so that only the ECR source and its main equipments (power supplies, RF transmitter, and gaz control) are placed on the platform. The required area is then rather reduced and can be a simple concrete floor ($13m^2$) supported by 9 insulators, with just a grounded external enclosure.

The ECRIS controls (RF, powers, gaz flow , oven heating, etc ...) are carried through a VAX workstation via a first U135 Siemens automat at ground potential, linked to a corresponding one on the platform by means of optical fibers.

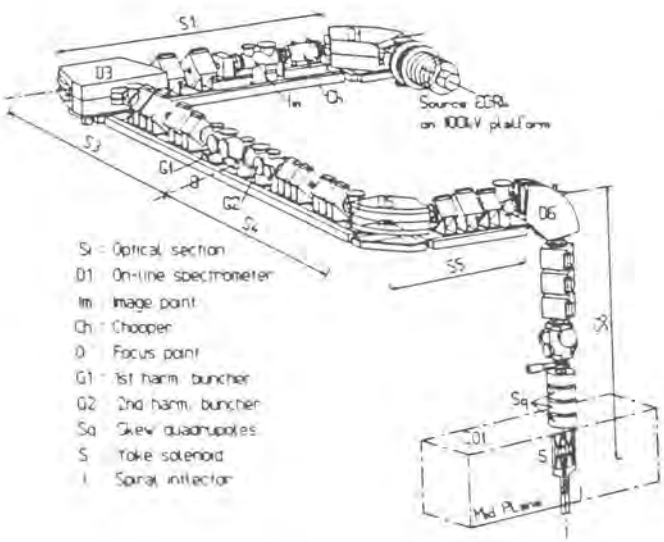


Figure 2 : General layout of the beam line

All the difficulties encountered during the first months of commissioning, were related to the platform :

- At first, a lack of experience in such high voltage led us to reconsider some ground links and equipment protections.

- Secondly, the new industrial equipments use now more and more synthetic caps and cases so that the electronic circuits become more sensitive to electromagnetic perturbations. The connection between the two automats was frequently disturbed and the ECRIS control completely lost.

- Finally, another critical point is a frequent Penning discharge in the first gap. Reducing the emission aperture diameter from 20 mm to 7 mm minimizes this effect as well as the pollution of the puller. Nevertheless, a permanent control of this current is required.

All these difficulties are now over come, and two beams (Ne and Ta) have been delivered to the experimental areas.

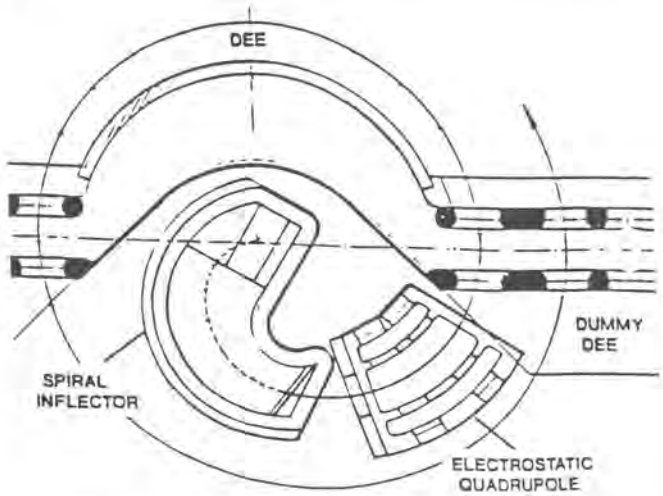


Figure 3 : Central region for the 100 kV injection

2. EXPERIMENTAL RESULTS

2.1. Beam transport efficiency

In the first measurements, the beam transmission from the platform to the entrance of the NCO1 yoke was only 60 to 70% in the 60 π x 60 π mm.mrad NCO1 acceptance.

From the on-line emittance measurements at point O (figure 2) computations performed backwards using the FOCA code [4] indicate that the initial conditions are not in good agreement with the expected ones : the beam is convergent at the puller output (20 kV) and the "waist" is shifted by about 7 cm towards the analyzing dipole. These results confirm the conclusions of the preliminary tests carried out with the total direct beam just after the column and also the observations made on the ion source test-bench.

They also show that a large suspicion has to be put on the "pepper-pot measurements" which gave us wrong initial conditions.

Ion	HV	After analyzing magnet	Yoke entrance		Beam transmission	Comments
	(kV)	Current (eμA)	Current (eμA)	Emittance π mm.mrad		
Ar^{8+}	50	322	200	60 x 60	62%	(a)
Ar^{9+}		300	200	" "	66%	(b)
Xe^{20+}	63	12	6.5	30 x 30	54%	(")
			8.6	60 x 60	72%	(")
			9.7	83 x 83	81%	(")
			10.0	100 x 100	83%	(b)
Ta^{22+}	68	33	26	60 x 60	79%	(b) (c)
	81	11	9	" "	82%	
O^{2+}	67	104	87	60 x 60	84%	(b) (c)
Ne^{6+}	74	55	45	60 x 60	82%	(b) (c)

(a) : with the theoretical HV distribution on the 4-electrode column -(b) : after adjustment of the HV distribution - (c) : emissionaperture diameter : 7 mm (previous value 20 mm)

Table 1. : Beam transmission from the platform to the entrance of the NCO1 yoke

On the other hand, measurements also show that the total emittance is rather large (over 90% of particles in 130 π mm.mrad at 20 kV). By reducing the emission aperture diameter from 20 mm down to 7 mm (mainly to prevent the perturbation described previously), the total emittance decreases to ≅ 110 π mm.mrad and the waist is pushed back near the puller entrance.

Table 1 shows some significant results : by adjusting the potential distribution and after reducing the aperture , the beam transmission raises to 80-90%.

2.2. NCO1 Injector cyclotron and axial injection efficiencies

The central region geometry and matching conditions were determined from beam dynamic studies [1,4].

They are shown respectively on figure 3 and in table 2. The beam matching at the entrance of the first gap is obtained with the beam line sections 4, 5, 6 together with the bunchers which give the required ± 6° phase extension. Theoretically, in these conditions, 68% of the initial beam could be accelerated and extracted from the cyclotron without any losses.

$\varepsilon_r = \varepsilon_v$	= 60 π mm.mrad	
Δr_{max} = ± 2 mm	$\Delta r'_{max}$ = ± 30 mrad	$r_{21} = 0$
Δz_{max} = ± 6 mm	$\Delta z'_{max}$ = ± 0.4 mrad	r_{43} = - 2.87
$\Delta\phi_{max}$ = ± 6°	$C_{r'\phi}$ = 3.3 mrad/°	

Table 2 : Matching conditions at injection

(r_{21}, r_{43} and $C_{r'\phi}$ are the usual correlation coefficients as in the TRANSPORT code).

In the first tests with Xe^{20+}, Ar^{5+}, O^{2+} and Ta^{22+} beams injected with a first set of calculated beam line parameters, efficiencies of only 30 to 50% were obtained.

More refined calculations taking into account the real magnetic field pattern along the injection path (solenoid and inflector) gave us a new set of beam line parameters fulfilling the same matching conditions. Using this new tuning, 66 to 75% transmissions were achieved for a Ne^{6+} beam depending on its intensity.

These results are summarized in the table 3. The turn pattern of the accelerated beam inside the cyclotron are shown on figures 4 and 5 respectively for a Ne^{6+} and a Ta^{24+} beam corresponding to two extreme values of the main field level (respectively 0.97 T and 1.4 T). In the case of Ta, the monotonous decrease of the intensity (20%) is due to a very poor vacuum (1.3 x 10^{-7} mbar). Taking into account this loss, the normal efficiency would be 75%, as for the Ne^{6+} beam.

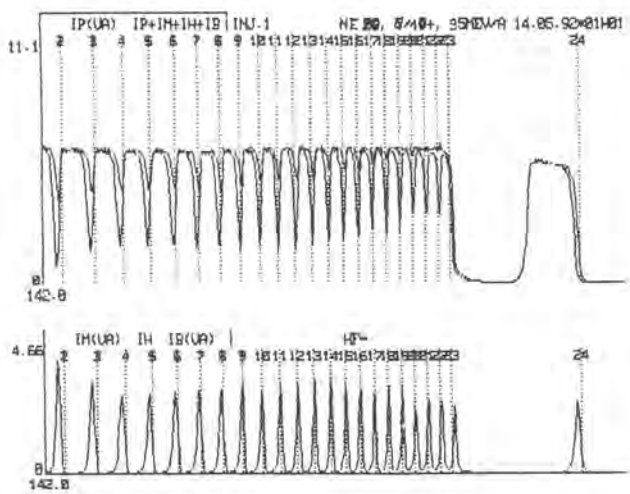


Figure 4 : Turn pattern of Ne in the cyclotron

When the injected beam current is increased (Cf. table 3, Ne^{6+} 36 eμA), the efficiency decreases due to the space charge effects but still reaches 66.7%. Of course, in these conditions, the tuning of the beam line has to be

readjusted : mainly the voltages of the two bunchers and the parameters of the sections 4 and 5.

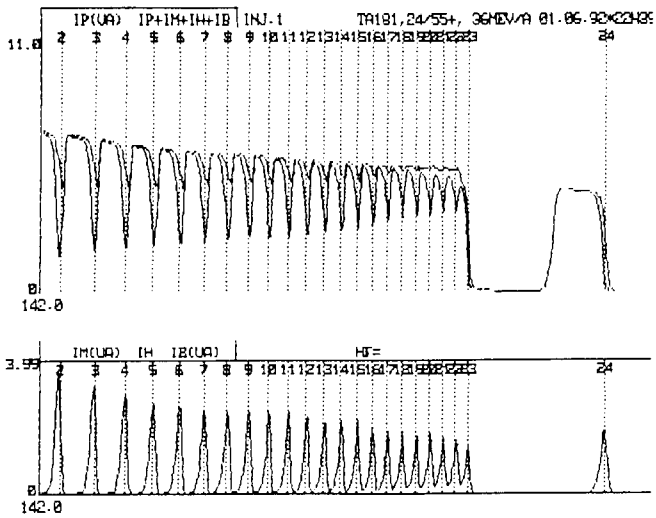


Figure 5 : Turn pattern of Ta in the cyclotron

Ions	H.V (kV)	CO1 Yoke entrance (eμA)	Extracted (eμA)	Efficiency
$_{132}Xe^{20+}$	60	2.9 (30 π x 30 π)	1	34% (a)
$_{181}Ta^{22+}$	70	20 (60 π x 60 π)	6	30% (a)
$_{40}Ar^{5+}$	75	16 (50 π x 50 π)	8	50% (a)
$_{16}O^{2+}$	75	50 (60 π x 60 π)	22	44% (a)
$_{20}Ne^{6+}$	80	16.8 (60 π x 60 π)	12.6	75% (b) (Fig. 4)
"	"	19 (60 π x 60 π)	13.77	72.5% (b)
"	"	36 (60 π x 60 π)	24	66.7%
$_{181}Ta^{24+}$	77	9 (60 π x 60 π)	5	55% (b) (Fig.5)

(a) : with initial computed parameters
(b) : adjustments taking into account the B value

Table 3 : NCO1 injector cyclotron and axial injection efficiencies

2.3. Beam qualities

The characteristics of the extracted Ne^{6+} and Ta^{24+} beams were measured. They are equivalent despite the difference of the energy and extracted current (1 MeV/u, 24 eμA Ne^{6+} and 0.42 MeV/u 5 eμA Ta^{24+}) :
ε_r (uncorrelated) ≅ ε_z ≅ 45 π mm.mrad
ε_L (ΔW/W.Δφ uncorrelated) = 8 π deg.%
(with ΔW/W ≅ ± 1.6%).

The numerical simulations which have been performed gave smaller values (at the last turn, before ejection : ε_r (correlated) = 26 π mm.mrad, ε_z= 10 π mm.mrad, Δφ = ± 6°, ΔW/W = ± 4 x 10^{-3}).

We have still no definite explanation for these discrepancies, we can observe on figures 4 and 5 a difference between the theoretical and measured positions of the successive turns associated with an amplitude modulation. These patterns can be explained by an error of ≅ 35 mrad on the injection angle $\dot{r}_0$ which will have to be corrected.

3. CONCLUSION

The NCO1 injector was connected to the SSC's and two beams, Ta and Ne, have already been used for experiments. For 5 and 3 days respectively, 4 eμA of Ta^{24+} and 24 eμA of Ne^{6+}were extracted from NCO1, 50 to 60% of these beams suitable for further acceleration through the SSC's. The stability and the availability of these beams on the target were excellent.

Two main conclusions can be drawn from the results :

- Concerning the available intensities out of NCO1 we obtain for the heaviest ions at least a factor of 10 higher than with NCO2, which was one of our goals.
- Concerning the very high intensities needed for exotic ion production either by fragmentation of by the ISOL method, we are still faced with the large emittances of the beams extracted from NCO1. The large values of transverse emittances (≅ 40 - 50 π mm.mrad) and of the energy dispersion (≅ 1.5%) do not fit the SSC's acceptance for an acceleration with manageable losses.

Therefore, we will have either to cut in the beam in front of SSC1 or, better, to understand and cure the causes of these large emittances.

References

(1) - M.P. Bourgarel et al.- "Modification of the GANIL injectors" - Proceedings of the 12th. Int. Conf. Cyclotrons (Berlin-1989)
(2) - R. Beck et al.- "Six dimensional beam matching for axial injection into a cyclotron" - Proceedings of the 12th. Int. Conf. Cyclotrons (Berlin-1989)
(3) - Ch. Ricaud et al.- "Preliminary design of a new high intensity injection system for GANIL" - Proceedings of the 12th. Int. Conf. Cyclotrons (Berlin-1989)
(4) - Ch. Ricaud et al.- "Status of the new high intensity injection system for GANIL" - Proceedings of the 2nd. European Particle Accelerator Conference (Nice 1990)
(5) - M.P. Bourgarel et al.- "Proposals for a radioactive ion beam facility at GANIL" - Proceedings of the 6th. Int. Conf. on Electrostatic Accelerators and Associated Boosters" - (Legnaro 1992)
(6) - P. Bricault et al.- "An on-line isotopic separator test bench at GANIL" - This conference
(7) - M.P. Bourgarel et al.- " A review of the GANIL activity with the 14.6 GHz ECR ion sources" - Proceedings of the 4th. Int. Conf. on Ion Sources (Bensheim 1991)

A FORMULATION OF SPIRAL INFLECTOR DESIGN AND ITS APPLICATION TO SF CYCLOTRON

M. Sekiguchi, Y. Shida, Y.Ohshiro, M. Fujita,
T. Yamazaki, N. Yamazaki and M. Nishiguchi

Institute for Nuclear Study, University of Tokyo, 3-2-1 Midori-cho, Tanashi-shi,
Tokyo, 188, Japan

ABSTRACT

Ion trajectories through a spiral inflector are analyzed. In the case of a uniform magnetic field, it is shown that the central trajectory can be expressed as a simple analytical form, which includes all the inflector types already known. By using a curvelinear coordinate along the central trajectory, the equations of motion of non-central ions are modified to describe the ion motion in the transverse and longitudinal planes. A method is presented to expand the electric potential around the central trajectory to calculate the electric field to be used in the equations of motion. In the method, an electric potential thus obtained is used instead of the electric field, which guarantees the energy conservation of the ions through the inflector. Numerical studies have been carried out for design of an inflector for the SF cyclotron at the Institute for Nuclear Study, University of Tokyo.

1. INTRODUCTION

With advent of excellent external ion sources, such as ECR sources for heavy ions, more cyclotrons are equipped with them. Most cyclotrons are designed recently from the beginning to employ only them. It has been proved that the ions are most effectively injected along the main magnetic field of the cyclotron into its center. They must be deflected into the median plane in order for them to be accelerated successfully in the cyclotron.

In the early stage of the development of the modern cyclotron, many studies have been carried out for devices to inflect the ions injected along the main magnetic field into the median plane.[1-4] Nowadays, most cyclotrons employ a device called a spiral inflector [2,3,5,6] or an electrostatic mirror. [8] It is essential that a good optical device should be employed to accept ions effectively from the ion source.

A spiral inflector for ions may be defined as a device with a pair of electrodes which produce an electric field always perpendicular to the velocity of the ions moving in a given magnetic field. The ion velocity at its entrance is parallel to the magnetic field, while at its exit the velocity should have been turned into a direction perpendicular to the magnetic field. Although it is not evident whether such a device generally exists in any given shape of magnetic field, spiral inflectors can be actually manufactured for cyclotrons, in which the main magnetic field is along the initial ion velocity, whereas the final ion velocity should be in the median plane of the cyclotron.

In this paper, firstly, the central trajectory of an ion through the spiral inflector is reviewed by using a uniform magnetic field approximation. Secondly, the equations of motion for the non-central ions are modified in a curvelinear coordinate with the central trajectory as the reference curve to integrate them numerically. Thirdly, trajectory as the reference a method to expand the electric potential produced by the inflector electrodes around the central trajectory is presented. These formulae are applied to study the inflector design for the SF cyclotron at the Institute for Nuclear Study.

2. CENTRAL TRAJECTORY AND CENTERING OF THE CYCLOTRON ORBIT

The equations of motion of an ion with mass m and charge e, moving in a magnetic field $\boldsymbol{B}$ and electric field $\boldsymbol{E}$ with velocity v, can be written as

$$\boldsymbol{t}' = K\boldsymbol{e} - F\boldsymbol{n} + [\boldsymbol{t} \times \boldsymbol{b}], \tag{1}$$

where the prime designates differentiation with respect to the length s along the orbit, $\boldsymbol{b}$ is the magnetic curvature vector,

$$\boldsymbol{B} = \frac{mv}{e}\boldsymbol{b},$$

K and F are the electric curvatures,

$$\boldsymbol{E} = \frac{mv^2}{e}(K\boldsymbol{e} - F\boldsymbol{n}),$$

$\boldsymbol{t}$ is the tangent unit vector, $\boldsymbol{e}$ and $\boldsymbol{n}$ are unit vectors perpendicular to $\boldsymbol{t}$ and $\boldsymbol{n} = \boldsymbol{t} \times \boldsymbol{e}$.

We will find solutions of the equations of motion by using $\boldsymbol{t}$, $\boldsymbol{e}$ and $\boldsymbol{n}$. The other two vectors should satisfy the following simultaneous equations

$$\boldsymbol{e}' = -K\boldsymbol{t} + G\boldsymbol{n} + [\boldsymbol{e} \times \boldsymbol{b}]$$

and

$$\boldsymbol{n}' = -G\boldsymbol{e} + F\boldsymbol{t} + [\boldsymbol{n} \times \boldsymbol{b}],$$

together with Eq.(1). The curvature G is also a function of s. K and F determine the bending electric field and G determines the rotation of the electric field along the trajectory.

By definition, the electric field acts just as the magnetic field or *vice versa* so long as the central trajectories are concerned, since it exerts force in the perpendicular direction to the ion velocity. This fact is incorporated into these equations. If the magnetic field distribution $\boldsymbol{b}$ and the functions K, F and G are given as functions of position of the ion, we can integrate above three equations to obtain the central orbit.

In the case of a uniform magnetic field B, it can be shown that the equations have simple solutions containing only trigonometric functions in the case

$$K = C_e, F = C_f \sin\alpha, G = -C_f \cos\alpha$$

and

$$\alpha = C_e s + \alpha_0,$$

where C_e and C_f are constants specifying the electric curvatures and α_0 is a constant determining the phase of the rotation of the electric field. Let us introduce the following notation: $R_0 = (1/B)\sqrt{2mV_d/e}$, $R_m = \sqrt{K_i}R_0$, $C_m = 1/R_m$, and $K_i = V_i/V_d$, where V_i and V_d are the injection voltage and dee voltage, respectively. The strength of the electric field is given by

$$E = 2V_i \left\{C_e^2 + C_f^2 \sin^2(C_e s + \alpha_0)\right\}^{1/2}.$$

This solution contains all of the types of the spiral inflectors so far studied in addition to new ones. With our notation, they are as follows:

normal [2]	: $C_e \neq 0$, $C_f = 0$, $\alpha_0 = 0$
slanted [2]	: $C_e \neq 0$, $C_f \neq 0$, $\alpha_0 = 0$
hyperboloid [3]	: $C_e = C_m/\sqrt{6}$, $C_f = -C_m/2$, $\alpha_0 = 0$
paraboloid [3]	: $C_e = C_m/2$, $C_f = -C_m/2$, $\alpha_0 = 0$.

It is known that the *hyperboloid* and *paraboloid* has no free parameters, while *normal* has one free parameter and the *slanted* has two free parameters. In the general case described above, we have three free parameters, C_e, C_f and α_0 in general. In the *normal* case, the strength of the electric field is constant along the trajectory and so is the gap between the electrodes. Among many possible combinations of parameters, we should note the case: $C_e = 0$, $C_f \neq 0$ (let's call this *parallel*, since the electric field is constant and the electrodes are parallel even if they are twisted). When $\alpha_0 = \pi/2$, this solution is the same as the *slanted*, except that the axis is rotated by $\pi/2$, but we can choose α_0 at will according to the requirement. This solution has also a constant gap and still has another free parameter.

After exit of the inflector, the ion orbit should be centered appropriately for further acceleration. In a simple approximation of a uniform magnetic field and the narrow-gap limit of acceleration, the tangent at the inflector exit should be the tangent of a circle with radius R_m. The center of this circle should be located properly for further acceleration in the cyclotron. This requirement determines one of the three parameters or the injection voltage.

3. OPTICAL PROPERTIES

For the non-central trajectories, we trace the ion orbits in a curvelinear coordinate system referring to the central trajectory as the reference curve. As in the theory of particle accelerator with large dimension, it is convenient to separate particle orbit in the transverse and longitudinal directions. For this purpose, let's introduce a vector in the transverse plane

$$\boldsymbol{q} = \boldsymbol{r} - \boldsymbol{r}_c$$

such that

$$\boldsymbol{q} \cdot \boldsymbol{t} = 0. \tag{2}$$

In order to trace the ion motion along the reference curve, let's introduce another vector

$$\boldsymbol{p} = \frac{d\boldsymbol{r}}{du} - \boldsymbol{t},$$

which describes the difference of the ion velocity with respect to the reference one. The quantity u has a dimension of length, $u = vt$, where v is the velocity of the reference ion and t is the time elapsed after entering the inflector. It is a function of s and corresponds to the flight time of the non-central ion in question. By differentiating Eq.(2), we obtain the equation for u:

$$u' = \frac{\lambda}{1 + \boldsymbol{p} \cdot \boldsymbol{t}}, \tag{3}$$

where

$$\lambda = 1 - (\boldsymbol{t}' \cdot \boldsymbol{e})(\boldsymbol{q} \cdot \boldsymbol{e}) + (\boldsymbol{n}' \cdot \boldsymbol{t})(\boldsymbol{q} \cdot \boldsymbol{n}).$$

With these vectors, we can rewrite the equations of motion in the following form:

$$\boldsymbol{q}' = u'\boldsymbol{p} + (u' - 1)\boldsymbol{t} \tag{4}$$

and

$$\begin{aligned}\boldsymbol{p}' = {} & (u' - 1)\{\boldsymbol{C}_c + [\boldsymbol{t} \times \boldsymbol{b}_c]\} \\ & + u'\{(\boldsymbol{C} - \boldsymbol{C}_c) + [\boldsymbol{t} \times (\boldsymbol{b} - \boldsymbol{b}_c)]\} + u'[\boldsymbol{p} \times \boldsymbol{b}],\end{aligned} \tag{5}$$

where the suffix c refers to the central trajectory and $\boldsymbol{C}$ is the electric curvature vector. It is easy to rewrite these vector equations into those for the components (q_e, q_n) of $\boldsymbol{q}$ and (p_e, p_n, p_t) of $\boldsymbol{p}$.

Up to present, we have not assumed that the magnetic field is uniform. If the magnetic and electric field distributions are given in the space and the central trajectory is given, we can integrate these equations to calculate the ion trajectories of non-central ions.

The energy conservation is easily verified in these equations if we use appropriate electric potential and electric field described in the next section. It should be noted that the longitudinal electric field appears for the non-central ions that are absent on the central trajectory. In the calculations using these equations, we can use the energy conservation as the checks for the calculations at each step of integration. When calculating transmission efficiency or acceptance of the inflector, we can check if an ion hit the inflector electrode or not by looking at the electric potential at each point in question.

4. ELECTRIC FIELD AND SHAPE OF ELECTRODE SURFACE

Since we are using a curvelinear coordinate moving with the central trajectory, the electric potential becomes somewhat complicated due to the twisting of the reference curve. In the transverse plane, the relation of the electric potential and the electric field is as usual:

$$\boldsymbol{E} \cdot \boldsymbol{e} = -\frac{\partial \phi}{\partial q_e}$$

and

$$\boldsymbol{E} \cdot \boldsymbol{n} = -\frac{\partial \phi}{\partial q_n}.$$

In the longitudinal direction, the electric field is given by

$$\begin{aligned} \boldsymbol{E} \cdot \boldsymbol{t} &= -\frac{1}{\lambda}\partial_s \phi \\ &\equiv -\frac{1}{\lambda}\left\{(e' \cdot \boldsymbol{n})\left(q_n \frac{\partial \phi}{\partial q_e} - q_e \frac{\partial \phi}{\partial q_n}\right) + \frac{\partial \phi}{\partial s}\right\}. \end{aligned}$$

The Laplace equation then becomes

$$\begin{aligned} \Delta\phi &= \frac{1}{\lambda}\left\{\frac{\partial}{\partial q_e}\left(\lambda \frac{\partial \phi}{\partial q_e}\right) + \frac{\partial}{\partial q_n}\left(\lambda \frac{\partial \phi}{\partial q_n}\right)\right\} \\ &\quad + \frac{1}{\lambda}\partial_s\left(\frac{1}{\lambda}\partial_s \phi\right) \\ &= 0. \end{aligned}$$

We can expand the potential ϕ around the central trajectory as a power series of $\boldsymbol{q}$ by using a polar coordinate (q, θ) in the transverse plane:

$$\phi = \sum_{n \geq 0} \phi_n,$$

where

$$\phi_n = Real\left\{a_n(s) q^n e^{in\theta} + \sum_{n<k, m \leq k-2} c_{nkm}(s) q^k e^{im\theta}\right\},$$

a_n and c_{nkm} are complex functions of s, and m is an odd or even non-negative integer as n is. Note that the factor $q^n e^{in\theta}$ is a solution of the Laplace equation when the reference curve is a straight line. The coefficient a_0 must be independent of s since the electric field is perpendicular to the reference curve and a_1 is determined by K and F. The other coefficients a_n introducing the $2n$-pole electric potential are free parameters for the shape of the inflector electrodes.

It should be noted that this expansion is only valid near the central trajectory: it is valid for small $C_m q$, $C_e q$ and $C_f q$.

5. DESIGN STUDY FOR THE INS SF CYCLOTRON

The SF cyclotron[9] at the Institute for Nuclear Study, University of Tokyo, has been using a mirror to deflect the ions both from a polarized-ion source and from an ECR ion source.[10] The cyclotron was designed and constructed to be used mainly with internal PIG sources. The transmission through the vertical injection line is not good(1-5%), which is the main motivation of the present study. It is an ordinary AVF cyclotron with an extraction radius of 730 mm. Usually it employs a constant orbit acceleration with 250 turns up to extraction: thus R_0 = 33 mm. The dee voltage used for usual operation lies in the range 20 - 60 kV. Since the magnetic field is uniform within 0.5% in the region of interest, the uniform field approximation may be adequate.

Numerical calculations have been carried out by using the polynomial expansion of the potentials up to 5th order in qC_m, qC_e and qC_f. Four types of potentials have been generated: two deflector types in $\boldsymbol{e}$ and $\boldsymbol{n}$ directions, two quadrupole types with hyperbolic shapes. The equations of motion, Eqs.(3-5), were integrated numerically for each ion starting at a point generated randomly in the phase space. The Monte Carlo calculations were performed for each combination of these potentials.

The numerical values of the potential thus obtained show distortion of the electrode surfaces due to the twist of the central trajectory. In the case of the *normal* type with a value of V_i = 0.3, radii of the magnetic and electric curvatures are 18 mm and 41 mm, respectively, the surfaces of the electrodes deviate from a straight horizontal line by about 0.5 mm at a point 5 mm apart from the central trajectory. Conversely, if we machine the electrode surface as a straight line in this case, considerable strength of the quadrupole and/or higher-order components of the electric potential is introduced inevitably at the edges of the electrode width, although it is not clear that these components improve or deteriorate the optical properties.

It was found that the *parallel* type has large freedom for choosing the injection voltage: V_i changes widely by changing α_0 for a given path length as shown in Fig.1. Note that $\alpha_0 = 90°$ is equal to the *normal* case. In our cyclotron, the injection energy of the ions must be varied widely, since the injection voltage is proportional to the dee voltage once the inflector structure is fixed. This point is an advantage of this type, because more ions with better emittance can be extracted usually from the ion sources and the ions with higher energy are less affected by disturbance such as stray field during the beam transport.

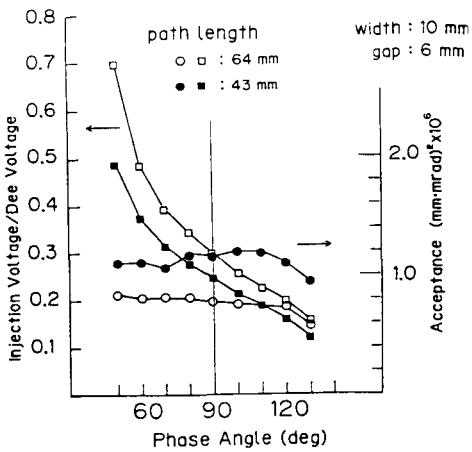


Fig. 1. Ratio of the injection voltage to the dee voltage and acceptance as a function of α_0 for the two different cases of the path length.

In the figure, the values of C_f were so changed that the path length has two different values of 64 mm and 43 mm for each α_0. The former is a realistic value having a height of about 40 mm and the latter, having a height of 30 mm, seems too small in our case.

Acceptance is also shown in Fig.1, calculated by the Monte Carlo method mentioned above. A waist with a radius covering the physical aperture and with an angular spread of 100 mrad was assumed for the beam at the entrance. It can be seen that the acceptance depends little on α_0, which allows us to select an adequate injection voltage without affecting the acceptance.

As expected, calculations show that acceptance is primarily determined by the path length of the central trajectory. The values of the acceptance shown in Fig.1 appear to be large enough, but calculations show that the two transverse motions and the longitudinal motion are highly coupled in the inflector that the transmission should be calculated for individual design of the inflector.

For simplicity, we have determined to start from the simplest type of the inflector, the *normal* type.

6. SUMMARY

The formulation of the central trajectory described in this paper can classify and compare several kinds of inflector types already known in the uniform field approximation. It can be used for compact-type cyclotrons in which the magnetic field is almost uniform in the central region of the cyclotron. It can be modified or used as a starting point of estimation also for separated-sector type cyclotrons in which the field changes considerably. It should be noted that the three free parameters allows us to choose a best central orbit for a specific requirement at a cost of difficulty of machining.

Our formulation of the non-central orbit is more transparent than those of other works by guaranteeing the energy conservation, when used with appropriate electric potentials. However, we don't believe that we have clarified the optical properties sufficiently by present numerical calculations because of the inherent complexity of the problem. Further numerical studies seem to be necessary.

7. REFERENCES

1) Powell, W. B. and Reece, B., L., "Injection of Ions into a Cyclotron from an External Source," Nucl.Instrum. Meth., **32**, 325(1965).
2) Belmont, J. L. and Pabot, J. L., "Study of Axial Injection for the Grenoble Cyclotron," IEEE Trans.Nucl.Sci., **NS-13**, 191(1966).
3) Müller, R. W., "Novel Inflectors for Cyclic Accelerators," Nucl.Instrum.Meth., **54**, 29(1967).
4) Hazewindus, N., "Calculation of Particle Trajectories in a Cyclotron Axial Injection System with an Electrostatic Deflector," Nucl.Instrum.Meth.,**76**, 273(1969).
5) Root, L. W., "Design of an Inflector for the TRIUMF Cyclotron," M. Sc. Thesis, Univ. of British Columbia, Vancouver, 1972.
6) Root, . W., "Experimental and Theoretical Studies of the Behaviour of an H^- Ion Beam during Injection and Acceleration in the TRIUMF Central Region Model Cyclotron," Ph.D. Thesis, Univ. of British Columbia, Vancouver, 1974.
7) Balden, R. J. *et al.*, "Aspects of Phase Space Dynamics in Spiral Inflectors," in **Proc. 12th Int. Conf. on Cyclotrons and their Applications** (World Scientific, Singapore, 1989) pp.435–438.
8) Bellomo, G. *et al.*, "On the Feasibility of Axial Injection in Superconducting Cyclotrons," Nucl.Instrum. Meth.,**83**, 19(1983).
9) Hirao, Y. *et al.*, "The INS 176cm Sector Focusing cyclotron," in **Proc. 7th Int. Conf. on Cyclotrons and their Applications**, (Birkhauser, Basel, 1975), pp103-106.
10) Ueda, N. *et al.*, "Acceleration of the Polarized Proton and Deuteron at the INS SF Cyclotron," in **Proc. 5th Int. Symp. on Polarization Phenomena in Nuclear Physics**, (American Institute of Physics, New York, 1981), pp.901-903.

PRELIMINARY DESIGN OF A NEW CENTRAL REGION FOR THE LNS SUPERCONDUCTING CYCLOTRON

M-H MOSCATELLO
Laboratorio Nazionale del Sud, Catania, Italy

ABSTRACT

This paper presents the preliminary design of a new central region for the LNS superconducting cyclotron, for the h = 2 mode, and with the use of a spiral inflector. The geometry of the electrodes has been determined by three dimensional calculations, and will be verified later on by electrolytic tank measurements. The results concerning the vertical motion and the radial envelopes are also presented and show that the emittances of a beam injected via a spiral inflector fit the acceptance of the cyclotron.

1. INTRODUCTION

A new central region for the LNS superconducting cyclotron is under study, with a spiral inflector which presents several advantages with respect to the mirror inflector, used in the previous design.[1] The central region design has been optimized for the h = 2 mode, corresponding to the energy range 8 MeV/A to 100 MeV/A,[2] and is foreseen to operate in a constant orbit mode. The present dees are machined down to the radius of 9 cm and must be designed from this radius inwards. All the design calculations were carried out for the ion with Q/A = 0.5, B_0 = 31.3 kgauss, f = 48 MHz, which corresponds to a final energy of 100 MeV/A. This ion corresponds to the highest voltages of the dees and of the ECR source. To get the constant orbit mode for other ions, it will be sufficient to apply a factor proportional to the product $fB\rho$.

2. CHOICE OF THE SPIRAL INFLECTOR

The spiral inflector has been chosen for the many advantages it presents when compared to the others (electrostatic mirror and hyperboloidal inflector):

- the electrostatic mirror deteriorates too much the incident beam properties;
- the hyperboloidal inflector does not enable an injection on the axis of the machine, which is very inconvenient for a superconducting cyclotron, and has only one variable parameter, the magnetic curvature;
- the spiral inflector occupies little space and has two variable parameters (magnetic curvature and "slant" angle). Its drawback is nevertheless a difficult machining.

For the design of the central region, the initial conditions, that is the conditions at the exit of the inflector, are the theoretical ones, obtained from the fundamental equations:[3]

$$\text{position:} \quad \begin{aligned} x &= 2K\lambda \sin(K\pi) - \lambda \\ y &= -2K\lambda \cos(K\pi) \\ z &= 0 \end{aligned} \qquad (1)$$

$$\text{velocity:} \quad \begin{aligned} V_x &= V_o \sin\theta\cos(2K\theta) \\ V_y &= V_o \sin\theta\sin(2K\theta) \\ V_z &= -V_o \cos\theta \end{aligned} \qquad (2)$$

with the usual definitions of K and λ.

The condition at the exit of the inflector is that $V_z = 0$ (corresponds to $\theta = \pi/2$) and from the study made in Milan[4]:

K = 1.1, A = 20.24 mm, V electrodes = ±5 kV

V_{inj} (source voltage) = 20 kV for Q/A = 0.5

which produces the following conditions:

r = 1.41 cm, p_r = 330 mrad, E_o = 0.01 MeV/A.

The radial space occupied by the inflector and its shielding has been chosen equal to the MSU's one.[5]

3. ELECTRIC FIELD AND ORBIT CALCULATIONS

The electric field calculations have been made with RELAX3D.[6] A cubic mesh, 1 mm size, covering a region of 160x160 mm in the X and Y horizontal directions and 17 mm in the Z vertical direction has been used. Starting from spiraled dees down to the radius of 1 cm, several geometries have been tried, and tested with the central orbit calculation made with the dynamics program CYCLONE 3D.[7] The geometry retained is presented in

Fig. 1:

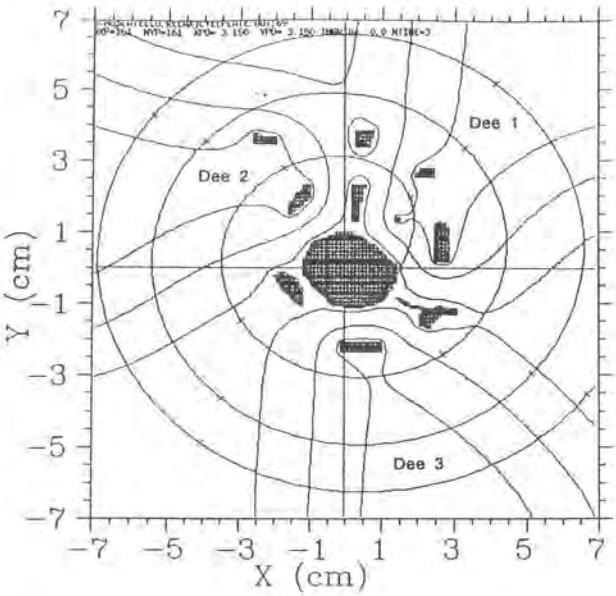


Fig. 1. Central region geometry and central orbit

mum clearance of the whole beam is of 1 mm.

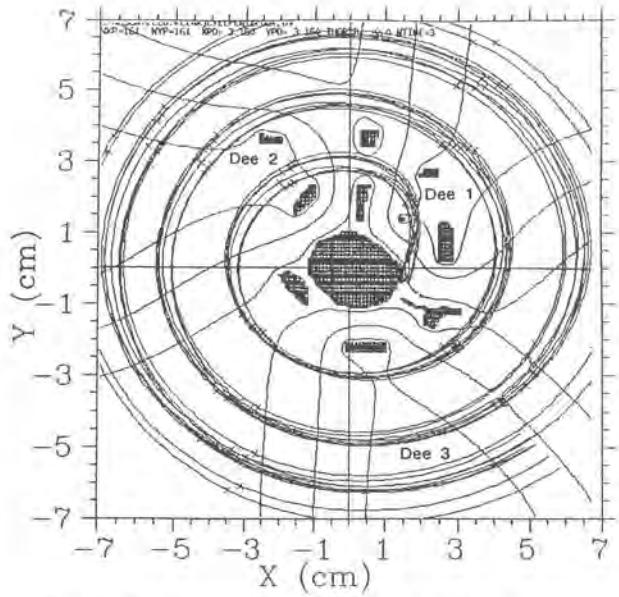


Fig. 2. Trajectory of a beam with a radial emittance of 100π mm-mrad

All the electrodes on the dees and on the dummy-dees cross the median plane. The grounded electrodes should be sufficient to obtain low couplings between the dees.The electric gaps are all equal to 10 mm minimum,in order to have an electric field always smaller than 100 kV/cm.

A calculation of the central orbit was made with an injection voltage of 15 kV instead of 20 kV, and the off-centering is of the order of 2 mm, an acceptable value when the source is operated at a lower voltage.

The starting phase of the beam is in advance of 40° on the RF phase, to compensate the delay taken in the first half turn.

4. RADIAL AND VERTICAL MOTIONS

4.1. Radial motion

The radial phase space study has been made for an emittance $\varepsilon = 100\pi$mm·mrad,greater than the emittance transmitted by a spiral inflector. Figure 2 presents the trajectory of this beam, where it appears that the minimum clearance of the whole beam is of 1 mm.

The beam is represented by 8 particles of a radial ellipse obtained from the eigen-ellipse and then traced back to the centre of the cyclotron, and 2 particles distant ±20° RF from the central particle(Fig.3).

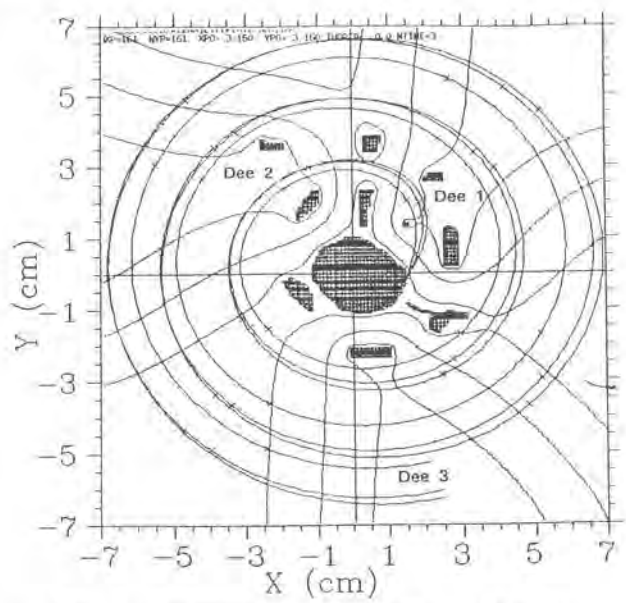


Fig. 3. Trajectory of the central particle and 2 particles distant of $\Delta\phi = \pm 20°$ RF.

The evolution of the beam in the radial phase space during the first turns is presented in Fig. 4.

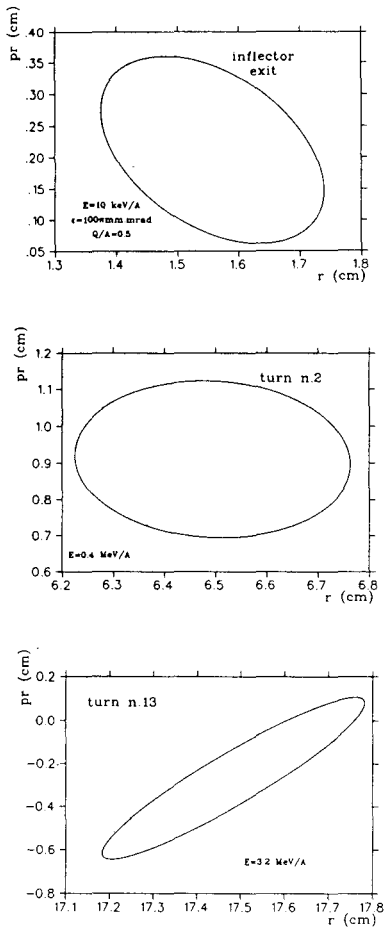


Fig. 4. Evolution in the radial phase space

4.2. Vertical motion

The vertical motion has been studied for an emittance $\epsilon = 100\pi$mm·mrad, and a total height of the beam equal to 4 mm at the exit of the inflector. To get a sufficient vertical focusing during the first turn, some vertical reductions have been added at the locations indicated in Fig.5 (horizontal hatched areas). In these places the vertical gap is of 14 mm instead of the nominal 25 mm. The vertical focusing is rather sensitive to the starting phase.

These radial and vertical emittances accepted by the central region do not take into account the correlations which could be added by the structure of the injection line. When the injection line is designed as well as the inflector, more calculations will have to be made to know the real acceptance of the central region.

4.3. Beam centering

The beam centering has to be improved by a few mm, being up to now of the order of 5 mm at the radius r=18 cm, by slightly modifying the shape of the dees near the centre. Indeed such a value cannot be accepted; ν_r being close to 1, this leads to a substantial increase in the radial dimension of the beam. Of course the harmonic 1 coils can be used to re-centre the beam, but must be considered as a fine adjustment tool.

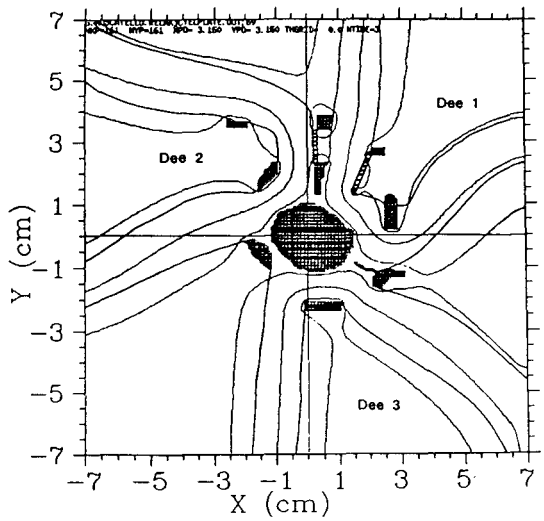


Fig. 5. Central region with the vertical reductions

5. CONCLUSION

This preliminary design shows that the main requirements are reached, although the beam centering must be refined. This work will be followed by a precise calculation of the spiral inflector, with the program RELAX3D, including a fine modelization of the inflector RF shielding, and the construction of a model. Meanwhile, it is intended to build a model of the central region to proceed to electrolytic tank measurements, and to verify that the coupling between the dees at the centre is low enough.

6. REFERENCES

1) G. Bellomo and L. Serafini, "Design of the central region for axial injection in the Milan superconducting cyclotron", in Proc. 11th Int. Conf. on Cyclotrons and their Applications (Ionics, Tokyo, 1987) pp. 507 - 510.
2) E. Fabrici and A. Salomone, "Acceleration studies for the Milan superconducting cyclotron", Report INFN/TC - 83/9 (1983).
3) S. Chell, thesis "Etude de l'injection axiale d'un faisceau d'ions lourds dans un cyclotron compact", Report GANIL/T89.02 (1988).
4) A. Thalmeir, thesis "Design and test of a spiral inflector for the axial injection in the Milan superconducting cyclotron", Università di Milano, July 1990.
5) F. Marti and A. Gavalya, "Axial injection in the K500 superconducting cyclotron", in Proc. 11th Int. Conf. on Cyclotrons and their Applications (Ionics, Tokyo, 1987) pp. 484 - 487.
6) C. J. Kost and F. W. Jones, "RELAX3D User's guide and reference manual", Report TRI-CD-88-01 (1988).
7) F. Marti et al., "Design calculations for the central region of the NSCL 500 MeV superconducting cyclotron", in Proc. 9th Int. Conf. on Cyclotrons and their Applications (Caen, 1981).

NON-LINEAR BEAM TRANSPORT EFFECTS IN HIGHLY CHARGED POSITIVE ION BEAMS EXTRACTED FROM ECR ION SOURCES

Timothy A Antaya *
National Superconducting Cyclotron Laboratory, Michigan State University, East Lansing MI 48824-1321, USA

and

Z.Q. Xie
Lawrence Berkeley Laboratory, Berkeley CA 49720, USA

ABSTRACT

Using ECR ion sources, heavy ions with charge as high as 39+ have been injected directly into cyclotrons at intensities of a few hundred nanoampheres, as well as nearly fully-stripped light ions at intensities of a few hundred microampheres for cyclotron or synchrotron injection. These are not ion beam intensities normally considered to be space charge dominated. However, experimentally it is observed that both extremes– highly charged ions at low intensities and low charge ions at high intensities, exhibit sharp non-linear emittance growth in beam transport systems. In extreme cases, the overall beam transmission has actually been observed to decrease sharply with increasing beam intensity[1]. A correct interpretation of this emittance growth, as being a direct consequence of a non-linear growth in the beam envelope due to space charge forces, will be demonstrated using theory, simulations and experimental measurements. For proper matching of ECR ion source beams to accelerators, an aberration-free maximum beam intensity must be built into the beam transport system.

1. RTECR EMITTANCE MEASUREMENTS

Emittance measurements on the RTECR at NSCL can be made in either transverse coordinate before or after the analysis magnet. We have made 2D 'pepper pot' emittance measurements at each location, but we find a 'wire scanner' measurement at a single M/Q, after analysis in the dispersion plane of the dipole, to be most useful. Such an emittance measurement for Argon 10+ ions is shown in Fig. 1. This measurement shows an emittance with a central core and a high divergence tail. Similar measurements have been made on other ECR ion sources[2,3] . The 90% emittance is $245 mm \cdot mrad$, but there is an equal emittance in the 10% intensity tail. The 90% and 100% intensity emittances for Argon 2+ through 10+ ions are shown in Fig. 2. The emittance increases with Q, while the intensity decreases with Q. In each case, fully 1/2 of the emittance is in the 10% intensity tail. (To make such large emittance measurements, the analysis slits have been fully opened.)

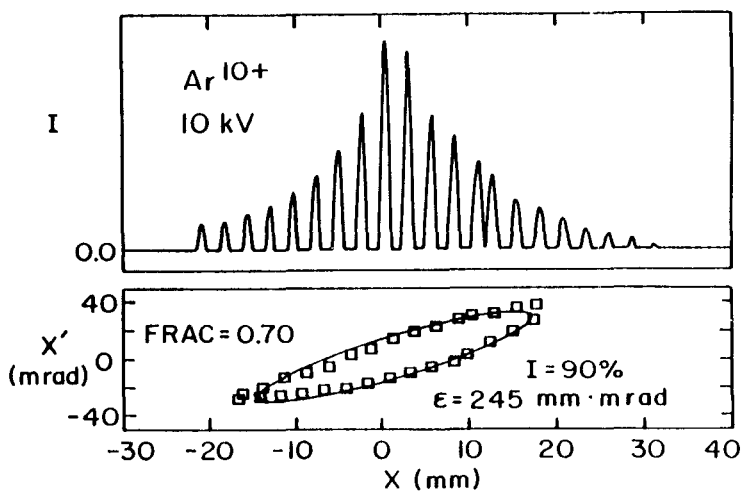


Fig. 1. The emittance of Argon 10+ ions. The 90% current level includes only about one half of the total emittance.

2. THEORETICAL ANALYSIS

Heretofore, ECR ion source beam emittance measurements like those in Fig. 2. have resisted explanation. The first question then is, how large

should the emittance from an ECR ion source be?

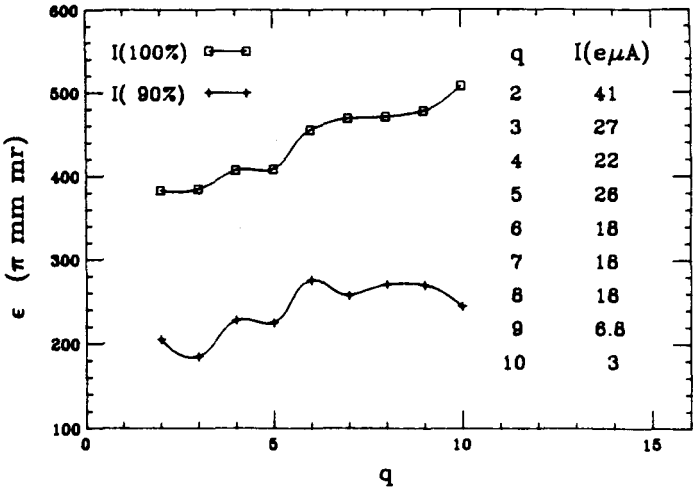


Fig. 2. Both 90% and 100% current level emittances are shown for Argon 2+ through 10+ ions extracted from the RTECR ion source.

In ECR sources, ions are extracted from the approximate maximum of the exit magnetic mirror, in a circular aperture of radius a. ECR ion sources have 3D minimum B magnetic structures[4], and in the RTECR, this is obtained through the superposition of a 30cm bore $SmCo_5$ hexapole with a warm bore tandem magnetic mirror[5]. Since a=0.8cm for the RTECR, $\vec{A} = A_\phi(r,z)\hat{\phi}$ is valid within the radius of the extraction aperture, the hexapole notwithstanding.

To estimate the emittance analytically, one assumes that the electrostatic potential has azimuthal symmetry, including both the extraction fields and the beam space charge, and that in the LEBT, the positive dc beam intensity neutralizes. One can show that the maximum emittance is determined by ions starting at the maximum starting radius r=a. Further, taking $K_Q \ll QV_{ex}$, and introducing a thermodynamic temperature T_Q, we may write the transverse emittance as

$$\epsilon = \epsilon_{xx'} = \epsilon_{yy'} = a[(\frac{T_Q}{2QV_ex})^{1/2} + A_\phi(a,o)\left(\frac{Q}{2MV_{ex}}\right)^{1/2}] \quad (1)$$

There are two limiting cases:

$$\text{Hot Ions} \qquad \epsilon \simeq a\left(\frac{T_\phi}{2QV_{ex}}\right)^{1/2} \quad (2)$$

$$\text{Cold Ions} \qquad \epsilon \simeq a^2 Q B_z(a,o)\left(\frac{Q}{2MV_{ex}}\right)^{1/2} \quad (3)$$

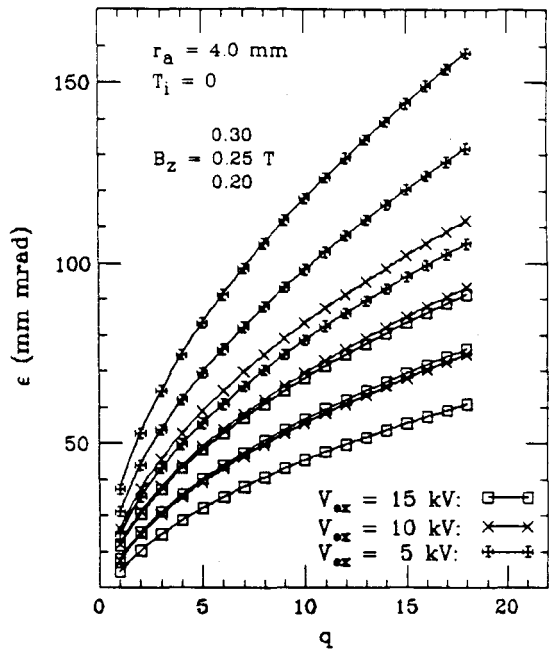


Fig. 3. Theoretical emittances of argon ions extracted from the RTECR, in the cold ion limit, for various extraction voltages and magnetic fields.

The measured thermal energy of ions extracted from the RTECR is about $6eV \times Q$ [6], and hence high ion energies are not sufficient to explain the large measured emittances, so we cannot take the hot ion limit of Eq. 2.

Figure 3 shows the magnetic field and extraction voltage dependence of argon ion beam emittance for $T_i = 0$, the limit of Eq. 3. At 10 kV, and $B_z(a,o) = 0.25T$, the predicted emittance is$70mm \cdot mrad$ for Ar^{10+}. The experimental numbers (from Fig. 2) are, in comparison $245mm \cdot mrad$ for the core, and $500mm \cdot mrad$ when including the tail, about seven times larger!

3. EXTRACTION SIMULATIONS

The acceptance of the RTECR beam transport system is $200mm \cdot mrad$ in both transverse planes [7], but the measured emittances exceed this design acceptance. Therefore, aberrations may be causing an emittance growth —but what is driving the

aberrations?

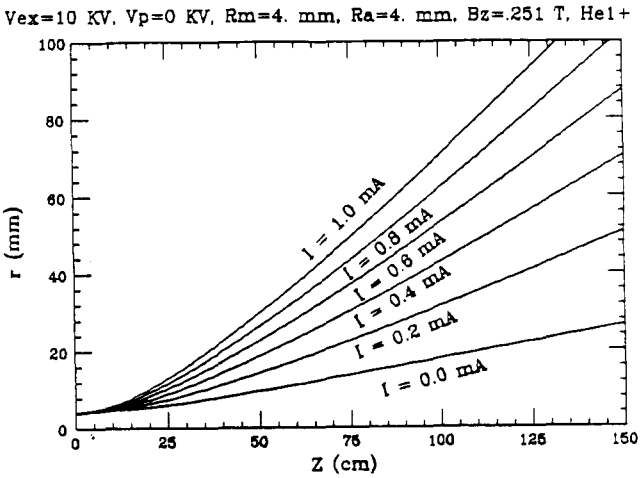


Fig. 4. As the maximum divergence increases with drift distance z, the beam envelope radius must increase with z^2. This is a significant effect, even for short drift distances, for high space charge beams.

Beam simulations with BEAM3D [8] do explain the measured emittances if we assume that there is zero neutralization of the extracted beam, as we will demonstrate. It is useful first to review how this is possible. When we view the dc beam as an ensemble of ions, then the total radial space charge force is a summation over all particles. It can be shown that the transverse divergence $\alpha_\perp$ for an ion on the edge of a drifting azimuthally symmetric beam is

$$\alpha_\perp = \left[\frac{P_\phi^2}{M^2 v_z^2 r_M^2} + \frac{Q}{\pi M \epsilon_o v_z^2} \ln\left(\frac{r}{r_m}\right) \sum\left(\frac{I_i}{v_{zi}}\right)\right]^{1/2} \quad (4)$$

Eq. 4 shows that the beam surface will have a constant maximum transverse divergence if the space charge force is zero, that is $\sum(I_i/v_{zi}) = 0$. This is of course the normal assumption in the LEBT design for ECR sources. However, with space charge, the maximum beam divergence has a strong dependence on the beam intensity. To determine the beam radius dependence on drift distance, we integrate Eq. 4 once with respect to r, and find that

$$\int_{r_m}^{r} \left[\frac{P_\phi^2}{M^2}\left(\frac{1}{r_m^2} - \frac{1}{r^2}\right) + \frac{Q}{\pi M \epsilon_o} \ln\left(\frac{I_i}{v_{zi}}\right)\right]^{-1/2} dr = t \quad (5)$$

There exists no analytical solution for the left side of Eq. 5, but numerical integration techniques can be used to estimate the integral. Let $r = r_m + x$ and assume that x is small (i.e., a short drift distance). We have, after performing the integration

$$r - r_m = \frac{1}{4}\left[\frac{2P_\phi^2}{M^2 r_m^3} + \frac{Q}{\pi M \epsilon_o r_m} \sum\left(\frac{I_i}{v_{zi}}\right)\right] \frac{z^2}{v_z^2} \quad (6)$$

Figure 4 shows the growth of a He^+ ion beam envelope for various intensities. In a 1 meter drift, there is a 4-fold increase in beam radius for a 1 emA He^+ beam over a beam with zero net space charge. The consequence of this non-linear radial space charge induced growth is that the beam expands faster than would be the case assuming a constant maximum divergence.

4. SPACE CHARGE AND HELIUM 1+ TRANSIT OF THE FIRST FOCUSSING SOLENOID

To study the radial space charge question, we simulated the beam formation process in the RTECR with BEAM3D, through the transit of the first focussing solenoid, up to the entrance of the analysis dipole. To study the extraction from the RTECR, we use He^+ beams of various intensities.

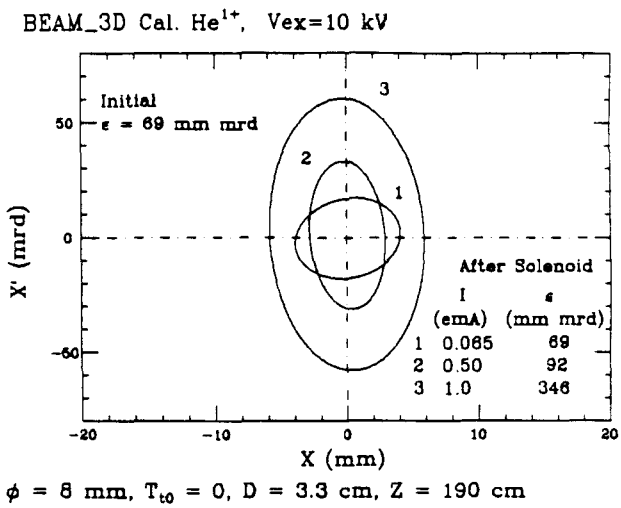


Fig. 5. The effective emittance of He^{1+} after crossing the focussing solenoid for various beam intensities. In each case, the extraction is space charge limited, the beam energy is of 10keV, and the emittance after extraction is $69mm \cdot mrad$.

We have found that it is possible to tune this ion source to produce He^+ beams over a wide range of

intensities (0.01–1.5 emA), without producing significant He^{2+} intensities, which would complicate the analysis. Helium is the only species for which it is possible to produce an approximately mono-charged total extracted current in the RTECR.

Figure 5 shows the BEAM3D estimate of emittance growth due to space charge for He^{+} beams when crossing the focussing solenoid. This emittance growth is the result of spherical aberration due to the space charge growth of the beam envelope before entering the solenoid. As is seen, no emittance growth is observed at $65e\mu A$ intensity, while at 1emA, the emittance growth is nearly 6-fold. Hence, theoretically, the radial space charge force could cause a large emittance growth due to aberrations in the transit of the focussing solenoid, but does that happen?

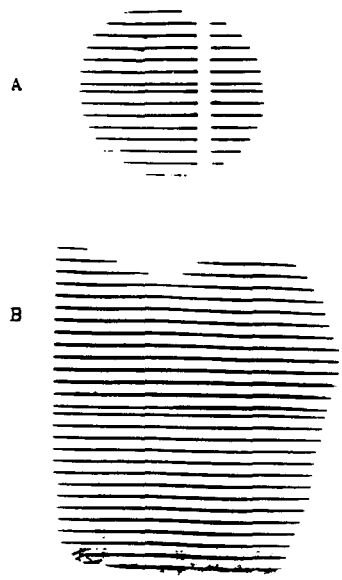


Fig. 6. A and B are Kapton foil burns after the RTECR focussing solenoid with He^{+} beams of 65 and 550 $e\mu A$ respectively.

Figure 6 shows actual kapton foil burns for $65e\mu A$ and $550e\mu A$ He^{+} beams after transit of the solenoid. The $65e\mu A$ He^{+} shows a round image of the RTECR extraction aperture, while the $550e\mu A$ beam completely fills the $10cm \times 10cm$ kapton foil, in good agreement with the prediction of Fig. 7. Further, the emittance of the $65e\mu A$ He^{+} beam of Fig. 6 can be extracted, and is measured to be is $69mm \cdot mrad$, in exact agreement with the calculated starting emittance of Fig. 5. Such an emittance corresponds to the cold ion limit given in Eq. 3. The emittance of the $550e\mu A$ beam cannot be obtained from Fig. 6, since the left boundary of the beam cannot be determined, but is greater than $250mm \cdot mrad$.

5. SUMMARY AND CONCLUSIONS

The main point here is that dc beams extracted from ECR ion sources, like the RTECR, do not neutralize. Then the beam envelope growth will depend quadratically on the product of the drift distance z and the total intensity in the LEBT: $\Delta r \propto I\Delta z^2$. All LEBT designs for ECR ion sources assumed $\Delta r \propto \alpha\Delta z$, where α is the starting transverse divergence. Hence all focussing magnets are too far 'downstream'. The beam envelopes are then larger than anticipated, filling magnet apertures, exciting aberrations, and diluting the phase space and LEBT transmission. To correct this effect, proper LEBT requires 'designing in' the desired maximum beam current to be transported, which essentially means increasing the focussing.

This paper began with a measurement of Ar^{10+} emittance that had a central core and a high divergence tail. We can now say that the starting emittance is dominated by the fact that the ions are extracted from a magnetic field. However, the measured emittance (after analysis) is dominated by second order aberrations during the transverse of the analysis dipole—again due to space charge blow up of the beam, as we will demonstrate in a future paper.

6. REFERENCES

1) Baron, E., Cyclotron '86, Tokyo, Ionics., (1986) p. 234.
2) Clark, D., Int. Conf. ECR ion sources, (MSU, East Lansing, Michigan, 1987), p. 433.
3) Hagedoorn, H., Int. Conf. ECR Ion Sources, (MSU East Lansing, Michigan, 1987), p. 389.
4) Geller, R., 8th Int. Conf. on Cyclotrons, (Bloomington Indiana, 1978), p. 2120.
5) Antaya, T., 7th Workshop on ECR Ion Sources, (Julich Germany, 1986), p. 72.
6) Antaya, T., Proc. Int. Conf. ECRs, (Grenoble, France, 1988), p. 707.
7) Harwood, L.H., Cyclotron '86, Tokyo, Ionics., (1986) p. 488.
8) Xie, Z.Q., MSUCP-60, (1989).

NUMERICAL STUDIES FOR SUPPRESSION OF VERTICAL OSCILLATIONS IN THE K1200 CYCLOTRON

K. Joh, F. Marti, and J.A. Nolen
NSCL, Michigan State University, East Lansing, MI 48824-1321, U.S.A.

ABSTRACT

Calculations using vertical electric deflectors to eliminate the coherent vertical oscillations in the K1200 cyclotron are presented. A central region code is used to track individual particles through 3-dimensional electric fields of deflecting plates. The results are promising, indicating that this method could be used if simpler methods of reducing the vertical oscillations are unsuccessful.

1. INTRODUCTION

A new internal beam probe[1] in the K1200 cyclotron based on CCD TV camera is yielding information about the internal beam structure and dynamics in much greater detail than previously available.

Initial results show that the intrinsic beam height in the cyclotron is about 1 mm, but its effective size is dominated by vertical oscillation with a peak-to-peak amplitude of typically 4 mm. This oscillation increases the transverse beam emittance of the extracted beam in the axial direction.

Some experimental studies of correcting the oscillations have been done by moving the spiral inflector vertically and/or unbalancing trim coil 0. Preliminary measurements with trim coil 0 were promising, but it is not clear if this method will work for all beams. This simple method will be pursued further. The present paper presents an alternative technique.

Calculations have been carried out to show if some small electrostatic vertical deflection plates are added to the central region the vertical oscillations could be tuned. For these calculations the NSCL central region code CYCLONE[2] has been modified to include 3-dimensional electric fields of deflecting plates calculated with the code RELAX3D.[3]

2. SIMPLIFIED THEORY

The underlying idea to eliminate the coherent vertical oscillations is to use two electrostatic deflectors on successive hills near the central region. The 1st electric deflector applies an impulse to make the central ray in a beam pass through the magnetic median plane in the 2nd electric deflector. Then the 2nd deflector applies another impulse to keep the ray on the median plane. As a result the coherent oscillation of the beam would disappear if the phase space distribution is symmetric about the central ray in $z - p_z$ space. While in some cases one deflector is enough, two are needed to make the method general.

The impulse by a static electric field E_z to a particle of electric charge q, mass m, and orbital frequency ω is

$$\Delta p_z = \int \frac{qE_z}{\omega} d\theta \,, \tag{1}$$

where

$$\omega = \frac{d\theta}{dt} \,. \tag{2}$$

We define associated length units $\tilde{p}$ and a as

$$\tilde{p} \equiv \frac{p}{m\omega} \tag{3}$$

$$a \equiv \frac{c}{\omega} \,, \tag{4}$$

where c is the velocity of light.

If the electric field and orbital angular frequency are constant, the impulse to the particle of charge q and atomic mass A is given in the cyclotron units by:

$$\Delta \tilde{p}_z \;\propto\; \frac{q}{A} a^2 E_z \Delta\theta \,. \tag{5}$$

The vertical motion over a small radial range can be approximated by

$$z = z_0 \cos(\nu\theta + \varphi) \tag{6}$$

$$\tilde{p} = -z_0 \nu \sin(\nu\theta + \varphi) \,, \tag{7}$$

where ν is the vertical tune and φ is initial phase. z_0 and ν are not constant in general but are nearly so for a range of several turns.

If we assume that the electric fields are localized in the centers of the two electric deflectors positioned at θ_1

and θ_2 respectively, then we can consider the impulse by the electric field as a momentum kick.

Now position and momentum in the 1st electric deflector are given by:

$$z_1(\theta_1) = z_{10}\cos(\nu\theta_1+\varphi) \quad (8)$$
$$\tilde{p}_1(\theta_1) = -z_{10}\nu\sin(\nu\theta_1+\varphi)+\Delta\tilde{p}_1\ , \quad (9)$$

where $\Delta\tilde{p}_1$ is the momentum kick by the 1st electric field.

Or with a redefined phase φ_1 and amplitude z^*_{10}:

$$z^*_1(\theta_1) = z^*_{10}\cos(\nu\theta_1+\varphi_1) \quad (10)$$
$$\tilde{p}^*_1(\theta_1) = -z^*_{10}\nu\sin(\nu\theta_1+\varphi_1)\ . \quad (11)$$

And position and momentum in the 2nd electric deflector are given by:

$$z_2(\theta_2) = z_{20}\cos(\nu\theta_2+\varphi_1) \quad (12)$$
$$\tilde{p}_2(\theta_2) = -z_{20}\nu\sin(\nu\theta_2+\varphi_1)+\Delta\tilde{p}_2\ , \quad (13)$$

where $\Delta\tilde{p}_2$ is the momentum kick by the 2nd electric field. (Note that z_{20} is equal to z^*_{10})

And with another redefined phase φ_2 and amplitude z^*_{20}:

$$z^*_2(\theta_2) = z^*_{20}\cos(\nu\theta_2+\varphi_2) \quad (14)$$
$$\tilde{p}^*_2(\theta_2) = -z^*_{20}\nu\sin(\nu\theta_2+\varphi_2)\ . \quad (15)$$

Since $\tilde{p}^*_1=\tilde{p}_1$ and $z^*_1=z_1$ at θ_1, $\frac{\tilde{p}^*_1(\theta_1)}{z^*_1(\theta_1)} = \frac{\tilde{p}_1(\theta_1)}{z_1(\theta_1)}$ gives

$$-\nu\tan(\nu\theta_1+\varphi_1) = \frac{-z_{10}\nu\sin(\nu\theta_1+\varphi)+\Delta\tilde{p}_1}{z_{10}\cos(\nu\theta_1+\varphi)}\ . \quad (16)$$

If the ray passes through the magnetic median plane in the 2nd electric deflector i.e. $z_2(\theta_2)=0$, so it follows that from eq. 12 that

$$\nu\theta_2+\varphi_1 = (n+\frac{1}{2})\pi\ \cdots\ , \quad (17)$$

where $n = 0, 1, 2, \cdots$

Therefore, the required momentum kick in the 1st electric deflector to make the ray pass through the magnetic median plane in the 2nd electric deflector can be found from eq. 16 and eq. 17:

$$\Delta\tilde{p}_1 = \nu z_{10}\{\sin(\nu\theta_1+\varphi)-\cos(\nu\theta_1+\varphi)\cot(\nu(\theta_2-\theta_1))\}\ . \quad (18)$$

3. DESIGN CONSIDERATIONS

Eq. 18 has absolute values of minima(zeros) at $(\nu\theta_1+\varphi)+(\nu(\theta_2-\theta_1)) = \frac{1}{2}\pi, \frac{3}{2}\pi, \frac{5}{2}\pi, \cdots$. But in general the above conditions can not be satisfied since the locations of deflectors are not movable and tunes are also not fixed values for all beams. And from the characteristic of $\cot(\nu(\theta_1-\theta_2))$ the points of $\nu(\theta_2-\theta_1) = \pi, 2\pi, 3\pi, \cdots$ should be avoided. Therefore, it would be reasonable and safe to minimize only the second term of eq. 18 to include all beams of various tunes.

Then the appropriate positions of two deflectors would exist around

$$\nu(\theta_2-\theta_1) = \frac{1}{2}\pi, \frac{3}{2}\pi, \frac{5}{2}\pi, \cdots\ . \quad (19)$$

Let Δn be the difference of turns at two deflectors. For example $\Delta n = 1$ if $\theta_2 = \theta_1 + 2\pi$. Then we have

$$(\theta_2-\theta_1) = 2\pi\Delta n\ . \quad (20)$$

From eqs.(19)-(20), the relative positions of two deflectors can be rewritten

$$\Delta n = \frac{(m+\frac{1}{2})\pi}{2\nu}\ , \quad (21)$$

where $m = 0, 1, 2, \cdots$

Since the locations of two deflectors are not movable, the values of tunes of various beams between them are important. Figure 2 shows the curve of tunes and relative positions of deflectors. If we go too far from the central region, the tune becomes larger and the gap between turns becomes smaller. Therefore, it might not be easy to find an appropriate solution, if the electric fields of the deflectors are not well confined to include just a few turns.

For example, in the K1200 cyclotron the vertical tunes of most of beams are $0.1 \le \nu \le 0.14$ near the central region(about $2.5 \sim 5$ inches in radius from the center). So the oscillations of all beams could be suppressed with relatively well optimized conditions for $\Delta n \approx 2$ from Fig. 2.

Now let's consider the required magnitude of electric fields for the deflectors. If the relative positions of two deflectors are relatively well optimized, then from eq. 18 we have

$$\Delta\tilde{p}_1 \approx \nu z_0\sin(\nu\theta_1+\varphi)\ . \quad (22)$$

Therefore the required momentum kicks in both deflectors are proportional to the tune and the amplitude z_0 of z motion. For a given beam the angular frequency ω is constant, and $z_0^2\nu \approx$ constant the required electric fields for two deflectors are from eq. 5 in the nonrelativistic limit:

$$E_1,\ E_2 \propto \frac{(T/A)}{(q/A)\Delta\theta}\sqrt{\nu}\ , \quad (23)$$

where (T/A) is the final kinetic energy per nucleon of a beam.

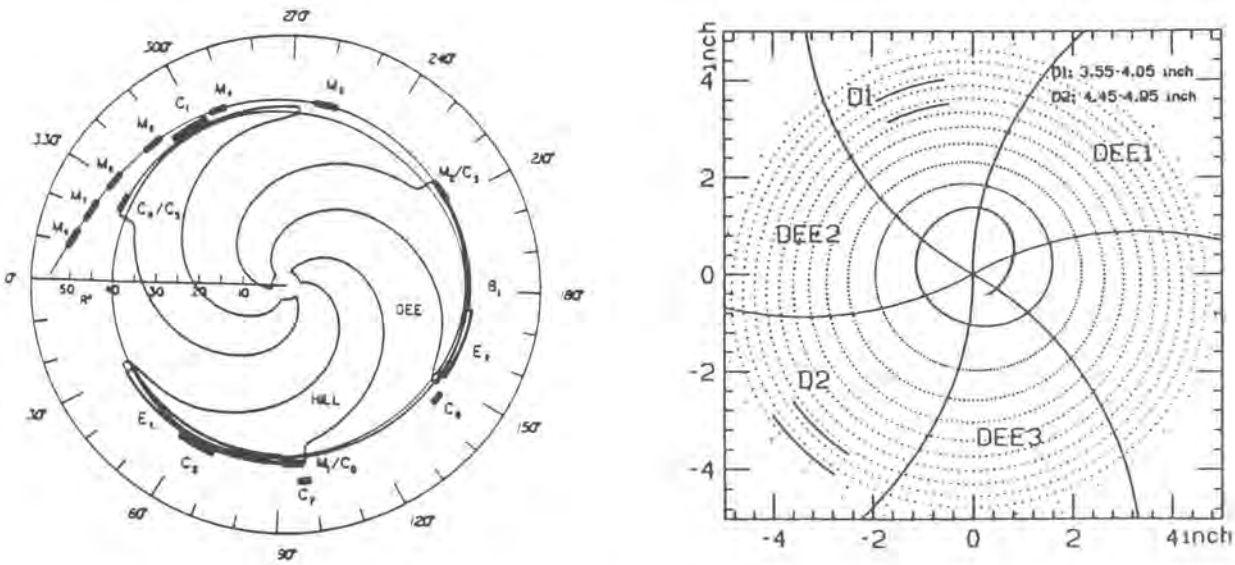


Fig. 1. Section view of the median plane of the K1200 cyclotron(left) and the enlarged top view of central region(right). The spiral dotted line shows a particle trajectory and D1, D2 are the electric deflectors locations.

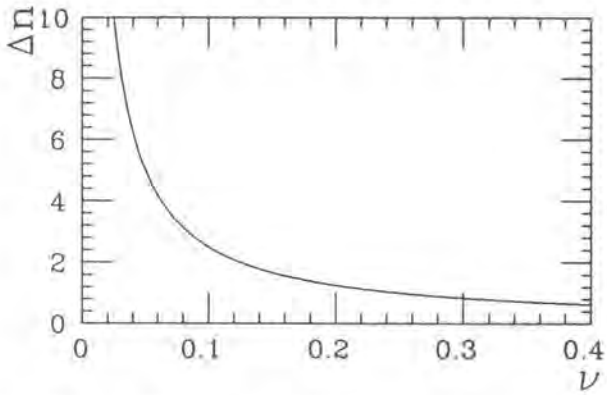


Fig. 2. The relative turns between two electric deflectors vs. the vertical tune with relatively well optimized conditions in eq. 21.

4. COMPUTER SIMULATION

The code RELAX3D[3] is a FORTRAN program to solve the three dimensional Helmholtz-Laplace equation. RELAX3D was used to calculate the 3-dimensional electric field distribution of a realistic electric deflector. The deflector has a sector shape with an angular width of 20 degrees, plate thickness of 0.225 inch, and a radial width of 1.5 inches. Edges of the deflector are rounded to reduce peak electric fields. (see Figure 3) The gap between the electric plates of the deflectors was taken to be 0.6 inch.

The raytracing was done with the NSCL central region code CYCLONE modified to include additional electric fields of two electric deflectors calculated from RELAX3D. One electric deflector was put on the hill between the 1st and 2nd dees at the radius of 3.80 inches from the center of the K1200 to the center of the deflector, while the other was put between the 2nd and 3rd dees at the radius of 4.70 inches.(see Figure 1)

The initial phase space for the beam in the vertical direction(see Figure 4) was guessed from the TV beam probe[1] data mentioned above. Figure 5 shows individual particle trajectories of nine rays with different initial phase space coordinates for $^4He^{1+}$ of 40 MeV/u. The coherent vertical oscillation(upper) was eliminated almost completely after passing the 2nd deflector(lower) to reduce the effective size of a beam by about two times. The required deflector voltages were -0.55 kV and -0.70 kV for the 1st and the 2nd deflectors, respectively.

5. DISCUSSION

The electric deflector method to eliminate undesirable coherent vertical oscillations is promising in these calculations. Alternative methods of correcting the oscillations, such as moving the spiral inflector vertically, with or without unbalancing trim coil 0, would not require new hardware, but needs further investigation to determine their range of usefulness in the K1200 cyclotron.

Research supported by the US National Science Foundation.

6. REFERENCES

1) F. Marti et al. A CCD Camera Probe for a Superconducting Cyclotron. In Proc. of the 1991 Particle Accelerator Conference, San Francisco, pp. 1163-1165.

2) M.M. Gordon, S. Motzny, and J. Bishop, Revised Cyclone Program for Central Region Orbit Calculations, MSU Annual Report 1977-78.
F. Marti, M.M. Gordon et al., Design Calculations for the Central Region of the NSCL 500 MeV Superconducting Cyclotron, In Proceedings of the Ninth Int. Conf. on Cyclotrons, Caen (France), 1981, pp. 465-468.

3) H. Houtman, C.J. Kost, A Fortran Program(RELAX-3D) to solve the 3-Dimensional Poisson(Laplace) Equation, In Proceedings of Computing in Accelerator Design and Operation, Berlin 1983, pp. 98-109.

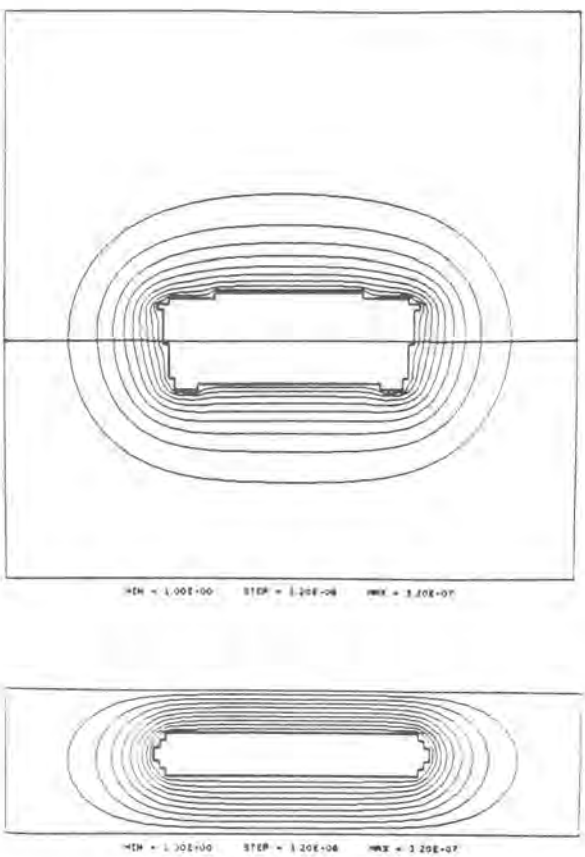


Fig. 3. A RELAX3D field calculation of a deflector plate showing equipotential lines both for top view(upper) and for cross sectional view(lower). The top solid line in the sectional view(lower) is the copper hill cover and the bottom solid line is the magnetic median plane.

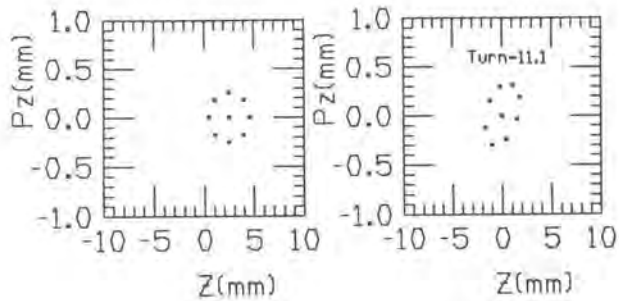


Fig. 4. Phase space coordinates of 9 rays at the beginning (left) and at turn=11.1 after passing the 2nd electric deflector(D2). The central ray has moved to the origin.

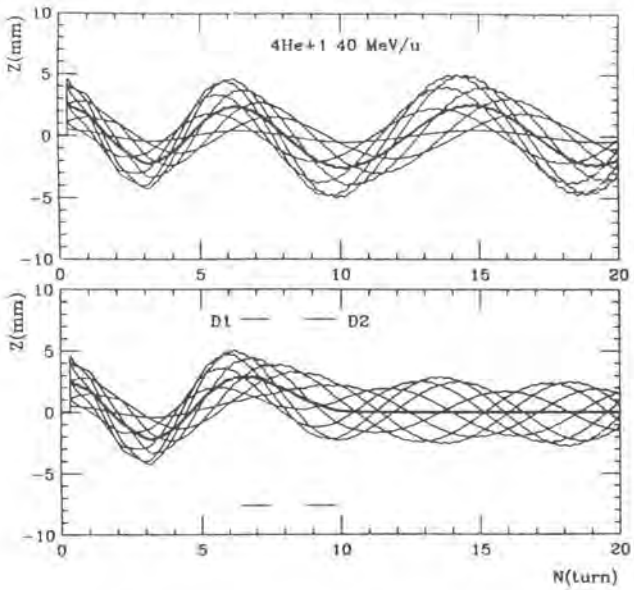


Fig. 5. Individual particle trajectories with different initial conditions as a function of turn number. A coherent vertical motion is simulated in the upper part. The lower part illustrates the calculated effect of the two vertical deflection plates. Also note that the central ray(the thick solid line) is on the median plane after passing the 2nd plate.

EXPERIMENTS ON THE AXIAL INJECTION SYSTEM OF THE CYCLOTRON U-120M

Z. Trejbal, M. Křivánek, J. Kučera, V. Bejšovec, J. Štursa
Nuclear Physics Institute, Czechoslovak Academy of Sciences
250 68 Řež, Czechoslovakia

ABSTRACT

The basic parameters of the axial injection system of the isochronous cyclotron U-120M were tested using an ion beam of low emittance and intensity as well. The transmission of the 17keV deuteron beam including the capture into acceleration reached 40% while the transmission of the 19keV proton beam was only 12%. Several measured characteristics are presented and the connection with different injector efficiency is discussed.

1. INTRODUCTION

The isochronous cyclotron U-120M has been working in the Nuclear Physics Institute in Řež near Prague since 1977. It accelerates ions in the range of the mass to charge ratio A/Z =1–2.8 up to the maximal energy given by K=40. The physical and biological measurements are carried out there. About 30% of the operational time is scheduled for irradiation of the targets for the production of isotopes. The axial injection system[1)] installed on cyclotron in January 1992 will extend the cyclotron's experimental possibilities to the range of heavier ions, polarised ions and ions H^-, D^-.

The measurements were done in two different regimes: the first one for deuterons with maximal attainable energy 20MeV (regime D), that is very close to the regime for the acceleration of heavy ions and the second one for the protons of energy 25MeV (regime P). The main parameters of the accelerated ion beams of these two regimes are given in the table 1. The resulting coeficient of the transmission is 3.3 times higher in the regime D than in the regime P and it can be easily reproduced.

2. DESCRIPTION OF THE INJECTOR

The arrangement of the described injector[1)] is given on Fig. 1. Its basic components are: (1) - radio-frequency ion source with low emittance (normalized emittance 0.29 π mm·mrad), (2) - 5-gap acceleration structure supplemented by an einzel lens, (3) - 2000 l/s diffusion pump, (4) - the first correction magnet that compensates a stray magnetic field produced by the cyclotron, (5),(10) - diagnostic units consisting of Faraday cup, exchangeable collimation diaphragm of a circular shape and illuminated shade, (6) - double focusing bending magnet ($\alpha = 90^o$, $\beta = 26.5^o$), (7) - the two-gap first harmonic buncher, (8) - the second correction magnet with an adjustable orientation around the vertical axis, (9),(12) - the first and second water-cooled magnetic focusing B-channels, (13) - spiral inflector (Belmont-Pabot type) with an 8 mm gap between electrodes.

Table 1. Parameters of the accelerated deuterons (D) and protons (P).

ACCELERATED PARTICLES	D	P
energy of injection, keV	17	19
energy after acceleration, MeV	20	25
magnetic field in the cyclotron center, T	1.82	1.36
beam current measured between two B-channels, μA	6	22
beam current measured on the inflector, %	90	80
buncher switched off:		
accelerated beam current (R=100mm), %	36	6.8
accelerated beam current (R=150mm), %	19	5.2
accelerated beam current (R=500mm), %	10	2.8
buncher switched on:		
accelerated beam current (R=500mm), %	40	12
acceptance without inflection, mm·mrad	459π	398π
acceptance with acceleration, mm·mrad	$< 126\pi$	$< 65\pi$

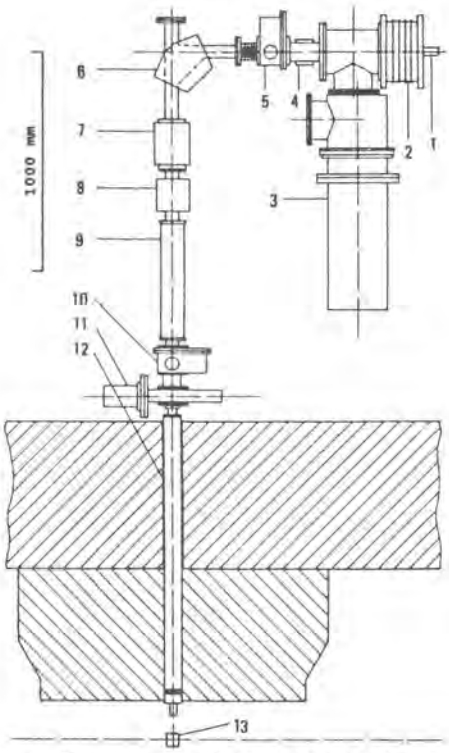


Fig. 1. Components of the axial injection system

3. EXPERIMENTAL RESULTS

3.1. Measuring of the acceptance

The acceptance of the system was measured by means of two equally oriented dipole magnets (6), (8) located in different distances before the entrance of the first B-channel (9). The point of the x-x'transverse phase-space plane which represents the center of the injected beam can be displaced in this plane in a wide interval employing these magnets. The characteristics of the injected beam current i_0 on the current I_c of the second correction magnet (8) were measured for different currents I_b of the bending magnet (6), see fig. 2.

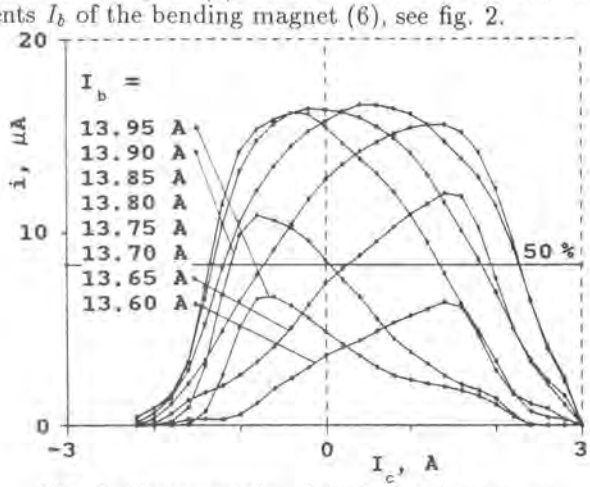


Fig. 2. Characteristics of the injected beam current i_0 on the current I_c for different currents I_b.

The acceptance of the injection line between the pair of the magnets and the place where the beam is measured was evaluated basing on these characteristics. We can see flat parts of the highest curves. They arise when the beam's emittance is fully placed inside the region of the acceptance. The points, where the measured current of the beam is 50% of the maximal current of the beam, correspond to the contour of the acceptance. For these measurements the beam current was measured on the bottom inflector electrode, negative voltage was connected to the upper inflector electrode. The measured acceptance demonstrate the focusing capability of the vertical line.

The acceptance of the whole system including capture and acceleration was considerably lower. In this case the flat parts are missing on the curves analogous to the curves on fig. 2. The measured characteristics represent rather the beam emittance. The acceptance is lower.

The acceptance figures for regimes D and P are shown on fig. 3. The larger areas represent the acceptance of the vertical line consisting of two magnetic B-channels together with an inlet diaphragm of the diameter of 7 mm. The smaller regions contain the acceptance of the whole system including acceleration. All graphs are calculated for the beam at the entrance of the first B-channel.

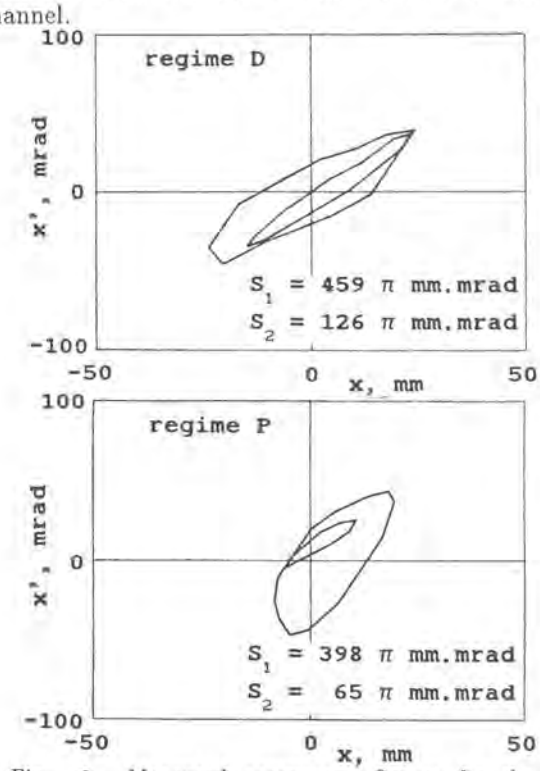


Fig. 3. Measured acceptance figures for the regimes D and P

3.2. Central region

The spiral inflector is the main element which determines setting-up parameters of the injector. The injection energy and optical elements of the whole injection

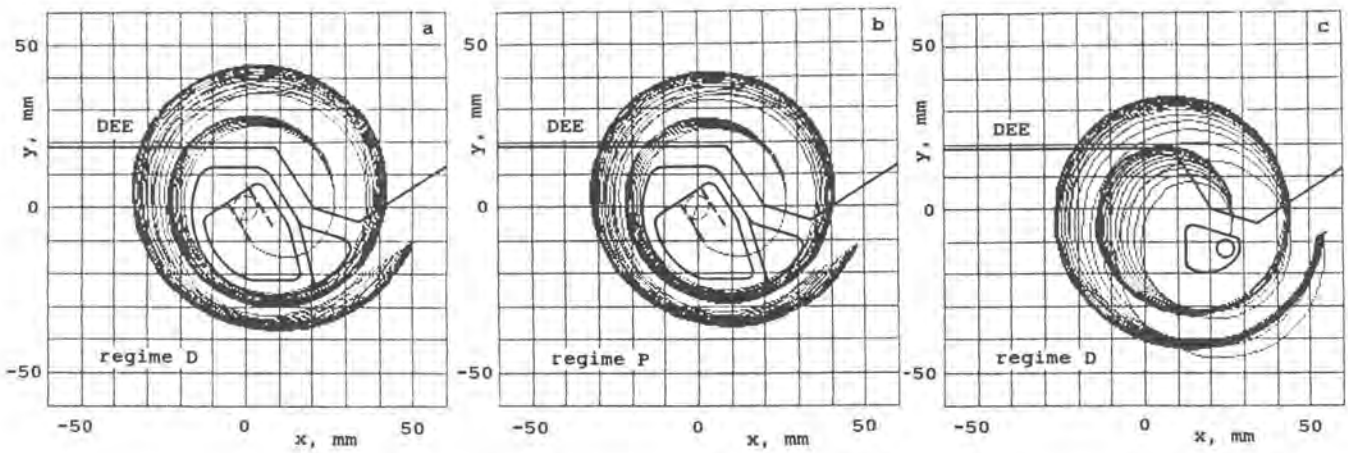


Fig. 4. Positions of the first beam orbits and the central regions in: a) regime D with inflector b) regime P with inflector c) regime D with inner ion source

line must be matched to its parameters. A supporting construction of our inflector had to enable us a simple replacement of the inflector with an inner radially mounted ion source without any additional constructional modifications. This is why the inflector was fixed to the supporting rods of the same construction like the rods of the inner radial ion source. The difference in positions of the beam orbits for the inner ion source and for the inflector is small. The amplitudes of betatron oscilations were reduced to the amplitude less than 2 mm in both regimes by a small correction of the current in the harmonic coils. Positions of the first uncentered beam orbits are shown on fig. 4. Three different figures are presented: a) injection of the deuterons (regime D) into the cyclotron by means of the inflector, b) injection of the protons (regime P) also with the inflector and c) extraction of the deuterons in regime D from the inner ion source. The ion trajectories were calculated for input h-f phases in the range from -45° to $+45^o$ (step 5°). The amplitude of the dee voltage was 34 kV.

One of the reasons for higher beam losses in regime P is the fact that a vertical emittance of the beam which exits from the inflector is not matched with a vertical acceptance of the cyclotron acceleration system.[2] This fact is obvious from the graph of the accelerated beam current i_{500} on the voltage U_{-inf} of the upper inflector electrode, see fig. 5. The displayed characteristics were measured by two methods: a) the beam current was tuned by the voltage U_{+inf} of the bottom spiral electrode and b) the voltage U_{+inf} was constant. The point marked by an arrow is the point in which the voltage of the spiral electrodes are the same but of the opposite sign. The flat parts of the curves would mean here, as well as in the measurements of the acceptance of the vertical channel, that the vertical cyclotron acceptance is bigger than the vertical beam emittance. These curves could be used for the determination of the vertical cyclotron acceptance. Because there are no flat parts, we suppose that there are enormous vertical losses of the beam on the first orbits.

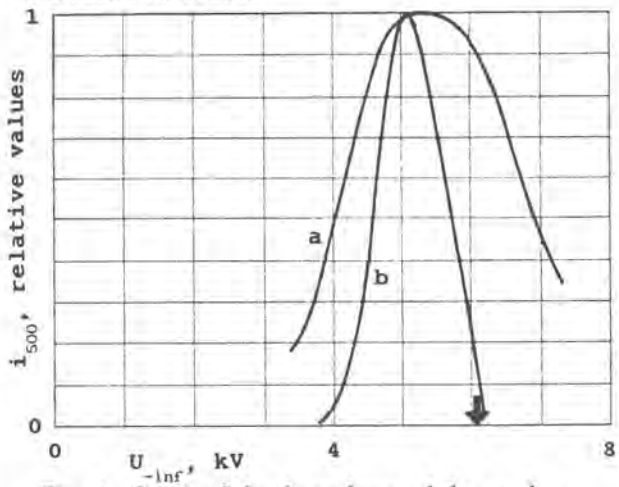


Fig. 5. Graph of the dependence of the accelerated beam current i_{500} on the voltage U_{-inf} for two cases: a) voltage U_{+inf} was tuned b) U_{+inf} was constant.

3.3. Beam in the magnetic B-channel

There are three elements used for focussing of the beam along the axis of the injection: the einzel lens placed in the acceleration structure behind the R-F ion source and the two magnetic B-channels placed in the vertical part. Magnetic B-channel is a classical solenoid supplemented by a system of cylindrical rings from ferromagnetic and nonmagnetic materials, alternately arranged in a row along the axis of injection. Maximum intensity of the transferred beam can be well reproduced. Characteristics of the accelerated beam current i_{500} on

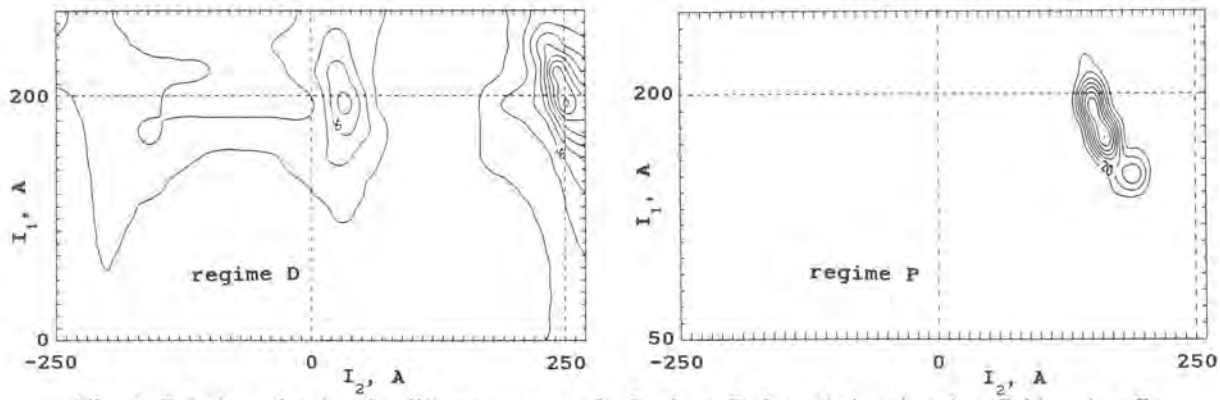


Fig. 6. Relative value i_{500} for different currents I_1, I_2 of two B-channels in: a) regime D b) regime P

currents I_1, I_2 in the first and second B-channels for D and P regimes are shown on fig. 6.

The resulting magnetic field of the second B-channel is a superposition of the monotonous component of the stray axial magnetic field in the central hole of the cyclotron yoke and the periodical axial magnetic field of the B-channel. In the regime D, when the magnet of the cyclotron is almost saturated, the monotonous component of the magnetic field in the second B-channel is much higher then in the regime P, see fig. 7.

Beam envelopes of the injected beam were calculated using the program TRANSPORT. These calculations were done for the transport of the particles from the interior of the inflector back to the entrance of the second B-channel, providing the beam is focussed at the center of the inflector. The envelopes differ in the number of wavelengths in the second B-channel, see fig. 8. The same character of the envelopes as in the more successful deuteron regime can be obtained in the proton regime only with current I_2, for which the coil of the second B-channel cannot be sufficiently cooled because of the small rate of water flow. Another possibility of improving the transmission for regime P is a vertical change of the position of the second B-channel. This change is

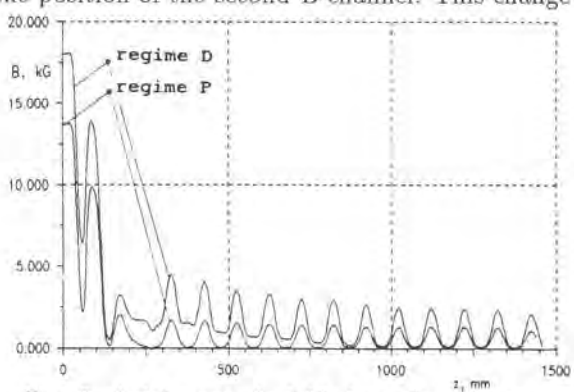


Fig. 7. Axial magnetic field along the axial hole of the second B-channel in: a) regime D (current of the cyclotron's magnet I_0=556A, current of the second B-channel I_2=250A b) regime P (I_0=279A, I_2=150A)

not possible without complex disassembly of the whole system.

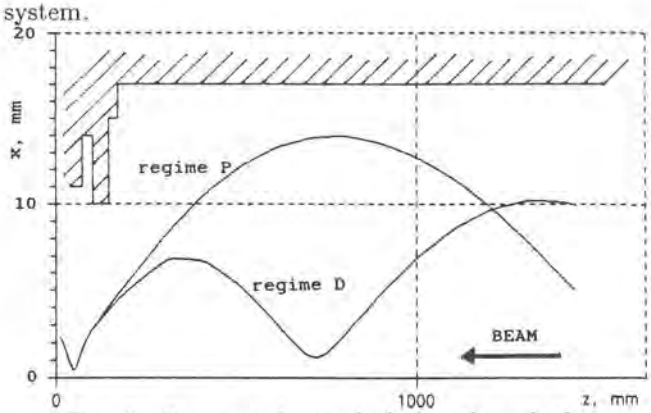


Fig. 8. Beam envelope calculation through the second B-channel in: a) regime D b) regime P

4. CONCLUSION

The basic parameter of the injector is a transmission efficiency of the injected beam from an outer ion source to the final cyclotron orbit. The transmission efficiency of our injector, measured for deuteron regime D with the beam of low intensity, gives a good chance to accelerate fully ionized particles, whereas the efficiency of the transmission in the regime P is approximately 3.3 times lower. The reason for the decrease of the transmission efficiency is bad matching of the beam emittance with the vertical acceptance of the accelerating system in the place of inflector. Installation of a correction quadrupole in front of the second magnetic B-channel would improve this situation. Another possibility is to change the position of the second B-channel with the respect to the strong magnetic lens created by the hole in iron plug at the entrance to vacuum chamber. The acceptance of the vertical line is sufficient.

5. REFERENCES

1) J. Štursa et al., The axial injection system of the isochronous cyclotron, Proc. Europ. Part. Accel. Conf., Berlin, Germany, 24-28 march, 1992
2) R. Baartman, Proc. Europ. Part. Accel. Conf., Rome, Italy, 7-11 June, pp.947-948.

THE NEW PHASE DETECTION SYSTEM OF THE COSY-INJECTOR

K. Kennepohl, M. Herschbach, D. Maeckelburg,
Zentrallabor für Elektronik,
W. Bräutigam,
Institut für Kernphysik,
Forschungszentrum Jülich GmbH (KFA), D-5170 Jülich, Germany.

ABSTRACT

For the Julic isochronous cyclotron JULIC a new beam phase detection system has been developed on the basis of the heterodyne principle using rf-signal mixing and filtering, rf-disturbance compensating techniques and 50Ω striplines, similar to the old phase measuring equipment (set to work in 1978). The new equipment detects and analyses the beam signals within a beam current range of 20nA to 50μA with satisfying accuracy. In addition to the old phase measuring system the new one is controlled by computer and able to determine the beam phase angle and beam intensity for continuous and pulsed beams (down to approx. 5msec beam on). Furthermore the new equipment includes a facility for calibrating the total beam phase detection system by a rf-signal decoupled from a dee. Testbench measurements, showing the linearity over the full dynamic range, as well as measurements with beam are presented.

1. INTRODUCTION

The cyclotron JULIC is undergoing extensive upgrading in order to serve as injector for the new Cooler synchrotron COSY-Jülich.[1)2)] Part of the upgrading is the installation of the new **PHASe Measuring Equipment** PHASME II. The upgrading of the existing PHASME I[3)] was necessary to get a much faster handling of the measured beam signals and especially to measure the phase in a pulsed beam mode needed for injection into the COSY-ring. The phase detection system should work over the full cyclotron frequency range from 20 to 30Mhz. The accuracy should be better than $\pm 1^0$ over the total dynamic range. In order to get an automatic noise voltage suppression a compensating unit is installed. The detection system is able to handle internal beam currents from 20nA to 50μA.

2. LAYOUT OF THE PHASE DETECTION SYSTEM

The beam signals are decoupled by 24 probes mounted above and below the medium plane of the cyclotron. The probes are 50Ω striplines where the upstream end is open. The length of each probe is 15cm, the width 15mm

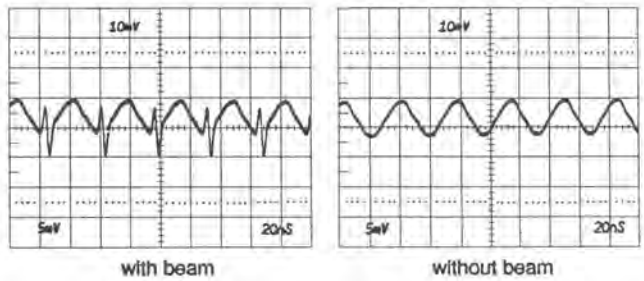


Fig. 1. measured signal of pickup pair 6

and the distance between the upper and lower probes is 20 mm.[3)] Together with the beam signals disturbing rf-voltages from the acceleration system are picked up. The noise comes from the accelerating rf-voltage, about 45 kV when JULIC is operated at maximum energy, resulting in a noise amplitude of about 10 mV at the pickup output. The disturbances can be much greater than the beam signals. As they are opposite in phase and almost equal in amplitude, the addition of the upper and lower probe sig-

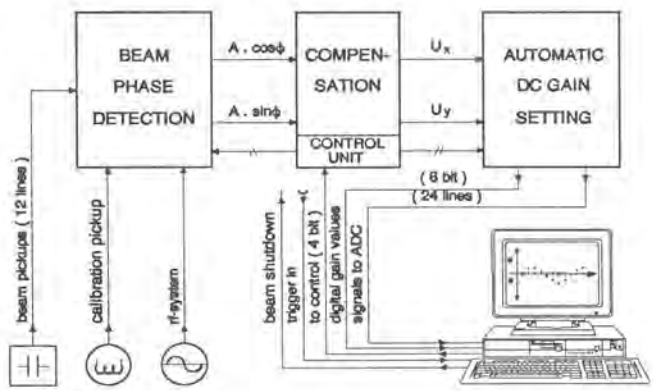


Fig. 2. schematic of PHASME II

nals is a first step to reduce these voltages. Since on the other hand the beam signals are equal in phase on the corresponding probes, their output is simultaneously doubled. Figure 1 shows the output voltage for one probe pair with and without beam.

Even if the beam signal to rf-disturbance ratio on the average is better for higher harmonics, we decided to work on the 2nd harmonic for the following reason: As

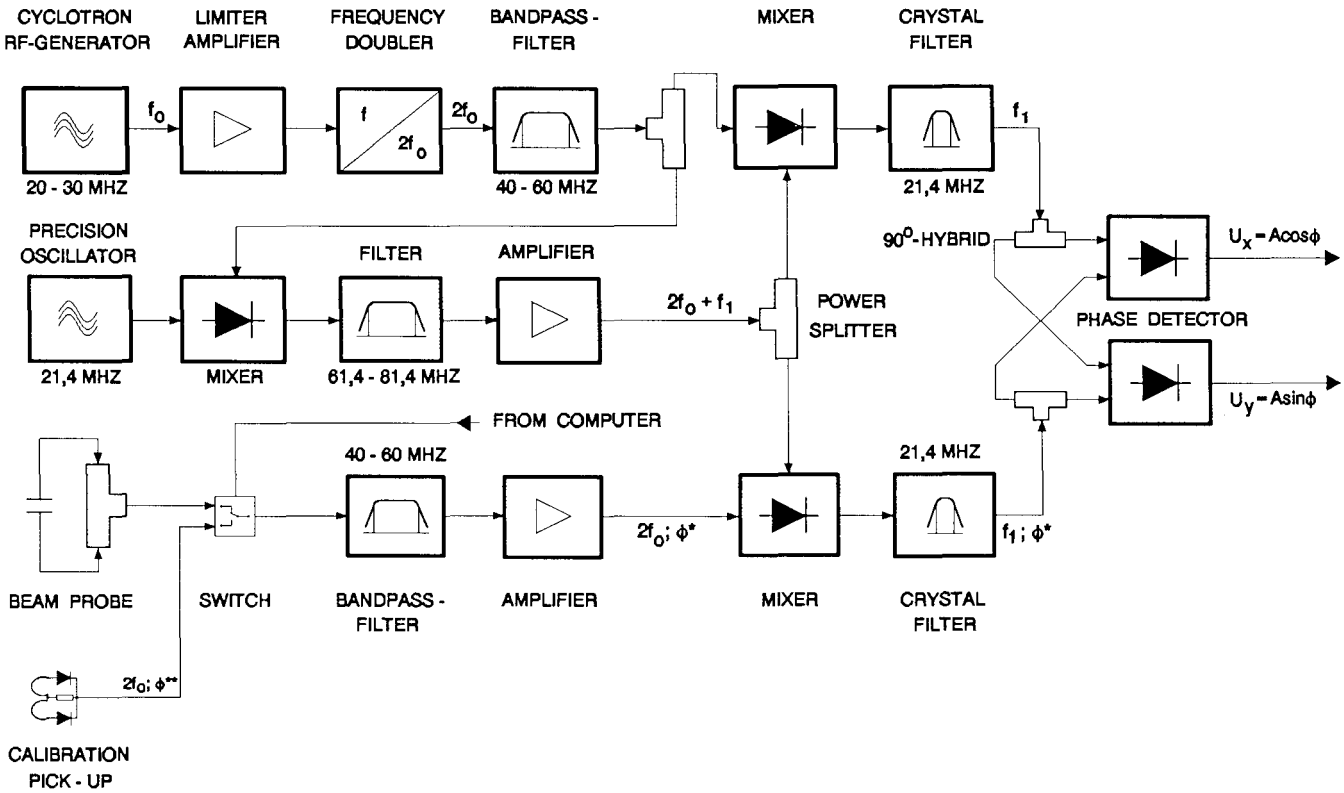


Fig. 3. blockdiagram of the rf-part

the measured phase angle of the beam is multiplied by the harmonic number, the possible range of $-90^0 < \varphi_{beam} > +90^0$ is converted to $-180^0 < \varphi > +180^0$ which can be detected directly without ambiguity.

Figure 2 shows a schematic of PHASME II. The major subsystems are the "beam phase detection", "the compensation" including the "control unit", the "automatic DC gain setting" as well as a PC. In order to get phase information along the cyclotron radius, 12 independent pickup pairs are used together with 12 parallel operating phase detection channels. After adequate amplification the 24 DC-signals - X-Y-components of 12 phase vectors - are fed to two ADC's in the PC. Likewise the corresponding digital gain values are fed to the PC. The PC drives the central control unit, digitizes, calculates and displays the measured beam phase signals and angles of the 12 pick-ups along the cyclotron radius. By a trigger signal from the central clock of the COSY-ring the PC and PHASME II are synchronized to the pulsed beam. Compared to the old system PHASME I[3] all 12 channels can be read out in parallel without channel multiplexing. Thus the beam phase can be measured in continuous as well as in pulsed beam mode. The shortest pulse width is approx. 5msec. An extra pickup mounted in the dee provides the possibility to eliminate phase response differences between the 12 rf-signal handling channels and a method for calibrating the system to the beam zero phase. PHASME II works over the full cyclotron frequency range.

The rf-circuit design was based on commercially available rf-components as power splitters, double balanced mixers, frequency doublers, hybrids, crystal filters, amplifiers and GaAsFet-switches. Bandpass filters and amplifiers for signal and impedance matching were developed in our laboratory. The internal rf-connections and the thirteen 33m long pickup lines are realized in form of semi-rigid coaxial cables. The whole PHASME II has been built into the mechanical system EUROPACK.

2.1 Details of the RF-part

Like in the old PHASME I also in PHASME II we make use of the heterodyne principle, which in the past already allowed a precise and reliable beam phase detection (Fig. 3). Just as for PHASME I we use the two DC-output signals of the phase detectors, which are components of a vector in rectangular coordinates, to determine the phase angles and the beam intensity. This vector still has an inherent error, which is induced by the 2nd harmonic content of the accelerating voltage in the pickup signals and by a small DC-offset voltage of the phase detector outputs themselves. This error will be compensated when the beam is switched off.

The basic rf-signal handling of PHASME II already has been described earlier.[3] In order to avoid a frequency synthesizer[3] we insert an additional frequency mixing stage and choose an intermediate fixed frequency of $f_1 =$ 21.4Mhz. By this frequency conversion the required signal $2f_0 + f_1$ is generated with the output signal of a 21.4Mhz fixed frequency oscillator and a $2f_0$ signal derived from the reference channel.

The GaAsFet-switch in the information channel input allows to connect the following bandpass filter either with the beam signal or the output signal of the calibration pickup.

The phase detection is similar to that of PHASME I, but the needed 90^0-phase shift now has been realized by hybrids, which are commercially available. Both DC-signals of the phase detectors are amplified by a factor of about 100, so that for internal beam currents of 50μA the DC-signals are nearly 10V.

By the calibration pickup, mounted in the cyclotron dee, a signal is decoupled from the rf-system, then doubled in frequency and simultaneously fed to the 12 switches in the information channels. There the probe signals can be replaced by the signal, derived from the calibration pickup. The cables are in both cases equal in electrical length. So a frequency independent phase response test of the information channels is possible. Without beam the phase behavior can be measured by PHASME II and taken into account for the calculation of the beam phase angles. Because the output voltage of the calibration pickup in the dee has a constant, frequency independent phase offset to the accelerating voltage, we use this feature for calibration.

2.2 The Readout Electronics

The inherent error of the 24 phase detector output signals will be compensated by the "compensation" of PHASME II (Fig. 2) a few msec before the beam is switched on. This section mainly contains 24 parallel operating analog auto-zeroing circuits modified for our application. All circuits and also the following 24 DC-amplifiers are activated synchronously by the control unit and the PC.

In order to cover the dynamic range of the rf-section and to be free from gain setting by the PC the 24 DC-signals of the X-Y-vector components now are amplified by the "automatic DC gain setting" which consists of 12 pairs of X- and Y-autoranging amplifier stages. Their amplification factors can be automatically set from 1 to 4096 in steps of 1, 4, 16, ... To get sufficient accuracy for the data conversion, the DC-signals are amplified in such a way that always voltages between $\pm$2.5V and $\pm$10V will be fed to the 12bit ADC's in the PC. Parallel to this the gain steps, 4bit data words, are transmitted to the PC, where they are used for the calculation of the phase angles as well as the intensity of the internal beam.

3. RESULTS OF THE TESTBENCH

Due to the width of 15mm the pickups take depending on radius position signals from about 2 to 9 beam orbits. This results in a measured sensitivity of about 100μV/μA (DC beam current).[3] The allowed 2nd harmonic beam signal voltages must lie in the range from 2μV to 5mV. That means, with PHASME II we can detect beam currents from 20nA to 50μA.

In order to measure the linearity of the rf-part within the dynamic range, we fed two rf-signals to PHASME II, one to the f_0 input with the cyclotron frequency $f_0 =$ 25Mhz and an amplitude of 250mV, the other to a probe

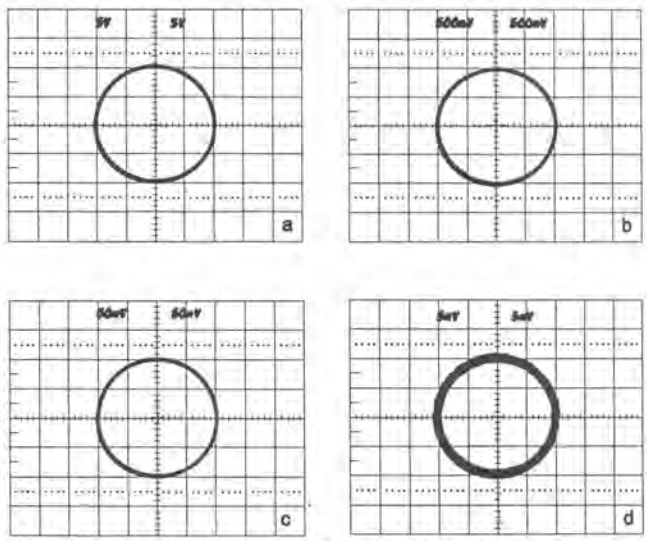


Fig. 4. amplitude linearity ($f_0 =$ 25Mhz)

input as a 2nd harmonic probe signal $2f_0$ but with a frequency lag of 1kHz and variable amplitude. In Fig. 4a the beam amplitude was adjusted in such a way that on a X-Y-scope the two output signals of the corresponding phase detector form a circle. In Fig. 4b-4d the beam signal was reduced by a factor of 10 from picture to picture. It is obvious from the circles that PHASME II works very well within a dynamic range of 60db with sufficient amplitude linearity. For the given amplification of the rf-part of nearly 3000 (a factor of about 30 for the information channels and about 100 for the DC-output signals of the phase detectors) the 10mV output signal is due to an 2nd harmonic probe signal voltage of about 3.5μV.

In Tab. 1 the output phase is shown for different input signals varying in amplitude and phase. The cyclotron test frequency f_0 is 27.316Mhz. The output phase was measured with the complete system, including the numeric data handling of the PC. For an input signal of about 3μV the phase accuracy is $\pm 0.5^0$, whereas for the maxi-

mum allowed input signal the accuracy is $\pm 0.25^0$. As appears from Tab. 1 the phase reading follows precisely the input phase. Please note, that without 2nd harmonic disturbances the phase detector outputs of their own have an DC-offset in the range of ±0.2mV to ±0.5mV. Comparing this offset to the amplified signals of about 5mV to 10mV for the lowest input signals and regarding to the mentioned phase accuracy the compensation must work sufficiently. For Fig. 4 and Tab. 1 two different frequencies were chosen in order to demonstrate the frequency variability of PHASME II.

Tab. 1. phase linearity of PHASME II

ϕ_o[...°] / ϕ_{in}[...°]	$U_{in}(2f_0)$ 3620µV (-36dbm)	$U_{in}(2f_0)$ 362µV (-56dbm)	$U_{in}(2f_0)$ 36,2µV (-76dbm)	$U_{in}(2f_0)$ 3,62µV (-96dbm)	accuracy within 60dbm
0	172,95	173,05	172,75	172,40	± 0,39
30	143,21	143,20	142,69	142,90	± 0,31
60	112,82	113,05	112,82	112,70	± 0,25
90	82,72	82,70	82,8	83,05	± 0,23
120	53,05	53,05	52,92	53,10	± 0,12
150	22,80	22,85	22,60	22,90	± 0,19
180	-7,19	-7,35	-7,08	-7,32	± 0,15
accuracy within 180°	± 0,28	± 0,29	± 0,19	± 0,41	average deviation [...°]

ϕ_{in} = input phase; ϕ_o[...°]= measured output phase;
$U_{in}(2f_0)$ = second harmonic input voltage ; test frequency f_0 = 27,316Mhz

4. TEST WITH BEAM

For a first test PHASME II was connected to the 12 probe pairs in the cyclotron.

In Fig. 1 the signals from probe pair 6 are shown on an oscilloscope with and without beam for an internal cyclotron beam of about 6µA.

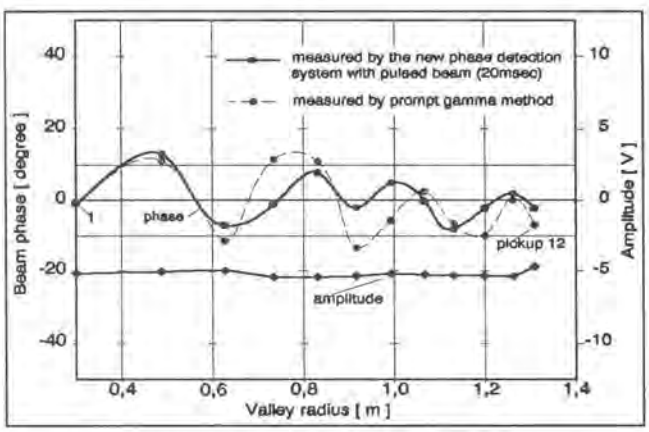


Fig. 5. measurement with beam

In Fig. 5 the amplitude of the beam phase vector, representing the beam intensity, and the beam phase are shown along the different probe positions for an internal pulsed cyclotron beam of about 15µA. The pulse length was 20msec with a repetition rate of 2 Hz. The phase information is compared with an independent beam disturbing phase measurement done by prompt gamma rays. The agreement of both curves is obvious and acceptable for a first test. The amplitude is nearly constant over the 12 probes, although the number of beam orbits and the beam energy is varying along the radius, from the inner pickup (r = 0.3m) to the outer one (r = 1.53m) by a factor of about 26 (from 1.45 MeV/a to 38MeV/a).

The cyclotrons operating parameters for both measurements are: U_{rf}= 35kV, f_0= 27.316Mhz, 76MeV H_2^+, external beam current about 8µA.

5. POSSIBLE FUTURE OUTLOOK

Due to the broadband properties of the probes the analysed signals in the time domain can give information about the bunch shape. Therefore the rf-noise signal must be known in amplitude and phase. The bunch shape then can be elaborated by reconstruction methods.[4)]

With PHASME II we get the 2nd harmonic beam signal, which is related to the beam current. If it should be possible to measure simultaneously the sum and difference of the upper and lower pickup signals in spite of severe rf-interference with the accelerating voltage, there is in principle a possibility to detect vertical beam positions.

6. ACKNOWLEDGEMENT

The authors thank K. Bongardt for many fruitful discussions about pickup properties and especially about further options with PHASME II.

7. REFERENCES

1)W. Bräutigam, H. Beuscher, H. G. Böge, R. Brings, R. Maier, M. Rogge, P. Wucherer, "Commissioning of the Injector Complex of the COSY-Jülich", Proceedings of this Conference

2) R. Maier, U. Pfister for the COSY-team, "COSY-Jülich, a synchrotron and storage ring for medium high energie physics", Proceedings of this Conference

3) W. Bräutigam, M. Herschbach, K. Kennepohl, J. Reich, "Beam phase detection with a fixed intermediate frequency system at JULIC", IEEE Trans. o. Nu. Sc., Vol. NS-26 No. 2, April 1979, pp. 2375-2378

4) K. Bongardt, K. Kennepohl, "Determination of 100psec short linac bunches by broadband pickups and reconstruction technique", Proceedings of the first European Particle Accellerator Conference EPAC, Rome (Italy), 7-11 June 1988, pp. 976 - 978, Vol 2., Wourld Scientific Publishing Co., Singapore

HIGH-SENSITIVE IONIZATION DETECTORS OF TRANSVERSE DISTRIBUTION OF ACCELERATED PARTICLES BEAM

V.G.Mikhailov, V.A.Rezvov, A.A.Roshchin, V.I.Sklyarenko, L.I.Tudin

I.V.Kurchatov Institute of Atomic Energy,
Moscow, 123182, Russian Federation

ABSTRACT

Devices for the high-sensitive contactless diagnostics of accelerated particle beam, using residual gas ionization products, were considered. Similar facilities make it possible to measure effectively the beam profile, position of a center of gravity and its displacement, to assess the beam averaged density distribution via its cross-section. The ionization sensor developed at IAE was described. The sensor provides an operative representation of a real cross-section of the accelerated particle beam with information display on a TV screen, as well as a monitoring of the beam impulse and average currents. The sensor beam cross-section sensitivity is about 10^{-8} A, the resolution at visual check - 1 mm, the dimension of a region under control - 40x40 mm. The results of the beam cross-section sensor operation are presented at various accelerators.

1. INTRODUCTION

Practically any operation with the use of an accelerated beam is associated with the necessity of measurements of its sizes and position. Among a variety of sensors of these parameters [1] one can single-out sensors based on detection of electrons or ions arising at ionization by a residual gas beam in a path of accelerated aparticles transportation. The interest in them is caused by their complete transparency for a controlled beam the lack of additional radiation backgrounds and high potentialities.

In the simplest case electrons or ions of residual gas are transferred by a transverse electric field to a collector. To record a distribution of the residual gas ionization particles current density over a profile of the beam under investigation use is made of screen covered by phosphor. An optical image of the current density distribution over its profile is TV reflected on a telemonitor by means of a TV camera. Simile censors are used in synchrotrons operating at relatively high beam currents - 10^{12} - 10^{13} particles in the cycle of acceleration [2,3]. To reduce the effect of the beam space charge a combination of electric and magnetic field is used sometimes.

According to data on ionization losses for particles with energies of 10-100 MeV [4], which are typical of the majority of cyclotron beams, assessments were performed of the number of N electron-ion pairs generated on the 1 cm path at a pressure of 10^{-5} torr by various particles (Fig.1). Using these estimations it is easy to see that at the protons current J = 1 mkA with energy of 30 MeV on the 1 cm path 10^{8} electron-ion pairs are generated for 1 sec. This means that in cyclotrons operating, as a rile, with mean currents of 10^{-5} - 10^{-8} A, an output current of ionization sensors is so low that is direct recording is very difficult. In this connection there appears the problem of increasing the ionization sensors sensitivity.

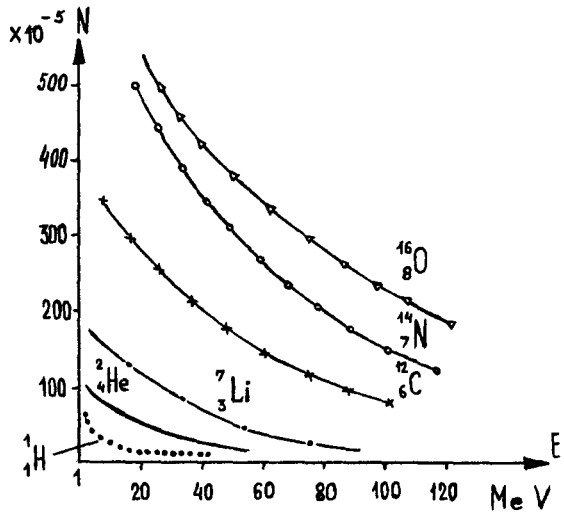


Fig.1. The calculated dependence of ionization power on a beam energy for various particles.

2. IONIZATION PROFILOMETERS WITH OUTPUT CURRENT MULTIPLICATION

An illustration of the possibilities of increasing the ionization sensor output current can be profilometers of DESY III and PETRA II installations whose data were published in the late eighties [5]. The DESY III installation profilometer diagram is presented in Fig.2. Here in the working volume between the anode and cathode a homogeneous electric field was formed. Ionized Residual gas electrons are shifted to the anode, ions - towards the cathode having a secondary emission ratio of 2-3. A glow of the phosphor screen placed in the anode plane can be caused by both ionization and secondary-emission electrons. The beam profile picture is read-out by the TV camera for a further presentation and processing. Various operating conditions of the profilometer were investigated, which are distinguished by voltage distributions between electrodes. Optimum results were obtained while using secondary-emission electrons only the amount of which correspondingly by 2-3 times exceeds the amount of ionization ones. In these conditions a voltage on electrodes amounts to U_{G1} = +1 kV, U_{G2} = -1 kV, U_A = + 18 kV, U_K = - 18 kV.

In the PETRA II installation profilometer one microchannel plate (MCP) of 60x60 mm size is

placed in the anode plane, which allowed the sensor output current to be increased by $3 \cdot 10^3$ times. In conformity with this the results of measurements of the beam profile at the DESY III synchrotron given in the publications, were obtained at proton current of 20 mA, on the PETRA II accumulator - at proton current of 20 mkA. The measurements were carried out under conditions of almost identical vacuum and beam energy - 10^{-8} and $2.5 \cdot 10^{-8}$ mbar, 5 and 7.5 GeV, respectively.

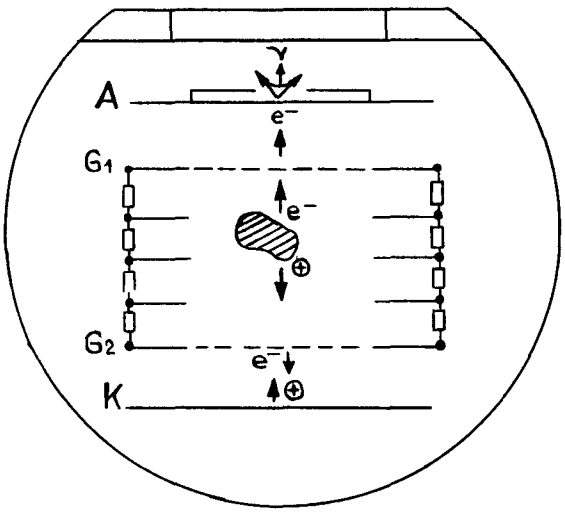


Fig.2. The DESY III installation profilometer diagram.

Thus, the radical way to increase the output current of ionization sensors is the use of position-sensitive electron micro-channel plate multipliers on. To the authors'knowledge, the first suggestion on the use of MCP to increase the output current of ionization sensors of cyclotron parameters beam was made in [6]. To develop this suggestion in [7] was described the ionization profilometer of cyclotron beam with an amplifier on cheron out of two MCP and with a TV watch and presentation of information (Fig.3). The MCP size is 90x70 mm, the sensor aperture is restricted only in one coordinate by a gap between the deflector and the MCP and is 70 mm. The ion component of the ionized residual gas is transferred to the MCP by the plane-parallel electric field. An amplified current of secondary-emission electrodes creates on the phosphor a bright picture of the studied beam intensity distribution over a profile. The profile image is displayed by the TV camera on a TV monitor in order to be effectively presented to an operator. At the same time a signal from the TV camera is processed by a microprocessor. Digited information is transmitted to a colored display where the envelope of profile is presented for the given moment as well as (in another color) the shape and position of the envelope of profile during several last measurements. The sensor sensitivity for a beam of protons with energy of 30 MeV at a vacuum of 10^{-5} torr comes up to 10^{-8} A, the spatial resolution - 1 mm.

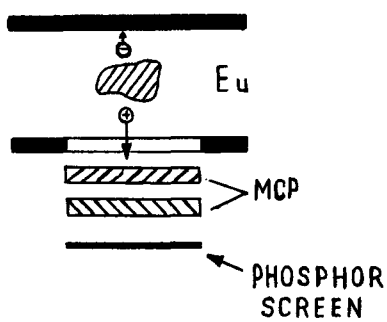


Fig.3. The cyclotron extracted beam profilometer.

The works on the cyclotron beam profile diagnostics have been developed creating a high sensitive profilometer for a fast-cyclic heavy-ion synchrotron [8]. The block diagram of this profilometer is analogous to that depicted in Fig.3. Here use was made of two MCP the gap between which is shifted to a closed state and is opened during a measurement of a driving pulse. The pulse duration is regulated from a few microseconds to a time of the acceleration cycle. The pulse is delayed with respect to a beginning of the cycle and synchronized with an accelerating h.f. voltage. Such a regime makes it possible to follow the dynamics of the beam profile in the cycle of acceleration.

The particularity of the profilometer is the application of non-standard operating conditions of the TV camera photodetector based on a matrix charge-coupled device (CCD) array. The CCD matrix lines are oriented perpendicularly to an ion-conductor. A charge previously distributed over all lines of the matrix storage section. Such a regime of matrix increases the instrument sensitivity by more than one order of magnitude in comparison with a usual TV regime. Besides, in the matrix storage section lines information is accumulated on several sequential measurements of the beam profile per one cycle of acceleration, which later on is read-out by processing and representation units it a tempo of these unit operation. This makes it possible to follow the dynamics of the beam evolution in every cycle of acceleration.

On the accelerator model at a vacuum of $5 \cdot 10^{-8}$ torr an ultimate sensitivity was reached which was limited by the number of input events per time of exposure, which was sufficient for a statistical description of the beam profile. Assuming that to describe the beam profile 10^3 events are sufficient and in terms of the beam of protons with energy of 30 MeV during an exposure time being equal to the TV frame duration of 40 m.sec, 10^8 particles should pass through the profilometer working gap, which corresponds to the beam current of 10^{-10} A. A spatial resolution depends on a deflector voltage and at an extracting field voltage of 1 kV/cm has the value less of 1 mm.

3. THE IONIZATION SENSOR AT ACCELERETED PARTICLES BEAM TRANSVERSE CROSS-SECTION

The units considered above make it possible to detect vertical and horizontal beam profiles but unable to control a real beam distribution over a cross-section. A practice shows, however, tham complicated systems for cyclotron beam with allowance for multicirculation of release can form beams of rather complicated shape which cannot be restored by measuring simultaneously the horizontal and vertical profiles. Besides, the simultaneous measurement of the beam profile via two orthogonal directions is associated with the necessity to place of an additional equipment in the beam transportation path. Therefore, a creation of a beam transverse cross-section sensor having all advantages of ionization profilometers seems to be actual.

One of the first proposals on observation of a two-coordinate beam distribution over cross-section by means of the ionization sensor has been given in [9], sufficiently long ago; however, its practical realization, in any event for cyclotron beams, has become possible only with an appearance of microchannel plates.

In [10,11] the authors have suggested the method and construction of sensor (Fig.4) for an operative observation of the beam transverse cross-section based on spatial and energy analyses of residual gas products ionized by the beam.

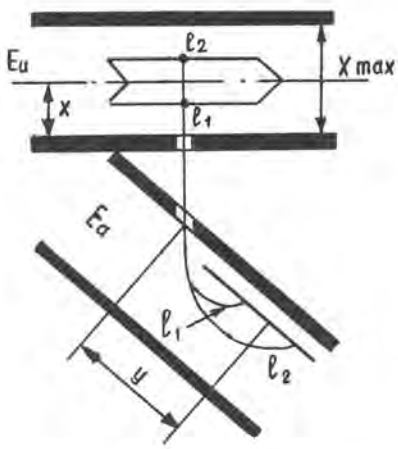


Fig.4. The transverse beam cross-section sensor diagram.

The sensor contains extracting and analyzing condensers, a current collector made as electron-optical convertor (EOC) with a microchannel plate-base amplifier and appropriate power sources. Residua gas ions are accelerated by a plane electric field towards extracting electrode provided with a forming slit of 1x50 mm size directed across the ion-conductor axis. Pathing through the forming slit the accelerated ions form a sheet beam in which a spatial distribution of particles in the direction along the slit corresponds to the distribution of particles in the controlled beam in this direction. Energy distribution of extracted ions corresponds to the distribution of the investigated beam over the other orthogonal coordinate. The analysis of this energy distribution is accomplished by the electric field of the analyzing condenser. As a result, on the current collector screen of EOC is formed the two-coordinate optic image of extracted ions distribution, corresponding to the transverse distribution of particles in the accelerated particles beam under control. The location of the analyzed condenser at an angle of 45 to the direction of extraction and plane of the extracted electrode provides a linear coupling between sizes of the obtained image and controlled beam sizes. the image size Y corresponding to the beam size X in the direction of extraction is linked by the dependence:

$Y = 2 \cdot X \cdot E_u / E_\alpha$, where E_u and E_α are strengths of the extracting and analyzing fields, respectively. Record of the optic image of the beam transverse cross-section is performed by the commercial TC camera.

The standard device to control sizes and displacement of an accelerated beam has presently been developed on the IAE cyclotron. Structural elements of the beam cross-section contactless sensor are placed in the standard diagnostic section with external dimensions of 230x230x230 mm and diameter of flange holes of 166 mm. Admission of supply voltage is accomplished via the flange on which the extracting electrode and analyzing condenser with EOC are fixed. A record of an optical image of the beam cross-section is performed by the TV camera.

From one of lateral sides of the diagnostic box a remote-controllable drive was placed ensuring mounting of the fluorescent screen into the gap of the extracting condenser. This makes it possible to conduct pretuning of the beam using traditional diagnostics means. Photo fig.5 shows the example of the complex form beam cross-section from the EOC screen.

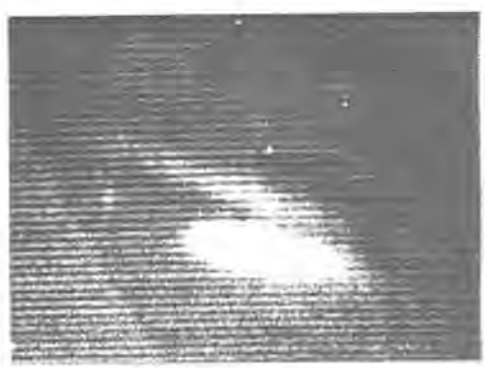


Fig.5. The example of the complex form beam cross-section from EOC screen.

The sensor design makes it possible to monitor the controlled beam intensity. To this end, it is sufficient to measure current on the EOC screen. However, the device sensitivity depends on pressure in the beam transportation path. In [12] to exclude this dependence it was suggested to change transmission factor of the MCP multiplier in accordance with changes in pressure in the beam transportation path.

Additional conveniences for user creates the unit of quasi-colored representation of TV signal. In this case on the monitor screen a colored image of the beam cross-section is formed, and the shape of colored closed bands of each color corresponds to intensity distribution of the investigated beam on the present level of comparison. Processing of cross-section parameters of the beam controlled is provided by means of computer.

The main parameters of the beam cross-section contactless sensor are given in Table

Size of controlled region	40x40 mm
Aperture	60 mm
Spatial distribution at visual check	< 1x1 mm
Sensitivity of 30 MeV proton beam	10^{-8}A
Working pressure range in ion conductor	< 3*10 torr
Feed source voltage	10 kV
Utilized current	100 muA
MCP multiplier amplification factor	10
Time of image formation	100 nsec

4. CONCLUSION

At the present time similar beam cross-section sensors have been tested on cyclotrons and tandems and are successfully operated at I.V.Kurchatov IAE (Moscow), INR (Kiev), INF (Rzez in the environs of Prauge), ZfK (Rossendorf in the environs of Drezden); the same sensor was passed to the University of Jyvaskyld (Finland). A part of these sensors was made in the ISO standard used at European accelerator centers. A sensor design was developed for an investigation of a beam with energy of a few kilovolts. Measures were taken in it on compensating a beam displacement in the transportation path due to the effect of extracting voltage of the sensor deflector. The sensor to control uniformity of the tandem scanning beam was also developed in producing nuclear filters [13]. Thus, it is seen that ionization sensors of accelerated particles beam cross section find more and more increasing use of various accelerators.

REFERENCES

1. V.A.Rezvov, L.I.Yudin. Diagnosis of particle beams in cyclotrons (Review). Instruments and experimental techniques. Vol. 33, No.6, part 1, 1990. Translated from Russian.

2. V.Agoritsas, S.Batisti, K.D.Johnson, G.Shnaider. Methods for measuring accelerated particle beam parameters. Proc. II All-Union Conf. on Charged Particle Accelerators; vol. II, p.82. M., Nauka, 1972.

3. L.Rezzonico. Beam diagnostic at SIN. XI Intern. Conf. on Cycl. and their Appl. pp.457-461, 1987, Jonics Publishing Comp. Tokyo

4. N.N.Pucherov, S.V.Romanovskii, T.D.Chesnokova. Tables of mass retardin ability and pathes of particles with energy of 1-100 MeV. Kiev, Naukovadumka, 1975.

5. W.Hain, F.Horstra, A.Lazos at all. Beam profile monitors for HERA proton acceleration. Proc. EPAC 90, Nice, June 12-16, v.1, p. 759-761, 1990

6. V.A.Rezvov, I.N.Serikov, L.I.Yudin, et al. Possibilities of use of ionization sensors to control a cyclotron beam. Proc. All-Union Conf. on Low and mean energy ion accelerators, p. 68, Kiev, Naukova dumka, 1982.

7. P.Yu.Komissarov, V.G.Mikhailov, V.A.Rezvov et al. Proc. X All-Union Conf. on charged particle accelerators. JINR, D9-87-105, vol. 1, p. 61, Dubna, 1987.

8. V.G.Mikhailov, V.A.Rezvov, A.A.Roshchin et al. The high-sensitive profilometer for a heavy-ion synchrotron. Proc. IX All-Union Conf. on charged particle accelerators, vol.1, p.83, Dubna, 1986.

9. V.V.Elyan. The method for measurement of a transverse density distribution in charged particle beams. - Cert. of Authorship SSSR No. 556697, BOJ No.39, p.230, 1977.

10. V.A.Rezvov, L.I.Yudin. the method for measurement of a transverse distribution of charged particle beam density. Cert. of Authorship SSSR No. 1392645. OI No.16, 1988, p. 32.

11. V.G.Mikhailov, V.A.Rezvov, V.I.Sklyarenko, L.I.Yudin. The ionization sensor of charged particle beam density distribution over a cross section. Cert. of Authorship, SSSR No. 1462521 OI, No.8, 1989, p. 294.

12. P.Yu. Komissarov, V.G.Mikhailov, V.A.Rezvov et al. The contactless control a transverse distribution of accelerated beam particles. Proc. XI All-Union Conf. on charged particle accelerators, vol. I, p. 87, Dubna, 1989.

13. S.T.Latushkin, V.A.Rezvov, L.I.Yudin. The contactless sensor of charged particle accelerated beam parameters. Cert. of Authorship USSR No. 10009219. BOI, 1984, No. 7, P. 211.

14. V.G.Mikhailov, V.A.Rezvov, V.I.Sklyarenko et al. The device for control of beam parameters in the course of irradiation of nuclear filters. X All-Union Conf. on exchange of operation experience and improvement of electrostatic accelerators, November, 1991.

A BEAM PROFILE MONITOR USING THE IONIZATION OF RESIDUAL GAS

J.M. Schippers and H.H. Kiewiet *
Kernfysisch Versneller Instituut
Zernikelaan 25, 9747 AA Groningen
the Netherlands

ABSTRACT

A non intercepting beam-profile monitor for the beam-guiding system of AGOR has been designed and tested successfully. By detecting the ions created by the beam in the residual gas, a one dimensional intensity distribution of the beam is obtained. The device is suitable for a wide range of beam intensities, but especially at beam intensities below several nanoAmps it has proven to be much more sensitive than e.g. scintillation screens.

1. INTRODUCTION

A new monitor that measures the beam-intensity profile in one direction and without intercepting the beam, has been designed and tested. It is designed to be suitable for all AGOR beams. After testing a prototype version[1] also experiments with the version that will be mounted in the actual beam pipe had to be performed. Especially the life time of the device during realistic operation conditions was tested during the last months of operation of the Philips cyclotron at KVI.

2. OPERATION PRINCIPLE

The residual gas beam-profile monitor (RG-BPM) uses the ions that are created by beam particles traversing the residual gas in the beam tubes. The ions are extracted from the beam tube with a homogeneous electric field and drifted towards a pair of micro channel plates (MCP's) acting as a charge multiplier. The electrons generated in the MCP's are collected on strips parallel to the beam, so that a position sensitive readout is obtained in a direction perpendicular to the beam. By varying the amplification of the MCP's the signal magnitude can be changed, so that a large dynamic range is achieved.

It can be shown that the MCP's should operate with an amplification larger than 4×10^4 for a 200 MeV proton beam of 1 nA traversing a residual gas of $10^{-7} - 10^{-6}$ mbar. The produced ions (about 135 ions s^{-1} cm^{-1}) will then give a final signal current of at least 1pA. Since the amplification factor of MCP's can be set from 1 to 10^6, this current can be measured quite easily.

*This work was performed as part of the research program of the "Stichting voor Fundamenteel Onderzoek der Materie" (FOM) with financial support from the "Nederlandse Organisatie voor Wetenschappelijk Onderzoek" (NWO).

At several positions along the beam lines the desired accuracy of beam position measurements is 0.3mm, so that the drift field has to be very homogeneous. For the prototype[1] this was rather easy to achieve; the final design discussed here, however, has to be mounted in a standard reference block in the beam pipe. The inner diameter of such a block is only 65 mm so that detailed calculations on the field shaping had to be performed.

3. DESCRIPTION OF THE DESIGN

In Fig.1. a drawing is shown of the RG-BPM. The drift field of 0.5 kV/cm is created by the field shaping electrodes: copper strips, evaporated on a flexible printed circuit board, shaped as the inner side of the vacuum chamber. A resistor chain provides the correct voltage on the strips. A free aperture of 55 mm is available for the beam. To allow convenient assembly the length of the strips has been limited by the length of the reference blocks (10 cm). Field calculations show that the field lines in the central region (length of 2 cm) are not distorted more than approx. 1 mm. Therefore the limit on the position resolution will be approximately 1 mm. However, if necessary this can be improved by using longer field shaping electrodes.

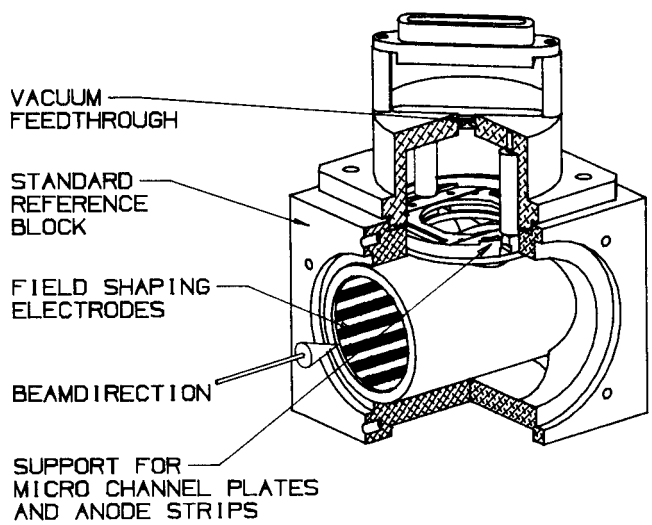


Fig.1. The Residual gas beam-profile monitor, mounted in an accurate position-reference block of the AGOR beam line.

The MCP's (Galileo; active area $\emptyset$ =42 mm), are mounted in a chevron geometry on top of the tube with the field shaping electrodes. A position sensitive anode is mounted on top of the upper MCP. It consists of 40 strips, 0.9 mm wide and spacing 0.1 mm, etched on a printed circuit board. The MCP's were operated at 600-800V each, resulting in a total gain of $10^4 - 10^6$.

Each anode strip was connected to a current to voltage amplifier.[2] The outputs of the amplifiers are multiplexed, digitized and sent to a BitBus line via a micro controller acting as an interface. Presently a PC interfaced to the BitBus system is used for displaying the beam profiles. Ten times per second the screen is refreshed and a new profile is made visible. If the statistics is very poor, an average over many cycles can be made and background subtraction is also possible. The conversion gain of the ADC can be adjusted from the PC. With this set of electronics also the beam-profile monitors normally used ("harps": 48 wires, spacing 1 mm, on which the secondary emission current is measured) are read out, allowing a nice flexibility.

4. PERFORMANCE

Tests on a prototype[1] have already shown that the signal height is in agreement with the expected values mentioned in section 2. The final version of the RG-BPM has been tested during a half year of the normal beam-time program with the Philips cyclotron at the KVI. Measurements on various beams at different intensities (0.1-200 nA) have been performed.

The detector was mounted in a reference block 50 cm before a harp and a viewing screen, so that beam profiles could be compared. A quadrupole doublet 1.5 m before the RG-BPM was used for adjustment of the beam size. The gas pressure in the beam pipe was usually 10^{-6} mbar. Typical convenient signal currents were in the order of several times 10 pA per nA beam current, summed over all strips.

The result of a measurement of a beam profile, taken with the RG-BPM is shown in Fig.2. The position resolution has been measured by comparing the widths of the peaks obtained from the RG-BPM and the harp, taking into account the beam divergence. Usually a resolution of about 2 mm FWHM was found.

During its half-year operation the dependence of the operating characteristics on the strength of the drift field, the amplification and beam intensity, as well as the time dependence of its characteristics have been studied systematically. It was found that the device has a constant behaviour approximately 10-20 min after switching on. Therefore a continuous operation mode is necessary.

The sensitivity of the RG-BPM has been clearly demonstrated at low beam currents. The cyclotron operators frequently used the RG-BPM in cases where the viewing screens gave a poor (or no) image.

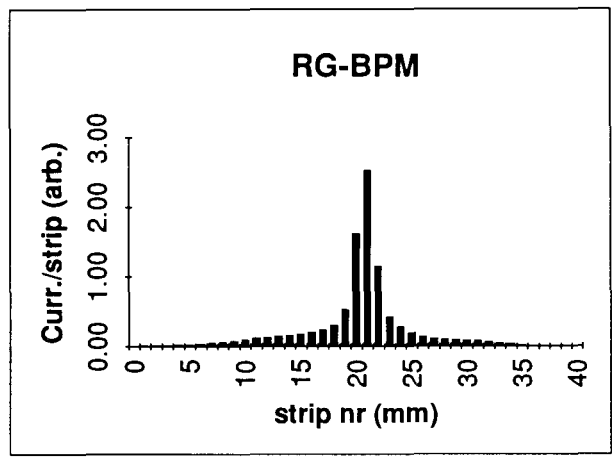


Fig.2. A beam profile, measured with the RG-BPM. The beam width was approx. 2 mm FWHM.

5. CONCLUSIONS

The beam-profile monitor based on the principle of the detection of ions created in the residual gas in the beam lines has shown to be a reliable device, suitable for all AGOR beams, especially at low intensities. Several of these profile monitors will be installed in the AGOR beam lines.

An advantage of such a non interceptive beam profile measurement, is that the amount of neutron- and gamma radiation created during the measurements is minimized. This may be very important for some of the nuclear physics studies planned with AGOR; we have experienced that even the radiation produced by other types of monitors, e.g. harps, contributes significantly to the background observed in experiments using neutron- or gamma ray detectors. Furthermore we have observed that beam particles scattered from the wires of a harp, dominate the background in several measurements at zero degree, performed with a magnetic spectrograph. Therefore they will be mainly used as last-profile measuring devices, installed before the target stations. An on-line continuous monitoring of the target spot is then possible, without interference with the experiments.

6. REFERENCES

1) J.M. Schippers, H.H. Kiewiet and J. Zijlstra, Nucl. Instr. and Meth. A310 (1991) 540.
2) Ch. Olivetto, AGOR internal report NT-DIA-29-09-88

EMITTANCE MEASUREMENTS IN THE HIRFL BEAM LINE

Hongwei Zhao, Zhiqing Shen, Baowen Wei
Institute of Modern Physics, Academia Sinica, P.O. Box 31, LanZhou, 730000, China

ABSTRACT

The transverse emittance in the HIRFL beam line has been measured using two different methods. One is the "Three-Position Method" in which the beam sizes at three different locations in a field-free drift space are measured by Three Secondary Emission Multi-Wire Profile Monitors. The other is the "Three-Gradient Method" in which the beam sizes at a particular location are measured by the profile monitor,as a function of the strength of an upstream quadrupole. The emittance calculations,measurement error analysis, the best beam configuration for making optimum emittance measurements, and results of experimental measurements for both methods in the HIRFL beam line are presented in this paper.

1. INTRODUCTION

The optical matching of various HIRFL subsystem as well as the optimization of beam parameters in HIRFL beam line requires accurate determination of the beam emittance and ellipsoid(σ -matrix) at key poits.The phase space and emittance at the exit of SSC also serve as a figure of merit for its operation. Assuming that particle transfer can be treated with the matrix formalism and no coupling motion exists in each transverse degree of freedom,the transverse phase space of a beam then can be characterized by three parameters which define the emittance boundary ellipse in horizontal or vertical direction. In the HIRFL beam line two different methods were used to measure the beam emittance . One is the "Three-Position Method".[1] The other is the "Three-Gradient Method" .[2-3]

2. ERROR ANALYSES

2.1. Three-Position Method

Consider a beam in a field-free drift space. If there are three measurement poits A, B, and C along the beam line at axial position z_1, z_2 , and z_3 respectively,define the origin of coordinates to be at B so that $z_1 = -l_1$, $z_2 = 0$, and $z_3 = l_2$. The beam sizes at the three poits are denoted by r_1, r_2 , and r_3 . Three profile monitors will be set at the three poits to measure the beam sizes. From theory of transfer matrix the beam emittance (horizontal or vertical) is given by

$$\begin{aligned}\varepsilon &= \{2l_1^2 r_3^2[l_2^2 r_1^2 + (l_1+l_2)^2 r_2^2] - l_1^4 r_3^4 \\ &\quad -[l_2^2 r_1^2 - (l_1+l_2)^2 r_2^2]^2\}^{\frac{1}{2}} / [2l_1 l_2 (l_1+l_2)]\end{aligned} \tag{1}$$

The standard deviation of emittance is then calculated from the following formulas:

$$\delta\varepsilon = [(\frac{\partial\varepsilon}{\partial r_1})^2 \delta r_1^2 + (\frac{\partial\varepsilon}{\partial r_2})^2 \delta r_2^2 + (\frac{\partial\varepsilon}{\partial r_3})^2 \delta r_3^2]^{\frac{1}{2}} \tag{2}$$

From Eq.2 we can derive that the $\delta\varepsilon$ is minimum when l_1 is equal to l_2 .

If $l_1 = l_2 = L$, the standard deviation of emittance is

$$\begin{aligned}\delta\varepsilon &= \frac{4}{\sqrt{2}\varepsilon}[r_1^2(r_1^2 - 4r_2^2 - r_3^2)^2 \delta r_1^2 \\ &\quad +16 r_2^2 (r_1^2 - 4r_2^2 + r_3^2)^2 \delta r_2^2 \\ &\quad +r_2^2 (r_1^2 + 4r_2^2 - r_3^2)^2 \delta r_3^2]^{\frac{1}{2}}\end{aligned} \tag{3}$$

With the aid of Eq.3 and theory of transfer matrix ,the beam configuration for making optimum emittance measurements can be found. The error in emittance measurements has a great dependence upon the location of a beam waist, the waist size and the separation for the three profile monitors.

The effect on the deviation of emittance measurement by moving the location of the beam waist is shown in Fig.1 ,which is corresponding to different waist sizes and a fixed separation for three profile monitors. Figure 1 illustrates that it is alwayse best to have the waist near the center measurement poit ($z_0 = 0$),although for some r_0 this requirement is not as critical. Figure 1 also indicates that for fixed z_0 ,there is a dependence of $\delta\varepsilon$ on r_0 .This is shown explicitly in Fig.2 , which gives the relation between $\delta\varepsilon$ and r_0 for z_0 =0, and several different L . The optimum value of beam size at waist r_0 as a function of L is shown in Fig.3 . Finally, with r_0 at its optimum value and $z_0 = 0$, the minimum deviation of emittance measurement as a function of L is displayed in Fig4 .

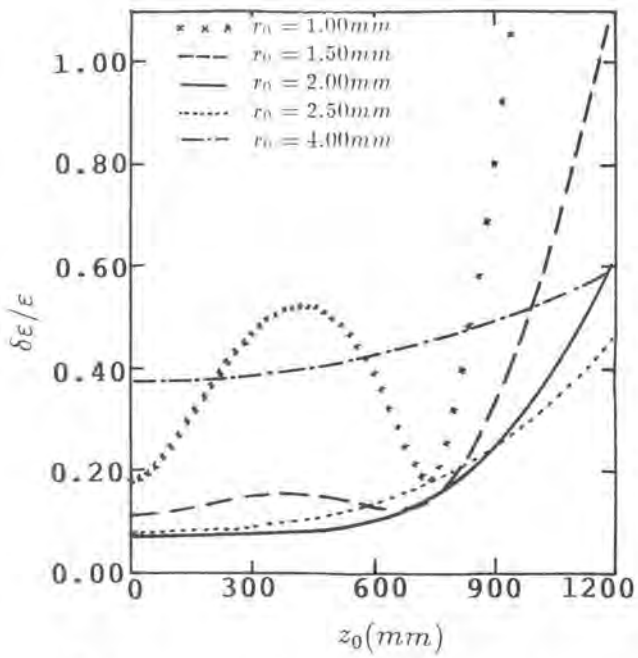


Fig.1. Deviation of emittance measurement $\delta\varepsilon$ versus location of beam waist z_0, for different waist sizes r_0. Here $L = 750.0mm$ and $\varepsilon = 8.00mm\ mrad$ The measurement error of the beam size at each poit is taken to be $\delta r = 0.13mm$ from the profile monitor and other consideration.

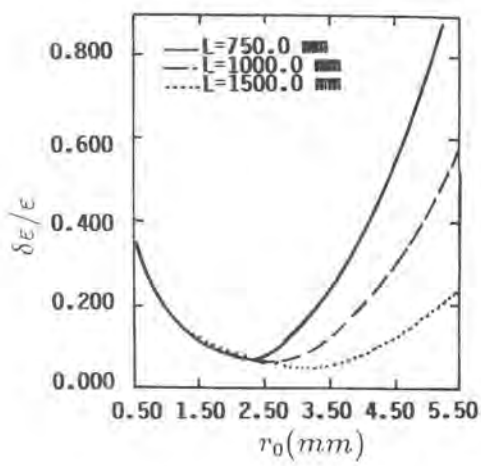


Fig.2. Deviation of emittance measurement $\delta\varepsilon$ versus waist size r_0, for different profile monitor separation L. Here $z_0 = 0.00mm, \varepsilon = 8.00mm\ mrad, \delta r = 0.13mm$.

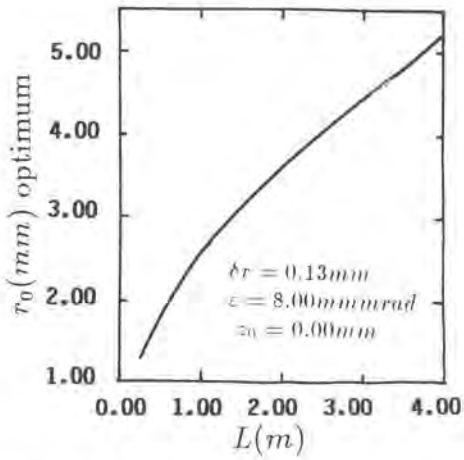


Fig.3. Waist size r_0 for optimum emittance measurement versus profile monitor separation L.

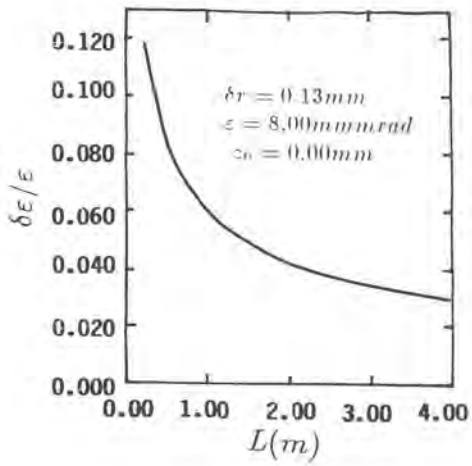


Fig.4. deviation of emittance measurement $\delta\varepsilon$ at optimum waist size r_0 and optimum waist location z_0 , as a function of profile monitor separation L.

2.2. Three-Gradient Method

Consider a section of a beam line in which a quadrupole is separated from a downstream profile monitor by a field-free region. In beam transfer principle,any three independent settings of the quadrupole are corresponding to three independent beam sizes at the profile monitor and three different transfer matrixs , and this can be used to solve for the three unknowns σ_{11} , σ_{12} , and σ_{22} , from which the beam emittance can be calculated. But in practice the emittance measurement is sensitive to the accuracy in determining the beam size. A series of profile measurements are taken by varying the strength of the quadrupole so that we could try to solve for those three unknowns by the least square method.

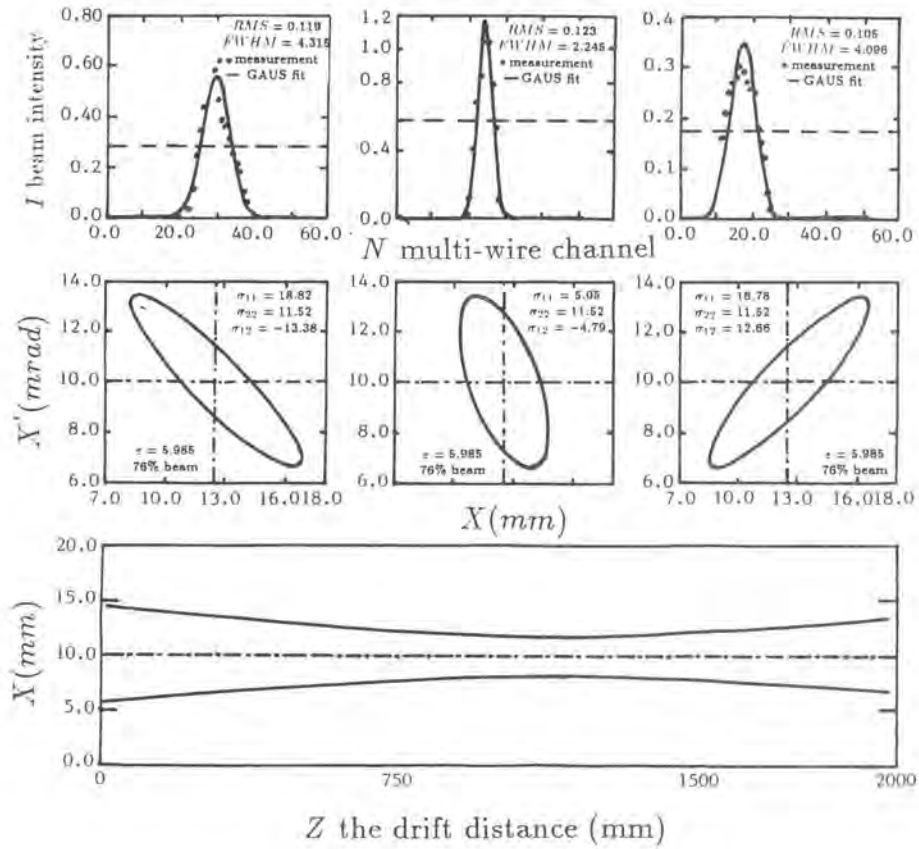


Fig.5. Display of emittance measurement results in horizontal direction.top: beam profiles at the three locations,middle:the beam ellipses. bottom: beam envelope in the measurement chamber.

With the use of the least square method and standard propagation of error calculations, the error in the emittance measurement is given by

$$\begin{aligned}\delta\varepsilon &= (\sigma_{11}^2\delta\sigma_{22}^2+\sigma_{22}^2\delta\sigma_{11}^2+4\sigma_{12}^2\delta\sigma_{12}^2 \\ &\quad -4\sigma_{11}\sigma_{12}\rho_{1222}\delta\sigma_{12}\delta\sigma_{22} \\ &\quad +2\sigma_{11}\sigma_{22}\rho_{1122}\delta\sigma_{11}\delta\sigma_{22} \\ &\quad -4\sigma_{12}\sigma_{22}\rho_{1112}\delta\sigma_{11}\delta\sigma_{12})^{\frac{1}{2}}/2\varepsilon \end{aligned} \quad (4)$$

where $\varepsilon = (\sigma_{11}\sigma_{22}-\sigma_{12}^2)^{\frac{1}{2}}$

in which $\delta\sigma_{ij}$ is the error in determination of σ_{ij} and ρ_{ijkl} is the coefficient of interrelation between σ_{ij} and σ_{kl} .

3. EXPERIMENTAL RESULTS

Emittance measurements in the HIRFL beam line ,based on the above analyses, are made with an automatic emittance measuring system. In order to determine the beam size from the beam profile a Gaussian distribution is fitted to the profile data.

In the emittance measurements with "Three-Position Method", the profile monitors seperation in the measurement chamber is only 750.00 mm. So we should try to make the beam waist near the center profile monitor and take the waist size to be $1.9-2.3mm$ as possible as we could. Figure 5 shows the results of emittance measurements in horizontal direction with the "Three-Position Method". From Fig.5 we can see that the beam configuration is not in the best state. This is a main source that error comes from. The results will be better if the profile seperation is greater.

In the emittance measurements with "Three-Gradient Method", fourteen settings of the quadrupole have been performed to get a series of profile measurements at one location. Figure 6 indicates the dependence of the beam size at the profile monitor on the quadrupole strength in the "Three-Gradient Method". Both experimental results and theory fitting from matrix elements are presented in Fig.6. Experiments indicate that in order to get a good result in the "Three-Gradient Method", the range of the quadrupole strength should generate a

waist at the profile monitor and cover both sides of the waist equally.

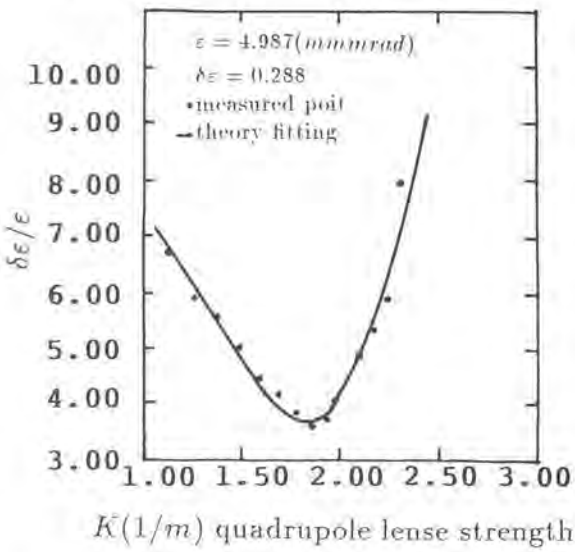


Fig.6. Dependence of the beam size at the profile monitor on the quadrupole strength.

The dependence of beam emittance on the beam percentage is shown in Fig.7, in which both experimetal results measured with "Three-Gradient Method" and theory curve based on Gaussian ditribution are provided.

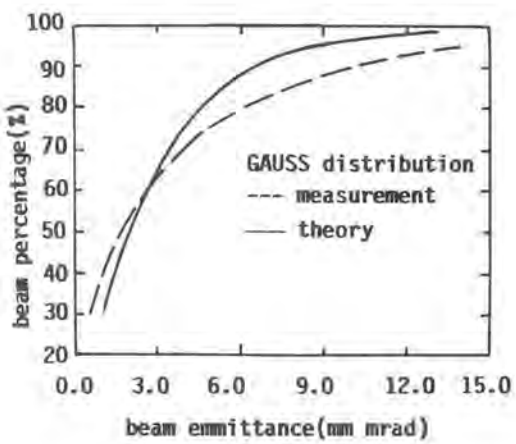


Fig.7. Dependence of emittance on the beam percentage in horizontal direction.

4. SUMMARY

Emittance measurements in the HIRFL beam line have been made using two different methods. From measurement results of the two methods it seems that they are not in very good agreement with each other. But some calibrations and revisions can be made to the measurement results if we take various errors into accout. After revisions,the horizontal emittances measured with two methods are as follows:
with Three-Position Method :

$$\varepsilon = 5.43 \ mm \ mrad \qquad 76\% \text{ beam}$$

with Three-Gradient Method :

$$\varepsilon = 4.99 \ mm \ mrad \qquad 76\% \text{ beam}$$

So we think the emittance measurement results using the two methods are consistent with each other in the error permission. Another emittance measuring system using slit and multi-wire profile monitor will also be put into operation in the near future.

5. REFERENCES

1) Jacobs.K.D, "Emittance Measurements at the Bates Linac" in **Proceedings of 1989 IEEE Particle Accelerator conference**(Chicago,1989) pp.1526-1528 .

2) Strehl.p , "Beam Diagnostic Devices for a Wide Range of Currents" Presented at the Ninth international Conference on cyclotrons and their Applications, pp.545-554.

3) Sheppard.J.C, "Emittance Calculations for the Stanford Linear Collider Injector" IEEE Trans.on Nucl. Sci. **NS-30,NO.4**, 2161(1983).

HIGH SENSITIVITY ELECTRONIC SYSTEM FOR THE PHASE PROBES OF THE LNS/MILANO SUPERCONDUCTING CYCLOTRON

A. Bosotti, D. Corti, C. Pagani, G. Varisco, F. Zibra
INFN and University of Milano, LASA, Via F.lli Cervi 201,
Segrate (Mi) 20090 Italy

and

M. Di Giacomo
INFN, LNS, V.le A. Doria (ang. Via S. Sofia)
Catania 95125 Italy

ABSTRACT

A computer controlled electronics has been developed to process the signals induced by the beam on the phase probes installed in the LNS/Milano K800 Cyclotron. The system works in the frequency range 30 to 96 MHz, corresponding to the 2nd harmonic of the RF voltage. Circuits schemes together with layout solutions and system performances are reported in this paper.

1. SYSTEM DESCRIPTION

The LNS/Milano Superconducting Cyclotron[1] is equipped with 14 non intercepting probes to measure the phase of the beam bunches with respect to the accelerating voltage. This phase detection would assure a precise adjustment of the magnetic field topology for all particles and energy. The required phase reproducibility is ± 0.3°, for an absolute error below ± 1°. The probes are placed inside proper groves carved over two adjacent liner hills.

A photograph of a phase probe is shown in Fig. 1.



Fig. 1. Photograph of a phase probe.

Each probe converts the beam charge into a pulse, whose repetition frequency is that of the accelerating voltage (15 - 48 MHz)[2].

A high sensitivity electronic system converts the signal picked up by the probe into a phase information, via the extraction of its 2nd harmonic. The electronic system block diagram is shown in Fig. 2.

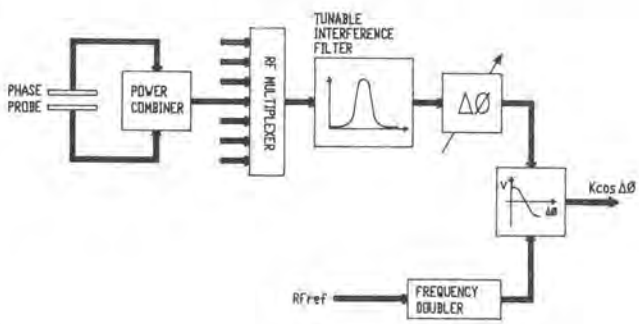


Fig. 2. Control Electronics block diagram.

The high spectral density RF signal induced on each probe is fed to a power combiner to increase the signal to noise ratio[3]. In this way the 1st harmonic noise, due to stray coupling with the accelerating voltage is expected to be reduced. A sixteen channels RF multiplexer is used to select the desired probe signal and to connect it to the control electronics, which is one for all the probes.

A tuneable filter is used to extract 2nd harmonic of the signal. The filtered signal is then amplified and compared with a reference one to detect the beam phase.

The phase detector working point (i.e. its bias) has to be chosen in such a way that the detected phase difference of all isochronous beams, with respect to the phase reference, is independent from the probe position and the signal frequency. A frequency doubled sample of the accelerating voltage is used as phase reference.

A DC voltage, proportional to the cosine of the ion beam phase, is the output of the phase detector. This signal is interfaced to the computer control via a INTEL 4410 microcomputer board.

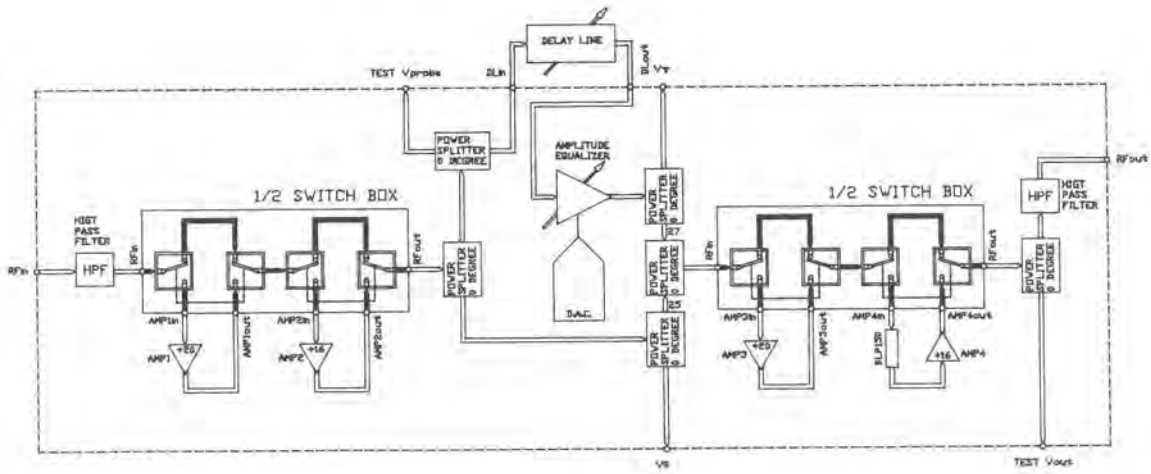


Fig. 4. Filtering section scheme.

1.1. Probe selection system

The probe selection system block diagram is shown in Fig. 3.

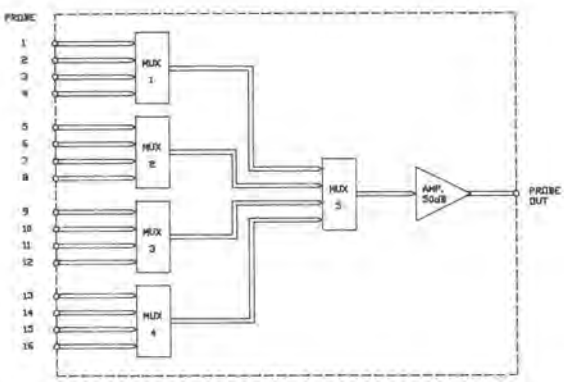


Fig. 3. Probe selection system. The 50 dB RF amplifier is also shown.

The RF multiplexer is a microstrip based device. RF relays shunt the transmission lines to perform channel selection, while the non selected channels are loaded with 50 ohm resistors. The multiplexer main characteristics are: VSWR < 1.5 (Z_o = 50 Ω) and insertion loss < 2 dB.

The desired channel is selected by the computer control through a digital interface board.

A 50 dB RF amplifier is used after the multiplexer to provide amplitude gain before the signal enters into the interference filter, to improve the signal to noise ratio .

The problems of noise and electromagnetic interference has been a crucial aspect in the mutiplexer-amplifier system design and construction. In fact the amplitude of the signal can be so low to be comparable with the stray TTL noise from digital boards and with RF picked up signals from radio waves. Special assembling techniques have been used to reduce these dangerous stray signal interferences. These techniques involve a combination of: filtration of input and output lines, careful layout and grounding, extensive electrostatic and magnetic shielding. High frequency circuits are enclosed in metallic boxes to shield them from logic circuits and the rack itself is fully enclosed in metallic walls to avoid RF pick up from the environment. Noise power level has been reduced below -90 dBm with these improvements.

1.2. Filtering section

The filtering section scheme is shown in Fig. 4.

The interference filter is the most crucial part of the phase probe control electronics system. The extraction of the bunch pulse 2nd harmonic from a high spectral density RF signal is in fact performed by this device. The principle of operation is the following.

The phase probe signal is split by a 0° two ways power divider and one of the two lines is than tuned in such a way that, at the recombination point, the odd harmonics differ by kπ and cancels while the even ones differ by 2kπ and add. A low pass filter after the "odd harmonic rejection filter" cancel the even harmonics higher than the second. A variable length delay line performs the required phase delay all over the operating range (15-48 MHz). This device is a modular six bits computer controlled stepping line (1 ns step for 63 ns maximum delay) together with a continuously variable length line used for fine adjustment in between two adjacent steps.

The delay line has been assembled using six pieces of RG58 coaxial cable of different length, shunted by six RF relays. The continuously variable length line is a microstrip trombone line with a motorized sliding short.

An amplitude equalizer is inserted after the delay line to ensure high degree of rejection in spite of signal amplitude variations .

Four RF amplifiers are also included in the filter rack. These amplifiers are optionally inserted via a system of pin diode switches to cover the required 80 dB working

range; in fact the probe detected signals span from some μV (heavy ions injected from the Tandem) to some mV (axially injected light ions).

1.3. Phase detection system

The phase detection system, shown in Fig. 5, is designed around the Mini Circuits RPD 1 frequency mixer.

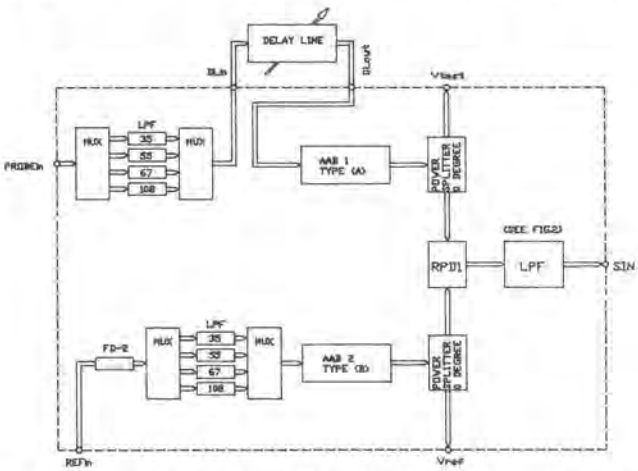


Fig. 5. Phase detection system. The frequency doubling system is also shown.

The phase detector sensitivity must be independent of signal frequency and amplitude and this is not the case of a mixer output signal that is strongly influenced by input signal levels. One applied solution is to overdrive the input ports (P_{in}> +7 dBm) and to use the device saturated[4]. Unfortunately this solution can not be applied in our case because of the device linearity reduction.

So that we have chosen to control the level of input signals, obtaining the curve presented in Fig. 6, where a linear output characteristic is confronted to a saturated one. The former curve has been obtained with +3 dBm and +1 dBm input power on the LO and RF ports respectively, the actual phase detector working point.

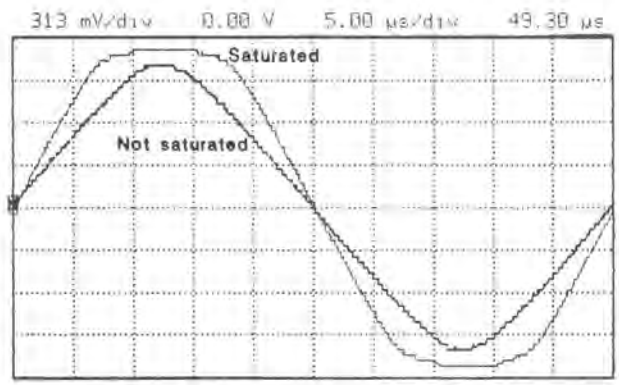


Fig. 6. Phase detector output characteristics, taken from a HP 54201A/D digitizing oscilloscope.

A vector analyzer is used to control the input signal levels, which are set to the right value by two computer controlled attenuation/amplification boxes[5]. A stepping delay line before the mixer RF port sets the proper phase detector working point, independently from the working frequency.

The frequency doubling system (based on a Mini Circuits FD2 RF doubler) is also inserted in the phase detector rack. A low pass filter, after the frequency doubler, cancels the stray high harmonic signals generated by the frequency doubling.

2. SYSTEM PERFORMANCE

Probe sensitivity calculations have been carried out before performing system testing. Particles are supposed to be packed in short bunches (less than 10° RF long) in which the electric charge is uniformly distributed. We have to consider the case of radial injection separately from the case of the axiall one.

Axially injected particles follow the same trajectories and the probes always see the same number of orbits. So that the sensitivity does not depend on the kind of accelerated particle and its computed value is:

$$V_{s2}/I_{dc} = 540\ \mu V/\mu A$$

where: V_{s2} is the amplitude of the 2nd harmonic signal and I_{dc} is the DC current intensity.

Conversely, for radial injection, different particle beams follow different trajectories, and consequently the probes detect different numbers of orbits, being the accelerated voltage amplitude fixed at 100 kV. The probe sensitivity varies from a minimum of 270 μV/μA for the heaviest ions, to a maximum of 540 μV/μA for the lightest particles.

Typical probe detected RF signal have been generated to test the electronic system (Table 1). Radial injection only has been considered.

Table 1. Typical beams

Ion	MeV/n	Z/A	V_{s2}[mV]	f[MHz]
C	100	0.5	79	48
C	60	0.5	47	38
O	100	0.5	105	48
O	60	0.5	62	38
Cu	30	0.34	92	28
Cu	60	0.34	181	38
I	10	0.22	21	16
I	30	0.22	63	28
U	16	0.143	50	21
Cu	40	0.34	123	32

The probe induced voltages are simulated synthesizing a short pulse whose repetition frequency and 2nd harmonic signal amplitude are chosen from Table 1

for the desired particle beam. Signal expected spectrum when accelerating copper ions is shown in Fig. 7 Accelerating voltage frequency is 38 MHz and the beam final energy is 60 MeV/nucleon[6].

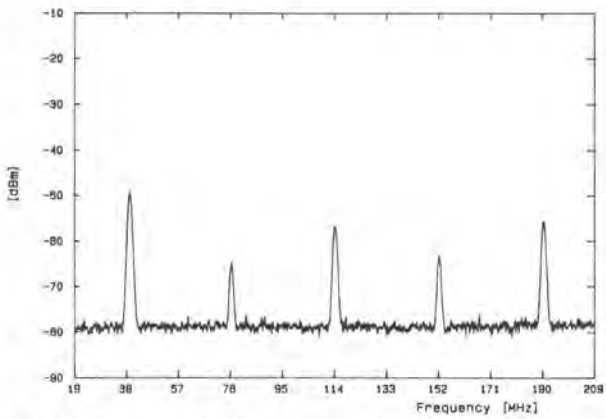


Fig. 7. Filter input signal spectrum. This signal is a simulation of a probe detected voltage when accelerating copper ions.

Signal after the interference filter is shown in Fig. 8 Note that a nearly 50 dB first harmonic rejection has been reached.

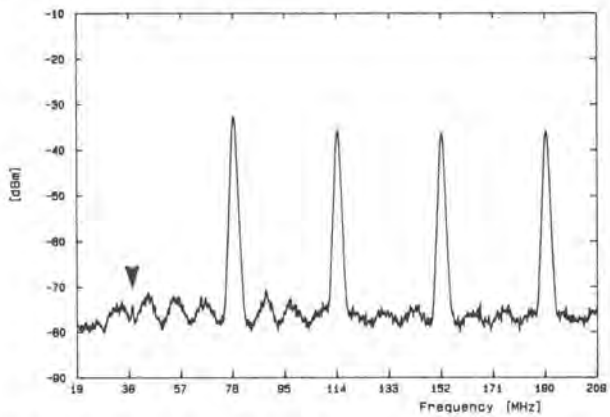


Fig. 8. Signal after interference filter.The arrow shows 1st harmonic power level.

Phase detection system output is shown in Fig. 9. This curve was taken varying the "beam phase" in the full operating range, i.e. ± 90° RF, with respect to the reference signal.

A wide linear range, covering nearly the full working region, is shown in Fig. 9, the phase detector sensitivity being ~ 14 mV/° RF.

The analog signal coming from the phase detector is converted in a digital signal via a SBX 311 12 bit A/D converter, mounted upon a Intel 4410 board. The A/D converts phase information with 494 μV resolution, corresponding to about 0.05°.

At the same time the phase is read, with a lower phase resolution, by the vector analyzer connected at the phase detector input.

As an example a picture of the phase detector rack, showing the internal layout, is shown in Fig. 10.

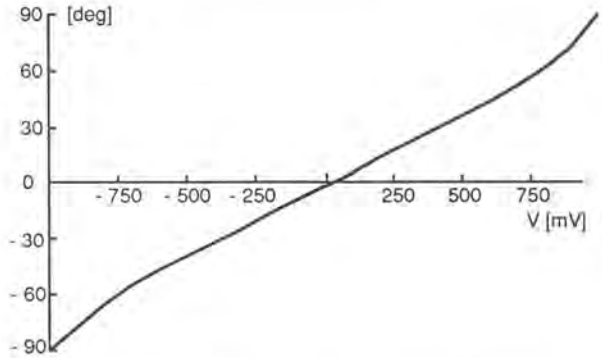


Fig. 9. Phase detection system output .This graph is obtained after phase detector output signal processing.

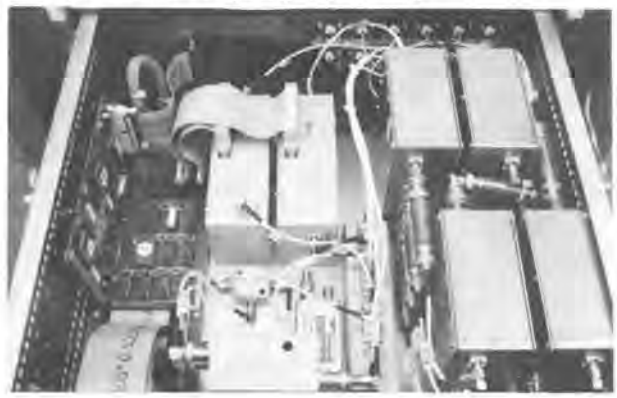


Fig.10. Internal layout of the phase detection section. Assembling techniques to reduce electromagnetic interference are shown.

3. REFERENCES

1) Acerbi, E. et al., "Conceptual design and test of the phase probes for the Milan K800 Cyclotron", in Proceedings of the 12th Conference on Cyclotrons (World Scientific, Berlin, 1989) pp. 287-290.

2) Pagani, C., "RF System of the Milan K800 Cyclotron", in Proceedings of the X International Conference on Cyclotrons (IEEE cat. N. 84CH 1966-3, East Lansing, 1984) pp. 305-310.

3) Van Heusden, G. et al., "Signals levels of phase probes", IEEE Trans. on Nucl. Science, Vol. NS-26 n. 2, 2209 (1979).

4) Legramandi, S.,"Sistema diagnostico per la rivelazione della fase delle particelle accelerate con il ciclotrone superconduttore", Thesis in Physics, University of Milano (1990) pp. 32-35.

5) Bosotti, A. et al.,"New developments in the control electronics for the Milan Superconducting Cyclotron RF system"in Proceedings of the 12th Conference on Cyclotrons (World Scientific, Berlin, 1989) pp. 216-219.

6) Calabretta, L. et al.,"Radial injection into the superconducting cyclotron at LNS", in Proceedings of the 2nd EPAC (Editions Frontieres, Nice,1990) pp. 1240-1242.

THE DIAGNOSTICS SYSTEM FOR THE AGOR SUPERCONDUCTING CYCLOTRON

B. Launé, C. Olivetto*, J. M. Kaplanski, B. Montsanglant, P. Dambre, D. Vincent
Institut de Physique Nucléaire
91406 Orsay Cedex, France†

ABSTRACT

Although the diagnostics needs had been included in the design at an early stage of the project, the compactness and the energy/particle range of AGOR required special care in the design of the different probes: a set of 3 centering probes, an array of 13 phase probes, a straight radial probe (multihead, removable without breaking the machine vacuum), extraction probes (each extraction element has a profile monitor, multiwire or scanning wire, at the entrance and a beamstop at its exit). Full use of the Bitbus interface has been made in the design of the electronics (multiwire BPM, current and phase measurement).

1. INTRODUCTION

The compactness of superconducting cyclotrons requires that the diagnostics needs be included in the design at an early stage of the project: space constraints would forbid further addition of probes. From the beginning it was decided to implement a complete system in order to make tuning as easy as possible and to be able to reach the desired beam quality.[1)] As a matter of fact, this is almost compulsory considering the broad energy/particle range of AGOR (6 MeV/nucleon heavy ions up to 200 MeV protons) and the accordingly complex extraction. In addition, radiation resistant harware had to be used. As will be described in details, automatic tasks are foreseen that make full use of the computer control system and the Bitbus interface. The layout of the internal beam diagnostics systems is shown in Figure 1 and consist in i) three dedicated centering probes ii) an array of 13 phases probes iii) a radial probe with interchangeable heads iv) extraction probes. This system will now be decribed in details, after having recalled the axial injection line diagnostics hardware.

2. AXIAL INJECTION LINE

The axial injection line has been described elsewhere[2)] and the diagnostics equipment is the following:

- current measurement units (I/V converters) connected to Faraday cups and slits,
- beam Profile Monitor (BPM) : 32-wire harps,

For both systems the same electronics as for the internal probes will be used, but with different ranges. See the electronics section for a complete description.

3. BEAM CENTERING

3.1. Principle

Beam centering is essential for beam quality; measurement and control of centering is highly desirable in order to ensure efficient extraction. The principle of the centering determination is the following:

Assuming that ν_r=1 and that acceleration is continous, one can write the beam radius at azimuth θ_i:

$$R(\theta_i) = R_0 + A\sin\theta_i + B\cos\theta_i + \frac{\theta_i}{2\pi}\Delta r \qquad (1)$$

A and B represent the centering error, R_0 a reference radius and Δr the energy gain per turn. At least three different angles θ_i are necessary to find A and B. It was then decided to implement three dedicated probes at 120°. As far as radius is concerned, measurements should occur when the turns are well separated but on the other hand correction has to be accomplished and checked: trim coils 2 and 3 are used to produce a first harmonic such as their combined effects vanish at the measurement location. The selected radial range is therefore 250-300 mm. Beam centering will be made by measuring the effect of one given first harmonic and the same dephased by 90°, enabling the calculation of the correction matrix. Computer simulation has shown that a reasonable precision can be achieved in this way. The radial probe will be used to stop the beam and be sure that one selects the right turns to solve system 1.

*Present address: Centre de Physique des Particules de Marseille, Luminy, Marseille, France.
†Work jointly supported by the Institut de Physique Nucléaire et de Physique des Particules (IN^2P^3), France and the Stichting voor Fundamenteel Onderzoek der Materie (FOM), the Netherlands.

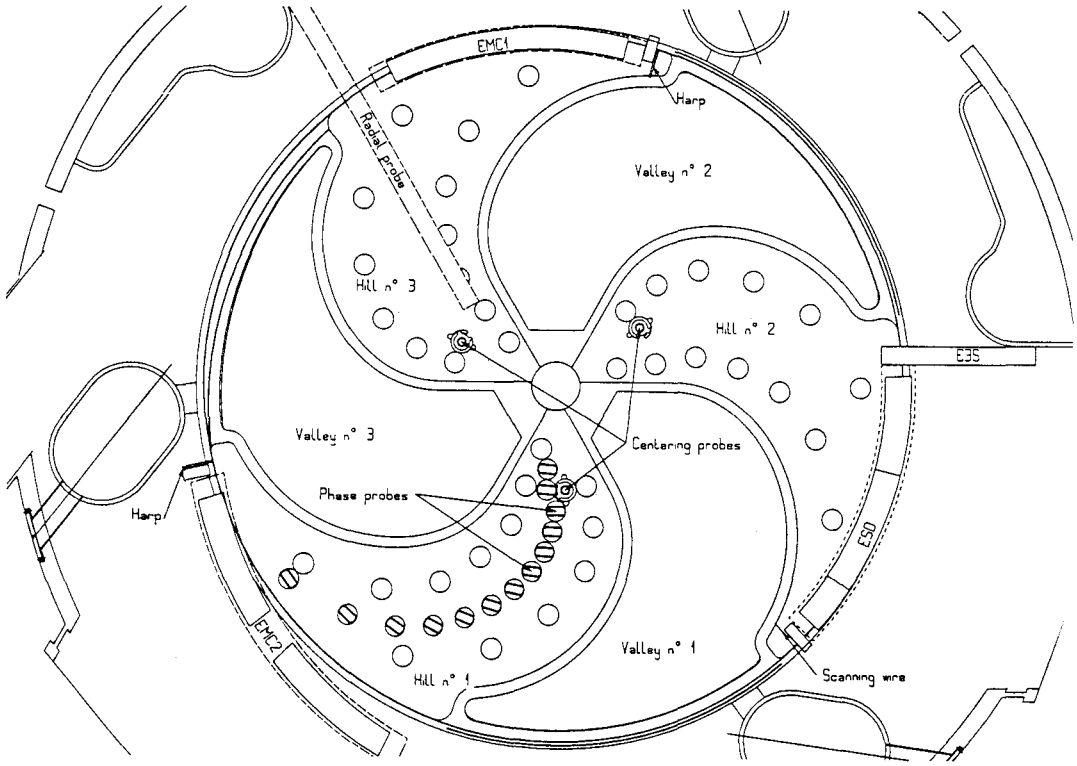


Fig. 1. Layout of the beam diagnostics equipment.

3.2. Centering probes

The lack of space in the center of the cyclotron makes the design of a probe very difficult. A first design was based on a trolley pulled by a string, actuated through a hole in the yoke. A step in the track made the wire flip. A prototype has been built and tested, but failed to sustain a sufficient number of travels. It was then decided to use a different principle: the new one is based on rotation instead of translation and Fig. 2 shows pictures of the probe where the wire is at rest and in a measurement position. The probe is bolted into the vacuum chamber and rotation is accomplished by a tube through the yoke, on top of which a stepping motor is located.

4. PHASE PROBES

A set of 13 non interceptive electrostatic pick-up probes has been implemented in one hill, taking advantage of the "little valley". The probes are bolted into the massive copper vacuum chamber; a 50 Ω coaxial feedtrough and a metallic seal ensure vacuum tightness.

As it is already implemented in others cyclotrons,[3] the data of the phase measurement will be used on-line by a program to calculate the corrections to apply to the main and trim coils in order to obtain the desired phase law; the program has been written and tested using simulated data.

5. RADIAL PROBE

The purpose of the radial probe is to stop and measure the beam from the center up to the extraction radius (see Fig. 3). The low hill spiralisation allowed a straight travel from a radius of 180 mm up to the exit of the extraction elements: electrostatic deflector ESD or first electromagnetic channel EMC1, as the probe has two possible locations. Multihead system was mandatory, considering the functions to be fulfilled and the kind of accelerated beams. The heads are common with the E3S extraction probe (see below); an absolute/differential and a five-finger probe heads have been built (see Fig. 4).

The motion has been divided in two:

- a measurement motion (770 mm), powered by a DC-current motor, the position is given by an absolute encoder and vacuum tightness ensured by bellows.
- a withdrawal motion (1400 mm), powered by a stepping motor, with a sliding seals sytem, that allows the insertion of a valve for head changes.

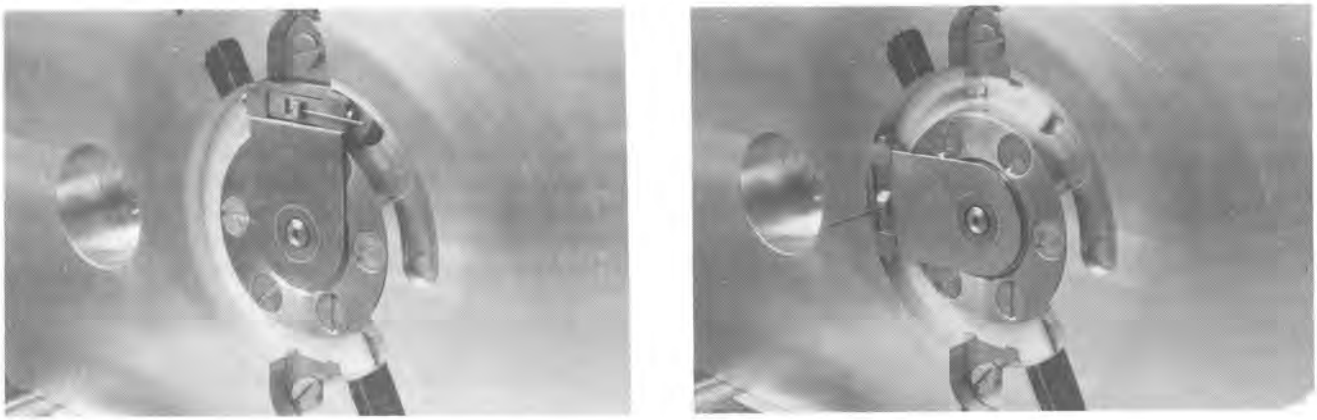


Fig. 2. The centering probe shown at rest (left) and at a measuring position (right).

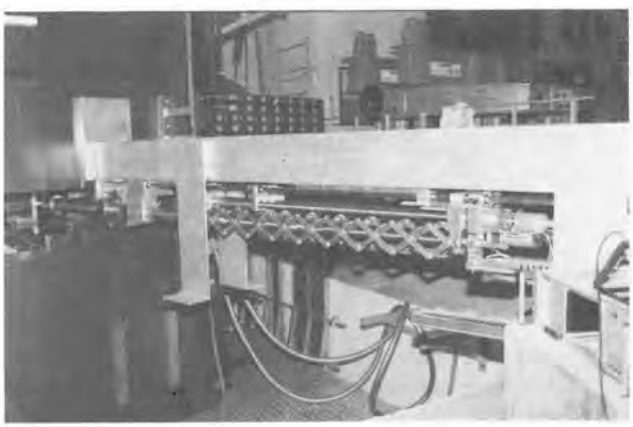


Fig. 3. The radial probe aligned on the cyclotron.

6. EXTRACTION PROBES

Considering the difficulty of the extraction system, a efficient diagnostics system would be particularly helpful. The following guidelines have been followed:

- measurement at entrance and exit of each element,
- beam profile and position at the entrance,
- beam stop at the exit,
- monitoring of losses on each entrance collimator.

We will now review in detail each extraction element:

6.1. ESD

At the entrance, a fast scanning wire allows the control of the beam separation and of the bump tuning, a dedicated probe (E3S) stops and measures the beam at its exit (this probe is compatible with the radial probe, but with a reduced travel: 80 mm); the probe follows the motion of ESD as turn separation between internal and extracted beams is small, it also checks the internal current, allowing efficiency measurement.

6.2. EMC1

The profile and position at the entrance with respect of the channel will be measured by a BPM, based on secondary emission (32-wire harp), that can be withdrawn (see Fig. 5). The compactness of the multiwire board has required construction of a prototype. The beam is mesured and stopped at the exit by the radial probe.

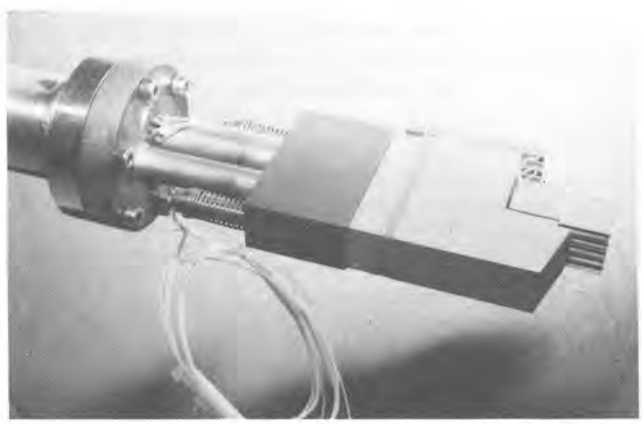


Fig. 4. Five-finger head mounted on the E3S probe.

6.3. EMC2

At the entrance, there is the same sytem as for EMC1, but because of space limitation, no probe could be located at the exit of this superconducting channel.

6.4. QP's

BPM's measure the beam horizontal position and profile at the entrance and exit, while vertical ones are checked at the exit. Beam stopping is accomplished by a Faraday cup located after the second quadrupole.



Fig. 5. 32-wire harp located in front of EMC1.

7. ELECTRONICS

7.1. Current measurement

High precision, wide range units are necessary to measure the current on both axial injection and accelerated beam probes. I/V converters have been built to be mounted directly on a Bitbus crate. Commuting the counter-reacted resistor allows the range selection: only three different resistors are necessary by using 16-bit Analog-to-Digital Converters, that are also self-calibrated and have built-in digital filters (10 Hz cut-off frequency). Test currents (to be sent to the probe, checking in that way the cabling and the whole measurement chain) and possibility to command an actuator are also included in the card. A Bitbus controller commands at the same time the measurement unit and the motor controller, speeding up the scanning of a probe for a profile acquisition.

7.2. Profile measurement

A modular set of 5 cards on Europe-size crate is assembled for each BPM:

- an I/V conversion card, with 32 amplifiers, a multiplexer followed by a variable amplifier providing the dynamic range. SMC technology and four-layer, double sided boards are used,
- a second I/V card if both vertical and horizontal profiles are measured,
- an ADC card,
- a Bitbus interface card,
- a power card.

The value of the resistors are 500 kΩ for the axial injection units and 50 MΩ for extracted beam ones. Tests performed on the KVI beam lines showed a noise of 2.5 pA. The local intelligence in the Bitbus controller can perform operations such as averaging or elimination of off-sets by measurement without beam.

7.3. Phase measurement

The principle of the measurement follows GANIL's one[3] (see Fig. 4):

- a multiplexer selects the probe number, signals from top and bottom are then summed,
- due to the position of the probe, a large pick-up at the fondamental of the RF frequency is expected:
  - measurement is made at twice the RF frequency,
  - a front-end filter cancels the fondamental. Its principle is to split the signal in two, delay one way by the amount that corresponds to 180° at the fondamental and recombine: all odd components should be eliminated. In order to avoid the use of an expensive delay line, a system based on a combination of fixed delay and variable phase shifter operating at a fixed frequency (160 MHz) will be tested.
- the phase measurement is made at a fixed frequency: 21.4 MHz (heterodyne method) by multiplying the signal with the resonator reference at 0° and 90°, producing signals proportionnal to the sine and cosine of the dephasing (I/Q detector), values that are converted in digital by the same ADC as used in the I/V's, then delivered to Bitbus,
- doubling of the reference will use a Phase Lock Loop to improve the spectral purity if necessary.

8. REFERENCES

1) AGOR: Cyclotron Design Report, October 1986.
2) M. Malard et al., "AGOR Axial Injection, using a Positive Light Ion Multicusp Source", in **Proceedings of the Twelfth International Conference on Cyclotrons and their Applications**, Berlin, 1989.
3) A. Chabert, F. Loyer, J. Sauret, "Beam Tuning and Stabilization using Beam Phase Measurements at GANIL" in **Proceedings of the Tenth International Conference on Cyclotrons and their Applications**, East Lansing, 1984.

BEAM DIAGNOSTICS IN THE RCNP RING CYCLOTRON

T. Itahashi, T. Saito and I. Miura
Research Center for Nuclear Physics, Osaka University,
Mihogaoka 10-1, Ibaraki, Osaka 567, Japan

and

S. Ichida
Quantum Equipment Division, Sumitomo Heavy Industries, Ltd.,
Niihama, Ehime 792, Japan

ABSTRACT

Various beam diagnostic devices showed sufficient performances for commissioning of the RCNP ring cyclotron. They worked successfully for an acceleration of 300 MeV proton or polarized proton at a limited current less than 1 nA. By adding filter circuits, more r.f. and static shields and by changing the wire assemblies of monitor head, enough signal to noise ratio was obtained. Beam phase was monitored with a heterodyne method by using a frequency of 5/3 multiple of acceleration frequency for a few nA proton beam, while the width was measured with nuclear gamma-ray and r.f. coincidence via time to amplitude converter.

1. INTRODUCTION

"RCNP Ring Cyclotron Facility" consists of a six-separated sector cyclotron (400 q^2/A) and a beam circulation ring linked to a ultra-high precision dual magnetic spectrograph system.[1] The beam extracted from the RCNP AVF cyclotron (140 q^2/A) are transported through one of the beam lines and injected into the ring cyclotron.

2. TRANSVERSE PLANE

The beam shape and position are measured with three wire profile monitor (TPM-1, -2, -3, -4,

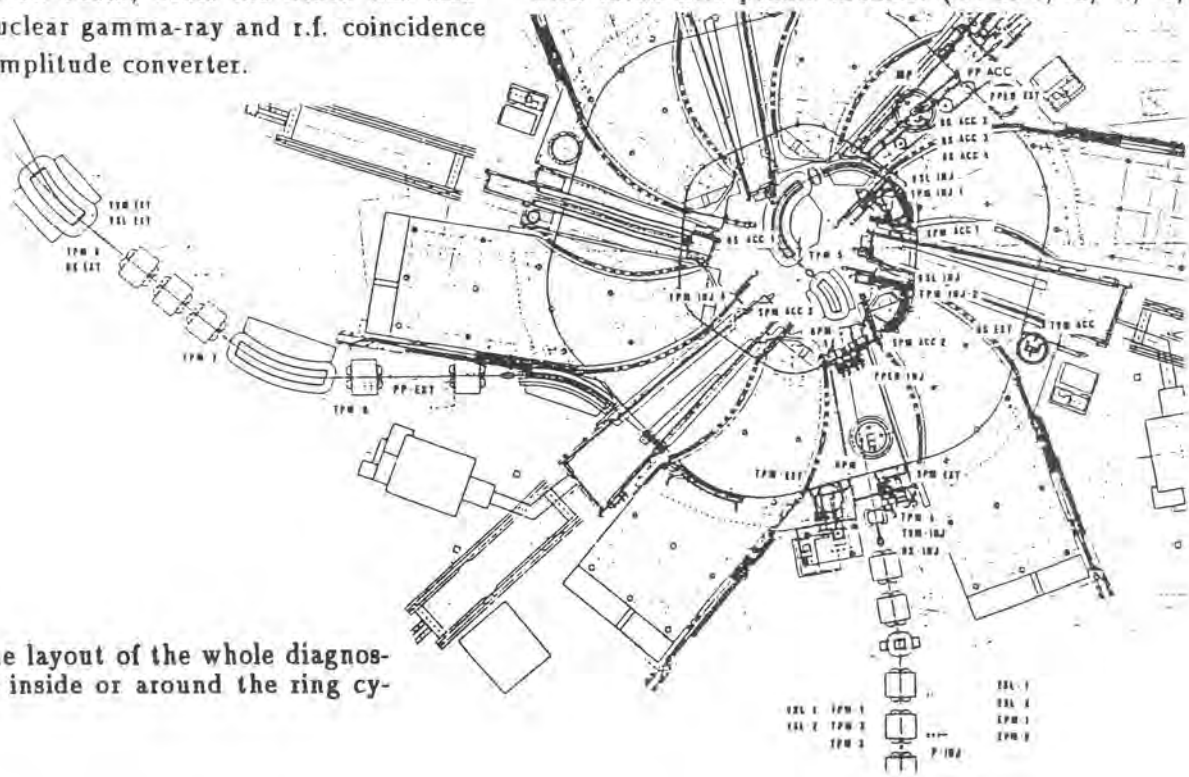


Fig. 1. The layout of the whole diagnostic devices inside or around the ring cyclotron.

-5) at several points of the injection line as shown in Fig. 1. They are installed into the beam duct 45° direction in the vertical plane. The head uses 0.1 mmϕ Au plated tungsten wires. At the total current of about 10nA it gives us the resolution for position of 0.1 mm and for width of 0.2 mm respectively. It is driven by stepping motor over 100mm stroke with about five seconds. Every 0.2mm steps, digitized current data are stored into a register and quickly transferred and displayed to color monitor scope as shown in Fig. 2.

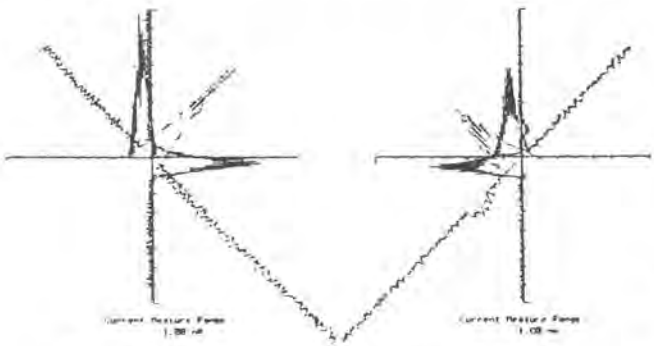


Fig. 2. Beam profiles obtained by three wire profile monitors (TPM-3, -4) in the injection line of the Ring Cyclotron. current range is 1 nA.

In order to obtain good signal to noise ratio for weak beam current down to 1nA, a 30 Hz and 5th order low pass filter circuit is supplemented to the multiplexer after the pre-amplifier in the current monitor system. An integrated circuit of switched capacitor filter (LTC1062) attenuates 30dB for 60-Hz noise component.

The intrusion of higher frequency components from three main cavities and flat top cavity are protected by π-type filter just between the device connector and the signal cable to the current amplifier.

2.1. Injection orbit

Original design of all three-wire profile monitor head employs 0.1 mmϕ gold plated tungsten wire as a sensing tool of current that gave us not enough signal for the beam current less than a few nA in the injection orbit. Thus, we convert this wire to 0.3 mmϕ platinum wire for TPM-INJ-1, 2, 3 and 0.1 mm thick and 1.5 mm wide tantalum ribbon for TPM-EXT (where the vertical wire only). Moreover, geometry of the wiring, where the magnetic field exists near the sector, is crucial to release the electrons produced by the energetic particles. Therefore, these tomography wire should be inclined 10~15 degree vertically to the beam direction. It is noted that cabling between these wire or ribbon to the vacuum feed-through made spurious signal if the cables vibrate accompanied by its stroke movement with a pulse motor accutuator. We improve shielded cables to fix the supporting rods tightly.

From the entrance of the first magnetic inflection channel (MIC-1) on about 2/3 of circumference for the 1st orbit, three three-wire profile monitors, three single-wire monitor (SPM-1,2,3) and one radial beam stop give us precise and sufficient data to match the orbital acceptance. The three spectra taken with the SPM-ACC-1,2,3 determines the vertical position of injected beam after passing the sector magnet 1, 2 and 4 as shown in Fig. 3. Its mechanical movement of 1 mmϕ single wire is ensured by quick rotation of 10 mmϕ aluminum tube via ferrofluidic seal coupled to the pulse motor actuator.

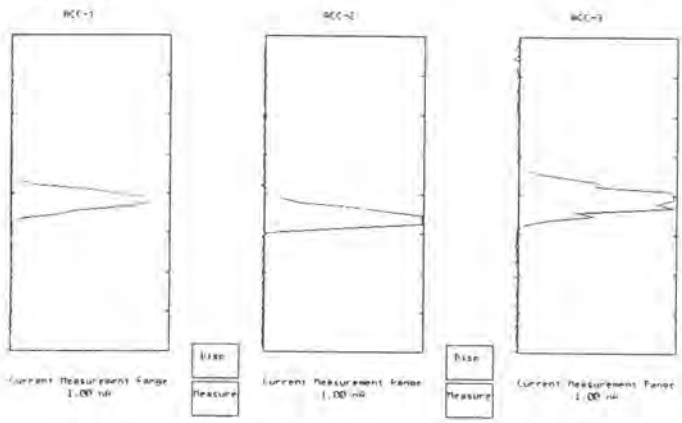


Fig. 3. Three spectra taken with single wire profile monitor at the injection orbit. Full stroke is ±20 mm from the median plane. SPM(ACC)-3 intercepts two or three accelerated beam orbits.

2.2. Accelerated beam orbit

The radial distribution during the acceleration can be properly observed with a main probe (M.P.) which has a 2000mm stoke. It is shown in Fig. 4. It measures the current and the transverse shape of the accelerated beam. It consists of tomog-

raphy head of three thin platinum wires and ribbon and an indirectly cooled beam stop. The probe can be adjusted for the head to face the tangential direction of the beam orbit at any radius. The driving speeds can be chosen between 20mm/sec and 200mm/sec (it is helpful to use it in a smaller radial position).

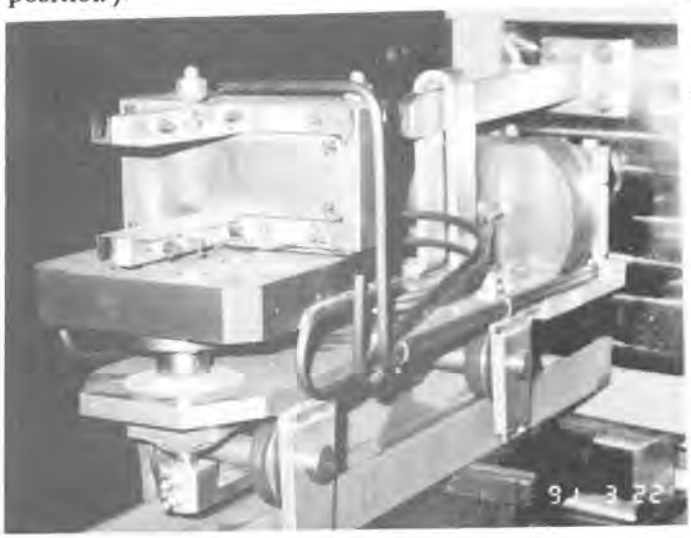


Fig. 4. Main probe.

2.3 Extraction orbit

Along the extraction orbit, TV-monitor (TVM-ACC), single-wire profile monitor (SPM-EXT) and three wire profile monitor (TPM-EXT) can observe the turn separation of the final few turns around the extraction orbit and behavior of a radial gain per turn by varying the r.f. phase or by tuning the phase history with correction of the magnetic field defect upon the radius $\delta B(r)$. The main probe is also useful to measure these features by repeating stroke around this region with a short intervals.

3. LONGITUDINAL PLANE

The phase acceptance of the ring is 20° for a flat-topping acceleration mode with beam energy resolution 10^{-4} while the value is 10° to do the neutron time of flight experiment. Especially for the axial injection mode, new dee-insert played very effective role to reduce the width at moderate current reduction.[2)]

3.1. Beam phase width

An r.f. and gamma-ray coincidence technique was applied for the phase width measurement at a beam current less than 10 nA. Spectrum of the time to amplitude converter is shown in Fig. 5. Time width for the injected beam obtained so far is less than 1.1ns. In these measurements, instrumental time resolution is less than 0.5 ns.

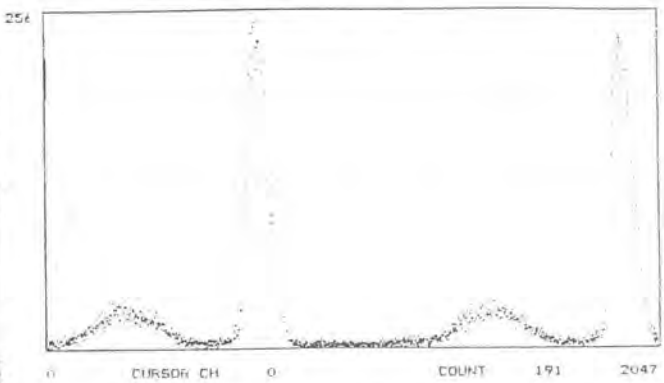


Fig. 5. An r.f.-gamma coincidence spectra obtained at the final radius of the AVF cyclotron. Two peaks is separated by 63.8 ns.

3.2. Beam phase relative to the acceleration r.f.

The actual phase of the beam from the injector cyclotron relative to the acceleration r.f. can be measured by a non-intercepting capacitive pick-up (PP-INJ) when the beam not less than 10 nA

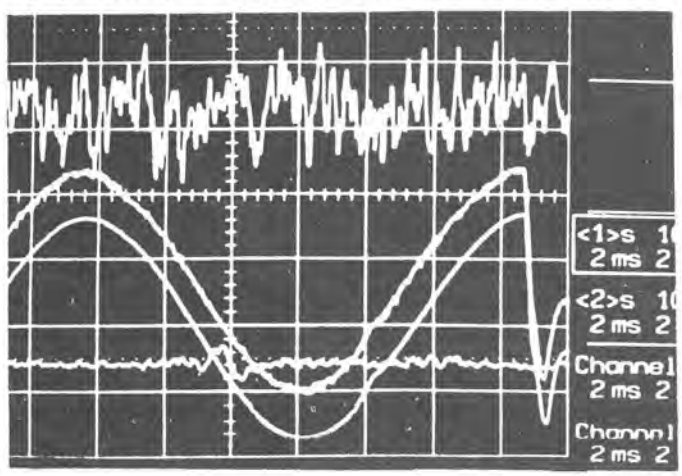


Fig. 6. Beam phase relative to the acceleration r.f. observed with a non-intercepting capacitive pick-up (PP-INJ) when the current was about 50 nA.

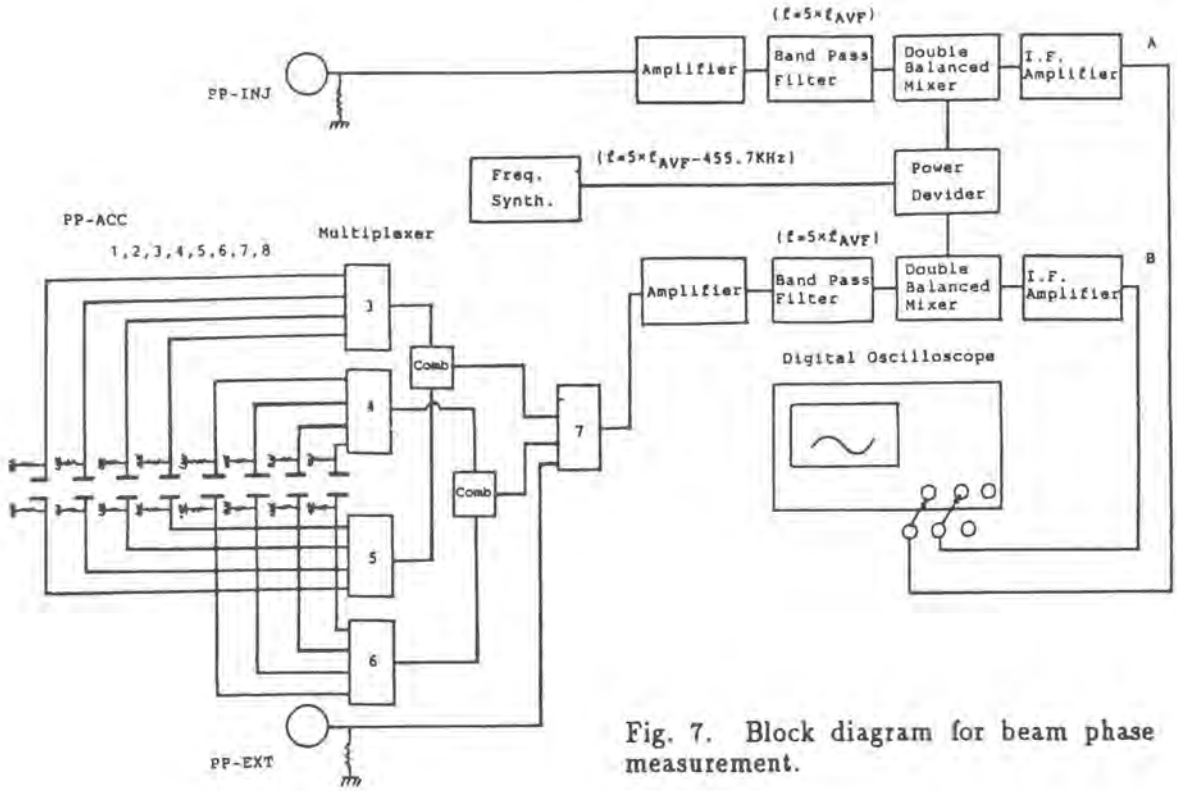


Fig. 7. Block diagram for beam phase measurement.

is injected; rf. caused from three main cavities and flat-top cavities interfered the beam signal severely. It used the sampling pulse circuits and digital oscilloscope. Fig. 6 shows beam phase observed with PP-INJ, when the current was about 50 nA. Beam signal was obtained after averaging and subtracting two signals with a injected beam and without the beam each other.

The beam phases relative to the acceleration r.f. are measured with eight parallel plate detectors (PP-ACC), which are separated by 300 mm each other on a same carriage. Superheterodyne technique applied for measurements gives good signal to noise ratio in existence of large r.f. background. They are measured with the 5th harmonic component of the beam signal. It is designed so as to use 455 KHz for IF stage to any cyclotron frequency: it uses a crystal filter in the IF amplifier. The output signals are averaged by a digital oscilloscope to reduce a thermal noise. The block diagram of the total circuits is shown in Fig. 7.

4. ACKNOWLEDGMENTS

We would like to thank Dr. M. Kase for his useful comments on operational experiences of diagnostic devices for RIKEN cyclotron (RRC). Special thank to Dr. W. Joho (PSI) for his contribution to Kikuchi summer school and his comment.

REFERENCES

1) Ikegami, H. "The RCNP Ring Cyclotron Facilities" in Proc. 12th Int. Conf. on Cyclotrons and Their Applications, 1989, pp.30~39.
2) Miura, I, Itahashi, T. "New Dee-insert system to select the longitudinal phase width assisted by an r.f. intrusion" to be published in Nucl. Instr. & Method.
3) Itahashi, T. "Beam diagnostics in the ring cyclotron", Proc. 12th Int. Conf. on Cyclotrons and their Applications, 1989, pp. 301-304.

Signal Processing for Internal Phase Probe in the TRIUMF cyclotron

K. Fong
TRIUMF, 4004 Wesbrock Mall, Vancouver, B.C., Canada V6T 2A3

ABSTRACT

In the TRIUMF cyclotron, the beam cavity is sandwiched between the rf resonant cavity, with several parasitic modes that are in the vicinity of the operating frequency. Rf fields that are present in the beam cavity are orders of magnitude higher than cyclotrons of other designs. Phase probes in this region must be able to extract the beam signal from the significant amount of contaminating rf noise that is present. With a combination of hardware and software adaptive noise cancelling techniques, it is possible to obtain accurate beam phase information at a signal-to-noise ratio of less than one, corresponding to a beam current of 5 μA.

INTRODUCTION

In the TRIUMF 500 MeV H^- cyclotron the beam induced signals from the internal phase probes are completely masked by the pick up of extraneous signals due to rf fields generated through excitation of parasitic modes and random electrical discharges in the accelerating dee structure. The cavity in which the beam travels can support parasitic modes that can be excited through misalignments of the resonators at the dee gap. These parasitic mode fields with frequency components consisting of 23.06 MHz fundamental dee excitation frequency plus its harmonics and the inherent wide band noise due to discharge lead to extraneous fields ranging from 1kV/m to more than 10 kV/m depending on dee alignment. These fields generate interfering signals on the capacitive probes used for non-intercepting detection of the beam. By signal processing at the second rf harmonic the interference is reduced significantly while still permitting a wide operating range of 180° for beam phase measurement. Direct conversion from the 46 MHz harmonic into base-band using a vector demodulator is used to extract beam phase information. The effect of residual rf leakage is removed by pulsing the beam so that the phase of the beam can be obtained from subtracting the beam-on vector from the beam-off vector. The beam-off vector is continuously updated to allow for long time drifts in the system. Using the combination of the above techniques, we have been able to obtain beam phase information for peak current as low as 5 μA at 50 % duty cycle.

PHASE PROBE FRONT-END

A non-intercepting phase probe is simply a metal plate over which a charged beam bunch passes. The beam induces a voltage on the plate which is proportional to the amount of charges in the beam pulse. Stray electric fields that are present near the plate also induce voltages in the plate, contaminating the beam signal. To improve the signal-to-noise ratio, an opposing upper and lower probe pair is used. Most of the rf leakage picked up by the two probes have vertical electric fields that induce voltage in the upper and lower probes that are 180° out of phase. On the other hand, the beam induces voltages in the probes that are in phase. Therefore, by summing the two probe signals the leakage component will be suppressed and the beam component enhanced. The existing probe pair is located inside the vacuum tank behind the resonator, starting at a radius of 272 inches. The front surface of each plate is covered with aquadag to suppress electron emission from occurring at its surface. The plates are surrounded by grounded shields, isolated from ground by ceramic stand-offs and connected to the detection electronics by 50 Ω coaxial cables. The turn separation of the beam at the radii of the phase probes is of the order of 1.5 mm, so the induced voltage is the sum of more than 60 turns. For a 100 μA beam, the measured second harmonic component of the signal is 10 mV_{p-p}. This is close to the predicted value when cable losses are taken into account. The second harmonic component of the rf leakage voltage is typically 10 mV_{p-p}, with noise bursts up to 30 mV_{p-p}. Due to the presence of non-vertical fields, cancellation of rf leakage by this standard method is not complete. The residual noise consists of random bursts of less than 1 μs in duration (Figure 1). The origin of these noise bursts is discharges in either the rf resonator or the rest of the vacuum tank which generates rf noises that are able to propagate to the phase probes. Vibrations of the resonator support structure further modulate the amplitude of the residue noise with a 5 Hz component. The amplitude of the residual noise is typically 2 mV_{p-p}, which can still pose a significant interference to the beam signal at lower beam current.

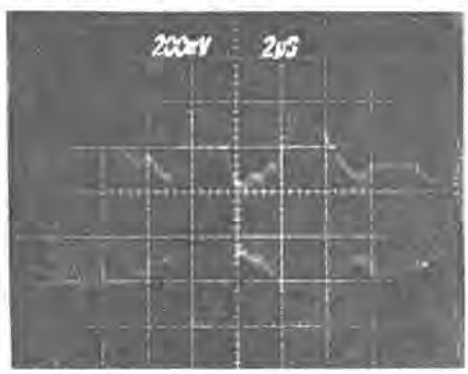


Figure 1. 46MHz component of noise bursts from a single phase probe. The signal is amplified 30 times. The average amplitude is 600 mV_{p-p}, with a modulation of greater than 50 %.

DETECTION ELECTRONICS

The second harmonic of 46 MHz is chosen for phase probe signal processing because of its low leakage values as well as its wide operating range. A schematic of the vector demodulator is given in Figure 2. Direct conversion of the phase signal from rf to base-band is employed. The reference signal is derived directly from the rf system itself. Since the rf accelerating field is amplitude controlled but not phase

controlled, vibrations in the support structure of the resonant cavity changes the tune of the cavity and causes a time-varying phase shift between the amplifier and the cavity. The reference phase for the detector is obtained from an electric field probe located inside the resonator near the accelerating gap where the electric field is

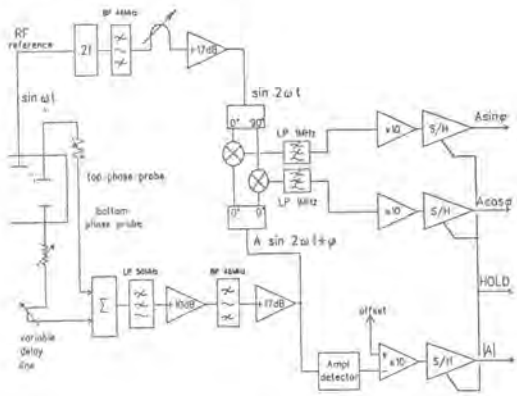


Figure 2. Block diagram of vector demodulator for the phase probe.

in phase with the accelerating field. Since the probe is located inside the resonator, the induced voltage consists of the 23 MHz signal with all other frequencies at least 60 dB weaker. For this reason no filtering is needed before the dee probe signal is frequency doubled by mixing with itself to obtain a 46 MHz phase reference. The other mixing products are removed by bandpass filters. The reference 46 MHz signal is amplified and split into two equal parts : the I (in-phase) and Q (quadrature) components. The signals from the upper and lower phase probes are bandpass filtered to accept only the 46 MHz components. These consist of the Fourier component of the beam signal, the second harmonic rf leakage and the 46 MHz component of wideband discharges. The relative amplitudes and phases of the filtered signals are adjusted to obtain the maximum cancellation of the rf leakage. Filtering before combining the two signals enables each of the signal to be monitored individually with an oscilloscope. The relative amplitudes and phases of the two signal can then be adjusted for cancellation. The combined signals are monitored by a directional coupler installed after the combiner. Fine cancellation is performed by minimizing the voltage at this point with the beam switched off. A small amount of the signal is tapped off to a tuned amplitude detector for beam intensity measurements. The main portion of the signal is split and mixed with the I and Q reference signals. A pair of diplexers at the output of the mixers provides constant terminating impedance in order to minimize inter-modulation products. The 500 KHz low frequency branches of the diplexers extract the I and Q information of the phase probe signal. The I,Q and amplitude signal are then amplified and digitized. Track-and-Hold amplifiers are used before the digitizer to assure that the digitized information from all the channels are acquired simultaneously. The information at this stage is the vector sum of the leakage and the beam pick-up phasors. Frequency response at this stage extends from dc to the response of the post detection amplifiers which are approximately 100 KHz.

Using the I,Q information, Figure 3 shows the two clusters of sampled data in the I-Q plane with a 180 μA beam pulsed at 50 % duty cycle. The beam-off cluster is located at the centre of the picture and the beam-on cluster at the right side.



Figure 3. I-Q diagram showing the data clusters of demodulated beam phase signal. The distance between the two clusters is proportional to the magnitude of the beam current and the angle the beam phase.

The sizes of clusters are indications of the amount of noise that is contaminating the measurements. The 5 Hz AM noise from the resonator support structure vibration can cause the centroid of the cluster to move in unison without affecting the angle between them. Actual beam phase modulation due to the vibration can cause the beam-on measurement to rotate about the beam-off measurement. It is apparent from the figure that the phase resolution of the phase probe is determined by the size of the clusters and their separation. The cluster sizes depend on the noise generated by the rf system and on the effectiveness of the cancellation. The separation between the cluster is proportional to the beam intensity. For a given cluster size, when the beam intensity is reduced, the beam-on cluster moves towards the beam-off cluster, and the uncertainty in the beam phase angle increases almost linearly with the reciprocal of the separation until the two clusters overlap, at which point the uncertainty in beam phase is approximately 45°. Generally speaking, this uncertainty can be reduced by averaging the data points for each of the clusters at the expense of the frequency response. This is performed in software as described in the next section.

SIGNAL ANALYSIS SOFTWARE

After digitization, the beam signals are processed by software. The signals are digitized in a CAMAC module and read by a general purpose computer through a CAMAC branch highway, with the consequence that real time information of the signal is lost. The main objective of the software is to calculate the phase angle and to remove the time varying background noise. To accomplish this, the software consists of two main parts: the adaptive beam detection logic and the angle calculation. The main logic blocks are indicated in Figure 4. During angle calculation, the code keeps running averages of the sines and cosines during beam-on and beam-off intervals as determined by the beam detection logic, and uses these values to calculate the actual beam phase angle ϕ. The averaging are performed by one pole Infinite Impulse

Response filters. More sophisticated filters can be used if necessary.

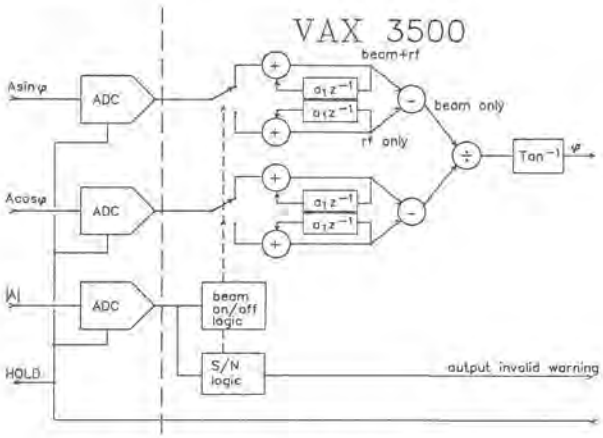


Figure 4. Software logic block diagram for the beam phase angle calculation.

The adaptive beam detection logic is used to determine the presence or absence of the beam signal. The signal which occurs during the absence of the beam is used for background subtraction. At the start of the measurement, a sample of beam intensity values which consists of both beam-on and beam-off values is collected. This set of numbers are histogrammed and their values smoothed by a 9-point quadratic smoothing routine[1]. The peaks corresponding to the maximum and minimum intensities are determined by fitting to Gaussian profiles, and their standard deviations determined. This information is used to set the centers and widths of windows of acceptance for the subsequent data. Spurious data caused by transients due to sparks in the ion source, the injection line, the main acceleration rf, as well as the rising and falling edge of the pulsing beam-on period which can result in intensity values falling outside the window of acceptance are rejected by the detection system. These data windows are not set a priori but are derived from the beam to compensate for the varying beam intensities and tuning conditions of the cyclotron, which tend to drift slowly. Furthermore, the centers and widths of the acceptance windows are updated in each data acquisition cycle in the form of running averages, which enable them to adapt the variations in the rf leakage or the beam intensity. In this way as long as the beam or the rf leakage does not suddenly change by more than two standard deviations within the averaging interval, the detection logic is able to track these changes and adjust the acceptance windows accordingly. Care must be taken in tracking the widths of the peaks since the acceptance/rejection process is intrinsically unstable for the width. The growth rate can be made very small, however, by an appropriate choice of the tracking parameters. The acceptance windows are chosen to be 3 standard deviations from the peaks to include 99 % of the valid data.

MEASUREMENTS

A series of measurement were performed at various beam intensities. It was found that the minimum current required for phase measurement depended on the stability of the rf system, since this is manifested in the amplitude of noise bursts picked up by the phase probes. During a period of stable rf operation, accurate phase information was obtained from beam currents as low as 3 μA.

Figure 5 shows the phase measurement when there were instabilities in the rf system during the course of the measurement. During this measurement the beam current was increased from 36 μA to 60 μA in 2 increments of 12 μA. The calculated phase remained stable at 59±2° for beam current of 36 and 48 μA. At approximately the 160th count, the current was increased to 60 μA. Shortly afterward a spark occurred and brought down the rf system. After it was restarted the rf became unstable and the rf leakage increased in amplitude and fluctuated wildly, as observed in the figure. Even though the signal increased as a result of the increase in beam intensity, the signal-to-noise ratio decreased by a large amount due to the wild fluctuation in the rf leakage. Correspondingly the calculated phase in Figure 5 became unreliable and showed phase fluctuations of more than 7°.

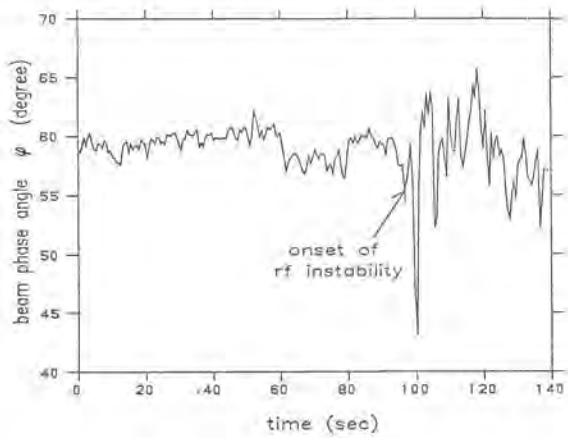


Figure 5. Beam phase angle before and after unstable rf operation.

CONCLUSION

It is possible to extract good beam phase information from a high rf leakage background by adequate signal processing. In order to track the time varying background for background subtraction, the beam must be able to pulse off regularly. Under stable rf operations, beam phase information can be obtained from contaminated signal with a signal-to-noise ratio of less than one, corresponding, for the TRUMF case, beam currents as low as 5 μA.

REFERENCE

1. A. Savitzky and M. Golay, Anal. Chem. 36,8, 1627 (1964)

A DC Current Transformer for TRIUMF

Yan Yin
TRIUMF, University of British Columbia
4004 Wesbrook Mall, Vancouver, V6T 2A3, Canada

ABSTRACT

A DC current transformer (DCCT) has been designed to operate over the current range of ± 20 mA, with a resolution and accuracy of 2 μA. The long term drift has been measured at less than 3 μA over 30 hours.

A test has been done using H^- beam CRM 2" cusp ion source to compare the readings of DCCT and the Faraday Cup. The test shows that they both agree within 3 μA.

1. The Principle of the DCCT

The DCCT consists of 2 toroids which are wound with 1 mil supermalloy tape. The diameter is 8.5" O.D, 7.875" I.D, the height is 0.313". The two toroids are matched with each other. The permeability is as high as 60000.

There are 5 coils. Each toroid has a 30 turn drive-coil driving it to saturation. The two drive coils are connected in series but with opposite polarity. So the two toroids will be driven into saturation in opposite directions. A 100 turns sense coil is wound around the two toroids. The DCCT measures the magnetic field of the beam. When there is no current going through the toroids, the sense coil will sense nothing. But when there is current going through the toroids, the current will bias the saturation of the toroids, the difference of them is proportional to the current to be measured. A feedback coil is used to balance the sense signal, so that the current going through the feedback coil will build up a voltage on the standard resistors to be readout.

The circuit is a modification of the CERN[1)] type DCCT circuit. The circuit consists of Drive, Receiver, De-modulator, Feedback, Calibration and Output. The driving signal is a 1.7 KHz square wave.

2. A Test with ion source

The device was installed in the injection line of the Central Region Model cyclotron and its output compared with the current read by a Faraday cup equipped with ring plates biased to repel stripped and secondary electrons, The DCCT was inserted into the beam pipe with an nylon pipe spacer to cut off the wall current which flowed through wires bridging the gap and outside the DCCT. With this arrangement, the DCCT will be able to detect the beam signal. Fig.1. A 2" cusp ion source delivered a steady current of H^- or D^- ions accelerated to 15 KeV.

Three tests have been done. The first one compared the DCCT reading with the Faraday cup reading with H^- beam. The vacuum close to the the Faraday cup was 4×10^{-7}. Due to current limit of the ion source, the measurement was only done up to 950 μA. The measurement showed that the DCCT read a current 5% smaller than the Faraday Cup did, Fig.2, where " □ " represents H^-, "+" represents D^-.

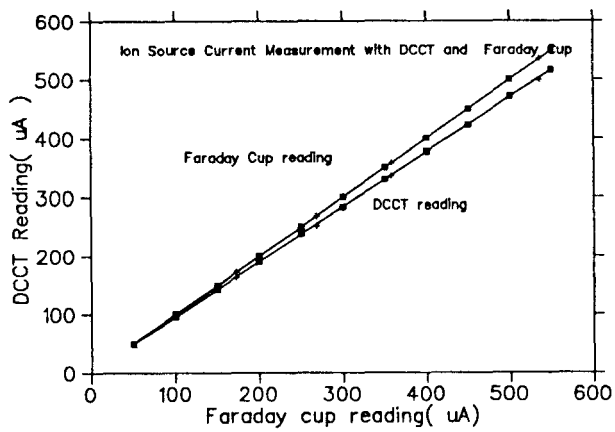


Fig.2. Ion current measured by Faraday Cup and DCCT

To understand the discrepancy of the two readings, the second and the third tests were done. The second test measured the currents from Faraday Cup and the Bias while keeping the voltage of the bias at -300 volts but changing the beam current. This test was done with D^- beam due to the ion source set-up at the time. The test showed that the current on the bias was increasing

when the beam current was increasing. The difference between the Faraday Cup and the bias current is just the reading of DCCT, see Fig.3, symbol "+". Although the DCCT was not installed at the second and third test, by interpolating from the Faraday Cup reading, , the corresponding data which fitted the the DCCT reading curve obtained from the first test, can be gotten. The difference is less than 3 μA as following table shows.

$I_{Faraday}$	$I_{Faraday}$-I_{bias}	$I_{interpolated}$=DCCT
173	165	164.62
268	253.5	254.56
301	283.4	284.92
358	337.2	337.52
400	377.1	377
536	500.7	503.4

The current unit in above table is μA.

The third test measured the currents from Faraday Cup and the Bias while keeping the beam constant and changing the voltage of the bias from 0 to -350 V. The vacuum in the beam pipe before the Faraday Cup was 2.6×10^{-7}. This test showed that the difference between both was constant although both readings were changing, Fig.3. But when the voltage was higher than 10 volts, the change was very small.

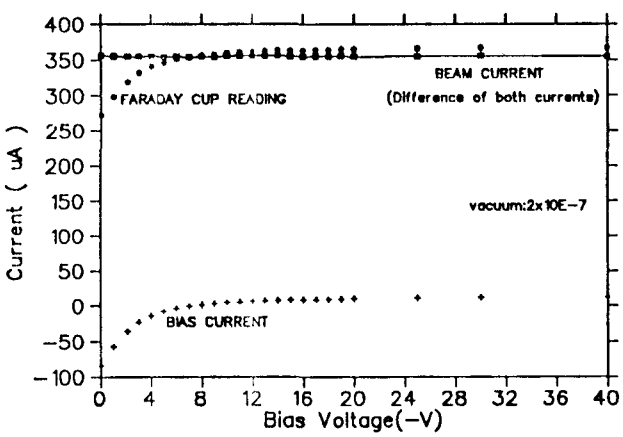


Fig. 3. The Bias, Faraday cup and DCCT

This phenomenon is related to secondary emission and backscattering. When the voltage of the bias is higher than -8 volts, the electrons due to secondary emission or gas stripping were repelled and can not reach the bias plate, but when the voltage is lower than -8 volts, the electrons will be able to hit the bias plate to form the negative current. When the bias voltage is higher than 8 volts, there is a positive current going through the bias plates, this is because the bias with negative voltage will attract the positive charges due to ion stripping and the backscattering. If the beam current is increasing, this part will be also increasing proportionally to the beam current.

3. The drift and sensitivity to the magnetic field of the DCCT

The DCCT was tracked over several days to measure the drift. The DCCT was placed in Trailer GG for a long weekend and the zero reading was collected by the computer.

The measurement started on Nov.8, Friday, 5:30 PM, ended on Nov.11, Monday, which was a long weekend. On Nov.10th 7:00 AM, the main magnet was turned on, the DCCT detected the magnetic field change, Fig.4. Each division of Y is equivalent to 10 μA. during the first 7 hours, DCCT drifted about 10 μA; it then stayed at $\pm2\mu$A. If the temperature change in the room was about 5°C, the drift related to temperature is 0.8 μA/°C. The DCCT reads current by measuring the magnetic field of the current. The μ of the toroid is 60000, so every mA current will produce 1.2 Gauss magnetic field in the toroid, which will be converted to the DC current reading. So the sensitivity to the magnetic field is about 0.83 mA/Gauss. This is consistent to the observation of the DCCT reading change when it was on the roof of the Proton Hall with the main magnet turned on.

4. The wall current influence to the DCCT

Although the DCCT measures the beam current by detecting the magnetic field, the non-metal material spacer is still needed nearby. Since when the beam goes through the pipe, the wall current will go along the pipe on the opposite direction, cancelling each other, and the DCCT will not be able to detect beam signal. Also because the beam pipe is like a long antenna, with many interference induced in it, this gives DCCT a big false reading. A test has been done to prove this. Even without the beam, the DCCT read about 4 mA which was jumping and could not be set to zero.

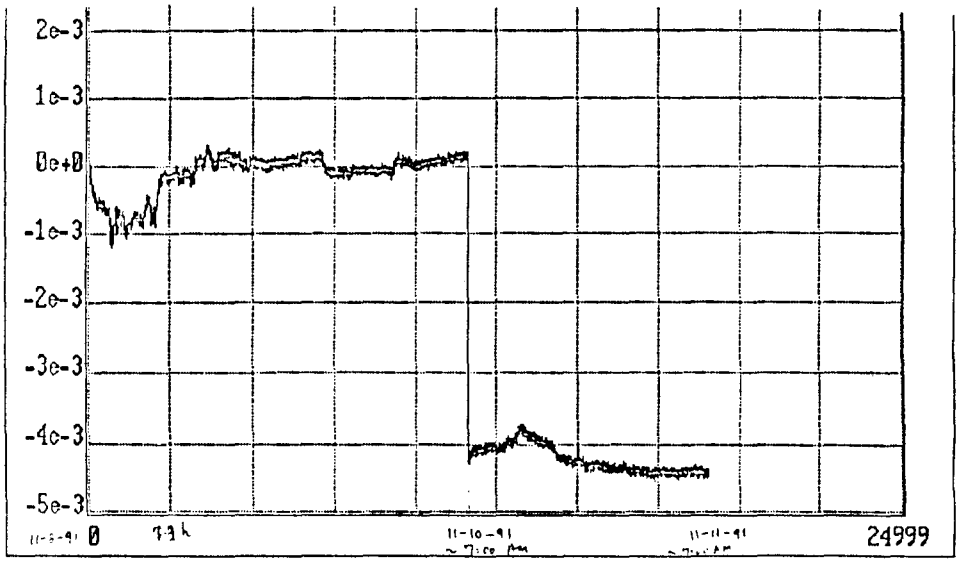


Fig.4. The drifting test and the influnce of the magnetic field

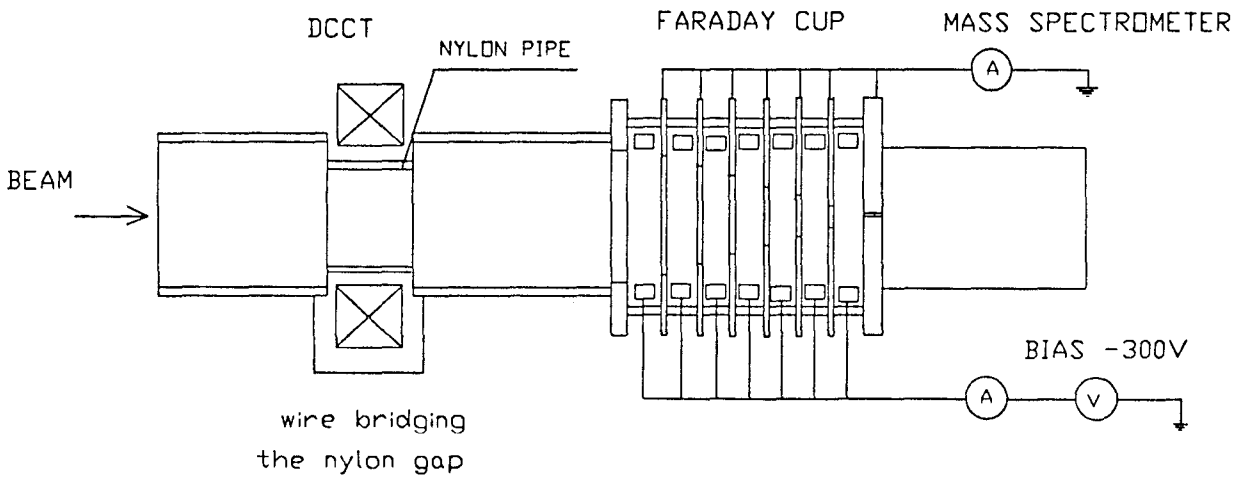


Fig. 1. IRM 2" cups ion source set up for DCCT test

5. Acknowledgments

The author gives her thanks to Dick Yuan for doing the experiment with CRM ion source, for Brian Evans for helping with DCCT drifting tracking measurement, also thanks for John Fraser and Bill Rawnsley for the discussion to better understanding of the results.

6. REFERENCES

1) K.B.Unser, *Beam Current Transformer with DC to 200 MHz Range*, IEEE ,NS-16, p.934-938, June 1969

ADVANCES IN RF TECHNOLOGY FOR CYCLOTRONS

C. Pagani

University of Milano and INFN
LASA, Via F.lli Cervi 201, 20090 Segrate (Milano), Italy.

ABSTRACT

The wide number of cyclotron applications and the different physics requirements have produced a variety of machine designs, especially of the RF cavities which have to support the Dees, and depend strongly on the magnet design. In this paper few recent RF systems are discussed with emphasis on the cavity design improvements, mainly based on new ideas, designer's imagination and advances in allowable technology. Some suggestion on the way to make profit from the use of computer are also given, together with some general ideas on how to design the control electronics and the RF power amplifiers.

1. INTRODUCTION

In the cyclotron history many cases can be found in which the RF system was considered just when the general machine design (that is mainly the magnet) was practically frozen. As a consequence a number of RF systems suffer the fact that some of the imposed constraints, which limited the possible solutions and sometime the best envisaged performances, were not strictly necessary. In these cases a minor modification of the machine design would possibly have produced a much performing RF.

In this paper I will describe few recent RF systems which were designed with discussed boundary conditions, that is whose parameters have been optimized together with the general machine parameters. To do that the RF designer must have a serious knowledge on beam dynamics and techniques related to magnetic field design, while the project leader must have a good competence on RF related problems.

I am convinced that most of the RF performances are dominated by the cavity design[1,2], including the coupling element. In fact few companies can deliver a very good amplifier, the problem being eventually the price. Again modern electronics allows to design performing controls which match phase and amplitude stability requirements and can be operated via computer. But in the case of meson factories, with very strong beam loading, electronic controls can be considered like cyclotron independent. This concept means that, adapting the frequency range and the software compatibility, a good electronic control, designed for a multi-cavity machine, can in principle be used for any other cyclotron whose cavities have no major limitations.

In the next paragraph I will briefly discuss five recent cavities, pointing out the major design choices together with the solutions adopted, based on the development of original designs for critical components and on the use of special technologies, which could be widely applied in cavity realization to improve the system reliability and performance. The eventual impact on the overall machine cost is discussed too.

In the third paragraph few comments and personal opinions are given on the way to make profit from a proper use of the allowable computer codes and more generally from the computer itself.

Finally in each of the last two paragraphs one example will be given, respectively of control electronics and RF amplifier. These two examples can be considered as a reference, in the sense that they include most of the important, or just useful, choices which would have to be done when a RF system is designed.

2. CAVITY DESIGN EXAMPLES

Among all the built cavities, I have chosen few recent examples to discuss the most interesting technologies applied or developed together with the design criteria, related to the machine specs and constraints. I will also use these examples to sketch how design, ideas and technical solutions are going together all over the time of the machine construction; so that most of the comments expressed for a specific RF system have to be considered as general comments referred to most of the RF systems.

2.1 The AGOR Cavity

The superconducting cyclotron AGOR[3,4] has three vertical and identical cavities, symmetrically placed with respect to the machine median plane. The conceptual design of this cavity has been conceived together with the magnet design, with the aim to obtain the best compromise from the machine point of view. Particularly, with respect to the other three sectors superconducting cyclotrons[5-8], the chosen frequency range is considerably higher (24 to 62 MHz), asking for a different harmonic operation. In this case the majority of ion energies per atomic mass unit (10 to 72 MeV/amu) are accelerated using the 3rd harmonic instead of the 2nd

(LNS/Milano) or the 1st, like in the others cases. The use of the 4th harmonic for energies below 10 MeV/amu increases the minimum RF frequency up to 24 MHz.

The major impacts on the magnet and RF designs produced by the chosen frequency range can be summarized as in the following:

a) Each magnet pole has three very large (Φ=500 mm) vertical holes, tangent to the hill profile, but no other holes are supplied for coupling and fine tuning. A careful design of the valley shimming[3] was necessary to compensate for the big holes. In the other similar machines this magnet design has not been accepted or proposed. A schematic drawing of the AGOR pole face, where the large RF holes are visible, is presented in Fig. 1.

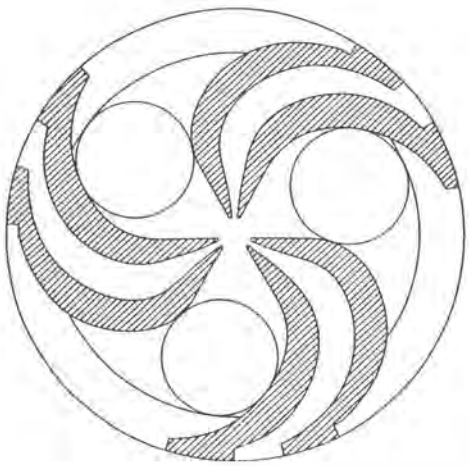


Fig. 1. Schematic drawing of the AGOR pole face with the large RF holes tangent to the hill profile.

b) The RF cavities can be much shorter (~ 2 m) and no ceramic insulator between the HV electrode and the outer coaxial line is supposed to be needed[9]. For a lower RF power and Dee voltage, a compact and performing sliding short has been developed, able to slide under power and vacuum, and to include variable inductive coupling and fine tuning[10]. Very tight general tolerances and external multi-axis adjustments are needed too.

Once defined the frequency range and the general design criteria - based on the previously mentioned compromise supported by first order calculations and technological considerations - as for the other machine components, the RF boundary conditions become practically frozen and the detailed design starts, including the items and the fabrication technologies which need to be implemented or developed. In the case of the AGOR RF system I will list in the following the major characteristics of the cavity design[9,10] and technology, pointing out the most interesting solutions, which could be eventually applied for other machines.

• Because of the absence of the mechanical support given by the ceramic feedthrough, the cavity length has been minimized at low frequency, while increasing the minimum distance of the sliding short circuit from the beam plane. These two effects have been together obtained maximizing the characteristic impedance of the coaxial part (just limited by mechanical rigidity and current density considerations), while reducing the impedance of the dee-liner region, by a careful shaping of the HV electrode and of the valley part of the liner. The reduction of the impedance of the dee-liner region slightly increases the average current density on the sliding short, the effect being screened by a more homogeneous distribution[10].

• Coarse tuning, fine tuning and variable inductive coupling are performed via two symmetrical multi-function sliding shorts, one carrying the coupling loop. A schematic drawing of the multi-function sliding short carrying the coupling loop is presented in Fig. 2. Particularly: coarse tuning is accomplished by mean of a symmetrical and rigid movements of the two sliding shorts; the coupling loop is matched varying the distance between the two concentric rings, in which the short is split; fine tuning is done and maintained acting (during operation via a feedback system) on the position of the outer ring of the sliding short not involved in the coupling loop matching.

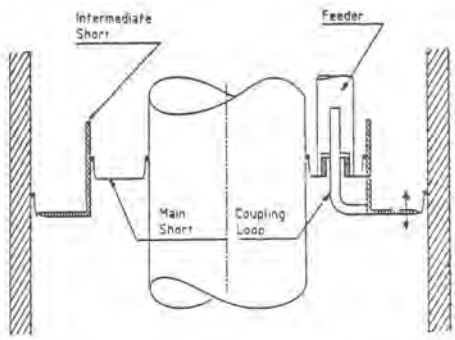


Fig. 2. Schematic drawing of the AGOR cavity sliding short which carries the coupling loop.

• Many technologies have been used to fulfil the tight requirements on the general mechanical tolerances and stability against induced vibrations and thermal deformations. Moreover the very compact solution chosen for the sliding short contacts (based on the developments of carefully optimized finger contacts), while supporting the needed current density (~ 40 A/cm @ 60 MHz), with a 50% safety margin[10], asks for overall tolerances between the two coaxials of the order of ± 0.5 mm. As a consequence, compared to the other cavities for similar cyclotrons[5,6,11], this one needed more engineering and the total cost has been higher. Each dee half is EB welded to the inner coaxial and can not be disassembled. Again numerically controlled multi-axis machining has been widely used (together with EB

welding) to guarantee the mechanical tolerances needed for the dee position (central region, extraction and lip plane) and for a safe operation of the sliding contacts all over the frequency range.

2.2 The LNS/Milano Cyclotron Cavity

While the operating diagram of the LNS/Milano cyclotron is very similar to that of AGOR, the general design is quite different[7,8]. As mentioned above the majority of ion energies per atomic mass unit (8.5 to 100 MeV/amu) are accelerated using the 2nd harmonic instead of the 3rd, the RF frequency range being 15 to 48 MHz.

The compromise between magnet and RF has been different: for a less sophisticated coil design, the large holes (Φ = 500 mm) on the pole valleys have been accepted just up to a minimum distance of 600 mm from the median plane. As a consequence the 3rd harmonic, with frequencies up to 72 MHz was impossible, and we decided to put all the efforts to have a 2nd harmonic operation covering almost all the operating diagram up to 100 MeV/amu. Moreover the 2nd harmonic (with respect to the 3rd) has the advantage to reduce the phase precession problem at the extraction, for a 13 % lost of the peak dee voltage.

Among these discussed boundary conditions, the cavity was designed to fulfil the specs with a reasonable cost and development[11-14]. In the following I will list the rationals of some choices, together with the conceptual design of few special items, trying to sketch how they are sometime dictated by theory and experience, and sometime by personal feeling, optimism or imagination.

• Dee shape has been defined with the aim to minimize the overall capacitance and reduce the high field regions to those considered unavoidable (at the centre and at the extraction; see the photograph of Fig. 6). An aluminium bulk structure has been chosen for the dee to minimize its volume and weight for the same stiffness A copper cone, which can be disassembled, assures the connection to the dee stem, while housing the cryopump cold head. A brazing technique had to be developed to connect the Cu cooling pipes to the Al dee.

• Being the hole shape in the magnet yoke a boundary condition (see Fig. 3), the transition region, between the valley part of the cavity and the uniform coaxial part, was designed to get the maximum required frequency (48 MHz), while optimizing (see below for the criteria) the insulator region in the allowable space. Once understood and taken into account the behaviour of the cavity characteristic impedance into this strongly perturbed region and how it affects the overall cavity parameters (maximum frequency, power dissipation, etc,), the main criteria to perform the optimization of the insulator region can be summarised in a careful control of the following three parameters:

- maximum electric surface field on the corona ring; ≤ 30 kV/cm for a dry controlled atmosphere.
- maximum electric surface field at the ceramic edges: ~ 2 kV/cm, to strongly simplify the vacuum tight ceramic to Cu connection (done by a simple Viton OR seal)
- maximum power dissipation inside the insulator: ~ 200 W, together with a proper distribution to minimize the insulator equilibrium temperature (a minimum insulator Q = 5000 is in this case accepted).

After measurements on the cavity prototype a second order optimization has been performed (see § 3) using the computer code SUPERFISH, which was implemented for this purpose. A maximum frequency of 49.5 MHz was reached for the cavity supporting the most capacitive dee (that is the dee between the two electrostatic deflectors), instead of 47 MHz, as measured on the cavity prototype (one MHz below the computed value). A drawing of the upper half of the LNS/Milano cavity is presented in Fig. 3.

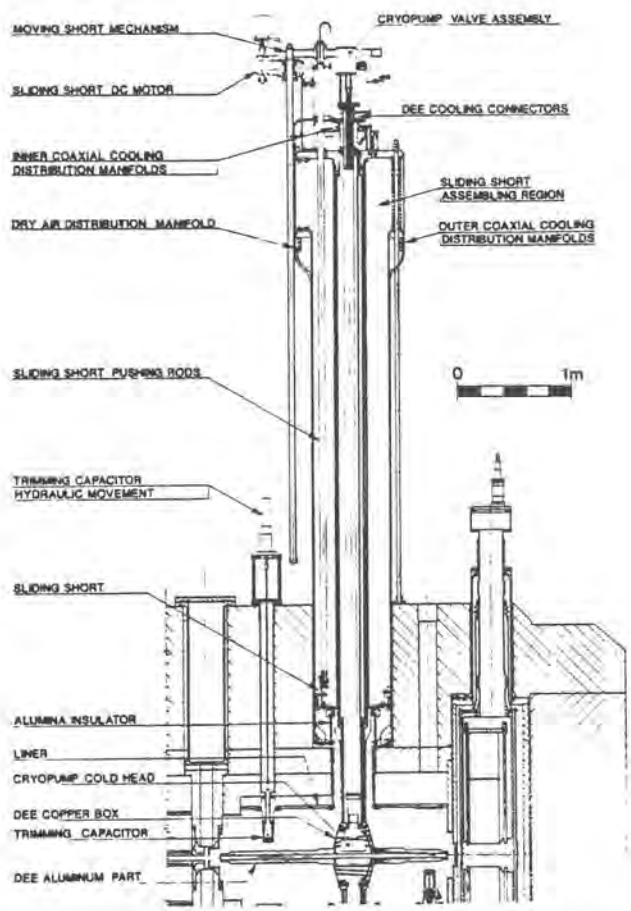


Fig. 3. Schematic drawing of the upper half of the LNS/Milano cavity fitted into the magnet.

• The characteristic impedance of the uniform coaxial part of the cavity, which does not appreciably affect the maximum frequency and the maximum dissipated power (in such a cavity being always associated to the highest

frequency), has been determined as a compromise between the cavity length and the maximum current density to be accepted by the sliding short contacts. I want to point out that a rms current density of more than 40 A/cm @ 50 MHz, together with reasonable mechanical tolerances (greater than ± 1 mm to limit the cavity cost), was at that time already optimistic and well above the existing technology. Nevertheless, if the high performance ball based sliding short[15] was at that time already developed, a different optimization would have been done, reducing the cavity length (and the sliding short stroke) of at least half a metre!

• A drawing of the high performance ball based sliding short, which was developed to fulfil the specs, is presented in Fig. 4. Being the item designed around a completely new idea[15], its performances, as optimistically expected, resulted to be much higher than needed. Since a more detailed discussion on the basic idea, experimental results and technologies involved is available in Ref. [15], in the following I will just list the major performances and characteristics of the actual sliding short, as a reference for other projects on what can be reliably done today. In particular its characteristics are:

- Maximum current density (rms, @ 50 MHz) > 200 A/cm
- Accepted mechanical tolerances ± 2.5 mm
- Sliding distance before ball maintenance > few km
- Under vacuum operation (~ 10^{-7} mbar) allowed
- Sliding at full current allowed

• The last interesting item I want to mention is the coupling capacitor, whose drawing is presented in Fig. 5. Its main peculiarity are:

- The inner conductor is coaxially water cooled up to the edge of the cylindrical alumina insulator;
- The coupling head has a stroke of 50 mm;
- An especially designed tee (6 1/8") is used for a reliable access of water pipes and rotary actuator ceramic staff.

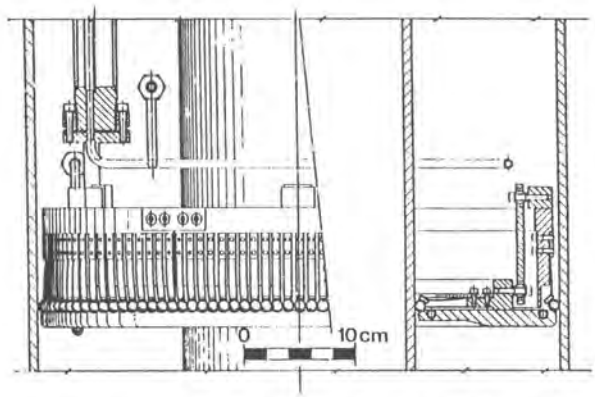


Fig. 4. Drawing of the very high performance, ball based, sliding short of the LNS/Milano cavity.

A thin layer of Ti (~ 60 Å), deposited on the insulator surface exposed to vacuum, can be used to prevent damages from static charges, like usually done in SC cavity main couplers[16]. This technique has not been already adopted for the couplers of cyclotron cavities, but it would improve their reliability.

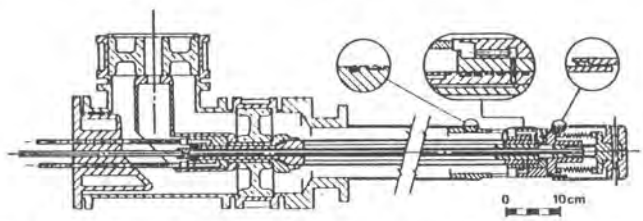


Fig. 5. Schematic drawing of the variable, coaxially cooled, coupler of the LNS/Milano cavity.



Fig. 6. Picture of one of the LNS/Milano liners covering the magnet pole, the three alluminum dee halves being assembled in their final position. On the top of the hills the special groves carved for beam dyagnostic and stripper are also visible.

Among the unusual technologies adopted to solve some critical feature[11], I want to mention:

- Electroforming of outer coaxials, to have together tolerances, thickness and surface quality;
- EB welding of the major Cu components of the coaxials, to be not limited on their thickness (that is on the general cavity stiffness);
- Inner coaxial cooling by coaxial stainless steel tubes, the external one supporting an especially shaped rubber joint, helically placed with a variable pass (see Fig. 11);
- TIG welding (with a proper He-Ar atmosphere) of the two Cu-OFHC liners, composed of thin (3 mm) sheets for the vertical parts and thick (18 mm) sheets for the horizontal ones (hill and valley covering). This solution, presented in Fig. 6, while mechanically stiff, gives the possibility to locate beam probes into special groves (carved into the hill covers) and to precisely work (with a numerically controlled machine) all the critical parts like the dee lining and the vacuum tight connections with the outer coaxial, the trimmer, the coupler and the central plug. A similar technique has been adopted for the AGOR liners, which have to support atmospheric pressure[10].

2.3 The GANIL SSC Cavity

I want to mention the GANIL SSC cavity[17-19], also if its design is not very recent, because it is an example of imagination to better fulfil the machine requirements, discussed in advance, with a reasonably compact and quite reliable structure. In this case, for an envisaged frequency range very low and wide (6.4 to 14.2 MHz), a dee voltage almost proportional to the frequency was required. Again, to have a favourable phase compression, a dee voltage increasing with the machine radius was strongly recommended. Conversely the only limitation imposed by the magnets was to fit in the region between two sectors.

With these requirements, a cavity of the coaxial type (tuned by sliding shorts) is not a good solution; in fact the usual behaviour of such a cavity type would produce these major effects:

- a dissipateed power strongly increasing with the frequency (dee voltage being a constant), that is with a behaviour opposite to that suggested by dee voltage vs frequency required low;
- the need of a vertical symmetrical structure, because of the required voltage vs radius behaviour,
- an enormous vertical dimension for a power dissipation which is negligible at low frequency, with respect to that required at high frequency.

So that the GANIL SSC cavity, whose schematic drawing is presented in Fig. 7, while being symmetrical with respect to the beam plane, is more similar to a lumped circuit than a coaxial cavity. In fact, referring to Fig. 7, the two folded (to reduce the vertical dimension) dee stems behave like two parallel inductances, resonating with the dee capacitance. Starting from the highest one, frequency range is covered increasing the dee capacitance, by mean of a very large wave panel. As a result, at the price of an almost constant power dissipation, in spite of the dee voltage vs frequency low, a very compact and reliable cavity has been realized.

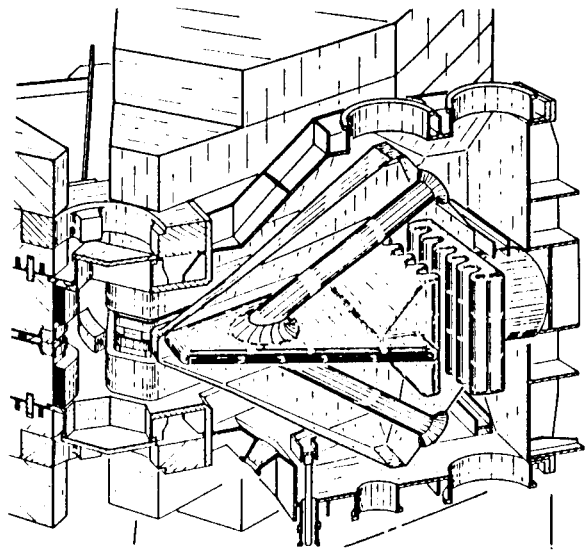


Fig. 7. Pictorial view of the GANIL SSC cavity in its operational position between two magnet sectors.

I want to mention a possible problem which comes with this type of structure, that is the existence of a strong, radial and high Q high order mode, involving the dee, the capacitive panel and its stem. In the case of the GANIL cavity, this mode, which was computed and measured, can be excited by the 3rd harmonic of the fundamental, the last being tuned at a frequency closed to 9 MHz. Nevertheless, in the GANIL operation, this parasitic mode has never been a limitation, because of the combination of the weak coupling performed to this mode by the main coupler and of the good harmonic rejection performed by the RF amplifier output circuit, together with the matching line.

2.4 The RIKEN Ring Cyclotron Cavity

Among the many cavities designed and constructed for large separated sector cyclotrons I want also to quote the cavity of RIKEN[20,21], because of its unusual and very interesting design which could be taken as a reference when a high (with respect to that of GANIL) and wide RF frequency range is required, for a frequency independent peak dee voltage. Particularly, for the RIKEN cavity, the frequency range is 20 to 45 MHz, for a dee voltage of 250 kV. A sketch of the movable box RIKEN resonator is presented in Fig. 8.

As can be evinced from the drawing of Fig. 8, the cavity is a vertical half-wavelength (that is two time $\lambda/4$) coaxial resonator, the tuning being performed by two symmetrical, very low characteristic impedance, movable

boxes, instead of by sliding shorts, as usual and envisaged in the preliminary design. The effect of the low impedance boxes[22] can be understood thinking that the effect of a characteristic impedance jump on the length of a λ/4 coaxial resonator depends on the standing wave longitudinal phase at the jump position, according to the first order equation[22]:

$$\Delta\alpha = \frac{Z_{0o} - Z_{0i}}{2\,Z_{0i}} \sin 2\alpha_i$$

where: $\Delta\alpha$ is the phase advance due to the jump (in the direction from the open edge to the shorted one), Z_{0i} and Z_{0o} are respectively the characteristic impedance before and after the jump and α_i is the phase just before the jump. Because a box produces two opposite jumps at two different phase positions, that is weighted by two different values of sin2α, the effect of the box movement, which has a fixed geometrical length, is that to tune a constant length cavity all over a frequency range. We note that, in this case, the effect of the dee to box cpacitance is also important to compute the cavity behaviour.

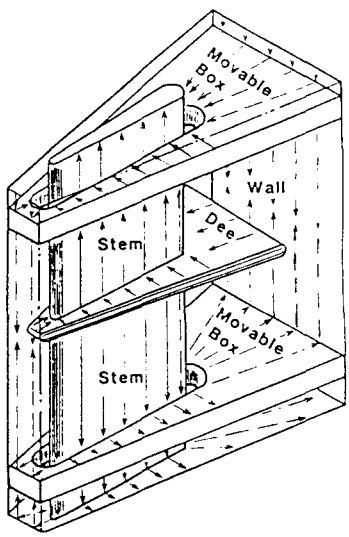


Fig. 8. Schematic drawing of the box tuned cavity for the RIKEN ring cyclotron. The arrows show the RF surface current behaviour.

Once optimized the box dimensions, the main advantages of this tuning system, with respect to the use of symmetrical sliding shorts, are:

- the overall cavity length is reduced,
- the demands on the box sliding shorts are much less severe and so the position of the dee stem can be set for a radial increase of the dee voltage, to take advantage of the induced beam phase compression,
- the stroke of the box is smaller with respect to an equivalent sliding short.

Conversely the most important disadvantage is that of the total power dissipation which, for a wide tuning range, is significantly increased all over the frequency range.

2.5 The Tritron SC Cavity

Tritron is based on a quite original concept, very promising for compact accelerators[23]. As discussed in Ref. 23, this machine is called Tritron because it has typical features of a cyclotron, a syncrotron as well as a linac. In particular, the beam performs separated orbits, guided by 238 superconducting magnetic channels, for a total of almost 20 turns. Radial and axial focusing are produced by the alternating gradient of the channels, while, as in a conventional cyclotron, the condition of isochronism is fulfilled by the radial dependence of B_z. Also longitudinal focusing will occurs in this machine.

Concerning the accelerating system, the Tritron concept asks for very compact, and properly shaped, superconducting cavities, able to fit the magnetic channels structure, while supplying to the beam an accelerating voltage per turn ranging from 1.4 to 3 MV, at injection and extraction respectively. Conversely, the use of high harmonic numbers (harmonic number h ranging from 14 to 55), allowed because of the longitudinal focusing, sets the cavity frequency to 170 MHz. A drawing of one of the six Tritron cavities is presented in Fig. 9.

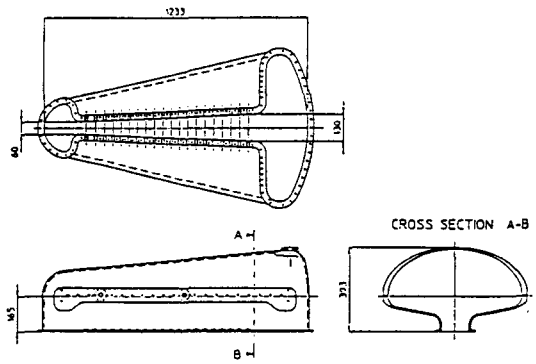


Fig. 9. Drawing of the 170 MHz superconducting cavity for the Tritron cyclotron.

Since all the details are available in Ref. [24], I want just to mention two very unusual and promising technologies which have been developed to fulfil the cavity specs and could be considered for other new machines, namely:

- Electroforming of the Cu cavity halves. The major steps of this technique are: a solid plastic model of the cavity inside, a mold which encloses the model exactly, a number of fibreglass shells (one for each cavity half) sprayed with a conducting layer, electroforming of the cavity halves, final machining of the symmetry planes.
- Electroplating of the superconducting PbSn layer (4 at % Sn). This was performed by the Tritron group with a commercially available bath, the electrodes being made by a set of platinum plated titanium roads.

As a result six superconducting cavities have been realized, able to hold an accelerating voltage higher than the design value (250 kV at the injection and 530 kV at the extraction), for a heat dissipation well below 6 W.

3. COMPUTER CODES IN CAVITY DESIGN

The need of a very large 3D electromagnetic code is not felt by most of the cyclotron community. In fact, as can be understood from the above examples (but the TRITRON CAVITY), the geometry of a cyclotron cavity is usually very complex and completely three dimensional. Moreover to define the general behaviour of the fundamental, accelerating, mode the design method based on the transmission line schematization and model measurements[1] is well established and can give very good results: the limit of a cavity usually being determined by technological problems. Thus the design of good existing cavities would probably have been almost the same even if a large electromagnetic code had been used.

The use of large electromagnetic codes (2D and 3D) is eventually useful if an envisaged (or built) structure has serious problems coming from the excitation of high order (parasitic) modes by the harmonics of the fundamental. One example of two computed dangerous high order modes[25], standing inside the accelerating electrode of the TRIUMF cavity, is presented in Fig. 10

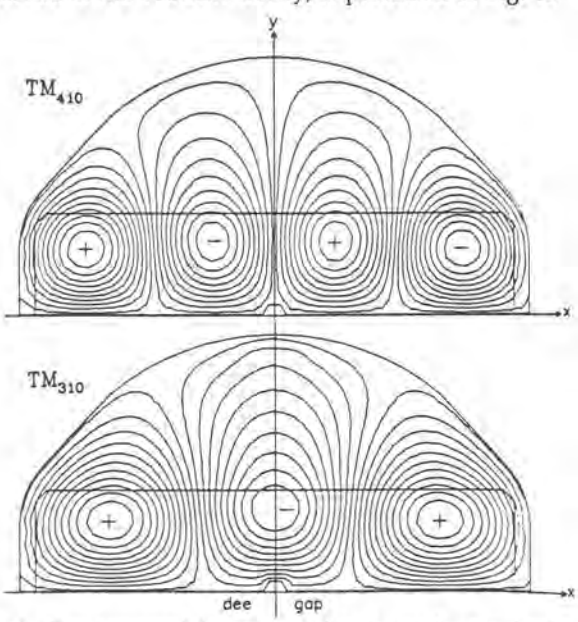


Fig. 10. Two computed dangerous high order modes, standing inside the accelerating electrode of the TRIUMF cavity.

In variable frequency machines, the excitation of high order modes by harmonics of the fundamental takes place at some specific frequency and usually can not be avoided all over the frequency range.

Nevertheless, with a careful design of the cavity and its coupling element, the effect on the beam, produced by the eventual excitation of some parasitic mode, becomes negligible (see § 2,3). Particularly, using a proper electromagnetic code, the position and the field shape of the critical modes (for the beam dynamics or for the cavity) can be evaluated, together with a rough estimation of their frequency.

Usually minor modifications of the cavity design and a proper position and shape of the main coupler have the effect to strongly reduce the coupling between harmonics and parasitics. A very general and also useful design criterion is, for example, that to limit the vertical dee aperture to the value strictly necessary for the beam, having in mind that each centimetre is paid with an increase either of the RF power and of the coupling of possibly dangerous high order modes.

Finally, a good direct way to simplify the parasitic induced problems is that to design a RF amplifier (possibly in class B) with a very low harmonic content (see § 5).

In the recent cyclotron cavities, computers play an important role in the transmission line method[1]. In particular existing codes are used or new more performant codes have been written[26]:

- to manipulate the line equations;
- to compute the characteristic impedance of unfamiliar sections (via a 2D electrostatic code), together with the expected current distribution;
- to speed up the comparison of different cavity shapes which could be used;
- to speed up the optimization of a cavity, whose shape has been already decided, including the eventual modifications dictated by mechanical problems;
- to speed up the iteration procedures for fixed length cavities;

Nevertheless I want to point out that, using the transmission lines approach for cavities of unusual shape (see for example the cavities presented in Figs 3, 7 and 8), most of the errors are introduced at the level of the choice of the line schematization, which must be done by the RF designer according to the envisaged shape and position of the wave propagation surfaces[1]. Moreover a careful correction of the current distribution in each constant impedance section, according to the current previous history, is mandatory for a good estimation of the power dissipation and a good design of the cooling system.

In two peculiar cases[6,11] - both referring to cavities for superconducting cyclotrons - a 2D electromagnetic code (SUPERFISH) has been widely used to perform a second order optimization of an already designed and tested cavity[27,28] (see § 2,2). In the following a brief description of the work performed for the LNS/Milano cyclotron to increase the maximum frequency of the cavity prototype[11] (47 MHz instead of 48 MHz) ant to improuve the design of the ceramic insulator region, is given.

As can be seen in Fig. 3, the cavity has a cylindrical geometry (i.e. a 2D geometry), but in the dee region. The basic idea[27,28] is that to find, by trial and error, a 2D model for the 3D region, able to produce for the cylindrical part of the cavity the proper boundary conditions over the frequency range. It is worthwhile that the matching surface (between the model and the real cavity) has to be a

propagation surface where the field is that typical of a cylindrical transmission line. In such a way the whole structure can be studied by means of 2D finite element procedure such as the code SUPERFISH, which performs a discretization of the Helmoltz equation over an irregular triangular mesh.

It is important to point out that an a priori knowledge of the cavity frequency behaviour is required in order to check the simulating 2D model throughout the frequency range. In the present case the measurements on the cavity prototype of the frequency versus the sliding short position have been used for this purpose.

Since a more detailed discussion is available in Ref. [28], only a few computer outputs are presented here to give an idea of the use of this procedure in improving the understanding of the cavity behaviour.

An enlarged view of the ceramic insulator region before (left - cavity prototype) and after (right - final cavity) the optimization is presented in Fig. 11.

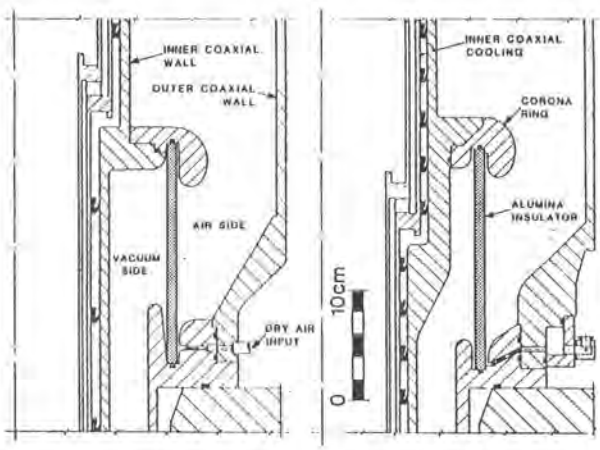


Fig.11. Enlarged view of the ceramic insulator region before (left) and after (right) the optimization.

The plot presented in Fig. 12 (which refers to the cavity prototype @ 47 MHz, see Fig. 11) is based on the Slater theorem which, in a perturbative approximation, gives the frequency shift, Δf, due to the removal of a small volume, ΔV, from a cavity of volume V, according to the formula:

$$\frac{\Delta f}{f} = \frac{\int_{\Delta V} (\mu H^2 - \varepsilon E^2)\, dV}{\int_{V} (\mu H^2 + \varepsilon E^2)\, dV} = \frac{\int_{\Delta V} (\mu H^2 - \varepsilon E^2)\, dV}{4W}$$

where W is the total stored energy. The numbers shown on the lines give the shift of the resonant frequency [kHz/cm^2] due to a 1 cm^2 reduction of the cavity area in the r-z section. This system of lines is very useful to evaluate quickly the effect on the resonant frequency of any tapering applied to the cavity, simply adding the contribution of each elementary square in which the tapering can be subdivided. All the numbers in the plot of Fig. 12 are positive because, at that frequency, the region is inductive ($\alpha > \pi/4$).

In Fig. 13 a comparison between the boundary of the ceramic insulator region of the cavity prototype (dashed line) and of the optimized cavity (solid line) is given. The volume reduction, which mainly determines the frequency increase from 47 to 49.5 MHz, is clearly visible. The sliding short, shown on the right side of Fig. 13, is in both cases at the minimum distance from the corona ring.

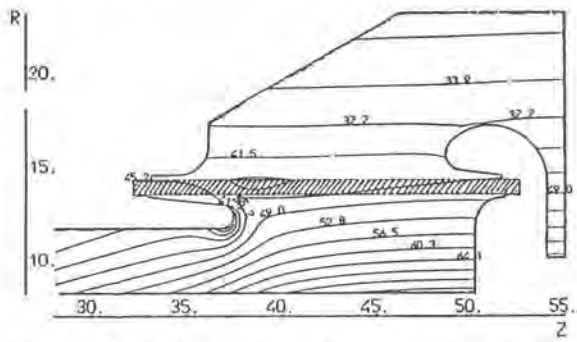


Fig.12. Plot @ 47 MHz, referring to the cavity prototype and based on the Slater theorem (see text for details).

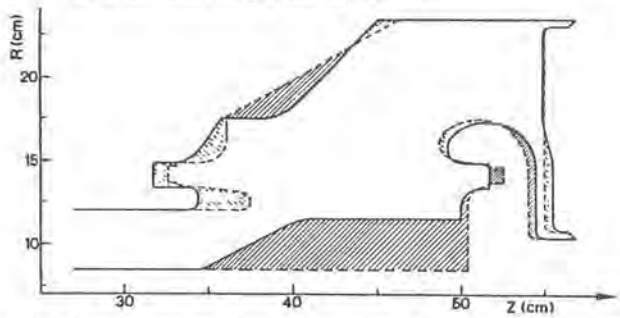


Fig.13. Comparison between the boundary of the ceramic insulator region of the cavity prototype and of the optimized one.

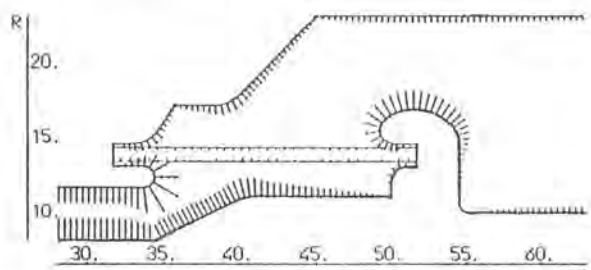


Fig.14. Electric field on the surface of the two coaxial in the region close to the ceramic insulator (@ 15 MHz, worst case).

The electric field on the surface of the two coaxials in the ceramic insulator region (@15 MHz) is shown in Fig. 14. The arrows represent just the electric field vectors on the surface; each segment marked by the scale on the arrows represents a field value of 10 kV/cm. Because the electric field amplitude on the surface can not be

computed precisely by SUPERFISH, a new routine has been added to have a better numerical solution of the equation:

$$|E| = \frac{\sqrt{\mu_o/\varepsilon_o}}{k\,\varepsilon_r}\,\frac{\partial(rH)}{r\,\partial l}$$

where: k=ω/c and l is the path coordinate along the cavity boundary. This routine is very useful to optimize the metal to ceramic connection and the voltage holding capability of that critical region. Particularly, limiting the electric field to less than 2 kV/cm at the ceramic to copper connection, no metallization and brazing was needed, a conventional vacuum sealing (by Viton O-ring) being sufficient and fully reliable. A similar solution has being adopted for the main coupler (~ 600 kW) to be realized for the new high power cavities of the PSI ring cyclotron[29].

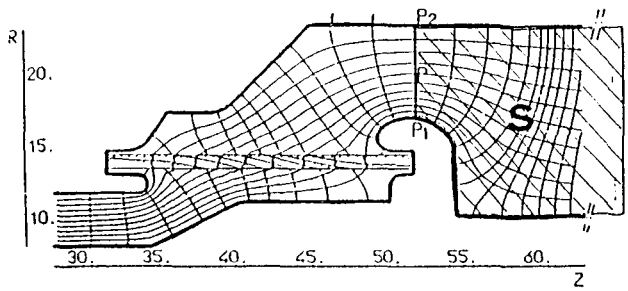


Fig.15. Plot of electric field lines and "equipartitional lines". S is the surface used to compute the voltage (see text for details).

A very interesting field pattern is presented in Fig. 15 (for the usual example @ 32.2 MHz) where two orthogonal systems of lines are plotted. The first one consists of the electric field lines[28], spaced at a constant increase of the voltage between the two coaxials (as calculated along an electric field line). The second one consists on the "equipartitional lines", which connect the points of the electric field lines having the same voltage fraction, with respect to the total voltage difference as computed along the field line itself. To have a precise value of the electric field integral (voltage) along a field line, the Stokes's theorem is applyed, the computing surface for the magnetic field flux being that limited by the coaxials, the short circuit and the electric field line itself.

This way to present the electromagnetic field of a resonant coaxial cavity has a lot of interesting properties, among them I mention:

- The lines of the two systems are orthogonal to each other, like field lines and equipotentials in an electrostatic field.
- The ratio V_P/V corresponds, in the dynamic case, to the electrostatic potential;
- Each curvilinear rectangle links the same magnetic flux.
- The ratio between the dimensions of each curvilinear rectangle is related to the local impedance of the cavity.
- A cavity limited by any two "equipartitional lines" has the same resonant frequency as the actual cavity.

All these properties should offer the possibility of a very powerful definition for the generalized characteristic impedance along the cavity, as a function of the wave phase advance.

4. CONTROL ELECTRONICS

As mentioned above, the block diagrams of the RF control electronics for multi-cavity cyclotrons are now very similar[30,34], major differences being at the level of the internal layout of a single block. Since this topik is extensively discussed in a dedicated papar at this conference[35] - where a special enphasis is given to the more diffilcult problem related to the very high beam loading, typical for a mason factory - I will just present in Fig. 16, as a typical example, the block diagram of one chain of the RF control electronics, designed for the operation of each cavity of the LNS/Milano cyclotron.

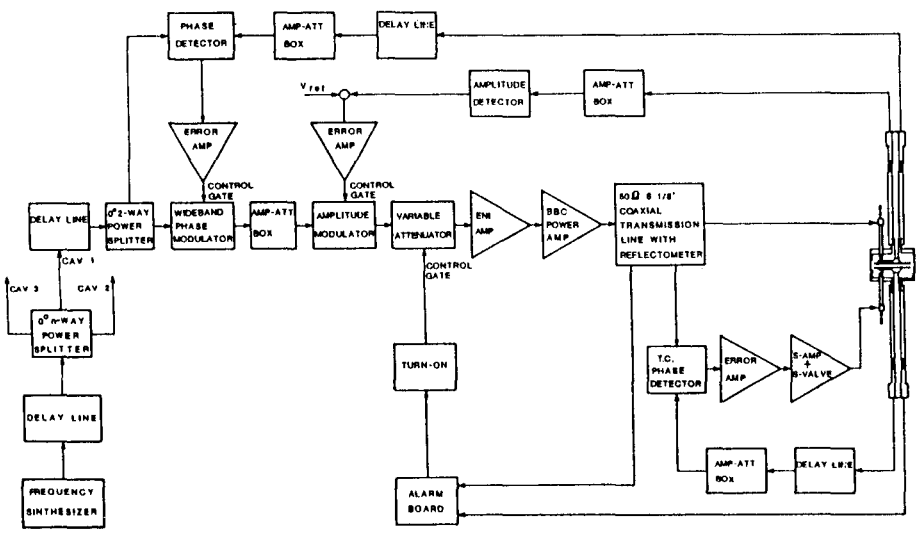


Fig.16. A typical example of RF control electronics block diagram (LNS/Milano SC cyclotron).

5. RF POWER AMPLIFIER

This very short paragraph is just to mention a number of general considerations which are important when a new machine has to be designed.

Because the RF power amplifiers are usually purcased and their cost is not negligible, often some money is saved reducing the specs required to those which are strictely necessary (i.e. output power and frequency range), with a less enphasis on the other characteristics. In particular, according to my experience, I will give in the following some suggestions which, while increasing a bit the RF amplifier cost, are very usefull and would improve the overall RF system performances and reliability. In particular:

- Grounded grid configuration is strongly preferred for the power stage to overcome neutralization problems.
- Class B operation is also preferred, because of better linearity (the coltrol electronics becomes easier) and of lower harmonic content (the risk to excite cavity parasitic modes is reduced)
- To have both, L and C, separately tunable in the output tank circuit is usefull to easily suppress eventual parasitics (this is really helping if the frequency range is wide).
- A Class B driver, with a broad band input, relaxes the power requirement (that is the price) for the broad band solide state pre-amplifier, the total number of tunable elements staying constant.

The scheme of a well designed amplifier, which fulfil the specs given above, is presented in Fig. 17.

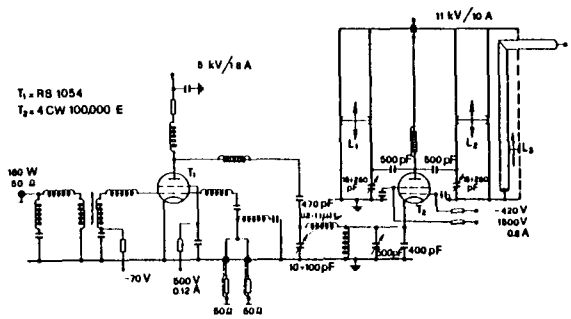


Fig.17. 90 kW, class B, two stages (final grounded grid) RF power amplifier for the LNS/Milano SC cyclotron (made by BBC).

6. CONCLUSIONS

As a conclusion I want to remember that, being the cyclotron the first of the circular accelerators, since 1930 more than one hundred of different machines have been built and others are under construction. Cyclotron RF system performances are dominated by the cavity design and technology, choices being mainly based on the machine parameters, on the designer's imagination and on the allowable money and/or man power. Nevertheless, the support, on money and man power, given to the other ancillary equipments, like amplifiers and control electronics, is also very important for a good and reliable RF system. In particular, while for a good amplifier money is enough (few companies being qualified to deliver excellent RF amplifiers), for a good control electronics competent peoples are needed.

REFERENCES

[1] C. Pagani, Cyclotron Cavities, CERN Acc. School on RF, Oxford, April 1991, CERN report, to be published.
[2] C. Bieth, Proc. 10th Int. Conf. on Cycl., IEEE Catalog No. 84CH1996-3, p. 294.
[3] S. Gallès, Proc. 11th Intern. Conf. on Cyclotrons, Ionics Pub., Tokyo, 1987, p. 184.
[4] H.W. Schreuder, Proc. 12th Int. Conf. on Cycl., Berlin, May 1989, World Scientific Pub., Singapore, 1991, p. 21.
[5] H. Blosser et al., Proc. 11th Int. Conf. on Cycl., Ionics Pub., Tokyo, 1987, p. 157.
[6] D.P. May et al., Proc. 11th Int. Conf. on Cycl., Ionics Pub., Tokyo, 1987, p. 195.
[7] E. Acerbi et al., Proc. 9th ICC, Les Editions de Physique Pub., France, 1981, p. 169.
[8] E. Acerbi et al., Proc. 10th Int. Conf. on Cycl., IEEE Catalog No. 84CH1996-3, p. 251.
[9] C. Bieth, AGOR internal report, 1985
[10] S. Brandenburg, C, Bieth et al., Proc. 12th Intern. Conf. on Cycl., Berlin, May 1989, World Scientific Pub., Singapore, 1991, p. 21.
[11] C.Pagani, Proc. 10th Int. Conf. on Cycl., IEEE Catalog No. 84CH1996-3, p. 305.
[12] C.Pagani et al., Proc. 9th ICC, Les Editions de Physique Pub., France, 1981, p. 423.
[13] C.Pagani et al., Report INFN/TC-83/18, Nov. 1983.
[14] C.Pagani et al., Proc. 11th Int. Conf. on Cycl., Ionics Pub., Tokyo, 1987, p. 271.
[15] C.Pagani et al., Proc. 11th Int. Conf. on Cycl., Ionics Pub., Tokyo, 1987, p. 361.
[16] B. Dwersteg, Qiao Yufang, Proc. 4th Workshop on RF Superconductivity, KEK Report 89-21, January 1990, p.605.
[17] C. Bieth, Report GANIL 78R/053/HF/02, Caen, France, 1978.
[18] C. Bieth et al., IEEE Trans. Nucl. Sci., NS-26, June 1979, p. 4117.
[19] C. Bieth et al., Rep. GANIL 80R/148/HF/23, Caen, France, 1980.
[20] T. Fujisawa et al., Proc. 10th Int. Conf. on Cycl., IEEE Catalog No. 84CH1996-3, p. 311.
[21] H. Kamitsubo, Proc. 11th Int. Conf. on Cycl., Ionics Pub., Tokyo, 1987, p. 17.
[22] G.Fausti, C.Pagani, M.Puglisi, Rep. INFN/TC-72/9, Nov. 1972.
[23] U. Trinks, Proc. 10th Int. Conf. on Cycl., IEEE Catalog No. 84CH1996-3, p. 605 and These Proceedings.
[24] T. Grundey et al., Nucl. Instr. and Meth. A306 (1991), p. 21.
[25] V. Pacak et al., Proc. 10th Part. Acc. Conf., IEEE Catalog No. 89CH2669-0, p. 174.
[26] F. Pigeaud, NSCL internal report, RF Note 111.
[27] R.C. Rogers, Proc. 10th Int. Conf. on Cycl., IEEE Catalog No. 84CH1996-3, p. 299.
[28] L.Serafini, S.Gustafsson and C.Pagani, Proc. 11th Int. Conf. on Cycl., Ionics Pub., Tokyo, 1987, p. 365.
[29] P. Sigg, private communication.
[30] A. Bosotti et al., Proc. 12th Int. Conf. on Cycl., Berlin, May 1989, World Scientific Pub., Singapore, 1991, p. 216.
[31] D.R. Haenni et al., Proc. 12th Int. Conf. on Cycl., Berlin, May 1989, World Scientific Pub., Singapore, 1991, p. 264.
[32] A. Joubert et al, Proc. 10th Part. Acc. Conf., IEEE Catalog No. 89CH2669-0, p. 367.
[33] J. Riedel and J. Vincent, Proc. 10th Part. Acc. Conf., IEEE Catalog No. 89CH2669-0, p. 315.
[34] T. Fujisawa et al, Proc. 11th Int. Conf. on Cycl., Ionics Pub., Tokyo, 1987, p. 329.
[35] P. Sigg, These Proceedings.

THE RF COUPLING SYSTEM OF THE VINCY CYCLOTRON

B. Bojovic, M. Josipovic, A. Susini
VINCY group, PS Division, CERN, Geneva, Switzerland

ABSTRACT

The main parameters of the VINCY cyclotron RF system are presented. A possibility to tune the λ/2 primary resonator only by action of a variable capacitor is discussed. A design procedure based on transformer equations has been verified by model measurements.

1. INTRODUCTION

The main parameters of the VINCY Cyclotron have been already presented[1] (k_b=150, both physical and medical purposes,...). In this isochronous cyclotron, the acceleration of ions on the first, second and fourth harmonic is accomplished by two dees settled in two opposite magnet valleys. The resonator type is implied by the basic design constraints. The use of the magnet based on the modification of the CEVIL magnet from Orsay, France, implies application of horisontal λ/4 type resonator cavities. The design of the cavities is based on the use of the prototype cavities of the LNS Catania Superconducting Cyclotron [2]. A short circuiting piston is used to tune the cavities thruoghout the frequency range. The main parameters of the RF system are:

Table 1.

Accelerating dees	2 x 30°
Min. RF gap	10 mm
Frequency range	17-31 MHz
Piston excursion	2 m

In order to avoid complex matching system, each power amplifier is directly coupled to the corresponding resonator cavity, thus enabling the use of only one variable vacuum capacitor as a matching element. Each amplifier makes a part of a λ/2 primary resonator, inductively coupled with the cavity. The λ/2 resonators were chosen in order to locate the power amplifiers in a low stray magnetic field zone (fig 1.) where the power tubes could be efficiently screened.

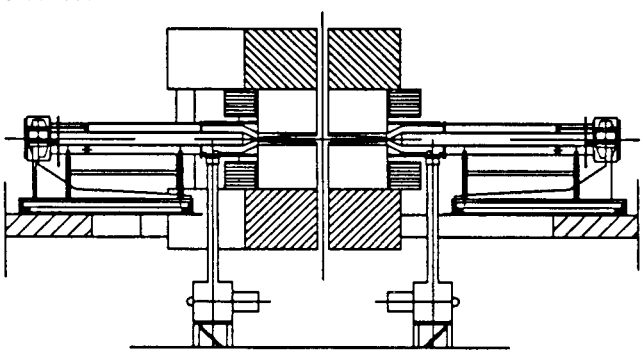


Fig. 1. The section layout of the VINCY cyclotron.

Having chosen inductive coupling, one has the choice between two solutions.

a) *Tuned primary, tuned secondary.* The obvious drawbacks are first a need of moving the mechanical coupling loop inside the vacuum to adjust the primary impedance level and second, a need for a fast electronic device to protect the power tube in case of arc sparking at the dee. The advantages are that the isolated tuning frequencies of both resonators coincide with the accelerating frequency.

b) *Detuned primary.* The coupling loop is fixed, the impedance level is obtained by detuning considerably the primary resonator. The reactive energy required by this resonator can be delivered only by the secondary one which, in turn, is also detuned, in the opposite sense, though by a much smaller amount. It follows that the isolated resonant frequencies of the primary and secondary, ω_{n1}, ω_{n2}, must be known beforehand. Any subsequent adjustment of the primary impedance (which is easily obtained with the variable condenser on the primary) requires an adjustment on the secondary as well. If this cannot be obtained by the fine tuning paddle only, the piston position should be corrected - a risky action at full power operation.

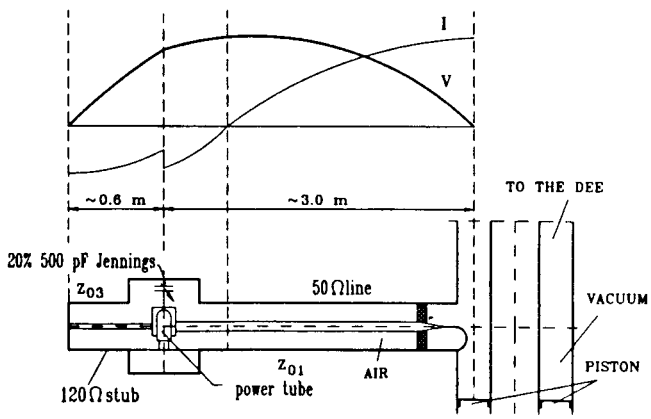


Fig. 2. How the resonators are coupled.

An other important fact is that the coupling loop size is noticeably larger than in a) and that there is a limitation due to mechanical constraints (sparking danger between the loop and the secondary stem).

For these reasons and in order to check the feasibility of the arrangement over the whole RF band, an analysis has been developed which shows the mechanism of the coupling phenomena and, by means of simple expressions, calculates

the characteristic and the criticity of the components involved.

2. THE TRANSFORMER EQUATIONS

Instead of the standard approach by using Kirchhoff equations, we have preferred one which highlights the feedback action between primary and secondary resonators as a function or the coupling coefficient k. This leads to the primary impedance as seen by the power tube:

$$Z_1(S) = \frac{\omega_n Z_{n1v}}{2} \frac{S+\sigma_2}{(S+\sigma_1)(S+\sigma_2)+\Omega^2} \qquad [2.1]$$

As explained[4], the expression is approximate and it is acceptable for bandwidths of the order less than 10% and Q's of the order of 1000. Z_{nv} is a proportionality constant between top dee voltage V_1 squared and energy content E:

$$Z_{n1v} = \frac{V_1^2}{2\omega_n E} \qquad [2.2]$$

σ is the 3-db half-bandwidth : $\sigma = \omega_n/2Q$ and

$$S = s - j\omega_n \qquad [2.3]$$

is the complex displacement from the nominal frequency $j\omega_n$. Though not absolutely necessary, reduced variable S is used (narrow band approximation)[4], which cuts by half the degree of the polynomials at the price of systematic errors. It is found that, as in our case, when the Q's are of the order of several thousands and the relative bandwidths less than 10%, the errors are tolerable.

Ω is a frequency related to the coupling coefficient k

$$k = \frac{\omega_n}{\sqrt{Z_{n2i\text{-}loop} Z_{n1i\text{-}loop}}} M$$

$$\Omega = \omega_n k/2 \; ; \qquad M = \frac{\mu_o A}{2\pi r} \qquad [2.4]$$

(r = distance of the coupling loop gravity centre from the linear axis; A the loop surface).

An other constant, which appears in the coupling coefficient k, is Z_{ni} defined via the internal circulating current i:

$$Z_{n1i} = \frac{2\omega_n E}{i^2} \qquad [2.5]$$

Both Z_n's have the dimension of an impedance and are functions of the point x where the resonator is measured.

The advantage of using the Z_n's instead of the equivalent inductances and capacitances is that the former are simple figures of the order of 50 Ω, independent of the frequency. For our purpose, only the dee top and the loop position are interesting. For the secondary, which is a non-uniform transmission line, all $Z_{nv}(x)$ and only $Z_{ni\text{-}short}$ can be measured with the perturbation method or calculated by means of the section method[5] and also by means of modern codes[2]; $Z_{ni\text{-}loop}$ can only be obtained by calculation.

For the primary, if the power amplifier can be considered as a lumped capacitance tuning a φ long transmission line Z_o, we find :

$$\begin{cases} Z_{nv\text{-}anode} = 4Z_o \sin^2\varphi / (\sin 2\varphi + 2\varphi) \\ Z_{nv\text{-}loop} = Z_o \, (\sin 2\varphi + 2\varphi)/4 \end{cases} \qquad [2.6]$$

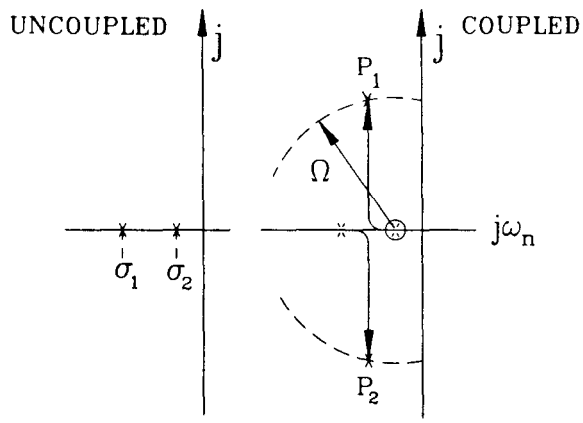


Fig 3. The singularities of the tuned primary arrangement

3. THE TUNED PRIMARY CASE

The denominator of Eq. [2.1] could be factorized as:

$$Z_1 = \frac{\omega_n Z_{n1v}}{2} \frac{S+\sigma_2}{(S-P_1)(S-P_2)} \qquad [3.1]$$

where $$P_{1,2} = -\frac{\sigma_1+\sigma_2}{2} \pm j\sqrt{\Omega^2 - (\frac{\sigma_2-\sigma_1}{2})^2} \qquad [3.2]$$

therefore, the locus of the coupled poles (Fig. 3) show that by increasing k, the poles move vertically still staying on a circle centered at $j\omega_n - \sigma_2$ with radius Ω. A zero appears where there was previously the uncoupled pole at $-\sigma_2$. The exact Kirchhoff solution would indicate a zero at $j\omega_n/\sqrt{1-k^2}$ and a pair of poles at $j\omega_n/\sqrt{1-k}$ and $j\omega_n/\sqrt{1+k}$. The lack of geometrical symmetry is due to the narrow band approximation. A plot of amplitude and phase is shown in Fig. 4. The impedance is real at $\pm j\Omega$ and at centre. Letting S = 0 in Eq. [2.1], the resulting $Z_1(0)$ is the parallel between the primary R_p : $R_p = \omega_n Z_{niv}/2\sigma$ and the reflected secondary impedance Z_R :

$$Z_R(0) = \frac{\omega_n Z_{n1v}}{2} \frac{\sigma_2}{\Omega^2} \qquad [3.3]$$

This expression, together with the energy equation, leads to the desired transforming ratio V_2/V_1 :

$$\tau = \sqrt{\frac{Z_{n2v}}{Z_{n1v}}}\,\frac{\Omega}{\sigma} \qquad [3.4]$$

Both t and Z_R depend on Ω, and so finally on the cross section A of the loop.

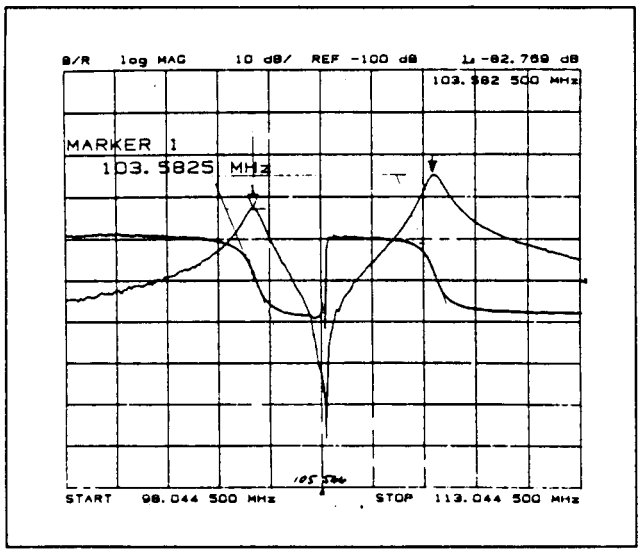


Fig. 4. The phase and amplitude function.

4. DETUNING THE PRIMARY

Because the poles were located in the S plane at $j0 - \sigma$, the terms $S + \sigma$ appeared in Eq. [2.1]. If the primary had been resonant at $\omega_n - \delta$ (detuned), then the pole, still in the S plane would have been located at $-j\delta - \sigma$ and a term $S + \sigma + j\delta$ would have appeared at the denominator instead. To facilitate the discussion, the primary pole is supposed to be affected by a real part $\sigma_1 = \sigma_2 = \sigma$. In the obvious case where $\sigma_1 > \sigma_2$ a resistance $R_p = \omega_n Z_{n1}/2(\sigma_1 - \sigma_2)$, which does not participate to the energy transfer, will be considered to be in parallel to the primary. For the same reason, the power tube internal resistance has to be neglected. It should, however, be taken into account in those cases where the beam load transfers energy to the accelerating secondary, because instabilities could occur[4].

Since the primary resonator is tuned at $\omega_n - \delta$, the coupled primary impedance is

$$Z_1(S) = (\omega_n - \delta) Z_{n1v} \frac{S+\sigma}{(S+\sigma)(S+\sigma+j\delta)+\Omega^2} \qquad [4.1]$$

with roots : $$P_{1,2} = -\left(\sigma + j\frac{\delta}{2}\right) \pm j\sqrt{\Omega^2 + \delta^2/4} \qquad [4.2]$$

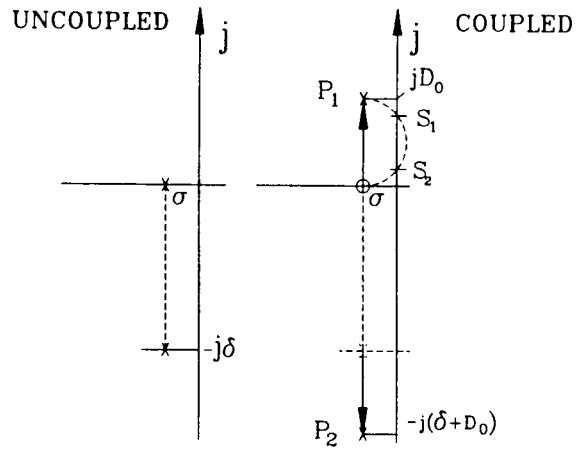


Fig 5. The singularities of the detuned primary arrangement

Again, there are three frequencies where the impedance is real : close to P_1, close to S = 0 and at $P_2 = -j(d + D_0)$. From figure 5 it appears that:

$$D_0 = \sqrt{\Omega^2 + \delta^2/4} - \delta/2 \quad \Rightarrow \quad D_0(D_0 + \delta) = \Omega^2 \qquad [4.3]$$

The frequency at P_2 is the primary mode, non interesting since no significant energy is transmitted to the secondary.

The two other frequencies with phase zero are found at the intersection between the circle diameter D_0 with the j axis. Generally, S_2 leads to excessively low impedances whereas

$$S_1 = D_0 - \sigma^2/D_0 \qquad [4.4]$$

is the useful one, provided of course that

$$D_0 >> 2\sigma \qquad \text{(say} \qquad D_0 = N\sigma)$$

It is found that for N = 3 the upper phase margin is less than 20° and it is doubtful that the automatic tuning system could work satisfactorily in the presence of a noise or transients.

The relation between D_0 and δ can be obtained from energy considerations : there are two resonators, the primary tuned at $-j\delta$ and the secondary at j0; both are excited at $j(D_0 - \sigma^2/D_0)$. No reactive power is delivered by the amplifier at $S = S_1$. The energy is balanced between the two resonators since at S_1 there is a 180° phase shift. Therefore, it must be :

$$\frac{V_2^2}{2}\,\mathrm{Im}(Y_2(S1)) = \frac{V_1^2}{2}\,\mathrm{Im}(Y_1(S1)) \qquad [4.5]$$

which leads to :

$$\frac{V_2^2}{\omega_n Z_{n2v}}\left(D_0 - \frac{\sigma^2}{D_0}\right) = \frac{V_1^2}{(\omega_n - \delta) Z_{n1v}}\left(D_0 + \delta - \frac{\sigma^2}{D_0}\right) \qquad [4.6]$$

and finally: $$\delta\left(\frac{1}{D_0 - \sigma^2/D_0} + \frac{\tau^2}{\omega_n}\frac{Z_{n1v}}{Z_{n2v}}\right) = \tau^2 \frac{Z_{n1v}}{Z_{n2v}} \qquad [4.7]$$

5. THE VINCY ARRANGEMENT

In our primary resonator shown schematically in Fig. 2, the amplifier is located in the second half of the resonant transmission line Z_{01}. The characteristic impedance Z_{03} of the tuning stub and its length x_3 can be negotiated to keep the amplifier sufficiently far from the median plane and compatible with the physical dimension of the power cabinet.

To calculate Z_{nv} and Z_{ni} for this arrangement, from Eqs. [2.2] and [2.5]:

$$\frac{1}{Z_{nv\text{-}anode}} = \frac{1}{Z_{nv\text{-}line1}} + \frac{1}{Z_{nv\text{-}line3}} \qquad [5.1]$$

Since $$I_{loop\text{-}line1} = V_{anode} / Z_{01} \sin\varphi_1 \qquad [5.2]$$

whereas the energy is: $$E = V^2_{anode} / (2Z_{nv\text{-}anode}) \qquad [5.3]$$

gives: $$Z_{ni1\text{-}loop} = Z^2_{01} \sin^2\varphi_1 / Z_{nv2\text{-}anode} \qquad [5.4]$$

Once the Q's are known, the Z_{nv}'s give the shunt resistances

$$R_p = Z_{nv}\, Q \qquad [5.5]$$

and the power in function of the applied voltages.

a) *Primary*. It has been shown in Figs. 1 and 2. The power tube is a SIEMENS type RS1084CJ tetrode in grounded grid configuration. The anode d.c. voltage is 10 kV, then V_{rf1} = 8.5 kV. As the maximum dee voltage will be V_{rf2}= 100 kV, independent of the frequency, then the transforming ratio is $\tau = 11.7$

A wooden model of the cabinet with tuning lines and coupling loop indicate that the primary resonator can be considered as a x_1 = 2.77 m long 50 Ω line terminated at its open end with x_3 = 0.6 m long 120 Ω line in parallel with a variable vacuum capacitor variable between 20 and 423 pF at 31 and 17 MHz respectively.

Then, from Eq. [2.5, 2.6] one gets (Table 2.):

Table 2.

f (MHz)	31	17
$Z_{n1v\text{-}anode}$ (ohm)	26.26	16.73
$Z_{ni1\text{-}loop}$ (ohm)	90.17	104.22

b) *Secondary* The dimensions of the secondary resonator are such that r = 0.225 m. The other parameters, calculated and measured[2] are (Table 3.) :

Table 3.

f (MHz)	31	17
Z_{n2v} (ohm)	42.25	52.98
$Z_{n2i\text{-}loop}$(ohm)	31.5	58.73
σ(kHz)	2.25	1.42
Q_2	6880	5980
R_{p2} (ohm)	291	317
W_2(kW)	17.2	15.7

c) *With the tuned primary* coupling, one obtains

Table 4.

f (MHz)	31	17
Ω (kHz)	22.9	9.36
A (cm^2)	5.42	11.0

which requires a mechanical displacement or rotation in vacuum of the coupling loop.

d) *With detuned primary* one starts at low frequency choosing D_0 sufficiently higher, though not excessively, then σ. From the phase plot it has been adopted N = 7. From Eq. [4.4] one gets:

$D_0 = 7 \times 1.42 = 9.94$ kHz.

From Eq. [4.5] we get : $\delta = 213$ kHz; $S_2 = 9.73$ kHz.

From Eq. [4.2] and [2.9]: Ω = 47 kHz and A = 50,7 cm^2.

At high frequencies, introducing the same value D_0 we get A = 19.5 cm^2. By iteration, it is found that D_0 = 22.5kHz leads to the previous value for A :

δ = 2030 kHz; S_2 = 25.25 kHz; Ω = 228.9 kHz; A = 50.7 cm^2.

6. CONCLUSION

It has to be observed that tuning the dee over the whole band as well as changing the transforming ratio τ can be performed by a unique action on the variable vacuum capacitor provided the dee fine tuning facility succeeds to retune from S_2 to zero i.e. at ω_n. Otherwise, the piston of the dee line has to be displaced.

7. REFERENCES

1) Neskovic N. et al. "Tesla accelerator installation", EPAC-Berlin, 24 - 28th March 1992.
2) Bojovic B. et al, "Status report of the rf system for the VINCY Cyclotron", EPAC-Berlin, 24-28th March, 1992.
3) Pagani, C. et al., "Very high performance sliding short ....", Cyclotron 1986, Tokyo, Japan, October 1986, pp. 365-369.
4) Susini A., "A novel equation for magnetic coupled rf resonators", TRIUMF-Vancouver, TRI-DN-92-K202, 26.5.1992 (Internal Paper).
5) Kannowade H., "Methoden zur Entwicklung ... Nucl. Inst. & Method 41, Vol. 41 pp. 208 - 212 - 1966.

DUAL FREQUENCY RESONATOR SYSTEM FOR A COMPACT CYCLOTRON

M. Eiche, K.L.Erdman
Ebco Technologies Ltd., 7851 Alderbridge Way, Richmond, B.C., Canada V6X 2A4

and

P. Lanz, M. Lipnicki, M. Zach
TRIUMF, 4004 Wesbrook Mall, Vancouver, B.C., Canada V6T 2A3

ABSTRACT

A dual frequency resonator system operating at 74/37 MHz used in a proton/deuteron isotope production cyclotron is described. The available design options are discussed, the selected concept is described, and results of model measurements are presented.

1. INTRODUCTION

A compact cyclotron for isotope production is under construction at Ebco Technologies in Vancouver. The design is similar to the existing TR30 H^- machine now in operation at Nordion International[1] (Fig. 1), and it is again undertaken with the technical and design assistance of TRIUMF. The main difference between the two cyclotrons is the added capability to accelerate deuterons so that the rf system must operate at 74 and 37 MHz respectively. The design options for this dual frequency system are the content of this paper.

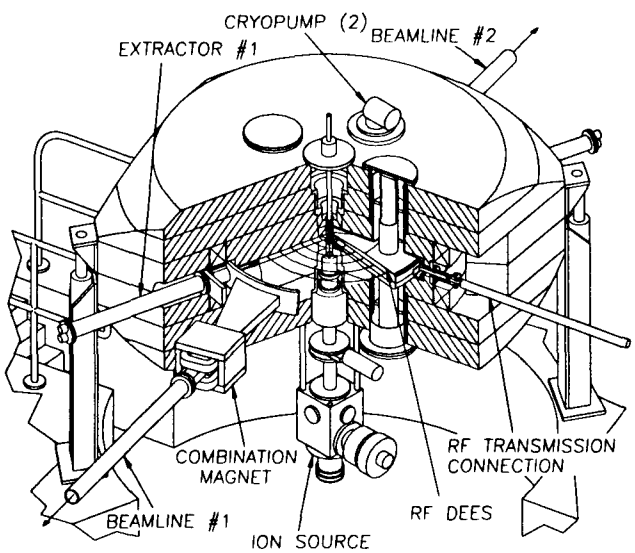


Fig. 1. TR30 cyclotron.

2. SPECIFICATIONS

Mode	Frequency	Dee Voltage
H^-	73.169 MHz	50 kV
D^-	36.654 MHz	25 kV

3. DESIGN CONSIDERATIONS

- it is advantageous to retain as many features of the proven design of the existing TR30 cyclotron as possible, mainly the dees and the diameter of the opening in the magnet yokes
- to resonate a system with a constant dee shape and capacity at both frequencies one must increase the inductive reactance of the stem for the 37 MHz mode
- the necessary increase of the stem length must not extend far beyond the magnet; ease of assembly and disassembly is imperative
- the structure must be mechanically and thermally stable (vibrations, frequency drift)
- switching between modes must be done remotely, and under vacuum;
- coarse and fine frequency tuning mechanisms are required

The layout of the system is shown in Fig. 2.

4. DESIGN OPTIONS

Three options have been considered and investigated using analytical calculations, computer modelling and model measurements.

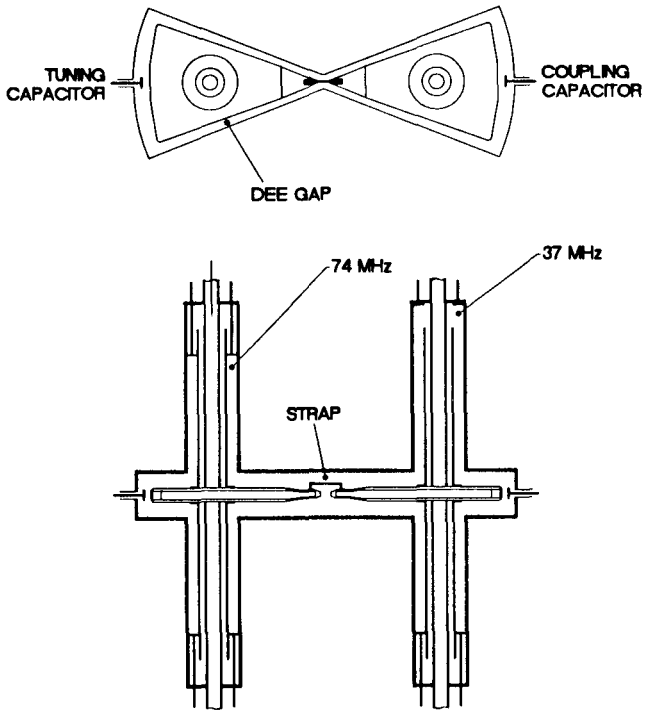


Fig. 2. Schematic diagram of the dual frequency resonator system.

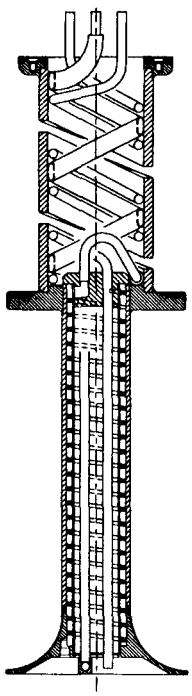


Fig. 3. Stem extension by a helix.

4.1. Stem Extension with a Helix

Figure 3 shows the inner conductor with the helix extension. A cooling line is run on the inside of the helix without crossing the gap. Not shown is a tuning and switching mechanism. By using this helical construction, the total weight of the inner system, including the dee, is supported by the lower helix which is then mechanically unstable. There are several possible solutions to this problem. The obvious one is a ceramic insulator inside the helix, or increasing the helix stiffness by using composite materials etc.

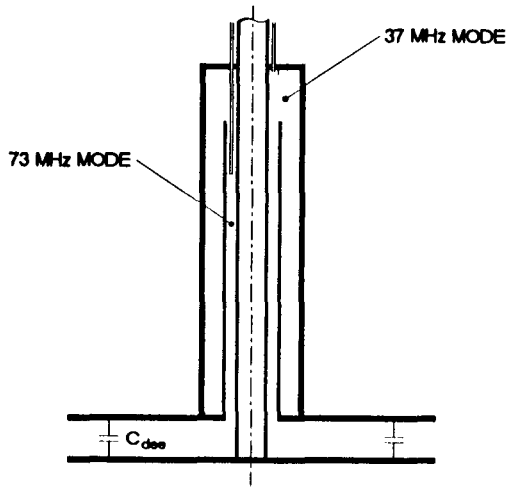


Fig. 4. Folded cavity.

4.2. Folded Line

4.2.1. Version A

The shortening of the line for 37 MHz operation can be achieved by "folding" it as shown in Fig. 4, which is self explanatory. In both cases the frequency can be adjusted by moving the shorting plate; when operating at 37 MHz the tuning is achieved by the capacitive effect of the shorting plate, still adjustable within limits.

For the geometry as shown and for D = 20 cm, d_1 = 11 cm, d_2 = 6 cm, then at f = 37 MHz and with a dee capacity C_{load} = 70 pF, simple calculations indicate that with equal characteristic impedances $Z_1 = Z_2 = 36\ \Omega$ the total resonator length is l_{res} = 134 cm.

When operating the same system in the 74 MHz mode the length reduces to 45.5 cm, bringing the difference in length between the modes to 21.5 cm. The current amplitude at the short is $I_0 = U_0/Z$ = 1426 A; for the specified voltage of 50 kV the power for one quarter of the system is ~7 kW or ~28 kW of total power. The system was also modelled by SUPERFISH and the above results confirmed.

The limitation in the resonator diameter does not allow for an increase of the characteristic impedance, and hence in a reduction in the power.

4.2.2. Version B

It is possible to modify the system such that at 74 MHz the dee is resonated using the shorted outer half of the folded cavity as in Fig. 5, where the radii of

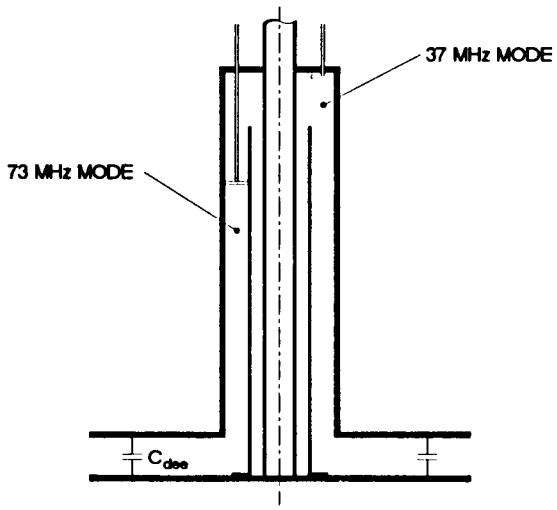


Fig. 5. Low loss folded cavity.

the coaxial line are large. Under those conditions for the same dimensions, characteristic impedances and loading capacity the skin loss is reduced by the ratio D/d_1 to ~4 kW, or for the total system to ~16 kW, in agreement with SUPERFISH results. This concept yields the shortest stems, and it appears to be the most elegant solution to the problem. On the other hand no model measurements and feasibility studies have been made so far (mechanical stability, tuning, cooling, and voltage holding); they are planned for the future.

4.3. Straight Transmission Line

A straight transmission line represents at 74 MHz a solution with the smallest skin loss due to the highest characteristic impedance (72 Ω) achievable within the available space.

For the same dee capacity of 70 pF the computed lengths are 26 cm and 91 cm at 74 and 37 MHz respectively. In order to switch between modes, the system length must change by ~65 cm. This is achieved by means of a newly developed coaxial switch which capacitively foreshortens the line in the middle, operates with a stroke of only 10 cm, and thus does not significantly increase the total mechanical length of the system (Fig. 6). The switch can be operated under vacuum in both the 37 and 74 MHz modes, and it is used firstly for adjusting the electrical balance of all four parts of the rf resonator, and also for fine frequency tuning during operation at either frequency.

In Fig. 7 is an equivalent circuit of a $\lambda/4$ resonator at 37 MHz. Figure 8 shows the dual frequency system installed in the magnet.

4.4. Model Measurements

Some results from test measurements on a copper-clad plywood model of the system are summarized below.

1. Voltage distribution at the acceleration gap (Fig. 9)
2. Voltage distribution along the coaxial line (Fig. 10)

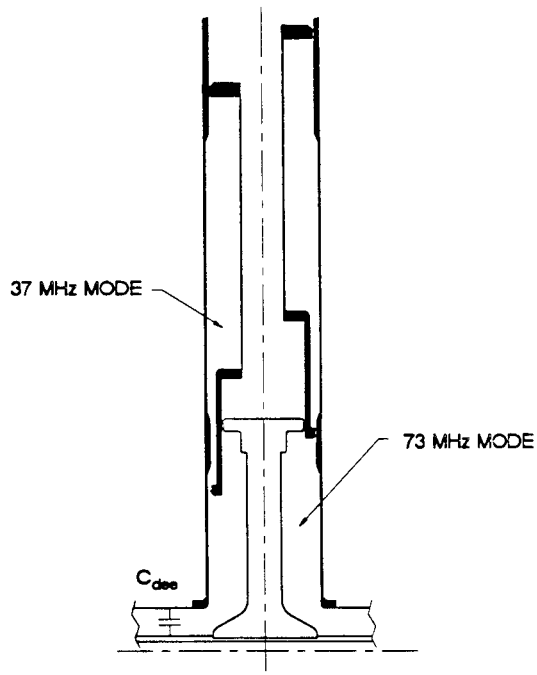


Fig. 6. Solution using a coaxial switch.

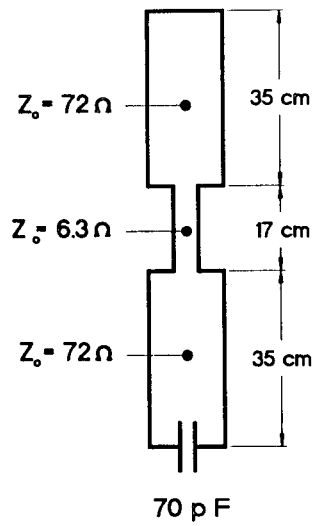


Fig. 7. Impedance diagram.

5. CONCLUSIONS

The straight transmission line option gives the lowest power requirement and highest mechanical stability for the resonator system as well as providing tuning at both frequencies. The capacity loading of the line in the middle at the 37 MHz frequency gives an overall line length of ~87 cm. The skin loss for an accelerating voltage of 50 kV is ~11 kW. The properties of the system at 74 MHz are the same as for the Nordion TR30 cyclotron.

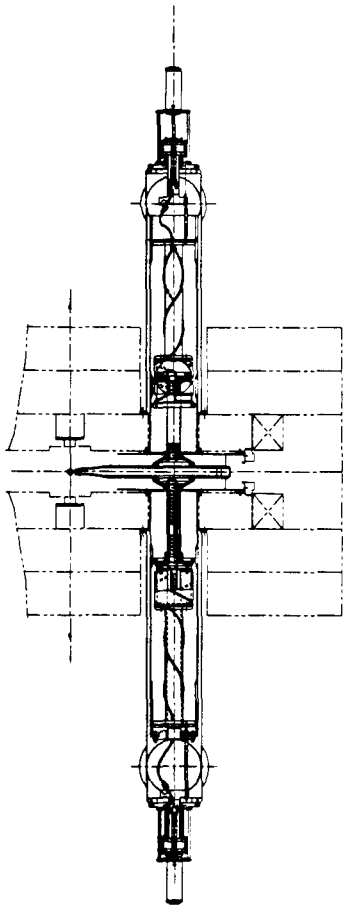


Fig. 8. One half of the TR30/15 resonator.

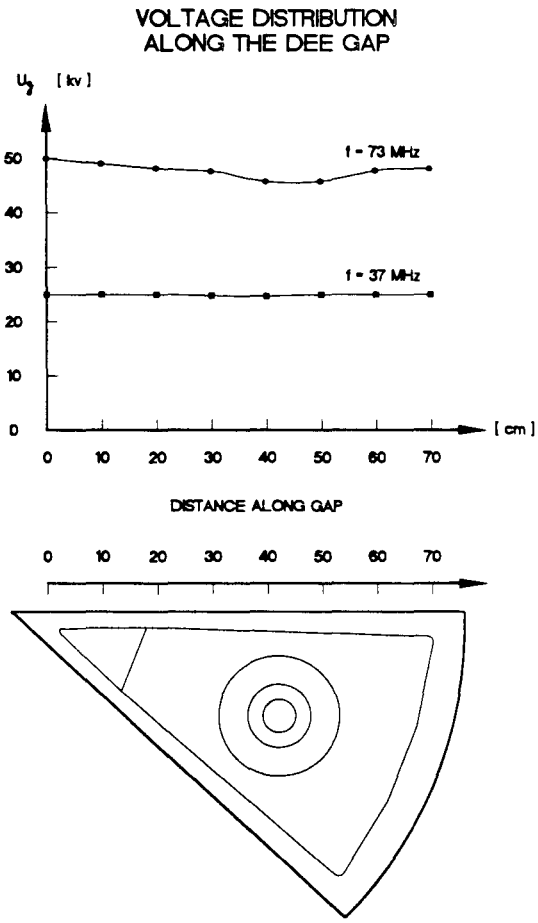
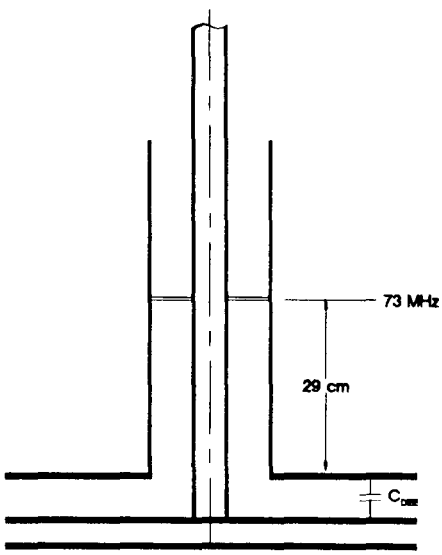


Fig. 9. Voltage measured at dee gap.

6. REFERENCES

1) B.F. Milton *et al.*, *First beam in a new compact intense 30 MeV H^- cyclotron for isotope production*, Proc. of the European Particle Accelerator Conference, Nice (1990) p.1812.



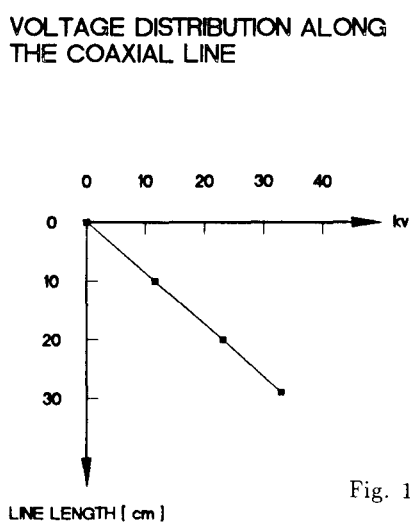


Fig. 10. Voltage measured along stem.

THE RF-SYSTEM FOR A VICKSI INJECTOR CYCLOTRON

W. Pelzer
Hahn-Meitner-Institut, Bereich Schwerionenphysik
Glienicker Straße 100, W-1000 Berlin 39
Germany

ABSTRACT

One alternative to the existing electrostatic injectors of VICKSI is a small compact cyclotron. The ions from an external ECR-source shall be axially injected and accelerated by an RF system with the same basic features as that of the existing K = 130 separated sector cyclotron. This means there will be two dees, located in two of the four magnetic field valleys opposite to each other, with an angle of 36° each, working either in push/push or push/pull mode in the frequency range of 10 to 20 MHz. The resonator volume is kept below 0.5 m^3 by the use of coils instead of a dee stem. This compact design concept allows a maximum dee voltage of 70 kV with a power loss of less than 6 kW.

1. GENERAL IDEAS

Nuclear physics at VICKSI[1] usually demand rather low beam intensity in the range of nano- and pico-amperes. But during the past few years, VICKSI experienced a growing demand of beam time for solid state physics experiments, often requiring higher beam currents than available. Today, the VICKSI beams are limited with respect to intensity mainly due to ion source characteristics and stripping efficiencies. Heavy ion beams with micro-amperes of current are produced only at low charge states. Since the "energy booster" cyclotron asks for a minimum charge to mass ratio $q/A \geq 1/8$, stripping is necessary before injection. At best, 30% of the delivered injector beam intensity is stripped to the right charge state. For highest beam energies, stripping efficiencies as low as 0.1% are encountered.

ECR-sources[2] deliver tens of micro-amperes of beam current directly at these high charge states necessary for our cyclotron, which would eliminate the need of a stripper. With the proposed new injector cyclotron, existing ECR-technology can be used to produce most VICKSI-beams at roughly tenfold intensity.

1.1. Basic Machine Layout

The new injector cyclotron will have an extraction radius of 43 cm, which corresponds to the injection radius of the booster cyclotron: The injector runs with the same mean magnetic field of 0.8 T at maximum. Then with the same pole shape symmetry and acceleration system every injected beam is automatically perfectly matched to the booster. Therefore the matching condition directly suggests to choose all the basic machine layout as it is at the booster:

- 4 straight magnetic sector poles with an angle of 50° each.
- 2 accelerating dees, 36° wide each, in two opposite magnetic field valleys, driven either push/push or push/pull at 10 to 20 MHz operating RF frequency (harmonic number 2 to 7).

The ECR-source beams are preaccelerated by a 100 kV platform and axially injected to a radius of 8 cm. The four magnetic poles are attached to a common yoke, which will have small outer dimensions of just 2x1x1 m. The k-factor is k = 8.

This paper deals especially with RF design aspects. Several resonator options have been compared in order to reach small overall machine dimensions.

2. RF DESIGN CONSIDERATIONS

As mentioned in 1.1., most of the basic RF layout is already set by beam matching considerations.

To find the necessary maximum dee voltage level, injection- and extraction-conditions are examined. For single turn extraction a minimum turn separation of 8 mm should be reached. At injection, the first turn radius of 80 mm should be increased by the dee voltage to at least 110 mm for the second turn. Both conditions are met with a dee voltage level of 70 kV even for worst case operation (2nd harmonic and $q/A = 0.5$). To limit the necessary amount of driving power, a high Q resonating structure is mandatory. Complete high vacuum environment is chosen.

The dee structure has been calculated to represent a capacitive load of roughly 55 pF by the use of code EFEBER, which is derived from an old code named EFICAL[3]. The configuration has a minimum dee gap width of 14 mm and a clearance for the beam passage of 20 mm in height.

An unloaded quarter wave resonator at an operating frequency of 10 MHz means a conductor length of 7.5 m. Capacitive loading with up to 260 pF cuts such a resonator of coaxial type down in length to about 2 m at cost of an increase in driving power by roughly a factor of 5. Still 2 m-resonators with 1.5 m outer diameter are large units if compared to the small overall yoke dimensions. A large cost reduction for the project is expected if the injector size can be kept small enough to be realized within existing buildings. Therefore alternative types of resonator construction have been investigated, capable of driving the same dee structure with still low losses but reduced requirement of space.

2.1. Comparison of Resonator Options

The simple quarter wave resonator, a piece of coaxial line connected horizontally to the rear of the dee, has been compared to a half wave structure with vertical dee-connection, and to another quarter wave system with the inner line conductor wound up to a coil.

2.1.1. Horizontal quarter wave coaxial line resonator

Length reduction of this type of resonator is limited by geometrical reasons. In order to limit the decrease of voltage versus increasing machine radius within the dee area, additional capacitive resonator loading should not be applied along the dee. Since the dee tip area is occupied by magnet poles and injection elements, space is available only at the rear of the dee. For 200 pF at a gap of 20 mm a capacitive plate area of $0.5 m^2$ needs to be provided around the dee stem, which means another meter of stem length. Therefore less than 2 meters of total resonator length cannot be achieved.

There are about 1 kW of power losses for 70 kV dee voltage at the open end of an unloaded shorted coaxial quarter wave line, with copper surfaces, outer diameter D = 1.5 m, stem diameter d = D/10, operated between 10 to 20 MHz. If tuned by shorting piston and loaded by a fixed 260 pF, this resonating line will be cut in length to less than half at cost of an increase of losses of up to 5 kW. With capacitive tuning only, the power loss amounts to a maximum of 3 kW.

Table 1. Coaxial line quarter wave resonator

Dee-capacity (includes fine tuning)	100 pF
Resonator outer diameter	1.5 m
Stem diameter	0.15 m
Resonator stem length	4.09 m
Dee-length	0.52 m
Coarse tuning via shorting piston/piston path length	2.84 m
Power losses at 70 kV dee voltage (copper surfaces)	1.45 kW (10 MHz) 1.8 kW (20 MHz)

Less ambitions with respect to length reduction permit the straightforward design-data given in table 1. At reduced dee voltage of 50 kV less than 1 kW of driving power is necessary, which would allow to run without a special power amplifier, and to use already existent drivers.

2.1.2. Vertical half wave coaxial line resonator

A large capacitive tuning range with a movable plate facing the rear of the dee is achieved easier, if the stem connects elsewhere. Vertical connection of two quarter wave stems through the magnet yoke has been considered, which results in a similar type of resonator as built for the two GANIL SSC's. With this solution the outer line diameter is limited to 0.5 m by the yoke/pole-dimensions. With 5 cm stem diameter, 215 pF tuning capacity and 55 pF dee capacity the results are: Up to 18 kW of driving power for 70 kV dee voltage and 2 m vertical space above and below the beam plane have to be provided.

2.1.3. Helical inner conductor

Smaller resonator dimensions are possible with the replacement of the inner conductor of a quarter wave coaxial line by a coil. Chapter 3 deals with special mechanical and electrical problems encountered with such a resonator; a feasible layout is shown in Fig. 1 and explained with Table 2. The resonator extends only 0.5 m beyond the magnet yoke and will give 70 kV of dee voltage with about 6 kW of losses.

3. SPECIAL FEATURES

A coil cannot support the dee structure mechanically. Cooling is not easily provided, and high currents must be handled at the shorting point.

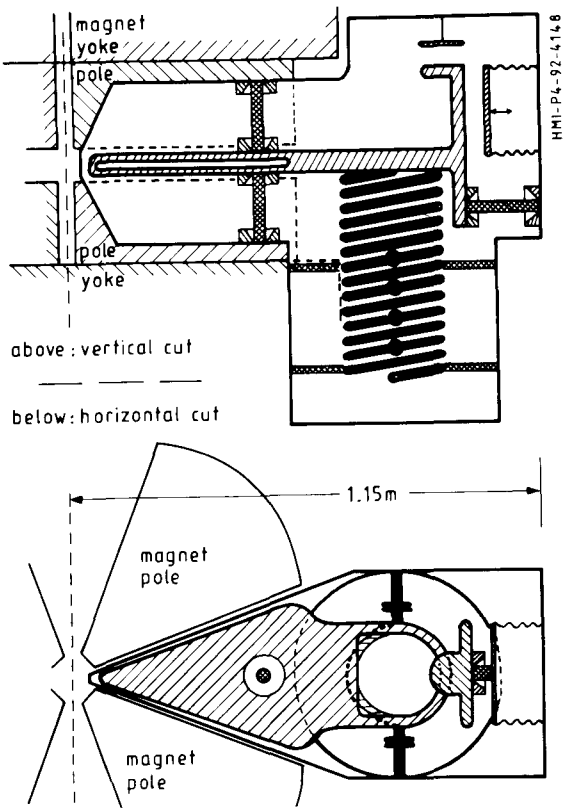


Fig. 1. Quarter wave resonator with helical inner conductor

Table 2. Double-helix quarter wave resonator

Dee-capacity:	55 pF
Tuning capacity (rear of dee)	10 to 40 pF
Coupling:	capacitive
Dee support: 3 BeO rod insulators/length 17.5 cm/ diameter 3 cm / protected by corona rings	
Coil: Double-helix in shielding box / Box diameter 0.5 m / Each coil is made from silvered, unmagnetic stainless steel tube with 2 cm tube diameter and 0.6 cm bore-radius / Coil-mean-diameter 22 cm, turn-pitch 7.2 cm / Both coils are turned into each other to form a double-helix with the connections oriented by 180° to the rear of the dee / Coil support by BeO rod insulators / Coil Q ~5000 (at 20 MHz) and ~4000 (at 10 MHz)	
Frequency-tuning: capacitively within four sub-bands by tuning plate facing the rear of the dee / Sub-band selected by pressing two ground studs to one out of the four pairs of taps on the double-helix	
Power loss at 70 kV dee voltage:	4 kW (10 MHz) 6 kW (17 MHz) 4,5 kW (20 MHz)
Shorting current, at 70 kV/17 MHz	700 A, total
divided to two studs, 10 cm contacts	35 A/cm

To support the dee and the coil mechanically, rod insulators have been used. At the metal / insulator-junction the electrical fields are strongly reduced with conical metal rings. With BeO as insulator material, the maximum losses per rod amount to about 60 W. This gives a maximum temperature rise of 20° K between the midpoint of the rod and the cooled end surfaces.

Cooling water is brought through the coil to the dee. In fact, two identical coils are used, fitted together as a double-helix with the hot ends connected to the rear ring of the dee at 180° apart from each other. This parallel connection allows the one coil tube being used as water feed, the other as drain.

Model measurements on a prototype double-helix showed the coil Q to be increased by about 10% over the single-helix case. The minimum Q-value is 4000. This results in 700 A of shorting current at 70 kV dee voltage, which excludes the use of sliding coil taps for frequency tuning. Therefore only a frequency sub-band is selected at the double-helix coil by means of switching one out of four fixed tap-pairs at the lowest four windings. The total maximum of 700 A divides onto two taps, one for each helix, with a contact ring of 10 cm in circumference. During RF operation the contact rings are under pressure, which gives a large safety margin over the anticipated maximum current load of 35 A/cm. Frequency tuning within the sub-bands is achieved with a movable capacitive plate facing the rear of the dee. To cover the sub-bands completely, a maximum capacity change of about 22 pF must be provided.

4. CONCLUSION

One important problem for the construction of an injector cyclotron for VICKSI is the design of the RF system.

The quarter wave coaxial line resonator described in table 1 is the simplest solution. It just requires space, which in turn easily means as much additional costs for a new building as the complete expenses for the injector alone. In the tradeoff between a simpler RF design with high building costs and a more complicated but smaller double-helix resonator the latter is favoured. With this solution the overall dimensions of the injector cyclotron are mainly defined by the magnet yoke and kept very small.

REFERENCES

1) Busse, W., Martin, B., Michaelsen, R., Pelzer, W. and Ziegler, K, "The heavy ion accelerator facility VICKSI", EPAC 88 (World Scientific, Singapore, 1989), Vol. 1, pp. 448-450
2) Geller, R., "Multiply charged ECR ion sources for particle accelerators", CYCLOTRON '86 TOKYO (Ionics Publishing Company, Tokyo, 1987), pp. 699-706
3) Ianovici, M.; "A computer program for the solution of the Laplace equation in two dimensional cartesian coordinates", EPUL Lausanne, 1974

LOW FREQUENCY RF SYSTEM FOR THE INDIANA UNIVERSITY COOLER RING

X. Pei

and

S. Anderson, V. Derenchuk, G. East, D. Friesel, D. Jenner, D. McCammon, T. Sloan
Indiana University Cyclotron Facility, Bloomington, IN 47408, U.S.A.

ABSTRACT

A low frequency rf system working at the orbiting frequencies of particles ($h=1$) has been built at the IUCF Cooler ring. The cavity design features a new ferrite biasing scheme proposed by S. Papureanu and has a wide tuning range. Application of the fundamental mode rf operation in the cooled rf stacking injection is discussed.

MOTIVATION

The Indiana University Cooler is a 3.6 T-m electron-cooled storage ring and synchrotron designed primarily for internal target nuclear physics experiments. Upon its commissioning in 1987, it was equipped with an rf system that covered a frequency range of 6 to 17 MHz and was ferrite-bias tunable for a 2:1 frequency ratio for synchrotron acceleration of $\beta<1$ ion particles. With a ring circumference of 86.8 m, the rf system had to run with modes of harmonic number 6 or higher for a typical proton beam with injection energies from 45 to 200 MeV.

In a ring with electron or stochastic cooling, if the cooling energy is set at the center of the rf bucket, all the beam will eventually converge to a small longitudinal emittance area in the center of the rf bucket due to the combined action of rf and cooling forces. Fig.1 is the computer simulation of the converging process of the beam[1].

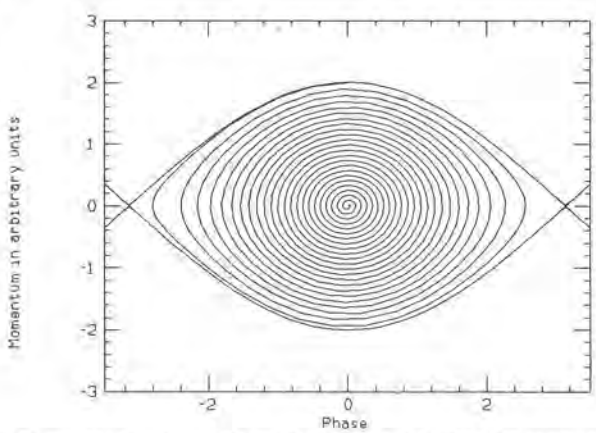


Fig. 1. Computer simulation shows that beam spirals into the center of the rf bucket with combined forces of cooling and rf.

Fundamental mode of rf operation thus has a unique capability to precisely place the beam in a single well defined azimuthal position. This was of particular interest to the cooled rf stacking injection for reasons that will be explained later in this article. Design and construction of a fundamental frequency rf system was thus proposed and accomplished.

THE RF CAVITY

A low frequency limit of 0.5 MHz was chosen to cover most of the beam types and energies that the cyclotron injects into the Cooler. At this frequency range, ferrite-loaded quarter-wavelength coaxial cavity is compact and easy to build.

It is also desired that the cavity has a wide tuning range to follow the synchrotron acceleration of $\beta<1$ particles such as proton and helium. Without a wide continuous frequency coverage, a beam has to be accelerated with a higher harmonic number first and then be rebunched at a lower harmonic number at an intermediate energy. Such a process adds complication to operation and often leads to beam loss.

Ferrite biased tuning is a widely used method to electronically tune an rf cavity. The permeability μ of ferrites decreases as the magnetic field increases. By adding a "biasing" DC or low-frequency magnetic field, the μ or the resonant frequency of the cavity can be changed. This biasing field, however, usually has to be quite strong and must be minimized where the beam goes through. The existing IUCF Cooler PPA cavity (salvaged from the Pennsylvania Proton Accelerator), for example, uses its enclosure as a single turn coil and needs a 4000 A power supply. For the low frequency cavity, an efficient biasing scheme proposed by S. Papureanu was used. The biasing magnet is a quadrupole and is placed outside the ferrite. The field in the center (where the beam line is located) is zero due to quadrupole cancellation. Fig.2 is an illustration of the biasing structure. This approach was first adopted by a cavity design at Max Planck Institute and hence this cavity at the IUCF Cooler was named MPI cavity. With 40 turns of windings on each magnet tip, a 20 A power supply

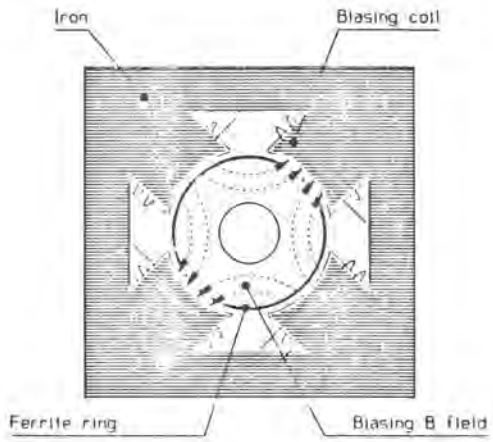


Fig. 2. Principle of ferrite biasing with a quadrupole magnet.

covers a frequency tuning ratio of 7:1, which is more than sufficient to cover the synchrotron acceleration frequency change of $\beta<1$ particles. In Fig.4, the frequency versus current plot of the MPI cavity is shown.

The ferrite rings are stacked with half an inch gaps in between. The enclosure which forms the outer conductor of the coaxial transmission line is made of copper straps instead of solid copper to minimize machining for construction. The spacings between the copper straps allow air flow into the gaps of the ferrites to remove heat buildup. Fig.3 is a cut-away view of the cavity structure.

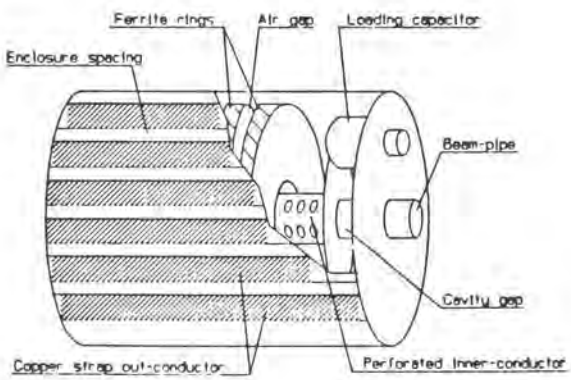


Fig. 3. Cutaway picture of the MPI cavity showing its internal structure.

A 4100 pf variable capacitor is loaded to the gap of the cavity to provide additional tuning range. With 4100 pf of capacitative loading and zero biasing, the cavity resonance is slight below 0.5 MHz.

A cavity merit factor "gap resistance" is defined as R_g as follows:

$$R_g = \frac{V_g^2}{2P} \qquad (1)$$

where V_g is the peak rf voltage developed across the cavity gap with a drive-power of P. R_g is thus the equivalent shunt loss resistance across the tank circuit. Fig.4 also shows a plot of R_g at various frequencies.

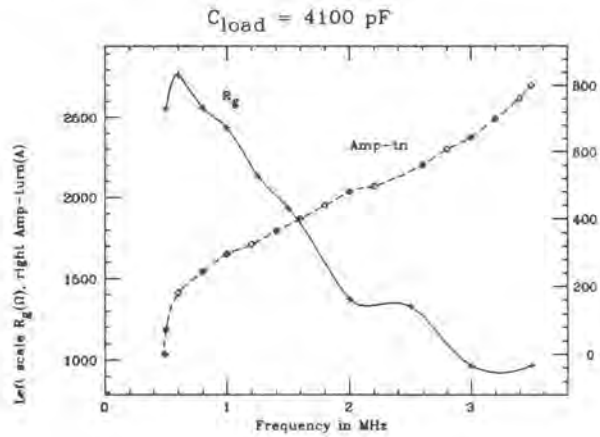


Fig. 4. Bias Ampere-turn and gap resistance versus frequency plot of MPI cavity.

AMPLIFIER, FREQUENCY SOURCE AND CONTROLS

In the $h=1$ mode, sufficient bucket size can be created with a relatively low rf voltage, as[1,2]:

$$\frac{\Delta p_{max}}{p} = \sqrt{\frac{2QeV}{\pi\beta^2 Eh\eta}} \qquad (2)$$

where Δp_{max} is the maximum momentum deviation from the synchronous momentum p that can be captured by the rf bucket, E the energy of the particle, and η the "frequency slipping factor" defined as $1/\gamma^2 - 1/\gamma_t^2$. γ_t is the "transition γ" of the ring. A ring is isochronous at $E=\gamma_t mc^2$.

A 150 Watt solidstate power amplifier is used to drive the cavity to obtain a gap voltage of 500 Volts peak or higher, sufficient to cover the typical cyclotron beam energy spread of $\Delta p/p = \pm 0.03\%$.

Fig.5 is a block diagram of the IUCF Cooler low frequency rf system. The sweeping frequency source is made of a direct digital frequency synthesizer (DDS) that

has sub-microsecond frequency switching speed with phase and amplitude continuity. Automatic tuning is achieved by comparing the phase of the rf drive at the cavity to the phase of rf electric field across the cavity gap. The phase information is used to drive a servo loop that controls a power supply to maintain proper cavity biasing field for correct tuning. Other feedback loops control the amplitude and phase of the cavity.

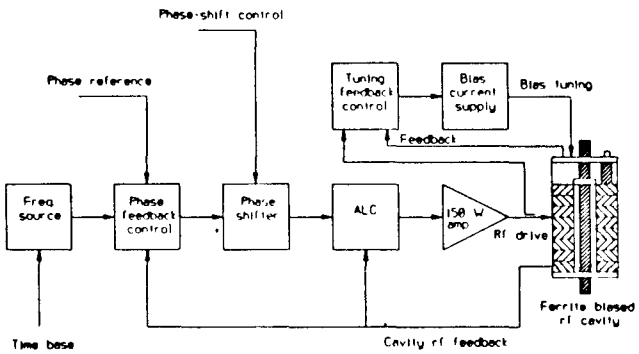


Fig. 5. Block diagram of the IUCF low frequency rf system.

APPLICATION

As an example of the application of the cavity, its use in the multiturn rf stacking injection of the Cooler ring is illustrated as follows.

Detailed description[1,2] of the whole rf stacking process is beyond the scope of this paper so we assume that there already is accumulated beam in the ring. In order for fresh beam injection to occur, a pair of matched kickers must be fired. Because the kickers are placed 180 degree betatron oscillation phases apart, they theoretically only cause a localized orbit distortion in the ring. However, precise matching of kickers is not possible and the stored beam will experience transverse-heating led beam loss while going through the kickers. With the stored beam bunched by electron cooling and the fundamental rf bucket, however, the stored beam can either stay away from the kickers when they fire or go through the kickers at a better behaved time, such as the flattop of the kicker pulse (Fig.6). The kicker firing does need to be synchronized to the rf phase for this operation. Beam experiments showed that with the fundamental frequency bunching, kicker-heating induced beam loss was greatly reduced[3].

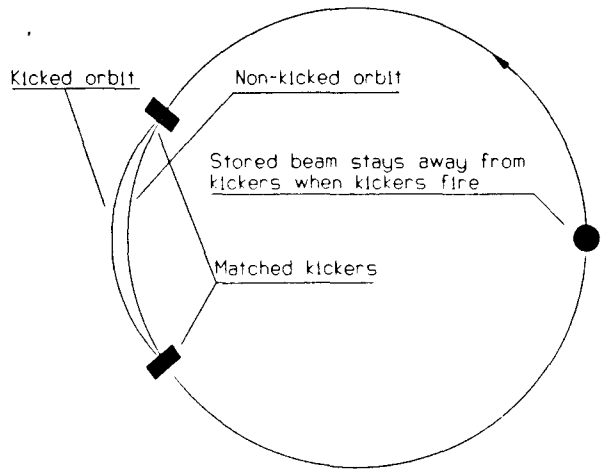


Fig. 6. The low frequency cavity bunches the beam at an azimuthal angle away from the kickers when kickers fire. Lower beam loss can also be achieved by letting beam go through the kickers at the flattop of the kicker pulse.

ACKNOWLEDGEMENTS

This work was supported by the U.S. National Science Foundation under grant NSF PHY9015957. The authors wish to thank R. E. Pollock for suggesting the MPI cavity design and calculating the key specifications.

REFERENCES

1) Pei, X., "Cooled Rf stacking Injection in the IUCF Cooler," Ph.D. Dissertation, Indiana University, 1991.
2) Pollock, R.E., "Cooler Design Notes," IUCF, 1988.
3) IUCF Cooler Logbook No.10.

A MODIFIED RF SYSTEM OF JAERI AVF CYCLOTRON

Y. Kumata, Y. Fukumoto
Sumitomo Heavy Industries, Ltd.
Niihama, Ehime 792 Japan,

M. Fukuda, K. Arakawa, T. Karasawa
Japan Atomic Energy Research Institute
Takasaki, Gunma 370-12, Japan

and

A. Shimizu
Research Center for Nuclear Physics Osaka University
Mihogaoka, Ibaraki, Osaka 567, Japan

ABSTRACT

A $\lambda/4$ coaxial cavity with a movable short has been developed in the JAERI AVF cyclotron. The original model of this cyclotron had the movable panel type resonator, of which maximum voltage was not sufficient for accelerating 90 MeV protons. The maximum voltage of the modified coaxial cavity is 60 kV at 21.14 MHz. The resonant frequency range is 10.6 to 22.0 MHz, and the fine tunable frequency $\Delta f/f$ is 1.6 %. The voltage and phase stability is $\pm 1 \times 10^{-3}$ and 0.5° respectively.

1. INTRODUCTION

The JAERI AVF cyclotron[1,2] (K-number=110) has been constructed for the purpose of extensive application of ion beams to R&D for radiation technology. Various kinds of ions from proton to xenon in a wide range of energy are required for fundamental research in materials science and bio-technology. We have two types of ion sources[3] in order to meet the requirement of producing light to heavy ions; one is a multicusp type ion source for generating protons, deuterons and helium ions, the other is an ECR type ion source mainly for heavy ions from proton to xenon. The ions with charge-to-mass ratio of 1 to 6.5 can be accelerated in a broad energy range: 5 to 90 MeV for protons, 5 to 53 MeV for deuterons, 10 to 108 MeV for $^4He^{2+}$, and 2.5 to $(110 \times (Q/M)^2)$ MeV/u for heavy ions.

The JAERI AVF cyclotron is of the model 930 of Sumitomo Heavy Industries, Ltd. (SHI). The cyclotron is basically the same model as the CYCLONE (Université Catholique de Louvain, Belgium), the IRE cyclotron (Institut National des Radioelements, Belgium) and NIRS-Chiba cyclotron (National Institute of Radiological Sciences, Japan). The latter three cyclotrons have a movable-panel type resonator with rf peak voltage of 35 kV at 21 MHz. A higher acceleration voltage of 60 kV was required for accelerating 90 MeV protons when the external ion sources were used. However, it is hard to get 60 kV by using the movable-panel type resonator owing to the power limit on the stem. The asymmetrical structure of the cavity causes the partial current concentration on the stem facing the movable panel, and then causes over-heated trouble on the stem and movable panel. The power consumption of the cavity was predicted to be 80 kW so as to operate at 60 kV and 21.14 MHz.

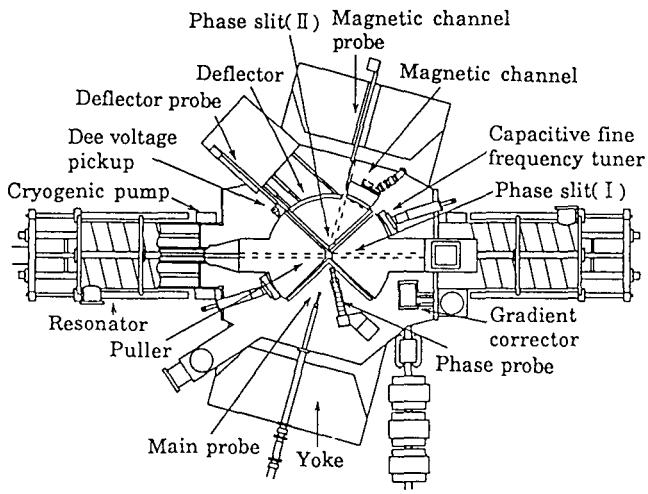


Fig. 1. Schematic drawing of the AVF cyclotron.

To avoid such a problem, the coaxial cavity with a movable short has been developed. The symmetrical structure of the cavity is more advantageous for the current density on the stem. The Q-value of the coaxial cavity, therefore, is higher than that of the movable-panel type cavity. Consequently, the power of 30 kW required for the amplifier is much less than before.

2. RF CAVITY

A schematic drawing of the cyclotron is shown in Fig. 1 and the specification of the rf system is summarized in Table 1. Two dees with a dee angle 86° are made of 10 mm thick oxygen free copper (OFC) so as to maintain a good thermal conductivity. Cooling water

Table 1. Specification of the rf system.

Number of dees	2
Dee angle	86°
Maximum dee voltage	60 kV
RF frequency	10.6 ~ 22.0 MHz
Resonator	Movable-short type
Harmonic number	1, 2, 3
Vertical aperture inside dee	40 mm
Gap between dee and ground plate	42 mm
Movable range of shorting plate	1350 mm
Inner tube diameter	300 mm
Inside diameter of outer tube	1000 mm
Full relative frequency change $\Delta f/f$	1.6 %
RF voltage stability	$< \pm 1 \times 10^{-3}$
RF phase stability	$< \pm 0.5^{\circ}$
Pre-amplifier	EIMAC 4CW800B
Final amplifier	EIMAC 4CW50000E
Power feeder	inductive coupling
Maximum output power	50 kW×2

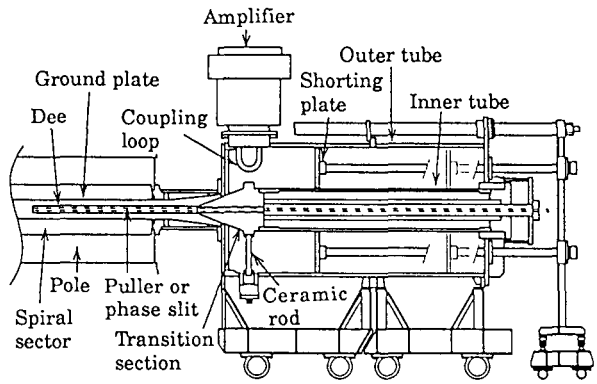


Fig. 2. Schematic view of the coaxial resonator with a movable shorting plate.

pipes are soldered on the inner surface of the dee. The gap between the dee and the ground plate is 42 mm, which is sufficient for the maximum voltage of 60 kV. The ground plate covering the trim coils is cooled indirectly.

The beam aperture inside of the dee is 40 mm. The acceleration gap in the center region is 17 mm and is increased radially up to 56 mm at r = 920 mm. The capacitive fine frequency tuner is located on the outer side of the dee. The tuner gap is adjustable from 8 mm to 50 mm automatically. The dee voltage is detected with a capacitive divider of which the ratio is 1/1000.

A puller extracting ions from inflector is inserted along the coaxial line of the cavity in contact with the inside surface of the dee. One of two phase slits is also inserted along the coaxial line of the other cavity and is movable radially.

A schematic view of the coaxial cavity is shown in Fig. 2. The dee is connected through the transition section to the inner coaxial line. The one end of the inner line is supported with a ceramic rod and the other end is supported with the end plate of the cavity. The outer diameter of the inner coaxial line is 300 mm and the inner diameter of the outer coaxial line is 1000 mm. The length of the cavity is approximately 2000 mm. They are made of OFC. The inner line is composed of three tubes so as to keep a go-and-return path of the cooling water and the space for the puller or the phase slit. The outer cavity is cooled by copper pipes which are wound around it. The outer cavity can be separated into front and rear parts when the maintenance of the movable short is necessary. The stroke of the movable short is 1350 mm so as to cover the required frequency range from 10.6 MHz to 22.0 MHz. The shorting plate has many contact fingers made of the Be-Cu. They are pressed to the inner and outer coaxial line with the pneumatic bellows. The contact piece on the finger is made of silver containing 5 % graphite. The final amplifier is directly mounted on the front part of the outer cavity and is coupled with the resonator by a loop coupling. The loop, made of 40 mm diameter copper pipe, is cooled by water. A couple of the cryogenic pumps (4000 l/s each) are mounted on the bottom of the cavity. An rf shield consisting of copper pipes was attached on the each pumping port to shield the leakage of rf power from the cavity to the pump.

3. CHARACTERISTICS OF THE RESONATOR

The electrical characteristics of the resonator have been measured by using a network analyzer (HP-8753A). A low level rf power was fed through a small capacitor facing to the final tetrode so as to avoid perturbation, and dee voltage was detected with capacitive divider. The resonant frequency is shown in Fig. 3 as a function of the movable short position. The frequency range adjusted by fine tuner is shown in Fig. 4 as a function of the tuner gap. The relative frequency range is 1.6 % for 10.585 MHz and 22.237 MHz.

The measured Q-value and the shunt impedance are shown in Fig. 5 and Fig. 6 as a function of resonant frequency. The shunt impedance was measured by a perturbation method using a small capacitor of which the capacitance was measured exactly. 75 % of the calculated values are shown with solid lines in Figs. 5 and 6, and are well consistent with measured values. The one-dimensional transmission line model is used for the calculation. For the comparison, the measured values of the movable panel type cavity are shown in dashed lines in Figs. 5 and 6. The shunt impedance in higher frequency region has been much improved by approximately 4 times.

4. AMPLIFIER

A schematic diagram of the amplifier is shown in Fig. 7. The amplifier is composed of one solid-state amplifier and two stage tetrodes (EIMAC 4CW800B and 4CW50,000E). They are used as grounded-cathode configuration to raise higher power gain. The all pass net-

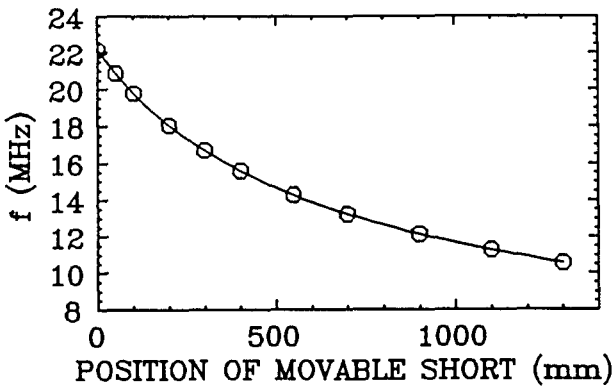


Fig. 3. Resonant frequencies of the resonator as a function of position of the movable shorting plate.

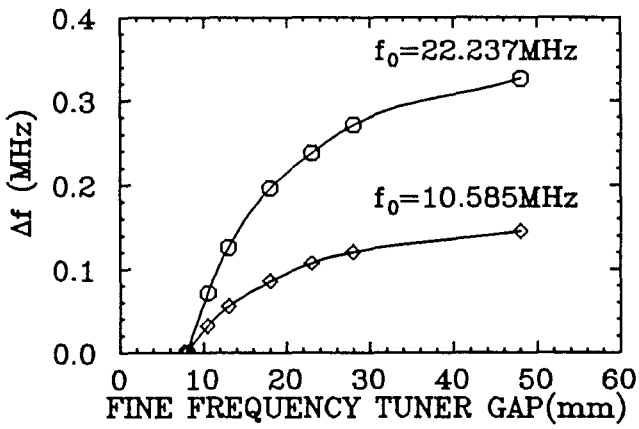


Fig. 4. Adjustable frequency by the capacitive tuner at 22.237 MHz and 10.585 MHz. The full relative frequency change is 1.6 %.

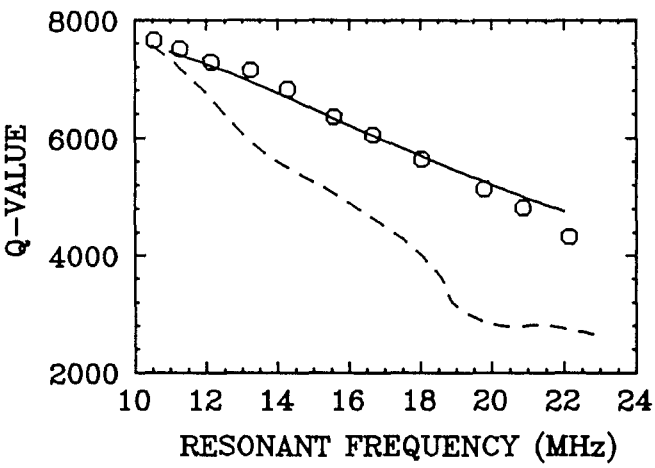


Fig. 5. Frequency dependence of Q-value. The solid line shows 75 % of the calculated value based on one-dimensional transmission line approximation. The dashed line shows the measured value of the movable panel type cavity.

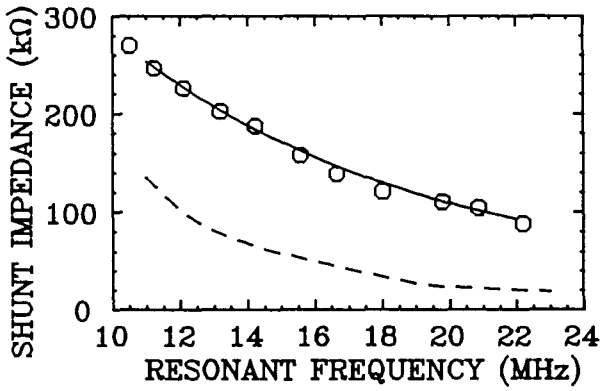


Fig. 6. Frequency dependence of shunt impedance. The solid line shows 75 % of the calculated value based on one-dimensional transmission line approximation. The dashed line shows the measured value of the movable panel type cavity.

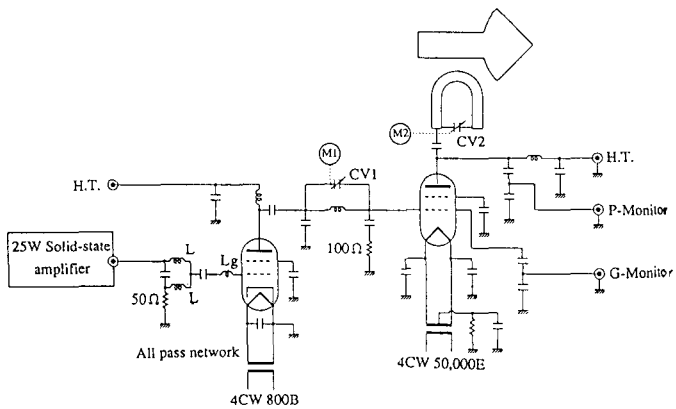


Fig. 7. Schematic diagram of the amplifier system.

work[4] is adopted for the input matching circuit of the pre-amplifier. This circuit has the advantage that no adjustment is required in the frequency range from 10 to 22 MHz. The final tetrode is coupled directly to the cavity through a loop coupling. A variable vacuum capacitor connected parallel to the loop is used for the adjustment of the coupling impedance.

5. LOW LEVEL CONTROL SYSTEM

The block diagram of the low level control system is shown in Fig. 8. The rf signal from a master oscillator (HP-8656B) is divided into three ways: the main rf system, a buncher system and a chopper system. The phase modulator stabilizes the absolute phase between the master oscillator and the No.1 dee on which the puller is mounted. The following phase shifter controls the relative phase between the two dees. The amplitude of the rf signal was controlled with the amplitude modulator.

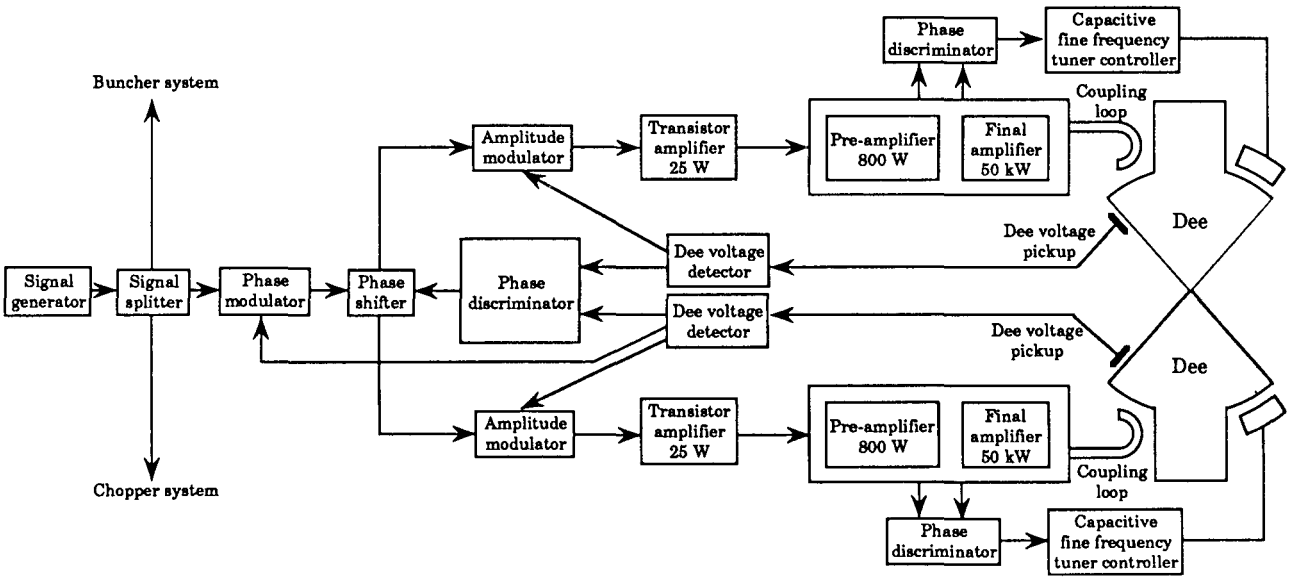


Fig. 8. Block diagram of the rf control system.

The rf signal is amplified with three-stage amplifier system: a 25 W solid-state amplifier and two tetrodes. The dee voltage is detected with capacitive pick-up method and fed to the dee voltage detector. The signal is divided and fed back to the phase discriminator, the amplitude modulator and the phase modulator. The capacitive fine tuner is controlled by the phase discriminator detecting phase difference between the grid and plate rf voltages of the final tetrode.

The operation sequence of the rf system is controlled automatically by a micro processor named "Universal Device Controller" (UDC).[5] The UDC is communicated with a host computer by optical fiber.

6. POWER TEST AND OPERATION

The power test has been carried out successfully in the frequency range of 10.6 MHz to 22.0 MHz. The required voltage in every frequency point has been achieved as shown in Fig. 9. The maximum voltage of 60 kV has been achieved at 21.14 MHz with a low power consumption of 22 kW measured by calorimetric method. The voltage and phase stability are better than $\pm 1 \times 10^{-3}$ and $\pm 0.5°$ respectively over the whole frequency range. The dee voltage ripple is less than 1×10^{-3} and the phase ripple 0.3°. In the early days of operation, it took some minutes to overcome multipactorings in pulse mode operation. But in these days, it is easy to start up the rf system. The operation time so far is approximately 2000 hours and no serious trouble has been suffered.

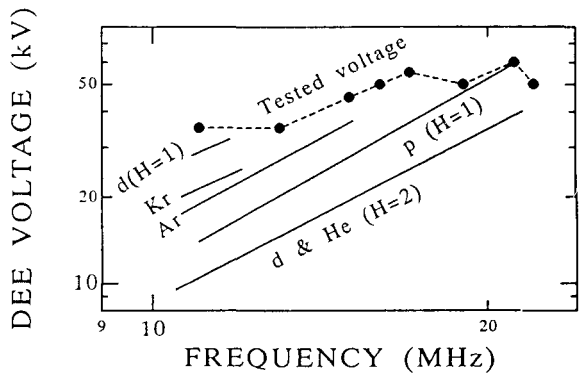


Fig. 9. The required dee voltage and tested voltage as a function of frequency.

7. REFERENCES

1) Tanaka, R. et al., "JAERI AVF cyclotron for research of advanced radiation technology," presented at the Conference on Cyclotrons and Their Applications, Berlin, Germany, May 8-12, 1989.
2) Arakawa, K. et al., "Construction and first year's operation of the JAERI AVF cyclotron," presented at this conference.
3) Yokota, W. et al., "Operation of ion sources and beam transport to JAERI AVF cyclotron," presented at this conference.
4) Mosko, S.W., Raylander, J.D., Shulze, G.K., "ORIC rf system preparation for HHIRF", IEEE Trans. Nucl. Sci., **NS-24**, pp. 1786-1788, June 1977.
5) Okumura, S. et al., "Control system for JAERI AVF cyclotron," presented at this conference.

MULTI-POINT CAVITY EXCITATION

E. Zaplatin
KFA, D-5170 Juelich, Germany

ABSTRACT

To simplify the solution to transfer and input of high rf power in the accelerating system it is proposed to excite a cavity at several points by independent loops and power generation systems, the rf power being then summed directly in the accelerating cavity. The theoretical and experimental study of this excitation has been carried out for development of an RF system for the project "Supercyclotron"[1] with the RF power to be about 20 MW per cavity.

1. ONE-LOOP CAVITY EXCITATION.

When one deals with a high power level, it is important to minimize the power of the wave reflected from the excitation system, i.e. good matching of the loop and the excitation circuit. Let us represent the cavity and the excitation system as a system of coupled circuits (Fig.1).

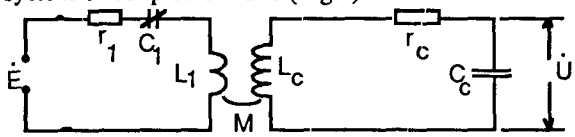


Fig. 1. RF system as the coupled circuit system.

Then the matching conditions are written as

$$x_1+x_c=0\,, \qquad (1a)$$

$$r_1+r_c=Z_0\,, \qquad (1b)$$

where r_1, x_1 are the natural active and reactive resistances of the loop, r_c, x_c are the activ and reactive components of the cavity impedance coupled into the power supply circuit, Z_0 is the wave resistance of the coupling feeder. If $r_1 \ll r_c$, which is practically always so, then

$$r_c=Z_0\,, \qquad (2a)$$

$$x_1=-x_c=2\Delta f Q Z_0/f\,. \qquad (2b)$$

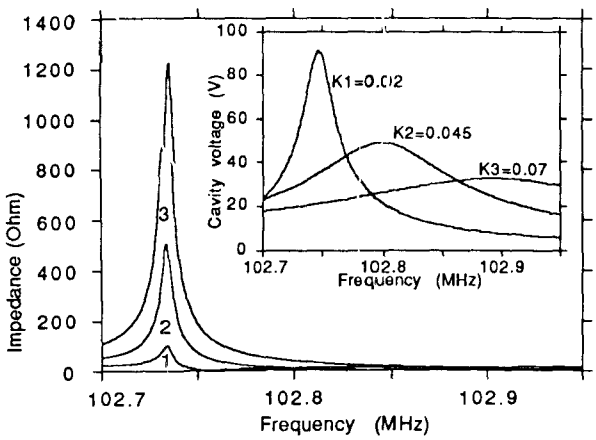


Fig. 2a. Coupling loop resonance characteristics.

Eq.1a is realized by connecting the compensating capacitor C_1 in series with the coupling loop inductor L_1 (Fig.1). Eq.1b can be realized by changing the interaction between the excitation system and the cavity.

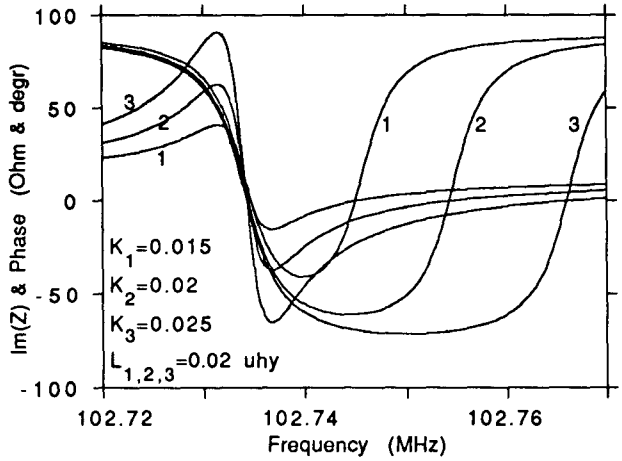


Fig. 2b. Reactance & Phase of coupling loop.

Theoretical analysis of the matching conditions was provided by means of the PSpice program.[2] Let's represent the scheme without compensating capacitor. On Fig.2a,b there are typical frequency functions of the cavity voltage and the coupling loop resonance characteristics at different coupling coefficient values. There are the cavity quality factor fall because of the increasing of the coupling system influence and the impedance grew coupled from the cavity for the generator.

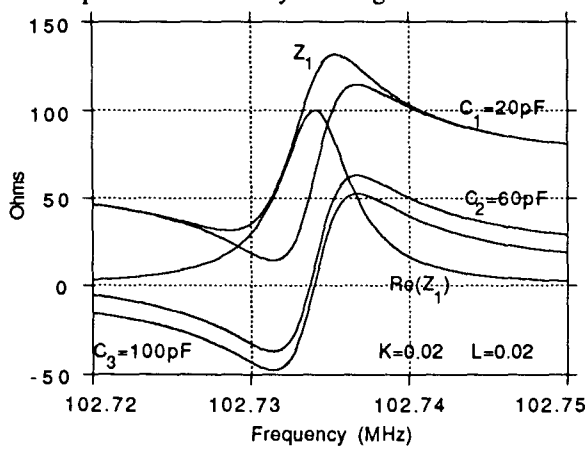


Fig. 3. Compensation of coupling system inductance.

At the presence of the compensating capacitor C_1 there is an additional parameter allowing to change coupling system characteristics. The frequency dependences of the excitation system reflecting the influence of the C_1 value - step by step compensation of the system inductance at the resonance frequency, are represented on Fig. 3.

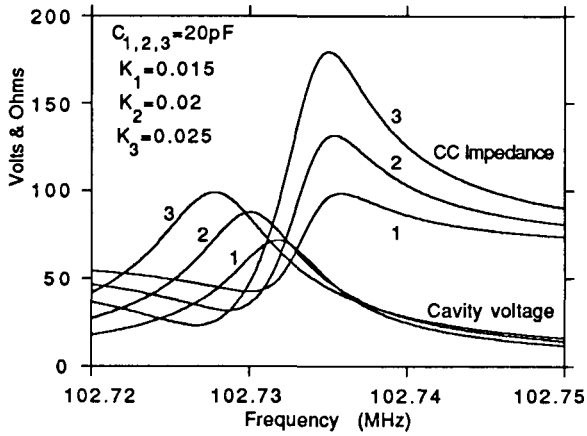


Fig. 4a.

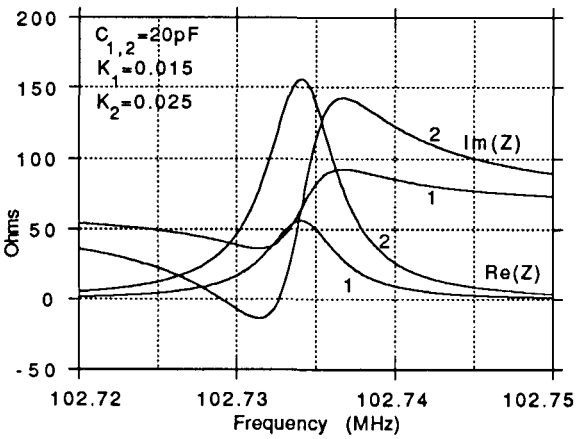


Fig. 4b. Exciting circuit frequency characteristics.

Now, the behavior of the exciting circuit frequency characteristics at the coupling change is shown on Fig.4a,b. Figure 5 demonstrates the principle of the coupling system tuning on the activ resistance 50 Ohm.

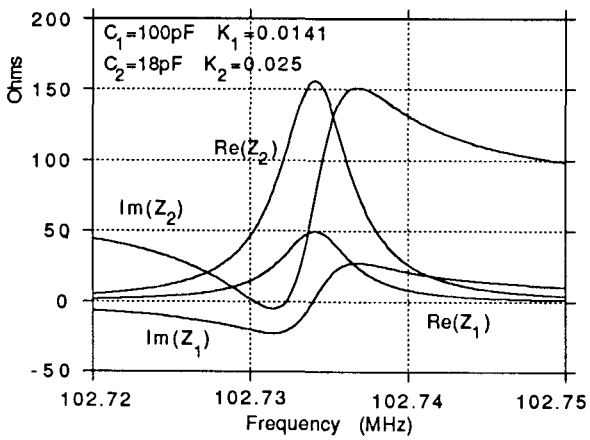


Fig. 5. Coupling system tuning.

Changing the coupling with the cavity and the compensating capacitor value it is possible to achieve the matching on different frequencies. It may be useful when the cavity frequency tune without its geometry change is needed.

The experimental unit for this study is a model of the "Supercyclotron" accelerating cavity 1/4 of full size[3-4] with a system of excitation loops, an rf generator with five independent outputs and a measuring system for rf parameters. The loop assembly includes the loop itself and 50-Ohm section of a feeder connected to the loop. To neutralise internal inductance of the loop, a polycylindrical variable capacitor is connected in series with the internal conductor of the feeder. The loop assembly can rotate round the axis, which allows one to change the coupling of the excitation system with the cavity. The zero angle α of loop rotation corresponds to the minimal coupling with the cavity.

In Fig.6 there are typical frequency functions of the activ and reactiv resistances measured at the connector of the coupling system. The functions are measured for different loop rotation angles, which changes the value of the coupled impedance from the cavity. The capacitance of the compensating capacitor is constant C_1=5.1. It is measured in relative units (turns of the capacitor tuning screw).

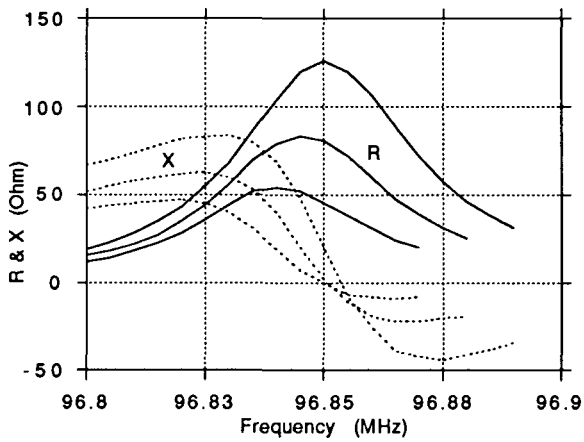


Fig. 6. Active & reactive resistances of coupling loop.

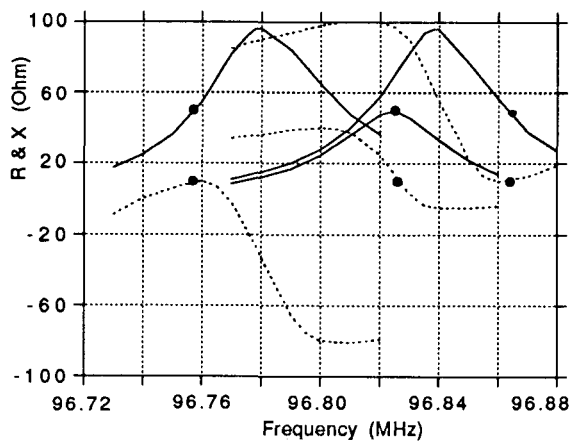


Fig. 7. Active & reactive resistances of coupling loop matched with cavity.

The system was tuned to matching by means of a vector voltmeter and a reflectometer which allowed us to check amplitudes of the incident and reflected waves in the excitation circuit and their phase difference. Tuning the compensating

capacitor and the coupling with the cavity, we set the reflected wave voltage to a minimum and the phase difference to zero, which corresponded to Eq.2.

In Fig.7 there is the family of curves, each of them corresponding to the matching regime for a certain frequency at different C_1 and α. The matching points are highlighted.

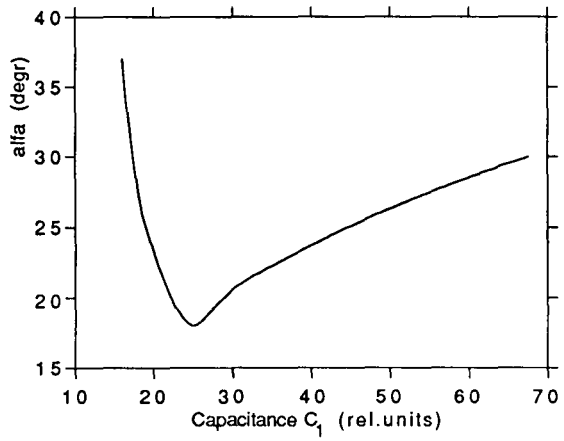


Fig. 8. Angle of loop vs compensating capacity.

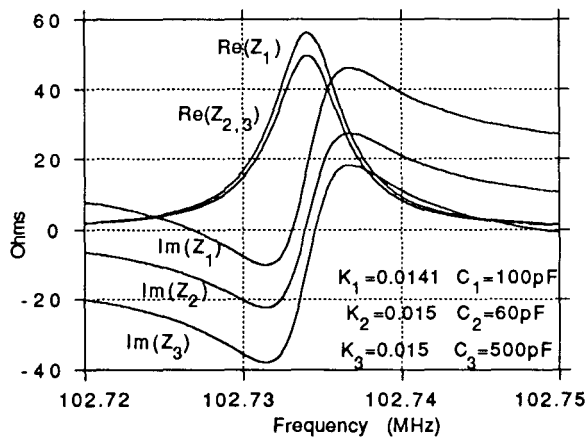


Fig. 9. Capacitance variation at the same coupling factor.

A specific feature of cavity excitation using a compensated coupling loop is that for one rotation angle α there are two values of the capacitance C_1 which allow matching. On Fig.8 the experimental curve of the angle α rotation versus compensating capacitor value C_1 and on Fig.9 the theoretical analysis of this effect are represented.

The explanation is as follows. At the moment when the value $C_1=C_0$ corresponds to the angle α we have an exact resonance, i.e. $x_{Cres}=x_{Lres}$, and C_1 compensates only for the internal inductance of the coupling loop. If $C_1<C_0$, the loop inductance is compensated for by detuning the cavity, so that to couple an additional capacitance C_{res}. If $C_1>C_0$, an additional inductance L_{res} is coupled to compensate for the excess capacitance C_1. This is how the mechanism of the matching frequency "detuning" is determined. However, shifting the frequency in this or that direction we also change the coupled active resistance. So we have to change the interaction with the cavity, i.e. the angle α, to satisfy Eq.2a. Thus, each point of the curve in Fig.9 corresponds to a resonant characteristic in Fig.8. The frequency shift of the matching moment depends on the loop area and the compensating capacitor parameters.

Thus, one can choose the matching moment for the cavity and the excitation system in a rather wide frequency range. If Eq.2 are satisfied, the magnitude of the transfer coefficient is

$$|\dot{K}| = \frac{|\dot{U}|}{|\dot{E}|} = \frac{1}{\omega C_c \sqrt{r_c Z_0}} \qquad (3)$$

i.e. the voltage in the cavity is independent of the coupling system parameters and depends only on the cavity itself. In agreement with this, we experimentally obtained the shift of the resonant characteristic of the voltage as large as six bandwidths of the cavity model without its amplitude reduction.

2. MULTI-LOOP CAVITY EXCITATION.

To find the excitation loop area satisfying Eq.2a, we shall make use of the fact that the loop dimensions are very small as compared with the cavity dimensions and the wave length, so H=const within the loop and

$$S = \frac{\sqrt{2 r_c P}}{\omega_0 \mu_0 H \sin(\alpha)} \qquad (4)$$

where S is the loop area, P is the power applied to the cavity, α is the angle of the loop plane with the lines of the magnetic field H counted off from the position of the minimal interaction between the excitation system and the cavity.

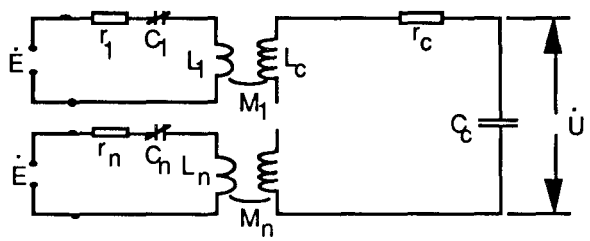


Fig.10. Simplyfied diagram of multi-loop cavity excitation.

If we have N similar loops (Fig.10), each matched to the excitation circuit at 90^0 and assume that the power applied to the cavity is uniformly distributed over all excitation circuits then the rotation angle of each loop must be

$$\alpha = \arcsin(1/N^{1/2}) \qquad (5)$$

for Eq.2 to be satisfied in the case of simultaneous excitation of the cavity by all loops.

Those results were got also using PSpice. On Fig.11,12 two-loop and three-loop excitation correspondently are represented.

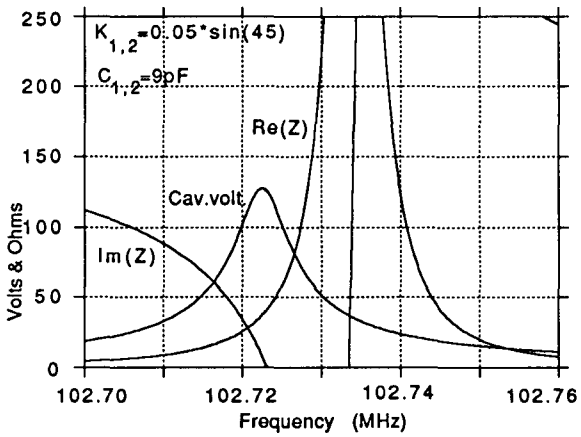


Fig. 11. Two-loop excitation.

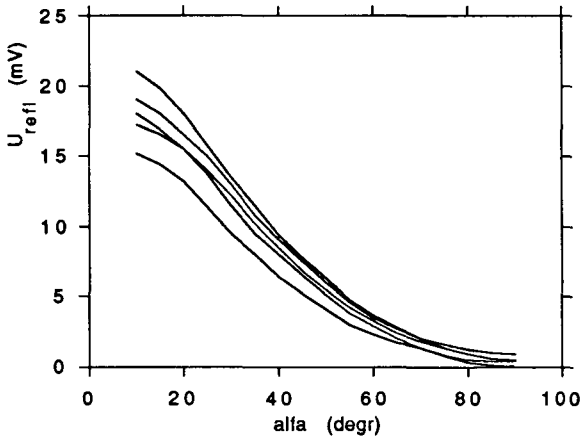


Fig. 13. Reflected wave vs loop angle.

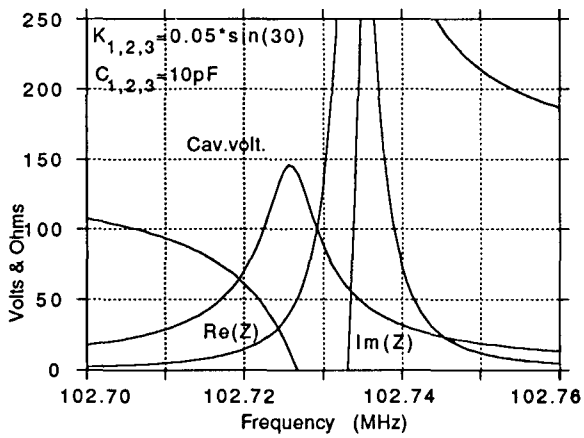


Fig. 12. Three-loop excitation.

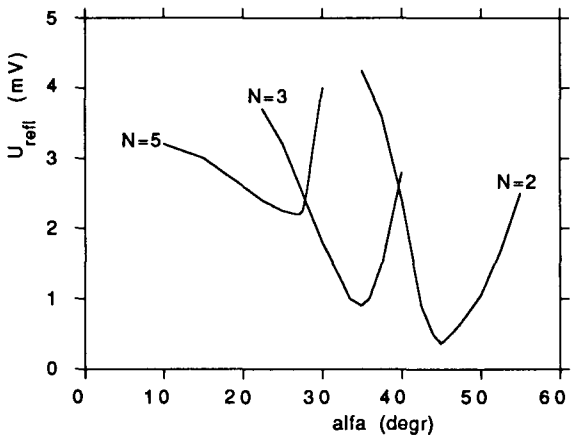


Fig. 14. Reflected wave vs angle of loops.

Showing the dependence of the reflected wave amplitude on the loop rotation angle, the experiment curves in Fig.13 characterize the results of tuning the matching of each of the five excitation channels. The non-identity of the excitation channels is seen to be 3 kHz in frequency and 5% in the reflection coefficient.

If we install several loops in the cavity, the dependence of the reflected wave amplitude on the simultaneous rotation of all loops will be as in Fig.14. The resonant voltage maximum is also shifted over the angle according to Eq.3. The tuning criterion was the maximal running wave factor in all excitation circuits. The fact that the running wave factor worsens as the number of loops increases is due to growing difficulty in tuning. Our investigations showed that the summed resonant voltage in excitation of the cavity by each loop separatly differs by 5% from the voltage in excitation by the five loops used together.

3. REFERENCES.

1) Glazov, A.A. et al. Proc. of All-Union Conf. on Particle Accelerators, "Nauka", Moscow, 1977, v.1.
2) Tuinenga, P.W. "A Guide to Curcuit Simulation and Analysis Using PSpice", Prentice Hall, Englewood Cliffs, New Jersey 07632, 1988.
3) Glazov, A.A. et al. JINR, 9-81-682, Dubna, 1981.
4) Glazov, A.A. and Zaplatin, E.N. JINR, 9-80-46, Dubna, 1980.

EXPERIENCE WITH THE PSI- CYCLOTRON RF-SYSTEM UNDER HEAVY BEAM LOADING

P. K. Sigg, J. Cherix, H. Frei, M. Märki
RF-Group, Paul Scherrer Institute,
CH-5232 Villigen, Switzerland

ABSTRACT

The projected proton beam of 1.5 mA from the 590 MeV ring cyclotron requires extensive replacement of RF-system components. Up to now, one of four amplifier chains on the accelerating cavities has been upgraded to provide for the necessary beam power as well as a 40% higher accelerating voltage. This required a new RF-control system and a new, more powerful final amplifier stage. In addition, everything but the cavity had to be replaced on the flattopping system; this in view of the expected heavy beamloading.
Both of these systems are now operational, and first experience with beam intensities up to 500 μA has been gained.
Serious restrictions will be imposed on our existing acceleration cavities. A new copper cavity design is therefore under investigation, with a first 1:3 scale prototype ready for power testing in 1993.

1. INTRODUCTION

The concept and reasons for expanding the PSI - meson facility to very high beam currents have been described previously.[1)2)] Furthermore, a paper presented at this conference by T. Stammbach[3)] deals with the current status of our upgrading program.
This paper will concentrate on the RF-system of the 590 MeV ring cyclotron and discuss the necessary improvements as well as our first operational experience with beam currents up to 500 μA.
These beam currents were obtained with only one accelerating cavity equipped with the new amplifier chain and operating at an increased cavity voltage of 700 kV_p; this corresponds to a power dissipation of approx. 300 kW. It is an increase of 40% in voltage (and 100% in power) over the existing RF-cavities, which continue to operate at their previous voltage levels of 480 kV_p, until they too, will be equipped with new equipment at the rate of one new system per year. One problem remains to be solved by that time, however: the RF-power coupling loops on the cavities work quite reliably at the previously required power levels of <220 kW (including beam power), but now, at at power levels >350 kW, the loop on cavity #1 fails often.
The flattopping cavity, operating at 150 MHz, also received a completly new amplifier chain, RF-transmission line with power divider, absorber and RF-control system.

2. ACCELERATING CAVITIES, 50 MHz

Cavity #1 was the first one to be equipped with a new amplifier chain and control system. The previously used final stage with 250 kW output power was converted into a driver stage for the new 800 kW final stage. At the same time, the location of the final stage was changed from inside the accelerator vault (close to the cavity) to a location outside and above the vault, about 40 m away, and a new transmission line of higher power rating was installed. This was done in view of the anticipated, much higher radiation dose levels at higher beam currents.

2.1. RF-Control System

The control system is an upgraded and adapted version of the modular concept that has been designed for the Injector 2 cyclotron. It consists of the RF-amplitude, phase, and resonance tuning circuits. The amplitude controller has been expanded by a beam- intensity controlled fast clipping circuit, which limits the maximum output power. This is necessary because of the high output power potential of the new final amplifier. For protection, the maximum power limiter always rides 20 kW **above** the required power level, which will vary from 300 kW (no beam) to about 520 kW @ 1.5 mA beam current. Measurements have shown that the specified amplitude- and phase stability limit (better than 10^{-4}_{pp} resp. less than 0.01^{o}_{pp}) is not exceeded at 500 μA beam current. Figure 1 shows amplitude voltage rest modulation spectrum, at 500 μA, measured with an **independent** pickup loop and demodulator on cavity #1.
In addition to the increased noise modulation, loop gain is reduced as a function of the beam current; if we neglect an eventual effect of variing load impedance on the final amplifier gain, we get:
$\Delta G = -4.8\,dB, \quad @ \quad I_{beam} = 1.5\,mA.$
Looking at the gain margin in our measured spectrum again (Fig. 1), we see that this gain reduction still keeps all spectral components below the specified limit of 10^{-4}_{pp}.

2.2. Power Amplifiers

The 800 kW final amplifier stage is built in a 'grounded grid' configuration; the advantage of this concept lies mainly

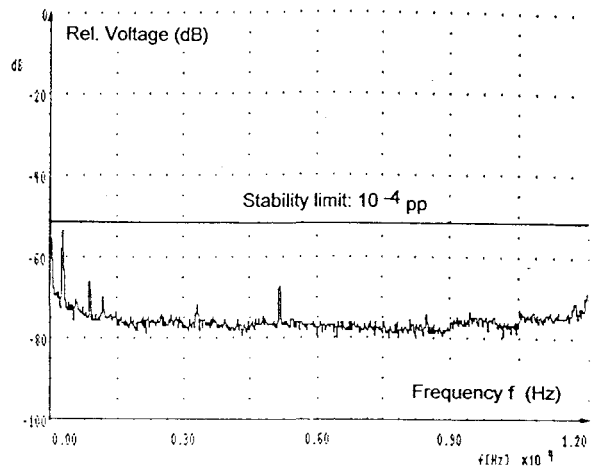


Fig. 1. Cavity voltage rest modulation spectrum, measured on cavity #1, @ $I_{beam} = 500\mu A$

in a more stable mode of operation, that is, less tendency to oscillate at parasitic frequencies, and a wider range of tolerable mismatch, since load variations of 1:2 will have to be handled in the future. Furthermore, no neutralisation network is necessary. The disadvantage of reduced power gain (G = 11..12 dB) can be countered by using the 'old' grounded cathode type final amplifier as a driver; it can easily provide the necessary driving power of ~60 kW. Since this stage is equipped with the same type of power tetrode [RS 2074 HF by Siemens] as the new final stage, older tubes with decreasing cathode emission can be transferred from the final- to the driver stage to extend their lifetime. This concept permits the reuse of all existing RF-amplifiers; they were of course rebuilt and power supplies and interlock systems were replaced by new designs.
The amplifier chain has been operated successfully into a wideband 50 Ω load at power levels up to 850 kW, and has delivered 400 kW into the cavity with only minor adjustments.

2.3. Results of first Operation, Problems

After commisioning of the cavity #1 RF-system in June 1991, beam current was gradually increased over the next half year, up to 500 μA (at an increased cavity #1 voltage of 700 kV_p) for about 2 weeks at the end of the year.
The new system performed remarkably well, this is especially true for the 800 kW amplifier, which, up to now has a perfect record.
Unfortunately, the same cannot be said about the RF-power coupling loop on the cavity: it has been an almost continuous source of trouble by causing a lot of unscheduled down time on the accelerator. This loop , which has been improved over the years to perform reliably on the existing power amplifiers, seems to have reached a limit in power-handling capacity. This despite the fact that we have continuously made improvements and modifications to eliminate weak spots over the past year. Some of these were:

- 'Field gradient rings' at both ends of the ceramic cylinder to lower E-field gradients and shield the edges of the ceramic-to-metal seal. These rings are made of the same material (Vacon) as the water-cooled metal rings at the ends, in order to have identical thermal expansion characteristics; and are silver-plated. The rings have been installed on all 4 acceleration cavities.
- Ionisation detection electrode; a DC voltage of 400 V connected to an electrode near the coupling loop, equipped with current monitoring to shut off the RF-drive if a certain 'dark current' is exceeded. This system proved to be effective in detecting multipacting and sparking in the coupling loop region. In fact, since it has been installed on the other 3 cavities, we have not let the machine up to air accidentally by cracking ceramic windows. Unfortunately, it did nothing to improve life expectancy at higher power levels in cavity #1; that is: it prevented breaking the vacuum all right, but shut off continuously.
  At inspection, the ceramic cylinder then turned out to be partially metal-film coated, and traces of pitting could be seen on metal parts.
- Additional water cooling at the base plate of the coupling loop installation, effective RF-filtering and shielding of the DC-bias connection.
- Amplitude clamp electronics: modifications to prevent up to 30% cavity voltage overshoot after a 'microspark'.

Tests on a loop indicated that overvoltage or multipacting at the loop could not be responsible for the failures. It is now suspected that the problems are caused, at least partially, by the high RF-currents in the cavity wall around the coupling hole.
Temperature tests show that dielectric losses in the ceramic material cannot be the sole source of the problem; we found temperatures of the ceramic cylinder (vacuum side) to be between 110° and 140° C, and lower everywhere else, due to the extensive water cooling.
Since it is doubtful that the existing design can ever reach the required power handling capacity in excess of 500 kW, a completely new concept has to be considered. Some ideas are:

- Remove the ceramic vacuum window (cylinder) from the inside of the cavity back into the coaxial transmission line; this has been tried before with a disk-shaped window, with catastophic results due to multipacting.
- Use two coupling loops of the present type, and install them symmetrically about the median plane, with a power splitter in the RF-feed line.

- Change the dimension of the ceramic cylinder in the present design, that is: make it **longer** or **change** the diameter, or both.

3. FLATTOPPING CAVITY, 150 MHz

In April 1992, the new flattopping amplifier - system became operational. It contains several completely different components, compared to the 50 MHz systems. The reason is that the flattopping cavity has to **absorb** power induced by the beam at the rate of $\sim 65\,kW/mA$; this figure has to be compared to the resonator losses of $< 75\,kW$, at $320\,kV_p$ flattopping voltage. A simplified block diagram can be seen in Fig. 2. One key element in this concept is an high power $50\,\Omega$ load, coupled to the transmission line between final amplifier and cavity via a variable ratio 'power divider': a system of $\lambda/4$ - impedance transformation sections and variable length $50\,\Omega$- line sections. A detailed description can be found in.[4)]

The basic idea of the concept is to lower the Q - value of the cavity such that the critical limit (that is: when the beam - induced power gets into the range of the loaded resonator losses), shifts towards higher beam currents. Above this limit (1 mA), the amplifier tube should act as a variable resistive load to maintain the proper cavity voltage.

The amplifier has to deliver maximum power at no - beam condition and becomes 'unloaded' as beam power is tranferred to the cavity. It is important in this configuration that the line length be adjusted such that the electrical length between cavity and tube is $n \cdot \lambda/2$ (1 : 1 transformation). The cavity impedance always remains resistive due to the resonance tuning system. Even so, the amplifier works into a (resistive) mismatch except at one operating point. The transmission lines have to be considerably overrated to handle the high SWR. Nominal power losses on a mismatched transmision line are by a factor SWR (> 1) **higher** than with a matched line; this requires careful load coupling adjustments to keep transmission line dimensions (and costs) to reasonable levels.

Another problem develops even before the final stage is operated in absorbtion mode: the amplitude - and phase control loops will loose 'controllability' of the cavity voltage. Therefore, in order to keep the amplitude controller in its linear range and operate it in the small signal domain, we **subtract** from the RF - signal between controller and amplifier stages a second RF - signal, with an amplitude proportional to the beam current. This is done with a $0°/180°$ power combiner, as can be seen in Fig. 2. Such a concept has been successfully operated (at lower overall power levels) on our Injector 2 cyclotron; and although the system on the ring cyclotron has only worked at low beam currents up to $500\,\mu A$, we feel confident about its performance above the critical level of ~ 1 mA.

3.1. Control System

In principle, the control system is composed of the same modular units as are used in our 50 MHz controls, although

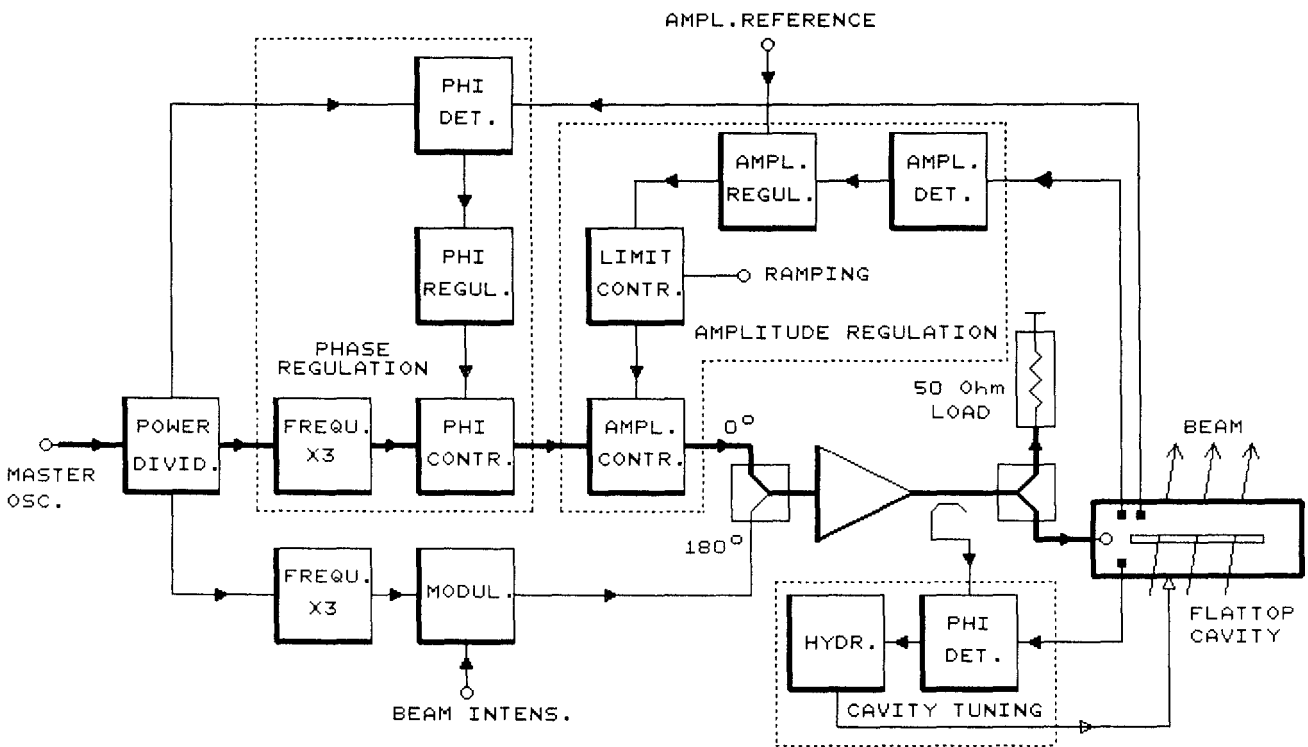


Fig. 2. Simplified block digram of the 150 MHz flattopping cavity control system

some modules had to be adapted to 150 MHz operation. The block diagram (Fig. 2) shows the differences; these are mainly: $3 \cdot f_0$ frequency multiplier, phase locked to the fundamental frequency f_0 , as well as the beam intensity modulator circuit and the $0°/180°$ power combiner used to subtract the beam intensity vector from the (modulated) RF-signal.

3.2. Power Amplifier

A new power amplifier has been designed and built; it uses the same tube as our previous flattopping amplifier, that is: a Siemens power tetrode, type RS 2004 J. Its configuration is 'grounded grid', the mechanical layout is very similar to the 50 MHz amplifier, and the RF-power output is 120 kW @ 150 MHz into a 50 Ω load. In absorbtion mode, the maximum absorbed power is limited by the max. plate dissipation and comes out to be ~42 kW (RF).

3.3. Test Results

There is only limited experience available with the new flattop- system, because beam current in the ring cyclotron was limited to about 500 μA. The flattopping voltage is not yet at its full level; it always operates at ~11% of the total accelerating voltage (ideal flattopping).
The weak element is again the coupling loop; the situation is even more critical than in the 50 MHz cavities, even though total power levels are considerably lower (< 75 kW). Shortly after starting up again after the long shutdown in mid-1991, and still operating with the old amplifier system, the loop failed. Metal surfaces of the loop assembly were coated with a flaky, magnetic film which easily could be wiped off. The 'metal films' were created when arcing caused sputtering of stainless steel and 'Vacon' surfaces. A second failure at the end of 1991 showed similar effects, so a replacement loop will be equipped with an ionisation detector (electrode) similar to the concept used in the 50 MHz loops. (comp. Section 2.3)
This coupling loop is hampered by its smaller size compared to the 50 MHz types used in accelerating cavities; this is due to the high field at the loop location plus the fact, that it has to provide 50 Ω coupling impedance for matching of the cavity to the transmission line at 150 MHz. One way to improve that situation is to increase the overall size of the loop by designing it for a higher coupling impedance, of say, 118 Ω, and then add a λ/4-transformation section ($l = 0.5$ m, $Z_0 = 77\ \Omega$) to the outside of the coupling loop flange to match it to the 50 Ω transmission line.
Another method might be to move the loop to a different location (with less field) on the cavity.

4. NEW ACCELERATION CAVITY (PROTOTYPE)

The present cavity voltage of 700 kV_p is considered to be the maximum safe voltage for continuous operation. The corresponding power dissipation of 300 kW presents a thermal and mechanical limit. The original concept was designed to dissipate 130 kW, it was built from aluminum, with integrated cooling. This makes the cavity very sensitive to changes in atmospheric pressure and temperature; furthermore, temperature gradients across the cavity walls make it impossible to turn on the cavity to the higher operating voltage in one step. Instead, a two step (or ramping) turn- on procedure has to be followed each time the cavity has been turned off for more than 1/4 hr. This will produce lenghty interruptions in beam production at a time when all four cavities will be operating at full accelerating voltage. Should one cavity fail mechanically, there is no spare available; for that reason alone, we are quite interested in a new cavity. The following points should be considered and improved in a new cavity design:

- The mechanical support structure designed to hold up the cavity against an atmospheric pressure has to be separated from the cooling system, this should drastically reduce thermal influences on the resonance tuning system.
- Using copper instead of aluminum for the cavity's inner surface as well as changing the shape of the cavity allows us to obtain a calculated 10 to 15 % higher Q-value, which translates into considerable savings in RF power.
- Integrated acceleration gap electrodes, instead of bolted-on units as in our present design, allow direct water cooling and eliminate the present contact- and thermal conductance problems.

We hope that using copper as our RF-surfaces, as well as a different geometry, will lead to an improvement in multipacting behaviour and turn-on characteristics as well.
We are at present in the design stage of a 1:3 model cavity prototype for power testing, since we now have a spare 150 MHz/60 kW amplifier chain available. It will furthermore allow some limited coupling loop design testing. The cavity prototype is scheduled to be available for first measurements by the end of 1992, and power testing should hopefully start sometime in 1993.

5. REFERENCES

1) W. Joho, "High Intensity Beam Acceleration with the SIN Cyclotron Facility", **Proc. of the 11th Int. Conference on Cyclotrons and their Applications,** (Tokio, Oct. 1986)
2) U. Schryber et al., "Upgrading the PSI- Accelerator Facility for High Intensity Operation", **Proc. of the 3rd Europ. Particle Accelerator Conf.,** (Berlin, March 1992)
3) T. Stammbach, "Experience with the High Current Operation of the PSI-Cyclotron Facility", **these proceedings,** (Vancouver, July 1992)
4) M. Märki, "Die 120 kW/ 150 MHz Zweiweg-Anlage der Ringmaschine", **PSI-Internal Report, TM-12-89-03,** (Villigen, July 1989), [in German]

INITIAL OPERATION OF THE RF SYSTEM FOR THE RCNP RING CYCLOTRON

T. Saito, A. Shimizu, M. Uraki and I. Miura
Research Center for Nuclear Physics, Osaka University,
Mihogaoka 10-1, Ibaraki, Osaka 567, Japan

ABSTRACT

The RF system for the RCNP ring cyclotron is described. The RF system consists of three single gap acceleration cavities and a single gap flat-topping cavity. The RF system operates satisfactorily and proton beams were successfully accelerated.

1. INTRODUCTION

The cyclotron cascade project of RCNP approved in 1986 and was completed in 1991. General features of the cyclotron are described elsewhere.1) Excellent phase and amplitude stability of the RF system are required to get high quality beam with the ring cyclotron.

2. ACCELERATION SYSTEM

Characteristics of the acceleration system and the flat- topping system are summarized in Table 1. The acceleration cavity is variable frequency single gap resonator. The resonant frequency is varied by rotating a pair of tuning plates. The plates are electrically connected to a wall of the cavity through current-carrying hinges and silver contacts. The hinge is consists of thin copper plates.2) Maximum current density at the plates is 20A/cm. The copper plates operate satisfactorily but silver contacts were replaced newly designed ones after 6 months operation. Each cavity is powered by a power amplifier capable of delivering 250kW in a frequency range of 30-52 MHz. The RF power is fed through a 50 Ω coaxial line which is coupled with the resonator by means of variable coupling loop. The forward and the reverse power signals are used for automatic tuning of the cavity. The fine tuning is done by changing the inductance with two cylindrical trimmers. The dynamic range of the trimmer is more than 0.2% in frequency.

The walls of the cavity are made of stainless steel 50mm in thickness with water cooled copper lining. The side walls of the cavity are not strong enough to support atmospheric pressure. The walls

Table 1
Characteristics of the RF system.

	acceleration	flat-topping
RF frequency	30～52MHz	90～155MHz
Harmonic Number	6, 10, 12, 18	
Number of cavities	3	1
RF power	250kW/cavity	45kW
1st stage (TR wideband)	500W	500W
2nd stage	RS2012CJ	4CW3500A
Final stage (grounded grid)	RS2042SK	4CW50,000E
Resonator	single gap	single gap
Power feeder	inductive coupling	inductive coupling
Beam aperture	30mmx2310mm	30mmx2310mm
Acceleration gap	200～300mm	50mm

are supported by the neighboring magnet chambers. Fig.1 shows photograph of the acceleration cavity and power amplifier. Fig.2 shows Q-value and angle of the tuning plates vs. resonant frequency.

A single gap resonator is also used for the flat-topping cavity. The mechanical structure of the cavity wall is similar to that of the acceleration cavity. Resonant frequency is changed by sliding the upper and lower walls of the cavity. The flat-topping cavity is designed to get similar voltage distributions to those of the acceleration cavity. Fig.3 shows voltage distributions of the acceleration cavity and the flat-topping cavity.

Frequency conversion method and intermediate frequency (0.455MHz) is employed on the control circuits of the RF system.2) These circuits are working fairly well but it remains final adjustments for better stability.

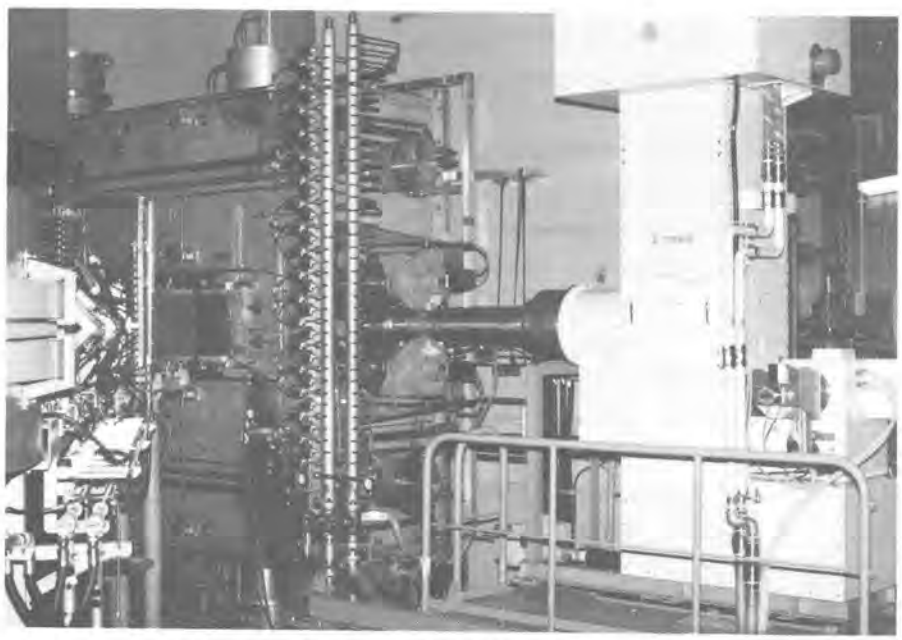


Fig. 1. Photograph of the acceleration cavity and the power amplifier.

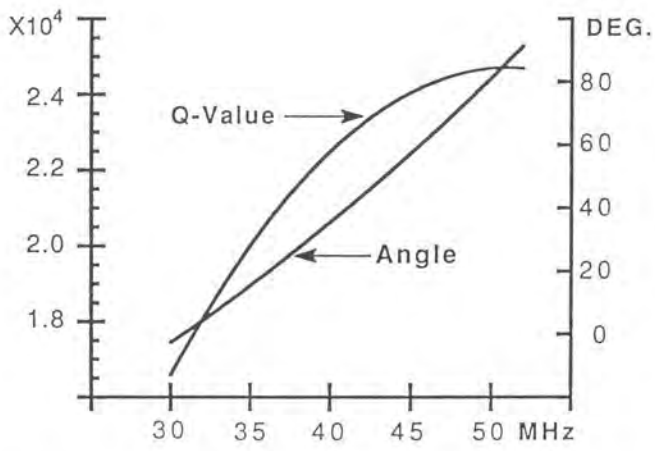


Fig. 2. Q-value and angle of the tuning plates of the acceleration cavity vs. resonant frequency.

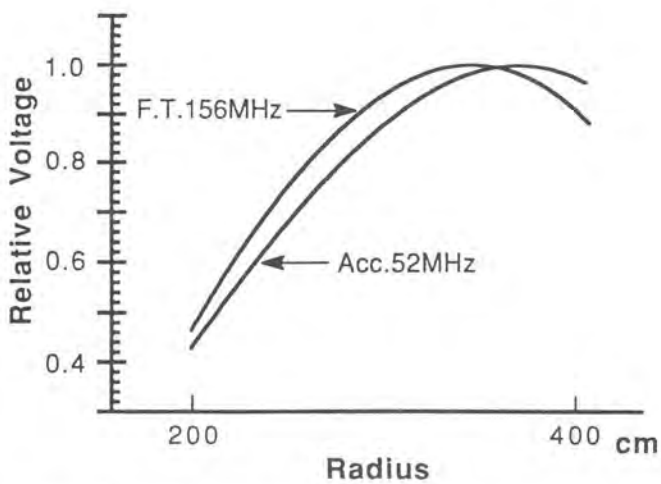


Fig. 3. Voltage distributions of the acceleration cavity and the flat-topping cavity.

3. POWER OPERATION

The power amplifiers have been tested separately on dummy loads in 1990, and proved to be able to generate enough power and have sufficient open loop stability at every frequency. After full assemble of the ring cyclotron, full power test of the RF system was started. The cavities were excited with pulse mode operation during conditioning. After about 10 hours of conditioning, CW operation of the acceleration cavities were enabled and less conditioning time was needed for the flat- topping cavity. After conditioning, the cavities were excited up to more than enough voltage for acceleration.

Typical data of operation of the RF system are shown in Table 2. Effect of mechanical vibration on stability of the acceleration voltage is observed. Mechanical strength of the tuning plates is strong enough for stable operation, the influence is not a serious problem. Stabilities of the acceleration voltage and phase will be improved in August.

The RF leakage power from the beam aperture of the flat-topping cavity caused serious damage to the trim coil feeds-through. RF shields for the trim coil feed-through were set on the both sides of the flat-topping cavity. The leakage RF signal also disturbs another electric instruments of the cyclotron. The leakage is induced by vertical asymmetry of the resonator, symmetric settings of the sliding walls are very important.

4. BEAM BUNCHER

A post-injector beam buncher being settled between the injector cyclotron and the ring cyclotron is also completed and used for the beam tuning. To inject longitudinally focused beam into the ring cyclotron, the buncher is essentially required in the achromatic beam line between two accelerators. The bunching is achieved by beam velocity modulation given by a synchronized higher harmonics RF voltage at two gaps of the buncher drift tube. The buncher resonator is a quarter wave variable frequency (60-104 MHz) coaxial type. A π-mode drift tube and the coaxial tuner made of polished OFHC copper is mounted on a cylindrical copper chamber. RF power is fed into the resonator through an adjustable capacitor to be matched to the 50 Ω coaxial feeder from the grounded grid power amplifier (4CW 25,000) mounted 1.5m apart from the resonator. To achieve phase focusing along with

Table 2
Typical operating data of the RF system.

Acceleration system (Ep=400MeV)	
Frequency	50.5361MHz
RF peak voltage(power)	520kV (115kW)
RF voltage stability	5×10^{-4}
	(goal 1×10^{-4})
RF phase excursion	less than $\pm1°$
	(goal $\pm0.1°$)
Flat-toppig system (Ep=300MeV)	
Frequency	138.75MHz
RF peak voltage(power)	120kV (25kW)
RF voltage stability	10^{-3}
RF phase excursion	less than $\pm1°$
	(goal $\pm0.1°$)

80m injection line drift space, the RF voltage required is 150kV with H_B=6 (102MHz) for the injection of 65MeV protons (400MeV from ring cyclotron). Fig.4 shows photograph of the resonator of the beam buncher.

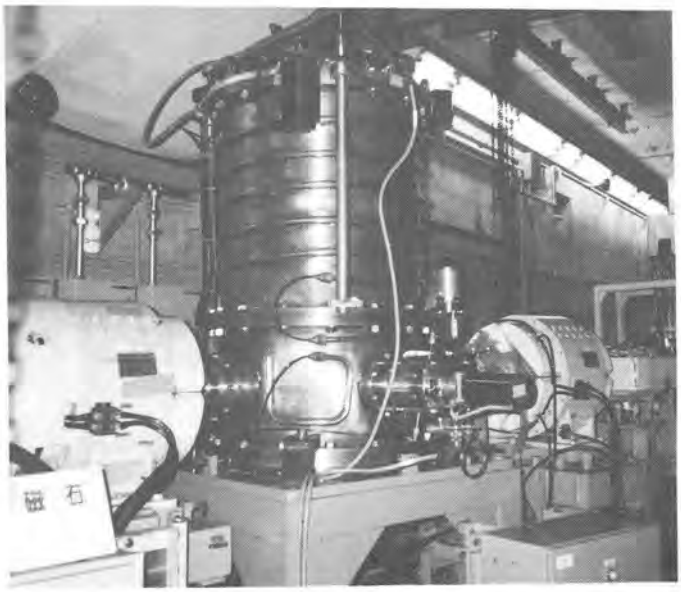


Fig. 4. Photograph of the resonator of the beam buncher.

5. REFERENCES

1) I. Miura et al., in these proceedings.
2) T. Saito, et al.,"The RF system for the RCNP ring cyclotron", in Proceedings of the 12th Conf. on Cyclotrons and Their Applications, (Berlin,1989)pp.201-204.

RF TRANSMITTER FOR ECR ION SOURCES

R. Boux, JP Ichac and M Soudée
THOMSON TUBES ELECTRONIQUES
BP 121 - 78148 VELIZY CEDEX - FRANCE

1. ABSTRACT

A growing number of accelerators, mainly cyclotrons, are using ECR ion sources to extend their possibilities. In ECR sources, the plasma which generates the ion beam is created by RF power. The microwave tube which delivers the RF power must be able to withstand large amounts of reflected power, due to mismatching induced by the plasma.

An especially designed transmitter, manufactured by TTE, can withstand continuous total reflection. It delivers 2 kW CW RF power, regulated at 0.1 %, and can also operate in pulsed mode.

This transmitter was built for the GANIL (Grand Accelerateur National d'Ions Lourds)

2. REQUIREMENTS FOR THE RF GENERATOR

The ECR (Electron Cyclotronic Resonance) ion source generates an ion beam by means of a plasma. About 2 kW of RF power is required to create the plasma.
When the source is tuned with stable operating conditions, the plasma operates as a matched load for the incident RF power.
The source cannot be tuned for RF matching under all operating conditions, for instance :

- when restarting the source after the vacuum chamber has been opened.

- With special tuning as for metallic ion production from solid samples.

In these cases, the RF power may be totally reflected by the plasma.

In a conventional transmitter, the microwave tube is protected from reflected RF by an interlock.

When feeding an ECR Source, the generator must operate normally regardless of any reflected power.



FIGURE 1 - TRANSMITTER CABINET

3. CARACTERISTICS OF THE 2 kW - 14.5 GHz GENERATOR

3a) CW mode

- Frequency : 14.5 GHz
- RF output power range : 10 W..2 kW
- RF output power adjustement : potentiometer on front panel.
- VSWR : any
- Power stability (line ± 5 %) : 0.1 %
- Power regulation response time : 1 ms
- Klystron cathode voltage : 9 kV.
- Klystron cathode current : 1.2 A

3b) Pulsed mode

- Minimum pulse width : 1 ms
- Maximum pulse repetition frequency : 1 kHz
- Maximum switching time (10 % to 90 % of amplitude) : 1 µs

3c) AC Line

- Line : 400 VAC - 50 Hz - 3 phases
- Power : 15 kVA

3d) Dimensions and weight (see fig. 1)

- Height : 1.510 m
- Width : 0.6 m
- Depth : 0.8 m
- Weight : 205 kg

4. PRINCIPLE

4.1. RF chain (See fig. 2)

Fig. 2 shows the principle of the RF chain.

- The power amplifier is a medium power klystron P/N TH 2464.
- A circulator at the RF output protects the klystron from the reflected RF. The matched load of the circulator can dissipate the full 2 kW of reflected power.
- The amplitude loop controls the low level amplitude by means of a PIN diode variable attenuator.
- The interlocks switch off the RF by means of a PIN diode RF modulator.

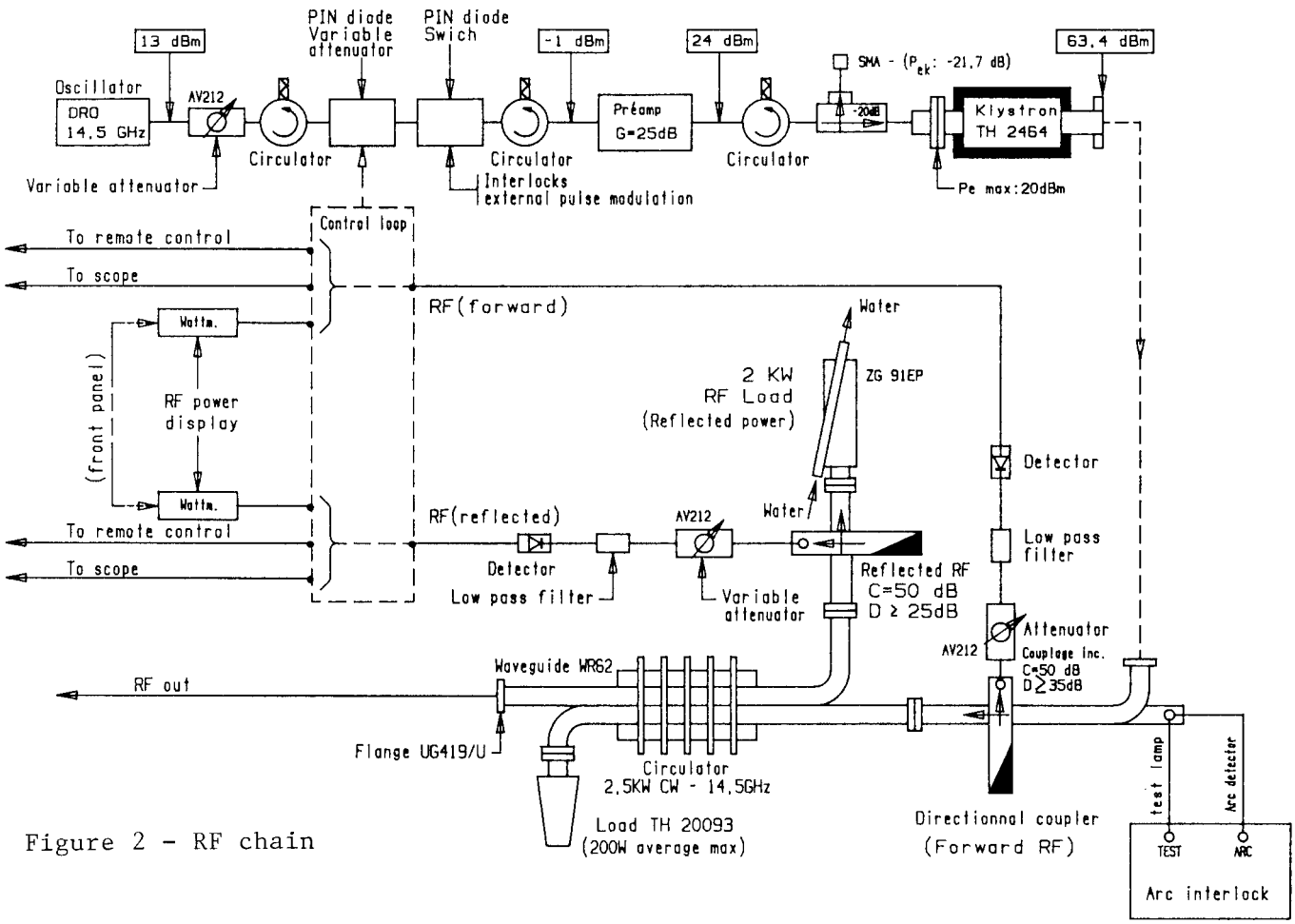


Figure 2 - RF chain

4.2. High voltage power supply

To achieve high stability of the RF power, the HVPS must have a low ripple.

The switching mode power supply results in both a low ripple and a low value of the energy stored in the filtering capacitor. Thus, a crowbar is not required.

A resonant switching mode is used, to reduce high frequency noise.

The switching mode power supply has small dimensions, compared to a conventionnal HV supply. The complete generator may therefore fit in a standard cabinet.

4.3. Power amplifier

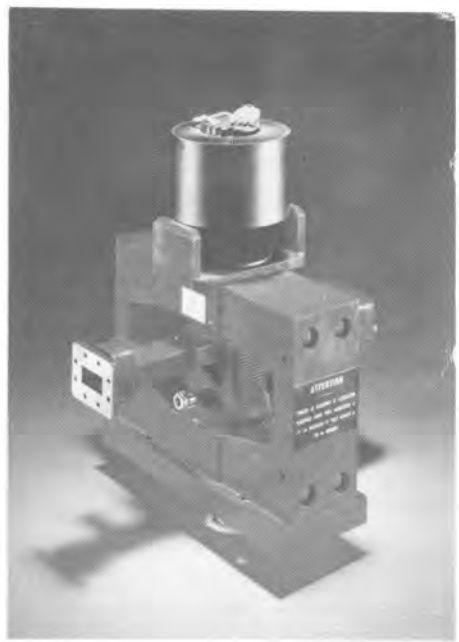
Medium power klystrons are the right choice to obtain a significant amount of CW power at frequencies required by present ECR ion sources. They are self-focused by permanent magnet, and can be fed by rugged and efficient power supplies ; they can work on a large dynamic range, are easy to install and reach a really high reliability.

The characteristics of medium power klystrons manufactured by TTE for ECR ion sources ar given hereafter ; with minor modifications, TH 20482 transmitter fits with all these klystrons and permits a larger flexibility for a long term and a cost effective investment of research laboratories.

P/N	Frequency (GHz)	CW RF Power (kW)	Cathode Voltage (kV)	Beam current (A)	Cooling
TH2462	5.85-6.45	2	8.3	1.3	Forced Air
TH2461	7.9-8.4	1.65	7.2	0.63	Forced Air
TH2477A	9.5-10	2.5	10	0.9	Water
TH2477B	10-10.5	2.5	10	0.9	Water
TH2464	14-14.5	2	8.5	0.5	Forced Air
TH2463	18	1.5	12	0.5	Forced Air



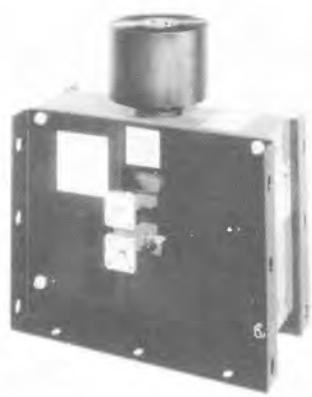
TH 2477



TH 2462



TH 2464



TH 2463

TRIUMF CYCLOTRON RF SYSTEM IMPROVEMENTS

G. C. Blaker, A. K. Mitra, R. L. Poirier
TRIUMF, 4004 Wesbrook Mall, Vancouver, B.C. V6T 2A3

ABSTRACT

The 1.8 MW, 23 MHz RF system for the TRIUMF cyclotron has been in operation since 1974. In order to improve reliability, ease maintenance, and increase efficiency of the power amplifiers, a program of upgrading some system components and retuning the four amplifier, three combiner system has been undertaken. Measurements were made on the amplifier input/output circuits and combiner circuits to understand their theory of operation and to determine the modifications and retuning required. Analysis of these measurements, modifications incorporated and future modifications required are reported.

1. INTRODUCTION

The TRIUMF cyclotron RF system has undergone many improvements over the original system supplied by Continental Electronics[1] in the early seventies. This system has been described in many papers[2], but many of the modifications have not been reported. Many of these changes have come about as a result of fault diagnosis, and some have evolved from a need to more easily tune, service and repair the RF system.

A simplified diagram of the system is shown in Fig. 1. The RF system consists of a solid state preamp driving a two stage intermediate power amplifier up to the 30 kW level. This power is then split four ways through a pi network phasing circuit to drive four power amplifiers. The 250kW outputs of these amplifiers are then recombined using three 4-port hybrid combiners.

Tuning the amplifier input circuits, output circuits and combiners has been very difficult due to a lack of diagnostic signals and a less than full understanding of the circuitry. Diagnostics have been installed and extensive measurements taken to ease this difficulty.

2. PA INPUT CIRCUIT

The power amplifier input circuit consists of a pi network

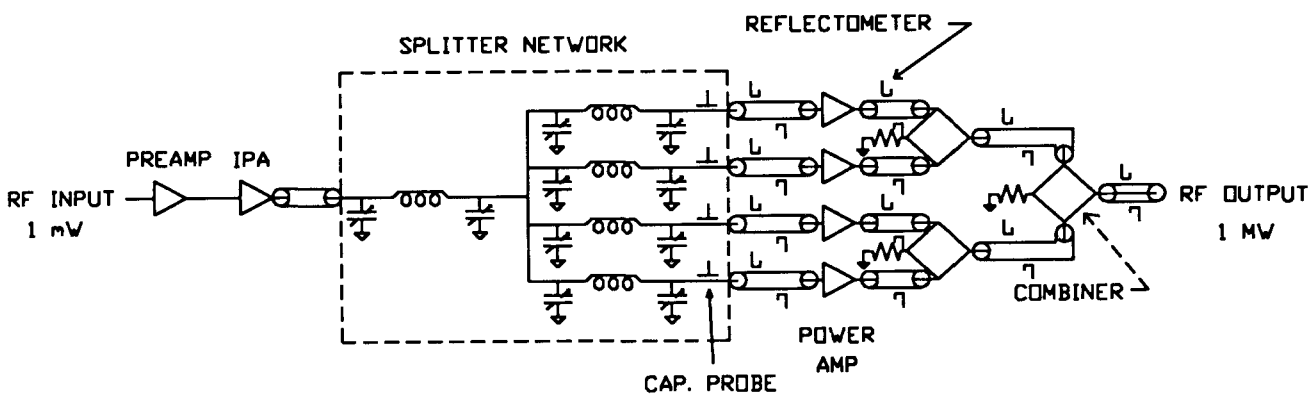


Figure 1. RF System Diagram

with a toroidal transformer to match the 50 ohm input to the push pull grounded grid tubes. Although simple in principle, the circuit is much more complex in practice.

Signal level measurements and tuning revealed many resonances and some unpredicted behavior. In order to tune the input circuit at signal level, it is necessary to place external loads between the grids and cathodes of the tubes to simulate the dynamic operating impedance of the tubes. Since one cannot physically place the calculated dynamic load impedance inside the tube, it must be transformed through the various structures to the point where the external load can physically be connected. However, determining what this external dynamic load should be was the result of many hours of measurements and computer modeling. Network analyser and vector impedance measurements were taken in order to develop a model of the input circuit[3]. A computer program was written to simulate the response of the circuit, and predict the external dynamic load values. The simulation proved to be very close to the measured parameters, and yielded a value of 22 ohms in series with 80pF for the needed external dynamic load.

3. REFLECTOMETERS & PROBES

In order to balance the outputs of the four power amplifiers and tune the combiners, reflectometers were installed in all of the 9 inch transmission lines, as shown in Fig. 1. These reflectometers allow precise adjustment of the amplitude and phase of the RF at each port of the amplifier-combiner system and the input impedance of the combiners to 50 ohms.

Each reflectometer signal is brought to a patch panel via identical cable lengths so that phase accuracy is maintained. In addition, capacitive probes located at the splitter outputs, PA cathodes, and PA anodes provide additional signals at the patch panel. A permanently mounted vector voltmeter and an oscilloscope adjacent to the patch panel allow easy measurement of power level, phase at any point in the system, the VSWR on any line, the phase shift through any components, and the power level at dirrerent points along the amplifier chain.

4. COMBINERS

A schematic of the four port combiner is shown in Fig. 2. The capacitance is provided by Jennings vacuum capacitors and the inductance by 1.5 inch diameter copper pipe, which makes the connections between the ports requiring an inductive path. Not shown in the schematic are 4 parasitic mode dampers which are required because of the arrangement of the components in a large volume housing.
A 50 ohm resistive load , refered to as a waster load is required at the port opposite the output port to provide a dissipative load for unbalanced currents and in the event of a failure in one of the input amplifiers. The waster loads which were supplied with the original RF equipment are a

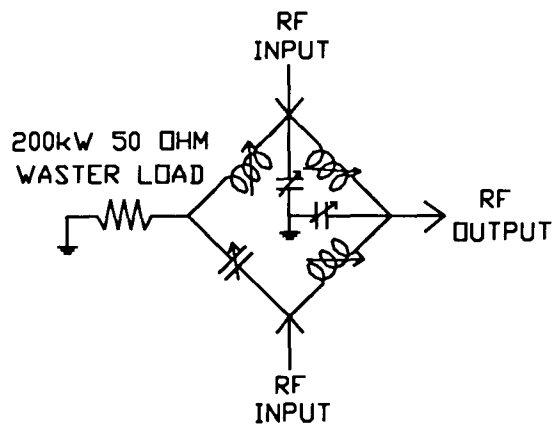


Figure 2. Combiner Schematic

circulating column of water doped with sodium nitride to provide a 50 ohm impedance. When the combiner is properly tuned and terminated the input ports should provide a 50 ohm load for the amplifiers and minimun power should be dissipated into the waster load.

Initial measurements with the reflectometers clearly indicated that the input impedances were not 50 ohms and that the combiners needed retuning. Because of the mechanical design of the combiners, terminating the ports with 50 ohms was not possible without dismantling and moving around long lengths of nine inch transmission line. A scheme was developed where the soldered-in transitions from the nine inch lines to the combiner circuit were replaced with removable brass cones using finger stock contacts. These allowed the easy termination of any of the combiner ports, the termination of the power amplifiers, and the ability to disconnect the output transmission line to the cyclotron for resonator measurements. Special fixtures were fabricated to allow easy connection of BNC cables and 50 ohm loads to the combiners.

Extensive measurements were then taken using an HP network analyzer and vector impedance meter. A 50 ohm matching point at the input ports of the combiners could not be attained because the inductances in the phasing and matching networks were too large. A new mechanical design of the combiner is being developed to reduce this inductance as well as hopefully reducing some of the parasitic modes also present in the combiners. However the above modifications enabled the matching at the input ports to be greatly improved from the initial values.

The impedance of the sodium nitrite waster loads used as the load for each combiner is very sensitive to temperature variations, and consequently they would not present a 50 ohm load to the combiner under all operating conditions, especially when trying to tune at signal levels. These waster loads have been replaced with Altronics 57200 BE6 water cooled 200 kW resistor loads, which are not only extremely clean and simple, but also present 50 ohms to the combiner at all times.

The original waster loads were designed for up to 600 kW of power dissipation, while the new loads are only rated for 200 kW. In order to protect these loads, interlocked water flow meters are installed in the cooling lines, as well as power level sensing and trip circuits which disable the RF drive if too much power is fed to the loads.

With the aid of the new reflectometers, the amplifier system can be tuned so that there is less than 1 kW dissipated in each load during normal operation.

5. PLATE CIRCUIT

The power amplifier plate circuit was difficult to tune due to lack of a reliable method of measuring the plate impedance of the amplifier, and an easy way of terminating the amplifier with a 50 ohm load.

The plate circuit output transformer primary is attached to the anode of the tube at one point only, causing anode current to flow asymmetrically on the anode ring. As a result the impedance measured at the anode varied substantially at different points around the anode ring. A jig was fabricated to ensure that the HP vector impedance meter probe was held at a particular position on the tube's anode for all measurements so that consistent measurements could be taken. The plate circuits were tuned for 600 ohms plate to ground at 23 MHz, to correspond to the value calculated from the characteristics of the tube and the tube's operating currents. This resulted in an amplifier efficiency increase from 50% to 62%.

Mechanical modification to the combiners with quick disconnect connectors has made terminating the amplifier with 50 ohms much easier.

6. OTHER IMPROVEMENTS

There have also been several other small but significant improvements made to the RF system. The tube sockets were completely overhauled, and were reassembled using Dow Corning DC4 silicone on all Kapton bypass capacitor surfaces. In addition Dow Corning 3140 RTV silicone was used on all external edges and bolt holes in an effort to waterproof the sockets. These measures have proven very successful and have eliminated the need to overhaul a socket in the event of a water leak on to the socket.

An intermittent parasitic oscillation in the screen circuits of the amplifiers, which would usually damage the screen power supply and choke, was damped successfully with two Ferroxcube 3C8 torroids placed over the screen series resistor.

The RF controls were modified so that the RF drive was cut off when a resonator spark was detected. This was supposed to be how the original controls were designed, but the circuit did not work properly, and tried to increase drive in closed loop to regulate the resonator voltage. The result was often a crowbar in the high voltage plate power supply, but sometimes a spark and water leak in an amplifier would also occur. Since this repair, no similar sparks or leaks have occurred.

7. CONCLUSIONS

The modifications described have proven extremely useful in both diagnosing RF system faults and reducing beam off time due to RF failures. It is now possible to easily measure many system parameters which were difficult or impossible before, thereby making tuning a straightforward task. Amplifier efficiency has improved, components run cooler and last longer. Measurements have shown a need to redesign the combiners, and this task is now proceeding. For further improved reliability, two power amplifier operation with two amplifiers on standby is also being investigated.

8. ACKNOWLEDGEMENTS

The authors wish to acknowledge the contributions of Norman Carlson, Vojta Pacak and Robert Worsham to the work described.

9. REFERENCES

1) TRIUMF RF Manual, Continental Electronics Manufacturing Co., Dallas Texas.

2) K.L. Erdman et al., "TRIUMF Amplifier and Resonator System", Proc. 6th Int Cyclotron Conf., AIPCP#9 (AIP,1972) p.451

3) A.K. Mitra and G.C. Blaker, "Input Matching of Power Amplifiers of Main RF System of TRIUMF Cyclotron", Triumf Design Note DN-92-15

IMPROVEMENTS TO THE RF SEPARATOR IN THE M9 MUON CHANNEL AT TRIUMF

G. C. Blaker, A. K. Mitra, R. L. Poirier
TRIUMF, 4004 Wesbrook Mall, Vancouver, B.C. V6T 2A3

ABSTRACT

The M9A secondary beamline at TRIUMF incorporates an RF cavity driven at the cyclotron frequency to separate pions and electrons from the muons required at the experiment target. The RF system has undergone a major upgrade in the last 3 years in order to improve its operating reliability and ease of operation. The 23 MHz cavity was completely overhauled, and a new 150 kW amplifier system was built at TRIUMF. In order to locate the amplifier away from the radioactive experimental area, the amplifier is connected to the cavity via a 20 meter rigid six inch coaxial transmission line. When powering a high Q resonant cavity at the end of a long line, the line's electrical length is critical. Measurements made to determine the proper length in order to avoid exciting transmission line resonances are presented. The major features of the RF system are described and operational experience reported.

1. INTRODUCTION

The RF Separator[1] is a device incorporated in the M9A beamline which is used to select either pions or muons, produced near the T2 production target, by deflecting unwanted particles whose time of flight causes them to be out of phase with respect to the RF frequency. The system consists of a pair of electrodes mounted parallel to the beam and connected to quarter wave resonant cavity structures, which are driven by a 150 kW RF amplifier at the cyclotron frequency of 23 MHz. The RF power is coupled to the cavity via a 50 ohm coupling loop mounted in the upper resonator. The phase of the separator RF is varied with respect to the beam phase in order to deflect the unwanted particles, while allowing the desired particles through to the experimental target and detectors.

2. AMPLIFIER RELOCATION

The first Separator amplifier was the original TRIUMF cyclotron center region model amplifier manufactured by Continental Electronics[2]. It was located next to the RF cavity, and was connected to the cavity by a length of transmission line and two capacitors in shunt. This arrangement presented problems in servicing the amplifier due to the high radiation fields in the experimental area, and the vacuum capacitors used to tune the transmission line were unreliable and difficult to replace. The new amplifier was relocated to the mezzanine above the experimental area, and was connected to the cavity via a 20 meter length of six inch transmission line, with no tuning capacitors. In order to eliminate the tuned line, the coupling loop was redesigned to be 50 ohms, and was moved from the bottom resonator to the top.

3. POWER AMPLIFIER DESIGN

The power amplifier was designed and built at TRIUMF, and uses an Eimac 4CW150000 power tetrode operating in grounded grid configuration. With 1.5 kW of drive power, the amplifier delivers 100 kW to the cavity. The schematic for the amplifier is shown in Fig. 1.
The anode tank circuit is a quarter wave resonant cavity, with an adjustable loading

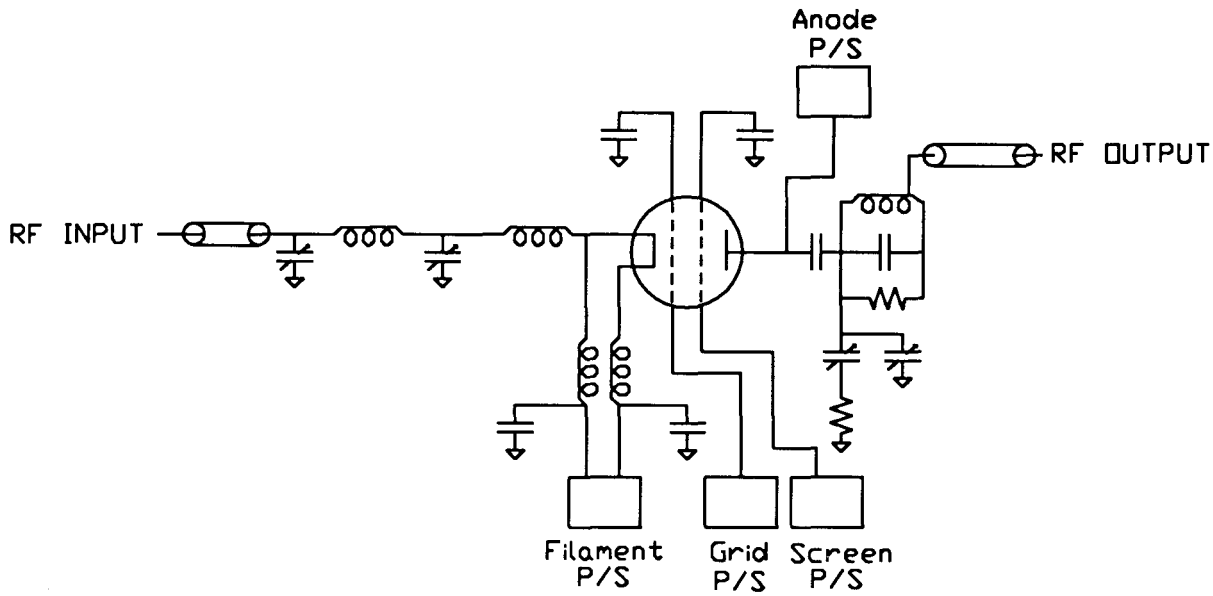


Figure 1. Power Amplifier Simplified Schematic

capacitor and adjustable galvanic coupling to the 50 ohm output transmission line. The tube output impedance is tuned to approximately 1000 ohms.

The input circuit is a pi network consisting of Jennings variable vacuum capacitors and a copper inductor. This circuit matches the 50 ohm source impedance of the driver amplifier to the 22 ohm impedance of the grid-cathode circuit.

The tube is biased to operate class A-B, with a plate idle current of 6 amps and a plate voltage of 18 kV. There is an air cooled damping resistor capacitively coupled to the anode to suppress parasitic modes caused by the long transmission line. The damping resistor dissipates about 1kW of RF power at 100 kW output.

4. SOLID STATE DRIVER AMPLIFIER

Figure 2 shows the schematic for a driver amplifier module. The driver is also a TRIUMF designed and built unit. It is a 2 kW solid state amplifier, with a gain of 67 dB. This amplifier consists of a preamp whose 20 watt output is split 8 ways to drive 8 250 watt amplifier modules. These outputs are then recombined to give 2000 watts using a TRIUMF designed 8 input water cooled combiner. The amplifier modules use Motorola MRF151G TMOS FET devices and conventional ferrite RF transformers. The circuit boards are designed with built-in stripline reflectometers to provide signals for the amplifier protection circuits.

Each amplifier module is mounted on a water cooled copper heatsink, and incorporates overvoltage, over current, over temperature and VSWR protection.

The driver amplifier is capable of operating with one module tripped, delivering 1600 watts, which is sufficient to drive the separator to full power. Two or more tripped modules shut off the separator through an interlock to the main control circuits.

The amplifier has been constructed in a modular fashion, so that replacement of failed amplifier modules is quick and simple, and so that similar modules can be used in other applications at TRIUMF.

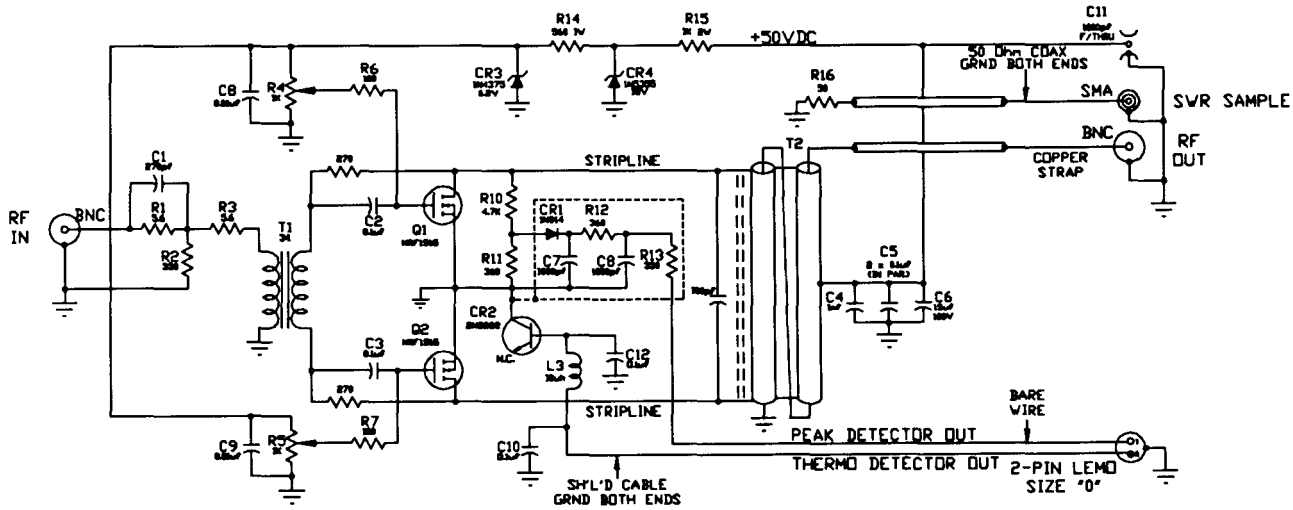


Figure 2. Driver Amplifier Module

5. TRANSMISSION LINE

The power amplifier is connected to the cavity via a 20 meter length of 6 inch copper 50 ohm transmission line. The line was initially installed with the shortest length possible, but after operating for a short time, it was clear that amplifier stability was not satisfactory. The screen current was higher than expected from the tube characteristic curves, and was very unstable, causing many screen power supply trips. This problem was traced to the length of transmission line, which was an arbitrary length, and was transforming the cavity impedance back to the amplifier such that the amplifier was seeing a sharp impedance variation with frequency. This caused the load impedance of the tube to change significantly with small frequency changes. The proper length of line was calculated using a computer circuit analysis code NODE[3], and was verified with low level network analyzer measurements of the system, as shown in Fig. 3. The extra length of line was installed, and immediately improved the stability of the system. No further problems with the transmission line have been encountered.

6. METERING & CONTROLS

The separator amplifier controls are based on conventional relay ladder logic, and incorporate latching interlocks for the various cooling water and air circuits, voltage proves for all amplifier power supplies, cavity vacuum, cavity magnet, and driver amplifier status. Metering is provided for all amplifier power supplies, as well as driver and power amplifier forward and reflected power signals. The separator cavity frequency and cyclotron RF frequency are also displayed.

The RF low level controls for the separator consist of an STD based supervisory and control computer linked to analog circuitry for the amplitude and phase regulating loops and the cavity tuning loop[4) 5)].

7. PERFORMANCE

The separator has been operating extremely well since the upgrade program was undertaken. There have been many weeks of data taking in the M9 muon channel with very little lost time due to separator problems. The system is largely operated by experimentalists with little training on the system, but because of its

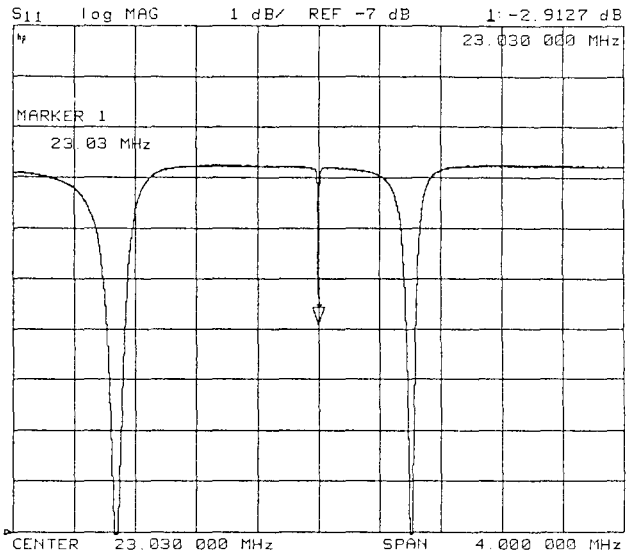


Figure 3. Cavity & transmission line modes.

simplicity, has been of little problem for the users. Initial problems with the original commercial driver amplifier have been solved with the new driver, which has performed very well.

8. CONCLUSIONS

The upgrading of the RF separator has been a great success. The system is now easier for the experimenters to use, requires no tuning by the users and is much more reliable than the original system. The expertise gained in developing the driver and power amplifiers in-house has proven extremely worthwhile, and this knowledge has been applied to other applications at TRIUMF.

9. ACKNOWLEDGEMENTS

The authors wish to acknowledge the work of Slawomir Kwiatkowski, Vojta Pacak and Robert Worsham on the power amplifier and transmission line, Joseph Lu for his work on the solid state driver, and Richard Shanks and Bruce Whiteside for their work on the amplifier controls. Also, Josef Holek, Eberhart Knappe and Gus Mannes for their expert mechanical work.

10. REFERENCES

1)E.W. Blackmore *et al.*, "An RF Separator for Cloud Muons at TRIUMF," Nuclear Instruments & Methods in Physics Research A234(1985) pp.235-243.

2)Continental Electronics Manufacturing Company, Dallas, Texas

3)K Fong, "NODE Users Guide," TRIUMF Design Note TRI-CD-89-33

4)R. Burge *et al.*, "Amplitude and Phase Regulation of the RF Separator," presented at the 1989 Particle Accelerator Conference, March 20-23, Chicago IL.

5)R. Burge, "RF Separator Control," TRIUMF Design Note TRI-DN-90-15

THE RF SYSTEM OF THE GUSTAF WERNER CYCLOTRON/SYNCHROCYCLOTRON

B.Lundström and B. Holmgren
The Svedberg Laboratory, University of Uppsala,
Box 533, S-751 21 Uppsala, Sweden

ABSTRACT

The RF system of the reconstructed cyclotron has two modes of operation, CW mode (isochronous cyclotron) and FM mode (synchrocyclotron). In CW mode the two dee resonators work on f_{rf}/f_{ion}=1, 2 or 3. The RF frequency is variable in the range 12.25-24.5 MHz and the maxiaml dee voltages are 50 kV. In FM mode, which must be used for protons above 105 MeV, the same two dee resonators are used on fundamental frequency in the range 17-24.5 MHz as "broadband" systems without synchronously tuned cavities with FM bandwidths up to 2.2 MHz and dee voltages up to approx. 15 kV. The dee electrodes are phase locked during the FM sweep and are also used to stretch the beam macro pulse, a duty cycle of 50 % has so far been achieved for 180 MeV protons. Power consumption per system is 50 kW in CW mode and 140 kW in FM mode. The system has been in use in CW mode since 1987 and in FM mode since 1991.

1. GENERAL CHARACTERISTICS

The old Gustaf Werner Synchrocyclotron (operating from 1949 to 1977) was a conventional synchrocyclotron with a single dee tuned by a rotating capacitor from 33 MHz at start of acceleration to 26 MHz at extraction. The repetition rate was limited by the capacitor to 250 Hz, and could accelerate protons only to a fixed energy of 185 MeV. The improved accelerator should be able to accelerate a variety of ions to variable energies, and the solution found was a combination of isochronous cyclotron and sector focussed synchrocyclotron. For the RF system it was chosen to use two dee electrodes each covering an electrode angle from 72 degreees at centre to 45 degrees at full radius (Figure 1).[1] This permits operation on fundamental frequency as well as on harmonic numbers 2,3 and possibly 4 with a reasonable energy gain per turn (Fig. 2).

The introduction of sector focussing and cylindrical trimcoils makes isochronous acceleration possible for all particles except protons above 105 MeV and $^3He^{2+}$ above 260 MeV where frequency modulation still is required, but with a much smaller bandwidth. For 180 MeV protons the rel. bandwidth reduced from 24 % to 9 %[2]. This makes it possible to avoid synchronously tuned dee cavities and instead use the power tubes as a broadband amplifiers.

All equipment inside the cyclotron vault is the same in both modes of operation with exception for the dee tips, which together with the other parts of the central region can be exchanged using an air lock and a remote handling mechanism. The RF synthesizer, detectors, modulators and preamplifiers are at present completely exchanged between FM and CW operation (the RF coaxial cables to and from the cyclotron vault are simply reconnected from one system to the other). The block diagram is esentially the same for the two modes of operation (Fig. 3).

2. THE DEE RESONATOR

The shape of the dee electrode was determined after full scale model tests. The dee is supported from the vacuum feedthrough and consists of a stainless steel structure clad by copper. The dee has an equivalent capacitance of approx. 300 pF and is tuned to $\lambda/4$ resonance by a shorted coaxial line outside the vacuum feedthrough with a movable short circuit plate (inner conductor 220 mm diameter, outer a rectangular box 1100x700 mm resulting in a characterisitc impedance of 120 Ω). The tuning range is 12.25 -24.5 MHz, and the Q value is at 24 MHz approx. 1600. Highest required dee voltage is 50 kV peak, corresponding to a short circuit current of 2500 A peak and a power loss of 30 kW. The short circuit plate (movable only with RF off) has beryllium copper spring contacts to the outer conductor and a pneumatic system to the inner conductor, where the linear current density is 36 A/cm. The vacuum feedthrough is equipped with a system to "swing" the dee with beam on to optimize the position of the dee with respect to the central region. A damping system dissipating up to 40 kW used in FM operation is located close to the inner end of the tuning box, and a fine tuning system (a plunger from the short circuit plate) is used in CW mode (Figs. 4 and 5).

3. THE FINAL AMPLIFIER

The final amplifier uses the tetrode Eimac 4CW100,000E in grounded cathode configuration. The filament has DC heating (3-phase full wave rectifier) and is RF grounded by kapton disc capacitors. The control grid is tuned to resonance by a variable stub and is terminated to 50 Ω, which gives a bandwidth sufficient for the FM operation. The anode is tuned by a variable vacuum capacitor and is coupled to the dee resonator through a tapered air coaxial line ending in a variable stub inside the dee resonator, serving as an inductance mutual to both cavities. The final amplifier moves together with the tuning plate of the dee resonator. The power supplies for the control grid bias (200-500 V, 100 mA), screen grid (1500 V, 1.2 A) and anode (4-12 kV, 15A) are all located more than 50 m from the cyclotron. The DC cables for anode and control grid enter their cavities from the low voltage end and require no RF

chokes, only DC blocking capacitors (a cylindrical 5000 pF kapton capacitor built on coppered soft iron couples the anode to the resonator line, and also serves as a magnetic shield for the tube, which has to operate in a position where the stray field exceeds 200 gauss). A problem in the final amplifier was a self oscillation at 1.1 GHz, which was solved by filling the volume between control and screen grid connecting rings of the tube with ferrite.

4. THE RF SYSTEM IN ISOCHRONOUS MODE

The CW system is a conventional master oscillator-power amplifier system. The two coupled tuned circuits (anode and dee) produce an anode impedance curve vs. frequency with two peaks, and in CW mode operation is normally on a peak close to the dee resonator frequency, whereas the anode is detuned a few MHz to give the desired voltage transformation between anode and dee electrode. The RF amplitude and phase control is "standard" with voltage pickups (both inductive and capacitive) on the dee resonators used for control loops for amplitude and dee-dee phase together with other pickups (anode, control grid etc.). Fine tuning during operation is achieved by a servo system using the anode-to-grid phase signal as input. The fine tuning range is small, it corresponds to a movement of 1 mm on the main shorting plate at all frequencies, and the reponse time is of the order of a few seconds, which is enough to cover for the temperature drift but not for mechanical vibrations. The voltage stability is of the order 1/10000 and the dee voltage control loop has a bandwidth exceeding 10 kHz. The CW system has been in operation since 1987.

5. THE RF SYSTEM IN SYNCHROCYCLOTRON MODE

The FM system is more unique. There are no variable tuning elements used during the FM sweep, the frequency modulation is performed electronically. This has been performed previously in a smaller scale at CERN in the Micro-SC with a single dee electrode. The frequency source in the FM mode is a numerically controlled oscillator (NCO, Stanford Telecommunications STEL-2172) operated with a 2^{28} Hz (268.435456 MHz) clock oscillator (Fig. 6). The NCO is programmed during the frequency sweep by a computer memory 32 bits wide (of which 28 bits used for frequency program and the rest for triggers) and 32k long clocked at 1/40 of the master clock, giving a time resolution of 150 ns for the frequency program and a max. sweep time of 5 ms. Additional memories (clocked at 1/8 of the frequency program clock, time resolution 1.2 μs) are used to load six 12-bit DACs to give the analog waveforms required for dee voltage reference programs etc. The memories are loaded from an IBM compatible PC. The RF signal is amplified in broadband transistor preamplifiers with a peak output power of 4 kW.

In FM mode the dee resonators and the anodes are tuned to the centre frequency of the FM band, giving an anode impedance with two peaks, one close to the initial frequency and one close to the final frequency. Approx. 40 kW can be added to the dee resonator losses at 15 kV dee voltage by damping systems consisting of a pickup loop, a varaiable series capacitor and a water cooled 50 Ω resistor. This reduces the Q value from 1600 to 160 and gives a smoother shape on the phase transitions from input RF signal to dee voltage which occur when a peak is passed during the FM sweep (Fig. 7). Since the two dees have to be phase locked during FM acceleration the differences between the two systems must be minimized to allow the dee-dee phase control loop to be able to handle the phase transitions.

Broadband systems are very power consuming, the power is proportional to the equivalent electrode capacitance and the FM bandwidth[3]. The dee capacitance (approx. 300 pF, reduced as much as possible by cut-back of electrode angle, reduced aperture where possible and by mounting supporting structure and cooling pipes on the outside of the dee). Using fixed anode voltage supplies (so far the two anode supplies have been used in series operation in FM mode to provide a DC voltage of more than 20 kV) a max. dee voltage of 16 kV peak over a band 24.2 to 22 MHz would require more than 250 kW per system. Since the anode can tolerate only 100 kW and the dee resonator 40 kW some means to reduce power is necessary. The simplest solution is to reduce the time of operation at full dee voltage. Since most physics experiments require a beam macro duty factor better than that normally achieved in a synchrocyclotron beam stretching is necessary. To achieve this the FM frequency source is programmed to reduce df/dt during extraction and simultaneously the accelerating voltage is reduced to approx. 5 kV, keeping the phase stable "bucket area" constant. RF power is thus reduced to negligible levels during this time, which is an order of magnitude longer than the acceleration time, and hence the necessary reduction in duty cycle of the RF system is achieved (Fig. 8). A future solution for experiments requiring higher beam currents and higher repetition rates will be the use of amplitude modulation on the anode supply voltage using a pulse width modulation system similar to that of modern high power AM transmitters.

During 1991 first beams to experiments where delivered using the FM system. Typical extracted beam currents so far have been 1nA/Hz, and repetition rates up to 300 Hz have been used for short beam pulses and 170 Hz with macro duty cycle exceeding 50 % (Fig. 9).

6. REFERENCES

1) S. Dahlgren et al., "Conversion studies for the Uppsala Synchrocyclotron" in Proc. 7th Int. Conf. on Cyclotrons and their Applications (Birkhäuser, Basel, 1975) p.127-131
2) S.Holm, P-U Renberg, Magnetic field design for a combined fixed frequency and frequency modulated cyclotron, GWI-PH 8/78,1978
3) R. Giannini, A. Susini: Optimisation des paramètres des systèmes accélérateurs HF à large bande, CERN 68-18, 1968

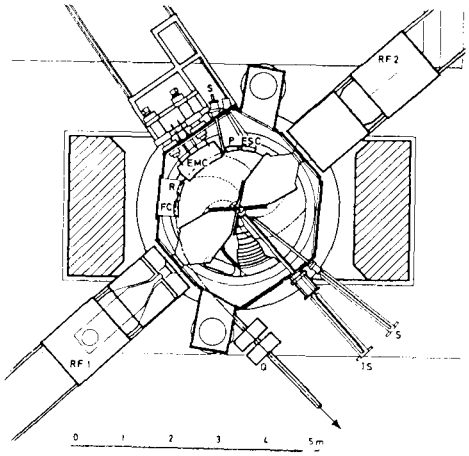


Figure 1. General layout of the cyclotron and the dee electrodes

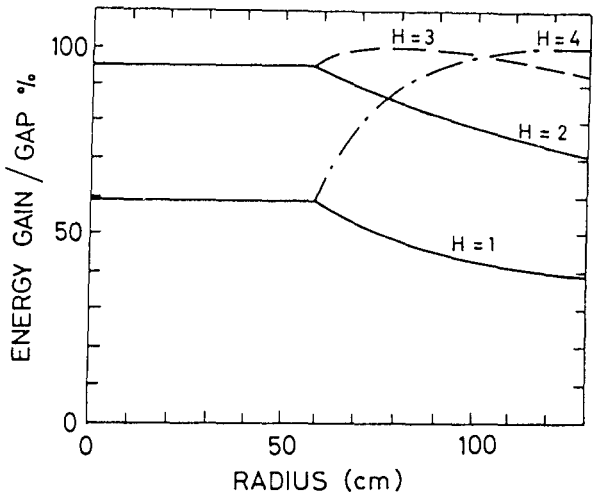


Figure 2. Energy gain per turn vs. radius for different values of $H = f_{rf}/f_{ion}$

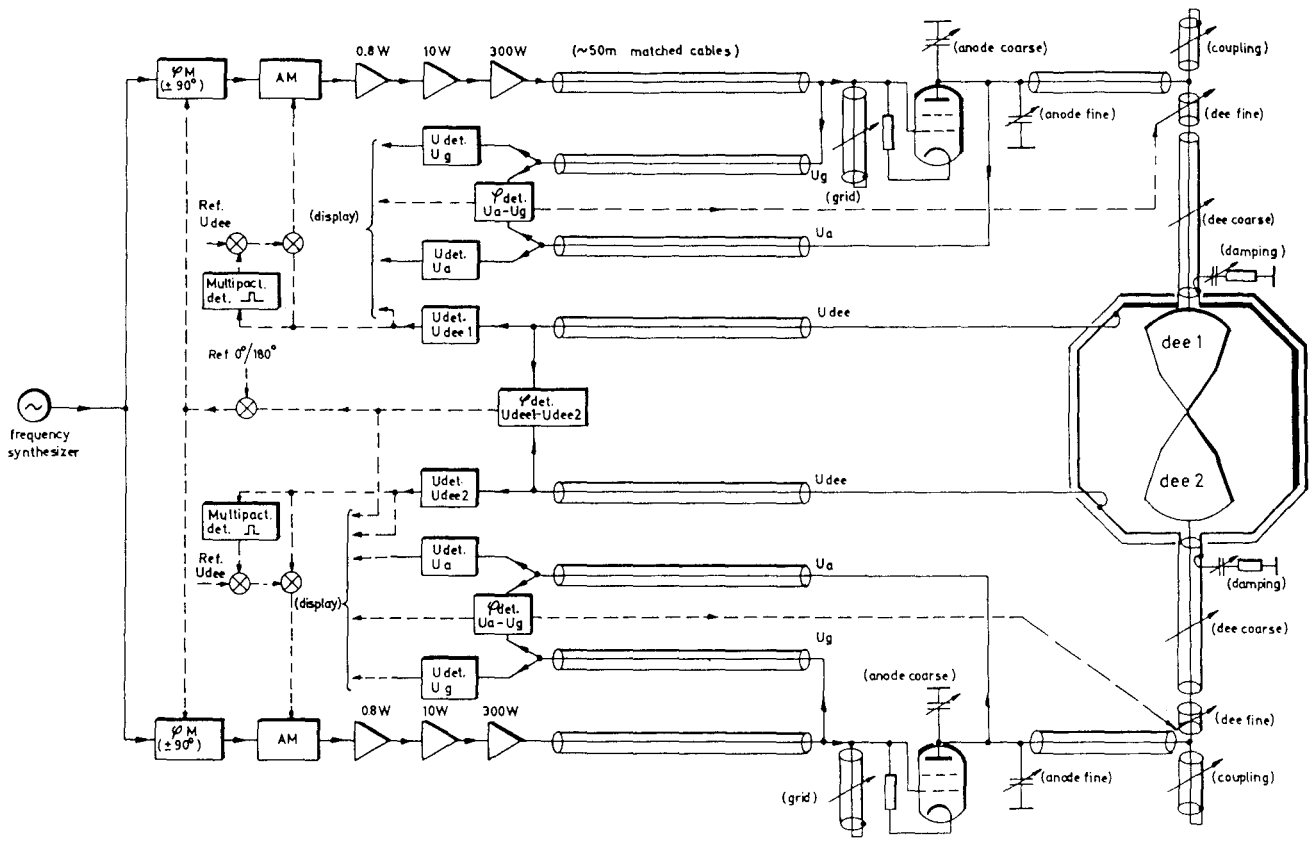


Figure 3. Block diagram of the RF system (CW mode)

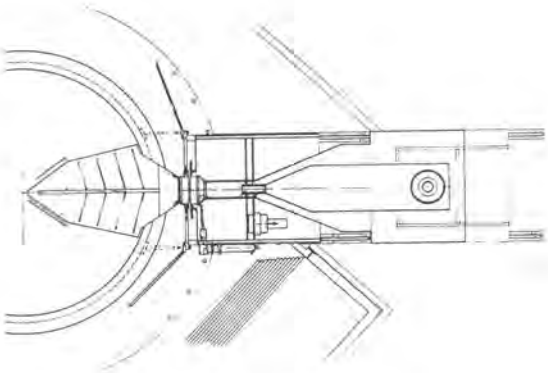


Figure 4. Top view of one RF system.

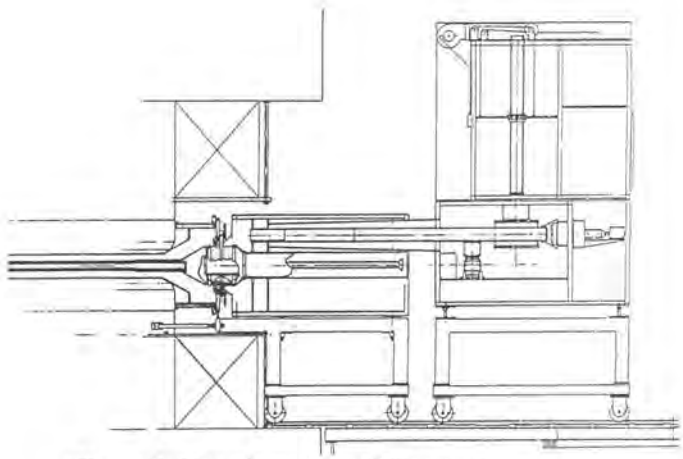


Figure 5. Side view of one RF system.

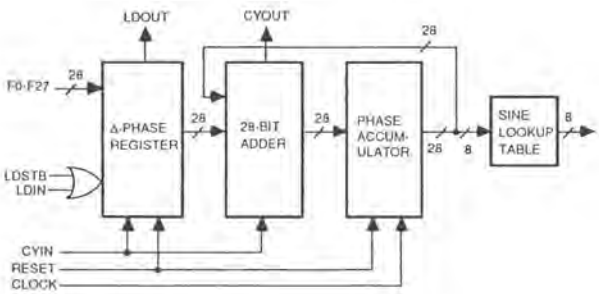


Figure 6. Numerically controlled oscillator (FM source).

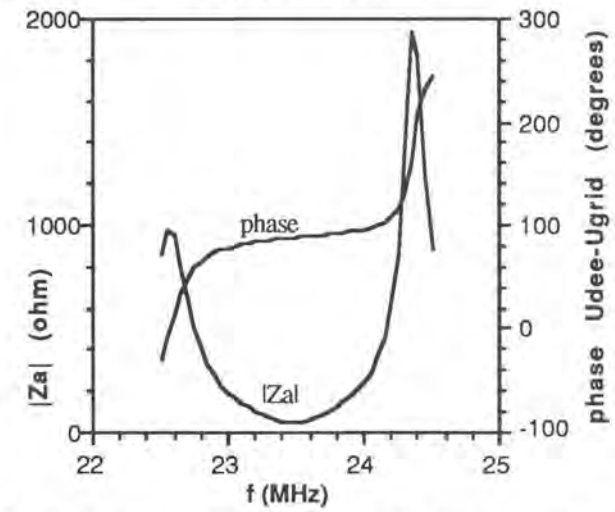


Figure 7. Anode impedance and phase between dee voltage and control grid.

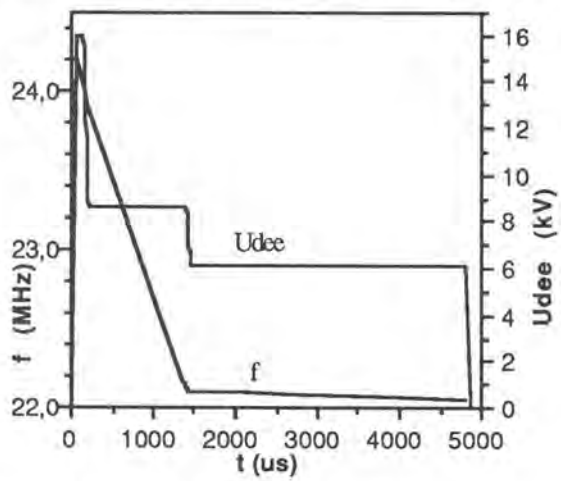


Figure 8. Programs for f(t) and $U_{dee}(t)$ used for 180 MeV protons with macro duty cycle of 50 %.

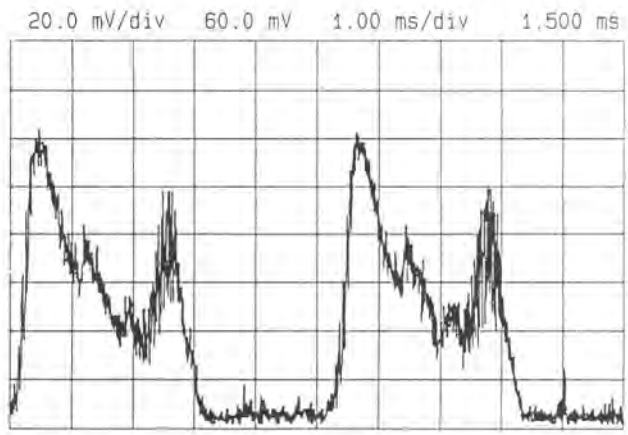


Fig. 9. Faraday cup measurement of a stretched 180 MeV proton beam with approx. 50 % duty cycle.

LOW TEMPERATURE TESTS OF THE AGOR SUPERCONDUCTING COIL SYSTEM

K. Pieterman, J.A.M. Dam, C. Commeaux* and C. Penco+

Cryocon B.V., P.O. Box 685, 3800 AR Amersfoort, The Netherlands
*IPN, P.O. Box 1, 91406 Orsay Cedex, France
+Ansaldo Componenti Srl, Via N. Lorenzi 8, Genoa, Italy

ABSTRACT

In the period from November 1991 till June 1992 low temperature tests have been performed on the AGOR coils and cryostat first in Genoa where early December the factory tests were succesfully done by reaching the contractual point X where in air the maximum specified attracting force between the coils are obtained (4.5 MN). After warm up and transport the coils and cryostat were installed inside the yoke in Orsay where final acceptance tests are underway. The performance of the cryogenic system will be described in this paper.

1. GENERAL INTRODUCTION

AGOR, the joint project of the Dutch organisation FOM and the French organisation IN2P3 has now reached the phase of final testing of the different subsystems. The general overview of those systems is given in another paper[1]. Here we will focus on the superconducting coil system and its cryogenic support system that are presently under final acceptance test in Orsay. A general description of this system has been presented earlier[2,3]. Final assembly of the coils and cryostat has been realised at the premises of Ansaldo Componenti Srl in Genoa Italy, the company that has been responsible for this contract.

During final assembly of the four different coils special attention was paid to the relative positioning of the coils to obtain the close tolerances that were specified in the contract. After shrinking on the 40 mm thick hoop stress cylinders the magnetic axis and the medium plane of the coils were measured magnetically by running a small current through the coils. Based on those measurements mechanical references were machined in the outer diameter of the hoop stress cylinder both for axis and plane. Those refences have been used for the final machining and mounting of the upper and lower halves of the coil system. Before connecting the upper and lower coil sets additional magnetic measurements were done to obtain the optimum relative positioning of the two parts. Final positioning of the coils was realised within the specified 0.2 mm tolerance field.

Final assembly of the coils, radiation shields and cryostat was done in August and September 1991. During assembly some minor modifications have been made especially on connecting cryogenic tubing, to assure enough space between the different temperature levels as in general mounting space was very limited. Figure 1 shows the system during assembly. After completion of the system the external cryogenic connections were made and the pumping of the cryostat vacuum started on November 1, 1991.



Figure 1. The AGOR cryostat during assembly.

2. FACTORY ACCEPTANCE TESTS

2.1. Cooldown

After a final check of all subsystems including a 1 kV test on the isolation of the coil system to ground cooldown started on November 4, 1991. The cold gas flow was regulated to keep the temperature gradient over the coils below 40 K to avoid high thermally induced stresses on the coil system. A maximum of 5 K for the temperature gradient over the coils and 20 K between adjacent coils were also set but we found that the maximum gradient of 40 K over the complete coil system was sufficent to regulate the cooldown. The coils superconducting state was reached on November 29, 1991. The cooldown time was in agreement with the calculated time of 3 weeks taking into account a few regulation problems with the liquefier. With the shields filled with liquid Nitrogen we observed a small cold

spot in the oval medium plane support at 35°. The cryostat vacuum was 2×10^{-6} mbar and a check with the helium leak detector showed that there were no helium cold leaks.

2.2. 4K Operation.

Stabilizing the helium level inside the cryostat turned out to be difficult and could only be obtained by keeping a constant warm gas return flow of about 4 Nm^3 per hour in addition to the warm gas return of the current leads. A measurement of the losses of the cryostat was done by closing the liquid helium filling line as well as the cold gas return and adjusting the warm gas return valves in such a way that a constant pressure inside the cryostat was maintained. Table 1 gives the specified and measured values.

Table 1: losses of the cryostat.

Temp. level	Specified	Measured
80 K	190 W	71 W
4 K cold return	10,1 W	18,4 W
4 K warm return	6,5 l/h	6,1 l/h

After a final 1 kV to ground test energising of the coil system could start.

2.3 Coil Performance.

The coil tests were performed using the AGOR dual power supply (900 A,10 V and 1800 A,15 V) delivered by Foeldi, Switserland. Due to transport damage the slow dump cabinet could not be used during these tests. As primary security the quench detector that was part of the delivery of Ansaldo was used. At currents up to 100 A the behaviour of the power supply and quench detector were tested. To gain experience with the operation of the power supplies we used a software program that allowed full manual control. Strong disturbances were observed on the quench detector from the voltage regulation during charging of the coils. By carefully regulating the voltage steps of the power supply and small modifications to the quench detector the coils could be charged to higher currents.

The voltage taps on the coils are measured in such a way that the four coils form a measuring bridge. An amplifier mounted close to the cryostat amplifies the bridge signal by a factor of 25. The quench detector gives a warning signal if a voltage peak of 1 V (40 mV on the coils) is detected. A quench is regarded as occurred if the integral of the signal over 1 second is greater than 1 V or a voltage level of 3 V is surpassed disregarding the peak width. A signal of 40 mV from the coils roughly corresponds with a normal zone length of one winding. Taking into account the propagation velocity of the normal zone this was regarded as sufficient[4].

The coils were charged towards the contractual point X (I1 = 450 A, I2 = 900 A, see Fig. 2) the attracting force between the coils reach the same value

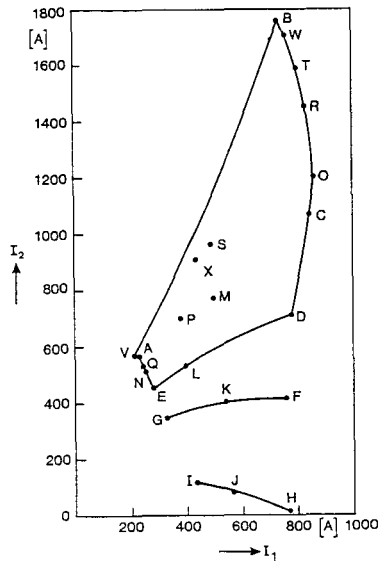


Figure 2. Operating diagram of the AGOR coil system.

(4.5 MN) as at point B (the maximum field operating point with iron). At the point where the power supply started to regulate in order to stabilize the current at this level (I1 = 445 A, I2 = 850 A) an opening of the breakers was observed. Analysis showed that no quench has occured neither at the opening of the breakers nor afterwards during the fast dump. By adjusting manually the voltage regulation we obtained a stable current level at I1 = 445 A and I2 = 895 A on December 6, 1991. At this point field maps were made to check both the radial off centering of the coils and the magnetic medium plane. The results obtained are given in table 2.

Table 2: Magnetic coil behaviour at point X.

offcentering	coils 1 (mm)	coils 2 (mm)
radial absolute	0.76 @ 296°	0.82 @ 298°
relative	0.06	
medium plane absolute	-0.41	-0.37
relative	0.04	
magnetic	specified (mT)	measured(mT)
C1 (Bz)	0.17	0.007
C2 (Bz)	0.55	0.007
C1 (Br)	0.17	0.196
mean Br	0.17	-0.097

Only the first harmonic C1 (Br) of the radial field is higher than the specified value due to a local anomaly at 240°. Figure 3 shows the measured Bz at point X.

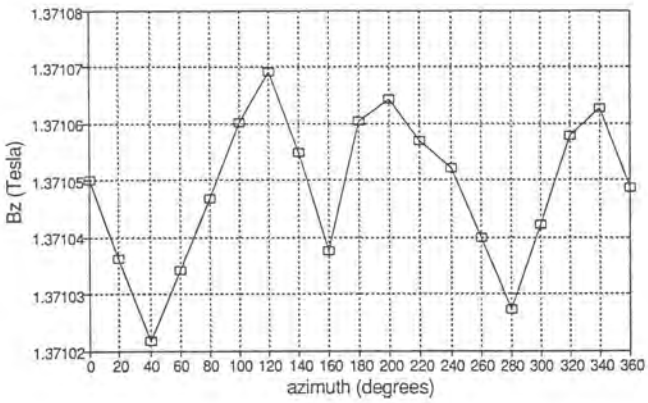


Figure 3. Bz modulation at maximum attracting force

The modulation can be explained by a coil deformation under the maximum attracting force of 0.06 mm. This deformation is about a factor two lower than foreseen in the original design calculation.

To test the breaker system we externally activated the quench detection system at point X. At this point an induced partial quench was detected at the lower coil B2, where a maximum temperature of 8.5 K was observed. The total stored energy in the system at point X (deducted from the measured inductances L1 = 16.3 H, L2 = 12.4 H and M = 6.8 H) was 11.9 MJ. 98.5% of this energy was dumped inside the fast dump resitors and 1.5% inside the coil system.

2.4. Factory Tests Conclusions.

Apart from the small anomaly in the radial field measurements the magnetic coil performance was excellent. The high accuracy in coil winding and assembly realised by Ansaldo made it possible to meet the tight tolerances specified by AGOR.

To optimize the stabilisation of the level inside the cryostat it was decided to modify slightly the internal cold gas return circuit of the cryostat to better equalize the pressures between the Helium volume at the liquid inlet and the current leads.

After analysing the cryogenic performance we found two main reasons as for why the 4 K losses were higher than expected. First the anchoring temperature of the upper spport (185 K) was too high with respect to the design value and secondly we found that three small 80 K covers at the oval medium plane support were mistakenly not mounted. The combined effect of this could well explain the difference with the specified losses at 4 K. The 80 K losses were considerably less than expected, partly because of the higher anchoring temperature and indicating a good efficiency of the applied superinsulation.

Some anomalies were observed in the read out of the upper tie rod strain gauges that was believed to be a torsion effect. It was decided to mount four instead of two of these sensors to form a compensated bridge.

Essential experimental data were obtained with the regulation of the power supplies to develop the final software for this system.

3. FINAL ACCEPTANCE TESTS IN ORSAY.

The AGOR coils and cryostat were delivered to their temporary site in Orsay on February 14, 1992, with the modifications that resulted from the factory tests implemented. Figure 4 shows the cryostat before mounting inside the yoke. Seven weeks after arrival

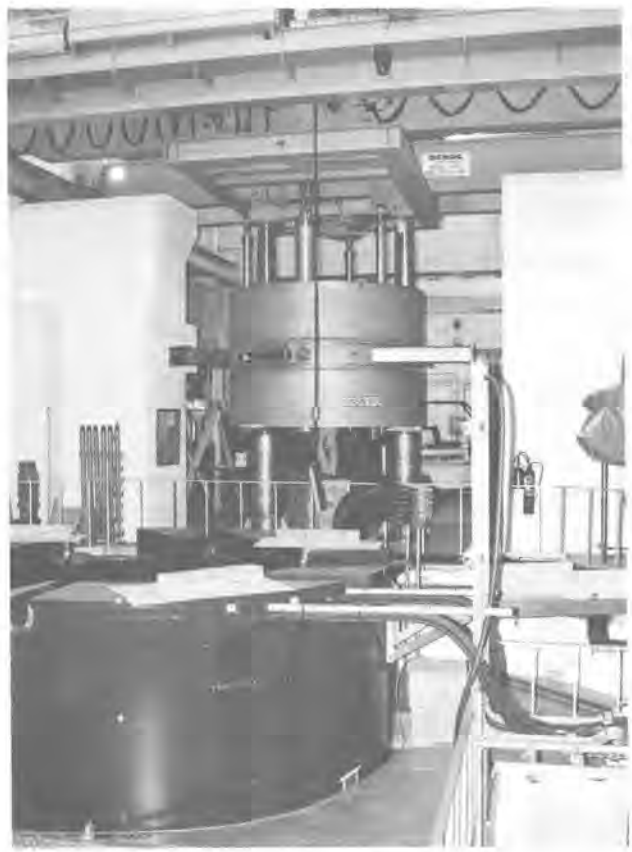


Figure 4. The AGOR cryostat at the Orsay test site

the system was mounted inside the yoke, the external cryogenic system connected and all electrical connections made and tested. The second system cooldown using the AGOR refrigeration system delivered by Sulzer, Switserland was started on April 6, 1992. As it was the first full scale use of the complete cryogenic system it took somewhat longer than expected to reach the 4 K level. Expecially during the final cooldown from 80 K to 4 K a number of minor modifications were made to the control software before we were able to operate the system in full automatic mode. Despite of a careful repositioning of the shields during the mounting procedure in Orsay we still observed a small coldspot at the same position as during the factory tests. By attaching a 25 W heater to the spot we could avoid condensation and ice formation.

Normal operation of the system at 4 K level was obtained on May 12, 1992. The modifications of the internal cold gas circuit made by Ansaldo proved to be succesfull as liquid Helium level stabilisation was obtained without any problem. Also the 80 K recondensor that has not been used before, operated as expected. A first measurement of the 4 K losses of the cryostat was

done by isolating the cryostat from the liquefier and keeping a constant level and pressure in the cryostat by transferring Helium from the 1000 liter dewar and returning all gas at room temperature to the suction side of the compressor. The total loss at 4 K level was 29 W, including transferline and valve box losses. The latter were not measured seperately but taking their expected losses we may conclude that also in this respect the modifications to the system realised after the factory tests were succesful. A check on the cryostat vacuum with the leak detector revealed a Helium level of 10^{-6} mbarl/s that seems to be decreasing. Further checks are necessary on this point.

At low field level (2.5 T) a number of tests were carried out with the newly implemented control program for the power supplies that proved to be very succesfull as no inacceptable disturbances were observed on the quench detector. Adjustement of the coil position both with respect to medium plane position and radial centering was done with the results obtained from the AGOR fieldmapping system.

On June 24, after having proved that all subsystems operated satisfactory, high field tests were started. Around the maximum field strength we observed a sharp rizing of the tension in the radial tie rods indicating a strong increase in offcentering force. At 3.8 T the secondary safety system activated a slow dump as the force on the tie rods surpassed rapidly the 45 kN level that was used in the protection system (25% of the maximum allowed force). The maximum force observed was 110 kN indicating the strong destabilizing effect of the offcentering force. Nonetheless the coils remained perfectly stable and no quench was induced by the activation of the slow dump circuit at this field.

We obtained stable operation of the system at a field strength of slightly over 4 T on July,1 by adjusting the radial tie rods as good as the mechanical system allowed. Up to this point, almost at maximum specified field and stored energy no irregularities in the superconducting system were observed.

4. CONCLUSIONS

The coils show perfect stability towards the maximum obtained field strength at present (4 T). The signal of the quench detector is very stable and no disturbances were observed. Even at the activation of the slow dump circuit at high field the system remained stable.

After having solved some minor regulation problems in the refrigeration system it performs very well in automatic mode. The overall losses both at 4 K and 80 K are comfortably within the capacity of the refrigeration system, giving us more reserve capacity than foreseen for the cooling of the superconducting extraction elements.

The only remaining points of concern are the fact that we still have a cold spot at the medium plane inside the beam vacuum that at the moment is heated away and the fact that Helium was detected inside the cryostat vacuum. Those points will be addressed when the system is to be dismantled for final transportation to the KVI in Groningen. We are also considering to mount stronger radial tie rods to reduce their stress level caused by the offcentering force. With the experience obtained sofar however we feel secured that the system performance is more than sufficient to allow for the beam tests foreseen in Orsay.

5. REFERENCES

1) Schreuder, H.W., "AGOR: Recent Achievements", presented at the **13th International Conference on Cyclotrons and their Applications**, Vancouver, Canada, July 6-10,1992.
2) Pieterman, K., et.al.,"The AGOR Cryogenic system" Proceedings of the **11th International Conference on Cyclotrons and their Applications**, Tokyo, Japan, 1986, p. 548.
3) Pieterman, K., et al, "AGOR cryogenics: A Status Report", Proceedings of the **12th International Conference on Cyclotrons and their Applications**, Berlin, Germany, 1989, p. 220.
4) AGOR design report, KVI/IPN Orsay October 1986.

A PERMANENT MAGNET SYSTEM FOR A CYCLOTRON USED AS A MASS SPECTROMETER

C.Y. Li, M. Cooper, K. Halbach, W.B. Kunkel, K.N. Leung, R.P. Wells, and A.T. Young
University of California, Lawrence Berkeley Laboratory
Berkeley, CA 94720 USA

ABSTRACT

The design of a compact, low energy cyclotron used as a mass spectrometer is presented. The instrument is designed for high resolution, high sensitivity detection of trace isotopes. It features the use of permanent magnets to excite the soft iron pole pieces which provide the magnetic field of the cyclotron. Tuning magnets are used to enable the field to be varied. This significantly improves the operational requirements of the instrument when compared to one which uses electromagnets. The cyclotron will use a spiral inflector for axial injection.

1. INTRODUCTION

High sensitivity, high resolution mass spectroscopy has applications in many fields. Among them are archaeology, biomedicine, geology and geochemistry, and environmental research. One method used to achieve these goals is Accelerator Mass Spectroscopy. In this technique, the sample is ionized and accelerated to high energy. Using this technique, detection of trace isotopes at a level of 1 part in 10^{15} has been achieved. In general, most AMS facilities use high energy tandem accelerators with energies in excess of 1 MeV. However, it has been recently demonstrated that high resolution can also be obtained by using a compact, relatively low energy cyclotron as the accelerator.[1] This technique is called Cyclotron Mass Spectrometry (CMS).

At Lawrence Berkeley Laboratory (LBL), a program is underway to develop CMS into an easy to use, inexpensive instrument which is widely available. An overview of this program is given in another paper in these proceedings. [2] . This paper presents the design of the cyclotron vacuum structure and magnet design.

2. CYCLOTRON DESIGN .

2.1 Magnet Design

This cyclotron mass spectrometer has been optimized for the detection of ^{14}C, the isotope of most widespread interest in the AMS community. The magnetic field in the midplane is 1T. For high mass resolution, the orbits need to be isochronous, therefore a flat, uniform field must be maintained throughout the acceleration region. The field in the midplane should be uniform to better than 1 part in 10^4.

These parameters can be obtained by using permanent magnet material to energize soft iron poles pieces. This is shown schematically in fig 1. Magnet material, such as samarium cobalt, is placed in contact with the iron pole pieces. The iron concentrates and directs the magnetic flux to the pole faces. For one pole, the magnets are oriented so that the magnetization vector points toward the pole face. For the other pole piece, the magnets are oriented so that the magnetization points away from the pole face. A magnetic flux return ('yoke') connects the magnets to complete the circuit. The midplane of the accelerator is placed between these poles. With careful design, the uniformity of the field will not be set by the magnetic uniformity of the magnet material or where it is placed, but rather by the quality of the finish on the pole faces and the accuracy of the spacing between the poles.

Based on the desired mid-plane B-field, the remanent field of the permanent magnet material, and the geometry of the poles, (i.e. pole diameter and gap width), the amount of permanent magnet material needed is calculated.[3] Material

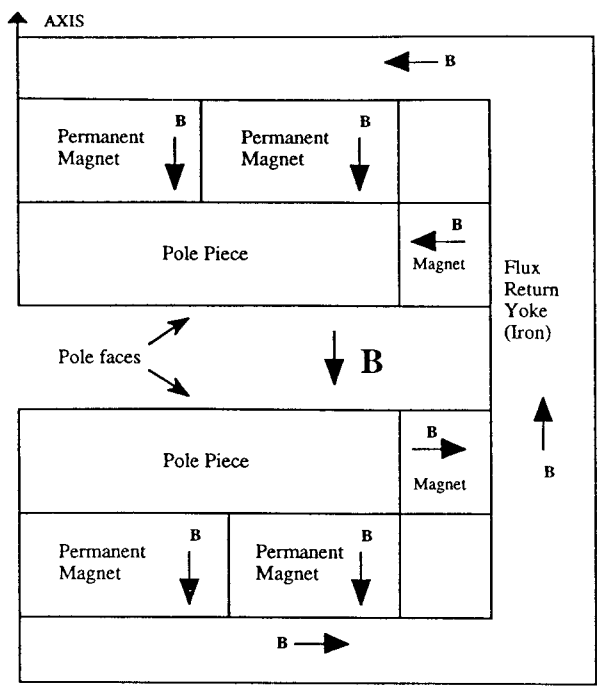


Figure 1 Conceptual design of a permanent magnet excited magnetic field.

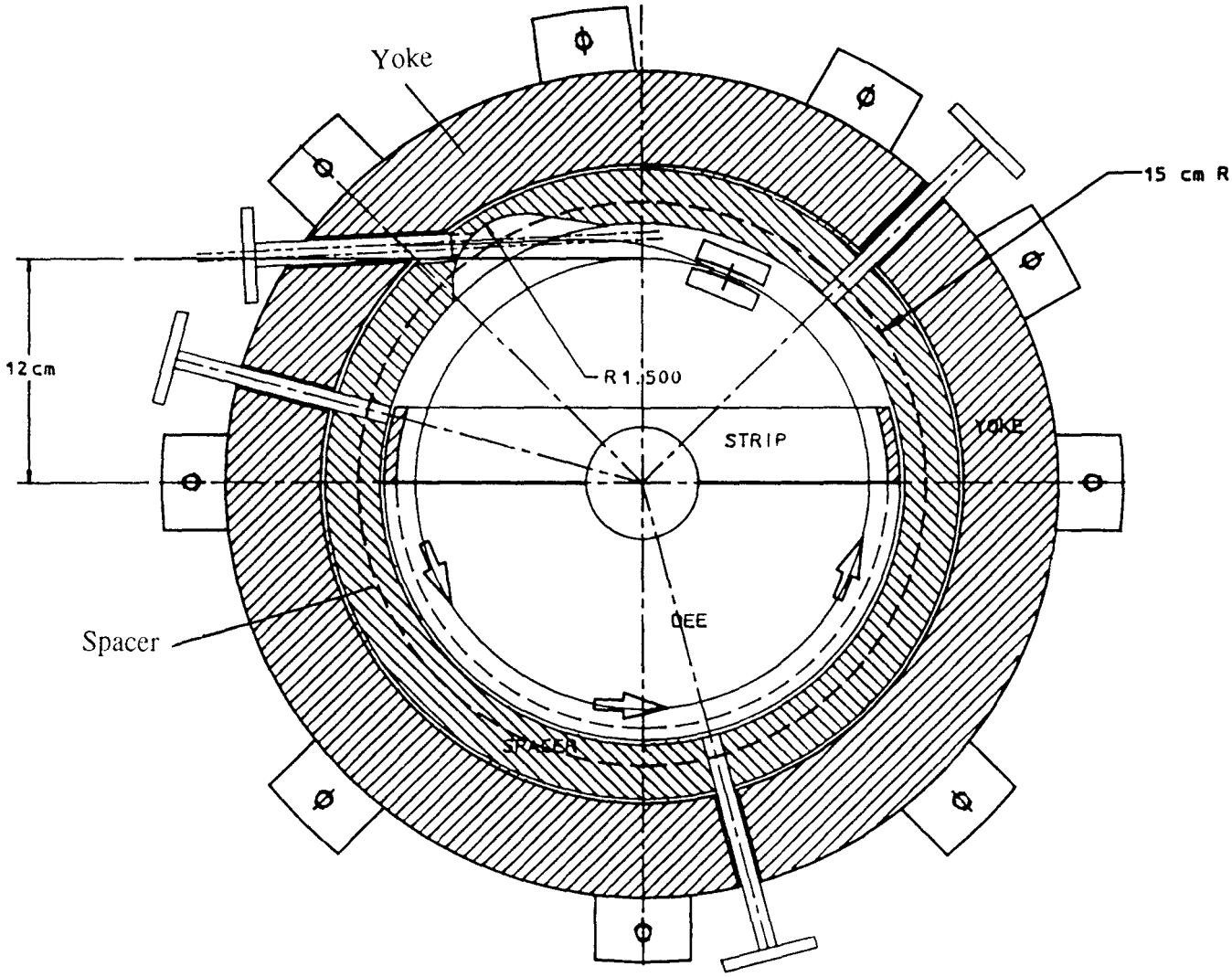


Figure 2 Top View of the Cyclotron Mass Spectometer (CMS)

can be placed on both the sides of the poles, with the magnetic field vectors pointing radially, and the top and bottom of the poles, with the fields directed axially. Calculation of the magnetic field using the computer program POISSON verified that the field was uniform to better than 1 part in 10^4 throughout the acceleration region.

2.2 Machine Parameters

The overall size of the machine is dictated by the species to be measured, the injection energy of the ion, and the mass resolution needed. For ^{14}C, a mass resolution of about 1800 is needed; this is sufficient to separate ^{14}C from ^{13}CH. The resolution of a CMS is determined by

$$R \approx 3 \times n \times H \qquad (1)$$

where n is the number of orbits the particles make before extraction and H is the harmonic of the fundamental cyclotron frequency that the accelerating RF is operating on. For ^{14}C in a 1T field, the fundamental frequency is 1 MHz. H might typically be 15, so that the minimum number of orbits would be 40. With modest energy gain per turn, ≤500 V, it is possible to achieve this figure with an extraction radius of ≤ 9 cm. We have conservatively designed the instrument for an extraction radius of up to 12 cm.

Vacuum requirements are determined by the amount of stripping and scattering of the C^- there is by the residual gas molecules within the accelerator structure. Assuming a stripping cross section on the order of 2×10^{-15} cm,[4] a vacuum level in the mid 10^{-7} torr range will be acceptable.

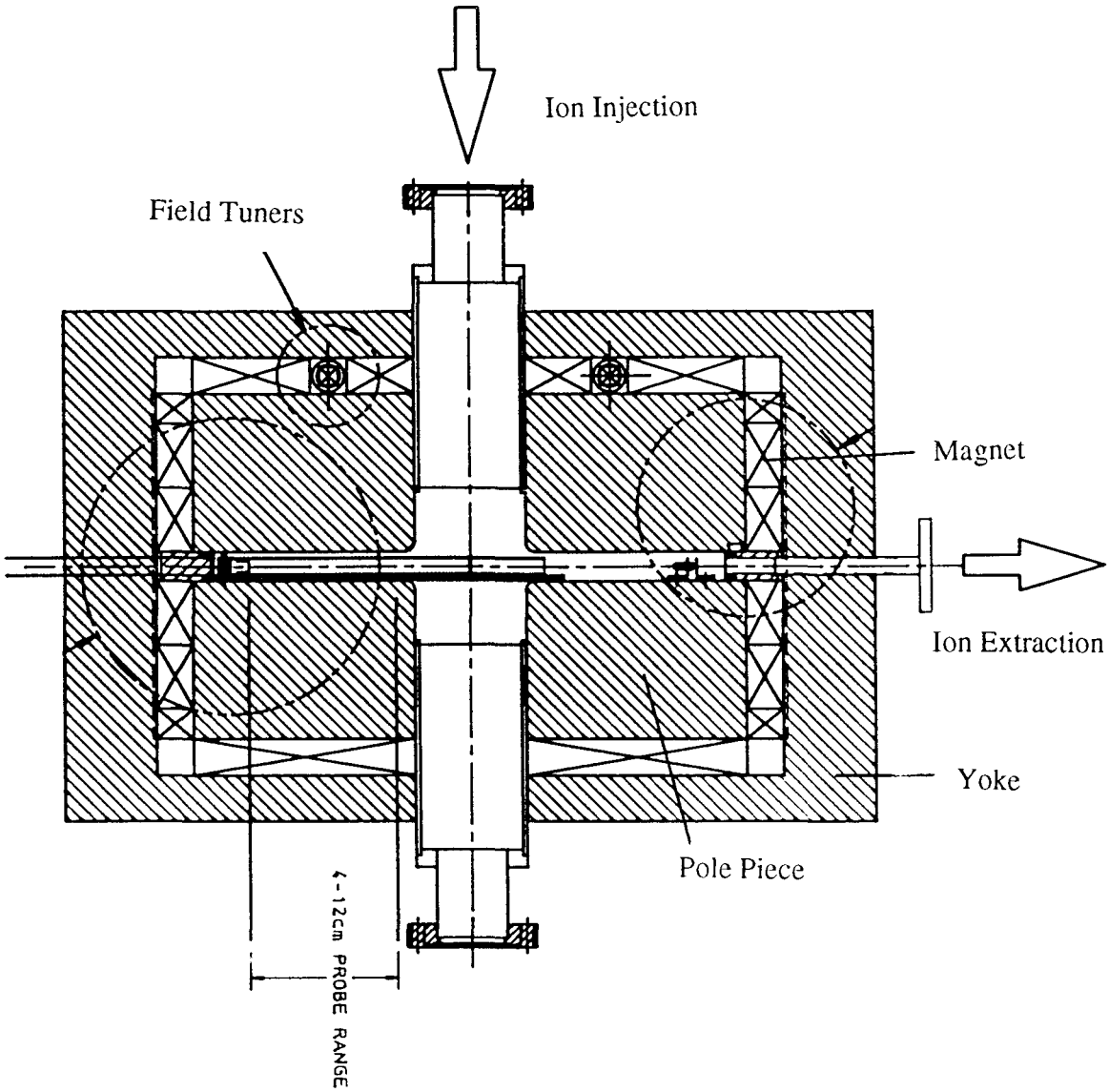


Figure 3 Side view of the CMS

Design parameters for the CMS are summarized in Table 1.

3. DESIGN DETAILS

Figures 2 and 3 show the top and side views of the cyclotron vacuum structure and magnet assembly. The soft iron pole pieces are 15 cm in radius, with an axial hole of about 2.5 cm radius machined into them to provide access for the axial ion injector and pumping ports. The pole pieces are kept apart by an aluminum spacer ring which has an inside diameter of 13.5 cm and a thickness equal to the desired pole gap, 1.6 cm. In this design, the inner pole surfaces are exposed to the high vacuum. This configuration was chosen to reduce the distance between the pole faces, an important consideration to minimize the magnet material needed to achieve the desired midplane magnetic field. Although the magnet material has good vacuum properties, it has been excluded from the vacuum by o-ring seals in the spacer ring and by welding the beam entrance tube and the vacuum exhaust tube to the pole faces. This minimizes outgassing and virtual leaks.

Accelerated C^- is extracted using an electrostatic channel and directed out of the cyclotron through a tangential hole in the spacer ring. Additional radial holes in the spacer ring provide access for three 'dee' probes used to measure the ion beam current and position. These probes are mounted on bellows and can move radially from the injection radius to the extraction radius. In addition, they are segmented

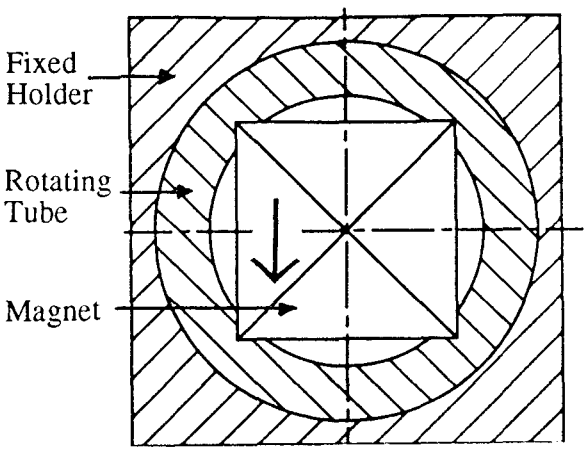


Fig. 4 Cross section of a magnetic field tuner. Arrow is aligned with the magnet's field, which rotates with the rod.

vertically to provide information on the beam properties in that dimension.

The samarium cobalt magnet material is purchased as larger blocks and cut and ground to the desired dimensions. The individual magnets are glued to the flux return yoke for permanent mounting. Approximately 200 individual magnets are used in this design, with a total volume of about 6000 cm^3. Magnet material does not completely fill the annular gap between the outer radius of the pole faces and the inner surface of the yoke. This would have required arc-shaped wedges. Instead, the annulus is filled with segments of rectangular magnets. Viewed from the top, the magnets in the annulus appear as an 18-sided polygon with small wedge shaped gaps where the magnet corners on the inner radius touch each other while the outer corners do not. Small ledges are machined in the yoke to aid in the alignment and assembly of these magnets.

Although the top (bottom) of the upper (lower) pole piece also has magnets attached, there are areas on these surfaces where there is no magnet material. This occurs for a variety of reasons, such as for the penetration for the axial injection line. In addition, magnets can be left out to coarsely adjust the magnetic field strength in the midplane. These voids do not affect the field homogeneity as the pole piece 'smoothes' out these non-uniformities.

Minor adjustments in the magnetic field will be made by using 'field tuners,' movable magnets which can be oriented such that their magnetic field is parallel, antiparallel, or any angle with respect to the existing field. A cross section of the tuners is shown in fig 4. They consist of rectangular magnets which are placed in tubes. The magnetization vector is radially directed. The tubes are then placed in rectangular holders which will lie across chords in the top and bottom magnet volumes, taking the place of the normal magnets. The rods are free to rotate within the holder, and depending upon the angle between the rod's B-field and the existing field, the tuner may either increase or decrease the midplane field.

Table 1 Design Parameters of the CMS

Pressure	3×10^{-7} torr
Injection Method	Spiral Inflector
Injection Radius	4 cm
Magnet Material	Samarium Cobalt
Pole Radius	15 cm
Pole Gap	1.6 cm
Pole Material	1005 Steel

4. SUMMARY

The design of a permanent magnet cyclotron has been presented. This instrument has been design for use as a highly sensitive and selective mass spectrometer, optimized for the detection of ^{14}C. The instrument is now under construction, with completion scheduled by 1993. Initial tests will be conducted with a cesium sputter source, but experiments with an advanced ion source are also planned.[5)]

5. ACKNOWLEDGMENTS

This work has been supported by the U.S. Department of Energy, Division of Advanced Energy Projects, Office of Basic Energy Sciences under contract number DE-AC03-76SF00098.

6. REFERENCES

1) Bertsche, K.J., Karadi, C.A., Muller, R.A. and Paulson, G.C. Nucl. Instr. and Methods, B52, (1990) 398
2) Young, A.T., Bertsche, K.J., Clark, D.J., Halbach,K., Kunkel,W.B., Leung, K.N., and Li, C.Y., these proceedings
3) Li, C.Y., Halbach, K, and Young, A.T., in preparation
4) Tsuji, H., Ishikawa, J., Maekawa, T., and Takagi, T., Rev. Sci. Instru. 61 (1990) 427
5) Leung, K.N., Bachman, D.A., McDonald, D.S., and Young, A.T., these proceedings are references therein

SECTOR MAGNET OF THE RCNP RING CYCLOTRON AND THE ISOCHRONIZATION

K. Hosono, M. Kibayashi and I. Miura
Research Center for Nuclear Physics, Osaka University,
Mihogaoka 10-1, 567 Ibaraki Osaka, Japan

ABSTRACT

The RCNP six-sector ring cyclotron is in operation for nuclear physics experiments. We briefly recall the sector magnet of the ring cyclotron. Then we present the method of the magnetic field setting for isochronization and the results.

1. SECTOR MAGNET

A schematic mid plane view of the sector magnets of the ring cyclotron including injection and extraction devices is shown in Fig. 1. The parameters of the sector magnet are listed in Table 1. Figure 2 shows a photograph of the sector magnets installed in the cyclotron vault. A vacuum chamber made by SUS is welded at the side faces of the pole. Figure 3 shows the schematic cross sectional view of the pole edge section.

The maximum magneto-motive force was estimated to be about 1.4×10^5 ampere-turns to obtain the maximum field strength of 17.5 kG. The main coil and the auxiliary coil consist of 80 turns and 20 turns of copper hollow conductors, respectively. We can control the magnetic field strength of 500 Gauss for each sector by the auxiliary coil. The 36 pairs of trim coils are fixed on each pole face of the sector magnet. Two pairs among them are used as harmonic coils. Each trim coil is coated with alumina-ceramics ($A\ell_2O_3$) for insulation and is fixed on the pole face by SUS-Fe welded volts to reduce the magnetic perturbation due to bolt holes.

High current stability is required for the power supplies of main, auxiliary and trim coils to obtain a high quality beam. In order to acieve high stability, a precision shunt resistance made of germanium-manganese-copper alloy (ZERAMIN) is used as a current sense. The temperature coeffi-

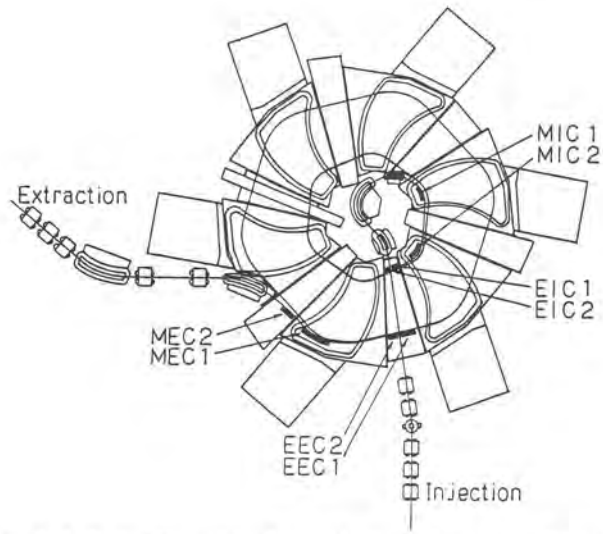


Fig. 1. Schematic mid plane view of the magnet system of the ring cyclotron.

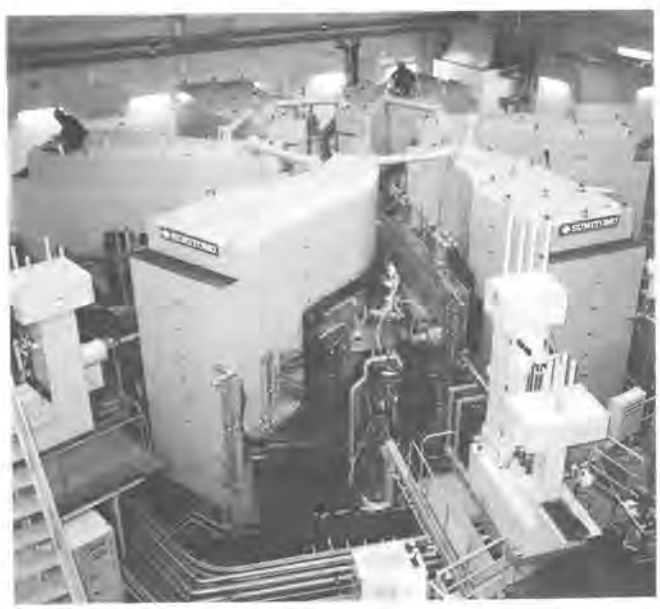


Fig. 2. Photograph of sector magnets installed in the cyclotron vault.

cient of the shunt resistance is less than 3 ppm/°C. The shunt resistance of the main and auxiliary coils are cooled by temperature controlled water kept at 27.0 ± 0.1°C. In this condition, the current stability of $\pm 2 \times 10^{-6}$ is obtained at main coil currents of 650A and 400A.

2. FIELD MAPPING

We used the non magnetic pneumatically driven system for field mappings. Twenty Hall generators were fixed along a radial arm. With the mapping apparatus, we can measure field maps with radial interval of 10 mm or 20 mm step between 1600 mm and 4300 mm and with azimuthal interval of 0.4° step over the whole region of 360°. A computer (μ-VAXII) is used for arm driving system, data acquisition system and control system of power supplies. The details of the measuring system have been described elsewhere.[1)]

3. MAIN RESULTS OF THE FIELD MAPPINGS

Various modes of the field setting procedure have been examined to reproduce field strength and distribution as quickly as possible. In a cycling procedure, it takes about 1.5 hour for higher field strength than 13 kG and 2-4 hours for low one. Excitation characteristic of a sector magnet is shown in Fig. 4.

Measurement of the base field distributions of six sectors was carried out for seven main coil current of 250A, 350A, 400A, 450A, 500A, 550A and 650A. The main coil currents correspond to the field strength of 8.5 kG, 11.7 kG, 13.2 kG, 14.5 kG, 15.6 kG, 16.3 kG and 17.5 kG, respectively. The injection and extraction elements were excited during the measurement.

The base field distributions along the center line of the No.5-sector magnet for the seven levels of main coil current and the relative strength are shown in Fig. 5. There is at most 0.2% difference in the field shape among the seven levels. In order to obtain the required isochronous field distribution along the sector-center line, we have adopted a method similar to that used at GANIL.[2)] Equilibrium orbits are calculated using the measured base field distributions and the ratios between the field

Table 1
Parameters of the spiral sector magnet.

Number of sector magnets	6
Sector angle	22° ~27.5°
Gap width	60 mm
Height of magnet	5.26 m
Overall diameter	14.4 m
Total weight	~2200 tons
Injection radius	2 m
Extraction radius	4 m
Maximum magnetic field	17.5 kG
Maximum ampere turns	1.4×10^5 A.T
Maximum current	900 A
Maximum power	440 kW
Number of trim coils	36 pairs×6
Maximum current	500 A
Total trim coil power	~350 kW

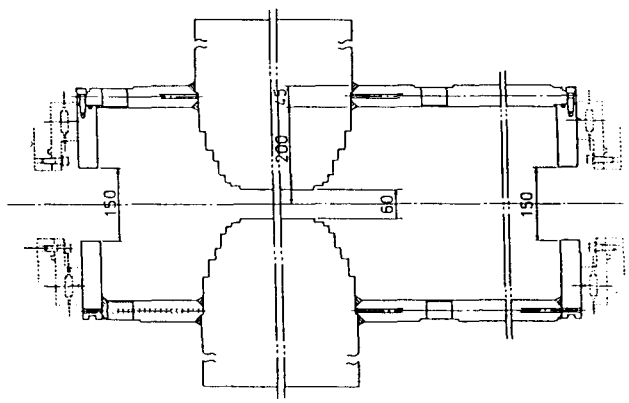


Fig. 3. Schematic cross sectional view of the pole edge section.

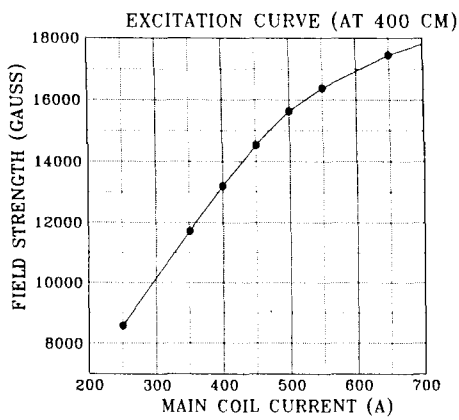


Fig. 4. Excitation characteristic of a sector magnet.

strength and the radius averaged along the closed orbit ($\bar{B}$ and $\bar{R}$) and those at the sector-center line (B_c and R_c) $K_b = B_c/\bar{B}$ and $K_r = R_c/\bar{R}$ are calculated. The K_b and K_r values of No.5-sector at the seven levels of main coil currents are shown in Fig. 6 and those of the six sectors at 500A (14.5 kG) excitation are shown in Fig. 7. Perturbation due to the injection and extraction elements was observed, more or less, in all sector magnets.

4. TRIM COIL FIELD

Measurement of the trim coil fields was performed for the No.5-sector magnet only at the base fields of the main coil current of 250A, 450A, 550A and 650A. In order to obtain the non-linear effectiveness of the trim coil field, four kinds of the measurement were carried out for each base level of the main coil current. The field gradient of the isochronous radial field distribution is positive for protons of higher energy than 200 MeV and is negative for all energies of heavier ions than protons. In the measurement, the current was fed to each trim coil to make the radial field gradient corresponding to the gradient of the isochronous field distributions of 300 MeV and 400 MeV protons (positive gradient) and 400 MeV and 100 MeV alpha particles (negative gradient). Figure 8 shows examples of the trim coil field distributions along the sector center line in the case of the field gradients corresponding to 400 MeV proton and to 400 MeV alpha particle field gradients at the 450A base field, respectively. In order to estimate the difference of the effectiveness of the trim coil fields among the six sectors, the field maps with the field gradients were also measured for each sector.

5. ISOCHRONIZATION

An isochronous field distribution along the center line of each sector magnet can be calculated by using the measured data of $B_c(N, I, r)$, $K_r(N, I, G, r)$ and $K_b(N, I, G, r)$, and the optimum currents of the main and trim coils to reproduce isochronous field distribution can be obtained by using the data of B_c, $B_T(I, G, r)$ and $\Delta B_T(N, I, G, r)$, where B_c, K_r, K_b, B_T and ΔB_T are main level field along the sector center-line, $K_r = r_c/\bar{r}$, $K_b = B_c/\bar{B}$, trim coil effective field of the No.5-sector magnet and the

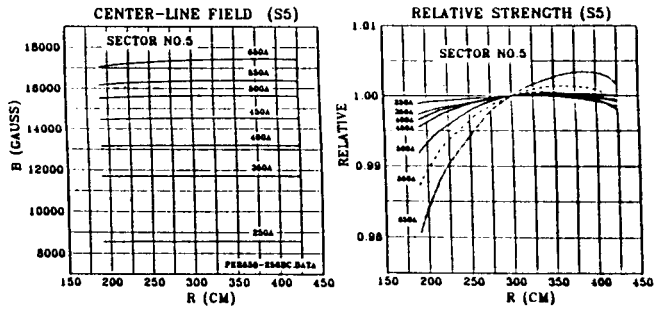


Fig. 5. Base field distributions along the center line of the No.5-sector and the relative strength.

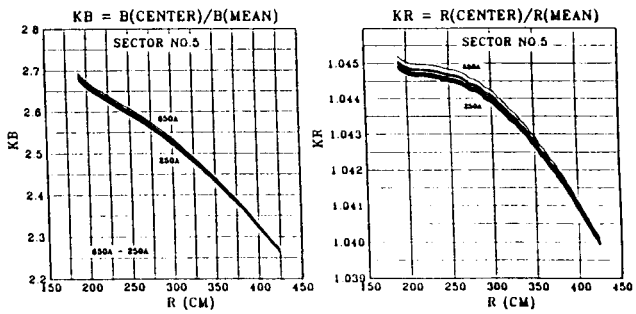


Fig. 6. K_b and K_r values of the No.5-sector at the seven main coil levels.

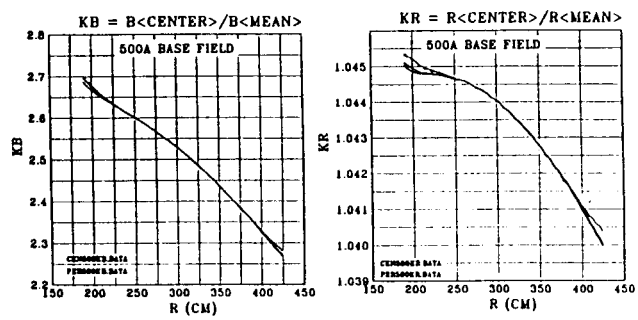


Fig. 7. Comparison of K_b and K_r values among the six sectors at 500A excitation.

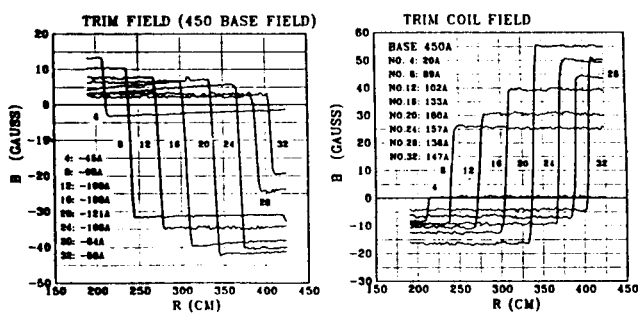


Fig. 8. Examples of the trim coil field distributions along the sector center line at the field gradients corresponding to the 400 MeV protons 400 MeV alpha particles at 450A base field.

difference of the all time coil effectiveness among the six sectors, respectively. These are dependent on sector (N) main coil current (I), gradient of the isochronous field (G) and radius of the sector center-line (r).

When a particle and the acceleration energy are given, our code calculates the isochronous field and determines first the required main field level on the sector center-line and then interpolates the B_c, K_r, K_b between the measured main levels to give $B_c^0(N,r)$, $K_r^0(N,r)$ and $K_b^0(N,r)$ at the required level and field gradient. The required field distribution for acceleration of each sector can be calculated using the B_c^0, K_r^0 and K_b^0 values. Next, the main and trim coil currents are calculated in order to reproduce the isochronous field. We have no data of trim coils fields for the other sector magnets except No.5-sector. Therefore the required field distributions for the sector magnets except No.5-sector can be obtained by taking account of the ΔB_T^0 at the required level and field gradient which are given by interpolation of ΔB_T measured at various levels and gradients. The optimum coil currents are automatically searched with a computer code.

6. ACCELERATION

After cycling of the magnets, the calculated coil currents are fed to the coils. We have accelerated protons to 300 MeV (E_{inj}=52.7 MeV).

Figure 9 shows measured beam currents on a 1 mm wire of the main probe from the injection radius to the extraction radius. Figure 10 shows the particle phase excursion from the injection to the extraction by a dotted line in the case of setting the calculated coil currents and by a solid line in the case of a slight correction of the trim coil currents.

7. CONCLUSION

Magnetic field distributions of the sector magnet of the RCNP ring cyclotron were measured. The values of B_c, K_r, K_b, B_T and ΔB_T were obtained at various combinations of the main levels, field gradients, trim coil, currents, etc. These data bases are used to reproduce isochronous fields of various ions and energies. We have accelerated protons to 300 MeV by setting the calculated coil currents. We have no serious problems which occur on setting the calculated coil currents, through the phase excursion appears in acceleration. The phase excursion can be corrected by a slight adjustment of trim coil currents.

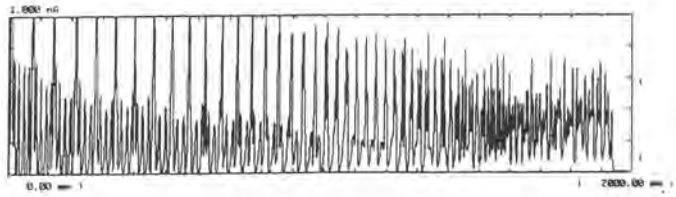


Fig. 9. Beam current measured by a wire probe from injection radius to extraction radius.

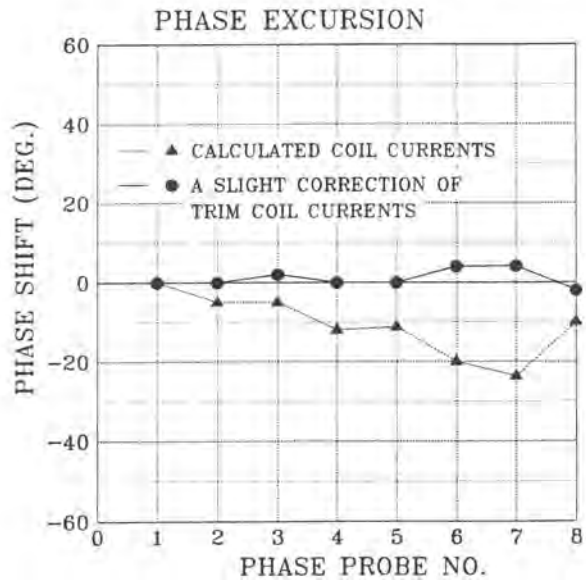


Fig. 10. Phase excursion.

REFERENCES

1) K. Hosono et al., RCNP-Annual Report 1989, p.179.
2) M. Barre et al., Proc. of the 9th Int. Conf. on Cyclotron and Their Applications, Caen (1981), p.371.

THE ELECTROSTATIC DEFLECTOR FOR THE CHALK RIVER SUPERCONDUCTING CYCLOTRON

W.T. Diamond, C.R. Hoffmann, G.R. Mitchel and H. Schmeing
AECL Research, Chalk River Laboratories,
Chalk River, Ontario, Canada, K0J 1J0

ABSTRACT

The electrostatic deflector is the first extraction element in the Chalk River superconducting cyclotron. The design goal of the deflector is a field of 143 kV/cm, to be obtained with a voltage of 100 kV across a gap of 7 mm. This has proven to be very difficult to achieve. The tight space constraints of a compact superconducting cyclotron, high-temperature operation imposed by stray rf fields and problems associated with very strong magnetic fields all contribute to this difficulty. In an effort to reach the design goal, we have investigated many aspects of the physics and technology of high-voltage vacuum insulation. Various choices of materials and surface treatments were tested. The results from this extensive research effort have led to changes in the design of the deflector, and we now routinely exceed the design field, but at a reduced gap of 5 to 5.5 mm. While the reduced gap reduces the transmission for some ion beams, the present deflector performance has led to successful cyclotron commissioning.

1. INTRODUCTION

The electrostatic deflector is a critical component in the extraction system of the Chalk River superconducting cyclotron. It must operate at an electric field in excess of 140 kV/cm for all operating conditions of the cyclotron. These include magnetic fields from 2.5 to 5 T, and residual rf fields from the high power (100 kW) rf system. The deflector, mounted inside a dee, is subject to significant heating from residual rf fields. Tight space constraints limit the maximum vertical spacing to 76 mm, with just over 24 mm between the high-voltage electrode and the sparking plates. These conditions have made progress toward the design goal difficult. We undertook several approaches to improve performance.[1-4] We used the cyclotron as a test bed for some development and built three test stands, including one with a magnetic field, to develop insulators, test electrode materials and study alternative electrode configurations. The wealth of results generated over two years has led to a re-design of most parts of the deflector and, in particular, to the present choice of materials for deflector electrodes. Only the geometrical appearance did not change substantially. The resulting performance level proved sufficient for the cyclotron to be commissioned.

In this paper we give a brief description of the present design and also a summary of some of the results that have led to these choices. Finally, we give a summary of the deflector performance at this time.

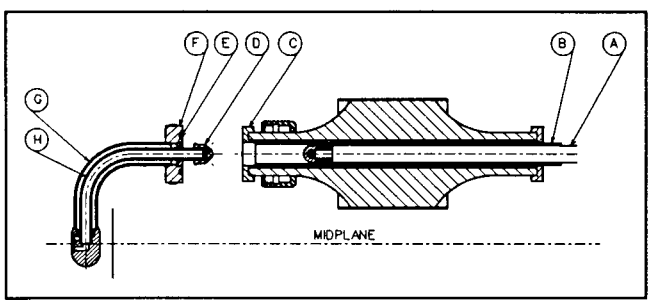


Fig. 1 Cross section of the high-voltage electrode and feed insulator. Details are explained in the text.

2. DEFLECTOR DESIGN

Figure 1 shows a schematic cross-sectional view of the electrostatic deflector, and its feed insulator. We had determined previously that, under the operating conditions of the cyclotron, elevated temperatures of any deflector component led to substantial reductions in performance. Consequently, we decided to cool, as directly as possible, all components that are subject to heating from residual rf or the ion beam. The figure shows in detail how this is done for the high-voltage electrode.

High-resistivity (about 15 MΩ • cm) water is circulated between the high-voltage cable (A) and a teflon tube (B). The water passes through fitting (D) to the high-voltage electrode through tube (H). The electrode is cooled over its entire length. The water returns through tube (G), exits through small holes in (F), and passes on the outside of the teflon tube (B), completing circulation back to the external water system. Flange (C) is part of a teflon liner that is installed inside the ceramic insulator. It captures a smoothly contoured metal fitting that is used to join the insulator to the high-voltage electrode. The teflon is etched and epoxied to the ceramic, with a joint near the center of the insulator. Both the O-ring joint (E), between (C) and (F), and the insulators have proven to be very reliable.

A 2 cm water column between the high-voltage cable and the electrode provides a large (30 MΩ) reliable isolation resistor. Operation without this resistor leads to much greater spark damage and rapid failure of the deflector.

3. REVIEW OF VACUUM DISCHARGE REGIMES

An electrostatic deflector is a vacuum-insulated high-voltage gap operating in a strong perpendicular magnetic field. A vast literature exists on high-voltage discharge phenomena in vacuum gaps, but little research has been done on such discharges in a magnetic field.[5] It is useful to review the physics of discharges, to put our problem into context.

Figure 2 shows the measured breakdown voltage of a plane-parallel high-voltage vacuum gap.[6] Note that this is for an electrode profile minimizing electric field enhancements at the edge and for high-quality electrode materials such as stainless steel or titanium. The breakdown voltage is dominated by different phenomena as the gap is increased. For gaps up to about 1 mm, it increases linearly with gap. The discharge is initiated by Field-Emitted Electrons (FEE) that leave the cathode and cross the gap. The FEE current increases exponentially with the electric field and, at some current, a spark occurs. Sparking may help condition an electrode, leading to operation at higher electric fields. As the voltage is increased, irreversible damage finally occurs.

For gaps greater than a few centimeters, microdischarges limit the breakdown voltage. These involve lumps of material pulled from either electrode by the electric field. They cross the gap and impact on the other electrode. As the voltage is increased, the microdischarge can initiate a spark.

For gaps between 5 and 8 mm, the region of interest to our deflector operation, there is a transition region in which both phenomena may be active. To put our requirements into perspective, a line labelled "deflector operation" in Fig. 2 corresponds to 140 kV/cm for gaps from 5 to 8 mm. It shows that our design goal lies only a factor of 2 below what is achievable under ideal conditions, and in the absence of strong magnetic fields or electrode heating. We calculate a field enhancement of about 15 % for the deflector because the electrodes can not be made with ideal profiles.

For gap dimensions that lie in this region, it is difficult to determine if the precursor for a spark is field-emitted electrons or microdischarge activity. Much of our research tends to support anode-originated microdischarges as an important activity. However, if a damaging spark occurs, a region of enhanced field emission is produced on the cathode. FEE current increases exponentially, with a tenfold increase in current for a 20 percent increase in electric field. This high FEE current generally determines the maximum electric field that can be sustained.

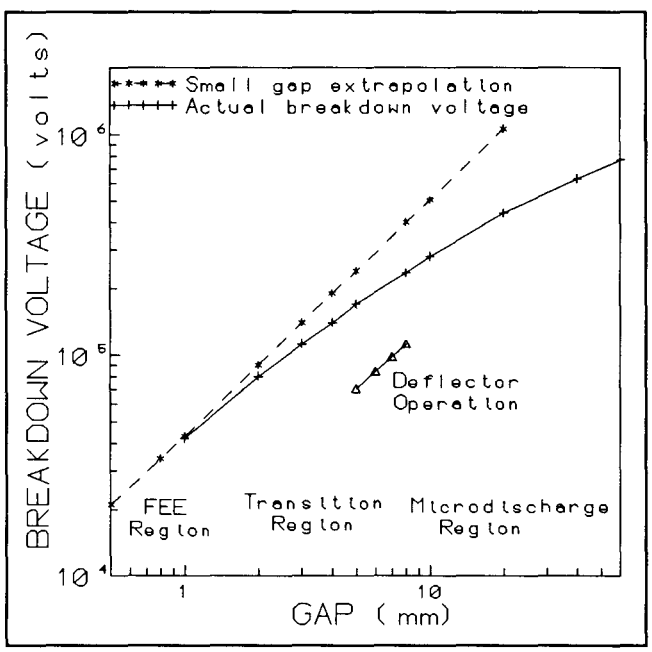


Fig. 2 Breakdown voltage of a vacuum gap as a function of the gap spacing.

3.1 Test Stand Results

Table 1 presents results of measurements[3] with plane-parallel copper, stainless steel or titanium electrodes for either anode or cathode. Electrodes of 19 mm diameter were machined and polished with 600 grade silicon carbide paper. They were cleaned ultrasonically with detergent and ethyl alcohol and installed with a 2.5 mm gap. After evacuation, the voltage was increased from about 40 kV in 2 kV increments until irreversible damage was done. This is the breakdown voltage shown in Table 1. Typically, 1 to 3 samples were tested for each entry and the data represents averages were more than one sample was tested.

Table 1. Breakdown voltage (kV) for combinations of copper, stainless steel and titanium electrodes.

Cathode Material	**Anode Material**		
	Copper	**Stainless Steel**	**Titanium**
Copper	64	92	98
Stainless Steel	74	96	110
Titanium	72	88	110

The table shows the strong effect of the anode on the breakdown voltage. If field-emitted electrons from the cathode were the main precursor for a damaging spark, one would not expect the large observed increase in breakdown voltage when a copper cathode is matched with a stainless-steel or titanium anode. This conclusion is also supported by data obtained when one or both electrodes are

electropolished. These data are shown in Table 2.

Table 2. Breakdown voltage (kV) for copper and stainless-steel electrodes that have been electropolished (E.P.). The gap is 2.5 mm.

Cathode Material		Copper Anode	
		E.P.	Not E.P.
Copper	E.P.	98,96	64
	Not E.P.	85	
Stainless Steel	E.P.		
	Not E.P.	94,94	

Electropolishing both copper electrodes made a dramatic improvement in the maximum breakdown voltage. It was observed that there was a great reduction in microdischarge activity and fewer conditioning sparks as the voltage was increased. When only the cathode was electropolished, there was no improvement, while treating the anode but not the cathode produced a large improvement. Tests with two electropolished stainless-steel electrodes showed only a modest improvement in the breakdown voltage, but there was much less microdischarge activity and fewer sparks as the voltage was increased. This reduced electrical activity in a gap operated at voltages well below the breakdown level is an important consideration in deflector operation.

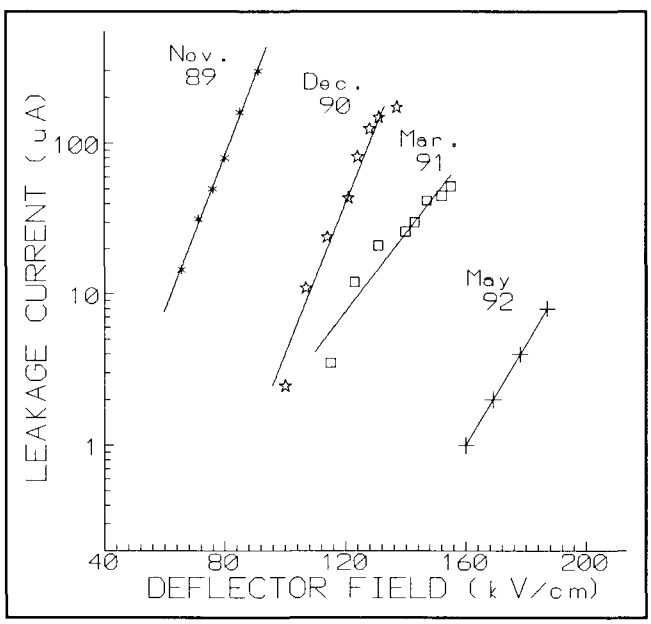


Fig. 3 Lowest deflector leakage current for the dates indicated.

4. DEFLECTOR PERFORMANCE

Results obtained from test-stand experiments have guided the development of the deflector. Significant improvements were made when we replaced the molybdenum used in the original deflector for sparking plates and the septum with stainless steel.[1] This was an unconventional choice of materials which was based on the observation that a spark could result in the transfer of a small sample of molybdenum from the anode to the cathode, where it became the site of enhanced field emission. The observation of increased FEE current for a heated cathode[3] led to the design of the water-cooled high-voltage electrode shown in Fig. 1. The results shown in Tables 1 and 2 pointed to the importance of the anode in high-voltage discharges (with a 2.5 mm gap). We used this as guidance in the choice of electropolished stainless steel for the septum, sparking plates and the supporting rails that hold the septum. Below we summarize some relevant features for optimum performance of the deflector.

The high-voltage electrode was redesigned with a geometry that minimized the electric field enhancements at curved portions and near the ends. We have chosen its thickness and height to be as large as possible, consistent with the restricted space available. Two-dimensional calculations show that there is less than a 15% electric field enhancement for the choices that we have made, but we have not attempted to calculate the field enhancement at the ends where there are compound radii.

It is important to minimize the stored energy in the deflector. We use the water resistor for this purpose.

The vacuum quality of the cyclotron is also important. We observed poor operation of the deflector, which was traced to a minor contamination of the midplane vacuum with roughing pump oil. The oil was cracked into elemental carbon by the rf and deposited on the deflector electrodes. Small flakes on the cathode served as sources of enhanced field-emission. A substantial effort was expended to clean the deflector and the midplane before deflector performance was restored.

The results of all these efforts are shown in Fig. 3. It shows the progress in improving the deflector as a function of time. The data show the best operation at the dates shown. All of the data were obtained with the magnet on at about 3 T and no rf. The deflector gap was 7 mm for the 1989 measurement and about 5 mm for the other measurements. The most recent curve, May 92, was the same with the magnet on or off, but we did not attempt to operate above 85 kV (170 kV/cm) with the magnet and rf in operation. Operation at 85 kV with a magnetic field of 3.5 T and 90 kV with the magnet off were for periods of 18 to 24 hours. The peak performance was at 94 kV (188 kV/cm), and this was achieved for several hours before the voltage was reduced.

The improvement between November, 1989, and December, 1990, was from the change from molybdenum to stainless steel sparking plates and septum, and changes in the geometry to reduce field enhancements. Electropolished cathodes were tested during this period with some success,[3] but anodes were not electropolished.

The water-cooled high-voltage electrode was tested between December, 1990, and March, 1991. This led to better peak performance and increased reliability for operation near the peak levels of performance.

The performance shown for May, 1992, was obtained after a meticulous cleanup following the vacuum contamination that was discussed previously. We also started to electropolish all of the stainless steel anode components during this cleanup. These data were taken during a slow conditioning of the deflector after re-assembly. The conditioning included slow increase of the voltage to 85 kV during a 24 hour period and operation at 90 kV (180 kV/cm) for a second 24 hour period followed by an increase to 94 kV for several hours, all with the magnet off. The voltage was increased to 85 kV with the magnet at 3.5 T for 18 hours and then rf power was turned on. The deflector voltage was lowered to about 40 kV while the dees were conditioned to their operating level. The deflector voltage was then increased to 85 kV with the rf and magnet in operation. This deflector then operated routinely under conditions of high rf power and a magnetic field of 3.5 T during a recent one week experiment at about 135 kV/cm and with only a few μA of FEE current.

5. SUMMARY

A water-cooled high-voltage electrode attached to an alumina feed insulator has been in use for over a year and has operated reliably. We believe that microdischarge activity originating from the anode is an important precursor to electrical breakdown of the gap. Appropriate surface treatments, such as electropolishing both the anode and cathode, appear to reduce microdischarges and sites of field-emitted electrons. We have adopted these procedures for all parts of the deflector that can be treated. We also carefully cleaned the inner surfaces of the dee that form a copper anode and we used a slow conditioning procedure with the magnet off after the deflector had been re-assembled. These meticulous procedures have permitted us to increase the maximum electric field that can be sustained to greater than 180 kV/cm with a 5 mm gap during pre-run testing, and to operate the deflector reliably at electric fields up to 150 kV/cm during cyclotron operation. We intend to test if fields of about 150 kV/cm can be used reliably with a gap of at least 6 mm.

6. ACKNOWLEDGEMENTS

The authors would like to acknowledge the skillful machining of N. Bray and T. Sprake, and the valuable technical assistance of R.E. Milks, J.F. Mouris, D.R. Proulx and R.R. Tremblay.

7. REFERENCES

1) Diamond, W.T., Mitchel, G.R., Almeida, J. and Schmeing, H., Proceedings of the 1991 Particle Accelerator Conference, San Francisco, Ca., (1991), p. 979.

2) Hoffmann, C.R. and Mouris, J.F., Proceedings of the 1991 Particle Accelerator Conference, San Francisco, Ca., (1991), p. 2397.

3) Diamond, W.T., Hoffmann, C.R., Mitchel, G.R. and Schmeing, H., XIV International Symposium on Discharges and Electrical Insulation in Vacuum, Santa Fe, New Mexico, (1990), p. 630.

4) Hoffmann, C.R. and Mouris, J.F., these proceedings.

5) Broggi, F., De Martinis, C. and Ferrari, A., Twelfth International Conference on Cyclotrons and their Applications, Berlin, (1989), p. 350.

6) Latham, R.V., "High Voltage Vacuum Insulation: The Physical Basis", Academic Press Inc. (London), (1981), p. 39.

POTENTIAL ENHANCEMENT OF MAGNETIC DEFLECTION IN THE CHALK RIVER SUPERCONDUCTING CYCLOTRON EXTRACTION SYSTEM

C.R. Hoffmann and E.H. Lindqvist
AECL Research, Chalk River Laboratories
Chalk River, Ontario, Canada K0J 1J0

ABSTRACT

The electrostatic deflector in the Chalk River superconducting cyclotron is often required to operate at its high-voltage limit. To ease the operating constraints this limit imposes, a study has been undertaken to explore the potential effects of increasing the intrinsic magnetic deflection that is available in iron extraction elements (hill lenses), immediately following the deflector. Modifications to the hill lens geometry and compensation elements have been identified that significantly increase the magnetic steering. Beam orbit calculations show that a 20% reduction in deflector voltage may be possible, in principle, for ion beams of interest when the dipole fields in the hill lenses are changed by about 0.1 T. However, resulting perturbation effects must be well compensated to avoid substantially reducing the benefit.

1. INTRODUCTION

One of the limits to beam extraction from the Chalk River superconducting cyclotron[1] is reliable high-voltage operation of the electrostatic deflector, which often runs at its performance limit. Deflector development work at Chalk River has pursued several options to improve overall performance. Companion papers at this conference report on improvements made to the existing deflector,[2] and on an alternative deflector configuration that has electrodes between the conventional sparking plates and the high-voltage electrode.[3] This paper describes results of a study to reduce the beam deflection required in the electrostatic deflector by enhancing the magnetic deflection available in extraction elements (two hill lenses) immediately downstream from the deflector along the extraction trajectory. In the following sections the layout of the extraction system is briefly described, some guidelines for changes are given, hill lens modifications and corresponding changes to magnetic field compensation are identified, and the calculated performance is presented.

2. EXTRACTION SYSTEM

Figure 1 shows schematically the extraction system in the cyclotron midplane and identifies the major elements, which are fixed. Briefly, the beam entering the deflector (A) in a dee gets an electrical push outwards, to escape the confining magnetic field and enter the magnetic channel (D,E), contained within magnet cryostat (G). The hill lenses (B,C) generate a radial gradient in the axial magnetic field, to provide radial focusing to offset the strong radial defocusing of the fringe field of the magnet. The hill lenses also produce a significant dipole field that steers the beam. The magnetic channel contains superconducting coils and passive iron structures, to provide radial focusing and steering. The iron elements generate perturbation fields in the midplane acceleration region that must be adequately compensated, especially for first harmonic perturbations in the regions where $\nu_r = 1$. Iron bars (F) opposite the hill lenses, and (H) opposite the iron of the channel, provide the compensation. The superconducting coils are designed with compensation windings included. The extracted beam exits the cyclotron through a hole in the iron yoke (I).

Figure 2(a) gives the cross section of the iron elements of lens 1 (B in Fig. 1). The cross section of lens 2 (C in Fig. 1) is identical to that of lens 1, except that each of the bars on the right-hand side has its vertical height reduced from 12 mm to 11.25 mm. Each lens subtends an azimuthal width of 10 degrees at the cyclotron centre, and a space 16 degrees wide separates the two lenses. Stainless steel brackets mounted on the cryostat wall hold the lenses in

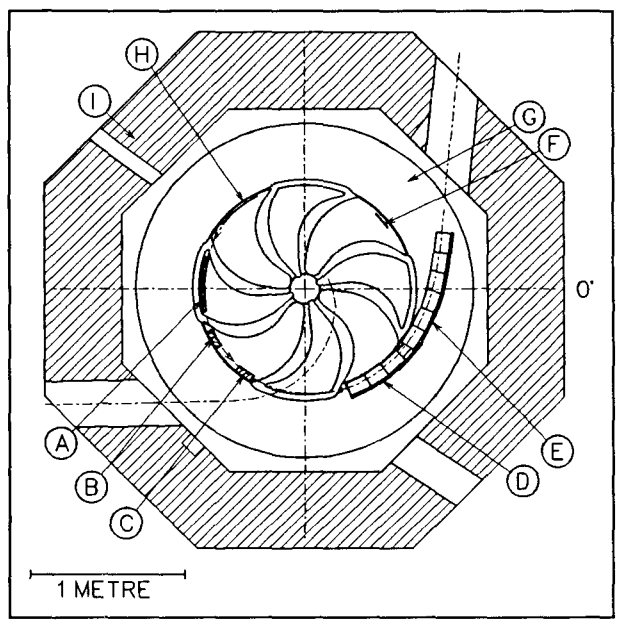


Fig. 1 Extraction system midplane layout.

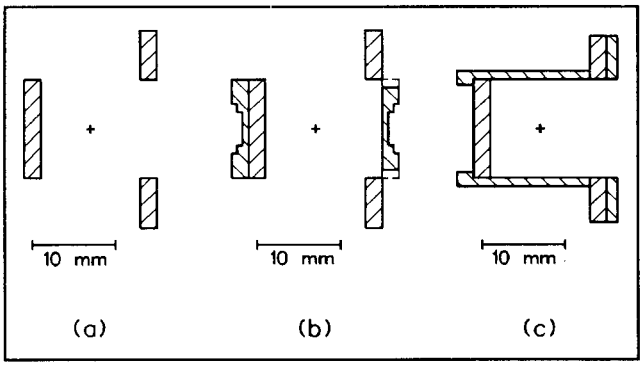


Fig. 2 Cross section of hill lenses: (a) lens 1 without modifications; (b) modified lens 1; (c) modified lens 2.

place in a hill gap.

2.1 Requirements

It is highly desirable for operational reasons that any changes to the extraction elements have as small an impact as possible on the beam circulating in the acceleration region. In particular, the co-ordinates of the beam entering the deflector should not be altered appreciably, especially the radial momentum.

Extraction of beams with the revised system should not require magnetic channel winding currents that are significantly different from those required in the unmodified system. This means that the radial momentum at the channel entrance for a given beam must not be altered appreciably. By providing radially outward deflection, both hill lenses make the radial momentum at the channel entrance more positive; i.e., the beam is directed outwards more. This increased radial momentum would require channel currents outside the operating range for some beams. The remedy is to steer the beam radially inwards in lens 2 after it has experienced strong outward steering in lens 1. In effect, the beam should be "dog-legged" in the revised system by the changed iron in the hill lenses.

3. LENS MODIFICATIONS

3.1 Lens Additions

Initial calculations with the code SUPERGOBLIN,[4] modified to allow superposition of uniform dipole fields on the extraction region field maps for the unmodified hill lenses, showed that field changes of about 0.1 T could lead to an interesting reduction in the deflection required in the electrostatic deflector. However, the field changes would have to act over longer lengths of beam path than the existing lenses. The fields would be reduced in lens 1 and increased in lens 2 by roughly equal magnitudes, and the path lengths over which the fields act would be adjusted to maintain the radial momentum of the beam at the channel entrance so that it is essentially the same as the value without the modifications.

To identify the shape of iron pieces that could be added to the lenses to get the desired field changes at the azimuthal middle section of the lenses, infinitely long, straight iron bars of rectangular cross section, magnetically saturated, were modelled analytically as current sheets.[5] Vertical surfaces of the cross sections were aligned with the background magnetic field, which ranged from about 2 to 5 T. The cross section for required iron was built up by trial and error, to give the desired dipole field in the azimuthal middle section. Once the cross section of the iron additions was defined, calculations were performed using a two-dimensional code, EXMAP, based on the Biot-Savart law, to verify that the dipole fields were acceptable when the curved shape and finite length of the lenses were taken into account. The resulting cross sections for the iron changes are shown in Fig. 2(b) for lens 1, and Fig. 2(c) for lens 2. The azimuthal extent of the iron additions to lens 1 is from 204 degrees to 225 degrees. Lens 2 modifications extend from 225 degrees to 240 degrees. EXMAP was used to calculate maps of the fields generated in the acceleration region and along the extraction path. These maps were combined with the maps for the unmodified pieces, to give a composite set of maps to use in SUPERGOBLIN.

3.2 Compensation of Perturbations

After detailed field maps were calculated for the extraction region, and used in SUPERGOBLIN to verify that the magnetic geometry produced the desired effects along the extraction path, the perturbation fields in the acceleration region were calculated and Fourier analyzed. The perturbation fields requiring correction were the average field change and the first harmonic.

The compensation strategy was to first identify iron pieces that adequately cancel the first harmonic perturbations introduced by the iron additions to the hill lenses. Then, iron additions to deal with the average field perturbations were sought. These pieces were added to the system in diametrically opposite pairs, which avoided the generation of additional first harmonic fields. All iron additions are made in a symmetrical fashion about the midplane, to preserve the midplane symmetry. This process leads to an inevitable increase in second harmonic perturbations. Compensation of second harmonics is not easily dealt with, because suitable locations for appropriate compensators are not available.

The compensator for the first harmonic was an iron bar, rectangular cross section 2.5 mm high by 0.5 mm thick, bent to have the inner surface on an arc of radius 664 mm. It subtends 10 degrees at the machine centre. This piece is

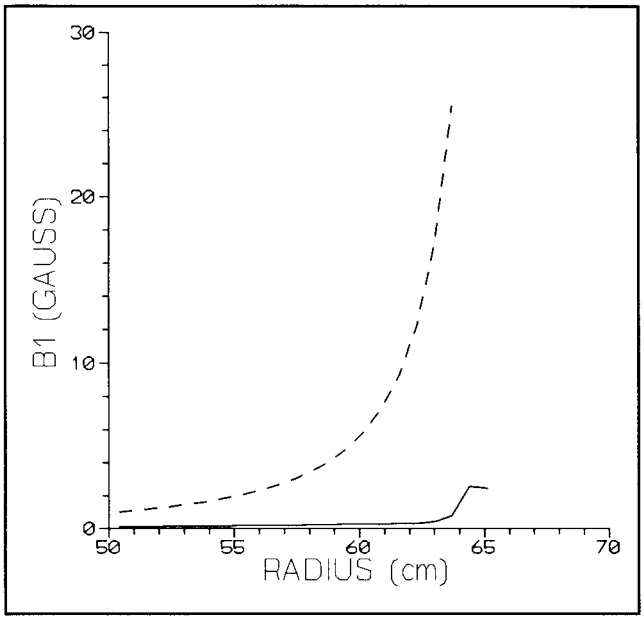


Fig. 3 Plot of first harmonic perturbation fields B1 from the iron additions to the hill lenses; dashed line, uncompensated; solid line, compensated.

a simple addition to the existing compensating bar for the hill lenses. Figure 3 shows the first harmonic perturbations from the modifications to the lenses, before and after the compensation was added. The residual first harmonic at 63 cm radius generated by the iron additions exceeds 18 G, but is reduced to 0.4 G when compensation is added.

Figure 4 gives the midplane layout and the cross section of the compensator for the average field perturbations that the lens modifications generate. One pair of these pieces, arranged symmetrically about the midplane (Z=0), is located radially in front of the modified lenses, and another pair is 180 degrees away, radially in front of the first harmonic compensator. Figure 5 shows the compensation of the changes to the average field. The poorest compensation is at the inner edges of the iron (see Fig. 4).

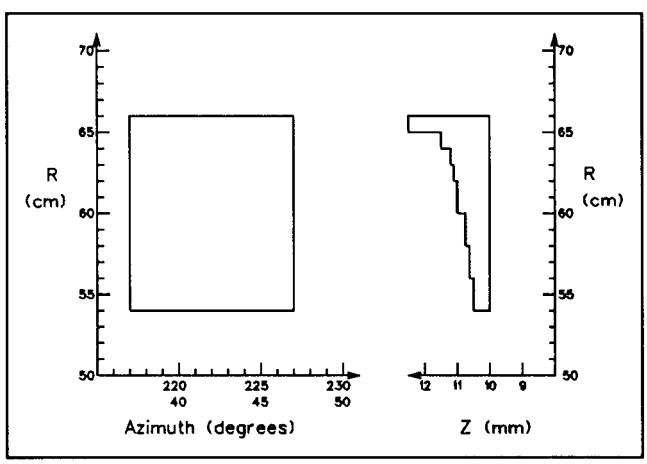


Fig. 4 Schematic of the iron used to compensate average field perturbations caused by the hill lens modifications.

4. RESULTS

Extensive calculations were performed with SUPERGOBLIN using the composite field maps generated for the revised hill lenses. Two kinds of calculations were done. First, a wide selection of beams, with an average field ranging from 2.5 to 5.0 T, was run through the extraction system, starting at the entrance of the deflector. The setup of the cyclotron and the beam initial co-ordinates were those of the originally calculated beams for no modifications to the hill lenses. Second, calculations were done for several different beams, starting at injection of the beam into the cyclotron, followed by foil stripping, and acceleration out to the deflector entrance. The average field ranged from 2.5 to 3.2 T. Again, cyclotron setup and the beam initial co-ordinates were those for the system with the original hill lenses. However, the field maps contained the perturbations from the modifications to the lenses. Dee voltage was adjusted for entry into the deflector on the same turn as in the unperturbed calculation.

Figure 6 illustrates the general trend of the calculated results. The upper curve represents the case with no perturbations in the acceleration region. About a 20% decrease in deflector voltage occurs for beams such as 45 MeV/u carbon, which has an average midplane field of 3.0 T. However, when the beam experiences the perturbations in the acceleration region from the additional iron, it is evident that the benefit may be decreased substantially. This situation arises because the radial

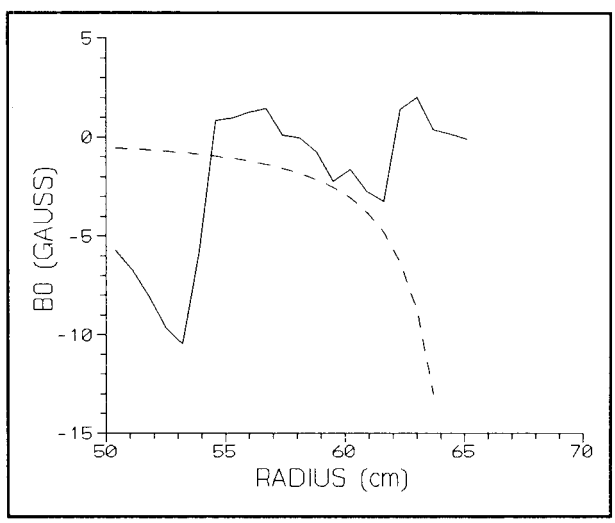


Fig. 5 Plot of the average field perturbations generated by the hill lens modifications; dashed line, uncompensated; solid line, compensated.

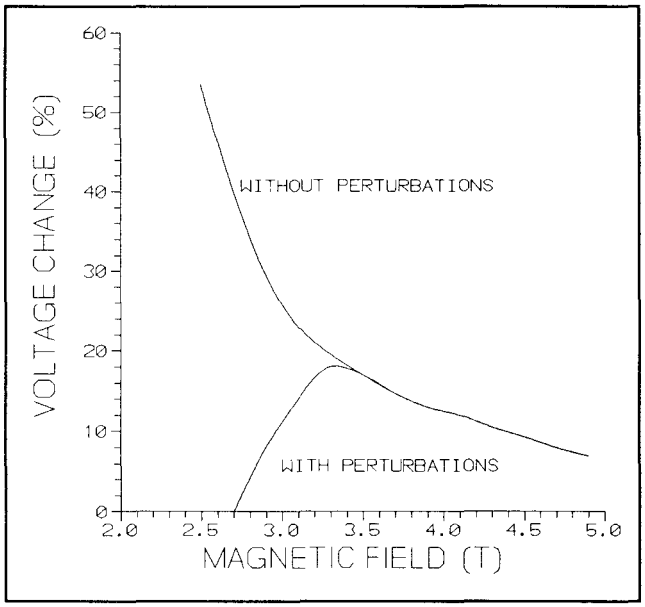


Fig. 6 Plot of the deflector voltage change resulting from enhanced magnetic deflection in the hill lenses.

momentum at the deflector entrance is more negative than in the unperturbed case, and thus results in a smaller decrease in deflector voltage.

Figure 7 displays some examples of the outer 10 turns for carbon (45 MeV/u, 3.0 T) and chlorine (8.5 MeV/u, 2.5 T) beams with and without the additions to the lenses.

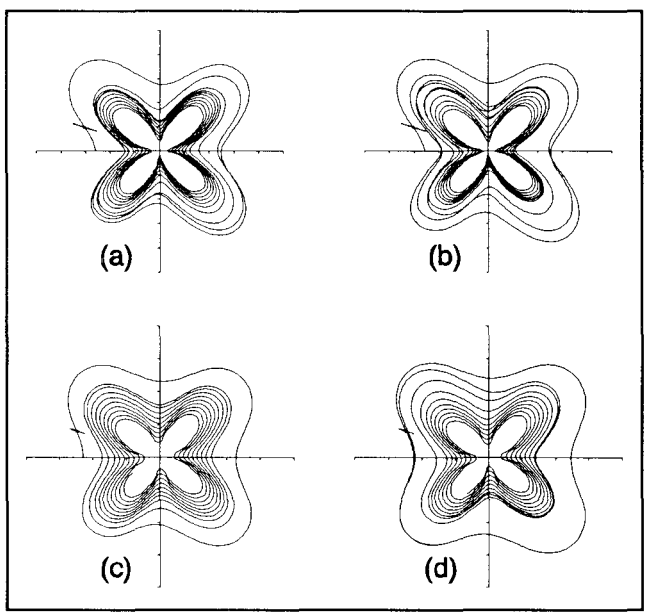


Fig. 7 Orbit plots for C, 45 MeV/u without (a) and with (b) lens modifications; and for Cl, 8.5 MeV/u without (c) and with (d) lens modifications. Scale interval: (a) and (b), 1 cm; (c) and (d), 2 cm.

The origins are at radii of 62 and 60 cm for the carbon and chlorine plots respectively. The short, slanted line in the second quadrants indicates the entrance face of the deflector. (The entrance midpoint is at a radius of 65.2 cm.) The orbit sensitivity to the small changes in the perturbations is evident. Calculations for several beams, with the average field B0, first harmonic B1 or second harmonic B2 perturbations removed from the perturbation field maps, showed that the B0 and B1 perturbations were consistently detrimental. However, B2 perturbations had radial momentum at the deflector entrance increased for some beams.

We have reported the preliminary results from this study for compensating the incremental perturbation fields arising from iron added to the extraction system. Future work on this method of enhancing magnetic deflection will consider improved compensation for all of the extraction system perturbations, and the implications for redetermining the setup parameters for the more than 50 different ion beams that have been extracted to date.

5. ACKNOWLEDGEMENT

It is a pleasure to acknowledge technical assistance from D.R. Proulx.

6. REFERENCES

1) Bigham, C.B., Davies, W.G., Heighway, E.A., Hepburn, J.D., Hoffmann, C.R.J., Hulbert, J.A., Ormrod, J.H. and Schneider, H.R., "First operation of the Chalk River superconducting cyclotron", Nucl. Instr. and Methods, **A254**, p237, (1987).

2) Diamond, W.T., Hoffmann, C.R., Mitchel, G.R. and Schmeing, H., "The electrostatic deflector of the Chalk River superconducting cyclotron", these proceedings.

3) Hoffmann, C.R. and Mouris, J.F., "Potential enhancement of magnetic deflection in the Chalk River superconducting cyclotron extraction system", these proceedings.

4) Heighway, E.A. and Hoffmann, C.R., "SUPERGOBLIN - The Accelerated Orbit Code in Use for the Chalk River Superconducting Cyclotron", IEEE Trans. Nucl. Sci. **NS-32**, p2522, (1985). Also, AECL Report, AECL-8792, (1985).

5) Hoffmann, C.R., "Extraction System for the Chalk River Superconducting Heavy-Ion Cyclotron", IEEE Trans. Nucl. Sci. **NS-24**, p1470, (1977).

MODEL STUDY OF AN ELECTROSTATIC DEFLECTOR CONFIGURATION WITH AN INTERMEDIATE ELECTRODE

C.R. Hoffmann and J.F. Mouris
AECL Research, Chalk River Laboratories
Chalk River, Ontario, Canada K0J 1J0

ABSTRACT

As part of a development program for electrostatic deflectors in the Chalk River superconducting cyclotron, an alternative electrode configuration has been studied, which has a set of electrodes between the high-voltage electrode and sparking plates of the traditional deflector geometry. These intermediate electrodes are driven by an independent power supply at half the deflector voltage and have a series water resistor for isolation. They grade the potential between main electrode and sparking plates and reduce the maximum energy available to main electrode sparks occurring along the magnetic field lines. A model was built and tested in a modest magnetic field of 0.5 T.

1. INTRODUCTION

The first element in the extraction system for the Chalk River superconducting cyclotron[1] is an electrostatic deflector, located in one of four dees. The electrode configuration is the traditional one of a negative, high-voltage electrode and a grounded septum, which bound the extracted beam path in the midplane. A cross section of this configuration is shown schematically in Fig. 1(a). Above and below the high-voltage deflector electrode are sparking plates, to provide refractory surfaces that resist spark damage. Insulators off the midplane support the deflector electrode.[2] One of the insulators contains a column of high-resistivity flowing water that isolates a spark from the energy stored in the high-voltage cable and power supply,[3] and provides a source of cooling to the deflector electrode.[4] The present status and recent developments of this system are reported in a companion paper at this conference.[5] One of the remaining challenges in this system is to develop the deflector system to the point of reliable operation at voltages above 90 kV and apertures greater than 5 mm.

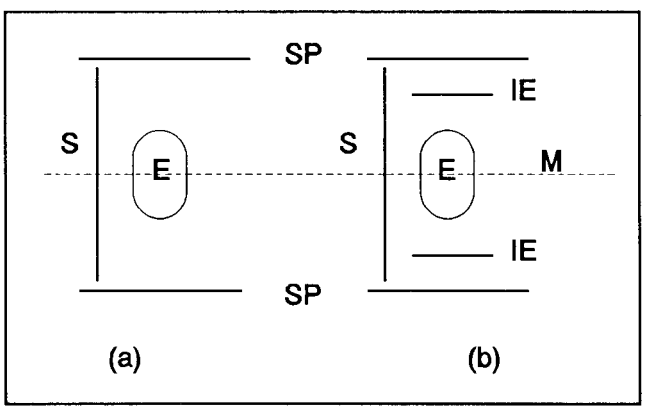


Fig. 1 Schematic of the deflector electrodes, (a) traditional arrangement, and (b) with intermediate electrodes (IE). E - deflector electrode; M - cyclotron midplane; S - septum; SP - sparking plates.

Work at Chalk River has followed several avenues in pursuit of better deflector performance. While development of the existing electrode design progressed, a study was undertaken to assess the potential reduction in deflector voltage requirements that could arise if magnetic elements following the deflector in the extraction path were altered to obtain more magnetic deflection of the beam.[6]

Also, other electrode geometries were investigated in the search for reliable, higher voltage operation. This paper reports work on a model study of an alternative electrode configuration illustrated schematically in Fig. 1(b). This configuration has electrodes placed at an intermediate position between the deflector electrode and the sparking plates of the conventional deflector configuration. This intermediate electrode system is described in the following sections along with the high-voltage system and insulators required; results are given for operation of a model in a 0.5 T magnetic field.

2. INTERMEDIATE ELECTRODE

As shown in Fig.1 the configuration studied here is basically the traditional deflector geometry, with a pair of planar electrodes added in the gaps between sparking plates and deflector electrode. These electrodes (IE) are held at a common potential that is half that of the main deflector electrode (E). The intermediate electrode segments divide the vertical space between deflector electrode and sparking plates in half. Consequently, the intermediate electrodes define the potential at their locations to be 50% of the original gap potential (between electrode E at 100% and a sparking plate SP), rather than about 75% without the electrodes, as predicted by two-dimensional electrostatic calculations. This grading of the gap potential significantly reduces the electric field on the deflector electrode, and presumably any resulting field emission of electrons. The intermediate electrodes are wide enough to have all of the

magnetic shadow of the deflector electrode fall on them. (The magnetic shadow is defined by the magnetic field lines that pass through the deflector electrode.) Because the charged particles of a typical spark are confined by the magnetic field lines, the intermediate electrodes will intercept all sparks originating at the main deflector electrode, and as a result the maximum energy available to particles in the spark is limited to half of what it would be without the intermediate electrodes. This should lead to reduced sparking damage.

2.1. Intermediate Electrode Model Deflector

Figure 2 shows the cross section of the model. Cross-section dimensions are full size, but the model length is 20% of the deflector in the cyclotron. The metal components are stainless steel, and electrical surfaces are polished. The sparking plates (A) cover the pole tips of the magnet and are insulated from their surroundings with thin layers of Kapton. Each sparking plate is connected to ground through a 1 kΩ resistor, to monitor leakage current. The pole tips fit into the top and bottom surfaces of a vacuum chamber that enclose the model. The vertical gap between sparking plates is 76 mm. Insulator posts (B) are alumina (99.5%), coated with Cr_2O_3 for reduction of secondary electron emission.[7] Their length is 10 mm. The septum plate (D) is wide, to support the sparking plates

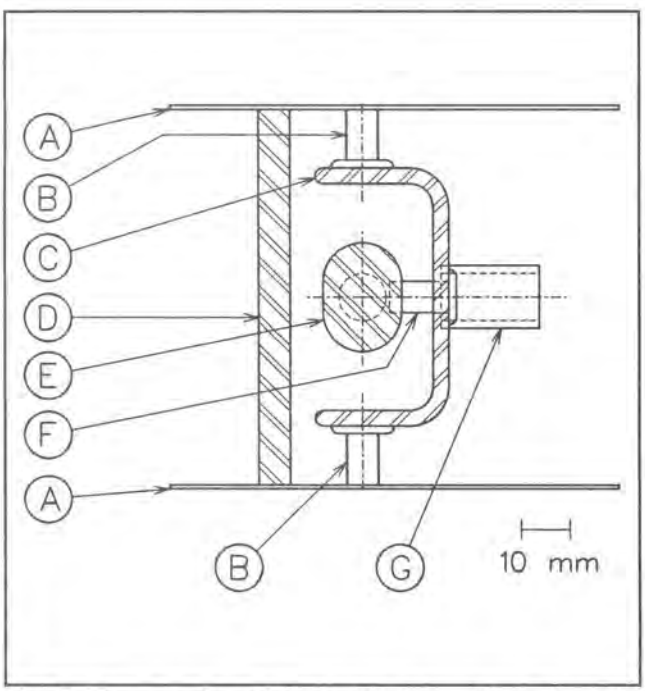


Fig. 2 Cross section of the model intermediate electrode. A - sparking plates; B - insulator; C - intermediate electrode; D - septum; E - deflector electrode; F - insulator; G - metal post.



Fig. 3 Photograph of the intermediate electrode model.

against the magnet pole tips and vacuum chamber walls. The gaps between septum and intermediate electrodes are 5 mm, and the gap between septum and deflector electrode is 6 mm. The high-voltage connection to the intermediate electrode (E) is made on a metal post (G), which slips into a high-voltage termination. A high-voltage connection is made to the deflector electrode (E) at a hole in the end of the electrode. Insulator F is identical with insulator B, but has a length of 6 mm. The edges of the intermediate electrodes facing the septum have a 1.5 mm radius.

Figure 3 is a photograph of the model and the feed insulators that provide high voltage to the electrodes. The electrode assembly fits between the poles of the magnet and the insulators fit into appropriate housings attached to the walls of the vacuum chamber. The chamber walls, sparking plates, and septum form the ground plane.

2.2. High-Voltage System

Figure 4 gives the basic electrical configuration. The

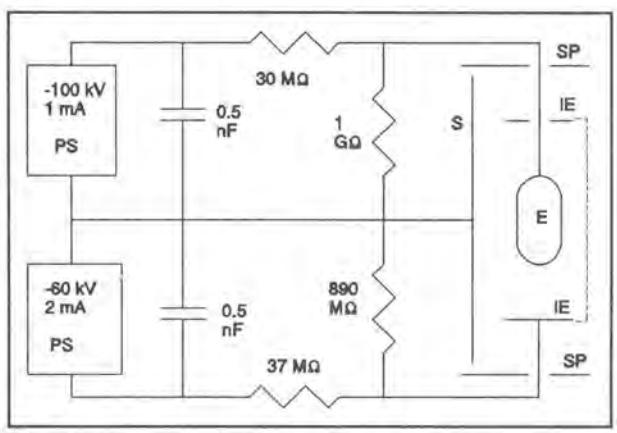


Fig. 4 Schematic of the system to supply high voltage to the model deflector electrode and the intermediate electrodes.

major features are the power supplies, the isolation resistors, and the electrode configuration. The power supplies are standard switching units with small energy storage. They are usually operated from a control module that maintains a two-to-one ratio between their output voltage settings, with the smaller voltage on the intermediate electrode. The resistors shown in Fig. 4 are formed in flowing water in the interior of the custom-designed insulators. The high-voltage feed insulator for the deflector electrode has been described previously.[2,3)]

2.3. Feed Insulator

High voltage to the intermediate electrode is supplied through the bore of an alumina (99.5%) insulator that contains a column of flowing, high-resistivity water. The insulator is 15.9 mm outside diameter and is 36 mm long between the cathode and anode terminations. Figure 5 displays the insulator cross section. It has similar water circuitry to the feed insulator used for the main deflector electrode. A Teflon sleeve (B), vacuum-epoxied to the alumina, separates the water from contact with the alumina and provides a barrier to possible water leaks if the alumina body should crack. One end of the sleeve has an electrode (C) sealed into it with an O-ring (D), and the other end of the sleeve has a flange to seal for vacuum and water. The outer surface of the alumina (F) is coated with a thin layer of Cr_2O_3, to reduce secondary emission of electrons near the cathode end (A) of the insulator.[7)] The high-voltage cable (L) is contained within a thin-walled Teflon tube (K), which in turn is within the insulator bore and the interior of a standard-size length of copper tubing (J) (inside diameter 7.9 mm; wall thickness 3.5 mm). Water flows to and from the insulator bore in the annular regions formed by the insulator/tubing, the Teflon tubing (inside diameter 6.7 mm and wall thickness 0.4 mm) and the high-voltage cable (dielectric diameter 6.0 mm). Tubing and cable of these dimensions is readily available commercially. The isolation resistor (E) formed between the end of the cable and the output voltage termination is 10 mm long. The whole insulator assembly is mounted on a flange (H) and sealed to the vacuum chamber wall (G). Three sets of O-rings (I) provide sealing. The metal post (G) in Fig. 2 fits into the end of terminal (A).

3. PERFORMANCE

Figure 6 gives the current-voltage characteristic for the isolation resistor in the intermediate electrode feed insulator. The water resistor performed reliably at the maximum voltage applied across it of -57 kV.

The intermediate electrode deflector model was installed in a small vacuum chamber inside the poles of a dc magnet. X-rays were monitored outside one of the chamber ports, and leakage currents were monitored for the sparking plates and the deflector electrode feed insulator surface. Also, the septum plate was isolated with Kapton and the current collected on it was measured. Current and voltage from the power supplies were measured with precision digital panel meters. The vacuum pressure was typically 1×10^{-4} Pa, and the resistivity of the water to the insulator isolation resistors was in the range of 12 to 14 MΩ • cm.

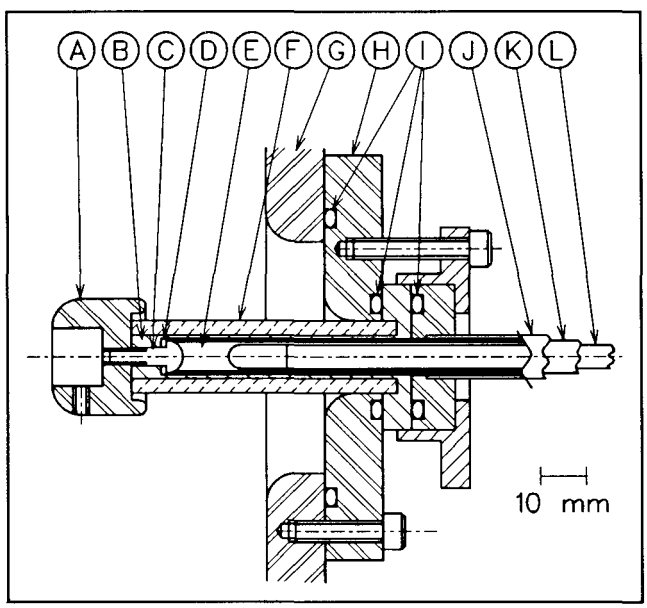


Fig. 5 Schematic of the high-voltage feed insulator for the intermediate electrodes.

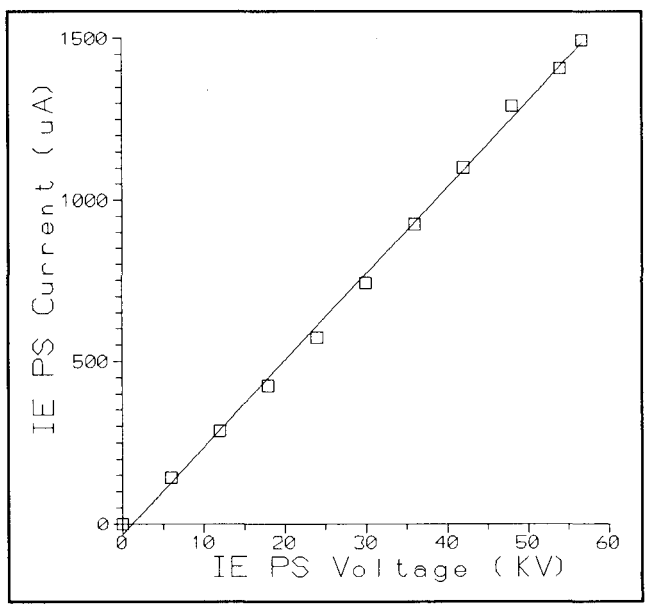


Fig. 6 Feed insulator characteristic for the intermediate electrodes.

Several variations of the configuration shown in Fig. 2 were studied. They include the electrodes with the support insulators (B), the electrodes with insulator (F), and the full configuration displayed in Fig. 2. Holes in the electrodes were filled as required with stainless steel inserts. Conditioning of these configurations to voltages of -100 kV on the main electrode and -50 kV on the intermediate electrode was straightforward, and was performed with the magnet off. With one exception discussed below, leakage currents to septum and sparking plates usually did not exceed a few microamperes during conditioning microdischarges, which were accompanied by X-ray emission. When the magnet was turned on, the septum leakage current was extinguished and X-ray emission ceased. Leakage current to the sparking plates increased, but subsequently decayed away to about 50 nA or less, which is consistent with the surface resistivity of the coatings on the insulator posts. The surface resistance on the insulator posts depends on the thickness of the Cr_2O_3 coating (which was not controlled), but is usually the order of 10^{11} Ω per square.

Attempts were made to measure the intermediate electrode voltage directly with a high-voltage resistive divider (total resistance of 2 GΩ). The presence of the divider invariably led to enhanced sparking that did not condition away. The divider could be connected to either the intermediate or deflector electrode through a port in the vacuum chamber, via a 4.5 metre length of high-voltage cable and appropriate fittings, with no isolation resistor at the electrode end. Sparks occurred inside the vacuum chamber and discharges in air occurred in a bushing near the top of the divider. This divider had been used previously in another system with a similar connection method without such breakdown, but with a connecting cable about 0.5 m long. The energy storage in the full-length divider cable is the order of 1 joule. It appears possible that the availability of this stored energy might influence the sparking behaviour.

The model deflector with an intermediate electrode operated satisfactorily in a 0.5 T magnetic field. Successful operation of the intermediate electrode feed insulator demonstrated a plausible system to provide another high-voltage source in the cyclotron dee with excellent isolation resistance essentially next to the electrodes. Such water isolation resistors of small physical dimensions have been used for about 7 years in the Chalk River superconducting cyclotron, and have been reliable.

The next step in this development is to test an intermediate electrode assembly in the cyclotron. The preferred configuration is the one with only the post insulators (F) in Fig. 2. It is believed that a rigid electrode assembly can be designed that can be supported in the same fashion as the existing deflector electrode in the cyclotron. The feed insulator would occupy the space of the existing support insulator. However, a second high-voltage input system to the deflector dee is required in a region where space constrains are severe.

4. ACKNOWLEDGEMENTS

It is a pleasure to acknowledge technical assistance from J.E. Anderchek, D.G. Hewitt and D.R. Proulx.

5. REFERENCES

1) Bigham, C.B., Davies, W.G., Heighway, A.E., Hepburn, J.D., Hoffmann, C.R.J., Hulbert, J.A., Ormrod, J.H. and Schneider, H.R., "First operation of the Chalk River superconducting cyclotron", Nucl. Instr. and Methods, **A254**, p237, (1987).

2) Hoffmann, C.R. and Mouris, J.F., "Development and performance of electrostatic deflector insulators for the Chalk River superconducting cyclotron", Proceedings of the 1991 IEEE Particle Accelerator Conference, IEEE catalog no.91CH3038-7, p2337, (1991). Also, AECL Report, AECL-10414, (1991).

3) Hoffmann, C.R. and Bigham, C.B., "Electrostatic deflector high-voltage system for the Chalk River superconducting cyclotron", Proceedings of the 1987 IEEE Particle Accelerator Conference, IEEE catalog no. 87CH2387-9, **3**, p1567, (1987). Also, AECL Report, AECL-9374, (1987).

4) Diamond, W.T., Mitchel, G.R., Almeida, J. and Schmeing, H., "Electrostatic deflector development at the Chalk River superconducting cyclotron", Proceedings of the 1991 IEEE Particle Accelerator Conference, IEEE catalog no.91CH3038-7, p979, (1991).

5) Diamond, W.T., Hoffmann, C.R.J., Mitchel G.R. and Schmeing, H., "The electrostatic deflector of the Chalk River superconducting cyclotron", these proceedings.

6) Hoffmann, C.R. and Lindqvist, E.H., "Potential enhancement of magnetic deflection in the Chalk River superconducting cyclotron extraction system", these proceedings.

7) Sudarshan, T.S. and Cross, J.D., "The effect of chromium oxide coatings on surface flashover of alumina spacers in vacuum", IEEE Trans. Electrical Insulation, **EI-11**, p32, (1976).

PERFORMANCE OF BEAM CHOPPING SYSTEM FOR JAERI AVF CYCLOTRON

W. Yokota, M. Fukuda, K. Arakawa, Y. Nakamura, T. Nara, T. Agematsu, S. Okumura, I. Ishibori
Japan Atomic Energy Research Institute,
1233, Watanuki, Takasaki, Gunma, 370-12, Japan

and

T. Tachikawa, Y. Hayashi, Y. Kumata
Sumitomo Heavy Industries, Ltd.,
5-2, Sobiraki, Niihama, Ehime, 792, Japan

ABSTRACT

A beam chopping system was installed for the JAERI AVF cyclotron with external ion sources to supply pulse beams with a wide variety of pulse interval, acceleration energy and ion species. A combination of a pulse voltage chopper in the injection line and a sinusoidal voltage chopper after the exit of the cyclotron was adopted to extract a single beam pulse from the cyclotron beam. Beam deviation by the choppers and time spectrum of chopped beam were measured. This paper presents observed separate and total performance of a couple of choppers in comparison with the designed performance.

1. INTRODUCTION

The JAERI AVF cyclotron provides various ion beam characteristics in order to meet a number of requirements for beam utilization in the research program.[1] Pulsed beam irradiation is one of the important characteristics and is planned mainly for the in-situ analysis of elementary process in irradiated materials and for basic research on radiation chemical reaction process.

The chopping system was designed and made to reduce repetition of naturally bunched beam from the cyclotron (11 MHz - 22 MHz) down to 1 kHz - 1 MHz. A pulse voltage chopper (P-chopper) was installed in the injection line to chop DC beams from the ion sources[2] into pulse beams with intervals of 1 μs - 1 ms and with duration several times as long as the RF period of the cyclotron. A sinusoidal voltage chopper (S-chopper) was installed after the exit of the cyclotron to extract a single beam pulse from a train of plural beam pulses. Both choppers are of the parallel-plate electrode type. The design of the chopping system was reported in last the conference.[3]

Table 1. Design parameters of the chopping system

	P-chopper	S-chopper
elecrode length (cm)	13	120
electrode gap (cm)	8	4
drift length (cm)	60	80
slit gap (cm)	2.4	0.4
maximum voltage (kV)	1.5	40
frequency (MHz)	0.001 - 1.0	1-3
reduction rate 1/m	–	1/4,1/5,1/6

$*$ maximum H^+ energy
for a single pulse extraction : 75 MeV!

Test operation has been carried out since October 1991 to evaluate chopping system performance using H^+ and He^{2+} beam. The time spectrum of chopped beam was measured by two different methods; one is oscilloscopic observation by a Faraday cup, the other is detection of prompt γ-ray induced by nuclear reaction in target materials. Multi-turn extraction was estimated by comparing the duration of beam pulse chopped by the P-chopper with that of a beam pulse train from the cyclotron. Finally we extracted a single beam pulse of 50 MeV He^{2+} beam using a couple of choppers.

2. BRIEF REVIEW OF CHOPPING PROCESS

A geometrical arrangement of the chopping system and the beam chopping process is illustrated in Fig. 1. The DC beams from ion sources are chopped by the P-chopper into beam pulses with 1 μs to 1 ms intervals and total time width T several times as long as the RF period of the cyclotron τ_c. The period of zero volt of P-chopper voltage τ_p is chosen so that the duration at the maximum beam current equals the effective bunching phase time t_b (assumed at 150 degrees of τ_c): τ_p-t_l=t_b, where t_l is the ion transit time through the P-chopper electrodes). The resultant beam pulse is modulated by the buncher into plural bunches, followed by injection into the cyclotron. The bunches are separated into a pulse train by natural bunching during the acceleration. Each pulse is further divided into plural pulses (n pulses) by multi-turn extraction at the deflector. Time length of the extracted beam train is longer than beam pulse

width after the P-chopper due to additional pulses from the multi-turn extraction.

The period of the sinusoidal voltage wave is $2m\tau_c$ (1/m: reduction rate), and the length of a beam pulse train must be shorter than the period to extract a single beam pulse from the train. This is realized when T is shorter than $T_{max}=2m\tau_c-(n-1)\tau_c-t_b$, as shown in Fig. 1. The design parameters of the chopping system are listed in Table 1.

3. MEASUREMENT OF BEAM DEVIATION AND TIME SPECTRUM

We measured the beam deviation at the baffle slit, the wave form of chopper voltage, that of a beam pulse after the baffle slit and time spectrum of resultant beam pulses from the cyclotron. The beam deviation was measured by a three-wired beam profile monitor 7 cm upstream from the baffle slit. The wave form of the chopper voltage was observed by an oscilloscope through a capacitive pickup. Chopped beams were detected by a Faraday cup after the baffle slit and the wave form of the beam pulses was observed by an oscilloscope. Though the level of random and non-random noises was high in this measurement, averaging and subtracting functions of background reduced it significantly and signals were observed very clearly.

The pulse beam from the cyclotron bombarded an alumina target. The γ-rays emitted from the target were detected by a plastic scintillation counter and the spectra of time difference between the γ-ray signal and the P-chopper trigger signal were observed without any influence of noise. The time length of the beam pulse train was obtained from the spectra. During the measurement of the P-chopper performance, beams were well focused at the baffle slit with a beam diameter smaller than the designed slit gap (24 mm).

We ensured that beam deviation by the S-chopper was large enough at the baffle slit gap, by observing one of every m beam pulses appeared in the γ-ray time spectra, since we have no beam monitor for the S-chopper.

4. PERFORMANCE OF P-CHOPPER

4.1. Beam Deviation and Wave Form of Beam Pulse

Deviation of 12.5 keV H^+ beam at the baffle slit was measured over the range of the P-chopper voltage V_{pmax} from 500 V to 800 V. The measured deviation is larger than the designed one by about 30% for all the preset value of V_{pmax}. This suggests the difference of the preset and the actual V_{pmax}.

The chopper voltage falls linearly with time from V_{pmax} to zero in 150 ns independently of V_{pmax} and τ_p, and the fall time is shorter than that in the design (200 ns). On the other hand, the voltage rises slowly like a logarithmic function and it takes 350 ns from 10% to

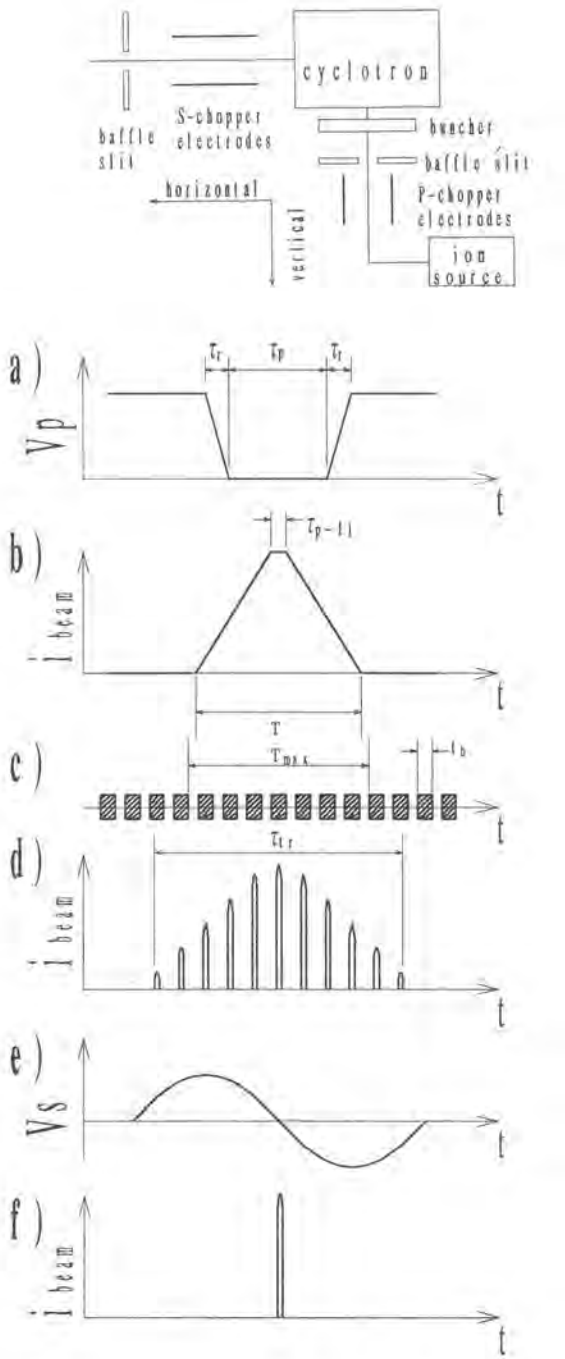


Fig. 1 Geometrical arrangement of the chopping system and diagram of beam chopping process.
t_l:ion transit time through P-chopper electrodes.
τ_r:rise and fall time of P-chopper voltage.
t_b:effective buncher phase.
a) P-chopper voltage.
b) Beam pulse after passing through P-chopper.
c) Acceleration phase.
d) A train of plural beam pulses from cyclotron.
e) S-chopper voltage.
f) Beam pulse after S-chopper.

90% for V_{pmax}. The sum of the fall and the rise times is 100 ns longer than that designed (400 ns).

Signal-to-noise ratio is good in the wave form measurement on pulsed beam by the P-chopper, however, there is a reflection 1 μs after the signal, and this makes it difficult to extract total pulse width from the wave form. Therefore, we adopted full width at twentieth maximum $\tau_{1/20}$ as total width. The observed full width at half maximum and $\tau_{1/20}$ are plotted in Fig. 2 in comparison with those designed. The figure also shows the result of calculation on the wave form of beam pulse using the observed chopper voltages. For full width at half maximum, the observed and calculated widths are roughly close to those in the design. While the full widths from the calculation τ_{cl} are close to those in the design, the values of $\tau_{1/20}$ are different. In the observed wave form, the steep fall of the beam pulse suddenly becomes moderate below half maximum, and it does not agree with the result of the calculation. This may be a reason of the difference between $\tau_{1/20}$ and τ_{cl}. As a result, the total width T is not defined clearly from the obtained data, and is uncertain between $\tau_{1/20}$ and τ_{cl}.

4.2. Estimation of Multi-turn Extraction

The time spectra of the pulse train were measured for 50 MeV He^{2+} with the P-chopper voltage on and the S-chopper voltage off. The structure of the spectrum changed drastically by tuning the base magnetic field of the cyclotron. This indicates the importance of cyclotron tuning to minimize multi-turn extraction. Clear correlation was not observed between the time spectrum and beam extraction efficiency at the deflector.

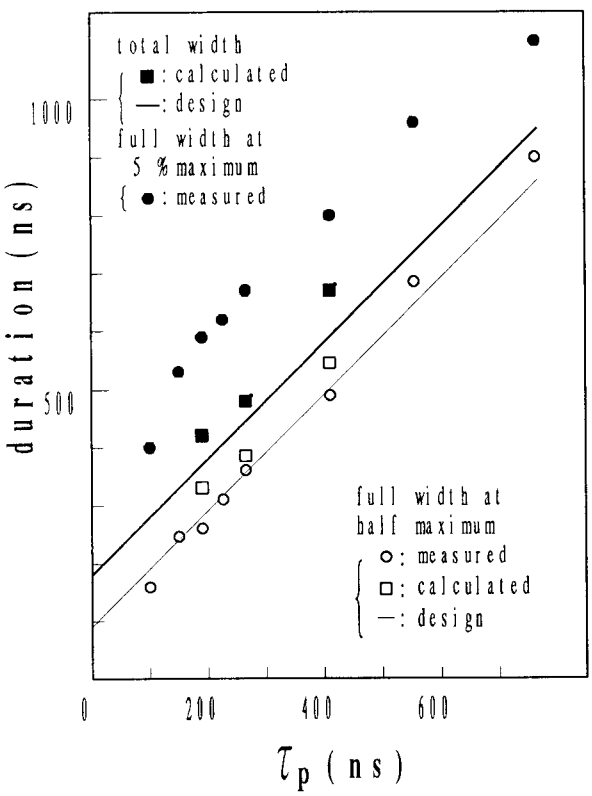


Fig. 2 Duration of 17 keV He^{2+} beam pulse after the P-chopper.

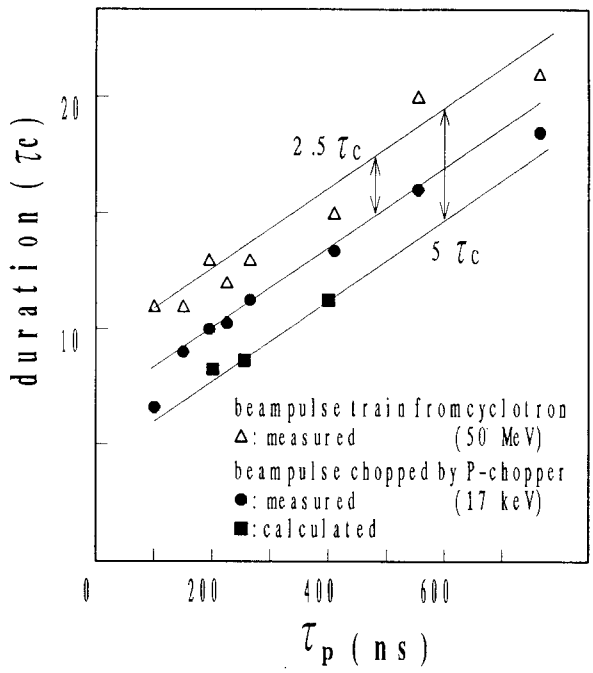


Fig. 3 Estimation of multi-turn extraction from difference between He^{2+} beam pulse width after the P-chopper and pulse train duration from the cyclotron.

The number of multi-turn extraction n is deduced from the difference between the total pulsed beam width after the P-chopper and the duration of a pulse train from the cyclotron τ_{tr}. The observed τ_{tr}, under well tuned cyclotron condition, is compared with $\tau_{1/20}$ and τ_{cl} as function of τ_p in Fig. 3. They increase linearly with the τ_p and the differences are almost constant over a wide range of τ_p. This suggests that we can clearly define the number of multi-turn extraction n from the data. The difference of τ_{tr} from $\tau_{1/20}$ and from τ_{cl} are about $2.5\tau_c$ and $5\tau_c$, respectively, and n is estimated to be 4 to 6. As a result, it turned out that the assumption of n=5 in the design was reasonable.

5. TOTAL PERFORMANCE

5.1. Performance of S-chopper

At the baffle slit for the S-chopper, it is important that the accelerated beam is well focused and its diameter is smaller than the slit gap. The slit gap of the S-chopper baffle was set at 4 mm according to the design. The minimum beam diameter was slightly larger

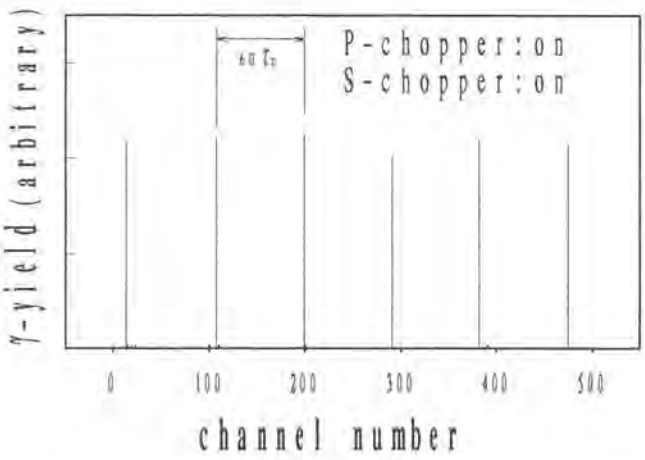


Fig. 4 Beam pulses with a long interval of 3.5 μs obtained by using the P- and the S-chopper.

than the slit gap because about 10% of the total beam current hit the slit edge. We measured the minimum chopper voltage which allowed complete 1/m reduction of beam pulses for m=4,5,6 without the P-chopper voltage. It turned out from the result that the observed voltages satisfied the designed performance.

5.2. Total Performance

The result of beam deviation for each chopper showed the performance as designed or better. The only problem is that the beam pulse width after the P-chopper is uncertain between $\tau_{1/20}$ and τ_{cl} in our measurement. If $\tau_{1/20}$ is the actual total width (T=$\tau_{1/20}$), T is longer than T_{max} and a single pulse cannot be extracted from a beam pulse train using designed reduction rate of the S-chopper. However, T can be reduced if we remove the condition $\tau_p=t_l+t_b$ for maximizing the intensity of the single beam pulse and/or we use higher V_{pmax}. Moreover, the observed τ_{tr} is close to that in the design. Therefore, it is considered that observed performance satisfies the most critical requirement for the total chopping system: $T<T_{max}$.

The single pulse extraction was made for 50 MeV He^{2+} using a couple of choppers, with the P-chopper voltage interval of $60\tau_c$ (3.5 μs) and 1/6 reduction rate of the S-chopper. In Fig. 4, beam pulses with $60\tau_c$ interval are shown under high signal-to-noise ratio and the γ-yields of neighboring peaks are less than a hundredth of those for the extracted beam pulse.

As a result, if the actual T is longer than that in the design within the uncertainty, it is not a serious problem, and the single pulse extraction from a pulse train is considered possible over a wide energy range and a variety of ion species in the design.

6. CONCLUSION

The chopping system was designed and made to reduce repetition of naturally bunched beam from the cyclotron down to 1 kHz - 1 MHz, which consists of a pulse voltage chopper installed in the injection line and a sinusoidal voltage chopper after the exit of the cyclotron. The choppers were tested separately and as the overall performance.

The observed beam deviation is close to that in the design for both choppers. The observed duration of the beam chopped by the P-chopper is also in good areement with that in the design in full width at half maximum. On the other hand, for the total width, there is uncertainty of two and a half times the period of the cyclotron RF. Even if the width is longer than that in the design within the uncertainty, it is not serious for overall performance of the chopping system, because shorter width can be obtained by using higher voltage and/or shorter zero-voltage duration of the P-chopper, and also the observed duration of a pulse train after the cyclotron is close to that in the design.

The number of multi-turn extraction strongly depended on tuning of the cyclotron. We could minimize it by tuning base magnetic field, and the number of multi-turn extraction was estimated at 4 to 6 under well tuned cyclotron conditions, from comparing beam pulse duration after the P-chopper with the duration of a beam pulse train after the cyclotron. We assumed it at 5 in the design and this turned out to be reasonable.

Realization of pulsed beams of 50 MeV He^{2+} with 3.5 μs interval was observed under high signal-to-noise ratio. The single pulse extraction is considered possible over a wide range of energy and a wide variety of ion species in the design.

7. REFERENCES

1) Arakawa, K., Nakamura, Y., Yokota, Y., Fukuda, M., Nara, T., Agematsu, T., Okumura, S., Ishibori, I., Karasawa, T., Tanaka, R., Shimizu, A., Tachikawa, T., Hayashi, Y., Ishii, K., Satoh, T., "Construction and first year's operation of the JAERI AVF cyclotron", presented at this Conference.
2) Yokota, W., Nara, T., Arakawa, K., Nakamura, Y., Fukuda, M., Agematsu, T., Okumura, S., Ishibori, I., Karasawa, T., Tachikawa, T., Hayashi, Y., Ishii, K., "Operation of ion sources and beam transport to JAERI AVF cyclotron", presented at this Conference.
3) Yokota, W., Arakawa, K., Nakamura, Y., Kamiya, T.,Fukuda, M., Tanaka, R., Tachikawa, T., Mita, T., Satoh, T., "Design of beam chopping system for JAERI AVF cyclotron", in Proceesings of the Twelfth International Conference on Cyclotrons and their Applications (World Scientific, Singapore, 1991) pp.388-391.

THE AGOR SUPERCONDUCTING EXTRACTION CHANNEL EMC2

K. Pieterman, J.A.M. Dam, H.J.H. ten Kate* and S. Gustafsson+

Cryocon B.V., P.O. Box 685, 3800AR Amersfoort, The Netherlands
* T.U. Twente, P.O. Box 217, 7500AE Enschede, The Netherlands
+ IPN, P.O. Box 1, 91406 Orsay Cedex, France

ABSTRACT

Only recently, one of the two elements of EMC2 was completed and was tested with liquid Helium to measure its performance in a varying transversal magnetic background field of maximum 3T. It was found that all superconducting coils are capable of handling at least 150A at 3T, although the main coil set shows training above 100A at 3T. Compared with the 150A at 5T for the single superconducting wire, this result is quite good.
Further it was found that with a local heat input of 15W continuously, the quench current is still 100A at 3T. Since the coils are operated at a maximum of 80A at 4T, the thermal stability of the Aluminum mandrel and its cooling seems to be good enough to keep the coils superconducting under all operational conditions of the cyclotron.
Up to this date the production of both elements of EMC2 is almost completed.

1. INTRODUCTION

In 1989 the lay-out of a superconducting electromagnetic extraction channel for the AGOR cyclotron was presented[1,2]. EMC2, being one of the two electromagnetic channels of the cyclotron, is devided into two almost identical elements named EMC2-1 and EMC2-2. Both elements contain a main dipole coil set, a gradient coil set and a correction coil set. All corresponding coil sets are electrically connected in series and are powered by a separate power supply.
The position of the two elements in the median plane of the cyclotron is adjustable for good alignment with the beam that is to be accelerated. The total (almost radial) adjustment possibility is in the order of +-9mm.
By now EMC2 is almost completely manufactured* and a preliminary version of EMC2-2 has been build for testing. The test results are presented in this paper.

2. MAGNETIC STRUCTURE

The mandrel of both EMC2 elements are machined out of a single piece of Aluminum. The superconducting coils are wound and impregnated on separate mandrels and later pressed into the Aluminum structure. The coils are cooled by conduction only. For that purpose two liquid Helium channels are made, one located below the coils one located above the coils. Small holes drilled through the structure connect both Helium channels and form a feedthrough for the conductors of the lower coil set. Liquid Helium enters the element in the lower channel and leaves the element through the upper channel. All electrical connections are placed in the upper liquid Helium channel and glued there in place.
The completed EMC2 elements are then closed by means of electron beam welding. Figure 1 shows a section of the EMC2-2 structure.

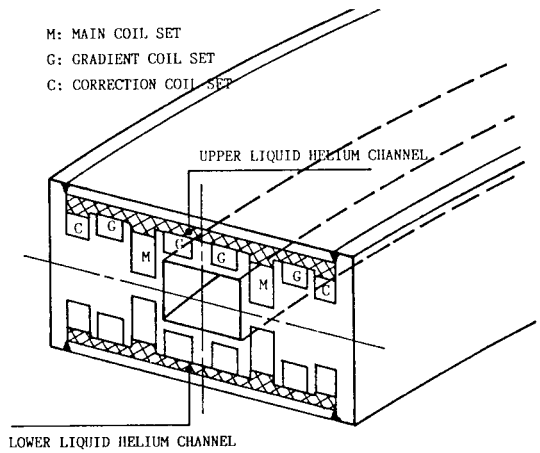


Figure 1: The geometry of the EMC2 coil system

3. MECHANICAL STABILITY

Extensive mechanical calculations using the three dimensional CAE program PATRAN showed that under normal operating conditions the Von Mises stress level is not more than 16N/mm^2 where as the maximum deflection is less than 0.2mm (operational point B of the cyclotron, B=4.05T). Since the forces acting on EMC2 differ both in direction and magnitude (especially

* The superconducting coils and elements are build by the University of Twente, The Netherlands, The cryostat and moving mechanism is build by Leybold Woerden, The Netherlands.

under fault conditions) the mechanical stability of the structure is a point of great concern in the design. Figure 2 shows the maximum forces on the elements of EMC2 and the corresponding deformation of the structure.

POINT	FORCE (N) EMC2-1	FORCE (N) EMC2-2	THETA deg EMC2-1	THETA deg EMC2-2	STRESS (N/mm^2)	DEFLECTION (mm)
B	676	890	110	142	16.0	0.20
B corr. coils only	3092	2835	118	143	53.9	0.62
E	274	38	-93	-84	13.7	0.14
E corr. coils only	2800	1949	-63	-37	43.4	0.50

Note: The 330^0 degree line of the cyclotron is roughly the line through the center of the cyclotron and the center of EMC2-2

Figure 2: Maximum forces with corresponding stress level and deflections of EMC2

The positioning of EMC2 relative to the beam makes a guide/slide mechanism to connect EMC2 to the world necessary. Three motor driven guide/slide constructions make a +-9mm positioning parallel to the 330^0 line of the cyclotron possible (see figure 2). The position of EMC2-1 relative to EMC2-2 is achieved by linking both elements using a hinge construction. Figure 3 gives the construction of these guide/slide mechanisms.

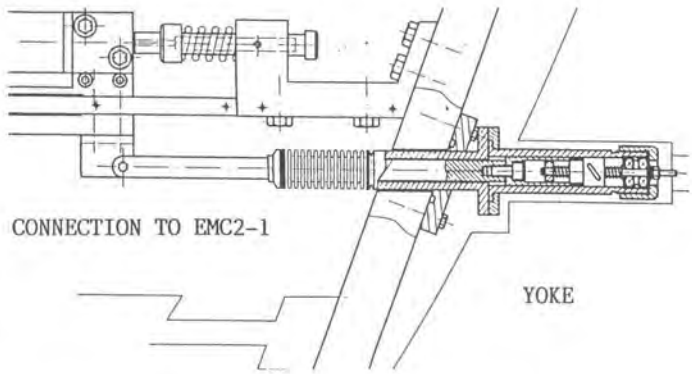


Figure 3: The mechanical construction of a guide/slide mechanism

Figure 4 shows the hinge construction connected to the 80K radiation shield. Via a glass-epoxy thermal bridge EMC2-1 and EMC2-2 are firmly connected to one side of the 80K radiation shield. The guide-slide mechanism is connected to the other side of the 80K shield.
FEM thermal calculations showed that without additional cooling the equilibrium temperature of the 80K shield would be 175K. Therefore, the 80K shield is connected to the 13bar, 80K cooling circuit of the system main Helium liquefier thus keeping the outer radiation shield of EMC2 at a temperature of approximately 70K.

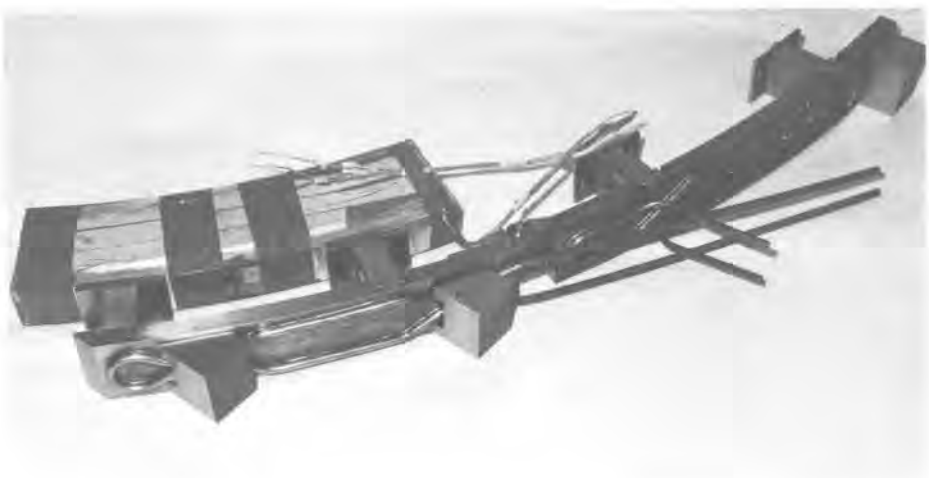


Figure 4: EMC2-1 connected to the 80K shield. The hinge construction between EMC2-1 and EMC2-2 is visible

4. QUENCH BEHAVIOUR AND THERMAL PERFORMANCE

To gain production experience and for doing quench test measurements, EMC2-2 is build on a full scale. The results of the quench tests for the different coil sets are given in figure 5.

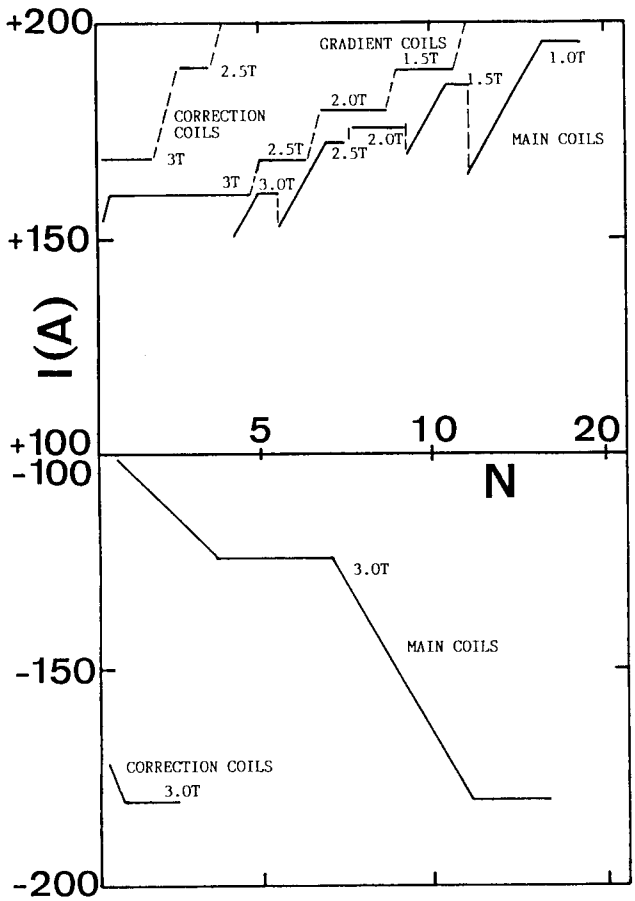


Figure 5: Results of the quench test done on EMC2-2

From figure 5 it is clear that all coils are able (after training) to carry at least 150A at 3T transversal magnetic background field. The main coil set is the least stable since the cross-section of this coil is not constant. However also for this coil training only occurs above 100A at 3T. Since for the superconducting wire 150A at 5T is given by the manufacturer, and keeping in mind that the maximum coil current is 80A at 4T, the results are fully acceptable.

From the viewpoint of thermal heat loads on the elements, there are in the first place radiative and conductive heat loads. Conductive heat loads are reduced by introducing glass-epoxy elements between 4.2K and 300K, radiative heat losses are reduced by introducing an outer 80K radiation shield all around the EMC2 elements and an inner radiation shield in the beam bore of the elements. This inner shield not only reduces the radiative heat load from 300K, but also reduces the radiative heat load of the beam by a factor of 10. Since the beam has an energy between 100W/mm^2 and 200W/mm^2, and a certain percentage of this energy is lost in EMC2, this inner shielding is a must.

Figure 6 gives the results of the quench test performed while heating the bore of EMC2-2 using small heaters (dimensions 20mmx20mm, the background field is 3T).

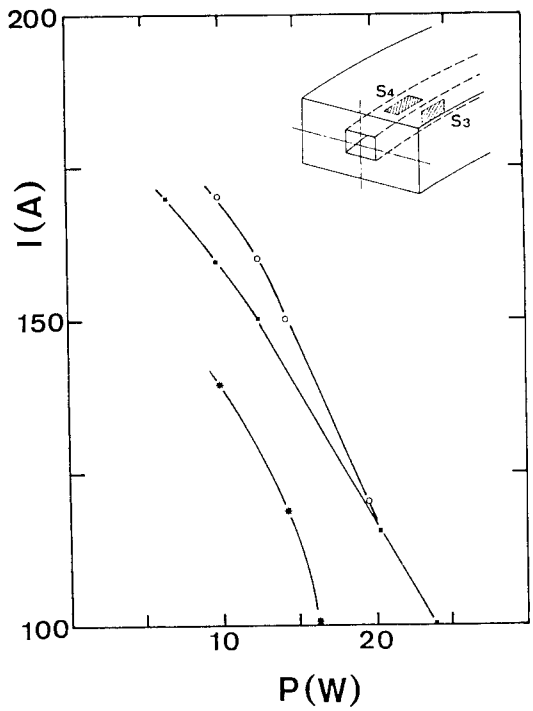


Figure 6: Quench current of EMC2-2 in relation to a simulated beam load on the bore of the element

The thermal stability of the Aluminum structure assures a quench current in the order of 100A at 15W heater power in 3T background field. This thermal stability seems enough to garantee the operation of EMC2 under all normal operating conditions of the cyclotron.

5. PRESENT STATUS

The construction of both EMC2-1 and EMC2-2 as well as the outer cryogenic system is almost completed. Planning is that the assembly of the

total structure is done in August 1992, followed by a total system test at the IPN in Orsay in september 1992.

REFERENCES

1) S. Gustafsson, "A superconducting electromagnetic channel for AGOR", Proc. 12th Int. Conf. on Cyclotrons and their applications, Berlin 1989, pp354-357.
2) K. Pieterman et al., "A design study for a superconducting extraction element for AGOR", Proc. 12th Int. Conf. on Cyclotrons and their applications, Berlin 1989, pp358-360.

MATERIAL CONSIDERATION FOR MAGNETIC CHANNELS

J. Sura, L. Calabretta, G. Di Biasi, P. Gmaj, D. Rifuggiato
I.N.F.N., Laboratorio Nazionale del Sud
V.le A. Doria ang. S.Sofia, 95123 Catania, Italy

1. INTRODUCTION

In the attempt to optimize the extraction system of the LNS CS cyclotron we were looking for a two-bar passive magnetic channel which could fit the CS requirements for the beam extraction system.

Three sets of two-bar channels were tried: two sets - same geometry but different materials, one - different geometry. The results of theoretical estimates and measurements are discussed.

2. THEORETICAL ESTIMATES

For the theoretical estimates we used the simple model given in the paper by B.Carbonel et. al..[1] We adopted their formulae with notations shown in Fig. 1.

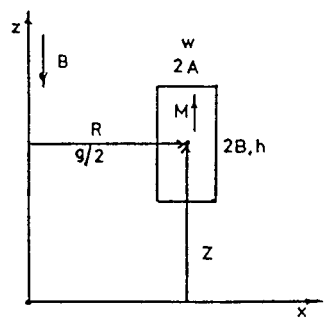


Fig. 1. Schematic explaining the used notations for a single bar. Capital letters - used in formulae, lower case letters - in the text.

For a single bar we have the axial field component $B = B_z(x, 0)$

$$B = M[\arctan\frac{x_1}{c_1} - \arctan\frac{x_2}{c_1} - \arctan\frac{x_1}{c_2} + \arctan\frac{x_2}{c_2}] \quad (1)$$

and for the gradient $G = \frac{\partial B}{\partial x}$

$$G = M\{\frac{1}{c_1[1+(\frac{x_1}{c_1})^2]} - \frac{1}{c_1[1+(\frac{x_2}{c_1})^2]} - \frac{1}{c_2[1+(\frac{x_1}{c_2})^2]} + \frac{1}{c_2[1+(\frac{x_2}{c_2})^2]}\}$$

where

$$\begin{aligned} x_1 &= x - R - A \\ x_2 &= x - R + A \\ c_1 &= Z + B \\ c_2 &= Z - B \end{aligned}$$

For the magnetization M at full saturation we adopted the experimental value M=0.2770 Tesla from MSU data.

The two-bar field in this model is a simple superposition of the single bar fields .

The obtained estimates are discussed below in comparison with measured results.

3. EXPERIMENTAL SETUP

We are looking for a field distribution in a narrow aperture g=8mm. The bulk size of the probe is of the same order of magnitude. The only possibility to get nearly point readings was to cut a groove in the bars which let the probe pass through the bar set. A precise

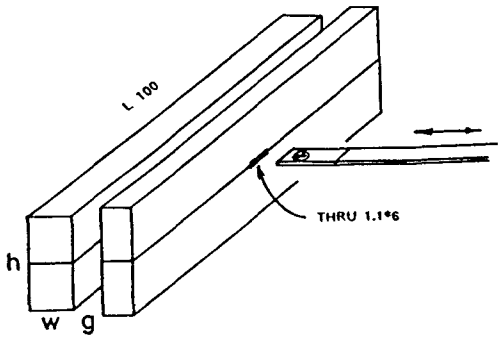


Fig. 2. A two- bar channel. The groove is to let pass thru the Hall probe.

machining of this groove meeting the probe sizes is rather difficult. That is why we decided to design each bar in two pieces. Figure 2 shows the schematic design. The bars are being held in a frame made up of brass. The cross-section of the frame at the groove position is shown in Fig. 3. A set of alignment plates and fixing screws is holding the bars in the test position. The whole setup is put in a test magnet equipped with a precise probe moving mechanism (precision within 0.1 mm).

4. RESULTS

First we measured the magnetic field of bars made up of soft iron with dimensions shown in the upper part of Fig. 4.

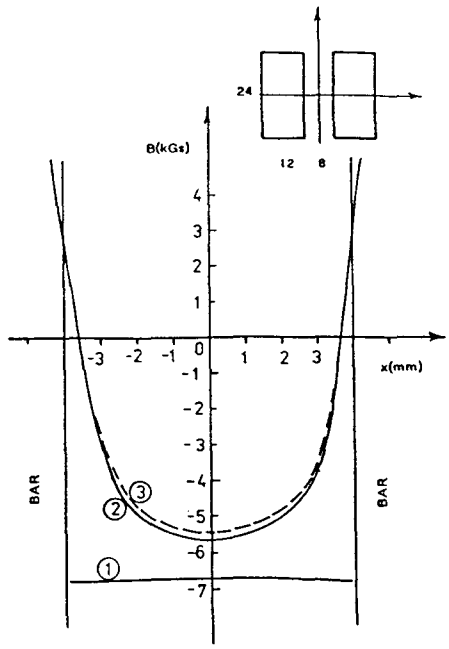


Fig. 4. Results for a symetric two- bar channel. The bar dimensions in milimeters are shown in the upper part. 1- theoretical field, 2- Armco iron, 3- soft- iron.

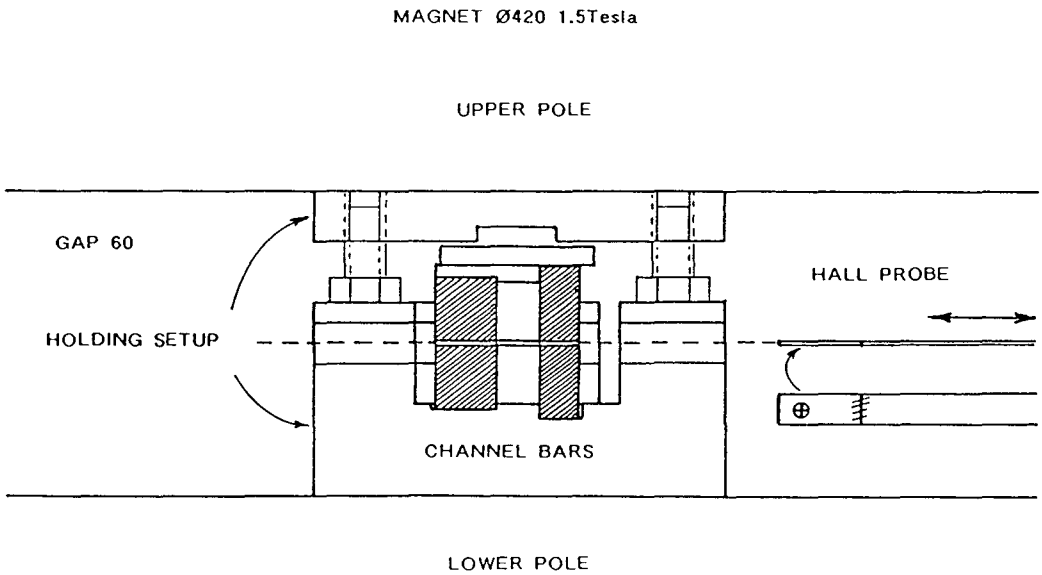


Fig. 3. The two- bar channel fixed by a holding setup in the gap of the test- magnet.

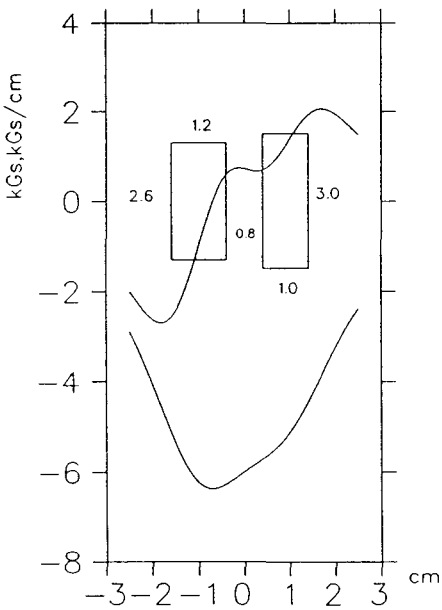
The measured magnetic field represents the dashed curve 3. The minimum field is by -5.54 kGs lower than the unperturbed magnet field (which is 15.336 kGs). The solid line 2 gives the field obtained with Armco iron bars. This gives a slightly lower field i.e. -5.69 kGs. The curve 1 shows the calculated field. Its value in the middle of the gap is -6.71 kGs.

We see that the real field is "smeared" against the theoretical distribution. It might be considered homogenous within an aperture of 3 to 4 mm . The second channel was made up of Armco iron and the bars have different dimensions. It was expected to get both diminished field and a given gradient. The sizes of the bars are shown in the left part of Fig. 5 as well as the calculated field gradient. The resulting measured field is given in the right part of this figure. The "smearing" effect is also well pronounced. For comparison the minimum field is -4.14 kGs and slightly shifted to the left of the middle point of the gap.

5. CONCLUSIONS

Theoretical estimates fail using the model[1] and bidimensional computer simulation by Poisson program is probably needed.

The chosen materials do not differ substantially.



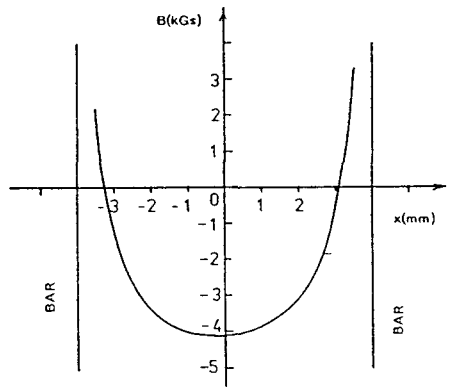


Fig. 5. Results for an asymetric two- bar channel. The bars are made up of Armco- iron. Left side - the theoretical estimates, right part - measured magnetic field.

REFERENCES

1) B. Carbonel et al., "Calculation of the geometry of magnetic channels for synchrocyclotrons and cyclotrons," Nucl. Instr. Meth. 84, 144-146 (1970).

DESIGN OF PASSIVE MAGNETIC CHANNELS

G. Bellomo
University of Milan and I.N.F.N. – Sez. Milano
L.A.S.A. – Via Fratelli Cervi, 201
20090 Segrate (MILANO), Italy

ABSTRACT

Passive magnetic channels are extensively used as magnetic shield or focusing devices for the extraction of beams from cyclotrons. The field properties in the beam aperture can be analyzed using a multipole expansion of the field in a two dimensional approximation, owing to the large length over aperture ratio.

Analytical formulas, assuming uniform saturation of the iron, are given to calculate the multipole coefficients. The basic configuration for dipole e/o quadrupole are evaluated and compared.

1. INTRODUCTION

Passive magnetic channels, providing partial shielding of the main field and radial focusing, have been introduced in the 60's for the beam extraction from sincrocyclotrons[1] and have been subsequently used also in many cyclotrons.

The most recent application of these devices is in the extraction system of superconducting cyclotrons like the K500, K1200 of MSU and of LNS/Milan.[2] In these machines a considerable number of passive magnetic channels (up to 10) are spaced all the way along the beam extraction path. They provide partial shielding of the main field (up to 3 kG) and radial focusing (gradients up to 4 kG/cm) .

The geometry of these channels (called also focusing bars) is similar to the one given in Fig. 3 and indicated as type I. Owing to the large value of the main field (in the range 15–50 kG) of superconducting cyclotrons uniform magnetization of the iron bars can be safely assumed.

Analytical formulas for the computation of the magnetic field produced by rectangular block of saturated iron are well known.[3] An extensive analysis of the field properties of focusing bars is given in ref.[4] in terms of the multipole coefficients obtained by numerical evaluation from the computed fields.

An alternative approach based on a direct analytical evaluation of the multipole coefficients is presented in the following.

2. MULTIPOLE GENERATION WITH SATURATED IRON BARS

K. Halbach has developed a technique for the generation of multipoles using permanent magnets.[5] The multipole is made using equal blocks (rectangular, trapezoidal, ring sector) spaced around a circle and with a changing direction of the magnetization. The multipole coefficients are evaluated for a standard block placed on the X axis (see Fig.1) and for a given magnetization orientation.

The multipoles coefficients for all the other blocks are then obtained by the reference block considering the rotation of the block (angle ϕ of Fig. 1) and the orientation of the magnetization.

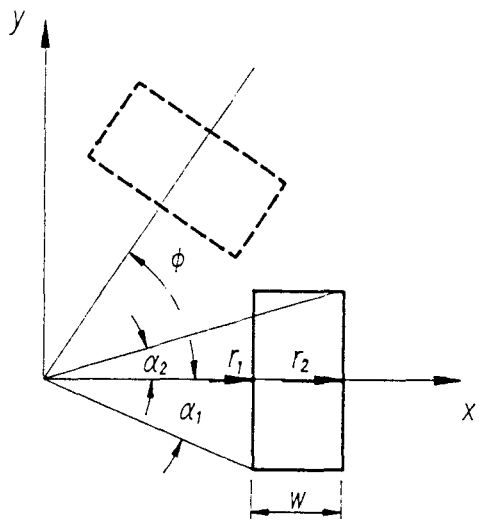


Fig. 1. Coordinate system and parameters of a standard block.

The calculation is two dimensional, i.e. the multipole is assumed to have infinite length in the direction of the beam path.

In the case of passive channels for cyclotrons the length over aperture ratio (tipical values are 10 cm and 1 cm aperture diameter) justify the two dimensional approach; example are given in ref..[4]

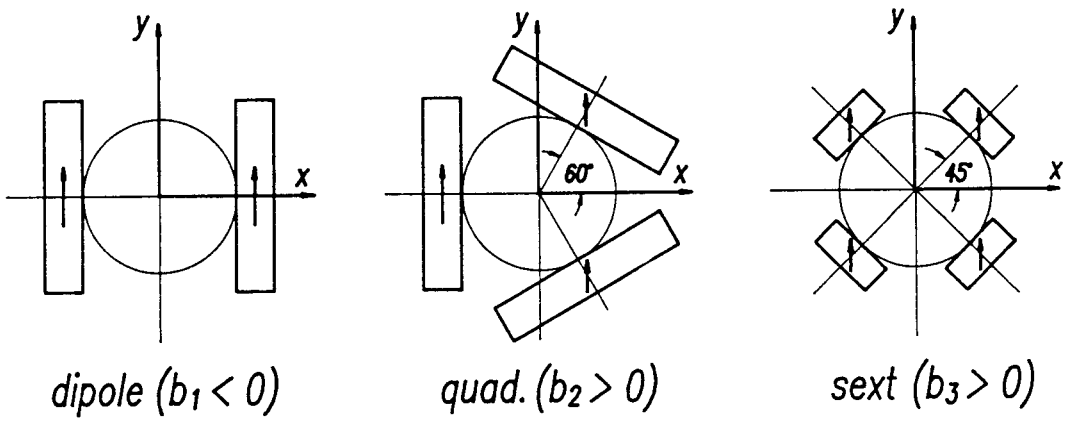


Fig. 2. Geometries of the bars for the generation of dipole, quadrupole and sextupole field.

Assuming midplane symmetry (y =0), uniform saturation in the positive Y direction and the rectangular type block of Fig. 1, the formulas given by Halbach[5] can be simplified as

$$B_y(x, y=0) = \sum_n b_n \left(\frac{x}{\rho}\right)^{(n-1)} \qquad (1)$$

where the field expansion is valid inside a circle of radius ρ not enclosing iron. (i.e. $\rho \leq r_1$) . The multipole coefficients b_n are given by ($\rho = r_1$):

$$b_1 = \frac{B_s}{\pi}(\alpha_2 - \alpha_1) \qquad (2)$$

$$b_n = -\frac{B_s}{\pi}\frac{1}{n-1}\left(\cos^{n-1}\alpha_1 \sin(n-1)\alpha_1 - \left(\frac{r_1}{r_2}\cos\alpha_2\right)^{n-1}\sin(n-1)\alpha_2\right) \qquad (3)$$

with B_s the saturated field in the positive Y direction. Rotation of an angle ϕ of the reference block gives new values of the multipole coefficients

$$b_n(\phi) = b_n(\phi = 0)\cos(n+1)\phi \qquad (4)$$

The geometry of the basic multipoles, dipole, quadrupole, sextupole, are presented in Fig. 2 with the appropiate sign of the multipoles to obtain shielding ($b_1 < 0$), radial focusing ($b_2 > 0$) and to correct the sextupole component of the main field.

The general properties of the multipole using saturated iron are the following:

- to generate multipole of order N are required (N+1) bars
- maximum efficiency for given bar thickness is obtained for $\alpha = \pi/(2(N+1))$ where $\alpha = (\alpha_1+\alpha_2)/2$. These values are exact for block of trapezoidal shape and are only a good approximation for rectangular block
- only multipole coefficients of order $N + k(N+1)$, $k = 0, 1, 2\ldots$ are generated with decreasing values. Therefore:

dipole $\alpha = \pi/4$ $b_1, b_3, b_5, \ldots$
quad $\alpha = \pi/6$ $b_2, b_5, b_8, \ldots$
sext $\alpha = \pi/8$ $b_3, b_7, b_{11}, \ldots$

- The multipole coefficient of order $N + (N+1)$ can be eliminated using $\alpha = \pi/(2N+1)$

dipole $b_3 = 0$ $\alpha = \pi/3$
quad $b_5 = 0$ $\alpha = \pi/5$
sext $b_7 = 0$ $\alpha = \pi/7$

with a modest reduction of efficiency.

- change of sign of the multipole coefficient of order N can be obtained rotating the all system by the angle of $\pi/(N+1)$

3. FOCUSING BARS

As already mentioned passive magnetic channel providing shield ($b_1 < 0$) and radial focusing ($b_2 > 0$) are normally indicated as focusing bars.

The basic geometry is similar to the type I given in Fig. 3, although channels made with bars of circular cross section have been employed.

The desirable feature of these channel should be, beside providing dipole and quadrupole components, to eliminate or minimize the other main components, i.e. sextupole b_3 and possibly octupole b_4.

Analytical evaluation of the multipole coefficients can be made, with the formulas presented in Section 2, considering the two bars on the rigth side (positive X axis) as the sum of a bar of height H with positive magnetization (positive Y axis) and a bar of height h with negative magnetization.

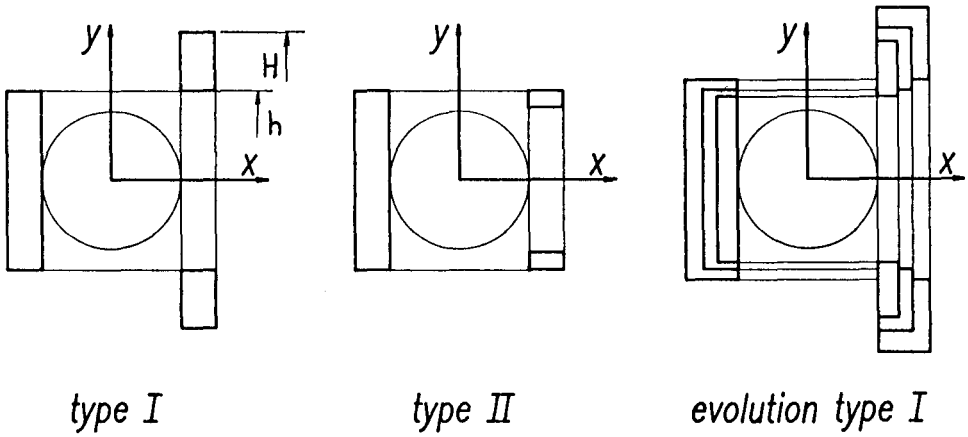


Fig. 3. Geometries of the focusing bars producing dipole (shield) and quadrupole fields.

Imposing the condition $b_3 = 0$, $b_4 = 0$ the solution can be numerically found and generally implies an height of the left bar not equal to h.

Table 1. Multipole coefficients (kG) for various magnetic channels

n	type I	type II	dipole	quad
1	-0.845	-0.944	-1.691	0.0
2	1.228	0.848	0.0	3.174
3	0.0	0.0	0.0	0.0
4	0.0	0.0	0.0	0.0
5	0.028	0.080	0.057	0.0
6	-0.192	-0.119	0.0	0.0
7	-0.005	-0.043	-0.017	0.0
8	0.018	0.002	0.0	-0.387

Three specific cases can however be evaluated quite easily;

- setting $H = \infty$ a pure quadrupole field ($b_2 > 0, b_1 = b_3 = 0$) is obtained. The height h can be chosen to have $b_4 = 0$. This corresponds to $\alpha = 45°$ for the left bar; the value is exact for block of trapezoidal shape and only a good approximation for the rectangular shape.
- for the type I configuration the sextupole component b_3 depend only on the value of H; therefore $b_3 = 0$ using $\alpha = 60°$. The value of h can be chosen to obtain $b_4 = 0$; this corresponds to $\alpha = 47°$
- for the type II configuration the octupole coefficient b_4 depends only on the value of h; selection of $\alpha = 45°$ gives $b_4 = 0$. The value of H can be chosen to have $b_3 = 0$, i.e. $\alpha = 50°$.

Type I and type II focusing bars represent practically the extremes of the useful range for this type of configuration. Type I is limited by the total height H which increase with the bar thickness as shown in Fig. 3. Type II is instead limited by the small vertical dimension $(H - h)$ of the bars on the right side for reasonable values of bar thickness.

The multipole coefficients up to b_8 for type I and type II focusing bars are given in Table 1 for a selected case : aperture $r_1 = 0.6$ cm, bar thickness 0.2 cm and saturation field $B_s = 21.4$ kG.

The main difference between type I and type II geometry is the value of the quadrupole component which is almost 50% higher for type I case. The dipole component is instead 10% higher for the type II. For both cases the main imperfection multipole is the dodecapole component b_6.

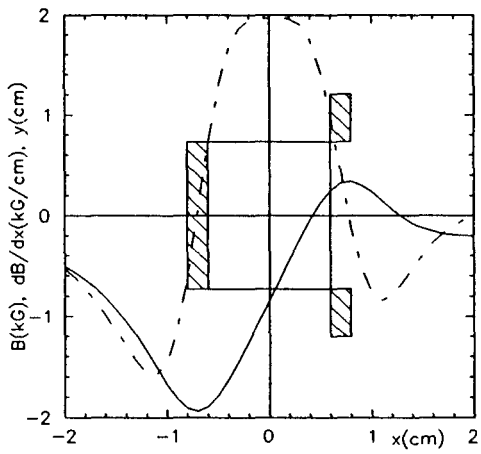


Fig. 4. Fields and gradients for type I geometry. Solid line field, dashed line gradient.

The midplane fields and gradients for the two type of focusing bars are plotted in Figs. 4,5. Uniformity of the gradients is within 10% or better inside a region covering

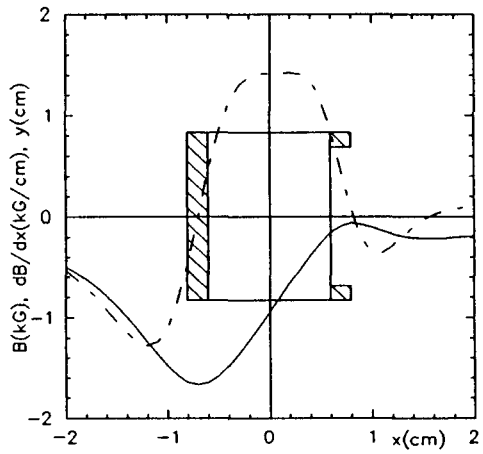


Fig. 5. Fields and gradients for type II geometry. Solid line field, dashed line gradient.

2/3 of the aperture. The uniformity normally increases (up to 5%) with increasing bar thickness.

The possible ranges of b_1, b_2, varying the bar thickness, for type I and type II configuration are presented in Fig. 6 for the reference case; maximum bar thickness is 1 cm.

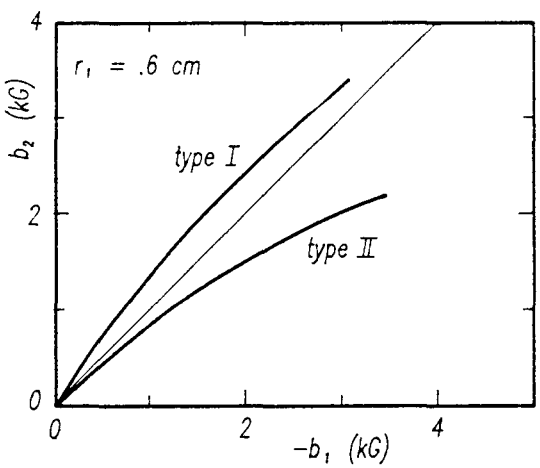


Fig. 6. Dipole (b_1) and quadrupole (b_2) multipole coefficients produced by type I and II focusing bars, varying the bar thickness.

4. COMPARISON OF THE GEOMETRIES

For the extraction of the beam from the cylotron partial shielding of the main field as well as radial focusing is needed. They can be provided separately, using a set of multipoles of the Halbach type, or combined in a single device like in the case of the focusing bars.

In Table I are reported the multipole coefficients of the dipole and quadrupole channel of the Halbach type (see also Fig. 2) for an aperture $r_1 = 0.6$ cm and bars thickness 0.2 cm.

The multipole components of order $N + (N + 1)$ has been eliminated by appropriate selection of the bar height as indicated in Section 2.

For the dipole there is a gradient of 0.100 kG/cm at 2/3 aperture. In the case of the quadrupole the uniformity of the gradient is better than 10% for 2/3 of the aperture.

As apparent from the Table, the type I focusing bars has half strength of the pure dipole and one third strength of the pure quadrupole.

The use of individual multipoles seems therefore more efficient, for a given aperture and bar thickness, of the type I focusing bars. Furthermore, the focusing bars are not flexible enough for the independent selection of the dipole and quadrupole strength.

The obvious, and perhaps dominant, advantages of the focusing bars are the simplicity of the device and the possibility to combine the two components (dipole, quadrupole) in a single channel of very short length.

5. REFERENCES

1) Danilov, V.I., Savchenko, O.V., Instr. Exp. Tech. **3**, 363 (1959); Suwa, S. et al., Nucl. Instr. and Meth. **5**, 189 (1959).
2) Fabrici, E.M. et al, Nucl. Instr. and Meth., **184**, 301 (1981); Fabrici, E.M., Salomone, A. in **Proceedings of the IX International Cyclotron Conference** (Caen, 1981) p. 501.
3) Carbonel, B. et al, Nucl. Instr. and Meth., **84**, 144 (1970).
4) Gordon, M.M. and Taivassalo V., Nucl.Instr. and Meth. **A247**, 423 (1986) .
5) Halbach K., Nucl. Instr. and Meth. **169**, 1 (1980), and Halbach K., Nucl. Instr. and Meth. **189**, 213, (1982) .

DEFLECTOR DEVELOPMENT FOR THE K1200 CYCLOTRON

Thomas Kuo* and Jerry Nolen†
National Superconducting Cyclotron Laboratory
Michigan State University
East Lansing, Michigan 48824, USA

ABSTRACT

Certain progress has been made for the electrostatic deflectors of the K1200 cyclotron. At present, 80 kV at subμA leakage current can be achieved. The system has been operated in a stable, very few sparks and almost zero current mode for about a year and a half. The progress is attributed to a better understanding of various discharge phenomena at high magnetic field and the treatments to eliminate them. The future plan is to further improve the voltage holding capability to 100 kV, so that 80 kV would be obtained routinely and reliably.

1. INTRODUCTION

The voltage holding capability of the electrostatic deflectors had been one of the limiting factors of extracting higher energy beams. For K1200, the field strength required for the extraction of the 200 MeV/n, q/A=0.5 ions and the 135 MeV/n, q/A=0.33 ions is about 140 kV/cm (84kV at 6mm). The early performance of two deflectors used for K1200 was not able to meet this requirement. About two and half years ago, highest priority was set for improving these deflectors to acquire the capability of this field strength reliably thus to remove the limitation on extractable beam energy.

Progress has been gradual in small steps but in pace with the demands of beam requirement. At present, 80 kV with subμA leakage current is reachable. Below 60 kV, the deflector operation has been very stable,very few sparks with very low leakage. Breakdown occurance and unscheduled repair has also been down to minimal. This progress was possible mainly due to a better understanding on the high voltage discharge mechanisms in the deflector of a particular design. Some hardware improvement was important at the begining but became less critical later on as our techniques of handling discharges are better developed.

In the following sections, various discharge modes and the corresponding techniques of treatment are described. Future development to further improve the voltage holding capability to 100 kV and to handle high external beam operation for secondary/radioactive beams production is also proposed.

*present address: TRIUMF.
†present address: ATLAS, Argonne National Lab.

2. DISCHAGRE MECHANISMS

The origins and the characteristics of the discharges come from several subsystems in different modes. In terms of hardware the deflector system can be divided into three subsystems, namely:

—HV power supply and feedthrough,
—Supporting insulators and mountings and
—HV electrode and anode plates structure.

During our development, these three subsystems were studied and improved in the above listing sequence. In terms of the nature of discharges, they can be classified into two basic classes. The first is the random,short burst modes and the second the CW discharge modes. It turns out that the random modes are easier to be recognized and therefore easier to handle, but the CW modes are much more subtle thus the solutions to eliminate them are more elaborate. The following sections will discuss these individual modes in some details.

2.1. Random Discharges

Microscopic emissions It has been theorized that under high negative bias an electrode with macroscopic smooth surface will undergo micro-explosion[1)] due to defects or fornign materials in submicron sites where the local polarizing field is so strong that the material around these sites are exploded away. These micro-explosions continue until the sites of defect is exhausted under a given bias. A new series of explosions will be initiated when the bias is raised to a higher level.

Microscopic protrusions are also formed under high electric field resulting field emissions. The initial electrons collide with residue gas molecules and bombard the anode surface. Ions from the residue gas and from the contaminations on the anode surface are drawn back to the cathode releasing secondary electrons. If the magnetic field is very strong, say 5T, these ions will be concentrated onto the original emission sites, triggering intense secondary electrons and in turn intense ion emissions. This process eventually leads to a plasma discarge. A weaker magnetic field will allow this process to develop slower and to have higher possibility to melt off the protrusion. The behavor of this process is recognizable by its gradual current buildup prior to a spark or a gradual current decrament.[2)]

If the bias voltage increases slowly and constraint of current flow is added, these micro-explosions and micro-

protrusion emissions would not be too harmful. In fact, one wants to control these discharges at a rate that conditioning to a higher voltage can be done without damage by heavy discharges. However, if the bias voltage increases in big steps, avalanching sequence of microdischarge would occur and major discharge events are triggered. Although deflector is considered a DC device, it acts like an unmatched transmission line during discharge. Standing wave of high currents up to thousands of amperes in amplitude rings back and forth. Many major discharges will follow if the oscillation are not heavily damped.

Gas emission discharges Gas desorption from the metal lattice of the cathode also contributes to random discharges while the gas released from the anode surrounding seems to be less eventful. It is inferred that when a burst of gas is released from the negative electrode, a glow discharge is formed which further induces more gas release. These mini glow discharges have been observed through a window of a test facility. A very clean observation was obtained as follow. A cathode coated with non-absorptive glass was cycled with pressurization and evacuation after the typical conditioning had been carried out. Usually no recondition was needed to resume the voltage holding capability already reached. On the other hand, another cathode coated with Alumina layer (slightly porous) needed to be reconditioned for every cycle.

Macroscopic defects Random discharges stemed from macroscopic defects usually identify themselves by major discharge intensity and light emitting events. For K1200 deflectors, we have encountered defects coming from many sources. Examples are:

- material defects in supporting insulators.
- defects in component fabrication, system assembly.
- deterioration of negative electrode surface smoothness.
- deterioration and damage on anode surface.
- local sharp edges.
- non-conductive dust particles or fibers attracted to the cathode.

Some items also cause discharges in CW mode while those defects contribute to CW mode only are omitted here.

Discharges induced by dynamic EM fields It has been observed that violent discharges occur in the deflector during RF sparking when the deflector is set at a voltage beyond which it has not yet been conditioned to. In other words, the deflector is unstable in this condition. Similar effect takes place when the magnetic field is ramping up or down. One inferred that the RF penetrated into the deflector induces an RF voltage superimposed on the DC voltage. Likewise the change of magnetic field induced an EMF voltage. In both cases,the resulting field is higher than the level the deflector has attained, consequently discharges are triggerd. After repeated confirmation of this phenomenum the simultaneous conditioning of RF and deflector has been avoided. It is also manditory that when the deflector is being conditioned, ramping up/down magnet or bring up RF are excluded.

2.2. CW Discharges

The CW discharges (CWD) distinguish themselves from the random discharges by the continual current drainage. Currents start at a takeoff voltage then rise very rapidly with respect to voltage increase. Typical events are from defects such as whiskers developed on the cathode or from damage (craters and ridges) on the anode plates. There are situations in which several CWD start from different sites but at different takeoff voltages and they might superimpose with several types of random discharges. So the circumstance might be quite complex. Not all CWD are the consequence of the uncontrolled random events. For example, metallic chips might migrate to the vicinity of the cathode and eventually be attracted to the cathode surface. Once this happens, the performance of the deflector will be severely hampered.

Defects listed in the random discharge section are also sources of CWD. In addition to macroscopic defects, a few other discharge mechanisms exist even if the deflector is in its *perfect mechanical* condition. They are called Reverse Penning, ExB and Thermal field emission modes.

Reverse Penning mode This CW mode occurs as a consequence of a twofold symmetric electrical geometry imerged in a strong magnetic field perpendicular to the axis of the symmetry. The discharge is entirely symmetric from the negative electrode to the upper and lower anode plates up to very minor detail, as shown in Fig. 1. This mode take place most frequently at the locations where the highest electric field exists, e.g. the semicircle edge of the endtips of the electrode at the median plane. The process ignites like an arc formation and once it has started the 'arc' current could be up to a few hundred microamps. The arc is able to self sustain even if the current is limited to 10 μA. We found that this discharge is most destructive and it is necessary to turn off the high voltage to extinguish it. Due to limitation of space, we shall offer the explanation in a separate publication.



Fig. 1. The etching on the upper and lower sparking plates by CW reverse Penning mode. Note the complete symmetry of the crescent shape.

ExB mode Fig. 2 shows an image of ExB discharge. The electric field is 140 kV/cm at 100 kV and the magnetic field is about 1T. The plane of moment of the intense electron core lies in the deflector median plane but the pattern was captured symmetrically on both the upper and lower anode plates. The carbon tracks were produced by the hydrocarbon particles ionized by the ExB electrons. The electric and magnetic field made them record the image of the electron paths on the anode plates.

Electrons are initiated from a site (see the fine line of the first half circle and the sharp begining point) and contained by the magnetic field. Upon returning to the electrode the electrons are repelled again. Positive ions produced very close to the electrode and also energetic enough are pulled onto the electrode, otherwise they are pulled to the anodes. The secondary electrons follow the trace of the primary ones and this process continues until a spark is triggered. Many isolated tracks were observed indicating that this process is common. ExB electrons are very destructive to the supporting insulators located at the median plane particularly at the metal-insulator interface.



Fig. 2. Image of ExB electrons. note the spark damage from random discharge mode.

Thermal field emissions Operation experience shows that the E1 deflector with bare electrodes (vs. coated) performed perfectly at the begining of extracting about half μA of Oxygen ${}_{18}O^{6+}$ at 80 MeV/n, but started to draw current after two hours. If special attention were not given, the deflector currents might grow to an unacceptable level. The leakage decreased slowly after the beams was turned off. The time interval between beam on and leakage starting depends on how long the beams has been off, how high the beam currents and how the cyclotron is tuned. Subsequent inspection on the deflector indicated that the current flow was in the form of thin but long electron sheet along the front surface of the electrode. The etching on the anode plates was very narrow (0.2mm) but very long (about 30 cm), symmetric on upper and lower plates. Before the cooling for the deflector system is added, a set of coated electrodes was used. The symptom of this thermal field emission was much improved, but how high can a beam current be extracted remained unanswered.

3. HARDWARE IMPROVEMENT

In the previous section, we concentrated on the description of various discharge mechanisms but deferred the corresponding treatemnts for the sake of continuity and clearity. One might wonder that if that many discharge modes are recognized, the deflector problems would have already been half solved. This indeed is the case. Almost all of these discharges have been handled either by complete elimination or by minimization to a great degree (see Fig. 3. next page). The HV feedthrough and the supporting insulators were studied and improved first, then the anode plates and the negative electrodes. Basically, the development for the one-segment E2 is completed as far as the 80 kV capability is concerned. The three-segment E1 is more involved due to its complex mechanical structure.

3.1. High Voltage Feedthrough

The version of HV feedthrough used for the K500[3] superconducting cyclotron consists of a long metal rod mounted coaxially with a 5 cm diameter spark tube. The rod is terminated by a large corona ring which is isolated from ground by a quartz tube. Sparks between the center rod and the spark tube had been a problem. A new design adapted by the K1200 replaced the vacuum coaxial line by a solid coaxial cable at atmospheric pressure. Fig. 4 shows the schematic of this design. The HV cable connects directly to the HV power supply and to the tip of the feedthrough which is latched into a hinge in the negative electrode. The HV tip and the ground tube are separated by a 15 cm long macor tube. The tip is made of Titanium and is brazed onto the macor tube by glass bonding. This bonding technique is developed at NSCL and is considered necessary because any metallic bonding would create macroscopic sharp points. The ground end of the macor tube is tapered so that the ground surface is gradually flared away to avoid abrupt field change at the cable-macor-ground tube interface.

The center conductor of the HV cable is removed as suggested by Bob Roger of Texas A & M University Cyclotron Institute.[4] The remaining carbon rubber layer provides about 6 kΩ/in resistivity so a cable of 10 feet has a resistance of 720 kΩ. The resistive cable reduces the spark damage but additional resistance, in the order of 50 MΩ made by a string of resistors, is found needed to make the sparks non-destructive. However, this series limiting resistance can not stop the damage by the CW mode discharges. In the event that the leakage currents exceed 10 μA during routine operation, the 50 MΩ string can be replaced with a 5 MΩ string in order to reduce the voltage fluctuation.

Besides being used as HV feeding, the feedthrough is also used for deflector position drive. After 4 years of operation, our experience with this type of feedthrough has been very satisfactory. No HV or mechanical difficulty was encountered.

3.2. Supporting Insulators

The original sapphire insulators[3] are being phased out for the reason that some of them glow to cherry red at 50-60 kV with large leakage currents. This is consistant with the observation that some insulators were found coated with thin metallic film at the HV end and

high temperature colorations were printed on the anode plates. The brazing joint was found depleted due to the evaporation of brazing compound from high temperature. The metallic coating and the imperfection in fabrication of seating contributed to frequent flashovers. In other words, there existed volume defect, surface defect and sharp point defect associated with the use of the sapphire insulators. Before the new version of insulator was developed, only those which could sustain 80kV without glowing were selected. In the meantime, the problem of sharp point defect was corrected as much as possible (It could not be corrected completely because the original design called for sharp 90 degree fabrication).

Several versions of insulator made of Macor were developed. Macor is chosen for its machinability to achieve complex configuration, particularly for making ExB electron barrier. Sharp edge design was removed and the metallic brazing was replaced by glass bonding. One version increased the insulator cross-section about 50 % and the binding area to the cathode 150 % for stronger mechanical strength. All versions have been tested and used in the K1200 cyclotron. Their performance has been very satisfactory.

3.3. Cathode Electrode and Anode Plates

We have isolated the deflector system in three parts and studied them in operational sequence. With the first two parts free of discharges and difficulties we were able to concentrate on the deflector channel where the cathode electrode and the anode plates interact under the influence of a strong magnetic field. As we shall see later the effort to minimize the spark frequency and spark damage leads to the complete elimination of sparks on the anode plates which in turn leads to the complete suppression of the CW Penning mode and ExB mode. The thermal field emission is greatly reduced but not completely suppressed yet since the development of cooling capability has just begun.

Conditioning technique Spark cleaning has been the conventional or usual method of voltage conditioning. The voltage holding capability is the prime object while the current drainage is considered secondary. In the situation of K1200, a moderate spark strength or a small current drain results in high power density on the anode plates because of the high magnetic field. Damage may develop very rapidly leading to a failure at low operating voltage.[5)]

A new technique for conditioning was then developed in order to minimize the spark damage. At first we added large series limiting resistors in the HV feedthrough to damp the high current ringings during a spark and clamp the maximum macroscopic pulsed currents under 20 μA. The characteristics of leakage currents or spark currents were monitored vs. time with resolution better than 0.2 second using a program called Fmon. The voltage is to increase in very small and gentle steps to smooth the micro defects. Each step begins with zero current, stops once a small current is seen. Several seconds to several minutes may be needed to bleed out the micro-emissions, mostly from gas desorption at lower voltage. At higher voltage pulsed discharges from a few μA to 10 μA (electronically clamped) followed by a continual bleeding are seen. If no CW mode discharge is initiated, currents will fall back to zero for each step.

The steps are in a few hundred volts increment at lower voltage decreasing to 10 to 20 volts per step at the higher end. This procedure repeats for three cycles. The first is with the magnet current off (some residue field exists in the location of the deflectors). This cycle is used to clean the cathode (sites of micro-explosion, field protrusions and gas desorption), usually takes about 4-6 hours to reach 60 kV for a bare electrode and about an hour for a coated one. The second is with magnetic field at about 1 to 2 tesla to clean the anode plates and to melt off residue field protrusion and gas desorption sites. The third cycle is for final conditioning at full operating field. Using this procedure, we usually obtain conditioning without the high risk of damaging the deflector. This is demonstrated in Fig. 3.

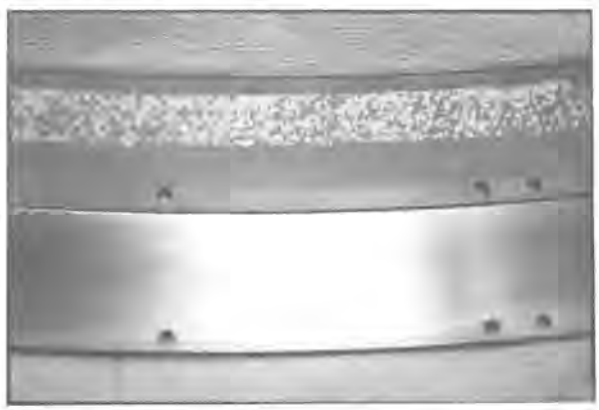


Fig. 3. The contrast of sparking condition between using the new technique (lower) to the traditional method (upper).

Anode sparking plates reflectory metals such as Tungsten have been used for sparking plates for many deflector designs. One must emphysize that the tungsten plates must be of high purity and of high performance grade. The lower grade made by powder metallurogy will not work well because of its high impurity contents which contribute to the endless emission of ions of contamination. In addition, droplets of tungsten are sputtered off easily by the spark energy. These droplets are ionized and are attracted to the negative electrode. This action deteriorates the smoothness of the negative electrode hence triggers more sparks.

Lower melting point alloy with strong modular strength such as stainless steel might be useful as sparking plate material. At NSCL we have explored the use of s.s. as an option over the high grade tungsten for its ease in fabrication and the simpler construction it allows. Sparking tests show that the s.s. evaporates in the form of metal gas and coats the negative electrode evenly when a major spark occurs. The craters created by the sparks show smoothier boundary edges. Encouraged by this result the material was then used to make sparking plates for the E2 deflector. As a result, the negative electrode has maintained its smoothness ever since. Later on, the new conditioning technique and the use of electropolished s.s. anode plates made the complete elimination of random discharges possible.

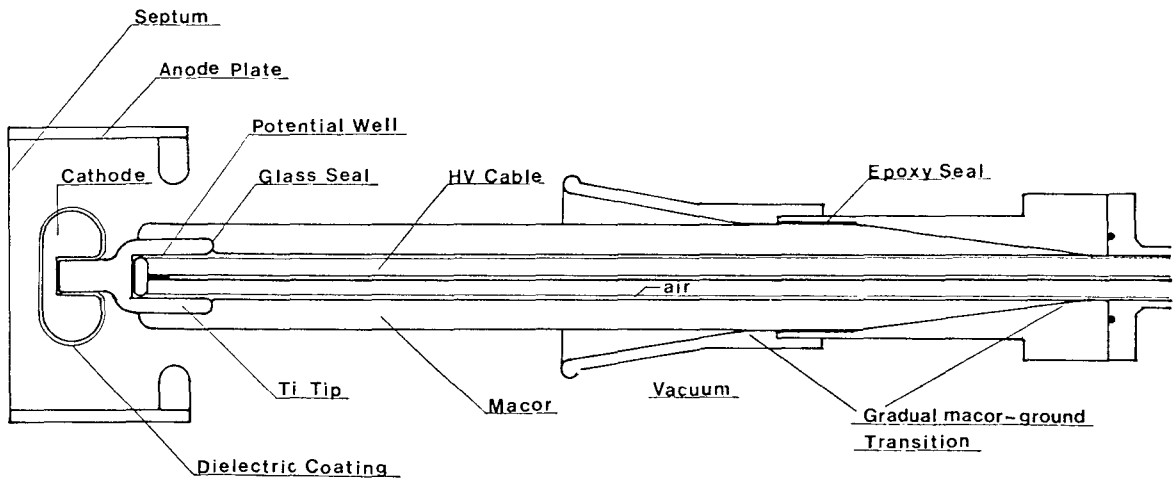


Fig. 4. The deflector channel structure and the main features of the new feedthrough design. Note the cathode is wrapped around cpmpletely by a layer of dielectric coating.

The ChalkRiver group also explored s.s., Ti and Mo as alternative anode material. Their conclusion is that Ti is the best when tested in a teststand.[6] Further development at NSCL indicated that although s.s. works well in handling the random discharges, but on the other hand is not satisfactory in handling CW mode. We shall see in the following paragraphs that how this problem is solved.

Surface treatment for cathodes As we have discussed in section 2, the reverse Penning CW mode is field geometry dependent. It can be ignited even if the deflector is in perfect condition. Although we have succeeded in suppressing almost all random mode discharges, this most destructive CW mode is still at large. We then decided to eliminate all electron emissions from the cathode by coating the negative electrode with dielectric material. This method has been used for the high energy electrostatic separators at CERN.[7]

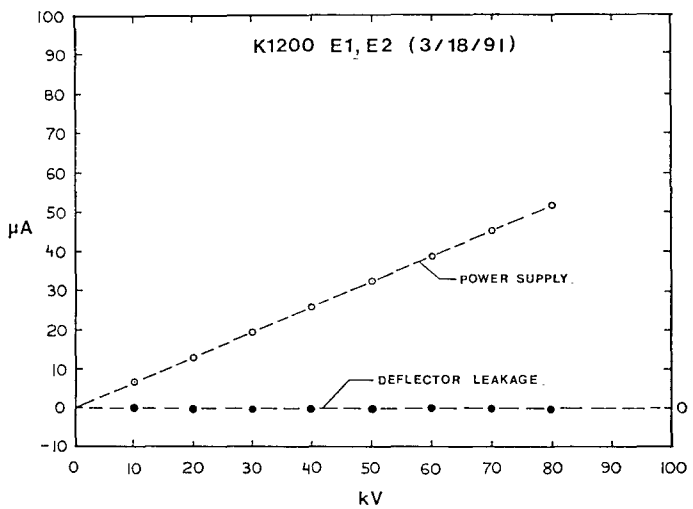


Fig. 5. Both E1 and E2 achieved 80 kV with near zero current leakage using glass coated cathode endtips.

The coating development progressed in phases and lasted about a year. At first, one endtip of a test electrode was coated with binding glass while the other end was left bare. The test electrode was put into a brute force spark test up to 110 kV. The result showed that the coated end was completely free of any discharge while the bare end went through the usual spark action as expected. In the second phase the end tips of the electrodes used for K1200 were coated. On March 18, 1992 both E1 and E2 were able to hold 80 kV at near zero leakage current in stable condition *for the first time*. The leakage current vs. applied voltage is shown in Fig. 5. Since then both E1 and E2 have been routinely operated with high reliability.

Still of concern was the fact that much of the electrode surface was uncoated. Thermal or non-thermal field emissions, emissions from attracted dirts and ExB CW mode were not yet eliminated. The third phase of this operation is to develop a technique to coat the entire length of the electrode except for a 6 mm band in the median plane. The fully coated electrode works extremely well for the single-segment E2. *All* discharge modes are suppressed. No sign of spark or CW mode damage is detected on the anode plates after 6 months of operation. The plates are found undistinguishable from a new set.

For the three-segment unit E1, the electrostatic performance is also excellent. However, the beam height in the E1 channel is taller than the uncoated bandwidth. The coating reacts to the impinging beams in some uncontrollable manner. Many micro-explosions from the surface of the glass occurred until the glass layer is eventually cleaned by the beams. The E1 finally takes beam up to half μA at stable operating condition.

The glass coating technique requires high level skill to implement, and the high quality coating is quite difficult to obtain. Industry produced anodized Aluminium surface might be a better alternative. Such electrode was prepared and put into E2 for test. The electrostatic performance is the best so far—very easy to condition to 80 kV, can be turned on full voltage like turning on

RF, etc. It is observed that the electron emission under beam bombardment seems to be much higher than the glass coated counterpart. The aluminium atoms in the oxide compound may be displaced by the impinging beams thus contribute to the higher electron emission. More operation experience will be acquired in the next few months.

4. CONCLUSION AND FUTURE PLAN

The R & D study on the K1200 deflector for the past few years provided us the basic understandings on various discharge mechanisms. The treatments to eliminate these discharges led to a 80 kV capability. The 80 kV with near zero current is chosen as an intermediate goal at this stage of development, since 60-65 kV is required for certain beam energies specified by experimenters. The future demand calls for a reliable 80-90 kV and a stable operation for extracting high external beams. Thus the goal should be a voltage holding capability of 100 kV. To achieve this goal,it is necessary to take a complete review and assessment over the quality of every subsystems. For hardware improvement, the immediate efforts will be:

1. Adding cooling capability to E1 negative electrodes
2. Special treatment for E1 on the hinge joints and beam entrance collimation
3. Acquisition of higher rating HV power supplies (120kV, 25nA)
4. Further refinement in making dielectric coating, support insulators and HV feedthrough.

In addition, the relationship of beam quality, beam tuning and extraction efficiency to the performance of deflector at high beam extraction will be studied. Further research on the HV discharge in vacuum under the influence of high magnetic field and the bombardment of high energy heavy ions will be continued.

5. ACKNOWLEDGEMENT

The authors wish to thank the NSCL operation group for their constant cooperation and assistance given to the deflector test program. Thanks also go to the design department and the machine shop who responded to our shop requests promptly. Numerous helpful discussions with Dr. Diamond of Chalk River, practical suggestions from Dr. Roger of Texas A & M are deeply appreciated. Finally we want to thank Prof. Austin and Prof. Blosser, Directors of NSCL, for their vision to set this program at 1st priority.

6. REFERENCES

1) Mesyats, G.A. and Proskurosky, D.I., **Pulsed Electrical Discharge in Vacuum** (Springer-Verlag, Berlin, 1989), ch.8.
2) Latham, R.V., "Prebreakdown Characteristics of HV Electrodes", presented at the 14th Int. Sym. on Discharges and Electrical Insulation in Vacuum, Santa Fe, New Mexico, Sept. 17-20, 1990.
3) Nolen, J.A., et.al, "Status of electrostatic deflector of the MSU K500 cyclotron," Proceedings of the 10th Int. Conf. on Cyc. E. Lansing, April 29-May 3, 1984, p.571.
4) Private communication.
5) De Martinis, C. and Ferrari, A., "High Voltage Experiments for the Electrostatic Deflector of the Milan Superconducting Cyclotron", presented at the 11th Int. Conf. on Cyclotrons and Their Applications, Tokyo, Oct. 13-17, 1986.
6) Diamond, W.J. et. al., "The Electrostatic Deflector of Chalk River Superconducting Cyclotron", presented at the 13th Int. Conf. on Cyclotrons and Their Applications", Vancouver, July 6-10, 1992.
7) Rohrbach, F., "Investigation of the Properties of Oxide-Coated Aluminium Electrodes", Proceeding of the 1st Symposium on Insulation of High Voltages in Vacuum, 1964, pp.393.

RESULTS FROM THE DEFLECTOR TEST STAND AT TEXAS A&M UNIVERSITY

D. May, G. Derrig, W. Dewees, P. Smelser, D. Tran and R. C. Rogers
Cyclotron Institute, Texas A&M University, College Station, Texas,
77843-3366, U. S. A.

ABSTRACT

The new room-temperature deflector test stand has recently been put in operation. We are beginning to test new insulator designs, new increased pumping-speed septa, and various conditioning strategies. Results of these tests and experiences with bringing these results to cyclotron operation will be presented.

1. INTRODUCTION

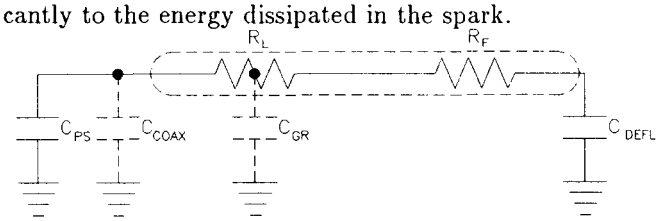
The electrostatic extraction elements (deflectors) for the K500 cyclotron are the primary limitation on the maximum extracted particle energy. This is the direct result of a limited long-term voltage holding capability of approximately 65 kV. At higher voltages sparking inevitably leads to damage to the insulators that results in complete failure to hold voltage without excessive drain current.

The room-temperature deflector test stand was built to provide an opportunity to observe the deflector under sparking conditions and test various techniques for improving the voltage holding capability. Although the magnetic field in the test stand is only 0.7 Tesla, damage similar to that experienced in the K500 has been reproduced.

A few insulator designs, spark shield materials and septa designs have been tested and are discussed below.

2. STORED ENERGY CONSIDERATIONS

Fig. 1 shows the equivalent electrical circuit of the deflector assembly. The power supplies being used are a special low stored energy type, Glassman High Voltage, Inc. model PS/LG100N-0.5X76, with an equivalent output capacitance of 200 pF. With a total distributed capacitance of 372 pF for the complete assembly, the maximum stored energy is 1.86 joules. The spark detection circuitry of the power supply turns the supply output off in less that 10 μseconds, so it does not add significantly to the energy dissipated in the spark.



C_{PS} – POWER SUPPLY OUTPUT CAPACITANCE – 200 pF
C_{COAX} – CAPACITANCE OF FLEXIBLE COAXIAL CABLE – 74 pF
C_{GR} – CAPACITANCE OF GLASS INPUT ROD – 46 pF
C_{DEFL} – CAPACITANCE OF DEFLECTOR ELECTRODE – 52 pF
R_L – DISTRIBUTED RESISTANCE OF LINE – 230 KΩ
R_F – FIXED RESISTOR, 270 KΩ

Fig. 1 Equivalent circuit of deflector, input assembly and power supply.

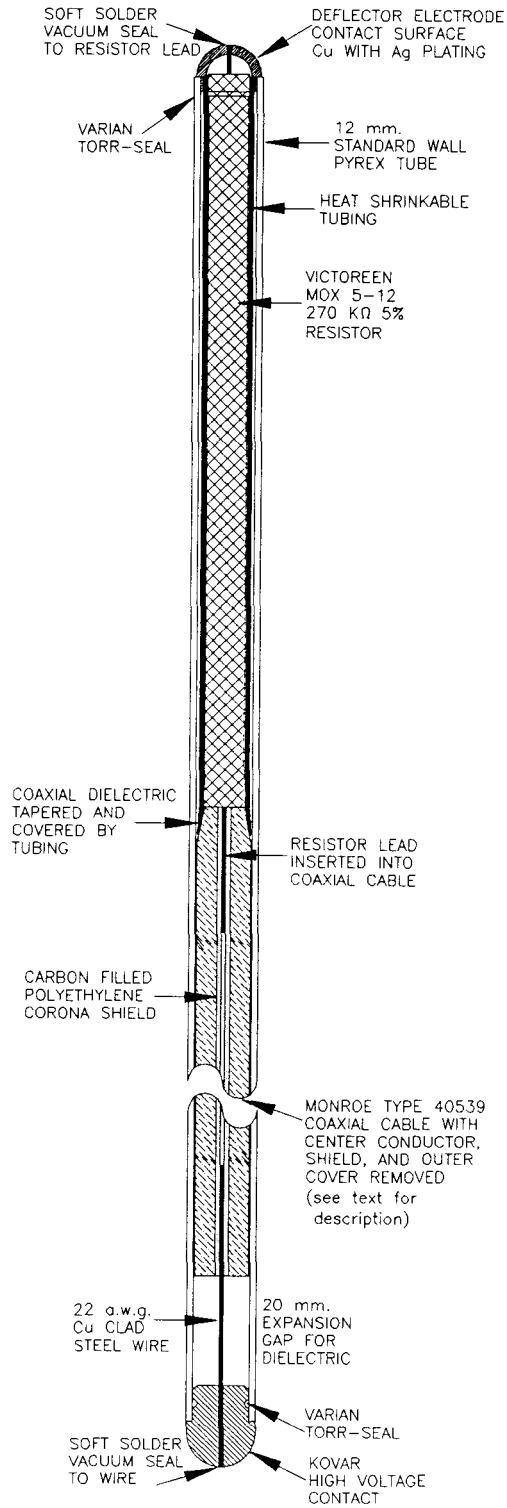


Fig. 2 Glass encapsulated high voltage input rod.

The "glass rod" referred to in Fig. 1 and shown in detail in Fig. 2 is the high voltage input to the deflector. This assembly was developed to cope with the small diameter tube which passes through the cryostat of the main magnet. The small inside diameter of the tube leads to, even with an optimally sized center rod, unacceptably high gradients at the surface of a metal rod that would result in sparking. The assembly consists of a Pyrex tube that encloses a length of high voltage rated coaxial cable, Monroe type 40539, from which the outer sheath and ground braid have been removed. The center lead is almost fully withdrawn from the cable to take advantage of the resistivity of the carbon loaded corona shield. The resistance of the cable plus the fixed resistor at the deflector end of the assembly gives a total resistance of 500 KΩ. This resistance helps dissipate some of the stored energy during sparking. The overall length of the rod is 1.03 meters.

3. FAILURE CHARACTERISTICS

It has been found in the K500 environment that voltages in excess of 65 kV lead to sparking that results in damage to the insulators. This implies that a spark of only 0.75 joules causes enough effluent to be generated at the spark impact point to cause a conductive coating to be deposited on the insulator surfaces. This appears to be the dominant failure mode and can be reproduced in the test stand even at its much lower level of magnetic field.

In addition to the leakage that is caused by sparking, another leakage mechanism seems to be the direct result of coating of the insulators with hydrocarbons. It is thought that this is the result of the use of turbomolecular pumps with poorly trapped backing pumps. Although a cryopanel has been added to the K500, it is used to augment the pumping of the turbomolecular pumps. There is room for two more cryopanels that are scheduled for installation in the latter part of 1992. Improved traps are being added to the backing pumps to reduce the possibility of backstreaming pump oil into the system.

4. INSULATOR DESIGN

The original design of the insulator followed that of the MSUNSCL as shown in Fig. 3. This design performed well in the test stand at MSU but had difficulty in the higher field of the K500. Further, this insulator is difficult to make because of the brazed connection between the sapphire and the metal end electrode.

Fig. 4 is a modification to the original MSU design that features recessed end electrodes. This design was based on a suggestion[1] that leakage along the surface from the high gradient point formed at the junction of the metal to the sapphire would be reduced. This design did not show the expected improvement but performed about the same as the original design. It did give some operating experience using the epoxy bonding technique that showed an inability to accept side loads in this configuration.

Fig. 5 is the present design being used in the K500 and undergoing continued testing. This design continues the idea of recessing the contacts but has a much larger surface area for the epoxy bond for increased strength. It also uses MACOR as the insulator material. This design has shown no particular improvement in resistance to damage but does show some improved ability to in situ cleaning by gas. This process is discussed below.

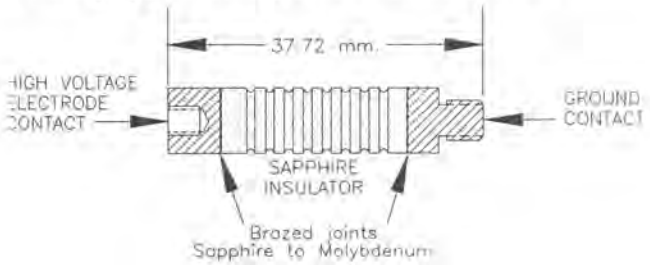


Fig. 3 Original insulator design.

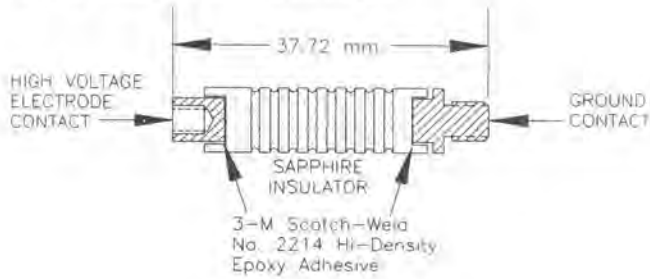


Fig. 4 Insulator with recessed contacts.

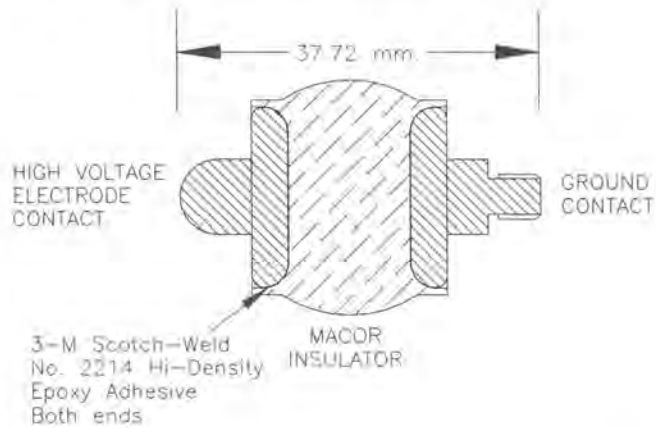


Fig. 5 Insulator now in use in the first deflector of the K500.

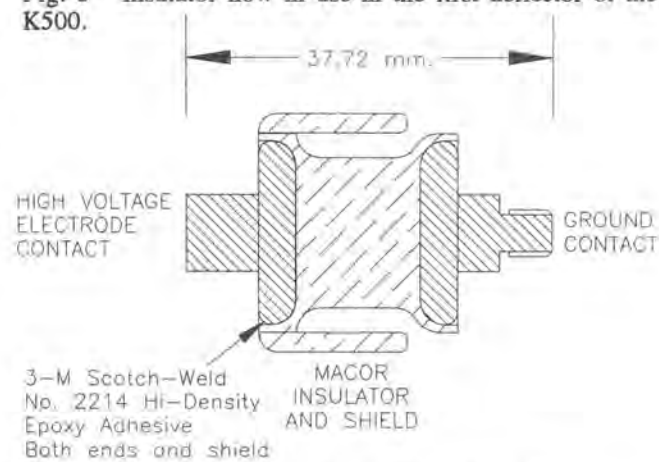


Fig. 6 Proposed self shielding insulator design.

Fig. 6 is a proposed design that attempts to cope with the plating problem by having an integral insulator shield.

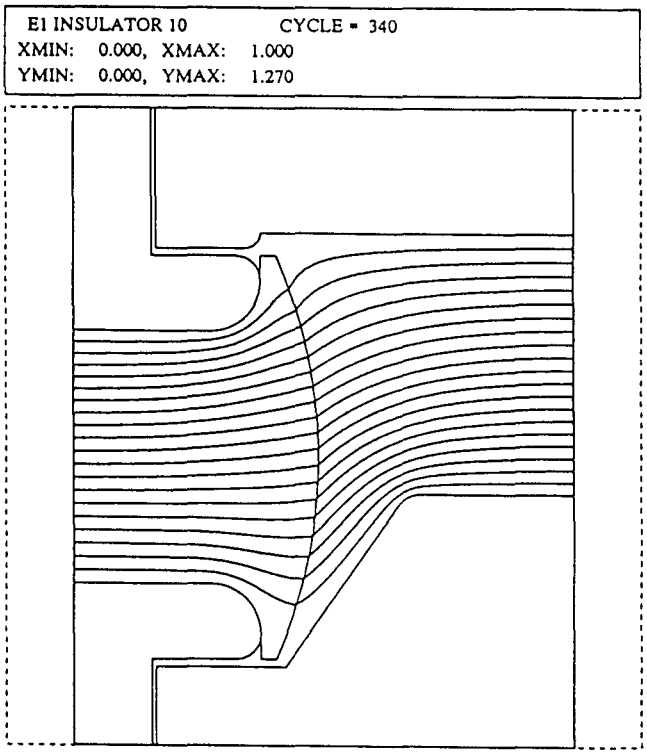


Fig. 7 POISSON field calculation of insulator in Fig. 5.

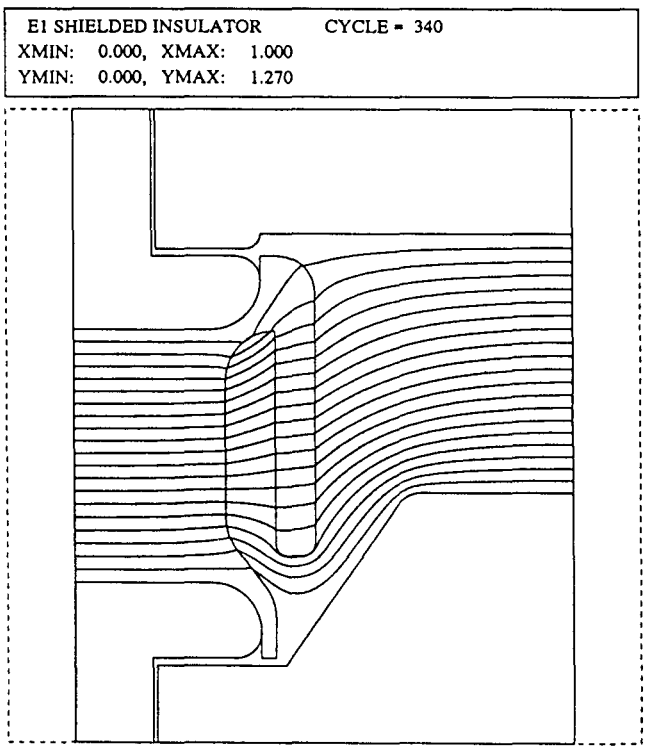


Fig. 8 POISSON field calculation of proposed self-shielding insulator.

Fig. 7 and Fig. 8 show POISSON plots of the fields for the designs in Fig. 5 and Fig. 6, respectively. The equipotential lines are in 5% increments. The shield does not appear to cause serious distortion to the field.

5. SLOTTED SEPTUM

It was suggested[1] that better pumping in the sparking region might help remove some of the effluent caused by the sparks. To improve the pumping, a slotted septum as shown in Fig. 9 was built. The septum showed no unusual behavior in the test stand so it was installed in the K500. There has been no noticeable improvement with this design but there is some indication that the deflector is more susceptible to the effects of the r.f. fields.

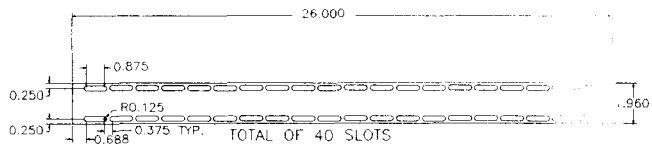


Fig. 9 Slotted system for improved pumping in deflector housing.

6. SPARK SHIELDS

From the beginning of operation, tungsten spark shields have been used above and below the high voltage electrode. Stainless steel shields have been tried in the K500 but seem to damage more easily. Shields made of 97% alumina were tried in the test stand. The maximum voltage that could be attained with no magnetic field was only 90 kV. Further, when the alumina shields were removed it was found that the surfaces exposed to the high voltage had acquired a yellow color. This apparently was not a hydrocarbon coating on the surface because it could not be removed by vigorous scrubbing. It has been suggested that the color may be the result of x-rays produced by the sparking.

7. IN-SITU GAS CLEANING

A technique for in-situ cleaning of the deflector insulators was developed by the MSUNSCL.[2] This consists of flowing a small amount of gas across the insulators while increasing the voltage and monitoring the leakage current. In practice, the gas flow is set by monitoring the pressure in the cyclotron and typically is about 3×10^{-5} torr. Several types of gas have been used: air, N_2, O_2, Ar and H. The higher molecular weight molecules seem to give quicker results in reducing the leakage current. It is possible, for light ion beams which do not require low operating pressures, to allow the gas to flow continuously during operation to suppress the leakage current.

A different technique has been attempted on the test stand. The gas is introduced at a sufficient rate to raise the pressure to the range of 40 to 500 microns. At these pressures glow discharges can be initiated. It has been found that cleaning in this manner with dry O_2 can improve the voltage holding capability of the insulators but only for a limited period of time. Further, it was found that attempting the same technique with H_2 resulted in a film of fine powder being produced throughout the deflector housing. The physical appearance of the deflector after scrubbing with O_2 was extremely clean with no evidence of any residue being created.

8. CONCLUSIONS

Several different approaches to improve the deflector have been tried in the test stand but to this point only marginal improvements have been achieved. The test stand has been a valuable tool in that it allows rapid changes of configuration and has been most successful in duplicating the failure mechanisms of the K500.

9. REFERENCES

1) Proskurovsky, D., FSU Academy of Sciences, Siberian Division, Institute of High Current Electronics, 4, Akademichesky Avenue SU-634055 Tomsk, Russia, private communications.

2) Miller, P., Michigan State University, NSCL, private communication.

SOME PERSPECTIVES IN THE BEAM TRANSPORT AND ANALYZING SYSTEM DESIGN FOR THE U-250 CYCLOTRON

L.E. Korolev
The D.V. Efremov Scientific Research Institute of Electrophysical Apparatus
St. Petersburg, 189631, Russia

ABSTRACT

The existing beam transport system for the U-250 cyclotron is designed in a traditional manner. Because of this the system does not allow the full experimental possibilities of the accelerator, especially in nuclear physics investigations. Electromagnetic equipment design experience acquired by specialists of the institute may be utilized in the design of the beam analyzing system, including that of the magnetic analyzer installed in the external beam line and of the broad range spectrograph for the analysis of nuclear reaction products. Such additions will change the U-250 complex into a universal research center.

1. DESIGN CONCEPTS FOR THE BEAM TRANSPORT SYSTEM

A multichannel beam transport system is necessary for the successful realization of the research programme of the U-250 cyclotron. It is desirable for any trend of cyclotron investigations to be provided with its own beam transport channel. Omitting the discussion on scientific directions, it may be remarked that the beam transport system of the U-250 cyclotron has to have at least 10 transport channels, each with its own target device. It is not necessary to install every target in a separate room, especially for targets equipped with remote control devices for their dismantling and transport.

It's unlikely to qualify the accelerator center as universal if nuclear spectroscopy and nuclear reaction studies are not provided with the appropriate equipment. Progress in this direction is possible only for a beam transport system equipped with a magnetic analyzer for the cyclotron beam and a broad-range magnetic spectrograph for secondary-particle analysis.

2. MAGNETIC ANALYZER PROJECTS FOR THE U-250 CYCLOTRON

The criteria are widely known to appreciate the characteristics of various types of magnetic analyzers. The most important qualities of any analyzer are defined by its optical parameters and its cost. A real magnetic analyzer project makes a compromise between these considerations. High resolution force is the main desirable physical parameter for a cyclotron beam analyzer, while a large solid angle and momentum acceptance may be required for satisfactory physical results from a secondary-particle analyzer.

The production characteristics of an analyzer depend on its design features that define the costs of analyzer manufacturing, installation and instrumentation.

The main optical schemes of magnetic analyzers are widely known. It is a suitable moment to remark that in spite of their simplicity, single magnet analyzer projects with homogeneous magnetic fields are objects of the past because of their unsatisfactory physical characteristics. Similarly, an $n = 0.5$ magnetic analyzer is not a suitable construction for a modern accelerator center. This leads to the questions: What magnetic schemes are available? Are they the combinations of some magnets united in a general assembly? Evidently this direction is a perspective one although, frankly speaking, it is not "terra incognita"– various assembly analyzers are also known[1–3]. Study of these references shows the attempts of assembly-analyzer designers to achieve a workable compromise between the high optical parameters of the analyzing device and a low production cost. Everybody may estimate the results of such attempts in different ways, but it is the author's opinion that these designers deserve great respect.

Magnet assembly analyzers are seldom used as a cyclotron beam analyzing system although an example of such a project is not difficult to name[1]. In the author's opinion, a 270° magnetic analyzer may be considered an acceptable alternative to an assembly analyzer for the U-250 cyclotron beam. This type of analyzer was produced by NIIEFA in two versions:

a) as the MSP-133, an experimental model with a central radius of $R = 0.6$ m[4];

b) as the SP-017 analyzer of the U-240 cyclotron, with a central radius of $R = 2.0$ m.

The magnetic scheme of the SP-017 analyzer is shown in Fig. 1. Its basic parameters are: inhomogenity field index $n = 0.872$, central radius $R = 2$ m, design resolution force $F_p = 22600$ (at 1 mm source width). The field inhomogenity is produced by pole faces that slope at a definite angle. Sextupole lenses are installed at the magnet edges for correction of second-order aberrations.

I would like to put forward some arguments to substantiate such a selection. The main argument for its preference is the large resolution force obtained; the second one is its compactness. Some doubts may arise about the simplicity of the manufacturing procedure for the device. However, it is necessary to take into account the NIIEFA available know-how in the production and the fitting of such equipment. It is evident that the beam analyzer for the U-250 cyclotron has to realize the main design ideas of the SP-017 analyzer but not to copy one in all of the details. In the author's opinion, keeping the principles reported above will guarantee the effective design of a magnetic beam analyzer for the U-250 cyclotron.

Among the secondary-particle analyzers, the assembly ones are sufficiently extended because of their sharp optical parameters. On the other hand, the split-pole spectrograph (Enge spectrograph) is known as a design alternative for an assembly analyzer[5]. A secondary-particle magnetic analyzer was designed by NIIEFA specialists on the basis of the constructive features of the split-pole spectrograph. As a result the stepped-pole spectrograph MSP-144 has been produced at NIIEFA[6]. In this analyzer two homogeneous magnetic zones and straight boundary lines create suitable conditions for both broad-range momentum acceptance and large solid angle. Comparative characteristics of the Enge and MSP-144 spectrographs are given in table 1.

It may be seen from these data that in optical characteristics the stepped-pole spectrograph is similar to the Enge spectrograph. However, the manufacturing features of the MSP-144 make it a simpler device than a split-pole analyzer.

Table 1
Comparative characteristics of the Enge and MSP-144 spectrographs

	Enge spectrograph	MSP-144 spectrograph
Magnetic rigidity (T-m)	1.3	1.25
Momentum ratio accepted simultaneously P_{max}/P_{min}	2.6	2.7
Solid angle (msr)	4–7	3.3–7.7
Resolution force (for 1 mm width source)	$(3-4.7)10^3$	$(3.4-4.2)10^3$

The experimental possibilities of the MSP-144 device were checked by specialists of LNR JINR (Dubna, Russia). Positive results of such checking have been expressed in the following production of four MSP-144 units for LIN JINR needs. A photograph of the MSP-144 analyzer is shown in Fig. 2. Data analysis of the stepped-pole spectrograph shows that this is an acceptable design basis of a broad-range magnetic spectrograph for the U-250 cyclotron.

3. SOME COMMON REMARKS TO THE BEAM TRANSPORT PROJECT

Generally speaking, the layout of the beam transport equipment is a problem of minor importance in comparison with the beam transport content problem. A symmetrical beam transport scheme is used in the U-250 project where switch magnets are installed in the central transport line. Because of this it is natural to arrange the analyzing-magnet equipment as some supplementary block that may be added to the available beam transport system without essential changes in the cyclotron equipment layout. It is evident that the cyclotron beam analyzer has to be arranged in such a manner as to provide their operation both together and apart.

One further remark should be made about the beam transport project. The words "some perspectives" are in the title of this report. This expression is usually said in Russian when a real possibility takes place for their creation. Someone may put a question: Is it justly for the U-250 beam transport project? The author of the report has no doubts of the expediency of this project and he would be ready to cooperate with every specialist or firm if they would have an interest in these ideas.

4. REFERENCES

1) Hints, R.E., Selph, F.B., Flood, W.S. et al., "Beam analyzing system for variable energy cyclotron", Nucl. Instr. and Meth. **72**, 61-71 (1969).
2) Wiender, C.A., Goldshmidt, M., Ricor, D. et al., "Performance of a QDDD spectrograph", Nucl. Instr. and Meth. **105**, 205-210 (1971).
3) Kato, S., Hasegawa, T. and Tananka, M., "A QDD-type magnetic spectrometer", Nucl. Instr. and Meth. **154**, 19-28 (1978).
4) Basargin, Yu.G., Boldin, N.I., Korolev, L.E. et al., "Ion optics and performance of a double focussing magnetic analyzer", Nucl. Instr. and Meth. **102**, 125-129 (1972).
5) Spencer, J.E. and Enge, H.A., "Split-pole magnetic spectrograph for precision nuclear spectroscopy", Nucl. Instr. and Meth. **49**, 181-193 (1967).
6) Basargin, Yu.G.,Boldin, N.I. and Korolev, L.E., "A broad range stepped-pole magnetic spectrograph", Nucl. Instr. and Meth. **126**, 413-416 (1975).

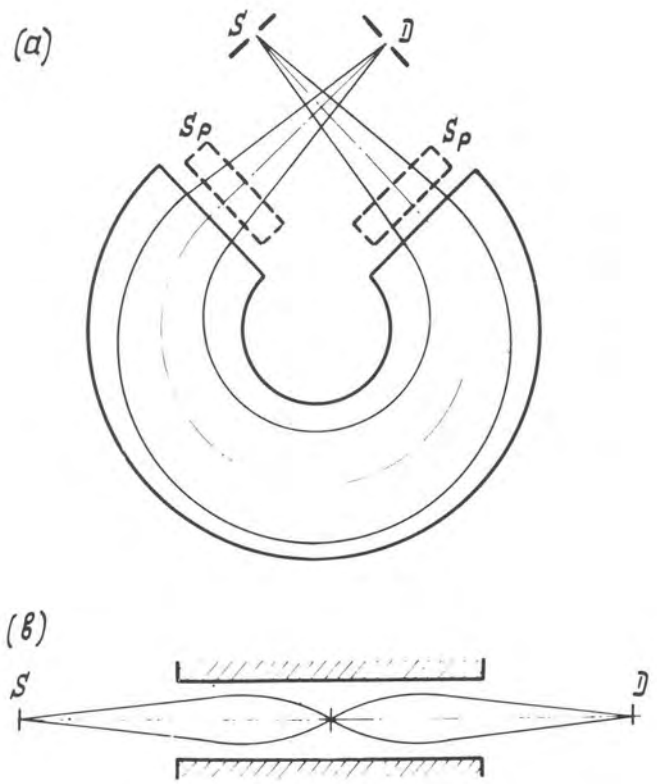


Fig. 1. Optical scheme of the 270° magnetic analyzer for horizontal (a) and vertical (b) planes. (Sp – sextupole lenses, S – source slit, D – analyzing slit).

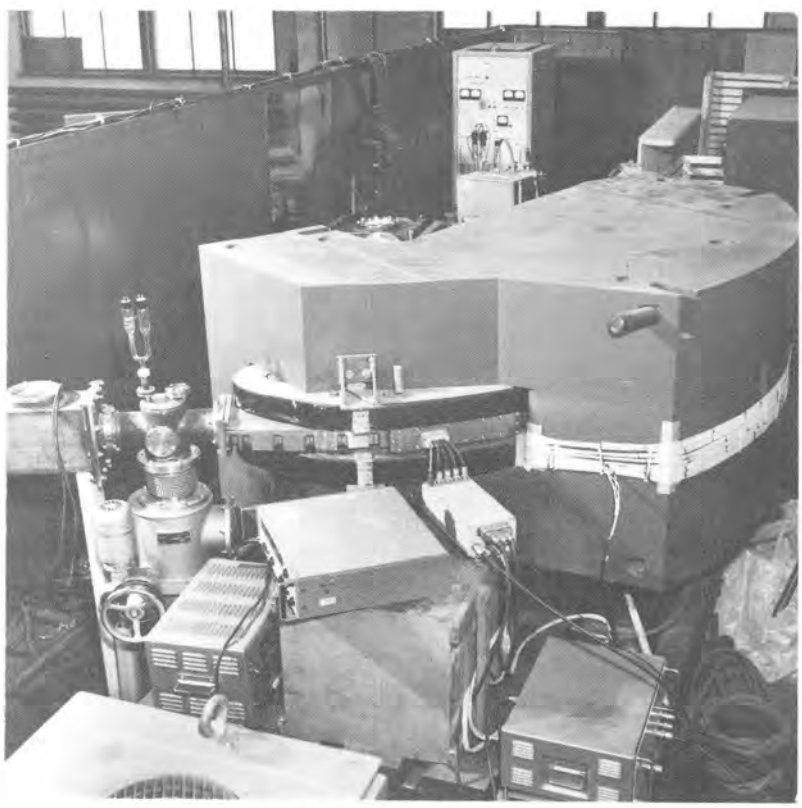


Fig. 2. NIIEFA made MSP-144 spectrograph.

BEAM TRANSPORT SYSTEM FOR THE IUCF HIGH INTENSITY POLARIZED ION SOURCE

W.P. Jones, T.J.P. Ellison, M.S. Ball, J.C. Collins, D. DuPlantis, D.L. Friesel, B. Hamilton, J.W. Hicks, and P. Schwandt*
Indiana University Cyclotron Facility
2401 Milo B. Sampson Lane
Bloomington, IN 47408 USA

ABSTRACT

The new High Intensity Polarized Ion Source[1)] (HIPIOS) being built at IUCF is designed to increase the intensity of polarized beams by approximately an order of magnitude. The 30 m long beam transport system which connects the 600 kV ion source terminal to the cyclotrons, has been designed with the goal of increasing the transmission of beam from the source to extraction from the main stage cyclotron by another factor of five. In this paper we will discuss the new beamline design and improvements to the beam bunching and injection systems which should provide this increase in transmission efficiency. The beam diagnostic system and procedures planned for tuning the beamline are discussed.

1. GENERAL DESCRIPTION OF SYSTEM

The beamline (BL1) consists of three 90 degree sections with a dispersion free double waist at the end of each. The third section is followed by two quadrupole doublets coupling the line to the injector cyclotron. Each 90 degree section consists of 5 quadrupoles and two dipoles. The first two are quite similar, with the magnets in the sequence QQDQDQQ. The quadrupole between the dipoles will be used to zero dispersion and its derivative; the other four will be used to adjust the location and size of the double waist in the straight section. The third section was designed to splice into an existing beamline and its optics are somewhat different. Its magnets are in a QDQQDQQ configuration. Rf bunching will take place in the straight section at the end of the first 90 degree section, and polarization measurements will be made in the second. The second straight section will also contain slit systems to produce a pencil beam and steerers to use this pencil beam to map out the acceptance of the cyclotron. The quadrupoles and dipoles have been designed to have apertures of twice the expected beam envelope. Because of the low rigidity of the beams in the line this has not had a significant impact on magnet costs.

*Work supported in part by the National Science Foundation under Grant Nos. NSF PHY-8914400 and NSF PHY-9015957

2. BEAM DIAGNOSTIC SYSTEMS

2.1. Introduction

The beam diagnostic systems include a nonintercepting beam position monitoring (BPM) system, phase pickups and longitudinal profile monitors; these latter two systems will be discussed in the section on beam bunching. Since the beam intensity will be so high (in the range from 1 to 100 μA), all these systems will be able to process information with high bandwidths (100 kHz) while still providing excellent (60 dB) signal to noise. Consequently, they will be used in high speed hardware feedback loops to keep the ion optical parameters optimized.

2.2. The BPM System

The BPM system, although based upon our previous designs for the Cooler and present cyclotron beamlines, has been completely redesigned. The systems will process information at rates up to 100 kHz, have a nominal accuracy of 0.1 mm, and precision of 0.02 mm. The entire system (pre-amplification and vector sum and differences of the rf signals, rf-IF conversion, and signal processing) is all contained on a single 4 layer board. Although the board will accept signal with frequencies as high as 60 MHz and will operate with an IF as high as 1 MHz, there are no standard "rf" components with exception of mixers. Instead, high speed operational amplifiers are used in both in the rf and IF sections. Such a design would not have been possible, or would have been prohibitively expensive, 5 years ago. The board has 6 analog inputs and 4 analog outputs. The input signals consist of: 4 information signals from the 0.05 m length electrodes (vertical top and bottom, and horizontal left and right); the local oscillator; and a calibration signal which can be switched on the board to any of the four signal inputs. The board also outputs 4 information signals (corresponding to the 4 input information signals):

the horizontal and vertical beam positions, beam intensity, and quadrupole moment.

3. EMITTANCE MEASUREMENT

At the entrance to BL1, a quadrupole and wire scanner are being used to measure emittance of the beam entering the line by measuring beam size as a function of quadrupole strength. This information will then be input to a TRANSPORT calculation to determine the settings of the quadrupoles needed to bring the beam around the first corner with the desired properties.

3.1. Measuring Beam Envelopes

After the emittance has been measured, we will be in a position to use the BPM system to measure beam envelopes even though the BPM's are only measuring the centroid of the beam. The procedure planned is to use two x-y steerers located in the drift space before the first quad to sweep the beam along the surface of an ellipse that has the same shape and has one fourth the area of the beam. By making synchronous measurements of the beam centroids and steerer settings the shape and size of the beam ellipse at each BPM will be obtained.

4. BEAM STEERING AND CENTERING

BL1 has been designed so that, starting at the beginning of the line, pairs of steerers and BPM's are located approximately every 90 degrees in betatron phase advance (in both traverse planes) along the beamline. Redundancy is provided by the fact that each BPM measures both horizontally and vertically and there are some BPM locations that are used for vertical information with the horizontal information being a secondary consideration.

It is planned to steer the beam by stepping down the beamline using each steerer in turn to zero the beam's position at the BPM 90 degrees downstream of the steerer. Although this procedure can be easily performed in a "manual" mode, the entire operation will be automated.

5. QUADRUPOLE TUNING PROCEDURES

5.1. Dispersion Control

BL1 is designed to have zero dispersion in the straight sections. For the first two corners which have a quadrupole magnet centered between the dipoles, there is a unique setting of that quadrupole which will zero the dispersion everywhere in the subsequent straight section. The BPM at the entrance to the quadrupole following the second dipole in the corner will be used to measure the change in horizontal position while the control computer is varying the two dipole fields. The sensitivity of this method is such that a 1% error in quadrupole strength will give a 0.8 mm position shift at the BPM when the dipoles are being varied by +/- 1%. This position amplitude is about 50 times the BPM system resolution, and thus it should be possible to set these quadrupoles with a precision of about 0.01%.

Setting the quadrupoles in the third corner is somewhat more complicated because there are two quadrupoles between the corner dipoles. However the effect on dispersion of one of the quadrupoles is four times than that of the other. Thus by using the sensitive quad in an analogous way to those in the first two corners, it will be possible to zero the dispersion in the last straight section in a straightforward manner.

5.2. Focussing Adjustments

In order to provide control of the position and sharpness of the waists in the straight sections, software controls for combinations of quadrupoles will be created. It is possible to generate four combos (linear combinations) which independently adjust the position of the x or y waist and the sharpness of the x or y waist. Combo's of the readouts from the beam sweeping system will provide a measurement of each of these parameters. Consequently there will be a unique readout for every control, leading to simple "manual" or automatic setting of quadrupoles.

6. BEAM BUNCHING AND PHASE CONTROL

6.1. Overview

There is a two-stage bunching system. In the ion source terminal there is a gridded single-gap buncher with a ramp waveform. This buncher will operate at the cyclotron frequency, or the 2nd or 3rd subharmonic for beam pulse-selection. This system pre-bunches up to 90% of the beam into a 60 degree width bunch for further bunching by a resonant klystron buncher in the beamline. This second buncher has an adjustable length to maximize the transit time factor for any beam species and any cyclotron rf frequency. The location of this buncher determines the ratio of the beam energy spread to phase spread at the injector cyclotron. It is located 21 m upstream of the cyclotron to provide beams with an energy spread of +/- 1.5 keV and +/- 4 degrees.

6.2. Buncher System Beam Diagnostics

Both bunchers will be phase-locked to the beam, consequently automatically compensating for the myriad of mechanisms which can cause a change in the beam phase with respect to the bunchers. The voltage of the high energy buncher needs to be scaled as a constant plus an amount proportional to the square root of the beam current due to space charge effects; this will be done in hardware using a beam intensity monitor and fast signal processor to send a beam current dependent reference signal to the automatic level controller (ALC).

At the entrance to the cyclotron, the beam bunches will be about 0.005 m in length. To measure their length

we are using a Longitudinal Profilometer (LPM) which consists of 3 parallel chemically-etched grids, separated by 0.002 m, mounted with their surfaces normal to the beam direction. The outer two grids will be grounded to prevent the center grid from sensing the electric field from the beam before its arrival. The signal will be taken from the center grid. We do not have instrumentation capable of resolving such high frequency signals; instead, a Bunching Factor Diagnostic (BFD) will calculate the bunching factor by comparing the amount of power detected at multiple harmonics of the fundamental frequency.

We may, in addition, have automatic tuning of the buncher amplitude and phase. The buncher amplitude would be controlled by modulating the amplitude and synchronously detecting the output of the BFD to generate an error signal. A similar system would modulate the buncher phase and synchronously detect the beam current at the output of the cyclotron.

7. MATCHING TO INJECTOR CYCLOTRON

The injection system for the Injector Cyclotron consists of two electrostatic cylindrical inflectors. The first element is used to compensate for the fringe fields of the cyclotron magnets and bends the beam in the opposite direction as the second element. The gap in this element has been increased by 25% to minimize its restrictions on the beam and provide greater flexibility in steering. The second element has been one of the primary restrictions for the present beamlines and because of voltage holding capabilities in a confined space it is not possible to increase its gap. In the current system, the distance between the inflection elements and the rf buncher is much less than in the new system and as a result the energy spread in a beam of a given pulse length is much larger than in the new system (+/- 5.0% rather than +/- 0.3%). This places a significant limit on the transmission from existing beamlines to the cyclotron.

Four tuning combos will be generated using the last four quadrupoles to adjust the positions of the two waists and their sizes inside the cyclotron.

8. BEAM INTENSITY MODULATION SYSTEM (BIMPS)

An electrostatic quadrupole which is located after the junction of the new beam line with two existing injection lines will be used to modulate the beam intensity when beam is being shared by users with significantly different intensity requirements. This quadrupole, which will be off for the high intensity operation, will be pulsed on to blow up the beam when the switching magnet is set to bring beam to the secondary user who requires a less intense beam. This system has already been tested and found to be very effective in the present beamline, providing modulation of the beam current by a factor of 1000 on a 1 μs time scale.[2)]

9. SUMMARY

The beamline has been designed to incorporate diagnostics which can, in essence, provide an error signal for each variable in the line. This will lead to a significant reduction in the time needed for manual setup of the beamline and will make it possible to fully automate systems as they are commissioned.

10. REFERENCES

1) Derenchuk, V. et al., these procedings.
2) M. S. Ball, B. Hamilton, private communication.

SUPERCONDUCTING FOCUSSING CHANNEL FOR THE AGOR CYCLOTRON

H.W.Schreuder* P.Blache, C.Commeaux, S.Gustafsson, A.Lafoux, M.Mormiche and R.Panvier
Institut de Physique Nucléaire, 91406 Orsay, France†

ABSTRACT

The AGOR cyclotron will be equipped with a focussing channel consisting of two superconducting coil systems, placed inside a shielding tube. The channel will focus the beam during its passage through the magnet yoke. Magnetic, cryogenic and mechanical aspects of the design are discussed.

1. INTRODUCTION

Extraction of the beam from the AGOR cyclotron is performed by three channels: an electrostatic deflector (ESD), a room-temperature electromagnetic channel (EMC-1) and a electromagnetic channel with superconducting coils (EMC-2). The lay-out of these channels is shown schematically in fig.1.

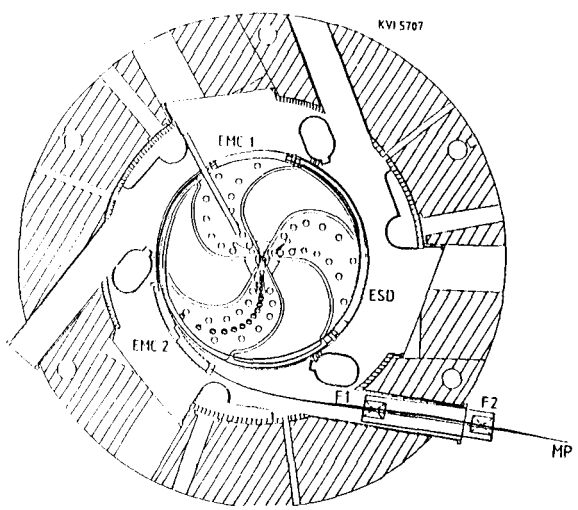


Fig.1. Median plane section of AGOR, showing the elements of the extraction system.

*permanent address: Kernfysisch Versneller Instituut, Zernikelaan 25, 9747 AA Groningen, Netherlands.

†Work jointly supported by the Institut de Physique Nucléaire et de Physique des Particules (IN2P3), France and the Stichting voor Fundamenteel Onderzoek der Materie (FOM), the Netherlands.

After the exit of EMC-2, the beam enters a passage through the magnet yoke through which it passes to the outside of the machine. In order to provide focussing for the beam on its 3.4 m long trajectory between the exit of EMC-2 and the beginning of an external beam guiding system, a set of two quadrupoles is foreseen inside the yoke passage. Various aspects of the design have been described in AGOR internal reports, one of which[1] presents a summary with references to the other reports.

2. FOCUSSING AND BENDING DURING THE YOKE PASSAGE

2.1. Beam Focussing

The first order optics of the extracted beam along the extraction path bears resemblance to a periodic structure with a FD lattice. The extraction channels EMC-1 and EMC-2 provide horizontal focussing by means of their gradient coils, the fringe field being horizontally defocussing. The first focussing element, located at the entrance of the yoke passage, is horizontally focussing, the second, situated just after the beam has left the magnet yoke, provides vertical focussing. Since the orbits of the different ions are not far apart geometrically, focussing strengths could be chosen to be approximately proportional to beam rigidity with a maximum gradient of 36 T/m at a magnetic length of 0.2 m.

2.2. Beam Bending

The degree of saturation of the magnet yoke varies considerably over the operation range of the magnet. For the lowest excitations, associated with the acceleration of protons, the magnetic field in the yoke passage is nearly zero. However, at the maximum cyclotron field of 4 T the field in the yoke passage is 0.22 T. The trajectories of different beams in this passage therefore have different radii of curvature. In order to allow alignment of the beam onto the axis of the external beamline, the deflection produced by the final extraction channel EMC-2 is adjusted in such a way that all beams, regardless of magnetic rigidity, pass through one common point on

this axis. At this location, situated 1 m beyond the magnet yoke and called the 'Meeting Point' (MP), a small bending magnet is foreseen to provide alignment with the axis of the beam line. Inside the yoke passage, the variations in orbit curvature are associated with a spread in the transverse position of the different central orbits at the entrance of the first quadrupole, requiring a corresponding positioning range for this element. Calculations[2] have indicated the feasibility of reducing the positioning requirement by the introduction of a soft iron shielding tube inside the yoke passage, inside which both quadrupoles are mounted. The calculated remaining field inside the tube is only 7.8 mT, resulting in straight trajectories inside the shielding tube leading to a reduced positioning requirement at the channel entrance of 18 mm. In addition, since all (straight) orbits pass through the MP, positioning is equivalent to a rotation around this point.

3. STEERING

Since the strength of the magnetic field along the trajectories of the extracted beams will not be known with adequate precision until measured field maps are available, the calculated field strengths in the extraction channels necessarily have a certain margin of uncertainty. In addition, the cyclotron's magnetic field may prove to have horizontal field components, due to misalignments or constructional tolerances, leading to vertical deflection of the beam. It is therefore necessary to provide steering in both horizontal and vertical planes before the beam leaves the cyclotron. For this purpose, a horizontally steering dipole coil, capable of a deflection of 5 mrad, is integrated in the first quadrupole. In addition, 2.5 mrad of vertical steering will be provided in each of the quadrupoles by operating the upper and lower coil sets at different currents.

4. DESIGN

4.1. Coil Configuration

Figure 2 shows a cross-section of the shielding tube at the location of the first focussing element.

The beam aperture is 30 x 20 mm. All coils have a racetrack shape. The four windings with a flat cross-section constitute the steering dipole, which can produce a maximum field of 0.1 T. The focussing gradient inside the beam aperture consists of the stray fields produced by the two sets of four windings at both sides of the beam aperture, which simply are dipole coils with fields of opposite signs.

Each winding carries 49000 Ampere×turns at the nominal gradient of 36 T/m, which is constant within 1% over a total width of 20 mm. The difference in current between upper and lower coils for the required 2.5 mrad of vertical steering is 10%.

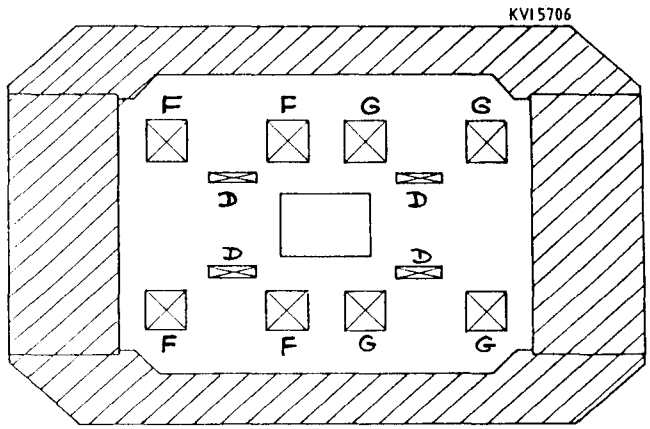


Fig.2. Cross-section of shielding tube and first focussing element. F and G are gradient coils, D is the dipole coil.

4.2. Cryogenic Design

The coils will be fabricated in-house, using the wet-winding technique using wire with a diameter of 0.5 mm, including insulation. The wire itself has 561 NbTi filaments with a diameter of 10.3 μm and a copper to superconductor ratio of 2.4. The need for unequal currents in the upper and lower coils, required for vertical beam steering, implies that three current leads are required for each focussing element, one of the leads being shared between top and bottom coils. Two additional leads are used for the dipole coil in the first element. The cryogenic equipment associated with the channel is housed in a vertical cylinder connected to the beam pipe at the outside of the magnet yoke. It has a reservoir for liquid helium, the level of which will be regulated. The coil mandrels receive their liquid helium from this reservoir, the tube for the return gas being connected to the same volume, which also houses the current leads. A separate tube supplies cold gas from this volume to the thermal shield surrounding the coil mandrels. The return gas from the shield cooling and the gas emanating from the current leads is returned at room temperature to the suction side of the compressors of the helium liquifier. The liquid helium consumption of the channel is estimated at 4 l/h.

4.3. Mechanical Design

The mechanical structure of the channel has been designed to satisfy the positioning requirements, to cope with the magnetic forces and with the weight of the system. As explained in section 2, positioning is reduced to a rotation about the MP. This point, however, is not physically accessible since it is the location of the first steering magnet in the external beam line. Also, the location of the MP is defined with respect to the magnet pole, while the vacuum tube in which the channel is located is part of the main cryostat, whose position with

respect to the magnet is not accurately known. As shown in fig.3, these problems were solved by cantilevering the shielding tube containing the lenses from a picture frame support outside the magnet.

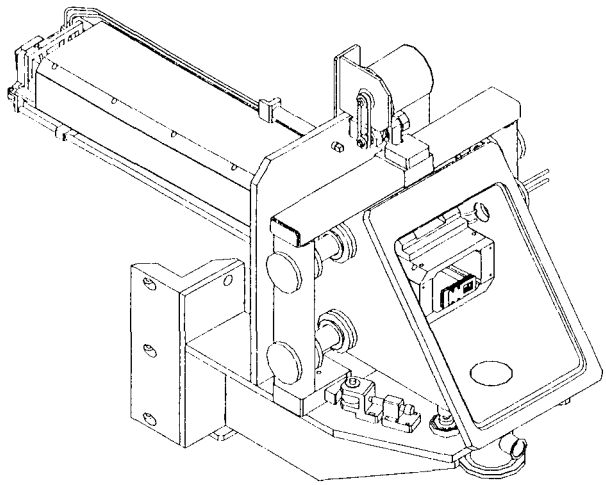


Fig.3. Perspective view of the channel with its support structure. The buffer volume for liquid helium is not shown.

This frame is positioned on a short section of a circular track centered on the MP and supported by the magnet yoke. In this way, positioning is done with respect to the magnet, independently of the walls of the cryostat beam pipe. The shielding tube, located in the machine vacuum, is fixed to the picture frame, which is in air, by means of two horizontal rods passing through the vacuum wall using bellow seals.

5. DIAGNOSTICS

In operation, the beam must pass on the axis of the channel. The beam position with respect to the axis must therefore be measured at the entrance and at the exit of the channel. At the entrance, the channel is aligned on the beam by a rotation around the MP and the steering dipole in the first quadrupole is used to aim the beam at the MP. This dipole may turn out to be redundant, since the deflection produced by EMC-2 can also be used for horizontal steering. In the vertical plane, the vertical steering capability of the first lens is used to position the beam on axis at the location of the second quadrupole. The vertical steering of this element is then used to align the beam to the geometric median plane. The vertical position must therefore be measured at the second quadrupole and at a point further down the beam line.

In summary, the following diagnostic equipment will be integrated in the channel:

At the channel entrance : one harp for horizontal beam position. At the channel exit : one harp for horizontal beam position, one harp for vertical beam position.

The quadrupoles will be protected from incident beam by means of a diaphragm at their entrance. The diaphragm will be equipped with beam current read-out and is be capable of safely accepting the dissipation of 200 W of beam power.

6. REFERENCES

1) H.W.Schreuder, "The Quadrupole Channel" AGOR technical note NT/EXT/14/02/92.
2) S.Gustafsson, "Proposition de quadrupole supraconducteur blindé." AGOR technical note NT/AIM/15/10/90 (in French).

THE BEAM-GUIDING SYSTEM OF AGOR

J.M. Schippers *
Kernfysisch Versneller Instituut,
Zernikelaan 25, 9747 AA Groningen,
the Netherlands

ABSTRACT

The design and status of the beam guiding system between the AGOR cyclotron and two target stations (among which a magnetic spectrometer) is discussed. An overview of the optics and the matching of the extracted beams is given. Examples of beam-transport calcualtions are shown and some devices for beam diagnostics are discussed.

1. INTRODUCTION

In 1994 the super-conducting cyclotron AGOR will be installed at the KVI in Groningen. It will replace the existing Philips cyclotron. Within the existing building, a new layout of the experimental area is made and new experimental setups will be installed at new target stations: a large scattering chamber "Huygens Vat" and a new QQD-type magnetic spectrometer (resolution $\Delta p/p = 2 \times 10^{-4}$). For the moment only the new beam lines to the QQD spectrometer and to the Huygens Vat have been designed in detail. In a later stage also beam lines to other target stations (for polarization experiments, gamma-ray spectroscopy, applied research and a facility for radio-therapy with protons) are foreseen.

2. THE DESIGN OF THE BEAM-LINE OPTICS

2.1. Global Description

The beam lines are designed for particles with momentum rigidities up to 3.7 Tm. For the two target stations different types of beam-transport are possible:
QQD spectrometer:
-High resolution transport, dispersion matched beam.
-Achromatic transport, mainly intended for heavy ions.
Huygens Vat:
-Achromatic transport, mainly intended for heavy ions.

The beam lines are separated into several optical sections. In Fig. 1 the layout of the beam lines is shown. Globally the following functions are assigned to different sections:

1) From extraction until Slit-1 the phase-space of the beam is matched using five quadrupoles. The extracted beams may be regarded as originating at a virtual waist in the extraction channel. The horizontal and vertical waists have been chosen as object points for the transport calculations. These object points are imaged to the center of a small bending magnet, located at the position where all extracted beams will meet, each at a slightly different angle. Using the small bending magnet at the meeting point and the steering properties of the first two Q-poles in the extraction channel, the extracted beams can be aligned onto the optical axis of the beam guiding system. A triplet following the bending magnet makes an image at slit-system Slit-1.

2) In addition to the betatron motions of the extracted particles, there exist large correlations between the momenta and horizontal positions of the particles. The correlations correspond to dispersions between 1.6 and 5.0 cm/(%$\Delta p/p$) and may have a large uncertainty.

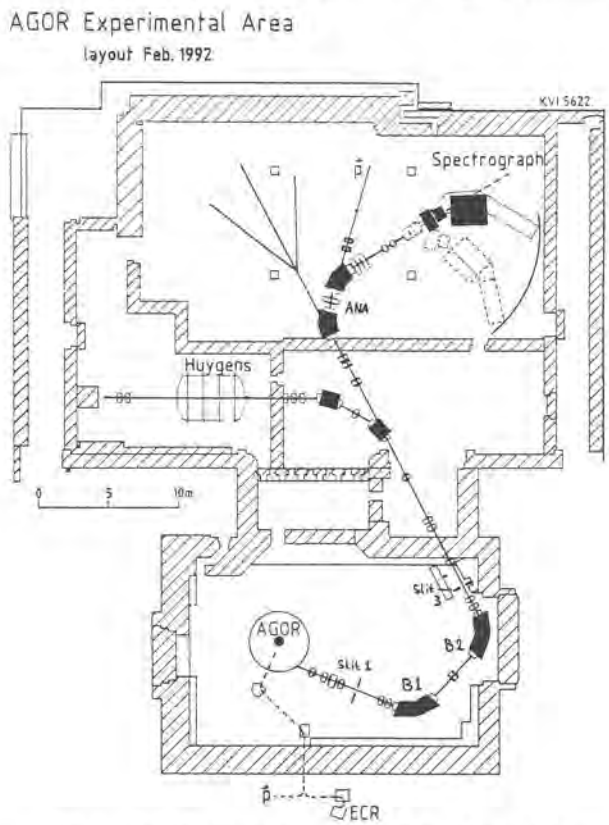


Fig.1. AGOR experimental area and beam-line layout at the KVI.

*This work was performed as part of the research program of the "Stichting voor Fundamenteel Onderzoek der Materie" (FOM) with financial support from the "Nederlandse Organisatie voor Wetenschappelijk Onderzoek" (NWO).

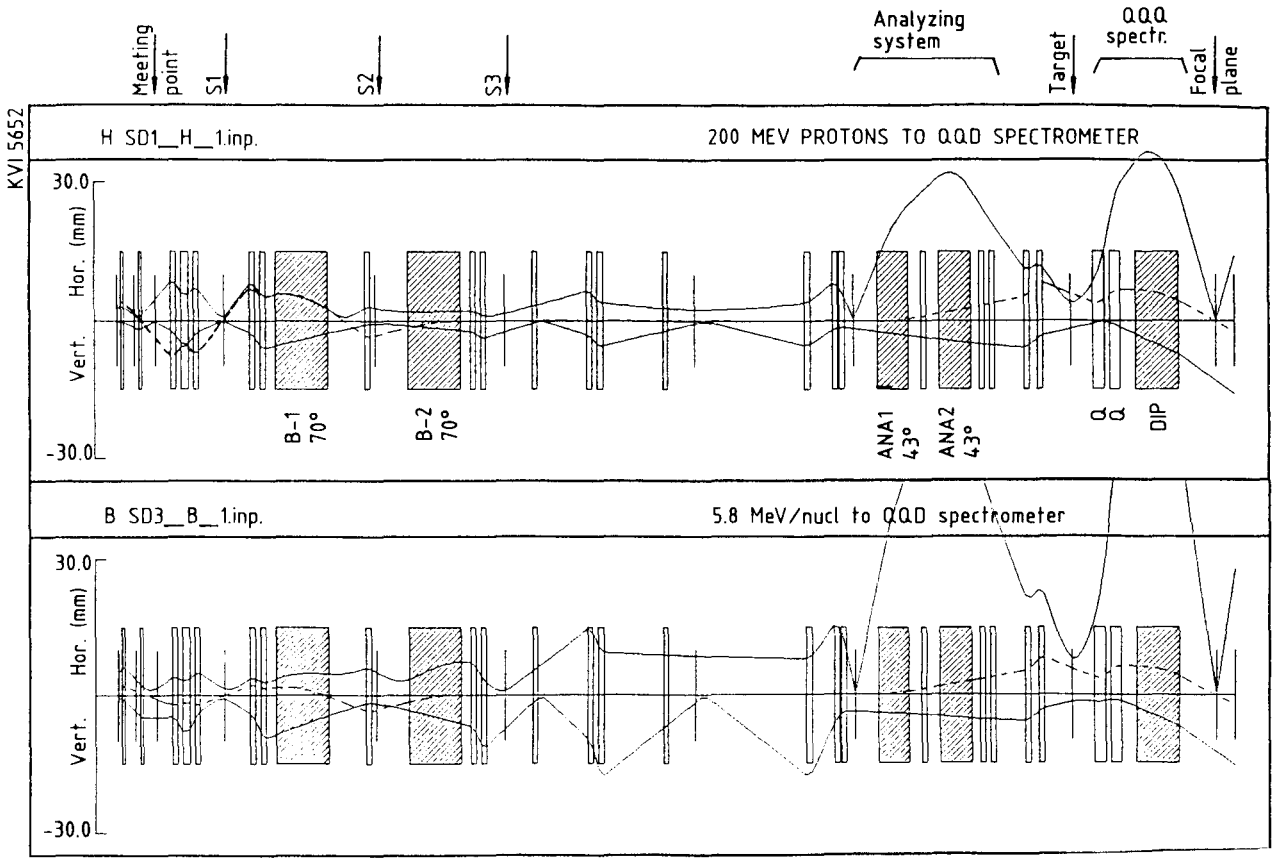


Fig. 2. Envelopes and dispersion lines (dashed) for two AGOR beams in high-resolution mode to the QQD magnetic spectrometer.

These correlations could easily cancel the dispersion of the analyzing system necessary for high resolution experiments. Therefore, after Slit-1 the momentum correlations in the extracted beam are compensated using the system with the two bending magnets B1 and B2. Then at Slit-3 (located just before the exit of the cyclotron vault) there are no correlations between particle momenta and horizontal positions anymore.

3) Slit-3 serves as a new object point for the transport to the targets. Starting at this point the beam transport is the same for all AGOR beams so that, for the optical mode selected, the magnet settings just scale with beam momentum.

4) Matching to the target conditions is performed in the last sections.[1)]

-The beam is transported to the Huygens Vat in an achromatic mode. For heavy ion beams the target-spot size depends strongly on the dispersion at the target, which should therefore be minimized.

-At the QQD target the momentum dispersion $D_a \approx 5.6$ cm/(%$\Delta p/p$) due to the analyzing magnets ANA1+2 can be matched to the QQD dispersion and the reaction kinematics, so that the spread in beam momentum does not contribute to the spot size in the focal plane. Slit-3 is imaged with a magnification factor $M = 1/5$ to the target. Then at the target the dispersion R_{16} is:

$$R_{16} = M \cdot D_{slit3} + D_a$$

In this way the effect of a possible error D_{slit3} in the compensation of the momentum correlations, is decreased with a factor 5. Further more, a large slit opening decreases the contribution of slit scattering, which is very important for experiments at zero-degree. It is also possible to tune the analyzing system as an achromat, allowing a larger acceptance and a smaller target-spot size, which may be important for heavy ion beams.

2.2. Transport Calculations

Beam-transport calculations have been performed using the characteristics of 11 different beams at extraction, as calculated by the AGOR theory group. For these beams, scattered over the whole operating diagram of AGOR, the phase space properties have been calculated and the positions of the virtual waists have been derived.

In Fig. 2. TRANSPORT calculations of the envelopes of 200 MeV proton- and 5.6 MeV/nucl. heavy ion beams to the QQD spectrometer are shown (point H and B in the AGOR operating diagram). In the figure the dashed line represents the dispersion. The compensation of the dispersion present in the extracted beam is

performed with B1 and B2. As can be seen, at the focal plane of the spectrometer the dispersion equals 0.0, reflecting the effect of dispersion matching at the target. It is possible to change the lateral and angular dispersion, the horizontal and the vertical spot size at the target within certain ranges, which may be necessary to compensate for reaction kinematics.[2)]

In general, only in the first part of the beam line the magnet setting depends on the beam properties. It has been found that only 4 different "basic settings" are needed for the beam transport to Slit-1, while the setting of the lenses between Slit-1 and Slit-3 is directly related to the type of basic setting used before. After Slit-3 in principle only a choice has to be made between an achromatic- or a dispersion-matched setting.

Second order transport calculations have shown that aberrations induced by the analyzing magnets and two 3°-bending magnets, used for shifting the beam axis 35 cm in the vertical direction, increase the incoherent spot-size at the QQD-target more than a factor 3. However, by adding two small sextupoles to the analyzing system these second order aberrations can be compensated sufficiently.

3. BEAM DIAGNOSTICS AND CONTROL

Beam diagnostics will be performed with beam-profile monitors, non-intercepting beam-current monitors, electrostatic pick-up electrodes and direct beam current measurements with Faraday cups and slit systems. The beam profile monitors are mostly "harps": grids of 48 wires of 20μm mounted on an actuator. Measurement of the secondary-emission current on the wires gives a spatial beam-intensity distribution. Also several non intercepting beam-profile monitors using the residual gas in the beam pipe[3)] will be used.

The read-out electronics for the profile monitors has been bought at the IPN at Orsay and it has arrived this year. The electronics for the pick-up electrodes is designed and prototypes have been tested succesfully.

A non-intercepting beam current measurement device has been tested successfully. Basically it is a toroid with a high-μ_r core, surrounding the beam pipe. It serves as a current transformer, with the (chopped) beam current as the primary current. With electronics developed at the KVI, beam currents from 1eμA down to one enA. can be measured by integrating the secondary current in the toroid, see Fig. 3. Several pieces of this device have been built at the KVI.

Signals from the instruments for beam diagnostics will be sent to a Micro-Vax of the central control system,[4)] via a BitBus line. Also the power supplies of the magnets will be controlled with BitBus. The control system is based on a local micro-controller, serving as a BitBus node. Every instrument (e.g. power supply or harp) is, in principle, interfaced to one node. In this way the central control system is relieved from details (of the instruments at the nodes; only the principal messages (e.g. "set current" or "give profile") are sent and received via BitBus.

The beam line has been divided into several vacuum sections and the PLC of the vacuum control system can also be connected via BitBus to a Micro Vax of the central control system. Then the PLC is also regarded as one BitBus node.

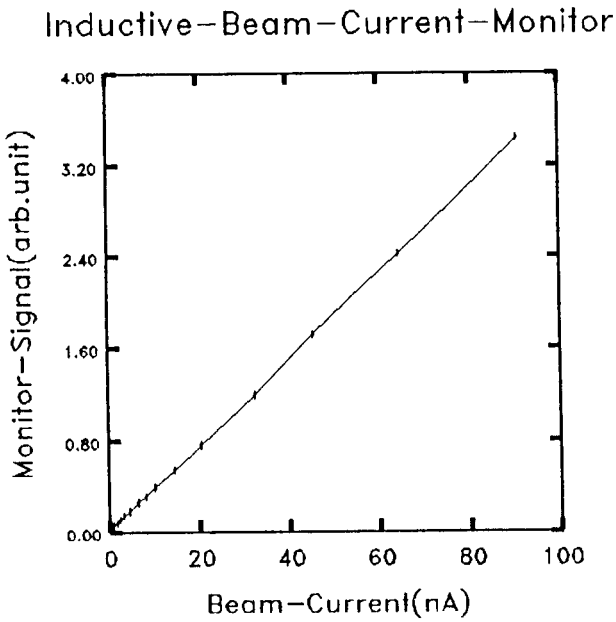


Fig.3. Signal from the inductive beam-current monitor, measured as function of beam intensity, simulated by a chopped current.

4. PRESENT STATUS OF THE BEAM LINES

In march 1992 the manufacuring of the magnets has started at Danfysik. The first batch of magnets is expected to be delivered in the autumn of 1992, at which date the building phase of the beam lines will start.

The manufacturing of almost all necessary components for diagnostics and the vacuum system has been completed now.

The design and first tests of the control of the vacuum system has started. Local pump control-stations have been built and are ready for installation now.

5. REFERENCES

1) J.M. Schippers, "The optics of the AGOR beam guiding- and analyzing system for high resolution transport", AGOR-beta TN-BUN-21-5-91.
2) J.M. Schippers, "The first order beam conditions at the QQD target", AGOR-beta TN-BUN-25-9-91.
3) J.M Schippers and H.H. Kiewiet, "A beam-profile monitor using residual gas", these procedings.
4) P.A. Kroon et al., The control system of the AGOR cyclotron, Proc. Europhysics. Conf. on Control Systems, CERN 90-08 (1990).

BUNCHER IN THE BEAM LINE FROM ECR TO SFC

J.Z.Jiang, X.H.Zhou, Q.Wang, F.Wang, W.M.Jiang
IMP,Academia Sinica,P.O. Box 31, LanZhou,730000, China

ABSTRACT

A buncher was used to produce the required bunched beams at the entrance of SFC. The buncher consists of two parallel mash plates. It is excited by an RF voltage with a saw-tooth waveform produced directly from a waveform convertor without combining RF sine wave with different higher harmonics. There are significant advantages for using waveform convertor at the lower operating frequencies. The peak-to-peak amplitude of the saw-tooth wave is about 800v. The stabilities of the voltage amplitude and the phase are less than $\pm 1 \times 10^{-3}$ and $\pm 0.5^0$ respectively.The maximum reguired RF power is 500 W.

1. INTRODUCTION

To achieve high energy resolution of the output beam from HIRFL. The beam injected into SSC must be bunched to three degrees in RF phase. This corresponds to 1.3 ns to 0.6 ns bunches for the 6.5 to 14 MHz frequency range of SSC RF and this exacting requirements must be established at the injection orbit by the external bunching system. The bunching system consists of a buncher B_0 and two rebunchers B_1, B_2 (rebuncher is not described in this paper), see Fig.1.

The new ECR ion source was installed and tested in the injection beam line. It is able to provide variant beams with continuons microwave into SFC. But the RF accelerating phase is about only few degrees in the injector SFC accelerating gap. Most of beams must be lost if the continuous beams are injected derectly into SFC from ECR ion source. The buncher was designed and constructed to modulate the continuous beams from the ECR ion source and to match the RF accelerating phase with SFC in RF phase.

2. BUNCHER

The single gap buncher consists of two parallel mesh plates. The two electrodes with hexagonal mesh are made of copper plates by photo etching and are insulated with ceramics. The size of hexagon is 2 mm. Both width and thickness of the mesh are 0.1 mm. The gap between two electrodes is 5 mm and the diameter of the mesh section is 60 mm. Aligning the meshes of the two electrodes may increase the beam transmission of the two grids almost to that of a single grid. The efficiency of beam transmission is more than 83%.

The buncher is excited by an RF voltage with sawtooth-like waveform as indicated in Fig.2, it is produced directly by a waveform convertor without combining RF sine wave with different higher harmonics. There are significant advantages for using the waveform convertor to produce the sawtooth waveform at the lower operating frequencies.

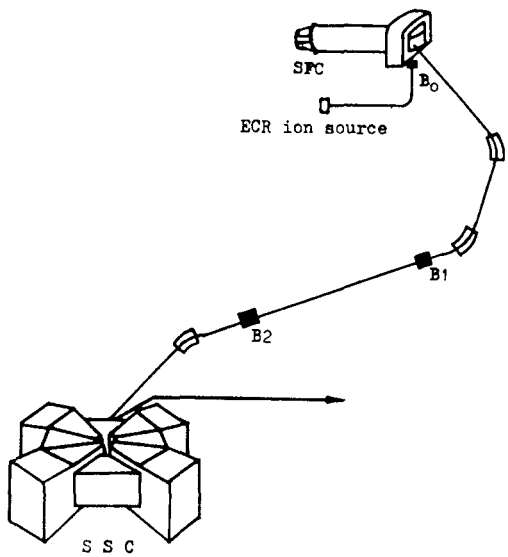


Fig.1 Schematic layout of the buncher B_0 and the rebunchers B_1, B_2

3. WAVEFORM CONVERTOR

Combination with higher sine wave harmonics is a normal way to produce the sawtooth wave. For example, using fundamental and second, third harmonics with the

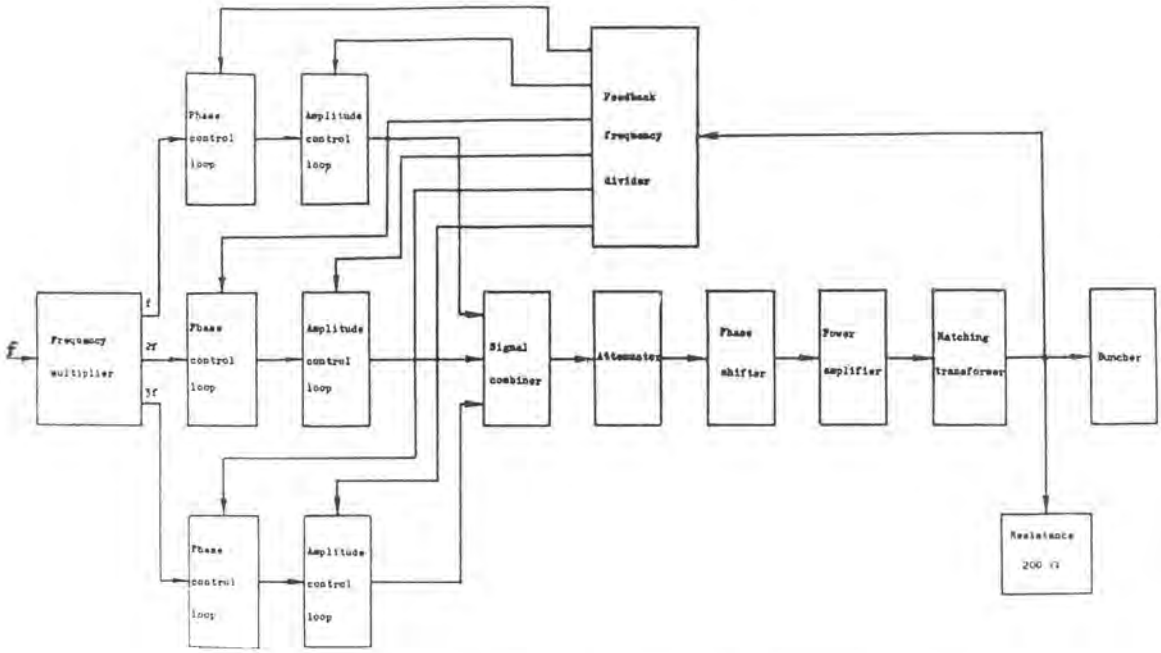


Fig.3 Block diagram of the buncher circuit for the sawtooth waveform.it produced by combining RF sine wave with the first three harmonics.

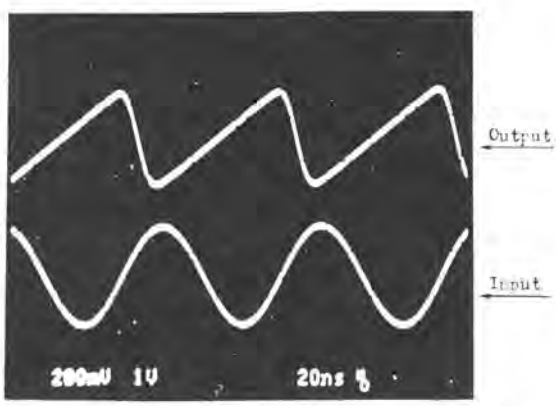


Fig.2 Sawtooth waveform convertor as seen on oscilloscope in control room

definite amplitude and phase relationship can combine sawtooth waveform, as shown in Fig.3. The shape of the sawtooth waveform depends on how many harmonics were joined to combine. Although increasing the number of the higher sine wave harmonics may get the ideal sawtooth waveform, the respective phase and amplitude control loops for every frequency must be built, and the many filters in the frequency multiplier and feedback divider are also difficult to make for wide band operating frequencies. In this case, the whole system is very complicated and expensive.

A waveform convertor was designed and constructed in order to improve the technique of the combining sawtooth waveform in the bunching system in HIRFL. Figure 4 shows the block diagram of the waveform convertor and the waveform at the different points. The narrow pulses with width τ were formed by "shaper–differentiator–shaper" circuits at the plus crossing points of the input sine wave. T is the period of the input sine wave. The capacitor C is charged with constant current I when $U_d = 0$. The capacitor C is discharged quickly during the narrow pulses occur. As a result the sawtooth waveform was formed directly. There are only one amplitude and one phase control loops in whole system and without any filters. $(T - \tau)/T$ is used to evaluate the bunching efficiency of the sawtooth wave. This value is about 70 % for combining sawtooth waveform with three harmonics and without regard to the frequency (see Fig. 5). But the $(T - \tau)/T$ value is from 91 % to 73 % correspondent frequencies from 6 to 18 MHz for the sawtooth waveform produced by the waveform convertor as shown in Fig.2. Here τ is 15 ns and this is compromise consideration. Although the smaller τ is, the better, the sawtooth waveform contains rich high harmonics with minimal τ value. It is difficult to amplify such sawtooth wave with rich harmonics. It needs more wide band power amplifier and better matching, but these are more difficult problems.

Obviously, using waveform convertor are more sim-

ple and much cheaper than combining to produce the sawtooth waveform voltage. The shape of the sawtooth waveform is better than it is combined.

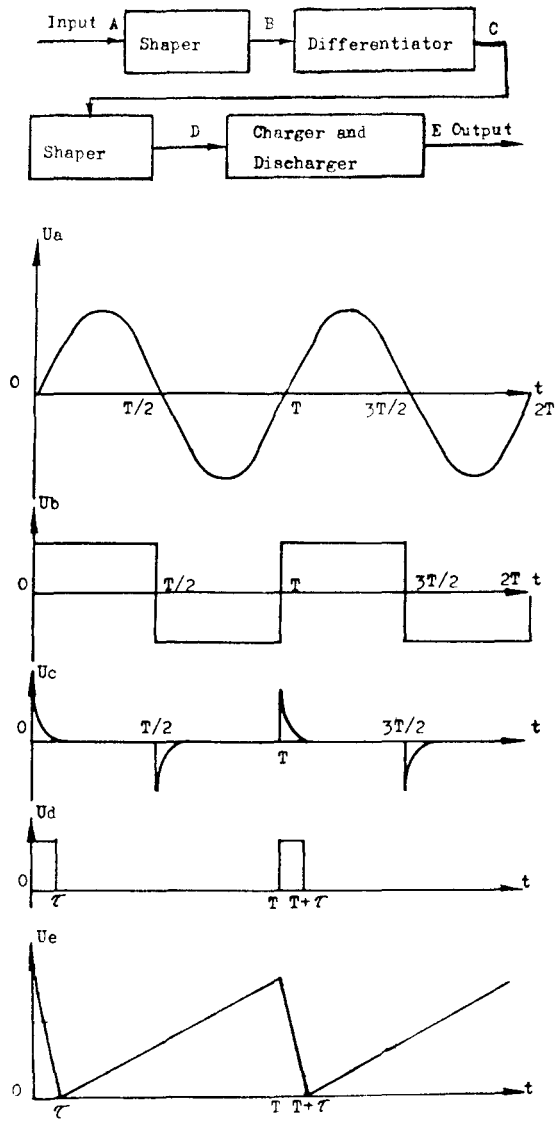


Fig.4 Block diagram of the waveform convertor and waveforms at the different points.

4. RF SYSTEM OF THE BUNCHER

Figure 6 shows the block diagram of the buncher RF system. The RF signal from synthesizer is split into the waveform convertor in which the sawtooth wave is produced with the RF frequency range as same as the injector SFC drive frequencies (6–18 MHz). The RF signal with sawtooth waveform is amplified by a 500 W wide band power amplifier and passes through a matching transformer to one of the two electrodes to which a resistance of 200Ω is connected in parallel.

The peak–to–peak amplitude of the sawtooth waveform in the accelerating gap is about 800 V. The gap voltage is monitored by a resistance divider. The amplitude stability of the voltage is less than $\pm 1 \times 10^{-3}$. The relative phase between the mesh signal and the reference signal is stable to better than 0.5 degree.

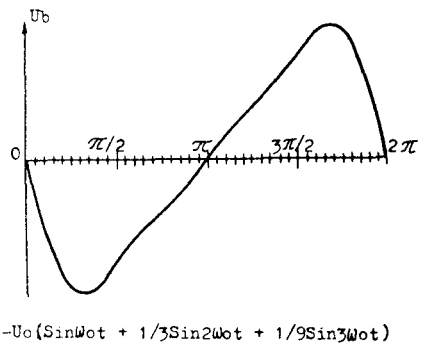


Fig.5 Sawtooth waveform produced by combining RF sine waves with fundemental, second and third harmonic frequencies

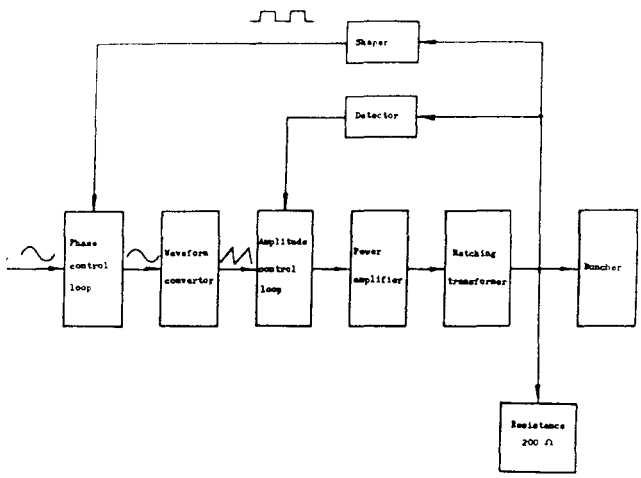


Fig.6. Block diagram of the buncher circuit for the sawtooth waveform produced by a waveform convertor

BEAMLINES FOR A SECOND INJECTOR CYCLOTRON AT NAC

John C Cornell, J Lowry Conradie and Dirk T Fourie

National Accelerator Centre, PO Box 72, FAURE, 7131 Republic of South Africa.

ABSTRACT

A second solid-pole injector cyclotron (SPC2) is at present being constructed to provide pre-accelerated heavy ion beams and polarized hydrogen ions for acceleration into the K=200 MeV sector cyclotron (SC) at NAC. The transfer beamlines from an ECR source to SPC2, and from a polarized ion source to SPC2 are described, as is the transfer beamline from SPC2 to the SC.

1. INTRODUCTION

The large sector cyclotron (SC) at NAC[1] is designed to accelerate protons to some 200 MeV, and also to accelerate a variety of light and heavy ions. It has operated successfully for several years now, with the solid-pole injector cyclotron SPC1 providing the necessary pre-acceleration of light-ion beams from its internal hooded-arc PIG ion source. A second injector cyclotron SPC2, very similar in size to SPC1, is now under construction[2] and will provide pre-accelerated heavy-ion and polarized-ion beams, produced in two external ion sources. The two injector cyclotrons are situated at ground level (datum level zero), with their horizontal median planes level with that of the SC, *i.e.* at +1.5 m height. The SC vault extends downwards to the basement, 4 metres below ground datum.

As can be seen from Fig. 1, these new ion sources are situated in the basement below the second injector SPC2, and on opposite sides of it. Both sources are arranged horizontally, with their beams produced at 1 metre above floor height, *i.e.* at 3 m below ground datum. Beam transport systems are therefore required to guide particle beams from both the ECR ion source and the atomic-beam polarized ion source, up into the common vertical axial injection beamline of SPC2.

On leaving SPC2, the pre-accelerated particle beams have then to be transported towards the SC, which means that the beamline must join that from SPC1, after which the injection path into the SC is the same.

2. THE ECR TRANFER LINE

The beamline from the ECR ion source has been described previously[3] in some detail. We briefly

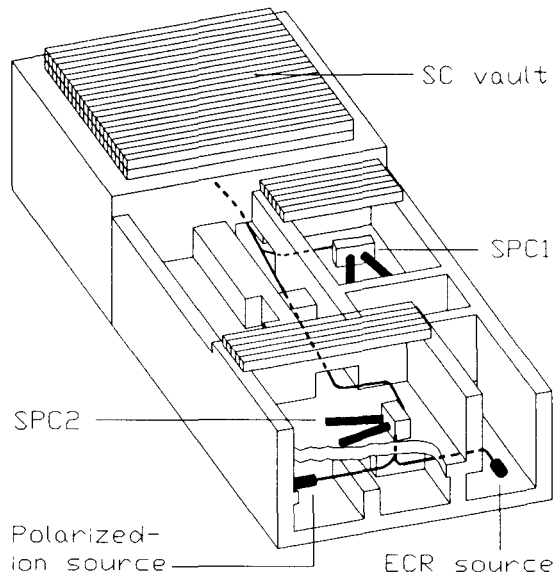


Fig. 1. Layout of the transfer beamlines at NAC.

summarize the design here for the sake of completion. This line is shown on the left of Fig. 2, part in plan and part in section, because the line is a "twisted achromat" with one 90° dipole B1Q operating in the horizontal plane, followed by a second (identical) dipole B2Q bending the beam into the vertical direction. A single (movable) solenoid lens L1Q controls the divergence and focuses the initial beam from the horizontal ECR source onto the objective slit aperture, where some initial (partial) rejection of unwanted charge-states takes place.

After the first 90° analysing magnet (Fig. 3) has completed the charge-state selection, the plane of dispersion is horizontal, and two pairs of solenoid lenses L2Q-L5Q then transport the selected particle beam along to the second dipole magnet. The first two lenses (L2Q and L3Q) are operated with opposing polarities, and therefore impart no net rotation to the dispersion plane. The next two lenses (L4Q and L5Q) are operated in the same sense, and impart approximately 90° of rotation, so that the plane of dispersion is vertical.

A solenoid "field lens", formed by two solenoids R1 and R2 with opposing fields so as to impart no net rotation, is placed at the symmetry point of this system

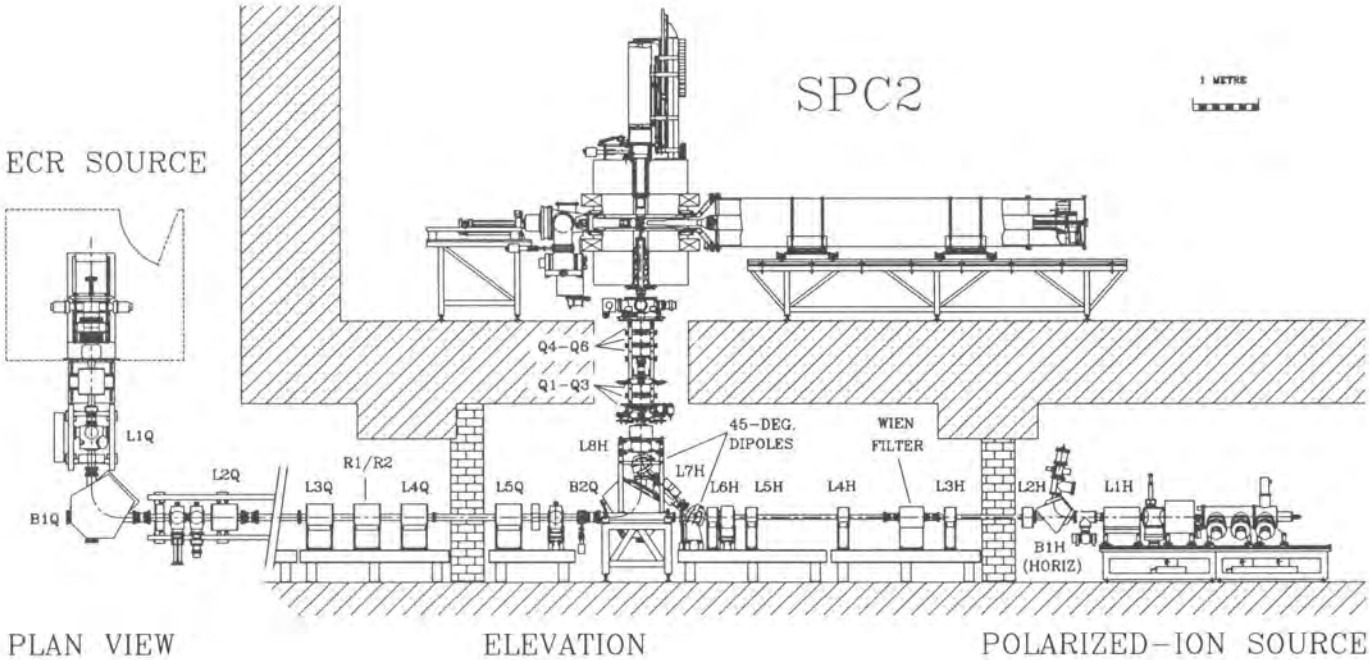


Fig. 2. The transfer beamlines between the ECR and polarized-ion sources and the injector cyclotron SPC2.

and allows us to focus the dispersed particles correctly, so that the entire system is achromatic. The midpoint of the system is also a horizontal and vertical waist, so that the focusing of the system as a whole is not affected by the operation of the field lens. As the focusing of the solenoid lenses may need fine-tuning, which would also affect the rotation of the plane of dispersion, we have manufactured the "field lens" in the form of an inner solenoid with two half-length solenoids on either end, which permits us to vary independently the focusing power and the absolute rotation imparted by this lens.

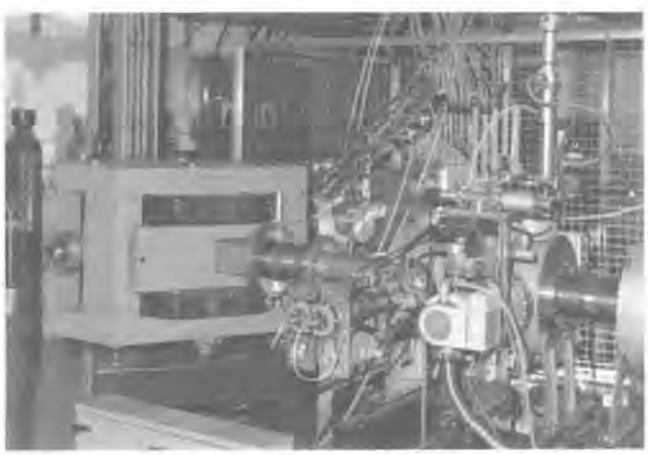


Fig. 3. The first 90° dipole of the "twisted achromat" in the beamline from the ECR source which is visible in the background.

3. THE AXIAL INJECTION BEAMLINE

Matching of the transverse phase-spaces of the beam to the requirements of SPC2 while taking account of the phase-space coupling which can occur in the spiral inflector requires a fairly versatile system. This has been provided by a system of 6 quadrupole magnets,



Fig. 4. Rotatable 2-triplet quadrupole telescope, prior to mounting in the axial injection beamline below SPC2.

arranged as two triplets, and mounted in an assembly which can rotate them around the axial injection beamline below SPC2. The completed quadrupole telescope is shown in Fig. 4, prior to installation The entire assembly itself has since been attached to the side of the opening in the 1.25 m thick floor slab, and pivoted so that it can be rotated out of the way to permit components of the axial injection line to be lowered from within the lower yoke of the cyclotron.

Within the cyclotron yoke will be two more solenoid lenses plus an *x-y* steering magnet and a non-invasive beam centroid detector. The *x-y* steering magnet is formed using commercially-available laminations for the stator of an electric motor, with two sets of sinusoidally-wound coils, oriented so that their dipole fields are at right angles to each other. A POISSON plot of this magnet can be seen in Fig. 5.

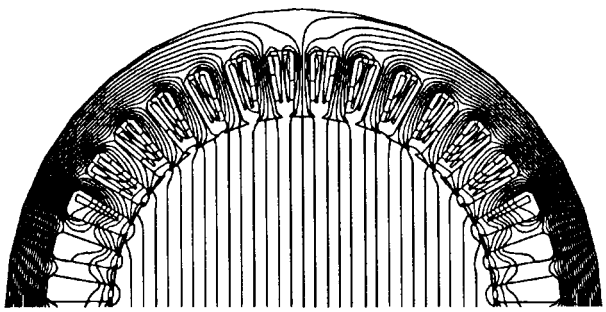


Fig. 5. POISSON plot of the field lines calculated for a sinusoidally wound *x-y* steering magnet, shown here operating in the *x*-direction only.

4. THE POLARIZED-ION TRANSFER LINE

The polarized-ion source is also located in the basement, like the ECR source, but with its extracted beam direction aimed towards the axis of the cyclotron projected down to the -3 m level. As shown in Fig. 2, the beamline which transfers the polarized ions into SPC2 joins up with that from the ECR source at the exit waist of the achromatic section discussed above. In order to achieve this, a smaller vertical achromatic system is used, consisting of two 45° dipoles together with several focusing solenoid lenses.

The source itself was supplied together with a solenoid lens just after extraction and a 120° analysing dipole magnet, used as a diagnostic tool to optimize the extraction of the analysed mass-1 beam by using a Faraday cup and a diagnostic "harp". For transfer into SPC2, the dipole B1H will be switched off so that the polarized beam can proceed through the dipole undeflected, until the waist formed by the solenoid L1H is reached. (An aperture here will also remove some of the unfocused mass-2 particles.) A pair of solenoid lenses L2H and L3H will then transport the beam to another waist, where a Wien filter will be located, followed by a second pair of identical solenoids L4H and L5H.

Thereafter the beam enters the achromatic system comprising two outer solenoid lenses and two 45° dipoles, with a solenoid "field lens" located at the symmetry point, *i.e.* in the middle of the 45° section. As before, the field lens is tuned so that the system is properley achromatic. The field lens is also divided into two halves, wired in series but with opposite polarities, so that no net rotation is imparted to the plane of dispersion. This trick is also used for the three solenoid lenses which lie between the Wien filter and the 45° dipoles, in order to preserve the direction of the polarization vector, discussed below.

4.1 Vertically Polarized Beams

The beam from the polarized ion source is polarized along the extracted beam axis, either forwards or backwards. The axis of polarization will then precess in the 45° dipoles. Polarized protons will precess through 251.4 degrees, while deuterons precess through 77.2 degrees. The Wien filter (or crossed-field analyser) will permit us to add to (or subtract from) the precession, by an appropriate amount, without deviating the beam from its path, so that when the particles reach the vertical axis of the injection system, the polarization vector is vertical. This vector is not expected to precess much in the axial fields of either SPC2 or the SC. The successive pairs of triplets of quadrupole lenses in the "high-energy" beamlines should also have limited depolarization effects, as they should tend to cancel out, preserving the "up" or "down" direction of the vertically polarized beam until the target is reached.

4.2 Polarization in the Horizontal Plane

There is no space available in the vertical section of beamline beneath SPC2 for a second Wien filter which could rotate the axis of polarization into the horizontal plane at any specified angle, and another approach was therefore needed. The solution chosen is to allow the Wien filter in the horizontal section of beamline leading from the polarized ion source to rotate. This can then serve in the normal way, as described above, for delivering a vertically polarized beam, and can also provide us with a horizontally polarized beam. For any arbitrary angle of polarization required in the horizontal plane in the vertical injection beamline, we can then calculate (a) the angle of rotation of the Wien filter (*i.e.* of the plane of polarization) about the horizontal beam axis, and (b) the angle of rotation of the polarization axis in the Wien filter.

As the particles traverse the vertical achromat, the polarization vector precesses about the direction of the magnetic field in each of the two 45° dipoles, so that the resultant vector ends up in the horizontal plane, and at the required angle. The subsequent solenoid lenses, and the axial dipole fields of SPC2 and the SC, as well as any dipole magnets encountered *en route* to the target area, will then cause the polarization vector to precess. For a horizontal vector this means that the vector will simply rotate in the horizontal plane, arriving at some angle on target, which can then be altered simply by changing the Wien filter's parameters.

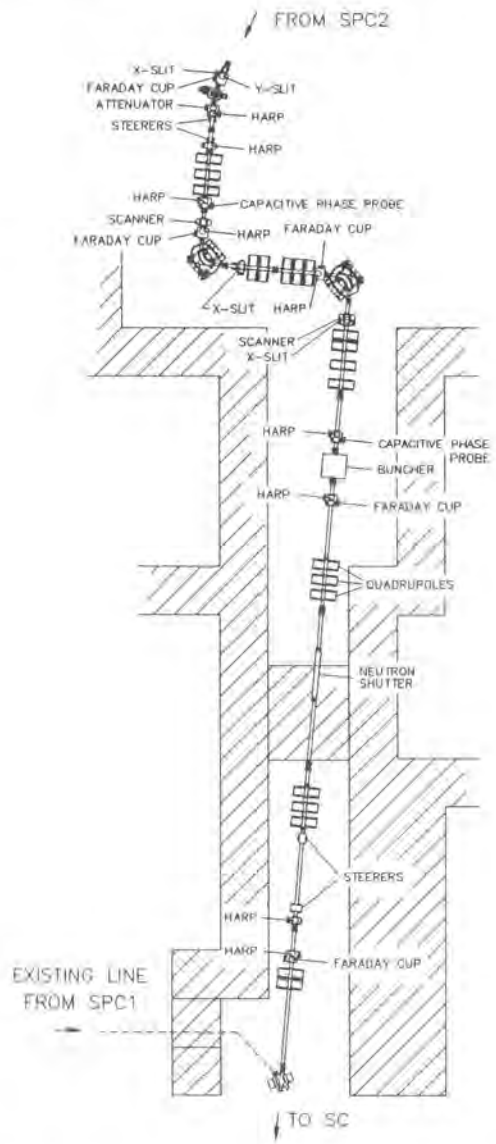


Fig. 6. The transfer beamline between SPC2 and the sector cyclotron, which joins the existing transfer beamline from SPC1.

5. TRANSFER FROM SPC2 TO THE SC

The beamline from SPC2 to the SC is shown schematically in Fig. 6, and is divided both physically and functionally into several sections. A triplet of quadrupole lenses prepares the beam initially by focusing it to a waist at the entrance to a zig-zag dipole achromat. The latter consists of two 90° dipole magnets, with a quadrupole doublet telescope between them, in order to provide the additional x and y waist needed to make the system non-dispersive. An analysing slit at the first waist makes provision for energy-selection, while another quadrupole is placed at the second waist to steer the dispersed particles correctly so that the system is achromatic. Diagnostic "harps" and scanners will be used together with Faraday cups for beam profile monitoring, as in the existing beamlines.

After the achromat, a non-symmetric arrangement of four quadrupoles reduces the divergence of the beam so that it can be transported (*via* a 2-triplet quadrupole telescope) down a tunnel alongside the existing injector cyclotron. A new buncher located in this section will be used together with the existing buncher in the next section of line to provide longitudinal phase-space matching to the SC. The beamline then passes through a shielding wall, and joins the existing beamline linking SPC1 and the SC. Matching of the transverse phase-spaces to the injection requirements of the SC will be carried in this latter section of the line, as is done at present with beams from SPC1.

All the magnets for this beamline have been manufactured, and the line is at present being built up. All the beam transfer systems discussed in this paper are on schedule for completion in time for accelerating the first beams in SPC2[2)]

6. REFERENCES

1) Botha, A.H. *et al.*, "Operation and development of the NAC accelerator facilities", in **Proceedings of the Twelfth International Conference on Cyclotrons and their Applications** (World Scientific, Singapore, 1989) pp. 80-83.

2) Du Toit, Z.B. *et al.*, "Progress with the NAC injector cyclotron for heavy and polarized ions", these Proceedings.

3) Conradie, J.L. *et al.*, "Tranfer beamlines for ECR and polarized-ion sources for a new injector at NAC", in **Proceedings of the Twelfth International Conference on Cyclotrons and their Applications** (World Scientific, Singapore, 1989) pp. 376-379.

BEAM TRANSPORT SYSTEM FOR THE HIMAC

K. Noda, H. Ogawa, E. Takada, A. Itano, M. Kanazawa, A. Kitagawa, M. Kumada,
T. Kohno, K. Sato, Y. Sato, M. Sudou, S. Yamada, T. Yamada and Y. Hirao
National Institute of Radiological Sciences
9-1, Anagawa 4-chome, Inage-ku, Chiba-shi, 263, Japan

and

K. Endo
National Laboratory for High Energy Physics
1 Oho-1, Tukuba-shi, Ibaragi, 305, Japan

ABSTRACT

The Heavy Ion Medical Accelerator in Chiba (HIMAC) will be the first heavy ion accelerator complex for the clinical treatment of tumor in Japan. This paper describes design considerations of the beam transport system for the HIMAC.

1. Introduction

The HIMAC is an accelerator complex for the clinical treatment of tumor and is now under construction at National Institute of Radiological Sciences (NIRS).[1] The ion species which are required for the clinical treatment range from He to Ar. The beam energy is designed to be variable from 100 MeV/u to 800 Mev/u for an efficient treatment. As shown in Fig. 1, Beam transport system of the HIMAC can be divided into three region area, i.e. INJBT, EXBT, and HEBT, of which the former two are to match with synchrotron requirements.

The injection beam transport system[2] (INJBT) between the linac cascade and two synchrotron rings is designed to transport the beam alternately by using a fast switching magnet to two rings, which are placed on two stages, in the same condition for multiturn injection. The upper and the lower extraction beam transport system (EXBT) are designed to match a beam optics of a slowly extracted beam from each ring independently to that of each high energy beam transport system (HEBT). The high energy beam transport system[3] is designed to transport the vertical beam from the upper and the lower ring as well as the horizontal one from the lower one. This design allows simultaneous irradiation by horizontal and vertical beam. In addition, beams can be switched from one treatment room to an other one in a short time, keeping the good reproducibility of the beam position.

2. Injection Beam Transport System

The design conditions of the INJBT are : i) to transport the beam with the maximum magnetic rigidity of 1.42 Tm corresponding to the energy of 6 MeV/u for ions with a charge to mass ratio of 1/4, ii) to obtain a good efficiency of beam transmission and iii) to be adjustable the beam to the optical condition of the multiturn injection. The acceptance for betatron oscillation and for momentum spread are designed to be 26.4πmm mrad and $\pm$0.3%, respectively.

The basic requirements for the INJBT are as follows.
(a) Beam should be injected alternately to two rings in the same condition.
(b) The Twiss parameters at the entrance of each ring should be easily adjustable to match the condition of multiturn injection.
(c) Ions with different charge to mass ratio should be separated and the momentum should be analyzed for an efficient transportation and an easy beam tuning in the ring.

A fast switching magnet is designed for the simultaneous operation of two rings. The rising and the falling time of its power supply are 140 msec. The stability at the 10 msec flat top is regulated to be less than $2\text{x}10^{-4}$, which is achieved in test by using a dummy load.

A required size of beam duct is determined by considering a centroid displacement of beam as well as an acceptance for the betatron oscillation and for the momentum spread. First, the beta and the dispersion function are calculated by using program MAGIC,[4] as shown in Fig. 2. Second, the position and the field strength of steering magnets and the position of profile monitors are determined for the centroid displacement caused by a misalignment and a field error of magnets to be suppressed within the size of 5 mm at a standard deviation. Third, for easy beam tuning procedure, a mirror symmetry optics is adopted to realize a waist to a waist transportation with a doubly achromatic condition. Finally, in the last section of the INJBT, a doubly achromatic condition can be realized by adjusting two quadrupole magnets, which ensures reducing an applied high voltage between a septum and an electrode of an inflector in each ring. Other additional four quadrupole magnets are prepared to match the beta function and its derivative at the entrance of the ring to the condition of the multiturn injection.

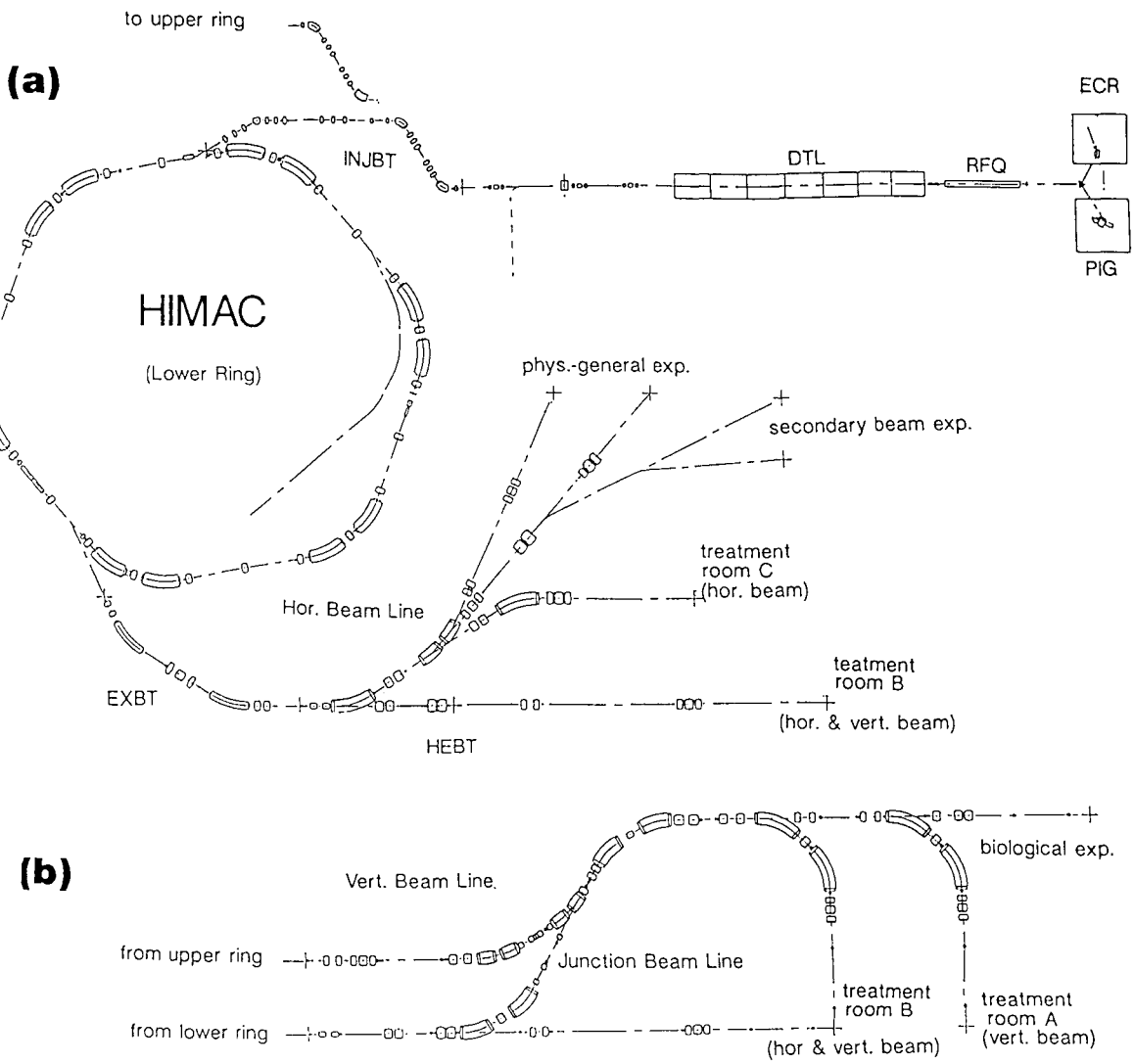


Fig. 1. (a) A plane view of the HIMAC. (b) A side view of the vertical beam line in the HEBT.

A beam momentum and a charge to mass ratio are analyzed by measuring the field strength of the first bending magnet with a NMR and by using two horizontal slits. The measurement result is referred to the field strength of the main magnets at a flat base of an excitation pattern of the ring.

3. Extraction beam transport system

The EXBT of each ring is designed to transport the slowly extracted beam to the HEBT and to match Twiss parameters to the condition at the entrance of the HEBT. The acceptance for the betatron oscillation and for the momentum spread in the EXBT and the HEBT are designed to be 10πmm mrad and $\pm 0.2\%$.

The beam optics from the entrance of the first electrostatic deflector in the ring to that of the HEBT is calculated as shown in Fig. 3, and the steering magnets and the profile monitors are assigned in the EXBT by the same manner as in the case of the INJBT.

In addition, the fast beam shutter is installed to assure an accurate irradiation dose for the clinical treatment and for the biological experiment. The beam is adjusted to an optimum condition for profile, centroid and a spill structure by using the profile monitors and the spill monitor and by tuning the beam extraction apparatuses in the ring before transportation to the HEBT.

4. High energy beam transport system

The HEBT system consists of a horizontal and a vertical beam line. The horizontal beam line is designed to transport the beam from the lower ring. The beams up to 800 MeV/u are provided to two treatment rooms (B,C) and two experimental rooms (for physics-general experiment and for secondary beam one).

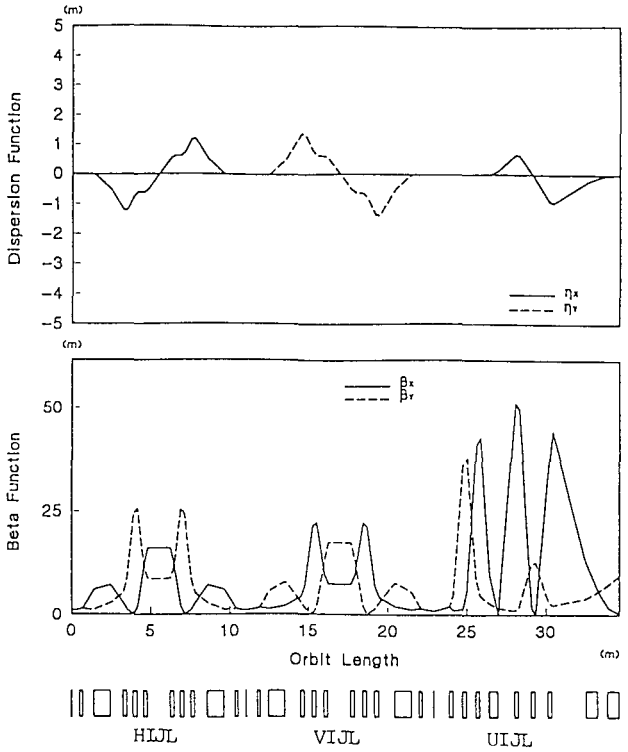


Fig. 2. Beta and dispersion functions in the INJBT to the upper ring.

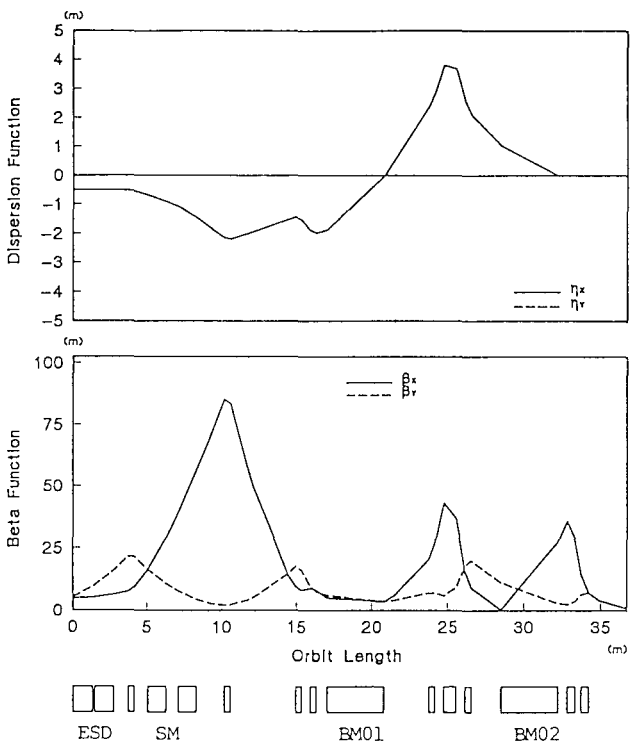


Fig. 3. Beta and dispersion functions in the EXBT.

On the other hand, The vertical beam line is designed to guide the beam from the upper ring and that from the lower one through a junction beam line. It can transport the beams up to 600 MeV/u to two treatment room (A,B) and a biological experiment room. It is possible for the same patient to be irradiated simultaneously by horizontal and vertical beam in the treatment room B. Further, the beam from the horizontal beam line can be guided to the vertical beam line by a switching magnet in the beam junction line. Therefore, the beams from the upper ring and the lower one can be transported alternately to the same target.

For achieving a required dose uniformity (±2%) in even the case of a broad beam (max. dia. of 220 mm) which is obtained by using scanner magnets and scatterer, the beam optics is designed such that the beam at each isocenter satisfies a doubly achromatic condition and is within the size of 10 mm. A typical calculation result is shown in Fig. 4. Further, this set of beam optics keeps the design acceptance of 10πmm mrad when the pole gap of all bending magnets are downsized to 60 mm for cost reduction.

In addition, the beam should be switched within 5 minutes from one course to the other by only adjusting the current of the switching magnet in order to obtain an efficient beam use for a treatment. The reproducibility of the beam position is required to be within ±2.5mm after beam switching. To satisfy the requirements, an excitation procedure of the magnet will be programmed for an initialization and setting the current, and its magnetic field will be precisely monitored by NMR. Further, a residual field of the switching magnet will be also compensated by using a small current source.

Beam profile monitors and steering magnets are assigned for the beam centroid displacement to be reduced within the size of 5 mm at a standard deviation. The beam profile monitor, which is a multiwire proportional chamber, was tested by using a proton beam of 70 MeV at NIRS and worked well in the intensity range corresponding to helium beams of 800 MeV/u at $1.4\text{x}10^{6}$~$1.4\text{x}10^{11}$.[5)]

The secondary beam line will be prepared for the study of diagnostic and therapeutic applications of a radioactive beam, which are separated from the primary and any other undesirable ions. Further, the momentum spread can be suppressed within ±0.2% by using a wedge degrader. The vertical beam line from the upper ring is also applicable for the same purposes. The produced radioactive beam is analyzed by four bending magnets and a slit, and is transported to the treatment room A or B. By using the radioactive beam, one can measure precisely the stopping point of the beam in a patient's body, and the treatment will be performed by using stable heavy ion beams with the same range as the radioactive beam.

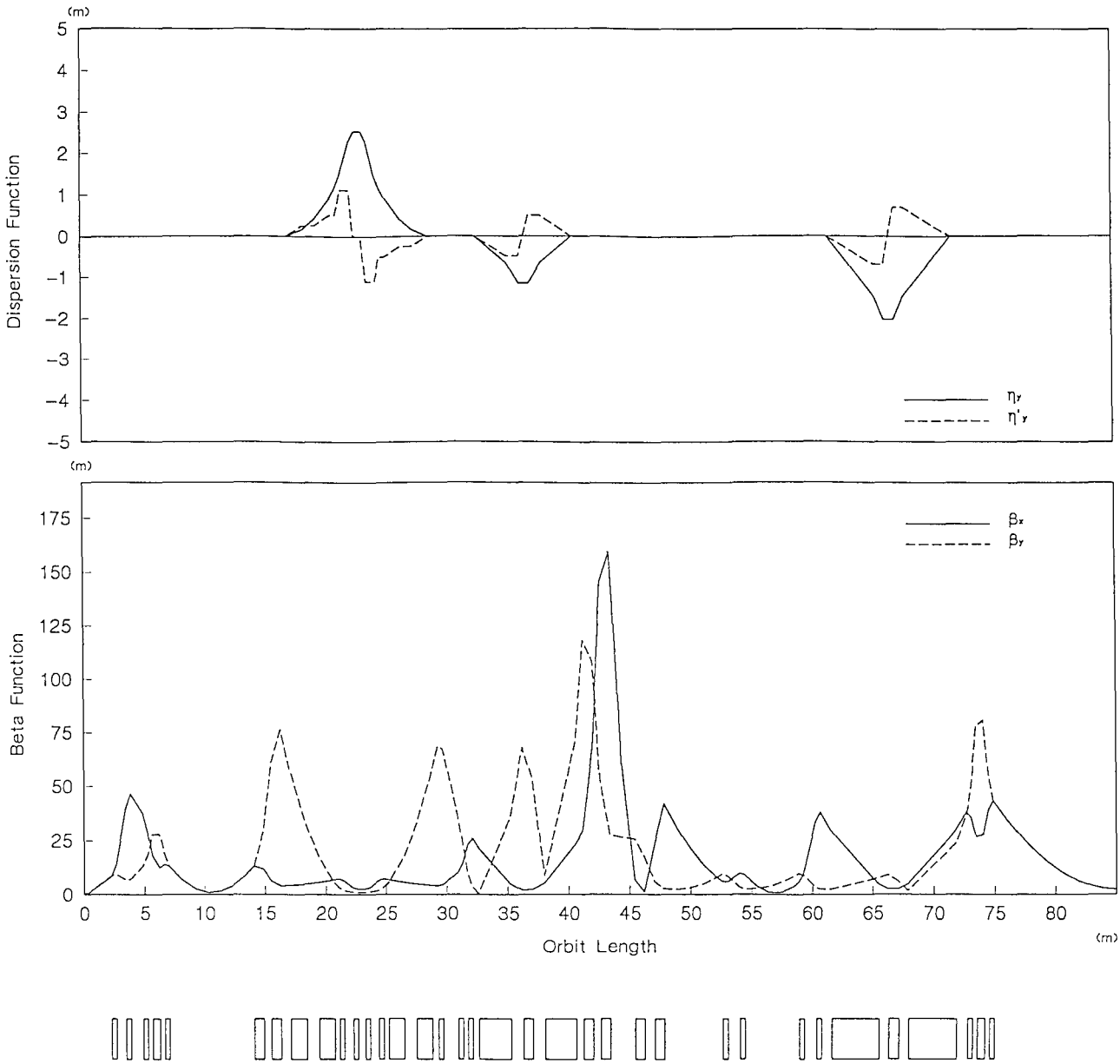


Fig. 4. Beta and dispersion function of the vertical beam line to the isocenter of the treatment room A.

5. Acknowledgment

The authors would like to express their sincere gratitude to Dr. K. Kawachi and the members of the Division of Accelerator Research of NIRS for their supports and helpful discussions. The authors also express thanks to the engineers of Toshiba Corp. and of Mitsubishi Electric Corp. for their useful assistance and discussion

6. REFERENCES

1) Y. Hirao, et al., "HEAVY ION SYNCHROTRON FOR MEDICAL USE" Nucl. Phys. **A538**,541c(1992)
2) K. Noda, et al., "INJECTION AND EXTRACTION BEAM TRANSPORT SYSTEM FOR THE HIMAC SYNCHROTRON" in Proc. 8th Symp. on Accel. Sci. and Tech., 1991, Saitama, pp.205-207.
3) H. Ogawa, et al., "BEAM DELIVERY SYSTEM OF HIMAC" in Proc. 7th Symp. on Accel. Sci. and Tech., 1989, Osaka, pp.48-50.
4) A. S. King et al., SLAC-183, 1975.
5) M. Torikoshi et al., "DEVELOPMENT OF BEAM PROFILE MONITOR FOR HIMAC" in Proc. 8th Symp. on Accel. Sci. and Tech., 1991, Saitama, pp.317-319.

DESIGN OF A BEAM BUNCHER USING A HALF-COSINE DRIVING FUNCTION

R. C. Rogers
Cyclotron Institute, Texas A&M University, College Station
Texas, 77843-3366, U. S. A.

ABSTRACT

A beam buncher design for the axial injection system on the K500 cyclotron is described. The buncher uses a unique, easily generated, driving waveform of repetitive half cycles of a cosine function. The effect on the beam velocity profile is to mimic the action of a true saw-tooth waveform. Considerations of single and multiple gap performance and their effect on the velocity profile and power demand are presented.

1. INTRODUCTION

The K500 cyclotron uses an external Electron Cyclotron Resonance Ion Source (ECRIS) and axial injection system to provide particles for acceleration. Figure 1 is a schematic drawing of the axial injection transport line showing the major elements of the system. The particles are extracted from the ECRIS by a d. c. voltage that provides a continuous current to the cyclotron. The particles can be more efficiently used if they are collected into "bunches" that are injected into the machine in synchronism with the accelerating voltage. As shown in the figure, the buncher is the last active element before the particles enter the hole through the upper pole cap of the cyclotron.

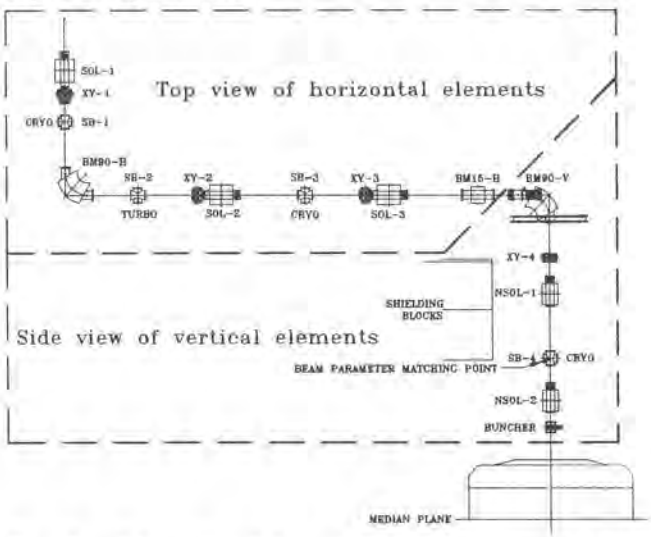


Fig. 1. Schematic of the axial injection system for the K500 cyclotron.

The action of a buncher using a sawtooth waveform has been previously described.[1] Efforts to generate and support this waveform on several types of bunching structures have met with little success owing to the wide bandwidths and power requirements of the final amplifier. Most successful bunching has been achieved through the use of single-gap devices, using either a single sinusoidal waveform or two waveforms[2] operating on the first and second or first and third harmonics. Multiple-gap systems that use several harmonics to construct the sawtooth waveform have also been successful.[3] Single-frequency devices typically recover about 30% of the original d. c. current while multiple-gap systems can recover as much as 70-80%, depending upon the number of harmonics used.

The bunching structure described here is a single gap type using a driving waveform that is more easily generated than a sawtooth while yielding the same result.

2. BUNCHER GAP EFFECT

Figure 2 shows a sectional drawing of the bunching structure with an active gap constructed of two closely spaced grids with attached field shaping cones, driving voltage inputs and load resistors. The gap voltage is a sinusoidal waveform operating at the frequency of the cyclotron and at some fixed phase relative to the dee voltage.

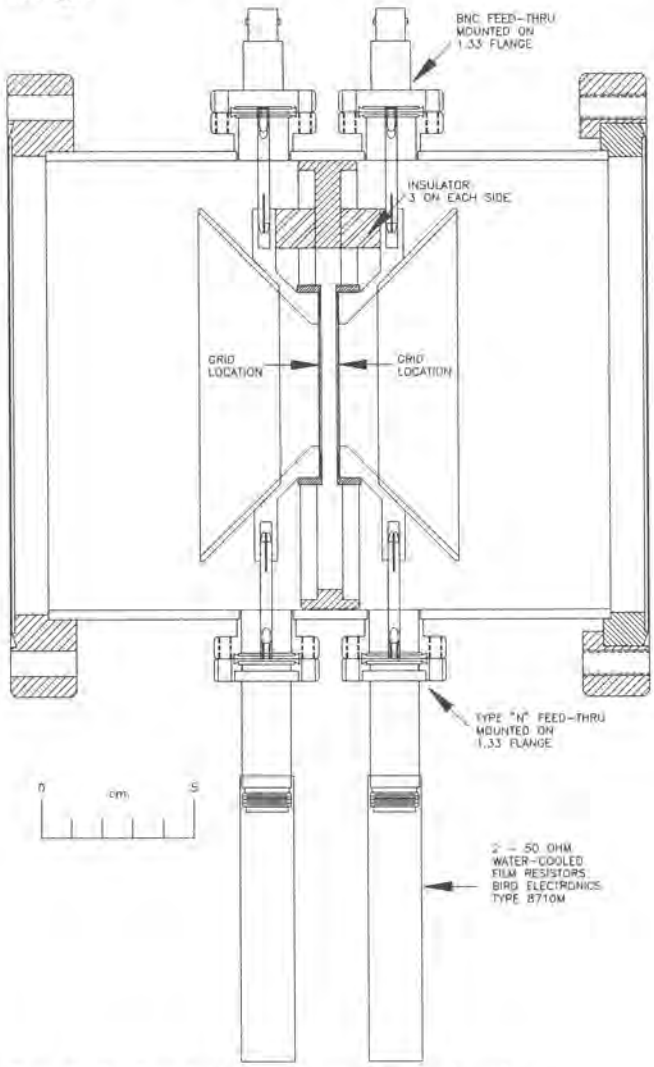


Fig. 2. Sectional view of the single gap buncher.

The K500 cyclotron accepts the external beam through a helical inflector that has an output aperture at a fixed radius from the center of the machine. The velocity of the beam is adjusted to match the central magnetic field of the cyclotron and the radius of the inflector aperture. From this a beam wavelength can be defined as

$$\lambda_b = \frac{v_i}{f} = 2\pi r_i \qquad (1)$$

where v_i is the injection velocity, r_i is the radius of the inflector aperture and f is the cyclotron frequency. Since r_i is fixed the beam wavelength is constant. It is useful to discuss some features of the buncher in terms of this number λ_b.

The velocity of the particles after exiting the gap is given by

$$v_g = v_o \frac{V_g}{2V_e} \frac{\sin\frac{\pi}{\lambda_b}s}{\frac{\pi}{\lambda_b}s} \sin\left(\omega f + \frac{\pi}{\lambda_b}S\right) \qquad (2)$$

where v_g is the output velocity from the gap, v_o is the input velocity, V_g is the peak voltage across the gap, V_e is the ECRIS extraction voltage, s is the distance across the gap and ω is the radian frequency of the gap voltage. This result assumes that the change in velocity in the gap is very small compared to the input velocity and that the electric field in the gap is uniform.

A normalized plot of the effect of the gap as a function of the gap distance, in terms of λ_b, is shown in Fig. 3. Any single gap buncher of the type shown in Fig. 2 has, in fact, three gaps. There is a long input gap, a short active gap and a long output gap. From Fig. 3 it is apparent that the long gaps, e.g., five wavelengths or more, have very little effect on the beam velocity. This effect can be further reduced if the grids are driven in a bi-phase or push-pull mode. In most cases the fields in the input and output gaps are not uniform, so the actual effect of these gaps must be evaluated on a cases-by-case basis.

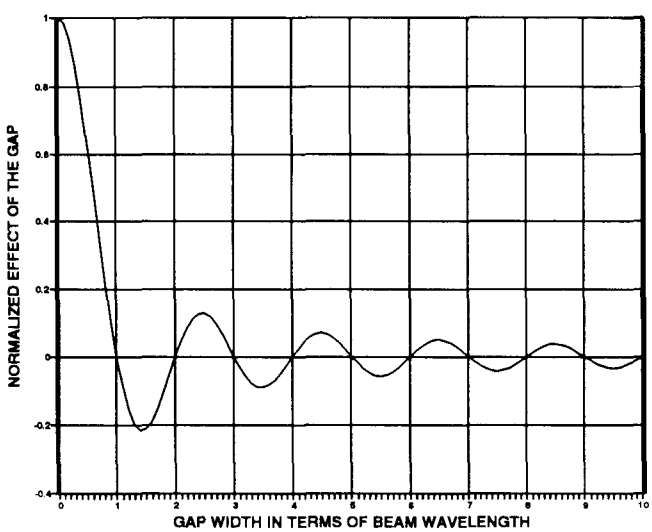


Fig. 3. Normalized gap effectiveness as a function of gap width.

3. WAVEFORM ANALYSIS

The arguments for using a sawtooth waveform for bunching were presented in Ref. 1. However, this waveform is generated at small signal levels and must be amplified. The fast risetime and amplitude that are required for effective bunching place very large demands on the amplifiers in terms of power output capability and bandwidth. An alternative to the sawtooth waveform is that of a half cycle of a cosine wave. This signal is simple to generate at low power and a scheme will be presented for high power generation.

Figure 4 shows a comparison of an ideal sawtooth waveform to an ideal half-cosine wave. The peak amplitude of the cosine wave is 0.7854 times the peak

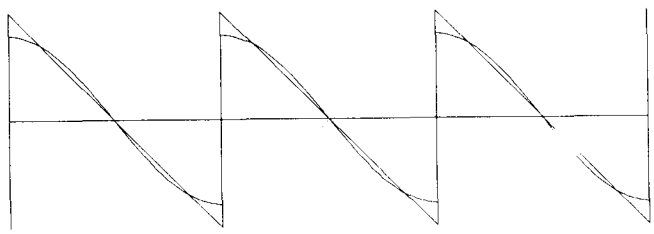


Fig. 4. Idealized sawtooth and half-cosine wave forms.

amplitude of the sawtooth. This amplitude gives the least average error fit of the cosine to the sawtooth over the period. Figure 5 shows more realistic signals with nominal risetimes of 10% of the period for both signals and the same amplitude relationship. It is clear that the half-cosine wave very closely approximates the sawtooth.

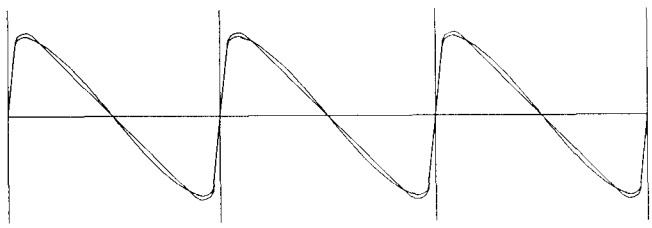


Fig. 5. Sawtooth and half-cosine wave forms with 10% risetimes.

Fourier decomposition of the two signals with 10% risetimes gives the following relation between their harmonic components.

Table 1.

Harmonic	Sawtooth	Half-cosine
1	0.777	0.836
2	0.344	0.314
3	0.190	0.181
4	0.113	0.116
5	0.070	0.075
6	0.046	0.048
7	0.030	0.030
8	0.018	0.017

The harmonic content of the two waveforms is almost identical with the higher harmonics being virtually equal since both signals have equal risetimes.

Equation 2 can be modified to include the harmonic terms as

$$v_g = v_o \frac{V_g}{2V_e} \frac{\sin\frac{n\pi s}{\lambda_b}}{\frac{n\pi s}{\lambda_b}} \sin(n\omega t + \frac{n\pi}{\lambda_b} S) \qquad (3)$$

where the term n represents the harmonic number. The effect of the gap on each of the harmonic components can therefore be evaluated and the components recombined to give the resulting velocity profile.

The active gap in the buncher under consideration is 0.25 inches long which is equal to $0.126\lambda_b$ for the K500 cyclotron. The gap effect for each of the harmonics above is shown in the following.

Table 2.

Harmonic	Gap effect
1	0.974
2	0.899
3	0.781
4	0.632
5	0.464
6	0.292
7	0.131
8	-0.008

Figure 6 shows both the reconstructed half-cosine wave and the resulting velocity profile with each compared to its ideal waveform. The loss of risetime in the velocity profile is the result of the gap effect attenuating the higher frequency components. This effect is discussed in Ref. 1 and is repeated in this form to provide quantifying values for this particular buncher configuration.

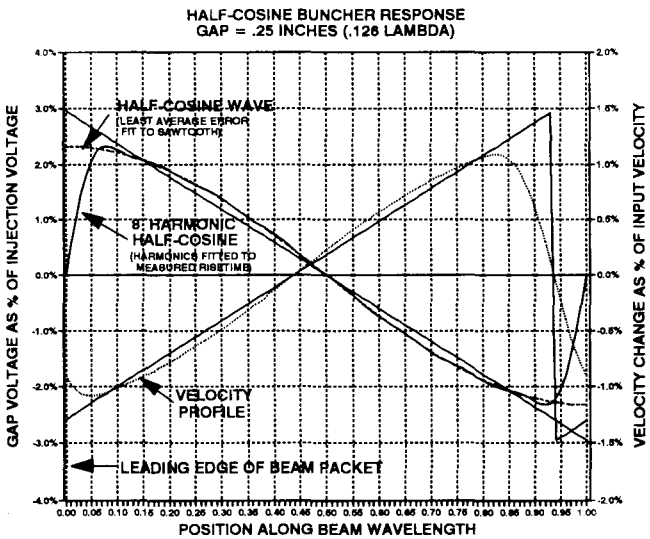


Fig. 6. Half-cosine voltage wave form and particle velocity profiles reconstructed from Fourier components. Velocity profile is constructed from gap effect modified components.

4. POWER CONSIDERATIONS

The power required for the buncher grids is dependent on the ECRIS extraction voltage and the distance to the inflector aperture, i.e., the drift path over which the bunching action takes place. For the location of the buncher shown in Fig. 1, the drift path is approximately 34 wavelengths. For an ideal sawtooth waveform that is symmetric about zero volts, this implies a peak voltage across the gap of 2.96% of the ECRIS extraction voltage. For the half-cosine wave a peak voltage of 2.32% (0.7894 x 2.96 from Section 3 above) would be required. Because the grids are driven in a push-pull manner the peak voltage for each grid is then 1.16% of the ECRIS extraction voltage.

From Fig. 2 above or from the block diagram shown in Fig. 7 below, it can be seen that a 50Ω load resistor is connected to each grid of the buncher. This resistor provides the wide bandwidth load required to match the multi-harmonic driving voltage. The maximum extraction voltage required to match the K500 center region is approximately 18 kV. From the voltage calculated above, this leads to a maximum power requirement of 435 watts per grid.

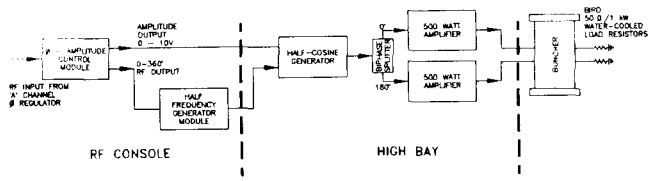


Fig. 7. Block diagram of buncher electronics system.

The power demand can be reduced by half by adding a second active gap one wavelength away. This will result in further degradation of the risetime of the velocity profile to the point where the result is little different from the use of a single frequency driving voltage.

5. LOW POWER SIGNAL GENERATION

Figure 7 shows the overall view of a buncher control system. The driving R.F. signal is derived from the phase regulator for the initial accelerating dee. This insures that the buncher signal has a properly phased signal for injection. The first module provides an amplitude control to the half-cosine generator and an adjustable phase R.F. signal to the half-frequency generator. The half-frequency generator divides the frequency of the input signal by two and provides a high purity sine wave of f/2 to the half-cosine generator.

Figure 8 is a schematic diagram of the half-cosine generator. The half-frequency signal is applied to the input of a quadrature hybrid signal divider to provide two signals that are 90° out of phase. One signal is then

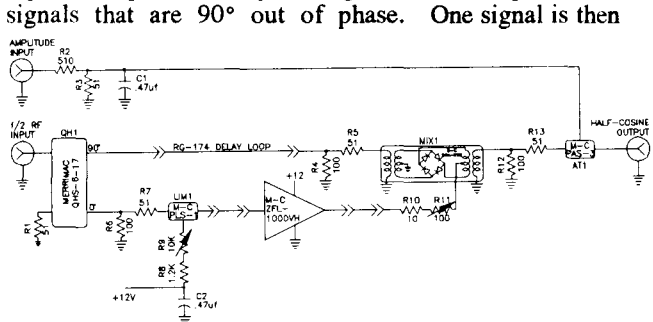


Fig. 8. Schematic diagram of half-cosine wave generator.

applied to a limiter to generate a square wave that is amplified and applied to the i.f. output terminal of a mixer. Note that this square wave is operating symmetrically about zero volts. The other signal from the quad hybrid is applied, through a delay line, to the r.f. input of the mixer. The delay is required to account for the delay in the limiter and amplifier. The half-cosine wave is then available at the l.o. input terminals of the mixer. The square wave first biases the ring modulator diodes in a direction so that the output from the l.o. terminals is in-phase with the r.f. input signal. When the square wave switches, it biases the diodes so that the output is 180° out-of-phase with the input signal. Because the switching takes place at the peak of the input signal and happens each half cycle, the resulting signal is a half-cosine wave with a period equal to the period of the original r.f. signal. Another way of looking at this is that two signals of equal frequency, f/2, have been mixed with the result that the signal of cyclotron frequency, f, has been recovered. Further, the high frequency harmonics necessary for the fast risetime were supplied by the square wave. The final circuit provides amplitude control of the half-cosine signal.

From Fig. 7 above, it can be seen that the half-cosine wave is split in a 180° power divider to provide the bi-phase or push-pull driving signals to the amplifier chain and thus to the buncher grids.

The design of this system was based on the proliferation of wide bandwidth high power amplifiers designed around the Motorola MRF151G power MOSFET. Although many amplifiers of this basic design are available and are advertised as being "linear" amplifiers, none that have been tested to this time should be represented as "linear". In fact, all the amplifiers of this design are operating in a Class AB mode and cannot support the half-cosine waveform. One amplifier has been found which can provide the proper amplification, Amplifier Research Model 1000L. However, this amplifier, available at a list price of $44,000 (U. S. currency) each, is prohibitively expensive for this application.

6. HIGH POWER SIGNAL GENERATION

Because of the extreme cost of amplification of the small signal waveform some design work has been done on methods of generating the half-cosine wave at high power levels. Fig. 9 is a diagram of a circuit that uses the MRF151G in a switching mode. This takes advantage of the device's high current capability and fast switching speed without the demand for wide bandwidth linear gain.

The operation of this circuit is to apply a high power full-wave rectified signal to the center tap on the switching transformer. The gate switching waveform is applied so that the switching takes place when the current through the switching transformer is at a peak. This reverses the current through the transformer and gives the fast reversal of phase necessary to produce the risetime required for the half-cosine waveform. The rectification of the input signal is required to maintain positive voltage on the drain inputs of the N-channel MOSFET. The transformers for this type of application follow the design given in Ref. 4.

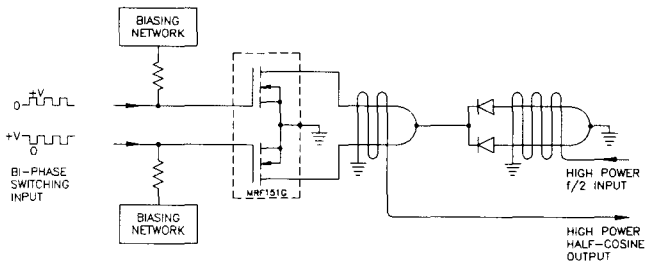


Fig. 9. Preliminary circuit design for a high power half-cosine generator.

A SPICE analysis of this circuit has been done and the important waveforms are shown in Fig. 10. Reading from top to bottom of the figure are the following signals:

1. Half-frequency high power input wave,
2. Rectified signal applied to switching transformer,
3. Gate 1 drive signal,
4. Gate 2 drive signal,
5. Half-cosine output signal.

Note that the gate drive signals are at frequency f, not f/2. Also, the output half-cosine wave has essentially the same peak amplitude as the input wave. This indicates that it may be possible to switch the power through the circuit with very low loss.

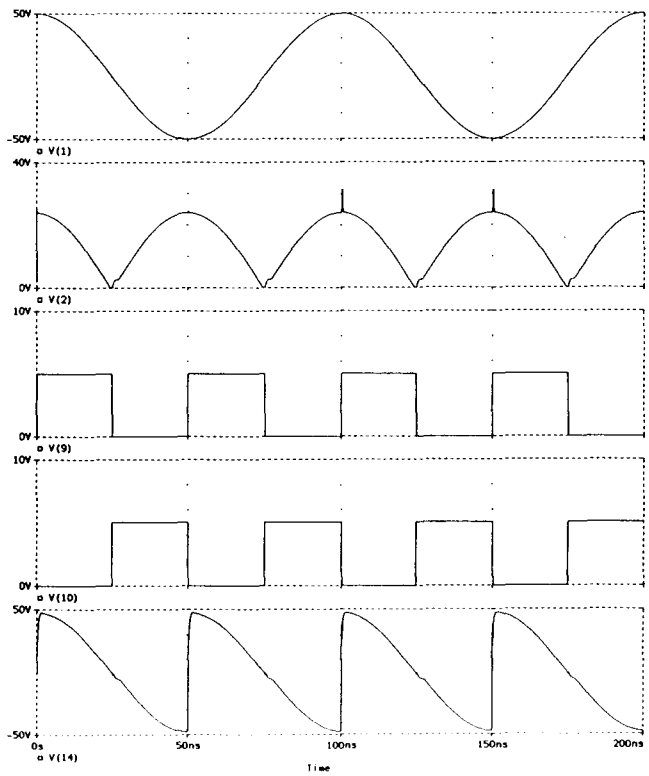


Fig. 10. SPICE analysis waveforms for circuit shown in Fig. 9.

The high power input for the signal generation is supplied from an amplifier of modest bandwidth. For the K500 cyclotron the amplifier need only cover the frequency range from 4.5 MHz to 13.75 MHz. Amplifiers of this bandwidth and nominal 500 watt capability are available at costs in the $10,000 price range.

There are a few different power MOSFET devices available and the MRF151G may not be the best choice but this remains to be investigated.

7. PRESENT STATUS AND CONCLUSION

The buncher mechanical structure shown in Fig. 2 is installed and operating with a push-pull sinusoidal wave while work continues on developing a high power half-cosine signal generator.

While the sawtooth waveform remains as an ideal choice for buncher applications, the half-cosine waveform must be considered because of its simplicity of generation. If high power generation techniques can be found, then the half-cosine waveform can potentially replace many expensive and complex multiple-gap, multiple harmonic systems.

8. ACKNOWLEDGEMENT

The author would like to thank Robert A. Gutierrez for assistance with the high power generation circuit design and SPICE analysis. Also, thanks go to John Vincent of the MSUNSCL for software for the Fourier analysis of the waveforms.

9. REFERENCES

1) Resmini, F. and Clark, D. J., "A Proposed Sawtooth Buncher for the 88-Inch Cyclotron Axial Injection System," UCRL-18125, University of California, Berkeley Radiation Laboratory, March 1968.
2) Lynch, F.J. et. al., "Beam Buncher for Heavy Ions," Nucl. Instr. and Methods **159**, 245-263 (1979).
3) Ratzinger, U. et. al., "The Three-harmonics Double-drift Buncher at the Munich Heavy Ion Postaccelerator," Nucl. Instr. and Methods **205**, 381-386 (1983).
4) Granberg, H. O., "Building Push-Pull, Multioctave, VHF Power Amplifiers," Motorola Application Note AR305 (1987).

INTEGRATED TOOLS FOR CYCLOTRON OPERATION

W. Busse
Hahn-Meitner-Institut, Bereich Schwerionenphysik
Glienicker Straße 100, W-1000 Berlin 39
Germany

ABSTRACT

With reference to the generally accepted architecture of modern control systems a review of facilities as implemented for cyclotrons presently being commissioned will be compared to commercially available control packages and tools. An attempt is made to point out their qualification to integration, their interoperability and present drawbacks.

1. INTRODUCTION

Modern process control systems use embedded distributed intelligence which is based on well defined hardware standards and more or less standardized software. Data bases hold all the necessary configurational static or dynamic views. More modern systems even implement software standards and integrate tools. Future control systems will be generated and run by fully integrated tool kits. These are the highlights which you might take along from control conferences and working group meetings. But where are we today? What in fact is a control system in this context? What are integrated tools? Are there any such tools available for accelerator, or more specially for cyclotron controls?

An abstracted view of a machine control system is given by fig.1. The process in view and the product it has to deliver are part of the lowermost level. It may be called the SHAPING level where the manipulation of producing objects is carried out and where views of the resulting states or of the transitions between them are generated. The uppermost level, which could be called the REASONING level, comprises all the activities like DESIGN, MODELING, SIMULATION, OPERATION etc., which in general still involve human brains and human intervention. The area between these two levels is the TRANSACTION level, which transfers requests of the REASONING into appropriate actions of the SHAPING level and vice versa, according to well defined rules of interference. This intermediate level is the translator of functions and data according to their level-dependent meaning and representation; it has appropriately defined access interfaces to the upper and lower levels respectively. The process Control System is the vehicle for all the transactions. A good control system is completely transparent and offers the flexibility and expandability needed to adapt to changing functionality in either level.

2. TOOLS FOR DESIGN AND IMPLEMENTATION

The analysis of the functional requirements has presumably always been the basis of any control system design. However, the final implementation often had to decide on acceptable drawbacks because of technological limitations or even man-power or financial constraints. It must be admitted,however, that the need for more functionality has motivated and pushed technological development and that the advent of new technologies has opened the view for refinements in both, design and implementation.

Whilst the system architecture is based on the functional requirements through the question 'what do we want to achieve?', the implementation of the hardware and a software architectures is based on 'how do we want to achieve this aim?'. Again both have functional components which should reflect the overall system functionality. Although logically interrelated, the topology within the architectural schemes need not necessarily be the same, e.g. a given hardware architecture can be the basis of different software architectures and vice versa [1].

Presently all but the smallest systems use distributed computing. The underlying hardware and software architectures are surprisingly similar and can largely be divided into three logical layers as symbolized by fig. 1.

Hardware:

- an upper layer made up of the operator interface and the application computers,
- a middle layer of processors distributed around the accelerator dealing with sets of equipment,
- a lower layer of processors which interface to dif-

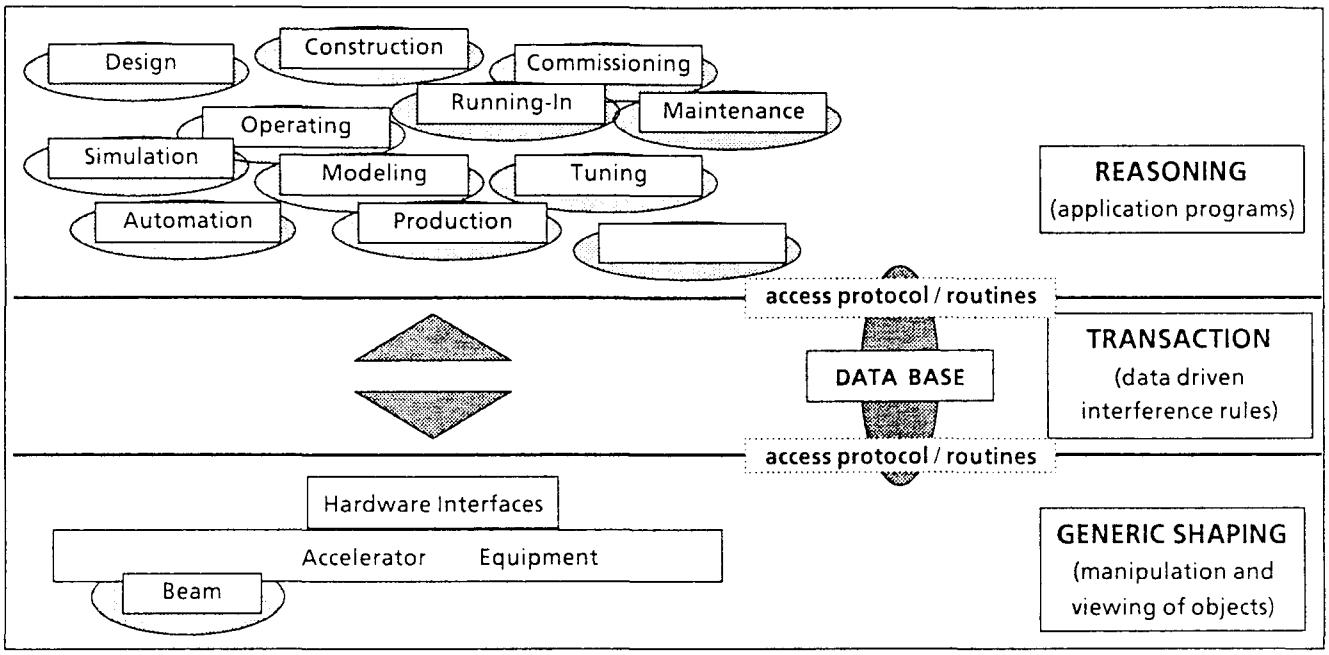


Fig.1: Schematic view of logical control system levels

ferent types of equipment.

The layers are interconnected by a communication network as the backbone. In most cases this is a local-area network for the upper and middle layers with multidrop or individual links connecting the middle layer processors to those of the lower level (cf fig. 2).

Software:

- an upper level comprising the application processing, including the operator interface,
- a middle level, transferring operational actions into hardware interface actions and vice versa (in general data driven),
- and a lower level of equipment driving and hardware access routines.

A (distributed) data base is the backbone, with its access routines from and to the upper and lower levels. It allows to separate the upper and lower levels from each other and to make them independent of each other by operational protocols which only deal with 'meaningful' operational parameters and which are transparent with regard to distribution and specific hardware.

The hardware architecture is generally supported by accepted standards with written specifications. The hardware is commercially available and may often be chosen from a variety of products according to the actual needs.

The same is, or is becoming, true for what I would like to call the control system firmware, i.e. the computer and microprocessor operating systems, the network communication software and the software development environment.

It goes without saying, that increased empha-

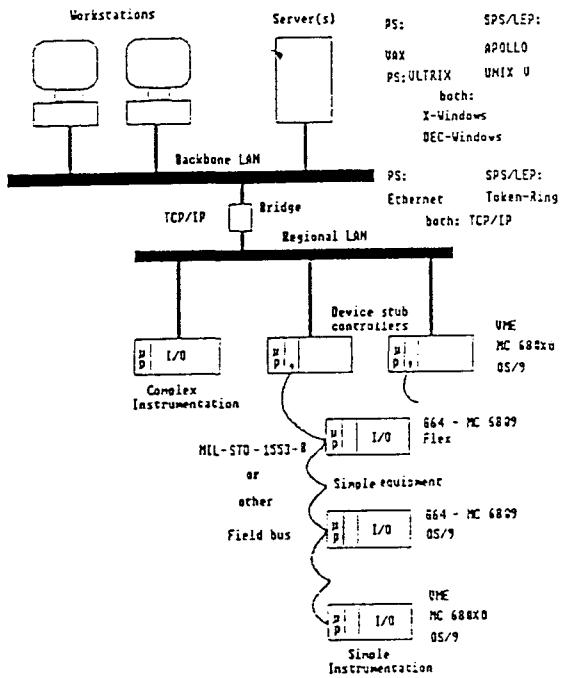


Fig.2: Simplified view of the hardware architecture for CERN accelerator control [1)]

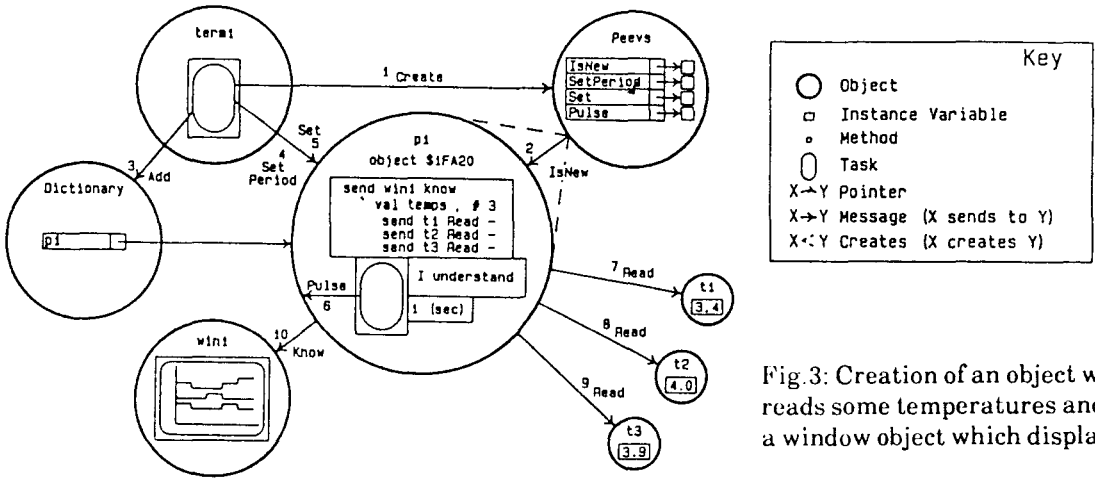


Fig.3: Creation of an object which periodically reads some temperatures and sends the values to a window object which displays them graphically

sis is now put on techniques for designing software in a more formalized way in order to reduce the increasing cost of ever more sophistication.

Given the fact of the commercially available hard- and firmware mentioned above, the idea is to base the underlying control system design on a higher level of abstraction. Initial discussions should not concern specific hard- and software architectures and implementations, but should regard the system as being primarily independent of such aspects.

A notion of L.Chapman[15] may serve as an example. His basic vision of a control system is a sea of objects spread over a computer network, organized logically and somewhat independently of the physical organization of the network. That is, any particular processor might contain one or more logical groups of objects, and an object group might be spread over multiple processors. These objects send each other messages in a simple, uniform way, regardless of whether these objects are nearby (e.g. in the same processor) or distant (e.g. on a different network node). Figure 3 illustrates a detail of an implementation which is based on these ideas

Tools are supposed to help their user achieving the aim in mind in a smooth and easy way. With wrong or badly adapted tools he will not succeed. With the aim of refinement good tools can be used to produce new more sophisticated tools intended for more sophisticated operations, and so on.

Integrated tools produce an output which can be directly used as input for the next step. They are plug-compatible to a common backbone like hardware modules to their standard bus. They are the basis of interoperability.

Assuming that the hard- and firmware for a control system implementation is commercially available as mentioned above, tools for their production, e.g. CAD/CAM-techniques, need not be looked at. It is still felt, however, that there still is little choice among tools helping with the design and implementation of the software architecture or even tool-kits representing a tailorable control system which can be tuned to the user's needs.

Commercially available tools exist e.g. to facilitate software implementation: language sensitive editors, version management and control, graphical editors, program development environment for programmable local controllers (development on host computer, down-loading, remote debugging) often even menu-driven via graphical user interfaces, test managers. These tools are in general part of the software delivered by the computer manufacturers.

The next higher level of commercial support is by Computer Aided Software Engineering (CASE) tools. Various companies offer packages which they like to call *workbenches* and which lead the user with the help of graphical desk user interfaces through analyzing, architecturing, designing and programming phases. Code generation is not necessarily available. The integrating backbone is a project database which often may be a different manufacturer's product. These packages are mostly model based and implement methodologies like *Structured Analysis* (SA)[2], *Real-time Structured Analysis* (RT/SA)[3] and *Structured Design* (SD)[4], the so-called SASD techniques. More modern implementations are based on *Object Oriented* principles, which seem to be more adequate to process control systems. However, *object orientation* is today where SASD was about ten years ago. An application of these techniques is discussed is discussed by G.Ludgate and E.Osberg[5]. In summary, these tools completely integrate their sub-tools, run on many commercially available platforms, but in general do not produce the code to let you directly use the product which is designed with their help.

The nest group of tools to be discussed consists

of products with embedded executable software for a specified range of applications. They offer graphical editors to let the user choose objects from given selections, choose their attributes and their interconnections. The next paragraph will describe tools of this group in more details.

3. SELECTED COMMERCIAL TOOLS AND APPLICATION EXAMPLES

The following examples were chosen to illustrate commercially available tools which can indeed help with implementing or generating an accelerator control system. Their common feature is the generation of animated synoptics for operator interaction, nevertheless their internal features and their range of completeness in the context of a process control system are totally different.

3.1 DATAVIEWS, SL-GMS

DATAVIEWS [6] and SL-GMS [7] (SL Graphical Modeling System) are two of the more complete development systems for building and managing graphics screens which can be (easily) embedded in user applications. Both products enable the user to generate sophisticated graphical user interfaces to any application, e.g. monitoring and control, modeling, simulation. Apart from a very powerful drawing tool the user is supplied with a prototyping package (no programming is needed) and a library of run-time routines for programming access to views, sub-views, graphical objects and their attributes, screen management etc. Programming access is provided for most standard languages such as C, Fortran, Pascal, Ada.

Figure 4 illustrates the positioning of these tools within an imagined control system as *application*. For *monitoring* the interface receives input from the application in form of application data, the interface then delivers output to the user in the form of graphical data displays. For *control* the interface receives input from the user in form of keystrokes, mouse picks or other locator events which is delivered as output to the application in form of control data. The data exchange can either be done by intermediate files or by direct delivery to or from the product internal data structures using calls to the respective library routines. In the first case a description of the file structure must be maintained in both, the application and the interface, the second needs a sort if integrating gateway between either data structures.

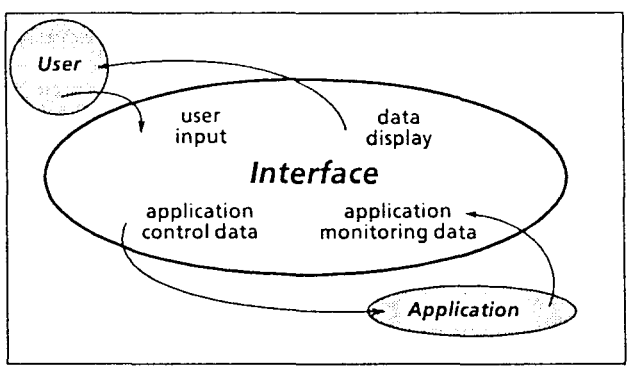


Fig.4: Illustration of the dialogues of a visualization and interaction interface with user and application

Both products support a large number of platforms, operating systems and graphical interfacing standards. DATAVIEWS seems to be the more industrial and stable product being based on classical design concepts, the design of SL-GMS follows the more modern object oriented principles but still is less ergonomic. [8]

Mind, however, that these products produce visualization and interaction interfaces, they do not generate a runnable process control system.

3.2 Vsystem

Vsystem [9], the Vista Control system software, is developed to control a given specifiable process through a CAMAC or VME hardware interface using Digital Equipments VAX-computers with the manufacturer's VMS and ELN operating systems. Devices to be connected to the system have to be described in a data base of text entries which is afterwards converted into binary format, the run-time data base.for use by the control software. A graphics interface based on window software provides control and monitoring functions, referred to as channels. The system incorporates a comprehensive toolkit to create operator displays, to connect device-channels to parts of the displays and to access information in the runtime data base.

Before the system can be put into service, the system manager must provide a *handler* for each hardware interface describing its characteristics (if not delivered by VISTA) and he must specify a data base entry for each channel in the system which also includes the handler name for the hardware channel.

Vsystem offers a variety of features which are known to be useful in process control systems, such as generic readers and reader banks, data logging, "strip-charts", alarms for specified channels. A sequencer package is available to the operator to perform sentence-like instructions on specified channels in a certain sequence.

As any other commercial company in the field VISTA is continuously implementing enhancements

and new features [10].

Various accelerator control systems have implemented partial systems generated by the Vsystem package or are evaluating for future use. Figure 5 is an operator interaction display of the TRIUMF Beam Line 2C vacuum system [11].

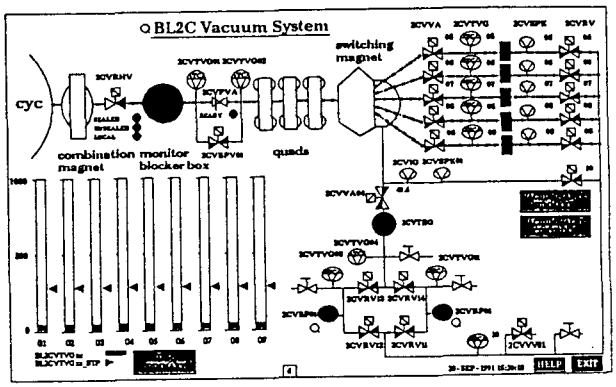


Fig.5: Vsystem operator display of TRIUMF beam line 2C vacuum system

Assuming that all the hardware handlers mentioned above are available, the user of this package need not write any software, unless he wants to integrate features which are not yet offered (e.g. model support, simulation). In this case, however, the user is either compelled to stay with the VAX hardware and VMS/ELN software and especially with the system data base or he has to undergo a considerable integration job where data integrity can be an issue.

3.3 SYSTEMS BASED ON INDUSTRIAL PROGRAMMABLE CONTROLLERS

Various industrial systems within this group provide the highest degree of commercially available tool integration. This is due to the fact that one manufacturer delivers proven hardware and software which can be configured to the costumer's requirements. Hardware and software configuration is achieved by putting together prefabricated modules with the aid of graphical tools, appropriately engineered for each level of the process control system hierarchy.

The outstanding advantages of such sysstems are proven and guaranteed reliability in an industrial environment, determined and stable behaviour even under extreme conditions, possibility of interconnection and point-to-point communication. Programming, which means logical assembly of appropriate building objects, is done by integrated 'programming tools' which can be used by 'programmers' of all levels. The packages also integrate 'programmable' user interfaces. Complete compatability between hardware and software is guaranteed on all levels, documentation is automatic and maintenance is assured by the manufacturer.

Generally speaking slower processing is the price to be paid for the reliability of such systems within industrial environment. Limited memory space which was an inconvenience of early implementations is being overcome.

Complete knowledge of the process to be monitored and/or controlled is another basic requirement for these systems to be appropriate. No modeling or basic research about the internal process behaviour is appreciated. Hence, these systems are favorable candidates for the implementation of turn-key systems.

The industrial example chosen here is the SIMATIC-S5[12] system with the STEP-5[12] and COROS[12] programming and production tools. Figure 6 is a pop-up of the base-level I/O-modules, function generators and signal processing modules, their

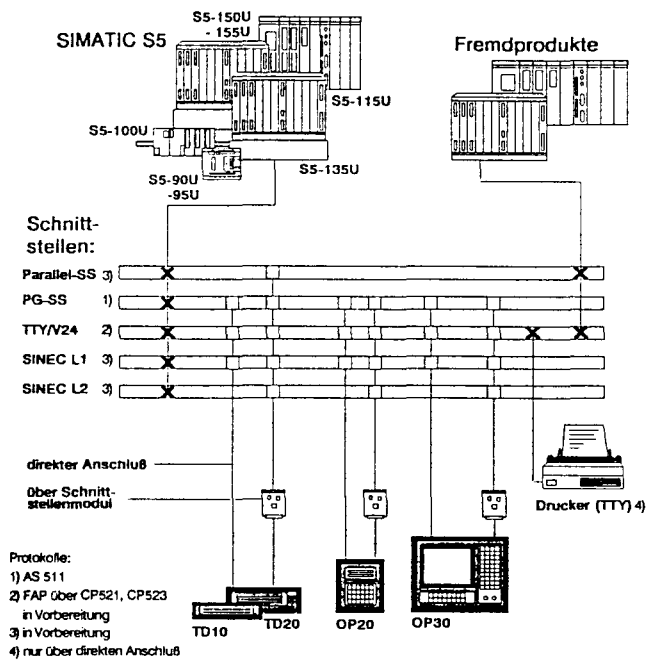


Fig.6: Base level hardware of the SIMATIC-S5 system

bus systems and interconnections as well as base-level local operator interfaces. Programming on this level is done with the tool package STEP-5 which offers a symbolic editor to define and name (globally uniquely) input- and output-signals or functions and to produce or to correct graphical views of their logical interconnection with the help of ladder logic. COROS provides the tool to interconnect base-level equipment of subsystems, subsystems to site-systems and sites to central monitoring and control.

Commands to exchange data between processors and process image as well as reactions to be carried out in case of data changes can be defined. Messages and reaction strategies on alarms, alarm analysis and automatic archiving can be set up to the user's requirements.

In the accelerator field the SIEMENS tool kit has been successfully applied to e.g. the control system of the compact cyclotron Cyclone 30 at the Catholic University of Louvain, Belgium[13]. Figure 7 is a schematic view of the system. The following functionality is offered to the user: automatic startup and rundown to a standby state, automatic change of source

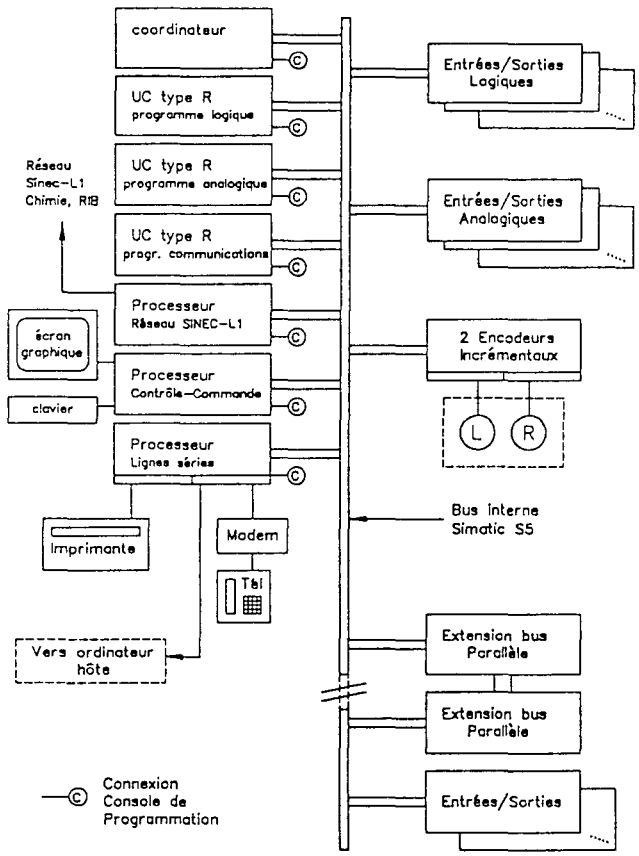


Fig.7: SIMATIC-S5 system as implemented for CYCLONE 30. The system also provides 2 shaft encoders to fine-tune parameter settings.

or target material on operator request, intensity monitoring, intensity reduction if preset limits are exceeded, calculation of extraction energy, automatic adjustment and shift compensation of the main magnetic field, calculation and proposal of setting values for extraction of new beams, automatic call of the person in charge in case of a failure. The setting values for different beams are held in an archive for downloading if required.

Keitel et al.[14] report on a similar system implemented for the TRIUMF TR30 cyclotron on the basis of Allen Bradley PLC's.

4. CONCLUSIONS

Highly integrated tool kit solutions comprising hardware and software exist for well defined processes. Due to their reliability and robustness they can be used in industrial environment and are applicable to turn-key systems. Some have been implemented for compact cyclotrons and other ion implanting machines.

Partial solutions exist for systems where some flexibility and extensibility to new requirements or research about the process itself is desirable. Often more computing power and fast signal processing is mandatory in such cases. These solutions have been evaluated or implemented for medium scale systems.

No complete example exists for the application of the above mentioned tools in large scale complex machines. On the contrary, while the complexity of these systems has increased several orders of magnitude over the last twenty years the ability to reliably specify them and manage their implementation has not kept pace.

5. REFERENCES

1) Rausch, R. et al., "Common Control System for the CERN PS and SPS Accelerators", ICALEPCS'91, Tsukuba, Japan Japan, Nov. 11-15, 1991 (Proceedings to be published)
2) De Marco, T., "Structured Analysis and System Specification", Yourdon Press, 1978, ISBN 0-13-854380-1
3) Ward, P.T., and Mellor, S.J., "Structured Development for Real-time Systems", Yourdon Press, 1985, ISBN 0-917072-51-0
4) Yourdon, E., and Constantine, L.L., "Structured Design", Prentice Hall, 1979, ISBN 0-13-854471-9
5) Ludgate, G.A., Osberg, E.A., "Contemporary Approaches to Control System Specification and Design Applied to KAON, contribution to this conference
6) DATAVIEWS, product and trademark of V.I. Corporation, Northampton, Ma 01060
7) SL-GMS, product and trademark of SL Corporation, Coste Madera, California 94925
8) Lugnet, J. et al., "Evaluation de Produits d'Animation de Synoptiques", Technical Report No. 91/012 of CEN SACLAY DPhN-STAS-STP

9) Vsystem, product and trademark of VISTA Control Systems Inc., Los Alamos, NM 87544
10) Clout, P. et al., "Past, Present and Future of a Commercial, Graphically Oriented Control System", ICALEPCS'89, Vancouver, Canada, Nucl.Instr. and Meth. A293, pp. 456-459, 1990
11) Wilkinson, N.A., Ludgate, G. A., "Experience with the Application of Object Oriented Techniques in the TRIUMF Beam Line 2C Control System", contribution to this conference
12) SIMATIC-S5, STEP-5, COROS are products and trademarks of the SIEMENS AG, Berlin, Germany
13) Lacroix, M., "Il est possible de contrôler un cyclotron compact avec des processeurs industriels, en vue d'en rendre le fonctionnement automatique", thesis submitted to the Catholic University of Louvain, Belgium, 1989
14) Keitel, R. and Dale, D., "The TR30 Control System a Case for Off-the-Shelf Software", ICALEPCS'91, Tsukuba, Japan, Nov. 11-15, 1991 (Proceedings to be published)

THE IUCF HIGH INTENSITY POLARIZED ION SOURCE CONTROL SYSTEM*

T. Capshew, J.C. Collins, D.W. Frame, D. DuPlantis, J. Graham, D.D. Reid

Indiana University Cyclotron Facility
2401 Milo B. Sampson Lane
Bloomington, IN 47408-0768

ABSTRACT

A high intensity polarized ion source (HIPIOS), capable of producing 100μA of protons at 600keV with $\geq$75% polarization is presently under construction at IUCF. An overview of the control system is presented, with a brief explanation of the bakeout and vacuum subsystems. HIPIOS will utilize a control architecture new to IUCF. Implementation through the use of VME hardware and programmable logic controllers, all under control via the VAX-based Vista^{tm} graphical user interface, and results from initial bench tests will be discussed.

1. INTRODUCTION

IUCF is developing HIPIOS to improve substantially polarized beam intensity in the Cooler Ring[1]. The existing accelerator complex is controlled by PDP-11s driving DACs, ADCs and parallel I/O over a system built in-house from a long obsolete commercial standard[2]. While it is possible, for many reasons it is not prudent to further expand this system. Since HIPIOS and its associated beamline (BL1C) can be operated independently of the IUCF accelerators and other beamlines, we chose to use them as an opportunity to become familiar with new controls equipment. HIPIOS and BL1C will be controlled through VMEbus, commercial VME cards, PLCs, GPIB, workstations and a commercial software system. Figure 1 presents a schematic representation of the HIPIOS control system.

2. CONTROL SYSTEM COMPONENTS

2.1 Software

As in any computer intensive project, software costs eventually dominate, as long as manpower costs are accounted for. Recognizing this in our own control system and knowing that we could not afford to create our own graphical user interface system, we examined a number of existing systems. We chose the Vista[3] software system as best fitting our requirements and limitations. Vista provides the GUI framework and basic device access mechanisms. We need only create control displays for the operator using Vista tools and write that software which is unique to our equipment.

The distributed control system uses ethernet and fiber optics to connect data acquisition nodes to graphics generating nodes and operator X-window terminals. All operator interaction will use X-terminals, not hardwired panels. Our operations staff have insisted that knobs be included at all control stations. (They do not want to use on-screen sliders.) Our goal is to have sufficient tools on hand at commissioning that neither knobs nor sliders will be necessary.[4]

2.2 Hardware

The basic unit of the control system is a 21 slot 6U VME crate built by VERO to our specifications so that crate power supplies can be serviced from the front. Most crates contain an AEON VME300 CPU board which includes an rtVAX300, 8Mb of memory, and VMEbus and ethernet interfaces, running the VAXELN operating system. Crates operated in hostile environments, such as inside HIPIOS, are driven by Augment fiber optic backplane extenders from a ground potential station and do not contain a cpu. There will also be a reboot link between the terminal and ground which

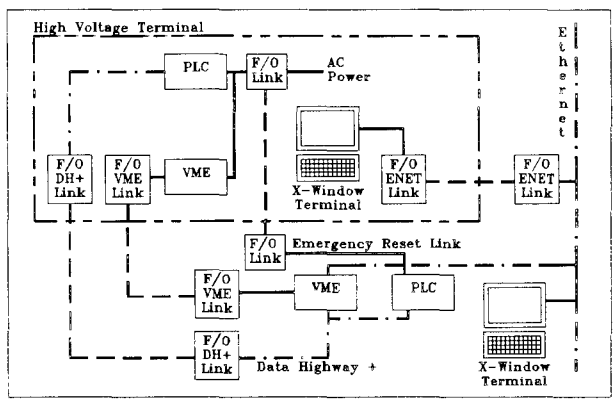


Fig. 1. Controls block diagram

*Work supported by the U.S. National Science Foundation under grant NSF PHY 90-15957

will allow the operator to reset all controls systems in the terminal.

2.2.1 PLC

The hardware in the new controls system which provides us a qualitative advance over the old system is the Programmable Logic Controller (PLC). We have decided on the Allen-Bradley PLC5/VME, a PLC5/15 equivalent in a VME form-factor. We use 32-point 24v input modules (A/B #1771-IBN) for status/interlock inputs, 32-point contact closure output modules (A/B #1771-OWNA) for device actuation outputs and 8-point thermocouple input modules (A/B #1771-IXE) for temperature readout. For spark protection, the PLC5/VME resides in the ground station VME crate and communicates with the HIPIOS high voltage platform via the fiber optic converter modules (A/B #1771-AF) and remote I/O adapter modules (A/B #1771-ASB).

On/Off control, interlocks and status for power supplies, vacuum devices, bakeout devices, RF devices and stops are handled in the PLC. Commands from the control computers are treated as requests by the PLC. If the pre-defined interlocks and conditions are satisfied, the PLC will honor the request via a contact opening or closure. All interlocks are hardwired or implemented under PLC ladder logic; controls computers do no interlock checking on their own.

Programming the PLC is done with ICOM Ladder Logistics software running on a PC. Currently a desktop PC is used, but we are ordering a laptop PC since portability will be important in diagnosing control problems in the future.

Communication between the PLC and a controls computer is provided through a block of PLC memory accessible from the VMEbus. To reduce software overhead, the device handler divides this memory into blocks for treating reads, writes and error reporting. Because obtaining a data block from the PLC is comparatively slow, the handler supports a deferred read function where execution returns to the calling program immediately after a read command is issued. The program may later execute a handler call to return the last data block read or wait until it becomes available. The handler uses multiple read blocks so that multiple programs may have simultaneously active read requests.

2.2.2 Analog I/O

In choosing components for the analog section of the control system, multi-function cards were rejected as too costly to maintain in the long run. Standard commercial components were chosen where-ever possible.

For analog acquisition we use ADAC 7000MF series ADC cards. These twelve bit (7010MF) and sixteen bit (7040MF) VME cards allow their inputs to be multiplexed through an external chassis (5305ENV) using 4012HLEX multiplexer cards. In this way one can have up to eighty analog inputs per VME slot. Inputs are differential to avoid common mode voltage problems with power supplies. Few sixteen bit inputs are needed so multiplexers are not used with the 7040MF cards.

For analog control we chose Datel's DVME-626 and DVME-628 DAC cards for fourteen bit and twelve bit resolutions, respectively. (Although the DVME-626 is a sixteen bit card, it is only monotonic to fourteen bits.) These cards were chosen primarily for their thermal stability (8ppm/°C).

2.2.3 Isolation

The DAC cards are not isolated from digital (VME) ground, while the supplies we are controlling require the outputs to be isolated from digital and frame ground. To cut costs, we decided to design and build an analog isolation subsystem ourselves; the isolator card (CYC-V01) is the only non-commercial component we are using. It is a 160x233mm Eurocard which fits into a VME crate, using it's P2 connector for power and output connections. Inputs for the CYC-V01 come through DB-25 connectors on the front panel. The CYC-V01 uses Burr Brown ISO-102 amplifiers and PWM740 DC-DC conversion components to provide eight isolated outputs per card. The bandwidth of the system is limited to 6Hz to eliminate any switching noise from the ISO-102. We implement these cards in VERO KM6 subracks to save expansion space on the VME backplane.

2.2.4 EMI Shielding

We have invested considerable thought to trying to protect expensive electronics in the hostile environment of the HIPIOS high voltage terminal. Because of the industrial ruggedness of the PLC components and the bandwidth limits and analog isolation for the DAC channels and because of costs, we shield only analog inputs, GPIB and serial lines. We are using ferrite beads, a 100 Ohm series resistor, a 1.5KE18CA transzorb and an Oxley FLT/P/5000 on each signal connection. There is a filter assembly on both signal and return connections for all signals attached to the VME crate. The filter assemblies will be mounted in the rear doors of a General Devices EMI shielded rack. Tests have been done using a proto-type which show that, by using these filter assemblies, damage to our electronics from typical discharge events should be minimized.[5]

2.2.5 Motors, GPIB and serial links

Motors will be driven by Oregon Micro Systems VME8 eight-axis controller boards interfacing to SD3 motor drivers. This combination can handle a wide variety of motors with programmable velocity and acceleration profiles.

We are using National Instruments GPIB-1014 for a GPIB interface and FORCE ISIO-2 for a serial interface supporting both RS-232 and RS-422 protocols. Both devices are serviced by separate programs rather than device handlers, even though interrupts are used to signal command completion. This does make new applications less convenient to create, but the variety in serial and GPIB devices is too great to admit a simple common service routine.

3. OPERATIONAL SYSTEMS

3.1 Bakeout

A bakeout system is needed to improve the vacuum conditions for source operation. Each chamber of HIPIOS has its own bakeout sub-system, consisting of two heaters, two thermocouples and two temperature sensing klixons. All klixons are wired in series and pass the drive voltage for the main 110 VAC contactor. When any klixon reaches 170° F, it opens, shutting off power to all heating elements, providing highly reliable protection against overheating.

The PLC is programmed to keep the temperature of each chamber within a range defined by the user. If either thermocouple reads above the high setpoint, the PLC turns off the heating elements. When both thermocouples are below the low setpoint, the PLC turns the heaters back on. This algorithm protects against driving the system to an undesired temperature should one of the thermocouples fail.

The bakeout system uses only one control display. A pair of temperature bar graphs, an ON/OFF control button, an indicator showing when the heaters are actually energized, a fault indicator and a strip chart showing temperatures vs. time form a group of controls which is repeated on the display for each of the HIPIOS chambers. There are also indicators for the emergency stop button and the klixon circuit and a fault acknowledge button. Most faults are not reset until this last button is activated to show that the user is aware of the fault. Display data is updated at 1Hz.

3.2 Vacuum

The vacuum control system must deal with a wide variety of devices, including a PLC system for on/off, interlocks and status for vacuum and water valves and flow switches, RS-422 for convectron gauge controllers[6], GPIB for cryotemp monitors (Lake Shore Cryotronics model 819), and ADCs for cold cathode ion gauge controllers (MKS Instruments series 421) and flow/ratio controllers (Vacuum General model 80-4). The convectrons have alarm setpoints and outputs (contact closures) which feed directly into the PLC system for interlocking (of cold cathode ion gauge high voltages, for example). The cryotemp monitors have alarm outputs (contact closure) fed to the PLC for interlocking of cryo gate valves.

The vacuum system uses a number of control displays, some of them arranged hierarchically showing ever finer details of the system. Valve control is performed by placing the cursor on the proper valve and clicking a mouse button. Bar graphs provide pressure readings. Special buttons are provided to open or close sets of valves which experience has shown are often used together. We intend to automate pumpdown and venting procedures via the Vista command sequencer.

4. CONCLUSIONS

To date the new control system has met our goals. We have been quite pleased with how quickly bakeout and vacuum control have been implemented, considering that it is all new technology for us.

5. ACKNOWLEDGMENTS

We are indebted to the IUCF Computer and Electronics Technicians Group for their efforts in constructing and helping us troubleshoot the new systems.

6. REFERENCES

1) V. Derenchuk, et al., "Performance of the IUCF High Intensity Polarized Ion Source", these proceedings
2) J. Collins, et al., "The IUCF Cooler Ring Control System", 12th Inter. Conf. on Cyclotrons and Their Applications, Berlin, Germany, 1989, p.244
3) P. Clout, et al., "Past, present and future of a commercial, graphically oriented control system", Accelerator and Large Experimental Physics Control Systems, Vancouver, B.C., 1989, p.456
4) W.P. Jones, et al., "Beam Transport System for the New IUCF Polarized Ion Source", these proceedings
5) J. Budnick, IUCF, private communication
6) D. Dale, TRIUMF, private communication

AN OPERATOR ASSISTANCE SYSTEM FOR THE AVF CYCLOTRON

Tetsuya Okamura and Tohru Murakami
Systems Engineering Laboratory, Sumitomo Heavy Industries, 2-4-15 Yato-cho, Tanashi City, Tokyo 188, Japan

Toshiki Tachikawa
Quantum Equipment Div., Sumitomo Heavy Industries, 5-2 Soubiraki-cho, Niihama City, Ehime 792, Japan

Takashi Agematsu, Susumu Okumura and Kazuo Arakawa
Takasaki Radiation Chemistry Research Establishment, Japan Atomic Energy Research Institute, 1233 Watanuki-machi, Takasaki City, Gunma 370-12, Japan

ABSTRACT

A computer-based operator assistance system installed at the AVF cyclotron in Japan is described. This system provides CRT display of cyclotron beam trajectories, feasible setting regions (FSRs), and search traces designed to enhance beam parameter adjustments. A system evaluation experiment was conducted and the operation time to reach required beam conditions was reduced by approximately 65%. In addition, results of an operator questionnaire survey indicated high system operability.

1. INTRODUCTION

A computer-based operation system which assists inexperienced operators has been implemented at the AVF (Azimuthally Varying Field) cyclotron of the Japan Atomic Energy Research Institute (JAERI)[1,2]. Cyclotron start-up operations require dozens of adjustable parameters to be finely tuned to maximize beam extraction efficiency. Veteran operators use their experience and relatively easily perform a trial-and-error procedure. On the other hand, inexperienced operators have a difficult time because operator consoles displaying measured beam parameters, alarm information, component status, etc. do not provide enough information to guide these new operators.

This operator assistance system provides three visual human interfaces to support beam adjustment of the axial injection and central and extraction regions, i.e.,

(1) Beam trajectory is rapidly calculated and graphically displayed whenever the operators change the cyclotron parameters.
(2) Feasible setting regions (FSR) of the parameters that satisfy the cyclotron's beam acceptance criteria are indicated.
(3) Search traces, being a historical visual map of beam current values represented by various colored blocks, are superimposed on the FSRs.

Since the above visual information is based on ap-

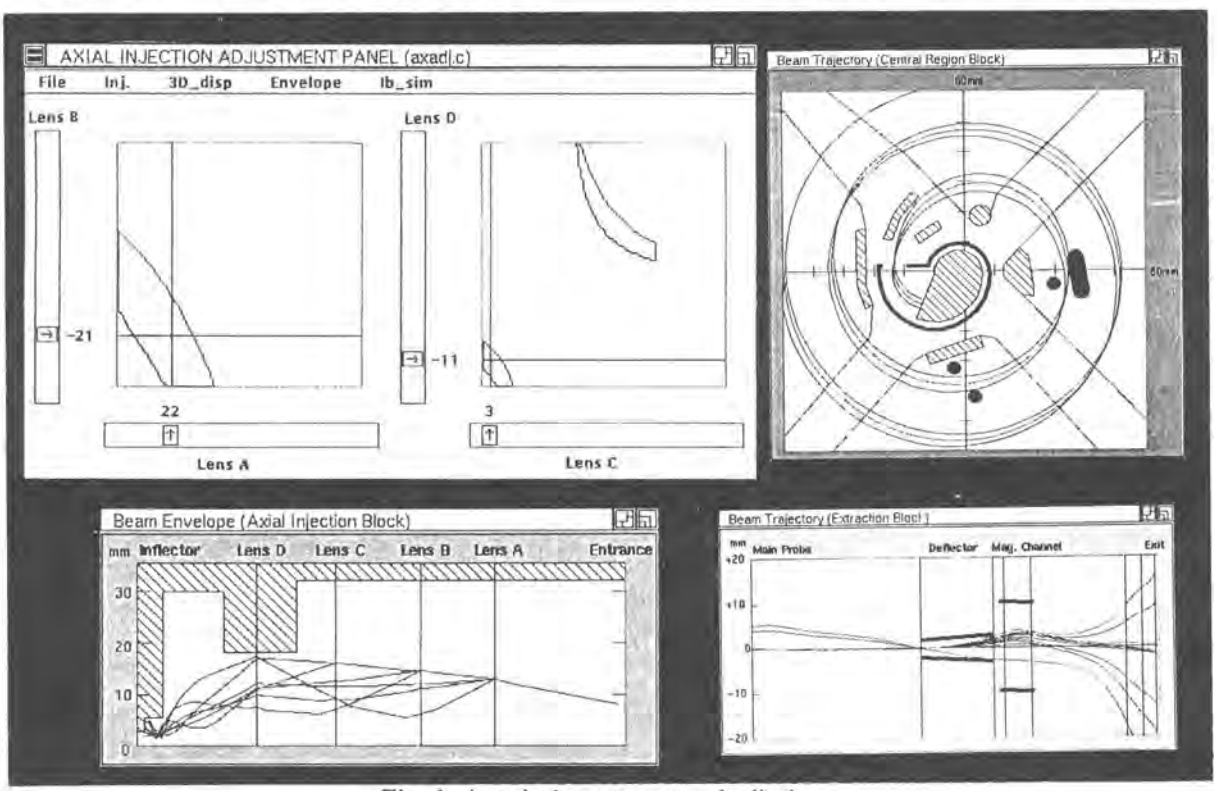


Fig. 1. A typical operator console display.

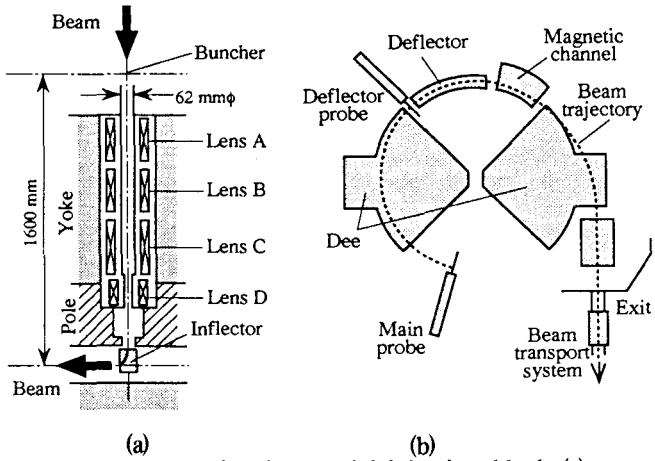


Fig. 2. Schematic of the axial injection block (a) and the extraction region (b).

plicable theoretical equations and numerical simulations, operators are able to quickly gain valuable operation experience which ultimately leads to a reduction of the time to reach the planned cyclotron conditions. This systematic combination of the computer computational power and human intuitive ability is the primary advantage of our assistance system.

The present study describes details concerning these three interface displays, and also discusses the results of a system evaluation experiment and an operator questionnaire survey on system operability.

2. VISUAL INTERFACES

2.1. Beam Trajectory Display

Veteran operators normally infer the beam trajectory parameters using their knowledge of the beam's internal behavior. The beam adjustment interface calculates the beam trajectories/envelopes using actual parameters and displays them on a CRT, thus whenever an operator changes the adjustable parameters, a graphical image is created which is similar to the expert's mental model.

In Fig. 1, showing a typical operator console display, the bottom left CRT display shows a typical beam envelope of the axial injection block,[3] the region between the entrance to the yoke and the inflector (Fig. 2(a)). The resultant envelopes are calculated within several milliseconds from the coil currents of four glazer lenses (A-D) and the magnetic field distribution using the transfer matrix method.[4] The top right display shows the central region beam trajectories which occur between the inflector and the second phase slit, being calculated within 3-4 s by the Runge-Kutta-Gill (RKG) method.[5,6] In addition, the layout of the phase slits is dynamically updated whenever they are changed. The bottom right display shows the extraction region which is between the deflector and the beam exit (Fig. 2(b)), where the x-axis represents the ideal trajectory. Before calculating the extraction region trajectory, the trajectory entering the deflector is infered by measuring the position of the final turn using both the main probe and the deflector probe. Similarly to the phase slits, the layout of the deflector and the magnetic channel have a dynamically updated display.

2.2. FSR Display[7]

Veteran operators generally know the approximate range of parameter values; hence a real-time display of FSRs is provided. The FSR represents the parameter range which allows the beam to pass through its respective region without hitting any components. By taking into account the spatially dependent beam acceptance criteria determined by the internal components, the FSR is derived by solving an inverse problem of the trajectory model.

The procedure to calculate the FSR for the axial injection block is presented as an example. The acceptance of the inflector in the x-θ phase plane is shown in Fig. 3(a), whereas Fig. 3(b) shows that occurring just after lens D, being considered as the adjustment target. The acceptance after lens D is approximated by the interior of a parallelogram defined by the four lines

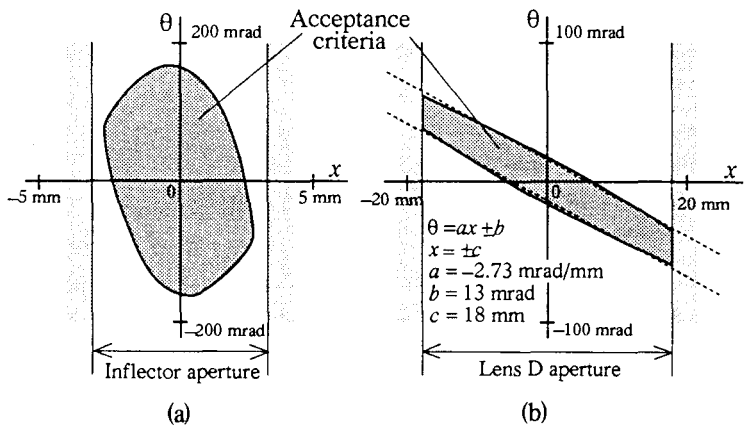


Fig. 3. Acceptance criteria of the axial injection block. (a) For inflector (b) following lens D.

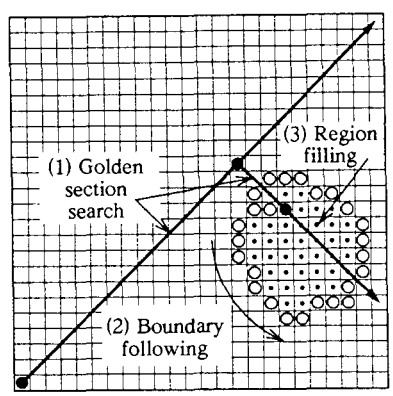


Fig. 4. Process used by the "search method" to obtain an FSR.

$$x = \pm c \quad (1)$$

$$\theta = ax \pm b \quad (2)$$

On the other hand, the beam is represented by an ellipse

$$\sigma_{22}x^2 - 2\sigma_{12}x\theta + \sigma_{11}\theta^2 = \sigma_{22}\sigma_{11} - \sigma_{12}^2 \quad (3)$$

where σ_{ij} are the x-θ elements of the sigma matrix for this beam state, being determined by functions of the adjustable focal lengths of the lenses (F_a, F_b, F_c, and F_d).

For the injected beam to pass through the inflector, the ellipse in Eq. 3 can not intersect the acceptance characteristics in Eqs. 1 and 2. This condition is derived from the discriminant of a quadratic equation, i.e.,

$$w_1 = \sigma_{11} - c^2 < 0 \quad (4)$$

$$w_2 = \sigma_{22} - 2\sigma_{12}a + \sigma_{11}a^2 - b^2 < 0 \quad (5)$$

Where w_1 and w_2 represent the degrees of insufficiency which satisfy the conditions of Eqs. 4 and 5.

Determining combinations of the focal length values (F_a, F_b, F_c, and F_d) which satisfy Eqs. 4 and 5 is analytically difficult, although a nonlinear minimization problem can be formulated. An objective function $w(F_a,F_b,F_c,F_d)$ is defined by

$$w(F_a,F_b,F_c,F_d) = \begin{cases} 0 & (w_1 \le 0 \text{ and } w_2 \le 0) \\ \sqrt{\alpha w_1^2 + \beta w_2^2} & (w_1 > 0 \text{ or } w_2 > 0) \end{cases} \quad (6)$$

where α and β are respectively the weights of w_1 and w_2. The FSR is defined as an area where the objective function is zero.

To visualize an FSR in a two-dimensional plane, we developed a "search method" in which a fast search algorithm is applied to a gridded search plane. This new method combines nonlinear programming and image processing techniques. Figure 4 shows the process used by the search algorithm. A golden section search, a type of line search algorithm, is first carried out to find a point where w=0. Then, starting from this point, the boundary of the region where w=0 is searched for. Next, the boundary is tracked (boundary following) using an image processing boundary following technique. Finally, it is assumed that w=0 at all points inside the boundary (boundary filling). The resultant region and its boundary is an FSR. The top left display in Fig. 1 shows typical FSRs for the axial injection block. Operators change the displayed parameter by pointing/clicking a mouse on the desired search plane.

The FSR also represents the sensitivity of each parameter and their mutual relation. A parameter's sensitivity is determined by the length of the cursor lines inside the FSR, where a shorter length indicates a more sensitive parameter. The mutual relation between parameters is indicated by the gradient of the FSR, e.g., an FSR sloping downward to the right indicates that the lens A and B will give the almost same effect on the beam.

Using a VAX-station 3100, 200 ms is required to search for and display an FSR for a particular plane, thereby providing real-time beam information.

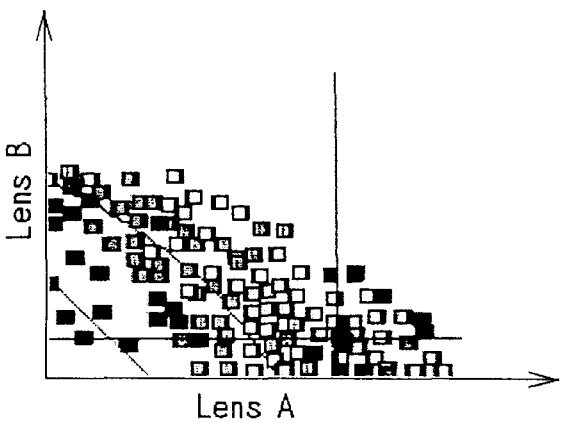


Fig. 5. Search trace display showing colored blocks of the measured beam current values superimposed on the FSR display.

2.3. Search Trace Display[7]

It is believed that operators are able to visualize, i.e., generate a mental map, of the beam current values in the operation space by memorizing action-response-sequences. To complement an operator's short term memory, search traces are superimposed on an FSR (Fig. 5). This display shows a historical summary of measured beam current values after any parameter "setting" adjustment by an operator. The beam current values are converted to a color scale and plotted as colored blocks at a position corresponding to the measured beam values. It should be noted that the search trace display indicates the cyclotron's actual condition, whereas the FSR shows the theoretical one. Operators can refer to either display, correct the differences between them, and search for the optimum set point which provides maximum beam current.

2.4. Operation Flow Using the Interfaces

Figure 6 is a block diagram of the information flow between the operator, assistance system, and cyclotron. The operator initially performs parameter setting adjustment by pointing/clicking the mouse at any position on the displayed search plane. The computer simultaneously calculates the new FSRs and beam trajectory, and

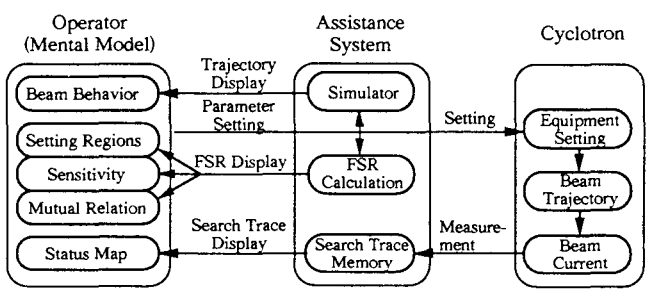


Fig. 6. Block diagram of information flow in the operator assistance system.

the assistance system transmits the setting values to the cyclotron components and measures the new beam current, which is then displayed on the search trace display as a colored block at the corresponding value. The operator can search inside or in the neighborhood of the regions by referring to the colored blocks. The three displays enable operators to feel as if they are actually interfacing with the beam, even though it is not visible.

3. SYSTEM EVALUATION

To evaluate system effectiveness, the search time required to reach maximum beam current conditions was measured. In addition, system operability was evaluated using written questionnaires.

Nine operators (1 expert, 4 trainees, and 4 novices) were asked to obtain maximum beam current by performing adjustments of the axial injection block by tuning the four lenses using three different interface modes:

Mode 1: Using the existing console with four dials and a beam current meter.

Mode 2: Using the assistance system without the FSR display.

Mode 3: Using the full assistance system.

Table 1 summarizes the resultant search times for the three modes and give their medians. All values were normalized by mode 1.

In mode 2, the average search time was reduced by ≈ 80% of that in mode 1. This improvement in operation is attributed to the search trace display and the ability to make beam settings using a mouse.

Operational improvements were increased an additional 15% using the full assistance system (mode 3), i.e., the search time was reduced by ≈ 65% in comparison to mode 1. The FSR display decreased the search time because an operator searches a smaller parameter area than without the display; thus more quickly reaching the desired optimal setting even though the theoretical model does not exactly represent the actual cyclotron conditions.

Table 2 summarizes the results of an operator questionnaire survey given to 7 operators (1 expert, 4 trainees, and 2 novices) to evaluate system effectiveness. Five system functions are considered and scored from 1 (not effective) to 5 (very effective). Since scores ranged from 4.0-4.7, the operators highly evaluated the effectiveness of system operability.

4. CONCLUSION

Three human interface, real-time CRT displays used for cyclotron beam adjustment are described, i.e., beam trajectories, FSRs, and search traces. The beam trajectory display enables operators to feel as if they are directly interacting with the beam, while the FSR display provides a visible expression of constraints among the adjustable parameters. The search trace display gives operators a visual feedback of their beam set point adjustment.

Results of a system operation experiment showed that the search time to reach specific beam conditions was significantly reduced using these displays. The written questionnaires survey showed the operators highly evaluate system operability.

Table 1 Summary of search times using three inteface modes.

Operator	Level[a]	Mode 1	Mode 2	Mode 3
1	E	1.0	1.07	0.59
2	T	1.0	0.76	0.86
3	T	1.0	0.68	0.63
4	T	1.0	0.97	0.73
5	T	1.0	0.67	0.46
6	N	1.0	0.92	0.85
7	N	1.0	0.95	0.80
8	N	1.0	0.65	0.42
9	N	1.0	0.47	0.34
Median		**1.0**	**0.76**	**0.63**

[a] Level: E; Expert, T; Trainee, N; Novice.

Table 2 Questionnaire results on the effectiveness of the operator assistance system.

Function	Ave. Score	Histogram 5	4	3	2	1
(1) Trajectory display	4.29	2	5			
(2) FSR display	4.00	2	3	2		
(3) Search trace display	4.14	3	3			
(4) Display layout	4.71	5	2			
(5) Operation by mouse	4.14	2	4	1		

5. REFERENCES

1) Okamura, T. and Murakami, T., "A Support System for Beam Adjustment of Cyclotron Based on Fuzzy Grading Model and Texture Display," **Proc. 11th Automatic Control World Congress, vol. 4**, pp.57-62 (1990).
2) Arakawa, K. et al., "Construction and First Year's Operation of the JAERI AVF Cyclotron", presented at this conference.
3) Ryckewaert, G.H., "Axial Injection Systems for Cyclotrons," **Proc. 9th Int. Conf. on Cyclotron and their Applications**, pp.241-247 (1981).
4) Brown, K.L. et al., "TRANSPORT," CERN, Tech. Rep. CERN 80-04, pp.129-195 (1981).
5) Kost, C.J., The Computer Code "TRIWHEEL", TRIUMF, Univ. of British Columbia.
6) Bellomo, G. and Serafini, L., "Design of the Central Region for Axial Injection in the Milan Superconducting Cyclotron," **Proc. 11th Int. Conf. on Cyclotrons and their Applications**, pp.507-510 (1987).
7) Okamura, T. and Murakami, T., "An Operator Assistance System for Beam Adjustment of a Cyclotron," IEEE Trans. on Nucl. Sci., **NS-39**, 1, pp.13-20 (1992).

CONTROL SYSTEM FOR JAERI AVF CYCLOTRON

S. Okumura, T. Agematsu, W. Yokota, T. Kamiya, M. Fukuda, Y. Nakamura, T. Nara, I. Ishibori, and K. Arakawa
Takasaki Radiation Chemistry Research Establishment, Japan Atomic Energy Research Institute
1233 Watanuki-machi, Takasaki, Gunma, 370-12, Japan

and

M. Maruyama, K. Iso, K. Hoshika, and M. Tachibana
Quantum Equipment Division, Sumitomo Heavy Industries, Ltd.
5-2 Soubiraki-cho, Niihama, Ehime, 792, Japan

ABSTRACT

The computer control system of the JAERI AVF cyclotron has been developed, and is now in operation. This system is a distributed computer system and is composed of a central computer serving man-machine interfaces, two subcomputers executing sequential device controls, and device controllers installed in each device. The central computer and the subcomputers are linked through an Ethernet. A device controller is connected to a subcomputer by a signal-multiplexed communication system. One operator can easily control the cyclotron through this control system. To assist an operator, a knowledge based operation assist system has been developed. This system provides sequences of operation, simulated beam trajectories, etc.

1. INTRODUCTION

The JAERI AVF cyclotron[1)] has been constructed to accelerate many kinds of ions over a wide range of energies mainly for various fields of materials science research. It is required that beam condition can be changed rapidly and frequently for effective use of the cyclotron. The computer control system of the cyclotron was designed so that an operator can control devices smoothly without thinking about computers and programming. Using a man-machine interface and automated sequential programs, the operator can turn the cyclotron on or off and adjust device parameters efficiently. Such functions reduce the beam production time.

The system is divided into three layers. The top layer provides the man-machine interface and manages lower layers. The middle layer executes the control sequences of device groups. The bottom layer controls each component device.

In the cyclotron operation, theoretical and empirical knowledge is required for efficient beam production. To assist an operator with this knowledge, an operation assist system has been developed.

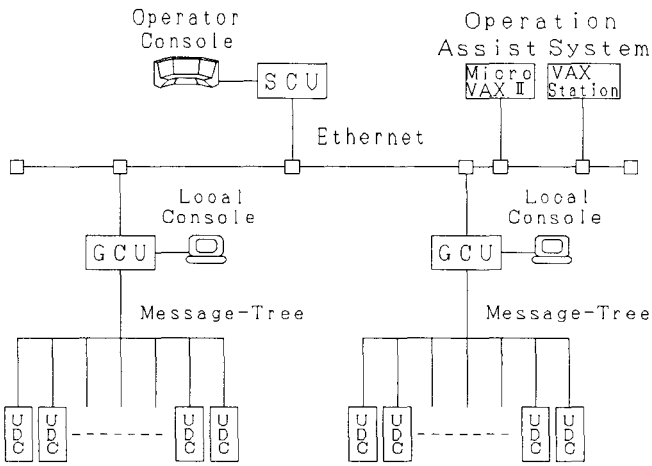


Fig. 1. Architecture of the JAERI AVF cyclotron control system

2. SYSTEM ARCHITECTURE

The system is composed of computer networks like a tree structure and is divided into three layers, as shown in Fig.1. In the top layer, a central computer named system control unit (SCU) manages the whole system and serves operators with man-machine interfaces and operation functions. In the middle layer, two subcomputers named group control unit (GCU) control groups of devices. In the bottom layer, universal device controller (UDC), single-board computers, are installed in each device for specific control.

SCU, GCU's and the operation assist system are connected to each other through an Ethernet. GCU communicates with UDC's through a signal-multiplexed communication system named Message-Tree.

2.1. System Control Unit (SCU)

SCU comprises a central processing unit (Micro VAX 3500), two hard disks, and several kinds of interface devices. Using touch-screens, rotary-encoders and graphic displays provided by SCU, the operator can control devices smoothly. SCU manages device conditions and control processes, communicating with GCU's. Various files such as program files and parameter files are stored and maintained in SCU. For a new beam production, SCU calculates a new set of parameters from stored parameter files of accelerated beams.

2.2. Group Control Unit (GCU)

Two GCU's (rt VAX1000) execute control sequences for each group of devices according to commands of SCU. All devices are divided into four groups: ion sources, the injection system, the cyclotron, and the beam transport system. One GCU manages the first three groups, and the other manages the last group through Message-Tree. Local consoles can connect with a GCU to control devices directly from GCU for construction and maintenance.

2.3. Universal Device Controller (UDC)

A UDC is an eight-bit single-board computer, as shown in Fig.2, standardized for easy development and maintenance. 420 UDC's are used in the whole system. Table 1 gives the specification of the UDC hardware. System and application software is programmed into two ROM's. A UDC controls each device intelligently through optically isolated 32-bit digital inputs, 32-bit digital output and 16-bit parallel input/output by executing up to eight tasks (including communication task). Devices can be operated directly using a local panel connected with UDC, as shown in Fig.3. The local panel indicates preset and actual values of the device, and provides several buttons for operation.

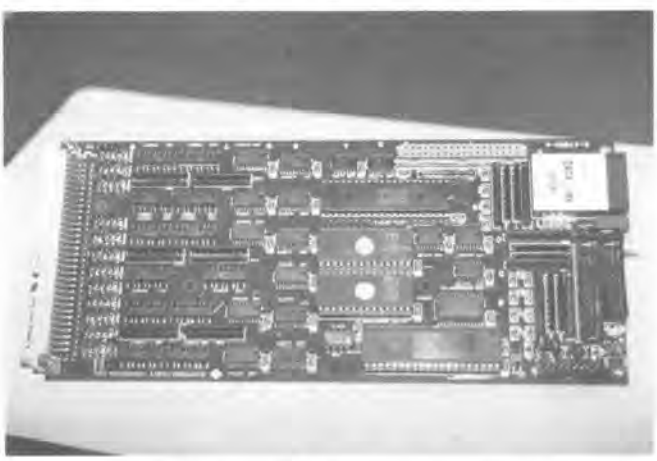


Fig. 2. Universal device controller (UDC)

Table 1. Specification of the UDC hardware

MPU	i8344(Intel)
Clock frequency	12 MHz
Memory	16 kbyte ROM
	32 kbyte ROM
	32 kbyte RAM
Serial interface	SDLC 1port
	iSBX 1port
Board size	100mm×220mm
	(Euro card)
Connector	DIN41612(96pin)



Fig. 3. Local panel of UDC

2.4. Message-Tree

A Message-Tree is a signal-multiplexed communication system between GCU and UDC's, and consists of an interface board installed in GCU, named message tree communicator (MTC), a signal distributor named message tree brancher (MTB) and UDC's, as shown in Fig.4. Fifty UDC's can be connected to a MTC through a Message-Tree, and five MTC's can be connected to a GCU.

Message-Tree is a polling-addressing communication system; an MTC is a master and UDC's are slaves. MTC sends order messages to all UDC's through an MTB. An MTB distributes the messages to all connected UDC's. UDC's receive the message identified by the UDC number and send response messages including only changed status data for reducing communication loads. These communications are executed every 100 ms. The major features of Message-Tree are the following:

- electromagnetic noise immunity by using optical-fiber cables;

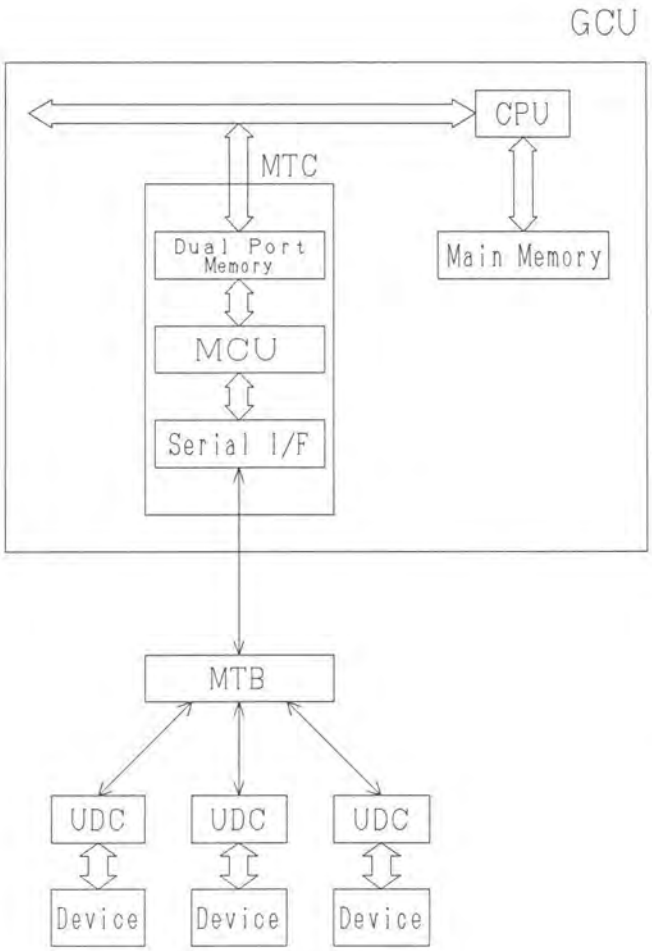


Fig. 4. Block diagram of Message-Tree

- transmission speed of 375 kbit/s;
- transmission capability of 2.6 km;
- synchronous data-link control(SDLC) protocol.

3. OPERATION

3.1. Operator Console

The cyclotron is normally operated using an operator console in the control room, as shown in Fig.5. The operator console consists of a pair of identical control units, and a monitor unit composed of a monitor TV for beam diagnostics, a 400 MHz oscilloscope for fast-signal measurement, etc. Each control unit provides a display-panel (20-inch CRT), an operation-panel (14-inch CRT), an adjustment-panel (14-inch CRT), the touch-screens on these panels, and four rotary-encoders, as shown in Fig.6. An operator can control devices by touching color-coded cells on the displays in combination with four



Fig. 5. Control room of the JAERI AVF cyclotron



Fig. 6. Control unit

rotary-encoders. The response time from a change of parameter to the display of changed actual parameter is about 250 ms. The cyclotron is operated efficiently using two control units simultaneously.

3.2. Operation Procedure

In normal operation, an operator has to go through two operational steps: starting up devices and adjusting device parameters. The former can be executed by auto- start mode starting up all devices sequentially. The latter can be accomplished through operator's efforts to search for the optimum condition. Without any care of running programs the operator can control devices by touching cells on the displays for the following ways:

1. selecting the beam condition such as the beam energy;
2. loading the preset parameters into devices;
3. starting up groups of devices;
4. assigning a rotary-encoder for adjusting a device parameter;
5. adjusting the parameter with turning the rotary-encoder.

When a fault occurs, a fail-safe sequence is executed automatically and the alarm is given in sound and display. An operator can receive information about the fault to clear up the causes.

Various data for every run of beam acceleration, such as ion species, acceleration energy and device parameters, are recorded in a log-file which is useful to refer records of past operations for next beam production.

4. SAFETY SYSTEM

An interlock system always monitors the status of devices and irradiation rooms to reject the wrong operation and to stop devices immediately whenever any failure occurs. To prevent serious failures, a hardware interlock composed of relay circuits is used in combination with software one. For more serious failures, an emergency switch which turns off the whole system was installed on the operator console. The beam current is always monitored so as not to exceed the limit of radiation safety.

To protect crews and visitors from accidents, the announcement with a public- address system and the display with graphic panel give them information about the status of the cyclotron, and the operator can watch the insides of target rooms through a monitor TV from the control room.

5. SOFTWARE

The operating system of SCU is VMS, and that of GCU is VAXELN, and C language is mainly used in these systems. Since GCU has no magnetic disk, the control programs and device information stored in SCU are loaded into GCU's at system start-up.

The programs for GCU are described in a concurrent interpretive language for sequence control of accelerators, named OPELA (OPEration Language for Accelerator).[2] Sequence programs are described in this language and executed concurrently. These programs can be debugged and modified easily and executed fast by using the intermediate codes. In these programs devices are treated by using logical names to set and refer to parameter values.

The operating system of UDC (UDC44) has been developed for multitask programming to control devices. UDC44 consists of a kernel, a basic I/O system (BIOS) and a serial interface unit (SIU) handler. The kernel can manage eight tasks, and the BIOS manages communication registers and input-output ports. The SIU handler is a communication task for Message-Tree. Application programs can be written in a high-level language PL/M51.

6. OPERATION ASSIST SYSTEM

Adjustment of cyclotron parameters requires a lot of theoretical and empirical knowledge. To provide operators with the knowledge an operation assist system is developed. The system is composed of two systems: a knowledge based expert system (Micro VAX II) and a beam trajectory simulation system (VAXstation 3100).[3]

The knowledge based expert system is programed by OPS83. This system shows the operational sequences for parameter adjustment when operators need advice. These sequences, written in the IF-THEN form, are stored in the knowledge base and referred according to the operational condition. The sequences of operation are divided into eight blocks from axial injection to extraction of the cyclotron, so that even an inexperienced operator can understand the sequences clearly. This system can be more powerful by acquiring the knowledge of operations from experienced operators.

The beam trajectory simulation system visualizes beam trajectories and correlations among parameters. Beam trajectories are calculated and displayed graphically for axial injection, central region and extraction of the cyclotron, whenever operators change cyclotron parameters. Allowable setting range of parameters that satisfies acceptance of the cyclotron is indicated on multi-dimensional graphs.

7. REFERENCES

1) Arakawa, K., et al., "Construction and First Year's Operation of the JAERI AVF Cyclotron," presented at this conference.
2) Iso, K., et al., "A Concurrent Interpretive Language for Sequence Control of Accelerators", in **Proc. of First Workshop on Control Systems** (Tsukuba, Japan, 1987), pp.100–103.
3) Okamura, T., et al., "An Operation Assistance System for AVF Cyclotron", presented at this conference.

AUTOMATIC CONTROL SYSTEM OF MAGNETIC SEPARATOR FOR KURCHATOV IAE CYCLOTRON

V.Buranov, N.Venikov, O.Gotovtsev,
L.Iudin, P.Komissarov, V.N.Unezhev.

ABSTRACT

An automatic control system for a magnetic achromatic separator of exotics (MASE) designed to investigate with a cyclotron the neutron-physical processes of small cross-section as well as to produce beams of radioactive nuclei is described. The characteristics of the MASE installation are given; hardware and software ensuring automation of its control are described. The automation system was developed on the basis of CAMAC modules controlled by a personal computer IBM PC/AT. The fibre-optics data exchange systems are used to connect the hardware with controlled objects. The system makes it possible to adjust automatically the magnetic field for the standard operation modes of the MASE installation, to detect the failures of individual units as well as to calculate and select new operation modes. Automation of the MASE installation allows a physicist-experimenter to change over the installation directly during experiment. The system considered can be used in other electrophysical installations.

1. INTRODUCTION

A magnetic achromatic separator of exotic nuclei (MASE) was proposed and implemented for the first time in I.V.Kurchatov IAE [1]. The separator is designed to perform the following experiments:
-investigation of processes running with a small cross-section, study of the properties of exotic nuclei;
- production of secondary radioactive beams;
- correlation measurements in investigating the decay modes of giant resonances and other nuclear states.

The schematic diagram of the installation is presented in Fig.1. A beam of charged particles with various masses in the whole energy range which exits from a target along the MASE longitudinal axis is formed by an aperture diaphragm within a required angular interval. The required dimensions of the beam at the target (an optical source) are ensured in an ion-optical system of cyclotron beam transport to be X ≤3 mm and ZY ≤ 2 mm.A crossover in the horizontal plane is formed at the MASE center in the area of an analyzing diaphragm to separate in the best way the beam of a given energy range. The formation is performed by a doublet of quadruple lenses and a dipole magnet. This magnet is involved in analyzing the particles for momenta (the turning angle of the axial trajectory in it is 30°). The effect of the achromatic aberration of the separator on its energy resolution is eliminated by the analyzing diaphragm placed at an angle of 6° with the beam axis.

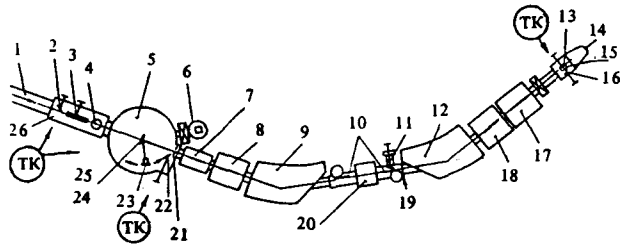


Fig.1. The schematic diagram of the MASE installation: 1 - ion guide; 2, 11, 16, 22, 25 - scintillators; 3 - collimator; 4 - profilometer; 5,14 - target chambers; 6 - lock; 7,8,17,18 - quadruple doublets; 9 - analyzing magnet; 10 - analyzing diaphragm; 12 - collecting magnet; 13, 23 - telescopes ΔE-E; 15,26 - diagnostic units; 19 - foil; 20 - quadruple singled - symmetrizing lens; 21 - aperture diaphragm; 24 - target.

The beam trajectories are symmetrized relative to the MASE center (energy focusing) by a symmetrizing lens representing a quadruple magnet focusing in a plane of analysis (horizontally).

The second part of the MASE ion-optical system is reflection-symmetrical to the first one and intended for collection of particles having been analyzed and their transport to the second target (or a detector).

The character of experiments to be made in the MASE sets high requirements to its reliability, stability of operation, operative, change-over efficiently of diagnostics and quality of operator's work. One of the ways for improving the above characteristics of the cyclotron and the MASE installation consists in development of an automatic control system.

2. THE CONTROLLED OBJECTS

The controlled components of the MASE installation include the power supply devices for the magnets of its ion-optical system. To compact quadruple magnets having a high field gradient invariable over the whole aperture better than within 1% guarantee good conservation of the phase volume of the beam during its transport through the installation.

The parameters of these magnets are listed in Table 1.

All magnets are energized from commercial reversible thyristor converters (RTCs) with a specially-developed stabilization system [2]. The converters are about 100 m distant from a control room. Water-cooled manganin instrument shunts are disposed near the RTCs.

Parameter of magnet	Magnet index		
	56k2	38k21	38k13
Diameter of aperture, mm	56	38	38
Length of pole, mm	210	210	130
Supply current, A	1000	1000	1000
Voltage, V	60	85	100
Magnet weight, kg	48	24	15
Magnetic field gradient, T/m	25	35	23

Table 1. Parameters of MASE magnets.

All devices for the control of the magnet current have the conventional negative-feedback stabilization scheme. The voltage from the instrument shunt is applied to the input of an error amplifier through an MDM converter to decouple conductively the power supply and the measuring circuits. Program-controlled digital-to-analog converters (DACs) ensure the control over the reference voltage at the input of the error amplifier and, therefore, the current in the windings within $2 \cdot 10^{-5}$.

3. THE STRUCTURE OF THE AUTOMATIC CONTROL SYSTEM

The Kurchatov IAE cyclotron uses a structure of automatic control with the control functions distributed among individual subsystems. The control system of the MASE installation is a constituent part of the cyclotron complex.

A standard control station was developed on the basis of the CAMAC modules [4]. The station includes measuring equipment to record analog signals in a range of -10 V to +10V and to control analog parameters within 10^{-3}, units for control over discrete parameters and interface modules connecting the equipment with a control computer and peripherals used for operator-system interaction.

Wide use of commercial fiber-optics data-exchange systems is the important feature of the station [5]. The hardware comprise a digital data transmission systems "Elektronika MS-4101", an analog data collection systems "Elektronika MS-8201" and an analog data distribution systems "Elektronika MS-8401". Each system consists of a transmitter and a receiver connected by a fiber-optics line (FOL) up to 300 m long and ensuring the transfer of information with a rate of up to 8 Mbit/s.

Use of such multichannel devices connected through the input and output registers evidently allows one to eliminate the conductive coupling between the control equipment and the controlled objects, to guarantee reliable protection of the communication lines from electromagnetic fields, to increase considerably their reliability and to bring ADCs and DACs nearer to the controlled objects, which essentially improves the performance of the system in terms of error probability.

An IBM PC/AT computer controlled by an MS-DOS 3.31 operation system is used as a control computer. The complex of control and checking programs is written in Turbo-Pascal 5.5 and occupies about 200 kbite in the main memory. The structure of the system is shown in Fig.2.

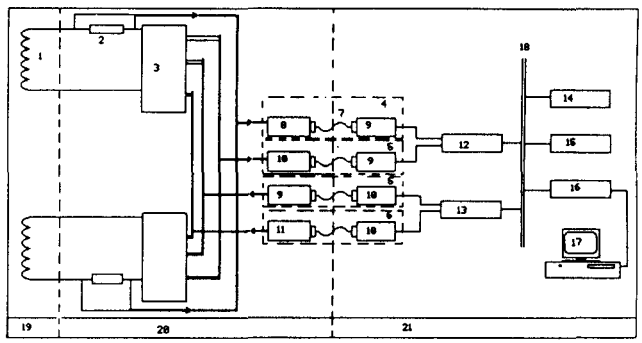


Fig.2. The structure of the automatic control system for the cyclotron and MASE magnets: 1 - magnet; 2 - shunt; 3 - RTC; 4 - analog data collection system; 5 - digital data transmitting system; 6 - analog data distribution system; 7 - fiber optic line; 8 - collection module; 9 - receiver; 10 - transmitter; 11 - distribution module; 12 - input register; 13 -output register; 14,15 - functional CAMAC modules; 16 - crate controller; 17 - computer; 18 - CAMAC bus; 19 - cyclotron hall; 20 - electrotechnical hall; 21 - control room.

The control computer, the CAMAC equipment as well as the digital receivers and transmitters of the fiber-optics systems are in the control room. The FOLs are laid from the systems to an electrotechnical hall 100 m distant from the control room. The response parts of the fiber-optics systems connected directly to the controlled objects and transducers are in this hall.

4. SOFTWARE FEATURES

The automatic control program for the power supply of the isochronic cyclotron and MASE installation magnetic circuits realizes the interaction with the RTCs setting the current in the windings of the magnets. The controlled parameters involve the voltages of the outer reference-voltage sources, "ION", and the signal of current polarity and energizing of the converters "REVERS". The checked parameters are the voltages across the RTC shunts "SHUNT" and a signal "STATUS" showing the presence of the RTC outer control authorization "STATUS". The values of the parameter "SHUNT" determining unambiguously the magnetic field configuration can be set by an operator or automatically in accordance with data stored in the computer.

The whole complex of programs is controlled by a menu system (Fig.3) which fixes a certain current state of the dialog environment and offers several alternative paths of transition from this state. The main menu allows one

- to start the program of setting the magnet currents;

- to calculate a new mode of magnet operation;
- to select a precalculated mode from the mode database;
- to start a program changing the channel display form;
- to exit from the program.

The example presented shows the graphical copy of the display screen - the case when the



Fig.3. The fragment of the operator menu system.

operator selects the mode of 77-MeV ^{7}Be beam production by the MASE installation. The CTCs are controlled by a program "Setting of current". The character of interaction of the operator with the controlled devices is determined by three basic operation modes of the system: (1) monitoring and automatic adjustment, (2) general control and (3) channel control. Each RTC has a cell on the monitor screen, "a channel window", to display the RTC and its magnet numbers, the RTC purpose and the status signals in the form of colored pictograms. The analogous variables are represented in the following way: the signals "SHUNT" and "ION" by colored columns with a length proportional to the magnitude of the signal, the stored values by colored marks on the scale. Figure 4 shows an example of representing the status of the controlled and adjusted parameters corresponding to one of the real operation modes of the cyclotron magnetic systems. The MASE magnets work in the computer-controlled mode, all other magnets are only diagnosed.

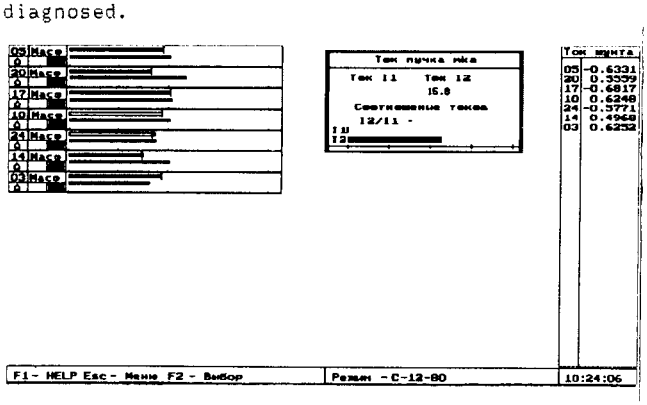


Fig.4. The information to be output onto the monitor screen in the mode of automatic adjustment of currents (example of representation).

The mode of monitoring and automatic adjustment ensures successive measurement of voltages across the shunts in all controlled channels and automatic fine adjustment of the voltages in accordance with their set values as well as indication of the most important status information. The 0.1% deviations of the measured parameter from its set value after being stored attract the operator's attention because of the change in color of the "SHUNT" column from blue to red-framed blue; the 1% deviation changes the blue color to the red one. When the deviation is 0.5%, automatic adjustment of the changed parameter is initiated. If the system is not able for any reasons to correct the changed parameter, it attracts the operator's attention by a sound signal. In mode (1) the system works without operator's intervention, the keyboard is blocked to protect from stray keystrokes. An encapsulated directive is provided for the system change-over in the general control mode.

The general control mode ensures the control over a selected group of channels which can be used to execute the following operations: setting of voltages, reset write-in, storage-to-mode menu writing, transition to the channel scan mode, output to the main menu, prompt call. In the pauses between the directives specified by the operator and after the execution of each directive the systems scans in turn the channels representing the information about their status and the voltage across the shunts. The general control mode is intermediate between modes (1) and (3).

The channel control mode ensures the control of any selected individual channel. This mode makes it possible:

- to activate or deactivate the mode of automatic adjustment of currents;
- to correct the currents coarsely or finely;
- to write in the values of current;
- to set the current in accordance with its stored value;
- to select other channel;
- to go over into the mode of successive call of channels.

All above operations are executed by pressing so-called "operative intervention key".

Simultaneously with the main modes the logic pickups are tested for status of locking. In the case of disconnection in the locking circuit the display indicates both the channel number where the locking has operated and the concrete reason. Moreover, the sound signal from the display will attract the operator's attention to the information about the failure.

5. CALCULATION OF THE MASE MODES

A program of automatic mode change was developed to automate some experiments to be made with the cyclotron and the MASE installation. The results of magnetic measurements were used as a basis to derive the analytical dependences of the quadruple lens gradients and the dipole magnet induction on the currents in the excitation windings, G(I) and B(I), and the inverse

functions I1=f(G) and I2=f(B), where I1 and I2 are the currents in the MASE windings. Using the well-known relationships between the field gradient and the magnetic rigidity of focused particles (depending on their type and energy) we obtain the expressions:

$$G = \omega^2 \sqrt{(E^2 + 2EE_0)} / q \cdot c ,$$

$$B = \rho^2 \sqrt{(E^2 + 2EE_0)} / q \cdot c$$

where ρ is the radius of turning in the dipole magnet; ω is the focusing force of the lens; E is the kinetic energy of an ion; E_0 is the ion rest energy; q is the ion charge; c is the velocity of light.

It is convenient to express the ion rest energy through the parameters:

$$E \approx \{ A + [0,01 \cdot (A-100)^2 - 64] \cdot 10^{-3} \} \cdot 931,141 - (Z-N) \cdot 0,51$$

where A is the mass number; Z is the number of protons in the nucleus; N is the multiplicity of the ion charge. Substituting the calculated values of R and B into the derived dependences of the excitation currents it is not difficult to obtain their values for setting the specified operation mode of the MASE installation. The results of the calculations are written by the operator's command in the MASE mode menu. After this corresponding currents are automatically set.

To identify the spectrum of nuclear reaction products separated by the MASE installation during experiment it is essential to know the range of their energies. Such calculations are mode operatively during the setting of the magnet currents. For this purpose a certain feature of magnetic rigidity separation of wanted ($B\rho_1$) and accompanying ($B\rho_i$), particles is used. Using the known dependence $B\rho = f(A,Q,N,E)$ (where A is the number of nucleons of the particle; Q is the ion charge; N is the nuclear charge; E is the kinetic energy of the particle) we obtain the equation with a single unknown quantity

$$f(A_1,Q_1,N_1,E_1) - f(A_i,Q_i,N_i,E_i) = 0$$

The prepared program allows the solution of this equation for a particle of any type and the representation of the calculated data as a table of possible energy ranges of transmission in the MASE for given types of particles.

The automation of the MASE allows a physicist-experimenter to change over the installation directly during experiment without intervention of a cyclotron.

6. CONCLUSION

At present the automatic control system for the magnetic circuits of the cyclotron and the MASE installation ensures on-line control and monitoring of the analog variables within $2 \cdot 10^{-5}$, check of the pickups of served equipment logic state, automatic change-over to the standard operation modes, acquisition of data on the operation time of the power supply systems and their stability, etc. The considered automation system is being operated successfully in I.V.Kurchatov Institute of Atomic Energy and can be used for other electrophysical installations. In particular, a modification of the developed hardware and software complex will be used to create a control system for a mini-cyclotron being developed now for medical research [6].

7. REFERENCES

1. V.V.Buranov, N.I.Venikov, A.M.Dobychin et al. Diagnostics and adjustment of the MASE installation. - VANT, ser. Obshchaya i Yadernaya Fizika, 1988, vyp. 2(42), p. 61.
2. A.N.Bryukhanov, A.I.Bel'kov, I.I.Kakunov et al. Stabilized power supply sources with length modulation. - IAE Preprint No. 4024/14m Moscow, 1984.
3. V.V.Buranov, P.Yu.Komissarov, M.V.Kuznetsov et al. Automation of control of the Kurchatov IAE cyclotron. - Modular information computer systems (Book of Abstracts). VII All-Union Symposium, Novosibirsk, 1989, p.18.
4. P.Yu.Komissarov, M.V.Kuznetsov, S.T.Latushkin, L.I.Yudin. A microprocessor control station for the functional units of a cyclotron. - All-Union Scientific-Technical Conference (Book of Abstracts), VNIIE, Moscow, 1985, p. 33.
5. M.A.Ananyan, I.I.Tursukov. Fiber-optics information-exchange systems. - Elektronnaya Promyshlennost, vyp. 3, 1984, p. 27.
6. K.D.Burbeza, N.I.Venikov, P.Yu.Komissarov et al. State of works on a minicyclotron for PET in IAE. - Transactions of II International Meeting on Cyclotron and Their Use, Behine, Czechoslovakia, 1989, p. 107.

THE NEW DISTRIBUTED CONTROL SYSTEM OF THE NAC

H F Weehuizen, R K Fisch, E J S Franklin, M E Hogan, I H Kohler, J P Rogers, P J Theron
National Accelerator Centre, P O Box 72, Faure, South Africa

ABSTRACT

A microprocessor based distributed control system is being developed for a 200 MeV cyclotron and two injector cyclotrons. The system will be based on at least 25 IBM compatible PC/AT microcomputers grouped into functions of operator consoles, instrumentation controllers and database nodes communicating over an Ethernet LAN. The aims of the system design are flexibility of use, ease of configuration allowing for changing hardware and user requirements, and ready availability of data for performance analysis.

1. INTRODUCTION

The National Accelerator Centre (NAC) operates a 200 MeV Separated Sector Cyclotron together with two injector cyclotrons. One of the latter is a light ion injector while the other which is still under construction will be used to accelerate both heavy and light ions.[1] The control system presently used to control these cyclotrons consists of the classical computer control architecture of a centralized computer controlling remote hardware which has little or no intelligence. Failure of the computer results in failure of the complete system. The present design is also such that the addition of extra operator consoles significantly increases the load on the system and thus impacts its performance. The most important limitation of the present system is that the number of processes that can simultaneously be handled by the minicomputers has a fixed upper limit and this is less than that required to control the cyclotron facility as it is finally envisaged.

There is thus a need to develop a new system that can cope with all the future requirements of the NAC control system. These are as follows:

a) It must be readily expandable to at least double the capacity of the present system.

b) It must be sufficiently flexible to cope with the changing requirements of a partly experimental facility such as at the NAC.

c) Hardware failures should have a minimal effect on the system.

A distributed system inherently offers these advantages. New processes and functions required of the system are usually handled by new nodes which can be optimally configured to handle the new requirements. Expansion of existing facilities by the addition of new nodes means increased parallelism in the operation of the system thus providing minimal impact on the performance of the latter.

Failure of a node results only in the loss of access to, and control of hardware related to the node, allowing the rest of the system to function normally. The only node whose failure could affect the viability of the system is the database node. In this instance a second node acts as the backup and mirrors the image of the active database node.

2. THE NEW SYSTEM

The new system, in keeping with control strategy, is designed to be as homogeneous as possible. It can be divided into four major functions, namely network, instrumentation nodes, console nodes, and database nodes. Figure 1 illustrates the system in block diagram form.

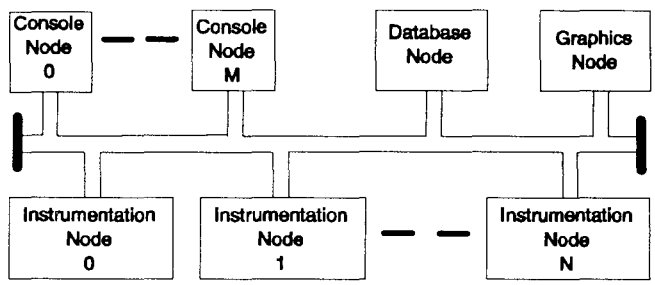


Fig. 1 A block diagram of the new control system.

2.1. The Network

There are three major types of network in use today. Two of these are bussed networks, namely CSMA/CD [2] characterized by Ethernet, and the token bus[3] characterized by MAP or mini-MAP. The third is the token ring[4] and is characterized by the IBM ring. The latter is the least suited to the present application because of the complexities of wiring a ring structure and because the node interface is of the active type, reducing its reliability.

A frequently chosen network for the control environment is that of the token bus, because of the bus structure and because the transmission delay is predictable.[5] However the hardware is costly and the transmission delay is significant because of the long

circulation time of the token.[6,7]

Ethernet is attractive because it is a mature standard and the hardware is relatively inexpensive. The transmission delay is short in a lightly loaded network and is in fact shorter than that of the equivalent token bus up to a network loading of 50%. The major criticism of this network is the probabilistic nature of the transmission delay arising from the randomized contention resolution mechanism that it uses. This can be excessive in a heavily loaded network, but provided that the network loading is carefully controlled it gives a performance superior to that of the token bus. Thus the latter network was chosen.

Because the transmission delay of the network can be affected by network loading, it will be worthwhile at this point to see how the behaviour of the control system can affect the network load. Typically a single processor, real time system is event driven, i.e. every time an external status changes, an interrupt is generated in the computer which demands a response. It is up to the designer to ensure that the processor is not overwhelmed by external events in periods of high activity. The situation is aggravated in a distributed system communicating over a shared network where a high proportion of the actions will result in network activity. This will result in high loading of the network resulting in indeterminate delays which will impact both the behaviour of the system and its speed of operation. An alternative which is currently favoured by some of the real time community[8,9] is to use a state driven system. Here the status of node parameters is broadcast over the network at regular intervals resulting in a constant load on the network, thus making transmission delays predictable.

The method adopted at the NAC is to combine the two techniques. System status parameters are communicated at regular intervals of once per second as long as events are occurring at a rate greater than or equal to this. At lower event rates, an update occurs at the occurrence of an event or once every 10 seconds if events occur less frequently. The latter determines the maximum time interval that the state of health of each node is checked.

For the transmission of operator commands, the virtual circuit facility of the transport layer is used to ensure the integrity of the command data. This is an event driven operation which is an acceptable compromise because the rate at which a human operator can generate inputs to the system is low and easily controllable.

2.2. The System Nodes

The IBM PC compatible computer is being used in a variety of applications for which it was never envisaged purely because it offers reasonable performance at a low price. Its reliability is good because of the extensive use of LSI technology. While its architecture is rather limiting, it is still economic to use more or bigger systems to offset its shortcomings.

In an application such as is described here, a multitasking, pre-emptive scheduling operating system is essential. The networked environment together with a good graphical user interface and access to good database facilities are further requirements of the operating system. Currently there are several operating systems to choose from, such as a real time Unix, RMX for Windows, OS/2 or possibly Windows NT when it becomes available. OS/2 has been available for some time and currently provides the most effective solution to our requirements. However its future development in relation to our needs is not yet clear and a migration to one of the alternative systems is still a possibility.

The PC systems used to run this software are 25 MHz 386 AT systems with 8 Mbytes of memory and 16 bit peripheral cards for the instrumentation and console nodes while 33 MHz 486 AT machines will be used for the graphical interfaces and those nodes that require more performance.

2.3. The Instrumentation Nodes

These consist of the system as described above and use an expansion I/O bus that was originally conceived as an 8 bit microcomputer bus. The main processors of this bussed system rapidly outgrew the performance of the bus to become the standard PC as described above. Concurrently the I/O cards increased in sophistication and became based on the 8051 micro controller. Thus the original bus has evolved into a byte wide parallel communication medium between the host and intelligent I/O interfaces.

The function of the instrumentation node is centred around a variable table which holds all the current values of the parameters controlled by the node. There are several values for each parameter. The first group of values consist of a set point reference value and its associated status. The second group would hold the actual value of a variable and its status, including an error status if relevant. Further fields are used for housekeeping and link requests to the variable in the table. Application tasks are activated when any change to the reference group occurs and they perform the appropriate actions on the related hardware. Similar tasks continuously update the actual value and status group of the table from the hardware status.

A communication task transfers information between the network and the variable table. At the request of a console node, this task can continuously communicate the

contents of the variable table over the network to update the actual values displayed at the consoles. It was originally intended that this communication would take the form of multicasting to the console nodes, but unfortunately the network software in use does not support this facility, so data broadcasting is currently being used. Unfortunately this loads the communication processors of all the nodes in the network, so point to point communication is going to be tried as an alternative. This will only increase the load of the transmitting node if more than one console selects the same page of variables, an infrequent occurrence during normal operation of the system.

The communication task also receives commands from the console nodes to control the reference values of the variables. Before the process of reference value change can begin, a request must be made to allow control of the variable. Requests can come from several sources in the system but only one may control it, so any contention for access must be resolved at this point. Thus the source whose request is received first is granted access and all subsequent requests are refused until the source granted access releases control, or a communications failure occurs. The request/grant action is uninterruptible, thus avoiding ambiguity in assigning access.

Alarm conditions requiring operator action can be spontaneously broadcast by this task as well. These would be repetitively sent at one second intervals until a response is received.

Functions such as acquisition of dynamic data would be handled by a separate process as these would be application specific, although the data communication format is standard.

2.4. The Console Nodes

The present control system controls approximately 1000 variables. These are logically divided into pages of approximately 20 variables each which can be displayed on a video screen. The display consists of the variable name, its reference value, actual value and status. Four analogue meters are available to provide an analogue display of the actual values of variables selected by the operator. In a similar manner the operator can link two set point units and a touch panel to the reference value fields of the displayed variables. The set point units are used to provide infinitely variable control of the selected variables while the touch panel is used to select predefined states. While the present console is effective it is cumbersome and expensive, thus obviating the use of mobile consoles.

The new system offers similar facilities but presented in a different way. The facilities of the Presentation Manager are used to emulate the functions of the present system. Because the graphical user interface is used, it is easy to configure the displayed page and to include bar and line graphics. Graphical instruments are easily included, substituting for the analogue displays of the present system with no loss in useability.

Initial trials of the system using a mouse as the input device produced mixed reactions. Some operators liked the use of the mouse while others complained that interaction with the system was too slow as repetitive sequences of operations required considerable movements of the mouse. If instruments other than the main video screen were being monitored while the cyclotrons were being adjusted, it was difficult to keep the mouse within the correct adjustment field. Simultaneous use of the set point function and the touch panel emulated on the screen was also not possible.

A new interface is being developed which offers facilities somewhere between those of the full emulation just described and the discrete controls of the present system. A reduced function keyboard is being developed. This will provide direct page selection and numeric value entry for setpoint values. Included will be a joystick to allow the adjustment of set points and a LCD graphics display with optical sensors will provide touchpanel entry. These will all interface via the standard PC keyboard input allowing the use of standard software. This provides an economic solution and maximum flexibility in that either the new keyboard or a standard keyboard may be used. Mobile or temporary consoles can thus be standard computers.

Central to the console software is a large variable table holding a copy of the information in the instrumentation nodes together with the names of the nodes from which they originate. This table is updated by the transmission of variable data from the various instrumentation nodes. When a page is displayed on the console the variable information is selected from the local table. Operator actions at the console are transferred to the local table process from where the commands are directed via virtual circuits to the correct instrumentation node.

At startup the page layouts and variable groupings are fetched from the database node and held in memory thus forming a local memory resident database. It is held memory resident because network or disc operations would cause the console response to operator commands to be too slow.

2.5. The Database Nodes

The control system is required to be flexible in that the facilities at the NAC are still expanding and the equipment controlled by the system is subject to alteration. It is thus a requirement of the system that it be easily configurable. The hardware of a distributed system lends

itself naturally to reconfiguration, but the software must be designed to be so. The logical way to provide flexibility is to hold all the system variables in a database. The system may then be reconfigured by modifying the database. Commercial database packages for networked systems are based on a central file server serving the workstations over the network. This is not ideal for a control system as the access of a disc based database over a network is too slow for real time response. However the convenience of a single point of entry for configuration information is important.

At startup, subsets of the main database are transferred to each node on the system as required and remain memory resident for access by the local node. The console nodes each have a complete list of all the page configurations and display formats of each variable and its logical address. The instrumentation nodes receive a list of the variables pertinent to their respective nodes.

Another function of the database node is to log the status of the system at regular intervals for collecting trending information and for system status recovery after interruptions in operation or return to operation at a previously used energy level.

The use of the database node is such that it is not crucial to the operation of the control system. If it did fail, operation of the system would continue, but several important facilities would be lost. Thus a mirrored disc is used on a separate node which is able to take over the functions of the main node should the latter fail.

2.6. The Graphics Node

This node has a 20 inch, high resolution colour graphics display which will be used initially to display the beam profiles derived from data collected by harp and scanner devices situated in the various beamlines throughout the facility. Up to six devices will be displayed simultaneously on the screen which will be refreshed at the rate of four to six traces per second. A laser printer will provide hard-copies of the screen information.

The node will run application specific software under the supervision of the control nodes. The former will communicate with the instrumentation nodes that control the diagnostic hardware. These will send data across the network to the graphics node where it will be prepared for display. A virtual circuit connection will be used here to provide flow control over the network as the graphics display task is computation intensive and thus will be slower than the data acquisition task.

3. CONCLUSIONS

The new control system offers several advantages over the old system which has now become obsolete. It is readily expandable with an upper limit beyond that required to run the present cyclotron facility. The data handled by the system is readily accessible to personal computers attached to the network so off line analysis of performance data is easily achievable.

Because of the distributed nature of the system, its integrity is not dependent on any single node in the system. Failure of a node thus results in loss of a facility rather than the whole system. Equipment maintenance is facilitated through local control and through the nearly continuous availability of the control system as there is no need to stop the entire control system for maintenance purposes.

The reliability of the new system is currently equal to that of the present system and is orders of magnitude better than that of the present system in its early stages of operation.

4. REFERENCES

1) Burdzik, G.F. et al, "Decentralisation of the NAC Control System" in **Proceedings of the 11th Int. Conf. on Cyclotrons and Their Applications,** (Ionics Publishing, Tokyo, Japan, October 1986) pp. 422-425.
2) **IEEE Standard for Local Area Networks: Carrier Sense Multiple Access with Collision Detection. Std 802.3-1988 and supplements** (IEEE, New York).
3) **IEEE Standard for Local Area Networks: Token Passing Bus Access Method. Std 802.4-1990** (IEEE, New York).
4) **IEEE Standard for Local Area Networks: Token Ring Access Method. Std 802.5-1989** (IEEE, New York).
5) **MAP: General Motors Manufacturing Automation Protocol, Version 3.0,** (GM Technical Center, Warren, Michigan, 1987).
6) Weehuizen,H.F., Rodd, M.G. and McLaren, S.G.,"The Simulated Performance of Practical Ethernet and MAP Networks" in **Proceedings of 7th IFAC Workshop on Distributed Computer Control Systems** (Pergamon Press, London, 1987) pp.73-77.
7) Damsker, D.J.,"A Critique to MAP and Proway", ibid.
8) Meyer, S.P., McLeod, I.M. and Rodd, M.G.,"The design of Shoptalk, a Distributed Multiprocessor Computer Control System", ibid.
9) Izikowitz, I., Rodd, M.G. and Guo-Feng Zhao, "A Real Time OSI Based Network: Is it Possible?" in **Proceedings of 9th IFAC Workshop on Distributed Computer Control Systems** (Pergamon Press, London, 1990) pp.9-16.

ION SPECTRA IDENTIFICATION SOFTWARE FOR THE ECR ION SOURCE AT NAC

E J S Franklin and J G de Villiers
National Accelerator Centre, PO Box 72, Faure, South Africa

ABSTRACT

A microprocessor based software package to aid in ion identification has been developed at the NAC. The package automates the scanning process and aids species identification by displaying theoretical peak positions. The analysing magnet current is accurately controlled giving high resolution scans over any analysing magnet current range. Provision is made for automatic recording of beam stability. Complete ion source setup information as well as the graph is recorded. It uses a graphical user interface and runs on top of the OS/2 multitasking operating system. A description of the system is presented.

1. INTRODUCTION

The National Accelerator Centre (NAC) operates a 200 MeV separated sector cyclotron (Main Cyclotron) together with two injector cyclotrons (SPC1 and SPC2)[1]. The latter has two ion sources: an electron cyclotron resonance (ECR) ion source and an ion source for spin aligned ions (ISI) (see Fig. 1).

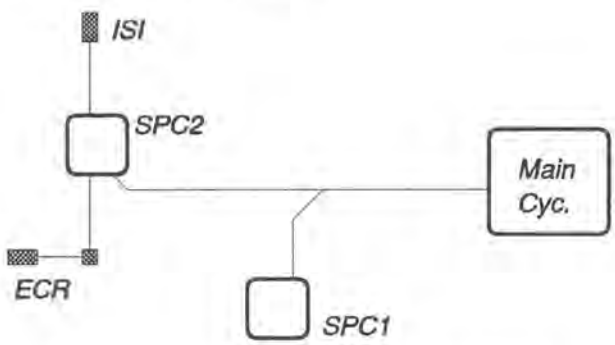


Fig. 1. Schematic Layout of NAC Cyclotrons.

Figure 2 illustrates the ECR ion source. The analysing magnet is used to select the ion with the required mass number and charge state.

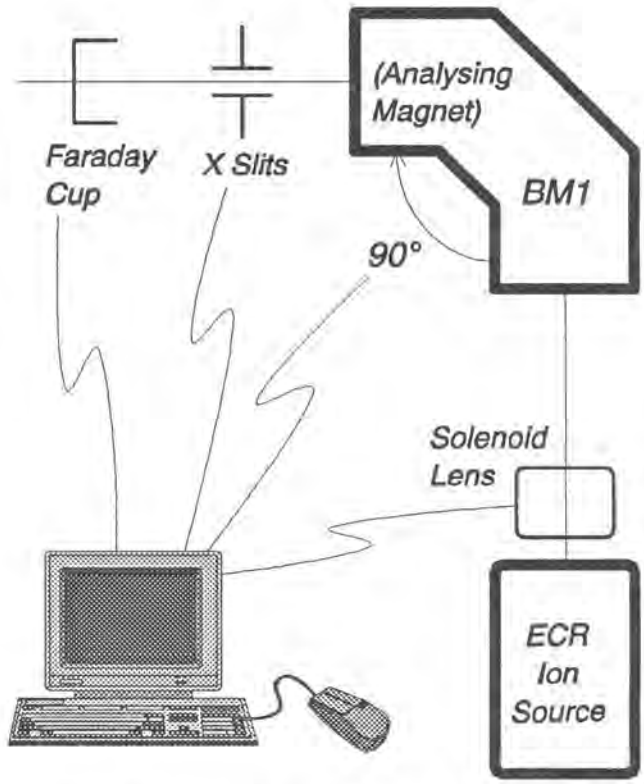


Fig. 2. Schematic Layout of the ECR Ion Source.

It was with a view to aiding the selection process that a program capable of controlling the analysing magnet and recording beam intensity on a Faraday cup was written.

2. ORIGINAL METHOD

Tests of the ECR Ion source were done with a 104° analysing magnet with its object focus point on the extractor and the image focus point on a Faraday cup. Currents measured on the cup were viewed on a storage oscilloscope. For a permanent record photographs of the ion spectrum were taken and ion source settings had to be tabled by hand.

The ECR ion source at the NAC has a solenoid lens located between the 90° analysing magnet and the ion source to focus the beam. The analysing magnet can be scanned from 0.0A to 10.0A. A set of slits in front of the Faraday cup can be adjusted to cut off unwanted beam or

to obtain better definition of mass numbers of a certain charge state, for example Kr^{9+}.

The spectra of the first heavy ion beam were recorded on an X-Y plotter. Ion source settings once again had to be tabled by hand and corresponding plots attached, taking care not to mis-identify charge states.

The major disadvantages of this approach were:

- the difficulty in matching observed peaks with an ion;
- the possibility of making a mistaken identification, and
- identification was time consuming.

3. COMPUTER AIDED METHOD

3.1 Principle

As a PC was already in place for controlling the slits and the solenoid lens, it seemed reasonable to put it to work on the ion source as well. The idea was essentially simple: to store ion source settings along with the corresponding graphical spectra on disk and to be able to recall those settings and spectra for later reference. The computer must set the analysing magnet coil current (it should also read a return signal confirming the actual value) and read the beam current (on a Faraday cup).

In order to investigate the entire ion spectrum the software performs an automated scan by varying the magnet coil current between two user specified values (for example, from 0.0A to 10.0A) and plots the beam current *vs.* magnet current, which is displayed on the video screen.

Once the operator has identified at least two peaks of an element, for example helium, a constant K for the system can be calculated; viz.:

$$\frac{q}{m} = K\frac{V}{I^2} \qquad (1)$$

where
V is the extraction voltage,
I is the magnet current,
q is the charge on the ion, and
m is the mass of the ion.

With this constant the program can calculate the positions of the charged states of any isotope and display these theoretical positions as an overlay on the graph. The analysing magnet current can then be set to the desired peak within 1mA and the operator can optimise the ion source. A rescan - usually over a much smaller range - will update the beam spectrum, and the graph and setup parameters of the ion source can be saved to disk.

Once K has been found for each of the various extraction voltages it can be used thenceforward without recalculation.

3.2 Further Advantages

After installation of the software in its basic form as described above, it was apparent that the presence of the computer could help with a few other aspects.

3.2.1 Beam stability analysis

While the scanned graph is displayed on the video screen, a free-moving 'dot' indicates the present magnet and beam currents being measured. This dot can leave 'high' and 'low' markers behind to indicate the peaks and troughs of beam current. These markers are made to persist for a while so the operator can get an idea of the stability of the beam and so that variations too fast for the eye to follow are nevertheless noticed.

To make this feature more useful the software keeps a record over time of these maxima and minima averaged over a user specified period. This is then displayed as a plot of maximum, minimum and average beam current *vs.* time (see Fig. 3). The plot is saved to disk along with the scan information and ion source parameters.

3.2.2 Data storage/retrieval

Obviously being able to save data to disk is a tremendous advantage. Not only can previous graphs be called up for comparison, but all information pertaining to the ion source itself can be retrieved enabling the operator to quickly reproduce the same beam.

3.2.3 Fine adjustment of magnet current

An unexpected advantage was the improvement in control over the analysing magnet coil current. The manual method relied on a rotary dial which provided good fine adjustment. Computer control via the DAC* is, however, much easier to use. With the mouse the operator can smoothly sweep the current through a range of values (using the dial the current tends to jump around) as well as directly set a specific value.

3.2.4 Distributed control system

The NAC is in the process of converting its control system to a distributed set of microprocessors linked via

* Digital to analogue converter.

an Ethernet LAN[2]. The presence of this computer at the ECR ion source lends itself to connection to the new control system as an instrumentation node. It is conceivable that the graphical data could be displayed on the central graphics node and the entire source operated under remote control.

3.3 Results

Figure 3 is an example of a typical screen display after an automatic scan.

In this case the analysing magnet was scanned from 3.20A to 4.30A in 200 steps. At the right side of the plot can be seen the value of the calibration constant, K = 2.7235. Above the graph itself are displayed some overlays for He, O, N and C. It can immediately be seen how these overlays help in identifying the ion species present.

To the right of the graph the word *SLOW* indicates that the operator has chosen to use the slower and more accurate DAC which updates the screen only twice per second. A *FAST* setting uses a slightly lower accuracy DAC but updates ten times each second. The number below (e.g. *3.950*) indicates the actual setting of the analysing magnet current. This value is set via the mouse: a digit is selected by double-clicking and then is made to run up and down with the two mouse buttons. This proved to be a most satisfactory way of adjusting the current. Above this, *Im* and *Ib* refer to the actual magnet and beam current values.

When the mouse pointer is moved into the graph area a crosshair appears and the beam current and magnet current corresponding to the crosshair position are indicated (the cross-hair has been removed to prevent clutter in an illustration that has been much reduced in size). Also visible on the $^{14}N^{5+}$ peak (a bit below the maximum) is the 'dot' which indicates the present beam and magnet currents.

The broken lines running across the graph near the top are an example of a beam stability plot: in this case the minimum, maximum and average beam value were recorded from 13:58:25 to 14:08:33. When a beam stability plot is displayed the time corresponding to the crosshair position is also displayed.

Along the top of the screen are a number of menu options available to the operator. These are chosen by mouse (or with keyboard accelerator keys). For example, a scan will be started from a menu option.

Lastly, it should be pointed out that plots on the colour computer screen are naturally clearer and can show more information than can be reproduced here.

Figure 4 illustrates the ECR ion source parameters stored for each plot; this particular set pertains to the plot of Fig 3 (optimised for $^{14}N^{5+}$).

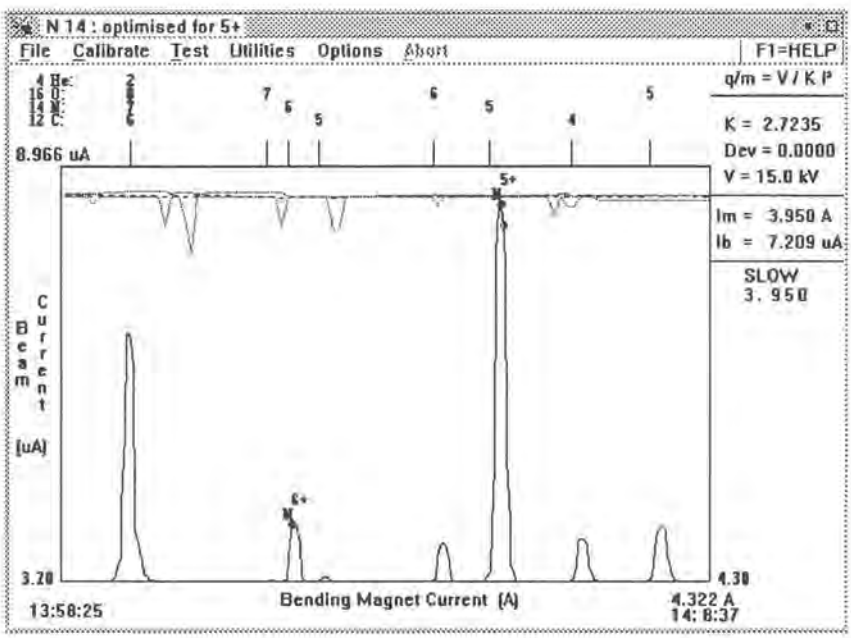


Figure 3. ECR ion source plot for a $^{14}N^{5+}$ beam.

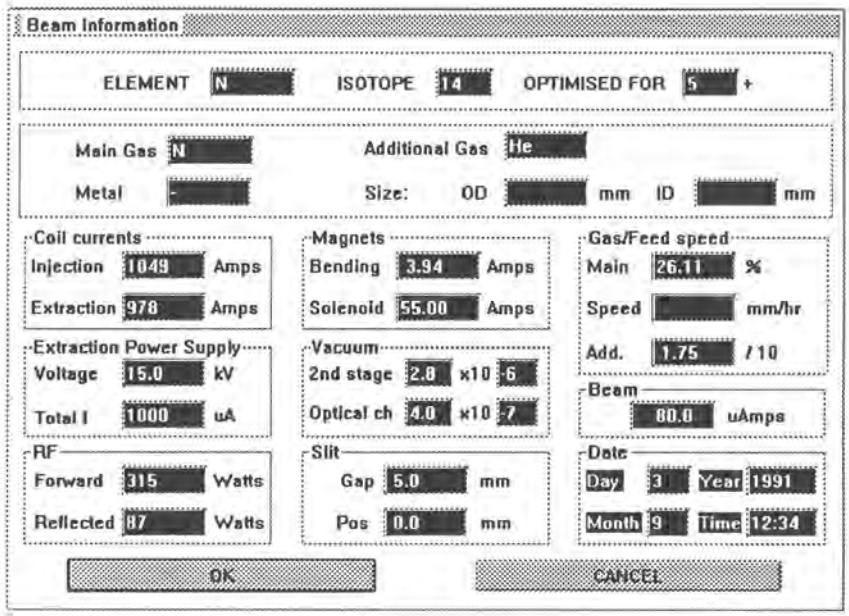


Fig. 4. ECR ion source information stored for each beam.

Figure 5 is included to illustrate a plot for Krypton in which each charge state has been resolved further showing the different mass numbers, namely ^{82}Kr, ^{83}Kr, ^{84}Kr and ^{86}Kr.

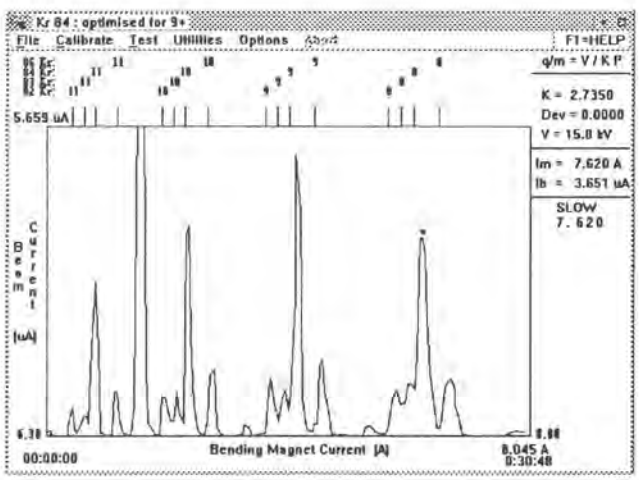


Figure 5. Plot illustrating different mass numbers.

3.5. Hardware

The microprocessor is a 25MHz Intel 80386DX with 8MB of RAM running the OS/2 v1.3 operating system. It has a 40MB hard disk drive and VGA screen. Input is via a mouse and keyboard.

Locally developed hardware is used for controlling the analysing magnet power supply as well as for reading the beam current. This hardware resides in a separate crate (SABUS crate) and communication from the crate to the PC is via locally developed differential drivers. Naturally the analysing magnet power supply must be electronically controllable.

4. CONCLUSIONS

The major initial objective of this software was to aid in the identification of ion species, the manual method of comparing plots with pre-prepared schematic graphs being cumbersome and prone to error. Not only was this objective achieved but a number of other advantages came to light; namely, improved control of the analysing magnet, automatic recording of beam stability, easy retrieval of past data (both graph and ion source parameters) and the possibility of remote control.

5. REFERENCES

1) du Toit, Z. B. et al, "Progress with the NAC Injector Cyclotron for Heavy and Polarised Ions", this conference.
2) Weehuizen, H.F. et al, "The New Distributed Control System of the NAC", this conference.

MICRO-CONTROLLED VACUUM SYSTEMS AT NAC

P.J. Celliers and E.J.S. Franklin

National Accelerator Centre, P.O. Box 72, FAURE, 7131 Republic of South Africa

ABSTRACT

The vacuum systems for both the 'beam swinger' and the newly-installed spectrometer at NAC are controlled by an OS/2-based 386 micro-computer (PC). The operating system's multitasking environment allows both vacuum control programs to run simultaneously and its graphical capabilities provide an intuitive and easy-to-use interface for the operator. Graphical layouts of the systems, showing pump and valve states and beamline pressures, are displayed on the colour monitor, while a pointing device enables an operator to communicate with the system directly on the monitor. A local-area network allows control of the systems from any node on the network. A description of the hardware and software of the two vacuum systems is presented here.

1. INTRODUCTION

The new system for vacuum control is the third-generation of such systems being used at NAC. The first was an electronic system with a mimic panel to display the state of the system and press buttons to operate pumps and valves. The interlocking was done electrically. The second[1-3] is a microprocessor controlled system with a station-dependent mimic panel, a specialized keyboard and an alpha-numerical display for communications. The third generation has the following features:

(a) dynamic display of the layout and state of the system,
(b) simplified operator control via a mouse,
(c) software access for later enhancements in the layout or control of the system,
(d) standardization in hardware and communication, and
(e) multitasking.

A layout of the beamlines and cyclotron facility at NAC is depicted in reference 4. The systems under discussion are on the right of the figure.

2. CONTROL

The control for the new system uses a 386 micro-computer, a cardcage with the SABUS interface backplane to hold all the necessary modules, a mouse and a VGA colour monitor (see Fig. 1). The layout of the vacuum system(s) is displayed on the monitor. The pressures measured by all the gauges and the states of the various pumps and valves are displayed in various colours at the appropiate positions on the screen. Green symbolizes a "closed" or "off" state and red an "open" or "on" state. Black symbolizes a valve state which is neither "open" nor "closed". It is therefore very easy for the operator to establish the state of the vacuum system.

The computer communicates with the hardware by means of two differential drivers, one in the computer and the other in the SABUS crate. This crate holds the four 32-bit relay output modules, the four 80-bit opto-isolator input modules and the 32-channel analogue (ADC) input module. Each relay output module consists of 2.5 V reed relays which latch 220 V relays thus enabling the system to switch pumps on/off or to close/open valves. An electronic watchdog has been installed on each module which will cause the relays to unlatch if they are not addressed within 22 s. The 24 V opto-isolator modules are responsible for reading the limit-switches on the pumps and valves. The 2.5V ADC input module reads the analogue signals for the gauges and translates them to pressure readings.

Each element (bit) on the modules can be addressed by means of the port addresses on the motherboard, the addresses of the modules and addresses within the modules. Correct wiring of these modules ensures that each vacuum element can thus be addressed. All these modules were designed and manufactured at the NAC.

The computer communicates with the operator by means of messages on the screen. Changes in vacuum system state are represented by colour changes of the pump and valve symbols and a display of the pressure at the corresponding positions. Under OS/2 Presentation Manager a 'window' for each symbolic pump, valve and meter is generated on the screen. Any change in the vacuum state is reflected by writing to the respective window using its software window 'handle'.

The operator communicates with the system by means of the mouse which is easy and intuitive to use. To change the state of a pump or valve the mouse cursor is moved to the desired window (pump or valve) and the left mouse button is depressed. This causes a request flag to be set. A white dot or square on the relevant window indicates that a request was made. If the

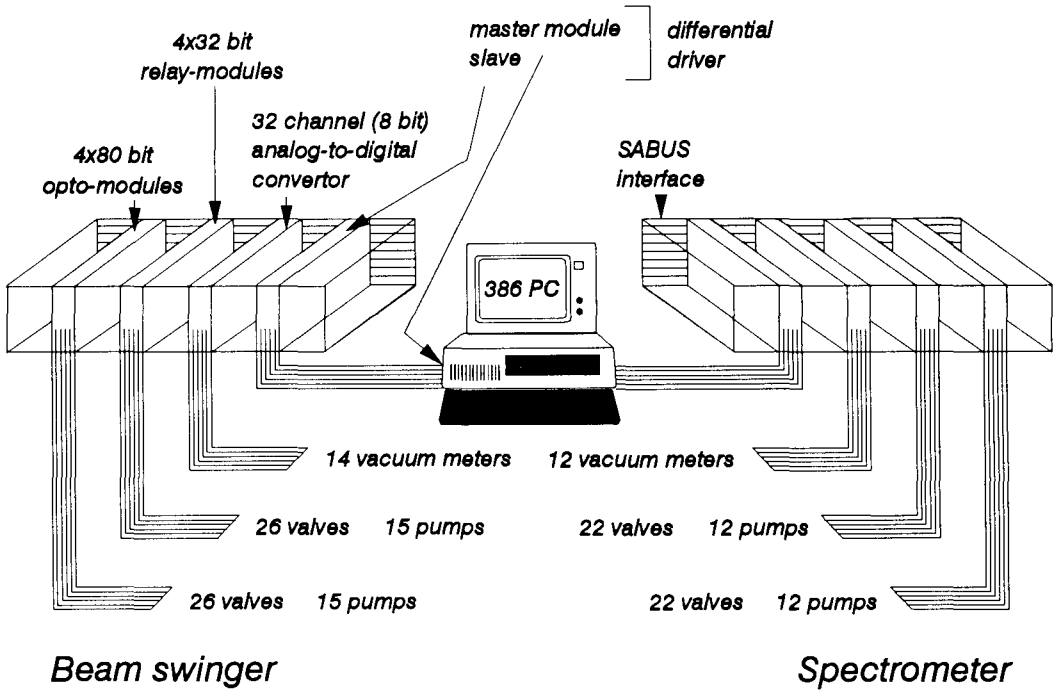


Fig. 1. A scematic view of the instrumental node for the two vacuum systems.

interlocking conditions are met the state is changed. The right button is used to switch off any pump or close a valve immediately without considering the interlocking conditions or to reset the request before it was executed.

The system is fully automatic by utilizing five OS/2 threads in the program. They continiously monitor the pressure and limit switches, control the screen display and the relays, and handle all network communication.

In addition to the monitoring, the following active procedures are also initiated as a result of a change of the state of the system:

- Valves will close on any unacceptable rise in pressure. Because the request flag remains set the valve will open if the pressure decreases sufficiently again.
- Valves are also protected from the particle beams. If a beam is passing through a beamline and the valves are closed for any reason, signals sent to the cyclotron interlocking system will result in stopping the beam on Faraday cups.
- Turbopumps will be switched off if signals indicating malfunctions are received. If a turbopump fails to start, the fore-pump will be switched off in 20s.

3. MULTITASKING

The computer is supported by the OS/2 operating system with Presentation Manager as the graphical user interface. The programs are written in the C language. The multitasking environment allows more than one complete vacuum control system to run concurrently on one machine. Multiple windows and icons provide for a convenient display. One or both vacuum systems can be displayed on the screen in separate windows. The one that is displayed is graphically active and is identified by its title bar located on the top of the window. Messages can be sent or received from this window. To select

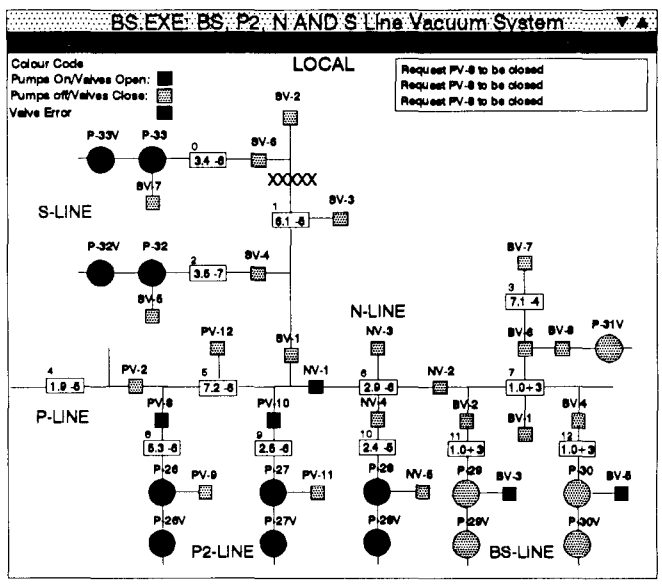


Fig. 2. A screen copy of the colour monitor video display of the 'beam swinger' vacuum system.

another window to become active, the operator must shrink the active window by pointing the mouse to the 'minimize' box at the top hand right corner of the present window and press the mouse button. Next, the mouse cursor is pointed to the icon which represents the program to be viewed and whose name is displayed at its bottom and the button is pressed to maximize the icon.

The two vacuum systems mentioned above are the beam swinger and associated beam lines and the spectrometer beamline[4]. The computer layouts for the two vacuum systems are shown in Fig. 2 and 3.

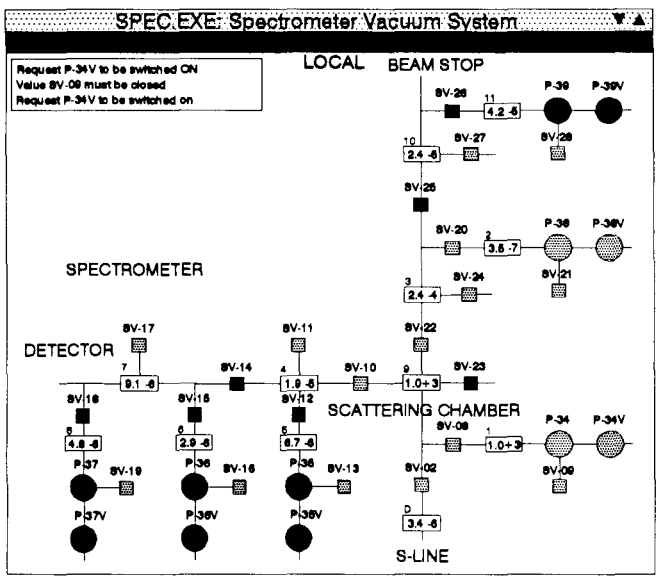


Fig. 3. A copy of the colour monitor video display of the spectrometer vacuum system.

4. LOCAL AREA NETWORK

The network consists of a thick Ethernet baseband cable connected to the nodes via transceivers and cluster boxes where the nodes are closely spaced. The local computer with its hardware (known as the instrumentation node), the console computer and any other nodes are connected to these multiport transceivers by means of the Ethernet communication interface as shown in Fig. 4. By means of the interface, data is sent to or received from the network. Data packages are sent at a rate of 10 Mbits/s and consist of data, the destination and source address.

The local node controls the vacuum systems which are in turn being controlled by one or more console nodes. Each instrumentation node has a memory-resident table which is a dynamic database of all the actual values of vacuum system parameters at that local station. Any change in the state of the vacuum system is written to the local table and is transmitted to all the nodes on the network. The table in the local node can

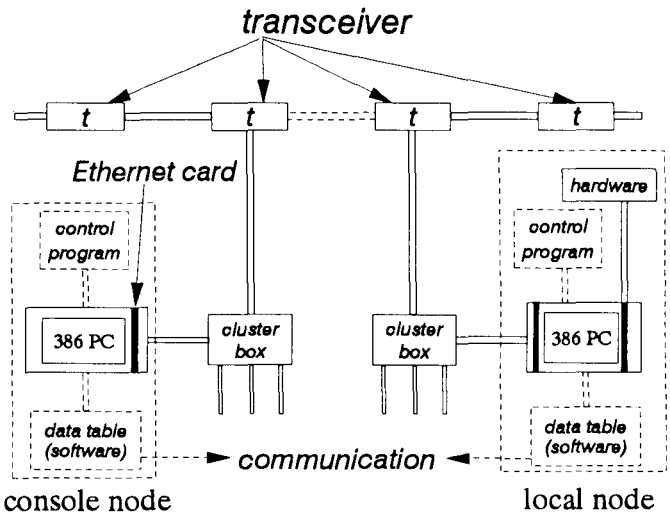


Fig. 4. A schematic representation of the Ethernet network.

also receive commands from the console nodes via the network, update the variables and then controls the instrumentation accordingly.

The console node has the same programs as the instrumentation node, namely the vacuum control program and the console table program for the database. The console table is updated via the network when changes in the hardware are written to the local table and then transmitted to the console nodes. The latter then displays the updated vacuum system parameters on the colour monitor by writing the latest pressure and displaying the correct state of the pumps or valves. The table program can also display the actual and reference values of all the parameters in the database in a page format.

We are now running two independent vacuum systems on the local computer. In addition there is a console node situated in the control room from which both vacuum systems can be controlled. Control of the system from any other node has also been demonstrated. A detailed description of the NAC distributed control system, which includes the vacuum control, is given in the present proceedings[5].

5. INTERLOCKING

The interlocking function is only accessed when a request has come from an operator or if a system parameter such as the pressure or a limit-switch position, has changed. The interlocking conditions are specified for pumps and for valves. The pumps have separate conditions for fore-pumps and for high-vacuum pumps. The conditions for the valves are classified according to whether they are isolation valves (between beam lines),

ventilation valves, or valves connecting pumps to beam lines.

The interlocking principle is as follows. Each parameter is identified by its state, its requested state and the number of requests. In the case of valves an additional value, the differential pressure across the valve, is set. To operate a pump or valve, all these various values (software flags) for the affected valve(s), pump(s) and pressure difference(s) are grouped together in a byte. If this value corresponds to a pre-calculated value then a pre-defined action is taken and messages are written to the display window.

The maximum pressure difference (MPD) allowed across the valves mentioned above, is set to change according to the geometrical average pressure difference across the valve. This is to ensure that the MPD will always have a realistic value. The relation is given by

$$MPD = \frac{100 \times \sqrt{(P_1 \times P_2)}}{\sqrt{(1 + P_1 \times P_2)}} \text{ mbar.}$$

P_1 and P_2 are the pressures on each side of the valves. For high pressures (1000 mbar) the maximum difference is high (100 mbar) and for low pressure (1×10^{-6} mbar) the maximum difference is low (100×10^{-6} mbar).

These interlocking conditions were tested in the laboratory on an electric system of switches, LEDs and potential dividers before the program was installed on the various computers.

6. METERS

The software is designed to accomodate two sets of meters. One set has two voltage signal outputs and therefore two ADC channels are used, one for each of the Pirani and Penning gauge signals. Two tables of 128 values each are also necessary for converting the voltage signals to pressure in mbar.

The other set, which was built at NAC, supplies only one output signal and the relation for converting the signal to pressure is very simple. If the voltage is given by a 3-digit, 2 decimal figure, which we can write as A.BC volts, then the pressure is given by $B.C \times 10^{-(A-9)}$ mbar.

The pressure is only recorded if the output voltage of the gauges change with 2/128 V. The accuracy of measuring the pressure is 1/128.

7. TROUBLE SHOOTING

The majority of problems are caused by valves which close unexpectedly. This is mainly due to faulty gauges or meters. On rare occasions some of the output relays malfunction, inhibiting pump or valve operations. A chart is available to locate the faulty relays very easily.

8. CONCLUSION

After two years of experience with the beamswinger system and a few months with the spectrometer system for it is evident that the performance is very good. The new NAC vacuum-meters also behave very well. Similar vacuum control systems will be installed in future systems for the second injector (SPC2) and associated beamlines[4].

9. ACKNOWLEDGEMENTS

The authors wish to thank Mr Hanekom for his assistance in preparing the computer-processed diagrams in this paper.

10. REFERENCES

1) Visser, K. and Mostert, H., "Vacuum control systems at the NAC cyclotrons," in **Proceedings of the 11th Int. Conf. on Cyclotrons and their Applications** (Ionics Publishing, Tokyo, Japan, 1986) pp 426-427.

2) NAC Annual Report 1984, NAC/AR/84-01, pp. 81.

3) NAC Annual Report 1985 NAC/AR/85-01, pp. 91.

4) Botha, A.H. *et al.*, "Commissioning of the NAC Separated-Sector Cyclotron", in **Proceedings of the 11th Int. Conf on Cyclotrons and their Application** (Ionics Publishing, Tokyo, Japan, 1986) pp 9-16.

5) Weehuizen, H.F. *et al.*, "The new distributed control system of NAC", (these proceedings).

TWO DIMENSIONAL SCANS WITH ADAPTIVE DOMAIN CONTROL

Stefan Adam and Anton C. Mezger
Paul Scherrer Institute (PSI)
5232 Villigen, Switzerland

ABSTRACT

Methods to investigate the combined effect of two parameters being varied, can be helpful for online optimization of the beam setup in an accelerator complex. Compared to single parameter scans, twodimensional scans provide more insight into the way how parameter changes can modify the accelerator performance.
For onedimensional scans it is common practice to monitor the beam losses while scanning and to cut back the interval originally forseen when the beam losses exceed a critical value. In the program described in this paper, the principle of adaptating the interval to be scanned, is extended to the twodimensional case: The domain of allowable parameter variations is built up during the process of scanning. With this new method, twodimensional scanning is not anymore bound to the disadvantage of using extremely narrow scanning intervals, nor does it run the risk of producing too many beam shutoffs.

1. THE NAME OF THE GAME

The program for two-dimensional scanning presented in this paper was given the name "GEISS". This name is neither an acronym, nor does it point back to greek origins, it is simply the Swiss-German name for a goat. The name of this animal was felt to fit the idea of the program, for goats are curious and they are able to find distributed parts of herbs in the mountains without falling down a slope. A short name that is easy to remember can also help to make a program popular with the control crew.

2. THE ORIGINAL SCOPE OF THE PROGRAM

For the control system of the PSI accelerator complex[1),2)] a series of individual programs for onedimensional scanning had been summarized in a single scanning program of general applicability due to selectable parameter-files.

Some programs for twodimensional scanning were in use, but their replacement by a single program appeared to be difficult. These programs had differences in their functionality, in particular with respect to the shape of the twodimensional domain to be scanned. In addition to differences between individual programs, most of the twodimensional scanning programs had a common problem: when the scanning domain was fixed before the start of the scanning, the size of this domain had to be chosen carefully finding a compromise between using only small parameter variations and running the risk of a beam shutoff (interlock). The task to construct a generally applicable program for twodimensional scanning therefore started with the search for a solution to the problem of the scanning domain.

In one dimension the solution is evident: while the active variable is changed stepwise, some passive parameters that give an indication on beam losses are continuously monitored along with the main passive parameter recorded by the scan. If the beam losses become higher than a predefined critical level, the scanning stops, even if the parameter variation has not yet reached the end of the scanning range forseen at the start. Such a scheme of adapting the range while scanning had to be realized in the twodimensional case as well: the scanning domain had to be built-up online.

3. REALIZING THE BASIC FUNCTIONALITY

In most of the cases of twodimensional scanning for parameter optimisation in a accelerator, one can clearly distinguish between the primary and the secondary parameter to be varied e.g. parameter changes of RF devices are much more reproducible than changes of the current in a big magnet. The parameter that is more reproducible is considered as primary parameter, which is changed up and down many times, while the secondary parameter is changed by single steps only. The different role of the two active parameters is the reason why the program "Geiss" is based on a sequence of onedimensional scans which is quite an asymmetric way of treating the two scanning parameters.

The main framework of the program "Geiss" is based on the principle of extendability of a onedimensional scan (see fig. 1).

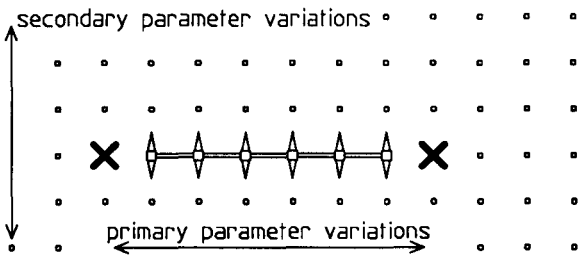


Fig. 1. **Candidates for domain extension.** The changes of the secondary parameter by one step up and down from a successfull point within a line segment of primary parameter scanning are the set of candidates for domain extension from this elementary subdomain.

A onedimensional scan that has been completed, varying the primary parameter, represents a horizontal line-interval in the twodimensional plane, hence an elementary subdomain where scanning has proven to be possible. This elementary subdomain cannot be extended to the left nor to the right hand side, because the onedimensional scan has been done with limit-checking. In the vertical direction however, from each point of this subdomain, an extension upwards and downwards is feasible. Such movements, which represent changes of the secondary parameter by one step up or down, while the primary parameter remains within the range of the scan-line, form the set of candidates for domain extension.

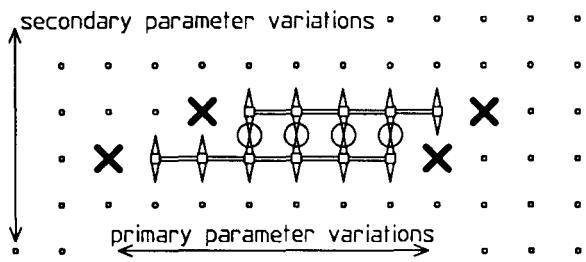


Fig. 2. **Cancellation of candidates pointing towards each other.** Extension candidates that point upwards from the lower scan-line cancel with their counterpart pointing down from the upper scan-line.

During the build-up of the domain in the twodimensional scanning process the program tries to extend the known subdomain using candidates for domain extension. If the elementary movement of domain extension leads to excessive beam losses, the parameter is stepped back, this candidate is eliminated and another candidate has to be tried. If a candidate for extension is successful, it becomes the starting point for a new horizontal (primary parameter) scan.

Two adjacent horizontal scan lines always have some pairs of extension candidates that cancel each other (see fig. 2). These pairs have to be eliminated from the list of candidates after every onedimensional scanning, except for the very first. Candidates of domain extension that have no counterpart from the neighbouring scan, but which point to an endpoint of a neighbouring scan-line have to be eliminated as well because this endpoint, in the previous scan, has proven to lie outside the allowed region. After these bookkeeping operations are done, another attempt to extend the domain via an extension candidate follows. When the list of extension candidates has become empty, the process of twodimensional scanning is complete.

The main working cycle of this twodimensional scaning can be summarized as follows:

A) initialisations
B) do the first primary parameter scan
C) cycle, while there are extension candidates:
  1) try candidates (secondary parameter steps)
    a) discard candidate upon warning
    b) else take as new starting point
  2) do a primary parameter scan (warning limited)
  3) update list of candidates (add new, cancel pairs)
D) display the scanning results

4. FUNCTIONALITY EXTENSIONS

The basic functionality described in the previous section is not sufficient to get a useful program. An elementary additional requirement is that in spite of the automatic domain control based on loss warnings the twodimensional scanning range must be confined. Absolute minima and maxima of the active parameters have to be given and the program has to treat these absolute limits in a different way than the loss warning limits.

The aim to avoid beam interlocks requires that beween two primary parameter scans, when both active parameters are varied, to move to the starting point of the next extension candidate, this travelling path should remain inside the allowed domain. To make this "good-path" option work, the program has to maintain a table describing the valid domain. This table records all the successful scans sequentially including their vertical positions and their horizontal limits. It is independent of the candidate list which gets empty at the end while the domain table steadily grows.

Another important entry in this domain table is the "father" pointer indicating from which scan line the extension link originated that lead to the present scan line. These pointers bring a tree organisation into the domain table. Travelling inside the domain from one scan line to another corresponds to motions along branches of this tree. The tree of scan lines has an unusual structure. Compared to tree structures used for commercial data processing it has extremely few branching nodes. Most of the nodes in this tree have just one father and one son, but if a branching occurs, there is no principal limit to its multiplicity. The strange structure of the tree of scan lines reflects the fact that this tree is an image of the topology of the domain (see fig. 3).

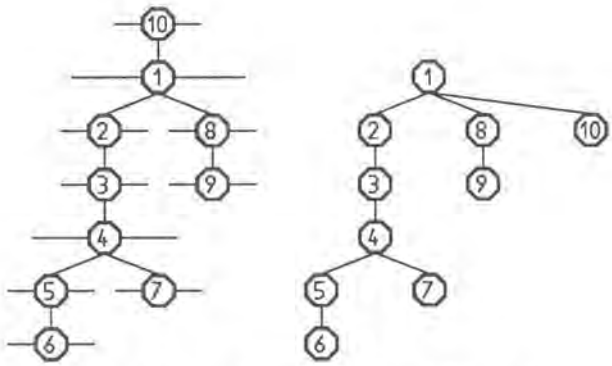


Fig. 3. An example of a domain with a complicated shape and of the corresponding tree structure describing the topology of the interconnections between scan lines.

In the description of the basic functionality a symbolic program step requires "to choose a candidate", but it leaves open how this choice is implemented. Several strategies for selecting the next extension candidate have been tested. Aiming at a minimal number of non-scanning steps, mainly for the secondary parameter, the following scheme appeared to be quite favourable:

The highest priority is given to domain extension candidates starting from a scan line located as near as possible to the present scan line (wrt. to chronological order). If this criterion is still ambiguous, the selection strategy tries to use the same direction for the extension of the domain as for the previous scan. With these two criteria there is still no priority difference among a group of adjacent, parallel extension candidates; in that case the middle one is selected.

5. TEST FUNCTIONS

The program "Geiss" is organized in a way that all scanning and moving operations in the twodimensional space of parameter variations are requested by calling a single function. This central moving and measuring function can therefore be replaced by a test function that gives a similar response to the calling program, but does not vary any real parameter. The requests to change active parameters are just used to update the coordinates of the current point. These coordinates then serve as independent variables in a mathematical formula calculating the value of the passive parameter to be passed back. A loss warning is simulated by the test function when the passive parameter gets larger than a critical value.

Several of these test functions have been used where each one is conceived to demonstrate a different part of the program functionality. The "fourdip" function was the first of those test functions, it was made to test the ability of the program "Geiss" to find the boundaries of a non convex domain (see fig. 4). The functions "nautilus" (with a spiral shaped domain) and "snake" primarily checked the "goodpath" option, requiring that parameter movements must remain inside the valid domain. The "sta-logo" test and also the "snake" are examples that define domains where the connections between scan lines have a complicated topology.

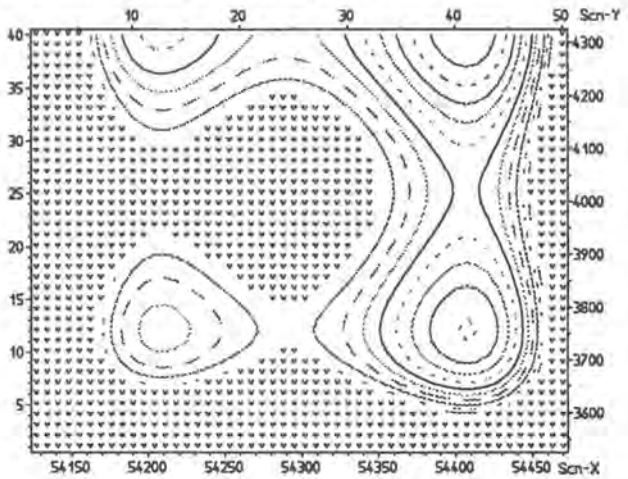


Fig. 4. The domain and the contour lines of a twodimensional simulated scan using the test function "fourdip".

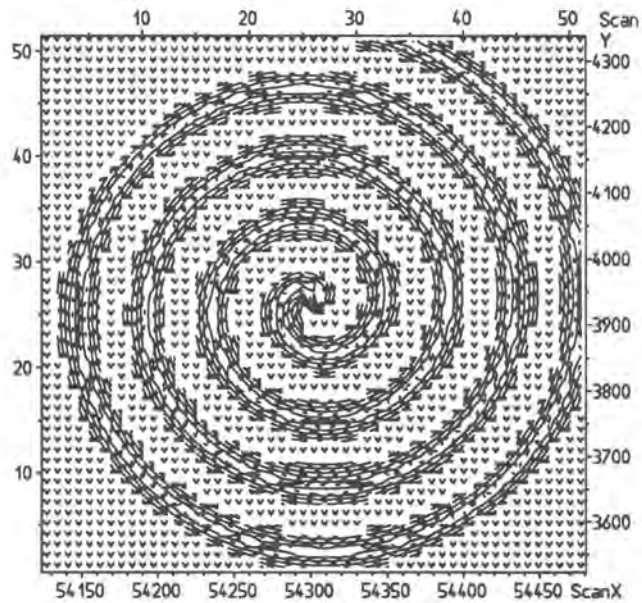


Fig. 5. **A scan with the "nautilus" test function.** Running the program "Geiss" with this test function checks that parameter motions remain inside the valid domain.

6. RUNNING EXPERIENCE AND IMPROVEMENTS

A very early version of the program was tried out with real beam during machine development and was successful in finding the allowed domain avoiding interlocks. After some more test with real beam a wishlist for

improvements came up. An urgent requirement was to inhibit multiple scanning of the same domain. In some scanning experiments, the fact that beam losses are not reproducible, and therefore the beam loss limits are varying, made the program scan the same parts many times. This fault was cured by restricting the scanning range not only to the absolute parmeter limits, but to the part of the horizontal line that has not been scanned before. The "diagonal band" test function was programmed to check the multiple scanning inhibition offline. It uses a simple mathematical function, but includes a random function component.

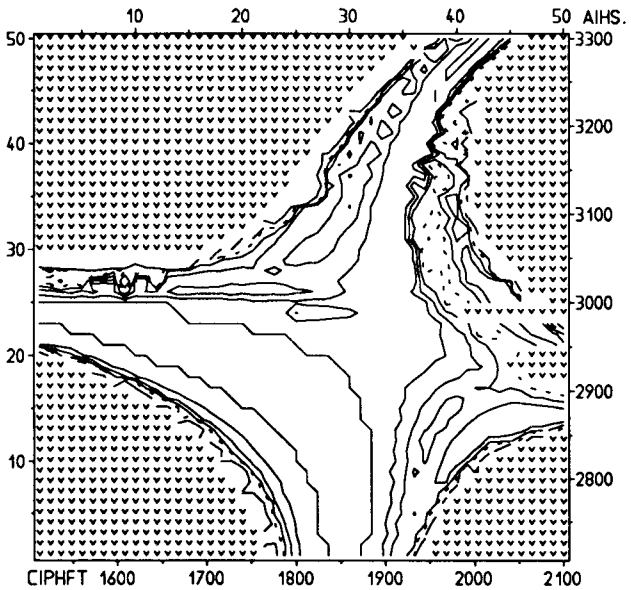


Fig. 6. **A twodimensional scan of flattop phase and main magnet excitation recording extraction losses.** The strange shape of the domain where scanning is possible reveals the advantage of a program that finds this domain automatically.

As twodimensional scanning can take quite some time, a way to abort the running program was introduced. Beam interlocks can occur any time, also in the middle of a running scan. The scan then stops and the operator can decide whether he wants the program to exit or to continue. A special option allows to continue scanning, but avoid the region having been scanned at the moment of the interlock. In studies of extraction losses the contour lines were concentrated at the boundary of the scanned domain giving no information on the loss structure inside the area. This drawback could be avoided using a new procedure to select the contour levels. It makes a statistics on the distribution of measured values and divides the integral curve – number of measured points vs. measured parameter values – into equal slots wrt. to the number of measured points in order to get the set of parameter values for contouring.

In order to reduce the total scanning time without loosing much information an option was introduced that can diminish the number of tries to extend the domain. An entry in the list of extension candidates is deleted by this option when the number of adjacent candidates is smaller than a critical width that can be specified.

An example of a twodimensional scan result with real beam is shown in figure 6.

7. THE USER INTERFACE

Before a twodimensional scan can be started, a long list of options and parameter values must be available to the program. This list includes e.g. the device names for active, passive and loss monitoring parameters, the absolute limits, the critical values for warnings as well as step size and time delay for the active parameters. If the operator would have to type in all this data for each measurement, the program "Geiss" would never be used. Complete sets of these running parameters are stored in individual parameter files, the operator has just to select one of the sample cases from a list and tell the program to start scanning.

Using the multi-window techniques of the OSF-motif (Open Software Foundation) display system on the VAX Workstation, the operator could be given a good overwiew and full control over the activities of the program. Selecting a predefined case, changing critical values, and changing device lists can easily be done with pointing to items in well separated scroll windows. Start and stop of the program and continuation after an interlock can be steered with click buttons.

The continuous display of the domain accumulated so far and of the current parameter values (position in the domain) had been forseen for testing only, but as twodimensional scanning can be quite slow this display was kept for the application case. It steadily informs the operator on what the scan is doing.

8. CONCLUSIONS

The twodimensional scanning program "Geiss" has become a good tool for beam optimisation. The method to build up the valid domain while scanning has proven to work well and makes the program much more useful than previous ones with a fixed scanning domain. The window based user interface and the online graphic display are essential to the success of this program.

9. REFERENCES

1) Blumer, T. et al., "The PSI Accelerator Control System: A Status Report." Proc of the Int. "Conf. on Accelerator and Large Experimental Physics Control Systems", Vancouver BC, Canada, 1989
2) Stammbach, Th., "Experience with the High Current Operation of the PSI Cyclotron Facility." this conference.

CONSTRUCTION AND SYSTEM TUNING OF CONTROL SYSTEM FOR THE RCNP RING CYCLOTRON AND BEAM LINES

T. Yamazaki, K. Tamura, A. Ando, K. Hosono, T. Itahashi,
M. Kibayashi, I. Miura, K. Nagayama, T. Saito, A. Shimizu, M. Uraki and H. Ogata
Research Center for Nuclear Physics, Osaka University,
Mihogaoka 10-1, Ibaraki, Osaka 567, Japan

and

M. Maruyama, S. Yamada, Y. Kimura, K. Aoki, K. Kodaira* and M. Tachibana
Quantum Equipment Division, Sumitomo Heavy Industries,
Soubiraki 5-2, Niihama, Ehime 792, Japan

ABSTRACT

The control system for the RCNP ring cyclotron and beam lines was designed in 1987, and the constructions of individual device control units and their softwares were completed in 1990. The control system was installed in the new ring cyclotron building in autumn of 1990, and final adjustments and operational tests were executed by using the softwares of control computers. After the accelerated proton beam from the injector AVF cyclotron was injected to the ring cyclotron, the computer control system has been used for the beam acceleration of the ring cyclotron. The software of this control system performs its basic facilities almost satisfactory under actual cyclotron operation.

1. INTRODUCTION

The control system consists of a computer network with a central computer (a system control unit SCU using microVAX 3500), four computers (group control units GCU using a microVAX II and three diskless rtVAX 1000's) and many control cabinet racks.[1] The SCU computer has charge of a concentrated control of the total system, file managements and a man-machine interface. The RING-GCU subsystem (microVAX II) covers the controls of injection beam line, cyclotron magnets and injection-extraction system. The RF-GCU subsystem (rtVAX 1000) covers the covers the controls of RF system, vacuum system and cooling system. The BT-GCU subsystem (rtVAX 1000) covers the control of magnets of the beam lines. The DIAG-GCU subsystem (rtVAX 1000) covers the control of beam diagnostic devices. Each group control computer is also connected to many device controllers by an optical communication system.

The control cabinets located in the cyclotron vault, experimental halls and power supply areas, and contain universal device controllers (UDC's) which control component devices, associated local panels, the drivers of the stepping motors and AC motors, input signal multiplexers, analog-to-digital converters and interlock relays.

2. POWER SUPPLIES OF MAGNET COILS

The UDC's and associated local control panels are installed within power supplies of the cyclotron coils, i.e., main coil, auxiliary coils, trim coils and magnetic-channel coils. The communication data between GCU computer and UDC are stored in the memories of UDC named a communication register (CRG).

The power supply of the ring cyclotron main coil uses a high precision digital-to-analog converter for the coil current setting, and its CRG has unique status bit corresponding to the GP-IB interface. The firmware of the power supply control for the main magnet coil consists of six tasks. Task1 starts at 200 ms intervals to initialize the GP-IB port, output a preset value, and read the current value. Task2 is a communication task, and uses the CRG as the communication area. Task3 starts at 10 ms intervals to calculate the output current value depending its cycling mode which set the ratio of the output value to the final preset value. Task4 starts at 10 ms intervals for the operation of the sequence control depending on the present status and setting commands. They are the startup and shutdown sequences, the polarity change of the output current, and the interlock and status monitorings and correspoding status transition operations. Task7 starts at 100 ms intervals for the local panel controls. Task8 starts at 100 ms intervals for the GP-IB input-output processings.

3. POWER SUPPLIES OF THE RF SYSTEMS

Power supplies of intermediate stage and final stage amplifiers were constructed since 1987 in the early stage of the construction of the ring cyclotron, the designs to control the power supplies by using UDC's were not in time. Therefore the control units including UDC's were connected externally to the power supplies already completed. On the contrary other power supplies were designed by considering the controls using UDC's together with associated local control panels, and control units

*Systems Engineering Development Department, Sumitomo Heavy Industries, Yato 2-4-15, Tanashi, Tokyo 188, Japan

containing UDC's and local control panel were included inside the power supply cabinets. The power supplies of the RF system amplifiers can be operated locally without using UDC, but other power supplies such as magnet coils of the ring cyclotron and the beam lines cannot be operated without UDC even in a local control mode.

The firmware of the power supply controls for the amplifiers of RF system consists of five tasks. They are input of actual values from an analog-to-digital converter, a communication task, output of preset value to a digital-to-analog converter, sequence controls including startup and shutdown of the power supply and checking functions of interlock and status signals, and local input-output controls.

The harmonic numbers of accelerations at the ring cyclotron are 6, 10, 12 and 18, and ratios of the RF frequencies of the ring cyclotron to the AVF cyclotron are 3 and 5.[2] These relations determine the RF phase differences between three accelerating cavities and a flat-topping cavity. The UDC for the phase adjustment of RF low level system reads the detected phase values and outputs new setting value for RF phase. The UDC for an automatic tuning of RF low level system reads an injected power from the final stage amplifier, a reflected power from a cavity, an amplitude and a phase of the input impedance to cavity.



Fig. 1. Central operator console.

4. CONTROLS OF STEPPING MOTORS AND AC SERVOMOTORS

The stepping motors are used for the open loop controls of the positions of electro-static channels, frequency tuning devices of RF power amplifiers and cavities, variable width slits and beam probes.

At power-on time, the UDC for the driving of stepping motor has no pulse value corresponding to the present position. Then a GCU subcomputer downloads the pulse value for the position at power-off time, or it sets new pulse value at either limit position used for a calibration. One UDC can control upto four stepping motors. When the UDC receives a drive command from the GCU subcomputer or a local control panel, the UDC controls the positions of a device by outputting control pulses to the driver module of a stepping motor. The UDC controls hold and brake functions and also interlock conditions if necessary.

Some position controls of RF cavities use AC servomotors with a closed loop control. One UDC can control upto four AC motors. After selecting motor number, the UDC reads the present position from a potentiometer through analog-to-digital converter, determines driving direction by comparing the present value with a preset value, and outputs driving signals until reaching to final preset position by checking interlocks relating the driving direction.

5. ADJUSTMENT OF DEVICE PARAMETERS AND DISPLAY OF DEVICE STATUS

Device states can be displayed on two twenty-inch CRT displays with touch panels of the central operator console.(Fig. 1) The screens for device status, not ready device list, fault device list and dynamic parameter value are prepared. These values are also displayed on the computer console terminals of GCU subcomputers, and are useful to check the control functions for not only maintenance aids but also daily operations.

In the early stage of the construction operational tests of the device control systems were performed at the local panels of the control units in the cabinet racks installed in and near the cyclotron vault and experimental halls. After completing installations and checks of the device control systems, their control functions were confirmed at GCU subcomputers and finally at SCU main computer.

All the control informations of each device is displayed on a memory of the UDC called communication register CRG. The subcomputers GCU's usually have updated copies of the CRG data of UDC's. According to the requests from the tasks of the SCU and the operator console, the main computer SCU gets necessary CRG data from the corresponding GCU. For each control information a proper name called operation name is assigned, the main computer and subcomputers can refer CRG data by using the operation name. After defining the operation names on SCU, the device control functions are checked from the computer console terminal of the GCU by using not bit images of the CRG but more familiar names based on the operation name. In this process the validity of the operation names can be checked. Next the control functions are checked from the operator console by using the main computer SCU. Twenty-nine processes run on the SCU with issuing mails between processes, and total software system is rather complicated. Therefore it is often to run a particular process with a debugging mode for checking purpose. After finishing these procedures, the control software itself becomes open to general operators of the ring cyclotron system in spring

of 1991.

During the checking procedures of the control functions it is often to use the displays of GCU and the operator console simultaneously. A device control is initiated from the operation screen of the operator console by selecting particular cell. Then the following control result is displayed on the display of GCU, and the control function can be confirmed. They are performed by comparing device states, preset values and measured actual values on both GCU and SCU (operator console).

6. INTERLOCK SYSTEM

Device status signals used for external interlocks to other devices are collected in an interlock control unit through a signal distributer box with terminal boards and status display lights. The control unit contains a UDC and relays to output the signals for an interlock circuit. The interlock system for power supplies, a beam handling and an interface to the radiation protection system and the injector cyclotron are constructed by using hardwiring and conservative relays. Software interlocks using sequence programs, written by a basiclike interpreter-type language, are also supplementarily executed on GCU subcomputers. Processes of SCU main computer also contain software interlock facility.

Devices are controlled by UDC, and hardwired interlock signals are also connected to UDC's in an interlock unit. Many interlock units are distributed to control cabinet racks: two units for cyclotron magnet coils, eight units for RF cavities and amplifiers, two units for injection and extraction devices, six units for beam lines, and also for beam diagnostic devices and radiation protection system. The UDC for interlock handles 48 digital input signals and 16 digital output signals. Interlock signals such as flow switches of magnet coils are inputed to digital input port of the UDC in addition to the hardwired interlock circuits. These signal data are sent to GCU subcomputers and the SCU main computer. The digital output port of the UDC is an interface between the hardware interface and the software interface.

The software interlock conditions are created in GCU computers and the SCU main computer. Each digital output signal of the UDC has operation name correspondig to its function, and the software interlock conditions are outputed to UDC's by referring operation names. The digital outputs are taken into hardware interlock relay circuits. Excess beam current on slits at beam lines and in the ring cyclotron will stop beam before acceleration by using this software interlock function. After this interlock system sends an information on a selected beam line to the radiation protection system, the control system receives additional interlock data concerning a safety condition on transporting beam to the specific beam course in experimental hall. The degree of vacuum data can be also used as software interlock. Compared with the hardware interlocks the flexibility of the software interlock function is very useful for the dynamic change of interlock threshold values to actual parameters.

Another type of the software interlocks is a direct output of the interlock conditions to the UDC of power supplies and motor drives. Fault sequence programs in GCU subcomputers can control the status of power supplies and other devices by using their operation names.

7. SEQUENTIAL STARTUP AND SHUTDOWN

Operations of the ring cyclotron and beam lines consist of parameter setting to devices according to a beam condition, device startups, parameter adjustments, shutdowns and fault status handlings. For realizing an automatic sequential operation it is convenient to grouping many devices. Considering an operation unit of the ring cyclotron and beam lines, control facilities are divided to a few groups. Individual group consists of a few blocks, and each device belongs to one block. Startup and shutdown procedures of the system can be performed by three methods: operations in unit of group, operations in unit of block and operations in unit of device.

The RING-GCU subcomputer covers the controls of injection beam line, cyclotron magnets and injection-extraction system. Devices connected to the RING-GCU subcomputer belong to INJBT group or RING group. The INJBT group consists of INJBT1 block and INJBT2 block. Power supplies in the upperstream part of the injector beam line belong to the INJBT1 block, and power supplies in the downstream part of the injector beam line belong to the INJBT2 block. The RING group consists of MAINC block (power supply of main coil), AUXC block (power supplies of auxiliary coils), TRIMC block (power supplies of trim coils), MICMEC block (power supplies of injection and extraction magnetic channels), EIC block (injection electrostatic channels) and EEC block (extraction electrostatic channels).

During the coil current setting a cycling function of the coil current has been introduced as a firmware of the UDC's. In the case of the RING group startup, at first the startup sequence (ON sequence) of the MAINC block runs. When the cycling state of the main coil becomes the third state, the ON sequences of remaining AUXC and other blocks begin to run. Then the field distributions of the sector magnets of the ring cyclotron become to the desired distributions. A fault state processing procedure for discharges in the electrostatic channels is included in the UDC firmwares.

8. TREND DISPLAY

Variations of coil currents, degrees of vacuum and temperatures of cooling water can be displayed graphically on the trend display screen of twenty-inch CRT display. Three screens for the trend displays are prepared and each display shows eight parameters.

For the startup procedure of the power supplies of the ring cyclotron magnet coils, one can use the ON sequence operation of the RING group and the trend display of magnet coils. A cycling pattern of the main coil

current together with auxiliary and trim coil currents can be recorded on this trend display. On the operations of electrostatic channels and RF systems one can use the trend display to show the relation between the degree of vacuum, high voltages and leakage currents for a diagnostic purpose.

9. COMMUNICATION WITH CONTROL SYSTEM FOR EXPERIMENTAL INSTRUMENTS

By using a power-line connection system one power supply can change its connection to magnet coils in beam lines and experimental instruments. Many devices in the beam lines are controlled by the SCU main computer. However it is also necessary to control some devices that are connected to SCU from experimental side for some specific precesses such as a dispersion matching beam handling.

The communication function between the SCU main computer and a control computer for experimental instruments is realized by a process named PCP (communication process with personal computers and VAX computer by DECnet). This process opens a link to other computers with a name of PCP-PORT, and it is necessary that the control computer for experimental instruments establishes a logical link to this port.

The PCP process treats functions such as connection-disconnection of the communication, conversion from operation names to operation name numbers for the speedup of data access, device parameter transmission and adjustment, device on/off operation, device status monitoring and operation and data transmission of beam profile monitors.

A VAX computer in the counting room performs the man-machine interface of the control system for experimental instruments and is connected with intelligent VME crates for the control of experimental instruments and the SCU computer. The uses of control functions by this remote VAX computer are now open to users of experimental instruments.

10. INITIAL OPERATIONS OF THE RING CYCLOTRON

Software of the control system has been constructed assuming the usage at final stage of the particle acceleration. For example, the interlock checks is to be executed from beam injection to beam dumps in the experimental halls. However an initial beam test of the ring cyclotron was restricted to the beam injection part, and it is necessary to modify both hardware and software interlock sequences depending on particular test purpose.

The group and block start/stop facilities have been used partly at initial beam acceleration period. The start and stop sequences of injection beam line group and cyclotron magnet group have been executed several times upto now, but the startup procedure of devices for RF system is executed manually one by one. The data of accelerated particles and their energies are limited to a few cases for the present and the data on frequency and position relations of cavities and relating devices have not been included in the software properly. Therfore an automatic frequency tuning procedure for RF system is not yet completed now.

During the initial startup procedures the use of a trend display is very useful for the checks of operation itself and firmware contents of the UDC's such as cycling procedure at startup time of the power supplies of magnet coils. For the startup procedure of high voltages of RF cavities and electrostatic channels rather complicated time sequences are considered, and their operations were confirmed together with the variation of degree of vacuum in the cyclotron chamber and also leakage currents.

Interlock system concerning with beam stopper and radiation protection system was tested for hardware wiring only using actual ring cyclotron operation, and the tests for software interlocks is left for future beam acceleration. Trivial troubles on the operations at the central operator console were temporarily fixed by using the console terminals of the GCU subcomputers, and the softwares of the SCU computer are updated later by including this operational experience.

During a beam injection process of the ring cyclotron many beam diagnostic devices such as slits, beam profile monitors and beam viewers have been applied, and many checks on device position and beam current measurement including noise current observation were done. For slight beam current the lack of beam viewers in injection part of the cyclotron made the beam tranport procedure to be difficult. Continuous measurements on reliability and reproducibility of the control system are necessary for the present particle accerelation period.

11. CONCLUSION

The accerelated proton beam from the injector AVF cyclotron has been injected to the ring cyclotron and the computer control system is used for the beam accerelation of the ring cyclotron. The software of this control system performs its basic facilities almost satisfactory under actual cyclotron operation.

12. REFERENCES

1) Yamazaki, T. *et al.*, "Design of distributed control system for the RCNP ring cyclotron" in Proceedings of Twelfth International Conference on Cyclotrons and Their Applications, Berlin, 1989, (World Scientific, 1991) pp.252-256.
2) Ikegami, H., "The RCNP Ring Cyclotron Facilities" in Proceedings of Twelfth International Conference on Cyclotrons and Their Applications, Berlin, 1989, (World Scientific, 1991) pp.30-39.

EARLY EXPERIENCE WITH DECWINDOWS/MOTIF IN THE TRIUMF CENTRAL CONTROL SYSTEM

S.Kadantsev
Joint Institute for Nuclear Research, Dubna,
Head Post Office, P.O.Box 79, Moscow, 101000, Russia

and

M.Mouat
TRIUMF, 4004 Wesbrook Mall, Vancouver, B.C., V6T 2A3, Canada

ABSTRACT

Early experience in the implementation and porting of several control programs to the DECwindows/Motif environment in the TRIUMF Central Control System (CCS) is presented. A description is included of the separation of form and function under the Motif windowing system, and how applications were easily implemented using the UIL interface description language and the VUIT interface builder. Several operator interface (OPI) issues and different ways of graphical data representation in a control system are discussed. Applications involving two cyclotron sub-systems, a fourth harmonic RF cavity and the laser control system of an optically pumped H^- polarized ion source, have been adapted to the new environment. The evolution included porting applications under VMS from UIS to XUI and then to Motif.

1. INTRODUCTION

In the world of workstations there have been a number of window managers and graphical systems with which software developers have plied their trade. In the past, systems have mostly been proprietary and quite limited in their platform interoperability. A major change occurred in these areas when personnel from the Massachusetts Institute of Technology (MIT) and Digital Equipment Corporation (DEC) developed the X Window System (commonly referred to as X). Currently "It is widely recognized as a standard for network-based window systems and is supported by a consortium of well-known, highly respected companies...".[1)]

The X window system has been commercially available since first release of MIT X11 in 1986 but until approximately the beginning of 1990 there had not been a widely accepted, non-proprietary (open) X based window manager. Motif is just such X based graphical user interface. It is the product of the Open Software Foundation (OSF) which is a non-profit organization founded in 1988.

The experience with Motif windows within TRIUMF's Controls Group has been gained mostly but not exclusively from two projects, development of the RF booster remote OPI and a port of the optically pumped ion source's laser OPI. These two projects presented different perspectives of using Motif given that one project was a development from scratch and the other was a port from an old window manager and graphics environment known as VAX Workstation Software/User Interface Services (VWS/UIS).

2. THE HISTORY OF GRAPHICS PACKAGES AND WINDOW MANAGERS IN THE CCS

VWS/UIS is an early windowing and graphics system from DEC that runs on the VMS operating system. In 1987 within TRIUMF's Cyclotron Division, a project was started to explore using a workstation as an operator control console. The original plan was to provide local control for the laser sub-system of a polarized H^- ion source. A VAXstation II/GPX running VMS and VWS/UIS was acquired and used successfully.

VWS/UIS supports many of the features that are now commonly expected with windowing systems. From the initial release of VWS/UIS there were some major restrictions. The product is not an open system and thus has the constraints of proprietary packages. The basic omission is the ability to redirect input and output between workstations. Graphics from a VWS workstation can only be displayed locally. The efficiency of generating interfaces was also found to be a problem. In describing VWS DEC states "Its procedural interface, the User Interfaces Services (UIS), provides a high-level programming interface to the graphic subsystem"[2)] but this avoids the issue of efficiency in producing graphics applications. Although a high-level programming interface is provided, the interface elements (graphic objects), are quite low level and it requires relatively a lot of effort to construct higher level components such as data plots. This issue of efficiency would be aided by some type of interactive interface editor but none is provided. VWS/UIS seems to have been recognized by DEC at an early time as being a dead end product and from their in-

volvement in the development of the X Window System, a new package called DECwindows/XUI was made available. The migration from VWS/UIS to DECwindows is quite difficult because the systems are very different. A guide to migration and some tools are available to help the process of moving to the new system but our experience has been that that is it best to re-examine the application in view of the X perspective rather than try and port the older VWS/UIS ideas.

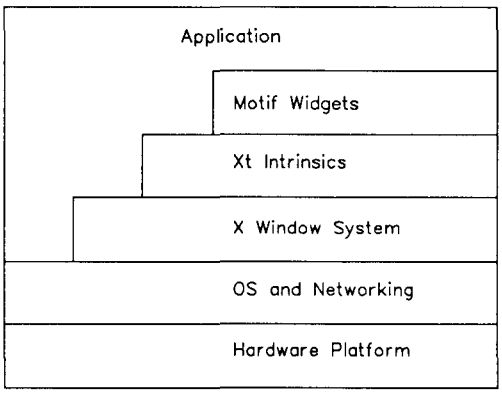


Fig. 1. User Interface Development Model

DECwindows/XUI is a blend of a proprietary window manager and the open X Window System. It addresses some of the open/proprietary issues and takes advantage of the advances of X. One particularly important suppliment to the X Window System is the User Interface Language (UIL). This is a higher level of abstraction than exists in X and provides for the separation of form and function within a graphics application. UIL helps in the topics of efficiency, by allowing a high level of specification of graphics objects (widgets/gadgets), and in organization, by letting you separate the layout and appearance of the application from the functions provided. Again, no interface builder/editor has been included to increase development efficiency. A separate issue is the standardization of the look and feel of applications between various vendors' platforms. The solution to this problem was the need for an open window manager. As mentioned in the Introduction, one answer to this came from OSF with the product Motif. DEC has embraced the Motif window manager with a product called DECwindows/Motif. A migration from DECwindows/XUI to DECwindows/Motif was undertaken on the laser control workstation. Motif is currently available from a number of vendors, for various hardware platforms and operating systems.

The main Motif components are as follows:

1. Style Guide.[3] Describes the principles, philosophy, and components used to build consistent and well-integrated applications.
2. Window Manager. Allows user to manipulate multiple applications on the screen. Plays the principal role of enforcing style guidelines. Includes configurability of appearance and behavior. Provides for consistancy.
3. Interface Toolkit. Provides a library of graphical objects which can be consistently used by all applications.
4. User Interface Language. Allows application developers to describe the presentation characteristics of the interface independently from the application code itself - separate form and function.
5. Documentation. Includes Style Guide, programmer and user documentation.

The migration from DECwindows/XUI to DECwindows/Motif is relatively easy. Typically, procedure and parameter names are straight substitutions and only occasionally are the number of parameters in a call different. Tools are available to make these translations but only some languages are supported, fortran is not one of them. DECwindows/Motif is somewhat faster at drawing graphics than DECwindows/XUI which is somewhat faster than VWS/UIS but in general the hardware platform is a bigger factor in graphics speed than the software being used so although the increased performance is welcome, it is not such a critical issue. A common feature between DECwindows/XUI and Motif is that applications can make use of a multilayer development model (see Fig. 1).

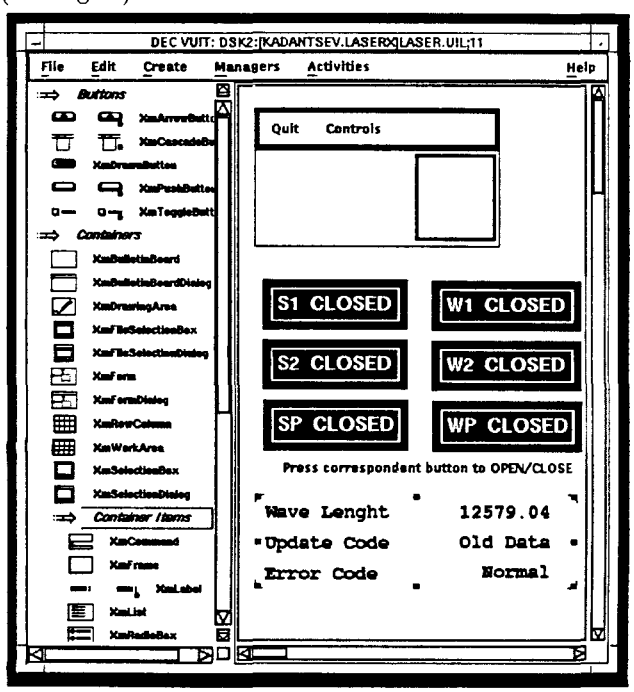


Fig. 2. Using the VUIT Interface Builder

The various levels of abstraction allow developers to accommodate the tradeoffs between performance and

special needs at the low end, and the efficiency of development and maintenance at the high end. In particular, it is worth examining two features at the high end of the abstractions. Concepts within the User Interface Language and the availability of interactive interface builders have been found to be important aids in application development.

UIL is a specification language that describes the characteristics of the graphical interface. This specification describes the graphical objects, known generically as widgets and gadgets, in the interface and specifies the procedures to be called (callbacks) when a change of state occurs as a result of a user action or other event. There is a UIL compiler that translates the UIL source module into a User Interface Description (UID) binary file. When the application executes, the resource manager reads in the UID file and builds the run-time structures necessary to create the user interface. This means that the UID file can be changed to alter the appearance and structure of the interface without altering the executable image and its flow. The result is a separation of form and function. A simple example of this is to have several UID files with text in different languages and only one executable image. The UIL level of abstraction is very useful and has been enhanced by the availability from several sources of interactive interface editors that build UIL. DEC's product which has been used by the TRIUMF Controls Group is called VUIT.

This is a WYSIWYG-style editor that greatly enhances a developers ability to build, test and modify Motif application interfaces. DEC VUIT generates and imports Motif standard UIL which is non-proprietary so the interface's form is portable between environments. Having an interface editor that generates UIL allows the interface to be developed separately as opposed to it being included in the application program. The UIL file which is created contains a static definition of the user interface but at the user's request a simulation of the run-time appearance and behavior of the interface can be obtained using the simulation feature.

Interface builders such as VUIT increase productivity in a number of ways:

1. Laying out an interface with the builder is faster than writing UIL or Xt Intrinsics code and a continual view of the interface is available so the edit/compile/run/adjust cycle is eliminated.
2. Standard UIL and X Window System interfaces mean that applications can be used on a variety of hardware and software platforms without modifications or enhancements.
3. The interface builder checks the legality of resources and relationships and then restricts the user to legal choices, the user does not have to know or look up this information.
4. Portions of existing interfaces can be copied, exported and imported to allow re-use of previous work.
5. Resources are easily configured into the widget definition.
6. Changes made to a single widget in the work area can be propagated to multiple widget definitions throughout an interface via literals and lists.
7. The builder's default parts box can be extended to include the user's own widgets.
8. Extensive, on-line, context-sensitive Help is available.
9. A widget tree browser is available to help manage and navigate the interface and aid in understanding the hierarchy of an unfamiliar interface.

3. LASER APPLICATION

A polarized H^- ion source (I4) has been developed that relies on lasers[4] for optical pumping of a rubidium vapour charge exchange cell. The laser control system continues to evolve from a VAXstation/CAMAC setup using VWS/UIS for local control to a local and remotely operated system using Motif. Figure 3. shows the simplifide block diagram of the I4 laser control system. The local VAXstation connects to CAMAC and can run autonomously and remote X windows servers can connect to that VAXstation via ethernet.

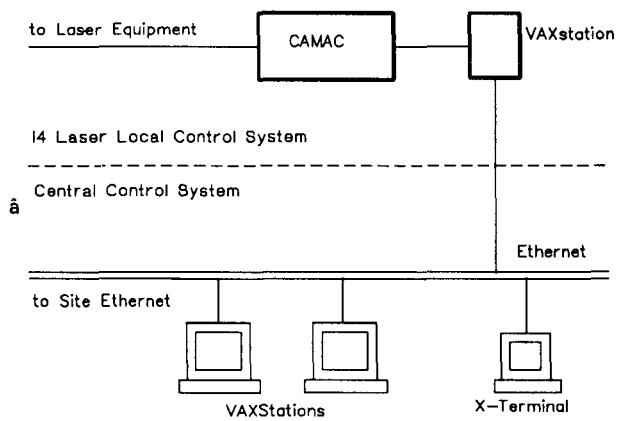


Fig. 3. Simplified Block Diagram of the I4 Laser Remote/Local Control System

3.1. Laser Operator Interface Evolution

Early developments used a VAXstation II/GPX, VWS and UIS. That software is easy to use but low level. It is slow to modify and does not allow remote operation but it allowed the requirements to be fulfilled. The decision was made later to use DECwindows/XUI to provide support for remote operation.

At the end of 1991, DECwindows/Motif superseded DECwindows/XUI and migration was done from XUI to Motif. The early XUI windows had been done at the UIL and Xt Intrinsics level while Motif windows used VUIT. In the near future all VWS/UIS will be phased out and Motif will be used for both local and remote operation.

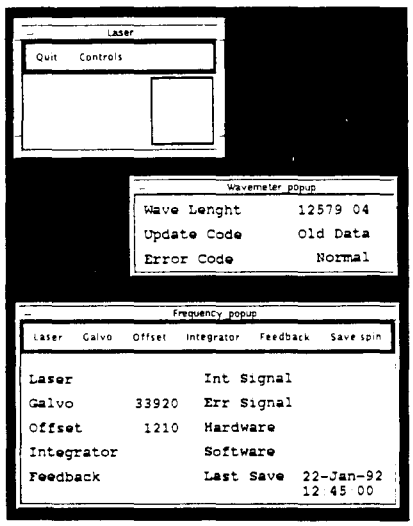


Fig. 4. Parts of the I4 Operator Interface.

3.2. Lessons Learned

When the decision to move from VWS/UIS to Decwindows/XUI was made, a re-evaluation of the old OPI was made by the software developers and the primary user. Several salient points came out of the discussions:

1. Make simplifying the window interface a high priority.
2. Minimize descriptive text and where possible put text on buttons, etc.
3. Remove diagnostic information from the top level interface.
4. Add Help via a pulldown menu.

Running both the VWS/UIS software locally for the end user and simultaneously running X for remote development has allowed the system to be used while the new development was underway. In addition, X allows multiple connections so more than one developer was able to be working on the new interfaces while the old system continued to run. The use of VUIT later on made the prototyping cycle between developer and end user much easier because changing the interface was then simpler than editting UIL code.

4. RF BOOSTER APPLICATION

The 160 KV, 92 MHz booster cavity is amplitude and phase regulated by a VME/PC-AT based local control system.[5] This control system is partitioned into three subsystems: digital, analog, and rf. It also includes automatic power-up sequencing, cavity conditioning and tuning functions. These and other parameters can be controlled locally through soft buttons and knobs in conjunction with a plasma discharge display. Some functions can be controlled remotely from Central Control System using a DECwindows/Motif based OPI.

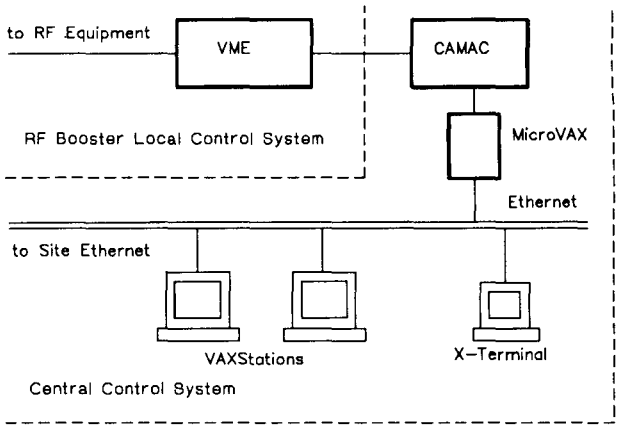


Fig. 5. Simplified Block Diagram of the RF Booster Local/Remote Control System.

Figure 5. shows the simplified block diagram of the RF Booster Control System. VAXes in the CCS communicate with the RF VME crate via a CAMAC-to-VME link.

4.1. RF Booster Operator Interface

The primary goal of the interface design was to create an operator interface that is consistent and easy to use. The main guidelines were as follows:

1. Adopt the operator perspective. Take operator's point of view. Involve operators and RF engineers in the design.
2. Give the operator control. Provide multiple ways for operators to access application functions. Use progressive disclosure.
3. Use real-world metaphors. Allow direct manipulation. Provide rapid response.
4. Keep the interface natural. Provide natural colors and screen elements' positions.
5. Keep the interface consistent. Keep intra-application and inter-application consistency.
6. Communicate application actions to the operator. Provide feedback, anticipate errors, provide warnings.

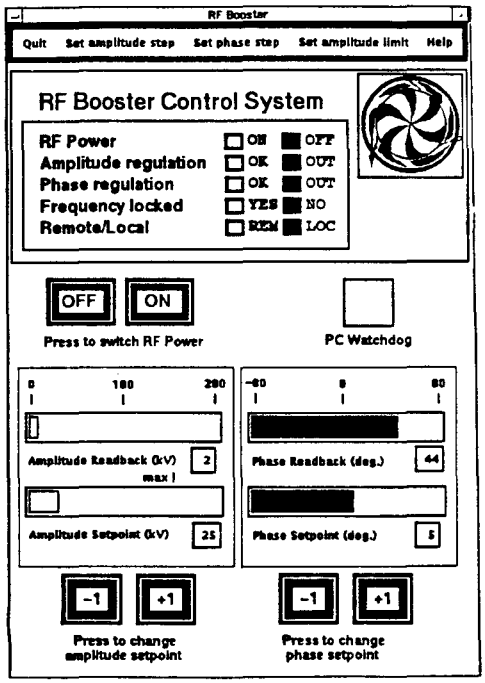


Fig. 6. RF Booster Operator Interface.

4.2. Lessons Learned

During the prototyping, a close liaison was maintained with the RF engineers and the cyclotron operators. A number of interesting requests came out of this work:

1. Push buttons were desired instead of sliders for varying the setpoints.
2. Binary status indicators were setup in groups so that abnormal conditions can be seen at a glance without having to read the specific text.
3. Some indication that the interface is active was included.
4. Setpoints and readbacks were paired as vectors with the same scaling so that abnormalities can be identified without having to read a textual number, just compare the vectors for equal length.

A beneficial point of doing development using an X based system is that most of the work, including the OPI, can be done from the sanctity of the developer's office with their local workstation instead of working in the often unpleasant environment of the laboratory's subsystems. This aspect is another area of increased efficiency.

5. CONCLUSIONS

Our early experience shows that developing an operator interface with a graphical interface builder such as VUIT is more productive than using the toolkit directly. Having some experience in using VUIT and having implemented callback routines, one can build the graphical user interface for a small (2-3 controlled object) application in an hour.

Motif and its environment has some favourable features, among them:

1. Documented standards from many sources.
2. Available from many vendors (it's open).
3. Interface builders available from many sources.
4. It's object oriented.
5. Multilayer implementation (layers of abstraction).
6. Separation of form and function.
7. Interoperability between hardware and software platforms.

Motif's problem areas seem to be the following:

1. Low level software is complex.
2. No specialized widgets for data visualization (graph, histogram, etc.).
3. No suitable means to display help information.
4. Strongly associated to C programming language, so other languages are not a good fit, in particular, the XUI to Motif porting tools do not support applications written in Fortran.

6. REFERENCES

1) McMinds, D.L., **Mastering OSF/Motif Widgets** (Addison-Wesley Publishing Company, Inc., Massachusetts, 1992), p.XXV.
2) **DECwindows/X11 Server for VWS Installation and User's Guide** (Digital Equipment Corporation, 1989), p.1-1.
3) **OSF/Motif Style Guide. Release 1.1** (Prentice Hall, New Jersy, 1991).
4) Levy, C.D.P., Burge, R., Dehaven, R., Mouat, M., Sarkar, S., Schmor, P.W., Wilkinson, N. and Zelenskii, A.N., "The laser system of the optically pumped ion source at TRIUMF," in **Proceedings of the International Workshop on Polarized Ion Sources and Polarized Gas Jets** (KEK Report 90-15, November 1990) pp.180-186.
5) Fong, K., Laverty, M., "RF control system for the TRIUMF booster cavity," presented at the EPAC Conference, Berlin, March 1992.

APPLICATION OF OBJECT ORIENTED TECHNIQUES IN THE TRIUMF BEAM LINE 2C CONTROL SYSTEM

N.A. Wilkinson, E.A. Osberg* and G.A. Ludgate
TRIUMF, 4004 Wesbrook Mall, Vancouver B.C., Canada, V6T 2A3

ABSTRACT

The KAON Factory central control system study employed a uniform approach to requirements analysis, architectural design and programming based on well established object oriented principles. These principles were applied to the successful analysis, design and implementation of the control system for the TRIUMF Beam Line 2C Solid Target Facility. The specification for this control system was created in collaboration with Beam Line 2C equipment management experts and, once the analysis models were validated, an approach was developed for the direct translation of these models into C code. A commercial real time database was central to this translation, as inter-object data and control flows are implemented by channels in the database. This paper focuses on the experience gained in the use of object oriented techniques during the complete analysis–design–implementation cycle of a working control system and on the utility of implementing such a system using a commercial real time database and graphical interface.

1. INTRODUCTION

Beam Line 2C[1] uses a proton beam from the TRIUMF Cyclotron to produce radioisotopes. The Beam Line 2C *Solid Target Facility* (BL2C STF) irradiates solid targets and consists of a water system, a beam energy degrader and various pipes, pumps, valves, sensors and actuators. The water system is a significant component of the STF and is composed of an *elevating* water subsystem, a *cooling* water subsystem, a nine metre water column and associated hardware. The elevating water subsystem is used to insert and remove the solid target, and the cooling water subsystem is used to provide shielding and cooling while the solid target is being irradiated.

When a solid target is to be irradiated, it is mounted on a float and water from the elevating system reservoir is pumped into the water column until it is full. The assembled target and buoyant float are placed in the water column and the elevating water is drained from the water column. As the water drains from the water column, the target/float assembly descends with the water until it reaches the irradiation level, where it is latched in position. Once the column is empty of elevating water, water from the cooling water system is pumped in and continually circulated through the water column while the target is being irradiated.

The water column accepts water from both water subsystems. However, mixing of cooling and elevating water in the water column must be avoided because the cooling water may be radioactive and the volume of water in the two water subsystems exceeds the reservoir capacity of each subsystem. A spill of radioactive cooling water may result if water originating in the reservoir of one subsystem is inadvertently drained from the water column into the reservoir of the other subsystem. One of the responsibilities of the STF control system is to ensure that this does not happen.

2. OBJECT ORIENTED ANALYSIS

The Beam Line 2C control system requirements were specified via an object oriented methodology which was developed during the KAON Factory Project Definition Study.[2)3)] This object oriented methodology uses the notation of the Yourdon methodology with Ward-Mellor extensions[4)] to describe objects according to their static characteristics, their dynamic characteristics and their mutual interactions.

The static characteristics of an object can be identified when the object is not changing as a consequence of interactions with its environment.* These characteristics include the object's name, its attributes, its relationships with other objects and its potential relationships with other objects. Since the extended entity relationship diagram[5)] (EERD) graphically represents entities, their attributes, their relationships and their potential relationships, the EERD is suitable for modelling the static characteristics of objects.

In contrast to static characteristics, the dynamic characteristics of an object can be identified by observing an object's response to stimulation from its environment. Since *behaviour* is defined as *anything an [object] does involving action and response to stimulation*,[6)] it is clear that an object's behaviour is key to any description of its dynamic characteristics. The dynamic response to an external stimulus is *mode* dependent. For instance, a person who is unconscious will respond to a different set of stimuli than the same person would when conscious. The state transition diagram[7)] (STD) can be used to represent this mode dependent behaviour. When an external stimulus occurs, the STD indicates whether or not the object will respond to the stimulus. The STD also indicates *how* the object will respond by identifying what actions will be done and/or what activities will be started or stopped.

A complete description of an object is obtained using the object structure diagram (OSD), which is shown in Figure 1. On the OSD, object behaviour is represented by a behaviour transform, object actions and ac-

*Present address: Superconducting Super Collider Laboratory, 2550 Beckleymeade Ave., Dallas, TX, USA 75237

*i.e. when the object is in *equilibrium*

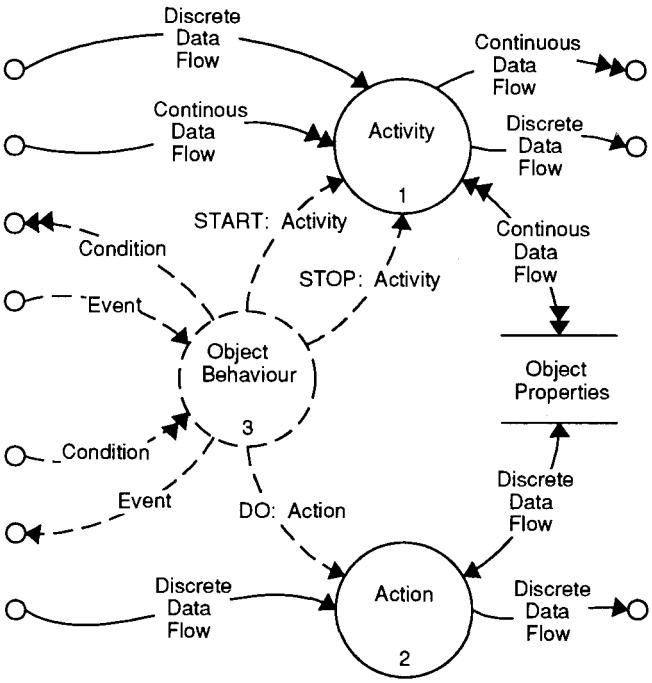


Figure 1. **Sample Object Structure Diagram**

tivities are represented by data transforms, the object's static properties are represented by a data store and information flows are represented by directed arrows. The behaviour transform encapsulates a state transition diagram, and the data store encapsulates the object EERD. OSD information flows are classified according to their persistence over time and their information content. Information flows which persist over time are represented with double arrowheads; information flows which do not persist over time are represented with single arrowheads. An information flow which contains data is classified as a data flow and is represented with a solid line. Events, conditions and activation prompts are represented by dotted lines. Conditions and continuous data flows persist over time. Discrete data flows, events and activation prompts do not persist over time. The small bubbles on Figure 1 indicate information flows which cross the object's boundaries. Whereas data flows, events and conditions may cross object boundaries, activation prompts are always confined within objects. (Activation prompts start or stop object activities and/or activate object actions.)

Object interactions are modelled on an object interaction diagram (OID). On the OID, the representation of inter-object information flows is the same as on the OSD. However, it is on the OID that objects which transform mass and energy (*terminator* objects) are distinguished from objects that transform information (*system* objects). Each terminator object on an OID is represented by a box and each system object is represented by a data transform†. Each terminator object is paired with a system object, and this system object mediates between the terminator object and other system objects.

3. BL2C CONTROLS REQUIREMENTS

The uniform, object oriented methodology described in Section 2 was applied to the requirements for the BL2C STF Control System. As the only CASE tool available on site was DECdesign, a CASE tool from Digital Equipment Corporation, this tool was used to prepare the BL2C STF models. The strict Yourdon–Ward–Mellor methodology implemented by this tool did not accommodate some aspects of the object oriented methodology. For instance, the OID should show both system and terminator objects, but DECdesign only allows terminator objects to appear on the Context Diagram. As a consequence of this inadequacy, only EERDs and STDs were used to describe the BL2C STF objects. The OID and the object OSDs were inferred from the EERDs and STDs.

To determine the BL2C STF controls requirements, BL2C equipment management experts were interviewed in detail. Their responses were analysed to identify BL2C STF objects, their static characteristics and their dynamic characteristics. EERDs and STDs were used to describe these characteristics and were subject to ongoing review and verification by the equipment management personnel.

During object model verification, additional objects were identified. The initial analysis of the BL2C STF produced an EERD which showed only a single, monolithic water system. This view did not adequately describe the two water subsystems and the water column. As the requirements analysis progressed, it was evident that the water system model should reflect this structure. In retrospect, more effort should have been devoted to the analysis of the static characteristics of the STF.

4. THE LOW LEVEL BL2C CONTROLS

The BL2C hardware is accessed via serial and parallel CAMAC systems. Concurrent with the analysis process, a low level interface to the BL2C STF system was created using a VAX/VMS commercial real time database and screen generator obtained from Vista Control Systems (VCS). This interface enabled the BL2C equipment management experts to run the system by direct manipulation of the CAMAC hardware. The VCS real time database is made up of a number of *channels*. Each channel may represent an analogue, binary, or integer value or an array of values. Periodically‡, a program updates the database and the corresponding hardware to ensure that they are consistent with each other. VCS provides an X windows screen generator to allow development of graphical interfaces to database channels. VCS also provides libraries of system calls which can be made from user software (in C or Fortran) for access to

†which explodes to the object's OSD

‡typically at 1 second intervals

database channels. One of the many facilities offered by the VCS system calls is the ability for a user supplied VMS Asynchronous System Trap (AST) handler to be *attached* to a database channel. Once an AST handler is attached to a channel, it will be called whenever the value of the channel changes. Upon being called, the AST handler may be passed a parameter, which is defined by the user when the AST handler is attached to the channel.

5. IMPLEMENTING BL2C OBJECTS

Once the object models were validated, inter-object information flows, including flows from terminator objects, were defined as channels in the real time database. Control flows and conditions were implemented as binary channels. Discrete data flows and continuous data flows were implemented as analogue channels. Inter-object communication is implemented by attaching an AST handler from each object to the relevant channels in the real time database. The AST parameter mentioned in Section 4 is used to identify the corresponding information flow. This mechanism ensures that each object is informed of the arrival of events and discrete data flows or of the change in a condition or a continuous data flow.

STF object behaviour is implemented by direct translation of the object STD into a state–event–action table, which is described by a C structure. The object instance state is maintained in private memory and a transition condition on an STD becomes one or more events associated with database channels. The transition actions associated with each state–event pair are implemented by a C function. Using this translation schema, each BL2C STF object is composed of:

- a private data structure describing the object instance. Included in this data structure is a record of the object instance state, a list of the database channels accessed by the object and their values, and a state–event–action table.
- the VMS Asynchronous System Trap (AST) handler, which serves as a transaction centre for object events and/or conditions, and
- the C functions which implement the object's actions and activities.

When an AST occurs, the associated event is indicated by the AST parameter. The event and the current object instance state serve as an index into the state–event–action table. The AST handler uses this index to look up the new state and the address of the C function which implements the actions associated with the state–event pair. The new state is recorded as the current object instance state and the associated C function is called. The AST handler then checks for transition conditions which may now be valid. If a valid transition condition is found, the AST handler again looks up and

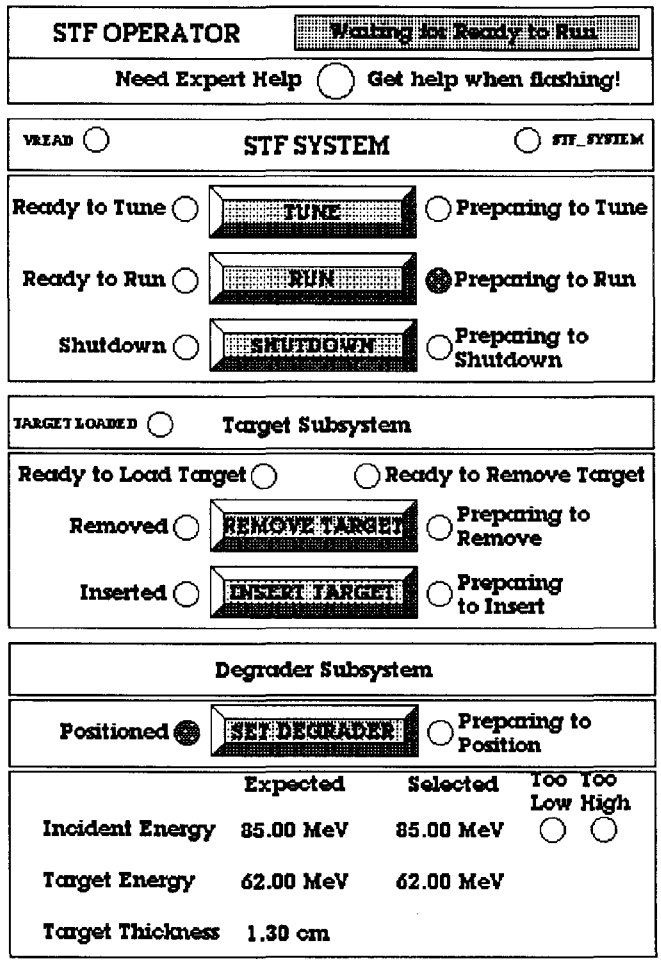


Figure 2. **STF Operator Control Panel**

calls the C function associated with the transition and updates the object instance state. When no more transition conditions are satisfied, the AST handler exits.

The considerable overheads inherent in VAX/VMS process creation precludes creation of separate processes for object methods which are continuously active. Instead, continuous activities are emulated by calling any enabled activities during execution of the AST handler.

6. DISCUSSION

A significant aspect of the analysis was the modelling of the BL2C Solid Target Facility Operator. Modelling human behaviour is challenging because of the large number of modes involved and because of the wide range of behaviour which, typically, must be modelled. However, if the specialist knowledge about how to operate a system can be captured and accurately modelled in an STD, the STD can be implemented. By capturing this information and implementing the operator *as a system object*, the complex sequences and interactions which would require an expert operator can be considerably simplified to the point that a non-expert can safely operate the system. In the case of the BL2C STF opera-

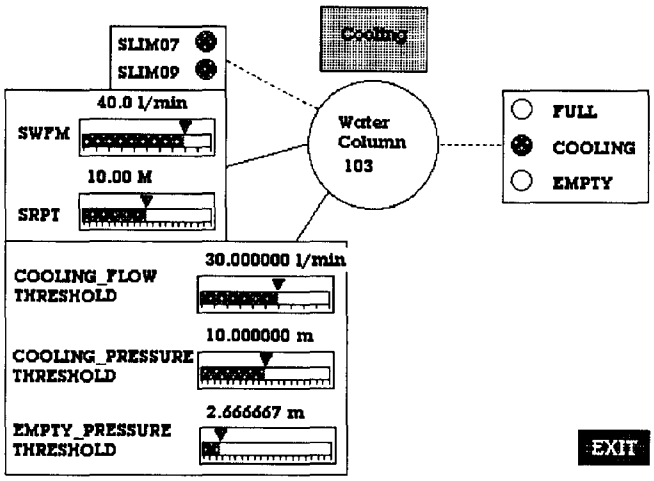


Figure 3. **Water Column Object Test Page**

tor model, the interactions required to operate the BL2C Solid Target Facility were reduced to only six pushbuttons and three numerical inputs, as shown on Figure 2.

The STF operator *object* can recognise dangerous or unsafe situations and, by popping up a dialogue box, inform the operator that an equipment management expert is required. Other dialogue boxes are used to inform the operator of the necessity to manually load or remove a target/float assembly.

The use of real time database channels for information flows between objects enabled concurrent and independent code development and testing during the BL2C implementation phase. Since all inter-object information flows are defined as database channels, each object refers to appropriate database channels for its information flows, rather than to the objects from which the information flows originate. Thus, the coding and testing of objects did not depend on the existence of other objects and could proceed concurrently on an object-by-object basis.

Figure 3 illustrates a test page used for verification of object behaviour during code development. This test page represents a fragment of the BL2C OID. By convention, all input information flows to the water column object are shown on the left hand side of the test page and all output flows are shown on the right hand side. The water column object is represented by the large circle on Figure 3 and the water column state (*Cooling*) is shown in the box above this circle. The small circles labelled *SLIM07* and *SLIM09* are pushbuttons controlling binary channels. These channels can be toggled by clicking the mouse on the corresponding circle. In this manner, events and condition changes may be simulated. The remaining inputs to the object are analogue channels which represent data flows. These may be changed by mouse and/or keyboard input, again simulating an input to the object. The water column object behaviour can be *exercised* by simulating the various combinations of input events, conditions and data flows. As the inputs change, the state changes and output information flows can be observed and verified by direct comparison with the object's STD. This technique facilitated the thorough testing of each object in isolation, rather like component testing of an electronic assembly. Only when an object passed its component test was it installed in the system.

7. CONCLUSIONS

The object oriented analysis of the BL2C STF control system produced a requirements specification which could be directly translated into code. In particular, the information captured by modelling operator behaviour allowed implementation of the complex operator control sequences required to operate the facility as part of the operator *object*. This enables safe operation of the system by non-experts.

The use of the real time database from Vista Control Systems to implement inter-object information flows allowed concurrent and independent implementation of the BL2C STF control system objects. This implementation would have taken a single programmer nine months. Instead, three programmers were able to use the object oriented requirements specification to concurrently implement the STF control system objects in only three months.

8. REFERENCES

1) D R Pearce. "A Facility for Radioisotope Production at TRIUMF with 70/110 Mev Protons". Submitted to: *XIII International Conference on Cyclotrons and their Applications, Vancouver, British Columbia, Canada, 6-10 July 1992.*
2) D A Dohan, G A Ludgate, E A Osberg, S Koscielniak, and C Inwood. "Definition Study of the TRIUMF KAON Factory Control System Project". *Nuclear Instruments and Methods in Physics Research*, A293(1,2):6–11, 1990.
3) C Inwood, G A Ludgate, D A Dohan, E A Osberg, and S Koscielniak. "Domain-driven Specification Techniques Simplify the Analysis of Requirements for the KAON Factory Central Control System". *Nuclear Instruments and Methods in Physics Research*, A293(1,2):390–393, 1990.
4) Paul T. Ward and Stephen J. Mellor. *Structured Development for Real-Time Systems*, volume 1. Yourdon Press, 1985.
5) E A Osberg, G A Ludgate, S Koscielniak, and D A Dohan. "Dynamic Object Modelling as Applied to the KAON Control System". *Nuclear Instruments and Methods in Physics Research*, A293(1,2):394–401, 1990.
6) Frederick C. Mish, editor. *Webster's Ninth New Collegiate Dictionary.* Merriam-Webster, Springfield, Mass, USA, 1988.
7) Paul T. Ward and Stephen J. Mellor. *Structured Development for Real-Time Systems*, volume 1, chapter 7, pages 64–80. Yourdon Press, 1985.

THE TR30 CONTROL SYSTEM - A CASE FOR OFF-THE-SHELF SOFTWARE

R. Keitel, D. J. Dale, and B. F. Milton
TRIUMF, 4004 Wesbrook Mall, Vancouver, B.C.
V6T 2A3, Canada

ABSTRACT

The TR30 is a 30 MeV high intensity H^- cyclotron for medical isotope production. The control system for this machine was implemented using commercial software and hardware wherever possible. An Allen Bradley PLC programmed in ladder logic was used as the control processor. The console supervisory system consisted of two IBM PCs running the Allen Bradley ControlView software. With this approach, a very low software to hardware cost ratio of 1:2 was achieved with no penalty in functionality.

1. INTRODUCTION

The TR30 is a compact cyclotron for production of radionuclides for medical use. The first machine of this type was designed and built on the TRIUMF site under a technology transfer agreement between TRIUMF and Ebco Technologies Inc. of Vancouver, B.C. The machine accelerates H^- ions up to an energy of 30 MeV. Two high intensity proton beams – up to 350 μA total current – of different energies can be extracted simultaneously.

2. REQUIREMENTS

2.1. Control System Scope

The TR30 control system looks after the cyclotron from the ion source to the ends of the beam lines. This includes all aspects of device and machine protection. Independent systems are responsible for the control of the RF feed-back system, the target stations, site services, and the enforcement of personnel safety, especially with respect to high voltage and radiation. These systems are beyond the scope of the control system and this paper.

2.2. Required Features

The control system has to provide operator access for control and diagnostics to all elements of the TR30 vacuum system, to the power supplies of the injection line, to the main magnet, to the two beam lines, to extraction and diagnostic probes, and to all beam diagnostic elements. In addition, control and status information must be exchanged with up to six target stations, the RF feed-back control system, and the radiation safety system. The control system uses 700 digital and 220 analog control channels. All device protection is carried out by the control system thus avoiding hard-wired interlocks. With commercial applications in mind, emphasis was placed on reliability and ease of operation and maintenance.

3. DESIGN AND IMPLEMENTATION

Over the past years, with the increased performance of personal computers, a wide variety of commercial products for process monitoring and control has become available.[1)] For various reasons these systems have not been widely used for accelerator control, although the progress in technology makes them more and more attractive.

In the TR30 project, it was decided at an early stage to base the control system on one of these commercially available software/hardware solutions. Expected benefits from this approach were

a) greatly reduced software costs by being able to concentrate on application programming and by avoiding system programming tasks,

b) the industrial ruggedness and quality of the final product, and

c) simplification of documentation and maintenance.

It was felt that these benefits would by far outweigh the limitations of a general-use software package over a tailor-made in-house solution, provided the commercial system was "open", i.e. allowed the addition of user-written code to add missing functionality.

After evaluation of a variety of commercial systems, the TR30 control system was based on an Allen Bradley solution: a programmable logic controller (PLC) and the ControlView * console software package.

*ControlView is a trademark of Allen Bradley Corp.

3.1. Concept

The control system uses three networked processors in a two-layer architecture, a *device control layer* at the lower level and a *supervisory layer* at the higher level.

The device control layer implements the functions for basic device control such as analog and digital device readout, device switching, setpoint change and device interlocks. It provides fast beam trips and vacuum trips, some sequencing and fast closed-loop control, as well as the interface to the safety system, target stations, etc. When this layer is shut down, e.g. for software or hardware servicing, all devices are switched to a safe state. This is necessary because all interlocks are provided by this layer. In general, valves are closed, all other devices are switched off. Exceptions are made for the gate valves to the probe housings and for the five cryo-pumps which do not change state if the control system is brought down. This prevents damage to the probes and maintains the high vacuum in the cyclotron tank and in the beam lines during control system service.

The supervisory layer provides the operator interface through graphics screens a pointing device, and and alphanumeric keyboard. Higher level functions such as alarming, data logging, trend displays, slow closed-loop control and some automation are also provided in this layer.

3.2. Hardware

The device control layer hardware consists of one PLC 5/25 processor, four crates of 1771 series I/O modules at ground potential, and one I/O crate at the ion source potential of approximately 25 kV. The ion source crate is connected to the rest of the system by a fibre-optics link. There is no redundancy in this layer.

The supervisory layer consists of two IBM compatible PCs (80386), each equipped with 4 MBytes of memory and a 60 MByte hard disk drive. The PCs are located in the operator console. Each drives one colour screen, one monochrome screen, and a printer. Control of the TR30 is possible using only one of the console computers although there is some loss of convenience.

The two layers are networked with the Allen Bradley Data Highway Plus, a serial token-passing bus with a speed of 57.6 kbits/sec. Figure 1 shows a schematic diagram of the hardware setup.

3.3. Software

Reading and writing of the I/O modules and the communication between the PLC and the console processors are all part of the PLC system firmware. The PLC application program for the TR30 device control layer was developed using the Ladder Logistics † package of the AI Series software from ICOM Incorporated. The application is developed on a PC, e.g. one of the

†Ladder Logistics is a trademark of ICOM Inc.

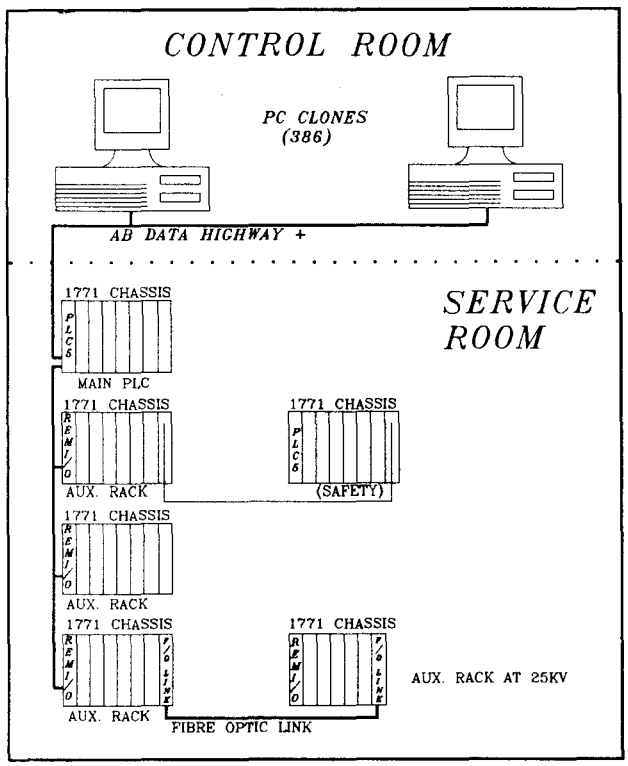


Figure 1. Overview of the Control System Hardware Configuration

console PCs, and downloaded into the PLC5 user memory where it can also be modified on-line. The program is "written" in *ladder logic*, a programming paradigm which is borrowed from drawing relay logic diagrams. This method of programming is highly intuitive for controls engineers and technicians. As a result, software and hardware implementation are closely coupled. The programmer draws the diagrams using the interactive ladder editor of the Ladder Logistics software. The assembling of the diagrams into machine code is taken care of by the programming software. An short example of ladder logic code as it looks to the programmer in the ladder editor is shown in Fig. 2.

The supervisory control layer uses the ControlView software package from Allen Bradley. ControlView consists of a core, a proprietary real-time operating system for the PC and optional application modules. The core maintains a current value data base of user-designated PLC variables ("tags"). Raw values are periodically scanned, i.e. read from the PLC, and scaled according to information which the programmer provides when configuring the data base. The data base and the update rates for different scan classes are configured by filling in forms. The application modules are set up in a similar way. No programming skills are required. The TR30 system uses the ControlView modules for alarming, data logging, trending, derived tags, and event detection.

A special application module is the ControlView

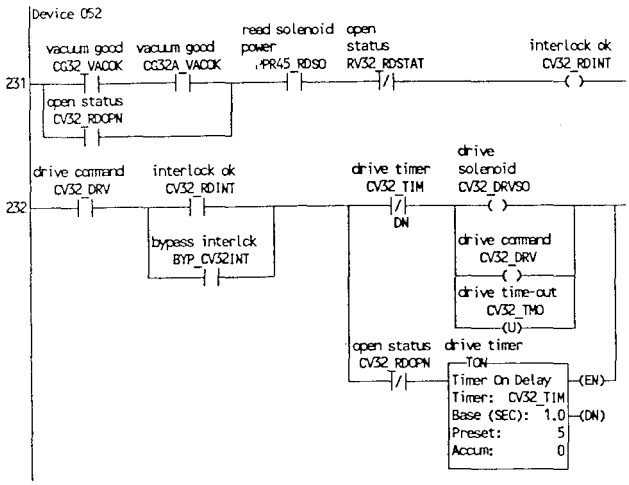


Figure 2. Section of ladder logic code. A processor bit is represented as a relay with an arbitrary number of contacts.

graphics editor which is used to design the graphics pages for the operator interface. One can assign attributes like colour, visibility etc. to the objects on a graphics page. These attributes may depend on and change with tag values in the current value data base. Lists of function key commands can also be attached to graphics objects. Again, these assignments are done interactively. Graphics pages can be modified while the control system is operating.

ControlView is an open system due to the C-Toolkit library option which allows the user to develop custom tasks and easily integrate them into the system.

3.4. Operator Interface

The operator interfaces to the ControlView system using a pointing device such as mouse, trackball or touchscreen, and the PC keyboard.

For the TR30, a mouse was chosen as the pointing device and the user interface was designed so that the operator runs the machine essentially from pictures and menus. This can also be done by using function keys and command line input from the keyboard only. Using the ControlView tools, a set of sub-system pages and device control panels was developed which are accessed through a customized menu system. A sub-system page, e.g. for the vacuum system or a beam line, shows a graphical outline of the sub-system. The operator selects and operates devices with the mouse or function keys. In addition, complete information for each device, including the state of all its interlocks, can be obtained by calling up the device's control panel. Figure 3 shows a hard copy of a beam line page.

3.5. Implementation Experience

Only one of us (DJD) had previous experience with PLC programming. The ControlView package was a newly released product. In both cases the learning curve was very short. Most of the desired functionality was easily achieved with the features available in the ladder logic and ControlView. Custom C code was written to accommodate the non-linear scaling of the vacuum gauges, to generate customizable alphanumeric display pages on the monochrome screens, to provide an on-line diagnostic probe scan, and to develop a command procedure processor with more functionality than provided by the ControlView macro processor.

For a new product, ControlView proved to be quite complete, mature and bug-free. Missed were tools for more tightly integrating the development of the ladder logic and the ControlView application as well as tools for monitoring and optimizing the use of ControlView resources.

As the TR30 was the first machine of its type, the control system implementation was done in two stages: At the start of commissioning, an open loop system was provided. During commissioning and as operating experience was gained on the machine, more operator support was added such as closed loops in the PLC, event driven adjustments in ControlView, and command procedures for routine operational tasks.

The Ladder Logistics package contains extensive on-line diagnostics features. The actual state of all inputs and outputs and internal program variables as well as the activity of the ladder rungs can be inspected on-line in real-time. This proved invaluable during commissioning of the system.

In ControlView, fixing application bugs and upgrading the system was very easy as it mainly involved interactive changes of screens or configuration form entries. Due to the layered system architecture and the redundancy at the console level, there was very little downtime due to control system work. This was especially important as all interlocks were provided through the device control layer.

Of course there are limits in any off-the-shelf system. On the hardware side, only DACs with 12-bit resolution were available. Therefore higher resolution interfaces to the power supplies for the cyclotron magnet and four beam line dipole magnets had to be developed. The control circuitry of a few other power supplies had to be modified to match the Allen Bradley signal levels. On the software side, the C-Toolkit allowed straightforward work-arounds in the few cases where we encountered difficulties, such as inadequacies in the ControlView expression syntax and in the macro processor. The low Data Highway speed and database update rates created problems for diagnostic probe scans which were solved by data buffering in PLC memory and slightly delayed readout carried out by a C-Toolkit task.

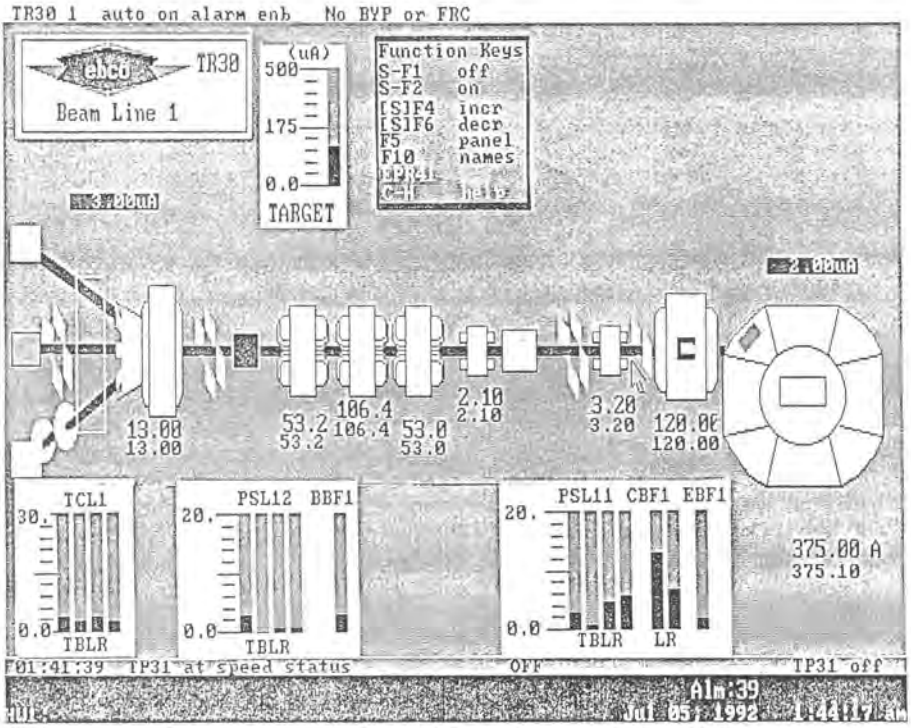


Figure 3. Example of a beam line sub-section page

Although the restriction to EGA resolution in the graphics displays is of mainly aestetic importance, it should be corrected in a future ControlView release.

4. Summary

In summary, the decision to build the TR30 control system based on a PLC and commercial software proved to be very successful. The control system was built on schedule and on budget. An unusually low ratio between overall software and hardware cost was achieved without loss of functionality. This was mainly due to the high "entry level" which both the ControlView and Ladder Logistics packages provide for the system designer. Since the initial commissioning of the system several functionality upgrades have increased the amount spent on software and pushed the ratio from 1:3 closer to 1:2. Figure 4 shows a break-down of the control system costs.

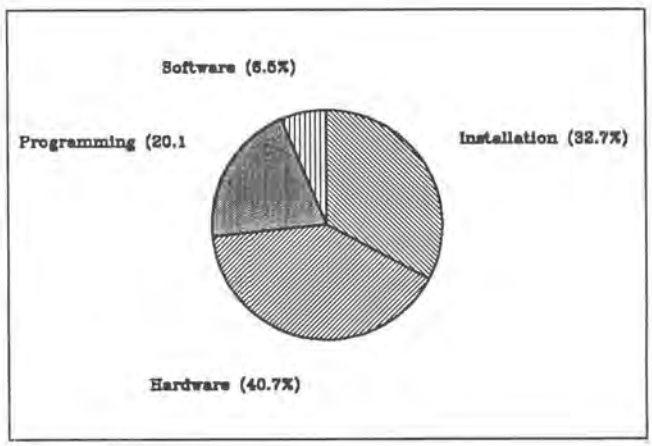


Figure 4. Control system cost breakdown

5. Acknowledgements

Although this paper emphasizes software aspects, the authors would like to acknowledge the essential contributions of T. Ewert and D. Harrison to the success of this project on the hardware side. TRIUMF is operated under a grant from the National Research Council of Canada.

6. REFERENCES

1) "Process Monitoring and Control Software Listings", Control Engineering, **Vol.39 No.3**, 16 (1992).

FORMAL SPECIFICATIONS FOR A CYCLOTRON CONTROL SYSTEM

Jonathan Jacky and Ruedi Risler

Department of Radiation Oncology,
University of Washington,
Seattle, WA 98195, USA

ABSTRACT

We are preparing a comprehensive specification for the computer control system of a cyclotron and treatment facility that provides particle beams for cancer treatments with fast neutrons, production of medical isotopes, and physics experiments. The informal (prose) specification describes the control system as thoroughly as is practical using standard technical English, supplemented by tables, diagrams, and some algebraic equations. We are supplementing the prose specification with a formal (mathematical) specification. Potential advantages of formal specifications are discussed, and experiences writing and using formal specifications are described.

1. INTRODUCTION

The Clinical Neutron Therapy System (CNTS) at the University of Washington is a cyclotron and treatment facility that provides particle beams for cancer treatments with fast neutrons, production of medical isotopes, and physics experiments. The facility was installed in 1984, and includes a computer control system provided by the cyclotron vendor.[1] The University is now developing a new, successor control system. This development project is motivated by requirements to make the system easier and quicker to use, easier to maintain, and able to accomodate future hardware and software modifications.[2]

We are attempting to achieve high reliability and safety by applying rigorous software development and quality assurance practices. Modern recommendations for the development of safety-critical computer-based systems[3,4] emphasize the need for an explicit statement of functional and safety requirements, and a development process that can be shown to produce an implementation that meets the requirements. A central idea is that developers should provide a functional specification that allows system outputs to be predicted if system inputs are described.

We determined that our first step in this project should be the production of a comprehensive specification for the new control system, to serve as an authoritative and complete guide for software development, testing, and instruction of facility users.

2. THE INFORMAL SPECIFICATION

We first prepared an informal (prose) specification, expressed in standard technical English, supplemented by tables, diagrams, and some algebraic equations.

The informal specification consists of four parts. Part I is an overview of the system that describes the facility, the hardware organization of controls, and introduces much of the vocabulary used in subsequent parts. It comprises almost 100 pages of single-spaced text. Part II is a detailed specification of operations which users perform at video terminals and control consoles. It comprises over 250 pages, including many illustrations of displays. Part III will be a detailed specification of internal operations involving the cyclotron and therapy apparatus itself, which are only indirectly visible to users, and will comprise about 100 pages. Part IV will be a largely tabular presentation of numerical operating parameters whose values can be changed independently of the rest of the specification. We plan to maintain these tables in a relational database.

Parts I and II have been prepared for distribution outside our department as technical reports[5,6] and we anticipate releasing the other parts as they are completed in coming months.

3. FORMAL SPECIFICATIONS

The prose specification is organized to help facility users read and understand it, so they can offer meaningful reviews. However, this organization is not necessarily the best for purposes of programming and analysis. An alternative is to make greater use of mathematical nota-

tions, annotated sparingly with English. Such specifications are called *formal* specifications.

Formal specifications are distantly related to popular design notations based on data flow diagrams, which have been applied to acclerators.[7] We are investigating notations that provide more mathematical rigor, in the sense that they allow more properties to be inferred or calculated.

There are potential advantages to developing programs from formal specifications. They can be more precise and compact than English specifications, and can be automatically checked for certain kinds of errors. They can be used to prove or calculate whether the specificied behavior is consistent with certain intended properties, such as safety. Formal specifications can support systematic software development methods where every development step can be justified and checked.

4. A FORMAL CASE STUDY

We have prepared a formal specification for computations that calculate control system state variables from input/output device register contents (and vice-versa). Specified behaviors include scaling and offsetting analog quantities to match data converters (ADC's and DAC's), adjusting analog quantities according to calibration curves, encoding groups of digital signals as discrete variables, and detection of errors (where clients invoke operations with invalid parameters) and faults (where input/output devices report inconsistent data).

Our specification is motivated by our facility but is quite generic and should be widely applicable. It is parameterized so that an implementation can be adapted to different control systems by providing tables of configuration data, rather than changing executable code. The specification is not merely descriptive, but is also used in the formal development of a detailed design.

We used a formal notation called Z[8,9] (pronounced *zed*) for this work because it is a good match to our chosen table-driven strategy. Some of our preliminary experiments with Z have appeared,[10] and we have prepared a detailed report of the present work.[11] Excerpts appear in the following subsections. This brief report does not permit much explanation, so these excerpts will not be meaningful to readers unfamiliar with Z; they are only included to show what a formal specification looks like.

4.1. The System Configuration and the System State

At the lowest level, input/output is accomplished by data converter hardware. Data converters accomodate *signals* connected to the controlled process. Signals may be digital or analog, and carry information which is input or output with respect to the computer.

Data converters contain *registers*. Every register is identified by a unique *address*, and holds *contents* that encode the value of one signal in a form intelligible to the computer. In any particular configuration, a fixed set of addresses is populated with registers.

We distinguish register contents from control program *state variables*. While registers hold contents, *variables* have *values*.

Expressed in Z, we have:

$$[ADDR, CONTENTS, VAR, VALUE]$$

$$\begin{array}{|l} ioreg : \mathbb{P}\ ADDR \\ iovar : \mathbb{P}\ VAR \\ map : VAR \leftrightarrow ADDR \\ \hline map(\!|iovar|\!) \subseteq ioreg \end{array}$$

Sys

$$\begin{array}{|l} register : ADDR \pfun CONTENTS \\ variable : VAR \pfun VALUE \\ \hline \mathrm{dom}\ register = ioreg \\ \mathrm{dom}\ variable \cap \mathrm{dom}\ map \subseteq iovar \end{array}$$

The sets *ioreg* and *iovar*, and the relation *map* model some of the tables that describe the configuration. We have actually specified a whole family of control systems, where each assignment of values to *ioreg*, *iovar* and *map* determines a particular control system that belongs to the family.

4.2. Translating between Registers and State Variables

The function *encode* determines the translation between variable values and register contents. The operation *Translate* uses *encode* to calculate variable values from register contents (or vice versa):

$$\begin{array}{|l} encode : \\ (ADDR \pfun CONTENTS) \pfun VAR \pfun VALUE \end{array}$$

Translate

$$\begin{array}{|l} \Delta Sys \\ vars? : \mathbb{P}\ VAR \\ \hline variable' = variable \oplus vars? \lhd encode\ register' \end{array}$$

This schema can be specialized in each direction.

$$Encode \mathrel{\widehat=} [\ Translate \mid register' = register\ ]$$

$$Decode \mathrel{\widehat=} [\ Translate \mid variable' = variable\ ]$$

4.3. Formal Development

We have not yet shown how the all-important function *encode* is constructed. In the full report[11] we construct the function *encode* from configuration tables, calibration formulas and other available information. A series of representations for *encode* are presented, where each successive version provides more detail. We find that *encode* can be expressed:

$$encode\ register\ v = translate\_seq\ (class\ v)\ (addr\_seq\ v \fatsemi register)$$

This suggests an efficient implementation in an imperative programming language, as explained in the full report.[11]

4.4. Non-constructive Definitions

Formal specifications bear a superficial resemblance to executable programs, but there is an important difference: programs must be constructive, but specifications can be *non-constructive*. This is an advantage because non-constructive definitions can be concise and expressive. For example, they make it easy to define inverse operations, as in the definition of the *Decode* operation that translates state variable values to register contents (section 4.2). However, at some point it is necessary to show how items so defined can be implemented; this requires converting them to constructive form, as demontrated in the full report.[11]

4.5. Handling Errors and Faults

In most computing applications, it is expected that programs should detect and report errors (where clients invoke operations with invalid parameters), but it is left to the users to deal with faults (where operations fail despite valid invocation by the client). Control systems differ from other computing applications in part because they are expected to handle some faults.

An advantage of a formal specification is that it isn't necessary to rely solely on inspiration to discover potential errors and faults; some of them can be calculated. The *precondition* of an operation describes the set of initial states for which a final state is defined. States which do not satisfy the precondition of an operation are usually those that designers consider erroneous or faulty. It is poor practice to implement operations that admit such states, since their response to errors and faults is undefined. For our operation *Encode*, the precondition is:

$$PreEncode \mathrel{\widehat=} \exists\, Sys' \bullet Encode$$

The expression on the right can be expanded:

PreEncode

$$Sys$$
$$vars? : \mathbb{P}\ VAR$$
$$vars? \subseteq iovar$$
$$\exists\, reg : \mathbb{P}\ register \bullet RegValid$$

The first line in the predicate deals with the input parameter *vars?*; failure to satisfy this predicate is an error. The second deals with the contents of *register*; failure to satisfy this predicate is a fault.

We must extend the specification to deal with such conditions. When an error or fault is detected, it should be reported, but the system state must not otherwise change, for example:

BadReg

$$\Xi Sys$$
$$vars? : \mathbb{P}\ VAR$$
$$status : STATUS$$
$$status = badreg$$
$$\neg\, (\exists\, reg : \mathbb{P}\ register \bullet RegValid)$$

A similar schema *BadVar* describes the case where the input variables are not valid. Then the *Encode* operation can be extended:

$$T\_Encode \mathrel{\widehat=} (Encode \wedge Success) \vee BadVar \vee BadReg$$

These three outcomes exhaust all possibilities. Therefore, the operation *T_Encode* is defined in every possible state.

4.6. Checking the Development

An important advantage of formal development is that each step can be calculated, inferred or otherwise formally justified, and then checked. This ability to check each intermediate development step, rather than having to wait until an executable program can be produced and tested, distinguishes formal development from more intuitive software development methods.

In addition to checking each step in turn, the entire development can be checked against the original requirements. For example, we would like to claim,

> "All possible inputs will be handled properly"

but this statement is much too vague to relate to our formal specification. Trying again, we say,

> "If the configuration tables are accurate, then valid input signals will be translated to the proper state variable values, and invalid input signals will be detected."

Here the features of the formal specification begin to emerge, but we need still more detail. Trying once again, we begin,

> "If a group of signals are entered into the routing table, and the addresses to which the signals are connected are populated, and the signals are found in the tables to be members of recognized classes, and the value of each signal falls within the permitted range for its class membership, and ..."

Rather than press on in this vein, we resort to formal notation. We are trying to state a hypotheses about signals:

$$
\begin{array}{|l}
\textit{SigValid} \\
\hline
sigs : \mathbb{P}\ SIGNAL \\
scontents : SIGNAL \pfun CONTENTS \\
\hline
sigs = \mathrm{dom}\ scontents \\
routing(\!|sigs|\!) \subseteq ioreg \\
member(\!|sigs|\!) \subseteq \mathrm{ran}\ classdef \\
\exists\ RegValid \bullet \\
\quad sigs = signal(\!|vars?|\!) \land \\
\quad scontents = \{\ a : \mathrm{dom}\ reg \bullet routing^{\sim} a \mapsto reg\ a\ \} \\
\hline
\end{array}
$$

Other parts of the hypothesis can be formalized in the same way. A formal conjecture which expresses the requirement, "All valid signals will be handled properly", is:

$$
\begin{array}{l}
SigValid \land SigMatchVar \land Encode \vdash \\
\forall\ v : vars? \bullet \exists\ c : CLASS \bullet c = class\ v \land \\
\quad variable'\ v = \\
\quad\quad translate\ c\ \{s : sigs \bullet member\ s \mapsto scontents\ s\}
\end{array}
$$

Proving this conjecture could check for errors in the development, and provide confidence that the formal specification expresses the intended requirements.

5. FUTURE WORK

The first formally-specified subsystem scheduled for implementation is the controller for the leaf collimator that is used to shape the therapeutic neutron beam.[2] The program will be written in a Pascal dialect[12] and will run on a Digital Equipment Corporation MicroVAX II computer.

6. REFERENCES

1) Ruedi Risler, Jüri Eenmaa, Jonathan P. Jacky, Ira J. Kalet, Peter Wootton, and S. Lindbaeck. Installation of the cyclotron based clinical neutron therapy system in Seattle. In *Proceedings of the Tenth International Conference on Cyclotrons and their Applications*, pages 428 – 430, IEEE, East Lansing, Michigan, May 1984.
2) R. Risler, P. Wootton, F. Ziai, J. Jacky, S. Brossard, and I. Kalet. Continued operation of the Seattle clinical cyclotron facility. (This proceedings).
3) Great Britain Health and Safety Executive. *Programmable Electronic Systems in Safety Related Applications. Volume 1: An Introductory Guide. Volume 2: General Technical Guidelines.* Her Majesty's Stationery Office, London, 1987.
4) Nancy G. Leveson. Software safety: what, why and how. *ACM Computing Surveys*, 18(2):125–163, June 1986.
5) Jonathan Jacky, Ruedi Risler, Ira Kalet, and Peter Wootton. *Clinical Neutron Therapy System, Control System Specification, Part I: System Overview and Hardware Organization.* Technical Report 90-12-01, Radiation Oncology Department, University of Washington, Seattle, WA, December 1990.
6) Jonathan Jacky, Ruedi Risler, Ira Kalet, Peter Wootton, and Stan Brossard. *Clinical Neutron Therapy System, Control System Specification, Part II: User Operations.* Technical Report 92-05-01, Radiation Oncology Department, University of Washington, Seattle, WA, May 1992.
7) G. A. Ludgate, B. Haley, L. Lee, and Y. N. Miles. The use of structured analysis and design in the engineering of the TRIUMF data acquisition and analysis system. *IEEE Transactions on Nuclear Science*, NS34(1):157 – 161, 1987.
8) J. M. Spivey. *The Z Notation: A Reference Manual.* Prentice-Hall, New York, 1989.
9) Ben Potter, Jane Sinclair, and David Till. *An Introduction to Formal Specification and Z.* Prentice Hall International (UK) Ltd, Hemel Hempstead, Hertfordshire, 1991.
10) Jonathan Jacky. Formal specifications for a clinical cyclotron control system. In Mark Moriconi, editor, *Proceedings of the ACM SIGSOFT International Workshop on Formal Methods in Software Development*, pages 45 – 54, Napa, California, USA, May 9 – 11 1990. (also in *ACM Software Engineering Notes*, 15(4), Sept. 1990).
11) Jonathan Jacky. *Formal Specification and Development of Control System Input/Output.* Technical Report 92-05-02, Radiation Oncology Department, University of Washington, Seattle, WA, May 1992.
12) Digital Equipment Corporation. *VAXELN Technical Summary.* Digital Equipment Corporation, Maynard, MA, 1984.

THE SUPERCONDUCTING SEPARATED–ORBIT CYCLOTRON TRITRON

U. Trinks

Physik Department, Technische Universität München,
D–8046 Garching, Germany

ABSTRACT

The Tritron will be a separated–orbit cyclotron with superconducting channel magnets and superconducting accelerating cavities. All magnets and cavities are manufactured, the assemblage is going on. The Tritron design is expected to overcome the focusing problems and current limitations of other types of cyclotrons. It seems to be a promising candidate for providing high cw–currents of protons and heavy ions up to specific energies of $\simeq$ 600 MeV/u at rather low cost.

1. THE TRITRON DESIGN

The Tritron project is a study of a new type of cyclotron, a superconducting separated-orbit cyclotron with a MP-tandem as injector .[1,2] A separated–orbit cyclotron was proposed first by F.M. Russell .[3,4] The Tritron shall increase the ion energies by a factor of 5. The beam is guided by 238 superferric, independently adjustable channel magnets with alternating gradients along a spiral orbit with almost 20 turns. The spiral consists of 30°–arcs and drift lengths between them. The turn separation outside the channel magnets is $\Delta r = 4$ cm. Radially neighbouring channels are joined into 12 flat sectors (see Fig.1). In each second of the intermediate free sectors a superconducting rf–cavity with fixed frequency $\nu_{rf} = 170$ MHz provides for the rather strong accelerating voltage corresponding to the turn separation. In the remaining intermediate sectors beam position probes for both transverse coordinates are installed to control the current setting of the channel magnets, when centering the beam along the spiral orbit.

The specific feature of the Tritron design is the strong transversal and longitudinal focusing .[5,6] The betatron oscillation numbers can be chosen far from the stability limits, resonances can be avoided. Longitudinal focusing is caused by the fact, that the magnetic field will

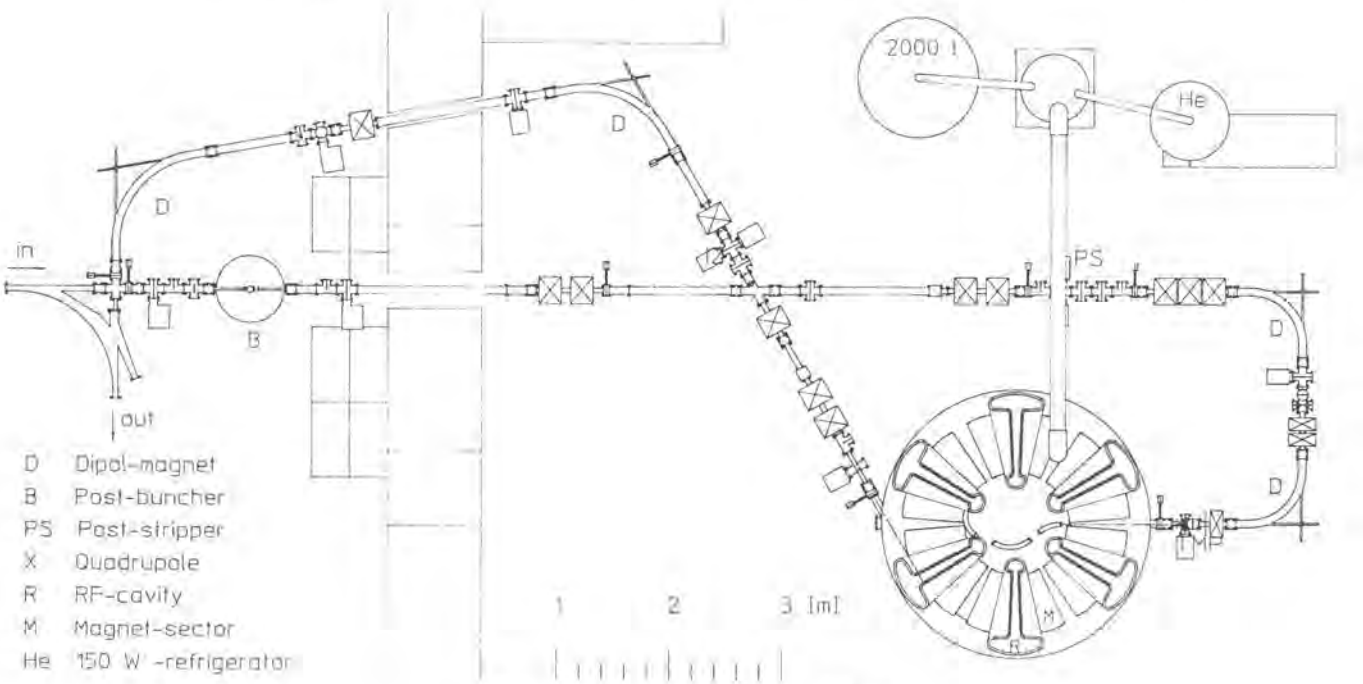


Fig. 1. Plan view of the Tritron hall.

not be isochronous for non–central particles. The relative variation of the revolution frequency $\Delta\nu/\nu_o$ is given by the variation of the velocity and of the mean orbit radius r (turn length over 2π):

$$\frac{\Delta\nu}{\nu_o} = \frac{\Delta v}{v_o} - \frac{\Delta r}{r} \qquad (1)$$

$\nu_o = \nu_{rf}/h$ with the harmonic number h is a subharmonic of the fixed rf–frequency. v_o is the velocity of the isochronous particle running along the orbit, that is with $\Delta r = 0$ and $\Delta v = 0$. If the field levels of all channel magnets are adjusted properly, the central particle in the bunch will move with $\Delta r = 0$. However the energy of the central particle may differ from the isocronous energy, so that $\Delta v \neq 0$. Then the resulting frequency deviation $\Delta\nu$ will lead to stationary coherent energy and phase oscillations of the whole bunch with respect to a particle moving isochronously, if the slope of the accelerating voltage as function of the phase is positive. The oscillation numbers are approximately $Q_{coh} \simeq 0.3$ per turn. Noncentral particles with $\Delta r \neq 0$ will execute incoherent synchrotron oscillations with respect to the centre of the bunch. Due to the difference concerning the Δr – term in Eq.1 the oscillation numbers Q_{inc} are about $0.7 \cdot Q_{coh}$.

The beam centering procedure starts at the first position probe. Here the beam is assumed to be centered already, however with a horizontal angle error of the beam axis, which will not be measured by the probes. Then the currents in both succeeding channel magnets will be changed equally, until the beam is centered at the next position probe, too. If the first channel is radially focusing (positive gradient) and the second radially defocusing (negative gradient), then the angle error will be reduced automatically, as shown in Fig.2.

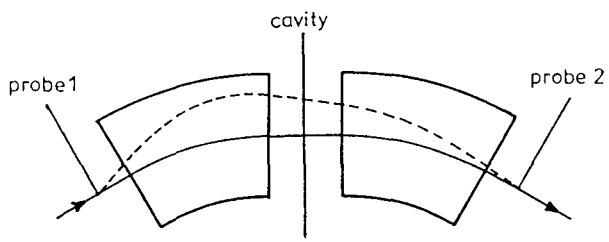


Fig. 2. Centering the beam at probe 2 causes a reduction of angle error, if the first magnet has radially increasing and the second decreasing field.

The injection is made simply by three superconducting channel magnets. The third one imposes the bending limit for the Tritron, because it has the smallest bending radius with $\varrho_{inj} = 30$ cm, compared to $\varrho_1 = 43$ cm for the channel magnets on the first turn. For extraction no element is needed at all. In principle several rings of the Tritron type with increasing radii could be combined to achieve specific energies of the ions of several 100 MeV/u.

All main components of the Tritron were new developments with uncertain results. Therefore the final energy was chosen to be rather moderate: e.g. for protons a maximum energy of $\simeq$ 43 MeV corresponding to an maximum accelerating voltage of $\simeq$ 0.53 MV per cavity was planned. In the meantime all cavities and channel magnets are manufactured (except the first two of three injection magnets) and partly tested with much better results than expected originally. Best values so far for the unloaded quality factor Q_o, for the maximum voltage U_{max}, and for the maximum gap field E_{gap} in the cavities are: $Q_o = 1.9 \cdot 10^9$, $U_{max} = 1.2$ MV and $E_{gap} = 10.6$ MV/m. The maximum current in the main coils of the channel magnets, achieved without any training, was 2000 A (design value 1450 A). Thus the magnetic induction can be as high as $B_{max} \simeq 1.9$ T in the sector channels respectively $\simeq 2.4$ T in the third injection channel, which was made from FeCo. Due to these encouraging test results maximum energies of $\simeq$ 74 MeV for protons respectively $\simeq$ 6 MeV/u for the very heavy ions may be obtained, provided that the terminal voltage of the tandem is at least $\simeq$ 15 MV.

The fixed rf–frequency causes the revolution frequency $\nu_o = \nu_{rf}/h$ as well as the final energy T_2 to have discrete values. Due to the longitudinal focusing harmonic numbers h ranging from $\simeq$ 14 to $\simeq$ 55 can be used. In the upper right quarter of Fig.3 the corresponding energy levels T_2 are shown as horizontal bars with h as parameter. The density of the levels increases strongly with growing values of h. By the choice of the initial energy and rf–phase a distinct stationary coherent energy oscillation will be stimulated, so that the final energy can be varied somewhat (yet $\Delta r = 0$ for the centre of the bunch!). Thus the gaps between neighbouring levels can be filled partially (not shown in Fig.3). While the right ends of the bars are meaningless, the left ends give (on the horizontal axis) the effective accelerating voltage $Q/A \cdot U_{max}$ needed at least per cavity, according to:

$$\frac{Q}{A}U_{max} = T_o\beta^2\gamma^3\frac{\Delta r}{r_2}\cdot\frac{1}{T_{rans}} \qquad (2)$$

Here Q/A and T_o are the specific charge and rest energy. β and γ correspond to T_2 at the mean extraction radius $r = r_2 = 1.45$ m. T_{rans} is the transittime factor. Neglecting T_{rans}, from Eq.2 follows $Q/A \cdot U_{max} \sim T_2$ in non–relativistic approximation. For small values of h the linear dependence is apparent. At high numbers h the decreasing transittime factor requires higher accelerating voltages.

In the upper left quarter of Fig.3 the final energy is plotted versus the injection energy T_1:

$$T_2 = \frac{\gamma_2}{\gamma_1}\left(\frac{r_2}{r_1}\right)^2 T_1 \qquad (3)$$

In non–relativistic approximation this again has a linear dependence: with $r_1 = 0.66$ m follows $T_2 \simeq 4.9\ T_1$.

In the lower left quarter of Fig.3 the specific charge (vertical axis) is given, which is needed to bend the ions with the energy T_1 along the third injection channel,

either with $B_{inj} = 2.4$ T or 2.0 T (bending limit), according to

$$T_1 = \sqrt{\left(\frac{Q}{A}\right)^2 (e \cdot c \cdot \varrho_{inj} \cdot B_{inj})^2 + T_o^2} - T_o \qquad (4)$$

In non-relativistic approximation T_1 is proportional to $(Q/A)^2 \cdot B_{inj}^2$. In the lower right quarter of Fig.3 the effective accelerating voltage is shown for given Q/A and cavity voltage U_{max}.

Figure 3 demonstrates the limits imposed on the different types of particles. Protons with Q/A = 1 could be injected by $B_{inj} < 2.4$ T without problems for all harmonic numbers $h \geq 11$, however the limitation of the cavity voltage U_{max} will lift the minimum h to h = 14 corresponding to $U_{max} = 0.81$ MV and $T_2 = 74.7$ MeV. Light ions with Q/A = 0.5 would need $B_{max} > 2.4$ T for $h \leq 20$, the bending limit sets the minimum to h = 21 corresponding to $T_2 = 31.2$ MeV/u and a cavity voltage of at least $U_{max} = 0.77$ MV. Energies near to the Coulomb barrier of about 5.5 MeV/u can be obtained for $h \simeq 49$ with $Q/A \cdot U_{max} = 0.16$ MV. The injection energy would be $T_1 = 1.16$ MeV/u. Due to the very low yield of ions with specific charge $Q/A \geq 0.215$ for ^{238}U, ^{208}Pb or even ^{198}Au at this low energy, the induction $B_{max} = 2.4$ T in the injection channel is of crucial importance for the very heavy ions, which are of special interest for physics. The accelerating voltage in the cavities then has to be $U_{max} \geq 0.73$ MV.

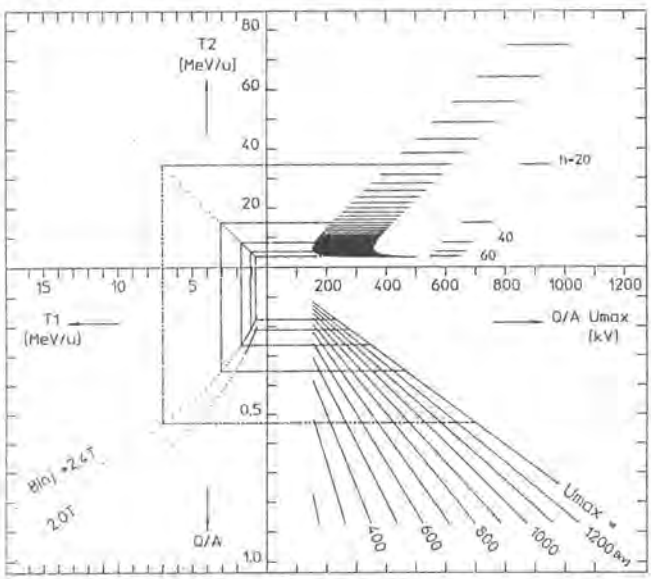


Fig. 3. Characteristics of the Tritron. Explanations see text.

2. THE MAGNETS

The channel magnets are of the window-frame type with the coils bent up and down at the ends (Fig.4) .[7] The entrance and exit edges are not tilted. The bending radius of the innermost channels is $\varrho_1 = 43$ cm. It increases from turn to turn by $\Delta\varrho = 26.94$ mm. All sectors (sector angle 20°) are of equal geometrical shape except the last two, where one channel is removed for injection respectively extraction. Cooling is made indirectly by cooling pipes (thermal siphon). Each sector

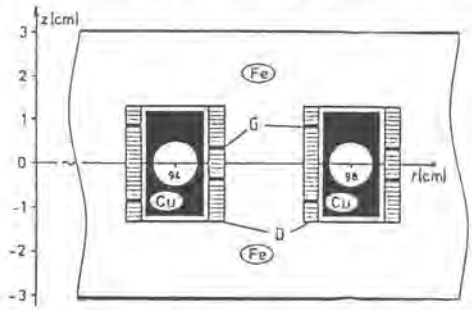


Fig. 4. Cross section through a magnet sector with two adjacent channels. G gradient windings, D insulating layers.

consists of two steel sheets (Fe with 1.8% Si), each 30 mm thick, with curved slots every 4 cm (width 22 mm, depth 15.5 mm). All pieces from steel are Ni plated to avoid rust. The maximum induction is limited by the saturation of the steel to about $B_{sat} \simeq 2$ T. Thus the overall current density in the superconducting coils can be chosen ≥ 600 A/mm^2, and the radial width of the coil can be made small ($\simeq 3$ mm). The coils consist of 2 × 13 windings (including a separate gradient winding in each half-coil) of a Rutherford-type cable (0.69 × 2.88 mm^2, 14 strands, each diam. 0.4 mm and 54 filaments, Cu/Nb = 1.4, 2 insulating layers of glass cloth with prepreg, each 0.1 mm thick). The half-coils were wound directly into the slots by a computer controlled winding machine (640 half-coils within 17 months)and then vacuum impragnated with epoxy in situ. A copper profile (with a 11 mm bore for the beam) shields the coil from beam losses. Flat disc springs between the copper profile and the coil prevent the coil from cracking. The total effective width of the coils and the walls of the shield is 9 mm. So one gets for the maximum radial geometrical aperture a_x:

$$a_x = \frac{\Delta r}{1 + \frac{B_{max}}{B_{sat}}} - 9\,mm \qquad (5)$$

The normalized field gradients are $\frac{\delta B}{\delta \varrho} \cdot \frac{1}{B} = 3.6$ m^{-1} in the radially and −4.9 m^{-1} in the axially focusing channels, if the gradient windings are operated without current: $I_g = 0$. The field indices $n = \frac{\delta B}{\delta \varrho} \cdot \frac{\varrho}{B}$ increase linearly with the turn number (see Fig. 5). The betatron oscillation numbers range from $Q_x \simeq 1.3$ to 1.6 and $Q_y \simeq 0.8$ to 1.7 for $I_g = 0$. Axial misalignments of the magnetsectors with a first harmonic amplitude of 0.3 mm would cause a strong increase of the axial betatron amplitudes at the $Q_y = 1$ resonance. To shift the field indices of the 10 innermost turns upward, the corresponding channels could be operated with a current $I_g \neq 0$, opposite to the current

in the main coils. In order to correct even non–resonant axial deflections from misalignments, small superconducting magnets ($\int B\delta s \leq 5 \cdot 10^{-3}$ Tm) with radially directed fields will be inserted into the six intermediate sector gaps in front of the position probes. The distribution of

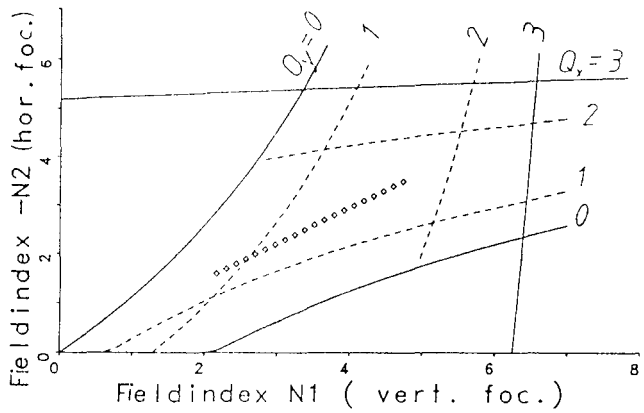


Fig. 5. The field indices n_1 and n_2.

the cables in the coil cross section should be as uniform as possible to avoid disturbing field terms of higher order than the linear one from the gradients. Quadratic contributions of $\left|\frac{\Delta B}{B}\right| > 5 \cdot 10^{-3}$ at $x = \pm 4$ mm apart from the central orbit would cause the dynamic aperture to be less than the geometrical. Negative quadratic contributions at the ends of the coils, where both half–coils spread apart, can be compensated by positive terms introduced by proper choice of the distance of the gradient windings from the central plane of symmetry and by additional insulating layers between the half–coils and the ground of the slots in the steel ($\simeq 0.5$ mm). Field measurements showed, that the relative quadratic contributions, averaged along the channels, stay below $1.5 \cdot 10^{-3}$ at $x = \pm 4$ mm for $I_g = 0$.

The local magnetic field inside the superconducting coil induce persistent screening currents in those filaments, which are not yet occupied by a transport current. The resulting dipol fields depend on the present and previous current settings and cause the gradient to depend on the current too. Above $\simeq 500$ A, the variations of the gradients by these magnetization effects were measured to be less than 5%. The effect on the quadratic field contributions is negligible. These results are in agreement to those obtained from a computer model calculation.

In order to guide the beam along the central orbit the current of each of the 238 channels has to be adjusted individually. The difference between maximum and minimum current of all channels is less than $\simeq 170$ A. All main coils will be connected in series. Each half of a main coil has a superconducting switch with superconducting contacts in parallel, which will be turned to the superconducting state as soon as the appropriate current of the coil is achieved. Further variation of the current from the power supply will be shared between the switch and the coil, according to the ratio of the inductances. The switches are made of superconducting wires (hairpin shape) with the copper matrix etched off along $\simeq 3$ cm, which can be heated above the critical temperature with an Allen–Bradley resistor. The filaments at the ends of the switch are mixed with those of all strands of the coil cable and pressed within a copper tube (pressure $\simeq 5 \cdot 10^4$ N/cm^2) to form the superconducting contacts.

From voltage measurements across a complete sector and across individual channels the inductances of the channels were determined to range from 1 to $3 \cdot 10^{-4}$ H in agreement with values calculated from the field energy. The mean inductance of the 40 superconducting switches was $2.6 \cdot 10^{-7}$ H. From this one expects a current variation in the main coils of some 10^{-3} of the variation of the switch current. Indeed a relative change of the field of $< 6 \cdot 10^{-4}$ in channel 19 e.g. was observed, when the main current in channel 18 was lowered from 1000 A to 850 A, while the switches of all other channels (including that of channel 19) were superconducting. If the main current of several neighbouring channels was changed simultaneously, the field variation in the channel with the switch superconducting was larger, indicating an increased 'cross talking'. This effect will not set in, when the beam is thread through succeeding channels, because then the main current of only one channel per sector will be changed.

The rate of current change in the superconducting switches could be as high as 20 A/sec without quenches for currents in the switches below 220 A. At a rate of 0.5 A/sec no switch quenched below 310 A. The total resistance of all normal conducting joints between adjacent coils was less than $2.7 \cdot 10^{-7}\Omega$ corresponding to a mean value less than $7 \cdot 10^{-9}\Omega$ per joint. The total dissipated heat in the joints would be less than 1 W per sector at the maximum current of 1800 A.

When energizing all channels at the same time, extended eddy current loops are induced in the steel, which are linked to all channels and which decay with a time constant of the order of several minutes. If only one channel is energized while the flux is kept constant in all others by the superconducting switches, then no long lasting eddy currents are observed.

3. THE CAVITIES

The six rf–cavities with a radial length of 120 cm are of the reentrant type with radially prolonged accelerating lips, forming a wedge–shaped gap of 62 mm length at the first beam hole and 128 mm at the last, see Fig.6. The accelerating lips are $\simeq 90$ cm long and $\simeq 15$ cm high. The surrounding bulge for the magnetic rf–flux was chosen as big as possible to keep the surface fields and thus the losses small. All radii of curvature were made sufficiently large to get the electrical peak field not more than 1.5 of the maximum field in the gap. The beam hole diameters are 13 mm, the length of the cutoff bores in the accelerating lips is 30 mm. The radial field and voltage characteristics are shown in Fig.7. The radial

increase of the voltage due to that of the gap length corresponds approximately to the requested curve according to Eq.2 (β and γ according to $r_1 \leq r \leq r_2$). So far a maximum voltage U_{20} = 1.2 MV was obtained at the last beam hole corresponding to a maximum electrical gap field at the 13th hole of 10.6 MV/m and a maximum surface induction of $\simeq$ 0.023 T near to the first beam hole.

The cavities are operated in the fundamental mode at

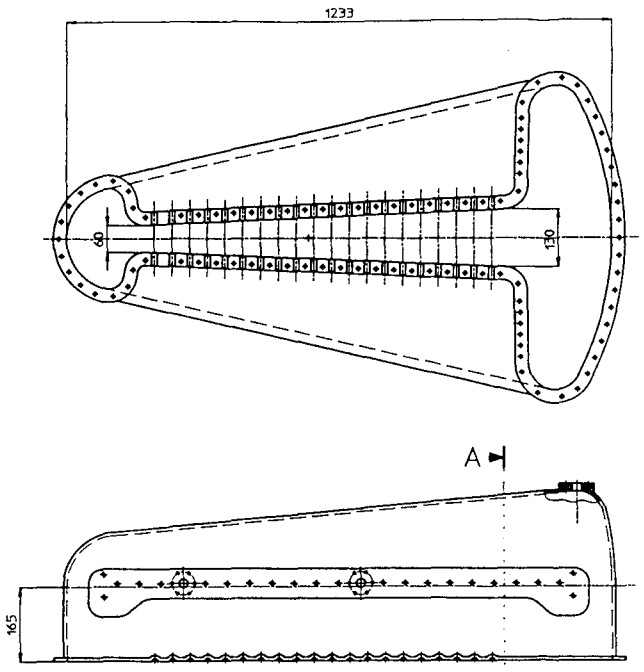


Fig. 6. Cross sections of the upper half of a cavity. Numbers in mm.

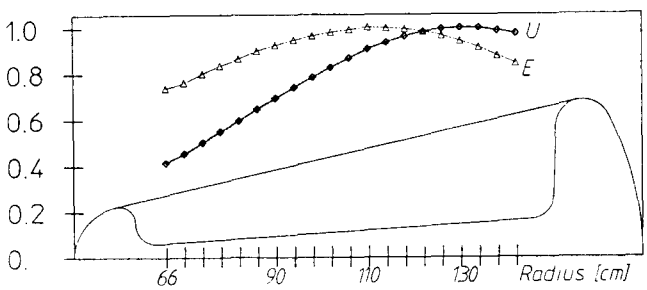


Fig. 7. The radial characteristics of the normalized voltage U and gap field E.

a frequency of ν_{rf} = 170 MHz. No currents should cross the horizontal plane of symmetry. Therefore the cavities can be made from two halves, which are connected simply by a flat joint. The cavity halves were fabricated by electroplating copper (for the most parts 10 mm thick) onto fibre–glass shells, which were removed afterwards .[9] The copper halves were electroplated with a $\simeq$ 5μm thick layer of PbSn (4 Sn, 96 Pb atoms), which has a critical temperatur of T_c = 7.5 K. Two O–shaped cooling pipes are attached on both sides of the cavity. During a test more than 100 W dissipated rf–power were removed without quenching the cavity.

Due to rather small mechanical tolerances the frequencies of the cavities are equal within $\pm 3 \cdot 10^{-4}$. Tuning is made in three steps: coarse (20 kHz) by mechanical deformation (at the arrow in Fig.6), fine (300 Hz) by moving sapphire rods into the rf–field volume, and final phase corrections by a fast electronic control system adapted from the S–DALINAC .[10] Sapphire has a low rf–loss factor and high thermal conductivity at low temperature. The frequency shift due to electromagnetic pressure was –230 Hz at a maximum voltage U_{20} = 1200 kV at the last beam hole. Frequency variations due to acoustic vibrations are less than 10 Hz, partially owing to the fact, that the cavities are supported very near to the nodes of the fundamental vibration (frequency: $\simeq$ 170 Hz).

PbSn is a better superconductor than pure Pb because of its enhanced stability against chemical reactions, the lower BCS resistance and better throwing power during the electroplating procedure .[11] The temperature dependent part of the surface resistance is given by

$$R_{BCS} = 6.85 \cdot 10^{-5}\, \nu^{1.9} \cdot \frac{1}{T} e^{\frac{-15.1}{T}} \qquad (6)$$

with R_{BCS} in Ω, ν in GHz and T in K. Due to the rather low frequency of 170 MHz the cavity needs not to be cooled down below 5 K. At T = 5 K one has $R_{BCS} = 2.3 \cdot 10^{-8}\Omega$, which gives the unloaded quality factor $Q_o = G / R_{BCS} = 4.1 \cdot 10^9$, where G = 95 Ω is the geometry factor of the cavity. This Q_o–value represents an upper limit. Additional contributions R_{RES} to the surface resistance R_S, which are independent from temperature, e.g. dielectric layers, normal–conducting spots or magnetic flux causing persistent currents will lower the Q_o–value. The stray fields of the channel magnets and current leads have to be shielded by thin steel sheets below $\simeq 10^{-4}$ T.

In Fig.8 some measurements of the Q_o–values versus U_{20} respectively the maximum gap field E_{max} at the 13th beam hole are shown. The temperature was below 5 K, the background induction $\leq 8 \cdot 10^{-5}$ T. The cavities were electroplated with the PbSn–layers in alphabetical order. The improvement of the later Q–values indicates the progress in the surface preparation technique. The curves slope at low voltages slightly, at those above $\simeq$ 600 kV more steeply due to starting field emission. The dotted curves are for constant dissipated heat, 6 W respectively 12 W per cavity. The broken line gives the limiting value mentioned above. The best measurements are not far from this limit. Up to now the quality factor showed no degradation during several months, though the cavities were exposed to air each time, when the vacuum vessel was opened. The insulating vacuum is not separated from the beam vacuum in the Tritron. This good results in spite of the large total surface of $\simeq$ 3 m^2 per cavity can be explained by the fact, that the heat, dissipated in small normal–conducting spots e.g., will be led

away from the thin PbSn layer into the copper body very effectively, causing a rather small temperature increase and preventing the spot to grow, at least below a certain maximum power input. In addition the skin depth of the rf–fields in normal–conducting PbSn exceeds the thickness of the layer considerably.

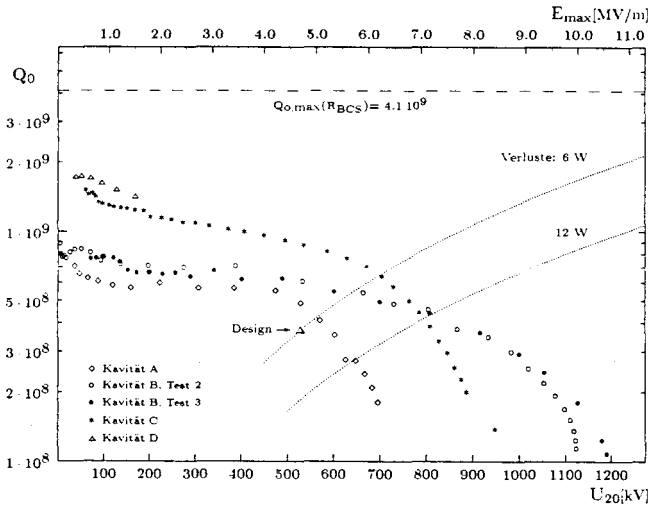


Fig. 8. Unloaded quality factor Q_o versus the voltage U_{20} resp. the maximum gap field.

4. PRESENT STATUS

The assemblage of all parts inside the vacuum vessel is going on. The cryosystem including the refrigerator (150 W at 4.6 K) is operating well. Evacuation of the vessel needs about 24 h. Cooling down from 300 K to 4.2 K was accomplished within 50 h with somewhat reduced refrigerator power, up to now with $\simeq$ 40% of the final mass ($\simeq$ 6 tn). The beam guiding system between the tandem and the Tritron is ready except the post–buncher [13], which is under test. The computer control system of the tandem and Tritron is in an advanced state. First beam entering the Tritron is expected at the end of this year.

5. FUTURE DEVELOPMENTS

The Tritron development was started to overcome the limitations of the conventional cyclotron on the energy due to transverse resonance and focusing problems, and on the beam intensity due to the missing longitudinal focusing and the extraction problems. The maximum proton current of the 590 MeV – ring cyclotron at the Paul Scherrer Institute in Villigen/Switzerland is expected to be 1.5 mA .[14] With cyclotrons of the Tritron type proton energies as high as 1 GeV and currents comparable to those in linacs ($\geq$ 100 mA) appear to be attainable in principle. A 500 MeV proton beam with a current of 10 mA, that is a beam power of 5 MW, would give a spallation neutron source with a thermal neutron flux of 10^{15} n/(cm^{2}sec), which is comparable to the highest flux from a nuclear reactor (at the Institute Laue Langevin in Grenoble). While the flux from a reactor hardly can be increased much above this value due to cooling problems in the core (power density $\simeq$ 3 MW/l), the power density in the target of a 500 MeV spallation source would allow currents of more than 100 mA. Of special interest on the long–term will be the possibility to produce energy by fission without the safety problems of nuclear plants, avoiding radioactive waste with long lifetimes by transmutation. For this purpose superconductivity improves the efficiency considerably. Of course, there will be many steps in the development of high intensity Tritron rings before, therefore the following design considerations are restricted to a proton current of 10 mA.

A system of two Tritron rings will be investigated. The extraction radius of the first shall be equal to the injection radius of the second ring: $r^I_{ex} = r^{II}_{in}$. The total beam losses shall not exceed 10 W or 10^{-6} in relative units to avoid quenching of the superconducting elements as well as high activation levels. Then the geometrical aperture $a_{x,y}$ should be at least 10 standard deviations $\sigma_{x,y}$, assuming a gaussian particle density. With the turn separation Δr = 10 cm, B_{max} = 1.75 T and B_{sat} = 1.9 T one gets from Eq.5 a_x = 43 mm (LAMPF: 19.1 mm, PSI–injection cyclotron: a_y = 35 mm).

All cavities are assumed to be equal and about twice as large as the present Tritron cavities. Larger cavities with a weight of $\geq$ 3 tn would be difficult to handle and to produce with the present electroforming technique. The accelerating gap length shall range from 20 cm at the first and 40 cm at the last beam hole. 16 beam holes with a radial distance of 150 cm from the first to the last are planned. The accelerating lips are vaulted asymmetrically with respect to the radial axis, so that one flat magnet sector could be installed in the concave side without loosing space at a most dense packing of the cavities along the ring, as shown in Fig.9. The cut–off bores in the accelerating lips with a diameter of 43 mm will have a length of 120 mm. The overall length of the cavities will be about 3 m, the frequency in the fundamental mode is estimated to be $\nu_{rf} \simeq$ 90 MHz. At the last beam hole a maximum voltage U_{16} = 2 MV is assumed, corresponding to a field in the gap E_{16} = 5 MV/m respectively a maximum gap field E_{max} = 5.8 MV/m near the 10th beam hole. The dissipated heat in the cavity walls is given by

$$P_w = 2\pi \cdot \nu_{rf} \cdot E_{cav} \cdot \frac{R_s}{G} \qquad (7)$$

Here E_{cav} is the electromagnetic energy stored in the cavity, and $R_s = R_{BCS} + R_{RES}$ is the surface resistance. The dissipated heat in the existent Tritron cavities is about $P_w \simeq$ 6 W at a field level of $E_{max} \simeq$ 5.8 MV/m (see Fig.8). The dissipated heat in the walls of a new cavity is estimated to be at most about P_w = 36 W, assuming for ν_{rf}/G about one half and for E_{cav} about 12

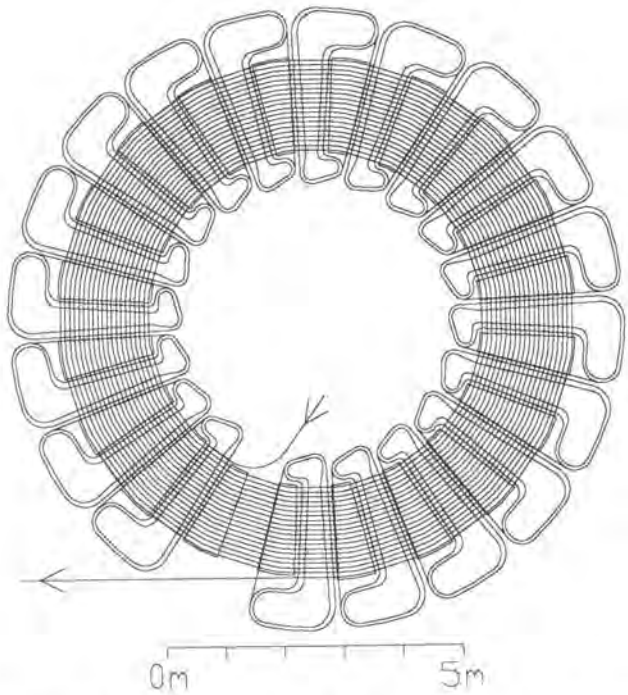


Fig. 9. Schematic plan view of a large Tritron ring for 500 MeV protons.

times the value of the old cavities. R_s is assumed to stay constant.

The mean orbit radius at extraction is given by

$$r_{16} = \varrho + \frac{N_{sec}\,(l_{gap} + 2d_{rift})}{2\pi} \tag{8}$$

with the bending radius

$$\varrho = \frac{m_o \cdot c}{e} \cdot \frac{\beta \cdot \gamma}{B_{max}} \tag{9}$$

l_{gap} = 40 cm is the length of the accelerating gap at the 16th beam hole. d_{rift} = 18 cm is the drift length between the effective edges of the accelerating gap and the succeeding channel magnet.

$$N_{sec} = f \cdot \frac{U^*}{U_{16}} \tag{10}$$

is the minimum number of sectors, with U_{16} = 2 MV, and U^* according to Eq.2 (Q/A = 1 for protons and T_{rans} = 1). The factor f ≃ 1.15 takes into account, that some overvoltage is needed for accelerating at a phase below $\pi/2$, and that the cavity of one sector will be omitted to leave space for the injection channel. Combining Eq.2,8,9, and Eq.10 gives r_{16} as function of γ at extraction

$$r_{16} = \sqrt{\gamma^2 - 1}\;\frac{m_o \cdot c}{2e \cdot B_{max}} \cdot \left\{1 + \sqrt{1 + \frac{2e \cdot f}{\pi\, m_o\, U_{16}}\,(l_{gap} + 2d_{rift}) \cdot B_{max}^2 \cdot \Delta r \cdot \gamma}\right\} \tag{11}$$

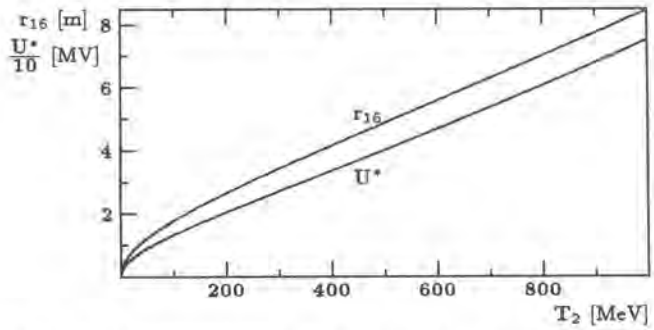


Fig. 10. The extraction radius r_{16} and the accelerating voltage U^* versus the extraction energy T_2

Figure 10 shows r_{16} and U^* versus the final energy T_2. Both curves are almost straight lines for $T_2 > 200$ MeV. Due to Eq.10 the number of sectors and the number of cavities $N_{cav} = N_{sec} - 1$ depend linearly on T_2. In table 1 some data of three systems are summarized, each consisting of two Tritron ring, with the final energy 500 MeV, 750 MeV and 1000 MeV. r^I_{in} and r^{II}_{in} indicate the injection radius of the first resp. the second ring, r^{II}_{ex} the extraction radius of the second ring. The number of sectors is assumed to be 16, of course detailed beam dynamic calculations may lead to somewhat smaller numbers. The maximum power, which has to be transmitted to a 10 mA proton beam per cavity, is less than 190 kW. Present input couplers for superconducting cavities are operated at up to ≃200 kW. The limiting effects for the beam

Table 1. Some data of 2–ring systems for 500 MeV, 750 MeV and 1000 MeV

	a)	b)	c)
$T\left(r^{II}_{ex}\right)$ [MeV]	500	750	1000
$T\left(r^{II}_{in}\right)$	151	271	393
$T\left(r^{I}_{in}\right)$	33	101	180
r^{II}_{ex} [cm]	486	663	845
r^{II}_{in}	326	503	685
r^{I}_{in}	166	343	525
$U^*\left(r^{II}_{ex}\right)$ [MV]	40	57	75
$U^*\left(r^{II}_{in}\right)$	12	16	20
$U^*\left(r^{I}_{in}\right)$	4	7	9
N^I_{sec}	16	16	16
N^{II}_{sec}	22	32	42
N_{cav}	21 + 7	31 + 9	41 + 15
N_{mag}	608	768	928
ν [MHz]	7.4	6	4.9
$h = \nu_{rf}/\nu_o$	12	15	18

current are similar to those known from proton storage rings. The beam creates fields, the space charge fields and those from image currents on the beam tube walls, which act back on the beam itself. All related effects depend mainly on the longitudinal and transverse coupling

impedances. Pure inductive and capacitive impedances cause real, intensity dependent shifts of the betatron and synchrotron oscillation numbers, and some change of the bunch dimensions. A resistive impedance causes imaginary frequency shifts $\Delta\omega$ and eventually instabilities, with the time constant of groth given by $\tau = -1/\Im(\Delta\omega)$. In the Tritron the beam runs either in a copper tube inside the channel magnets or in a cavity gap. The influence of the slits between the tubes and the cutoff bores of the cavities is assumed to be negligible.

The resistive wall effect of the copper tubes is expected to be much less compared to that of stainless steel vacuum chambers normally used in storage rings. The surface resistance of cold copper at 500 MHz for example is about 40 times less than that of stainless steel at room temperature (anomalous skin effect). Furthermore each individual bunch traverses one ring within $16/\nu_o \simeq 3 \cdot 10^{-6}$ sec. This limits the time for the development of an instability. The reactive part of the impedance in the Tritron is mainly determined by the space charge effect. It decreases strongly with increasing particle energy. It can be overcome by choosing the injection energy sufficiently high. In addition, in the Tritron rather large shifts of the betatron oscillation numbers are admissible due to the insensibility to resonance problems. Longitudinally the high accelerating voltage per turn causes unusual high synchrotron oscillation numbers, so that rather large shifts are admissible here also.

The superconducting cavities are traversed by 16 bunches in parallel, radially distributed along a large range. So the exitation of higher order modes by the beam has to be expected. Some special features of the Tritron cavities may be helpful to overcome these problems. First the cavities are single cells, resulting in a simple line spectrum without broad passbands. Thus there will be a certain chance to detune the cavity with respect to the frequency of a special higher order mode, which may be excited by the beam. Secondly, the quality factor of all modes with surface currents crossing the horizontal plane of symmetry are reduced due to the poor flat rf–joint. Finally, the cavity volume is accessible from all sides to install higher order mode couplers in an effective manner, avoiding trapped modes as in some multicell cavities. The interaction of several parallel high intensity bunches with a superconducting Tritron cavity can be investigated experimentally by triggered electron pulses through the beam holes, theoretically by means of computer codes. So far various storage rings with superconducting multicell cavities operate stably with beams above 10 mA. In HERA at DESY a current of 60 mA is envisaged for the near future.

6. ACKNOWLEDGEMENTS

Thanks are given to all members of the Tritron group, especially to M.Arnold, A.Cazan, G.Hinderer, R.Kratz, and P.Schütz, who have made important contributions to this work. Sincere thanks also to V.P.Dmitrievsky and S.B.Vorozhtsov from JINR / Dubna for fruitful discussions during many years.

This work was funded by the German Federal Minister for Research and Technology (BMFT) under the contract number 06 TM 189.

7. REFERENCES

1) Trinks, U., Assmann, W., Hinderer, G., "The Tritron: A superconducting separated–orbit cyclotron", Nucl. Instr. Meth., **A244**, 273 (1986),
2) Hinderer, G. and Trinks, U., "Beam dynamics in the Tritron", Nucl. Instr. Meth., **A244**, 283 (1986),
3) Russell, F.M., "A fixed–frequency, fixed–field, high–energy accelerator", Nucl.Instr.Meth.23, **229** (1963),
4) Martin, J.A., "The separated-orbit cyclotron", IEEE Trans. Nucl. Sci.**NS-13**, 288 (1966),
5) Trinks, U., "Longitudinal particle dynamics in the Tritron", Nucl. Instr. Meth. **A306**, 27 (1991),
6) Hinderer, G., Rieß, C., Trinks, U., "Transverse beam dynamics and coupling effects in the Tritron", Nucl. Instr. Meth. (1992),
7) Kratz, R., Hinderer, G., Junger, J., Labedzki, J., Trinks, U., "The superconducting Tritron magnets", IEEE Part. Accel. Conf., May 6-9, 1991, San Francisco, 2254,
8) Schütz, P., Grundey, T., Labedzki, J., Trinks, U., "The superconducting cavities for the Tritron", IEEE Part.Accel.Conf.,May 6-9, 1991,San Francisco, 2450,
9) Grundey, T., Labedzki, J., Schütz, P., Trinks, U., "The superconducting accelerating cavities for the Tritron", Nucl. Instr. Meth. **A306**, 21 (1991),
10) Aab, V.,et al., "The superconducting 130 MeV electron accelerator at Darmstadt", Proc. European Part. Accel. Conf., 1988, Rome, 335,
11) Dietl, L., Trinks, U., "The surface resistance of a superconducting lead–tin alloy", Nucl. Instr. Meth. **A284**, 293 (1989),
12) Hinderer, G., Leu, M., "The beam matching for the tandem–Tritron accelerator system", Nucl. Instr. Meth. **A287**, 287 (1990),
13) Rohrer, L., Schnitter, H., Walchshäusl, B., "The tandem Tritron control system", Nucl. Instr. Meth. **A287**, 170 (1990),
14) Joho, W., "High intensity problems in cyclotrons", 9th Int. Cycl. Conf.,Caen 1981,337

STUDY OF AN FFAG SYNCHROCYCLOTRON FOR A PULSED NEUTRON SOURCE

S.A. Martin, E. Zaplatin†
Institut für Kernphysik, Forschungszentrum Jülich GmbH Postfach 1913, D-5170 Jülich, Germany

P. F. Meads, Jr.
7053 Shirley Drive, Oakland, CA 94611-1631 USA

G. Wüstefeld
Berliner Elektronenspeicherring-Gesellschaft für Synchrotronstrahlung mbH, Lentzeallee 100, D-1000 Berlin 33, Germany

K. Ziegler
Hahn Meitner Institut Berlin GmbH, Glienicker Strasse 100, D-1000 Berlin 39, Germany

ABSTRACT

A series of workshops has been held during the last year discussing the accelerator technical background for a new European pulsed spallation neutron source (ESS).[1)] The basic design parameters are discussed for a high power (5MW), high current (1.7mA) FFAG synchrotron as a possible solution for the accelerator.

1. INTRODUCTION

The specification for the source was based on the requirements for future use of neutrons in condensed matter research. An average beam power of 5 MW is chosen to give an average thermalized flux of about 10^{15} n/cm^2/s, equivalent to the High Flux Reactor at ILL Grenoble. The required pulse length is less than 3 μs at a repetition rate of 50 Hz. The operation of such a source will require the highest standards in terms of availability (greater than 90%). Five different schemes have been considered as possible accelerator systems that might meet the source requirements:

1) A linear induction accelerator.
2) A linac followed by collector rings and rapid and medium cycling synchrotrons accelerating a relatively low current (125 μA) to a rather high energy (40 GeV).
3) A linac followed by a rapid cycling synchrotron.
4) A linac followed by a number of compressor rings.
5) A linac followed by a Fixed Field Alternating Gradient (FFAG) synchrotron.

Here the FFAG alternative is discussed in terms of its basic design parameters as well as a more general listing of its advantages and disadvantages. Preliminary calculations of the magnets demonstrate the feasibility of such complex magnets.

2. GENERAL FEATURES OF FFAG TYPE ACCELERATORS

We first list the advantages and disadvantages of an FFAG for a 5 MW beam power, 50 Hz repetition rate facility with less than 3 μs pulse length.

2.1 Advantages:

About 80% of the total beam power is gained in the FFAG ring. This makes the power of the injector linac rather low, and the neutron flux associated with injection losses also relatively low.

The time structure of the injector linac is relaxed, because the adiabatic trapping makes the chopping of the linac beam unnecessary. The chopper system, which is required for the compressor ring solution, provides a time structure in the linac beam to minimize the losses associated with the injection into the compressor rings. It provides a zero-intensity interval of about 100 ns every microsecond; this means a substantial fraction of the beam will be delivered during transient portions of the rf field.

A higher energy means a lower number of particles for the equivalent power. This results in smaller transverse apertures and smaller peak current per pulse, or shorter pulses.

The losses for charge exchange injection are less critical the lower the beam power and energy at injection into the ring is. These losses are mainly caused during the trapping right after injection.

The larger the energy gain in the FFAG the lower are the losses during the trapping procedure.

The beam losses during the acceleration process are very small relative to the rapid-cycling synchrotron option because:

† Guest scientist from JINR, Dubna, Moscow, Russia

—The main field is dc (no pulsed magnets).
—The radial aperture is large.
—The momentum acceptance is very large.
—The shimming of dc magnets is easy.

Good stability conditions: the beam does not see the ferrites of the extraction kickers except for the last few turns, therefore coherent instabilities are relaxed.

The stacking of beam at an energy between injection and extraction is a future option for intensity upgrading.

A higher repetition frequency can easily be realized at a later stage.

2.2 Disadvantages:

The FFAG is not an existing machine. The evaluation of reliability and performance needs special discussion.

The magnets are very large, with a high flux up to 4 Tesla. The radial type magnets are not complicated, but so far no prototypes have been studied.

The working point is determined by the hardware of the magnets. Special systems (e.g., pole-face windings) need to be built for the fine tuning.

The operation of superconductors in the radiation field requires special attention to the losses.

Ferrite-tuned cavities require large ceramic windows for the acceleration gap.

Concepts for non ferrite loaded RF systems such as rotating capacitors (ROTCO) need additional study.

The high beam intensity requires special studies of beam loading effects.

The shielding for higher energy is more costly.

The operational costs for the FFAG cannot be based on existing operating machines.

3. BASIC DESIGN FEATURES AND OPTIMIZATION OF THE BASIC PARAMETERS

In the range of 1-3 GeV, the required proton beam power for a given thermal neutron flux is approximately independent of the incident proton energy. The repetition rate of 50 Hz is specified by the user community. The rf harmonic is the first or second in order to avoid coupled bunch instabilities.

If we assume $2 \cdot 10^{14}$ accelerated ions—a figure achieved at the CERN ISR—the final energy must be 3.12 GeV; a 50% increase in the number of accelerated ions would reduce the maximum energy to 2 GeV. The higher energy means higher bending magnet strength, but it does provide a number of advantages. For comparable Laslett tune shifts, the injection energy for $2 \cdot 10^{14}$ would be 430 MeV, whereas that for $3 \cdot 10^{14}$ would be 560 MeV. Choosing the lower intensity means a power gain in the FFAG of a factor of 7 rather than 4.

From experience at both the Rutherford and Los Alamos neutron sources, the most severe particle losses are at the injection energy. This is partially due to losses in the charge-exchange injection process and partially due to incomplete longitudinal trapping into the rf bucket. Both machines are limited by activation due to these losses. We expect such losses in the FFAG to be much smaller because the dc magnetic field provides ample time for careful trapping, and the injected beam will make few traversals of the stripping foil due to the brightness of the beam and short injection time. Because the threshold for the most damaging neutron-producing events is 100 MeV, the neutron production in the FFAG due to injection losses will be only about one tenth that for comparable losses in the compressor ring option.

There should be virtually no losses after the trapping is completed because there is no changing magnetic field to track. The vacuum chamber will be very smooth over most of the accelerating range, and the extraction kicker magnet will not be seen by the beam until it reaches full energy; coherent instabilities should be much less severe than for a comparable normal synchrotron.

In a scaling FFAG, the average magnetic field increases with average radius as $\langle r \rangle^k$. Gamma transition is given by $\gamma_{tr} = \sqrt{(k+1)}$. We would like to choose ring parameters to avoid the crossing of γ_{tr} in order to avoid the possible exciting of strong longitudinal beam oscillations, possible emittance blow-up, and, in the worst case, particle losses. Because the relativistic γ at 3 GeV is 4.197, we consequently desire that the field index, k, should not be less than 20. The radial tune will be close to γ_{tr} and thus around 4-5. For the optimum phase advance of 70° or so (to insure a small and smooth beam envelope), we will need about 20 sectors. The radius should be larger than 40 m in order to provide adequate room for the rf cavities, the injection and the extraction systems. The radial magnet width is determined by the field index, k, and the injection and extraction energies. For the values, k=25, T_{inj}=500 MeV, and T_{ext}=3 GeV, the radial aperture is 2.5 m.

4. BEAM DYNAMICS CALCULATIONS

The sector model used comprises one positive magnet placed between two negative magnets to enhance the flutter and consequently the vertical focusing. The field between the two magnets is assumed to follow a COSINE curve from 0 to π with a width appropriate to the magnet gap, and the separation is arbitrary. On the outer side of the negative magnets, the field is assumed to go zero as a COS^2 function with an arbitrary width. The length of the plateau region of the negative magnets is specified, and that of the positive magnet is calculated to provide the required net bending

angle. In the absence of a return yoke, the field from one coil pair would have this qualitative shape.

The ORBIT program was originally written during 1983-1985 to study FFAGs for the German SNQ program.[2] It calculates quickly, by orbit integration, the properties of a general *scaling* FFAG (where all orbits are photographic enlargements of a reference orbit). The exact equations of motion are used, and the axial field at the reference orbit, which is entirely arbitrary, is input. The code has been recently extended to treat the model currently considered by surveying the parameter space and calculating the dynamic aperture. A new option to include terms to the fifth power in the axial displacement shows that the effects of these terms on the dynamic aperture are small—typically less than 1%.

Injection will be done by charge exchange of H^- ions from a linac. For a 100 mA beam, the current requirement of the FFAG is reached in 0.32 msec or about 262 turns. The linac beam is already so bright that we do not wish to place more than one turn in a given volume of phase space, and thus we will arrange the injection such that most ions will pass through the stripping foil only one time.

Extraction will be done in a single turn with a fast kicker. The kicker impedance is seen by the beam near full energy only at the end of the acceleration cycle.

5. MAGNET DESIGN

Vertical focusing in a radial FFAG is due primarily to the alternating gradient created by the presence of negative gradient magnets; that in a spiral FFAG is due to the edge angles as is the case in a typical isochronous cyclotron. Because of orbit scalloping there is some edge angle focusing in a pure radial machine. In the absence of negative field magnets, there must be strong spiral angles (60-70°), and such large spiral angles induce significant nonlinearities. Although these nonlinearities are beneficial in expanding the tune spread to provide Landau damping, they do significantly reduce the single particle stability limits. As was already shown in 1985, a pure radial machine becomes reasonably compact if strong magnetic fields of 4 T are used.[3] Thus we here seek a compromise of a machine with a modest spiral angle (~30°), a feasible positive field (~4T), and an easily obtained negative "gully" field (~ -2T).

The basic design for a radial type FFAG magnet has been studied[4] using the 3-D program PROFI.[5] The detailed design is of a magnet with a main pole 1.0 m (azimuthal) by 3.2 m (radial) and two poles carrying the return field. The field varies in radial direction between 1.16 and 3.5 Tesla, corresponding to a field index of k=15; the ratio of positive to negative bending is 3.02. The azimuthal field distribution through one half of the magnet

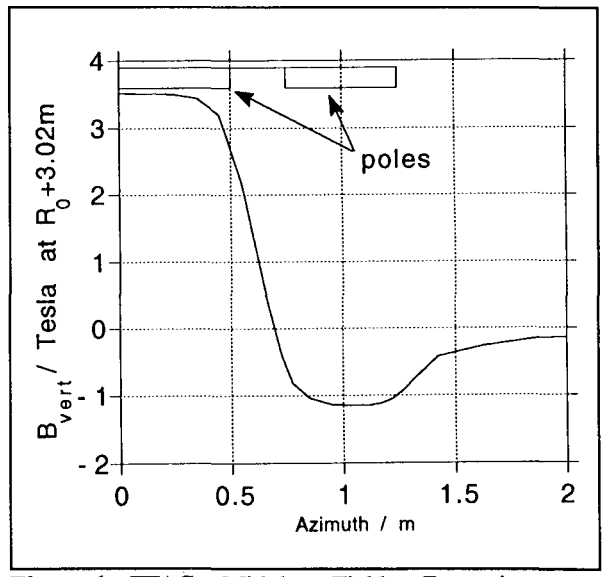


Figure 1. FFAG—Midplane Field at Extraction

is shown in Figure 1. The remaining flux, which is not used for the gully fields, is guided back through a return yoke. Additional calculations demonstrate the possibility of going up with the maximum field to 4.4 Tesla, of realizing a field index of k=26, and of adjusting the ratio of peak to gully field between 2 and 5. More detailed design studies will be done after the optical parameters of the FFAG are fixed.

6. RF STUDIES

The main characteristics of the accelerating system in an FFAG are the existence of a large accelerating gap in the radial direction (2.5 m)—as in a cyclotron—and, at the same time, the need to modulate the resonant frequency—as in synchrotrons. The first, together with a relatively low frequency (less than 2 MHz), implies large geometric dimensions of the cavity. If we accept the standard method of changing frequencies employed in conventional synchrotrons, then ferrites would be used to increase the cavity frequency. In this case, the large cavity volume will require a large ferrite volume resulting in a high price. Such a structure was suggested for the MINI ASPUN project of ANL.[6] An accelerating system for ESS, based on this report, was presented during EPAC-1992.[7] This cavity is a rectangular box extending a quarter wave along the beam path with specially shaped accelerating electrodes in the radial beam plane. The variation of the resonant frequency is accomplished through a polarization current wrapped around the ferrites. Ceramic insulators may be used in the

accelerating gap to separate the vacuum volume from that containing the ferrites. However, the creation of the 2m long insulator to hold high vacuum with high reliability is expected to be a very complicated design problem.

The main parameters of this structure are contained in Table I.

Table I Properties of the FFAG rf system.

frequency range	1.66-2.06	Mhz
harmonic number	2	
accelerating Voltage/ turn	200	keV
cavity voltage	20	kV
number of cavities	10	
$B_{ferrite}$	0.0150	Tesla
ferrite volume/cavity	2.4	m^3
ferrite μ	64.9-100	
shunt impedance	8800	Ohm
maximum current	230	A
stored power	0.22	MVA
power losses/cavity	23	kW
peak power density lost	94	(kW/m^3)

The possibility of varying the resonant frequency by means of a rotating capacitor may be taken into account as well. In this case, there should be a special design to reduce the resonant line down to 3-5 m length. The weakest component and most complicated design task of such a structure would be the rotating condenser (ROTCO). Taking into account that the highest voltage achieved on the ROTCO plates is 40 kV[8], one would need at least five such accelerating cavities. One advantage of this scheme is the reduction in power (less than 100 kW required). This compares favorably with the ferrite loaded cavities, where substantially more power is required. We will also consider a hybrid system containing both a rotating condenser and biased ferrites to provide tuning variability.

The frequency can be reset very quickly so that capture and acceleration of a new bunch can start virtually immediately after the extraction of the previous bunch. After capture and bunching, the maximum voltage is applied for the duration of the cycle in contrast to the sinusoid used in a conventional synchrotron. These considerations yield a substantially reduced cavity voltage for a given repetition rate as compared to a normal synchrotron.

If a faster acceleration time should turn out to be advisable to limit the time over which instabilities act, more rf power can be added. With such an increase, the repetition rate could be increased to obtain a greater current throughput.

7. ACKNOWLEDGEMENTS

We wish to thank G. Hinderer, U. Trinks (T.U. Munich), H. Klein, A. Schempp, (Univ. Frankfurt), G. Bauer (PSI), H. Conrad, G. Müller, U. Sieling (KFA Jülich), H. Henke (TU Berlin), W. Pelzer (HMI), I. S. K. Gardner, M. Harold, C. W. Planner, G. H. Rees (RAL), V. Vaccaro (U. Naples), A. Susini (CERN), V. Dimitriewski (Dubna), J. Botman (TU Eindhoven), Y. Cho, R. Kustom, F. Mills (ANL), and K. Erdmann (UBC).

8. REFERENCES

1) Martin, S. and Planner, C., "Accelerator Design Parameters for a European Pulsed Spallation Neutron Source", European Particle Accelerator Conference, Berlin, 1992 (to be published)

2) Meads, P. F., "A New FFAG Orbit Code", IEEE Trans. Nucl. Sci. **NS-32**, p. 2243 (1985).

3) Meads, P. and Wüstefeld, G., "An FFAG Compressor and Accelerator Ring Studied for the German Spallation Neutron Source", IEEE Trans. Nucl. Sci. **NS-32**, p. 2697 (1985).

4) G. Müller and U. Sieling, KFA Jülich, Germany, private communication.

5) PROFI-Engineering, D-6100 Darmstadt, Germany

6) Kustom, R. L., Proc. of Advanced Neutron Sources Conf., 1988, Inst. Physics Conf. Series **97**, Bristol, New York (1989).

7) Zaplatin, E., Fourth Accelerator Meeting for the EPNS, Berlin, 24-MAR-92, EPNS/AW4/3/92.

8) Vasilenko, A. T. et al, "'F' Facility Status Report", Proc. of the Xth All-Union Acc. Conf. **2**, Dubna, p. 228 (1987).

Design of a Compact Permanent Magnet Cyclotron Mass Spectrometer for the Detection and Measurement of Trace Isotopes.

A. T. Young, K.J. Bertsche*, D.J. Clark, K. Halbach, W.B. Kunkel, K.N. Leung and C.Y. Li
University of California,
Lawrence Berkeley Laboratory
Berkeley, California 94720, USA

ABSTRACT

A technique for the detection of trace amounts of rare isotopes, Cyclotron Mass Spectrometry (CMS), is described. This technique uses the relationships between particle mass, charge, magnetic field strength and cyclotron orbital frequency to provide high mass resolution. The instrument also has high sensitivity and is capable of measuring isotopes with abundances of $< 10^{-12}$. Improvements now being implemented will lead to further increases in the sensitivity and enhance operating parameters such as cost, portability, and sample throughput.

1. INTRODUCTION

Measuring the abundance of trace isotopic constituents has applications in many fields. In biomedicine, the use of carbon-14 (^{14}C) has an important role in studying the metabolism of drugs and DNA sequencing. Archaeological applications include the radiodating of carbon containing samples to obtain accurate ages of fossils and anthropologic artifacts. In planetary geology, the abundance of the isotopes of iridium in past geological periods has given rise to the "catastrophe" theory of mass extinctions. Environmental applications of the trace detection of isotopes also abound, such as in the measurement of the CO_2 content of ice cores and deep ocean water or measuring the distribution of combustion byproducts in the atmosphere. In general, these applications require a very high sensitivity and selectivity. The combination of the samples being very dilute in the isotope desired ($<10^{-9}$) and containing other atoms and molecules with almost the same atomic or molecular weight makes essential a detection scheme with high sensitivity *and* specificity (or resolution.)

One method of high-sensitivity detection has been Accelerator Mass Spectrometry (AMS). [1] In this technique, the sample of interest is ionized, and a charged-particle accelerator is used to detect single atoms of the isotope of interest. The first use of an accelerator as a mass analyzer was made in 1939 by Alvarez, who measured ^3He at natural abundance using a cyclotron. The "modern" era of AMS began in 1977, when Muller proposed using a cyclotron for carbon and beryllium measurements[2,3], and the groups at the University of Rochester, and McMaster University demonstrated ^{14}C detection with tandem accelerators[4,5]. AMS has developed over the last decade and a half into a powerful tool for use in the detection of trace quantities of materials., having been employed in a variety of environmental, archaeological, and geological studies. Virtually all work is performed on large tandem accelerators. By using the high energy (≥ 1 million electron-volts) inherent in these accelerating schemes and ion detection techniques capable of measuring a single particle, analysis of isotopes which are present in samples at a level of 1 part in 10^{15} has been achieved.

Unfortunately, the use of AMS is not widespread. AMS measurements are performed at central, multimillion dollar facilities, with experimenters bringing or shipping their samples to the site to be analyzed. There are several reasons for this. First, the facilities are large and expensive to acquire, operate, and maintain. The utility requirements are substantial, and a multi-person crew is required to operate the instrument. Second, because of the large accelerating voltages used, substantial amounts of radiation are produced, necessitating heavy shielding. Third, the sample preparation is complicated, requiring the production of solid samples suitable for use in sputter ion systems. Combined, these factors have made AMS a relatively expensive technique with low sample throughput.

To retain the advantages of conventional AMS without the disadvantages of the large accelerator facilities, the original idea of using a cyclotron as the accelerator has been revived, with the new wrinkle that the cyclotron be small and that the accelerating voltages be modest. In this incarnation, the technique has been dubbed Cyclotron Mass Spectrometry (CMS.) Here, the large cumbersome accelerator has been replaced by a compact, low-energy cyclotron. Previous work at LBL [6,7] has demonstrated the principle of these devices and has shown that CMS can have significant detection advantages over the scintillation methods used routinely in biomedical research for ^{14}C. As a result, several small cyclotron spectrometers are now

*present address: University of California Lawrence Livermore National Laboratory, Livermore, CA 94704

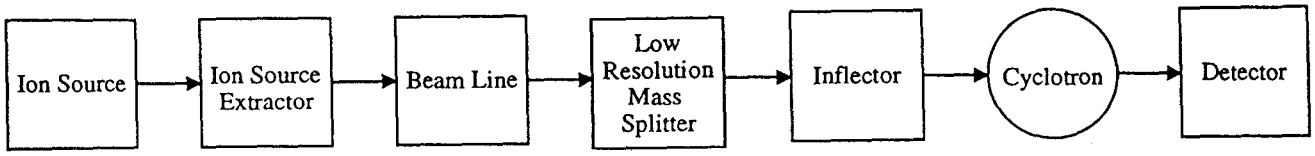


Fig 1 Schematic diagram of the cyclotron mass spectrometer

under development around the world. However, the utility requirements, sampling methods, and sensitivity of CMS are still such that widespread application of the technique to common problems is not currently feasible.

This paper describes the development program now underway at Lawrence Berkeley Laboratory (LBL) to improve the performance and operating characteristics of CMS. The new CMS system will be more compact, less expensive, and have a higher sample throughput than existing AMS and CMS instruments. To meet these goals, improvements are now being undertaken in the ion source, the injector system, and the cyclotron magnet system. In this paper, these improvements are briefly described and the general operating characteristics of the new machine presented.

2. CMS IMPROVEMENT PROGRAM

Figure 1 shows a schematic diagram of the LBL CMS system. To improve the performance over existing devices, changes are being made in the ion source and beam transport and injection line. This will lead to enhanced sensitivity and increased sample throughput. In order to reduce the size, weight, and complexity of the system, the magnetic field of the cyclotron will be produced by permanent magnets rather than electromagnets. These improvements are described below.

The ion source typically used in AMS (and present CMS) is a cesium sputter ion source. A solid sample (graphite for ^{14}C analysis) is prepared and bombarded by an atomic cesium beam. The resulting ions are then collected and sent to the accelerator. This type of source can produce modest ion currents with modest beam quality. However, sample preparation, i.e. the production of a solid sample, can be laborious and time consuming, leading to low sample throughput. In addition, the many steps in preparing the sample make contamination of the sample more likely.

At LBL, substantial experience has been obtained in developing negative ion sources for fusion and ion implantation applications using magnetic multicusp sources.[10] In these devices, medium-density, low temperature electric discharge plasmas are used to directly produce negative ions from gas phase precursors. These sources have high negative ion emission yields and superior beam emittance. Recent experiments have shown that C^- can be formed in these sources as well. Figure 2 shows the negative ion yield from a multicusp source using CO_2 as the precursor gas. As can be seen, a substantial fraction of the ions produced is C^-. Further research is underway to optimize this type of source for C^- production. If successful, this source will provide a simple to operate, high throughput source of negative ions without the need for complicated processing procedures.

After their production, the ions are transported to the cyclotron analyzer. In a previous instrument, the ions were radially injected. Although this radial injection system was relatively straightforward to implement, it introduced losses to the ion beam. As the sensitivity of the detection depends on the ion current available, it is important to minimize these losses.

One method to possibly improve the transmission of the beam is to use axial rather than radial injection of the ions. Axial injection, in general, is very efficient, and may be simpler than undergoing the several bounces needed for radial injection. To this end, trajectory calculations have been performed to design a spiral inflector, an electrostatic channel which twists or "tilts" as it guides the ions down the axis of the machine and into the midplane. Several designs have been produced. Figure 3 exhibits one candidate, showing one of the two parallel electrodes. All these designs guide the ions to the cyclotron midplane with ion orbits centered on the machine axis, but the inflectors differ in the detailed

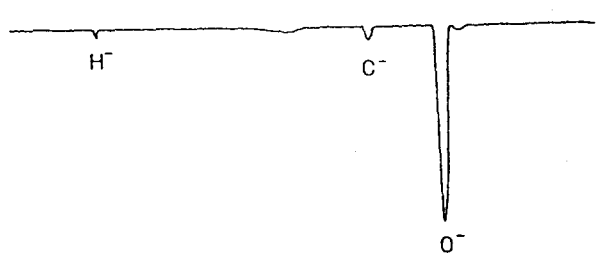


Fig 2 C^- ion output from a magnetic multicusp source

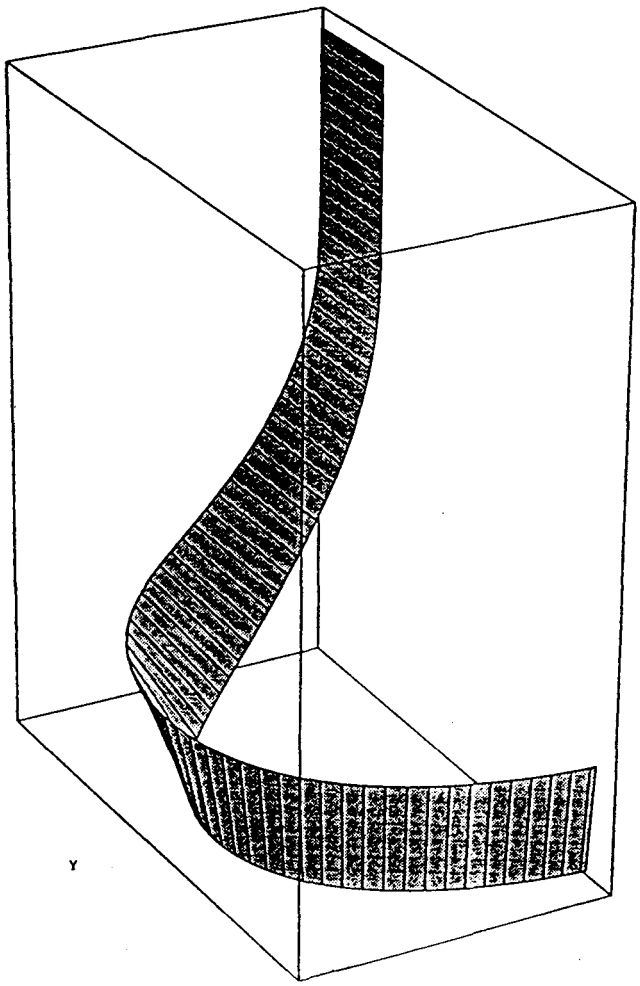


Fig 3 Inflector design for axial injection of ions into the cyclotron.

specification of the tilt angles and electric field. Acceptance calculations are being performed to optimize the design.

The third improvement now being implemented in the CMS will substitute permanent magnets for the existing electromagnet now used in producing the magnetic field. This change has several important advantages. First, the overall size and weight of the magnet structure is reduced, as the magnet coils and power supplies are eliminated. Second, the electrical power and cooling water consumption of the instrument is minimized. With permanent magnets, the CMS will be quite portable and could be placed aboard aircraft, small boats, or out in field locations. It will also reduce operational costs. Using samarium cobalt as the magnetic material, a design for the magnet structure has been produced which has both the required field (1 T) and uniformity (1 part in 10^4). Figure 4 shows a view of the

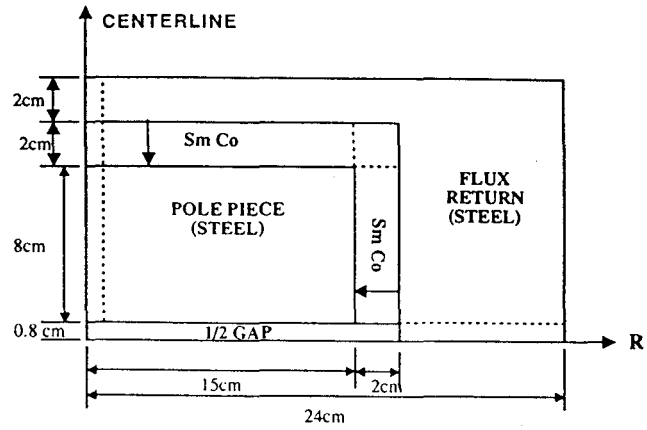


Fig 4 Schematic diagram of permanent magnet systme for the cyclotron.

design. This figure shows one quadrant of the machine. The cyclotron has axial symmetry about the centerline. The midplane (marked R in the figure) is a mirror plane, with the exception that the magnet field vectors in the SmCo points away from the pole face in the lower half of the machine. In this concept, the pole faces of the magnet are part of the vacuum vessel. A more detailed description of this design appears elsewhere in these proceedings. [11]

3. SYSTEM CHARACTERISTICS AND PROJECT STATUS

The advanced CMS is being designed and optimized for use with ^{14}C. Some of the operating characteristics are shown in Table 1. Construction of the permanent magnet structure and the axial injection system should be finished by the end of 1992. Ion source development is occurring concurrently, with integration of the source and cyclotron to take place in 1993.

In addition to these developments, additional improvements are anticipated. In particular, improvements to the beam transport and low resolution mass selector will be made to decrease their size. Earlier devices used a Wien filter for this purpose, but a bending magnet analyzer may be used instead. In addition, advanced accelerator structures may also be used, such as the dee structure proposed by Chen et al.[8] This advance would allow for an even higher mass resolution in the same cyclotron structure.

4. CONCLUSIONS

Cyclotron mass spectrometry (CMS) is a potentially powerful analytical technique with applications ranging from studies of global warming constituents to the biological metabolism of pollutants and pathogens. A

Parameter	Value
Ion source	Magnetic multicusp
Species	14C
Injector type	Spiral inflector
Injection energy	5 kV
First orbit radius	4 cm
Extraction radius	12 cm
Extraction energy	< 50 kV
Pole face radius	15 cm
Pole gap	1.6 cm
Magnetic Field	1 T
Field Source	SmCo Magnets

Table 1 Cyclotron design Parameters

development program is now underway which will increase the sensitivity and improve operational characteristics, such as portability and sample preparation, while at the same time reducing the cost of the instrument and its operation. These improvements will make CMS more widely available for routine analysis of trace materials.

5. ACKNOWLEDGMENTS

The authors would like to thank Bruce Milton and Corrie Kost of TRIUMF for help in obtaining some of the ion trajectory codes. This work has been supported by the Director, Division of Advanced Energy Projects, Office of Basic Energy Sciences, of the U.S. Department of Energy.

References

[1] Litherland, A.E., in Ann. Rev. Nucl. Part. Sci. 30 437-73 (1980).

[2] Muller, R.A., Science 196 (1977) 489.

[3] Muller, R.A., Stephenson, E.J., Mast, T.S., Science 201 (1978) 347.

[4] Nelson,D.E., Korteling,R.G., and Stott,W.R., Science 198, 507 (1977)

[5] Bennett et al, Science 198, 508 (1977)

[6] Welch, J.J., Bertsche, K.J., Friedman, P.G., Morris, D.E., Muller, R.A., and Tars, P.P., Nucl. Instr. and Methods B5 (1984) 230.

[7] Bertsche, K.J., Karadi, C.A., Muller, R.A., and Paulson, G.C., Nucl. Instru. and Methods, B52 (1990) 398, Bertsche, K.J., .Karadi, C.A., and Muller, R.A., Nucl. Instr. and Methods, A301, (1991) 358 and Bertsche, K.J., Nucl. Instr. and Methods, A301, (1991) 171.

[8] Chen, M.B., Xu, S.L., Li, D.M., Zhabg, X.L., Chen, G.S., and Gao, W.Z., Nucl. Instru. and Methods, A297 (1990) 47.

[9] Subotic, K.M., J. Physics G - Nucl. and Part. Physics 17S, S363.

[10] Leung, K.N., Anderson, O.A., Chan, C.F., Cooper, W.S., deVries, G.J., Hauck, C.A., Kunkel, W.B., Kwan, J.W., Lietzke, A.F., Purgalis, P., and Wells, R.P., Rev. Sci. Instru. 61 (1990) 9, also see Leung, K.N., these Proceedings.

[11] Li, C.Y., *et al.* these proceedings

A NEW DESIGN PROPOSAL FOR A 200 MEV SUPERCONDUCTING RING-CYCLOTRON MAGNET

H N Jungwirth and J G de Villiers

National Accelerator Centre, P.O. Box 72, Faure, 7131 Republic of South Africa

ABSTRACT

A new magnet design for a superconducting ring-cyclotron with proton energies in the 200 MeV range is presented and discussed. The proposal features four separate 30-ton iron sectors at room temperature and superconducting coils which are confined to each sector and located between the poles and return yoke, outside extraction. The design characteristics of the magnet configuration are examined using results obtained by numerical field computation and orbit integration. A preliminary analysis of these results confirms that the proposal is feasible and can be used to develop a superconducting ring-cyclotron for clinical proton therapy.

1. INTRODUCTION

The interest in radiotherapy with proton beams in the energy range from 200 to 250 MeV and efforts to provide suitable facilities for this purpose have increased dramatically during the past decade [1-5]. A trend from multidisciplinary to fully dedicated accelerators has emerged for such applications, and it is now more important than ever to establish and examine all machine options available. Traditionally the proton energies and beam properties required for radiotherapy fall into the realm of cyclotrons, and indeed most pioneering work in this field has made use of synchrocyclotrons. A superconducting 250 MeV synchrocyclotron for application in hospitals already has been studied[6]. Existing isochronous superconducting cyclotrons have difficulty in reaching the required energy range owing to problems with beam focusing, and their operational characteristics are also less attractive for the demands of clinical treatment schedules. Recently a more conventional isochronous cyclotron has been proposed as an alternative, therefore, which retains the layout and features of superconducting cyclotrons but employs normal coils[7].

Proton-therapy programmes also are supported on a multidisciplinary basis by several ring cyclotrons (a designation which is assumed to include separated-sector cyclotrons in this paper). The better quality and CW characteristic of the beam which can be obtained from such machines hold important advantages for proton therapy, but existing ring-cyclotron facilities are far too complex and expensive to rate as a suitable choice for dedicated radiotherapy centres. Inherently superconducting ring-cyclotrons (SRC) should be well-suited for such applications, because they would combine a relatively compact size and good beam properties with reliable and cost-effective operational characteristics. The complexity could be kept within acceptable limits for a fixed energy SRC operating in the stand-alone mode without the requirement for pre-acceleration, transfer and matching of the beam. A crucial issue is the magnet design for such a machine, because comparable magnets do not exist at present and stringent requirements must be met with simple solutions. A promising design option employing S-coils[8] is currently being studied at the National Accelerator Centre, and the results obtained thus far are presented and discussed below.

2. CYCLOTRON CONSIDERATIONS

The SRC layout is adopted from existing 200 MeV room-temperature ring cyclotrons and features four 34° sector magnets and two $\lambda/2$ rf-resonators. The resonators have triangular ($\leq 47°$) dees located in opposite valleys between the sector magnets and operate at the 4th harmonic of the orbit frequency ν_0. The choice of $\nu_0 = 26$ MHz essentially determines the machine size as well as the rf and magnetic field requirements. The rf-system works at a fixed frequency of 104 MHz (FM broadcasting range) and the magnetic field in the cyclotron centre just exceeds 1.7 tesla. The 200 MeV orbit radius is close to 1.04 m and requires an average field of ~2.1 tesla.

The radial field shape is determined by isochronism which must be maintained with extremely high accuracy ($\delta B / B < 10^{-4}$) and inherently yields good radial beam focusing. The azimuthal field shape has to provide sufficient and suitable (resonances) vertical beam focusing to overcome the defocusing effect of the isochronous radial field increase. In order to achieve this without spiral geometries, the field at extraction must typically vary from about 4 tesla in the sectors to ≤ 1 tesla in the valleys. The iron mass of the magnets should not exceed 120 metric tons under these conditions[9], and superconducting coils are necessary to produce such fields. The relatively low magnetic field in the valleys permits the efficient use of conventional electric and magnetic extraction devices.

A special feature of such an SRC is that the beam would be accelerated right from the centre, most probably by making use of a small internal ion source. Assuming a dee voltage of 60 kV and considering that only a low beam current at fixed energy is required, the magnetic field in this region is acceptable for this purpose. The resonators should be made such that the peak acceleration voltage increases to $\geq$ 200 kV at full radius, thus relaxing magnetic field tolerances significantly and providing strong phase compression of the beam to improve the extraction efficiency. Access to the central region is possible from the valleys which are not occupied by rf-structures. Obviously, an extensive design study would be necessary to determine the details of the central region layout, but it should be less difficult to find a suitable solution here than in conventional superconducting cyclotrons. The essential requirement is that the isochronous magnetic field can be produced and maintained right from the cyclotron centre.

3. MAGNET CONFIGURATION

The design concept, employing S-coils in the proposed magnet configuration, is shown schematically in Fig. 1. Its most attractive feature is that the coils are removed completely from the valleys to a place where they do not take up space which is needed for other cyclotron components, in particular in the central region and at extraction. This characteristic allows the sector geometry to extend right to the cyclotron axis as in conventional superconducting cyclotrons, but retains the conceptual advantages of ring cyclotrons with regard to vertical focusing and extraction of the beam.

The magnet configuration has a diameter of 4.2 m and is 3 m high. A pole radius of 1.15 m was selected to place the onset of the radial fringe field beyond the 200 MeV orbit. A constant pole gap of 20 mm allows sufficient vertical space for the anticipated beam intensities, but excludes trim coils from this region. Each sector magnet features one pair of superconducting excitation coils which are located in a cryostat between the poles and return yoke. The cryostat is accessible from either side of the magnet, and a space of ~100 mm between the warm magnet surfaces and the coils at 4.2 °K should make ample provision for its structures.

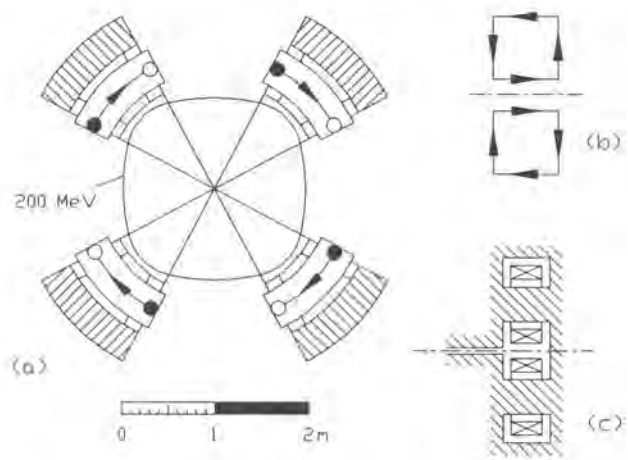


Fig. 1. The schematic lay-out of the proposed sector magnets showing the S-coils (a) located between the poles and return yoke, and in (b) radial elevation and (c) radial section.

The eight identical coils have a simple compact geometry and are relatively easy to fabricate. The azimuthal coil width is just over 1 m and a height of 1 m was found to be adequate. Average current densities in the range of 40 A/mm^2 should be acceptable for coils of this size if the magnetic field does not become too high. A current-carrying coil section of 400 mm × 175 mm was chosen to allow a maximum excitation of the magnets in the order of 2 × 3 MA. The dimensions result in a sturdy coil structure which facilitates mechanical support from the surrounding magnet parts. The substantial electromagnetic forces expected to act on the coils can be reduced by filling the core region of each coil with iron. A filler piece bridging the gap between pole and return yoke through an opening in the cryostat is suggested for this purpose. Alternatively the coils can be wound directly on a full core of magnet steel which is then included in the cryostat and thus cannot extend to the warm magnet parts. Such a design reduces the field in the coils even more and seems to be technologically advantageous.

4. FIELD ANALYSIS AND ORBIT PROPERTIES

The theoretical assessment of S-coil fields is facilitated by considering that the two coil-sets above and below the median plane are essentially short octupoles with regard to the cyclotron axis, but have opposite polarity and azimuthal conductor sections which result in strong dipole components. On the cyclotron axis and in the median plane only axial components of the dipole field remain, and the field at the axis can be calculated analytically. It is also quite simple to evaluate the field in the median plane if the coils are represented by filaments. A typical result obtained in this way is shown in Fig. 2 and clearly illustrates the characteristic field properties of S-coils in the median plane. Off the axis and median plane the analysis of the coil field becomes much more involved, except for the azimuthally averaged field components to which multipoles cannot contribute, by definition. However, fully 3-dimensional numerical field computations are necessary to evaluate the radial as well as azimuthal field properties of sector magnets with S-coil excitation.

A three-dimensional field analysis of the magnet configuration was carried out at the Paul Scherrer Institute[10] by making use of the TOSCA codes[11].

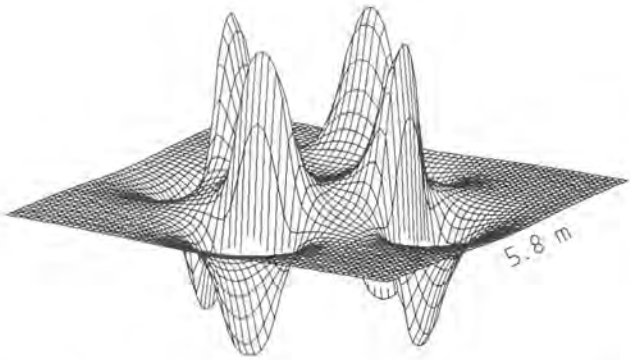


Fig 2. The magnetic field computed in the median plane for a filament representation of four symmetric 34° wide S-coils at a radius of 1.45 m. The filaments with clockwise and anticlockwise current directions are located 1.01 m and 0.19 m away from the median plane respectively.

The field obtained in the median plane for a mean current density of 46.3 A/mm^2 in the S-coils is shown in Fig. 3. Perhaps the most unusual result is that the magnetization contributes up to ~2.5 tesla in the pole gap at smaller radii, but only 1.7 tesla near extraction. This effect is a consequence of the extremely inhomogeneous field produced by the S-coils which use the magnet steel to 'pump' as much as possible magnetic flux into the central region of the cyclotron. It is remarkable that the magnetization field contributed near extraction does not change more than usually over the azimuthal range of the pole gap, in spite of the influence of the high octupole currents and although the iron is fully saturated.

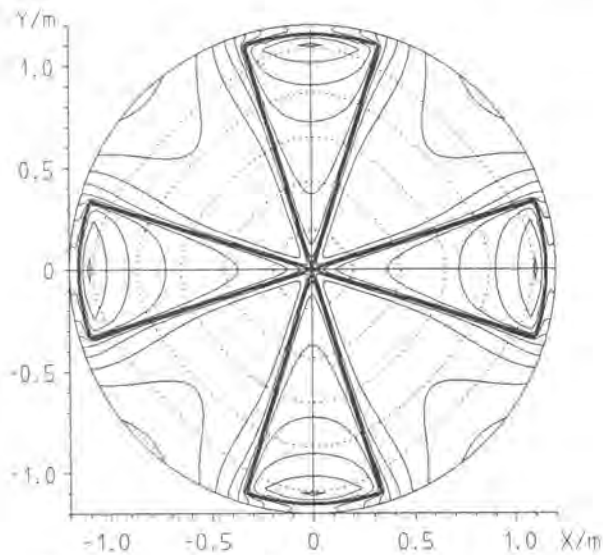


Fig. 3 The magnetic field computed in the median plane of the proposed sector magnets; equi-field contours at 0.3 tesla intervals are shown from 0.6 to 4.2 tesla within a radius of 1.2 m, together with five equilibrium orbits.

Results obtained by numerical orbit integration in this field are summed up in Fig. 4, for orbital frequencies of 26, 26.5 and 27 MHz. The field is too high for all three frequencies, but it becomes approximately isochronous within ~1% when it is multiplied with appropriate scaling factors which correspond to average current densities of 42.7, 44.3 and 46 A/mm^2 respectively in the coils. The apparent 2% field increase in the central region is most probably due to the discretization used in the calculation of the field, but there can be little doubt that only minor modifications of the poles are needed to correct the remaining deviations from isochronism or possible field aberrations which might occur in practice.

The focusing properties are satisfactory for the beam requirements and no unusual resonances are encountered by the beam in the ν_x/ν_z-diagram. For orbital frequencies of 26 and 27 MHz the extraction energy is limited to ~205 MeV by the onset of the radial fringe field or by losing vertical beam focusing, but a maximum proton energy of $\geq$ 220 MeV could be reached for 26.5 MHz if the radial fringe field is used to extract the beam. Under these conditions the fringe field is entered beyond 216 MeV and the $\nu_x=1$ resonance is

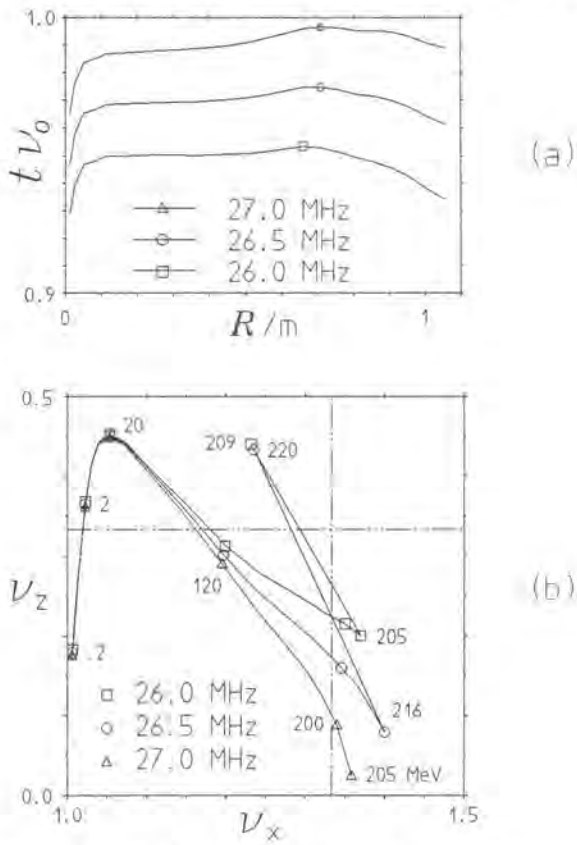


Fig. 4 The radial slope of the normalized revolution time (a) computed for orbital frequencies ν_0 of 26, 26.5 and 27 MHz respectively, and (b) the focusing characteristics obtained for the beam when the field has been made isochronous accordingly.

passed at $\nu_z = 0.75$ between 221 and 222 MeV. The average phase slip is only about 1.5° (rf) per turn in this region and the orbit separation increases to $\geq$ 2.5 mm/MeV in the process. This could be enhanced further to a value between 5 and 7 mm/MeV with the help of coherent beam oscillations at $\nu_x = 1$ which provides favourable conditions for making effective use of extraction devices in a 4-sector machine.

5. MAGNET STRUCTURE

Construction and assembly of the magnets is facilitated considerably by their reduced size, which also has structural advantages. A preliminary assessment of different assembly options indicates that the magnet poles should be integrated into a single cylindrical vacuum chamber by mounting them on the inside of the top and bottom lid of the chamber. The individual pole pieces are ~0.9 m high for such a design and suitable spacers can be inserted on the radial rim of the pole gap to provide the necessary support. The yoke sections and pole pieces of each magnet also must be bolted together to ensure structural integrity, but the requirements are quite conservative. Calculations show that the attraction between the poles will not exceed 1.6 MN per sector at full excitation, and that the deformation of the pole gap is insignificant under these conditions. The strongest structural forces are those transferred from the S-coils which push the magnets radially outwards. Suitable links must be provided between the four magnets at the top and bottom yoke sections to ensure their radial stability.

Without doubt the most difficult mechanical problem is to prevent the S-coils from moving excessively within the confinement of the cryostat. The Lorentz force acting on the coils when they are perfectly positioned has been analysed using the field computed with TOSCA, and the results are presented in Fig. 5. The maximum field across the superconductors does not exceed 5.4 tesla for a mean current density of 44.3 A/mm^2 in the coils, but overall the forces are quite high. Each coil is pushed radially away from the cyclotron axis with 3.8 MN and pulled towards the median plane with 0.9 MN. A force of 4.2 MN acts azimuthally on the vertical coil sections. Although the resulting stresses are far within the acceptable limit for potted coils, the total forces clearly demonstrate how important it is to reduce the field in the coils as much as possible by optimizing the magnet design. Winding the coils directly on a full iron core and increasing the area of the return yoke somewhat would help considerably to attain this goal. The moments acting on the coils for deviations from the ideal position still have to be investigated, and the whole cryogenic design needs proper attention, but it should be technologically feasible to develop and operate such magnets successfully.

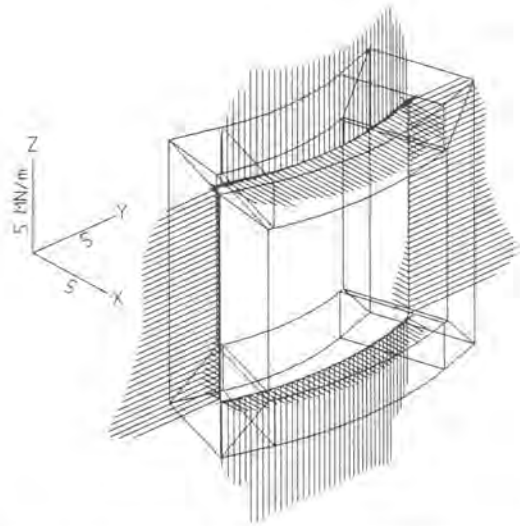


Fig. 5. The Lorentz force components calculated on the centre line of the S-coil above the median plane of the proposed sector magnet for a mean current density of 44.3 A/mm^2.

6. ACKNOWLEDGEMENTS

We would like to thank Dr U Schryber and Mr B Berkes of PSI for making the field calculations possible, Mr D P Brombach of PSI for his untiring efforts to bring them to a successful conclusion, Mr W A G Nel of NAC for carrying out the orbit calculations and Dr A H Botha of NAC for his essential support and discussions concerning the cyclotron.

7. REFERENCES

1) Chuvilo, I.V. *et al.*, **Proc. 11th Int. Conf. on Cycl. and their Applic.** (Tokyo, 1986) pp. 693-696.
2) Cole, R. *et al.*, **Proc. 1989 IEEE Part. Acc. Conf.**, Vol. 2 (Chicago, 1989) pp. 737-740.
3) Mandrillon, P., **Proc. 2nd Eur. Part. Acc. Conf.** (Nice, 1990) pp. 263-267.
4) Fukumoto, S. *et al.*, **Proc. 8th Symp. on Acc. Sci. and Techn.** (Saitama, 1991) pp. 456-458.
5) Inoue, M. *et al.*, ibid, pp. 459-461.
6) Blosser, H.G. *et al.*, **Proc. 11th Int. Conf. on Cycl. and their Applic.** (Tokyo, 1986) p. 165.
7) Jongen, Y. *et al.*, **Proc. 2nd Eur. Part. Acc. Conf.** (Nice, 1990) pp. 274-276.
8) Jungwirth, H.N and Brombach, D.P., **Proc. 12th Int. Conf. on Cycl. and their Applic.** (Berlin, 1989) pp. 498-501.
9) Jungwirth, H.N., **Proc. 11th Int. Conf. on Cycl. and their Applic.** (Tokyo, 1986) pp. 325-328.
10) Brombach, D.P., private communications.
11) Trowbridge, C.W., **Proc. 12th Int. Conf. on Cycl. and their Applic.** (Berlin, 1989) pp. 422-431.

Accelerated Radioactive Nuclear Beams: Existing and Planned Facilities

J. Michael Nitschke
Nuclear Science Division, Lawrence Berkeley Laboratory, Berkeley
CA, 94702, USA

ABSTRACT

An over-view of existing and planned radioactive nuclear beam facilities world-wide is given. Two types of production methods are distinguished: projectile fragmentation and the on-line isotope separator (ISOL) method. While most of the projectile fragmentation facilities are already in operation, almost all the ISOL-based facilities are in still the planning stage.

1. INTRODUCTION

The advent of intense Radioactive Nuclear Beams (RNB) in this decade may rival in importance the development of heavy ion beams in the 1960s. Radioactive beams were mentioned, for the first time, during the concluding discussion of the Symposium on Nuclides far of Stability in Lysekil in 1966 where J.P. Bondorf pointed out "the rich field of information that would be opened by a future use of unstable targets and projectiles in nuclear reaction studies".[1] The first radioactive beams were produced in 1969 by a group from LRL (later LBL), Berkeley, that accelerated fission fragments from a ^{252}Cf source placed in the MIT MP Van De Graaff.[2] The idea was kept alive in Europe mainly by members of the CERN/ISOLDE group. However, even as recently as 1977, a CERN Workshop on Intermediate Energy Physics concluded that there was not a sufficiently strong physics case to warrant a major RNB construction project.[3] This has now changed profoundly, as a host of scientific questions has been raised that can only be addressed with radioactive beams. What is even more important, several crucial technological advances have occurred in the preceding years that allow the generation of *intense* RNBs for meaningful physics experiments.

The science of RNBs has been discussed at several workshops and conferences.[4-11] The key new physics feature is that the neutron-to-proton ratio of radioactive projectiles can be varied over a wide range for experiments in the nuclear-, astrophysical-, atomic-, and material sciences. For example, in stellar processes at elevated temperatures the time for nuclei to β-decay toward more stable configurations may be long compared to the time it takes these nuclei to undergo nuclear reactions. This may lead to the synthesis of heavier elements from lighter precursors. An understanding of this process requires the measurement of a large number of nuclear reaction- and structure parameters, many of them involving radioactive beams or targets. RNBs may themselves have extreme nuclear matter distributions, if they are located near the neutron- or proton drip lines, and may produce even more exotic nuclei in compound nucleus or transfer reactions. This could provide access to new closed shells or regions of deformation, new nuclear shapes, and new forms of collectivity. Hyper deformed (axis ratio 3:1) and "banana" shaped nuclei have been predicted for nuclei that can only be studied with RNBs. The flexibility in the choice of the neutron to proton ratio offered by RNBs will allow the exploration of isospin dependent nuclear properties over a wide range of isotopes and isotones (and explains why the RNB facility proposed for North America has been given the name IsoSpin Laboratory). For details about these fascinating scientific questions the reader is referred to the above mentioned conference- and workshop proceedings.

2. PRODUCTION METHODS

There are two methods of producing high intensity RNBs: one is based on the fragmentation of high energy *heavy* ion projectiles on a light target and the second on the fragmentation, spallation, or fission of heavy targets by energetic *light* ion beams, followed by the post-acceleration of the radioactive species. The two methods are the kinematic inverses of each other and in many ways complementary. Projectile fragmentation has been used successfully in several laboratories while the second approach -- termed ISOL method -- is still in the development stage. The ISOL method derives its name from the fact that the central part of the RNB facility is similar to an Isotope Separator On-Line. A third method[12-13] using peripheral reactions at low energies and a superconducting solenoid spectrometer has been used to produce RNBs of modest intensities; it will, however, not be discussed here in detail.

2.1 Projectile Fragmentation

Projectile fragmentation (PF) is a reaction process in which the heavy ion projectile reacts peripherally with

the target nucleus, leaving the projectile with much of its initial momentum and a small angular spread. The cross section for PF becomes a significant fraction of the total reaction cross section for heavy ion beam energies of ~50MeV/u to several GeV/u. The projectile fragments are characterized by a wide distribution in A and Z and need to be purified in magnetic spectrometers to become useful for nuclear physics experiments. Due to overlapping charge-to-mass ratios a purely electro-magnetic separation is inadequate and a Z dependent ion-optical element in the form of a degrader has to be added. Many RNBs produced by PF in the past have been used at the full projectile energy. For other experiments, however, lower energies are needed and the RNBs have to be decelerated by passage through an absorber or -- after injection into a storage ring -- by an RF system. To avoid severe degradation of the beam quality during deceleration stochastic- and/or electron cooling has to be applied.

The advantages of using the PF method for RNB production are: short separation times (~μs) and therefore no losses due to radioactive decay, no chemical selectivity (the release of the radioactive species from the target is independent of Z), simple production targets (no large amounts of unwanted radioactivity are produced), high product collection efficiency (≳50%) due to forward kinematic focusing, and reliable operation. Some disadvantages are: low primary beam intensity compared to the ISOL method, target thickness limited by the acceptable momentum spread of the secondary beam, high projectile energies necessary for fully stripped ions in the separator (50-500MeV/u), poor secondary beam emittance (depending on the production mechanism and the target thickness), moderate beam purity, and difficult deceleration without intensity loss. The RNB production luminosity of a modern PF facility can reach 3×10^{35} $cm^{-2}s^{-1}$. A recent survey of the PF method has been given by Sherrill.[14)]

2.2. ISOL Method

Compared to PF, the ISOL method takes a complementary approach to RNB production. A high energy beam of light ions (typically protons) impinges on a thick target and creates radioactive species through target fragmentation, spallation or fission reactions. The products are produced with low kinetic energies and stop in the target. Target materials vary greatly, depending on the intended reaction mechanism, the chemical properties, and the half-life of the desired isotope: pure metals like Ta, La, Nb, V, and compounds like UC, ThO, and Hf_5Si_3 are used in solid-, liquid-, foil-, or powder form. To facilitate the removal of the activity from the target, transport to the ion source, and ionization, all parts with which the radioactive element comes into contact are kept elevated temperatures (up to ~2500C). If desired, a limited Z selection can be obtained by varying the temperature of the transport line to the ion source. The radioactivity is introduced into an ion source in gaseous form and singly or multiply charged ions are produced. They are accelerated to energies of a few tens of keV and mass-analyzed by an isotope separator. The function of the separator is to provide beams for post-acceleration that are free of unwanted isotopes, isobars, ionic charges, and molecular ions.

The most effective method for post-acceleration is a series of LINACs operating at ~100% duty factor, since they have excellent transmission and good beam quality. To make the acceleration process more economical the ions are, in general, stripped at intermediate energies. Most planned ISOL-based RNB facilities intend to provide beam energies of at least 1.2MeV/u and some may go as high as 30MeV/u. The RNB production luminosities are very high ($\lesssim10^{39}$ $cm^{-2}s^{-1}$) which is one of the main advantages over PF-based facilities. Other advantages are the high beam purity, ease of energy variation, and excellent beam quality characterized by small transverse and longitudinal emittances. Some disadvantages of the ISOL method are: RNB yields that are strongly dependent on the target/product chemistry, losses due to radioactive decay caused by delays associated with diffusion and effusion, the generation of large amounts of unwanted radioactivity, and the need for a post-accelerator. A recent survey of the ISOL method has been given by Ravn.[15)]

3. EXISTING AND PLANNED PROJECTILE FRAGMENTATION FACILITIES

3.1 Bevalac, Berkeley

The Bevalac has been considered the "grandfather" of the projectile fragmentation method. (For a detailed account of its capabilities see Ref. 16.) Using primary ion beams as heavy as ^{238}U with energies of up to 2.1GeV/u radioactive beam experiments have been carried out since the early 1970s.[17)] Primary intensities of 10^8/pulse can be routinely obtained at a pulse rate of one per 6s. The potential of the PF method was shown in a pioneering experiment in 1979 when over 64 isotopes formed in the fragmentation of ^{48}Ca were observed, many of them for the first time.[18)] Presently four beam lines are dedicated to RNB research: one for the radiotherapy treatment program, two for low- and medium mass nuclear science studies, and a fourth line for higher mass ($A \lesssim 100$) experiments. The latter is connected to the Bevalac's Heavy Ion Superconducting Spectrometer. All beam lines are operated in a dispersive mode that allows the separation of RNBs according to A/Z and Z. Additional selectivity can be obtained through time-of-flight selection. In favorable cases up to 1% of the primary beam can be

converted to RNBs. Polarized- and low-energy beams have been produced for magnetic and life-time measurements.[19)]

3.2. RIKEN, Japan

The primary beam accelerator for the RIKEN RNB facility is a K=540 separated sector cyclotron injected by a heavy ion LINAC and an AVF cyclotron. High intensities of high charge state ions from ECR sources result in a variety of heavy ion primary beams with energies of ~100MeV/u. The facility has produced RNBs since 1990 and was recently described in Ref. 20. A second-generation projectile fragment separator for RNBs (RIPS) has been constructed as an achromatic spectrometer in which the projectile fragments are analyzed by a combination of magnetic and energy loss elements. The strong kinematic forward focusing characteristic of the PF process and large geometric- (5msr) and momentum (6%) acceptances of the spectrometer result in high intensity secondary beams. The maximum rigidity of RIPS is 65% larger than that of the cyclotron, which allows the analysis even of very neutron rich fragments at the highest primary beam energies. An example of typical conditions for the production of light, neutron-rich RNBs is: a primary beam of ^{18}O at 100 MeV/u with an intensity of 100 pnA and a converter target of Be with a thickness of 1.1 g/cm^2. Under these conditions the following RNB intensities were observed: 1.7×10^5 ^{8}He/s, 2.8×10^4 ^{11}Li/s, and 4.4×0^3 ^{14}Be/s. These beam intensities have allowed secondary reaction studies with cross sections as low as 1mb. Recently a spectrometer system has been added to RIPS for the exclusive measurement of secondary reaction products. Also, low energy RNBs to ~5MeV/u can be obtained with a degrader technique. An intermediate-energy PF reaction mechanism is used to obtain spin-polarized RNBs with $\lesssim$5% polarization.[21)] The polarized RNBs are emitted off the forward direction and are guided into RIPS by a beam swinger.

3.3. GSI, Germany

At GSI RNBs are produced through the fragmentation of heavy ion projectiles up to U from a synchrotron (SIS18), with typical energies of 0.5-1GeV/u. The secondary beams are analyzed in a large zero-degree achromatic spectrometer (FRS)[22)] and can either be studied directly in its focal plane or injected into a storage ring (ESR). Eventually, the ESR will be able to reinject beams into SIS18 for acceleration to higher energies. The FRS uses the energy-degrader technique and a combination of dipoles and quadrupoles to achieve A and Z resolution and to spatially separate individual isotopes. Its resolving power is 1.5×10^3 for 20π mm mrad beam emittance and its efficiency for projectile fragments is ~60%. Its luminosity for fragment production is $\lesssim3\times10^{35}$ cm^{-2}s^{-1}.[22)] The feature of the GSI facility that is unique among the PF installations is the coupling of the FRS to the storage ring. It allows the direct observation of the decay of accumulated RNBs, measurements of their masses, and the study of their interaction with an internal gas target. Cooling the circulating beam with electrons results in a 10^7 fold improvement in the phase space density (a momentum spread of $\Delta p/p=2\times10^{-6}$ has been observed).[23)] Cooling is necessary for the successful deceleration of the beam due to the momentum dependence of the emittances. It is expected that beams can be decelerated from ~500MeV/u to <5MeV/u, and low energy RNBs thus would become available not only from ISOL- but also from PF- based facilities. There are, however, two effects that curtail the usefulness of this technique: one is the space charge forces in the ring that limit the number of circulating ions to ~10^6-10^7, and the other is the time it takes to cool the beam, which is on the order of several seconds, and rules out the deceleration of very short lived isotopes.

3.4. GANIL, France

The primary heavy ion beams at GANIL are produced with two K=400 cyclotrons that can be operated independently or in tandem. In the latter case stripping between the cyclotrons is employed to obtain higher charge states and final energies of 30-100 MeV/u. Beam intensities are well above 10^{12} ions/s and a one-order-of-magnitude upgrade is planned. A novel beam focusing- and reaction-product-collection device named SISSI has recently been installed at the target position. It increases the RNB intensities by a factor ~10.[24)]

The principal instrument for the production and study of secondary radioactive beams is LISE, a zero degree spectrometer consisting of two dipoles and several quadrupoles.[25-26)] The first dipole analyses the projectile fragments according to A/Z, a slit in the dispersion plane selects the desired momentum bite, and the second, symmetric dipole compensates the dispersion of the first one. Consequently, the spectrometer is doubly achromatic in angle and position, and the flight path between the target and the final focus is independent of the emission angle of the reaction products. By introducing an energy degrader of variable thickness in the dispersive plane, q/A ambiguities can be resolved and the spectrometer operates as an isotope separator. To improve further the isotopic selection a "Wien filter" has recently been added that separates the nuclei according to their velocity. Using the LISE spectrometer, all existing neutron-deficient nuclei up to Ti (Z=22) have been studied. Recent results from LISE3

are reported in Ref. 27. A second spectrometer at GANIL, SPEG, is particularly well suited for the measurement of masses of exotic nuclei. It combines high resolution time-of-flight with magnetic analysis and achieves a mass resolution of m/Δm=1000. Mass measurements have also been discussed using the two coupled K=400 cyclotrons.[28)]

3.5. NSCL, East Lansing

At the National Superconducting Cyclotron Laboratory (NSCL) primary ion beams in the energy range 50-200MeV/u are produced by a K=1200 superconducting cyclotron. A beam analysis device, A1200, connects the cyclotron to the experimental areas. With suitable targets installed at its "object" position the A1200 also can be used to collect and separate RNBs produced by PF and deliver them to several experimental devices. The A1200 was designed as an achromatic device with two intermediate images that allows for momentum measurements and the placement of degrader foils, as discussed for the other PF facilities.[29)] The A1200 has a resolving power that ranges from 0.7 to 1.5×10^3 depending on the chosen solid angle in the range from 4.3 to 0.8msr. Despite the good resolution very exotic nuclei can only be produced with modest purity. For example, for ^{65}As the expected RNB purity is $\sim5\times10^{-4}$. However, since the production rate is only ~10/s the flight time relative to the cyclotron RF cycle can be used to discriminate against unwanted nuclei. Currently, the construction of a large superconducting solenoid is underway that will allow the production of RNBs through transfer reactions with primary beams of ≲50MeV/u.[30)]

3.6. Planned PF Facilities

In Italy two laboratories have plans for radioactive beams. At the "Laboratorio Nazionale del Sud," Catania, a K=800 superconducting cyclotron will be injected by a 15MV MP-Tandem. RNBs can be produced from medium light ions at energies of 50-80MeV using the PF method.[31)] A fragment recoil separator is used to analyze the secondary beams and supply them to the experimental areas.

At the same laboratory low energy RNBs can be obtained by operating the cyclotron in a stand-alone mode, using an external ECR source, and transporting light ion beams with 50-80MeV/u energy to the Tandem area where they will be used to bombard a thick target. Target recoils will be attached to aerosols, transported to a negative-ion source and extracted by a 150kV potential. After isotope separation the ions are injected into the Tandem, which will provide RNBs with energies up to 8MeV/u and projected intensities of ≲10 pnA.

The second Italian project is at the Legnaro Laboratory associated with the ADRIA facility.[32)] It has two accelerator rings that have a maximum magnetic rigidity of 22.3Tm. The first synchrotron can deliver ion beams with intensities in excess of 10^{11} s^{-1} and energies of 1-2.5GeV/u to a production target for PF. The secondary beams are injected into the second ring and cooled stochastically or by electrons. After accumulation of a sufficient number of radioactive ions (~10^7) deceleration to the Coulomb barrier is planned. The extracted beams will be used for nuclear structure studies.

A large PF facility is under construction for the Dubna Laboratory, FSU, using two coupled cyclotrons that will provide beams from H to U with intensities of ≲10^{13} s^{-1} and energies of 100-20 MeV/u.[33-34)] The RNBs will be analyzed and studied with several instruments: a projectile fragment separator (COMBAS), a time projection chamber, a He-filled neutron counter, and a 4π γ- and charged particle spectrometer. The separator is preceded by a beam swinger to allow the production of spin-aligned secondary fragments. Future expansion of the Dubna facility will include two storage rings (K4 and K10) with maximum rigidities of 4 and 10Tm, respectively.[35)] Both rings are equipped with electron coolers. RNBs produced by PF of the primary beam from the K4 ring can be injected into the K10 ring through a projectile fragment separator. The authors of the proposal (Ref. 35) "specify the main purpose of the project by dedicating it to the production of high precision RNBs."

At the Research Center for Nuclear Physics, Osaka University, Japan, a secondary beam channel is under construction.[36)] Its central instrument is a fragment separator employing the degrader technique described earlier. Calculations show that a mass resolution m/Δm≈330 and a Z resolution Z/ΔZ≈200 can be expected. The separator receives its primary beam of medium heavy ions from a K=400 cyclotron.

4. EXISTING AND PLANNED ISOL-BASED RNB FACILITIES

In contrast to the PF situation, there is only one ISOL-based RNB facility in operation. Yet, as of this writing, (June 1992) there are twelve proposals for ISOL facilities in nine countries. The proposals are in various stages of development and no attempt will be made to judge their merits or chances of realization. Only very brief descriptions can be given here.

4.1. Louvain-la-Neuve, Belgium

The RNB facility at Louvain-la-Neuve has successfully produced pure RNBs of ^{13}N and ^{19}Ne for astrophysical experiments.[37-38] This was done by coupling together two cyclotrons: the first, using a beam of up to 500μA of 30MeV protons and suitable targets, produces large amounts of light radioactive isotopes near stability. The radioactive species emanate from the hot target and are ionized in an ECR source. The second cyclotron accelerates them to ~1MeV/u for astrophysical experiments. Measured intensities for ^{13}N and ^{19}Ne have exceeded 50 ppA. The high mass resolution of the second cyclotron was crucial for obtaining high RNB purities.

There are plans to expand the facility at Louvain-la-Neuve to produce other intense RNBs for nuclear-, astrophysical-, and solid-state studies (ARENAS^3).[39] The upgrade is mainly based on the development of efficient ECR sources for high charge states that will allow the production of RNBs near the Coulomb barrier. For astrophysical studies a post-acclerator with an energy range of 0.1-1.0MeV/u is under study.

4.2. PRIMA, ISOLDE/CERN, Switzerland

The ISOLDE facility is presently being reconstructed at a new experimental hall where it will make use of a 1GeV proton beam from the CERN PS Booster. In 1989 a detailed proposal (PRIMA) for the post-acceleration of radioactive ions from the ISOLDE facility was presented.[40] The physics motivation for PRIMA came predominantly from astrophysicists and has influenced the specifications: mass range 6-30u, energy $\lesssim$1MeV/u, and intensities ~$10^9 s^{-1}$. Radioactive beams from ISOLDE3 would be accelerated in a pre-stripper RFQ accelerator, stripped at ~200keV/u, and further accelerated in a system of four LINACs of the interdigital H-type with magnetic focusing. To extend the mass and energy range in the future, higher charge states are needed and the use of an electron beam stripper combined with a superconducting booster LINAC is being investigated.

4.3. PSI, Switzerland

Plans are being discussed to construct an RNB facility at the Paul Sherrer Institut (PSI).[41] A primary production beam of 590MeV protons with a current of $\lesssim$1mA is available. Contrary to most other ISOL-based projects, it is proposed to focus on the "thin target" approach. In this method the target thickness is kept thin enough (~0.2-10mg/cm^2) to let the proton-induced reaction products recoil into a stopping gas. Compared to the thick target method there is a loss in target thickness of ~10^4. To compensate partially for this, the PSI proposal envisions using up to 1000 targets of 0.2mg/cm^2 in a gas volume of 2ℓ (STP). Another approach uses a 1m long gas target at 10 bar with a volume of 20ℓ. In both cases the radioactive atoms are separated from the bulk of the gas by a skimmer technique and introduced into an ECR source. The post-acceleration could be accomplished with an existing K=120 cyclotron to give RNB energies of 1.0-30MeV/u. It is often assumed that the thin target approach is insensitive to chemical discrimination since the release from the target does not involve diffusion or desorption processes, and that it can, therefore, deliver elements that are usually inaccessible to the ISOL method. It should, however, be kept in mind that much of the chemical discrimination takes place in the *ion source* and depends strongly on its operating temperature. ECR sources, in particular, have, thus far, not been developed for high temperatures.

4.4. ISIS, Rutherford Laboratory, England

At the Rutherford Appleton Laboratory (RAL) a proton beam of 800Mev and 100μA (200μA after upgrade) is available for RNB production. It has been proposed to construct an RNB facility following the technologies developed at ISOLDE/CERN.[42] In a first option RNBs with masses up to A=80 and q=1 will be accelerated in a series of RFQs and LINACs to energies of 6.5 MeV/u. By going to q>1 and boosting the heavy ion LINAC, RNBs up to mass A=180 would become available. In a second option the RFQ injects directly into a fast-cycling synchrotron that would deliver light RNBs with energies up to 20MeV/u. In a future development the synchrotron could inject ions back into the ISIS ring and RNBs with 40.6 and 120 MeV/u energy could be obtained for light and heavy ions, respectively. It has been discussed to combine the ISOLDE/PRIMA proposal with the RAL plans to create a "European High Intensity Radioactive Nuclear Beam Facility."[43]

4.5. RNB, Moscow, Russia

An RNB facility at the Moscow Meson Factory is under discussion.[44] The proposal differs in several regards from other ISOL-based facilities. It is planned to use the full-intensity 600MeV-1mA proton beam on *thick* porous or liquid targets. To cope with the large amounts of radioactivity a purification step using gas-phase chemistry is interspersed between the target and the ion source. The chemical system also serves to transport the activities at the velocity of sound to a remotely located ion source that produces multiply charged ions. The post-acceleration proceeds in two steps: an isochronous injector cyclotron (K=208) coupled to a separated sector cyclotron (K=600). This accelerator complex will yield energies above the Coulomb barrier ($\gtrsim$5MeV/u) for masses A$\lesssim$150. As an alternative, a system of CW LINACs for the acceleration of

RNBs from 1keV/u to 6.5MeV/u is being developed.[44] Eventually a storage ring with cooling and acceleration may be added.

4.6. GANIL, France

GANIL has been at the forefront of radioactive beam research for several years using the PF method. There is now a proposal to add a unique ISOL-based facility using light ions as primary beams.[45-46] This will be facilitated by an upgrade yielding beam intensities close to 5×10^{13} and 5×10^{12} for Ar and Kr, respectively. The arguments for using light ions as primary beams are that the cross sections for producing nuclei far from stability are larger, and that thinner targets can be used that will shorten the diffusion time and, therefore, reduce decay losses. (This will, however, not affect desorption-limited delays.) The basic features of the proposal are: the use of light C or Ar beams at energies of 100MeV/u with intensities of ~5×10^{13} s^{-1} on thick targets, ionization of the radioactive species in an ECR source, and post-acceleration with a combination of RFQs and LINACs. The final beams will have energies >25MeV/u and can be injected into the main beam line at GANIL to make optimal use of the experimental areas. Another method of post-acceleration is to use the combination of an injector cyclotron and a separated-sector cyclotron similar to the "standard" GANIL design.[46] The two cyclotrons also would serve as a powerful spectrometer.

4.7. PIAFFE, Grenoble, France

A second RNB facility in France (PIAFFE) is proposed for the high flux reactor at the Institut Laue Langevin in combination with the SARA accelerator complex at Grenoble.[47] The goal is to produce beams of neutron-rich nuclei in the mass range of A=70-150u with energies of 2-10 MeV/u (≲20MeV/u for masses A≲85u). The expected beam intensities are 10^5-10^9 s^{-1} depending on the nuclear species. The production target consists of ~(1-3)g of ^{235}U immersed in a thermal neutron flux of (1-3)×10^{14} neutrons/cm^2/s. One of the advantages of using neutrons for RNB production is that target heating by the beam is negligible; the only heat source is the fission process. Two target arrangements are contemplated: A thick hot target where the release of the radioactive species is based on diffusion, and a series of thin targets where the activity recoils into a stopping gas (He). In the first case the ion source is ~1m from the target at the end of a transfer tube. For the He-jet system a skimmer arrangement is used to separate the transport gas from the activity that is then introduced into an ECR source outside the biological shield of the reactor. After mass separation q=+1 ions with 30 keV energy are transported (under vacuum) 450m(!) to the SARA accelerating complex, which consists of two coupled cyclotrons with K=88 and 160. With a new extraction system the 2-10MeV/u energy range of interest in nuclear physics could be covered. The over-all efficiency of the facility is estimated to be ~10^{-4}. The projected intensities for certain neutron-rich isotopes compare favorably with those expected from some proton machines. The factor limiting the RNB intensities is, apparently, the safety of the reactor.

4.8. E-Arena, INS, Japan

An update of the Japanese plans for an RNB facility at the Japanese Hadron Project (JHP) was given recently by T. Nomura[48] (see also Ref. 49). The primary beam is H^- with an energy of 1GeV and a maximum average current of 400μA. Standard ISOL techniques are used to generate the radioactive ions that are then accelerated to a maximum energy of 6.5 MeV/u by a series of RFQs and LINACs. The planned mass ranges are A≲60 for ions with q=+1, and A≲120 for q=+2. Substantial developments have been carried out to accelerate "slow" (1keV/u) ions to 45keV/u. For N_2^+ ions a transmission of 92% through a Split-Coax RFQ operating with a 30% duty factor has been obtained. In preparation for the E-Arena at the JHP a development project is underway that makes use of a 45 MeV primary proton beam from the INS K=68 cyclotron. RNBs of light isotopes of interest in astrophysics will be produced with energies ≲1MeV/u. A high resolution mass separator is an integral part of the project; it has achieved a resolution of m/Δm=5000.

4.9. ISAC, TRIUMF, Canada

One of the earliest proposals for a radioactive beam facility (ISAC) was made by Canadian researchers.[50] Recent updates were given in Ref. 51 and 52. ISAC will make use of the variable energy proton beam (185-505MeV) at TRIUMF. Variable primary energy could be useful to enhance the production of desired nuclei while suppressing the "background" of unwanted ones. It is planned to couple the target/ion source via a high-resolution separator to an RFQ pre-accelerator, followed by a stripper and a drift-tube LINAC as post-accelerator. The final energy of ≲1.5MeV and the mass range of A≲60 were chosen mainly to study astrophysical problems. Presently, a Test Isotope Separator On-Line (TISOL) is in operation. One of its unique features is an on-line ECR source. This and other developments carried out at TISOL are intended not only to support a future ISAC proposal but also the plans for an IsoSpin Laboratory in North America discussed below.

The specifications of a TRIUMF-based RNB facility are in flux, depending on the fate of KAON. If KAON gets built, locating ISAC at a 3 or 30GeV beam line has been discussed.[51] Higher primary beam energies would have the advantage of larger cross sections for nuclei far from stability and reduced energy deposition in the target.

4.10. OREB, Oak Ridge

At the Oak Ridge National Laboratory an RNB facility is under construction that could, in principle, provide 95 proton-rich isotopes between ^{6}He and ^{84}Rb with energies >5MeV/u.[53] The facility is based on the ORIC cyclotron (K=105) as a light ion (LI) primary beam accelerator. The maximum energies for ^{1}H, ^{2}H, ^{3}He, and ^{4}He are 55, 52, 140, and 105 MeV, respectively, and the desired nuclei are typically formed in (LI; xn,yp) reactions. Negative(!) radioactive ions are generated by one of two methods: for elements with electron affinities greater than ~2eV direct surface ionization on hot LaB_6 can be used, for other elements a charge-exchange vapor cell may be employed. After extraction the ions are accelerated to 300keV and injected into the existing 25MV Tandem electrostatic accelerator. Ref. 53 gives details about expected RNB intensities and the planned physics program. As is true of the TISOL facility at TRIUMF, some of the work at OREB is undertaken to support plans for a future full-scale RNB facility in North America.

4.11. The IsoSpin Laboratory, North America

In 1989, as contribution to the Long Range Plan for Nuclear Science,[54] the author proposed the construction of a High Intensity Radioactive Nuclear Beam Facility in North America, later named IsoSpin Laboratory (ISL). The scientific case for such a facility was discussed at several meetings.[55] [8-9] A Steering Committee for the ISL has been formed that has published a report[56] detailing the research opportunities at the ISL and showning its technical feasibility in the form of a "bench-mark facility" (BMF). The "design philosophy" for the ISL is to push the technologies for producing and accelerating radioactive species to their limits to obtain the highest RNB intensities feasible. Accordingly, the intensity of the primary 0.5-1GeV light ion beam (~100pμA) will be considerably above the ~2pμA that have traditionally been used, for example, at ISOLDE/CERN. The primary beam intensity is limited by the power density in the target to $\lesssim$1kW/cm^2 for many materials (total power ~40kW). Besides the conventional surface- and plasma sources ECR- and Laser sources will play a major role in the ISL. The characteristics of the target matrix and the ion source must be matched to the chemical nature and the half-life of the radioactive isotope to maximize its yield. To cope with the large amounts of unwanted radioactivity a chemical/physical purification step is interspersed between the target and the ion source, and a high resolution isotope separator will reduce isobaric contamination of the desired RNBs. The post-acceleration, as proposed for the BMF, starts with a low-β RFQ, stripping at ~100keV, followed by a drift-tube LINAC, stripping at ~1.2MeV/u, and final acceleration to ~10MeV/u with a superconducting LINAC. Acceleration to higher energies and the addition of a storage ring are being discussed. To minimize beam losses, the goal is to obtain close to 100% transmission for all ion-optical elements and accelerating structures. It may be possible to eliminate stripping losses with a device proposed by Cramer.[57] Expected RNB intensities and further technical and scientific details are given in Ref. 56.

It is hoped that funding for several planned RNB facilities will become available in this decade, allowing us to open new and exciting chapters in nuclear- and astrophysics, atomic physics, and material science.

This work was performed under DoE contract DE-AC03-76SF00098.

5. REFERENCES

1) *Nuclides far off the Stability Line,* Proceedings of the Lysekil Symposium, 1966, Session XII, W. Forsterling, C.J. Herrlander, and H. Ryde eds., Lysekil, Sweden (Almquist & Wiksell, Stockholm, 1967) p.681.

2) E. Cheifetz et al., Phys. Rev. Lett. **24**, 148 (1970).

3) G.Hansen, Proceedings of the CERN Workshop on Intermediate Energy Physics, Far unstable Nuclei, and Radioactive Ion Beams (1977) CERN PS-CDI/77-43.

4) J.M. Nitschke, Proceedings of the Symposium on Heavy Ion Physics From 10 to 200 MeV/AMU, J. Barrette and P.D. Bond eds., Brookhaven National Laboratory, 1979, BNL-51115, p.325.

5) Proceedings of the TRIUMF-ISOL Workshop, J. Crawford and J.M. D'Auria eds., Mont Gabriel, Québec, 1984, TRI-84-1, p.230.

6) Proceedings of the Workshop on Prospects for Research with Radioactive Beams from Heavy Ion Accelerators, J.M. Nitschke ed., Washington DC, 1984, LBL 18187, CONF-8404154.

7) J.M. Nitschke, Proceedings of the Workshop on Intermediate Energy Heavy Ion Physics, ORNL, 1985, p.K-1.

8) Proceedings of the First International Conference on Radioactive Nuclear Beams, W.D. Myers, J.M. Nitschke, and E.B. Norman eds., Berkeley, 1989 (World Scientific, Singapore, 1990).

9) Proceedings of the Workshop on the Science of Intense Radioactive Ion Beams, J.B. McClelland and D.J. Vieira eds., Los Alamos NM, 1990, LA-11964-C.

10) Proceedings of the Second International Conference on Radioactive Nuclear Beams, Th. Delbar ed., Louvain-la-Neuve, August 19-21, 1991 (Adam Hilger, 1992).

11) Proceedings of the International Workshop on the Physics and Techniques of Secondary Nuclear Beams, Dourdan, France, March 23-25 (1992) to be published.

12) F.D. Becchetti et al., Nucl. Instr. and Meth. **B56/57**, 554 (1991).

13) T. Yamagata et al., Phys. Rev. **C39**, 873 (1989).

14) B.M. Sherrill, Ref. 10, p.3.

15) H.L. Ravn, Ref. 10, p.85.

16) G.F. Krebs, J.R. Alonso, B. Feinberg, and J.G. Kalnins, Ref. 10, p.59.

17) H.H. Heckman et al., Phys. Rev. Lett. **28**, 926 (1972).

18) G. Westfall et al., Phys. Rev. Lett. **43**, 1859 (1979).

19) K. Matsuta, Hyp. Int. **61**, 1387 (1990).

20) T. Kubo et al., Ref. 10, p.65.

21) K. Asahi et al., Phys. Lett. **B251**, 488 (1990).

22) G. Münzenberg et al., Ref. 8, p.91.

23) G.Münzenberg et al., Ref. 11.

24) W. Mittig, Ref. 8, p.583.

25) J.P. Dufour et al., Nucl. Instr. and Meth. **A248**, 268 (1986).

26) A. Mueller and R. Anne, Ref. 8, p.132.

27) V. Borrel et al., Ref. 10, p.179.

28) P. Auger et al., Ref. 8, p.465.

29) B. Sherrill et al. Ref. 8, p.72.

30) F. Becchetti et al., *A Proposal to the DoE for a Large Superconducting Solenoid*, Univ. of Michigan, 1989.

31) E. Mignecoet al., Ref. 11.

32) L. Tecchio, Ref. 11.

33) R.Ts. Oganessian, Proc. 12th Int. Conf. on Cyclotrons and their Applications, Tokyo, Japan, (1986) p.566.

34) A.G. Artukh, Ref. 10, pp.21, 27, and 33.

35) *Heavy Ion Storage Ring Complex K4-K10*, Dubna, 1992, JINR Report E9-92-15.

37) P. Decrock et al., Ref. 10, p.121.

38) D. Darquennes et al., Phys. Rev. **C42** R804 (1990).

39) P. Decrock et al., Ref. 11.

40) H. Haas et al., Ref. 8, p.59.

41) H. Gäggeler et al., Ref. 11.

42) T.G. Walker, Nucl. Instr. and Meth. in Phys. Research, **B56/57**, 521 (1991).

43) H. L. Ravn, Ref. 11.

44) V.A. Andreev et al., Ref. 10, p.101; and A.S. Iljinov, V.M. Lobashev, and Yu.Ts. Oganessian, Ref. 8, p.23.

45) Report GANIL P 91.12

46) A. Chabert et al., Ref. 10, p.115.

47) J.L. Belmont et al.,Ref. 11.

48) T. Nomura et al., Ref. 11.

49) T. Nomura, Ref. 8, p.13.

50) *The TRIUMF-ISOL Facility*, Aproposal for an Intense Radioactive Beam Facility, TRIUMF, 1985.

51) L. Buchmann et al., Ref. 8, p.46.

52) L. Buchmann et al., Ref. 10, p.109.

53) A Proposal for Physics with Exotic Beams at the Holfield Heavy Ion Research Facility, J.D. Garrett and D.K. Olsen eds., February 1991, Physics Div. ORNL.

54) *Nuclei, Nucleons, Quarks* Nuclear Science in the 1990's. A Long Range Plan by the DOE/NSF Nuclear Science Advisory Committee, December 1989, U.S. DoE and NSF.

55) Transcript of the Workshop to Discuss Plans for a National High Intensity Radioactive Nuclear Beam Facility, J.M. Nitschke ed., Berkeley CA, 1989, LBL-28470.

56) *The IsoSpin Laboratory*, Research Opportunities with Radioactive Beams, LALP91-51.

57) J.G. Cramer, Nucl. Instr. and Meth. **130**, 121 (1975).

A CONCEPTUAL DESIGN FOR A PRIMARY CYCLOTRON FOR THE ISL RADIOACTIVE BEAM PROJECT*

D. J. Clark
Nuclear Science Division, Lawrence Berkeley Laboratory, Berkeley
CA, 94720, USA

ABSTRACT

A design for a 600 MeV proton cyclotron is described. Features include a single stage with external ion source, a normal conducting magnet coil with 2 T peak field in the hills, and dees in valleys. The design can be extended to 800 and 1000 MeV.

1. INTRODUCTION

The report on the IsoSpin Laboratory (ISL)[1] describes a "benchmark" reference design for a facility for the production of radioactive nuclear beams in North America. The primary accelerator is required to produce protons at an energy of .5-1.0 GeV and an intensity of 100 μA, while a secondary accelerator will accelerate radioactive beams from the target up to 10 MeV/u. The primary accelerator can be a cyclotron such as the PSI ring or TRIUMF. Because of the high beam power an essential requirement for this cyclotron is that of minimizing the beam lost at high energy inside the cyclotron, to prevent component damage and reduce radiation exposures during maintenance. This in turn requires very high extraction efficiency either by good turn separation at extraction or by use of negative ions. This paper presents a primary cyclotron design which minimizes cost while maintaining high extraction efficiency.

2. DESIGN CHOICES

A principal design choice is that between positive and negative ion acceleration. The negative ion choice (TRIUMF) is attractive because of easy beam extraction. However it requires low field to prevent electromagnetic stripping, and thus a large radius magnet. Also some beam is lost during acceleration, causing component activation. The positive ion choice (PSI ring) is attractive because of the very low beam losses and the smaller diameter magnet, but very careful beam handling and good turn separation are necessary. The large turn separation requires large energy gain per turn. The PSI design uses separate sectors, allowing space for 4-550 kV cavities giving over 2 MV/turn. The separate sector design requires an injector cyclotron. This paper combines features of both these cyclotrons. A positive ion design is chosen because of its smaller magnet and low beam losses. A compact magnet, rather than separated sectors, is used because it requires only one main coil, and eliminates the injector stage.

The requirement of good turn separation implies a large radius at full energy, since the turn separation at extraction is proportional to this radius for a given maximum energy. Large radius also means higher cost, since all the components are larger, and more magnet steel is required. So a compromise must be used to optimize cost and turn separation.

The magnet and rf design are closely related. Two styles of rf design are the "dees over hills and valleys" used at TRIUMF, and "dees or cavities in valleys" used at PSI. The dees in valleys design is chosen here because the hill gaps can be made small, just larger than the beam size, giving acceleration out to near the edge of the magnet, and easier extraction. Also the magnet power is lower with a small gap. These factors reduce the cost for a given energy. Dees in the valleys at this energy require the resonators to be in the valleys also, since the radial length of the dees is the order of 1/4 wavelength. The highest acceleration is required near extraction, so additional dees can be added there.

The number of sectors should be large enough to avoid the essential radial resonance at Nur=2 for small sector number. This requires at least 6 sectors for an energy of 600 MeV. A review of resonances is given by Richardson[2]. A sector number of 8 gives the possibility of accelerating through Nur=2, as demonstrated in an electron model at ORNL, Analogue II[3].

The sector number of 8, with dees in valleys, would cause problems of low axial focusing and large rf transit time near the center of the cyclotron. One solution is to start with 4 sectors near the center and have a transition to 8 sectors part way out in radius. Examples of this design are shown in Figs. 1 and 2. These are for illustration only, and use no spiral. They represent a region near the center, and spiral could be added if necessary. The flutter has not been evaluated. The design of 4 straight valleys, Fig. 1, would be simpler for the dee system. The design of 4 straight hills, Fig. 2, would be simpler for the magnet structure, but the dees would be rather complicated. The 4 sector, dee-in-valley design has been used very successfully by IBA in their 30 MeV proton cyclotron[4]. It uses axial injection at 30 kV with H^- ions, accelerates on harmonic 4 and produces 500 μA of external beam.

The ion source is assumed to be external, with an injection energy of about 50 kV. An external source allows bunching into the required phase width for turn separation at extraction. The energy and particle would be fixed. In a special design one might also accelerate other light ions by changing magnet level and harmonic number of the rf.

3. PRESENT DESIGN

The present design for 600 MeV protons is shown in Fig. 3. As mentioned above it is a compact design using a single main coil. The maximum radius is about 3/4 of that of the PSI ring design. 8 sectors are used to avoid the Nur=2 resonance of 3 or 4 sectors and to allow valleys for small dees near extraction. This figure doesn't show the N=4 center region of Fig. 1, but that design is an option. The ion source is mounted below. Extraction is shown schematically, since no calculations have been done. It will use electrostatic and magnetic channels.

The hill field is assumed maximum at 2 T at maximum radius, and made proportional to gamma at smaller radius by varying the gap. The hill gap is .1 meter at the edge, and the beam accelerates to within .1 meter of the pole edge in the hill. The return yoke is assumed cylindrical outside the pole edge. The magnet yoke is split at the midplane, and the upper half can be lifted for maintenance.

The main dees operate at harmonic 4, 44 MHz, and extend in to the center. 1/4 wavelength of rf is 1.7 m, only about 1/2 the extraction radius, so the resonators must be in the valleys, with vertical dee stems. The rf amplifiers can feed from the side. Small dees, ED, indicated near extraction radius in Fig. 3, increase the energy gain/turn there and give the option of flat-topping for better turn separation. For acceleration they can operate at harmonic 8. For example, 4 dees at 250 kV, harmonic 8 would give about 2 MV/turn.

The orbit calculations used the simple formula for the axial focusing[5]:

$$Nuz^2 = F^2 (1 + 2 \tan^2 Eps) - \mu'$$

where Nuz is axial frequency, F^2 is flutter, Eps is spiral angle and μ' is the gradient term. A hard edge hill and valley boundary is assumed, and the valley field is assumed zero because of the large valley depth. In this case $F^2 = (1/f_h) - 1$. The hill fraction, f_h, is set equal to .6 and is assumed constant vs. radius. This gives $F^2 = .67$ at all radii. The spiral tan Eps is assumed proportional to radius squared to give a Nuz of about .8 at all radii. The actual soft edge F^2 will be smaller than assumed, but can be compensated with an increase in spiral angle. For example the PSI ring F^2 is about 20% less than the hard edge value. This would require a 3 degree increase in spiral angle in the present design. Nur is approximately equal to gamma: 1-1.6 for 0-600 MeV. Small trim coils on the hills can be used to produce the isochronous field.

Extraction will require some increase in turn separation beyond the natural value for an isochronous field. Since turn separation at extraction is proportional to radius, for fixed maximum energy, both the radius and the turn separation are 3/4 of the PSI ring values. It is assumed that the turn separation can be sufficiently increased to give nearly 100% extraction, by using high energy gain/turn, precession, letting the field fall below isochronism at extraction, and using the Nur=1.5 resonance. PSI uses these techniques to get a turn separation of 9 mm at extraction[6].

Table 1 gives some of the parameters of the present design. The maximum values of gamma, and spiral angle are given. The total angle of turning of the hills, theta, is shown and the weight is given. Also shown in Table 1 are higher energy designs at 800 and 1000 MeV, using the same assumptions of hill fraction of .6, maximum hill field of 2 T and valley field of zero. The 1000 MeV design would require accelerating through Nur=2, which appears possible, as mentioned earlier.

4. ACKNOWLEDGMENTS

The author wishes to extend thanks for the helpful discussions with W. Joho and H. Blosser, and for the information received from B. Milton and S. Adam on computer programs and magnetic fields.

5. REFERENCES

1) The IsoSpin Laboratory (ISL), LALP 91-51, North American Steering Committee of the ISL, 1991.
2) J. Reginald Richardson, "Sector Focusing Cyclotrons", in **Progress in Nuclear Techniques and Instrumentation**, V. 1 (North Holland, Amsterdam, 1965) pp. 58-61.
3) J. A. Martin, F. M. Russell, E. G. Richardson, Jr. and H. L. Dickerson, "Beam Extraction From Analogue II", CERN 63-19 (CERN, Geneva, 1963) pp. 52-58.
4) Y. Jongen, J. L. Bol, A. Chevalier, M. Lacroix and G. Ryckewaert, "Construction of the Louvain-la-Neuve 30 MeV 500 μA H^- Cyclotron", in Proc. 11th Int. Conf. on Cyclotrons and their Applications (Ionics, Tokyo, 1987) pp. 275-278.
5) Ref. 2, pp. 1-21.
6) W. Joho, "Recent and Future Developments at S.I.N.", in IEEE Trans. Nucl. Sci. **Vol. 26**, (2), 1950 (Apr. 1979).

*This work was supported by the Director, Office of Energy Research, Division of Nuclear Physics of the Office of High Energy and Nuclear Physics of the U.S. Department of Energy under Contract DE- ACO3-76SF00098.

Table 1.

E(MeV)	B-Rho (Txm)	Gamma	R_{pole} (m)	Spiral (deg)	Nuz	Theta (deg)	Magnet Wgt. (Met.T)
600	4.06	1.64	3.49	48	.8	36	1200
800	4.88	1.85	4.17	53	.8	41	1700
1000	5.65	2.07	4.81	57	.7	54	2300

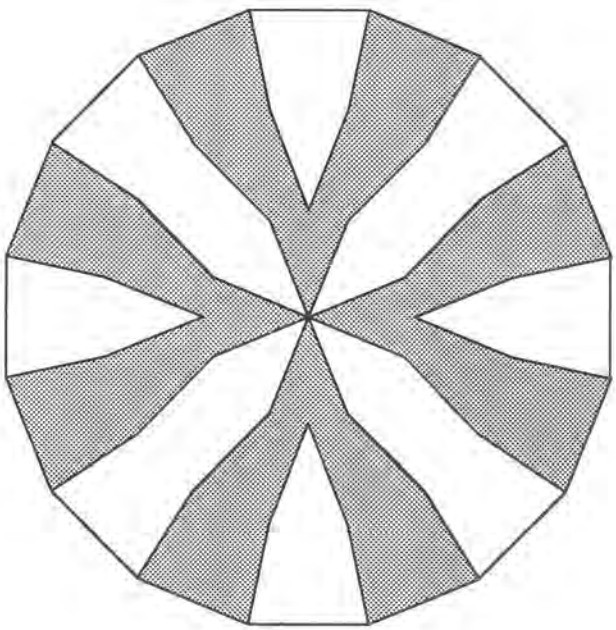


Fig. 1. N=4 center, N=8 edge. 4 valleys straight.

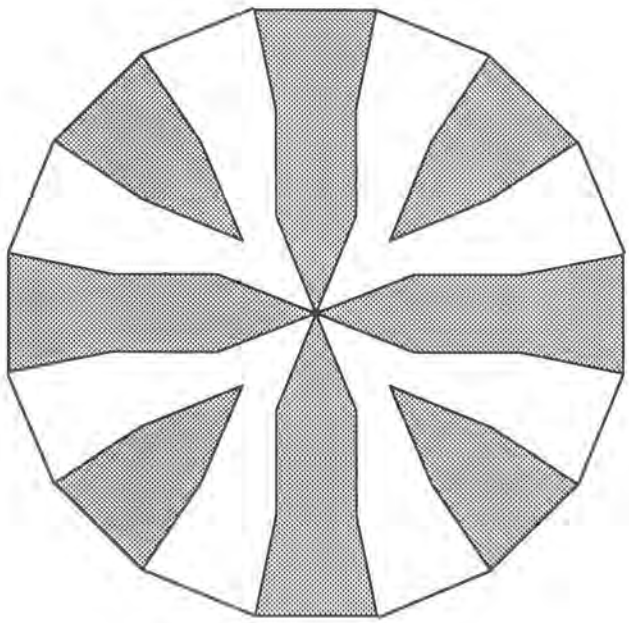


Fig. 2. N=4 center, N=8 edge. 4 hills straight.

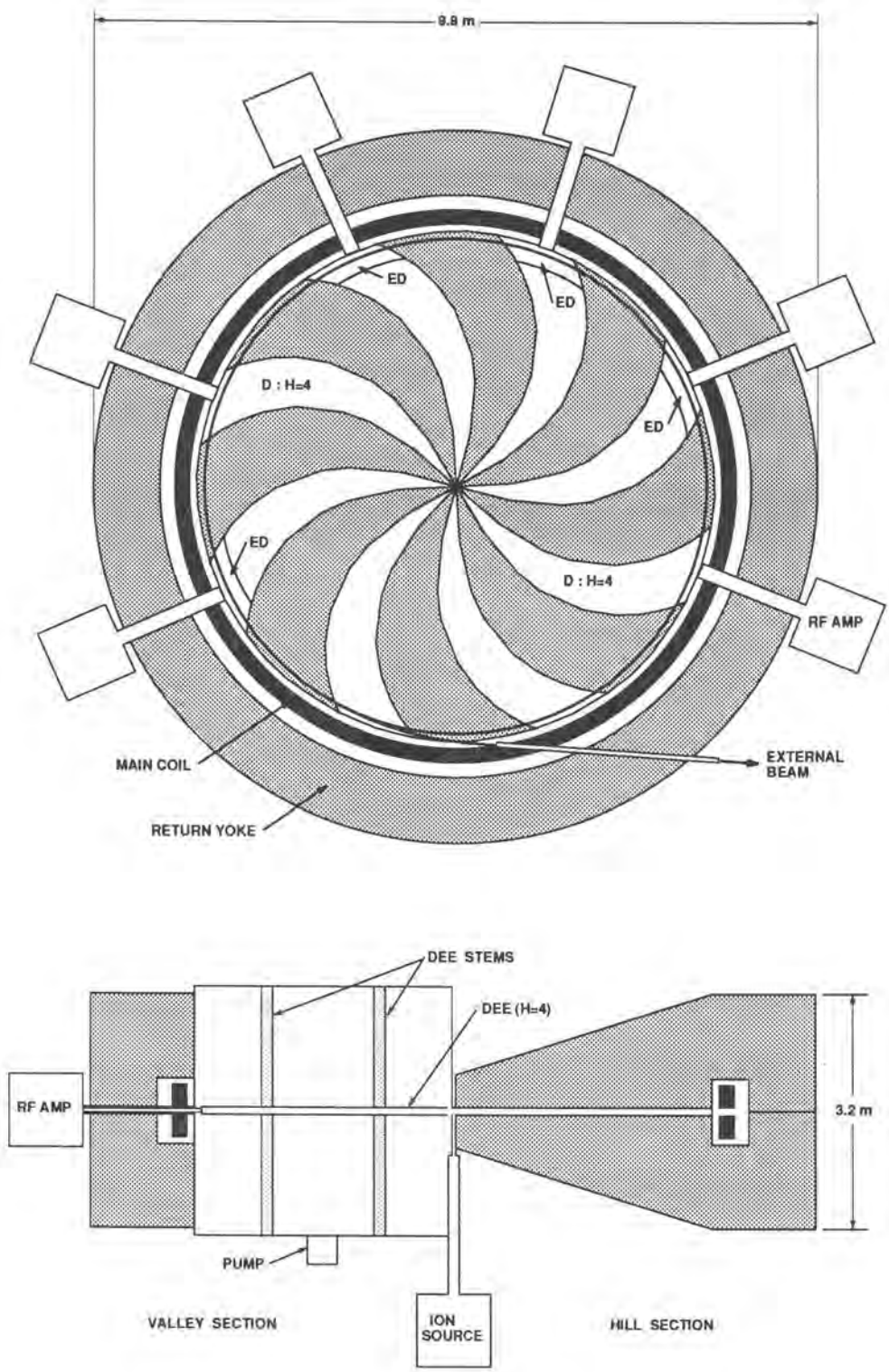


Fig. 3. 600 MeV proton cyclotron, plan and elevation views.

AN ON-LINE ISOTOPIC SEPARATOR TEST BENCH AT GANIL

P. Bricault, R. Leroy, M. Lewitowicz, J.Y. Pacquet, M.G St-Laurent, P. Sortais,

GANIL, B.P. 5027, 14021,CAEN, FRANCE,

A.C. Mueller, J. Obert, J.C. Putaux
IPN, 91406, ORSAY, FRANCE,

Liang C.F., P. Paris
CSNSM, 91406, ORSAY, FRANCE

and
J.C. Steckmeyer
LPC-ISMRA, 14050, CAEN, FRANCE.

ABSTRACT

A brief description of an isotopic separator test bench installed at GANIL is given. This test bench is equipped with a very compact ECR ion source made entirely from permanent magnets, operating at 10 GHz. Results obtained during the first run with a ^{20}Ne beam at 95 A*MeV on a MgO thick target are presented.

1. INTRODUCTION

There is over the last years a growing worldwide interest on the possible use of radioactive nuclear beams for a variety of fundamental and applied sciences studies. In our project we use the high energy heavy ion beams provided by the GANIL cyclotrons facility to produce "exotic" beams. For the moment the primary beam intensities are limited to 2 10^{12} pps for light ions. With the new high intensity axial injection system the primary beam intensity will be multiplied by a factor of 10 for light ions from ^{12}C to ^{40}Ar[1].

In order to determine if heavy ions can be competitive compare to high energy protons for the production of "exotic" nuclei we have built an isotopic separator on-line test bench. This test bench is equipped with a very compact ECR ion source made entirely from permanent magnets, operating at 10 GHz. All over the year we will measure the production rate using other heavy ion beams such as ^{24}Mg, ^{86}Kr, ^{12}C, etc. on various target materials.

For future applications of "exotic" nuclei, we plane to post-accelerate them up to a few tenth MeV per nucleon. There are two major solutions under study, the linear accelerator based on super conducting cavities and a compact cyclotron.

In section 2 general layout description of the separator is given. The target assembly and the ECR ion source is described in section 3.2 and 3.3 respectively. In section 4 we will present the first results obtained with this separator.

2.GENERAL LAYOUT OF THE SEPARATOR

A schematic top view of the separator is given in fig. 1. The ion beam from the accelerator makes an angle of 73° to the axis of the separator beam. Reaction products are thermalized in the target and subsequently ionized in the ion source. The reaction products are extracted axially from the ion source. The accelerating voltage is usually 15 kV, but it can go up to 20 kV. The extraction system is the same as the one used on the ECR ion source used at GANIL. The extraction electrode is at the ground potential. In order to compensate the space charge effect observed during the first runs a new extraction system is under studies.

The separator beam travels through the 102° magnet into a collection chamber. The collection chamber is equipped with diagnostic instrumentations, in particular a Faraday cup and a profile monitor mounted on a remote control mechanism.

Low intensity stable beams and radioactive beams can be guided through a narrow slits aperture and after continuing through a quadrupole doublet, comes to a second focus in another collection chamber. This collection chamber is equipped with various instrumentation for final diagnosis and collection, including a tape transport system and detectors for radioactive species identification

The separator beam lies in a horizontal plane, coplanar with the acceleration beam lines. The separator is located in an experimental room, so the second collection chamber is not shielded enough from the accelerator beam lines. This brings some problems during the detection of the radioactive species, so the primary beam must be pulsed to avoid high level of background.

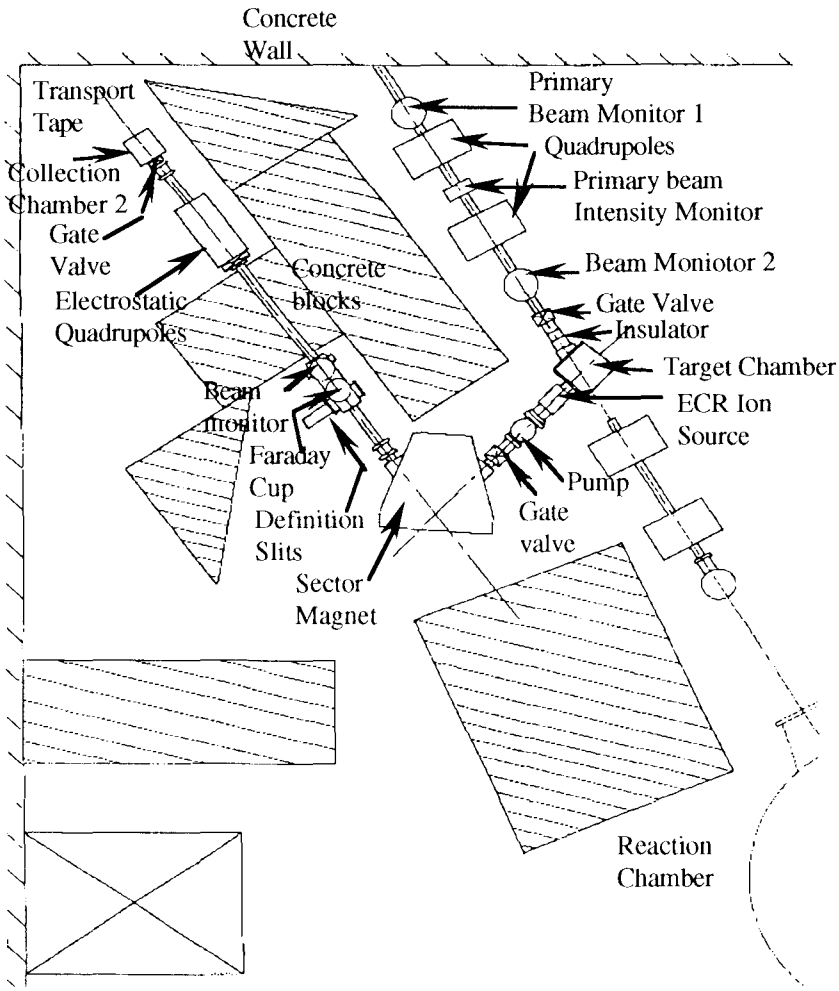


Fig.1 Schematic top view of the separator test bench installed in the experimental room D2 at GANIL.

3. DETAILS OF THE SYSTEM

3.1 The sector magnet

Due to the requested short delay of realization we have chosen for our separator, the same magnet as the one used for the ECR ion source test bench[2]. The magnet was built with an H configuration under the following specifications: radius of curvature r_0= 350 mm, sector angle 102°, the pole face angle are 26°. The resolving power R defined by R=M/δM, where δM is the full width at half maximum of a peak at mass M is about 100 for low masses (A<20).

3.2. The target chamber

In the on line mass separator discussed in this paper the reaction products are always brought to rest before being ionized. We have to separate continuously the product nuclei from a huge amount of target nuclei and transfer them into the gas phase to the ion source. This is done by heating a low vapour pressure target material to a sufficiently high temperature at which the nuclei of interest are released by diffusion and desorption process.

The transfer process is governed entirely by element specific diffusion, desorption and chemical processes.

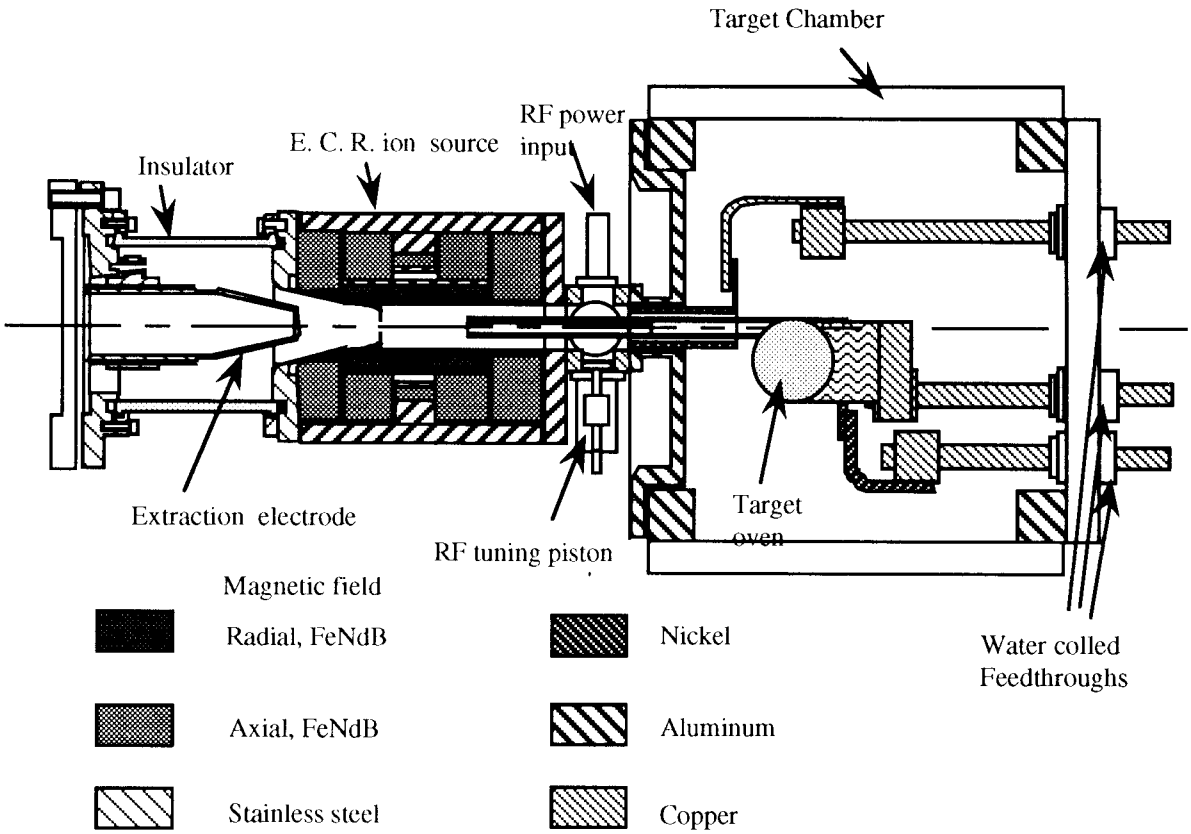


Fig 2 Schematic view of the target and ECR ion source.

We used the same target as the one constructed by the ISOCELE group at Orsay[3]. Fig. 2 shows a schematic view of the target chamber and the coupling to the ECR ion source.

The target is on high voltage (20 kV) mounted on a flange of the vacuum chamber.

The nickel target oven is a 7.5 cm long cylinder heated by resistive heating up to the maximum temperature of about 1200 °C. The current feedthroughs are water cooled copper. Inside the oven is the target crucible supported on boron nitride insulators which holds the target material. The wall of the crucible are made from a very thin grid allowing the gaseous products to escape. The oven is connected to a nickel transfer line.

The transfer line is a 25 cm long, 5 mm diameter nickel tube. This tube can be also heated to several hundred ° C by resistive heating independently of the target oven.

3.3 The ECR ion source

The ion source selected for the on line mass separator is a single stage electron cyclotron resonance ion source (ECRIS). ECRIS showed high efficiencies in ionizing various species and as well demonstrated long running times without any maintenance being necessary. In addition, to post accelerate the radioactive ions up to several tenth MeV per nucleon, a high charge state obtained directly from the ion source will reduce considerably the cost of the planned post accelerator. For this reason it was decided to couple an ECRIS to our test bench.

We have built a completely new ECRIS, the axial field is made using FeNdB permanent magnets. The mirror ratio is 2.9 at the injection and 2.7 at the extraction. This difference is due to the shape of the plasma chamber at the extraction (Fig. 2). An octupole, also made from FeNdB permanent magnets provide the radial electron confinement. The surface field is 0.6 T. Our ion source is 17 cm long and 13 cm of diameter. Such very small ECRIS can only be done by using permanent magnets.

The radio frequency power is brought by a 10 GHz klystron powered amplifier. The rf injection is done using a coaxial line tuned by a small piston. The gas is fed in the ECRIS through the copper tube of the coaxial rf injection. The injection of the vapour directly into the ECR zone seems to lead to very good ionization efficiencies. We plan in a very near future to measure the ionization efficiency using calibrated leak. This can also be done using a similar technic as the one described by

R. Kirchner[4], a stable incoming beam is brought at rest in the target. The ions after neutralization are released to the ion source, ionized and subsequently they are accelerated. Then, we can obtain the release profile I_{out}/I_{in}, where I_{in} is the primary and the secondary beam intensities.

The extraction chamber of the ECRIS is pumped by a 450 l/s turbomolecular pump. Typical pressures achieved in the extraction chamber are of the order of $5x10^{-6}$ mbar or lower.

3.4 Detection system

The collection chamber at the end of the separator beam line is a cube. It is equipped with a Faraday cup and a tape transport system from ISOCELE[3]. The tape transport system is operated in primary vacuum, except for the collection point placed in a secondary vacuum.

The collected beam is moved periodically to one of the two different detector locations. In the first one two NaI detectors are used to detect in coincidence the two gammas produced by the annihilation of the β^+. At the other location we have placed a plastic scintillator and a Ge detectors. We can make single γ detection or coincidence between the plastic and the Ge for delayed γ emitter.

For the both detection systems the informations on particle energies and the characteristic decay time were registered for each studied isotopes.

All information are send to the GANIL acquisition system consisting of VAX computers for further off-line analysis.

Table 1 Summary of the observed isotopes.

Isotope	Half life (s)	Primary beam (nA_p)	Yield (particle/s/μA_p)①
$^{19}Ne^{1+}$	17.2	35	$4,8\ 10^7$
$^{19}Ne^{2+}$	"	35	$8,9\ 10^6$
$^{19}Ne^{3+}$	"	32	$1,6\ 10^6$
$^{18}Ne^{2+}$	1,67	95	$1,9\ 10^6$
$^{18}Ne^{4+}$	"	90	$1,9\ 10^5$
$^{23}Ne^{1+}$	37,5	100	$6,310^5$
$^{24}Ne^{1+}$	$2,0\ 10^2$	110	$1,5\ 10^5$
$^{13}N^{1+}$	$6,0\ 10^2$	40	$3,8\ 10^5$

① This the yield observed on the transport tape, the efficiency of the transport system is not take into account.

4. RESULTS AND DISCUSSIONS

The first run was in march 1992, we have used a 95 A*MeV ^{20}Ne beam impinging a thick target of natural MgO. We succeeded to extract and ionize the $^{18,19}Ne$, $^{23,24}Ne$ and ^{13}N. The results are summarized in Table 1.

The intensity on the target was limited to $1\mu A_e$ for handling and damages cause on the thin window at the entrence of the target.

This results are very promising since this is the very first attempt to produce radioactive species with the on-line isotopic separation method at GANIL.

A new location is under study in order to avoid problems coming from the slow neutrons and background in the experimental room. A new separator is also under consideration, the resolving power should be much greater, of the order of few thousands, in order to separate properly masses in the region of mass 100.

Following the magnet we will place a cylindrical electrostatic deflector in order to separate off neutral components. The new beam line will pass through a concrete wall and the second collection chamber will be well shielded behind 4 m of concrete.

5. REFERENCES

1) C. Ricaud, M. P. Bourgarel. "Commissioning of the New High Intensity Axial Injection System for GANIL", paper presented at this conference.

2) L. Bex, M. Bisch, M.P. Bourgarel, Y. Bourgouin, E. Baron, "First results with the GANIL ECR ion Source", presented at the Workshop in the Sixth Int. ECR ion Source, Lawrence Berkeley Laboratory, Jan, 1985.

3) P. Paris, V. Berg, A. Caruette, J. Obert, J.C. Putaux, J.L. Sarrouy, "Development ot the ORSAY High Current On-Line Separator ISOCELE", NIM 139 (1976) 251-256.

4) R. Kirchner, "On the release and ionization efficiency of catcher-ion-source systems in isotope separation on-line", presented at the conference on Electromagnetic Isotope Separation, Sendai, Japan, Sept 2-6, 1991.

THE PIAFE PROJECT AT GRENOBLE : BEAM TRANSPORT AND ACCELERATION

J.L.Belmont, J.F. Bruandet, J.M. de Conto, M. Fruneau, G. Gimond, K. Golovanivsky,
E. Liatard, J.M. Loiseaux, H. Nifenecker, A. Savalle, B. Vignon
Institut des Sciences Nucléaires - IN2P3 - Université Joseph Fourier
53, avenue des Martyrs 38026 Grenoble Cedex, France

P. Briand
Centre d'Etudes Nucléaires de Grenoble - DRFMC/PSI
B.P. 85X 38041 Grenoble Cedex, France

ABSTRACT

SARA, the two cyclotrons of the Institut des Sciences Nucléaires de Grenoble (ISN) is close to the Institut Laue Langevin (ILL) high flux reactor. This unique opportunity leads us to the PIAFE project: the exotic atoms - or ions - (fission products: neutron rich nuclei, mass mainly between 80 and 150) should be extracted from an Uranium 235 target put into a 10^{14} neutrons/cm^2/s flux and, after mass separation, should be transported to the cyclotrons and accelerated. We expect from several 10^5 to more than 10^8 ions per second, depending on production rate and energy needed (from 2 MeV/amu to 10 MeV/amu or up to 20 MeV for masses close to 80).

INTRODUCTION

Grenoble is characterized by the existence, in nearby sites, of a possible source of exotic nuclei, the high flux reactor of the Institut Laue Langevin (ILL) and of a low to medium energy accelerator complex SARA, the two cyclotrons of the Institut des Sciences Nucléaires de Grenoble (ISN).

The aim of the "PIAFE" project[1)2)] (in French : Production, Ionisation, Acceleration de Faisceaux Exotiques) is to produce neutron rich nuclei with masses between 80 and 150 and energies between 2 and 10 MeV/amu (up to 20 MeV/amu for masses around 80). The accelerated intensities will depend on the production rates, extraction efficiencies and final energies, and should range between 10^5 and 10^9 particles per second. We have to take into account the half-life times of these elements wich are close to the *second*.

In the following we give a more detailed overview of the project as it stands today, and which may still be subject to change.

Figure 1 shows a sketch of the production, ionization and acceleration complex and expected efficencies.

1 - OUTLINE OF THE EXOTIC ION PRODUCTION

1.1 - The fission source

The fission source should be as intense as possible, conform to security requirements, and as high a proportion of fission fragments as possible should escape from it. To fix ideas we consider an ensemble of ten 100 cm^2 U^{235} layers, with a thickness of 1 mg/cm^2, alternating with 10 mg/cm^2 graphite layers, placed in a 10^{14} neutrons/cm^2/sec flux.

The total amount of 1 gram of U^{235} would lead to approximately 10^{14} fissions/sec. This number compares favorably to that expected from a 100 µA beam of 1 GeV protons. The power produced in the target would be about 4 KW, to be compared to more than 20 KW for the proton case. The power dissipation could be used to heat the source up to 2000° C. in order to maximize the diffusion of elements like alkalines and rare gases out of the graphite.

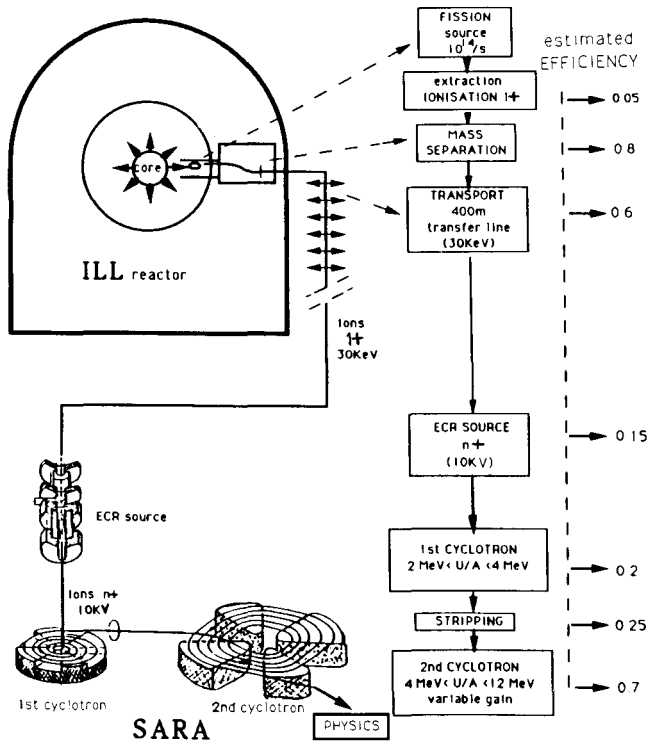


Fig.1. Schematic diagram of the projected production, ionization, acceleration of exotic beams facility P.I.A.F.E. at Grenoble

The target heating will probably be the limiting factor of the production rates. Here the thermal neutron production scheme has a distinct advantage over all other competing methods since target heating due to the incident beam is negligible.

1.2 - Ionisation and mass separation steps

The more easily obtained beams should probably be either rare gases or alkalines. Alkalines could be obtained as singly charged ions using the thermoionization effect directly from the source[3)]. Diffusion times of 0.2 s and 0.8 s for Rb and Cs respectively have been reported.

For rare gases one has to rely on a separated ionization step. Rare gases would be pumped through an ionization source of the plasma or ECR type, and singly ionized. Efficiencies in the range of a few percent are expected.

After acceleration by around 30 kilovolts, the singly charged ions should be mass analysed in a standard mass spectrograph, directly situated outside the reactor biologicial shield. It is of great importance to ensure the confinement of dangerous species like Sr^{90} or Cs^{137}.

2 - TRANSPORT

The q = 1^+ ions would be transported under vacuum and focused by quadrupoles from the mass separator output to the SARA site, where they would be injected into the ECR source. The transit time would be, typically, around 1.5 ms for 400 meters.

It is important to reduce, as much as possible, the cost of the transfer line, since it will be the major component of the total cost of the project. A careful optimization of all elements involved in the transfer is needed : Vacuum,number and positions of beam diagnostics, corrections of alignment defects.

Due to the length of the transfer line, rather good vacuum, in the 10^{-7} torr range, is needed. The attenuation of the beam by charge exchange processes during the transport will depend on the nature of the ions.

The total effect of scattering on the residual gas and charge exchange is smaller if we transport (1^+) ions instead of multicharged ions. Due to scattering, the emittance grows during the transport and the aberrations of a long series of lenses disturbs the apparent emittance at the exit. But these effects are without consequence since the 1^+ beam will be injected into the high charge state ECR source of the SARA axial injection system. We consider a scheme in which the beam would impinge on a heated catcher within the high charge ECR source from which the atoms would be evaporated into the plasma. In this way, the emittance would be regenerated, and energy and charge would be adapted to axial injection in the first cyclotron.

During the transfer, the activity of the beam has to be taken into account, for the shortest periods, but it would not exceed 10 microcuries per meter. However careful monitoring should ensure that the beam is not accidently lost, since, in such a case, local activities in the Curie range could be produced. Monitoring should also ensure that no long life chain is sent to the accelerator.

Two schemes of beam handling are proposed.The first scenario is the use of a FODO lattice. The design of any transport line, but especially of a long one, must provide a good acceptance (maximum value of emittance acceptable by the line, for a given geometrical aperture), without being too sensitive to structure defects, like misalignments of quadrupoles. Without defects, the acceptance of a such structure versus the transversal oscillation phase advance μ per cell, is maximum for μ = 76 degrees. However, the misalignment of quadrupoles induces the decentring of the central trajectory of the beam and then decreases the acceptance. In such a case, optimum values for cell length, geometrical aperture and betatron phase advance have to be found. For example, we have considered a 200 m structure made of 3 metre long FODO cells put on 6 meter long girders (4 quadrupoles per girder). The quadrupoles have a transverse positionning precision of 0.3 mm RMS, the girders have an angle positionning precision of 0.15 mrad RMS along the axis and the relative positionning error from girder to girder is 0.9 mm RMS, the geometrical aperture remains 2 * 40 mm.

We intend to use Panofsky style quadrupoles[4] which reduce effects of remanent fields for low field quadrupoles and can give high quality fields without complex machining. We need 500 A in each one conductor coil with 0.4 m long quadrupoles (gradient = 0.36 T/m). With a baked vacuum chamber, a getter pump each 40 m should ensure a 10^{-7} torr vacuum.

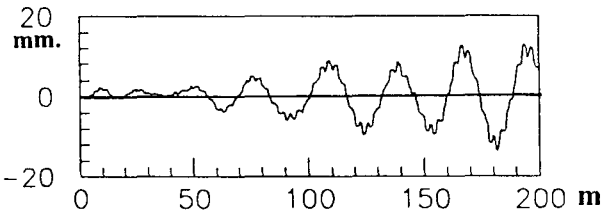


Fig. 2. The central trajectory is plotted along a 200 m FODO structure and for one set of mispositionnings (see text).

The effect of one particular set of mispositionnings is illustrated in figure 2, where the central trajectory is plotted along a 200 m FODO structure: the trajectory draws progressively away from the theoretical axis, reducing the real available acceptance. Corrections can help to compensate that effect.

Figure 3 shows the acceptance of the line **without** mispositionning (maximum at μ = 76 degrees per cell) and **with** mispositionnings of elements: in this case the acceptance is maximum for μ = 40 degrees. A result of the simulations using this configuration is given by figure 4 which shows the acceptance of the line (center of the figure) for 200 sets of mispositionnings. For 1000 sets the confidence level to get at least a reasonably large remaining acceptance available before correction ($\approx 60\pi$ mm.mrad) is 0.999. Simulations performed for many values of μ have shown that the best compromise is always around μ = 40 degrees.

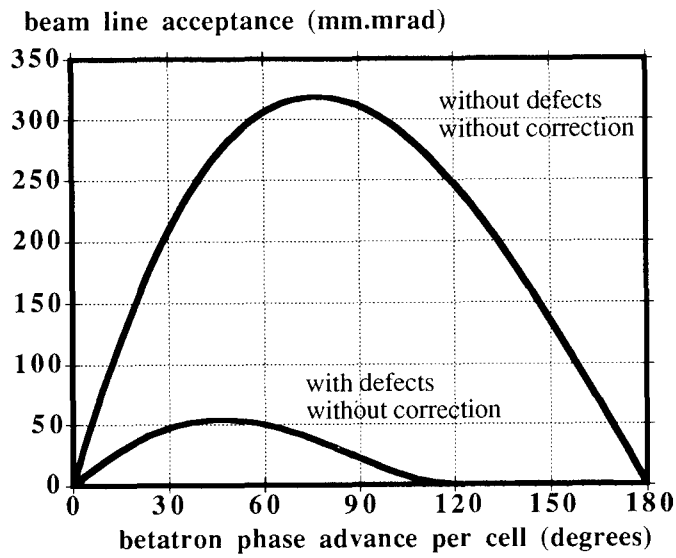


Fig. 3. Acceptance of a 200 m long beam handling made of FODO cells with or without defects on quadrupole positions (see text). Our channel having 400 m we will have to recenter the beam along the path.

The quadrupole alignment of 0.3 mm R.M.S. could be achieved with a method proposed by the SLC[4] : turning off successively the quadrupoles by consecutive pairs procures a set of relations between quadrupole misalignments and beam excentration measured at a few points. These relations permit the estimation of the misalignments. As an example, fig. 5

shows the real and estimated defects with that method over 100 m. The quads are originally decentered by 0.7 mm R.M.S and only three beam position monitors are used.

Another scenario is the use of a high frequency continuous quadrupole guide, working around 0.1 MHz with an electric gradient of around 100 V/cm. It might alleviate alignment problems and should be cheaper if vacuum design remains simple.

We will test these two different schemes of tranfer lines from the ILL to SARA with the aim to minimize the costs.

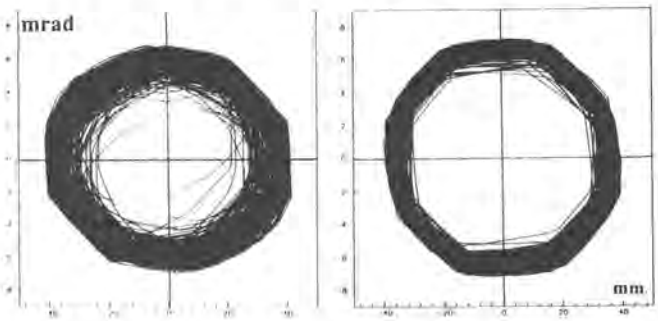


Fig. 4. Acceptances of a FODO 200m long line for 200 sets of mispositionnings (see text for conditions).before and after recentring of the beam after each 50m, taking into account of the 1 mm RMS error of monitor positionning.

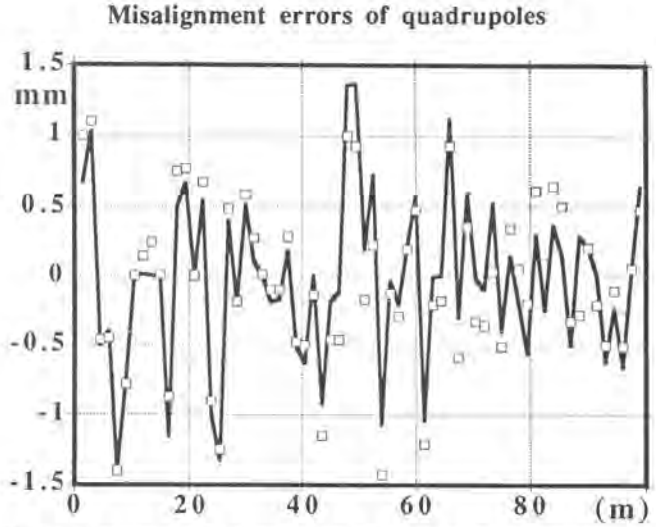


Fig. 5. Example of a simulation of a set of misalignments of quadrupoles over 100 m : real values (arbitrary linked by a solid line) and estimated values (square points) (see text for conditions)

3 - TRANSFORMATION OF THE 1^+ BEAM.

The q/A value of injected ions inside the first cyclotron must be higher than 0.15. In order to couple the 30 keV ion beam to an ECR Ion Source (ECRIS) plasma, we project to implant radioactive ions into a catcher outgassing because of its high temperature : thermal atoms immediately after desorption are facing a magnetized plasma.

Due to the characteristics of the injection line into the first cyclotron, the voltage of the ECRIS cannot exceed 10 Kilovolts. The 1^+ beam will have a rigidity close to eight times that of multicharged ions. We are studying two solutions for changing the 1+ beam into a high charge one

In the first solution the 30 keV 1^+ beam (rigidity $\approx$ 0.3 T.m) crosses transversely the magnetic field (0.06 T) in the central part of a first ECRIS[6]. After exit from the catcher the atoms will be singly ionized again inside this first ECRIS, working with two 2.45 GHz cavities,where the plasma could have the rather high density of 10^{12} cm^{-3} and which serves as a large first stage of a high performance 16 GHz ECRIS.. The plasma of the 2.45 GHz source could be guided to the 16 GHz ECRIS by a magnetic field smoothly and continously increasing from the first source to the second one.

In a second solution, the 1^+ beam is injected in the 16 GHz ECRIS axis through the extraction electrodes: it is decelerated from 30 keV to 20 keV and slightly focused by the magnetic field at the other side of the source where we put the catcher. In this design the exotic atoms after desorption from the catcher facing the plasma should be multiply ionized. These multicharged extracted ions and 1+ beam travel in opposite directions and are easely separated by a small magnet close to the extraction.

The global efficiency of the ECRIS, for a given final charge state is estimated to be around 15 %. The time delay induced by the ionization process in the ECRIS has been measured to be less than 1 ms per charge unit[4], i.e. between 20 and 30 ms for the ions of interest here.

4 - ACCELERATION

The SARA acceleration complex has two cyclotrons, one compact with K = 88MeV and one of the separated sector type with a K = 160 MeV.

The multiply charged ions are injected into the first cyclotron and the energies produced range between 1.9 and more than 4 MeV/amu, depending upon the charge states.

The second cyclotron acts like an amplifier with a gain in energy given by the square of the ratio of extraction and injection radii. The present gain is equal to 5.4. This gain is not optimum for physics with exotic beams since it gives a *lower* limit of achievable energies of 10.3 MeV/amu. (1.9 * 5.4). We plan to modify the extraction system in order to make the gain continuously varying between 2.1 and 4.1 (see figure 6). The gain variation would be obtained by a change of the extraction radius. The energy change will be much easier and quicker, not far from that of a tandem !

The idea is simple but we have to remove one of the two RF resonators and to replace it by a movable electrostatic extractor positionned at the needed radius, used to push the beam into the septum magnet after the next magnetic sector. If we succeed in putting this magnet in two articulated parts (and may be in reinstalling the second cavity at 90° with respect to the first one) we will obtain the full range of energy gain : 2.1 to 5.4. The first harmonic due to this design could be easely compensated by correcting coils[7].

Factors limiting the masses accelerated by the second cyclotron are the stripping efficiency and the maximum of the rigidity accepted at the injection by this machine (K = 33MeV). Figure 6 shows energy ranges of the machines for Xenon.

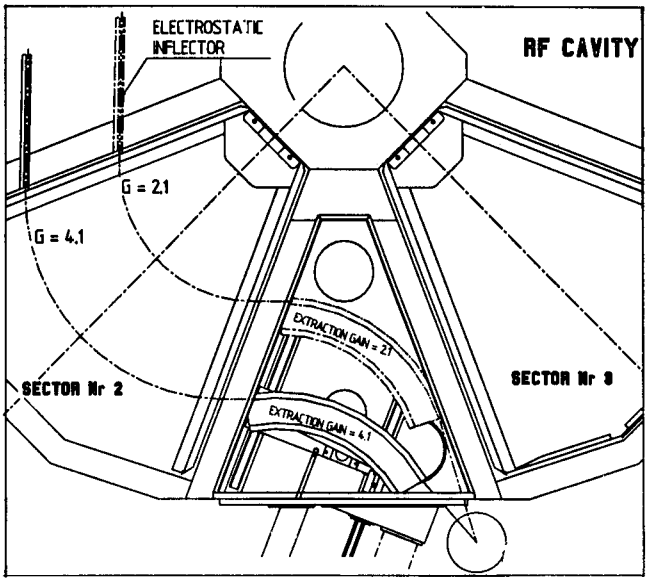


Fig. 6. The proposed extraction system allows the second cyclotron having a continuously varying gain between 2.1 and 4.1.

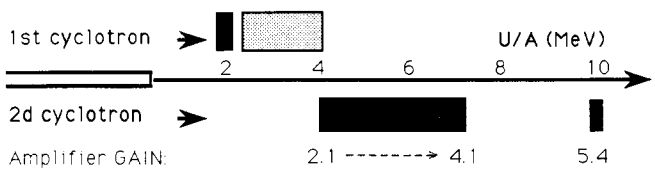


Fig. 7. Energies for Xenon.4 MeV/amu is directly obtained with the first cyclotron. Presently energy gain G of the second cyclotron is G = 5.4, allowing only 10.5 MeV/amu. It is expected a variable extraction : 2.1 < G < 4.1 allowing to cover the energy range of 4 to 7.8 MeV/amu (and 10.5). Because stripping effect is not large enough, only 1.9 MeV/amu from the first cyclotron can be injected in the second one.

Nucleus	$T_{1/2}$ sec.	Usable beam First cyclotron	Usable beam Second cyclotron
Rb^{93}	0.58	2.10^9	3.10^8
Kr^{93}	1.29	9.10^7	$1.7\ 10^7$
Cs^{142}	1.8	2.10^9	$3.4\ 10^8$
Cs^{144}	1.02	$1.7\ 10^8$	3.10^7
Xe^{144}	1.2	2.10^7	$3.4\ 10^6$

Table 1 - Estimated usable beam intensities ion pps at the output of the first and second cyclotrons.

CONCLUSION

The association of the high flux reactor of the ILL to the SARA accelerator system opens the perspective of intense neutron rich isotope beams, with masses between 80 and 150 and intensity of exotic ions gets 10^9pps (see table 1).

Development work has been started on different critical points of the project : in-pile fission source, transfer line and injection of a singly charged ion beam into a high charge state ECR source.

ACKNOWLEDGEMENTS

We would like to thank the member of the institut ISN and ILL for theirs collaboration to the PIAFE project. Particularly we thank Dr. R.Geller for helpful discussions Dr. E. Baron, from GANIL, for his help about charge exchange and stripping problems, Dr. S.Albrand for calculations.

BIBLIOGRAPHY

1) J.L. Belmont et al. Presented at the Dourdan conference (march 1992).

2) J.L. Belmont et al. "The Grenoble scheme for accelerating neutron rich nuclei" to be published in Proceeding of conference of Crime (october 1991).

3) G. Rudstam et al. Radiochimica Acta 49 (1990) 155 and references included.

4) P. Emma "Beam based alignment" SLAC-PUB 5787 1992.

5) L. Harwood et al. "Magnet design for Cebaf", EPAC 1992.

6) K. Golovanisvky, et al., "ECRIC the ECR ion converter for the PIAFE project at ISN" - Grenoble, Internal report n° 92.50, May 1992.

7) S. Albrand et al., "Statuts report of SARA", this conference.

HIGH INTENSITY SUPERCONDUCTING CYCLOTRON BEAMS FOR A RADIOACTIVE ION BEAM FACILITY

L. Calabretta, D. Rifuggiato
I.N.F.N., Laboratorio Nazionale del Sud,
v.le A. Doria ang. S. Sofia, 95123 Catania, Italy

ABSTRACT

One of the major limits to the beam intensity in the Superconducting Cyclotron is presently set by the extraction system, which consists of an electrostatic deflector. A valid alternative to electrostatic extraction could be extraction by stripping. The feasibility of this method has been studied taking into account the major constraints of the machine and particularly of the cryostat. This study includes some investigation on the magnetic channel system to be used in the extraction trajectory and on the consequent perturbation of the three-fold symmetric field.

1. INTRODUCTION

In the project for a Radioactive Ion Beam (R.I.B.) facility at L.N.S.[1] the Superconducting Cyclotron is planned to be employed as the primary accelerator, delivering ion beams with energies up to 100 MeV/a.m.u.

Of course many efforts have to be made in order to achieve a reasonably high intensity of the primary beam. Several efficiency factors have in fact to be taken into account when estimating the total intensity of the radioactive beam delivered in the target, due to the production, transportation, ionization, mass analysis and acceleration processes.

The S. C. is by now strongly intensity-limited by the extraction process, which is performed by electrostatic deflection: in order to extract fully stripped ions at the maximum energy (focusing limit: 100 MeV/a.m.u.), the gap size of the deflector must be 6 mm to obtain the electric field of 140 kV/cm planned in the design. Then the probability for the whole beam to hit the deflector increases; in the case an intense beam (some pμA) is to be extracted, the beam power exceeds the expected limit, which is about 0.5 kW.

Moreover the electrostatic solution gets more and more worrying the more intense is the beam to be extracted: space charge effects produce distortions of the emittance figure in the transverse phase space when the beam is electrostatically deflected.

Therefore an extraction method leaving out the electrostatic deflector would be desirable. The feasibility of extraction by stripping in the Superconducting Cyclotron is studied for some cases and here discussed.

2. EXTRACTION TRAJECTORIES WITH THE STRIPPING METHOD

The extraction by stripping method has already been adopted in a compact isochronous cyclotron[2] for heavy ions. During the feasibility study for the Superconducting Cyclotron, a fundamental constraint has been considered: the cryostat is not to be modified. An immediate consequence of this assumption is that the extraction trajectory has to be similar to the trajectory in the electrostatic extraction: the beam has to enter the yoke and exit through the extraction channel (Fig. 1[3]).

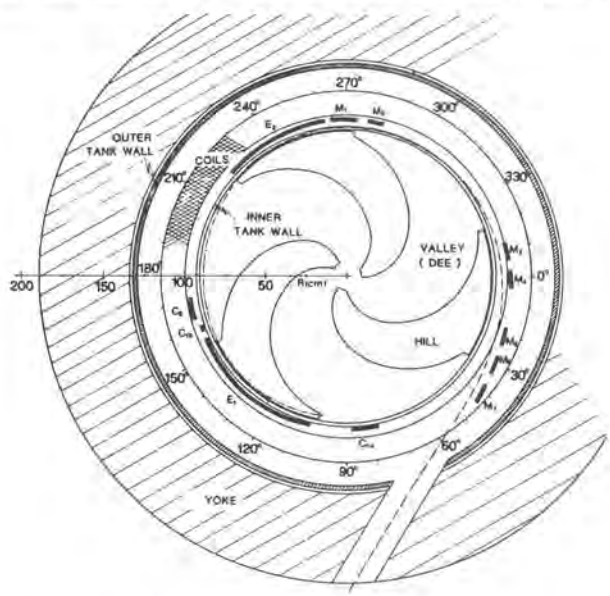


Fig. 1. Beam trajectory in the electrostatic extraction system.

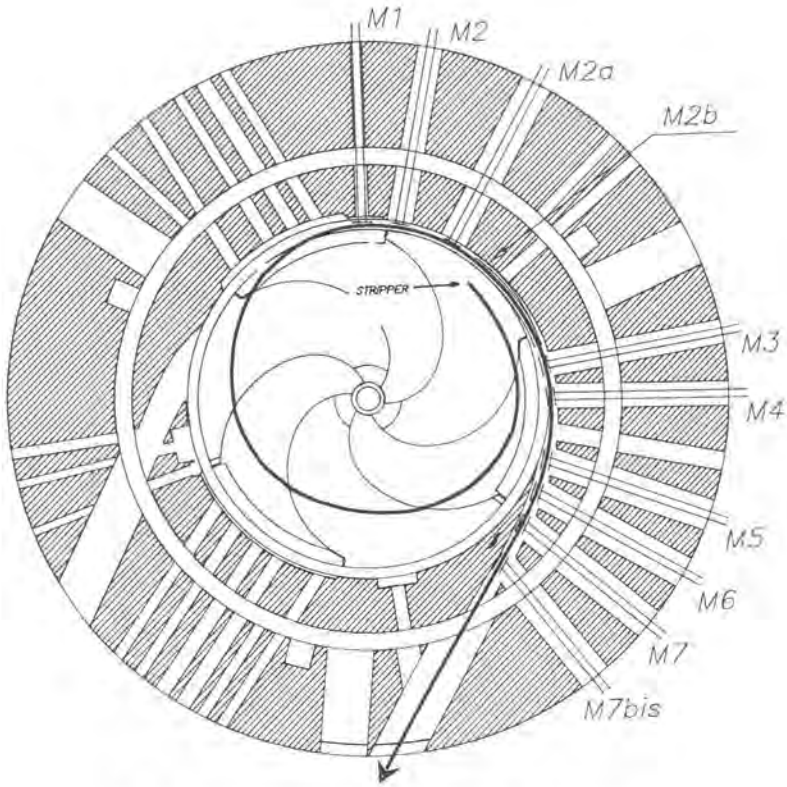


Fig. 2. Extraction trajectory with the stripping method.

A one-two units charge change of the ion at the end of the acceleration process makes the orbit go inward in about half a turn and then outward in the following half turn. Depending on the stripping radius and angle, and on the charge "jump", after one turn the stripped ion can either go inward or definitely and abruptly exit from the Cyclotron. The second possibility cannot be accepted if the extraction channel has to be penetrated: then, according to the first case, at the position where the orbit reaches the maximum radius after one turn, before going inward, it is extracted by magnetic channels (Fig. 2).

In the original project of the Cyclotron, a set of iron channels is planned to radially focuse and help to deflect the beam along the extraction path. Two channels are placed immediately after the second deflector, six channels are placed along the extraction channel (Fig. 1).

The "Spiral Gap" code[4] was used to simulate the acceleration of the ion, starting from the equilibrium orbit at 30 MeV/a.m.u., until the stripper. Another code,[3] using the same integration routine, takes into account the effect of the field decreasing channels and allows to simulate the extraction trajectory.

The behaviour of the beam along the extraction path has been studied in the radial and axial phase space after having ascertained that there is no destructive effect on the beam in the path between the stripper and M1. The eigen-ellipse at 30 MeV/a.m.u., calculated at the position 0°, was transported until the extraction point (θ=92°, r=~216 cm). The emittance was calculated supposing that the beam emittance injected by an E.C.R. source is 100π mm·mrad.

Keeping in mind the final purpose of this study, i.e. the employment of the Cyclotron as the primary machine in a R.I.B. facility, we decided to begin the feasibility study considering an ion with mass A<30. Since at the Cyclotron energies every ion with A<30 hitting a foil stripper becomes fully stripped, the extraction efficiency reaches almost 100%.

As it can be easily understood, the strength of the magnetic channels is as small as the difference between the charges before and after stripping is small. Then the first case to be investigated was ^{16}O, q_i=7, q_f=8, q_i and q_f being the charge states before and after stripping. According to recent results an E.C.R. source can produce $^{16}O^{7+}$ with intensity of 25 pμA.[5]

In order to study the case mentioned, the field at the center of the machine was assumed to be B_o=32.2 kGauss, which corresponds to a maximum energy of 78 MeV/a.m.u for the 7^+ ion. In this case we found that:

- the stripper should be placed at r_s=81.6 cm, θ_s=316° (Fig. 2), where the beam energy is about 75 MeV/a.m.u., to allow the beam to reach the radial range (90.0-91.6 cm) of M1 at its angular position (θ=264°);
- all the magnetic channels planned have to be used, including M2bis and M7bis;

- an extra channel has to be employed between M2bis and M3; since there is no hole for magnetic channels, a fixed device should be designed;
- the strength values of the channels is around 6 kGauss, apart from M1 and M2, which maintain the same values as in the electrostatic extraction case (1-2 kGauss) because they are definitely assembled inside the cryostat;
- the magnetic channels have to provide a certain field gradient to focuse the beam; in Fig. 3 a possible, not optimized, solution shows that assuming field gradients of 1-3 kGauss/cm, the beam is much smaller than the extraction channel size (~3 cm height, ~4 cm width).

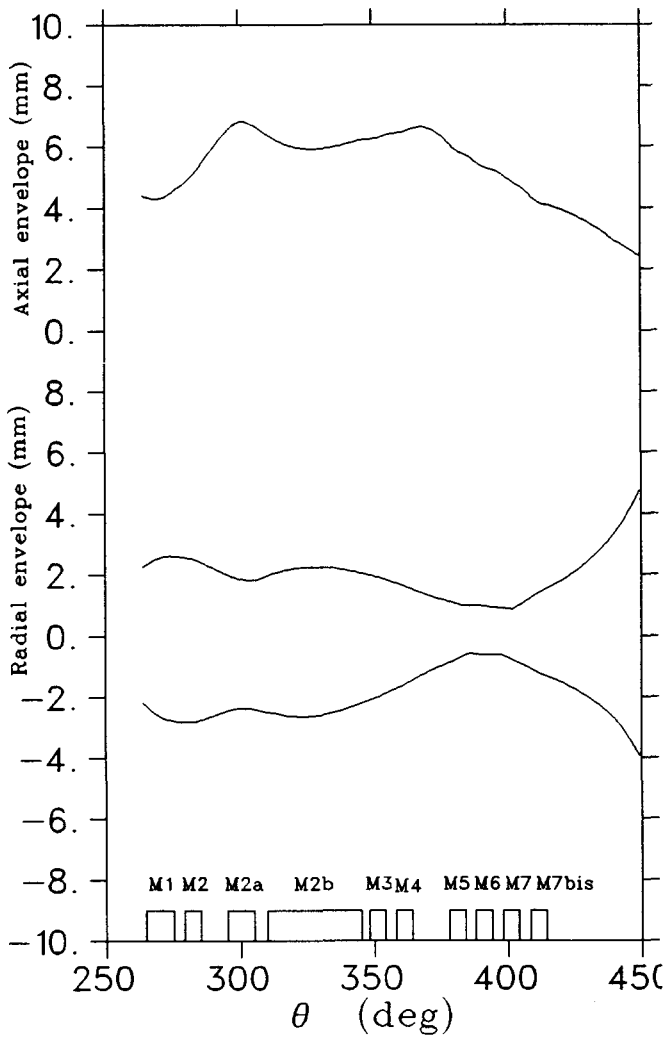


Fig. 3. Radial and axial beam envelope along the extraction trajectory.

3. MAGNETIC CHANNELS

An attempt was done to design iron magnetic channels whose strength is about 6 kGauss. Since the width of the extraction channel is ~4 cm, the three-bar configuration, adopted for the mainly focusing channels of the electrostatic extraction, was discarded, not allowing to achieve a considerable strength. Two two-bar configurations, which seemed to fulfil the requirements, were realized. The first one was a not focusing, two equal bars channel, which should provide a field of about 6.8 kGauss in the gap according to the calculations[6]; the second one was a two different bars channel, which should provide a constant gradient of ~1 kGauss/cm in the gap (8 mm) and a field of 6.0 kGauss in the center.

As explained in,[7] the measurement of the field inside the gap showed that the difference between the calculated and the measured field is about 1 kGauss in the zero-gradient channel and 2 kGauss in the other one; moreover in the second one the gradient is not constant. A separated functions solution (with only focusing and only deflecting magnetic channels) would require the strength of the only deflecting channels to be more than 6 kGauss.

The use of passive channels produces a relevant problem concerning the beam dynamics of the Cyclotron: the perturbation of the three-fold symmetric field. In fact the first harmonic produced by two-bar 6 kGauss channels at r~82 cm, which is more or less the radial position of the resonance ν_r=1, ranges from some gauss to tens of gauss, depending on the azimuthal extent of the channel. Therefore, it has to be compensated by iron bars appropriately placed in the available holes of the yoke. However the first harmonic contribution of the fixed channel can hardly be compensated by simple iron bars.

Since many problems arise, as noticed, from the use of passive channels, we think that efforts should be devoted to look for the possibility of employing active channels.

4. STUDY OF SOME CASES

In order to verify the statement done before on the relationship between the charge change and the channels strength, we studied the case ^{16}O, q_i=6, q_f=8: we found that the stripped beam reaches the radial range of M3 at its angular position (θ=348°) after about one turn, but it is not possible to make the beam go through the extraction channel due to the big change in magnetic rigidity.

Another confirmation comes from the study of the case ^{20}Ne, q_i=9, q_f=10. The charge state 9^+ is produced with an intensity of ~1 pμA,[8] but higher intensities are expected in future. A Ne beam is particularly good to be employed in a R.I.B. facility as a primary beam. The magnetic field at the center of the Cyclotron was assumed to be 31.4 kGauss, which corresponds to a maximum energy of 78 MeV/a.m.u for the 9^+ ion. The stripper position results to be r_s=82.6 cm, θ_s=318°, which is not so different from the Oxygen case. However, in this case we found that the strength of the channels is about 5 kGauss, lower than in the previous case.

5. CONCLUSIONS

The theoretical feasibility study of the new extraction method proposed needs to be extended to a wide set of ion species that can be produced with high intensity by E.C.R. sources.

More important, the technological feasibility must be ascertained: the possibility of realizing magnetic channels with the mentioned requirements has particularly to be verified. Finally, the possibility of placing the stripper system in the position found out by the calculation needs some investigation.

6. REFERENCES

1) Migneco, E. et al., "Design of the Radioactive Ion Beam Facility at the LNS," presented at the III E.P.A.C., Berlin, Germany, March 24-28, 1992
2) Oganessian, R.Ts., "105 cm heavy ion isochronous cyclotron for applied research," in **Proceedings of E.P.A.C.** (Frontières, Nice, 1990) pp. 455–457.
3) Fabrici, E. and Salomone, A., "The extraction system for the Superconducting Cyclotron at the University of Milan," in **Proceedings of the 9th Int. Conf. on Cyclotrons and their Applications** (Les Éditions de Phisique, Caen, 1981) pp. 501–503.
4) Gordon, M.M., "Effects of spiral electric gaps in Superconducting Cyclotrons," Nucl. Instr. and Meth. **169**, 327–336 (1980).
5) Briand, P., private communication
6) Carbonel, B., et al., "Calculation of the geometry of magnetic channels for synchrocyclotrons and cyclotrons," Nucl. Instr. and Meth. **84**, 144–146 (1970).
7) Sura, J., et al., "Material consideration for magnetic channels," presented at this Conference.
8) Jacquot, B. and Pontonnier, M. "La source Caprice 10 GHz en mode harmonique $2(\omega_{HF}-\omega_{ce})=0$," Nucl. Instr. and Meth. **A287**, 341–347 (1990).

RADIOACTIVE ION BEAM PRODUCTION USING THE LOUVAIN-LA-NEUVE CYCLOTRONS : PRESENT STATUS AND FUTURE DEVELOPMENTS

G. Ryckewaert, M. Loiselet and N. Postiau,
Centre de Recherches du Cyclotron,
Université catholique de Louvain,
2, Chemin du Cyclotron,
B-1348 Louvain-la-Neuve, Belgium

ABSTRACT

CYCLONE 30, the high intensity 30 MeV H^- cyclotron, is used to produce large quantities of short lived radioactive isotopes. These are extracted on-line from the target, ionized in an ECR-source and accelerated with CYCLONE. Isobaric contamination is eliminated in the acceleration and ejection process without loss of intensity. Pure radioactive beams of $^{13}N^{+1}$ and 2^+, $^{19}Ne^{+2}$, 3^+ and 4^+ are now accelerated routinely in the energy range between 0.56 and 4.5 MeV/AMU with intensities reaching 2 10^9 pps. They are used for nuclear astrophysics and nuclear physics experiments. To overcome a number of limitations due to CYCLONE the design of a dedicated postaccelerator cyclotron has been started. In this paper, recent developments of the present system and design features of the new cyclotron are described.

1. GENERAL DESCRIPTION

The installation for the production of intermediate energy RIB has been described earlier.[1] In this paragraph we summarize the main features of the subsystems and their recent developments.

1.1. The production of radioactive elements

The radioisotopes of interest are produced selectively on specific targets. In this way, only small quantities of unwanted (eventually long lived) activity are formed, allowing still relatively simple ways to manipulate the production targets.

A special beamline transports the proton beam from CYCLONE 30 to the target, located in the shielding wall between the two cyclotrons. It consists of a 90° doubly focusing magnet, tilted up 32°, a quadrupole doublet, steering magnets and a 50 Hz wobbling magnet. Table 1 lists a number of radioactive elements of interest that could be produced with CYCLONE 30 and the respective production reactions. The first target developed, for the production of ^{13}N, consisted of a solid disk made of enriched ^{13}C, fixed on a watercooled target holder. The target assembly is isolated from the beamline vacuum by a thin carbon window. However, other target materials such as LiF, B_2O_3, BN, could not be used this way. Therefore we developed closed graphite containers, filled with the respective materials, and which are outgassed before being placed on the watercooled target holder. Even the operating ^{13}C-target for ^{13}N-production is now made this way.

Several sweeping gases are being tried out for the different elements. ^{19}Ne production is special in two aspects : it does not require any sweeping gas and since it is not cryopumped itself, an additional purification is achieved by passing the target gas flow through a cryopump. In this way very low pressures are obtained in the ECR-source yielding high ionization efficiencies even for relatively high (4^+, 5^+) charge states. It should be noted that in the LiF-target the ^7Be activity ($T_{1/2}$ = 53 d) builds up slowly.

1.2 Ionization

A single stage ECR-source working at 6.4 GHz was built and its ionization efficiency for the light elements was carefully optimized. To obtain the maximum beam current for a given isotope at a given charge state, it is important that all accessible source parameters, such as axial field, microwave power, source-to-puller gap be carefully adjusted. The pressure in the source is crucial : it must be as low as possible. In the case a carrier gas is to be used with the production target, an optimum flow rate has to be found since the extraction efficiency from the target usually requires increased flow whereas the ionization efficiency requires the lowest possible flow. Using a source aperture of 10 mm this optimum lies around 0.1 cc/min.

Element	$T_{1/2}$	Production reaction	Target material	Contaminant/ analogous beam	$\frac{\Delta Q/M}{Q/M}$	Reaction	Energy MeV/AMU
^{6}He	0.8 s	$^{7}Li(p,2p)$	Li	^{6}Li, ^{12}C	6.10^{-4}	$^{6}He(\alpha,n)^{9}Be$	0.4
^{7}Be	53d	$^{7}Li(p,n)$	LiF	^{7}Li, ^{14}N	$1.3.10^{-4}$	$^{7}Be(\alpha,\gamma)^{11}C$	0.4
^{8}Li	0.8 s	$^{9}Be(p,2p)$		^{16}O	3.10^{-3}	$^{8}Li(\alpha,n)^{11}B$	0.4
						$^{8}Li(d,n)^{9}Be$	0.6
^{11}C	20 min	$^{11}B(p,n)$	B_2O_3	^{11}B, ^{22}Ne	2.10^{-4}	$^{11}C(p,\gamma)^{12}N$	0.6
		$^{14}N(p,\alpha)$	BN				
^{13}N	10 min	$^{13}C(p,n)$	enriched ^{13}C	^{13}C	2.10^{-4}	$^{13}N(p,\gamma)^{14}O$	0.6
^{14}O	70 s	$^{14}N(p,n)$	BN	^{14}N	4.10^{-4}	$^{14}O(\alpha,p)^{17}F$	0.6
^{15}O	2 min	$^{19}F(p,\alpha n)$	LiF	^{15}N	2.10^{-4}	$^{15}O(\alpha,\gamma)^{17}F$	0.3
^{19}Ne	17 s	$^{19}F(p,n)$	LiF	^{19}F	2.10^{-4}	$^{19}Ne(p,\gamma)^{20}Na$	0.5

Table 1 : Some radioactive beams, their production reactions, contaminants and nuclear reactions of interest for astrophysics.

1.3. Acceleration and isobaric separation

The low energy beam is injected axially in CYCLONE and accelerated on 6th harmonic mode. The limited resolution in M/Q (40) of the low energy analyzing system eliminates neighbouring charge states and contaminants but not those particles that have nominally the same M/Q (see table 1).

To achieve the required purity of the final beam, various physical and chemical methods have been tried out, all rather unsuccessfully.

Finally it was tried to use the cyclotron as a high resolution mass spectrometer. Let us recall here briefly how this could work.[2)]

Consider an isochronous field in which a particle with a given Q/M is accelerated to full energy in N_0 turns with an accelerating voltage working at the Hth harmonic of the particle revolution frequency. Consider another particle whose charge to mass ratio differs slightly from the first by an amount $\Delta(Q/M)$. The change in phase, ϕ, during acceleration between the two particles will be given by :

$$\Delta\sin\phi = 2\pi\, H\, N_0\, \Delta(Q/M)/(Q/M) \qquad (1)$$

When the absolute phase of the particle with respect to the RF reaches 90° the acceleration will stop. The condition to eliminate the wrong particle from the beam, is that this should happen before the extraction radius is reached. Remember that $\Delta\sin\phi$ means $(\sin\phi e - \sin\phi b)$ where e means end of acceleration and b means beginning of acceleration. Depending on the starting phases of the particles, $\Delta\sin\phi$ will be somewhere between 0 and 2. Defining the resolution $R = (Q/M)/\Delta(Q/M)$ gives then :

$$R = 2\pi\, H\, N_0 / \Delta\sin\phi \qquad (2)$$

This relation shows that the mass resolution of a cyclotron is not an unambiguous quantity. It depends for example strongly on the starting conditions in the central region. If starting phases around 0° are considered then the resolution R_0 becomes :

$$R_0 = 2\pi\, H\, N_0 \qquad (3)$$

If for some reason (axial focusing e.g.) starting phases far from 0° have to be adopted then the resolution for wrong particles with larger or smaller Q/M values will be totally different. As an example let us take a starting phase of 30°. In the case of a slightly heavier particle $\Delta\sin\phi$ equals 1.5, in the opposite case 0.5 or a factor of 3 difference in the resolution for a given cyclotronsetting. This situation was experimentally verified with CYCLONE and illustrated in Fig. 1.

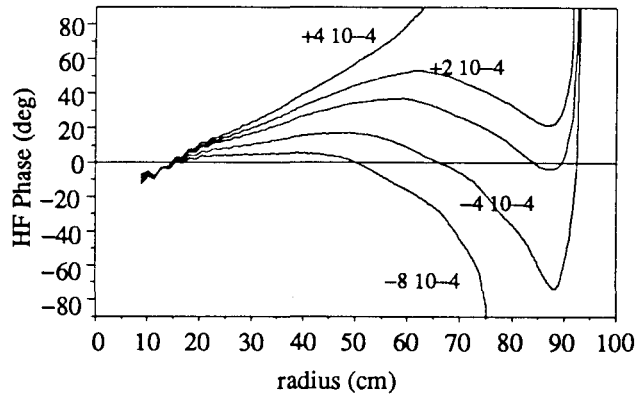


Figure 1 : Phase histories for a given particle in the reference field and fields with $\Delta B/B$ = +2, +4, - 4 and -8 10^{-4}.

Another effect is illustrated in Fig. 2 : even when some of the wrong particles reach the extraction radius and start their way through the deflector, they never reach the cyclotron exit because they do not fall into the extraction system's acceptance.

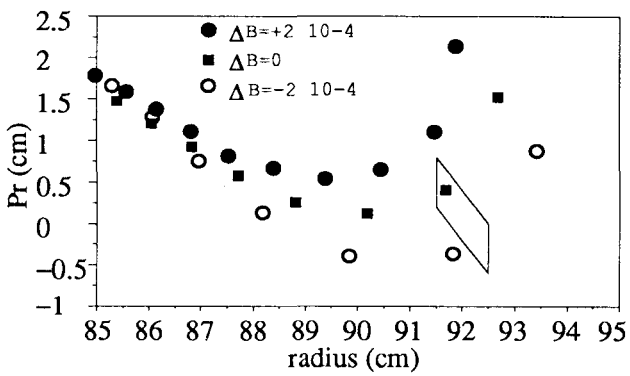


Figure 2 : Acceptance of the extraction system and trajectories of a particle in the reference field and fields with $\Delta B/B$ = +2 and -2 10^{-4}.

Using systematically these effects we have been able to suppress contaminant beams by factors of 10^5 or more without loss of the radioactive beam intensity although their respective Q/M ratios differ only by less than 2 parts in 10^4.

2. OPERATIONAL ASPECTS

Arrangements have been made so that production, transport and acceleration can be optimized independantly. In a first step,the gas flow from the production target can be pumped to a counting station outside the cyclotron vault. This way, the initial outgassing does not have to go through the source and the extraction efficiency can be checked. New targets can be tested.

When the target conditions have been optimized, the gas flow is directed to the source. To optimize the source conditions and to check the ionization efficiency, the low energy beam is stopped and focused on a plate at some distance behind the first Glaser lens. The beam current measured at this point represents essentially the intensity of the contaminant beams. To get an idea of the radioactive beam intensity this beam stop has also been equipped with a β^+ detector. This detector is well shielded from the background generated by the proton beam. At this point the overall efficiency (production + ionization) can be optimized. This works particularly well with the short lived elements (^{19}Ne e.g.).

Transport from the source to the cyclotron, axial injection, acceleration and transport to the experimenter's target are adjusted using a stable beam having the almost identical Q/M value (see Table 1). If the natural contamination in the source is not sufficient, gas is fed to the source. Finally, before switching to the radioactive beam, the mass resolution is checked carefully and the cyclotron is eventually retuned to make sure that a pure radioactive beam is obtained. Table 2 lists the intensities of radioactive beams obtained until now.

Element	Charge State	Intensity [pps]	Maximum Energy [MeV]
^{13}N	1+	$4x10^8$	8.5
($T_{1/2}$ = 10 min)	2+	$3x10^8$	34
^{19}Ne	2+	$1.9x10^9$	23
($T_{1/2}$ = 17 s)	3+	$(10^9)^*$	52
	4+	$5x10^8$	93

* expected

Table 2 : Intensities and energies of the radioactive beams which are presently available at the Louvain-la-Neuve facility.

Figure 3 shows the operating diagram of CYCLONE in the area of interest.

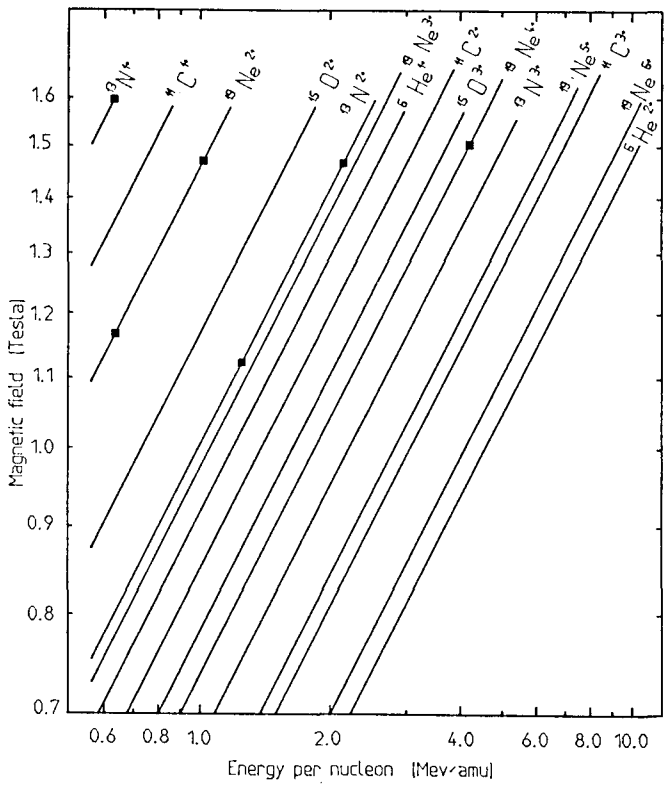


Figure 3 : Operating diagramme for RIB acceleration with CYCLONE.

3. A DEDICATED POSTACCELERATOR FOR RADIOACTIVE ION BEAMS

The actual system suffers two major drawbacks with respect to the requirements for nuclear astrophysics experiments. First, the lower energy limit in H = 6 mode is 0.56 MeV/AMU. Higher harmonic modes seem out of the question. However, as Table 1 shows, there are a number of reactions to be measured at lower energies. Secondly, some of the cross sections to be measured are extremely low so that a minimal intensity is required to make the experiments feasible. This intensity will not be reached: the losses (50 to 80%) due to insufficient vacuum are too high and the matching in the central region is poor. It is very difficult to improve these parameters significantly because of the basic design and operational modalities of CYCLONE.

We have proposed to build a dedicated postaccelerator for radioactive beams. Earlier proposals by other groups comprise a combination of an RFQ and a linac or a tandem for the postacceleration of Isotope Separator On Line (ISOL) beams. In this case very high resolution separators together with ion sources of very high optical qualities are needed at the low energy side to eliminate any isobaric contamination.[3] In our case we want to use an ECR-source because of its high ionization efficiency and high charge state yield for the light elements : higher charge states imply a reduced size for the accelerator. For the metal and alkali elements however, a solution has still to be developed to transfer the activity from the production target to the ECR-source. The emittance of ECR-sources is also larger by a factor of 10 to 100, compared with the classical ISOL-sources.

A cyclotron which combines a large acceptance with a high Q/M resolving power has been chosen. In order to achieve a high acceleration efficiency, special attention has to be paid to the vacuum in the cyclotron and to the matching of the cyclotron acceptance with the source emittance. Harmonic modes 4 and 6 have been chosen: this allows a reasonable size for the RF-resonators, a low effective number of turns which reduces the losses due to stripping whilst assuring a large Q/M resolution. The cyclotron parameters have been redefined as shown in Table 3. Design and construction are planned for the period 1992-1996.

Energy constant	33 MeV
Energy range	0.2 - 0.8 MeV/AMU
M/Q (max)	13
Resolution in Q/M	10 000
Magnet structure	4-sector
Average Field (max)	1.6 T
(min)	0.7 T
Extraction radius	0.52 m
RF-system	2 DEES, 30° wide
Frequency range	11 - 15 MHz
Max DEE voltage	20 kV
Harmonic modes	4,6

Table 3 : Characteristics of the new postaccelerator cyclotron.

4. REFERENCES

1) Berger, G. et al., "Acceleration and mass-separation of radioactive ion beams in an isochronous cyclotron", 1991 IEEE PAC, San Francisco 1991, pp. 2610-2612.
2) Clark, D.J., "Cyclotrons as mass spectrometers", Proc. of the 10th Int. Conf. on Cyclotrons and their Applications, (IEEE, New York, 1984) pp. 534-539.
3) Wollnik, H., et al., "The proposed JHP-ISOL and its expected performance," Proc. of the 1st Int. Conf. on RIB (World Scientific, Singapore,1990) pp. 603-609.

THE ORNL RADIOACTIVE ION BEAM PROJECT WITH THE ORIC ACCELERATOR

D. K. Olsen, G. D. Alton, C. Baktash, D. T. Dowling, J. D. Garrett, D. L. Haynes, C. M. Jones, R. C. Juras, S. N. Lane, I. Y. Lee, M. J. Meigs, G. D. Mills, S. W. Mosko, B. A. Tatum, and K. S. Toth

Oak Ridge National Laboratory*
P. O. Box 2008
Oak Ridge, Tennessee 37831

and

H. K. Carter and J. Kormicki

Oak Ridge Associated Universities
Oak Ridge, Tennessee 37831

ABSTRACT

The ORNL project to produce medium-intensity, proton-rich, radioactive ion beams (RIBs) for astrophysics, nuclear physics, and applied research with the Holifield Heavy Ion Research Facility (HHIRF) accelerators has been approved. Radioactive atoms will be produced by fusion reactions in an Isotope Separator On-Line (ISOL)-type target-ion source assembly using light ion beams from the Oak Ridge Isochronous Cyclotron (ORIC). The radioactive atoms will be converted to negative ions using either (1) direct-surface ionization or (2) charge exchange following positive ionization. After acceleration to approximately 300 keV from a high-voltage platform, these negative ions will be injected into the 25-MV tandem accelerator for acceleration to higher energies. Beams of up to mass 80 will be accelerated to energies greater than 5 MeV/nucleon. For some radioactive beams, intensities greater than 1 pnA are possible.

1. INTRODUCTION

During the last few years, substantial interest has developed in the scientific opportunities presented with accelerated radioactive ion beams. This interest has led to the development and proposed development of RIB facilities in North America, Europe, and Asia; international conferences on RIBs at Berkeley [1] and Louvain-la-Neuve [2]; and many workshops on specific aspects of RIB technology and science. This paper describes the ORNL RIB project [3] which has been recently approved.

The reconfiguration of the two accelerators of the HHIRF will provide a quick and inexpensive first-generation, proton-rich, medium-intensity, ISOL-type RIB facility for North America. In the past, ORIC has served as an energy booster for stable heavy ions produced by the 25-MV tandem accelerator. To produce RIBs, this process will simply be reversed: the tandem accelerator will be injected with radioactive heavy ions produced by ORIC. In this case, the two accelerators will be coupled by an ISOLDE-type [4] thick-target and ion source assembly, mass separator, and charge exchange canal, all mounted on a 250-kV high-voltage platform in an existing shielded room. Light ions from ORIC, with an internal ion source, will produce radioactive heavy ions for tandem injection. Moreover, the existing UNISOR on-line isotope separator allows the timely development of the target-ion source hardware and chemistry.

2. EXISTING COMPONENTS

A central feature of the ORNL RIB project is that most of the main components already exist. The new hardware required for this RIB reconfiguration is shown in Fig. 1. The existing components include:

2.1 ORIC Accelerator

The k = 100 ORIC was designed for the acceleration of both light and heavy ions and was used initially for intense light-ion beams in the first years after its completion in the early 1960s. In the 1970s, ORIC was used mostly for heavy ion acceleration, and in the 1980s, ORIC was used mostly as an energy booster. ORIC was originally designed to accelerate 1 mA of 75-MeV protons. Thus, ORIC is an ideal driver for the intense light-ion primary beams needed to produce RIBs. For RIB intensity estimates in the ORNL proposal, H and He beams were limited to 2 kW of extracted beam power and Li and B beams were limited to 10 pμA of extracted beam current. For first operation, 0.5 kW of extracted beam power seems readily achievable. Table 1 lists the main parameters of the cyclotron.

2.2 UNISOR

This on-line isotope separator has been operating since 1971, is managed and used by a consortium of university physicists, and provides extensive in-house experience. UNISOR, with its high-efficiency FEBIAD ion source, has allowed the immediate investigation and development of the thick-target and ion-source materials, geometry, chemistry, and procedures required to produce RIBs for subsequent acceleration. In particular, experiments have started in which elements for future RIBs are implanted in thick target materials of interest. The chemistry and physics of the subsequent thermal diffusion, desorption, and ionization can, therefore, be studied without actual production of RIBs. [5]

* Research sponsored by the U.S. Department of Energy under contract DE-AC05-84OR21400 with Martin Marietta Energy Systems, Inc.

2.3 Tandem Accelerator

The tandem terminal presently operates at 25 MV, which is the highest electrostatic accelerator voltage in the world. The charge state fractions and transmission efficiencies through the tandem accelerator have been extensively measured and are well understood. With gas stripping, beams of mass 52 can be accelerated above 5 MeV/A with a total efficiency of 20%. With foil stripping, beams of mass 80 can be accelerated above 5 MeV/A with a total efficiency of over 8%. Beams of lower masses can be accelerated to higher energies with total efficiencies approaching 50%.

The tandem accelerator has some very important advantages for RIBs. No modifications would be required for service as a RIB accelerator. Since it is inherently a dc machine, no bunching is required for the injected beam, thus maximizing the dc beam available from the RIB target ion source. In addition, other inherent advantages, such as simplicity, reliability, and excellent beam quality, are also available. One of the main difficulties with RIBs is the separation of analog and isobaric beams. The folded configuration of the tandem allows the separation of analog beams. More importantly, the excellent emittance ($< 1\ \pi$ mm mrad) and low energy spread ($< 1 \times 10^{-4}$) of the tandem beam will allow convenient use of the existing energy analyzing magnet for some separation of isobaric beams.

2.4 Shielded Space

The shielding for the original ORIC vault and target rooms was designed for 75-MeV, 1-mA proton beams. These rooms are also equipped with single-pass HVAC systems appropriate for high-radiation areas. In the present plan, room C111, shown in Fig. 1, will house the target-ion source, mass separator, and charge exchange canal on a 250-kV high-voltage platform system. In order to reduce potential radiation damage to electronic components during high-intensity operation, the platform system will consist, in fact, of two platforms, one for mechanical equipment and one for electronic equipment, connected by a HV conduit and separated by a radiation shielding wall. No new civil construction is required for the ORNL RIB project.

3. ADDITIONAL EQUIPMENT

The additional equipment required to produce RIBs is shown in Fig. 1. Except for a necessary change in elevation, the mechanical high-voltage platform could be fed by an existing 13-m-long beam line from ORIC. The high-voltage platform will be specified to operate at potentials up to 250 kV and with the ISOLDE-type source potential of 20 to 50 kV with respect to platform ground, will provide the nominal 300-keV energy which is presently used for tandem injection. Recent measurements with various beams have shown that the tandem transmission efficiency is essentially independent of injection energy between 200 and 300 kV. The ORIC beams will be transported from ground potential to the platform and the ISOLDE-type target-ion source through 250-kV and 50-kV acceleration tubes. Depending on the RIB, either positive or negative ions will be formed in the target-ion source. These ions will be accelerated to platform potential and mass analyzed to a single mass number with a first-stage magnetic mass analyzer. This mass-analyzed beam will be charge exchanged, if required, and accelerated to ground potential, ready for tandem injection. A 23-m-long beam line at an elevation of 2.3 m will be built to transport the negative ion beam through the east experimental room from the high-voltage platform to the tandem accelerator. Injection will be accomplished by merging the beam through the existing, de-energized, mass-analyzing tandem injector magnet. Figure 2 shows a vertical view of the new equipment required for RIB acceleration in the tandem. This new beam line will be reconfigured to be a second stage in the mass analyzing system.

4. EXPECTED ENERGY AND INTENSITY

The maximum intensities and energies for RIBs from the tandem accelerator for some of the most interesting and intense beams are listed in Table 2 for an initial ORIC beam power of 0.5 kW. With single stripping, masses up to about 80 can be accelerated to energies above 5 MeV/nucleon. The maximum currents for these beams are much more difficult to estimate, and depend on the product of a number of factors. These factors can be divided into a thick target production rate for radioactive atoms and the overall efficiency for converting these atoms to beam on target. The thick target production rates were estimated using fusion cross sections based on measured nuclear systematics and stopping powers. Production rates for C, O, F, Na, Si, P, S, Cl, K, Cu, Ga, Ge, As, Se, Br, and Rb RIBs were calculated using (H, xn) (He, xn), (Li, xn), (B, xn), and (p, αxn) reactions on Be, C, N, O, Mg Al, Si, S, Ca, Zn, Ni, Ge, and Sr target atoms contained in BeO, BN, C, MgO, AlB_2, SiO_2, Zr_5Si_3, CeS_2, CaO, ZnO, NiO, Zr_5Ge_3, and SrO refractory target materials.

The overall efficiency for converting extracted atoms to accelerated beam on target is listed in Table 3 and is a simple measure of the system merit. Two methods are considered for negative ion formation: direct surface ionization and charge exchange. Direct surface ionization is applicable to elements with large electron affinities and efficiencies were estimated from the Langmuir-Saha relation for a LaB_6 surface ionizer operated at 1370 K. Efficiencies using charge-exchange are the product of two factors: the efficiency for positive ionization and the efficiency for conversion of positive to negative ions. The positive ion efficiencies were estimated by scaling the probability for electron impact ionization of the element in question to that of calcium which has a 30% measured efficiency. The efficiencies for sequential charge exchange are based on measured results. In addition, a 50% loss factor has been included to account for transport losses. The transmission efficiency through the tandem accelerator is well understood and based on experience. The average overall conversion efficiency from radioactive atoms to

beam on target is about 1% and varies widely, depending on the element.

The product of these overall conversion efficiencies with the thick target yields for some of the most interesting RIBs are listed in Table 2. Examination of this table shows that many of the RIBs listed have intensities greater than 0.1 pnA, the intensity that presently can be used at the HHIRF for experiments with 4π detector systems. Fluorine and chlorine, which combine favorable production reactions, surface negative ionization, and acceleration efficiencies, are expected to be the most intense RIBs. It should be emphasized that Table 2 does not contain decay loss or release rate factors. In addition, high positive ionization efficiencies for low-mass RIBs will require an ECR ion source. Figure 3 shows a summary of the process with average efficiencies with 2.0 kW of ORIC beam power for a generic "good case" radioactive beam. It will require about 1000 protons to produce one radioactive atom in a thick target and these radioactive atoms, with the tandem accelerator, should be delivered as beam on target with about a 1% efficiency, giving a factor of 10^5 between the RIB beam intensity and the ORIC beam intensity.

5. WORK IN PROGRESS

Presently, a substantial amount of work is in progress at ORNL to develop a RIB capability. Internal ion source operation of the ORIC accelerator is being restored and central region calculations have been completed [6] to optimize the ion source geometry in order to minimize beam losses and maximize extracted light-ion beam. UNISOR implantation studies have been initiated [5] and the engineering for an ISOLDE-type FEBIAD target-ion source is nearly completed. An exhaustive study of the various locations and configurations for the HV platform system and the overall layout has been completed. Numerous other tasks and studies are in progress. Studies have shown that the tandem accelerator acceptance is relatively insensitive to injection energy between 200 and 300 keV and that the new tandem potential stabilizer system will provide the long-term stability required for very low intensity beam operation, as well as isobar separation, while operating in the generating voltmeter mode.

In principle, several isobars with the same mass number could be produced in the target-ion source and accelerated through the tandem accelerator, giving a mixed beam of isobars on target. Up to and including the mass 80 region, isobars tend to be separated in mass by approximately one part in 10,000. Recent experimental studies have shown that with gas stripping, the tandem energy analyzing system may be capable of this mass resolution.

6. CONCLUSIONS

It appears that accelerator-based nuclear physics which, only a few decades ago, moved, in part, from light-ion to heavy-ion beams, is now starting to move, in part, from stable-heavy-ion to radioactive-heavy-ion beams. It also appears that the ORIC will start its fourth decade of operation as the light-ion driver for the first accelerated RIB facility in North America.

REFERENCES

[1] Proc. First Int. Conf. on Radioactive Nuclear Beams, Berkeley, CA, October 1989, eds. W. D. Myers, J. M. Nitschke, and E. B. Norman (World Scientific, Singapore, 1990).

[2] Proc. Second Int. Conf. on Radioactive Nuclear Beams, Louvain-la-Neuve, Belgium, August 1991, ed. by Th. Delbar (Adam Hilger, Bristol, 1992).

[3] "A Proposal for Physics with Exotic Beams at the Holifield Heavy Ion Research Facility," eds. J. D. Garrett and D. K. Olsen (ORNL, February 1991).

[4] H. L. Ravn and B. W. Allardyce, *Treatise on Heavy Ion Science*, ed. D. A. Bromley, Vol. VIII, *Nuclei Far From Stability* (Plenum Press, New York, 1989), p. 363.

[5] G. D. Alton, H. K. Carter, I. Y. Lee, C. M. Jones, J. Kormicki, and D. K. Olsen, Nucl. Instr. and Meth. B66 (1992) 492.

[6] H. Blosser, L. Lee, and F. Marti, private communication, 1992.

Table 1. Oak Ridge Isochronous Cyclotron (ORIC) Parameters

Bending Limit (ME/q2)	100
Focusing Limit (ME/q)	75
Magnet System	
Pole face diameter	76 in
Number of compact sectors	3
Maximum spiral angle	30°
Minimum gap/maximum field	7.5 in/23.8 kG
Maximum gap/minimum field	28. in/13.2 kG
Main Coil Conductor	250 turns Al
Main Coil Power Supply	5000 A–350 V
Trim coils	10 pairs
Harmonic coils	4 pairs per valley
Weight	210 tons
RF System	
Configuration	Single 180° dee to ground
Maximum voltage per gap	70 kV
Maximum RF power	200 kW
Frequency range	6.7–20.1 MHz
Vacuum System	
Operating pressure	1×10^{-6} Torr
Pumps	Two 80-cm oil DP
	One 50-cm oil DP
	One 50-cm cryopump
Internal Ion Source	Cold cathode Penning
Extraction Channel	
One 60 cm long, 70 kV/cm, electrostatic deflector	
One 25 cm long, 3 kG, 5000 A, coaxial, sepum magnet	
One 100 cm long, 6.5 kG, 3000 A-3000 A, compensated iron, magnet channel	

Table 2. Estimated Maximum Beam Intensities and Energies from the ORNL Radioactive Ion Beam Facility*

Isotope	Beam Intensity (ions/s)	Maximum Beam Energy (MeV/Amu)	Isotope	Beam Intensity (ions/s)	Maximum Beam Energy (MeV/Amu)
^{10}C	4.3 x 10^{7}	13.0	^{63}Ga	1.8 x 10^{5}	6.1
^{11}C	5.0 x 10^{7}	13.0	^{64}Ge	1.8 x 10^{6}	6.0
^{14}O	1.4 x 10^{8}	13.0	^{68}As	1.1 x 10^{9}	5.9
^{15}O	3.3 x 10^{8}	13.0	^{69}As	1.3 x 10^{9}	5.9
^{17}F	1.1 x 10^{10}	12.7	^{70}As	1.0 x 10^{9}	5.8
^{18}F	5.8 x 10^{9}	12.3	^{70}Se	1.9 x 10^{8}	5.8
^{21}Na	4.3 x 10^{7}	11.2	^{71}Se	9.3 x 10^{7}	5.7
^{22}Na	4.3 x 10^{7}	10.7	^{72}Se	1.9 x 10^{8}	5.6
^{26}Si	1.2 x 10^{9}	8.8	^{74}Br	3.3 x 10^{7}	5.5
^{27}Si	1.0 x 10^{9}	8.8	^{76}Br	1.7 x 10^{7}	5.3
^{33}Cl	2.5 x 10^{10}	7.8	^{77}Br	6.8 x 10^{6}	5.3
^{34}Cl	2.2 x 10^{10}	7.5	^{77}Rb	1.4 x 10^{5}	5.3
^{37}K	6.5 x 10^{8}	7.0	^{78}Rb	1.2 x 10^{5}	5.2
^{38}K	3.3 x 10^{7}	6.8	^{79} Rb	1.2 x 10^{5}	5.2
^{58}Cu	1.0 x 10^{9}	6.3			

* These estimates are for 0.5 kW of ORIC beam power, isotopically pure targets, and do not include any decay, target release, or surface sticking losses.

Table 3. Estimated Overall Efficiency from Atoms to Accelerated Beam.[a]

Element	Electron Affinity (eV)	Negative Ion Production Method[c]	Positive Ion Efficiency (%)[d]	Negative Ion Efficiency (%)[e]	Tandem Transport Efficiency (%)[f]	Overall Efficiency (%)[g]
He	0.08[b]	CE	2.4	1.5	80 G	0.01
Li	0.62	CE	14	9	80 G	0.50
Be	0.19[b]	CE	9.3	3	70 G	0.10
B	0.28	CE	11	12	60 G	0.40
C	1.27	CE	8.9	42	47 G	0.88
N	<0					
O	1.46	CE	8.5	45	35 G	0.67
F	3.40	SI		100	32 G	16.0
Ne	<0					
Na	0.55	CE	27	5	30 G	0.20
Mg	<0					
Al	0.46	CE	25	14	28 G	0.49
Si	1.39	CE	19	60	28 G	1.60
P	0.74	CE	15	70	28 G	1.37
S	2.08	SI		15.6	28 G	2.05
Cl	3.62	SI		100	25 G	12.5
Ar	<0					
K	0.50	CE	42	1.8	24 G	0.09
Ca	0.04	CE	30	0.4	23 G	0.01
Sc	<0					
Ti	0.2	CE	29	4	21 G	0.12
V	0.5	CE	31	10	21 G	0.33
Cr	0.66	CE	31	10	21 G	0.33
Mn	<0					
Fe	0.25	CE	27	6	11 F	0.09
Co	0.70	CE	28	12	10 F	0.17
Ni	1.15	CE	29	60	11 F	0.96
Cu	1.23	CE	30	60	9.5 F	0.86
Zn	<0					
Ga	0.3	CE	40	7	9.0 F	0.13
Ge	1.20	CE	31	62	8.6 F	0.83
As	0.80	CE	26	75	8.5 F	0.83
Se	2.02	CE	26	75	8.2 F	0.80
Br	3.36	SI		100	8.2 F	4.10
Kr	<0					
Rb	0.49	CE	64	0.8	8.0 F	0.02

[a]Excluding decay and target release losses.
[b]Metastable state.
[c]SI denotes direct surface ionization. CE denotes charge exchange.
[d]Scaled as discussed in the text.
[e]Measured efficiencies.
[f]F or G denotes gas or foil stripping in the tandem terminal.
[g]Includes an additional 50% reduction to account for transport losses to the tandem accelerator.

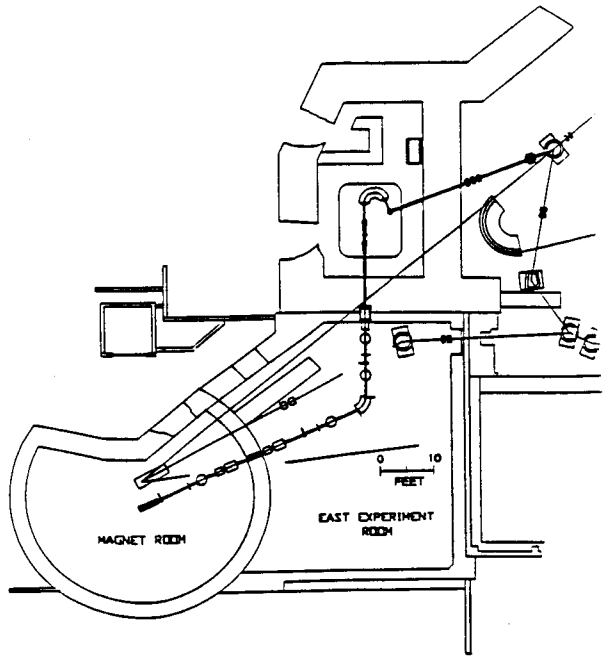


Figure 1. Additional hardware required to reconfigure the ORNL accelerator system to produce RIBs.

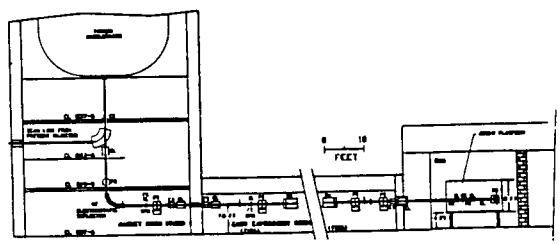


Figure 2. Elevation view of the ORNL RIB facility showing the HV platform and negative-ion transfer line to the tandem accelerator.

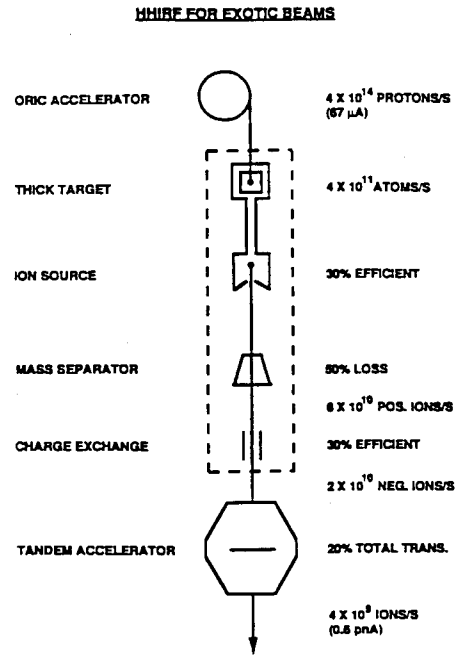


Figure 3. Summary of the ORNL concept and average efficiencies for a "good case" RIB produced with 67 μA of 30-MeV protons. About 10^{-6} of the primary beam of 0.6 pnA of RIBs would be produced as beam on target.

RESEARCH AND DEVELOPMENT STUDIES WITH RADIOACTIVE BEAMS AT TRIUMF

J.M. D'Auria[1], M. Dombsky[1], L. Buchmann[2], H. Sprenger[2], J. Vincent[2], J. King[3], P. McNeely[4] and G. Roy[4]

[1]Dept. of Chemistry, Simon Fraser University, Burnaby, B.C. Canada, V5A 1S6
[2]TRIUMF, 4004 Wesbrook Mall, Vancouver, B.C. Canada, V6T 2A3
[3]Dept. of Physics, University of Toronto, Toronto, Ontario, Canada, M5S 1A7
[4]Dept. of Physics, University of Alberta, Edmonton, Alberta, Canada, T6G 2E9

ABSTRACT

In 1985 a detailed conceptual plan was proposed for the installation at TRIUMF of a high intensity accelerated radioactive beams facility (ISAC) involving an on-line isotope separator and a LINAC post-accelerator. Masses up to A=60 were to be accelerated to energies between 0.2 and 1.5 MeV/u and the facility devoted mainly to studies in nuclear astrophysics. While awaiting a decision on this proposal, a prototype isotope separator, TISOL, has been successfully installed and is now available as a limited production facility, servicing an experimental program. This paper will provide a status of the ISAC proposal, a general description of the TISOL radioactive beams facility now operating at TRIUMF, and a summary of the future plans of these programs including a revised ISAC proposal.

1. INTRODUCTION

The TRIUMF cyclotron is an optimal facility for the intense production of a wide range of radioisotopes, which can then be accelerated appropriately to result in a low energy radioactive beams facility. This was recognized some years ago as a proposal was submitted in 1985 to install a high intensity, accelerated radioactive beams facility at TRIUMF. This low energy, facility (ISAC) was to consist of an on-line isotope separator followed by a LINAC post-accelerator to boost the energies of the separated radioisotopic ion beams to 1.5 MeV/u.[1,2] This was the pioneer proposal of the two accelerator type which has now spawned a number of similar proposed or operational facilities. ISAC was delayed due to the presense of the KAON proposal, but TRIUMF did authorize the installation of a thick target, on-line separator (TISOL) for research and development studies with radioactive beams. The TISOL facility has been in operation for several years both as a test system and now as a production facility servicing a modest experimental program. Based upon the experience and expertise developed with TISOL, and depending upon a final decision on KAON, a revised ISAC could be implemented at TRIUMF. A description of the TISOL facility will be presented herein along with aspects of the experimental and developmental program; a conceptual plan for a revised ISAC will also be described.

2. THE TISOL FACILITY

2.1. General Description

TISOL is a vertically mounted, thick target, on-line isotope separator located at the 500 MeV proton facility, TRIUMF. Such energetic protons are ideal for the production of a wide range of radioisotopes, and the thick target combined with the high intensity of the TRIUMF beam leads to relatively high production rates for the resulting radioactive nuclear beams. Figure 1 displays an elevation view of TISOL as it exists today, having evolved from a much smaller version which was installed originally.[3] The target is positioned just before the beam dump and beam intensities up to 1.5 μA can be used. Target handling has been performed mainly by personnel up to now, but a new remote target changing system is being installed to allow for changing of the very hot target systems. A halo monitor is used upstream of the target to monitor the beam position while a secondary electron emission monitor is located behind the target to monitor the proton beam intensity. A new experimental area with the three beam lines is located at ground level, well shielded from proton beam radiation. A detailed description of the facility can be found elsewhere.[3–6]

2.2. Ion Sources

There are presently two working ion sources available at TISOL, an ECR (Electron Cyclotron Resonance) source and a standard heated surface, thermal source; these have been described in detail elsewhere.[5,6] While the latter source does provide some degree of elemental selectivity (species of low ionization potentials) in its ionization, the ECR source will ionize any species, elemental or molecular, which reaches it, to a range of charge states, e.g., recently the isotope ^{18}N was observed at a

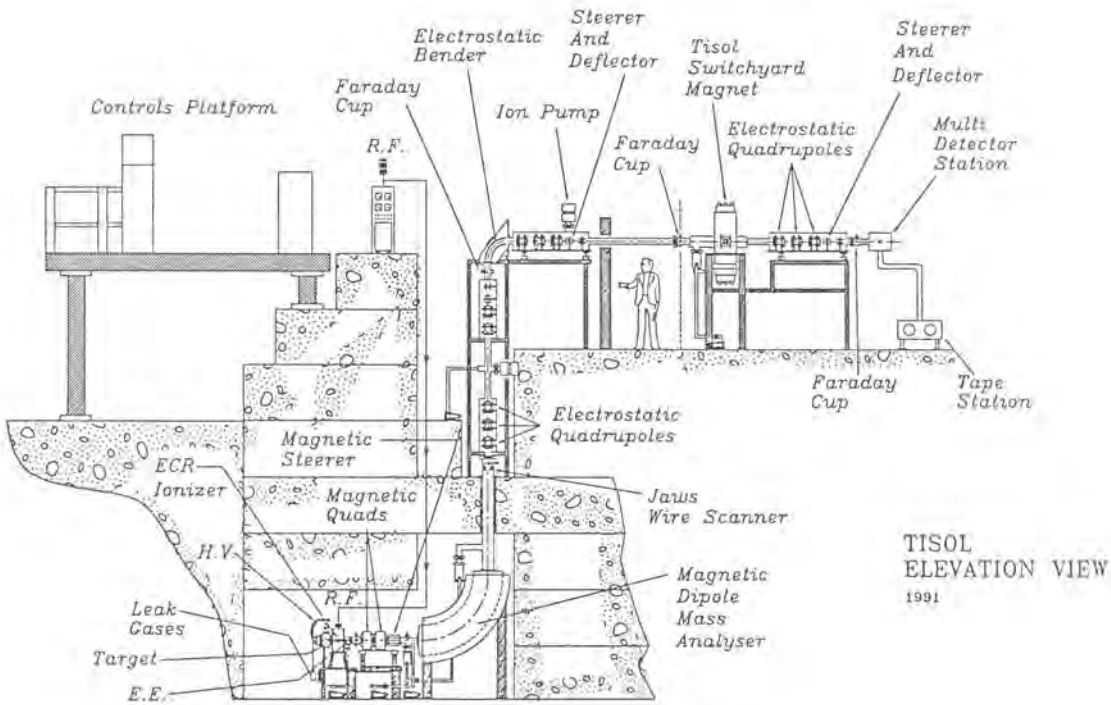


Fig. 1. Elevation view of TISOL.

mass position of 16 as the species $(^{18}N^{14}N)^{++}$. Some selectivity can be obtained by using a non-heated transfer line between the source and the target, eliminating non-volatile species.

Improvements are planned to allow for ion changes quickly (one hour), and this combined with the target changing system will further reduce personnel doses. The ECR system will also incorporate ceramic insulating flanges.

2.3. Target Materials and Radioactive Beams

A range of target materials have been used at TISOL and these are summarized in Table 1. Ion beams of radioactive isotopes from all of these elements have been observed. Intensities vary depending upon the target, its thickness, the reaction involved, the stability of the species and operating parameters of the facility; intensities as high as 10^9 p/sec per μA of production proton beam have been observed. Observed production rates can be found elsewhere.[4–6]

The zeolite (commonly called molecular sieve) target material is unique for an ISOL target. The type used here is 13X ($NaA1SiO_4$) and has openings of the order of nm. The target elements are optimal for producing low Z products on both sides of stability. In order to be useful as a target, it must be heated under vacuum for several days and the temperature should not exceed about 600°C to prevent break-down of the structure. This material, when properly conditioned, has proven to be optimal for the production of nitrogen beams when coupled with the ECR source; oxygen, carbon and helium beams

Table 1.

Target Source	Form	Operating Temp (°C)	Elements Observed
			a) ECR Source
A1N	Powder	1050	He,Ne,N
CaO	Chunks	1100	C,He,Se,N
CaO	Powder	1100	Ar,C,Ne,N
LaC_2	Chunks	1700	He,Ne,Xe
MgO	Chunks	1300	C,He,Ne,N
MgO	Pellets	1300	C,Ne,N
MgO	Powder	1300	C,Ne,N
$Mg^{18}O$	Powder	1300	C,He,Ne,N
SiC	Pellets	1500	Ne,O
Ti	Foils	1500	Ne,Ar,Cl,He
UO_2/C	Pellets	2000	C,Kr,He,Xe,Se,O,Sn
Zeolite*	Spheres	500	Ar,C,He,Ne,N,O
			b) Re Surface Source
Hf	Foils	1800	Cs,K,Li,Na,Rb,Yb
Nb	Foils	1900	K,Li,Na,Rb,Sr
Nb	Powder	2000	Rb
SiC	Pellets	1500	Al,Li,Na
Ti	Foils	1500	Al,K,Li,Na
Ti	Foils	1500	Al,K,Li,Na
$U0_2/C$	Pellets	2000	Al,Cs,Ga,In,Li,Na,Rb
Zr	Foils	1000	K,Na,Rb,Sr
ZrC	Pellets	2000	Al,K,Li,Na,Rb,Sr

*($NaAlSiO_4$)

have also been observed. The cation, e.g., Na^+ for 13X, can be exchanged relatively easy for heavier substances and this material could then be used for heavy A, radioactive beams production.

2.4. The Experimental Program

The TISOL facility is now also used as a production facility, servicing an experimental program. There are now five approved studies and a brief summary of some is given herein.

While Exp. 617 (Studies of Light Rb Isotopes) has obtained publishable results in 1991, problems in the data acquisition system have forced remeasurement this year. Significant results have been obtained for Exp. 589, a major experimental study on the beta delayed alpha emission of ^{16}N. This decay is the inverse of the important astrophysical reaction, $\alpha + {}^{12}C$, and approximately 4 weeks of continuous use of TISOL have resulted in the observation of new, important results.[7] The new zeolite target released the highest yields of ^{16}N available anywhere, and over 1.25 × 106 coincidence events (^{12}C and α) have been observed.

3. FUTURE GOALS

3.1. Future Plans at TISOL

It is difficult to describe future plans without reference to the proposed KAON facility at TRIUMF. It is planned to continue with research and development studies on TISOL, independent of the final decision on KAON. If KAON is finally funded properly, the TISOL facility can continue in its present location as beam line 4A should still be in operation although at a slightly lowered beam energy (450 MeV) and in intensities up to 15 μA.

In the planning and development of the suggested ISL (IsoSpin Laboratory),[8] it is expected that TISOL will be available for target development studies using proton beam intensities up to 10 μA. These studies would be in addition to the continuation of the present TISOL scientific program mentioned above.

3.2. A Revised ISAC Facility

In the scenario of a positive decision on KAON, there is a possibility that an ISAC facility will be considered for installation on the 3 GeV beam line. Figure 2 presents a layout of the revised ISAC. However, given the large manpower demands and costs of KAON, this has to be considered remote. In the case of a negative, final decision on KAON, there is a good possibility that ISAC will be a centerpiece of the new TRIUMF facility. Considerations thus have been given to the previous ISAC proposal and possible changes depending upon the previous ISAC proposal, the world situation in the field of accelerated radioactive beams, and the interest shown by potential users, especially in North America. It is important to preface any such remarks by a close look at the reasons why TRIUMF is considered a good location for ISAC.

3.2.1. Why at TRIUMF?

It is important to indicate clearly the advantages of locating a low energy, high intensity accelerated radioactive beams facility at TRIUMF. The presence of the high intensity, 500 MeV proton facility makes it the obvious choice, since thick targets can be used leading to high production rates. The personnel at TRIUMF are also quite experienced in working with the very high radiation fields expected to be generated by the ISOL device when using beams up to 100 μA. This gives this lab a considerable edge when compared to labs who may have possible post-accelerators on site but lack such experience. TRIUMF has developed expertise in working with such thick target facilities given the presence of the TISOL facility. Finally, the TRIUMF cyclotron itself is an important consideration. It is a reliable, cost-effective machine which produces an essential CW beam, ideal for ISOL types of targets, with good beam emittance properties. Several beams can be extracted simultaneously which allows for beam availability to several high priority facilities.

3.2.2. Specifications

The specifications for the revised ISAC facility are presented in Table 2 and have been developed over a period of years. It is believed that these specifications are all technically achievable with either presently existing technology or with some modest upgrades in present systems.

3.2.3. Research and Development Areas (TISOL and Elsewhere)

Certain areas do require some developmental studies prior to finalizing the design of ISAC. These include:

- development of a low beta, RFQ accelerating structure for CW operation;
- development and test of a thick target which can handle high proton beam intensities;
- optimization of an ECR ion source to produce high relative yields of multiply charged ions of masses with A>60;
- development of an optimal stripping system for such low intensity, low energy beams.

Some of these activities can be done on the TISOL facility which must remain as a test and experimental station during construction of ISAC. In addition, various labs around the world have indicated their willingness and interest to collaborate in such studies including LAMPF, CRNL, Argonne, ISL, and Oak Ridge.

Table 2: Specifications for ISAC (Revised)

Production System		
Projectile	-	protons (200-500 MeV)
Intensities	-	<100 μA
Target Stations	-	2
Target Thicknesses	-	20 cm
Products	-	A<240, Z<93
Separation System		
Ion Sources	-	for charge state, Q = 1± [plasma, thermal, ECR]; for q>1+ charge states, [ECR];
Mass Separators	-	two medium mass resolution systems with two mass beams extractable; one high mass resolution (M/M=30,000)
Extraction Voltage	-	60 kV
Post Acceleration System		
Injection Specs	-	E = 60 keV, q/A>1/60
Output Energy	-	variable, 0.2–10 MeV/u
Energy Resolution	-	<1%
Energy Increments	-	<0.1%
Mass Range	-	A<60–(A>60 for q>1+) expandable up to A = 240 (q/A = 1/240)

4. CONCLUSION

TRIUMF remains active in the field of radioactive beams with the operating TISOL facility. With a decision on KAON, the future of the proposed ISAC, the high intensity, low energy, accelerated radioactive beams facility of the ISOL/PA type can then be ascertained.

5. REFERENCES

1) Buchmann, L., D'Auria, J.M., King, J.D. Mackenzie, G., Schneider, H., Moore, R.B. and Rolfs, C., Nucl. Instrum. Meth. in Phys. Res. **B26**, 151 (1987).
2) Proposal, "The TRIUMF-ISOL Facility: A Proposal for an Intense Radioactive Beams Facility", submitted to TRIUMF, June 1985.
3) Oxorn, K. *et al.*, Nucl. Instrum. Meth. **B26** (1987).
4) Dombsky, M. *et al.*, Nucl. Instrum. Meth. **A295**, 291 (1990).
5) Buchmann, L., Vincent, J., Sprenger, H. Dombsky, M., D'Auria, J.M., McNeely, P. and Roy, G., Nucl. Instrum. Meth. **B62**, 521 (1992).
6) Dombsky, M., Ph.D. Thesis, Simon Fraser University, 1991.
7) Buchmann, L. *et al.*, "The β-delayed α spectrum of ^{16}N and the low-energy extropolation of the $^{12}C(\alpha,\gamma)^{16}O$ cross section; submitted to Conf. on Chaos in the Cosmos, Karlsruhe, Germany, July 1992, preprint.
8) "The IsoSpin Laboratory: Research Opportunities with Radioactive Nuclear Beams", prepared by the North American Steering Committee for the ISL Laboratory, LALP 91-51 (1992).

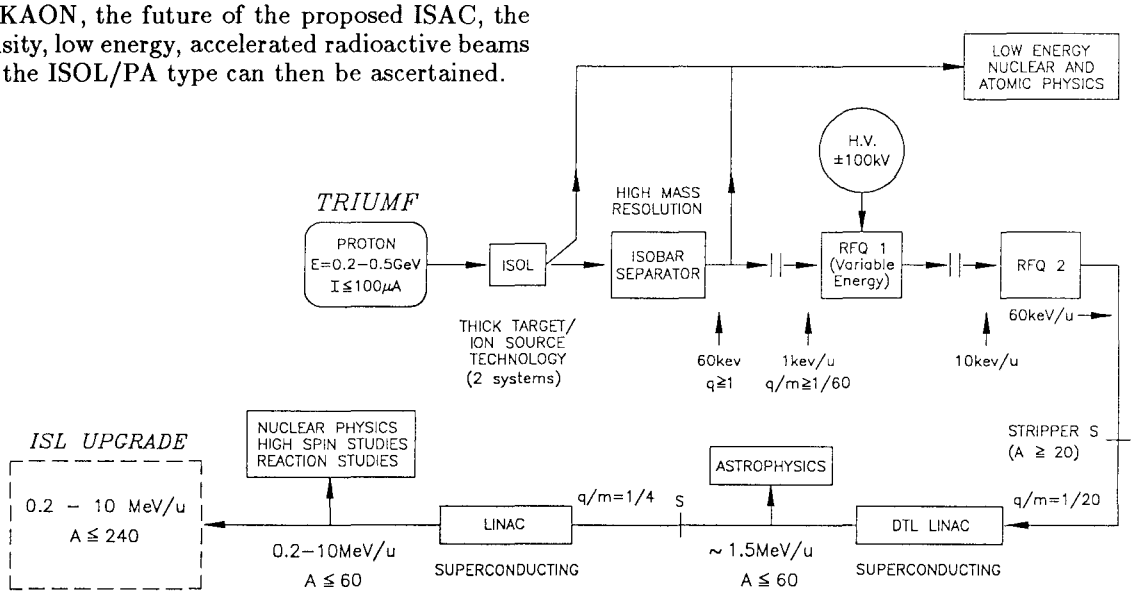


Fig. 2. Schematic representation of a revised ISAC Facility

POST-ACCELERATOR STUDIES FOR THE ISOL FACILITY AT TRIUMF

L. Root, H.R. Schneider, and J.S. Fraser
TRIUMF, 4004 Wesbrook Mall, Vancouver
British Columbia, Canada V6T 2A3

ABSTRACT

A conceptual design for an ISOL post-accelerator, based on superconducting linac structures developed at Argonne National Laboratory was described in earlier papers. Periodic focusing provided by 7 T solenoids spaced at 8 cell intervals could maintain adequate transverse focusing only if the accelerating gradients were kept well below the demonstrated 6 MV/m capability of the SC structures. To permit higher accelerating gradients several variations of the solenoid focusing as well as RFQ focusing elements have been investigated. The RFQ elements are $\beta\lambda$ long and act like a quadrupole doublet with time dependent fields that can be much higher than in an electrostatic quadrupole. Using RFQ focusing with 93 kV/cm peak fields in a 1 cm radius bore, spaced at eight cell intervals, it was found that adequate focusing to compensate for the rf defocusing associated with 6 MV/m accelerating gradients could be achieved. The 5.6 m drift-tube linac length in stage 1 of the previous conceptual design could then be reduced to 3.1 m.

1. INTRODUCTION

In an earlier paper we described the conceptual design of a post accelerator (ISAC) for radioactive beams generated in an isotope separator on line (ISOL) at TRIUMF.[1] As illustrated in Fig. 1, it consisted of a room temperature RFQ to capture, bunch, and accelerate the singly charged ISOL ion beam (with $A \leq 60$) to an energy of 60 keV/u, followed by a stripper to raise the ion charge to mass ratio (q/A) to at least 1/20 before further acceleration to 1.6 MeV/u in two stages of a superconducting interdigital linac. Twelve four gap interdigital tanks of the ANL type,[2] operating at 50 MHz made up the first stage, while the second stage, operating at 100 MHz consisted of 21 four gap interdigital modules. Superconducting solenoid lenses installed at two tank intervals in the first stage and three tank intervals in the second stage, provided the transverse focusing for the beam. The magnetic induction in the solenoids was chosen to be 7 T, and solenoid lengths varied from .3 m to .45 m.

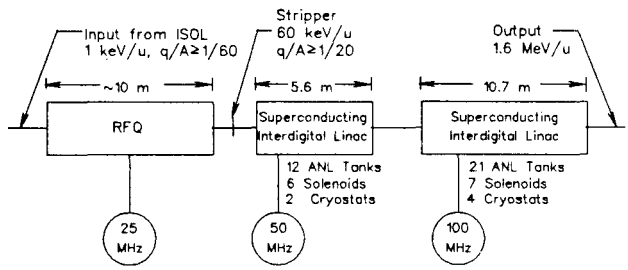


Fig. 1. Conceptual design of ISAC

To limit rf defocusing in the accelerating gaps it was found, in this design, that in addition to choosing a relatively small synchronous phase angle of $-15°$, it was also necessary to choose accelerating gradients in the 50 MHz section well below the demonstrated capabilities of the ANL interdigital structures. Thus the accelerating gradient was limited to 2 MeV/m in the first tank of stage 1, and allowed to ramp up in succeeding tanks, ending at 4.8 MeV/m in the last tank of this stage, still below the 6 MeV/m achieved in such structures.

In the current study two approaches to increase the transverse focusing strength, and hence allow higher accelerating gradients, have been investigated. In one case various options involving solenoid focusing have been reexamined and optimized, while in the other, the possible use of focusing RFQ elements has been investigated. The objective in either case was to attempt to reduce the overall length of the linac, or more particularly, to reduce the required number of superconducting modules.

2. SOLENOID FOCUSING

Several options are possible for increasing the focusing strength using solenoids. These include a) increasing the periodicity from tank-tank-solenoid to tank-solenoid, b) increasing the solenoid lengths (within limits as discussed later), and c) increasing the solenoid strength.

Case No.	Focusing Periodicity	B_s	Solenoid Length	Accel. Field	Output Emittance	Beam Rmax	Linac Length	No. Tanks
		T	cm	MV/m	cm·mrad	cm	cm	
1	TK-TK-SOL	7	25-35	2-4.8	1.2π	1.0	560	12
2	TK-TK-SOL	8	25	4.8	2.4π	1.0	380	8
3	TK-SOL-TK	7	25	4.8	$.91\pi$	.5	480	8
4	TK-TK-SOL	7	40,50,60	6.0	2.6π	1.0	400	6

Table 1. Summary of solenoid focusing cases studied for the 50 MHz linac section.

Starting with a beam from the RFQ, with an energy of 60 keV/u, an emittance of 4.2π cm-mrad, and q/A=1/20, the time dependent code PARMION was used to generate linac geometries for the 50 MHz section and trace particles through them for various solenoid focusing schemes. In all cases a tank is considered to be a four gap ANL type interdigital structure.[2] Drift space allowances between tanks, and between a tank and solenoid are 10 cm and 5 cm respectively.

Table 1 contains a summary of the solenoid focusing cases studied for the 50 MHz linac section. The first case in this list is the conceptual design described previously.[1] Cases 2 and 3 with relatively short solenoids similar to that used in the previous study, show that by either increasing the solenoid induction to 8 Tesla or by increasing the focusing periodicity to Tank - Solenoid - Tank with 7 Tesla solenoids, a constant accelerating gradient of 4.8 MV/m could be accommodated. For the last case listed the solenoid lengths were chosen to maximize their focusing strength. To determine the appropriate lengths, a simple analytical treatment to describe solenoid focusing in linacs was used.

If B_s is the solenoid magnetic induction, l is the length of the solenoid, and $B\rho$ is the magnetic rigidity of the ion, and we define $\theta = B_s l/(B\rho)$, $C = \cos(\theta/2)$, and $S = \sin(\theta/2)$, $\alpha = \theta/(2l)$, then, provided we rotate the exit coordinates by an an angle $\theta/2$, one finds that the the transfer matrix for a solenoid[3] is equivalent to a thin lens with focal strength $-\alpha S$ included between two drift spaces of length $(1-C)/(\alpha S)$. For a given ion energy and magnetic induction, the maximum equivalent thin lens focal strength is achieved when the solenoid length L_{max} is equal to $\pi/(2\alpha)$.

The defocusing action of an acceleration gap may be approximated by a thin lens of focal strength Δ, given by,

$$\Delta = \frac{-qET}{m_o c^2 \beta^2} \sin(\phi)(1-\beta^2) \qquad (1)$$

where, E is the peak accelerating field in the gap, T is the transit time factor(slightly less than 1 for our case), ϕ is the gap crossing phase measured relative to the peak of the r.f. voltage, and β is the usual relativistic factor.[4]

Assuming now that the defocusing effects of the N accelerating gaps preceding a solenoid lens can be approximated with the defocussing effect of a a single thin lens having a focal strength $G = N\Delta$, and using the standard solenoid transfer matrices, we derive an expression for the maximum value of the Twiss parameter β describing the transverse motion within a matched periodic (thin lens)-(drift space)-(solenoid)-(drift space) structure and obtain;

$$\beta_{max} = \frac{\left|\frac{S}{\alpha}(DG+1) + \frac{1-C}{2\alpha^2}G + \frac{C+1}{2}D(2+DG)\right|}{\sqrt{1-(\frac{SG}{2\alpha} + C[DG+1] - \frac{\alpha DS}{2}[2+DG])^2}} \qquad (2)$$

where D is the drift space between the solenoid and the defocusing thin lens, and C, S and α are the solenoid

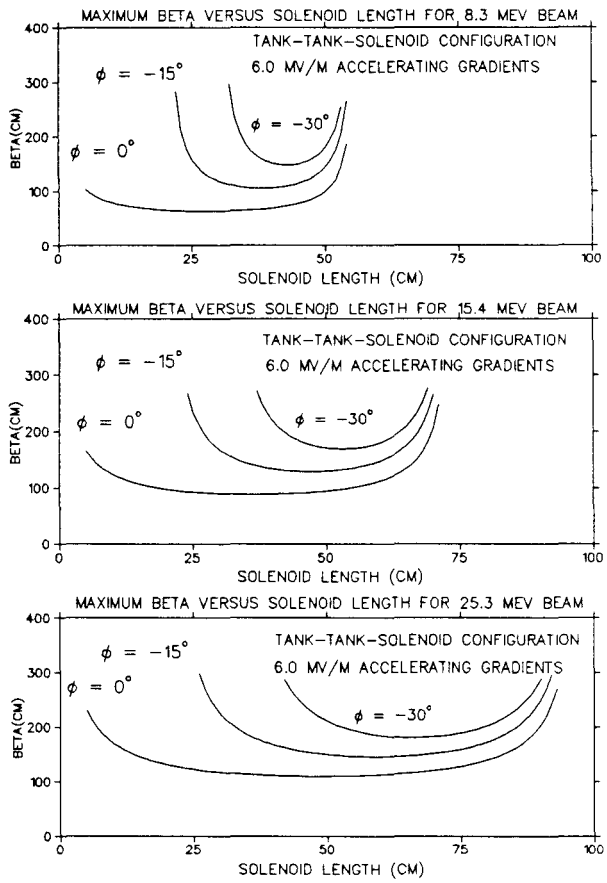


Fig. 2. Maximum values of β versus solenoid length for various beam energies.

transfer matrix parameters defined earlier*. In Fig. 2 β_{max} is plotted as a function of solenoid length for three beam energies that correspond roughly to the energies after 8, 16, and 24 accelerating gap crossings with $E_{acc} =$ 6 MV/m. From this we see a rather broad minimum for β_{max} over the range of gap crossing phases of -30° to 0° with optimum solenoid lengths of approximately 40, 50, and 60 cm for beam energies of 8.3, 15.4, and 25.4 MeV respectively. Using these values in the PARMION[1] calculations results in the linac that is summarized as case 4 in Table 1.

3. RFQ FOCUSING

Use of electric focusing is often advantageous in beam transport systems for low velocity ion beams such as those found in the first stage of the ISAC interdigital linac. Here we consider a special type of electric focusing element, namely an RFQ with no vane modulation and of length $\beta\lambda$ producing, in the quasi-static approximation, a time varying potential of the form

$$V(x, y, z, t) = K(x^2 - y^2)\sin(\omega t + \psi) \qquad (3)$$

where x and y are the transverse coordinates, $K = V_p/a^2$ is the RFQ strength constant evaluated in terms of the peak voltage V_p on one of the electrodes and the electrode aperture a, ω is the r.f. frequency, and ψ is an r.f. phase angle. Such a device will only have transverse electric fields(provided we ignore fringe field effects near the entrance and exit), and will act as an electric quadrupole doublet. The rf fields with higher sparking limits than in the electrostatic case can provide relatively strong focusing in the two orthogonal transverse phase space planes.

To investigate the application of this type of focusing to the ISAC linac, the PARMION[1] code was modified to include an RFQ element for which the particle equations of motion are solved using the fourth order Runge-Kutta method. With the modified PARMION, the phase dependent focal properties of RFQ lenses could be calculated. Fig. 3 shows the focusing strength versus the angle $\omega t + \psi$ of the RF voltage when the ion enters the RFQ. The focussing is strongest for the 0° phase ions and decreases as the phase is increased or decreased. It is anticipated that the phase acceptance of the first interdigital stage of ISAC will be approximately 30°, and we see from the figure that the phase dependence of the focusing will be small over such an interval provided the interval is centered near 0°.

In order to do a preliminary assessment of the feasibility of using RFQs as focusing elements in the 50 MHz section of ISAC, a series of analytic calculations similar to those described in the previous section were carried out. The acceleration tank configuration was assumed

*Since the beam envelope is equal to $\sqrt{\beta\epsilon}$ where ϵ is the beam's emittance, for a fixed emittance, minimizing β will minimize the beam envelope.

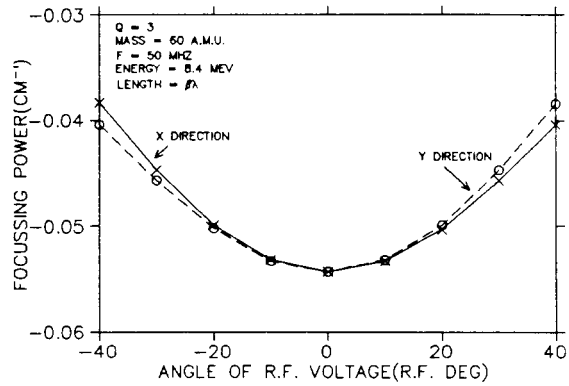


Fig. 3. RFQ focussing power versus angle of r.f. voltage

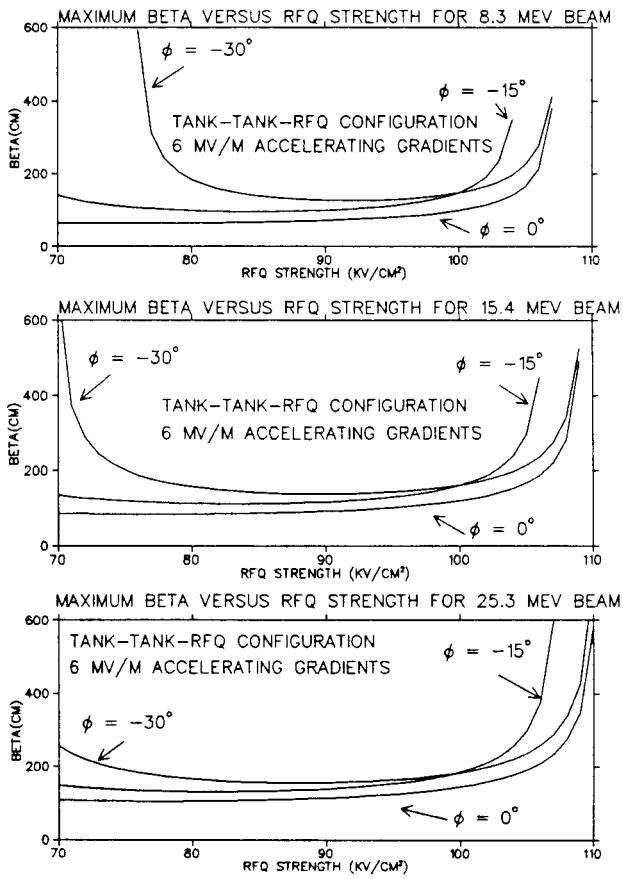


Fig. 4. Maximum values of β versus RFQ strength for various beam energies.

Focussing Periodicity	RFQ Strength Const. kV/cm^2	Accelerating Field MV/m	Output Emittance cm·mrad	Beam Rmax cm	Linac Length cm	No. Tanks
TK-TK-RFQ	93.8	6.0	2.4π	1	310	6

Table 2 Summary of RFQ focussing case studied for the 50 MHZ linac section

to be the same as in case 4 of the solenoid focusing study described earlier. Using the same thin lens approximations for the defocusing at the acceleration gaps and the same periodic transport system assumptions but with an RFQ replacing the solenoid, β_{max} was calculated and is shown in Fig. 4 as a function of the RFQ strength constant K. Plots in Fig. 4 for particle phases of $-30°$, $-15°$, and $0°$ relative to the rf in the accelerating structure show that within this phase band β_{max} has a very broad minimum centered approximately about $K = 90$ kV/cm^2.

Calculations with the RFQ modified version of PARMION were carried out to verify that it would be possible to build a 50 MHz linac section using RFQ focusing elements with $K \approx 90$ kV/cm^2 as predicted above. Table 2 summarizes the results of these computations. The beam envelopes and the emittances obtained are similar to those obtained with the optimized solenoid example shown as case 4 in Table 1.

In order to determine the feasibility of constructing an RFQ lens with $K \approx 90$ kV/cm^2 and $a \approx 1$cm, we must estimate the surface electric fields on the electrodes. Assuming hyperbolic electrodes, the profiles of the cross-sections will satisfy equations of the form $a^2 = x^2 - y^2$. Using this result along with the electric field intensity derived from equation 2, we find that the peak surface field E_s is given by

$$E_s = 2K\sqrt{2x_{max}^2 - a^2} \qquad (4)$$

where x_{max} is the maximum extent of the electrodes in the x direction. Assuming $x_{max} \approx 2a$ gives $E_s \approx 480$ kV/cm for the case under consideration †. This is well below the peak fields of over 1000 kV/cm achieved at ANL in a 64 MHz test RFQ structure.[5]

4. DISCUSSION

Taking focusing power per unit length as a figure of merit, a plot of this against energy, in the energy range covered by 50 MHz linac section, is shown in Fig. 5. This illustrates the potential advantage of RFQ focusing over solenoid focusing at the lower energies. At higher energies the two focusing approaches are roughly equivalent.

†A second estimate of the surface fields may be obtained by considering the peak surface electric field on the surface of two circular cylinders of radius a with sufficient spacing to approximate the geometry of the RFQ vanes. Using this approximation, a calculation by one of the authors indicates that $E_s \approx 2.7V_p/a$ which is about 240 kV/cm in our case.

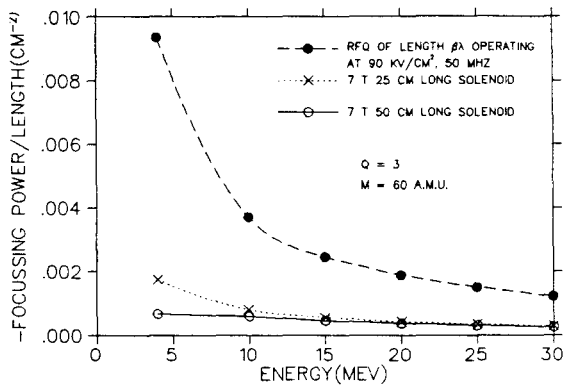


Fig. 5. Comparison of figures of merit for RFQ and solenoid

Using either solenoids with optimized lengths, or RFQ elements for focusing, would permit accelerating gradients of up to 6 MV/m in the 50 MHz section of the present conceptual design for ISAC. This reduces the number of tanks in this section to 6 from 12 in the previous design, and reduces the overall length of the section by up to 2.5 m. The penalty paid for this improvement is an approximate doubling of the output beam emittance.

5. REFERENCES

1) J. S. Fraser, and H. R. Schneider, "Design of A Superconducting Interdigital Accelerator Structure For Radiosactive Ions", in **Proc. 1990 Linear Accel. Conf.**(Los Alamos, Albuquerque, 1990)pp. 88-90
2) K. W. Shepard, "Development of a very low velocity superconducting linac", in **Proc. 1987 Part. Accel. Conf.** (I.E.E.E., Washington, D.C., 1987)p. 1812
3) A. P. Banford, **The Transport of Charged Particle Beams**(E. & F. N. Spon Limited, London, 1966) Ch. 7, p. 133
4) J. J. Livingood, **Principles of Cyclic Particle Accelerators**(D. Van Nostrand Co., Princeton, N.J., 1961) Ch. 14, p. 283
5) J. R. Delayen, and K. W. Shepard, "First Tests of a Superconducting RFQ Structure", in **Proc. 1990 Linear Accel. Conf.**(Los Alamos, Albuquerque, 1990) pp. 76-78

FUTURE CYCLOTRONS

H.G. Blosser, NSCL, East Lansing, Michigan, USA

CONTRIBUTION NOT RECEIVED

THE USE OF CYCLOTRONS FOR PHYSICS EXPERIMENTS, PAST, PRESENT AND FUTURE

J.C. Hardy, Atomic Energy of Canada, Chalk River, Ontario, Canada

CONTRIBUTION NOT RECEIVED

PHYSICS WITH STORAGE RINGS

R. E. Pollock
Physics Department and IUCF, Indiana University
Swain Hall West, Bloomington, IN, USA 47405

ABSTRACT

In the past few years, new storage rings with cooled beams have appeared in several cyclotron laboratories and also in other locations. A few examples of the physics emerging from such storage rings are presented, in the context of future prospects for this technology.

1. INTRODUCTION

Beam storage was first a technology for attaining a maximum collision energy. Now storage rings are being constructed for a wider variety of purposes. The ring may be thought of as a processing device interposed between the traditional accelerator and the beam user. With the ring, beam properties can be altered to increase their usefulness.

Several of the new rings which have begun operation within the past four years incorporate beam cooling systems. Cooling was originally developed to improve beam accumulation to obtain stored beams of higher intensity. Beam cooling however endows the beam stored in a ring with a number of attractive properties. As the cooled metastable equilibrium state of the beam evolves, memory of initial conditions is lost. The beam user is thus isolated from fluctuations in the beam properties of the injecting accelerator. The phase space volume of the equilibrium state may be reduced by several orders of magnitude from conditions on injection. This bright intense beam with its reduced energy spread and emittance can make possible more precise experiments.

A particle beam is one of the ubiquitous tools of twentieth-century physics. The composition of atoms, nuclei and "elementary" particles has been probed through the interaction of particle beams with an appropriate target. A stored cooled beam may be used in this manner, but the nature both of the cooling process and of the beam-target interaction processes places constraints on the amount of target material which can be tolerated. Thus the event rate in an experiment is not as high as expected from the high stored current.

The event rate in a typical fixed-target experiment is the dimensionless product of four factors:

beam intensity - beam particles/second;

target thickness - target particles (eg. atoms)/unit area;

detector coverage - solid angle & efficiency;

interaction probability - cross sectional area/unit solid angle.

The product of the first two factors is commonly referred to as the luminosity L. The goals of the experiment determine an acceptable range for the magnitude of L. For an experiment in atomic physics, for example, where the cross section might be on the order of a megabarn, an L of 10^{24} cm^{-2} s^{-1} might be ample. For nuclear physics with a strongly-interacting primary beam and total cross sections of order of a barn, L = 10^{30} cm^{-2} s^{-1} might suffice. For an electromagnetic probe, add about two orders of magnitude for the fine structure constant. To create a secondary beam of useful intensity, the primary luminosity would have to be much higher. Factories may be designed for L = 10^{36} cm^{-2} s^{-1} or more.

The luminosity attainable with an internal target in a cooled storage ring depends on beam and target species, on beam energy, and to some extent on the ring design. For light targets and light beams of intermediate energy, L = 10^{31} cm^{-2} s^{-1} has been demonstrated, and the ultimate limit is probably at least an order of magnitude higher. In broad terms, the luminosity attainable in rings is ample for atomic physics, acceptable for many strong interaction studies, but too low to consider their use in secondary beam production.

If beam is extracted after processing, a much thicker target may be used, but the average beam current is limited to the number of particles stored divided by the beam processing time. In general this will lead to a lower luminosity than for the direct beam from the injector, although the external target

mode can still be useful as the processing may include acceleration to a much higher energy.

A more detailed discussion of the processes limiting performance of cooling rings is outside the scope of this paper. Further information on these facilities and their properties may be obtained from a recent review 1).

Abbreviated names, institutes and locations of cooling rings which are referred to in the following sections:

LEAR - CERN Geneva
Cooler - IUCF Bloomington
TSR - MPI für Kernphysik, Heidelberg
TARN II - INS Tokyo
CELSIUS - TSL, Uppsala
ASTRID - Århus University
ESR - GSI Darmstadt
CRYRING - MSI Stockholm
CoSy - FZ(KFA) Jülich

2. STRONG INTERACTION PHYSICS

2.1 Thresholds and Resonances

The creation of a meson in a nucleon-nucleon collision is a fundamental inelastic process. Studies of this process with accelerator beams began about forty years ago, and a considerable body of data has resulted. Near the threshold, the restricted phase space makes the cross section small and strongly energy-dependent. Target impurities can give a large background. For these reasons measurements near threshold have been more difficult and the information obtained has been of poorer quality.

A storage ring with cooling offers almost the ideal environment for threshold studies. The windowless internal targets are free of impurities, the cooled beam is nearly monoenergetic and the energy is readily varied in small or large steps. The luminosity attainable is sufficient for detailed measurements of sub-microbarn cross sections with detector arrays of good angular coverage. It is therefore not surprising that several of the new cooling rings have meson threshold measurements as a part of their planned research programs.

Experiments in the first years of operation of the IUCF Cooler have verified that the combination of cooled beam with a pure thin target can result in vastly improved measurements of pion threshold channels. The $pp \rightarrow pp\pi^0$ channel was observed by reconstruction of the event from the four-momenta of the two outgoing protons. The missing mass spectrum contained a useful sample of pp bremsstrahlung events as well. The results have been published 2). Data of comparable quality which has been obtained in the past year for the $pp \rightarrow pn\pi^+$ and $pd \rightarrow pd\pi^0$ processes will appear shortly.

An experiment of comparable luminosity has been carried out with antiprotons near the charm threshold with an internal target in the Fermilab stochasticly-cooled accumulator ring. An experimental resolution of 0.5 MeV is obtained for the narrow peak at the 3 GeV J/ψ resonance, and widths of other peaks with cross section as small as 1 nb have been measured 3). Internal target experiments with the JETSET detector in LEAR are in progress. Internal and external target experiments at the Λ-$\bar{\Lambda}$ threshold at that facility exploit the good beam quality of the variable beam energy antiproton beam.

A comparably elaborate detector at the CELSIUS ring is being readied for studies of decay modes of the η^0 and π^0 mesons 4). The CoSy ring now under construction has measurements planned in the energy region of strange particle thresholds and nucleon resonances. Electron cooling technology does not at present extend to the energy range above 0.6 GeV, so the beam for these measurements will be precooled prior to acceleration.

2.2 Polarized Beams and Targets

Experiments can be performed in storage rings with polarized beam or polarized targets or both. A scattering experiment on scattering asymmetry in the Coulomb-nuclear interference region, performed with 185 MeV polarized protons and an unpolarized proton target in the IUCF Cooler has been reported 5, 6). A byproduct of this measurement was the observation that cooling does not reduce the polarization of the stored beam (a lower bound of polarization lifetime of several hours).

A new ^{3}He polarized target is operational at IUCF and has been used within the past month for the first "triple-scattering" measurements with an accelerated and cooled polarized proton beam. Within the ^{3}He nucleus, proton spins are antiparallel so polarization effects at some level of approximation reflect largely the spin of the unpaired neutron.

A polarized hydrogen target has been installed this past spring in the TSR where it will be used to demonstrate that an initially unpolarized beam may acquire a polarization by selective depopulation in

interaction with a polarized target. A polarized hydrogen target is also in preparation for scattering and reaction measurements in the IUCF Cooler.

2.3 Heavy Ion Nuclear Reactions

At GSI, a measurement of half-life and mass of an unstable beam has been reported [7]. In this measurement, an external target bombarded by the SIS synchrotron beam created the radioactive isotope. After filtering by a fragment separator, the particles of interest were injected into ESR for storage and cooling. In this mode the ring functions as a precise measuring instrument following the production process. All stored species are cooled to the same velocity by electron cooling, but exhibit slightly different orbit frequencies even at the same nominal charge/mass ratio because of small differences in nuclear binding energies. The mass of the unstable species can then be directly compared to that of nearby reference ion peaks. A mass determination accuracy of 80 keV was reported.

Stored and cooled heavy ions can also be used in a mode with internal target interactions. At low beam energies, charge-changing processes have such large cross sections that nuclear reactions are difficult to observe. Experiments with internal targets are practical however at intermediate energies with fully-stripped beams. In this regime the cross section for a charge-changing event in the target is not too large.

The ESR at Darmstadt has demonstrated that the spallation products from the interaction of a stored beam with an Argon cluster jet target can be observed as accumulated and cooled secondary beams [8]. Satellite peaks are observed in the Schottky frequency spectrum.

Reactions of stored radioactive beams with light targets are planned, offering the study of conventional reactions with inverse kinematics.

The CELSIUS ring has recently stored a beam of ^{16}O at 100/Mev/amu. Heavy ion reaction studies are planned both there and at CoSy.

3. ATOMIC PHYSICS

The cooling electron beam may be employed as a target. Observations of radiative dissociation of H_2^+ at TARN II [9] and D_2^+ at CELSIUS[10] have been reported.

Radiative electron capture (REC) in the cooling region has been used as a monitor of the cooling process for light ions. The loss of beam through this process is normally less important than through interactions with residual gas in the ring. The cross section for REC increases with beam atomic number Z approximately as Z^2, so the electron density must be reduced for heavy ion beams to maintain a long beam lifetime. The capture may be stimulated by a pulsed laser [11] Rate enhancement factors of about 60 have been reached [12].

If the ring design accepts a substantial enough band of magnetic rigidities, charge-changing processes may not lead to beam loss. The preparation of a Bi^{80+} beam for dielectronic recombination (DR) studies by injecting Bi^{82+} into the ESR ring and then collecting the products of one and two electron pickup have been reported [7]. The injected beam serves as a reservoir, feeding the charge state of interest to maintain its population during the measurement. DR observations with a cooled ^{12}C beam at TSR [13] and with an uncooled ^4He beam at IUCF have been made.

TSR, ASTRID and the newly-completed CRYRING (which has accelerated and electron-cooled beams in recent months [14]) are examples of smaller storage rings with significant programs of atomic physics research.

4. ACCELERATOR PHYSICS

4.1 Spin Manipulation Studies

While polarized beams have been accelerated in strong-focussing synchrotrons for some time, there are problems with depolarizing resonances that can become severe at high energies or slow ramp rates. The use of spin rotators to ease the passage through resonances was proposed in 1977 but few rings have been constructed with the long open space required for a spin inverter. The rings designed for internal target experiments tend to have long straight sections to house targets and detectors. This fact has led to a sequence of measurements on spin rotators mounted in the IUCF Cooler [15] which establish the usefulness of such "Siberian Snakes", especially for the passage through imperfection resonances. In the course of these studies it has also been established that a partial snake may be employed to produce a stable in-plane polarization component at an internal target, and that the solenoids, toroids and correcting dipoles in the cooling section may conspire to produce a significant shift in the energy of depolarizing resonances[16, 17]. More recently an rf solenoid has

been used to demonstrate that the spin direction of a stored beam can be reversed in an "nmr" process. Reversals during a measurement are important for control of systematic errors.

4.2 Laser Cooling

Fast cooling of selected stored ion species has been obtained with lasers. Experiments at TSR with Be^+ and with metastable Li^+ ions have demonstrated very low longitudinal temperatures of below 0.02 Kelvin [12]. Electron precooling to reduce the transverse emittance, and careful mechanical stabilization of photon transport structures to reduce vibration were needed to reach this temperature.

4.3 Collective Phenomena

At ASTRID a very cold Li^+ beam injected for laser cooling studies was observed to heat itself up rapidly through intrabeam scattering. Short length beam pulses showed an additional growth of kinetic energy through a Coulomb explosion. As the pulses lengthened, the stored potential energy was converted to kinetic form. The same system showed a curious implosion phenomenon for long pulses. The inflector could be used to fill most of the ring circumference, leaving a short gap in the beam azimuthal density distribution. Instead of the gap simply closing, it was found to split into two short gaps which maintained a constant width while moving away from each other [19].

The electron-cooled beam at LEAR shows collective instabilities for stored particle number N above about $N = 5\ 10^9$. Application of fast feedback damping circuits for coherent betatron motion in both transverse planes has raised this limit about one order of magnitude [20]. The control system of LEAR allows the dampers to distinguish between incipient unstable betatron motion and the closed orbit changes encountered during energy changes so the dampers can be employed in antiproton deceleration. Other cooling rings show similar thresholds for coherent instabilities.

4.4 Orbit Dynamics Studies

A cooled beam has suppressed Landau damping, which means that coherent motion persists for a rather long time before smearing into emittance growth. Beam phase space phenomena may be explored by kicking the cooled beam and tracking the coherent motion with position detectors. The technique generates, for example, almost textbook examples of phase space motion around islands of stability near non-linear resonances [21].

4.5 Injection Studies

It is clear that almost any kind of accelerator can serve as a cooling ring injector. Cyclotrons are used as injectors at several laboratories, although the continuous output of such machines is not an ideal match to the intermittent filling requirements of a storage ring. Other facilities employ synchrotrons, linacs, or electrostatic injectors.

Each of the cooling rings seems to contribute one or two new methods of cooled injection to a growing inventory of such techniques. Cooling eliminates phase space volume constraints on the filling process, replacing these by a rate limit set by the strength of the cooling force. If enough time is available, the ring can be filled to the limit of cooled beam stability.

When filling is rate-limited, the optimum luminosity is in general not obtained with the thickest target. If small angle scattering causes beam loss, choose a target thin enough that the emittance remains small compared to the ring acceptance.

5. PROSPECTS FOR FUTURE FACILITIES

The glimpses of very useful output which have emerged from the early years of operation of cooled beam storage rings indicate that an interesting decade or more of their exploitation lies ahead. It is perhaps no longer premature to ask whether the concept might be extended in other new directions.

One field of significant current interest is the use of radioactive beams. The ESR is in a unique position to process beams of all masses up to some hundreds of MeV per nucleon. A proposal for a new two-ring facility at JINR Dubna is under review. This facility has a goal of collecting products of reactions between a cooled beam of about 150 MeV/amu and a rare isotope target.

The extension of the cold storage concept to lighter beams and lower energies eventually runs into the charge-changing problem. An electron pickup in an internal target leads to a lost beam particle if the changed magnetic rigidity lies outside the ring acceptance. Possibly a ring of greater topological complexity should be designed, one in which discrete paths are provided for distinctly different rigidities. This concept has been advanced as a method for

improving the efficiency of strippers [22], but also may be used to increase the efficiency of beam use with internal targets and heavy ion beams, lowering the threshold energy for which this mode is useful.

A natural limit to cooling of radioactive species is set by the relation between decay lifetime and cooling time. Very short-lived species are not amenable to cooled beam storage. However when the production rate is very low, it is conceivable to apply particle-by-particle feedforward methods to reduce the phase space density in flight. The idea has been advanced for slow muons [23] but may have applicability also to more exotic species.

A second direction for possible future extension is toward higher beam energies. Electron cooling in the present machine generation is limited to about 0.3 MeV, which can cool beams to about 0.6 GeV/amu. Pressurized electrostatic terminals may extend this limit in future by about one order of magnitude, provided that non-trivial problems of efficient electron collection and beam confinement can be solved for this energy range. Stochastic cooling has no such energy bounds. The internal target experiments near the charm threshold [3] show the promise of this physics. A proposal for a "superLEAR" facility has been under discussion [24].

The possibility of a cooled light facility for higher energy cooled polarized beams has been suggested at IUCF. This would be a slow-cycling device, filled from the present Cooler, with ample space for internal targets, spin manipulation elements, and cooling systems. Injection at about 400 MeV after acceleration in the IUCF Cooler should raise the beam current limit by an order of magnitude.

The target heating-beam cooling equilibrium which determines the thickest useful target requires further careful study before a luminosity limit for this unexplored energy region with cooled beams can be predicted with confidence. One thing that is clear is that the small angle Rutherford scattering that provides the dominant loss process for light ion beams of lower energy is negligible above a few GeV. The stored beam may therefore be used to create nuclear reactions with great efficiency.

6. ACKNOWLEDGMENTS

This work was supported in part by the U. S. National Science Foundation under grant NSF PHY 90-15957 and by Indiana University.

7. REFERENCES

1) Pollock, R. E., An. Rev. Nucl. Part. Sci. **41** 357 (1991).
2) Meyer, H.-O. et al, Nucl. Phys. **A539** 633 (1992); v. Przewoski, B. et al, Phys Rev. **C45** 2001 (1992).
3) Armstrong, T. A. et al, Intersections between Nuclear and Particle Physics, Tucson 1991, A. I. P. Conf. Proc. **243** (1992), p. 79.
4) The Svedberg Lab Progress Report 1987/91, p 84.
5) Pitts, W. K. et al, Phys. Rev. **C45** R1 (1992).
6) Pitts, W. K. , Phys. Rev. **C45** 455 (1992).
7) Geissel, H. et al, Phys. Rev. Lett **68** 3412 (1992).
8) Franzke, B., International Workshop on Physical Experiments and First Results on the Heavy Ion Storage and Cooler Rings, Smolenice CSR, June 1/5, 1992.
9) Tanabe, T. et al, Proc. 19th INS Symposium on Cooler Rings and Their Applications, T. Katayama, A. Noda, ed., World Scientific (1991), p 69.
10) see ref. 4, p 95.
11) Schramm, U. et al, Phys. Rev. Lett. **67** 22 (1991).
12) Grimm, R. , see ref. 7.
13) Kilgus, G. et al, Phys. Rev. Lett. **64** 737 (1990).
14) Herrlander, C. J., see ref. 7.
15) Goodwin, J. E. et al, Phys. Rev. Lett. **64** 2779 (1990).
16) Pollock, R. E., Nucl. Instrum. Methods **A300** 210 (1991).
17) Minty, M. et al, Phys. Rev. **D44** R1361 (1991).
18 Schröder, S. et al, Phys. Rev. Lett. **64** 2901 (1990).
19) Berg-Sørensen, K. et al, see ref. 10, p 80.
20) Bosser, J., see ref. 7.
21) Lee, S. Y. et al, Phys. Rev. Lett **67** 3768 (1991).
22) Cramer, J. G., Nucl. Instrum. Methods **130** 121 (1975).
23) Taqqu, D., Nucl. Instrum. Methods **A247** 288 (1986).
24) LeFevre, P., Proc. Sixième Journées d'Études Saturne, Le Mont Sainte-Odile, May 18/22, 1992.

CONFERENCE SUMMARY*

D. J. Clark
Nuclear Science Division, Lawrence Berkeley Laboratory, Berkeley
CA, 94720, USA

1. CONFERENCE ORGANIZATION AND SETTING

The TRIUMF group put together an interesting and smooth-running conference. Mike Craddock served as Chairman of the Conference and of the International Organizing Committee. He was also chairman of the Local Committee, which coordinated the secretariat, exhibits, budget, proceedings and social events. Gerardo Dutto was Chairman of the Program Committee, which held a number of meetings to select the invited and other oral papers. This committee even had a newsletter to keep members up to date.

The setting was the beautiful city of Vancouver, surrounded by mountains, rivers, inlets and the sea. The Hotel Vancouver had good conference and poster rooms on the same floor. It had comfortable rooms, fast elevators and a health club and pool. Its breakfast buffet served an international fare of exotic delicacies such as pickled prawns and Pepsi-Cola glazed ham. The opening welcome address by Erich Vogt (Dr. KAON), invited the audience to tear up their return tickets and stay in this magical area of Vancouver, which was Indian territory not so long ago.

The TRIUMF tour on Monday afternoon was preceded by talks by Dutto on developments at TRIUMF, and by Craddock on the proposed KAON Factory. The cyclotron has been improved by the addition of a cavity at large radius, which has been shown to increase the energy gain per turn and thus reduce the electromagnetic stripping. It can also be used in the flat top mode to improve beam quality and H^- extraction. The support for KAON has been growing, with the assistance of Dr. KAON, Mr. KAON and KAON Kim. The tour was organized in a flexible way to allow people to either follow a guide to all the stations or take a self guided tour, spending more time at points of individual interest by following the map provided. The magnetic field strength of the TRIUMF magnet was demonstrated by a guide on top of the cyclotron shielding, who suspended a quarter and a dime from another quarter. (This doesn't work with U.S. money).

2. TECHNICAL PROGRAM

The following summary of the Conference covers the larger projects or those having some new design feature. It thus omits discussion of many interesting results and important contributions of the more than 190 papers, which can be found in these Proceedings.

The early sessions were devoted to papers describing the initial operation of new or upgraded cyclotron facilities. The facilities which were completed since the last International Conference in Berlin in May 1989, are listed Table 2. A superconducting isotope production cyclotron without a return yoke, similar to that of the Oxford Instruments design, was proposed in an abstract by the Belgrade group, but the paper was not submitted to the Conference. In Table 3 are found projects which were completed before the Berlin Conference but have undergone important commissioning work since that time. Table 4 shows projects which are under construction and Table 5 shows new projects which are proposed or under study. Table 6 lists the storage rings and synchrotrons injected with cyclotrons. There are of course many other rings with other types of injectors. In Table 7 are listed radioactive beam projects associated with cyclotrons. Finally a list of cyclotrons shut down since the Berlin Conference is given in Table 8. They have lived productive careers.

2.1. Invited Review Papers

There were a number of invited review talks on topics of interest to the cyclotron community. The speakers were selected for their experience in their areas and their ability to present the topic to the audience. They are listed in Table 1.

The reviews of non-medical and medical applications gave cyclotron designers an insight into the beam requirements in these fields. The review of compact cyclotrons showed the important application of cyclotron principles to compact commercial machines, where negative ion acceleration is becoming more important because of its easy extraction of high beam currents. New designs or operation of compact cyclotrons for isotope production, some with both proton and deuteron beams, are reported at this Conference. They include the Kurchatov MPC-10 for 10 MeV p using H^-, the EBCO TR-30 and TR-13 for 30 and 13 MeV p using H^-, the 16 MeV proton Scanditronix PETtrace 2000 using H^-, the Nagoya/Japan Steel 22 MeV proton machine, the Dubna/Tashkent 20 MeV proton design with internal target, and the IBA Cyclone-3 with 3.6 MeV deuterons. The review of beam instrumentation for cooler facilities described the feedback

Table 1. Invited Review Papers

BECHTOLD	Commercially Available Compact Cyclotrons for Isotope Production
ZIEGLER	Material Research with Beams at Cyclotron Energies
WAGNER	The Clinical use of Radioisotopes
RUTH	The Production of Radionuclides for the Biosciences
PEDRONI	Accelerators for Charged Particle Therapy: Performance Criteria from the User Point of View
THORNTON	Current and Potential Clinical Indications of Proton Irradiation
ELLISON	Beam Instrumentation for Cyclotron-Based Cooler Synchrotron Facilities
LYNEIS	ECR Ion Sources for Accelerators
SCHMOR	A Review of Polarized Ion Sources for Cyclotrons
DAVIES	Advantages of Differential-Algebra and Lie-Algebra in the Orbit Dynamics of Cyclotrons
PAGANI	Advances in Rf Technology for Cyclotrons
BUSSE	Integrated Tools for Cyclotron Operation
NITSCHKE	Accelerated Radioactive Nuclear Beams: Existing and Planned Facilities
BLOSSER	Future Cyclotrons
HARDY	The Use of Cyclotrons for Physics Experiments, Past, Present and Future
POLLOCK	Physics with Storage Rings

Table 2. Projects with First Operation since Berlin Conference.

Laboratory	Facility	Description
RCNP, Osaka	K400 6-sector ring cyclotron	First beam 12/91. Protons accelerated to 300 MeV. Designed for 400 MeV protons and He^{2+}. Injected by older K140 cyclotron.
Dubna, Russia	U400M cyclotron	First beam 5/91 with a He^{1+} beam accelerated to 30 MeV/u. Coupled to U400 it will accelerate all ions, with uranium going to 20 MeV/u.
Jyvaskyla, Finland	K130 cyclotron	First beam 1/92. Design is for heavy ions and 85 MeV protons. Furthest north cyclotron.
JAERI, Japan	K110 cyclotron	First beam 3/91. Designed for heavy ions and 90 MeV protons.
MEDICYC, Nice, France	K65 cyclotron	First beam 12/90. Using 65 MeV protons for proton therapy and will also do neutron therapy.
KFA, Julich	K180 cyclotron	Upgrade, including RF and trim coils, as injector for storage ring COSY.
Uppsala, Sweden	K200 cyclotron	FM mode now in operation in addition to CW mode, giving 180 MeV protons at up to 60% duty factor. Only FM/CW cyclotron.
PSI, Switzerland	Injector II cyclotron for ring.	Increased average beam current to 1.5 mA at 72 MeV, with special attention to defining slits, bunching and space charge.
Oxford Instruments	K12,17 cyclotrons	Superconducting without return yoke. NMR magnet technology. For isotope production and neutron radiography. Not reported at Conference.

and operator assistance systems needed for these machines. The ion source reviews gave surveys of this important area. The addition of an ECR source can increase the heavy ion performance by an amount approaching that of another acceleration stage. ECR developments include the unique high field 10 GHz source CAPRICE at Grenoble, the superconducting source at MSU, and electron injection with either a biased disk as at Grenoble or with an electron gun as at LBL. With the electron gun the LBL AECR source has produced 1 eμA CW beam for each of Ar^{16+}, Kr^{26+}, Xe^{31+} and Bi^{35+}. Polarized source developments include ECR ionizers for atomic beam sources. Differential and Lie Algebras are an alternative formalism to the conventional orbit analysis, and a lively discussion was held after this talk. The reviews of rf and control

Table 3. Projects with Major Commissioning since Berlin Conference.

Laboratory	Facility	Description
HIRFL, Lanzhou	K450 ring	Commissioning of ring and K69 injector cyclotron. Carbon beam at 75 MeV/u.
MSU/Harper Hospital	K96 cyclotron	Superconducting "flying cyclotron" in full operation for neutron therapy in a hospital on a rotating gantry. Uses pulsed rf.
RIKEN, Japan	K70 cyclotron	Developed as 2nd injector for K540 ring cyclotron. Light ion energies increased, with protons at 210 MeV.
GANIL	C02 injecting SSC1, SSC2 ring cyclotrons	Higher energies available from OAE and new metallic ions from ECR.
MSU, NSCL	K1200 cyclotron	Superconducting. New tuning methods and diagnostics, including TV probe. ECR source development includes super gas mixing and space charge studies. U^{39+} accelerated to 25 MeV/u.
Texas A&M	K500 cyclotron	Superconducting. Deflector development, main coil positioning, ECR first operation. Many new beams.
Chalk River	K520 cyclotron	Superconducting. Deflector development to study effect of insulators, materials and surface treatment. Many new beams.

Table 4. Projects under Construction

Laboratory	Facility	Description
Tech. Univ., Munich	TRITRON	Separated Orbit Cyclotron, x5 energy gain as post-accel. for tandem, superconducting magnet and rf.
Groningen and Orsay	AGOR	K600 superconducting cyclotron, reached 4 T in magnet.
Catania/Milan	K800 cyclotron	Superconducting cyclotron. Magnet cool-down measurements and tandem tests.
St. Petersburg and Tashkent	U250 cyclotron	K200 cyclotron. A/Q = 2-10. Heavy ion cyclotron.
Gatchina, Russia	2 m cyclotron	Heavy ions and 75 MeV H^-. Nuclear physics and isotope production.
NAC, Faure, South Africa	K11 injector	Injector cyclotron will use ECR and polarized sources.
Dubna, Russia	U400 plus U400M	Connection of cyclotrons will give ions H to U at 100-20 MeV/u.
PSI, Switzerland	Ring beam increase	Intensity will go from .5 mA to 1.5 mA for 590 MeV protons with upgrade of rf power.
LBL, Berkeley	K=0.05 cyclotron	First permanent magnet cyclotron. For cyclotron mass spectroscopy: ^{14}C, etc.

systems gave up to date information in this area. The review of radioactive nuclear beams described production methods and facilities planned and operating throughout the world. The talk on future cyclotrons described the challenges of new designs and showed a simple spread sheet program on a personal computer to do conceptual designs, parameter studies and preliminary cost estimates on proposed cyclotrons. The nuclear physics applications of cyclotrons and storage rings were described in the last 2 talks.

2.2. Challenges for the Future

The challenges for the future lie in the extension of the technology and of the limits of performance of present cyclotrons. These can be seen in the projects under construction and those in the proposal/study stages, Tables 4,5,6,7 and in some of the review papers, Sec. 2.1.

Table 5. Projects Proposed or under Study

Laboratory	Facility	Description
HMI, Berlin KFA, Julich Bessy,Berlin	FFAG ring	Accel. from 500 MeV to 3 GeV, 1 mA, 50 Hz, for neutron spallation source. This is a type of synchro-cyclotron.
IBA - Sumitomo	K230 cyclotron	230 MeV protons for therapy. Energy variation by degrading to as low as 70 MeV. Zero hill gap at edge.
Alma Ata	K600 ring	Heavy ion cyclotron.
NAC, Faure South Africa	K200 cyclotron	Superconducting cyclotron with "S-Coils" in return yoke area, for proton therapy.

Table 6. Storage Rings and Synchrotrons Injected by Cyclotrons

Laboratory	Facility	Description
Operating		
Indiana	Cooler Ring	Electron cooling. Polarized protons. Injected by K215 ring cyclotron.
INS, Tokyo	Tarn II	Accel. to 220 MeV/u, electron cooling. Injected by K68 cyclotron
Uppsala	CELSIUS	Electron cooling. Injection by stripping and multi-turn. Can accel. protons to 1.3 GeV. Injected by K200 cyclotron.
Under Construction		
KFA, Julich	COSY	Electron and stochastic cooling, slow extraction, K2500. Injected by K180 cyclotron.
Proposed or under Study		
TRIUMF	KAON	Accel. 100 μA to 30 GeV with 2 synchrotrons and 3 storage rings. H^- extraction from TRIUMF cyclotron using auxiliary cavity.
RCNP, Osaka	K1800 ring	Ring injected by K400 ring cyclotron.
Kiev	2 rings	Booster synchrotron plus storage ring, with accel. up to 300 MeV/u, electron cooling, protons-xenon. Injected by U240 cyclotron. Radioactive beams.
Dubna	2 rings	"K4" storage ring and "K10" ring with electron cooling. Ring rigidities are 4 and 10 Tm. Injected by U400 plus U400 M complex.

We can look at projects under construction, Table 4. The TRITRON will be the first Separated Orbit Cyclotron (SOC), an idea that started in the 1960's with the "Beehive" three dimensional design of F. M. Russell of the U.K. TRITRON will also be the first cyclotron with superconducting rf. Like some other designs it has a superconducting magnet, but with the unusual feature of the return flux flowing between particle turns. Examples were given of designs up to 1000 MeV. Cyclotron intensity limits are being extended by the PSI cyclotrons, with the next challenge being the injection of the 1.5 mA available from Injector II into the Ring, and its acceleration from 72 to 590 MeV. A new technology for very small cyclotrons is being developed at Berkeley with a permanent magnet cyclotron.

We then have projects in the proposed/study status, Table 5. The FFAG ring proposed in Germany to accelerate protons from 500 MeV to 3 GeV would be the highest energy cyclotron, actually a synchro-cyclotron. This technology comes from the MURA studies in the U.S.A. The IBA/Sumitomo 230 MeV proton therapy design faces the challenge of fast energy variation by degrading, in competition with synchrotrons, and extracting the beam at high magnetic field by having zero magnet gap at the edge. The S-Coils proposed by NAC for a superconducting proton cyclotron at 200 MeV, are an interesting new coil configuration. In an abstract the Belgrade group proposed 2 large superconducting cyclotrons, 4 m diameter, without return yokes, for heavy ion acceleration, ISOL or acceleration/deceleration. Unfortunately this group did not attend the Conference and the paper was not received.

The challenge for storage ring and synchrotron systems, Table 6, is to fully develop electron and stochastic cooling, and target systems, and provide upgraded control

Table 7. Radioactive Beam Projects Using Cyclotrons

Laboratory	Facility	Description
Operating		
TRIUMF	TISOL	ISOL facility with isotopes produced by TRIUMF cyclotron, ionized in ECR or surface ioniz. sources, used for physics expts. R&D to support proposed ISAC post accelerator and ISL facilities described below.
Louvain, Belgium	K30 plus Cyclone	ISOL primary beam with 500 μA p K30 cyclotron. ECR ionization and accel. with K130 Cyclone. $^{13}N^{1,2+}$, $^{19}Ne^{2,3+}$ to .6 MeV/u, up to 50 ppA. New post accel. K33 cyclotron funded.
GANIL	C02, SSC1, SSC2	Fragments produced by C02 + SSC1 are accel. in SSC2, identified and mass measured by SSC2 to $5x10^{-6}$. Also LISE-3 and SPEG spectrometers.
RIKEN, Japan	K540 ring	Fragmentation beams up to 100 MeV/u. "RIPS" spectrometer to separate fragments. Energies down to 5 MeV/u with degrader.
MSU, NSCL	K1200 cyclotron	Fragmentation products separated by A1200 spectrometer for delivery to experimental area. Superconducting solenoid under construction for <50 MeV/u.
Under Construction		
Oak Ridge	OREB	ISOL facility using K100 ORIC cyclotron for production, negative ion source, 25 MV tandem for accel. Ion masses <80, >5 MeV/u, <10 pnA.
INS, Japan	ISOL facility	Primary beam from present K68 cyclotron: protons at 45 MeV. High resolution separator with m/Δm=5000. R&D for Japanese Hadron Project (JHP).
Osaka	K400 cyclotron	Fragment separation by secondary channel with degrader.
Dubna	U400 plus U400M	Fragmentation of all mass beams at 100-20 MeV/u. Analyzer "COMBAS". Later will use storage rings K4 and K10.
Proposed or under Study		
TRIUMF	ISAC	ISOL facility using TRIUMF or KAON beam, high-resolution separator, RFQ plus drift tube linac post-accel. to give 1.5 MeV/u for A<60.
ISL, North America	ISOL facility	Will produce all masses, with energies up to 10 MeV/u at $<10^{12}$ p/s. Primary accelerator for 100-200 μA light ions at 500-1000 MeV can be a cyclotron.
GANIL	ISOL facility	Primary beam of 100 MeV/u , 10 pμA for A up to 40, from present K400 coupled cyclotrons. Thick target, ECR source. Option for secondary accel. is a compact plus a ring cyclotron, similar to present GANIL designs.
PSI, Switzerland	ISOL facility	590 MeV p at up to 1 mA from ring, ECR source, existing K120 cyclotron secondary accel.
Moscow	ISOL facility	Linac primary accel. Coupled cyclotrons: K208 injecting K600 ring considered for secondary accel. to give >5 MeV/u for A<150.
Grenoble	PIAFE	Fission products, A=70-150, from ILL reactor to ECR source, charge +1 ions 450 meters at 30 kV to SARA coupled cyclotrons. Accel. to 2-20 MeV/u, $<10^{9}$ p/s.
Catania/Milan	K800 cyclotron	Fragmentation beams at 50-80 MeV/u. Also ISOL facility using cyclotron for production and 15 MV Tandem for acceleration up to 8 MeV/u.

systems so that the potential physics can be fully realized. The KAON facility has the challenge of extracting 100 μA of H^- beam and matching it to the succeeding synchrotron rings at 3 and 30 GeV.

In the radioactive beam field, Table 7, the challenge is to provide usable beams of a wide variety of radioactive species, so that interesting physics can be done with them. A start has been made by TRIUMF, Louvain, GANIL, RIKEN and MSU. New beams will be provided by Oak Ridge, INS, Osaka and Dubna, and later hopefully by ISAC at TRIUMF, ISL, GANIL, PSI, Moscow, Grenoble and Catania/Milan.

The review papers of section 2.1 pointed out some challenges also. In applications, better communication is needed between the cyclotron "builder/operator" and the "user" so that new innovative uses and funding sources can be found. The ion source challenge is to improve beam intensities with an acceptable quality. For ECR sources better understanding is needed of rf coupling, electron injection, magnetic field and frequency optimization, so that higher charge states can be produced. Technical

Table 8. Cyclotrons Shut Down Since the Berlin Conference - R.I.P.

Laboratory	Facility	Description
CERN	K600 synchro-cyclotron	600 MeV proton synchro-cyclotron. Decommissioning plan paper at Conference.
AERE, Harwell	K86 cyclotron	Heavy ion cyclotron, high beam intensities from internal source.
Groningen	K160 cyclotron	Heavy ion cyclotron. Shut down to prepare for installation of AGOR (Table 3). Will be used for shielding.
McGill	K100 synchro-cyclotron	p, d, He-3, He-4 beams.

challenges in cyclotron design and operation continue, such as producing higher magnetic fields and deflector electric fields, and improving operator controls.

3. SPECIAL AWARD

The Conference Summary speaker (DJC) announced a special award based on his experience as a member of the Program Committee in reading the abstracts submitted to the Conference. Its text is shown in Fig. 1.

4. SOCIAL EVENTS

The Conference social events included 2 receptions, 2 dinners and a choice of 5 excursions on Wednesday afternoon. The salmon barbecue was held on Monday evening at the picnic area of the impressive site of the UBC Museum of Anthropology, where guests could tour the Museum after dinner.

The Conference Dinner was held on Thursday evening at the Hotel Vancouver. The master of ceremonies was Mike Craddock, who also filled in as banquet speaker. He extended the congratulations of the cyclotron community to Henry Blosser and Bob Pollock, who had been awarded the American Physical Society Bonner Prize for contributions which included superconducting cyclotron construction and a cyclotron-injected storage ring. In his speech Craddock pointed out that his research has revealed that there are two classes of accelerators, "proper" and "improper". The proper machines are of course cyclotrons, with their rotational periodic symmetry due to their sector structure. An example of an improper machine is the synchrotron, with its frequent deviations from symmetry due to straight sections of unequal length. He didn't explain how he got involved in a synchrotron project such as KAON. He also noted that the TRIUMF group had mystically arranged the weather at the Conference, so that the occasional rain fell at times during the sessions, while on the important social occasions such as the salmon barbecue and the Wednesday excursions the weather was fine. This kind of weather control is unknown outside Super, Natural British Columbia.

5. PREDICTIONS FROM THE PAST

In Henry Blosser's talk "Future Cyclotrons" at the last session of the Conference he made some predictions about future improvements in cyclotron design. Following the historians, it is useful to look to the past for important clues about the future directions for cyclotron development. We have often heard about ancient astronauts, but seldom hear of ancient cyclotron designers. Two examples will show the importance of this field of study.

The first is taken from Athens (Greece, not Ohio). Fig. 2 shows a design found on stone at an agora near the Acropolis[1]. This early design shows a three sector magnet whose spiral sectors are remarkably similar to those of modern designs such as the Jyvaskyla cyclotron, Fig. 3, which just came into operation (Table 2). It is also similar to other modern era designs such as the LBL 88-Inch Cyclotron and the MSU/Harper Cyclotron (Table 3).

The second example, Fig. 4, is a high-spiral design by the Maori people of New Zealand[3]. It was found on one of their meeting houses. The use of 2 sectors gives high flutter near the center. Apparently they had solved the problem of the NuR = 2/2 radial resonance which has caused more cautious later designers to believe that we need at least 3 sectors. Also this design appears to operate without an rf system.

So we have much to learn from these ancient cyclotron designers, and I suggest that we include Athens and New Zealand on our list of potential locations for future cyclotron conferences.

6. ACKNOWLEDGMENTS

The author wishes to thank M. Craddock and G. Dutto for their helpful comments on this paper.

7. REFERENCES

1) Courtesy of D. Stiver, LBL, member of the Voluntary (No DOE funding) International Historical Cyclotron Task Force for the Investigation of Ancient Cyclotrons.

2) Esko Liukkonen, "The Jyvaskyla K130 Cyclotron Project", in Proc. Twelfth Int'l Conf. on Cyclotrons and their Applications (World Scientific, Singapore, 1991) pp. 40-42.
3) Courtesy of D. Clark, Chairman of the Board of the Task Force of Ref.1).

*This work was supported by the Director, Office of Energy Research, Division of Nuclear Physics of the Office of High Energy and Nuclear Physics of the U.S. Department of Energy under Contract DE- ACO3-76SF00098.



Fig. 2. Three sector design, Athens, Greece.

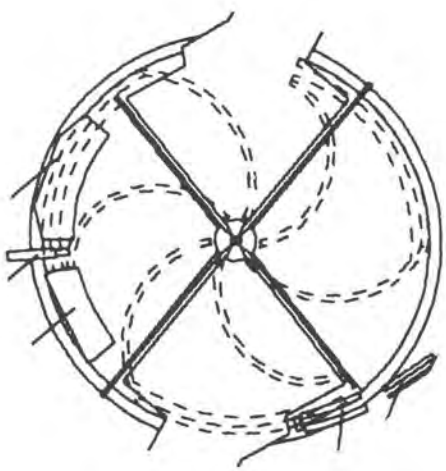


Fig. 3. Jyvaskyla K130 magnet pole[2].

FIRST TRIENNIAL AWARD

FOR

THE MOST LIVELY ABSTRACT

TO

HENRY BLOSSER

FOR

"FUTURE CYCLOTRONS"

"..IN 1972 THE AUTHOR PREDICTED A MINOR ROLE FOR SUPER-CONDUCTIVITY IN .. CYCLOTRONS. NOW 20 YEARS LATER, .. ALL .. PREDICTIVE RESOURCES WILL .. BE USED (ORDERED TRANSPARENT SPHERES, ASTRONOMICAL SYNCHRONISITIES, 3D COMPUTER CALCULATIONS, TEA LEAVES, ETC.).. "

A subcommittee will determine the nature of the award.

Fig. 1. Special award.



Fig. 4. Maori high spiral design, New Zealand.

PROPER AND IMPROPER ACCELERATORS – IN PRAISE OF CYCLOTRONS AND THEIR BUILDERS*

M.K. Craddock
Physics Department, University of British Columbia, Vancouver, B.C., V6T 1Z1
and
TRIUMF, 4004 Wesbrook Mall, Vancouver, B.C., Canada, V6T 2A3

Ladies and Gentlemen – Finding a speaker for this evening has been something of a saga. I had hoped to be able to introduce a distinguished Canadian scientist, renowned for his erudition and wit. Unfortunately, our invitee was forced to cancel and we were unable to find an appropriate replacement. Last week, therefore, we arranged some musical entertainment, but once again fate struck and the day before the conference I learned that the father of one of the duo had died, and that they would be unable to perform today, the funeral day. So the long and short of it is that you are stuck with me for the rest of the evening. At least I have the consolation of knowing from your applause for the Trio Grazioso that you enjoyed the entertainment provided earlier this evening by this group, all ex-students from the University of British Columbia School of Music.

Because of our lack of control over the human element in the program, we felt it necessary to demonstrate that at least the conference organizers were in full control of inanimate factors. In this respect many delegates have noted our successful control of the weather – how the rain stopped in time for the outdoor barbecue at UBC on Monday, how it rained again during the sessions on Tuesday, and how the clouds cleared as the buses left for the Wednesday afternoon excursions. A number of people have commented on this "good luck" with the weather. Some of the the organizers were deeply offended by such lack of recognition of their tour de force in weather control, but most took it in good part, realizing that in many places such skills are totally unknown. Any fool can organize a whole week of unbroken sunshine – they do it all the time in California – but it takes real skill to arrange rain for the week of the conference when there has been a drought for several months, and then interrupt it exactly at the time of the excursions. In case any of you have to organize conferences, I can recommend it as a real crowd-pleaser – the sunshine is all the better appreciated for being uncertain until the last moment.

Well, putting aside the tribulations and triumfs of conference organization, I had to select a theme that would be popular with the listeners, and ideally even keep them awake. With an audience of the world's experts on cyclotrons, what could be more popular than speaking "In praise of cyclotrons and their builders"? Cyclotrons I will leave until a little later, when there will be time to explain how their design entitles them to be described as "proper" accelerators, as opposed to other, somewhat "improper" ones. But first, ever courting popularity, praise for the builders! And in praising the explorers of physics, it may be helpful – or at least topical – to refer to some famous explorers of the globe. This year it is maritime explorers who have been particularly in the public eye. In his welcoming remarks on Monday, Professor Vogt pointed out that 1992 is not only the 500th anniversary of Columbus' exploration of the Caribbean, but the 200th anniversary of Vancouver's exploration of the Pacific Northwest. Captain George Vancouver was an Englishman with Dutch ancestors who had sailed as a boy with Captain Cook. In describing this, the last inhabitable coastline in the world to be discovered and settled by Europeans, Vancouver wrote[1]:

> "To describe the beauties of this region, will on some future occasion, be a very grateful task to the pen of a skilful panegyrist. The serenity of the climate, the innumerable pleasing landscapes, and the abundant fertility that unassisted nature puts forth, require only to be enriched by the industry of man with villages, mansions, cottages, and other buildings, to render it the most lovely country that can be imagined; whilst the labour of the inhabitants would be amply rewarded, in the bounties which nature seems ready to bestow on cultivation."

I am sure that those of you who have an opportunity to explore this region following the conference will agree that Vancouver's description is still recognizable and his prophecies largely fulfilled – even to such sophisticated bounties as cyclotrons.

You will understand then that George Vancouver is to B.C. what Christopher Columbus is to the USA. The

*Based on remarks made following the Conference dinner in the Hotel Vancouver

name of British Columbia is of course in itself a celebration of Columbus. And mentioning Columbus gives me an opportunity to come back to cyclotron builders by way of the memorable analogy made by Weisskopf[2]:

> "Instrument construction was and will remain for some time the most important precondition to further progress of our knowledge of the basic structure of matter. High Energy Physics today is an exploratory science; it is still far from its explanatory stage. It may appear surprising to an outside observer that, in spite of this, theorists dominate the field and the names of the instrument builders do not appear on the title pages of the publications of discoveries.
> The situation has been compared to Columbus' trip to the West in 1492: The accelerator physicists are the ship-builders and navigators who made possible the crossing of oceans; the experimental physicists are the people who stepped upon the new territories exploring the plains, mountains, streams, and the strange people and animals; the theorists are those who remained in Madrid and predicted that Columbus would land in India."

While we "ship-builders and navigators" all bask in the praise of accelerator builders as a group, this is also an appropriate occasion for us to praise three individuals among us tonight. I mean of course Reg Richardson, Henry Blosser and Bob Pollock, who have recently been awarded major prizes by the American Physical Society. It is surely a tribute to the degree of genius within this small cyclotron community that recognition has come so generously from the wider physics world. You will notice that I have inveigled all three of the prize winners to sit with me this evening – I am still hoping that some of their genius will brush off!

Starting with the most senior, everyone at TRIUMF was delighted last year to learn that Professor J. Reginald Richardson, (Figure 1) ex-director of the UCLA and TRIUMF cyclotrons, had been awarded the 1991 Robert R. Wilson prize, jointly established by the APS Divisions of Particles & Fields and Physics of Beams "to recognize and encourage outstanding achievement in the physics of particle accelerators". The citation reads:

> "For his original contributions to the development of cyclotrons. These include the first experimental demonstration of phase stability, the first synchrocyclotron, and the first sector-focused cyclotron. This work is the basis of numerous cyclotrons that have had and continue to have major impact on nuclear physics, solid state physics, chemistry and medicine."

It's a particular pleasure to be able to recognize this award in Vancouver, which is essentially Reg's home town. Although born in Edmonton, across the mountains, his family soon moved to Vancouver and he spent



Figure 1: Reg Richardson

his boyhood years just a few blocks from here, close to Stanley Park. Then at the age of 12 he moved with his family to California, later enrolling at Berkeley and, already showing that talent for recognizing the best scientific opportunities available, acquiring Ernest Lawrence as his Ph.D. supervisor. The rest, as they say, is history. The phase-stability principle itself should have been enough for one man. After all, all high-energy accelerators, up to and beyond the SSC, depend on it for their operation, and without it virtually nothing of modern particle physics would have been discovered.

But Reg's achievements have not only been demonstrations of principle. The major facilities he has built have themselves led to the opening up of new fields in science and medicine. Chief among these facilities of course is the TRIUMF cyclotron – unfortunately only a mere shadow of its original conception as a 750 MeV meson factory for UCLA. I count myself fortunate to have been here in 1964, in time to take a significant role in selecting Reg's design for TRIUMF, and thereby to have had some hand in bringing him back permanently to his old haunts. In fact the B.C. connection was already there, in that Reg had maintained a summer home on Galiano Island, 40 km from here across the Strait of Georgia, since the 1940s. (Galiano, incidentally, was the Spanish captain whose meeting with Vancouver near UBC in June 1792 he commemorated with the local place names Spanish Banks and English Bay.) Indeed, the TRIUMF cyclotron was conceived on Galiano Island, so it seems not inappropriate that it should be built close by. But even the meson factory was not enough. Hardly had Reg retired as director but another relaxing summer on Galiano produced schemes of kaon factories. And the ink on the 30 GeV KAON proposal was hardly dry before he had schemes afoot for the addition of a superconducting ring to reach 100 GeV.

Reg, you are the dean of the cyclotron community. As you approach your 80th birthday later this year we offer our heartiest congratulations to you on the award of the Wilson Prize, and our best wishes to you and Louise

for the future. And please slow down, the rest of us can't stand the pace!

Now I turn to the joint winners of the 1992 Bonner Prize of the APS Division of Nuclear Physics, Henry Blosser and Robert Pollock. These are the second-generation cyclotron builders – the precision men and introducers of new technologies! Their citation reads:

> "For their pioneering development of innovative accelerator configurations which have allowed new levels of precision and flexibility for nuclear physics research. The room temperature and superconducting cyclotron developments and the novel beam cooling techniques have formed the basis for a new generation of facilities throughout the world which are currently providing important tools to advance our understanding of nuclear and particle properties in the medium energy regime. Their developments have also led to important advances in accelerator techniques for the neighbouring disciplines of atomic and medical physics."

Henry Blosser (Figure 2) obtained his Ph.D. from the University of Virginia and was introduced to the mysteries of the then-novel sector focusing cyclotron while subsequently working at Oak Ridge. Fired by its possibilities, he moved to Michigan State University in 1958 and there built a 56 MeV cyclotron which became a byword for precision in both construction and performance. In doing so he gathered around him a group of talented physicists and engineers, and founded what has become the leading school of cyclotron design and innovation in the USA. Henry then made the memorable mistake (at the Vancouver conference 20 years ago – perhaps it was the air?) of predicting[3]:

> "Superconductivity then seems unlikely to make a contribution to cyclotrons in the foreseeable future, primarily because there is no overriding problem which would thereby be solved such as is the case for synchrotrons and linacs."



Figure 2: Henry Blosser

However, he has since redeemed himself handsomely by constructing a whole series of cyclotrons using superconducting magnets. The first of these, the K500 heavy ion machine, was of course the first to be brought into operation anywhere – much to the honour of Henry, but to the chagrin of the Canadian team at Chalk River who had started earlier but run into funding problems during construction. This was followed by the K1200, bigger and better for heavy ion physics, and the compact "flying" cyclotron, which can be swung around the patient to alter the beam direction, now in regular use for neutron therapy at the Harper Hospital. Meanwhile, these developments had led to the dedication of the National Superconducting Cyclotron Laboratory, with Henry as its first director.

Henry, we salute you for demonstrating that cyclotrons can be precision tools, for vastly extending the capabilities of cyclotrons by introducing the economies of superconductivity, and for generating a steady stream of graduate students to maintain the health of the community. You and Mamar have all our good wishes for the future. I should also add that Henry has taught me all I know about the use of a hand bell by a conference chairman.

Bob Pollock (Figure 3) is another Canadian, a graduate of the University of Manitoba, and a member of a family prominent in the early settlement of that province. After a Ph.D. and teaching at Princeton he moved on to Indiana University and became director of IUCF, where he supervised the construction of the two ring cyclotrons and various spectrometers, and the development of a very productive laboratory for light ion physics. Perhaps it was the complete separation of the sector magnets in these rings that freed his mind from conventional cyclotrons, perhaps it was the success of the Intersecting Storage Rings at CERN and the plans for a Low Energy Antiproton Ring there; whatever the reason, he conceived the brilliant notion of building a cooling and acceleration ring as the third stage of IUCF, to produce ultra-high-quality beams and raise the proton energy to 500 MeV. He then led the design and successful construction of this ring, the progenitor of a number of storage rings built for nuclear and atomic physics. While he has become a consum-



Figure 3: Bob Pollock

mate expert in accelerator design and has plans for even bigger rings in the future, he has always maintained a strong involvement in nuclear experiments, particularly meson production near threshold, and is now busy meeting the challenges posed by performing experiments in a circulating beam.

Bob has one other talent that should not pass unmentioned and uncelebrated – he can pack more information on a viewgraph than anyone else I have been exposed to in a lifetime of lecture attendance. Most of the skills cultivated by cyclotron builders and nuclear physicists are too esoteric to be of interest to the general public – but here is one that could surely make it into the Guinness Book of Records. Writers of the Lord's Prayer on the head of a pin – beware – your fame is about to be eclipsed!

Bob, we congratulate you on this prize, which is a tribute to that deep understanding of accelerator design and flare for innovation which have given us the first ring cyclotron and first cooling ring dedicated to light ions. At TRIUMF you served long and faithfully on our Advisory Board and we hope you are now enjoying your retirement from that duty.

It is a special pleasure that two out of the three prize winners have Canadian roots. It is of course only an historical accident – the magnanimity of the Canadians in returning Detroit and its hinterland to the USA after the war of 1812 – that we do not lay claim to the third as well.

Having praised their builders, let's move on to the cyclotrons themselves – the first of the circular accelerators and the embodiment of all those principles which entitle them to be referred to as proper, as opposed to improper, accelerators. What do I mean by a "proper" accelerator? I mean one whose design is characterized by simplicity and symmetry. The beauty of circularity has been recognized from time immemorial – in the shapes and orbits of the sun and moon, in the paths of the planets, in the stone circles of Stonehenge in England and British Block in Alberta, in the dome of the Pantheon ... Early synchrotrons exhibited circular symmetry in perhaps a more perfect form, since they had no trace of the spirality inherent in cyclotrons, but modern machines have deviated sadly from the ideal. Linear accelerators also have a symmetry which entitles them to be called "proper", but what a clumsy and unimaginative symmetry that is, requiring separate radiofrequency fields and equipment to be provided for every step of acceleration! The linac is straight, both literally and colloquially, but not smart.

The cyclotron is not only properly symmetric, but by making repetitive use of the same accelerating system, achieves compactness and elegance of design as well. The construction of a classical cyclotron illustrates a classic response to a major design challenge, incorporating several disparate elements in a compact assembly, somewhat in analogy to nature's elegant solution to the design of fruit in spherical layers working out from the seed to the skin. Thus around the particle beam we build the accelerating structure, around that the vacuum chamber, and around that, finally, the magnet.

I have to admit, of course, that people have not been content with this classic simplicity. They have played around, complicating the design in the name of "improvements". They have allowed the radiofrequency to vary, forcing the cyclotron to operate in fits and starts as a so-called "synchrocyclotron", they have broken the magnet into separate sectors, forcing the ions to orbit in a drunken way around Lawrence's beautiful circles, they have distorted the magnet sectors from straight radial edges to contorted spirals, they have even cut out the centre – the heart – to form a "ring" cyclotron, all with the excuse of attaining higher energies. And I'm sorry to say that some of our most respected colleagues, even including Reg Richardson here, have been involved in this mad race for progress. But through it all some symmetry has been retained, maybe three-fold or six-fold rather than perfect axial symmetry, but enough for the cyclotron to retain its claim to dignity as a proper accelerator.

Freedoms beyond these, however, amount to nothing more nor less than license. The rot began with the synchrotron, once the accelerator with the most perfect circular symmetry, with the addition of short straight sections to accommodate accelerating cavities and beam transfer equipment, and by the division of the magnet into alternate focusing and defocusing sections; but at least these changes retained some higher-order axial symmetry. The process accelerated, however, with the adoption of "separated function" designs, in which focusing and bending magnets were completely separated, and with the advent of storage rings, requiring long straight sections for particle detectors, cooling systems, Siberian snakes, and so on.

Nowadays we seem to have arrived at a free-form school of design, in which an accelerator is nothing more than a beam transport line bent into a loop. In these designs it seems possible to arrange the elements almost randomly, simply for convenience, rather than in obedience to some higher principle. An early example of this dangerous trend, I'm sad to say, was perpetrated by one of our prize winners, Bob Pollock. If his cooler ring for IUCF had retained that hexagonal symmetry with which it was apparently originally conceived, there would be no question but that it should be counted as proper; but with the sides lengthened here and shortened there to meet merely practical needs, it teeters on the edge of impropriety. Then there is the Main Injector proposed at Fermilab, in which almost no signs of symmetry remain; it is true that the two long straights are parallel, but they are displaced lengthwise as if the two sides of the ring had suffered an earthquake shear. This is certainly an improper accelerator.

These tendencies are usually justified as making accelerators "easier" to design and build. Here we see a parallel with modern society, in which easiness is counted

as a virtue – surely an unmistakable sign of a decadent civilization. The freedom that takes away constraints also takes away the challenges. When the dipoles and quadrupoles and correction magnets and rf cavities and vacuum chambers and injection systems and extraction systems can all be designed independently of each other, where are the challenges needed to transform our talented young graduates into the master craftsmen of the future? Considering this transition from formalism to freedom in accelerator design, it may be instructive to draw some parallels with the transition from classic to modern art. In music we have come from Bach to Boulez, in drama from Sophocles to Samuel Beckett, in painting from Piero de la Francesca to Pablo Picasso – analogies demonstrating that uncontrolled freedom simply leads to anarchy.

In the case of cyclotrons we have not yet reached this terminal stage, and there is even some indication of a return to basics. Dangerous flights of imagination still occasionally occur, however, even among our most sage colleagues. For instance, I was shocked earlier this week to see a poster by David Clark, in which one of the cyclotron designs considered had four sectors at the centre, dividing into eight in the outer region. I am glad to report that this was rejected in favour of a simple 8-sector spiral.

The return to basics that I mentioned and commended above has been brought about largely by the demand for superconducting cyclotrons for nuclear physics, for neutron therapy, and for radioisotope production. This is a perfect demonstration of how challenges are necessary to bring out the best in people. The advantages of using superconducting magnets are normally said to be economies of size and of dollars, but this misses the whole point. Finance is always a secondary consideration for the true craftsman. The really important factor here is the miniaturization, which sets major challenges not only for the mechanical engineering but for the voltage-holding on both rf cavities and electrostatic deflectors. So Henry Blosser at MSU, and Harvey Schneider, Clarence Hoffmann and their colleagues at Chalk River, didn't go superconducting because it was cheaper, but because it was more difficult! Here we can draw a parallel with the great sculptors of the Renaissance, who delighted in demonstrating their virtuosity by casting bronzes of greater and greater complexity, in the hope that their rivals couldn't match them. And so it is with master cyclotron builders. Great men can only demonstrate their greatness by overcoming great challenges – and this they have done best of all when working within the constraints imposed on cyclotrons as "proper" accelerators.

I will close by wishing you all success in meeting the challenges of designing and building new and better cyclotrons – provided of course they remain "proper" accelerators. And as this is the 20th anniversary of the 1972 conference held in Vancouver, we hope that if you follow this advice we can look forward to cyclotrons flourishing for another twenty years and the 2012 conference returning to Vancouver again. Perhaps we should regard this hotel as a particularly appropriate venue. In the lobby downstairs you will notice that the chandeliers are supported from mouldings clearly representing the 8 sectors of very proper sector-focused cyclotrons (Figure 4).

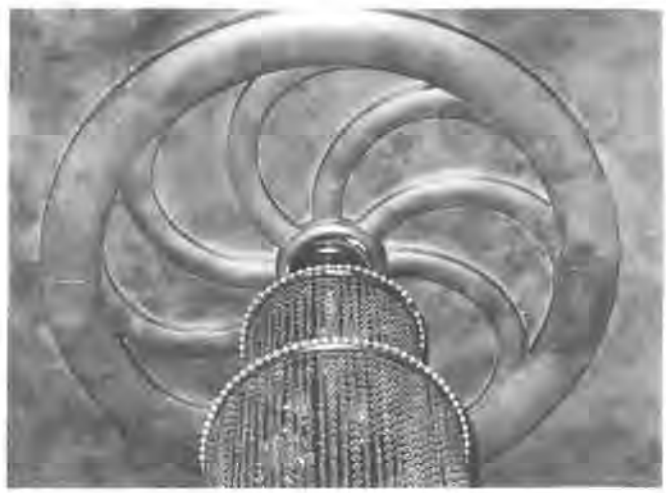


Figure 4: Ceiling moulding – Hotel Vancouver (Photo credit – Tallulah)

REFERENCES

1. G. Vancouver, "Voyage of Discovery to the North Pacific Ocean and Around the World" (London, 1798) Vol. I, 259.
2. V. Weisskopf, IEEE Trans. Nucl. Sci. **NS 22**, 1948 (1975).
3. H. Blosser, **Cyclotrons'72**, (ed. J.J. Burgerjon, A. Strathdee), AIP Conf Proc. **9**, 24 (1972).

Keyword Index

A

acceleration
accumulation
AGOR
ALICE

B

background
beam-losses
beam-transport
betatron
BNL
booster
bunching

C

cathode
cavity
CERN
closed-orbit
controls
COSY
coupling
cryogenics
cyclotron

D

diagnostics
dipole

E

ECR
ECRIS
electromagnetic-fields
electron
emittance
extraction

F

factory
feedback
focusing

H

heavy-ion
high-voltage

I

impedance
injection
insertion
instrumentation
interlocks
ion
ion-source
ISAC
ISOL
isotope-production

J

JAERI

K

kaon
kicker
klystron

L

laser
lattice
light-ion
linac
luminosity

M

MCP
micro-particles
microtron
monitoring
multipole

N

neutron

O

octupole
optical-matching
optics

P

permanent-magnet
photon
pick-up
plasma
polarization
positron
power-supply
proton

Q

quadrupole

R

radiation
radioactivity
resonance
rf-amplifier
rfq

S

scattering
septum
sextupole
shielding
simulation
site
solenoid
space-charge
status
storage-ring
survey
synchro-cyclotron
synchrotron

T

tandem-accelerator
target
TRIUMF

V

vacuum